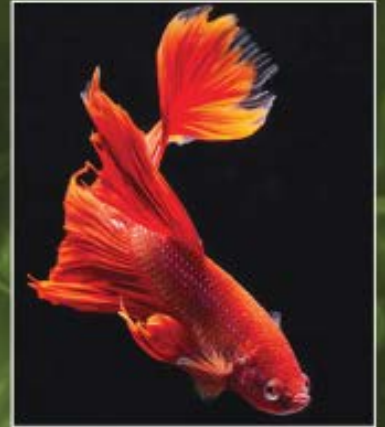# Animal Models for the Study of Human Disease

Edited by **P. Michael Conn**

ANIMAL MODELS FOR THE STUDY OF HUMAN DISEASE

Second Edition

Dedicated to the memory of P. Michael Conn
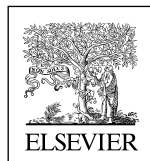
ANIMAL MODELS FOR THE STUDY OF HUMAN DISEASE

Second Edition

Edited by

P. MICHAEL CONN
Senior Vice President for Research
Associate Provost and Professor of Internal Medicine and Cell Biology-Biochemistry
Texas Tech University Health Sciences Center, Lubbock, TX, United States

Notices
Knowledge and best practice in this field are constantly changing. As new research and experience broaden our understanding, changes in research methods, professional practices, or medical treatment may become necessary.

Practitioners and researchers must always rely on their own experience and knowledge in evaluating and using any information, methods, compounds, or experiments described herein. In using such information or methods they should be mindful of their own safety and the safety of others, including parties for whom they have a professional responsibility.

To the fullest extent of the law, neither the Publisher nor the authors, contributors, or editors, assume any liability for any injury and/or damage to persons or property as a matter of products liability, negligence or otherwise, or from any use or operation of any methods, products, instructions, or ideas contained in the material herein.

For information on all Academic Press publications visit our website at
https://www.elsevier.com/books-and-journals

Working together
to grow libraries in
developing countries

www.elsevier.com • www.bookaid.org

Dedication

I began working for Dr. P. Michael Conn in his research laboratory in September 1984, and had continued to work with him until his untimely passing in November 2016. Dr. Conn was a superb mentor, friend, and human being. He mentored numerous postdoctoral fellows, graduate students, and staff throughout his research career, and, in turn, many of the fellows and students have successful careers and hold Dr. Conn in very high regard.

Dr. Conn was known for his research involving the mechanisms of action of gonadotropin-releasing hormone in the pituitary, and therapeutic approaches that restore misfolded protein functioning. He authored and coauthored over 350 publications in his field and wrote and edited over 200 books, including texts in neurosciences, molecular biology, and endocrinology. He was recognized with a MERIT Award of the National Institutes of Health; the J.J. Abel Award of the American Society for Pharmacology and Experimental Therapeutics; the Weitzman, Oppenheimer, and Ingbar Awards of the Endocrine Society; the Miguel Aleman Prize; Mexico's National Science Medal; and the Stevenson Award of Canada. He was the recipient of the Oregon State Award for Discovery, the Media Award of the American College of Neuropsychopharmacology, and was named distinguished Alumnus of Baylor College of Medicine in 2012. Dr. Conn served as the editor of numerous professional journals and book series: *Endocrinology*, *Journal of Clinical Endocrinology and Metabolism*, *Endocrine*, *Methods*, *Progress in Molecular Biology and Translational Science*, and *Contemporary Endocrinology*. He was an advocate for the value of animal research and the dangers posed by animal extremism. He was the coauthor of *The Animal Research War* (2008) and wrote many opinion editorials for the public and academic community, which appeared in *The Washington Post*, *The LA Times*, *The Wall Street Journal*, the *Des Moines Register*, and elsewhere.

I am honored that I spent 32 years learning and working with Dr. Conn, a true friend.

Dr. P. Michael Conn will be sorely missed. Rest in peace my friend!

Jody Janovick
Texas Tech University Health Sciences Center,
Lubbock, TX, United States

Page left intentionally blank

Contents

Part A
ETHICS, RESOURCES, AND APPROACHES

Part B
VISION

Part E
SKIN

Part F
URINARY TRACT, KIDNEY, AND BOWEL

Part J
EARLY LIFE

Part K
VIRAL DISEASE

33. Animal Models of Human Viral Diseases

SARA I. RUIZ, ELIZABETH E. ZUMBRUN, AYSEGUL NALCA

Part L
CANCER

34. Modeling Cancer Using CRISPR-Cas9 Technology

SANDRA RODRIGUEZ-PERALES, MARTA MARTINEZ-LAGE, RAUL TORRES-RUIZ

35. Modeling Breast Cancer in Animals— Considerations for Prevention and Treatment Studies

JOELLEN WELSH

Part M
SCLEROSIS

36. Animal Models of Systemic Sclerosis

TOSHIYUKI YAMAMOTO

Part N
PSYCHIATRIC AND NEUROLOGICAL DISEASE

Page left intentionally blank

List of Contributors

Bernhard Aigner   Molecular Animal Breeding and Biotechnology; Center for Innovative Medical Models (CiMM), Ludwig-Maximilian University, Munich, Germany

W. Ted Allison   University of Alberta, Edmonton, AB, Canada

Roberto Andreatini   Federal University of Paraná, Centro Politécnico, Curitiba, PR, Brazil

Marta Antonelli   Institute of Cellular Biology and Neuroscience "Prof Dr. Eduardo de Robertis", Buenos Aires University, Buenos Aires, Argentina

Saskia S. Arndt   Utrecht University, Utrecht, The Netherlands

Amazon Austin   King's College London, London, United Kingdom

Cristin Brand   Institute of Reproductive and Regenerative Biology, Centre of Reproductive Medicine and Andrology, University Clinics, Münster, Germany

Joanna Bukowska   Institute of Animal Reproduction and Food Research, Polish Academy of Sciences, Olsztyn, Poland

Andrew C. Caprariello   University of Calgary, Hotchkiss Brain Institute, Canada

Rachel E. Carlisle   McMaster University and St. Joseph's Healthcare Hamilton, Hamilton, ON, Canada

Lucas M. Chaible   Meyerhofstr, Heidelberg, Germany

Li Chen   Merck Research Laboratories, Merck & Co., Inc., West Point, PA, United States

Mengqi Chen   Centre of Excellence for Alzheimer's Disease Research and Care, Edith Cowan University, Joondalup, WA, Australia

Thomas Chi   University of California, San Francisco, CA, United States

Mohammed E. Choudhury   Ehime University Graduate School of Medicine, Shitsukawa, Shitsukawa, Toon-shi, Ehime, Japan

Iain J. Clarke   Monash Biomedical Discovery Institute, Monash University, Clayton, VIC, Australia

Kristine Coleman   Oregon National Primate Research Center, Beaverton, OR, United States

Gabriela D. Colpo   University of Texas Health Science Center at Houston, Houston, TX, United States

Oliver S. Damm   Institute of Reproductive and Regenerative Biology, Centre of Reproductive Medicine and Andrology, University Clinics, Münster, Germany

Catherine M. Davis   Johns Hopkins University School of Medicine, Baltimore, MD, United States

Erica E. Davis   Center for Human Disease Modeling, Duke University Medical Center, Durham, NC, United States

Luis de Lecea   Stanford University, Stanford, CA, United States

Aline S. de Miranda   Biological Institute, Federal University of Minas Gerais (UFMG), Belo Horizonte, MG, Brazil

Diogo B. de Souza   State University of Rio de Janeiro, Rio de Janeiro, RJ, Brazil

Jeffrey G. Dickhout   McMaster University and St. Joseph's Healthcare Hamilton, Hamilton, ON, Canada

Paul J. Donaldson   NZ National Eye Centre; University of Auckland, Auckland, New Zealand

Geoffrey A. Donnan   Florey Neuroscience Institutes, Melbourne Brain Centre, University of Melbourne, Heidelberg, VIC, Australia

Yuko Emoto   Kansai Medical University, Hirakata, Osaka, Japan

David Feifel   University of California, San Diego, La Jolla, CA, United States

Marcus A. Finzi Corat   University of Campinas, Campinas, São Paulo, Brazil

Martin G. Frasch   University of Washington, Seattle, WA, United States

Ryutaro Fukumura   RIKEN BioResource Center, Tsukuba, Ibaraki, Japan

Toshio Fukusato   Teikyo University School of Medicine, Tokyo, Japan

John-Paul Fuller-Jackson   Monash Biomedical Discovery Institute, Monash University, Clayton, VIC, Australia

Sharyl Fyffe-Maricich   University of Pittsburgh, Rangos Research Center, Pittsburgh, PA, United States

Barbara Gawronska-Kozak   Institute of Animal Reproduction and Food Research, Polish Academy of Sciences, Olsztyn, Poland

Godfrey S. Getz   Ben May Institute for Cancer Biology, University of Chicago, Chicago, IL, United States

Yoichi Gondo   RIKEN BioResource Center, Tsukuba, Ibaraki, Japan

Belinda A. Henry   Monash Biomedical Discovery Institute, Monash University, Clayton, VIC, Australia

David W. Howells   Florey Neuroscience Institutes, Melbourne Brain Centre, University of Melbourne, Heidelberg, VIC; University of Tasmania, Hobart, TAS, Australia

Sumit Jamwal   I.S.F College of Pharmacy, Moga, Punjab, India

Jiro Kasahara   Institute of Biomedical Sciences, Graduate School of Pharmaceutical Sciences, Tokushima University, Shoumachi, Tokushima, Japan

Nicholas Katsanis   Center for Human Disease Modeling, Duke University Medical Center, Durham, NC, United States

Matthew W. Kemp   The University of Western Australia, Perth, Australia; Tohoku University Hospital, Sendai, Japan

Barbara Kessler   Molecular Animal Breeding and Biotechnology; Center for Innovative Medical Models (CiMM), Ludwig-Maximilian University, Munich, Germany

Imran Khan   Curtin Health Innovation Research Institute—Biosciences, Curtin University, Bentley; The University of Western Australia, Crawley; Hollywood Medical Centre, Nedlands, WA, Australia

Aileen King   King's College London, London, United Kingdom

Denise Kinoshita   Ibirapuera University, Interlagos, São Paulo, Brazil

Nikolai Klymiuk   Molecular Animal Breeding and Biotechnology; Center for Innovative Medical Models (CiMM), Ludwig-Maximilian University, Munich, Germany

Ryuta Koyama   Graduate School of Pharmaceutical Sciences, The University of Tokyo, Tokyo, Japan

Doris Kretzschmar   Oregon Institute of Occupational Health Sciences, Oregon Health & Sciences University, Portland, OR, United States

Puneet Kumar   I.S.F College of Pharmacy, Moga, Punjab, India

Jitka Kuncova   Biomedical Center, Charles University, Pilsen, Czech Republic

Maki Kuro   Kansai Medical University, Hirakata, Osaka, Japan

Mayuko Kurome   Molecular Animal Breeding and Biotechnology; Center for Innovative Medical Models (CiMM), Ludwig-Maximilian University, Munich, Germany

Michael Lardelli   University of Adelaide, Adelaide, SA, Australia

Heather A. Lawson   Washington University School of Medicine, St. Louis, MO, United States

Lars Lewejohann   University of Münster, Münster, Germany

Julie C. Lim   NZ National Eye Centre; University of Auckland, Auckland, New Zealand

David M. Lyons   Stanford University, Stanford, CA, United States

Malcolm R. Macleod   University of Edinburgh, Edinburgh, United Kingdom

Shigeru Makino   RIKEN BioResource Center, Tsukuba, Ibaraki, Japan

Marta Martinez-Lage   Spanish National Cancer Research Centre—CNIO, Madrid, Spain

Renita M. Martis   NZ National Eye Centre; University of Auckland, Auckland, New Zealand

Ellen Meijer   Utrecht University, Utrecht, The Netherlands

Gerlinde A.S. Metz   Canadian Centre for Behavioural Neuroscience, University of Lethbridge, Lethbridge, Alberta, Canada

Robert H. Miller   George Washington University, Washington, DC, United States

Yuichiro Miura   The University of Western Australia, Perth, Australia

Zahraa Mohammed-Ali   McMaster University and St. Joseph's Healthcare Hamilton, Hamilton, ON, Canada

Gabrielle C. Musk   Animal Care Services, The University of Western Australia, Perth, Australia

Samera Nademi   McMaster University and St. Joseph's Healthcare Hamilton, Hamilton, ON, Canada

Aysegul Nalca   Center for Aerobiological Sciences, United States Army Institute of Infectious Diseases (USAMRIID), Fort Detrick, Frederick, MD, United States

Morgan Newman   University of Adelaide, Adelaide, SA, Australia

Yu Nie   King's College London, London, United Kingdom

Noriko Nishikawa   Ehime University Graduate School of Medicine, Shitsukawa, Shitsukawa, Toon-shi, Ehime, Japan

Masahiro Nomoto   Ehime University Graduate School of Medicine, Shitsukawa, Shitsukawa, Toon-shi, Ehime, Japan

Rebecca E. Nordquist   Brain Center Rudolf Magnus; Utrecht University, Utrecht, The Netherlands

Victoria E. O'Collins   Florey Neuroscience Institutes, Melbourne Brain Centre, University of Melbourne, Heidelberg, VIC, Australia

Masatoshi Ogawa   Institute of Biomedical Sciences, Graduate School of Pharmaceutical Sciences, Tokushima University, Shoumachi, Tokushima, Japan

Marco A. Pereira-Sampaio   State University of Rio de Janeiro, Rio de Janeiro; Fluminense Federal University, Niteroi, RJ, Brazil

Jean-Paul Praud   Université de Sherbrooke, Sherbrooke, QC, Canada

João Quevedo   University of Southern Santa Catarina (UNESC), Criciúma, Santa Catarina, Brazil; Center for Experimental Models in Psychiatry, The University of Texas Medical School at Houston, Houston, TX, United States

Catherine A. Reardon   Ben May Institute for Cancer Biology, University of Chicago, Chicago, IL, United States

Christopher P. Regan   Merck Research Laboratories, Merck & Co., Inc., West Point, PA, United States

Simone Renner   Molecular Animal Breeding and Biotechnology; Center for Innovative Medical Models (CiMM), Ludwig-Maximilian University, Munich, Germany

Fabiola M. Ribeiro   Institute of Biological Sciences, Federal University of Minas Gerais, (UFMG), Belo Horizonte, MG, Brazil

Natalia P. Rocha   University of Texas Health Science Center at Houston, Houston, TX, United States

Sandra Rodriguez-Perales   Spanish National Cancer Research Centre—CNIO, Madrid, Spain

Sara I. Ruiz   Center for Aerobiological Sciences, United States Army Institute of Infectious Diseases (USAMRIID), Fort Detrick, Frederick, MD, United States

Masatoshi Saito The University of Western Australia, Perth, Australia; Tohoku University Hospital, Sendai, Japan

Francisco J.B. Sampaio State University of Rio de Janeiro, Rio de Janeiro, RJ, Brazil

Steven J. Schapiro The University of Texas MD Anderson Cancer Center, TX, United States; The University of Copenhagen, København, Denmark

Alan F. Schatzberg Stanford University, Stanford, CA, United States

Jay Schulkin University of Washington, Seattle, WA, United States

Angela L. Shamchuk University of Alberta, Edmonton, AB, Canada

Richard P. Shannon University of Virginia, Charlottesville, VA, United States

You-Tang Shen University of Pennsylvania, Philadelphia, PA, United States

Paul D. Shilling University of California, San Diego, La Jolla, CA, United States

Milan Stengl Biomedical Center, Charles University, Pilsen, Czech Republic

Marshall L. Stoller University of California, San Francisco, CA, United States

Stephen R. Stürzenbaum King's College London, London, United Kingdom

Jitka Sviglerova Biomedical Center, Charles University, Pilsen, Czech Republic

Kazumi Taguchi University of California, San Francisco, CA, United States; Nagoya City University Graduate School of Medical Sciences, Nagoya, Japan

Yoshihisa Takahashi Teikyo University School of Medicine, Tokyo, Japan

Akie Tanabe Institute of Biomedical Sciences, Graduate School of Pharmaceutical Sciences, Tokushima University, Shoumachi, Tokushima, Japan

Junya Tanaka Ehime University Graduate School of Medicine, Shitsukawa, Shitsukawa, Toon-shi, Ehime, Japan

Jerrold Tannenbaum University of California, Davis, Davis, CA, United States

Antônio L. Teixeira University of Texas Health Science Center at Houston, Houston, TX, United States

Jeffrey M. Testani Yale University, New Haven, CT, United States

Keith B. Tierney University of Alberta, Edmonton, AB, Canada

Raul Torres-Ruiz Spanish National Cancer Research Centre—CNIO, Madrid, Spain

Airo Tsubura Kansai Medical University, Hirakata, Osaka, Japan

Ryosuke Tsuji Institute of Biomedical Sciences, Graduate School of Pharmaceutical Sciences, Tokushima University, Shoumachi, Tokushima, Japan

David T. Tzou University of California, San Francisco, CA, United States

Haruo Usuda The University of Western Australia, Perth, Australia; Tohoku University Hospital, Sendai, Japan

Samira S. Valvassori University of Southern Santa Catarina (UNESC), Criciúma, Santa Catarina, Brazil

Franz J. van der Staay Brain Center Rudolf Magnus; Utrecht University, Utrecht, The Netherlands

Roger B. Varela University of Southern Santa Catarina (UNESC), Criciúma, Santa Catarina, Brazil

Giuseppe Verdile Curtin Health Innovation Research Institute—Biosciences, Curtin University, Bentley; The University of Western Australia, Crawley; Hollywood Medical Centre, Nedlands, WA, Australia

Irene Vorontsova University of California, Irvine, Irvine, CA, United States

Jessica P. Wayhart Washington University School of Medicine, St. Louis, MO, United States

James L. Weed Comparative Medicine Branch, National Center for Emerging and Zoonotic Infectious Diseases, Centers for Disease Control and Prevention, Atlanta, GA, United States

JoEllen Welsh Cancer Research Center, University at Albany, Albany, NY, United States

Steffi Werler Institute of Reproductive and Regenerative Biology, Centre of Reproductive Medicine and Andrology, University Clinics, Münster, Germany

Joachim Wistuba Institute of Reproductive and Regenerative Biology, Centre of Reproductive Medicine and Andrology, University Clinics, Münster, Germany

Eckhard Wolf Molecular Animal Breeding and Biotechnology; Center for Innovative Medical Models (CiMM); Gene Center, Ludwig-Maximilian University, Munich, Germany

Annegret Wünsch Molecular Animal Breeding and Biotechnology; Center for Innovative Medical Models (CiMM), Ludwig-Maximilian University, Munich, Germany

Toshiyuki Yamamoto Fukushima Medical University, Fukushima, Japan

Hironori Yokoyama Institute of Biomedical Sciences, Graduate School of Pharmaceutical Sciences, Tokushima University, Shoumachi, Tokushima, Japan

Katsuhiko Yoshizawa Kansai Medical University, Hirakata, Osaka; Mukogawa Women's University, Nishinomiya, Hyogo, Japan

Maria L. Zaidan Dagli School of Veterinary Medicine and Animal Science, University of São Paulo, São Paulo, Brazil

Jennifer Y. Zhang Duke University Medical Center, Durham, NC, United States

Yu Zhou Institute of Biomedical Sciences, Graduate School of Pharmaceutical Sciences, Tokushima University, Shoumachi, Tokushima, Japan

Elizabeth E. Zumbrun United States Army Institute of Infectious Diseases (USAMRIID), Fort Detrick, Frederick, MD, United States

Page left intentionally blank

Preface

The key to use animal models is to select ones that have similarities to human tissues or disease states. Some models have the advantage that the reproductive, mitotic, development, or aging cycles are more rapid compared with those in humans, facilitating study; others are utilized because individual proteins may be studied in an advantageous way and have human homologs. Other organisms are facile to grow in laboratory settings, lend themselves to convenient analyses or have defined properties that are important.

The collection of systems represented in this volume is an effort to reflect the diversity and utility of models that are used to study human disease. That utility is based on the consideration that observations made in particular organisms provide insight into the workings of other, more complex systems. Even the cell cycle in the simple yeast cell has similarities to that in humans and regulation with similar proteins occurs.

We have included sections on ethics and animal care, and the ethics of research; both are important in our view.

Some models will have been omitted due to page limitations and we have encouraged the authors to use tables and figures to make comparisons of models so that observations not available in primary publications can become useful to the reader.

We thank the authors for the timely submission of chapters so that this volume could be published while it is still fresh and to the staff at Academic Press for shepherding the process of publication.

P. Michael Conn
Lubbock, TX, United States

Page left intentionally blank

ETHICS, RESOURCES, AND APPROACHES

Page left intentionally blank

1

Ethics in Biomedical Animal Research: The Key Role of the Investigator[a]

Jerrold Tannenbaum

University of California Davis, Davis, CA, United States

[a]Some content in this chapter has been reproduced from Tannenbaum, J., 2017. Ethics in the Use of Animal Models of Seizures and Epilepsy. In: Pitkänen, A., et al. (Eds). Models of Seizures and Epilepsy, Chapter 5, pp. 47-68.

1 NATURE AND SCOPE OF THE CHAPTER

This chapter presents an overview and explanation of ethical principles that are of crucial importance in the use of animal models for the study of human disease. The chapter is intended primarily for, and is written from the perspective of, scientists who conduct biomedical animal research. Like the other chapters in this volume, the discussion of animal research ethics presented here focuses on matters that are directly relevant to the design and implementation, by investigators, of animal research projects.

The chapter begins with a consideration of the nature of biomedical animal research ethics. The chapter reviews the reasons investigators should engage in ethical assessment of their work, and explains why they are uniquely qualified to do so. The discussion presents a number of fundamental principles of biomedical animal research ethics, and offers guidelines for putting these principles into practice. The chapter then highlights several ethical issues regarding which members of the biomedical research community have exhibited some lack of clarity or disagreement. The discussion concludes with recommendations for participation by investigators in ethical discussion of their work, and of biomedical animal research generally.

The chapter does not provide a detailed description of ethical theories that have been applied to biomedical animal research by academic philosophers or legal theorists. Nor does the chapter summarize the large (and growing) scholarly literature in animal research ethics. I suggest below that animal researchers become familiar with some of this literature. However, attempting to present comprehensive descriptions of ethical theories or the animal research ethics literature would preclude a discussion that is useful to investigators. Aside from the fact that many different arguments and conclusions have been offered by different thinkers, much of the animal research ethics literature focuses on a question that has *already* been answered by scientists who conduct biomedical animal research, and by society generally. As stated by one philosophical discussion, "at the heart of the wide-ranging and seemingly unending controversy over the use of animals in biomedical science, whether in basic or applied research, toxicity testing, drug production, or education, is one burning question: Are we humans ethically *justified* in such a use of animals, in general and in particular cases?" (Donnelly and Nolan, 1990, p. 8) Clearly, there would be no need for this chapter, or more importantly for biomedical animal research ethics, if there were no significant ethical issues relating to the use of animals in biomedical research. However, it is simply a fact that among the most fundamental ethical tenets of contemporary society is not just that humans *are* justified in using animals to understand and combat human disease, but that we are often ethically *obligated* to do so.

As used in the chapter, the term "investigator" refers to principal and coprincipal investigators, and also includes scientific colleagues who participate significantly in formulating the goals and design of an animal research project. The central theme of the chapter is that investigators—not animal care and use committees, attending veterinarians, or government agencies—play the primary role in ensuring the ethical conduct of biomedical animal research.

2 THE SUBJECT MATTER OF BIOMEDICAL ANIMAL RESEARCH ETHICS

Biomedical animal research ethics has three essential features in addition to its concern with the use of animals in scientific research.

First, biomedical animal research ethics involves issues that pertain to whether animals employed in research are

used and treated properly from an ethical standpoint in ways that accord with human ethical obligations *to the animals*. Many important ethical questions raised by uses of animals in biomedical research are not issues of biomedical animal research ethics. For example, potential employment of the CRISPR gene editing technique to produce animals with transplantable human organs has raised questions about whether the technique itself could lead to the editing of the human germ line and to the engineering of humans with supposedly desirable characteristics (Baltimore et al., 2015; Lanphier et al., 2015), or could result in unintended organisms that might harm public health or the environment (Caplan et al., 2015). These are not questions of biomedical animal research ethics because they do not ask whether the animals in such research are being used properly, from the standpoint of the interests of the animals themselves. In contrast, it would be a matter of biomedical animal research ethics to ask whether animals produced using CRISPR will experience problematic pain or distress: during research procedures, as a result of their genetic make up, or because of how they might be bred and raised to provide human organs or tissues (Combes and Balls, 2014; Hyun et al., 2007).

Second, biomedical animal research ethics addresses questions that pertain to animals employed in research intended to address *medical* issues in humans or animals. Biomedical animal research ethics is a subset or branch of animal research ethics, which deals with ethical obligations to animals used in all kinds of scientific animal research, including, for example, use of animals to test the safety of household products, chemicals used in industrial processes, and cosmetics; research intended to understand how various species can be preserved in the wild; and agricultural experiments aimed at breeding animals that produce nutritious and palatable food. These uses of animals sometimes involve facts, ethical issues, and ethical principles that are significantly different from those that pertain to using animal models to study human disease. Biomedical animal research ethics considers research directed at improving animal health because animals are sometimes intended beneficiaries of animal research (Quimby, 1998).

Third, as generally defined, biomedical animal research ethics (like animal research ethics) relates to the use and treatment of *live* animals that are *sentient*, in the sense of being capable of experiencing unpleasant or pleasant sensations or feelings. Questions in biomedical animal research ethics can be asked regarding whether live animals should be killed. For example, some people believe that certain species (e.g., chimpanzees) should never be killed in research, and it can be asked whether it is morally wrong (and not just a waste of resources) to euthanize many more mice for their tissues than is required for a given study. These are questions in biomedical animal research ethics because they ask whether there is an ethical obligation to certain animals to allow them to live.

This chapter considers issues in biomedical animal research ethics relating to the proper treatment of animals employed in scientific research that aims at discovering methods of preventing, alleviating, or curing human disease.

3 WHY INVESTIGATORS SHOULD CARE ABOUT BIOMEDICAL ANIMAL RESEARCH ETHICS

Some investigators may be suspicious of advice (sometimes offered by nonscientists) that they should devote valuable time and energy to ethical assessment of their research. Biomedical research is science, and science deals with objectively verifiable facts and hypotheses. In contrast, ethics is a matter of value judgments, about which there can be disagreement, even when there is an agreement about the facts. For example, some people believe that it is unethical to use animals in research, even when such research results in the prevention or cure of serious disease (Regan, 2004). It is difficult enough to conduct productive scientific research, the results of which *are* subject to objective empirical verification. Leave us alone to do our experiments, some investigators might say, and let others worry about demonstrating that what we do is ethical.

3.1 Investigators are Already Committed to High Ethical Standards

One reason investigators should engage in ethical assessment of their work is that they have *already* committed themselves to high ethical standards in their use of animals. Biomedical animal research is founded on an enormously important ethical principle (which is discussed in detail later in the chapter): *It is among the most noble and imperative of human endeavors to employ scientific research to prevent, alleviate, and cure the pain, suffering, distress, fear, anxiety, disability, infirmity, and death associated with human disease.* The decision to use animals to fight disease is motivated by this high ethical ideal. Having already committed themselves to engaging in one of the most virtuous endeavors known to humankind, investigators who use animal models are logically and unavoidably committed to ethical behavior in all aspects of their work, including their use and treatment of animals.

3.2 Ethical Treatment of Animals is Required by Law

Perhaps the most immediate and direct reason investigators should want to adhere to high ethical standards is that they must follow the laws of their respective countries relating to animal research. Many of these laws

impose straightforwardly *ethical* requirements. Failure to comply with these requirements can result in disapproval of a proposed animal research project by an institutional animal care and use committee (IACUC) or in some countries a government official or licensing authority; disciplinary action, such as public censure or a fine; or in extreme cases termination of research (APHIS, 2016a; Home Office, 2014; NIH, 2015a, Part II §8.5).

3.2.1 General Commitment to Ethical Behavior

Laws in many countries assert a general commitment to ethics in the use and care of research animals. For example, the 2010 *European Directive on the Protection of Animals Used for Scientific Purposes* (*EU Directive*), which represents the official policies of the European Parliament and the Council of the European Union, states that "(a)nimals have an intrinsic value which must be respected" (European Union, 2010, Preamble para. 12). In the United States, the National Resources Council *Guide for the Care and Use of Laboratory Animals* (the *Guide*) (NRC, 2011) must be followed in all research on live vertebrates that is funded by one of the institutes or centers of the National Institutes of Health (NIH) [HREA, 1985, §289d(c)]. In a section titled "Ethics and Animal Use," the *Guide* reminds investigators that they do not have a legal right to conduct animal research. The use of animals is a *privilege* afforded by government, which it can withdraw. As the *Guide* observes, this privilege is conditioned on the use and care of research animals in accordance with ethical standards, some of which exceed those specifically required by law:

> The decision to use animals in research requires critical thought, judgment, and analysis. Using animals in research is a privilege granted by society to the research community with the expectation that such use will provide either significant new knowledge or lead to improvement in human and/or animal well-being. (references omitted). It is a trust that mandates responsible and humane care and use of these animals. ... Ethical considerations discussed here and in other sections of the *Guide* should serve as a starting point; readers are encouraged to go beyond these provisions. NRC (2011, p. 4)

3.2.2 Legal Requirements Reflecting General or Specific Ethical Principles

Many laws, regulations, and government agency policies that pertain to animal research state explicitly, or reflect, very general ethical ideals or requirements. Underlying the US Animal Welfare Act (AWA, 2013), for example, is the general principle of biomedical animal research ethics that investigators must minimize pain or distress experienced by animal subjects. The *EU Directive* requires that any harm caused to animals in a research project must be justified by expected benefits of the research [European Union, 2010, Art. 38 para. 2(d)]. A well-known

set of nine general ethical principles for biomedical animal research (some of which are included in substance in the fundamental ethical principles presented later in the chapter) is enunciated in the *US Government Principles for the Utilization and Care of Vertebrate Animals Used in Testing, Research, and Training* (*US Principles*) (OLAW, 2015b, pp. 4–5), which must be followed by investigators conducting research governed by the Health Research Extension Act of 1985 (HREA) and its incorporated *Public Health Service Policy on Humane Care and Use of Laboratory Animals* (*PHS Policy*) (OLAW, 2015b, para. I). Certain laws state more specific ethical rules, such as the requirement of the US AWA [AWA, 2013, §2143(a)(3)(B)] and the AWA Regulations [AWAR, 2015, §2.31(d)(1)(ii)] that investigators consider alternatives to procedures likely to produce pain or distress in research animals. Some laws state even more specific ethical requirements, such as the requirement of the AWA that, unless scientifically necessary, animals should not be subjected to multiple major invasive procedures [AWA, 2013, §2143(a)(3)(D)].

3.3 Ethical Treatment of Animals Promotes Sound Scientific Results

As is discussed in this chapter, among the central principles of biomedical animal research ethics are that animals should not experience more pain or distress than necessary for the scientific aims of an experiment, and that they should be provided housing environments and general care that are appropriate for their species and contribute (consistent with experimental aims) to their health and comfort. Studies have long established that unnecessary animal pain or distress during experiments can affect and invalidate experimental results (Russell and Burch, 1959), and that removal of stressors from housing environments can improve the validity and repeatability of data (Garner, 2005; Weed and Raber, 2005).

3.4 Ethical Treatment of Animals is Required by Funding Bodies

Government agencies that fund animal biomedical research require adherence to ethical standards as a condition of support. In the United States, applicants to the NIH must certify that projects will meet the ethical requirements of the Vertebrate Animals Section of the grant application (OLAW, 2016b), which includes the pain and distress minimization principle (discussed below) and justification of the use of animals and the proposed species. Moreover, no NIH-funded animal research may begin, or continue, without determination by the IACUC that the project complies with the ethical standards of the *PHS Policy* (OLAW, 2015b, para. II), and of the *Guide* [OLAW, 2015b, para. IV(A)(1)]. Animal research funded

by the National Science Foundation must also meet the standards applied by the *PHS Policy* to NIH-funded animal research (OLAW, 2015a).

Private funding bodies also require grant recipients to meet various ethical standards. For example, the American Cancer Society (ACS, 2016, p. 6), the American Epilepsy Society (AES, 2016), and the American Heart Association (AHA, 1985) require applicants to certify that animal research projects have received approval from their IACUC, which in the United States includes a determination that all legally required ethical standards will be followed. These organizations also specifically require adherence to the *PHS Policy* and its ethical standards. In the United Kingdom, major funding organizations, including the Association of Medical Research Charities (AMRC, 2015), the Biotechnology and Biological Sciences Science Council (BBSRC, 2013), the Medical Research Council (MRC, 2016), and the Wellcome Trust (2016) require that animal research be conducted only when no feasible nonanimal alternative exists; that applicants employ the "3Rs" of replacement, reduction, and refinement (discussed below), and that appropriate Home Office licenses and certificates are followed. These organizations also require grantees to follow the ARRIVE Guidelines of the UK National Centre for the Replacement Refinement & Reduction of Animals in Research (NC3Rs, 2010), which are intended to assist investigators in preparing manuscripts submitted for publication and are considered below.

3.5 Ethical Treatment of Animals is Required by Peer-Reviewed Journals

Virtually all journals that publish reports of animal research require that authors state, when submitting manuscripts or sometimes in the manuscripts themselves, that they have adhered to specified ethical standards. These journals always include in such standards, observance of all applicable laws and approval of the research by the investigator's IACUC or other legally required review body or government official. As noted earlier, these laws contain fundamental principles of biomedical animal research ethics. Some journals include ethical standards adherence to which might not be legally required in given cases. For example, although the HREA requires that NIH-funded projects follow the ethical standards of the *PHS Principles* and the *Guide*, many journals require adherence to the ethical standards in these documents for all research on live vertebrates, however funded. Some journals mention specific ethical requirements already implied by the general requirement of following all laws and government agency policies. Such journal requirements typically include that the minimum number of animals was

used (e.g., Journal of Neuroscience; PLoS One) and that animal pain, suffering, or distress were prevented or minimized (e.g., Neuroscience; Neuroscience Research; PLoS One). Some journals require adherence to the ethical standards of the professional association under whose auspices these journals are edited. The *Journal of Neuroscience*, for example, requires that all reported animal experimentation be conducted in accordance with the Society for Neuroscience *Policies on the Use of Animals in Neuroscience Research* (SfN, 2016), which mandate observance of the *PHS Policy* and the *Guide* for all experiments on live vertebrate animals.

3.5.1 The ARRIVE Guidelines

The ARRIVE Guidelines (NC3Rs, 2010), mentioned earlier, contain a checklist of 20 directives for the preparation of manuscripts reporting animal research projects. The Guidelines are widely regarded as an effective vehicle not just for promoting standardized, transparent descriptions of animal use that can be evaluated by the scientific community, but also for facilitating the use of animals in ethically as well as scientifically sound ways (du Sert, 2011; Eisen et al., 2014; Reynolds et al., 2012; Rice et al., 2013.) Among the directives of the Guidelines are that the investigator "(e)xplain how and why the animal species and model being used can address the scientific objectives and, where appropriate, the study's relevance to human biology" (NC3Rs, 2010, para. 3b); "(p)rovide details of the animals used, including species, strain, sex, developmental stage (e.g., mean or median age plus age range) and weight (e.g., mean or median weight plus weight range)" (para. 8a); "(p)rovide details of housing (type of facility, e.g., specific pathogen free (SPF); type of cage or housing; bedding material; number of cage companions; tank shape and material etc. for fish)" (para. 9a); "(e)xplain how the number of animals was arrived at. Provide details of any sample size calculation used." (para. 10b); "(p)rovide details of the statistical methods used for each analysis" (para. 13a); "(d)escribe any implications of your experimental methods or findings for the replacement, refinement or reduction (the 3Rs) of the use of animals in research" (para. 18c); and "(c)omment on whether, and how, the findings of this study are likely to translate to other species or systems, including any relevance to human biology" (para. 19).

At the time of this writing, more than 600 journals have recommended that authors follow the ARRIVE Guidelines (Cressey, 2016). However, relatively few journals require compliance, and one study found that few investigators followed the Guidelines even when encouraged to do so (Baker et al., 2014). In light of the support of the ARRIVE Guidelines by journal editors, it seems inevitable that all high-impact journals eventually will make compliance mandatory. It is, therefore,

at the very least prudent for investigators to become used to incorporating the Guidelines into their experiments and manuscript preparation. More importantly, following the ARRIVE Guidelines will assist investigators in conducting scientifically and ethically sound experimentation.

3.6 Ethical Treatment of Animals is Essential for Public Support

A very important reason investigators should be sensitive to ethical aspects of their work is that without public support most biomedical animal research would cease. The great majority of this research is funded by government agencies (FASEB, 2016a), which receive the money they disburse from the public. Moreover, underlying government acceptance and regulation of animal research is the general view of society that biomedical animal research is valuable and is conducted ethically. Were the public to reject this view, it would likely demand an end to government funding, and perhaps to biomedical animal research altogether.

Public approval of biomedical animal research cannot be taken for granted and in some countries may be declining. Polls conducted by the Pew Research Center (2015, p. 141) found that in 2009, 52% of US adults "favored," and 43% "opposed," "the use of animals in scientific research." By 2014, those in favor dropped to 47%, and those opposed rose to 50%. The annual Gallup Poll on moral attitudes of Americans (Gallup, 2016) found that in 2016, 53% of the public believed that "medical testing on animals" is "morally acceptable" and 41% that it is "morally wrong." In 2006, the percentages were 61 and 32%, respectively.

Governments worldwide have recognized that public support for animal research depends upon the public's knowledge that experimental animals are treated in accordance with high ethical standards. For example, in enacting the 1985 amendments to the AWA (2013), the US Congress declared (Public Law 99-198, 1985) that "measures which help meet the public concern for laboratory animal care and treatment are important in assuring that research will continue to progress." In passing the HREA (1985) Congress stated (House Conference Report, 1985, p. 747) that although humane standards of animal care "will change in the future as science advances ... the consultation inherent in the review of the care and treatment of animals by animal care committees is essential. Within such a framework, the public can have confidence that the proper sensitivity, whatever the sensitivity may be, to the care and treatment of animals will occur." The *EU Directive* recognizes the importance of "the ethical concerns of the general public as regards the use of animals in procedures" (European Union, 2010, Preamble para. 12).

3.7 Ethical Treatment of Animals is the Right Thing to Do

Finally, and surely most importantly, investigators should conduct ethical animal research because this is simply the right thing to do. If animals are to be used to understand human disease, they should always be used for ethically sound reasons and in ethically appropriate ways. We owe this to them, as well as to the humans who benefit from their use in research and who should rest assured that this use is ethically appropriate.

4 ASPECTS OF ANIMAL USE AND CARE RELEVANT TO BIOMEDICAL ANIMAL RESEARCH ETHICS

Most issues in biomedical animal research ethics pertain to the conduct of individual animal research projects, that is, to how experiments or research procedures are designed and executed. Ethical questions can arise in all stages of a project, beginning with whether there is sufficient rationale for the use of animals or a particular species, to whether the project treats the animals appropriately during experimental procedures, to when and how the animals' lives may or should be ended, to what should be done with animals that survive experimentation. Although such questions typically arise in the context of particular projects, biomedical animal research ethics sometimes address them generally. Thus, one can ask when certain kinds of physical restraint might be unacceptable for certain species, or when it is ethically acceptable to withhold pain relief from animals (Tannenbaum, 1999). Answers or general approaches to such questions may then sometimes be applied in particular animal research projects.

Biomedical animal research ethics is also concerned with the treatment of animals when they are not undergoing research procedures. Many, perhaps most, research animals spend the majority of their time housed in facility animal quarters, before or after procedures are conducted on them. To be sure, many animals are never off-study, if, for example, effects on their physiology or behavior while in the animal quarters are of direct interest in the research, or if what they are fed or how they are housed is part of the study. However, even these animals can be affected by conditions of housing and care that are not part of the research. Ethical issues relating to housing and general care of animals include whether the size, constituent materials, and physical layout of cages or other enclosures are sufficient to meet certain behavioral needs, whether animals receive adequate care from veterinarians and support staff to address health or welfare problems,

and whether and to what extent research facilities are ethically obligated to provide enriched housing environments.

Biomedical animal research ethics also deals with general issues that pertain to whether it is ethically acceptable to use certain kinds of animals in any, or in various kinds of, research. One such issue is whether chimpanzees may be used in biomedical research (IOM, 2011). Another is whether researchers are ethically obligated to use purpose-bred cats or dogs rather than random-source former pets obtainable from shelters or commercial dealers (NRC, 2009b). These are questions in animal research ethics because they ask whether using such animals in research or in certain kinds of research would accord with investigators' or society's ethical obligations to these animals.

5 USE OF PRIVATELY OWNED ANIMALS IN BIOMEDICAL RESEARCH

It is helpful at this stage of the discussion to consider two general aspects of biomedical animal research: use of privately owned animals, and the nature of basic animal research.

Presently, the vast majority of biomedical animal research is conducted in facilities on animals owned by these facilities or investigators. Recently there has been an increase in the use of privately owned animals, primarily pet cats and dogs, that aims at understanding medical problems not just of these species, but also of humans (Alvarez, 2014; Christopher, 2015a,b; Khanna et al., 2009; Kol et al., 2015; Lairmore and Khanna, 2014). Among the advantages of this research are said to be that certain diseases are already present in many pets and thus need not be induced in laboratories in healthy animals; that certain kinds of ailments of humans and pets are sometimes easier to study in pets; and that what can be learned about certain kinds of diseases in privately owned animals can shed light on identical or virtually identical human ailments (Kol et al., 2015).

Biomedical research on pets is subject to some of the same ethical requirements explored in this chapter, for example, the pain and distress and harm minimization principles. However, there are distinctive ethical issues raised by research on such animals. These issues include how investigators should obtain informed consent from pet owners who may be more interested in helping their animals than contributing to soundly designed experiments; whether and when investigators may enroll an animal in an experiment if there already exists an effective treatment for the animal's condition, or a treatment the success of which is predictably at least as good as that of the experimental procedure; whether a beloved pet should be kept on an experimental treatment that is not working or is not working as well as a treatment other animals in a study are receiving; and whether owners are ethically entitled to a portion of profits that might result from the development of drugs or techniques based on use of their animals.

Also central in the ethical assessment of research projects using privately owned animals is the issue of when these animals are good experimental subjects from a *scientific* standpoint. As is discussed later in this chapter, an important rule of biomedical animal research ethics is that sound science contributes to the ethical use of animals and poor science is likely to cause ethical problems. For example, as will be noted below, if in an experiment too few animals are used to obtain valid results, the use of any of the animals will be pointless at best and at worst could cause pain or distress that is unjustified. There are surely often scientific advantages in employing laboratory animals, such as the ability to use a sufficient number of animals with characteristics (including genetic make-up or disease condition) tailored to an experiment; to perform all scientifically appropriate procedures (including production of a precise disease state and use of controls); and to euthanize animals at scientifically appropriate times.

As of this writing, a few published articles have addressed some of the ethical issues raised by use of privately owned animals in research also aimed at understanding human disease (Baneux et al., 2014; Habing and Kaneene, 2011; Kol et al., 2015, p. 6.) However, there is not yet anything approaching a developed literature on these issues. One reason may be the fact that, at least in the United States, laws governing biomedical animal research do not apply to experiments conducted by veterinary clinicians on privately owned animals. As is discussed earlier, legal requirements relating to animal research tend to express fundamental, widely accepted ethical principles regarding how animals should be treated. In the absence of laws relating to research on privately owned animals, the scientific community may lack strong motivation to address all the ethical issues this kind of research can raise.

Proponents of the use of privately owned animals are hopeful that much of this work will produce important knowledge that can lead directly to clinical trials in humans, and that will produce important advances in understanding human diseases (Kol et al., 2015). Time will tell whether this will be so, and whether ethical questions raised by such research will receive sufficient attention. The remainder of this chapter considers ethical issues that relate to animal experimentation conducted in laboratories, which currently constitutes the great preponderance of biomedical animal research.

6 THE NATURE OF BASIC ANIMAL RESEARCH

Many investigators who use animals in biomedical research describe their research as "basic." It is important that they are clear about what they mean by this term. There are two different senses of "basic" research commonly employed in the scientific literature, which raise very different ethical issues.

6.1 "Basic" Research as the Search for Knowledge for its Own Sake

Historically the first, and possibly still the predominant, definition characterizes basic research as "directed towards increase of knowledge … where the primary aim of the investigator is a fuller knowledge or understanding of the subject under study, rather than a practical application thereof" (NSF, 1959, p. 368); as "uncommitted research, prompted by disinterested curiosity, and aimed primarily at the extension of the boundaries of knowledge" (American Council on Education, 1954, p. 49); as aimed at "the extension of knowledge for its own sake" (OECD, 1966, p. 24); or as motivated by "intellectual curiosity (where) the motivating force is not utilitarian goals, but a search for a deeper understanding of the universe and of the phenomena within it" (Seaborg, 1963, p. 1383). I shall call this the *subjective* sense of "basic" research because it identifies investigators' *motivation* as the key factor in whether their research is so classified.

There is a long-standing and sizeable body of thought that rejects intellectual curiosity and knowledge for its own sake as acceptable reasons for animal experimentation, and certainly for causing experimental animals any pain, suffering, or distress (Bowd, 1980; Midgley, 1981; Rollin, 1992, p. 170; Ryder, 1971). Although these thinkers accept knowledge for its own sake as a justification for scientific inquiry, and accept some curiosity-driven research that does not cause animals pain (e.g., purely observational studies of animals in natural habitats), they argue that it is profoundly unethical to cause an animal any pain or distress so that scientists can obtain and enjoy knowledge for its own sake. Louis Goldman, who for many years led the Royal Society for the Prevention of Cruelty to Animals (RSPCA), expressed this view as follows.

> Experiments which cause pain and suffering demand special justification. That special justification cannot merely be that scientists are entitled to do anything that might increase the sum total of knowledge or bring about a medical advance in the remote future. There has to be a direct benefit, a good and immediate relevant reason—one which most people would accept as adequate.
>
> I believe that most people would accept the use of animals to test a new vaccine or a new drug before it is given to man.

> I believe that most people accept that new surgical procedures like transplant operations should first be tested on animals. … (But) some scientific problems are not really worth solving. We don't really need proof that inhaling a mixture of air and alcohol produces a state of addiction in mice. Nor do we need proof that animals can be trained to avoid a part of a cage where they received electric shocks to their feet. The link between the experiment and a possible benefit to mankind is so remote as to be almost invisible. Goldman (1979, pp. 191–2).

This viewpoint is, I would suggest, widespread. Many people are unlikely to accept experiments that cause animals pain or distress in order to discover something that is solely of intellectual interest, and that does not offer *some* possibility of ultimately benefiting humankind.

Appreciating the general hostility to curiosity-driven research that can cause animals pain or distress, some defenders of such research argue that it will *eventually* benefit human health (Miller, 1985; Morrison, 2009; Thomas, 1974). According to sleep investigator Adrian Morrison, for example,

> the basic researcher seeks to understand a biological phenomenon for the sake of understanding it, not in an attempt to solve a particular problem. … Nonetheless, basic research is the very first step toward solving a clinical problem, often without a specific disease in mind, because so many bits of information from varied and often improbable sources will ultimately come together to provide a solution to a diseased condition. In other words, good and successful basic research will usually end up solving a problem that the researcher did not originally intend to solve. Morrison (2009, p. 69)

Morrison and others find support for this view in the famous study of physiologists Julius Comroe and Robert Dripps (1976), which concluded that many important clinical advances treating cardiac and pulmonary disease resulted from animal experiments in which investigators had no interest in discovering knowledge with potential clinical relevance. However, this study was retrospective, and was able to identify successful experiments that did lead to clinical advances. The claim that all or most curiosity-driven animal research will in the future benefit human health is not supported by the Comroe and Dripps (1976) study, and seems intuitively false. There is surely no connection *simply* between *any* researcher's *interest* in certain biological phenomena and any probability that the research will lead to health benefits. A number of recent literature surveys has shown that, in fact, many animal experiments (whether or not classified as "basic") have not yet translated into clinical applications (Hackam and Redelmeier, 2006; Henderson et al., 2013; van der Worp et al., 2010). It is important to note that the studies just cited do not claim, or show, that animal research is not necessary or useful in combating human disease. Rather, the authors of the studies call for better understanding of aspects

of animal projects that might increase their probability of discovering effective clinical applications. One of the primary aims of the new and rapidly expanding science of translational medicine is not only finding potential clinical applications of completed animal research, but identifying kinds of animal research that might lead to clinical applications (Reed et al., 2012; Zerhouni, 2007; Zucker, 2009). This new science recognizes, as have investigators in a number of fields of biomedical research (Galanopoulou et al., 2013), that the record of translation of animal studies has sometimes been disappointing and that it is no longer acceptable to support animal experiments on the grounds that one cannot predict what discoveries will eventually contribute to clinical applications.

6.2 "Basic" Research as the Search for Fundamental, Underlying Mechanisms, and Causes

There is another sense of the term "basic" research employed by scientists that does not tie basic animal research, by definition, to the search for knowledge for its own sake. "Basic" research in this second sense is sometimes referred to as "fundamental" research, because it seeks to understand foundational, underlying mechanisms or causes that it is hoped might eventually explain much, if not all, of a wide range of phenomena. So defined, basic research typically does not expect to quickly make discoveries with specific relevance to practical results, precisely because the research seeks to find causes and explanations of matters that are not yet well understood. It is sometimes said that basic research in this sense seeks to discover knowledge that is widely applicable to multiple scientific fields, or is so significant and central to a specific field that it might contribute to a changed and greatly improved way of looking at that field (Calvert, 2006; Kidd, 1959; Reagan, 1967). I shall call this the *objective* sense of "basic" research because it identifies features of research itself and not investigators' motivation as the key factor in whether research is classified as basic. An animal experiment that constitutes basic research in the objective sense can have as *part* of its motivation the discovery of knowledge for its own sake, but this is not what makes such research basic. Basic research in the objective sense can—and in the biomedical sciences almost always does—aim at fighting disease and improving health. It is the objective sense of "basic" research, coupled with this practical aim, that the NIH employs when it states (NIH, 2015b) that its "mission is to seek fundamental knowledge about the nature and behavior of living systems and the application of that knowledge to enhance health, lengthen life, and reduce illness and disability."

6.3 What Investigators Mean by "Basic" Animal Research

Some investigators who characterize their animal research as "basic" do not indicate clearly what they mean by the term. Scientists who conduct biomedical animal research almost always have as their ultimate goal understanding and conquering human or animal disease. Therefore, if asked which definition of the term "basic" they employ, most investigators would likely endorse the objective sense. However, like Morrison in the passage quoted earlier, some animal researchers who comment about the nature of basic animal research do appear to employ the subjective sense of "basic research," although they go on to express confidence that curiosity-driven animal research will eventually lead to clinical advances. Some scientists who speak about the nature of basic animal research seem to want to employ both the subjective and the conflicting objective sense of the term. For example, the eminent epilepsy animal researcher Philip Schwartzkroin appears to adopt the objective definition when he writes that "technological invention drives modern science, and the findings from 'basic' laboratory (and clinical) research drive technical innovation. … It is *often* the technological advance that is the ultimate goal of even the most basic forms of research" (Schwartzkroin, 2012, pp. 2–3, author's italics). However, he also asserts that the primary if not the sole motivation for many epilepsy researchers who use animals is intellectual curiosity. He states that "many young researchers are attracted to epilepsy research *simply* because the problems are intellectually fascinating, the phenomena are dramatic, and the potential experimental approaches allow/encourage the use of a broad array of technical weaponry" (p. 4, author's italics). He also writes that "(o)btaining knowledge for its own sake is an old and sacred pursuit … Because of the uncertainty about what insights might become important in the future, because what seems irrelevant or unusable at one time might provide the basis for important future developments, 'basic research' without specific practical rationale should be encouraged and supported" (p. 3).

6.4 Recommendations

The view that it is wrong to cause animals pain, distress, or other severe harms in experiments that are motivated solely or primarily by curiosity does not imply that it is wrong for investigators who conduct basic animal research in the objective sense to enjoy solving intellectual problems, or to believe that biological knowledge is worth obtaining for its own sake. Nor, for reasons discussed below, do all ethically conducted basic animal research projects require a demonstration of immediate or likely clinical applications. However, in

light of the hostility that many have to animal experimentation that causes animals pain or distress and is motivated by the desire to discover knowledge for its own sake, several things seem clear. First, investigators should not express or endorse the subjective definition of "basic" animal research out of a mistaken assumption that basic research must be defined as motivated by the search for knowledge for its own sake. Second, in communicating with members of the public, funding agencies, government regulators, and IACUCs, investigators should make clear that they are using the objective sense of "basic" research. Finally, even if intellectual curiosity comprises part of their motivation for using animals in basic research, investigators should indicate clearly that the primary and ultimate aim of their research is, as the NIH characterizes its mission in funding fundamental research, "to enhance health, lengthen life, and reduce illness and disability" NIH (2015b). This statement surely reflects how the vast majority of biomedical animal researchers who conduct basic studies view their work.

7 WHY INVESTIGATORS PLAY THE KEY ROLE IN ENSURING THE ETHICAL CONDUCT OF ANIMAL RESEARCH PROJECTS

Some investigators may be reluctant to become involved in ethical discussion of their work, or of biomedical animal research generally because their distinctive professional expertise relates not to ethical theory but to scientific investigation. In fact, animal researchers are uniquely qualified and situated to engage in ethical evaluation of biomedical animal research.

7.1 The Nature of Principles of Biomedical Animal Research Ethics

A helpful starting point for investigators who may think that their scientific background does not qualify them to engage in ethical assessment of animal research, is to consider the nature of fundamental ethical principles that apply to biomedical animal research. Most such principles are general and require *factual* information to be applied to actual circumstances. For example, as discussed later, one of the central principles of animal research ethics (which I call "the pain and distress minimization principle") is that *an animal research project should cause no more pain or distress to the animals than is necessary to achieve the scientific goals of the research.* This principle sometimes requires investigators to ask questions about procedures used in experiments, and may sometimes necessitate changes in project design and implementation. However, the principle cannot by itself generate any specific conclusions or courses of action without the

asking of questions that are empirical in nature and the consideration of which involves scientific knowledge and expertise.

For example, one issue to which the pain and distress minimization principle applies is whether in a given experiment, it is ethically acceptable to allow animals to die on their own, in pain or distress, or whether they should be euthanized at some point prior to death. What the pain and distress minimization principle requires when this question is asked will depend on a number of facts about the experiment, which can include the following: (1) what the project aims to discover; (2) whether the animal model used in the study is a good model from a scientific standpoint to achieve the project's goals; (3) whether the study correctly employs the model; (4) whether the model, or the results sought in the study, require death as the endpoint or can allow the euthanasia of at least some of the animals; and (5) how much pain or distress the animals actually experience. These are all empirical questions, consideration of which does not involve value judgments.

7.2 The Need for Scientific Expertise in Applying General Ethical Principles

The pain and distress minimization principle illustrates why animal researchers should not be reluctant to consider ethical issues relating to their work. First, the principle is (like the other fundamental ethical rules presented in this chapter) immediately and intuitively compelling. Although more can be said about the ethical foundations of the principle, a great deal of theoretical discussion is not required to demonstrate its persuasiveness. Investigators should be entirely comfortable endorsing and applying it. Second, the pain and distress minimization principle cannot be applied correctly to an animal research project without knowledge and expertise possessed uniquely by *scientists* who are familiar with the kinds of questions asked by the project; with the applicability to these questions of various kinds of experiments or research techniques; with the nature and effects of possible ways of using the animals on what they experience; and with techniques for preventing or minimizing their pain or distress. These are all matters of science and not ethical theory.

7.3 The Investigator as Captain of the Experimental Ship

The primary reason investigators must play the *central* role in ensuring the ethical conduct of animal research projects is that they play the central role in determining project goals, and in designing and implementing their experiments to achieve these goals.

7.3.1 Primacy of Project Goals

One crucial reason the investigator plays the key role in ensuring that an animal experiment is ethically appropriate is that the investigator formulates the aim or aims of the experiment. Even if a government official or funding agency, for example, is authorized to, or might convince, an investigator to modify a project's goals for scientific or ethical reasons, it is the investigator who must accept these goals if the project is to be conducted. Likewise, animal housing and care, even if modified by an IACUC or facility veterinarian for welfare reasons, must be consistent with the investigator's experimental goals.

Intuitively, it is clear that the goals of an animal research project must determine how the animals are used. For the primary purpose of an animal experiment aimed at understanding a human disease is not to use or treat animals in certain ways, but to understand the disease. Animals used in research projects must be treated ethically, and as is discussed below, it can be possible that a research project ought not to be done because how it treats the animals is not justified by the value of the project. Nevertheless, how animals are used will always remain subservient to, and be controlled by, project goals.

W.M.S. Russell and R.L. Burch, who introduced the concepts of the "3Rs," (discussed below) recognized the primacy of project goals in the ethical design and implementation of biomedical animal experiments. As they stated in their original discussion of the 3Rs, the "central problem" faced by investigators is how to minimize animal pain and distress "without prejudice to scientific and medical aims" (Russell and Burch, 1959, p. 14). This means that the scientific aims of an experiment must determine whether, to what extent, and how pain or distress can be minimized. Put another way, an investigator must *first* determine the aims of an experiment, support these aims on scientific grounds, and *then*, consistent with these aims, ask whether pain or distress can be eliminated or lessened. Put yet another way, elimination or lessening of pain or distress, or other harms to animals, is not an independent goal that is to be balanced *against* the aims of an experiment, so that the aim of a project should be changed if there is another aim that might cause less animal pain or distress. If live animals must be used in an experiment that is justifiable scientifically, they should be used. If they must be caused some pain, distress, or other harm it will be appropriate to cause such harm, provided the harm is minimized consistent with project aims and this minimized harm is ethically justified.

The formulation of scientifically sound project goals, before minimization of pain or distress is implemented, is both a scientific and ethical requirement. It is a scientific requirement because changing or compromising project aims to lessen animal pain or distress could produce results that are not scientifically valuable, or not as valuable as those that would be produced by pursuing the original aims. It is an ethical requirement because causing animals pain or distress in a poorly designed experiment that likely will not produce good scientific results is causing unnecessary and unjustifiable pain or distress, and even when there is no pain or distress can involve a waste of resources and a pointless ending of animals' lives.

Russell and Burch's insistence on the primacy of experimental aims is reflected in the requirement of the US AWA that each "principal investigator considers alternatives to any procedure likely to produce pain to or distress in an experimental animal" [AWA, 2013, §2143(a)(3)(B)]. To enforce this provision, the US Department of Agriculture (USDA) has adopted the following policy that defines and sets forth requirements for investigators regarding consideration of such "alternatives."

> Alternatives or alternative methods, as first described by Russell and Burch in 1959, are generally regarded as those that incorporate some aspect of replacement, reduction, or refinement of animal use in pursuit of the minimization of animal pain and distress *consistent with the goals of the research*. These include methods that use non-animal systems or less sentient animal species to partially or fully replace animals (for example, the use of an in vitro or insect model to replace a mammalian model), methods that reduce the number of animals to the minimum required to obtain scientifically valid data, and methods that refine animal use by lessening or eliminating pain or distress and, thereby, enhancing animal well-being (for example, the use of appropriate anesthetic drugs). However, *methods that do not allow the attainment of the goals of the research are not, by definition, alternatives.* USDA (2016, Policy #12, p. 12.1, author's italics)

7.3.2 Design and Implementation of Experimental Procedures

It is also the investigator who designs and implements the scientific procedures employed to fulfill project aims. If an IACUC, review body, or government official is authorized to demand a modification in experimental procedures, the investigator must be satisfied that changes will not compromise the scientific goals of the project. It is also the investigator and the investigator's research staff who perform experimental procedures and are, therefore, responsible for ensuring that all scientifically and ethically appropriate procedures are carried out.

7.3.3 The Importance of Sound Science in Ensuring Ethical Animal Experimentation

There is another, and critically important, reason investigators play the key role in ensuring that their projects are conducted ethically. As will be discussed in detail later, the central ethical question raised by any biomedical animal experiment is whether what is done with or to the animals is justified by the *value* of the experiment.

For reasons explained later in the chapter, the key task in ensuring that an animal research project has sufficient value to justify its use of animals is typically designing and implementing a project that is *scientifically* sound. It is the investigator, in setting project goals and designing and implementing the experiment to achieve these goals, who ultimately determines its level of scientific soundness.

7.4 The Role of Review Committees and Government Officials in Assessing the Ethical Appropriateness of Animal Experiments

In some countries, local or national review committees or government officials are legally authorized to assess the ethical appropriateness of biomedical animal research projects, and can deny investigators permission to conduct an experiment that in their view does not meet certain ethical requirements. In the European Union, one foundation of such legal authority is the provision of the 2010 *EU Directive* that "the project evaluation" must include "a harm-benefit analysis of the project, to assess whether the harm to the animals in terms of suffering, pain and distress is justified by the expected outcome taking into account ethical considerations, and may ultimately benefit human beings, animals or the environment" [European Union, 2010, Art. 38 para. 2(d)]. The UK ASPA requires that the Home Office official who must license a procedure "carry out a harm-benefit analysis of the programme of work to assess whether the harm that would be caused to protected animals in terms of suffering, pain and distress is justified by the expected outcome, taking into account ethical considerations and the expected benefit to human beings, animals or the environment" [ASPA, 1986, §5B(3)(d)].

7.4.1 Ethical Review in the United States

In recent years there appears to have been increasing acceptance in the United States of the view that IACUCs are legally authorized, and indeed required, to engage in ethical assessment of proposed animal research projects. Some commentators believe that language in the AWA and the HREA requiring the humane or proper treatment of animals authorizes IACUCs to reject animal research projects they find to be scientifically and hence ethically unjustifiable, on the grounds that animals cannot be treated humanely or properly if they are used in scientifically unsound experiments (Mann and Prentice, 2004). Acceptance of the view that American IACUCs are constituted by law as ethics review committees appears to have been furthered by the official position of the Association for Assessment and Accreditation of Laboratory Animal Care International (AAALAC) that an IACUC in its accredited institutions must conduct a "harm/benefit analysis," in which it would "weigh the potential

adverse effects of the study against the potential benefits that are likely to accrue as a result of the research" (AAALAC, 2015). To support this position, AAALAC cites (Newcomer, 2012, p. 296) the statement in the *Guide* that "due to their potential for unrelieved pain or distress or other animal welfare concerns," in certain protocols "the IACUC is obliged to weigh the objectives of the study against other potential animal welfare concerns" (NRC, 2011, p. 27). Conferences and workshops on animal research in the United States routinely include sessions on how IACUCs should engage in harm–benefit analysis and ethical review of research protocols.

It is beyond the ability of this discussion to settle definitely whether IACUCs are permitted or obligated by US law to reject biomedical animal experiments they find ethically unjustified. This matter may need to be resolved by the courts, the conclusions of which are not always predictable. However, a discussion of ethical assessment of biomedical animal research in the United States would be remiss if it did not observe that Congress, in enacting both the HREA and the AWA, expressed its intention that IACUCs must never review the ethical appropriateness of animal research projects. The HREA directs the NIH to issue guidelines to ensure "(t)he proper *care* of animals to be used in biomedical and behavioral research" [§289d(a)(1), author's italics] and "the proper *treatment* of animals while being used in such research" [§289d(a)(2), author's italics]. The statute also states that any guidelines or regulatory actions "shall not be construed to prescribe methods of research" [§289d(a)(2)]. In explaining the meaning of these provisions, Congress declared that "the animal care committees have *no authority to interfere with research decisions, goals, or methods*. The committees have *no authority to 'second guess' or review the appropriateness of research*. The authority of the committees is limited to review of the care and treatment of animals pursuant to guidelines established by the NIH" (House Conference Report, 1985, pp. 746, author's italics).

Likewise, the AWA prohibits the USDA from promulgating "rules, regulations, or orders with regard to the design, outlines, or guidelines of actual research or experimentation by a research facility as determined by such research facility" [AWA, 2013, §2143(a)(6)(A)(1)(i)]. The USDA policy on alternatives, quoted earlier, reflects the guiding principle of the AWA that IACUCs may review and require changes in scientific aspects of animal research projects, but only when, *consistent with the scientific goals of a project*, modifications in project design or implementation would better fulfill the animal welfare aims of the statute. In further explaining its policy on alternatives quoted earlier, the USDA states that investigators must demonstrate to the IACUC that they have searched relevant databases and other appropriate sources for alternatives. If an adequate search would identify "a bona fide alternative method (one that could

be used to *accomplish the goals of the animal use proposal*), the IACUC may and should ask the PI to explain why an alternative that had been found was not used. The IACUC, in fact, can withhold approval of the study proposal if the Committee is not satisfied with the procedures the PI plans to use in his study" (USDA, 2016, Policy #12, p. 12.1, author's italics). However, if any methods that might lessen pain or distress would interfere with the attainment of project goals, these methods need not be used; as indicated in the policy statement quoted earlier, they would not be called "alternatives" (id.).

There are a number of arguments supporting the wisdom of Congress' prohibition of IACUC ethical assessment of experimental goals. As is discussed below, the scientific soundness or merit of an animal experiment is a central determinant in whether it is ethically justified. IACUCs in the United States typically do not have the scientific expertise to assess the scientific merit of all protocols they must consider. Regarding experiments covered by the HREA, those with the responsibility for scientific merit review—and who have expertise to conduct such review—are NIH-appointed scientific review groups (SRGs) (NIH, 2016b).

More importantly, allowing IACUCs to reject project goals on ethical grounds would likely lead to discord and confusion in the biomedical research community, and could hinder potentially beneficial experimentation. There are as yet no universally accepted or legally mandated standards of what constitutes ethically good or bad goals for animal experiments. Moreover, some ethical issues relating to the ethical appropriateness of animal research are difficult, complex, and contentious in their own right. Thus, different IACUCs with different ethical views could reach different conclusions about whether the same or similar kinds of animal experiments would be permitted in their institutions.

Imagine, for example, a hypothetical project that proposes to simulate cigarette smoking in monkeys to determine whether various new potential therapeutic agents can alleviate or reverse the resulting emphysema in these animals, and ultimately in people. The IACUC at one institution regards the goal of the experiment and what will be done to the animals as ethically justified, on the grounds that many people around the world smoke cigarettes, develop emphysema, and need relief. An IACUC at another institution rejects precisely this kind of study. This IACUC maintains that smoking-related emphysema can most effectively be eliminated or reduced if people simply stop smoking, and believes it is not fair to monkeys to give them the disease to help people who should not have smoked in the first place. However, this IACUC tells the investigator that if monkeys are to be used, the animals will have to be subjected to the equivalent of secondhand smoke; such an experiment would be ethically justifiable, this IACUC believes, because many

people (such as children of smokers) who contract lung disease as a result of smoking by others cannot be held responsible for their illness. An IACUC at a third institution rejects this latter kind of study as unethical, on the grounds that nonhuman primates should not be used in any kind of tobacco research, but tells the investigator that if the experiment is modified to study first- or secondhand smoke in mice, it would be ethically justified and would be approved. Another IACUC will approve only studies of secondhand smoke on mice, for the same reason the second IACUC mentioned earlier rejects firsthand smoke studies on monkeys. These hypothetical IACUCs (like many actual IACUCs) concede that they are unqualified to assess the scientific merit of these experiments. Their conclusions reflect their differing views about whether, all things considered, it is *right* to use the animals in the studies, or put another way, whether what is done to these animals would be justified ethically by the value of the experiments.

The claim advanced here is not that there would be disparities in IACUC ethical determinations relating to all or even most kinds of biomedical animal research projects. As is clear from the discussions in this chapter, there is a great deal of agreement in the research community about general fundamental ethical principles relating to biomedical animal research and about how these principles should be applied in many kinds of circumstances. However, there are many kinds of ethically difficult or societally controversial animal experiments regarding which different IACUCs could, and probably will, come to different ethical conclusions about whether experiments will be permitted. Funding agencies might be prevented by IACUC ethical disapprovals from considering studies they would find to be of high scientific merit. Investigators might be forced to leave institutions with IACUCs that reject their work on ethical grounds. Perhaps some institutions would compete for investigators on the basis of their IACUCs' acceptance of certain kinds of animal research, or would appoint IACUC members whose ethical views will not chase away investigators and funding. At some institutions, whether certain kinds of research are approved or rejected could continually change, as different people with different ethical opinions about such research become IACUC members.

To prevent such disparities and changes, government authorities would presumably need to find a way of ensuring consistent IACUC ethical conclusions. Perhaps the *PHS Policy* or the AWA regulations would contain rules not only relating to research animal care and treatment, but also setting forth ethically acceptable research goals and methods. One commentator (who recognizes that current US law does not allow IACUC review of ethical merit) argues that the best way to ensure nationwide ethical consistency is for Congress to establish a national

commission that would issue ethical policies and rules binding on all IACUCs and investigators in the country (Brody, 1989).

One argument sometimes offered to support the legality of IACUC ethical review in the United States is the claim that such review is required by Principle II of the *US Principles* (OLAW, 2015b, pp. 4–5). This principle states that "(p)rocedures involving animals should be designed and performed with due consideration of their relevance to human or animal health, the advancement of knowledge, or the good of society." As is explained below, Principle II is reasonably interpreted to express the most general ethical principle of animal research ethics: whatever is done to animals in a research project must be justified by the project's value. IACUCs are required by the HREA to ensure that research projects covered by the statute conform to the *PHS Policy* (OLAW, 2015b, para. IV.C.1, p. 13), and the *PHS Policy* is "intended to implement and supplement" the *US Principles* (OLAW, 2015b, para. I, p. 7). Therefore, it might seem plausible to conclude that the *PHS Policy*, via the *US Principles*, requires IACUCs to determine whether the goals of animal research projects are sufficiently worthy to justify how these projects use and treat animals.

The *US Principles* were adopted in 1985 by a number of federal agencies (including the NIH) primarily for use in animal research conducted intramurally by these agencies (Laboratory Animal Welfare, 1985). Congress subsequently passed the HREA, which applies to NIH-funded animal research conducted in nongovernment institutions. The HREA directed the NIH to establish guidelines for enforcing the statute [HREA §289d(a)]. The NIH adopted the *US Principles* and the *PHS Policy*, originally intended to apply in its own facilities, as guidelines for NIH-funded animal research in nongovernment institutions. In exercising the authority given to it by Congress, the NIH could not then, and cannot now, contradict or override the legislative intent of Congress in passing the HREA, including Congress' stated prohibition of IACUC review of scientific goals and ethical appropriateness of animal research projects. This means that nothing in the *US Principles* or the *PHS Policy* can allow or require an IACUC to reject or demand changes in a project because in the IACUC's view the project does not provide sufficient ethical justification for its use of animals.

Proponents of IACUC ethical review also point to the *Guide* and certain statements by the NIH Office of Laboratory Animal Welfare (OLAW), which administers the HREA and the *PHS Policy*. One statement in particular in the *Guide* is thought by some to require IACUC review. As noted earlier, the *Guide* asserts that "due to their potential for unrelieved pain or distress or other animal welfare concerns," in certain protocols "the IACUC is obliged to weigh the objectives of the study against other potential animal welfare concerns" (NRC, 2011,

p. 27). As discussed below, this is a statement of what I call the harm justification principle, one of the most important principles of biomedical animal research ethics. OLAW has also indicated that it expects experiments to be rejected if found by IACUCs to be scientifically and hence ethically inappropriate. For example, OLAW asserts that

> Although not intended to conduct peer review of research proposals, the IACUC is expected to include consideration of the U.S. Government Principles in its review of protocols. Principle II calls for an evaluation of the relevance of a procedure to human or animal health, the advancement of knowledge, or the good of society. Other PHS Policy review criteria refer to sound research design, rationale for involving animals, and scientifically valuable research. Presumably a study that could not meet these basic criteria is inherently unnecessary and wasteful and, therefore, not justifiable. OLAW (2016a, D.12)

Time will tell to what extent IACUCs in the United States reject experiments on ethical grounds; whether investigators and institutions that feel aggrieved by such determinations challenge them administratively or in the courts; and what the results of any such challenges might be. If, as has been argued here, in enacting the HREA and the AWA Congress forbade IACUCs from rejecting or modifying research projects or goals on ethical grounds, the ability or obligation of IACUCs to engage in such behavior cannot be conferred by any language contained in the *US Principles*, the *PHS Policy*, the *Guide*, or any document or policy statement issued or endorsed by the NIH or the USDA.

Although IACUCs do not appear to be permitted to reject or demand modifications of project goals they find unethical, current US law does assign crucial ethical functions to IACUCs. By requiring, consistent with project goals, minimization of pain and distress, IACUCs ensure application by investigators of the pain and distress minimization principle (discussed below). IACUCs in the United States also have legal authority to assure compliance with the species-appropriate housing and appropriate care principles (discussed below). Correct application of these fundamental principles of biomedical animal research ethics is essential in ensuring that animal experiments are conducted ethically.

US law, as characterized here, leaves it ultimately to the investigator to choose project goals that, together with experimental procedures to implement these goals (which IACUCs do have limited authority to modify), provide sufficient ethical justification for a project's use of animals. As already noted, court decisions are sometimes unpredictable. It is, therefore, worth observing that even if the US legal system should determine that the HREA or the AWA allows or obligates IACUCs to reject or modify animal experiments they find ethically unjustified, it would still be the investigator who is best able to articulate why a project has sufficient scientific value

to justify its use and treatment of animals. It would still be the investigator who sets project goals, and who must accept any modifications of these goals if the project is to proceed. It will still be the investigator who is responsible for putting into effect an experiment with sufficient value to assure that it justifies its use of animals.

8 SOURCES OF GUIDANCE FOR INVESTIGATORS IN CONDUCTING ETHICAL RESEARCH

In designing and applying an animal model, an investigator will want to consult accurate and up-to-date published sources (such as the chapters in this book) that consider the value of the model in studying the disease or aspect of the disease under investigation. Readers of this chapter are also likely, and reasonably, to ask what published sources they can consult to evaluate *ethical* claims about animal research, and to make sound decisions regarding ethical issues relating to their projects.

8.1 Scientific Resources

Most published sources animal researchers will want to consult to ensure that their projects are ethically sound are wholly scientific in nature, and are indeed very same kinds of materials investigators already consult. These are resources that address issues pertaining to the scientific soundness of the design and implementation of a project, including the choice of project goals that are appropriate to investigating a given disease or aspect of a disease, the animal model to be employed, and experimental means of applying the model. Such materials assist investigators in designing projects that are strong from a scientific, and for reasons discussed later, are therefore likely to be strong from an ethical, standpoint. Investigators already consult scientific sources that are relevant to ensuring that projects meet legal requirements relating to animal welfare, such as publications that indicate whether there are available methods that would lessen animal pain or distress consistent with project goals.

8.2 Ethical and Ethically Relevant Resources

There are numerous resources that address ethical issues more directly and that investigators will find helpful in considering how to apply various ethical principles in developing and employing animal models.

8.2.1 Legally Mandated Ethical Principles

As observed earlier, one important source of ethical rules relating to biomedical animal research are the ethical requirements that government agencies impose on researchers, IACUCs, and research facilities. Most ethical standards relating to animal research required by law in the United States are set forth in statutes, primarily the AWA (2013) and the HREA (1985); in regulations or rules that are applied by the government agencies that administer these statutes, for the AWA, the AWA Regulations in the Code of Federal Regulations (AWAR, 2015), and for the HREA, the *PHS Policy* (OLAW, 2015b); and in various policies adopted by these agencies, for the AWA, by the USDA Animal and Plant Health Inspection Service (APHIS), and for the HREA, by OLAW. In the United Kingdom, ethical as well as technical standards are contained in the general statute governing animal research, the Animals (Scientific Procedures) Act 1986 or ASPA (1986). The Home Office, which enforces the Act, issues guidance documents and policy statements to assist investigators and to explain legally mandated ethical and technical animal research standards to the public (Home Office, 2014, 2015, 2016a,b). In the European Union, the fundamental legal documents governing animal research are the *European Convention for the Protection of Vertebrate Animals Used for Experimental and Other Scientific Purposes* (*European Convention*) (Council of Europe, 1986) and the *EU Directive* (European Union, 2010), which contain ethical principles member nations are expected to acknowledge and enforce.

Only a representative sampling of legally mandated ethical principles can be provided here. The AWA indicates [AWA, 2013, §2143(b)(3)] that its general aim is to ensure that "(p)rocedures involving animals will avoid or minimize discomfort, distress, and pain to the animals." To achieve this ethical goal the AWA and AWA Regulations impose a number of more specific ethical requirements. These include requirements that the "principal investigator considers alternatives to any procedure likely to produce pain to or distress in an experimental animal" [AWA, 2013, §2143(a)(3)(B)]; "(t)he principal investigator has provided written assurance that the activities do not unnecessarily duplicate previous experiments" [§2.31(d)(1)(iii)]; "(p)rocedures that may cause more than momentary or slight pain or distress to the animals will … (b)e performed with appropriate sedatives, analgesics or anesthetics, unless withholding such agents is justified for scientific reasons, in writing, by the principal investigator and will continue for only the necessary period of time" [§2.31(d)(1)(iv)(A)]; paralytics without anesthesia shall not be used [§2143(a)(3)(C)(iv)]; "(n)o animal will be used in more than one major operative procedure from which it is allowed to recover, unless ... (j)ustified for scientific reasons by the principal investigator, in writing" [AWAR, 2015, §2.31(d)(1)(x)]; and "(a)nimals that would otherwise experience severe or chronic pain or distress that cannot be relieved will be painlessly euthanized at the end of the procedure or, if appropriate, during the procedure" [§ 2.31(d)(1)(v)].

Perhaps the best-known legally mandated ethical rules for animal research in the United States are the *US Principles* (OLAW, 2015b, pp. 4–5). The *Principles* include statements that "(p)rocedures involving animals should be designed and performed with due consideration of their relevance to human or animal health, the advancement of knowledge, or the good of society" (Principle II); "(t)he animals selected for a procedure should be of an appropriate species and quality and the minimum number required to obtain valid results. Methods such as mathematical models, computer simulation, and in vitro biological systems should be considered" (Principle III); "(p)roper use of animals, including the avoidance or minimization of discomfort, distress, and pain when consistent with sound scientific practices, is imperative. ..." (Principle IV); "(p)rocedures with animals that may cause more than momentary or slight pain or distress should be performed with appropriate sedation, analgesia, or anesthesia. Surgical or other painful procedures should not be performed on unanesthetized animals paralyzed by chemical agents" (Principle V); "(a)nimals that would otherwise suffer severe or chronic pain or distress that cannot be relieved should be painlessly killed at the end of the procedure or, if appropriate, during the procedure" (Principle VI); "(t)he living conditions of animals should be appropriate for their species and contribute to their health and comfort. ..." (Principle VII); and "(i) nvestigators and other personnel shall be appropriately qualified and experienced for conducting procedures on living animals ..." (Principle VIII).

The Preamble of the *EU Directive* (European Union, 2010) contains a large number of general principles of animal research ethics. These include statements that "(n)ew scientific knowledge is available in respect of factors influencing animal welfare as well as the capacity of animals to sense and express pain, suffering, distress and lasting harm. It is therefore necessary to improve the welfare of animals used in scientific procedures by raising the minimum standards for their protection in line with the latest scientific developments" (para. 6); "(w)hile it is desirable to replace the use of live animals in procedures by other methods not entailing the use of live animals, the use of live animals continues to be necessary to protect human and animal health and the environment" (para. 10); "(t)he methods selected should avoid, as far as possible, death as an end-point due to the severe suffering experienced during the period before death" (para. 14); "(f)rom an ethical standpoint, there should be an upper limit of pain, suffering and distress above which animals should not be subjected in scientific procedures. To that end, the performance of procedures that result in severe pain, suffering or distress, which is likely to be long-lasting and cannot be ameliorated, should be prohibited." (para. 23); "(t)o ensure the ongoing monitoring of animal-welfare needs, appropriate

veterinary care should be available at all times and a staff member should be made responsible for the care and welfare of animals in each establishment" (para. 30); and "(t)he accommodation and care of animals should be based on the specific needs and characteristics of each species" (para. 34).

8.2.2 Nongovernmental Documents Adherence to Which is Required by Law

As already noted, the *Guide* (NRC, 2011), though published by the nongovernmental National Research Council (NRC), is required by the *PHS Policy* to be followed in all research covered by the HREA (OLAW, 2015b, para. I, p. 7). The *Guide* (NRC, 2011, Appendix B, pp. 199–200), mandates adherence to the ethical rules in the *US Principles*. Most of the standards of animal use and care enunciated in the *Guide* are not ethical rules like those enunciated in the *Principles*. However, the *Guide* contains discussions that are relevant to considering ethical questions raised by various aspects of animal research. Among the many subjects with ethical implications considered in the *Guide* are choice of endpoints (pp. 27–28); physical restraint (pp. 29–30); multiple survival surgical procedures (p. 30); food and fluid regulation (pp. 30–31); pain and distress (pp. 120–121); anesthesia and analgesia (pp. 121-123); euthanasia (pp. 123–124); and environment, housing, and management in general and relating to various species (pp. 41–88). Investigators conducting research governed by both the AWA (USDA, 2016, Policy 3) and the *PHS Policy* (OLAW, 2015b, para. IV.C.1.g) must employ methods of euthanasia approved in the American Veterinary Medical Association (AVMA) *Guidelines on Euthanasia* (AVMA, 2013). This document contains discussions of ethical questions relating to when euthanasia should be performed in various circumstances. Although current US law requires investigators to use a euthanasia *method* approved in the AVMA guidelines, (and does not mandate adherence to ethical suggestions in the document), investigators will find its discussions of ethical issues useful.

8.2.3 Publications of Workshops, Study Committees, and Nongovernmental Entities

Another source of guidance in ethical assessment of animal research projects are publications of groups or special committees of nongovernment bodies that are requested or consulted by their respective governments. In the United States, these groups include the NRC of the National Academies of Science, and the NRC Institute for Laboratory Animal Research (ILAR). These publications tend not to offer detailed discussion of or arguments for ethical principles. However, these publications provide useful information about how to apply certain accepted ethical principles (such as the pain and distress minimization principle) to various situations

faced by researchers. Among such publications are the reports of the ILAR Committee on well-being of nonhuman primates on *The psychological well-being of nonhuman primates* (ILAR, 1998); the NRC Committee on *Guidelines for the care and use of mammals in neuroscience and behavioral research* (NRC, 2003); the NRC Committee on *Recognition and alleviation of distress in laboratory animals* (NRC, 2008); the NRC Committee on the *Recognition and alleviation of pain in laboratory animals* (NRC, 2009a); and the Federation of Animal Science Societies *Guide for the care and use of agricultural animals in research and teaching* (FASS, 2010). Discussion of general issues relating to the use or availability of certain animals for research can be found in the NRC report on *Scientific and humane issues in the use of random source dogs and cats in research* (NRC, 2009b) and the Institute of Medicine (IOM) report on the *Use of chimpanzees in biomedical and behavioral research* (IOM, 2011). The RSPCA has written or published a number of documents discussing ethical assessment of animal experiments, including *A resource book for lay members of ethical review and similar bodies worldwide* (Jennings and Smith, 2015). A useful, comprehensive treatment of animal research ethics is *The ethics of research involving animals*, published by the UK Nuffield Council on Bioethics (2005). An invaluable source of discussions with implications for ethical issues in biomedical animal research is the *ILAR Journal*, the leading-peer reviewed periodical in the United States focusing on research animal welfare. Issues of the journal are dedicated to specific human diseases, animal models, research techniques, or species of research animal.

8.2.4 Ethical Guidelines of Professional Associations

Among the most helpful sources of published principles in biomedical animal research ethics are official statements and policies of professional associations of scientists, laboratory animal veterinarians, and research animal care specialists. These statements sometimes assert ethical principles that focus on particular kinds of research, and sometimes apply general ethical principles to certain kinds of animal research or species. Investigators need not be a member of a particular association to find its ethical statements applicable to their research projects.

Among general ethical statements by professional scientific associations are those of the American Physiological Society (APS, 2016), the American Psychological Association (APA, 2012), the American Society of Primatologists (ASP, 2001), the Federation of American Societies for Experimental Biology (FASEB, 2016b), the Society for Neuroscience (SfN, 2016), and the Society of Toxicology (SOT, 2008).

Statements of veterinary associations of ethical principles relating to biomedical animal research,

sometimes accompanied by detailed suggestions for their application, can be found in statements or documents of, for example, the American College of Laboratory Animal Medicine (ACLAM, 2001, 2006, 2012a,b), the American Society of Laboratory Animal Practitioners (ASLAP, 2007, 2008, 2009), the AVMA (2016), the British Veterinary Association (BVA, 2016), and the Laboratory Animal Veterinary Association of the BVA (LAVA, 2016).

Professional associations whose focus is on the wide range of research animal use and care offer general ethical policies and sometimes specific guidance in implementing these policies. Such organizations include the American Association for Laboratory Animal Science (AALAS, 2014), the Basel Declaration Society (Basel Declaration, 2010), the Canadian Council on Animal Care (CCAC, 1989), the Federation of European Laboratory Animal Science Associations (FELASA, 2005; Guillen, 2012), and the International Council for Laboratory Animal Science (ICLAS, 2012). AAALAC (2016) includes in its accreditation requirements a number of its own ethical policies, as well as adherence to other documents containing ethical standards for animal research, including the *Guide* (NRC, 2011) and the *European Convention* (Council of Europe, 1986).

9 DEVELOPING USEFUL ETHICAL GUIDELINES

Whether contained in laws, regulations, or professional association documents, most current statements of principles of biomedical animal research ethics enunciate a relatively small number of ethical rules. Moreover, multiple ethical rules contained in many of these documents express the pain and distress minimization principle, either stating this principle generally or applying the principle to certain kinds of situations in which it is relevant. The latter is the intent, for example, of the third through the sixth of the *US Principles* (OLAW, 2015b), and of similar statements in the AWA and ethical guidelines of scientific and veterinary associations cited earlier. The ethical rules contained in current legal and professional documents also tend to be extremely general and often omit certain specific kinds of research or research procedures that, it can be argued, ought to be mentioned explicitly in any useful set of ethical rules. For example, one can ask whether statements of ethical principles that invoke the pain and distress minimization principle should at least mention—or perhaps include much more specific rules regarding—various issues that raise distinctive applications of the principle, such as choice of humane endpoints, physical restraint, and tumor burden.

That statements of biomedical animal research ethics tend to present a small number of very general principles allows these statements to apply to a wide range of research: on different diseases, employing different models and research procedures, and using different species. The generality of the principles also adds to their credibility. It is usually more difficult to find counter-examples to a very general rule (e.g., that research animal pain and distress should be minimized consistent with project goals) than to very specific guidelines that may not be persuasive in some situations (e.g., a rule that death as an endpoint may be used only in specified kinds of studies).

The major shortcoming of a limited number of general ethical principles is that general rules provide little practical guidance. Animal researchers might benefit from statements of ethical principles that are more detailed than those provided in current legal and professional documents. A useful set of principles probably should not contain a large number of very specific ethical rules. Too many specific rules might distract investigators from the necessary task of carefully examining the particulars of each project, and from considering how the project treats the animals during all of its stages. On the other hand, investigators might find it helpful to have dedicated ethical rules dealing with certain animal models, research techniques, or species. This might make ethical assessment of particular projects more persuasive and efficient by focusing attention on recurring ethical questions and by presenting possible answers to such questions.

Current legal and professional documents that enunciate ethical principles for biomedical animal research also do not provide supporting ethical *arguments* for these principles—perhaps because the principles are widely accepted in the biomedical research community and seem unquestionably correct to investigators and government regulators alike. However, as is demonstrated below, it is important to consider underlying ethical and empirical arguments for principles of biomedical animal research ethics. These arguments can be helpful in explaining the meaning of the principles and in motivating investigators to follow them.

It cannot be known what a more comprehensive set of principles of biomedical animal research ethics will contain until sustained work is done to offer and evaluate such principles. The rules presented in the remainder of this chapter serve as a core for the articulation of additional principles and practical guidelines. Absence in this discussion of any rule currently mandated by law or included in professional association ethical documents is not meant to suggest that such rules should not be followed by investigators, or should not be included in a comprehensive set of fundamental principles of biomedical animal research ethics.

10 FUNDAMENTAL PRINCIPLES OF BIOMEDICAL ANIMAL RESEARCH ETHICS

The following discussion presents 13 principles that express basic truths about animal research or about how it should be conducted. An ethical evaluation of any individual animal research project is likely not only to involve the application of one or more of these principles, but also to employ these principles to support the most important ethical conclusions relating to the project. Additionally, each of these principles applies to different aspects of many kinds of animal experiments. Thus, the principles can be said collectively to form the fundamental structure on which the ethical conduct of biomedical animal research rests. The principles are listed in Table 1.1, and for convenience of discussion are designated as F1–F13.

F1. The Biomedical Research Principle

It is among the most noble and imperative of human endeavors to employ scientific research to prevent, alleviate, and cure the pain, suffering, distress, fear, anxiety, disability, infirmity, and death associated with human disease.

What I call *the biomedical research principle*, deserves a prominent place in biomedical animal research ethics. The principle does more than reflect the central motivation of biomedical science in using animals to understand human disease. The principle also does more than commit animal researchers to conduct research for ethically sound reasons and in ethically sound ways—by proclaiming that biomedical research is driven by the highest of ethical ideals at its core. The biomedical research principle, together with the accompanying next two fundamental principles discussed below, implies a truth of critical importance. As indicated by the quotation early in the chapter from a philosophical discussion of animal research (Donnelly and Nolan, 1990, p. 8), many philosophers think that the primary question in biomedical animal research ethics is whether or to what extent the use of animals in research is justified. If what must be shown is that animal research *is* justified, the burden of argument is on those who think it is justified. However, if as is surely the case it is a noble and imperative endeavor to employ scientific research to understand and combat human disease, and if as is surely the case the development of knowledge necessary to understand and combat human disease often requires in vivo animal experimentation (see Principle F2 below), and if as is surely also the case animals should be used before humans in research on human disease when scientifically appropriate (see Principle F3 below), the ethical burden of proof is on those who think that biomedical animal research is *not* justified.

TABLE 1.1 Fundamental Principles of Biomedical Animal Research Ethics

1. *The biomedical research principle.* It is among the most noble and imperative of human endeavors to employ scientific research to prevent, alleviate, and cure the pain, suffering, distress, fear, anxiety, disability, infirmity, and death associated with human disease.
2. *The animal research principle.* "The development of knowledge necessary for the improvement of the health and well-being of humans, as well as other animals requires in vivo experimentation with a wide variety of animal species." Preamble, *US Principles* (OLAW, 2015b, p. 4).
3. *The Nuremberg principle.* Medical research on human subjects "should be so designed and based on the results of animal experimentation and a knowledge of the natural history of the disease or other problems under study that the anticipated results will justify the performance of the experiment." (Nuremberg Code, 1947, para. 3).
4. *The pain and distress minimization principle.* An animal research project should cause no more pain or distress to the animals than is necessary to achieve the scientific goals of the research.
5. *The pain and distress justification principle.* Any pain or distress that an animal research project will cause the animals must be justified by the value of the project, and the more pain or distress an animal research project will cause animals, the greater must be the value of the project to justify this pain or distress.
6. *The harm justification principle.* Any harm (including pain or distress) that an animal research project will cause the animals must be justified by the value of the project, and the greater the harms an animal research project will cause animals, the greater must be the value of the project to justify these harms.
7. *The harm minimization principle.* An animal research project should cause no more harm (including pain or distress) to the animals than is necessary to achieve the scientific goals of the research.
8. *The general justification principle.* Whatever is done with or to animals in a research project (including but not restricted to causing harms, such as pain and distress) must be justified by the value of the project.
9. *The 3Rs principle.* In designing and implementing animal experiments investigators should practice the "3Rs" of replacement, reduction, and refinement.
10. *The species-appropriate housing principle.* "The living conditions of animals should be appropriate for their species and contribute to their health and comfort." *US Principles*, Principle VII (OLAW, 2015b, p. 5).
11. *The appropriate care principle.* While housed in the research facility, animals must receive appropriate veterinary supervision and care, and the conscientious attention of trained animal care staff.
12. *The appreciation principle.* Research animals should be treated with kindness, compassion, and gratitude.
13. *The translation principle.* Investigators should support, stay informed about, and when appropriate engage in scientific and professional efforts aimed at improving the translation of animal experiments to clinical applications.

This does not mean that all animal research is ethically justified. Nor does it mean that for any given animal research project there is a presumption that the project is ethically appropriate, and that someone who might think otherwise has the burden of proving that this is so. For reasons explained below, it is primarily the task of investigators and others who are part of the general biomedical animal research endeavor to ensure that individual research projects are ethically appropriate.

F2. The Animal Research Principle

"*The development of knowledge necessary for the improvement of the health and well-being of humans as well as other animals requires in vivo experimentation with a wide variety of animal species.*" Preamble, *US Principles* (OLAW, 2015b, p. 4).

This statement, which I shall call *the animal research principle*, opens the *US Principles*. The animal research principle, together with the biomedical research principle, provides a critically important foundation for regarding animal research as generally ethically justified. For if it is imperative to understand and combat human disease, and if doing so requires animal research, then it is imperative (subject to additional scientific and ethical considerations) to conduct biomedical animal research. The animal research principle does not imply that all animal research projects are necessary for the improvement

of human health. It is incumbent on investigators to conduct animal research that *does* have the potential to understand and combat disease.

F3. The Nuremberg Principle

Medical research on human subjects "should be so designed and based on the results of animal experimentation and a knowledge of the natural history of the disease or other problems under study that the anticipated results will justify the performance of the experiment." (Nuremberg Code, 1947, para. 3).

The quoted portion of this principle is a key provision of the Nuremberg Code, widely regarded as the historical foundation of internationally accepted ethical principles relating to the use of humans in medical research (Annas and Grodin, 1992). I shall therefore call this *the Nuremberg principle.* The Nuremberg Code was written by the American judges who presided over the post-World War II trials of the so-called "Nazi doctors" who were prosecuted for crimes against humanity for conducting torturous experiments on concentration camp inmates. The Code's insistence on scientifically appropriate animal research prior to human experimentation reflects the recognition that animal models often facilitate the understanding of human disease. The Nuremberg Code also expresses the view that that research on humans that is conducted with the voluntary consent

of research subjects must—in fairness to these human subjects—have at least some possibility of discovering something useful. There must be good reason to ask these people to possibly forego an available treatment, or to experience potential pain, distress, or discomfort, or feelings of anticipation, hope, or disappointment that can be associated with participating in a clinical trial.

The Nuremberg Code also expresses the widely held view that humans are of greater worth and value than animals. What horrified the Nuremberg judges, and the entire civilized world, when evidence of the experimental atrocities was presented during the trials, was that the Nazi experimenters had no respect for the value of human life. As the chief prosecutor told the judges (Taylor, 1992, pp. 89–90), the experimenters did not even treat their human victims like animals; they treated them worse than research animals could be treated under German law. In requiring that animals be used before humans when scientifically appropriate, the Nuremberg Code reflects the view that certain things may and should first be done with animals because they are animals and not humans.

The Nuremberg principle does not condone subjecting animals to the pointless torture the Nazi experimenters inflicted on people. The Nuremberg Code was strictly a proclamation of *human* rights. The conduct of ethical animal research was not one of its concerns. The ethical requirement of proper treatment of animals in research preceding human testing was added to international research standards in the Declaration of Helsinki (World Medical Association, 2013), which expands upon the Nuremberg Code and is regarded as the most important contemporary comprehensive exposition of ethical principles relating to medical research on humans (Perley et al., 1992). Paragraph 21 of the Declaration states that "(m)edical research involving human subjects must conform to generally accepted scientific principles, be based on a thorough knowledge of the scientific literature, other relevant sources of information, and adequate laboratory and, as appropriate, animal experimentation. The welfare of animals used for research must be respected."

The Nuremberg principle calls upon investigators to employ animal models that *do* further the understanding of human diseases. For if a model that does not assist in understanding a particular disease leads to human clinical trials, and if investigators know or should know prior to such trials that this is not a good model for the disease, the human trials will not have sufficient scientific rationale, and human subjects who volunteer for these trials will not be treated fairly.

Because the Nuremberg principle is a statement about fundamental human rights as much as it is a foundation of biomedical animal research, in communicating with the public about their work (which is urged below),

animal researchers would do well not just to explain how animal research can help people who suffer from terrible diseases. Investigators should also emphasize that in using animal models they are seeking to protect the interests and rights of *people* whose participation in clinical trials is essential for progress in combating human disease.

F4. The Pain and Distress Minimization Principle

An animal research project should cause no more pain or distress to the animals than is necessary to achieve the scientific goals of the research.

This is what I have called *the pain and distress minimization principle*. Due to its prominence in rules of animal research ethics enunciated by government bodies and professional scientific associations, it is fair to say that the pain and distress minimization principle is often regarded in the biomedical research community as the most important principle of animal research ethics. For reasons explained below, this is not the case, although the principle is a key rule of animal research ethics and often figures centrally in the ethical assessment of individual animal experiments.

F4.1 Ethical Foundations of the Pain and Distress Minimization Principle

Although the principle is intuitively persuasive, it is useful to examine its ethical foundations. As I discuss in the context of pain research on animals (Tannenbaum, 1999), the ethical basis of the pain and distress minimization principle is the fact that, as significantly unpleasant experiences, pain and distress are harms or evils in themselves. Although pain is sometimes beneficial in signaling the presence of a problem, such as an injury, the experience of pain is bad in itself, which is why humans as well as animals do not like it and try to avoid it. If one is asked to explain *why* feeling pain or distress is a bad thing (a question that is rarely asked because its answer is obvious) one would respond that these experiences are bad because of how they feel: they are bad because they are pain or distress. In other words, one cannot provide a further reason why pain and distress are bad, it is just self-evident that they are evils and harms in themselves. Because pain and distress are evils, one ought not inflict them on animals unless one has a justification for doing so. A basic principle of ethics is that it is wrong to harm or cause an evil to a being without a justifiable reason.

From these considerations, it follows that if an investigator can achieve the scientific goals of an animal research project in a way that would cause animals less pain or distress than would another way of achieving these goals, the investigator is ethically obligated to choose the way that causes less pain or distress. To cause more pain or distress than is necessary to achieve these goals is to

cause pain or distress that is provided no legitimate reason or justification by the goals of the research.

F4.2 Qualifications to the Pain and Distress Minimization Principle

The pain and distress minimization principle requires two important qualifications to be applied persuasively.

UNCERTAINTY REGARDING MINIMIZATION

If an investigator knows with certainty that one practicable method of pursuing a project's aims will cause less pain or distress to the animals than another, it will be wrong to use the latter method. However, it may sometimes be impossible to *know* that a given method will in fact minimize pain or distress. For example, a research procedure may be so novel that one can only surmise but not be certain that one has designed the procedure so as to minimize the animals' pain or distress. In such a case, it would be unreasonable to criticize an investigator who has made good-faith efforts, based on available scientific and veterinary knowledge, to minimize the animals' pain or distress. In other words, reasonably interpreted, the pain and distress minimization principle sometimes obligates an investigator to *attempt* to cause no more pain or distress to animals than is necessary for the purposes of the research. Although one sometimes cannot fairly ask more of investigators than this, in accordance with typical statements of the pain and distress minimization principle, I have not phrased the principle in terms of making attempts. A good reason for this approach, I would argue, is that stating the obligation in terms of attempts rather than success might be interpreted by some as an expression of satisfaction with merely trying, and as lessening the importance of the need to try to *ensure* that pain and distress are minimized.

IMPRECISION IN ESTIMATES OF ANIMAL PAIN OR DISTRESS

It is also often impossible to apply the pain and distress minimization principle with a high degree of precision. Sometimes it will be clear that pain is being minimized. If, for example, an animal is fully anesthetized during surgery, its pain will be minimized during anesthesia. However, when animals must experience some unrelieved pain or distress because of research goals, it will sometimes be impossible to know whether a procedure has been designed or executed so as to cause *absolutely* the *minimum* amount of pain or distress necessary to pursue project goals. Animals are not capable of verbally expressing precisely the nature, duration, and severity of their pain or distress. Much has been and continues to be learned about pain and distress in various species (NRC, 2008, 2009a). Perhaps some day research into chemical and physiological aspects of animal pain and distress will enable very precise measurements, so that investigators can know that by employing some procedure or using some drug or behavioral technique, they can reduce the pain or distress of research animals even by just a small amount. However, at least at present, investigators must sometimes settle for somewhat imprecise estimates of how much and what kinds of pain or distress research animals experience.

F4.3 The Incompleteness of the Pain and Distress Minimization Principle

Despite its persuasiveness and importance, the pain and distress minimization principle can never be sufficient to justify any animal research project that causes animals pain or distress. For it can conceivably be the case that an experiment causes no more pain or distress to the animals than is necessary for accomplishing a project's scientific aims, but the project aims at discovering such unimportant knowledge that the discovery of this knowledge does not seem to justify causing animals *any* pain or distress. It can also conceivably be the case that an animal research project causes so much animal pain or distress that, even though this amount is the minimum required for accomplishing the project's scientific aims, and even though the project aims to discover something that would be regarded as having some value, the value of this knowledge does not seem to justify this amount of animal pain or distress.

F5. The Pain and Distress Justification Principle

Any pain or distress that an animal research project will cause the animals must be justified by the value of the project, and the more pain or distress an animal research project will cause animals, the greater must be the value of the project to justify this pain or distress.

To support any given animal research project that causes animals pain or distress, the pain and distress minimization principle must be supplemented by Principle F5, which I shall call *the pain and distress justification principle*. To be ethically acceptable, the value of a project must justify the pain or distress experienced by the animals, even if this pain and distress is the minimum necessary to achieve the goals of the research. Additionally, because more or more severe pain or distress is a greater evil for animals than less or less severe pain or distress, the more pain or distress an animal research project will cause animals, the stronger must be the justification for causing this pain or distress. Expressed another way, the more the pain or distress, the more the project must be *worth* the pain and distress from an ethical standpoint, that is, the greater must the *value* of the research (Tannenbaum, 1999).

F6. The Harm Justification Principle

Any harm (including pain or distress) that an animal research project will cause the animals must be justified by the value of the project, and the greater the harms an animal research project will cause animals, the greater must be the value of the project to justify these harms.

It is important in considering how the pain and distress justification principle functions in assessing the ethical appropriateness of research projects, to consider the more general principle of which the pain and distress justification principle is a specific application. This is Principle F6, which I call *the harm justification principle.*

The pain and distress minimization and justification principles derive their persuasiveness from the more general ethical principles that it is wrong to cause a harm or evil to an animal without justification for doing so, and that the greater the harm one causes an animal the stronger must be the justification. Pain and distress are harms or evils for animals. However, they are not the only possible harms to animals that may sometimes need to be justified by the value of animal research projects. For example, as Morton (1995) observes, there are unpleasant feelings or emotions other than pain or distress that at least some research animals seem capable of experiencing, such as severe stress, fear, boredom, and anxiety. If the negative feelings of pain and distress experienced by research animals must be justified by the value of research, and must be minimized, there seems to be no reason why other feelings that can be at least as unpleasant do not also require justification and minimization.

F6.1 Determining the Value of a Research Project

For the purpose of determining whether a project's value justifies any harms it may cause animals, it is useful to separate the value of animal research projects into two components, what I shall call their *medical value* and their *scientific value*.

MEDICAL VALUE OF THE PROJECT

In asking whether an animal research project justifies any harms it may cause animals, the first thing many people probably will want to consider is its "medical value." I use this term to refer to the value or importance of understanding the disease or aspect of the disease the project investigates. In determining the level of a project's medical value, one would consider the nature, severity, and duration of the pain and suffering, distress, discomfort, fear, anxiety, and infirmity associated with the disease. One would also consider, among other things, whether the disease or aspect of the disease under investigation is life threatening or terminal; it impairs the ability of sufferers to enjoy a decent quality of life; there are a large number of sufferers; the disease is transmissible or easily transmissible to others; it impairs the ability of

sufferers to be gainfully employed; there are currently effective treatments; the disease is currently treatable only with methods that have serious risks or side effects; changes in lifestyle and behavior can prevent people who do not yet have the disease from contracting it; how it affects family members of sufferers; and the extent to which the disease currently or will in the future impose financial costs on the healthcare system or the economy.

SCIENTIFIC VALUE OF THE PROJECT

Clearly, to justify any harms a project may cause to the animals, an animal research project must do more than seek to understand a disease or an aspect of a disease that it is important to understand. A study that has high medical value in seeking, for example, a cure for a currently incurable form of cancer, begins with a goal that *if reached* would justify a great deal more animal pain or distress than would a project that seeks to discover something trivial or unimportant. However, the former project would not justify *any* animal pain, distress, or other significant harm if it seeks to achieve its important goals by asking questions that are not scientifically relevant to achieving these goals, or by employing methodologies that are not scientifically appropriate to answering questions that are relevant to achieving these goals.

To comply with the harm justification principle, an animal research project must have something more than medical value. The project must also have "scientific value," by which I mean that it must be sound from a scientific standpoint. The concept of scientific soundness (often called *scientific merit*) is complex and impossible to define succinctly. Indeed, one of the most important and difficult questions that scientists ask is how to determine whether various kinds of research are scientifically sound. However, it can be said that in determining the extent to which a project's scientific value justifies any harms it causes to animals, among the things one would ask are whether (1) the scientific questions addressed by the project are relevant to understanding the disease or aspect of the disease under investigation, (2) the animal model is appropriate to this task, (3) the project design applies the model correctly, and (4) the experimental procedures have some likelihood of answering the questions posed by the project.

- **Relevance of the NIH Concept of "Scientific and Technical Merit"** Investigators who have sought funding from one of the institutes or centers of the NIH are familiar with the NIH concept of "scientific and technical merit" (to which I shall refer as *scientific merit*). A detailed discussion of this concept is not possible here. Nevertheless, it is important to note that the concept of "scientific value" employed here incorporates many—but not all—elements of the NIH concept of scientific merit.

As defined by the NIH (2016b, First Level of Review, para. B, Peer Review Criteria and Considerations), the scientific merit of a research project is comprised of five general major characteristics: significance, investigator(s), innovation, approach, and environment. During SRG peer review of a grant proposal, each of these aspects receives a separate score, which are used to reach a final score for the project's scientific merit. Significance and innovation pertain to the quality or value of the scientific goals of the project. Approach, investigator(s), and environment relate to the likelihood that the project will fulfill these goals. Because applying these criteria is complex, difficult, and impossible to capture in brief definitions or rules that do justice to the variety of projects that are reviewed, the NIH lists several questions that an SRG should ask in assessing a project's value for each of the five general considerations. In assessing *significance*, reviewers are to ask: "Does the project address an important problem or a critical barrier to progress in the field? Is there a strong scientific premise for the project? If the aims of the project are achieved, how will scientific knowledge, technical capability, and/or clinical practice be improved? How will successful completion of the aims change the concepts, methods, technologies, treatments, services, or preventative interventions that drive this field?" The following questions are listed for assessment of *innovation*: "Does the application challenge and seek to shift current research or clinical practice paradigms by utilizing novel theoretical concepts, approaches or methodologies, instrumentation, or interventions? Are the concepts, approaches or methodologies, instrumentation, or interventions novel to one field of research or novel in a broad sense? Is a refinement, improvement, or new application of theoretical concepts, approaches or methodologies, instrumentation, or interventions proposed?" Questions reviewers are to ask about *investigator(s)* include "Are the PD/PIs, collaborators, and other researchers well suited to the project? If Early Stage Investigators or New Investigators, or in the early stages of independent careers, do they have appropriate experience and training?" Questions relating to *approach* include whether "the overall strategy, methodology, and analyses (are) well-reasoned and appropriate to accomplish the specific aims of the project" and whether "potential problems, alternative strategies, and benchmarks for success (are) presented." Questions relating to *environment* include whether "the scientific environment in which the work will be done contribute to the probability of success? Are the institutional support, equipment, and other physical resources available to the investigators adequate for the project proposed?"

As is apparent from the questions relating to significance and innovation, the NIH concept of scientific merit includes some measure of "medical value" as I have defined it. For example, one reason an SRG might determine that a project "addresses an important problem" is that the disease the project investigates causes suffering and death to many people. One reason peer reviewers may favor a project that could "shift current research or clinical practice paradigms" is that current approaches used to understand and treat a devastating disease have not been successful. At least as applied to biomedical animal research (which typically seeks to provide scientific foundations for subsequent human trials), most of the questions used by the NIH in determining scientific merit relate to what I have called scientific value. This is not surprising. An SRG might review a number of proposed projects that seek to understand the same disease or aspect of a disease. It must, therefore, often be the quality of the science of these projects that distinguishes those with greater scientific merit and likelihood of funding from those with less.

The inclusion of what I have termed a project's "medical value" and "scientific value" in the NIH concept of "scientific merit" doubtlessly works well for the intended primary function of the NIH concept, which is to facilitate decisions about which of the competing grant proposals will receive funding (NIH, 2016b). However, for the purpose of *ethical* assessment of animal research projects, it is useful to assess a project's medical value and scientific value independently and separately. Determining the importance of understanding a disease involves considering issues about such matters as how many people suffer from a disease, the nature of this suffering, and the economic costs of the disease on the healthcare system and the general economy. Such questions range far beyond the design of an animal research project. Careful consideration and assessment of the medical value of the disease that an animal research project seeks to understand is more likely to occur if such consideration is kept separate from addressing questions that deal exclusively with the scientific soundness of the project, and that can be answered by considering the scientific quality of the questions the project asks and the methodologies it employs.

In sum, the definition of "scientific value" employed here for the purposes of applying the harm justification principle includes the NIH definition of "scientific merit," with the exception of considerations that relate to what I have called medical value. This understanding of scientific

value is not intended to restrict scientific value to components of the NIH definition of scientific merit. What constitutes scientific value is a matter for scientists to determine. However, it is useful to incorporate elements of the NIH concept of scientific merit that relate to scientific soundness in any understanding of the scientific value that must play a role in the ethical assessment of animal research projects. The NIH concept of scientific merit is widely accepted by scientists as providing criteria for determining sound science. Moreover, many animal researchers are already seeking to design projects that have high scientific value as defined here because they are already seeking to design projects that have scientific merit as defined by the NIH.

F6.2 Determining Whether the Value of a Project Justifies any Pain, Distress, or Other Harms Caused to the Animals

There has thus far been relatively little consideration in the biomedical animal research ethics literature regarding precisely how one should determine whether the value of a project justifies any pain, distress, or other harms it will cause to animals. The following discussion attempts to provide some guidance in approaching this difficult but nonetheless ethically imperative task.

ASSESSING THE PROJECT'S MEDICAL VALUE

In applying the harm justification principle to a research project, an investigator might begin by reviewing its medical value. This would involve considering the criteria for determining medical value discussed earlier, including the number of people who suffer from the disease or condition; the pain and suffering, distress, fear, anxiety, infirmity, or death associated with the disease; the need for further understanding of the disease; its impacts on society; and so on. For all the diseases discussed in this book, this process will result in a determination of high medical value.

ASSESSING THE NATURE AND EXTENT OF HARMS TO THE ANIMALS

To ensure that any pain or distress experienced by animals is justified by the value of the project, an investigator must determine as accurately as possible whether and to what extent the animals will experience pain, distress and other kinds of significant harms. This is to be sure an immensely important and sometimes difficult task.

THE PROJECT'S SCIENTIFIC VALUE AS THE JUSTIFICATORY LINK BETWEEN MEDICAL VALUE AND HARMS TO THE ANIMALS

There is still one major missing piece that must be provided before it can be determined whether the value of a project justifies any harms it causes the animals. There must be a connection or link between the medical value of the project on the one hand, and any pain, distress, or other harms to the animals on the other, which allows the former to justify the latter. This connection is provided *by the project itself and by its scientific value*. If a project does not ask scientifically sound questions that would assist in understanding the disease or aspect of the disease under investigation, does not propose scientifically appropriate methodologies to answer such questions, or cannot succeed because the investigator does not have adequate facilities or staffing, the medical value of understanding the disease and of the project will be disconnected as it were from any pain or distress or other harms the project may cause the animals. It will, therefore, be impossible to appeal to the medical value to justify the harms. In contrast, if a project asks scientifically relevant questions, proposes sound methodologies, and has some likelihood of answering its questions, it will have a high level of scientific value. There will then be a scientific link between the project's medical value and any harms caused to the animals that will allow a determination of whether the former justifies the latter. Although the project may be unable to promise likely clinical applications at the time it is proposed (see discussion below), if it is scientifically sound it might provide knowledge that eventually could contribute to a clinical application. Moreover, the higher the scientific value of the project, the more likely the project will seem worth how it uses and treats the animals. A project with indisputably very high medical value and with exceptionally high scientific value that causes animals little or no unrelieved pain or distress will seem clearly justified; and such a project is likely to seem justified, even when there is some unrelieved pain or distress, and even if such pain or distress is significant, if this pain or distress is necessary to achieve project goals.

PREDICTABILITY OF RESULTS AND SCIENTIFIC VALUE

It is beyond the scope of this discussion to consider in detail the many ways in which various kinds of biomedical animal research can have significant scientific value. For purposes of understanding the harm justification principle, it is helpful, however, to note the relevance of the predictability of results to the scientific value and justifiability of biomedical animal experiments. As is recognized by several of the NIH criteria for scientific merit, an animal experiment *will* have very high scientific value if it *is* likely to lead to an important clinical application, such as a new and effective cancer drug. However, investigators who employ animal models can rarely claim their experiments are likely to result in clinical applications in humans, not because there is necessarily something wrong with their experiments, but because biomedical animal experiments rarely can promise likely

clinical applications. There are several reasons for this, which relate to the nature of biomedical research itself.

LIKELY LIMITED IMPACT OF SUCCESSFUL EXPERIMENTAL RESULTS

First, it will almost always be inaccurate and inappropriate to try to justify the harm any single animal research project may cause animals by claiming that this harm will be outweighed by the benefits associated with understanding and being able to combat the disease under study. No one project is likely to result in a complete understanding or treatment of a disease. Many experiments that investigate a disease about which much more needs to be learned will likely, even when successful, discover something that will add only a limited amount of knowledge to the understanding of the disease. However, even this limited value can justify harms the project does to the animals. The best that most individual projects *can* do is to achieve limited understanding of a disease. Moreover, if a project does contribute to understanding and conquering a disease, it will often be the results of the experiment, *together with the results of other animal research projects often of other investigators as well*, that will lead to understanding the disease. It is, therefore, unrealistic to demand, as does philosopher Bernard Rollin (1992, p. 140), that an animal research project is ethically justifiable only if "the benefit to humans (or to humans and animals) clearly outweighs the pain and suffering experienced by the experimental animals."

VALUE OF UNSUCCESSFUL PROJECTS

Science sometimes progresses by not succeeding. A hypothesis that one hopes to verify may prove incorrect, a general line of inquiry may not lead to fruitful results. Animal research projects that can be described as unsuccessful for such reasons may clear the way for eventual success by ruling out certain hypotheses, theories, or general approaches. Therefore, that an animal research project that seemed worth doing and ethically justifiable when begun fails to achieve its goals, does not imply the project was really not worth doing and did not justify harms it caused to animals. Unfortunately, it is usually difficult for investigators to learn, before doing an experiment, that a kind of experiment or procedure has been conducted by someone else and failed to yield valid or useful results. Journals usually do not publish reports of negative findings or failed experiments (unless included in reports of approaches that succeeded). Some investigators might understandably be reluctant to want to publish accounts of unsuccessful experiments. One of the major recommendations of the 2012 International Translational Research Task Force on epilepsy research, which was established to improve translation of animal experiments to clinical treatments of the epilepsies, was the exploration of acceptable and useful ways of disseminating negative experimental results (Galanopoulou et al., 2013).

UNPREDICTABILITY OF THE IMPACT OF RESEARCH RESULTS

An animal research project aimed at understanding a human disease may obtain results, the significance of which is unclear at the time of discovery. As Comroe and Dripps (1976) demonstrated, it often takes years, sometimes decades, for knowledge discovered by animal research to contribute to the understanding of a disease, in part because discoveries must sometimes await the results of research yet to be conducted. If an animal experiment aimed at understanding a human disease yields results that are not clearly applicable in understanding this (or another) disease, it would be unreasonable to conclude that years or decades may need to pass before it can be determined whether the project was ethically appropriate.

F6.3 Problematic Expressions of the Harm Justification Principle: "Harm–Benefit Analysis"

Investigators must pay careful attention to the harm justification principle, and not just because some procedures cause unrelieved pain, distress, or other harms. A widely endorsed interpretation of the principle appears to make it impossible for many experiments to justify the pain, distress, or harms they sometimes must cause animals. It is, therefore, essential that animal researchers, especially those engaged in basic research, insist that the harm justification principle not be interpreted improperly.

The *Guide* asserts the harm justification principle when it states (NRC, 2011, p. 27) that "due to their potential for unrelieved pain or distress or other animal welfare concerns," in certain protocols "the IACUC is obliged to weigh the objectives of the study against other potential animal welfare concerns." Although this statement does not use the words "harm" or "value" it clearly intends to ask that harms to animals be weighed against the value of experiments. In speaking of animal welfare concerns *other* than unrelieved pain or distress, the *Guide* recognizes that harm is the more general category of welfare problems to which research animals can be subjected, and that pain and distress, though critically important, are not the only possible harms that must be justified.

The *Guide's* statement of the harm justification principle does not attempt to specify or restrict the kinds of value that would justify various uses of animals. However, major difficulties for biomedical animal experimentation are created by some well-known expressions of the harm justification principle. These statements of the principle use the term "benefits" to refer to what *must* justify harms research animals experience, and they use the term "harm–benefit analysis" to refer to the process of justifying these harms. Moreover, by "benefits" these statements of the

harm justification principle usually mean *practical benefits*, such as discovery of a treatment for a disease. Additionally, these statements of the harm justification principle not only require "benefits" in this sense, but also require any experiment that harms animals to have, at the time it is proposed, a *high probability* or *likelihood* of resulting in such benefits. For example, as noted earlier, AAALAC interprets the statement from the *Guide* quoted previously to require an IACUC to conduct a "harm/benefit analysis," in which it would "weigh the potential adverse effects of the study against the potential *benefits* that are *likely to accrue* as a result of the research" (AAALAC, 2015, author's italics). The *EU Directive* demands a high probability of practical benefits when it asserts that investigators and review committees must engage in "a harm-benefit analysis of the project, to assess whether the harm to the animals in terms of suffering, pain and distress is justified by the *expected outcome* taking into account ethical considerations, and may ultimately *benefit human beings, animals or the environment*" (European Union, 2010, Art. 38 para. 2(d), author's italics). According to the Federation of European Laboratory Animal Associations (FELASA), "ethical evaluation should take the form of a harm-benefit assessment" (FELASA, 2005, p. ii), which consists of "considering ethical justification in terms of the balance of *likely benefit* over harm" (*id*., p. 20, author's italics).

WHY THE HARM JUSTIFICATION PRINCIPLE WHEN PROPERLY INTERPRETED SHOULD NOT REQUIRE LIKELY BENEFITS

If interpreted to require that any animal experiment project that causes animal pain, distress, or other harms must be likely to result in practical benefits, the harm justification principle would reject a great deal of potentially important biomedical animal research as unethical. Much of animal research is basic (in the objective sense) and cannot promise practical benefits at the time an experiment is proposed. Paradoxically, because some of the knowledge that basic animal research would discover will play a role in eventual clinical advances, requiring all animal research that might harm animals to be likely to produce clinical advances, will ensure that many clinical advances will never be made.

Moreover, even in the rare instance in which an investigator has good reason to think that an animal experiment, before it is begun, might lead to a clinical treatment for humans, it will often be impossible to maintain that there is a *likelihood* that this treatment will result from the experiment. Indeed, even after an animal experiment has been completed, and appears to have discovered a successful treatment in experimental animals, it will often be impossible to predict, before human trials are conducted, that the experiment will likely result in an effective and safe clinical application for humans. This is why human clinical trials are conducted.

PROBLEMATIC RESPONSES TO THE PROBLEM FOR THE HARM–BENEFIT ANALYSIS OF BASIC ANIMAL RESEARCH

Investigators should avoid and oppose two common and persistent responses to the problem that so-called "harm–benefit" analysis could eliminate much if not all basic animal research. Some have attempted to solve the problem by expanding the definition of "benefits" to include knowledge that is valuable for its own sake irrespective of whether it might ever contribute to practical benefits. It is also claimed that all, most, or (typically) an unspecified proportion of basic biological research will eventually contribute to clinical applications.

For example, in interpreting the UK ASPA, the Animal Procedures Committee (APC) established by the Act states that

> The "advancement of knowledge in biological or behavioural sciences" is a permissible purpose under Section 5(3) of the Act. Moreover, under the Act, such gains in knowledge are considered to be intrinsically valuable, and do not have to be instrumentally beneficial in order to provide an acceptable reason for using animals. In other words, they are considered to be actual benefits; they are not being judged simply on the basis of the potential or possible benefits to which they might lead. APC (2003, p. 49)

As discussed earlier, the view that it is permissible to cause animals harms, such as pain or distress, to obtain "intrinsically valuable" knowledge is abhorrent to many people, and could result in substantial public opposition to animal research if widely endorsed in the scientific community.

The APC also states that sometimes,

> although particular practical applications are not envisaged in research classified as fundamental, such research is usually carried out in areas identified as being of strategic importance, in which better knowledge can influence work more obviously directed at a practical application. For example, work to understand central nervous system receptor sites for chemicals produced in the brain could be classified as fundamental research, because the work is not directed towards any clearly identified practical application. But it is nevertheless apparent that the knowledge generated by such work could be used in research that is directed towards particular health care benefits in the future. APC (2003, p. 49)

This kind of general justification of basic animal research accords entirely with the general account of the harm justification principle presented in this chapter. In proposing the sort of experiment discussed by the APC, an investigator would—doubtlessly—characterize the potential medical value of the project by identifying a number of specific brain diseases the understanding of which the kind of knowledge sought in the project might advance. The investigator would also—correctly— observe that because these diseases involve or can be

affected by the functioning of brain chemical receptor sites, some of the knowledge the project might discover could some day assist in treating one or more of the specified diseases. What is problematic about the APC's characterization of this kind of experiment is the claim that the project is justified by harm–benefit analysis, as delineated by the UK ASPA, the *EU Directive*, and other statements of harm–benefit analysis quoted earlier. It is simply incorrect, and unhelpful, to try to make the case that the study described by the APC can promise *likely* or *expectable* practical benefits. About such a project one can and should say that it is in a *general area* of research in which *some* experiments can be expected, for good scientific reasons, eventually to contribute to the understanding of certain neurological disorders. It is for this reason that such a project can have high scientific value, if it asks clearly relevant or innovative questions about chemical receptors in the brain and if it proposes and can implement scientifically sound procedures to address these questions. It is on such matters relating to medical and scientific value that a determination of ethical appropriateness will focus, not on speculative and unverifiable claims of likely or expected benefits.

In 2016, a working group convened by AALAS and FELASA released a two-part report intended to explain and provide guidance to review bodies and investigators regarding "harm–benefit analysis" (Brønstad et al., 2016; Laber et al., 2016). The report will stimulate a good deal of useful discussion. Although it is beyond the scope of this chapter to examine the report in detail, two of its contentions are noteworthy here.

According to the report, "(b)enefits for human, animal or environment health are regarded as acceptable benefits to justify animal use as long as there are no alternatives. The intrinsic uncertainty whether promised benefits will be realized or not, must be compensated by strengthening the quality of the study to optimize the possibility of reliable known benefits" (Brønstad et al., 2016, p. 17). The second sentence appears to accord with the account of the harm justification principle presented in this chapter, as long as it is understood that "optimize" does not mean "make highly probable or likely." However, the AALAS–FELASA report also maintains that among what it calls "primary benefits" that can directly justify harming animals in research is "the intrinsic value of knowledge itself and the relevance of this knowledge in applications that are directly beneficial to humans and other species or the global environment and that sustain the quality and diversity of life" (p. 8). This statement appears to assert that intrinsically valuable knowledge itself sometimes justifies harming animals. The report also includes among "secondary" benefits that can justify harming animals when there also present a likely primary benefit, the "quest for knowledge" (p. 17), respect for which reflects "recognition of the intellectual arena,

the exercise of our creative imagination, rationality and problem-solving skills in the pursuit of the animal-based branch of science, which is part of our culture" (p.10).

It is not clear from the report when intrinsically valuable knowledge is supposed to constitute a primary or a secondary benefit. Nor is it clear when knowledge and associated intellectual activities are a secondary benefit, how strongly they can add to the justification of animal research harms. However, as noted earlier, a great many people believe that it is *never* appropriate to cause an animal pain, distress, or other harm in the pursuit of knowledge for its own sake. This view does not preclude using animals in research part of the *motivation* of which is pursuing knowledge for its own sake. However, this view does not countenance knowledge for its own sake as a sufficient or supplementary ethical *justification* for causing animals pain, distress, or other serious harms.

Like some others who attempt to reconcile basic animal research with the harm–benefit analysis, the AALAS–FELASA report also appears to make the fallacious claim that because many currently available clinical advances would not have been developed without past basic animal experimentation, current basic animal experiments can be counted on eventually to produce practical benefits. According to the report, "(w)hile basic research is burdened with some uncertainty regarding direct benefits, we have a long history of experience showing that basic research is beneficial for the development of society, especially with regard to taking advantage of technological progress" (p. 14).

F6.4 Further Needed Discussion of the Harm Justification Principle

In sum, I have suggested that what is needed is not harm–benefit analysis, but harm–*value* analysis, which includes but is not restricted to considering likely or expected benefits as a justification for causing animals pain, distress, or other harms. Much more discussion is needed to explain and apply such an analysis, and the harm justification principle. For example, as is observed below, there is some disagreement regarding what constitutes "harms" as understood by the principle, and greater consideration is needed regarding kinds of "value" that can justify various experimental uses of animals.

Another general issue that would be useful to consider is the extent to which projects that have higher scientific value, thereby justify causing more harm to animals. Determining scientific value (or "scientific merit" as understood by the NIH minus what I call medical value) is complex and requires balancing different criteria. For example, of two projects, *A* and *B*, that both seek to understand the same disease or aspect of the disease and thus have the same level of medical value, *A* might be judged by peer reviewers to have somewhat

more scientific value than *B* because, while both projects score well for significance, *A* is more innovative, because it examines novel methodologies for treating the disease. In such a case, it might not seem reasonable to conclude that because project *A* has somewhat higher scientific value than *B*, project *A* is justified in causing a somewhat higher amount of pain or distress to animals. On the other hand, if project *A* has a great deal more scientific value than *B* because of *A*'s innovativeness, *A* might well seem justified in causing significantly more pain to animals than *B*. Addressing such questions probably would require consideration of a large number of examples of research projects that involve varying levels of the components of scientific value. We might conclude that it is sometimes impossible to correlate different levels of scientific value with correspondingly higher or lower levels of justified animal pain or distress. It may sometimes or often be possible only to conclude that a given animal research project has *sufficient* value to cause certain harms to animals.

F7. The Harm Minimization Principle

An animal research project should cause no more harm (including pain or distress) to the animals than is necessary to achieve the scientific goals of the research.

This principle, which I shall call *the harm minimization principle*, is the more general and underlying foundation of the pain and distress minimization principle (F4), just as the harm justification principle (F6) is the more general and underlying foundation of the pain and distress justification principle (F5). The harm minimization principle holds that whenever a project causes animals something that would be classified as a harm, this harm should be minimized consistent with the project's goals. This principle follows from the ethical principles, discussed earlier, that one should not cause a harm or evil to an animal without a justifiable reason for doing so, and that to cause animals more harm than is necessary to achieve a project's goals is to cause harm that is provided no legitimate reason or justification by the goals of the research.

F8. The General Justification Principle

Whatever is done with or to animals in a research project (including but not restricted to causing harms, such as pain and distress) must be justified by the value of the project.

Questions about ethical justification of animal research typically involve research that causes or can cause harms to animals. The focus of ethical analysis in such cases is usually on whether the value of the research justifies these harms. As is discussed below, there are disagreements regarding what should be included in the definition of a "harm" to research animals. The term is typically used to refer at least to pain or distress, and not to much less

unpleasant experiences, such as very slight and brief discomfort. Merely using animals in a research project is not generally regarded as harming them, nor is euthanasia. If this is how harming research animals is understood, the majority—surely the great majority—of biomedical animal research projects do not cause *any* harm to animals. The only statistics available in the United States regarding how many animals experience pain or distress are compiled by the USDA for AWA-covered animals, which presently do not include mice and rats. In 2015, 445,972 or approximately 58% of the 767,622 AWA-covered animals did not experience any pain or distress and were not given any drugs to eliminate any pain or distress; 252,618 or approximately 33% would have experienced pain had drugs not been administered; and 69,032 or approximately 9% experienced some unrelieved pain or distress (APHIS, 2016b). Statistics issued by the UK Home Office (2016b, pp. 17–18), which include all vertebrate species, as well as cephalopods, indicate that for all procedures completed in 2015, 24% involved what the Home Office classifies as causing "moderate" harms (defined as causing "a significant and easily detectable disturbance to an animal's normal state, but this is not life threatening. Most surgical procedures carried out under general anaesthesia and with good post-operative analgesia (i.e., pain relief) would be classed as moderate"). Six percent of all procedures were assessed as "severe" (defined as causing "a major departure from the animal's usual state of health and well-being. It would usually include long-term disease processes where assistance with normal activities such as feeding and drinking are required or where significant deficits in behaviours/activities persist. It includes animals found dead unless an informed decision can be made that the animal did not suffer severely prior to death").

It is not the case that an animal research project that does not cause animals any harms is necessarily ethically justified. If a project has absolutely no scientific value, it is difficult to see how it is appropriate to use animals at all—even if the project would not cause the animals any harms, such as pain or distress. An animal experiment might lack scientific value because, for example, using animals will clearly not assist in answering the questions posed by the project; the questions the project seeks to address using animals are not relevant to the disease or condition supposedly under investigation; or the project repeats without variation an experiment that has been done before and regarding which no rationale can be provided for such repetition. One can object to such experiments on the grounds that they would involve a waste of money and animals that could be allocated to potentially valuable research. It also seems reasonable to think that employing animals in projects in which there is no legitimate scientific rationale for doing so constitutes an inherent misuse of the animals themselves,

a complete waste of them and of their lives if they are euthanized.

There is a well-known and widely accepted ethical principle that expresses the need to ensure that all animal research projects—those that do and those that do not harm the animals—are ethically justified. This is Principle F8, which I call *the general justification principle.* This ethical rule is stated in Principle II of the *US Principles* (OLAW, 2015b, pp. 4–5), discussed earlier. In asserting that "(p)rocedures involving animals should be designed and performed with due consideration of their relevance to human or animal health, the advancement of knowledge, or the good of society," Principle II does not explicitly or implicitly speak of harms. Principle II is reasonably interpreted as declaring that *whatever* is done to research animals must be justified by the value of the research. (To be sure, Principle II also identifies goods that, in its view, comprise the categories of research value; these are not included in the broad statement of the general justification principle offered here.) The general justification principle is the most general fundamental principle of animal research ethics. For the general justification principle includes the pain and distress and harm justification principles, and additionally includes *anything* that could require justification by the value of a research project.

F8.1 Applying the General Justification Principle to Projects That do and Those That do not Cause Animals Harm

When applying the principle to projects that cause harms to research animals, one would employ the harm justification principle component of the general justification principle, using an appropriate methodology for applying the harm justification principle. When applying the general justification principle to animal research projects that do not harm animals, one would apply a similar general methodology. One could begin by assessing the medical value of a project, and identify the use or treatment of animals the project must justify. One could then determine whether the project has sufficient scientific value to provide a connection between its medical value and the animal use that allows the former to justify the latter.

F8.2 Why Many Projects That do not Harm Animals Will be Easily Justified

When the general justification principle is applied to research that does not cause animals harm, it will very often be relatively easy to conclude that the research is justified, precisely because the treatment of animals to be considered does not rise to the level of a harm. As is discussed below, some people believe that a stronger showing of the value of a project is required to use or kill certain species in research (e.g., nonhuman primates), even if the research does not cause the animals any

"harms" as usually defined. However, for many research animals (e.g., mice and rats), most people would surely say that to justify simply the use of animals, and even their euthanasia, in a project that will cause them no pain or distress, there is not a great deal that the medical and scientific value of the project must justify. All the project must have is a legitimate scientific rationale for the animal use, that is, a scientifically sound reason for thinking that the project requires the use of animals, and that the project may answer questions relevant to an aspect of the disease under investigation.

To illustrate, consider the following example of a common use of animals that does not cause them "harms" as usually defined: obtaining cells or tissue for examination or further experimentation. An experiment with the general aim of understanding vision in mammals and eventually humans, euthanized mice after their arrival in the laboratory and harvested their retinas (Coombs et al., 2006). The investigators sought to determine whether certain staining techniques are superior in studying mouse retinal ganglion cells, and hoped to discover morphological patterns in these cells common to mice. One rationale for using mice was the investigators' view that because of possibilities of genetic manipulation of mice, the mouse retina may prove to be a valuable model for vision research. Although the project obtained the desired results, it was clearly ethically justified when proposed by its scientifically supportable and potentially successful aim of furthering understanding of the structure of the mouse retina. That the experiment would not cause any animal pain or distress ensured that the project's treatment of the animals was justified by its demonstrable scientific and medical value. Indeed, this project would have seemed ethically justified even if the investigators could provide just *some* reason for thinking they *might* discover *something* that might *some day* prove relevant to understanding mammalian and thus perhaps ultimately human vision.

This experiment illustrates why discussions of animal research ethics tend to focus on projects or kinds of research that cause animals harms, such as pain or distress. Nevertheless, it would be useful to consider a range of examples of experiments that do not cause animals harm. Such an examination might reveal that the threshold of justification for such projects is very low, and that the strongest objection against using animals in scientifically pointless experiments usually is that doing them is a waste of resources that could be allocated to valuable research.

F9. The 3Rs Principle

In designing and implementing animal experiments investigators should practice the "3Rs" of replacement, reduction, and refinement.

The so-called "3Rs," introduced by Russell and Burch in 1959, are so widely accepted, and are featured so prominently in laws and statements of principles of biomedical animal research ethics worldwide, that they must be regarded as belonging in the fundamental principles of biomedical animal research ethics. However, as is discussed in detail elsewhere (Tannenbaum and Bennett, 2015), there is considerable misunderstanding regarding what Russell and Burch meant by replacement, reduction, and refinement. There is also significant lack of clarity and disagreement about how the 3Rs ought to be defined, and about their underlying ethical justifications.

For the purposes of this discussion, it is sufficient to emphasize that Russell and Burch viewed all 3Rs as tools for minimizing research animal pain, distress, and fear. Their discussion of the 3Rs begins with

> consideration of the ways in which inhumanity can be and is being diminished or removed. These ways can be discussed under the broad headings of Replacement, Reduction, and Refinement. … Replacement means the substitution for conscious living higher animals of insentient material. Reduction means reduction in the numbers of animals used to obtain information of given amount and precision. Refinement means any decrease in the incidence or severity of inhumane procedures applied to those animals which still have to be used. Russell and Burch (1959, p. 64)

As is indicated by the beginning of this passage, for Russell and Burch, the *only* purpose of *all* the 3Rs is to diminish or remove what they call "inhumanity." They define "inhumanity" as "pain or fear inflicted on animals by man" (p. 15), as well as "distress of a certain degree (of whatever origin) … *which, if protracted, would lead to the physiological stress syndrome*" (p. 24). This is why their definition of "refinement" refers to a decrease in the incidence or severity of "inhumane procedures." (They understand "humanity" or "humaneness" as the absence of pain, fear, or severe distress.) For Russell and Burch, refinement aims, by definition, at minimizing pain, fear, and distress. Reduction can minimize pain, fear, and distress by using fewer animals that experience pain, fear, or distress. Replacement aims at minimizing pain, fear, and distress by substituting "conscious living higher animals" with "insentient material" that cannot experience pain, fear, or distress. Russell and Burch did *not* define "replacement" as not using animals; accordingly, they included in replacement the use of completely anesthetized vertebrates that do not experience any pain or distress during experimentation (p. 70). Additionally, although Russell and Burch are commonly said to have used the term "alternatives" to refer to the 3Rs, the word does not appear in their book. Indeed, Russell (who was responsible for most of the volume) never accepted the term because his overriding goal was not finding experimental methods that are alternatives to using animals,

but preventing or lessening research animal pain, distress, or fear (Tannenbaum and Bennett, 2015).

F9.1 Redefinition of "Replacement"

More recently, many—often citing Russell and Burch—have defined "replacement" as not using animals in research. For example, in its official policy on animal research, the AVMA states that it "endorses the principles embodied in the '3R' tenet of Russell and Burch (1959)," and defines replacement as "replacement of animals with nonanimal methods wherever feasible" (AVMA, 2016). The UK National Centre for the Replacement Refinement & Reduction of Animals in Research, sponsor of the ARRIVE Guidelines, defines "replacement" as "methods that avoid or replace the use of animals defined as 'protected' under the Animals (Scientific Procedures) Act" (NC3Rs, 2016). The *EU Directive* defines "replacement" as ensuring that "wherever possible, a scientifically satisfactory method or testing strategy, not entailing the use of live animals, shall be used" (European Union, 2010, Art. 4, para. 1). Such definitions appear to view replacement not as, or not just as, a means of eliminating or minimizing animal pain or distress, but as an aim that should be sought in its own right (Tannenbaum and Bennett, 2015). Rowan, for example, states that the "three Rs provide a broad-based approach to reducing both laboratory animal numbers *and* laboratory animal suffering" (Rowan, 1984, pp. 261–262, author's italics).

Those who define and promote replacement in the sense of not using animals rarely explain *why* investigators should try to use no animals, independently of the goal of minimizing pain and distress. It can be maintained that using no animals would reduce the expense of research, and that this would be a good thing in itself or might allow more research using the same financial resources; indeed, in enacting the AWA, Congress stated [Public Law 99-198, 1985, §1751(3)] that "measures which eliminate or minimize the unnecessary duplication of experiments on animals can result in more productive use of Federal funds." It can be argued that using no (or fewer) animals is preferable because using animals in research can be difficult, time consuming, or inefficient. It can be argued that eliminating use of animals in research is preferred by the public and thus would enhance public support for biomedical research. Perhaps the reason that no animals should be used is supposed to be that research animals are confined, or that many of them are killed. One or more of these arguments, or others, might well support not using animals. However, proponents of "replacement" as not using animals typically advance no reasons for this position. Perhaps some believe that it is just self-evident that it is better not to use animals in research than to use them.

Importantly, those who view replacement as a goal entirely independent of the aim of minimizing pain or distress appear to think replacement in this sense must be a goal of *all* animal research. It is supposed to be ethically obligatory to use no animals even if animals that are used experience no pain or distress, have a much better life than they would in natural environments, are "happy" when used in research, or are not killed during or after research. Some who define "replacement" as not using animals appear to believe that it is inherently wrong to use animals in biomedical research, and that when animals must be used because there is no alternative way of understanding a disease process, such research is an unfortunate necessary evil. It is clear why people would view using animals in biomedical research as inherently wrong if they believe that *all* uses of animals for any human purposes (such as for food) are unethical on the grounds that any human use of animals violates their moral rights (Regan, 2004.) However, this latter position does not seem to be held by many people in the research community who view not using animals in research as an end in itself. Their reasons for holding this view need to be made clear and explained.

F9.2 Redefinition of "Refinement"

Some people have adopted definitions of "refinement" that also depart from Russell and Burch's original definition. The *Guide*, for example, defines "refinement" to include not only minimization of pain or distress, but also providing animals "well-being" (NRC, 2011, p. 5), by which the *Guide* sometimes appears to mean the presence of positive, pleasant experiences. Such a definition seems to reflect a view that those who use animals in research have a general ethical obligation to provide these animals positive experiences, irrespective of the ability of such positive experiences to prevent or counter pain or distress (Tannenbaum, 2001; Tannenbaum and Bennett, 2015). The *Guide* does not indicate *why* well-being should be included in the goals of refinement. Buchanan-Smith et al. (2005, p. 382) concede that Russell and Burch restrict the purpose of refinement to the elimination of adverse experiences, such as pain or distress, and propose a new definition of "refinement" that includes providing positive experiences, such as well-being and happiness. One reason for this inclusion, they maintain, is that a purpose of refinement is improving the quality of research results, and in their view, happy and healthy animals increase the value, validity, and accuracy of scientific results. They also claim, without further explanation, that their revised definition is "in line with new developments in animal ethics and animal welfare science" (p. 384). For reasons outlined below, the claim that research animals are entitled to well-being or happiness is hardly self-evident and requires considerable clarification and supporting argument.

F9.3 The Need for Clarity and Argument

It would be useful for the field of biomedical animal research ethics to consider in depth how the 3Rs should be defined and what their goal or goals should be (Tannenbaum and Bennett, 2015). Sustained ethical discussion might demonstrate the advisability of including some pleasurable feelings among the goals of refinement, and might provide persuasive reasons for viewing replacement and reduction as ethically obligatory, independent of their capacity to minimize pain or distress. However, the only support that proponents of such views tend to offer are citations to Russell and Burch, who in fact did not view the 3Rs as anything other than tools for eliminating or reducing research animal pain, fear, and distress.

F10. The Species-Appropriate Housing Principle

"The living conditions of animals should be appropriate for their species and contribute to their health and comfort." US *Principles*, Principle VII (OLAW, 2015b, p. 5).

This rule, which I shall call *the species-appropriate housing principle*, is included in many professional association statements of principles of animal research ethics, as well as in governmental documents, such as the *US Principles*. One persuasive ethical basis for the principle is the pain and distress minimization principle. Species-appropriate living conditions often prevent pain or distress that might result when animals do not live or behave in certain ways that are natural to their species. However, it is possible to argue that research animals deserve species-appropriate housing that contributes to health and comfort because such housing does more than prevent or minimize pain and distress. For this reason, the species-appropriate housing principle raises conceptual, scientific, and ethical questions that require attention.

F10.1 Definitions of and Ethical Arguments for Research Animal "Well-Being"

One source of questions regarding the species-appropriate housing principle is the contention, which appears to be widely accepted in the research community, that a purpose of providing species-appropriate living conditions is to promote and enhance animals' "well-being." The *Guide*, for example, is replete with statements to the effect that "(t)he design of animal facilities combined with appropriate animal housing and management are essential contributors to animal well-being, the quality of animal research and production, teaching or testing programs involving animals, and the health and safety of personnel" (NRC, 2011, p. 41). The *Guide* further states that "(t)he primary aim of environmental enrichment is to enhance animal well-being by providing animals with sensory and motor stimulation, through structures and resources that facilitate the

expression of species-typical behaviors and promote psychological well-being through physical exercise, manipulative activities, and cognitive challenges according to species-specific characteristics" (pp. 52-53). Although the *Guide* contains definitions of many terms, it does not define or indicate clearly what it means by "well-being." The omission is important not just because the term is used frequently in the document, but because there are two different conceptions of animal "well-being" that have been used in the animal research community. Each of these conceptions reflects a different underlying *ethical* argument for providing well-being and species-appropriate housing for research animals.

WELL-BEING AS ABSENCE OF PAIN OR DISTRESS

Some commentators define research animal "well-being" as the absence of pain or distress. For example, Reinhardt (1993, p. 1) interprets the 1985 amendment to the AWA mandating environments for nonhuman primates conducive to their "psychological well-being" to require "that the barren cage environment of laboratory non-human primates must be enriched in order to ameliorate the adverse effects attendant upon chronic understimulation." Weed and Raber (2005, p. 120) define "refinement" (which will be considered further below) as "the use of methods that lessen or eliminate pain and/or distress and therefore enhance an animal's well-being." The NRC *Guidelines for the care and use of mammals in neuroscience and behavioral research* offers the identical definition (NRC, 2003, p. 10). Likewise, "comfort" provided by species-appropriate environments can be understood to mean the absence of discomfort or other kinds of distressful or negative feelings. Those who adopt such definitions of "well-being" or "comfort" employ the pain and distress minimization principle to justify the species-appropriate housing principle. They believe that one way of minimizing pain or distress animals can experience in research facilities is by affording them species-appropriate housing.

WELL-BEING AS INCLUDING POSITIVE FEELINGS AND EXPERIENCES

In contrast, "well-being" is sometimes understood to mean not just absence of pain or distress, but also the presence of positive experiences, such as certain pleasures, contentment, or happiness. Likewise, "comfort" can be understood as including certain positive experiences and not just absence of feelings of distress or discomfort. Those who employ definitions of "well-being" and "comfort" that include positive or pleasurable feelings believe that research animals deserve living conditions appropriate to their species and conducive to their comfort, in addition to, and independently of, their entitlement to minimization of pain or distress. For example, Buchanan-Smith et al. (2005, p. 382) use "the term 'well-being' to relate to both the physical health of the animal and to its psychological wellbeing." "The aim," they say, "should be not only to avoid or minimise adverse effects, but also to maximise well-being. This means that we must take a proactive approach in promoting the positive elements of welfare, such as companionship, comfort, and security." Indeed, they hold that one component of well-being is research animal *happiness*, asserting that "the enhancement of well-being has potential benefits to the science; 'happy' and healthy animals increase the validity and accuracy of scientific results." Rollin maintains that "all animals kept in confinement for human benefit" should be provided environments conducive to their psychological well-being and that accordingly the research community must "begin to seek animal-friendly housing, care, and husbandry systems that allow the animals to live *happy lives* while being employed for human benefit" (Rollin, 1995, Preface, n.p.).

The *Guide* sometimes rejects housing conditions that are not species-appropriate on the grounds that they result in pain, distress, or other significantly unpleasant experiences. For example, it is stated (pp. 50–51) that "(e)nvironments that fail to meet the animals' needs may result in abnormal brain development, physiologic dysfunction, and behavioral disorders … that may compromise both animal well-being and scientific validity. The primary enclosure or space may need to be enriched to prevent such effects." However, the *Guide* appears to adopt a concept of "well-being" that includes more than absence of pain or distress. It defines "refinement" as "modifications of husbandry or experimental procedures to enhance animal well-being *and* minimize or eliminate pain and distress" (NRC, 2011, p. 5, author's italics.). The *Guide* does not indicate what kinds of positive feelings or experiences it presumably includes within animal "well-being" and endorses as a reason for providing species-appropriate living conditions.

QUESTIONS ABOUT PROVIDING POSITIVE EXPERIENCES TO RESEARCH ANIMALS

Because the pain and distress minimization principle is unquestionably persuasive, it provides convincing ethical support for the species-appropriate housing principle. However, serious questions must be asked about the contention that research animals are entitled to positive experiences, such as pleasure, contentment, or happiness (Tannenbaum, 2001). These questions include how terms, such as "pleasure," "contentment," and "happiness" should be defined as applied to animals; whether and when it can confidently be said that research animals of various species experience these mental states; and whether, when, and how possibly

greater or lesser amounts of these states can be determined for various species. It must also be asked whether requiring pleasures or happy lives for research animals, assuming we know what this means and how to provide it, would hinder or preclude valuable research by greatly increasing its economic cost. Moreover, if providing a "happy life" or even more limited pleasures for *all* research animals is ethically obligatory, any experiment that must cause some unrelieved pain or distress, or is not consistent with animal happiness, might be unethical. Perhaps sustained ethical discussion will demonstrate that it is conceptually and ethically appropriate to interpret the species-appropriate housing principle to require positive feelings of pleasure, contentment, or happiness, for all or for some research animals. However, this interpretation should not be accepted without clearly expressed and persuasive arguments.

F10.2 Environmental Enrichment

A second source of the need for further thinking about the meaning and ethical foundations of the species-appropriate housing principle is the fact that providing such housing is now widely understood to require not just basic conditions, such as clean air and water and sufficient cage space, but also environmental enrichment. Although the AWA requires enrichment only for nonhuman primates [AWA, 2013 §2143(a)(2)(B)], the *Guide* maintains (NRC, 2011, pp. 52–54) that species-appropriate housing includes environmental enrichment for all species covered by the *PHS Policy*. In the biomedical research community generally, understanding and applying enrichment techniques to all species used in research is regarded as a major priority (Wolfle, 2005).

DIFFERING DEFINITIONS OF "ENRICHMENT"

One reason inclusion of enrichment in the species-appropriate housing principle raises issues regarding how and why the principle should be applied is that there is disagreement about how "enrichment" should be defined. As Newberry (1995, p. 230) observes, the term is sometimes used to refer to certain kinds types of environmental change (such as group housing or various kinds of feeding mechanisms), is sometimes defined as an increase in environmental complexity, and sometimes refers to positive outcomes for the animals' welfare. Lack of uniformity in definitions can make it difficult to engage in a discussion of enrichment and its ethical foundations.

DIFFERING VIEWS OF THE AIMS OF ENRICHMENT

Another source of difficulty in considering whether and why certain kinds of enrichment might be ethically obligatory is the fact that proponents of enrichment differ about whether enriched environments are ethically obligatory solely because these environments can prevent or ameliorate pain or distress, or also because they may sometimes result in positive experiences, such as pleasures, contentment, or happiness. All the authors quoted earlier regarding the nature of and ethical arguments for animal "well-being" are discussing not just well-being, but environmental enrichment, which they view as promoting well-being. Thus, inclusion of enrichment in the species-appropriate housing principle raises the same issues discussed earlier regarding whether and why providing certain kinds of positive experiences to research animals might be ethically obligatory.

POTENTIAL EFFECTS ON RESEARCH RESULTS

Also important in considering when investigators may be ethically required to provide enriched environments is the fact that there have been conflicting claims regarding whether enrichments of various kinds impact research results positively, negatively, or not at all (Bayne, 2005). There is evidence that at least in certain kinds of studies and for certain kinds of animals, enrichment can lessen deleterious effects of captive environments and can improve the validity, reliability, and replicability of research results (Garner, 2005; NRC, 2011, p. 54). On the other hand, various ways in which enrichment can make the housing environment more complex are sometimes not conducive to animal welfare, or can introduce variables that might adversely affect the quality of experimental data. Benefiel et al. (2005, p. 103) concluded, after reviewing a wide range of enrichment techniques in various kinds of research, that "not all—and maybe not most—forms of supplementation are beneficial for laboratory animals or good for research." As is discussed earlier, the strongest justification for using animals in a research project, and for causing pain or distress when necessary, is that the project has medical and scientific value. If enriched housing conditions would jeopardize the scientific results of a project, the justification for using the animals can be weakened. Assuring that enriched environments are good for the research, as well as for the animals is, therefore, an ethical, as well as scientific imperative.

F11. The Appropriate Care Principle

While housed in the research facility, animals must receive appropriate veterinary supervision and care, and the conscientious attention of trained animal care staff.

This principle, which I shall call *the appropriate care principle*, is based at the very least on the pain and distress minimization principle. Insofar as animals may be ethically entitled to positive experiences, such as certain pleasures, contentment, or happiness, it can be argued

that these experiences constitute part of the reason they should be afforded good veterinary care and skilled attention from animal care staff. The ethical obligation to provide such care and attention is also implied by Principle F12, because being kind, compassionate, and grateful to research animals involves attending to their medical and behavioral needs.

F12. The Appreciation Principle

Research animals should be treated with kindness, compassion, and gratitude.

What I call *the appreciation principle* reflects the fact that research animals do not volunteer for experiments. Additionally, most are kept in confinement, few can exhibit all their natural behaviors, and some experience unrelieved pain or distress. This is almost always done not for their benefit, but ours. Although research animals are incapable of volunteering, or of understanding or entering into a contract or bargain, surely in return for what they give up and provide, they are entitled to kind and compassionate treatment and care.

Gratitude for what research animals make possible is also important. One cannot express gratitude to animals in ways that they would understand as gratitude. However, there are tangible ways, aside from proper treatment during research and in housing and general care, in which gratitude sometimes can be expressed. One issue of increasing interest in the research community is whether, to what extent, and how investigators and research facilities should deal with animals that survive research projects. Aside from euthanasia, possible options for animals that are not diseased or disabled can include transfer to another investigator in the facility for use in research; transfer to another research institution; resettlement in a sanctuary where they will not be used in research (as has been the case for some nonhuman primates); or for some kinds of animals, adoption as pets. A survey of research institutions in the United States found that 71 of 177 IACUCs permitted adoption of animals as pets after use in research under specified circumstances (Huerkamp and Archer, 2007, p. 222). Adoption can be a tangible way of thanking some animals for their service to research. Difficult questions can be raised about adoption and other options that do not involve killing animals, for example, about appropriate criteria for choosing adoptive owners; about who should pay for or engage in efforts to adopt or place animals no longer needed by an investigator or institution; and about whether and when it may not be ethically acceptable to subject usable animals to still more research (and the possibility of pain or distress) by reusing or sending them to another research institution.

F13. The Translation Principle

Investigators should support, stay informed about, and when appropriate engage in scientific and professional efforts aimed at effecting translation of animal experiments to clinical applications.

The most significant general development in recent years in biomedical research arguably has been the emergence and development of the field of translational science and medicine. This general scientific endeavor is universally endorsed by investigators, government regulators, and funding agencies. However, what I call *the translation principle* is not yet routinely included in government or professional association statements of fundamental rules of biomedical animal research ethics. The principle belongs in any such statement. The translation principle is as important as any ethical rule relating to biomedical animal research because following the principle will likely facilitate application of the pain and distress and harm justification principles.

In light of the inherent complexity of disease, and the ways in which biomedical research progresses, it is unrealistic and unreasonable to demand that all animal experiments, when proposed, be likely to result in clinical applications for humans. However, as observed earlier, any likelihood that an experiment will lead to clinical applications will enhance its scientific value in justifying harms it might cause to animals. Therefore, if investigators could know that certain kinds of animal experiments or certain kinds of experimental procedures might be likely—or more likely than other kinds of experiments or procedures—to lead to clinical applications, they might be able to conduct experiments that provide increased justification for using animals, and for harms the animals might experience. Similarly, if investigators could know that certain kinds of experiments or procedures are not likely—or less likely than other kinds of experiments or procedures—to lead to clinical applications, they might be able to spare animals unjustifiable harms by not conducting such experiments.

It cannot be known at present whether advances in translational science will lead to a decrease in the total number of animals used in biomedical research, and thereby to a decrease in the total amount of research animal pain, distress, and other harms. Perhaps improved translation will reduce research animal numbers. However, it is possible that in certain areas of research, use of animals will become so much more productive in developing and testing clinical applications that more and not fewer animal experiments will be conducted. There may also be forces independent of translatability that could lead to use of more animals in total, such as the need to breed large numbers

of transgenic mice; required testing of advances suggested by experiments on this or other species on animals higher on the phylogenetic scale; or the development of kinds of animal experimentation that are at present unpredictable. On the other hand, more efficient translation might lead to a lessening of even these numbers.

The translation principle not only aims at properly treating animals, it also seeks to benefit and ensure the ethical treatment of humans. In areas where translation from animal studies to clinical applications has thus far been disappointing, development of treatments can be hindered by the reluctance of pharmaceutical companies and other funders to invest in animal experiments that will be needed to develop and test such treatments (O'Brien et al., 2013). Generally, conducting animal experiments that are more likely to produce clinical applications should allow government and private funding agencies to allocate available resources more efficiently, so that experiments can be directed toward the widest possible range of disease states, and can be conducted by as many talented investigators as possible.

As noted earlier in the discussion of the Nuremberg principle, humans are not only beneficiaries of biomedical animal research, we also occupy an essential role in the link between animal experiments and clinical applications. At least at present, it can rarely be known with certainty what most human clinical trials will find. However, the more probable that animal studies on which such trials are based will lead to clinical applications, the stronger the case that can be made to enroll human volunteers in associated clinical trials. Moreover, the more that can be learned about potential translation of animal studies on which human clinical trials are based, the more that can be told to potential volunteers about possible risks and benefits to them, so that they can exercise the best possible informed consent before they participate in these studies (Kimmelman and London, 2011).

11 PRACTICAL ETHICAL GUIDELINES FOR INVESTIGATORS

The preceding discussion suggests a number of practical ethical guidelines for investigators. These practical guidelines are designated as P1–P10.

P1. Approach all phases and aspects of an animal research project with the aim of making the project ethically as well as scientifically sound

Particularly good times to review the ethical soundness of a project are when one is thinking about the project as a whole; for many investigators this will be during the preparation of a grant proposal and of an IACUC animal use application. After a project has begun, anything that would require notification to the IACUC of a significant change in the nature of the research, such as a change in project goals, procedures, or numbers of animals [AWAR, 2015, §2.31(d); OLAW, 2015b, para. IV.B.7, p. 13], should be accompanied by consideration of whether any of these changes would affect the project's ethical appropriateness.

P2. Appreciate that as the source of the project's scientific goals, you play the key role in determining whether the project will be conducted ethically

See the discussion of the ethical importance of project goals and of the harm justification principle (Principle F6) earlier in this chapter.

P3. Keep in mind that the central question in the ethical assessment of a project is whether its value justifies its use and treatment of animals; that the value of a project consists of its medical and scientific value; and that the greater the value of the project, the more likely the project will justify its use and treatment of the animals

See the discussion of the harm and general justification principles (Principles F6 and F8) earlier.

P4. To be able to make the strongest case for the medical value of the project, always keep up-to-date information and documentation, which is readily understandable by laypersons, regarding the nature, effects, and need for further understanding about the disease or the aspect of the disease under investigation

An investigator who conducts serious animal research regarding one of the diseases discussed in this book will already have extensive knowledge about why it is important to gain further understanding of the disease or the aspect of the disease under study. However, it is useful to be able to include in a complete argument for the ethical justification of a project current information and documentation that can establish its medical value beyond a doubt. A comprehensive and detailed account of a project's medical value, in language that is understandable by laypersons, can also help investigators explain to members of the public why their work is important.

P5. Design the project with the maximum possible scientific value, by framing sound scientific questions that relate to the medical value of the project, by designing scientifically sound research procedures aimed at answering these questions, and by assembling facilities and staff that will enable the project to achieve its goals

This is what biomedical scientists always seek to do in the conduct of high-quality science. See the discussion of the harm and general justification principles (Principles F6 and F8) earlier.

P6. If the project has the potential to cause harms to animals, specifically pain or distress, but also any other significant unpleasant experiences, assure yourself that these harms are not only necessary to achieve project goals, but are ethically justified in light of the value of the project

See the discussion of the pain and distress justification principle (Principle F5) and the harm justification principle (Principle F6) earlier.

P7. In designing and conducting the project, take all reasonable steps to minimize any pain or distress that the animals may experience, consistent with project goals

As I have suggested, minimization of pain or distress may well be a subject regarding which investigators would find it helpful to have a number of specific ethical rules. Aspects of project design and execution that the pain and distress minimization principle can impact are numerous, and include the following: animal identification methods; anesthesia during surgery; use of analgesics for pain prevention or relief; methods of sampling blood and other tissues; injection sites and methods; kinds and duration of physical restraint; tumor size and location; forced exercise; aversive behavioral stimuli; use of adjuvants; deprivation of food or water; minimization of pain and distress in control animals; determination of humane endpoints; euthanasia; and training of researchers and research staff regarding appropriate handling of animals in experimental procedures. In the absence of more specific practical ethical guidelines for minimizing pain or distress—and perhaps even if such guidelines become available—investigators might consider the general approach suggested by Carbone (2007, p. 163):

> First, visualize every step in the animal's life from the initial point of contact (birth at the facility or arrival into the facility) until the animal's euthanasia or departure from the institution.

List every reasonable source of significant pain or distress, whether related to housing or the experimental procedures. Each of these potential sources of pain or distress should then be addressed, whether in a targeted literature search, consultation with peers who have published on the methodology, or consultation with veterinarians and animal care specialists, and with as much creative thinking as the investigator can muster.

P8. Regard your attending veterinarian as a constant source of information and guidance during all stages of the project

Laboratory animal veterinarians have expertise in minimization of pain and distress and in animal housing and care. As members of or advisors to IACUCs, they keep abreast of regulatory requirements. They have knowledge of kinds of biomedical research and experimental techniques and effects of these techniques on research animals. Consultation with a veterinarian during project design can help ensure that subsequent modifications required by legal standards will not be necessary. Veterinarians can also help ensure that a project is conducted ethically by assisting in eliminating or minimizing potential harms to animals in a project's design or implementation.

P9. Collect, read, and regularly consult publications that enunciate or apply ethical principles relevant to your research

See the earlier discussion of sources ethical guidance in conducting ethical research.

P10. Although you should follow legal requirements applicable to the project, when such requirements impose only minimum ethical standards, appreciate that conducting research ethically may involve exceeding these standards

As observed earlier, legal requirements sometimes impose important, but nevertheless minimum, ethical standards. Investigators should not ignore or put aside reasonable ethical questions relating to a research project on the grounds that the project may meet all ethical expectations that are required by law. The fundamental ethical imperative of using animals for good reasons and treating them properly and the importance of assuring public support of animal research are the only two reasons for trying to exceed legal standards if ethical requirements demand more. Another is that if investigators are thought by regulators or the public to be violating ethical standards that are not yet mandated by law, the result may be additional regulations and government supervision of research. This may not always

be salutary for ethical discussion, much less for research. Some issues in animal research ethics are difficult and complex. Regarding such issues, ethical deliberation may sometimes be best left open to debate, with possible approaches emerging widely and voluntarily, after extended consideration of varying viewpoints, rather than being imposed by legal edict.

12 SOME CURRENT DIFFICULT ISSUES IN ANIMAL RESEARCH ETHICS

There are issues in biomedical animal research ethics regarding which there is a lack of clarity or disagreement in the research community, and that require considerable thought because of their complexity and potential implications. One such issue, discussed earlier, is whether, to what extent, and why research animals might be entitled to positive experiences, such as pleasures, contentment, or happiness. Other ongoing ethical issues include the following.

12.1 The Nature and Weight of Harms to be Justified by the Value of Animal Research Projects

The harm justification principle holds that any harm (including pain or distress) that an animal research project will cause animals must be justified by the value of the project, and the more harm an animal research project will cause animals, the greater must be the value of the project. There are difficult issues regarding what counts as "harms" to research animals and how much weight such harms should be given in determining whether they are justified by animal research projects.

Unpleasant Experiences Other Than Pain and Distress

Pain and distress are clearly harms to research animals, and their nature, intensity, and duration must be weighed against the value of a research project. I suggest earlier that if pain and distress count as harms that must be justified by the value of animal research projects, some other negative experiences, such as fear (which is included by Russell and Burch among such harms), anxiety, and boredom sometimes might also have to be counted as harms. Whether and to what extent research animals, or some research animals can experience such emotions is a matter for further empirical investigation (Tannenbaum, 2001). Ethical discussion is also needed to determine the extent to which such experiences would constitute harms, and the value that various kinds of animal experimentation might need to outweigh these harms.

Frustration of an Animal's Nature or Telos

Some philosophers and animal welfare advocates believe that, as Rollin (1992) argues, the inborn nature or to use the Aristotelian term *telos* of animals is entitled to respect by people who use animals for their benefit. According to this view, preventing animals from engaging in certain kinds of natural activities harms them, in addition to and independently of any pain, distress, or other unpleasant feelings they may experience as a result. Though sympathetic to this view, Thompson (2010) concedes it has problems, the significance of which have not yet been adequately examined. For example, allowing animals to engage in natural behavior is sometimes inimical to their welfare by subjecting them to risks of injury or disease. It is also doubtful, I would suggest, that natural tendencies, irrespective of distress or severe discomfort their frustration might cause, are entitled to respect in their own right. Humans are programmed by our inborn nature to grow old and die. Yet much of medical science seeks not only to change this process from what it would be if nature were allowed to take its course, but to postpone and perhaps even eliminate this natural process altogether. If some natural behaviors or tendencies are good and others are bad, it cannot be just the fact that they are natural that make them so. If there is something wrong in restricting some natural behaviors of research animals, other than the fact that animals may experience pain, distress, or other unpleasant feelings, what this is needs to be identified and explained. If preventing research animals from engaging in certain behaviors is in itself harming them, it also would have to be determined how strong such harms are and how strongly they might count against conducting certain kinds of research.

Killing Research Animals

There is a disagreement in the animal ethics and animal welfare literature regarding whether death in itself (i.e., death irrespective of whether it occurs with pain or distress) constitutes a harm to animals. Some thinkers (Regan, 1983, pp. 99–103) argue that death is a misfortune or harm for animals and that killing inflicts harm on them because it prevents them from having a future life. Others (Cigman, 1981, pp. 53–59; Webster, 1994, p. 15) maintain that killing animals does not harm them or their welfare because they do not have a concept of life and a desire to live, or a concept or a fear of death. The prevalent view in the research community appears to be that whether or not killing animals harms them, the fact that a research project kills animals is not relevant to determining whether the project is ethically justified. Cancer researcher Harold Hewitt (1981, pp. 169–170) accurately characterizes the prevailing position.

I must confess that my own concern is really not with the number of animals (used in an experiment), in the sense that I should be more upset by my having caused one animal to suffer by my neglect or ineptitude than I should be by administering euthanasia to 50 at the termination of an experiment in which none had been caused suffering. The question the prospective animal experimenter has to ask himself is whether he considers that the painless taking of animal life is itself an immoral act. For me it is not. ... I do not see the moral distinction between the taking of an animal life in the laboratory, in the slaughter house, or in the course of pest control.

This view is reflected in the AWA and HREA, neither of which requires that killing animals be justified on scientific grounds, and regarding killing require only that killing be done without causing pain or distress [AWAR, 2015, §1.1, §2.31(d)(xi); OLAW, 2015b, para. IV.C.1.g, p. 14]. In many years discussing animal research ethics with investigators, IACUC members, and veterinarians, I have encountered an increasing number of people who believe that killing certain kinds of animals, specifically nonhuman primates and cats and dogs, necessitates a stronger justification than does killing mice, rats, or fish, for example. If this view represents a trend in the research community and society generally, the issue of the ethical relevance of species will become increasingly important in discussions of biomedical animal research ethics.

12.2 Ethical Relevance of Species and Species Characteristics

The IOM Chimpanzee Report

In 2011, a committee appointed by the NRC IOM issued a report on the use of chimpanzees in biomedical and behavioral research (IOM, 2011). The committee recommended that chimpanzees be used in research only if the "knowledge gained is necessary to advance the public's health" and only if there is "no other research model by which the knowledge could be obtained, and the research cannot be ethically performed on human subjects." (p. 4) The committee also stated (p. 15) that "imposing requirements for justifying the use of higher species is an implicit recognition that use of higher animals comes at higher moral costs." In 2016, exceeding the restrictions on chimpanzee research recommended by the IOM report, the NIH (2016a) decided not to fund any new projects or renewals or revisions of ongoing projects involving chimpanzees, with the exception of projects involving noninvasive research. Among the matters the NIH regards as "noninvasive" are "visual observation," "behavioral studies designed to improve the establishment and maintenance of social groups," and "collections of biological materials (e.g., saliva, oral or other cavity specimens, urine, feces, or hair) obtained voluntarily from a chimpanzee that has been trained through positive reinforcement to cooperate in the collection. This excludes venipuncture or other more invasive methods."

The Relative Moral Cost View

Whether one agrees with the IOM committee's recommendations or the NIH's decision regarding chimpanzees, there are some, probably many, people who believe that using certain species in research requires stronger ethical justification than does using other species. I shall call this the "relative moral cost view." This view does not imply that harms, such as pain and distress, are less important to minimize and justify in certain species than in others. Pain and distress are evils for any animal that can experience them, and investigators are ethically obligated to cause only the minimum necessary amount of justifiable pain or distress to achieve research goals. Nor does the relative moral cost view involve the claim that because of their mental capacity some species (e.g., nonhuman primates) may be capable of experiencing more pain or distress than other species, and research causing pain and distress in these animals may, therefore, require a higher value to justify this higher level of pain or distress. As commonly expressed, the relative moral cost view holds that a stronger justification—that is, a higher value of a research project—is required simply to use or kill certain species, even if the research causes these animals no pain or distress.

Criteria for Ranking Species

The relative moral cost view raises many difficult questions. First, if species are to be ranked, persuasive criteria are needed for such ranking. In speaking of "higher animals," the IOM report appears to suggest that the criteria to be used relate to characteristics, such as mental sophistication and complex emotions. These criteria may effectively distinguish nonhuman primates from other animals, but may not do justice to all discriminations that many people seem to want to make. For example, doubtlessly many people think a stronger showing of the value of a research project must be made for using and killing dogs than pigs. However, pigs are extremely sophisticated mentally and socially, perhaps no less so than dogs. What seems to distinguish pigs from dogs is not that dogs are "higher" animals, but that in many countries dogs are beloved pets and pigs are food. Rowan and I have suggested (Tannenbaum and Rowan, 1985) a number of criteria for distinguishing species in ways that support demanding a stronger showing of the value of research in using certain species. These criteria include whether animals exhibit self-awareness, their mental complexity, the complexity of their natural social behavior, and whether and how they interact with human beings. These criteria support the widely held view that using

monkeys, cats, and dogs, for example, requires a stronger justification than using mice or rats. Moreover, the criteria suggest that many peoples' inclination to require a stronger justification for using dogs than pigs in research is supported by the regular (and often emotional) involvement of people with dogs. However, it is not clear why this cultural and historical preference for dogs over pigs would *justify* requiring a higher value of research for one of two species with comparable mental and behavioral capacities.

Number of Ranked Categories

If species are to be ranked, it must also be decided how many categories of ranking should be employed. It can be argued that if it makes scientific and ethical sense to rank species for the purpose of justifying their use, we should separately rank *all* species commonly used in research. This might involve placing all species along a spectrum, presumably with chimpanzees at the high end, with amphibians and fish, for example, far down the scale. One might then assign a different level of moral cost to the research use of each species, and require a stronger justification for use in research the closer each species is located toward the chimpanzee end of the spectrum. One can only begin to imagine the arguments this approach would engender. Some people might argue, for example, that baboons should be distinguished from and ranked higher than other monkeys. Some might argue that rabbits are higher on the scale than hamsters or guinea pigs, or that hamsters or guinea pigs are or are not higher than rats or mice, that rats are or are not higher than mice, and so on.

Alternatively, one could argue for a smaller number of ranked categories, some or all of which would consist of multiple species. Such an approach might place chimpanzees in the first category, other nonhuman primates next, dogs and cats in the next category, and then perhaps all other species. Perhaps baboons would be distinguished from other monkeys and placed in a separate category closer to the chimpanzee end of the spectrum. Perhaps rabbits would be recognized as a separate category closer to chimpanzees than guinea pigs or hamsters. These and other possible ways of recognizing ranked categories would presumably be based on whatever criteria are regarded as appropriate for ranking. There could well be vigorous disagreements about how many groupings there should be, and the species membership of these groups.

Research Implications of Species Rankings

Finally, if species are to be ranked, it must be determined how much moral cost is associated with each ranked group or species, so that it can be determined how much value a given animal research project must

have to outweigh this cost. Moreover, it might be necessary to determine whether certain ranked groups or species may be used in certain, but not other kinds of research. For example, it might be deemed appropriate to use monkeys in research aimed at understanding diseases, such as AIDS and Ebola, but not in certain kinds of behavioral studies.

The aim of this discussion is not to reject ranking or some ranking of research animals. What is needed is a great deal of further discussion and supporting argument, *if* we want persuasively and consistently to rank various species for the purpose of determining how strong a showing must be made of the value of experiments before these species may be used in research or certain kinds of research.

13 GENERAL SUGGESTIONS FOR INVESTIGATORS

The following suggestions are offered to investigators for engaging in activities beyond the laboratory setting.

S1. Communicate to the public the nature and potential benefits of your research, and the ethical values and standards you apply in all phases of your work

As observed earlier, public support is essential for the continued conduct and funding of biomedical animal research. No one can speak more knowledgeably and persuasively about the nature, potential benefits, and ethical conduct of biomedical animal research than investigators. No one can speak more knowledgeably and persuasively about the value and ethical appropriateness of individual biomedical animal experiments than the investigators who conduct these experiments (Nature, 2011; Ringach and Jentsch, 2009).

S2. Become familiar with some of the animal research ethics literature

Some investigators may find the animal research ethics literature inaccessible or unwelcoming. Much of this literature employs specialized philosophical or legal terminology and theories with which scientists may be unfamiliar. Moreover, as one philosopher (a critic of animal research) correctly observes, "more is written in moral opposition to animal experimentation than in its support" (Nobis, 2011, p. 298).

There are a number of reasons animal researchers should not avoid or ignore the academic animal research ethics literature. Animal activists who seek to eliminate all animal research derive their opposition and many of

their public relations and political tactics from the views of academic philosophers and lawyers (Conn and Parker, 2008; Miller, 2011; Regan, 2004; Smith, 2010). At the very least, researchers should be familiar with the underlying beliefs of animal research opponents.

Additionally, there is much in the animal research ethics literature to which investigators can respond on empirical grounds. Two fundamentally different approaches have been adopted by opponents of animal research. What is typically called the "animal rights" approach, maintains that using animals for the benefit of humans or other animals is an inherent violation of these animals' moral rights, whatever benefits such uses might bring to humans or other animals (Francione, 2000; Regan, 1983, 2004; Wise, 2001). There is some disagreement among proponents of this approach regarding what kinds of animals have such rights and why. However, all such animal rights proponents agree that is wrong to use mammals in research, even if this research results in medical benefits for people or animals, and even if the research causes the animals no pain or distress, or does not involve killing them. However, there are philosophers and other critics of animal research who base their opposition on what they claim in fact results from or happens to animals in research. For example, Peter Singer, the author of *Animal liberation* (1975), objects to animal research on the grounds that in his view it results in no medical benefits, or that benefits it does bring to people or animals are greatly outweighed by pain and suffering which (he claims) experimentation causes animals. Using their knowledge of animal research and of their own projects, investigators can argue against this kind of objection by pointing to what animal research has discovered and how research animals are actually treated.

Finally, as discussed earlier, there are unresolved difficult ethical issues in animal research ethics. Contributions to discussions of these issues by advocates of *all* viewpoints will be encouraged, if animal researchers take an active and continuing interest in philosophical and legal debates about animal use in general and animal research in particular.

There are publications that investigators will find accessible and that can ease one into the animal research ethics literature. Among these are general accounts of current and historical controversies (Conn and Parker, 2008; Rudacille, 2000; Smith, 2010), collections of papers that discuss general ethical issues in animal research (Kraus and Renquist, 2001; Paul and Paul, 2001), and the autobiography of a prominent animal researcher (Morrison, 2009). These publications are more sympathetic to biomedical animal research than is much of the philosophical literature, but for this reason provide good starting points for further reading.

S3. Participate in discussions of ethical issues relating to biomedical animal research

Investigators play the key role in ensuring the ethical conduct of biomedical animal research. It is, therefore, essential that you participate in discussions of ethical issues relating to animal research and contribute your perspectives and expertise to the debates. If you are at an academic institution, organize, participate in, or attend courses or lecture series that discuss animal research. If you are at an academic institution or conduct research in a corporation or a government agency, encourage your colleagues to sponsor seminars and discussions about biomedical animal research ethics. Organize or attend sessions on animal research ethics at meetings of professional associations. Wherever and whenever you can—as you conduct your projects, among scientific colleagues, in interactions with the public—be eager and ready to think and talk about the ethical principles that motivate and guide your work.

References

Alvarez, C.E., 2014. Naturally occurring cancers in dogs: insights for translational genetics and medicine. ILAR J. 55 (1), 16–45.

American Cancer Society. Research scholar grants policies and instructions. Available from: http://www.cancer.org/acs/groups/content/@researchadministration/documents/document/ac-spc-024104.pdf

American College of Laboratory Animal Medicine, 2001. Pain and distress in laboratory animals. Available from: http://www.aclam.org/Content/files/files/Public/Active/position_painanddistress.pdf

American College of Laboratory Animal Medicine, 2006. Guidelines for the assessment and management of pain in rodents and rabbits. Available from: http://www.aclam.org/Content/files/files/Public/Active/position_pain-rodent-rabbit.pdf

American College of Laboratory Animal Medicine, 2012a. Adequate veterinary care. Available from: http://www.aclam.org/Content/files/files/Public/Active/position_adeqvetcare.pdf

American College of Laboratory Animal Medicine, 2012b. Rodent surgery. Available from: http://www.aclam.org/Content/files/files/Public/Active/position_rodentsurgery.pdf

American Council on Education, 1954. Committee on Institutional Research Policy. Sponsored research policy of colleges and universities. American Council on Education, Washington, DC (Quoted in Shepard, H.A., 1956. Basic research and the social system of pure science. Philos. Sci. 23 (1), 48–57).

American Epilepsy Society, 2016. Rresearch and training fellowship for clinicians policies and procedures. Use of animals in research. Available from: https://www.aesnet.org/research/funding%20for%20junior%20investigators/clinical%20fellowships/policies_and_procedures

American Heart Association, 1985. Position of the American Heart Association on the use of research animals. Circ. Res. 57, 330–331.

American Psychological Association, 2012. Guidelines for ethical conduct in the care and use of nonhuman animals in research. Available from: http://www.apa.org/science/leadership/care/care-animal-guidelines.pdf

American Physiological Society, 2016. Guiding principles for the care and use of vertebrate animals in research and training. Available from: http://www.the-aps.org/mm/Publications/Info-For-Authors/Animal-and-Human-Research

American Society of Laboratory Animal Practitioners, 2007. Humane endpoints. Available from: http://www.aslap.org/Content/files/files/Public/ASLAP_Endpoints_2007.pdf

American Society of Laboratory Animal Practitioners, 2008. ASLAP animal care principles. Available from: http://www.aslap.org/Content/files/files/Public/ASLAP_Animal_Care_Principles_2008-12-23.pdf

American Society of Laboratory Animal Practitioners, 2009. Physical restraint of research animals. Available from: http://www.aslap.org/Content/files/files/Public/Physical_Restraint_of_Research_Animals_Position_Statement_11_8_09.pdf

American Society of Primatologists, 2001. Principles for the ethical treatment of non-human primates. Available from: http://www.asp.org/society/resolutions/EthicalTreatmentOfNonHumanPrimates.cfm

American Veterinary Medical Association, 2013. AVMA guidelines for the euthanasia of animals: 2013 edition. Available from: https://www.avma.org/KB/Policies/Pages/Euthanasia-Guidelines.aspx

American Veterinary Medical Association, 2016. Use of animals in research, testing, and education. Available from: https://www.avma.org/KB/Policies/Pages/Use-of-Animals-in-Research-Testing-and-Education.aspx

Animal and Plant Health Inspection Service, 2016a. Animal Welfare Act enforcement. Available from: https://www.aphis.usda.gov/aphis/ourfocus/animalwelfare/SA_AC_Enforcement_Actions/SA_AC_Enforcement_Actions_AWA

Animal and Plant Health Inspection Service, 2016b. Animal and Plant Health Inspection Service. Annual report animal usage by fiscal year. Fiscal year 2015. Available from: https://www.aphis.usda.gov/animal_welfare/downloads/7023/Annual-Reports-FY2015.pdf

Animal Procedures Committee, 2003. Review of cost-benefit assessment in the use of animals in research. Available from: http://science.rspca.org.uk/ImageLocator/LocateAsset?asset=document&assetId=1232712104105&mode=prd

Animal Welfare Act, 2013. 7 USC. §2131 et seq.

Animal Welfare Act Regulations, 2015. 9 C.F.R. Ch. 1. §1.1 et seq.

Animals (Scientific Procedures) Act, 1986. Available from: https://www.gov.uk/government/uploads/system/uploads/attachment_data/file/308593/ConsolidatedASPA1Jan2013.pdf

Annas, G.J., Grodin, M.A. (Eds.), 1992. The Nazi Doctors and the Nuremberg Code: Human Rights in Human Experimentation. Oxford University Press, New York, NY.

Association for Assessment and Accreditation of Laboratory Animal Care International, 2015. Accreditation: frequently asked questions. C.3. Harm-benefit analysis. Available from: http://www.aaalac.org/accreditation/faq_landing.cfm

Association for Assessment and Accreditation of Laboratory Animal Care International, 2016. Position statements. Available from: http://www.aaalac.org/accreditation/positionstatements.cfm

Association for the Advancement of Laboratory Animal Science, 2014. About AALAS. Available from: https://www.aalas.org/about-aalas

Association of Medical Research Charities, 2015. Animal Research. Available from: http://www.amrc.org.uk/our-work/animal-research

Baker, D., Lidster, K., Sottomayor, A., Amor, S., 2014. Two years later: journals are not yet enforcing the ARRIVE Guidelines on reporting standards for pre-clinical animal studies. PLoS Biol. 12 (1), e1001756.

Baltimore, D., Berg, P., Botchan, M., Carroll, D., Charo, R.A., Church, G., Corn, J.E., Daley, G.Q., Doudna, J.A., Fenner, M., Greely, H.T., Jinek, M., Martin, G.S., Penhoet, E., Puck, J., Sternberg, S.H., Weissman, J., Yamamoto, K.R., 2015. A prudent path forward for genomic engineering and germline gene modification. Science 348 (6230), 36–38.

Baneux, P.J.R., Martin, M.E., Allen, M.J., Hallman, T.M., 2014. Issues related to institutional animal care and use committees and clinical trials using privately owned animals. ILAR J. 55 (1), 200–209.

Basel Declaration Society, 2010. Basel Declaration. Available from; http://www.basel-declaration.org/basel-declaration/

Bayne, K., 2005. Potential for unintended consequences of environmental enrichment for laboratory animals and research results. ILAR J. 46 (2), 129–139.

Benefiel, A.C., Dong, W.K., Greenough, W.T., 2005. Mandatory "enriched" housing of laboratory animals: the need for evidence-based evaluation. ILAR J. 46 (2), 95–105.

Biotechnology and Biological Sciences Research Council, 2013. The use of animals in research—the position of the biotechnology and biological sciences research council. Available from: http://www.bbsrc.ac.uk/documents/animals-in-research-pdf/

Bowd, A.D., 1980. Ethical reservations about psychological research with animals. Psychol. Rec. 30, 201–210.

British Veterinary Association, 2016. Use of animals in research. Available from: https://www.bva.co.uk/News-campaigns-and-policy/Policy/Ethics-and-welfare/Animal-research/

Brody, M., 1989. Animal research: a call for legislative reform requiring ethical merit review. Harvard Environ. Law Rev. 13, 423–477.

Brønstad, A., Newcomer, C.E., Decelle, T., Everitt, J.I., Guillen, J., Laber, K., 2016. Current concepts of harm-benefit analysis of animal experiments—report from the AALAS–FELASA working group on harm–benefit analysis—part 1. Lab. Anim. 50 (Suppl. 1), 1–20.

Buchanan-Smith, H.M., Rennie, A.E., Vitale, A., Pollo, S., Prescott, M.J., Morton, D.B., 2005. Harmonising the definition of refinement. Anim. Welf. 14 (4), 379–384.

Calvert, J., 2006. What's special about basic research? Sci. Technol. Human Values 31, 199–220.

Canadian Council on Animal Care, 1989. CCAC policy statement on ethics of animal investigation. Available from: http://www.ccac.ca/en_/standards/policies/policy-ethics_animal_investigation

Caplan, A., Parent, B., Shen, M., Plunkett, C., 2015. No time to waste—the ethical challenges created by CRISPR. EMBO Rep. 16 (11), 1421–1426.

Carbone, L., 2007. Justification for the use of animals. In: Silverman, J., Suckow, M.A., Murthy, S. (Eds.), The IACUC Handbook. CRC Press, Boca Raton, FL, pp. 157–176.

Christopher, M.M., 2015a. A new decade of veterinary research: societal relevance, global collaboration, and translational medicine. Front. Vet. Sci. 2, 1.

Christopher, M.M., 2015b. One health, one literature: weaving together veterinary and medical research. Sci. Transl. Med. 7 (303), 303fs36.

Cigman, R., 1981. Death, misfortune, and species inequality. Philos. Public Aff. 10 (1), 47–64.

Combes, R.D., Balls, M., 2014. Every silver lining has a cloud: the scientific and animal welfare issues surrounding a new approach to the production of transgenic animals. Altern. Lab Anim. 42 (3), 137–145.

Comroe, J., Dripps, R., 1976. Scientific basis for the support of biomedical science. Science 192 (4235), 105–111.

Conn, P.M., Parker, J.V., 2008. The Animal Research War. Palgrave Macmillan, New York, NY.

Coombs, J., Van der List, D., Wang, G.-Y., Chalupa, L.M., 2006. Morphological properties of mouse retinal ganglion cells. Neuroscience 140 (1), 123–136.

Council of Europe, 1986. European convention for the protection of vertebrate animals used for experimental and other scientific purposes, Council of Europe (ETS 123). Available from: http://ec.europa.eu/world/agreements/downloadFile.do?fullText=yes&treatyTransId=1346

Cressey, D., 2016. Surge in support for animal-research guidelines. Nature Newsdoi: 10.1038/nature.2016.19274, (Available from: http://www.nature.com/news/surge-in-support-for-animal-research-guidelines-1.19274).

Donnelly, S., Nolan, K., 1990. Animals, science, and ethics. Hastings Cent. Rep. 20 (3), 1–32.

du Sert, N.P., 2011. Improving the reporting of animal research: when will we ARRIVE? Dis. Model. Mech. 4, 281–282.

Eisen, J., Ganley, E., MacCallum, C.J., 2014. Open science and reporting animal studies: who's accountable? PLoS Biol. 12 (1), e1001757.

European Union, 2010. Directive 2010/63/EU of the European Parliament and of the Council of 22 September 2010 on the Protection of Animals Used for Scientific Purposes. Available from: http://eur-lex.europa.eu/legal-content/EN/TXT/?uri=CELEX:32010L0063

Federation of American Societies for Experimental Biology, 2016a. Federal funding for biomedical and related life sciences research FY 2017. Available from: http://www.faseb.org/Portals/2/PDFs/opa/2016/Federal_Funding_Report_FY2017_FullReport.pdf

Federation of American Societies for Experimental Biology, 2016b. Statement of principles for the use of animals in research and education. Available from: http://www.faseb.org/Science-Policy-and-Advocacy/Science-Policy-and-Research-Issues/Animals-in-Research-and-Education.aspx

Federation of Animal Science Societies, 2010. Guide for the Care and Use of Agricultural Animals in Research and Teaching, third ed. Federation of Animal Science Societies, Champaign, IL.

Federation of European Laboratory Animal Associations, 2005. Principles and practice of ethical review of animal experiments across Europe. Available from: http://www.felasa.eu/media/uploads/Principles-practice-ethical-review_full%20report%20.pdf

Francione, G., 2000. Introduction to Animal Rights: Your child or Your Dog? Temple University Press, Philadelphia.

Galanopoulou, A.S., Simonato, M., French, J.A., O'Brien, T.J., 2013. Joint AES/ILAE translational workshop to optimize preclinical epilepsy research. Epilepsia 54 (Suppl. 4), 1–2.

Gallup Inc., 2016. Moral issues. Available from: http://www.gallup.com/poll/1681/moral-issues.aspx#2

Garner, J.P., 2005. Stereotypies and other abnormal repetitive behaviors: Potential impact on validity, reliability, and replicability of scientific outcomes. ILAR J. 46 (2), 106–117.

Goldman, L., 1979. Controversial aspects of current animal experimentation. In: Paterson, D., Ryder, R.A. (Eds.), Animals' Rights: A Symposium. Centaur Press, Fontwell, UK, pp. 187–193.

Guillen, J., 2012. FELASA guidelines and recommendations. J. Am. Assoc. Lab. Anim. Sci. 51 (3), 311–321.

Habing, G.C., Kaneene, J.B., 2011. Stopping rules in veterinary randomized clinical trials. J. Am. Vet. Med. Assoc. 239 (9), 1197–1199.

Hackam, D.G., Redelmeier, D.A., 2006. Translation of research evidence from animals to humans. JAMA 296 (14), 1731–1732.

Health Research Extension Act of 1985, 1985. 42 USC. §289d.

Henderson, V.C., Kimmelman, J., Fergusson, D., Grimshaw, J.M., Hackam, D.G., 2013. Threats to validity in the design and conduct of preclinical efficacy studies: a systematic review of guidelines for in vivo animal experiments. PLoS Med. 10 (7), e1001489.

Hewitt, H., 1981. The use of animals in experimental cancer research. In: Sperlinger, D. (Ed.), Animals in Research: New Perspectives in Animal Experimentation. John Wiley & Sons, Chichester, UK, pp. 141–174.

Home Office, 2014. Guidance on the Operation of the Animals (Scientific Procedures) Act 1986. Available from: https://www.gov.uk/government/uploads/system/uploads/attachment_data/file/291350/Guidance_on_the_Operation_of_ASPA.pdf

Home Office, 2015. The harm-benefit analysis process. Available from: https://www.gov.uk/government/uploads/system/uploads/attachment_data/file/487914/Harm_Benefit_Analysis__2_.pdf

Home Office, 2016a. Research and testing using animals. Available from https://www.gov.uk/guidance/research-and-testing-using-animals

Home Office, 2016b. Statistics of scientific procedures on living animals. Great Britain 2015. Available from: https://www.gov.uk/government/uploads/system/uploads/attachment_data/file/537708/scientific-procedures-living-animals-2015.pdf

House Conference Report, 1985. Joint Explanatory Statement of the Committee of Conference, H.R. Conf. Rep. 99–309, reprinted in 1985 United States Code Congressional and Administrative News (West 1985), 731–753.

Huerkamp, M.J., Archer, D.R., 2007. Animal acquisition and disposition. In: Silverman, J., Suckow, M.A., Murthy, S. (Eds.), The IACUC Handbook. CRC Press, Boca Raton, FL, pp. 189–225.

Hyun, I., Taylor, P., Testa, G., Dickens, B., Jung, K.W., McNab, A., Robertson, J., Skene, L., Zoloth, L., 2007. Ethical standards for human-to-animal chimera experiments in stem cell research. Cell Stem Cell 1 (2), 159–163.

Institute of Medicine, 2011. Chimpanzees in Biomedical and Behavioral Research: Assessing the Necessity. The National Academies Press, Washington, DC.

International Council for Laboratory Animal Science, 2012. ICLAS Ethical Guideline for Researchers. Available from: http://iclas.org/wp-content/uploads/2012/07/ICLAS-Ethical-Guidlines-Researcher.pdf

Institute for Laboratory Animal Research, 1998. The Psychological Well-Being of Nonhuman Primates. The National Academies Press, Washington, DC.

Jennings, M., Smith, J.A., 2015. A resource book for lay members of ethical review and similar bodies worldwide. Available from: http://science.rspca.org.uk/ImageLocator/LocateAsset?asset=document&assetId=1232713599355&mode=prd

Khanna, C., London, C., Vail, D., Mazcko, C., Hirschfeld, S., 2009. Guiding the optimal translation of new cancer treatments from canine to human cancer patients. Clin. Cancer Res. 15 (18), 5671–5677.

Kidd, C.V., 1959. Basic research—description versus definition: a definition of basic research in probability terms is useful, but statistics based thereon are not. Science 129 (3346), 368–371.

Kimmelman, J., London, A.J., 2011. Predicting harms and benefits in translational trials: ethics, evidence, and uncertainty. PLoS Med. 8 (3), e1001010.

Kol, A., Arzi, B., Athanasiou, K.A., Farmer, D.L., Nolta, J.A., Rebhun, R.B., Chen, X., Griffiths, L.G., Verstraete, F.J.M., Murphy, C.J., Borjesson, D.L., 2015. Translational scientist's new best friends. Sci. Transl. Med. 7 (308), 308ps21.

Kraus, A.L., Renquist, D. (Eds.), 2001. Bioethics and the Use of Laboratory Animals: Ethics in Theory and Practice. American College of Laboratory Animal Medicine, Chester, NH.

Laber, K., Newcomer, C.E., Decelle, T., Everitt, J.I., Guillen, J., Brønstad, A., 2016. Recommendations for addressing harm-benefit analysis and implementation in ethical evaluation—report from the AALAS-FELASA working group on harm-benefit analysis—part 2. Lab. Anim. 50 (Suppl. 1), 21–42.

Laboratory Animal Welfare, 1985. US Government Principles for the utilization and care of vertebrate animals used in testing, research, training. 50, Fed. Reg., 20864.

Laboratory Animals Veterinary Association, 2016. LAVA position statement on the use of animals in research. Available from: http://www.lava.uk.net/viewtopic.php?f=3&t=26

Lairmore, M.D., Khanna, C., 2014. Naturally occurring diseases in animals: contributions to translational medicine. ILAR J. 55 (1), 1–3.

Lanphier, E., Umov, F., Haecker, S.E., Werner, M., Smolenski, J., 2015. Don't edit the human germline. Nature 519 (7544), 410–411.

Mann, M.D., Prentice, E.D., 2004. Should IACUCs review scientific merit of animal research projects? Lab. Anim. 33 (1), 26–31.

Medical Research Council, 2016. Research involving animals. Available from: https://www.mrc.ac.uk/research/policies-and-resources-for-mrc-researchers/research-involving-animals/

Midgley, M., 1981. Why knowledge matters. In: Sperlinger, D. (Ed.), Animals in research: new perspectives in animal experimentation. John Wiley & Sons, Chichester, UK, pp. 319–336.

Miller, N.E., 1985. The value of behavioral research on animals. Am. Psychol. 40 (4), 423–440.

Miller, G., 2011. The rise of animal law. Science 332 (6025), 28–31.

Morrison, A.R., 2009. An Odyssey with Animals: A Veterinarian's Reflection on the Animal Rights and Welfare Debate. Oxford University Press, New York, NY.

Morton, D.B., 1995. Advances in refinement in animal experimentation over the past 25 years. Altern. Lab. Anim. 23 (6), 812–822.

National Centre for the Replacement Reduction & Refinement of Animals in Research, 2010. Animal research: reporting of in vivo experiments. The arrive guidelines. Available from: http://www.nc3rs.org.uk/ARRIVE

National Centre for the Replacement Reduction & Refinement of Animals in Research, 2016. The 3Rs. Available from: https://www.nc3rs.org.uk/the-3rs

National Institutes of Health, 2015a. Grants policy statement. Available from: http://grants.nih.gov/grants/policy/nihgps/nihgps.pdf

National Institutes of Health, 2015b. What we do. Mission and goals. Available from: http://www.nih.gov/about-nih/what-we-do/mission-goals

National Institutes of Health, 2016a. NIH research involving chimpanzees. NOT-OD-16-095. Available from: http://grants.nih.gov/grants/guide/notice-files/NOT-OD-16-095.html

National Institutes of Health, 2016b. Peer review process. Available from: http://grants.nih.gov/grants/peer_review_process.htm

National Research Council, 2003. Guidelines for the Care and Use of Mammals in Neuroscience and Behavioral Research. The National Academies Press, Washington, DC.

National Research Council, 2008. Recognition and Alleviation of Distress in Laboratory Animals. The National Academies Press, Washington, DC.

National Research Council, 2009a. Recognition and Alleviation of Pain in Laboratory Animals. The National Academies Press, Washington, DC.

National Research Council, 2009b. Scientific and Humane Issues in the Use of Random Source Dogs and Cats in Research. The National Academies Press, Washington, DC.

National Research Council, 2011. Guide for the Care and Use of Laboratory Animals, eighth ed. The National Academies Press, Washington, DC.

National Science Foundation, 1959. Federal funds for science, fiscal years 1956, 1957, and 1958 (Quoted in Kidd, C.V., 1959. Basic research—description versus definition: a definition of basic research in probability terms is useful, but statistics based thereon are not. Science, 129 (3346), 368–371).

Nature, 2011. Editorial: animal rights and wrongs. Nature 4707 (335), 435.

Newberry, R.C., 1995. Environmental enrichment: increasing the biological relevance of captive environments. Appl. Anim. Behav. Sci. 44 (2), 229–243.

Newcomer, C., 2012. The evolution and adoption of standards used by AAALAC. J. Am. Assoc. Lab. Anim. Sci. 51 (3), 293–297.

Nobis, N., 2011. The harmful, nontherapeutic use of animals in research is morally wrong. Am. J. Med. Sci. 344 (4), 297–304.

Nuffield Council on Bioethics, 2005. The ethics of research involving animals. Available from: http://www.nuffieldbioethics.org/wp-content/uploads/The-ethics-of-research-involving-animals-full-report.pdf

Nuremberg Code, 1947. Permissible medical experiments. Trials of War Criminals Before the Nuremberg Military Tribunals Under Control CouncilUS Government Printing Office, Washington, DC, (Law No. 10., Nuremberg October 1946–April 1947, pp. 181–182).

O'Brien, T.J., Ben-Menachem, E., Bertram, III, E.H., Collins, S.D., Kokaia, M., Lerche, H., Klitgaard, H., Staley, K.J., Vaudano, E., Walker, M.C., Simonato, M., 2013. Proposal for a "phase II" multicenter trial model for preclinical new antiepilepsy therapy development. Epilepsia 54 (Suppl. 4), 70–74.

Office of Laboratory Animal Welfare, 2015a. Memorandum of understanding between NIH and NSF concerning laboratory animal welfare. Available from: http://grants.nih.gov/grants/olaw/references/mou_nsf.htm

Office of Laboratory Animal Welfare, 2015b. Public Health Service policy on humane care and use of laboratory animals. National Institutes of Health, Bethesda, MD.

Office of Laboratory Animal Welfare, 2016a. Frequently asked questions: PHS Policy on humane care and use of laboratory animals. Available from: http://grants.nih.gov/grants/olaw/faqs.htm

Office of Laboratory Animal Welfare, 2016b. Vertebrate animals section. Available from: http://grants.nih.gov/grants/olaw/vertebrate_animal_section.htm

Organization for Economic Cooperation and Development, 1966. Ministerial Meeting on Science, Fundamental Research and the Policies of Government (Quoted in Sintonen, M., 1990. Basic and applied sciences—Can the distinction (still) be drawn? Sci. Stud. 3 (2), 23–31).

Paul, E.F., Paul, J. (Eds.), 2001. Why Animal Experimentation Matters: The use of Animals in Medical Research. Transaction Publishers, New Brunswick, NJ.

Perley, S., Fluss, S., Bankowski, Z., Simon, F., 1992. The nuremberg code: an international overview. In: Annas, G.J., Grodin, M.A. (Eds.), The Nazi Doctors and the Nuremberg Code: Human Rights in Human Experimentation. Oxford University Press, New York, NY, pp. 149–173.

Pew Research Center, 2015. Americans, politics and science issues. Available from: http://www.pewinternet.org/files/2015/07/2015-07-01_science-and-politics_FINAL.pdf

Public Law 99-198, 1985. Animal Welfare Act. Congressional findings of fact for the 1985 amendment. Public Law, 1985:99-198. Title XVII, subtitle F, §1751(4).

Quimby, F., 1998. Contributions to veterinary medicine from animal research. Appl. Anim. Behav. Sci. 59 (1), 183–192.

Reagan, M.D., 1967. Basic and applied research: a meaningful distinction? Science 155 (3768), 1383–1386.

Reed, J.C., White, E.L., Aubé, J., Lindsley, C., Li, M., Sklar, L., Schreiber, S., 2012. The NIH's role in accelerating translational sciences. Nat. Biotechnol. 30 (1), 16–19.

Regan, T., 1983. The Case for Animal Rights. University of California Press, Berkeley.

Regan, T., 2004. Empty Cages: Facing the Challenge of Animal Rights. Rowman & Littlefield, Lanham, MD.

Reinhardt, V., 1993. Foraging enrichment for caged macaques: a review. Lab. Primate Newslett. 32 (4), 1–4.

Reynolds, P., Wall, P., van Griensven, M., McConnell, K., Lang, C., Buchman, T., 2012. Shock supports the use of animal research guidelines. Shock 38 (1), 1–3.

Rice, A.S.C., Morland, R., Huang, W., Currie, G.L., Sena, E.S., Macleod, M.R., 2013. Transparency in the reporting of in vivo pre-clinical pain research: The relevance and implications of the ARRIVE (Animal Research: Reporting in Vivo Experiments) guidelines. Scand. J. Pain 4 (2), 58–62.

Ringach, D.L., Jentsch, J.D., 2009. We must face the threats. J. Neurosci. 29 (37), 1147–1148.

Rollin, B.E., 1992. Animal Rights and Human Morality. Prometheus Books, Amherst, NY.

Rollin, B.E., 1995. The Experimental Animal in Biomedical Research-CRC Press, Boca Raton, FL.

Rowan, A.N., 1984. Of Mice, Models, and Men: A Critical Evaluation Of Animal Research. State University of New York Press, Albany, NY.

Rudacille, D., 2000. The Scalpel and the Butterfly: The War Between Animal Research and Animal Protection. Farrar, Straus and Giroux, New York, NY.

Russell, W.M.S., Burch, R.L., 1959. The Principles of Humane Experimental Technique. Methuen & Co., London.

Ryder, R.A., 1971. Experiments on animals. In: Godlovitch, S., Godlovitch, R., Harris, J. (Eds.), Animals, Men, and Morals. Victor Gollanz Ltd., London, UK, pp. 41–82.

Schwartzkroin, P.A., 2012. Why—and how—do we approach basic epilepsy research? In: Noebels, J.L., Avoli, M., Rogawski, M.A., Olsen, R.W., Delgado-Escueta, A.V. (Eds.), Jasper's Basic Mechanisms of The Epilepsies. fourth ed. National Center for Biotechnology Information, Bethesda, MD, pp. 1–15.

Seaborg, G.T., 1963. Statement of Glenn T. Seaborg, Chairman, US Atomic Energy Commission, at the hearing on Federal Research and Development Programs before the House Select Committee on Government Research, 88th Congress, 1st Session, quoted in Reagan, M. D. (1967). Basic and applied research: a meaningful distinction? Science 155 (768), 1383–1386.

Singer, P., 1975. Animal Liberation. Avon Books, New York, NY.

Smith, W.J., 2010. A rat is a pig is a dog is a boy: the human cost of the animal rights movement. Encounter Books, New York, NY.

Society for Neuroscience, 2016. Policies on the use of animals and humans in neuroscience research. Available from: http://www.sfn.org/Advocacy/Policy-Positions/Policies-on-the-Use-of-Animals-and-Humans-in-Research

Society of Toxicology, 2008. Guiding principles in the use of animals in toxicology. Available from: http://www.toxicology.org/pubs/statements/Guiding_Principles.pdf

Tannenbaum, J., 1999. Ethics and pain research in animals. ILAR J. 40 (3), 97–110.

Tannenbaum, J., 2001. The paradigm shift toward animal happiness. Society 39 (6), 24–36.

Tannenbaum, J., Bennett, B.T., 2015. Russell and Burch's 3Rs then and now: the need for clarity in definition and purpose. J. Am. Assoc. Lab. Anim. Sci. 54 (2), 120–132.

Tannenbaum, J., Rowan, A.N., 1985. Rethinking the morality of animal research. Hastings Cent. Rep. 15 (5), 32–43.

Taylor, T., 1992. Opening statement of the prosecution, December 9, 1946. In: Annas, G.J., Grodin, M.A. (Eds.), The Nazi Doctors and the Nuremberg Code: Human Rights in Human Experimentation. Oxford University Press, New York, NY, pp. 67–93.

Thomas, L., 1974. The future impact of science and technology on medicine. BioScience 24 (2), 99–105.

Thompson, P.B., 2010. Animal ethics and public expectations: The North American outlook. J. Vet. Med. Educ. 37 (1), 13–21.

United States Department of Agriculture, 2016. Animal Care Policy Manual. Available from: https://www.aphis.usda.gov/animal_welfare/downloads/Animal%20Care%20Policy%20Manual.pdf

van der Worp, H.B., Howells, D.W., Sena, E.S., Porritt, M.J., Rewell, S., O'Collins, V., Macloed, M.R., 2010. Can animal models of disease reliably inform human studies? PLoS Med. 7 (3), e1000245.

Webster, J., 1994. Animal Welfare: A Cool Eye Towards Eden. Wiley-Blackwell, Oxford.

Weed, J.L., Raber, J.M., 2005. Balancing animal research with animal well-being: Establishment of goals and harmonization of approaches. ILAR J. 46 (2), 118–128.

Wellcome Trust, 2016. The use of animals in medical and veterinary research. Available from: https://wellcome.ac.uk/funding/managing-grant/use-animals-medical-and-veterinary-research

Wise, S., 2001. Rattling the Cage: Toward Legal Rights for Animals. Perseus Books, New York, NY.

Wolfle, T., 2005. Environmental enrichment. ILAR J. 46 (2), 79–82.

World Medical Association, 2013. Declaration of Helsinki Ethical Principles for medical research involving human subjects. 2013 rev. Available from: http://www.wma.net/en/30publications/10policies/b3/index.html

Zerhouni, E.A., 2007. Translational research: moving discovery to practice. Clin. Pharmacol. Ther. 81 (1), 126–128.

Zucker, D.R., 2009. What is needed to promote translational research and how do we get it? J. Investig. Med. 57 (2), 468–470.

2

Psychological Environmental Enrichment of Animals in Research

Kristine Coleman*, James L. Weed**, Steven J. Schapiro[†,‡]

*Oregon National Primate Research Center, Beaverton, OR, United States
**Comparative Medicine Branch, National Center for Emerging and Zoonotic Infectious Diseases,
Centers for Disease Control and Prevention, Atlanta, GA, United States
[†]**The University of Texas MD Anderson Cancer Center, TX, United States**
[‡]**The University of Copenhagen, København, Denmark**

1 INTRODUCTION

Behavioral management is a term that entered the lexicon of animal care at the end of the last century (Weed and O'Neill-Wagner, 2006). Broadly, it refers to animal care practices and items that we provide to captive animals to manage their psychological and behavioral needs. It incorporates both social and nonsocial environmental enrichment, as well as positive reinforcement training (PRT), facilities design, positive interactions between caretakers and animals, and behavioral monitoring and assessment to promote psychological well-being

for captive animals (Bloomsmith and Else, 2005; Keeling et al., 1991; Weed and Raber, 2005). All animals evolved distinct behavioral patterns and repertoires, including social behaviors, foraging behaviors, and antipredator behaviors, to promote survival in a complex environment. Compared to natural environments, captive settings are usually rather simple, and do not always allow for the expression of all of these behaviors, which can lead to frustration, boredom, stress, and even the development of abnormal behaviors. Enrichment provides a way to functionally simulate the natural environment of captive animals, in an effort to increase opportunities for the expression of species-specific behaviors.

Environmental enrichment (EE) is just one component of a comprehensive behavioral management program for addressing the behavioral and psychological needs of captive animals. Most institutions devote considerable resources to ensure that varied and species-appropriate behavioral management programs are provided for their animals. Further, many organizations, particularly those that house nonhuman primates (NHPs), have one or more staff members dedicated to providing enrichment for their animal subjects (Baker, 2016). Enrichment is now provided to all vertebrate animals; not only to mammals, but also to birds (Meehan et al., 2004; Nager and Law, 2010), reptiles (Almli and Burghardt, 2006), amphibians (Tinsley, 2010; Torreilles and Green, 2007), and fish (Kihslinger and Nevitt, 2006; Williams et al., 2009).

Enrichment as a field of scientific inquiry has undergone considerable growth over the past few decades. In the past, toys or other items were given to animals without much thought. Today, enrichment programs are recognized as integral components of animal care practices (National Research Council, 2011). Further, they are often approached from an empirical scientific perspective, with many, particularly those involving NHPs, overseen by PhD-level staff (Baker et al., 2007). The past decade or so has seen a dramatic increase in the number of published scientific papers that address environmental enrichment (Simpson and Kelly, 2011). A recent (2016) PubMed search using the keyword "environmental enrichment" produced over 1500 results, of which over 1100 were published in the past 10 years (unpublished data). Interestingly, the majority of these manuscripts were not authored by animal welfare scientists, but rather by biomedical scientists (de Azevedo et al., 2007), illustrating the dual applied and basic science natures of enrichment. Animal welfare scientists, including behaviorists, zoo biologists, and others, examine enrichment and its effects on the psychological well-being of captive animals, in an effort to improve the lives of these animals. Neuroscientists, and other biomedical scientists, utilize enrichment to model environmental effects on a variety of behavioral, neurobiological, and physiological outcome measures.

In this chapter we examine the use of environmental enrichment in both applied and basic science contexts; as a welfare tool and as an experimental model. We will briefly discuss whether enrichment increases variability in research protocols, and will present some practical tips on ways to implement an effective enrichment program for laboratory animals.

2 ENRICHMENT AND WELFARE

2.1 Why Enrich?

Two of the primary goals of enrichment are to reduce stress and improve the psychological well-being of research subjects. Animals living in a laboratory are exposed to a variety of stressors in their daily lives (Morgan and Tromborg, 2007). Some experimental procedures to which these animals are exposed can be aversive, and even common husbandry practices, such as cage changes or physical restraint, may be stressful. Environmental factors, such as lighting, noise, and temperature, may also cause stress for some species or individuals (Morgan and Tromborg, 2007). In addition, laboratory animals often live in enclosures that restrict their ability to express species-typical behaviors. EE can help alleviate the effects of potential stressors associated with captive conditions, enhancing both physical and mental health for subjects. Importantly, in addition to reducing stress, enrichment can also foster resiliency to stress (Novak and Suomi, 1988). It is neither possible nor, in many cases, desirable to eliminate all stress experienced by animals. Stressors are not intrinsically detrimental (Novak and Suomi, 1988), and can even be adaptive, relieving boredom, and helping animals learn to cope with various factors in their environment (Newberry, 1995). Enrichment and behavioral management techniques have been shown to mitigate stress responses to aversive stimuli (including predator odors) in a variety of species, including rodents (Benaroya-Milshtein et al., 2004), birds (Reed et al., 1993), and snakes (Almli and Burghardt, 2006). Enriched animals show less fear and are less responsive, both behaviorally and physiologically, to negative events, such as exposure to predators or certain experimental procedures, compared to animals in a nonenriched environment (Barbelivien et al., 2006; Klein et al., 1994; Moncek et al., 2004; Sampedro-Piquero et al., 2016). Responding appropriately to stress is widely considered an important indicator of well-being in captive animals (Novak and Suomi, 1988; Overall and Dyer, 2005). Not only can enrichment modulate the stress response, but it also may help to reverse the effects of early adverse experiences on hypothalamic-pituitary-adrenal (HPA) function (Francis et al., 2002).

There are both ethical and scientific motivations to provide the best possible environment for laboratory animals. Scientists using animal models in research recognize their ethical responsibility to attend to, and enhance, the psychological well-being of their subjects (Coleman, 2011; National Research Council, 2011). In addition, the reduction of potentially confounding captivity-related stressors, through the use of enrichment, can improve the quality and utility of animal models. It has long been established that highly stressed animals are not reliable subjects for most scientific studies except, perhaps, for those examining the effects of stress. Psychosocial and environmental stressors can alter the HPA axis, as well as cardiovascular function (Gerber et al., 2002; von Holst, 1998) in laboratory animals. Reproductive and immunological functions may also be compromised by emotional stress (Bethea et al., 2008; Rogers et al., 1999). These physiological and immunological changes can affect a variety of research outcomes. Because individuals can vary widely in their physiological and behavioral response to stress, it can increase experimental variability (Schapiro, 2000; Weed and Raber, 2005). Additionally, stressed or emotionally compromised animals have a greater risk of becoming ill or developing maladaptive behaviors, such as self-directed aggressive behavior (Novak, 2003), which can also adversely affect research. Therefore, identifying ways to reduce stress for laboratory animals is important to maximize scientific validity.

Not only does enrichment help to improve well-being, but it can also result in improved safety for caregivers. Working with calm, cooperative animals is safer for care staff than working with highly stressed, and potentially reactive, animals (Bloomsmith, 1992). Van de Weerd et al. (2002) found that mice from an enriched environment were easier to handle (e.g., exhibited more relaxed behavior) compared to mice from a standard environment. Dogs reared in an environment in which they were enriched with a great deal of human interaction were more outgoing, easier to work with, and less likely to bite handlers compared to those reared without human interaction (Adams et al., 2004; Fox and Stelzner, 1966).

2.2 Common Abnormal Behaviors Seen in Captivity

As mentioned earlier, one goal of enrichment is to reduce abnormal, or maladaptive, behaviors. Abnormal behaviors are generally defined as behaviors that deviate from those that are typical of the species (Garner, 2005). They can also include normal behaviors expressed at unnatural levels or at inappropriate times (Garner, 2005). Abnormal behaviors in laboratory animals can take many forms; it is beyond the scope of this chapter to provide a comprehensive review of these behaviors. Instead, we will provide a brief overview of those abnormal behaviors that are most common and/or most problematic to laboratory animals.

One of the more pervasive maladaptive behaviors seen in captive animals is stereotypical behavior (Garner, 2005). Stereotypies, often defined as repetitive behaviors without obvious function (Mason, 1991), are seen in numerous species of animals that live in a variety of captive settings, including zoos, sanctuaries, and research facilities (Mason and Latham, 2004). Pacing, or repetitive movement over the same path, and other whole-body locomotor behaviors, such as jumping, twirling, and rocking are common stereotypical behaviors for laboratory animals. Variations of these behaviors are seen in NHPs (Gottlieb et al., 2013a, 2015; Lutz et al., 2003), rodents (Garner, 2005; Latham and Mason, 2010; Würbel et al., 1998), pigs (Puppe et al., 2007), and birds (Meehan et al., 2004; Polverino et al., 2015), and have even been reported in fish (Kistler et al., 2011). Bar biting or mouthing is relatively common in rodents and pigs. Stereotypies can also include self-directed behaviors, such as hair pulling, eye poking, and self sucking, which have been reported in NHPs and dogs (Lutz et al., 2003). Regardless of its manifestation, the most commonly posited etiology is thought to be suboptimal housing conditions, such as a barren environment with insufficient external stimuli to meet the animals' behavioral needs (Meehan et al., 2004; Swaisgood and Shepherdson, 2006). For example, captive gerbils housed without substrate conducive to digging (an intrinsic behavior) often develop stereotypic digging behavior (Wiedenmayer, 1997).

Alopecia, or loss of hair, fur or feathers, is a relatively common condition for captive animals (Novak and Meyer, 2009). There are many potential etiologies for such loss of hair or fur, including bacterial or fungal infections, parasitic infestations, compromised immune function, and nutritional deficiencies (Honess et al., 2005; Kramer et al., 2010; Novak and Meyer, 2009; Steinmetz et al., 2005), as well as certain behavioral patterns. Behavioral etiologies for hair loss include self-epilating behaviors, such as hair pulling in primates (Honess et al., 2005), barbering in rodents (Garner et al., 2004; Kalueff et al., 2006), and feather pulling in birds (Garner et al., 2006; Grindlinger and Ramsay, 1991). Group-housed animals may execute these behaviors on conspecifics. Psychogenic alopecia, thought to arise from excessive grooming due to anxiety and conflict, is relatively common in dogs and cats (Gross et al., 2005). Social or environmental stresses have also been hypothesized as potential underlying factors in the development of alopecia (Reinhardt, 2005; Reinhardt et al., 1986; Steinmetz et al., 2006), although this is not a universal finding (Kramer et al., 2010). Regardless, alopecia, particularly in NHPs, is highly visible to

regulatory inspectors (e.g., USDA in the United States) and is thus of concern for many facilities.

The maladaptive behavior of greatest concern for laboratory animals is self-injurious behavior (SIB). Seen most commonly in NHPs, SIB includes behaviors such as self-biting, head banging, damaging hair plucking, and other behaviors that could cause injury to the individual (Novak, 2003). SIB can result in significant tissue or muscle damage and infection, and thus can compromise the well-being and welfare of the individual. Inadequate socialization early in life (e.g., rearing in a nursery without the mother) has been identified as the biggest risk factor for the development of SIB in macaques and other primates (Bellanca and Crockett, 2002; Novak, 2003; Rommeck et al., 2009). Common husbandry practices, such as relocating animals to new rooms, can exacerbate bouts of SIB in animals with a history of the behavior (Davenport et al., 2008). In rodents, SIB is typically induced by exposure to caffeine and other stimulants (Kies and Devine, 2004).

2.3 Types of Enrichment

Enrichment is often broken down into five basic and overlapping categories (Bloomsmith et al., 1991; Keeling et al., 1991); social (housing gregarious species in groups or pairs), physical (perches, platforms, huts, toys, and other objects that can be explored or manipulated), food (novel food items, or objects that increase foraging time), sensory (televisions, radio), and occupational (physical and mental activity, including PRT). These enrichment options are not utilized equally by all species. For example, television and radios are often provided for NHPs, but may not be of value to mice and rats. Ideally, laboratory animals should receive multiple forms of enrichment. In the following sections we provide selected examples of these types of enrichment, with some benefits and potential costs for each.

2.3.1 Social Enrichment

Most common laboratory animals are social, and live in complex societies in the wild [e.g., fish, rodents (Baumans, 2010; Koolhaas, 2010), rabbits (Cowan, 1987), dogs (Serpell, 1996), New (Fragaszy et al., 2004; Williams et al., 2010), and Old (Wolfensolm, 2010) World monkeys, and chimpanzees (Wrangham et al., 1994)]. For these species, housing them with compatible conspecifics is one of the most effective forms of enrichment. Such housing allows individuals to engage in many species-typical behaviors, including social play and social grooming (Hutchinson et al., 2005). It has also been shown to reduce abnormal behaviors in rabbits (Chu et al., 2004), dogs (Hubrecht et al., 1992), and NHPs (Reinhardt, 1999; Weed et al., 2003), and to improve wellness in NHPs. Rhesus macaques housed in groups (i.e., with social

enrichment) have enhanced immune function compared to those living in individual cages (Schapiro et al., 2000). Importantly, social housing can prevent abnormal behaviors (including SIB) from occurring in a number of species, including NHPs (Lutz and Novak, 2005), rabbits (Chu et al., 2004), and sheep (Dwyer, 2009). Further, social companionship can buffer individuals against external stresses (Balcombe, 2006; Epley, 1974; Gerber et al., 2002; Gust et al., 1994) and reduce cortisol levels (Fuentes and Newgren, 2008).

Social housing can be accomplished by housing animals in pairs or in groups. It is important to understand the behavioral biology of the target species before making decisions about how best to engage them in social housing. While many Old World monkey species live in multimale, multifemale groups, Hamadryas baboon groups have a harem structure, with only one male; multimale, multifemale groups in captivity would likely result in unacceptable levels of aggression.

While social housing can greatly improve the well-being of captive animals, it is not without risk, and can lead to aggression, as individuals establish their place in the dominance hierarchy. A certain degree of aggression is to be expected. Individuals do not always need to be separated at the first sign of fighting, even if there is some minor wounding. The benefit of social companionship often outweighs the cost of minor wounds to the individual. However, this may not be true for severe trauma or escalated aggression. The degree of "acceptable" aggression depends on many factors, including the species and the type of individuals (e.g., aggression might be less tolerable when infants or frail animals are involved). Refer to Olsson and Westlund (2007) for a review of social housing for rodents and NHPs.

Thus, it is important to find compatible partners. Many factors can influence compatibility, including the species, strain (Crawley et al., 1997), and sex (Latham and Mason, 2004) of the animals. Within rodent species, mice tend to be more aggressive than rats. Further, female mice tend to fight less than male mice, particularly during mating season. Adding enrichment (e.g., nesting material) can reduce aggression in socially housed male mice (Van Loo et al., 2002). Intrinsic traits, such as temperament, may also influence compatibility, at least in macaques. Female rhesus macaques tend to be more compatible with temperamentally similar, rather than temperamentally dissimilar, conspecifics (Capitanio et al., 2017; Coleman, 2012).

Humans can also serve as social enrichment for laboratory animals, particularly dogs and NHPs. Dogs are unique among laboratory animals in that they have evolved a well-developed bond with humans. As such, positive interaction with human handlers is an effective form of enrichment for laboratory dogs (Overall and Dyer, 2005). Socializing dogs with humans, particularly

when they are puppies, allows them to learn appropriate social cues and behaviors (Adams et al., 2004). It has also been shown to reduce stress in dogs. Simply petting a dog can increase affiliative neurotransmitters, including beta endorphins, for both the dog and the human (Odendaal and Meintjes, 2003). Further, socialization with humans can help to prevent the development of behavior problems (Hubrecht, 1995). NHPs can also benefit from positive interactions with human caretakers. Such interactions have been shown to reduce abnormal behavior, increase species-appropriate behaviors, such as grooming, and improve well-being in marmosets, macaques, and chimpanzees (Baker, 2004; Bayne et al., 1993a; Manciocco et al., 2009; Reinhardt, 1997; Waitt et al., 2002), among others. These relationships can also promote coping skills (Rennie and Buchanan-Smith, 2006) and help mitigate stress reactivity toward potentially stressful situations. Miller et al. (1986) found that chimpanzees were less anxious when confronted with novelty in the presence of their trusted caretaker than when the caretaker was absent. While less is known about the effects of human interactions on other animals, early handling by care staff can help reduce stress in rodents (Caldji et al., 2000; Cloutier et al., 2012; Plotsky and Meaney, 1993), pigs (Zupan et al., 2016), and rabbits (Swennes et al., 2011).

Because of the importance of socialization, social pairs or groups should remain intact and stable whenever possible. While most species of laboratory animals are gregarious in nature, some, such as sheep, are highly social. These animals can become extremely agitated in response to separation from the group (Dwyer, 2009), and are prone to displays of stereotypic behavior. The effects of such separations on such species can be attenuated by ensuring that other members of the social group are in visual contact.

2.3.2 Physical Enrichment

Physical enrichment generally refers to items designed to increase the complexity of the environment and promote species-normative behaviors. It includes substrate, nesting material, climbing structures, places to hide or rest, toys, and objects on which subjects can gnaw, to list just a few. These objects provide animals with choice (e.g., they can choose to use them or not) and some degree of control over their environment (Joffe et al., 1973). As with social enrichment, decisions concerning the utilization of specific enrichment items should be guided by an understanding of the natural behavior of the species. For example, many laboratory animals, including rodents and rabbits, are prey species, which shapes much of their behavior. When confronted with an aversive or frightening stimulus, their first reaction is to hide or burrow. Providing the animals with shelter (e.g., tunnels or huts) or substrate in which they

can dig, affords them with the ability to withdraw from aversive situations, which can alleviate fear and stress (Hutchinson et al., 2005). Fig. 2.1 illustrates some examples of structural enrichment.

Effective physical enrichment encourages species-typical behaviors, such as exploration and manipulation, play, nesting, burrowing, rooting, dust bathing, and locomotion. Certain items, such as visual barriers, can provide protection from aggressive conspecifics (Archard, 2012). Enrichment has also been shown to increase fecundity in fish (Wafer et al., 2016) and learning in elderly dogs (Milgram et al., 2005), and to induce positive affect in rats (Brydges et al., 2011; Richter et al., 2012) and pigs (Douglas et al., 2012). Enriched mice have higher natural killer cell activity levels (Benaroya-Milshtein et al., 2004) compared to mice that are not enriched, suggesting better immune function. Physical enrichment has even been found to improve wound healing rates in rats (Vitalo et al., 2012).

The benefits of enrichment may be related to the novelty and complexity of the items. Animals often lose interest in enrichment items with continuous exposure (Hubrecht, 1993; Lutz and Novak, 2005), and thus rotating and/or replacing items can promote their use (National Research Council, 2011; Rawlins et al., 2004). Complexity of enrichment may also be important. Recent work by Abou-Ismail and Mendl (2016) assessed the effect of enrichment novelty versus complexity in newly weaned male Wistar rats. Socially housed rats were exposed to five novel enrichment items (e.g., ladders, crawl balls, wood blocks, shelter, Nylabones) over a 5-week period. These enrichment items were either presented sequentially (novelty condition) or simultaneously (complexity condition). Rats in the novelty condition were provided with five copies of one enrichment item (e.g., five wood blocks) for 1 week, five copies of a different enrichment item (e.g., five Nylabones) the following week, and so on, while those in the complexity condition were provided with one of each of the five enrichment items for the entire 5 week period. The authors found that the animals in the complexity condition showed more signs of positive welfare, such as weight gain and species-normal behaviors, and fewer indicators of poor welfare, such as aggression and vocalizations, compared to those in the novelty condition. These results suggest that diversity of objects may be important to well-being (Abou-Ismail and Mendl, 2016).

Physical enrichment may also decrease abnormal behavior in a variety of species, including rodents and rabbits (Balcombe, 2006; Chu et al., 2004; Marashi et al., 2003; Renner and Rosenzweig, 1986; Wemelsfelder, 1990), pigs (Beattie et al., 1996), and NHPs (Gottlieb et al., 2014; Kessel-Davenport, 1998; Lam et al., 1991; Schapiro and Bloomsmith, 1995). For example, moving to an outdoor environment, which is arguably more

FIGURE 2.1   **Examples of housing with physical enrichment (including toys and structures for climbing, resting, and hiding)** (A) Enriched housing for guinea pigs, (B) enriched housing for dogs, (C) play structure for group housed rhesus macaques, *Macaca mulatta*, and (D) a "porch" on a rhesus macaque cage. *Source: (A) Photo courtesy of the Oregon National Primate Research Center; (B) photo courtesy of Novo Nordisk A/S, and reprinted from Ottesen, J.L., Weber, A., Gürtler, H., Mikkelsen, L.F., 2004. New housing conditions: improving the welfare of experimental animals. ATLA, 32, 397–404; (C) group housed rhesus, photo courtesy of the Oregon National Primate Research Center; (D) photo reprinted from Gottlieb, D.H., O'Connor, J.R., Coleman, K., 2014. Using porches to decrease feces painting in rhesus macaques (*Macaca mulatta*). J. Am. Assoc. Lab. Anim. Sci. 53 (6), 653–656 (Fig. 1, p. 654).*

complex and stimulating than an indoor environment, has been shown to reduce stress (Honess et al., 2005; Schapiro et al., 1995) and SIB in macaques (Fontenot et al., 2006). Further, there is some evidence that exposing mice to an enriched environment early in life can help prevent the development of stereotypical behavior when the mice are older, even after enrichment has been removed (Gross et al., 2012). However, these results are not universal. Several studies have found no discernible effect of simple enrichment devices on abnormal behavior (Line et al., 1991; Novak et al., 1998) or that the benefit was limited to the time till the apparatus was present (Lutz and Novak, 2005).

Care must be taken to avoid injuries related to enrichment items. Animals can injure themselves on certain types of hooks that are used to attach enrichment devices to the outside of cages. For example, juvenile or infant monkeys often put items in their mouths, and can injure themselves on "S-shaped" hooks. Ropes and wire used to hang devices or swings should be short and/or covered with a material (PVC tubing) that reduces the potential of the rope or wire accidentally encircling the animal's neck. Handmade devices should be sturdy, to minimize the likelihood of breakage and the exposure of sharp edges. It is important to ensure that enrichment items can be easily cleaned, to avoid spreading disease (Bayne, 2005; Bayne et al., 1993b). There may be other untoward consequences of physical enrichment, potentially increasing aggression among socially housed animals (Marashi et al., 2003), due to competition over favored

items. Providing multiple enrichment items and dispersing them, as opposed to clustering them, can also help reduce enrichment-related aggression (Akre et al., 2011).

2.3.3 Food Enrichment

Foraging, which includes searching for, procuring, and manipulating food (e.g., opening seeds), is a major part of the behavioral repertoire of many animals in the wild. Animals can spend more than 50% of their waking hours engaged in this behavior. Time spent foraging and eating is greatly reduced in a laboratory setting, where processed food items (biscuits, chow, pellets) are typically provided only once or twice a day, or even less frequently; rodent chow is often placed in a hopper at the top of the cage weekly. Feeding enrichment includes procedures and devices designed to increase time spent feeding and foraging. This kind of enrichment is almost universally utilized by animals. Indeed, given a choice, rodents and other animals will often choose to work to obtain their food, even if they could get it for "free" (Carder and Berkowitz, 1970), a concept known as "contrafreeloading."

Food enrichment can be as simple as hiding food in the substrate to promote foraging behaviors or providing whole foods to promote processing behaviors. Since the goal of food enrichment is to encourage species-typical foraging behaviors, food treats should be provided in ways that extend the time to find and procure food, and not simply handed to the animal.

Specialized manipulanda are often used to provide food enrichment for laboratory animals. These devices, which typically have a small opening for food, are manipulated by the animal to remove the food. While most commonly used for NHPs, similar manipulanda can be used for most species, including dogs and pigs (Huntsberry et al., 2008; Lutz and Novak, 2005; Figure 2.2). Foraging manipulanda have been found to decrease the occurrence of some abnormal behaviors, including stereotypies (Novak et al., 1998) and over-grooming (Schapiro and Bloomsmith, 1995) in NHPs, when they remain attached to the cage. However, the undesired behaviors tend to return after time, likely due to decreased interest in devices that remain attached to cages indefinitely.

With all feeding enrichment, care must be taken not to provide items that are high in "empty" calories. Weight gain and even obesity can be a problem for certain laboratory animals, particularly if they are not given ample opportunities to exercise. Further, if too many treats are provided to animals, they may not consume the nutritionally balanced components of their diets. There are ways to provide food enrichment without adding problematic additional calories. Putting a desired treat in ice can be effective feeding enrichment for dogs and NHPs. The animal's chow may also be provided in such a way as to be "enriching." For example, hamsters and gerbils

hoard their food naturally. For these species, scattering food on the substrate, as opposed to using a hopper, provides them with multiple opportunities to search for, gather, transport, and then hoard their food.

2.3.4 Sensory Enrichment

Animals in the wild are exposed to a variety of visual, auditory, tactile, gustatory, and olfactory stimuli, the diversity of which is often greatly reduced in laboratory conditions. Sensory enrichment is typically designed to provide stimulation for one or more of these senses. As with most other types of enrichment, it is important to take the species' capabilities into account when providing sensory enrichment. Olfactory stimuli are very important to certain species, but are of only minimal consequence to others. While many laboratory species, including rodents, rabbits, dogs, prosimians, and New World monkeys rely heavily on scent marking, it is not common in other species, such as birds, Old World monkeys, and apes.

Auditory enrichment often consists of music or natural habitat sounds. In addition to being used as enrichment, auditory stimuli may also be used to mask other, presumably stressful, sounds (e.g., animal handling and/or cage cleaning procedures). While certain kinds of music have been shown to be anxiolytic in humans (Wells, 2009), the results in animal studies are less clear. Music has been found to be reduce anxiety in mice (Chikahisa et al., 2007), guinea pigs (Wells, 2009), and dogs (Wells et al., 2002). It may also reduce aggression and agonistic behavior in chimpanzees (Howell et al., 2003). However, when given a choice, chimpanzees, tamarins, and marmosets frequently chose silence over "music" (McDermott and Hauser, 2007; Richardson et al., 2006). Further, while it is often assumed that "natural" sounds (i.e, those from an animal's natural environment) are enriching, this is not always the case. Such sounds may not be meaningful to the animals, or may actually be stressful (Wells, 2009). Auditory enrichment is subject to the greatest potential for "abuse" by animal caregivers. It is often difficult to determine whether the musical stimulation being provided is intended to enrich the subject animals or the humans responsible for their care (personal observation).

Visual enrichment can be provided in a variety of forms, including television or videos, computer screen savers and similar applications, or even simply a window. Several species of NHPs will watch videos presented to them (Bloomsmith and Lambeth, 2000; Platt and Novak, 1997), with individually housed primates spending more time "actively" watching than socially housed animals (Bloomsmith and Lambeth, 2000). Whether or not this kind of enrichment affects the welfare of subjects may depend on the degree of control available to subjects. The presentation of video stimuli over which

the animals have no control has not been shown to dramatically affect either the promotion of species-typical behavior or the reduction of abnormal behavior (Bloomsmith and Lambeth, 2000; Platt and Novak, 1997). However, Ogura and Matsuzawa (2012) found that visual stimuli that changed frequently and could be controlled by the subjects did reduce abnormal behavior in Japanese macaques. Television may be aversive if stressors, such as predators, appear on the screen.

2.3.5 Occupational Enrichment

Occupational enrichment includes physical activity and cognitive tasks. It provides opportunities for animals to obtain physical and/or mental stimulation. One of the most common forms of occupational enrichment for small laboratory animals is exercise. There is a large body of evidence suggesting that exercise can help reduce stress, improve overall health, and improve memory and learning in captive animals (Penedo and Dahn, 2005; Santos-Soto et al., 2013; Van Praag, 2009). While many laboratory animals will readily exercise when given the opportunity, others are less eager to do so. Further, providing opportunities for exercise can be challenging for some species. While providing exercise for dogs is mandated by the Animal Welfare Act (1991), it can be challenging to implement. Simply giving the dog an area in which to play may not be enough to promote exercise. Dogs generally do not exercise unless they have the stimulation of humans or other animals (Campbell et al., 1988).

Housing NHPs in large enclosures is one way to provide them with exercise. When this is not possible, activity cages can be utilized to provide exercise to NHPs (Wolff and Rupert, 1991). Indeed, the *Guide for Care and Use of Laboratory Animals* (National Research Council, 2011) recommends the intermittent use of such activity units for NHPs housed in cages, particularly if they are singly housed. These cages have been found to reduce abnormal behavior in baboons (Kessel and Brent, 1995), vervet monkeys (Seier et al., 2011), and rhesus macaques (Griffis et al., 2013), at least for the time that the animals are able to use them.

Cognitive-based enrichment provides animals with opportunities to solve problems. Such enrichment, often accomplished with computers or tablets, is gaining in popularity, at least for NHPs. In particular, tablets provide NHPs access to a wide range of games, known as apps, which can be easily changed and updated (O'Connor et al., 2015). There is currently a paucity of studies examining the effects of this kind of cognitive enrichment; however, a small number of studies have shown that tablets and apps positively affect welfare in NHPs and pigs. Pigs exposed to cognitive challenges showed decreased stereotypical behavior (Puppe et al., 2007) and fewer behavioral and physiological indices of stress compared to nonenriched pigs (Zebunke et al., 2013). Computer tasks have been found to reduce levels of stereotypies and other behavioral problems in rhesus and bonnet macaques (Lincoln et al., 1995; Platt and Novak, 1997; Washburn and Rumbaugh, 1992).

Another form of cognitive/occupational enrichment is positive reinforcement training (PRT). PRT techniques are a form of operant conditioning (Skinner, 1938) in which subjects are rewarded with something desirable (e.g., a food treat) for performing specific behaviors on command. The animals are not punished if they do not perform the behavior; they are simply not rewarded. In PRT, the subject is presented with a stimulus (e.g., a verbal command), responds by performing a specific behavior (e.g., move to the front of the cage and remain stationary), and is provided with reinforcement (e.g., food treat) when it has completed the specific behavior. Refer to Laule et al. (2003) and Pryor (1999) for an overview of PRT.

The use of PRT is recognized as an important tool for promoting well-being in captive species. It is most often used with dogs (Fugazza and Miklósi, 2015; Pryor, 1999) and NHPs (Coleman et al., 2008; McKinley et al., 2003; Prescott et al., 2005; Schapiro et al., 2003; Schapiro et al., 2005), although other species may benefit from this kind of training as well. Laboratory animals have been successfully trained to perform various husbandry or clinical tasks, including moving to a new part of an enclosure (Veeder et al., 2009), presenting a body part for an injection or another procedure (Priest, 1991; Schapiro et al., 2003), taking oral medications (Klaiber-Schuh and Welker, 1997) and remaining stationary for blood sampling (Coleman et al., 2008; Laule et al., 1996; Figure 2.3).

There are many benefits to using PRT. By allowing individuals to cooperate with various procedures, PRT can
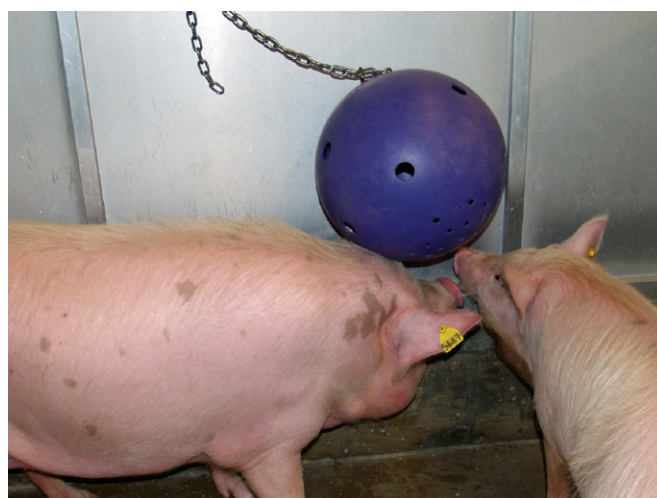
FIGURE 2.2 **Example of foraging device being utilized by two pigs (*Sus scrofa*).** *Source: Photo reprinted from Huntsberry, M.E., Charles, D., Adams, K.A., Weed, J.L., 2008. The foraging ball as a quick and easy enrichment device for pigs* (Sus scrofa). *Lab. Anim. 37 (9), 411–414.*

FIGURE 2.3 **Adult male rhesus macaque (*Macaca mulatta*) with arm in blood sleeve.** The monkey was trained to put his arm in the blood sleeve and hold onto the peg at the distal end and accept venipuncture. *Source: Photo reprinted from Coleman, K., Pranger, L., Maier, A., Lambeth, S.P., Perlman, J.E., Thiele, E., Schapiro, S.J., 2008. Training rhesus macaques for venipuncture using positive reinforcement techniques: a comparison with chimpanzees. J. Am. Assoc. Lab. Anim. Sci. 47 (1), 37–41 (Fig. 1, p. 38).*

reduce the stress associated with these procedures (Bassett et al., 2003; Laule et al., 2003; Schapiro et al., 2003). It can also increase well-being by decreasing boredom, and increase mental stimulation for subjects (Laule et al., 2003). Trained animals are often easier to work with than are untrained animals (Adams et al., 2004). In addition, training has been used to reduce abnormal behaviors, such as stereotypic behavior in NHPs (Coleman and Maier, 2010). While it may take time to train animals for specific tasks, the time invested will likely result in significant time savings when conducting procedures with trained subjects (McKinley et al., 2003; Veeder et al., 2009).

3 ENRICHMENT AND ANIMAL MODELS

Researchers have utilized EE as a model for the ways in which environmental factors affect physiological and biological outcomes for over 70 years, ever since Donald Hebb examined learning in the rats he kept as pets in his home. Compared to rats kept in cages in the laboratory, rats allowed to live as pets when young had better problem solving abilities later in life (Hebb, 1947). Since Hebb's studies, there have been many publications demonstrating that rats and mice living in an enriched

environment perform better than nonenriched conspecifics on a variety of standardized tests of memory and spatial learning, including the Morris water maze (Morris, 1984). Rodents provided with an enriched cage (including some sort of substrate, toys rotated on a regular basis, objects on which to climb, and a hut or other shelter), either with or without social partners, tend to perform better on these tests than do nonenriched conspecifics (Falkenberg et al., 1992; Renner and Rosenzweig, 1986; Schrijver et al., 2002).

Learning is certainly not the only area of research in which enrichment is used as a model. The effect of enrichment on research outcomes has been tested in many, if not most, models of human diseases. However, enrichment is a relative term; the exact characteristics of an "enriched environment" for rodents are not consistent across studies (Fox et al., 2006; Simpson and Kelly, 2011). Rodent enrichment can include items such as large cages, nestlets, or other material in which the rodents can nest, different types of substrates, toys, climbing structures, tunnels, wood objects on which the animals can gnaw, and exercise wheels. In some studies, the enriched condition consists of a few toys added to the cage, while in others, enrichment consists of large cages with structural complexity, including running wheels and other opportunities for exercise (Fox et al., 2006). In at least one study (Landers et al., 2011), the environmentally enhanced rodents lived in outdoor enclosures, and in others (Sparling et al., 2010) animals in an enriched environment had access to several floors of caging. Similarly, there is also variation in unenriched, control groups across studies, ranging from relatively barren enclosures with virtually no enrichment to enclosures with bedding and nestlets. Interestingly, this seems to be changing over time; what was considered an "enriched" condition in older studies is often considered the "control" condition today. Social enrichment (i.e., having more than one animal in the enclosure) also varies, with some authors considering "social enrichment" to be two animals cohoused, and others considering "social enrichment" to be larger groups (Simpson and Kelly, 2011). Despite these differences, there are many commonalities among studies involving EE. We present representative and relevant examples of some of this research below. For more exhaustive and comprehensive reviews of EE as a model for specific human conditions, see Bayne and Würbel (2012), Fox et al. (2006), Nithianantharajah and Hannan (2006), Renoir et al. (2013), Simpson and Kelly (2011), van Praag et al. (2000), and Will et al. (2004).

3.1 Neuroplasticity and Neurogenesis

There is a wealth of data demonstrating that environmental enrichment can increase brain plasticity through a variety of mechanisms (Simpson and Kelly, 2011).

EE has been shown to increase brain size and weight (Greenough, 1975) and increase the number of synapses per neuron (Benefiel and Greenough, 1998) in rodents. Further, several studies have demonstrated that enrichment can promote cell proliferation and neurogenesis in mice, rats (Kempermann et al., 1997; van Praag et al., 2000), and guinea pigs (Rizzi et al., 2011), which may also promote plasticity. Voluntary running on an exercise wheel promotes neurogenesis in the rat dentate gyrus at the same level as cage enrichment (van Praag et al., 1999), suggesting that several kinds of enrichment can affect neurogenesis. This neurogenesis in response to enhanced environmental conditions has also been observed in invertebrate species, including crickets (Lomassese et al., 2000) and crayfish (Ayub et al., 2011), suggesting it has been conserved across species. In addition to promoting neurogenesis, enrichment can decrease apoptosis or cell death (Young et al., 1999) in rodents and aged dogs (Siwak-Tapp et al., 2008).

The hippocampus, an area of the brain involved in learning, appears particularly sensitive to the effects of an enriched environment (Brown et al., 2003; Kempermann et al., 1997; Zhu et al., 2006). Kempermann et al. (2002) found that hippocampal neurogenesis in adult mice exposed to long-term enrichment was five-fold higher than nonenriched controls. Living in an enriched environment following early insult, such as neonatal alcohol exposure, can promote neurogenesis in the hippocampal dentate gyrus and reverse associated learning deficits (Hamilton et al., 2014). In contrast, lack of social enrichment (i.e, social isolation) can impair adult neurogenesis in the dentate gyrus (Lieberwirth et al., 2012).

The effects of enrichment on plasticity can be long lasting. EE has been found to mitigate age-related changes in neurogenesis (Kempermann et al., 1997, 2002), gliogenesis (Soffie et al., 1999), cortical thickness, and dendritic branching (Mohammed et al., 2002). These changes have been associated with improved learning and memory in aged rodents (Bennett et al., 2006; Kempermann et al., 2002) and dogs (Milgram et al., 2005).

3.2 Neurological Disorders

EE has also been used as a model to study the ways in which the environment interacts with specific neurological diseases. EE has been found to be neuroprotective when provided after insult in models of seizures (Dhanushkodi and Shetty, 2008), stroke (Mering and Jolkkonen, 2015), and Parkinson's disease (Faherty et al., 2005). It has also been found to be protective when provided prior to the insult (Williamson et al., 2012). In general, EE improves functional recovery after brain damage in a variety of models (Will et al., 2004), and has important implications for studies on degenerative

diseases, such as Alzheimer's (Jankowsky et al., 2005) and Huntington's disease (HD) (van Dellen et al., 2000). Exposure to enrichment has been shown to delay the onset of motor deficits (van Dellen et al., 2000), decrease cognitive deficits (Nithianantharajah et al., 2008), and decrease depressive behaviors (Pang et al., 2009) associated with HD in a transgenic mouse model. In addition, exercise (Pang et al., 2006) and cognitive enrichment (Martinez-Coria et al., 2015) have been found to have beneficial effects on HD, although the effects are often not as profound as those associated with physical enrichment (Mazarakis et al., 2014). Larger and more complex caging has also been found to mitigate detriments in learning and working memory associated with Alzheimer's disease (Arendash et al., 2004; Jankowsky et al., 2005). Studies such as these provide insight into the effects of environmental conditions on disease progression (Nithianantharajah and Hannan, 2006).

3.3 Affective Disorders

Affective and other psychiatric disorders often have an environmental component, and thus environmental enrichment is often used as a model in these studies. There are several studies examining the anxiolytic role of EE, both in applied and basic science. EE has been found to reduce behavioral and physiological signs of anxiety in rats (Ashokan et al., 2016; Mychasiuk et al., 2012), mice (Benaroya-Milshtein et al., 2004; Chapillon et al., 1999), and fish (Manuel et al., 2015). For example, mice living in an enriched environment appear less anxious in tests assessing anxiety, including the elevated plus maze and open field tests than to those in standard housing (Benaroya-Milshtein et al., 2004; Chapillon et al., 1999). Not only can enrichment function preventatively, it can also be therapeutic (Sampedro-Piquero et al., 2016). These findings are not universal. Leal-Galicia et al. (2007) found no difference in exploratory behavior between enriched and control animals on the open field test. However, the animals in this study were not provided with continuous enrichment, suggesting that enrichment may need to be continuous to be completely effective in this model (Simpson and Kelly, 2011).

Not only does enrichment affect the development of anxiety in animal subjects, but it can also affect the subjects' progeny. Mychasiuk et al. (2012) found that offspring of rats living in a highly enriched environment (i.e., large cages with toys, climbing structures, and food treats) showed more exploratory behavior in an open field than did offspring of rats living in standard housing. Pups from enriched parents also showed reduced global DNA methylation (which implies increased gene expression) in the hippocampus and frontal cortex compared to pups of control parents (Mychasiuk et al., 2012). This study suggests that prenatal enrichment can induce

epigenetic changes that can affect behavioral trajectories of offspring (Mychasiuk et al., 2012).

Relatively few studies have examined the effects of EE on other psychiatric disorders; however, EE has been shown to impact addiction. Several studies have demonstrated enriched animals self-administer decreased amounts of amphetamine compared to controls (Bardo et al., 2001; Green et al., 2002), and show reduced impulsivity-related behaviors when nose poking for a sucrose reward (Wood et al., 2006). Enrichment has also been shown to reduce schizophrenic-like behaviors in a mouse model for schizophrenia (Burrows et al., 2015; Santos et al., 2016).

3.4 Obesity

Researchers who study obesity often examine food intake. Unlike many other models of human behavior, there are a number of studies that demonstrate that exposure to enrichment has no effect on food intake. For example, Beale et al. (2011) found that environmental enrichment, consisting of chew sticks and/or black tubes, did not affect food intake, body weight, or behavior in rats. Similarly, Teske et al. (2016) found no difference in food intake between rats provided with bedding, a relatively basic form of enrichment, and those housed on a wire-bottom cage, nor did they find differences in hyperphagia following administration of orexin-A after animals were given a chewable enrichment device (Nylabone). However, in both of these studies, rats in the "enriched" condition were singly housed and had only basic enrichment (bedding and a toy). Thus, the lack of effect could be due to the relatively low levels of enrichment provided and/or the lack of social companionship.

In support of this concept, mice socially housed with additional enrichment had higher food intake and enhanced leptin sensitivity compared to those in a nonenriched environment (Mainardi et al., 2010). Interestingly, the effect of enrichment on food intake was only found when enrichment was provided to adult mice; mice reared in an enriched environment from birth did not differ from others in food intake. Thus, it is also possible that the timing of EE is important to food intake.

Regardless of the effect enrichment has on food intake, several authors have demonstrated that enriched animals tend to be leaner than their unenriched conspecifics (Cao et al., 2011). While exercise is known to reduce adiposity (Mainardi et al., 2010), physical enrichment, such as cage complexity, is also important to this process. Mice provided with an enriched environment, including toys, nesting material, and running wheels, showed significant reduction in white adipose tissue compared to both nonenriched mice and those given only a running wheel (Cao et al., 2011). It has been posited that the cognitive and physical stimuli associated with environmen-

tal enrichment promote transformation of white adipose tissue to brown adipose tissue through activation of brain-derived neurotrophic factor mediator(s) (Foglesong et al., 2016).

Enrichment can also help to mitigate some of the other negative consequences of obesity. EE can help reverse cognitive deficits caused by a high-fat diet in rats (Gergerlioglu et al., 2016). It can also reduce obesity-related liver streatosis and insulin resistance (Foglesong et al., 2016). Animals in an enriched environment are also less likely to suffer from various cancers associated with obesity than are control animals (Cao et al., 2010).

3.5 Cancer

EE has been found to be protective against certain types of cancer. Mice provided with a highly enriched environment, including both social and structural complexity, showed inhibited tumor growth in a melanoma and a colon cancer model (Cao et al., 2010). The effect of EE on the tumors was both preventative and therapeutic. Interestingly, this effect did not extend to exercise; voluntary wheel running in the absence of other enrichment was not found to have the same tumor suppressive effect as an enriched environment for mice in this study (Cao et al., 2010). EE has also been shown to augment the efficacy of immunotherapy in B cell lymphoma (Benaroya-Milshtein et al., 2007). Immunized mice housed in an enriched environment produced higher levels of antibodies and had more attenuated tumor growth compared to those in a standard environment.

Studies have also examined the effect of EE on models of breast cancer. EE reduced tumor growth in mice (Nachat-Kappes et al., 2012). Further, mammary gland development has been shown to be influenced by EE. Mice maintained in a highly enriched environment had fewer cyclooxygenase-2 (COX-2) positive cells, proinflammatory mediators implicated in the development of breast cancer, compared to those housed in a standard environment (Nachat-Kappes et al., 2012). Interestingly, mammary gland development in mice living in the standard environment was similar to that of mice fed with a high-fat diet, another known risk factor for tumor development (Nachat-Kappes et al., 2012).

While the aforementioned study examined the effects of physical enrichment on cancer, similar results have been found with social enrichment. Singly housed mice (Williams et al., 2009) and rats (Hermes et al., 2009) demonstrated increased cancer development compared to socially housed conspecifics. Similarly, lack of social companionship augments angiogenesis in colon cancer (Wu et al., 2000). In both cancer models, the reduction of stress associated with social and/or environmental enrichment was posited as the likely reason for the improvement.

4 ENRICHMENT AND EXPERIMENTAL VARIABILITY

The use of environmental enrichment and/or exercise is mandated by the Animal Welfare Act (1991) for captive primates and dogs, and therefore these animals tend to receive a fair amount of enrichment. However, despite the plethora of studies demonstrating the beneficial effects of EE on welfare and specific disease outcomes, enrichment for rodent species is still often rudimentary, frequently consisting of little more than bedding and some sort of shelter (e.g., hut). This minimal enrichment for rodents is due, in large part, to the concern that differences in enrichment practices across, and even within, laboratories will lead to increased variability in the data and an inability to replicate findings (Benefiel et al., 2005). It is believed that if environmental conditions are kept constant, reproducible results will follow (Richter et al., 2009, 2010). However, the *lack* of enrichment can also produce variability across laboratories (Weed and Raber, 2005). As discussed previously, enrichment can help attenuate stress responses to aversive stimuli. Given that individuals can vary greatly in their response to stress (Bartolomucci et al., 2005; De Kloet, 2004; Meaney et al., 1991), lack of enrichment can increase an animal's vulnerability to various stressors and thus, overall experimental variability (Weed and Raber, 2005). The provision of enrichment and other behavioral management techniques can reduce fear and anxiety associated with experimental procedures and the development of stress-related problems, and thereby increase the validity of experimental results. In addition, managing aspects of the behavioral environment can minimize the effects of previously uncontrolled factors that may confound the research project.

There is mounting evidence suggesting that the provision of enrichment does not lead to experimental variability. Richter et al. (2009, 2010) argue that environmental standardization may actually cause poor reproducibility in experimental outcomes. Wolfer et al. (2004) examined whether enrichment influenced between-laboratory variation in the behavior of female mice tested on four commonly utilized behavioral assessments (water maze, open field, object exploration, and elevated maze). There was significant within-group variation in behavioral measures, regardless of degree of enrichment. However, they did not find significant effects of the individual laboratory, suggesting that enrichment did not increase variation *across* laboratories (Wolfer et al., 2004).

It is also important to point out that living in a barren environment can interfere with normal brain development and behavior (Benefiel and Greenough, 1998; Renner and Rosenzweig, 1986) and can lead to the development of maladaptive behavior (Würbel, 2001).

Therefore, it can be argued that animals in these conditions are not appropriate subjects for neurobiological research, which should focus on modeling normal brain development (Olsson et al., 2003). In short, good science depends on animals that are physically and psychologically healthy. EE is a key component in accomplishing these goals.

5 IMPLEMENTING AN ENRICHMENT PLAN

It is beyond the scope of this chapter to describe how to implement enrichment plans for all laboratory species. There are many published papers and books that provide excellent overviews concerning methods for implementing enrichment, including Bloomsmith et al., 1991; Keeling et al., 1991; Markowitz, 1982; Ottesen et al., 2004; Shepherdson et al., 1998; Stewart, 2004; Young, 2003. Table 2.1 provides additional resources for some commonly utilized laboratory species. However, while specifics may change across species, there are general tenets of enrichment. We describe these in the following sections. We also present an example of an enrichment plan for a nontraditional species.

5.1 Understand the Natural History of the Species you are Trying to Enrich

As detailed throughout this chapter, one of the first and most important steps in designing an enrichment program is to understand the behavioral needs of the species to be enriched. Every species evolved under different environmental conditions, resulting in unique species-specific behavioral patterns. Most species retain these behavioral repertoires in captivity. Even rodents, which have been bred in laboratories for many generations, still maintain behaviors similar to their wild counterparts (Boice, 1977; Hutchinson et al., 2005), including nest-building, burrowing, hiding, and foraging. Therefore, knowledge of the natural behavioral biology of the species is important for the establishment of a successful enrichment program, and should inform decisions concerning the specific enrichment opportunities to be provided. For instance, while most rodents are social, golden hamsters are not, and should not be housed in groups. Owl monkeys (*Aotus sp.*) utilize nests in the wild, and should be provided with nest boxes in captivity; such nest boxes would be of little value to most macaque species. The Animal Welfare Information Center (United States Department of Agriculture) website (http://awic.nal.usda.gov/publications/bibliographies-and-resource-guides) contains useful information regarding the natural history and behavior of various laboratory animal species (Table 2.1).

TABLE 2.1 Resources on Behavioral Biology/Natural History and Enrichment Programs for Some Commonly Utilized Laboratory Animals

Animal	Behavioral biology	Overview of EE
Fish	Engeszer et al. (2007); Spence et al (2008)	Williams et al. (2009)
Amphibians	Tinsley (2010); Hayes et al. (1998)	Archard (2012)
Birds	Nager and Law (2010)	Nager and Law (2010)
Mice	Baumans (2010); Latham and Mason (2004)	Baumans (2005)
Rats	Koolhaas (2010)	Baumans (2005); Hutchinson et al. (2005)
Rabbits	Lidfors and Edström (2010)	Baumans (2005); Lidfors and Edström (2010)
Guinea pigs	Kaiser et al. (2010)	Kaiser et al., (2010)
Cats	Bradshaw et al. (2012)	Overall and Dyer (2005); Rochlitz (2000)
Dogs	Serpell (1996)	Hubrecht (1993); Overall and Dyer (2005); Wells (2004)
Pigs	Spinka (2009)	Spinka (2009)
Nonhuman primates	Brent (2001); Erwin et al. (1979); Rylands (1993); Wolfensoln (2010); http://pin.primate.wisc.edu/factsheets	Coleman et al. (2012); Novak and Petto (1991); National Research Council (1998); Wolfensohn and Honess (2005); http://www.nc3rs.org.uk/macaques/captive-management/enrichment/ http://www.marmosetcare.com/care-in-captivity/what-is-enrichment.html

Bradshaw, J.W.S., Casey, R.A., Brown, S.L., 2012. The Behaviour of the Domestic Cat, second ed. CABI, Oxford, UK.

Brent, L., 2001. The Care and Management of Captive Chimpanzees: Special Topics in Primatology. San Antonio, American Society of Primatologists.

Engeszer, R., Patterson, L.G.B., Rao, A.A., Parichy, D.M., 2007. Zebrafish in the wild: a review of natural history and new notes from the field. Zebrafish, 4, 21–38.

Erwin, J, Maple, T.L., Mitchell, G., 1979. Captivity and Behavior: Primates in Breeding Colonies, Laboratories and Zoos, NY: Van Nostrand Reinhold CompanyNew York,

Hayes, M.P., Jennings, M.R., Mellen, J.D., 1998. Beyond mammals: environmental

enrichment for amphibians and reptile. In: D. J. Shepherdson, J. D. Mellen, & M. Hutchins (Eds.), Second Nature: Environmental Enrichment for Captive Animals Smithsonian Press, Washington, DC, pp. 205–235.

Kaiser, S., Krüger, C., Sachser, N., 2010. The guinea pig. In R. Hubrecht, J. Kirkwood (Eds.), The UFAW Handbook on the Care and Management of Laboratory and Other Research Animals, eight ed. Wiley-Blackwell, Oxford, UK, pp. 380–398.

Lidfors, L., Edström, T., 2010. The laboratory rabbit. In: Hubrecht, R., Kirkwood, J., (Eds.), The UFAW Handbook on the Care and Management of Laboratory and Other Research Animals, eight ed. Wiley-Blackwell. Oxford, UK, pp. 399–471

National Research Council. 1998. The Psychological Well-Being of Nonhuman Primates. National Academy Press, Washington, DC.

Novak, M., Petto, A., 1991. Through the Looking Glass: Issues of Psychological Well-being in Captive Nonhuman Primates, American Psychological Association, Washington, D.C.

Rochlitz, I., 2000. Recommendations for the housing and care of domestic cats in laboratories. Lab Anim. 34, 1–9.

Rylands, A.B., 1993. Marmosets and Tamarins: Systematics, Behaviour, and Ecology. Oxford University Press, Oxford, UK.

Spence, R., Gerlach, G., Lawrence, C., Smith, C., 2008. The behaviour and ecology of the zebrafish Danio rerio. Biol. Rev. 83, 13–34.

Spinka, M., 2009. The behaviour of pigs. In: Jensen, P., (Ed.), The Ethology of Domestic Animals: An Introductory Text, second ed. CIBA, Oxford, UK, pp. 177–191

Wolfensohn, S., Honess, P., 2005. Handbook of Primate Husbandry and Welfare, Blackwell, Oxford, UK.

EE, Environmental enrichment.

Even within a species, enrichment needs may also vary by strain (Van de Weerd et al., 1994), age (Newberry, 1995), or gender (Welberg et al., 2006). In many species, young animals tend to be more exploratory and active than older animals, and should be provided with increased opportunities to explore and play. Other factors, such as individual temperament, may also play a role in the behavioral needs of animals. Most EE plans incorporate some sort of novelty. Toys and other items are often replaced and/or rotated on a regular basis, in an effort to promote the use of, and hence, the value of the enrichment (Hubrecht, 1993). However, highly anxious or inhibited individuals may respond to constant changes of EE differently than less inhibited conspecifics (Coleman, 2012; Fox and Millam, 2007; Freeman and Gosling, 2010). For these neophobic animals, frequent changing of enrichment items may actually cause, rather than reduce, stress (Coleman, 2012). Enrichment programs should account for these differences to the extent possible.

There is one caveat to this tenet, however. While it is important to keep in mind the natural history of the species, it is equally important to remember that the captive environment has limitations, particularly in terms of space and the ability to escape, which can preclude the expression of naturalistic behavior. Social behaviors may be especially vulnerable to captive conditions. For example, wild rabbits are known to be gregarious, but in captivity, adults, especially males, are often aggressive toward one another, making social introductions challenging (Morton et al., 1993). Conversely, hamsters are naturally solitary. However, captive hamsters seem to prefer social housing, spending more time in social contact with others than alone (Arnold and Estep, 1990). It is important to balance natural history with published literature on best care practices.

5.2 Devise Enrichment Plans With Specific Behavioral Outcomes in Mind

EE should be goal-based. In other words, it should be implemented so that it addresses particular needs. As an example, foraging, including food procurement and processing (e.g., finding food, opening shells, or coverings) is a significant part of the behavioral repertoire of many animals. The presentation of a pelleted diet in captivity is likely to substantially reduce time spent in these behaviors. Therefore, the goal of food enrichment should be to increase the amount of time animals spend finding, processing, and eating their food. It is not intended simply as a way to give animals treats. To meet food enrichment-related goals, desired food treats should not be handed out, but should be hidden or presented in ways that extend foraging time.

5.3 Do no Harm

As detailed earlier, an important factor to consider in providing enrichment is safety. Certain enrichment items may be problematic for specific individuals. While nesting material is used without problem in many rodent species, it can cause conjunctivitis in some genetically modified mice (Bazille et al., 2001). Therefore, enrichment options should be carefully researched prior to implementation, to ensure that they are appropriate for the species and strain being utilized. Further, new enrichment options should be tested in a small number of individuals prior to widespread implementation, to determine whether they are safe and/or may affect experimental outcomes.

5.4 Consider the Costs of the Enrichment

Enrichment should balance the benefits to the animals with the cost of the device. Some enrichment, including larger cages, exercise wheels, and commercially available devices can be prohibitively expensive. One way to provide such costly items is to allow animal's access to them on a rotating basis. Alternatively, many enrichment items (e.g., rodent tunnels) can easily be made with inexpensive and commonly available materials, such as PVC tubing. Cardboard tubes can also be used as an inexpensive enrichment device for rodents (Würbel et al., 1998).

Another cost associated with enrichment is the time of care staff. Enrichment should be somewhat challenging for the animals (to meet the goal of occupying their time), but not too challenging for the animal care staff to maintain. Enrichment items that take a longer time for staff to fill, put up, and clean than the time it takes the animals to use should be reconsidered. That being said, the human cost should not be overemphasized. Effective environmental enrichment programs must establish a workable balance between human convenience and the needs of the animals. Animal needs should be the primary factor driving decisions about enrichment programs.

5.5 "Listen" to the Animals to Determine Whether They Find the Enrichment Enriching

As detailed earlier, environmental enrichment should be goal-oriented. Typically, goals of enrichment, if not used as part of an experimental paradigm, include increasing behavioral diversity and decreasing or preventing abnormal behaviors. Enrichment offerings should be empirically evaluated to ensure they are meeting these goals. Items that do not have a demonstrable effect upon the well-being of the animals should be reconsidered, and probably replaced (Newberry, 1995). Enrichment items that are shown to have untoward effects (e.g., decreased reproduction, illness, maladaptive behaviors) should be eliminated. Even enrichment that has been effectively used for long periods should be regularly evaluated to ensure it is still achieving its desired behavioral goals.

Evaluation can be accomplished in several ways. Taking systematic observations on a subset of individuals is one way to evaluate the effectiveness of enrichment. These types of observations tend to assess whether the enrichment is affecting the expression of both normal and abnormal behaviors, as well as whether it is being utilized at all. As some individuals change their behavior in the presence of a human observer (Iredale et al., 2010), utilizing video cameras can be useful for these sorts of observations, with the caveat that analysis of video data is often quite time consuming. In addition to direct observations, the value of enrichment can be inferred from some physiological measurements. If multiple animals get hurt or sick from the enrichment, then obviously removal of the enrichment is likely to be necessary. Another way to evaluate enrichment is through the use of consumer demand approaches, such as preference tests, to determine how hard animals are willing to work to gain access to specific enrichment opportunities (Schapiro and Lambeth, 2007). Items for which animals are not willing to work should be reconsidered.

Recently, investigators have begun to use cognitive bias testing to evaluate how animals perceive enrichment (i.e., positively or negatively). Cognitive bias refers to the influence of affective state on information processing (Mendl et al., 2009). Multiple studies have demonstrated that, in humans, self-reported emotional states can influence cognitive processes, including attention, memory, and judgment. Specifically, individuals in a negative affective state show increased vigilance to threatening stimuli, are quicker to recall negative memories, and are more likely to have negative assumptions about future events or ambiguous stimuli compared to those in a positive emotional state (Eysenck et al., 1991).

Researchers have exploited this bias in information processing to develop cognitive bias tests to indirectly measure emotional states in nonhuman animals. These tests have been used to assess emotionality in animals living in enriched compared to unenriched environments in a variety of species, including rats (Brydges et al., 2011; Richter et al., 2012), pigs (Douglas et al., 2012), and starlings (Matheson et al., 2008). These studies demonstrated that enrichment induced positive emotionality. While still relatively new, this kind of testing offers a promising tool for assessing the effects of various kinds of enrichment.

5.6 Predictability is Important

As detailed earlier, there are many stressors in the environment of laboratory animals. Husbandry events, such as room cleaning, presence of new care staff, or sudden noises can be stressful for animals. Even "positive" events, such as feeding and provision of enrichment, can be a source of chronic stress to some individuals. These events occur daily, but their timing is often unpredictable for animals, leading to prolonged anticipation of husbandry events resulting in chronic stress. Making such events more predictable to animals can decrease stress and improve well-being (Gottlieb et al., 2013b; Stella et al., 2014; Ulyan et al., 2006; Waitt and Buchanan-Smith, 2001). Simply feeding animals their chow at the same time every day can effectively decrease behavioral indicators of stress in caged rhesus macaques (Gottlieb et al., 2013b). Thus, to the extent possible, provision of enrichment should be somewhat predictable to the animals. Similarly, it should also be consistent. Because enrichment can affect many research outcomes, care must be taken to ensure enrichment is given uniformly, and not haphazardly. Enrichment should be considered an integral part of animal care, and not as something extra to be done "when there is time" (Stewart, 2004).

5.7 Document

While not necessarily a tenet of enrichment, another important part of an enrichment plan is documentation. Information such as when and what kind of enrichment is provided should be recorded. Maintaining these records serves as a way to show that the animals have received enrichment opportunities. Further, systematic documentation can be used to help address unexpected results, and provides a way to ensure that enrichment is consistently being delivered.

Documentation can take several forms. Enrichment can be written on daily logs (Coleman et al., 2012), if they are utilized, or can also be entered directly into spreadsheets.

6 EXAMPLE OF AN ENRICHMENT PLAN: BLACK-TAILED PRAIRIE DOGS (CYNOMYS LUDOVICIANUS)

Enrichment plans should be tailored for each species housed in the laboratory. The point of writing an enrichment plan is to address the potential display of species-specific behavior while animals are housed under laboratory conditions. Inclusion into a study or protocol should not exclude animals from receiving EE or prevent them from displaying normative behavior for the duration of the project. The following is an example of an enrichment plan for a nontraditional laboratory species (adapted from the Compatative Medicine Branch, CDC, Behavioral management plan, 2015).

Prairie dogs are diurnal, burrowing rodents. They are a social species and may concentrate their burrow locations in one area and defend home burrows from neighboring colonies. Prairie dogs are primarily herbivorous and cache their food (Fink, 2004; Hoogland, 1995).

Coloniality is a hallmark of prairie dog societies. Each colony is made up of territorial family groups called a coterie. Thus, social housing (in groups) should be one of the first considerations in implementing an enrichment program for this species. Such housing allows individuals to engage in many species typical behaviors, including play and grooming. Groups of prairie dogs can be housed in relatively large indoor enclosures. If they must be single housed for scientific reasons approved by the Institutional Animal Care and Use Committee (IACUC), they should be arranged in a manner that permits animals to have visual, auditory, and possibly olfactory contact with conspecifics. Single housing should be the shortest duration possible.

Prairie dogs should be housed on Envirodry or similar type bedding which allows for the expression of burrowing and nest-building behavior. Providing the animals with shelter (e.g., tunnels or houses) or substrate in which to burrow affords them the ability to withdraw from aversive situations, which can alleviate fear and stress and tunnels. Many of these items (e.g., tunnels) can easily be made with commonly available materials, such as PVC tubing or cardboard sections cut from longer commercially available tubes.

In the wild, prairie dogs forage from dawn to dusk (Hoogland, 1995), and thus food enrichment is an important part of their enrichment program. Feeding enrichment can be as simple as hiding food in the substrate, which promotes foraging. This kind of enrichment should be provided as often as possible (i.e., at least 3–5 days a week). In the laboratory, food enrichment can include items such as apples, carrots, sweet potato, hay, sunflower seeds, peanuts, and mealworms. Mealworms can be placed into paper bags prior to delivery and tossed onto the floor of each colony room prior to feeding.

7 CONCLUSIONS

Animal models of human disease are key to finding new treatments, cures, and preventative measures for those afflicted. As such, captive animals will continue to play a key role in these efforts. We are morally, ethically, and, for many species legally responsible for providing the highest quality of care for the animals that contribute to our understanding of these disease processes and their treatments. The requirement that environmental enrichment be part of a comprehensive care program at any institute where animal research is conducted is a relatively new concept (Weed and O'Neill-Wagner, 2006), but it is one that has received a great deal of attention. With the publication of the 8th edition of the *Guide for Care and Use of Laboratory Animals* (National Research Council, 2011) the Association for the Assessment and Accreditation of Laboratory Animal Care, International (AAALAC, International), the NIH Office of Laboratory Animal Welfare (OLAW) and others have reiterated the importance of addressing the well-being of those animals used in research.

EE is an important refinement to many laboratory procedures. Along with *Reduction* and *Replacement*, *Refinement*, or practices that minimize stress and distress experienced by animals, make up Russell and Burch's 3Rs (Russell and Burch, 1959). The 3Rs have long been accepted as guiding principles for the ethical and humane use of animals in biomedical research (National Research Council, 2011). EE represents a significant refinement, insofar as it improves psychological well-being and welfare, and reduces stress for subjects.

Attending to the behavioral needs of animals also helps research endeavors. To provide the most reliable and valid data, subjects must be provided with the best physical and social environment conditions possible within the framework of the research. With few exceptions, animals evolved to live in complex environments, which can substantially differ from those experienced in captivity. Lack of environmental stimulation can cause stress for animals, which in turn can affect a wide range of physiological outcomes. Not only can this negatively impact welfare, but it can impact the research on which these animals participate. Addressing the species-specific needs of laboratory animals enhances the work conducted with every animal model, improves our understanding of basic biomedical questions and enhances our ability to seek valid answers and appropriate treatments.

Acknowledgments

References

Abou-Ismail, U.A., Mendl, M.T., 2016. The effects of enrichment novelty versus complexity in cages of group-housed rats (*Rattus norvegicus*). Appl. Anim. Behav. Sci. 180, 130–139.

Adams, K.M., Navarro, A.M., Hutchinson, E.K., Weed, J.L., 2004. A canine socialization and training program at the National Institutes of Health. Lab Anim. 33, 32–36.

Akre, A.K., Bakken, M., Hovland, A.L., Palme, R., Mason, G., 2011. Clustered environmental enrichments induce more aggression and stereotypic behaviour than do dispersed enrichments in female mice. Appl. Anim. Behav. Sci. 131 (3–4), 145–152.

Almli, L.M., Burghardt, G.M., 2006. Environmental enrichment alters the behavioral profile of ratsnakes (elaphe). J. Appl. Anim. Welf. Sci. 9 (2), 85–109.

Animal Welfare Act, 1991. Standards, Final Rule (Part 3, Subpart D: Specifications for the humane handling, care, treatment, and transportation of nonhuman primates). 56, 6495–6505.

Archard, G.A., 2012. Effect of enrichment on the behaviour and growth of juvenile xenopus laevis. Appl. Anim. Behav. Sci. 139, 264–270.

Arendash, G.W., Garcia, M.F., Costa, D.A., Cracchiolo, J.R., Wefes, I.M., Potter, H., 2004. Environmental enrichment improves cognition in aged Alzheimer's transgenic mice despite stable beta-amyloid deposition. Neuroreport 15 (11), 1751–1754.

Arnold, C.E., Estep, D.Q., 1990. Effects of housing on social preference and behavior in male golden hamsters (*Mesocricetus auratus*). Appl. Anim. Behav. Sci. 27, 253–261.

Ashokan, A., Hegde, A., Mitra, R., 2016. Short-term environmental enrichment is sufficient to counter stress-induced anxiety and associated structural and molecular plasticity in basolateral amygdala. Psychoneuroendocrinology 69, 189–196.

Ayub, N., Benton, J.L., Zhang, Y., Beltz, B.S., 2011. Environmental enrichment influences neuronal stem cells in the adult crayfish brain. Dev. Neurobiol. 71 (5), 351–361.

Baker, K.C., 2004. Benefits of positive human interaction for socially housed chimpanzees. Anim. Welf. 13, 239–245.

Baker, K.C., 2016. Survey of 2014 behavioral management programs for laboratory primates in the United States. Am. J. Primatol. 78 (8), 780–796.

Baker, K.C., Weed, J.L., Crockett, C.M., Bloomsmith, M.A., 2007. Survey of environmental enhancement programs for laboratory primates. Am. J. Primatol. 69 (4), 377–394.

Balcombe, J.P., 2006. Laboratory environments and rodents' behavioural needs: a review. Lab Anim. 40 (3), 217–235.

Barbelivien, A., Herbeaux, K., Oberling, P., Kelche, C., Galani, R., Majchrzak, M., 2006. Environmental enrichment increases responding to contextual cues but decreases overall conditioned fear in the rat. Behav. Brain Res. 169 (2), 231–238.

Bardo, M.T., Klebaur, J.E., Valone, J.M., Deaton, C., 2001. Environmental enrichment decreases intravenous self-administration of amphetamine in female and male rats. Psychopharmacology 155 (3), 278–284.

Bartolomucci, A., Palanza, P., Sacerdote, P., Panerai, A.E., Sgoifo, A., Dantzer, R., Parmigiani, S., 2005. Social factors and individual vulnerability to chronic stress exposure. Neurosci. Biobehav. Rev. 29 (1), 67–81.

Bassett, L., Buchanan-Smith, H.M., McKinley, J., Smith, T.E., 2003. Effects of training on stress-related behavior of the common marmoset (*Callithrix jacchus*) in relation to coping with routine husbandry procedures. J. Appl. Anim. Welf. Sci. 6 (3), 221–233.

Baumans, V., 2005. Environmental enrichment for laboratory rodents and rabbits: requirements of rodents, rabbits, and research. ILAR J. 46 (2), 162–170.

Baumans, V., 2010. The laboratory mouse. In: Hubrecht, R., Kirkwood, J. (Eds.), The UFAW Handbook on the Care and Management of Laboratory and Other Research Animals. eight ed. Wiley-Blackwell, Oxford, UK, pp. 276–310.

Bayne, K., 2005. Potential for unintended consequences of environmental enrichment for laboratory animals and research results. ILAR J. 46 (2), 129–139.

Bayne, K., Würbel, H., 2012. Mouse enrichment. In: Hedrich, H.J. (Ed.), The Laboratory Mouse. Elselvier, London, UK, pp. 547–566.

Bayne, K., Dexter, S.L., Strange, G.M., 1993a. The effects of food treat provisioning and human interaction on the behavioral well-being of rhesus monkeys. Contemp. Top. Lab. Anim. Sci. 32 (2), 6–9.

Bayne, K., Dexter, S.L., Strange, G.M., Hill, E.E., 1993b. Kong toys for laboratory primates: are they really an enrichment of just fomites? Lab. Anim. Sci. 43 (1), 78–85.

Bazille, P.G., Walden, S.D., Koniar, B.L., Gunther, R., 2001. Commercial cotton nesting material as a predisposing factor for conjunctivitis in athymic nude mice. Lab. Anim. 30 (5), 40–42.

Beale, K.E., Murphy, K.G., Harrison, E.K., Kerton, A.J., Ghatei, M.A., Bloom, S.R., Smith, K.L., 2011. Accurate measurement of body weight and food intake in environmentally enriched male Wistar rats. Obesity 19 (8), 1715–1721.

Beattie, V.E., Walker, N., Sneddon, I.A., 1996. An investigation of the effect of environmental enrichment and space allowance on the behaviour and production of growing pigs. Appl. Anim. Behav. Sci. 48, 151–158.

Bellanca, R.U., Crockett, C.M., 2002. Factors predicting increased incidence of abnormal behavior in male pigtailed macaques. Am. J. Primatol. 58 (2), 57–69.

Benaroya-Milshtein, N., Hollander, N., Apter, A., Kukulansky, T., Raz, N., Wilf, A., et al., 2004. Environmental enrichment in mice decreases anxiety, attenuates stress responses and enhances natural killer cell activity. Eur. J. Neurosci. 20 (5), 1341–1347.

Benaroya-Milshtein, N., Apter, A., Yaniv, I., Kukulansky, T., Raz, N., Haberman, Y., et al., 2007. Environmental enrichment augments the efficacy of idiotype vaccination for B-cell lymphoma. J Immunother. 30 (5), 517–522.

Benefiel, A.C., Greenough, W., 1998. Effects of experience and environment on the developing and mature brain: implications for laboratory animal housing. ILAR J. 39 (1), 5–11.

Benefiel, A.C., Dong, W.K., Greenough, W.T., 2005. Mandatory enriched housing of laboratory animals: the need for evidence-based evaluation. ILAR J. 46 (2), 95–105.

Bennett, J.C., McRae, P.A., Levy, L.J., Frick, K.M., 2006. Long-term continuous, but not daily, environmental enrichment reduces spatial memory decline in aged male mice. Neurobiol. Learn. Mem. 85 (2), 139–152.

Bethea, C.L., Centeno, M.L., Cameron, J.L., 2008. Neurobiology of stress-induced reproductive dysfunction in female macaques. Mol. Neurobiol. 38 (3), 199–230.

Bloomsmith, M.A., 1992. Chimpanzee training and behavioral research: a symboitic relationship. AAZPA/CAZPA, 403–410.

Bloomsmith, M.A., Else, J.G., 2005. Behavioral management of chimpanzees in biomedical research facilities: the state of the science. ILAR J. 46 (2), 192–201.

Bloomsmith, M.A., Lambeth, S.P., 2000. Videotapes as enrichment for captive chimpanzees (*Pan troglodytes*). Zoo Biol. 19 (6), 541–551.

Bloomsmith, M.A., Brent, L.Y., Schapiro, S.J., 1991. Guidelines for developing and managing an environmental enrichment program for nonhuman primates. Lab. Anim. Sci. 41 (4), 372–377.

Boice, R., 1977. Burrows of wild and albino rats: effects of domestication, outdoor raising, age, experience, and maternal state. J. Comp. Physiol. Psychol. 91 (3), 649–661.

Brown, J., Cooper-Kuhn, C.M., Kempermann, G., Van Praag, H., Winkler, J., Gage, F.H., Kuhn, H.G., 2003. Enriched environment and physical activity stimulate hippocampal but not olfactory bulb neurogenesis. Eur. J. Neurosci. 17 (10), 2042–2046.

Brydges, N.M., Leach, M., Nicol, K., Wright, R., Bateson, M., 2011. Environmental enrichment induces optimistic cognitive bias in rats. Anim. Behav. 81 (1), 169–175.

Burrows, E.L., McOmish, C.E., Buret, L.S., Van den Buuse, M., Hannan, A.J., 2015. Environmental enrichment ameliorates behavioral impairments modeling schizophrenia in mice lacking metabotropic glutamate receptor 5. Neuropsychopharmacology 40 (8), 1947–1956.

Caldji, C., Francis, D., Sharma, S., Plotsky, P.M., Meaney, M.J., 2000. The effects of early rearing environment on the development of GABAA and central benzodiazepine receptor levels and novelty-induced fearfulness in the rat. Neuropsychopharmacology 22 (3), 219–229.

Campbell, S.A., Hughes, H.C., Griffin, H.E., Landi, M.S., Mallon, F.M., 1988. Some effects of limited exercise on purpose-bred beagles. Am. J. Vet. Res. 49 (8), 1298–1301.

Cao, L., Liu, X., Lin, E.J., Wang, C., Choi, E.Y., Riban, V., et al., 2010. Environmental and genetic activation of a brain-adipocyte BDNF/leptin axis causes cancer remission and inhibition. Cell 142 (1), 52–64.

Cao, L., Choi, E.Y., Liu, X., Martin, A., Wang, C., Xu, X., During, M.J., 2011. White to brown fat phenotypic switch induced by genetic and environmental activation of a hypothalamic-adipocyte axis. Cell Metab. 14 (3), 324–338.

Capitanio, J.P., Blozis, S.A., Snarr, J., Steward, A., McCowan, B.J., 2017. Do birds of a feather flock together or do opposites attract? Behavioral responses and temperament predict success in pairings of rhesus monkeys in a laboratory setting. Am. J. Primatol. 79, 1–11.

Carder, B., Berkowitz, K., 1970. Rats' preference for earned in comparison with free food. Science 167 (922), 1273–1274.

Chapillon, P., Manneche, C., Belzung, C., Caston, J., 1999. Rearing environmental enrichment in two inbred strains of mice: 1. Effects on emotional reactivity. Behav. Genet 29 (1), 41–46.

Chikahisa, S., Sano, A., Kitaoka, K., Miyamoto, K., Sei, H., 2007. Anxiolytic effect of music depends on ovarian steroid in female mice. Behav. Brain Res. 179 (1), 50–59.

Chu, L.-r., Garner, J.P., Mench, J.A., 2004. A behavioral comparison of New Zealand White rabbits (*Oryctolagus cuniculus*) housed individually or in pairs in conventional laboratory cages. Appl. Anim. Behav. Sci. 85 (1–2), 121–139.

Cloutier, S., Panksepp, J., Newberry, R.C., 2012. Playful handling by caretakers reduces fear of humans in the laboratory rat. Appl. Anim. Behav. Sci. 140 (3–4), 161–171.

Coleman, K., 2011. Caring for nonhuman primates in biomedical research facilities: scientific, moral and emotional considerations. Am. J. Primatol. 73 (3), 220–225.

Coleman, K., 2012. Individual differences in temperament and behavioral management practices for nonhuman primates. Appl. Anim. Behav. Sci. 137 (3–4), 106–113.

Coleman, K., Maier, A., 2010. The use of positive reinforcement training to reduce stereotypic behavior in rhesus macaques. Appl. Anim. Behav. Sci. 124 (3–4), 142–148.

Coleman, K., Pranger, L., Maier, A., Lambeth, S.P., Perlman, J.E., Thiele, E., Schapiro, S.J., 2008. Training rhesus macaques for venipuncture using positive reinforcement techniques: a comparison with chimpanzees. J. Am. Assoc. Lab. Anim. Sci. 47 (1), 37–41.

Coleman, K., Bloomsmith, M.A., Crockett, C.M., Weed, J.L., Schapiro, S.J., 2012. Behavioral management, enrichment and psychological well-being of laboratory nonhuman primates. In: Abee, C.R., Mansfield, K., Tardif, S., Morris, T. (Eds.), Nonhuman Primates in Biomedical Research. Academic Press, London, UK, pp. 149–176.

Cowan, D.P., 1987. Aspects of the social organisation of the European wild rabbit (*Oryctolagus cuniculus*). Ethology 75 (3), 197–210.

Crawley, J.N., Belknap, J.K., Collins, A., Crabbe, J.C., Frankel, W., Henderson, N., et al., 1997. Behavioral phenotypes of inbred mouse strains: implications and recommendations for molecular studies. Psychopharmacology 132 (2), 107–124.

Davenport, M.D., Lutz, C.K., Tiefenbacher, S., Novak, M.A., Meyer, J.S., 2008. A rhesus monkey model of self-injury: effects of relocation stress on behavior and neuroendocrine function. Biol. Psychiatry 63 (10), 990–996.

de Azevedo, C.S., Cipreste, C.F., Young, R.J., 2007. Environmental enrichment: a GAP analysis. Appl. Anim. Behav. Sci. 102 (3–4), 329–343.

De Kloet, E.R., 2004. Hormones and the stressed brain. Ann. NY. Acad. Sci. 1018, 1–15.

Dhanushkodi, A., Shetty, A.K., 2008. Is exposure to enriched environment beneficial for functional post-lesional recovery in temporal lobe epilepsy? Neurosci. Biobehav. Rev. 32 (4), 657–674.

Douglas, C., Bateson, M., Walsh, C., Bédué, A., Edwards, S.A., 2012. Environmental enrichment induces optimistic cognitive biases in pigs. Appl. Anim. Behav. Sci. 139 (1–2), 65–73.

Dwyer, C., 2009. The behaviour of sheep and goats. In: Jensen, P. (Ed.), The Ethology of Domestic Animals: An Introductory Text. second ed. CABI, Oxford, UK, pp. 161–176.

Epley, S.W., 1974. Reduction of the behavioral effects of aversive stimulation by the presence of companions. Psychol. Bull. 81 (5), 271–283.

Eysenck, M.W., Mogg, K., May, J., Richards, A., Mathews, A., 1991. Bias in interpretation of ambiguous sentences related to threat in anxiety. J. Abnorm. Psychol. 100 (2), 144–150.

Faherty, C.J., Raviie Shepherd, K., Herasimtschuk, A., Smeyne, R.J., 2005. Environmental enrichment in adulthood eliminates neuronal death in experimental Parkinsonism. Mol. Brain Res. 134 (1), 170–179.

Falkenberg, T., Mohammed, A.K., Henriksson, B., Persson, H., Winblad, B., Lindefors, N., 1992. Increased expression of brain-derived neurotrophic factor mRNA in rat hippocampus is associated with improved spatial memory and enriched environment. Neurosci. Lett. 138 (1), 153–156.

Fink, R.S., 2004. Medical management of prairie dogs. In: Quesenberry, K.E., Carpenter, J.W. (Eds.), Ferrets, Rabbits, and Rodents. Saunders, St. Louis, Mo, pp. 226–273.

Foglesong, G.D., Huang, W., Liu, X., Slater, A.M., Siu, J., Yildiz, V., et al., 2016. Role of hypothalamic VGF in energy balance and metabolic adaption to environmental enrichment in mice. Endocrinology 157 (3), 983–996.

Fontenot, M.B., Wilkes, M.N., Lynch, C.S., 2006. Effects of outdoor housing on self-injurious and stereotypic behavior in adult male rhesus macaques (*Macaca mulatta*). J. Am. Assoc. Lab. Anim. Sci. 45 (5), 35–43.

Fox, R.A., Millam, J.R., 2007. Novelty and individual differences influence neophobia in orange-winged Amazon parrots (*Amazona amazonica*). Appl Anim. Behav. Sci. 104 (1–2), 107–115.

Fox, M.W., Stelzner, D., 1966. Behavioural effects of differential early experience in the dog. Anim. Behav. 14 (2), 273–281.

Fox, C., Merali, Z., Harrison, C., 2006. Therapeutic and protective effect of environmental enrichment against psychogenic and neurogenic stress. Behav. Brain Res. 175 (1), 1–8.

Fragaszy, D.M., Visalberghi, E., Fedigan, L.M., 2004. The Complete Capuchin. Cambridge University Press, Cambridge, UK.

Francis, D.D., Diorio, J., Plotsky, P.M., Meaney, M.J., 2002. Environmental enrichment reverses the effects of maternal separation on stress reactivity. J. Neurosci. 22 (18), 7840–7843.

Freeman, H.D., Gosling, S.D., 2010. Personality in nonhuman primates: a review and evaluation of past research. Am. J. Primatol. 72 (8), 653–671.

Fuentes, G.C., Newgren, J., 2008. Physiology and clinical pathology of laboratory New Zealand white rabbits housed individually and in groups. J. Am. Assoc. Lab. Anim. Sci. 47 (2), 35–38.

Fugazza, C., Miklósi, Á., 2015. Social learning in dog training: the effectiveness of the do as I do method compared to shaping/clicker training. Appl. Anim. Behav. Sci. 171, 146–151.

Garner, J.P., 2005. Stereotypies and other abnormal repetitive behaviors: potential impact on validity, reliability, and replicability of scientific outcomes. ILAR J. 46 (2), 106–117.

Garner, J.P., Weisker, S.M., Dufour, B., Mench, J.A., 2004. Barbering (fur and whisker trimming) by laboratory mice as a model of human trichotillomania and obsessive-compulsive spectrum disorders. Comp. Med. 54 (2), 216–224.

Garner, J.P., Meehan, C.L., Famula, T.R., Mench, J.A., 2006. Genetic, environmental, and neighbor effects on the severity of stereotypies and feather picking in Orange-winged Amazon parrots (*Amazona amazonica*): an epidemiological study. Appl. Anim. Behav. Sci. 96 (1–2), 153–168.

Gerber, P., Schnell, C.R., Anzenberger, G., 2002. Behavioral and cardio-physiological responses of common marmosets (*Callithrix jacchus*) to social and environmental changes. Primates 43 (3), 201–216.

Gergerlioglu, H.S., Oz, M., Demir, E.A., Nurullahoglu-Atalik, K.E., Yerlikaya, F.H., 2016. Environmental enrichment reverses cognitive impairments provoked by Western diet in rats: role of corticosteroid receptors. Life Sci. 148, 279–285.

Gottlieb, D.H., Capitanio, J.P., McCowan, B., 2013a. Risk factors for stereotypic behavior and self-biting in rhesus macaques (*Macaca mulatta)*: animal's history, current environment, and personality. Am. J. Primatol. 75 (10), 995–1008.

Gottlieb, D.H., Coleman, K., McCowan, B., 2013b. The effects of predictability in daily husbandry routines on captive rhesus macaques (*Macaca mulatta*). Appl. Anim. Behav. Sci. 143 (2–4), 117–127.

Gottlieb, D.H., O'Connor, J.R., Coleman, K., 2014. Using porches to decrease feces painting in rhesus macaques (*Macaca mulatta*). J. Am. Assoc. Lab. Anim. Sci. 53 (6), 653–656.

Gottlieb, D.H., Maier, A., Coleman, K., 2015. Evaluation of environmental and intrinsic factors that contribute to stereotypic behavior in captive rhesus macaques (*Macaca mulatta*). Appl. Anim. Behav. Sci. 171, 184–191.

Green, T.A., Gehrke, B.J., Bardo, M.T., 2002. Environmental enrichment decreases intravenous amphetamine self-administration in rats: dose-response functions for fixed- and progressive-ratio schedules. Psychopharmacology 162 (4), 373–378.

Greenough, W.T., 1975. Experiential modification of the developing brain. Am. Sci. 63 (1), 37–46.

Griffis, C., Martin, A.L., Perlman, J.E., Bloomsmith, M.A., 2013. Play caging benefits the behavior of singly housed laboratory rhesus macaques (*Macaca mulatta*). J. Am. Assoc. Lab. Anim. Sci. 52, 534–540.

Grindlinger, H.M., Ramsay, E., 1991. Compulsive feather picking in birds. Arch. Gen. Psychiatry 48 (9), 857.

Gross, T.L., Ihrke, P.J., Walder, E.J., Affolter, V.K., 2005. Skin Diseases of the Dog and Cat: Clinical and Histopathologic Diagnosis, second ed. Blackwell Science Ltd., Oxford, UK.

Gross, A.N., Richter, S.H., Engel, A.K., Würbel, H., 2012. Cage-induced stereotypies, perseveration and the effects of environmental enrichment in laboratory mice. Behav Brain Res. 234 (1), 61–68.

Gust, D.A., Gordon, T.P., Brodie, A.R., McClure, H.M., 1994. Effect of a preferred companion in modulating stress in adult female rhesus monkeys. Physiol. Behav. 55 (4), 681–684.

Hamilton, G.F., Jablonski, S.A., Schiffino, F.L., St Cyr, S.A., Stanton, M.E., Klintsova, A.Y., 2014. Exercise and environment as an intervention for neonatal alcohol effects on hippocampal adult neurogenesis and learning. Neuroscience 265, 274–290.

Hebb, D.O., 1947. The effects of early expeirence on problem-solving at maturity. Am. Psychol. 2, 306–307.

Hermes, G.L., Delgado, B., Tretiakova, M., Cavigelli, S.A., Krausz, T., Conzen, S.D., McClintock, M.K., 2009. Social isolation dysregulates endocrine and behavioral stress while increasing malignant burden of spontaneous mammary tumors. Proc. Natl. Acad. Sci. USA 106 (52), 22393–22398.

Honess, P., Gimpel, J., Wolfensohn, S., Mason, G., 2005. Alopecia scoring: the quantitative assessment of hair loss in captive macaques. Altern. Lab. Anim. 33 (3), 193–206.

Hoogland, J.L., 1995. The Black-Tailed Prairie Dog. University of Chicago Press, Chicago, IL.

Howell, S., Schwandt, M., Fritz, J., Roeder, E., Nelson, C., 2003. A stereo music system as environmental enrichment for captive chimpanzees. Lab. Anim. 32 (10), 31–36.

Hubrecht, R.C., 1993. A comparison of social and environmental enrichment methods for laboratory housed dogs. Appl. Anim. Behav. Sci. 37 (4), 345–361.

Hubrecht, R.C., 1995. Enrichment in puppyhood and its effects on later behavior of dogs. Lab. Anim. Sci. 45 (1), 70–75.

Hubrecht, R.C., Serpell, J.A., Poole, T.B., 1992. Correlates of pen size and housing conditions on the behaviour of kennelled dogs. Appl. Anim. Behav. Sci. 34 (4), 365–383.

Huntsberry, M.E., Charles, D., Adams, K.A., Weed, J.L., 2008. The foraging ball as a quick and easy enrichment device for pigs (*Sus scrofa*). Lab. Anim. 37 (9), 411–414.

Hutchinson, E., Avery, A., VandeWoude, S., 2005. Environmental enrichment for laboratory rodents. ILAR J. 46 (2), 148–161.

Iredale, S.K., Nevill, C.H., Lutz, C.K., 2010. The influence of observer presence on baboon (*Papio* spp.) and rhesus macaque (*Macaca mulatta*) behavior. Appl. Anim. Behav. Sci. 122 (1), 53–57.

Jankowsky, J.L., Melnikova, T., Fadale, D.J., Xu, G.M., Slunt, H.H., Gonzales, V., et al., 2005. Environmental enrichment mitigates cognitive deficits in a mouse model of Alzheimer's disease. J. Neurosci. 25 (21), 5217–5224.

Joffe, J.M., Rawson, R.A., Mulick, J.A., 1973. Control of their environment reduces emotionality in rats. Science 180 (93), 1383–1384.

Kalueff, A.V., Minasyan, A., Keisala, T., Shah, Z.H., Tuohimaa, P., 2006. Hair barbering in mice: implications for neurobehavioural research. Behav. Processes 71 (1), 8–15.

Keeling, M.E., Alford, P.L., Bloomsmith, M.A., 1991. Decision analysis for developing programs of psychological well-being: a bias-for-action approach. In: Novak, M.A., Petto, A.J. (Eds.), Through the Looking Glass. American Psychological Association, Washington, D.C, pp. 57–65.

Kempermann, G., Kuhn, H.G., Gage, F.H., 1997. More hippocampal neurons in adult mice living in an enriched environment. Nature 386 (6624), 493–495.

Kempermann, G., Gast, D., Gage, F.H., 2002. Neuroplasticity in old age: sustained fivefold induction of hippocampal neurogenesis by long-term environmental enrichment. Ann. Neurol. 52 (2), 135–143.

Kessel, A.L., Brent, L., 1995. An activity cage for baboons, part II: long-term effects and management issues. Contemp. Top. Lab. Anim. Sci. 34 (6), 80–83.

Kessel-Davenport, A., 1998. Cage toys reduce abnormal behavior in individually housed pigtail macaques. J. Appl. Anim. Welf. Sci. 1 (3), 227–234.

Kies, S.D., Devine, D.P., 2004. Self-injurious behaviour: a comparison of caffeine and pemoline models in rats. Pharmacol. Biochem. Behav. 79 (4), 587–598.

Kihslinger, R.L., Nevitt, G.A., 2006. Early rearing environment impacts cerebellar growth in juvenile salmon. J. Exp. Biol. 209 (Pt 3), 504–509.

Kistler, C., Hegglin, D., Würbel, H., König, B., 2011. Preference for structured environment in zebrafish (*Danio rerio*) and checker barbs (*Puntius oligolepis*). Appl. Anim. Behav. Sci. 135 (4), 318–327.

Klaiber-Schuh, A., Welker, C., 1997. Crab-eating monkeys can be trained to cooperate in non-invasive oral medication without stress. Primate Rep. 47, 11–30.

Klein, S.L., Lambert, K.G., Durr, D., Schaefer, T., Waring, R.E., 1994. Influence of environmental enrichment and sex on predator stress response in rats. Physiol. Behav. 56 (2), 291–297.

Koolhaas, J.M., 2010. The laboratory rat. In: Hubrecht, R., Kirkwood, J. (Eds.), The UFAW Handbook on the Care and Management of Laboratory and Other Research Animals,. eight ed. Wiley-Blackwell, Oxford, UK, pp. 311–326.

Kramer, J., Fahey, M., Santos, R., Carville, A., Wachtman, L., Mansfield, K., 2010. Alopecia in rhesus macaques correlates with immunophenotypic alterations in dermal inflammatory infiltrates consistent with hypersensitivity etiology. J. Med. Primatol. 39 (2), 112–122.

Lam, K., Rupniak, N.M., Iversen, S.D., 1991. Use of a grooming and foraging substrate to reduce cage stereotypies in macaques. J Med. Primatol. 20 (3), 104–109.

Landers, M.S., Knott, G.W., Lipp, H.P., Poletaeva, I., Welker, E., 2011. Synapse formation in adult barrel cortex following naturalistic environmental enrichment. Neuroscience 199, 143–152.

Latham, N., Mason, G., 2004. From house mouse to mouse house: the behavioural biology of free-living *Mus musculus* and its implications in the laboratory. Appl. Anim. Behav. Sci. 86 (3–4), 261–289.

Latham, N., Mason, G., 2010. Frustration and perseveration in stereotypic captive animals: is a taste of enrichment worse than none at all? Behav. Brain Res. 211 (1), 96–104.

Laule, G.E., Thurston, R.H., Alford, P.L., Bloomsmith, M.A., 1996. Training to reliably obtain blood and urine samples from a young, diabetic chimpanzee (*Pan troglodytes*). Zoo Biol. 15, 587–591.

Laule, G.E., Bloomsmith, M.A., Schapiro, S.J., 2003. The use of positive reinforcement training techniques to enhance the care, management, and welfare of primates in the laboratory. J. Appl. Anim. Welf. Sci. 6 (3), 163–173.

Leal-Galicia, P., Saldivar-Gonzalez, A., Morimoto, S., Arias, C., 2007. Exposure to environmental enrichment elicits differential hippocampal cell proliferation: role of individual responsiveness to anxiety. Dev. Neurobiol. 67 (4), 395–405.

Lieberwirth, C., Liu, Y., Jia, X., Wang, Z., 2012. Social isolation impairs adult neurogenesis in the limbic system and alters behaviors in female prairie voles. Horm. Behav 62 (4), 357–366.

Lincoln, 3rd, H., Andrews, M.W., Rosenblum, L.A., 1995. Pigtail macaque performance on a challenging joystick task has important implications for enrichment and anxiety within a captive environment. Lab. Anim. Sci. 45 (3), 264–268.

Line, S.W., Morgan, Kathleen N., Markowitz, H., 1991. Simple toys do not alter the behavior of aged rhesus monkeys. Zoo Biol. 10, 473–484.

Lomassese, S.S., Strambi, C., Strambi, A., Charpin, P., Augler, R., Aouane, A., Cayre, M., 2000. Influence of environmental stimulation on neurogenesis in the adult insect. J. Neurobiol. 45, 162–171.

Lutz, C.K., Novak, M.A., 2005. Environmental enrichment for nonhuman primates: theory and application. ILAR J. 46 (2), 178–191.

Lutz, C.K., Well, A., Novak, M., 2003. Stereotypic and self-injurious behavior in rhesus macaques: a survey and retrospective analysis of environment and early experience. Am. J. Primatol. 60 (1), 1–15.

Mainardi, M., Scabia, G., Vottari, T., Santini, F., Pinchera, A., Maffei, L., et al., 2010. A sensitive period for environmental regulation of eating behavior and leptin sensitivity. Proc. Natl. Acad. Sci. USA 107 (38), 16673–16678.

Manciocco, A., Chiarotti, F., Vitale, A., 2009. Effects of positive interaction with caretakers on the behaviour of socially housed common marmosets (*Callithrix jacchus*). Appl. Anim. Behav. Sci. 120, 100–107.

Manuel, R., Gorissen, M., Stokkermans, M., Zethof, J., Ebbesson, L.O., van de Vis, H., et al., 2015. The effects of environmental enrichment and age-related differences on inhibitory avoidance in zebrafish (*Danio rerio* Hamilton). Zebrafish 12 (2), 152–165.

Marashi, V., Barnekow, A., Ossendorf, E., Sachser, N., 2003. Effects of different forms of environmental enrichment on behavioral, endocrinological, and immunological parameters in male mice. Horm. Behav. 43 (2), 281–292.

Markowitz, H., 1982. Behavioral Enrichment at the Zoo. Van Nostrand Reinhold, New York.

Martinez-Coria, H., Yeung, S.T., Ager, R.R., Rodriguez-Ortiz, C.J., Baglietto-Vargas, D., LaFerla, F.M., 2015. Repeated cognitive stimulation alleviates memory impairments in an Alzheimer's disease mouse model. Brain Res. Bull. 117, 10–15.

Mason, G.J., 1991. Stereotypies: a critical review. Anim Behav. 41 (6), 1015–1038.

Mason, G.J., Latham, N.R., 2004. Can't stop, won't stop: is stereotypy a reliable animal welfare indicator? Anim Welf. 13 (Suppl. 1), S57–S69.

Matheson, S.M., Asher, L., Bateson, M., 2008. Larger, enriched cages are associated with optimistic response biases in captive European starlings (*Sturnus vulgaris*). Appl. Anim. Behav. Sci. 109 (2–4), 374–383.

Mazarakis, N.K., Mo, C., Renoir, T., van Dellen, A., Deacon, R., Blakemore, C., Hannan, A.J., 2014. 'Super-enrichment' reveals dose-dependent therapeutic effects of environmental stimulation in a transgenic mouse model of Huntington's disease. J. Huntington's Dis. 3 (3), 299–309.

McDermott, J., Hauser, M.D., 2007. Nonhuman primates prefer slow tempos but dislike music overall. Cognition 104 (3), 654–668.

McKinley, J., Buchanan-Smith, H.M., Bassett, L., Morris, K., 2003. Training common marmosets (*Callithrix jacchus)* to cooperate during routine laboratory procedures: ease of training and time investment. J. Appl. Anim. Welf. Sci. 6 (3), 209–220.

Meaney, M.J., Viau, V., Bhatnagar, S., Betito, K., Iny, L.J., O'Donnell, D., Mitchell, J.B., 1991. Cellular mechanisms underlying the development and expression of individual differences in the hypothalamic-pituitary-adrenal stress response. J. Steroid Biochem. Mol. Biol. 39 (2), 265–274.

Meehan, C.L., Garner, J.P., Mench, J.A., 2004. Environmental enrichment and development of cage stereotypy in orange-winged Amazon parrots (*Amazona amazonica)*. Dev. Psychobiol. 44 (4), 209–218.

Mendl, M., Burman, O.H.P., Parker, R.M.A., Paul, E.S., 2009. Cognitive bias as an indicator of animal emotion and welfare: emerging evidence and underlying mechanisms. Appl. Anim. Behav. Sci. 118 (3–4), 161–181.

Mering, S., Jolkkonen, J., 2015. Proper housing conditions in experimental stroke studies-special emphasis on environmental enrichment. Front Neurosci. 9, 106.

Milgram, N.W., Head, E., Zicker, S.C., Ikeda-Douglas, C.J., Murphey, H., Muggenburg, B., et al., 2005. Learning ability in aged beagle dogs is preserved by behavioral enrichment and dietary fortification: a two-year longitudinal study. Neurobiol. Aging 26 (1), 77–90.

Miller, C.L., Bard, K.A., Juno, C.J., Nadler, R.D., 1986. Behavioral responiveness of young chimpanzees to a novel environment. Folia Primatol. 47, 128–142.

Mohammed, A.H., Zhu, S.W., Darmopil, S., Hjerling-Leffler, J., Ernfors, P., Winblad, B., et al., 2002. Environmental enrichment and the brain. Prog. Brain Res. 138, 109–133.

Moncek, F., Duncko, R., Johansson, B.B., Jezova, D., 2004. Effect of environmental enrichment on stress related systems in rats. J. Neuroendocrinol. 16 (5), 423–431.

Morgan, K.N., Tromborg, C.T., 2007. Sources of stress in captivity. Appl Anim. Behav. Sci. 102 (3–4), 262–302.

Morris, R., 1984. Developments of a water-maze procedure for studying spatial learning in the rat. J. Neurosci. Methods 11 (1), 47–60.

Morton, D.B., Jennings, M., Batchelor, G.R., Bell, D., Birke, L., Davies, K., et al., 1993. Refinements in rabbit husbandry. Second report of the BVAAWF/Frame/RSPCE/UFAW joint working group on refinement. Lab. Anim. 27, 301–329.

Mychasiuk, R., Zahir, S., Schmold, N., Ilnytskyy, S., Kovalchuk, O., Gibb, R., 2012. Parental enrichment and offspring development: modifications to brain, behavior and the epigenome. Behav. Brain Res. 228 (2), 294–298.

Nachat-Kappes, R., Pinel, A., Combe, K., Lamas, B., Farges, M.C., Rossary, A., et al., 2012. Effects of enriched environment on COX-2, leptin and eicosanoids in a mouse model of breast cancer. PLoS One 7 (12), e51525.

Nager, R.G., Law, G., 2010. The zebra finch. In: Hubrecht, R., Kirkwood, J. (Eds.), The UFAW Handbook on the Care and Management of Laboratory and Other Research Animals. eight ed. Wiley-Blackwell, Oxford, UK, pp. 674–685.

National Research Council, 2011. Guide for the Care and Use of Laboratory Animals. National Academies Press, Washington, D.C.

Newberry, R.C., 1995. Environmental enrichment: increasing the biological relevance of captive environments. Appl. Anim. Behav. Sci. 44 (2–4), 229–243.

Nithianantharajah, J., Hannan, A.J., 2006. Enriched environments, experience-dependent plasticity and disorders of the nervous system. Nat. Rev. Neurosci. 7 (9), 697–709.

Nithianantharajah, J., Barkus, C., Murphy, M., Hannan, A.J., 2008. Gene-environment interactions modulating cognitive function and molecular correlates of synaptic plasticity in Huntington's disease transgenic mice. Neurobiol. Dis 29 (3), 490–504.

Novak, M.A., 2003. Self-injurious behavior in rhesus monkeys: new insights into its etiology, physiology, and treatment. Am. J. Primatol. 59 (1), 3–19.

Novak, M.A., Meyer, J.S., 2009. Alopecia: possible causes and treatments, particularly in captive nonhuman primates. Comp. Med. 59 (1), 18–26.

Novak, M.A., Suomi, S.J., 1988. Psychological well-being of primates in captivity. Am. Pscyhol. 43 (10), 765–773.

Novak, M.A., Kinsey, J.H., Jorgensen, M.J., Hazen, T.J., 1998. Effects of puzzle feeders on pathological behavior in individually housed rhesus monkeys. Am. J. Primatol. 46 (3), 213–227.

O'Connor, J.R., Heagerty, A., Herrera, M., Houser, L.A., Coleman, K., 2015. Use of a tablet as enrichment for adult rhesus macaques. Am. J. Primatol. 77 (S1), 122.

Odendaal, J.S., Meintjes, R.A., 2003. Neurophysiological correlates of affiliative behaviour between humans and dogs. Vet. J. 165 (3), 296–301.

Ogura, T., Matsuzawa, T., 2012. Video preference assessment and behavioral management of single-caged Japanese macaques (*Macaca fuscata*) by movie presentation. J. Appl. Anim. Welf. Sci. 15 (2), 101–112.

Olsson, I.A.S., Westlund, K., 2007. More than numbers matter: the effect of social factors on behaviour and welfare of laboratory rodents and non-human primates. Appl. Anim. Behav. Sci. 103 (3–4), 229–254.

Olsson, I.A.S., Nevison, C.M., Patterson-Kane, E.G., Sherwin, C.M., Van de Weerd, H., Wurbel, H., 2003. Understanding behaviour: the relevance of ethological approaches in laboratory animal science. Appl. Anim. Behav. Sci. 81 (3), 245–264.

Ottesen, J.L., Weber, A., Gürtler, H., Mikkelsen, L.F., 2004. New housing conditions: improving the welfare of experimental animals. ATLA 32, 397–404.

Overall, K.L., Dyer, D., 2005. Enrichment strategies for laboratory animals from the viewpoint of clinical veterinary behavioral medicine: emphasis on cats on dogs. ILAR J. 46 (2), 202–215.

Pang, T.Y., Stam, N.C., Nithianantharajah, J., Howard, M.L., Hannan, A.J., 2006. Differential effects of voluntary physical exercise on behavioral and brain-derived neurotrophic factor expression deficits in Huntington's disease transgenic mice. Neuroscience 141 (2), 569–584.

Pang, T.Y., Du, X., Zajac, M.S., Howard, M.L., Hannan, A.J., 2009. Altered serotonin receptor expression is associated with depression-related

behavior in the R6/1 transgenic mouse model of Huntington's disease. Hum. Mol. Genet. 18 (4), 753–766.

Penedo, F.J., Dahn, J.R., 2005. Exercise and well-being: a review of mental and physical health benefits associated with physical activity. Curr. Opin. Psychiatry 18 (2), 189–193.

Platt, D.M., Novak, M.A., 1997. Videostimulation as enrichment for captive rhesus monkeys (*Macaca mulatta*). Appl. Anim. Behav. Sci. 52 (1–2), 139–155.

Plotsky, P.M., Meaney, M.J., 1993. Early, postnatal experience alters hypothalamic corticotropin-releasing factor (CRF) mRNA, median eminence CRF content and stress-induced release in adult rats. Mol Brain Res. 18 (3), 195–200.

Polverino, G., Manciocco, A., Vitale, A., Alleva, E., 2015. Stereotypic behaviours in Melopsittacus undulatus: behavioural consequences of social and spatial limitations. Appl. Anim. Behav. Sci. 165, 143–155.

Prescott, M.J., Bowell, V.A., Buchanan-Smith, H.M., 2005. Training of laboratory-housed non-human primates, part 2: resources for developing and implementing training programmes. Anim. Technol. Welf. 4 (3), 133–148.

Priest, G.M., 1991. Training a diabetic drill (*Mandrillus leucophaeus*) to accept insulin injections and venipuncture. Lab. Primate Newslett. 30, 1–4.

Pryor, K., 1999. Don't Shoot the Dog: The New Art of Teaching and Training. Simon & Schuster, New York.

Puppe, B., Ernst, K., Schön, P.C., Manteuffel, G., 2007. Cognitive enrichment affects behavioural reactivity in domestic pigs. Appl. Anim. Behav. Sci. 105 (1–3), 75–86.

Rawlins, J.M., Johnson, J.G., Coleman, K., 2004. The effect of novelty on device use in female rhesus macaques. Contemp. Top. Lab. Anim. Sci. 43, 96.

Reed, H.J., Wilkins, L.J., Austin, S.D., Gregory, N.G., 1993. The effect of environmental enrichment during rearing on fear reactions and depopulation trauma in adult caged hens. Appl. Anim. Behav. Sci. 36 (1), 39–46.

Reinhardt, V., 1997. Refining the traditional housing and handling of laboratory rhesus macaques improves scientific methodology. Primate Rep. 49, 93–112.

Reinhardt, V., 1999. Pair-housing overcomes self-biting behavior in macaques. Lab. Primate Newslett. 38 (1), 4–5.

Reinhardt, V., 2005. Hair pulling: a review. Lab. Anim. 39 (4), 361–369.

Reinhardt, V., Reinhardt, A., Houser, D., 1986. Hair pulling and eating in captive rhesus monkey troops. Folia Primatol. 47 (2–3), 158–164.

Renner, M.J., Rosenzweig, M.R., 1986. Social interactions among rats housed in grouped and enriched conditions. Dev. Psychobiol. 19 (4), 303–314.

Rennie, A., Buchanan-Smith, H., 2006. Refinement of the use of non-human primates in scientific research Part 1: the influence of humans. Anim. Welf. 15, 203–213.

Renoir, T., Pang, T.Y., Hannan, A.J., 2013. Effects of environmental manipulations in genetically targeted animal models of affective disorders. Neurobiol. Dis. 57, 12–27.

Richardson, A.S., Lambeth, S.P., Schapiro, S.J., 2006. Control over the auditory environment: a study of music preference in captive chimpanzees (*Pan troglodytes*). Int. J. Primatol. 27, 423.

Richter, S.H., Garner, J.P., Wurbel, H., 2009. Environmental standardization: cure or cause of poor reproducibility in animal experiments? Nat. Methods 6 (4), 257–261.

Richter, S.H., Garner, J.P., Auer, C., Kunert, J., Wurbel, H., 2010. Systematic variation improves reproducibility of animal experiments. Nat. Methods 7 (3), 167–168.

Richter, S.H., Schick, A., Hoyer, C., Lankisch, K., Gass, P., Vollmayr, B., 2012. A glass full of optimism: enrichment effects on cognitive bias in a rat model of depression. Cogn. Affect. Behav. Neurosci. 12 (3), 527–542.

Rizzi, S., Bianchi, P., Guidi, S., Ciani, E., Bartesaghi, R., 2011. Impact of environmental enrichment on neurogenesis in the dentate gyrus during the early postnatal period. Brain Res. 1415, 23–33.

Rogers, C.J., Brissette-Storkus, C.S., Chambers, W.H., Cameron, J.L., 1999. Acute stress impairs NK cell adhesion and cytotoxicity through CD2, but not LFA-1. J. Neuroimmunol. 99 (2), 230–241.

Rommeck, I., Anderson, K., Heagerty, A., Cameron, A., McCowan, B., 2009. Risk factors and remediation of self-injurious and self-abuse behavior in rhesus macaques. J. Appl. Anim. Welf. Sci. 12 (1), 61–72.

Russell, W.M.S., Burch, R.L., 1959. The Principles of Humane Experimental Technique. Methuen, London.

Sampedro-Piquero, P., Castilla-Ortega, E., Zancada-Menendez, C., Santin, L.J., Begega, A., 2016. Environmental enrichment as a therapeutic avenue for anxiety in aged Wistar rats: effect on cat odor exposition and GABAergic interneurons. Neuroscience 330, 17–25.

Santos, C.M., Peres, F.F., Diana, M.C., Justi, V., Suiama, M.A., Santana, M.G., Abilio, V.C., 2016. Peripubertal exposure to environmental enrichment prevents schizophrenia-like behaviors in the SHR strain animal model. Schizophr. Res. 176 (2–3), 552–559.

Santos-Soto, I.J., Chorna, N., Carballeira, N.M., Velez-Bartolomei, J.G., Mendez-Merced, A.T., Chornyy, A.P., Pena de Ortiz, S., 2013. Voluntary running in young adult mice reduces anxiety-like behavior and increases the accumulation of bioactive lipids in the cerebral cortex. PLoS One 8 (12), e81459.

Schapiro, S.J., 2000. A few new developments in primate housing and husbandry. Lab. Anim. Sci. 27, 103–110.

Schapiro, S.J., Bloomsmith, M.A., 1995. Behavioral effects of enrichment on singly-housed yearling rhesus monkeys: an analysis including three enrichment condtitions and a control group. Am. J. Primatol. 35, 89–101.

Schapiro, S.J., Lambeth, S.P., 2007. Control, choice, and assessments of the value of behavioral management to nonhuman primates in captivity. J. Appl. Anim. Welf. Sci. 10 (1), 39–47.

Schapiro, S.J., Porter, L.M., Suarez, S.A., Bloomsmith, M.A., 1995. The behavior of singly-caged, yearling rhesus monkeys is affected by the environment outside of the cage. Appl. Anim. Behav. Sci. 45 (1–2), 151–163.

Schapiro, S.J., Nehete, P.N., Perlman, J.E., Sastry, K.J., 2000. A comparison of cell-mediated immune responses in rhesus macaques housed singly, in pairs, or in groups. Appl. Anim. Behav. Sci. 68 (1), 67–84.

Schapiro, S.J., Bloomsmith, M.A., Laule, G.E., 2003. Positive reinforcement training as a technique to alter nonhuman primate behavior: quantitative assessments of effectiveness. J. Appl. Anim. Welf. Sci. 6 (3), 175–187.

Schapiro, S.J., Perlman, J.E., Thiele, E., Lambeth, S., 2005. Training nonhuman primates to perform behaviors useful in biomedical research. Lab. Anim. 34 (5), 37–42.

Schrijver, N.C., Bahr, N.I., Weiss, I.C., Wurbel, H., 2002. Dissociable effects of isolation rearing and environmental enrichment on exploration, spatial learning and HPA activity in adult rats. Pharmacol. Biochem. Behav. 73 (1), 209–224.

Seier, J., de Villiers, C., van Heerden, J., Laubscher, R., 2011. The effect of housing and environmental enrichment on stereotyped behavior of adult vervet monkeys (*Chlorocebus aethiops*). Lab. Anim. 40 (7), 218–224.

Serpell, J., 1996. The Domestic Dog: Its Evolution, Behaviour and Interactions with People. Cambridge University Press, Cambridge, UK.

Shepherdson, D.J., Mellen, J.D., Hutchins, M. (Eds.), 1998. Second Nature: Environmental Enrichment for Captive Animals. Smithsonian Institution Press, Washington, D.C.

Simpson, J., Kelly, J.P., 2011. The impact of environmental enrichment in laboratory rats—behavioural and neurochemical aspects. Behav. Brain Res. 222 (1), 246–264.

Siwak-Tapp, C.T., Head, E., Muggenburg, B.A., Milgram, N.W., Cotman, C.W., 2008. Region specific neuron loss in the aged canine

hippocampus is reduced by enrichment. Neurobiol. Aging 29 (1), 39–50.

Skinner, B.F., 1938. The Behavior of Organisms. Appleton-Century-Crofts, New York.

Soffie, M., Hahn, K., Terao, E., Eclancher, F., 1999. Behavioural and glial changes in old rats following environmental enrichment. Behav. Brain Res. 101 (1), 37–49.

Sparling, J.E., Mahoney, M., Baker, S., Bielajew, C., 2010. The effects of gestational and postpartum environmental enrichment on the mother rat: a preliminary investigation. Behav. Brain Res. 208 (1), 213–223.

Steinmetz, H.W., Kaumanns, W., Neimeier, K.A., Kaup, F.J., 2005. Dermatologic investigation of alopecia in rhesus macaques (*Macaca mulatta*). J. Zoo Wildl. Med. 36 (2), 229–238.

Steinmetz, H.W., Kaumanns, W., Dix, I., Heistermann, M., Fox, M., Kaup, F.J., 2006. Coat condition, housing condition and measurement of faecal cortisol metabolites—a non-invasive study about alopecia in captive rhesus macaques (*Macaca mulatta*). J. Med. Primatol. 35 (1), 3–11.

Stella, J., Croney, C., Buffington, T., 2014. Environmental factors that affect the behavior and welfare of domestic cats (*Felis silvestris catus*) housed in cages. Appl. Anim. Behav. Sci. 160, 94–105.

Stewart, K., 2004. Development of an environmental enrichment program utilizing simple strategies. Anim. Welf. Info. Cent. Newslett. 12, 1–7.

Swaisgood, R., Shepherdson, D., 2006. Environmental enrichment as a strategy for mitigating stereotypies in zoo animals: a literature review and meta-analysis. Mason, G.J., Rushen, J. (Eds.), Stereotypic Animal Behaviour: Fundamentals and Applications to Welfare, vol. 2, CABI, Oxfordshire, pp. 256–285.

Swennes, A.G., Alworth, L.C., Harvey, S.B., Jones, C.A., King, C.S., Crowell-Davis, S.L., 2011. Human handling promotes compliant behavior in adult laboratory rabbits. J. Am. Assoc. Lab. Anim. Sci. 50 (1), 41–45.

Teske, J.A., Perez-Leighton, C.E., Noble, E.E., Wang, C., Billington, C.J., Kotz, C.M., 2016. Effect of housing types on growth, feeding, physical activity, and anxiety-like behavior in male Sprague-Dawley rats. Fronteirs Nutr. 3, 4.

Tinsley, R., 2010. Amphibians, with special reference to *Xenopus*. In: Hubrecht, R., Kirkwood, J. (Eds.), The UFAW Handbook on the Care and Management of Laboratory and Other Research Animals. eight ed. Wiley-Blackwell, Oxford, UK, pp. 741–759.

Torreilles, S., Green, S.L., 2007. Refuge cover decreases the incidence of bite wounds in laboratory South African clawed frogs (*Xenopus laevis*). J. Am. Assoc. Lab. Anim. Sci. 46 (5), 33–36.

Ulyan, M.J., Burrows, A.E., Buzzell, C.A., Raghanti, M.A., Marcinkiewicz, J.L., Phillips, K.A., 2006. The effects of predictable and unpredictable feeding schedules on the behavior and physiology of captive brown capuchins (*Cebus apella*). Appl. Anim. Behav. Sci. 101 (1–2), 154–160.

Van de Weerd, H.A., Baumans, V., Koolhaas, J.M., van Zutphen, L.F., 1994. Strain specific behavioural response to environmental enrichment in the mouse. J. Exp. Anim. Sci. 36 (4–5), 117–127.

Van de Weerd, H.A., Aarsen, E.L., Mulder, A., Kruitwagen, C.L., Hendriksen, C.F., Baumans, V., 2002. Effects of environmental enrichment for mice: variation in experimental results. J. Appl. Anim. Welf. Sci. 5 (2), 87–109.

van Dellen, A., Blakemore, C., Deacon, R., York, D., Hannan, A.J., 2000. Delaying the onset of Huntington's in mice. Nature 404 (6779), 721–722.

Van Loo, P.L.P., Kruitwagen, C.L.J.J., Koolhaas, J.M., Van de Weerd, H.A., van Zutphen, L.F.M., Baumans, V., 2002. Influence of cage enrichment on aggressive behaviour and physiological parameters in male mice. Appl. Anim. Behav. Sci. 76 (1), 65–81.

Van Praag, H., 2009. Exercise and the brain: something to chew on. Trends Neurosci. 32, 283–290.

van Praag, H., Kempermann, G., Gage, F.H., 1999. Running increases cell proliferation and neurogenesis in the adult mouse dentate gyrus. Nat. Neurosci. 2 (3), 266–270.

van Praag, H., Kempermann, G., Gage, F.H., 2000. Neural consequences of environmental enrichment. Nat. Rev. Neurosci. 1 (3), 191–198.

Veeder, C.L., Bloomsmith, M.A., McMillan, J.L., Perlman, J.E., Martin, A.L., 2009. Positive reinforcement training to enhance the voluntary movement of group-housed sooty mangabeys (*Cercocebus atys atys*). J. Am. Assoc. Lab. Anim. Sci. 48 (2), 192–195.

Vitalo, A.G., Gorantla, S., Fricchione, J.G., Scichilone, J.M., Camacho, J., Niemi, S.M., et al., 2012. Environmental enrichment with nesting material accelerates wound healing in isolation-reared rats. Behav. Brain Res. 226 (2), 606–612.

von Holst, D., 1998. The concept of stress and its relevance for animal behavior. Moller, A.P., Milinski, M., Slater, P.J.B. (Eds.), Stress and Behavior, vol. 27, Academic Press, San Diego, CA, pp. 1–109.

Wafer, L.N., Jensen, V.B., Whitney, J.C., Gomez, T.H., Flores, R., Goodwin, B.S., 2016. Effects of environmental enrichment on the fertility and fecundity of zebrafish (*Danio rerio*). J. Am. Assoc. Lab. Anim. Sci. 55 (3), 291–294.

Waitt, C., Buchanan-Smith, H.M., 2001. What time is feeding? How delays and anticipation of feeding schedules affect stump-tailed macaque behavior. Appl. Anim. Behav. Sci. 75, 75–85.

Waitt, C., Buchanan-Smith, H.M., Morris, K., 2002. The effects of caretaker-primate relationships on primates in the laboratory. J. Appl. Anim. Welf. Sci. 5 (4), 309–319.

Washburn, D.A., Rumbaugh, D.M., 1992. Testing primates with joystick-based automated apparatus: lessons from the Language Research Center's Computerized Test System. Behav. Res. Methods 24 (2), 157–164.

Weed, J.L., O'Neill-Wagner, P.L., 2006. Animal behavior research findings facilitate comprehensive captive animal care: the birth of behavioral management. Environmental Enrichment for Nonhuman Primates Resource Guide. Retrieved from https://www.nal.usda.gov/awic/environmental-enrichment-nonhuman-primates-resource-guide-animal-behavior-research-findings

Weed, J.L., Raber, J.M., 2005. Balancing animal research with animal well-being: establishment of goals and harmonization of approaches. ILAR J. 46 (2), 118–128.

Weed, J.L., Wagner, P.O., Byrum, R., Parrish, S., Knezevich, M., Powell, D.A., 2003. Treatment of persistent self-injurious behavior in rhesus monkeys through socialization: a preliminary report. Contemp. Top. Lab. Anim. Sci. 42 (5), 21–23.

Welberg, L., Thrivikraman, K.V., Plotsky, P.M., 2006. Combined pre- and postnatal environmental enrichment programs the HPA axis differentially in male and female rats. Psychoneuroendocrinology 31 (5), 553–564.

Wells, D.L., 2004. A review of environmental enrichment for kennelled dogs *Canis familiaris*. Appl. Anim. Behav. Sci. 85 (3–4), 307–317.

Wells, D.L., 2009. Sensory stimulation as environmental enrichment for captive animals: a review. Appl. Anim. Behav. Sci. 118 (1–2), 1–11.

Wells, D.L., Graham, L., Hepper, P.G., 2002. The influence of auditory stimulation on the behaviour of dogs housed in a rescue shelter. Anim. Welf. 11 (4), 385–393.

Wemelsfelder, F., 1990. Boredom and laboratory animal welfare. In: Rollin, B.E. (Ed.), The Experimental Animal in Biomedical Research, vol. I. A Survey of Scientific and Ethical Issues for Investigators. CRC Press, Inc, Boca Raton, FL, pp. 243–272.

Wiedenmayer, C., 1997. Causation of the ontogenetic development of stereotypic digging in gerbils. Anim. Behav. 53 (3), 461–470.

Will, B., Galani, R., Kelche, C., Rosenzweig, M.R., 2004. Recovery from brain injury in animals: relative efficacy of environmental enrichment, physical exercise or formal training (1990–2002). Prog. Neurobiol 72 (3), 167–182.

Williams, T.D., Readman, G.D., Owen, S.F., 2009. Key issues concerning environmental enrichment for laboratory-held fish species. Lab. Anim. 43 (2), 107–120.

Williams, L.E., Brady, A.G., Abee, C.R., 2010. Squirrel monkeys. In: Hubrecht, R., Kirkwood, J. (Eds.), The UFAW Handbook on the Care and Management of Laboratory and Other Research Animals. eight ed. Wiley-Blackwell, Oxford, UK, pp. 564–578.

Williamson, L.L., Chao, A., Bilbo, S.D., 2012. Environmental enrichment alters glial antigen expression and neuroimmune function in the adult rat hippocampus. Brain Behav. Immun. 26 (3), 500–510.

Wolfensolm, S., 2010. Old World monkeys. In: Hubrecht, R., Kirkwood, J. (Eds.), The UFAW Handbook on the Care and Management of Laboratory and Other Research Animals. eight ed. Wiley-Blackwell, Oxford, UK, pp. 592–617.

Wolfer, D.P., Litvin, O., Morf, S., Nitsch, R.M., Lipp, H.P., Wurbel, H., 2004. Laboratory animal welfare: cage enrichment and mouse behaviour. Nature 432 (7019), 821–822.

Wolff, A., Rupert, G., 1991. A practical assessment of a nonhuman primate exercise program. Lab. Anim. 20, 36–39.

Wood, D.A., Siegel, A.K., Rebec, G.V., 2006. Environmental enrichment reduces impulsivity during appetitive conditioning. Physiol. Behav. 88 (1–2), 132–137.

Wrangham, R.W., McGrew, W.C., de Waal, F.B.M., Heltne, P.G., 1994. Chimpanzee Cultures. Harvard University Press, Cambridge, MA.

Wu, W., Murata, J., Murakami, K., Yamaura, T., Hayashi, K., Saiki, I., 2000. Social isolation stress augments angiogenesis induced by colon 26-L5 carcinoma cells in mice. Clin. Exp. Metastasis 18 (1), 1–10.

Würbel, H., 2001. Ideal homes? Housing effects on rodent brain and behaviour. Trends Neurosci 24 (4), 207–211.

Würbel, H., Chapman, R., Rutland, C., 1998. Effect of feed and environmental enrichment on development of stereotypic wire-gnawing in laboratory mice. Appl. Anim. Behav. Sci. 60 (1), 69–81.

Young, R.J., 2003. Environmental Enrichment for Captive Animals. Blackwell Publishing, Oxford, UK.

Young, D., Lawlor, P.A., Leone, P., Dragunow, M., During, M.J., 1999. Environmental enrichment inhibits spontaneous apoptosis, prevents seizures and is neuroprotective. Nat. Med. 5 (4), 448–453.

Zebunke, M., Puppe, B., Langbein, J., 2013. Effects of cognitive enrichment on behavioural and physiological reactions of pigs. Physiol. Behav. 118, 70–79.

Zhu, S.W., Yee, B.K., Nyffeler, M., Winblad, B., Feldon, J., Mohammed, A.H., 2006. Influence of differential housing on emotional behaviour and neurotrophin levels in mice. Behav. Brain Res. 169 (1), 10–20.

Zupan, M., Rehn, T., de Oliveira, D., Keeling, L.J., 2016. Promoting positive states: the effect of early human handling on play and exploratory behaviour in pigs. Animal 10 (1), 135–141.

Further Reading

Olsson, I.A., Dahlborn, K., 2002. Improving housing conditions for laboratory mice: a review of environmental enrichment. Lab. Anim. 36 (3), 243–270.

Page left intentionally blank

Large Farm Animal Models of Human Neurobehavioral and Psychiatric Disorders: Methodological and Practical Considerations

Franz J. van der Staay*,**, Rebecca E. Nordquist*,**,
Saskia S. Arndt*

*Utrecht University, Utrecht, The Netherlands
**Brain Center Rudolf Magnus, Utrecht University, Utrecht, The Netherlands

O U T L I N E

1 ANIMAL MODELS

In order to gain insight into human behavioral dysfunctions and neurologic and psychiatric disorders, it is of utmost importance that appropriate animal models are used in the behavioral neurosciences, such as neurobiology, biopsychology, neurology, and psychiatry. Animal model approaches have a long history in biomedical (Ericsson et al., 2013; Franco, 2013) and neuroscience research (Cowan et al., 2000), where the models have been developed to investigate brain–behavior relations. The aim has been to gain insight into human behavior and its underlying neuronal and neuroendocrinological processes, their role in neurological and neuropsychiatric diseases and their treatment.

Animal models in neuroscience research are mainly used for two purposes:

- for gaining insight in the processes and mechanisms underlying neurobehavioral disorder, which is primarily an area of basic research, but may also be a first step in translational research, and
- for identifying new therapeutic options and testing their efficacy and safety (van der Staay, 2006; van der Staay et al., 2009, 2014). For evaluating the safety and efficacy of interventions, translational research using (large) animal models alongside clinical trials is necessary (Drolet and Lorenzi, 2011).

In this chapter, we shall address the subject "large animal models." First, the theoretical framework of performing animal experimental studies will be discussed and a definition of animal models will be given. Then, the position of (large) animal models in the translational chain will be discussed. Next, we direct our attention to selecting an appropriate animal model for addressing a scientific question. Some aspects of performing research using large animal models are challenging, compared to rodent models. We will address these challenges and their implications. Large model animal species need an adapted infrastructure for housing and testing. Also, we pay particular attention to methodological questions associated with the use of large animal models, such as considerations about the experimental unit. The most efficient use of large animal models may imply multiple testing and multiple readouts to obtain a maximum of information. Similarly, reuse of animals within a study and/or reuse in successive (possibly unrelated studies) is discussed. Finally, the advantages and disadvantages of studies with large model animal species will be contrasted.

2 WHY ANIMAL EXPERIMENTAL STUDIES?

The possibilities to investigate the processes underlying behavioral dysfunctions and psychiatric disorders in the brain of humans are restricted, except when they are assessed in a clinical setting with patients as subjects. However, the extent and location of the damage [although emerging imaging techniques broaden the possibilities (Mier and Mier, 2015)], and its "history," are often unclear, and the neurobiological variables associated with behavioral dysfunctions cannot be controlled sufficiently to achieve meaningful and interpretable results. Comparative approaches (Brenowitz and Zakon, 2015; Mehta and Gosling, 2008) relying on animal models could be used to answer questions about behavioral dysfunctions and their underlying neural substrate. Animals with a known and reproducible dysfunction or damage may help us to understand brain dysfunctions and their effects on behavior (Blanchard et al., 2013).

The comparative approach is based on the evolutionary theory and the assumption that fundamental aspects of the behavior of humans have a genetic basis with a common evolutionary trajectory that are shared with other species. A central intention of comparative behavioral sciences is to identify "(…) animal species with behavioral or psychological repertories similar to humans so that the results of experiments with these animal models may throw light on seemingly related behavior in human beings" (Lickliter, 2004, pp. 27–28). Whereas animals are in most instances intended as a model for humans, one animal species may also serve as model organism for another species. Studies, however, which

explicitly compared behavior across species, are rare in neuroscience (Sharbaugh et al., 2003).

We define animal models of neurobehavioral disorders as follows:

> An animal model with biological and/or clinical relevance in the behavioral neurosciences is a living organism used to study brain–behavior relations under controlled conditions, with the final goal to gain insight into, and to enable predictions about, these relations in humans and/or a species other than the one studied, or in the same species under conditions different from those under which the study was performed. *van der Staay, 2006*, *pp. 133–134*

3 ANIMAL MODELS IN BIOMEDICAL RESEARCH

Animal models are used during the entire cascade from proof of concept (POC) through efficacy testing, safety, teratology, and toxicology evaluations of candidate drugs to translational research to product-related research. POC, also called proof of principle (POP) is objective evidence supporting the functionality of a principle, concept, or theory and its potential for real-world application. In preclinical trials using appropriate animal models, the efficacy and safety of a drug is determined (Lalonde et al., 2007). Safety pharmacology aims to detect the liability of adverse effects, determine safety margin calculation, and monitor clinical safety (Pugsley et al., 2008). Teratology or developmental toxicology assesses agent-induced abnormal development (Vorhees, 1989), whereas toxicology is the study of the effects of (putative) poisonous chemicals or drugs on living beings. Finally, product-related research is performed during experimental research preceding and/or following the introduction of, for example, a therapeutic drug into the market. Its purpose is to fully tap the potential of a therapeutic substance at advanced stages in the clinical development and of the products that have already been launched onto the market (to our knowledge, this element of the cascade has not yet been addressed in scientific publications). All steps in the cascade of drug development are performed using animals as subjects, in particular rodent species. However, large animal models are increasingly being used and may change the cascade of animal experiments from basic research to research intended to develop new therapeutic principles.

4 CONCERNS ABOUT THE TRANSLATABILITY OF FINDINGS FROM ANIMAL EXPERIMENTAL STUDIES

The relevance of results from preclinical animal studies for developing new therapeutics and the translational value of preclinical animal studies has been criticized (Plath et al., 2011; Pratt et al., 2012). Many putative new therapeutics turn out to be ineffective or not effective enough in clinical trials, whereas they showed good efficacy and safety in animal models (Gribkoff and Kaczmarek, in press; Macleod, 2011; van der Worp et al., 2010). Consequently, the translatability of result of animal studies to humans has been described as poor (Garner, 2014; Ioannidis, 2008; Macleod, 2011; van der Worp et al., 2010).

Many putative causes have been identified for the poor translatability of results from animal experimental studies (Sabroe et al., 2007), in particular ascribed to methodological flaws, such as underpowered studies, low group sizes, and/or lack of blinding, to name only a few (van der Worp et al., 2010). Awareness is increasing that animal studies can be flawed in multiple ways, and recommendations to increase the predictive validity of animal model-based research have been published (Ioannidis et al., 2014). Notably, it has hardly ever been questioned in this distending stream of critical reviews addressing lack of translatability, whether the appropriate model animal species have been used and whether a change of animal model species from rodents to large animals may improve translatability (presumably not in all, but probably in some areas of neuroscience research).

5 TRANSLATIONAL RESEARCH

Whereas research for identifying new therapeutic principles and putative therapeutics may be considered as basic research, using validated animal models to develop novel therapeutics may be considered translational research, where translation refers to the process in which knowledge generated in one area of research is applied in another area of research to advance goals in that area (Abernethy and Wheeler, 2011).

McGarland Rubio et al. defined translational research as follows:

> Translational research fosters the multidirectional integration of basic research, patient-oriented research, and population-based research, with the long-term aim of improving the health of the public. T1 research expedites the movement between basic research and patient-oriented research that leads to new or improved scientific understanding or standards of care. T2 research facilitates the movement between patient-oriented research and population-based research that leads to better patient outcomes, the implementation of best practices, and improved health status in communities. T3 research promotes interaction between laboratory-based research and population-based research to stimulate a robust scientific understanding of human health and disease. *McGartland Rubio et al., 2010*, *p. 471*

The European Society for Translational Medicine (TM) defined translational medicine as "an interdisciplinary branch of the biomedical field supported by

three main pillars: benchside, bedside and community. The goal of TM is to combine disciplines, resources, expertise, and techniques within these pillars to promote enhancements in prevention, diagnosis, and therapies." (Cohrs et al., 2015, p. 88).

Animal models are the first step in the translational continuum that has been described as consisting of three (Abernethy and Wheeler, 2011; Drolet and Lorenzi, 2011; McGartland Rubio et al., 2010), four (Lander and Atkinson-Grosjean, 2011), or five (Waldman and Terzic, 2010) distinct stages (Trochim et al., 2011). For our

purposes, the first translational stage(s) (T0 and T1) are of relevance. Fig. 3.1 depicts the chain of research from basic to translational. Nowadays, many if not most researchers using animal models in biomedical research denote their work as "translational." The T0 stage (Waldman and Terzic, 2010) in Fig. 3.1 may cover this use of "translational."

Translational animal models can be considered as a subset of the more general concept of "generalizability." The "translational value" and "translational relevance" of an animal model, and the concept of "predictive validity" are connected, or may be conceived as basically
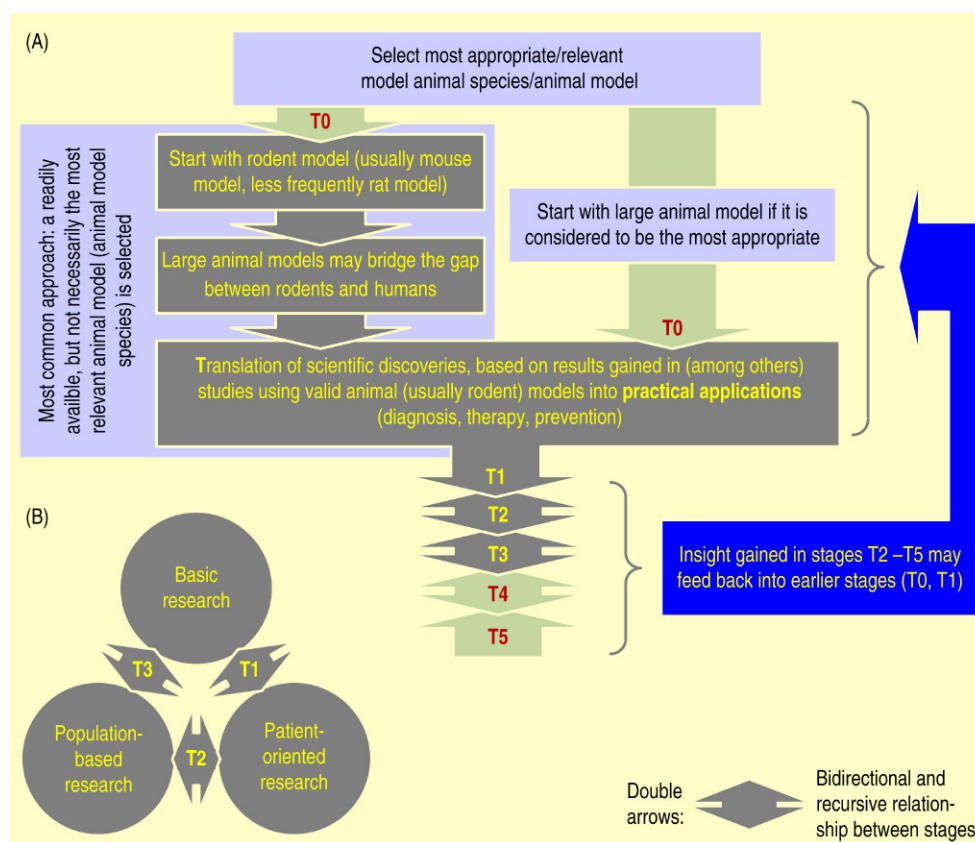
FIGURE 3.1   **The position of animal models in the stages from basic (bench) to applied (bedside) translational research and the decision about the animal model species/animal model(s) to be used.** Translational research distinguishes different stages, most commonly T1–T3 [panel (B) Drolet and Lorenzi, 2011; McGartland Rubio et al., 2010, p. 472], which may be considered as the basic concept. Others, however, distinguish more stages, for example, T1–T4 (Trochim et al., 2011), or T0–T5 (Waldman and Terzic, 2010). In all systems, the first stage (T1) or the first two stages (T0, T1) involve animal experimental research (in particular proof of concept research, Hostiuc et al., 2016). Proof of concept research may start using rodent experiments [panel (A) upper left] or may be performed using large animals, if the large animal model is considered as more appropriate/relevant, eventually completely skipping rodent experiments [panel (A) upper right]. T1 is "the transfer of new understandings of disease mechanisms gained in the laboratory into the development of new methods for diagnosis, therapy, and prevention and their first testing in humans" (Woolf, 2008, p. 211). Waldman and Terzic (2010) suggested to add the stages T0, preclinical research (in vitro research and in vivo animal model-based research), which may start as basic research, and T5, improving the wellness of populations by reforming suboptimal social structures. Basic research is performed for gaining scientific insight without the primary intention of practical application of the knowledge, whereas T0 already considers practical applicability. The bidirectional and recursive relationship between animal models, translation to applications, and reverse translation to animal models is indicated by the *double-headed arrows*. Also, insight gained in later stages may feed back to the first stage(s) of translational research (T0 or T1, depending on the classification of stages used). Stages T0, T4, and T5, which have been added to the original concept of three translational stages shown in panel B, are depicted as *green arrows* or *double arrows* in panel A. *Source: Panel (A) modified from van der Staay, F.J., Arndt, S.S., Nordquist, R.E., 2014. Developing mouse models of neurobehavioral disorders: when is a model a good model? In: Pietropaolo, S., Sluyter, F., Crusio, W.E. (Eds.), Behavioral Genetics of the Mouse, vol. 2. Cambridge University Press, United Kingdom, pp. 3–17; panel (B) modified from McGartland Rubio, D., Schoenbaum, E.E., Lee, L.S., Schteingart, D.E., Marantz, P.R., Anderson, K.E., et al., 2010. Defining translational research: implications for training. Acad. Med. 85 (3), 470–475.*

the same concept. "Translational," however, has a clear focus on applicability (diagnosis, therapy, prevention). By comparing the effects of a new therapeutic with a compound with proven efficacy in the clinic, the predictive validity of an animal model can be determined experimentally. Likewise, the "translational value" or "translational relevance" of a (large) animal model is determined retrospectively: insights derived by using the animal model must successfully be translatable to practice.

Using models with proven construct validity may increase the probability of successful translation of animal research-based preclinical findings to clinical applications (Kimmelman and London, 2011; Pratt et al., 2012). The translatability can further be increased by using a broader range of relevant models (Pratt et al., 2012), for example, by using animals that show comorbidity (Libby, 2015), by applying a treatment regime that closely matches that of clinical practice (Green et al., 2011), and by applying appropriate behavioral tests that can distinguish between different behavioral domains and endophenotypes (Homberg, 2013). The "translational value" and "translational relevance" of large animal models largely depends on the degree to which they mimic the dysfunction/disease under study and the availability of reliable testing methods.

Translational research is bidirectional (Donaldson and Hen, 2015). It may start with clinical observations and characterizing disease-relevant endophenotypes in patients which are then reverse translated to animal models, that is, clinical findings inseminate basic research (Holschneider et al., 2011). This can be considered as a process of induction in the process of developing animal models (van der Staay, 2006). Sinha et al. (2011) assessed whether neuropharmacological findings in humans yield new insights, that is, whether they can be reverse translated to investigating underlying mechanisms in an appropriate animal model. Reverse translational approaches thus may contribute to conceiving and developing new animal models or to refining established ones. For developing translationally relevant animal models (Pratt et al., 2012), an intensive interaction of animal research scientists and clinical researchers is fundamental (Markou et al., 2009).

"The model's circular structure suggests that research is a continuing cycle, and its bidirectional arrows emphasize that new knowledge and hypotheses are generated at each step. Some basic research and population-based research is translational, but neither type of research is by definition translational. In contrast, patient-oriented research fundamentally addresses issues that have the potential to translate to clinical practice and, therefore, affect health." (McGartland Rubio et al., 2010, p. 472).

Animal models intended for use in basic research and animal models in translational research should,

in principle, fulfill the same criteria to be valid and relevant. However, translational animal models may need to fulfill additional criteria if they are applied in translational stage 1 (T1) (van der Staay et al., 2014). Whereas the key definitions per stage may differ for different classifications of the translational continuum, they all describe translational research as a process that moves from basic/preclinical research [T1 or T0/T1 that include(s) animal models] to the clinical application of the knowledge gained in animal experiment, and finally, to public health (Fig. 3.1). This process is bidirectional (Trochim et al., 2011) and in some instances, can be recursive.

6 CHOICE OF APPROPRIATE ANIMAL MODEL

In most instances, if authors reflect on the choice of an appropriate animal model, they are looking for models with rodents, and do not consider *nonrodent* species, that is, they usually mean *rodent model*, or *mouse model* when referring to *animal model*. Manger et al., 2008 discussed the consequences of the disproportionate use of rodent model, and particularly mouse models in basic neuroscience research. This extreme bias may hinder "(...) the discovery of novel aspects of brain structure and function that would be of importance in understanding both the evolution of the human brain and in selecting appropriate animal models for use in clinically related research." (Manger et al., 2008, p. 2).

There has been a steady increase of using rodent species, mainly mice, whereas in nonrodent species, in this decade, the use of pigs has overtaken that of rabbits and dogs as model species in biomedical research (Ericsson et al., 2013; Table 3.1). Recently, the use of large animal models appears to increase owing to the development of genetically modified farm animals. For example, genetically modified pigs are being developed as models for human diseases, such as Alzheimer's disease (Søndergaard and Herskin, 2012).

The reasons for sticking to rodent models, where nonrodent models might be more appropriate are mainly nonscientific:

- The researcher is mainly experienced with performing rodent studies. Rand (2008) cautions against selecting an animal model solely based on the familiarity of the researcher with a model, its availability and its costs.
- The question "which model species is the most suited for my research" very often is not even asked. This should, however, be one of the first questions when planning to perform animal experimental studies (Rand, 2008; von Rechenberg, 2012),

TABLE 3.1   Advantages and Disadvantages of the Reuse of Animals in Different Tests in the Same Study, Yielding Multiple Readouts From the Same Animals, or of the Same Animals in Successive, Unrelated Studies

	Disadvantages	
Advantages	Reuse of animals in one study (multiple tests and/or repeated testing)	Reuse of animals in successive, unrelated studies (which may comprise of one test or multiple tests, and eventually, repeated testing)
Fewer animals are needed for research (Reduction)	If nonrepresentative samples of the population are used, then this may affect the results of all experiments and/or tests with the same animals	If the samples are not representative for the population from which they were drawn, then this may affect all experiments/tests performed with the same animals
Animals are handled and accustomed to being tested; less habituation or training trials are needed; animals are used to be handled and tested; lower stress level	Animals may not be "test naïve" in later tests or experiments, that is, previous testing may affect results of subsequent tests and/or experiments; excessive reuse of animals may compromise their welfare (depending on the degree of discomfort induced by the testing methods used, Festing et al., 1998)	Excessive reuse of animals may compromise their welfare (depending on the degree of discomfort induced by the testing methods used, Festing et al., 1998); reuse may necessitate transportation, mixing (introduction into a new group due to random assignment to treatment conditions), housing in an unfamiliar animal room
Animals are test experienced. Successive testing provides opportunities to adapt to different environmental demands and challenges; behavioral consistency may increase with age, due to experience with testing (Bell et al., 2009); less likely "Casper Hauser" individuals with unchallenging life (van der Staay et al., 2010)	Animals may not be "test naïve" in later tests or experiments; altered behavioral baseline; prior testing may alter effects of treatment (Holmes et al., 2001b); this may complicate comparison with studies that used test naïve animals; previous testing may interfere with subsequent testing (proactive interference)	Animals may not be "test naïve" in later tests and/or experiments; prior testing may alter effects of treatment (Holmes et al., 2001b); this may complicate comparison with studies that used "test naïve" animals; previous testing may interfere with subsequent testing (proactive interference)
Knowledge accumulates with each test/ experiment, providing a more complete picture, and allowing investigation of relationships between variables (readouts) (Reduction, Refinement)	Animals are older in successive tests (age cannot strictly be controlled); animals may reach "ceiling" performance level, reducing sensitivity to detect treatment effects; correction of P-values for multiple comparisons may reduce sensitivity to detect (subtle) effects	Animals are inevitably older in each successive study (age cannot strictly be controlled)
Testing may act as enrichment	Testing per se may overshadow the effects of experimental manipulations (Westlund, 2014a,b)	Testing per se may overshadow the effects of experimental manipulations (Westlund, 2014a,b)

where the appropriateness of the selected animal model species should be the first consideration (Held, 1983).

- Conservatism of rodent researchers may withhold them from considering alternative animal model species. In this connection, Libby (2015) coined the term *Murine "model" monotheism*, which is a nice label for the bias toward rodent models.
- Neglecting publications that used nonrodent animal models (perhaps best described as "reading bias").
- In most research institutes, facilities other than those needed for housing and testing rodents are unavailable.

Instead, the selection of rodent and nonrodent species for preclinical assessment of, for example, the efficacy and/or safety of new putative therapeutics, should

always be based on scientific and ethical justifications. Animal models must fulfill a set of scientific criteria and should thoroughly be validated (Belzung and Lemoine, 2011; Markou et al., 2009; van der Staay, 2006; van der Staay et al., 2009, 2014). Of course, these criteria are closely connected with the research question(s) that the animal study is supposed to answer. Besides this very specific consideration, general questions must be addressed to help finding the animal model best fitting one's research question(s). This implies that the selection of an animal model species and the animal model should be considered on a case-by-case basis (Colleton et al., 2016; Rand, 2008). Based on Rand's (2008) listing of scientific and practical criteria, the following questions need to be answered before selecting an animal model and starting a study. The first questions are related to the experimental approach to be chosen:

- What is known about the problem under consideration (based on a thorough review of the scientific literature, for example, via a systematic review, Hooijmans and Ritskes-Hoitinga, 2013, or via less time-consuming rapid reviews, Featherstone et al., 2015)?
- Has the selected model been validated and is it deemed to be the most appropriate for answering the research question(s)? How closely, for example, does the animal replicate the human disease (Søndergaard and Herskin, 2012)?
- What kind of model is it: does the model animal express naturally occurring or experimentally induced deficits (for different classifications of "animal models," see Rand, 2008; van der Staay, 2006)?
- What are the ethical implications of this choice (similar considerations as, e.g., for stroke models in primates Sughrue et al., 2009, may be relevant in other large animal model species)?
- How many animals are needed to answer the research question(s), that is, which group sizes are needed to ensure sufficient power?

Next, questions concerning availability, animal housing, and animal care must be answered, such as:

- Is the animal model species chosen readily available. In most instances, availability should not be a major problem in research using large farm animals.
- Can the animals be housed appropriately? This may be a concern in large animal research because they may need considerably more space and must be housed in stables/pens that fulfill their species-specific needs.
- Are the researchers and animal caretakers trained to work with large model animal species and provide special care, if necessary?

Finally, a number of specific questions must be answered:

- Do animals with genetic homogeneity or heterogeneity best serve the research question(s)? Most large model animal species are heterogeneous lines/breeds, that is, homogeneous (inbred) lines are not yet readily available. However, for most farm animal species, a large variety of breeds is available.
- Is the selected model animal species testable, both in terms of ease of handling, as well as in terms of availability of well-established and validated test methods and test equipment (see also Chapter 39)?
- Does the size of the animal facilitate taking samples from the animal (blood, hair, tissues)? Is it crucial that organ size is similar to that of humans?

- Should the animal be tested during ontogeny, (e.g., early postpartum, as juvenile), as adult, or during senescence. Whereas large animal species may be specially suited for pre-, peri-, and early postnatal experimental manipulations, they may be less suited for aging research, due to poor availability of aged subjects and the high life expectancy of many of these species.
- Recently, the "sex bias" in neurosciences and biomedical sciences in general attracts increasing attention (Beery and Zucker, 2011; Zakiniaeiz et al., 2016). It has to be decided whether males, females, or both sexes should be included. Due to the extra space, special equipment, well-trained personnel needed to perform experiments using large model animal species, inclusion of both sexes may overburden available resources.

7 WHERE IN THE PROCESS OF MODELING HUMAN DISEASES AND DEVELOPING PUTATIVE THERAPEUTICS HAVE LARGE ANIMAL MODELS BEEN USED?

Large animal models may be relevant for research that aims to improve production of animal-derived products (not considered further in this chapter), for animal health and welfare, and for translational biomedical research (Gonzalez-Bulnes et al., 2016; Ireland et al., 2008; Koopmans and Schuurman, 2015), that is, they can be considered as multiple purpose models. Large animal models are well accepted in the area of orthopedic and xenotransplantation research (Cook et al., 2014; Gregory et al., 2012; Harding et al., 2013). They are, however, only sporadically used in neuroscience, where they are mainly applied in stroke and traumatic brain injury studies (Boltze et al., 2008; Duhaime, 2006; Margulies et al., 2015; Mehra et al., 2012; Platt et al., 2014; Wells et al., 2012).

Most of the efficacy, toxicology, teratology, and safety studies use rodents species as subjects. However, in particular in toxicology, teratology, and safety studies a considerable proportion of animals used are large animals (e.g., dogs and miniature pigs). In particular in safety pharmacology/toxicology/teratology studies, the minipig is gaining importance (Bode et al., 2010; Forster et al., 2010a,b,c; Svendsen, 2006; van der Laan et al., 2010).

Other than in risk assessment studies, the use of large animal model species is still negligible in drug testing, be it in POC studies or in studies, which aim to test the efficacy of a new compound preclinically, compared with rodents.

8 WHICH MODEL ANIMAL SPECIES ARE CLASSIFIED AS LARGE IN SCIENTIFIC RESEARCH?
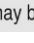
One may distinguish between "small (e.g., mouse, rat)," "midsized" (e.g., dove, chicken, rabbit, guinea pig, marmoset, cats) and "large" (e.g., pig, dog, rhesus monkey, baboon, chimpanzee) animals. However, Hagen et al. (2012) categorize companion animals, such as cats, dogs, rabbits, and ferrets, farm animals, such as pigs, goats, sheep, cows, and horses, chickens, ducks, goose, etc. as "large" animals, if compared with the most commonly used species in scientific research, mice and rats (Fig. 3.2).

The designation of specific species as "small," "midsized," or "large" animals depends in part on the system under study. Rodents are virtually always considered "small" animals, while dogs, sheep, swine, and primates are typically considered "large" animals. Chickens and cats can be included in either group, depending on the specific system studied.

For purposes of brain research, it may be useful to ask which feature in humans one is attempting to reconstruct in a given model. In a study of experimentally induced brain injury one may, for example, try to model one or more of the following features: the mechanistic forces that caused the brain injury, the resultant morphological changes in the brain, the effects of age (maturation) and aging on these changes, and/or the effects of treatment with putative therapeutics on the development and final extent of the damage (Duhaime, 2006).

The size of the model animal species and of its brain may crucially determine the resolution at which these changes in the afflicted brain can be studied. Consequently, big is sometimes better. For example, bigger brains contain more tissue for analysis, nuclei and areas

(A)	(B)	Species		Approximate brain weight	Gyri and sulci
		Human	5 cm	1300–1400 g	Gyrencephalic
Large animal model species	Large animal model species	Cow		480 g	Gyrencephalic
		Sheep		175 g	Gyrencephalic
		Pig		80–180 g (large variation between breeds)	Gyrencephalic
		Dog		70–130 g (large variation between breeds)	Gyrencephalic
	mid-sized	Cat		30 g	Gyrencephalic
small*		Chicken		2.5–4.5 g (large variation between breeds)	Lissencephalic
	small*	Rat		2 g	Lissencephalic
		Mouse		0.5 g	Lissencephalic

aNote: quail and pigeons may be considered as small model animal species

FIGURE 3.2 Classification of animal model species as large, midsized, or small (columns A and B), and weight (g) of the brain of adults of these species, from mice to humans. In pigs and dogs, the variability is high, due to selection on, among others, body size. *Source: Silhouette of brains of human, sheep, pig, dog, cat, rat, mouse, and chicken redrawn from photographs: Welker, W., Johnson, J. I., Noe, A., 1995. Comparative mammalian brain collections: major national resources for study of brain anatomy. The University of Wisconsin, Michigan State University, and the National Museum of Health and Medicine. Dept. of Physiology, University of Wisconsin. Available from: http://www.worldcat.org/title/comparative-mammalian-brain-collections-major-national-resources-for-study-of-brain-anatomy-the-university-of-wisconsin-michigan-state-university-and-the-national-museum-of-health-and-medicine/oclc/37416838#details-allauthors; brain of cow redrawn from photograph: Wouterlood, F., Voorn, P., 2010. The bos taurus brain. Department of Anatomy & Neurosciences, VUMC Amsterdam, Amsterdam, The Netherlands. Available from: http://www.anatomie-amsterdam.nl/sub_sites/kalfshersenen/start.htm. Modified from Gieling, E.T., Schuurman, T., Nordquist, R.E., van der Staay, F.J., 2011. The pig as a model animal for studying cognition and neurobehavioral disorders. Curr. Top. Behav. Neurosci. 7, 359–383.*
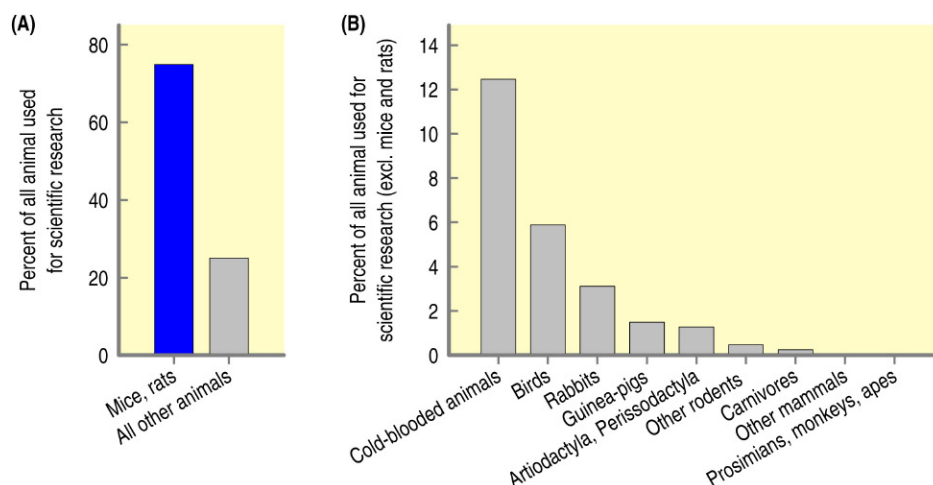
FIGURE 3.3 **Animal use in the European Union in 2011.** Panel (A) shows that the majority of studies are performed using mice and rats. In panel (B), "All other animals" from panel (A) is subdivided. Note that chickens are included in "Birds." The Perissodactyla include horses, donkeys, and their crossbreds. The Artiodactyla include pigs, goats, sheep, and cattle (European Commission, 2013). Unfortunately, the different reporting schedules, classifications of model animal species, and inclusion/exclusion of model species preclude a one-to-one comparison between statistics about experimental animal use in the EU and the USA (USDA, 2015).

of interest are bigger, allowing more precise lesioning of target structures, local injections of test compounds via cannulas, electrophysiological stimulation or recordings in deep brain structures, or electroencephalography from the surface of the brain or skull.

The use statistics of different animal model species in scientific research in the European Union in 2011 (European Commission, 2013) are depicted in Fig. 3.3. Large animal use represents only a very low percentage of the total use of experimental animals.

9 WHICH TYPES OF (LARGE) ANIMAL MODELS ARE AVAILABLE?

A number of classifications of animal models have been proposed. These classifications typically distinguish between normal animals, animals with spontaneously occurring deficits, and animals with experimentally induced deficits (Gamzu, 1985; van der Staay, 2006), but other classifications have also been proposed (Rand, 2008). The classification can be applied to rodent and nonrodent (e.g., farm animal) models.

Normal subjects, that is, animals without observable (behavioral) deficit are useful for assessing the safety/toxicology risk of putative therapeutics (Dixit and Boelsterli, 2007), for assessing the putative abuse liability of a compound, and for investigating the neurobiological specificity of compounds and their mechanisms of action.

Spontaneous models are, for example, old animals, animals showing spontaneously and endogenously

occurring psychiatric or neurological conditions, spontaneously occurring mutations, genetic lines (inbred strains and their crossings), and lines resulting from selective breeding, and selected extremes from a particular animal population (Hudler, 2007; van der Staay, 2006).

Induced models are healthy animals in which the pathological condition is induced experimentally, for example, transgenic and knockout animals, selection lines resulting from selective breeding, animals with disruptions induced, for example, by stimulation with electric currents, pharmacological treatments, or by inducing hypoxia or anoxia. This class also includes animals with neuro- or immunotoxic, radiofrequency, cryogenic CNS-specific lesions, and lesions induced by aspiration or ablation (knife cuts). Finally, this class contains animals with experimentally induced cerebral ischemia or hemorrhagic stroke.

Rand (2008) in addition distinguishes negative models and orphan models. Negative models may be useful to investigate the mechanisms behind disease resistance because they are characterized by insusceptibility to disease or chemical stimulation. The opposite of negative models are orphan models. These animals show a disease/deficiency/dysfunction for which no correspondence has yet been described in humans. As soon as a similar disease has been identified in humans, an orphan model may become the basis of a spontaneously or naturally occurring, or an induced model (e.g., sheep suffering from scrapie, now may serve as model human spongiform encephalopathies).

A considerable number of rodent models have been developed for at least the first three classes. However,

they have not yet been established broadly in large model animal species.

Already 4.5 decades ago, Douglas (1972) summarized arguments why the pig may be a useful animal model species for human biomedical research, predominantly based on hematological and organ similarities between pigs and humans. However, he also noted that "Apart from the biological side, the pig must not be considered stupid. The pig can be used for the observation of many well-defined patterns of individual and group behavior (…)" (Douglas, 1972, p. 232), a first hint that this species may also be useful in neuroscience research. Reasons why large animal models should be used are given by Bähr and Wolf (2012), de Groot et al. (2005), Gieling et al. (2011b), Reynolds (2009), and Roberts et al. (2009). They all agree that "(…) the validity of an animal model as a predictor of human response depends on how closely the model resembles humans for the specific characters being investigated." (Festing and Altman, 2002, p. 246).

10 SPECIAL ASPECTS IN USING LARGE FARM ANIMAL MODELS

Large animal models need more housing and testing space than rodent species (Fig. 3.4, panel A). Also, test procedures and equipment must be adapted from rodent studies or must be developed and validated.

New equipment and new tools for large animal models are being developed. For example, stereotaxic atlantes and stereotaxic frames (Marcilloux et al., 1989; van Eerdenburg and Dierx, 2002) are available for many large animal species. For about a decade, the stereotaxic, histology-based atlas by Félix et al. (1999) and the magnetic resonance imaging-based atlas by Watanabe et al. (2001) were the only source of stereotaxic coordinates of the pig brain. Recently, higher resolution three-dimensional representation of the pig brain have been published (Göttingen minipig, Andersen et al., 2005; neonatal pig, Conrad et al., 2014; commercial pig, Saikali et al., 2010). A stereotaxic atlas for the chicken brain has been published a decade ago (Puelles et al., 2007), whereas for sheep (and for a number of other species), three-dimensional representations became recently available online (Johnson et al., 2016).

For pigs, a large number of tests to assess emotion (reviewed by Murphy et al., 2014) and cognition (reviewed by Gieling et al., 2011a) have been developed. Similarly, an increasing repertoire of behavioral test is being developed for sheep (e.g., judgment bias, Doyle et al., 2011; face and object discrimination learning, Kendrick et al., 1996, 2001; spatial learning, Lee et al., 2006), although progress is slow. The repertoire of tests for assessing learning and memory in chicks is still limited, but expanding (e.g., the spatial holeboard task, Nordquist et al., 2011; Tahamtani et al., 2015; Fig. 3.5, panel B).
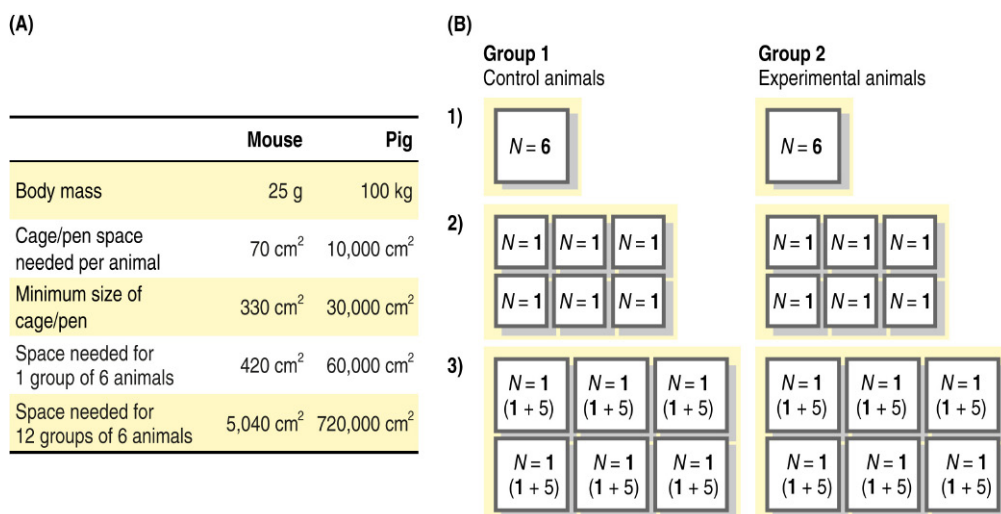
FIGURE 3.4 **Space requirements and examples of different experimental setups of the same study.** In panel (A), the space requirements for housing 6 mice or pigs individually or as group are tabulated in cm^2. In the example depicted in the panel (B), each of 12 animals is randomly assigned to one of two treatment groups (assuming that a group size of 6 animals is sufficient to address the scientific questions of the experiment). Although it cannot be excluded that cage is a confound variable that might codetermine or even cause differences between treatments in setup 1, the mere assumption leads to a huge increase in animals used, if a "state of the art" experimental setup (setup 3) is applied. Note, that the 6 pens per condition in setup 3 do not provide 100% identical environments for the 6 experimental animals per treatment group. Instead, strict standardization of the housing conditions (i.e., of the two cages in setup 1) could be applied, reducing the number of animals to 12. In social species, setup 1, but not setup 2 is an alternative for setup 3. Note: none of the setups is able to control all putative intervening variables. The number of control or experimental animals per cage/pen is printed bold (the *squares* representing cage/pen areas are on scale and correspond to the tabulated values; based on Forbes et al., 2007).
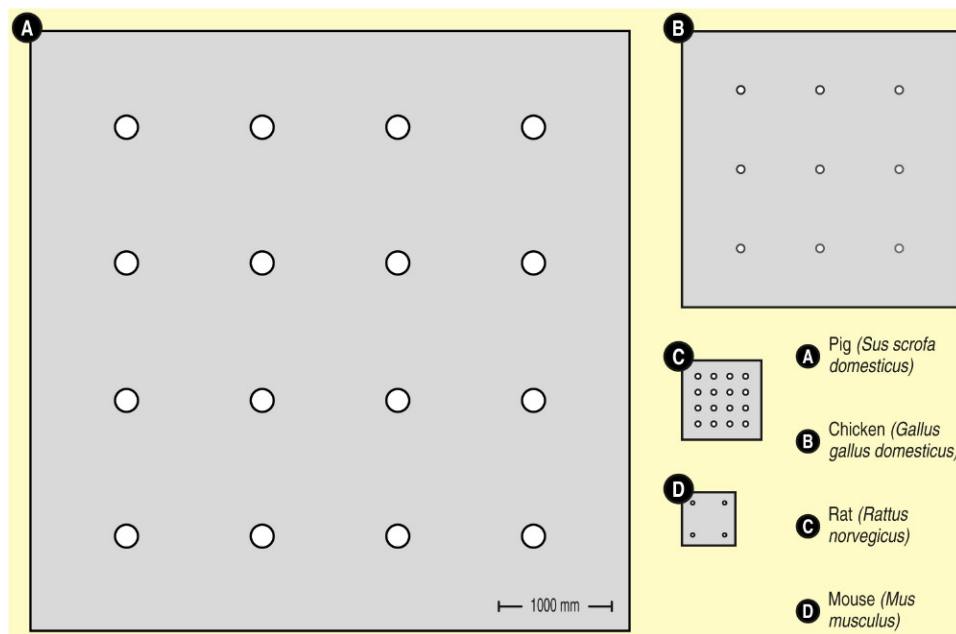
FIGURE 3.5 Comparison of holeboard arena's used to test spatial learning in two large animal model species [(A) pigs, Antonides et al., 2015a; Gieling et al., 2013; (B) chickens, Nordquist et al., 2011; Tahamtani et al., 2015] and two small animal model species [(C) rats, van der Staay, 1999; (D) mouse, Kuc et al., 2005].

Many of these tests have been developed for assessing cognitive functions in farm animal species, and have only sporadically been used in biomedical studies. They still need scientific validation but they provide a basis for testing learning and memory in disease models using large animal model species. However, it is obvious that additional tests must be developed to increase the usability and relevance of large animal models of neurobehavioral and psychiatric disorders.

The test equipment for large animals must fulfill a number of special requirements. First, obviously, it must fit the size of the animal species to be tested (Fig. 3.5). This may require a room which exceeds the size of a standard rodent laboratory. Second, the equipment must be stable enough to resist destruction by the tested animals. Our test apparatuses for pigs (Fijn et al., 2016; Gieling et al., 2014; Murphy et al., 2013; van Eck et al., 2016) were constructed by a stable builder according to our specifications, using standard material that normally is used to construct pig pens. Stable builders know how to construct pig-proof equipment.

Also, testing procedures and methods need to be suited for the species to be tested. For example, pigs must thoroughly be habituated to the test environment, the experimenter(s), and to being alone in the test apparatus (Gieling et al., 2011a; Murphy et al., 2014) (see also Chapter 39). The habituation and training period can be time consuming, before formal testing starts.

11 EXPERIMENTAL UNIT

Most animal experimental studies do not explicitly define the experimental unit. It needs to be stressed that *experimental unit is not* the same as *unit of analysis*. Depending on the experimental design used, there may be multiple units of analysis. Whereas in a basic single-level experiment the *experimental unit* would be considered the *unit of analysis*, a multilevel design may have more than one unit of measurement (Festing, 2006; Festing and Altman, 2002; Perrett, 2012).

An "experimental unit" is defined as the smallest division of the experimental material that allows any two experimental units to receive different treatments (Festing, 2006, 2011), or as Bate and Clark define it, "An experimental unit for a treatment factor is the smallest unit which a level of the treatment can be applied to." (Bate and Clark, 2014, p. 37). An experimental unit is one member or a set of animals that are initially similar on the measure(s) of interest, with each animal then subjected to one of several experimental treatments (Fig. 3.6, panels A–D). An experimental unit can also be a part of an animal (e.g., skin patches that undergo different treatments; Fig. 3.6, panel E). Each treatment represents one of a set of different experimental conditions. The effects of these different conditions are assessed experimentally.

For some, it must be possible to treat an animal independently from all other animals involved in the study *at any time*, that is, "The experimental unit may be defined
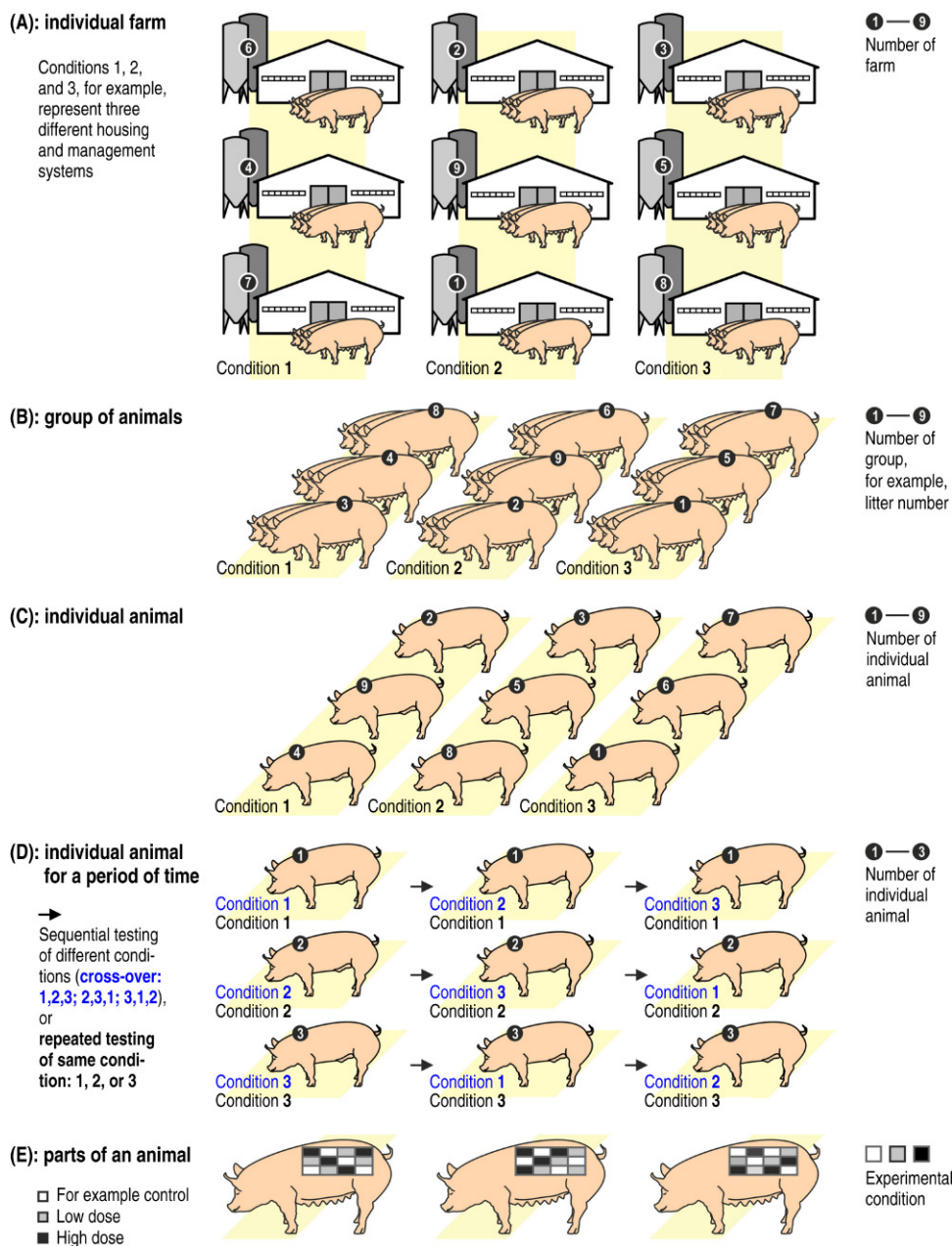
FIGURE 3.6 **Experimental units in animal research.** "Condition" refers to experimental condition (treatment or control). While it is unusual to depict pigs instead of rodents as experimental animals, studies with large animals may pose additional challenges that need to be addressed when designing and performing an experiment. *Source: Modified from Gieling, E.T., Schuurman, T., Nordquist, R.E., van der Staay, F.J., 2011. The pig as a model animal for studying cognition and neurobehavioral disorders. Curr. Top. Behav. Neurosci. 7, 359–383, Fig. 4.*

as the object independently treated in an experiment." (Perrett, 2012, p. 3). For others, this may refer to random assignment or placement to one of the experimental conditions *at the start of an experiment*, before the animals undergo their assigned experimental manipulations. According to Cheng, following a definition of Cox from 1958 "In general, an experimental unit can be defined as the smallest division of the experimental material such

that different units may receive different treatments." (Cheng, 2013, p. 1) (see Figs. 3.6 and 3.7 for schematic overviews of experimental units). Random assignment is the procedure by which animals are allotted to different treatment groups (treatment conditions), or to an untreated control group (control condition; note that some studies comprise more than one control group). It is assumed that as a result of random assignment to
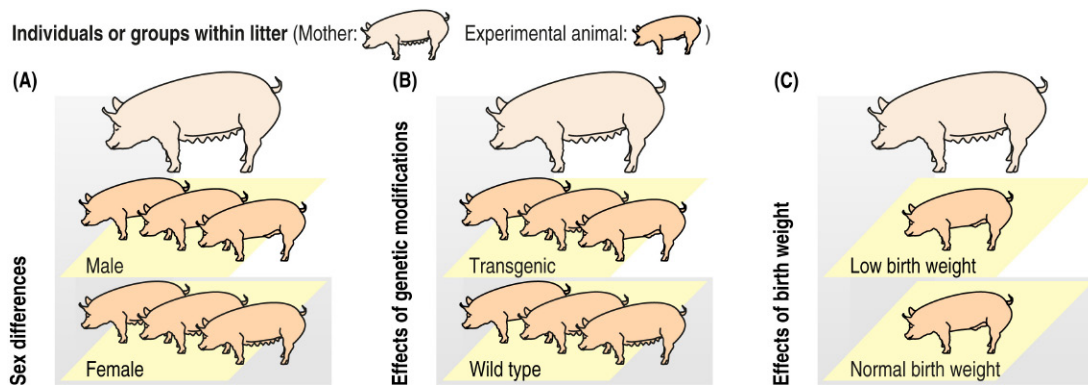
FIGURE 3.7 **Examples of individuals or groups within litter (i.e., offspring of the same sow) are shown, where litter is the experimental unit.** Instead of litter, the experimental unit may be pen, herd, compound in a zoo, etc. In (A) male and female pigs are selected from the same litter for assessing sex differences. In (B) transgenic and wild-type pigs are derived from the same litter to investigate the effects of genetic manipulations, whereas in (C) low birth weight (LBW) and normal birth weight (NBW) pigs are selected for investigating the effects of birth weight. In all examples, a study comprises a number of litters. Note that in these examples, random assignment of individuals to a group is not possible, but random selection of animals from a larger pool (e.g., selection of one or a few males in a litter from a larger number of male littermates) to a study is possible.

treatment conditions, the different treatment groups will be initially similar; differences between the treatment groups (conditions) are likely not due to differences between the groups that already existed before the start of the experimental manipulations. Once an individual has been assigned to a particular experimental condition, it may be impossible to treat that individual animal independently from the other animals in the same group during the term of the experiment. Due to space requirements and space restrictions, this is a problem inherent in studies using large animal model species.

Most large model animal species produce litters with multiple offspring. It is advisable to use this in designing experiments. There are two ways to assign littermates to experimental groups (conditions): either all littermates are assigned randomly to the same experimental group, a nested design, or the littermates are randomly assigned to different experimental groups, a randomized blocks design (Denenberg, 1984). In the nested design (Fig. 3.6, panel B and Fig. 3.7) litter must be considered as experimental unit because littermates are not independent. As Lazic and Essioux (2013) pointed out, litter effects are common and usually large. Consequently, replication of findings is difficult if this source of variation is ignored when analyzing the data and the translational value of the study may be low.

Mixed model analyses of variance may be used to account for nested effects. They have been developed to account for "nested (multiple observations within a single subject/animal in a given condition) and crossed (subjects/animals observed in multiple conditions) structure of the data" (Boisgontier and Cheval, 2016). Unfortunately, this statistical approach has not yet been fully appreciated in the neurosciences.

In the randomized block design of a one-factorial study consisting of an experimental and a control condition one might use pairs of littermates from a number of different litters equal to the number of animals per group used. Then, one sibling per pair is assigned randomly to the experimental group, the other to the control group. Fig. 3.7 (panels A–C) shows a different design in which a *group of littermates within litter* is assigned randomly to the experimental condition, and *another group of littermates within the same litter* to the control condition. In these designs, accounting of litter effects helps to obtain a better estimate of the effects of the experimental manipulation (Denenberg, 1984; Healy, 1972).

12 EXPERIMENTS USING SOCIAL ANIMALS REQUIRING GROUP HOUSING

Fig. 3.4 (panel B) shows a schematic overview of different experimental setups for studying the effects of experimental manipulations on social animals (here: pigs). Assuming that six animals per treatment condition are sufficient for sound statistical interference about the effects of the experimental intervention(s) and that a group size of six animals fulfills the need to live in a group, and strictly following the previously given definition of "experimental unit" (Festing, 2006), the state of the art setup of the study is depicted as setup 3. Note, that this setup needs 5 times more animals than the 2×6 animals assigned randomly to the treatments groups in setups 1 and 2. In setups 2 and 3, each of the 2×6 experimental animals can be treated independently. In large animal research, setup 3 may already exceed the possibilities of appropriate housing of the animals. Instead,

one may house each of the 2 × 6 animals individually in smaller pens (Fig. 3.4, panel B, setup 2), adhering to the postulation of independent treatment. However, still the space requirements for housing all animals are high (Fig. 3.4, panel A). In addition, welfare of the animals may be at stake because social animals should be housed in groups.

In setup 1, all animals of the same treatment group are housed in one pen. In this case it is impossible to treat each individual animal independently from the pen mates, that is, the other animals undergoing the same experimental intervention. Consequently, according to the definition, the pen is the experimental unit and it is impossible to perform proper statistics on the effects of the experimental manipulation(s), as $N = 1$. However, the animals are housed socially and not individually as in setup 2, and no surplus animals are used, as in setup 3.

We discuss the implications of the definition of experimental unit, of housing animals in groups, and of repeated testing and/or reuse of animals against the background of principles of two (Reduction, Refinement) of the 3Rs (the third one being Replacement: Russell and Burch, 1959).

What are the consequences for the majority of studies performed, in which animals are housed in groups? For example, pigs are group housed in a barren or an enriched pen to assess the effects of environmental enrichment (Bolhuis et al., 2013; Grimberg-Henrici et al., 2016). A strict definition of "experimental unit" may have major implications for studies with socially housed animals, and may lead to an undesirable increase in the number of animals used. It also may considerably increase the costs of a study, in particular if large animals are involved (e.g., pigs, sheep, cattle, horses), but also if rodents are kept under special condition, such as isolators or ventilated cages.

Finally, we address the question what the welfare consequences are of collecting a multitude of measures in the same animal, of testing the animal repeatedly in the same study, and of reusing the animal in subsequent (unrelated) studies.

13 PUTATIVE ADVANTAGES AND DISADVANTAGES OF GROUP HOUSING

Group housing and environmental enrichment are common measures to improve the welfare of social animals. Most large animal model species (in particular the farm animals, such as chickens, pigs, sheep) are social animals that live in groups/herds (Estevez et al., 2007). Compulsory group housing might reduce the number of experimental units (i.e., cages/pens) and may consequently increase the number of animals needed (even if a

part of the penmates are not tested). Individual housing of these animals with the aim to increase the number of experimental units, compromises their welfare (Fig. 3.4, panel B, setup 2).

When using social animals, it is mandatory to apply group housing from an animal welfare perspective. Some Ethics Committees routinely demand group housing, even in cases where individual housing would be more appropriate, for example, if highly aggressive male mice are used in a study, despite the fact that this practice may compromise the experimental results (Poole, 1997). Older, sexually mature minipig boars, for example, should be housed individually to prevent fierce fighting, whereas younger boars can be kept in groups (Ellegaard et al., 2010).

One of the disadvantages of group housing and testing more than one member of the group or all group member, effects of test order, have been documented by Kask et al. (2001) for rats and by Arndt et al. (2009), and Takao et al. (2016) for mice. In rats, cohort removal induced anxiogenic like effects (Kask et al., 2001). In the study by Takao, cohort removal induced an increase in body temperature, pain sensitivity, and anxiety-like behavior in mice. Cohort removal also increased the plasma corticosterone concentration in mice (Takao et al., 2016). Arndt et al. (2009) observed a within cage order effect on the hormonal stress response (corticosterone) in socially housed female C57BL/6 mice. Whether similar effects may occur in other group-housed animals species as well (Fig. 3.4, panel B, setup 1) needs to be investigated. A thorough habituation of group-housed animals to the test environment and to being tested alone might help to forestall test-order effects.

14 PRINCIPLES OF THE 3R—REPLACEMENT, REDUCTION, REFINEMENT

Replacement is the "the use of non-animal methods, such as cell cultures, human volunteers and computer modeling instead of animals to achieve a scientific aim." (Richmond, 2000, p. 84). Under certain conditions, in vitro studies may replace in vivo studies, or insentient lower creatures may replace higher animals, that is, it should be obvious that we are not dealing with Replacement when discussing large animal models. Using, for example, pigs instead of dogs in regulatory toxicology studies cannot be seen as Replacement according to the 3Rs, as they do not replace or avoid animal use (Russell and Burch, 1959; Webster et al., 2010). However, many people have severe objections against using pet animals, such as dogs (Hasiwa et al., 2011) in scientific research laboratories. These objections may be less severe if pigs are used instead (Fig. 3.8).
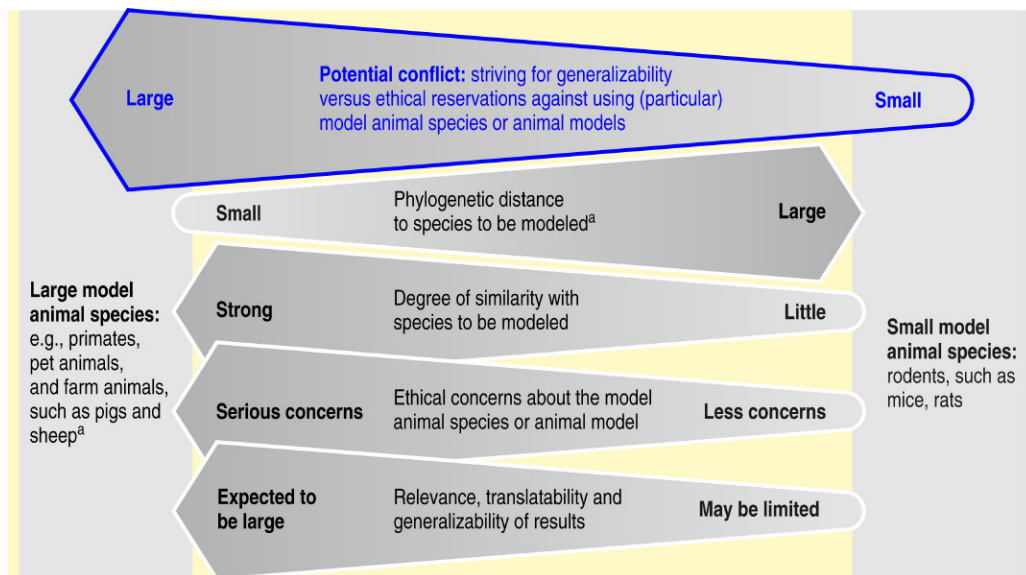
FIGURE 3.8   General characteristics of large animal models versus rodent models for studying human disease, area of potential conflict between the model animal species/animal model, and the expected degree of generalizability of results are compared. [a]Note that the phylogenetic distance between some large animal model species, such as domestic artiodactyls (which include cattle and pigs) and humans is larger than that between rodents and humans (Varga, 2012), whereas they may share more anatomical and physiological similarities with humans than rodents (Bähr and Wolf, 2012). *Source: Modified from van der Staay, F.J., Arndt, S.S., Nordquist, R.E., 2009. Evaluation of animal models of neurobehavioral disorders. Behav. Brain Funct. 5, 11., Fig. 4.*

Reduction is "Any approach in scientific research, product testing or education that leads directly or indirectly to a decrease in the number of animals used while meeting the scientific requirements." (Consensus definition in: de Boo and Hendriksen, 2005, p. 376). Reduction thus refers to the minimum number of animals necessary to answer a scientific question. The National Centre for the Replacement, Refinement, and Reduction of Animals in Research adds to this definition methods that enable researchers to obtain comparable levels of information from fewer animals or to obtain *more information from the same number of animals*, thereby avoiding further animal use (Wellcom Trust, 2013).

Refinement is "Any approach which avoids or minimizes the actual or potential pain, distress and other adverse effects experienced at any time during the life of the animals involved, and which enhances their wellbeing" (Buchanan-Smith et al., 2005, p. 381). Remarkably, Refinement does not include the measures that improve the quality of experiments, which, by reducing the number of poor experiments, reduces the number of animals that is necessary for gaining solid scientific insight.

Note that the 3Rs are a somewhat one-sided view on the use of animals in scientific experiments (for critical notes about the 3Rs see Ibrahim, 2006). Refinement, for example, is considered exclusively in the context of pain, distress, adverse effects. However, Refinement of procedures and methods may yield clearer, replicable results which answer the research questions without the need of performing an endless series of additional experiments. Using the most appropriate animal model species thus may in fact reduce the use of animals as well. Approaches to the evaluation and improvement of animal models have extensively been described (Belzung and Lemoine, 2011; van der Staay, 2006; van der Staay et al., 2009, 2010). Developing valid large animal models may contribute to reducing animal experimentation in the long run.

15 GETTING THE MOST OUT OF AN ANIMAL EXPERIMENTAL STUDY

Experiments should be designed in a way that a maximum of relevant information can be derived. This may have considerable implications for the study design, the number of animals used, and the statistical analysis of data. Repeated testing and/or reuse in related or unrelated experiments are means to increase the amount of information derived from the same animal, and to reduce the number of animals in experimental research. Repeated testing may also be applied for determining onset, progression of neurobehavioral dysfunctions, neurologic and psychiatric conditions, their duration, and their reversibility by treatment with putative therapeutics. Similarly, this testing schedule may be used for assessing onset, progression, duration, and reversibility of neurotoxic injury (Henck et al., 2016).
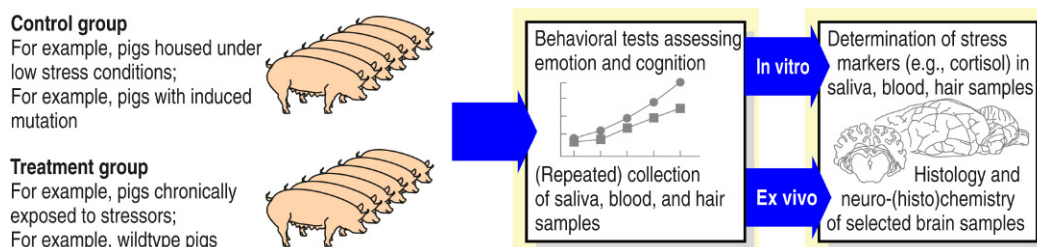
FIGURE 3.9 **Example of multiple readouts (dependent variables) in a single animal experimental study.** After chronic exposure to stressors, pigs are subjected to behavioral tests of emotion and cognition, each of which may reveal a large number of measures. In addition, saliva, blood, and hair samples are collected to determine stress markers ex vivo. The animals are sacrificed at the end of the study, and brain and organ samples are taken for a variety of analyses, for example, for assessing the correlation between stress markers and cognitive performance.

An advantage of measuring multiple variables is that more information can be gained from a study, without increasing the number of animals needed (see Fig. 3.9 for a hypothetical example, which, however, is inspired by Antonides et al., 2015a). The approach may be considered as contributing to Refinement and Reduction according to the principles of the 3Rs.

In an attempt to reduce the number of animals employed in experimental studies, one may decide to reuse animals. Reuse may refer to using animals in one particular study in successive experiments to address additional scientific questions within the study or in successive studies that may address scientific questions unrelated to those of the first study. The gain of information must be weighed ethically against an increase of discomfort that the animal may experience, as must be any reuse of the same animals in subsequent studies. Festing (1998) cautions against possible welfare consequences of the wish to reduce animal use, for example, through excessive reuse of animals. Such a practice may threaten the animal's welfare, depending on the discomfort caused by each of the tests employed. The reuse of animals has a number of advantages and disadvantages (Table 3.1).

16 NEED TO CORRECT FOR MULTIPLE COMPARISONS?

Without doubt, there is a higher probability of false positive results in studies with multiple dependent variables. On the statistical level, multiple read-out variables and multiple testing in the same study (Fig. 3.9) imply that the P-values must be corrected for multiple comparisons, that is, that the P-value for accepting the alternative hypothesis (incorrect rejection of the null hypothesis) becomes more stringent. Consequently, when performing a large number of statistical tests of significance, a correction for multiple testing (e.g., the Bonferroni correction for multiple testing) must be applied. This approach, however, leads to a loss of sensitivity (Benjamini et al., 2001; Storey, 2002). Therefore, a more sophisticated

approach, such as controlling the "false discovery rate" (FDR) is indicated (Benjamini and Yekutieli, 2001).

In studies with an exploratory character, all differences/correlations with associated probabilities <0.05 are considered, without making provisions for multiple testing through applying a Bonferroni correction or controlling the FDR (Bender and Lange, 2001; Sainani, 2009).

17 REPLICATION STUDIES

The risk of false positive results for the main question(s) of a study (e.g., does an experimental intervention affect working memory and/or reference memory performance in a cognitive holeboard task, Antonides et al., 2015a,b), is unaffected by analyzing additional variables obtained from the same subjects. These ancillary variables may provide valuable information about the study (Gaines Das, 2002) and thus may help to understand and discuss the results of a study. The additional variables measured might be treated as "exploratory."

Subsequent replication studies must be performed to corroborate the effects found in the exploratory studies (van der Staay et al., 2010), that is, the repeatability and robustness of findings across studies should be investigated. One should consider all findings as tentative, until they have been corroborated in additional, independent studies (Feise, 2002; van der Staay et al., 2010). Replication studies help to determine the generalizability of previous findings (van der Staay et al., 2010). These studies should, however, not be exact replications. Instead, they should be extended replications (partial, systematic or differential, conceptual, or quasireplications; van der Staay et al., 2010). Extended replications are based on a wider notion of replication, namely the repetition of a test of a hypothesis or a result of earlier work with different methods (Schmidt, 2009).

In "partial" replications (slight) procedural modifications are introduced whereas all other aspects closely mimic the original study. "Conceptual replications"

investigate the same relationships/constructs as the original study, using different procedures. "Systematic or differential replications" induce variations in major independent variables, for example, in rearing, housing, and/or test conditions, or gender. This type of replication may even extend to seminatural or natural environments. In "quasireplications" species different from the one used in the original study are tested (Palmer, 2000). Quasireplications are often performed using large animal models to fill the gap between rodent studies and humans.

For example, in a study addressing the effects of different levels of environmental enrichment, all animals undergoing the same level of environmental complexity may be housed in the same cage/pen/enclosure. Under this condition, of course, the level of environmental enrichment cannot be manipulated per individual animal (Fig. 3.4, panel B). Comparing the effects of experimental manipulations in wildlife populations in different territories or in groups of animals in different zoos suffers from the same restriction.

18 IDENTIFICATION OF POSSIBLE CONFOUNDS

"A primary function of research design is to maximize the validity of the conclusions (…), i.e. to minimize the number of alternative hypotheses that are consistent with the data." (Altmann, 1974, p. 15). A main purpose of designing the experimental conditions is the identification and marginalization of the influence of confounding variables (MacVittie, 2014), for example, through a systematic inventory of the factors that affect an animal during its life that may affect its behavior in a study (Hendrick, 1991) (Fig. 3.10, panel A). Unfortunately, some of these putative confounds are not under control of the experimenter, and their effects may remain undetected
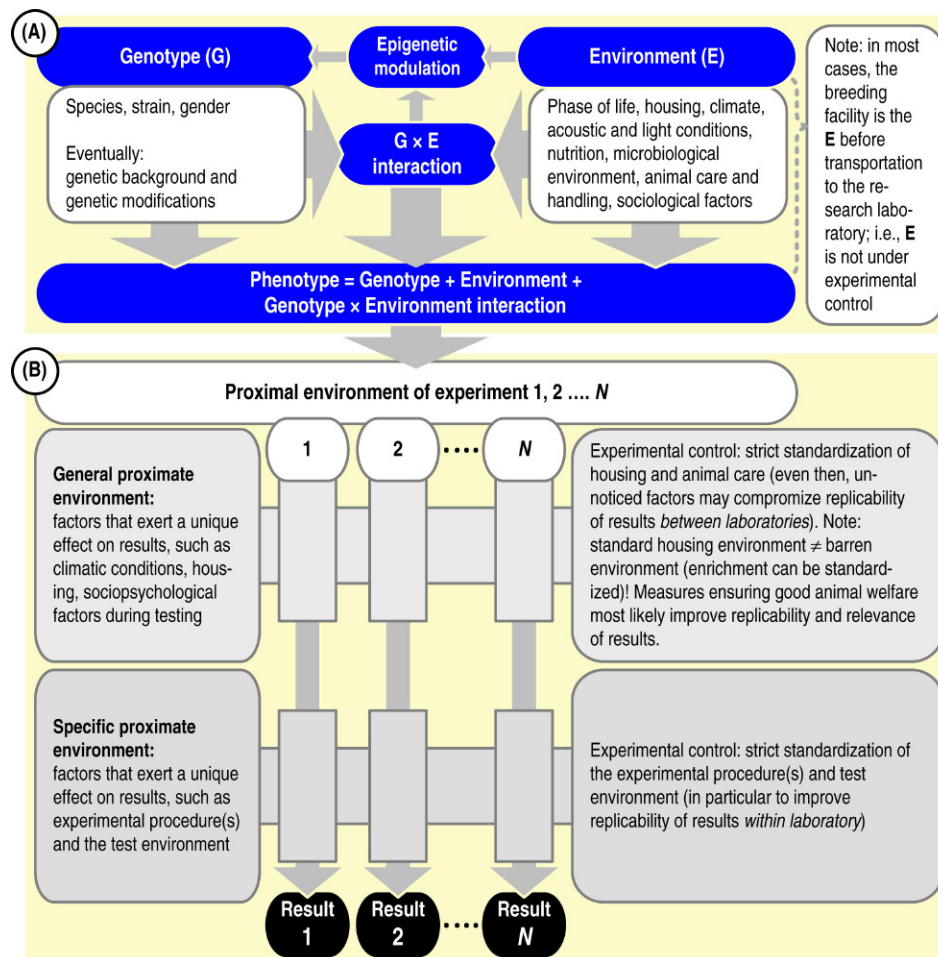
FIGURE 3.10 **Factors affecting results of animal experimental studies, and how to control them.** Variations in responses to experimental conditions are caused by the interplay between the phenotype and the effects of the response-eliciting proximate environment that in turn consists of the testing environment and testing procedures (Nomura et al., 2008; Russell and Burch, 1959). *Source: Modified from van der Staay, F.J., Arndt, S.S., Nordquist, R.E., 2014. Developing mouse models of neurobehavioral disorders: when is a model a good model? In: Pietropaolo, S., Sluyter, F., Crusio, W.E. (Eds.), Behavioral Genetics of the Mouse, vol. 2. Cambridge University Press, United Kingdom, pp. 3–17.*
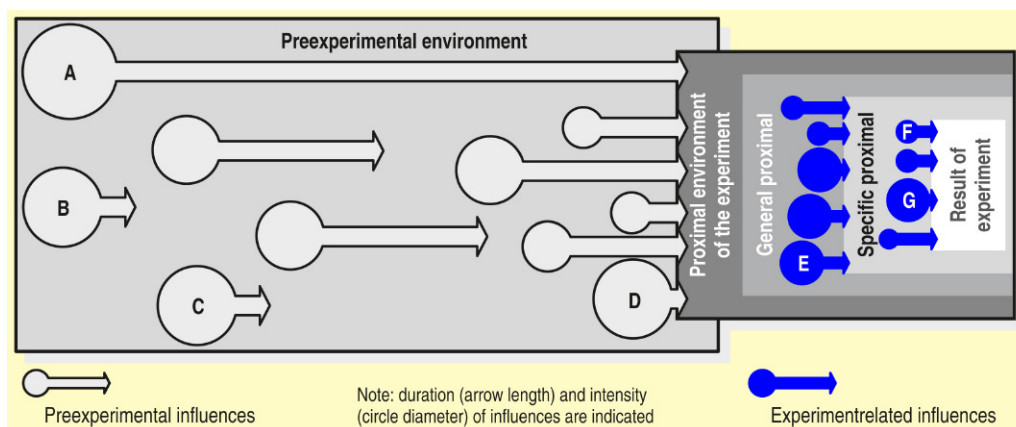
FIGURE 3.11   **Factors affecting experimental results (Fig. 3.10B).** Factors are, for example, (A) housing conditions and animal care routines, (B) maternal care, (C) weaning and mixing, (D) transport from breeder to animal laboratory, (E) construction clatter due to structural alteration works in the building housing the laboratory, (F) change of experimenter during testing, (G) order of testing animals housed in the same cage (Arndt et al., 2009; Takao et al., 2016). Note that, although a factor may have affected the experimental animals during a narrow time period, its effects may extend into the testing phase.

or defy statistical control, that is, their contribution to test results cannot properly be estimated.

Other factors are part of the proximate experimental environment (Gáspár et al., 1991; Fig. 3.10, panel B). Already more than half a century ago, Russell and Burch (1959) directed attention to the role of the testing environment and testing conditions, using the concept called "dramatype." More recently, these thoughts were adopted in the elaboration of the concept of "response action pattern" by Nomura et al. (2008).

Both concepts—"dramatype" and "response action pattern"—are poorly defined, nor have they broadly been adopted by animal behavioral scientists. According to Hino (2004), they stand for how the animal presents itself in the experiment as evidenced by the test results derived from it. Nevertheless, this concept has focused attention on the *general* and *specific proximate environment* of an experiment (Fig. 3.10, panels A and B, and Fig. 3.11).

In brief, both concepts act on the assumption that the variations in responses to experimental conditions are caused by the interplay between the phenotype and the effects of the response-eliciting proximate environment that in turn consists of the testing environment and testing procedures (Nomura et al., 2008; Russell and Burch, 1959). Since even slight variations in the proximate environment may affect the results of an experiment, it is important to identify, and eventually control these factors (Fox, 1986; Russell and Burch, 1959; van der Staay et al., 2010, 2014). Schellinck et al., 2010 summarized the potential confounding factors in mouse studies. Many of these factors may also act as confounds in animal studies using other species than the mouse. Recently, Nevalainen (2014) directed attention to the effects of laboratory animal husbandry praxis as an integral

part of the experimental design. It can cause major interference with the results, whereas these influences can easily be overlooked (Fig. 3.11). If these confounds are undetected but relevant for the test scores obtained, then only robust effects may be detectable (van der Staay et al., 2010), or the study may yield false positive or false negative results.

The genetic makeup of the experimental animal is relatively stable and thus controllable; in particular if animals with a defined genotype are used, such as inbred strains or the first filial generation (F1) form crossings between inbred strains. However, even then they may be subject to epigenetic modulation. The environment is less well controllable and subject to change (Hino, 2004).

For studies using large animal model species, availability of inbred strains is still extremely limited (Fang et al., 2012; Meurens et al., 2012). Developing inbred strains in farm animals, that is, strains established by brother by sister mating for 20 or more consecutive generations (Staats, 1976) can be a long-standing undertaking, in particular due to the slow succession of generations in many large species (Bähr and Wolf, 2012).

19 EFFECTS OF OBESITY ON EXPERIMENTAL RESULTS

A putative intervening variable in animal experimental research, that has been neglected, is obesity in the experimental animals. Martin et al. (2010) discussed the effects of obesity in laboratory rodents on the results of scientific experiments. Instead of moving around and foraging during the major part of the period of wakefulness, rodents in the laboratory live in a very restricted area, with food and water available *ad libitum*. Under

FIGURE 3.12 **Minipigs are prone to becoming obese.** The left panel shows a lean and an obese minipig side by side. The right panel shows group housing of Göttingen minipigs. *Source: Photographs courtesy Ellegaard Göttingen Minipigs, DK.*

these conditions, they are overweight to obese. A direct consequence is that laboratory rodents may develop insulin resistance, hypertension, and that their life expectancy is reduced (Gibbs and Smith, 2016), compared with animals living in a larger enriched cage, fed a restricted diet where food is provided intermittently. Restricted feeding retards the development of neurological disorders (e.g., Parkinson's and Huntington's disease), compared with overfed conspecifics. Also, the brains of overfed rodents may be more vulnerable to stroke and traumatic brain injury. All these factors may affect the outcome of drug testing and may contribute to a lack or translatability of results to humans (Martin et al., 2010) and consequently, overfeeding and obesity should be avoided.

In particular commercial pigs and minipigs (Fig. 3.12) are also prone to obesity if fed *ad libitum* (making them interesting animal models in obesitas research, Johansen et al., 2001; Koopmans and Schuurman, 2015). Even more pronounced this is also true for the parental lines of broiler chickens. To control their weight gain and to avoid obesity-associated problems, these birds are kept on a strict and severe diet. Until they reach adulthood, they are fed ≤50%, then approximately 90% of the quantity that they would consume if feed were available *ad libitum* [broiler breeder may be interesting for studying (abnormal) regulation of feed intake, Buzała et al., 2015; D'Eath et al., 2009; Richards et al., 2010]. This may lead to similar effects as discussed for rodent studies. Therefore controlled restricted feeding to prevent obesity is indicated in minipigs (Bollen et al., 2005; Boonen et al., 2014). Restricted feeding can induce a chronic sensation of hunger that may reduce welfare, but not health (Bollen and Ritskes-Hoitinga, 2007). However, the sensation of hunger per se does not impair welfare: it is a natural motivational state that triggers foraging and eating behavior (Tolkamp and D'Eath, 2016). Therefore contrary to the Farm Animal Welfare Council (FAWC, 2103) that defined welfare as, among others, "freedom from hunger and

thirst", we assume that animal welfare is not at stake as long as an animal can adequately react to hunger, thirst, or incorrect food (Ohl and van der Staay, 2012).

20 TESTING UNDER UNIFORM CONDITIONS IN THE LABORATORY VERSUS TESTING IN A HETEROGENEOUS ENVIRONMENT, SUCH AS A FARM

If experiments are not highly standardized, environmental influences, in particular the proximal environment of the experiment, are probably the major source of variation between experiments (Nomura et al., 2008). This may reduce the replicability of results (van der Staay et al., 2010) *within* and *between* laboratories (Fig. 3.13).

The reason why setup 1 in Fig. 3.4, panel B is not considered appropriate is that pen or cage may act as confound. "For example, if one cage held all the control animals and another all the animals treated with some test substance and a difference was found between the means of the two cages for some character of interest, this might be due to the effect of the treatment, or it might be because the animals in one cage had been fighting, or had a sub-clinical infection not found in the other cage. In such cases any treatment effect is "confounded" or inextricably mixed with an environmental effect." (Festing, 2011, p. 3). Unfortunately, this is a procedure that is used in a large proportion of animal experimental studies, either because this is common use in a laboratory [especially in research using (mutant) mice as subjects and in research in which rodents are kept in ventilated cages], or because of space restrictions, for example, in biomedical studies using large animals, such as farm animals.

When deciding which experimental setup to choose—more pens with fewer animals or fewer pens with more animals, or many pens with many animals of which only
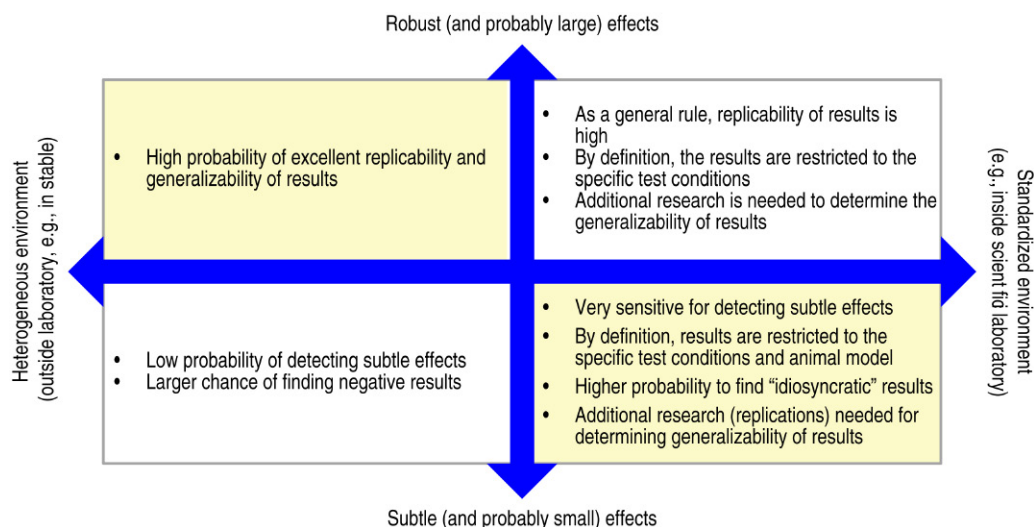
FIGURE 3.13 **Consequences of strict standardization versus heterogenization of the experimental environment for the detection of effects of experimental manipulations.** Highly standardized conditions can be realized in a laboratory setting, whereas, for example, experiments on farm are more likely performed under heterogeneous (and less well controllable) environmental conditions.

one serves as experimental animal (Fig. 3.4, panel B)—two sources of (uncontrolled) variation may affect the results:

1 between pen variation (Demétrio et al., 2013), which may be experimentally controlled by strict standardization of housing and testing conditions, and
2 between animal within-pen variation (Demétrio et al., 2013), which may be controlled by random assignment or random matched assignment of animals to the pens/conditions, on characteristics that might imbalance the groups, such as the weight of the animals, age (which often correlates with weight), or the sex ratio in the group.

Consequently, experimental control through strict standardization (van der Staay, 2006; van der Staay and Steckler, 2002; van der Staay et al., 2009, 2010) may increase the confidence in the conclusions drawn from an experiment. Unfortunately, this problem is more complex and the setup of an experiment depends on whether the expected effects are large or small, and on the desired degree of generalizability of results (Fig. 3.13).

21 TRAINING AND TESTING MAY ACT AS ENVIRONMENTAL ENRICHMENT

Coleman et al., 2013 distinguish between different classes of enrichment, among them social, physical, food, sensory, and occupational enrichment, the latter including mental activity and training). If, for example, training and testing act as (cognitive) enrichment, they may overshadow the effects of experimental manipulations, such as housing in barren versus enriched environments

(Grimberg-Henrici et al., 2016; Westlund, 2014a,b). Cognitive enrichment may improve animal welfare (Boissy and Lee, 2014; Boissy et al., 2007; Špinka and Wemelsfelder, 2011). It may also ameliorate disease-associated cognitive deficits, similar to the effects of environmental enrichment. More research is needed to learn about the effects of (extended) behavioral training and testing. To circumvent this putative confound in large animal models of neurobehavioral deficiencies, new, short-lasting cognitive tests are urgently needed, that do not necessitate extended training before testing can start (Roelofs et al., 2016).

22 MODELING EARLY LIVE EVENTS THAT AFFECT SUBSEQUENT DEVELOPMENT

Large animal models may be especially suited for investigating long-term effects of pre-, peri-, and early postnatal adverse events on functioning later in life, for example, events that might adversely affect (brain) development (see also Chapter 39), which is already vulnerable during gestation. The gestation length is approximately 21 days in rats, varies between 142 and 152 days in sheep, is approximately 115 days in pigs, and 280 days in humans (Fig. 3.14). Moreover, within the framework of neurobiological investigations on factors affecting early brain development, rodents deviate more from humans than, for example, pigs and sheep. If a study aims to investigated the effects of putative adverse factors on brain development during its most vulnerable period, the brain growth spurt, then pigs are especially suited as model for humans. The growth spurt in pigs starts prenatally and peaks around birth, similar
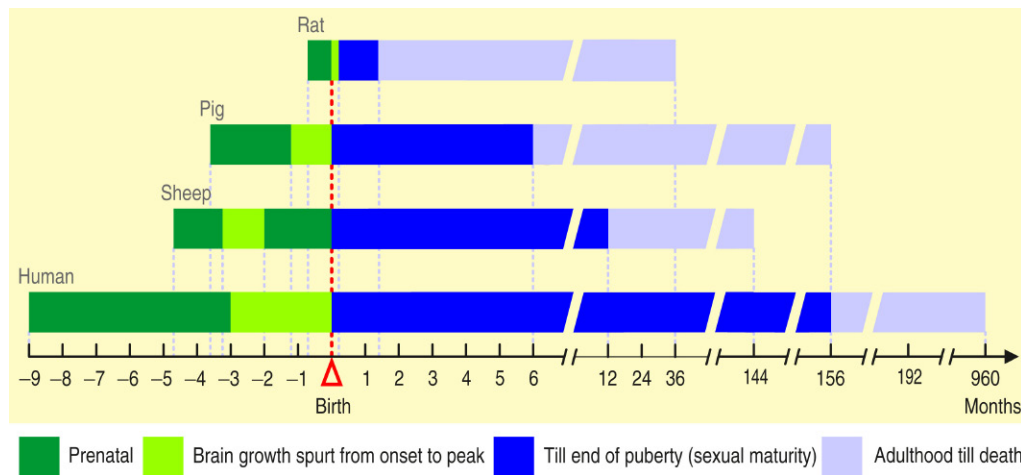
FIGURE 3.14 **Brain growth spurt in rats, sheep, pigs and humans.** Whereas the brain growth spurt in rats occurs after birth, it starts before birth in sheep, pigs and humans, and pigs. Note that the timing of events between conception and birth within species is quite invariable, but may vary considerably between breeds and individuals within breeds of pigs and sheep postnatally. Also in humans, the variability is large postnatally. Rats can be considered as postnatal brain developers, sheep are prenatal brain developers, whereas pigs and humans might be categorized as perinatal brain developers, with the strongest brain growth spurt peaking around birth (Dobbing and Sands, 1979). Note that for proliferation, synaptogenesis, subplate neurons and myelination of rats, sheep and humans, a similar overview is given by Yager (2004, Fig. 3.1, p. 33). The natural life expectancies of pigs and sheep have not systematically been documented and are therefore estimates primarily based on anecdotal evidence.

to that in humans. On the other hand, the growth spurt in sheep starts and peaks much earlier during pregnancy, and in rodent species, such as rats it starts after birth (Dobbing and Sands, 1979). Using more advanced techniques, this proposed timing of events in brain development seems generally to be corroborated (Clancy et al., 2001). Clancy et al., 2007 created a website that enables fast comparison of neurodevelopmental stages in a number of mammalian species (unfortunately, chickens and pigs are not included).

23 BRAIN INFARCTION, HEMORRHAGE, TRAUMATIC BRAIN INJURY

Large animal models have proven relevance in research on brain infarction, hemorrhage, and traumatic brain injury. Cai and Wang (2016), Mehra et al. (2012), and Mergenthaler and Meisel (2012) compared the advantages and disadvantages of using rodent versus large animal models for studying stroke. Duhaime (2006) performed a similar comparison for models of traumatic brain injury. Regional imaging techniques, such as nuclear magnetic resonance spectroscopy and imaging, and functional imaging, are easier to perform in large gyrencephalic animals, that is, in animals with a cerebral cortex that has convolutions (gyri). Also, advanced physiological monitoring can repeatedly and simultaneously be performed, eventually supplemented with neurological examinations, neurobehavioral tests, and neurochemical and neuropathological analyses (Traystman, 2003). Many techniques to induce infarc-

tion [e.g., middle cerebral artery occlusion (MCAO), Platt et al., 2014], hemorrhage (James et al., 2008), and traumatic brain damage (Margulies et al., 2015) have been developed. Large animal models may be especially suited to assess the effects of early (neonatal) stroke (Duhaime, 2006) and traumatic head injury (Friess et al., 2007, 2009).

24 AGING AND AGING-RELATED DISEASES

Aging research using large (farm) animal species may not easily be realized. For farm animal species, the anticipated average life is unknown, and estimates are based on anecdotal evidence at the best (Fig. 3.14). Aged pet animals could provide an alternative. With their owners consent, these animals could be used in noninvasive and nonaversive studies to assess naturally occurring age-related and/or disease (e.g., beta amyloid pathogenesis)-related neurobehavioral dysfunctions and putative therapeutic options to treat them (e.g., dogs, Martin et al., 2011).

Combined with an *Animal donor codicil* (Faculty Veterinary Science, University Utrecht, 2016), this approach may even make postmortem examinations possible. This approach, arguably, would only be applicable for a restricted number of research questions because it largely depends on the cases presented in a veterinary practice, the willingness of the pet owner to allow scientific investigations on his/her animal, the existence of a signed codicil, and timely offering of the dead animal to the research institution. Postmortem MRI

and other suitable techniques may then provide insight into the brain tissue integrity (Dawe et al., 2016). This approach may allow to investigate the effects of sex, age, strain, and comorbidities, to name a few. Although this approach can be considered as "Reduction" in the spirit of the 3Rs, as it spares laboratory animal use (Russell and Burch, 1959), many putative intervening variables cannot properly be controlled (Fig. 3.11).

25 TRANSGENIC LARGE ANIMAL MODELS

The development of techniques for experimentally manipulating genes gave a boost to the use of mice in biomedical and translational research. Newly developed and validated techniques for manipulating genes in large animal model species (Aigner et al., 2010; Bähr and Wolf, 2012; Klymiuk et al., 2012), in particular swine, could stand at the cradle of developing sophisticated, translatable large animal models of human disease. Transgenic pig models of neurodegenerative diseases, such as Huntington's disease (Baxa et al., 2013), Parkinson's disease, and Alzheimer's disease are under development or have been developed (Holm et al., 2016). The development of inducible gene expression in large model animal species is a further milestone for deriving at relevant and translational biomedical models (Klymiuk et al., 2012) of human diseases.

26 DISCUSSION

26.1 State of Large Animal Model Development and Research

Appropriate animal experimental studies can contribute to unraveling mechanisms and processes underlying human diseases, and to detecting and developing putative therapeutics for the treatment of these diseases. Recently, the lack of translatability of animal experimental studies to humans has severely been criticized. "(…) livestock models have been underutilized in translational research. This has been partially due to the slow realization of their advantages and value and to the perceived expense and difficulty of using livestock models." (Roth and Tuggle, 2015, p. 5).

Can large animal models fill the gap between rodent studies and clinical testing in humans? For example, in stroke research, lissencephalic rodents are generally used, rather than gyrencephalic species (Fig. 3.2). The brains of gyrencephalic species show a greater resemblance with the human brain (Gribkoff and Kaczmarek, in press).

We are just beginning to appreciate the value of large animal model species for biomedical research and for

gaining insight into disease processes and their cure. The available knowledge about a putative animal model species is a determining factor in the choice of using this species (Clancy et al., 2007). Also, available information that helps to closely compare results between species (preferentially including humans) affects the selection of an animal model species. Comparative studies provide valuable information to close this gap (Clancy et al., 2007; de Vere and Kuczaj II, 2016; MacLean et al., 2012; Workman et al., 2013) and facilitate interpretation and generalization of results.

26.2 Factors Specifically Associated With Large Animal Models

False positive or negative findings may be caused by use of an inappropriate animal model (Belzung and Lemoine, 2011; van der Staay, 2006; van der Staay et al., 2009), an inappropriate experimental design, and/or inappropriate statistical analyses. In principle, the criteria with respect to the reliability and validity of rodent models also apply to large animal models. However, researchers using large animal models are confronted with practical questions, which are related to the specific infrastructure needed, such as space for housing and testing the animals. These practical problems and their solutions may also raise methodological/scientific questions, such as about the experimental unit, the reuse of animals in order to reduce the number of animals needed and/or to collect as much information as possible from a study.

Provided an appropriate animal model was used and effects of an experimental intervention were demonstrated, then replicability of result may be compromised by differences in the proximal experimental conditions in subsequent studies (van der Staay et al., 2010). We have proposed a replication strategy to corroborate (and extend) experimental findings (van der Staay et al., 2010), depending on the type of replication (Nuzzo, 2014).

In this chapter, we focused on methodological and practical considerations with respect to the development and application of large animal models for biomedical research and for human neurobehavioral and psychiatric disorders. A number of these considerations may also be relevant for rodent models, and as such are not specific and unique for large animal models. However, because large animal models need an infrastructure for performing studies that cannot be delivered by the standard rodent housing and testing facilities, many of the points raised in this chapter are of special relevance for studies using large animal model species.

26.3 Small Sample Sizes and Reuse of Animals

Owing to the infrastructure needed and higher costs, group sizes in experiments using large animal models are generally small. Reduction of animal use is one

of the principles of the 3Rs (Russell and Burch, 1959). However, these principles are not objectives in itself, but directed by the goal of the experiment. This set of principles should not restrict the validity and generalizability of results by, for example, reducing the number of subjects per treatment group to such an extent that an experiment becomes underpowered (Button et al., 2013). Such underpowered experiments, that is, experiments designed with a too small number of animals, run an increased risk of failing to detect an effect of the treatment (false negative result) or to detect an effect that essentially is a chance finding (false positive result) (Eisen et al., 2014). Consequently, the animals in underpowered experiments have been used/sacrificed unnecessarily. This type of studies thus only contributes to increasing the number of subjects needed to answer a question scientifically because additional (and better) experiments with sufficient statistical power will be required.

On the other hand, reuse of animals reduces the number of animals for animal experimental studies. Repeated testing within a study can be considered as a special variant of reuse of animals. This approach introduces an extra dimension, namely within subject comparisons, sometimes on a timeline (e.g., progress of learning across training sessions; changes due to aging processes, due to therapeutic interventions, etc.).

26.4 Practical and Methodological Consequences of Mandatory Group Housing

Farm animals, such as chickens, sheep, goats, and pigs are social, living in groups, often with a well-established hierarchy (Estevez et al., 2007). Testing of group-housed animals consists of separating one group member at the time from the group, and returning it to the group after testing. It has been shown in group-housed mice, that sequential removal of an individual for testing and reintroduction into the group may have adverse effects, such as stress or anxiety (Arndt et al., 2009; Takao et al., 2016). Similar effects might be expected to occur in large social, group-housed farm animals, such as sheep, goats, and pigs (although systematic studies about this topic in using farm animals are still missing). Minimizing the effects of testing outside the group may necessitate extensive habituation of the animals to the housing conditions, the experimenters, the testing environment and the test procedures (Antonides et al., 2015a). Some of these factors are depicted under "general proximal environment and "specific proximal environment" in Fig. 3.10, panel B).

26.5 Multiple Readout Parameters

For a better understanding of an animal's behavior in a test, but also to derive maximal advantage of experiments with large animal species, we may need to consider multiple variables, which may represent multiple underlying mechanisms, such as learning, memory, motivation, and sensorimotor capacities (Kapadia et al., 2016; van der Staay et al., 2012). Many behavioral tests yield more than one read-out parameter. For example, holeboard-type tasks may provide dependent parameters that reflect different components of spatial memory, such as working and reference memory, or the food search strategy adopted, the animal's motor abilities and their motivation (van der Staay et al., 2012). More than one readout parameter may necessitate correction for multiple measurements, that is, the P-values may be corrected to more stringent testing of effects.

26.6 Advantages and Disadvantages of Using Large Animal Models

Using large animal models has a number of advantages and disadvantages both at the scientific and the practical level (Rand, 2008). Is should be noted, that the subsequent lists of advantages and disadvantages are not exhaustive. Depending on future developments, more items may be listed or items may be delisted because problems may be solved.

Advantages of the use of farm animals as model species:

- Larger farm animal species (e.g., pig, sheep) show a closer resemblance to humans (size matters) with presumably higher translational value than the usual rodent models, although the phylogenetic distance between large animal model, such as domestic artiodactyls (which includes cattle and pigs) and humans is larger than that between rodents and humans (Varga, 2012) (Fig. 3.8). This also holds true for the phylogenetic distance between Galliformes (e.g., chickens, junglefowl, turkeys, quails, and pheasants) and humans (Maximino et al., 2015). However, large model animal species may be more similar to humans than rodents in many respects (e.g., physiology, anatomy) (Gieling et al., 2011b). Mammalian large model species may more faithfully replicate human disease than do rodent species (Pinnapureddy et al., 2015).
- Many large animal model species have larger, *gyrencephalic* brains, in which the cerebral cortex has convolutions formed by gyri and sulci, than the commonly used rodent species, which have *lissencephalic brains,* in which the cerebral cortex is smooth, without gyri and sulci (Figs. 3.2 and 3.8). Gyrencephalic brains are generally larger than lissencephalic brains and thus provide higher resolution images using, for example, imaging techniques, such as MR, positron emission tomography, and CT scanners (Mehra et al., 2012).

- Large farm animal models may serve as "second species" in preclinical drug development, in particular in risk assessment studies (Hasiwa et al., 2011), filling the gap between rodents and humans. Minipigs, for example, may replace dogs as frequently used species in risk assessment studies (e.g., safety pharmacology, toxicology, Bode et al., 2010; Forster et al., 2010c; Swindle et al., 2012; Vamathevan et al., 2013; van der Laan et al., 2010). As far as prenatal development is concerned, chickens may also be useful for safety studies (Bjørnstad et al., 2015).
- Large animals may be used in comparative approaches to identify and characterize differences and similarities between various species. "The standard model species represent a vanishingly small percentage of the total biological diversity." (Brenowitz and Zakon, 2015, p. 273). "Convergence on selected model species often carries an implicit assumption that mechanisms observed in one species are characteristic of all related species. A focus on any single species, however, fails to encompass the diversity of mechanistic adaptations present in even closely related species that differ behaviorally." (Brenowitz and Zakon, 2015, p. 274).
- The number of behavioral tests for assessing emotion and cognition in a number of farm animal species is increasing (Gieling et al., 2011a; Kornum and Knudsen, 2011; Murphy et al., 2014).
- Generalizability and translatability of results may increase through replication studies with other species than the rodent species that most likely were used previously (van der Staay et al., 2010).
- Nearly unrestricted availability of a large number of species/strains from controlled suppliers and well-defined sources (e.g., for Göttingen minipigs see Simianer and Köhn, 2010).
- Unlike rodent studies in which experiments are short lasted because of the short life expectancy, experiments with large animal models can be long lasting. This allows performance of longitudinal studies in, for example, the area of gene therapy (Casal and Haskins, 2006).
- Large animal model species, such as chickens (approximately 275 eggs per layer hen per year) and pigs (approximately 30 piglets per sow per year) produce many progenies.
- Special miniature pig and commercial pig breeds are available for biomedical research (Smith and Swindle, 2006) with known/controlled health status [e.g., conventional, specific pathogen free, or gnotobiotic, that is, germ-free or formerly germ-free animal with fully defined composition of its associated microbial flora (Miniats and Jol, 1978)].
- Higher level of acceptance of general public—in particular if farm animals are used as large animal model instead of primates or pet animals, such as cats and dogs (Hagen et al., 2012; Ormandy and Schuppli, 2014; van der Staay et al., 2009) (Fig. 3.8). Moreover, farm animals may be returned to the food chain for human consumption provided they were not treated with compounds that might endanger the human consumer.
- Studies using large model animal species extend knowledge about farm animals that may be relevant for farm animal health and welfare (Reynolds et al., 2009).

Large animal models are less well established than rodent models. This entails some disadvantages, in particular caused by gaps in our knowledge, such as lack of comprehensive ethograms. A number of the listed disadvantages are expected to dissipate with increasing experience and use of these models:

- Less "historical" data are available for large farm animal model species than for "classical" model species [e.g., rodents (efficacy, safety, toxicology), dogs (safety)], although relevant information is increasingly available for pigs (in particular Göttingen minipigs) in risk assessment (teratology, toxicology) research (Swindle et al., 2012).
- Lack of external funding opportunities for research and technological development (Chiba et al., 1994; Golden et al., 2012; Ireland et al., 2008; Reynolds, 2009; Roberts et al., 2009).
- Lack of validated models, that is, models that have survived a validation process (van der Staay, 2006; van der Staay et al., 2009).
- Lack of validated tests (e.g., for pigs reviewed by Gieling et al., 2011a; Murphy et al., 2014).
- Lack of test equipment; only very few commercial suppliers offer test equipment for large animals; testing equipment very often is custom made (see also Chapter 39). Special demands regarding the testing equipment, for example, pig-proof apparatus (e.g., barn builders have expert knowledge for constructing pig-proof equipment).
- The current education of scientists and technicians is "rodent" centered (Libby, 2015). Using large model animal species increases the need for trained technicians.
- Large model animal species require special housing conditions, such as large stables and pens. Nearly all farm animal species are social (Estevez et al., 2007), requiring group housing.
- Associated with group housing in cages/pens is the issue of "experimental unit" (Fig. 3.6 and 3.7).
- Studies using large-animal models may be more expensive than studies using rodent models (e.g., purchase of the animals, housing facilities, testing equipment).

- Many large animal model species grow fast (e.g., the daily weight gain of pigs in the grower-finisher period: approximately 800–1000 g, Pardo et al., 2013; Vautier et al., 2013, and the brain volume of pigs doubles between 2 and 24 weeks of age, Conrad et al., 2012). Moreover, the high body mass in adulthood, for example, in pigs (Lind et al., 2007) may thwart their handling, drug administration (voluntary oral administration may be preferred, Turner et al., 2011), and behavioral testing.

- Compared with rodent research, large amounts of investigational drugs are needed when testing efficacy, safety, and toxicology in large animal models. In neuropharmacological research, it is worthwhile to investigate whether this may eventually be solved by intracerebroventricular (ICV) administration of centrally acting drugs. Such an approach may also prevent development of peripheral side effects. A disadvantage of ICV injections is the need to supply the animal with a cannula (Yao et al., 2014), which will need surgical interventions (e.g., stereotaxic placement), and which, in fast-growing species, eventually may grow out if implanted before they are full grown.

- One of the largest risk factors for many human diseases is aging (Harman, 1991; Niccoli and Partridge, 2012). Unfortunately, the life expectancy and longevity of large animal model species has not yet been documented well, but appears to be much higher than that of rodent species, making aging research with large animal models less feasible (Mitchell et al., 2015) (Fig. 3.14). Avian species, such as chickens are estimated to have a life expectancy considerably exceeding that of equally sized mammals (Holmes et al., 2001a; Wasser and Sherman, 2010).

Summarizing, existing models need to be modified to better serve their goals and new models need to be developed. They must undergo rigorous evaluation to ascertain their reliability and validity (Belzung and Lemoine, 2011; van der Staay et al., 2009). They must also measure up to high standards of preclinical evaluation to improve and ensure their translational value. "There is no single, perfect animal model that can completely predict the outcome of clinical trials. The challenge is to collect relevant and sufficient information from as many models as are required to make an informed decision regarding the potential benefits and risks to patients." (Cibelli et al., 2013, p. 274). We are not advocating the use of large animal models *instead* of rodent models. We advocate use of the animal model that best suits the aim of a study and that best informs the researcher.

References

Abernethy, A.P., Wheeler, J.L., 2011. True translational research: bridging the three phases of translation through data and behavior. Transl. Behav. Med. 1 (1), 26–30.

Aigner, B., Renner, S., Kessler, B., Klymiuk, N., Kurome, M., Wünsch, A., Wolf, E., 2010. Transgenic pigs as models for translational biomedical research. J. Mol. Med. 88 (7), 653–664.

Altmann, J., 1974. Observational study of behaviour: sampling methods. Behaviour 49 (3/4), 227–267.

Andersen, F., Watanabe, H., Bjarkam, C., Danielsen, E.H., The, DaNeX., Study Group, Cumminga, P., 2005. Pig brain stereotaxic standard space: mapping of cerebral blood flow normative values and effect of MPTP-lesioning. Brain Res. Bull. 66, 17–29.

Antonides, A., Schoonderwoerd, A.C., Nordquist, R.E., van der Staay, F.J., 2015a. Very low birth weight piglets show improved cognitive performance in the spatial cognitive holeboard task. Front. Behav. Neurosci. 9 (43), 10.

Antonides, A., Schoonderwoerd, A.C., Scholz, G., Berg, B.M., Nordquist, R.E., van der Staay, F.J., 2015b. Pre-weaning dietary iron deficiency impairs spatial learning and memory in the cognitive holeboard task in piglets. Front. Behav. Neurosci. 9 (291), 16.

Arndt, S.S., Laarakker, M.C., van Lith, H.A., van der Staay, F.J., Gieling, E.T., Salomons, A.R., et al., 2009. Individual housing of mice—impact on behaviour and stress responses. Physiol. Behav. 97 (2–3), 385–393.

Bähr, A., Wolf, E., 2012. Domestic animal models for biomedical research. Reprod. Domest. Anim. 47 (1), 59–71.

Bate, S.T., Clark, R.A., 2014. The Design and Statistical Analysis of Animal Experiments. Cambridge University Press, New York, (http://dx.doi.org/10.1017/CBO9781139344319).

Baxa, M., Hruska-Plochan, M., Juhas, S., Vodička, P., Pavlok, A., Juhasova, J., et al., 2013. A transgenic minipig model of Huntington's disease. J. Huntingtons Dis. 2, 47–68.

Beery, A.K., Zucker, I., 2011. Sex bias in neuroscience and biomedical research. Neurosci. Biobehav. Rev. 35, 565–572.

Bell, A.M., Hankison, S.J., Laskowski, K.L., 2009. The repeatability of behaviour: a meta analysis. Anim. Behav. 77 (4), 771–783.

Belzung, C., Lemoine, M., 2011. Criteria of validity for animal models of psychiatric disorders: focus on anxiety disorders and depression. Biol. Mood Anxiety Disord. 1 (9), 14.

Bender, R., Lange, S., 2001. Adjusting for multiple testing—when and how? J. Clin. Epidemiol. 54, 343–349.

Benjamini, Y., Yekutieli, D., 2001. The control of the false discovery rate in multiple testing under dependency. Ann. Stat. 29 (4), 1165–1188.

Benjamini, Y., Drai, D., Elmer, G., Kafkafi, N., Golani, I., 2001. Controlling the false discovery rate in behavior genetics research. Behav. Brain Res. 125 (1–2), 279–284.

Bjørnstad, S., Austdal, L.P.E., Roald, B., Clinton Glover, J., Paulsen, R.E., 2015. Cracking the egg: potential of the developing chicken as a model system for non-clinical safety studies of pharmaceuticals. J. Pharmacol. Exp. Ther. 355 (3), 386–396.

Blanchard, D.C., Summers, C.H., Blanchard, R.J., 2013. The role of behavior in translational models for psychopathology: functionality and dysfunctional behaviors. Neurosci. Biobehav. Rev. 37, 1567–1577.

Bode, G., Clausing, P., Gervais, F., Loegsted, J., Luft, J., Nogues, V., Sims, J., 2010. The utility of the minipig as an animal model in regulatory toxicology. J. Pharmacol. Toxicol. Methods 62 (3), 196–220.

Boisgontier, M.P., Cheval, B., 2016. The ANOVA to mixed model transition. Neurosci. Biobehav. Rev. 68, 1004–1005.

Boissy, A., Lee, C., 2014. How assessing relationships between emotions and cognition can improve farm animal welfare. Rev. Sci. Tech. 33 (1), 103–110.

Boissy, A., Manteuffel, G., Jensen, M.B., Oppermann Moe, R., Spruijt, B., Forkman, B., et al., 2007. Assessment of positive emotions in animals to improve their welfare. Physiol. Behav. 92, 375–397.

Bolhuis, J.E., Oostindjer, M., Hoeks, C.W.F., de Haas, E.N., Bartels, A.C., Ooms, M., Kemp, B., 2013. Working and reference memory of pigs (*Sus scrofa domesticus*) in a holeboard spatial discrimination task: the influence of environmental enrichment. Anim. Cogn. 16, 845–850.

Bollen, P., Ritskes-Hoitinga, M., 2007. The welfare of pigs and minipigs. The Welfare of Laboratory Animals, vol. 2, Springer, pp. 275–289.

Bollen, P.J.A., Madsen, L.W., Meyer, O., Ritskes-Hoitinga, J., 2005. Growth differences of male and female Göttingen minipigs during ad libitum feeding: a pilot study. Lab. Anim. 39, 80–93.

Boltze, J., Förschler, A., Nitzsche, B., Waldmin, D., Hoffmann, A., Boltze, C.M., et al., 2008. Permanent middle cerebral artery occlusion in sheep: a novel large animal model of focal cerebral ischemia. J. Cereb. Blood Flow Metab. 28, 1951–1964.

Boonen, H.C.M., Moesgaard, S.G., Birck, M.M., Christoffersen, Berit, Berit Østergaard, C., Cirera Salicio, S., et al., 2014. Functional network analysis of obese and lean Göttingen minipigs elucidates changes in oxidative and inflammatory networks in obese pigs. Pflügers Archiv 466 (12), 2167–2176.

Brenowitz, E.A., Zakon, H.H., 2015. Emerging from the bottleneck: benefits of the comparative approach to modern neuroscience. Trends Neurosci. 38 (5), 273–278.

Buchanan-Smith, H.M., Rennie, A.E., Vitale, A., Pollo, S., Prescott, M.J., Morton, D.B., 2005. Harmonising the definition of refinement. Anim. Welf. 14, 379–384.

Button, K.S., Ioannidis, J.P.A., Mokrysz, C., Nosek, B.A., Flint, J., Robinson, E.S.J., Munafò, M.R., 2013. Power failure: why small sample size undermines the reliability of neuroscience. Nat. Rev. Neurosci. 14, 365–376.

Buzała, M., Janicki, B., Czarnecki, R., 2015. Consequences of different growth rates in broiler breeder and layer hens. Poult. Sci. 94 (4), 728–733.

Cai, B., Wang, N., 2016. Large animal stroke models vs. rodent stroke models, pros and cons and combination? Applegate, R.L., Chen, G., Feng, H., Zhang, J.H. (Eds.), Brain Edema XVI—Translate Basic Science Into Clinical Practice, vol. 121, Springer International Publishing, Switzerland, pp. 77–81.

Casal, M., Haskins, M., 2006. Large animal models and gene therapy. Eur. J. Hum. Genet. 14, 266–272.

Cheng, C.S., 2013. The Theory of Factorial Design. Single- and Multistratum Experiments. Monographs on Statistics & Applied Probability. CRC Press, Chapman & Hall, Boca Raton, London, New York.

Chiba, A.A., Kesner, R.P., Reynolds, A.M., 1994. Memory for spatial location as a function of temporal lag in rats: role of hippocampus and medial prefrontal cortex. Behav. Neural Biol. 61 (2), 123–131.

Cibelli, J., Emborg, M.E., Prockop, D.J., Roberts, M., Schatten, G., Rao, M., et al., 2013. Strategies for improving animal models for regenerative medicine. Cell Stem Cell 12 (3), 271–274.

Clancy, B., Darlington, R.B., Finlay, B.L., 2001. Translating developmental time across mammalian species. Neuroscience 105 (1), 7–17.

Clancy, B., Finlay, B.L., Darlington, R.B., Anand, K.J.S., 2007. Extrapolating brain development from experimental species to humans. NeuroToxicology 28, 931–937.

Cohrs, R.J., Martin, T., Ghahramani, P., Bidaut, L., Higgins, P.J., Shahzad, A., 2015. Translational medicine definition by the European Society for translational medicine. New Horiz. Transl. Med. 2 (3), 86–88.

Coleman, K., Weed, J.L., Schapiro, S.J., 2013. Environmental enrichment for animals used in research. In: Conn, P.M. (Ed.), Animal Models for the Study of Human Disease. Elsevier Inc, Amsterdam, pp. 75–94, (Part I: Ethics, resources and approaches; Chapter 4).

Colleton, C., Brewster, D., Chester, A., Clarke, D.O., Heining, P., Olaharski, A., Graziano, M., 2016. The use of minipigs for preclinical safety assessment by the pharmaceutical industry: results of an IQ DruSafe minipig survey. Toxicol. Pathol. 44 (3), 458–466.

Conrad, M.S., Dilger, R.N., Johnson, R.W., 2012. Brain growth of the domestic pig (*Sus scrofa*) from 2 to 24 weeks of age: a longitudinal MRI study. Dev. Neurosci. 34 (4), 291–298.

Conrad, M.S., Sutton, B.P., Dilger, R.N., Johnson, R.W., 2014. An in vivo three-dimensional magnetic resonance imaging-based averaged brain collection of the neonatal piglet (*Sus scrofa*). PLoS One 9 (9), e107650.

Cook, J.L., Hung, C.T., Kuroki, K., Stoker, A.M., Cook, C.R., Pfeiffer, F.M., et al., 2014. Animal models of cartilage repair. Bone Joint Res. 4, 89–94.

Cowan, W.M., Harter, D.H., Kandel, E.R., 2000. The emergence of modern neuroscience: some implications for neurology and psychiatry. Annu. Rev. Neurosci. 23, 343–391.

D'Eath, R.B., Tolkamp, B.J., Kyriazakis, I., Lawrence, A.B., 2009. "Freedom from hunger" and preventing obesity: the animal welfare implications of reducing food quantity or quality. Anim. Behav. 77, 275–288.

Dawe, R.J., Yu, L., Leurgans, S.E., Schneider, J.A., Buchman, A.S., Arfanakis, K., et al., 2016. Postmortem MRI: a novel window into the neurobiology of late life cognitive decline. Neurobiol. Aging 45, 169–177.

de Boo, J., Hendriksen, C., 2005. Reduction strategies in animal research: a review of scientific approaches at the intra-experimental, supra-experimental and extra-experimental levels. ATLA 33, 369–377.

de Groot, J., Boersma, W., van der Staay, F.J., Niewold, T., Stockhofe, N., Koopmans, S.J., et al., 2005. Development of domestic animal models for the study of the ontogeny of human disease. In: Hodgson, D.M., Coe, C.L. (Eds.), Perinatal Programming: Early Life Determinants of Adult Health & Disease. CRC Press, Taylor & Francis, London, pp. 117–128.

de Vere, A.J., Kuczaj II, S.A., 2016. Where are we in the study of animal emotions? Wiley Interdiscip. Rev. Cogn. Sci. 7, 354–364.

Demétrio, C.G.B., Menten, J.F.M., Leandro, R.A., Brien, C., 2013. Experimental power considerations—Justifying replication for animal care and use committees. Poult. Sci. 92 (9), 2490–2497.

Denenberg, V.H., 1984. Some statistical and experimental considerations in the use of the analysis-of-variance procedure. Am. J. Physiol. Regul. Integr. Comp. Physiol. 246 (4), R403–R408.

Dixit, R., Boelsterli, U.A., 2007. Healthy animals and animal models of human disease(s) in safety assessment of human pharmaceuticals, including therapeutic antibodies. Drug Discov. Today 12 (7–8), 337–342.

Dobbing, J., Sands, J., 1979. Comparative aspects of the brain growth spurt. Early Hum. Dev. 311 (1), 79–83.

Donaldson, Z.R., Hen, R., 2015. From psychiatric disorders to animal models: a bidirectional and dimensional approach. Biol. Psychiatry 77, 15–21.

Douglas, W.R., 1972. Of pigs and men and research. A review of applications and analogies of the pig, *Sus scrofa*, in human medical research. Space Life Sci. 3 (3), 226–234.

Doyle, R.E., Lee, C., Deiss, V., Fisher, A.D., Hinch, G.N., Boissy, A., 2011. Measuring judgement bias and emotional reactivity in sheep following long-term exposure to unpredictable and aversive events. Physiol. Behav. 102 (5), 503–510.

Drolet, B.C., Lorenzi, N.M., 2011. Translational research: understanding the continuum from bench to bedside. Transl. Res. 157 (1), 1–5.

Duhaime, A.-C., 2006. Large animal models of traumatic injury to the immature brain. Dev. Neurosci. 28, 380–387.

Eisen, J.A., Ganley, E., MacCallum, C.J., 2014. Open science and reporting animal studies: who's accountable? PLoS Biol. 12 (1), e1001757.

Ellegaard, L., Cunningham, A., Edwards, S., Grand, N., Nevalainen, T., Prescott, M., Schuurman, T., 2010. Welfare of the minipig with special reference to use in regulatory toxicology studies. J. Pharmacol. Toxicol. Methods 62 (3), 167–183.

Ericsson, A.C., Crim, M.J., Franklin, C.L., 2013. A brief history of animal modeling. Missouri Med. 110 (3), 201–205.

Estevez, I., Andersen, I.-L., Nævdal, E., 2007. Group size, density and social dynamics in farm animals. Appl. Anim. Behav. Sci. 103, 185–204.

European Commission, 2013. Seventh report on the statistics on the number of animals used for experimental and other scientific purposes in the member states of the European Union. Report From the Commission to the Council of the European Parliament No. COM(2013) 859 final, Brussels. Available from: http://eur-lex.europa.eu/legal-content/EN/TXT/PDF/?uri=CELEX:52013SC0497&from=EN.

Faculty Veterinary Science, 2016. Animal donor codicil. University Utrecht. Available from: http://www.ivd-utrecht.nl/en/ethical-animal-experiments/animaldonorcodicil/.

Fang, X., Mu, Y., Huang, Z., Li, Y., Han, L., Zhang, Y., et al., 2012. The sequence and analysis of a Chinese pig genome. GigaScience 1 (16).

FAWC, 2103. The farm animal welfare committee. Annual Review 2012–2013. London. Available from: https://www.gov.uk/government/uploads/system/uploads/attachment_data/file/317786/FAWC_Annual_Review_2012-2013.pdf.

Featherstone, R.M., Dryden, D.M., Foisy, M., Guise, J.-M., Mitchell, M.D., Paynter, R.A., et al., 2015. Advancing knowledge of rapid reviews: an analysis of results, conclusions and recommendations from published review articles examining rapid reviews. Syst. Rev. 4 (50), 8.

Feise, R.J., 2002. Do multiple outcome measures require p-value adjustment? BMC Med. Res. Methodol. 2 (8).

Félix, B., Léger, M.-E., Albe-Fessard, D., 1999. Stereotaxic atlas of the pig brain. Brain Res. Bull. 49 (1/2), 1–138.

Festing, M.F.W., 2006. Design and statistical methods in studies using animal models of development. ILAR J. 47 (1), 5–14.

Festing, M.F. W., 2011. How to reduce the number of animals used in research by improving experimental design and statistics (No. ANZCCART Fact Sheet RT10, revised and republished September, 2011). The University of Adelaide South Australia, Adelaide. Available from: https://www.adelaide.edu.au/ANZCCART/publications/T10_HowtoReducetheNumberFactSheet.pdf.

Festing, M.F.W., Altman, D.G., 2002. Guidelines for the design and statistical analysis of experiments using laboratory animals. ILAR J. 43 (4), 244–258.

Festing, M.F.W., Baumans, V., Combes, R.D., Halder, M., Hendriksen, C.F.M., Howard, B.R., et al., 1998. Reducing the use of laboratory animals in biomedical research: problems and possible solutions—the report and recommendations of ECVAM workshop 291,2,3. ATLA 26, 283–301.

Fijn, L., Antonides, A., Aalderink, D., Nordquist, R.E., van der Staay, F.J., 2016. Does litter size affect emotionality, spatial learning and memory in piglets? Appl. Anim. Behav. Sci. 178, 23–31.

Forbes, D., Blom, H., Kostomitsopoulos, N., Moore, G., Perretta, G., 2007. EUROGUIDE. On the Accommodation and Care of Animals Used for Experimental and Other Scientific Purposes. FELASA: Federation of European Laboratory Animal Science Associations, London.

Forster, R., Ancian, P., Fredholm, M., Simianer, H., Under the Auspices of the Steering Group of the RETHINK Project, 2010a. The minipig as a platform for new technologies in toxicology. J. Pharmacol. Toxicol. Methods 62, 227–235.

Forster, R., Bode, G., Ellegaard, L., van der Laan, J.W., Steering Group of the RETHINK Project, 2010b. The RETHINK project—minipigs as models for the toxicity testing of new medicines and chemicals: an impact assessment. J. Pharmacol. Toxicol. Methods 62, 158–159.

Forster, R., Bode, G., Ellegaard, L., van der Laan, J.-W., 2010c. The RETHINK project on minipigs in the toxicity testing of new medicines and chemicals: conclusions and recommendations. J. Pharmacol. Toxicol. Methods 62, 236–242.

Fox, M.W., 1986. Laboratory Animal Husbandry. Ethology, Welfare and Experimental Variables. SUNY Press, Albany.

Franco, N.H., 2013. Animal experiments in biomedical research: a historical perspective. Animals 3, 238–273.

Friess, S.H., Ichord, R.N., Owens, K., Ralston, J., Rizol, R., Overall, K.L., et al., 2007. Neurobehavioral functional deficits following closed head injury in the neonatal pig. Exp. Neurol. 204, 234–243.

Friess, S.H., Ichord, R.N., Ralston, J., Ryall, K., Helfaer, M.A., Smith, C., Margulies, S.S., 2009. Repeated traumatic brain injury affects composite cognitive function in piglets. J. Neurotrauma 26, 1111–1121.

Gaines Das, R.E., 2002. Role of ancillary variables in the design, analysis, and interpretation of animal experiments. ILAR J. 43 (4), 214–222.

Gamzu, E., 1985. Animal behavioral models in the discovery of compounds to treat memory dysfunction. Ann. NY Acad. Sci. 444, 370–393.

Garner, J.P., 2014. The significance of meaning: why do over 90% of behavioral neuroscience results fail to translate to humans, and what can we do to fix it? ILAR J. 55 (3), 438–456.

Gáspár, E., Heeringa, M., Markel, E., Luiten, P.G.M., Nyakas, C., 1991. Behavioral and biochemical effects of early postnatal cholinergic lesion in the hippocampus. Brain Res. Bull. 28, 65–71.

Gibbs, V.K., Smith Jr, D.L., 2016. Nutrition and energetics in rodent longevity research. Exp. Gerontol. 86, 90–96.

Gieling, E.T., Nordquist, R.E., van der Staay, F.J., 2011a. Assessing learning and memory in pigs. Anim. Cogn. 14, 151–173.

Gieling, E.T., Schuurman, T., Nordquist, R.E., van der Staay, F.J., 2011b. The pig as a model animal for studying cognition and neurobehavioral disorders. Curr. Top. Behav. Neurosci. 7, 359–383.

Gieling, E.T., Wehkamp, W., Willigenburg, R., Nordquist, R.E., Ganderup, N.-C., van der Staay, F.J., 2013. Performance of conventional pigs and Göttingen miniature pigs in a spatial holeboard task: effects of the putative muscarinic cognition impairer biperiden. Behav. Brain Funct. 9, 4–14.

Gieling, E.T., Mijdam, E., van der Staay, F.J., Nordquist, R.E., 2014. Lack of mirror use by pigs to locate food. Appl. Anim. Behav. Sci. 154, 22–29.

Golden, B.L., Benson, M.E., Wulster-Radcliffe, M., McCurry Schmidt, M., Hamernik, D.L., 2012. Letter to the editor: innovative approaches and culture changes to meet the challenge. J. Anim. Sci. 90, 4161–4163.

Gonzalez-Bulnes, A., Astiz, S., Ovilo, C., Lopez-Bote, C.J., Torres-Rovira, L., Barbero, A., et al., 2016. Developmental origins of health and disease in swine: implications for animal production and biomedical research. Theriogenology 86, 110–119.

Green, A.R., Gabrielsson, J., Fone, K.C.F., 2011. Translational neuropharmacology and the appropriate and effective use of animal models. Br. J. Pharmacol. 164, 1041–1043.

Gregory, M.H., Capito, N., Kuroki, K., Stoker, A.M., Cook, J.L., Sherman, S.L., 2012. A review of translational animal models for knee osteoarthritis. Arthritis 2012, 764621.

Gribkoff, V. K., Kaczmarek, L. K. (in press). The need for new approaches in CNS drug discovery: why drugs have failed, and what can be done to improve outcomes. Neuropharmacology. doi: j.neuropharm.2016.03.021

Grimberg-Henrici, C.G., Vermaak, P., Bolhuis, J.E., Nordquist, R.E., van der Staay, F.J., 2016. Effects of environmental enrichment on cognitive performance of pigs in a spatial holeboard discrimination task. Anim. Cogn. 19 (2), 271–283.

Hagen, K., Schnieke, A., Thiele, F., 2012. Editorial "Does size matter". Graue Reihe 51, 6–12.

Harding, J., Roberts, R.M., Mirochnitchenko, O., 2013. Large animal models for stem cell therapy. Stem Cell Res. Ther. 4 (23).

Harman, D., 1991. The aging process: major risk factor for disease and death. Proc. Natl. Acad. Sci. USA 88, 5360–5363.

Hasiwa, N., Bailey, J., Clausing, P., Daneshian, M., Eileraas, M., Farkas, S., et al., 2011. Critical evaluation of the use of dogs in biomedical research and testing in Europe. ALTEX 28 (2), 326–340.

Healy, M.J.R., 1972. Animal litters as experimental units. J. Royal Stat. Soc. C 21 (2), 155–159.

Held, J.R., 1983. Appropriate animal models. Ann. NY Acad. Sci. 406, 13–19.

Henck, J.W., Elayan, I., Vorhees, C., Fisher, Jr., J.E., Morford, L.L., 2016. Current topics in postnatal behavioral testing. Int. J. Toxicol 35, 499–520.

Hendrick, C., 1991. Replications, Strict Replications and Conceptual Replications: Are They Important? Sage Publications, Newbury Park, pp. 41–49.

Hino, O., 2004. Studies of familial tumors using models: genotype, phenotype, and drama type in carcinogenesis. Int. J. Clin. Oncol. 9 (4), 257–261.

Holm, I.E., Alstrup, A.K.O., Luo, Y., 2016. Genetically modified pig models for neurodegenerative disorders. J. Pathol. 238, 267–287.

Holmes, D.J., Flückiger, R., Austad, S.N., 2001a. Comparative biology of aging in birds: an update. Exp. Gerontol. 36 (4–6), 869–883.

Holmes, A., Iles, J.P., Mayell, S.J., Rodgers, R.J., 2001b. Prior test experience compromises the anxiolytic efficacy of chlordiazepoxide in the mouse light/dark exploration test. Behav. Brain Res. 122, 159–167.

Holschneider, D.P., Bradesi, S., Mayer, E.A., 2011. The role of experimental models in developing new treatments for irritable bowel syndrome. Expert Rev. Gastroenterol. Hepatol. 5 (1), 43–57.

Homberg, J.R., 2013. Measuring behaviour in rodents: towards translational neuropsychiatric research. Behav. Brain Res. 236, 295–306.

Hooijmans, C.R., Ritskes-Hoitinga, M., 2013. Progress in using systematic reviews of animal studies to improve translational research. PLoS Med. 10 (7), e1001482.

Hostiuc, S., Moldoveanu, A., Dascălu, M., Unnthorsson, R., Jóhannesson, Ó.I., Marcus, I., 2016. Translational research—the need of a new bioethics approach. J. Transl. Med. 14 (16), 20.

Hudler, P., 2007. The use of animals in biomedical research. Slov. Vet. Res. 44 (3), 55–62.

Ibrahim, D. M., 2006. Reduce, refine, replace: the failure of the three R's and the future of animal experimentation. Arizona Legal Studies Discussion Paper No. No. 06-17. The University of Arizona, James E. Rogers College of Law, Tucson Arizona, pp. 191–225. Available from: http://ssrn.com/abstract=888206.

Ioannidis, J.P.A., 2008. Why most discovered true associations are inflated. Epidemiology 19 (5), 640–648.

Ioannidis, J.P.A., Greenland, S., Hlatky, M.A., Khoury, M.J., Macleod, M.R., Moher, D., et al., 2014. Increasing value and reducing waste in research design, conduct, and analysis. Lancet 383, 166–175.

Ireland, J.J., Roberts, R.M., Palmer, G.H., Bauman, D.E., Bazer, F.W., 2008. A commentary on domestic animals as dual-purpose models that benefit agricultural and biomedical research. J. Anim. Sci. 86, 2797–2805.

James, M.L., Warner, D.S., Laskowitz, D.T., 2008. Preclinical models of intracerebral hemorrhage: a translational perspective. Neurocrit. Care 9, 139–152.

Johansen, T., Hansen, H.S., Richelsen, B., Malmlöf, K., 2001. The obese Göttingen minipig as a model of the metabolic syndrome: dietary effects on obesity, insulin sensitivity, and growth hormone profile. Comp. Med. 51 (2), 150–155.

Johnson, J. I., Sudheimer, K. D., Davis, K. K., Kerndt, G. M., Winn, B. M., 2016. The sheep brain atlas. Michigan State University, Brain Biodiversity Bank. Available from: https://msu.edu/~brains/brains/sheep/index.html.

Kapadia, M., Xu, J., Sakic, B., 2016. The water maze paradigm in experimental studies of chronic cognitive disorders: theory, protocols, analysis, and inference. Neurosci. Biobehav. Rev. 68, 195–217.

Kask, A., Nguyen, H.P., Pabst, R., von Hörsten, S., 2001. Factors influencing behavior of group-housed male rats in the social interaction test. Focus on cohort removal. Physiol. Behav. 74 (3), 277–282.

Kendrick, K.M., Atkins, K., Hinton, M.R., Heavens, P., Keverne, B., 1996. Are faces special for sheep? Evidence from social and object discrimination learning tests showing effects of inversion and social familiarity. Behav. Processes 38, 19–35.

Kendrick, K.M., da Costa, A.P., Leigh, A.E., Hinton, M.R., Peirce, J.W., 2001. Sheep don't forget a face. Nature 414, 165–166.

Kimmelman, J., London, A.J., 2011. Predicting harms and benefits in translational trials: ethics, evidence, and uncertainty. PLoS Med. 8 (3), e1001010.

Klymiuk, N., Böcker, W., Schönitzer, V., Bähr, A., Radic, T., Fröhlich, T., et al., 2012. First inducible transgene expression in porcine large animal models. FASEB J. 26, 1086–1099.

Koopmans, S.J., Schuurman, T., 2015. Considerations on pig models for appetite, metabolic syndrome and obese type 2 diabetes: from food intake to metabolic disease. Eur. J. Pharmacol. 759, 231–239.

Kornum, B.R., Knudsen, G.M., 2011. Cognitive testing of pigs (*Sus scrofa*) in translational biobehavioral research. Neurosci. Biobehav. Rev. 35 (3), 437–451.

Kuc, K.A., Gregersen, B.M., Gannon, K.S., Dodart, J.-C., 2005. Hole-board discrimination learning in mice. Genes Brain Behav. 5 (4), 355–363.

Lalonde, R.L., Kowalski, K.G., Hutmacher, M.M., Ewy, W., Nichols, D.J., Milligan, P.A., et al., 2007. Model-based drug development. Clin. Pharmacol. Ther. 82 (1), 21–32.

Lander, B., Atkinson-Grosjean, J., 2011. Translational science and the hidden research system in universities and academic hospitals: a case study. Soc. Sci. Med. 72, 537–544.

Lazic, S.E., Essioux, L., 2013. Improving basic and translational science by accounting for litter-to-litter variation in animal models. BMC Neurosci. 14 (37), 11.

Lee, C., Colegate, S., Fisher, A.D., 2006. Development of a maze test and its application to assess spatial learning and memory in Merino sheep. Appl. Anim. Behav. Sci. 96, 43–51.

Libby, P., 2015. Murine "model" monotheism. An iconoclast at the altar of mouse. Circ. Res. 117, 921–925.

Lickliter, R., 2004. The aims and accomplishments of comparative psychology. Dev. Psychobiol. 44, 26–30.

Lind, N.M., Moustgaard, A., Jelsing, J., Vajta, G., Cumming, P., Hansen, A.K., 2007. The use of pigs in neuroscience: modeling brain disorders. Neurosci. Biobehav. Rev. 31, 728–751.

MacLean, E.L., Matthews, L.J., Hare, B.A., Nunn, C.L., Anderson, R.C., Aureli, F., et al., 2012. How does cognition evolve? Phylogenetic comparative psychology. Anim. Cogn. 15 (2), 223–238.

Macleod, M., 2011. Why animal research needs to improve. Nature 477, 511.

MacVittie, T.J., 2014. Editorial—the MCART consortium animal models series: an evolving MCART. Health Phys. 106 (1), 1–6.

Manger, P.R., Cort, J., Ebrahim, N., Goodman, A., Henning, J., Karolia, M., et al., 2008. Is 21st century neuroscience too focussed on the rat/mouse model of brain function and dysfunction? Front. Neuroanat. 2 (5), 7.

Marcilloux, J.-C., Rampin, O., Felix, M.-B., Laplace, J.-P., Albe-Fessard, D., 1989. A stereotaxic apparatus for the study of the central nervous structures in the pig. Brain Res. Bull. 22, 591–597.

Margulies, S.S., Kilbaugh, T., Sullivan, S., Smith, C., Propert, K., Byro, M., et al., 2015. Establishing a clinically relevant large animal model platform for TBI therapy development: using cyclosporin A as a case study. Brain Pathol. 25, 289–303.

Markou, A., Chiamulera, C., Geyer, M.A., Tricklebank, M., Steckler, T., 2009. Removing obstacles in neuroscience drug discovery: the future path for animal models. Neuropsychopharmacol. Rev. 34, 74–89.

Martin, B., Ji, S., Maudsley, S., Mattson, M.P., 2010. "Control" laboratory rodents are metabolically morbid: why it matters. Proc. Natl. Acad. Sci. USA 107 (14), 6127–6133.

Martin, S.B., Dowling, A.L.S., Head, E., 2011. Therapeutic interventions targeting beta amyloid pathogenesis in an aging dog model. Curr. Neuropharmacol. 9, 651–661.

Maximino, C., do Carmo Silva, R.X., de Nazaré Santos da Silva, S., do Socorrodos Santos Rodrigues, L., Barbosa, H., Silva de Carvalho, et al., 2015. Non-mammalian models in behavioral neuroscience: consequences for biological psychiatry. Front. Behav. Neurosci. 9, 233.

McGartland Rubio, D., Schoenbaum, E.E., Lee, L.S., Schteingart, D.E., Marantz, P.R., Anderson, K.E., et al., 2010. Defining translational research: implications for training. Acad. Med. 85 (3), 470–475.

Mehra, M., Henninger, N., Hirsch, J.A., Chueh, J., Wakhloo, A.K., Gounis, M.J., 2012. Preclinical acute ischemic stroke modeling. J. Neurointerv. Surg. 4, 307–313.

Mehta, P.H., Gosling, S.D., 2008. Bridging human and animal research: a comparative approach to studies of personality and health. Brain Behav. Immun. 22, 651–661.

Mergenthaler, P., Meisel, A., 2012. Do stroke models model stroke? Dis. Model Mech. 5, 718–725.

Meurens, F., Summerfield, A., Nauwynck, H., Saif, L., Gerdts, V., 2012. The pig: a model for human infectious diseases. Trends Microbiol. 20 (1), 50–57.

Mier, W., Mier, D., 2015. Advantages in functional imaging of the brain. Front. Hum. Neurosci. 9 (249), 6.

Miniats, 0.P., Jol, D., 1978. Gnotobiotic pigs—derivation and rearing. Can. J. Comp. Med. 42 (4), 428–437.

Mitchell, S.J., Scheibye-Knudsen, M., Longo, D.L., de Cabo, R., 2015. Animal models of aging research: implications for human aging and age-related diseases. Annu. Rev. Anim. Biosci. 3, 283–303.

Murphy, E., Nordquist, R.E., van der Staay, F.J., 2013. Responses of conventional pigs and Göttingen miniature pigs in an active choice judgement bias task. Appl. Anim. Behav. Sci. 148 (1–2), 64–76.

Murphy, E., Nordquist, R.E., van der Staay, F.J., 2014. A review of behavioural methods to study emotion and mood in pigs, *Sus scrofa*. Appl. Anim. Behav. Sci. 159, 9–28.

Nevalainen, T., 2014. Animal husbandry and experimental design. ILAR J. 55 (3), 393–398.

Niccoli, T., Partridge, L., 2012. Ageing as a risk factor for disease. Curr. Biol. 22, R741–R752.

Nomura, T., Tamaoki, N., Takakura, A., Suemizu, H., 2008. Basic concept of development and practical application of animal models for human diseases. In: T., Nomura, T., Watanabe, S., Habu, (Eds.), vol. 324. Springer Verlag, Berlin.

Nordquist, R.E., Heerkens, J.L.T., Rodenburg, T.B., Boks, S., Ellen, E.D., van der Staay, F.J., 2011. Laying hens selected for low mortality: behaviour in tests of fearfulness, anxiety and cognition. Appl. Anim. Behav. Sci. 131, 110–122.

Nuzzo, R., 2014. Statistical errors. Nature 506 (7487), 150–152.

Ohl, F., van der Staay, F.J., 2012. Animal welfare: at the interface between science and society. Vet. J. 192, 13–19.

Ormandy, E.H., Schuppli, C.A., 2014. Public attitudes toward animal research: a review. Animals 4, 391–408.

Palmer, A.R., 2000. Quasireplications and the contract of error: lessons from sex ratios, heritabilities and fluctuating asymmetry. Annu. Rev. Ecol. Syst. 31, 441–480.

Pardo, C.E., Kreuzer, M., Bee, G., 2013. Effect of average litter weight in pigs on growth performance, carcass characteristics and meat quality of the offspring as depending on birth weight. Animal 7 (11), 1884–1892.

Perrett, J.J., 2012. A case study on teaching the topic "experimental unit" and how it is presented in advanced placement statistics textbooks. J. Stat. Educ. 20 (2), 1–14.

Pinnapureddy, A.R., Stayner, C., McEwan, J., Baddeley, O., Forman, J., Eccles, M.R., 2015. Large animal models of rare genetic disorders: sheep as phenotypically relevant models of human genetic disease. Orphanet J. Rare Dis. 10 (107), 8.

Plath, N., Lerdrup, L., Larsen, P.H., Redrobe, J.P., 2011. Can small molecules provide truly effective enhancement of cognition? Current achievements and future directions. Expert Opin. Investig. Drugs 20 (6), 795–811.

Platt, S.R., Holmes, S.P., Howerth, E.W., Duberstein, K.J.J., Dove, C.R., Kinder, H.A., et al., 2014. Development and characterization of a Yucatan miniature biomedical pig permanent middle cerebral artery occlusion stroke model. Exp. Transl. Stroke Med. 6 (5), 14.

Poole, T., 1997. Happy animals make good science. Lab. Anim. 31, 116–124.

Pratt, J., Winchester, C., Dawson, N., Morris, B., 2012. Advancing schizophrenia drug discovery: optimizing rodent models to bridge the translational gap. Nat. Rev. Drug Discov. 11 (7), 560–579.

Puelles, L., Martinez-de-la-Torre, M., Paxinos, G., Watson, C., Martinez, S., 2007. The Chick Brain in Stereotaxic Coordinates: An Atlas Featuring Neuromeric Subdivisions and Mammalian Homologies. Academic Press, Amsterdam, London.

Pugsley, M.K., Authier, S., Curtis, M.J., 2008. Principles of safety pharmacology. Br. J. Pharmacol. 154, 1382–1399.

Rand, M.S., 2008. Selection of biomedical animal models. In: Conn, P.M. (Ed.), Sourcebook of Models for Biomedical Research. Humana Press, Totowa, NJ, pp. 9–15.

Reynolds, L.P., 2009. Perspectives: the decline of domestic animal research in agriculture and biomedicin. J. Anim. Sci. 87, 4181–4182.

Reynolds, L.P., Ireland, J.J., Caton, J.S., Bauman, D.E., Davis, T.A., 2009. Commentary on domestic animals in agricultural and biomedical research: an endangered enterprise. J. Nutr. 139, 1–2.

Richards, M.P., Rosebrough, R.W., Coon, C.N., McMurtry, J.P., 2010. Feed intake regulation for the female broiler breeder: In theory and in practice. J. Appl. Poult. Res. 19, 182–193.

Richmond, J., 2000. The 3Rs—past, present and future. Scand. J. Lab. Anim. Sci. 27 (2), 84–92.

Roberts, R.M., Smith, G.W., Bazer, F.W., Cibelli, J., Seidel, Jr., G.E., Bauman, D.E., et al., 2009. Farm animal research in crisis. Science 324 (5926), 468–469.

Roelofs, S., Boleij, H., Nordquist, R.E., van der Staay, F.J., 2016. Making decisions under ambiguity: judgment bias tasks for assessing emotional state in animals. Front. Behav. Neurosci. 10 (119), 16.

Roth, J.A., Tuggle, C.K., 2015. Livestock models in translational medicine. ILAR J. 56 (1), 1–6.

Russell, W.M. S., Burch, R.L., 1959. The Principles of Humane Experimental Technique. Methuen, London (Reprinted by UFAW, 1992: 8 Hamilton Close, South Mimms, Potters Bar, Herts EN6 3QD England. Available from: http://altweb.jhsph.edu/pubs/books/humane_exp/het-toc.

Sabroe, I., Dockrell, D.H., Vogel, S.N., Renshaw, S.A., Whyte, M.K.B., Dower, S.K., 2007. Identifying and hurdling obstacles to translational research. Nat. Rev. Immunol. 7, 77–82.

Saikali, S., Meuriceb, P., Sauleau, P., Eliat, P.-A., Bellaud, P., Randuineau, G., et al., 2010. A three-dimensional digital segmented and deformable brain atlas of the domestic pig. J. Neurosci. Methods 192, 102–109.

Sainani, K.L., 2009. The problem of multiple testing. PM&R 1, 1098–1103.

Schellinck, H.M., Cyr, D.P., Brown, R.E., 2010. How many ways can mouse behavioral experiments go wrong? Confounding variables in mouse models of neurodegenerative diseases and how to control them. Adv. Study Behav. 41, 255–366.

Schmidt, S., 2009. Shall we really do it again? The powerful concept of replication is neglected in the social sciences. Rev. Gen. Psychol. 13 (2), 90–100.

Sharbaugh, C., Viet, S.M., Fraser, A., McMaster, S.B., 2003. Comparable measures of cognitive function in human infants and laboratory animals to identify environmental health risks to children. Environ. Health Perspect. 111 (13), 1630–1639.

Simianer, H., Köhn, F., 2010. Genetic management of the Göttingen minipig population. J. Pharmacol. Toxicol. Methods 62, 221–226.

Sinha, R., Shaham, Y., Heilig, M., 2011. Translational and reverse translational research on the role of stress in drug craving and relapse. Psychopharmacology 218, 69–82.

Smith, A.C., Swindle, M.M., 2006. Preparation of swine for the laboratory. ILAR J. 47 (4), 358–363.

Søndergaard, L.V., Herskin, 2012. Does size matter—considerations of importance for choice of animal species in a transgenic model for Alzheimer's disease. Graue Reihe 51, 84–99.

Špinka, M., Wemelsfelder, F., 2011. Environmental challenge and animal agency. In: Appleby, M.C., Mench, J.A., Olsson, I.A.S., Hughes, B.O. (Eds.), Animal Welfare. second ed. CAB International, Wallingford, pp. 27–43.

Staats, J., 1976. Standardized nomenclature for inbred strains of mice: sixth listing. Cancer Res. 36, 4333–4377.

Storey, J.D., 2002. A direct approach to false discovery rates. J. Royal Stat. Soc. B 64 (3), 479–498.

Sughrue, M.E., Mocco, J., Mack, W.J., Ducruet, A.F., Komotar, R.J., Fischbach, R.L., et al., 2009. Bioethical considerations in translational research: primate stroke. Am. J. Bioeth. 9 (5), 3–12.

Svendsen, O., 2006. 3rd European congress of toxicologic pathology, 2005, Copenhagen, Denmark—the minipig in toxicology. Exp. Toxicol. Pathol. 57, 335–339.

Swindle, M.M., Makin, A., Herron, A.J., Clubb, Jr., F.J., Frazier, K.S., 2012. Swine as models in biomedical research and toxicology testing. Vet. Pathol. 49 (2), 344–356.

Tahamtani, F.M., Nordgreen, J., Nordquist, R.E., Janczak, A.M., 2015. Early life in a barren environment adversely affects spatial cognition in laying hens (Gallus gallus domesticus). Front. Vet. Sci. 2 (3), 11.

Takao, K., Shoji, H., Hattori, S., Miyakawa, T., 2016. Cohort removal induces changes in body temperature, pain sensitivity, and anxiety-like behavior. Front. Behav. Neurosci. 10, 99.

Tolkamp, B.J., D'Eath, R.B., 2016. Hunger associated with restricted feeding systems. Phillips, C.J.C. (Ed.), Nutrition and the Welfare of Farm Animals, vol. 16, Springer International Publishing, Switzerland, pp. 11–27.

Traystman, R.J., 2003. Animal models of focal and global cerebral ischemia. ILAR J. 44 (2), 85–95.

Trochim, W., Kane, C., Graham, M.J., Pincus, H.A., 2011. Evaluating translational research: a process marker model. Clin. Transl. Sci. 4 (3), 153–162.

Turner, P.V., Brabb, T., Pekow, C., Vasbinder4, M.A., 2011. Administration of substances to laboratory animals: routes of administration and factors to consider. J. Am. Assoc. Lab. Anim. Sci. 50 (5), 600–613.

USDA., 2015. Annual report animal usage by fiscal year—2014. United States Department of Agriculture—Animal and Plant Health Inspection Service. Available from: https://speakingofresearch.files.wordpress.com/2008/03/animals-used-in-research-2014.pdf.

Vamathevan, J.J., Hall, M.D., Hasan, S., Woollard, P.M., Xu, M., Yang, Y., et al., 2013. Minipig and beagle animal model genomes aid species selection in pharmaceutical discovery and development. Toxicol. Appl. Pharmacol. 270, 149–157.

van der Laan, J.W., Brightwell, J., McAnulty, P., Ratky, J., Stark, C., 2010. Regulatory acceptability of the minipig in the development of pharmaceuticals, chemicals and other products. J. Pharmacol. Toxicol. Methods 62, 184–195.

van der Staay, F.J., 1999. Spatial working and reference memory of Brown Norway and WAG rats in a holeboard discrimination task. Neurobiol. Learn. Mem. 71 (1), 113–125.

van der Staay, F.J., 2006. Animal models of behavioral dysfunctions: basic concepts and classifications, and an evaluation strategy. Brain Res. Rev. 52 (1), 131–159.

van der Staay, F.J., Steckler, T., 2002. The fallacy of behavioral phenotyping without standardisation. Genes Brain Behav. 1 (1), 9–13.

van der Staay, F.J., Arndt, S.S., Nordquist, R.E., 2009. Evaluation of animal models of neurobehavioral disorders. Behav. Brain Funct. 5, 11.

van der Staay, F.J., Arndt, S.S., Nordquist, R.E., 2010. The standardization-generalization dilemma: a way out. Genes Brain Behav. 9, 849–855.

van der Staay, F.J., Gieling, E.T., Espitia Pinzón, N., Nordquist, R.E., Ohl, F., 2012. The appetitively motivated "cognitive" holeboard: a family of complex spatial discrimination tasks for assessing learning and memory. Neurosci. Biobehav. Rev. 36, 379–403.

van der Staay, F.J., Arndt, S.S., Nordquist, R.E., 2014. Developing mouse models of neurobehavioral disorders: when is a model a good model? Pietropaolo, S., Sluyter, F., Crusio, W.E. (Eds.), Behavioral Genetics of the Mouse, vol. 2, Cambridge University Press, United Kingdom, pp. 3–17.

van der Worp, H.B., Howells, D.W., Sena, E.S., Porritt, M.J., Rewell, S., O'Collins, V., Macleod, M.R., 2010. Can animal models of disease reliably inform human studies? PLoS Med. 7 (3), e1000245.

van Eck, L.M., Antonides, A., Nordquist, R.E., van der Staay, F.J., 2016. Testing post-weaning food motivation in low and normal birth weight pigs in a runway and operant conditioning task. Appl. Anim. Behav. Sci. 181, 83–90.

van Eerdenburg, F.J.C.M., Dierx, J.A.J., 2002. A new technique for long term, stress free, cannulation of the lateral ventricle in postpubertal, freely moving, pigs. J. Neurosci. Methods 121, 13–20.

Varga, O.E., 2012. Predictive validity of animal models and the question of size. Graue Reihe 51, 113–125.

Vautier, B., Quiniou, N., van Milgen, J., Brossard, L., 2013. Accounting for variability among individual pigs in deterministic growth models. Animal 7 (8), 1265–1273.

von Rechenberg, B., 2012. The right question and the corresponding animal model in light of the 3 R's. Graue Reihe 51, 100–112.

Vorhees, C.V., 1989. Concepts in teratology and developmental toxicology derived from animal research. Ann. NY Acad. Sci. 562, 31–41.

Waldman, S.A., Terzic, A., 2010. Clinical and translational science: from bench-bedside to global village. Clin. Transl. Sci. 3 (5), 254–257.

Wasser, D.E., Sherman, P.W., 2010. Avian longevities and their interpretation under evolutionary theories of senescence. J. Zool. 280, 103–155.

Watanabe, H., Andersen, F., Simonsen, C.Z., Evans, S.M., Gjedde, A., Cumming, P., & DaNeX Study Group, 2001. MR-based statistical atlas of the Göttingen minipig brain. NeuroImage 14, 1089–1096.

Webster, J., Bollen, P., Grimm, H., Jennings, M., 2010. Ethical implications of using the minipig in regulatory toxicology studies. J. Pharmacol. Toxicol. Methods. 62 (3), 160–166.

Wellcom Trust, 2013. Responsibility in the Use of Animals in Bioscience Research: Expectations of the Major Research Councils and Charitable Funding Bodies. NC3Rs, London, (https://www.nc3rs.org.uk/the-3rs).

Wells, A.J., Vink, R., Blumbergs, P.C., Brophy, B.P., Helps, S.C., Knox, S.J., Turner, R.J., 2012. A surgical model of permanent and transient middle cerebral artery stroke in the sheep. PloS One 7 (7), e42157.

Westlund, K., 2014a. Is training zoo animals enrichment? A letter to the editor. Appl. Anim. Behav. Sci. 152, 100–102.

Westlund, K., 2014b. Training is enrichment—and beyond. Appl. Anim. Behav. Sci. 152, 1–6.

Woolf, S.H., 2008. The meaning of translational research and why it matters. JAMA 299 (2), 211–213.

Workman, A.D., Charvet, C.J., Clancy, B., Darlington, R.B., Finlay, B.L., 2013. Modeling transformations of neurodevelopmental sequences across mammalian species. J. Neurosci. 33 (17), 7368–7383.

Yager, J.Y., 2004. Animal models of hypoxic-ischemic brain damage in the newborn. Semin. Pediatr. Neurol. 11 (1), 31–46.

Yao, Y., Su, J., Zhang, F., Lei, Z., 2014. Effects of central and peripheral administration of neuropeptide S on the level of serum proinflammatory cytokines in pigs. Neuroimmunomodulation 21, 45–51.

Zakiniaeiz, Y., Cosgrove, K.P., Potenza, M.N., Mazure, C.M., 2016. Balance of the sexes: addressing sex differences in preclinical research. Yale J. Biol. Med. 89, 255–259.

Further Reading

Salaberger, T., Millard, M., El Makarem, S., Möstl, E., Grünberger, V., Krametter-Frötscher, R., et al., 2016. Influence of external factors on hair cortisol concentrations. Gen. Comp. Endocrinol. 233, 73–78.

VISION

Page left intentionally blank

4

Animal Models in Cataract Research

Julie C. Lim,**, Irene Vorontsova†, Renita M. Martis*,**,
Paul J. Donaldson*,***

*University of Auckland, Auckland, New Zealand
**NZ National Eye Centre, University of Auckland, Auckland, New Zealand
†University of California, Irvine, Irvine, CA, United States

1 INTRODUCTION

Cataract is the leading cause of blindness worldwide and accounts for approximately half of all forms of vision loss (Bourne et al., 2013). Currently, the only way to treat cataracts is by surgery. However, with an aging population and an increase in the number of people affected by diabetes, the demand for surgery and the need for cost-effective alternative solutions are growing exponentially. To reduce the need for cataract surgery, alternative medical therapies to delay cataracts are urgently required, as it has been predicted that delaying the onset of cataract by 10 years will halve its incidence (Brian and Taylor, 2001).

Research with human tissue offers the best possibilities of designing an anticataract therapy that is effective in humans. Unfortunately, there are a myriad of difficulties associated with working with human donor lenses. This includes the limited availability of human donor lenses and intact cataractous lenses, the narrow age range, postmortem delay between death and tissue processing, and the inherent variability between donors (genetic variation, systemic disease, cause of death, exposure to environmental risk factors). As a result, this has led to researchers to turn to animal models of lens cataract to investigate the mechanisms underlying cataract formation and to test the efficacy of therapies for their potential use in humans.

There is a large number of animal models currently in use, and with the uptake of transgenic technologies, this number is increasing. These models have been used to either study the cataract pathogenesis or to trial anticataract therapies with the long-term view to reduce the incidence of cataract in humans. While one experimental system cannot entirely replicate the cataract process in humans, investigators need to be mindful of selecting an appropriate animal model. However, it is often unclear what form of human cataract these animal models are trying to replicate.

As a recent review has assessed and evaluated animal models for studying age-related nuclear cataract (Lim

et al., 2016), the aim of this chapter is to focus on identifying the most appropriate animal models for studying diabetic cataract. To do this, we will describe reported changes in human diabetic lenses in terms of lens physiology, cellular structure, and biochemistry, and then use this set of parameters to determine which animal models are the most appropriate for mimicking the cataract process in humans.

2 CATARACT TYPES

Clinically four main forms of lens cataract are recognized in humans. Three of these: nuclear, cortical, and subcapsular are named on the regions in the lens where the light-scattering cataract first originates (Fig. 4.1). While the light scattering normally originates in one of these three regions of the lens, over time, the cataract may spread to other lens regions to produce a mixed-cataract phenotype, the fourth major class of cataract.

Of these four subtypes of cataract, nuclear cataract is the most common (Age-Related Eye Disease Study Research Group, 2001). Age is the major risk factor for nuclear cataract formation and accounts for 50% of the total cataract cases. Age-related nuclear (ARN) cataract is characterized by the depletion of the antioxidant glutathione (GSH) in the lens nucleus, resulting in the extensive oxidation of proteins and lipids in this region of the lens (Truscott, 2005), without any obvious damage to the lens fiber structure (Al-Ghoul et al., 1996). ARN cataracts involve the gradual opacification of the lens nucleus, and are graded by the extent of nuclear brunesence (Fig. 4.2) and nuclear opalescence (Chylack et al., 1984). While age is also a risk factor for cortical and posterior subcapsular (PSC) cataracts, both of these cataract subtypes are also strongly associated with diabetes (Bron et al., 1993). Cortical cataracts initially appear in the lens cortex, often with wedge-shaped spokes (Fig. 4.2); however, as the cataract matures, the entire lens becomes opaque (Bron et al., 1993). PSCs are disc-shaped opacities that develop
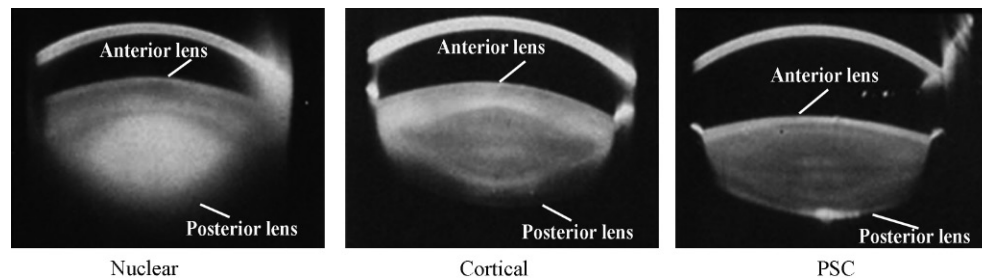
FIGURE 4.1 **Location of cataract subtypes.** Scheimpflug slit-lamp photographic images showing the three main types of cataract: nuclear, cortical, and posterior subcapsular (PSC). *Source: Taken from Datilles III, M.B., Ansari, R.R., 2006. Clinical evaluation of cataracts. Duane's Ophthalmology, vol. 1. Lippincott Williams and Wilkins, Baltimore, MD, USA (Chapter 73B).*
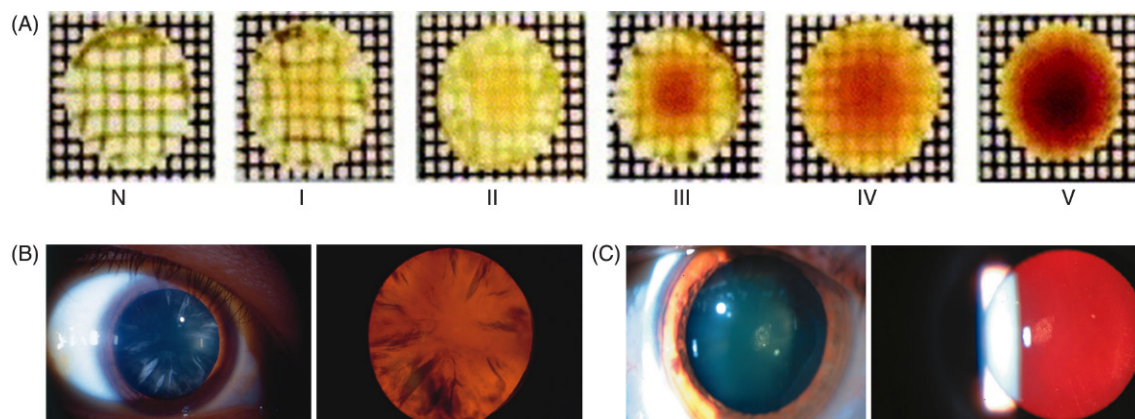
FIGURE 4.2 **Characterization of cataract subtypes.** (A) Human age-related nuclear (ARN) cataract lenses graded by nuclear color according to the Pirie classification system. *N*, Normal; type *I–V* cataracts. (B) Cortical cataract using direct illumination *(left panel)* and retroillumination *(right panel)*. Cortical cataracts usually start in the lens periphery, encroach into the visual axis, and interfere with central vision. Opacities are visible as dark shapes that are typically wedge-shaped and oriented radially. (C) PSC cataract using direct illumination (*left panel*) and retroillumination (*right panel*). PSCs usually start centrally and extend toward the periphery, interfering with visual function, causing early glare disability. *Source: Image taken from (A) Truscott, R.J.W., 2005. Age related nuclear cataract-oxidation is the key. Exp. Eye Res. 80 (5) 709–725; (B–C) taken from Datilles III, M.B., Ansari, R.R., 2006. Clinical evaluation of cataracts. Duane's Ophthalmology, vol. 1. Lippincott Williams and Wilkins, Baltimore, MD, USA (Chapter 73B).*

at the posterior pole of the lens. They appear as a dense, circular plaque in the central posterior part of the lens (Fig. 4.2) and are surrounded by vacuoles and smaller areas of degenerated lens material (Adrien Shun-Shin et al., 1989).

3 AGE-RELATED NUCLEAR CATARACT

In this section, we will briefly describe the pathogenesis of ARN cataract in humans, as it is the most common cataract type. The pathophysiological mechanisms that lead to ARN cataract formation are well established in the human lens, and as a result, we have a firm understanding of changes to lens physiology (Duncan and Bushell, 1975), cellular structure (Al-Ghoul et al., 1996; Costello et al., 1992), and biochemistry (Fujii et al., 2012; Garner and Spector, 1980a,b; Hooi et al., 2013a,b; Lou, 2003; Lou and Dickerson, 1992; Spector and Roy, 1978; Takemoto, 1996; Truscott and Augusteyn, 1977a,b,c) that occur during ARN cataract formation. These changes have been extensively reviewed by many (Lim et al., 2016; Lou, 2003; Michael and Bron, 2011; Truscott, 2005) and are, therefore, only summarized in this chapter (Table 4.1).

It is well established that oxidation is the hallmark of ARN cataract and that depletion of GSH, the principal antioxidant in the lens, specifically in the nucleus (<2 mM), but not the lens cortex, appears to trigger a cascade of events that precedes cataract formation (Truscott, 2005). This includes the extensive loss of protein sulfhydryl groups, with over 90% of cysteine residues and ~50% of methionine residues oxidized in nuclear proteins in lenses obtained from patients with ARN cataract (Garner and Spector, 1980a; Spector and Roy, 1978; Truscott and Augusteyn, 1977a,b). This loss of protein sulfhy-

dryl groups is accompanied by an increase in protein-thiol mixed disulfides (Lou and Dickerson, 1992; Lou et al., 1990, 1999), and an increase in the water-insoluble fraction (Pirie, 1968; Truscott and Augusteyn, 1977a), which culminate in the formation of protein–protein disulfides (PSSP), and other cross-linkages that lead to protein aggregation, light scattering, and ultimately cataract.

As a number of ARN cataract animal models have been recently reviewed and assessed for their ability to replicate changes in human ARN cataract (Lim et al., 2016), we will concentrate on the mechanisms of human diabetic cataract formation and the identification of the most appropriate animal models for studying human diabetic cataract in the following sections.

4 DIABETIC CORTICAL CATARACT

Diabetes is characterized by chronic hyperglycemia resulting from defects in insulin secretion, insulin action, or both. There are different types of diabetes with the most common types being type 1 and type 2 diabetes.

Type 1 diabetes is most commonly diagnosed in children in a rapidly progressive form, but can be detected as a slowly progressive form in adults. Type 1 diabetes is an autoimmune disease that leads to the destruction of the insulin-producing pancreatic β cells, resulting in insulin deficiency (King, 2012). Type 1 diabetic patients are usually not obese, and there is a genetic predisposition for the autoimmune destruction of β cells.

Type 2 diabetes is most commonly diagnosed in middle-aged adults and while there is a hereditary component, the risk of development of type 2 diabetes increases proportionally with increasing body mass index

TABLE 4.1   Summary of Human Lens-Related Changes in ARN and Diabetic Cataract

Human lens changes	ARN cataract	Diabetic cataract
Morphology	• No major fiber disruptions or extracellular debris in the lens nucleus • Signs of intracellular space distension between adjacent fibers with electron microscopy • Increased frequency of multilamellar bodies	• Distinct localized zone of cell swelling in the lens cortex • Globular bodies, water clefts, vacuoles in the deeper cortex region, with unaltered structural changes in the superficial cortex and nuclear layers
Physiology	• No changes in Na^+, K^+, and Ca^{2+} in the lens nucleus	• Increased Na^+ and Ca^{2+} and decreased K^+
Biochemistry	• Depletion of GSH in the lens nucleus • Significant loss of PSH groups • Increase in protein mixed disulfides bound to GSH (PSSG) or cysteine (PSSC) formation • Significant loss of water-soluble protein in the lens nucleus • Cataract-specific modifications to crystallin proteins	• Increase in glucose and sorbitol • Decrease in GSH • Activation of Ca^{2+}-dependent proteases • Cleavage of cytoskletelon proteins • Decrease in Na^+/K^+ ATPase activity • Increase in glycated proteins (AGEs) • Increase in disulfide cross-linked proteins • Decrease in ATP and NADPH • Decrease in amino acid uptake and amino acid content

GSH, Glutathione; PSH, protein sulfhydryl; PSSC, protein–cysteine disulfide; PSSG, protein–glutathione disulfide.

(Lehtovirta et al., 2010). Type 2 diabetes is associated with insulin resistance and a lack of appropriate compensation by the β cells, leading to insulin deficiency (King, 2012).

A frequent complication of both type 1 and type 2 diabetes is cataract. Diabetic patients are at a greater risk, 2–5 times, for cataract formation and are more likely to get cataracts at an earlier age (Klein et al., 1995a,b). A number of epidemiological studies (Delcourt et al., 2000; Klein et al., 1995a; Leske et al., 1999; Rotimi et al., 2003; Rowe et al., 2000) have reported up to a fivefold increase in the prevalence of cortical and/or PSCs in diabetic subjects (type 1 and type 2) compared with nondiabetics. In addition, the onset of cataract develops at an earlier age (Leske et al., 1991) and progresses faster in diabetics compared to nondiabetics (Caird and Garrett, 1962).

4.1 Mechanism of Action

In contrast to those of ARN cataract, the mechanisms of human diabetic cataract formation have largely been determined using animal models. Historically, two animal models in particular have been responsible for our understanding of the molecular pathways involved in diabetic cataract formation. These two models are the streptozotocin (STZ) rat, a model used to chemically induce type 1 diabetes by destroying pancreatic β cells (Bond et al., 1996; Chatzigeorgiou et al., 2009; Obrosova et al., 2010; Perry et al., 1987; Suryanarayana et al., 2005, 2007; Varsha et al., 2014; Wang et al., 2016), and galactose-fed animals, a model for obese type 2 diabetes (Bond et al., 1996; Kador, 1988; Kador et al., 1979, 2006, 2007; Perry et al., 1987; Robison et al., 1990, 1995; Sato et al., 1998; Sippel, 1966; Suryanarayana et al., 2005, 2007; Varsha et al., 2014; Wang et al., 2016). These models have been very popular with researchers because diabetes or galactosemia can be induced rapidly and effectively in animals resulting in formation of "fast" sugar lens cataract. These acute models replicate the fast development of cataract that occurs in diabetic patients with uncontrolled hyperglycemia. However, most diabetic patients are able to control their blood glucose reasonably well and, therefore, such acute cataract development is rarely seen.

From these animal models, however, a general consensus was reached among researchers on the mechanism of diabetic cataract formation in humans. The long-standing traditional view has been that high levels of the impermeable osmolyte, sorbitol, produced from excess glucose by the enzyme aldose reductase (AR), initiates osmotic stress, resulting in the attraction of fluid, lens fiber cell swelling, and tissue liquefaction (Kinoshita, 1965, 1974). Based on this view, considerable attention was focused on the development and testing of AR

inhibitors. These inhibitors have proven to be very successful in ameliorating diabetic cataract in rats and dogs (Drel et al., 2008; Kador et al., 2006, 2007, 2010, 2016; Matsumoto et al., 2008), but an anticataract therapy in humans remains elusive.

Rodents and, in particular, rats have been the most commonly employed experimental model for studying diabetic cataract. However, distinct biochemical differences exist between humans and rats with respect to AR activity and polyol accumulation. Adult rat lenses have very high levels of AR activity and low levels of SDH activity (Jedziniak et al., 1981; Varma and Kinoshita, 1974). This is the opposite of human lenses, which exhibit low AR activity and high SDH activity (Jedziniak et al., 1981; Varma and Kinoshit, 1974). In addition, the amount of sorbitol present in human diabetic cataractous lenses is considerably less than that found in STZ-injected and galactose-fed rats (Chylack et al., 1979).

While these animal models have undoubtedly been instrumental in identifying enzymes and signaling pathways involved in the pathogenesis of diabetic cataract, they have also led to a misleading view, particularly on the importance of AR in the human lens. More recent research is now focused on identifying additional pathways that may contribute to cataract formation and, as a result, has prompted a reevaluation of the current animal models of diabetic cataract. However, to determine which animal models are most likely to be of relevance for studying human diabetic cataract, it is important to first identify the key changes to the human lens as a result of diabetic cataract formation.

4.2 Lens Changes in Human Diabetic Cataracts

In this section, we describe changes at the physiological, morphological, and biochemical level of lenses from diabetic patients and have summarized these findings in Table 4.1.

4.2.1 Physiology

Studies on human lenses have shown that there is an increase in the membrane permeability of lens cells with age that leads to an increase in internal sodium and calcium content (Duncan et al., 1989). In cortical cataract, there is a progressive alteration in ionic content, with lens sodium and calcium content further increasing (Duncan and Bushell, 1975). The effects of increased intracellular calcium have been studied using organ-cultured human donor lenses incubated in the presence of inomycin, a calcium ionophore (Sanderson et al., 2000). In this study, the increased calcium content increased lens wet weight, activated calcium-dependent cleavage and cross-linking of vimentin by calpain and transglutaminase, and induced cortical opacification (Sanderson et al., 2000).

Interestingly, this was also accompanied by an efflux of protein into the media and a loss of soluble lens proteins (Sanderson et al., 2000). This finding is consistent with a study from mature human cortical cataracts, which exhibited a loss of crystallins from the soluble fraction by insolubilization and efflux into the aqueous humor (Sandberg, 1976).

4.2.2 Morphology

While sorbitol accumulation in adult human diabetic lenses is unlikely to be sufficient to initiate osmotic stress over the entire lens, it is proposed that localized osmotic stress cannot be ruled out (Kador et al., 2016). In support of this, morphological analyses of human diabetic lenses reveals that the major cellular damage is typically observed in a localized zone in the deeper lens cortex that is surrounded by relatively undamaged cells in the superficial cortex and nucleus (Obrosova et al., 2010). The major damage to the restricted area fiber is suggested to correlate with the high levels of expression of AR in the epithelium and cortex and, therefore, the localized accumulation of sorbitol (Jedziniak et al., 1981). Numerous morphological alterations have been documented. These include globular bodies, such as extracellular Morgagnian globules or intracellular globules containing α-, β-, and γ-crystallin and actin (Creighton et al., 1978); cellular degeneration and breakdown of lens fibers (Vrensen, 2009); swelling of the broken ends of cortical fibers (Vrensen, 2009); undulating and folded fibers at the borders between the cortex and nucleus (Michael et al., 2008); and small fluid-filled water clefts close to the folded fibers (Michael et al., 2008). These changes tend to be present in the deeper cortex with no changes in the fiber cell morphology and cytoplasmic texture evident in the nuclear regions (Al-Ghoul and Costello, 1996). Several reports have also documented a decrease in cell density in the lens epithelium of type 2 diabetic patients (Takamura et al., 2000; Tkachov et al., 2006).

4.2.3 Biochemistry

A correlation between AR gene markers and susceptibility to develop complications among diabetic patients has been reported, suggesting that AR is also involved in the pathogenesis of diabetic complications in humans (Chung and Chung, 2003). However, in contrast to animal studies, there is currently no direct evidence of AR in the pathogenesis of human diabetic cataract. However, it is likely that the polyol pathway does play a contributory role. Recent studies suggest that the polyol pathway activity contributes to diabetic lesions in a number of ways, including osmotic, glycation, and oxidative stress (Chung and Chung, 2003; Nakamura et al., 2001; Szwergold et al., 1990). Each of these is discussed further.

4.2.3.1 INCREASED POLYOL PATHWAY ACTIVITY

It has been proposed that excess glucose enters the sorbitol pathway in diabetes, where AR catalyzes the NADPH-dependent reduction of glucose to its sugar alcohol, sorbitol. Sorbitol dehydrogenase (SDH) then catalyzes the NAD-dependent oxidation of sorbitol to fructose. As sorbitol does not readily diffuse out of the cells, and its oxidation to fructose is slow, the accumulation of sorbitol as a result of hyperglycemia increases the intracellular osmotic pressure, promoting cell swelling. Although it is well established that the sorbitol pathway leads to sugar cataract in animal lenses (Kinoshita, 1974), its role in the etiology of diabetic cataract in human lenses is uncertain. This is due to conflicting results on the levels of sorbitol and fructose measured in human lenses obtained from diabetic and nondiabetic patients, and from inconsistent and limited data regarding the levels of enzyme activity of AR and SDH in human lenses [summarized by Jedziniak et al. (1981)]. Some studies report comparable levels of sorbitol and fructose in both nondiabetic lenses and diabetic lenses (Heaf and Galton, 1975; Kuck, 1965; Pfaffenberger et al., 1976), while other studies found no sorbitol and decreased levels of fructose in nondiabetic lenses, but increased levels of sorbitol in the diabetic lens (Pirie and Vanheyningen, 1964; Varma et al., 1979). In cases where sorbitol has been measured in the human diabetic lens, the amounts of sorbitol detected have been quite low, and in some studies, deemed insufficient on a lens mass basis to account for the observed osmotic damage (Varma et al., 1979). Fructose levels are increased in human diabetic lenses and appear to be related to the degree of blood glucose levels (Jedziniak et al., 1981; Varma et al., 1979) and the extent of circulating hemoglobin glycation (Lerner et al., 1984). Consistent with this finding of higher fructose in diabetic human lenses, measurement of the enzymes involved in the polyol pathway has shown AR activity to be very low in human lens and SDH activity to be high, relative to animal lenses, indicating that the sorbitol pathway in the adult human lens is different from that in the animal lenses (Jedziniak et al., 1981). Comparison of the AR and SDH activity between human nondiabetic lenses and diabetic lenses revealed that AR and SDH levels were not significantly higher in the diabetic lenses relative to the nondiabetic lenses (Jedziniak et al., 1981). The lack of elevated AR activity in human diabetic lenses is in stark contrast to studies performed on diabetic rat lenses (Varma and Kinoshit, 1974). However, it has been postulated that despite low AR activity in the human lens, significant osmotic effects could be generated if the sorbitol was localized to specific regions of the lens. The localization and activity of AR in the human lens is highest in the epithelium and superficial cortical fiber cells (Jedziniak et al., 1981). Such a specific localization of AR and the associated localized accumulation of sorbitol

could explain the localized cellular swelling observed in the diabetic lens.

4.2.3.2 NONENZYMATIC GLYCATION

Nonenzymatic glycation has been implicated in the pathogenesis of diabetic cataract (Obrosova et al., 2010), and occurs when free amino groups of proteins react nonenzymatically with the acyclic form of glucose via an Amadori rearrangement (John and Lamb, 1993). Over time, the Amadori product undergoes dehydration and cleavage reactions in a process known as the Maillard reaction, in which the product forms stable adducts on proteins known as advanced glycation end products (AGEs) that manifest as protein brunescene and/or an increase in the fluorescent properties of the glycated protein (Bucala et al., 1992). Lens proteins, in particular crystallin proteins, are particularly susceptible to AGE formation for two reasons. First, as the lens is not dependent on insulin for glucose uptake, it is constantly exposed to high glucose concentrations (Pokupec et al., 2003), and second, as crystallin proteins have little or no turnover, they are particularly susceptible to posttranslational changes, such as modification by AGE formation (Pokupec et al., 2003). Advanced glycation occurs during normal aging in the human lens, but is significantly increased in diabetic cataract (Ahmed, 2005; Vlassara et al., 1994), with an overall increase in fluorescence in lens proteins and an increase in nonenzymatic lens brunescene (Monnier and Cerami, 1981; Oimomi et al., 1988; Stevens et al., 1978). AGEs have been shown to accumulate in human diabetic lenses (Ahmed et al., 2003; Franke et al., 2003; Pokupec et al., 2003), and include pentosidine and carboxymethyllysine (AGES formed oxidatively) and imidazolone (AGE formed nonoxidatively) (Franke et al., 2003). However, in another study, no differences in carboxymethyllysine content were identified between nondiabetic and diabetic lenses (Lyons et al., 1991). AGE structures modify crystallin proteins and in doing so cause conformational changes that lead to altered structure and function (Luthra and Balasubramanian, 1993). Modification of α-crystallin, for example, by the AGE precursor methylglyoxal, causes altered chaperone-like activity, partial protein unfolding, enhanced proteolysis, and subsequent protein insolubilization (Biswas et al., 2006, 2008). The glycation of lens proteins in vitro has been shown to result in the formation of dimers, trimers, and polymers, as well as high–molecular weight protein aggregates (Liang and Rossi, 1990), which would act to scatter light and result in cataract formation (Kasper and Funk, 2001).

4.2.3.3 OXIDATIVE STRESS

Oxidative stress is detected in the human diabetic lens and manifests early as a depletion of GSH (Ozmen et al., 1997). The depletion of GSH is most likely due to a decrease in the availability of NADPH, which is necessary for its regeneration from glutathione disulfide (GSSG) by glutathione reductase (GR) (Fig. 4.3). The depletion of NADPH results from its excessive consumption during the conversion of glucose to sorbitol (Bron et al., 1993). This implies that the pentose phosphate pathway, which is the main regenerative source of NADPH, fails to restore NADPH levels. This view is supported by the observation that the activity of glucose-6-phosphate dehydrogenase, the key regulatory enzyme of the pentose phosphate pathway, decreases in the diabetic lens (Donma et al., 2002; Nishikawa et al., 2000). Other signs of increased oxidative stress in the diabetic lens includes the accumulation of lipid peroxidation products, such as malondialdehyde (MDA) (Altomare et al., 1995); an increase in GSSG (oxidized GSH), depletion of other nonenzymatic antioxidants, such as ascorbate and taurine (Anthrayose and Shashidhar, 2004); as well as a decrease in activity of antioxidant defense enzymes, such as superoxide dismutase, catalase, and glutathione peroxidase (Donma et al., 2002; Ozmen et al., 2002). In diabetic patients, it is suggested that the efficiency of these enzymes might be compromised due to decreased availability of GSH, NADPH cofactors, and/or reduced activity of the these enzymes by AGE formation that is known to cause structural changes that reduce enzyme activity (Shin et al., 2006). While there is evidence to show that diabetic cataract in humans is associated with increased oxidative stress, the source of this oxidative stress remains unclear. Glucose autoxidation and nonenzymatic glycation are thought to contribute to an increase in free radicals in the diabetic lens (Ansari et al., 1996; Nagaraj et al., 1991; Wolff and Dean, 1987), which interestingly in turn, further accelerate the process of glycation (Loske et al., 2000). SDH, the second enzyme in the polyol pathway that converts sorbitol to fructose has also been suggested to contribute to oxidative stress. The oxidation of sorbitol to fructose increases the rate of formation of NADH, resulting in an increased cytosolic ratio of free NADH to NAD. As NADH is a substrate for NADH oxidase, an increase in NADH results in the generation of reactive oxygen species (ROS). In addition, large increases in NADH will also inhibit glycolysis (Rose and Warms, 1966), and thus limit the availability of pyruvate for the regeneration of NAD. Due to the inhibition of glycolysis, more glucose will enter the polyol pathway, further altering the cytosolic NAD:NADH ratio. Finally fructose and its metabolites fructose-3-phosphate and 3-deoxyglucosone are more potent nonenyzmatic glycation agents than glucose (Chung et al., 2003). Therefore more glucose entering the polyol pathway increases AGE formation and exacerbates oxidative stress.

Taken together, it is clear that osmotic stress alone does not account for the slow development of cataracts
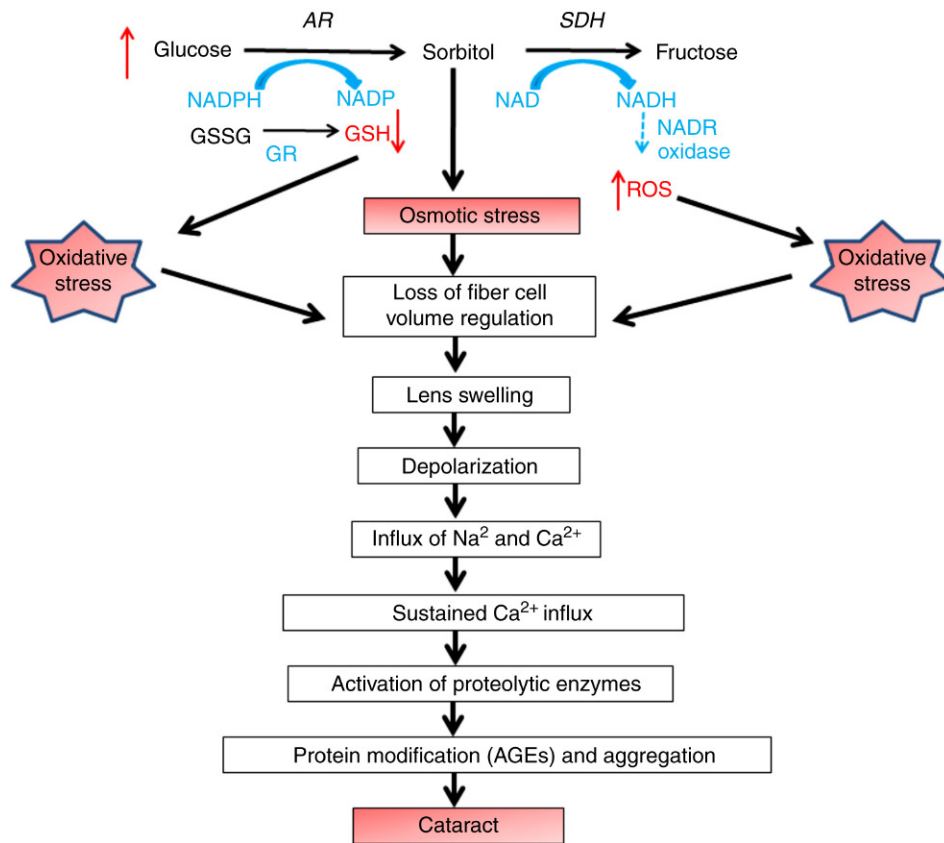
FIGURE 4.3 **Molecular mechanisms involved in the pathogenesis of diabetic cataract.** Osmotic and oxidative stress work synergistically to result in loss of fiber cell volume regulation. This triggers a series of events that lead to cell swelling, depolarization, and an influx of sodium and calcium ions. The accumulation of calcium ions results in the activation of calcium-dependent proteases, which targets cytoskeletal and crystallin proteins. In parallel, proteins are further modified by the formation of advanced glycation end products (AGEs), which are known to alter the structure and function of crystallins. As a result, there is an increase in insoluble proteins, the subsequent formation of high–molecular weight aggregates, and ultimately cataract. *AR*, Aldose reductase; *GR*, glutathione reductase; *GSSG*, glutathione disulfide; *NADP*, nicotinamide adenine dinucleotide phosphate; *NADPH*, reduced form of nicotinamide adenine dinucleotide phosphate; *ROS*, reactive oxygen species; *SDH*, sorbitol dehydrogenase.

that is typically seen in the majority of adult diabetic patients (Chan et al., 2008). Rather, the emerging view is that hyperglycemia results in increased polyol activity, which generates osmotic stress and oxidative stress in the diabetic lens (Chung et al., 2003). While the initiating mechanism in the development of diabetic cataract results in osmotic stress, there is evidence that the lens is able to regulate its volume through an osmoregulatory mechanism that can accommodate small changes in cellular osmotic pressure (Cammarata et al., 2002). However, over time, the ability of the lens to actively regulate its volume becomes impaired (Chan et al., 2008), and coupled with oxidative stress, these two pathways converge and contribute to cataract formation (Fig. 4.3). With this new view of diabetic cataract formation, we will now assess and evaluate current diabetic animal models for their ability to replicate the slow development of cataract formation observed in the human lens.

5 ANIMAL MODELS OF DIABETIC CATARACT

The STZ rat and galactose-fed animals both represent acute models for replicating the fast development of cataract that occurs in some diabetic patients with uncontrolled hyperglycemia. It is clear that these models possess similar hallmarks of human diabetic cataract and have increased our understanding of the contribution of the polyol pathway to osmotic stress in diabetic cataract significantly. However, moving forward, to develop anticataract therapies that will be effective in humans, we must identify diabetic animal models that develop slow-forming cataracts, which represent a more typical scenario in adult diabetic cataract formation than the traditional acute models. In humans, diabetic cataract can take 10–20 years to develop. Therefore, in animal cataract models where cataracts develop slowly, it is unlikely that these lenses would experience a rapid and

significant increase in polyol accumulation that would cause serious osmotic stress. Rather, the contribution of oxidative stress from increased polyol pathway activities is likely to be an important factor for chronic cataract development.

Excellent reviews of animal models in diabetes research are described by Chatzigeorgiou et al. (2009) and King (2012). From these diabetic animal models, a small subset has been used to study diabetic cataract and of this subset, a few describe the development of slow-forming cataracts. These models are discussed further.

5.1 Obese Models of Type 2 Diabetes

Animal models of type 2 diabetes tend to include models of insulin resistance and/or models of β cell failure (King, 2012). Many animal models of type 2 diabetes are obese, which reflects the human condition where obesity is closely linked to type 2 diabetes development. From these obese models, there were two models in particular that caught our attention due to the development of slow-forming cataracts, as well as the exhibition of morphological and biochemical changes reminiscent of that in human diabetic cataract.

5.1.1 Zucker Diabetic Fatty (ZDF) Rat

The Zucker fatty rat is used as a model of human obesity accompanied with hyperlipidemia and hypertension. Inbreeding of the Zucker fatty rat for hyperglycemia gave rise to the ZDF rat strain, which are less obese than the Zucker fatty rat, but have more severe insulin resistance (Pick et al., 1998). Diabetes develops in males at 8 weeks of age, but females do not develop overt diabetes (Peterson et al., 1990; Srinivasan and Ramarao, 2007; Wohlfart et al., 2014). Cataract in male ZDF rats is observed at ~15 weeks with the appearance of peripheral vesicles in the lens, which progress to cortical opacities and the development of a mature cataract by 21 weeks (Kim et al., 2011a,b; Shibata et al., 2000) Immunohistochemistry of ZDF lenses revealed large areas of tissue liquefaction, fiber cell swelling, as well as multiple membrane ruptures in the cortex (Kim et al., 2011b). At the biochemical level, lenses of the ZDF rats exhibited 3-fold increase in glucose and fructose, and a 22-fold increase in sorbitol levels (McCaleb and Sredy, 1992), as well as significantly higher AR activity relative to control rats. Lenses also exhibited a decrease of GSH (2.5-fold) in the ZDF rats relative to control rats (Coppey et al., 2002). Labeling for argpyrimidine, a methylglyoxal-derived AGE, and apoptotic molecules revealed that AGEs were highly accumulated in the epithelium (Kim et al., 2012). In addition, expression of the apoptotic factor nuclear factor kappaB (NFκB) was increased in the lens epithelium, as well as the mRNA expression of iNOS (Kim et al., 2010), indicating the involvement of the AGEs/NFκB/iNOS in the alteration of lens epithelial cells in diabetes.

5.1.2 Otuska Long Evans Tokushima Fatty (OLETF) Rat

The OLETF rat develops obesity-induced diabetes, but compared to other obese rodent models, the OLETF rat is only mildly obese. The OLETF rat comes from an outbred colony of Long Evans rats. Male OLETF rats are more susceptible to developing type 2 diabetes, with diabetes apparent at 18–25 weeks (Kawano et al., 1992). Hyperglycemia and hyperinsulinemia are exhibited in the early phases of the disease as a result of islet cell hyperplasia and peripheral insulin resistance (Ishida et al., 1995; Sato et al., 1995). As such OLETF rats are used as a model of human type 2 diabetes (Kawano et al., 1992, 1994). However, very few studies have used the OLETF rat as a model to study diabetic cataract (Bhutto et al., 2002; Kubo et al., 2001; Nagai et al., 2011). In the studies that have been reported, all male OLETF rats develop bilateral cortical cataracts after 60 weeks of age (Bhutto et al., 2002). At 40 weeks, swelling of the lens fibers was observed in the anterior and PSC fibers (Kubo et al., 2001), and at 60 weeks, vacuoles and cell swelling were observed in the equatorial cortex and supranuclear fibers (Kubo et al., 2001) These morphological changes in the OLETF rats resemble those in the galactosemic- and STZ-induced diabetic rats (Fukushi et al., 1980; Kinoshita, 1974), but occur much later in the OLETF rat. Sorbitol levels and AR and SDH activity in the lenses of OLETF rats were also increased (Kubo et al., 2001). Interestingly, SDH activity was greater than AR activity in the 60-week-old OLETF rat lens and this resulted in a net sorbitol conversion to fructose (Kubo et al., 2001), demonstrating that the polyol pathway is a factor in the development of sugar cataract. Other studies, which examined apoptosis and epithelial cell density in OLETF rat lenses have reported that markers of apoptosis, such as interferon-γ (IFN-γ) and interlukin-18 (IL-18), were markedly increased in the OLETF lenses relative to control (Nagai et al., 2011). This indicates that the decreased lens epithelial cell density reported in human diabetic cataract may be due to activation of IL-18 (Awasthi and Wagner, 2004; Nagai et al., 2011) Given that cataract becomes apparent in older animals and that a number of morphological and a few biochemical changes are apparent that resemble those observed in human diabetic cataract, the OLETF rat may be a potentially useful model for studying the chronic pathways that lead to cataract formation in type 2 diabetic patients.

5.2 Nonobese Models of Type 2 Diabetes

As type 2 diabetes can also manifest in the absence of an obese phenotype, the development of nonobese

models is also important for studying the etiology of this disease. Of the nonobese models commonly used by researchers, there are two particular models that slowly develop lens cataract formation and exhibit some evidence of the physiological, morphological, and biochemical features that are the hallmarks of human diabetic cataract.

5.2.1 Spontaneous Diabetic Torri (SDT) Rat

SDT rats spontaneously develop hyperglycemia and glucose intolerance due to decreased insulin secretion and accompanying β cell degeneration. The male SDT rat develops diabetes from about 20 weeks of age (Masuyama et al., 2003), while female SDT rats develop diabetes from 40 weeks of age (Shinohara et al., 2004). In male and female SDT rats, cataracts were observed at 40 weeks of age or older. Lens clouding begins at the posterior pole of lens and progresses to mature cortical cataract in which severe swelling, vacuolation, disintegration of the lens fibers, and formation of Morgagnian globules in the lens cortex are observed (Sasase, 2010). Eventually nuclear sclerosis and opacification of the lens cortex are both observed (Sasase, 2010), along with the extrusion of the lens nucleus into the vitreous chamber as a result of rupture of the posterior lens capsule (Shoda et al., 2007). Few female rodent models currently exist for type 2 diabetes, as in most diabetic models, it is only the males who develop diabetes. Therefore, the female SDT rat may be a useful animal model to study diabetic cataracts, especially for studies in females.

5.2.2 Wistar Bonn/Kobori (WBN/Kob) Rats

The WBN/Kob rat is an animal model for spontaneous diabetic syndrome and retinal degeneration (Mori et al., 1990). Cataracts are apparent at ~12 months of age in males only and appear in the lens periphery with cell swelling and disorder of lens fibers (Miyamura and Amemiya, 1998; Mori et al., 1992). In male WBN/Kob rats, total lens calcium increased at 18 months, and this was accompanied by activation of calpain 2 and 10 and proteolysis of α spectrin (Sakamoto-Mizutani et al., 2002). Although human lenses contain approximately 3% of the calpain activity found in rat lenses, calpain 2 has been suggested to be a major endopeptidase in human lenses (David et al., 1989). There is some evidence to support a role for calpain 2 in human diabetic cataract (Thampi et al., 2002a,b), suggesting that the enzyme might play a role in human diabetic cataract. The WBN/Kob model may, therefore, be useful for elucidating the roles of calpain 2 (and 10) in human cataractogenesis.

5.3 Transgenic or Knockout Mice

Transgenic and knockout mice enable researchers to study the role of a particular gene in disease. However,

diabetic mice are resistant to developing cataract and the levels of AR in the mouse lens are very low (Varma and Kinoshita, 1974). As a consequence, while mouse transgenic models have been used to study other diabetic complications, it is not a readily used model for studying diabetic cataract. However, they do offer an important role for identifying new pathogenic mechanisms brought about by genetic manipulation of the polyol pathway.

5.3.1 Aldose Reductase Transgenic (AR-Tg) Mice

The AR-Tg mice express high levels of human AR specifically in the lens. No morphological lens abnormalities were detected, indicating that overexpression of AR per se does not have any deleterious effect on the lens (Lee et al., 1995). However, when mice were induced to become galactosemic by the introduction of a 50% galactose diet, cataract developed ~1–2 days later, with the appearance of vacuoles detected at the periphery of the lens. (Lee et al., 1995). After 12–14 days, vacuoles covered the entire lens and fused together to produce a completely opaque lens by ~2–3 weeks after the initial administration of the galactose diet (Lee et al., 1995). Measurement of polyol accumulation in these lenses revealed a 20–30 fold increase in galactitol, indicating that the rapid accumulation of this polyol was the cause of the observed galactose-induced cataract (Lee et al., 1995).

AR-Tg mice injected with STZ to induce diabetes first develop cataracts at 7–14 days postinjection, which progresses to complete opacification by ~2–3 weeks (Lee et al., 1995). Lens sorbitol increased under hyperglycemic condition, but much lower than the galactitol levels under galactosemic conditions, reflecting faster accumulation of galactitol. In another study, diabetes-induced AR-Tg mice were used to study whether AR was involved in the generation of oxidative stress (Lee and Chung, 1999). The study revealed that the lenses had a significant decrease in GSH levels and a significant increase in the levels of MDA, indicative of oxidative stress (Lee and Chung, 1999), suggesting that AR is a major contributor to diabetes-induced oxidative stress. Furthermore, blocking the conversion of sorbitol to fructose by a SDH mutation, leads to higher levels of sorbitol accumulation, reduced oxidative stress, and development of cataract faster than mice with a normal SDH, indicating that SDH also contributes to oxidative stress (Lee et al., 1995).

5.3.2 Sorbitol Dehydrogenase–Deficient Mice

The SDH-deficient mouse represents a model that can simulate slow-developing cataract in diabetic patients, but is not diabetic itself (Chan et al., 2008). Cataract first developed at around 6 months of age in 5% of the mice, with ~70% of mice having cataracts at 16–17 months

(Chan et al., 2008). Cataract initially appeared as small vacuoles or clefts, followed by opacities that appeared to spread into the lens nucleus (Chan et al., 2008). Cataract development in the nondiabetic SDH deficient mice was unexpected because the mouse lens has very low AR levels and AR was thought to only be active in hyperglycemic animals due to its high K_m for glucose (Wermuth et al., 1982). While a lack of SDH did not affect lens glucose levels, the levels of sorbitol were dramatically increased in the lens (Chan et al., 2008). These findings demonstrate that the polyol pathway is active even in the nondiabetic mouse lens and that the increase in sorbitol levels most likely contributes to cataract development (Chan et al., 2008). There was no difference in GSH, MDA, or mRNA levels of antioxidant enzymes between wildtype and SDH-deficient mice, indicating that SDH deficiency did not overtly affect oxidative stress levels (Chan et al., 2008). However, introduction of a null mutation of the antioxidant enzyme glutathione peroxidase-1 (Gpx-1) into SDH-deficient mice accelerated cataract development relative to age-matched SDH-deficient mice and Gpx-1 knockout mice, indicating that oxidative stress contributes to cataract formation in SDH-deficient mice. Finally, measurement of ^{86}Rb uptake, an indicator of Na^+/K^+ ATPase activity, revealed that SDH-deficient mice had 50% lower Na^+/K^+ ATPase activity than wildtype mice, and that treatment of SDH-deficient mice with vitamin E prevented the loss of Na^+/K^+ ATPase activity (Chan et al., 2008). These findings suggest that chronic oxidative stress impairs the osmoregulatory mechanisms of the lens and may explain why diabetic patients who control their blood glucose moderately well are still susceptible to the cataract development.

6 ASSESSMENT OF DIABETIC CATARACT ANIMAL MODELS

While a number of diabetic animal models are used in diabetes research (Chatzigeorgiou et al., 2009; King, 2012), the majority of these animal models have not be used to study diabetic cataract. As such, existing models that are routinely used to study other diabetic complications could be reexamined to investigate the effects diabetes on the lenses of these animals.

While the STZ-induction appears to the model of choice for investigating type 1 diabetic cataract formation, there are also a number of animal models of spontaneous type 1 diabetes that could be explored for their use in studying diabetic cataract (Chatzigeorgiou et al., 2009). These include the diabetes-prone BB rat, which was developed from a colony of outbred Wistar rats in Canada (Nakhooda et al., 1977), the Long Evan

Tokushima Lean (LETL) rat (Kawano et al., 1991), the LEW-iddm rat (Jorns et al., 2004), and the Komeda diabetes prone (KDP) rat (Yokoi et al., 2003).

More options are available for researchers studying cataract formation in type 2 diabetes. The models in which cataracts develop slowly and thus appear in older animals are of interest. In light of this, the OLETF rat, an obese type 2 diabetic model is a promising model in which onset of cataract is first detected at 40 weeks (10 months), with bilateral cortical cataracts being formed by 60 weeks (15 months). The slow formation of cataract in the OLETF rat, the appearance of cell swelling and vacuoles in the lens cortex, and increased SDH activity relative to AR activity, bears similarities to characteristics of human diabetic lenses. Another model that would warrant further investigation is the WBN/Kob rat, a nonobese type 2 diabetic model that develops cataract at 12 months of age. Cell swelling is evident in the lens cortex and elevated calcium and calpain activation have also been demonstrated. Surprisingly, for both of these models, there is limited research on their lens physiology and biochemistry, opening up opportunities for researchers to assess the real potential of these models for studying obese and nonobese type 2 diabetic cataract formation.

7 CONCLUSIONS

Although these is much debate about the true value of using animal models in the study of diabetes and diabetic cataract, experimental models are essential tools for understanding the molecular basis, the pathogenic mechanism, and the utility of therapeutics agents in a multifactorial disease. It is unlikely that there is one animal model that entirely replicates the cataract process in humans. However, we have identified some animal models that mimic key characteristics of human diabetic cataract formation. The future use of these more relevant animal models will not only increase our understanding of human diabetic cataract formation, but will also aid our future development of anticataract therapies. The selection of an appropriate animal model(s) is, therefore, vitally important if we are to be successful in developing medical therapies to delay the onset of cataract and avoid the imminent cataract epidemic posed by our increasing diabetic population.

Acknowledgments

References

Adrien Shun-Shin, G., Brown, N.P., Bron, A.J., Sparrow JM, 1989. Dynamic nature of posterior subcapsular cataract. Br. J. Ophthalmol. 73, 522–527.

Age-Related Eye Disease Study Research Group, 2001. Risk factors associated with age-related nuclear and cortical cataract: a case-control study in the Age-Related Eye Disease Study, AREDS Report No. 5. Ophthalmology 108, 1400–1408.

Ahmed, N., 2005. Advanced glycation endproducts—role in pathology of diabetic complications. Diabetes Res. Clin. Pract. 67, 3–21.

Ahmed, N., Thornalley, P.J., Dawczynski, J., Franke, S., Strobel, J., Stein, G., Haik, G.M., 2003. Methylglyoxal-derived hydroimidazolone advanced glycation end-products of human lens proteins. Invest. Ophthalmol. Vis. Sci. 44, 5287–5292.

Al-Ghoul, K.J., Costello, M.J., 1996. Fiber cell morphology and cytoplasmic texture in cataractous and normal human lens nuclei. Curr. Eye Res. 15, 533–542.

Al-Ghoul, K.J., Lane, C.W., Taylor, V.L., Fowler, W.C., Costello, M.J., 1996. Distribution and type of morphological damage in human nuclear age-related cataracts. Exp. Eye Res. 62, 237–251.

Altomare, E., Vendemiale, G., Grattagliano, I., Angelini, P., Micelli-Ferrari, T., Cardia, L., 1995. Human diabetic cataract: role of lipid peroxidation. Diabetes Metab. 21, 173–179.

Ansari, N.H., Wang, L., Erwin, A.A., Church, D.F., 1996. Glucose- dependent formation of free radical species in lens homogenate. Biochem. Mol. Med. 59, 68–71.

Anthrayose, C.V., Shashidhar, S., 2004. Studies on protein and taurine in normal, senile and diabetic cataractous human lenses. Indian J. Physiol. Pharmacol. 48, 357–360.

Awasthi, N., Wagner, B.J., 2004. Interferon-gamma induces apoptosis of lens alphaTN4-1 cells and proteasome inhibition has an anti-apoptotic effect. Invest. Ophthalmol. Vis. Sci. 45, 222–229.

Bhutto, I.A., Lu, Z.Y., Takami, Y., Amemiya, T., 2002. Retinal and choroidal vasculature in rats with spontaneous diabetes type 2 treated with the angiotensin-converting enzyme inhibitor cilazapril: corrosion cast and electron-microscopic study. Ophthal. Res. 34, 220–231.

Biswas, A., Miller, A., Oya-Ito, T., Santhoshkumar, P., Bhat, M., Nagaraj, R.H., 2006. Effect of site-directed mutagenesis of methylglyoxal-modifiable arginine residues on the structure and chaperone function of human alphaA-crystallin. Biochemistry 45, 4569–4577.

Biswas, A., Wang, B., Miyagi, M., Nagaraj, R.H., 2008. Effect of methylglyoxal modification on stress-induced aggregation of client proteins and their chaperoning by human alphaA-crystallin. Biochem. J. 409, 771–777.

Bond, J., Green, C., Donaldson, P., Kistler, J., 1996. Liquefaction of cortical tissue in diabetic and galactosemic rat lenses defined by confocal laser scanning microscopy. Invest. Ophthalmol. Vis. Sci. 37, 1557–1565.

Bourne, R.R., Stevens, G.A., White, R.A., Smith, J.L., Flaxman, S.R., Price, H., Jonas, J.B., Keeffe, J., Leasher, J., Naidoo, K., Pesudovs, K., Resnikoff, S., Taylor, H.R., Vision Loss Expert G, 2013. Causes of vision loss worldwide, 1990-2010: a systematic analysis. Lancet Glob. Health 1, e339–e349.

Brian, G., Taylor, H., 2001. Cataract blindness—challenges for the 21st century. Bull. World Health Organ. 79, 249–256.

Bron, A.J., Sparrow, J., Brown, N.A., Harding, J.J., Blakytny, R., 1993. The lens in diabetes. Eye 7 (Pt. 2), 260–275.

Bucala, R., Vlassara, H., Ceramin, A., 1992. Advanced glycosylation end product. Harding, J.J., Crabbe, M.J.C. (Eds.), Post-Translational Modifcations of Proteins, vol. 2, CRC Press, Boca Raton, pp. 53–59.

Caird, F.I., Garrett, C.J., 1962. Progression and regression of diabetic retinopathy. Proc. Royal Soc. Med. 55, 477–479.

Cammarata, P.R., Schafer, G., Chen, S.W., Guo, Z., Reeves, R.E., 2002. Osmoregulatory alterations in taurine uptake by cultured human and bovine lens epithelial cells. Invest. Ophthalmol. Vis. Sci. 43, 425–433.

Chan, A.W., Ho, Y.S., Chung, S.K., Chung, S.S., 2008. Synergistic effect of osmotic and oxidative stress in slow-developing cataract formation. Exp. Eye Res. 87, 454–461.

Chatzigeorgiou, A., Halapas, A., Kalafatakis, K., Kamper, E., 2009. The use of animal models in the study of diabetes mellitus. In Vivo 23, 245–258.

Chung, S.S., Chung, S.K., 2003. Genetic analysis of aldose reductase in diabetic complications. Curr. Med. Chem. 10, 1375–1387.

Chung, S.S., Ho, E.C., Lam, K.S., Chung, S.K., 2003. Contribution of polyol pathway to diabetes-induced oxidative stress. J. Am. Soc. Nephrol. 14, S233–S236.

Chylack, Jr., L.T., Henriques, 3rd, H.F., Cheng, H.M., Tung, W.H., 1979. Efficacy of Alrestatin, an aldose reductase inhibitor, in human diabetic and nondiabetic lenses. Ophthalmology 86, 1579–1585.

Chylack, Jr., L.T., Ransil, B.J., White, O., 1984. Classification of human senile cataractous change by the American Cooperative Cataract Research Group (CCRG) method: III. The association of nuclear color (sclerosis) with extent of cataract formation, age, and visual acuity. Invest. Ophthalmol. Vis. Sci. 25, 174–180.

Coppey, L.J., Gellett, J.S., Davidson, E.P., Dunlap, J.A., Yorek, M.A., 2002. Changes in endoneurial blood flow, motor nerve conduction velocity and vascular relaxation of epineurial arterioles of the sciatic nerve in ZDF-obese diabetic rats. Diabetes/Metab. Res. Rev. 18, 49–56.

Costello, M.J., Oliver, T.N., Cobo, L.M., 1992. Cellular architecture in age-related human nuclear cataracts. Invest. Ophthalmol. Vis. Sci. 33, 3209–3227.

Creighton, M.O., Trevithick, J.R., Mousa, G.Y., Percy, D.H., McKinna, A.J., Dyson, C., Maisel, H., Bradley, R., 1978. Globular bodies: a primary cause of the opacity in senile and diabetic posterior cortical subcapsular cataracts? Canadian J. Ophthalmol. 13, 166–181.

David, L.L., Varnum, M.D., Lampi, K.J., Shearer, T.R., 1989. Calpain II in human lens. Invest. Ophthalmol. Vis. Sci. 30, 269–275.

Delcourt, C., Cristol, J.P., Tessier, F., Leger, C.L., Michel, F., Papoz, L., 2000. Risk factors for cortical, nuclear, and posterior subcapsular cataracts: the POLA study, Pathologies Oculaires Liees a l'Age. Am. J. Epidemiol. 151, 497–504.

Donma, O., Yorulmaz, E., Pekel, H., Suyugul, N., 2002. Blood and lens lipid peroxidation and antioxidant status in normal individuals, senile and diabetic cataractous patients. Curr. Eye Res. 25, 9–16.

Drel, V.R., Pacher, P., Ali, T.K., Shin, J., Julius, U., El-Remessy, A.B., Obrosova, I.G., 2008. Aldose reductase inhibitor fidarestat counteracts diabetes-associated cataract formation, retinal oxidative-nitrosative stress, glial activation, and apoptosis. Int. J. Mol. Med. 21, 667–676.

Duncan, G., Bushell, A.R., 1975. Ion analyses of human cataractous lenses. Exp. Eye Res. 20, 223–230.

Duncan, G., Hightower, K.R., Gandolfi, S.A., Tomlinson, J., Maraini, G., 1989. Human lens membrane cation permeability increases with age. Invest. Ophthalmol. Vis. Sci. 30, 1855–1859.

Franke, S., Dawczynski, J., Strobel, J., Niwa, T., Stahl, P., Stein, G., 2003. Increased levels of advanced glycation end products in human cataractous lenses. J. Cataract Refract. Surg. 29, 998–1004.

Fujii, N., Sakaue, H., Sasaki, H., Fujii, N., 2012. A rapid, comprehensive liquid chromatography-mass spectrometry (LC-MS)-based survey of the Asp isomers in crystallins from human cataract lenses. J. Biol. Chem. 287, 39992–40002.

Fukushi, S., Merola, L.O., Kinoshita, J.H., 1980. Altering the course of cataracts in diabetic rats. Invest. Ophthalmol. Vis. Sci. 19, 313–315.

Garner, M.H., Spector, A., 1980a. Selective oxidation of cysteine and methionine in normal and senile cataractous lenses. Proc. Natl. Acad. Sci. USA 77, 1274–1277.

Garner, M.H., Spector, A., 1980b. Sulfur oxidation in selected human cortical cataracts and nuclear cataracts. Exp. Eye Res. 31, 361–369.

Heaf, D.J., Galton, D.J., 1975. Sorbitol and other polyols in lens, adipose tissue and urine in diabetes mellitus. Clin. Chim. Acta 63, 41–47.

Hooi, M.Y.S., Raftery, M.J., Truscott, R.J.W., 2013a. Accelerated aging of Asp 58 in alpha A crystallin and human cataract formation. Exp. Eye Res. 106, 34–39.

Hooi, M.Y.S., Raftery, M.J., Truscott, R.J.W., 2013b. Age-dependent racemization of serine residues in a human chaperone protein. Prot. Sci. 22, 93–100.

Ishida, K., Mizuno, A., Min, Z., Sano, T., Shima, K., 1995. Which is the primary etiologic event in Otsuka Long-Evans Tokushima Fatty rats, a model of spontaneous non-insulin-dependent diabetes mellitus, insulin resistance, or impaired insulin secretion? Metab. Clin. Exp. 44, 940–945.

Jedziniak, J.A., Chylack, Jr., L.T., Cheng, H.M., Gillis, M.K., Kalustian, A.A., Tung, W.H., 1981. The sorbitol pathway in the human lens: aldose reductase and polyol dehydrogenase. Invest. Ophthalmol. Vis. Sci. 20, 314–326.

John, W.G., Lamb, E.J., 1993. The Maillard or browning reaction in diabetes. Eye 7 (Pt 2), 230–237.

Jorns, A., Kubat, B., Tiedge, M., Wedekind, D., Hedrich, H.J., Kloppel, G., Lenzen, S., 2004. Pathology of the pancreas and other organs in the diabetic LEW.1AR1/Ztm- iddm rat, a new model of spontaneous insulin-dependent diabetes mellitus. Virchows Arch. 444, 183–189.

Kador, P.F., 1988. The role of aldose reductase in the development of diabetic complications. Med. Res. Rev. 8, 325–352.

Kador, P.F., Betts, D., Wyman, M., Blessing, K., Randazzo, J., 2006. Effects of topical administration of an aldose reductase inhibitor on cataract formation in dogs fed a diet high in galactose. Am. J. Vet. Res. 67, 1783–1787.

Kador, P.F., Randazzo, J., Babb, T., Koushik, K., Takamura, Y., Zhu, W., Blessing, K., Kompella, U.B., 2007. Topical aldose reductase inhibitor formulations for effective lens drug delivery in a rat model for sugar cataracts. J. Ocular Pharmacol. Ther. 23, 116–123.

Kador, P.F., Webb, T.R., Bras, D., Ketring, K., Wyman, M., 2010. Topical KINOSTAT ameliorates the clinical development and progression of cataracts in dogs with diabetes mellitus. Vet. Ophthal. 13, 363–368.

Kador, P.F., Wyman, M., Oates, P.J., 2016. Aldose reductase, ocular diabetic complications and the development of topical Kinostat(R). Progr. Retinal Eye Res. 54, 1–29.

Kador, P.F., Zigler, J.S., Kinoshita JH, 1979. Alterations of lens protein synthesis in galactosemic rats. Invest. Ophthalmol. Vis. Sci. 18, 696–702.

Kasper, M., Funk, R.H., 2001. Age-related changes in cells and tissues due to advanced glycation end products (AGEs). Arch. Gerontol. Geriatr. 32, 233–243.

Kawano, K., Hirashima, T., Mori, S., Natori, T., 1994. OLETF (Otsuka Long-Evans Tokushima Fatty) rat: a new NIDDM rat strain. Diabetes Res. Clin. Pract. 24 (Suppl), S317–S320.

Kawano, K., Hirashima, T., Mori, S., Saitoh, Y., Kurosumi, M., Natori, T., 1991. New inbred strain of Long-Evans Tokushima lean rats with IDDM without lymphopenia. Diabetes 40, 1375–1381.

Kawano, K., Hirashima, T., Mori, S., Saitoh, Y., Kurosumi, M., Natori, T., 1992. Spontaneous long-term hyperglycemic rat with diabetic complications. Otsuka Long-Evans Tokushima Fatty (OLETF) strain. Diabetes 41, 1422–1428.

Kim, J., Kim, O.S., Kim, C.S., Sohn, E., Jo, K., Kim, J.S., 2012. Accumulation of argpyrimidine, a methylglyoxal-derived advanced glycation end product, increases apoptosis of lens epithelial cells both in vitro and in vivo. Exp. Mol. Med. 44, 167–175.

Kim, J., Kim, C.S., Sohn, E., Kim, H., Jeong, I.H., Kim, J.S., 2010. Lens epithelial cell apoptosis initiates diabetic cataractogenesis in the Zucker diabetic fatty rat. Graefe's Arch. Clin. Exp. Ophthalmol. 248, 811–818.

Kim, J., Kim, C.S., Sohn, E., Kim, H., Jeong, I.H., Kim, J.S., 2011a. KIOM-79 prevents lens epithelial cell apoptosis and lens opacification in Zucker diabetic fatty rats. J. Evid. Based Complementary Altern. Med., 2011.

Kim, J., Kim, C.S., Sohn, E., Lee, Y.M., Kim, J.S., 2011b. KIOM-79 inhibits aldose reductase activity and cataractogenesis in Zucker diabetic fatty rats. J. Pharm. Pharmacol. 63, 1301–1308.

King, A.J., 2012. The use of animal models in diabetes research. Br. J. Pharmacol. 166, 877–894.

Kinoshita, J.H., 1965. Cataracts in galactosemia. The Jonas S. Friedenwald Memorial Lecture. Invest. Ophthalmol. 4, 786–799.

Kinoshita, J.H., 1974. Mechanisms initiating cataract formation. Proctor Lecture. Invest. Ophthalmol. 13, 713–724.

Klein, B.E., Klein, R., Moss, S.E., 1995a. Incidence of cataract surgery in the Wisconsin Epidemiologic Study of Diabetic Retinopathy. Am. J. Ophthalmol. 119, 295–300.

Klein, B.E., Klein, R., Wang, Q., Moss, S.E., 1995b. Older-onset diabetes and lens opacities. The Beaver Dam Eye Study. Ophthal. Epidemiol. 2, 49–55.

Kubo, E., Maekawa, K., Tanimoto, T., Fujisawa, S., Akagi, Y., 2001. Biochemical and morphological changes during development of sugar cataract in Otsuka Long-Evans Tokushima fatty (OLETF) rat. Exp. Eye Res. 73, 375–381.

Kuck, Jr., J.F., 1965. Carbohydrates of the lens in normal and precataractous states. Invest. Ophthalmol. 4, 638–642.

Lee, A.Y.W., Chung, S.S.M., 1999. Contributions of polyol pathway to oxidative stress in diabetic cataract. FASEB J. 13, 23–30.

Lee, A.Y.W., Chung, S.K., Chung, S.S.M., 1995. Demonstration that polyol accumulation is responsible for diabetic cataract by the use of transgenic mice expressing the aldose reductase gene in the lens. Proc. Natl. Acad. Sci. USA 92, 2780–2784.

Lehtovirta, M., Pietilainen, K.H., Levalahti, E., Heikkila, K., Groop, L., Silventoinen, K., Koskenvuo, M., Kaprio, J., 2010. Evidence that BMI and type 2 diabetes share only a minor fraction of genetic variance: a follow-up study of 23,585 monozygotic and dizygotic twins from the Finnish Twin Cohort Study. Diabetologia 53, 1314–1321.

Lerner, B.C., Varma, S.D., Richards, R.D., 1984. Polyol pathway metabolites in human cataracts. Correlation of circulating glycosylated hemoglobin content and fasting blood glucose levels. Arch. Ophthalmol. 102, 917–920.

Leske, M.C., Chylack, Jr., L.T., Wu, S.Y., 1991. The lens opacities case-control study. Risk factors for cataract. Arch. Ophthalmol. 109, 244–251.

Leske, M.C., Wu, S.Y., Hennis, A., Connell, A.M., Hyman, L., Schachat, A., 1999. Diabetes, hypertension, and central obesity as cataract risk factors in a black population. The Barbados Eye Study. Ophthalmology 106, 35–41.

Liang, J.N., Rossi, M.T., 1990. In vitro non-enzymatic glycation and formation of browning products in the bovine lens alpha-crystallin. Exp. Eye Res. 50, 367–371.

Lim, J.C., Umapathy, A., Donaldson, P.J., 2016. Tools to fight the cataract epidemic: a review of experimental animal models that mimic age related nuclear cataract. Exp. Eye Res. 145, 432–443.

Loske, C., Gerdemann, A., Schepl, W., Wycislo, M., Schinzel, R., Palm, D., Riederer, P., Munch, G., 2000. Transition metal-mediated glycoxidation accelerates cross-linking of beta-amyloid peptide. Eur. J. Biochem. 267, 4171–4178.

Lou, M.F., 2003. Redox regulation in the lens. Progr. Retinal Eye Res. 22, 657–682.

Lou, M.F., Dickerson, Jr., J.E., 1992. Protein-thiol mixed disulfides in human lens. Exp. Eye Res. 55, 889–896.

Lou, M.F., Dickerson, Jr., J.E., Garadi, R., 1990. The role of protein-thiol mixed disulfides in cataractogenesis. Exp. Eye Res. 50, 819–826.

Lou, M.F., Dickerson, Jr., J.E., Tung, W.H., Wolfe, J.K., Chylack, Jr., L.T., 1999. Correlation of nuclear color and opalescence with protein S-thiolation in human lenses. Exp. Eye Res. 68, 547–552.

Luthra, M., Balasubramanian, D., 1993. Nonenzymatic glycation alters protein structure and stability. A study of two eye lens crystallins. J. Biol. Chem. 268, 18119–18127.

Lyons, T.J., Silvestri, G., Dunn, J.A., Dyer, D.G., Baynes, J.W., 1991. Role of glycation in modification of lens crystallins in diabetic and non-diabetic senile cataracts. Diabetes 40, 1010–1015.

Masuyama, T., Fuse, M., Yokoi, N., Shinohara, M., Tsujii, H., Kanazawa, M., Kanazawa, Y., Komeda, K., Taniguchi, K., 2003. Genetic analysis for diabetes in a new rat model of nonobese type 2 diabetes, spontaneously diabetic torii rat. Biochem. Biophys. Res. Commun. 304, 196–206.

Matsumoto, T., Ono, Y., Kuromiya, A., Toyosawa, K., Ueda, Y., Bril, V., 2008. Long-term treatment with ranirestat (AS-3201), a potent aldose reductase inhibitor, suppresses diabetic neuropathy and cataract formation in rats. J. Pharmacol. Sci. 107, 340–348.

McCaleb, M.L., Sredy, J., 1992. Metabolic abnormalities of the hyperglycemic obese Zucker rat. Metabolism 41, 522–525.

Michael, R., Bron, A.J., 2011. The ageing lens and cataract: a model of normal and pathological ageing. Philos. Transact. Royal Soc. London B 366, 1278–1292.

Michael, R., Barraquer, R.I., Willekens, B., van Marle, J., Vrensen, G.F., 2008. Morphology of age-related cuneiform cortical cataracts: the case for mechanical stress. Vis. Res. 48, 626–634.

Miyamura, N., Amemiya, T., 1998. Lens and retinal changes in the WBN/Kob rat (spontaneously diabetic strain). Electron-microscopic study. Ophthal. Res. 30, 221–232.

Monnier, V.M., Cerami, A., 1981. Nonenzymatic browning in vivo: possible process for aging of long-lived proteins. Science 211, 491–493.

Mori, Y., Yokoyama, J., Nishimura, M., Kurata, H., Miura, J., Ikeda, Y., 1990. Diabetic strain (WBN/Kob) of rat characterized by endocrine-exocrine pancreatic impairment due to distinct fibrosis. Pancreas 5, 452–459.

Mori, Y., Yokoyama, J., Nishimura, M., Oka, H., Mochio, S., Ikeda, Y., 1992. Development of diabetic complications in a new diabetic strain of rat (Wbn/Kob). Pancreas 7, 569–577.

Nagai, N., Murao, T., Ito, Y., Okamoto, N., Okamura, H., 2011. Involvement of interleukin 18 in lens opacification of Otsuka Long-Evans Tokushima Fatty rats, a model of human type 2 diabetes. Curr. Eye Res. 36, 497–506.

Nagaraj, R.H., Sell, D.R., Prabhakaram, M., Ortwerth, B.J., Monnier, V.M., 1991. High correlation between pentosidine protein cross-links and pigmentation implicates ascorbate oxidation in human lens senescence and cataractogenesis. Proc. Natl. Acad. Sci. USA 88, 10257–10261.

Nakamura, J., Kasuya, Y., Hamada, Y., Nakashima, E., Naruse, K., Yasuda, Y., Kato, K., Hotta, N., 2001. Glucose-induced hyperproliferation of cultured rat aortic smooth muscle cells through polyol pathway hyperactivity. Diabetologia 44, 480–487.

Nakhooda, A.F., Like, A.A., Chappel, C.I., Murray, F.T., Marliss, E.B., 1977. The spontaneously diabetic Wistar rat. Metabolic and morphologic studies. Diabetes 26, 100–112.

Nishikawa, T., Edelstein, D., Du, X.L., Yamagishi, S., Matsumura, T., Kaneda, Y., Yorek, M.A., Beebe, D., Oates, P.J., Hammes, H.P., Giardino, I., Brownlee, M., 2000. Normalizing mitochondrial superoxide production blocks three pathways of hyperglycaemic damage. Nature 404, 787–790.

Obrosova, I.G., Chung, S.S., Kador, P.F., 2010. Diabetic cataracts: mechanisms and management. Diabetes/Metab. Res. Rev. 26, 172–180.

Oimomi, M., Maeda, Y., Hata, F., Kitamura, Y., Matsumoto, S., Baba, S., Iga, T., Yamamoto, M., 1988. Glycation of cataractous lens in non-diabetic senile subjects and in diabetic patients. Exp. Eye Res. 46, 415–420.

Ozmen, D., Mutaf, I., Ozmen, B., Mentes, J., Bayindir, O., 1997. Lens lipid peroxides and glutathione concentrations in diabetic cataract. Ann. Clin. Biochem. 34 (Pt. 2), 190–192.

Ozmen, B., Ozmen, D., Erkin, E., Guner, I., Habif, S., Bayindir, O., 2002. Lens superoxide dismutase and catalase activities in diabetic cataract. Clin. Biochem. 35, 69–72.

Perry, R.E., Swamy, M.S., Abraham, E.C., 1987. Progressive changes in lens crystallin glycation and high-molecular-weight aggregate formation leading to cataract development in streptozotocin-diabetic rats. Exp. Eye Res. 44, 269–282.

Peterson, R.G., Shaw, W.N., Neel, M.-A., Little, L.A., Eichberg, J., 1990. Zucker diabetic fatty rat as a model for non-insulin-dependent diabetes mellitus. ILAR J. 32, 16–19.

Pfaffenberger, C.D., Szafranek, J., Horning, E.C., 1976. Gas chromatographic study of free polyols and aldoses in cataractous human lens tissue. J. Chromatogr. 126, 535–545.

Pick, A., Clark, J., Kubstrup, C., Levisetti, M., Pugh, W., Bonner-Weir, S., Polonsky, K.S., 1998. Role of apoptosis in failure of beta-cell mass compensation for insulin resistance and beta-cell defects in the male Zucker diabetic fatty rat. Diabetes 47, 358–364.

Pirie, A., 1968. Color and solubility of the proteins of human cataracts. Invest. Ophthalmol. 7, 634–650.

Pirie, A., Vanheyningen, R., 1964. The effect of diabetes on the content of sorbitol, glucose, fructose and inositol in the human lens. Exp. Eye Res. 3, 124–131.

Pokupec, R., Kalauz, M., Turk, N., Turk, Z., 2003. Advanced glycation endproducts in human diabetic and non-diabetic cataractous lenses. Graefe's Arch. Clin. Exp. Ophthalmol. 241, 378–384.

Robison, Jr., W.G., Houlder, N., Kinoshita, J.H., 1990. The role of lens epithelium in sugar cataract formation. Exp. Eye Res. 50, 641–646.

Robison, Jr., W.G., Laver, N.M., Jacot, J.L., Glover, J.P., 1995. Sorbinil prevention of diabetic-like retinopathy in the galactose-fed rat model. Invest. Ophthalmol. Vis. Sci. 36, 2368–2380.

Rose, I.A., Warms, J.V., 1966. Control of glycolysis in the human red blood cell. J. Biol. Chem. 241, 4848–4854.

Rotimi, C., Daniel, H., Zhou, J., Obisesan, A., Chen, G., Chen, Y., Amoah, A., Opoku, V., Acheampong, J., Agyenim-Boateng, K., Eghan, Jr., B.A., Oli, J., Okafor, G., Ofoegbu, E., Osotimehin, B., Abbiyesuku, F., Johnson, T., Fasanmade, O., Doumatey, A., Aje, T., Collins, F., Dunston, G., 2003. Prevalence and determinants of diabetic retinopathy and cataracts in West African type 2 diabetes patients. Ethnicity Dis. 13, S110–S117.

Rowe, N.G., Mitchell, P.G., Cumming, R.G., Wans, J.J., 2000. Diabetes, fasting blood glucose and age-related cataract: the Blue Mountains Eye Study. Ophthal. Epidemiol. 7, 103–114.

Sakamoto-Mizutani, K., Fukiage, C., Tamada, Y., Azuma, M., Shearer, T.R., 2002. Contribution of ubiquitous calpains to cataractogenesis in the spontaneous diabetic WBN/Kob rat. Exp. Eye Res. 75, 611–617.

Sandberg, H.O., 1976. Alpha-crystallin content of aqueous-humor in cortical, nuclear, and complicated cataracts. Exp. Eye Res. 22, 75–84.

Sanderson, J., Marcantonio, J.M., Duncan, G., 2000. A human lens model of cortical cataract: Ca^{2+}-induced protein loss, vimentin cleavage and opacification. Invest. Ophthalmol. Vis. Sci. 41, 2255–2261.

Sasase, T., 2010. Pathophysiological characteristics of diabetic ocular complications in spontaneously diabetic torii rat. J. Ophthalmol. 2010, 615641.

Sato, T., Asahi, Y., Toide, K., Nakayama, N., 1995. Insulin resistance in skeletal muscle of the male Otsuka Long-Evans Tokushima Fatty rat, a new model of NIDDM. Diabetologia 38, 1033–1041.

Sato, S., Mori, K., Wyman, M., Kador, P.F., 1998. Dose-dependent prevention of sugar cataracts in galactose-fed dogs by the aldose reductase inhibitor M79175. Exp. Eye Res. 66, 217–222.

Shibata, T., Takeuchi, S., Yokota, S., Kakimoto, K., Yonemori, F., Wakitani, K., 2000. Effects of peroxisome proliferator-activated receptor-alpha and -gamma agonist, JTT-501, on diabetic complications in Zucker diabetic fatty rats. Br. J. Pharmacol. 130, 495–504.

Shin, A.H., Oh, C.J., Park, J.W., 2006. Glycation-induced inactivation of antioxidant enzymes and modulation of cellular redox status in lens cells. Arch. Pharm. Res. 29, 577–581.

Shinohara, M., Oikawa, T., Sato, K., Kanazawa, Y., 2004. Glucose intolerance and hyperlipidemia prior to diabetes onset in female spontaneously diabetic torii (SDT) rats. Exp. Diabesity Res. 5, 253–256.

Shoda, T., Shinohara, M., Takahashi, T., Miyajima, K., Kakehashi, A., Miyakawa, Y., 2007. Histopathological features of diabetic ocular complications in the spontaneously diabetic torri (SDT) rat. J. Toxicol. Pathol. 20, 179–183.

Sippel, T.O., 1966. Changes in the water, protein, and glutathione contents of the lens in the course of galactose cataract development in rats. Invest. Ophthalmol. 5, 568–575.

Spector, A., Roy, D., 1978. Disulfide-linked high molecular weight protein associated with human cataract. Proc. Natl. Acad. Sci. USA 75, 3244–3248.

Srinivasan, K., Ramarao, P., 2007. Animal models in type 2 diabetes research: an overview. Indian J. Med. Res. 125, 451–472.

Stevens, V.J., Rouzer, C.A., Monnier, V.M., Cerami, A., 1978. Diabetic cataract formation: potential role of glycosylation of lens crystallins. Proc. Natl. Acad. Sci. USA 75, 2918–2922.

Suryanarayana, P., Saraswat, M., Mrudula, T., Krishna, T.P., Krishnaswamy, K., Reddy, G.B., 2005. Curcumin and turmeric delay streptozotocin-induced diabetic cataract in rats. Invest. Ophthalmol. Vis. Sci. 46, 2092–2099.

Suryanarayana, P., Saraswat, M., Petrash, J.M., Reddy, G.B., 2007. *Emblica officinalis* and its enriched tannoids delay streptozotocin-induced diabetic cataract in rats. Mol. Vis. 13, 1291–1297.

Szwergold, B.S., Kappler, F., Brown, T.R., 1990. Identification of fructose 3-phosphate in the lens of diabetic rats. Science 247, 451–454.

Takamura, Y., Sugimoto, Y., Kubo, E., Takahashi, Y., Akagi, Y., 2000. Immunohistochemical study of apoptosis of lens epithelial cells in human and diabetic rat cataracts. Jpn. J. Ophthalmol. 44, 569–570.

Takemoto, L., 1996. Increase in the intramolecular disulfide bonding of alpha-A crystallin during aging of the human. Exp. Eye Res. 63, 585–590.

Thampi, P., Hassan, A., Smith, J.B., Abraham, E.C., 2002a. Enhanced C-terminal truncation of alphaA- and alphaB-crystallins in diabetic lenses. Invest. Ophthalmol. Vis. Sci. 43, 3265–3272.

Thampi, P., Zarina, S., Abraham, E.C., 2002b. alpha-Crystallin chaperone function in diabetic rat and human lenses. Mol. Cell. Biochem. 229, 113–118.

Tkachov, S.I., Lautenschlager, C., Ehrich, D., Struck, H.G., 2006. Changes in the lens epithelium with respect to cataractogenesis: light microscopic and Scheimpflug densitometric analysis of the cataractous and the clear lens of diabetics and non-diabetics. Graefe's Arch. Clin. Exp. Ophthalmol. 244, 596–602.

Truscott, R.J., 2005. Age-related nuclear cataract-oxidation is the key. Exp. Eye Res. 80, 709–725.

Truscott, R.J., Augusteyn, R.C., 1977a. Changes in human lens proteins during nuclear cataract formation. Exp. Eye Res. 24, 159–170.

Truscott, R.J., Augusteyn, R.C., 1977b. Oxidative changes in human lens proteins during senile nuclear cataract formation. Biochim. Biophys. Acta 492, 43–52.

Truscott, R.J., Augusteyn, R.C., 1977c. The state of sulphydryl groups in normal and cataractous human lenses. Exp. Eye Res. 25, 139–148.

Varma, S.D., Kinoshit, J.H., 1974. Sorbitol pathway in diabetic and galactosemic rat lens. Biochim. Biophys. Acta 338, 632–640.

Varma, S.D., Kinoshita, J.H., 1974. The absence of cataracts in mice with congenital hyperglycemia. Exp. Eye Res. 19, 577–582.

Varma, S.D., Schocket, S.S., Richards, R.D., 1979. Implications of aldose reductase in cataracts in human diabetes. Invest. Ophthalmol. Vis. Sci. 18, 237–241.

Varsha, M.K.N.S., Raman, T., Manikandan, R., 2014. Inhibition of diabetic-cataract by vitamin K1 involves modulation of hyperglycemia-induced alterations to lens calcium homeostasis. Exp. Eye Res. 128, 73–82.

Vlassara, H., Bucala, R., Striker, L., 1994. Pathogenic effects of advanced glycosylation: biochemical, biologic, and clinical implications for diabetes and aging. Lab. Invest. 70, 138–151.

Vrensen, G.F., 2009. Early cortical lens opacities: a short overview. Acta Ophthalmol. 87, 602–610.

Wang, F., Ma, J., Han, F., Guo, X., Meng, L., Sun, Y., Jin, C., Duan, H., Li, H., Peng, Y., 2016. DL-3-*n*-butylphthalide delays the onset and progression of diabetic cataract by inhibiting oxidative stress in rat diabetic model. Sci. Rep. 6, 19396.

Wermuth, B., Burgisser, H., Bohren, K., von Wartburg, J.P., 1982. Purification and characterization of human-brain aldose reductase. Eur. J. Biochem. 127, 279–284.

Wohlfart, P., Lin, J., Dietrich, N., Kannt, A., Elvert, R., Herling, A.W., Hammes, H.-P., 2014. Expression patterning reveals retinal inflammation as a minor factor in experimental retinopathy of ZDF rats. Acta Diabetol. 51, 553–558.

Wolff, S.P., Dean, R.T., 1987. Glucose autoxidation and protein modification. The potential role of 'autoxidative glycosylation' in diabetes. Biochem J. 245, 243–250.

Yokoi, N., Namae, M., Fuse, M., Wang, H.Y., Hirata, T., Seino, S., Komeda, K., 2003. Establishment and characterization of the Komeda diabetes-prone rat as a segregating inbred strain. Exp. Anim. 52, 295–301.

N-Methyl-N-Nitrosourea Animal Models for Retinitis Pigmentosa

Airo Tsubura*, Yuko Emoto*,
Maki Kuro*, Katsuhiko Yoshizawa*,**

*Kansai Medical University, Hirakata, Osaka, Japan
**Mukogawa Women's University, Nishinomiya, Hyogo, Japan

Animal Models for the Study of Human Disease.

1 INTRODUCTION

Retinitis pigmentosa (RP) is a well-known clinical entity that was named by German physician Franz Cornelius Donders in 1857. It is characterized by early night blindness followed by peripheral visual field alterations (tunnel vision) and eventually blindness. The incidence of RP is estimated to be 1 in 4000, which makes it one of the most common causes of severe visual impairment in humans (Hartong et al., 2006). The first type of photoreceptors to be lost is the rods, which provides black-and-white vision and functions in dark or dim light. The loss of rods initially occurs in the equatorial zone and then extends peripherally and centrally. Cones, which are responsible for color vision and function in bright light, are lost after the rods. Photoreceptor cell loss is followed by perivascular pigment deposition within the retina (Hartong et al., 2006). The fundus of an RP patient typically shows intraretinal pigmentation, referred to as bone-spicule deposits, which are created by the migration of retinal pigment epithelial (RPE) cells and their deposition around retinal vessels. RP is a heterogeneous group of retinal disorders with autosomal dominant inheritance (30%–40%), autosomal recessive inheritance (50%–60%), or X-linked inheritance (5%–15%). Although RP is primarily a genetic disease, some sporadic cases are known. RP is mostly observed in isolation (nonsyndromic) but may also occur in the following syndromes: Usher (an autosomal recessive disorder associated with deafness); Laurence-Moon-Bardet-Biedl (an autosomal recessive disease associated with obesity, hypogonadism, mental retardation, and dysmorphic extremities); Kearns-Sayre (a usually sporadic disease that is associated with progressive external ophthalmoplegia); Batten (autosomal recessive disease accompanied with neurodegenerative disease); Refsum (autosomal recessive disorder accompanied with cerebellar ataxia and chronic polyneuropathy); and Senior-Loken (autosomal recessive disease accompanied with kidney failure) (Bhatti 2006; Fleischhauer et al., 2005). RP is a noninflammatory, bilateral, progressive, degenerative pigmentary retinopathy of genetic origin. Thus, the word "retinitis" is a misnomer because retinal inflammation does not play a major role. More than 160 different mutations in genes that encode proteins with remarkably diverse functions result in rod photoreceptor degeneration (www.sph.uth.tmc.edu/retnet). Although various genes are involved in RP, the final common pathway is apoptotic cell death of the rod photoreceptors (Koenekoop, 2009). Vitamin A (Berson, 2007), vitamin A in combination with docosahexaenoic acid (DHA), an n-3 polyunsaturated fatty acid (PUFA) found in fish (Shintani and Klionsky, 2004), and lutein found in green leafy vegetables (Berson et al., 2010) can slow the progression of human. However, there is currently no cure or effective therapy for RP.

Animal models of retinal degeneration are important for a better understanding of human RP, particularly in regard to the search for treatments (Dalke and Graw, 2005; Rivas and Vecino, 2009). Mice carrying the *rd* (rodless retina or retinal degeneration) gene (now *Pde6b*), a defect in the β subunit of cyclic guanosine monophosphate phosphodiesterase (cGMP PDE), develop retinal degeneration early in life. Retinal development in *rd* mice is comparable to that in normal mice at 8 days of age; however, a reduction in the number of photoreceptor cells becomes apparent at 11 days of age, and photoreceptor cells are completely missing or reduced to a single layer of cells by 20 days of age (Nambu et al., 1996). In *rds* (retinal degeneration slow) mice carrying mutations in the *peripherin/rds* gene (now *Prph2*), photoreceptor cell loss starts at 2 weeks of age and progresses slowly with complete loss occurring 1 year after birth (Sancho-Pelluz et al., 2008). The *RCS* (Royal College of Surgeons) rat has a deletion in the gene encoding a receptor tyrosine kinase (*Mertk*) expressed in RPE cells, and the inability to phagocytize rod outer segment debris leads to photoreceptor degeneration by apoptosis (Perche et al., 2008); this degeneration begins at 20 days of age, and there are almost no detectable photoreceptors by 60 days of age. The *rd*, *rds*, and *RCS* animals are spontaneous animal models for RP that have heterogeneous genetic defects that lead to photoreceptor apoptosis, which is characterized by internucleosomal cleavage and fragmentation (Chang et al., 1993; Portera-Cailliau et al., 1994; Tso et al., 1994). Importantly, mutations in these genes have been detected in patients with RP (Perche et al., 2008; Sancho-Pelluz et al., 2008). In addition to isolated models for RP, the tubby mouse carrying a mutation in the *tub* gene (Kong et al., 2007) is an animal model for Usher syndrome, the most common syndrome associated with RP (Fleischhauer et al., 2005). In addition to spontaneous animal models, transgenic animal models of RP are available and have been used to understand the mechanisms of the disease and develop therapeutic strategies (Chader, 2002; Dalke and Graw, 2005; Rivas and Vecino, 2009). However, the establishment of additional animal models, resembling human RP, is desired for the further understanding of disease progression, the analysis of disease mechanisms, and the development of treatments.

In addition to genetic models of RP, light induces photoreceptor cell damage and death through phototoxic mechanisms (Organisciak and Vaughan 2010), and certain chemicals can artificially cause photoreceptor cell damage in animals. Mammalian eyes are highly sensitive to toxic substances, and several chemicals induce retinal degeneration in animals (Voaden, 1991). Among these chemicals, *N*-methyl-*N*-nitrosourea (MNU), an alkylating agent, exhibits its cytotoxicity by transferring its methyl group to nucleobases in nucleic acids. MNU

selectively damages photoreceptor cells and may be a good candidate for the induction of retinal degeneration. Importantly, apoptosis is the final common pathway of photoreceptor cell death in RP animal models, as well as RP patients. Thus, if MNU-induced photoreceptor cell damage is due to apoptosis, it may represent another animal model for RP.

2 TIME-COURSE PROGRESSION OF MNU-INDUCED RETINAL DEGENERATION

Herrold (1967) first described retinal degeneration in Syrian golden hamsters that received two intravenous (IV) 5-mg doses of MNU per week and were sacrificed between 4 and 7 months of age. These MNU-treated animals exhibited photoreceptor cell loss that resulted in the inner nuclear layer being in direct contact with the choroid. A single 40 mg/kg dose of MNU to F344 rats and Japanese white rabbits by an intraperitoneal (IP) and IV route, respectively, caused severe destruction of photoreceptor cells after 3 days and complete photoreceptor cell loss after 5 or more weeks (Ogino et al., 1993). A single IV 15 mg/kg dose of MNU (given together with 20 mg/kg ketamine but not MNU alone) to cats caused distinctive loss of photoreceptor cells in 7 days (Schaller et al., 1981). We tried to shorten the time-course progression of MNU-induced retinal degeneration in rats, which are frequently used for toxicological studies. The

dose of MNU needed to cause photoreceptor cell loss in 7 days was determined in albino (Sprague-Dawley) and pigmented (Brown-Norway) rats.

Fig. 5.1 illustrates the time-course progression of MNU-induced retinal degeneration in Brown-Norway rats. In both pigmented and albino rats, IP administration of 60 or 75 mg/kg MNU caused time-dependent retinal damage in which photoreceptor cell loss occurred over a 7-day course (Nakajima et al., 1996a,b; Yoshizawa et al., 1999, 2000). Although age-matched control (MNU-untreated) rat retina exhibited ordered retinal layers, rats treated with MNU displayed retinal photoreceptor cell loss in a characteristic pattern. Twenty-four hours after MNU administration, photoreceptor cells showed pyknosis and karyorrhexis of the nuclei, shortening of the inner segment, and disorientation of the outer segment. The destruction of photoreceptor segments can be easily recognized by the periodic acid-Schiff (PAS)-negative inner segment and PAS-positive outer segment. At this time point, the pigment deposition in the RPE cells was irregular. After 48 h, karyorrhexis of the photoreceptor cells progressed, and widespread destruction of the photoreceptor layer occurred. At 72 h, photoreceptor cell destruction had progressed to include widespread destruction of the photoreceptor segments and detachment of the RPE cells from Bruch's membrane. At this time point, cells presumed to be Müller cells with mitotic figures were present within the dying photoreceptor cells and in the inner nuclear layer. At day 7, active
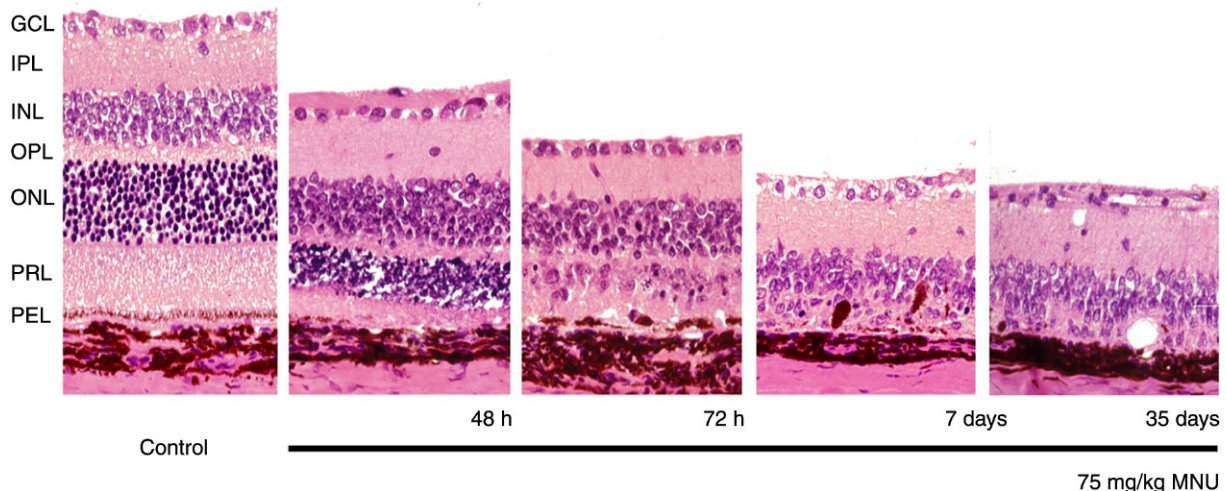
FIGURE 5.1 **Time-course progression of retinal damage after a single systemic administration of 75 mg/kg N-methyl-N-nitrosourea (MNU) to 7-week-old pigmented Brown-Norway rats.** GCL, Ganglion cell layer; INL, inner nuclear layer; IPL, inner plexiform layer; ONL, outer nuclear layer; OPL, outer plexiform layer; PEL, pigment epithelial cell layer; and PRL, photoreceptor cell layer. At 48 h after MNU administration, photoreceptor cells show pyknosis and karyorrhexis and the destruction of the inner and outer segments. At 72 h, the destruction of photoreceptor cells and photoreceptor segments had progressed, the migration of the melanin-containing retinal pigment epithelial (RPE) cells began, and mitotic cells among the photoreceptor cells appeared. At day 7, active signs of photoreceptor cell destruction were indistinct because almost all of the photoreceptor cells were lost, and the inner nuclear cells were either in direct contact with choroids or separated by a few layers of cells. At day 35, vacuole formation (cystoid degeneration) was observed within the retina (hematoxylin and eosin). *Source: Reprinted with permission from Tsubura, A., et al., 2010. Histol. Histopathol. 25(7), 933–944.*
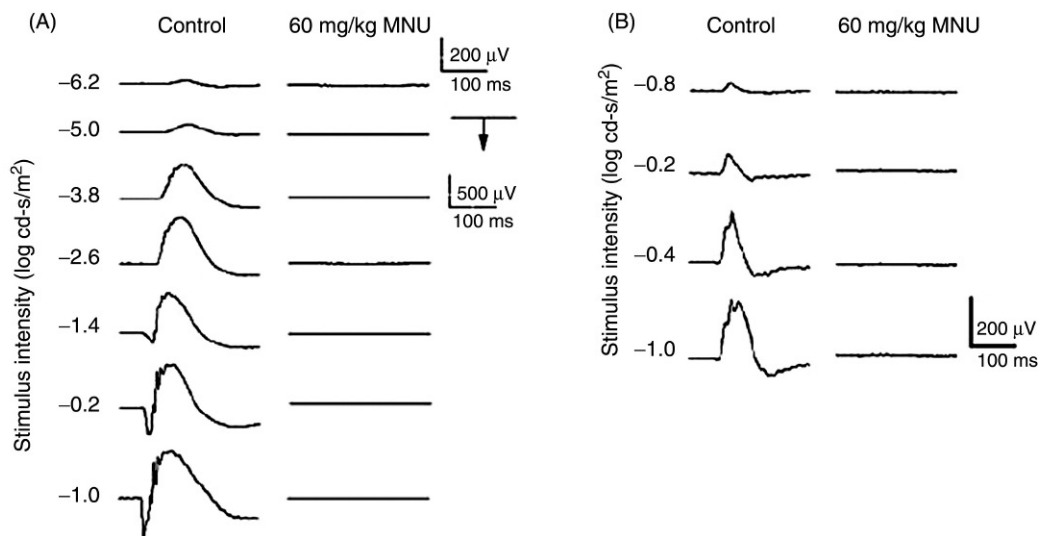
FIGURE 5.2   **Electroretinogram *(ERG)* recording 7 days after a single systemic administration of 60 mg/kg of MNU to an 8-week-old albino Sprague-Dawley rat and an age-matched MNU-untreated control.** (A) Scotopic waveforms. (B) Photopic waveforms. Both the scotopic and photopic ERG responses became undetectable in the MNU-treated rats. *Source: Reprinted with permission from Tsubura, A., et al., 2010. Histol. Histopathol. 25(7), 933–944.*

signs of photoreceptor degeneration were indistinct due to photoreceptor cell loss, and the PAS-positive outer segment was diminished. At this time point, scotopic and photopic electroretinogram (ERG) responses were undetectable, suggesting the functional loss of the retina (Fig. 5.2) (Kiuchi et al., 2003). Thus, MNU caused complete photoreceptor cell death, as observed structurally and functionally, in a 7-day course.

At 21 and 35 days, the inner nuclear layer was either in direct contact with the choroid or was separated from it by a few layers of cells. At these time points, RPE cell migration occurred within the retina, and vacuole formation (cystoid degeneration) occurred in the inner nuclear layer and inner plexiform layer. In rats, although the migration of RPE cells was observed within all layers of the retina, direct contact to intraretinal vascular cells was indistinct even 150 days after MNU administration. When a lower dose of MNU (50 mg/kg) is applied to Sprague-Dawley rats, photoreceptor cell loss requires a longer period of time (Jeong et al., 2011). In addition to these histopathological analyses, optic coherence tomography has been used to obtain cross-sectional noninvasive images to monitor the progression of MNU-induced retinal degeneration in animals (Yamauchi et al., 2011).

3 RETINAL DEGENERATION CAUSED BY MNU IN VARIOUS ANIMAL SPECIES

In Sprague-Dawley and Brown-Norway rats, photoreceptor cell loss occurred over a 7-day period after 60 or 75 mg/kg of MNU was administered to young mature animals at 7 weeks of age (Nakajima et al., 1996a,b;

Yoshizawa et al., 1999, 2000). A single systemic administration of MNU-induced retinal degeneration in both female and male mammals including the house musk shrew *Suncus murinus* (Insectivora), mice of the BALB/c, GRS/A, and C57BL strains, rats of the Sprague-Dawley, Lewis, Brown-Norway, Long-Evans, and Copenhagen strains (Emoto et al., 2016a), the Syrian golden hamster (Rodentia), cat (Carnivora), and nonhuman primates (monkey; *Macaca fuscata and Macaca fascicularis*) (Kinoshita et al., 2015; Tsubura et al., 1998). Rodent studies indicate that retinal susceptibility to MNU does not show strain differences (Emoto et al., 2016a; Tsubura et al., 1998). However, the dose of MNU necessary for the induction of retinal degeneration in a 7-day period differed among species (Table 5.1). In mice, both systemic IP administration of 60 mg/kg MNU or topical intravitreal (IVT) administration of 3 mg/kg MNU cause retinal degeneration within a week (Rösch et al., 2014). Although systemic MNU administration affects both eyes, topical administration only affects the injected eye. Moreover, although the photoreceptor cell loss required more than 7 days, MNU causes retinal degeneration in Japanese white rabbits (Lagomorpha) (Ogino et al., 1993) and Sudanian grass rats (Rodentia) (Boudard et al., 2010, 2011). Interestingly, MNU together with ketamine (but not MNU alone) was necessary for the development of photoreceptor cell damage in cats (Schaller et al., 1981). Ketamine blocks calcium channels associated with *N*-methyl-D-aspartate (NMDA) receptors, which prevents the influx of ions and subsequent photoreceptor cell death in adult rabbits (Paques et al., 2006). In contrast, ketamine enhances neuronal cell death in rats by compensatory upregulation of NMDA

TABLE 5.1   Retinal Degeneration Induced by *N*-Methyl-*N*-Nitrosourea (MNU) in Different Animal Species

Vertebrata	Species	Age or body weight	MNU (mg/kg)	Route of administration	Site of origin	Migration of retinal pigment epithelial cells	References
Mammal	Monkey	Young adult	40	IV	Equatorial zone	No migration	Tsubura et al. (1998)
	Cat	5–10 months	15[a]	IV	ND	ND	Schaller et al. (1981)
	Rabbit	2.3–2.5 kg	40[b]	IV	ND	ND	Ogino et al. (1993)
	Hamster	7 weeks	90	IP	Posterior pole	Contact with intraretinal blood vessels	Taomoto et al. (1998)
	Grass rat	2–6 months	150[c]	IP	ND	ND	Boudard et al., 2010
	Rat	7 weeks	60	IP	Posterior pole	Intraretinal migration without contact with blood vessels	Nakajima et al. (1996b); Yoshizawa et al. (2000)
	Mouse	7 weeks	60	IP	Posterior pole	No migration	Yuge et al. (1996)
	Shrew	7 weeks	65	IP	Posterior pole	No migration	Tsubura et al. (1998)
Fish	Zebrafish	12–24 months	150 mg/L	IMMR	ND	No migration	Tappeiner et al. (2013)

[a]*Photoreceptor cell loss develops when MNU is given together with IV administration of 20 mg/kg ketamine. Photoreceptor cell loss is complete in 7 days.*
[b]*Photoreceptor cell loss takes 5 weeks.*
[c]*Photoreceptor cell loss takes 20 days.*
IMMR, Immerse; *IP*, intraperitoneal; *IV*, intravenous; *ND*, not described.

receptors in the developmental stage (Zou et al., 2009). In an unpublished experiment performed by our laboratory, ketamine hydrochloride diluted in physiologic saline was subcutaneously (SC) injected into 7-day-old and 12-week-old Sprague-Dawley rats. A dose of 0, 10, 20, and 40 mg/kg was administered 6 times at 2-h intervals. Rats were sacrificed 24 h after the first injection. In 7-day-old rats, dose-dependent single cell necrosis of the brain occurred, and single cell necrosis of the retinal ganglion cells (not photoreceptor cells) occurred in all groups (unpublished observation). The number of rats with single cell injury in the inner retina was 2 of 11 rats in the 0 mg/kg group; 3 of 12 rats in the 10 mg/kg group; 3 of 15 rats in the 20 mg/kg group; and 4 of 13 rats in the 40 mg/kg group. Ketamine did not cause retinal ganglion cell injury in these rats. Ketamine at a dose of 40 mg/kg was lethal in 7-day-old animals (10 of 13 animals), whereas 12-week-old animals treated with ketamine did not die or exhibit damage to the brain or retina. Thus, the effects of ketamine on photoreceptor cells may be species-specific. Insectivora are considered to be the most primitive class of primates and also considered to be related to rodents (Romer and Parson, 1978). Among the insectivora, the house musk shrew *Suncus murinus*, which belongs to the family Soricidae, is widely distributed throughout the tropical regions of Asia and the Far East, and also inhabits southern Japan. Shrews have morphological and functional phenotypes that are similar to those of primates, and some of these phenotypes may closely reflect those of humans; therefore, the shrew is a valuable experimental animal from a

phylogenetic point of view (Tsubura et al., 1995). Thus, phylogenetically, MNU-induced retinal degeneration observed from shrews to monkeys may suggest that MNU-induced retinal degeneration is a universal phenomenon in mammals. Similar to human RP, degeneration originates from the equatorial zone in monkeys, whereas degeneration originates from the central retina (posterior pole) and extends to the peripheral retina in shrews, mice, rats, and hamsters (Kinoshita et al., 2015; Tsubura et al., 1998). Rats and mice are nocturnal rod-dominant animals (98 and 96% rods, respectively) with a sparse distribution of cones across the retina. Although the total number of cones in the human retina is of the same order ($\sim$5%), many are concentrated in the central macular zone. This difference in the distribution of rods and cones among different animal species might explain the differences in the initiation site of photoreceptor cell damage. Moreover, in addition to mammals, MNU targets fish photoreceptor cells. Zebrafish incubated in fresh water containing 150 mg/kg MNU in 10 mM phosphate-buffered saline (PBS; pH 6.3) for 1 h exhibit photoreceptor cell loss over a 7-day period (Tappeiner et al., 2013). Unlike mammals, zebrafish displays persistent retinal neurogenesis throughout their life. Characteristically, within a month after photoreceptor cell degeneration, zebrafish photoreceptor cells regenerate from Müller cells. In rats, Müller cells express rodopsin and synaptophysin in response to MNU damage (Wan et al., 2008), but further study is required to determine whether these rodopsin- and synaptophysin-positive cells, which are presumed to be Müller cell-derived photoreceptor

cells, acquire functional properties. Cultured human Müller cells retain the capacity to express photoreceptor-specific markers; however, confirmation is necessary to determine whether they obtain functional properties when transplanted to athymic mouse retina (Giannelli et al., 2011). Unlike zebrafish, mammals do not exhibit persistent retinal neurogenesis throughout life.

In human RP, cone disappearance occurs secondary to rod loss. Cones can be assessed using peanut agglutinin staining. Light damage to the retina causes rod loss followed by cone loss in transgenic T17M rhodopsin mice (Krebs et al., 2009). The retinal damage in mice caused by IP injection of 60 mg/kg MNU consists of rod disappearance in parallel with the progressive disappearance of peanut agglutinin-labeled cones from the central retina to the periphery (Krishnamoorthy et al., 2008). In diurnal cone-rich Sudanian grass rats that receive an IP injection of 150 mg/kg MNU, cone loss is delayed relative to rod loss (Boudard et al., 2010). MNU-induced cone disappearance secondary to rod loss is similar to that observed in human RP. However, MNU only targets rod cells in cone-rich zebrafish (Tappeiner et al., 2013), with MNU inducing rod cell but not cone cell loss, although photoreceptor function is impaired in both rod and cone cells in monkeys (Kinoshita et al., 2015). In parallel to photoreceptor cell loss, intraretinal migration of melanin-containing RPE cells occurred in rats and hamsters (Table 5.1); however, RPE cells in contact with blood vessels were observed only in hamsters (Taomoto et al., 1998). Interestingly, RPE migration did not occur in monkeys, mice, shrews, or zebrafish (Tappeiner et al., 2013; Tsubura et al., 1998; Yuge et al., 1996).

4 AGE-RELATED PHOTORECEPTOR CELL DAMAGE AND SENSITIVITY TO MNU

In contrast to the MNU-induced photoreceptor cell loss in young mature animals, MNU administered transplacentally (Smith and Yielding, 1986) or to newborn animals (Nambu et al., 1998a,b) resulted in retinal dysplasia characterized by the progressive disorganization of neuroblasts, which led to rosette formation in the outer neuroblastic/nuclear layer (Fig. 5.3). Retinal dysplasia characterized by rosettes is a developmental anomaly present at birth (Godel et al., 1981). In C57BL mice, retinal dysplasia developed when 60 mg/kg MNU was administered to 0- or 3-day-old pups but not to pups that were 5 days old or older (Nambu et al., 1998a). In contrast, retinal degeneration occurred when MNU was given to mice that were 11 days old or older. Interestingly, no structural alteration of the retina occurred when 60 mg/kg MNU was administered to 5- and 8-day-old mice. MNU administered in the proliferative phase of retinal development led to retinal dysplasia, but MNU had no effect on the retinal developmental stage when administered after the proliferation of neuroblastic cells had ended. However, after retinal tissue had differentiated into specialized cells, photoreceptor cells became susceptible to MNU. In the mature retina of Lewis rats, photoreceptor cell loss occurred over a 7-day period when >90, >50, and ≥35 mg/kg MNU was given to 21-, 50-, and 150-day-old animals, respectively (Nambu et al., 1998b). Ontogenetically, the sensitivity of photoreceptor cells to MNU-induced retinal degeneration increased with age. This increased sensitivity in parallel to
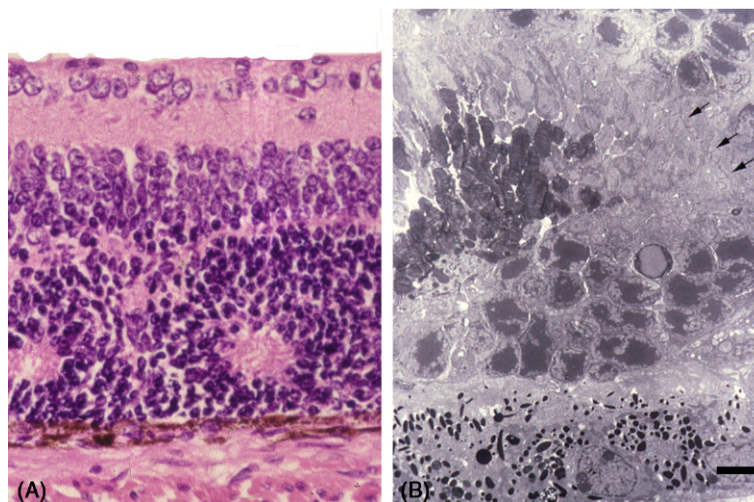
FIGURE 5.3 **Retinal dysplasia after a single systemic administration of 60 mg/kg MNU to 0-day-old C57BL mice.** (A) Retinal rosette in the outer nuclear layer at 8 days of age (hematoxylin and eosin). (B) Electron micrograph of the retinal rosette at 20 days of age. In some areas the photoreceptor segments radiated toward the center, and in other areas the photoreceptor cell nuclei directly face the center. A single layer of pigment epithelial cells was observed above the Bruch's membrane. *Arrowheads* indicate the outer limiting membrane. Bar = 4 μm. *Source: Reprinted with permission from Nambu, H., et al., 1998. Pathol. Int. 48(3), 199–205.*

aging may be caused by the accumulation of DNA damage with age. However, regardless of the time of MNU administration to rats that are at least 21 days old (after the retina has matured), the loss of photoreceptor cells was a selective phenomenon in that no other neural cells in the retina were affected by MNU.

5 PHOTORECEPTOR CELL DEATH, CELL DEBRIS REMOVAL, AND RPE CELL MIGRATION

5.1 Photoreceptor Cell Death

Apoptosis and autophagy-associated cell death are the two fundamental types of programmed cell death (Hotchkiss et al., 2009). Apoptosis (type I programmed cell death) is characterized by condensation of the cytoplasm and nucleus, accompanied by chromatin condensation, nuclear fragmentation, and the formation of plasma membrane blebs. Autophagic cell death (type II programmed cell death) is characterized by the accumulation of autophagosomes and autolysosomes. Autophagosomes fuse with lysosomes to form autolysosomes, in which acid hydrolases catabolize the ingested material into metabolic substrates. Paradoxically, autophagy may function as an essential survival mechanism by producing energy from the breakdown of deleterious products and organelles (Mizushima, 2007). In most normal tissues and cells, autophagy occurs at basal levels (basal autophagy) and contributes to the routine turnover of cytoplasmic components. In disease conditions, autophagy contributes to cell damage but can also protect cells from injury (Shintani and Klionsky, 2004). Photoreceptor degeneration in several animal models for RP occurs through apoptosis (Chang et al., 1993; Portera-Cailliau et al., 1994; Tso et al., 1994).

An apoptotic mechanism is responsible for MNU-induced retinal degeneration in rats (Nakajima et al., 1996b) and other species (Taomoto et al., 1998; Yuge et al., 1996). Light microscopy studies of MNU-treated rat retina revealed that the dying photoreceptor cell nuclei appeared hyperchromatic after 24 h and that the degree of hyperchromatic nuclei progressed after 72 h (Fig. 5.4A). Among the dying photoreceptor cells and in the inner nuclear layer, scattered mitotic cells, presumed to be Müller cells, were observed. Dying photoreceptor cells were selectively labeled with terminal deoxynucleotidyl transferase-mediated dUTP nick-end labeling (TUNEL) 24 and 72 h after MNU (Fig. 5.4B). Electron microscopy showed photoreceptor cell nuclei to be pyknotic while Müller cell nuclei remained viable (Fig. 5.4C). In addition, internucleosomal DNA fragmentation was detected in the retina 12 and 24 h after MNU administration; the fragmentation peaked 72 h after

MNU administration and was almost negligible at day 7 (Fig. 5.4D). These findings suggest that an apoptotic mechanism is responsible for photoreceptor cell death.

In normal photoreceptor cells, besides the intermittent shedding of the disk from outer segments, autophagy functions as a degradative pathway in photoreceptor metabolism. Autophagic vacuoles are mainly encountered in the myoid portion of the inner segments of photoreceptor cells with dense material (Remé et al., 1999). In BALB/c mice, autophagosomes were detected in the myoid portion of the inner segment of the photoreceptor cells in untreated controls (Fig. 5.5). However, autophagosomes were barely detectable 72 h after the administration of 75 mg/kg MNU when the level of apoptosis peaked (Kuro et al., 2011). Decreased levels of basal autophagy concomitantly occurred during the course of apoptosis progression in photoreceptor cells of MNU-treated mice. Several animal models for RP indicate that defects in retinal genes encoding rod proteins initiate the pathogenesis of RP leading to the apoptotic rod cell death, which is followed by the loss of cones. In contrast to rods, cone loss is due to nutritional deficiencies, starvation, and autophagy (Punzo et al., 2009). The role of autophagy in photoreceptor cells appears to be complex.

5.2 Removal of Apoptotic Photoreceptor Cells

Clearance of apoptotic cells is mediated by professional phagocytes, such as macrophages and nonprofessional phagocytes, which are cells near apoptotic cells in which phagocytosis is not their principal function (Erwig and Henson, 2008). Macrophages, Müller cells, and RPE cells participate in the clearance of damaged retinal neuronal cells (Chang et al., 2006; Strauss, 2005). During the course of photoreceptor cell apoptosis caused by 75 mg/kg MNU in rats, mitotic cells appeared in the inner nuclear layer and within dying photoreceptor cells 72 h after MNU administration when apoptosis peaked (Fig. 5.4A). Cells not undergoing apoptosis contained proliferating cell nuclear antigen (PCNA) in their nucleus (Fig. 5.6A) and glial fibrillary acidic protein (GFAP) and/or vimentin in their proliferating cell processes (Fig. 5.6B); these characteristics are indicative of Müller cells. These cells appeared 48 h after MNU administration and peaked at 72 h. Proliferating Müller cell processes contained numerous phagocytic inclusions derived from apoptotic photoreceptor cells (Fig. 5.6C). The role of Müller cell proliferation and the extension of their processes within damaged areas may also participate in stabilizing and preserving the damaged retina. At days 7 and 21 after MNU administration, there was an influx of ED1-positive and ED2-negative bone marrow-derived microglia/macrophages within the retina (Fig. 5.6D) (Kaneko et al., 2008; Nakajima et al., 1996a,b). Therefore, Müller cells, macrophages, and RPE cells with
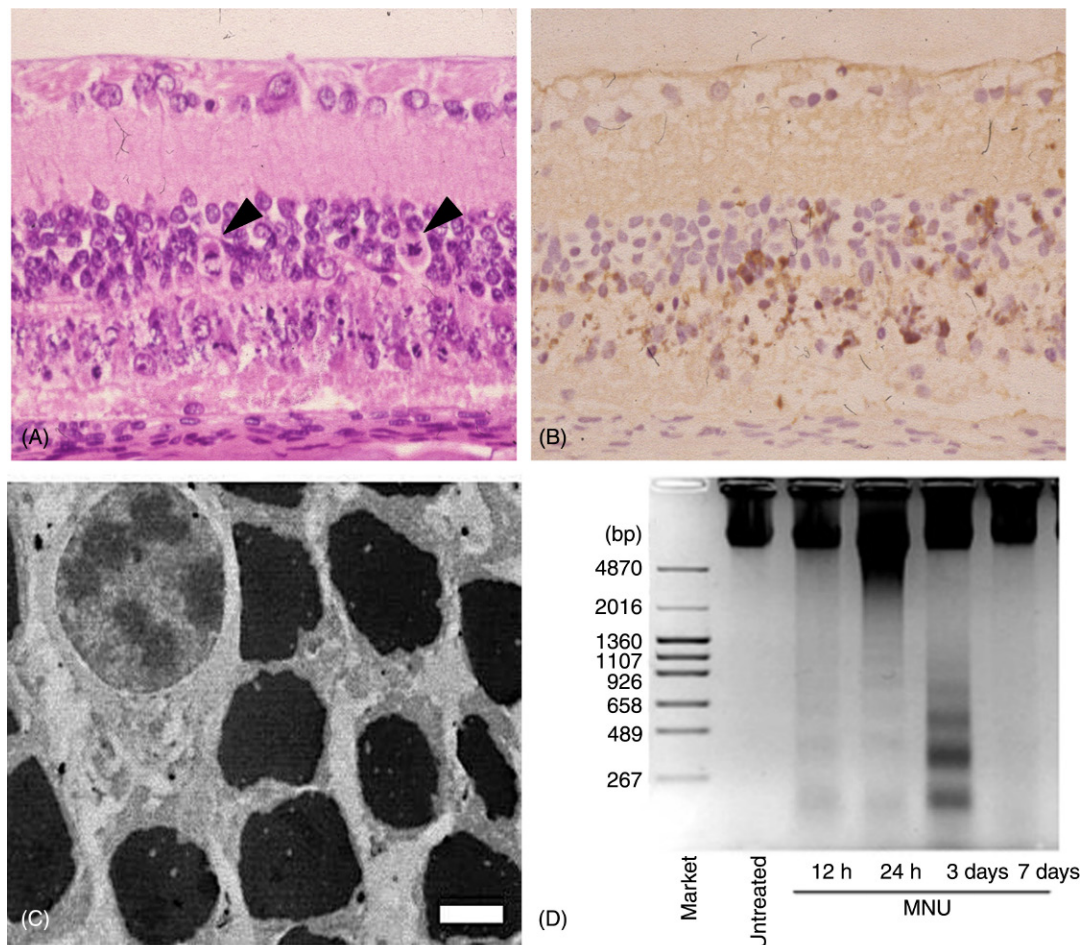
FIGURE 5.4   Apoptosis characteristics of photoreceptor cell death induced by MNU. (A) Pyknotic photoreceptor cell nuclei were observed in 75 mg/kg MNU-treated Sprague-Dawley rats 72 h after MNU treatment. Mitotic cells presumed to be Müller cells *(arrowheads)* are indicated (hematoxylin and eosin). (B) Terminal deoxynucleotidyl transferase-mediated dUTP nick-end labeling (TUNEL). TUNEL-positive signals are restricted to photoreceptor cell nuclei of Sprague-Dawley rats 72 h after administration of 75 mg/kg MNU. (C) Electron micrograph. MNU-treated rat retina showed hyperchromatic photoreceptor cell nuclei, leaving Müller cells located in the upper left corner intact. Retinal tissue was from Sprague-Dawley rats 24 h after administration of 75 mg/kg MNU. Bar = 3.5 μm. (D) DNA fragmentation in the retina of Lewis rats treated with 60 mg/kg MNU and untreated controls. DNA ladders appeared in MNU-treated retina 12 and 24 h after MNU and peaked 72 h after MNU; the ladder was negligible at day 7. *Source: Reprinted with permission from Tsubura, A., et al., 2010. Histol. Histopathol. 25(7), 933–944.*

FIGURE 5.5   Autophagy in photoreceptor cells. (A) Schematic presentation of the formation of autophagic vacuoles in the inner segment of photoreceptor cells. Segregation (1–3) and degradation (4–6) stages of an autophagic vacuole. (B) Autophagosomes are observed in the myoid portion of the inner segment of photoreceptor cells in untreated control retina in a BALB/c mouse. In contrast, autophagic vacuoles are virtually absent in 75 mg/kg MNU-treated mice 72 h after treatment. *White arrowheads*, autophagic vacuoles; *N*, photoreceptor nucleus. Bar = 1 μm. *Source: Reprinted with permission from Kuro, M., et al., 2011. In Vivo 25(4), 625–631.*
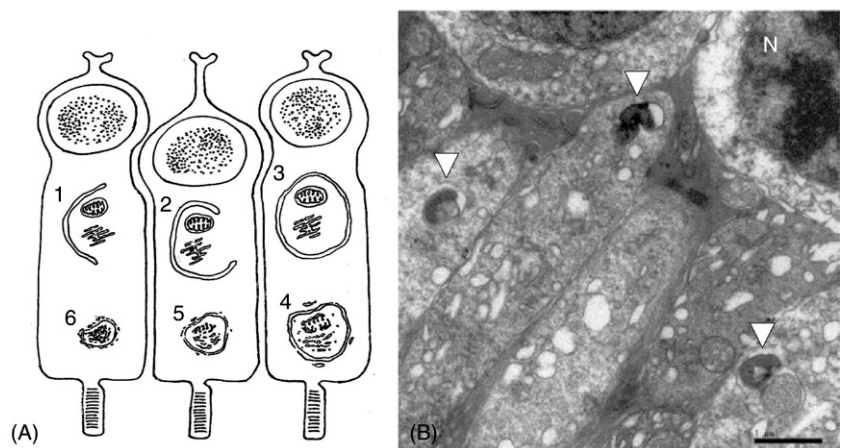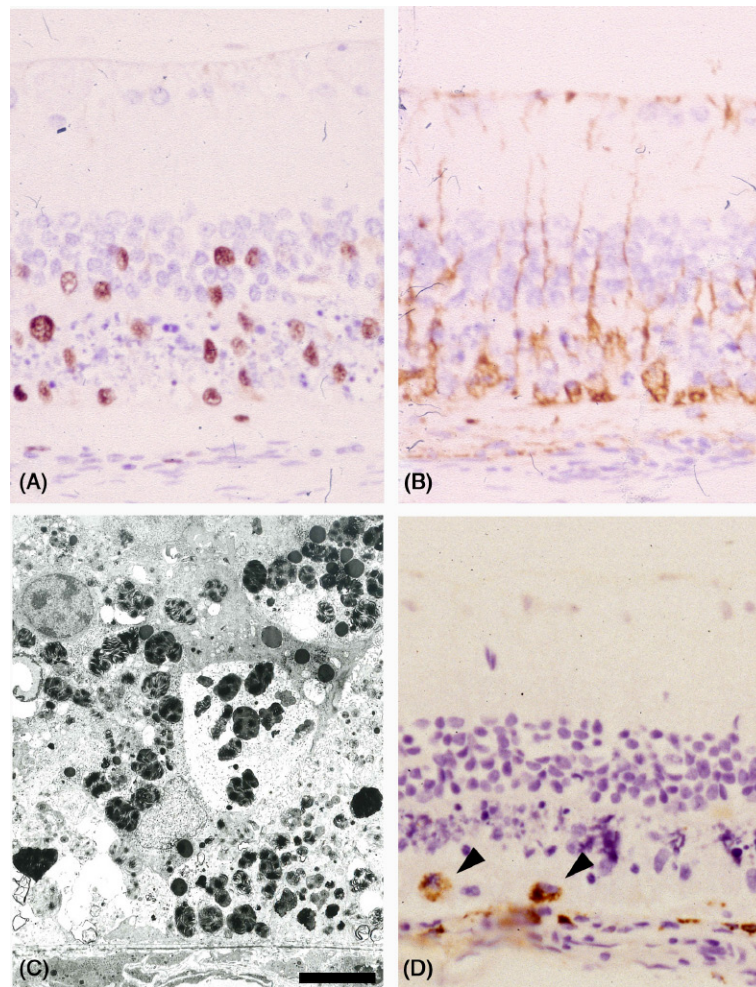
FIGURE 5.6   Cell debris removal after MNU insult. Proliferation of Müller cells is indicated by: (A) Proliferating cell nuclear antigen (PCNA)-positive nuclei *(PCNA)*, (B) vimentin-positive cytoplasm (Vimentin), and (C) electron micrograph. Proliferating Müller cell processes contain numerous phagocytic inclusions. Bar = 4 μm. (D) ED-1-positive migrating macrophages *(arrowheads)* are observed within the injured outer retina (ED-1). *Source: Reprinted with permission from Nakajima, M., et al., 1996b. Am. J. Pathol. 148(2), 631–641.*

phagocytic function were involved in the removal of apoptotic photoreceptor cells, which were characterized by marked cytoplasmic and nuclear condensation and fragmentation into membrane-bound bodies. No inflammatory response was observed in these processes.

5.3 Bone Spicule Pigmentation

Fundus pictures of RP patients show a pale, waxy optic nerve head, attenuated retinal blood vessels, and characteristic bone spicule pigment in regions of photoreceptor degeneration (Li et al., 1995). The bone spicule pigment corresponds to melanin-containing RPE cells clustered around branching blood vessels in the inner retina. Translocated RPE cells in contact with retinal blood vessels are a distinctive feature of human RP. Although photoreceptor cell loss by apoptosis occurs in various vertebrate species, a phenotypically similar

model can only be reproduced in MNU-treated hamsters (Taomoto et al., 1998). When Syrian golden hamsters received a single IP injection of 90 mg/kg MNU at 7 weeks of age, photoreceptor cell apoptosis developed 24 h after the treatment and resulted in photoreceptor cell loss at day 7. On day 5, when the photoreceptor cells were almost lost, the migration of RPE cells to the photoreceptor layer started. After day 7, and during 2–20 weeks after MNU injection, RPE cells migrated and reached all layers of the retina, and some were in contact with retinal vessels (Fig. 5.7A–B). Rhodopsin knockout ($rho^{-/-}$) mice on a C57BL/6 background, a murine homolog of an autosomal recessive form of human RP, completely lack rod outer segments and functional rods. Rod photoreceptor cells are quickly lost in these mice, followed by progressive cone degeneration at approximately 3 months of age (Jaissle et al., 2010). After the loss of all photoreceptor cells, the inner retinal vessels are in direct
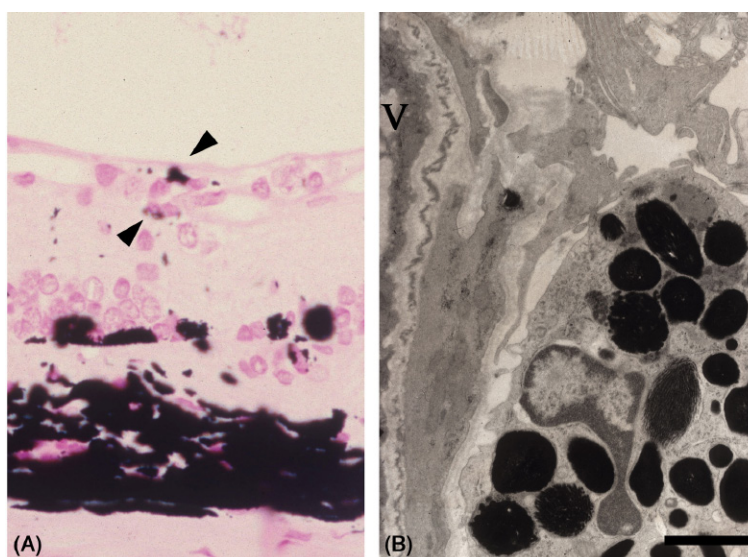
FIGURE 5.7　**Bone spicule pigment formation in 90 mg/kg MNU-treated Syrian golden hamster 20 weeks after MNU treatment.** (A) Note translocated Fontana-Masson-positive cells *(arrowheads)* are in contact with an intraretinal blood vessel (Fontana-Masson). (B) Translocated pigment epithelial cells are in contact with basal lamina of a retinal vessel (V). Bar = 1 μm. *Reprinted with permission from Taomoto, M., et al., 1998. Graefe's Arch. Clin. Exp. Ophthalmol. 236(9), 688–695.*

contact with migrated RPE cells. Different results were found in conventional C57BL mice treated with 60 mg/kg MNU and monitored for 21 days. The photoreceptor nuclei and rod/cone layer were destroyed, resulting in the inner nuclear layer being in direct contact with RPE cells. A single layer of RPE cells was preserved above Bruch's membrane. There was no evidence of RPE cell migration far into the retina, and the RPE cells did not contact the intraretinal vessels (Yuge et al., 1996). Thus, the rhodopsin knockout genotype may be involved in the bone-spicule phenotype in C57BL mice. Although the fate of RPE cells differs among species, photoreceptor cell loss by apoptosis is the primary event in human RP and MNU-induced retinal degeneration in animals.

6 MOLECULAR MECHANISMS IN PHOTORECEPTOR CELL DEATH CAUSED BY MNU

6.1 DNA Adduct Formation

Photoreceptor cell death is the major hallmark of RP, although the mechanisms leading to photoreceptor apoptosis remain poorly understood. MNU is an alkylating agent that interacts with DNA to yield a variety of reaction products. The predominant adduct (70%–90%) following the reaction of methylating agents with DNA is at the 7-position of guanine, which yields the 7-methyldeoxyguanosine (7-medGua) adduct (Degan et al., 1988). While 7-medGua does not appear to be directly mutagenic, it is useful for the detection of methylating agent

exposure because it is more stable than mutagenic O^6-methyldeoxyguanosine. Immunohistochemically, 7-medGua DNA adducts were selectively detected in the photoreceptor cell nuclei of F344 and Sprague-Dawley rats and C57BL mice 3, 6, 12, and 24 h after MNU exposure, with a gradual decrease at days 3 and 7 (Kiuchi et al., 2002; Ogino et al., 1993; Yoshizawa et al., 1999). Accumulated DNA adducts in the photoreceptor cell nuclei might suppress DNA synthesis, causing photoreceptor cell death. After DNA adduct accumulation, photoreceptor cell apoptosis was confirmed by DNA laddering, TUNEL signals, and ultrastructural nuclear images.

6.2 PARP Activity

Poly(ADP-ribose) polymerase (PARP) is an abundant nuclear enzyme involved in DNA repair. DNA damage induced by alkylating agents activates PARP, which repairs DNA damage by using nicotinamide adenine dinucleotide (NAD^+) as a substrate (Carson et al., 1986). PARP hyperactivation results in the depletion of cellular NAD^+ pools, leading to ATP deficiency, energy loss, and subsequent cell death. After Sprague-Dawley rats were treated with 60 mg/kg MNU, the PARP activity in retinas, as evaluated by the expression of poly(ADP-ribose) (PAR), which is the product of PARP, increased at 12 and 24 h and peaked at 72 h. PAR immunoreactivity at 24 h was restricted to degenerative photoreceptor cell nuclei (Uehara et al., 2006). PARP overactivation is also observed in photoreceptor cells of P23H and S344ter transgenic rats carrying rhodopsin mutations (Kaur et al., 2011). In retinal explant cultures derived

from PARP knockout and wild-type animals, the wild-type retina subjected to *Pde6b* inhibition to imitate the *rd* mouse condition shows massive photoreceptor cell degeneration, while cell death is reduced in the PARP knockout culture (Sahaboglu et al., 2010). PARP activation plays a pivotal role in mediating photoreceptor cell apoptosis not only in the MNU model but also in an inherited mouse model of retinal degeneration. PARP regulates transcription through its interaction with transcription factors, such as nuclear factor-κB (NF-κB) and activator protein-1 (AP-1) (Aguilar-Quesada et al., 2007; Andreone et al., 2003; Chiarugi, 2002; Skaper, 2003).

6.3 Transcription Factors

Transcription factors serve as pivotal regulators of cell survival or cell death. NF-κB is a ubiquitous transcription factor that acts as a master regulator of stress responses and plays an essential role in cell injury. NF-κB activity is regulated at multiple levels (Vermeulen et al., 2002). In its latent form in the cytoplasm, NF-κB is bound to IκB, which prevents its translocation into the nucleus. Phosphorylation of IκB at serine 32 is necessary for the release of active NF-κB. Phosphorylation of the NF-κB p65 subunit at serine 276 is necessary for NF-κB to be constitutively active in the nucleus and exert efficient transcriptional activity. The administration of 60 mg/kg MNU to Sprague-Dawley rats did not increase the phosphorylated-IκB (serine 32) protein levels. However, phosphorylated-NF-κB (serine 276) protein levels were significantly decreased 12, 24, and 72 h after MNU administration (Miki et al., 2007). NF-κB is constitutively active in cultured 661W mouse photoreceptor cells, and light exposure decreases NF-κB activity, leading to photoreceptor cell death; thus, the preservation of NF-κB activity in photoreceptor cell nuclei is necessary for photoreceptor cells survival (Krishnamoorthy et al., 1999). In contrast, the activation and nuclear translocation of NF-κB p65 occurs during the course of the retinal degeneration of *rd* mice (Zeng et al., 2008). NF-κB activation can induce both anti- and proapoptotic effects, depending upon the specific model of retinal degeneration and the pathological stimuli.

AP-1 is a dimeric complex mainly composed of c-Jun and c-Fos, and it is closely associated with intracellular signals for cell cycle, differentiation, and apoptosis. Increased AP-1 activity in the retinas of light-exposed c-fos^{+/+} mice implicates the contribution of AP-1 to apoptosis induction. Retinas from c-fos^{−/−} mice have unchanged AP-1 activity and are resistant to apoptosis. These results indicate that c-Fos is essential for the light-induced apoptotic pathway (Wenzel et al., 2000). A gene expression analysis of retinas from MNU-treated rats, consisting of microarray analysis and real-time RT-PCR, showed that c-Fos was upregulated by MNU (Yang

et al., 2007). However, in contrast to light exposure, MNU exposure causes photoreceptor apoptosis in both c-fos^{+/+} and c-fos^{−/−} mice (Wenzel et al., 2000). c-Jun and the phosphorylation of its N-terminus at serine 63 and serine 73 by c-Jun N-terminal kinase (JNK) are associated with neural apoptosis (Estus et al., 1994; Xia et al., 1995). In parallel to photoreceptor cell apoptosis induced by a single IP injection of 60 mg/kg MNU to Sprague-Dawley rats, the phosphorylation of JNK peaked at 12 h and the phosphorylation of c-Jun peaked at 24 h, followed by a gradual decrease. The induction of AP-1 (c-Jun and c-Fos) was observed at 12 h, peaked at 24 h, and then gradually decreased at 3 and 7 days. These results indicate the importance of JNK/AP-1 in the MNU-induced apoptotic pathway (Uehara et al., 2006). However, in an apparent contradiction, phosphorylated c-Jun is not required for MNU-induced photoreceptor apoptosis in mice (Grimm et al., 2001). The lack of a requirement for phosphorylated c-Jun may be due to the shorter observation period (2 h after MNU exposure) or species differences. NF-κB and JNK are closely linked, and JNK plays a key role by interacting with the Bcl-2 family of apoptosis regulator proteins (Liu and Lin, 2005; Okuno et al., 2004).

p53 is a transcription factor that plays a crucial role against genotoxic stress and is a major regulator of cell death in response to DNA damage (Donehower and Bradley, 1993). Eight-week-old p53^{−/−}, p53^{+/−}, and p53^{+/+} mice generated in 129/Sv-derived embryonic stem cells backcrossed onto a C57BL background received an IP injection of 60 mg/kg MNU and were sacrificed after 7 days (Yoshizawa et al., 2009). Regardless of the p53 gene status, equivalent levels of photoreceptor cell loss were observed, indicating that MNU-induced photoreceptor cell degeneration was p53-independent. In agreement with this observation, photoreceptor cell apoptosis is p53-independent in *rd* mice (Wu et al., 2001) and *rds* mice (Ali et al., 1998), as well as following light-induced retinal damage (Marti et al., 1998).

6.4 Bcl-2 Family Proteins

The Bcl-2 family proteins are important determinants of apoptosis. Bcl-xL and Bcl-2 prevent apoptosis, whereas Bax induces apoptosis. Sprague-Dawley rats were given a single IP injection of MNU. At 40 mg/kg, MNU caused upregulation of Bax and Bcl-xL, which peaked at 24 h. The Bax/Bcl-xL ratio also increased and peaked 24 h after MNU (Yang et al., 2007). At 60 mg/kg, MNU caused upregulation of Bax, which peaked after 72 h and remained high for 7 days, while Bcl-2 expression was unchanged (Uehara et al., 2006). However, it was reported that 60 mg/kg MNU caused upregulation of Bax and downregulation of Bcl-2 after 24 h (Xu et al., 2008). After 12 h, a 75 mg/kg dose of MNU caused downregulation of Bcl-2 and upregulation of Bax, which peaked 24 h after

MNU (Yoshizawa et al., 1999). Cell destructive stimuli caused by different levels of MNU may evoke varying effects on the Bcl-2 family proteins involved in apoptosis, but the proapoptotic/antiapoptotic ratio seems to rise after MNU injection.

6.5 Caspase Activation

Caspases (cysteine aspartate-specific proteases) coordinate and execute the apoptotic process. The substrates cleaved by caspases include members of the Bcl-2 family of apoptosis regulator proteins. The caspase family plays a decisive role in the execution of retinal apoptosis in that the caspase-3/CPP32, caspase-6/Mch2, and caspase-8/FLICE protease activities peaked 72 h after 75 mg/kg MNU administration to Sprague-Dawley rats (Yoshizawa et al., 1999). Similarly, in 40 mg/kg MNU-treated Sprague-Dawley rats, caspase-3 activity significantly increased at 24 h, peaked at 72 h, and decreased at day 7 (Gao et al., 2010). However, in 45 mg/kg MNU-treated C57BL mice, caspase-3-positive staining and a change in caspase-3 mRNA values were not detected at 1, 3, and 7 days after MNU treatment (Zulliger et al., 2011). Other apoptotic pathways may be involved in MNU-damaged photoreceptor cells.

6.6 Calcium Overload and Calpain Activation

Cytotoxic stimuli result in a massive calcium (Ca^{2+}) influx into the target cells, and increased cellular Ca^{2+} concentrations cause calpain (calcium-dependent cysteine protease) activation (Goll et al., 2003). Ca^{2+} overload, calpain activation, and increased caspase-3 activity occur in the rd model of photoreceptor degeneration (Doonan et al., 2005; Sharma and Rohrer, 2004). Ca^{2+} influx, membrane depolarization, and energetic collapse caused by a depletion of ATP and NAD^+ are frequently associated with neuronal cell death (Kristián and Siesjö, 1998; Nicholls and Ward, 2000). PARP overactivation and the resulting energetic collapse trigger apoptosis-inducing factor (AIF)-mediated photoreceptor cell death in rd mice (Paquet-Durand et al., 2007). Calpain does not directly cause chromatin condensation, but an activated form of AIF participates in DNA fragmentation and photoreceptor cell death (Sanges et al., 2006). DNA damage-induced PARP activation further dysregulates Ca^{2+}, resulting in calpain activation and AIF induction, which are followed by cell death (Vosler et al., 2009). In 60 mg/kg MNU-treated Sprague-Dawley rat retina, total retinal Ca^{2+} significantly increases 24 h after MNU treatment and continuously increases over 7 days, compared with MNU-untreated rat retina (Oka et al., 2007). The 280 kDa intact form of α-spectrin is ubiquitously localized in both the inner and outer retina, and calpain activity can be detected by the presence of calpain-induced

α-spectrin proteolysis products at 150 kDa (proteolyzed by caspase-3 and calpain) and 145 kDa (proteolyzed by calpain) (Shimazawa et al., 2010). In the retinas of BALB/c mice, calpain activity was increased 24 h after 60 mg/kg MNU treatment (Kuro et al., 2011). In the retinas of 60 mg/kg MNU-treated Sprague-Dawley rats, total retinal Ca^{2+} significantly increases and calpain activity dramatically increases at 1 and 3 days after MNU administration, respectively, and these levels decrease at day 7 (Oka et al., 2007). Cyclin-dependent kinase 5 (Cdk5) is a protein serine/threonine kinase requiring the regulatory subunit p35 for activity (Lew et al., 1994; Tsai et al., 1994). Conversion of p35 to p25 by calpain and prolonged activation of Cdk5/p25 may be a possible downstream mechanism for photoreceptor cell death (Oka et al., 2007). The calpain cascade is involved in retinal degeneration after MNU treatment, as well as in rd retina.

6.7 Reactive Oxygen Species Production

Oxidative stress contributes to the pathogenesis of neurodegenerative disorders, and reactive oxygen species (ROS) production in response to oxidative stress is implicated in photoreceptor cell death, including retinal DNA damage in rd mice (Sanz et al., 2007). When 100 μg/mL MNU is added to cultured murine 661W photoreceptor-derived cells or mouse RGC-5 ganglion cell line, MNU induces radical generation (as measured by intracellular ROS levels) in 661W cells, but not in RGC-5 cells. Oxidative stress is involved in photoreceptor cell death in MNU-induced retinal degeneration in rodents (Emoto et al., 2013, 2014; Tsuruma et al., 2012). MNU treatment increases the levels of the oxidative stress markers 8-hydroxy-2-deoxyguanosine (8-OGdG) and heme oxygenase-1 (HO-1) compared with untreated controls (Emoto et al., 2013, 2016b). Thus, MNU selectively elevates ROS in photoreceptor cells and induces photoreceptor cell death in vitro and in vivo.

6.8 Autophagic Cascade

Microtubule-associated protein light chain 3 (LC3), which is the mammalian homolog of yeast Atg8, is the best-characterized autophagic marker. LC3 has two forms, LC3-I (18 kDa), which is localized to the cytosol, and its proteolytic derivative, LC3-II (16 kDa), which is localized to the autophagosome membrane (Kabeya et al., 2000). LC3-II levels have been correlated to the number of autophagosomes and autophagic activity (Kabeya et al., 2000; Mizushima, 2004). In BALB/c mice treated with 60 mg/kg MNU, caspase-3 activity gradually increased, while LC3 activity gradually decreased during 72 h after MNU administration (Fig. 5.8). In contrast to the gradual increase in apoptosis, the gradual decrease in
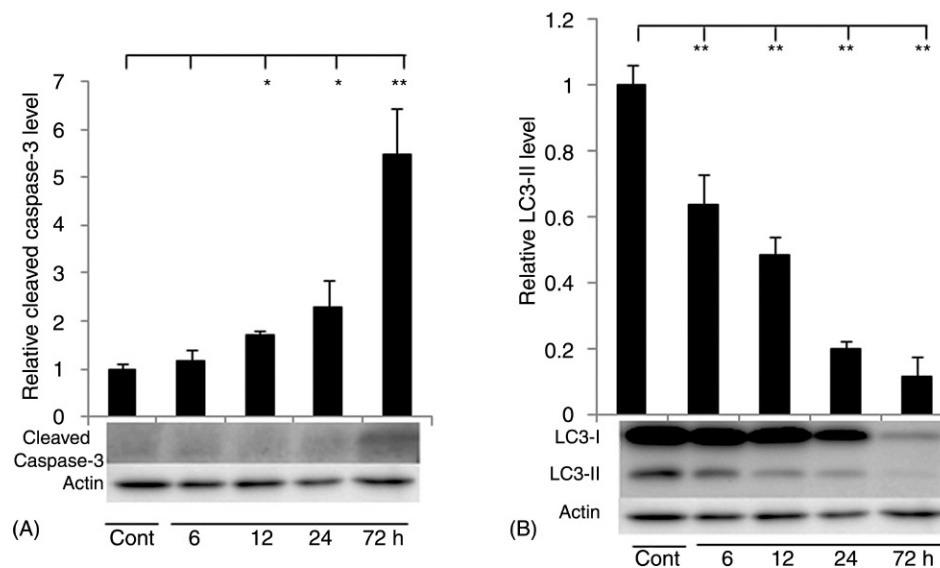
FIGURE 5.8 *N*-methyl-*N*-nitrosourea (MNU, 75 mg/kg) accelerates apoptosis and suppresses autophagy in BALB/c mouse retina. Over the 72 h post-MNU treatment period: (A) Caspase-3 expression is gradually increased. (B) LC3 expression is gradually decreased. *Source: Reprinted with permission from Kuro, M., et al., 2011. In Vivo, 25(4), 625–631.*

basal autophagy was noteworthy in the course of MNU-induced retinal degeneration. In normal photoreceptor cells, besides the intermittent disk shedding from the outer segments, autophagy functions as a degradative pathway in photoreceptor cell metabolism. As shown in Fig. 5.5, autophagic vacuoles are mainly encountered in the myoid region of the inner segment of the photoreceptor cells with dense material (Remé et al., 1999). The loss of autophagosomes and autolysosomes in MNU-treated mouse retinas, as determined by electron microscopy, indicates the suppression of basal autophagy (Kuro et al., 2011). The role of autophagy in cell death is controversial. However, in quiescent cells, such as neurons, the suppression of basal autophagy causes neurodegeneration in mice (Hara et al., 2006); thus, autophagy in neuronal cells plays a cell-protective role. Therefore, both increased apoptosis and decreased autophagy may accelerate the MNU-induced photoreceptor cell death in mice.

Possible death signals caused by MNU are summarized in Fig. 5.9. MNU causes DNA adduct formation restricted to photoreceptor cell nuclei, followed by increased PARP activity that leads to the inactivation of NF-κB and activation of JNK/AP-1, causing downregulation of Bcl-2, upregulation of Bax, and the activation of caspase-3, -6, and -8. Also, calpain activity is increased by Ca^{2+} dysregulation, leading to the prolonged activation of Cdk5/p25. Together, these observations indicate that the generation of ROS is involved in photoreceptor cell apoptosis. MNU also suppresses basal autophagy, which may also contribute to the acceleration of photoreceptor apoptosis. These molecular events may partially explain

MNU-induced photoreceptor cell apoptosis. Fig. 5.9 also shows possible strategies for photoreceptor rescue with therapeutic agents.

7 THERAPEUTIC TRIALS AGAINST MNU-INDUCED PHOTORECEPTOR APOPTOSIS

7.1 PARP Inhibitors

Our laboratory performed therapeutic trials in an MNU-induced animal model for RP, and the results are summarized in Table 5.2. Seven- or 3-week-old animals received 40–60 mg/kg MNU. Nicotinamide (NAM), a water-soluble B group vitamin (vitamin B3/niacin), was SC injected at a dose of 1000, 25, 10, or 0 mg/kg immediately after 60 mg/kg MNU administration, and animals were sacrificed 7 days later. NAM significantly suppressed MNU-induced photoreceptor cell loss in a dose-dependent manner (Kiuchi et al., 2002), as evaluated by the photoreceptor cell ratio [(photoreceptor cell thickness/total retinal thickness) ×100] in HE-stained sections of the central retina (Yoshizawa et al., 2000). The photoreceptor cell ratio after treatment with 1000, 25, 10, and 0 mg/kg NAM was 33, 34, 22, and 6%, respectively. The percent inhibition of the photoreceptor cell ratio, which was determined as [(NAM-treated—NAM-untreated animals)/NAM-treated animals) × 100], was 82, 82, and 73% in the 1000, 25, and 10 mg/kg NAM-treated groups. Treatment with 1000 mg/kg NAM yielded no side effects. Functionally, scotopic and photopic ERGs
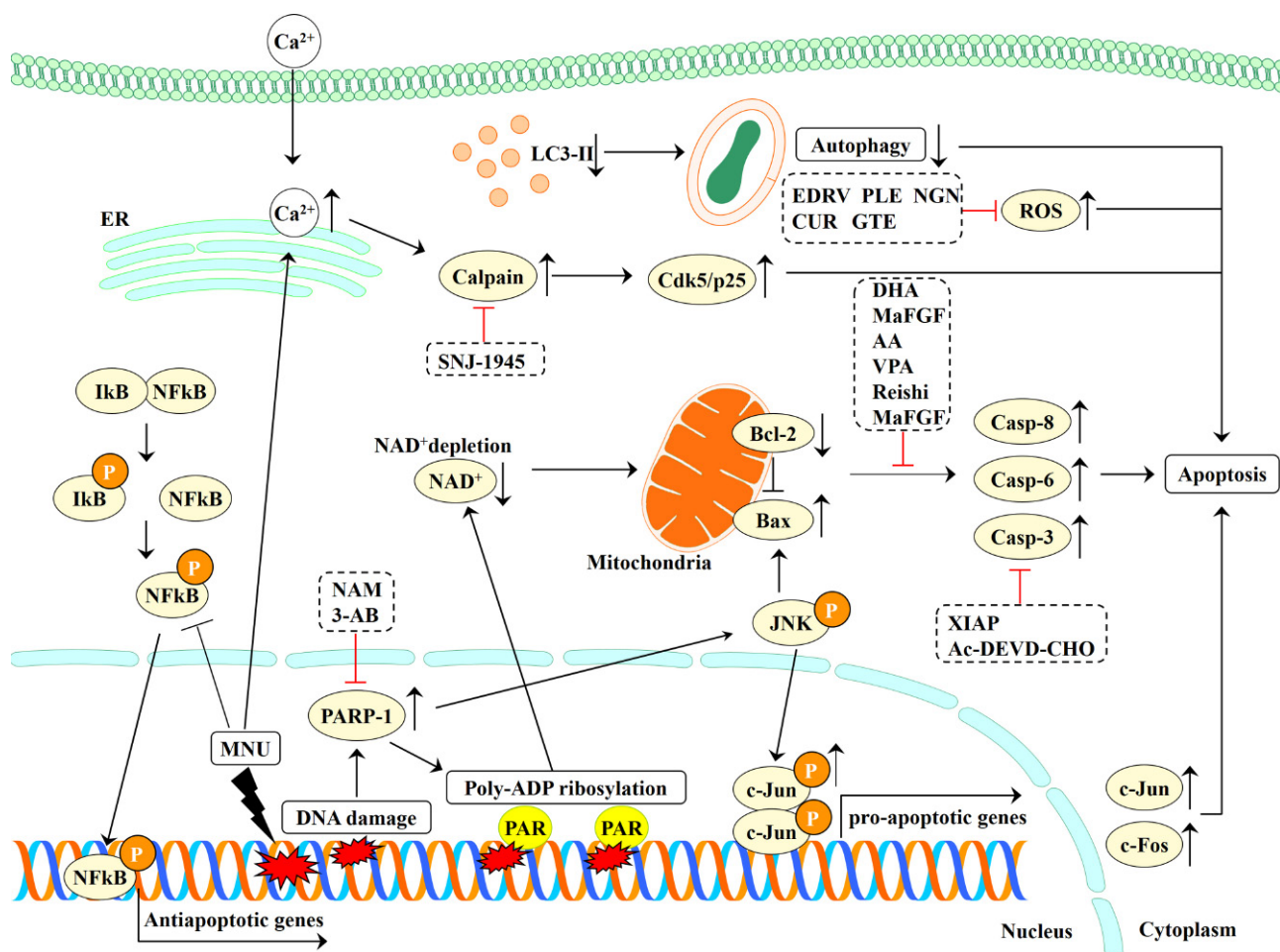
FIGURE 5.9 Possible molecular signaling events occurring in response to MNU-induced photoreceptor apoptosis and therapeutic intervention. *AA*, Arachidonic acid; *3-AB*, 3-aminobenzamide; *Ac-DEVD-CHO*, caspase-3 inhibitor; *CUR*, curcumin; *DHA*, docosahexaenoic acid; *EDRV*, edaravone; *GTE*, green tea extract; *MaFGF*, mutant of acidic fibroblast growth factor; *NAM*, nicotinamide; *NGN*, nargenin; *PLE*, persimmon leaf extract; *Reishi*, Ganoderma lucidum; *SNJ-1945*, calpain inhibitor; *VPA*, valproic acid; and *XIAP*, X-linked inhibitor of apoptosis.

showed that 1000 mg/kg NAM protected both rods and cones from MNU damage (Kiuchi et al., 2003). The suppression of photoreceptor cell loss by 1000 mg/kg NAM was confirmed structurally and functionally. Moreover, NAM at a dose of 1000 mg/kg significantly suppressed photoreceptor cell loss when administered up to 6 h after MNU; however, NAM administered 12 h after MNU was ineffective (Kiuchi et al., 2002). NAM did not reduce the levels of 7-medGua DNA adducts. Therefore, NAM did not prevent DNA damage; rather, the DNA damage appeared to be repaired. NAM, a precursor of NAD$^+$, may block the depletion of NAD$^+$ or inhibit PARP activation (Purnell and Whish, 1980). When 1000 mg/kg NAM was administered at the same time as MNU, PARP activation was diminished, and the level of downstream JNK/AP-1 expression was compatible to that in untreated animals (Uehara et al., 2006). Therefore, the mechanism by which NAM suppressed MNU-induced retinal damage involved PARP inhibition through the JNK/AP-1 signaling

pathway. These results indicate that PARP inhibition can block MNU-induced photoreceptor cell apoptosis. The beneficial effect of PARP inhibition against MNU injury was confirmed by using the PARP inhibitor 3-aminobenzamide (3-AB).

3-AB suppressed 60 mg/kg MNU-induced photoreceptor apoptosis (Miki et al., 2007). An SC injection of 50 or 30 mg/kg 3-AB, administered concurrently with MNU, significantly suppressed photoreceptor cell loss. The photoreceptor cell ratio after treatment with 50, 30, and 0 mg/kg 3-AB was 48, 38, and 18%, respectively. The percent inhibition of the photoreceptor cell ratio was 63 and 53% in the 50 and 30 mg/kg 3-AB-treated groups, respectively. Retinal damage can also be expressed as the retinal damage ratio [(length of damaged retina/whole retinal length) × 100] (Yoshizawa et al., 2000). Damage to the retina was defined as the presence of less than four rows of photoreceptor nuclei in the outer nuclear layer. The retinal damage ratio was 0, 11, and 70% in animals

TABLE 5.2 Percent Inhibition of Retinal Damage After Therapeutic Trials of Different Agents Against MNU Injury in Rats and Mice

| | Animal | MNU | Test chemicals | | | Photoreceptor cell ratio (%) | | Retinal damage ratio (%) | | |
Spices	Age (weeks)	Dose		Dose	Frequency/duration	Route	Untreated/ treated	Inhibition (%)	Treated/ untreated	Inhibition (%)	References
Rat	7	60	NAM	1000 mg/ kg BW	×1	SC	6/33	82			Kiuchi et al. (2003)
				25 mg/kg BW	×1	SC	6/34	82			
				10 mg/kg BW	×1	SC	6/22	73			
Rat	7	60	3-AB	50 mg/kg BW	×1	SC	18/48	63	0/70	100	Miki et al. (2007)
				30 mg/kg BW	×1	SC	18/38	53	11/70	84	
Rat	7	60	AC-DEVD-CHO	4000 ng	×2	IVT	3/12	75	54/99	45	Yoshizawa et al. (2000)
Mouse	7	60	SNJ-1945	80 mg/kg BW	×8	IP	20/34	41	35/79	56	Kuro et al. (2011)
Rat	7	60	DHA	9.5% w/w·diet	14 days before MNU	PO			38/88	57	Moriguchi et al. (2004)
				9.5% w/w·diet	7 days after MNU	PO			46/88	48	
				9.5% w/w·diet	14 days before and 7 days after MNU	PO			47/88	47	
Rat	3	50	AA	0.50% w/w·diet	28 days before MNU	PO	19/47	60	3/40	93	Yoshizawa et al. (2013)
				2.01% w/w·diet	28 days before MNU	PO	19/44	57	6/40	85	
Rat	7	40	CUR	200 mg/kg BW	×10	IP	5/23	78	37/66	44	Emoto et al. (2013)
Rat	7	40	GTE	250 mg/kg BW	×10	PO	10/17	41	61/88	31	Emoto et al. (2014)

Animals received intraperitoneal injection of MNU and were sacrificed 7 days later; photoreceptor cell ratio at the central retina is calculated as (photoreceptor cell thickness/total retinal thickness) × 100; percent inhibition of photoreceptor cell ratio is calculated as the photoreceptor cell ratio as [(reagent-treated–untreated animals)/reagent-treated animals × 100]. Retinal damage ratio is calculated as [(retinal length composed of less than four rows of photoreceptor cells/total retinal length) × 100]; Percent inhibition of retinal damage ratio is calculated as the retinal damage ratio in [(untreated–reagent-treated animals)/ untreated animals × 100]. *AA*, Arachidonic acid; *3-AB*, 3-aminobenzamide; *Ac-DEVD-CHO*, caspase-3 inhibitor; *BW*, body weight; *CUR*, curcumin; *DHA*, docosahexaenoic acid; *GTE*, green tea extract; *IP*, intraperitoneal; *IVT*, intravitreal; *NAM*, nicotinamide; *PO*, peroral; *SC*, subcutaneous; *SNJ-1945*, calpain inhibitor. All values (photoreceptor cell ratio and retinal damage ratio) were statistically significant between treated and untreated groups.

that received 50, 30, and 0 mg/kg 3-AB, respectively. MNU-induced retinal damage proceeds from the central retina to the peripheral retina, indicating that 3-AB suppressed and/or delayed the progression of photoreceptor cell damage. 3-AB treatment preserved NF-κB activity and resulted in photoreceptor cell survival (Miki et al., 2007). In contrast to NAM (Kiuchi et al., 2002), 3-AB administration 4 or 6 h after MNU did not rescue photoreceptor damage (Miki et al., 2007). NAM is a PARP inhibitor, a NAD^+ precursor, and a vasodilator (Huang and Chao, 1960). Thus, in addition to PARP inhibition, the two other mechanisms may also contribute to the retinal protection provided by NAM. PARP is activated in rd retinas, and the PARP inhibitor (N-(6-oxo-5,6-dihydrophenanthridin-2-yl)-N,N-dimethylacetamide × HCl) (PJ34) has a therapeutic effect in an ex vivo model with rd retinal explants (Paquet-Durand et al., 2007). Thus, PARP inhibition can be included in RP therapy.

7.2 Caspase Inhibitors

It is theoretically possible to suppress photoreceptor cell apoptosis by inhibiting the apoptosis cascade. The apoptosis cascade converges on a family of cysteine proteinases known as caspases. X-linked inhibitor of apoptosis (XIAP) inhibits caspases 3, 7, and 9 to confer resistance to apoptosis (Liston et al., 1996). Subretinal injection of recombinant adeno-associated virus encoding XIAP 6 weeks prior to 60 mg/kg MNU administration suppresses MNU-induced photoreceptor cell apoptosis structurally and functionally when examined 24, 48, and 72 h, and 7 days after MNU administration (Petrin et al., 2003). Overall, XIAP-treated eyes show histologic protection of the outer nuclear layer in 66% (4/6) of the rats at each time point. XIAP-treated eyes in 2 of 4 animals showing morphologic protection had a diminished but recordable ERG response. XIAP gene therapy is effective against photoreceptor cell apoptosis caused by genetic mutation, as well as by MNU stress. P23H and S344ter rhodopsin transgenic rats carry rhodopsin mutations that affect the protein folding and sorting of rhodopsin, respectively. In these transgenic rats, XIAP gene therapy provides long-term neuroprotection of photoreceptor cells structurally and functionally by inhibiting the action of caspase-3, -7, and -9 (Leonard et al., 2007).

IVT administration of Z-YVAD-FMK and Z-DEVD-FMK, caspase-1/4 and 3/7 inhibitors, respectively, as well as Z-VAD-FMK, a broad spectrum caspase inhibitor, transiently suppresses photoreceptor apoptosis and preserves photoreceptor function in RCS rats (Perche et al., 2008). Z-VAD-FMK and Z-DEVD-FMK protect, while Z-YVAD-FMK shows no protective effect, against light-induced retinal degeneration in rats (Perche et al., 2007). In rd/caspase-3 double-mutant mice, although rods eventually die in the absence of caspase-3,

the lack of caspase-3 does not abolish but reduces the number of apoptotic cells (Zeiss et al., 2004). Ac-DEVD-CHO, a caspase-3 inhibitor, was IP administered at a dose of 2 mg/kg to rd mice every other day from 8 days of age (Yoshizawa et al., 2002). Photoreceptor cells were significantly preserved in Ac-DEVD-CHO-treated mice at 13 days of age, but the effect was lost at 17 days of age. Thus, the caspase-3 inhibitor transiently delayed the progression of retinal degeneration in rd mice. In Sprague-Dawley rats, two IVT injections of 4000 ng Ac-DEVD-CHO dissolved in PBS were administered 0 and 10 h after the IP administration of 60 mg/kg MNU (Yoshizawa et al., 2000). Ac-DEVD-CHO suppressed MNU-induced photoreceptor cell apoptosis as evaluated by TUNEL labeling 24 h after MNU and ameliorated retinal damage 7 days after MNU administration. The TUNEL index 24 h post-MNU was 79.5% in the peripheral retina and 83.7% in the central retina, while Ac-DEVD-CHO significantly reduced the TUNEL index to 59.7 and 71.8%, respectively. Total retinal thickness and outer retinal thickness 7 days after MNU was 38 and 2 μm in the peripheral retina and 75 and 2 μm in the central retina, respectively, while Ac-DEVD-CHO treatment increased these values to 71 and 31 μm and 77 and 9 μm, respectively. The retinal damage ratio 7 days after MNU administration was significantly decreased from 99% to 54% by Ac-DEVD-CHO treatment. Caspase inhibitors are likely to be useful for the treatment of human RP. However, apoptotic retardation in the absence of caspase-3 implies the presence of caspase-independent mechanisms (Doonan et al., 2003).

7.3 Calcium Channel Blockers

Apoptotic photoreceptor cells in rd mice have increased levels of intracellular calcium (Doonan et al., 2005). In rd mice, the calcium channel blockers D-cis-diltiazem (Frasson et al., 1999) and nilvadipine (NVP; 5-isopropyl-3-methyl 2-cyano-1,4-dihydro-6-methyl-4-(3-nitrophenyl)-3,5-pyridinedicarboxylate) (Takano et al., 2004) are able to preserve photoreceptor cells from degeneration. NVP also delays apoptotic progression of photoreceptor cells in rds mice (Takeuchi et al., 2008). In 75 mg/kg MNU-treated Lewis rats, daily IP administration of 0.05 mg/kg NVP starting 7 days before MNU until 1 or 3 days after MNU provides no retinal protection at 1 and 3 days after MNU (Maruyama et al., 2001). The ineffectiveness of NVP in the MNU model may be explained by the use of a higher dose of MNU (75 mg/kg instead of 60 mg/kg), which might have caused excessive DNA damage in photoreceptor cells that was beyond the rescue capacity. Therefore, we repeated the experiment in Sprague-Dawley rats that received daily IP administration of 0.1 or 1.0 mg/kg NVP dissolved in a mixture of ethanol:polyethylene glycol 400:distilled water (2:1:7).

The NVP treatment was started 7 days before the administration of 60 mg/kg MNU and continued until 7 days after MNU administration. Again, retinal protection was not achieved (unpublished observation).

7.4 Calpain Inhibitors

Although the calpain inhibitor *N*-acetyl-leu-leu-norleucinal (ALLN) does not protect against photoreceptor degeneration in *rd* retinal explants (Doonan et al., 2005), the calpain inhibitors ALLN and *N*-acetyl-leu-leu-methioninal (ALLM) prevent the activation of AIF and reduce apoptosis in *rd* mice photoreceptor cells in vivo. The knockdown of AIF expression completely blocks apoptosis in *rd* photoreceptor cells in vitro (Sanges et al., 2006). In *RCS* rats, the calpain inhibitors ALLN and PD150606 effectively inhibit photoreceptor apoptosis (Mizukoshi et al., 2010), while Mu-Phe-hPhe-FMK (MuhPhe) does not reduce photoreceptor apoptosis (Perche et al., 2008). The calpain inhibitor ((1S)-1-[([(1S)-1-benzyl-3-cyclopropyl-amino-2,3-di-oxopropyl]amino)carbonyl]-3-methylbutyl) carbamic acid 5-methoxy-3-oxapentyl ester (SNJ-1945) has good penetration into the retina when perorally (PO) administered (Shirasaki et al., 2006) and has a low level of side effects (Oka et al., 2006). At a dose of 100 mg/kg IP or 200 mg/kg PO 30 min before and just after light exposure, SNJ-1945 significantly protects photoreceptor cell loss in ddY mice (Imai et al., 2010). In 60 mg/kg MNU-treated BALB/c mice, 80 mg/kg SNJ-1945 was administered IP 3 h prior to MNU and thereafter once daily for 7 days (Kuro et al., 2011). The photoreceptor cell loss was significantly prevented as compared with MNU-treated mice that did not receive SNJ-1945. The photoreceptor cell ratio at the central retina (20.0± 2.1 vs. 33.7± 4.6) and the retinal damage ratio (79.3± 6.4 vs. 34.5± 12.7) revealed that the photoreceptor cell preservation caused by SNJ-1945 was significant. In MNU-treated Sprague-Dawley rats, a retinal protective effect was observed with PO administration of 200 mg/kg SNJ-1945 within 30 min after MNU, and once daily for 7 days (Oka et al., 2007). Thus, both IP and PO administration of SNJ-1945 is effective, and SNJ-1945 ameliorates MNU-induced photoreceptor cell loss in rats and mice.

7.5 Polyunsaturated Fatty Acids

Although there are no established standard treatment modalities for RP, vitamin A and DHA supplementation slows the progression of retinal degeneration in RP patients (Shintani et al., 2009). Patients with RP had mean decreased values of red blood cell DHA concentrations, and serum levels were correlated with retinal levels. Decreased amounts of DHA and arachidonic acid (AA) in plasma phospholipids are observed in Usher syndrome (Bazan et al., 1986). Photoreceptor membranes are richly endowed with DHA (22:6n-3), an n-3 PUFA, and AA (20:4n-6), an n-6 PUFA, indicating that these fatty acids play an integral role in photoreceptor cells. *rd* mice have lower levels of DHA in the retina and in photoreceptor cells (Scott et al., 1988). Seven-week-old Sprague-Dawley rats were fed an AIN-76A (basal) diet or a DHA diet, in which 5% corn oil and 5% corn starch from the AIN-76A diet were replaced by 9.5% DHA and 0.5% linoleic acid (LA), for 2 weeks. Then, the rats received 60 mg/kg MNU and continued to receive the same diet or were switched to the opposite diet for 3 or 7 days until they were sacrificed (Moriguchi et al., 2004). Three days after MNU administration, the progression of photoreceptor damage was delayed in parallel with serum DHA levels. Seven days after MNU administration, although the damage was not delayed in parallel with serum DHA levels, the retinal damage ratio was significantly lower in rats fed DHA at some point compared to rats fed the basal diet throughout the experimental period. The retinal damage ratio was 38% in rats who received the DHA diet for 14 days before MNU administration, 46% in rats who received the DHA diet 7 days after MNU administration, and 47% in rats who received the DHA diet 14 days before and 7 days after MNU administration; in contrast, the retinal damage ratio was 88% in rats who received the basal AIN-76A diet (without DHA) throughout the experimental period. Thus, the DHA diet likely delayed the onset and suppressed the progression of photoreceptor cell apoptosis. DHA interferes with pro- and antiapoptotic proteins of the Bcl-2 family and protects photoreceptor cells from apoptosis (Rotstein et al., 2003).

Seven-week-old Sprague-Dawley rats were given MNU at a dose of 50 mg/kg, which is lower than the dose needed to cause photoreceptor cell loss within 7 days in all treated animals. Thereafter, the rats received one of five diets containing the following fatty acids: 10% LA (LA diet); 9.5% palmitic acid (PA) and 0.5% LA (PA diet); 9.5% eicosapentaenoic acid (EPA) and 0.5% LA (EPA diet); 4.75% EPA, 4.75% DHA, and 0.5% LA (DHA plus EPA diet); or 9.5% DHA and 0.5% LA (DHA diet) (Moriguchi et al., 2003). The rats were observed for 20 weeks after MNU administration. The degree of retinal lesions varied significantly among the five diet groups. The incidence of retinal damage [(number of rats with retinal degeneration/total number of rats) ×100] and the retinal damage ratio for each diet was: LA diet, 88 and 61%; PA diet, 41 and 18%; EPA diet, 73 and 40%; EPA plus DHA diet, 53 and 24%; and DHA diet, 0 and 0%, respectively. Thus, the DHA diet completely suppressed retinal damage, while the EPA diet, which is rich in another n-3 PUFA, did not suppress retinal damage. The DHA plus EPA diet had a weaker retinal protective effect, whereas the lesions were accelerated in rats fed the LA diet. DHA is significantly enriched in the retinas

of diurnal Sudanian grass rats as compared to the retinas of Brown-Norway rats, resulting in a relative resistance to MNU-induced damage (Boudard et al., 2011). Thus, the role of DHA in the adult retina seems to be important. In contrast to the beneficial effects of dietary DHA, conjugated DHA, a mixture of positional and geometric isomers of DHA, did not evoke beneficial effects against MNU-induced photoreceptor damage (unpublished observation). In cultured retinal neurons, DHA supplementation decreased photoreceptor cell death, whereas PA, oleic acid, or AA was unable to decrease photoreceptor cell death (Politi et al., 2001; Rotstein et al., 1996).

DHA and AA are highly concentrated in the phospholipid bilayer of biologically active brain and retinal neural membranes, and supplementation of DHA and AA may protect infants from visual problems (Brémond-Gignac et al., 2011). Lower levels of AA have been found in the retinas of *rd* mice (Cagianut et al., 1985). When *rd* mice were fed diets containing various doses of AA (control diet, 0.008% AA; low-dose AA diet, 0.13% AA; medium-dose AA diet, 0.50% AA; and high-dose AA diet, 2.01% AA) through the last 2/3 of pregnancy and the lactation period, the retinal degeneration of the pups sacrificed at 12 or 18 days of age was not affected (unpublished observation). Sprague-Dawley rats were fed diets containing various doses of AA (same diets as listed earlier) beginning 2 weeks prior to mating and continuing through gestation (3 weeks) and the lactation period (3 weeks). Then, the 3-week-old male pups were given 50 mg/kg MNU IP, fed the same diet their mothers had received for 1 week, and subsequently sacrificed (Yoshizawa et al., 2013). AA dose-dependently ameliorated retinal injury, as shown by the photoreceptor cell ratios and retinal damage ratios in each group: control diet, $19.4 \pm 11.9\%$ and $39.5 \pm 14.4\%$; low-dose AA diet, $32.0 \pm 16.2\%$ and $21.2 \pm 17.4\%$; medium-dose AA diet, $46.7 \pm 2.8\%$ and $2.7 \pm 3.7\%$; and high-dose AA diet, $43.6 \pm 8.8\%$ and $6.1 \pm 6.7\%$, respectively. The medium- and high-dose AA groups showed significant retinal improvement compared to the control diet group. Thus, AA supplementation ($\geq 0.5\%$ in the diet) during the prenatal, perinatal, and neonatal period is effective in suppressing MNU-induced retinal degeneration. Toward optimizing human vision, it has been recommended that infants receive at least 0.3% fatty acids from DHA with at least 0.3% AA (Hoffman et al., 2009). However, these AA diets given to 10-week-old male Sprague-Dawley rats for 6 weeks did not improve retinal damage caused by 60 mg/kg MNU administered at 15 weeks of age to animals that were sacrificed at 16 weeks of age. Thus, the role of AA in the infant retina (but not the adult retina) seems to be important.

Valproic acid (VPA), a short-chain fatty acid that is a heat shock protein (HSP) 70 inducer, suppresses MNU-induced photoreceptor cell death through inhibition of apoptotic caspase signals; HSP70 may also modulate photoreceptor apoptosis through the calpain pathway (Koriyama et al., 2014).

7.6 Health Supplements

Resveratrol (3,5,4'-trihydroxystilbene), a polyphenolic phytoalexin, is a naturally occurring product found in grape skin and red wine that has various bioactivities including anticarcinogenic effects (Nakagawa et al., 2001). Light-induced photoreceptor cell damage in BALB/c mice is significantly reduced both structurally and functionally by prior treatment with resveratrol at a dose of 50 mg/kg daily for 5 days by gastric intubation (Kubota et al., 2010). The retinal protective effect of resveratrol is via inhibition of retinal AP-1 activity as measured by c-Fos levels. However, seven daily doses of 50 mg/kg resveratrol dissolved in 0.3% carboxymethyl cellulose solution (administered PO from 3 days prior to 3 days after MNU administration) could not rescue retinal damage caused by 60 mg/kg MNU in Sprague-Dawley rats that were sacrificed and examined 7 days after MNU administration (unpublished observation).

Anthocyanins are plant pigments that are widely distributed in berries, dark grapes, cabbages, and other pigmented foods, plants, and vegetables. They belong to the widespread class of phenolic compounds collectively named flavonoids. Although the mechanisms of action have not been described, when anthocyanins extracted from black soybean seed coat (50 mg/kg/day) were PO administered daily for 4 weeks (but not 1 or 2 weeks) to 50 mg/kg MNU-treated 10-week-old male Sprague-Dawley rats, retinal damage was reduced, as determined by ERG responses and retinal morphology (Paik et al., 2012).

Ganoderma lucidum, known as Reishi or Lingzhi, is a medical mushroom used for more than 4000 years in China to promote health and longevity. Sprague-Dawley rats received ganoderma spore lipid (GSL) at a dose of 0, 0.5, 1, 2, and 4 g/kg each day for 3 days via the intragastric route; then, the rats received an IP injection of 40 mg/kg MNU and were sacrificed 1, 3, 7, or 10 days later (Gao et al., 2010). GSL at a dose of 2 g/kg inhibited the decrease of a- and b-wave amplitudes and suppressed photoreceptor cell apoptosis through Bax, Bcl-xl, and caspase-3 regulation. A daily 2 g/kg dose of GSL or 2 g/kg dose of fish oil (containing 70% n-3 PUFAs, of which DHA accounted for 54% and EPA for 7%) exerted a similar potency in suppressing MNU-induced retinal damage (Gao et al., 2011).

7.7 Neurotrophic Factors

Neurotrophic factors protect neurons and initiate their growth. These factors are neuroprotective in a

range of diseases including retinal disease (Thanos and Emerich, 2005). IVT injection of 500 ng of basic fibroblast growth factor (bFGF, FGF-2) in 1 μL PBS at 23 days of age when photoreceptor cell degeneration starts in *RCS* rats results in photoreceptor cell rescue 2 months after the injection (Faktorovich et al., 1990). IVT injection of 1150 ng of bFGF in 1 μL of PBS to F344 rats 2 h prior to constant light exposure reduces the progression of photoreceptor degeneration (Faktorovich et al., 1992). IVT injection of 1 μg of bFGF in 1 μL of PBS into BALB/c mice 3 h prior to light damage affords photoreceptor protection from light-induced damage (O'Driscoll et al., 2008). Acidic FGF (aFGF, FGF-1) ameliorates ischemic injury of the rat retina (Cuevas et al., 1998), but the use of aFGF requires caution because of its mitogenic activity (Galzie et al., 1997). In this context, mutant aFGF (MaFGF), which is a nonmitogenic form of human aFGF, has been developed and applied to the MNU model (Wu et al., 2005) by IVT injections at 0 and 12 h after MNU administration (Xu et al., 2008). In 60 mg/kg MNU-treated Sprague-Dawley rats, IVT administration of MaFGF at a dose of 1.25 and 2.5 μg protects MNU-induced retinal damage in rats 7 days after MNU through upregulating Bcl-2 and downregulating Bax. The apoptotic index 24 h post-MNU was 38.1 ± 3.6% in the peripheral retina, while it was 27.5 ± 2.5% and 21.1 ± 1.9% after MaFGF treatment at a dose of 1.25 and 2.5 μg, respectively. Total retinal thickness and outer retinal thickness 7 days after MNU in the peripheral retina were 37 ± 2 and 3 ±1 μm, while 1.25 and 2.5 μg MaFGF increased these values to 44 ± 2 and 15 ± 2 μm, and 55 ± 3 and 22 ± 2 μm, respectively. The central retina was beyond the rescue capacity of MaFGF treatment. The apoptotic index 24 h post-MNU was 38.1 ± 3.6% in the peripheral retina, while it was 27.5 ± 2.5% and 21.1 ± 1.9% after MaFGF treatment at a dose of 1.25 and 2.5 μg, respectively.

7.8 Antioxidants

Edaravone (EDRV) is a potent antioxidant and free-radical scavenger. At a dose of 1 μM, EDRV reduces MNU-induced free-radical production in cultured murine 661W photoreceptor-derived cells (Tsuruma et al., 2012). After adult ddY mice were treated by IP injection of 60 mg/kg MNU, EDRV at a dose of 0, 0.3, or 1.0 mg/kg was IV injected immediately and 6 h after MNU treatment. Seven days after MNU treatment, the vertical length of the outer nuclear layer relative to the inner nuclear layer was compared, and EDRV at 1.0 mg/kg (but not 0.3 mg/kg) significantly suppressed the reduction in the outer nuclear thickness compared to mice not treated with EDRV. EDRV inhibits MNU-induced photoreceptor cell death by its ROS-scavenging activity. Many phytochemicals possess antioxidant activity and may be useful in suppressing retinal damage caused by MNU.

Prevention of MNU-induced retinal damage was observed following oral administration of persimmon leaf extract (PLE) in mice (Kim et al., 2015), and topical treatment (eye drops) with naringenin (NGN, found in citrus and grape fruit) in rats (Lin et al., 2014), both of which have antioxidant activity. Curcumin (CUR), a yellow pigment of turmeric and a constituent of curry powder, and green tea extract (GTE), which mainly contains the potent antioxidant epigallocatechin gallate (EGCG), were effective in suppressing MNU-induced retinal damage (Emoto et al., 2013, 2014). Seven-week-old rats were given daily IP injection of 200 mg/kg CUR or PO administration of 250 mg/kg GTE for 10 days, starting 3 days prior to 40 mg/kg MNU, and retinas were examined 7 days after MNU. CUR and GTE treatment suppressed MNU-induced photoreceptor apoptosis with no side effects. Significant increases in oxidative stress markers, such as nitrotyrosine and S-nitro-cysteine, occur in photoreceptor cells after mice are treated with MNU (Chen et al., 2014). CUR and GTE treatment lowered the levels of the oxidative stress marker 8-OHdG and HO-1 following MNU administration in rats (Emoto et al., 2013, 2016b). In an effort to identify potential synergistic interactions between CUR and GTE, 7-week-old rats were treated with daily IP injection of either 100 mg/kg CUR and PO administration of 125 mg/kg GTE (low dose antioxidant), or 200 mg/kg CUR and 250 mg/kg GTE (high dose antioxidant) for 10 days starting 3 days prior to 40 mg/kg MNU, and retinas were examined 7 days after MNU (unpublished observation). However, no synergistic effects were observed. In high-dose, low-dose, antioxidant-free MNU-treated rats, and untreated control rats, photoreceptor ratios were 13.2, 11.4, 11.3, and 44.5%, and retinal damage ratios were 67.5, 72.0, 71.2, and 0%, respectively. Potential synergic interactions between CUR and DHA were examined in 7-week-old rats by IP injection of 200 mg/kg CUR and PO administration of 2 mL DHA for 10 days starting 3 days prior to 40 mg/kg MNU. Retinas were examined 7 days after MNU (unpublished observation) treatment, and no synergistic effects were evident.

7.9 Autophagy Preservation

Rapamycin is a negative regulator of mammalian target of rapamycin and has been used to induce autophagy. BALB/c mice received IP injections of 10 mg/kg rapamycin during the 10-day light damage period (Kunchithapautham et al., 2011), which significantly improved photoreceptor rod survival and function and reduced apoptosis. As decreased basal autophagy in photoreceptor cells occurs along with apoptosis after MNU treatment, rapamycin was utilized in the MNU model. Daily doses of 2 mg/kg rapamycin (dissolved in 0.4% ethanol and 1.6% cremophore EL) were IP injected into

7-week-old BALB/c mice for 7 days before and 7 days after 60 mg/kg MNU administration. Seven days after MNU treatment, mice were sacrificed and examined, and photoreceptor cell survival was not promoted by this protocol (unpublished observation). In cones, autophagy suppression might be necessary for cone-cell survival because reduced cone-cell function secondary to rod-cell loss is due to autophagic cell death through stimulation of the insulin/mammalian target of rapamycin pathway (Punzo et al., 2009).

7.10 Cell Transplantation

In addition to the pharmacological approaches described earlier, degenerative photoreceptors can be repaired and retinal function rescued if the damaged photoreceptors can be replaced with healthy cells that make appropriate synaptic connections with the remaining functional circuitry within the retina. Photoreceptor cells and stem/progenitor cells can be used for cell transplantation. Photoreceptor cell loss caused by MNU can be repaired by cell transplantation. Synapses between transplanted neurons and host retina are formed, and partial functional recovery is achieved when dissociated photoreceptors are transplanted concomitantly with chondroitinase ABC, a bacterial enzyme that degrades the chondroitin sulfate proteoglycan side chain, 1 day after MNU treatment in adult C57BL mice (Suzuki et al., 2007). Chondroitinase ABC, which degrades chondroitin sulfate proteoglycans in the extracellular matrix, may help eliminate the barrier between photoreceptor transplants and host retina and may increase the neurite-extending activity. Some of the progeny of the Müller glia in adult rat retina undergo gliosis and proliferate in response to photoreceptor cell loss caused by MNU, and they express a rod-specific marker and synaptic proteins (Wan et al., 2008). Cultured Müller cells that are transplanted show a regenerative capacity by migrating into the MNU-induced damaged retina and expressing a rod-specific marker. Müller cells have progenitor/stem-cell properties and can be used for cell replacement therapy.

8 CONCLUDING REMARKS

A single systemic administration of MNU induces photoreceptor cell loss in various mammalian species, from insectivora to primates, and fish (zebrafish). Disease progression is rapid in that the active signs of photoreceptor cell apoptosis end by day 7. MNU causes DNA adduct formation in photoreceptor nuclei, followed by increased PARP activity that leads to the activation of JNK/AP-l and inactivation of NF-κB, causing the downregulation of Bcl-2, upregulation of Bax, and the activation of caspase-3, -6, and -8. In addition, increased intracellular Ca^{2+} levels activate calpain, leading to prolonged activation of Cdk5/p25. Furthermore, MNU leads to ROS production in response to oxidative stress. Collectively, these molecular events appear to cause photoreceptor cell apoptosis. In parallel to a gradual increase in photoreceptor cell apoptosis, there is a gradual decrease in basal autophagy essential for cell survival. Many novel approaches have been applied to control MNU-induced photoreceptor cell death (Fig. 5.9). MNU-induced photoreceptor apoptosis can be suppressed by the following agents: PARP inhibitors, such as NAM and 3-AB; DHA, AA, VPA, Reishi, and MaFGF, which may interfere with pro- and antiapoptotic molecules; caspase inhibitors XIAP and Ac-DEVD-CHO; calpain inhibitor SNJ-1945; and free-radical scavenger and antioxidants EDRV, CUR, GTE, NGN, and PLE. In addition to pharmacological manipulation, cell transplantation may possibly rescue MNU-induced retinal damage. MNU-induced photoreceptor cell death is a valuable animal model for human RP. Although the potency of agents that suppress MNU-induced photoreceptor cell death in animals does not guarantee that these agents will be effective in humans, it may be worthwhile to extrapolate these results to RP patients. Special techniques useful for the establishment and evaluation of MNU-induced retinal damage are described later in the chapter.

9 APPENDIX: SPECIAL TECHNIQUES

9.1 MNU Preparation and Administration

MNU (Fig. 5.10) is a direct-acting alkylating agent that does not require metabolic activation to be effective and is known to methylate DNA. MNU is sensitive to humidity and light, and storage at temperatures below −10°C is recommended. The purity of MNU obtained from the manufacturer can differ between lots. Therefore, the equivalent purity must be considered in every occasion. MNU must be stored at −20°C in the dark, and since MNU stability depends on the pH of the medium, it is dissolved in physiological saline containing 0.05% or 0.1% acetic acid immediately before use. This solution should be kept on ice and shielded from light. A 23-G needle is used for administration to rodents. The dose of MNU (per kg of body weight of animals) needed to cause complete loss of photoreceptors in 7 days depends on the animal species (Table 5.1). The half-life of MNU
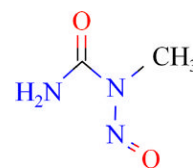
FIGURE 5.10   Chemical structure of MNU.

under physiological conditions is <1 h (Weisberger and Williams, 1975), and the half-life in plasma is only 5–15 min (Smith and Yielding, 1986). Therefore, the injection solution must be freshly prepared every 15 min.

9.2 Eyeball Fixation and Processing for Light Microscopy

Immediately after sacrifice, eyes are removed, and a hole is made in the corneal edge through the anterior chamber with a 27-G needle to facilitate entry of fixative to the retina. For light microscopic examination, one eye is fixed overnight in neutral-buffered formalin, and the other eye is fixed overnight in methacarn (60% methanol, 30% chloroform, and 10% acetic acid). The fixed tissues are then embedded in paraffin and cut into sections. The sections are cut at the center of the retina, parallel to the optic axis and optic nerve. The sections are stained with hematoxylin and eosin (HE) or other special stains or are used for immunohistochemistry. Formalin-fixed but not methacarn-fixed eye specimens easily develop separation of the outer layers of the retina from the underlying retinal pigment epithelium, whereas formalin fixation can only be suitable for certain staining. Therefore, both fixatives must be used properly according to their purpose.

9.3 Electron Microscopy

After eyeballs are fixed for 1.5 h in 0.5% Karnovsky fixative, the cornea and lens of each eye are removed for better penetration of the fixative. Then, the eyes are post-fixed in 2% OsO_4 and embedded in Luveak-812. Semi-thin sections (thickness, 1 μm) stained with toluidine blue are used to locate areas to be examined by electron microscopy. Thin sections stained with uranyl acetate and lead citrate are examined by transmission electron microscopy.

9.4 Immunohistochemistry

Antibodies useful in retinal immunohistochemistry, along with their clone name and source, suitable fixative, the necessity of preincubation, and the expression site of their target protein, are listed in Table 5.3. Anti-7-methyldeoxyguanosine (7-medGua) detects the DNA adducts produced by MNU (Yoshizawa et al., 1999), and antipoly(ADP-ribose) (PAR) labels activated PARP in cells damaged by MNU (Uehara et al., 2006). Antiphosphodiesterase (PDE) 6β and antirhodopsin label photoreceptor outer segments (Emoto et al., 2014). Antivimentin and antiglial fibrillary acidic protein (GFAP) can be used to stain proliferating Müller cell processes, and antiproliferating cell nuclear antigen (PCNA)

TABLE 5.3 Antibodies Used to Detect Retinal Pathology Caused by MNU in Animals

Antibody	Clone	Source	Fixative	Preincubation	Expression site	References
7-methyldeoxyguanosine	Polyclonal	Gift from PC Wild, Univ. of Leeds, UK	Amex[a]	Yes[b]	Disrupted photoreceptor nuclei	Yoshizawa et al. (1999)
Poly(ADP-ribose)	10H	Trivingen, Gaithersberg, MD, USA	Methacarn	No	Disrupted photoreceptor nuclei	Uehara et al. (2006)
Phosphodiesterase 6β	Polyclonal	Abcam, Cambridge, UK	Formalin	Yes[c]	Photoreceptor outer segments	Emoto et al. (2014)
Rhodopsin	RET-P1	Millipore, Temecula, CA, USA	Formalin	Yes[c]	Photoreceptor outer segments	Emoto et al. (2014)
Vimentin	V9	Dako, Glostrup, Denmark	Methacarn	No	Proliferating Müller cells	Nakajima et al. (1996b)
Glial fibrillary acidic protein	Polyclonal	Dako	Methacarn	No	Proliferating Müller cells	Nakajima et al. (1996b)
Proliferating cell nuclear antigen	PC10	Novocastra, Newcastle upon Tyne, UK	Methacarn	No	Proliferating Müller cells	Nakajima et al. (1996b)
Rat macrophage and monocyte	ED1	Serotec, Oxford, UK	Formalin	Yes[d]	Infiltrating macrophage	Nakajima et al. (1996b)
Rat macrophage	ED2	Serotec	Formalin	Yes[d]	Resident macrophage	Nakajima et al. (1996b)

[a] Amex, Acetone methylbenzoate xylene (Sato et al., 1986).
[b] 0.05N sodium hydroxide in 40% ethanol for 5 min, 5% acetic acid in 40% ethanol for 15 s, and 1% nonfat milk in PBS-saline for 1 h.
[c] Heat treatment in 0.01M citrate buffer pH 6.0 in 115°C for 10 min.
[d] 0.1% trypsin for 15 min.

can be used to stain proliferating Müller cell nuclei (Nakajima et al., 1996b). Anti-ED-1 stains macrophages that have infiltrated the retina, while anti-ED2 stains resident macrophages (Nakajima et al., 1996b). Immunohistochemistry can be performed by using a labeled streptavidin biotin (LSAB) staining kit (Dako, Carpinteria, CA, USA), 3,3'-diaminobenzidine (DAB, Wako Pure Chemical, Osaka, Japan) for antigen visualization, and hematoxylin for counterstaining. Also, cross-reactivity data for each antibody is needed before utilization with animal tissues.

9.5 In Situ Apoptotic Cell Detection

Apoptotic cells can be identified by using the TUNEL assay and by performing formamide-induced DNA denaturation and staining with a monoclonal antibody (MoAb) against single-stranded DNA (formamide-MoAb). TUNEL detects the DNA fragmentation caused by apoptotic signaling cascades. The assay relies on the presence of nicks in the DNA that can be identified by terminal deoxynucleotidyl transferase, an enzyme that will catalyze the addition of dUTPs that are secondarily labeled with a marker. Formalin-fixed, paraffin-embedded specimens can be utilized in the TUNEL assay by using a commercially available apoptosis detection kit (ApopTag, Millipore, Billerica, MA, USA) according to the manufacturer's instructions (Nakajima et al., 1996b). The formamide-MoAb technique can be performed by using the protocol of Frankfurt and Krishan (2001). Briefly, formalin-fixed, paraffin-embedded retinas are sectioned, and the sections are deparaffinized. Each section is incubated with PBS containing 0.1 mg/kg saponin and 20 µg/mL proteinase K for 20 min, rinsed in PBS, rinsed in distilled water, and heated in 50% formamide (diluted with distilled water) at 56–60°C for 20 min. After heating, sections are transferred into ice-cold PBS, in which they are incubated with mouse monoclonal anti-single-stranded DNA antibody (clone F7-26, Chemicon, Temecula, CA, USA) diluted ×10 with Tris-buffered saline-containing Tween 20 (TBST: 0.05 M Tris-HCl (pH 7.6) buffer containing 0.1% Tween 20). The sections are then stained by using an LSAB staining kit. In both methods, DAB is used as the chromogen, and hematoxylin is used as the counterstain (Miki et al., 2007).

9.6 Internucleosomal DNA Fragmentation Assay

Eyes are excised from the sacrificed animals. The corneas and lenses are removed, and the retinal DNA is isolated by the digestion of cells with proteinase K at a concentration of 0.2 µm/µL in tissue lysis buffer solution [50 mM Tris-HCl (pH 8.0), 10 mM EDTA (pH 8.0), 0.5% SDS] at 50°C for 2 h. RNase A, at a concentration of 0.2 µg/µL, was then added to the lysate and incubated for 1 h, followed by extraction with phenol/chloroform. Ten µg of DNA are analyzed by electrophoresis in 1.5% (w/v) agarose gel and visualized under UV light after staining with ethidium bromide (Uehara et al., 2006).

9.7 Western Blot Analysis

For western blot analysis, a protein extract is prepared by homogenizing the retinas in lysis buffer solution [50 mM Tris-HCl (pH 8.0), 125 mM NaCl, 1 mM sodium fluoride, 1 mM sodium orthovanadate, 10 mM sodium pyrophosphate, and 1 mM PMSF] containing the protease inhibitors leupeptin, pepstatin, and aprotinin, each at a final concentration of 1 µg/mL. The homogenates are sonicated and then centrifuged at $110 \times g$, and the resulting pellets are discarded. Protein concentrations are measured by using the DC protein assay method (BioRad, Hercules, CA, USA). Aliquots of lysates equivalent to 80 µg of protein are electrophoresed through polyacrylamide gels and transferred to Hybond-P PVDF membranes (Amersham Biosciences, Buckinghamshire, UK). The membranes are blocked with 5% nonfat powdered milk and then incubated with the primary specific antibody. Then, the blots are washed and incubated with the appropriate secondary antibody. Antiactin antibody can be used as the loading control (Uehara et al., 2006).

9.8 Morphometric Analysis

Methacarn-fixed, paraffin-embedded, and HE-stained sections obtained from the central part of the eyeball, which is parallel to the optic axis and nerve, including the ora serrata and optic nerve, should be used for morphometric evaluation. Total retinal thickness (from the internal limiting membrane to the pigment epithelium) and outer retinal thickness (from the outer nuclear layer to the pigment epithelial layer) are measured by using NDP.view (Yoshizawa et al., 2009). The measurements are collected at the central retina (approximately 400 µm from the optic nerve) and the peripheral retina (approximately 400 µm from both sides of the ciliary bodies) (Fig. 5.11). The photoreceptor cell ratio is calculated as [(outer retinal thickness/total retinal thickness) × 100]. To determine the area of retinal damage, the entire length of the retina and the length of the damaged area (dotted space located in the central retina around the optic disk in rodents) in HE preparations are measured. A damaged retina is designated as the presence of less than four rows of photoreceptor nuclei in the outer nuclear layer, and the retinal damage ratio is calculated as [(length of damaged retina/whole retinal length) × 100] (Yoshizawa et al., 2000).
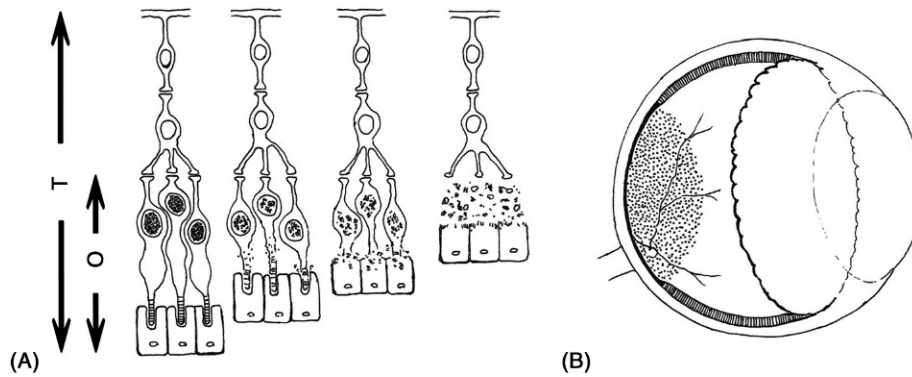
FIGURE 5.11 Morphometric analysis of photoreceptor cell ratio and retinal damage ratio. (A) The photoreceptor cell ratio is calculated as [(outer retinal thickness/(total retinal thickness) $\times$ 100]. *O*, Outer retinal thickness; *T*, total retinal thickness. (B) To determine the retinal damage ratio, the entire length of the retina and the length of the damaged area are measured. The damaged retina is designated as the presence of less than four rows of photoreceptor nuclei in the outer nuclear layer, and the retinal damage ratio is calculated as [(length of damaged retina/whole retinal length) $\times$ 100]. The *dotted* region in the scheme indicates the injured area at the central retina around the optic nerve, leaving the peripheral retina intact.

9.9 Electroretinogram Recording

ERG recording in rats is performed as follows (Kiuchi et al., 2003). First, the animals are dark-adapted for 12 h and prepared under dim red light. Next, the rats are anesthetized with an intramuscular injection of ketamine and xylazine. Then, pupils are dilated with topical tropicamide and phenylephrine HCl, and the rats are then placed on a heating pad. ERGs are recorded with a gold wire loop on the cornea by using tetracaine topical anesthesia and a drop of methylcellulose. A gold wire electrode is placed on the sclera 1 mm from the temporal limbus. The ground electrode is placed on the ear. Signals are band-pass amplified (range, 1–1000 Hz) by using a computer-assessed signal averaging system (Power Lab, AD Instruments, Castle Hill, Australia). Scotopic ERG responses are averaged with a stimulus interval of 3–60 s (depending on intensity), and 20–30 photopic responses are averaged with a stimulus interval of 1 s. Strobe flash stimuli are presented in a Ganzfeld bowl (Model GS2000, LACE Electronica sel via Marmiccilo, Pisa, Italy). The maximum luminance of the stimulus is 1.0 log cd-s/m^2 (photopic unit), and neutral density filters are used to reduce the stimulus intensity. Six stimulus levels, at equal log intervals, ranging from -6.2 to 1.0 log cd-s/m^2, are used for the scotopic ERG recording. Four stimulus levels, at equal intervals, ranging from -0.8 to 1.0 log cd-s/m^2, are used for the photopic ERG recording on a rod-desensitizing white adapting background of 1.3 log cd-s/m^2.

Acknowledgments

References

Aguilar-Quesada, R., Muñoz-Gámez, J.A., Martín-Oliva, D., Peralta-Leal, A., Quiles-Pérez, R., Rodríguez-Vargas, J.M., Ruiz de Almodóvar, M., Conde, C., Ruiz-Extremera, A.J., Oliver, F.J., 2007. Modulation of transcription by PARP-1: consequences in carcinogenesis and inflammation. Curr. Med. Chem. 14 (11), 1179–1187.

Ali, R.R., Reichel, M.B., Kanuga, N., Munro, P.M., Alexander, R.A., Clarke, A.R., Luthert, P.J., Bhattacharya, S.S., Hunt, D.M., 1998. Absence of p53 delays apoptotic photoreceptor cell death in the rds mouse. Curr. Eye Res. 17 (9), 917–923.

Andreone, T.L., O'Connor, M., Denenberg, A., Hake, P.W., Zingarelli, B., 2003. Poly(ADP-ribose) polymerase-1 regulates activation of activator protein-1 in murine fibroblasts. J. Immunol. 170 (4), 2113–2120.

Bazan, N.G., Scott, B.L., Reddy, T.S., Pelias, M.Z., 1986. Decreased content of docosahexaenoate and arachidonate in plasma phospholipids in Usher's syndrome. Biochem. Biophys. Res. Commun. 141 (2), 600–604.

Berson, E.L., 2007. Long-term visual prognoses in patients with retinitis pigmentosa: the Ludwig von Sallmann lecture. Exp. Eye Res. 85 (1), 7–14.

Berson, E.L., Rosner, B., Sandberg, M.A., Weigel-DiFranco, C., Brockhurst, R.J., Hayes, K.C., Johnson, E.J., Anderson, E.J., Johnson, C.A., Gaudio, A.R., Willett, W.C., Schaefer, E.J., 2010. Clinical trial of lutein in patients with retinitis pigmentosa receiving vitamin A. Arch. Ophthalmol. 128 (4), 403–411.

Bhatti, M.T., 2006. Retinitis pigmentosa, pigmentary retinopathies, and neurologic diseases. Curr. Neurol. Neurosci. Rep. 6 (5), 403–413.

Boudard, D.L., Acar, N., Bretillon, L., Hicks, D., 2011. Retinas of the diurnal rodent Arvicanthis ansorgei are highly resistant to experimentally induced stress and degeneration. Invest. Ophthalmol. Vis. Sci. 52 (12), 8686–8700.

Boudard, D.L., Tanimoto, N., Huber, G., Beck, S.C., Seeliger, M.W., Hicks, D., 2010. Cone loss is delayed relative to rod loss during induced retinal degeneration in the diurnal cone-rich rodent Arvicanthis ansorgei. Neuroscience 169 (4), 1815–1830.

Brémond-Gignac, D., Copin, H., Lapillonne, A., Milazzo, S., on behalf of the European Network of Study and Research in Eye Development (ENSRED), 2011. Visual development in infants: physiological and pathological mechanisms. Curr. Opin. Ophthalmol. 22 (Suppl.), S1–S8.

Cagianut, B., Sandri, G., Zilla, P., Theiler, K., 1985. Studies on hereditary retinal degeneration. The rd gene in the mouse. Graefe's Arch. Clin. Exp. Ophthalmol. 223 (1), 16–22.

Carson, D.A., Seto, S., Wasson, D.B., Carrera, C.J., 1986. DNA strand breaks, NAD metabolism, and programmed cell death. Exp. Cell Res. 164 (2), 273–281.

Chader, G.J., 2002. Animal models in research on retinal degenerations: past progress and future hope. Vis. Res. 42 (4), 393–399.

Chang, G.Q., Hao, Y., Wong, F., 1993. Apoptosis: final common pathway of photoreceptor death in rd, rds, and rhodopsin mutant mice. Neuron 11 (4), 595–605.

Chang, M.L., Wu, C.H., Chien, H.F., Jiang-Shieh, Y.F., Shieh, J.Y., Wen, C.Y., 2006. Microglia/macrophages responses to kainate-induced injury in the rat retina. Neurosci. Res. 54 (3), 202–212.

Chen, Y.Y., Liu, S.L., Hu, D.P., Xing, Y.Q., Shen, Y., 2014. N-methyl-N-nitrosourea-induced retinal degeneration in mice. Exp. Eye Res. 121, 102–113.

Chiarugi, A., 2002. Poly(ADP-ribose) polymerase: killer or conspirator? The 'suicide hypothesis' revisited. Trends Pharmacol. Sci. 23 (3), 22–29.

Cuevas, P., Carceller, F., Redondo-Horcajo, M., Lozano, R.M., Giménez-Gallego, G., 1998. Systemic administration of acidic fibroblast growth factor ameliorates the ischemic injury of the retina in rats. Neurosci. Lett. 255 (1), 1–4.

Dalke, C., Graw, J., 2005. Mouse mutants as models for congenital retinal disorders. Exp. Eye Res. 81 (5), 503–512.

Degan, P., Montesano, R., Wild, C.P., 1988. Antibodies against 7-methyldeoxyguanosine: its detection in rat peripheral blood lymphocyte DNA and potential applications to molecular epidemiology. Cancer Res. 48 (18), 5065–5070.

Donders, F.C., 1857. Beitra ge zur pathologischen Anatomie des Auges. Pigmentbildung inder Netzhaut. Albrecht Von Graefes Archiv für klinische und experimentelle Ophthalmologie 3 (1), 139–165, (in German).

Donehower, L.A., Bradley, A., 1993. The tumor suppressor p53. Biochim. Biophys. Acta 1155 (2), 181–205.

Doonan, F., Donovan, M., Cotter, T.G., 2003. Caspase-independent photoreceptor apoptosis in mouse models of retinal degeneration. J. Neurosci. 23 (13), 5723–5731.

Doonan, F., Donovan, M., Cotter, T.G., 2005. Activation of multiple pathways during photoreceptor apoptosis in the rd mouse. Invest. Ophthalmol. Vis. Sci. 46 (10), 3530–3538.

Emoto, Y., Yoshizawa, K., Kinoshita, Y., Yuki, M., Yuri, T., Tsubura, A., 2016a. Susceptibility to N-methyl-N-nitrosourea-induced retinal degeneration in different rat strains. J. Toxicol. Pathol. 29 (1), 66–71.

Emoto, Y., Yoshizawa, K., Kinoshita, Y., Yuki, M., Yuri, T., Tsubura, A., 2016b. Green tea extract attenuates MNU-induced photoreceptor cell apoptosis via suppression of heme oxygenase-1. J. Toxicol. Pathol. 29 (1), 61–65.

Emoto, Y., Yoshizawa, K., Kinoshita, Y., Yuri, T., Yuki, M., Sayam, K., Shikata, N., Tsubura, A., 2014. Green tea extract suppresses N-methyl-N-nitrosourea-induced photoreceptor apoptosis in Sprague-Dawley rats. Graefe's Arch. Clin. Exp. Ophthalmol. 252 (9), 1377–1384.

Emoto, Y., Yoshizawa, K., Uehara, N., Kinoshita, Y., Yuri, T., Shikata, N., Tsubura, A., 2013. Curcumin suppresses N-methyl-N-nitrosourea-induced photoreceptor apoptosis in Sprague-Dawley rats. In Vivo 27 (5), 583–590.

Erwig, L.P., Henson, P.M., 2008. Clearance of apoptotic cells by phagocytes. Cell Death Differ. 15 (2), 243–250.

Estus, S., Zaks, W.J., Freeman, R.S., Gruda, M., Bravo, R., Johnson, Jr., E.M., 1994. Altered gene expression in neurons during programmed cell death: identification of c-jun as necessary for neuronal apoptosis. J. Cell Biol. 127 (6 Pt 1), 1717–1727.

Faktorovich, E.G., Steinberg, R.H., Yasumura, D., Matthes, M.T., LaVail, M.M., 1990. Photoreceptor degeneration in inherited retinal dystrophy delayed by basic fibroblast growth factor. Nature 347 (6288), 83–86.

Faktorovich, E.G., Steinberg, R.H., Yasumura, D., Matthes, M.T., LaVail, M.M., 1992. Basic fibroblast growth factor and local injury protect photoreceptors from light damage in the rat. J. Neurosci. 12 (9), 3554–3567.

Fleischhauer, J., Njoh, W.A., Niemeyer, G., 2005. Syndromic retinitis pigmentosa: ERG and phenotypic changes. Klinische Monatsblatter für Augenheilkunde 222 (3), 186–190.

Frankfurt, O.S., Krishan, A., 2001. Identification of apoptotic cells by formamide-induced DNA denaturation in condensed chromatin. J. Histochem. Cytochem. 49 (3), 369–378.

Frasson, M., Sahel, J.A., Fabre, M., Simonutti, M., Dreyfus, H., Picaud, S., 1999. Retinitis pigmentosa: rod photoreceptor rescue by a calcium-channel blocker in the rd mouse. Nat. Med. 5 (10), 1183–1187.

Galzie, Z., Kinsella, A.R., Smith, J.A., 1997. Fibroblast growth factors and their receptors. Biochem. Cell Biol. 75 (6), 669–685.

Gao, Y., Deng, X.G., Li, N., Luo, G.W., Chung, P.C., 2011. The comparative protective effects of Ganoderma spores lipid and fish oil on N-methyl-N-nitrosourea-induced photoreceptor cell lesion in rats. Evid. Based Complement. Alternat. Med. 2011, 903261.

Gao, Y., Deng, X.G., Sun, Q.N., Zhong, Z.Q., 2010. Ganoderma spore lipid inhibits N-methyl-N-nitrosourea-induced retinal photoreceptor apoptosis in vivo. Exp. Eye Res. 90 (3), 397–404.

Giannelli, S.G., Demontis, G.C., Pertile, G., Rama, P., Broccoli, V., 2011. Adult human Müller glia cells are a highly efficient source of rod photoreceptors. Stem Cells 29 (2), 344–356.

Godel, V., Nemet, P., Lazar, M., 1981. Retinal dysplasia. Doc. Ophthalmol. 51 (3), 277–288.

Goll, D.E., Thompson, V.F., Li, H., Wei, W., Cong, J., 2003. The calpain system. Physiol. Rev. 83 (3), 731–801.

Grimm, C., Wenzel, A., Behrens, A., Hafezi, F., Wagner, E.F., Remé, C.E., 2001. AP-1 mediated retinal photoreceptor apoptosis is independent of N-terminal phosphorylation of c-Jun. Cell Death Differ. 8 (8), 859–867.

Hara, T., Nakamura, K., Matsui, M., Yamamoto, A., Nakahara, Y., Suzuki-Migishima, R., Yokoyama, M., Mishima, K., Saito, I., Okano, H., Mizushima, N., 2006. Suppression of basal autophagy in neural cells causes neurodegenerative disease in mice. Nature 441 (7095), 885–889.

Hartong, D.T., Berson, E.L., Dryja, T.P., 2006. Retinitis pigmentosa. Lancet 368 (9549), 1795–1809.

Herrold, K.M., 1967. Pigmentary degeneration of the retina induced by N-methyl-N-nitrosourea. An experimental study in Syrian hamsters. Arch. Ophthalmol. 78 (5), 650–653.

Hoffman, D.R., Boettcher, J.A., Diersen-Schade, D.A., 2009. Toward optimizing vision and cognition in term infants by dietary docosahexaenoic and arachidonic acid supplementation: a review of randomized controlled trials. Prostaglandins Leukot. Essent. Fatty Acids 81 (2–3), 151–158.

Hotchkiss, R.S., Strasser, A., McDunn, J.E., Swanson, P.E., 2009. Cell death. New Engl. J. Med. 361 (16), 1570–1583.

Huang, T.F., Chao, C.C., 1960. The effect of niacinamide on cerebral circulation. Proc. Soc. Exp. Biol. Med. 105 (3), 551–553.

Imai, S., Shimazawa, M., Nakanishi, T., Tsuruma, K., Hara, H., 2010. Calpain inhibitor protects cells against light-induced retinal degeneration. J. Pharmacol. Exp. Ther. 335 (3), 645–652.

Jaissle, G.B., May, C.A., van de Pavert, S.A., Wenzel, A., Claes-May, E., Giessl, A., Szurman, P., Wolfrum, U., Wijnholds, J., Fischer, M.D., Humphries, P., Seeliger, M.W., 2010. Bone spicule pigment formation in retinitis pigmentosa: insights from a mouse model. Graefe's Arch. Clin. Exp. Ophthalmol. 248 (8), 1063–1070.

Jeong, E., Paik, S.S., Jung, S.W., Chun, M.H., Kim, I.B., 2011. Morphological and functional evaluation of an animal model for the retinal degeneration induced by *N*-methyl-*N*-nitrosourea. Anat. Cell Biol. 44 (4), 314–323.

Kabeya, Y., Mizushima, N., Ueno, T., Yamamoto, A., Kirisako, T., Noda, T., Kominami, E., Ohsumi, Y., Yoshimori, T., 2000. LC3, a mammalian homologue of yeast Apg8p, is localized in autophagosome membranes after processing. EMBO J. 19 (21), 5720–5728.

Kaneko, H., Nishiguchi, K.M., Nakamura, M., Kachi, S., Terasaki, H., 2008. Characteristics of bone marrow-derived microglia in the normal and injured retina. Invest. Ophthalmol. Vis. Sci. 49 (9), 4162–4168.

Kaur, J., Mencl, S., Sahaboglu, A., Farinelli, P., van Veen, T., Zrenner, E., Ekström, P., Paquet-Durand, F., Arango-Gonzalez, B., 2011. Calpain and PARP activation during photoreceptor cell death in P23H and S334ter rhodopsin mutant rats. PLoS One 6 (7), e22181.

Kim, K.A., Kang, S.W., Ahn, H.R., Song, Y., Yang, S.J., Jung, S.H., 2015. Leaves of Persimmon (Diospyros kaki Thunb.) Ameliorate *N*-Methyl-*N*-nitrosourea (MNU)-induced retinal degeneration in mice. J. Agric. Food Chem. 63 (35), 7750–7759.

Kinoshita, J., Iwata, N., Maejima, T., Imaoka, M., Kimotsuki, T., Yasuda, M., 2015. *N*-Methyl-*N*-nitrosourea-induced acute alteration of retinal function and morphology in monkeys. Invest. Ophthalmol. Vis. Sci. 56 (12), 7146–7158.

Kiuchi, K., Kondo, M., Ueno, S., Moriguchi, K., Yoshizawa, K., Miyake, Y., Matsumura, M., Tsubura, A., 2003. Functional rescue of *N*-methyl-*N*-nitrosourea-induced retinopathy by nicotinamide in Sprague-Dawley rats. Curr. Eye Res. 26 (6), 355–362.

Kiuchi, K., Yoshizawa, K., Shikata, N., Matsumura, M., Tsubura, A., 2002. Nicotinamide prevents *N*-methyl-*N*-nitrosourea-induced photoreceptor cell apoptosis in Sprague-Dawley rats and C57BL mice. Exp. Eye Res. 74 (3), 383–392.

Koenekoop, R.K., 2009. Why do cone photoreceptors die in rod-specific forms of retinal degenerations? Ophthal. Genet. 30 (3), 152–154.

Kong, L., Tanito, M., Huang, Z., Li, F., Zhou, X., Zaharia, A., Yodoi, J., McGinnis, J.F., Cao, W., 2007. Delay of photoreceptor degeneration in tubby mouse by sulforaphane. J. Neurochem. 101 (4), 1041–1052.

Koriyama, Y., Sugitani, K., Ogai, K., Kato, S., 2014. Heat shock protein 70 induction by valproic acid delays photoreceptor cell death by *N*-methyl-*N*-nitrosourea in mice. J. Neurochem. 130 (5), 707–719.

Krebs, M.P., White, D.A., Kaushal, S., 2009. Biphasic photoreceptor degeneration induced by light in a T17M rhodopsin mouse model of cone bystander damage. Invest. Ophthalmol. Vis. Sci. 50 (6), 2956–2965.

Krishnamoorthy, R.R., Crawford, M.J., Chaturvedi, M.M., Jain, S.K., Aggarwal, B.B., Al-Ubaidi, M.R., Agarwal, N., 1999. Photo-oxidative stress down-modulates the activity of nuclear factor-kappa B via involvement of caspase-1, leading to apoptosis of photoreceptor cells. J. Biol. Chem. 274 (6), 3734–3743.

Krishnamoorthy, V., Jain, V., Cherukuri, P., Baloni, S., Dhingra, N.K., 2008. Intravitreal injection of fluorochrome-conjugated peanut agglutinin results in specific and reversible labeling of mammalian cones in vivo. Invest. Ophthalmol. Vis. Sci. 49 (6), 2643–2660.

Kristián, T., Siesjö, B.K., 1998. Calcium in ischemic cell death. Stroke 29 (3), 705–718.

Kubota, S., Kurihara, T., Ebinuma, M., Kubota, M., Yuki, K., Sasaki, M., Noda, K., Ozawa, Y., Oike, Y., Ishida, S., Tsubota, K., 2010. Resveratrol prevents light-induced retinal degeneration via suppressing activator protein-1 activation. Am. J. Pathol. 177 (4), 1725–1731.

Kunchithapautham, K., Coughlin, B., Lemasters, J.J., Rohrer, B., 2011. Differential effects of rapamycin on rods and cones during light-induced stress in albino mice. Invest. Ophthalmol. Vis. Sci. 52 (6), 2967–2975.

Kuro, M., Yoshizawa, K., Uehara, N., Miki, H., Takahashi, K., Tsubura, A., 2011. Calpain inhibition restores basal autophagy and suppresses MNU-induced photoreceptor cell death in mice. In Vivo 25 (4), 617–623.

Leonard, K.C., Petrin, D., Coupland, S.G., Baker, A.N., Leonard, B.C., LaCasse, E.C., Hauswirth, W.W., Korneluk, R.G., Tsilfidis, C., 2007. XIAP protection of photoreceptors in animal models of retinitis pigmentosa. PLoS One 2 (3), e314.

Lew, J., Huang, Q.Q., Qi, Z., Winkfein, R.J., Aebersold, R., Hunt, T., Wang, J.H., 1994. A brain-specific activator of cyclin-dependent kinase 5. Nature 371 (6496), 423–426.

Li, Z.Y., Possin, D.E., Milam, A.H., 1995. Histopathology of bone spicule pigmentation in retinitis pigmentosa. Ophthalmology 102 (5), 805–816.

Lin, J.L., Wan, Y.D., Ma, Y., Zhong, C.M., Zhu, M.R., Chen, W.P., Lin, B.Q., 2014. Protective effects of naringenin eye drops on *N*-methyl-*N*-nitrosourea-induced photoreceptor cell death in rats. Int. J. Ophthalmol. 7 (3), 391–396.

Liston, P., Roy, N., Tamai, K., Lefebvre, C., Baird, S., Cherton-Horvat, G., Farahani, R., McLean, M., Ikeda, J.E., MacKenzie, A., Korneluk, R.G., 1996. Suppression of apoptosis in mammalian cells by NAIP and a related family of IAP genes. Nature 379 (6563), 349–353.

Liu, J., Lin, A., 2005. Role of JNK activation in apoptosis: a double-edged sword. Cell Res. 15 (1), 36–42.

Marti, A., Hafezi, F., Lansel, N., Hegi, M.E., Wenzel, A., Grimm, C., Niemeyer, G., Remé, C.E., 1998. Light-induced cell death of retinal photoreceptors in the absence of p53. Invest. Ophthalmol. Vis. Sci. 39 (5), 846–849.

Maruyama, I., Ohguro, H., Maeda, T., Takano, Y., Nakazawa, M., 2001. Study of mechanism of retinal damage by *N*-methyl-*N*-nitrosourea. J. Eye 18, 539–542, (In Japanese, Abstract in English).

Miki, K., Uehara, N., Shikata, N., Matsumura, M., Tsubura, A., 2007. Poly (ADP-ribose) polymerase inhibitor 3-aminobenzamid rescues *N*-methyl-*N*-nitrosourea-induced photoreceptor cell apoptosis in Sprague-Dawley rats through preservation of nuclear factor-kappaB activity. Exp. Eye Res. 84 (2), 285–292.

Mizukoshi, S., Nakazawa, M., Sato, K., Ozaki, T., Metoki, T., Ishiguro, S., 2010. Activation of mitochondrial calpain and release of apoptosis-inducing factor from mitochondria in RCS rat retinal degeneration. Exp. Eye Res. 91 (3), 353–361.

Mizushima, N., 2004. Methods for monitoring autophagy. Int. J. Biochem. Cell Biol. 36 (12), 2491–2502.

Mizushima, N., 2007. Autophagy: process and function. Genes Dev. 21 (22), 2861–2873.

Moriguchi, K., Yoshizawa, K., Shikata, N., Yuri, T., Takada, H., Hada, T., Tsubura, A., 2004. Suppression of *N*-methyl-*N*-nitrosourea-induced photoreceptor apoptosis in rats by docosahexaenoic acid. Ophthal. Res. 36 (2), 98–105.

Moriguchi, K., Yuri, T., Yoshizawa, K., Kiuchi, K., Takada, H., Inoue, Y., Hada, T., Matsumura, M., Tsubura, A., 2003. Dietary docosahexaenoic acid protects against *N*-methyl-*N*-nitrosourea-induced retinal degeneration in rats. Exp. Eye Res. 77 (2), 167–173.

Nakagawa, H., Kiyozuka, Y., Uemura, Y., Senzaki, H., Shikata, N., Hioki, K., Tsubura, A., 2001. Resveratrol inhibits human breast cancer cell growth and may mitigate the effect of linoleic acid, a potent breast cancer cell stimulator. J. Cancer Res. Clin. Oncol. 127 (4), 258–264.

Nakajima, M., Nambu, H., Shikata, N., Senzaki, H., Miki, H., Tsubura, A., 1996a. Pigmentary degeneration induced by

N-methyl-N-nitrosourea and the fate of pigment epithelial cells in the rat retina. Pathol. Int. 46 (11), 874–882.

Nakajima, M., Yuge, K., Senzaki, H., Shikata, N., Miki, H., Uyama, M., Tsubura, A., 1996b. Photoreceptor apoptosis induced by a single systemic administration of N-methyl-N-nitrosourea in the rat retina. Am. J. Pathol. 148 (2), 631–641.

Nambu, H., Taomoto, M., Ogura, E., Tsubura, A., 1998a. Time-specific action of N-methyl-N-nitrosourea in the occurrence of retinal dysplasia and retinal degeneration in neonatal mice. Pathol. Int. 48 (3), 199–205.

Nambu, H., Yoshizawa, K., Yang, J., Yamamoto, D., Tsubura, A., 1998b. Age-specific and dose-dependent retinal dysplasia and degeneration induced by a single intraperitoneal administration of N-methyl-N-nitrosourea to rats. J. Toxicol. Pathol. 11 (2), 127–131.

Nambu, H., Yuge, K., Shikata, N., Tsubura, A., Matsuzawa, A., 1996. Fas-independent apoptosis of photoreceptor cells in C3H mice. Exp. Anim. 45 (4), 309–315.

Nicholls, D.G., Ward, M.W., 2000. Mitochondrial membrane potential and neuronal glutamate excitotoxicity: mortality and millivolts. Trends Neurosci. 23 (4), 166–174.

O'Driscoll, C., O'Connor, J., O'Brien, C.J., Cotter, T.G., 2008. Basic fibroblast growth factor-induced protection from light damage in the mouse retina in vivo. J. Neurochem. 105 (2), 524–536.

Ogino, H., Ito, M., Matsumoto, K., Yagyu, S., Tsuda, H., Hirono, I., Wild, C.P., Montesano, R., 1993. Retinal degeneration induced by N-methyl-N-nitrosourea and detection of 7-methyldeoxyguanosine in the rat retina. Toxicol. Pathol. 21 (1), 21–25.

Oka, T., Nakajima, T., Tamada, Y., Shearer, T.R., Azuma, M., 2007. Contribution of calpains to photoreceptor cell death in N-methyl-N-nitrosourea-treated rats. Exp. Neurol. 204 (1), 39–48.

Oka, T., Walkup, R.D., Tamada, Y., Nakajima, E., Tochigi, A., Shearer, T.R., Azuma, M., 2006. Amelioration of retinal degeneration and proteolysis in acute ocular hypertensive rats by calpain inhibitor ((1S)-1-((((1S)-1-benzyl-3-cyclopropylamino-2,3-di-oxopropyl)amino)carbonyl)-3-methylbutyl)carbamic acid 5-methoxy-3-oxapentyl ester. Neuroscience 141 (4), 2139–2145.

Okuno, S., Saito, A., Hayashi, T., Chan, P.H., 2004. The c-Jun N-terminal protein kinase signaling pathway mediates Bax activation and subsequent neuronal apoptosis through interaction with Bim after transient focal cerebral ischemia. J. Neurosci. 24 (36), 7879–7887.

Organisciak, D.T., Vaughan, D.K., 2010. Retinal light damage: mechanisms and protection. Prog. Retinal Eye Res. 29 (2), 113–134.

Paik, S.S., Jeong, E., Jung, S.W., Ha, S.W., Kang, S., Sim, S., Jeon, J.H., Chun, M.H., Kim, I.B., 2012. Anthocyanins from the seed coat of black soybean reduce retinal degeneration induced by N-methyl-N-nitrosourea. Exp. Eye Res. 97 (1), 55–62.

Paques, M.W., Guizzo, R., Siqueira, R.C., Silva, A.R., Cardillo, J.A., Scott, I.U., Flynn, Jr., H.W., Santos, W.F., Jorge, R., 2006. Neuroprotective effects of intramuscular ketamine in rabbit retinas after pars plana vitrectomy and silicone oil injection. Retina 26 (2), 196–201.

Paquet-Durand, F., Silva, J., Talukdar, T., Johnson, L.E., Azadi, S., van Veen, T., Ueffing, M., Hauck, S.M., Ekström, P.A., 2007. Excessive activation of poly(ADP-ribose) polymerase contributes to inherited photoreceptor degeneration in the retinal degeneration 1 mouse. J. Neurosci. 19 (38), 10311–10319.

Perche, O., Doly, M., Ranchon-Cole, I., 2007. Caspase-dependent apoptosis in light-induced retinal degeneration. Invest. Ophthalmol. Vis. Sci. 48 (6), 2753–2759.

Perche, O., Doly, M., Ranchon-Cole, I., 2008. Transient protective effect of caspase inhibitors in RCS rat. Exp. Eye Res. 86 (3), 519–527.

Petrin, D., Baker, A., Coupland, S.G., Liston, P., Narang, M., Damji, K., Leonard, B., Chiodo, V.A., Timmers, A., Hauswirth, W., Korneluk, R.G., Tsilfidis, C., 2003. Structural and functional protection of photoreceptors from MNU-induced retinal degeneration by the X-linked inhibitor of apoptosis. Invest. Ophthalmol. Vis. Sci. 44 (6), 2757–2763.

Politi, L., Rotstein, N., Carri, N., 2001. Effects of docosahexaenoic acid on retinal development: cellular and molecular aspects. Lipids 36 (9), 927–935.

Portera-Cailliau, C., Sung, C.H., Nathans, J., Adler, R., 1994. Apoptotic photoreceptor cell death in mouse models of retinitis pigmentosa. Proc. Natl. Acad. Sci. USA 91 (3), 974–978.

Punzo, C., Kornacker, K., Cepko, C.L., 2009. Stimulation of the insulin/mTOR pathway delays cone death in a mouse model of retinitis pigmentosa. Nat. Neurosci. 12 (1), 44–52.

Purnell, M.R., Whish, W.J., 1980. Novel inhibitors of poly(ADP-ribose) synthetase. Biochem. J. 185 (3), 775–777.

Remé, C.E., Wolfrum, U., Imsand, C., Hafezi, F., Williams, T.P., 1999. Photoreceptor autophagy: effects of light history on number and opsin content of degradative vacuoles. Invest. Ophthalmol. Vis. Sci. 40 (10), 2398–2404.

Rivas, M.A., Vecino, E., 2009. Animal models and different therapies for treatment of retinitis pigmentosa. Histol. Histopathol. 24 (10), 1295–1322.

Romer, A.S., Parson, T.S., 1978. Who's who among vertebrates. In: Romer, A.S., Parson, T.S. (Eds.), The Vertebrate Body. fifth ed. Saunders, Philadelphia, pp. 75–91.

Rösch, S., Johnen, S., Mataruga, A., Müller, F., Pfarrer, C., Walter, P., 2014. Selective photoreceptor degeneration by intravitreal injection of N-methyl-N-nitrosourea. Invest. Ophthalmol. Vis. Sci. 55 (3), 1711–1723.

Rotstein, N.P., Aveldaño, M.I., Barrantes, F.J., Politi, L.E., 1996. Docosahexaenoic acid is required for the survival of rat retinal photoreceptors in vitro. J. Neurochem. 66 (5), 1851–1859.

Rotstein, N.P., Politi, L.E., German, O.L., Girotti, R., 2003. Protective effect of docosahexaenoic acid on oxidative stress-induced apoptosis of retina photoreceptors. Invest. Ophthalmol. Vis. Sci. 44 (5), 2252–2259.

Sahaboglu, A., Tanimoto, N., Kaur, J., Sancho-Pelluz, J., Huber, G., Fahl, E., Arango-Gonzalez, B., Zrenner, E., Ekström, P., Löwenheim, H., Seeliger, M., Paquet-Durand, F., 2010. PARP1 gene knock-out increases resistance to retinal degeneration without affecting retinal function. PLoS One 5 (11), e15495.

Sancho-Pelluz, J., Arango-Gonzalez, B., Kustermann, S., Romero, F.J., van Veen, T., Zrenner, E., Ekström, P., Paquet-Durand, F., 2008. Photoreceptor cell death mechanisms in inherited retinal degeneration. Mol. Neurobiol. 38 (3), 253–269.

Sanges, D., Comitato, A., Tammaro, R., Marigo, V., 2006. Apoptosis in retinal degeneration involves cross-talk between apoptosis-inducing factor (AIF) and caspase-12 and is blocked by calpain inhibitors. Proc. Natl. Acad. Sci. USA 103 (46), 17366–17371.

Sanz, M.M., Johnson, L.E., Ahuja, S., Ekström, P.A., Romero, J., van Veen, T., 2007. Significant photoreceptor rescue by treatment with a combination of antioxidants in an animal model for retinal degeneration. Neuroscience 145 (3), 1120–1129.

Sato, Y., Mukai, K., Watanabe, S., Goto, M., Shimosato, Y., 1986. The AMeX method. A simplified technique of tissue processing and paraffin embedding with improved preservation of antigens for immunostaining. Am. J. Pathol. 125 (3), 431–435.

Schaller, J.P., Wyman, M., Weisbrode, S.E., Olsen, R.G., 1981. Induction of retinal degeneration in cats by methylnitrosourea and ketamine hydrochloride. Vet. Pathol. 18 (2), 239–247.

Scott, B.L., Racz, E., Lolley, R.N., Bazan, N.G., 1988. Developing rod photoreceptors from normal and mutant Rd mouse retinas: altered fatty acid composition early in development of the mutant. J. Neurosci. Res. 20 (2), 202–211.

Sharma, A.K., Rohrer, B., 2004. Calcium-induced calpain mediates apoptosis via caspase-3 in a mouse photoreceptor cell line. J. Biol. Chem. 279 (34), 35564–35572.

Shimazawa, M., Suemori, S., Inokuchi, Y., Matsunaga, N., Nakajima, Y., Oka, T., Yamamoto, T., Hara, H., 2010. A novel calpain inhibitor, ((1S)-1-((((1S)-1-benzyl-3-cyclopropylamino-2,3-di-oxopropyl)

amino)carbonyl)-3-methylbutyl)carbamic acid 5-methoxy-3-oxapentyl ester (SNJ-1945), reduces murine retinal cell death in vitro and in vivo. J. Pharmacol. Exp. Ther. 332 (2), 380–387.

Shintani, T., Klionsky, D.J., 2004. Autophagy in health and disease: a double-edged sword. Science 306 (5698), 990–995.

Shintani, K., Shechtman, D.L., Gurwood, A.S., 2009. Review and update: current treatment trends for patients with retinitis pigmentosa. Optometry 80, 384–401.

Shirasaki, Y., Yamaguchi, M., Miyashita, H., 2006. Retinal penetration of calpain inhibitors in rats after oral administration. J. Ocular Pharmacol. Ther. 22 (6), 417–424.

Skaper, S.D., 2003. Poly(ADP-ribosyl)ation enzyme-1 as a target for neuroprotection in acute central nervous system injury. Curr. Drug Targets CNS Neurol. Dis. 2 (5), 279–291.

Smith, S.B., Yielding, K.L., 1986. Retinal degeneration in the mouse. A model induced transplacentally by methylnitrosourea. Exp. Eye Res. 43 (5), 791–801.

Strauss, O., 2005. The retinal pigment epithelium in visual function. Physiol. Rev. 85 (3), 845–881.

Suzuki, T., Akimoto, M., Imai, H., Ueda, Y., Mandai, M., Yoshimura, N., Swaroop, A., Takahashi, M., 2007. Chondroitinase ABC treatment enhances synaptogenesis between transplant and host neurons in model of retinal degeneration. Cell Transplant. 16 (5), 493–503.

Takano, Y., Ohguro, H., Dezawa, M., Ishikawa, H., Yamazaki, H., Ohguro, I., Mamiya, K., Metoki, T., Ishikawa, F., Nakazawa, M., 2004. Study of drug effects of calcium channel blockers on retinal degeneration of *rd* mouse. Biochem. Biophys. Res. Commun. 313 (4), 1015–1022.

Takeuchi, K., Nakazawa, M., Mizukoshi, S., 2008. Systemic administration of nilvadipine delays photoreceptor degeneration of heterozygous retinal degeneration slow (rds) mouse. Exp. Eye Res. 86 (1), 60–69.

Taomoto, M., Nambu, H., Senzaki, H., Shikata, N., Oishi, Y., Fujii, T., Miki, H., Uyama, M., Tsubura, A., 1998. Retinal degeneration induced by *N*-methyl-*N*-nitrosourea in Syrian golden hamsters. Graefe's Arch. Clin. Exp. Ophthalmol. 236 (9), 688–695.

Tappeiner, C., Balmer, J., Iglicki, M., Schuerch, K., Jazwinska, A., Enzmann, V., Tschopp, M., 2013. Characteristics of rod regeneration in a novel zebrafish retinal degeneration model using *N*-methyl-*N*-nitrosourea (MNU). PLoS One 8 (8), e71064.

Thanos, C., Emerich, D., 2005. Delivery of neurotrophic factors and therapeutic proteins for retinal diseases. Exp. Opin. Biol. Ther. 5 (11), 1443–1452.

Tsai, L.H., Delalle, I., Caviness, Jr., V.S., Chae, T., Harlow, E., 1994. p35 is a neural-specific regulatory subunit of cyclin-dependent kinase 5. Nature 371 (6496), 419–423.

Tso, M.O., Zhang, C., Abler, A.S., Chang, C.J., Wong, F., Chang, G.Q, Lam, T.T., 1994. Apoptosis leads to photoreceptor degeneration in inherited retinal dystrophy of RCS rats. Invest. Ophthalmol. Vis. Sci. 35 (6), 2693–2699.

Tsubura, A., Shikata, N., Oyaizu, T., Takahashi, H., 1995. Experimental models for carcinogenesis in the house musk shrew, Suncus murinus insectivora. Histol. Histopathol. 10 (4), 1047–1055.

Tsuruma, K., Yamauchi, M., Inokuchi, Y., Sugitani, S., Shimazawa, M., Hara, H., 2012. Role of oxidative stress in retinal photoreceptor cell death in *N*-methyl-*N*-nitrosourea-treated mice. J. Pharmacol. Sci. 118 (3), 351–362.

Tsubura, A., Yoshizawa, K., Miki, H., Oishi, Y., Fujii, T., 1998. Phylogenetic and ontogenetic study of retinal lesions induced by *N*-methyl-*N*-nitrosourea in animals. Anim. Eye Res. 17 (3–4), 97–103, (in Japanese, Abstract in English).

Uehara, N., Miki, K., Tsukamoto, R., Matsuoka, Y., Tsubura, A., 2006. Nicotinamide blocks *N*-methyl-*N*-nitrosourea-induced photoreceptor cell apoptosis in rats through poly (ADP-ribose) polymerase activity and Jun N-terminal kinase/activator protein-1 pathway inhibition. Exp. Eye Res. 82 (3), 488–495.

Vermeulen, L., De Wilde, G., Notebaert, S., Vanden Berghe, W., Haegeman, G., 2002. Regulation of the transcriptional activity of the nuclear factor-kappa B p65 subunit. Biochem. Pharmacol. 64 (5–6), 963–970.

Voaden, M.J., 1991. Retinitis pigmentosa and its models. Prog. Retinal Eye Res. 10, 293–331.

Vosler, P.S., Sun, D., Wang, S., Gao, Y., Kintner, D.B., Signore, A.P., Cao, G., Chen, J., 2009. Calcium dysregulation induces apoptosis-inducing factor release: Cross-talk between PARP-1- and calpain-signaling pathways. Exp. Neurol. 218 (2), 213–220.

Wan, J., Zheng, H., Chen, Z.L., Xiao, H.L., Shen, Z.J., Zhou, G.M., 2008. Preferential regeneration of photoreceptor from Müller glia after retinal degeneration in adult rat. Vision Res. 48 (2), 223–234.

Weisberger, J., Williams, G., 1975. Metabolism of chemical carcinogens. Becker, F. (Ed.), Cancer: A Comprehensive Treatise, vol. 1, Plenum Publishers, New York, pp. 185–234.

Wenzel, A., Grimm, C., Marti, A., Kueng-Hitz, N., Hafezi, F., Niemeyer, G., Remé, C.E., 2000. c-fos controls the "private pathway" of light-induced apoptosis of retinal photoreceptors. J. Neurosci. 20 (1), 81–88.

Wu, J., Trogadis, J., Bremner, R., 2001. Rod and cone degeneration in the rd mouse is p53 independent. Mol. Vision 7, 101–106.

Wu, X., Su, Z., Li, X., Zheng, Q., Huang, Y., Yuan, H., 2005. High-level expression and purification of a nonmitogenic form of human acidic fibroblast growth factor in *Escherichia coli*. Protein Expr. Purif. 42 (1), 7–11.

Xia, Z., Dickens, M., Raingeaud, J., Davis, R.J., Greenberg, M.E., 1995. Opposing effects of ERK and JNK-p38 MAP kinases on apoptosis. Science 270 (5240), 1326–1331.

Xu, H., Yang, J.N., Li, X.K., Zheng, Q., Zhao, W., Su, Z.J., Huang, Y.D., 2008. Retina protective effect of acidic fibroblast growth factor after canceling its mitogenic activity. J. Ocular Pharmacol. Ther. 24 (5), 445–451.

Yamauchi, Y., Kimura, K., Agawa, T., Tsukahara, R., Mishima, M., Yamakawa, N., Goto, H., 2011. Correlation between high-resolution optical coherence tomography (OCT) images and histopathology in an *N*-methyl-*N*-nitrosourea-induced retinal degeneration rat model. Br. J. Ophthalmol. 95 (8), 1161–1615.

Yang, L., Li, D., Chen, J., Yang, J., Xue, L., Hu, S., Wu, K., 2007. Microarray expression analysis of the early *N*-methy-*N*-nitrosourea-induced retinal degeneration in rat. Neurosci. Lett. 418 (1), 38–43.

Yoshizawa, K., Kiuchi, K., Nambu, H., Yang, J., Senzaki, H., Kiyozuka, Y., Shikata, N., Tsubura, A., 2002. Caspase-3 inhibitor transiently delays inherited retinal degeneration in C3H mice carrying the *rd* gene. Graefe's Arch. Clin. Exp. Ophthalmol. 240 (3), 214–219.

Yoshizawa, K., Kuwata, M., Kawanaka, A., Uehara, N., Yuri, T., Tsubura, A., 2009. *N*-Methyl-*N*-nitrosourea-induced retinal degeneration in mice is independent of the p53 gene. Mol. Vision 15, 2919–2925.

Yoshizawa, K., Nambu, H., Yang, J., Oishi, Y., Senzaki, H., Shikata, N., Miki, H., Tsubura, A., 1999. Mechanisms of photoreceptor cell apoptosis induced by *N*-methyl-*N*-nitrosourea in Sprague-Dawley rats. Lab. Invest. 79 (11), 1359–1367.

Yoshizawa, K., Sasaki, T., Kuro, M., Uehara, N., Takada, H., Harauma, A., Ohara, N., Moriguchi, T., Tsubura, A., 2013. Arachidonic acid supplementation during gestational, lactational and post-weaning period rescues retinal degeneration in a rodent model. Br. J. Nutr. 109 (8), 1424–1432.

Yoshizawa, K., Yang, J., Senzaki, H., Uemura, Y., Kiyozuka, Y., Shikata, N., Oishi, Y., Miki, H., Tsubura, A., 2000. Caspase-3 inhibitor rescues *N*-methyl-*N*-nitrosourea-induced retinal degeneration in Sprague-Dawley rats. Exp. Eye Res. 71 (6), 629–635.

Yuge, K., Nambu, H., Senzaki, H., Nakao, I., Miki, H., Uyama, M., Tsubura, A., 1996. *N*-Methyl-*N*-nitrosourea-induced photoreceptor apoptosis in the mouse retina. In Vivo 10 (5), 483–488.

Zeiss, C.J., Neal, J., Johnson, E.A., 2004. Caspase-3 in postnatal retinal development and degeneration. Invest. Ophthalmol. Vis. Sci. 45 (3), 964–970.

Zeng, H.Y., Tso, M.O., Lai, S., Lai, H., 2008. Activation of nuclear factor-kappaB during retinal degeneration in rd mice. Mol. Vision 14, 1075–1080.

Zou, X., Patterson, T.A., Sadovova, N., Twaddle, N.C., Doerge, D.R., Zhang, X., Fu, X., Hanig, J.P., Paule, M.G., Slikker, W., Wang, C.,

2009. Potential neurotoxicity of ketamine in the developing rat brain. Toxicol. Sci. 108 (1), 149–158.

Zulliger, R., Lecaudé, S., Eigeldinger-Berthou, S., Wolf-Schnurrbusch, U.E., Enzmann, V., 2011. Caspase-3-independent photoreceptor degeneration by *N*-methyl-*N*-nitrosourea (MNU) induces morphological and functional changes in the mouse retina. Graefe's Arch. Clin. Exp. Ophthalmol. 249 (6), 859–869.

CARDIAC AND CARDIOVASCULAR

Page left intentionally blank

CHAPTER

6

Animal Models for Cardiovascular Research

You-Tang Shen**, Li Chen*, Jeffrey M. Testani†, Christopher P. Regan*, Richard P. Shannon‡

*Merck Research Laboratories, Merck & Co., Inc., West Point, PA, United States
**University of Pennsylvania, Philadelphia, PA, United States
†Yale University, New Haven, CT, United States
‡University of Virginia, Charlottesville, VA, United States

1 INTRODUCTION

Cardiovascular diseases are the leading cause of mortality and morbidity in the United States. Although the incidence has been declining over the past decades, the mechanisms of diseases are still incompletely understood and developments of new therapeutic approaches are required. Both of these critical activities rely heavily on basic and preclinical research in which highly relevant animal models are required for accurate translational research from novel discovery at the bench to treatment at the bedside. Currently, more than 90% of all laboratory animals are mice and rats. Obviously, there are several advantages of using rodent species. First, it is easy to maintain and also costs less compared to larger animal species. Second, mice and rats reproduce quickly and have a short lifespan. Most importantly, rodent, particularly mice, are easily amenable to genetic manipulation, either through conventional gene knockout, knock-in, transgenic expression, and/or inducible systems where genes expression can be altered at specific times. Because of this, the vast majority molecular and genomic mechanistic insight into cardiovascular development and diseases has come from genetically-engineered

mouse models. However, it has been recently noticed that many potential exciting therapeutic interventions have ultimately failed in clinical trials; thus, exposing a significant gap between preclinical research data and clinical trial results (Arrowsmith, 2011; Mullard, 2011; Prinz et al., 2011). Additionally, irreproducibility between different laboratories has increased significantly (Arrowsmith, 2011; Mullard, 2011; Prinz et al., 2011). Besides the major species difference between rodent and human as one of the answers, multiple physiological measurements from different directions are difficult to be performed and also less reproducible in the rodent species, which also contribute to the inconsistency between laboratories, as well as between these small animals and humans. Anesthesia and recent surgical trauma is another important factor to influence laboratory results. Accordingly, a suitable larger animal model, such as dogs and pigs, under conscious state with appropriate direct measurements of cardiovascular function is needed to complement early rodent studies and to serve as a better translational research tool. It should be further pointed out that contradictory results in drug discovery, as well as cardiovascular control can even be found between nonhuman primates and other larger mammals (Shen, 2010). To conduct experiments in nonhuman primates, it requires special resources, techniques, expertise, and consideration of welfare concerns; hence, medical research using nonhuman primates currently only represents <0.3% of the laboratory animals used. Nevertheless, nonhuman primates still to be considered as important translatable model, as it has unique advantage of significant physiological, metabolic, biochemical, and genetic similarity with humans (Shen, 2010; Shen et al., 2008a). Current chapter is focused on, but not exclusive to, surgically manipulated larger animal models including nonhuman primates. Equally important, several factors that influence model characteristics, as well as considerations for accurate preclinical cardiovascular measurements and correct data interpretation are also discussed. Genetically engineered and chemically or diet-induced animal models are beyond the scope of this chapter.

2 MYOCARDIAL ISCHEMIC MODELS

2.1 Brief Coronary Artery Occlusion-Induced Myocardial Stunning

Coronary artery spasm, myocardial revascularization, and coronary artery bypass grafting often produce a consequence of a brief myocardial ischemia with a reversible, but prolonged, regional myocardial dysfunction for hours to days in patients. This clinical phenomenon has been termed as "myocardial stunning." The first post-

ischemia induced myocardial dysfunction in conscious dog model was described by Heyndrickx et al. (1975). During the past three decades, myocardial stunning was extensively studied in different animal species, primarily dogs, pigs, rabbits, and nonhuman primates (Bolli and Marban, 1999; Shen and Vatner, 1996). Brief coronary artery occlusion and reperfusion can be achieved by transiently inflating and deflating a surgically-implanted hydraulic occluder around either the left circumflex or left anterior descending coronary artery. The duration of coronary artery occlusion should not be more than 15 min to avoid irreversible myocardial injury. The regional myocardial dysfunction is closely correlated with the duration of coronary artery occlusion. Thus, the confirmation of complete coronary artery occlusion and reperfusion is critical for a reproducible consistent pattern of myocardial dysfunction within and among experiments when same ischemic protocol is utilized. Ideally, a coronary blood flow probe proximal to the occluder needs to be implanted for continuously monitoring of coronary blood flow during the entire experiment. The regional myocardial function in both potential ischemic zone and contralateral nonischemic zone, which is the end point for myocardial stunning, can be measured directly using a transit time dimension gauge technique (Shen and Vatner, 1996; Shen et al., 2008a). Concomitant continuous measurements of both coronary blood flow and regional myocardial function are essential for the study of myocardial stunning. Other physiological measurements should be also considered which include arterial pressure, heart rate, as well as left ventricular (LV) pressure, and its first derivative (dP/dt). These parameters along with regional myocardial function and coronary blood flow provide a comprehensive profile for assessment of myocardial stunning. Fig. 6.1 illustrates the changes in continuous waveforms of LV pressure, LV dP/dt, wall thickness of posterior and anterior left ventricular walls, coronary blood flow, and heart rate in a chronically instrumented conscious dog during brief coronary artery occlusion.

The degree of myocardial stunning is characterized by both the level of regional myocardial dysfunction and the duration of myocardial function recovery. There are several factors to affect the degree of myocardial stunning, which can lead to increase variability or lack of reproducibility. First, incomplete coronary artery occlusion, even residual leak of coronary blood flow, can result in significantly less myocardial stunning as compared to a complete coronary artery occlusion. Usually, this can be easily detected from coronary blood flow and regional myocardial function in the ischemic zone. However, the change in regional function can also be induced by opening collateral channels, rather than incomplete coronary artery occlusion, particularly in dog species, where coronary precollateral channels are present.
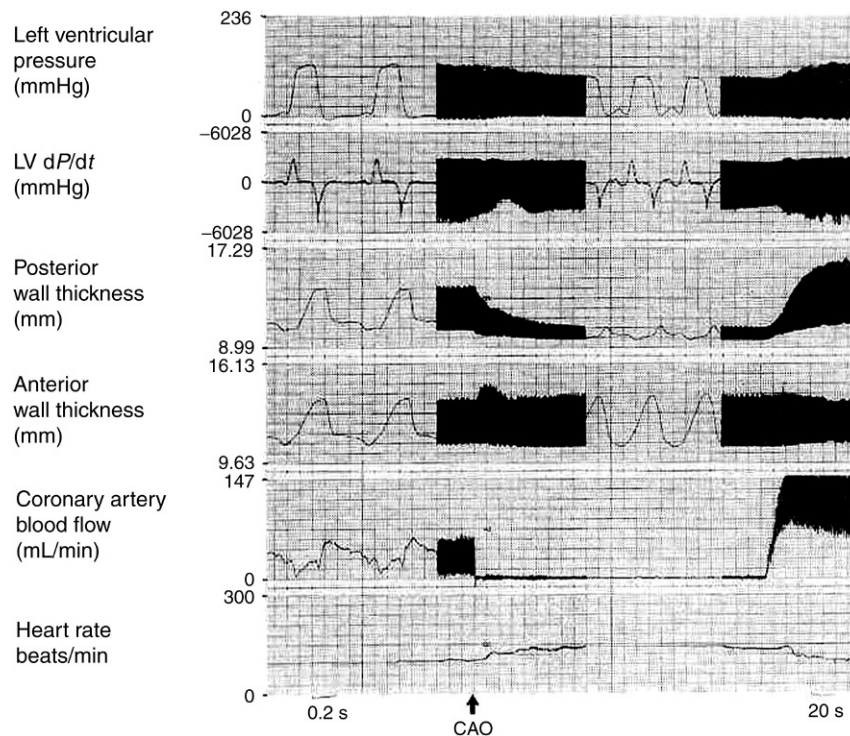
FIGURE 6.1 **Effects of brief left circumflex coronary artery occlusion on systolic wall thickening in posterior ischemic and anterior nonischemic walls.** Note that wall thickening in the posterior wall was diminished during the coronary artery occlusion which was confirmed by complete loss of coronary blood flow (Shen et al., 1988).

Second, where regional myocardial function is measured within the ischemic area can produce marked variability of myocardial stunning in different animals. The closer the center of ischemic area the more severity of myocardial dysfunction is. When the location of myocardial function measured is close to boarder zone, the myocardial stunning often cannot be clearly detected. Thus, it is important to know the exact potential ischemic zone and then find the center of ischemic zone for measurement of regional myocardial function before study is performed. This can be easily achieved by a brief coronary artery occlusion, that is, less than 10 s during the surgery, to induce a temporal color change of epimyocardium to outline of the ischemic zone. The dimension gauge should be placed as close to central ischemic zone as possible. A representative regional myocardial function recording in a chronically instrumented conscious dog during control, left circumflex coronary artery occlusion, and after coronary artery reperfusion is shown in Fig. 6.2.

Noninvasive techniques, such as echocardiograph, are more limited in sensitivity. It is also relatively difficult to repeatedly measure the regional myocardial function in the exact same location over the time, a limitation not present with the direct measurement via fixed, chronically implanted ultrasonic dimension gauge. Further, when longitudinal or repeated myocardial stunning data are compared in the same animal, the slight change in location of measurement via noninvasive techniques should be carefully considered.

Although myocardial stunning in the dog model has been studied extensively, one of the major concerns for this particular species is that myocardial stunning cannot be reproduced when the same experiment is performed several days later. Our previous study demonstrated that reductions in regional myocardial function, assessed by systolic wall thickening via surgically implanted dimension gauge, were significantly less in the 2nd and 3rd myocardial stunning experiments as compared to the 1st experiment (Shen and Vatner, 1996). Interestingly, the same repeated ischemic protocol studied in pigs does not show the "preconditioning-like effects" as seen in the dog model (Shen and Vatner, 1996). The effects of three separate 10-min coronary artery occlusions, each 2 days apart, on systolic wall thickening in both ischemic and nonischemic zone in conscious dogs and pigs are shown in Figs. 6.3 and 6.4, respectively. Clearly, repeated myocardial stunning performed in dog model results in a great variability compared to that observed in pigs. Understanding the different characteristics of myocardial stunning in different species is important for choosing a right model to meet goals of different studies.

Myocardial stunning can also be performed in conscious or tranquilized nonhuman primate models, that is, monkey or baboon. The basic implanted transducers
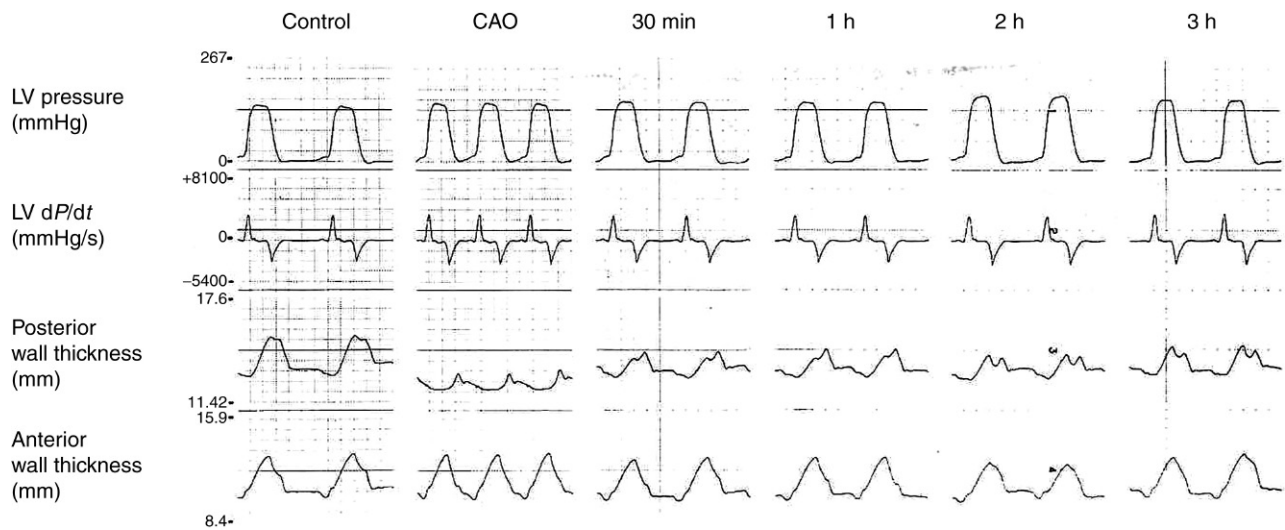
FIGURE 6.2	**Phasic waveforms of left ventricular (LV) pressure, rate of change of LV pressure (dP/dt), and posterior and anterior wall thickness in a conscious dog subjected to 10 min of coronary artery occlusion (CAO) followed by 3 h of coronary artery reperfusion.** Note there was no major effect on systolic wall thickening in nonischemic (anterior) zone, whereas systolic wall thickening in ischemic (posterior) wall zone reversed to wall thinning during CAO and was depressed at 3 h of CAR (Shen and Vatner, 1996).
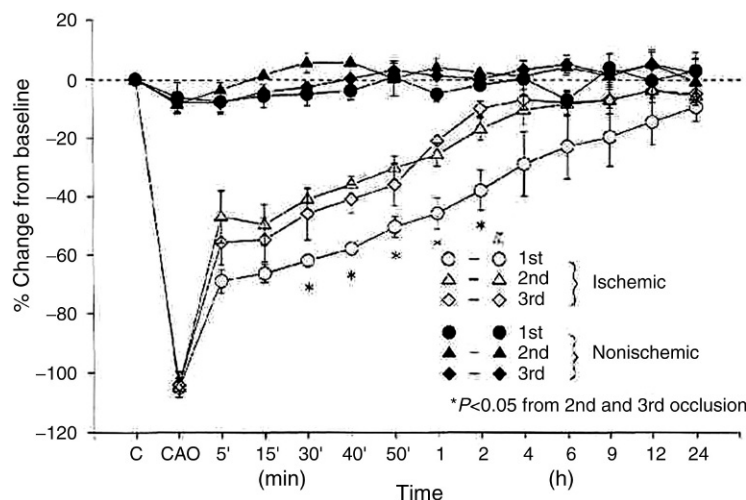
FIGURE 6.3	**Three separate 10 min of coronary artery occlusion (CAO) and reperfusion, performed 2 days apart, in conscious dogs.** Note that following coronary artery reperfusion, depression of systolic wall thickening in the ischemic zone was more severe and prolonged after 1st coronary occlusion than after 2nd and 3rd occlusions. *$P < 0.05$, 1st versus 2nd and 3rd coronary occlusions (Shen and Vatner, 1996).

and experimental protocols are similar to those used in dog or pig models. Since left ventricular wall thickness in nonhuman primates are often smaller than those seen in dogs and pigs, regional myocardial function usually is assessed using left ventricular segmental length, rather than wall thickness, via implanted ultrasonic dimension gauges in the remote, adjacent, and central risk areas. Fig. 6.5 shows a schematic illustration for instrumentation and direct measurements for cardiac global and regional myocardial segmental length in a conscious monkey subjected to a brief coronary artery occlusion. A typical experimental set up in conscious nonhuman primates is shown in Fig. 6.6.

2.2 Chronic Coronary Stenosis

Coronary artery stenosis is one of the most common symptoms in patients with heart disease. It is usually caused by chronic atherosclerosis accumulation on the inner linings of arteries, which restricts coronary blood flow to the myocardium. Since the pathophysiological process of coronary artery stenosis has been well understood, it is relatively easy to use a highly atherogenic diet to induce a chronic arterial stenosis model in different species (Moghadasian, 2002). The limitation, however, is that the model development requires a long period of time. Recent transgenic/knockout animal models have
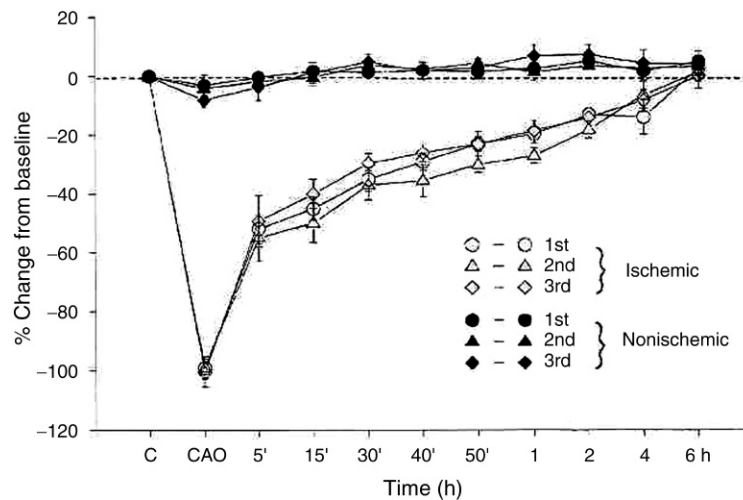
FIGURE 6.4 **Three separate 10 min of coronary artery occlusion (CAO) and reperfusion, performed 2 days apart, in conscious pigs.** Note that following coronary artery reperfusion, depression of systolic wall thickening in the ischemic zone was similar among three separate performed coronary artery occlusion and reperfusion. (Shen and Vatner, 1996).
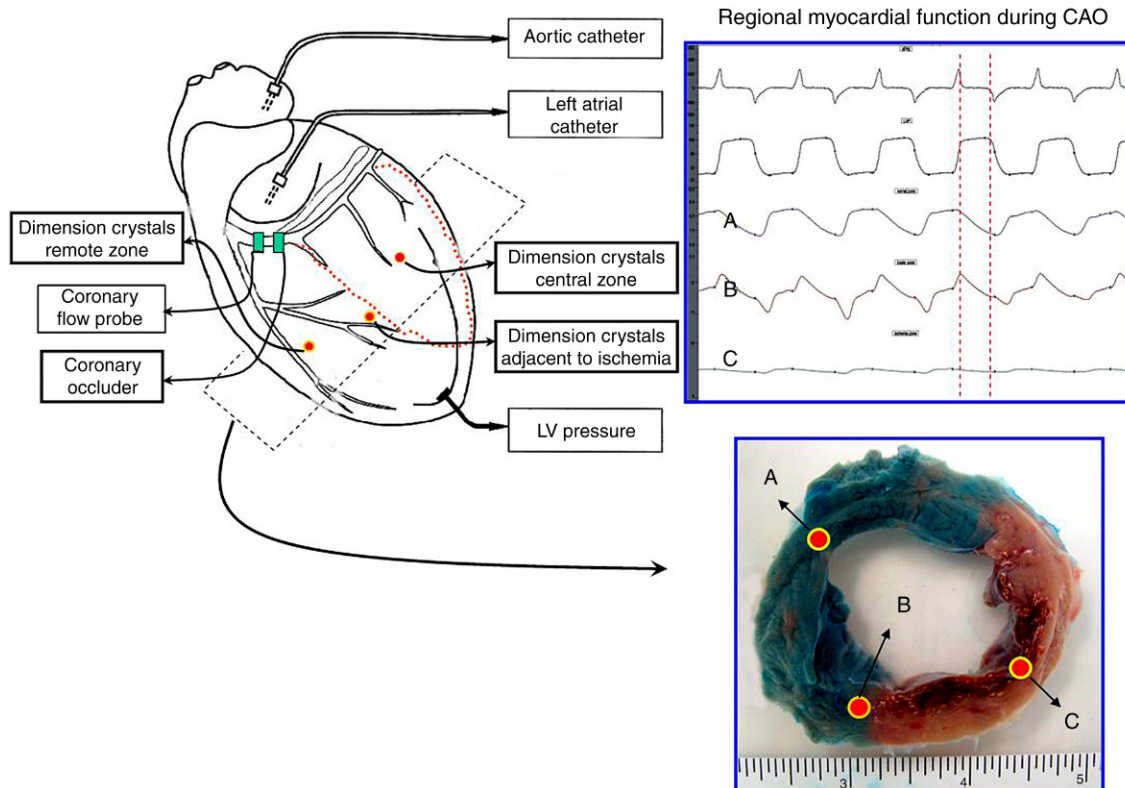
FIGURE 6.5 During brief coronary artery occlusion (CAO), there was a complete loss of regional segmental length in the central ischemic zone (C) during systolic phase, while remote nonischemic zone was reduced normally (A). The function in the adjacent to ischemic zone (B) became nonsynchronous, as compared to the remote nonischemic zone (unpublished report).

the advantage to develop atherogenesis faster without special diet need, but are limited to rodent, where physiological measurements are difficult to be made as stated earlier. In the current section, two chronic coronary artery stenosis models in conscious pigs are described. It is well accepted that the pig is a better model for chronic myocardial ischemic studies, as compared to dog models which has well established, preexisting collateral channels that can significantly alter myocardial function and extent of stenosis-induced ischemia.

Ameroid constrictor, a special device for gradual reduction in coronary blood flow, has been used extensively

Diagram of the tether system
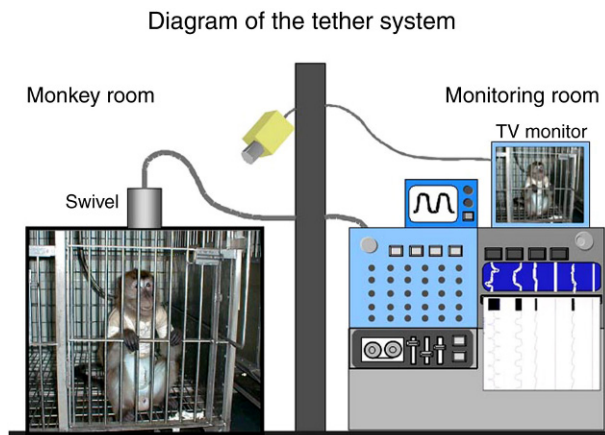
FIGURE 6.6 **Illustration of experiment conducted in conscious monkey via a tether system (unpublished report).**

for studies of coronary artery stenosis in pigs over past several decades. The constrictor is made by casein inside a ring of stainless steel, which swells at a predictable rate over time as it absorbs body fluid and eventually blocks the lumen of ring. The lumen diameter of constrictor is usually from 2–4 mm depending on the size of coronary artery. Because of the properties of this device, the coronary stenosis is progressively increased leading to complete or almost complete coronary artery occlusion after the device is implanted for weeks to months. The Ameroid constrictor can be implanted around either left circumflex or left anterior descending coronary arteries. In order to prevent surgically induced preconstriction, the coronary artery should be isolated longer than the width of the Ameroid constrictor. The size of Ameroid constrictor selected should be very similar to the diameter of vessel. However, the diameter of coronary artery is often significantly less, soon after it is isolated owing to the phenomenon of mechanically-induced constriction from the surgical isolation procedure in pig. Because if this, the correct diameter of coronary artery should be determined at least 10–15 min after the dissection is completed. To help the coronary artery restore to its initial condition, applying a few drops of lidocaine on the surface of coronary artery is often helpful.

The speed of gradual lumen closure from the Ameroid constrictor has been studied in vitro (Elzingz, 1969; Monnet and Rosenberg, 2005). Using a constant perfusion system to simulate in vivo coronary blood flow rate, Elzingz demonstrated that the flow through Ameroid constrictor placed in a warm saline bath was reduced to minimal level, that is, 3 ± 1 mL/min, from a baseline of 47 ± 0 mL/min after 10 days. When the Ameroid constrictor was coated with silicone, the flow reduction was significantly slower, that is, 20 ± 2, 11 ± 2, and 7 ± 2 from baseline of 46 ± 0 mL/min at 10, 20, and 40 days, respectively (Elzingz, 1969). A report by Monnet and Rosenberg showed that Ameroid constrictors incubated in saline or

plasma diluted with saline to obtain a different protein concentrations were not completely closed at 27 days and lumen diameter was 0.21 ± 0.22 mm from baseline of 3.5 mm. The experiments further indicated that the high plasma protein concentrations caused more rapid closure than the others (Monnet and Rosenberg, 2005). These in vitro data provide direct evidence for better understanding of the changes in lumen diameter in vivo. However, the real change in vivo can be different from those fixed in vitro conditions, as several factors could affect the pattern of coronary stenosis, for example, the size of Ameroid constrictor selected, level of body fluid and/or blood accumulated in the location of the Ameroid constrictor placed, etc. Ideally, a hydraulic occluder distal to the Ameroid constrictor should be implanted along with other measurements in the myocardial area perfused by the coronary artery in order to determine the degree of coronary stenosis. First, the changes in blood flow and regional function can be observed, but not precisely, in resting condition when the Ameroid constrictor progressively reduces the diameter of coronary artery. Next, when the hydraulic occluder is applied for several seconds to minutes, either blood flow or regional myocardial function should change significantly if the coronary blood flow is not altered by the Ameroid constrictor, that is, very early time postimplantation of Ameroid constrictor. When the Ameroid constrictor progressively reduces the diameter of coronary artery, the brief coronary artery occlusion induced changes in blood flow or function should be also gradually less. By using combination of hydraulic occluder with flow/function measurements, the degree of Ameroid constrictor induced coronary stenosis in conscious pigs was demonstrated in our previous study (Shen and Vatner, 1995). Examples of the effects of brief coronary artery occlusion on regional myocardial function and myocardial blood flow during progressive coronary stenosis in conscious pigs are shown in Figs. 6.7 and 6.8. At day 1 of Ameroid constrictor implanted, a time point when the constrictor should have no effect of coronary artery diameter, brief coronary artery occlusion resulted in maximal changes in both regional function (Fig. 6.7) and blood flow (Fig. 6.8). At 20 days after the Ameroid constrictor was implanted, the baseline regional function, but not blood flow, was depressed compared to day 1. Further, coronary artery occlusion did not suppress the blood flow to minimum. The regional function was also detected, indicating that partial blood flow still passed the Ameroid constrictor. The amount of blood flow detected was from contralateral myocardium via newly developed collateral circulation due to chronic coronary stenosis. At 32 days, baseline myocardial function was returned toward the level of baseline at Day 1 and brief coronary artery occlusion did not induce significant changes in both function and blood flow, indicating that collateralization has been
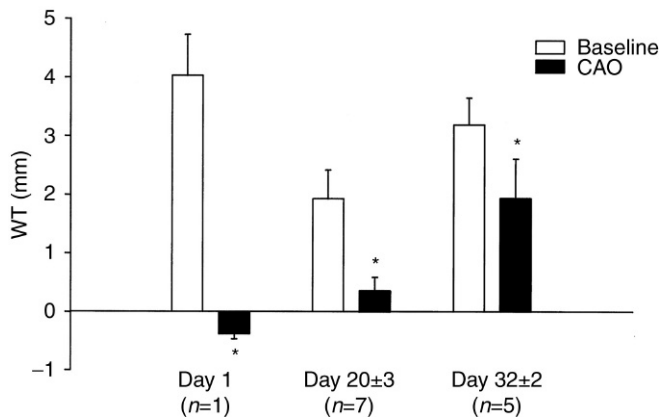
FIGURE 6.7 **Effects of brief coronary artery occlusion (CAO) using hydraulic occluder placed distal to Ameroid contractor on left circumflex coronary artery on systolic wall thickening (WT) at day 1, day 20, and day 32 in conscious pigs.** Note that CAO induced progressively less of a deficit in systolic WT as the stenosis gradually increased and collateral developed (Shen and Vatner, 1995).

well developed and the Ameroid contractor was almost completely closed, which cannot play any role in control regional myocardial function and blood flow.

Our prior study provides a comprehensive picture of the relationship between Ameroid constrictor and degree of coronary stenosis in conscious animal model. Since this model produces a progressive, but nonsustained, stenosis leading to almost complete coronary artery occlusion, it cannot represent a typical chronic coronary stenosis induced myocardial hibernation seen in patients (Shen and Vatner, 1995). On the other hand, this model is useful to study coronary revascularization as the collateral vessels are rapidly developed by myocardial ischemia induced by severe coronary stenosis.

Chronic coronary stenosis can also be induced in pig model using either a hydraulic occluder (Kim et al., 2003; Shen et al., 2008b; St. Louis et al., 2000) or a fixed diameter device (Fallavollita et al., 2001; Page et al., 2008). The surgical preparation is similar to those from the Ameroid constrictor induced stenosis model. Either left circumflex or left anterior descending coronary arteries can be used. The results from several laboratories have shown that the coronary blood flow can be reduced 30%–90% for hours when a hydraulic occluder was applied (Kim et al., 2003; Shen et al., 2008b; St. Louis et al., 2000). Studies from fixed diameter devices, that is, 1.5–2.0 mm, implanted on coronary artery demonstrated that both myocardial function and blood flow were reduced substantially at 2–3 months after surgery, suggesting a hibernating myocardium developed (Fallavollita et al., 2001; Page et al., 2008).

However, it should be pointed out that one important phenomenon of coronary circulation is autoregulation mechanism, a unique intrinsic ability to maintain a constant myocardial blood flow when the perfusion pressure is changed. Briefly, when the coronary artery is partially occluded, the coronary artery pressure distal to the occlusion initially reduced and myocardial blood flow in this area also falls. The blood flow then returns toward baseline within few minutes, as the coronary vasculature dilates (i.e., coronary vascular resistance decreased). In most circumstances, new established steady-state blood flow could be very close to baseline, that is, before coronary stenosis, despite the reduced perfusion pressure induced by partial occlusion. Only when the perfusion pressure is beyond the range of coronary autoregulation, blood flow decreases passively in parallel with
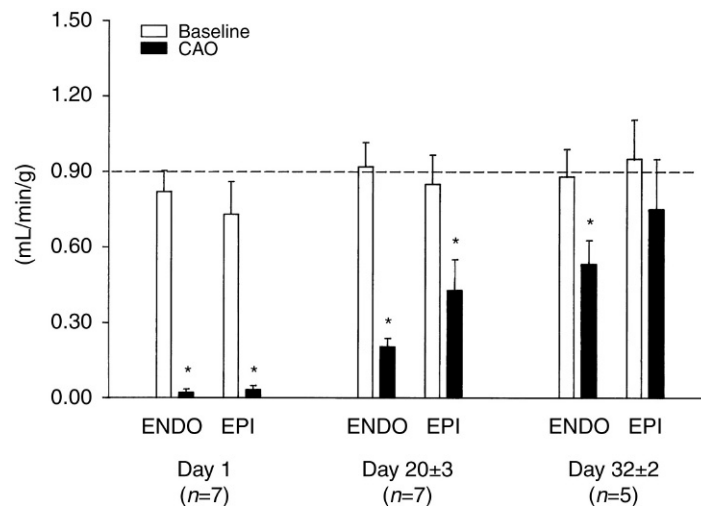
FIGURE 6.8 **Effects of brief coronary artery occlusion (CAO) using hydraulic occluder placed distal to Ameroid contractor on left circumflex coronary artery on regional myocardial blood flow in endo- (ENDO) and epi-(EPI) myocardium systolic wall thickening (WT) at day 1, day 20, and day 32 in conscious pigs.** Note that CAO reduced blood flow in both layers, and still decreased blood flow at 20 days, indicating that coronary artery was not occluded. However, CAO only slightly decreased ENDO but not EPI blood flow at 32 days, indicating that collateral had developed extensively (Shen and Vatner, 1995).

the reduction in perfusion pressure. Based upon this well-established concept of autoregulation, it is unlikely to keep a sustained reduction in coronary blood flow when a hydraulic occluder or fixed diameter device are used. Indeed, our prior experiments using a hydraulic occluder to maintain coronary stenosis found that coronary blood flow cannot be controlled at a fixed reduction level. In fact, the reduction in coronary blood flow during short period of time, that is, less than 15 min period, varied from 35% to 45% even with repeated and precise stenosis adjustments made (Shen et al., 2008b). This was also described in the study by St. Louis et al. (2000). Despite of the limitation of this model, partial coronary stenosis that does not significantly induce collateralization provides a model to study the hibernating myocardium. In addition, the difference between these models versus human hibernating myocardium is the absence of atherosclerotic vascular disease.

2.3 Prolonged Coronary Artery Occlusion With and Without Reperfusion-Induced Myocardial Infarction

Myocardial infarction (MI) refers to the interruption of coronary blood supply to certain myocardial area which leads to irreversible myocardial tissue death. Most commonly seen MI in patients comes from complete blockage of a coronary artery following the rupture of a vulnerable atherosclerotic plaque. The extent to which MI is developed depends upon duration and location of the

coronary artery occlusion. Animal models of MI can be achieved by direct occlusion of coronary artery using either reversible hydraulic occluder or ligation. Numerous studies from different species including, mice, rat, rabbit, dog, pig, and nonhuman primates, have been reported previously. Since the procedure to produce MI seems to be straightforward, the detailed description of the procedure in different species is not included in this section. Since myocardial infarct size can be easily influenced by several factors including assessment of infarct size, these areas are particularly emphasized in the current section.

Protocols for induction of MI vary from permanent coronary artery occlusion to coronary artery occlusion followed by reperfusion. The minimal time required for coronary artery occlusion-induced MI in most species should not be less than 20–30 min, which provides a clear and minimal size of MI. It is well known that the infarct size is closely correlated with the duration of coronary artery occlusion. However, the relationship does not appear to be linear, particularly when the time of occlusion is beyond 90 min in most species. Our previous studies in a conscious dog model showed that a 40- and 90-min of coronary artery occlusion resulted in about 16 and 32% of infarct size, respectively (Shen et al., 1996a), while 24 h of coronary artery occlusion induced about 45% of infarct size (Shen et al., 1988) as shown in Fig. 6.9. The relationship between the duration of coronary artery occlusion and infarct size in conscious pig model blunted compared to the dog model. Our previous results found that the infarct size was 46, 54, and 53% from the 40, 60,
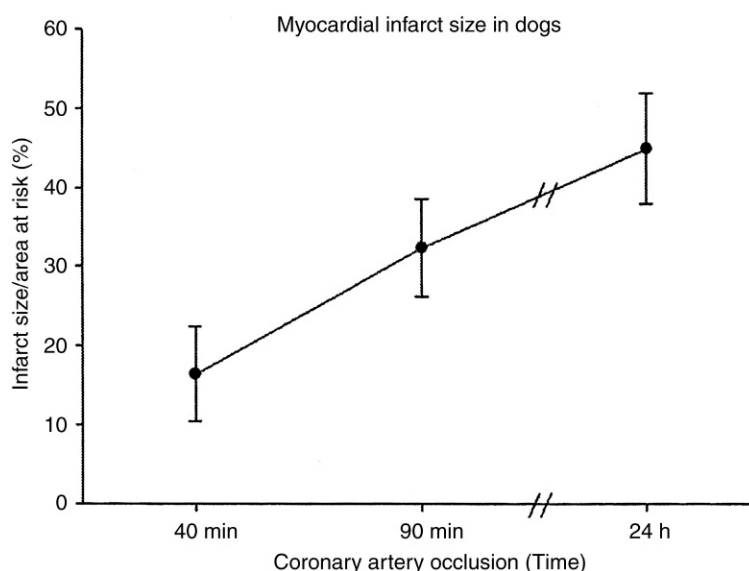
FIGURE 6.9   **Effects of different time of coronary artery occlusion on infarct size, expressed by infarct size/area at risk, in conscious dogs.** Note that there is a nonlinear relationship between the duration of coronary occlusion and infarct size. *Source: Replotted based on data from Shen, Y-T., Fallon, J.T., Iwase, M., Vatner, S.F., 1996b. Innate protection of baboon myocardium following coronary artery occlusion and reperfusion. Am. J. Physiol. 270, H1812–H1818; Shen, Y-T, Knight, D.R., Vatner, S.F., Randall, W.C., Thomas, J.X., Jr, 1988. Responses to coronary artery occlusion in conscious dogs with selective cardiac denervation. Am. J. Physiol. 255, H525–H533.*
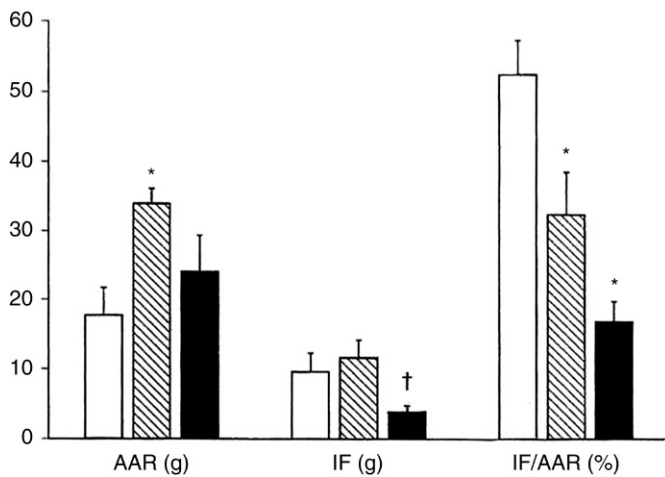
FIGURE 6.10 **Effects of 90 min of coronary artery occlusion (CAO) and reperfusion (CAR) on area at risk (AAR), infarct size (IF), and IF expressed as percentage of AAR (IF/AAR) in conscious pigs** *(open bars),* **dogs** *(hatched bars),* **and baboons** *(filled bar).* The IF/AAR was greatest in pigs and least in baboons (Shen et al., 1996a).

and 90 min of coronary artery occlusion, respectively (Chen et al., 2011; Shen et al., 1996a).

Our prior study demonstrated that there are major species differences in infarct size among conscious dogs, pigs, and nonhuman primates (Shen et al., 1996a). As shown in Fig. 6.10, a 90-min of coronary artery occlusion resulted in a significantly greater infarct size in pigs compared to dogs and baboons. It is not surprising the difference between dog and pig species, because of the difference in preexisting collateral channels. Interestingly, both baboons and pigs are characterized by similar collateral circulation, but show a significant difference in infarct size (Shen et al., 1996a). Although the mechanism of the major difference in infarct size between these two species is unclear, the difference could be partially attributed to natural protective mechanisms and/or less coronary reperfusion-induced myocardial injury in baboon, as evidenced by more blood flow in the endomyocardial layers during the time of reperfusion in baboons compared to pigs (Shen et al., 1996a). Also, it should be mentioned that the same species but different strain could also make the difference in infarct size, for example, beagle would have a greater infarct size than mongrel dogs (Uemura et al., 1989).

Several other factors are also involved in development of infarct size. The site of coronary artery occlusion or ligation is an obvious one, that is, the more proximal to the origin of coronary artery; the more infarct size would be. In larger animal species, it is not difficult to identify a similar location for coronary artery occlusion in different animals, as coronary branches can be identified easily. However, this is difficult in small animal species, such as mice and rats. More importantly, slight difference in location for coronary occlusion would result

in a great difference in infarct size as the heart is very small. Because of the importance of location for coronary artery occlusion, the infarct size in all species should be expressed as a function of area at risk (IF/AAR), rather a percentage of left ventricular mass (IF/LV), which rely on the anatomic area at risk that is decided by surgeon or possibly difference between individual animals.

Another factor that influences infarct size during the procedure of coronary artery occlusion is incomplete coronary artery occlusion, which has been also discussed in the section of myocardial stunning. The confirmation of complete occlusion before reperfusion is critical. In larger animal species, this can be accomplished by monitoring coronary blood flow and regional myocardial function in the ischemic zone, and comparing those with the same measurements at very beginning time after coronary artery occlusion. For example, the time points at about 5 and 85 min during the coronary artery occlusion is often used for a 90 min of coronary artery occlusion protocol. If the physiological measurements show difference between these two points, the experiment usually should not be considered as valid in animals that do not have preexisting collateral channels, such as pigs and nonhuman primates. In dog models, however, myocardial function could be slightly changed at the later compared to the early time points, because of collateral channels. This can particularly happen when the measurement of regional myocardial function is in the risk, but adjacent to boarder zone, which easily recruits blood from the contralateral area via the preexisting collateral channels. Accordingly, an ideal method for confirmation of coronary artery occlusion should include both regional myocardial blood flow, measured by either radioactive or colored microsphere techniques, and coronary blood flow in the species that have preexisting collateral channels. Furthermore, the infarct size in those animal species should be expressed by using the slope of transmural collateral blood flow versus IF/AAR, which helps to exclude all influences from collateral channels. Apparently, it is difficult to be performed in small animal models.

Our preliminary unpublished data found that coronary occlusion on left anterior descending coronary in pig or dog models appears to be much more vulnerable to ventricular arrhythmias leading to ventricular fibrillation compared to those from occlusion on left circumflex coronary artery. The left anterior descending coronary artery occlusion also induced a relative larger infarct size as compared to those from left circumflex coronary occlusion. Consistent with what we found, Becker et al. (1983) also reported that permanent occlusion of left anterior descending coronary in anesthetized dogs produced a significant larger infarct size (52%) than those from left circumflex coronary artery occlusion (32%) with a similar size of risk area. Using

microsphere technique to measure regional myocardial blood flow in this study, the collateral blood flow was found to be markedly lower in left anterior descending coronary artery perfused area compared to the area of left circumflex coronary artery, demonstrating that relatively lower level of collateral blood flow is the factor to be responsible for larger infarct size developed (Becker et al., 1983).

Another important factor that affects myocardial infarct size during coronary artery occlusion is the change in myocardial demand. This is important when the coronary artery occlusion is conducted in conscious animals, in which heart rate and arterial blood pressure can be changed markedly via the intact autonomic control. Several previous studies failed to show that the myocardial demand, as expressed by indirect measurement of rate pressure product, affected myocardial infarct size in anesthetized animals (Miura et al., 1987; Reimer et al., 1985), but did affect the infarct size in conscious animals (Reimer et al., 1985). Also, different anesthesia along with recent surgical trauma not only affects cardiovascular control, but also alters the biochemical system, as well as, myocardial calcium handling (Li et al., 1993; Pagel et al., 1993).

MI can be usually detected within the area at risk by gross examination with histochemical tetrazolium stains (TTC) for identifying infarcted tissue from salvaged tissue, as well as, the tissue from nonischemic area. Thus, it is important and also is the first step to identify the area at risk before any staining technique is used, as the infarct size should be expressed as a percentage of area at risk, rather than total left ventricular mass. In larger animal species, a dual perfusion system is often used (Shen et al., 1988, 1996a). In order to prevent blood clot in coronary circulation, animal needs to be first heparinized prior to euthanasia. Immediately after the whole heart is removed, the ascending aorta is cannulated (distal to the sinus of Valsalva) and perfused retrogradely with blue dye, such as Evans, Alcian blue, etc. Simultaneously, the coronary artery at the site of occlusion is cannulated and perfused with saline. The pressure for the perfusion apparatus should be maintained at 100–150 mmHg via a reservoir for both cannulas. The simultaneous perfusion should be maintained until the nonischemic area is clearly stained with blue dye. In small animal species, such as rat and mice, a similar concept, but modified procedure can be carried out in vivo. After animal is heparinized and euthanized, saline should be perfused retrogradely via aorta proximal to the heart while its distal to the heart is ligated. Once all blood is washed out, the site of coronary artery occlusion/reperfusion should be ligated again. The blue dye can be delivered via either aorta or directly slow injection through the apex of left ventricle. After completion of perfusion procedure, the heart is sectioned at the atrioventricular junction and the right ventricle can be kept or removed. Usually the ventricle can be divided into 5–8 rings for larger animal species, and 3–5 rings for small animal species. The individual ring should be carefully labeled, weighed, and then imagined using a digital camera for both sides of each ring. At this point, the coronary artery perfused territory from each ring, that is, anatomical area at risk, should clearly show native color, whereas the remainder of the areas shows the blue stain. One of example from a mouse heart subjected to 60 min of coronary artery occlusion is shown in Fig. 6.11. After TTC staining, the area at risk was no longer detected. Thus, it is extremely important to perfuse the heart using blue dye first before TTC staining in order to obtain the anatomic area at risk.

TTC is one of the most popular histochemical stains used in the quantification of infarct size; it stains viable myocardium red (TTC positive), but does not react with infarcted myocardium (TTC negative) because of lack of dehydrogenase enzymes. The concentration of the TTC is about 1% in phosphate buffer to achieve the level of pH 7.4. All rings are incubated in the TTC solution at 37–38°C for several minutes until the nonischemic myocardial tissue becomes clearly red. TTC stain can also be perfused at the same time when the heart perfusion is performed. The major advantage of this method compared to the incubated rings is that the tissue can be stained entirely, rather than the exposed surface from each ring. However, it is important that the TTC solution can be only perfused in the coronary occluded area while the nonischemic areas still need to be perfused with either saline or blue dye with equal perfusion pressure. This will prevent the tissue from nonischemic region from being stained with TTC and thus retain a clear area at risk. Due to the technical limitation, the perfusion of TTC is not possible in small animal species.

Although TTC is sensitive to differentiate the irreversible infarcted myocardium from nonischemic myocardium, several factors often result in "false positive" or "false negative" results. Downey (1990) reported that assessment of MI using TTC often has the limitation when tested agents, for example, free radical scavenger, are used. Thus, the TTC stain should not be used when any agents that may have potential effects on cardiac enzymes, which would directly react with TTC to cause "false positive." Early studies utilized conventional histological method also found other important limitations of using TTC. Vivaldi et al. (1985) demonstrated that myocardial infarction in rodent species can be identified by TTC at 30 min after coronary artery occlusion. Six hours after coronary occlusion in rodent species, however, the differentiation of reversibly from irreversibly infarcted tissue at the 1–2 mm
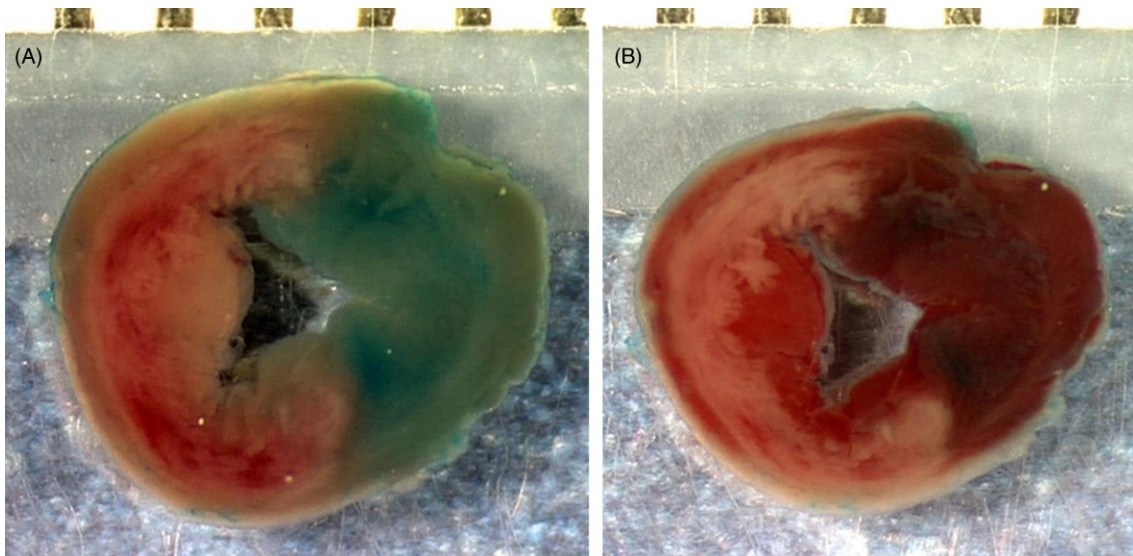
FIGURE 6.11 Example of slice of heart from a mouse subjected to 60 min of coronary artery occlusion before (A) and after TTC staining (B). Note that the infarct tissue can be easily detected after TTC staining. Anatomic area at risk was no longer clearly visible after TTC (unpublished data).

peripheral margin of the infarct became less sharp. At the macroscopic boundary of the infarcted tissue, myocardium not stained with TTC always had irreversibly salvaged myocytes, while the myocardial tissue stained with TTC often had a narrow zone of mixed salvaged and irreversible damaged tissue adjacent to the infarct (Vivaldi et al., 1985), indicating that the TTC is ideal for the early detection of MI.

The reason why TTC stain should not be used too long after occlusion is that myocardial remodeling has commenced. The myocardial mass in ischemic area starts to shrink within a few days following coronary artery occlusion and reperfusion. As a matter of fact, the infarcted tissue can be directly observed from the risk area without any staining methods during the time between 4 and 7 days following coronary artery occlusion/reperfusion. Fig. 6.12 shows a pig heart subjected to coronary artery occlusion for 90 min followed by 4 days of reperfusion. The irreversible infarcted tissue mixed with hemorrhage and necrosis located in endo- and midmyocardial layer can be differentiated from salvaged tissue located in epimyocardial layer in the risk area, while the nonischemic tissue was stained with blue dye. When the reperfusion time was extended to 7 days, the infarcted tissue was much clearer and sharp as compared to 5 days of reperfusion. Fig. 6.13 shows a pig heart 7 days after coronary artery reperfusion. The mixed hemorrhage and necrosis was a lot less compared to 4 days of reperfusion.

The total weight of infarcted tissue normalized by the area at risk for the infarct size (IF/AAR) from each animal can be calculated using planimetry from all sliced rings with or without TTC stain. Numerous computer-assisted planimetry techniques are now available. Both surface areas of each ring of heart should be measured and averaged. Based upon the infarct area, areas at risk and nonischemic area along with the weight from each ring, infarct size can be obtained. In chronic coronary artery occlusion and reperfusion animal models, that is, longer than 1 week, the infarct size will be difficult to be obtained using the earlier method because of myocardial remolding. Usually, the infarct size can be determined by measuring the circumferences of the left ventricle and the infarcted region, and then expressed as a percentage
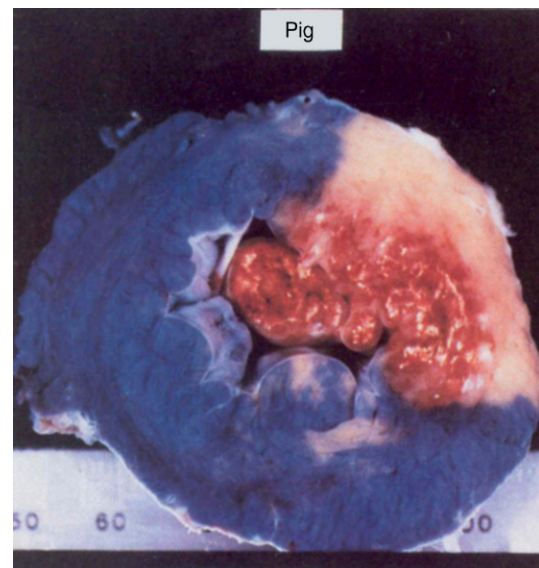
FIGURE 6.12 **A slice of heart from a pig subjected to left circumflex coronary artery occlusion followed by 4 days of reperfusion.** Note that the infarct tissue can be differentiated from salvaged tissue within the area at risk without any staining procedure (Shen et al., 1996a).
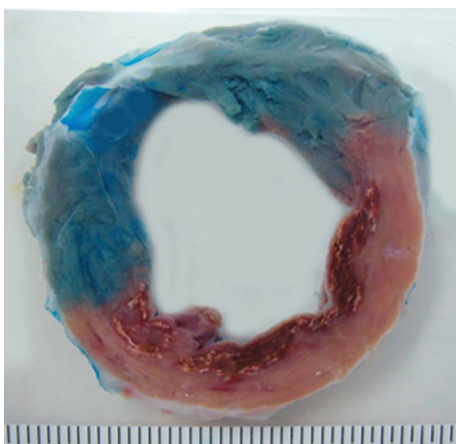
FIGURE 6.13   **A slice of heart from a pig subjected to 60 min of left circumflex coronary artery occlusion followed by 7 days of reperfusion.** Comparing with 4 days of reperfusion shown in Fig. 6.12, the infarct tissue within the area at rick was much clearer and sharper while the mass of entire risk area had not been reduced (unpublished report).

FIGURE 6.14   **A slice of heart from a pig 6 weeks after left circumflex coronary artery occlusion.** Note that the infarct was clearly different from normal myocardium (unpublished report).

of the LV perimeter. Fig. 6.14 shows an example of one slice of pig heart 6 weeks after coronary artery occlusion. Clearly, the remodeling process completely changed the ratio between infarcted and salvaged tissue within the area at risk. Without knowing the exact area at risk, the infarct size could be significantly influenced by the site of coronary occlusion. Thus, when a protocol for study of a cardioprotective agent involves prolonged reperfusion, the results can be affected significantly by inconsistency in the site of coronary artery occlusion between animals.

3 HYPERTENSION AND LEFT VENTRICULAR HYPERTROPHY MODELS

3.1 Hypertension

One in every three adults in the United States has hypertension, a major risk factor for cerebral, cardiac, and renal events. More than 90% of cases are categorized as essential (primary) hypertension, which does not have a clear underlying cause, but has been known to contain a significant genetic component. Remaining 5%–10% of cases are categorized as secondary hypertension, which can be induced by several conditions, such as renal disease, adrenal gland dysfunction, pregnancy, or medication. Because of complex and unknown mechanisms of hypertension, creating an animal model to mimic clinical hypertension is difficult.

Several genetically induced hypertensive models, primarily in small animal species have been developed and characterized. One of the most notable models is the spontaneously hypertensive rat (SHR) which represents the essential hypertension. The SHR strain was produced as early as 1960s by Okamoto and Aoki (1963). Subsequently, double transgenic mice and rat models, for example, the stroke-prone spontaneously hypertensive (SHRSP) model, as well as, other genetically engineered models have been developed. In addition, mineralocorticoid deoxycorticosterone salt sensitive models have also been developed in rodent, which provides another pathway for the study hypertension (Johns et al., 1996). Due to the limitation of small animal species for comprehensive physiological measurements, a larger animal model of hypertension is required. The most direct method to mimic the pathological changes in hypertensive patients is to use surgical manipulation by either kidney wrapping or renal artery stenosis. The surgical procedure for perinephritic hypertension can be performed via a left flank incision (Kirby and Vatner, 1987; Uemura et al., 1993). After perinephric fat is removed, the kidney can be wrapped by an unbleached silk pouch. Care should be taken to avoid inadvertent stenosis of the renal artery. The procedure for renal vascular stenosis uses either suture or a metal clip to reduce diameter of renal artery by approximately 50%. Based on our prior experience, both procedures only produce a minimal to moderate level of hypertension in dog models. In conscious nonhuman primates, monkey model, however, we found renal artery stenosis produces more stable hypertension compared to the dog model. In order to achieve a sustained moderate to severe hypertension, a contralateral nephrectomy is needed which can be performed at the same time or 1–2 weeks after initial surgical procedure is completed (Kirby and Vatner, 1987; Uemura et al., 1993).

3.2 Pulmonary Hypertension

Like systemic arterial hypertension, pulmonary hypertension is also divided into primary and secondary pulmonary arterial hypertension. In contrast to systemic arterial hypertension, secondary pulmonary hypertension is much more common than primary pulmonary hypertension. The causes of pulmonary hypertension include blood clots, artery constriction, and/or heart and lung dysfunction. Several animal models have been studied. The most commonly used models in small animal species are the hypoxia or chemical-induced pulmonary hypertension (Stenmark et al., 2009). More recently, genetically manipulated mouse models have been generated which provides insight into the role of specific molecules in the pulmonary hypertensive process (Stenmark et al., 2009). We adapted both hypoxia and thromboxane induced pulmonary hypertension procedure to a larger animal, pig, model in our previous studies (Ho et al., 2012). Briefly, hypoxia is induced under anesthesia with ventilation by changing fraction of inspired O_2 to the level about 0.1% via introducing N_2 into the inspiratory limb of the ventilator. The mean pulmonary artery pressure is elevated by 5–10 mmHg from baseline level in the pig model. Chronic infusion of thromboxane-induced pulmonary hypertension resulted in a greater increase in pulmonary artery pressure compared to hypoxia induced hypertension. The major limitation of these models is that the mechanism of hypertension is very different from human pulmonary hypertension.

It is known that acute pulmonary embolism is also a major cause of pulmonary hypertension which can be mimicked by administration of air, blood clots, or synthetic microspheres in animal models (Marsboom and Janssens, 2004). We have modified the microsphere injection method and made it possible for direct and repeated administration of microspheres directly into the pulmonary circulation in a chronically instrumented conscious pig model. Under continuous monitoring of cardiac output, pulmonary, systemic arterial, right and left atrial pressure along with SPO_2, glass microspheres can be infused multiple times, several hours to days apart. The increase in mean pulmonary artery pressure and pulmonary vascular resistance can be doubled, but it returns toward the baseline level within few hours, which is the major limitation of this model. Repeated injections for 5–6 times within a 2-week period resulted in a chronic elevation of mean pulmonary artery pressure. By using a chronically implanted catheter technique, this model can be studied under fully conscious state. Preliminary results from our pilot study are shown in Figs. 6.15 and 6.16. Clearly, systemic hemodynamics were not changed significantly, while pulmonary arterial pressure, pulmonary vascular resistance, and right atrial pressure were elevated markedly compared to control, suggesting that pulmonary embolism alone selectively causes right ventricular dysfunction, while left ventricular function was still preserved.

3.3 Left Ventricular Hypertrophy

Left ventricular hypertrophy is an adapted response to physiological or pathological stress, such as hypertension, MI, neurohormonal dysfunction, and valve defection. Much progress has been recently made in the development of left ventricular hypertrophy linked with molecular and genetic basis. Most common methods for development of left ventricular hypertrophy are through MI, chronic hypertension, or aortic stenosis. As described in the section of MI, myocardial remodeling occurs following MI. Myocardial wall thickness in the ischemic region becomes thinned and also enlarged due to the tissue shrinking, while the contralateral nonischemic region gradually hypertrophies via the constantly enhanced contractile force to compensate the function loss from ischemic region. Fig. 6.17 shows a left ventricular cross section from one pig at 6 weeks after left circumflex coronary artery occlusion (Fig. 6.17B) compared to the pig with the same protocol but without coronary artery occlusion (Fig. 6.17A). The wall thickness from nonischemic region, particularly at the adjacent to ischemic region, appears to be greater as compared to the remote area of nonischemic region, as well as to control pig.

In nonhuman primates, about 2 months after left anterior descending coronary artery ligation, left ventricular mass/body weight is slightly increased. However, given the reduction in myocardial mass in the infarcted region, the degree of hypertrophy should be greater than observed (Shen et al., 2005). Hypertension is another approach to induce left ventricular hypertrophy. Using a perinephritic hypertension dog model, left ventricular mass during developing hypertension, that is, 2–4 week, was increased by more than 20% (Uemura et al., 1993). Overall, both MI and hypertension induced hypertrophy in larger animal species should be considered as a physiological response to stress which does not reach a pathological alternation in myocardium.

Aortic banding is an optimal approach to induce left ventricular hypertrophy which is much more severe compared to ischemia and hypertension induced models. In dogs, aortic banding often produces a moderate to severe hypertrophy, that is, more than 40% up to 80% increase in left ventricular weight/body weight (Hittinger et al., 1992, 1994). The banding procedure is performed in mongrel puppies at 8–10 weeks of age. Briefly, through a right thoracotomy at the third or fourth intercostal space, the ascending aorta 0.5–1.0 cm above the coronary
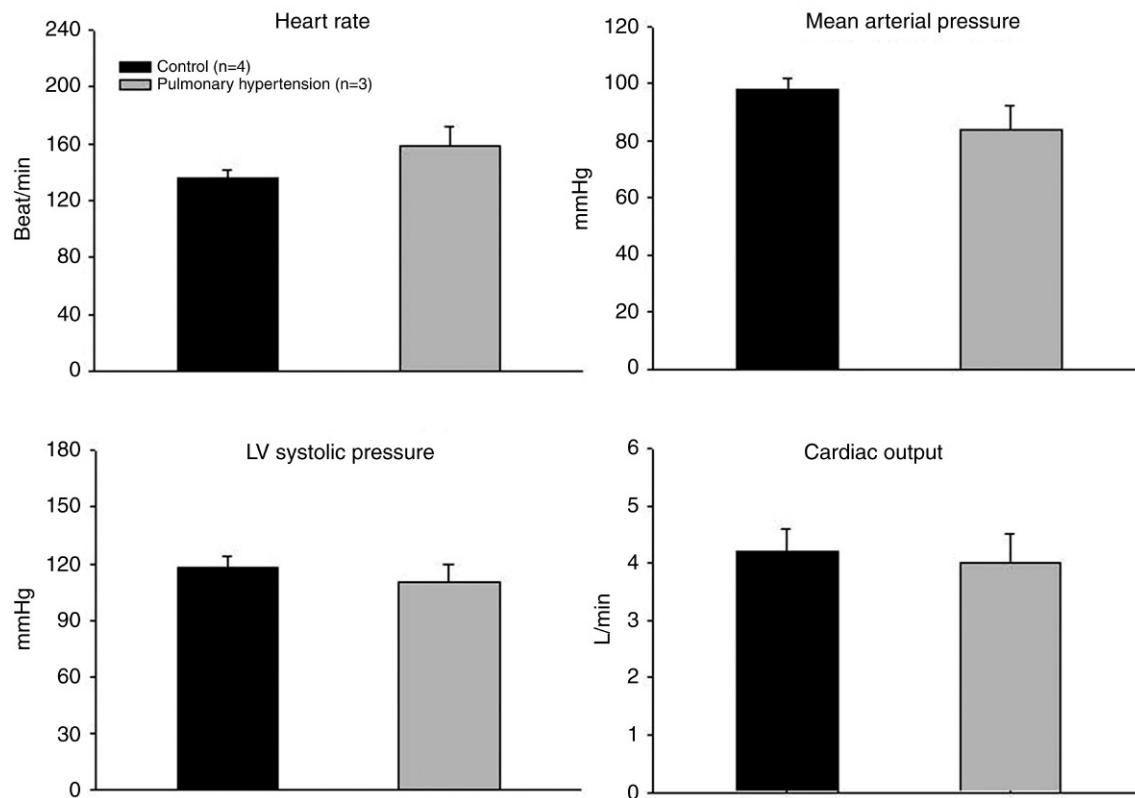
FIGURE 6.15 **Effects of pulmonary embolism on heart rate, mean arterial pressure, LV systolic pressure, and cardiac output in conscious pigs.** There was a slight change in all these indices compared to control (unpublished data).
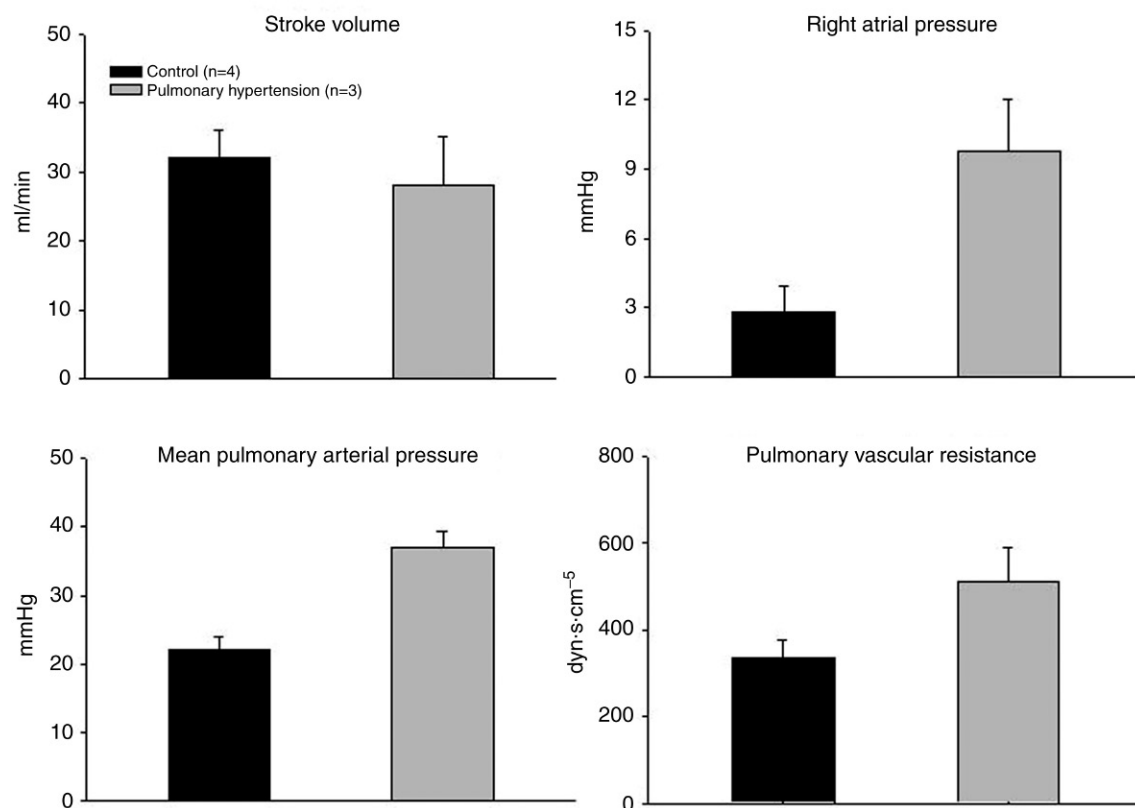
FIGURE 6.16 **Effects of pulmonary embolism on stroke volume, right atrial pressure, mean pulmonary arterial pressure, and pulmonary vascular resistance in conscious pigs.** There was a marked increase in pulmonary artery pressure and resistance, along with increased right atrial pressure, while stroke volume was unchanged compared to control (unpublished data).
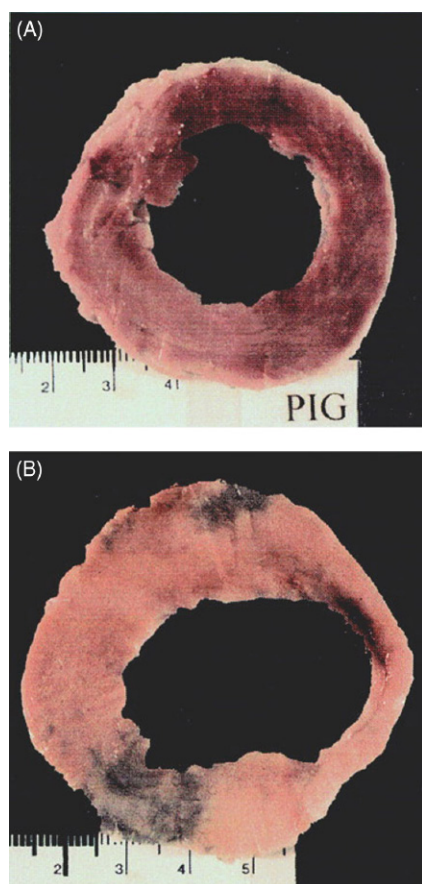
FIGURE 6.17 Representative left ventricular (LV) cross sections from two pigs with (B) and without (A) myocardial infarction. Note that the wall thickness, particularly adjacent to myocardial infarction is enlarged compared to that without myocardial infarction (Shen et al., 1999).

arteries is dissected free of surrounding tissue. A 10-mm wide Teflon cuff is placed around the aorta and tightened until a thrill could be palpated over the aortic arch. The Teflon band creates a fixed supravascular aortic lesion, which produces progressive increasing stenosis as the puppies grow. Animals are studied for about 1 year after banding (Hittinger et al., 1992, 1994). The left ventricular and aortic pressure gradient in this model could reach 100–150 mmHg. Global and regional myocardial function and coronary blood perfusion in response to stress are clearly impaired (Bishop et al., 1996; Hittinger et al., 1994). The aortic banding induced hypertrophy can be also used in adult animal, but the degree of aortic stenosis should be less than used in puppies. The degree of hypertrophy is also much less severe as compared to the chronic banding model in puppies. The left ventricular and aortic pressure gradient should be controlled to less than 100 mmHg to avoid acute decompensation (von Harsdorf et al., 1997). The aortic banding procedure can also be used in rodent species for the development of left ventricular hypertrophy. Following anesthesia and

mechanical ventilation in mouse models, a left thoracotomy can be performed via the second intercostal space. Aortic stenosis is induced by tying a 7-0 polyester braided suture ligature against an appropriately sized needle, to provide a reproducible transverse aortic constriction of 65%–70% when the needle is removed. Chronic left ventricular hypertrophy also can be induced in nonhuman primates via multiple, progressive coronary artery occlusion followed by repeated rapid ventricular pacing. Detailed experimental protocol and results is shown in the section of heart failure.

4 HEART FAILURE MODELS

Heart failure is a final pathway from different cardiovascular diseases, which is the leading cause of cardiovascular mortality and morbidity in the United States. The most common cause of heart failure in patients is the ischemic cardiomyopathy resulting from insufficient myocardial perfusion associated with complex neurohormonal activation. Heart failure generally can be characterized by a decrease in cardiac function, increase in systemic vascular tone, and sodium retention. The most extensively used heart failure animal models are the MI in all animal species (Ellis et al., 1964; Nuttall et al., 1985; Pfeffer and Pfeffer, 1988; Sabbah et al., 1991; Van der Giessen et al., 1989) and the rapid ventricular pacing (Armstrong et al., 1986; Chow et al., 1990; Hendrick et al., 1990; Wilson et al., 1987) in larger animal species. Recently, many transgenic knockout or overexpression of heart failure models in small animal models has also been developed.

4.1 Heart Failure Induced by Ischemia

Previous studies showed that ligation of coronary artery in rats induce a significant impairment of left ventricular function leading to heart failure. In those studies, the infarct size can reach to the level of 35%–50% of the left ventricle (Pfeffer and Braunwald, 1990; Pfeffer and Pfeffer, 1988; Shen et al., 1996b). However, the level of infarct size in rats is difficult to reproduce in larger animal species, because of sudden death due to uncontrolled acute cardiogenic shock or ventricular fibrillation. Although several previous studies reported that chronic heart failure can be induced in pig models a few weeks after coronary artery occlusion (Van der Giessen et al., 1989; Van Woerkens et al., 1993), there are no significant changes in left ventricular contractile function as assessed by left ventricular dP/dt in these studies. Since the infarct size can be variable, it is reasonable to characterize all animals after MI, and then divide them into different subgroups, in order to obtain the animals that meet the criteria of the diagnosis of systolic heart failure.

A prior study shows that left ventricular end diastolic pressure was only slightly increased even in the most severe group (Zhang et al., 1996); further indicating that heart failure induced by coronary artery occlusion alone in larger animal models is different from those observed in small animals.

It has been reported that unlike coronary artery occlusion produced by either occluder or ligation, multiple intravascular microembolization in dogs can induce progressive myocardial injury that leads to heart failure (Nuttall et al., 1985; Sabbah et al., 1991). However, the procedure requires intracoronary injection technique often conducted under anesthesia in a catheterization laboratory or a special catheter chronically implanted in coronary artery. Furthermore, it is difficult to find a consistent protocol for the number of injections and amount of microembolization. Thus, this model cannot be easily produced by most laboratories.

4.2 Heart Failure Induced by Rapid Ventricular Pacing

Rapid pacing produces a fast and significant decrease in cardiac function which meets the hemodynamic criteria of heart failure. Rapid pacing can be produced using pacing leads located at atrium, right or left ventricles. Most prior studies in larger animal species have used right ventricular pacing via pacing leads implanted in the free wall of right ventricle. The pacing rate, controlled by a programmable internal or external cardiac pacemaker, ranges of 200–300 bpm depending on species, for example, 220–230 bpm in pigs (Shen et al., 1998), 230–240 bpm in dogs (Shannon et al., 1993; Shen et al., 2000), 280–290 bpm in monkeys (Park et al., 2009; Shen et al., 2005, 2008a), and 320–340 bpm in rabbits (Liu et al., 2001). The duration of the pacing varies from few days to weeks. The severity of cardiac dysfunction depends on both the rate and duration of pacing. The major limitation of the pacing model is that the cardiovascular hemodynamics, as well as, biochemical alterations, progressively revert to near baseline levels after pacing is ceased (Larosa et al., 1993; Shannon et al., 1993), indicating that the mechanisms of pacing model are different from those of the irreversible failing heart seen in humans. Thus, the definition of pacing model in general should be considered as a severe, but reversible injury leading to dilated cardiomyopathy.

4.3 Myocardial Ischemia Super Imposed with Pacing

Given the limitation of the reversible nature of rapid pacing alone, we developed a pig heart failure model induced by sequential coronary artery occlusion followed by rapid ventricular pacing (Shen et al., 1999). Unlike either intervention alone, left ventricular dysfunction and abnormal systemic hemodynamics are severe and do not progressively reverse after cessation of pacing, suggesting that the underlying mechanism following combined MI and rapid ventricular pacing is different from pacing or ischemia alone-induced heart failure. It is conceivable that the nonischemic myocardium can compensate for the loss of regional function after coronary artery occlusion and maintain global left ventricular performance. In the presence of MI, rapid ventricular pacing increases the energy demand of the nonischemic myocardium possibly beyond the range of compensation. Consequently, compensatory mechanisms presumably operating particular within the border zone may be insufficient, resulting in irreversible myocardial damage. Thus, MI followed by rapid ventricular pacing should be considered as a better mimic of the process of heart failure observed in human.

Fig. 6.18 shows a schematic illustration of surgically implanted instrumentations and the protocol for induction of heart failure in this model. The progressive MI in the pig model can be performed by two left circumflex coronary artery occlusions. The first occlusion is performed using the occluder implanted distally to the origin of its first margin branch, which results in about infarct size less than 20% of left ventricle (Shen et al., 1999). The second occlusion is performed 48 h after the first occlusion by using the second occluder implanted at the proximal circumflex coronary artery, resulting in about the infarct size more than 30% of left ventricle. By using this stepwise manner, the acute mortality during the coronary artery occlusion can be minimized with maximizing the infarct size. The rapid right ventricular pacing at a rate of 220 bpm usually can be initiated 2 days after the second coronary artery occlusion.

Figs. 6.19 and 6.20 show the comparison of cardiovascular function in the rapid ventricular pacing protocol with and without sequential coronary artery occlusions induced MI. The changes in cardiac function as expressed by cardiac output, left ventricular dP/dt, and left ventricular fractional shortening are similar with pacing, which are clearly depressed. However, during the 3 weeks recovery period, that is, cessation of pacing, cardiac function returns toward control level in the pacing group without myocardial ischemia. In contrast, in the group with myocardial ischemia and pacing, the cardiac function remained depressed.

Models of heart failure induced by myocardial ischemia superimposed with rapid ventricular pacing have been studied in other larger animal species, such as dogs (Shen et al., 2010) and nonhuman primates, monkeys (Park et al., 2009; Shen, 2010). The induction of heart failure in conscious monkey model is different from that used for pigs and dogs. The detailed experimental protocol is shown in Fig. 6.21. MI is induced by permanent
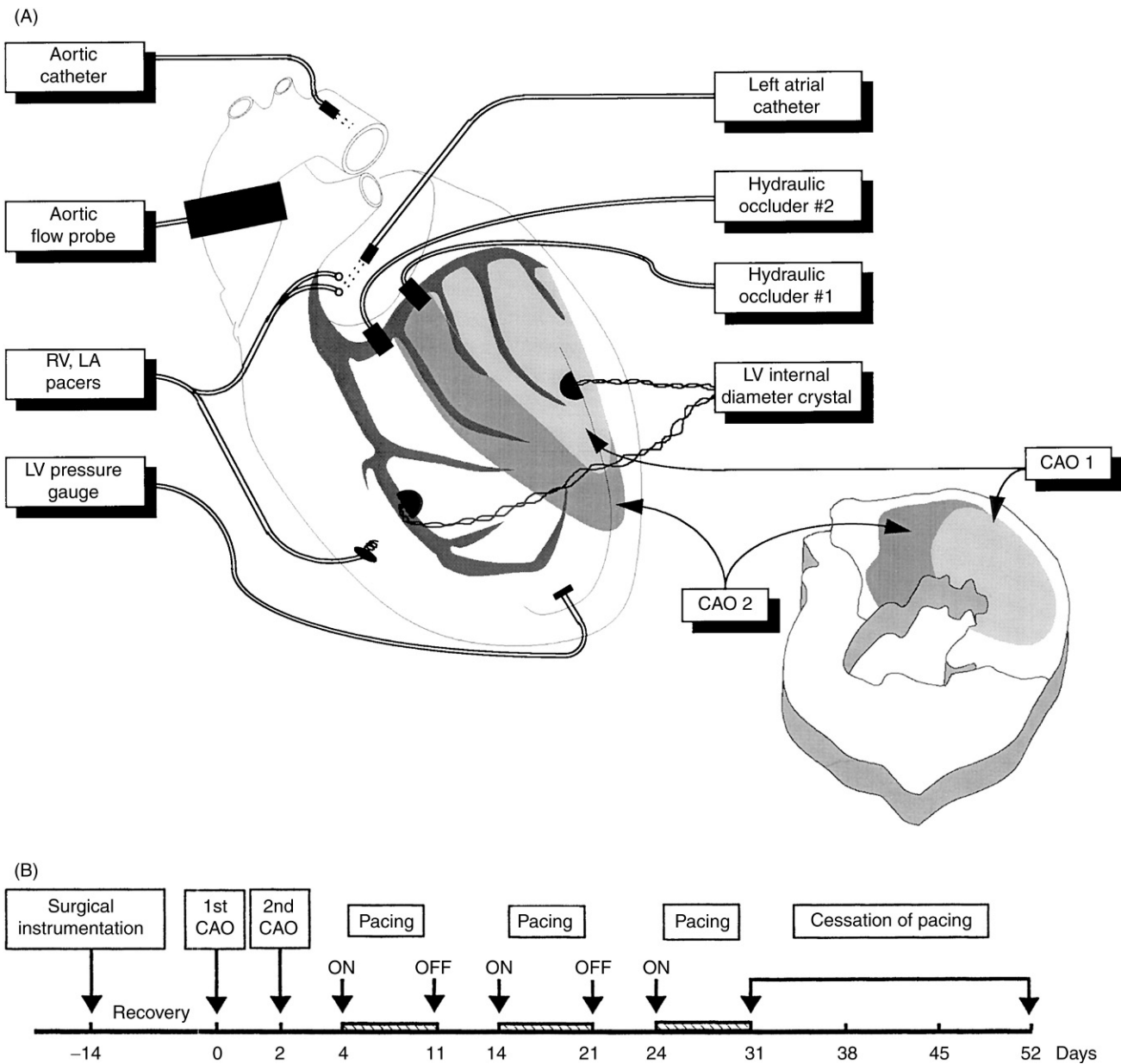
FIGURE 6.18 (A) Schematic illustrations of instrumentation implanted for measurements of cardiac and systemic dynamics. One section of left ventricle (LV) depicting progressive myocardial infarction after two sequential left circumflex coronary artery occlusions (CAO). *RV*, right ventricle; *LA*, left atrium; (B) experimental protocol for heart failure model in conscious pigs (Shen et al., 1999).

ligation of the left anterior descending coronary artery at half the distance from its origin in combination with ligation of all branch vessels via thoracotomy at the fourth/fifth intercostal space. In addition to the ligation of the coronary artery, instrumentations to record hemodynamics along with pacing leads can be implanted selectively, as needed.

Approximately 2 months after coronary artery ligation surgery, rapid ventricular pacing is applied at approximately 220–290 bpm for 3–4 weeks. Our previous studies (Park et al., 2009; Shen, 2010; Shen et al., 2005)

demonstrated that before rapid pacing is applied (i.e, 2 months after coronary ligation), LV dP/dt was slightly decreased compared with control, indicating that MI even after 2 months does not cause a significant reduction in left ventricular function. Following rapid ventricular pacing, LV dP/dt was significantly reduced, while left ventricular end-diastolic pressure was significantly increased. Using this model, left ventricular mass, based on the direct measurement of LV/body weight ratios, was demonstrated to be increased compared with control, indicating that left ventricular hypertrophy is also
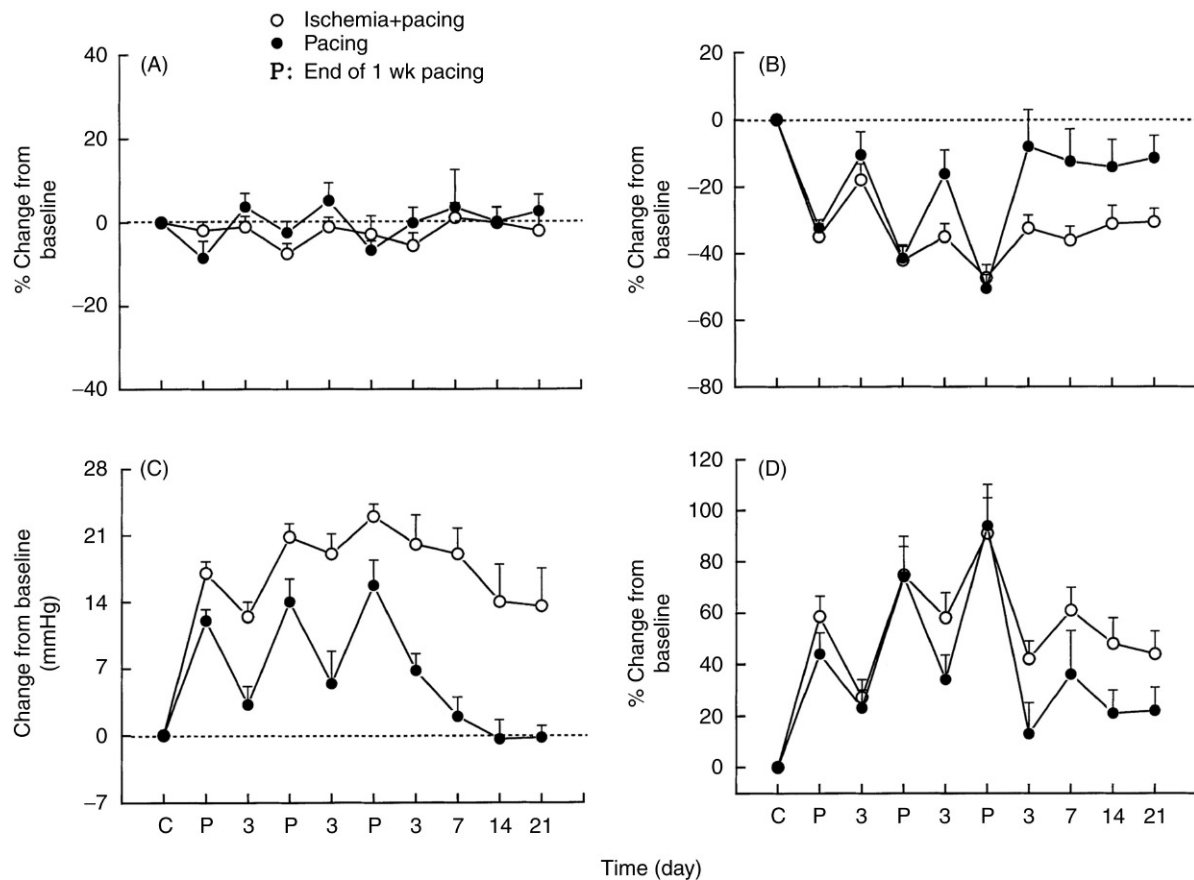
FIGURE 6.19   Time course if changes in mean arterial pressure (A), cardiac index (B), mean left atrial pressure (C), and total peripheral resistance (D) before (C) and after three 1-week periods of pacing (P) separated by 3 days of rest and during a 21-day postpacing recovery period in conscious pigs. Note that there were differences in all indices except for mean arterial pressure during the recovery period between pacing alone and pacing combined with myocardial ischemia groups (Shen et al., 1999).

produced. Given the reduction in cardiac mass induced by scar formation, the degree of hypertrophy is likely to be greater than that suggested by the cardiac weight alone (Shen, 2010; Shen et al., 2005). Fig. 6.22 shows the results of cardiac function and LV /body weight in conscious monkey model with heart failure. Clearly, the nonhuman primate model enables the investigation of all stages of heart failure, from initial myocardial ischemia to compensated left ventricular hypertrophy leading to end-stage of decompensated heart failure. This model provides a unique opportunity for elucidation of cardiovascular disease mechanisms and also the evaluation of novel interventions.

By using the same concept, the heart failure model can also be induced by pressure overloaded, that is, banding aorta, induced left ventricular hypertrophy followed by rapid pacing (Shen et al., 2010). Table 6.1 shows that left ventricular hypertrophy (LVH), just like MI alone, does not reduce baseline cardiac function. However, when myocardial ischemia or left ventricular hypertrophy combined with pacing, significantly decreased left ventricular dP/dt and increased left ventricular end

diastolic pressure is observed. The combination of two different approaches generates a better model for study of heart failure.

4.4 Cardio-Renal Syndrome Induced by Biventricular Dysfunction

A number of interactions between heart and kidney disease have been described and are termed the cardio-renal syndrome. The interaction is bidirectional, that is, heart or kidney can induce acute or chronic dysfunction in the other organ. It has been well accepted that this cardiovascular disorder is often much worse than isolated heart or kidney dysfunction alone. Despite severe left ventricular contractile dysfunction, animal models of heart failure are often associated with preserved renal function until the terminal stages of heart failure. Clinical studies have demonstrated an association between renal dysfunction in heart failure and right, rather than left ventricular dysfunction (Damman et al., 2009; Mullens et al., 2009; Testani et al., 2010). This observation is likely explanation why animal models fail to exhibit
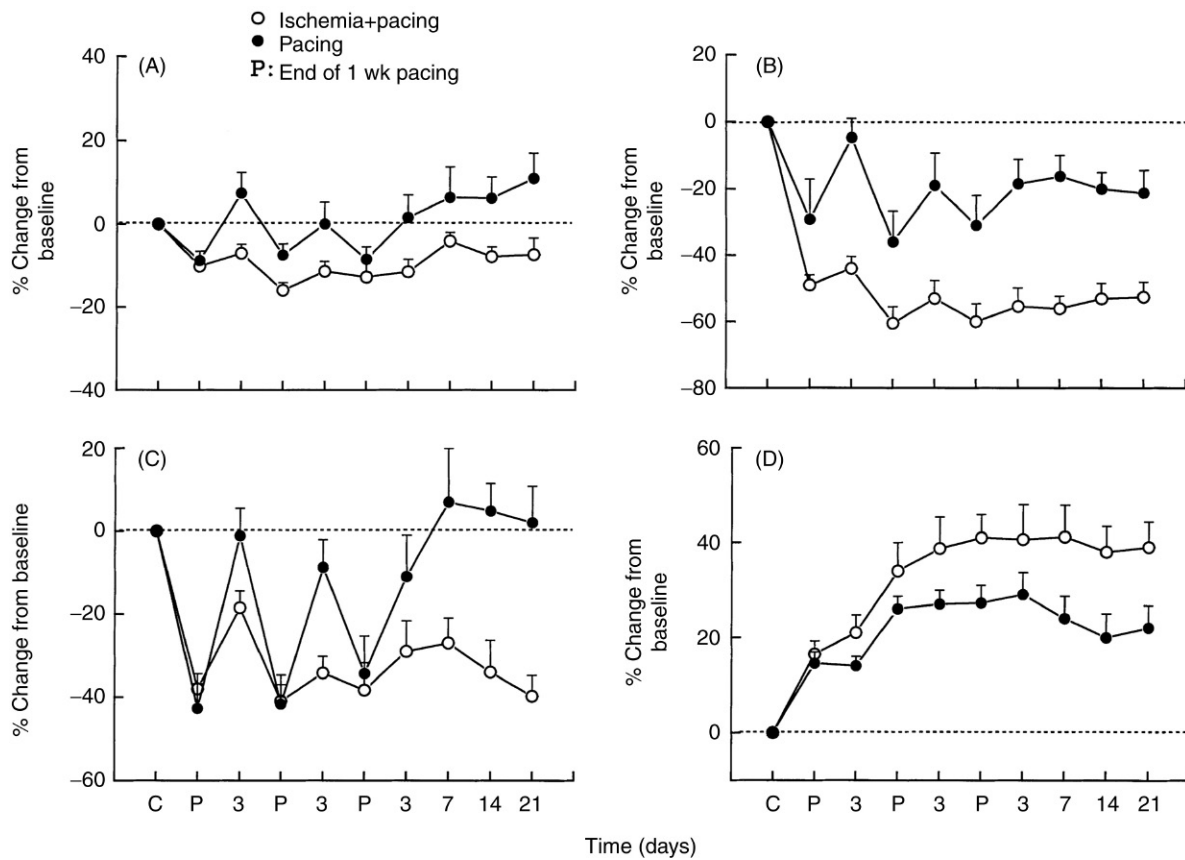
FIGURE 6.20 Time course if changes in left ventricular (LV) systolic pressure (A), LV fractional shortening (B), LV dP/dt (C), and LV end diastolic dimension (D) before (C) and after three 1-week period of pacing (P) separated by 3 days of rest and during a 21-day postpacing recovery period in conscious pigs. Note that all indices were stable after cessation of pacing in the pacing combined with myocardial ischemia, compared to pacing alone groups (Shen et al., 1999).
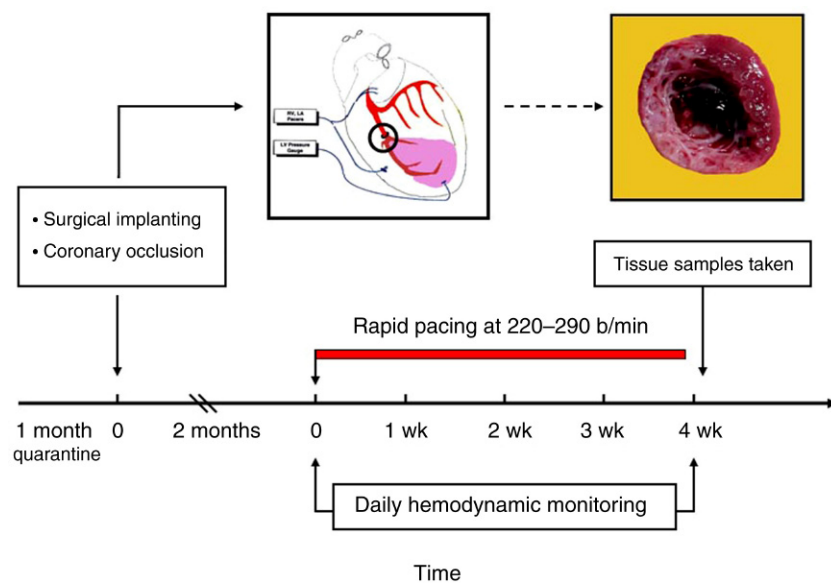
FIGURE 6.21 Experimental protocol for heart failure model in conscious monkeys (Shen et al., 2005).

Hemodynamic and LV/body weight in control and heart failure monkeys
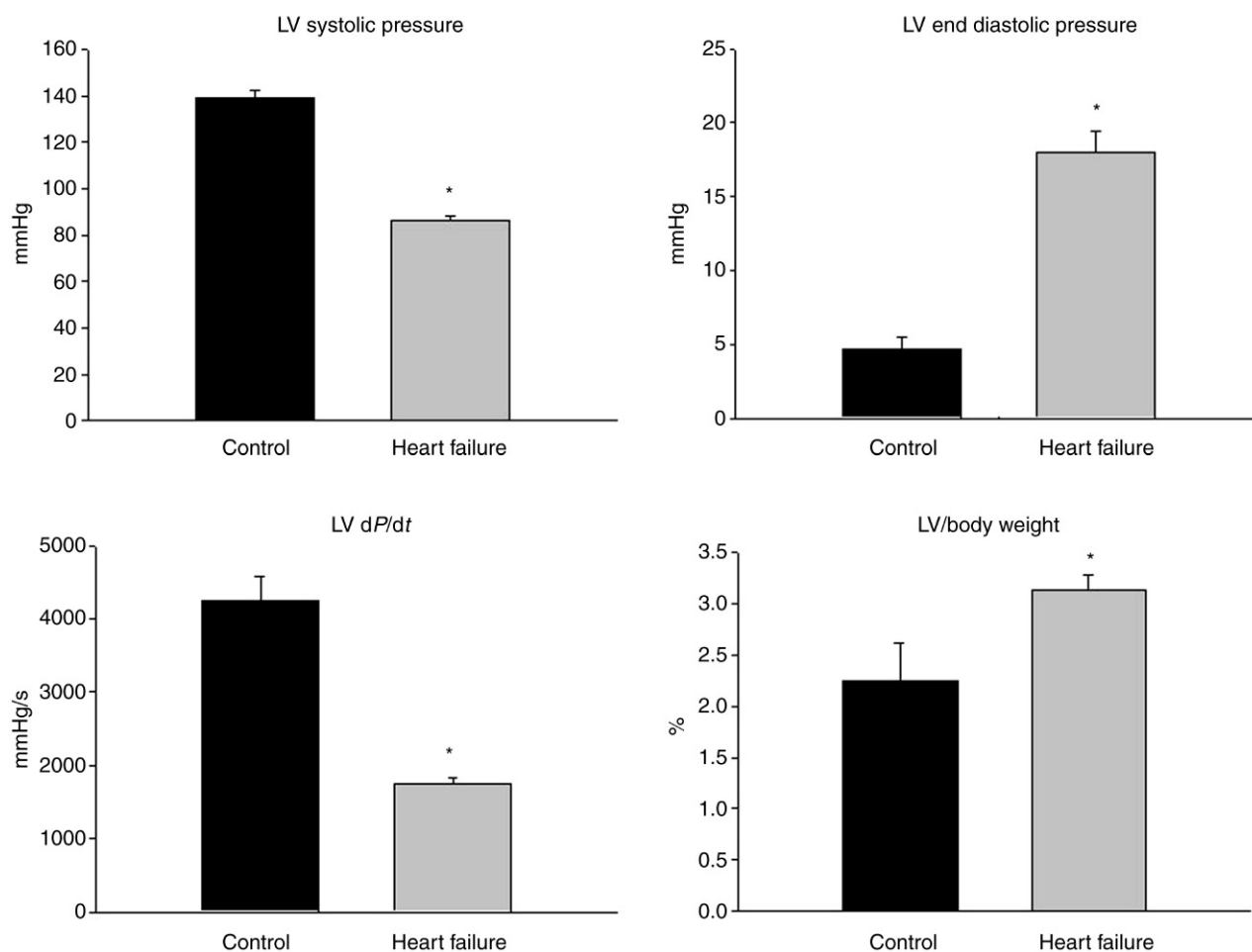
FIGURE 6.22 **Averaged date from monkey model of heart failure.** Note that LV function, as assessed by LV systolic pressure, LV dP/dt, and LV end diastolic pressure, were significantly altered at the end of stage of heart failure compared to control. LV/body weight was also elevated significantly (Shen et al., 2005).

TABLE 6.1 Baseline Values in Conscious Dogs Before Pacing (Normal, MI, and LVH) and in Conscious Dogs After Pacing (MI-sHF and LVH-sHF) (Shen et al., 2010)

	Before Pacing			After Pacing	
	Normal ($n = 4$)	MI ($n = 5$)	LVH ($n = 7$)	MI-sHF ($n = 6$)	LVH-sHF ($n = 5$)
Mean arterial pressure (mm Hg)	92 ± 6.6	88 ± 2	93 ± 1.8	87 ± 5.0	89 ± 5.3
Heart rate (bpm)	90 ± 7.2	116 ± 11[†]	123 ± 3.4*	143 ± 7.1*	142 ± 7.2*
Mean left atrial pressure (mm Hg)	3.4 ± 1.0	6.8 ± 1.5	4.6 ± 0.5	25 ± 0.9*[†]	22 ± 2.1*[†]
LV systolic pressure (mm Hg)	115 ± 4.7	110 ± 1.5	188 ± 6.6*	101 ± 5.2	133 ± 11
LV end-diastolic pressure (mm Hg)	7.3 ± 1.7	7.6 ± 0.7	11 ± 0.9	28 ± 2.4*	29 ± 2.5*
LV dP/dt max (mm Hg/s)	2861 ± 180	3425 ± 215	3705 ± 281	1663 ± 111*	1780 ± 93*

* $P < 0.05$ versus normal.
† There is 1 less animal in this measurement than for all others in this group.

renal dysfunction, since existing animal models manifest predominantly left ventricular dysfunction. Accordingly, we have accomplished and characterized a combined microembolization in pulmonary circulation followed by rapid ventricular pacing in pig species to induce biventricular dysfunction which mimics the cardiorenal syndrome seen in patients.

A schematic illustration of surgically-implanted instrumentations and the experimental protocol are shown in Figs. 6.23 and 6.24, respectively. After recovery from surgery, repeated infusions of glass microspheres into the pulmonary circulation via pulmonary artery catheter is performed for about a month. The rapid ventricular pacing at a rate of 220–230 bpm is initiated after the first week of glass microspheres is injected. Cardiac and renal vascular dynamics are monitored twice a week during the development of biventricular dysfunction. Fig. 6.25 shows a representative waveform record from a conscious pig subjected to microsphere injection followed by 3 weeks of rapid ventricular pacing. Both left and right ventricular functions, that is, LV dP/dt, right atrial pressure, as well as, renal blood flow were significantly changed compared to baseline. The average cardiac and renal vascular dynamic results are shown in Fig. 6.26 (A and B). These data support the notion that right ventricular dysfunction is important for interaction between heart and kidney. One of major limitations for this model development is that the amount of microspheres and number of injections are variable between the individual animal. Therefore, adjustment of the injection requires the hemodynamic monitoring continuously during the
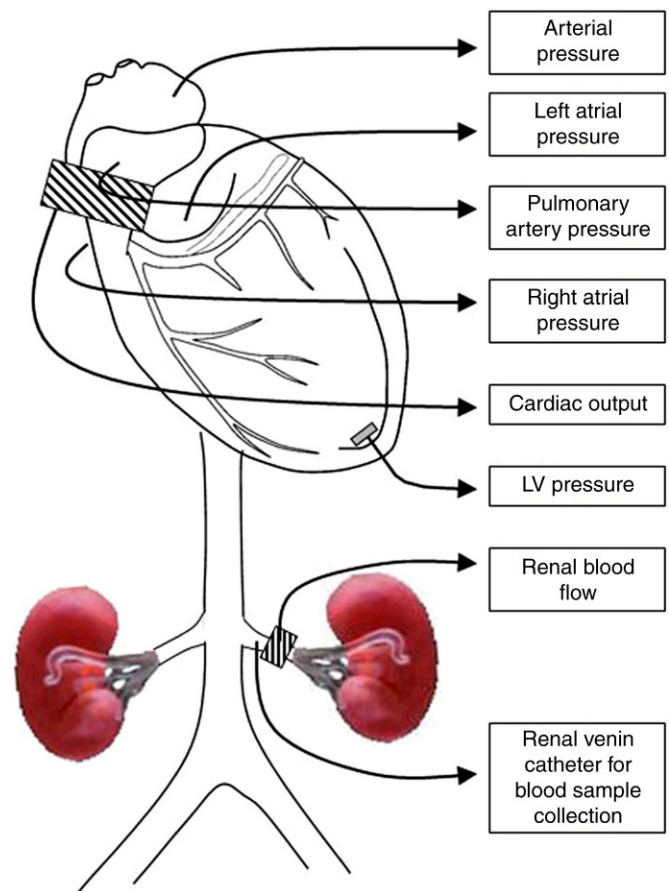
FIGURE 6.23 Schematic illustrations of instrumentation implanted for measurements of left ventricular (LV) pressure gauge, ascending aortic and renal blood flow probes along with catheters for different pressure measurements (unpublished data).
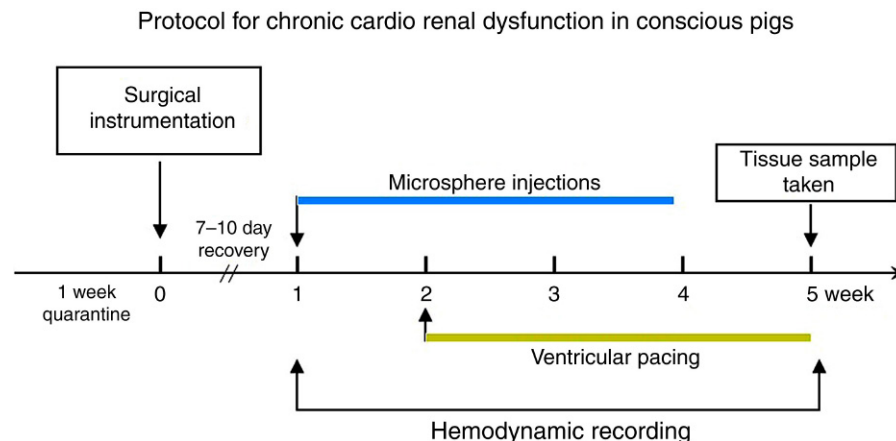
FIGURE 6.24 Experimental protocol for biventricular dysfunction induced cardiorenal syndrome in chronically instrumented conscious pigs (unpublished data).

Chronic conscious pig model with cardio-renal syndrome
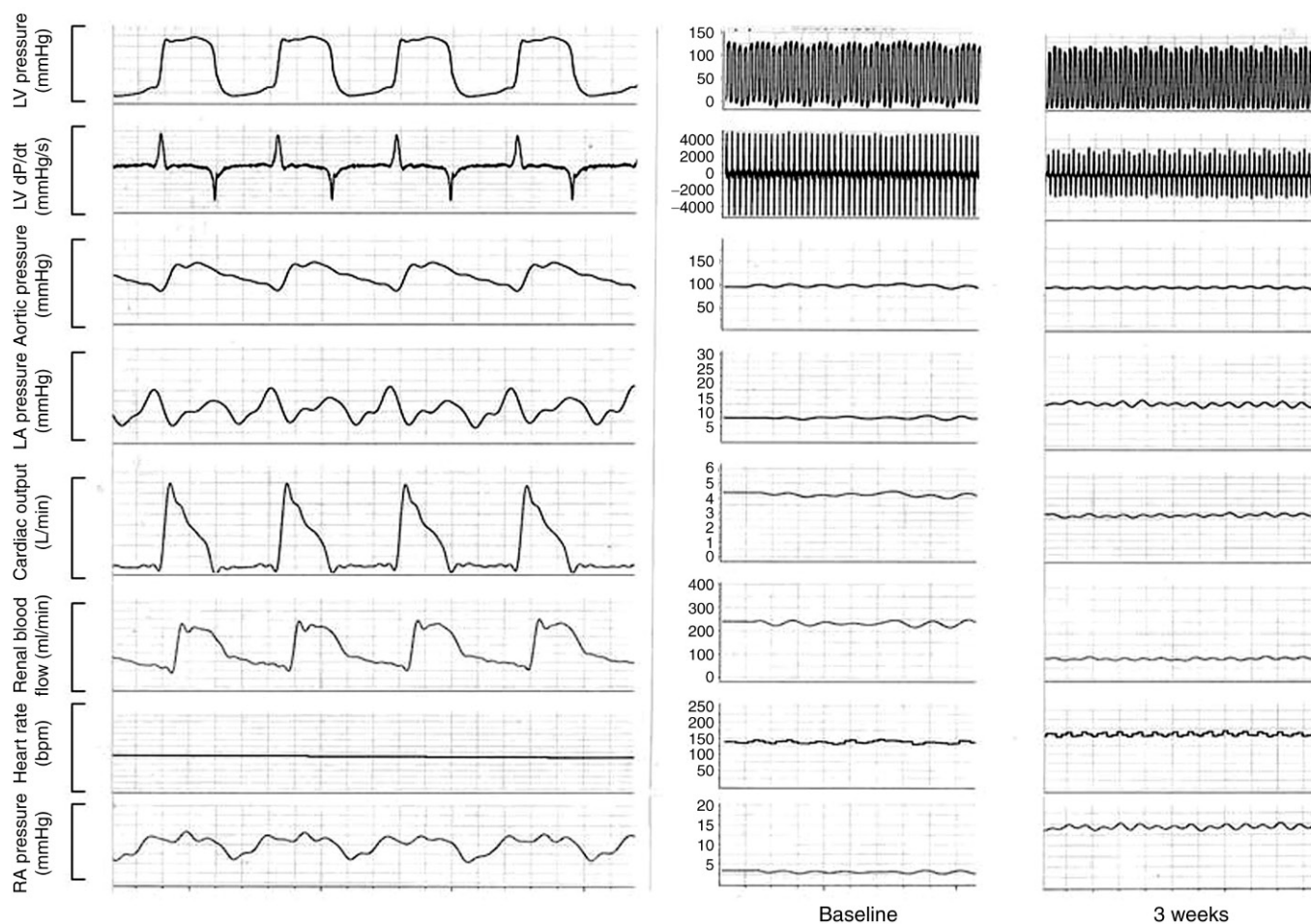
FIGURE 6.25 **Phasic waveforms of left ventricular (LV) pressure, LV (dP/dt), aortic, left and right atrial pressure, ascending aortic (cardiac output), and renal blood flow, and heart rate in a conscious pig subjected to microsphere injection followed by 3 weeks of pacing.** Note that both left and right ventricular function was impaired along with a markedly decrease in renal blood flow (unpublished data).

time of each injection and then frequently monitored during the entire course of model development. To optimize the protocol and achieve a consistent and predictable result, further studies are needed.

5 MODELS WITHOUT CARDIOVASCULAR DISEASES

5.1 Vascular Stiffness in Aging and Gender

It has been recognized increased vascular stiffness with aging represents an independent cardiovascular risk factor (O'Leary et al., 1999). Although rodent species can be served as a useful model for study of aging, major limitation is the species difference between rodent and human. In addition, due to the size of vessel from rodent species, a direct physiological measurement of vascular stiffness in conscious animals, which requires both pulse pressure and vascular diameter, is not possible. A schematic illustration of surgically implanted instrumentations for study of vascular stiffness in non-human primates, specifically rhesus monkeys, is shown in Fig. 6.27. All instrumentations implanted are similar to those described in the previous section. Aortic diameter is measured with miniature piezoelectric ultrasonic dimension crystals. Experiments can be conducted in fully conscious animals using the same set up system as shown in Fig. 6.6.

Aortic strain is calculated as systolic aortic diameter—diastolic aortic diameter (Dd)/Dd. Pressure strain (Ep) is calculated as K $\times$ (systolic blood pressure − diastolic blood pressure)/aortic strain (K = 1333). Aortic stiffness (β) is computed by In(Ps/Pd)/aortic strain (Qiu et al., 2007; Zhang et al., 2016). Baseline of aortic stiffness in male young and old, female young and old monkeys are shown in Fig. 6.28. Pulse pressure was increased in

(A)

(B)
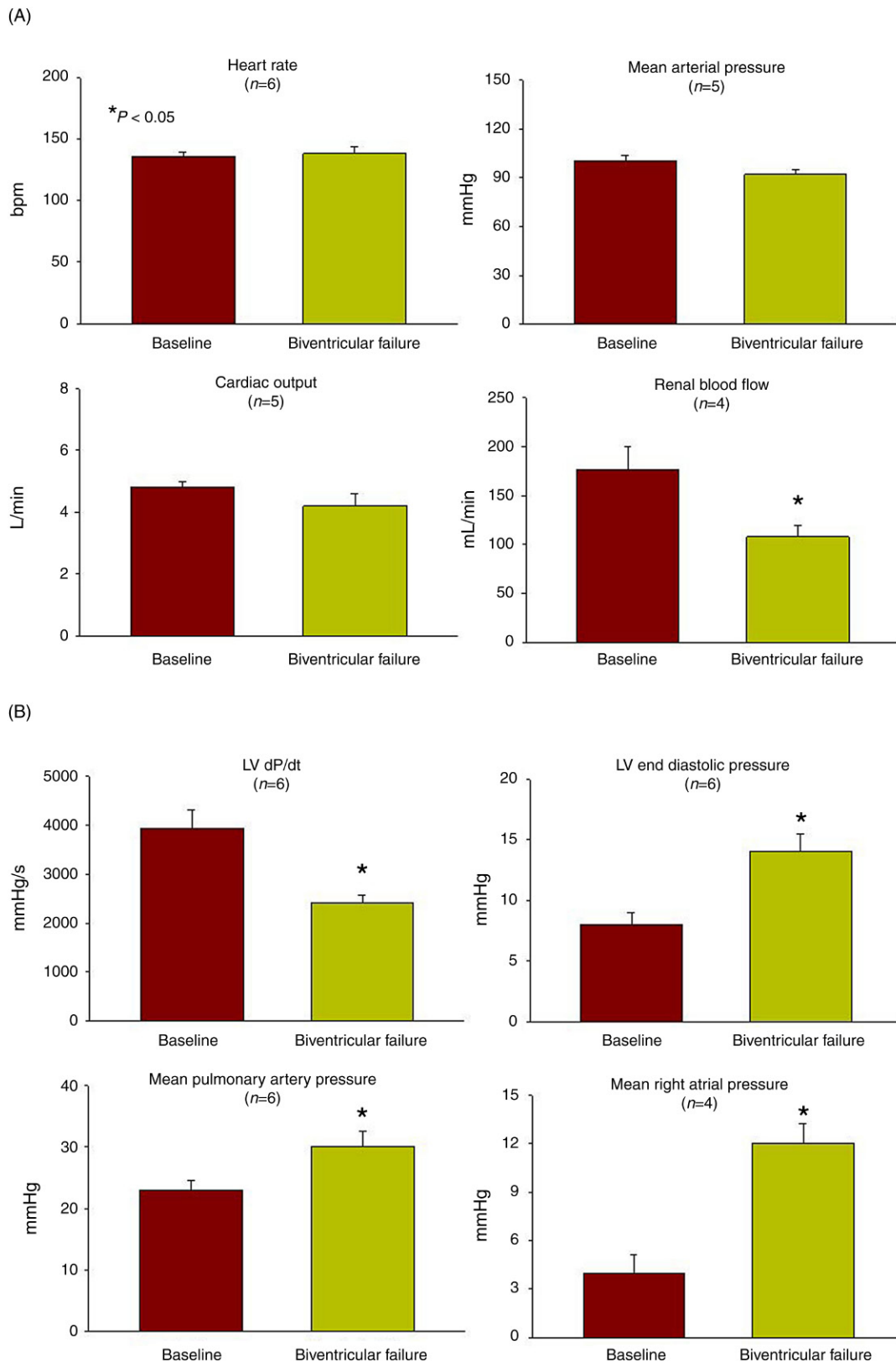
FIGURE 6.26 **Averaged cardio and renal vascular dynamic values from conscious pigs with biventricular dysfunction.** (A) Cardiovascular dynamics in conscious pigs before and after development of biventricular failure. (B) Cardiovascular dynamics in conscious pigs before and after development of biventricular failure. Note that both left and right ventricular function along with renal hemodynamic were impaired significantly compared to baseline (unpublished data).
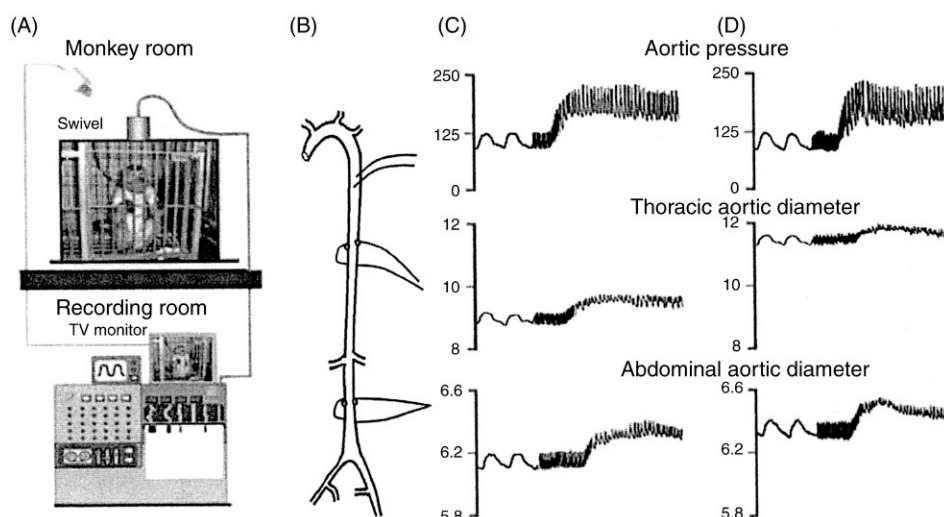
FIGURE 6.27 (A) A chronically instrumented, conscious monkey was connected to a tether system; (B) the aorta was instrumented with descending thoracic aortic catheter for measurement of aortic pressure and ultrasonic dimension crystals on opposing surface of the thoracic and abdominal aorta for measurements of aortic diameters. Examples of response to acute phenylephrine-induced hypertension are shown in young monkey, (C) and in old monkey (D) (Zhang et al., 2016).
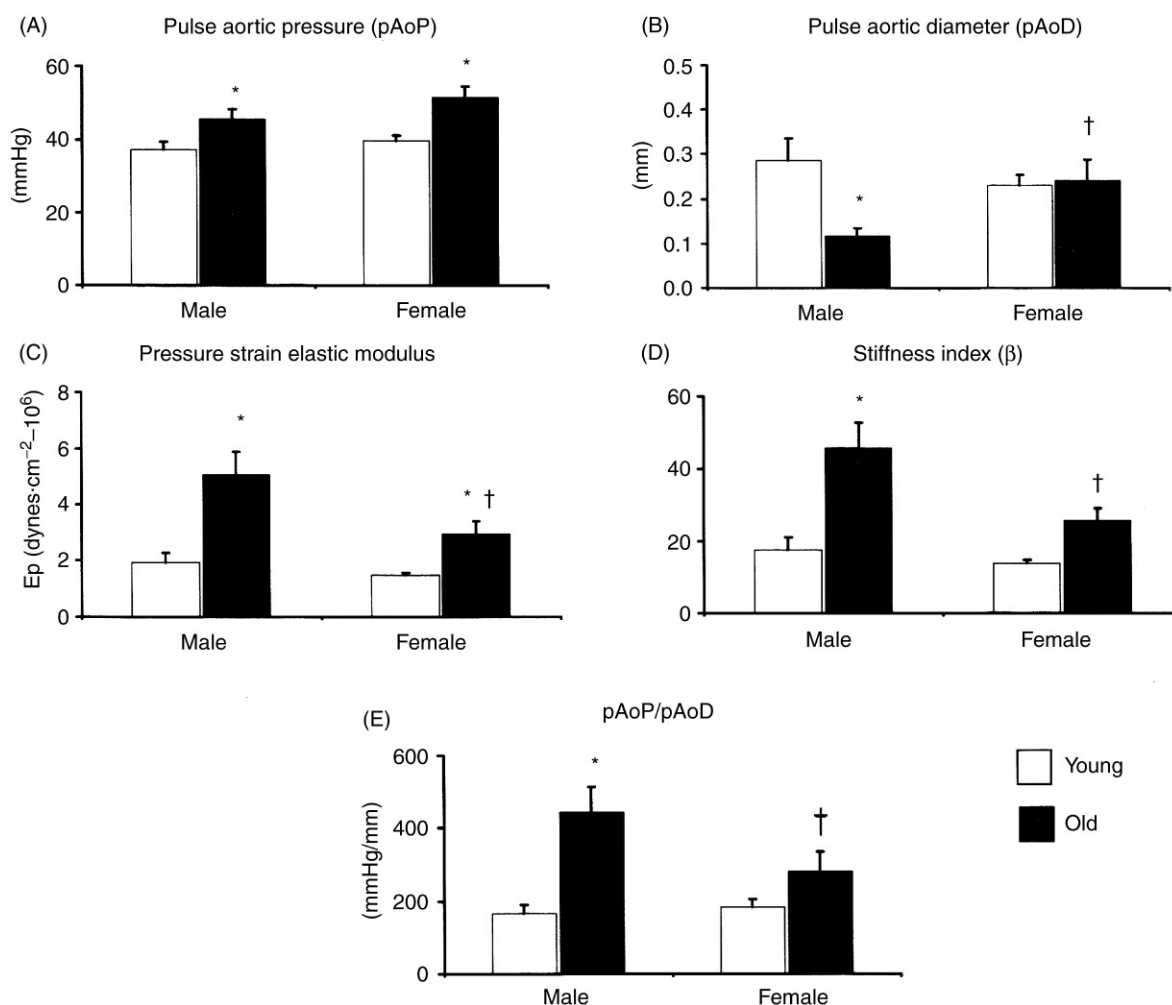
FIGURE 6.28 **Baseline aortic stiffness in young and old male, young and old female conscious monkeys.** Measurement of pulse aortic pressure (pAoP; A), pulse aortic diameter (pAoD; B), pressure strain elastic modulus (Ep; C), stiffness index (β; D), and ratio of pAoP to pAoD (E) are compared in these 4 groups. *$P < 0.05$ versus corresponding young monkeys; [†] $P < 0.05$ versus corresponding old male monkeys (Qiu et al., 2007).

both male and female old monkeys, while mean aortic pressure was similar among the four groups. Pulse diameter was greater in old females than old males. These differences in pulse diameter account for the greater increase in the pressure strain elastic modulus (Ep) and the stiffness index (β) in old male monkeys compared with old female monkeys, which reflects the increased stiffness with aging in male monkeys.

5.2 Cardiovascular Denervation

Heart transplantation is an alternative approach for patients with end stage of heart failure. It is well-known that all nerves from the original heart will be destroyed and replaced by donor heart nerves without external nerve supply. Therefore, heart transplantation has also been considered as a surgical procedure of total cardiac denervation. In patients with severe coronary artery stenosis leading to coronary artery occlusion, bypass surgery, that is, coronary artery bypass graft, has been also extensively used to restore blood supply in patients. This surgical procedure, however, also partially or completely destroys the innervation of myocardium that are perfused by the coronary artery, since majority of cardiac sympathetic nerve fibers are located subepicardially and travel along the routes of major coronary arteries. Thus, total or selective cardiac denervated animal models are required to model these clinical surgical approaches. In addition, it is important to unitize denervated animal models to understand the role and mechanism of cardiovascular control in preclinical drug research and development.

5.2.1 Selective Regional Left Ventricular Denervation

Regional ventricular denervation can be performed in either posterior or anterior left ventricular wall in larger animal species, as long as main and branch of coronary arteries can be surgically dissected and separated from myocardium. The procedure often requires a combination of surgical and chemical techniques (Kudej et al., 2006; Randall and Ardell, 1985). There are three major steps to complete the procedure, for example, posterior left ventricular denervation. First, the ventrolateral cardiac nerve at the point of the left superior pulmonary vein needs to be isolated and sectioned completely. Second, the left circumflex coronary artery from all is surrounding tissue starting at proximal to the left marginal branch and continuing to the posterior descending coronary arteries. The last procedure is to apply phenol to the atrioventricular groove above the isolated portion of the left circumflex coronary artery, all the way down the posterior groove to the apex and also down the marginal branch of the left circumflex coronary artery to the apex. The phenol can be given by using a small cotton-tripped

applicator to carefully apply to the surface of dissected areas. The procedure for anterior left ventricular wall denervation is similar to the posterior wall denervation. The confirmation of the regional denervation can be accomplished by examination of tissue norepinephrine level from the denervated area compared to innervated contralateral area. In the tissue from denervated area should be essentially depleted compared to contralateral area of tissue.

5.2.2 Left Ventricular Denervation

Left ventricular denervation can be performed by using either a combination of surgical and chemical techniques as described earlier or the surgical technique alone (Randall and Ardell, 1985; Shen et al., 1988, 1990a). Basically, the surgical procedure consists of dissection across the superior surface of the left atrium and sectioning of the ventrolateral cardiac nerves and then stripping the adventitial layers of the main pulmonary artery distal to its origin on the side facing the left atrial surface. The next step is to remove all nerves located between the aorta and pulmonary artery that project onto the surface of the left ventricle over the left main coronary artery. The phenol can be applied around the circumference of the atroventricular groove and to the triangular-shaped fat pad above the coronary sinus on the posterior wall as an optional approach. If the surgical procedure is well accomplished, the application of phenol is not necessary. Total ventricular denervation can be confirmed at the time of surgery by lack of increase in left ventricular contraction and rate during direct electrical stimulation of the left and right ansae subclaviae at a 10 Hz, 5 ms with 5–7 V, which is completely different from what is observed before the surgical denervation procedure is started. The denervation can be further confirmed using tissue norepinephrine level as described earlier.

5.2.3 Total Cardiac Denervation

Total cardiac denervation can be performed by either chronic permanent (Randall et al., 1980; Shen et al., 1990b) or acute reversible procedures (Arndt et al., 1981; Dorward et al., 1983; Shen et al., 1991). The chronic total cardiac denervation procedure is to use the intrapericardial denervation technique by surgically stripping the adventitia and nerve fibers from the main pulmonary artery, left superior pulmonary vein, and right pulmonary artery; sectioning the left ventrolateral cardiac nerve and the pericardial reflection in the transverse sinus and azygos vein. Furthermore, dissection around the pericardial reflection at the bifurcation of the right pulmonary artery needs to be completed. The completeness of the total cardiac denervation can be verified at surgery by confirming the lack of ECG response to bilateral stellate ganglion stimulation at a 10 Hz, 5 ms with 3–5 Vor bilateral vagal stimulation at a 20 Hz, 5 ms with 3–5 V. The denervation can be further

confirmed by tissue norepinephrine level from both right and left ventricles. Acute reversible total cardiac denervation is a relatively easy and fast approach for studies to compare the presence and absence of total cardiac denervation in same animals. The procedure only requires implanting a catheter in the pericardial space and acute denervation can be induced by injection of anesthetics, for example, procaine or lidocaine, into the pericardial space periodically during the experiment. The amount of anesthetics and duration between two injections depend on the size of heart and drug half-life.

The total cardiac denervation both chronic and acute models can be also examined by a pharmacological approach, that is, elimination of the reflex heart rate changes induced by either efferent or afferent stimulations. Usually, a vasodilator and vasoconstrictor, for example, phenylephrine and nitroglycerin, can be administered intravenously. Also, injection of veratridine alkaloid via the left atrium to determine reflex cardiovascular actions mediated from receptors in the myocardium (Shen et al., 1990b).

5.2.4 Sinoaortic Baroreceptor Denervation

Sinoaortic baroreceptor located in aorta and carotid arteries plays important role in regulating arterial blood pressure and blood volume. The denervation procedure needs to be performed in both areas with a combination of surgical and chemical approaches. Aortic denervation is accomplished by stripping all nerve fibers and connective tissue from the aortic root to the second intercostal artery (Shen et al., 1990b, 1991). The brachiocephalic and the subclavian arteries are also stripped from the aorta cranially to the second set of branches. After that, the carotid sinus denervation needs to be performed in both right and left common carotid arteries. Both arteries should be carefully isolated and stripped of nerve fibers and connective tissue all the way past the bifurcation of the internal and external carotid arteries. Phenol is applied to all stripped surfaces of the vessel. The confirmation of sinoaortic baroreceptor denervation can be determined by a similar pharmacological method as described earlier. The lack of reflex heart rate changes in response to alterations of arterial blood pressure can be observed when either a vasodilator or vasoconstrictor is injected intravenously. However, the response to left atrial injection of veratridine alkaloid should remain intact, indicating that the cardiac receptor is not affected by the surgical procedures (Shen et al., 1990b).

6 FUTURE DIRECTIONS

With advances in molecular and genomic research offering novel insights into the cardiovascular diseases, many transgenic mouse models have been developed and characterized. The major advantage of genetically engineered models is that a specific cellular target can be manipulated, and its role in pathogenesis established. This has led to an explosion of potential targets for therapeutic intervention. In the current chapter, we emphasize the need to validate novel targets in well-characterized, larger animal models that provide better potential for clinical translatability. Without this important translational step, many exciting research discoveries from mouse models could fail to translate into improved clinical outcomes in human studies, which has unfortunately become the norm rather than the exception. As such, it is reasonable to rethink our research strategy to include validation in clinically relevant larger animal models before proceeding to clinical trials. We have highlighted most of the existing larger animal models that can be studied in the conscious, chronically instrumented state. This unique experimental approach is vital to the accuracy and validity of experimental findings. Furthermore, advances in the development of larger animal models with multiple disorders, rather than single disorders, allow the examination of important clinical syndromes, such as cardiorenal syndrome and diabetic cardiomyopathy.

Importantly, these cardiovascular syndromes are often much worse than heart or kidney disease alone. Our preliminary and feasibility studies presented in this chapter are to call attention for future direction of translation cardiovascular medicine. Thus, while reductionist approaches are useful identifying cardiovascular targets of therapeutic interest, larger animal models of cardiovascular disease and syndromes are essential in the study of disease mechanisms, as well as target validation.

References

Armstrong, P.W., Stopps, T.P., Ford, S.E., deBold, A.J., 1986. Rapid ventricular pacing in the dog: pathophysiologic studies of heart failure. Circulation 74, 1075–1084.

Arndt, J.O., Pasch, U., Samodelov, L.F., Wiebe, H., 1981. Reversible blockade of myelinated and non-myelinated cardiac afferents in cats by instillation of procaine into the pericardium. Cardiovasc. Res. 15, 61–67.

Arrowsmith, J., 2011. Phase II failures: 2008-2010. Nat. Rev. Drug Discov. 10, 328–329.

Becker, L.C., Schuster, E.H., Jugdutt, B.I., Hutchins, G.M., Bulkley, B.H., 1983. Relationship between myocardial infarct size and occluded bed size in the dogs: difference between left anterior descending and circumflex coronary artery occlusions. Circulation 67, 549–557.

Bishop, S.P., Powell, P.C., Hasebe, N., Shen, Y.-T., Patrick, T.A., Hittinger, L., Vatner, S.F., 1996. Coronary vascular morphology in pressure-overload left ventricular hypertrophy. J. Mol. Cell. Cardiol. 28, 141–154.

Bolli, R., Marban, E., 1999. Molecular and cellular mechanisms of myocardial stunning. Physiol. Rev. 79, 609–634.

Chen, L., Lizano, P., Zhao, X., Sui, X., Dhar, S.K., Shen, Y.-T., Vatner, D.E., Vatner, S.F., Depre, C.J., 2011. Preemptive conditioning of the swine heart by H11 kinase/Hsp22 provides cardiac protection through inducible nitric oxide synthase. Am. Physiol. Heart Circ. Physiol. 300, H1303–H1310.

Chow, E., Woodard, J.C., Farrar, D.J., 1990. Rapid ventricular pacing in pigs an experimental model of congestive heart failure. Am. J. Physiol. 258, H1603–H1605.

Damman, K., van Deursen, V.M., Navis, G., Voors, A.A., van Veldhuisen, D.J., Hillege, H.L., 2009. Increased central venous pressure is associated with impaired renal function and mortality in a broad spectrum of patients with cardiovascular disease. J. Am. Coll. Cardiol. 53, 582–588.

Dorward, P.K., Flaim, M., Ludbrook, J., 1983. Blockade of cardiac nerves by intrapericardial local anesthetics in the conscious rabbit. Aust. J. Exp. Biol. Med. Sci. 61, 219–230.

Downey, J.M., 1990. Free radicals and their involvement during long-term myocardial ischemia and reperfusion. Annu. Rev. Physiol. 52, 487–504.

Ellis, Jr., P.R., Bailas, N.J., Viskos, J.D., Wong, S.H., Hyland, J.W., 1964. Experimental heart failure in dog. Arch. Surg. 89, 299–306.

Elzingz, W.E., 1969. Ameroid constrictor: uniform closure rates and a calibration procedure. J. Appl. Physiol. 27, 419–421.

Fallavollita, J.A., Logue, M., Canty, Jr., J.M., 2001. Stability of hibernating myocardium in pigs with a chronic left anterior descending coronary artery stenosis: absence of progressive fibrosis in the setting of stable reductions in flow, function and coronary flow reserve. J. Am. Coll. Cardiol. 37, 1989–1995.

Hendrick, D.A., Smith, A.C., Kratz, J.M., Crawford, F.A., Spinale, F.G., 1990. The pig as a model of tachycardia and dilated cardiomyopathy. Lab. Anim. Sci. 40, 495–501.

Heyndrickx, G.R., Millard, R.W., McRitchie, R.J., Maroko, P.R., Vatner, S.F., 1975. Regional myocardial functional and electrophysiological alterations after brief coronary artery occlusion in conscious dogs. J. Clin. Invest. 56, 978–985.

Hittinger, L., Shen, Y.-T., Patrick, T.A., Hasebe, N., Komamura, K., Ihara, T., Manders, W.T., Vatner, S.F., 1992. Mechanisms of subendocardial dysfunction in response to exercise in dogs with severe left ventricular hypertrophy. Circ. Res. 71, 423–434.

Hittinger, L., Patrick, T., Ihara, T., Hasebe, N., Shen, Y.-T., Kalthof, B., Shannon, R.P., Vatner, S.F., 1994. Exercise induces cardiac dysfunction in both moderate, compensated and severe hypertrophy. Circulation 89, 2219–2231.

Ho, D., Chen, L., Zhao, X., Durham, N., Pannirselvam, M., Vatner, D.E., Morgans, D.J., Malik, F.I., Vatner, S.F., Shen, Y.-T., 2012. Muscle myosin inhibition; a novel therapeutic approach for pulmonary hypertension. PLoS One. 7 (5), e36302.

Johns, C., Gavras, I., Handy, D.E., Salomao, A., Gavras, H., 1996. Models of experimental hypertension in mice. Hypertension 28, 1064–1069.

Kim, S.-J., Peppas, A., Hong, S.-K., Yang, G., Huang, Y., Diaz, G., Sadoshima, J., Vatner, D.E., Vatner, S.F., 2003. Persistent stunning induces myocardial hibernation and protection. Flow/function and metabolic mechanism. Circ. Res. 92, 1233–1239.

Kirby, D., Vatner, S.F., 1987. Enhanced responsiveness to carotid baroreceptor unloading in conscious dogs during development of perinephritic hypertension. Circ. Res. 61, 678–686.

Kudej, R., Shen, Y.-T., Peppas, A., Huang, C.-H., Chen, W., Yan, L., Vatner, D.E., Vatner, S.F., 2006. Obligatory role of cardiac nerves and alpha1-adrenergic receptors for the second window of ischemic preconditioning in conscious pigs. Circ. Res. 99, 1270–1276.

Larosa, G., Armstrong, P.W., Seeman, P., Forster, C., 1993. beta adrenoceptor recovery after heart failure in the dog. Cardiovasc. Res. 27, 489–493.

Li, X.Y., McCay, P.B., Zughaib, M., Jeroudi, M.O., Triana, J.F., Bolli, R., 1993. Demonstration of free radical generation in the "stunned" myocardium between conscious and open-chest dogs. J. Clin. Invest. 92, 1025–1041.

Liu, J.L., Pliquett, R.U., Brewer, E., Cornish, K.G., Shen, Y.-T., Zucker, I.H., 2001. Chronic endothelin-1 blockade reduces sympathetic nerve activity in rabbits with heart failure. Am. J. Physiol. Regul. Integr. Comp. Physiol. 280, R1906–R1913.

Marsboom, G.R., Janssens, S.P., 2004. Models for pulmonary hypertension. Drug Discov. Today Dis. Model. 1 (3), 289–296.

Miura, T., Yellon, D.M., Hearse, D.J., Downey, J.M., 1987. Determinants of infarct size during permanent occlusion of a coronary artery in the closed chest dog. J. Am. Coll. Cardiol. 9, 647–654.

Moghadasian, M.H., 2002. Experimental atherosclerosis—a historical overview. Life Sci. 70, 855–865.

Monnet, E., Rosenberg, A., 2005. Effects of protein concentration on rate of closure of ameroid constrictor in vitro. Am. J. Vet. Res. 66, 1337–1340.

Mullard, A., 2011. Reliability of 'new drug target' claims called into question. Nat. Rev. Drug Discov. 10, 643–644.

Mullens, W., Abrahams, Z., Francis, G.S., Sokos, G., Taylor, D.O., Starling, R.C., Young, J.B., Tang, W.H., 2009. Importance of venous congestion for worsening of renal function in advanced decompensated heart failure. J. Am. Coll. Cardiol. 53, 589–596.

Nuttall, A., Smith, H.J., Loveday, B.E., 1985. A clinically relevant model of heart failure: effects of ticlopidine. Cardiovasc. Res. 19, 187–192.

O'Leary, D.H., Polak, J.F., Kronmal, R.A., Manolio, T.A., Burke, G.L., Wolfson, Jr., S.K., 1999. Carotid-artery intima and media thickness as a risk factor for myocardial infarction and stroke in older adults: Cardiovascular Health Study Collaborative Research Group. N. Eng. J. Med. 340, 14–22.

Okamoto, A.K., Aoki, 1963. Development of a strain of spontaneously hypertensive rat. Jap. Circ. J. 27, 282–293.

Page, B., Young, R., Iyer, V., Suzuki, G., Lis, M., Korotchkina, L., Patel, M.S., Blumenthal, K.M., Fallavollita, J.A., Canty, Jr., J.M., 2008. Persistent regional downregulation in mitochondrial enzymes and upregulation of stress proteins in swine with chronic hibernating myocardium. Circ. Res. 102, 103–112.

Pagel, P.S., Kampine, J.P., Schmeling, W.T., Warltier, D.C., 1993. Reveral of volatile anesthetic-induced depression of myocardial contractility by extracellular calcium also enhances left ventricular diastolic function. Anesthesiology 78, 141–154.

Park, M., Shen, Y.-T., Gaussin, V., Heyndrickx, G.R., Bartunek, J., Resuello, R.R.G., Natividad, F.F., Kitsis, R.N., Vatner, D.E., Vatner, S.F., 2009. Apoptosis predominates in nonmyocytes in heart failure. Am. J. Physiol. Heart Circ. Physiol. 297, H785–H791.

Pfeffer, M.A., Braunwald, E., 1990. Ventricular remodeling after myocardial infarction. Experimental observations and clinical implications. Circulation 81, 1161–1172.

Pfeffer, J.M., Pfeffer, M.A., 1988. Angiotensin converting enzyme inhibition and ventricular remodeling in heart failure. Am. J. Med. 84 (Suppl. 3A), 37–44.

Prinz, F., Schlange, T., Asadullah, K., 2011. Believe it or not: how much can we rely on published data on potential drug targets? Nat. Rev. Drug Discov. 10, 712–713.

Qiu, H., Depre, C., Ghosh, K., Rossi, F., Peppas, A., Shen, Y.-T., Vatner, D.E., Vatner, S.F., 2007. Mechanism of gender-specific differences in aortic stiffness with aging in nonhuman primates. Circulation 116, 669–676.

Randall, W.C., Ardell, J.L., 1985. Differential innervation of the heart. In: Zipes, D., Jalife, J. (Eds.), Cardiac Electrophysiology and Arrhythmias. Grune & Stratton, New York, pp. 137–144, Chapter 15.

Randall, W.C., Kaye, M.P., Thomas, J.X., Barber, M.J., 1980. Intrapericardial denervation of the heart. J. Surg. Res. 29, 101–109.

Reimer, K.A., Jennings, R.B., Cobb, F.R., et al., 1985. Animal models for protecting ischemic myocardium: results of the NHLBI cooperative study. Comparison of unconscious and conscious dog models. Circ. Res. 56, 651–665.

Sabbah, H.N., Stein, P.D., Kono, T., Gheorghiade, M., Levine, T.B., Jafri, S., Hawkins, E.T., Glodstein, S., 1991. A canine model of chronic heart failure produced by multiple sequential coronary microembolizations. Am. J. Physiol. 260, H1379–H1384.

Shannon, R.P., Komamura, K., Shen, Y.-T., Bishop, S.P., Vatner, S.F., 1993. Impairment in regional subendocardial coronary flow and vasodilator reserve in conscious dogs with pacing-induced heart failure. Am. J. Physiol. 265, H801–H809.

C. CARDIAC AND CARDIOVASCULAR

Shen, Y.-T., 2010. Primate models for cardiovascular drug research and development. Curr. Opin. Invest. Drugs 11, 1025–1029.

Shen, Y.-T., Vatner, S.F., 1995. Mechanism of impaired myocardial function during progressive coronary stenosis in conscious pigs: hibernation vs. stunning. Circ. Res. 76, 479–488.

Shen, Y.-T., Vatner, S.F., 1996. Difference in myocardial stunning following brief coronary artery occlusion in conscious pigs and dogs. Am. J. Physiol. 270, H1312–H1322.

Shen, Y.-T., Knight, D.R., Vatner, S.F., Randall, W.C., Thomas, Jr, J.X., 1988. Responses to coronary artery occlusion in conscious dogs with selective cardiac denervation. Am. J. Physiol. 255, H525–H533.

Shen, Y.-T., Knight, D.R., Thomas, Jr., J.X., Vatner, S.F., 1990a. Effects of selective cardiac denervation on collateral blood flow after coronary artery occlusion in conscious dogs. In: Heusch, G., Ross, Jr., J. (Eds.), Adrenergic Mechanism of Myocardial Ischemia. Steinkopff Verlag Darmstadt Springer-Verlag, New York, pp. p229–p239.

Shen, Y.-T., Knight, D.R., Thomas, Jr., J.X., Vatner, S.F., 1990b. Relative Roles of cardiac receptors and arterial baroreceptors during hemorrhage in conscious dogs. Circ. Res. 66, 397–405.

Shen, Y.-T., Cowley, A.W., Vatner, S.F., 1991. Relative roles of cardiac and arterial baroreceptors in vasopressin regulation during hemorrhage in conscious dogs. Circ. Res. 68, 1422–1436.

Shen, Y.-T., Fallon, J.T., Iwase, M., Vatner, S.F., 1996a. Innate protection of baboon myocardium following coronary artery occlusion and reperfusion. Am. J. Physiol. 270, H1812–H1818.

Shen, Y.-T., Wiedmann, R.T., Lynch, J.J., Grossman, W., Johnson, R.G., 1996b. Replacement of growth hormone fails to improve ventricular function in hypophysectomized rats with myocardial infarction. Am. J. Physiol. 271, H1721–H1727.

Shen, Y.-T., Wiedman, R.T., Greenland, B.D., Lynch, J.J., Grossman, W., 1998. Combined effects of angiotensin converting enzyme inhibition and angiotensin II receptor antagonism in conscious pigs with congestive heart failure. Cardiovasc. Res. 39, 413–422.

Shen, Y.-T., Lynch, J.J., Shannon, R.P., Wiedmann, R., 1999. A novel heart failure model induced by sequential coronary artery occlusions and tachycardiac stress in awake pigs. Am. J. Physiol. 277, H388–H398.

Shen, Y.-T., Buie, P.S., Lynch, J.J., Krause, S.M., Ma, X-L, 2000. Chronic therapy with an ETa/b receptor antagonist in conscious dogs during progression of congestive heart failure. Intracellular Ca^{++} regulation and nitric oxide mediated coronary relaxation. Cardiovasc. Res. 48, 332–345.

Shen, Y.-T., Lin, Y., Depre, C., Resuello, R.R.G., Natividad, F., Peppas, A., Rossi, F., Takao, N., Vanter, D.E., Vatner, S.F., 2005. A novel nonhuman primate model of myocardial infarction, left ventricular hypertrophy and congestive heart failure. FASEB J. 19 (4), A243.

Shen, Y.-T., Rossi, F., Vatner, S.F., 2008a. Nonhuman primate models for cardiovascular research. In: Daniel Acosta, Jr. (Ed.), Cardiovascular Toxicology. fourth ed. Informa Healthcare, New York, NY, USA, pp. 133–152.

Shen, Y.-T., Depre, C., Yan, L., Park, J.Y., Tian, B., Jain, K., Chen, L., Zhang, Y., Kudej, R.K., Zhao, X., Sadoshima, J., Vatner, D.E., Vatner, S.F., 2008b. Repetitive ischemia by coronary stenosis induces a novel window of ischemic preconditioning. Circulation 118, 1961–1969.

Shen, Y.-T., Malik, F.I., Zhao, X., Depre, C., Dhar, S.K., Abarzua, P., Morgans, D.J., Vatner, S.F., 2010. Improvement of cardiac function by a cardiac myosin activator in conscious dogs with systolic heart failure. Circ. Heart Fail. 3, 522–527.

St. Louis, J.D., Hughes, G.C., Kypson, A.P., DeGrado, T.R., Donovan, C.L., Coleman, R.E., Yin, B., Steenbergen, C., Landolfo, K.P., Lowe, J.E., 2000. An experimental models of chronic myocardial hibernation. Ann. Thorac. Surg. 69, 1351–1357.

Stenmark, K.R., Meyrick, B., Galie, N., Mooi, W.J., McMurtry, I.F., 2009. Animal models of pulmonary arterial hypertension: the hope for etiological discovery and pharmacological cure. Am. J. Physiol. Lung Cell. Mol. Physiol. 297, L1013–L1032.

Testani, J.M., Khera, A.V., St John Sutton, M.G., Keane, M.G., Wiegers, S.E., Shannon, R.P., Kirkpatrick, J.N., 2010. Effect of right ventricular function and venous congestion on cardiorenal interactions during the treatment of decompensated heart failure. Am. J. Cardiol. 105, 511–516.

Uemura, N., Knight, D.R., Shen, Y.-T., Nejima, J., Cohen, M.V., Thomas, J.X., Vatner, S.F., 1989. Increased myocardial infarct size due to reduced coronary collateral blood flow in beagles. Am. J. Physiol. 257, H1798–H1803.

Uemura, N., Vatner, D.E., Shen, Y.-T., Wang, J., Vatner, S.F., 1993. Increased alpha$_1$-adrenergic vascular sensitivity during the development of hypertension in conscious dogs. Am. J. Physiol. 264, H1259–H1268.

Van der Giessen, W.J., van Woerkens, L.J., Duncker, D.J., Roelandt, J.T.C., Verdouw, P.D., 1989. The acute hemodynamic effects of nisoldipine and pimobendan in conscious pigs with chronic heart failure. J. Cardiovasc. Pharmacol. 14, 653–658.

Van Woerkens, L.J., van der Giessen, W.J., Verdouw, P.D., 1993. Cardiovascular effects of dopamine and dobutamine in conscious pigs with chronic heart failure. Crit. Care Med. 21, 420–424.

Vivaldi, M.T., Kloner, R.A., Schoen, F.J., 1985. Triphenyltetrazolium staining of irreversible ischemic injury following coronary artery occlusion in rat. Am. J. Pathol. 121, 522–530.

von Harsdorf, R., Edward, J.G., Shen, Y.-T., Kudej, R.K., Dietz, R., Leinwand, L.A., Nadal-Ginard, B., Vatner, S.F., 1997. Identification of a Cis-acting regulatory element conferring inducibility of the atrial natriuretic factor gene in cardiac hypertrophy. J. Clin. Invest. 100, 1294–1304.

Wilson, J.R., Douglas, P., Hickey, W.F., Lanoce, V., Ferrard, N., Muhammad, A., Reichek, N., 1987. Experimental congestive heart failure produced by rapid ventricular pacing in the dog: cardiac effects. Circulation 75, 857–867.

Zhang, J., Wilke, N., Wang, Y., Zhang, Y., Wang, C., Eijgelshoven, M.H.J., Cho, Y.K., Murakami, Y., Ugurbil, K., Bache, R., From, A.H.L., 1996. Functional and bioenergetic consequence of postinfarction left ventricular remodeling in a new porcine model. MRI and ^{31}P-MRS study. Circulation 94, 1089–1100.

Zhang, J., Zhao, X., Vatner, D.E., McNulty, T., Bishop, S., Sun, Z., Shen, Y.-T., Chen, L., Meininger, G.A., Vatner, S.F., 2016. Extracellular matrix disarray as a mechanism for greater abdominal versus thoracic aortic stiffness with aging in primates. Arterioscler. Thromb. Vasc. Biol. 36 (4), 700–706.

Further Reading

Moe, G.W., Stopps, T.P., Howard, R.J., Armstrong, P.W., 1988. Early recovery from heart failure: insight into the pathogenesis of experimental chronic pacing-induced heart failure. J. Lab. Clin. Med. 112, 426–432.

Cardiovascular Models: Heart Secondarily Affected by Disease (Diabetes Mellitus, Renal Failure, Dysfunctional Sympathetic Innervation)

Jitka Sviglerova, Jitka Kuncova, Milan Stengl

Biomedical Center, Charles University, Pilsen, Czech Republic

1 THE HEART AND DIABETES MELLITUS

Diabetes mellitus represents a serious medical problem with increasing prevalence in both developed and developing countries that has reached a global epidemic level with significant social and economic consequences. Diabetes mellitus may be classified as type 1 diabetes (insulin-dependent) or type 2 diabetes (noninsulin-dependent). Type 1 diabetes is characterized by a complete (or almost complete) lack of endogenous insulin due to destruction of β-cells in pancreatic islets of Langerhans. This chapter will be focused on animal models of type 1 diabetes mellitus and cardiovascular complications that accompany the disease. The cardiovascular diseases are the primary cause of death in diabetic patients and the prevalence of and mortality from cardiovascular

diseases are several fold higher in patients with diabetes mellitus than in the general population. One of the most important cardiovascular complications is a diabetic cardiomyopathy characterized by an early diastolic and later systolic dysfunctions, (Mahgoub and Abd-El-fattah, 1998) microangiopathy, hypertrophy of cardiac myocytes, (Gargiulo et al., 1998), and finally by heart failure (Jarret, 1989). The possible mechanisms of diabetic cardiomyopathy include metabolic disturbances, myocardial fibrosis, small vessel disease, cardiac autonomic neuropathy, and insulin resistance (Fang et al., 2004).

Various experimental models may be used for studying the type 1 diabetes mellitus and associated complications. Spontaneous hyperglycemia and ketoacidosis occur in BB rats, in which pancreatic insulitis rapidly followed by selective destruction of β-cells develops between 50 and 90 days of age (Mordes et al., 1987). Another model of spontaneous autoimmune diabetes is the nonobese diabetic (NOD) mouse (Makino et al., 1980). These mice develop insulitis at the age of 5 weeks and by 7 months 80% of female and 20% of male mice become diabetic. Beside these spontaneous models, the β-cell may be destroyed by experimental viral, surgical, or pharmacological interventions. The viral induction of diabetes was demonstrated with encephalomyocarditis virus or Kilham rat virus in rats (Jordan and Cohen, 1987; Yoon and Jun, 2006). For pharmacological induction of diabetes, usually alloxan or streptozotocin are used (Dunn et al., 1943; Rakieten et al., 1963). This chapter will further focus on streptozotocin-induced diabetes mellitus in laboratory animals with special emphasis on the rat model of streptozotocin-induced diabetes mellitus.

2 METHODOLOGICAL ASPECTS

Streptozotocin (2-deoxy-2-(3-methyl-3-nitrosoureido)-D-glukopyranose), an antibiotic with antineoplastic effects produced by *Streptomyces achromogenes* bacteria, destroys selectively the β-cells of pancreatic islets of Langerhans (Fig. 7.1) (Junod et al., 1967). Streptozotocin induces DNA strand breaks and DNA alkylation that leads to necrosis of pancreatic β-cells (Elsner et al., 2000; Yamamoto et al., 1981). Streptozotocin is transported inside the β-cell by the glucose transporter GLUT2 and expression of GLUT2 is therefore required for the toxic effect (Elsner et al., 2000; Schnedl et al., 1994). The signaling pathways of the toxic effect of streptozotocin involve activation of inducible NO-synthase, increase in NO concentration, (Flodström et al., 1999) increased H_2O_2 generation (Takasu et al., 1991).

Development of diabetes mellitus after the application of streptozotocin is very fast, especially in the rat. The sensitivity of β-cells to glucose is significantly reduced already 2 h after application of streptozotocin, the destruction and significant reduction of the number of β-cells occurs in several hours after application (West et al., 1996). This is accompanied by changes in glucose and insulin plasma levels: 2 h after application a hyperglycemia with no changes in plasma and pancreatic insulin levels develops, followed by hypoglycemia with increased plasma levels of insulin but no change in pancreatic insulin level. One day after application of streptozotocin, the rats show all characteristic symptoms of diabetes including hyperglycemia, glycosuria, polyuria, reduced plasma, and pancreatic insulin levels (Junod et al., 1969).

Streptozotocin may be applied in a single dose or in repeated manner, usually dissolved in citrate buffer (pH 4.5), by intravenous, intraperitoneal, or intraarterial injection. In our experiments, diabetes was reliably induced by a single intravenous injection of streptozotocin dissolved in citrate buffer in tail vein at dose of 65 mg/kg body weight. The dose necessary for diabetes induction in rats varies between 40 and 60 mg/kg body weight, although higher values are sometimes reported (Ganda et al., 1976). The diabetic symptoms correlate well with the dose used. In general, in doses below 40 mg/kg body weight only slight changes in glycemia, glycosuria, and insulin plasma levels are observed and
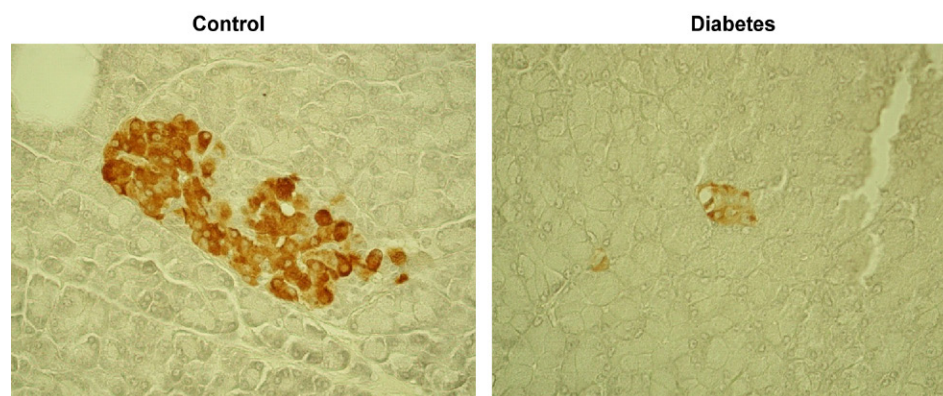
FIGURE 7.1 **Histology and immunohistochemistry of the pancreatic islets of Langerhans in control** *(left panel)* **and streptozotocin-induced diabetic** *(right panel)* **rats.** In diabetic rats, the number and size of islets was reduced and the immunoreactivity for insulin was diminished.

these slight changes tend to normalize spontaneously in up to 25% of animals (Junod et al., 1969). With a sufficient dose of streptozotocin, the induction of diabetes in rats is easy, fast, and reliable. In a majority of studies employing this rat model, however, the pathogenesis of diabetes and associated symptoms were usually studied just for several weeks or months during which diabetes is fully developed and maintained. The long-term effects of streptozotocin and possible recovery from streptozotocin-induced diabetes are explored much less. In our experiments, we followed the rats with streptozotocin-induced diabetes for one year and a recovery was observed in a significant portion of animals. All 152 rats showed fully blown diabetes for the first 6 months of experiment. In the second half of the year, two different groups could be clearly distinguished. In the diabetic group ($n = 92$) the glycemia remained high (above 18 mmol/L), the body weight did not grow, plasma levels of insulin were kept low, and histological analysis revealed reduction in number and size of pancreatic islets with a lack of insulin-secreting cells. In contrast, the recovery group ($n = 60$) showed in the second half of the year significant differences that were not present in the first 6 months of experiment: lower glycemia (below 12 mmol/L), steadily growing body weight, higher plasma levels of insulin that approached values found in control animals (Fig. 7.2). Also, the histological structure of pancreatic islets was similar to control animal with a number of well-preserved β-cells. Therefore,

after 6 months there was a significant group of animals (~40%) that showed a significant recovery with a number of parameters approaching values in control, nondiabetic animals. The only test that was able to reliably distinguish the recovery animals from nondiabetic controls was the glucose tolerance test. The glucose tolerance test was performed in the 9th and 12th month of the experiment and the curve clearly showed pathological values similar to the diabetic group and significantly different from those of control nondiabetic animals. Both streptozotocin groups responded by a decreased secretion of insulin. In conclusion, the streptozotocin-induced diabetes mellitus in rats was stable for 6 months, afterward, however, a significant recovery developed in ~40% animals. The functional insufficiency of the recovery in this period (7–12 months after streptozotocin application) may be uncovered by the glucose tolerance test. The insulin secretion in recovery animals is probably sufficient at rest, however, an increased glucose load unmasks the still impaired glucose tolerance (Fig. 7.3). In majority of animals (~60%) no recovery was observed and severe diabetes persisted throughout the period of 12 months. A spontaneous recovery from streptozotocin-induced diabetes was already described in neonatal rats, in which streptozotocin was applied at birth, (Garofano et al., 2000) or in adult animals but with low dose streptozotocin (Rakieten et al., 1976; Su et al., 2000).

Beside rat, streptozotocin is used for induction of diabetes also in other species. In mice, the type 1 diabetes
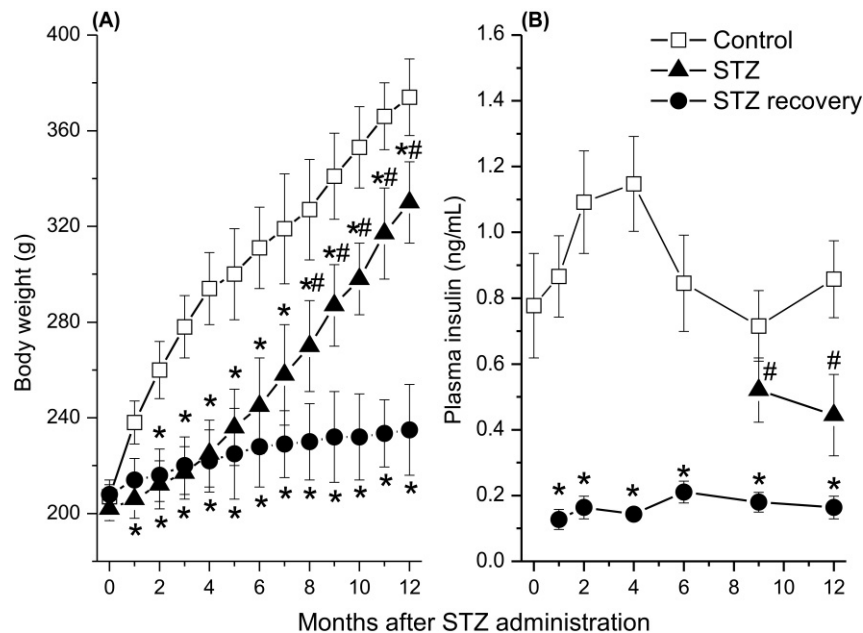
FIGURE 7.2 Body weight (A) and plasma insulin concentration (B) in control and STZ-diabetic rats. *Open squares*, control rats; *filled triangles*, STZ-diabetic rats having blood glucose level above 18 mmol/L at least 6 month after STZ administration and below 12 mmol/L 9 and 12 months after STZ administration (recovery), *filled circles*, STZ-diabetic rats having blood glucose above 18 mmol/L during the whole experimental period. *$P < 0.01$ compared with control rats, #$P < 0.01$ compared with animal being hyperglycemic during the whole experimental period.
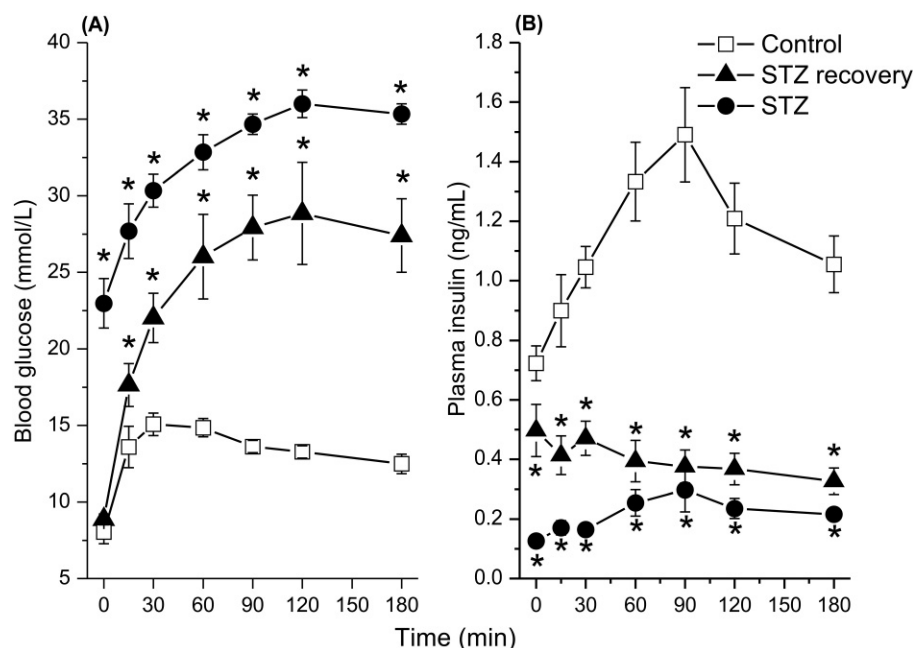
FIGURE 7.3   Blood glucose (A) and plasma insulin concentration (B) after intraperitoneal administration of glucose (2 g/kg) 12 month after STZ administration. *Open squares*, control rats; *filled triangles*, STZ-diabetic rats having blood glucose level above 18 mmol/L at least 6 month after STZ administration and bellow 12 mmol/L 9 and 12 months after STZ administration (recovery), *filled circles*, STZ-diabetic rats having blood glucose above 18 mmol/L during the whole experimental period. *$P < 0.01$ compared with control rats.

may be induced either by a single higher dose of streptozotocin or by repeated application of lower doses, both applied intraperitoneally. In case of single dose application, a reliable induction is described for doses of 200 mg/kg (Anderson et al., 1974; Guz et al., 2002). A serious disadvantage of single dose application is very high immediate lethality (up to 90% for 180 mg/kg in our hands). Repeated application of streptozotocin is usually performed with doses of 40–50 mg/kg daily applied for five consecutive days (Carlsson et al., 2000). The characteristic diabetic symptoms (hyperglycemia, glycosuria, stagnant body weight) develops after application of the last dose. The mice typically show significant intergender differences: in male mice the plasma levels of glucose after streptozotocin application were significantly higher than in female mice. Since testosterone administration is known to increase the hyperglycemic response in castrated males and females, as well as in noncastrated females, it probably contributes to the diabetogenic effects of streptozotocin (Rossini et al., 1978).

The diabetogenic effects of streptozotocin in guinea pig are controversial. According to some studies, guinea pigs are resistant to the diabetogenic effects of streptozotocin (Kushner et al., 1969). In contrast, other studies describe a reliable guinea pig model of streptozotocin-induced diabetes on basis of reduced growth rate, beta cell dysfunction, polydipsia, polyuria, and glycosuria (Schlosser et al., 1987). Differences in the experimental methods of diabetes induction, especially dosing and application, may be responsible for these discrepancies. The most recommended methods include intracardiac application of streptozotocin (200 mg/kg) preceded by insulin administration, (Aomine et al., 1990) intracardiac injection of streptozotocin (150 mg/kg) without insulin, (Schlosser et al., 1987) or intravenous application of streptozotocin (Gorray et al., 1986). Based on differences in the method of diabetes induction, also the diabetic parameters, the time course of the disease or associated lethality differ between the models. In our experimental conditions, whereas the intraperitoneal application of streptozotocin (300 mg/kg) did not induce any diabetic symptoms, the intravenous administration of streptozotocin (150 mg/kg) lead to significant glycosuria. The histological analysis of pancreas did not reveal any signs of destruction of islets regardless of the method of streptozotocin administration. Even the glycosuria observed after intravenous administration of streptozotocin may not be the diabetic symptom but rather a result of a direct nephrotoxic effect of streptozotocin that was described in patients. This hypothesis is supported by the fact that a daily administration of insulin (5 i.u./kg) did not prevent the glycosuria.

With regard to the rabbit model of diabetes, the studies using the alloxan-induced model clearly prevail. The studies with streptozotocin-induced diabetes in rabbit are rare and contradictory. There is some evidence about diabetogenic effects of streptozotocin in adult rabbits, as well as fetuses but other studies argue

against this possibility (Chaffin et al., 1995; Kedar and Chakrabarti, 1983; Kushner et al., 1969; Lazarus and Shapiro, 1972; Lazar et al., 1968).

From large mammals, streptozotocin was successfully used to induce diabetes in dog and pig. In dog the application of streptozotocin was associated with high mortality and therefore several techniques were developed to reduce the dose of streptozotocin and the associated mortality. Freyse et al. (1982) combined partial pancreatectomy and low dose (2 mg/kg) streptozotocin infusion into the superior pancreaticoduodenal artery. Other techniques include a combined intravenous administration of streptozotocin and alloxan or suprarenal intraarterial infusion of streptozotocin and alloxan after balloon occlusion of the juxtarenal abdominal aorta (Liu et al., 2000; Salis et al., 2001). Another large mammal species sensitive to the diabetogenic effects of streptozotocine is pig (and minipig). For a reliable diabetogenic effect of streptozotocin in both pig and minipig a dose of 100–150 mg/kg is needed (Gäbel et al., 1985). In minipigs a successful induction of diabetes by two low doses (40 mg/kg) was also reported (Rolandsson et al., 2002).

3 EXPERIMENTAL RESULTS IN THE RAT MODEL OF STREPTOZOTOCIN-INDUCED DIABETES

3.1 Diabetes and Cardiac Contractility

Effects of chronic (16 weeks) streptozotocin-induced diabetes on cardiac contractility were investigated using the right ventricle papillary muscles (Svíglerová et al., 2005). Streptozotocin-induced diabetes decreased the contraction force of the papillary muscles considerably. Furthermore, the dependence of the contraction force on stimulation frequency was reduced, especially at lower rates (<1 Hz). The kinetics of contraction were also influenced, diabetes prolonged significantly both the time to peak contraction and relaxation time. Next, the effects of insulin on cardiac contractility were investigated in both control and diabetic animals. Surprisingly, insulin reduced the contraction force in both control and diabetic groups (Fig. 7.4). To elucidate the negative inotropic effects of diabetes and of insulin in more detail, additional experiments aimed at various stages of excitation–contraction coupling were performed.

First, the rest potentiation of cardiac contraction was tested. In rats, the first contraction after a period of rest is increased. This phenomenon is called post-rest potentiation of contraction and it mainly reflects function of the Na^+/Ca^{2+} exchange and of the sarcoplasmic reticulum Ca^{2+} pump (Bers and Christensen, 1990; Shattock and Bers, 1989). Steady-state stimulation (1 Hz) was interrupted by a rest period of variable duration and the first postrest contraction was always increased (Fig. 7.5). In diabetic myocardium the postrest potentiation of contraction was preserved, however, the increase in postrest contraction was less pronounced (Fig. 7.5). Furthermore, the dependence of potentiation on the duration of the resting period was flatter in diabetic rats than in control rats. Insulin did not influence the postrest potentiation in control rats but it significantly enhanced the
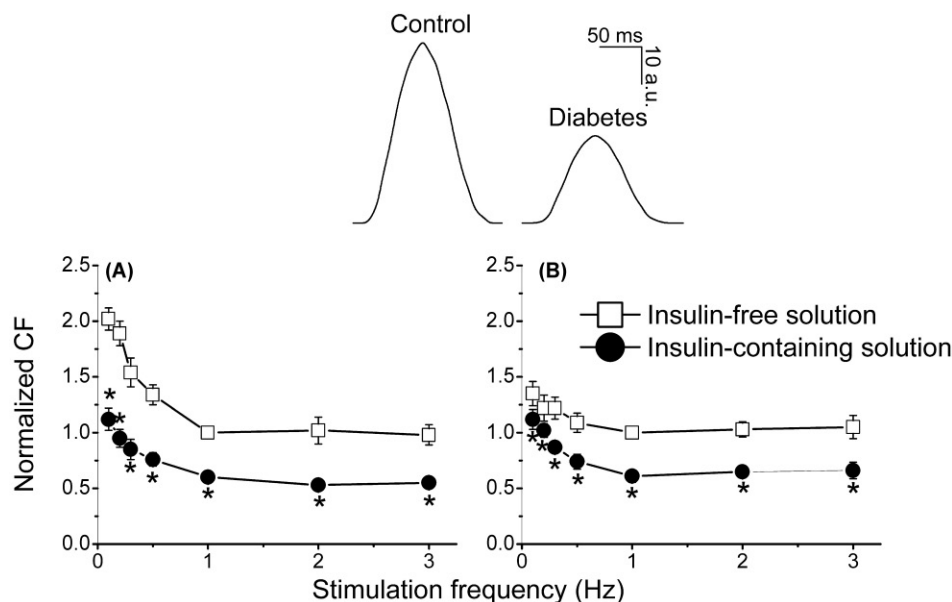
FIGURE 7.4 **The effect of insulin on the contraction force in control and diabetic rats.** The dependence of contraction force (CF) on stimulation frequency in control (A) and diabetic rats (B). Values were normalized to the contraction force at 1 Hz in baseline solution. *Open squares*, baseline; *filled circles*, effect of insulin (80 i.u./L). * Significantly different from baseline ($P < 0.05$). Upper inset: representative examples of contraction of the right ventricle papillary muscle in the rat at stimulation rate of 1 Hz. *Left*, control animal; *right*, diabetic rat. a.u., arbitrary units.
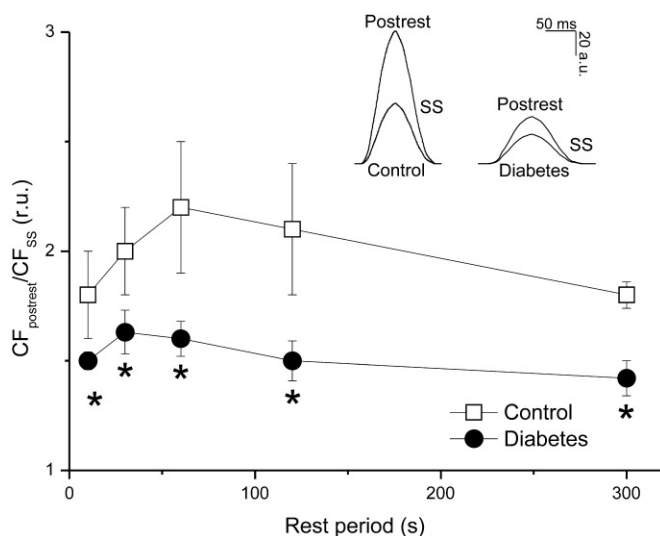
FIGURE 7.5 **The postrest potentiation of contraction in control and diabetic rats.** *Open squares*, control rats; *filled circles*, STZ-diabetic rats. *, significantly different from control rats (*P* < 0.05). The upper inset: the last steady-state contraction (SS) and the first postrest contraction (postrest) of the right ventricle papillary muscle in the rat. Left, control animal; right, diabetic rat. a.u., arbitrary units.

phenomenon in diabetic rats. This strongly suggests that the negative inotropic effect of insulin is not mediated by influencing processes of sarcoplasmic reticulum Ca^{2+} loading.

To verify this further, pharmacological interventions with cyclopiazonic acid, a selective blocker of sarcoplasmic reticulum Ca^{2+} pump (SERCA2) and with nifedipine, a blocker of sarcolemmal Ca^{2+} transport through L-type Ca^{2+} channels (L-type Ca^{2+} current, ICaL), were employed. Cyclopiazonic acid (3 μmol/L) showed a negative inotropic effect, this effect being similar in both control and diabetic animals. Cyclopiazonic acid also slowed down the relaxation, especially the second half of it. Administration of insulin on top of cyclopiazonic acid further decreased the contraction, again in both control and diabetic rats. The insulin-dependent decrease of contraction in the presence of cyclopiazonic acid was similar to that in the absence of it. This again suggests that the Ca^{2+} uptake to sarcoplasmic reticulum by SERCA2 is not a major determinant of the negative inotropic effect of insulin and that different mechanisms must be involved. Nifedipine (3 μmol/L) diminished the contraction force in both experimental groups and this effect was strongly dependent on stimulation frequency as reported previously being much more pronounced at high frequencies (Schouten and ter Keurs, 1991). Administration of insulin on top of nifedipine did not affect the contraction further. This lack of effect of insulin in the presence of nifedipine was also observed at low frequencies of stimulation, in which the reduction of contraction by nifedipine was only minor. These data suggest that

insulin inhibits ICaL and the reduction of ICaL leads to the negative inotropic effect. In the presence of nifedipine, which binds to ICaL channels, this inhibitory action of insulin would be prevented. However, the effect of insulin on ICaL was investigated directly using the patch-clamp method in rat isolated ventricular myocytes (Aulbach et al., 1999). In contrast to the aforementioned hypothesis, no inhibition but stimulation of ICaL by insulin was found. If this is also the case in our experimental conditions of multicellular preparation, the impairment of triggering SR Ca^{2+} release by ICaL (decreased efficiency of this process) remains as the most likely mechanism. The central finding of the negative inotropic effect of diabetes corresponds well with other studies that indicate a vast number of cellular mechanisms contributing to this phenomenon: depression of sarcoplasmic reticulum Ca^{2+}-ATPase and its enhanced inhibition by phospholamban, (Ganguly et al., 1983; Teshima et al., 2000; Vasanji et al., 2004) defective sarcolemmal Ca^{2+}-ATPase, (Heyliger et al., 1987; Makino et al., 1987) depression of Na$^+$-Ca^{2+} exchanger, (Chattou et al., 1999; Makino et al., 1987) reduced L-type calcium current, (Chattou et al., 1999; Lee et al., 1992) decreased number of sarcoplasmic reticulum ryanodine-sensitive Ca^{2+} channels, (Teshima et al., 2000; Yu et al., 1994) and alterations of contractile proteins, such as diminished Ca^{2+} sensitivity, shifts in myosin isoenzymes (from V1 myosin with high ATPase activity to V3 myosin with low ATPase activity), (Malhotra and Sanghi, 1997) reduced cross-bridge cycle rate, (Ishikawa et al., 1999) altered myosin heavy chain isoform expression (Rundell et al., 2004).

3.2 Diabetes and Autonomic Cardiac Innervation

Cardiovascular autonomic neuropathy is one of the most common diabetes-associated complications and it contributes significantly to the increased morbidity and mortality of diabetic patients (Kuehl and Stevens, 2012). In the rat model of streptozotocin-induced diabetes the autonomic neuropathy was demonstrated by functional studies, for example, blunted chronotropic responses to both nadolol and atropine suggesting diminished vagal and sympathetic control, diminished circadian variation in the heart rate and altered baroreflex sensitivity (Chang and Lund, 1986; Hicks et al., 1998). We have investigated how diabetes affects the content, release, and uptake of norepinephrine in cardiac sympathetic nerves in early and later stages of streptozotocin-induced diabetes in female rats (Kuncová et al., 2003). In isolated atria, the diabetic state significantly affected norepinephrine concentrations. An initial significant increase (1 month after onset of diabetes) was followed by a sustained decline in tissue noepinephrine concentrations that became significantly different 7 months from the onset of disease

(Fig. 7.6A). Both basal and potassium-evoked releases of norepinephrine were significantly increased 4 months from the onset of disease. The neuronal uptake blocker desipramine significantly reduced both basal and potassium-evoked releases of norepinephrine 4 months from the onset of diabetes suggesting that a substantial portion of norepinephrine release was due to a calcium-independent carrier-mediated process. In experiments with calcium-free solution in the presence of desipramine the potassium-evoked release of norepinephrine was nearly abolished in control rats. In diabetic rats (4 and 7 months from the induction) the potassium-evoked release was still significantly higher than the basal one.
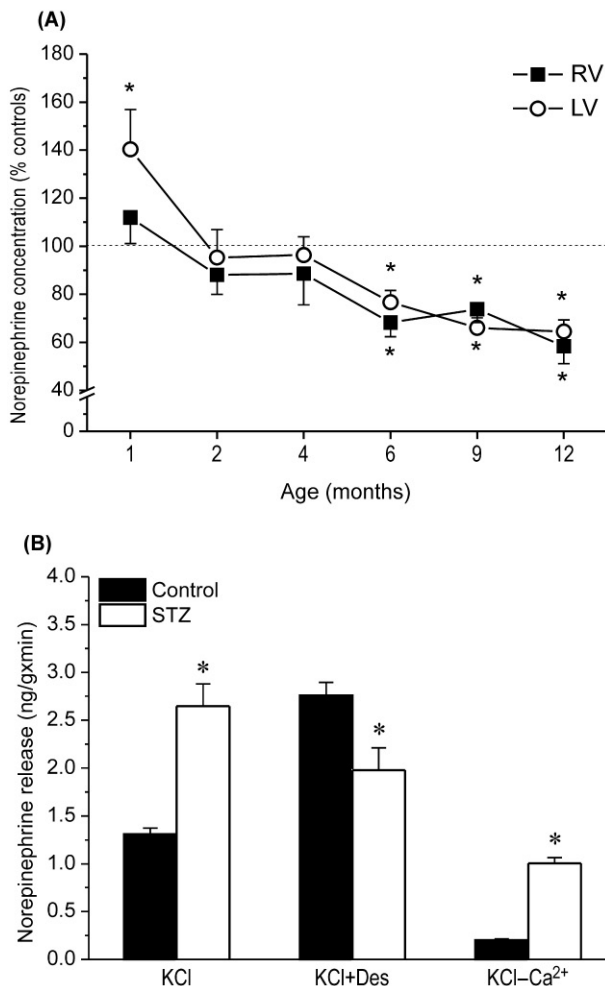
FIGURE 7.6 The impact of STZ-induced diabetes on norepinephrine concentrations in the free walls of the right (RV) and left ventricles (LV) expressed in percentage of the respective control values (*dashed line*) (A). Values are means ± SEM (*n* = 6). *P* < 0.05 compared to the respective control rats. Norepinephrine (NE) release from the atria of STZ-diabetic rats (B). KCl-evoked release of NE in the control atria and preparations from STZ-diabetic rats 4 months after the onset of diabetes (KCl), NE KCl-evoked release in the presence of neuronal uptake blocker desipramine (10–6 mol/L) (KCl + Des), KCl-evoked release of NE in the absence of calcium ions (KCl−Ca^{2+}). Error bars = SEM. *P* < 0.05 compared to the respective control value, *n* = 5.

Therefore, the norepinephrine-releasing mechanisms may remodel in the time course of chronic diabetes and may contribute to the decreased norepinephrine concentration in the atria of rats with streptozotocin-induced diabetes. The increased potassium-evoked release of norepinephrine from the diabetic atria might be attributed to the abnormal function of neuronal transporter (Fig. 7.6B).

Next we focused on the peptidergic innervation of the heart. The cardiac sensory nerve fibers may, in addition to conveying impulses toward the CNS, upon stimulation directly release neuropeptides from their peripheral terminal located within the heart. This mode of action has been termed the local effector function of sensory nerve terminals (Holzer, 1988). Calcitonin gene-related peptide (CGRP) is the major neuropeptide released from such nerve terminals in the heart (Franco-Cereceda and Lundberg, 1988). CGRP was described to exert a number of effects in the heart: CGRP increases heart rate and contractile force in the isolated rat atrium, (Wang and Fiscus, 1989) it is a powerful vasodilator increasing coronary artery perfusion, (Miyauchi et al., 1987; Saito et al., 1987) and it is involved in ischemic preconditioning (Källner and Franco-Cereceda, 1998). Diabetes was reported to abolish the protective effects of ischemic preconditioning and this effect may be related to the reduction in CGRP release in diabetic heart (Kersten et al., 2000; Lu et al., 2001; Tosaki et al., 1996). We therefore analyzed the quantitative changes in cardiac CGRP content and expression of its receptor during diabetes development. CGRP concentrations in diabetic ventricles increased significantly, reaching approximately twofold levels of control at 16 weeks after application of streptozotocin. Also the GRP content of both atria increased in diabetic rats, but the increase was less marked. Immunohistochemistry revealed the known distribution of CGRP immunoreactive varicose nerve fibers around the ascending aorta and coronary vessels, in the atrial myocardium, subendocardial layer including valves, papillary muscles, and within cardiac ganglia. The distribution was not visibly altered by diabetes. The expression of mRNA for the ligand-binding subunit of CGRP receptor, the calcitonin receptor-like receptor, was increased two- to threefold after 4 weeks of diabetes in the right atrium and ventricle and declined thereafter to fall below control levels 16 weeks from the onset of diabetes. The same pattern, although quantitatively less pronounced, was also observed in the left ventricle. The time pattern of the calcitonin receptor-like receptor was different in the left atrium with a decreased expression in the initial phase of diabetes (4 weeks from induction). In contrast to our findings of increased cardiac CGRP content and an unchanged innervation pattern of the heart by CGRP-immunoreactive fibers, the rat sensory dorsal root ganglion neurons were reported to respond to streptozotocin-induced

diabetes with decreased expression of the CGRP precursor (Diemel et al., 1994; Rittenhouse et al., 1996). These discrepant observations are best explained by impaired CGRP release from nerve terminals, leading to intraaxonal accumulation of the peptide despite a reduced supply from the perikaryon. The alterations of the CGRP signaling system in experimentally induced diabetic cardiomyopathy that include both the ligand and its receptor may contribute to functional impairment of cardioprotective mechanisms that involve CGRP released from sensory nerve terminals.

Another peptide that is present in cardiac innervation is neuropeptide Y (NPY). NPY is the most abundant neuropeptide in the cardiac innervation. It is produced by cleavage from a large precursor, preproNPY, and its most prominent source in the heart are the postganglionic sympathetic axons that originate from cell bodies located in the cervicothoracic sympathetic chain ganglia like the stellate ganglion (Gu et al., 1983). NPY elicits multiple effects in the heart: induction of vasoconstriction, (Pernow et al., 1987) modulation of intracellular calcium in endocardial endothelial cells, (Jacques et al., 2003) regulation of protein turnover and of constitutive gene expression in hypertrophying cardiomyocytes, (Nicholl et al., 2002) presynaptic inhibition of noradrenaline release from sympathetic axons, (Lundberg et al., 1984), and induction of angiogenesis (Zukowska-Grojec et al., 1998).

Our analysis by radioimmunoassay revealed a decrease of rat heart NPY content in long-term (6–12 months) streptozotocin-induced diabetes (Kuncová et al., 2005). NPY concentrations in the atria of diabetic rats did not differ from those in age-matched control rats 1, 2, 4, 6 months in the right atria and even 9 months after diabetes induction in the left atria. A significant decrease in NPY levels in the right and left atria was only observed 9 and 12 months after streptozotocin administration, respectively. In the ventricles, NPY concentrations were significantly decreased 6 months after the onset of diabetes. Interestingly, partial spontaneous recovery of diabetes was associated with increased NPY levels in the atria. These data suggest that the cardiac NPY signaling system is affected in diabetes mellitus, which may be of relevance for the pathogenesis of the functional and structural impairment of the heart during progression of the disease. To further test this hypothesis, we investigated the quantitative changes in ligand (preproNPY) and receptor expression within the different chambers of the heart, as well as the extrinsic ganglia that supply axons to the heart. Since neuronal mRNA expression is restricted to the area of the cell bodies, separate analysis of the stellate ganglion and of upper thoracic dorsal root ganglia allowed us to discriminate between changes in the sympathetic and the sensory nerve supply to the heart (Chottová Dvoráková et al., 2008). Ventricular, but not atrial innervation density by NPY immunoreactive

fibers was diminished, and preproNPY expression was transiently (26 weeks) reduced in left atria, but remained unchanged in sympathetic neurons and was not induced in DRG neurons. In all ganglia and heart compartments, Y1 receptor expression dominated over Y2 receptor, and Y1 receptor immunoreactivity was observed on cardiomyocytes and neuronal perikarya. Atrial, but not ventricular Y1 receptor expression was upregulated after 1 year of diabetes. Therefore, at the level of sympathetic and spinal sensory neurons, residing in the stellate ganglion and upper thoracic dorsal root ganglia, respectively, the capacity to express preproNPY and prejunctional receptors (Y1, Y2 receptors) is maintained even 1 year after onset of diabetes. Ventricular sympathetic terminals, however, appear to be affected by long-term diabetes (6 months to 1 year), as revealed by a diminished ventricular NPY content and a reduced innervation density documented by immunohistochemistry (Kuncová et al., 2005). The data indicate that the imbalance of the cardiac intrinsic and extrinsic neuronal NPY-Y1/Y2 receptor signaling system develops slowly in the course of streptozotocin-induced diabetes and that the atria and ventricles are affected differentially. This is in line with a well-known imbalance in diabetic cardiac autonomic neuropathy, in which the parasympathetic branch of the autonomic nervous system is affected more than the sympathetic one and in which the atria and the ventricles are affected differentially (Pourmoghaddas and Hekmatnia, 2003).

3.3 Conclusions and Clinical Implications

In general, the ideal animal model should mimic the human subject metabolically and pathophysiologically and should develop end-stage disease comparable to those in humans (Russell and Proctor, 2006). Obviously, with regard to the complexity of the organism and the multifactorial nature of the disease, there will always be some differences between the animal model and clinical situation and the translation from the model must be very careful. With this limitation in mind, the model of streptozotocin-induced diabetes corresponds to the human diabetes prior to the proper diagnosis and therapy. It allows obtaining important information about early changes developing in various tissues that may later result in serious impairment/failure of organ function. The model is suitable for studying diabetic cardiomyopathy in early stages after induction of the disease but less appropriate for investigating diabetic macroangiopathy (Tomlinson et al., 1992). The diabetic autonomic neuropathy in streptozotocin-induced diabetes resembles the diabetic complication in patients; however, the contribution of underlying mechanisms is probably different: the role of the polyol pathway being probably less important in patients than in diabetic rat (Nakamura et al., 2002;

Pfeifer et al., 1997). With regard to the cardiovascular system, a number of differences between man and rat exist in physiological conditions and these discrepancies may be further accentuated by the disease, for example, in contrast with human disease the diabetic rats show a low blood pressure, a pronounced bradycardia and increased baroreflex sensitivity. In conclusion, the rat model of streptozotocin-induced diabetes provides information that is relevant for the clinical situation, especially about the early stages of diabetes development. However, a number of differences in the organ physiology, as well as in the pathogenesis of the disease must be considered when translating the experimental findings to clinic.

3.4 The Heart and Renal Failure

Renal failure is the inability of the kidneys to excrete waste products and to keep water, electrolyte, and acid-base balance under basal conditions. Renal failure is divided into two types: acute failure characterized by sudden loss of kidney function which can be eventually recovered to normal and chronic failure caused by slow progressive loss of kidney function. Chronic renal failure (CRF) is the end stage of many chronic renal diseases including glomerulopathy, tubulointerstitial nephritis, polycystic kidney disease etc.

CRF is associated with higher risk of cardiovascular complications including hypertension, arteriolosclerosis, arrhythmia, impairment of the cardiac autonomic innervation, and disorder of ventricular myocardium (mainly of the left ventricle). Cardiovascular disorders like ischemic heart disease, heart failure, and sudden cardiac death resulting from aforementioned complication are the leading causes of death in CRF population and account for approximately 50% of all death (London, 2003). The incidence of cardiovascular death in patients with CRF younger than 30 years is even 150 times higher compared to general population (Johnstone et al., 1996). Since CRF has rising incidence and prevalence (the prevalence of CRF in all stages increased from 10% in 1988–94 to 13.1% in 1999–2004 in US adult population) it has become a global health problem (Castro and Coresh, 2009).

3.5 Animal Models of Chronic Renal Failure

To better understand CRF and its complications the experimental animal models were introduced into biomedical research. CRF can be induced by many methods divided into chemical nephrectomy and the remnant kidney model achieved by either vascular ligation (infarction model) or surgical nephrectomy in which approximately 1/6 of the functional renal tissue is preserved. For the chemical nephrectomy the immunological techniques or the nephrotoxic agents like doxorubicin, (Allison et al., 1974; Yoneko et al., 2007) cisplatin, (Heidemann

et al., 1990) uranyl nitrate, (Fukuda and Kopple, 1980), or aristolochic acid are used (Debelle et al., 2004). Vascular ligation model is based on the unilateral nephrectomy followed by ligation of vessel supplying the renal poles of the contralateral kidney (Purkerson et al., 1976). The most frequently used model of CRF is a surgical partial (usually five-sixth) nephrectomy consisting of the unilateral total nephrectomy followed by contralateral partial nephrectomy, by contralateral unilateral renal cortex destruction with electrocoagulation, (Boudet et al., 1978) by cryosurgery, (Kumano et al., 1986) or by contralateral papillectomy (Kroon et al., 1962). The chemical induction of CRF is relatively easy but disadvantages of this method are obvious—a lot of undesirable effect including cardiotoxicity, lower reproducibility, and lower similarity to the human disease (Chow et al., 2003). On the other hand the remnant kidney model is associated mainly with the technical difficulties—hemorrhage and higher mortality due to operative and postoperative complications in surgical nephrectomy and heterogeneity of ligation model due to anatomical variations of the renal artery and possible formation of collateral vessel that bypass the ligated vessel (Liu et al., 2003). The advantages of both the methods, that is, homogeneity in the surgical model and lower mortality of the ligation technique, are connected in the method of renal mass reduction by ligation of the renal parenchyma (Perez-Ruiz et al., 2006).

The first animal partial surgical nephrectomy was performed by Thodore Tuffier in dog at the end of 19th century but no changes in the elimination of urine or urea were found despite the loss of kidney mass (Tuffier, 1889). Since then the surgical method was refined to achieve a characteristic signs of renal failure and the technique was gradually applied in other species including mice, (Gagnon and Gallimore, 1988) rats, (Chanutin and Ferris, 1932; Liu et al., 2003; Platt et al., 1952) rabbits, (Brown et al., 1990) cats, (Adams et al., 1994) piglets, (McKenna et al., 1992) sheep, (Eschbach et al., 1980) cattle, (Vogel et al., 2011) etc. Based on many experiments the surgical partial nephrectomy performed in two steps became a standard method for induction of renal failure. In our laboratory, the surgical 5/6 nephrectomy model in rat was used to study and describe the basic features of this model and the progressive changes in cardiovascular functions.

4 EXPERIMENTAL RESULTS IN RAT MODEL OF RENAL FAILURE

4.1 Chronic Renal Failure Induced by Partial Nephrectomy

Four-months-old Wistar male rats (Velaz, Prague, Czech Republic) were randomly allocated into subtotal nephrectomy (NX) and control groups. All operations

were performed under total anesthesia by intraperitoneal injection of sodium pentobarbital (100 mg/kg, i.p., Sigma Aldrich, Czech Republic) and xylazine (10 mg/kg, i.p., Rometar, Bioveta, Czech Republic). In NX group the anaesthetized rat was placed on its abdomen with fixed limbs and the left dorsolateral incision (approximately 2–3 cm wide) was made into the skin. The exposed back muscles were moved aside and the left kidney was carefully pulled out of the retroperitoneal space. The surrounding connective tissue of the kidney was removed with special care in the upper pole to prevent damage to the adrenal gland. The renal vessels were clamped by an atraumatic microvascular clamp and both poles (2/3 of the functional kidney mass) were resected by cuts perpendicular to the longitudinal axis of the kidney (Fig. 7.7). The cut surface was cauterized and then treated by hemostat Lyostypt (B. Braun, Germany). After bleeding was stopped the microvascular clamp was removed and the renal stump was returned into the retroperitoneum. Two weeks after the partial nephrectomy the right kidney was exposed by the previously described procedure. The renal pedicle was ligated by nonabsorbable multifilament suture (PremiCron, B. Braun, Germany)

and the total right nephrectomy was done to achieve 5/6 reduction of the total renal mass. The sham operation in control rats consisted of renal evacuation, decapsulation, and returning the intact kidney into the abdominal cavity performed bilaterally in a two-week interval. In both experimental groups the strict aseptic rules were respected, the incisions were sutured in two layers by monofilament suture (Premilene, B. Braun, Germany) and covered by a liquid bandage. After each operation, rats were treated by one-time subcutaneous application of antibiotic marbofloxacinum (5 mg/kg, s.c., Marbocyl, Vétoquinol, Czech Republic) and housed individually with free access to food and water. The presented results were obtained 10 weeks after the second step of surgery if not stated otherwise.

A significant increase of creatinine and urea concentrations in serum, polyuria and a decrease in glomerular filtration rate measured by creatinine clearance indicated a severe impairment of the kidney functions (Table 7.1). Functional markers of CRF (appearing already one week after the second step of surgery and remaining almost unchanged for weeks) were associated with morphological changes in the remnant kidney. The renal stump
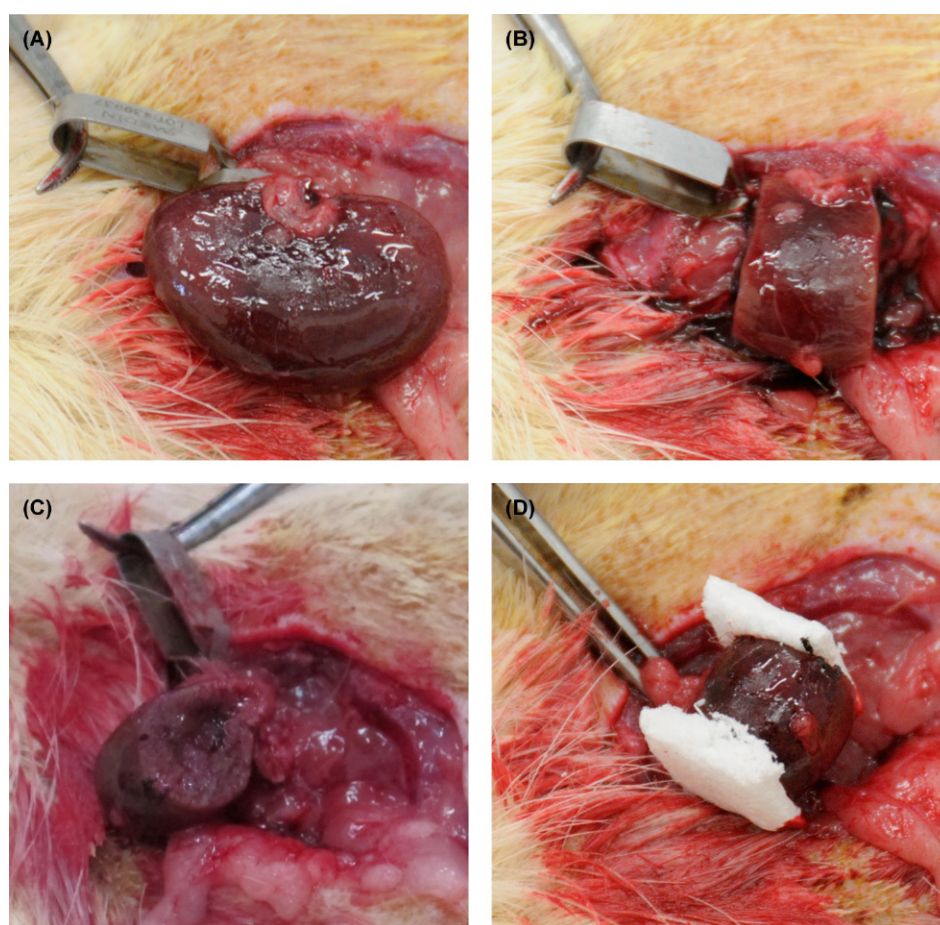
FIGURE 7.7 **Unilateral partial surgical nephrectomy in the adult rat.** (A) Clumping of renal vessel by an atraumatic clamp. (B) Renal stump after removal of both poles. (C) Cut surface of the kidney after cauterization. (D) Cut surfaces treated by hemostat.

TABLE 7.1 Renal Functional Parameters of Control and Partially Nephrectomized Rats

	sham	NX
S-creatinine (µmol/L)	52.1 ± 2.18	146 ± 9.90*
S-urea (mmol/L)	6.7 ± 0.91	25.6 ± 3.08*
S-potassium (mmol/L)	5.57 ± 0.09	6.26 ± 0.07*
U-urea (mmol/24 h)	14.66 ± 0.78	12.26 ± 0.43
U-potassium (mmol/24 h)	3.89 ± 0.17	3.43 ± 0.20
U-sodium (mmol/24 h)	1.44 ± 0.07	1.58 ± 0.12
Urine volume (mL/24 h)	15.67 ± 1.17	39.44 ± 3.15*
Creatinine clearance (mL/min)	2.58 ± 0.18	0.99 ± 0.09*
Body weight (g)	489.6 ± 24.31	431.5 ± 15.42*
(Remnant) kidney weight (g)	1.4 ± 0.03	2.1 ± 0.01*
(Remnant) kidney weight/body weight (g/kg)	3.32 ± 0.03	5.57 ± 0.05*

Renal functional parameters in serum (S) and urine (U), body weight and absolute and relative kidney weights of control (sham) and partially nephrectomized (NX) rats 10 weeks after surgery.
* Significantly different from sham-operated rats, $P < 0.05$.

had an atypical pale color, its wet weight was significantly higher than a single kidney of healthy controls (Table 7.1) and displayed typical remodeling of the renal tissue (Fig. 7.8). The capsular surface of the operated kidneys of the partialy nephrectomized rats was depressed in several areas. No necrotic areas were found, but the medullary pyramids were distorted.

In contrast to the infarction method in which declined glomerular filtration rate varies in rather wide range, surgical nephrectomy gives more reproducible values of glomerular filtration rate probably owing to precise control of renal ablation (Liu et al., 2003). Moreover, surgical nephrectomy enables to induce a standardized, stable uremia at predetermined levels—mild uremia (due to 3/4 nephrectomy), moderate uremia (5/6 nephrectomy), and severe uremia produced by 7/8 reduction of the functional renal mass (Ormrod and Miller, 1980).

Both systolic and diastolic pressures measured by tail-cuff method were significantly increased in NX rats 3 weeks after surgery and further while no difference in blood pressure between sham and nephrectomized groups was found 1 week after surgery, for example, in the acute phase of renal failure (Fig. 7.9).
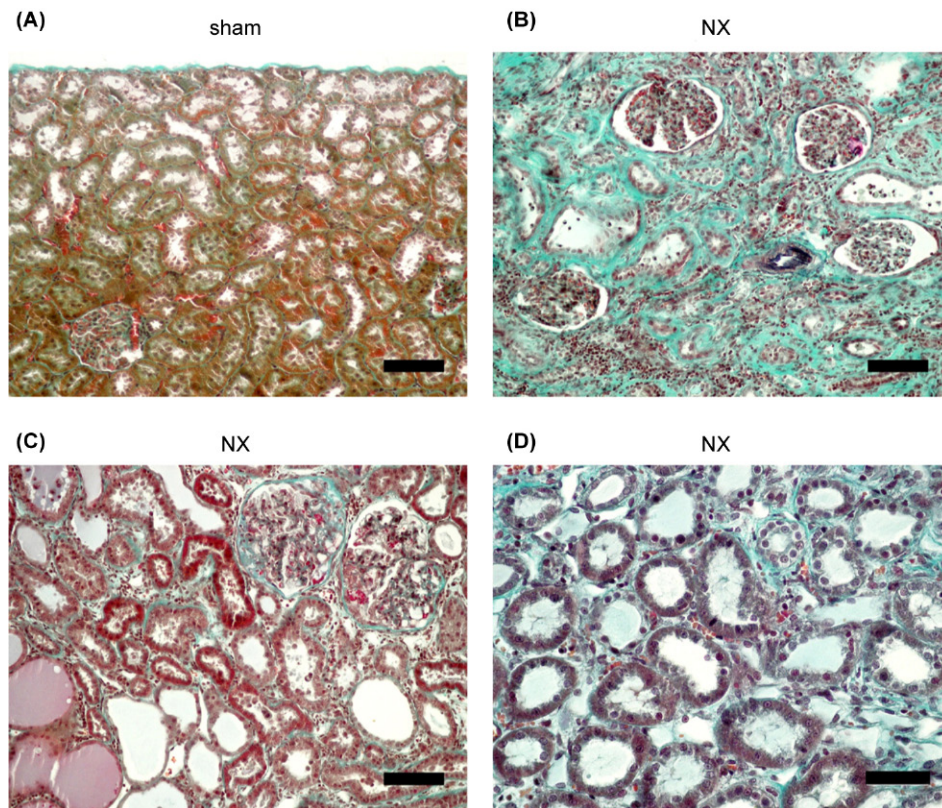
FIGURE 7.8 **Microscopic changes of the kidney 10 week after partial nephrectomy.** Unlike in sham-operated rats (A), the superficial cortex of the operated kidneys (B) of the nephrectomized (NX) rats was severely disorganized. The loss of tubules resulted in a crowding together of the glomeruli, and the interstitial tissue was considerably expanded, severely fibrosed and heavily infiltrated by chronic inflammatory cells. In the deeper and juxtamedullary cortex of the NX rats (C), proximal and distal the tubules were dilated and some of them contained densely eosinophilic casts. The medullary tubules of the operated kidneys (D) seemed to be recovered. Verhoeff's hematoxylin and green trichrome stain, scale bar 100 µm (A, B, C), and 50 µm (D).
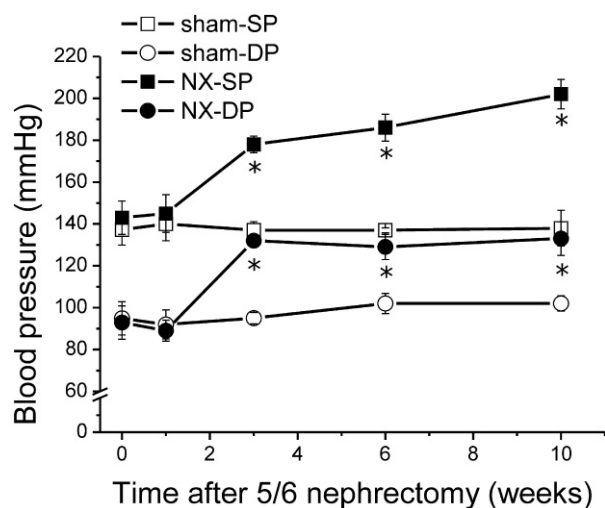
FIGURE 7.9   **Systolic (SP) and diastolic (DP) pressures in control (sham) and partially nephrectomized (NX) rats.** *Open symbols*, conrols; *filled symbols*, NX, * Significantly different from control rats, $P < 0.05$.

FIGURE 7.10   **The left ventricle (LV) cross sections of control (sham) and partially nephrectomized (NX) rats demonstrates the considerable concentric hypertrophy of LV in NX group 10 weeks after the surgery.**

4.2 Cardiovascular Parameters of the Rat Model

The morphological and functional impairment of the myocardium resulting from CRF is called uremic cardiomyopathy characterized by the left ventricular hypertrophy associated with systolic and diastolic dysfunctions (Parfrey et al., 1991; Zoccali et al., 2004). The myocardium impairment leads to a decrease in cardiac contractility followed by a drop in cardiac output caused by the diminished left ventricular compliance (Johnstone et al., 1996). Factors contributing to the pathogenesis of the uremic cardiomyopathy are hemodynamic (pressure overload due to hypertension and arteriolosclerosis and volume overload caused by water and sodium retention, arteriovenous shunt and anemia), (London and Parfrey, 1997; Kalantar-Zadeh et al., 2009) nonhemodynamic or metabolic (activation of renin-angiotensin system, ischemia, electrolyte dysbalance, the effect of uremic toxins including parathyroid hormone, advanced glycation end products, reactive oxygen species, cytokines, asymmetric dimethylarginine etc.) (Vanholder et al., 2003).

Structural, contractile, and electrophysiological remodeling was also observed in the hearts of partially nephrectomized rats. Both absolute and relative heart weights were significantly higher in NX rats compared to sham-operated ones. Since the weights of the left ventricle including septum (LV) and LV weight to body weight ratio were significantly increased, the change in weight of the uremic heart resulted probably from the hypertrophy of LV. The apparent concentric hypertrophy of LV (Fig. 7.10) developing already 10 days after the surgery was verified by the morphometric immunohistological analysis of cardiac cells showing the increase in the cross-sectional area of cardiac myocytes in LV of NX group (Table 7.2).

TABLE 7.2   Cardiac Parameters of Control and Partially Nephrectomized Rats, 100 Weeks After Surgery

	sham	NX
Heart weight (g)	0.935 ± 0.033	1.158 ± 0.047*
Left ventricle + septum (g)	0.753 ± 0.022	0.942 ± 0.062*
Right ventricle (g)	0.182 ± 0.012	0.217 ± 0.034
Heart weight/body weight (g/kg)	1.92 ± 0.03	2.7 ± 0.17*
Left ventricle/body weight (g/kg)	1.55 ± 0.04	2.21 ± 0.19*
Right ventricle/body weight (g/kg)	0.37 ± 0.01	0.49 ± 0.07
Cross-sectional area of LV myocytes (μm^2)	431.32 ± 21.54	597.67 ± 23.56*,#
Cross-sectional area of RV myocytes (μm^2)	396.01 ± 36.91	460.89 ± 21.29

LV, left ventricle; RV, right ventricle.
* Significantly different from sham-operated rats.
# Significantly different from RV, $P < 0.05$.

Contraction force (CF) measured on papillary muscles in control Tyrode solution was significantly higher in the left ventricle (LV) compared to the right ventricle (RV) in control animals at stimulation frequencies 0.5, 1, 2, and 3 Hz. In NX rats, the contractile remodeling was different in LV and RV—CF was significantly augmented in RV but significantly reduced in LV compared to age-matched controls at all stimulation frequencies tested (Fig. 7.11A). Fifty percent substitution of extracellular sodium with lithium (an intervention stimulating the reverse mode of sodium-calcium exchanger), had a significant positive inotropic effect only in LV of NX animals
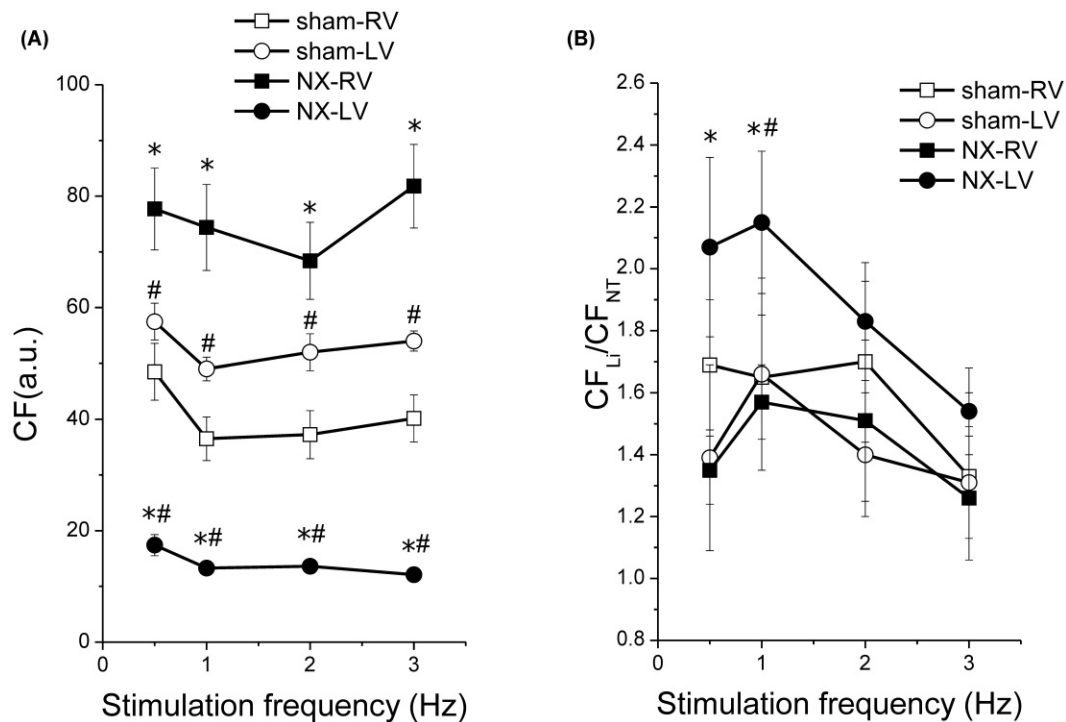
FIGURE 7.11 **Steady-state contraction (CF) of papillary muscles in control (sham) and partially nephrectomized rats (NX).** (A) The dependence of CF on stimulation frequency in the right *(RV, squares)* and left *(LV, circles)* ventricles in control *(open symbols)* and NX *(filled symbols)* rats in control Tyrode solution. (B) The effects of lithium substitution on CF: the ratio of CF in solution with 50% Li$^+$ substitution (Li) and in control Tyrode solution (NT) in the right *(RV, squares)* and left *(LV, circles)* ventricles in control *(open symbols)* and NX *(filled symbols)* rats. a.u., arbitrary units. * Significantly different from control rats, # significantly different from RV, $P < 0.05$.

but neither in RV nor in both ventricles sham-operated rats (Fig. 7.11B).

The rest-potentiation phenomenon reflecting the function of Na$^+$/Ca^{2+} exchanger (i.e., the increase in contraction force after period of rest characteristic for rat myocardium) was more pronounced in LV than in RV. Nephrectomy further enhanced the relative rest-potentiation in LV, but suppressed it in RV (Fig. 7.12A) regardless of the duration of period of rest (10–300 s). The rest-potentiation phenomenon compensated the interventricular changes in steady-state CF described in NX group: enhanced rest-potentiation for reduced steady-state contraction in LV and reduced rest-potentiation for increased steady-state contraction in RV (Fig. 7.12B).

Time to peak of contraction (TTP) in LV and time parameters of relaxation, that is, time from peak of contraction to 50% relaxation (R50) and time from peak of contraction to 90% relaxation (R90) in both ventricles were significantly prolonged due to partial nephrectomy at all stimulation frequencies tested. Nephrectomy also led to shortening of action potential duration at 50% (APD50) and 90% (APD90) level of repolarization in both ventricles. In contrast to the contractile functions the electrophysiological remodeling and the prolongation of relaxation in NX rats was similar in both ventricles (Table 7.3).

Cardiovascular autonomic dysfunction (CAD) contributes to higher incidence of arrhythmias, blood pressure disturbances and sudden cardiac death in patients suffer from CRF (Robinson and Carr, 2002). CAD is characterized by decreased baroreceptor sensitivity, increased sympathetic tone but decreased parasympathetic one (Zoccali et al., 1982). The sympathetic hyperactivity is explained by the abnormal stimulation of sensory renal nerves innervating the affected kidney which is potentiated by cumulation of adenosine in the ischemic renal tissue. These afferent signals integrated in central nervous system together with stimulation of renin-angiotensin system, alteration of NO metabolism, and the effect of uremic toxins results in a higher sympathetic outflow (Schlaich et al., 2009). In contrast to the sympathetic nervous system, little is known about the pathogenesis of the uremic impairment of the parasympathetic cardiac innervation.

The resting heart rate values obtained from conscious animals by electrocardiography progressively increased in NX rats to be significantly different from controls 10 weeks after surgery (Fig. 7.13A). Cardiac parasympathetic tone measured by an increase in the heart rate after application of muscarinic blocker atropine to animal pretreated by beta-blocker metipranolol was significantly lower in NX rats showing the alteration of cardiac parasympathetic innervation due to CRF (Fig. 7.13B).
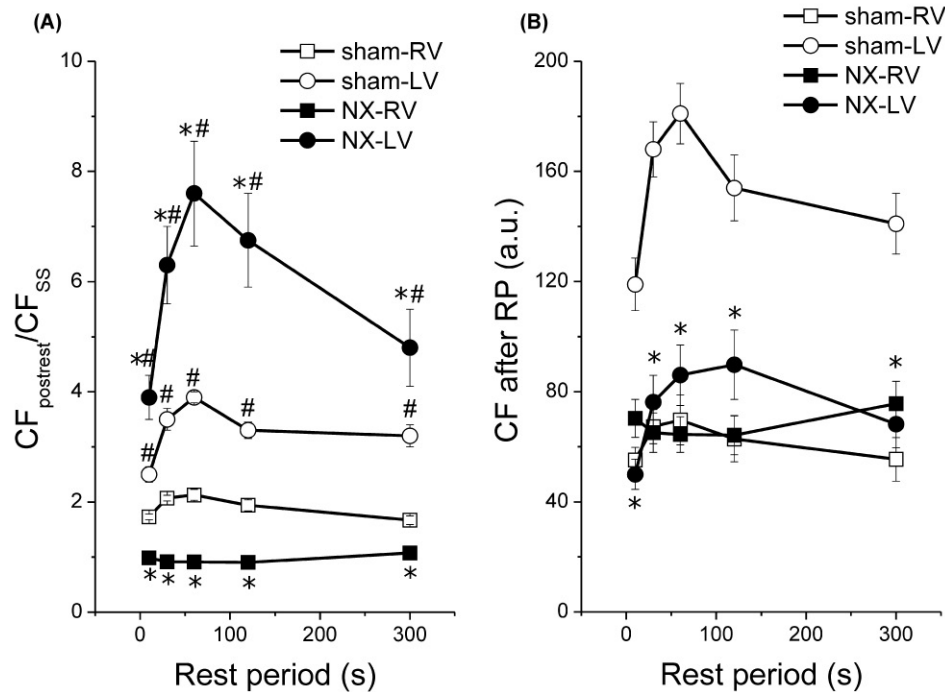
FIGURE 7.12   Rest-potentiation of contraction (CF) of papillary muscles in control Tyrode solution in control (sham) and partially ne-phrectomized rats (NX). (A) The dependence of rest potentiation (ratio of first postrest CF and steady state CF) on duration of rest period in the right *(RV, squares)* and left *(LV, circles)* ventricles in control *(open symbols)* and NX *(filled symbols)* rats. (B) The dependence of CF of the first postrest contraction on duration of rest period in the right *(RV, squares)* and left *(LV, circles)* ventricles in control *(open symbols)* and NX *(filled symbols)* rats. * Significantly different from control rats, # significantly different from RV, $P < 0.05$.

TABLE 7.3   Time Parameters of the Contraction-relaxation Cycle and Action Potential Duration

	sham		NX	
	LV	RV	LV	RV
TTP (ms)	$67.18 \pm 1.28^{\#}$	57.01 ± 4.12	$87.33 \pm 2.11^{*,\#}$	63.82 ± 3.54
R_{50} (ms)	$49.35 \pm 1.95^{\#}$	36.18 ± 2.3	$67.79 \pm 2.92^{*,\#}$	$42.67 \pm 2.57^{*}$
R_{90} (ms)	$87.12 \pm 1.3^{\#}$	61.58 ± 3.64	$125.88 \pm 4.64^{*,\#}$	$77.82 \pm 4.38^{*}$
APD_{50} (ms)	$32.06 \pm 1.19^{\#}$	19.96 ± 3.05	$24.62 \pm 1.57^{*,\#}$	12.76 ± 0.63
APD_{90} (ms)	$91.96 \pm 5.32^{\#}$	56.18 ± 4.92	$75.76 \pm 3.26^{*,\#}$	$41.57 \pm 4.92^{*}$

Time parameters of contraction-relaxation cycle and action potential duration in left (LV) and right (RV) papillary muscles of control (sham) and partially nephrectomized (NX) rats at stimulation frequency 1 Hz. TTP, time to peak of contraction, R_{50}, time from peak of contraction to 50% relaxation, R_{90}, time from peak of contraction to 90% relaxation, APD_{50}, duration of action potential at 50% level of repolarization, APD_{90}, duration of action potential at 90% level of repolarization.
*Significantly different from control rats,
#Significantly different from RV, $P < 0.05$.

In vitro experiments, the muscarinic agonist carbachol exerted a negative chronotropic effect on the isolated rat heart atria (Fig. 7.14A) and a negative inotropic effect on the papillary muscles in both rat ventricles (Fig. 7.14B) without the significant difference between control and NX groups. No differences between sham-operated and nephrectomized rats were also revealed in negative chronotropic responses to the stimulation of

vagus nerve (Fig. 7.15), the relative expression of muscarinic M2 receptors in all cardiac chambers and in the relative expression of high affinity choline transporter, vesicular acetylcholine transporter, and choline acetyltransferase in left atria.

Rat uremic myocardium showed the characteristic signs of uremic cardiomyopathy—hypertrophy and contractile dysfunction of LV. Occurrence of LV hypertrophy prior to hypertension and the absence of RV hypertrophy suggest that pressure and volume overloads are not the critical contributors to the development of LV hypertrophy in NX rats and the humoral factors should be considered. Partial recovery of contractile function of LV by rest-potentiation and by lithium substitution of extracellular sodium indicates the role Na^+/Ca^{2+} exchanger in the different interventricular cardiac remodeling of the heart in partially nephrectomized rats (Švíglerová et al., 2012). Cardioacceleration present in rats with CRF resulted probably from the decreased tone of cardiac parasympathetic innervation what corresponds with findings in a number of human studies proving that the alteration of parasympathetic division of autonomic nervous system more than sympathetic one contributes to uremic autonomic neuropathy (Giordano et al., 2001; Zoccali et al., 1982). Since the intact intrinsic cardiac cholinergic signaling system the impairment of the central parasympathetic activity partially nephrectomized rats is suspected (Kuncová et al., 2009).
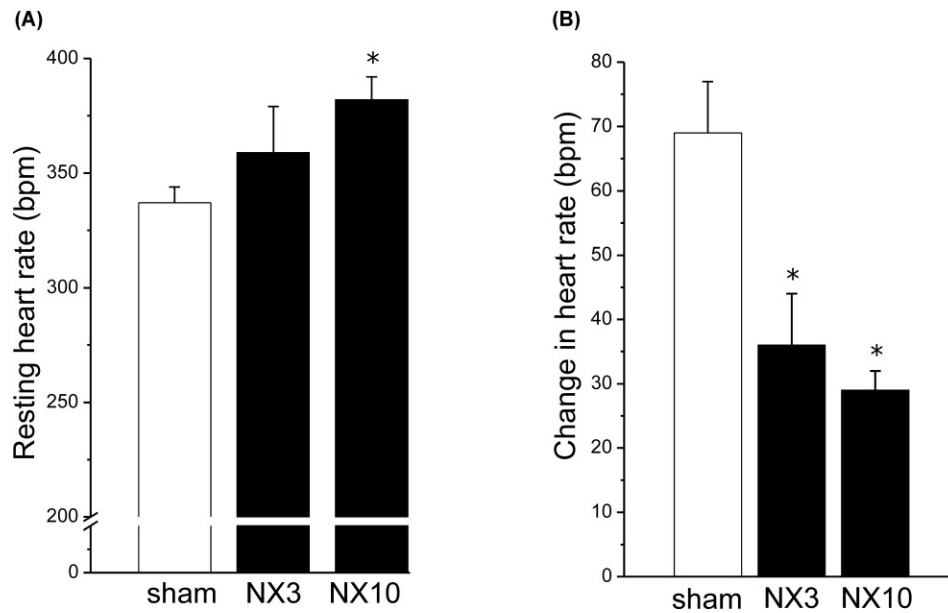
FIGURE 7.13 **Heart rate in control (sham) and partially nephrectomized (NX) rats.** (A) Resting heart rate. (B) Change in heart rate after atropine administration (4 mg/kg of body weight) to animals pretreated by metipranolol (2 mg/kg). *Open bars*, controls; *filled bars*, NX; *NX3*, 3 weeks; *NX10*, 10 weeks after the second step on nephrectomy, * Significantly different from control rats, $P < 0.05$.
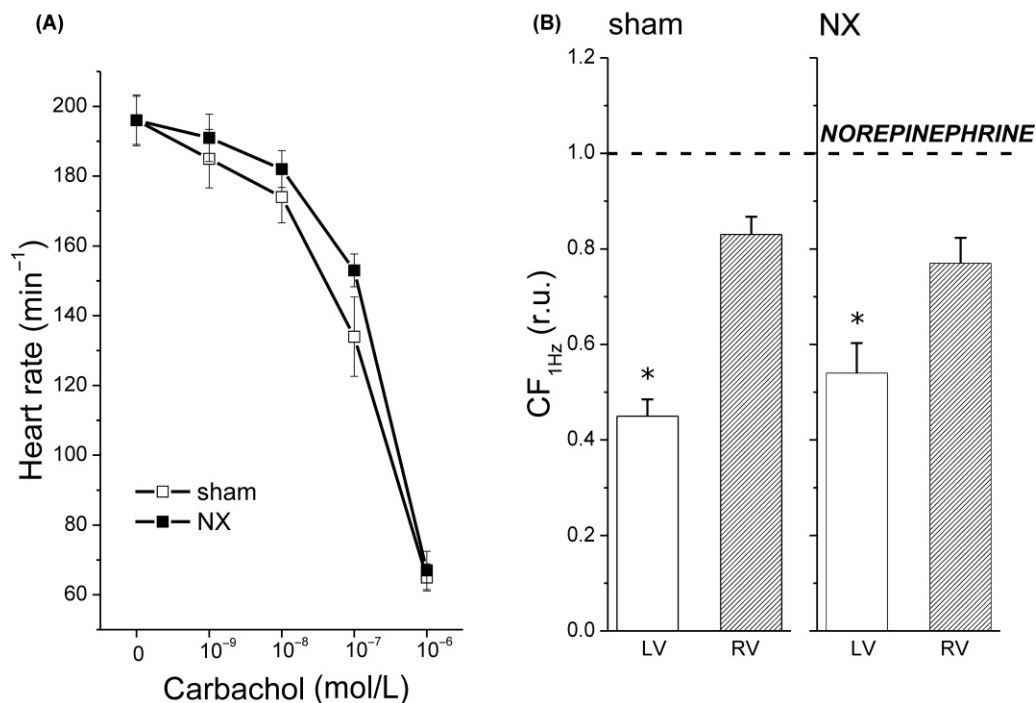
FIGURE 7.14 **The chronotropic and inotropic effects of carbachol in control (sham) and partially nephrectomized rats (NX).** (A) The effect of carbachol on beating rate of the isolated rat heart atria. *Open squares*—sham, *filled squares*—NX. (B) The effect of carbachol (10–4 mol/L) on contraction force (CF) of papillary muscle from left *(LV, empty bars)* and *right (RV, hatched bars)* ventricles measured at stimulation frequency 1 Hz in the presence of noradrenaline (10–4 mmol/L) in control *(left panel)* and NX *(right panel)* rats. The negative inotropic effect of carbachol was more pronounced in LV of both control and NX rats. *r.u.*, relative units (values are normalized to CF in carbachol-free solution with norepinephrine. * Significantly different from RV, $P < 0.05$.

4.3 Conclusions

The presented model of 5/6 surgical nephrectomy in rat performed in two steps displays the typical features of uremia including reduced glomerular filtration rate, increased serum levels of urea and creatinine and arterial hypertension. The model also simulates cardiovascular complications of human CRF—hypertrophy and systolic dysfunction of the left ventricle and the impairment of
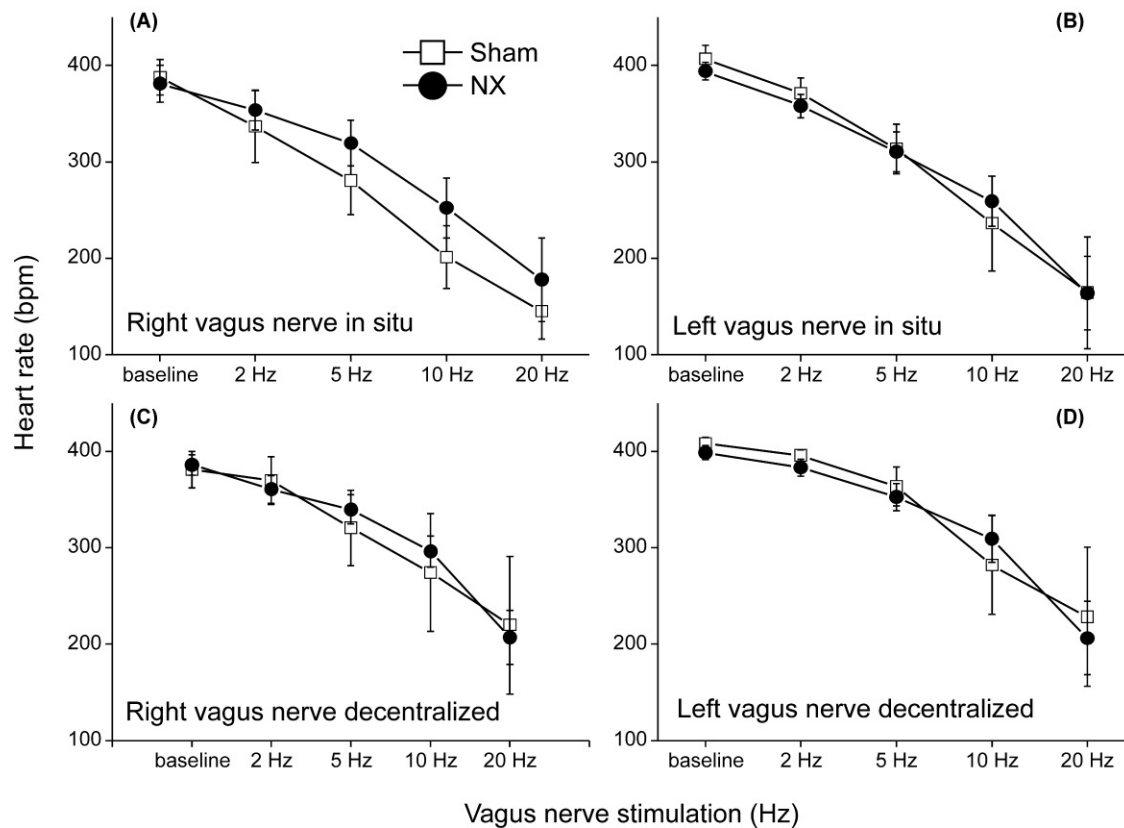
FIGURE 7.15   **Chronotropic effect of the vagus nerve stimulation.** The right (A, C) and left (B, D) vagus nerves were stimulated in situ (A, B) or after decentralization (C, D). *Sham*, control rats; *NX*, subtotally nephrectomized rats.

autonomic cardiac innervation. The advantages of this model like similarity to human diseases, homogeneity, reproducibility and stability of uremia, precise control of renal mass reduction, and minimum undesirable effects exceed disadvantages including a higher risk of mortality, rather fast onset of uremia compared to slow progression in humans and the difficulty of technique.

In the clinical application of research findings the earlier mentioned disadvantages of rat model of partial nephrectomy and presently known differences between rat and human myocardium should be considered. Under physiological conditions, shorter duration of action potential, inverted force-frequency relationship, insignificant role of Na/Ca exchanger in calcium removal from cytoplasma, faster heart rate are typical for rat heart (Grossman, 2010). Atherosclerosis characteristic for human CRF occurs only rarely in rats (Ritskes-Hoitinga and Beynen, 1988). Moreover cardiovascular diseases resulted from CRF develop slowly in human patients which are usually older, multimorbid and both gender are represented whereas animals used in research are usually young and healthy, the onset of cardiovascular complications is relatively rapid and the majority of experiments is performed on males. Taken together, the rat model of CRF induced by 5/6 surgical nephrectomy plays important role in the study of chronic renal diseases and their cardiovascular complications

nevertheless the experimental results must be implicated in human medicine with caution.

5 THE HEART AND DYSFUNCTIONAL SYMPATHETIC INNERVATION

Cardiac sympathetic innervation plays an important role in the regulation of the cardiac functions, particularly heart rate, contractility, and velocity of conduction. Removing the sympathetic nerves supplying the cardiovascular system could be important for the understanding the heart function in clinical conditions affecting the neural control of the heart. In the experimental practice, the variety of sympathectomy methods is used, including surgical ablation of the sympathetic chains, immunosympathectomy, and chemical damaging of the sympathetic neurons. Among them, chemical sympathectomy is the most suitable method for small laboratory animals, such as rat and mice (Picklo, 1997). In the classical view, the only source of norepinephrine in the mammalian heart is postganglionic sympathetic fibers. However, recent experimental evidence suggests that norepinephrine is distributed in the heart in at least three additional sources:

1. Intrinsic ganglion neurons of the cardiac nerve plexus that express tyrosine hydroxylase (TH) and

dopamine β-hydoxylase (DBH), that is, enzymes essential for norepinephrine synthesis (Slavikova et al., 2003). In the rat heart, the cell bodies of ganglion neurons are located in the atria, particularly the left one, but not in the ventricles (Batulevicius et al., 2003).

2. Intrinsic catecholaminergic (ICA) cells that are diffusely distributed throughout the heart including both atria and ventricles contribute to the total cardiac content of norepinephrine and epinephrine by 18, and 13%, respectively (Huang et al., 1996). ICA cells do not have neuronal or chromaffin cell ultrastructural morphology on electron microscopic analysis and are capable of catecholamine uptake and release (Huang et al., 2005).

3. Negligible portion of norepinephrine in the atria could be localized in two additional cell types: small intensely fluorescent (SIF) cells and glomus-like bodies (GLB) displaying moderate or week DBH immunoreactivity, respectively, suggesting the presence of norepinephrine (Kummer et al., 1986).

In addition, catecholamines dopamine and epinephrine could also contribute to the regulation of the cardiac function in a more complex way than recognized to date. Classically, epinephrine is secreted by the adrenal medulla and reaches the heart via the circulation. Epinephrine release from the heart after sympathetic nerves stimulation was concomitantly attributed to the uptake of this catecholamine by norepinephrine transporter and its subsequent release (Lameris et al., 2002). However, an expression of phenylethanolamine *N*-methyltransferase (PNMT), enzyme decisive in epinephrine synthesis was demonstrated in the heart, both in neuronal and nonneuronal elements (Huang et al., 1996; Ebert and Taylor, 2006).

Finally, dopamine regarded so far as mere norepinephrine precursor, seems to be involved in the cardiac catecholaminergic system in a more intriguing manner. Dopamine can be detected in the cardiac ganglia and SIF cells (Slavikova et al., 2003). Dopamine receptors that are distinct from α- and β-adrenoreceptors, are expressed in the heart, suggesting that dopamine could mediate cardiospecific effects (Emilien et al., 1999). Norepinephrine-independent dopamine release has been already demonstrated (Ilebekk et al., 1983).

With regard to the novel and complex view on the organization of the cardiac catecholaminergic system, we aimed to review our results of the studies dealing with two methods of chemical sympathectomy, that is, neonatal administration of guanethidine and 6-hydroxydopamine to rats and the impact of these interventions on various cardiovascular parameters.

6 METHODS OF CHEMICAL SYMPATHECTOMY

6-hydroxydopamine (6-OHDA) was the first chemical recognized to cause selective damage to the noradrenergic neurons (Thoenen and Tranzer, 1973). It enters the cells via norepinephrine transporter, undergoes a series of chemical transformations to reactive quinone compounds that stimulate free radicals production, membrane disintegration, and neuronal death. Guanethidine is also a substrate of norepinephrine transporter in the sympathetic nerve endings. It replaces norepinephrine in the synaptic vesicles, causes swelling of mitochondria and increase in protein content in the sympathetic ganglia followed by lymphocyte infiltration and concomitant retraction of the whole sympathetic postganglionic neurons (Burnstock et al., 1971).

In our studies, both chemicals were applied in doses reported to cause permanent loss of the sympathetic postganglionic neurons. After birth, rats received subcutaneously 6-OHDA (100 mg/kg) dissolved in 0.9% NaCl solution containing 0.1% ascorbic acid on postnatal days 1–7, 14, 21, and 28 or guanethidine sulfate (50 mg/kg) dissolved in 0.9% NaCl solution on postnatal days 1–21. The control group received equal volumes of solvent at the same time points. All rats were used for further experiments at the ages of 20, 40, 60, 90, and 150 postnatal days.

7 EXPERIMENTAL RESULTS IN THE RAT MODEL OF CHEMICAL SYMPATHECTOMY

7.1 Concentrations of Norepinephrine, Epinephrine, and Dopamine in the Heart

Both sympathotoxins, guanethidine and 6-OHDA enter the sympathetic nerve endings via norepinephrine transporter and cause degeneration of the whole sympathetic neurons. It is thus interesting that guanethidine sympathectomy was repeatedly reported to be more extensive than that using 6-OHDA and that not all cells expressing norepinephrine transporter display the same susceptibility to the toxins (Burnstock et al., 1971; Johnson et al., 1976). Therefore, we have determined norepinephrine, epinephrine, and dopamine levels in all heart compartments of denervated rats at the ages of 20–150 postnatal days to compare the efficacy of both regimens. Catecholamines levels were assayed in tissue extracts by radioimmunoassay using commercial kits (IBL Hamburg, FRG).

In the control animals, all catecholamines concentrations were relatively stable in the whole course of experiment (Table 7.4).

Fig. 7.16 shows the effect of chemical ablation of the cardiac sympathetic nerves on norepinephrine concentrations in the heart compartments. Guanethidine

TABLE 7.4 Norepinphrine, Epinephrine, and Dopamine Concentrations in the Heart of Control Rats

Age (days)		RA (ng/g)	LA (ng/g)	RV (ng/g)	LV (ng/g)
20	NE	1263 ± 110	1095 ± 95	791 ± 81	610 ± 54
	DA	95 ± 9	102 ± 8	37 ± 5	25 ± 3
	EPI	57 ± 6	62 ± 7	44 ± 5	29 ± 4
40	NE	1104 ± 97	1049 ± 110	625 ± 45	520 ± 49
	DA	90 ± 8	114 ± 12	38 ± 4	24 ± 3
	EPI	68 ± 7	74 ± 8	30 ± 4	20 ± 2
60	NE	1338 ± 111	987 ± 89	735 ± 67	612 ± 59
	DA	89 ± 10	98 ± 10	45 ± 6	31 ± 2
	EPI	71 ± 8	62 ± 7	44 ± 5	29 ± 4
90	NE	1289 ± 95	1085 ± 104	655 ± 52	541 ± 48
	DA	104 ± 6	125 ± 7	56 ± 6	34 ± 4
	EPI	56 ± 7	47 ± 6	32 ± 4	27 ± 3
150	NE	1315 ± 121	1225 ± 95	811 ± 62	630 ± 51
	DA	95 ± 7	116 ± 12	44 ± 5	29 ± 2
	EPI	62 ± 6	45 ± 5	41 ± 5	31 ± 3

DA, dopamine; EPI, epinephrine; LA, left atrium; LV, free wall of left ventricle; NE, norepinephrine; RA, right atrium, RV, free wall of right ventricle. Control rats aged 20–150 days. Data expressed as mean ± S.E.M.; n = 5–8 per group and age category.
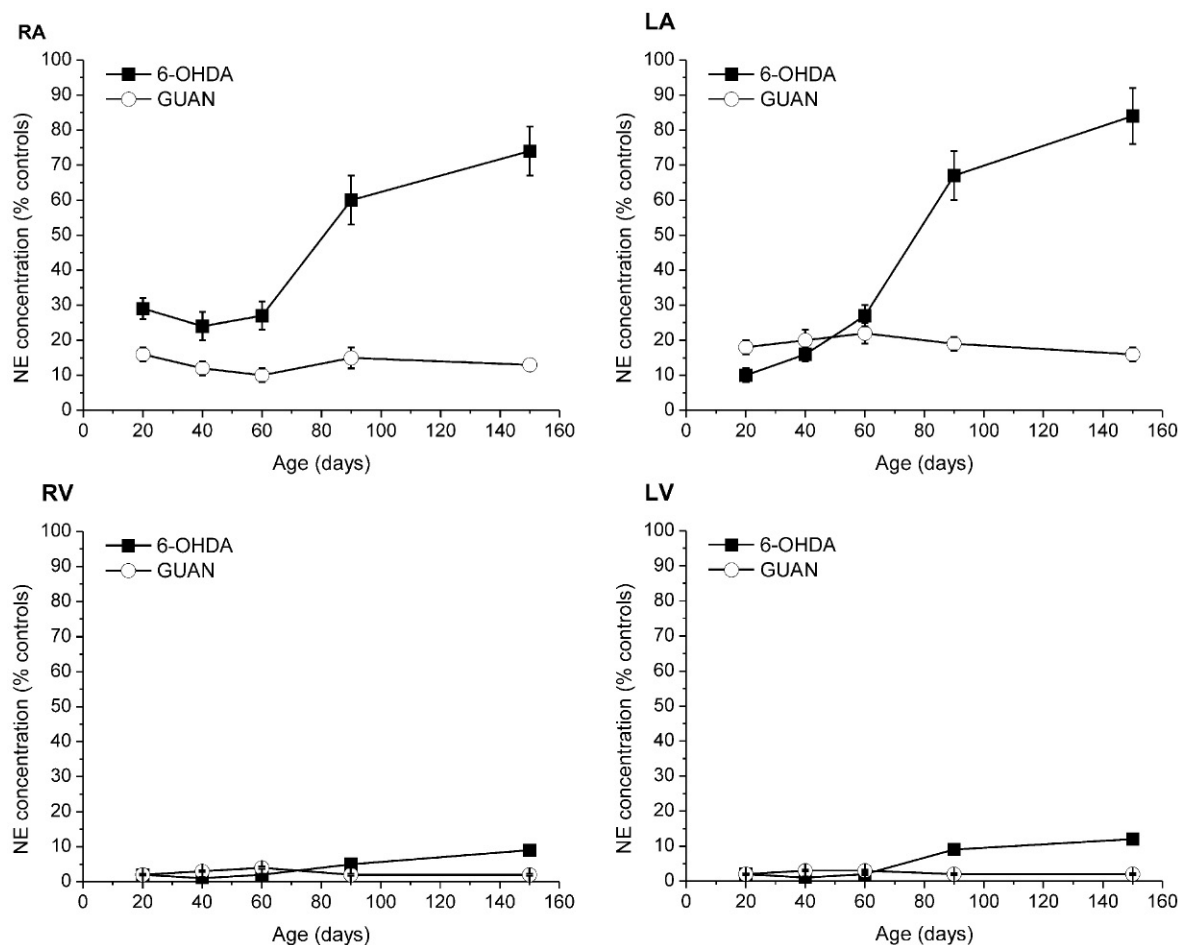
FIGURE 7.16 **Norepinephrine (NE) concentrations in the right and left atria (RA, LA, respectively) and free walls of the right (RV) and left (LV) ventricles of 20-, 40-, 60-, 90-, and 150-day-old rats sympathectomized by 6-hydroxydopamine (6-OHDA) or guanethidine (GUAN).** Data are expressed in percentage of the control values as mean ± S.E.M., n = 6–9 per group and age category.

sympathectomy resulted in more profound depletion of norepinephrine in the heart, although catecholamine content remained slightly higher in the atria than in the ventricles. In addition, partial recovery of norepinephrine tissue stores could be observed in rats treated by 6-OHDA in the atria, but not in the ventricles.

The effects of both treatments on dopamine concentrations in the heart are shown in Fig. 7.17. Whereas in 6-OHDA treated animals, dopamine levels completely restored to control values at the age of 90 days, in rats denervated by guanethidine, dopamine concentrations ranged around 30% throughout the whole experiment. However, relative reduction in dopamine concentration after both interventions was smaller than that of norepinephrine suggesting dopamine tissue stores not accessible by both neurotoxins.

Epinephrine concentrations in the denervated atria restored to control values after 6-OHDA treatment and remained significantly lower than in controls after guanethidine administration. In the ventricles, both compounds had similar effect—epinephrine tissue levels were significantly lower than in the age-matched controls being more extensively reduced after guanethidine (Fig. 7.18).

7.2 Neuropeptide Y and Calcitonin-Gene Related Peptide Concentrations

Although norepinephrine is the principal neurotransmitter of the sympathetic postganglionic nerve fibers supplying the heart, neuropeptide Y (NPY), which is costored with norepinephrine in most sympathetic nerves, also exerts multiple effects on the heart (Zukowska et al., 2003). Besides the true sympathetic neurons, NPY is localized in the intrinsic cardiac ganglia that contain nerve cell bodies both positive and negative to norepinephrine transporter
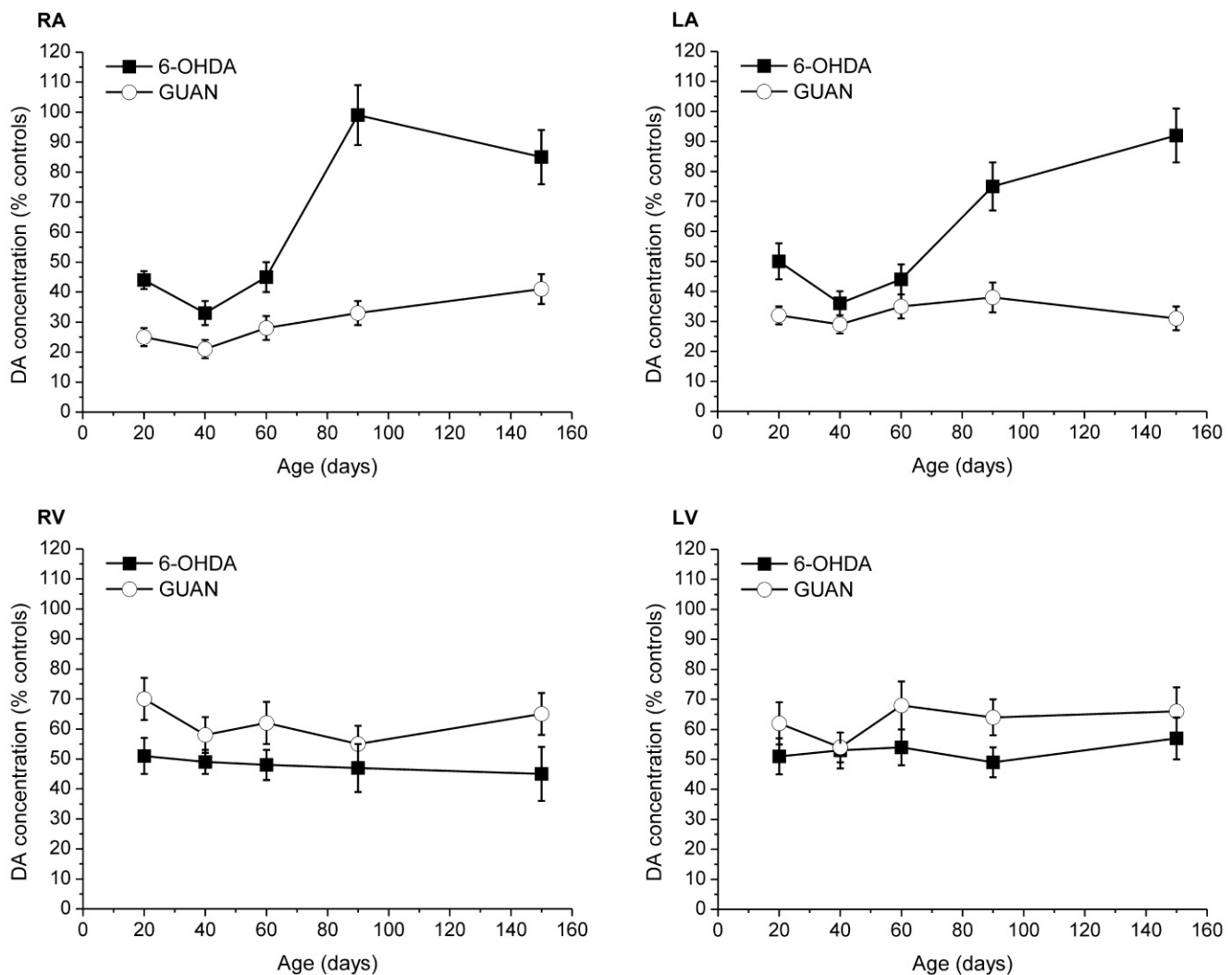
FIGURE 7.17 Dopamine (DA) concentrations in the right and left atria (RA, LA, respectively) and free walls of the right (RV) and left (LV) ventricles of 20-, 40-, 60-, 90-, and 150-day-old rats sympathectomized by 6-hydroxydopamine (6-OHDA) or guanethidine (GUAN). Data are expressed in percentage of the control values as mean ± S.E.M., n = 6–9 per group and age category.
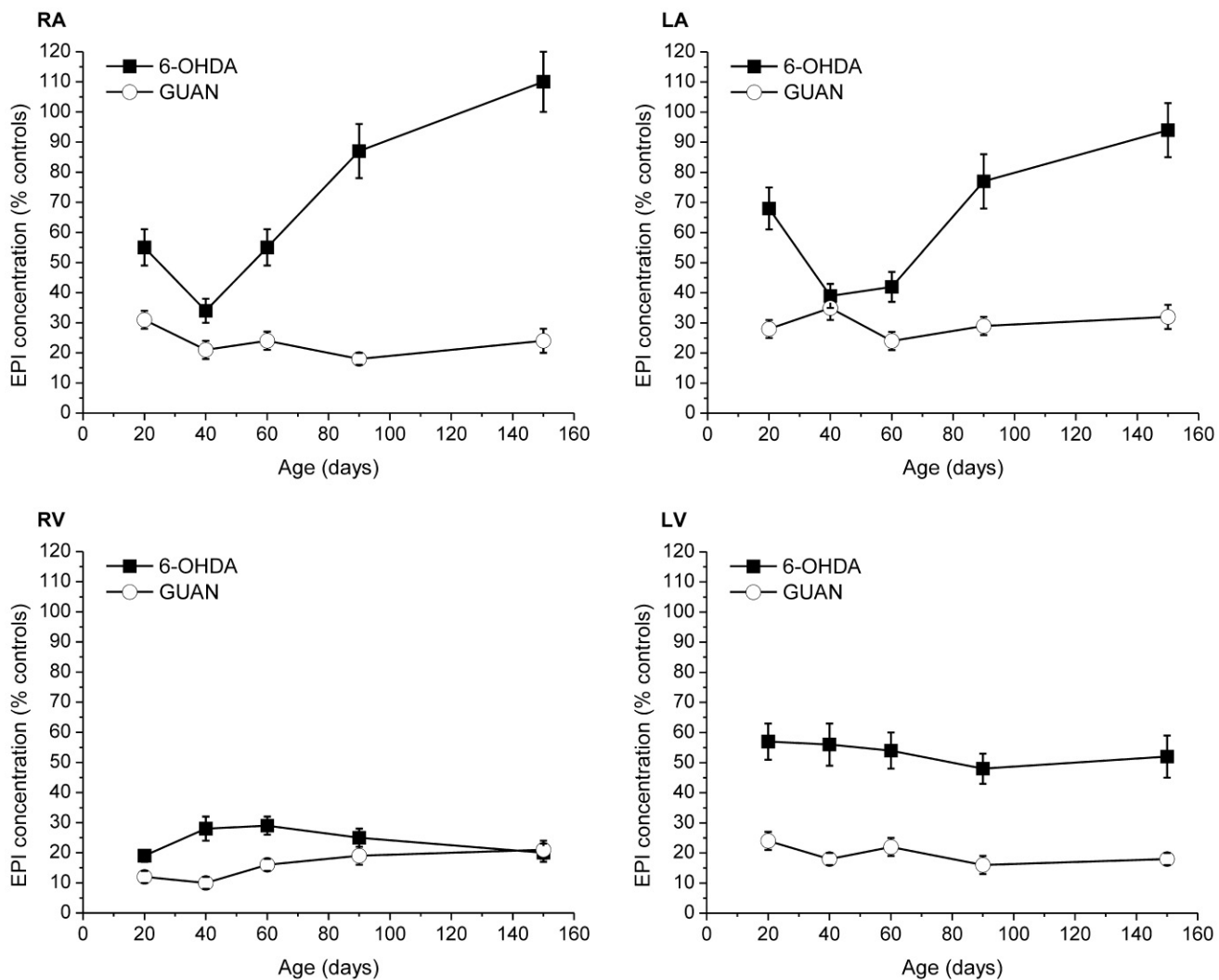
FIGURE 7.18   Epinephrine (EPI) concentrations in the right and left atria (RA, LA, respectively) and free walls of the right (RV) and left (LV) ventricles of 20-, 40-, 60-, 90-, and 150-day-old rats sympathectomized by 6-hydroxydopamine (6-OHDA) or guanethidine (GUAN). Data are expressed in percentage of the control values as mean ± S.E.M., $n = 6$–9 per group and age category.

immunoreactivity (Palomar et al., 2011). Moreover, NPY has been recently demonstrated in the endothelial and endocardial cells (Abdel-Samad et al., 2007). Contribution of the individual pools of the peptide to its total content in the heart is not precisely known. Fig. 7.19 shows the time course of NPY concentrations assayed by RIA using commercial kits (Phoenix Pharmaceuticals, CA, USA, and IBL Hamburg, FRG) after both types of sympathetic denervation. Relatively high NPY levels seem to prove NPY localization outside the sympathetic nerves. Restoration of catecholamines and NPY concentrations after 6-OHDA, but not guanethidine could be at least partly explained by the different sensitivity of the intrinsic ganglia to both toxins.

Calcitonin gene-related peptide (CGRP) is a principal neurotransmitter of the sensory neurons and it exerts multiple effects on the cardiomyocytes and coronary vasculature (Giuliani et al., 1992). It has been repeatedly

reported that neonatal sympathectomy is associated with an abrupt increase in CGRP levels in the heart (Rubino et al., 1997). Table 7.5 shows CGRP concentrations in the individual heart compartments after 6-OHDA and guanethidine treatments. Administration of both toxins led to significant increase in CGRP levels in both atria and ventricles. However, in 6-OHDA treated rats, there could be observed a trend of decreasing CGRP levels with age.

8 FUNCTIONAL PARAMETERS

8.1 Resting Heart Rate and Chronotropic Responses to Atropine and Metipranolol

The rats were placed in a small chamber with electrodes in the floor that were connected to an electrocardiograph. (EKG Seiva Praktik, Prague, Czech Republic).
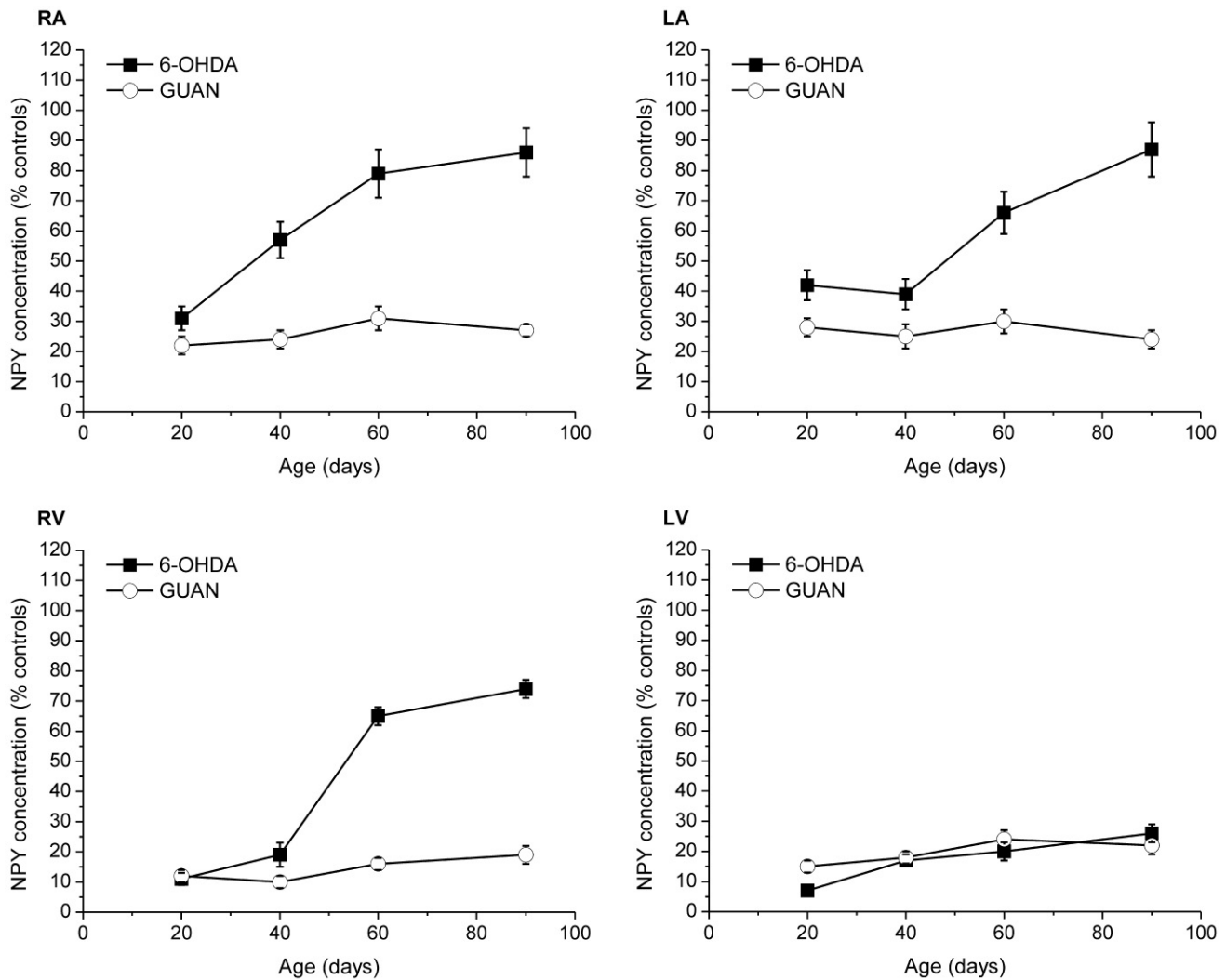
FIGURE 7.19 **Neuropeptide Y (NPY) concentrations in the right and left atria (RA, LA, respectively) and free walls of the right (RV) and left (LV) ventricles of 20-, 40-, 60-, and 90-day-old rats sympathectomized by 6-hydroxydopamine (6-OHDA) or guanethidine (GUAN).** Data are expressed in percentage of the control values as mean ± S.E.M., n = 5–8 per group and age category.

TABLE 7.5 Relative CGRP Concentrations in the Rat Heart

Age (days)		RA (% controls)	LA (% controls)	RV (% controls)	LV (% controls)
20	GUAN	119 ± 9	252 ± 12	452 ± 11	548 ± 32
	6-OHDA	563 ± 60	366 ± 40	432 ± 35	392 ± 25
40	GUAN	307 ± 25	261 ± 26	703 ± 15	588 ± 45
	6-OHDA	306 ± 32	226 ± 29	340 ± 31	460 ± 31
60	GUAN	260 ± 23	204 ± 12	550 ± 19	452 ± 32
	6-OHDA	231 ± 25	205 ± 19	351 ± 29	248 ± 19
90	GUAN	312 ± 31	230 ± 18	502 ± 44	410 ± 21
	6-OHDA	293 ± 31	186 ± 14	183 ± 18	197 ± 21

LA, left atrium; LV, free wall of left ventricle; RA, right atrium; RV, free wall of right ventricle. Rats sympathectomized by 6-hydroxydopamine (6-OHDA) or guanethidine (GUAN), aged 20–90 days. category. Data are expressed in percentage of the control age-matched values as mean ± S.E.M.; n = 6 per group and age category.
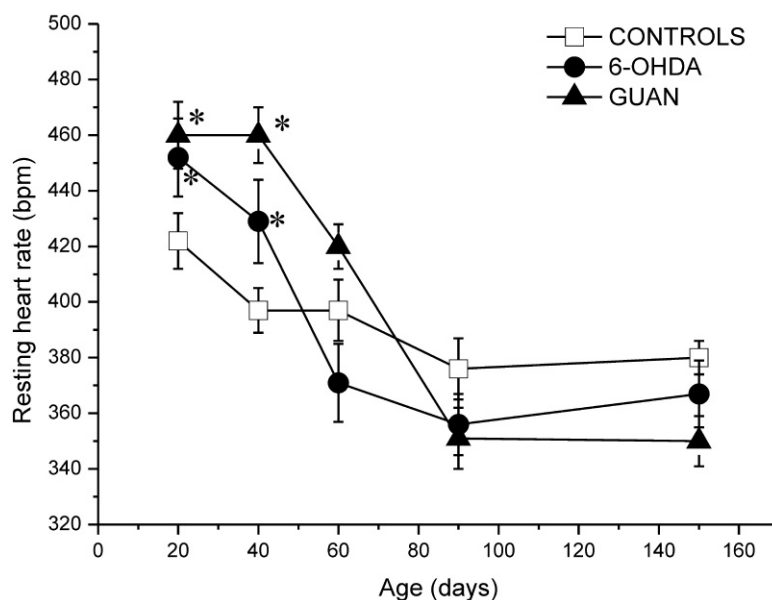
FIGURE 7.20   Resting heart rate in the rats sympathectomized by 6-hydroxydopamine (6-OHDA) or guanethidine (GUAN) and the age-matched controls aged 20–150 days. Data are expressed as mean ± S.E.M., n = 8–10 per group and age category, *P < 0.05, compared to the respective control value.

To estimate the tonic influence of the cardiac sympathetic innervation on the heart rate, the β-adrenergic receptor antagonist metipranolol (Hoechst-Biotika, Martin, Slovac Republic; 2 mg/kg, s.c.) was administered subcutaneously after pretreatment with the muscarinic receptor blocker atropine (atropine sulphate, Sigma Aldrich, Prague, Czech Republic; 4 mg/kg of body weight).

As shown in Fig. 7.20, the resting heart rate was significantly higher in the sympathectomized animals at the ages of 20 and 40 days and then it did not significantly differ from the age-matched controls.

The effect of metipranolol after previous administration of atropine suggested that estimated tonic effect of the sympathetic nerves on the heart rate was lower after both types of sympathectomy and that chemical ablation of the sympathetic nerves resulted in lower but not negligible tonic β-adrenergic effect (Fig. 7.21). This finding cannot be explained by an expected increase in the
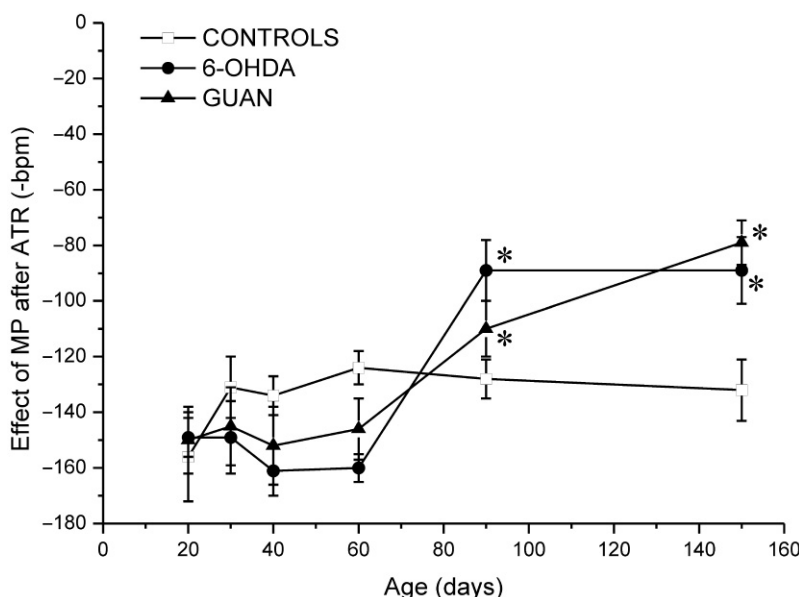
FIGURE 7.21   The net effect of metipranolol (MP) after previous atropine (ATR) administration estimating the "sympathetic tone" in the control rats and animals sympathectomized by 6-hydroxydopamine (6-OHDA) or guanethidine (GUAN) aged 20–150 days. Data are expressed as mean ± S.E.M., n = 8–10 per group and age category. *P < 0.05, compared to the respective control value.

density and/or sensitivity of cardiac beta-adrenergic receptor signaling system following chemical sympathetic denervation, since denervation supersensitivity could be observed when ablation of the sympathetic nerves is performed in adult, but not neonatal animals (Slotkin et al., 1995).

8.2 Beating Rate of the Isolated Right Atria

The heart rate was further analyzed on the isolated right atria of 6-OHDA rats in the modified Tyrode solution without and with tyramine, substrate of norepinephrine transporter that replaces it in the synaptic vesicles causing its release (Sulzer et al., 2005). As shown in Fig. 7.22, tyramine had no or significantly lower effect in the sympathectomized atria of all age categories. However, at the age of 90 days, tyramine had

significant positive chronotropic effect that was blocked by β-adrenergic blocker propranolol.

8.3 Contraction Experiments

Inotropic properties of the denervated cardiac tissue were measured on the isolated papillary muscles in an experimental chamber with Tyrode solution using an isometric force transducer F30 (Hugo Sachs, Germany). The resting tension was set so that the developed twitch tension reached 90%–95% of maximum at stimulation frequency of 1 Hz. After a stabilization period, steady-state contractions at various stimulation frequencies (3, 2, 1, 0.5, 0.3, 0.2, and 0.1 Hz) were recorded. Contractions were measured in arbitrary units (a.u.). Time course of contraction was characterized using time-to-peak (time from resting tension to the peak of contraction, TTP)
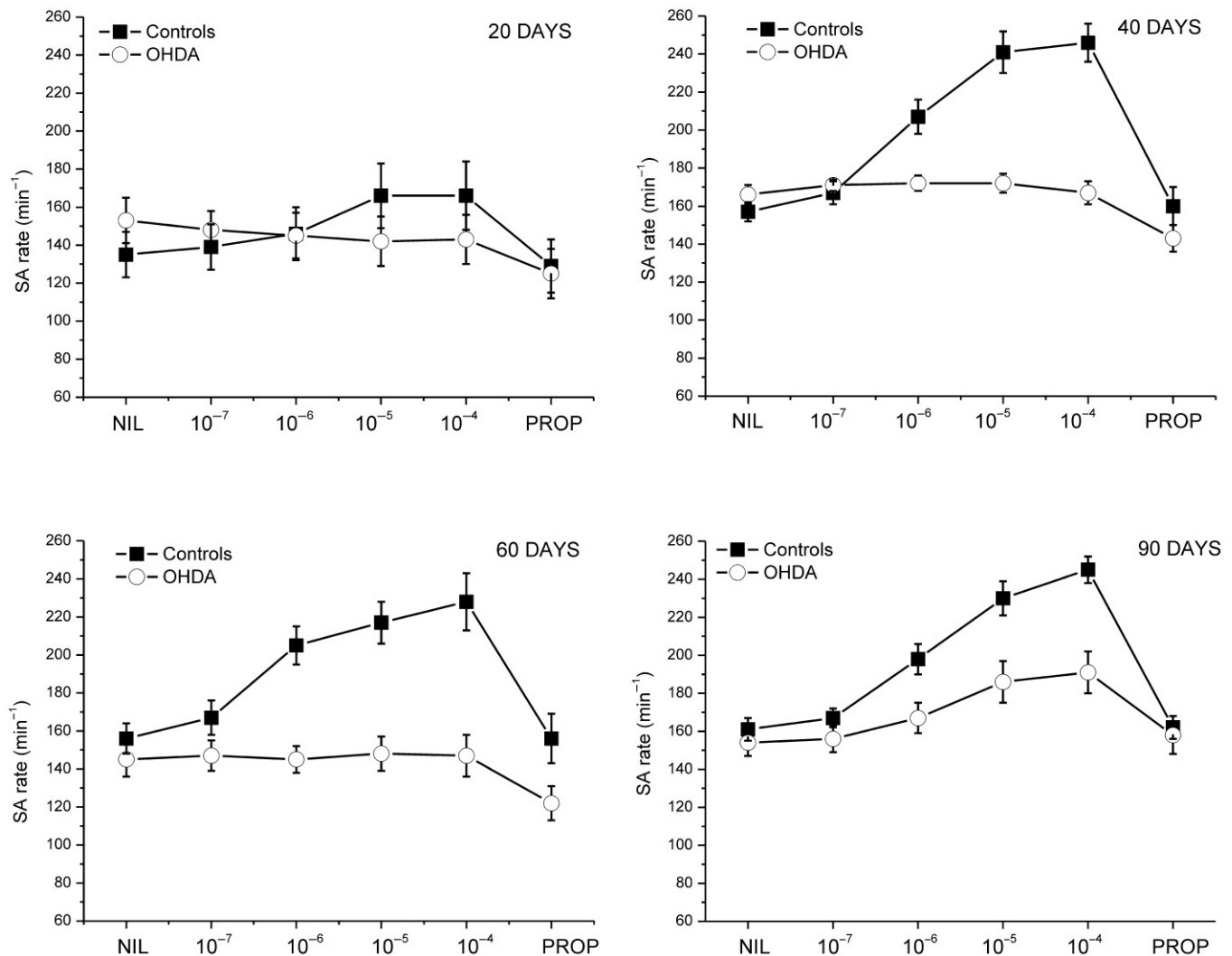
FIGURE 7.22 The effect of tyramine on the beating rate of the isolated right atrium (SA rate) in the control and sympathectomized rats aged 20–90 days. Data are expressed as mean ± S.E.M., n = 8–10 per group and age category.
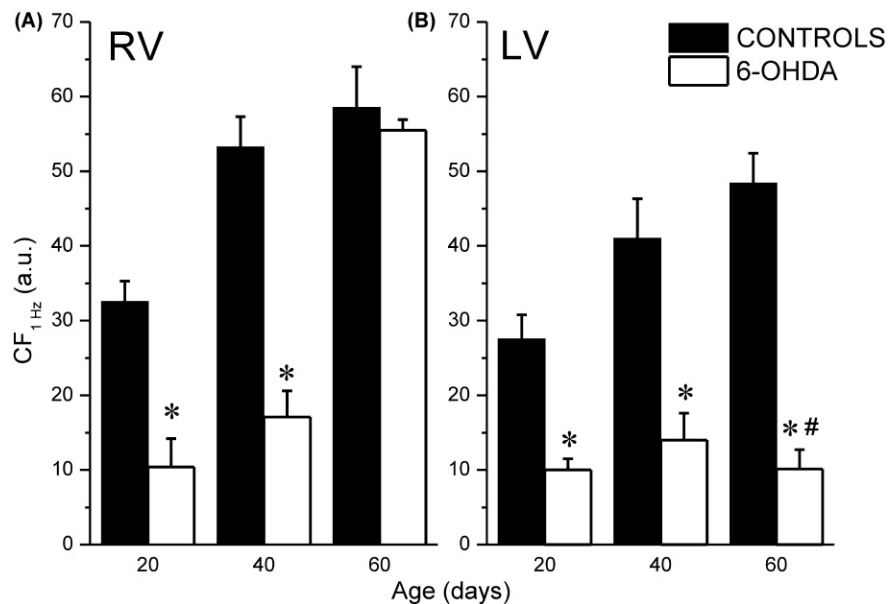
FIGURE 7.23 **The contraction force of the control and sympathectomized (6-OHDA) rats aged 20, 40, and 60 days.** (A) Contraction force (CF) of papillary muscles from the right ventricles (RV) in control ($n = 6$) and sympathectomized rats ($n = 5$). (B) Contraction force (CF) of papillary muscles from the (LV) ventricles in control ($n = 6$) and sympathectomized ($n = 5$) rats. Stimulation frequency was 1 Hz. a.u., arbitrary units. *$P < 0.01$, compared to the respective control value, #$P < 0.01$, compared to the respective value in the right ventricle.

and half-maximal relaxation time (R/2) parameters. The resting tension was taken as zero. Chemical sympathectomy significantly decreased the contraction force of the papillary muscle in all age categories in the left ventricle and in 20- and 40-day-old rats in the right ventricle and (Fig. 7.23). At day 60, however, this reduction disappeared and the contraction force of the right papillary muscle was comparable to control. The effect of the chemical sympathectomy on the contraction force was well expressed at all stimulation frequencies tested (0.1–3 Hz), that is, the force of contraction of papillary muscles in denervated rats was always significantly lower than in control rats except the right ventricle papillary muscles at the age of 60 days.

In both control and denervated rats, time to peak of contraction (TTP) shortened with increasing frequency of stimulation in all age groups. Neither chemical sympathectomy nor age of animals affected TTP. Similarly, half-maximal relaxation time shortened with increasing frequency of stimulation and there was no difference between the intact and sympathectomized rats at any age (data not shown).

In the control rats, administration of tyramine significantly increased the contraction force of papillary muscles from both ventricles independent of age. The values of the contraction force of the right and left ventricular papillary muscles after application of β-adrenergic blocker propranolol (10–4 mol/L) on top of tyramine (10–4 mol/L) were not significantly different from values in tyramine-free solution in any age group. In contrast, both right and left ventricle papillary muscles of sympathectomized rats were insensitive to both tyramine and propranolol in all age groups (Fig. 7.24).

8.4 Experimental and Clinical Implications

Taken together, neonatal chemical sympathectomy leads to profound, but differential changes in concentrations of catecholamines and neuropeptides in the rat heart compartments. Guanethidine-induced sympathectomy seems to have long-term effect on the norepinephrine tissue stores. However, with regard to novel findings in the organization of the catecholaminergic system in the heart, the precise cell types attacked by the compound could be better analyzed by quantitative immunohistochemical analysis. Norepinephrine and NPY tissue content was completely or partially restored in the atria of 6-OHDA treated rats and the same trend could be observed in the ventricles. In contrast, guanethidine effect on the cardiac levels of sympathetic neurotransmitters was stable and no tendency to recovery could be observed. It is thus tempting to speculate that intrinsic ganglion cells containing norepinephrine and NPY and displaying norepinephrine transporter immunoreactivity could serve as a source of these recovering tissue stores in 6-OHDA treated rats and that the stable and profound effect of guanethidine might occur due to its more complex toxic effect not only on extrinsic postganglionic neurons but also on noradrenergic and NPY-ergic nerve structures of the intrinsic ganglion plexus of the rat heart.
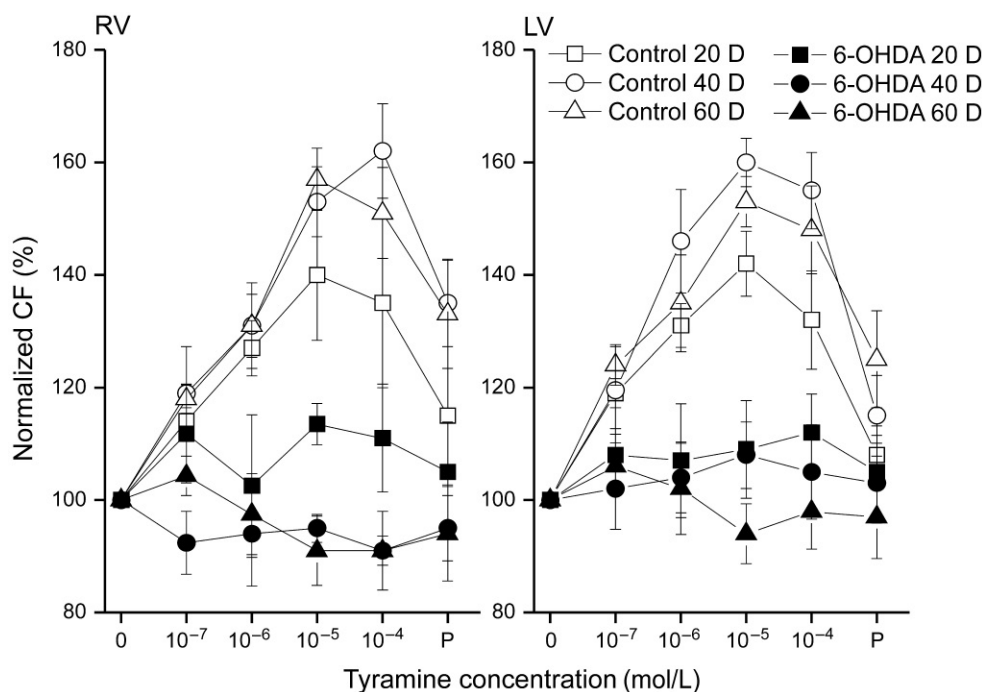
FIGURE 7.24 **The effect of tyramine and propranolol on contraction force of the control and sympathectomized rats.** Contraction force (CF) of papillary muscles from the right (RV) and left ventricles (LV) in control rats and rats sympathectomized by 6-hydroxydopamine (6-OHDA). Values were normalized to the CF in tyramine-free solution. Stimulation frequency was 1 Hz. D = age in days. P = administration of propranolol (concentration 10^{-4} mol/L) on top of tyramine (concentration 10^{-4} mol/L).

Neonatal chemical sympathectomy seems to be an excellent tool to analyze neurotransmitter equipment of individual cell types; it could help to study mutual trophic effects of cardiac neurons and myocardial cells. It is also a simple method to study the impact of neuronal activity on the postnatal development of chronotropic and inotropic properties of the heart. However, with regard to various clinical conditions affecting the sympathetic nerves (diabetes mellitus, amyloidosis, Parkinson disease, drug and alcohol abuse etc.), the results of these studies should be interpreted with caution, since the early postnatal degeneration of the sympathetic nerves or even some intrinsic ganglion neurons leads to an excessive growth of the sensory nerves, which is not finding typical for the previously listed diseases. Nevertheless, the ability of the heart to restore its catecholaminergic system after previous denervation and at least some functional parameters could be important in the investigation of various degenerative and hereditary autonomic neuropathies and the regulation of the heart function after the transplantation.

Acknowledgment

References

Abdel-Samad, D., Jacques, D., Perreault, C., et al., 2007. NPY regulates human endocardial endothelial cell function. Peptides 28, 281–287.

Adams, L.G., Polzin, D.J., Osborne, C.A., O'Brien, T.D., Hostetter, T.H., 1994. Influence of dietary protein/calorie intake on renal morphology and function in cats with 5/6 nephrectomy. Lab. Invest 70, 347–357.

Allison, M.E., Wilson, C.B., Gottschalk, C.W., 1974. Pathophysiology of experimental glomerulonephritis in rats. J. Clin. Invest. 53, 1402–1423.

Anderson, T., Schein, P.S., McMenamin, M.G., Cooney, D.A., 1974. Streptozotocin diabetes. Correlation with extent of depression of pancreatic islet nicotinamide adenine dinucleotide. J. Clin. Invest. 54, 672–677.

Aomine, M., Nobe, S., Arita, M., 1990. The making of diabetic guinea pigs by streptozotocin and high incidence of triggered activity in the ventricular muscle. Jpn. J. Physiol. 40, 651–663.

Aulbach, F., Simm, A., Maier, S., Langenfeld, H., Walter, U., Kersting, U., Kirstein, M., 1999. Insulin stimulates the L-type Ca^{2+} current in rat cardiac myocytes. Cardiovasc. Res. 42, 113–120.

Batulevicius, D., Pauziene, N., Pauza, D.H., 2003. Topographic morphology and age-related analysis of the neuronal number of the rat intracardiac nerve plexus. Ann. Anat. 185, 449–459.

Bers, D.M., Christensen, D.M., 1990. Functional interconversion of rest decay and ryanodine effects in rabbit and rat ventricle depends on Na/Ca exchange. J. Mol. Cell. Cardiol. 22, 715–723.

Boudet, J., Man, N.K., Pils, P., Sausse, A., Funck-Brentano, J.L., 1978. Experimental chronic renal failure in the rat by electrocoagulation of the renal cortex. Kidney Int. 14, 82–86.

Brown, J.H., Lappin, T.R., Elder, G.E., Bridges, J.M., McGeown, M.G., 1990. The metabolism of erythropoietin in the normal and uraemic rabbit. Nephrol. Dial. Transplant. 5, 855–859.

Burnstock, G., Evans, B., Gannon, B.J., et al., 1971. A new method of destroying adrenergic nerves in adult animals using guanethidine. Br. J. Pharmacol. 43, 295–301.

Carlsson, P.O., Flodström, M., Sandler, S., 2000. Islet blood flow in multiple low dose streptozotocin-treated wild-type and inducible nitric oxide synthase-deficient mice. Endocrinology 141, 2752–2757.

Castro, A.F., Coresh, J., 2009. CKD surveillance using laboratory data from the population-based National Health and Nutrition Examination Survey (NHANES). Am. J. Kidney Dis. 53, S46–S55.

Chaffin, D.G., Clark, R.M., McCracken, D., Philipps, A.F., 1995. Effect of hypoinsulinemia on growth in the fetal rabbit. Biol. Neonate. 67, 186–193.

Chang, K.S., Lund, D.D., 1986. Alterations in the baroreceptor reflex control of heart rate in streptozotocin diabetic rats. J. Mol. Cell. Cardiol. 18, 617–624.

Chanutin, A., Ferris, E.B., 1932. Experimental renal insufficiency produced by partial nephrectomy. Arch. Intern. Med. 49, 767–787.

Chattou, S., Diacono, J., Feuvray, D., 1999. Decrease in sodium-calcium exchange and calcium currents in diabetic rat ventricular myocytes. Acta Physiol. Scand. 166, 137–144.

Chottová Dvoráková, M., Wiegand, S., Pesta, M., Slavíková, J., Grau, V., Reischig, J., Kuncová, J., Kummer, W., 2008. Expression of neuropeptide Y and its receptors Y1 and Y2 in the rat heart and its supplying autonomic and spinal sensory ganglia in experimentally induced diabetes. Neuroscience 151, 1016–1028.

Chow, K.M., Liu, Z.C., Chang, T.M., 2003. Animal remnant kidney model of chronic renal revisited. Hong Kong J. Nephrol. 5, 57–64.

Debelle, F.D., Nortier, J.L., Husson, C.P., De Prez, E.G., Vienne, A.R., Rombaut, K., Salmon, I.J., Deschodt-Lanckman, M.M., Vanherweghem, J.L., 2004. The renin-angiotensin system blockade does not prevent renal interstitial fibrosis induced by aristolochic acids. Kidney Int. 66, 1815–1825.

Diemel, L.T., Brewster, W.J., Fernyhough, P., Tomlinson, D.R., 1994. Expression of neuropeptides in experimental diabetes; effects of treatment with nerve growth factor or brain-derived neurotrophic factor. Brain Res. Mol. Brain Res. 21, 171–175.

Dunn, J.S., Sheehan, H.L., McLethie, N.G.B., 1943. Necrosis of islets of Langerhans produced experimentally. Lancet 1, 484–487.

Ebert, S.N., Taylor, D.G., 2006. Catecholamines and development of cardiac pacemaking: an intrinsically intimate relationship. Cardiovasc. Res. 72, 364–374.

Elsner, M., Guldbakke, B., Tiedge, M., Munday, R., Lenzen, S., 2000. Relative importance of transport and alkylation for pancreatic beta-cell toxicity of streptozotocin. Diabetologia 43, 1528–1533.

Emilien, G., Maloteaux, J.M., Geurts, M., et al., 1999. Dopamine receptors—physiological understanding to therapeutic intervention potential. Pharmacol. Ther. 84, 133–156.

Eschbach, J.W., Adamson, J.W., Dennis, M.B., 1980. Physiologic studies in normal and uremic sheep: I. The experimental model. Kidney Int. 18, 725–731.

Fang, Z.Y., Prins, J.B., Marwick, T.H., 2004. Diabetic cardiomyopathy: evidence, mechanisms, and therapeutic implications. Endocr. Rev. 25, 543–567.

Flodström, M., Tyrberg, B., Eizirik, D.L., Sandler, S., 1999. Reduced sensitivity of inducible nitric oxide synthase-deficient mice to multiple low-dose streptozotocin-induced diabetes. Diabetes 48, 706–713.

Franco-Cereceda, A., Lundberg, J.M., 1988. Actions of calcitonin gene-related peptide and tachykinins in relation to the contractile effects of capsaicin in the guinea-pig and rat heart in vitro. Naunyn Schmiedebergs Arch. Pharmacol. 337, 649–655.

Freyse, E.J., Hahn von Dorsche, H., Fischer, U., 1982. Low dose streptozotocin diabetes after partial pancreatectomy in dogs. Histological findings in a new type of experimental diabetes. Acta Biol. Med. Ger. 41, 1203–1210.

Fukuda, S., Kopple, J.D., 1980. Chronic uremia syndrome in dogs induced by uranyl nitrate. Nephron 25, 139–143.

Gäbel, H., Bitter-Suermann, H., Henriksson, C., Säve-Söderbergh, J., Lundholm, K., Brynger, H., 1985. Streptozotocin diabetes in juvenile pigs. Evaluation of an experimental model. Horm. Metab. Res. 17, 275–280.

Gagnon, R.F., Gallimore, B., 1988. Characterization of a mouse model of chronic uremia. Urol. Res. 16, 119–126.

Ganda, O.P., Rossini, A.A., Like, A.A., 1976. Studies on streptozotocin diabetes. Diabetes 25, 595–603.

Ganguly, P.K., Pierce, G.N., Dhalla, K.S., Dhalla, N.S., 1983. Defective sarcoplasmic reticular calcium transport in diabetic cardiomyopathy. Am. J. Physiol. 244, E528–E535.

Gargiulo, P., Jacobellis, G., Vaccari, V., Andreani, D., 1998. Diabetic cardiomyopathy: pathophysiological and clinical aspects. Diab. Nutr. Metab. 11, 336–346.

Garofano, A., Czernichow, P., Bréant, B., 2000. Impaired beta-cell regeneration in perinatally malnourished rats: a study with STZ. FASEB J. 14, 2611–2617.

Giordano, M., Manzella, D., Paolisso, G., Caliendo, A., Varricchio, M., Giordano, C., 2001. Differences in heart rate variability parameters during the post-dialytic period in type II diabetic and non-diabetic ESRD patients. Nephrol. Dial. Transplant. 16, 566–573.

Giuliani, S., Wimalawansa, S.J., Maggi, C.A., 1992. Involvement of multiple receptors in the biological effects of calcitonin gene-related peptide and amylin in rat and guinea-pig preparations. Br. J. Pharmacol. 107, 510–514.

Gorray, K.C., Baskin, D., Brodsky, J., Fujimoto, W.Y., 1986. Responses of pancreatic b cells to alloxan and streptozotocin in the guinea pig. Pancreas 1, 130–138.

Grossman, R.C., 2010. Experimental models of renal disease and the cardiovascular system. Open Cardiovasc. Med. J. 4, 257–264.

Gu, J., Polak, J.M., Adrian, T.E., Allen, J.M., Tatemoto, K., Bloom, S.R., 1983. Neuropeptide tyrosine (NPY)—a major cardiac neuropeptide. Lancet 1, 1008–1010.

Guz, Y., Torres, A., Teitelman, G., 2002. Detrimental effect of protracted hyperglycaemia on beta-cell neogenesis in a mouse murine model of diabetes. Diabetologia 45, 1689–1696.

Heidemann, H.T., Hoffmann, K., Inselmann, G., 1990. Long-term effects of acetazolamide and sodium chloride loading on cisplatin nephrotoxicity in the rat. Eur. J. Clin. Invest. 20, 214–218.

Heyliger, C.E., Prakash, A., McNeill, J.H., 1987. Alterations in cardiac sarcolemmal Ca^{2+} pump activity during diabetes mellitus. Am. J. Physiol. 252, H540–H544.

Hicks, K.K., Seifen, E., Stimers, J.R., Kennedy, R.H., 1998. Effects of streptozotocin-induced diabetes on heart rate, blood pressure and cardiac autonomic nervous control. J. Auton. Nerv. Syst. 69, 21–30.

Holzer, P., 1988. Local effector functions of capsaicin-sensitive sensory nerve endings: involvement of tachykinins, calcitonin gene-related peptide and other neuropeptides. Neuroscience 24, 739–768.

Huang, M.H., Friend, D.S., Sunday, M.E., et al., 1996. An intrinsic adrenergic system in mammalian heart. J. Clin. Invest. 98, 1298–1303.

Huang, M.H., Bahl, J.J., Wu, Y., et al., 2005. Neuroendocrine properties of intrinsic cardiac adrenergic cells in fetal rat heart. Am. J. Physiol. Heart Circ. Physiol. 288, H497–H503.

Ilebekk, A., Andersen, F.R., Kjeldsen, S.E., et al., 1983. Dopamine release from the porcine myocardium. Acta Physiol. Scand. 119, 197–201.

Ishikawa, T., Kajiwara, H., Kurihara, S., 1999. Alterations in contractile properties and Ca^{2+} handling in streptozotocin-induced diabetic rat myocardium. Am. J. Physiol. 277, H2185–H2194.

Jacques, D., Sader, S., Perreault, C., Fournier, A., Pelletier, G., Beck-Sickinger, A.G., Descorbeth, M., 2003. Presence of neuropeptide Y and the Y1 receptor in the plasma membrane and nuclear envelope of human endocardial endothelial cells: modulation of intracellular calcium. Can. J. Physiol. Pharmacol. 81, 288–300.

Jarret, R.J., 1989. Cardiovascular disease and hypertension in diabetes mellitus. Diabetes Metab. Rev. 5, 547–558.

Johnson, Jr., E.M., O'Brien, F., Werbitt, R., 1976. Modification and characterization of the permanent sympathectomy produced by the administration of guanethidine to newborn rats. Eur. J. Pharmacol. 1, 45–54.

Johnstone, L.M., Jones, C.L., Grigg, L.E., Wilkinson, J.L., Walker, R.G., Powell, H.R., 1996. Left ventricular abnormalities in children, adolescents and young adults with renal disease. Kidney Int. 50, 998–1006.

Jordan, G.W., Cohen, S.H., 1987. Encephalomyocarditis virus-induced diabetes mellitus in mice: model of viral pathogenesis. Rev. Infect. Dis. 9, 917–924.

Junod, A., Lambert, A.E., Orci, L., Pictet, R., Gonet, A.E., Renold, A.E., 1967. Studies of the diabetogenic action of streptozotocin. Proc. Soc. Exp. Biol. Med. 126, 201–205.

Junod, A., Lambert, A.E., Stauffacher, W., Renold, A.E., 1969. Diabetogenic action of streptozotocin: relationship of dose to metabolic response. J. Clin. Invest. 48, 2129–2139.

Kalantar-Zadeh, K., Regidor, D.L., Kovesdy, C.P., Van Wyck, D., Bunnapradist, S., Horwich, T.B., Fonarow, G.C., 2009. Fluid retention is associated with cardiovascular mortality in patients undergoing long-term hemodialysis. Circulation 119, 671–679.

Källner, G., Franco-Cereceda, A., 1998. Aggravation of myocardial infarction in the porcine heart by capsaicin-induced depletion of calcitonin gene-related peptide (CGRP). J. Cardiovasc. Pharmacol. 32, 500–504.

Kedar, P., Chakrabarti, C.H., 1983. Effects of jambolan seed treatment on blood sugar, lipids and urea in streptozotocin induced diabetes in rabbits. Indian J. Physiol. Pharmacol. 27, 135–140.

Kersten, J.R., Toller, W.G., Gross, E.R., Pagel, P.S., Warltier, D.C., 2000. Diabetes abolishes ischemic preconditioning: role of glucose, insulin, and osmolality. Am. J. Physiol. 278, H1218–H1224.

Kroon, D.B., Jongkind, J.F., Wisse, J.H., 1962. Resection of the renal papillae in rats. Experientia 18, 581–583.

Kuehl, M., Stevens, M.J., 2012. Cardiovascular autonomic neuropathies as complications of diabetes mellitus. Nat. Rev. Endocrinol. 8, 405–416.

Kumano, K., Kogure, K., Tanaka, T., Sakai, T., 1986. A new method of inducing experimental chronic renal failure by cryosurgery. Kidney Int. 30, 433–436.

Kummer, W., Addicks, K., Heym, C., 1986. Heterogeneity of supracardiac paraganglia. J. Auton. Nerv. Syst., 289–293.

Kuncová, J., Slavíková, J., Svíglerová, J., 2003. Norepinephrine release in the heart atria of diabetic rats. Gen. Physiol. Biophys. 22, 397–410.

Kuncová, J., Svíglerová, J., Tonar, Z., Slavíková, J., 2005. Heterogenous changes in neuropeptide Y, norepinephrine and epinephrine concentrations in the hearts of diabetic rats. Auton. Neurosci. 121, 7–15.

Kuncová, J., Švíglerová, J., Kummer, W., Rajdl, D., Chottová-Dvořáková, M., Tonar, Z., Nalos, L., Štengl, M., 2009. Parasympathetic regulation of heart rate in rats after 5/6 nephrectomy is impaired despite functionally intact cardiac vagal innervation. Nephrol. Dial. Transplant. 24, 2362–2370.

Kushner, B., Lazar, M., Furman, M., Lieberman, T.W., Leopold, I.H., 1969. Resistance of rabbits and guinea pigs to the diabetogenic effect of streptozotocin. Diabetes 18, 542–544.

Lameris, T.W., de Zeeuw, S., Duncker, D.J., et al., 2002. Epinephrine in the heart: uptake and release, but no facilitation of norepinephrine release. Circulation 106, 860–865.

Lazar, M., Golden, P., Furman, M., Lieberman, T.W., 1968. Resistance of the rabbit to streptozotocin. Lancet 2, 919.

Lazarus, S.S., Shapiro, S.H., 1972. Streptozotocin-induced diabetes and islet cell alterations in rabbits. Diabetes 21, 129–137.

Lee, S.L., Ostadalova, I., Kolar, F., Dhalla, N.S., 1992. Alterations in $Ca^{(2+)}$-channels during the development of diabetic cardiomyopathy. Mol. Cell. Biochem. 109, 173–179.

Liu, S., Wang, W., Luo, X.M., Ye, B., 2000. Chemically induced (streptozotocin-alloxan) diabetes mellitus in dogs. Hunan Yi Ke Da Xue Xue Bao 25, 125–128.

Liu, Z.C., Chow, K.M., Chang, T.M., 2003. Evaluation of two protocols of uremic rat model: partial nephrectomy and infarction. Ren. Fail. 25, 935–943.

London, G.M., 2003. Cardiovascular disease in chronic renal failure: pathophysiologic aspects. Semin. Dial. 16, 85–94.

London, G.M., Parfrey, P.S., 1997. Cardiac disease in chronic uremia: pathogenesis. Adv. Ren. Replace. Ther. 4, 194–211.

Lu, R., Hu, C.P., Peng, J., Deng, H.W., Li, Y.J., 2001. Role of calcitonin gene-related peptide in ischaemic preconditioning in diabetic rat hearts. Clin. Exp. Pharmacol. Physiol. 28, 392–396.

Lundberg, J.M., Stjarne, L., Neuropeptide Y, 1984. (NPY) depresses the secretion of 3H-noradrenaline and the contractile response evoked by field stimulation, in rat vas deferens. Acta Physiol. Scand. 120, 477–479.

Mahgoub, M.A., Abd-Elfattah, A.S., 1998. Diabetes mellitus and cardiac function. Mol. Cell. Biochem. 180, 59–64.

Makino, S., Kunimoto, K., Muraoka, Y., Mizushima, Y., Katagiri, K., Tochino, Y., 1980. Breeding of a non-obese, diabetic strain of mice. Jikken Dobutsu 29, 1–13.

Makino, N., Dhalla, K.S., Elimban, V., Dhalla, N.S., 1987. Sarcolemmal Ca^{2+} transport in streptozotocin-induced diabetic cardiomyopathy in rats. Am. J. Physiol. 253, E202–E207.

Malhotra, A., Sanghi, V., 1997. Regulation of contractile proteins in diabetic heart. Cardiovasc. Res. 34, 34–40.

McKenna, P.H., Khoury, A.E., McLorie, G.A., Reid, G., Churchill, B.M., 1992. A surgical model for normotensive chronic renal failure in the growing piglet. J. Urol. 148, 756–759.

Miyauchi, T., Ishikawa, T., Sugishita, Y., Saito, A., Goto, K., 1987. Effects of capsaicin on nonadrenergic noncholinergic nerves in the guinea pig atria: role of calcitonin gene-related peptide as cardiac neurotransmitter. J. Cardiovasc. Pharmacol. 10, 675–682.

Mordes, J.P., Desemone, J., Rossini, A.A., 1987. The BB rat. Diabetes Metab. Rev. 3, 725–750.

Nakamura, J., Hamada, Y., Chaya, S., Nakashima, E., Naruse, K., Kato, K., Yasuda, Y., Kamiya, H., Sakakibara, F., Koh, N., Hotta, N., 2002. Transition metals and polyol pathway in the development of diabetic neuropathy in rats. Diabetes Metab. Res. Rev. 18, 395–402.

Nicholl, S.M., Bell, D., Spiers, J., McDermott, B.J., 2002. Neuropeptide Y Y(1) receptor regulates protein turnover and constitutive gene expression in hypertrophying cardiomyocytes. Eur. J. Pharmacol. 441, 23–34.

Ormrod, D., Miller, T., 1980. Experimental uremia. Description of a model producing varying degrees of stable uremia. Nephron 26, 249–254.

Palomar, A.R., Larios, B.N., De Sánchez, V.C., et al., 2011. Expression and distribution of dopamine transporter in cardiac tissues of the guinea pig. Neurochem. Res. 36, 399–405.

Parfrey, P.S., Harnett, J.D., Barre, P.E., 1991. The natural history of myocardial disease in dialysis patients. J. Am. Soc. Nephrol. 2, 2–12.

Perez-Ruiz, L., Ros-Lopez, S., Cardús, A., Fernandez, E., Valdivielso, J.M., 2006. A forgotten method to induce experimental chronic renal failure in the rat by ligation of the renal parenchyma. Nephron. Exp. Nephrol. 103, e126–e130.

Pernow, J., Lundberg, J.M., Kaijser, L., 1987. Vasoconstrictor effects in vivo and plasma disappearance rate of neuropeptide Y in man. Life Sci. 40, 47–54.

Pfeifer, M.A., Schumer, M.P., Gelber, D.A., 1997. Aldose reductase inhibitors: the end of an era or the need for different trial designs? Diabetes 46, S82–S89.

Picklo, M.J., 1997. Methods of sympathetic degeneration and alteration. J. Auton. Nerv. Syst. 62, 111–125.

Platt, R., Roscoe, M.H., Smith, F.W., 1952. Experimental renal failure. Clin. Sci. 11, 217–231.

Pourmoghaddas, A., Hekmatnia, A., 2003. The relationship between QTc interval and cardiac autonomic neuropathy in diabetes mellitus. Mol. Cell. Biochem. 249, 125–128.

C. CARDIAC AND CARDIOVASCULAR

Purkerson, M.L., Hoffsten, P.E., Klahr, S., 1976. Pathogenesis of glomerulopathy associated with renal infarction in rats. Kidney Int. 9, 407–417.

Rakieten, N., Rakieten, M.L., Nadkarni, M.V., 1963. Studies on the diabetic action of streptozotocin. Cancer Chemother. Rep. 29, 91–98.

Rakieten, N., Gordon, B.S., Beaty, A., Cooney, D.A., Schein, P.S., Dixon, R.L., 1976. Modification of renal tumorigenic effect of streptozotocin by nicotinamide: spontaneous reversibility of streptozotocin diabetes. Proc. Soc. Exp. Biol. Med. 15, 356–361.

Ritskes-Hoitinga, J., Beynen, A.C., 1988. Atherosclerosis in the rat. Artery 16, 25–50.

Rittenhouse, P.A., Marchand, J.E., Chen, J., Kream, R.M., Leeman, S.E., 1996. Streptozotocin-induced diabetes is associated with altered expression of peptide-encoding mRNAs in rat sensory neurons. Peptides 17, 1017–1022.

Robinson, T.G., Carr, S.J., 2002. Cardiovascular autonomic dysfunction in uremia. Kidney Int. 62, 1921–1932.

Rolandsson, O., Haney, M.F., Hagg, E., Biber, B., Lernmark, A., 2002. Streptozotocin induced diabetes in minipig: a case report of a possible model for type 1 diabetes? Autoimmunity 35, 261–264.

Rossini, A.A., Williams, R.M., Appel, M.C., Like, A.A., 1978. Sex differences in the multiple-dose streptozotocin model of diabetes. Endocrinology 103, 1518–1520.

Rubino, A., Ralevic, V., Burnstock, G., 1997. Calcitonin gene-related peptide (CGRP)-evoked inotropism during hyper- and hyposensory-motor innervation in rat atria. J. Auton. Pharmacol. 17, 121–127.

Rundell, V.L., Geenen, D.L., Buttrick, P.M., de Tombe, P.P., 2004. Depressed cardiac tension cost in experimental diabetes is due to altered myosin heavy chain isoform expression. Am. J. Physiol. 287, H408–H413.

Russell, J.C., Proctor, S.D., 2006. Small animal models of cardiovascular disease: tools for the study of the roles of metabolic syndrome, dyslipidemia, and atherosclerosis. Cardiovasc. Pathol. 15, 318–330.

Saito, A., Ishikawa, T., Kimura, S., Goto, K., 1987. Role of calcitonin gene-related peptide as cardiotonic neurotransmitter in guinea pig left atria. J. Pharmacol. Exp. Ther. 243, 731–736.

Salis, A.I., Peterson, R.G., Stecker, M.S., Patel, N.H., Willis, L.R., Galley, P., Eclavea, A.C., Dreesen, R.G., 2001. Suprarenal intraarterial infusion of alloxan and streptozotocin during balloon occlusion of the juxtarenal abdominal aorta: a simple technique for inducing diabetes mellitus in canines with reduced mortality. Acad. Radiol. 8, 473–477.

Schlaich, M.P., Socratous, F., Hennebry, S., Eikelis, N., Lambert, E.A., Straznicky, N., Esler, M.D., Lambert, G.W., 2009. Sympathetic activation in chronic renal failure. J. Am. Soc. Nephrol. 20, 933–939.

Schlosser, M.J., Kapeghian, J.C., Verlangieri, A.J., 1987. Selected physical and biochemical parameters in the streptozotocin-treated guinea pig: insights into the diabetic guinea pig model. Life Sci. 41, 1345–1353.

Schnedl, W.J., Ferber, S., Johnson, J.H., Newgard, C.B., 1994. STZ transport and cytotoxicity. Specific enhancement in GLUT2-expressing cells. Diabetes 43, 1326–1333.

Schouten, V.J., ter Keurs, H.E., 1991. Role of ICA and Na^+/Ca^{2+} exchange in the force-frequency relationship of rat heart muscle. J. Mol. Cell. Cardiol. 23, 1039–1050.

Shattock, M.J., Bers, D.M., 1989. Rat vs. rabbit ventricle: Ca flux and intracellular Na assessed by ion-selective microelectrodes. Am. J. Physiol. 256, C813–C822.

Slavikova, J., Kuncova, J., Reischig, J., et al., 2003. Catecholaminergic neurons in the rat intrinsic cardiac nervous system. Neurochem. Res. 28, 593–598.

Slotkin, T.A., Lorber, B.A., McCook, E.C., et al., 1995. Neural input and the development of adrenergic intracellular signaling: neonatal denervation evokes neither receptor upregulation nor persistent supersensitivity of adenylate cyclase. Brain Res. Dev. Brain Res. 88, 17–29.

Su, E.N., Alder, V.A., Yu, D.Y., Yu, P.K., Cringle, S.J., Yogesan, K., 2000. Continued progression of retinopathy despite spontaneous recovery to normoglycemia in a long-term study of streptozotocin-induced diabetes in rats. Graefes Arch. Clin. Exp. Ophthalmol. 238, 163–173.

Sulzer, D., Sonders, M.S., Poulsen, N.W., et al., 2005. Mechanisms of neurotransmitter release by amphetamines: a review. Prog. Neurobiol. 75, 406–433.

Svíglerová, J., Kuncová, J., Stengl, M., 2005. Negative inotropic effect of insulin in papillary muscles from control and diabetic rats. Physiol. Res. 54, 661–670.

Švíglerová, J., Kuncová, J., Nalos, L., Holas, J., Tonar, Z., Rajdl, D., Štengl, M., 2012. Cardiac remodeling in rats with renal failure show interventricular difference. Exp. Biol. Med. 237, 1056–1067.

Takasu, N., Komiya, I., Asawa, T., Nagasawa, Y., Yamada, T., 1991. Streptozocin- and alloxan-induced H_2O_2 generation and DNA fragmentation in pancreatic islets. H_2O_2 as mediator for DNA fragmentation. Diabetes 40, 1141–1145.

Teshima, Y., Takahashi, N., Saikawa, T., Hara, M., Yasunaga, S., Hidaka, S., Sakata, T., 2000. Diminished expression of sarcoplasmic reticulum Ca^{2+}-ATPase and ryanodine sensitive Ca^{2+} channel mRNA in streptozotocin-induced diabetic rat heart. J. Mol. Cell. Cardiol. 32, 655–664.

Thoenen, H., Tranzer, J.P., 1973. The pharmacology of 6-hydroxydopamine. Annu. Rev. Pharmacol. 13, 169–180.

Tomlinson, K.C., Gardiner, S.M., Hebden, R.A., Bennett, T., 1992. Functional consequences of streptozotocin-induced diabetes mellitus, with particular reference to the cardiovascular system. Pharmacol. Rev. 44, 103–150.

Tosaki, A., Engelman, D.T., Engelman, R.M., Das, D.K., 1996. The evolution of diabetic response to ischemia/reperfusion and preconditioning in isolated working rat hearts. Cardiovasc. Res. 31, 526–536.

Tuffier, T., 1889. Études Expérimentelles Sur La Chirurgie Du Reis. G. Steinheil, Paris.

Vanholder, R., Glorieux, G., Lameire, N., 2003. Uraemic toxins and cardiovascular disease. Nephrol. Dial. Transplant. 18, 463–466.

Vasanji, Z., Dhalla, N.S., Netticadan, T., 2004. Increased inhibition of SERCA2 by phospholamban in the type I diabetic heart. Mol. Cell. Biochem. 261, 245–249.

Vogel, S.R., Desrochers, A., Babkine, M., Mulon, P.Y., Nichols, S., 2011. Unilateral nephrectomy in 10 cattle. Vet. Surg. 40, 233–239.

Wang, X., Fiscus, R.R., 1989. Calcitonin gene-related peptide increases cAMP, tension, and rate in rat atria. Am. J. Physiol. 256, R421–R428.

West, E., Simon, O.R., Morrison, E.Y., 1996. Streptozotocin alters pancreatic beta-cell responsiveness to glucose within six hours of injection into rats. West Indian Med. J. 45, 60–62.

Xiao, Z.S., Li, Y.J., Deng, H.W., 1996. Ischemic preconditioning mediated by calcitonin gene-related peptide in isolated rat hearts. Zhongguo Yao Li Xue Bao 17, 445–448.

Yamamoto, H., Uchigata, Y., Okamoto, H., 1981. Streptozotocin and alloxan induce DNA strand breaks and poly(ADP-ribose) synthetase in pancreatic islets. Nature 294, 284–286.

Yoneko, M., Kamei, J., Ito, C.F., Kojima, J., 2007. New approach for chronic renal failure model by direct kidney injection of doxorubicin in rats. Methods Find. Exp. Clin. Pharmacol. 29, 389–394.

Yoon, J.W., Jun, H.S., 2006. Viruses cause type 1 diabetes in animals. Ann. N Y Acad. Sci. 1079, 138–146.

Yu, Z., Tibbits, G.F., McNeill, J.H., 1994. Cellular functions of diabetic cardiomyocytes: contractility, rapid-cooling contracture, and ryanodine binding. Am. J. Physiol. 266, H2082–H2089.

Zoccali, C., Ciccarelli, M., Maggiore, Q., 1982. Defective reflex control of heart rate in dialysis patients: evidence for an afferent autonomic lesion. Clin. Sci. 63, 285–292.

Zoccali, C., Benedetto, F.A., Tripepi, G., Mallamaci, F., 2004. Cardiac consequences of hypertension in hemodialysis patients. Semin. Dial. 17, 299–303.

Zukowska, Z., Pons, J., Lee, E.W., et al., 2003. Neuropeptide Y: a new mediator linking sympathetic nerves, blood vessels and immune system? Can. J. Physiol. Pharmacol. 81, 89–94.

Zukowska-Grojec, Z., Karwatowska-Prokopczuk, E., Rose, W., Rone, J., Movafagh, S., Ji, H., Yeh, Y., Chen, W.T., Kleinman, H.K., Grouzmann, E., Grant, D.S., 1998. Neuropeptide Y: a novel angiogenic factor from the sympathetic nerves and endothelium. Circ. Res. 83, 187–195.

Page left intentionally blank

8

Animal Models of Atherosclerosis

Godfrey S. Getz, Catherine A. Reardon

Ben May Institute for Cancer Biology, University of Chicago, Chicago, IL, United States

In this chapter, we will primarily focus on models of atherosclerosis and myocardial infarction.

Atherosclerosis is a complex vascular inflammatory disease that underlies most clinical cardiovascular diseases. This includes coronary artery disease with complicating myocardial infarction, many subtypes of stroke, peripheral vascular disease, and aortic aneurysms. For coronary arterial disease, the risk factors are many; foremost of which are elevated LDL cholesterol levels, reduced HDL cholesterol levels, increased inflammation as measured by plasma levels of C-reactive protein and serum amyloid A, and leukocytosis, especially monocytosis. In some cases, it is unclear to what extent the factors are biomarkers as distinct from etiologic mediators. In what follows we pay attention to how one can modify these and other potential risk factors in the variety of animal models to determine the answer to the preceding question. Each model has advantages and disadvantages, though we recognize that no animal model can faithfully duplicate the situation in human patients. Recent development of advanced technologies can however, mitigate some but not all of the differences, especially those that are reflective of the fundamental physiological features of the model (species). Regardless, animal mod-

els are of particular value for the preclinical testing of potential therapeutic agents. Atherosclerosis is often enhanced in obese and diabetic subjects. These additional risk relationships, which may or may not operate via the traditional risk factors mentioned earlier, will not be discussed in this chapter, as they will be taken up in other chapters of this collection.

Atherosclerosis is a complex, focal, chronic inflammatory reaction of the intima of large and medium sized arteries. The features of the atherosclerotic plaque depend upon the maturation state of the lesion. The focality of lesion development is determined by the local hemodynamic pattern. Lesions preferentially develop in areas of disturbed flow, with regions of vessels experiencing laminar flow being relatively protected from lesion development. Lesion development depends on the interaction of global factors, for example, hyperlipidemia, with the focal environment in susceptible areas of vessel wall. The endothelium in the atherosclerosis prone and atherosclerosis protected regions of the vessel wall exhibits differences in barrier function and gene expression. An established risk factor that mediates the initiation of atherogenesis is high plasma levels of LDL. The near wall concentration of LDL is higher in the areas of disturbed

flow than it is in areas of laminar flow. Atherogenesis is initiated by the influx of plasma LDL into the intima at the susceptible sites where the lipoprotein is retained by interaction with intimal proteoglycans. ApoB100 on the LDL has a specific binding site for proteoglycans. The retained LDL in the intima may be modified by digestion with acid sphingomyelinase resulting in aggregation of the lipoprotein or by oxidation. Oxidized LDL initiates a number of proinflammatory processes. Its interaction with endothelial cells alters gene expression, including the upregulation of adhesion molecules resulting in the influx of monocytes that differentiate into macrophages within the intimal microenvironment. The macrophages take up the modified LDLs via their scavenger receptors or by macropinocytosis of aggregates of lipoproteins and in the process becoming lipid laden foam cells. The lipoprotein cholesterol liberated from the lipoprotein in the endosomal compartments traffics to the endoplasmic reticulum or to cell membranes where it may contribute to enhanced signaling. Most of the sterol in the endoplasmic reticulum is esterified by acyl cholesterol acyl transferase and is stored in the lipid droplets of the foam cells. There is a notable change in gene expression and protein levels in the lipid loaded cells. This includes upregulation of proteins that promote cholesterol efflux and proinflammatory cytokines and chemokines that among other things attract lymphocytes to the plaque. The result is a soup of cytokines and chemokines that are responsible for communication among the cells of the plaque microenvironment. The accumulation of free cholesterol in the endoplasmic reticulum of the macrophage foam cell can elicit the unfolded protein response and then apoptosis of these cells, which are removed by other macrophages by a process known as efferocytosis. However, with inefficient efferocytotic removal of these apoptotic cells, they undergo secondary necrosis (Tabas et al., 2015), which among other effects results in the liberation of the stored lipid droplets, creating a pool of extracellular lipid. The modified LDL may also function as a neoantigen eliciting an adaptive immune response. Macrophages in the plaque may function as antigen presenting cells, presenting modified peptides derived from the endocytosed LDL, eliciting an immune response to such potential autoantigens.

Among the consequences of macrophage signaling is the production of growth factors that promotes the proliferation of lesion macrophages. Other factors act on smooth muscle cells to promote their migration from the media into the intima where they proliferate and produce matrix and fibrous proteins that contribute to the formation of the fibrous cap over the intimal plaque. This contributes to the stable plaque phenotype. The plaque may be destabilized by the action of a variety of proteases secreted from macrophages and other inflammatory cells in the plaque. Disruption of the fibrous plaque can result in platelet aggregation and activation, which can lead to occlusion of the lumen and the interruption of the blood supply. This atherothrombosis is the critical unfavorable clinical sequelae of atherosclerosis. Prior to such an event, most of the features of the evolving atherosclerotic plaque are clinically silent. Thus most preventive approaches to dealing with atherosclerotic cardiovascular disease are directed at lowering the risk factors. Although the earlier description suggests a linear progression of lesion development, this is not necessarily the case in vivo.

It is 103 years since Anitschkov in his seminal studies first drew attention to cholesterol in eliciting arterial lesions in the rabbit (Steinberg, 2013). His studies were surprisingly thoughtful and perceptive. As it turns out the rabbit is particularly sensitive to a dietary cholesterol load. These observations could not be duplicated in rodents or dogs, which required the addition of cholate or thiouracil, respectively, to elicit both hypercholesterolemia and modest arterial lesions. With the subsequent large volume of work in animal models, our understanding of the process of atherogenesis has advanced immensely. This has involved both large animal models and murine models, especially the genetic manipulation of the mouse (Table 8.1).

1 PRIMATE MODELS

With the goal of understanding the human disease, one might expect many studies of the species that are closest in evolutionary distance, namely nonhuman primates, to have been undertaken. Indeed atherosclerosis in baboons, chimpanzees, rhesus monkeys, Cynomolgus monkeys, and African green monkeys has been studied (Getz and Reardon, 2012; Phillips et al., 2014). Nonhuman primates have a lipoprotein profile that closely resembles that of humans, with significant baseline concentrations of VLDL and LDL and heterogeneous HDL particles. Their hemodynamic profile and heart rate resembles that in humans. Upon the feeding of fat and cholesterol enriched diets, these animals develop lesions in the major arteries, including coronary arteries. Cynomolgus monkeys have been employed to explore the role of gender on the development of coronary artery atherosclerosis. As with humans, coronary artery lesions in Cynomolgus monkeys are more frequent in males than in females, but ovariectomy restores the equivalence of lesion frequency between the genders. The social behavior of these animals also allows for the analysis of social stress on coronary artery lesions. When subject to recurrent reorganization of social groups, dominant males have increased coronary lesions compared to subordinate males. However when in stable social groups, dominant males have fewer lesions, though not significantly so. On the other

TABLE 8.1   Animal Models of Atherosclerosis

Species	Advantages	Disadvantages
Nonhuman primates	Human-like lipoprotein profile	Ethical considerations of using this species, including genetic manipulations
	Human-like atherosclerotic lesions, including in coronary artery	Long time frame for lesion development
	Capable of sampling tissues/cells from vessels	Expense
Pigs	Human-like lipoprotein profile except for HDL subclasses	Currently few genetically modified models, although through the development of new techniques this limitation may be reduced
	Human-like atherosclerotic lesions, including in coronary artery	Expense
	Capable of sampling tissues/cells from vessels	
	Can be imaged noninvasively	
Rabbits—wild type		
	Cholesterol sensitive	Largely foaming lesions
	Express CETP (all rabbits)	β-VLDL is primary lipoprotein
		Hepatic lipase deficient (all rabbits)
	Can be imaged noninvasively	Currently few genetically modified models, although through the development of new techniques this limitation may be reduced
Rabbits—WHHL	Human-like lipoprotein profile	
	Spontaneously develop human-like lesions, including coronary lesions	
Mice—wild type	Multiple inbred strains with different susceptibility to atherosclerosis	Development of atherosclerosis requires a cholesterol and cholate containing diet
		Lipoprotein profile is significantly different from humans
Mice—genetically modified	More human-like lipoprotein profile in $Ldlr^{-/-}$ mice except for HDL subclasses	$Apoe^{-/-}$ mice accumulate remnant particles
	Atherosclerosis develops over a relatively short period of time	Lack of complex human-like atherosclerotic lesions
	Ease of breeding to generate transgenic/knockout/knockin or conditional knockout of specific genes on atherogenic background	Seldom observe coronary lesions except in complex models
		Limited ability to sample tissues/cells from vessel wall
		Limitations for noninvasive imaging

hand, dominant females always have fewer lesions than subordinate females (Kaplan et al., 2009).

Primates have the further advantage of their size allowing for the examination of arterial tissues and cells. However, there are several disadvantages to the use of these animals. Recently there has emerged a moral and ethical concern about whether these sentient animals should be used for experiments requiring their sacrifice as the endpoint of the study. The expense of the husbandry is substantial and few laboratories can bear this expense. Their life cycle and thus time line for development of atherosclerosis is long compared to that for other animal models and their susceptibility to genetic modulation is very limited, although modern technologies are beginning to overcome this particular barrier to experimentation (Niu et al., 2014).

2 PORCINE MODELS

A more tractable large animal model that does not pose the moral or ethical problems of the nonhuman primates is the pig, which has both similarities and modest differences from humans. Pigs have a similar cardiac

anatomy and develop atherosclerosis in a distribution similar to that seen in humans, including the coronary arteries. The pig resembles humans in having an apoB dependent lipoprotein profile. However, the pig does not express either cholesteryl ester transfer protein (CETP) or apo(a) and its HDL is homogeneous. Unstable plaques are also not characteristic of the arterial lesion in this species, perhaps related to differences in the thrombotic systems in pigs and humans (Vilahur et al., 2011). In seminal studies, Ross Gerrity (1981) followed the trajectory of monocytes into the atherosclerosis sensitive areas and their conversion to macrophage foam cells in the intima of swine using scanning electron microscopy. The ratio of monocytes to macrophage foam cells in the intima declined as the lesion matured. Atherosclerosis sensitive areas of increased permeability were defined by their ability to take up Evans blue dye.

Initial reports on the genetics of the lipoprotein system of the pig came from the laboratory of Jan Rapacz. First was the report of an apoB epitope change that led to hypercholesterolemia with elevated buoyant LDL and increased atherosclerosis in the coronary, iliac, and femoral arteries (Prescott et al., 1991). A later report concerned the finding of a point mutation in the ligand-binding domain of the LDL receptor (R84C) leading to recessive hypercholesterolemia (Hasler-Rapacz et al., 1998). The advent of recent genetic technologies involving the transplant of mutated somatic nuclei into the zygote have shown the proof of principle for the creation of new strains of Yucatan minipigs with specific genetic alterations. One of these involved the use of the Sleeping Beauty transposition system to create a somatic cell bearing a gain of function mutation in the proprotein convertase subtilisin/Kexin type 9 (PCSK9) gene that leads to reduced surface presentation of the LDL receptor in the liver and consequent reduced clearance of LDL (Al-Mashhadi et al., 2013). With high fat, high cholesterol diet, LDL levels were significantly increased and atherosclerosis formed in coronary arteries, aortic arch, and abdominal aorta in the PCSK9 mutant expressing pig, with lesion histology resembling human lesions. The atherosclerotic plaques in the pigs could be noninvasively imaged, suggesting that this transgenic pig may be useful model for preclinical testing of drugs or devices in an atherogenic environment. A second example is the use of AAV8 to reduce the expression of the LDL receptor in a somatic cell followed by nuclear transplant into zygote. The resultant minipig had elevated LDL levels and consequent atherosclerosis (Davis et al., 2014). Peter Davies has taken advantage of the size of the minipig to isolate endothelial cells from atherosclerosis sensitive aortic regions, including in the coronary artery, and atherosclerosis resistant regions within the same vessel to define the endothelial transcriptome (Civelek et al., 2011). Perhaps not surpris-

ingly, the transcriptomes differ significantly from one another.

3 RABBIT MODELS

As mentioned earlier, the feeding of cholesterol to rabbits, which are very sensitive to dietary cholesterol, has been fairly widely used for atherosclerosis research. Indeed until the description of mice deficient in apoE or the LDL receptor, rabbits, were the most frequently used animal models for atherosclerosis research (Fan et al., 2015). This includes cholesterol fed rabbits, particularly New Zealand White (NZW) rabbits and Japanese White rabbits, and the Watanabe Heritable Hyperlipidemic (WHHL) rabbits that develop atherosclerosis on a chow diet. The rabbit is a medium sized animal that is relatively inexpensive, easily bred, and housed, and shares advantages with larger animals with respect to tissue sampling and analysis of lesions. The WHHL rabbits were described in the early 1980s (Tanzawa et al., 1980). These rabbits have defective LDL receptor function due to a 12 nucleotide deletion (four amino acids) in the region of the gene encoding the cysteine rich ligand binding domain of the LDL receptor (Kita et al., 1982) and thus are defective in clearance of plasma LDL. But the receptor plays no role in the clearance of methylated LDL (Bilheimer et al., 1982). The lipoprotein profile of cholesterol fed NZW rabbits is distinct from that of the WHHL rabbits. The predominant lipoprotein in WHHL rabbit plasma is LDL, while in cholesterol fed rabbits this is β-VLDL. HDL levels are low in the WHHL rabbit. Comparing human and rabbit lipoprotein, there are similarities and differences. In both species, apoB is not edited in the liver, CETP is present in the plasma and HDL is heterogeneous, but the rabbit HDL does not contain apoA-II (Fan et al., 2015). Atherosclerotic lesions in cholesterol fed rabbits are largely foam cell lesions, although advanced lesions with calcification are also present. On the other hand, in the WHHL lesions are more like the complex lesions seen in human arteries. The advanced lesions in the aorta of the WHHL rabbit aged about 1 year have necrotic and lipid cores overlaid with a fibrous cap. While lesions develop in the coronary arteries of cholesterol fed rabbits, their distribution is not the same as in the WHHL rabbits and only in the WHHL rabbits do the coronary artery lesions advance to an obstructed artery resulting in myocardial infarction (Fan et al., 2015). The analysis of the whole genome of NZW, Japanese White, and WHHL rabbits has just been reported along with an analysis of the transcriptome in the liver and aorta of control and cholesterol fed NZW animals (Wang et al., 2016). Despite the differences in lipoproteins discussed earlier, the transcriptome of the aorta of cholesterol fed NZW and WHHL was surprisingly similar. One needs to note a caveat that this may not be found in older

animals with more advanced lesions. In the liver transcriptome, however, many more differentially expressed genes were noted in the cholesterol fed rabbits than in the WHHL rabbits, in keeping with previous reports that cholesterol was deposited in several tissues of the fed animals in contrast to the WHHL rabbits (Buja et al., 1983).

The range of plasma cholesterol levels is much narrower for the WHHL rabbits than for the cholesterol fed NZW rabbits. This makes the former rabbits very valuable for the assessment of therapeutic approaches, particularly for hypercholesterolemia. Additional genetic models have been created. At least 16 transgenic lines have been established affecting apoproteins, and enzymes influencing plasma lipoprotein metabolism, as well as a few genes affecting the vascular wall (Fan et al., 2015). This review points out the potential for creating gene knockouts in rabbits using modern targeting technologies, such as ZFN (zinc finger nucleases), TALEN (Transcription Activator Like Effector Nucleases), and CRISPR/Cas9 (Clustered Regularly Interspaced Palindrome Repeats/CRISPR Associated nucleases).

4 MOUSE MODELS AND ATHEROSCLEROSIS

4.1 Cholesterol and Lipoproteins

Unlike rabbits, rats and mice are relatively resistant to dietary cholesterol induced hypercholesterolemia, probably because of the capacity of their liver to readily convert cholesterol to bile acids, which are excreted into the bile. This process can be attenuated by the feeding of the bile acid cholate or by the administration of thiouracil. Thus, feeding rats a cholate containing cholesterol enriched diet resulted in modest lesions in rats (Wissler et al., 1954). Beverly Paigen used a similar diet in mice. The diet contains 15% fat derived either from milk fat or cocoa butter, 1%–1.25% cholesterol and 0.5% cholic acid or sodium cholate (Ishida et al., 1991; Paigen, 1995) and is often referred to as the Paigen diet. Inbred strains of mice fed the Paigen diet showed considerable variability in their susceptibility to diet induced aortic sinus atherosclerosis, which did not correlate with the plasma lipid responses to the diet. Among the strains studied, C57BL/6 was the most susceptible and this is the strain most widely employed in the experimentation on murine atherosclerosis. Indeed fully backcrossing genetically manipulated mice onto this background to evaluate its role in atherosclerosis is important, except in those instances when evaluating genetic differences across inbred strains is the goal of the study. The mouse has important advantages and disadvantages as a suitable model for atherosclerosis studies. It is small, easily bred and housed, inexpensive and highly susceptible to genetic manipulation. However, it's small size makes it difficult to sample arterial tissue for analysis. Its lipoprotein profile is also distinct from humans. In mice, HDL is their major lipoprotein and it is relatively homogeneous compared to human HDL. The atherosclerosis that develops in mice on the Paigen diet is limited and is confined to the apex of the aortic sinus. To induce robust atherosclerosis in mice, the lipoprotein profile must be substantially altered genetically to one in which there is a predominance of apoB containing lipoproteins. However, mice do not express CETP. But even in these genetically modified mice, atherosclerosis is not identical to that seen in primates. The distribution of the atherosclerotic lesions is different. Lesions are readily induced in the aortic sinuses in mice but not humans. This is probably related to the rapid heart rate in mice and the consequent flow disturbance around the aortic valves. Obstructive coronary lesions are very rarely seen except in certain complex genetic models to be discussed later. Also the lesions are relatively stable, seldom revealing the instability that is seen in advanced human lesions and that accounts for the clinical sequelae, including thrombosis that is so characteristic of human atherosclerotic heart disease.

Preclinical atherosclerosis research was greatly stimulated by the description of mice lacking either apoE or the LDL receptor in the early 1990s (Ishibashi et al., 1993; Plump et al., 1992; Zhang et al., 1992). These two models have been widely employed to gain understanding of the cells and genes/proteins that are important participants in atherogenesis (Hopkins, 2013; Tabas et al., 2015). As useful as are these two models, they nevertheless exhibit important differences especially in their lipoprotein composition and the mechanism by which the absence of the proteins promotes atherosclerosis. We have recently reviewed these differences (Getz and Reardon, 2016). Many cell types produce apoE and its absence impacts several metabolic processes. In lipoprotein metabolism, apoE is an important ligand for the uptake of lipoproteins by cell surface receptors on hepatocytes. Intestinally derived chylomicrons acquire apoE in the plasma, primarily from HDL. During the lipolysis of the triglycerides in chylomicrons in the circulation, chylomicron remnants are formed. Their clearance is mediated by apoE binding to three hepatic receptors; the LDL receptor, the LDL receptor related protein (LRP1), and heparan sulfate proteoglycans. The three receptors have some modest measure of functional redundancy. Hence, $Apoe^{-/-}$ mice are hyperlipidemic, whether on chow or high fat diets, primarily due to the accumulation of cholesteryl ester rich apoB48-containing chylomicron remnants. On the other hand, $Ldlr^{-/-}$ mice have profoundly elevated LDL levels with apoB100 as its major apoprotein that is increased on high fat diet fed animals along with an increase of triglyceride-rich VLDL.

$Apoe^{-/-}$ mice develop extensive atherosclerotic lesions even when fed chow, though of course lesion development and maturation are accelerated with the feeding of a high fat, high cholesterol Western type diet (in the absence of cholate). The more advanced lesions resemble human lesions. On the other hand, very little lesion development occurs in $Ldlr^{-/-}$ mice fed standard chow. A high cholesterol diet is required, with or without high fat, to elicit significant lesions. With added dietary fat $Ldlr^{-/-}$ mice are insulin resistant. Mice are unusual in that the apoB100 mRNA is edited in the liver to produce hepatic apoB48, which is produced only in the intestine in other species. The global removal of this activity, coupled with LDL receptor deficiency results in another model ($Ldlr^{-/-}Apobec^{-/-}$) that develops atherosclerosis while being fed a standard chow diet (Powell-Braxton et al., 1998).

It is very difficult to assess the comparability of atherogenesis in these two models because of the differences in their lipoprotein classes, size, and lipid and protein composition. In order to assess the relative atherogenicity of these particles, Stephen Young and coworkers created animals that express only apoB100 in both the $Apoe^{-/-}$ and the $Ldlr^{-/-}$ backgrounds (Veniant et al., 2008). Fortuitously, female animals of each of these genotypes had very similar total plasma cholesterol levels. In the apoE deficient background the cholesterol was carried in a smaller number of cholesterol rich large particles, while in the LDL receptor deficient background, the cholesterol was transported in a larger number of smaller particles, each of which carries a lower load of sterol. When fed a standard chow diet the $Ldlr^{-/-}apoB^{100/100}$ animals had more atherosclerosis. Increased permeability of these smaller lipoproteins across the vascular endothelium may be the mechanism.

4.2 Endothelial Cells

The major cell types that have been implicated in the atherogenic process are endothelial cells, monocyte/ macrophages and their subsets, and a variety of lymphocytes. The endothelial cells represent the cellular barrier to the influx of macromolecules and cells into the subendothelial space in the arterial wall. Endothelial cells are activated by hyperlipidemia and exhibit distinct gene expression profiles depending upon their flow exposure patterns. As pointed out earlier, atherogenesis localizes to sites of blood flow disturbance in the macrovascular arteries. The atherosclerosis resistant areas express important flow dependent genes, such as endothelial nitric oxide synthase (eNOS) with the production of high levels of nitric oxide and flow dependent activation of the transcription factors KLF4 and KLF2 that integrate antiinflammatory and antithrombotic gene expression in the endothelium at these sites. Thus the knockout of

these molecules in atherogenic mouse models results in an increment in atherosclerosis (Tabas et al., 2015). The atherosclerosis sensitive areas are distinct from their atherosclerosis resistant counterparts in that they express adhesion molecules that participate in the temporary sequestration of the cells in the blood, for example, monocytes on the surface of the endothelial cells. Such molecules include vascular cell adhesion molecule (VCAM) and platelet endothelial cell adhesion molecule (PECAM), although the role of this latter molecule in atherosclerosis is complex (Getz and Reardon, 2016).

4.3 The Monocyte/Macrophage

The macrophage is the core cell of the atherosclerotic plaque. Crossing of $Apoe^{-/-}$ mice with the $Mcsf1^{-/-}$ mice reinforced this. M-CSF1 (op) is the prime growth factor for monocytes and macrophages and the double knockout mice have a lower blood monocyte level and significantly lower atherosclerosis, especially in female mice, despite markedly elevated plasma cholesterol levels (Smith et al., 1995). Bone marrow transplantation has been employed to elucidate the contribution of bone marrow derived cells, especially monocyte/ macrophages, to atherogenesis. Transplantation of wild type bone marrow (expressing apoE) into apoE deficient hosts repairs the hyperlipidemia and atherosclerosis phenotype of $Apoe^{-/-}$ mice (Boisvert et al., 1995; Linton et al., 1995). Macrophage derived apoE is not unique in its ability to reduce the atherosclerosis phenotype. This is accomplished with transgenic expression of apoE at low levels in the adrenals, even with little effect on the hyperlipidemia (Thorngate et al., 2000). However, comparable plasma levels of apoE derived from adipose tissue is ineffective in repairing either the hyperlipidemia or the atherosclerosis (Huang et al., 2013). In contrast to the results with apoE expressing bone marrow, the transplantation of wild type bone marrow (expressing the LDL receptor) into $Ldlr^{-/-}$ recipients has virtually no effect on the atherosclerosis or the hyperlipidemia (Herijgers et al., 1997).

The adherent cells are attracted into the underlying intima by chemotactic gradients, the most important of which is that between CCL2 (MCP-1) and CCR2, a receptor highly expressed on major subsets of monocytes, notably the Ly6c^{hi} or inflammatory monocytes, which are the major monocyte subset involved in atherogenesis. The monocytes sequestered in the intima differentiate into macrophages, which participates in both the oxidative modification of the retained lipoproteins and their uptake by the scavenger receptors of the cells, forming foam cells. The loading of macrophages with cholesterol results in a variety of responses. These include the activation of cells to produce a variety of cytokines and chemokines that regulate the activation of endothelial cells and smooth muscle cells in the vessel wall. The chemokines

include CCL2 that attracts further monocytes from the blood, growth factors that promote the proliferation of macrophages, and others that stimulate the migration of smooth muscle cells into the intima. With the loading with cholesterol, some of this sterol may crystallize, and these crystals have been shown to activate the inflammasomes, which promotes the activation of caspase 1 and the production of IL-1β (Duewell et al., 2010).

Cholesterol loading results in changes in the expression of a network of proteins designated in the macrophage cholesterol responsive network (Becker et al., 2010). This network was identified by mass spectrometry using peritoneal macrophages from $Ldlr^{-/-}$ mice fed a Western type diet or standard chow. The proteins in this network belonged to several functional groups, including immune function, proteases, and complement proteins. The nuclear receptor liver X receptor (LXR) is also activated in cholesterol-loaded cells. Among the LXR stimulated proteins are several involved in reverse cholesterol transport, for example, ABCA1 and ABCG1, which may contribute to the limitation of cholesterol overload. It is evident that the cholesterol homeostasis in macrophages is complex, in which feedback mechanisms play an important regulatory role. One aspect of this regulation is the balance between incoming total cholesterol and the extent of its reesterification. Some free cholesterol is transported to the plasma membrane of the cell, where it can promote lipid raft formation, a microdomain important for signal transduction. Enrichment of the endoplasmic reticulum with free cholesterol in cholesterol-loaded macrophages can activate the unfolded protein response and subsequent apoptosis (Tabas et al., 2015). In the early stages of atherosclerosis, the apoptotic cells are removed by the efferocytotic activity of neighboring macrophages. The phagocytosed apoptotic cells contribute to the cholesterol load of the phagocytosing macrophage, so setting in motion a complex feed forward mechanism. If and when efferocytosis is no longer effective, for example, when Mertk, the apoptotic receptor on the cell surface of the efferocyte, is cleaved by the macrophage secreted proteases, the apoptotic cells may undergo secondary necrosis, forming the necrotic core of the more advanced plaques.

The enrichment of lipid rafts results in the concentration within these membrane microdomains of many enzymes and signaling molecules, including growth factor receptors and Toll Like Receptors (TLR), especially TLR2 and 4. The latter can serve as a receptor for minimally modified LDL, that is, LDL with modest extents of oxidative modification. The polyunsaturated fatty acids in minimally modified LDL are oxidized by the macrophage lipoxygenase. It's binding to TLR4 signals to the cell to produce inflammatory cytokines and to refashion the actin cytoskeleton, resulting in the macropinocytosis of the LDL products in the microenvironment (Miller et al., 2011). TLR4 signaling may also stimulate the production of reactive oxygen species. Growth factor receptor enrichment facilitates the proliferation of macrophages within the plaque.

Recent work has highlighted the importance of monocytosis and neutrophilia as positive risk factors for the development of atherosclerotic heart disease (Tall and Yvan-Charvet, 2015). One of the major influences on the production of these white blood cells is cholesterol homeostasis in their progenitor cells. The enrichment of cholesterol in these progenitor cells leads to increased expression of the common β subunit of IL-3/GM-CSF receptor and increased levels of these growth factor receptors and M-CSF receptor in lipid rafts. This results in the proliferation of the hematopoietic stem progenitor cells (HSPC) in response to IL-3, GM-CSF, and M-CSF giving rise to GMP and CMP cells, precursors of monocytes and granulocytes, respectively (Murphy et al., 2014). Monocytosis is more profound in $Apoe^{-/-}$ mice than in $Ldlr^{-/-}$ mice, probably due to apoE functioning in a cell autonomous fashion to promote cholesterol efflux in the HSPCs by its binding to cell surface heparan sulfate proteoglycans (Murphy et al., 2011). In this location, apoE serves as an acceptor for the efflux cholesterol.

4.4 Smooth Muscle Cells

As atherosclerotic plaques progress, smooth muscle cells migrate from the media into the intima, where they are responsible for the production of matrix proteins and the formation of the fibrous cap that provides a barrier against the activation of platelet by interaction with matrix proteins. One of the disadvantages of the $Apoe^{-/-}$ and $Ldlr^{-/-}$ models of atherosclerosis is that it is rare to observe unstable lesions with accompanying thrombosis as a result of the disruption of the fibrous cap that is seen in humans and several larger animal models. The basis for the lesion stability is not clear. These are the general views of the role of smooth muscle cells in atherogenesis. However, recent work with $Apoe^{-/-}$ animals has cast some ambiguity about this description (Tabas et al., 2015). This is because of the apparent ability of both smooth muscle cells and possibly macrophages to undergo phenotypic switching, so that the origin of the foam cells and smooth muscle like cells in the intima is uncertain. Thus smooth muscle cells that migrate into the intima may lose some of their characteristic markers and acquire macrophage markers and may become lipid-loaded. In addition, some apparent smooth muscle cells seem to be derived from the bone marrow. The ambiguity of these identifications awaits more definitive work.

4.5 Lymphocytes

The earlier discussion relates to the participation of the innate immune system in atherogenesis. The striking

increased incidence of cardiovascular diseases in patients with autoimmune diseases, such as systemic lupus erythematosus and rheumatoid arthritis suggests a strong involvement of the adaptive immune system as well (Witztum and Lichtman, 2014). The adaptive immune system is composed of a variety of T cell and B cell subsets. Some T cell subsets are found in atherosclerotic plaques. Th1 cells are proinflammatory, produce IFNγ and may provide help for antibody production. The inflammatory contribution of Th2 and Th17 cells is less clear. The action of the proinflammatory cells is countered by the antiinflammatory regulatory T cells (Tregs), which produce IL-10 and/or TGFβ. There is an extensive literature on the complex participation of T and B cells in atherogenesis, which we cannot detail here (Witztum and Lichtman, 2014). The atherosclerotic effect of the elimination of these adaptive immune cells depends upon the balance between the proinflammatory cells and their antiinflammatory counterparts, so that the outcome may not be predictable and straightforward. Both $Apoe^{-/-}$ mice and $Ldlr^{-/-}$ mice have been crossed with $Rag^{-/-}$ (recombination activating gene) mice that lack T and B cells. Both $Apoe^{-/-}Rag^{-/-}$ and $Ldlr^{-/-}Rag^{-/-}$ mice have reduced plasma cholesterol and reduced aortic root atherosclerosis but not innominate artery atherosclerosis (Reardon et al., 2001, 2003). The latter findings suggest that the balance between pro- and antiinflammatory immune cells may differ in different arterial beds. The specific removal of FOXP3+ Tregs in the $Ldlr^{-/-}$ background (Getz and Reardon, 2014; Klingenberg et al., 2013) leads to an increment in plasma cholesterol, mainly in the VLDL fraction, and also an increase in aortic sinus atherosclerosis. A model of autoimmune disease is seen in $Ldlr^{-/-} Apoa1^{-/-}$ mice that manifests as skin inflammation, lymphadenopathy, and a relative depletion of Tregs (Wilhelm et al., 2010; Zabalawi et al., 2007). This may contribute to the enhanced atherosclerosis observed in these mice.

A minor subset of T cells are natural killer T (NKT) cells, which bridge the innate and adaptive immune system, but are relevant because of they respond to lipid antigens. There are two classes of NKT cells. The major subset has relatively invariant T cell receptors, which in mice are Vα14Jα18 and a restricted set of β-chains. These are designated invariant NKT cells (iNKT). A second less frequent subset have a more diverse set of T cell receptor chains. The iNKT cells recognize glycosyl sphingolipid antigens presented by CD1d, a MHC class 1-like molecules, that is expressed on dendritic dells and macrophages and even on epithelial cells. The activating antigen may be endogenous or be derived from microorganisms, including those in the gut microbiome, though the precise nature of the endogenous antigen is not clear. These cells are readily activated without the necessity for prior education. Upon activation, they secrete IL-4 and IFNγ.

The liver and adipose tissue are enriched in iNKT cells. In the liver, iNKT cells make up as much as 40%–50% of the total T cells under "normal" conditions but the level of iNKT may vary quite widely depending upon the physiological circumstances. The adoptive transfer of splenocytes from Vα14 transgenic mice that are enriched in iNKT cells into immune deficient recipients ($Ldlr^{-/-}Rag^{-/-}$ mice) shows these cells to be proatherogenic (VanderLaan et al., 2007). This observation is consistent with findings using CD1d or Jα18 deficient mice crossed with either $Ldlr^{-/-}$ or $Apoe^{-/-}$ mice (Getz et al., 2011). Vα14tg/$Ldlr^{-/-}$ mice fed a high fat, high sucrose, cholesterol containing diet develop increased obesity, and atherosclerosis (Subramanian et al., 2013). A recent study indicates that the atherogenic activity of NKT cells is dependent on the cytotoxicity of the perforin and granzyme B secreted by the NKT cells (Li et al., 2015). IL-4 and IFNγ are not required for this effect. The perforin/granzyme B induces apoptosis in the lesional cells resulting in increased secondary necrosis in the lesion.

Like T cells, there are multiple subclasses of B cells. B2 cells are conventional antibody producing B cells that are probably proatherogenic, though their role is not without controversy (Tsiantoulas et al., 2014). Perhaps their precise activity depends on whether they are marginal zone or follicular B2 cell subsets. B1a cells produce germ line encoded natural antibodies of the IgM subtype and are found in the peritoneal cavity and spleen. A major set of B1a cells recognizes phosphocholine of bacterial cell wall and the phosphocholine head group of oxidized phosphatidylcholine. This antibody, designated T15/EO6, is found at high levels in $Apoe^{-/-}$ mice. These natural antibodies are thought to be atheroprotective, as exemplified by the increased atherosclerosis in $Ldlr^{-/-}$ mice that have cell surface IgM that is not secreted (i.e. soluble IgM deficient)(Lewis et al., 2009). It is noteworthy that these mice have an otherwise intact immune system. This may be relevant since the adoptive transfer of B1 cells producing "normal " levels of IgM to immune deficient $Ldlr^{-/-} Rag^{-/-}$ mice has no effect on atherosclerosis (Reardon CA, unpublished). Another minor subset of B cells is the B regulatory cells whose impact on atherosclerosis is unexplored.

4.6 Murine Models of Atherosclerosis Based on Expression of ApoE Variants

There are three common allelic variants of human apoE with the three protein isoforms designated as apoE2, apoE3, and apoE4. The isoforms differ by the amino acids at residues 112 and 158. Cysteine is present in both these positions in apoE2, while arginine occupies both positions in apoE4. ApoE3, the most frequent, "normal" isoform, has cysteine at position at 112 and arginine at 158. These amino acid variations result

in different protein conformations, which contributes to their functional differences. This has been reviewed by Mahley et al. (2009). In humans, some individuals homozygous for *APOE2* exhibit type III hyperlipoproteinemia and atherosclerosis, as well as xanthomatosis. This phenotype is thought to be attributable to the poor interaction of apoE2 with the LDL receptor and the consequent accumulation of VLDL remnants in the plasma. The reason why all *APOE2* homozygotes do not manifest this phenotype is not clear and is thought to require some additional genetic or environmental factor or factors. In human plasma, apoE3 preferentially associates with HDL, while apoE4 preferentially associates with VLDL. The differential lipoprotein association is primarily due to the interaction between residues 255 (glutamic acid) and 61(arginine) in apoE4, an interaction that is permitted by the presence of arginine at position 112. ApoE4 has a higher affinity for the LDL receptor than does apoE3. As a result, cholesterol-rich lipoproteins are more readily taken up by hepatocytes leading to the downregulation of the synthesis of the LDL receptor. Thus *APOE4* homozygotes tends to be hypercholesterolemic and more susceptible to atherosclerosis than *APOE3* homozygotes. In order to further explore the function of the isoforms, Maeda and coworkers created isoform replacement mice (Pendse et al., 2009), that is, mice expressing each of the human apoE isoforms in place of endogenous murine apoE. The *APOE2* replacement mice manifest a phenotype very similar to that seen in human subjects with type III hyperlipoproteinemia, including increased atherosclerosis. The *APOE4* replacement mice have a complex phenotype that also manifests an increased tendency to develop atherosclerosis. Thus, these replacement mice offer further opportunities for the exploration of the functions of the isoforms in a tractable experimental context.

Mouse apoE has an amino acid sequence similar to human apoE4 with respect to the amino acid at positions 112 and 158, but unlike the latter it has threonine at position 61 rather than arginine. Weisgraber and Raffai attempted to humanize mouse apoE by converting Thr61 to Arg61 (Raffai et al., 2001). In the course of this mutation they inserted a neomycin gene between two loxP sites in intron 3 of the apoE gene. This construct resulted in low expression of apoE (2%–5% of normal levels), so the resultant mice were designated "hypomorphic." Hypomorphic apoE mice fed chow exhibited a normal lipoprotein profile, but they were particularly sensitive to diet induced (containing cholate) hyperlipidemia and atherosclerosis (Raffai and Weisgraber, 2002). When the neomycin gene was excised by inducing Cre-mediated recombination, the mice had normal lipoproteins even on the atherogenic diet. *Apoe*$^{-/-}$ mice and hypomorphic apoE mice were crossed with *Ldlr*$^{-/-}$ mice. The resulting strains of mice were equally hypercholesterolemic on

chow diet and developed atherosclerosis, but the small amount of apoE in the hypomorphic cross was sufficient to reduce atherosclerosis (Gaudreault et al., 2012).

An additional atherogenic model based on a variant of apoE is the APOE*3 Leiden transgenic mouse (Lutgens et al., 1999; van Vlijmen et al., 1994). ApoE*3 Leiden has low affinity for the LDL receptor. The mice are less hyperlipidemic than *Apoe*$^{-/-}$ mice but develop atherosclerosis when fed an atherogenic diet.

4.7 Gene Identification by Strain Crosses

As mentioned earlier in this chapter, inbred strains of mice vary greatly in their susceptibility to develop atherosclerosis. In attempts to identify genes that might regulate atherosclerosis, *Apoe*$^{-/-}$ or *Ldlr*$^{-/-}$ mice in a sensitive genetic background (e.g., C57BL/6) have been crossed with *Apoe*$^{-/-}$ or *Ldlr*$^{-/-}$ mice in a resistant background (e.g., FVB). Several quantitative trait loci (QTL) were found from such crosses (Stylianou et al., 2012). However, after many studies, a single risk gene has been positively identified, *Raetle*, a major histocompatibility gene (Rodriguez et al., 2013). Given the advance in recent genetic technologies, it is not clear that this is the most cost effective approach. That said, a few crosses have been informative. Comparing C57BL/6 *Apoe*$^{-/-}$ with 129 *Apoe*$^{-/-}$ *mice*, aortic root lesions develop much more rapidly in the C57BL/6 strain, while aortic arch lesions develop more quickly in the 129 *Apoe*$^{-/-}$ strain. An intercross between these two strains identified a QTL that is associated with the increased aortic arch lesions that is also associated with the angle of the aortic arch bend in the 129 strain, likely producing different hemodynamic profiles at this aortic site in the two strains (Maeda et al., 2007; Tomita et al., 2010). An intercross of DBA *Apoe*$^{-/-}$ and 129 *Apoe*$^{-/-}$ revealed different QTLs for aortic root and aortic arch lesion development (Kayashima et al., 2014, 2015).

4.8 Experimental Myocardial Infarction in Mice

The most clinically important outcome of unstable atherosclerosis is coronary artery thrombosis and myocardial infarction. The most straightforward method to experimentally induce myocardial infarction is by the ligation of the left coronary artery, which is easily accomplished in the mouse because of its distinct coronary anatomy (Kumar et al., 2005). Myocardial infarction has been studied in *Apoe*$^{-/-}$ mice, in which it was shown that the healing of the infarct takes place in two stages. The first stage involves the influx of inflammatory monocytes (Ly6c^{hi}), followed by a predominance of healing monocytes (Ly6c^{lo}) at the infarct site. However, this switch may not be by influx of Ly6c^{lo} monocytes, but rather by the conversion of Ly6c^{hi}cells to Ly6c^{lo} cells in

situ (Dutta and Nahrendorf, 2015). The use of $Apoe^{-/-}$ mice for these experiments enabled the investigators to assess the effect of myocardial infarction on ongoing atherosclerosis. They showed that the cardiac injury indeed increased atherosclerosis, perhaps by the promotion of monocytosis, a known risk factor for atherosclerosis (Dutta et al., 2012). The increment in blood monocytes probably derives from the bone marrow under the influence of the stimulation of the sympathetic nervous system signaling (Dutta et al., 2012) and also the spleen, where extramedullary hematopoiesis is promoted (Robbins et al., 2012; Swirski et al., 2009). It is noteworthy that unlike the monocytosis induced by cholesterol loading of hematopoietic stem cells in the bone marrow (see earlier) when there was an accompanying neutrophilia, the response to myocardial infarction only involved the monocytes.

One of the striking features of the two models of murine atherosclerosis ($Apoe^{-/-}$ and $Ldlr^{-/-}$) is that they do not develop significant lesions in the main coronary arteries. However, more complex genetic models based on these two backgrounds do in fact develop these lesions (Table 8.2). This was first seen dramatically in mice deficient in both apoE and the B type scavenger receptor, SR-BI (Braun et al., 2002). These double knockout mice, even when fed standard chow, survived only to about 8 weeks of age. They had occlusive coronary artery lesions, evidence of platelet activity, myocardial fibrosis, and left ventricular cardiac dysfunction. SR-BI promotes the selective uptake of cholesteryl ester from HDL. It is widely expressed including on HSPC and this expression is required for the regulation of monocytosis and leukocytosis by apoA-I and HDL (Gao et al., 2014). The biogenesis of platelets is influenced by hypercholesterolemia, in part by promoting the conversion of megakaryocyte progenitors to mature platelets and by activating platelets (Wang and Tall, 2016). The ABC transporter ABCG4 is involved in the regulation of platelet production. In its absence, cholesterol accumulates in the

platelet and the thrombopoietin receptor is more highly expressed on the surface of megakaryocytes (Murphy et al., 2013). Elevated HDL reduces platelet biogenesis by promoting cholesterol efflux via ABCG4. SR-BI mediates the increase in eNOS activity in endothelial cells induced by HDL. SR-BI deficiency also leads to a change in the ratio of free to ester cholesterol in HDL and may not be as efficient in promoting cholesterol efflux. It is not possible to be certain which of the actions of SR-BI is most important in determining the phenotype seen in the $Apoe^{-/-}Srb1^{-/-}$ double knockout mice.

Variations on the SR-BI double knockout approach have also been associated with coronary artery occlusion and myocardial infarction. The binding of HDL to SR-BI initiates the activation of the downstream signaling: the adaptor protein PDZK1 (PDZ domain containing protein), Akt1 (Protein kinase B serine threonine kinase), and eNOS are activated. In fact when any of these proteins is eliminated in association with apoE deficiency, a very similar cardiac phenotype is observed as in the $Apoe^{-/-}Srb1^{-/-}$ mice, but only when an atherogenic diet is fed (Trigatti and Fuller, 2015). SR-BI deficiency has also been coupled with the hypomorphic apoE model. Such double mutant mice are normal when fed chow, but develop the coronary artery and cardiac phenotype when fed an atherogenic diet containing cholate (Zhang et al., 2005). In this model, transplantation of bone marrow expressing SR-BI rescues the coronary artery atherosclerosis, fibrosis, and cardiomegaly but not the lipoprotein dyslipidemia, underlying the importance of the receptor on some of the bone marrow derived cells (Pei et al., 2013). $Srb1^{-/-}Ldlr^{-/-}$ mice also develop occlusive coronary artery atherosclerosis and myocardial infarction (Fuller et al., 2014). This model is sensitive to the diet composition, being most obvious with diets enriched in cholesterol. The frequency of platelet markers in the occluding lesion was highest in mice fed the Paigen diet that contains cholate. There is little correlation between the atherosclerotic lesions in the coronary arteries and the aortic root.

$Apoe^{-/-}$ $Ldlr^{-/-}$ mice also exhibit coronary artery atherosclerosis and myocardial infarct when fed a Western type diet (Caligiuri et al., 1999). The overexpression of urokinase in macrophages on an $Apoe^{-/-}$ background leads to coronary artery lesions and myocardial infarction (Cozen et al., 2004). Thus, it is possible to generate murine models of coronary artery atherosclerosis and its consequent myocardial infarction by a variety of complex pathways based on either the $Apoe^{-/-}$ or the $Ldlr^{-/-}$ models. Both the ligation approach and genetic approach to coronary artery atherosclerosis and myocardial infarction provide models for preclinical testing of various therapies, though the latter has the virtue of working in the context of ongoing atherosclerosis which both contributes to and results from the therapeutic strategy.

TABLE 8.2   Mouse Models that Develop Coronary Artery Atherosclerosis and Myocardial Infarct

Genetic mouse model	Comments
$Apoe^{-/-}Srb1^{-/-}$	Survive only until 8 weeks of age
$Apoe^{-/-}Pdzk1^{-/-}$	Requires atherogenic diet
$Apoe^{-/-}Akt1^{-/-}$	Requires atherogenic diet
$Apoe^{-/-}Enos^{-/-}$	Requires atherogenic diet
$Ldlr^{-/-}Srb1^{-/-}$	Requires diets enriched in cholesterol
$Apoe^{-/-}Ldlr^{-/-}$	Requires atherogenic diet
Hypomorphic apoE, $Srb1^{-/-}$	Requires atherogenic diet with cholate

5 CONCLUDING COMMENTS

In this chapter, we have described a variety of large and small animal models that are used for the study of atherosclerosis. Each of these models has its unique advantages and limitations, not the least of which relates to husbandry issues. None of them fully duplicates the human condition and no doubt investigators appreciate this. The development of the new genetic technologies briefly referred to in this narrative will in the near future greatly expand our capacities to fashion new models based on what has been learned from analyses of disease related variations in the human genome of patients with cardiovascular disease. The limitations notwithstanding, the mouse models in particular have been of great value in uncovering potential mechanisms of atherogenesis, a very complex inflammatory disease that changes substantially over time. In the earlier narrative, we have tended to emphasize aspects of the cell biology of atherogenesis rather than the detailed biochemical interactions between cells and lipoproteins and their respective cross talk. Details of the latter can be found in excellent reviews (Hopkins, 2013; Tabas et al., 2015).

References

Al-Mashhadi, R.H., Sorensen, C.B., Kragh, P.M., Christoffersen, C., Mortensen, M.B., Tolbod, L.P., et al., 2013. Familial hypercholesterolemia and atherosclerosis in cloned minipigs created by DNA transposition of a human PCSK9 gain-of-function mutant. Sci. Transl. Med. 5 (166), 166ra161.

Becker, L., Gharib, S.A., Irwin, A.D., Wijsman, E., Vaisar, T., Oram, J.F., Heinecke, J.W., 2010. A macrophage sterol-responsive network linked to atherogenesis. Cell Metabol. 11 (2), 125–135.

Bilheimer, D.W., Watanabe, Y., Kita, T., 1982. Impaired receptor-mediated catabolism of low density lipoprotein in the WHHL rabbit, an animal model of familial hypercholesterolemia. Proc. Natl. Acad. Sci. USA 79 (10), 3305–3309.

Boisvert, W.A., Spangenberg, J., Curtiss, L.K., 1995. Treatment of severe hypercholesterolemia in apolipoprotein E-deficient mice by bone marrow transplantation. J. Clin. Invest. 96 (2), 1118–1124.

Braun, A., Trigatti, B.L., Post, M.J., Sato, K., Simons, M., Edelberg, J.M., et al., 2002. Loss of SR-BI expression leads to the early onset of occlusive atherosclerotic coronary artery disease, spontaneous myocardial infarctions, severe cardiac dysfunction, and premature death in apolipoprotein E-deficient mice. Circ. Res. 90 (3), 270–276.

Buja, L.M., Kita, T., Goldstein, J.L., Watanabe, Y., Brown, M.S., 1983. Cellular pathology of progressive atherosclerosis in the WHHL rabbit. An animal model of familial hypercholesterolemia. Arteriosclerosis 3 (1), 87–101.

Caligiuri, G., Levy, B., Pernow, J., Thoren, P., Hansson, G.K., 1999. Myocardial infarction mediated by endothelin receptor signaling in hypercholesterolemic mice. Proc. Natl. Acad. Sci. USA 96 (12), 6920–6924.

Civelek, M., Manduchi, E., Riley, R.J., Stoeckert, Jr., C.J., Davies, P.F., 2011. Coronary artery endothelial transcriptome in vivo: identification of endoplasmic reticulum stress and enhanced reactive oxygen species by gene connectivity network analysis. Circ. Cardiovasc. Genet. 4 (3), 243–252.

Cozen, A.E., Moriwaki, H., Kremen, M., DeYoung, M.B., Dichek, H.L., Slezicki, K.I., et al., 2004. Macrophage-targeted overexpression of urokinase causes accelerated atherosclerosis, coronary artery occlusions, and premature death. Circulation 109 (17), 2129–2135.

Davis, B.T., Wang, X.J., Rohret, J.A., Struzynski, J.T., Merricks, E.P., Bellinger, D.A., et al., 2014. Targeted disruption of LDLR causes hypercholesterolemia and atherosclerosis in Yucatan miniature pigs. PloS One 9 (4), e93457.

Duewell, P., Kono, H., Rayner, K.J., Sirois, C.M., Vladimer, G., Bauernfeind, F.G., et al., 2010. NLRP3 inflammasomes are required for atherogenesis and activated by cholesterol crystals. Nature 464 (7293), 1357–1361.

Dutta, P., Nahrendorf, M., 2015. Monocytes in myocardial infarction. Arterioscler. Thromb. Vasc. Biol. 35 (5), 1066–1070.

Dutta, P., Courties, G., Wei, Y., Leuschner, F., Gorbatov, R., Robbins, C.S., et al., 2012. Myocardial infarction accelerates atherosclerosis. Nature 487 (7407), 325–329.

Fan, J., Kitajima, S., Watanabe, T., Xu, J., Zhang, J., Liu, E., Chen, Y.E., 2015. Rabbit models for the study of human atherosclerosis: from pathophysiological mechanisms to translational medicine. Pharmacol Ther. 146, 104–119.

Fuller, M., Dadoo, O., Serkis, V., Abutouk, D., MacDonald, M., Dhingani, N., et al., 2014. The effects of diet on occlusive coronary artery atherosclerosis and myocardial infarction in scavenger receptor class B, type 1/low-density lipoprotein receptor double knockout mice. Arterioscler. Thromb. Vasc. Biol. 34 (11), 2394–2403.

Gao, M., Zhao, D., Schouteden, S., Sorci-Thomas, M.G., Van Veldhoven, P.P., Eggermont, K., et al., 2014. Regulation of high-density lipoprotein on hematopoietic stem/progenitor cells in atherosclerosis requires scavenger receptor type BI expression. Arterioscler. Thromb. Vasc. Biol. 34 (9), 1900–1909.

Gaudreault, N., Kumar, N., Posada, J.M., Stephens, K.B., Reyes de Mochel, N.S., Eberle, D., et al., 2012. ApoE suppresses atherosclerosis by reducing lipid accumulation in circulating monocytes and the expression of inflammatory molecules on monocytes and vascular endothelium. Arterioscler. Thromb. Vasc. Biol. 32 (2), 264–272.

Gerrity, R.G., 1981. The role of the monocyte in atherogenesis: I. Transition of blood-borne monocytes into foam cells in fatty lesions. Am. J. Pathol. 103 (2), 181–190.

Getz, G.S., Reardon, C.A., 2012. Animal models of atherosclerosis. Arterioscler. Thromb. Vasc. Biol. 32 (5), 1104–1115.

Getz, G.S., Reardon, C.A., 2014. The mutual interplay of lipid metabolism and the cells of the immune system in relation to atherosclerosis. Clin. Lipidol. 9 (6), 657–671.

Getz, G.S., Reardon, C.A., 2016. Do the Apoe$^{-/-}$ and Ldlr$^{-/-}$ mice yield the same insight on atherogenesis? Arterioscler. Thromb. Vasc. Biol. 36 (9), 1734–1741.

Getz, G.S., Vanderlaan, P.A., Reardon, C.A., 2011. Natural killer T cells in lipoprotein metabolism and atherosclerosis. Thromb. Haemost. 106 (5), 814–819.

Hasler-Rapacz, J., Ellegren, H., Fridolfsson, A.K., Kirkpatrick, B., Kirk, S., Andersson, L., Rapacz, J., 1998. Identification of a mutation in the low density lipoprotein receptor gene associated with recessive familial hypercholesterolemia in swine. Am. J. Med. Genet. 76 (5), 379–386.

Herijgers, N., Van Eck, M., Groot, P.H., Hoogerbrugge, P.M., Van Berkel, T.J., 1997. Effect of bone marrow transplantation on lipoprotein metabolism and atherosclerosis in LDL receptor-knockout mice. Arterioscler. Thromb. Vasc. Biol. 17 (10), 1995–2003.

Hopkins, P.N., 2013. Molecular biology of atherosclerosis. Physiol. Rev. 93 (3), 1317–1542.

Huang, Z.H., Reardon, C.A., Subbaiah, P.V., Getz, G.S., Mazzone, T., 2013. ApoE derived from adipose tissue does not suppress atherosclerosis or correct hyperlipidemia in apoE knockout mice. J. Lipid Res. 54 (1), 202–213.

Ishibashi, S., Brown, M.S., Goldstein, J.L., Gerard, R.D., Hammer, R.E., Herz, J., 1993. Hypercholesterolemia in low density lipoprotein receptor knockout mice and its reversal by adenovirus-mediated gene delivery. J. Clin. Invest. 92 (2), 883–893.

Ishida, B.Y., Blanche, P.J., Nichols, A.V., Yashar, M., Paigen, B., 1991. Effects of atherogenic diet consumption on lipoproteins in mouse strains C57BL/6 and C3H. J. Lipid Res. 32 (4), 559–568.

Kaplan, J.R., Chen, H., Manuck, S.B., 2009. The relationship between social status and atherosclerosis in male and female monkeys as revealed by meta-analysis. Am. J. Primatol. 71 (9), 732–741.

Kayashima, Y., Tomita, H., Zhilicheva, S., Kim, S., Kim, H.S., Bennett, B.J., Maeda, N., 2014. Quantitative trait loci affecting atherosclerosis at the aortic root identified in an intercross between DBA2J and 129S6 apolipoprotein E-null mice. PloS One 9 (2), e88274.

Kayashima, Y., Makhanova, N.A., Matsuki, K., Tomita, H., Bennett, B.J., Maeda, N., 2015. Identification of aortic arch-specific quantitative trait loci for atherosclerosis by an intercross of DBA/2J and 129S6 apolipoprotein E-deficient mice. PloS One 10 (2), e0117478.

Kita, T., Brown, M.S., Bilheimer, D.W., Goldstein, J.L., 1982. Delayed clearance of very low density and intermediate density lipoproteins with enhanced conversion to low density lipoprotein in WHHL rabbits. Proc. Natl. Acad. Sci. USA 79 (18), 5693–5697.

Klingenberg, R., Gerdes, N., Badeau, R.M., Gistera, A., Strodthoff, D., Ketelhuth, D.F., et al., 2013. Depletion of FOXP3+ regulatory T cells promotes hypercholesterolemia and atherosclerosis. J. Clin. Invest. 123 (3), 1323–1334.

Kumar, D., Hacker, T.A., Buck, J., Whitesell, L.F., Kaji, E.H., Douglas, P.S., Kamp, T.J., 2005. Distinct mouse coronary anatomy and myocardial infarction consequent to ligation. Coron. Artery Dis. 16 (1), 41–44.

Lewis, M.J., Malik, T.H., Ehrenstein, M.R., Boyle, J.J., Botto, M., Haskard, D.O., 2009. Immunoglobulin M is required for protection against atherosclerosis in low-density lipoprotein receptor-deficient mice. Circulation 120 (5), 417–426.

Li, Y., To, K., Kanellakis, P., Hosseini, H., Deswaerte, V., Tipping, P., et al., 2015. CD4+ natural killer T cells potently augment aortic root atherosclerosis by perforin- and granzyme B-dependent cytotoxicity. Circ. Res. 116 (2), 245–254.

Linton, M.F., Atkinson, J.B., Fazio, S., 1995. Prevention of atherosclerosis in apolipoprotein E-deficient mice by bone marrow transplantation. Science 267 (5200), 1034–1037.

Lutgens, E., Daemen, M., Kockx, M., Doevendans, P., Hofker, M., Havekes, L., et al., 1999. Atherosclerosis in APOE*3-Leiden transgenic mice: from proliferative to atheromatous stage. Circulation 99 (2), 276–283.

Maeda, N., Johnson, L., Kim, S., Hagaman, J., Friedman, M., Reddick, R., 2007. Anatomical differences and atherosclerosis in apolipoprotein E-deficient mice with 129/SvEv and C57BL/6 genetic backgrounds. Atherosclerosis 195 (1), 75–82.

Mahley, R.W., Weisgraber, K.H., Huang, Y., 2009. Apolipoprotein E: structure determines function, from atherosclerosis to Alzheimer's disease to AIDS. J. Lipid Res. 50, S183–188.

Miller, Y.I., Choi, S.H., Wiesner, P., Fang, L., Harkewicz, R., Hartvigsen, K., et al., 2011. Oxidation-specific epitopes are danger-associated molecular patterns recognized by pattern recognition receptors of innate immunity. Circ. Res. 108 (2), 235–248.

Murphy, A.J., Akhtari, M., Tolani, S., Pagler, T., Bijl, N., Kuo, C.L., et al., 2011. ApoE regulates hematopoietic stem cell proliferation, monocytosis, and monocyte accumulation in atherosclerotic lesions in mice. J. Clin. Invest. 121 (10), 4138–4149.

Murphy, A.J., Bijl, N., Yvan-Charvet, L., Welch, C.B., Bhagwat, N., Reheman, A., et al., 2013. Cholesterol efflux in megakaryocyte progenitors suppresses platelet production and thrombocytosis. Nat. Med. 19 (5), 586–594.

Murphy, A.J., Dragoljevic, D., Tall, A.R., 2014. Cholesterol efflux pathways regulate myelopoiesis: a potential link to altered macrophage function in atherosclerosis. Front. Immunol. 5, 490.

Niu, Y., Shen, B., Cui, Y., Chen, Y., Wang, J., Wang, L., et al., 2014. Generation of gene-modified cynomolgus monkey via Cas9/RNA-mediated gene targeting in one-cell embryos. Cell 156 (4), 836–843.

Paigen, B., 1995. Genetics of responsiveness to high-fat and high-cholesterol diets in the mouse. Am. J. Clin. Nutr. 62 (2), 458s–462s.

Pei, Y., Chen, X., Aboutouk, D., Fuller, M.T., Dadoo, O., Yu, P., et al., 2013. SR-BI in bone marrow derived cells protects mice from diet induced coronary artery atherosclerosis and myocardial infarction. PloS One 8 (8), e72492.

Pendse, A.A., Arbones-Mainar, J.M., Johnson, L.A., Altenburg, M.K., Maeda, N., 2009. Apolipoprotein E knock-out and knock-in mice: atherosclerosis, metabolic syndrome, and beyond. J. Lipid Res. 50, S178–182.

Phillips, K.A., Bales, K.L., Capitanio, J.P., Conley, A., Czoty, P.W., t Hart, B.A., et al., 2014. Why primate models matter. Am. J. Primatol. 76 (9), 801–827.

Plump, A.S., Smith, J.D., Hayek, T., Aalto-Setala, K., Walsh, A., Verstuyft, J.G., et al., 1992. Severe hypercholesterolemia and atherosclerosis in apolipoprotein E-deficient mice created by homologous recombination in ES cells. Cell 71 (2), 343–353.

Powell-Braxton, L., Veniant, M., Latvala, R.D., Hirano, K.I., Won, W.B., Ross, J., et al., 1998. A mouse model of human familial hypercholesterolemia: markedly elevated low density lipoprotein cholesterol levels and severe atherosclerosis on a low-fat chow diet. Nat. Med. 4 (8), 934–938.

Prescott, M.F., McBride, C.H., Hasler-Rapacz, J., Von Linden, J., Rapacz, J., 1991. Development of complex atherosclerotic lesions in pigs with inherited hyper-LDL cholesterolemia bearing mutant alleles for apolipoprotein B. Am. J. Pathol. 139 (1), 139–147.

Raffai, R.L., Weisgraber, K.H., 2002. Hypomorphic apolipoprotein E mice: a new model of conditional gene repair to examine apolipoprotein E-mediated metabolism. J. Biol. Chem. 277 (13), 11064–11068.

Raffai, R.L., Dong, L.M., Farese, Jr., R.V., Weisgraber, K.H., 2001. Introduction of human apolipoprotein E4 "domain interaction" into mouse apolipoprotein E. Proc. Natl. Acad. Sci. USA 98 (20), 11587–11591.

Reardon, C.A., Blachowicz, L., White, T., Cabana, V., Wang, Y., Lukens, J., et al., 2001. Effect of immune deficiency on lipoproteins and atherosclerosis in male apolipoprotein E-deficient mice. Arterioscler. Thromb. Vasc. Biol. 21 (6), 1011–1016.

Reardon, C.A., Blachowicz, L., Lukens, J., Nissenbaum, M., Getz, G.S., 2003. Genetic background selectively influences innominate artery atherosclerosis: immune system deficiency as a probe. Arterioscler. Thromb. Vasc. Biol. 23 (8), 1449–1454.

Robbins, C.S., Chudnovskiy, A., Rauch, P.J., Figueiredo, J.L., Iwamoto, Y., Gorbatov, R., et al., 2012. Extramedullary hematopoiesis generates Ly-6C(high) monocytes that infiltrate atherosclerotic lesions. Circulation 125 (2), 364–374.

Rodriguez, J.M., Wolfrum, S., Robblee, M., Chen, K.Y., Gilbert, Z.N., Choi, J.H., et al., 2013. Altered expression of Raet1e, a major histocompatibility complex class 1-like molecule, underlies the atherosclerosis modifier locus Ath11 10b. Circ. Res. 113 (9), 1054–1064.

Smith, J.D., Trogan, E., Ginsberg, M., Grigaux, C., Tian, J., Miyata, M., 1995. Decreased atherosclerosis in mice deficient in both macrophage colony-stimulating factor (op) and apolipoprotein E. Proc. Natl. Acad. Sci. USA 92 (18), 8264–8268.

Steinberg, D., 2013. In celebration of the 100th anniversary of the lipid hypothesis of atherosclerosis. J. Lipid Res. 54 (11), 2946–2949.

Stylianou, I.M., Bauer, R.C., Reilly, M.P., Rader, D.J., 2012. Genetic basis of atherosclerosis: insights from mice and humans. Circ. Res. 110 (2), 337–355.

Subramanian, S., Turner, M.S., Ding, Y., Goodspeed, L., Wang, S., Buckner, J.H., et al., 2013. Increased levels of invariant natural killer T lymphocytes worsen metabolic abnormalities and atherosclerosis in obese mice. J. Lipid Res. 54 (10), 2831–2841.

Swirski, F.K., Nahrendorf, M., Etzrodt, M., Wildgruber, M., Cortez-Retamozo, V., Panizzi, P., et al., 2009. Identification of splenic reservoir monocytes and their deployment to inflammatory sites. Science 325 (5940), 612–616.

Tabas, I., Garcia-Cardena, G., Owens, G.K., 2015. Recent insights into the cellular biology of atherosclerosis. J. Cell Biol. 209 (1), 13–22.

Tall, A.R., Yvan-Charvet, L., 2015. Cholesterol, inflammation and innate immunity. Nat. Rev. Immunol. 15 (2), 104–116.

Tanzawa, K., Shimada, Y., Kuroda, M., Tsujita, Y., Arai, M., Watanabe, H., 1980. WHHL-rabbit: a low density lipoprotein receptor-deficient animal model for familial hypercholesterolemia. FEBS Lett. 118 (1), 81–84.

Thorngate, F.E., Rudel, L.L., Walzem, R.L., Williams, D.L., 2000. Low levels of extrahepatic nonmacrophage ApoE inhibit atherosclerosis without correcting hypercholesterolemia in ApoE-deficient mice. Arterioscler. Thromb. Vasc. Biol. 20 (8), 1939–1945.

Tomita, H., Zhilicheva, S., Kim, S., Maeda, N., 2010. Aortic arch curvature and atherosclerosis have overlapping quantitative trait loci in a cross between 129S6/SvEvTac and C57BL/6J apolipoprotein E-null mice. Circ. Res. 106 (6), 1052–1060.

Trigatti, B.L., Fuller, M., 2015. HDL signaling and protection against coronary artery atherosclerosis in mice. J. Biomed. Res. 30, 94–100.

Tsiantoulas, D., Diehl, C.J., Witztum, J.L., Binder, C.J., 2014. B cells and humoral immunity in atherosclerosis. Circ. Res. 114 (11), 1743–1756.

van Vlijmen, B.J., van den Maagdenberg, A.M., Gijbels, M.J., van der Boom, H., HogenEsch, H., Frants, R.R., et al., 1994. Diet-induced hyperlipoproteinemia and atherosclerosis in apolipoprotein E3-Leiden transgenic mice. J. Clin. Invest. 93 (4), 1403–1410.

VanderLaan, P.A., Reardon, C.A., Sagiv, Y., Blachowicz, L., Lukens, J., Nissenbaum, M., et al., 2007. Characterization of the natural killer T-cell response in an adoptive transfer model of atherosclerosis. Am. J. Pathol. 170 (3), 1100–1107.

Veniant, M.M., Beigneux, A.P., Bensadoun, A., Fong, L.G., Young, S.G., 2008. Lipoprotein size and susceptibility to atherosclerosis--insights from genetically modified mouse models. Curr. Drug Targets 9 (3), 174–189.

Vilahur, G., Padro, T., Badimon, L., 2011. Atherosclerosis and thrombosis: insights from large animal models. J. Biomed. Biotechnol. 2011, 907575.

Wang, N., Tall, A.R., 2016. Cholesterol in platelet biogenesis and activation. Blood 127 (16), 1949–1953.

Wang, Z., Zhang, J., Li, H., Li, J., Niimi, M., Ding, G., et al., 2016. Hyperlipidemia-associated gene variations and expression patterns revealed by whole-genome and transcriptome sequencing of rabbit models. Sci. Rep. 6, 26942.

Wilhelm, A.J., Zabalawi, M., Owen, J.S., Shah, D., Grayson, J.M., Major, A.S., et al., 2010. Apolipoprotein A-I modulates regulatory T cells in autoimmune LDLr−/−, ApoA-I−/− mice. J. Biol. Chem. 285 (46), 36158–36169.

Wissler, R.W., Eilert, M.L., Schroeder, M.A., Cohen, L., 1954. Production of lipomatous and atheromatous arterial lesions in the albino rat. AMA Arch. Pathol. 57 (4), 333–351.

Witztum, J.L., Lichtman, A.H., 2014. The influence of innate and adaptive immune responses on atherosclerosis. Annu. Rev. Pathol. 9, 73–102.

Zabalawi, M., Bharadwaj, M., Horton, H., Cline, M., Willingham, M., Thomas, M.J., Sorci-Thomas, M.G., 2007. Inflammation and skin cholesterol in LDLr−/−, apoA-I−/− mice: link between cholesterol homeostasis and self-tolerance? J. Lipid Res. 48 (1), 52–65.

Zhang, S.H., Reddick, R.L., Piedrahita, J.A., Maeda, N., 1992. Spontaneous hypercholesterolemia and arterial lesions in mice lacking apolipoprotein E. Science 258 (5081), 468–471.

Zhang, S., Picard, M.H., Vasile, E., Zhu, Y., Raffai, R.L., Weisgraber, K.H., Krieger, M., 2005. Diet-induced occlusive coronary atherosclerosis, myocardial infarction, cardiac dysfunction, and premature death in scavenger receptor class B type I-deficient, hypomorphic apolipoprotein ER61 mice. Circulation 111 (25), 3457–3464.

Page left intentionally blank

OBESITY, DIABETES, METABOLIC, AND LIVER

Page left intentionally blank

9

Animal Models of Metabolic Syndrome

Jessica P. Wayhart, Heather A. Lawson

Washington University School of Medicine, St. Louis, MO, United States

1 INTRODUCTION AND OVERVIEW

The metabolic syndrome (MetS) is a suite of metabolic complications including central obesity, hypertension, insulin resistance, impaired fasting glucose, dyslipidemia, and inflammation that, in some combination, increases an individual's risk of developing type-2 diabetes (T2D) and/or cardiovascular disease (CVD). Each of these metabolic complications is rising worldwide due to factors such as increasing population size, population aging, urbanization, excess caloric intake, and decreased physical activity. Prevalence of MetS currently exceeds 20% in the United States (for a review, see Eckel et al., 2005 and references within). While aspects of most expert definitions of MetS overlap, there is no single internationally accepted clinical definition because diagnostic criteria used to identify individual risk factors vary among populations, Table 9.1 (Einhorn et al., 2003; Grundy et al., 2005; International Diabetes Federation (IDF), 2006; Parikh and Mohan, 2012; The European Group for the study of Insulin Resistance (EGIR), 2002; World Health Organization (WHO), 1999). For example, intraabdominal fat deposits can lead to severe insulin resistance and T2D in some South Asian populations at body mass indexes that are not considered obese in Western populations (Spiegel and Hawkins, 2012). Variations in diagnostic criteria make it difficult to compare results of studies across populations, and worldwide prevalence of MetS per se is not well quantified. The lack of a single accepted definition has led some investigators to favor keeping individual metabolic complications separate for clinical management. However, others believe that identifying individuals with an aggregation of metabolic complications provides information that

TABLE 9.1　Multiple Expert Definitions of the Metabolic Syndrome (MetS)

Group	Diagnostic criteria
American Association of Clinical Endocrinologists (AACE)	Based on clinical judgment, some combination of the following: • Central obesity • High blood pressure • Hypertriglyceridemia • Impaired glucose tolerance • Inflammation • Low HDL-C
American Heart Association/National Cholesterol Education Program Adult Treatment Panel III (AHA/NCEP ATP III)	Three or more of the following: • Central obesity • High blood pressure • High fasting glucose • Hypertriglyceridemia • Low HDL-C
European Group for the Study of Insulin Resistance (EGIR)	Elevated plasma insulin plus two or more of the following: • Central obesity • High blood pressure • High fasting glucose • Hypertriglyceridemia
International Diabetes Federation (IDF)	Central obesity plus two or more of the following: • High blood pressure • High fasting glucose • Hypertriglyceridemia • Low HDL-C
World Health Organization (WHO)	Glucose intolerance, impaired glucose tolerance or diabetes and/or insulin resistance plus two or more of the following: • Central obesity • High blood pressure • Hypertriglyceridemia • Microalbuminuria

should guide clinical management (Eckel et al., 2005; Grundy, 2008; Kahn et al., 2005; Simmons et al., 2010).

Although clinical definitions of MetS are disputed, the frequent clustering of certain metabolic complications has been a recognized phenomenon since the 1920s (Kylin, 1923). Over time, this clustering has been referred as *syndrome X*, *the deadly quartet*, and the *insulin resistance syndrome* and represents a premorbid condition that is a substantial biomedical and public health challenge. Knowing how and why multiple metabolic complications cluster in some individuals and not in others will greatly improve clinical prevention, management and therapy of TD2 and CVD. To this end, research using animal models has provided key insights into MetS etiology and pathophysiology with the goal of uncovering potential therapeutic targets.

Animal models provide complex biological systems that can be controlled, manipulated, sampled, and studied under conditions and at scales that are not ethical or practical for human studies. While some physiological features of MetS components vary among species, the units of research translation are the underlying genes, biological processes, and/or physiological pathways that can alter normal metabolic phenotypes (Kraja et al., 2008). MetS is complex, involving nonlinear interactions among multiple organs such as adipose tissue, brain, gut, liver, pancreas, and skeletal muscle. Animal models provide an opportunity to examine interorgan cross talk in a whole organism and to directly sample relevant tissues. Even when an animal model does not faithfully mimic the human disorder, novel biological insights can be gained from an in vivo approach. For example, the mouse- and rat-based characterizations of the genes encoding the hormone leptin, *Lep*, and the leptin receptor, *Lepr*, identified mutations affecting lipid metabolism that result in extreme obesity in rodents (Chung et al., 1998; Cool et al., 2006; Kurtz et al., 1989; Varga et al., 2009). In humans, mutations in the orthologous genes LEP and LEPR represent extremely rare cases of obesity (Bergman et al., 2006; Gesta et al., 2007). Yet this animal-based research was essential to further research characterizing leptin metabolism and to identify the hypothalamic pathways controlling signals of satiety and the neural pathways in the brain's striatal region that control perceptions of reward associated with food intake (Belgardt et al., 2009; Elmquist et al., 1999; Konner et al., 2009).

This chapter provides an overview of animal models of MetS that are used to understand etiology and pathophysiology to inform potential therapies. Research aimed at understanding MetS etiology can identify and protect at risk individuals. Research aimed at understanding pathophysiology can shed light on how the clustering of different MetS components increases an individual's risk of developing T2D and CVD. It is important to note that these two broad categories —etiology and pathophysiology—are not mutually exclusive. Rather each informs the other and each is used to develop further research efforts aimed at testing therapeutic strategies to guide appropriate clinical interventions. Animal models of MetS tend to focus on specific metabolic components although, as is seen in humans diagnosed with MetS, individual metabolic complications will often cluster in any given model. For example, obesity and insulin resistance generally coincide in most rodent models, and increased adiposity is associated with dyslipidemia and insulin resistance in both nonhuman primate and porcine models.

2 CHOOSING AN ANIMAL MODEL OF MetS

Rodents, especially mice, are the most commonly used animal model for studying MetS, particularly for genetic studies, because they are relatively easy to

breed and maintain, have highly standardized phenotyping protocols, and high-coverage whole-genome sequences are available for the most commonly studied inbred strains. Table 9.2 lists the most frequently used mouse metabolic phenotyping tests and the data collected for each test. When studying MetS, multiple tests are performed on the same animal to study correlations among different phenotypes that mimic the clustering of metabolic complications in humans. An exciting new technology for assaying multiple measurements simultaneously in rodents is the PhenoMaster system (TSE Systems, Germany). The system uses intrahome-cage technology, and is capable of indirect calorimetry, as well as measurement of food consumption, fluid intake, and activity.

TABLE 9.2 Common Mouse Phenotyping Tests for MetS

Phenotyping test	Data collected
Euglycemic-hyperinsulinemic clamp	Insulin action and glucose metabolism
Intraperitoneal insulin sensitivity test (IPIST)	Insulin resistance, glucose tolerance, glucose disposal
Intraperitoneal glucose tolerance test (IPGTT)	Insulin secretion, glucose tolerance, glucose disposal
Oral glucose tolerance test (OGTT)	Insulin secretion, glucose tolerance, glucose disposal
Fasted bleed (4–6 h)	Glucose, insulin, blood biochemistry, other hormones (e.g., leptin, glucagon, peptide-YY)
Metabolic caging	Food intake, water intake, urine and feces production, urine biochemistry and glucose
Noninvasive intestinal fat absorption	Fecal fat absorption
Echocardiography	Myocardial performance
Cardiac telemetry	Blood pressure, heart rate, pulse pressure, activity
Indirect calorimetry	Metabolic rate (oxygen consumption, carbon dioxide production, respiratory quotient)
Meal pattern analysis	Food intake
Lipid profiles	Triglycerides, total cholesterol, phospholipids, free fatty acids
Fast protein liquid chromatography	Lipoproteins, lipids, apolipoproteins
Quantitative magnetic resonance	Fat mass, lean mass, water content
Tail cuff	Blood pressure
Running wheels	Energy expenditure, circadian activity
Measuring animal	Body weight, body length, fatpad and organ weights (at necropsy)

Several obese, diabetic, and hypertensive mouse strains are well characterized and have been used for decades of biomedical research. Further, transgenic and knockout mouse resources are commercially available (these are discussed in Section 4.1). Other species, including nonhuman primates and larger mammals, such as dogs, pigs, and sheep have also made important contributions to understanding MetS. In some cases these other species may be more appropriate animal models than rodents (Varga et al., 2009). For example, rodent fat depots are not directly translatable to humans (Pond and Mattacks, 1987). Thus the most common measurements used in human anthropometric studies (e.g., waist circumference) are not equivalent in mouse studies of obesity and adiposity. Additionally, there are important biochemical distinctions in adipose tissue between humans and mice. For example, levels of the adipokine adipsin are low in obese mice, but high in obese humans. High levels of the adipokine resistin impairs glucose tolerance in mice, but does not appear to do so in humans (Arner, 2005). Further, mouse lipoprotein profiles are composed mainly of high-density lipoprotein (HDL), which is atheroprotective, whereas humans carry mostly low-density lipoprotein (LDL). Pigs have similar LDL levels to humans, develop atherosclerotic plaques at the same sites as humans (in the aorta and carotid artery), and have similar hemodynamic parameters (Kalt et al., 2008; Turk and Laughlin, 2004). Pigs are frequently used to model CVD and atherosclerosis because their cardiovascular system is morphologically and functionally similar to humans (Litten-Brown et al., 2010). Certain breeds of pigs (namely the Ossabaw minipigs and domestic Piebalds) develop obesity, hypertension, and insulin resistance that fit some definitions of MetS in humans (Spurlock and Gabler, 2008).

Precise criteria to diagnose T2D in mice are not established, however, many aspects of blood glucose control are similar between mice and humans, so mice are frequently used to model glucose homeostasis and regulation of glucose metabolism. Notably, nonhuman primates develop T2D with similar pathological features as humans, including increased plasma triglyceride levels and total cholesterol concentrations (Wagner et al., 2006). Increased levels of adiposity in both baboons and rhesus macaques is associated with insulin resistance and dyslipidemia, similar to humans diagnosed with MetS (Comuzzie et al., 2003). Further, obesity and its associated metabolic complications have been extensively studied in dogs, since domestic dogs have experienced their own obesity "epidemic." There exists a wealth of pathological data available for many different breeds, and dogs exhibit variation in metabolic traits similar to that seen among human populations. Thus dog represents a potentially fruitful large animal model for testing biomedical hypotheses because of the

abundant physiological information available through veterinary data (Edney and Smith, 1986). Additionally, canine models provide a resource for longitudinal data collection that is not possible in smaller animal models (Ionut et al., 2010; Zheng et al., 2010).

Larger mammals may represent more physiologically faithful models of the individual metabolic complications comprising MetS. However, the expense, housing requirements, longer lifespan, relatively less standardized phenotyping protocols, and species-specific ethical considerations, particularly with nonhuman primates, make large scale studies using these animal models impractical. Thus when choosing an animal model of MetS, one must consider its relevant strengths and, when possible, integrate multiple lines of evidence. For example, results identified through discovery research using a rodent model can inform, be integrated with, and ideally validated by, small-scale follow-up studies using a larger mammalian system, which can then be a bridge toward designing relevant human studies.

3 ANIMAL MODELS OF MetS ETIOLOGY

Understanding MetS etiology is important for implementing prevention strategies, as well as for prescribing appropriate therapeutic interventions. The rising prevalence of metabolic complications among human populations is environmental in origin yet there is clearly an important genetic component reflected in variations in prevalence between the sexes and among ethnic groups (Eckel et al., 2005). Given the same environment, some individuals will develop metabolic complications while others will not, indicating that standing genetic variation modifies the effects of the environment on phenotype. In some cases, but not others, metabolic complications will cluster resulting in MetS. For example, common complications that cluster with obesity (and in some combinations define MetS, as discussed earlier) include insulin resistance, dyslipidemia, and increased blood pressure. Data from 1994 to 2004 of National Health and Nutrition Examination Survey (NHANES) found that approximately 32% of obese adults were "metabolically healthy" based on measures of blood pressure, homeostasis model assessment of insulin resistance (HOMA-IR), and plasma triglycerides and HDL-cholesterol concentrations (Wildman et al., 2008). Heritability estimates for individual MetS components are up to 70% for body mass index (BMI), 50%–90% for T2D, 22%–62% for systolic blood pressure, 20%–66% for diastolic blood pressure, 8%–72% for total cholesterol, and 19%–72% for total triglycerides (Bogardus, 2009; Clee and Attie, 2007; Elder et al., 2009; Permutt et al., 2005; Song et al., 2006; Walley et al., 2009). Clearly much phenotypic variability in these metabolic parameters can be attributed to

heritable genetic variation, and animal models are fundamental in discovering the genetic underpinnings of these parameters and of their relationships to each other. Animal models of MetS etiology allow both genetic and environmental factors to be controlled for, manipulated, and monitored in study populations of known origin (Lawson and Cheverud, 2010). This facilitates the discovery of genetic mechanisms, the testing of environmental influences, and the investigation of how these two factors—genetics and environment—sometimes interact and result in MetS.

4 GENETIC FACTORS

4.1 Common Rodent Genetic Models

Genetic studies using classic rodent models of obesity, such as the ob/ob and db/db mice and the Zucker fa/fa rats have identified single genes, namely leptin, *Lep* (ob/ob and Zucker fa/fa rats), and the leptin receptor, *Lepr* (db/db), with major variants leading to extreme obesity and other metabolic complications. Leptin is an adipose tissue derived protein hormone that binds to, and decreases the activity of, neuropeptide Y neurons. This signals satiety, and mutated forms of leptin results in an inability to feel sated leading to hyperphagia and obesity (for a comprehensive review of leptin biology, see Havel, 2004). In addition to extreme obesity, each of these animals to some degree are hyperinsulinemic, insulin resistant, and exhibit defective thermogenesis (Chung et al., 1998; Cool et al., 2006; Kurtz et al., 1989). The leptin-deficient mouse model, $Lep^{ob/ob}$, arose from a spontaneous mutation at the Jackson Laboratory (Ingalls et al., 1950). These mice are obese by 4 weeks of age, and can weigh up to 4 times that of their littermate controls on a standard chow diet. In addition to hyperphagia, reduced energy expenditure and extreme obesity, $Lep^{ob/ob}$ mice have elevated serum cholesterol levels. However, this elevation is in HDL-rather than in LDL-cholesterol, so they are actually protected from developing diet-induced atherosclerosis (Nishina et al., 1994). An additional metabolic abnormality in $Lep^{ob/ob}$ mice involves disregulation of the hypothalamic-pituitary-adrenal axis, of which leptin is an important regulating hormone (Malendowicz et al., 2007). A complication with this model is that $Lep^{ob/ob}$ are infertile, which impedes collecting appropriate samples sizes (Kennedy et al., 2010). Leptin receptor-deficient mice, $LepR^{db/db}$, have nearly identical metabolic profiles and hypothalamic-pituitary-adrenal axis and reproduction problems as $Lep^{ob/ob}$ mice. The significant difference between the two models is that $LepR^{db/db}$ mice have pronounced concentrations of circulating leptin while the $Lep^{ob/ob}$ mice have none at all. Thus the $LepR^{db/db}$ model is frequently used to study

how leptin concentrations affect different cell types in metabolic studies (Surmi et al., 2008). Finally, the leptin receptor-deficient obese Zucker fa/fa rat model is significantly hyperphagic compared to its lean littermates by as early as 17-days old (Kava et al., 1990). These rats are hyperlipidemic and hyperinsulinemic, but are relatively normoglycemic. They are frequently used to study adipose tissue in obesity and the physiological effects of disregulation of leptin signaling (Miranville et al., 2012; Pico et al., 2002).

The Agouti lethal yellow mouse model, $A^{y/a}$, has several spontaneous mutations affecting expression of the agouti protein, transcribed by the agouti gene, A. The agouti protein acts as an antagonist of the melanocortin-signaling pathway, which mediates leptin action. These mice display variation in coat colors and develop adult onset obesity and insulin resistance due to hyperphagia and hypoactivity. Obese $A^{y/a}$ mice are hypertensive but they do not form atherosclerotic lesions on high fat diets (Burgueno et al., 2007). It is easier to obtain offspring and appropriate sample sizes from $A^{y/a}$ than from either $Lep^{ob/ob}$ or $LepR^{db/db}$ because $A^{y/a}$ remain fertile until approximately 4 months of age (Kennedy et al., 2010). Other commonly used single-gene rodent models of obesity and insulin resistance include the fat/fat (variants responsible for the phenotype have been characterized in carboxypeptidase E, Cpe) and tub/tub (variants responsible for the phenotype have been characterized in the tubby candidate gene, Tub) mice (Carroll et al., 2004; Coleman and Eicher, 1990; Naggert et al., 1995).

The low-density lipoprotein receptor-deficient mouse, $LdlR^{-/-}$, is a model of hyperlipidemia that has elevated atherogenic LDL lipoprotein levels similar to that seen in humans with hypercholesterolemia (Ishibashi et al., 1993). These mice will become obese and develop insulin resistance in response to high fat diets (Wu et al., 2006). The apolipoprotein E-deficient mouse, $apoE^{-/-}$, is another frequently used model that develops severe hyperlipidemia, but generally does not become obese and insulin resistant, even on a high fat diet (Hofmann et al., 2008). APOE is a lipoprotein ligand that is recognized by multiple receptors in the liver. Mutant forms of APOE result in elevated very low-density lipoprotein (VLDL). To better approximate the clustering of metabolic complications of MetS, $A^{y/a}$, $Lep^{ob/ob}$, and $LepR^{db/db}$ mice can be crossed with $LdlR^{-/-}$ or $apoE^{-/-}$ mice (Hasty et al., 2001).

When designing an experiment using these classic monogenic models it is important to consider strain background (Coleman and Hummel, 1973). Each strain has a unique combination of alleles and therefore of disease susceptible loci. Different mouse strains vary for different phenotypic traits and when considering complex, polygenic traits, such as those comprising MetS, genetic background—that is, strain effects—can

confound results. This is because of epistatic and/or compensatory interactions among loci. For example, when the Lep^{ob} mutation is bred into a BTBR (black and tan, brachyuric strain) background, the $Lep^{ob/ob}$ mice develop severe diabetes (Clee et al., 2005). However, in the C57BL/6J (the most widely used of all inbred strains and the $Mus\ musculus$ reference genome strain) background, $Lep^{ob/ob}$ mice present as mildly hyperglycemic between 8 and 12 weeks of age, but then glucose levels return to near normal (Coleman and Hummel, 1973). In contrast to other strains, BALB $Lep^{ob/ob}$ mice are fertile (Clee and Attie, 2007). FVB (friend virus B strain) $LepR^{db/db}$ mice have more severe hyperinsulinemia and hyperglycemia than C57BL/6J $LepR^{db/db}$ mice (Chua et al., 2002). $A^{y/a}$ mice are generally studied on C57BL/6J or KK (originally generated from wild-derived ddY mice in Japan) backgrounds, and the MetS phenotype is more extreme in the KK strain, with KK $A^{y/a}$ animals exhibiting age-onset obesity, hypertension, insulin resistance, and diabetic nephropathy (Okazaki et al., 2002).

The models described previously represent some of the most commonly used monogenic rodent models of metabolic complications. However, single-gene mutations account for a very small percentage of the overall heritable variation of any MetS component, and account for a negligible percentage of MetS cases in human populations (Bogardus, 2009). Polygenic rodent models have also been developed that include, but are not limited to, the NZO, TallyHo, and KK inbred mouse strains and the OM, WOKW, and SHR rats (Bielschowsky and Goodall, 1970; Clee and Attie, 2007; Dulin and Wyse, 1970; Fisler et al., 1993; Kloting et al., 2006; Noda et al., 2010; Song et al., 2006). Each of these models is frequently used to study the genetic inheritance of individual MetS components and how these components correlate. NZO, the New Zealand obese strain, is a spontaneous model of polygenic obesity and insulin resistance. It is frequently used as a model of MetS because in addition to being obese, animals are hyperinsulinemic, show reduced insulin-stimulated glucose uptake in muscle and adipose tissues, have high serum triglyceride levels, and present with elevated blood pressure. TallyHo is a naturally occurring model of obesity and diabetes that also displays hyperlipidemia. KK mice (of which there are many substrains) are obese, hyperleptinemic, severely hyperinsulinemic, and animals display insulin resistance in both adipose and muscle tissues. OM, the Osborne–Mendel rat, is susceptible to dietary obesity and develops cardiac hypertrophy and hyperinsulinemia (Fitzgerald et al., 2001). WOKW, the Wistar Ottawa Karlsburg W rat, is obese and exhibits decreased insulin sensitivity and insulin-stimulated glucose uptake in adipose tissue. WOKW animals also display dislipidemia and hyperleptinemia and are frequently crossed with disease-resistant rat strains for studying

MetS (Kovacs et al., 2000). SHR, the spontaneously hypertensive rat, is the most frequently used animal model of blood pressure and hypertension, but it is commonly used to study MetS because these animals also display insulin resistance, hypertriglyceridemia, and obesity (van den Brandt et al., 2000). Recently, a new rat model of MetS, the UCD-T2DM, was generated by researchers at the University of California-Davis by crossing the obese Sprague-Dawly rat with lean Zucker diabetic fatty rats. The UCD-T2DM rat develops polygenic obesity with insulin resistance, impaired glucose tolerance and beta-cell decomposition (Cummings et al., 2008).

Polygenic models may be better suited than monogenic models for studying the genetic underpinnings of MetS etiology, because most of the metabolic complications comprising the individual MetS components are the result of many interacting genes of individually small effects. The Jackson Labs provides a comprehensive catalog of mouse models of MetS components including both monogenic and polygenic models for CVD, T2D, and obesity (http://www.jax.org). Their catalog provides information on strain history, phenotypes, health and husbandry, as well as their susceptibility to diseases. Further, the Jackson Labs provides an online version of the book "Biology of the Laboratory Mouse," which provides information on mouse biology, as well as husbandry (http://www.informatics.jax.org/greenbook/). Additionally, the Mouse Phenome Database provides phenotypic information across mouse strains. The Rat Genome Database (http://rgd.mcw.edu/) provides genotypic and phenotypic information on rat models, and provides multiple tools for researchers to mine rat-generated genomic and phenotypic data. These resources include valuable information for designing and executing rodent model studies, which are not only aimed at understanding MetS etiology, using the aforementioned described monogenic or polygenic models, but also aimed at identifying the genetic underpinnings of MetS components through targeted candidate gene approaches or through genetic mapping studies that identify quantitative trait loci (QTL) and novel genes associated with variation in metabolic parameters.

Recently, the number of whole genome sequences for individual mouse strains has expanded immensely. The Wellcome Trust's Mouse Genomes Project has made the complete genomes of 36 inbred strains available for the scientific community's use (http://www.sanger.ac.uk/science/data/mouse-genomes-project). Their database includes raw sequence data in addition to characterized polymorphisms, such as SNPs, indels, and structural variants. Additionally, whole genome sequences for the FVB/NJ (Wong et al., 2012), LG/J, and SM/J (Nikolskiy et al., 2015) inbred strains are available, including strain specific variants relative to the reference C57BL/6J strain. Further, the Mouse Diversity Array measures

~600,000 genotypes and has been applied to several hundred laboratory strains (Yang et al., 2009). These data significantly improve researchers' ability to relate genotype to phenotype and elucidate underlying molecular mechanisms (Keane et al., 2011).

4.2 Candidate Gene Approaches: Testing Biological Hypotheses

Candidate gene approaches can be used to test hypotheses about the genetic basis of a trait, based on a priori knowledge of that trait and some biological evidence that a focal gene of interest affects phenotype. Candidate genes are usually studied in animal models by targeted manipulation using genetic engineering technologies in embryonic stem cells to knockout (to remove or disrupt transcription of the gene of interest) or to knock-in (to mutate or to insert a variant of the gene of interest), and then to monitor any phenotypic consequences in mice heterozygous and/or homozygous for the targeted gene. Knockout (KO) models can provide key insights into target gene actions, and knock-in (KI) mice are useful for assessing subtle effects of mutations on protein structure or function. KO and KI mice are produced by incorporating the modified embryonic stem cells into the germ line, and then by interbreeding animals that develop with one copy of the targeted gene in their cells to generate animals that are homozygous for the manipulated gene. A key problem with genetic manipulation approaches is that manipulation of the targeted gene may result in embryonic death, preventing study of its effects on offspring or adult phenotype. Another problem is that genetic manipulations can induce compensatory changes, where other mechanisms take over the targeted gene's action and the targeted gene appears to have little phenotypic effect, even if it is important. Still, targeted manipulation of candidate genes is a powerful way to test biological hypotheses because mutations can be selectively targeted to specific tissues, cells, and/or particular developmental stages allowing physiological, developmental and/or behavioral complications to be studied. Manipulation of the mouse genome has been possible for over 20 years, and there are many resources available for planning and executing such experiments (Capecchi, 1989a,b; Nadeau et al., 2001). For example, The International Mouse Phenotyping Consortium (http://www.mousephenotype.org/) is working to mutate every protein-coding gene in the mouse, and Mouse Genome Informatics (http://www.informatics.jax.org/) provides a collection of phenotypes and mutagenesis community resources (Collins et al., 2007).

Recently, CRISPR/Cas9 technology has allowed for generation of null, conditional, precisely mutated, reporter, or tagged alleles in mice (Jinek et al., 2012; Singh et al., 2015). This gene-editing technique is being used

to generate new KO mice, via a CRISPR (clustered regularly interspersed short palindromic repeats) mediated nonhomologous end joining approach. This approach utilizes single guide RNAs, which are directly injected into embryos along with Cas9 mRNA. This results in mice bearing frame-shifting mutations (insertion/deletions) that disrupt target genes. KI mice use CRISPR mediated homology directed repair. This approach utilizes a single-stranded oligonucleotide or a plasmid template, which is coinjected with single stranded RNAs and Cas9 mRNA. Generation of Cre-recombinase-dependent Cas9 allows tissue-specific or conditional gene editing (Yang et al., 2013). The Jackson Labs has generated close to 200 CRISPR/Cas9 mediated mouse models on multiple genetic backgrounds (www.jax.org/mouse-search).

4.3 Thrifty Genes

One hypothesis proposed to explain the genetic underpinnings of MetS, and which has motivated many candidate gene studies, is the "thrifty genotype hypothesis". The thrifty genotype hypothesis proposes that for most of evolutionary history, high-caloric foods were rare relative to the energy that was required to acquire them (Neel, 1962). Genetic variation that was efficient at stowing away excess calories in adipose tissue may have led to survival and fertility advantages that were advanced by natural selection over time. This hypothesis assumes that these "thrifty" genetic variants predispose an individual to metabolic complications in an environment where high-caloric foods are easily obtained. Candidate gene approaches testing the thrifty genotype hypothesis focus on genes involved in physiological processes necessary for energy balance, storage, and nutrition partitioning.

For example, the peroxisome proliferator-activated receptors (PPARs) are lipid-activated nuclear receptors that are necessary for multiple physiological processes important for energy balance (Lodhi and Semenkovich, 2014; Wang, 2010). These include fatty-acid catabolism (PPARα), thermoregulation and insulin homeostasis (PPARδ), and lipid metabolism and glucose homeostasis (PPARγ) (Barbier et al., 2002; Grimaldi, 2005; Wahli et al., 1995). $Ppar\alpha^{-/-}$ mice have decreased expression of fatty-acid oxidation genes and have a fatty liver phenotype indicating that $Ppar\alpha$ regulates hepatic lipid catabolism (Akiyama et al., 2001; Aoyama et al., 1998; Sugden et al., 2002). $Ppar\delta$ adipose-specific knockout mice have compromised thermoregulation. Analysis of $Ppar\delta$ deficient brown fat cells generated from mice containing floxed [a method of conditional targeting wherein one or more of a candidate gene's exons are flanked by lox P sites, allowing the gene to be manipulated by Cre recombinase action (reviewed in Brault et al., 2007)] $Ppar\delta$ alleles show downregulated expression of fat-burning

genes, indicating that $Ppar\delta$ is important in brown fat metabolism (Pan et al., 2009). Additionally, $Ppar\delta$ skeletal muscle-specific knockout mice have increased weight and insulin resistance relative to controls (Schuler et al., 2006). $Ppar\gamma$ adipose-specific knockout mice show lipodystrophy, high serum free-fatty acids and triglyceride levels, and decreased leptin and adiponectin levels (He et al., 2003). $Ppar\gamma$ muscle-specific knockout mice show increased adiposity and insulin resistance (Hevener et al., 2003; Norris et al., 2003). These studies have demonstrated that the PPARs play a substantial role in energy balance and metabolism, and that disruption of normal PPAR transcription can contribute to multiple metabolic complications clustering as MetS. These genes have been implicated in human association studies for both obesity and T2D (Kunej et al., 2012). However, more research is required to understand the detailed molecular mechanisms by which the PPARs interact with each other and with other genes in their transcriptional pathways.

Another candidate gene studied to test the thrifty gene hypothesis is the melanocortin-4 receptor, MC4R. The central melanocortin system mediates leptin action and plays an important role in energy homeostasis (Cone, 2005). Variations in MC4R cause obesity in humans (Marti et al., 2003; Willer et al., 2009). $Mc4\text{-}R^{-/-}$ mice develop the obese, hyperglycemic, and hyperinsulinemic phenotypes that are typical of MetS; however, their triglycerides appear to be normal and they tend to be hypotensive (Tallam et al., 2005). The obesity in these mice is behavioral, resulting from hyperphagia, but the hyperinsulinemia is only partially due to obesity as young $Mc4\text{-}R^{-/-}$ animals have elevated circulating insulin levels prior to becoming obese (Fan et al., 2000). A final example of this candidate gene approach tested the thrombosponin receptor, CD36. CD36 first identified as associated with insulin sensitivity and hypertension in SHR rats discussed earlier (Aitman et al., 1999; Pravenec et al., 2001). Insulin sensitivity affects the body's ability to use stored fat for energy and reduced insulin sensitivity or insulin resistance is a precursor for T2D. Further studies in $Cd36$ knockout mice revealed that this gene plays an important role in lipid processing, in insulin action, and atherogenesis (Drover et al., 2005; Goudriaan et al., 2005; Varga et al., 2009). Follow-up studies in human populations confirm that mutations affecting CD36 expression play a role in MetS risk (Griffin et al., 2001; Ma et al., 2004; Miyaoka et al., 2001).

Mouse models focused on testing biological hypotheses about candidate genes have advanced the study of MetS etiology by identifying a large number of physiologically plausible genes and pathways. However, as discussed earlier, strain background is important for assessing phenotypic consequences of candidate gene effects. For example, 85% of C57BL/6J mice heterozygous

for the insulin receptor knockout ($InsR^{+/-}$) and heterozygous for the insulin receptor substrate-1 ($Irs-1^{+/-}$) develop apparent diabetes by 6 months of age. However, only 64% of DBA mice and only 2% of 129Sv mice with the same mutations do (Kulkarni et al., 2003). Thus strain background must be considered along with the use of appropriate controls when designing candidate gene experiments.

4.4 Candidate Gene Approaches: Translating Human GWAS Results

Related to the candidate gene approach to test specific hypotheses about thrifty genes is the use of mouse models to directly test hypotheses about variants that were identified in human genome-wide association studies (GWAS). The idea is to translate variants that are significantly associated with common diseases in human studies to an animal model, with the goal of identifying the disease-causing gene within a GWAS linkage block. Variants identified in GWAS are part of linkage blocks, or sequences that are nonrandomly inherited together, and the disease-associated variant is usually not obvious and can often be found in noncoding sequence far from annotated genes (Wellcome Trust Case Control Consortium, 2007). An example of this candidate gene approach used mouse models to test the fat mass and obesity associated FTO locus. Multiple GWAS identified FTO as associated with T2D (although the association with T2D was lost once body mass index was controlled for) (Cox and Church, 2011; Dina et al., 2007; Frayling et al., 2007; Scuteri et al., 2007). *Fto* knockout mice showed a lean phenotype, reduced adipose tissue, and increased energy expenditure, despite being hyperphagic relative to controls. These animals also exhibited increased postnatal lethality and growth retardation (Fischer et al., 2009). An experiment that incorporated a missense mutation into the gene, causing loss of *fto* demethylase function, resulted in mice with reduced adipose tissue but without the additional phenotypic complications of the knockout (Church et al., 2009). Finally, over expression of the *fto* gene in mice resulted in extreme obesity due to hyperphagia (Church et al., 2010). Targeted manipulation of *fto* in these mouse models suggests FTO plays a role in energy homeostasis. This supports the GWAS results indicating that certain variants in human populations put an individual at risk for developing obesity and other obesity-related metabolic complications of MetS.

Another focused candidate approach targeted a linkage peak (containing multiple genes) on human chromosome 3 that is associated with a combined obesity-insulin factor in multiple human studies (Kraja et al., 2012). The researchers integrated the human linkage results with results from a mouse genetic mapping study that identified a significant association with serum insulin and glucose levels in the syntenic region of mouse chromosome 6. The researchers then performed a targeted association analysis in the focal human chromosome 3 region. By using the mouse results to "protect" the focal region in the human data from the extreme burden of multiple tests correction (essentially using the mouse results as an a priori hypothesis), novel genetic associations with multiple MetS components were identified.

The National Center of Biotechnology Information (NCBI) provides a database of genotypes and phenotypes (dbGaP) that both archives and distributes results of GWAS and other human genotype to phenotype studies, including many studies focused on metabolic complications (http://www.ncbi.nlm.nih.gov/sites/entrez?db=gap). As discussed in Section 1, the exact same variant is unlikely to affect humans and other species in the exact same way, but the units of research translation are the underlying genes, biological processes, and/or physiological pathways the genes interact in that can alter normal metabolic phenotypes. An assumption of this candidate approach is that these units of research translation have a similar function in humans and other species with respect to the disease process. Developing animal models that target variants underlying GWAS loci represents a powerful translational tool for identifying potential causal genes and elucidating how they function in disease and/or disease risk. Additionally, because human/mouse homology is well defined, using mouse results to protect homologous regions in these archived human data for correlated phenotypes will increase statistical power and identify new variants in candidate regions associated with disease and/or disease risk. Incorporating the candidate gene approach with GWAS results is a powerful method of identifying potentially relevant variants associated with MetS and rodent, especially mouse, models have proven invaluable tools for characterizing function and deconstructing molecular mechanisms (Fig. 9.1). Other genetic studies using animal models aim to identify novel MetS associated variants through hypothesis-free genetic mapping studies.

4.5 Identifying Quantitative Trait Loci and Novel Genes

Genetic mapping studies in animal models allow large numbers of offspring to be generated from relatively few founders of known genomic background. When the founders crossed differ in the trait of interest, for example, in levels of adiposity, phenotypic variation in the offspring can be correlated with genotypic variation in markers scored in the same individuals to identify QTL. Common markers used in QTL mapping are single-nucleotide polymorphisms, SNPs, but other
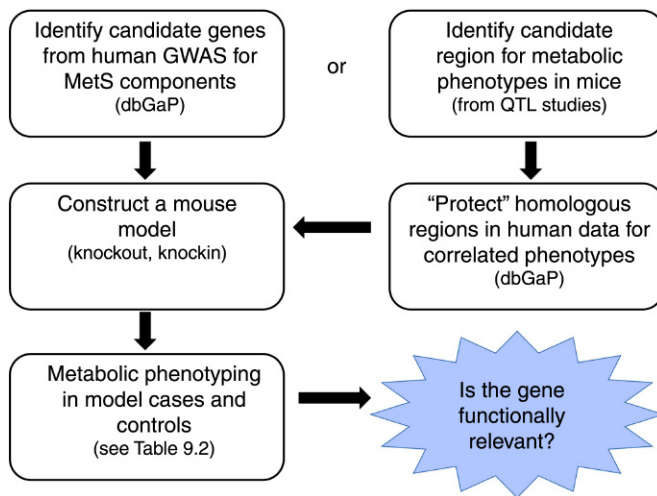
FIGURE 9.1 **A candidate gene approach for translating human GWAS results.** Associations identified in human studies can be directly tested in a mouse model to determine if the candidate gene affects the phenotype. Alternatively, mouse QTL regions can be used to mine GWAS results for correlated phenotypes and protect human syntenic regions from strict genome-wide multiple tests corrections. Candidate genes that are significant in the protected region (but that may have only been suggestive at the genome-wide level) can then be tested for functional relevance by going back to the mouse.

FIGURE 9.2 **An example QTL.** LOD scores (limit of detection, *y*-axis) are plotted along a chromosome (illustrated here in centiMorgans, *x*-axis) and represent the strength of a genomic association with phenotypic variance in a population. A higher LOD score indicates a lower probability that the association is by chance. A significance threshold is determined based on the number of genomic markers tested. The highest LOD score indicates the peak of the QTL and a support interval is defined (generally a 1-LOD drop from the peak position) to identify a physical region of the genome that can be interrogated for candidate genes. Note the cartoon chromosome refers to a generic mouse chromosome. All mouse chromosomes are acrocentric.

markers that vary within the experimental population, for example, microsatellites, can be used. In QTL studies, smaller sample sizes are required to find associations that can explain more than 50% of the heritable variation of a trait. In humans, thousands of individuals are required and findings typically explain a very small portion of the heritable variance. QTL represent physical locations on a chromosome in which genetic variants associate with phenotypic variation that was measured in the experimental population, illustrated in Fig. 9.2. As with candidate gene approaches, most QTL associated with MetS components have been identified and characterized in rodent, especially mouse, models (reviewed in: Lawson and Cheverud, 2010).

For rodent QTL mapping studies, the general experimental design is to first cross two inbred strains that are phenotypically distinct for the trait of interest (appropriately distinct strains can be identified using the Mouse Phenome Database and the Jackson Labs catalog as discussed earlier). The F_1 offspring are then either bred to each other to generate an F_2 intercross population, or bred back to one or both parental strains to generate a backcross population. An intercross between two genetically identical F_1 animals will result in F_2 animals with recombination on both transmitted chromosomes. An F_2 intercross, by having all possible combinations of genotypes represented at each locus, can provide information on both additive and dominance genetic effects. One-half of the chromosomes in

backcross offspring will be recombinants from the F_1 parents. Backcross offspring are either heterozygote or homozygote for one parental allele at each locus, and can therefore provide information on alleles acting in a dominant fashion. In addition to using backcross or intercross experimental populations, QTL are commonly mapped in recombinant inbred (RI) strains, chromosome substitution strains or outbred stocks (for detailed discussion on these types of mice, refer to the Jackson Labs' "Biology of the Laboratory Mouse" online reference: http://www.informatics.jax.org/greenbook/). In a QTL study, mapping resolution (the power to localize an association) is a function of the number of recombination events that occur between genotyped markers. For example, an F_{16} Advanced Intercross population has 8 times the recombination of an F_2 intercross and QTL support intervals will be much smaller, containing 10s rather than 100s of genes to interrogate, as illustrated in Fig. 9.3 (Lawson and Cheverud, 2010).

Mouse Genome Informatics (http://www.informatics.jax.org/) archives and maintains a database of mouse QTL under their Genes and Markers Query form. This resource can be used to determine if intervals identified in a QTL mapping study replicate (have been identified in mapping studies using other strains of mice), lending higher confidence to the region. There are currently 326 QTL associated with obesity, 212 with T2D, 340 with serum lipid traits, and 33 with hypertension listed in the database (Lawson and Cheverud, 2010). For studying
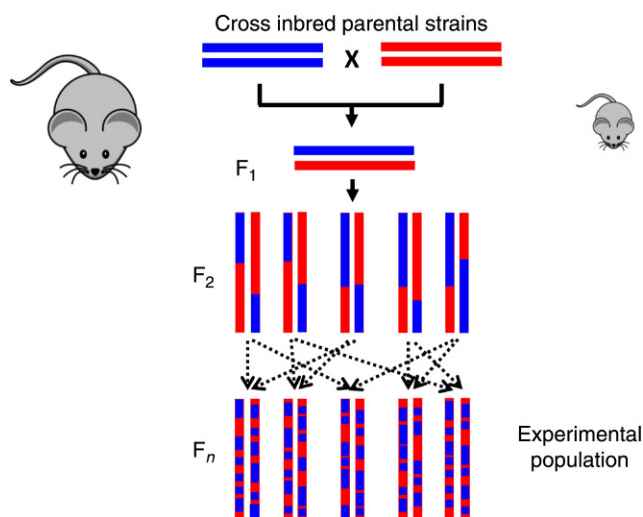
FIGURE 9.3 **Recombination increases the power to identify candidate genes.** When designing a QTL mapping study, the F1 offspring will be genetically identical. Brother-sister mating in the F1 will result in recombination and QTL can be identified in an F2 population. However, support intervals can be enormous, composed of hundreds of genes. Further interbreeding will increase recombination in every subsequent generation, which will narrow QTL support intervals and reduce the number of candidate genes to interrogate.

MetS, the most relevant QTL will be those associated with variation in multiple metabolic components.

For practical reasons the mouse is the animal model of choice for QTL mapping, but other studies have identified QTL associated with MetS components using pedigreed populations of baboons and pigs. The Southwest National Primate Research Center (SNPRC) at the Texas Biomedical Research Institute (San Antonio, TX) houses a large captive, pedigreed and genotyped baboon population (http://txbiomed.org/primate-research-center/). Baboons are used extensively in biomedical research and there are many physiological and genetic similarities between old-world monkeys and humans that make baboons an ideal model for MetS. SNPRC collects multiple metabolic data on their pedigreed colony (which is a mixture of yellow, *Papio hamadrayas cynocephalus*, and olive, *Papio hamadrayas anubis*, baboons) including measures of body composition (e.g., fat mass, fat-free mass, and waist circumference) and blood serum parameters. Approximately 10% of these animals become obese despite the population's uniform environment. Studies have found that increased adiposity in these baboons is significantly associated with dyslipidemia and insulin resistance, indicating this population is a good model for MetS (Comuzzie et al., 2003). Similar clustering of metabolic complications is also observed in studies of the rhesus macaque, another old-world primate frequently used in biomedical research (Bodkin et al., 1993). The SNPRC baboons have been used

to quantify heritabilities of multiple metabolic traits (Cai et al., 2004; Cole et al., 2003; Comuzzie et al., 2003). Research integrating the rich phenotype and genotype data collected in this pedigreed population have identified QTL associated with metabolic traits, such as HDL cholesterol (Cox et al., 2007), LDL cholesterol (Kammerer et al., 2002), adipocyte volume (Bose et al., 2010), and cholecytokinin, a major satiety signaling protein (Voruganti et al., 2007).

Pigs have been studied for fat and meat production in agriculture for decades, and pigs are becoming more frequently used animal models in biomedical research. The Ossabaw minipig and the Pietrain domestic pig are particularly promising porcine models for MetS research because obesity, insulin resistance and hypertension cluster in these two breeds. Combining metabolic phenotypes with genotyped markers in pig mapping studies has identified QTL for lipid metabolism in a Duroc x Pietrain intercross (Uddin et al., 2011), for obesity in a Meishan x Large White intercross (Bidanel et al., 2001), and for serum glucose and lipid levels in a White Duroc x Erhualian intercross (Chen et al., 2009). The Animal QTLdb (http://www.animalgenome.org/QTLdb/app) has a searchable pig QTL database that stores published pig QTL results and phenotypic parameters for different breeds, including phenotypes that are biomedically relevant to MetS (fat and adipose traits are listed as "meat quality traits") (Hu et al., 2005).

QTL mapping is powerful in that it requires no a priori knowledge of genes that may be involved in the trait. This is important for multifactorial conditions, such as MetS, which have complex etiologies and likely result from interactions of many genes of individually small effects. QTL mapping can thus lead to discovery of novel genes and genetic variants associating with phenotypic variation that can subsequently become targets of focused candidate gene studies. The UCSC Genome Browser has multiple mammalian genomes available to query, including low-coverage assemblies, such as the pig (*Sus scrofa*). Genes located in a QTL interval submitted to the browser can be identified (http://genome.ucsc.edu/index.html) and interrogated. The human genomic position homologous to the QTL region identified in an animal model study can be evaluated using NCBI Homology tools (http://www.ncbi.nlm.nih.gov/guide/homology/). Once a QTL is identified in an animal model mapping study, genes within the support interval can be interrogated using public databases, such as the National Center For Biotechnology Information: Entrez Gene (http://www.ncbi.nlm.nih.gov/gene) and PubMed (http://www.ncbi.nlm.nih.gov/pubmed) to identify and rank order the most plausible candidate quantitative trait genes for further interrogation of function (using methods discussed in Sections 4.2 and 4.4).

4.6 GWAS in Model Organisms

GWAS in model organisms can deconstruct the genetic underpinnings of metabolic disorders with improved power of detection and resolution over QTL mapping. GWAS are now feasible in mice given the breadth of variants characterized across phenotypically diverse strains as discussed earlier in Section 4.1. New strains, such as those generated by the collaborative cross, as well as commercially available outbred strains, such as the diversity outbred mice, provide gene-level resolution for mapping complex traits (Churchill et al., 2004; Svenson et al., 2012). GWAS in mice have identified loci involved in MetS components including lipids and blood pressure (Bennett et al., 2010; Zhang et al., 2012). Incorporation of additional phenotypic information, for example, of metabolites, has allowed researchers to place GWAS associated genes into specific metabolic pathways and identify correlations among metabolic parameters. For example, researchers were able to establish that insulin resistance and plasma arginine levels are related in mice (Parks et al., 2015). Identifying such correlations could help establish biomarkers for the complex relationships among MetS components.

A proposed approach for using GWAS in dogs is to identify loci associated with obese and lean dogs within breeds prone to obesity, followed by crossbreed comparison of variants (Switonski and Mankowska, 2013). In swine, there is a spectrum of fatness and body size phenotypes bred for agriculture. Selective genotyping of animals at the far ends of the phenotypic spectrum allows a reduction of sample size and an increase in cost efficiency (Fowler et al., 2013). As dogs and pigs are both appreciated models for human disease, any advancement in our understanding of their genetic susceptibility to MetS is beneficial to medical research.

4.7 Identifying Epigenetic Signatures Associated with MetS Components

Imprinting is defined as the unequal expression of an allele depending on its parent-of-origin. Over 80 imprinted genes have been identified in humans, and ≈30% of these genes overlap with genes demonstrated to be imprinted in mice (Herrera et al., 2011). Bioinformatic studies predict that several hundred more genes are likely to be imprinted in both species (Luedi et al., 2005, 2007). Most direct observations of imprinting have been carried out through analysis of monoallelic expression in reciprocal matings of inbred mouse strains. Imprinted genes are known to be involved in metabolic functions (Rampersaud et al., 2008), and failures in imprinting can result in metabolic complications by altering expression of growth and cellular differentiation factors. Genomic imprinting failures have been associated with

rare genetic syndromes having extreme forms of obesity (e.g., Prader–Willi syndrome) and mapping studies have identified imprinted genes (e.g., *GNAS*) affecting metabolic complications, such as obesity and insulin resistance in both humans and mice (Butler, 2009; Dong et al., 2005). QTL mapping studies in mice have identified loci having parent-of-origin effects on multiple MetS components, and some of these loci may be imprinted (Cheverud et al., 2011; Lawson et al., 2011a,b; Lawson et al., 2010). A striking result from these murine mapping studies is that parent-of-origin effects on metabolic traits is complex: in addition to the better characterized paternal and maternal patterns, polar and bi-polar dominance patterns were frequently observed. Polar dominance occurs when there are no additive genetic effects, so the two homozygote trait values are the same, yet there is a difference in the trait values between the two heterozygotes such that one class of heterozygote is in line with the homozygotes and the other is not, depending on parent of origin. In bi-polar dominance, again there is no significant difference between the two reciprocal homozygotes, but a pronounced difference occurs between the two reciprocal heterozygotes such that one class of heterozygote has the highest trait value of any other genotype class and the other class of heterozygote has the lowest trait value of any other genotype class as illustrated in Fig. 9.4 (for a detailed explanation of complex parent-of-origin patterns, including mathematical derivation, see Wolf et al., 2008). This complex pattern is rarely documented in human studies due to lack of sufficient genotypic information or statistical power, but
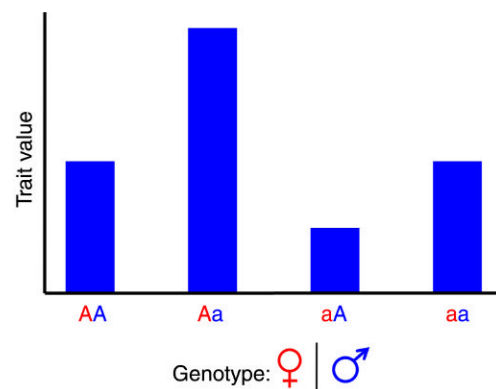
FIGURE 9.4 **An example of a bi-polar dominance parent-of-origin effect** In this example, trait value is the *y*-axis (trait value can be weight, cholesterol level, etc.) and the genotype classes are depicted on the *x*-axis. Parent-of-origin of alleles is known with *red* indicating a maternally derived allele and *blue* indicating a paternally derived allele. At this locus, there are no additive genetic effects (no difference in trait value between individuals belonging to the two homozygote classes), but there is a difference between the two reciprocal heterozygotes such that one class has the lowest trait value of any other genotypic class and the other has the highest trait value. Thus the same allele can be both protective and a potential risk factor depending upon parent-of-origin.

it does occur. For example, a study using the Icelandic genealogy database showed that the same genetic variant increases T2D risk when paternally inherited but decreases T2D risk when maternally inherited (Kong et al., 2009). This is consistent with a bipolar dominance parent-of-origin effect.

Epigenetic modifications, cell-specific changes in DNA chemistry that do not alter the DNA sequence itself, can affect gene expression and may underlie some of the parent-of-origin effects associated with MetS components found in mouse mapping studies. Commonly studied molecular epigenetic signatures include DNA methylation, histone modification, and small noncoding RNA interference. Tissue and T2D disease-stage specific altered methylation patterns were found in the Zucker diabetic fatty rat model relative to controls (Williams and Schalinske, 2012). A genome-wide methylation analysis in pig adipose and muscle tissues identified methylation patterns that segregated by breed (the researchers compared methylomes among three breeds: Landrace, Rongchang, and Tibetian), by sex, by tissue, and by fat depot (Li et al., 2012a). This work also identified regions that were "differentially methylated," meaning one allele is methylated while the other allele is not. This pattern is suggestive of parent-of-origin methylation, which may affect expression of genes in a parent-of-origin manner, and is a signature of imprinting (Harris et al., 2010). An exciting direction for future research is to combine results identified in animal QTL mapping studies with whole-genome epigenetic profiling.

4.8 Mouse ENCODE

The Mouse ENCODE Consortium was developed as a counterpart to the human Encyclopedia of DNA Elements (ENCODE). Using similar technologies and pipelines, Mouse ENCODE maps functional elements of the mouse genome, such as transcription, transcription factor binding, chromatin modifications, and replication domains. These data were mapped in a wide range of mouse tissues and cell types, mostly generated from C57BL/6J and are available to the research community at www.mouseencode.org.

The public availability of these data sets has significantly impacted comparative studies of mouse and human genomes. Studies have revealed conservation of some basic regulatory systems between humans and mice, as well as high levels of divergence in gene expression and regulation (Yue et al., 2014). Washington University in St. Louis houses an epigenome browser with which researchers can explore these existing datasets, or upload their own data to visualize a candidate region's genomic context (http://vizhub.wustl.edu/). Identification of patterns of epigenetic effects in animal models can be translated to human studies and will provide a framework for clarifying the relationship between DNA sequence variation and metabolic complications. This is a step toward development of better therapeutic strategies for MetS.

5 ENVIRONMENTAL FACTORS

5.1 Fetal Programming

Maternal developmental environment has been shown to affect not only fetal and early postnatal growth, but also adult susceptibility to MetS (Barker, 2007). Compromised nutrition during fetal and early postnatal life increases susceptibility to metabolic complications later in life because of "fetal programming" during critical periods of development and a mismatch between early and adult nutritional environments. The precise mechanism(s) through which this phenomenon occurs is unknown, but recent work suggests that epigenetic modifications of DNA affect many molecular processes related to intrauterine growth and development (Aagaard-Tillery et al., 2008; Heerwagen et al., 2010). Research in guinea pigs found that mothers fed moderately restricted diets throughout their pregnancies (70% of ad libitum intake/kg body wt.) gave birth to small pups and their adult male offspring were hyperinsulinemic (Kind et al., 2003). A similar study in guinea pigs found that mildly restricting maternal diet (85% of ad libitum) increased both total cholesterol and LDL cholesterol levels in male offspring (Kind et al., 1999). Maternal undernutrition is associated with increased arterial blood pressure in offspring that persists into adulthood in both sheep and rat models (McMillen and Robinson, 2005). Offspring of rat mothers fed restricted protein diets (50% less protein than standard chow-fed controls) had poor pancreatic beta-cell proliferative capacity at birth. When the low protein diet was maintained, weanlings, pancreatic islet morphology, and insulin content was found to be reduced (Bertram and Hanson, 2001). Recent rodent models have shown that maternal high fat diet, or overnutrition, also increases offspring susceptibility to developing adult metabolic complications (Liang et al., 2009; Morris and Chen, 2009; Odaka et al., 2010). When mothers consume a high fat diet their offspring tend toward obesity as adults, regardless of offspring diets. However, other research suggests that it is maternal adiposity and not dietary fat consumed that affects offspring susceptibility to adult metabolic complications (White et al., 2009). In sheep, maternal obesity and overnutrition results in metabolic complications in adult offspring (Long et al., 2011). Further, ovine models suggest that overnutrition affects adult offspring risk in two stages: first during the periconceptional period and second in late pregnancy (George et al., 2010). Studies

in nonhuman primates support findings from rodents and sheep. In baboons, preweaning overnutrition resulted in permanently increased adiposity in females (Lewis et al., 1986). In macaques, maternal high fat diet predisposed adult offspring to adult nonalcoholic fatty liver disease, which is highly correlated with MetS (McCurdy et al., 2009). Additionally in macaques, maternal overnutrition before and during pregnancy resulted in increased postnatal adiposity in offspring (Grayson et al., 2010). Thus the pattern of susceptibility to adult metabolic disease resulting from fetal programming is U-shaped, with both maternal undernutrition and overnutrition affecting offspring MetS risk (Taylor and Poston, 2007). Work in the rhesus macaque also showed that offspring of high fat fed mothers had increased proopiomelanocortin mRNA expression and decreased agouti-related protein mRNA expression, suggesting that maternal overnutrition during pregnancy may activate proinflammatory cytokines that could alter melanocortin activity (Grayson et al., 2010). Evidence in rodent models suggest molecular epigenetic mechanisms, such as those discussed in Section 4.7, underlie at least some of these effects (Lillycrop et al., 2005; Vickers et al., 2005). Identifying variation in epigenetic marks that associate with variation in maternal effects on fetal programming is a fruitful avenue for further research.

Maternal effects on fetal programming are generally considered environmental because they are not a function of the offspring's genome. Rather they result from the maternally produced developmental environment. Nearly all studies in mouse model systems have focused exclusively on maternal environmental effects using genetically uniform C57BL/6J mothers and offspring. But maternal genetic variations are also responsible for substantial variability in the fetal and neonatal developmental environment (although the effect is environmental with respect to the offspring). Murine maternal effect QTL associated with early offspring growth in a cross-fostered F_3 generation of a LG/J x SM/J intercross showed that variation in maternal genotype accounted for >30% of among litter offspring variation (Wolf et al., 2002). Another mouse study measured maternal genetic effects on multiple MetS components and found that variation in maternal genotype accounted for up to 10% of adult offspring phenotypic variation (Jarvis et al., 2005).

5.2 Nutrition

Animal models are ideal for studying the effects of nutrition on MetS etiology because commercial diets are readily available, allowing dietary composition to be precisely monitored. Further, specialized high fat and high sucrose diets have been developed that mimic the human "Western" diet hypothesized to underlie the past 30 years' rising rates of metabolic disease. In mouse, strains have been characterized by whether they become obese on a Western diet [referred to as diet-induced obesity (DIO) strains] or not (referred to as dietary-resistant strains). Variation in high fat dietary response has been quantified in 43 inbred strains for 10 phenotypic traits, including metabolic parameters in blood serum levels and adiposity (Svenson et al., 2007). Another study quantified variation in macronutrient diet self-selection across different inbred mouse strains (Smith et al., 2000). This study is interesting in that it shows that individual preference for certain macronutrients vary according to genetic background. Consistent with rodent results, dietary studies in nonhuman primates show that some species become obese and/or develop other metabolic complications while other species do not. For example, squirrel monkeys fed high fat, high sucrose diets became obese, while cebus monkeys fed the same diet did not (Ausman et al., 1981). This supports results from rodent models indicating that genetic background is an important factor of dietary risk. A recent study in rhesus macaques provided with a 500 mL/day 15% fructose-sweetened beverage showed that animals developed multiple MetS components including central obesity, dyslipidemia, inflammation, and insulin resistance. A subset of these animals developed overt T2D (Bremer et al., 2011), indicating that rhesus macaque is a good model for studying variation in dietary response and MetS. Further, the rhesus macaque genome has been sequenced at relatively high coverage, providing an opportunity to study gene by dietary–environment interactions in a nonhuman primate model of MetS (Gibbs et al., 2007). An exciting avenue of research uses animal models to study dietary influences on gut microbiota and the metabolic consequences of upsetting gut microbial diversity. Studies in rodents indicate that dietary environment can lead to bacterial disruptions that influence energy extraction from food, fat storage, serum lipid levels, and insulin resistance. This suggests that the gut microbiome is an important link between dietary environment and MetS (for a review, see Tilg and Kaser, 2011 and references within). However, much of this research has been conducted in rodent knockout or germ-free models, so the translational application to human subjects remains to be explored.

5.3 Gene by Dietary Environment Interactions

As discussed previously, standing genetic variation can modify the effects of the environment on expression of phenotype. Characterizing gene by environment, particularly gene by dietary environment, interactions are essential to understand MetS etiology and for identifying potential risk factors in the context of personalized medicine. These interactions are challenging to parse

from human studies where environmental factors can be difficult to accurately measure or, in the case of GWAS, can be computationally prohibitive to analyze. However, some studies have successfully characterized gene by diet interactions in human populations and there is an effort to archive these results as they pertain to metabolic traits (Lee et al., 2011). Animal models can dissect gene by environment interactions and the most frequently studied model is the mouse, using the targeted or discovery methods discussed earlier in Sections 4.2 and 4.4, but with an added dietary parameter in the model (Lawson and Cheverud, 2010). As discussed earlier, genetic background (strain or species) needs to be taken into account when designing such studies.

For example, a targeted knockout approach demonstrated that high fat fed $Ppar\alpha^{-/-}$ mice accumulated significantly higher lipid concentrations in their livers relative to wild-type controls. Interestingly, $Ppar\alpha^{-/-}$ mice that were fasted for 24 h developed additional metabolic complications including hypoketonemia, hypoglycemia, impaired thermoregulation, and increased serum free fatty acid (FFA) levels. This result indicates that $Ppar\alpha$ plays a role in regulating the fatty acid oxidation response to fasting (Kersten et al., 1999; Leone et al., 1999). QTL have been identified in crosses between inbred mouse strains fed with high fat diets (e.g., Taylor et al., 2001; West et al., 1995; York et al., 1996). However, generally these studies do not map variation in metabolic traits in high fat versus low fat diets, which is necessary to characterize the gene by diet interaction. Recently, gene by diet interactions (high fat vs. low fat isocaloric diets) were characterized for multiple MetS components in studies of an F_{16} generation of an Advanced Intercross between the LG/J and SM/J inbred mouse strains (Cheverud et al., 2011; Lawson et al., 2010, 2011a,b). A major finding from these studies was that interactions are not consistent between the sexes or among the traits studied: for adiposity and serum lipid levels, high fat fed females were the most affected cohort and for diabetes-related traits, high fat fed males were the most affected cohort. These studies also demonstrated that if context was not taken into account in the mapping model (context referring to the sex and/or dietary environment), genetic associations are missed. For example, if a genetic effect is found only in high fat fed females, the lack of genetic effects in the other sex by diet cohorts will wash the association out if the entire population is pooled together in the analysis. Additionally, if the additive genetic effects between two cohorts in a population are of opposite directions (the homozygote genotypes change ranks in different environments), the association will be washed out if the two cohorts are pooled (Fig. 9.5). This result has important implications for human studies.

Gene-by-dietary-environment interactions that are identified in rodent models have potential to inform
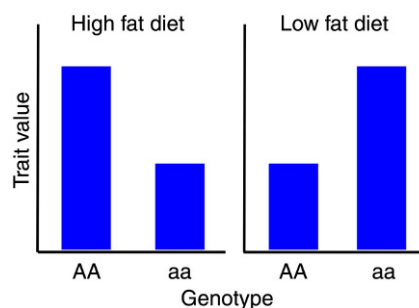
FIGURE 9.5 **An example of a gene-by-diet interaction with homozygote genotypes changing rank order in different dietary environments.** This figure illustrates that genetic associations can be missed if environment is not taken into account. In this example, trait value is the *y*-axis and homozygote genotypes are depicted on the *x*-axis. On a high fat diet, individuals with the AA genotype at the marker locus have a higher trait value than individuals with the aa genotype. The opposite is true for individuals on a low fat diet. If individuals of both diets are pooled together in an analysis, the opposite genetic effects of the two cohorts will wash each other out, despite a clear genetic association with the trait and gene by diet interaction. This result has been found in mouse models of MetS (Lawson et al., 2011a) and has implications for human studies.

human studies and potentially increase their power to identify patterns of interactions in populations of human subjects (using methods described in Sections 4.2 and 4.4). The idea is to identify biomarkers with dietary effects on metabolic parameters that may be context-dependent and that are relevant to the clinical reality of MetS in a nutritional genomics context. The promise of nutritional genomics is that it can provide personalized dietary recommendations based on an individual's genetic make-up at loci found to interact with diet. Personalized dietary recommendations aimed at prevention and therapy represent a practical clinical translation of animal model research to public health, particularly for MetS components, such as dyslipidemia or insulin resistance that could be delayed or even prevented through dietary modifications (Bouchard and Ordovas, 2012).

6 ANIMAL MODELS OF MetS PATHOPHYSIOLOGY

Understanding MetS pathophysiology in animal models can shed light on why some obese individuals develop metabolic complications while others do not. Further, animal models may also shed light on why some lean individuals develop multiple MetS components in the absence of obesity. Most animal models focused on pathophysiology attempt to understand the link between obesity and insulin resistance, which is an important risk factor for developing T2D and CVD. Physiological studies generally focus on the roles of adipose tissue, endocrine function, and fatty acid metabolism in metabolic complications, although each of these

factors is interrelated. Recently, the role of autophagy in obesity has been garnering attention. This is important because some fat depots (visceral adipose tissue) are correlated with increased risk of developing insulin resistance whereas others (subcutaneous adipose tissue) are actually correlated with decreased risk (reviewed in: Hardy et al., 2012), yet the mechanisms underlying these correlations are unknown. Animal models that test mechanistic hypotheses are the first step toward gaining new biological insight into MetS. Physiological studies inform genetic studies (and are also informed by genetic studies), and candidate gene studies can be designed based on physiological results with the idea that identifying molecular mechanisms underlying metabolic complications can lead to the discovery of novel biomarkers and the development of better therapeutic strategies for MetS.

6.1 Adipose Tissue: Hormones, Remodeling and Inflammation

The role of leptin in MetS is discussed earlier in Section 4.1. Adiponectin is another adipose tissue derived protein hormone that was discovered shortly after leptin was characterized in a mouse model (Havel and Bremer, 2010). Adiponectin has been shown to be a key factor linking visceral adipose tissue to MetS. It is the most abundant protein secreted by adipocytes, and high circulating levels of adiponectin is correlated with increased insulin sensitivity and resistance to metabolic complications (Scherer, 2006). Low circulating adiponectin levels is correlated with insulin resistance in rhesus monkeys (Hotta et al., 2001) and in rodent models (Cummings et al., 2008; Nawrocki et al., 2006). A recent study used RNA-sequencing to profile genes expressed in liver in both adiponectin knockout and wild-type mice (Liu et al., 2012). This study found differential expression in genes involved in several glucose and lipid pathways that are fruitful targets for focused candidate gene studies aimed at identifying functional pathways regulated by adiponectin.

Adipose tissue remodeling and inflammation is likely involved in the pathogenesis of MetS. The accumulation of large adipocytes is associated with increasing rates of adipocyte death, inflammation, and insulin resistance. Macrophages localize to the dead adipocytes and form crown-like structures that envelope and ingest the adipocyte and its lipid droplet (Cinti et al., 2005). This clearance of dead adipocytes by macrophages is an initial remodeling event that promotes proinflammatory activation of macrophages, and results in a bimodal distribution of both large and small adipocytes. DIO mice show marked increases in adipocyte size, death, and macrophage content (Strissel et al., 2007). This is positively correlated with insulin resistance, dylipidemia, and non-

alcoholic fatty liver disease (Ferrante, 2007). Mice with loss of function mutations in monocyte chemoattractant protein-1 (*Mcp1*) and its receptor (*Ccr2*) have decreased adipose macrophage content and appear to be protected from high fat diet induced insulin resistance (Kanda et al., 2006; Weisberg et al., 2006). Further, mice overexpressing *Mcp1* have increased levels of adipose tissue macrophages and increased insulin resistance. At baseline, mouse adipose tissue macrophages show low expression of macrophage differentiation markers. Overnutrition results in a macrophage population "shift," with increasing levels of monocytes being recruited from circulation into the adipose tissue (Lumeng et al., 2007), indicating that DIO results in adipose tissue remodeling and remodeling-associated inflammatory response. Expression studies in rodent models are illuminating some of the genes involved in the intercellular communication among adipose tissue cell types, including TNF, SFRP5, and WNT5a (among others). A promising avenue of research using animal models is aimed at inhibiting the infiltration of monocytes into adipose tissue and potentially ameliorating the inflammatory response and preventing insulin resistance (Ouchi et al., 2011; Suganami and Ogawa, 2010 for a review of macrophages in adipose tissue remodeling and inflammation). It is worth noting that adiponectin is considered an antiinflammatory adipokine, and circulating levels decrease as inflammation increases. Recent pharmaceutical based research in mice has found that inhibiting *Mcp1* expression both reduces inflammation and increases adiponectin levels in adipose tissue (Vinolo et al., 2012).

6.2 Free Fatty Acid Metabolism

Altered FFA metabolism is an important factor in the pathogenesis of insulin resistant glucose metabolism, dyslipidemia, and possibly inflammation associated with obesity in MetS (Boden, 2006; Shulman, 2000). Excess plasma FFA concentration impairs the ability of insulin to stimulate muscle glucose uptake and suppresses hepatic glucose production (Ferrannini et al., 1983). Increased FFA delivery to the liver increases hepatic VLDL-triglyceride production and plasma triglyceride concentrations (Lewis et al., 1995). This increases the transfer of triglycerides from VLDL to HDL, which leads to increased HDL clearance and results in decreased plasma HDL concentrations (Hopkins and Barter, 1986). Visceral adiposity is associated with lipid accumulation in the liver and insulin resistance. It has been hypothesized that FFAs released during lipolysis of visceral adipose tissue causes insulin resistance because these fatty acids enter the portal vein and are directly delivered to the liver, leading to hepatic insulin resistance, triglyceride accumulation and increased secretion of atherogenic lipoproteins (Despres and Lemieux, 2006).

This so-called "Portal Theory" of MetS has been tested in canine models at both molecular and physiological levels. Dog intraabdominal fat depots are easily measured using magnetic resonance imaging, and invasive procedures, such as portal vein cannulation and omentectomy (surgical removal of the greater omentum and its constituent visceral adipose tissue) are easier to perform in larger mammals than in rodents, although recently a rat model has been developed with a chronically implanted portal vein catheter to quantify pulsatile insulin secretion (Matveyenko et al., 2008). As is observed in human populations, dogs naturally exhibit wide variance in fat deposition and increased levels of visceral adiposity is highly correlated with insulin resistance in dogs (Bergman et al., 2006, 2007; Kim et al., 2003). Differential expression of several important genes involved in FFA metabolism (LPL, HSL, and PPARγ) in both visceral fat and liver tissue was observed between high fat fed dogs and controls. Liver insulin receptor binding was decreased by 50% in the high fat fed dogs, providing circumstantial molecular evidence supporting the portal theory (Kabir et al., 2005). Omentectomy in a dog model has been demonstrated to improve insulin sensitivity, supporting the association between visceral fat and insulin resistance, however, the FFA-portal vein link between visceral fat and insulin resistance was not supported in this model (Lottati et al., 2009). Further, isotope tracer data from human subjects suggests that only 20% of FFAs delivered to the liver derive from visceral fat, indicating that it is unlikely that the delivery of fatty acids via the portal vein underlies the strong correlation between visceral fat and insulin resistance (Nielsen et al., 2004). Thus more research is required to test the FFAs hypothesis in the context of visceral fat and insulin resistance, and animal models will be integral to understanding this connection in the context of MetS pathophysiology.

6.3 Gastrointestinal Hormones

Hormones produced by the gastrointestinal tract are essential to glucose and lipid metabolism. These hormones are involved in short-term regulation of satiety and potentially in long-term regulation of adiposity and energy homeostasis (for a comprehensive review of endocrine regulation of energy balance, see Havel and Bremer, 2010; Suzuki et al., 2011). Animal models have been critical to understanding the roles of hormone action in MetS, and to characterizing receptor, and signaling pathways that can be manipulated for therapeutic intervention. Ghrelin is a peptide hormone produced by, and secreted from, endocrine cells of the stomach and proximal small intestine. It increases hunger and potentially stimulates food intake, although high circulating ghrelin concentrations are negatively correlated with body weight (Tschop et al., 2001). Nevertheless, direct administration of ghrelin has been found to increase food intake resulting in weight gain in a rat model (Tschop et al., 2000). Glucose-dependent insulinotropic polypeptide (GIP) is a hormone secreted by K-cells in the duodenum and proximal jejunum in response to carbohydrate ingestion. GIP receptors are located in pancreatic islets, brain, adrenal, and adipose tissues. GIP augments glucose-stimulated insulin secretion (D'Alessio et al., 2001). Ablating GIP producing K-cells in a mouse model appears to protect animals from dietary obesity, and administering a GIP receptor antagonist in high fat fed mice has been reported to reverse obesity and insulin resistance (Althage et al., 2008; McClean et al., 2007). Glucagon-like peptide-1 (GLP-1) is produced by L-cells in the ileum. Administering GLP-1 receptor antagonist has been shown to improve glucose tolerance in a baboon model (D'Alessio et al., 1996). GLP-1 is also produced in neurons in the hypothalamus. Administering GLP-1 directly into the brains of rats has been shown to inhibit feeding and result in weight loss (Tang-Christensen et al., 1996). Oxyntomodulin (OXM) is cosecreted with GLP-1 from L-cells in the ileum. Administration of OXM inhibits food intake in rats, likely by increasing energy expenditure (Dakin et al., 2002). Peptide-YY (PYY) is produced by L-cells in the ileum and colon. PYY concentrations rise after feeding, peak after 1–2 h, and remain elevated for several hours longer. Higher levels of PYY are secreted after fat ingestion than after either carbohydrate or protein ingestion (Suzuki et al., 2011). It has been observed in a mouse model that PYY administration inhibits food intake, promoting weight loss and fat oxidation (Adams et al., 2006), although this result has not been observed in other mouse studies (Tschop et al., 2004). These gastrointestinal hormones all converge on major signaling pathways in the brain, namely the arcuate nucleus of the hypothalamus and the dorsal motor nucleus of the vagus nerve in the brainstem. Each represents promising therapeutic targets for appetite regulation in the context of MetS. The fundamental knowledge derived from animal models of endocrine regulation can set the stage for planning appropriate and safe therapeutic manipulations of these signaling pathways in human subjects.

6.4 Autophagy

Autophagy is an intracellular process wherein cell cytoplasm constituents and structures are isolated by a phagophore, segregated from the cytoplasm into an autophagosome, which then fuses with a lysosome to form an autolysosome whose contents are degraded and recycled for use in the cell. Autophagy is a response to stress but it also plays a role in normal cell remodeling (Mizushima and Klionsky, 2007). Autophagy is inhibited by mTOR activation in the presence of insulin-like and

other growth factors (Jung et al., 2010). It is induced by a reduction in mTOR signaling, activating a protein serine/threonine kinase complex. Autophagy has recently been associated with metabolic function, including regulation of lipid metabolism (Singh et al., 2009) and obesity (Goldman et al., 2010; Zhang et al., 2009). Inhibiting autophagy leads to an increase in circulating triglyceride levels and a decrease in triglyceride breakdown, suggesting that accumulating lipids decreases autophagy, potentially leading to a deleterious positive feedback loop in the cell's physiology (Singh et al., 2009). Key genes involved in this process include: ATG1, ATG7, BCN1, LC3, and class III P13K among others. Recently, an adipose tissue specific *Atg7* knockout mouse model found that adipose-specific *Atg7*$^{-/-}$ animals weigh less and have reduced reproductive fat depots relative to wild-type controls (Zhang et al., 2009). The knockouts consumed food at the same rate as wild-type mice regardless of diet, yet they failed to develop obesity when on a high fat diet. Additionally, they were more active than wild-type controls. *Atg7*$^{-/-}$ animals exhibited lower serum triglyceride, cholesterol, FFA, and leptin levels, but normal adiponectin and glucose levels with decreased serum insulin levels and increased insulin sensitivity. At the cellular level, adipogenesis was less efficient in *Atg7*$^{-/-}$ primary mouse embryonic fibroblasts than in wild-type controls. Histological analysis showed that *Atg7*$^{-/-}$ adipocytes were smaller and often contained multiple small lipid droplets rather than the single large droplet found in wild-type cells. A recent study in an Ossabaw pig model found that inhibited myocardial autophagy was associated with development of MetS (Li et al., 2012b). Better understanding the pathophysiology and the molecular underpinnings of autophagy in metabolic traits in animal models could facilitate the exploration of this cellular process in human obese subjects with the idea that exploitation of this pathway has therapeutic potential for MetS.

7 CONCLUSIONS

To prescribe the right therapies for MetS, one needs to be able to predict phenotype from genotype to some degree. Animal models have advanced our understanding of the genotype-metabolic function relationship through testing hypotheses about genetic underpinnings and molecular pathophysiologies that lead to the clustering of metabolic complications putting an individual at risk of developing T2D and/or CVD. Bioinformatic tools and archived genomic and phenotypic data for different animal model systems make it possible to design and execute focused studies using the species or strains that most appropriately mimic the clinical reality of MetS. Exciting advances in genomics make it possible to explore both

genetic and epigenetic modes of gene regulation and to understand how genes modify environmental effects on phenotypic variation. Characterization of molecular physiological pathways in animal models—especially direct characterizations in disease-relevant tissues—can illuminate potential therapeutic targets. Patterns identified in animal models can be translated to studies of human subjects for the improvement of human health.

References

Aagaard-Tillery, K.M., Grove, K., Bishop, J., Ke, X., Fu, Q., McKnight, R., et al., 2008. Developmental origins of disease and determinants of chromatin structure: maternal diet modifies the primate fetal epigenome. J. Mol. Endocrinol. 41 (2), 91–102.

Adams, S.H., Lei, C., Jodka, C.M., Nikoulina, S.E., Hoyt, J.A., Gedulin, B., et al., 2006. PYY[3–36] administration decreases the respiratory quotient and reduces adiposity in diet-induced obese mice. J. Nutr. 136 (1), 195–201.

Aitman, T.J., Glazier, A.M., Wallace, C.A., Cooper, L.D., Norsworthy, P.J., Wahid, F.N., et al., 1999. Identification of Cd36 (Fat) as an insulin-resistance gene causing defective fatty acid and glucose metabolism in hypertensive rats. Nat. Genet. 21 (1), 76–83.

Akiyama, T.E., Nicol, C.J., Fievet, C., Staels, B., Ward, J.M., Auwerx, J., et al., 2001. Peroxisome proliferator-activated receptor-alpha regulates lipid homeostasis, but is not associated with obesity: studies with congenic mouse lines. J. Biol. Chem. 276 (42), 39088–39093.

Althage, M.C., Ford, E.L., Wang, S., Tso, P., Polonsky, K.S., Wice, B.M., 2008. Targeted ablation of glucose-dependent insulinotropic polypeptide-producing cells in transgenic mice reduces obesity and insulin resistance induced by a high fat diet. J. Biol. Chem. 283 (26), 18365–18376.

Aoyama, T., Peters, J.M., Iritani, N., Nakajima, T., Furihata, K., Hashimoto, T., et al., 1998. Altered constitutive expression of fatty acid-metabolizing enzymes in mice lacking the peroxisome proliferator-activated receptor alpha (PPARalpha). J. Biol. Chem. 273 (10), 5678–5684.

Arner, P., 2005. Resist: yet another adipokine tells us that men are not mice. Diabetologia 48 (11), 2203–2205.

Ausman, L.M., Rasmussen, K.M., Gallina, D.L., 1981. Spontaneous obesity in maturing squirrel monkeys fed semipurified diets. Am. J. Physiol. 241 (5), R316–R321.

Barbier, O., Torra, I.P., Duguay, Y., Blanquart, C., Fruchart, J.C., Glineur, C., et al., 2002. Pleiotropic actions of peroxisome proliferator-activated receptors in lipid metabolism and atherosclerosis. Arterioscler. Thromb. Vasc. Biol. 22 (5), 717–726.

Barker, D.J., 2007. The origins of the developmental origins theory. J. Intern. Med. 261 (5), 412–417.

Belgardt, B.F., Okamura, T., Bruning, J.C., 2009. Hormone and glucose signalling in POMC and AgRP neurons. J. Physiol. 587 (Pt 22), 5305–5314.

Bennett, B.J., Farber, C.R., Orozco, L., Kang, H.M., Ghazalpour, A., Siemers, N., et al., 2010. A high-resolution association mapping panel for the dissection of complex traits in mice. Genome Res. 20 (2), 281–290.

Bergman, R.N., Kim, S.P., Catalano, K.J., Hsu, I.R., Chiu, J.D., Kabir, M., et al., 2006. Why visceral fat is bad: mechanisms of the metabolic syndrome. Obesity 14 (Suppl. 1), 16S–19S.

Bergman, R.N., Kim, S.P., Hsu, I.R., Catalano, K.J., Chiu, J.D., Kabir, M., et al., 2007. Abdominal obesity: role in the pathophysiology of metabolic disease and cardiovascular risk. Am. J. Med. 120 (2 Suppl. 1), S3–S8, discussion S29–S32.

Bertram, C.E., Hanson, M.A., 2001. Animal models and programming of the metabolic syndrome. Br. Med. Bull. 60, 103–121.

Bidanel, J.P., Milan, D., Iannuccelli, N., Amigues, Y., Boscher, M.Y., Bourgeois, F., et al., 2001. Detection of quantitative trait loci for growth and fatness in pigs. Genet. Sel. Evol. 33 (3), 289–309.

Bielschowsky, M., Goodall, C.M., 1970. Origin of inbred NZ mouse strains. Cancer Res. 30 (3), 834–836.

Boden, G., 2006. Fatty acid-induced inflammation and insulin resistance in skeletal muscle and liver. Curr. Diab. Rep. 6 (3), 177–181.

Bodkin, N.L., Hannah, J.S., Ortmeyer, H.K., Hansen, B.C., 1993. Central obesity in rhesus monkeys: association with hyperinsulinemia, insulin resistance and hypertriglyceridemia? Int. J. Obes. Relat. Metab. Disord. 17 (1), 53–61.

Bogardus, C., 2009. Missing heritability and GWAS utility. Obesity 17 (2), 209–210.

Bose, T., Voruganti, V.S., Tejero, M.E., Proffit, J.M., Cox, L.A., VandeBerg, J.L., et al., 2010. Identification of a QTL for adipocyte volume and of shared genetic effects with aspartate aminotransferase. Biochem. Genet. 48 (5–6), 538–547.

Bouchard, C., Ordovas, J.M., 2012. Fundamentals of nutrigenetics and nutrigenomics. Prog. Mol. Biol. Transl. Sci. 108, 1–15.

Brault, V., Besson, V., Magnol, L., Duchon, A., Herault, Y., 2007. Cre/loxP-mediated chromosome engineering of the mouse genome. Handb. Exp. Pharmacol. (178), 29–48.

Bremer, A.A., Stanhope, K.L., Graham, J.L., Cummings, B.P., Wang, W., Saville, B.R., et al., 2011. Fructose-fed rhesus monkeys: a nonhuman primate model of insulin resistance, metabolic syndrome, and type 2 diabetes. Clin. Transl. Sci. 4 (4), 243–252.

Burgueno, A.L., Landa, M.S., Schuman, M.L., Alvarez, A.L., Carabelli, J., Garcia, S.I., et al., 2007. Association between diencephalic thyroliberin and arterial blood pressure in agouti-yellow and ob/ob mice may be mediated by leptin. Metabolism 56 (10), 1439–1443.

Butler, M.G., 2009. Genomic imprinting disorders in humans: a mini-review. J. Assist. Reprod. Genet. 26 (9–10), 477–486.

Cai, G., Cole, S.A., Tejero, M.E., Proffitt, J.M., Freeland-Graves, J.H., Blangero, J., et al., 2004. Pleiotropic effects of genes for insulin resistance on adiposity in baboons. Obes. Res. 12 (11), 1766–1772.

Capecchi, M.R., 1989a. Altering the genome by homologous recombination. Science 244 (4910), 1288–1292.

Capecchi, M.R., 1989b. The new mouse genetics: altering the genome by gene targeting. Trends Genet. 5 (3), 70–76.

Carroll, L., Voisey, J., van Daal, A., 2004. Mouse models of obesity. Clin. Dermatol. 22 (4), 345–349.

Chen, R., Ren, J., Li, W., Huang, X., Yan, X., Yang, B., et al., 2009. A genome-wide scan for quantitative trait loci affecting serum glucose and lipids in a White Duroc x Erhualian intercross F(2) population. Mamm. Genome 20 (6), 386–392.

Cheverud, J.M., Lawson, H.A., Fawcett, G.L., Wang, B., Pletscher, L.S., et al., 2011. Diet-dependent genetic and genomic imprinting effects on obesity in mice. Obesity 19 (1), 160–170.

Chua, Jr., S., Liu, S.M., Li, Q., Yang, L., Thassanapaff, V.T., Fisher, P., 2002. Differential beta cell responses to hyperglycaemia and insulin resistance in two novel congenic strains of diabetes (FVB- Lepr (db)) and obese (DBA- Lep (ob)) mice. Diabetologia 45 (7), 976–990.

Chung, W.K., Belfi, K., Chua, M., Wiley, J., Mackintosh, R., Nicolson, M., et al., 1998. Heterozygosity for Lep(ob) or Lep(rdb) affects body composition and leptin homeostasis in adult mice. Am. J. Physiol. 274 (4 Pt. 2), R985–R990.

Church, C., Lee, S., Bagg, E.A., McTaggart, J.S., Deacon, R., Gerken, T., et al., 2009. A mouse model for the metabolic effects of the human fat mass and obesity associated FTO gene. PLoS Genet. 5 (8), e1000599.

Church, C., Moir, L., McMurray, F., Girard, C., Banks, G.T., Teboul, L., et al., 2010. Overexpression of Fto leads to increased food intake and results in obesity. Nat. Genet. 42 (12), 1086–1092.

Churchill, G.A., Airey, D.C., Allayee, H., Angel, J.M., Attie, A.D., Beatty, J., et al., 2004. The collaborative cross, a community resource for the genetic analysis of complex traits. Nat. Genet. 36 (11), 1133–1137.

Cinti, S., Mitchell, G., Barbatelli, G., Murano, I., Ceresi, E., Faloia, E., et al., 2005. Adipocyte death defines macrophage localization and function in adipose tissue of obese mice and humans. J. Lipid Res. 46 (11), 2347–2355.

Clee, S.M., Attie, A.D., 2007. The genetic landscape of type 2 diabetes in mice. Endocr. Rev. 28 (1), 48–83.

Clee, S.M., Nadler, S.T., Attie, A.D., 2005. Genetic and genomic studies of the BTBR ob/ob mouse model of type 2 diabetes. Am. J. Ther. 12 (6), 491–498.

Cole, S.A., Martin, L.J., Peebles, K.W., Leland, M.M., Rice, K., VandeBerg, J.L., et al., 2003. Genetics of leptin expression in baboons. Int. J. Obes. Relat. Metab. Disord. 27 (7), 778–783.

Coleman, D.L., Eicher, E.M., 1990. Fat (fat) and tubby (tub): two autosomal recessive mutations causing obesity syndromes in the mouse. J. Hered. 81 (6), 424–427.

Coleman, D.L., Hummel, K.P., 1973. The influence of genetic background on the expression of the obese (Ob) gene in the mouse. Diabetologia 9 (4), 287–293.

Collins, F.S., Rossant, J., Wurst, W., 2007. A mouse for all reasons. Cell 128 (1), 9–13.

Comuzzie, A.G., Cole, S.A., Martin, L., Carey, K.D., Mahaney, M.C., Blangero, J., et al., 2003. The baboon as a nonhuman primate model for the study of the genetics of obesity. Obes. Res. 11 (1), 75–80.

Cone, R.D., 2005. Anatomy and regulation of the central melanocortin system. Nat. Neurosci. 8 (5), 571–578.

Cool, B., Zinker, B., Chiou, W., Kifle, L., Cao, N., Perham, M., et al., 2006. Identification and characterization of a small molecule AMPK activator that treats key components of type 2 diabetes and the metabolic syndrome. Cell Metab. 3 (6), 403–416.

Cox, R.D., Church, C.D., 2011. Mouse models and the interpretation of human GWAS in type 2 diabetes and obesity. Dis. Model. Mech. 4 (2), 155–164.

Cox, L.A., Birnbaum, S., Mahaney, M.C., Rainwater, D.L., Williams, J.T., VandeBerg, J.L., 2007. Identification of promoter variants in baboon endothelial lipase that regulate high-density lipoprotein cholesterol levels. Circulation 116 (10), 1185–1195.

Cummings, B.P., Digitale, E.K., Stanhope, K.L., Graham, J.L., Baskin, D.G., Reed, B.J., et al., 2008. Development and characterization of a novel rat model of type 2 diabetes mellitus: the UC Davis type 2 diabetes mellitus UCD-T2DM rat. Am. J. Physiol. Regul. Integr. Comp. Physiol. 295 (6), R1782–R1793.

Dakin, C.L., Small, C.J., Park, A.J., Seth, A., Ghatei, M.A., Bloom, S.R., 2002. Repeated ICV administration of oxyntomodulin causes a greater reduction in body weight gain than in pair-fed rats. Am. J. Physiol. Endocrinol. Metab. 283 (6), E1173–E1177.

D'Alessio, D.A., Vogel, R., Prigeon, R., Laschansky, E., Koerker, D., Eng, J., et al., 1996. Elimination of the action of glucagon-like peptide 1 causes an impairment of glucose tolerance after nutrient ingestion by healthy baboons. J. Clin. Invest. 97 (1), 133–138.

D'Alessio, D.A., Kieffer, T.J., Taborsky, Jr., G.J., Havel, P.J., 2001. Activation of the parasympathetic nervous system is necessary for normal meal-induced insulin secretion in rhesus macaques. J. Clin. Endocrinol. Metab. 86 (3), 1253–1259.

Despres, J.P., Lemieux, I., 2006. Abdominal obesity and metabolic syndrome. Nature 444 (7121), 881–887.

Dina, C., Meyre, D., Gallina, S., Durand, E., Korner, A., Jacobson, P., et al., 2007. Variation in FTO contributes to childhood obesity and severe adult obesity. Nat. Genet. 39 (6), 724–726.

Dong, C., Li, W.D., Geller, F., Lei, L., Li, D., Gorlova, O.Y., et al., 2005. Possible genomic imprinting of three human obesity-related genetic loci. Am. J. Hum. Genet. 76 (3), 427–437.

Drover, V.A., Ajmal, M., Nassir, F., Davidson, N.O., Nauli, A.M., Sahoo, D., et al., 2005. CD36 deficiency impairs intestinal lipid secretion and clearance of chylomicrons from the blood. J. Clin. Invest. 115 (5), 1290–1297.

Dulin, W.E., Wyse, B.M., 1970. Diabetes in the KK mouse. Diabetologia 6, 317–323.

Eckel, R.H., Grundy, S.M., Zimmet, P.Z., 2005. The metabolic syndrome. Lancet 365 (9468), 1415–1428.

Edney, A.T., Smith, P.M., 1986. Study of obesity in dogs visiting veterinary practices in the United Kingdom. Vet. Rec. 118 (14), 391–396.

Einhorn, D., Reaven, G.M., Cobin, R.H., Ford, E., Ganda, O.P., Handelsman, Y., et al., 2003. American College of Endocrinology position statement on the insulin resistance syndrome. Endocr. Pract. 9 (3), 237–252.

Elder, S.J., Lichtenstein, A.H., Pittas, A.G., Roberts, S.B., Fuss, P.J., Greenberg, A.S., et al., 2009. Genetic and environmental influences on factors associated with cardiovascular disease and the metabolic syndrome. J. Lipid Res. 50 (9), 1917–1926.

Elmquist, J.K., Elias, C.F., Saper, C.B., 1999. From lesions to leptin: hypothalamic control of food intake and body weight. Neuron 22 (2), 221–232.

Fan, W., Dinulescu, D.M., Butler, A.A., Zhou, J., Marks, D.L., Cone, R.D., 2000. The central melanocortin system can directly regulate serum insulin levels. Endocrinology 141 (9), 3072–3079.

Ferrannini, E., Barrett, E.J., Bevilacqua, S., DeFronzo, R.A., 1983. Effect of fatty acids on glucose production and utilization in man. J. Clin. Invest. 72 (5), 1737–1747.

Ferrante, Jr., A.W., 2007. Obesity-induced inflammation: a metabolic dialogue in the language of inflammation. J. Intern. Med. 262 (4), 408–414.

Fischer, J., Koch, L., Emmerling, C., Vierkotten, J., Peters, T., Bruning, J.C., et al., 2009. Inactivation of the Fto gene protects from obesity. Nature 458 (7240), 894–898.

Fisler, J.S., Warden, C.H., Pace, M.J., Lusis, A.J., 1993. BSB: a new mouse model of multigenic obesity. Obes. Res. 1 (4), 271–280.

Fitzgerald, S.M., Henegar, J.R., Brands, M.W., Henegar, L.K., Hall, J.E., 2001. Cardiovascular and renal responses to a high-fat diet in Osborne–Mendel rats. Am. J. Physiol. Regul. Integr. Comp. Physiol. 281 (2), R547–R552.

Fowler, K.E., Pong-Wong, R., Bauer, J., Clemente, E.J., Reitter, C.P., Affara, N.A., et al., 2013. Genome wide analysis reveals single nucleotide polymorphisms associated with fatness and putative novel copy number variants in three pig breeds. BMC Genomics 14, 784.

Frayling, T.M., Timpson, N.J., Weedon, M.N., Zeggini, E., Freathy, R.M., Lindgren, C.M., et al., 2007. A common variant in the FTO gene is associated with body mass index and predisposes to childhood and adult obesity. Science 316 (5826), 889–894.

George, L.A., Uthlaut, A.B., Long, N.M., Zhang, L., Ma, Y., Smith, D.T., et al., 2010. Different levels of overnutrition and weight gain during pregnancy have differential effects on fetal growth and organ development. Reprod. Biol. Endocrinol. 8, 75.

Gesta, S., Tseng, Y.H., Kahn, C.R., 2007. Developmental origin of fat: tracking obesity to its source. Cell 131 (2), 242–256.

Gibbs, R.A., Rogers, J., Katze, M.G., Bumgarner, R., Weinstock, G.M., Mardis, E.R., et al., 2007. Evolutionary and biomedical insights from the rhesus macaque genome. Science 316 (5822), 222–234.

Goldman, S., Zhang, Y., Jin, S., 2010. Autophagy and adipogenesis: implications in obesity and type II diabetes. Autophagy 6 (1), 179–181.

Goudriaan, J.R., den Boer, M.A., Rensen, P.C., Febbraio, M., Kuipers, F., Romijn, J.A., et al., 2005. CD36 deficiency in mice impairs lipoprotein lipase-mediated triglyceride clearance. J. Lipid Res. 46 (10), 2175–2181.

Grayson, B.E., Levasseur, P.R., Williams, S.M., Smith, M.S., Marks, D.L., Grove, K.L., 2010. Changes in melanocortin expression and inflammatory pathways in fetal offspring of nonhuman primates fed a high-fat diet. Endocrinology 151 (4), 1622–1632.

Griffin, E., Re, A., Hamel, N., Fu, C., Bush, H., McCaffrey, T., et al., 2001. A link between diabetes and atherosclerosis: glucose regulates expression of CD36 at the level of translation. Nat. Med. 7 (7), 840–846.

Grimaldi, P.A., 2005. Regulatory role of peroxisome proliferator-activated receptor delta (PPAR delta) in muscle metabolism. A new target for metabolic syndrome treatment? Biochimie 87 (1), 5–8.

Grundy, S.M., 2008. Metabolic syndrome pandemic. Arterioscler. Thromb. Vasc. Biol. 28 (4), 629–636.

Grundy, S.M., Cleeman, J.I., Daniels, S.R., Donato, K.A., Eckel, R.H., Franklin, B.A., et al., 2005. Diagnosis and management of the metabolic syndrome: an American Heart Association/National Heart, Lung, and Blood Institute Scientific Statement. Circulation 112 (17), 2735–2752.

Hardy, O.T., Czech, M.P., Corvera, S., 2012. What causes the insulin resistance underlying obesity? Curr. Opin. Endocrinol. Diab. Obes. 19 (2), 81–87.

Harris, R.A., Wang, T., Coarfa, C., Nagarajan, R.P., Hong, C., Downey, S.L., et al., 2010. Comparison of sequencing-based methods to profile DNA methylation and identification of monoallelic epigenetic modifications. Nat. Biotechnol. 28 (10), 1097–1105.

Hasty, A.H., Shimano, H., Osuga, J., Namatame, I., Takahashi, A., Yahagi, N., et al., 2001. Severe hypercholesterolemia, hypertriglyceridemia, and atherosclerosis in mice lacking both leptin and the low density lipoprotein receptor. J. Biol. Chem. 276 (40), 37402–37408.

Havel, P.J., 2004. Update on adipocyte hormones: regulation of energy balance and carbohydrate/lipid metabolism. Diabetes 53 (Suppl. 1), S143–S151.

Havel, P.J., Bremer, A.A., 2010. Endocrine regulation of energy homeostasis: implications for obesity and diabetes. In: Rios, M.S., Ordovas, J.M., Gutierrez-Fuentes, J.A. (Eds.), Obesity. McGraw Hill, New York, NY.

He, W., Barak, Y., Hevener, A., Olson, P., Liao, D., Le, J., et al., 2003. Adipose-specific peroxisome proliferator-activated receptor gamma knockout causes insulin resistance in fat and liver but not in muscle. Proc. Natl. Acad. Sci. USA 100 (26), 15712–15717.

Heerwagen, M.J., Miller, M.R., Barbour, L.A., Friedman, J.E., 2010. Maternal obesity and fetal metabolic programming: a fertile epigenetic soil. Am. J. Physiol. Regul. Integr. Comp. Physiol. 299 (3), R711–R722.

Herrera, B.M., Keildson, S., Lindgren, C.M., 2011. Genetics and epigenetics of obesity. Maturitas 69 (1), 41–49.

Hevener, A.L., He, W., Barak, Y., Le, J., Bandyopadhyay, G., Olson, P., et al., 2003. Muscle-specific Pparg deletion causes insulin resistance. Nat. Med. 9 (12), 1491–1497.

Hofmann, S.M., Perez-Tilve, D., Greer, T.M., Coburn, B.A., Grant, E., Basford, J.E., et al., 2008. Defective lipid delivery modulates glucose tolerance and metabolic response to diet in apolipoprotein E-deficient mice. Diabetes 57 (1), 5–12.

Hopkins, G.J., Barter, P.J., 1986. Role of triglyceride-rich lipoproteins and hepatic lipase in determining the particle size and composition of high density lipoproteins. J. Lipid Res. 27 (12), 1265–1277.

Hotta, K., Funahashi, T., Bodkin, N.L., Ortmeyer, H.K., Arita, Y., Hansen, B.C., et al., 2001. Circulating concentrations of the adipocyte protein adiponectin are decreased in parallel with reduced insulin sensitivity during the progression to type 2 diabetes in rhesus monkeys. Diabetes 50 (5), 1126–1133.

Hu, Z.L., Dracheva, S., Jang, W., Maglott, D., Bastiaansen, J., Rothschild, M.F., et al., 2005. A QTL resource and comparison tool for pigs: PigQTLDB. Mamm. Genome 16 (10), 792–800.

Ingalls, A.M., Dickie, M.M., Snell, G.D., 1950. Obese, a new mutation in the house mouse. J. Hered. 41 (12), 317–318.

International Diabetes Federation (IDF), 2006. Online Guideline/Report: International Diabetes Federation: The IDF consensus worldwide definition of the metabolic syndrome. Retrieved from http://www.idf.org/webdata/docs/IDF_Meta_def_final.pdf

Ionut, V., Liu, H., Mooradian, V., Castro, A.V., Kabir, M., Stefanovski, D., et al., 2010. Novel canine models of obese prediabetes and mild type 2 diabetes. Am. J. Physiol. Endocrinol. Metab. 298 (1), E38–E48.

Ishibashi, S., Brown, M.S., Goldstein, J.L., Gerard, R.D., Hammer, R.E., Herz, J., 1993. Hypercholesterolemia in low density lipoprotein receptor knockout mice and its reversal by adenovirus-mediated gene delivery. J. Clin. Invest. 92 (2), 883–893.

Jarvis, J.P., Kenney-Hunt, J., Ehrich, T.H., Pletscher, L.S., Semenkovich, C.F., Cheverud, J.M., 2005. Maternal genotype affects adult off-spring lipid, obesity, and diabetes phenotypes in LGXSM recombinant inbred strains. J. Lipid Res. 46 (8), 1692–1702.

Jinek, M., Chylinski, K., Fonfara, I., Hauer, M., Doudna, J.A., Charpentier, E., 2012. A programmable dual-RNA-guided DNA endonuclease in adaptive bacterial immunity. Science 337 (6096), 816–821.

Jung, C.H., Ro, S.H., Cao, J., Otto, N.M., Kim, D.H., 2010. mTOR regulation of autophagy. FEBS Lett. 584 (7), 1287–1295.

Kabir, M., Catalano, K.J., Ananthnarayan, S., Kim, S.P., Van Citters, G.W., Dea, M.K., et al., 2005. Molecular evidence supporting the portal theory: a causative link between visceral adiposity and hepatic insulin resistance. Am. J. Physiol. Endocrinol. Metab. 288 (2), E454–E461.

Kahn, R., Buse, J., Ferrannini, E., Stern, M., 2005. The metabolic syndrome: time for a critical appraisal: joint statement from the American Diabetes Association and the European Association for the Study of Diabetes. Diab. Care 28 (9), 2289–2304.

Kalt, W., Foote, K., Fillmore, S.A., Lyon, M., Van Lunen, T.A., McRae, K.B., 2008. Effect of blueberry feeding on plasma lipids in pigs. Br. J. Nutr. 100 (1), 70–78.

Kammerer, C.M., Rainwater, D.L., Cox, L.A., Schneider, J.L., Mahaney, M.C., Rogers, J., et al., 2002. Locus controlling LDL cholesterol response to dietary cholesterol is on baboon homologue of human chromosome 6. Arterioscler. Thromb. Vasc. Biol. 22 (10), 1720–1725.

Kanda, H., Tateya, S., Tamori, Y., Kotani, K., Hiasa, K., Kitazawa, R., et al., 2006. MCP-1 contributes to macrophage infiltration into adipose tissue, insulin resistance, and hepatic steatosis in obesity. J. Clin. Invest. 116 (6), 1494–1505.

Kava, R.A., Greenwood, M.R., Johnson, P.R., 1990. New rat models of obesity and type II diabetes. Inst. Lab. Anim. Res. 32 (3), 4–8.

Keane, T.M., Goodstadt, L., Danecek, P., White, M.A., Wong, K., Yalcin, B., et al., 2011. Mouse genomic variation and its effect on phenotypes and gene regulation. Nature 477 (7364), 289–294.

Kennedy, A.J., Ellacott, K.L., King, V.L., Hasty, A.H., 2010. Mouse models of the metabolic syndrome. Dis. Model. Mech. 3 (3–4), 156–166.

Kersten, S., Seydoux, J., Peters, J.M., Gonzalez, F.J., Desvergne, B., Wahli, W., 1999. Peroxisome proliferator-activated receptor alpha mediates the adaptive response to fasting. J. Clin. Invest. 103 (11), 1489–1498.

Kim, S.P., Ellmerer, M., Van Citters, G.W., Bergman, R.N., 2003. Primacy of hepatic insulin resistance in the development of the metabolic syndrome induced by an isocaloric moderate-fat diet in the dog. Diabetes 52 (10), 2453–2460.

Kind, K.L., Clifton, P.M., Katsman, A.I., Tsiounis, M., Robinson, J.S., Owens, J.A., 1999. Restricted fetal growth and the response to dietary cholesterol in the guinea pig. Am. J. Physiol. 277 (6 Pt 2), R1675–R1682.

Kind, K.L., Clifton, P.M., Grant, P.A., Owens, P.C., Sohlstrom, A., Roberts, C.T., et al., 2003. Effect of maternal feed restriction during pregnancy on glucose tolerance in the adult guinea pig. Am. J. Physiol. Regul. Integr. Comp. Physiol. 284 (1), R140–R152.

Kloting, N., Bluher, M., Kloting, I., 2006. The polygenetically inherited metabolic syndrome of WOKW rats is associated with insulin resistance and altered gene expression in adipose tissue. Diab. Metab. Res. Rev. 22 (2), 146–154.

Kong, A., Steinthorsdottir, V., Masson, G., Thorleifsson, G., Sulem, P., Besenbacher, S., et al., 2009. Parental origin of sequence variants associated with complex diseases. Nature 462 (7275), 868–874.

Konner, A.C., Klockener, T., Bruning, J.C., 2009. Control of energy homeostasis by insulin and leptin: targeting the arcuate nucleus and beyond. Physiol. Behav. 97 (5), 632–638.

Kovacs, P., van den Brandt, J., Kloting, I., 2000. Genetic dissection of the syndrome X in the rat. Biochem. Biophys. Res. Commun. 269 (3), 660–665.

Kraja, A.T., Province, M.A., Huang, P., Jarvis, J.P., Rice, T., Cheverud, J.M., et al., 2008. Trends in metabolic syndrome and gene networks in human and rodent models. Endocr. Metab. Immune. Disord. Drug Targets 8 (3), 198–207.

Kraja, A.T., Lawson, H.A., Arnett, D.K., Borecki, I.B., Broeckel, U., de Las Fuentes, L., et al., 2012. Obesity-insulin targeted genes in the 3p26-25 region in human studies and LG/J and SM/J mice. Metabolism 61 (8), 1129–1141.

Kulkarni, R.N., Almind, K., Goren, H.J., Winnay, J.N., Ueki, K., Okada, T., et al., 2003. Impact of genetic background on development of hyperinsulinemia and diabetes in insulin receptor/insulin receptor substrate-1 double heterozygous mice. Diabetes 52 (6), 1528–1534.

Kunej, T., D, J.S., Zork, M., Ogrinc, A., Michal, J.J., Kovac, M., et al., 2012. Obesity gene atlas in mammals. J. Genomics 1, 45–55.

Kurtz, T.W., Morris, R.C., Pershadsingh, H.A., 1989. The Zucker fatty rat as a genetic model of obesity and hypertension. Hypertension 13 (6 Pt 2), 896–901.

Kylin, E., 1923. Studies of the hypertension, hyperglycemia, hyperuricemia syndrome. Zentralblatt fuer Innere Medizin (44), 105–127.

Lawson, H.A., Cheverud, J.M., 2010. Metabolic syndrome components in murine models. Endocr. Metab. Immune. Disord. Drug Targets 10 (1), 25–40.

Lawson, H.A., Zelle, K.M., Fawcett, G.L., Wang, B., Pletscher, L.S., Maxwell, T.J., et al., 2010. Genetic, epigenetic, and gene-by-diet interaction effects underlie variation in serum lipids in a LG/JxSM/J murine model. J, Lipid Res, 51 (10), 2976–2984.

Lawson, H.A., Cady, J.E., Partridge, C., Wolf, J.B., Semenkovich, C.F., Cheverud, J.M., 2011a. Genetic effects at pleiotropic loci are context-dependent with consequences for the maintenance of genetic variation in populations. PLoS Genet, 7 (9), e1002256.

Lawson, H.A., Lee, A., Fawcett, G.L., Wang, B., Pletscher, L.S., Maxwell, T.J., et al., 2011b. The importance of context to the genetic architecture of diabetes-related traits is revealed in a genome-wide scan of a LG/J x SM/J murine model. Mamm, Genome 22 (3–4), 197–208.

Lee, Y.C., Lai, C.Q., Ordovas, J.M., Parnell, L.D., 2011. A database of gene-environment interactions pertaining to blood lipid traits, cardiovascular disease and type 2 diabetes. J, Data Mining Genomics Proteomics 2 (1).

Leone, T.C., Weinheimer, C.J., Kelly, D.P., 1999. A critical role for the peroxisome proliferator-activated receptor alpha (PPARalpha) in the cellular fasting response: the PPARalpha-null mouse as a model of fatty acid oxidation disorders. Proc. Natl. Acad. Sci. USA 96 (13), 7473–7478.

Lewis, D.S., Bertrand, H.A., McMahan, C.A., McGill, Jr., H.C., Carey, K.D., Masoro, E.J., 1986. Preweaning food intake influences the adiposity of young adult baboons. J. Clin. Invest. 78 (4), 899–905.

Lewis, G.F., Uffelman, K.D., Szeto, L.W., Weller, B., Steiner, G., 1995. Interaction between free fatty acids and insulin in the acute control of very low density lipoprotein production in humans. J. Clin. Invest. 95 (1), 158–166.

Li, M., Wu, H., Luo, Z., Xia, Y., Guan, J., Wang, T., et al., 2012a. An atlas of DNA methylomes in porcine adipose and muscle tissues. Nat. Commun. 3, 850.

Li, Z.L., Woollard, J.R., Ebrahimi, B., Crane, J.A., Jordan, K.L., Lerman, A., et al., 2012b. Transition from obesity to metabolic syndrome is associated with altered myocardial autophagy and apoptosis. Arterioscler. Thromb. Vasc. Biol. 32 (5), 1132–1141.

Liang, C., Oest, M.E., Prater, M.R., 2009. Intrauterine exposure to high saturated fat diet elevates risk of adult-onset chronic diseases in C57BL/6 mice. Birth Defects Res. 86 (5), 377–384.

Lillycrop, K.A., Phillips, E.S., Jackson, A.A., Hanson, M.A., Burdge, G.C., 2005. Dietary protein restriction of pregnant rats induces and folic acid supplementation prevents epigenetic modification of hepatic gene expression in the offspring. J. Nutr. 135 (6), 1382–1386.

Litten-Brown, J.C., Corson, A.M., Clarke, L., 2010. Porcine Models for the Metabolic Syndrome, digestive and bone disorders: a general overview. Animal 4 (6), 899–920.

Liu, Q., Yuan, B., Lo, K.A., Patterson, H.C., Sun, Y., Lodish, H.F., 2012. Adiponectin regulates expression of hepatic genes critical for glucose and lipid metabolism. Proc. Natl. Acad. Sci. USA 109 (36), 14568–14573.

Lodhi, I.J., Semenkovich, C.F., 2014. Peroxisomes: a nexus for lipid metabolism and cellular signaling. Cell Metab. 19 (3), 380–392.

Long, N.M., Ford, S.P., Nathanielsz, P.W., 2011. Maternal obesity eliminates the neonatal lamb plasma leptin peak. J. Physiol. 589 (Pt. 6), 1455–1462.

Lottati, M., Kolka, C.M., Stefanovski, D., Kirkman, E.L., Bergman, R.N., 2009. Greater omentectomy improves insulin sensitivity in non-obese dogs. Obesity 17 (4), 674–680.

Luedi, P.P., Hartemink, A.J., Jirtle, R.L., 2005. Genome-wide prediction of imprinted murine genes. Genome Res. 15 (6), 875–884.

Luedi, P.P., Dietrich, F.S., Weidman, J.R., Bosko, J.M., Jirtle, R.L., Hartemink, A.J., 2007. Computational and experimental identification of novel human imprinted genes. Genome Res. 17 (12), 1723–1730.

Lumeng, C.N., Bodzin, J.L., Saltiel, A.R., 2007. Obesity induces a phenotypic switch in adipose tissue macrophage polarization. J. Clin. Invest. 117 (1), 175–184.

Ma, X., Bacci, S., Mlynarski, W., Gottardo, L., Soccio, T., Menzaghi, C., et al., 2004. A common haplotype at the CD36 locus is associated with high free fatty acid levels and increased cardiovascular risk in Caucasians. Hum. Mol. Genet. 13 (19), 2197–2205.

Malendowicz, L.K., Rucinski, M., Belloni, A.S., Ziolkowska, A., Nussdorfer, G.G., 2007. Leptin and the regulation of the hypothalamic-pituitary-adrenal axis. Int. Rev. Cytol. 263, 63–102.

Marti, A., Corbalan, M.S., Forga, L., Martinez, J.A., Hinney, A., Hebebrand, J., 2003. A novel nonsense mutation in the melanocortin-4 receptor associated with obesity in a Spanish population. Int. J. Obes. Relat. Metab. Disord. 27 (3), 385–388.

Matveyenko, A.V., Veldhuis, J.D., Butler, P.C., 2008. Measurement of pulsatile insulin secretion in the rat: direct sampling from the hepatic portal vein. Am. J. Physiol. Endocrinol. Metab. 295 (3), E569–E574.

McClean, P.L., Irwin, N., Cassidy, R.S., Holst, J.J., Gault, V.A., Flatt, P.R., 2007. GIP receptor antagonism reverses obesity, insulin resistance, and associated metabolic disturbances induced in mice by prolonged consumption of high-fat diet. Am. J. Physiol. Endocrinol. Metab. 293 (6), E1746–E1755.

McCurdy, C.E., Bishop, J.M., Williams, S.M., Grayson, B.E., Smith, M.S., Friedman, J.E., et al., 2009. Maternal high-fat diet triggers lipotoxicity in the fetal livers of nonhuman primates. J. Clin. Invest. 119 (2), 323–335.

McMillen, I.C., Robinson, J.S., 2005. Developmental origins of the metabolic syndrome: prediction, plasticity, and programming. Physiol. Rev. 85 (2), 571–633.

Miranville, A., Herling, A.W., Biemer-Daub, G., Voss, M.D., 2012. Differential adipose tissue inflammatory state in obese nondiabetic Zucker fatty rats compared to obese diabetic zucker diabetic fatty rats. Horm. Metab. Res. 44 (4), 273–278.

Miyaoka, K., Kuwasako, T., Hirano, K., Nozaki, S., Yamashita, S., Matsuzawa, Y., 2001. CD36 deficiency associated with insulin resistance. Lancet 357 (9257), 686–687.

Mizushima, N., Klionsky, D.J., 2007. Protein turnover via autophagy: implications for metabolism. Annu. Rev. Nutr. 27, 19–40.

Morris, M.J., Chen, H., 2009. Established maternal obesity in the rat reprograms hypothalamic appetite regulators and leptin signaling at birth. Int. J. Obes. 33 (1), 115–122.

Nadeau, J.H., Balling, R., Barsh, G., Beier, D., Brown, S.D., Bucan, M., et al., 2001. Sequence interpretation. Functional annotation of mouse genome sequences. Science 291 (5507), 1251–1255.

Naggert, J.K., Fricker, L.D., Varlamov, O., Nishina, P.M., Rouille, Y., Steiner, D.F., et al., 1995. Hyperproinsulinaemia in obese fat/fat mice associated with a carboxypeptidase E mutation which reduces enzyme activity. Nat. Genet. 10 (2), 135–142.

Nawrocki, A.R., Rajala, M.W., Tomas, E., Pajvani, U.B., Saha, A.K., Trumbauer, M.E., et al., 2006. Mice lacking adiponectin show decreased hepatic insulin sensitivity and reduced responsiveness to peroxisome proliferator-activated receptor gamma agonists. J. Biol. Chem. 281 (5), 2654–2660.

Neel, J.V., 1962. Diabetes mellitus: a "thrifty" genotype rendered detrimental by "progress? Am. J. Hum. Genet. 14, 353–362.

Nielsen, S., Guo, Z., Johnson, C.M., Hensrud, D.D., Jensen, M.D., 2004. Splanchnic lipolysis in human obesity. J. Clin. Invest. 113 (11), 1582–1588.

Nikolskiy, I., Conrad, D.F., Chun, S., Fay, J.C., Cheverud, J.M., Lawson, H.A., 2015. Using whole-genome sequences of the LG/J and SM/J inbred mouse strains to prioritize quantitative trait genes and nucleotides. BMC Genomics 16, 415.

Nishina, P.M., Naggert, J.K., Verstuyft, J., Paigen, B., 1994. Atherosclerosis in genetically obese mice: the mutants obese, diabetes, fat, tubby, and lethal yellow. Metabolism 43 (5), 554–558.

Noda, K., Melhorn, M.I., Zandi, S., Frimmel, S., Tayyari, F., Hisatomi, T., et al., 2010. An animal model of spontaneous metabolic syndrome: Nile grass rat. FASEB J. 24 (7), 2443–2453.

Norris, A.W., Chen, L., Fisher, S.J., Szanto, I., Ristow, M., Jozsi, A.C., et al., 2003. Muscle-specific PPARgamma-deficient mice develop increased adiposity and insulin resistance but respond to thiazolidinediones. J. Clin. Invest. 112 (4), 608–618.

Odaka, Y., Nakano, M., Tanaka, T., Kaburagi, T., Yoshino, H., Sato-Mito, N., et al., 2010. The influence of a high-fat dietary environment in the fetal period on postnatal metabolic and immune function. Obesity 18 (9), 1688–1694.

Okazaki, M., Saito, Y., Udaka, Y., Maruyama, M., Murakami, H., Ota, S., et al., 2002. Diabetic nephropathy in KK and KK-Ay mice. Exp. Anim. 51 (2), 191–196.

Ouchi, N., Parker, J.L., Lugus, J.J., Walsh, K., 2011. Adipokines in inflammation and metabolic disease. Nat. Rev. Immunol. 11 (2), 85–97.

Pan, D., Fujimoto, M., Lopes, A., Wang, Y.X., 2009. Twist-1 is a PPARdelta-inducible, negative-feedback regulator of PGC-1alpha in brown fat metabolism. Cell 137 (1), 73–86.

Parikh, R.M., Mohan, V., 2012. Changing definitions of metabolic syndrome. Indian J. Endocrinol. Metab. 16 (1), 7–12.

Parks, B.W., Sallam, T., Mehrabian, M., Psychogios, N., Hui, S.T., Norheim, F., et al., 2015. Genetic architecture of insulin resistance in the mouse. Cell Metab. 21 (2), 334–346.

Permutt, M.A., Wasson, J., Cox, N., 2005. Genetic epidemiology of diabetes. J. Clin. Invest. 115 (6), 1431–1439.

Pico, C., Sanchez, J., Oliver, P., Palou, A., 2002. Leptin production by the stomach is up-regulated in obese (fa/fa) Zucker rats. Obes. Res. 10 (9), 932–938.

Pond, C.M., Mattacks, C.A., 1987. The anatomy of adipose tissue in captive Macaca monkeys and its implications for human biology. Folia Primatol. 48 (3–4), 164–185.

Pravenec, M., Landa, V., Zidek, V., Musilova, A., Kren, V., Kazdova, L., et al., 2001. Transgenic rescue of defective Cd36 ameliorates insulin resistance in spontaneously hypertensive rats. Nat. Genet. 27 (2), 156–158.

Rampersaud, E., Mitchell, B.D., Naj, A.C., Pollin, T.I., 2008. Investigating parent of origin effects in studies of type 2 diabetes and obesity. Curr. Diab. Rev. 4 (4), 329–339.

Scherer, P.E., 2006. Adipose tissue: from lipid storage compartment to endocrine organ. Diabetes 55 (6), 1537–1545.

Schuler, M., Ali, F., Chambon, C., Duteil, D., Bornert, J.M., Tardivel, A., et al., 2006. PGC1alpha expression is controlled in skeletal muscles by PPARbeta, whose ablation results in fiber-type switching, obesity, and type 2 diabetes. Cell Metab. 4 (5), 407–414.

Scuteri, A., Sanna, S., Chen, W.M., Uda, M., Albai, G., Strait, J., et al., 2007. Genome-wide association scan shows genetic variants in the FTO gene are associated with obesity-related traits. PLoS Genet. 3 (7), e115.

Shulman, G.I., 2000. Cellular mechanisms of insulin resistance. J. Clin. Invest. 106 (2), 171–176.

Simmons, R.K., Alberti, K.G., Gale, E.A., Colagiuri, S., Tuomilehto, J., Qiao, Q., et al., 2010. The metabolic syndrome: useful concept or clinical tool? Report of a WHO Expert Consultation. Diabetologia 53 (4), 600–605.

Singh, R., Kaushik, S., Wang, Y., Xiang, Y., Novak, I., Komatsu, M., et al., 2009. Autophagy regulates lipid metabolism. Nature 458 (7242), 1131–1135.

Singh, P., Schimenti, J.C., Bolcun-Filas, E., 2015. A mouse geneticist's practical guide to CRISPR applications. Genetics 199 (1), 1–15.

Smith, B.K., Andrews, P.K., West, D.B., 2000. Macronutrient diet selection in thirteen mouse strains. Am. J. Physiol. Regul. Integr. Comp. Physiol. 278 (4), R797–R805.

Song, Q., Wang, S.S., Zafari, A.M., 2006. Genetics of the metabolic syndrome. Hosp. Phys. 42, 51–61.

Spiegel, A.M., Hawkins, M., 2012. Personalized medicine to identify genetic risks for type 2 diabetes and focus prevention: can it fulfill its promise? Health Aff. 31 (1), 43–49.

Spurlock, M.E., Gabler, N.K., 2008. The development of porcine models of obesity and the metabolic syndrome. J. Nutr. 138 (2), 397–402.

Strissel, K.J., Stancheva, Z., Miyoshi, H., Perfield, 2nd, J.W., DeFuria, J., Jick, Z., et al., 2007. Adipocyte death, adipose tissue remodeling, and obesity complications. Diabetes 56 (12), 2910–2918.

Suganami, T., Ogawa, Y., 2010. Adipose tissue macrophages: their role in adipose tissue remodeling. J. Leukoc. Biol. 88 (1), 33–39.

Sugden, M.C., Bulmer, K., Gibbons, G.F., Knight, B.L., Holness, M.J., 2002. Peroxisome-proliferator-activated receptor-alpha (PPARalpha) deficiency leads to dysregulation of hepatic lipid and carbohydrate metabolism by fatty acids and insulin. Biochem. J. 364 (Pt. 2), 361–368.

Surmi, B.K., Atkinson, R.D., Gruen, M.L., Coenen, K.R., Hasty, A.H., 2008. The role of macrophage leptin receptor in aortic root lesion formation. Am. J. Physiol. Endocrinol. Metab. 294 (3), E488–E495.

Suzuki, K., Jayasena, C.N., Bloom, S.R., 2011. The gut hormones in appetite regulation. J. Obes. 2011, 528401.

Svenson, K.L., Von Smith, R., Magnani, P.A., Suetin, H.R., Paigen, B., Naggert, J.K., et al., 2007. Multiple trait measurements in 43 inbred mouse strains capture the phenotypic diversity characteristic of human populations. J. Appl. Physiol. 102 (6), 2369–2378.

Svenson, K.L., Gatti, D.M., Valdar, W., Welsh, C.E., Cheng, R., Chesler, E.J., et al., 2012. High-resolution genetic mapping using the mouse diversity outbred population. Genetics 190 (2), 437–447.

Switonski, M., Mankowska, M., 2013. Dog obesity—the need for identifying predisposing genetic markers. Res. Vet. Sci. 95 (3), 831–836.

Tallam, L.S., Stec, D.E., Willis, M.A., da Silva, A.A., Hall, J.E., 2005. Melanocortin-4 receptor-deficient mice are not hypertensive or salt-sensitive despite obesity, hyperinsulinemia, and hyperleptinemia. Hypertension 46 (2), 326–332.

Tang-Christensen, M., Larsen, P.J., Goke, R., Fink-Jensen, A., Jessop, D.S., Moller, M., et al., 1996. Central administration of GLP-1-(7-36) amide inhibits food and water intake in rats. Am. J. Physiol. 271 (4 Pt 2), R848–R856.

Taylor, P.D., Poston, L., 2007. Developmental programming of obesity in mammals. Exp. Physiol. 92 (2), 287–298.

Taylor, B.A., Wnek, C., Schroeder, D., Phillips, S.J., 2001. Multiple obesity QTLs identified in an intercross between the NZO (New Zealand obese) and the SM (small) mouse strains. Mamm. Genome 12 (2), 95–103.

The European Group for the study of Insulin Resistance (EGIR), 2002. Frequency of the WHO metabolic syndrome in European cohorts, and an alternative definition of an insulin resistance syndrome. Diab. Metab. 28, 364–376.

Tilg, H., Kaser, A., 2011. Gut microbiome, obesity, and metabolic dysfunction. J. Clin. Invest. 121 (6), 2126–2132.

Tschop, M., Smiley, D.L., Heiman, M.L., 2000. Ghrelin induces adiposity in rodents. Nature 407 (6806), 908–913.

Tschop, M., Weyer, C., Tataranni, P.A., Devanarayan, V., Ravussin, E., Heiman, M.L., 2001. Circulating ghrelin levels are decreased in human obesity. Diabetes 50 (4), 707–709.

Tschop, M., Castaneda, T.R., Joost, H.G., Thone-Reineke, C., Ortmann, S., Klaus, S., et al., 2004. Physiology: does gut hormone PYY3-36 decrease food intake in rodents? Nature 430 (6996), 162–165.

Turk, J.R., Laughlin, M.H., 2004. Physical activity and atherosclerosis: which animal model? Can. J. Appl. Physiol. 29 (5), 657–683.

Uddin, M.J., Duy do, N., Cinar, M.U., Tesfaye, D., Tholen, E., Juengst, H., et al., 2011. Detection of quantitative trait loci affecting serum cholesterol, LDL, HDL, and triglyceride in pigs. BMC Genet. 12, 62.

van den Brandt, J., Kovacs, P., Kloting, I., 2000. Metabolic features in disease-resistant as well as in spontaneously hypertensive rats and newly established obese Wistar Ottawa Karlsburg inbred rats. Int. J. Obes. Relat. Metab. Disord. 24 (12), 1618–1622.

Varga, O., Harangi, M., Olsson, I.A., Hansen, A.K., 2009. Contribution of animal models to the understanding of the metabolic syndrome: a systematic overview. Obes. Rev. 11 (11), 792–807.

Vickers, M.H., Gluckman, P.D., Coveny, A.H., Hofman, P.L., Cutfield, W.S., Gertler, A., et al., 2005. Neonatal leptin treatment reverses developmental programming. Endocrinology 146 (10), 4211–4216.

Vinolo, M.A., Rodrigues, H.G., Festuccia, W.T., Crisma, A.R., Alves, V.S., Martins, A.R., et al., 2012. Tributyrin attenuates obesity-associated inflammation and insulin resistance in high-fat-fed mice. Am. J. Physiol. Endocrinol. Metab. 303 (2), E272–E282.

Voruganti, V.S., Tejero, M.E., Proffitt, J.M., Cole, S.A., Freeland-Graves, J.H., Comuzzie, A.G., 2007. Genome-wide scan of plasma cholecystokinin in baboons shows linkage to human chromosome 17. Obesity 15 (8), 2043–2050.

Wagner, J.E., Kavanagh, K., Ward, G.M., Auerbach, B.J., Harwood, Jr., H.J., Kaplan, J.R., 2006. Old world nonhuman primate models of type 2 diabetes mellitus. ILAR J. 47 (3), 259–271.

Wahli, W., Braissant, O., Desvergne, B., 1995. Peroxisome proliferator activated receptors: transcriptional regulators of adipogenesis, lipid metabolism and more. Chem. Biol. 2 (5), 261–266.

Walley, A.J., Asher, J.E., Froguel, P., 2009. The genetic contribution to non-syndromic human obesity. Nat. Rev. Genet. 10 (7), 431–442.

Wang, Y.X., 2010. PPARs: diverse regulators in energy metabolism and metabolic diseases. Cell Res. 20 (2), 124–137.

Weisberg, S.P., Hunter, D., Huber, R., Lemieux, J., Slaymaker, S., Vaddi, K., et al., 2006. CCR2 modulates inflammatory and metabolic effects of high-fat feeding. J. Clin. Invest. 116 (1), 115–124.

Wellcome Trust Case Control Consortium, 2007. Genome-wide association study of 14,000 cases of seven common diseases and 3,000 shared controls. Nature (447), 661–678.

West, D.B., Waguespack, J., McCollister, S., 1995. Dietary obesity in the mouse: interaction of strain with diet composition. Am. J. Physiol. 268 (3 Pt. 2), R658–R665.

White, C.L., Purpera, M.N., Morrison, C.D., 2009. Maternal obesity is necessary for programming effect of high-fat diet on offspring. Am. J. Physiol. Regul. Integr. Comp. Physiol. 296 (5), R1464–R1472.

Wildman, R.P., Muntner, P., Reynolds, K., McGinn, A.P., Rajpathak, S., Wylie-Rosett, J., et al., 2008. The obese without cardiometabolic risk factor clustering and the normal weight with cardiometabolic risk factor clustering: prevalence and correlates of 2 phenotypes among

the US population (NHANES 1999–2004). Arch. Intern. Med. 168 (15), 1617–1624.

Willer, C.J., Speliotes, E.K., Loos, R.J., Li, S., Lindgren, C.M., Heid, I.M., et al., 2009. Six new loci associated with body mass index highlight a neuronal influence on body weight regulation. Nat. Genet. 41 (1), 25–34.

Williams, K.T., Schalinske, K.L., 2012. Tissue-specific alterations of methyl group metabolism with DNA hypermethylation in the Zucker (type 2) diabetic fatty rat. Diab. Metab. Res. Rev. 28 (2), 123–131.

Wolf, J.B., Vaughn, T.T., Pletscher, L.S., Cheverud, J.M., 2002. Contribution of maternal effect QTL to genetic architecture of early growth in mice. Heredity 89 (4), 300–310.

Wolf, J.B., Hager, R., Cheverud, J.M., 2008. Genomic imprinting effects on complex traits: a phenotype-based perspective. Epigenetics 3 (6), 295–299.

Wong, K., Bumpstead, S., Van Der Weyden, L., Reinholdt, L.G., Wilming, L.G., Adams, D.J., et al., 2012. Sequencing and characterization of the FVB/NJ mouse genome. Genome Biol. 13 (8), R72.

World Health Organization (WHO), 1999. Definition, Diagnosis and Classification of Diabetes Mellitus and its Complications. WHO: Geneva.

Wu, L., Vikramadithyan, R., Yu, S., Pau, C., Hu, Y., Goldberg, I.J., et al., 2006. Addition of dietary fat to cholesterol in the diets of LDL receptor knockout mice: effects on plasma insulin, lipoproteins, and atherosclerosis. J. Lipid Res. 47 (10), 2215–2222.

Yang, H., Ding, Y., Hutchins, L.N., Szatkiewicz, J., Bell, T.A., Paigen, B.J., et al., 2009. A customized and versatile high-density genotyping array for the mouse. Nat. Methods 6 (9), 663–666.

Yang, H., Wang, H., Shivalila, C.S., Cheng, A.W., Shi, L., Jaenisch, R., 2013. One-step generation of mice carrying reporter and conditional alleles by CRISPR/Cas-mediated genome engineering. Cell 154 (6), 1370–1379.

York, B., Lei, K., West, D.B., 1996. Sensitivity to dietary obesity linked to a locus on chromosome 15 in a CAST/Ei x C57BL/6J F2 intercross. Mamm. Genome 7 (9), 677–681.

Yue, F., Cheng, Y., Breschi, A., Vierstra, J., Wu, W., Ryba, T., et al., 2014. A comparative encyclopedia of DNA elements in the mouse genome. Nature 515 (7527), 355–364.

Zhang, Y., Goldman, S., Baerga, R., Zhao, Y., Komatsu, M., Jin, S., 2009. Adipose-specific deletion of autophagy-related gene 7 (atg7) in mice reveals a role in adipogenesis. Proc. Natl. Acad. Sci. USA 106 (47), 19860–19865.

Zhang, W., Korstanje, R., Thaisz, J., Staedtler, F., Harttman, N., Xu, L., et al., 2012. Genome-wide association mapping of quantitative traits in outbred mice. G3 2 (2), 167–174.

Zheng, D., Ionut, V., Mooradian, V., Stefanovski, D., Bergman, R.N., 2010. Portal glucose infusion-glucose clamp measures hepatic influence on postprandial systemic glucose appearance as well as whole body glucose disposal. Am. J. Physiol. Endocrinol. Metab. 298 (2), E346–E353.

Page left intentionally blank

Animal Models of Type 1 and Type 2 Diabetes Mellitus

Aileen King, Amazon Austin

King's College London, London, United Kingdom

1 INTRODUCTION

Diabetes mellitus is a metabolic disease characterized by hyperglycemia due to a relative or complete deficiency of the hormone insulin. This hormone, which is secreted from the beta cells in the pancreatic islets of Langerhans, is essential in the control of blood glucose concentrations by facilitating glucose uptake and metabolism in peripheral tissues, such as the liver, muscle, and adipose tissue. There are two main classifications of diabetes: Type 1 diabetes and Type 2 diabetes. Type 1 diabetes is caused by the autoimmune destruction of the beta cells, leading to insulin deficiency whereas Type 2 diabetes is characterized by insulin resistance and an inability of the beta cells to adequately compensate with

increased insulin secretion. Acute symptoms of the disease include fatigue, polydipsia, and polyuria. Due to a severe insulin deficiency, Type 1 diabetes patients can present with acute weight loss and in some severe cases ketoacidosis and coma. Chronic hyperglycemia can lead to a variety of complications, such as neuropathy, nephropathy, and retinopathy. Animal models are routinely used in diabetes research as blood glucose homeostasis is well preserved across different species. Rodents are most commonly used for ethical and practical reasons (Renner et al., 2016) although larger animals, such as pigs, cats, dogs, and primates are used for specific studies. Although the symptom of hyperglycemia connects different types of diabetes, the etiology and patient characteristics of each is diverse. The animal model

chosen will depend on whether a model of Type 1 or Type 2 diabetes is required. In addition, the choice will be influenced by the study design, for example, whether the aim is to understand more about the pathogenesis, prevent disease onset or to treat the disease (King and Bowe, 2016).

2 TYPE 1 DIABETES

Type 1 diabetes is most commonly diagnosed in children and young adults. At the time of diagnosis, patients have very little endogenous insulin production and thus require life-long insulin therapy. Both genetic and environmental factors play a role in the disease, evidenced by identical twin concordance of around 27% (Hyttinen et al., 2003). Disease susceptibility has been linked with various major histocompatibility complex (MHC) genes in which genetic variations can either protect or increase risk of disease (Erlich et al., 2008; Pociot et al., 2016). Environmental triggers of the disease are not well understood but viruses have been implicated in some cases (Rewers and Ludvigsson, 2016). The disease is mainly characterized by severe hyperglycemia due to a substantial reduction in insulin production due to autoimmune destruction of the pancreatic beta cells (Wilcox et al., 2016). Therefore animal models of Type 1 diabetes should ideally have a large reduction in beta cell mass by either replicating the autoimmune process or by other means. Some of the most commonly used rodent models of Type 1 diabetes are outlined in Table 10.1.

2.1 Spontaneous Models of Autoimmune Type 1 Diabetes

A key histopathological characteristic of Type 1 diabetes is insulitis, which is the immune cell infiltration of the pancreatic islets, ultimately leading to beta cell death (Campbell-Thompson et al., 2016). Another distinctive feature of Type 1 diabetes is the presence of autoantibodies, such as islet antigen 2 (IA2), glutamic acid decarboxylase, and zinc transporter 8 (ZnT8) (Knip et al., 2016). Spontaneous autoimmune diabetes has been discovered in several rodent strains, which have been further inbred to provide strains in which diabetes develops at a relatively high incidence (Mathews, 2005). Although these rodent models have some differences from the human condition, they have been very useful in understanding some key aspects of the disease, such as the pathogenesis of insulitis, as human pancreas samples are difficult to obtain.

2.1.1 Nonobese Diabetic Mouse

One of the most commonly used autoimmune models of Type 1 diabetes is the nonobese diabetic (NOD) mouse. This strain was originally developed from inbreeding a colony of cataract-prone outbred Jcl:ICR mice to create a model of spontaneous autoimmune Type 1 diabetes. These mice develop severe insulitis within 2–4 weeks in females and 5–7 weeks in males leading to beta cell destruction and hyperglycemia by 30 weeks in up to 80% of females and 30% of males (Makino et al., 1980). The progression of the disease within NOD mice is a complex interaction of immune cell responses with involvement from macrophages, dendritic cells, NK cells, B lymphocytes, and T lymphocytes (Jorns et al., 2014; Lee et al., 1988; Welzen-Coppens et al., 2013). By the time insulitis is fully established at around 12–14 weeks, T lymphocytes are the predominate cell infiltrating the islets (Magnuson et al., 2015) causing beta cell destruction and leading to overt diabetes (Jayasimhan et al., 2014).

It should be noted that the extent of insulitis differs from humans, with NOD mice showing severe insulitis in nearly all islets whereas in the human diabetic islets the insulitis is less pronounced and not all islets are not affected (Driver et al., 2011; In't Veld, 2014). One disadvantage of using the NOD mouse is the uncertainness of when overt diabetes will develop as it can range from 18

TABLE 10.1   Main Characteristics of Most Commonly Used Rodent Models of Type 1 Diabetes

Model of Type 1 diabetes	Onset	Age/time of induction	Immune cell involvement?	Useful to understand pathogenesis?	Useful in prevention studies?
Nonobese diabetic (NOD) mice	Spontaneous	12–30 weeks	Yes	Yes	Yes
Biobreeding (BB) rats	Spontaneous	8–16 weeks	Yes	Yes	Yes
Lew.1AR1-iddm rats	Spontaneous	~8 weeks	Yes	Yes	Yes
Komeda diabetic-prone (KDP) rats	Spontaneous	~8 weeks	Yes	Yes	Yes
Akita mice	Spontaneous	~4 weeks	No	Some aspects	No
Low dose streptozotocin	Induced	Within days	Yes	Some aspects	Some aspects
High dose streptozotocin	Induced	Within days	No	No	No
Alloxan	Induced	Within days	No	No	No

to 30 weeks. Several tools exist to induce a rapid-onset model. One is the injection of cyclophosphamide, in which one or two intraperitoneal injections can induce overt diabetes rapidly in prediabetic male and female NOD mice (Harada and Makino, 1984; Yasunami and Bach, 1988). Alternatively, if islets are transplanted from a young NOD mouse to an overtly diabetic mouse, the newly transplanted islets rapidly succumb to insulitis and thus can be studied in a more controlled time frame (Wang et al., 1992). Finally, adoptive transfer models can be used to induce a diabetic phenotype rapidly into another mouse (Christianson et al., 1993; Wicker et al., 1986).

The NOD mouse has been an important tool in understanding the genetic risk factors associated with the development of Type 1 diabetes. Several genetic loci have been shown to have contributing or protective effects on the development of diabetes in NOD mice (Driver et al., 2012; Pearson et al., 2016). One example of this is the MHC, which is highly important in both NOD mouse and human diabetes development (Nerup et al., 1974; Prochazka et al., 1987). Indeed in humans, it is the most robust genetic predictor of Type 1 diabetes susceptibility (Pociot et al., 2016). Other genetic predictors present in both NOD mice and humans include cytotoxic T-lymphocyte-associated protein 4 (CTLA-4) (Ueda et al., 2003). However, it should be noted that many susceptibility loci identified in NOD mice turned out not to have an effect on the development of Type 1 diabetes in humans (Driver et al., 2011). Due to the common immunogenic progression of diabetes between NOD mice and humans, these mice provide a valuable tool for assessing therapies that target the immune components of the disease, mostly aimed at either modulating immune cell communication or suppressing T cell activation (Atkinson and Leiter, 1999). However, despite NOD mice being a vital model for studying the disease, many factors strongly influence the NOD mouse's susceptibility to respond to intervention treatment. Diabetes development is prevented in NOD mice if they are not kept in a specific pathogen-free environment (Leiter, 1993), which has been attributed to the influence of gut microbiota in different environmental conditions (Alam et al., 2011; King and Sarvetnick, 2011). Therefore diabetes incidence can be affected by different husbandry practices. Another source of variation is the age of the mouse at the time of treatment as it has been suggested that young diabetic NOD mice are more likely to respond to treatment than older mice (Roep, 2007). It has thus become clear that different conditions play a part in the efficacy of treatments within NOD mice and may be the reason for a few therapies being effectively translated to human trials (Jayasimhan et al., 2014; Reed and Herold, 2015). In the example of the anti-CD3 and IL-1 combination therapy, a multicenter trial was conducted based on some previous work showing the benefit of this treatment in

NOD mice (Ablamunits et al., 2012); however, human trials were not able to completely replicate the results seen in NOD mice (Daifotis et al., 2013), which was attributed to dosing, choice of endpoints and the fact that some patients may not be "responders" to that specific treatment (Herold et al., 2013; Reed and Herold, 2015). Indeed it is worth noting that the underlying pathology of the disease may differ between different patients and it is possible that the NOD mouse model only represents one subset of Type 1 diabetes patients.

New experimental models using NOD mice have now been developed including humanized and genetically altered NOD mice (Pearson et al., 2016; Serreze et al., 2016). These advances have shown promising results, however, important differences still remain between Type 1 diabetes in the NOD mouse and humans which should be taken into consideration when designing studies (Pearson et al., 2016; Reed and Herold, 2015; Roep, 2007; Simpfendorfer et al., 2015). Nonetheless, NOD mice are still widely used and are an asset to investigating the complex mechanisms of Type 1 diabetes.

2.1.2 BB Rat

Biobreeder (BB) rats were created from a Wistar colony in which spontaneous autoimmune diabetes had occurred (Mathews, 2005). Two separate diabetes-prone strains were derived: the inbred BBDP/Wor and the outbred BBdp, as well as a diabetes resistant BB strain known as BBDR (Mordes et al., 2004). In the diabetes-prone BB rats, hyperglycemia develops between 8 and 16 weeks of age with 90% developing diabetes within the first 3 months (Mathews, 2005). In contrast to NOD mice, there is no bias toward either sex. However, incidence of diabetes varies depending on housing conditions, much like the NOD, with up to 50% becoming diabetic in normal conditions (Nakhooda et al., 1978) and up to 90% in viral antibody-free conditions (Like et al., 1991). The pathogenesis of diabetes in these rats involves B cells, dendritic cells, macrophages, NK cells, and T cells infiltrating the islets directly and leading to insulitis 2–3 weeks before overt diabetes is established (Hanenberg et al., 1989). The resulting diabetes can be quite severe and therefore the rats often need to be maintained on insulin to prevent ketoacidosis (Bortell and Yang, 2012). In contrast to NOD mice, the insulitis in BB rats is not preceded by periinsulitis and thus may be a better alternative for insulitis studies, as this pattern more closely resembles the pathology seen in humans (Mordes et al., 2004). As with NOD mice and humans, BB rat susceptibility to diabetes has been linked with MHC class II gene loci (Jacob et al., 1992). However, BB rats are lymphopenic with a substantial reduction in CD4+ T cells and very few CD8+ T cells (Jorns et al., 2014) and from this perspective differ from the human disease. This lymphopenia is caused by a frameshift mutation

in Gimap5 causing T cell apoptosis and is necessary for the development of Type 1 diabetes in the BB rats (MacMurray et al., 2002). BB rats have a reasonably predictable onset of diabetes so have been a useful model in which to dissect the serum factors linked to early stages of diabetes progression (Kaldunski et al., 2010). They have also proved useful in investigating novel therapies targeting disease progression (Gotfredsen et al., 1985; Like et al., 1984; Scott et al., 1997).

2.1.3 Lew.1AR1-iddm

The Lew.1AR1-iddm rat was derived from a colony of congenic Lewis rats in Hannover, Germany, in which a spontaneous mutation in Lew.1AR1 rats lead to a Type 1 diabetic phenotype (Lenzen et al., 2001). The original incidence of diabetes in these rats was 20% but subsequent inbreeding increased the incidence up to 80% (Jorns et al., 2005). Overt diabetes develops around 8–9 weeks of age in both genders and is preceded by insulitis in the pancreas only around a week before diabetes onset (Jorns et al., 2005). Cells identified in the insulitis include CD4+ and CD8+ lymphocytes, macrophages, NK cells, and B cells (Lenzen et al., 2001; Mathews, 2005). In contrast to NOD mice and BB rats, the Lew.1AR1-iddm rat does not show signs of other autoimmune diseases and unlike BB rats they are not lymphopenic. This model has been used to understand the mechanisms involved in development of Type 1 diabetes from both a genetic point of view (Weiss et al., 2008) and the pathogenesis of the insulitis (Jorns et al., 2004). In addition, intervention studies have been carried out on this rat model (Jorns et al., 2010, 2015).

2.1.4 Komeda Diabetes-Prone Rat

The Komeda diabetes-prone (KDP) rats were derived from the Long-Evans Tokushima Lean strain, which were selectively bred to create diabetes prone (Kawano et al., 1991) and diabetes free substrain (Komeda et al., 1998). These rats develop typical signs of Type 1 diabetes including polyuria, hyperglycemia, and weight loss at around 60 days (Komeda et al., 1998). In similarity to the other rodent autoimmune models of Type 1 diabetes, beta cell loss is due to insulitis, but in KDP rats the cytokine profile differs where interferon-γ and tumor necrosis factor-α rather than interleukin-1β predominates (Jorns et al., 2014). Although these animals are not lymphopenic like BB rats, they do show signs of autoimmunity to the salivary and lacrimal glands (Mordes et al., 2004). These rats have not been extensively studied outside of Japan, but they been used to understand genetic susceptibilities to Type 1 diabetes. As with other rodent models and humans, MHC class II has been shown to be important in the development of the disease (Yokoi et al., 2012). In addition, a non-MHC susceptibility gene was identified (Casitas B-lineage lymphoma b)

in which polymorphisms were subsequently identified in the human disease (Yokoi et al., 2002). Although the most common variants do not seem to be linked to Type 1 diabetes in humans, some rarer missense mutations have been identified in human Type 1 diabetes patients (Yokoi et al., 2008).

2.2 Spontaneous Models of Nonautoimmune Diabetes

2.2.1 Akita Mouse

Mice differ from humans as they have two genes for insulin: *Ins1* and *Ins2*. The Akita mouse, also known as the Ins2 mouse or MODY4 mouse, was derived from a C57Bl/6 colony in which a spontaneous mutation of the *Ins2* gene resulted in early onset diabetes (Yoshioka et al., 1997). The mutation is an autosomal dominant missense mutation which stops one of the crucial disulphide bonds forming between the A and B chains of insulin 2, leading to misfolding of the proinsulin-2 protein (Wang et al., 1999). Electron microscopy has shown that this misfolded protein appears to aggregate in enlarged endoplasmic reticulum (ER). These aggregates are C-peptide positive but are around twice the size of expected proinsulin and have been shown to be linked to chaperone proteins, such as binding immunoglobulin protein (BiP). As these proteins are not fit for secretion, the ER unfolded protein response is triggered to degrade the aggregates. With limited degradation capacity within the ER, this accumulation ultimately leads to ER stress and beta cell destruction by apoptosis, specifically by a proapoptotic factor Chop (Oyadomari et al., 2002). These mice develop hyperglycemia, insulinopenia, polydipsia, and polyuria within 4 weeks of age and so provide a solid model of Type 1 diabetes (Izumi et al., 2003). Male mice in particular develop severe hyperglycemia and may require insulin administration to survive. However, females show a much less pronounced hyperglycemia (Oyadomari et al., 2002), which may be due to the protective effect of estrogen (Le May et al., 2006). Therefore, these mice have been used in both Type 1 diabetes research and Type 2 diabetes research as the severe deficiency of functional insulin in males gives a Type 1 diabetes phenotype, whereas the role of beta cell ER stress in the pathogenesis is of interest in studies of Type 2 diabetes.

In Type 1 diabetes research, the inability of the Akita mouse beta cells to regenerate have made this model a useful tool in investigating the impact of islet transplantation therapies (Mathews et al., 2002).

2.3 Chemical Induction of Diabetes

Several compounds have been tested and have been shown to induce diabetes in animal models, however, the two most studied and routinely used are streptozotocin

(STZ) and alloxan, both of which are glucose analogs. STZ and alloxan both work through the glucose transporter GLUT2 found in beta cells (Elsner et al., 2002; Schnedl et al., 1994). They do, however, have differing downstream mechanisms but ultimately both lead to almost complete ablation of beta cells within the islets causing a severe deficiency in insulin production leading to hyperglycemia and weight loss and thus reproducing the main symptoms of Type 1 diabetes. These compounds have been used for many years in animals for several reasons including their predictable symptom onset and relative low-cost compared to breeding spontaneously diabetic animals. These compounds provide stable hyperglycemia in small animals within a week (Deeds et al., 2011) and provide an ideal platform to study ways to decrease hyperglycemia which are not beta cell dependent, for example, in new insulin therapies or when investigating the efficacy of islet transplantation. The kidney and liver also contain the GLUT2 transporter but have better protection against the effects of these toxins, nonetheless care should be taken to avoid overdose as it will cause toxic effects in these organs (Elsner et al., 2002; Schnedl et al., 1994). Due to their analogy to glucose, alloxan and STZ compete with glucose for uptake via GLUT2, which is why some investigators suggest fasting prior to administration. Although beta cell regeneration does not routinely occur after alloxan or STZ administration, it has been reported for both these compounds (De Haro-Hernandez et al., 2004; Yin et al., 2006) and therefore measures to control for this should be taken.

2.3.1 Alloxan

Alloxan [2,4,5,6-tetraoxypyrimidine; 5,6-dioxyuracil] is a pyrimidine derivative of uric acid, first discovered in 1818 by Brugnaletti and then again in 1838 by Wohler. This compound was first noted to have diabetogenic effects in 1943 when central islet necrosis was found in alloxan-treated rabbits (Dunn et al., 1943). From then on, it has been used to model Type 1 diabetes in animal experimentation. Doses vary between studies; however, it is suggested that single doses ranging from 50 to 150 mg/kg produce chronic hyperglycemia in rodents depending on administration route and strain (Leiter and Schile, 2013; Szkudelski, 2001). Alloxan has been shown to begin exerting its effects within 2 min (Szkudelski et al., 1998) as plasma insulin levels are seen to rise consequently giving a period of hypoglycemia preceding long-term hyperglycemia. This hyperglycemia has been shown to be chronic but has been occasionally shown to ameliorate over time with blood glucose concentrations normalizing and body weight returning or surpassing original levels (De Haro-Hernandez et al., 2004). This has been proposed to be due to superior beta cell regeneration with alloxan treated-compared to STZ-treated animals as was demonstrated in guinea pigs (Gorray

et al., 1986), although it should be noted that the islets from different animal species show different susceptibilities to this toxin (Tyrberg et al., 2001).

Alloxan's mechanism of action has been compiled over the years from in vitro and in vivo studies and it is now well established. The uptake of alloxan through GLUT2 transporters on the beta cells leads to rapid cell destruction. As alloxan enters the beta cell, reactive oxygen species reduce the alloxan to dialuric acid, which can then go on to reoxidize to alloxan and generate free radicals, such as superoxide. Superoxide can form hydrogen peroxidase, as well as reduce Fe^{3+} ions leading to hydroxyl radicals, both of which damage the DNA of the beta cells leading to fragmentation and ultimate cell death. The hydrogen peroxidase has also been suggested to be involved in causing a surge of intracellular calcium leading to the high initial peak in insulin levels following alloxan administration (Szkudelski, 2001) which can in itself cause damage to the beta cells. This cyclical destruction may account for the ongoing action of alloxan long after its clearance from the body with a half-life of only 1.5 min at 37°C (Lenzen and Munday, 1991). Alloxan also has a second mode of impact on the insulin secretion of the beta cells as it has high affinity for —SH containing groups most notably found on glucokinase, the glucose-sensing molecule within the beta cells. Binding of alloxan to glucokinase inactivates it and ultimately hinders glucose-stimulated insulin secretion (Lenzen et al., 1987).

2.3.2 Streptozotocin

Streptozotocin [2-Deoxy-2-({[methyl(nitroso)amino] carbonyl}amino)-β-D-glucopyranose] (STZ) is an antibiotic made by the fungus *Streptomycetes achromogenes* and can be used both in a single high dose or multiple low doses to provide chronic diabetes. STZ also works through the GLUT2 transporter and accumulates intracellularly forming the alkylating product diazomethane resulting in beta cell death through alkylation of the DNA within these cells. The destruction of the beta cells by STZ is multifactorial. STZ itself is a nitric oxide donor and this can directly impact the DNA and cause damage. In addition, STZ causes production of free radicals like superoxide, much like alloxan, which ultimately leads to hydrogen peroxidase and hydroxyl-induced DNA damage through disruption of ATP production in the mitochondria. This DNA damage causes activation of poly ADP-ribosylation reducing intracellular NAD^+ and further decreasing the available ATP in the mitochondria. This overall reduction in ATP leads to less insulin synthesis and secretion from the beta cells. The subsequent glucose overload then activates the PKC pathways and results in downstream glycation products resulting in further oxidative stress and cell apoptosis, necrosis and DNA damage (Goyal et al., 2016). STZ

also has the ability to both directly and indirectly activate NFκB, which in turn leads to cytokine production and mitochondrial dysregulation, contributing to beta cell disruption.

STZ has a half-life of 15 min and it is therefore recommended that it must be administered as a fresh preparation each time, dissolved in a pH 4.5-citrate buffer for maximum effect. There are many differences in the doses between species and strains with doses ranging from 100 to 300 mg/kg for single high dose and 30–80 mg/kg for multiple low dose injections (Deeds et al., 2011). In fact, other factors, such as age and sex also play a large role as younger rodents have been shown to be more susceptible to STZ than older animals (Leiter, 1982) and females have partial resistance to STZ due to estrogens which appear to attenuate STZ-induced hyperglycemia as shown in rats (Riazi et al., 2006). STZ seems to have a slightly better toxicity profile than alloxan with fewer deleterious effects, for example, in the liver (El-Hawari and Plaa, 1983), as well as having a large therapeutic window making it now a more favorable option for the induction of diabetes. It should also be noted that STZ can induce lymphopenia, which could affect the interpretation of islet transplantation studies in which immune tolerance could be involved (Muller et al., 2011).

2.3.2.1 SINGLE HIGH DOSE STZ

A single high dose of STZ in rodents ranges from 35 to 65 mg/kg for rats and between 100 and 300 mg/kg for mice depending on the strain and sex. There is an initial hyperglycemia phase within the first few hours followed by up to 8 h of hypoglycemia preceding the slow increase of blood glucose levels to the usually in the range of 400–600 mg/dL (22–33 mM) over the consecutive 3–5 days (Deeds et al., 2011; Goyal et al., 2016). The reports of hypoglycemia have given rise to some protocols recommending the administration of glucose within the early period following injection. However, recent data by King et al. (2016) using continuous glucose monitoring in rats has shown that STZ-induced diabetes within hours with no signs of hypoglycemia.

2.3.2.2 MULTIPLE LOW DOSE STREPTOZOTOCIN

Multiple low dose STZ treatment is used to model insulitis, as well as produce hyperglycemia in rats and mice. Multiple doses of STZ between 20 and 40 mg/kg are administered over 3–5 consecutive days leading to depletion of around 85% of beta cells. This type of dosing induces an inflammatory response leading to macrophage infiltration of the islets that ultimately leads to beta cell death by cytokine mediated damage (Lukic et al., 1991; Sandberg et al., 1994; Yang et al., 2003). It is likely that this occurs through an NFκB-dependent pathway as blocking this pathway genetically leads to fewer animals becoming diabetic (Mabley et al., 2002).

A dramatic loss of beta cell mass and secretory function occurs within 1 day followed by the maximum macrophage infiltration which is seen later at around day 3 (Bonnevie-Nielsen et al., 1981). Unlike in human Type 1 diabetes, the beta cell destruction occurs in the absence of T lymphocyte involvement and thus investigators should interpret results in this model cautiously and preferably use it together with a spontaneous autoimmune model of beta cell destruction.

2.4 Virus-Induced Models of Diabetes

Viruses have been implicated to be involved in the pathogenesis of some cases of Type 1 diabetes (van der Werf et al., 2007). Animal models have therefore been developed to recapitulate viral infection leading to beta cell destruction, which can occur either directly or indirectly (Jun and Yoon, 2003). A variety of viruses have been used in animal models including Coxsackie B virus (Kang et al., 1994), Encephalomyocarditis virus (Craighead and McLane, 1968), and Kilham rat virus (Guberski et al., 1991). The models are complicated by the results depending on timing and efficiency of the viral infection. Indeed, depending on the conditions, some viruses have been shown to protect rather that cause Type 1 diabetes (von Herrath et al., 2011). Nonetheless, these models show an important proof of principle that viruses can induce a Type 1 diabetes phenotype and have increased our knowledge of this process.

2.5 Large Animal Models of Type 1 Diabetes

In some studies of Type 1 diabetes, it is desirable to use a large animal model. Spontaneous diabetes in larger animal models is relatively uncommon and the onset is unpredictable making spontaneous models rather unpractical. Therefore beta cell ablation is usually used. This can be achieved by pancreatectomy or by chemically ablating the beta cells using STZ.

2.5.1 Pancreatectomy

Whereas it is not practical or ethical to use pancreatectomy in rodents with the sole aim of inducing hyperglycemia, it is more widely used in larger animals. When carried out by a skilled surgeon, pancreatectomy is a reliable method to induce hyperglycemia in pigs (Morel et al., 1991), dogs (Fisher et al., 2001), and primates (He et al., 2011). However, the ethical implications should be carefully considered, as this is an invasive procedure that can lead to a variety of side effects. One potential use is in islet transplantation studies where autotransplantation can be carried out in a pig (Emamaullee et al., 2009b) or primate model (Rajab et al., 2008) as these animals have a similar islet: portal vein size as humans.

2.5.2 Chemical Ablation of Beta Cells in Large Animals

STZ can be used in large animals to deplete beta cells and has primarily been used in pigs (Hara et al., 2008) and primates (Koulmanda et al., 2003). Although it is very effective in primates, pigs show a reduced response to STZ due to a low GLUT2 expression (Dufrane et al., 2006). Increasing the STZ dose can lead to renal and hepatic toxicity and thus in pigs a narrow therapeutic window makes effective beta cell ablation difficult to achieve. Some studies have reported a correcting of hyperglycemia within 4 weeks of the STZ injection into pigs and thus careful attention is required to make sure spontaneous recovery is not affecting the study outcome (Dufrane et al., 2006). Some investigators have combined a partial pancreatectomy with a reduced STZ dose in pigs (Wise et al., 1985). Multiple low dose STZ has been used on primates to try and come closer to modeling human pathogenesis in Type 1 diabetes. One study showed that rhesus monkeys administered low dose STZ showed both hyperglycemia and autoantibodies to insulin, which is a valuable tool for preclinical testing (Wei et al., 2011). However, it is worthy to note that it has been shown that cynomolgus monkeys administered STZ-developed lymphopenia, which could interfere with interpretation of transplantation studies (Nagaraju et al., 2014).

2.6 Choosing an Animal Model for Type 1 Diabetes

If the study aims to understand the pathogenesis of Type 1 diabetes, an autoimmune model should be used. The NOD mouse, BB rat, Lew.1AR.1-iddm rat, and KDP rat have all contributed to understanding more about the genetic susceptibility of the disease and, in varying degrees, the effector mechanisms in beta cell destruction. Likewise, one of these models would ideally be used in prevention studies that involve manipulation of the immune attack on the beta cells. The low dose STZ model could also be used in addition to prevent immune mediated attack on the beta cells, but should ideally be combined with a spontaneous model.

In investigations that aim to study new insulin formulations or beta cell replacement therapies, the beta cell ablation models of STZ or alloxan could be used as the lack of beta cells is a more important characteristic of the model than the process that led to it. In addition the male Akita mouse is an ideal model in that scenario, as beta cell regeneration does not occur.

2.7 Endpoints in a Type 1 Diabetes Study

2.7.1 Blood Glucose Concentrations and Weight

In prevention and curative studies, the most obvious endpoint is blood glucose concentrations. However, it is important that bodyweight is also monitored as blood glucose concentrations will fall if the animal is not eating properly which could give the false impression that the animal is curing when in fact they are sicker. To truly be convinced that blood glucose homeostasis is improved, weight gain should be seen in conjunction with a reduction in blood glucose concentrations. Normal blood glucose concentrations are not well defined in rodents, although it should be noted that mice tend to have higher blood glucose concentrations than rats and humans. In rodent studies of Type 1 diabetes, blood glucose concentrations greater than 300 mg/dL (16.7 mM) is often defined as diabetic, although 400 mg/dL (22.2 mM) or higher is also used. Defining when the animal has cured is more difficult. The most conservative studies define less than 200 mg/dL (11.1 mM) as cured, although other studies use below 300 mg/dL (16.7 mM). In reality one can regard mice with blood glucose concentrations between 200 and 300 mg/dL (11.1 and 16.7 mM) as neither fully diabetic nor fully cured. It is usual to confirm "diabetes" or "cure" with blood glucose measurements taken over the course of several days to avoid a single fluctuation giving a false result. It should be noted that blood glucose concentrations vary between strains (Leiter, 2009) and also depend on the time of day that blood glucose is measured. The timing of blood glucose concentration measurement is particularly relevant if using rats or mice as these nocturnal animals feed at night. Therefore blood glucose concentrations during the day are lower than at night and this variation is considerably magnified in models of Type 1 diabetes (King et al., 2016). In general, blood glucose concentrations should be measured as early in the morning as possible and at the same time point each day. Continuous blood glucose monitoring by telemetry is a way to circumvent this problem, but is rather expensive and invasive for everyday use. However, it could be a useful tool to use in optimized models to really show improvements in minute-to-minute blood glucose variations (King et al., 2016).

2.7.2 Insulitis Scoring

In therapies designed to prevent the autoimmune attack on the islets, scoring of insulitis in histological sections of the pancreas at the end of the study can provide evidence of successful manipulation of the immune response. Typically, islets are scored from 0 to 3 depending on extent of the immune infiltration (Yoon et al., 1999). It is important that scoring occurs blinded to prevent bias and ideally should be carried out by two independent researchers scoring each sample. A more refined method is fluorescence-activated cell sorting to analyze the phenotype of the infiltrating cells (Magnuson et al., 2015).

2.7.3 Immune Cell Phenotyping and Autoantibody Response

To characterize the immune response during the autoimmune attack, cells of the peripheral blood, spleen, or lymph nodes can be analyzed by fluorescence-activated cell sorting (Pontesilli et al., 1987). In addition, autoantibodies in the serum can be measured by ELISA, radiobinding assays (Lampasona et al., 2008), or electrochemiluminescence-based assays (Lo et al., 2011). Immune cell secretory products, such as cytokines can be measured by enzyme-linked immunospot (ELISpot) (Emamaullee et al., 2009a).

2.7.4 Ruling Out Regeneration of Endogenous Beta Cells

In chemically induced beta cell ablation models, regeneration of endogenous beta cells could confound results and should be therefore ruled out. This can be done by insulin staining of the pancreas or measuring insulin content of the pancreas at the end of the study. In studies where islets have been transplanted under the kidney capsule, nephrectomy can be used to remove the graft at the end of the study with a reversion to hyperglycemia expected to show the graft was responsible for normoglycemia (Rackham et al., 2011).

3 TYPE 2 DIABETES

Type 2 diabetes is caused by an inability of the beta cell to fully compensate to insulin resistance, leading to a relative deficiency in insulin and hyperglycemia (Weir and Bonner-Weir, 2004). The disease has a strong genetic link but it is clear that, environmental factors play an important role in disease development (Franks and Pare, 2016). Indeed, the incidence of Type 2 diabetes has increased rapidly with the global epidemic in obesity, which is one of the major risk factors to the disease (Kahn and Flier, 2000). Impaired glucose tolerance is usually caused by decreased insulin sensitivity and is an important stage in the development of Type 2 diabetes (Weir and Bonner-Weir, 2004). At this stage of the disease, some beta cell compensation is usually apparent and thus it is an ideal stage, during which the development of overt Type 2 diabetes can be prevented by intervention (Eriksson et al., 1999). Many preclinical studies, therefore use animal models of impaired glucose tolerance and thus these models will also be discussed as they form an important part of Type 2 diabetes research. Overt diabetes occurs in both human and animal models when beta cell function and/or mass are impaired to the extent that insulin production is no longer sufficient to compensate for insulin resistance (Masiello, 2006; Weir and Bonner-Weir, 2004). Some of the most commonly used rodent models in Type 2 diabetes are outlined in Table 10.2.

3.1 Obese Models

As obesity-induced insulin resistance is a major contributor to the pathogenesis of Type 2 diabetes, many animal models are either genetically obese or obesity is induced by manipulation of the diet. Although most of these obese models are characterized by insulin resistance, not all will necessarily develop overt diabetes and many model a prediabetic state of impaired glucose tolerance.

Many genetically obese mouse strains are monogenic, that is, obesity is caused by the mutation or manipulation of a single gene. Although monogenic mutations are a rare cause of human obesity, in rodent models they are often used to replicate the insulin resistant and glucose intolerant state that embodies some of the main characteristics of Type 2 diabetes. The two most commonly used monogenic mouse models (Lep$^{ob/ob}$ and Lep$^{db/db}$ mice) have an aberrant leptin signaling pathway, leading to hyperphagia and subsequent obesity (Wang et al., 2014). A disrupted leptin signaling pathway is also a key characteristic of the Zucker fatty rat and Zucker fatty diabetic rat. Other mouse and rat models display polygenic obesity (Joost and Schurmann, 2014). Although this more accurately reflects the human condition, it raises other problems including the lack of a genetically similar lean control. Obesity can also be induced in mice and rats by feeding them a high-fat or high-fat/high-sugar diet (Hariri and Thibault, 2010), which may reflect the pathogenesis of the human disease.

3.1.1 Monogenic Models of Obesity

3.1.1.1 LEP$^{OB/OB}$ MICE

A single autosomal recessive mutation on the gene encoding leptin causes the obese phenotype in Lep$^{ob/ob}$ mice (Zhang et al., 1994). The nonsense mutation leads to a lack of functional leptin and thus the satiety pathway in these mice is disrupted leading to extensive hyperphagia. Lep$^{ob/ob}$ mice gain weight rapidly from an early age and by 2–4 weeks of age the obese phenotype starts to become apparent (Lindstrom, 2007). This is coupled with hyperinsulinemia and glucose intolerance. There is no beta cell dysfunction and although beta cell mass increases to compensate for insulin resistance (Tomita et al., 1992); these animals can still become hyperglycemic. However, the diabetic phenotype is usually relatively mild and it is transient in nature with a peak in blood glucose concentrations at 3–5 months after which they fall (Lindstrom, 2007). In addition, these mice have a variety of comorbidities including hyperlipidemia and infertility. It should also be noted that they have reduced energy expenditure and reduced physical activity. As with other animal models of Type 2 diabetes, the background strain of the Lep$^{ob/ob}$ mice determines the severity of the diabetic phenotype and on the C57BLKS/J background a more severe phenotype is evident (Coleman and Eicher, 1990; Hummel et al., 1972).

TABLE 10.2 Key Characteristics of Rodent Models of Type 2 Diabetes

Type of model	Examples	Obese?	Islet phenotype
Monogenic obesity	Lep$^{ob/ob}$ mice	√	Background dependent—C57Bl/6: compensation, C57Bl/KS: inadequate compensation
	Lep$^{db/db}$ mice	√	Initial compensation then reduction in beta cell mass. Severity background dependent as for Lep$^{ob/ob}$ mice.
	Zucker diabetic fatty rats	√	Inadequate beta cell compensation
Polygenic obesity	KK-Ay mice	√	Some beta cell compensation
	OLETF rats	√	Progressive beta cell degeneration
	New Zealand obese mice	√	Reduced beta cell mass
	TallyHo/Jng mice	√	Some beta cell compensation
Diet manipulation	High-fat feeding	√	Some beta cell compensation
	High-fat/high sucrose feeding	√	Some beta cell compensation
	Psammomys obesus	√	Progressive beta cell degeneration
Planned strain development	Goto-Kakizaki rats	x	Beta cell mass or function compromised.
	NoncNZO10/Ltj mice	√	Initial compensation then reduction in beta cell mass
	Zucker diabetic Sprague Dawley rats	√	Initial compensation then reduction in beta cell function
	UC Davis Type 2 diabetes mellitus rat	√	Initial compensation then reduction in beta cell function
	Human islet amyloid polypeptide rat	x	Amyloid deposits leading to beta cell degeneration
	Human islet amyloid polypeptide mouse	x	Amyloid deposits leading to beta cell degeneration
Induced models of beta cell insufficiencies	Neonatal streptozotocin rat	x	Depletion then mass regeneration
	Pancreas injury models	x	Depletion then mass regeneration
	High-fat diet + streptozotocin	√	Initial compensation then reduction in beta cell mass

3.1.1.2 LEP$^{DB/DB}$ MICE

The cause of the obese phenotype in Lep$^{db/db}$ mice is a nonfunctional leptin receptor due to a single autosomal recessive mutation resulting in abnormal mRNA splicing (Chen et al., 1996). In similarity to Lep$^{ob/ob}$ mice, this leads to hyperphagia and obesity from early in life (Hummel et al., 1966). Animals are hyperinsulinemic (Coleman and Hummel, 1974) and this coupled with beta cell dysfunction (Berglund et al., 1978) leads to severe hyperglycemia depending on the background strain (Coleman, 1978). In similarity to the Lep$^{ob/ob}$ mice, the background strain of the Lep$^{db/db}$ mice can determine the severity of the diabetic phenotype with C57BL/KS mice becoming more severely diabetic to the extent that they can develop ketosis (Hummel et al., 1972). This may be due to the poor ability of this strain to compensate with increased beta cell replication (Swenne and Andersson, 1984).

3.1.1.3 ZUCKER FATTY RATS AND ZUCKER DIABETIC FATTY RATS

Zucker fatty rats have a mutated leptin receptor (Phillips et al., 1996) leading to hyperphagia (Kowalski et al., 1998) with obesity apparent from around 4 weeks of age (Wang et al., 2014). They are hyperinsulinemic (Trimble et al., 1986) and have poor glucose tolerance (Triscari et al., 1979) although are not overtly diabetic. The Zucker diabetic fatty (ZDF) rat is a substrain of the Zucker fatty rat, which was derived from hyperglycemic Zucker fatty rats to gain a model with diabetic features (Peterson et al., 1990). It is severely insulin resistant and males become overtly diabetic at 8–10 weeks, which is due to an inability of beta cells to compensate for insulin resistance, which is associated with changes in islet morphology (Tokuyama et al., 1995). Females do not tend to develop overt diabetes but diabetes can be induced by feeding a high-fat diet (Corsetti et al., 2000).

3.1.2 Polygenic Models of Obesity

There are several different rodent models of impaired glucose tolerance and diabetes that are induced by a polygenic obese phenotype. It could be argued that this more closely reflects obesity in humans that monogenic strains. Models, such as these have been used to identify genes involved in the development of obesity-induced diabetes in humans (Joost and Schurmann, 2014).

3.1.2.1 KK AND KK-AY MICE

KK mice are hyperleptinemic, mildly obese mice that develop impaired glucose tolerance characterized by severe insulin resistance and hyperinsulinemia (Clee and Attie, 2007). There are signs of beta cell compensation with increased pancreatic insulin content and islet hypertrophy (Nakamura and Yamada, 1967). The introduction of the *Ay* gene led to KK-Ay substrain, which is more severely hyperinsulinemic and is overtly diabetic (Suto et al., 1998).

3.1.2.2 OTSUKA LONG-EVANS TOKUSIMA (OLETF) RATS

This strain derives from a spontaneously diabetic rat discovered in a colony of Long-Evans rats (Kawano et al., 1994). Selective breeding leads to the OLETF strain, which is characterized by mild obesity, hyperinsulinemia, and late-onset hyperglycemia, which occurs after the age of 18 weeks (Moran, 2008). Males are prone to develop diabetes, which occurs after progressive degeneration of the islets. Initially, there is a period of islet hyperplasia up to the age of 40 weeks after which the islets become fibrotic, apoptosis is detected and beta cell mass is reduced (Hong et al., 2002).

3.1.2.3 NEW ZEALAND OBESE MICE

New Zealand Obese (NZO) mice are obese due to hyperphagia (Leiter and Reifsnyder, 2004). The cause of this is most likely a defect in leptin transport across the blood brain barrier as these mice are hyperleptinemic and resistant to peripherally administered leptin but respond to centrally administered leptin (Halaas et al., 1997). They are hyperinsulinemic as a result of insulin resistance and have increased hepatic glucose production (Andrikopoulos et al., 1993; Veroni et al., 1991). Impaired glucose tolerance worsens with age and approximately half of males develop overt diabetes (Haskell et al., 2002). In male mice that have overt diabetes, a reduced beta cell mass is evident (Lange et al., 2006). The NZO strain has been used in a carbohydrate intervention diet model, in which carbohydrates are initially restricted from weaning and then fed from 18 weeks leading to rapid beta cell loss and induction of hyperglycemia in the space of 16 days (Kluth et al., 2011).

3.1.2.4 TALLYHO/JNG MICE

This strain of mice was derived from selective breeding of hyperglycemic mice discovered in an outbred colony of Theiler original mice (Kim et al., 2001). These obese mice have characteristics often seen in obese patients including increased plasma triglycerides, cholesterol and free fatty acids (Kim and Saxton, 2012). Male mice develop hyperglycemia at around 10–14 weeks whereas females do not become overtly diabetic (Kim and Saxton, 2012). Hyperinsulinemia is evident with

resulting hypertrophied and degranulated beta cells (Leiter et al., 2013).

3.1.3 Diet-Induced Models of Obesity and Diabetes

Manipulation of the diet by feeding rodents a high-fat, high-energy diet is another means of inducing obesity in rodents. This model is relevant given it reflects the mechanism of obesity-induced diabetes in humans. It is especially a useful tool in knock-out and transgenic mice in an attempt to establish whether the gene of interest affects the ability of islet function to adapt to the obesogenic environment. In addition, diet manipulation during pregnancy can be used as it can lead to aberrations in blood glucose homeostasis in the offspring.

3.1.3.1 HIGH-FAT FEEDING IN MICE AND RATS

Obesity can be induced by feeding mice a high-fat diet. This entails increasing the fat content of their chow from about 11% fat to around 58% fat (Surwit et al., 1998). It was first described in C57Bl/6 mice in 1988 and since then has been used in numerous studies (Surwit et al., 1988). Although overt diabetes does not usually occur, insulin resistance leading to glucose intolerance is a characteristic of this model (Winzell and Ahren, 2004). It therefore models an obesity-induced prediabetic state. Although increased weight gain can be detected within a week of high-fat feeding (Winzell and Ahren, 2004), it is typically administered over a longer time period (8–12 weeks) (Muhlhausler, 2009). It should be noted that the susceptibility to diet-induced obesity varies between different rat and mouse strains and thus the strain should be chosen carefully before commencing a study (Almind and Kahn, 2004; Surwit et al., 1998). It has also been shown that there is a variation in the response to high-fat feeding within inbred strains and thus it is not only genetic factors determining the outcome (Burcelin et al., 2002). The C57Bl/6 mouse strain has been shown to be susceptible to obesity and mild hyperglycemia when fed a high-fat diet and thus is a popular strain to use (Winzell and Ahren, 2004). In rats, the Sprague Dawley and Wistar strains are often used although it has been reported that the Wistar rat is more susceptible to the metabolic phenotypes (Marques et al., 2016).

3.1.3.2 HIGH-FAT HIGH SUCROSE FEEDING IN MICE AND RATS

High-fat high sucrose diets are also used to induce aberrant blood glucose homeostasis in rodents (Fernandes-Santos et al., 2009; Sampath and Karundevi, 2014). For example, a diet with addition of lard and sucrose can induce differences in weight in Sprague Dawley rats by day 30 (Nakajima et al., 2015). By day 56, increased adiposity, insulin resistance and hyperglycemia were evident. It should be noted that although the overall calorie intake is increased in this diet overall food consumption

is reduced due to the high calorific value. This can lead to a protein deficiency and should be carefully controlled for. This combination of a high-fat and high-sugar diet is thought to most closely resemble the diet that has dramatically increased obesity levels in humans over the past few decades.

3.1.3.3 DIET-INDUCED OBESITY IN THE SAND RAT (*PSAMMOMYS OBESUS*)

The sand rat is lean in its natural desert habitat where it feeds on low calorie vegetation, but in a laboratory setting becomes obese, hyperinsulinemic, and ultimately hyperglycemic when fed a standard chow diet (Shafrir et al., 2006). This is due to its poor adaptation to excess nutrition and thus it serves as a model of the "thrifty gene effect" where it is hypothesized, that rapid evolution from scarcity to nutritional abundance in some developing countries has led to a diabetes epidemic (Joffe and Zimmet, 1998). The progression from normal blood glucose metabolism to diabetes in the sand rat has been described in four different stages. Stage A is normoglycemic and normoinsulinemic, stage B is normoglycemic and hyperinsulinemic, stage C is hyperglycemic and hyperinsulinemic, and finally stage D is hyperglycemic and insulinopenic. Progression from stage A to C can be prevented by restricting the diet but stage D is characterized by beta cell attrition and is nonrecoverable (Shafrir et al., 2006). These pathophysiological changes reflect the progress of the disease in some patients and reflect a model of over nutrition and subsequent failure of beta cell adaptation.

3.1.3.4 PRENATAL DIET MANIPULATIONS

Developmental origins of metabolic diseases have been demonstrated in humans. For example, studies of children born just after the Dutch Winter Famine showed that in adulthood there were increased incidences of impaired glucose tolerance (de Rooij et al., 2006). In addition, an inappropriately high nutrient supply in utero has also been shown to lead to increased incidence of Type 2 diabetes later in life (Pettitt and Knowler, 1998). It is therefore clear that nutrient supply in utero is important and either restriction or oversupply of nutrients can lead to disturbed glucose homeostasis in adulthood.

3.1.3.4.1 MATERNAL LOW-PROTEIN MODEL IN RATS Pregnant dams fed a low protein diet (8% rather than 20%) give birth to growth-restricted offspring with a low body weight, which develop symptoms of Type 2 diabetes later in life (Muhlhausler, 2009). After birth, there is a period of rapid postnatal growth (Ozanne, 2001) and this has also been implicated as an important component of the model. Insulin sensitivity is initially enhanced but in adulthood insulin resistance develops leading on to a Type 2 phenotype (Ozanne et al., 2005).

Indeed, protein restriction during pregnancy has been shown to affect the offspring's islets, as well as insulin sensitive tissues, such as liver, fat, and muscle (Ozanne et al., 2005; Thompson et al., 2007). Islets in neonates are smaller than control animals and have higher levels of apoptosis (Petrik et al., 1999). A postnatal high-fat diet exacerbates the phenotype and in these animals (Claycombe et al., 2013).

3.1.3.4.2 MATERNAL OVER NUTRITION IN RATS High-fat feeding of pregnant dams has been associated with increased obesity and impaired blood glucose homeostasis in adulthood in the offspring (Srinivasan et al., 2006). The consequent obesity in the offspring may directly affect blood glucose homeostasis, although it has been suggested that abnormal development of the beta cells may also contribute to the phenotype (Cerf et al., 2007). Indeed offspring have hyperinsulinemia and impaired glucose tolerance (Srinivasan et al., 2006), as well as impaired beta cell function (Cerf et al., 2007; Taylor et al., 2005).

3.2 Planned Strain Development

Although many models of diabetes have been discovered through inbreeding of spontaneously diabetic rodents, some newer models have been created through planned breeding or genetic engineering to obtain a strain with Type 2 diabetes features.

3.2.1 Goto-Kakizaki Rats

Goto-Kakizaki (GK) rats were established by repeated breeding of glucose intolerant Wistar rats (Goto et al., 1976), which led to a nonobese rat model of Type 2 diabetes. In contrast to obese models, insulin resistance is not the main initiator of hyperglycemia in GK rats; the aberrant blood glucose homeostasis is largely due to an insufficient insulin response (Ostenson and Efendic, 2007; Portha et al., 2001). The cause of this varies between colonies, with the Stockholm and Dallas colonies presenting with defects in insulin secretion whereas in the Paris colony the rats have a 60% reduced beta cell mass (Portha et al., 2009). In addition, the islets in the Paris colony of GK rats show signs of inflammation and fibrosis and therefore have some features of islets in Type 2 diabetes patients (Homo-Delarche et al., 2006).

3.2.2 NoncNZO10/Ltj Mice

The NoncNZO10/Ltj mouse strain was specifically developed at the Jackson Laboratory by combining independent diabetes risk-conferring quantitative trait loci from two different NZO strains with a nonobese nondiabetic mouse strain (NON/Lt) which had a propensity for high nonfasting blood glucose concentrations (Leiter et al., 2013). The model is characterized by severe insulin

resistance in the liver and skeletal muscle which is evident from 8 weeks and hyperglycemia develops from around 12 weeks of age (Cho et al., 2007). Although islet mass initially increases to compensate for the insulin resistance, beta cell loss then occurs leading to overt diabetes (Leiter et al., 2013).

3.2.3 UC Davis Type 2 Diabetes Mellitus Rat

The UC Davis Type 2 diabetes mellitus rat (UCD-T2DM rat) was developed by breeding insulin-resistant obese Sprague Dawley rats with ZDF lean rats. The outcome of this breeding strategy was the creation of a strain that was characterized by adult-onset obesity, insulin resistance, and impaired glucose tolerance ultimately leading to diabetes due to beta cell loss (Cummings et al., 2008). It has been suggested that this closely mimics the disease progression in Type 2 diabetes. Diabetes develops in both males and females, although females develop the disease approximately 3–4 months after males with males developing overt diabetes at around 26 weeks and females at 40 weeks.

3.2.4 Zucker Diabetic Sprague Dawley Rats

Zucker diabetic Sprague Dawley (ZDSD) rat strain was developed by crossing ZDF rats with a substrain of Sprague Dawley rat, which was selectively bred for its susceptibility to obesity induced by high-fat feeding (Peterson et al., 2015). In contrast to the ZDF rat, this strain has a functional leptin pathway (Choy et al., 2016). However, when fed a specific diet (Purina 5008 chow), rats gain weight, which is coupled with a decrease in insulin sensitivity (Choy et al., 2016). There is an initial compensation in beta cell function but the disease progresses resulting in overt diabetes. In this model, onset of overt diabetes is variable between individual rats but at least half are overtly diabetic by 21 weeks (Reinwald et al., 2009). Due to the similar background of the rats, it is likely that ZDSD and UCD-T2DM rats have similar characteristics, but as far as we are aware, have not been directly compared.

3.2.5 Models of Amyloid Deposition

A characteristic of Type 2 diabetes is the deposition of amyloid with the islets, leading to altered structure and function (Clark, 1989). Amyloid is derived from islet amyloid polypeptide (IAPP); however, IAPP in rodents is not amyloidogenic and thus does not aggregate to form the histopathological fibrils (Hoppener et al., 1994). Therefore rodent models have been created to express human IAPP in order to recapitulate the human pathogenesis of islet amyloid deposition. The human islet amyloid polypeptide (HIP) rat develops islet amyloid and diabetes presents at between 5 and 10 months of age (Butler et al., 2004). The beta cell mass of the rats is reduced by 60%, primarily due to increased rates of apoptosis (Matveyenko and Butler, 2006a). In mice, human IAPP (hIAPP) expressed under the insulin promoter leads to deposition of human amyloid within the islets causing toxicity (Janson et al., 1996). The mice initially have impaired glucose-induced insulin secretion and a reduction in beta cell mass follows, resulting in hyperglycemia (Matveyenko and Butler, 2006b).

3.3 Induced Models of Beta Cell Insufficiencies

The role of the beta cell in the development of Type 2 diabetes has become increasingly apparent (Weir and Bonner-Weir, 2004). Even in states of severe insulin resistance, diabetes will not develop if the beta cell is able to compensate. Although an inability of the beta cell to compensate for insulin resistance is a feature of many of the Type 2 diabetes strains already discussed, it is sometimes of value to focus on the function and mass of beta cells in an induced model, which allows studies to be carried out in a more specific time frame.

3.3.1 Neonatal Streptozotocin Administration

STZ administration to neonatal rats (2 days old) induces hyperglycemia within 2 days (Portha et al., 1974). This is followed by regeneration of the beta cells and a return to normoglycemia is reached within 10 days. However, the regeneration process is not sufficient to meet the metabolic demands of the growing rat and by 6 weeks the rats revert to hyperglycemia (Bonner-Weir et al., 1981). The insulin inadequacy is thought be caused by a combination of beta cell dysfunction (Trent et al., 1984) and reduced beta cell mass (Trent et al., 1984) although insulin resistance has also been described in this model (Takada et al., 2007).

3.3.2 Pancreas Injury Models

Injury models, such as duct ligation and pancreatectomy lead to substantial and rapid beta cell regeneration. These models are therefore useful to understand beta cell proliferation and neogenesis. In rats, a 60% pancreatectomy does not lead to an increase in blood glucose concentration and regeneration is mild (Leahy et al., 1988). However, a 90% pancreatectomy leads to hyperglycemia and extensive beta cell regeneration (Bonner-Weir et al., 1983). Within a period of 4 weeks, the endocrine portion of the pancreas has increased by eightfold. In mice, 60% pancreatectomies are more commonly used due to technical difficulties of carrying out this procedure on such a small animal (Li et al., 2016). This leads to compensatory beta cell proliferation in a normoglycemic state, which is a useful tool to study beta cell mass regulation.

In rats, ligation of the tail portion of the pancreas, which accounts for 50%–60% of the pancreatic mass, leads to massive degeneration of this portion of the

pancreas (Wang et al., 1995). It is replaced by ductal structures by day 3 and by day 5 it consists of ductal structures interspersed with small islets in connective tissue. During the 1st week, the beta cell mass in the tail portion nearly doubles making it an ideal model in which to study beta cell regeneration. Hyperglycemia does not occur in this model, indeed blood glucose concentrations decreases, which may reflect the invasiveness of this procedure. However, in the mouse model of ductal ligation, no overall change in pancreatic mass occurs (Rankin et al., 2013) which indicates important species differences in mechanisms of beta cell regeneration.

3.3.3 *High-Fat Diet and Streptozotocin*

The high-fat fed and STZ rat model was originally described in 2000 by Reed et al. (2000). This model aims to combine inducing insulin resistance through diet with reducing beta cell mass to mimic the natural history and metabolic characteristics of Type 2 diabetes. In the original model, 7-week-old Sprague Dawley rats were high-fat fed for 2 weeks. At this stage glucose tolerance was normal compared to control fed rats, but insulin resistance was indicated by hyperinsulinemia in response to a glucose load. A single dose of 50 mg/kg STZ was administered to fasted rats, which leads to an induction of hyperglycemia. This model was then modified to use low dose STZ (Srinivasan et al., 2005; Zhang et al., 2008). This model has now been used in many studies, primarily using Sprague Dawley or Wistar rats. The age of initiation of high-fat feeding, length of high-fat feeding, and doses of STZ have varied somewhat, which could lead to different metabolic profiles of the model between different studies (Skovso, 2014). One potential controversy with this model is to what extent beta cell mass should be reduced to model Type 2 diabetes as, if the beta cell mass reduction is too severe, one could argue it more closely resembles an obese Type 1 diabetes model. Therefore the STZ dosing and frequency is an important component of the model, with low doses of STZ preferable. Overall a variety of factors affect the metabolic outcome of the rats with some studies modeling an early and others a late stage of Type 2 diabetes (Skovso, 2014).

3.4 Large Animal Models of Type 2 Diabetes

Some larger animals spontaneously develop Type 2 diabetes, making them ideal to study with regard to understanding the human condition. Others are suitable models for over nutrition and obesity. Cats develop diabetes in middle age, which is associated with obesity and insulin resistance (O'Brien, 2002). However, the most striking similarity is the deposition of amyloid in the islets as it is one of the few species other than old world monkeys that develop this feature of Type 2 diabetes (Henson and O'Brien, 2006; Hoenig, 2012). Indeed,

in similarity to humans, this leads to a loss of beta cell mass. Unlike cats, dogs do not spontaneously develop Type 2 diabetes (Rand et al., 2004) and thus diabetes has to be experimentally induced. High-fat feeding combined with STZ has been used in dogs to induce a Type 2 diabetes phenotype (Ionut et al., 2010). Feeding a highly palatable diet, which is high in fat and carbohydrate, induces obesity. Beta cell function compensates for the insulin resistance and therefore a second intervention is required where beta cell mass is reduced by administering STZ. Pigs have been used in Type 2 diabetes research for a variety of reasons. One is that they have anatomical and metabolic similarities to humans. Another major reason is their susceptibility to atherosclerosis, which makes it a suitable model in which to study cardiovascular complications of Type 2 diabetes (Bellinger et al., 2006). A wide variety of different pig strains have been used in studies. Differing degrees of aberrations in blood glucose homeostasis have been induced by high-fat feeding or a combination of high-fat feeding and chemically induced reductions in beta cell (Bellinger et al., 2006; Koopmans and Schuurman, 2015; Koopmans et al., 2006). Old-world nonhuman primates spontaneously develop Type 2 diabetes, which has many similarities to the human disease, including obesity-induced insulin resistance and islet amyloid deposition, which leads to impaired beta cell function and mass (Wagner et al., 2006). These primates have therefore provided a useful model in which to study the pathogenesis of Type 2 diabetes and pharmacological interventions.

3.5 Choosing an Appropriate Model for Type 2 Diabetes Research

Type 2 diabetes is a disease in which several different genetic and environmental factors contribute to the pathogenesis. Therefore one single animal model does not recapitulate the human disease, although many models have characteristics of Type 2 diabetes in humans. The choice of animal model will therefore depend whether the researcher is trying to understand the pathogenesis or whether trying to prevent or treat a specific aspect of the disease. It is appropriate in many studies to use an obese model, although this often models insulin resistance and a prediabetic state rather than overt diabetes. Insulin resistance is a key component of many obese models and often precedes overt diabetes and therefore may reflect an early stage of the disease. There are a variety of obese models to choose from including monogenic and polygenic models, as well as induction of obesity through dietary manipulation. In humans, loss of beta cell mass in Type 2 diabetes is an important factor in disease progression. Therefore animal models of beta cell insufficiencies are vital if this aspect of the disease is being investigated.

3.6 End Points in a Type 2 Diabetes Study

3.6.1 Glucose Tolerance Tests

In both humans and animal models of Type 2 diabetes, random blood glucose concentrations are often close to normal or only slightly elevated. Subsequently, glucose tolerance tests are often used to study blood glucose homeostasis under stimulated conditions. Animals are usually fasted prior to being administered the glucose load, to determine basal blood glucose concentration. In many studies, mice or rats are fasted overnight, although it has been suggested that this is inappropriate as these nocturnal animals feed overnight and thus rather than a fast it represents starvation (McGuinness et al., 2009). It has therefore been suggested that 6 h is a more appropriate time to fast rodents. Glucose can be administered intraperitoneally, intravenously, or orally by gavage and typically a dose of 1–2 g/kg is used. In normal nondiabetic mice, the blood glucose usually peaks at 15–30 min and reverts to basal levels by 120 min (Bowe et al., 2014). The definition of impaired glucose tolerance and diabetes is not clear in animal models. Impaired glucose tolerance is an inability to clear a bolus of glucose (often around 2 g/kg) from the blood supply in a defined time period (often 2 h). Many researchers regard glucose tolerance as "impaired" if it is significantly worse than in the control. Others regard it as abnormal if glucose concentrations have not returned to basal levels within the 2-h period.

3.6.2 Serum Insulin Concentrations

Measuring the concentrations of insulin in the blood can help determine whether beta cell function is impaired. Often glucose is injected into fasted animals to stimulate the beta cells and insulin is measured in serum removed prior to injection and at early (within the first 5 min) and later time points (around 30 min). Sensitive assays should be used, such as ELISA, which can measure accurate insulin concentrations in small blood volumes that can be ethically extracted from living mice. It should be noted that insulin concentrations per se cannot fully determine the cause of hyperglycemia in the animals.

3.6.3 Measuring Insulin Resistance

An approximate measure of insulin resistance can be obtained through carrying out insulin tolerance tests. Animals are often fasted for 6 h and insulin is injected and blood glucose measured over the next 60–90 min to determine how responsive the animal is to insulin. A more elegant measure of insulin sensitivity is the hyperinsulinemic-euglycemic clamp (DeFronzo et al., 1979) but this is less well used as the technique is invasive, technically demanding and usually requires the animals to be anaesthetized.

3.6.4 Ex Vivo Analysis

3.6.4.1 PANCREAS HISTOLOGY

It is often appropriate to study islet histology after the study ends. Islet and/or beta cell size and number can be investigated (Xu et al., 1999), as well as islet morphology (Arrojo e Drigo et al., 2015). In early stages of Type 2 diabetes, islets may appear larger than control animals whereas in late stages beta cell mass can be decreased. Beta cell proliferation rates can be determined by administering BrdU to the animals prior to the end of the study (Cordoba-Chacon et al., 2014) or using a proliferation marker, such as Ki67 (Jorns et al., 2014). In HIP rats and hIAPP transgenic mice islet morphology with regard to amyloid deposition can be studied using Congo Red to stain amyloid fibrils (Hoppener et al., 2008).

3.6.4.2 FUNCTION OF ISOLATED ISLETS

At the end of the study, islets from the pancreas can be isolated using a collagenase digestion technique. They can be used to study glucose-induced insulin secretion in either static or perifusion studies. Other parameters, such as glucose oxidation rates and insulin biosynthesis can also be measured. Such investigations allow beta cell function to be studied in detail in standardized conditions.

4 DIABETIC COMPLICATIONS

Diabetic complications, such as neuropathy, nephropathy, retinopathy, and cardiovascular disease arise in both Type 1 and Type 2 diabetes. In humans, these complications develop after chronic hyperglycemia and thus many rodent models do not develop complications due to the relatively short periods of hyperglycemia. STZ is often used in diabetes induction when studying complications, but the possibility of direct effects of the STZ on the specific organ should be considered. An example of this is in the study of neuropathies, where it has been shown that STZ directly stimulates the TRPA1 channels, which could complicate the interpretation of results (Andersson et al., 2015). The Akita mouse is an STZ-free alternative that has been used to study diabetic neuropathy (Islam, 2013), although many of the Type 2 models are also suitable for this purpose.

Models of retinopathy include STZ-induced models of hyperglycemia, as well as spontaneous Type 1 and Type 2 models, such as Akita mice, NOD mice, and Lep$^{db/db}$ mice (Lai and Lo, 2013). The pathogenesis of retinopathy can also be investigated by using normoglycemic models of proliferative retinopathy, such as oxygen-induced retinopathy.

A variety of different animal strains have been used to model nephropathy including OLETF rats, Lep$^{ob/b}$ mice, Lep$^{db/db}$ mice, Zucker fatty rats (Betz and Conway, 2016). STZ-induced diabetes has also been used, but possible

direct effects of STZ on the kidneys should be controlled for. Akita mice have also been used but the disease progression is limited so may not be the best model for late stage experiments (Alpers and Hudkins, 2011). It should be noted that susceptibility to diabetic nephropathy is strain dependent with the C57Bl/6 relatively resistant (Betz and Conway, 2016).

5 GENDER, STRAIN, AND AGE EFFECTS IN ANIMAL MODELS OF DIABETES

Many rodent models of diabetes show a gender bias in the severity and/or incidence of diabetes. In NOD mice, females have a higher incidence of diabetes than male mice, whereas in Akita mice, the male mice show a more severe phenotype, which is insulin dependent. Many Type 2 diabetes models also show a gender effect, with examples in which males are more insulin resistant and prone to diabetes. This is particularly noticeable in polygenic obese models and may be due to increased obesity leading to more severe insulin resistance. In addition, estrogen has been shown to have protective effects to beta cell damage (Le May et al., 2006). In addition, strain effects can be very prominent in metabolic research (Fontaine and Davis, 2016). This ranges from susceptibility to STZ (Wolf et al., 1984) to susceptibility to high-fat feeding (Almind and Kahn, 2004). In addition, there are strain differences in the ability of beta cells to compensate to insulin resistance (Hummel et al., 1972). Age should also be considered when carrying out an investigation in animal models of diabetes. In autoimmune models, it has been suggested that interventions at earlier ages are more successful than interventions in older mice (Roep, 2007). In obese animals, insulin resistance may progress with increasing age. However, beta cell compensation can also occur in older mice, meaning that the diabetic phenotype can lessen with increasing age. Ideally, several strains and both genders should be used to confidently demonstrate a given treatment has effect. The age of the animal at the time of the study should also be carefully considered. It is therefore of utmost importance that the strain, gender, and age of the rodent model is carefully chosen when embarking on a study within metabolic research.

6 CONCLUSIONS

There are numerous animal models available in which to study Type 1 and Type 2 diabetes. No single animal model accurately reflects the pathogenesis of either disease and thus the choice of animal model will depend on which aspect of the disease is relevant to the study. Ideally, more than one animal model should be used to convincingly demonstrate the effect of a potential therapy. Strain and gender effects should also be carefully considered during experimental design. Nonetheless, animal models of diabetes have clearly been of huge benefit in understanding the pathogenesis and treatment of this complicated disease.

References

Ablamunits, V., Henegariu, O., Hansen, J.B., Opare-Addo, L., Preston-Hurlburt, P., Santamaria, P., et al., 2012. Synergistic reversal of type 1 diabetes in NOD mice with anti-CD3 and interleukin-1 blockade: evidence of improved immune regulation. Diabetes 61 (1), 145–154.

Alam, C., Bittoun, E., Bhagwat, D., Valkonen, S., Saari, A., Jaakkola, U., et al., 2011. Effects of a germ-free environment on gut immune regulation and diabetes progression in non-obese diabetic (NOD) mice. Diabetologia 54 (6), 1398–1406.

Almind, K., Kahn, C.R., 2004. Genetic determinants of energy expenditure and insulin resistance in diet-induced obesity in mice. Diabetes 53 (12), 3274–3285.

Alpers, C.E., Hudkins, K.L., 2011. Mouse models of diabetic nephropathy. Curr. Opin. Nephrol. Hypertens 20 (3), 278–284.

Andersson, D.A., Filipovic, M.R., Gentry, C., Eberhardt, M., Vastani, N., Leffler, A., et al., 2015. Streptozotocin stimulates TRPA1 directly: involvement of peroxynitrite. J. Biol. Chem. 290, 15185–15196.

Andrikopoulos, S., Rosella, G., Gaskin, E., Thorburn, A., Kaczmarczyk, S., Zajac, J.D., Proietto, J., 1993. Impaired regulation of hepatic fructose-1,6-bisphosphatase in the New Zealand obese mouse model of NIDDM. Diabetes 42 (12), 1731–1736.

Arrojo e Drigo, R., Ali, Y., Diez, J., Srinivasan, D.K., Berggren, P.O., Boehm, B.O., 2015. New insights into the architecture of the islet of Langerhans: a focused cross-species assessment. Diabetologia 58 (10), 2218–2228.

Atkinson, M.A., Leiter, E.H., 1999. The NOD mouse model of type 1 diabetes: as good as it gets? Nat. Med. 5 (6), 601–604.

Bellinger, D.A., Merricks, E.P., Nichols, T.C., 2006. Swine models of type 2 diabetes mellitus: insulin resistance, glucose tolerance, and cardiovascular complications. ILAR J. 47 (3), 243–258.

Berglund, O., Frankel, B.J., Hellman, B., 1978. Development of the insulin secretory defect in genetically diabetic (db/db) mouse. Acta Endocrinol. (Copenh) 87 (3), 543–551.

Betz, B., Conway, B.R., 2016. An update on the use of animal models in diabetic nephropathy research. Curr. Diab. Rep. 16 (2), 18.

Bonner-Weir, S., Trent, D.F., Honey, R.N., Weir, G.C., 1981. Responses of neonatal rat islets to streptozotocin: limited B-cell regeneration and hyperglycemia. Diabetes 30 (1), 64–69.

Bonner-Weir, S., Trent, D.F., Weir, G.C., 1983. Partial pancreatectomy in the rat and subsequent defect in glucose-induced insulin release. J. Clin. Invest. 71 (6), 1544–1553.

Bonnevie-Nielsen, V., Steffes, M.W., Lernmark, A., 1981. A major loss in islet mass and B-cell function precedes hyperglycemia in mice given multiple low doses of streptozotocin. Diabetes 30 (5), 424–429.

Bortell, R., Yang, C., 2012. The BB rat as a model of human type 1 diabetes. Methods Mol. Biol. 933, 31–44.

Bowe, J.E., Franklin, Z.J., Hauge-Evans, A.C., King, A.J., Persaud, S.J., Jones, P.M., 2014. Metabolic phenotyping guidelines: assessing glucose homeostasis in rodent models. J. Endocrinol. 222 (3), G13–G25.

Burcelin, R., Crivelli, V., Dacosta, A., Roy-Tirelli, A., Thorens, B., 2002. Heterogeneous metabolic adaptation of C57BL/6J mice to high-fat diet. Am. J. Physiol. Endocrinol. Metab. 282 (4), E834–E842.

Butler, A.E., Jang, J., Gurlo, T., Carty, M.D., Soeller, W.C., Butler, P.C., 2004. Diabetes due to a progressive defect in beta-cell mass in rats transgenic for human islet amyloid polypeptide (HIP Rat): a new model for type 2 diabetes. Diabetes 53 (6), 1509–1516.

Campbell-Thompson, M., Fu, A., Kaddis, J.S., Wasserfall, C., Schatz, D.A., Pugliese, A., Atkinson, M.A., 2016. Insulitis and beta-cell mass in the natural history of type 1 diabetes. Diabetes 65 (3), 719–731.

Cerf, M.E., Williams, K., Chapman, C.S., Louw, J., 2007. Compromised beta-cell development and beta-cell dysfunction in weanling off-spring from dams maintained on a high-fat diet during gestation. Pancreas 34 (3), 347–353.

Chen, H., Charlat, O., Tartaglia, L.A., Woolf, E.A., Weng, X., Ellis, S.J., et al., 1996. Evidence that the diabetes gene encodes the leptin receptor: identification of a mutation in the leptin receptor gene in db/db mice. Cell 84 (3), 491–495.

Cho, Y.R., Kim, H.J., Park, S.Y., Ko, H.J., Hong, E.G., Higashimori, T., et al., 2007. Hyperglycemia, maturity-onset obesity, and insulin resistance in NONcNZO10/LtJ males, a new mouse model of type 2 diabetes. Am. J. Physiol. Endocrinol. Metab. 293 (1), E327–E336.

Choy, S., de Winter, W., Karlsson, M.O., Kjellsson, M.C., 2016. Modeling the disease progression from healthy to overt diabetes in ZDSD rats. AAPS J. 18, 1203–1212.

Christianson, S.W., Shultz, L.D., Leiter, E.H., 1993. Adoptive transfer of diabetes into immunodeficient NOD-scid/scid mice. Relative contributions of CD4+ and CD8+ T-cells from diabetic versus prediabetic NOD. NON-Thy-1a donors. Diabetes 42 (1), 44–55.

Clark, A., 1989. Islet amyloid and type 2 diabetes. Diabet. Med. 6 (7), 561–567.

Claycombe, K.J., Uthus, E.O., Roemmich, J.N., Johnson, L.K., Johnson, W.T., 2013. Prenatal low-protein and postnatal high-fat diets induce rapid adipose tissue growth by inducing Igf2 expression in Sprague Dawley rat offspring. J. Nutr. 143 (10), 1533–1539.

Clee, S.M., Attie, A.D., 2007. The genetic landscape of type 2 diabetes in mice. Endocr. Rev. 28 (1), 48–83.

Coleman, D.L., 1978. Obese and diabetes: two mutant genes causing diabetes-obesity syndromes in mice. Diabetologia 14 (3), 141–148.

Coleman, D.L., Eicher, E.M., 1990. Fat (fat) and tubby (tub): two autosomal recessive mutations causing obesity syndromes in the mouse. J. Hered. 81 (6), 424–427.

Coleman, D.L., Hummel, K.P., 1974. Hyperinsulinemia in pre-weaning diabetes (db) mice. Diabetologia 10 Suppl., 607–610.

Cordoba-Chacon, J., Gahete, M.D., Pokala, N.K., Geldermann, D., Alba, M., Salvatori, R., et al., 2014. Long- but not short-term adult-onset, isolated GH deficiency in male mice leads to deterioration of beta-cell function, which cannot be accounted for by changes in beta-cell mass. Endocrinology 155 (3), 726–735.

Corsetti, J.P., Sparks, J.D., Peterson, R.G., Smith, R.L., Sparks, C.E., 2000. Effect of dietary fat on the development of non-insulin dependent diabetes mellitus in obese Zucker diabetic fatty male and female rats. Atherosclerosis 148 (2), 231–241.

Craighead, J.E., McLane, M.F., 1968. Diabetes mellitus: induction in mice by encephalomyocarditis virus. Science 162 (3856), 913–914.

Cummings, B.P., Digitale, E.K., Stanhope, K.L., Graham, J.L., Baskin, D.G., Reed, B.J., et al., 2008. Development and characterization of a novel rat model of type 2 diabetes mellitus: the UC Davis type 2 diabetes mellitus UCD-T2DM rat. Am. J. Physiol. Regul. Integr. Comp. Physiol. 295 (6), R1782–R1793.

Daifotis, A.G., Koenig, S., Chatenoud, L., Herold, K.C., 2013. Anti-CD3 clinical trials in type 1 diabetes mellitus. Clin. Immunol. 149 (3), 268–278.

De Haro-Hernandez, R., Cabrera-Munoz, L., Mendez, J.D., 2004. Regeneration of beta-cells and neogenesis from small ducts or acinar cells promote recovery of endocrine pancreatic function in alloxan-treated rats. Arch. Med. Res. 35 (2), 114–120.

de Rooij, S.R., Painter, R.C., Roseboom, T.J., Phillips, D.I., Osmond, C., Barker, D.J., et al., 2006. Glucose tolerance at age 58 and the decline of glucose tolerance in comparison with age 50 in people prenatally exposed to the Dutch famine. Diabetologia 49 (4), 637–643.

Deeds, M.C., Anderson, J.M., Armstrong, A.S., Gastineau, D.A., Hiddinga, H.J., Jahangir, A., et al., 2011. Single dose streptozotocin-induced diabetes: considerations for study design in islet transplantation models. Lab. Anim. 45 (3), 131–140.

DeFronzo, R.A., Tobin, J.D., Andres, R., 1979. Glucose clamp technique: a method for quantifying insulin secretion and resistance. Am. J. Physiol. 237 (3), E214–E223.

Driver, J.P., Serreze, D.V., Chen, Y.G., 2011. Mouse models for the study of autoimmune type 1 diabetes: a NOD to similarities and differences to human disease. Semin. Immunopathol. 33 (1), 67–87.

Driver, J.P., Chen, Y.G., Mathews, C.E., 2012. Comparative genetics: synergizing human and NOD mouse studies for identifying genetic causation of type 1 diabetes. Rev. Diabet. Stud. 9 (4), 169–187.

Dufrane, D., van Steenberghe, M., Guiot, Y., Goebbels, R.M., Saliez, A., Gianello, P., 2006. Streptozotocin-induced diabetes in large animals (pigs/primates): role of GLUT2 transporter and beta-cell plasticity. Transplantation 81 (1), 36–45.

Dunn, J.S., Sheehan, H.L., McLetchie, N.G.B., 1943. Necrosis of islets of Langerhans produced experimentally. Lancet 1, 484–487.

El-Hawari, A.M., Plaa, G.L., 1983. Potentiation of thioacetamide-induced hepatotoxicity in alloxan- and streptozotocin-diabetic rats. Toxicol. Lett. 17 (3–4), 293–300.

Elsner, M., Tiedge, M., Guldbakke, B., Munday, R., Lenzen, S., 2002. Importance of the GLUT2 glucose transporter for pancreatic beta cell toxicity of alloxan. Diabetologia 45 (11), 1542–1549.

Emamaullee, J.A., Davis, J., Merani, S., Toso, C., Elliott, J.F., Thiesen, A., Shapiro, A.M., 2009a. Inhibition of Th17 cells regulates autoimmune diabetes in NOD mice. Diabetes 58 (6), 1302–1311.

Emamaullee, J.A., Merani, S., Toso, C., Kin, T., Al-Saif, F., Truong, W., et al., 2009b. Porcine marginal mass islet autografts resist metabolic failure over time and are enhanced by early treatment with liraglutide. Endocrinology 150 (5), 2145–2152.

Eriksson, J., Lindstrom, J., Valle, T., Aunola, S., Hamalainen, H., Ilanne-Parikka, P., et al., 1999. Prevention of type II diabetes in subjects with impaired glucose tolerance: the Diabetes Prevention Study (DPS) in Finland. Study design and 1-year interim report on the feasibility of the lifestyle intervention programme. Diabetologia 42 (7), 793–801.

Erlich, H., Valdes, A.M., Noble, J., Carlson, J.A., Varney, M., Concannon, P., et al., 2008. HLA DR-DQ haplotypes and genotypes and type 1 diabetes risk: analysis of the type 1 diabetes genetics consortium families. Diabetes 57 (4), 1084–1092.

Fernandes-Santos, C., Carneiro, R.E., de Souza Mendonca, L., Aguila, M.B., Mandarim-de-Lacerda, C.A., 2009. Pan-PPAR agonist beneficial effects in overweight mice fed a high-fat high-sucrose diet. Nutrition 25 (7–8), 818–827.

Fisher, S.J., Shi, Z.Q., Lickley, H.L., Efendic, S., Vranic, M., Giacca, A., 2001. Low-dose IGF-I has no selective advantage over insulin in regulating glucose metabolism in hyperglycemic depancreatized dogs. J. Endocrinol. 168 (1), 49–58.

Fontaine, D.A., Davis, D.B., 2016. Attention to background strain is essential for metabolic research: C57BL/6 and the International Knockout Mouse Consortium. Diabetes 65 (1), 25–33.

Franks, P.W., Pare, G., 2016. Putting the genome in context: gene-environment interactions in type 2 diabetes. Curr. Diab. Rep. 16 (7), 57.

Gorray, K.C., Baskin, D., Brodsky, J., Fujimoto, W.Y., 1986. Responses of pancreatic b cells to alloxan and streptozotocin in the guinea pig. Pancreas 1 (2), 130–138.

Gotfredsen, C.F., Buschard, K., Frandsen, E.K., 1985. Reduction of diabetes incidence of BB Wistar rats by early prophylactic insulin treatment of diabetes-prone animals. Diabetologia 28 (12), 933–935.

Goto, Y., Kakizaki, M., Masaki, N., 1976. Production of spontaneous diabetic rats by repetition of selective breeding. Tohoku. J. Exp. Med. 119 (1), 85–90.

Goyal, S.N., Reddy, N.M., Patil, K.R., Nakhate, K.T., Ojha, S., Patil, C.R., Agrawal, Y.O., 2016. Challenges and issues with streptozotocin-induced diabetes—a clinically relevant animal model to understand the diabetes pathogenesis and evaluate therapeutics. Chem. Biol. Interact. 244, 49–63.

Guberski, D.L., Thomas, V.A., Shek, W.R., Like, A.A., Handler, E.S., Rossini, A.A., et al., 1991. Induction of type I diabetes by Kilham's rat virus in diabetes-resistant BB/Wor rats. Science 254 (5034), 1010–1013.

Halaas, J.L., Boozer, C., Blair-West, J., Fidahusein, N., Denton, D.A., Friedman, J.M., 1997. Physiological response to long-term peripheral and central leptin infusion in lean and obese mice. Proc. Natl. Acad. Sci. USA 94 (16), 8878–8883.

Hanenberg, H., Kolb-Bachofen, V., Kantwerk-Funke, G., Kolb, H., 1989. Macrophage infiltration precedes and is a prerequisite for lymphocytic insulitis in pancreatic islets of pre-diabetic BB rats. Diabetologia 32 (2), 126–134.

Hara, H., Lin, Y.J., Zhu, X., Tai, H.C., Ezzelarab, M., Balamurugan, A.N., et al., 2008. Safe induction of diabetes by high-dose streptozotocin in pigs. Pancreas 36 (1), 31–38.

Harada, M., Makino, S., 1984. Promotion of spontaneous diabetes in non-obese diabetes-prone mice by cyclophosphamide. Diabetologia 27 (6), 604–606.

Hariri, N., Thibault, L., 2010. High-fat diet-induced obesity in animal models. Nutr. Res. Rev. 23 (2), 270–299.

Haskell, B.D., Flurkey, K., Duffy, T.M., Sargent, E.E., Leiter, E.H., 2002. The diabetes-prone NZO/HlLt strain. I. Immunophenotypic comparison to the related NZB/BlNJ and NZW/LacJ strains. Lab. Invest. 82 (7), 833–842.

He, S., Chen, Y., Wei, L., Jin, X., Zeng, L., Ren, Y., et al., 2011. Treatment and risk factor analysis of hypoglycemia in diabetic rhesus monkeys. Exp. Biol. Med. (Maywood) 236 (2), 212–218.

Henson, M.S., O'Brien, T.D., 2006. Feline models of type 2 diabetes mellitus. ILAR J. 47 (3), 234–242.

Herold, K.C., Gitelman, S.E., Ehlers, M.R., Gottlieb, P.A., Greenbaum, C.J., Hagopian, W., et al., 2013. Teplizumab (anti-CD3 mAb) treatment preserves C-peptide responses in patients with new-onset type 1 diabetes in a randomized controlled trial: metabolic and immunologic features at baseline identify a subgroup of responders. Diabetes 62 (11), 3766–3774.

Hoenig, M., 2012. The cat as a model for human obesity and diabetes. J. Diabetes Sci. Technol. 6 (3), 525–533.

Homo-Delarche, F., Calderari, S., Irminger, J.C., Gangnerau, M.N., Coulaud, J., Rickenbach, K., et al., 2006. Islet inflammation and fibrosis in a spontaneous model of type 2 diabetes, the GK rat. Diabetes 55 (6), 1625–1633.

Hong, E.G., Noh, H.L., Lee, S.K., Chung, Y.S., Lee, K.W., Kim, H.M., 2002. Insulin and glucagon secretions, and morphological change of pancreatic islets in OLETF rats, a model of type 2 diabetes mellitus. J. Korean Med. Sci. 17 (1), 34–40.

Hoppener, J.W., Oosterwijk, C., van Hulst, K.L., Verbeek, J.S., Capel, P.J., de Koning, E.J., et al., 1994. Molecular physiology of the islet amyloid polypeptide (IAPP)/amylin gene in man, rat, and transgenic mice. J. Cell Biochem. 55 Suppl., 39–53.

Hoppener, J.W., Jacobs, H.M., Wierup, N., Sotthewes, G., Sprong, M., de Vos, P., et al., 2008. Human islet amyloid polypeptide transgenic mice: in vivo and ex vivo models for the role of hIAPP in type 2 diabetes mellitus. Exp. Diabetes Res. 2008, 697035.

Hummel, K.P., Dickie, M.M., Coleman, D.L., 1966. Diabetes, a new mutation in the mouse. Science 153 (3740), 1127–1128.

Hummel, K.P., Coleman, D.L., Lane, P.W., 1972. The influence of genetic background on expression of mutations at the diabetes locus in the mouse. I. C57BL-KsJ and C57BL-6J strains. Biochem. Genet. 7 (1), 1–13.

Hyttinen, V., Kaprio, J., Kinnunen, L., Koskenvuo, M., Tuomilehto, J., 2003. Genetic liability of type 1 diabetes and the onset age among 22,650 young Finnish twin pairs: a nationwide follow-up study. Diabetes 52 (4), 1052–1055.

In't Veld, P., 2014. Insulitis in human type 1 diabetes: a comparison between patients and animal models. Semin. Immunopathol. 36 (5), 569–579.

Ionut, V., Liu, H., Mooradian, V., Castro, A.V., Kabir, M., Stefanovski, D., et al., 2010. Novel canine models of obese prediabetes and mild type 2 diabetes. Am. J. Physiol. Endocrinol. Metab. 298 (1), E38–E48.

Islam, M.S., 2013. Animal models of diabetic neuropathy: progress since 1960s. J. Diabetes Res. 2013, 149452.

Izumi, T., Yokota-Hashimoto, H., Zhao, S., Wang, J., Halban, P.A., Takeuchi, T., 2003. Dominant negative pathogenesis by mutant proinsulin in the Akita diabetic mouse. Diabetes 52 (2), 409–416.

Jacob, H.J., Pettersson, A., Wilson, D., Mao, Y., Lernmark, A., Lander, E.S., 1992. Genetic dissection of autoimmune type I diabetes in the BB rat. Nat. Genet. 2 (1), 56–60.

Janson, J., Soeller, W.C., Roche, P.C., Nelson, R.T., Torchia, A.J., Kreutter, D.K., Butler, P.C., 1996. Spontaneous diabetes mellitus in transgenic mice expressing human islet amyloid polypeptide. Proc. Natl. Acad. Sci. USA 93 (14), 7283–7288.

Jayasimhan, A., Mansour, K.P., Slattery, R.M., 2014. Advances in our understanding of the pathophysiology of Type 1 diabetes: lessons from the NOD mouse. Clin. Sci. (Lond) 126 (1), 1–18.

Joffe, B., Zimmet, P., 1998. The thrifty genotype in type 2 diabetes: an unfinished symphony moving to its finale? Endocrine 9 (2), 139–141.

Joost, H.G., Schurmann, A., 2014. The genetic basis of obesity-associated type 2 diabetes (diabesity) in polygenic mouse models. Mamm. Genome 25 (9–10), 401–412.

Jorns, A., Kubat, B., Tiedge, M., Wedekind, D., Hedrich, H.J., Kloppel, G., Lenzen, S., 2004. Pathology of the pancreas and other organs in the diabetic LEW.1AR1/Ztm-iddm rat, a new model of spontaneous insulin-dependent diabetes mellitus. Virchows Arch. 444 (2), 183–189.

Jorns, A., Gunther, A., Hedrich, H.J., Wedekind, D., Tiedge, M., Lenzen, S., 2005. Immune cell infiltration, cytokine expression, and beta-cell apoptosis during the development of type 1 diabetes in the spontaneously diabetic LEW.1AR1/Ztm-iddm rat. Diabetes 54 (7), 2041–2052.

Jorns, A., Rath, K.J., Terbish, T., Arndt, T., Meyer Zu Vilsendorf, A., Wedekind, D., et al., 2010. Diabetes prevention by immunomodulatory FTY720 treatment in the LEW.1AR1-iddm rat despite immune cell activation. Endocrinology 151 (8), 3555–3565.

Jorns, A., Arndt, T., Meyer zu Vilsendorf, A., Klempnauer, J., Wedekind, D., Hedrich, H.J., et al., 2014. Islet infiltration, cytokine expression and beta cell death in the NOD mouse, BB rat, Komeda rat, LEW. 1AR1-iddm rat and humans with type 1 diabetes. Diabetologia 57 (3), 512–521.

Jorns, A., Ertekin, U.G., Arndt, T., Terbish, T., Wedekind, D., Lenzen, S., 2015. TNF-alpha antibody therapy in combination with the T-cell specific antibody anti-TCR reverses the diabetic metabolic state in the LEW.1AR1-iddm rat. Diabetes.

Jun, H.S., Yoon, J.W., 2003. A new look at viruses in type 1 diabetes. Diabetes Metab. Res. Rev. 19 (1), 8–31.

Kahn, B.B., Flier, J.S., 2000. Obesity and insulin resistance. J. Clin. Invest. 106 (4), 473–481.

Kaldunski, M., Jia, S., Geoffrey, R., Basken, J., Prosser, S., Kansra, S., et al., 2010. Identification of a serum-induced transcriptional signature associated with type 1 diabetes in the BioBreeding rat. Diabetes 59 (10), 2375–2385.

Kang, Y., Chatterjee, N.K., Nodwell, M.J., Yoon, J.W., 1994. Complete nucleotide sequence of a strain of coxsackie B4 virus of human origin that induces diabetes in mice and its comparison with nondiabetogenic coxsackie B4 JBV strain. J. Med. Virol. 44 (4), 353–361.

Kawano, K., Hirashima, T., Mori, S., Saitoh, Y., Kurosumi, M., Natori, T., 1991. New inbred strain of Long-Evans Tokushima lean rats with IDDM without lymphopenia. Diabetes 40 (11), 1375–1381.

Kawano, K., Hirashima, T., Mori, S., Natori, T., 1994. OLETF (Otsuka Long-Evans Tokushima Fatty) rat: a new NIDDM rat strain. Diabetes Res. Clin. Pract. 24 Suppl., S317–320.

Kim, J.H., Saxton, A.M., 2012. The TALLYHO mouse as a model of human type 2 diabetes. Methods Mol. Biol. 933, 75–87.

Kim, J.H., Sen, S., Avery, C.S., Simpson, E., Chandler, P., Nishina, P.M., et al., 2001. Genetic analysis of a new mouse model for non-insulin-dependent diabetes. Genomics 74 (3), 273–286.

King, A., Bowe, J., 2016. Animal models for diabetes: understanding the pathogenesis and finding new treatments. Biochem. Pharmacol. 99, 1–10.

King, C., Sarvetnick, N., 2011. The incidence of type-1 diabetes in NOD mice is modulated by restricted flora not germ-free conditions. PLoS One 6 (2), e17049.

King, A., Austin, A., Nandi, N., Bowe, J., 2016. Diabetes in rats is cured by islet transplantation….but only during daytime. Cell Transplant. 26 (1), 171–172.

Kluth, O., Mirhashemi, F., Scherneck, S., Kaiser, D., Kluge, R., Neschen, S., et al., 2011. Dissociation of lipotoxicity and glucotoxicity in a mouse model of obesity associated diabetes: role of forkhead box O1 (FOXO1) in glucose-induced beta cell failure. Diabetologia 54 (3), 605–616.

Knip, M., Siljander, H., Ilonen, J., Simell, O., Veijola, R., 2016. Role of humoral beta-cell autoimmunity in type 1 diabetes. Pediatr. Diabetes 17 (Suppl. 22), 17–24.

Komeda, K., Noda, M., Terao, K., Kuzuya, N., Kanazawa, M., Kanazawa, Y., 1998. Establishment of two substrains, diabetes-prone and non-diabetic, from Long-Evans Tokushima Lean (LETL) rats. Endocr. J. 45 (6), 737–744.

Koopmans, S.J., Schuurman, T., 2015. Considerations on pig models for appetite, metabolic syndrome and obese type 2 diabetes: From food intake to metabolic disease. Eur. J. Pharmacol. 759, 231–239.

Koopmans, S.J., Mroz, Z., Dekker, R., Corbijn, H., Ackermans, M., Sauerwein, H., 2006. Association of insulin resistance with hyperglycemia in streptozotocin-diabetic pigs: effects of metformin at isoenergetic feeding in a type 2-like diabetic pig model. Metabolism 55 (7), 960–971.

Koulmanda, M., Qipo, A., Chebrolu, S., O'Neil, J., Auchincloss, H., Smith, R.N., 2003. The effect of low versus high dose of streptozotocin in cynomolgus monkeys (*Macaca fascilularis*). Am. J. Transplant. 3 (3), 267–272.

Kowalski, T.J., Ster, A.M., Smith, G.P., 1998. Ontogeny of hyperphagia in the Zucker (fa/fa) rat. Am. J. Physiol. 275 (4 Pt 2), R1106–R1109.

Lai, A.K., Lo, A.C., 2013. Animal models of diabetic retinopathy: summary and comparison. J. Diabetes Res. 2013, 106594.

Lampasona, V., Belloni, C., Piquer, S., Bonicchio, S., Furlan, R., Bonifacio, E., 2008. Radiobinding assay for detecting autoantibodies to single epitopes. J. Immunol. Methods 336 (2), 127–134.

Lange, C., Jeruschke, K., Herberg, L., Leiter, E.H., Junger, E., 2006. The diabetes-prone NZO/Hl strain. Proliferation capacity of beta cells in hyperinsulinemia and hyperglycemia. Arch. Physiol. Biochem. 112 (1), 49–58.

Le May, C., Chu, K., Hu, M., Ortega, C.S., Simpson, E.R., Korach, K.S., et al., 2006. Estrogens protect pancreatic beta-cells from apoptosis and prevent insulin-deficient diabetes mellitus in mice. Proc. Natl. Acad. Sci. USA 103 (24), 9232–9237.

Leahy, J.L., Bonner-Weir, S., Weir, G.C., 1988. Minimal chronic hyperglycemia is a critical determinant of impaired insulin secretion after an incomplete pancreatectomy. J. Clin. Invest. 81 (5), 1407–1414.

Lee, K.U., Amano, K., Yoon, J.W., 1988. Evidence for initial involvement of macrophage in development of insulitis in NOD mice. Diabetes 37 (7), 989–991.

Leiter, E.H., 1982. Multiple low-dose streptozotocin-induced hyperglycemia and insulitis in C57BL mice: influence of inbred background, sex, and thymus. Proc. Natl. Acad. Sci. USA 79 (2), 630–634.

Leiter, E.H., 1993. The NOD mouse: a model for analyzing the interplay between heredity and environment in development of autoimmune disease. ILAR J. 35 (1), 4–14.

Leiter, E.H., 2009. Selecting the "right" mouse model for metabolic syndrome and type 2 diabetes research. Methods Mol. Biol. 560, 1–17.

Leiter, E.H., Reifsnyder, P.C., 2004. Differential levels of diabetogenic stress in two new mouse models of obesity and type 2 diabetes. Diabetes 53 (Suppl. 1), S4–S11.

Leiter, E.H., Schile, A., 2013. Genetic and pharmacologic models for type 1 diabetes. Curr. Protoc. Mouse Biol. 3 (1), 9–19.

Leiter, E.H., Strobel, M., O'Neill, A., Schultz, D., Schile, A., Reifsnyder, P.C., 2013. Comparison of two new mouse models of polygenic type 2 diabetes at the Jackson Laboratory, NONcNZO10Lt/J and TALLYHO/JngJ. J. Diabetes Res. 2013, 165327.

Lenzen, S., Munday, R., 1991. Thiol-group reactivity, hydrophilicity and stability of alloxan, its reduction products and its N-methyl derivatives and a comparison with ninhydrin. Biochem. Pharmacol. 42 (7), 1385–1391.

Lenzen, S., Tiedge, M., Panten, U., 1987. Glucokinase in pancreatic B-cells and its inhibition by alloxan. Acta Endocrinol. (Copenh) 115 (1), 21–29.

Lenzen, S., Tiedge, M., Elsner, M., Lortz, S., Weiss, H., Jorns, A., et al., 2001. The LEW.1AR1/Ztm-iddm rat: a new model of spontaneous insulin-dependent diabetes mellitus. Diabetologia 44 (9), 1189–1196.

Li, W., Zhang, H., Nie, A., Ni, Q., Li, F., Ning, G., et al., 2016. mTORC1 pathway mediates beta cell compensatory proliferation in 60% partial-pancreatectomy mice. Endocrine 53 (1), 117–128.

Like, A.A., Dirodi, V., Thomas, S., Guberski, D.L., Rossini, A.A., 1984. Prevention of diabetes mellitus in the BB/W rat with Cyclosporin-A. Am. J. Pathol. 117 (1), 92–97.

Like, A.A., Guberski, D.L., Butler, L., 1991. Influence of environmental viral agents on frequency and tempo of diabetes mellitus in BB/Wor rats. Diabetes 40 (2), 259–262.

Lindstrom, P., 2007. The physiology of obese-hyperglycemic mice [ob/ob mice]. ScientificWorldJournal 7, 666–685.

Lo, B., Swafford, A.D., Shafer-Weaver, K.A., Jerome, L.F., Rakhlin, L., Mathern, D.R., et al., 2011. Antibodies against insulin measured by electrochemiluminescence predicts insulitis severity and disease onset in non-obese diabetic mice and can distinguish human type 1 diabetes status. J. Transl. Med. 9, 203.

Lukic, M.L., Stosic-Grujicic, S., Ostojic, N., Chan, W.L., Liew, F.Y., 1991. Inhibition of nitric oxide generation affects the induction of diabetes by streptozocin in mice. Biochem. Biophys. Res. Commun. 178 (3), 913–920.

Mabley, J.G., Hasko, G., Liaudet, L., Soriano, F.G., Southan, G.J., Salzman, A.L., Szabo, C., 2002. NFkappaB1 (p50)-deficient mice are not susceptible to multiple low-dose streptozotocin-induced diabetes. J. Endocrinol. 173 (3), 457–464.

MacMurray, A.J., Moralejo, D.H., Kwitek, A.E., Rutledge, E.A., Van Yserloo, B., Gohlke, P., et al., 2002. Lymphopenia in the BB rat model of type 1 diabetes is due to a mutation in a novel immune-associated nucleotide (Ian)-related gene. Genome Res. 12 (7), 1029–1039.

Magnuson, A.M., Thurber, G.M., Kohler, R.H., Weissleder, R., Mathis, D., Benoist, C., 2015. Population dynamics of islet-infiltrating cells in autoimmune diabetes. Proc. Natl. Acad. Sci. USA 112 (5), 1511–1516.

Makino, S., Kunimoto, K., Muraoka, Y., Mizushima, Y., Katagiri, K., Tochino, Y., 1980. Breeding of a non-obese, diabetic strain of mice. Jikken Dobutsu 29 (1), 1–13.

Marques, C., Meireles, M., Norberto, S., Leite, J., Freitas, J., Pestana, D., et al., 2016. High-fat diet-induced obesity Rat model: a comparison between Wistar and Sprague-Dawley Rat. Adipocyte 5 (1), 11–21.

Masiello, P., 2006. Animal models of type 2 diabetes with reduced pancreatic beta-cell mass. Int. J. Biochem. Cell Biol. 38 (5–6), 873–893.

Mathews, C.E., 2005. Utility of murine models for the study of spontaneous autoimmune type 1 diabetes. Pediatr. Diabetes 6 (3), 165–177.

Mathews, C.E., Langley, S.H., Leiter, E.H., 2002. New mouse model to study islet transplantation in insulin-dependent diabetes mellitus. Transplantation 73 (8), 1333–1336.

Matveyenko, A.V., Butler, P.C., 2006a. Beta-cell deficit due to increased apoptosis in the human islet amyloid polypeptide transgenic (HIP) rat recapitulates the metabolic defects present in type 2 diabetes. Diabetes 55 (7), 2106–2114.

Matveyenko, A.V., Butler, P.C., 2006b. Islet amyloid polypeptide (IAPP) transgenic rodents as models for type 2 diabetes. ILAR J. 47 (3), 225–233.

McGuinness, O.P., Ayala, J.E., Laughlin, M.R., Wasserman, D.H., 2009. NIH experiment in centralized mouse phenotyping: the Vanderbilt experience and recommendations for evaluating glucose homeostasis in the mouse. Am. J. Physiol. Endocrinol. Metab. 297 (4), E849–855.

Moran, T.H., 2008. Unraveling the obesity of OLETF rats. Physiol. Behav. 94 (1), 71–78.

Mordes, J.P., Bortell, R., Blankenhorn, E.P., Rossini, A.A., Greiner, D.L., 2004. Rat models of type 1 diabetes: genetics, environment, and autoimmunity. ILAR J. 45 (3), 278–291.

Morel, P., Kaufmann, D.B., Matas, A.J., Tzardis, P., Field, M.J., Lloveras, J.K., Sutherland, D.E., 1991. Total pancreatectomy in the pig for islet transplantation. Technical alternatives. Transplantation 52 (1), 11–15.

Muhlhausler, B.S., 2009. Nutritional models of type 2 diabetes mellitus. Methods Mol. Biol. 560, 19–36.

Muller, Y.D., Golshayan, D., Ehirchiou, D., Wyss, J.C., Giovannoni, L., Meier, R., et al., 2011. Immunosuppressive effects of streptozotocin-induced diabetes result in absolute lymphopenia and a relative increase of T regulatory cells. Diabetes 60 (9), 2331–2340.

Nagaraju, S., Bertera, S., Funair, A., Wijkstrom, M., Trucco, M., Cooper, D.K., Bottino, R., 2014. Streptozotocin-associated lymphopenia in cynomolgus monkeys. Islets 6 (3), e944441.

Nakajima, S., Hira, T., Hara, H., 2015. Postprandial glucagon-like peptide-1 secretion is increased during the progression of glucose intolerance and obesity in high-fat/high-sucrose diet-fed rats. Br. J. Nutr. 113 (9), 1477–1488.

Nakamura, M., Yamada, K., 1967. Studies on a diabetic (KK) strain of the mouse. Diabetologia 3 (2), 212–221.

Nakhooda, A.F., Like, A.A., Chappel, C.I., Wei, C.N., Marliss, E.B., 1978. The spontaneously diabetic Wistar rat (the "BB" rat). Studies prior to and during development of the overt syndrome. Diabetologia 14 (3), 199–207.

Nerup, J., Platz, P., Andersen, O.O., Christy, M., Lyngsoe, J., Poulsen, J.E., et al., 1974. HL-A antigens and diabetes mellitus. Lancet 2 (7885), 864–866.

O'Brien, T.D., 2002. Pathogenesis of feline diabetes mellitus. Mol. Cell Endocrinol. 197 (1–2), 213–219.

Ostenson, C.G., Efendic, S., 2007. Islet gene expression and function in type 2 diabetes; studies in the Goto-Kakizaki rat and humans. Diabetes Obes. Metab. 9 (Suppl. 2), 180–186.

Oyadomari, S., Koizumi, A., Takeda, K., Gotoh, T., Akira, S., Araki, E., Mori, M., 2002. Targeted disruption of the Chop gene delays endoplasmic reticulum stress-mediated diabetes. J. Clin. Invest. 109 (4), 525–532.

Ozanne, S.E., 2001. Metabolic programming in animals. Br. Med. Bull. 60, 143–152.

Ozanne, S.E., Jensen, C.B., Tingey, K.J., Storgaard, H., Madsbad, S., Vaag, A.A., 2005. Low birthweight is associated with specific changes in muscle insulin-signalling protein expression. Diabetologia 48 (3), 547–552.

Pearson, J.A., Wong, F.S., Wen, L., 2016. The importance of the non obese diabetic (NOD) mouse model in autoimmune diabetes. J. Autoimmun. 66, 76–88.

Peterson, R., Shaw, W., Neel, M., Little, L., Eichberg, J., 1990. Zucker diabetic fatty rat as a model for non-insulin-dependent diabetes mellitus. ILAR News 32 (3), 16–19.

Peterson, R.G., Jackson, C.V., Zimmerman, K., de Winter, W., Huebert, N., Hansen, M.K., 2015. Characterization of the ZDSD rat: a translational model for the study of metabolic syndrome and type 2 diabetes. J. Diabetes Res. 2015, 487816.

Petrik, J., Reusens, B., Arany, E., Remacle, C., Coelho, C., Hoet, J.J., Hill, D.J., 1999. A low protein diet alters the balance of islet cell replication and apoptosis in the fetal and neonatal rat and is associated with a reduced pancreatic expression of insulin-like growth factor-II. Endocrinology 140 (10), 4861–4873.

Pettitt, D.J., Knowler, W.C., 1998. Long-term effects of the intrauterine environment, birth weight, and breast-feeding in Pima Indians. Diabetes Care 21 (Suppl. 2), B138–B141.

Phillips, M.S., Liu, Q., Hammond, H.A., Dugan, V., Hey, P.J., Caskey, C.J., Hess, J.F., 1996. Leptin receptor missense mutation in the fatty Zucker rat. Nat. Genet. 13 (1), 18–19.

Pociot, F., Kaur, S., Nielsen, L.B., 2016. Effects of the genome on immune regulation in type 1 diabetes. Pediatr. Diabetes 17 (Suppl. 22), 37–42.

Pontesilli, O., Carotenuto, P., Gazda, L.S., Pratt, P.F., Prowse, S.J., 1987. Circulating lymphocyte populations and autoantibodies in non-obese diabetic (NOD) mice: a longitudinal study. Clin. Exp. Immunol. 70 (1), 84–93.

Portha, B., Levacher, C., Picon, L., Rosselin, G., 1974. Diabetogenic effect of streptozotocin in the rat during the perinatal period. Diabetes 23 (11), 889–895.

Portha, B., Giroix, M.H., Serradas, P., Gangnerau, M.N., Movassat, J., Rajas, F., et al., 2001. beta-cell function and viability in the spontaneously diabetic GK rat: information from the GK/Par colony. Diabetes 50 (Suppl. 1), S89–S93.

Portha, B., Lacraz, G., Kergoat, M., Homo-Delarche, F., Giroix, M.H., Bailbe, D., et al., 2009. The GK rat beta-cell: a prototype for the diseased human beta-cell in type 2 diabetes? Mol. Cell Endocrinol. 297 (1–2), 73–85.

Prochazka, M., Leiter, E.H., Serreze, D.V., Coleman, D.L., 1987. Three recessive loci required for insulin-dependent diabetes in nonobese diabetic mice. Science 237 (4812), 286–289.

Rackham, C.L., Chagastelles, P.C., Nardi, N.B., Hauge-Evans, A.C., Jones, P.M., King, A.J., 2011. Co-transplantation of mesenchymal stem cells maintains islet organisation and morphology in mice. Diabetologia 54 (5), 1127–1135.

Rajab, A., Buss, J., Diakoff, E., Hadley, G.A., Osei, K., Ferguson, R.M., 2008. Comparison of the portal vein and kidney subcapsule as sites for primate islet autotransplantation. Cell Transplant. 17 (9), 1015–1023.

Rand, J.S., Fleeman, L.M., Farrow, H.A., Appleton, D.J., Lederer, R., 2004. Canine and feline diabetes mellitus: nature or nurture? J. Nutr. 134 (8 Suppl.), 2072S–2080S.

Rankin, M.M., Wilbur, C.J., Rak, K., Shields, E.J., Granger, A., Kushner, J.A., 2013. beta-Cells are not generated in pancreatic duct ligation-induced injury in adult mice. Diabetes 62 (5), 1634–1645.

Reed, J.C., Herold, K.C., 2015. Thinking bedside at the bench: the NOD mouse model of T1DM. Nat. Rev. Endocrinol. 11 (5), 308–314.

Reed, M.J., Meszaros, K., Entes, L.J., Claypool, M.D., Pinkett, J.G., Gadbois, T.M., Reaven, G.M., 2000. A new rat model of type 2 diabetes: the fat-fed, streptozotocin-treated rat. Metabolism 49 (11), 1390–1394.

Reinwald, S., Peterson, R.G., Allen, M.R., Burr, D.B., 2009. Skeletal changes associated with the onset of type 2 diabetes in the ZDF and ZDSD rodent models. Am. J. Physiol. Endocrinol. Metab. 296 (4), E765–E774.

Renner, S., Dobenecker, B., Blutke, A., Zols, S., Wanke, R., Ritzmann, M., Wolf, E., 2016. Comparative aspects of rodent and nonrodent animal models for mechanistic and translational diabetes research. Theriogenology 86 (1), 406–421.

Rewers, M., Ludvigsson, J., 2016. Environmental risk factors for type 1 diabetes. Lancet 387 (10035), 2340–2348.

Riazi, S., Maric, C., Ecelbarger, C.A., 2006. 17-beta Estradiol attenuates streptozotocin-induced diabetes and regulates the expression of renal sodium transporters. Kidney Int. 69 (3), 471–480.

Roep, B.O., 2007. Are insights gained from NOD mice sufficient to guide clinical translation? Another inconvenient truth. Ann. NY Acad. Sci. 1103, 1–10.

Sampath, S., Karundevi, B., 2014. Effect of troxerutin on insulin signaling molecules in the gastrocnemius muscle of high fat and sucrose-induced type-2 diabetic adult male rat. Mol. Cell Biochem. 395 (1–2), 11–27.

Sandberg, J.O., Andersson, A., Eizirik, D.L., Sandler, S., 1994. Interleukin-1 receptor antagonist prevents low dose streptozotocin induced diabetes in mice. Biochem. Biophys. Res. Commun. 202 (1), 543–548.

Schnedl, W.J., Ferber, S., Johnson, J.H., Newgard, C.B., 1994. STZ transport and cytotoxicity. Specific enhancement in GLUT2-expressing cells. Diabetes 43 (11), 1326–1333.

Scott, F.W., Cloutier, H.E., Kleemann, R., Woerz-Pagenstert, U., Rowsell, P., Modler, H.W., Kolb, H., 1997. Potential mechanisms by which certain foods promote or inhibit the development of spontaneous diabetes in BB rats: dose, timing, early effect on islet area, and switch in infiltrate from Th1 to Th2 cells. Diabetes 46 (4), 589–598.

Serreze, D.V., Niens, M., Kulik, J., DiLorenzo, T.P., 2016. Bridging mice to men: using HLA transgenic mice to enhance the future prediction and prevention of autoimmune type 1 diabetes in humans. Methods Mol. Biol. 1438, 137–151.

Shafrir, E., Ziv, E., Kalman, R., 2006. Nutritionally induced diabetes in desert rodents as models of type 2 diabetes: *Acomys cahirinus* (spiny mice) and *Psammomys obesus* (desert gerbil). ILAR J. 47 (3), 212–224.

Simpfendorfer, K.R., Strugnell, R.A., Brodnicki, T.C., Wijburg, O.L., 2015. Increased autoimmune diabetes in pIgR-deficient NOD mice is due to a "Hitchhiking" interval that refines the genetic effect of Idd5.4. PLoS One 10 (4), e0121979.

Skovso, S., 2014. Modeling type 2 diabetes in rats using high fat diet and streptozotocin. J. Diabetes Investig. 5 (4), 349–358.

Srinivasan, K., Viswanad, B., Asrat, L., Kaul, C.L., Ramarao, P., 2005. Combination of high-fat diet-fed and low-dose streptozotocin-treated rat: a model for type 2 diabetes and pharmacological screening. Pharmacol. Res. 52 (4), 313–320.

Srinivasan, M., Aalinkeel, R., Song, F., Mitrani, P., Pandya, J.D., Strutt, B., et al., 2006. Maternal hyperinsulinemia predisposes rat fetuses for hyperinsulinemia, and adult-onset obesity and maternal mild food restriction reverses this phenotype. Am. J. Physiol. Endocrinol. Metab. 290 (1), E129–E134.

Surwit, R.S., Kuhn, C.M., Cochrane, C., McCubbin, J.A., Feinglos, M.N., 1988. Diet-induced type II diabetes in C57BL/6J mice. Diabetes 37 (9), 1163–1167.

Surwit, R.S., Wang, S., Petro, A.E., Sanchis, D., Raimbault, S., Ricquier, D., Collins, S., 1998. Diet-induced changes in uncoupling proteins in obesity-prone and obesity-resistant strains of mice. Proc. Natl. Acad. Sci. USA 95 (7), 4061–4065.

Suto, J., Matsuura, S., Imamura, K., Yamanaka, H., Sekikawa, K., 1998. Genetic analysis of non-insulin-dependent diabetes mellitus in KK and KK-Ay mice. Eur. J. Endocrinol. 139 (6), 654–661.

Swenne, I., Andersson, A., 1984. Effect of genetic background on the capacity for islet cell replication in mice. Diabetologia 27 (4), 464–467.

Szkudelski, T., 2001. The mechanism of alloxan and streptozotocin action in B cells of the rat pancreas. Physiol. Res. 50 (6), 537–546.

Szkudelski, T., Kandulska, K., Okulicz, M., 1998. Alloxan in vivo does not only exert deleterious effects on pancreatic B cells. Physiol. Res. 47 (5), 343–346.

Takada, J., Machado, M.A., Peres, S.B., Brito, L.C., Borges-Silva, C.N., Costa, C.E., et al., 2007. Neonatal streptozotocin-induced diabetes mellitus: a model of insulin resistance associated with loss of adipose mass. Metabolism 56 (7), 977–984.

Taylor, P.D., McConnell, J., Khan, I.Y., Holemans, K., Lawrence, K.M., Asare-Anane, H., et al., 2005. Impaired glucose homeostasis and mitochondrial abnormalities in offspring of rats fed a fat-rich diet in pregnancy. Am. J. Physiol. Regul. Integr. Comp. Physiol. 288 (1), R134–139.

Thompson, N.M., Norman, A.M., Donkin, S.S., Shankar, R.R., Vickers, M.H., Miles, J.L., Breier, B.H., 2007. Prenatal and postnatal pathways to obesity: different underlying mechanisms, different metabolic outcomes. Endocrinology 148 (5), 2345–2354.

Tokuyama, Y., Sturis, J., DePaoli, A.M., Takeda, J., Stoffel, M., Tang, J., et al., 1995. Evolution of beta-cell dysfunction in the male Zucker diabetic fatty rat. Diabetes 44 (12), 1447–1457.

Tomita, T., Doull, V., Pollock, H.G., Krizsan, D., 1992. Pancreatic islets of obese hyperglycemic mice (ob/ob). Pancreas 7 (3), 367–375.

Trent, D.F., Fletcher, D.J., May, J.M., Bonner-Weir, S., Weir, G.C., 1984. Abnormal islet and adipocyte function in young B-cell-deficient rats with near-normoglycemia. Diabetes 33 (2), 170–175.

Trimble, E.R., Bruzzone, R., Belin, D., 1986. Insulin resistance is accompanied by impairment of amylase-gene expression in the exocrine pancreas of the obese Zucker rat. Biochem. J. 237 (3), 807–812.

Triscari, J., Stern, J.S., Johnson, P.R., Sullivan, A.C., 1979. Carbohydrate metabolism in lean and obese Zucker rats. Metabolism 28 (2), 183–189.

Tyrberg, B., Andersson, A., Borg, L.A., 2001. Species differences in susceptibility of transplanted and cultured pancreatic islets to the beta-cell toxin alloxan. Gen. Comp. Endocrinol. 122 (3), 238–251.

Ueda, H., Howson, J.M., Esposito, L., Heward, J., Snook, H., Chamberlain, G., et al., 2003. Association of the T-cell regulatory gene CTLA4 with susceptibility to autoimmune disease. Nature 423 (6939), 506–511.

van der Werf, N., Kroese, F.G., Rozing, J., Hillebrands, J.L., 2007. Viral infections as potential triggers of type 1 diabetes. Diabetes Metab. Res. Rev. 23 (3), 169–183.

Veroni, M.C., Proietto, J., Larkins, R.G., 1991. Evolution of insulin resistance in New Zealand obese mice. Diabetes 40 (11), 1480–1487.

von Herrath, M., Filippi, C., Coppieters, K., 2011. How viral infections enhance or prevent type 1 diabetes-from mouse to man. J. Med. Virol. 83 (9), 1672.

Wagner, J.E., Kavanagh, K., Ward, G.M., Auerbach, B.J., Harwood, Jr., H.J., Kaplan, J.R., 2006. Old world nonhuman primate models of type 2 diabetes mellitus. ILAR J. 47 (3), 259–271.

Wang, T., Singh, B., Warnock, G.L., Rajotte, R.V., 1992. Prevention of recurrence of IDDM in islet-transplanted diabetic NOD mice by adjuvant immunotherapy. Diabetes 41 (1), 114–117.

Wang, R.N., Kloppel, G., Bouwens, L., 1995. Duct- to islet-cell differentiation and islet growth in the pancreas of duct-ligated adult rats. Diabetologia 38 (12), 1405–1411.

Wang, J., Takeuchi, T., Tanaka, S., Kubo, S.K., Kayo, T., Lu, D., et al., 1999. A mutation in the insulin 2 gene induces diabetes with severe pancreatic beta-cell dysfunction in the Mody mouse. J. Clin. Invest. 103 (1), 27–37.

Wang, B., Chandrasekera, P.C., Pippin, J.J., 2014. Leptin- and leptin receptor-deficient rodent models: relevance for human type 2 diabetes. Curr. Diabetes Rev. 10 (2), 131–145.

Wei, L., Lu, Y., He, S., Jin, X., Zeng, L., Zhang, S., et al., 2011. Induction of diabetes with signs of autoimmunity in primates by the injection of multiple-low-dose streptozotocin. Biochem. Biophys. Res. Commun. 412 (2), 373–378.

Weir, G.C., Bonner-Weir, S., 2004. Five stages of evolving beta-cell dysfunction during progression to diabetes. Diabetes 53 (Suppl. 3), S16–S21.

Weiss, H., Arndt, T., Jorns, A., Lenzen, S., Cuppen, E., Hedrich, H.J., et al., 2008. The mutation of the LEW.1AR1-iddm rat maps to the telomeric end of rat chromosome 1. Mamm. Genome 19 (4), 292–297.

Welzen-Coppens, J.M., van Helden-Meeuwsen, C.G., Leenen, P.J., Drexhage, H.A., Versnel, M.A., 2013. The kinetics of plasmacytoid dendritic cell accumulation in the pancreas of the NOD mouse during the early phases of insulitis. PLoS One 8 (1), e55071.

Wicker, L.S., Miller, B.J., Mullen, Y., 1986. Transfer of autoimmune diabetes mellitus with splenocytes from nonobese diabetic (NOD) mice. Diabetes 35 (8), 855–860.

Wilcox, N.S., Rui, J., Hebrok, M., Herold, K.C., 2016. Life and death of beta cells in Type 1 diabetes: a comprehensive review. J. Autoimmun. 71, 51–58.

Winzell, M.S., Ahren, B., 2004. The high-fat diet-fed mouse: a model for studying mechanisms and treatment of impaired glucose tolerance and type 2 diabetes. Diabetes 53 (Suppl. 3), S215–S219.

Wise, M.H., Gordon, C., Johnson, R.W., 1985. Intraportal autotransplantation of cryopreserved porcine islets of Langerhans. Cryobiology 22 (4), 359–366.

Wolf, J., Lilly, F., Shin, S.I., 1984. The influence of genetic background on the susceptibility of inbred mice to streptozotocin-induced diabetes. Diabetes 33 (6), 567–571.

Xu, G., Stoffers, D.A., Habener, J.F., Bonner-Weir, S., 1999. Exendin-4 stimulates both beta-cell replication and neogenesis, resulting in increased beta-cell mass and improved glucose tolerance in diabetic rats. Diabetes 48 (12), 2270–2276.

Yang, Z., Chen, M., Fialkow, L.B., Ellett, J.D., Wu, R., Nadler, J.L., 2003. The novel anti-inflammatory compound, lisofylline, prevents diabetes in multiple low-dose streptozotocin-treated mice. Pancreas 26 (4), e99–e104.

Yasunami, R., Bach, J.F., 1988. Anti-suppressor effect of cyclophosphamide on the development of spontaneous diabetes in NOD mice. Eur. J. Immunol. 18 (3), 481–484.

Yin, D., Tao, J., Lee, D.D., Shen, J., Hara, M., Lopez, J., et al., 2006. Recovery of islet beta-cell function in streptozotocin-induced diabetic mice: an indirect role for the spleen. Diabetes 55 (12), 3256–3263.

Yokoi, N., Komeda, K., Wang, H.Y., Yano, H., Kitada, K., Saitoh, Y., et al., 2002. Cblb is a major susceptibility gene for rat type 1 diabetes mellitus. Nat. Genet. 31 (4), 391–394.

Yokoi, N., Fujiwara, Y., Wang, H.Y., Kitao, M., Hayashi, C., Someya, T., et al., 2008. Identification and functional analysis of CBLB mutations in type 1 diabetes. Biochem. Biophys. Res. Commun. 368 (1), 37–42.

Yokoi, N., Hidaka, S., Tanabe, S., Ohya, M., Ishima, M., Takagi, Y., et al., 2012. Role of major histocompatibility complex class II in the development of autoimmune type 1 diabetes and thyroiditis in rats. Genes Immun. 13 (2), 139–145.

Yoon, J.W., Yoon, C.S., Lim, H.W., Huang, Q.Q., Kang, Y., Pyun, K.H., et al., 1999. Control of autoimmune diabetes in NOD mice by GAD expression or suppression in beta cells. Science 284 (5417), 1183–1187.

Yoshioka, M., Kayo, T., Ikeda, T., Koizumi, A., 1997. A novel locus, Mody4, distal to D7Mit189 on chromosome 7 determines early-onset NIDDM in nonobese C57BL/6 (Akita) mutant mice. Diabetes 46 (5), 887–894.

Zhang, Y., Proenca, R., Maffei, M., Barone, M., Leopold, L., Friedman, J.M., 1994. Positional cloning of the mouse obese gene and its human homologue. Nature 372 (6505), 425–432.

Zhang, M., Lv, X.Y., Li, J., Xu, Z.G., Chen, L., 2008. The characterization of high-fat diet and multiple low-dose streptozotocin induced type 2 diabetes rat model. Exp. Diabetes Res. 2008, 704045.

Page left intentionally blank

11

Model Nematodes in Obesity Research

Yu Nie, Stephen R. Stürzenbaum

King's College London, London, United Kingdom

1 OBESITY IS A GLOBAL CRISIS

The incidence of obesity is rising at an alarming rate, and presently affects a large proportion of the global population, in particular developed countries, such as the United States (the obesity rate is 35% among adults and 17% among children) and the United Kingdom (the adult obesity rate is about 20%). Besides, more than 40 million children under the age of five are overweight, which may lead to an increased chance of obesity (Wang et al., 2008a).

Abnormal or excessive fat accumulation occurs when energy intake is higher than the expenditure. Obesity is a complex trait caused by the interaction of genetic factors, an imbalanced dietary lifestyle, and other individual indispositions. Genetic susceptibility is the key contributing factor to the phenotypic variations in obesity. Indeed, animal mutants bearing defective metabolism pathways display various fat or skinny phenotypes.

The body mass index (BMI) is a basic predictor defining overweight (25–29.9 kg/m^2) and obesity (>30 kg/m^2). It is calculated by the following formula:

$$BMI = \frac{Weight\,(kg)}{\left[Height\,(m)\right]^2}$$

This is a simple measure that correlates well with densitometry measurements of fat mass. To distinguish

between fat mass and lean mass better, bioelectrical impedance quantifies the electrolyte solution resistance across the extremities. The waist-to-hip ratio (WHR) is an alternative approach that assesses the distribution of body fat. Skinfold thickness measures the size of the subcutaneous fat deposit.

The prevalence of obesity is accompanied with incalculable economic costs and social impacts. The healthcare cost linked to overweight and obesity has more than doubled every decade, and now accounts for one-sixth of the total health budget and a considerable consequential percentage loss of GDP (e.g., > 1% in United States and > 3.6% in China) (Popkin et al., 2006). Indeed, obesity facilitates the development of type 2 diabetes mellitus, hypertension, cardiovascular diseases, musculoskeletal disorders, respiratory problems, neurological damages, and cancers to name a few. Evidence suggests a "J-shaped" association between BMI and mortality (Berrington de Gonzalez et al., 2010). The notion that obesity can result in a lethal disease is unfortunately ignored by a large proportion of the population.

2 OBESITY: AN UNSOLVED MEDICAL PROBLEM

Timely, effective development and implementation of corrective therapies are needed, given that obesity remains a largely unsolved medical problem. Overweight and obesity can be managed by lifestyle changes or through the introduction of bariatric means; however, the success rate has been modest due to the low compliance with such regimes and limited availability. This has led to the development of effective pharmacological therapies that target weight loss.

The US Food and Drug Administration (FDA) requires that a suitable weight-loss drug demonstrate a minimum efficacy, namely to induce a loss of at least 5% of initial body weight over a 12-month period (Cooke and Bloom, 2006). Given the prevalence of obesity and the resulting financial potential, it is perhaps surprising that the pharmaceutical industries have not flooded the market. In the 1990s, the antiobesity drugs fenfluramine (Pondimin) and dexfenfluramine (Redux) were withdrawn from the market due to severe side effects linked to heart valve damage (Connolly et al., 1997), and similarly mazindol (Sanorex) was retracted in 2000 (Glazer, 2001). In 2008, rimonabant (Acomplia) was withdrawn due to its adverse effects on mental health, and 2 years later, sibutramine (Reductil) was withdrawn because of the associated severe contraindications, including tachycardia and hypertension (Williams, 2010). The only remaining FDA-approved antiobesity medications are phentermine (Adipex-p), phendimetrazine (Bontril), diethylpropion (Tenuate), and orlistat (Xenical). The first three appetite-

suppressants involve the short-term management of exogenous obesity (typically less than 12 weeks), but are characterized by restrictions due to the side effect profiles on the cardiovascular and neurological systems. Orlistat, a gastrointestinal tract and pancreatic lipase inhibitor, is the only remaining drug approved for long-term (>6 months) treatment. It is the saturated derivative of lipstatin, a potent natural inhibitor of pancreatic lipases isolated from the bacterium *Streptomyces toxytricini* (Barbier and Schneider, 1987). However, Orlistat's efficacy is moderate, leading to a 3%–4% reduction in body weight over a 2-year period, but is compounded by severe gastrointestinal side effects, such as steatorrhea and incontinence (Rucker et al., 2007).

In 2012, new drug applications of lorcaserin HCL (Belviq) (not approved in 2010 due to concerns over carcinogenicity observed in animals) and a combination of phentermine with the antiepileptic agent topiramate (Qnexa) (not approved in 2010 due to concerns over teratogenic potential) were resubmitted, and subsequently the FDA advisory committee supported its potential use for weight-management purposes (Kang and Park, 2012), notably some 13 years after the last weight-loss drug was approved. Although the benefits may outweigh the risks of a long-term application, the full approval is still pending, suggesting that regulatory committees are now more reluctant to approve novel treatments in the absence of long-term safety data.

3 MODEL ORGANISMS USED FOR BIOMEDICAL RESEARCH

"The Principles of Human Experimental Techniques" published in 1959 promoted the humane treatment of experimental animals, thereby defining the foundation of the replacement, reduction, and refinement (3R's) (Russell and Burch, 1959). In response to ethical concerns in the application of vertebrate animals, invertebrate models emerged. Examples include airborne insects (e.g., the fly *Drosophila*), terrestrial animals (e.g., the nematode *Caenorhabditis elegans*) and freshwater/marine life (e.g., planarians, crustaceans, and molluscs) (Wilson-Sanders, 2011) (Table 11.1).

Obesity is a challenging research topic, as homeostatic regulation of energy balance involves multiple tissues and molecular pathways, and is complicated by the complex interplay between the development/reproduction and lipid-storage capacity. One powerful model organism is the nematode *C. elegans* that can provide an insight into the feeding and defecating behavior, neuroendocrine signaling, mobilization, and a characterization of the genetic basis of lipid metabolism, and can, thereby, help tease apart the fundamental regulation of energy balance.

TABLE 11.1 Common Models Used to Study Fundamental Aspects of Diseases and Drug Discovery

Organism type	Species
Virus	T4 phage
	Phi X 174
Prokaryotes	*Escherichia coli*
	Bacillus subtilis
Eukaryotes	
Protists	*Chlamydomonas reinhardtii*
	Tetrahymena thermophila
Fungi	*Saccharomyces cerevisiae*
	Schizosaccharomyces pombe
Plants	*Arabidopsis thaliana*
	Lemna gibba
Animals	
Invertebrates	Nematode (*Caenorhabditis elegans*)
	Fruit fly (*Drosophila melanogaster*)
Vertebrates	Guinea pigs (*Cavia porcellus*)
	Zebrafish (*Danio rerio*)
	Chicken (*Gallus gallus domesticus*)
	Mouse (*Mus musculus*)
	Rat (*Rattus norvegicus*)
	Non-human primates (*Pan troglodytes*)
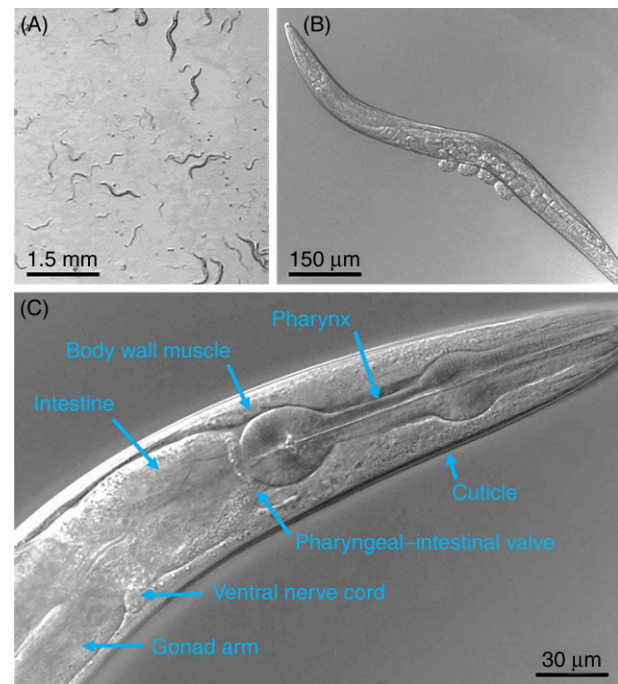
FIGURE 11.1 **A microscopic view of *C. elegans*.** (A) A population of mixed age on nematode growth media (NGM) agar. (B) A close-up of a single adult wild type worm, which has laid four eggs. (C) A high-resolution view of the head region of a hermaphrodite adult.

4 THE NEMATODE *CAENORHABDITIS ELEGANS*: SMALL IS BEAUTIFUL

C. elegans is a member of the phylum Nematoda and inhabits a wide range of habitats. The wild type strain (N2) originally isolated from Bristol (United Kingdom) and mutants can be maintained (using standardized protocols) in the laboratory on nematode growth media (NGM) plates supplemented with *Escherichia coli* (the food source) (Fig. 11.1). One of the key advantages of *C. elegans* is its short reproductive cycle (about 3 days) and life span (about 21 days) (Fig. 11.2).

C. elegans is, in many ways, an in vivo test tube. It is one of the simplest metazoan animals, only one millimeter in length, yet facilitating large-scale cultivation of thousands of staged animals. *C. elegans* is unsegmented, has a bilaterally symmetrical body tapering at both ends, and is transparent. The self-fertilizing hermaphrodite adult is made up of 959 somatic cells and produces homozygous progenies, which are genetically identical (bar spontaneous mutations). The male, which has a higher number of cells, one gonad and a tail with nine sensory palps to anchor the vulva, arises through a spontaneous nondisjunction in the hermaphrodite germ line, which is rare (typically less than 0.1% of a standard population) and can only copulate with its hermaphrodic counterpart. This feature represents an ideal tool for genetic crossing of two genotypes (Fig. 11.2).

The *C. elegans* genome is small and compact; it contains more than 20,000 protein-encoding genes assembled over 100 million base pairs. Although approximately only 1/30th the size of the human genome, many genes and core metabolic pathways are evolutionary conserved between the nematode and mammals (Hillier et al., 2005). *C. elegans* is thus primitive, and yet shares many of the most essential biological characteristics that are central to human biology (Table 11.2).

In 1963, Sydney Brenner introduced *C. elegans* as a model organism for developmental biology and neurobiology. Since then, the worm system has been applied to many fields, including genetics, cell biology, neuroscience, aging, stroke, muscle-associated disorders, metabolic diseases, cancer, embryogenesis, sex determination, and larval development (Markaki and Tavernarakis, 2010). Besides, the genome was fully sequenced in 1998 and the cell lineage of every single cell division, producing 959 somatic cells, was mapped in the 1980s. In addition, an RNA interference (RNAi) bacterial library containing 86% of the worm open reading frames has been constructed. Although injecting RNA into the body cavity of the animal induces gene silencing in most species, only *C. elegans* and a few other distantly related nematodes can take up RNAi molecules via the diet (Félix, 2008). Moreover, owing to its viability postfreezing, thousands of *C. elegans* strains are readily available (Table 11.3).
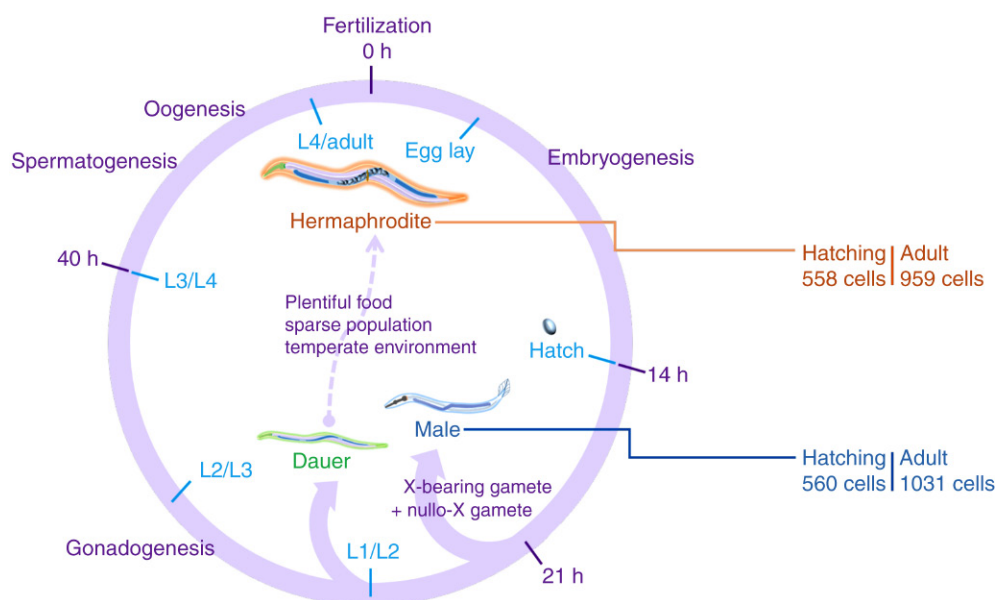
FIGURE 11.2 **The life cycle of *C. elegans* cultured at 25°C.** Under optimal growth conditions, the entire life cycle of hermaphrodite is completed within 3 days from the first larval stage (L1) to adulthood. Males arise from the fusion of nullo-X gametes (gametes that lack an X chromosome) and normal X-bearing gametes, at a rare frequency of less than 0.1%. When exposed to undesirable conditions (stress, crowding, or lack of food) the L1 enters "dauer," a stage that allows the worm to survive up to 4 months. Once conditions improve, the dauer animal develops to an L4 stage and oogenesis commences.

TABLE 11.2   A Comparison of the Genome and Proteome of Model Organisms

Species	Genome size (Mb)	% Of human genome	Protein count	% Of human protein
Homo sapiens **(human)**	**2,996.4**	**100**	**71,340**	**100**
Mus musculus (mouse)	2,671.8	89	39,412	55
Danio rerio (zebrafish)	1,391.7	46	47,861	67
Gallus gallus (chicken)	1,230.3	41	46,393	65
Drosophila melanogaster (fruit fly)	148.5	5	30,443	43
Caenorhabditis elegans **(nematode)**	**100.7**	**3**	**28,026**	**39**
Rattus norvegicus (Norway rat)	48.7	1.6	38,722	54
Saccharomyces cerevisiae (yeast)	12.3	0.4	5,404	8
Escherichia coli (bacterium)	5.2	0.2	4,931	7

Bold entries highlight the genome and proteome of human and *C. elegans* individually.
Source: Data taken from NCBI (https://www.ncbi.nlm.nih.gov/) .

TABLE 11.3   Scientific Contributions by Nobel Laureates Studying *C. elegans*

2002 Nobel Prize in Physiology or Medicine	
Sydney Brenner	Pioneering genetic studies
John Sulston	Elucidation of the embryonic cell lineage
Robert Horvitz	Definition of the molecular pathway of programmed cell death
2006 Nobel Prize in Physiology or Medicine	
Andrew Fire	Discovery of RNA interference during translation
Craig Mello	
2008 Nobel Prize in Chemistry	
Martin Chalfie	Application of green fluorescent protein as a marker for gene expression

TABLE 11.4 Examples of Popular Open-Access Worm Repositories

Website	Description
http://www.wormbase.org	A repository of biology and genomics of *C. elegans* and related nematodes
http://www.wormatlas.org	Handbooks focusing on the anatomy and behaviors of worms
http://www.wormbook.org	Peer-reviewed chapters covering the biology and protocols of *C. elegans* and other nematodes
http://www.wormbuilder.org	Provision of 294 worm strains carrying GFP markers at defined genomic locations
http://www.rnai.org	Provision of images, phenotypes, and graphic maps from RNAi studies in *C. elegans*
http://www.wormclassroom.org	An education and online learning community
http://cbs.umn.edu/cgc/home	Caenorhabditis Genetics Center, where worm strains are stored and sourced
http://shigen.nig.ac.jp/c.elegans/index.jsp	Provision of deletion worm mutants and the information regarding promoters and markers
http://www.acedb.org	A database for genome and bioinformatics data of various model organisms including *C. elegans*
http://www.wormmeeting-berlin.de	Organization of the European Worm Meeting
http://www.genetics-gsa.org/celegans	Organization of the International *C. elegans* Meeting

GFP, Green fluorescent protein; RNAi, RNA interference.

A comprehensive knowledge infrastructure has emerged over the past years, notably the strain and genome databases, such as those offered by the Caenorhabditis Genetics Center (http://cbs.umn.edu/cgc) or WormBase (http://wormbase.org). The abundance and open-access nature of resources have empowered worm researchers not only to focus on central biological issues, for example, aging, neurobiology, development, and evolution, but also other emerging fields, such as the biology of fat metabolism (Table 11.4).

5 THE BASIC BIOLOGY OF OBESITY: FROM A WORM'S PERSPECTIVE

Decades of genetic and physiological studies have focused primarily on murine lipid metabolism, which has contributed significantly to our knowledge of human energy homeostasis. *C. elegans* has been used to a lesser extent, nevertheless research has identified critical pathways, defined molecular mechanisms, uncovered new leads linked in particular to insulin signaling, the influence of serotonin on obesity, and the response to dietary glucose, feeding, and satiety (Zheng and Greenway, 2012). *C. elegans* lacks multifunctional adipocytes and certain fat-regulatory mechanisms, such as the leptin secretion from the white adipose tissue observed in mammals. It is also a cholesterol auxotroph, but is able to manufacture essential fatty acids (C18:2*n*6 and C18:3*n*3) endogenously and independent of dietary uptake (Mullaney and Ashrafi, 2009) (Fig. 11.3).

Setting aside the aforementioned physiological differences, many of the evolutionary conserved pathways governing energy metabolism have been identified in worms. The nuclear hormone receptor NHR-49 (the homolog of the human peroxisome proliferator–activated receptor-α, PPARα), for example, acts as a crucial regulator of metabolic gene transcription in worms (Chawla et al., 2001); social feeding is a sophisticated behavior, which depends on the worm homolog of the neuropeptide Y receptor NPY (a major regulator of mammalian feeding behavior) (De Bono and Bargmann, 1998); fat storage in *C. elegans* is also dependent on the AMP-activated protein and target of rapamycin (TOR) kinases, sterol regulatory element–binding protein (SREBP), and CCAAT/enhancer-binding protein (C/EBP) transcription factors (McKay et al., 2003); and a conserved set of lipases in worms have mammalian orthologs involved in the balancing of energy input and output via the liberation of triglycerides (Wang et al., 2008b). Other examples include the existence of fatty acid transporter homologs (CeFATPa and CeFATPb), to transport fatty acids between tissues (Grant and Hirsh, 1999) and lipid-binding proteins (Hirsch et al., 1998).

6 KEY FEATURES OF FAT METABOLISM IN *CAENORHABDITIS ELEGANS*

6.1 Dietary Uptake of Fatty Acids

The protein-coupled peptide transporter, PETP-1, increases intestinal proton influx, fatty acid absorption, and thus fat content. The sodium–proton exchanger, NHX-2, plays an essential role in the intestinal pH regulation and fatty acid transport, with the *nhx-2* mutant displaying a
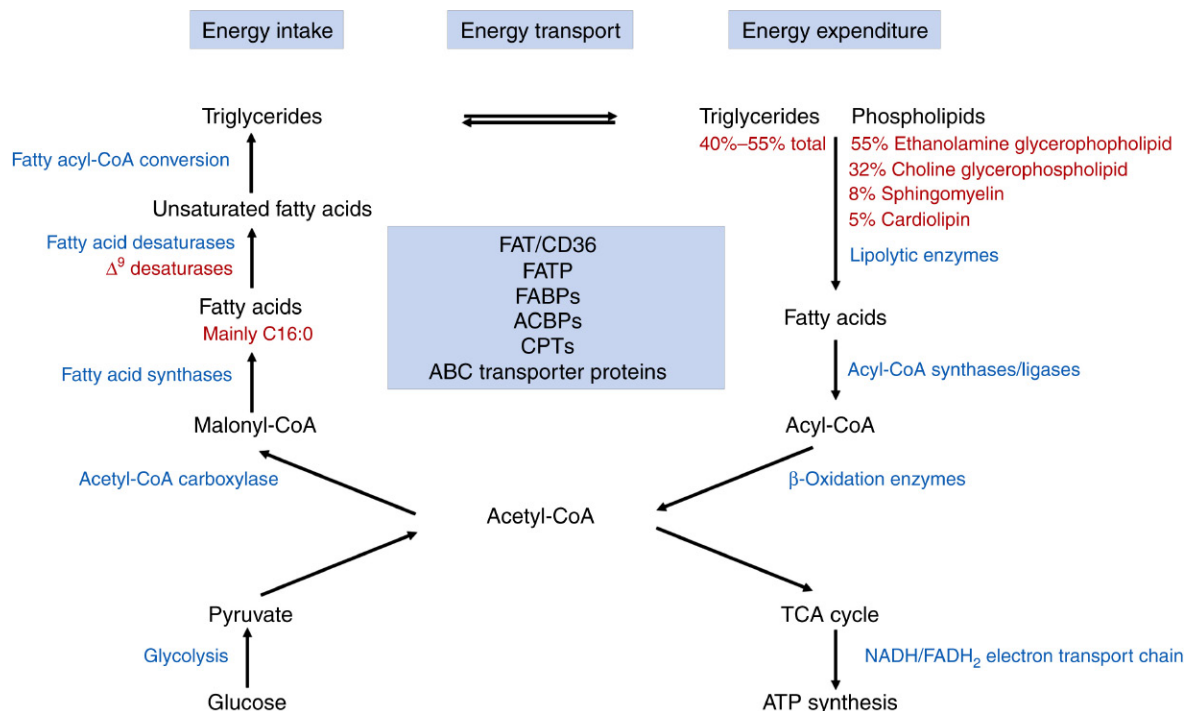
FIGURE 11.3 **Overview of the coordination of energy in** *C. elegans*, **involving the synthesis and breakdown pathways of mainly fat and sugar.** *ABC*, ATP-binding cassette; *ACBP*, acyl-CoA–binding proteins; *ATP*, adenosine triphosphate; *CPT*, carnitine–palmitoyl transferases; *FABP*, fatty acid–binding protein; *FADH₂*, flavin adenine dinucleotide; *FAT/CD36*, fatty acid translocase; *FATP*, fatty acid transport protein; *NADH*, nicotinamide adenine dinucleotide; *TCA*, tricarboxylic acid cycle.

low-fat profile. The import and activation of exogenous fatty acids is modulated by fatty acid transport proteins (FATPs) (i.e., ACS-20 and ACS-22, which are homologs of human FATP4). Acquired fatty acids and acyl-CoA are transported further by intracellular binding proteins, including LBP-1 to -9, FAR-1 to -8, and ACBP-1 to -7 for the degradation (Elle et al., 2010).

6.2 Synthesis of Fatty Acids

High levels of fatty acids originate from diet digestion, but some fatty acids, such as 7% of palmitic acid, 5% of palmitoleic acid and vaccenic acid, and 20% of oleic acid and polyunsaturated fatty acids are synthesized de novo in *C. elegans*, assisted by acetyl-CoA carboxylase (encoded by *pod-2*) and fatty acid synthase (encoded by *fasn-1* or *phi-46*) (Perez and Van Gilst, 2008). The monomethyl branched-chain fatty acids, in contrast, are mostly produced endogenously by worms. Monounsaturated fatty acids are converted by Δ^9 desaturases, which in worms are FAT-5, FAT-6, and FAT-7. FAT-2 and FAT-3 can desaturate monounsaturated fatty acids to polyunsaturated fatty acids (Brock and Watts, 2006).

6.3 Storage of Macronutrients

By binding to an insulin-link ligand, the nematode insulin receptor, DAF-2, activates the phospohinositide-3-kinase AGE-1 and the phosphorylation cascade via PIP3, ultimately leading to the phosphorylation of DAF-16 [Forkhead box O (FOXO) homolog] and its relocation. A loss of functional DAF-2 causes fat accumulation, as well as an altered life span, dauer formation, and stress responses (Mukhopadhyay and Tissenbaum, 2007). In comparison, the insulin receptor in mammals selectively increases fat deposits in adipocytes, while decreases fat content in muscles and neurons (Biddinger and Kahn, 2006). DAF-7 is a TGF-β–like ligand which, under nutrient deprivation, binds to the TGF-β receptor complex homologs: DAF-1 and DAF-4, thereby inhibiting the receptor-associated co-SMAD, DAF-3, subsequently regulating the feeding rate, fatty acid synthase activity, and lipid content. Under nutritional conditions, the expression of DAF-2 is downregulated, resulting in feeding rate changes and related dauer arrest along with lipid accumulation (Greer et al., 2008). Serotonin, a key neurotransmitter, is essential in maintaining the feeding rate in *C. elegans* via G-protein coupled receptors: SER-1 and -7. It also regulates the level of lipid storage via a β-oxidation relevant pathway, and depends on SER-6 and the serotonin-gated chloride channel, MOD-1. The synthesis of serotonin in neurons is activated by tryptophan hydroxylase TPH-1, and an impaired TPH-1 expression is linked to high-fat phenotypes (Srinivasan et al., 2008). Eukaryotic rapamycin (TOR) kinase targets protein complexes: TORC-1 and -2, and regulates the metabolic balance. RICT-1, a component of TORC-2, plays an important role in lipid regulation. An impaired function

TABLE 11.5 A Selection of Transcription Factors Involved in the Lipid Metabolism of *C. elegans*

Transcription factors	Mammalian homologs	Functional annotations
NHR-49	By sequence closely related to the mammalian HNF4α, while functionally similar to the PPARα	NHR-49 relocates to the nucleus and binds to promoter sequences containing hormone-response elements to regulate the transcription of target genes linked to lipid mobilization in *C. elegans*. A deletion of *nhr-49* induces profound changes in lipid synthesis, fatty acid β-oxidation, lipid saturation, glycolysis, and gluconeogenesis.
SBP-1	SREBP	SBP-1 is the only SREBP homolog in *C. elegans* and by homology, most closely related to mammalian SREBP-1c. The function of SBP-1 in lipogenesis of *C. elegans* is, however, yet to be delineated at a molecular level.
LPD-2	C/EBP	LPD-2 regulates the expression of lipogenic enzymes and plays a role in the development of *C. elegans*. The *lpd-2*–deficient worm mutant arrests at the larvae stage.
KLF-1/-2/-3	KLF-1 and -3 are homologs of human KLF-1; KLF-2 is the homolog of human KLF-7	The expression of KLFs regulates developmental functions, reproduction and lipid storage in *C. elegans*. KLF-3 in particular plays a role in fatty acid synthesis and degradation.
MDT-15	ARC105 as a subunit of the mediator complex	MDT-15 integrates several transcriptional regulatory pathways to monitor the availability and the nature of ingested materials in *C. elegans*.

ARC, Activator-recruited cofactor; C/EBP, CCAAT/enhancer binding protein; HNF4α, hepatocyte nuclear factor 4α; KLF, Krüppel-like factor; LPD, lipid depleted; MDT, mediator; NHR-49, nuclear hormone receptor 49; PPARα, peroxisome proliferator activated receptor α; SBP-1, sterol regulatory element–binding protein 1; SREBP, sterol regulatory element–binding protein.

of TORC-2, as a result of the depletion of RICT-1, induces lipid accumulation in worms (Jones et al., 2009).

6.4 Fat Catabolism

C. elegans stores fat, as mammals, mainly as triglycerides that are hydrolyzed into glycerol and fatty acid by a range of lipases to release energy. In dauer-stage animals, lipolysis is suppressed, which can be attributed to the downregulation of the *C. elegans* ortholog of the mammalian adipocyte triglyceride lipase. Another example is K04A8.5, a lipase whose intestinal expression significantly reduces lipid accumulation in vivo (Wang et al., 2008b). Likewise, worms on a restricted diet exhibit elevated levels of intestinal lipase, FIL-1 and -2, and thus a greater degree of triglyceride degradation (Jo et al., 2009).

Many mammalian transcription factors involved in energy homeostasis have functional counterparts in *C. elegans*, which are summarized in Table 11.5.

7 TECHNICAL ADVANCES DRIVING LIPID RESEARCH IN NEMATODES

One of the first methods to assess fat content utilized the lipophilic dye Sudan black, which allows the post-fix staining of worms (Kimura et al., 1997). Later, fluorescent dyes, such as LipidTOX, were used in place of Sudan black by a similar fixation protocol for easier visualization of the neutral lipids. Fat storage of worms was shown to take place mainly in the droplets/granules of intestinal and hypodermal cells (Wood, 1987).

Vital dye staining of fat in intact living animals was introduced to physically track the endogenous uptake and transport of lipids in a high-throughput manner. The most commonly used dyes are Nile red and fatty acid–conjugated BODIPY, both complement the microscopy-based methods of fat visualization (Greenspan et al., 1985).

However, fluorescent properties, though extremely sensitive, may not accurately reflect the endogenous fat levels. These limitations can be circumvented by means of biophysical techniques, such as coherent anti-Stokes Raman spectroscopy (CARS) and stimulated Raman scattering (SRS) (Hellerer et al., 2007).

Individual lipid species and parameters can also be defined by biochemical techniques (Watts, 2002), such as high performance liquid chromatography (HPLC), thin layer chromatography (TLC), gas chromatography (GC), and gas chromatography–mass spectrometry (GC-MS) analysis or via an enzymatic determination. Metabolic labeling strategies have helped to define individual contributions of de novo fat synthesis and dietary absorption to overall fat metabolism (Perez and Van Gilst, 2008).

Genetic screens have elucidated gene targets involved in fat-regulatory pathways. In addition, expression profiling and epistasis analysis have pinpointed specific components and pathways that are involved in β-oxidation, fatty acid synthesis, and acyl-CoA synthesis (Srinivasan et al., 2008). Owing to the power of the worm model, it is now possible to move beyond the study of overall fat content and examine the specific
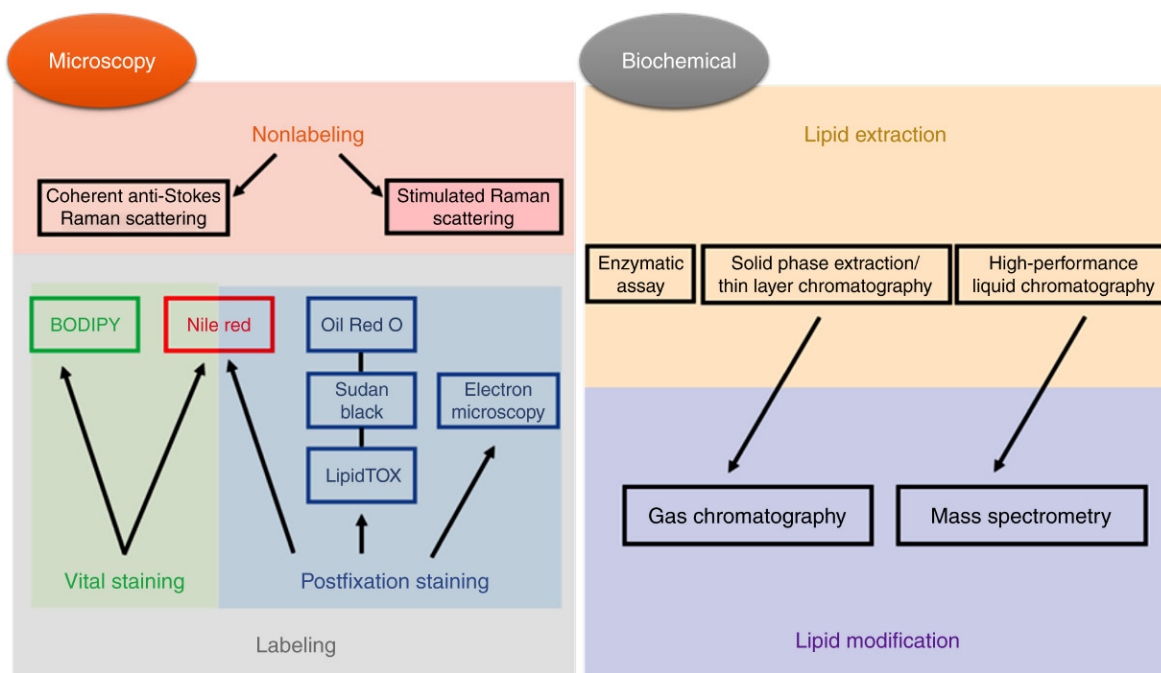
FIGURE 11.4   Overview of research techniques applied to track lipid storage and mobilization in *C. elegans*.

genetic targets that contribute to lipid homeostasis. Indeed, past experiments have included the mapping of obesity-related genes, targeted gene deletions, mutagenesis, and genome-scale RNAi screens, which in concert have uncovered over 400 genes that are involved in body fat regulation (Ashrafi et al., 2003) (Fig. 11.4).

8 THE INTESTINE: A DRIVER OF LIPID METABOLISM

In the absence of a dedicated liver and adipose tissue, the nematode's intestine has been suggested to act as a multifunctional organ. The entire intestine in an adult hermaphrodite is composed of merely 20 cells, with every 2 or 4 cells arranged in rings that enclose the lumen cavity spanning almost the entire length of the worm's body. Each of these intestinal cells is derived from a single embryonic blastomere (E) and the intestinal organogenesis is complete before the worm hatches.

The *C. elegans* intestine constitutes roughly one-third of the total somatic mass of the worm body. The digestive potential of worms is impressive: each cycle of defecation (a dynamic process that occurs in 45–50 s intervals) ejects up to half of the gut content. It is estimated that worms consume several million bacteria each day, while the average duration of a bacteria within the intestine is less than 2 min. Genes that are highly enriched in the intestine have helped to define the biology of digestion in *C. elegans*, for example, genes coding lysozymes and pore-forming proteins that ease the physical ingestion of

the bacterial diet, ATPases that acidify the intestinal lumen, and proteases/peptidases that catalyze the protein digestion.

Although the development of the intestine is programmed in a precise manner, its shape and function can be extremely flexible. The intestinal cytoplasm of long-lived dauer larvae is, for example, packed with electron-dense "cytosomes." The intestinal lumen constricts as part of an energy-restriction mechanism. These changes are reversed in worms that emerge from the dauer status.

C. elegans obtains fatty acids from its diet or by de novo synthesis to yield acetyl-CoA. The catabolism is realized through β-oxidation that takes place in two main sites: the mitochondria and peroxisome. Most peroxisomes are, therefore, found in the intestinal cells. Moreover, the nematode stores fat predominantly in intestinal lipid droplet (LD) organelles and lysosome-related organelles (LROs), the so-called "gut granules," which are involved in the intestinal differentiation and lipid metabolism. Serving as the primary triglyceride depot, the structural and biophysical characteristics of LDs or LROs are yet to be defined in detail.

9 THE LIPID DROPLETS ARE THE MAIN SITE OF TRIGLYCERIDE ACCUMULATION

LDs are characterized by the phospholipid monolayer membrane, which encases the lipid core. LDs are not inert fat particles, but rather dynamic organelles that function

in both energy storage and catabolism. They store neutral lipid triglycerides and polar lipids, including phospholipids and sterol esters, which help buffer cells from the toxic effects caused by excessive lipids. A disturbance of the lipid composition can result in larger LDs or they may break up into smaller units, facilitating the further digestion by lipases (Guo et al., 2008). Moreover, various enzymes required for the synthesis of triglyceride have been detected in isolated LDs, demonstrating their role in lipid anabolism (Fujimoto et al., 2007).

In mammals, LDs occupy adipocytes; however, the exact mechanisms that govern the distribution and mobilization of lipids in worms at the subcellular level are not clear. Lipophilic staining and physical approaches have identified that the intestine as the primary site and the hypodermis as the secondary site of energy storage, with additional deposits observed in maturing oocytes of the germ line, fertilized embryos, and in rare cases, muscle tissue. Accordingly, various classes of lipids are stored in distinct vesicular compartments, which can be differentiated by their electron densities (Chen et al., 2006; Hermann et al., 2005; Leung et al., 1999).

The LDs of nematode intestinal cells are typically large in size (spherical diameter > 10 μm), which is comparable to LDs in mammalian adipocytes. Excessive triglyceride in LDs are catabolized through β-oxidation in the mitochondria and peroxisome. A genetic defect in the peroxisomal β-oxidation pathway (e.g., in the *daf-22* lacking the terminal enzyme in peroxisomal fatty acid β-oxidation) results in a high-fat phenotype, namely an increase in the size of LDs (Zhang et al., 2010a). Transgenic DAF-22::GFP, which is expressed in the intestine, the hypodermis, and the body wall muscle of worms, is suppressed in *acs-22* and *dgat-2* mutants that lack fatty acyl-CoA synthetase and a diglyceride acyl transferase, respectively (Xu et al., 2012). This suggests that the mechanisms underlying the formation of LDs are conserved between worms and mammals. However, the mechanisms that govern the dynamic change in shape, size, or density of LDs are not yet fully understood.

10 THE NILE RED VITAL STAINING CONUNDRUM

Nile red was initially defined as a highly specific vital stain, allowing the detection of intracellular LDs in cultured aortic smooth muscle cells and peritoneal macrophages, as it selectively dissolves in the lipids and fluoresces with no local interaction with the tissue constituent (Greenspan et al., 1985). Ashrafi et al. (2003) reported how the Nile red assay could be applied to *C. elegans* to analyze fat storage and mobilization within a whole genome RNAi screen. As Nile red does not influence the growth rate, brood size, feeding, or lifespan of worms, it has since become a widely applied lipid proxy in nematodes. The accuracy of the methodology was, however, subsequently questioned as worms accumulated Nile red in lysosomal compartments rather than the major fat stores (Brooks et al., 2009; O'Rourke et al., 2009; Schroeder et al., 2007). A comprehensive comparison of fat-soluble vital dyes (BODIPY and Nile red), CARS, and standard biochemical triglyceride quantification found that CARS and the biochemical quantifications differed from the vital dyes that were limited to staining acidic organelles of lysosomal origin (Yen et al., 2010). An alternative to the vital dye staining method is staining in a postfixative manner. Fixation allows the direct penetration of the lipophilic dye to the hydrophobic targets.

The application of the vital Nile red staining is, in comparison to the fixative Oil Red O dye, more conducive, time efficient, and especially more suitable for high-throughput drug screening. Indeed, from a biophysical and biochemical perspective, Nile red–stained LROs were recently recognized to be the main location of cholesterol storage and a reduction of Nile red staining was noted to correlate with the bulk ratio of triglyceride to protein in nematodes (Zhang et al., 2010b). Likewise, lipid accumulation in endolysosomal compartments under pathophysiological conditions was observed (Schmitz and Grandl, 2009). The precise mechanisms of the uptake, transport, and turnover of these dyes are still not fully understood and further investigations are needed to provide a comprehensive understanding of the local interactions between exotic dyes and lipids/organelles in vivo. Any result derived from Nile red staining should, therefore, be validated by an alternative independent approach.

11 LYSOSOME-RELATED ORGANELLES PARTICIPATE IN LIPID MOBILIZATION

LROs can be stained by Nile red and are acidic, autofluorescent, birefringent, and express PGP-2, GLO-3, and FUS-1 as important functional proteins (Hermann et al., 2005). LROs may not be the main location of fat storage in *C. elegans*; however, this does not rule out that the LRO compartments play a role in the metabolism of lipid or physiologically relevant fats. Indeed, worms utilize energy reserves upon food deprivation via the recycling of LRO-mediated nutrients (Finn and Dice, 2006).

The Niemann–Pick type C disease in mammals underline the important role lysosomes play in the metabolism of cholesterol and sphingolipid (Futerman and Van Meer, 2004). Unlike mammalian cells, nematodes store cholesterol exclusively in LROs rather than LDs (Lee et al., 2015). Worms with a lysosomal storage disorder (*ncr* mutants) show diverse phenotypes, including a disturbed cholesterol trafficking and a hypersensitivity toward cholesterol derivation (De Voer et al., 2008).

Nematodes contain an essential gene that is a homolog of *Drosophila* SREBP. It is similar to those proteins regulating cholesterol levels in mammals and was reported to regulate enzymes for the synthesis of saturated fatty acids and phosphatidylethanolamine (Seegmiller et al., 2002).

Numerous studies in other organisms have highlighted the complex interaction(s) between LROs and LDs. Lipolysis and autophagy, for example, are both involved in nutrient deprivation–induced responses, namely lipids stored as triglycerides in LDs are hydrolyzed into fatty acids, and intracellular proteins and organelles sequestered in autophagosomes are transported to lysosomes as energy sources. This observation leads to the notion that LDs and LROs may be associated during starvation. Furthermore, an abnormal increase in intracellular lipid impairs the autophagic clearance, which traps cells in a harmful cycle with additional lipid retention. The therapeutic strategies to increase autophagic function have thus formed the basis of a new approach proposed to treat metabolic syndromes (Singh et al., 2009).

LRO can be observed in worms by means of specific acidic markers, including acridine orange and LysoTracker. The colocalization of Nile red and LysoTracker suggests that an interlinked mechanism underlies the LRO-regulated lipid metabolism. Following the death of a worm, LROs rupture and in turn result in a burst of strong autofluorescence, which greatly interferes with lipid visualization (De Duve, 1963).

12 INTESTINAL AUTOFLUORESCENCE: FRIEND OR FOE?

The majority of autofluorescence in worms is observed in granules of the intestinal cells. Histochemical staining of the autofluorescent granules suggested that they contain acid phosphatase, a lysosomal enzyme. Further, the autofluorescent granules accumulate exogenous material and concentrate a lysosomotropic weak base and are thus thought to act as secondary lysosomes (Clokey and Jacobson, 1986). The acidic intestinal compartments of the 1.5-fold stage embryo can be stained with acridine orange, which colocalize with birefringent gut granules; similarly, the autofluorescent and acidic LysoTracker Red–stained compartments colocalize with gut granules in newly hatched L1-stage larvae, confirming the birefringent, autofluorescent, and lysosomal identity (Hermann et al., 2005). Indeed, autofluorescence and lysosomal metabolism are interlinked. For example, progressive neurodegeneration and the accumulation of autofluorescent material are caused by mutations in lysosomal hydrolase genes (Futerman and Van Meer, 2004). In worms, defects in the expression of eight *glo* genes, namely *apt-6*, *apt-7*, *vps-16*, *vps-41*, *glo-1*, *glo-2*, *glo-3*, and *glo-4*, are responsible for the mislocalization of birefringent material into the intestinal lumen during embryogenesis, with the first four genes encoding proteins that are homologous to components of the AP-3–mediated Golgi-to-vacuole trafficking pathway (Odorizzi et al., 1998), while the latter are homologous to *Drosophila* eye pigmentation genes regulating the biogenesis of LROs (Dell'Angelica, 2004). LROs in *C. elegans* may, therefore, share some functional characteristics with the pigment granules in *Drosophila* and mammalian melanosomes (Hermann et al., 2005). Currently there are two main hypotheses regarding the chemical identity of the LRO fluorophore, namely that is lipofuscin like or anthranilic acid (AA) like.

12.1 Theory 1: Lipofuscin-Like Autofluorescence

The solubility of autofluorescent pigments closely resembles "lipofuscin" pigments (Clokey and Jacobson, 1986). They both accumulate during oxidative stress, and are marked by an extreme emission and diffusion in aged individuals (Katz and Robison, 2002). The spectra of both autofluorescence and lipofuscin overlap with most commonly used fluorophores (Kalyuzhny and Wessendorf, 1998). This broad excitation and emission characteristic suggests that lipofuscin-like pigments might be composed of a mixture of different, although related, fluorescent molecules (Steiner and Kirby, 1969).

12.2 Theory 2: Anthranilic Acid–Like Autofluorescence

According to a recent chemical analysis, the blue fluorescence observed within nematode intestinal cells is AA glucosyl ester, a product of the kynurenine pathway (Coburn et al., 2013). Altered intestinal fluorescence (*flu*) phenotypes can arise from mutations affecting the kynurenine pathway enzyme, such as *flu-1* and *flu-2*. The kynurenine pathway is known to be implicated in neurodegeneration and immunity (Munn et al., 1998; Sasaki et al., 2012). In *Drosophila*, kynurenines were hypothesized to contribute to aging; however, very little is known about the biology of kynurenines in nematodes. AA may harbor antibiotic properties to protect nematodes from a pathogen attack or may act as a photon protectant (Gems and Coburn, 2013).

Given the evolutionarily conserved role of electronlucent LDs and electron-opaque LROs in energy homeostasis, they are considered to be central in maintaining the energy balance. *C. elegans* offers unique opportunities to visualize fluorescence at a single-cell resolution in live animals, and combined with the plethora of genetic tools and biochemical assays, this model organism promises to advance our understanding of lipid metabolism in vivo.

13 A WHOLE GENOME APPROACH

C. elegans is amenable to high-throughput, genome-wide, and whole organism–association screens. For example, a genome-wide RNAi knockdown screen has identified around 400 genes that are linked to fat disturbance in worms. In addition, hundreds of genes are pleiotropic, causing multiple biological effects ranging from fat disorder, sterility, growth arrest, to lethality (Ashrafi et al., 2003). Extending this effort, a microscopic analysis of more than 300 RNAi-treated worms pinpointed evolutionary conserved genes that are associated with embryonic lipids (Schmökel et al., 2016).

A high-throughput phenotypic assay may lead to the discovery of genes not previously associated with metabolic process. Indeed, Oil Red O staining in tandem with high-volume image–based phenotyping allowed the efficient, rapid, and robust sample preparation and analysis of genetic/chemical perturbations in whole animals (Wählby et al., 2014).

A recent high-throughput study suggested that miR-NAs play a role in the lipid mobilization in worms. L4 larvae were subjected to a 12-h starvation period and 13 miRNAs were shown to be downregulated; however; the miR-35 family was upregulated 6–20 fold (Garcia-Segura et al., 2015).

A proteome analysis of lipid droplets isolated from wild type N2 and *daf-2* mutants identified 354 proteins that belong to various functional classes, including lipid metabolism, trafficking, transport, and signal transduction, to name a few. The top 100 most abundant LD proteins were studied further via RNAi knockdown and ACS-4 was characterized as a LD-associated protein (Vrablik et al., 2015). These recent studies carried out at the DNA, RNA, and protein level highlight the powerful quantitative phenotyping approaches that are possible with the invertebrate worm model.

14 NEW AVENUES OF LABEL-FREE METHODS

The challenges surrounding the inconsistencies of vial dye staining in nematodes have led to the development of new approaches for identifying the ubiquitous fat distribution and revealing lipid phenotypes stored in intestinal cells, gonads, germ line, and hypodermis. One exciting progress has been the application of biophysical tools, such as CARS microscopy, which demonstrated the advantages of a label-free method in comparison to standard fluorescence microscopy (Hellerer et al., 2007).

CARS allows the visualization of LDs by analyzing signals derived from the specific vibration of intrinsic carbon–hydrogen stretching. CARS imaging provides an accurate estimation of the size and number of LDs, as well as the dynamic monitoring of lipid molecules.

The order of polymethylene chains can be estimated by CARS by recording the asymmetric and symmetric CH_2 vibrations and their ratio: a higher ratio represents a gel phase of highly ordered methyl chains, while a lower ratio is linked to the liquid phase of less-ordered chains (Wurpel et al., 2002). Further subtraction of the background resonance improves the CARS spectra and allows a more accurate measurement of the lipid signal (Hagmar et al., 2008). By applying the spectral information from pointwise confocal Raman microspectroscopy, analysis of the fingerprint region of the CARS spectrum enables the detection of lipid-chain unsaturation and thus detailed phenotypes of worms from different genetic backgrounds. Subgroups of lipid-storage compartments can also be identified in the presence or absence of autofluorescence. Additionally, the differences in the amount of autofluorescent granules can be observed and quantified in worm strains (Le et al., 2010). The spectral interferometric polarization CARS (SIPCARS) allows the hyperspectral analysis of lipid phenotypes, as well as the quantification of lipid enrichment (Littleton et al., 2013).

SRS is another vibrational imaging technique typically employed for *C. elegans*. Signals can be recorded in nanosecond resolution and thus offer a high volume of pixel information and an exceptional optical sectioning capability. Moreover, the SRS signal exhibits a linear dependence on the underlying resonant bonds (as opposed to CARS, which typically returns a nonlinear output), thereby simplifying the extraction of quantitative features. An RNAi screen combined with quantitative imaging of lipids by means of single-frequency SRS yielded eight new genetic regulators of fat storage in worms (Wang et al., 2011). Likewise, a combination of hyperspectral SRS and multivariate analysis in the fingerprint vibration region resulted in the quantitative mapping of fat distribution, as well as the degree of lipid saturation, oxidation, and cholesterol enrichment in vivo in a whole worm. This approach confirmed that LROs are the main sites for storage of cholesterol in worms (Wang et al., 2014). SRS was further used in metabolic fingerprinting to probe the spatial–temporal dynamics of metabolites at the subcellular level, which revealed a lack of interaction between saturated and unsaturated fatty acids (Fu et al., 2014). One caveat of SRS is the difficulty to scale up to multiple channels, and, therefore, it is challenging to acquire the full spectral details of novel biological samples.

15 TRENDS AND CHALLENGES

To gain deeper insights into fat regulation, investigations from multiple aspects are called for, spanning signaling, transcription, neuronal circuits, development, behavior, and others. In addition to the LD–LRO interaction, further crosstalk between LDs and other subcellular

organelles, lipid species, nutrient factors, and additional bioactive molecules in various tissues, such as hypodermis and gonads, should be explored. The well-defined nervous system of worms offers unique avenues to decipher neural circuits that govern metabolism, feeding behaviors, and nutrient perception. Moreover, the nematode can provide an insight into physiological pathways and external factors, such as environmental perturbations.

Given the central role of the intestine in the uptake and storage of lipids, studies have mostly focused on gut cells to quantify and phenotype lipid molecules. It has been argued that the nematode intestine shares many features of the mammalian intestine and liver, while its hypodermal cells function as mammalian adipocytes (Lemieux and Ashrafi, 2015). One concern is that biochemically extracted lipids from hermaphrodites may comprise a considerable amount of intestinal yolk or embryonic lipid rather than genuine fat reserves that are needed for somatic structures. Therefore a detailed assessment of the dynamics of fat metabolism in different tissues is needed, as this will facilitate the quantitative phenotypic analysis of energy homeostasis in single worms and populations.

In summary, *C. elegans* is uniquely positioned, as it allows in vivo animal research at a single-cell resolution via a versatile experimental tool set. By acknowledging both its strengths and limitations, the nematode holds promise for the improvement and optimization of our knowledge base pertaining to lipid metabolism. Having said that, no single species can ever serve as a universal model. To advance of our knowledge of evolutionary conserved mechanisms of life, we should gather data from two or more organisms (Bolker, 2012).

References

Ashrafi, K., Chang, F.Y., Watts, J.L., Fraser, A.G., Kamath, R.S., Ahringer, J., Ruvkun, G., 2003. Genome-wide RNAi analysis of *Caenorhabditis elegans* fat regulatory genes. Nature 421 (6920), 268–272.

Barbier, P., Schneider, F., 1987. Syntheses of tetrahydrolipstatin and absolute configuration of tetrahydrolipstatin and lipstatin. Helv. Chim. Acta 70 (1), 196–202.

Berrington de Gonzalez, A., Hartge, P., Cerhan, J.R., Flint, A.J., Hannan, L., MacInnis, R.J., et al., 2010. Body-mass index and mortality among 1.46 million white adults. N. Engl. J. Med. 363 (23), 2211–2219.

Biddinger, S.B., Kahn, C.R., 2006. From mice to men: Insights into the insulin resistance syndromes. Annu. Rev. Physiol. 68, 123–158.

Bolker, J., 2012. Model organisms: there's more to life than rats and flies. Nature 491 (7422), 31–33.

Brock, T.J., Watts, J.L., 2006. Genetic regulation of unsaturated fatty acid composition in *C. elegans*. PLoS Genet. 2 (7), e108.

Brooks, K.K., Liang, B., Watts, J.L., 2009. The influence of bacterial diet on fat storage in *C. elegans*. PLoS One 4 (10), e7545.

Chawla, A., Repa, J.J., Evans, R.M., Mangelsdorf, D.J., 2001. Nuclear receptors and lipid physiology: opening the X-files. Science 294 (5548), 1866–1870.

Chen, C.C.H., Schweinsberg, P.J., Vashist, S., Mareiniss, D.P., Lambie, E.J., Grant, B.D., 2006. RAB-10 is required for endocytic recycling in the *Caenorhabditis elegans* intestine. Mol. Biol. Cell 17 (3), 1286–1297.

Clokey, G.V., Jacobson, L.A., 1986. The autofluorescent "lipofuscin granules" in the intestinal cells of *Caenorhabditis elegans* are secondary lysosomes. Mech. Ageing Dev. 35 (1), 79–94.

Coburn, C., Allman, E., Mahanti, P., Benedetto, A., Cabreiro, F., Pincus, Z., et al., 2013. Anthranilate fluorescence marks a calcium-propagated necrotic wave that promotes organismal death in *C. elegans*. PLoS Biol. 11 (7), e1001613.

Connolly, H.M., Crary, J.L., McGoon, M.D., Hensrud, D.D., Edwards, B.S., Edwards, W.D., Schaff, H.V., 1997. Valvular heart disease associated with fenfluramine-phentermine. N. Engl. J. Med. 337 (9), 581–588.

Cooke, D., Bloom, S., 2006. The obesity pipeline: current strategies in the development of anti-obesity drugs. Nat. Rev. Drug Discov. 5 (11), 919–931.

De Bono, M., Bargmann, C.I., 1998. Natural variation in a neuropeptide Y receptor homolog modifies social behavior and food response in *C. elegans*. Cell 94 (5), 679–689.

De Duve, C., 1963. The lysosome concept. Ciba Foundation Symposium-Lysosomes. John Wiley & Sons, Ltd, pp. 1–35.

De Voer, G., Peters, D., Taschner, P.E., 2008. *Caenorhabditis elegans* as a model for lysosomal storage disorders. Biochim. Biophys. Acta 1782 (7), 433–446.

Dell'Angelica, E.C., 2004. The building BLOC(k)s of lysosomes and related organelles. Curr. Opin. Cell Biol. 16 (4), 458–464.

Elle, I.C., Olsen, L.C.B., Pultz, D., Rødkær, S.V., Færgeman, N.J., 2010. Something worth dyeing for: molecular tools for the dissection of lipid metabolism in *Caenorhabditis elegans*. FEBS Lett. 584 (11), 2183–2193.

Félix, M.A., 2008. RNA interference in nematodes and the chance that favored Sydney Brenner. J. Biol. 7 (9), 1.

Finn, P.F., Dice, J.F., 2006. Proteolytic and lipolytic responses to starvation. Nutrition 22 (7), 830–844.

Fu, D., Yu, Y., Folick, A., Currie, E., Farese, Jr., R.V., Tsai, T.H., et al., 2014. In vivo metabolic fingerprinting of neutral lipids with hyperspectral stimulated Raman scattering microscopy. J. Am. Chem. Soc. 136 (24), 8820–8828.

Fujimoto, Y., Itabe, H., Kinoshita, T., Homma, K.J., Onoduka, J., Mori, M., et al., 2007. Involvement of ACSL in local synthesis of neutral lipids in cytoplasmic lipid droplets in human hepatocyte HuH7. J. Lipid Res. 48 (6), 1280–1292.

Futerman, A.H., Van Meer, G., 2004. The cell biology of lysosomal storage disorders. Nat. Rev. Mol. Cell Biol. 5 (7), 554–565.

Garcia-Segura, L., Abreu-Goodger, C., Hernandez-Mendoza, A., Dinkova, T.D.D., Padilla-Noriega, L., Perez-Andrade, M.E., Miranda-Rios, J., 2015. High-throughput profiling of *Caenorhabditis elegans* starvation-responsive microRNAs. PLoS One 10 (11), e0142262.

Gems, D., Coburn, C., 2013. The mysterious case of the *C. elegans* gut granule: death fluorescence, anthranilic acid and the kynurenine pathway. Front. Genet. 4, 151.

Glazer, G., 2001. Long-term pharmacotherapy of obesity 2000: a review of efficacy and safety. Arch. Int. Med. 161 (15), 1814–1824.

Grant, B., Hirsh, D., 1999. Receptor-mediated endocytosis in the *Caenorhabditis elegans* oocyte. Mol. Biol. Cell 10 (12), 4311–4326.

Greenspan, P., Mayer, E.P., Fowler, S.D., 1985. Nile red: A selective fluorescent stain for intracellular lipid droplets. J. Cell Biol. 100 (3), 965–973.

Greer, E.R., Perez, C.L., Van Gilst, M.R., Lee, B.H., Ashrafi, K., 2008. Neural and molecular dissection of a *C. elegans* sensory circuit that regulates fat and feeding. Cell Metab. 8 (2), 118–131.

Guo, Y., Walther, T.C., Rao, M., Stuurman, N., Goshima, G., Terayama, K., et al., 2008. Functional genomic screen reveals genes involved in lipid-droplet formation and utilization. Nature 453 (7195), 657–661.

Hagmar, J., Brackmann, C., Gustavsson, T., Enejder, A., 2008. Image analysis in nonlinear microscopy. J. Opt. Soc. Am. A 25 (9), 2195–2206.

Hellerer, T., Axäng, C., Brackmann, C., Hillertz, P., Pilon, M., Enejder, A., 2007. Monitoring of lipid storage in Caenorhabditis elegans using coherent anti-Stokes Raman scattering (CARS) microscopy. Proc. Natl. Acad. Sci. USA 104 (37), 14658–14663.

Hermann, G.J., Schroeder, L.K., Hieb, C.A., Kershner, A.M., Rabbitts, B.M., Fonarev, P., et al., 2005. Genetic analysis of lysosomal trafficking in Caenorhabditis elegans. Mol. Biol. Cell 16 (7), 3273–3288.

Hillier, L.W., Coulson, A., Murray, J.I., Bao, Z., Sulston, J.E., Waterston, R.H., 2005. Genomics in C. elegans: so many genes, such a little worm. Genome Res. 15 (12), 1651–1660.

Hirsch, D., Stahl, A., Lodish, H.F., 1998. A family of fatty acid transporters conserved from mycobacterium to man. Proc. Natl. Acad. Sci. USA 95 (15), 8625–8629.

Jo, H., Shim, J., Lee, J.H., Lee, J., Kim, J.B., 2009. IRE-1 and HSP-4 contribute to energy homeostasis via fasting-induced lipases in C. elegans. Cell Metab. 9 (5), 440–448.

Jones, K.T., Greer, E.R., Pearce, D., Ashrafi, K., 2009. Rictor/TORC2 regulates Caenorhabditis elegans fat storage, body size, and development through sgk-1. PLoS Biol. 7 (3), e1000060.

Kalyuzhny, A.E., Wessendorf, M.W., 1998. Relationship of µ-and δ-opioid receptors to GABAergic neurons in the central nervous system, including antinociceptive brainstem circuits. J. Comp. Neurol. 392 (4), 528–547.

Kang, J.G., Park, C.Y., 2012. Anti-obesity drugs: a review about their effects and safety. Diabetes Metab. J. 36 (1), 13–25.

Katz, M.L., Robison, W.G., 2002. What is lipofuscin? Defining characteristics and differentiation from other autofluorescent lysosomal storage bodies. Arch. Gerontol. Geriatr. 34 (3), 169–184.

Kimura, K.D., Tissenbaum, H.A., Liu, Y., Ruvkun, G., 1997. Daf-2, an insulin receptor-like gene that regulates longevity and diapause in Caenorhabditis elegans. Science 277 (5328), 942–946.

Le, T.T., Duren, H.M., Slipchenko, M.N., Hu, C.D., Cheng, J.X., 2010. Label-free quantitative analysis of lipid metabolism in living Caenorhabditis elegans. J. Lipid Res. 51 (3), 672–677.

Lee, H.J., Zhang, W., Zhang, D., Yang, Y., Liu, B., Barker, E.L., et al., 2015. Assessing cholesterol storage in live cells and C. elegans by stimulated Raman scattering imaging of phenyl-diyne cholesterol. Sci. Rep., 5.

Lemieux, G.A., Ashrafi, K., 2015. Insights and challenges in using C. elegans for investigation of fat metabolism. Crit. Rev. Biochem. Mol. Biol. 50 (1), 69–84.

Leung, B., Hermann, G.J., Priess, J.R., 1999. Organogenesis of the Caenorhabditis elegans intestine. Dev. Biol. 216 (1), 114–134.

Littleton, B., Kavanagh, T., Festy, F., Richards, D., 2013. Spectral interferometric implementation with passive polarization optics of coherent anti-Stokes Raman scattering. Phys. Rev. Lett. 111 (10), 103902.

Markaki, M., Tavernarakis, N., 2010. Modeling human diseases in Caenorhabditis elegans. Biotechnol. J. 5 (12), 1261–1276.

McKay, R.M., McKay, J.P., Avery, L., Graff, J.M., 2003. C. elegans: a model for exploring the genetics of fat storage. Dev. Cell 4 (1), 131–142.

Mukhopadhyay, A., Tissenbaum, H.A., 2007. Reproduction and longevity: secrets revealed by C. elegans. Trends Cell Biol. 17 (2), 65–71.

Mullaney, B.C., Ashrafi, K., 2009. C. elegans fat storage and metabolic regulation. Biochim. Biophys. Acta 1791 (6), 474–478.

Munn, D.H., Zhou, M., Attwood, J.T., Bondarev, I., Conway, S.J., Marshall, B., et al., 1998. Prevention of allogeneic fetal rejection by tryptophan catabolism. Science 281 (5380), 1191–1193.

Odorizzi, G., Cowles, C.R., Emr, S.D., 1998. The AP-3 complex: a coat of many colours. Trends Cell Biol. 8 (7), 282–288.

O'Rourke, E.J., Soukas, A.A., Carr, C.E., Ruvkun, G., 2009. C. elegans major fats are stored in vesicles distinct from lysosome-related organelles. Cell Metab. 10 (5), 430–435.

Perez, C.L., Van Gilst, M.R., 2008. A 13C isotope labeling strategy reveals the influence of insulin signaling on lipogenesis in C. elegans. Cell Metab. 8 (3), 266–274.

Popkin, B.M., Kim, S., Rusev, E.R., Du, S., Zizza, C., 2006. Measuring the full economic costs of diet, physical activity and obesity-related chronic diseases. Obesity Rev. 7 (3), 271–293.

Rucker, D., Padwal, R., Li, S.K., Curioni, C., Lau, D.C., 2007. Long term pharmacotherapy for obesity and overweight: updated meta-analysis. BMJ 335 (7631), 1194–1199.

Russell, W.M.S., Burch, R.L., 1959. The Sources, Incidence and Removal of Inhumanity. Methuen, London.

Sasaki, T., Mizuguchi, S., Honda, K., 2012. Growth inhibitory effects of anthranilic acid and its derivatives against Legionella pneumophila. J. Biosci. Bioeng. 113 (6), 726–729.

Schmitz, G., Grandl, M., 2009. Endolysosomal phospholipidosis and cytosolic lipid droplet storage and release in macrophages. Biochim. Biophys. Acta 1791 (6), 524–539.

Schmökel, V., Memar, N., Wiekenberg, A., Trotzmüller, M., Schnabel, R., Döring, F., 2016. Genetics of lipid-storage management in Caenorhabditis elegans embryos. Genetics 202 (3), 1071–1083.

Schroeder, L.K., Kremer, S., Kramer, M.J., Currie, E., Kwan, E., Watts, J.L., et al., 2007. Function of the Caenorhabditis elegans ABC transporter PGP-2 in the biogenesis of a lysosome-related fat storage organelle. Mol. Biol. Cell 18 (3), 995–1008.

Seegmiller, A.C., Dobrosotskaya, I., Goldstein, J.L., Ho, Y.K., Brown, M.S., Rawson, R.B., 2002. The SREBP pathway in Drosophila: Regulation by palmitate, not sterols. Dev. Cell 2 (2), 229–238.

Singh, R., Kaushik, S., Wang, Y., Xiang, Y., Novak, I., Komatsu, M., et al., 2009. Autophagy regulates lipid metabolism. Nature 458 (7242), 1131–1135.

Srinivasan, S., Sadegh, L., Elle, I.C., Christensen, A.G., Faergeman, N.J., Ashrafi, K., 2008. Serotonin regulates C. elegans fat and feeding through independent molecular mechanisms. Cell Metab. 7 (6), 533–544.

Steiner, R.F., Kirby, E.P., 1969. Interaction of the ground and excited states of indole derivatives with electron scavengers. J. Phys. Chem. 73 (12), 4130–4135.

Vrablik, T.L., Petyuk, V.A., Larson, E.M., Smith, R.D., Watts, J.L., 2015. Lipidomic and proteomic analysis of Caenorhabditis elegans lipid droplets and identification of ACS-4 as a lipid droplet-associated protein. Biochim. Biophys. Acta 1851 (10), 1337–1345.

Wählby, C., Conery, A.L., Bray, M.A., Kamentsky, L., Larkins-Ford, J., Sokolnicki, K.L., et al., 2014. High-and low-throughput scoring of fat mass and body fat distribution in C. elegans. Methods 68 (3), 492–499.

Wang, Y., Beydoun, M.A., Liang, L., Caballero, B., Kumanyika, S.K., 2008a. Will all Americans become overweight or obese? Estimating the progression and cost of the US obesity epidemic. Obesity 16 (10), 2323–2330.

Wang, P., Liu, B., Zhang, D., Belew, M.Y., Tissenbaum, H.A., Cheng, J.X., 2014. Imaging lipid metabolism in live Caenorhabditis elegans using fingerprint vibrations. Angew. Chem. Int. Ed. 53 (44), 11787–11792.

Wang, M.C., Min, W., Freudiger, C.W., Ruvkun, G., Xie, X.S., 2011. RNAi screening for fat regulatory genes with SRS microscopy. Nat. Met. 8 (2), 135–138.

Wang, M.C., O'Rourke, E.J., Ruvkun, G., 2008b. Fat metabolism links germline stem cells and longevity in C. elegans. Science 322 (5903), 957–960.

Watts, J.L., 2002. Genetic dissection of polyunsaturated fatty acid synthesis in Caenorhabditis elegans. Proc. Natl. Acad. Sci. USA 99 (9), 5854–5859.

Williams, G., 2010. Withdrawal of sibutramine in Europe. BMJ 340, c824.

Wilson-Sanders, S.E., 2011. Invertebrate models for biomedical research, testing, and education. ILAR J. 52 (2), 126–152.

Wood, W.B., 1987. The nematode *Caenorhabditis elegans*. Cold Spring Harb. Lab.

Wurpel, G.W., Schins, J.M., Müller, M., 2002. Chemical specificity in three-dimensional imaging with multiplex coherent anti-Stokes Raman scattering microscopy. Opt. Lett. 27 (13), 1093–1095.

Xu, N., Zhang, S.O., Cole, R.A., McKinney, S.A., Guo, F., Haas, J.T., et al., 2012. The FATP1-DGAT2 complex facilitates lipid droplet expansion at the ER-lipid droplet interface. J. Cell Biol. 198 (5), 895–911.

Yen, K., Le, T.T., Bansal, A., Narasimhan, S.D., Cheng, J.X., Tissenbaum, H.A., 2010. A comparative study of fat storage quantitation in nematode *Caenorhabditis elegans* using label and label-free methods. PLoS One 5 (9), e12810.

Zhang, S.O., Box, A.C., Xu, N., Le Men, J., Yu, J., Guo, F., et al., 2010a. Genetic and dietary regulation of lipid droplet expansion in *Caenorhabditis elegans*. Proc. Natl. Acad. Sci. USA 107 (10), 4640–4645.

Zhang, S.O., Trimble, R., Guo, F., Mak, H.Y., 2010b. Lipid droplets as ubiquitous fat storage organelles in *C. elegans*. BMC Cell Biol. 11 (1), 1.

Zheng, J., Greenway, F.L., 2012. *Caenorhabditis elegans* as a model for obesity research. Int. J. Obes. 36 (2), 186–194.

Animal Models for Manipulation of Thermogenesis

John-Paul Fuller-Jackson, Iain J. Clarke, Belinda A. Henry

Monash Biomedical Discovery Institute, Monash University, Clayton, VIC, Australia

1 INTRODUCTION

Metabolic function is a highly regulated process and, as for all physiological systems, it is governed by feedforward and feedback signals that maintain homeostatic balance. This metabolic balance is controlled by neuronal systems in the brain that regulate food intake and energy expenditure. Feedforward signals are provided by upregulation of orexigenic factors and downregulation of anorexigenic factors, to increase food intake and decrease energy expenditure. In response to starvation or reduced food intake, the activity of the orexigenic neurons, neuropeptide Y (NPY), and agouti-related protein (AgRP) increase and the activity of the anorexigenic proopiomelanocortin (POMC) neurons decrease. Peripherally derived feedback factors influence these central systems, examples being ghrelin, glucagon-like peptide 1 (GLP1) (from the gastrointestinal tract), and leptin (from adipose tissue). Ghrelin stimulates food intake, whereas leptin and GLP-1 are inhibitory. Ghrelin

levels are increased in low body weight conditions and leptin levels are reduced, allowing for homeostatic correction via stimulation of hunger and a reduction in energy expenditure.

Whereas there is significant knowledge of the systems that regulate food intake, relatively less is known about the control of energy expenditure. The rate of energy expenditure is substantially driven by sympathetic outflow from the brain to the peripheral organs/tissues, such as brown fat and skeletal muscle. Dogma stipulates that factors which increase food intake concurrently reduce energy expenditure and vice versa. Thus, elevation of NPY activity in the brain and reduction in melanocortin activity leads to increased food intake and reduced energy expenditure. A number of studies over recent years have targeted regulation of the systems controlling food intake, as a means of combating the global escalation in the incidence of obesity and Type II diabetes. Historically, these have not been successful for various reasons. In some instances, pharmacological agents have been used,

but virtually all of these act within the brain and have been withdrawn because of side effects. A new generation of pharmaceuticals, such as Contrave, Liraglutide, and Qsymia, have, however, produced some promising weight-loss effects. Lifestyle diet and exercise programs have not been successful because individuals who lose weight eventually drift back to their prior body weight/adiposity. This is because of the inherent "set-point" of individuals that is genetically determined. According to this theory, predisposition to obesity is genetically programmed and is typically unmasked by a poor-quality diet (high fat and/or high sugar) or sedentary behavior. Examples of predisposition to an obese phenotype can be readily observed when rodents are placed on a "junk food" diet, so some animals become obese (diet-induced obesity, DIO) and others do not (diet resistant, DR). This is also shown in the classical studies of Bouchard et al. (1990), whereby overfeeding by 1000 cal/day for 100 days resulted in highly variable weight gain across sets of twins, whereas there was a strong correlation between twins. This demonstrates that genetic factors not only determine the set-point body weight but that this is at least partly mediated via innate differences in energy expenditure.

With systematic failure to control obesity by controlling food intake, an important question is whether energy expenditure targets are more fruitful. The latter has various components, which will be discussed later, but one potential target that could yield significant results is thermogenesis. It has been generally accepted that thermogenesis occurs primarily in brown adipose tissue (BAT), because the brown adipocytes are rich in mitochondria and express uncoupling protein 1 (UCP1) (Cannon and Nedergaard, 2004; Lowell and Spiegelman, 2000). Furthermore, BAT is highly vascularized and receives profuse innervation from the sympathetic nervous system (SNS) (Cannon and Nedergaard, 2004; Lowell and Spiegelman, 2000). Activation of UCP1 via an increase in sympathetic activity results in the dissipation of energy through heat production (Cannon and Nedergaard, 2004; Lowell and Spiegelman, 2000). It was originally thought that BAT was exclusively found in neonates, and levels diminished in early life reaching negligible levels in adults, but we now know that this is not the case. Landmark imaging studies in humans revealed the presence of BAT in the clavicular, neck, and sternal regions of the body (Cypess et al., 2009; van Marken Lichtenbelt et al., 2009; Virtanen et al., 2009) and, as a result, this has become a more prominent therapeutic target. Recent studies have shown that BAT mass can be regulated by environmental factors, such as cold temperature. In addition, a long list of regulators of mitochondria and UCP1 function in BAT have been assembled. While the targeting of BAT might be a realistic way of controlling obesity, another approach could be to determine whether thermogenesis occurs in other tissues, through means other than BAT/UCP1. This would open up the possibility of manipulating thermogenesis and expenditure of energy through heat on a much larger scale than by the specific focus on BAT. Recent studies have indicated three very significant advances in this regard. Firstly, BAT is not confined to very small and focal depots within the body and can be found interspersed in white adipose tissue (WAT) (Cypess et al., 2009; Henry et al., 2010; Symonds et al., 2012; van Marken Lichtenbelt et al., 2009; Virtanen et al., 2009). Secondly, brown adipocytes can be "created" via the "browning" of WAT (Barbatelli et al., 2010; Petrovic et al., 2010). Furthermore, thermogenesis occurs in muscle, which may provide another fruitful target for manipulation of energy expenditure.

In this chapter, we examine animal models which have utility for the study of energy expenditure, particularly thermogenesis, and we indicate means of manipulation of energy expenditure.

2 THERMOGENESIS—A SIGNIFICANT DETERMINANT OF ENERGY EXPENDITURE

2.1 Brown Fat

As detailed earlier, BAT is frequently regarded as the primary thermogenic organ (Cannon and Nedergaard, 2004, 2010). Brown adipocytes are thermogenic due to their mitochondrial rich nature and specialized expression of UCP1. Activation of BAT occurs via the SNS whereby increased sympathetic activity increases noradrenaline (NA) release at brown adipocytes, activating cAMP, and leading to the intracellular mobilization of free fatty acids (Fig. 12.1). It is the mobilization of free fatty acids that activates UCP1 and initiates thermogenesis (Fig. 12.1). In order to support this thermogenic function, BAT is profusely innervated by the SNS and is highly vascularized (Cannon and Nedergaard, 2004; Lowell and Spiegelman, 2000). Within the mitochondria, the electron transport chain creates a proton gradient that is required for ATP synthesis. When activated, UCP1 creates proton leakage across the inner-mitochondrial membrane, "stealing" protons from ATP synthase, which ultimately reduces ATP synthesis but increases energy expenditure through the production of heat. This basic theory underlying the process of thermogenesis has been widely studied.

2.1.1 Derivation of BAT

A number of studies have sought to define the embryonic lineage of BAT. This is based on the premise that increasing levels of BAT could be beneficial for the
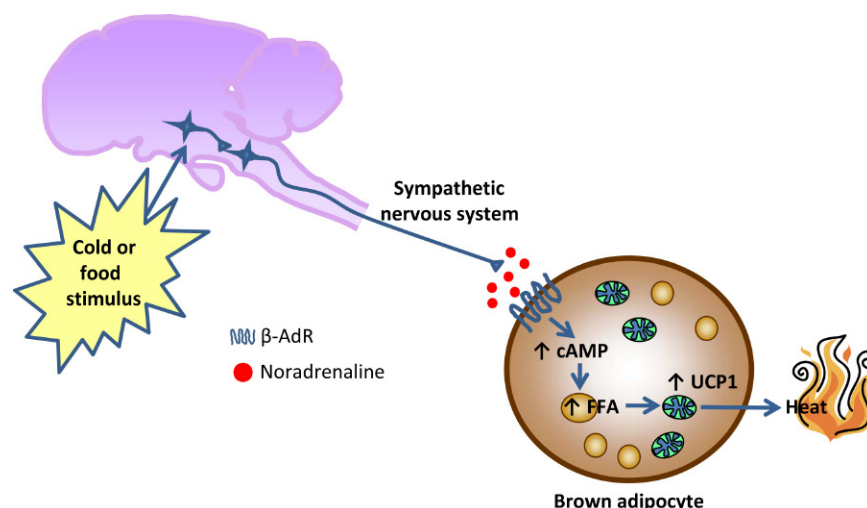
FIGURE 12.1 **The mechanism of brown fat activation and thermogenesis.** Dietary and cold stimuli are sensed by first-order neurons in the preoptic area and the hypothalamus. These stimuli are then relayed via the brainstem, causing activation of the sympathetic nervous system *(SNS)*. Activation of the SNS results in increased noradrenaline release within brown adipose tissue *(BAT)*, acting on β-adrenoceptors *(β-AdR)* located on brown adipocytes and activation of uncoupling protein 1 *(UCP1)*. The increase in UCP1 creates a proton leak across the mitochondrial membrane, uncoupling oxidative phosphorylation and leading to the dissipation of energy through thermogenesis.

development of novel antiobesity agents. Brown adipocytes are derived from a mesenchymal lineage similar to white adipocytes and myocytes (Kajimura et al., 2009; Seale et al., 2008). WAT and BAT are considered to be morphologically and functionally distinct tissues, but this requires revision as outlined later in the chapter. White adipocytes are unilocular, containing a single fat droplet and have few mitochondria, whereas the brown adipocyte is multilocular (containing many smaller lipid droplets) and contains numerous mitochondria. The primary function of white adipocytes is to store energy in the form of triglycerides, whereas brown adipocytes consume energy through the process of thermogenesis. In line with these differing functions, brown adipocytes are more closely related to myocytes than to white adipocytes. A "true" brown adipocyte is derived from a Myf-5 myocyte precursor, whereby the transcription factor PR-(PRD1-BF-1-RIZ1 homologous) domain containing protein 16 (PRDM-16) has been shown to inhibit myocyte development and enforce the development of brown adipocytes (Seale et al., 2008). Deletion of the gene that encodes PRDM-16 abolishes BAT development and results in skeletal muscle formation (Seale et al., 2008). A number of other factors also stimulate the expansion of BAT formation, including bone morphogenic protein 7 (BMP7), fibroblast growth factor 21 (FGF21), PPARγ and PGC1α agonists (Ahfeldt et al., 2012; Kajimura et al., 2009; Ohno et al., 2012; Schulz et al., 2011). PPARγ and PRDM16 exert synergistic effects via the CCAAT/enhancer-binding proteins (CEBPs) to promote BAT development (Lefterova et al., 2008). Overexpression of PRDM-16 in white subcutaneous fat results in the "browning" of WAT and the production of brown-like

adipocytes (see later). Although many studies have focused on increasing the *levels* of BAT to combat obesity, *activation* of BAT is also fundamentally important to this objective.

2.1.2 Neural Control of BAT

The SNS is integral to the activation of thermogenesis, whereby both cold and dietary stimuli increase thermogenesis via the localized release and action of NA. This effect is mediated via the β-adrenergic receptors (β-AdR) expressed by brown adipocytes. Indeed, all three isoforms of β-AdR are coexpressed in brown adipocytes and there is a general redundancy with regard to the control of thermogenesis (Collins et al., 2010). For example, gene deletion of all three β-AdR in the β-AdR-less mice causes obesity in the absence of hyperphagia and the obese phenotype is driven by a reduction in UCP1 and obliteration of thermogenesis (Bachman et al., 2002). The β-AdR-less mice show significant atrophy of BAT and an infiltration of white fat (Bachman et al., 2002). It has recently been shown, however, that under thermoneutral conditions chronic stress can increase BAT activity in the β-AdR-less mice (Razzoli et al., 2016). This stimulatory effect is independent of NA and is thought to be mediated via a purinergic SNS pathway (Razzoli et al., 2016). The neural network that governs the SNS and controls thermogenesis is complex. Injection of pseudorabies virus, a polysynaptic retrograde tracer, into the interscapular BAT of rats demonstrates that neurons arising from the preoptic area (POA), hypothalamus, and the brainstem all converge in an integrated network that projects to BAT (Oldfield et al., 2002). Neurons within the POA are essential to thermoregulation, receiving

information regarding ambient temperature upon skin cooling, and in turn exert effects on thermogenesis via a neuronal network involving the hypothalamus and brainstem. Overall, neurons within the POA activate BAT thermogenesis (Morrison and Nakamura, 2011). Earlier work identified a subset of cold-inhibited and warm-activated gamma-aminobutyric acid (GABA)-containing neurons in this region of the brain that mediate cold-induced activation of thermogenesis (Morrison et al., 2014; Nakamura and Morrison, 2008). These GABA-ergic neurons regulate BAT activity via projections to the dorsomedial hypothalamus (DMH) and the raphe pallidus (Cao and Morrison, 2006; Cao et al., 2004; Morrison et al., 2014; Nakamura et al., 2005). More recent work, using Designer Receptor Exclusivity Activated by Designer Drugs (DREADD) technology, however, shows that activation of GABA neurons in the POA had little effect on body temperature or energy expenditure (Yu et al., 2016). Indeed, the latter study provides strong evidence to suggest that leptin receptor-expressing neurons in the POA are central to the metabolic (food intake and energy expenditure) adaptations that occur in response to changes in ambient temperature (Yu et al., 2016). In addition to the POA, neural networks within the hypothalamus are known to be important in the dual control of food intake and energy expenditure.

Typically, neuropeptides that stimulate food intake also inhibit thermogenesis and vice versa (Verty et al., 2010). In this regard, the arcuate nucleus of the hypothalamus (ARC) is considered a primary center in the control of energy homeostasis. Within the ARC, two distinct neuronal populations regulate food intake and energy expenditure:

- The appetite-inhibiting cells, the POMC neurons, which produce melanocortins.
- The appetite-stimulating cells that contain NPY and agouti-related protein (AgRP).

NPY and AgRP inhibit thermogenesis (Billington et al., 1991; Small et al., 2003) and the melanocortins (α-, β-, and γ-melanocyte stimulating hormone encoded by the POMC gene) stimulate thermogenesis (Voss-Andreae et al., 2007). At least a subset of these neurons are located outside the blood brain barrier and therefore receive peripheral signals regarding nutritional state (Morita and Miyata, 2012); this includes endocrine signals, such as leptin, insulin, GLP-1, and ghrelin, as well as metabolic signals, such as glucose (Cone et al., 2001; Parton et al., 2007). The neurons of the ARC project to other hypothalamic regions, such as the lateral hypothalamus (LH), ventromedial hypothalamus (VMH), DMH, and the paraventricular nucleus (PVN), allowing for second order signaling (Gautron and Elmquist, 2011). In addition, signals, such as leptin can also cross the blood brain barrier and act

directly on neurons in hypothalamic nuclei beyond the ARC (Dhillon et al., 2006; Qi et al., 2010). In mice, leptin acts at the DMH to stimulate sympathetic output and increase BAT thermogenesis (Enriori et al., 2011; Simonds et al., 2014). Physiological studies and neural tracing studies have shown that neurons in the ARC and the LH (orexin—ORX and melanin-concentrating hormone—MCH neurons) are important in regulating not only food intake but also energy expenditure, especially thermogenesis (Pissios, 2009; Szekely et al., 2010). It is important to note that there are two ORX peptides (A and B), with approximately 50% sequence identity, produced by posttranslational processing of a single precursor protein. In a broad sense, ORX-A is thought to be more relevant to the control of energy homeostasis than ORX-B (Ferguson and Samson, 2003).

In rodents, intracerebroventricular (i.c.v.) infusion of ARC-derived peptides alters BAT thermogenesis. In particular, infusion of either NPY or AgRP stimulates food intake and inhibits thermogenesis in BAT, whereas infusion of the melanocortin, α-melanocyte stimulating hormone (α-MSH), inhibits food intake and stimulates thermogenesis in BAT (Voss-Andreae et al., 2007). Melanocortin action at both hypothalamic and nonhypothalamic sites (preganglionic cholinergic neurons of the SNS and parasympathetic nervous system) increases BAT thermogenesis (Berglund et al., 2014; Song et al., 2008). Furthermore, a recent study in male rats, showed that MC4R activation in the VMH with melanotan II (a nonspecific melanocortin receptor agonist) increased NA turnover and heat dissipation in skeletal muscle (Gavini et al., 2016), demonstrating that the melanocortin system regulates both BAT and muscle thermogenesis (discussed later). Retrograde labeling of neurons in the brain with pseudorabies virus tracers, which are transported across synapses, show that both NPY and POMC neurons project widely throughout the brain, especially the hypothalamus. Thus, BAT is under the control of hypothalamic neurons, through a polysynaptic network of neurons in the brain and ultimately through sympathetic outflow. NPY neurons project to a network in the hindbrain that controls sympathetic innervation to blood vessels within BAT, whereas POMC cells project directly to a neural network that innervates brown adipocytes (Oldfield et al., 2002). Studies in rodents have clearly elucidated a role for the melanocortins in the control of BAT thermogenesis and around 40% of POMC cells in the ARC coexpress virus when the polysynaptic retrograde tracer pseudorabies is injected into BAT (Oldfield et al., 2002). In rodents, central infusion of melanotan II increases BAT temperature (Song et al., 2008) and the melanocortin 4 receptor (MC4R) is expressed in numerous brain regions that constitute parts of a neuronal pathway that extend to BAT; these include the forebrain, hypothalamus, midbrain, and brainstem (Song et al., 2008). Thus, the central

melanocortin system is integral in the control of thermogenesis and this is exemplified in knockout mouse models for both POMC and MC4R (Butler and Cone, 2002; Butler et al., 2001); where impaired energy expenditure and thermogenesis is an important component leading to the obese phenotype.

As indicated earlier, neurons in the LH that produce ORX and MCH are also known to regulate thermogenesis. Both of these neuropeptides stimulate food intake, but exert differential effects in terms of the regulation of thermogenesis. Dichotomous findings have been obtained in studies of the effects of ORX on thermogenesis, which may be because ORX also regulates physical activity, and mutations in the ORX system (either the gene that encodes prepro-ORX or the ORX receptors) result in narcolepsy (Chemelli et al., 1999). Orexin also acts centrally to regulate food intake and energy expenditure, but these effects are thought to be secondary to those which regulate arousal and activity (Willie et al., 2001). Nevertheless, ORX neurons project into the brainstem and spinal cord and appear to be important in the regulation of thermogenesis (Marcus and Elmquist, 2005). In rats, around 30% of ORX-B and 50% of MCH neurons provide neural connections to the SNS innervating BAT (Adler et al., 2012). One study showed that blockade of the ORX-A receptor by i.c.v. infusion of the antagonist, SB-334867-A, increased BAT temperature in male rats, indicative of an endogenous effect of ORX to inhibit thermogenesis (Verty et al., 2010). This observation is, however, contradicted by a number of other studies, whereby i.c.v. infusion of ORX or direct injection into the rostral raphe pallidus increases BAT thermogenesis (Tupone et al., 2011). More recent work has also shown that deletion of orexin results in obesity and this is primarily caused by a deficit in thermogenesis due to diminished differentiation of brown adipocytes from preadipocytes (Mohammed et al., 2014; Sellayah et al., 2011). This clearly demonstrates that brain-derived ORX is important not only in the control of thermogenesis in adult animals but also in the embryonic development of BAT. It is clearly apparent that there is a complex neural network located within the hypothalamus that ultimately regulates sympathetic outflow and BAT function.

2.1.3 UCP1 Knockout Models—Alternative Pathways for Thermogenesis

Genetic models in mice have been used widely to characterize the cellular pathways that underpin thermogenesis in BAT, especially with respect to UCP1 function. As indicated earlier, cold and dietary stimuli act at the brain to activate the SNS, leading to an increase in the release of NA at BAT. Activated β-AdR on brown adipocytes, stimulates an increase in cAMP and the mobilization of intracellular free fatty acids. In turn, this activates UCP1 and adaptive thermogenesis (Cannon and Nedergaard, 2004; Lowell and Spiegelman, 2000). Rodent studies clearly support the notion that the level of activation of UCP1 is an important index of metabolic state and energy expenditure. Thus, physiological challenges that induce a state of negative energy balance, such as fasting and lactation inhibit UCP1 in BAT (Rothwell et al., 1984; Trayhurn and Jennings, 1988; Xiao et al., 2004). This is considered to be a part of the metabolic adaptation response, whereby UCP1 is reduced to inhibit energy expenditure and to restore energy balance. Accordingly, activation of UCP1 is an integral component of adaptive thermogenesis in rodents.

On this basis, it is hardly surprising that genetic deletion of UCP1 results in impaired tolerance to cold. On the other hand, it is surprising that some UCP1 knockout mice are not obese (Enerback et al., 1997). Neither do some UCP1-deficient mice display increased susceptibility to obesity when fed a high-fat diet (Enerback et al., 1997). One explanation for these observations is that UCP1 knockout mice have a compensatory increase in mitochondrial proton leakage within skeletal muscle, which prevents the development of an obese phenotype (Monemdjou et al., 2000). There is, however, no underpinning mechanism that may account for this altered muscle function, although, potential regulators of skeletal muscle thermogenesis have been identified (see later). More recent work in UCP1 knockout mice clearly demonstrates that ambient temperature is a predominant factor in the manifestation of an obese phenotype in this animal model (Feldmann et al., 2009). Previous studies (Enerback et al., 1997) housed animals below thermoneutral conditions and it is thought that increased energy expenditure, to maintain core body temperature, concealed the effects of UCP1 gene deletion on body weight. Recent work in animals housed at thermoneutrality show, however, that deletion of the UCP1 gene causes obesity in animals fed both chow and high-fat diet (Feldmann et al., 2009).

Ablation of BAT in mice has been achieved with the UCP-diphtheria toxin A chain (UCP-DTA) transgene, whereby a BAT-specific promoter was used to drive expression of DTA and reduce BAT levels; this causes marked effects on body weight and adiposity. UCP-DTA mice display reduced oxygen consumption at baseline and in response to stimulation with a β3-AdR-ligand (Klaus et al., 1998; Lowell et al., 1993). Thus, ablation of BAT by these means may have a greater effect on thermogenesis, body weight, and adiposity than seen in animals with global UCP1 KO. This suggests that mechanisms other than UCP1 in BAT may be operative in the retention of thermogenic function in UCP1 knockout animals. One possibility may be the activation of uncoupling protein-3 (UCP3), a factor that has more widespread distribution than its analog, UCP1. Indeed, allelic variation in intron 1 of the gene that encodes

UCP3 can impact on thermogenesis, cold tolerance, and the propensity to obesity. Thus, work in hamsters demonstrated an allelic variation in intron 1 that impacts on UCP3 expression in BAT and not in skeletal muscle. Impaired UCP3 expression in BAT reduces cold tolerance (Nau et al., 2008), and results in increased body weight in both males and females (Fromme et al., 2009). This suggests that, although UCP1 in BAT of rodents is integral to the control of body weight, it may not be the sole mediator of BAT function and other proteins, such as UCP3 may also be important, at least in hamsters.

2.1.4 BAT and Thermogenesis in Humans

As early as 1981, studies demonstrated the presence of multilocular adipose tissue and increased expression of mitochondrial markers within adipose tissue of the interscapular region of Scandinavian outdoor workers, in comparison to indoor workers (Huttunen et al., 1981), suggesting the presence of BAT in the former. The evolution of techniques using positron-electron tomography (PET)-scanning to measure fluorodeoxyglucose (FDG) uptake enabled the collection of the unequivocal evidence for functional and active BAT in at least some adult humans. PET-scanning has shown pockets or islands of adipose tissue that display high metabolic activity via increased FDG uptake, consistent with the presence of brown adipocytes (Cypess et al., 2009; Nedergaard et al., 2007; van Marken Lichtenbelt et al., 2009; Virtanen et al., 2009). These regions of metabolically active adipose tissue are located around the neck, clavicular, sternal, and paraspinal regions (Fig. 12.2), as verified by UCP1 expression in biopsies. The incidence of active BAT under warm conditions is unsurprisingly low, being less than 10% (Au-Yong et al., 2009; Cypess et al., 2009) but in protocols using mild cold exposure, the presence of functional BAT is found in up to 95% of subjects (Saito et al., 2009; van Marken Lichtenbelt et al., 2009). Nonetheless, biopsies of the fat tissue taken from the neck region in subjects who are not positive for BAT on PET-scanning still show higher expression of UCP1 and β3-Adr when compared to subcutaneous fat (Lee et al., 2011b). Thus, the incidence of functional BAT is likely to be underestimated by PET scanning. Even in the absence of demonstrable UCP1 expression, it has been shown in vitro that adipose samples from the neck region contain precursor cells for BAT and that brown adipocyte formation can be induced under tissue culture conditions (Lee et al., 2011a). Thus, it is now indisputable that BAT exists in adult humans and is likely to play a role in energy expenditure.

Various factors alter BAT thermogenesis including cold, age, adiposity, and a variety of metabolic hormones. Whereas BAT activity increases in response to cold exposure, the incidence of functional BAT is inversely related to levels of adiposity, BMI, and age
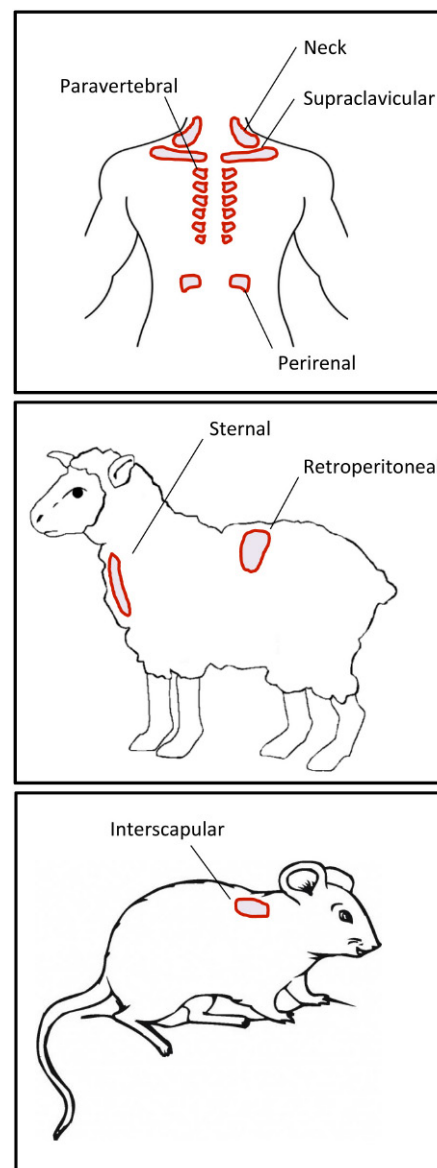
FIGURE 12.2　Distribution of BAT in humans, sheep, and rodents. Humans and sheep have brown adipocytes interspersed among white adipose tissue. In humans, brown adipocytes are primarily found in the neck, supraclavicular, and paraspinal regions. In sheep, UCP1 expression is abundant in sternal and retroperitoneal adipose tissue, which indicates that these fat depots are enriched in brown adipocytes. In contrast, rodents contain a defined brown fat depot, which is located in the interscapular region.

(Cypess et al., 2012, 2009; van Marken Lichtenbelt et al., 2009). In lean subjects (BMI <25); moderate cold exposure at 16°C activates BAT in virtually all subjects (97%), but with increasing age and adiposity the ability for cold to activate BAT is reduced (Orava et al., 2011; Ouellet et al., 2012; Saito et al., 2009; Virtanen et al., 2009; Yoneshiro et al., 2011b). Indeed, weight loss in morbidly obese subjects can increase the incidence of active BAT, although this is a moderate effect (Vijgen et al., 2012). Thus, variation in the levels of functional BAT may

determine the susceptibility of an individual to become obese and may influence the rate of weight gain associated with aging.

The amount of BAT is higher in neonates and declines across childhood, but may increase again across the pubertal transition (Gilsanz et al., 2012). This is, however, sex-dependent, being greater in males than in females. This sexual dimorphism relates to changes in muscle mass, so that males gain greater muscle and BAT mass across puberty (Gilsanz et al., 2012; Hu and Gilsanz, 2011). This observation is consistent with the derivation of BAT and the observation that myocytes and brown adipocytes share a common embryonic precursor (see earlier). In spite of the greater increase in BAT levels in males across puberty, female adults have greater BAT mass than males (Hu and Gilsanz, 2011). Accordingly, it has been hypothesized that gender differences in BAT activity are determined by sex differences in the levels of androgens, estrogens, and progesterone. Indeed, there is a reduction in BAT activity associated with the decline in estrogen levels in women that occurs at menopause (Quarta et al., 2012). In rodents, androgens induce weight gain and obesity (Clegg et al., 2006; Mauvais-Jarvis, 2011; McInnes et al., 2006; Moverare-Skrtic et al., 2006) whereas estrogen protects against this (Clegg et al., 2006; Mauvais-Jarvis, 2011). This may be partly mediated by the effects of sex steroids on thermogenesis (Clarke et al., 2012a; Quarta et al., 2012). Specifically, 17β-estradiol acts at estrogen receptor (ER) α expressing neurons within the VMH to increase BAT thermogenesis (Martinez de Morentin et al., 2014; Xu et al., 2011). In sheep, testosterone reduces thermogenesis in males but not females (Clarke et al., 2012a), clearly exemplifying sexual dimorphism in energy expenditure. The endocrine control of thermogenesis in humans is relatively unexplored, but insulin and thyroid hormone are known to increase glucose uptake in BAT (Orava et al., 2011). Other recent studies in humans have suggested that BAT may be an important buffering tissue to control glycaemia (Lee et al., 2016; Poher et al., 2015). Indeed, DIO causes insulin resistance in BAT of mice (Roberts-Toler et al., 2015). Additional endocrine factors that regulates BAT activity in humans are thought to include irisin, FGF21, and bone morphogenic proteins (BMPs) (Celi et al., 2015; Sidossis and Kajimura, 2015). In order to exploit BAT thermogenesis in the development of antiobesity therapies, it will be imperative to understand the endocrine control of this specialized tissue.

2.2 BAT and Thermogenesis in White Adipose Tissue

Whereas mice and rats maintain circumscribed brown fat depots that endure into adulthood, the majority of mammalian species exhibit brown adipocytes interspersed within white adipose beds (Nedergaard et al., 2010; Symonds et al., 2012) (Fig. 12.2). As indicated earlier, at least a proportion of humans display adipose tissue beds within the neck, clavicular, and paraspinal regions that are abundant in brown adipocytes and BAT-precursor cells (Cypess et al., 2009; van Marken Lichtenbelt et al., 2009; Virtanen et al., 2009). Similarly, sheep do not have a defined brown fat depot, but have regions of adipose tissue that are rich in UCP1, indicating the presence of brown adipocytes within these sites (Fig. 12.2). In lambs, UCP1 is highly expressed in the sternal, clavicular, pericardial, and retroperitoneal adipose depots. Temperature profiling in adipose depots of adult sheep indicates site-specific thermogenic differences, such that retroperitoneal fat exhibits greater thermogenic potential than subcutaneous gluteal fat (Henry et al., 2008). Typically basal temperature and UCP1 mRNA levels are lower in gluteal fat than in retroperitoneal fat (Henry et al., 2008, 2010). Furthermore, central administration of leptin or peripheral administration of estrogen increases heat production in peripheral tissues, indicative of thermogenesis (Clarke et al., 2013; Henry et al., 2008), and these stimulatory effects are greater in retroperitoneal fat than subcutaneous gluteal fat (Clarke et al., 2013; Henry et al., 2008). This suggests that diffuse adipose beds are thermogenic, most likely due to brown adipocytes interspersed among WAT. White adipocytes express UCP2 (a homolog of UCP1) and although initial reports suggested that this homolog could uncouple oxidative phosphorylation in mitochondria in vitro, this has not been replicated in vivo (Fleury et al., 1997). Indeed, rectal temperature is not altered in UCP2-deficient mice, consistent with a lack of effect on thermogenesis (Abdelhamid et al., 2014). WAT only displays thermogenic properties when UCP1 is overexpressed in adipocytes (Kopecky et al., 1995) or through the recruitment of brown-like adipocytes (described later in the chapter).

2.3 "Browning" of White Adipose Tissue

The recent description of beige or brite (brown in white) cells (Barbatelli et al., 2010; Petrovic et al., 2010) casts further complexity on the role of fat cells in thermogenesis. Beige cells are distinct from true brown fat cells, since they are not derived from the myf-5 lineage. In fact, beige cells are brown-like adipocytes that can be recruited in typically white fat depots and are most prevalent in subcutaneous fat (Barbatelli et al., 2010; Petrovic et al., 2010; Seale et al., 2011). Beige cells express essential thermogenic machinery, including UCP1 and PGC1α. Overexpression of PRDM-16 increases beige recruitment in subcutaneous fat of mice, leading to increased energy expenditure and relative protection against DIO (Seale et al., 2011). In addition to genetic manipulations, a number of physiological processes including β-adrenergic

stimulation and cold exposure, increase recruitment of beige cells within WAT. In rodents, exercise induces the recruitment of beige adipocytes, but data are lacking on the occurrence of this particular process in humans (Bostrom et al., 2012; Norheim et al., 2014; Stanford et al., 2015; Sutherland et al., 2009; Trevellin et al., 2014). The beige cell is morphologically distinct to both white and brown adipocytes and displays an intermediate phenotype, containing more mitochondria than white fat cells and being paucilocular, in that they do not contain a single fat droplet, but rather multiple droplets. Beige cells express PRDM-16, PGC1α, and UCP1, and recent studies have also identified short stature homeobox2 (Shox2), homeobox C9 (Hoxc9), Tmem26, Tbx1, and Cited1 as beige-specific markers (Lidell et al., 2013; Petrovic et al., 2010; Sharp et al., 2012; Walden et al., 2012; Wu et al., 2012). Although beige cells are derived from a different lineage to brown adipocytes, both are capable of utilizing energy, so that increasing the recruitment of beige cells has become a popular means of weight-loss therapy (Ishibashi and Seale, 2010). Importantly, beige cells are derived from bipotential precursors in that the precursors can develop into beige cells in response to cold or SNS stimulation (Jia et al., 2016; Lee et al., 2014b), or alternatively can become white adipocytes in response to a high-fat diet (Lee et al., 2012). To date, the majority of work investigating beige cells has been carried out in rodents and there are relatively few translational studies. In humans, beige cells have been identified in WAT depots (Jespersen et al., 2013; Sidossis et al., 2015) and adipose tissue of the neck and supraclavicular regions contain white, brown, and beige adipocytes (Jespersen et al., 2013).

It has long been thought that the beneficial effects of exercise are greater than the immediate energy spent during a bout of physical activity. In response to exercise the skeletal muscle of mice secretes irisin, a myokine that acts to increase beige cell recruitment in subcutaneous adipose tissue (Bostrom et al., 2012). Furthermore, in vivo treatment with irisin increases energy expenditure without any associated effect on food intake or physical activity (Bostrom et al., 2012). Irisin also improves glucose kinetics in DIO mice (Bostrom et al., 2012). Within adipocytes, irisin acts via the ERK and MAPK pathways to induce expression of the key thermogenic regular, PGC-1α (Zhang et al., 2014), but the cognate receptor for irisin has not been identified (Xie et al., 2015). Initial work produced contradictory findings in humans as irisin levels were not changed by exercise (Raschke et al., 2013). More recently, the use of tandem mass spectrometry has shown that irisin is indeed secreted by human skeletal muscle in response to exercise (Jedrychowski et al., 2015). In addition to irisin, in mice, meteorin-like hormone (metrnl) is increased in muscle in response to exercise and in adipose tissue

in response to cold-exposure (Rao et al., 2014). Metrnl acts via an eosinophil-dependent increase in interleukin 4, which promotes browning of WAT (Rao et al., 2014). There are no equivalent data in larger mammals on the effects of metrnl on thermogenesis. To date, studies in humans have failed to demonstrate any effect of exercise to induce "browning" or to recruit beige cells in white adipose depots (Hew-Butler et al., 2015; Scharhag-Rosenberger et al., 2014; Vosselman et al., 2015). Indeed, the physiological and pharmacological factors that may contribute to the recruitment of beige cells in humans remains largely unknown.

FGF21 is secreted from the liver and is upregulated in response to starvation. FGF21 induces the expression of thermogenic genes in WAT in mice (Fisher et al., 2012). The mechanistic link between FGF21 and BAT appears to be twofold, through the FGF receptor 1 and its coreceptor β-klotho (Yie et al., 2009), and via the SNS (Douris et al., 2015). At the cellular level, this leads to increased UCP1 expression and oxidative metabolism, as well as a systemic decrease in serum glucose and lipids, the latter being partially attributed to FGF21's induction of adiponectin secretion (Fisher et al., 2012; Holland et al., 2013; Kolumam et al., 2015; Lin et al., 2013). In humans, irisin and FGF21 are considered to be important in cold-induced activation of BAT thermogenesis (Lee et al., 2014a). Pharmacological administration of FGF21 causes weight loss and reverses insulin resistance, dyslipidaemia, and hepatic steatosis in rodent models of obesity (Xu et al., 2009; Zhang et al., 2013). In nonhuman primates, higher levels of endogenous FGF21 expression were associated with resistance to HFD (Nygaard et al., 2014). Initially this weight loss was thought to be primarily mediated via browning of WAT and the activation of BAT (Lee et al., 2015), since treatment with a long-acting FGF21 analog increased UCP1 in BAT and increased beige cell recruitment in inguinal fat (Talukdar et al., 2016), without accompanying changes in food intake. Nonetheless, FGF21 treatment causes equivalent weight loss in UCP1 knockout mice (Samms et al., 2015; Veniant et al., 2015), so the mechanisms of FGF21-induced weight loss remain unknown. Nonetheless, browning of WAT has clear beneficial metabolic effects via increasing energy expenditure and modulating glucose metabolism (Lee and Greenfield, 2015). It now becomes important to identify physiological and pharmacological means to either activate BAT or to induce functional beige cell formation in humans.

2.4 Skeletal Muscle

The notion that skeletal muscle is thermogenic has been contentious, largely due to the conflicting data across species. The brain provides a metabolic link to skeletal muscle via the SNS (Braun and Marks, 2011)

and this is likely to control thermogenic output (Henry et al., 2008). Mammalian skeletal muscle expresses both UCP2 and UCP3, with the latter being most abundant (10-fold higher than UCP2) (Clarke et al., 2012a; Henry et al., 2011). In addition, avian species do not possess UCP1 but retain an avian UCP (aUCP), which is expressed in skeletal muscle and shows greatest homology with mammalian UCP3 (Argyropoulos and Harper, 2002). Initial in vitro studies clearly demonstrate that UCP3 can uncouple oxidative phosphorylation in isolated mitochondria (Gong et al., 1997). Along with mitochondrial uncoupling, cellular pathways, such as futile calcium cycling and myosin-ATP turnover have also been suggested to underpin thermogenesis in skeletal muscle (Tseng et al., 2010). Here we review evidence for skeletal muscle thermogenesis in rodents, sheep, and humans.

2.4.1 Rodents

Studies investigating thermogenesis in skeletal muscle of rodents have produced conflicting data and it is generally considered that BAT is the primary or "sole" tissue capable of thermogenesis in such species (Cannon and Nedergaard, 2004, 2010). This consensus is challenged by consideration of the role of UCP3 in skeletal muscle. In mice, 3,4-methylenedioxymethamphetamine (MDMA or ecstasy)-induced hyperthermia is associated with an increase in UCP3 levels in skeletal muscle (Mills et al., 2003), indicative of a role for UCP3 in the control of thermogenesis and the regulation of body temperature. Initial gene knockout studies reported that ablation of the gene that encodes UCP3 attenuates cold tolerance but animals do not display a metabolic phenotype; these animals do not gain weight when fed a normal chow diet (Gong et al., 2000). Further studies implicated UCP3 in the maintenance of body weight in animals fed a high-fat diet as transgenic mice with overexpression of UCP3 in skeletal muscle were resistant to DIO (Tiraby et al., 2007). Ablation of UCP3 increases the propensity to weight gain when mice are fed a high-fat diet (Costford et al., 2008). Thus, a role for UCP3 in mediating thermogenesis and energy expenditure is unmasked when mice are exposed to an obesogenic diet.

In spite of the genetic studies, physiological studies have produced conflicting data. In vivo studies indicate that UCP3 levels typically reflect peripheral fatty acids and not the state of uncoupling or changes in energy expenditure. A good example of this is the effect of fasting on UCP3 expression. The catabolic state induced by fasting is associated with an increase in free fatty acids and also an increase in UCP3, which does not reflect the drive to conserve energy in states of negative energy balance (Cadenas et al., 1999). This contrasts with the demonstration that fasting reduces UCP1 expression in BAT consistent with the effort to conserve energy. The discordance between negative energy balance and UCP3 expression/function is not, however, always apparent. Lactation induces a catabolic state and this occurs in association with reduced UCP3 levels in skeletal muscle (Xiao et al., 2004). To further add complexity, changes in UCP3 levels in rodents often do not correlate to altered mitochondrial function (Cadenas et al., 1999). Deletion of the UCP1 gene increases UCP3 expression in skeletal muscle in cold-adapted animals, which suggests that a compensatory increase in the latter may improve cold tolerance in UCP1 knockout mice (Shabalina et al., 2010). In spite of this, the increase in UCP3 is not associated with an increase in uncoupled respiration in the skeletal muscle of UCP1 knockout animals (Shabalina et al., 2010). Furthermore, it has been suggested that any thermogenic potential of skeletal muscle in mice is derived from brown adipocytes interspersed among the muscle fibers (Almind et al., 2007). Indeed, stripping muscle tissue of these interspersed brown adipocytes is thought to abolish any thermogenic potential of muscle tissue (Almind et al., 2007). Although, more recent work has shown that isolated muscle fibers retain the ability to produce heat, but this occurs via calcium cycling (see later in the chapter) (Barclay, 2012). Thus in rodents, UCP3 may not be an important determinant in driving skeletal muscle thermogenesis. However, this may not be the case in larger mammals, such as sheep or humans and role for UCP3 in muscle thermogenesis will be discussed in detail later.

In general thermogenesis is thought to be due to altered mitochondrial function, whereby there is a switch that results in an increase in uncoupled or state 4 respiration. In skeletal muscle, however, additional metabolic and cellular pathways have been linked to heat production and energy expenditure (Kusminski and Scherer, 2012).

2.4.1.1 AMP-ACTIVATED PROTEIN KINASE

AMP-activated protein kinase (AMPK) is a metabolic fuel sensory kinase. Its primary function is the determination of the relative degree of glucose utilization and fatty acid oxidation; activation of AMPK in the skeletal muscle increases glucose utilization, fatty acid oxidation, and mitochondrial biogenesis (Kusminski and Scherer, 2012). Apart from this, phosphorylation of AMPK has been linked to an increase in muscle thermogenesis in rodents. Thus, administration of 3,5-diiodo-L-thyronine (T2) stimulates thermogenesis, associated with the activation of AMPK in skeletal muscle (Lombardi et al., 2008). Similarly, the A/J strain of mice, which is relatively resistant to DIO, displays associated elevated levels of AMPK activity and an increase in muscle thermogenesis (Kus et al., 2008). Other studies have linked the phosphorylation of AMPK to the thermogenic effect of leptin. Thus, leptin acts directly on mouse skeletal muscle to activate AMPK and to increase oxygen

consumption in vitro (Solinas et al., 2004). Other in vivo studies in mice show that peripheral and central administration of leptin activates AMPK (Minokoshi et al., 2002). In rats, the effect of direct application of leptin to phosphorylate AMPK in isolated muscle fibers is dependent on the fiber type, with activation occurring in white but not red fibers (Janovska et al., 2008). Thus, in rodents, various endocrine factors activate AMPK and this has been linked to skeletal muscle thermogenesis. This contrasts to the work in sheep, showing that a central infusion of leptin does not phosphorylate AMPK (Laker et al., 2011), but increases skeletal muscle thermogenesis (Henry and Clarke, 2008; Henry et al., 2008, 2011). Furthermore, direct infusion of AICAR into the femoral artery of ovariectomized ewes phosphorylates AMPK in skeletal muscle, but does not alter heat production (Henry et al., 2011). Hence, although the activation of AMPK has been linked to skeletal muscle thermogenesis in rodents, the same does not appear to be true for larger mammals, such as sheep.

2.4.1.2 FUTILE CALCIUM CYCLING

Calcium cycling occurs across the sarcoplasmic reticulum (SR) membrane in skeletal muscle and involves the ryanodine type 1 receptor (RyR1) and the sarco/endoplasmic reticulum calcium-dependent ATPases (SERCA). Skeletal muscle expresses SERCA1 and SERCA2a subtypes. The RyR1 pumps calcium from within the SR into the cytosol of the myocyte and activating mutations of RyR1 cause malignant hyperthermia (Lanner, 2012). Increasing the cytosolic calcium concentration either through release from the SR or across the cell membrane (i.e., through neurotransmitter stimulated opening of sodium channels) leads to activation of SERCA (Arruda et al., 2007; de Meis et al., 2005). In order to maintain intracellular calcium homeostasis SERCA is activated to pump calcium back across the SR membrane, which is dependent on the hydrolysis of ATP; this drives heat production (thermogenesis). Central administration of leptin increases SERCA2a levels in the skeletal muscle of rodents (Ukropec et al., 2006), which would increase in thermogenesis driven by futile calcium cycling. In rodents, the endogenous regulator of SERCA, sarcolipin, has been clearly linked to thermogenesis, energy expenditure, and the regulation of body weight. Sarcolipin binds to SERCA, which uncouples calcium transport from the hydrolysis of ATP, leading to an increase in the futile cycling of calcium and heat production. In the absence of BAT (surgical removal) or UCP1 (genetic deletion), sarcolipin increases muscle thermogenesis and is essential for cold-adaptation (Bal et al., 2012; Rowland et al., 2016). In mice, overexpression of sarcolipin in skeletal muscle increases oxygen consumption and fatty acid oxidation, which is associated with a relative resistance to weight gain in animals fed a high-fat diet (Maurya et al., 2015). Current work is investigating futile calcium cycling as a mode of thermogenesis in skeletal muscle in larger mammals and it is clear that postprandial elevation in muscle temperature is associated with upregulation of both RyR1 and SERCA2a (Clarke et al., 2012b).

2.4.2 Sheep

Sheep are a useful and novel model for the investigation of thermogenesis in skeletal muscle for various reasons. Being a larger species, it is possible to implant temperature recording devices in multiple tissues and to obtain serial blood samples to analyze circulating hormones and metabolic factors concomitantly. In addition, photoperiod has a profound effect on energy balance and this is a useful experimental model. In contrast to rodents, BAT depots are relatively low in adult sheep, so any thermogenic output of this tissue may be due to mechanisms other than the activation of UCP1 (Henry et al., 2011; Symonds et al., 2012). Alternatively, a series of studies show that heat production in skeletal muscle can be programmed by meal feeding, as well as various endocrine factors including leptin and the sex steroids.

Sheep are grazing species and eat continuously so they do not typically display meal-associated rhythms that are evident in humans. Placing sheep on a meal-feeding regime, however, where they are subjected to temporal food restriction, entrains a meal-associated rhythm. A good example of this is the preprandial rise in ghrelin levels, which is an orexigenic hormone secreted from the abomasum. Meal feeding in sheep can entrain a preprandial elevation of circulating levels of ghrelin in sheep, as is seen in humans (Solomon et al., 2008; Sugino et al., 2002). Similarly, meal-feeding in sheep entrains a postprandial elevation in heat production in peripheral tissues including adipose tissue and skeletal muscle (Henry et al., 2008). The heat production elicited in skeletal muscle is driven by intracellular mechanisms. Simultaneous measurement of femoral artery blood flow and skeletal muscle temperature demonstrates that feeding-associated rise in temperature occurs without an associated change in tissue perfusion (Clarke et al., 2012b). The postprandial response appears to be elicited by mitochondrial uncoupling and futile calcium cycling pathways. In isolated mitochondria, feeding increases uncoupled respiration, but this occurrs in the absence of any major shift in the expression of UCP3 (Clarke et al., 2012b). On the other hand, feeding increased the level of expression of RyR1 (mRNA), as well as SERCA2a protein levels (Clarke et al., 2012b). This clearly demonstrates that feeding activates futile calcium cycling and this may be a primary mechanism for the dissipation of excess calories at the time of feeding. Further study is required to investigate the role of sarcolipin controlling SERCA function and muscle thermogenesis in sheep.
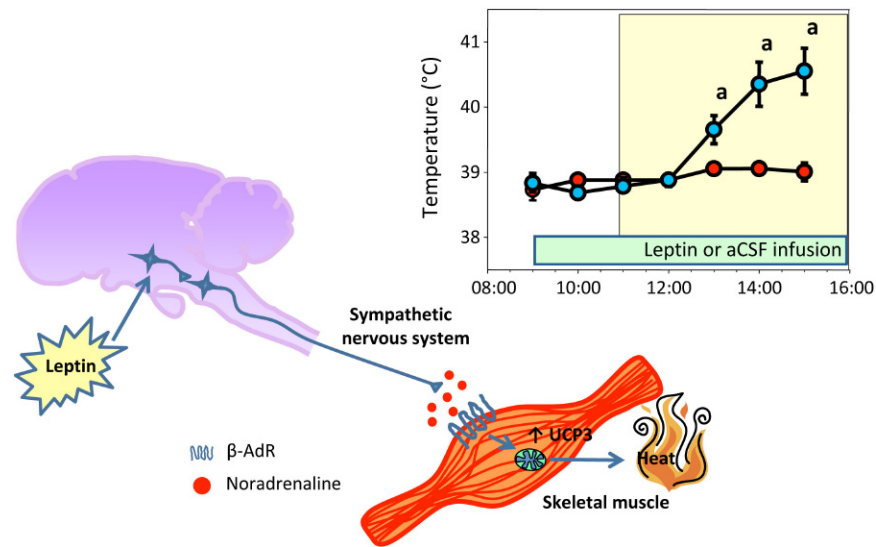
FIGURE 12.3 **Leptin acts at the brain to increase postprandial thermogenesis in skeletal muscle.** Intracerebroventricular infusion of lepton (*blue* symbols) increases heat production in skeletal muscle compared to control animals receiving artificial cerebrospinal fluid (*aCSF*: *red* symbols). Leptin-induced thermogenesis is associated with an increase in the expression of uncoupling protein 3 *(UCP3)* mRNA and protein in muscle. Thus, leptin acts win. The brain to increase sympathetic output resulting in increased noradrenaline release within muscle. Noradrenaline acts via the β-adrenergic system to increase UCP3 and activate thermogenesis. Feeding window is depicted by the *yellow* box. *β-AdR*, β-adrenoceptors. *Source: Adapted with permission from Henry, B.A., Dunshea, F.R., Gould, M., Clarke, I.J., 2008. Profiling postprandial thermogenesis in muscle and fat of sheep and the central effect of leptin administration. Endocrinology 149(4), 2019–2026.*

Central administration of leptin markedly enhances postprandial thermogenesis in skeletal muscle in sheep (Henry and Clarke, 2008; Henry et al., 2008, 2011) and this has been linked to altered mitochondrial function (Fig. 12.3). Indeed, the increase in skeletal muscle temperature in response to i.c.v. leptin treatment precedes any change in core body temperature, suggesting that the former drives the latter (Henry et al., 2008). Leptin-induced heat production is associated with an increase in UCP3 expression in skeletal muscle, without a coincident effect on UCP1 expression. Accordingly, postprandial heat production in muscle is unlikely to be due to increased thermogenesis within brown adipocytes interspersed among the muscle tissue. On the other hand, the increase in UCP3 levels supports the notion that myocytes are capable of thermogenesis via mitochondrial uncoupling. Indeed, uncoupled respiration is increased in mitochondria isolated from skeletal muscle of leptin-treated animals, in accordance with the biochemical hallmarks of thermogenesis. Thus, leptin acts at the brain to increase thermogenesis in skeletal muscle and this is associated with an increase in UCP3 expression and a switch toward uncoupled respiration.

In addition to leptin, thermogenesis in the skeletal muscle of sheep is regulated by sex steroids. Sexually dimorphic effects are seen, such that continuous testosterone treatment of castrated male sheep reduces skeletal muscle heat production (Clarke et al., 2012a), but does not do so in ovariectomized ewes. Importantly, testosterone did not alter the postprandial thermogenic response but acts to cause an overall downregulation of basal body temperature (Clarke et al., 2012a). It is possible, however, that the effect of testosterone on metabolism and energy balance are primarily effected via aromatization and are therefore due to actions of estrogen and not direct effects at the androgen receptor (Mauvais-Jarvis, 2011). In contrast, however, to the effects of testosterone, estrogen acts to increase skeletal muscle thermogenesis in females (Clarke et al., 2013). Thus, the effect of testosterone to inhibit muscle thermogenesis is via androgenic actions and most importantly is sexually dimorphic (Clarke et al., 2012a). Although testosterone and estrogen can modulate skeletal muscle temperature neither steroid impacts on the expression of UCP3, suggesting that effects of steroids on thermogenesis are mediated by alternative cellular systems, such as futile calcium cycling.

Overall, consistent data have been obtained in sheep, indicating that skeletal muscle is thermogenic and two distinct cellular pathways are important arbitrators of this response—mitochondrial uncoupling and futile calcium cycling across the SR membrane.

2.4.3 Humans

Prior to the recent reaffirmation that functional and active BAT is retained into adulthood in humans, it was thought that skeletal muscle may be the primary thermogenic tissue. Early work by Astrup (1986) demonstrated that skeletal muscle could account for up to 50% of ephedrine-induced thermogenesis, whereas adipose tissue accounts for approximately 5%. Although this original

paper did not characterize adipose depots that are now known to be rich in brown adipocytes, a recent paper substantiates this earlier work. Cypess et al. (2012) recently demonstrated that low dose ephedrine (1.5 mg/kg bodyweight) had no effect on BAT activity, but others have shown that high doses (2.5 mg/kg) could activate BAT (Carey et al., 2013). Despite this, chronic administration of low dose ephedrine reduces glucose uptake and BAT activity in humans (Carey et al., 2015). Glucagon can increase energy expenditure without an effect on BAT, further suggesting that alternative tissues are important in terms of adaptive thermogenesis and energy expenditure in humans (Salem et al., 2016). Because humans and other large mammals have relatively little BAT mass compared to rodent species, it has therefore been hypothesized that skeletal muscle thermogenesis is of considerable significance (Rowland et al., 2015). Variation in basal proton leakage within human skeletal muscle accounts for around 20%–50% of the variation in basal metabolic rate (Rolfe and Brown, 1997). As detailed later in the chapter, differences in UCP3 expression in skeletal muscle of obese females alters proton leakage and impairs weight loss (Harper et al., 2002). Thus, skeletal muscle, particularly the activity of UCP3 therein appears to be integral to adaptive thermogenesis and energy expenditure in humans. In spite of the earlier, the means by which thermogenesis in skeletal muscle mediates cold-adaption in humans is unclear. There is no doubt that exposure to cold activates UCP1-mediated BAT thermogenesis (van Marken Lichtenbelt et al., 2009; Vijgen et al., 2011; Wijers et al., 2010; Yoneshiro et al., 2011a), but an equivalent function in muscle is yet to be fully elucidated. Although the uptake of glucose by BAT is increased in response to cold exposure, skeletal muscle accounts for the vast majority of glucose utilization during this adaptive period (Blondin et al., 2015), but there is no associated change in UCP3 protein levels (Wijers et al., 2008). The cold-induced increase in energy expenditure is correlated with an increase in state 4 or uncoupled respiration in permeabilized muscle fibers, in spite of this (Wijers et al., 2008). This observation is similar to that displayed during the postprandial increase in muscle thermogenesis in sheep, whereby feeding increases uncoupled respiration without an effect of UCP3 gene or protein levels. To date, in humans (Blondin et al., 2015; Wijers et al., 2008) or in sheep (Clarke et al., 2012a), there have not been direct measurements of UCP3 activity and it remains possible that differences in mitochondrial uncoupling are not driven by changes in the level of gene expression but increased activity of UCP3. Whatever the mechanism, skeletal muscle represents 40% of body mass, which means that small increments in thermogenesis within this tissue would have significant effects on total energy expenditure. Given the paucity of evidence for skeletal muscle thermogenesis as a major contributor

of energy expenditure in rodents, other animals models, such as the sheep (and in humans) highlight the importance of this tissue and such species are ideal for studies to further delineate possible pathways and mechanisms that can be exploited for the development of antiobesity agents.

2.5 Models of Obesity

In humans, monogenetic forms of obesity are extremely rare, although a number of them have been reported. Mutations in the *obese (ob)* gene that encodes for the hormone leptin, result in profound obesity in humans and rodent species. Type II diabetes, immune dysfunction, and infertility are also displayed in individuals bearing such mutations (Farooqi, 2008; Farooqi and O'Rahilly, 2008). Nonetheless, *ob* mutations are rare in humans and the most common monogenic causes of obesity in humans are within the melanocortin system (Krude et al., 1998). Mutations in the melanocortin 4 receptor can account for as many as 6% of individuals with severe childhood obesity (Farooqi et al., 2003). Genetic models have been extensively studied in rodents (Boersma et al., 2012) and although this will not be considered here, thermogenesis is consistently reduced in these cases. For example, mutations in the leptin system (either the obese gene or in the signaling form of the leptin receptor) abolishes thermogenesis. Thus, the obese phenotype is driven not only by hyperphagia but also a concomitant reduction in thermogenesis and energy expenditure. Indeed, as early as 1977, both *ob/ob* mice and *fa/fa* rats were shown to be intolerant to cold exposure due to an inability to activate thermogenic pathways (Trayhurn et al., 1977). Furthermore, *ob/ob* mice develop obesity even when pair-fed with normal mice, demonstrating that a reduction in energy expenditure is a primary factor in the obese phenotype. Nevertheless, because human obesity is rarely caused by a monogenetic mutation, it is imperative that we characterize thermogenesis in polygenetic models. The application of quantitative genetics, to select for the polygenic condition of obesity or the reverse is well exemplified in the selection of mice for high heat loss (and consequent leanness) (Moody et al., 1999).

2.6 Diet-Induced Obesity and Thermogenesis

Long-term changes in adiposity impact on the neuroendocrine and neural networks that regulate energy homeostasis. Typically these changes reflect compensatory responses, in an effort to return body weight and levels of adiposity to normal. In sheep, low levels of adiposity increase the levels of appetite-stimulating peptides including NPY and MCH in an effort to drive food intake and reduce energy expenditure, ultimately increasing body weight (Barker-Gibb and Clarke, 1996;

Henry et al., 2000). With respect to the melanocortin system, long-term changes in adiposity also elicit compensatory effects to correct body weight toward normal. Low levels of adiposity will either decrease (Backholer et al., 2010) or have no effect on the levels of POMC mRNA; although there is minimal effect on POMC gene expression, low levels of adiposity alter POMC processing (Backholer et al., 2010). Chronic undernutrition and reduced adiposity inhibits the production of melanocortins and stimulates the synthesis of β-endorphin, thus there is an inhibition of the POMC-derived factors that inhibit food intake and an upregulation of those that stimulate food intake (Backholer et al., 2010). Ultimately, these changes in neuropeptide gene expression drive a correction in food intake through appetite drive but also impact on thermogenesis by means of a homeostatic mechanism, returning body weight back to the "set-point" of the individual.

It is generally held that increased rates of thermogenesis may be protective against weight gain. In humans and rodents, obesity is associated with an increase in sympathetic output, which would theoretically alter thermogenic output. A key component of obesity in mice is the development of leptin resistance, whereby exogenous leptin no longer inhibits food intake (Enriori et al., 2007; Munzberg et al., 2004; Myers et al., 2008), but the ability of leptin to activate the SNS and induce BAT thermogenesis is maintained; this is effected by direct action of leptin on the DMH (Enriori et al., 2011), although the target cells are not yet defined. Consistent with this, the majority of studies in rodents demonstrate that high fat feeding increases the expression of UCP1 in BAT, but there has been some discrepant data showing either no effect or a reduction in UCP1 expression in response to high fat feeding (Fromme and Klingenspor, 2011). This contrasts with data in humans, in whom BAT activity falls with increasing BMI and adiposity (van Marken Lichtenbelt et al., 2009); this is likely to confound weight loss and exacerbate the obese state. On the other hand, DIO has no effect on heat production in either adipose tissue or skeletal muscle in sheep (Henry and Clarke, unpublished data). In summary, animal models have not provided conclusive data demonstrating changes to thermogenesis that are representative of the condition of obesity in humans.

Innate differences in thermogenesis are seen to underlie the propensity to become obese and may also abrogate the ability of some individuals to lose weight. DIO rats have reduced BAT thermogenesis compared to their DR counterparts (Lockie et al., 2013). In women, lower UCP3 expression in skeletal muscle is associated with reduced mitochondrial uncoupling and an inability to lose weight (Harper et al., 2002). In addition, differences in weight loss compared to predicted weight loss in dieting humans have been ascribed to variations in diet-induced

thermogenesis (Goele et al., 2009). It is possible that reduced thermogenic potential may impact on the ability of individuals to maintain weight loss, but some individuals maintain a reduction in thermogenesis for up to 1 year after weight loss (Rosenbaum et al., 2008). In addition, DR strains of mice and rats display differential expression of UCP1 in response to high fat feeding compared to those that are susceptible to weight gain. DR strains of mice (AyJ and C57BLyKsJ) exhibit higher UCP1 expression in BAT during high fat feeding than DIO-prone strains (C57BLy6J) (Surwit et al., 1998). In addition to BAT, however, DR mice and rats increase ectopic expression of UCP1 in both skeletal muscle and WAT, particularly within subcutaneous WAT (Almind et al., 2007; Veyrat-Durebex et al., 2011). Indeed, in DIO animals, high fat feeding actually reduces UCP1 levels in subcutaneous fat and thus the ability to increase ectopic UCP1 may be a primary factor in determining susceptibility to obesity. Further work is required to measure ectopic expression of UCP1 in adipose tissue and skeletal muscle of larger mammals, such as sheep.

2.7 Photoperiod and Seasonality as Models of Metabolic Function

Domesticated and wild animals display marked seasonality in reproductive function, that is controlled by day length (Robinson, 1959), but also display seasonality in a number of other physiological processes. Animals are either long-day breeders or short-day breeders, such that the reproductive axis is activated by increasing day length or decreasing day length, respectively. Sheep are short-day breeders and hamsters are long-day breeders. With respect to "seasonality" of reproduction, it is firmly established that this is due to changing day length, "measured" by the perception of light through the eye, transmitting a signal to the suprachiasmatic nucleus (SCN). The signal is then relayed to the pineal gland, which secretes melatonin during the hours of darkness [reviewed in Boden and Kennaway (2006) and Kennaway (2005)]. CLOCK gene expression within the SCN is a fundamental driver of seasonality, being well characterized in numerous species including hamsters (Reiter, 1980) and sheep (Karsch et al., 1984; Lincoln et al., 2003). While seasonality of reproduction has been studied extensively, the impact of photoperiod and temperature on metabolic balance is less clearly deciphered. Seasonal changes in body weight and adiposity are displayed by many species including woodchucks (Young et al., 1982), squirrels (Zucker et al., 1983), hamsters (Wade and Bartness, 1984b), deer (Gaspar-Lopez et al., 2009), and sheep (Clarke et al., 2000), among other species. Although somewhat dampened, seasonality with respect to energy balance is also apparent in humans, with photoperiodic regulation of the occurrence

of BAT (Au-Yong et al., 2009). Interestingly, although both Syrian and Siberian hamsters breed during long-day photoperiod (LD), the former gain weight on short day photoperiod (SD) and the latter lose weight (vide infra). Importantly, however, studies in both species of hamsters have conclusively demonstrated a role for melatonin as a controller of metabolic function.

In Syrian hamsters, animals held on SD show a greater gain in weight than those held on LD, but the difference is greater in females than in males (Bartness and Wade, 1984). It was further demonstrated that in animals held on LD, afternoon injections of melatonin displayed an increase in body weight. SD and melatonin treatment of animals on LD increased BAT mass but there was an indication that norepinephrine-stimulated oxygen consumption (an index of thermogenesis) was lower in animals on SD. The curious lack of indication of statistical significance of the results in this paper render the data difficult to interpret, but there is a suggestion that the ability to gain weight on SD is due to reduced energy expenditure, as well as increased food intake as indicated by the increased amount of energy stored in the carcass. Similar data were presented in another paper on photoperiodic change and melatonin effect on body weight and fat accumulation in Syrian hamsters (Wade and Bartness, 1984b), emphasizing that the "seasonal obesity" is associated with a reduction in energy expenditure. It would be interesting to determine the effects of photoperiod on energy expenditure in this species with more sophisticated measures of energy expenditure.

In Siberian hamsters (Wade and Bartness, 1984a), SD reduces body weight in gonad-intact males, castrated males, and in gonad-intact females. The lack of effect in ovariectomized females led to the suggestion that the gonadal steroids are important for the response to photoperiod in this sex, but the same is not true for males. The reduction in body weight in response to SD, as well as melatonin injections in the afternoon on LD, were accompanied by a reduction in food intake by 4 weeks, but reduction in body weight preceded this by 2 weeks, suggesting that the photoperiod-induced change was due to alteration in energy expenditure. Consistent with this, both SD and melatonin treatment reduced the mass of interscapular BAT. These results with Siberian hamsters are at odds with two earlier communications on the same species (Heldmaier and Hoffmann, 1974; Heldmaier et al., 1981), which showed that SD or melatonin treatment *increases* BAT weight. Similar to this, a recent study in lean and obese Zucker diabetic rats, showed that melatonin could induce "browning" of the subcutaneous fat depot, irrespective of body weight (Jiménez-Aranda et al., 2013). Indeed, melatonin-induced browning coincided with increased heat production in inguinal fat and increased expression of UCP1 and PGC1α (Jiménez-Aranda et al., 2013), which supports the notion that the

effects of melatonin on body weight are due at least in part, to an upregulation of thermogenesis.

Photoperiod has been shown to regulate the expression of a number of clock genes in the SCN and the pars tuberalis of the Siberian hamster (Johnston et al., 2005), but this was not related to any changes in the expression of genes involved in appetite/energy expenditure control. More recent studies, however, suggest a role for CLOCK genes in both the brain and adipose tissue in the control of BAT activity in mice. Global deletion of *Bmal1* in mice increases BAT mass, increases UCP1 expression, and improves cold tolerance (Nam et al., 2015). Interestingly, specific deletion of *Bmal1* in WAT, mimics the phenotype of the global knockout (Nam et al., 2015). Similarly, targeted-ablation of *Bmal1* in SF-1 neurons on the VMH results in an increase in energy expenditure and enhanced thermogenic capacity of BAT in mice (Orozco-Solis et al., 2016). In this case, it was proposed that increased BAT thermogenesis is driven by enhanced SNS activity in the *Bmal1* mutant mice (Orozco-Solis et al., 2016). It is important to note that global deletion of any CLOCK gene would affect all cells in the body (all cells express CLOCK genes), leading to potential effects on SNS, free fatty acid and glucose production, production of transcription factors. This would be expected to have widespread ramifications on whole body metabolism and energy homeostasis. It is also likely that different CLOCK genes act in concert to control energy expenditure since global deletion of the Period2 (*Per2*) gene leads to the opposite phenotype to the *Bmal1* knockout animal. Mice that lack *Per2* are cold-intolerant and have lower body temperature at either 21 or 4°C compared to wild-type controls (Chappuis et al., 2013).

In sheep, a distinct seasonal cycle in appetite is apparent, as displayed in ovariectomized ewes (Clarke et al., 2000), which indicates that the effect of photoperiod is independent of changing levels of gonadal steroids between breeding to nonbreeding season. The nadir of food intake is seen in the Winter–Spring, which is consistent with an effect of SD to reduce appetite and body weight in gonad-intact Soay rams (Lincoln et al., 2001). The change in appetite in ovariectomized ewes was tightly correlated to changes in the expression of the gene for the orexigenic peptide, NPY in the ARC (Clarke et al., 2000), but not the level of expression of the POMC gene (Fig. 12.4). Another study of Soay rams recapitulated the effect of SD to reduce food intake (Fig. 12.5), also showing reciprocal changes in expression of the NPY and POMC, such that the former was reduced and the latter increased under SD (Fig. 12.6). Interestingly, the gonad-intact animals of this study became refractory to the SD and began to increase food intake after 16 weeks—this was directly related to changes in NPY and POMC gene expression that was not seen in the
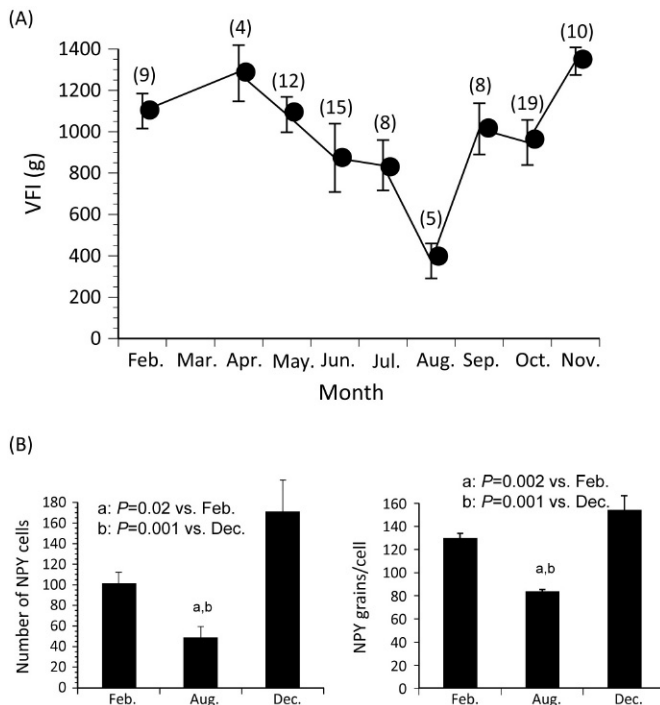
FIGURE 12.4 Changes in (A) voluntary food intake *(VFI)* and (B) expression of the neuropeptide Y *(NPY)* gene in the accurate nucleus of ovariectomized ewes across an annual cycle. Food intake declines on short-day photoperiod (Southern Hemisphere) and this is directly related to the level of expression of NPY. *Source: Adapted with permission from Clarke, I.J., Scott, C.J., Rao, A., Pompolo, S., Barker-Gibb, M.L., 2000. Seasonal changes in the expression of neuropeptide Y and pro-opiomelanocortin mRNA in the arcuate nucleus of the ovariectomized ewe: relationship to the seasonal appetite and breeding cycles. J. Neuroendocrinol. 12(11), 1105–1111.*

castrated rams. Another intriguing facet of these data is that, although castrated animals maintained a reduced level of food intake on SD, they gained adiposity. In other words, they became fat while food intake was minimal. Similar results were obtained in ovariectomized ewes, which were subject to normal seasonal cycles of photoperiod (adiposity increased at a time when food intake was reduced) (Anukulkitch et al., 2009). In both cases, the most likely explanation for this is a reduction in energy expenditure on SD. The only data which are available to support this notion were provided by one study which indicated changes in metabolic rate across seasons in Soay rams (Argo et al., 1999). Since this model shows such major changes with changing photoperiod, it may be instructive to interrogate the mechanisms underlying changes in energy expenditure.

Other studies in Siberian hamsters and in sheep, both of which display reduced food intake and body weight on SD, have yielded a wealth of information on expression of appetite-regulating genes in the hypothalamus. After exposure to SD, the following changes occur relative to LD:

- Plasma leptin levels and brain leptin receptor expression are lower in Siberian hamsters and Soay rams (Clarke et al., 2003; Marie et al., 2001; Mercer et al., 2000; Rousseau et al., 2003; Tups et al., 2004).
- POMC expression is lower in the arcuate nucleus of the hamster (Mercer et al., 2000; Reddy et al., 1999; Rousseau et al., 2003), but higher in the Soay ram (Clarke et al., 2003).
- NPY expression is lower in the ARC of Soay rams (Clarke et al., 2003) and ovariectomized ewes (Clarke et al., 2000), but no significant changes were seen in Siberian hamsters (Mercer et al., 2000; Reddy et al., 1999; Rousseau et al., 2003).
- Expression of AgRP is lower in Soay rams (Clarke et al., 2003), but in Siberian hamsters, expression is either elevated (Mercer et al., 2000) or unchanged (Rousseau et al., 2003).
- Melanin-concentrating hormone gene expression is higher in the perifornical area and the dorsomedial hypothalamic nucleus of Soay rams (Clarke et al., 2003), but there is no effect of photoperiod in the hamster (Mercer et al., 2000).
- The expression of cocaine and amphetamine-related transcript (CART) is higher in SD than LD in Siberian hamsters (Adam et al., 2000).

Expression of ORX and MCH genes are higher (in early summer/autumn) and reach a nadir, when voluntary food intake falls in late winter/early spring (Anukulkitch et al., 2009). Given that relative adiposity increases at the latter time point, when food intake is minimal, there is an obvious role of seasonal change in energy expenditure (thermogenesis?) that has not been detailed—the changes in expression of ORX and MCH may be salient to the potential change in energy expenditure at this time, for reasons indicated previously.

In summary, these studies show inconsistencies in the effects of photoperiod on expression of genes for appetite-regulating peptides in different species, but the data from sheep show changes more consistent with the observed changes in food intake. Information on the extent to which changes in energy expenditure are caused by photoperiod is rudimentary and some systematic studies with state-of-the-art equipment could yield interesting data on mechanisms.

2.7.1 Effect of Sex, Season, and Leptin Resistance

As indicated earlier, the effects of photoperiod on body weight differ in male and female hamsters, in accordance with gonadal status. In sheep and rodents, the satiety effect of leptin is greater in females than males (Clarke, 2001; Clegg et al., 2003, 2006). In addition, in sheep, the anorectic effect of leptin is greater in the
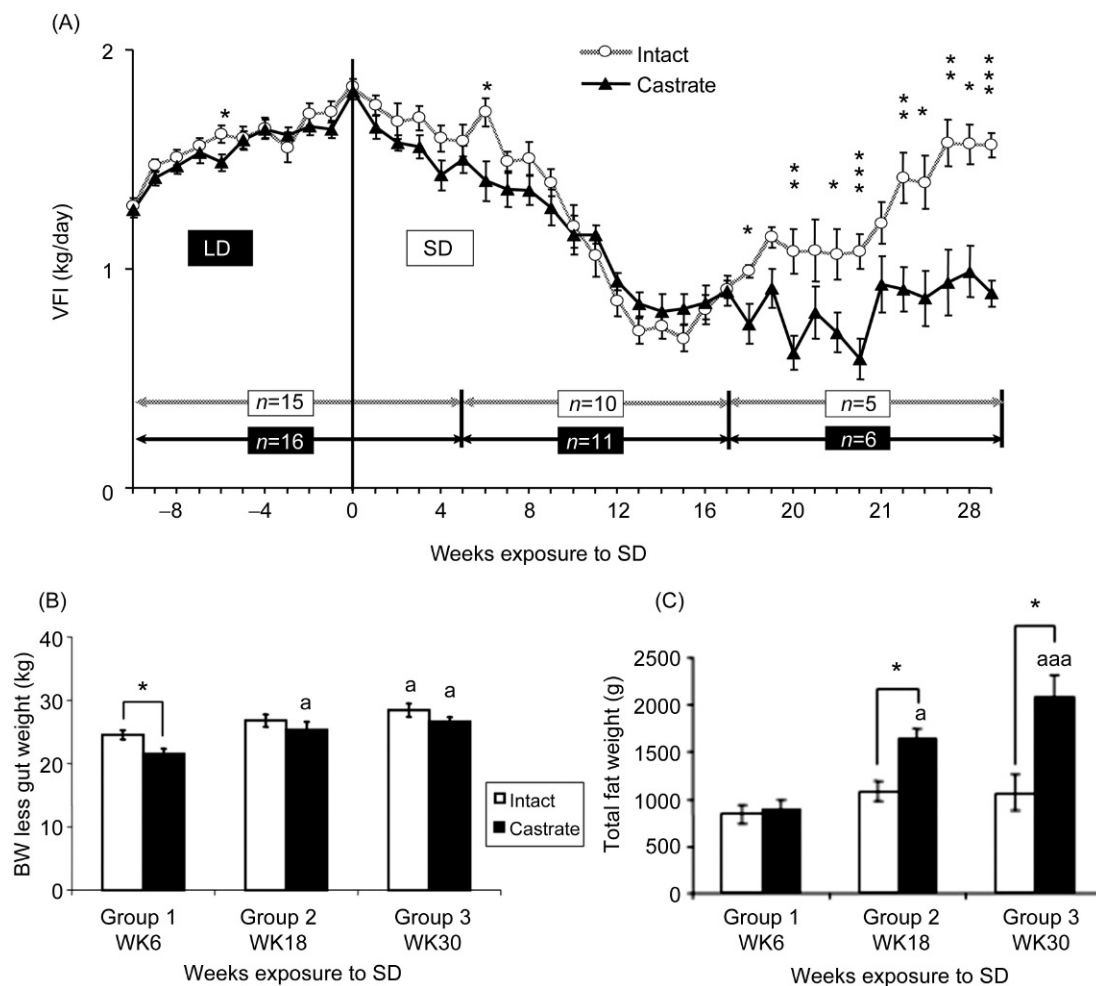
FIGURE 12.5 Effect of photoperiod on food intake, body weight, and adiposity in gonad-intact and castrated Soay rams. (A) Voluntary food intake (mean ± standard error) is reduced by short-day photoperiod *(SD)* dater transition from long-day photoperiod *(LD)*. This occurs in both gonad-intact animals and castrated animals, but the former eventually becomes photorefractory and food intake rises again, in spite of the SD. The numbers in each stage of the study were reduced because animals were taken to measure gene expression in the brain. (B) There are minimal changes in overall body weight *(BW)* less rumen weight (to account for differences in gut fill). (C) There are, however, significant photoperiod-dependent changes in adiposity. Note that castrated animals gain weight, while eating less food. *$P < 0.05$, **$P < 0.01$ for difference between groups indicated. [a]$P < 0.05$, [aa]$P < 0.01$, [aaa]$P < 0.001$ compared with week 6; and [b]$P < 0.05$, [bbb]$P < 0.001$ compared to week 18 within groups of the same gonadal status. *Source: Adapted with permission from Clarke, I.J., Rao, A., Chilliard, Y., Delavaud, C., Lincoln, G.A., 2003. Photoperiod effects on gene expression for hypothalamic appetite-regulating peptides and food intake in the ram. Am. J. Physiol. Regul. Integr. Comp. Physiol. 284(1), R101–R115.*

spring than the autumn (Clarke et al., 2001) (Fig. 12.7). Furthermore, the expression of the leptin receptor fluctuates across the year. Curiously, when the expression of leptin receptor is maximal food intake is greatest (at least 6 weeks after the summer solstice) (Anukulkitch et al., 2009). To add to the perplexity, transition from LD to SD also causes a reduction in leptin transport into the brain within 5 weeks (Adam et al., 2006) (Fig. 12.8). This may not have a great impact on the ability of leptin to regulate NPY and POMC neurons in the arcuate nucleus, which shows porosity to blood borne leptin (Faouzi et al., 2007), so transport to this level of the brain at least, may have only minimal impact on the ability of leptin to act on appetite-regulating systems.

As to whether altered leptin sensitivity or functionality leads to changes in energy expenditure in the sheep remains unknown.

2.7.2 The Role of Thyroid Hormone Action Within the Hypothalamus

One mechanism that may be highly relevant to metabolic change with photoperiod is metabolism of thyroid hormones in the hypothalamus. Type 2 iodothyronine deiodinase (Dio2) is an enzyme that converts T4 to the active form, T3, and is found in the hypothalamus. Original work in birds identified this enzyme as being regulated by photoperiod and being relevant to control of reproductive function (Yoshimura et al., 2003). This
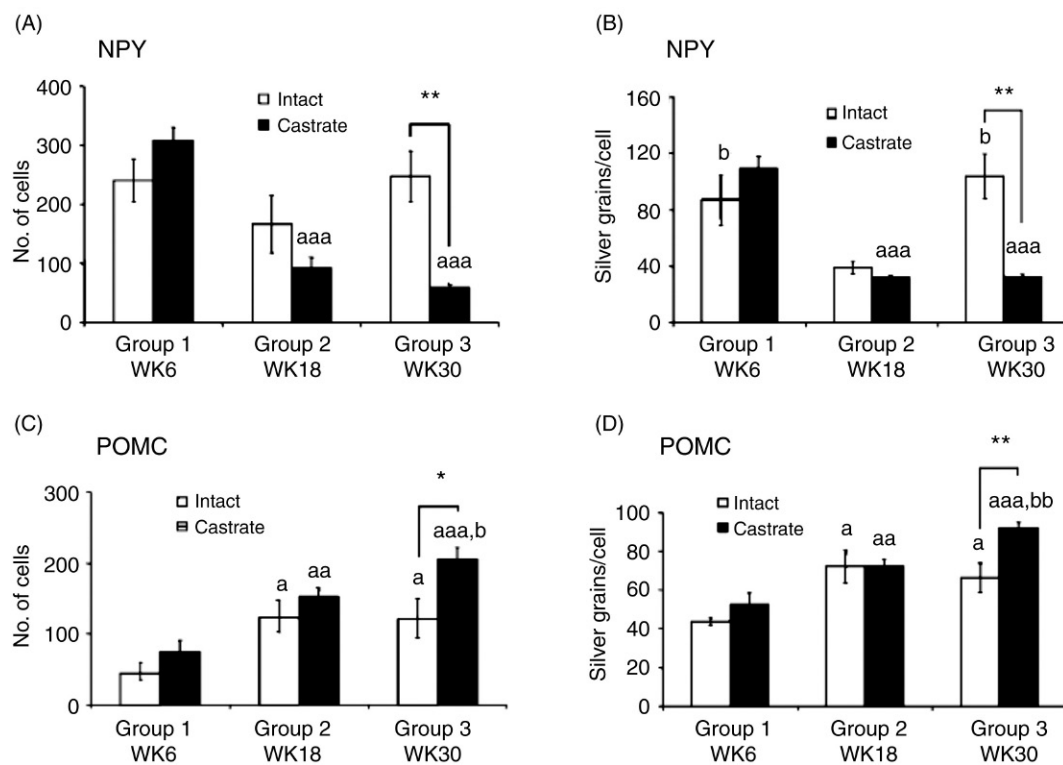
FIGURE 12.6 **Expression of the *NPY* and *POMC* genes in the arcuate nucleus for which data are shown in Fig. 12.5.** Note the close relationship between the expression of the gene for the orexigenic peptide (NPY) and the gene for the anorectic melanocortins (POMC) and the food intake of the animals displayed in Fig. 12.5. *Source: Adapted with permission from Clarke, I.J., Rao, A., Chilliard, Y., Delavaud, C., Lincoln, G.A., 2003. Photoperiod effects on gene expression for hypothalamic appetite-regulating peptides and food intake in the ram. Am. J. Physiol. Regul. Integr. Comp. Physiol. 284(1), R101–R115.*
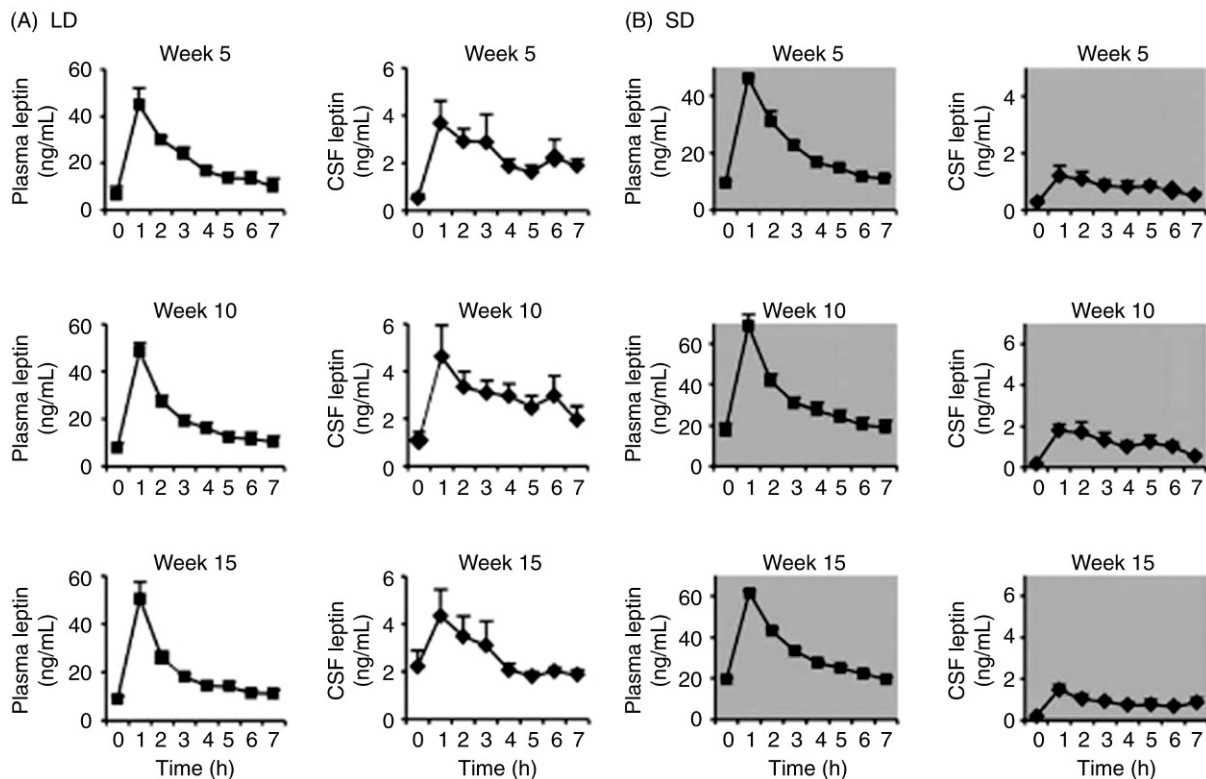
FIGURE 12.7 Plasma and cerebrospinal fluid *(CSF)* leptin concentration profiles in castrated, estrogen-treated male sheep before (time = 0 h) and after intravenous (5 mg) leptin injection at 5, 10, or 15 weeks in (A) LD photoperiod (clear background; *n* = 9) and (B) SD photoperiod (*gray* background; *n* = 9). Means ± standard error. Note that there are similar levels of leptin in plasma after injection, but there are lower levels in the CSF in animals injected during SD. *Source: Reproduced with permission from Adam, C.L., Findlay, P.A., Miller, D.W., 2006. Blood-brain leptin transport and appetite and reproductive neuroendocrine responses to intracerebroventricular leptin injection in sheep: influence of photoperiod. Endocrinology 147(10), 4589–4598.*
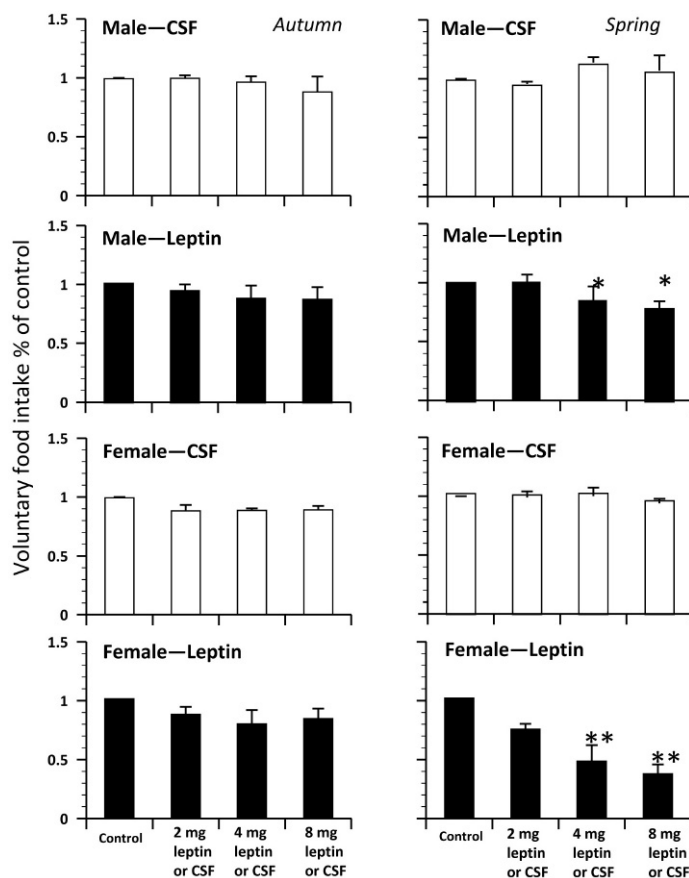
FIGURE 12.8   **Interaction between sex and season.** The effect of increasing doses of leptin (by intracerebroventricular injection), on voluntary food intake in castrated male and female sheep in spring and autumn. Note that the response is minimal in autumn and greater in spring. Also note that the response is greater in females than males. *Source: Reproduced with permission from Clarke, I.J., 2001. Sex and season are major determinants of voluntary food intake in sheep. Reprod. Fertil. Dev. 13(7–8), 577–582; Clarke, I.J., Tilbrook, A.J., Turner, A.I., Doughton, B.W., Goding, J.W., 2001. Sex, fat and the tilt of the earth: effects of sex and season on the feeding response to centrally administered leptin in sheep. Endocrinology 142(6), 2725–2728.*

finding was then replicated in mammals (Watanabe et al., 2004). In particular, the enzyme is found in the ependymal cell layer and the "cell-clear" zone overlying the tuberoinfundibular sulcus (Revel et al., 2006; Watanabe et al., 2004). In the Siberian hamsters, Dio2 is inhibited by SD or melatonin treatment (Watanabe et al., 2004). Similar results have been obtained in Syrian hamsters, but not in Wistar rats that are not photoperiodic (Revel et al., 2006). These studies also showed that the SD reduction in the expression of the enzyme is not affected by castration, but is upregulated by pinealectomy. Emphasizing that the enzyme is regulated by photoperiod, Yasuo et al. (2007) showed a response to photoperiod in Fischer 344 rats (photoperiodically regulated reproduction), but no similar response in Wistar rats. Saanen goats are SD breeders and, consistent with the notion that the activity of the enzyme relates to reproduction, Dio2 is inhibited by LD (Yasuo et al., 2006). In sheep, the notion that the expression of Dio2 is regulated by thyroid-stimulating hormone (TSH) has been investigated. TSH production is increased by LD (nonbreeding condition) and

TSH increases expression of Dio2 (Hanon et al., 2008). Again, this has been related to seasonal breeding but the question as to whether it relates to seasonal appetite/energy expenditure cycles is not known. Since Dio2 expression is affected in the same way by photoperiod in both Syrian and Siberian hamsters, whereas body weight responses to photoperiod are clearly different in the two species, it seems most likely that it relates more to reproductive function than metabolic control. This has, however, not been rigorously examined by, for example, administration of the inhibitor of Dio2, iopanoic acid. Differences between Syrian and Siberian hamsters extend to control of the seasonality of reproductive function (Bartness et al., 1993) as well, which may, at least in part, be due to the differences in the sites of action of melatonin. Thus, in Siberian hamsters, the SCN lesion prevents the inhibitory effect of exogenous melatonin infusions (Bartness et al., 1991), but this is not the case in Syrian hamsters (Bittman et al., 1989). As to how this extends to control of metabolic function, particularly thermogenesis, is not known.

2.7.3 Vitamin D and Photoperiod

In humans, low vitamin D is often associated with the obese state and insulin resistance (Soares et al., 2012), but little is known as to whether this is a cause or effect relationship. In humans, however, consumption of a breakfast high in vitamin D leads to increased fat oxidation and increased thermogenesis during the postprandial period (Ping-Delfos and Soares, 2011). This suggests that vitamin D may be important in modulating or increasing energy expenditure via activation of thermogenic pathways, at least in humans.

There are few data on the effect of vitamin D on energy expenditure or thermogenesis in animal models, but there is some suggestion of an inhibitory effect in rodents, in contrast to findings in humans. For example, mice that lack vitamin D or the vitamin D receptor exhibit a lean DR phenotype (Narvaez et al., 2009). Interestingly, food intake is slightly increased in the vitamin D receptor knockout animals and the lean phenotype appears to be at least partly driven by an increase in UCP1 in WAT (Narvaez et al., 2009). This is substantiated by targeted overexpression of the vitamin D receptor in the adipocytes of transgenic mice, which reduces UCP1 expression in BAT, reducing energy expenditure and leading to an obese phenotype (Wong et al., 2011).

As the vitamin D receptor is a nuclear receptor, it can act directly to alter expression of target genes, with specific findings pertaining to the repression of ELOVL3 in WAT (Ji et al., 2016). ELOVL3 is a BAT-specific marker, so reduced expression indicates that vitamin D is an inhibitor of BAT development and/or function in rodents. Interestingly, the central actions of vitamin D are completely opposite, causing reduced food intake and body weight in mice through the activation of POMC neurons within the ARC (Sisley et al., 2016). Such findings support the hypothesis that vitamin D deficiency is associated with obesity, but there are clearly disparate effects centrally and peripherally. There clearly appears to be a relationship between vitamin D, the control of body weight, and energy expenditure, but further investigation is required to try to address the apparent species differences, as well as the possible differences between central and peripheral effects on energy homeostasis.

2.8 Fetal Growth Retardation and Subsequent Effect on Metabolic Balance

Undernutrition during gestation is known to reduce birthweight and have long-term impact on body weight, body composition, and metabolic health. In humans, effects of maternal undernutrition on long-term weight regulation in progeny is dependent on the timing of undernutrition and the availability of food in the early postnatal period. Exposure to famine during the early stages of gestation increases the body weight of the offspring (Painter et al., 2005; Zeltser, 2015). Similar observations have been observed in sheep, where undernutrition during the first 3 months of gestation leads to increased adiposity and resultant obesity during adulthood (Gnanalingham et al., 2005). The similarities between sheep and humans are not surprising given that both are precocial newborns and thus the formation of neural circuits that regulate food intake and energy expenditure are largely formed prior to birth (Symonds, 2013).

The "Barker Hypothesis" (Barker and Osmond, 1986; Barker et al., 1989, 1993) states that early life events, especially prior to birth, have detrimental effects that are manifested in later life. In particular, this hypothesis focussed on the predisposition to heart disease, but it is now clear that early life events can lead to a number of adverse health issues, including cancer. This is reviewed in de Boo and Harding (2006), detailing the implications of fetal programming on disease in later life, as shown in Fig. 12.9. Animal models of the human disease have been developed, one being that of placental restriction (Robinson et al., 1979). This model, developed in sheep, involves the surgical removal of "caruncles" in the uterus that are the placental structures. Removal of caruncles leads to reduction in the growth of the fetus and a reduction in birthweight. As a consequence, the offspring have insulin resistance when young and glucose tolerance is compromised in the adults (De Blasio et al., 2007a,b, 2010, 2012; Gatford et al., 2008; Owens et al., 2007). In this model, insulin resistance appears to be due to reduced expression of genes related to insulin signaling and metabolic function in skeletal muscle, but not liver (De Blasio et al., 2012). It would be interesting to determine whether such fetal programming affects thermogenic function and alters energy expenditure in this way.

In rodents, the state of maternal nutrition clearly impacts on the developing neural circuitry that govern energy homeostasis (Zeltser, 2015). In rodents, which are altricial as newborns, the hypothalamic connections are primarily established during the postnatal period (Bouret, 2012). A primary driver of nutritional programming of hypothalamic circuitry appears to be circulating leptin levels. The neural projections extending from the ARC are disrupted in ob/ob mice (Bouret et al., 2004). Furthermore, this can only be reversed by leptin treatment during the neonatal period and not in adulthood; leptin replacement during postnatal days 4–12 restored AgRP- and αMSH-positive fiber density in the PVN (Bouret et al., 2004). The long-term consequences of altered synaptic development in the absence of postnatal leptin is unknown since ob/ob mice exhibit satiety in response to leptin treatment. It has also been hypothesized, that postnatal leptin levels are important for the development
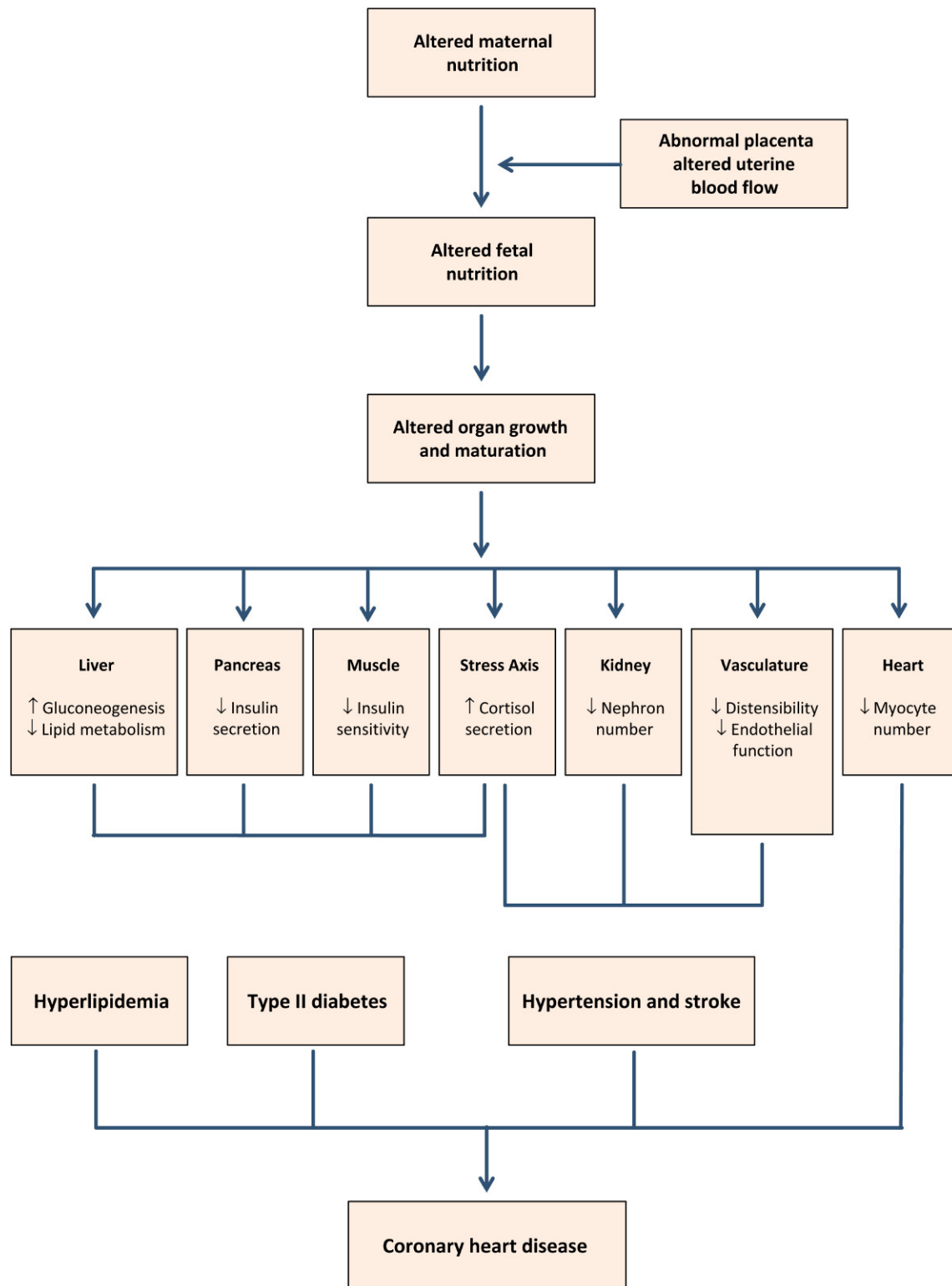
FIGURE 12.9 **Impact of early life programming on the prevalence of disease later in life.** *Source: Adapted with permission from de Boo, H.A., Harding, J.E., 2006. The developmental origins of adult disease (Barker) hypothesis. Aust. N Z J. Obstet. Gynaecol. 46(1), 4–14.*

of BAT (Zeltser, 2015). Interestingly, at postnatal day 10 the primary endogenous source of leptin is BAT and not WAT (Zhang et al., 2001). The effects of leptin on BAT development, however, are complex. In normal control or wild-type mice, neonatal leptin treatment inhibits BAT thermogenesis and increases the propensity to become obese (Vickers et al., 2008; Yura et al., 2005). In contrast, in states of leptin deficiency (ob/ob mice) or IUGR, neonatal leptin treatment improves BAT function (Bouyer and Simerly, 2013; Vickers et al., 2005). There is a lack of data on the effects of maternal programming on thermogenesis in tissues other than BAT. It would be most interesting to characterize the differential effects of maternal programming on thermogenesis in brown or beige adipocytes, as well as in skeletal muscle.

2.9 Transgenerational Effects of Obesity

In rats, female offspring, whose fathers had been rendered obese due to high-fat diet showed impaired insulin secretion and glucose tolerance, associated with altered gene profiles, particularly in the pancreatic islets (Ng et al., 2010). Hypermethylation of genes suggests epigenetic programming in these animals. Interestingly, the daughters did not have altered body weight, growth rate, energy intake, or energy efficiency, implying the unlikelihood of an impact on thermogenesis or overall energy expenditure. A study of mice born to obese fathers showed significant genetic perturbation in gametes of offspring and impaired fertility (Fullston et al., 2012). Increased body weight in F2 female offspring suggests that metabolic perturbations were transgenerational. Transcriptome analysis of pancreatic islet genes in female offspring of HFD fathers revealed alterations in the expression of 642 genes including those involved in ATP binding, the cytoskeleton and intracellular transport (Ng et al., 2010). Phenotypically this resulted in impaired glucose homeostasis possibly due to a decreased β-cell mass within the Islets of Langerhans. Another study based on the impact of paternal HFD on female offspring investigated transcriptional changes within retroperitoneal fat, as well as pancreatic cells, with 5108 genes having altered expression. Broadly speaking these changes were within pathways involved in responses to stress, cell survival, growth, and proliferation, which were hypothesized to be consistent with gene signatures characteristic of premature aging and degenerative disorders (Ng et al., 2014). What is exciting is that in the same model of transgenerational paternal metabolic influences, a short-term diet/exercise intervention can ameliorate insulin sensitivity and adiposity in female offspring. These changes are reflected at the molecular level. In HFD fathers, the expression of four X-chromosome-linked microRNAs (miRNAs) were reduced, however, with diet and/or exercise the expression profiles were restored comparable to that of controls (McPherson et al., 2015). These miRNAs are associated with early embryonic development and due to their link to the X chromosome any adverse effects as a result of altered miRNAs are more profound in females due effectively to the "double dose." These studies clearly demonstrate that maternal and paternal body weight and metabolic health are likely to have detrimental effects on progeny across a number of generations.

2.10 Polygenic Models of Obesity

Whereas single gene defects might lead to an obesity phenotype in humans and in animals, these do not account for the majority of cases in which body conformation is inherited. A large number of genes have been associated with obesity. In spite of this, it is seen that individual genes have a small influence on the obese phenotype as a whole. In a review of this topic (Walley et al., 2009), it was concluded that, in the search for single genes and gene linkage, "…our current methods are only identifying minor contributors to the genetic effect in obesity." This is most likely due to the fact that genetic determination of body conformation and propensity to become obese in an obesiogenic environment is polygenic in nature (Kunej et al., 2013). Accordingly, the application of quantitative genetics to selection of animals for obesity genotypes has provided useful animal models of the human condition. In this section we will discuss two ovine models that (1) have been selected for differences in adiposity or (2) the application of cortisol responsiveness as a marker for altered propensity to gain weight.

2.10.1 Models of Genetic Obesity

Polygenic models of obesity have been developed in chickens (Lilburn et al., 1982; Simon and Leclercq, 1982), pigs (Hetzer and Harvey, 1967; Hetzer and Miller, 1972, 1973) and sheep (McEwan et al., 2001; Morris et al., 1997; Suttie et al., 1991). Perhaps the most well-examined model is that in the sheep, which was based on the selection of animals with greater or lesser back-fat thickness and backcrossing of the animals of the two extremes; the lean and fat lines show a significant difference in adiposity, despite similar body weights and voluntary food intake (Alfonso and Thompson, 1996; Morris et al., 1997). Whereas the animals have a phenotype in the growth hormone axis (Francis et al., 1997, 1998a,b; French et al., 2006; Suttie et al., 1991), this may be only one factor contributing to the different phenotype. It is possible that the animals have different metabolic "set-point" and this might be exemplified in the steady-state level of gene expression for "appetite regulating peptides" in the hypothalamus. On a normal diet and at steady state, the level of gene expression for NPY in the arcuate nucleus is similar in
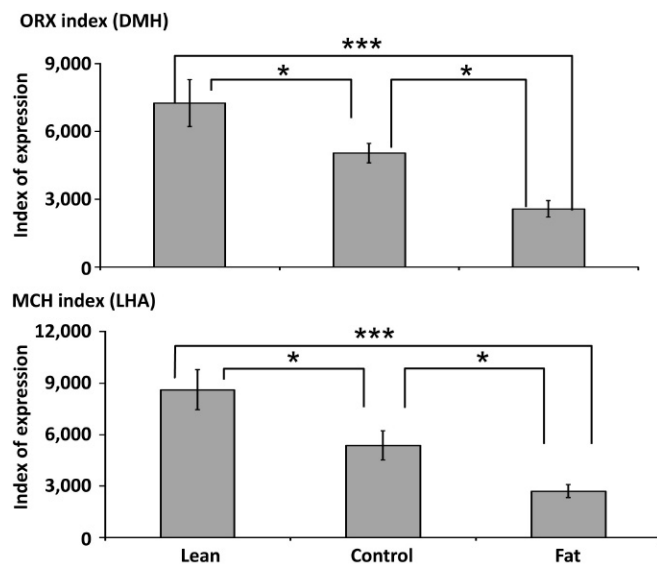
FIGURE 12.10 **Expression of genes for orexin *(ORX)* and melanin-concentrating hormone *(MCH)* in the hypothalamus of ewes selected for lean or fat phenotype.** Controls are animals from the same flock that were not selected. The animals were sampled on a normal diet, with no difference in food intake or body weight. The data are an index of expression which is obtained by the product of cell number and expression/cell. *Source: Adapted with permission from Anukulkitch, C., Rao, A., Dunshea, F.R., Clarke, I.J., 2009. A test of the lipostat theory in a seasonal (ovine) model under natural conditions reveals close relationship between adiposity and melanin concentrating hormone expression. Domest. Anim. Endocrinol. 36, 138–151.*

lean and obese animals (Anukulkitch et al., 2010), which contrasts the effects of diet-induced alterations in body weight where NPY expression is increased in normal (unselected) animals made lean by food restriction (Barker-Gibb and Clarke, 1996). This is not surprising, since the obese animals do not display leptin resistance; the reduction in food intake caused by central infusion of leptin is equivalent in genetically lean and obese animals (Henry et al., 2015). On the other hand, the expression of both ORX and MCH genes was altered. Thus, in the DMH, ORX gene expression was higher than control in lean animals and lower than control in fat animals (Fig. 12.10). A similar trend was seen for MCH gene expression in the lateral hypothalamus (Fig. 12.10). Since there is no difference in food intake in these lean and fat animals, the differences in steady-state gene expression may relate to differences in energy expenditure. Indeed, contemporaneous temperature recordings demonstrate that postprandial thermogenesis is attenuated in retroperitoneal adipose tissue of genetically obese sheep compared to their lean counterparts (Henry et al., 2015). The reduction in heat output in obese sheep is confined to adipose tissue (not skeletal muscle) and is associated with reduced UCP1 expression, supporting the notion that thermogenesis is reduced in the obese group (Henry et al., 2015). As mentioned before, MCH reduces energy

expenditure, whereas ORX increases the same (Astrand et al., 2004; Ito et al., 2003; Messina and Overton, 2007; Teske et al., 2008) and ablation of the ORX gene leads to obesity in mice (Hara et al., 2001), due to impaired development of BAT and reduced BAT thermogenesis (Sellayah et al., 2011). As to why there is a similar trend in the expression of MCH, being high in lean animals, is not known, since knockout of this gene in mice leads to accelerated weight loss (Willie et al., 2008). We propose that the altered expression of orexin may be important in determining altered thermogenesis and thus different body compositions in the genetically lean and obese sheep, but this requires further investigation.

2.10.2 Cortisol Responsiveness Marks Inherent Differences the Predisposition to Obesity

Glucocorticoids are well known to exert a broad range of metabolic effects on food intake, energy partitioning, and energy expenditure, but space does not allow these direct glucocorticoid effects to be described herein. Recent work, however, has suggested that the effects of glucocorticoids on thermogenesis differ between species. In humans, dexamethasone stimulates the differentiation and development of brown preadipocytes in adipose tissue samples from the clavicular region (Barclay et al., 2015). Furthermore, 3 days of prednisolone treatment enhanced cold-induced activation of BAT in healthy male volunteers (Ramage et al., 2016). This contrasts that seen in rodents, wherein glucocorticoids act, at least in the acute phase, to inhibit BAT function (Ramage et al., 2016). Further work is required to study the direct effects of glucocorticoids on thermogenesis in other tissues, such as skeletal muscle, and also in other large mammal models, such as pigs and sheep.

In humans, the secretion of cortisol is known to be altered in obese states, particularly in the case of abdominal or visceral obesity where cortisol levels are elevated (Duclos et al., 1999; Pasquali et al., 1993). Similarly, in sheep, DIO leads to increased secretion of cortisol in response to isolation restraint stress in comparison to their lean flockmates (Tilbrook et al., 2008). This initial work suggested that the obese state leads to dysfunction of the hypothalamo-pituitary-adrenal (HPA) axis. More recent work, however, suggests that inherent differences in cortisol responsiveness can be used to predict altered propensity to weight gain (Fig. 12.11). Initial studies identified rams as having either high or low cortisol responses to adrenocorticotropin (ACTH) with a greater response being correlated with lower feed-conversion efficiency (Knott et al., 2008, 2010). Marked differences in thermogenesis were revealed while using a similar protocol to identify high (HR) and low (LR) cortisol responders in female sheep. At baseline, in a steady nonstressed state, LR and HR eat similar amounts and have similar body composition, but HR accumulate more adipose tissue

High cortisol responsiveness
Increased CRF and AVP and decreased oxytocin
Increased POMC in anterior pituitary
Attenuated catabolic response to stress
Decreased thermogenesis in skeletal muscle
Impaired melanocortin signaling
Reactive behavioral coping strategy
= propensity to become obese

Low cortisol responsiveness
Decreased CRF and AVP and increased oxytocin
Decreased POMC in anterior pituitary
Elevated catabolic response to stress
Increased thermogenesis in skeletal muscle
Proactive behavioural coping strategy
Increased physical activity
Reduced fearfulness
= relative resistance to obesity

FIGURE 12.11 **Summary of the neuroendocrine, behavioral, and metabolic differences between animals selected for either low or high cortisol responsiveness.** Animals selected for high cortisol responsiveness exhibit increased food intake and reduced energy expenditure, which is associated with increased susceptibility to becoming obese. This figure summarizes the specific differences in neuroendocrine markers, the control of food intake, energy expenditure, and behavioral phenotypes in high or low cortisol responders. *AVP*, Arginine vasopressin; *CRF*, corticotrophin-releasing factor; and *POMC*, proopiomelanocortin. *Source: Adapted with permission from Hewagalamulage, S.D., Lee, T.K., Clarke, I.J., Henry, B.A., 2016b. Stress, cortisol, and obesity: a role for cortisol responsiveness in identifying individuals prone to obesity. Domest. Anim. Endocrinol. 56 Suppl., S112–S120.*

on a high-energy diet (Lee et al., 2014c). Furthermore, in the nonstressed basal state, LR and HR animals exhibit differences in the set-point of the HPA axis, with HR animals having increased expression of corticotrophin-releasing factor and arginine vasopressin, but reduced oxytocin levels in the PVN, as well as increased POMC mRNA in the anterior pituitary gland (Hewagalamulage et al., 2016a). Collectively these data demonstrate that high cortisol responsiveness can be used as a marker for increased susceptibility to obesity (Hewagalamulage et al., 2016b; Lee et al., 2014c,d).

Altered susceptibility to obesity in LR and HR is underpinned by a number of metabolic, neuroendocrine, and behavioral traits that ultimately lead to increased food intake (in response to stress) and reduced energy expenditure (Lee et al., 2014d). A key feature of increased propensity to weight gain in the HR animals is reduced postprandial thermogenesis in skeletal muscle (Lee et al., 2014c). HR animals also show an attenuated catabolic state in response to stress (Lee et al., 2014d). The reduction in food intake caused by psychosocial or immune stress is greater in LR than HR (Lee et al., 2014d). Furthermore, in response to lipopolysaccharide treatment the increase in muscle heat production is greater in LR, which suggests that energy expenditure is lower in HR animals (Lee et al., 2014d). Similar observations have been made in LR and HR women, where women characterized as HR tend to eat more and show greater

preference toward foods high in fat and sugar in response to stress than LR women (Adam and Epel, 2007; Epel et al., 2001; Tomiyama et al., 2011). These metabolic differences may be underpinned by altered melanocortin signaling in the PVN of the hypothalamus. Animals selected for HR, are resistant to the satiety effect of α-MSH and have reduced expression of the MC3R and MC4R in the PVN (Hewagalamulage et al., 2015). Indeed, previous work in sheep has shown the MC4R to be central to the reduction in food intake caused by immune challenge (Sartin et al., 2008). Thus selection for cortisol responsiveness, at least in sheep, identifies animals with innate differences in the melanocortin system.

In addition to the metabolic sequelae, LR and HR animals exhibit inherent behavioral differences. Animals characterized as LR display a proactive coping style in response to stress, which is exemplified by increased physical activity and reduced fearfulness (Lee et al., 2014d). This contrasts the HR animals that exhibit increased freezing, active avoidance behaviors, and increased fear, which are characteristic of a reactive coping style (Hewagalamulage et al., 2016b; Lee et al., 2014d). It has been hypothesized that proactive coping strategies are associated with increased physical activity and thus is another means by which LR animals may expend more energy than HR (Koolhaas et al., 1999, 2010).

In summary, selection for cortisol responsiveness identifies individuals with increased susceptibility to

become obese. This increased propensity to gain weight is underpinned by a suite of metabolic, behavioral, and neuroendocrine factors that ultimately lead to reduced energy expenditure and increased food intake (under certain conditions).

3 CONCLUDING REMARKS

The energy balance equation, in which energy intake and energy expenditure are factored is a crucial consideration for means of control of obesity. This chapter has sought to highlight the relevance of the latter and to examine models that might be useful in its interrogation. Thermogenesis is defined as the dissipation of energy through the specialized production of heat; this process occurs in brown and beige adipocytes, as well as skeletal muscle. To date, there has been a prominent focus on the role of BAT thermogenesis in the maintenance of energy balance and the control of body weight. The recent identification of beige adipocytes has sparked a great deal of interest. The ability to transform or recruit beige adipocytes within typical WAT depots is likely to have beneficial effects not only on body weight, but also on metabolic health (e.g., improved glucose metabolism). In order to advance this area of research it is imperative to not only understand how we might expand BAT or beige adipocytes, but how these tissues are effectively activated.

Larger animal models, such as the sheep have been useful in elucidating the role of skeletal muscle thermogenesis. This process primarily occurs via two distinct mechanisms, that is, mitochondrial uncoupling through UCP3 and futile calcium cycling. In sheep, feeding is associated with activation of both pathways and a concomitant increase in muscle heat production. Given the relative abundance of skeletal muscle in comparison to BAT in humans, agents that target muscle thermogenesis may have broader application in the development of antiobesity therapies.

It is clear from genetic models (genetically lean and obese sheep and selection for cortisol responsiveness) and other natural models (such as photoperiodic change) that thermogenesis can play a significant role in the determination of adiposity and that this is a potential target for manipulation. Furthermore, large animal models have allowed dissection of the differential contribution of BAT and skeletal muscle to total thermogenic capacity and the control of body weight. For example, genetic obesity in sheep coincides with impaired BAT thermogenesis in retroperitoneal fat, whereas reduced skeletal muscle thermogenesis is a key component of the increased propensity to become obese in animals characterized as high cortisol responders. Given that efforts to regulate energy intake have been unsuccessful, it is suggested that models of thermogenesis offer a realistic alternative.

References

Abdelhamid, R.E., Kovács, K.J., Nunez, M.G., Larson, A.A., 2014. After a cold conditioning swim, UPC2-deficient mice are more able to defend against the cold than wild type mice. Physiol. Behav. 135, 168–173.

Adam, C.L., Findlay, P.A., Miller, D.W., 2006. Blood-brain leptin transport and appetite and reproductive neuroendocrine responses to intracerebroventricular leptin injection in sheep: influence of photoperiod. Endocrinology 147 (10), 4589–4598.

Adam, C.L., Moar, K.M., Logie, T.J., Ross, A.W., Barrett, P., Morgan, P.J., et al., 2000. Photoperiod regulates growth, puberty and hypothalamic neuropeptide and receptor gene expression in female Siberian hamsters. Endocrinology 141 (12), 4349–4356.

Adam, T.C., Epel, E.S., 2007. Stress, eating and the reward system. Physiol. Behav. 91 (4), 449–458.

Adler, E.S., Hollis, J.H., Clarke, I.J., Grattan, D.R., Oldfield, B.J., 2012. Neurochemical characterization and sexual dimorphism of projections from the brain to abdominal and subcutaneous white adipose tissue in the rat. J. Neurosci. 32 (45), 15913–15921.

Ahfeldt, T., Schinzel, R.T., Lee, Y.K., Hendrickson, D., Kaplan, A., Lum, D.H., et al., 2012. Programming human pluripotent stem cells into white and brown adipocytes. Nat. Cell Biol. 14 (2), 209–219.

Alfonso, J., Thompson, J.M., 1996. Changes in body composition of sheep selected for high and low backfat thickness, during periods of ad libitum and maintenance feeding. Anim. Sci. 63, 395–406.

Almind, K., Manieri, M., Sivitz, W.I., Cinti, S., Kahn, C.R., 2007. Ectopic brown adipose tissue in muscle provides a mechanism for differences in risk of metabolic syndrome in mice. Proc. Natl. Acad. Sci. USA 104 (7), 2366–2371.

Anukulkitch, C., Rao, A., Dunshea, F.R., Clarke, I.J., 2009. A test of the lipostat theory in a seasonal (ovine) model under natural conditions reveals close relationship between adiposity and melanin concentrating hormone expression. Domest. Anim. Endocrinol. 36, 138–151.

Anukulkitch, C., Rao, A., Pereira, A., McEwan, J., Clarke, I.J., 2010. Expression of genes for appetite-regulating peptides in the hypothalamus of genetically selected lean and fat sheep. Neuroendocrinology 91 (3), 223–238.

Argo, C.M.S., Smith, J.S, Kay, R.N.B., 1999. Seasonal changes of metabolism and appetite in the Soay ram. Anim. Sci. 69, 191–202.

Argyropoulos, G., Harper, M.-E., 2002. Uncoupling proteins and thermoregulation. J. Appl. Physiol. (1985) 92 (5), 2187–2198.

Arruda, A.P., Nigro, M., Oliveira, G.M., de Meis, L., 2007. Thermogenic activity of Ca^{2+}-ATPase from skeletal muscle heavy sarcoplasmic reticulum: the role of ryanodine Ca^{2+} channel. Biochim. Biophys. Acta 1768 (6), 1498–1505.

Astrand, A., Bohlooly, Y.M., Larsdotter, S., Mahlapuu, M., Andersen, H., Tornell, J., et al., 2004. Mice lacking melanin-concentrating hormone receptor 1 demonstrate increased heart rate associated with altered autonomic activity. Am. J. Physiol. Regul. Integr. Comp. Physiol. 287 (4), R749–R758.

Astrup, A., 1986. Thermogenesis in human brown adipose tissue and skeletal muscle induced by sympathomimetic stimulation. Acta Endocrinol. Suppl. (Copenh.) 278, 1–32.

Au-Yong, I.T., Thorn, N., Ganatra, R., Perkins, A.C., Symonds, M.E., 2009. Brown adipose tissue and seasonal variation in humans. Diabetes 58 (11), 2583–2587.

Bachman, E.S., Dhillon, H., Zhang, C.-Y., Cinti, S., Bianco, A.C., Kobilka, B.K., et al., 2002. beta AR signaling required for diet-induced thermogenesis and obesity resistance. Science 297 (5582), 843–845.

Backholer, K., Bowden, M., Gamber, K., Bjorbaek, C., Iqbal, J., Clarke, I.J., 2010. Melanocortins mimic the effects of leptin to restore reproductive function in lean hypogonadotropic ewes. Neuroendocrinology 91 (1), 27–40.

Bal, N.C., Maurya, S.K., Sopariwala, D.H., Sahoo, S.K., Gupta, S.C., Shaikh, S.A., et al., 2012. Sarcolipin is a newly identified regulator of muscle-based thermogenesis in mammals. Nat. Med. 18 (10), 1575–1579.

Barbatelli, G., Murano, I., Madsen, L., Hao, Q., Jimenez, M., Kristiansen, K., et al., 2010. The emergence of cold-induced brown adipocytes in mouse white fat depots is determined predominantly by white to brown adipocyte transdifferentiation. Am. J. Physiol. Endocrinol. Metab. 298 (6), E1244–E1253.

Barclay, C.J., 2012. Quantifying Ca^{2+} release and inactivation of Ca^{2+} release in fast- and slow-twitch muscles. J. Physiol. 590 (23), 6199–6212.

Barclay, J.L., Agada, H., Jang, C., Ward, M., Wetzig, N., Ho, K.K., 2015. Effects of glucocorticoids on human brown adipocytes. J. Endocrinol. 224 (2), 139–147.

Barker, D.J., Osmond, C., 1986. Infant mortality, childhood nutrition, and ischaemic heart disease in England and Wales. Lancet 1 (8489), 1077–1081.

Barker, D.J., Osmond, C., Simmonds, S.J., Wield, G.A., 1993. The relation of small head circumference and thinness at birth to death from cardiovascular disease in adult life. BMJ 306 (6875), 422–426.

Barker, D.J., Winter, P.D., Osmond, C., Margetts, B., Simmonds, S.J., 1989. Weight in infancy and death from ischaemic heart disease. Lancet 2 (8663), 577–580.

Barker-Gibb, M.L., Clarke, I.J., 1996. Increased galanin and neuropeptide-Y immunoreactivity within the hypothalamus of ovariectomised ewes following a prolonged period of reduced body weight is associated with changes in plasma growth hormone but not gonadotropin levels. Neuroendocrinology 64 (3), 194–207.

Bartness, T.J., Goldman, B.D., Bittman, E.L., 1991. SCN lesions block responses to systemic melatonin infusions in Siberian hamsters. Am. J. Physiol. 260 (1 Pt 2), R102–R112.

Bartness, T.J., Powers, J.B., Hastings, M.H., Bittman, E.L., Goldman, B.D., 1993. The timed infusion paradigm for melatonin delivery: what has it taught us about the melatonin signal, its reception, and the photoperiodic control of seasonal responses? J. Pineal. Res. 15 (4), 161–190.

Bartness, T.J., Wade, G.N., 1984. Photoperiodic control of body weight and energy metabolism in Syrian hamsters (*Mesocricetus auratus*): role of pineal gland, melatonin, gonads, and diet. Endocrinology 114 (2), 492–498.

Berglund, E.D., Liu, T., Kong, X., Sohn, J.-W., Vong, L., Deng, Z., et al., 2014. Melanocortin 4 receptors in autonomic neurons regulate thermogenesis and glycemia. Nat. Neurosci. 17 (7), 911–913.

Billington, C.J., Briggs, J.E., Grace, M., Levine, A.S., 1991. Effects of intracerebroventricular injection of neuropeptide Y on energy metabolism. Am. J. Physiol. 260 (2 Pt 2), R321–R327.

Bittman, E.L., Crandell, R.G., Lehman, M.N., 1989. Influences of the paraventricular and suprachiasmatic nuclei and olfactory bulbs on melatonin responses in the golden hamster. Biol. Reprod. 40 (1), 118–126.

Blondin, D.P., Labbé, S.M., Phoenix, S., Guérin, B., Turcotte, É.E., Richard, D., et al., 2015. Contributions of white and brown adipose tissues and skeletal muscles to acute cold-induced metabolic responses in healthy men. J. Physiol. 593 (3), 701–714.

Boden, M.J., Kennaway, D.J., 2006. Circadian rhythms and reproduction. Reproduction 132 (3), 379–392.

Boersma, G.J., Salton, S.R., Spritzer, P.M., Steele, C.T., Carbone, D.L., 2012. Models and mechanisms of metabolic regulation: genes, stress, and the HPA and HPG axes. Horm. Metab. Res. 44 (8), 598–606.

Bostrom, P., Wu, J., Jedrychowski, M.P., Korde, A., Ye, L., Lo, J.C., et al., 2012. A PGC1-alpha-dependent myokine that drives brown-fat-like development of white fat and thermogenesis. Nature 481 (7382), 463–468.

Bouchard, C., Tremblay, A., Després, J.-P., Nadeau, A., Lupien, P.J., Thériault, G., et al., 1990. The response to long-term overfeeding in identical twins. N. Engl. J. Med. 322 (21), 1477–1482.

Bouret, S.G., 2012. Nutritional programming of hypothalamic development: critical periods and windows of opportunity. Int. J. Obes. Suppl. 2 (S2), S19–S24.

Bouret, S.G., Draper, S.J., Simerly, R.B., 2004. Trophic action of leptin on hypothalamic neurons that regulate feeding. Science 304 (5667), 108–110.

Bouyer, K., Simerly, R.B., 2013. Neonatal leptin exposure specifies innervation of presympathetic hypothalamic neurons and improves the metabolic status of leptin-deficient mice. J. Neurosci. 33 (2), 840–851.

Braun, T.P., Marks, D.L., 2011. Hypothalamic regulation of muscle metabolism. Curr. Opin. Clin. Nutr. Metab. Care 14 (3), 237–242.

Butler, A.A., Cone, R.D., 2002. The melanocortin receptors: lessons from knockout models. Neuropeptides 36 (2–3), 77–84.

Butler, A.A., Marks, D.L., Fan, W., Kuhn, C.M., Bartolome, M., Cone, R.D., 2001. Melanocortin-4 receptor is required for acute homeostatic responses to increased dietary fat. Nat. Neurosci. 4 (6), 605–611.

Cadenas, S., Buckingham, J.A., Samec, S., Seydoux, J., Din, N., Dulloo, A.G., et al., 1999. UCP2 and UCP3 rise in starved rat skeletal muscle but mitochondrial proton conductance is unchanged. FEBS Lett. 462 (3), 257–260.

Cannon, B., Nedergaard, J., 2004. Brown adipose tissue: function and physiological significance. Physiol. Rev. 84 (1), 277–359.

Cannon, B., Nedergaard, J., 2010. Thyroid hormones: igniting brown fat via the brain. Nat. Med. 16 (9), 965–967.

Cao, W.H., Fan, W., Morrison, S.F., 2004. Medullary pathways mediating specific sympathetic responses to activation of dorsomedial hypothalamus. Neuroscience 126 (1), 229–240.

Cao, W.H., Morrison, S.F., 2006. Glutamate receptors in the raphe pallidus mediate brown adipose tissue thermogenesis evoked by activation of dorsomedial hypothalamic neurons. Neuropharmacology 51 (3), 426–437.

Carey, A.L., Formosa, M.F., Van Every, B., Bertovic, D., Eikelis, N., Lambert, G.W., et al., 2013. Ephedrine activates brown adipose tissue in lean but not obese humans. Diabetologia 56 (1), 147–155.

Carey, A.L., Pajtak, R., Formosa, M.F., Van Every, B., Bertovic, D.A., Anderson, M.J., et al., 2015. Chronic ephedrine administration decreases brown adipose tissue activity in a randomised controlled human trial: implications for obesity. Diabetologia 58 (5), 1045–1054.

Celi, F.S., Le, T.N., Ni, B., 2015. Physiology and relevance of human adaptive thermogenesis response. Trends Endocrinol. Metab. 26 (5), 238–247.

Chappuis, S., Ripperger, J.A., Schnell, A., Rando, G., Jud, C., Wahli, W., et al., 2013. Role of the circadian clock gene Per2 in adaptation to cold temperature. Mol. Metab. 2 (3), 184–193.

Chemelli, R.M., Willie, J.T., Sinton, C.M., Elmquist, J.K., Scammell, T., Lee, C., et al., 1999. Narcolepsy in orexin knockout mice: molecular genetics of sleep regulation. Cell 98 (4), 437–451.

Clarke, I.J., 2001. Sex and season are major determinants of voluntary food intake in sheep. Reprod. Fertil. Dev. 13 (7–8), 577–582.

Clarke, S.D., Clarke, I.J., Rao, A., Cowley, M.A., Henry, B.A., 2012a. Sex differences in the metabolic effects of testosterone in sheep. Endocrinology 153 (1), 123–131.

Clarke, S.D., Clarke, I.J., Rao, A., Evans, R.G., Henry, B.A., 2013. Differential effects of acute and chronic estrogen treatment on thermogenic and metabolic pathways in ovariectomized sheep. Endocrinology 154 (1), 184–192.

Clarke, S.D., Lee, K., Andrews, Z.B., Bischof, R., Fahri, F., Evans, R.G., et al., 2012b. Postprandial heat production in skeletal muscle is associated with altered mitochondrial function and altered futile calcium cycling. Am. J. Physiol. Regul. Integr. Comp. Physiol. 303 (10), R1071–R1079.

Clarke, I.J., Rao, A., Chilliard, Y., Delavaud, C., Lincoln, G.A., 2003. Photoperiod effects on gene expression for hypothalamic appetite-regulating peptides and food intake in the ram. Am. J. Physiol. Regul. Integr. Comp. Physiol. 284 (1), R101–R115.

Clarke, I.J., Scott, C.J., Rao, A., Pompolo, S., Barker-Gibb, M.L., 2000. Seasonal changes in the expression of neuropeptide Y and pro-opiomelanocortin mRNA in the arcuate nucleus of the ovariectomized ewe: relationship to the seasonal appetite and breeding cycles. J. Neuroendocrinol. 12 (11), 1105–1111.

Clarke, I.J., Tilbrook, A.J., Turner, A.I., Doughton, B.W., Goding, J.W., 2001. Sex, fat and the tilt of the earth: effects of sex and season on the feeding response to centrally administered leptin in sheep. Endocrinology 142 (6), 2725–2728.

Clegg, D.J., Brown, L.M., Woods, S.C., Benoit, S.C., 2006. Gonadal hormones determine sensitivity to central leptin and insulin. Diabetes 55 (4), 978–987.

Clegg, D.J., Riedy, C.A., Smith, K.A., Benoit, S.C., Woods, S.C., 2003. Differential sensitivity to central leptin and insulin in male and female rats. Diabetes 52 (3), 682–687.

Collins, S., Yehuda-Shnaidman, E., Wang, H., 2010. Positive and negative control of Ucp1 gene transcription and the role of beta-adrenergic signaling networks. Int. J. Obes. (Lond.) 34 (Suppl. 1), S28–S33.

Cone, R.D., Cowley, M.A., Butler, A.A., Fan, W., Marks, D.L., Low, M.J., 2001. The arcuate nucleus as a conduit for diverse signals relevant to energy homeostasis. Int. J. Obes. Relat. Metab. Disord. 25 (Suppl. 5), S63–S67.

Costford, S.R., Chaudhry, S.N., Crawford, S.A., Salkhordeh, M., Harper, M.E., 2008. Long-term high-fat feeding induces greater fat storage in mice lacking UCP3. Am. J. Physiol. Endocrinol. Metab. 295 (5), E1018–E1024.

Cypess, A.M., Chen, Y.C., Sze, C., Wang, K., English, J., Chan, O., et al., 2012. Cold but not sympathomimetics activates human brown adipose tissue in vivo. Proc. Natl. Acad. Sci. USA 109 (25), 10001–10005.

Cypess, A.M., Lehman, S., Williams, G., Tal, I., Rodman, D., Goldfine, A.B., et al., 2009. Identification and importance of brown adipose tissue in adult humans. N. Engl. J. Med. 360 (15), 1509–1517.

De Blasio, M.J., Blache, D., Gatford, K.L., Robinson, J.S., Owens, J.A., 2010. Placental restriction increases adipose leptin gene expression and plasma leptin and alters their relationship to feeding activity in the young lamb. Pediatr. Res. 67 (6), 603–608.

De Blasio, M.J., Gatford, K.L., Harland, M.L., Robinson, J.S., Owens, J.A., 2012. Placental restriction reduces insulin sensitivity and expression of insulin signaling and glucose transporter genes in skeletal muscle, but not liver, in young sheep. Endocrinology 153 (5), 2142–2151.

De Blasio, M.J., Gatford, K.L., McMillen, I.C., Robinson, J.S., Owens, J.A., 2007a. Placental restriction of fetal growth increases insulin action, growth, and adiposity in the young lamb. Endocrinology 148 (3), 1350–1358.

De Blasio, M.J., Gatford, K.L., Robinson, J.S., Owens, J.A., 2007b. Placental restriction of fetal growth reduces size at birth and alters postnatal growth, feeding activity, and adiposity in the young lamb. Am. J. Physiol. Regul. Integr. Comp. Physiol. 292 (2), R875–R886.

de Boo, H.A., Harding, J.E., 2006. The developmental origins of adult disease (Barker) hypothesis. Aust. N. Z. J. Obstet. Gynaecol. 46 (1), 4–14.

de Meis, L., Arruda, A.P., Carvalho, D.P., 2005. Role of sarco/endoplasmic reticulum Ca(2+)-ATPase in thermogenesis [Review]. Biosci. Rep. 25 (3–4), 181–190.

Dhillon, H., Zigman, J.M., Ye, C., Lee, C.E., McGovern, R.A., Tang, V., et al., 2006. Leptin directly activates SF1 neurons in the VMH, and this action by leptin is required for normal body-weight homeostasis. Neuron 49 (2), 191–203.

Douris, N., Stevanovic, D.M., Fisher, F.M., Cisu, T.I., Chee, M.J., Nguyen, N.L., et al., 2015. Central fibroblast growth factor 21 browns white fat via sympathetic action in male mice. Endocrinology 156 (7), 2470–2481.

Duclos, M., Corcuff, J.B., Etcheverry, N., Rashedi, M., Tabarin, A., Roger, P., 1999. Abdominal obesity increases overnight cortisol excretion. J. Endocrinol. Invest. 22 (6), 465–471.

Enerback, S., Jacobsson, A., Simpson, E.M., Guerra, C., Yamashita, H., Harper, M.E., et al., 1997. Mice lacking mitochondrial uncoupling protein are cold-sensitive but not obese. Nature 387 (6628), 90–94.

Enriori, P.J., Evans, A.E., Sinnayah, P., Jobst, E.E., Tonelli-Lemos, L., Billes, S.K., et al., 2007. Diet-induced obesity causes severe but reversible leptin resistance in arcuate melanocortin neurons. Cell Metab. 5 (3), 181–194.

Enriori, P.J., Sinnayah, P., Simonds, S.E., Garcia Rudaz, C., Cowley, M.A., 2011. Leptin action in the dorsomedial hypothalamus increases sympathetic tone to brown adipose tissue in spite of systemic leptin resistance. J. Neurosci. 31 (34), 12189–12197.

Epel, E., Lapidus, R., McEwen, B., Brownell, K., 2001. Stress may add bite to appetite in women: a laboratory study of stress-induced cortisol and eating behavior. Psychoneuroendocrinology 26 (1), 37–49.

Faouzi, M., Leshan, R., Bjornholm, M., Hennessey, T., Jones, J., Munzberg, H., 2007. Differential accessibility of circulating leptin to individual hypothalamic sites. Endocrinology 148 (11), 5414–5423.

Farooqi, I.S., 2008. Monogenic human obesity. Front. Horm. Res. 36, 1–11.

Farooqi, I.S., Keogh, J.M., Yeo, G.S., Lank, E.J., Cheetham, T., O'Rahilly, S., 2003. Clinical spectrum of obesity and mutations in the melanocortin 4 receptor gene. N. Engl. J. Med. 348 (12), 1085–1095.

Farooqi, I.S., O'Rahilly, S., 2008. Mutations in ligands and receptors of the leptin-melanocortin pathway that lead to obesity. Nat. Clin. Pract. Endocrinol. Metab. 4 (10), 569–577.

Feldmann, H.M., Golozoubova, V., Cannon, B., Nedergaard, J., 2009. UCP1 ablation induces obesity and abolishes diet-induced thermogenesis in mice exempt from thermal stress by living at thermoneutrality. Cell Metab. 9 (2), 203–209.

Ferguson, A.V., Samson, W.K., 2003. The orexin/hypocretin system: a critical regulator of neuroendocrine and autonomic function [Review]. Front. Neuroendocrinol. 24 (3), 141–150.

Fisher, F.M., Kleiner, S., Douris, N., Fox, E.C., Mepani, R.J., Verdeguer, F., et al., 2012. FGF21 regulates PGC-1alpha and browning of white adipose tissues in adaptive thermogenesis. Genes Dev. 26 (3), 271–281.

Fleury, C., Neverova, M., Collins, S., Raimbault, S., Champigny, O., Levi-Meyrueis, C., et al., 1997. Uncoupling protein-2: a novel gene linked to obesity and hyperinsulinemia. Nat. Genet. 15 (3), 269–272.

Francis, S.M., Jopson, N.B., Littlejohn, R.P., Stuart, S.K., Veenvliet, B.A., Young, M.J., et al., 1998a. Effects of growth hormone administration on the body composition and hormone levels of genetically fat sheep. Anim. Sci. 67 (03), 549–558.

Francis, S.M., Veenvliet, B.A., Stuart, S.K., Littlejohn, R.P., Suttie, J.M., 1997. The effect of photoperiod on plasma hormone concentrations in wether lambs with genetic differences in body composition. Anim. Sci. 65 (03), 441–450.

Francis, S.M., Veenvliet, B.A., Stuart, S.K., Littlejohn, R.P., Suttie, J.M., 1998b. Growth hormone secretion and pituitary gland weight in suckling lambs from genetically lean and fat sheep. N. Z. J. Agric. Res. 41 (3), 387–393.

French, M.C., Littlejohn, R.P., Greer, G.J., Bain, W.E., McEwan, J.C., Tisdall, D.J., 2006. Growth hormone and ghrelin receptor genes are differentially expressed between genetically lean and fat selection lines of sheep. J. Anim. Sci. 84 (2), 324–331.

Fromme, T., Hoffmann, C., Nau, K., Rozman, J., Reichwald, K., Utting, M., et al., 2009. An intronic single base exchange leads to a brown adipose tissue-specific loss of Ucp3 expression and an altered body mass trajectory. Physiol. Genomics 38 (1), 54–62.

Fromme, T., Klingenspor, M., 2011. Uncoupling protein 1 expression and high-fat diets. Am. J. Physiol. Regul. Integr. Comp. Physiol. 300 (1), R1–R8.

Fullston, T., Palmer, N.O., Owens, J.A., Mitchell, M., Bakos, H.W., Lane, M., 2012. Diet-induced paternal obesity in the absence of diabetes diminishes the reproductive health of two subsequent generations of mice. Hum. Reprod. 27 (5), 1391–1400.

Gaspar-Lopez, E., Casabiell, J., Estevez, J.A., Landete-Castillejos, T., De La Cruz, L.F., Gallego, L., et al., 2009. Seasonal changes in plasma leptin concentration related to antler cycle in Iberian red deer stags. J. Comp. Physiol. B. 179 (5), 617–622.

Gatford, K.L., Mohammad, S.N., Harland, M.L., De Blasio, M.J., Fowden, A.L., Robinson, J.S., et al., 2008. Impaired beta-cell function and inadequate compensatory increases in beta-cell mass after intrauterine growth restriction in sheep. Endocrinology 149 (10), 5118–5127.

Gautron, L., Elmquist, J.K., 2011. Sixteen years and counting: an update on leptin in energy balance. J. Clin. Invest. 121 (6), 2087–2093.

Gavini, C.K., Jones, II, W.C., Novak, C.M., 2016. Ventromedial hypothalamic melanocortin receptor activation: regulation of activity energy expenditure and skeletal muscle thermogenesis. J. Physiol. 594, 5285–5301.

Gilsanz, V., Smith, M.L., Goodarzian, F., Kim, M., Wren, T.A., Hu, H.H., 2012. Changes in brown adipose tissue in boys and girls during childhood and puberty. J. Pediatr. 160 (4), 604–609, e601.

Gnanalingham, M.G., Mostyn, A., Symonds, M.E., Stephenson, T., 2005. Ontogeny and nutritional programming of adiposity in sheep: potential role of glucocorticoid action and uncoupling protein-2. Am. J. Physiol. Regul. Integr. Comp. Physiol. 289 (5), R1407–R1415.

Goele, K., Bosy-Westphal, A., Rumcker, B., Lagerpusch, M., Muller, M.J., 2009. Influence of changes in body composition and adaptive thermogenesis on the difference between measured and predicted weight loss in obese women. Obes. Facts 2 (2), 105–109.

Gong, D.W., He, Y., Karas, M., Reitman, M., 1997. Uncoupling protein-3 is a mediator of thermogenesis regulated by thyroid hormone, beta3-adrenergic agonists, and leptin. J. Biol. Chem. 272 (39), 24129–24132.

Gong, D.W., Monemdjou, S., Gavrilova, O., Leon, L.R., Marcus-Samuels, B., Chou, C.J., et al., 2000. Lack of obesity and normal response to fasting and thyroid hormone in mice lacking uncoupling protein-3. J. Biol. Chem. 275 (21), 16251–16257.

Hanon, E.A., Lincoln, G.A., Fustin, J.M., Dardente, H., Masson-Pevet, M., Morgan, P.J., et al., 2008,. Ancestral TSH mechanism signals summer in a photoperiodic mammal. Curr. Biol. 18 (15), 1147–1152.

Hara, J., Beuckmann, C.T., Nambu, T., Willie, J.T., Chemelli, R.M., Sinton, C.M., et al., 2001. Genetic ablation of orexin neurons in mice results in narcolepsy, hypophagia, and obesity. Neuron 30 (2), 345–354.

Harper, M.E., Dent, R., Monemdjou, S., Bezaire, V., Van Wyck, L., Wells, G., et al., 2002. Decreased mitochondrial proton leak and reduced expression of uncoupling protein 3 in skeletal muscle of obese diet-resistant women. Diabetes 51 (8), 2459–2466.

Heldmaier, G., Hoffmann, K., 1974. Melatonin stimulates growth of brown adipose tissue. Nature 247 (5438), 224–225.

Heldmaier, G., Steinlechner, S., Rafael, J., Vsiansky, P., 1981. Photoperiodic control and effects of melatonin on nonshivering thermogenesis and brown adipose tissue. Science 212 (4497), 917–919.

Henry, B.A., Andrews, Z.B., Rao, A., Clarke, I.J., 2011. Central leptin activates mitochondrial function and increases heat production in skeletal muscle. Endocrinology 152 (7), 2609–2618.

Henry, B.A., Blache, D., Rao, A., Clarke, I.J., Maloney, S.K., 2010. Disparate effects of feeding on core body and adipose tissue temperatures in animals selectively bred for nervous or calm temperament. Am. J. Physiol. Regul. Integr. Comp. Physiol. 299 (3), R907–R917.

Henry, B.A., Clarke, I.J., 2008. Adipose tissue hormones and the regulation of food intake. J. Neuroendocrinol. 20 (6), 842–849.

Henry, B.A., Dunshea, F.R., Gould, M., Clarke, I.J., 2008. Profiling postprandial thermogenesis in muscle and fat of sheep and the central effect of leptin administration. Endocrinology 149 (4), 2019–2026.

Henry, B.A., Loughnan, R., Hickford, J., Young, I.R., St John, J., Clarke, I.J., 2015. Differences in mitochondrial DNA inheritance and function align with body conformation in genetically lean and fat sheep. J. Anim. Sci. 93, 2083–2093.

Henry, B.A., Tilbrook, A.J., Dunshea, F.R., Rao, A., Blache, D., Martin, G.B., et al., 2000. Long-term alterations in adiposity affect the expression of melanin-concentrating hormone and enkephalin but not proopiomelanocortin in the hypothalamus of ovariectomized ewes. Endocrinology 141 (4), 1506–1514.

Hetzer, H., Harvey, W., 1967. Selection for high and low fatness in swine. J. Anim. Sci. 26 (6), 1244–1251.

Hetzer, H.O., Miller, R.H., 1972. Rate of growth as influenced by selection for high and low fatness in swine. J. Anim. Sci. 35 (4), 730.

Hetzer, H.O., Miller, L.R., 1973. Selection for high and low fatness in swine—correlated responses of various carcass traits. J. Anim. Sci. 37 (6), 1289–1301.

Hewagalamulage, S.D., Clarke, I.J., Rao, A., Henry, B.A., 2016a. Ewes with divergent cortisol responses to adrenocorticotropin (ACTH) exhibit functional differences in the hypothalamo-pituitary-adrenal (HPA) axis. Endocrinology 157, 3540–3549.

Hewagalamulage, S.D., Clarke, I.J., Young, I.R., Rao, A., Henry, B.A., 2015. High cortisol response to adrenocorticotrophic hormone identifies ewes with reduced melanocortin signalling and increased propensity to obesity. J. Neuroendocrinol. 27 (1), 44–56.

Hewagalamulage, S.D., Lee, T.K., Clarke, I.J., Henry, B.A., 2016b. Stress, cortisol, and obesity: a role for cortisol responsiveness in identifying individuals prone to obesity. Domest. Anim. Endocrinol. 56 Suppl., S112–S120.

Hew-Butler, T., Landis-Piwowar, K., Byrd, G., Seimer, M., Seigneurie, N., Byrd, B., et al., 2015. Plasma irisin in runners and nonrunners: no favorable metabolic associations in humans. Physiol. Rep. 3 (1), e12262.

Holland, W.L., Adams, A.C., Brozinick, J.T., Bui, H.H., Miyauchi, Y., Kusminski, C.M., et al., 2013. An FGF21-adiponectin-ceramide axis controls energy expenditure and insulin action in mice. Cell Metab. 17 (5), 790–797.

Hu, H.H., Gilsanz, V., 2011. Developments in the imaging of brown adipose tissue and its associations with muscle, puberty, and health in children. Front. Endocrinol. (Lausanne) 2, 33.

Huttunen, P., Hirvonen, J., Kinnula, V., 1981. The occurrence of brown adipose tissue in outdoor workers. Eur. J. Appl. Physiol. Occup. Physiol. 46 (4), 339–345.

Ishibashi, J., Seale, P., 2010. Beige can be slimming. Science 328 (5982), 1113–1114.

Ito, M., Gomori, A., Ishihara, A., Oda, Z., Mashiko, S., Matsushita, H., et al., 2003. Characterization of MCH-mediated obesity in mice. Am. J. Physiol. Endocrinol. Metab. 284 (5), E940–E945.

Janovska, A., Hatzinikolas, G., Staikopoulos, V., McInerney, J., Mano, M., Wittert, G.A., 2008. AMPK and ACC phosphorylation: effect of leptin, muscle fibre type and obesity. Mol. Cell Endocrinol. 284 (1–2), 1–10.

Jedrychowski, M.P., Wrann, C.D., Paulo, J.A., Gerber, K.K., Szpyt, J., Robinson, M.M., et al., 2015. Detection and quantitation of circulating human irisin by tandem mass spectrometry. Cell Metab. 22 (4), 734–740.

Jespersen, N.Z., Larsen, T.J., Peijs, L., Daugaard, S., Homoe, P., Loft, A., et al., 2013. A classical brown adipose tissue mRNA signature partly overlaps with brite in the supraclavicular region of adult humans. Cell Metab. 17 (5), 798–805.

Ji, L., Gupta, M., Feldman, B.J., 2016. Vitamin D regulates fatty acid composition in subcutaneous adipose tissue through Elovl3. Endocrinology 157 (1), 91–97.

Jia, R., Luo, X.Q., Wang, G., Lin, C.X., Qiao, H., Wang, N., et al., 2016. Characterization of cold-induced remodelling reveals depot-specific differences across and within brown and white adipose tissues in mice. Acta Physiol. (Oxf.) 217 (4), 311–324.

Jiménez-Aranda, A., Fernández-Vázquez, G., Campos, D., Tassi, M., Velasco-Perez, L., Tan, D.-X., et al., 2013. Melatonin induces browning of inguinal white adipose tissue in Zucker diabetic fatty rats. J. Pineal Res. 55 (4), 416–423.

Johnston, J.D., Ebling, F.J., Hazlerigg, D.G., 2005. Photoperiod regulates multiple gene expression in the suprachiasmatic nuclei and pars tuberalis of the Siberian hamster (Phodopus sungorus). Eur. J. Neurosci. 21 (11), 2967–2974.

Kajimura, S., Seale, P., Kubota, K., Lunsford, E., Frangioni, J.V., Gygi, S.P., et al., 2009. Initiation of myoblast to brown fat switch by a PRDM16-C/EBP-beta transcriptional complex. Nature 460 (7259), 1154–1158.

Karsch, F.J., Bittman, E.L., Foster, D.L., Goodman, R.L., Legan, S.J., Robinson, J.E., 1984. Neuroendocrine basis of seasonal reproduction. Recent Prog. Horm. Res. 40, 185–232.

Kennaway, D.J., 2005. The role of circadian rhythmicity in reproduction. Hum. Reprod. Update 11 (1), 91–101.

Klaus, S., Munzberg, H., Truloff, C., Heldmaier, G., 1998. Physiology of transgenic mice with brown fat ablation: obesity is due to lowered body temperature. Am. J. Physiol. 274 (2 Pt 2), R287–R293.

Knott, S.A., Cummins, L.J., Dunshea, F.R., Leury, B.J., 2008. Rams with poor feed efficiency are highly responsive to an exogenous adrenocorticotropin hormone (ACTH) challenge. Domest. Anim. Endocrinol. 34 (3), 261–268.

Knott, S.A., Cummins, L.J., Dunshea, F.R., Leury, B.J., 2010. Feed efficiency and body composition are related to cortisol response to adrenocorticotropin hormone and insulin-induced hypoglycemia in rams. Domest. Anim. Endocrinol. 39 (2), 137–146.

Kolumam, G., Chen, M.Z., Tong, R., Zavala-Solorio, J., Kates, L., van Bruggen, N., et al., 2015. Sustained brown fat stimulation and insulin sensitization by a humanized bispecific antibody agonist for fibroblast growth factor receptor 1/betaKlotho complex. EBioMedicine 2 (7), 730–743.

Koolhaas, J.M., de Boer, S.F., Coppens, C.M., Buwalda, B., 2010. Neuroendocrinology of coping styles: towards understanding the biology of individual variation. Front. Neuroendocrinol. 31 (3), 307–321.

Koolhaas, J.M., Korte, S.M., De Boer, S.F., Van Der Vegt, B.J., Van Reenen, C.G., Hopster, H., et al., 1999. Coping styles in animals: current status in behavior and stress-physiology. Neurosci. Biobehav. Rev. 23 (7), 925–935.

Kopecky, J., Clarke, G., Enerback, S., Spiegelman, B., Kozak, L.P., 1995. Expression of the mitochondrial uncoupling protein gene from the aP2 gene promoter prevents genetic obesity. J. Clin. Invest. 96 (6), 2914–2923.

Krude, H., Biebermann, H., Luck, W., Horn, R., Brabant, G., Gruters, A., 1998. Severe early-onset obesity, adrenal insufficiency and red hair pigmentation caused by POMC mutations in humans. Nat. Genet. 19 (2), 155–157.

Kunej, T., Jevsinek Skok, D., Zorc, M., Ogrinc, A., Michal, J.J., Kovac, M., et al., 2013. Obesity gene atlas in mammals. J. Genomics 1, 45–55.

Kus, V., Prazak, T., Brauner, P., Hensler, M., Kuda, O., Flachs, P., et al., 2008. Induction of muscle thermogenesis by high-fat diet in mice: association with obesity-resistance. Am. J. Physiol. Endocrinol. Metab. 295 (2), E356–E367.

Kusminski, C.M., Scherer, P.E., 2012. Mitochondrial dysfunction in white adipose tissue. Trends Endocrinol. Metab. 23 (9), 435–443.

Laker, R.C., Henry, B.A., Wadley, G.D., Clarke, I.J., Canny, B.J., McConell, G.K., 2011. Central infusion of leptin does not increase AMPK signaling in skeletal muscle of sheep. Am. J. Physiol. Regul. Integr. Comp. Physiol. 300 (2), R511–R518.

Lanner, J.T., 2012. Ryanodine receptor physiology and its role in disease. Adv. Exp. Med. Biol. 740, 217–234.

Lee, P., Bova, R., Schofield, L., Bryant, W., Dieckmann, W., Slattery, A., et al., 2016. Brown adipose tissue exhibits a glucose-responsive thermogenic biorhythm in humans. Cell Metab. 23 (4), 602–609.

Lee, P., Greenfield, J.R., 2015. Non-pharmacological and pharmacological strategies of brown adipose tissue recruitment in humans. Mol. Cell Endocrinol. 418 Pt 2, 184–190.

Lee, P., Linderman, J.D., Smith, S., Brychta, R.J., Wang, J., Idelson, C., et al., 2014a. Irisin and FGF21 are cold-induced endocrine activators of brown fat function in humans. Cell Metab. 19 (2), 302–309.

Lee, Y.H., Petkova, A.P., Mottillo, E.P., Granneman, J.G., 2012. In vivo identification of bipotential adipocyte progenitors recruited by beta3-adrenoceptor activation and high-fat feeding. Cell Metab. 15 (4), 480–491.

Lee, P., Swarbrick, M.M., Greenfield, J.R., 2015. The sum of all browning in FGF21 therapeutics. Cell Metab. 21 (6), 795–796.

Lee, P., Swarbrick, M.M., Zhao, J.T., Ho, K.K.Y., 2011a. Inducible brown adipogenesis of supraclavicular fat in adult humans. Endocrinology 152 (10), 3597–3602.

Lee, P., Werner, C.D., Kebebew, E., Celi, F.S., 2014b. Functional thermogenic beige adipogenesis is inducible in human neck fat. Int. J. Obes. (Lond.) 38 (2), 170–176.

Lee, T.K., Clarke, I.J., St John, J., Young, I.R., Leury, B.L., Rao, A., et al., 2014c. High cortisol responses identify propensity for obesity that is linked to thermogenesis in skeletal muscle. FASEB J. 28 (1), 35–44.

Lee, T.K., Lee, C., Bischof, R., Lambert, G.W., Clarke, I.J., Henry, B.A., 2014d. Stress-induced behavioral and metabolic adaptations lead to an obesity-prone phenotype in ewes with elevated cortisol responses. Psychoneuroendocrinology 47, 166–177.

Lee, P., Zhao, J.T., Swarbrick, M.M., Gracie, G., Bova, R., Greenfield, J.R., et al., 2011b. High prevalence of brown adipose tissue in adult humans. J. Clin. Endocrinol. Metab. 96 (8), 2450–2455.

Lefterova, M.I., Zhang, Y., Steger, D.J., Schupp, M., Schug, J., Cristancho, A., et al., 2008. PPARgamma and C/EBP factors orchestrate adipocyte biology via adjacent binding on a genome-wide scale. Genes Dev. 22 (21), 2941–2952.

Lidell, M.E., Betz, M.J., Leinhard, O.D., Heglind, M., Elander, L., Slawik, M., et al., 2013. Evidence for two types of brown adipose tissue in humans. Nat. Med. 19 (5), 631–634.

Lilburn, M.S., Leach, Jr., R.M., Buss, E.G., Martin, R.J., 1982. The developmental characteristics of two strains of chickens selected for differences in mature abdominal fat pad size. Growth 46 (2), 171–181.

Lin, Z., Tian, H., Lam, K.S., Lin, S., Hoo, R.C., Konishi, M., et al., 2013. Adiponectin mediates the metabolic effects of FGF21 on glucose homeostasis and insulin sensitivity in mice. Cell Metab. 17 (5), 779–789.

Lincoln, G.A., Andersson, H., Clarke, I.J., 2003. Prolactin cycles in sheep under constant photoperiod: evidence that photorefractoriness develops within the pituitary gland independently of the prolactin output signal. Biol. Reprod. 69 (4), 1416–1423.

Lincoln, G.A., Rhind, S.M., Pompolo, S., Clarke, I.J., 2001. Hypothalamic control of photoperiod-induced cycles in food intake, body weight, and metabolic hormones in rams. Am. J. Physiol. Regul. Integr. Comp. Physiol. 281 (1), R76–R90.

Lockie, S.H., Stefanidis, A., Oldfield, B.J., Perez-Tilve, D., 2013. Brown adipose tissue thermogenesis in the resistance to and reversal of obesity: a potential new mechanism contributing to the metabolic benefits of proglucagon-derived peptides. Adipocyte 2 (4), 196–200.

Lombardi, A., de Lange, P., Silvestri, E., Busiello, R.A., Lanni, A., Goglia, F., et al., 2008. 3,5-diiodothyronine rapidly enhances mitochondrial fatty acid oxidation rate and thermogenesis in rat skeletal muscle: AMP-activated protein kinase involvement. Am. J. Physiol. Endocrinol. Metab. 296, E497–E502.

Lowell, B.B., Spiegelman, B.M., 2000. Towards a molecular understanding of adaptive thermogenesis [Review]. Nature 404 (6778), 652–660.

Lowell, B.B., S-Susulic, V., Hamann, A., Lawitts, J.A., Himms-Hagen, J., Boyer, B.B., et al., 1993. Development of obesity in transgenic mice after genetic ablation of brown adipose tissue. Nature 366 (6457), 740–742.

Marcus, J.N., Elmquist, J.K., 2005. Orexin projections and localization of orexin receptors. In: Nishino, S., Sakurai, T. (Eds.), The Orexin/Hypocretin System: Physiology and Pathophysiology. Humana Press, Totowa, NJ, pp. 21–43.

Marie, M., Findlay, P.A., Thomas, L., Adam, C.L., 2001. Daily patterns of plasma leptin in sheep: effects of photoperiod and food intake. J. Endocrinol. 170 (1), 277–286.

Martinez de Morentin, P.B., Gonzalez-Garcia, I., Martins, L., Lage, R., Fernandez-Mallo, D., Martinez-Sanchez, N., et al., 2014. Estradiol regulates brown adipose tissue thermogenesis via hypothalamic AMPK. Cell Metab. 20 (1), 41–53.

Maurya, S.K., Bal, N.C., Sopariwala, D.H., Pant, M., Rowland, L.A., Shaikh, S.A., et al., 2015. Sarcolipin is a key determinant of the basal metabolic rate, and its overexpression enhances energy expenditure and resistance against diet-induced obesity. J. Biol. Chem. 290 (17), 10840–10849.

Mauvais-Jarvis, F., 2011. Estrogen and androgen receptors: regulators of fuel homeostasis and emerging targets for diabetes and obesity. Trends Endocrinol. Metab. 22 (1), 24–33.

McEwan, J.C., Morris, C.A., Fennessey, P.F., Greer, G.J., Bain, W.E., Hickey, S.M., 2001. Selection for high or low backfat depth in Coopworth sheep: breeding-ewe traits. Anim. Sci. 73, 241–252.

McInnes, K.J., Corbould, A., Simpson, E.R., Jones, M.E., 2006. Regulation of adenosine 5′,monophosphate-activated protein kinase and lipogenesis by androgens contributes to visceral obesity in an estrogen-deficient state. Endocrinology 147 (12), 5907–5913.

McPherson, N.O., Owens, J.A., Fullston, T., Lane, M., 2015. Preconception diet or exercise intervention in obese fathers normalizes sperm microRNA profile and metabolic syndrome in female offspring. Am. J. Physiol. Endocrinol. Metab. 308 (9), E805–E821.

Mercer, J.G., Moar, K.M., Ross, A.W., Hoggard, N., Morgan, P.J., 2000. Photoperiod regulates arcuate nucleus POMC, AGRP, and leptin receptor mRNA in Siberian hamster hypothalamus. Am. J. Physiol. Regul. Integr. Comp. Physiol. 278 (1), R271–R281.

Messina, M.M., Overton, J.M., 2007. Cardiovascular effects of melanin-concentrating hormone. Regul. Pept. 139 (1–3), 23–30.

Mills, E.M., Banks, M.L., Sprague, J.E., Finkel, T., 2003. Pharmacology: uncoupling the agony from ecstasy. Nature 426 (6965), 403–404.

Minokoshi, Y., Kim, Y.B., Peroni, O.D., Fryer, L.G., Muller, C., Carling, D., et al., 2002. Leptin stimulates fatty-acid oxidation by activating AMP-activated protein kinase. Nature 415 (6869), 339–343.

Mohammed, M., Ootsuka, Y., Yanagisawa, M., Blessing, W., 2014. Reduced brown adipose tissue thermogenesis during environmental interactions in transgenic rats with ataxin-3-mediated ablation of hypothalamic orexin neurons. Am. J. Physiol. Regul. Integr. Comp. Physiol. 307 (8), R978–R989.

Monemdjou, S., Hofmann, W.E., Kozak, L.P., Harper, M.E., 2000. Increased mitochondrial proton leak in skeletal muscle mitochondria of UCP1-deficient mice. Am. J. Physiol. Endocrinol. Metab. 279 (4), E941–E946.

Moody, D.E., Pomp, D., Nielsen, M.K., Van Vleck, L.D., 1999. Identification of quantitative trait loci influencing traits related to energy balance in selection and inbred lines of mice. Genetics 152 (2), 699–711.

Morita, S., Miyata, S., 2012. Different vascular permeability between the sensory and secretory circumventricular organs of adult mouse brain. Cell Tissue Res. 349 (2), 589–603.

Morris, C.A., McEwan, J.C., Fennessy, P.F., Bain, W.E., Greer, G.J., Hickey, S.M., 1997. Selection for high or low backfat depth in Coopworth sheep: juvenile traits. Anim. Sci. 65, 93–103.

Morrison, S.F., Madden, C.J., Tupone, D., 2014. Central neural regulation of brown adipose tissue thermogenesis and energy expenditure. Cell Metab. 19 (5), 741–756.

Morrison, S.F., Nakamura, K., 2011. Central neural pathways for thermoregulation. Front. Biosci. (Landmark Ed) 16, 74–104.

Moverare-Skrtic, S., Venken, K., Andersson, N., Lindberg, M.K., Svensson, J., Swanson, C., et al., 2006. Dihydrotestosterone treatment results in obesity and altered lipid metabolism in orchidectomized mice. Obesity (Silver Spring) 14 (4), 662–672.

Munzberg, H., Flier, J.S., Bjorbaek, C., 2004. Region-specific leptin resistance within the hypothalamus of diet-induced obese mice. Endocrinology 145 (11), 4880–4889.

Myers, M.G., Cowley, M.A., Munzberg, H., 2008. Mechanisms of leptin action and leptin resistance. Annu. Rev. Physiol. 70, 537–556.

Nakamura, K., Morrison, S.F., 2008. Preoptic mechanism for cold-defensive responses to skin cooling. J. Physiol. 586 (10), 2611–2620.

Nakamura, Y., Nakamura, K., Matsumura, K., Kobayashi, S., Kaneko, T., Morrison, S.F., 2005. Direct pyrogenic input from prostaglandin EP3 receptor-expressing preoptic neurons to the dorsomedial hypothalamus. Eur. J. Neurosci. 22 (12), 3137–3146.

Nam, D., Guo, B., Chatterjee, S., Chen, M.-H., Nelson, D., Yechoor, V.K., et al., 2015. The adipocyte clock controls brown adipogenesis through the TGF-β and BMP signaling pathways. J. Cell Sci. 128 (9), 1835–1847.

Narvaez, C.J., Matthews, D., Broun, E., Chan, M., Welsh, J., 2009. Lean phenotype and resistance to diet-induced obesity in vitamin D receptor knockout mice correlates with induction of uncoupling protein-1 in white adipose tissue. Endocrinology 150 (2), 651–661.

Nau, K., Fromme, T., Meyer, C.W., von Praun, C., Heldmaier, G., Klingenspor, M., 2008. Brown adipose tissue specific lack of uncoupling protein 3 is associated with impaired cold tolerance and reduced transcript levels of metabolic genes. J. Comp. Physiol. B 178 (3), 269–277.

Nedergaard, J., Bengtsson, T., Cannon, B., 2007. Unexpected evidence for active brown adipose tissue in adult humans. Am. J. Physiol. Endocrinol. Metab. 293 (2), E444–E452.

Nedergaard, J., Bengtsson, T., Cannon, B., 2010. Three years with adult human brown adipose tissue. Ann. N. Y. Acad. Sci. 1212 (1), E20–E36.

Ng, S.F., Lin, R.C., Laybutt, D.R., Barres, R., Owens, J.A., Morris, M.J., 2010. Chronic high-fat diet in fathers programs beta-cell dysfunction in female rat offspring. Nature 467 (7318), 963–966.

Ng, S.-F., Lin, R.C.Y., Maloney, C.A., Youngson, N.A., Owens, J.A., Morris, M.J., 2014. Paternal high-fat diet consumption induces common changes in the transcriptomes of retroperitoneal adipose and pancreatic islet tissues in female rat offspring. FASEB J. 28, 1830–1841.

Norheim, F., Langleite, T.M., Hjorth, M., Holen, T., Kielland, A., Stadheim, H.K., et al., 2014. The effects of acute and chronic exercise on PGC-1alpha, irisin and browning of subcutaneous adipose tissue in humans. FEBS J. 281 (3), 739–749.

Nygaard, E.B., Moller, C.L., Kievit, P., Grove, K.L., Andersen, B., 2014. Increased fibroblast growth factor 21 expression in high-fat diet-sensitive non-human primates (*Macaca mulatta*). Int. J. Obes. (Lond.) 38 (2), 183–191.

Ohno, H., Shinoda, K., Spiegelman, B.M., Kajimura, S., 2012. PPAR-gamma agonists induce a white-to-brown fat conversion through stabilization of PRDM16 protein. Cell Metab. 15 (3), 395–404.

Oldfield, B.J., Giles, M.E., Watson, A., Anderson, C., Colvill, L.M., McKinley, M.J., 2002. The neurochemical characterisation of hypothalamic pathways projecting polysynaptically to brown adipose tissue in the rat. Neuroscience 110 (3), 515–526.

Orava, J., Nuutila, P., Lidell, M.E., Oikonen, V., Noponen, T., Viljanen, T., et al., 2011. Different metabolic responses of human brown adipose tissue to activation by cold and insulin. Cell Metab. 14 (2), 272–279.

Orozco-Solis, R., Aguilar-Arnal, L., Murakami, M., Peruquetti, R., Ramadori, G., Coppari, R., et al, 2016. The circadian clock in the ventromedial hypothalamus controls cyclic energy expenditure. Cell Metab. 23(3), 467–478.

Ouellet, V., Labbe, S.M., Blondin, D.P., Phoenix, S., Guerin, B., Haman, F., et al., 2012. Brown adipose tissue oxidative metabolism contributes to energy expenditure during acute cold exposure in humans. J. Clin. Invest. 122 (2), 545–552.

Owens, J.A., Gatford, K.L., De Blasio, M.J., Edwards, L.J., McMillen, I.C., Fowden, A.L., 2007. Restriction of placental growth in sheep impairs insulin secretion but not sensitivity before birth. J. Physiol. 584 (Pt 3), 935–949.

Painter, R.C., Roseboom, T.J., Bleker, O.P., 2005. Prenatal exposure to the Dutch famine and disease in later life: an overview. Reprod. Toxicol. 20 (3), 345–352.

Parton, L.E., Ye, C.P., Coppari, R., Enriori, P.J., Choi, B., Zhang, C.Y., et al., 2007. Glucose sensing by POMC neurons regulates glucose homeostasis and is impaired in obesity. Nature 449 (7159), 228–232.

Pasquali, R., Cantobelli, S., Casimirri, F., Capelli, M., Bortoluzzi, L., Flamia, R., et al., 1993. The hypothalamic-pituitary-adrenal axis in obese women with different patterns of body fat distribution. J. Clin. Endocrinol. Metab. 77 (2), 341–346.

Petrovic, N., Walden, T.B., Shabalina, I.G., Timmons, J.A., Cannon, B., Nedergaard, J., 2010. Chronic peroxisome proliferator-activated receptor γ (PPARγ) activation of epididymally derived white adipocyte cultures reveals a population of thermogenically competent, UCP1-containing Adipocytes molecularly distinct from classic brown adipocytes. J. Biol. Chem. 285 (10), 7153–7164.

Ping-Delfos, W.C., Soares, M., 2011. Diet induced thermogenesis, fat oxidation and food intake following sequential meals: influence of calcium and vitamin D. Clin. Nutr. 30 (3), 376–383.

Pissios, P., 2009. Animals models of MCH function and what they can tell us about its role in energy balance. Peptides 30 (11), 2040–2044.

Poher, A.-L., Altirriba, J., Veyrat-Durebex, C., Rohner-Jeanrenaud, F., 2015. Brown adipose tissue activity as a target for the treatment of obesity/insulin resistance. Front. Physiol. 6, 4.

Qi, Y., Henry, B.A., Oldfield, B.J., Clarke, I.J., 2010. The action of leptin on appetite-regulating cells in the ovine hypothalamus: demonstration of direct action in the absence of the arcuate nucleus. Endocrinology 151 (5), 2106–2116.

Quarta, C., Mazza, R., Pasquali, R., Pagotto, U., 2012. Role of sex hormones in modulation of brown adipose tissue activity. J. Mol. Endocrinol. 49 (1), R1–R7.

Ramage, L.E., Akyol, M., Fletcher, A.M., Forsythe, J., Nixon, M., Carter, R.N., et al., 2016. Glucocorticoids acutely increase brown adipose tissue activity in humans, revealing species-specific differences in UCP-1 regulation. Cell Metab. 24 (1), 130–141.

Rao, R.R., Long, J.Z., White, J.P., Svensson, K.J., Lou, J., Lokurkar, I., et al., 2014. Meteorin-like is a hormone that regulates immune-adipose interactions to increase beige fat thermogenesis. Cell 157 (6), 1279–1291.

Raschke, S., Elsen, M., Gassenhuber, H., Sommerfeld, M., Schwahn, U., Brockmann, B., et al., 2013. Evidence against a beneficial effect of irisin in humans. PLoS One 8 (9), e73680.

Razzoli, M., Frontini, A., Gurney, A., Mondini, E., Cubuk, C., Katz, L.S., et al., 2016. Stress-induced activation of brown adipose tissue prevents obesity in conditions of low adaptive thermogenesis. Mol. Metab. 5 (1), 19–33.

Reddy, A.B., Cronin, A.S., Ford, H., Ebling, F.J., 1999. Seasonal regulation of food intake and body weight in the male Siberian hamster: studies of hypothalamic orexin (hypocretin), neuropeptide Y (NPY) and pro-opiomelanocortin (POMC). Eur. J. Neurosci. 11 (9), 3255–3264.

Reiter, R.J., 1980. The pineal and its hormones in the control of reproduction in mammals. Endocr. Rev. 1 (2), 109–131.

Revel, F.G., Saboureau, M., Pevet, P., Mikkelsen, J.D., Simonneaux, V., 2006. Melatonin regulates type 2 deiodinase gene expression in the Syrian hamster. Endocrinology 147 (10), 4680–4687.

Roberts-Toler, C., O'Neill, B.T., Cypess, A.M., 2015. Diet-induced obesity causes insulin resistance in mouse brown adipose tissue. Obesity 23 (9), 1765–1770.

Robinson, J.S., Kingston, E.J., Jones, C.T., Thorburn, G.D., 1979. Studies on experimental growth retardation in sheep. The effect of removal of a endometrial caruncles on fetal size and metabolism. J. Dev. Physiol. 1 (5), 379–398.

Robinson, T., 1959. The estrous cycle of the ewe and doe. Reprod. Domest. Anim. 1, 291–333.

Rolfe, D.F., Brown, G.C., 1997. Cellular energy utilization and molecular origin of standard metabolic rate in mammals. Physiol. Rev. 77 (3), 731–758.

Rosenbaum, M., Hirsch, J., Gallagher, D.A., Leibel, R.L., 2008. Long-term persistence of adaptive thermogenesis in subjects who have maintained a reduced body weight. Am. J. Clin. Nutr. 88 (4), 906–912.

Rothwell, N.J., Saville, M.E., Stock, M.J., 1984. Brown fat activity in fasted and refed rats. Biosci. Rep. 4 (4), 351–357.

Rousseau, K., Atcha, Z., Loudon, A.S., 2003. Leptin and seasonal mammals. J. Neuroendocrinol. 15 (4), 409–414.

Rowland, L.A., Bal, N.C., Periasamy, M., 2015. The role of skeletal-muscle-based thermogenic mechanisms in vertebrate endothermy. Biol. Rev. Camb. Philos. Soc. 90 (4), 1279–1297.

Rowland, L.A., Maurya, S.K., Bal, N.C., Kozak, L., Periasamy, M., 2016. Sarcolipin and uncoupling protein 1 play distinct roles in diet-induced thermogenesis and do not compensate for one another. Obesity 24 (7), 1430–1433.

Saito, M., Okamatsu-Ogura, Y., Matsushita, M., Watanabe, K., Yoneshiro, T., Nio-Kobayashi, J., et al., 2009. High incidence of metabolically active brown adipose tissue in healthy adult humans: effects of cold exposure and adiposity. Diabetes 58 (7), 1526–1531.

Salem, V., Izzi-Engbeaya, C., Coello, C., Thomas, D.B., Chambers, E.S., Comninos, A.N., et al., 2016. Glucagon increases energy expenditure independently of brown adipose tissue activation in humans. Diab. Obes. Metab. 18 (1), 72–81.

Samms, R.J., Smith, D.P., Cheng, C.C., Antonellis, P.P., Perfield, II, J.W., Kharitonenkov, A., et al., 2015. Discrete aspects of FGF21 in vivo pharmacology do not require UCP1. Cell Rep. 11 (7), 991–999.

Sartin, J.L., Marks, D.L., McMahon, C.D., Daniel, J.A., Levasseur, P., Wagner, C.G., et al., 2008. Central role of the melanocortin-4 receptors in appetite regulation after endotoxin. J. Anim. Sci. 86 (10), 2557–2567.

Scharhag-Rosenberger, F., Meyer, T., Wegmann, M., Ruppenthal, S., Kaestner, L., Morsch, A., et al., 2014. Irisin does not mediate resistance training-induced alterations in resting metabolic rate. Med. Sci. Sports Exerc. 46 (9), 1736–1743.

Schulz, T.J., Huang, T.L., Tran, T.T., Zhang, H., Townsend, K.L., Shadrach, J.L., et al., 2011. Identification of inducible brown adipocyte progenitors residing in skeletal muscle and white fat. Proc. Natl. Acad. Sci. USA 108 (1), 143–148.

Seale, P., Bjork, B., Yang, W., Kajimura, S., Chin, S., Kuang, S., et al., 2008. PRDM16 controls a brown fat/skeletal muscle switch. Nature 454 (7207), 961–967.

Seale, P., Conroe, H.M., Estall, J., Kajimura, S., Frontini, A., Ishibashi, J., et al., 2011. Prdm16 determines the thermogenic program of subcutaneous white adipose tissue in mice. J. Clin. Invest. 121 (1), 96–105.

Sellayah, D., Bharaj, P., Sikder, D., 2011. Orexin is required for brown adipose tissue development, differentiation, and function. Cell Metab. 14 (4), 478–490.

Shabalina, I.G., Hoeks, J., Kramarova, T.V., Schrauwen, P., Cannon, B., Nedergaard, J., 2010. Cold tolerance of UCP1-ablated mice: a skeletal muscle mitochondria switch toward lipid oxidation with marked UCP3 up-regulation not associated with increased basal, fatty acid- or ROS-induced uncoupling or enhanced GDP effects. Biochim. Biophys. Acta 1797 (6–7), 968–980.

Sharp, L.Z., Shinoda, K., Ohno, H., Scheel, D.W., Tomoda, E., Ruiz, L., et al., 2012. Human BAT possesses molecular signatures that resemble beige/brite cells. PLoS One 7 (11), e49452.

Sidossis, L., Kajimura, S., 2015. Brown and beige fat in humans: thermogenic adipocytes that control energy and glucose homeostasis. J. Clin. Invest. 125 (2), 478–486.

Sidossis, L.S., Porter, C., Saraf, M.K., Borsheim, E., Radhakrishnan, R.S., Chao, T., et al., 2015. Browning of subcutaneous white adipose tissue in humans after severe adrenergic stress. Cell Metab. 22 (2), 219–227.

Simon, J., Leclercq, B., 1982. Longitudinal study of adiposity in chickens selected for high or low abdominal fat content: further evidence of a glucose-insulin imbalance in the fat line. J. Nutr. 112 (10), 1961–1973.

Simonds, S.E., Pryor, J.T., Ravussin, E., Greenway, F.L., Dileone, R., Allen, A.M., et al., 2014. Leptin mediates the increase in blood pressure associated with obesity. Cell 159 (6), 1404–1416.

Sisley, S.R., Arble, D.M., Chambers, A.P., Gutierrez-Aguilar, R., He, Y., Xu, Y., et al., 2016. Hypothalamic vitamin D improves glucose homeostasis and reduces weight. Diabetes 65, 2732–2741.

Small, C.J., Goubillon, M.L., Murray, J.F., Siddiqui, A., Grimshaw, S.E., Young, H., et al., 2003. Central orexin A has site-specific effects on luteinizing hormone release in female rats. Endocrinology 144 (7), 3225–3236.

Soares, M.J., Murhadi, L.L., Kurpad, A.V., Chan She Ping-Delfos, W.L., Piers, L.S., 2012. Mechanistic roles for calcium and vitamin D in the regulation of body weight. Obes. Rev. 13 (7), 592–605.

Solinas, G., Summermatter, S., Mainieri, D., Gubler, M., Pirola, L., Wymann, M.P., et al., 2004. The direct effect of leptin on skeletal muscle thermogenesis is mediated by substrate cycling between de novo lipogenesis and lipid oxidation. FEBS Lett. 577 (3), 539–544.

Solomon, T.P., Chambers, E.S., Jeukendrup, A.E., Toogood, A.A., Blannin, A.K., 2008. The effect of feeding frequency on insulin and ghrelin responses in human subjects. Br. J. Nutr. 100 (4), 810–819.

Song, C.K., Vaughan, C.H., Keen-Rinehart, E., Harris, R.B., Richard, D., Bartness, T.J., 2008. Melanocortin-4 receptor mRNA expressed in sympathetic outflow neurons to brown adipose tissue: neuroanatomical and functional evidence. Am. J. Physiol. Regul. Integr. Comp. Physiol. 295 (2), R417–R428.

Stanford, K.I., Middelbeek, R.J.W., Goodyear, L.J., 2015. Exercise effects on white adipose tissue: beiging and metabolic adaptations. Diabetes 64 (7), 2361–2368.

Sugino, T., Yamaura, J., Yamagishi, M., Ogura, A., Hayashi, R., Kurose, Y., et al., 2002. A transient surge of ghrelin secretion before feeding is modified by different feeding regimens in sheep. Biochem. Biophys. Res. Commun. 298 (5), 785–788.

Surwit, R.S., Wang, S., Petro, A.E., Sanchis, D., Raimbault, S., Ricquier, D., et al., 1998. Diet-induced changes in uncoupling proteins in obesity-prone and obesity-resistant strains of mice. Proc. Natl. Acad. Sci. USA 95 (7), 4061–4065.

Sutherland, L.N., Bomhof, M.R., Capozzi, L.C., Basaraba, S.A., Wright, D.C., 2009. Exercise and adrenaline increase PGC-1{alpha} mRNA expression in rat adipose tissue. J. Physiol. 587 (Pt 7), 1607–1617.

Suttie, J.M., Lord, E.A., Gluckman, P.D., Fennessy, P.F., Littlejohn, R.P., 1991. Genetically lean and fat sheep differ in their growth hormone response to growth hormone-releasing factor. Domest. Anim. Endocrinol. 8 (2), 323–329.

Symonds, M.E., 2013. Brown adipose tissue growth and development. Scientifica 2013, 14.

Symonds, M.E., Pope, M., Sharkey, D., Budge, H., 2012. Adipose tissue and fetal programming. Diabetologia 55 (6), 1597–1606.

Szekely, M., Petervari, E., Balasko, M., 2010. Thermoregulation, energy balance, regulatory peptides: recent developments. Front. Biosci. (Schol Ed) 2, 1009–1046.

Talukdar, S., Zhou, Y., Li, D., Rossulek, M., Dong, J., Somayaji, V., et al., 2016. A long-acting FGF21 molecule, PF-05231023, decreases body weight and improves lipid profile in non-human primates and type 2 diabetic Subjects. Cell Metab. 23(3), 427–440.

Teske, J.A., Billington, C.J., Kotz, C.M., 2008. Neuropeptidergic mediators of spontaneous physical activity and non-exercise activity thermogenesis. Neuroendocrinology 87 (2), 71–90.

Tilbrook, A.J., Rivalland, E.A., Turner, A.I., Lambert, G.W., Clarke, I.J., 2008. Responses of the hypothalamopituitary adrenal axis and the sympathoadrenal system to isolation/restraint stress in sheep of different adiposity. Neuroendocrinology 87, 193–205.

Tiraby, C., Tavernier, G., Capel, F., Mairal, A., Crampes, F., Rami, J., et al., 2007. Resistance to high-fat-diet-induced obesity and sexual dimorphism in the metabolic responses of transgenic mice with moderate uncoupling protein 3 overexpression in glycolytic skeletal muscles. Diabetologia 50 (10), 2190–2199.

Tomiyama, A.J., Dallman, M.F., Epel, E.S., 2011. Comfort food is comforting to those most stressed: evidence of the chronic stress response network in high stress women. Psychoneuroendocrinology 36 (10), 1513–1519.

Trayhurn, P., Jennings, G., 1988. Nonshivering thermogenesis and the thermogenic capacity of brown fat in fasted and/or refed mice. Am. J. Physiol. 254 (1 Pt 2), R11–R16.

Trayhurn, P., Thurlby, P.L., James, W.P., 1977. Thermogenic defect in pre-obese ob/ob mice. Nature 266 (5597), 60–62.

Trevellin, E., Scorzeto, M., Olivieri, M., Granzotto, M., Valerio, A., Tedesco, L., et al., 2014. Exercise training induces mitochondrial biogenesis and glucose uptake in subcutaneous adipose tissue through eNOS-dependent mechanisms. Diabetes 63 (8), 2800–2811.

Tseng, Y.H., Cypess, A.M., Kahn, C.R., 2010. Cellular bioenergetics as a target for obesity therapy. Nat. Rev. Drug Discov. 9 (6), 465–482.

Tupone, D., Madden, C.J., Cano, G., Morrison, S.F., 2011. An orexinergic projection from perifornical hypothalamus to raphe pallidus increases rat brown adipose tissue thermogenesis. J. Neurosci. 31 (44), 15944–15955.

Tups, A., Ellis, C., Moar, K.M., Logie, T.J., Adam, C.L., Mercer, J.G., et al., 2004. Photoperiodic regulation of leptin sensitivity in the Siberian hamster, *Phodopus sungorus*, is reflected in arcuate nucleus SOCS-3 (suppressor of cytokine signaling) gene expression. Endocrinology 145 (3), 1185–1193.

Ukropec, J., Anunciado, R.V., Ravussin, Y., Kozak, L.P., 2006. Leptin is required for uncoupling protein-1-independent thermogenesis during cold stress. Endocrinology 147 (5), 2468–2480.

van Marken Lichtenbelt, W.D., Vanhommerig, J.W., Smulders, N.M., Drossaerts, J.M.A.F.L., Kemerink, G.J., Bouvy, N.D., et al., 2009. Cold activated brown adipose tissue in healthy men. N. Engl. J. Med. 360, 1500–1508.

Veniant, M.M., Sivits, G., Helmering, J., Komorowski, R., Lee, J., Fan, W., et al., 2015. Pharmacologic effects of FGF21 are independent of the "browning" of white adipose tissue. Cell Metab. 21 (5), 731–738.

Verty, A.N., Allen, A.M., Oldfield, B.J., 2010. The endogenous actions of hypothalamic peptides on brown adipose tissue thermogenesis in the rat. Endocrinology 151 (9), 4236–4246.

Veyrat-Durebex, C., Poher, A.L., Caillon, A., Montet, X., Rohner-Jeanrenaud, F., 2011. Alterations in lipid metabolism and thermogenesis with emergence of brown adipocytes in white adipose tissue in diet-induced obesity-resistant Lou/C rats. Am. J. Physiol. Endocrinol. Metab. 300 (6), E1146–E1157.

Vickers, M.H., Gluckman, P.D., Coveny, A.H., Hofman, P.L., Cutfield, W.S., Gertler, A., et al., 2005. Neonatal leptin treatment reverses developmental programming. Endocrinology 146 (10), 4211–4216.

Vickers, M.H., Gluckman, P.D., Coveny, A.H., Hofman, P.L., Cutfield, W.S., Gertler, A., et al., 2008. The effect of neonatal leptin treatment on postnatal weight gain in male rats is dependent on maternal nutritional status during pregnancy. Endocrinology 149 (4), 1906–1913.

Vijgen, G.H., Bouvy, N.D., Teule, G.J., Brans, B., Hoeks, J., Schrauwen, P., et al., 2012. Increase in brown adipose tissue activity after weight loss in morbidly obese subjects. J. Clin. Endocrinol. Metab. 97 (7), E1229–E1233.

Vijgen, G.H.E.J., Bouvy, N.D., Teule, G.J.J., Brans, B., Schrauwen, P., van Marken Lichtenbelt, W.D., 2011. Brown adipose tissue in morbidly obese subjects. PLoS One 6 (2), e17247.

Virtanen, K.A., Lidell, M.E., Orava, J., Heglind, M., Westergren, R., Niemi, T., et al., 2009. Functional brown adipose tissue in healthy adults. N. Engl. J. Med. 360 (15), 1518–1525.

Voss-Andreae, A., Murphy, J.G., Ellacott, K.L., Stuart, R.C., Nillni, E.A., Cone, R.D., et al., 2007. Role of the central melanocortin circuitry in adaptive thermogenesis of brown adipose tissue. Endocrinology 148 (4), 1550–1560.

Vosselman, M.J., Hoeks, J., Brans, B., Pallubinsky, H., Nascimento, E.B., van der Lans, A.A., et al., 2015. Low brown adipose tissue activity in endurance-trained compared with lean sedentary men. Int. J. Obes. (Lond.) 39 (12), 1696–1702.

Wade, G.N., Bartness, T.J., 1984a. Effects of photoperiod and gonadectomy on food intake, body weight, and body composition in Siberian hamsters. Am. J. Physiol. 246 (1 Pt 2), R26–R30.

Wade, G.N., Bartness, T.J., 1984b. Seasonal obesity in Syrian hamsters: effects of age, diet, photoperiod, and melatonin. Am. J. Physiol. 247 (2 Pt 2), R328–R334.

Walden, T.B., Hansen, I.R., Timmons, J.A., Cannon, B., Nedergaard, J., 2012. Recruited vs. nonrecruited molecular signatures of brown, "brite," and white adipose tissues. Am. J. Physiol. Endocrinol. Metab. 302 (1), E19–E31.

Walley, A.J., Asher, J.E., Froguel, P., 2009. The genetic contribution to non-syndromic human obesity. Nat. Rev. Genet. 10 (7), 431–442.

Watanabe, M., Yasuo, S., Watanabe, T., Yamamura, T., Nakao, N., Ebihara, S., et al., 2004. Photoperiodic regulation of type 2 deiodinase gene in Djungarian hamster: possible homologies between avian and mammalian photoperiodic regulation of reproduction. Endocrinology 145 (4), 1546–1549.

Wijers, S.L.J., Schrauwen, P., Saris, W.H.M., van Marken Lichtenbelt, W.D., 2008. Human skeletal muscle mitochondrial uncoupling is associated with cold induced adaptive thermogenesis. PLoS One 3 (3), e1777.

Wijers, S.L., Saris, W.H., van Marken Lichtenbelt, W.D., 2010. Cold-induced adaptive thermogenesis in lean and obese. Obesity (Silver Spring) 18 (6), 1092–1099.

Willie, J.T., Chemelli, R.M., Sinton, C.M., Yanagisawa, M., 2001. To eat or to sleep? Orexin in the regulation of feeding and wakefulness. Annu. Rev. Neurosci. 24, 429–458.

Willie, J.T., Sinton, C.M., Maratos-Flier, E., Yanagisawa, M., 2008. Abnormal response of melanin-concentrating hormone deficient mice to fasting: hyperactivity and rapid eye movement sleep suppression. Neuroscience 156 (4), 819–829.

Wong, K.E., Kong, J., Zhang, W., Szeto, F.L., Ye, H., Deb, D.K., et al., 2011. Targeted expression of human vitamin D receptor in adipocytes decreases energy expenditure and induces obesity in mice. J. Biol. Chem. 286 (39), 33804–33810.

Wu, J., Bostrom, P., Sparks, L.M., Ye, L., Choi, J.H., Giang, A.H., et al., 2012. Beige adipocytes are a distinct type of thermogenic fat cell in mouse and human. Cell 150 (2), 366–376.

Xiao, X.Q., Grove, K.L., Grayson, B.E., Smith, M.S., 2004. Inhibition of uncoupling protein expression during lactation: role of leptin. Endocrinology 145 (2), 830–838.

Xie, C., Zhang, Y., Tran, T.D., Wang, H., Li, S., George, E.V., et al., 2015. Irisin controls growth, intracellular Ca^{2+} signals, and mitochondrial thermogenesis in cardiomyoblasts. PLoS One 10 (8), e0136816.

Xu, Y., Lloyd, D.J., Hale, C., Stanislaus, S., Chen, M., Sivits, G., et al., 2009. Fibroblast growth factor 21 reverses hepatic steatosis, increases energy expenditure, and improves insulin sensitivity in diet-induced obese mice. Diabetes 58 (1), 250–259.

Xu, Y., Nedungadi, T.P., Zhu, L., Sobhani, N., Irani, B.G., Davis, K.E., et al., 2011. Distinct hypothalamic neurons mediate estrogenic effects on energy homeostasis and reproduction. Cell Metab. 14 (4), 453–465.

Yasuo, S., Nakao, N., Ohkura, S., Iigo, M., Hagiwara, S., Goto, A., et al., 2006. Long-day suppressed expression of type 2 deiodinase gene in the mediobasal hypothalamus of the Saanen goat, a short-day breeder: implication for seasonal window of thyroid hormone action on reproductive neuroendocrine axis. Endocrinology 147 (1), 432–440.

Yasuo, S., Watanabe, M., Iigo, M., Nakamura, T.J., Watanabe, T., Takagi, T., et al., 2007. Differential response of type 2 deiodinase gene expression to photoperiod between photoperiodic Fischer 344 and nonphotoperiodic Wistar rats. Am. J. Physiol. Regul. Integr. Comp. Physiol. 292 (3), R1315–R1319.

Yie, J., Hecht, R., Patel, J., Stevens, J., Wang, W., Hawkins, N., et al., 2009. FGF21 N- and C-termini play different roles in receptor interaction and activation. FEBS Lett. 583 (1), 19–24.

Yoneshiro, T., Aita, S., Matsushita, M., Kameya, T., Nakada, K., Kawai, Y., et al., 2011a. Brown adipose tissue, whole-body energy expenditure, and thermogenesis in healthy adult men. Obesity (Silver Spring) 19 (1), 13–16.

Yoneshiro, T., Aita, S., Matsushita, M., Okamatsu-Ogura, Y., Kameya, T., Kawai, Y., et al., 2011b. Age-related decrease in cold-activated brown adipose tissue and accumulation of body fat in healthy humans. Obesity (Silver Spring) 19 (9), 1755–1760.

Yoshimura, T., Yasuo, S., Watanabe, M., Iigo, M., Yamamura, T., Hirunagi, K., et al., 2003. Light-induced hormone conversion of T4 to T3 regulates photoperiodic response of gonads in birds. Nature 426 (6963), 178–181.

Young, R.A., Salans, L.B., Sims, E.A., 1982. Adipose tissue cellularity in woodchucks: effects of season and captivity at an early age. J. Lipid Res. 23 (6), 887–892.

Yu, S., Qualls-Creekmore, E., Rezai-Zadeh, K., Jiang, Y., Berthoud, H.-R., Morrison, C.D., et al., 2016. Glutamatergic preoptic area neurons that express leptin receptors drive temperature-dependent body weight homeostasis. J. Neurosci. 36 (18), 5034–5046.

Yura, S., Itoh, H., Sagawa, N., Yamamoto, H., Masuzaki, H., Nakao, K., et al., 2005. Role of premature leptin surge in obesity resulting from intrauterine undernutrition. Cell Metab. 1 (6), 371–378.

Zeltser, L.M., 2015. Developmental influences on circuits programming susceptibility to obesity. Front. Neuroendocrinol. 39, 17–27.

Zhang, Y., Hufnagel, C., Eiden, S., Guo, K.Y., Diaz, P.A., Leibel, R., et al., 2001. Mechanisms for LEPR-mediated regulation of leptin expression in brown and white adipocytes in rat pups. Physiol. Genomics 4 (3), 189–199.

Zhang, C., Shao, M., Yang, H., Chen, L., Yu, L., Cong, W., et al., 2013. Attenuation of hyperlipidemia- and diabetes-induced early-stage apoptosis and late-stage renal dysfunction via administration of fibroblast growth factor-21 is associated with suppression of renal inflammation. PLoS One 8 (12), e82275.

Zhang, Y., Li, R., Meng, Y., Li, S., Donelan, W., Zhao, Y., et al., 2014. Irisin stimulates browning of white adipocytes through mitogen-activated protein kinase p38 MAP kinase and ERK MAP kinase signaling. Diabetes 63 (2), 514–525.

Zucker, I., Boshes, M., Dark, J., 1983. Suprachiasmatic nuclei influence circannual and circadian rhythms of ground squirrels. Am. J. Physiol. 244 (4), R472–R480.

13

Animal Models of Liver Diseases

Yoshihisa Takahashi, Toshio Fukusato

Teikyo University School of Medicine, Tokyo, Japan

1 INTRODUCTION

Animal models are indispensable for the elucidation of pathogenesis mechanisms, the identification of potential therapeutic targets, and the development of novel therapies for various liver diseases. Although large animals (rabbits, dogs, chimpanzees, etc.) have occasionally been used, rodents (especially mice and rats) are used most frequently. Rodents (especially mice) have the following advantages: (1) maintenance and breeding are easy because their bodies are small, and their life spans and gestation periods are short; (2) they are genetically close to humans and genetic manipulation is easy; and (3) ethical restrictions are less stringent compared with those for primates. In 2010, a gold standard publication checklist (GSPC) for animal studies was presented to facilitate future systematic reviews and metaanalyses of animal studies, to allow others to replicate and build on work previously published, to diminish the number of animals needed in animal experimentation, to improve animal welfare, and to improve the quality of

scientific papers on animal experimentation (Hooijmans et al., 2010). Those who perform animal experiments in the future should consider GSPC for planning animal studies.

When using animal models, researchers need to understand their advantages and limitations. Compared with clinical studies, animal models have the following advantages: (1) an adequate number of specimens can be taken at various time points, (2) diseases develop in a shorter time, (3) a group with a homogenous genetic background can be examined, and (4) the roles of specific genes or signaling pathways can be analyzed by using genetically modified animals. Furthermore, compared with in vitro studies, studies using animal models have the following advantages: (1) functions of the liver as a complete organ can be examined, enabling analyses of cell–cell and cell–matrix interactions; and (2) immunologic, metabolic, and endocrinologic interactions between the liver and other organs can be analyzed. However, animal experiments have limitations. Experimental animals occasionally react differently to

noxious agents than humans do. For example, the hepatitis C virus does not infect rodent hepatocytes in the natural state (Mailly et al., 2013). Furthermore, it is difficult to induce alcoholic liver disease (ALD) in rodents because they have an aversion to alcohol (Mathews et al., 2014). Common bile duct ligation (CBDL) results in secondary biliary cirrhosis after only a few weeks in rodents, whereas month-long impairment of bile flow is needed to cause severe liver fibrosis in humans (Delire et al., 2015). As currently used animal models represent the characteristics of human diseases only partially, it is important to select an animal model that is suitable for the objective of the study. In this chapter, we present a systematic review of currently used animal models of various liver diseases, along with their advantages and disadvantages.

2 CLASSICAL MODELS OF LIVER FIBROSIS (TABLE 13.1)

Liver fibrosis and liver cirrhosis are the end-stage states of most chronic liver diseases. The cellular and molecular mechanisms of liver fibrogenesis have been extensively investigated using a wide variety of animal models. Most liver fibrosis models were first developed in rats and later adapted to mice, enabling genetic manipulation. In general, mice are more resistant to liver fibrosis than rats. However, susceptibility to fibrosis is highly variable among mouse strains; severe fibrosis can be induced in several strains by optimizing experimental procedures (Bissell, 2011; Hillebrandt et al., 2002).

2.1 Liver Fibrosis Models Created Using Hepatotoxic Chemicals

Repetitive administration of hepatotoxic agents is a classical method of inducing liver fibrosis. Carbon tetrachloride (CCl_4), thioacetamide (TAA), and diethyl or dimethyl nitrosamine (DEN or DMN) are the most commonly used hepatotoxic agents. It is relatively easy to create robust models using such agents. If all animals are given a similar effective dose of an inducing agent, the reproducibility is high.

2.1.1 Carbon Tetrachloride

CCl_4 is one of the most commonly used hepatotoxic agents for the induction of liver injuries in experimental animals. It directly impairs hepatocytes by altering the permeability of the plasma, lysosomal, and mitochondrial membranes (Liu et al., 2013; Starkel and Leclercq, 2011; Wu and Norton, 1996). CCl_4 is metabolized to the noxious trichloromethyl radical (CCl_3^-) by cytochrome P4502E1 (CYP2E1) in hepatocytes, and CCl_3^- causes lipid peroxidation and membrane damage leading to severe centrilobular liver necrosis. Acute and centrilobular hepatocyte necrosis occurs following a single dose of CCl_4; however, the liver subsequently recovers. When CCl_4 is administered repeatedly, liver fibrosis occurs in the centrilobular region, and subsequently progresses to bridging fibrosis, cirrhosis, and hepatocellular carcinoma (HCC) (Constandinou et al., 2005; Domenicali et al., 2009; Frezza et al., 1994). Significant fibrosis occurs after 2–4 weeks, severe bridging fibrosis after 5–7 weeks, and cirrhosis after 8–9 weeks of administration. After 10–20 weeks, micronodular cirrhosis, portal hypertension, and ascites progressively appear (Constandinou et al., 2005;

TABLE 13.1   Classical Animal Models of Liver Fibrosis

Animal models	Main features
CCl_4	Liver fibrosis occurs in the centrilobular region
	Liver injury can be induced by various administration methods
	Liver fibrosis is resolved after withdrawal of the agent
TAA	Damage in zone 1 is conspicuous
	Liver fibrosis persists for a long period even after withdrawal of TAA
	A relatively long period is required to induce significant fibrosis
DEN and DMN	Liver damage and necrosis occur in both centrilobular and periportal areas
	Liver fibrosis and cirrhosis progress even after cessation of these drugs
	Long-term administration of DEN causes HCC
CBDL	Biliary fibrosis develops within weeks
	Liver fibrosis can be resolved by biliodigestive anastomosis
	Surgical complications (e.g., bile leakage) may occur

CBDL, Common bile duct ligation; CCl_4, carbon tetrachloride; DEN, diethyl nitrosamine; DMN, dimethyl nitrosamine; HCC, hepatocellular carcinoma; TAA, thioacetoamide.

Domenicali et al., 2009; Starkel and Leclercq, 2011). However, the timing and severity of the lesions depend on the amount, route, frequency of CCl_4 administration, and on the species and strain of the animal. Liver injury can be induced by various administration methods, such as intraperitoneal injection, subcutaneous injection, oral gavage, and inhalation. When CCl_4 is administered by intraperitoneal injection, inflammation and necrosis may occur at the site of injection, which can impede the experiment. Although it requires special equipment and training, inhalation is an effective method when a noninvasive procedure is indispensable. Phenobarbitone, phospholipase D, and acetone potentiate liver injury by CCl_4 and promote liver fibrosis (Charbonneau et al., 1986; McLean et al., 1969; Ozeki et al., 1985). Liver fibrosis caused by CCl_4 is resolved after withdrawal of the agent (Iredale et al., 1998). Therefore, CCl_4 administration can be used both as a model of liver fibrosis and as a model of recovery from liver fibrosis.

2.1.2 Thioacetoamide

TAA itself is not toxic to the liver, but its metabolic intermediates (in particular TAA-S-oxide, a reactive oxygen species) covalently bind to hepatic macromolecules, leading to cellular damage and hepatocyte necrosis (Liu et al., 2013). Although TAA damages the hepatocytes of both zones 1 and 3, damage in zone 1 is more pronounced compared with that caused by other hepatotoxic agents. When low-dose TAA is administered for a long period, portal–portal or portal–central bridging fibrosis occurs and progresses to liver cirrhosis (Muller et al., 1988; Starkel and Leclercq, 2011; Zimmermann et al., 1987). Even after withdrawal of TAA, liver fibrosis persists for a long period (Muller et al., 1988). TAA administration over a long period also induces cholangiocarcinoma (CC) and HCC (Newell et al., 2008; Yang et al., 1998; Yeh et al., 2004). In addition to injection, TAA can be administered in drinking water. A drawback of this model is that a relatively long period is required to induce significant fibrosis. Several months are necessary to induce severe fibrosis/cirrhosis in mice or rats by administration of TAA (Muller et al., 1988; Reif et al., 2004; Salguero Palacios et al., 2008).

2.1.3 Diethyl Nitrosamine and Dimethyl Nitrosamine

DEN and DMN are hydroxylated by CYP2E1 in liver cells, yielding diazonium ions as the bioactive intermediates (Liu et al., 2013). These metabolites cause alkylating damage to nuclear acids, leading to hepatocyte necrosis and liver carcinogenesis. Liver damage and necrosis occur in both the centrilobular and periportal areas with subsequent formation of fibrotic septa (Liu et al., 2013). Liver fibrosis and cirrhosis progress even after the administration of DEN and DMN has ceased

(Jenkins et al., 1985; Tsukamoto et al., 1990). Furthermore, the long-term administration of DEN causes HCC (Newell et al., 2008; Poirier, 1975). Therefore, this model is suitable for the study of the progression from liver fibrosis/cirrhosis to HCC, although it is rarely used as a model of pure fibrosis.

2.2 Common Bile Duct Ligation

CBDL is a classical experimental model of secondary biliary fibrosis. Through bile acid toxicity, CBDL causes proliferation of biliary epithelial cells and oval cells, leading to the proliferation of bile ductules, portal inflammation, fibrosis, and eventually liver cirrhosis and liver failure (Geerts et al., 2008; Kountouras et al., 1984; Popov et al., 2010). Biliary fibrosis develops within weeks. Portal hypertension, hyperdynamic circulation, portosystemic shunting, and ascites develop in rats after 6–8 weeks (Geerts et al., 2008; Popov et al., 2010; Starkel and Leclercq, 2011; Tsukamoto et al., 1990). Liver fibrosis caused by CBDL can be resolved by biliodigestive anastomosis (Abdel-Aziz et al., 1990; Issa et al., 2001; Zimmermann et al., 1997). Therefore, CBDL can also be used as an experimental model of fibrosis reversibility. The main drawback of the CBDL model is the occurrence of surgical complications (e.g., bile leakage, rupture of a biliary cyst or gallbladder). This may occur more frequently in mice than in rats because of the more pronounced fragility of some mouse strains, especially transgenic mice, and the inevitable dilatation of the gallbladder (not present in rats) (Geerts et al., 2008). Therefore, CBDL is more commonly performed for rats, but it is occasionally adapted to mice.

3 ANIMAL MODELS OF SPECIFIC LIVER DISEASES

3.1 Animal Models of Primary Sclerosing Cholangitis (Table 13.2)

Primary sclerosing cholangitis (PSC) is a rare disease that predominantly affects males; it is characterized by chronic inflammation, fibrous thickening, and stricture of intrahepatic and extrahepatic bile ducts (Fallatah and Akbar, 2011). When it progresses, it develops into biliary cirrhosis due to chronic cholestasis, resulting in liver failure. Autoimmunity has been suggested as a possible mechanism, and PSC is associated with perinuclear antineutrophil cytoplasmic antibody (pANCA) in up to 90% of patients (Vierling, 2001). Ulcerative colitis (UC) is a complication in many cases. Pathologically, fibrous thickening and inflammatory cell infiltration, mainly due to lymphocytes and plasma cells, are observed in the walls of the extrahepatic and intrahepatic bile ducts.

TABLE 13.2 Animal Models of Primary Sclerosing Cholangitis (PSC)

Animal models	Main features
DDC diet	DDC-fed mice develop pericholangitis, periductal fibrosis, ductular reaction, and consequently portal–portal bridging fibrosis and segmental bile duct obstruction
$Abcb4^{-/-}$ mice	This model reflects the histopathological characteristics of human PSC well
	This model is not complicated with either UC or CC
	This model is complicated with hepatocellular neoplasia
$Cftr^{-/-}$ mice	$Cftr^{-/-}$ mice show progressive liver disease, with hepatosteatosis, focal cholangitis, inspissated secretion, and bile duct proliferation
	There is progression to focal biliary cirrhosis after 1 year of age

CC, Cholangiocarcinoma; DDC, 3,5-diethoxycarbonyl-1,4-dihydrocollidine; UC, ulcerative colitis.

When the disease progresses, fibrosis around the bile duct walls (onion skin–type fibrosis) becomes advanced, and the obstruction and destruction of bile ducts occur, eventually resulting in scar formation. CC may arise in ~15% of patients (Liu et al., 2013).

A perfect animal model that reflects all the characteristics of PSC has not yet been developed, but models that reflect some of the characteristics have (Fickert et al., 2014; Pollheimer and Fickert, 2015). Animal models for (primary) sclerosing cholangitis have been classified into six different groups: models of cholangitis induced chemically [e.g., by 2,4,6-trinitrobenzenesulfonic acid, α-naphthylisothiocyanate, or 3,5-diethoxycarbonyl-1,4-dihydrocollidine (DDC)]; knockout (KO) mouse models [e.g., using $Abcb4^{-/-}$ or cystic fibrosis transmembrane conductance regulator ($Cftr^{-/-}$) mice]; models of cholangitis induced by infectious agents (e.g., *Helicobacter hepaticus* or *Cryptosporidium parvum*); models of experimental biliary obstruction; models involving enteric bacterial cell wall components or colitis; and models of primary biliary epithelial and endothelial cell injury (Pollheimer and Fickert, 2015; Pollheimer et al., 2011). The $Abcb4^{-/-}$ KO mouse model is most appropriate for studying fibrosis (Delire et al., 2015).

3.1.1 The 3,5-Diethoxycarbonyl-1,4-Dihydrocollidine Diet Model

DDC is known to induce Mallory–Denk bodies, which are associated with cholestasis, ALD, and non-alcoholic steatohepatitis (NASH), in the hepatocytes of experimental animals (Fickert et al., 2002). DDC administration has also been proposed as a model of sclerosing cholangitis (Fickert et al., 2007). DDC-fed mice develop pericholangitis, periductal fibrosis, ductular reaction, and consequently portal–portal bridging fibrosis and segmental bile duct obstruction.

3.1.2 Abcb4$^{-/-}$ Mice

The *Abcb4* gene encodes phospholipid transporter multidrug resistant protein 2 (MDR2). $Abcb4^{-/-}$ mice

spontaneously develop cholangitis, ductular proliferation, onion skin–type periductal fibrosis, and portal inflammation and fibrosis (Fickert et al., 2004; Mauad et al., 1994; Pollheimer and Fickert, 2015). These features are most likely linked to the lack of biliary phospholipid secretion and consequently increased concentration of free nonmicellar-bound bile acids, which subsequently cause damage to bile duct epithelial cells (Halilbasic et al., 2009; Pollheimer and Fickert, 2015). This model reflects the histopathological characteristics of human PSC as well. However, it has the drawback that it is not complicated with UC or CC, but is complicated with hepatocellular neoplasia, which is rare in PSC patients (Pollheimer and Fickert, 2015).

3.1.3 Cftr$^{-/-}$ Mice

The histological features of the livers of PSC patients are similar to those observed in cystic fibrosis (Henckaerts et al., 2009). Durie et al. (2004) evaluated multiple organs of congenic C57BL/6J $Cftr^{-/-}$ mice and found that all the $Cftr^{-/-}$ animals showed progressive liver disease with hepatosteatosis, focal cholangitis, inspissated secretions, and bile duct proliferation; mice older than 1 year showed progression to focal biliary cirrhosis. In addition, a genetic analysis of PSC patients suggested that the CFTR gene might be implicated in the pathogenesis of PSC (Henckaerts et al., 2009).

3.2 Animal Models of Primary Biliary Cholangitis (Table 13.3)

Primary biliary cholangitis (PBC) is an autoimmune disease that is characterized by chronic nonsuppurative destructive cholangitis (CNSDC). It mainly occurs in middle-aged women, who are in their 40s or 50s. In PBC, interlobular bile ducts of less than 100 µm diameter gradually collapse and vanish; eventually, fibrosis around the portal tracts progresses, resulting in liver cirrhosis. Histologically, inflammatory cell infiltration, mainly by lymphocytes and plasma cells, is observed in

TABLE 13.3 Animal Models of Primary Biliary Cholangitis (PBC)

Animal models	Main features
NOD.c3c4 mice	NOD.c3c4 mice develop antibodies to PDC-E2 and histology like human PBC
	Extrahepatic biliary ducts are also affected unlike human PBC
	NOD.c3c4 mice develop biliary cysts that are not known in human PBC
dnTGF-βRII mice	These mice develop spontaneous production of AMAs
	Severe immunological abnormalities occur in multiple organs
	These mice have a relatively short life span
IL-2Rα$^{-/-}$ mice	These mice develop portal inflammation, biliary ductular damage, and AMAs
	These mice develop UC that are often seen in PSC, but not in PBC
	The life span is short
Ae2a,b$^{-/-}$ mice	Most *Ae2a,b$^{-/-}$* mice test positively for AMA
	The rate of mice showing histological features of PBC is low
	This mouse strain seems to be very difficult to breed
Scurfy mice	100% of scurfy mice exhibit high-titer serum AMA of all isotypes
	These mice have lymphocytic infiltrates surrounding portal areas
	These mice die as early as 16–25 days after birth
MRL/lpr mice	These mice have been used as a model for the study of SLE
	The target antigens of AMA are not PDC
	The rate of mice showing PBC-like pathology is rather low
2OA-immunized mice	High levels of AMAs are detected, and cholangitis and granulomas are observed
	Fibrosis occurs when these mice are exposed to α-GalCer
	Peritonitis occasionally occurs in association with intraperitoneal injection

AE2, Anion exchanger 2; AMA, antimitochondrial antigen; dnTGF-βRII, dominant-negative form of transforming growth factor beta receptor type II; α-GalCer, α-galactosylceramide; IL-2Rα, interleukin-2 receptor alpha; MRL/lpr, Murphy Roths large/lymphoproliferation; NOD, nonobese diabetic; 2OA, 2-octynoic acid; PDC, pyruvate dehydrogenase complex; PSC, primary sclerosing cholangitis; SLE, systemic lupus erythematosus; UC, ulcerative colitis.

portal tracts, and CNSDC and bile duct disappearance are observed to various degrees, often accompanied by epithelioid cell granulomas. The disease is classified into four stages: the florid duct lesion stage, the ductular proliferation stage, the precirrhosis stage, and the cirrhosis stage. Antimitochondrial antibodies (AMAs) that react with the pyruvate dehydrogenase complex (PDC), targeting the inner lipoyl domain of the E2 subunit (anti-PDC-E2), appear in the serum of almost all PBC patients (Liu et al., 2013).

Previously reported PDC-immunized mice, neonatally thymectomized mice, peripheral blood mononuclear cell administration, Murphy Roths large/lymphoproliferation (MRL/lpr) mice, and graft-versus-host-disease models are currently seldom used because they do not reflect the characteristics of human PBC sufficiently, or they require special technical skills. Newly introduced animal models of PBC can be roughly classified into spontaneous models and xenobiotic-immunized mice.

3.2.1 Spontaneous Mouse Models

3.2.1.1 NOD.c3c4 MICE

The NOD.c3c4 mouse, the first spontaneous mouse model of PBC, was generated by introgression of B6- and B10-derived insulin-dependent diabetes regions (idd loci) into a nonobese diabetic (NOD) mouse (Irie et al., 2006). NOD.c3c4 mice develop antibodies to PDC-E2 at 9–10 weeks. Histologically, lymphocytic and eosinophilic infiltration of portal tracts, destructive cholangitis, and granuloma formation are observed, as in human PBC patients. However, unlike in human PBC patients, in this model, extrahepatic biliary ducts are also affected. Furthermore, NOD.c3c4 mice develop biliary cysts, which are not known in human PBC (Moritoki et al., 2011; Nakagome et al., 2007).

3.2.1.2 dnTGF-βRII MICE

dnTGF-βRII mice are transgenic for directed expression of a dominant-negative form of transforming

growth factor (TGF)-β receptor type II under the direction of the CD4 promoter (Oertelt et al., 2006). These mice spontaneously produce AMAs, and histologically, lymphocytic liver infiltration with periportal inflammation is observed. Additionally, the serum cytokine profile of these mice mimics that found in human PBC. The main drawbacks of this model are that severe immunological abnormalities occur in multiple organs because of a defect in TGF-β signaling in T lymphocytes, and the mice have a relatively short life span (Tsuneyama et al., 2012). Colitis, which is not a characteristic feature of PBC but is a feature of PSC, occurs in these mice (Pollheimer and Fickert, 2015).

3.2.1.3 *IL-2R$\alpha$$^{-/-}$* MICE

Interleukin (IL)-2 is critical for the development and peripheral expansion of CD4(+)CD25(+) regulatory T cells, which promote self-tolerance by suppressing T-cell responses in vivo (Nelson, 2004). IL-2 receptor alpha (*IL-2Rα*)$^{-/-}$ mice develop portal inflammation (predominantly due to T cells) and biliary ductular damage similar to that found in human patients with PBC (Wakabayashi et al., 2006). Furthermore, *IL-2Rα*$^{-/-}$ mice develop AMAs with specificity for PDC-E2. The main drawbacks of this model are that the mice develop UC, which is often seen in PSC but not in PBC patients, and that their life span is short (Liu et al., 2013).

3.2.1.4 *Ae2a,b*$^{-/-}$ MICE

Cl^{-}/HCO$_3^{-}$ anion exchanger 2 (AE2) is involved in intracellular pH [pH(i)] regulation and transepithelial acid–base transport, including secretin-stimulated biliary bicarbonate excretion. *AE2* gene expression is reduced in liver biopsy specimens and blood mononuclear cells from patients with PBC (Medina et al., 1997; Melero et al., 2002; Pollheimer and Fickert, 2015). Accordingly, the suitability of *Ae2a,b*$^{-/-}$ mice as an animal model of PBC was determined (Salas et al., 2008). Most *Ae2a,b*$^{-/-}$ mice tested positive for AMA, and about one-third of the *Ae2a,b*$^{-/-}$ mice had extensive portal inflammation, with CD8+ and CD4+ T lymphocytes surrounding damaged bile ducts. Although the *Ae2a,b*$^{-/-}$ mouse model is considered useful for studying PBC, it has the drawback that the number of mice displaying the histological features of PBC is low. Moreover, this mouse strain seems to be very difficult to breed (Pollheimer and Fickert, 2015).

3.2.1.5 SCURFY MICE

Scurfy mice are those that have a mutation in the gene encoding the forkhead box 3 (Foxp3) transcription factor that results in a complete abolition of Foxp3(+) T regulatory cells. At 3–4 weeks of age, all scurfy mice exhibit high-titer serum AMA of all isotypes (Zhang et al., 2009). Furthermore, mice have moderate-to-severe lymphocytic infiltrates surrounding portal areas, with evidence of biliary duct damage, and dramatic elevation of cytokines in serum and messenger RNAs, which encode cytokines in liver tissue, including tumor necrosis factor (TNF)-α, interferon (IFN)-γ, IL-6, IL-12, and IL-23. Although the scurfy mouse model of PBC is interesting, it has the drawback that the mice die as early as 16–25 days after birth (Brunkow et al., 2001).

3.2.1.6 MRL/lpr MICE

MRL/lpr mice spontaneously develop lymphadenopathy, hypergammaglobulinemia, serum autoantibodies, and a generalized autoimmune disease, such as glomerulonephritis and arthritis, and have been used as a model for the study of systemic lupus erythematosus. Ohba et al. (2002) examined the suitability of MRL/lpr mice as an experimental autoimmune-mediated cholangitis model for PBC. They found that histopathologically, 24 of 47 (51%) older MRL/lpr mice showed evidence of cholangitis, compared with 2 of 20 (10%) younger MRL/lpr mice. In particular, epithelioid granuloma and/or bile duct loss were seen in 11 out of 47 (23%) older MRL/lpr mice, whereas such findings were seen in only 1 of 20 (5%) younger MRL/lpr mice. The target antigens of AMA were not the PDC, but the 2-oxoglutarate dehydrogenase complex and/or the branched-chain oxoacid dehydrogenase complex, as confirmed by immunoblotting. Currently, the MRL/lpr mouse model is seldom used to study PBC, mainly because the number of mice showing PBC-like pathology is rather low.

3.2.2 Chemical Xenobiotics–Immunized Mice

There is increasing evidence that environmental factors, such as bacterial infection and exposure to xenobiotics, are important in the pathogenesis of PBC. Wakabayashi et al. (2008, 2009) reported that C57BL/6 mice and NOD congenic strain 1101 (NOD.1101) mice that had been immunized with 2-octynoic acid (2OA) coupled to bovine serum albumin (BSA) showed pathological characteristics, similar to those found in human PBC. 2OA is a putative xenobiotic that is used as an additive for food and cosmetics. High levels of AMAs were detected in the animal models, and portal infiltrates enriched in CD8+ T lymphocytes, cholangitis, and liver granulomas were observed. Thereafter, it was reported that when the 2OA–BSA immunized mice were exposed to α-galactosylceramide (α-GalCer), an invariant natural killer T-cell activator, autoimmune cholangitis was exacerbated and fibrosis occurred (Wu et al., 2011). These models require simple techniques (intraperitoneal injection) and develop PBC-like pathological conditions with high reproducibility. However, it may be necessary to improve the method of administration because peritonitis occasionally occurs in association with intraperitoneal injection.

TABLE 13.4 Animal Models of Autoimmune Hepatitis (AIH)

Animal models	Main features
Con A hepatitis	Liver injury depends on the activation of T lymphocytes by macrophages
	Circulating autoantibodies are lacking
	Rapid hepatocyte damage occurs after a single-dose Con A injection
$TGF\text{-}\beta 1^{-/-}$ mice on BALB/c background	These mice develop a lethal necroinflammatory hepatitis
	Hepatitis is dependent on IFN-γ
	The mice usually die within a few weeks
NTx-$PD\text{-}1^{-/-}$ mice	These mice produce antinuclear antibodies and develop fatal hepatitis
	The hepatitis is characterized by CD4+ and CD8+ T-cell infiltration
	These mice usually die approximately 3 weeks after birth
Alb-HA/CL4-TCR mice	These mice spontaneously develop chronic autoimmune-mediated hepatitis
	Necroinflammatory lesions and hepatic fibrosis develop
	Hepatitis occurs only in males
Ad-2D6–infected mice	These mice develop persistent autoimmune liver disease
	Cellular infiltration, hepatic fibrosis, fused liver lobules, and necrosis are seen
	These mice generate type 1 liver kidney microsomal-like antibodies

Ad-2D6, Adenovirus expressing human CYP2D6; Alb-HA/CL4-TCR, albumin- hemagglutinin/CL4 T-cell receptor; Con A, concanavalin A; IFN, interferon; NTx-PD-1, neonatal thymectomy-programmed cell death 1; TGF-β1, transforming growth factor beta 1.

3.3 Animal Models of Autoimmune Hepatitis (Table 13.4)

Autoimmune hepatitis (AIH) is a chronic, active form of hepatitis that is associated with autoimmune mechanisms. Clinically, it occurs more commonly in women and is characterized by HLA-DR4, hypergammaglobulinemia, antinuclear antibody, antismooth muscle antibody, and the symptoms of chronic hepatitis. Histopathologically, it is characterized by lymphocyte and plasma cell infiltration of the portal tracts, interface hepatitis, and hepatocyte rosette formation in periportal areas. The difficulty in generating animal models of AIH exists in abolishing immune tolerance and maintaining the long-term immune alterations that are necessary for inducing chronic hepatitis.

3.3.1 Concanavalin A Hepatitis

Concanavalin A (Con A) is a plant lectin that is purified from jack beans. Con A binds to the mannose residues of various glycoproteins and activates lymphocytes. When Con A is administered to mice, liver injury that depends on the activation of T lymphocytes by macrophages occurs (Tiegs et al., 1992). Therefore, the model might allow the study of the pathophysiology of immunologically mediated hepatic disorders, such as AIH. TNF-α and IFN-γ play important roles in Con A–induced liver injury (Gantner et al., 1995; Kusters et al., 1996) and IL-10 prevents liver injury in this model (Di Marco et al., 1999; Louis et al., 1997). Blood levels of

IL-2, IL-4, and IFN-γ dramatically increase after administration of Con A (Wang et al., 2012). Major drawbacks of this model include the lack of circulating autoantibodies and rapid hepatocyte damage following a single-dose Con A injection, which is not a typical feature of chronic AIH (Liu et al., 2013).

3.3.2 BALB/c Strain TGF-β1$^{-/-}$ Mice

TGF-β1 exhibits various antiinflammatory activities and contributes to immune homeostasis and inhibition of autoimmunity. $TGF\text{-}\beta 1^{-/-}$ mice develop an excessive inflammatory response with massive infiltration of lymphocytes and macrophages into many organs (but primarily the heart and lungs), and they die when they are 3–4 weeks old (Kulkarni et al., 1993; Shull et al., 1992). BALB/c strain $TGF\text{-}\beta 1^{-/-}$ mice develop a lethal necroinflammatory hepatitis that is not observed in $TGF\text{-}\beta 1^{-/-}$ mice with a different genetic background (Gorham et al., 2001). This hepatitis is dependent on IFN-γ and epitomizes important aspects of AIH. The drawback of this model is that the mice usually die within a few weeks.

3.3.3 NTx-PD-1$^{-/-}$ Mice

Regulatory T cells regulate immunological tolerance. They play an important role in inhibiting excessive immunological response and maintaining immunological homeostasis. Kido et al. (2008) examined the regulatory roles of naturally arising regulatory T cells and programmed cell death 1 (PD-1)–mediated signaling

in the development of AIH. They subjected *PD-1*$^{-/-}$ mice to neonatal thymectomy (NTx), which severely reduces the number of regulatory T cells. As a result, the NTx-*PD-1*$^{-/-}$ mice produced antinuclear antibodies and developed fatal hepatitis characterized by CD4+ and CD8+ T-cell infiltration of the parenchyma with massive lobular necrosis. They concluded that the NTx-*PD-1*$^{-/-}$ mice could be used as the first model of spontaneous fatal AIH. However, these mice cannot be used in long-term experiments because they usually die of fulminant hepatic failure approximately 3 weeks after birth.

3.3.4 Alb-HA/CL4-TCR Mice

Zierden et al. (2010) generated transgenic mice expressing the influenza virus hemagglutinin (HA) autoantigen under the control of mouse albumin regulatory elements and α-fetoprotein enhancers (Alb) specifically in the liver (Alb-HA mice); the mice were crossed with mice that express a specific T-cell receptor (TCR) (CL4-TCR). As a result, the double-transgenic mice (Alb-HA/CL4-TCR) spontaneously developed chronic, autoimmune-mediated hepatitis characterized by necroinflammatory lesions, hepatic fibrosis, and increased levels of aminotransferase; these features resembled those of AIH. However, this model has the disadvantage that hepatitis occurs only in males.

3.3.5 Ad-2D6–Infected Mice

Cytochrome P450 2D6 (CYP2D6) is the major human autoantigen in type 2 AIH. Holdener et al. (2008) infected mice with adenovirus Ad5 expressing human CYP2D6 (Ad-2D6). As a result, Ad-2D6–infected mice

developed persistent autoimmune liver disease characterized by cellular infiltration, hepatic fibrosis, fused liver lobules, and necrosis. As with type 2 AIH patients, Ad-2D6–infected mice generated type 1 liver kidney microsomal-like antibodies that recognized the immunodominant epitope of CYP2D6. Interestingly, Ad-2D6–infected, wild-type FVB/N mice displayed exacerbated liver damage compared with transgenic mice expressing the identical human CYP2D6 protein in the liver, indicating the presence of a stronger immunological tolerance in CYP2D6 mice.

3.4 Animal Models of Alcoholic Liver Disease (Table 13.5)

ALD is a pathological condition of the liver that is caused by long-term (usually more than 5 years) and excessive alcohol consumption. Its symptoms, such as swelling of the liver and increased serum levels of aminotransferases and γ-glutamyl transpeptidase, are improved or normalized by abstinence from drinking. ALD is classified into alcoholic fatty liver, alcoholic hepatitis, alcoholic liver fibrosis, and alcoholic liver cirrhosis. To date, no animal model has been created that reflects all the features of ALD (Brandon-Warner et al., 2012; Mathews et al., 2014). In rodents, natural aversion to alcohol, absence of addictive behavior, spontaneous reduction in alcohol intake when acetaldehyde blood levels increase, a high rate of alcohol catabolism, and a high basal metabolic rate impair the ability to attain and maintain high blood alcohol levels over time; these factors explain the lack of hepatic damage (Brandon-Warner et al., 2012; Delire et al., 2015).

TABLE 13.5   Animal Models of Alcoholic Liver Disease (ALD)

Animal models	Main features
Acute binge ethanol–feeding model	The most commonly used dosage is 4–6 g/kg body weight
	This model affects hepatic mitochondrial function and oxidative stress
	This model induces only a mild elevation of serum AST and ALT levels
Liquid diet model	Animals are fed ethanol as part of a completely liquid diet
	This model is easy to use and causes fatty liver
	Severe inflammation, necrosis, and fibrosis of the liver do not develop
Intragastric ethanol infusion model	Severe and progressive fatty infiltration is observed in the liver
	Serum AST and ALT levels become markedly elevated
	This model requires advanced skills in catheter implantation
Chronic + binge ethanol–feeding model	This model induces liver injury, inflammation, and fatty liver
	This model reflects well a history of alcohol consumption in ALD patients
	This model is less time consuming compared to other models

ALT, Alanine aminotransferase; AST, aspartate aminotransferase.

3.4.1 Acute Binge Ethanol–Feeding Model

An acute binge of one or multiple doses of ethanol has been used by many laboratories to study the pathogenesis of alcoholic liver injury (Mathews et al., 2014; Shukla et al., 2013). The most commonly used dosage is 4–6 g ethanol/kg body weight, and acute feeding of ethanol has been shown to affect hepatic mitochondrial function, oxidative stress, and inflammatory responses. However, the acute binge ethanol–feeding model has not been used widely as an animal model of ALD, partly because it induces only mild elevation of serum aspartate aminotransferase (AST) and alanine aminotransferase (ALT) levels.

3.4.2 Liquid Diet Model

Ad libitum administration of alcohol in drinking water is the best and easiest way to emulate human behavior in experimental animals. However, rodents show a strong aversion to the taste and smell of ethanol. Due to this, in this method, the animals do not consume enough alcohol to produce significant liver pathology, even when using alcohol-preferring rodent strains (Liu et al., 2013). To overcome this, Lieber and DeCarli (1982, 1986) developed the technique of feeding ethanol as part of a totally liquid diet. This technique resulted in much higher ethanol intake than with conventional procedures, and it caused fatty liver. Moreover, the technique is simple. However, in this method, severe inflammation, necrosis, and fibrosis of the liver do not develop unless second hits of, for example, vitamin A are added (Leo and Lieber, 1983). Therefore, although this model may be appropriate for studying early-stage ALD, it is not useful for investigating the advanced disease.

3.4.3 Intragastric Ethanol Infusion Model (Tsukamoto–French Model)

As oral administration of alcohol does not induce liver injury that is more severe than fatty liver, Tsukamoto et al. (1985) developed an intragastric ethanol infusion model. In this model, a catheter was inserted into the stomach of each rat, and ethanol and a nutritionally defined low-fat liquid diet were infused continuously. As a result, blood alcohol levels were maintained at high levels, and severe and progressive fatty infiltration was observed in the liver. In addition, following 30 days of intoxication, one-third of the animals showed focal necrosis with mononuclear cell infiltration in the centrilobular areas of the livers. This was correlated with markedly elevated levels of serum AST and ALT in these animals. Dietary iron supplementation to the intragastric ethanol infusion exacerbated hepatocyte damage, promoted liver fibrogenesis, and produced evident cirrhosis in some rats (Tsukamoto et al., 1995). A high-fat (HF) diet in combination with this model also caused liver fibrosis (French et al., 1986). Later, Kono et al. (2000) adapted a long-term intragastric rat protocol to mice so that KO technology could be used to study the mechanisms of ALD. The main drawbacks of this model are that it requires constant monitoring and advanced skills in catheter insertion. However, it has the advantage that nutritional intake can be controlled accurately.

3.4.4 Chronic + Binge Ethanol–Feeding Model

Bertola et al. (2013a) developed a mouse model of alcoholic liver injury by chronic ethanol feeding (10-day ad libitum oral feeding with the Lieber–DeCarli ethanol liquid diet) plus single-binge ethanol feeding. This chronic plus single-binge ethanol–feeding protocol induces liver injury, inflammation, and fatty liver synergistically, which mimics acute-on-chronic alcohol liver injury in patients. This feeding protocol can also be extended to chronic feeding for longer periods (up to 8 weeks) plus single or multiple binges. The procedure upregulates the hepatic expression of IL-1β and TNF-α, and induces neutrophil accumulation in the liver (Bertola et al., 2013b). As ALD is often caused by recent heavy drinking on top of a chronic drinking habit, this model effectively reflects a history of alcohol consumption in ALD patients. Moreover, it is less time consuming compared with other conventional models.

3.5 Animal Models of Nonalcoholic Fatty Liver Disease (Table 13.6)

Like ALD, nonalcoholic fatty liver disease (NAFLD) is characterized by fatty liver, steatohepatitis, liver fibrosis, or liver cirrhosis, but it occurs in people who do not consume excessive quantities of alcohol. Obesity, diabetes, and dyslipidemia are important risk factors of the disease, and the resulting insulin resistance, fatty degeneration of the liver, and oxidative stress are thought to be involved in its pathogenesis. NAFLD is histopathologically classified into simple steatosis, which is just fat accumulation in the liver, and NASH, which comprises a necroinflammatory reaction and ballooning degeneration of hepatocytes, as well as steatosis. NASH is usually accompanied by fibrosis. The fibrosis usually begins as perisinusoidal fibrosis characterized by a chicken-wire pattern in zone 3, and portal fibrosis gradually develops, leading to portal–portal or portal–central bridging fibrosis (Takahashi and Fukusato, 2014). Long-standing NASH may progress to liver cirrhosis and HCC (Cohen et al., 2011; Harrison et al., 2003; Powell et al., 1990). NAFLD/NASH is currently the most common chronic liver disease in developed countries. Animal models of NAFLD/NASH are classified into genetic models, dietary models, and models combining genetic and nutritional factors.

TABLE 13.6   Animal Models of Nonalcoholic Fatty Liver Disease (NAFLD)

Animal models	Main features
Genetic models	
Ob/ob mice, db/db mice, and fa/fa rats	These animals have a mutation in the leptin or a leptin receptor gene
	The metabolic status of these animals reflects human NAFLD
	Neither hepatic inflammation nor hepatocellular damage occurs spontaneously
KK-A^y mice	These mice carry a heterozygous mutation of the agouti gene
	The metabolic status is similar to that of NAFLD patients
	Significant steatohepatitis does not occur spontaneously
PPARα$^{-/-}$ mice	Many genes encoding enzymes involved in β-oxidation are regulated by PPARα
	Fat does not accumulate in the liver of these mice under normal feeding condition
	Severe fat deposition occurs in the liver under fasting conditions
PTEN null mice	These mice show massive hepatomegaly and steatohepatitis
	These mice develop liver tumors (hepatocellular adenomas and carcinomas)
	These mice show insulin sensitivity
nSREBP-1c transgenic mice	Liver histology resembles human NASH
	These mice show disordered differentiation of adipose tissue
	The liver lesion might model steatohepatitis associated with lipodystrophy
AOX$^{-/-}$ mice	AOX is the first enzyme in the peroxisomal β-oxidation system
	Microvesicular fatty change in liver cells is evident at 7 days
	AOX$^{-/-}$ mice develop hepatocellular adenomas and carcinomas by 15 months of age
MAT1A null mice	These mice develop macrovesicular steatosis and mononuclear cell infiltration
	HCC develops
	Although these mice are hyperglycemic, their insulin levels are normal
TSOD mice	This model is regarded as a polygenic model of metabolic syndrome
	Liver tumors occur spontaneously
	The severity of steatosis and inflammation is mild
Dietary models	
MCD diet	MCD diet is easy to obtain and use
	This model induces more severe histopathology of NASH than other dietary models
	The metabolic profile is opposite to that in human NASH
HF diet	HF diet induces a metabolic profile that corresponds to NASH
	NAFLD/NASH induced by HF diet may be relatively mild and highly variable
	Administration of HF diet via an implanted gastrostomy tube effectively induces NASH
Atherogenic diet	Atherogenic diet containing cholesterol and cholate induces steatohepatitis
	The addition of a HF component accelerates the pathology of steatohepatitis
	Animals fed the atherogenic diet remain remarkably insulin sensitive
Fructose	Fructose consumption is a well-known risk factor for NAFLD
	A high-fructose diet induces macrovesicular steatosis and lobular inflammation
	Steatosis is mainly distributed in zone 1
Fast food diet	A fast food diet contains high levels of saturated fats, cholesterol, and fructose
	This model induces obesity and insulin resistance
	Histologically, steatohepatitis with ballooning and progressive fibrosis is observed

AOX, Acyl-CoA oxidase; HCC, hepatocellular carcinoma; HF, high fat; MAT1A, methionine adenosyltransferase-1A; MCD, methionine and choline deficient; NASH, nonalcoholic steatohepatitis; nSREBP-1c, nuclear sterol regulatory element–binding protein-1c; PPAR, peroxisome proliferator–activated receptor; PTEN, phosphatase and tensin homolog deleted on chromosome 10; TSOD, Tsumura–Suzuki obese diabetes.

3.5.1 Genetic Models

3.5.1.1 ob/ob MICE AND db/db MICE (OR fa/fa RATS)

Leptin is a satiety hormone synthesized by white adipose tissue; it regulates energy intake and expenditure. Ob/ob mice have a mutation in the gene that encodes leptin, and db/db mice and fa/fa rats have a mutation in the gene that encodes a leptin receptor (Ob-Rb) (Anstee and Goldin, 2006; Carmiel-Haggai et al., 2005; Lindstrom, 2007). Such animals are obese, hyperphagic, inactive, insulin resistant, and spontaneously develop hepatic steatosis and type 2 diabetes. Although the metabolic status of these animals reflects that found in human NAFLD, they do not spontaneously develop either hepatic inflammation or hepatocellular damage. One of the interesting features of ob/ob mice is that they are resistant to liver fibrosis even when CCl_4 or TAA is administered (Honda et al., 2002; Leclercq et al., 2002). This finding suggests that leptin is essential for hepatic fibrogenesis.

3.5.1.2 KK-A^y MICE

KK-A^y mice are a cross between diabetic KK and lethal yellow (A^y) mice, and carry a heterozygous mutation of the agouti gene (Liu et al., 2013). KK-A^y mice show altered adipokine expression, obesity, dyslipidemia, and insulin resistance; thus, their metabolic status is similar to that of NAFLD patients. Although KK-A^y mice develop mild hepatic steatosis, significant steatohepatitis does not occur spontaneously (Takahashi et al., 2012). KK-A^y mice exhibit increased susceptibility to methionine- and choline-deficient (MCD) diet–induced steatohepatitis, where hypoadiponectinemia probably plays a key role in the exacerbation of both inflammatory and profibrogenic responses (Ikejima et al., 2007; Okumura et al., 2006).

3.5.1.3 PPARα$^{-/-}$ MICE

Many genes encoding enzymes involved in the mitochondrial and peroxisomal fatty acid β-oxidation pathways in the liver are regulated by peroxisome proliferator–activated receptor α (PPARα) (Liu et al., 2013). Although fat does not accumulate in the livers of PPARα$^{-/-}$ mice under normal feeding conditions, under fasting conditions severe fat deposition occurs in the liver in association with dramatic inhibition of fatty acid uptake and oxidation (Kersten et al., 1999; Reddy, 2001).

3.5.1.4 PTEN NULL MICE

Phosphatase and tensin homolog deleted on chromosome 10 (PTEN) is a multifunctional phosphatase and tumor suppressor that serves as a negative regulator of several signaling pathways, including PI3K/Akt (Liu et al., 2013). Mice with a hepatocyte-specific null mutation of PTEN [AlbCrePten(flox/flox) mice] show massive hepatomegaly and steatohepatitis with triglyceride accumulation, a phenotype similar to that found in human

NASH (Horie et al., 2004). In one study, steatosis developed at 10 weeks of age, and steatohepatitis and fibrosis were present at 40 weeks of age. Importantly, the PTEN null mice developed liver tumors. By 44 weeks of age, 47% of the PTEN null mice had developed hepatocellular adenomas, and by 74–78 weeks of age, 100% of the PTEN null mice had hepatocellular adenomas and 66% had HCCs (Horie et al., 2004). Therefore, this model is considered suitable for studies on carcinogenesis associated with NASH. The main drawback of this model is that the mice retain insulin sensitivity, and therefore, their metabolic status is different from that of NAFLD patients.

3.5.1.5 nSREBP-1c TRANSGENIC MICE

Overexpression of the nuclear sterol regulatory element–binding protein-1c (nSREBP-1c) in cultured preadipocytes promotes adipocyte differentiation (Shimomura et al., 1998). nSREBP-1c transgenic mice develop marked fatty liver accompanied by hyperglycemia, hypoleptinemia, and hypoadiponectinemia (Nakayama et al., 2007). The liver histology in such mice is similar to that found in NASH, that is, steatosis, mononuclear cell infiltration, pericellular fibrosis, ballooning degeneration, and Mallory–Denk body formation are seen in the livers of these transgenic mice at 20 weeks or older. However, the mice show disordered differentiation of adipose tissue, marked insulin resistance, and diabetes mellitus; thus, the liver lesion might model steatohepatitis associated with lipodystrophy rather than normal NASH.

3.5.1.6 AOX$^{-/-}$ MICE

Acyl-CoA oxidase (AOX) is the first enzyme that is involved in the peroxisomal β-oxidation system. Mice deficient in fatty AOX (AOX$^{-/-}$ mice) develop specific morphological and molecular changes in the liver characterized by microvesicular fatty change, increased mitosis, spontaneous peroxisome proliferation, increased mRNA and protein levels of genes regulated by PPARα, and HCC (Cook et al., 2001). In AOX$^{-/-}$ mice, microvesicular fatty change in liver cells is evident at 7 days. At 2 months of age, livers show extensive steatosis and the presence in the periportal areas of clusters of hepatocytes with abundant granular eosinophilic cytoplasm rich in peroxisomes. However, a compensating increase in fatty acid oxidation is observed by 6–7 months of age, and hepatic steatosis recovers by the regeneration of hepatocytes. AOX$^{-/-}$ mice develop hepatocellular adenomas and HCCs by 15 months of age (London and George, 2007; Takahashi et al., 2012).

3.5.1.7 MAT1A NULL MICE

Methionine adenosyltransferase (MAT) 1A is a liver-specific enzyme that catalyzes the formation of S-adenosylmethionine, the principal biological methyl donor.

MAT1A KO mice are susceptible to choline-deficient diet–induced fatty liver at 3 months. At 8 months, *MAT1A* KO mice develop spontaneous macrovesicular steatosis and predominantly periportal mononuclear cell infiltration (Lu et al., 2001). HCC develops in more than half of the KO mice by 18 months of age (Martinez-Chantar et al., 2002). Although *MAT1A* KO mice are hyperglycemic, their insulin levels are normal and they do not appear to develop the other features of metabolic syndrome (Martinez-Chantar et al., 2002; Takahashi et al., 2012).

3.5.1.8 TSUMURA–SUZUKI OBESE DIABETES MICE

Tsumura–Suzuki obese diabetes (TSOD) male mice spontaneously develop diabetes mellitus, obesity, glucosuria, hyperglycemia, and hyperinsulinemia without any special treatments, such as gene manipulation. Therefore, TSOD is regarded as a polygenic model of metabolic syndrome. As NAFLD/NASH is associated with metabolic syndrome, Nishida et al. (2013) determined whether these mice develop NAFLD/NASH. They observed microvesicular steatosis, hepatocellular ballooning, and Mallory–Denk bodies in the livers of 4-month-old mice, with increasing severity over time. Interestingly, small liver nodules with high cellularity and the absence of portal tracts were frequently observed after 12 months. Most of the nodules showed nuclear and structural atypia, and mimicked human HCC. Recently, it has been suggested that splenic iron accumulation is involved in the development of NASH in TSOD mice (Murotomi et al., 2016). Although TSOD mice provide a natural model of NAFLD, the mice take a long time to develop the disorder, and the severity of steatosis and inflammation is mild.

3.5.2 Dietary Models

3.5.2.1 METHIONINE- AND CHOLINE-DEFICIENT DIET

MCD diet is a classical dietary model of NASH. Although the diet comprises high sucrose (40%) and fat (10%), it lacks methionine and choline, which are indispensable for hepatic mitochondrial β-oxidation and very low-density lipoprotein (VLDL) synthesis (Anstee and Goldin, 2006). As a result, an MCD diet induces hepatic steatosis. Furthermore, oxidative stress and changes in cytokines and adipocytokines occur, contributing to liver injury (Chowdhry et al., 2010; Larter et al., 2008; Leclercq et al., 2000; Takahashi et al., 2012). When animals are fed an MCD diet, they rapidly develop steatohepatitis; this is accompanied by pericellular fibrosis that appears as a chicken-wire pattern distributed mainly in zone 3, resembling that in human NASH (Fig. 13.1). In general, the MCD diet is easy to obtain and use, and it induces a more severe histopathology of NASH than other dietary models. The degree of liver injury induced by an MCD diet depends on the species, strain, and sex of the
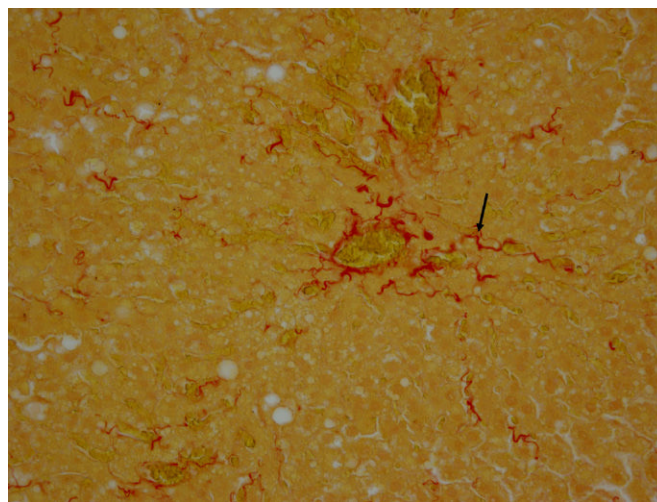
FIGURE 13.1　**Histological appearance of the liver of a mouse that was fed an MCD diet.** Pericellular fibrosis can be seen in intralobular zone 3 *(arrow)* (Sirius red stain, ×400).

animal. Kirsch et al. (2003) examined the responses of male and female Wistar, Long-Evans, and Sprague Dawley rats and C57BL6 mice to an MCD diet. The Wistar strain and male sex were associated with the greatest degree of steatosis in rats. Of the groups studied, male C57BL6 mice developed the most inflammation and necrosis, lipid peroxidation, and ultrastructural injury, and most closely approximated the histological features of NASH. The main drawback of the MCD diet model is that its metabolic profile is opposite to that found in human NASH. Rats or mice that are fed an MCD diet show significant weight loss and decreased serum triglyceride and cholesterol levels. Serum levels of insulin, leptin, and glucose are also decreased; serum adiponectin remains unchanged or even increases; and the animals are peripherally insulin sensitive, although they exhibit hepatic insulin resistance (Leclercq et al., 2007; Liu et al., 2013; Rinella and Green, 2004). Therefore, caution is required when interpreting the results of experiments using this animal model.

3.5.2.2 HIGH-FAT DIET

A HF diet is widely used to induce NAFLD/NASH in various experimental animals. Lieber et al. (2004) fed a HF liquid diet (71% of energy from fat, 11% from carbohydrates, and 18% from protein) to Sprague Dawley rats and examined the effects. The rats fed the HF diet ad libitum for 3 weeks developed panlobular steatosis. The diet caused abnormal mitochondria and mononuclear inflammation. Plasma insulin was elevated, which reflected insulin resistance, a pathogenic characteristic of NASH. It has subsequently been reported that the HF diet induced a metabolic profile (obesity and insulin resistance), serum data (abnormal aminotransferase activity, hyperglycemia, hyperinsulinemia, hypercholesterolemia,

and hypertriglyceridemia), and histopathology (hepatic steatosis, necroinflammation, mitochondrial lesions, hepatocyte apoptosis, and pericentral fibrosis) that corresponded to NASH in experimental animals (Ito et al., 2007; Svegliati-Baroni et al., 2006; Zou et al., 2006). However, other authors have reported that a HF diet did not induce hepatic steatosis or NASH in experimental animals (Romestaing et al., 2007). NAFLD/NASH induced by a HF diet may be relatively mild and highly variable, and may be affected by the composition and duration of the HF diet and by the species, strain, sex, and age of the animals. In a comparison of the effects of a HF diet between mouse strains, BALB/c male mice accumulated more hepatic lipid than C57BL/6J male mice, and middle-aged C57BL/6J mice increased the ratio of fat to body weight and hepatic lipid accumulation more than young mice (Nishikawa et al., 2007). To induce NASH more certainly using the HF diet, Deng et al. (2005) fed a HF diet to mice via an implanted gastrostomy tube for 9 weeks and increased the intake by up to 85% of the standard amount. As a result, overfed C57BL/6 mice progressed to obesity, with 71% larger final body weights. They had increased visceral white adipose tissue, hyperglycemia, hyperinsulinemia, hyperleptinemia, glucose intolerance, and insulin resistance. Of these mice, 46% developed steatohepatitis with increased plasma ALT, neutrophilic infiltration, and sinusoidal and pericellular fibrosis. Although this method seems to be the most certain way to induce NASH using the HF diet, it has the disadvantage that it requires specific equipment and special techniques.

Recently, various modified methods using the HF diet have been tried. The products of lipid peroxidation from oxidized low-density lipoprotein (OxLDL) are known to initiate intracellular oxidative stress (Maziere et al., 2000). It has been reported that OxLDL administration to HF diet–fed mice not only aggravates hepatic steatosis, fibrosis, and lipid metabolism, but also results in intense inflammation, including severe hepatic injury and inflammatory cell infiltration, which are the typical histological features of NASH (Yimin et al., 2012).

Ogasawara et al. (2011) determined whether mice treated with gold thioglucose—known to induce lesions in the ventromedial hypothalamus, leading to hyperphagia and obesity—and fed a HF diet had a comprehensive histological and dysmetabolic phenotype resembling human NASH. They found that gold thioglucose + HF induced dysmetabolism, with hyperphagia; obesity with increased abdominal adiposity; insulin resistance and consequent steatohepatitis with hepatocyte ballooning; Mallory–Denk bodies; and perivenular and pericellular fibrosis, as seen in adult NASH.

Fujii et al. (2013) established a reproducible NASH-HCC model in mice by combining a HF diet and the administration of streptozotocin, a naturally occurring chemical that is toxic to the insulin-producing β-cells of the mammalian pancreas. Neonatal male mice exposed to low-dose streptozotocin developed liver steatosis with diabetes after 1 week on a HF diet. A continuous HF diet decreased hepatic fat deposits but increased lobular inflammation with foam cell–like macrophages, which resembled NASH pathology. In parallel with the decreased phagocytosis of macrophages, fibroblasts accumulated to form chicken-wire pattern fibrosis. All the mice developed multiple HCC at approximately 20 weeks of age. Although this is an unnatural model, it has the advantage that HCC associated with NASH develops rather quickly.

3.5.2.3 ATHEROGENIC DIET (CHOLESTEROL AND CHOLATE)

An increase in the level of serum triglycerides and cholesterol is a risk factor for NAFLD/NASH and cardiovascular diseases. An atherogenic diet containing cholesterol and cholate induces steatohepatitis in experimental animals. Such a diet increases blood levels of AST, ALT, lactate dehydrogenase, and total cholesterol, and from a histopathological perspective, steatosis, macrophage infiltration, cellular ballooning, hepatic necrosis, myofibroblast proliferation, and hepatic fibrosis are also induced (Jeong et al., 2005; Matsuzawa et al., 2007). In one study, the addition of a HF component to the atherogenic diet caused hepatic insulin resistance and further accelerated steatohepatitis (Matsuzawa et al., 2007). Interestingly, the cholesterol and cholate components of the atherogenic diet were shown to induce distinct stages of hepatic inflammatory gene expression (Vergnes et al., 2003). The drawback of this model is that animals given the atherogenic diet remain remarkably insulin sensitive, reflecting a different metabolic status than that found in human NASH (Delire et al., 2015; Matsuzawa et al., 2007).

3.5.2.4 FRUCTOSE

Fructose consumption is a well-known risk factor for NAFLD (Ouyang et al., 2008). We showed that a high-fructose (70%) diet induced macrovesicular steatosis and lobular inflammation in rat livers (Kawasaki et al., 2009). However in this model, steatosis was mainly distributed in zone 1, a different pattern from that found in adult NAFLD patients (Fig. 13.2). Spruss et al. (2009) examined the effects of fructose on *toll-like receptor (TLR)-4* mutant mice and wild-type mice, and suggested that the onset of fructose-induced NAFLD was associated with intestinal bacterial overgrowth and increased intestinal permeability, subsequently leading to an endotoxin-dependent activation of hepatic Kupffer cells. Combining risk factors for metabolic syndrome by feeding mice trans fats and high-fructose corn syrup induced a metabolic profile and histological features similar to those found in NASH
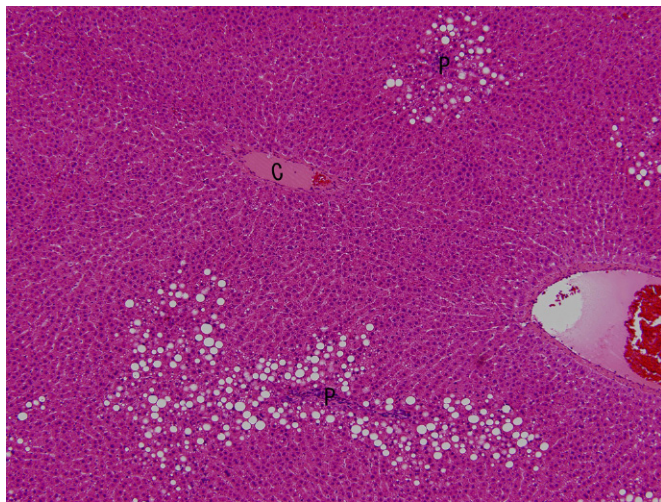
FIGURE 13.2　**NAFLD model of a mouse that was fed a high-fructose diet.** Steatosis, mainly distributed in zone 1 of hepatic lobules, was observed (×100). *C*, Central vein; *P*, portal tract.

patients (Tetri et al., 2008). Kohli et al. (2010) demonstrated that mice maintained on a HF, high-carbohydrate diet and water with 55% fructose and 45% sucrose (wt./vol.) became obese and experienced increased levels of hepatic reactive oxygen species and a NASH-like phenotype with significant fibrosis.

3.5.2.5 FAST FOOD DIET

Fast foods have high energy densities and glycemic loads, and are often served in excessively large portions; this may be one of the reasons for the increase in the number of overweight and obese people (Rosenheck, 2008). Charlton et al. (2011) examined the metabolic and histological effects of a fast food diet (high in saturated fats, cholesterol, and fructose). Mice that were fed fast food [40% energy as fat (12% saturated fatty acids and 2% cholesterol), supplemented with high levels of fructose] became obese and insulin resistant. Steatohepatitis with pronounced ballooning and progressive fibrosis (stage 2) was also observed in the mice. Therefore, it was suggested that a diet based on high levels of cholesterol, saturated fat, and fructose induces the features of metabolic syndrome and NASH with progressive fibrosis.

3.5.3 Combination Models (Genetic Modification Plus Dietary Manipulation)

Separate genetic and dietary models of NASH do not completely reflect all its pathological characteristics in humans. Therefore, numerous combination models, created by genetic and dietary manipulation, have been developed to more closely approximate the pathophysiology of human NASH. In general, these models show more severe histopathological changes and closer pathophysiology to human NASH than individual genetic or

dietary models. Some of the representative combination models are described here.

3.5.3.1 $LDLR^{-/-}$ MICE FED A HF DIET

The low-density lipoprotein receptor deficiency ($LDLR^{-/-}$) mouse is a widely used hypercholesterolemic atherosclerosis model. Gupte et al. (2010) showed that middle-aged male $LDLR^{-/-}$ mice fed a HF diet developed NASH associated with four of five metabolic syndrome components. As observed in humans, liver steatosis and oxidative stress promoted NASH development in these mice. Aging exacerbated the HF diet–induced NASH such that liver steatosis, inflammation, fibrosis, oxidative stress, and liver injury markers were greatly enhanced in middle-aged versus young $LDLR^{-/-}$ mice.

3.5.3.2 fa/fa RATS AND db/db MICE FED A HF DIET

Carmiel-Haggai et al. (2005) determined whether a HF diet can act as a second hit and cause progression to liver injury in obese fa/fa rats. Hyperglycemia and steatohepatitis occurred in the fa/fa rats fed the HF diet (60% calories as lard). This was accompanied by liver injury as assessed by ALT, hematoxylin and eosin staining, increased TNF-α and stellate cell–derived TGF-β, collagen deposition (periportal fibrosis), and upregulation of α-smooth muscle actin. Oxidative stress occurred in the fa/fa rats fed the HF diet because lipid peroxidation and protein carbonyl levels were elevated, whereas levels of glutathione and antioxidant enzymes were very low. We recently showed that db/db mice fed a HF diet develop the histopathology of NASH (Fig. 13.3) that is associated with increased serum levels of AST and ALT, although the metabolic status did not completely reflect that of human NASH (Takahashi et al., 2014).
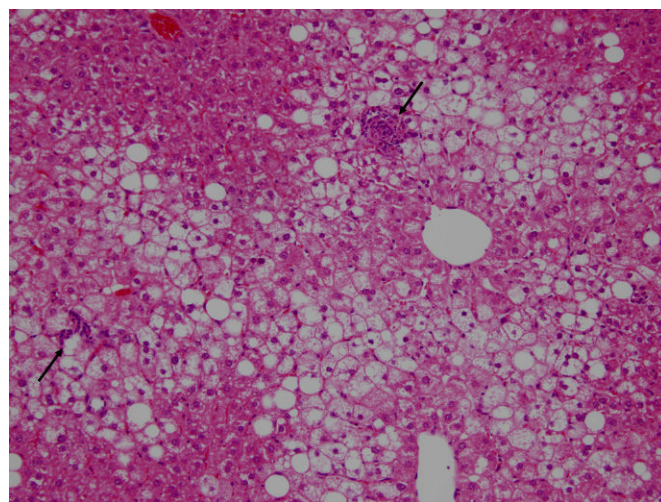
FIGURE 13.3　**Liver histology of a db/db mouse that was fed an HF diet.** Marked steatosis and scattered foci of lobular inflammation *(arrows)* and ballooned hepatocytes were observed (×200).

3.5.3.3 Foz/foz MICE FED A HF DIET

Foz/foz mice have a mutation in the *Alms1* gene that plays a role in intracellular trafficking, and they exhibit obesity, hyperinsulinemia, and diabetes (Arsov et al., 2006b). Foz/foz mice fed a HF diet develop serum ALT elevation and severe steatohepatitis with hepatocyte ballooning, inflammation, and fibrosis (Arsov et al., 2006a).

3.5.3.4 db/db OR *PPARα*$^{-/-}$ MICE FED AN MCD DIET

Sahai et al. (2004) fed db/db, ob/ob, and control mice an MCD diet and found that the MCD diet–fed db/db mice exhibited significantly greater histological inflammation and higher serum ALT levels than the ob/ob and control mice. Trichrome staining showed marked pericellular fibrosis in the MCD diet–fed db/db mice but no significant fibrosis in the ob/ob or control mice. Moreover, it has been reported that MCD diet–fed *PPARα*$^{-/-}$ mice developed more severe steatohepatitis associated with significantly higher serum AST levels compared with MCD diet–fed wild-type mice (Ip et al., 2003; Kashireddy and Rao, 2004).

3.6 Animal Models of Hepatitis C (Table 13.7)

HCV is an RNA virus that belongs to the Flaviviridae family and infects humans via blood transfusion or injection using an unsterilized needle. The virus encodes one long open reading frame that generates a single polyprotein precursor, which is subsequently processed into 10 individual gene products, including structural (C, E1, E2, and p7) and nonstructural (NS2, NS3, NS4A, NS4B, NS5A, and NS5B) protein subunits (Liu et al., 2013; Moradpour et al., 2007). Unlike hepatitis A or hepatitis B, hepatitis C frequently develops from acute to chronic hepatitis, and furthermore, progresses to liver cirrhosis and HCC. Chimpanzees are one of the few animals that tolerate natural HCV infection. Therefore, the chimpanzee has provided a valuable model for the study of HCV–host interactions and vaccine candidates, but its use is severely hampered by financial and ethical constraints (Vercauteren et al., 2014). As mice are naturally resistant to HCV infection, development of mouse models of hepatitis C has been challenging. However, to date, various mouse models of hepatitis C have been developed using molecular or immunological techniques.

3.6.1 Inducible-HCV Transgenic Mice

To study in vivo interactions between viral proteins and host cells, various transgenic mice models that overexpress HCV proteins have been generated. Several kinds of transgenic mice expressing HCV proteins have not provided evidence of liver pathology (Frelin

TABLE 13.7   Animal Models of Hepatitis C

Animal models	Main features
Inducible-HCV transgenic mice	Transgenic mice carrying the HCV core gene develop hepatic steatosis and HCC
	These mice are immunotolerant of HCV proteins
	Immunotolerance can be overcome using the Cre/loxP system
Immunotolerized rat model	Fetal rats are tolerized in utero with hepatocytes
	The rats support HCV gene expression and viral replication, and develop hepatitis
	A genuine adaptive immune response toward HCV cannot be expected
Human liver chimeric Alb-uPA/SCID mice	Human hepatocytes repopulate the mouse liver in a very organized fashion
	These mice show immunodeficiency
	Breeding efficacy is low and the time window for transplantation is narrow
FRG mice	These mice can be highly engrafted with human hepatocytes
	Mutant breeders of FRG mice are fully viable
	Hepatocyte repopulation can be achieved at any stage
Immunocompetent HCV-permissive mouse models	Human hematopoietic stem cells and hepatocyte progenitors are cotransfected
	These mice become infected with HCV and generate an immune response
	Viral RNA detection is low and hepatocyte repopulation is relatively poor
Genetically humanized mouse models	Human occludin and CD81 genes are expressed in these mice
	HCV infection is allowed in fully immunocompetent inbred mice
	Innate and adaptive immune responses restrict HCV infection in vivo

FRG, *Fah*$^{-/-}$/*Rag2*$^{-/-}$/*Il2rg*$^{-/-}$; HCC, hepatocellular carcinoma; HCV, hepatitis C virus; SCID, severe combined immunodeficiency; uPA, urokinase-type plasminogen activator.

et al., 2006; Kawamura et al., 1997; Koike et al., 1995; Pasquinelli et al., 1997). However, transgenic mice carrying the HCV core gene developed hepatic steatosis and HCC (Moriya et al., 1997, 1998), and HCV core–E1-E2 transgenic mice were predisposed to liver tumors (Kamegaya et al., 2005).

Transgenic mice with constitutive expression of HCV proteins have several drawbacks, such as a random transgene integration site, its artificial expression, and the potential influence of the mouse genetic background. However, one of the largest problems is that such mice are immunotolerant of HCV proteins, and therefore do not develop an immune response to them. To overcome this limitation, Wakita et al. (1998) developed efficient conditional transgene activation of HCV cDNA (nucleotides 294–3435) in transgenic mice using the Cre/loxP system. Efficient recombination was observed in transgenic mouse livers upon intravenous administration of an adenovirus that expresses Cre DNA recombinase. The findings in these mice suggested that the HCV proteins were not directly cytopathic and that the host immune response played a pivotal role in HCV infection. Thus, this HCV cDNA transgenic mouse model provides a powerful tool for the investigation of the immune responses and pathogenesis of HCV infection. Using these mice, the same group revealed that HCV proteins suppressed Fas-mediated apoptotic cell death, suggesting that HCV may cause persistent infection as a result of suppression of Fas-mediated cell death (Machida et al., 2001). Thereafter, the same group established HCV transgenic mice that expressed the full HCV genome in B cells (RzCD19Cre mice) and observed a 25.0% incidence of diffuse large B-cell non-Hodgkin lymphomas (22.2% in males and 29.6% in females) within 600 days of birth (Kasama et al., 2010). In the original method, the expression of HCV proteins was regulated by the Cre/loxP system and an adenovirus vector that expressed Cre DNA recombinase (Cre) controlled by the CAG promoter (AxCANCre). However, it was demonstrated that AxCANCre injection alone resulted in severe liver injury by the induction of the adenovirus protein IX gene. As a result, HCV protein expression in transgenic mice livers was only short term. To overcome this problem, the same group developed a Cre-expressing adenovirus vector that bore the EF1α promoter (AxEFCre) to express HCV protein in the transgenic mouse livers, and indicated that use of AxEFCre efficiently promoted Cre-mediated DNA recombination in vivo without a severe hepatitis response to the adenovirus vector (Chiyo et al., 2011).

3.6.2 Xenograft Models

3.6.2.1 IMMUNOTOLERIZED RAT MODEL

This model is based on the fact that the rat immune system does not develop until 15–17 days after gestation.

If human hepatocytes are transplanted into a rat during this period, tolerization of an immunocompetent rat can facilitate the transplantation and survival of functional human hepatocytes (Ouyang et al., 2001). Applying this principle, Wu et al. (2005) established an immunocompetent rat model of HCV infection and hepatitis. Fetal rats were tolerized in utero with 10^5 Huh 7 cells (hepatoma cell line). One day after birth, the rats received 5×10^6 Huh 7 cells, and 1 week later they were inoculated with HCV genotype 1. As a result, the HCV-inoculated immunocompetent rats supported HCV gene expression and viral replication, and provided biochemical and histologic evidence of hepatitis. However, a genuine adaptive immune response toward HCV cannot be expected in this model because of a mismatch between the rat immune system and the human major histocompatibility complex on the transplanted Huh 7 cells. Therefore, this model is only useful for studying some details of HCV infection, such as the involvement of receptors and intracellular host factors (Liu et al., 2013; Wu et al., 2005).

3.6.2.2 HUMAN LIVER CHIMERIC Alb-uPA/SCID MICE

Effective replacement of the mouse liver by human hepatocytes has become possible owing to the development of transgenic mice that overexpress hepatotoxic urokinase-type plasminogen activator (uPA) (Sandgren et al., 1991). To allow transplanted human hepatocytes to proliferate effectively in the mouse liver, mouse hepatocytes need to be destroyed. uPA is a type of protease. When the uPA gene is integrated under the control of the albumin promoter, it is exclusively expressed in the liver of the mouse and causes liver injury. uPA/severe combined immunodeficiency (SCID) mice are generated by crossing uPA transgenic mice with immunodeficient SCID mice. In these mice, transplanted human hepatocytes are not rejected; they proliferate and replace mouse hepatocytes.

Applying this technique, Mercer et al. (2001) generated mice with chimeric human livers by transplanting normal human hepatocytes into SCID mice carrying a plasminogen activator transgene (Alb-uPA). Homozygosity of Alb-uPA was associated with significantly higher levels of human hepatocyte engraftment, and these mice developed prolonged HCV infections with high viral titers after inoculation with infected human serum. Human hepatocytes repopulate the mouse liver in a very organized fashion with preservation of normal cell function in Alb-uPA/SCID mice (Meuleman et al., 2005). Once human hepatocytes are stably transplanted to Alb-uPA/SCID mice, the livers of the mice can be infected by HCV, HBV, and other viruses that infect the human liver. This model has been very useful for the study of the basic aspects of HCV pathogenesis, the evaluation of passive immunization strategies, and the assessment of novel antiviral

therapies (Akazawa et al., 2013; Meuleman et al., 2008; Singaravelu et al., 2014). However, Alb-uPA/SCID mice show immunodeficiency. As liver injury from hepatitis C is mainly caused by the host's immune response to the infection, sufficient chronic liver injury does not occur in Alb-uPA/SCID mice. Therefore, this model is not suitable for studying immune responses to HCV and related chronic liver injury. Moreover, the breeding efficacy of the mice is low, the time window for transplantation is narrow because of preweaning mortality, and the efficacy of human hepatocyte engraftment can be highly variable (Liu et al., 2013; Tateno et al., 2004; Turrini et al., 2006; Vercauteren et al., 2014).

3.6.2.3 $Fah^{-/-}/Rag2^{-/-}/il2rg^{-/-}$ MICE

Fumarylacetoacetate (Fah) is a metabolic enzyme that catalyzes the last step of tyrosine catabolism. Fah-deficient mice exhibit hypoglycemia and liver dysfunction owing to the accumulation of metabolites that are toxic to the liver (Grompe et al., 1993). The recombination-activating gene 2 KO ($rag2^{-/-}$) mouse is depleted of mature B and T lymphocytes. The IL-2 receptor, common γ-chain KO ($il2rg^{-/-}$) mouse has impaired B- and T-cell development and a complete absence of natural killer (NK) cell development. A triple KO ($Fah^{-/-}/Rag2^{-/-}/Il2rg^{-/-}$ or FRG) mouse model was created and examined to determine whether it is a superior repopulation model (Azuma et al., 2007; Bissig et al., 2007). The mice could be highly engrafted (up to 90%) with human hepatocytes from multiple sources, including liver biopsies. FRG mice have higher rates of liver chimerism than Alb-uPA/SCID mice, and propagate both HBV and HCV (Bissig et al., 2010). In contrast to Alb-uPA/SCID mice, FRG mutant breeders are fully viable, and hepatocyte repopulation can be carried out at any stage (Liu et al., 2013). More recently, other humanized chimeric mouse models of HCV (e.g., MUP-uPA SCID/Bg mice and TK-NOG mice) have been developed (Kosaka et al., 2013; Tesfaye et al., 2013).

3.6.2.4 IMMUNOCOMPETENT HCV-PERMISSIVE MOUSE MODELS

One of the major drawbacks of the human liver chimeric mouse models mentioned earlier is that they have to be immune deficient to prevent rejection of the engrafted human hepatocytes. The development of immunocompetent animal models is indispensable for the study of hepatitis C immunopathology. Washburn et al. (2011) developed humanized mice with a human immune system and liver tissues. To promote engraftment of human hepatocytes, they expressed a fusion protein of the FK506-binding protein and caspase 8 under the control of the albumin promoter (AFC8); this fusion protein induces liver cell death in BALB/c Rag2$^{-/-}$ γC-null mice. Cotransfection of human CD34+ human hematopoietic stem cells (HSC) and hepatocyte progenitors into the transgenic mice led to the efficient engraftment of human leukocytes and hepatocytes. The researchers then infected those humanized mice (AFC8-hu HSC/Hep) with primary HCV isolates and studied HCV-induced immune responses and liver diseases. They reported that the mice became infected with HCV, generated a specific immune response against the virus, and developed liver diseases that included hepatitis and fibrosis. Although this animal model of hepatitis C that includes the human immune system is promising, it has several drawbacks: a limited ability to detect viral RNA, relatively poor hepatocyte repopulation, and the lack of an efficient antibody response due to incomplete B-cell function (Liu et al., 2013).

3.6.3 Genetically Humanized Mouse Models

Human occludin and CD81 are entry factors that are necessary for HCV infection of murine cells (Ploss et al., 2009). Dorner et al. (2011) showed that the expression of the human genes that encode those two protein was sufficient to allow HCV infection of fully immunocompetent inbred mice. Later, the same group demonstrated that transgenic mice stably expressing human CD81 and occludin supported HCV entry, but innate and adaptive immune responses restricted HCV infection in vivo (Dorner et al., 2013). Blunting antiviral immunity in genetically humanized mice infected with HCV resulted in measurable viremia over several weeks. More recently, Chen et al. (2014) reported that HCV accomplished its replication cycle, leading to sustained viremia and infectivity for more than 12 months postinfection, with the expected fibrotic and cirrhotic progression in transgenic ICR strain mice that harbored both human CD81 and occludin genes.

3.7 Animal Models of Hepatitis B (Table 13.8)

HBV is a DNA virus that belongs to the Hepadnaviridae family and infects humans via body fluids, such as blood, semen, and saliva. HBV comprises 42 nm–sized round particles called Dane particles that possess a hepatitis B surface antigen (HBsAg), which corresponds to the viral envelope. Two kinds of antigens [hepatitis B core antigen (HBcAg) and hepatitis B e antigen (HBeAg)] exist in the core part. When HBeAg is positive, infective capacity is strong. A characteristic infection route of HBV is infection of the infant from the mother via the placenta or the birth canal, whereby the infant becomes a HBV carrier. Some HBV carriers do not develop hepatitis (healthy carriers), but others develop chronic hepatitis. Acute hepatitis B rarely progresses to chronic hepatitis. Although the prophylaxis of hepatitis B has become possible owing to the development of vaccines, hepatitis B remains one of the main causes of liver cirrhosis and HCC.

TABLE 13.8　Animal Models of Hepatitis B

Animal models	Main features
Animals that permit HBV infection and HBV-associated viruses that infect animals	Chimpanzees and tree shrews permit HBV infection
	WHV infects *Marmota monax* and DHBV infects ducks
	These models are not homologous to HBV infection in humans
HBV transgenic mice	
Transgenic mice that express a part of HBV genes	The influence of specific regions of HBV genes can be studied
	HBV does not replicate
	HBV cccDNA is not produced
Transgenic mice in which HBV replicates	These mice express all HBV proteins
	HBV reinfection is not observed
	HBV cccDNA is not expressed
Mice with transferred HBV genes	A recombinant adenovirus vector or hydrodynamic injection is used
	Adenovirus vector itself causes liver injury and immune response
	HBV virions that are released to the blood do not infect other hepatocytes
Human hepatocyte chimera mice	
Trimera mice	Human blood cells or tissues are implanted in irradiated mice or rats
	Viremia peaks between days 18 and 25
	This model enables the short-term evaluation of antiviral effects of drugs
Models in which human hepatocytes are transplanted to immunodeficient mice	Immortalized hepatocytes transfected with a HBV genome are used
	Engrafted cells secrete HBV virions, and HBsAg is detected in plasma
	Production of immortalized hepatocytes is difficult and time consuming
uPA/SCID mice	High-level and long-standing viremia is observed
	The mice are immunodeficient
	Mice are expensive and maintenance costs are high

cccDNA, Covalently closed circular DNA; DHBV, duck hepatitis B virus; HBsAg, hepatitis B surface antigen; HBV, hepatitis B virus; SCID, severe combined immunodeficiency; uPA, urokinase-type plasminogen activator; WHV, woodchuck hepatitis virus.

HBV is an enveloped virus. The HBV genome comprises of a partially double-stranded DNA of ~3.2 kb that is organized into four open reading frames (Liu et al., 2013). The covalently closed circular DNA (cccDNA) serves as the template for both viral transcription and replication. Infection and replication of HBV is possible in chimpanzees, but their use has become impossible for ethical reasons. Small animal models, especially mice, are preferred because they are easy to manage. To date, various animal models of HBV have been developed.

3.7.1 Animals That Permit HBV Infection and HBV-Associated Viruses That Infect Animals

Animals that permit HBV infection are very limited, and the chimpanzee is the only complete animal model. However, the chimpanzee has been classified as an endangered species, and its use in experiments on infectious diseases has been prohibited for ethical reasons.

The tree shrew (*Tupaia belangeri*) also permits HBV infection (Baumert et al., 2005). It is closely related to monkeys and has been used in experiments on HBV and HCV infection. However, the infectious efficacy of HBV in tree shrews is not high, and only temporary and low-titer infection occurs. Moreover, persistent infection does not occur. Although they can be kept in animal experiment institutions, tree shrews are difficult to breed, and wild tree shrews are usually used in experiments.

Woodchuck HBV (woodchuck hepatitis virus: WHV), which infects *M. monax*, and duck HBV (duck hepatitis B virus: DHBV), which infects ducks, have been investigated because they are similar to HBV; they have been used for viral infection experiments, the elucidation of viral life cycles, and the development of antiviral drugs (Korba et al., 2004). In woodchucks, vertical transmission of WHV causes chronic infection with high frequency, and after several years of persistent infection, almost all animals develop liver cancer. Therefore, the WHV

model has been regarded similar to the persistent infection and viral carcinogenesis caused by HBV. However, these models are not homologous to HBV infection in humans, so animal experiments using HBV are required.

3.7.2 HBV Transgenic Mice

HBV does not infect mice. However, transgenic mice in which a part of the HBV genome or the whole of the 1.3-fold long HBV genome is incorporated are useful for studying the association between HBV genes and HBV replication or carcinogenicity. HBV transgenic mice do not develop liver injury owing to immunotolerance arising from the expression of HBV proteins from the time of birth. Adenovirus vectors or hydrodynamic injection is used to introduce HBV genes to mice after birth.

3.7.2.1 TRANSGENIC MICE THAT EXPRESS A PART OF THE HBV GENOME

Transgenic mice in which a part of HBV genome is incorporated have been developed to study the influences of specific regions of HBV genes on persistent infection, immunological modification, or carcinogenicity. Chisari et al. (1987) developed transgenic mice containing the entire HBV envelope-coding region and showed that they developed ground glass hepatocytes, focal hepatocellular degeneration and necrosis, lobular macrophagic inflammation, and increased serum aminotransferase activity. Thereafter, Koike et al. (1994) studied the development of liver tumors in male HBx gene transgenic mice, and suggested that the continued expression of the HBx gene might initiate a complex progression to HCC by inducing DNA synthesis and subjecting large numbers of hepatocytes to secondary transformation events.

3.7.2.2 TRANSGENIC MICE IN WHICH HBV REPLICATES

Araki et al. (1989) produced transgenic mice that expressed and replicated the hepatitis B virus genome, and Guidotti et al. (1995) produced HBV transgenic mice whose hepatocytes replicated the virus at levels comparable to those in the infected livers of patients with chronic hepatitis. HBV possesses incomplete double-stranded circular DNA. The more than 1.3-fold long HBV genome was incorporated into the transgenic mice; therefore, they express all HBV proteins. They do not have a special promoter to express the incorporated genes, thus the expression of HBV genes is characteristically high in the liver and kidney. These mice have been used to examine the effects of antiviral drugs (e.g., nucleoside/nucleotide analogs, IFNs) or new antiviral therapies (Dang et al., 2009). These transgenic mice are suitable for studying the mechanisms of HBV replication and its relationship with host immunity in the in vivo system. However, HBV reinfection is not observed in these mice, so intracellular entry and diffusion of HBV cannot be studied. Furthermore, HBV cccDNA, which is a template for HBV replication, is not expressed. Therefore, studies on the complete elimination or the half-life of HBV are impossible.

3.7.2.3 MICE WITH TRANSFERRED HBV GENES

To overcome the limitations of the transgenic mice mentioned earlier, several researchers have transferred HBV genes to uninfected mice. Representative methods of gene transfer include the use of a recombinant adenovirus vector and the use of hydrodynamic injection of a HBV plasmid.

3.7.2.3.1 TRANSFER OF HBV GENES USING A RECOMBINANT ADENOVIRUS VECTOR Sprinzl et al. (2001) showed that adenovirus-mediated genome transfer initiates efficient HBV replication in cultured liver cells and in the experimental animals from an extrachromosomal template. To transfer hepadnavirus genomes across the species barrier, they developed adenovirus vectors in which 1.3-fold overlength human and duck HBV genomes were inserted. The adenovirus-mediated genome transfer efficiently initiated hepadnavirus replication from an extrachromosomal template in established cell lines, in primary hepatocytes from various species, and in mouse livers. Following the transfer, HBV proteins, genomic RNA, and all replicative DNA intermediates were detected. In addition, infectious virions were secreted into the sera of mice.

In contrast to transgenic mice, HBV DNA is not incorporated into the host genome in this model. Therefore, immune system–mediated viral clearance or antiviral treatment can be studied using the model. In addition, the replication of various HBV mutants can be investigated. However, long-term persistence of infection is difficult to achieve by the method using an adenovirus vector. In addition, liver histopathology is modified by the vector because the adenovirus vector itself causes liver injury and immune response. Improvements to the vector and technique are required.

3.7.2.3.2 TRANSFER OF HBV GENES BY HYDRODYNAMIC INJECTION OF HBV DNA Hydrodynamic injection is used as a method of transferring HBV genes to mouse hepatocytes without using virus vectors and without causing immune responses. In this method, plasmid DNA in which the target gene is incorporated is injected rapidly and massively to the mouse via the caudal vein; the method was established for HBV by Yang et al. (2002). After transfection of hepatocytes in vivo with a replication-competent, overlength, linear HBV genome, viral antigens and replicative intermediates were synthesized and the virus was secreted into the blood. Viral antigens disappeared from the blood as early as 7 days after transfection, coincident with the appearance of antiviral antibodies. HBV transcripts and replicative intermediates

disappeared from the liver by day 15, after the appearance of antiviral CD8+ T cells. In contrast, the virus persisted for at least 81 days after transfection of NOD/SCID mice, which lack functional T cells, B cells, and NK cells.

Although the expression of HBV genes is transient, immunomodulation by a vector is not present; thus, this model is useful for the verification of antiviral drugs and antiviral therapies. Verification of HBV elimination by treatment is also possible. Moreover, mutant HBV virions can be observed. However, in gene transfer by a vector or a plasmid, HBV virions that are released to the blood do not infect other hepatocytes, although HBV replication occurs. Therefore, the effects of antiviral drugs may be overestimated. In these methods, HBV cccDNA is produced in mouse hepatocytes; however, its significance in HBV replication requires confirmation.

3.7.3 *Human Hepatocyte Chimera Mice*

Even though HBV genes are incorporated, reinfection by HBV does not occur as long as the hepatocytes originate from the mouse. As long as hepatocytes of mice are used, it is difficult to elucidate the life cycle of HBV. To develop antiviral drugs, the diminution rate of the virus and the frequency of the occurrence of mutant strains need to be determined; the HBV replication system in mouse hepatocytes is not suitable for this purpose. Human hepatocytes are needed to carry out experiments in which HBV replicates and virions are released to infect other hepatocytes. Chimera mice that carry transplanted human hepatocytes have been generated to establish an experimental system with human hepatocytes.

3.7.3.1 TRIMERA MICE

Trimera mice (or rats) are created by the implantation of human blood cells or tissues into lethally irradiated mice (or rats), radioprotected with SCID mouse bone marrow cells. Ilan et al. (1999) first developed a mouse trimera model for human HBV infection. In this model, viremia is induced by transplantation of ex vivo, HBV-infected human liver fragments. Engraftment of the human liver fragments, evaluated by hematoxylin and eosin staining and human serum albumin mRNA expression, is observed in 85% of the transplanted animals 1-month postimplantation. HBV DNA in the serum is first detected 8 days after liver transplantation. Viremia peaks between days 18 and 25 when HBV infection is observed in 85% of the transplanted animals. This model enables the short-term evaluation of the antiviral effects of drugs. A trimera model for HCV infection has also been developed (Ilan et al., 2002).

3.7.3.2 MODELS IN WHICH HUMAN HEPATOCYTES ARE TRANSPLANTED TO IMMUNODEFICIENT MICE

To develop a murine model for HBV production, Brown et al. (2000) established an immortalized, cloned liver cell line by transferring the Simian Virus 40 large T antigen into primary human hepatocytes. These cells were stably transfected with a full-length HBV genome to generate a clone that expresses HBV genes and replicates HBV. The HBV-producing cells were transplanted into the livers of mice with combined immunodeficiency (Rag2 deficient) by intrasplenic injection. As a result, determination of plasma HBV DNA levels indicated that engrafted cells secreted 3×10^7 to 3×10^8 virions/mL into the blood, and HBsAg was detected in the plasma.

However, the production of immortalized hepatocytes is difficult and time consuming. In some cases, HBV genes are incorporated into the genome of the mouse as in transgenic mice. HBV replication is restricted, although persistent infection is achieved. Furthermore, sufficient substitution by human hepatocytes is difficult to achieve because proliferation of transplanted human hepatocytes is restricted.

3.7.3.3 uPA/SCID MICE

The uPA/SCID mouse is a useful model for HCV and HBV infection. Using this mouse model, Tsuge et al. (2005) performed transmission experiments on HBV. Human serum containing HBV and the virus produced in HepG2 cell lines that have been transiently or stably transfected with 1.4 genome length HBV DNA were inoculated. As a result, a high-level viremia (approximately 10^{10} copies/mL) was observed in mice inoculated with HBV-positive human serum samples. High-level and long-standing viremia was also observed in mice injected with the in vitro–generated HBV. The viremia continued for up to 22 weeks until death or killing. Passage experiments showed that the serum of these mice contained infectious HBV.

This experimental system may be used to accurately evaluate the direct therapeutic effects of antiviral drugs because HBV replication and diffusion are achieved. This model is useful for developing antiviral drugs that directly act on HBV, such as nucleoside/nucleotide analogs. However, analyses of immunological conditions are difficult because the mice are immunodeficient. The death rate of transgenic mice with homozygous uPA is high. Moreover, a supply of human hepatocytes is difficult to obtain and the passage of mice is difficult. Therefore, chimera mice with human hepatocytes are expensive. The cost of equipment and maintenance is also high because aseptic manipulation is necessary when handling mice, the administration of complement inhibitors is necessary for the prevention of renal impairment, and the supplementation of vitamin C, which human hepatocytes cannot produce, is necessary. The chimera mouse is an animal model in which HBV reinfection occurs effectively and with which the life cycle of HBV may be elucidated. The adoption of this model will require reductions in the cost of equipment and management.

3.8 Animal Models of Other Infectious Diseases

Hepatitis D virus (HDV), also called hepatitis delta virus, is an RNA virus that only infects hosts infected with HBV, and causes exacerbation of hepatitis. The surface of HDV is covered by HBsAg. Hepatitis D is mainly seen in the Mediterranean region. Transgenic mice, mice with humanized livers, and gene-delivery vectors have been developed for HDV, as for HBV or HCV (Aldabe et al., 2015). Various animal models for hepatitis A and E have also been developed (Krawczynski et al., 2011; Purcell and Emerson, 2001; Yugo et al., 2014). Schistosomiasis is a parasite-transmitted disease that may cause liver cirrhosis and portal hypertension. Mice infected with *Schistosoma mansoni* or *Schistosoma japonicum* develop egg-related granulomas and liver fibrosis, and can serve as a model of hepatic fibrosis (Bartley et al., 2006; Dunn et al., 1977).

4 CONCLUSIONS

In this chapter, we reviewed animal models of various liver diseases with an emphasis on their advantages and drawbacks. Many animal models for various liver diseases have been developed by genetic manipulation or exposure to external substances. No animal model completely emulates the human disease. However, animal models are very useful for elucidating certain aspects of liver diseases, such as their pathogenesis and pathophysiology, and they enable the development of novel prophylaxis or treatments. Each animal model has advantages and drawbacks; therefore, it is important to choose the most suitable model for the purpose of the study.

References

Abdel-Aziz, G., Lebeau, G., Rescan, P.Y., Clement, B., Rissel, M., Deugnier, Y., Campion, J.P., Guillouzo, A., 1990. Reversibility of hepatic fibrosis in experimentally induced cholestasis in rat. Am. J. Pathol. 137 (6), 1333–1342.

Akazawa, D., Moriyama, M., Yokokawa, H., Omi, N., Watanabe, N., Date, T., Morikawa, K., Aizaki, H., Ishii, K., Kato, T., Mochizuki, H., Nakamura, N., Wakita, T., 2013. Neutralizing antibodies induced by cell culture-derived hepatitis C virus protect against infection in mice. Gastroenterology 145 (2), 447–455.

Aldabe, R., Suarez-Amaran, L., Usai, C., Gonzalez-Aseguinolaza, G., 2015. Animal models of chronic hepatitis delta virus infection host-virus immunologic interactions. Pathogens 4 (1), 46–65.

Anstee, Q.M., Goldin, R.D., 2006. Mouse models in non-alcoholic fatty liver disease and steatohepatitis research. Int. J. Exp. Pathol. 87 (1), 1–16.

Araki, K., Miyazaki, J., Hino, O., Tomita, N., Chisaka, O., Matsubara, K., Yamamura, K., 1989. Expression and replication of hepatitis B virus genome in transgenic mice. Proc. Natl. Acad. Sci. USA 86 (1), 207–211.

Arsov, T., Larter, C.Z., Nolan, C.J., Petrovsky, N., Goodnow, C.C., Teoh, N.C., Yeh, M.M., Farrell, G.C., 2006a. Adaptive failure to high-fat diet characterizes steatohepatitis in Alms1 mutant mice. Biochem. Biophys. Res. Commun. 342 (4), 1152–1159.

Arsov, T., Silva, D.G., O'Bryan, M.K., Sainsbury, A., Lee, N.J., Kennedy, C., Manji, S.S., Nelms, K., Liu, C., Vinuesa, C.G., de Kretser, D.M., Goodnow, C.C., Petrovsky, N., 2006b. Fat aussie—a new Alstrom syndrome mouse showing a critical role for ALMS1 in obesity, diabetes, and spermatogenesis. Mol. Endocrinol. 20 (7), 1610–1622.

Azuma, H., Paulk, N., Ranade, A., Dorrell, C., Al-Dhalimy, M., Ellis, E., Strom, S., Kay, M.A., Finegold, M., Grompe, M., 2007. Robust expansion of human hepatocytes in Fah$^{-/-}$/Rag2$^{-/-}$/Il2rg$^{-/-}$ mice. Nat. Biotechnol. 25 (8), 903–910.

Bartley, P.B., Ramm, G.A., Jones, M.K., Ruddell, R.G., Li, Y., McManus, D.P., 2006. A contributory role for activated hepatic stellate cells in the dynamics of *Schistosoma japonicum* egg-induced fibrosis. Int. J. Parasitol. 36 (9), 993–1001.

Baumert, T.F., Yang, C., Schurmann, P., Kock, J., Ziegler, C., Grullich, C., Nassal, M., Liang, T.J., Blum, H.E., von Weizsacker, F., 2005. Hepatitis B virus mutations associated with fulminant hepatitis induce apoptosis in primary Tupaia hepatocytes. Hepatology 41 (2), 247–256.

Bertola, A., Mathews, S., Ki, S.H., Wang, H., Gao, B., 2013a. Mouse model of chronic and binge ethanol feeding (the NIAAA model). Nat. Protoc. 8 (3), 627–637.

Bertola, A., Park, O., Gao, B., 2013b. Chronic plus binge ethanol feeding synergistically induces neutrophil infiltration and liver injury in mice: a critical role for E-selectin. Hepatology 58 (5), 1814–1823.

Bissell, D.M., 2011. Therapy for hepatic fibrosis: revisiting the preclinical models. Clin. Res. Hepatol. Gastroenterol. 35 (8–9), 521–525.

Bissig, K.D., Le, T.T., Woods, N.B., Verma, I.M., 2007. Repopulation of adult and neonatal mice with human hepatocytes: a chimeric animal model. Proc. Natl. Acad. Sci. USA 104 (51), 20507–20511.

Bissig, K.D., Wieland, S.F., Tran, P., Isogawa, M., Le, T.T., Chisari, F.V., Verma, I.M., 2010. Human liver chimeric mice provide a model for hepatitis B and C virus infection and treatment. J. Clin. Invest. 120 (3), 924–930.

Brandon-Warner, E., Schrum, L.W., Schmidt, C.M., McKillop, I.H., 2012. Rodent models of alcoholic liver disease: of mice and men. Alcohol 46 (8), 715–725.

Brown, J.J., Parashar, B., Moshage, H., Tanaka, K.E., Engelhardt, D., Rabbani, E., Roy-Chowdhury, N., Roy-Chowdhury, J., 2000. A long-term hepatitis B viremia model generated by transplanting non-tumorigenic immortalized human hepatocytes in Rag-2-deficient mice. Hepatology 31 (1), 173–181.

Brunkow, M.E., Jeffery, E.W., Hjerrild, K.A., Paeper, B., Clark, L.B., Yasayko, S.A., Wilkinson, J.E., Galas, D., Ziegler, S.F., Ramsdell, F., 2001. Disruption of a new forkhead/winged-helix protein, scurfin, results in the fatal lymphoproliferative disorder of the scurfy mouse. Nat. Genet. 27 (1), 68–73.

Carmiel-Haggai, M., Cederbaum, A.I., Nieto, N., 2005. A high-fat diet leads to the progression of non-alcoholic fatty liver disease in obese rats. FASEB J. 19 (1), 136–138.

Charbonneau, M., Tuchweber, B., Plaa, G.L., 1986. Acetone potentiation of chronic liver injury induced by repetitive administration of carbon tetrachloride. Hepatology 6 (4), 694–700.

Charlton, M., Krishnan, A., Viker, K., Sanderson, S., Cazanave, S., Mc-Conico, A., Masuoko, H., Gores, G., 2011. Fast food diet mouse: novel small animal model of NASH with ballooning, progressive fibrosis, and high physiological fidelity to the human condition. Am. J. Physiol. Gastrointest. Liver Physiol. 301 (5), G825–G834.

Chen, J., Zhao, Y., Zhang, C., Chen, H., Feng, J., Chi, X., Pan, Y., Du, J., Guo, M., Cao, H., Chen, H., Wang, Z., Pei, R., Wang, Q., Pan, L., Niu, J., Chen, X., Tang, H., 2014. Persistent hepatitis C virus infections and hepatopathological manifestations in immune-competent humanized mice. Cell Res. 24 (9), 1050–1066.

Chisari, F.V., Filippi, P., Buras, J., McLachlan, A., Popper, H., Pinkert, C.A., Palmiter, R.D., Brinster, R.L., 1987. Structural and pathological effects of synthesis of hepatitis B virus large envelope polypeptide in transgenic mice. Proc. Natl. Acad. Sci. USA 84 (19), 6909–6913.

Chiyo, T., Sekiguchi, S., Hayashi, M., Tobita, Y., Kanegae, Y., Saito, I., Kohara, M., 2011. Conditional gene expression in hepatitis C virus transgenic mice without induction of severe liver injury using a non-inflammatory Cre-expressing adenovirus. Virus Res. 160 (1–2), 89–97.

Chowdhry, S., Nazmy, M.H., Meakin, P.J., Dinkova-Kostova, A.T., Walsh, S.V., Tsujita, T., Dillon, J.F., Ashford, M.L., Hayes, J.D., 2010. Loss of Nrf2 markedly exacerbates nonalcoholic steatohepatitis. Free Radic. Biol. Med. 48 (2), 357–371.

Cohen, J.C., Horton, J.D., Hobbs, H.H., 2011. Human fatty liver disease: old questions and new insights. Science 332 (6037), 1519–1523.

Constandinou, C., Henderson, N., Iredale, J.P., 2005. Modeling liver fibrosis in rodents. Methods Mol. Med. 117, 237–250.

Cook, W.S., Jain, S., Jia, Y., Cao, W.Q., Yeldandi, A.V., Reddy, J.K., Rao, M.S., 2001. Peroxisome proliferator-activated receptor alpha-responsive genes induced in the newborn but not prenatal liver of peroxisomal fatty acyl-CoA oxidase null mice. Exp. Cell Res. 268 (1), 70–76.

Dang, S.S., Jia, X.L., Song, P., Cheng, Y.A., Zhang, X., Sun, M.Z., Liu, E.Q., 2009. Inhibitory effect of emodin and Astragalus polysaccharide on the replication of HBV. World J. Gastroenterol. 15 (45), 5669–5673.

Delire, B., Starkel, P., Leclercq, I., 2015. Animal models for fibrotic liver diseases: what we have, what we need, and what is under development. J. Clin. Transl. Hepatol. 3 (1), 53–66.

Deng, Q.G., She, H., Cheng, J.H., French, S.W., Koop, D.R., Xiong, S., Tsukamoto, H., 2005. Steatohepatitis induced by intragastric overfeeding in mice. Hepatology 42 (4), 905–914.

Di Marco, R., Xiang, M., Zaccone, P., Leonardi, C., Franco, S., Meroni, P., Nicoletti, F., 1999. Concanavalin A-induced hepatitis in mice is prevented by interleukin (IL)-10 and exacerbated by endogenous IL-10 deficiency. Autoimmunity 31 (2), 75–83.

Domenicali, M., Caraceni, P., Giannone, F., Baldassarre, M., Lucchetti, G., Quarta, C., Patti, C., Catani, L., Nanni, C., Lemoli, R.M., Bernardi, M., 2009. A novel model of CCl4-induced cirrhosis with ascites in the mouse. J. Hepatol. 51 (6), 991–999.

Dorner, M., Horwitz, J.A., Donovan, B.M., Labitt, R.N., Budell, W.C., Friling, T., Vogt, A., Catanese, M.T., Satoh, T., Kawai, T., Akira, S., Law, M., Rice, C.M., Ploss, A., 2013. Completion of the entire hepatitis C virus life cycle in genetically humanized mice. Nature 501 (7466), 237–241.

Dorner, M., Horwitz, J.A., Robbins, J.B., Barry, W.T., Feng, Q., Mu, K., Jones, C.T., Schoggins, J.W., Catanese, M.T., Burton, D.R., Law, M., Rice, C.M., Ploss, A., 2011. A genetically humanized mouse model for hepatitis C virus infection. Nature 474 (7350), 208–211.

Dunn, M.A., Rojkind, M., Warren, K.S., Hait, P.K., Rifas, L., Seifter, S., 1977. Liver collagen synthesis in murine schistosomiasis. J. Clin. Invest. 59 (4), 666–674.

Durie, P.R., Kent, G., Phillips, M.J., Ackerley, C.A., 2004. Characteristic multiorgan pathology of cystic fibrosis in a long-living cystic fibrosis transmembrane regulator knockout murine model. Am. J. Pathol. 164 (4), 1481–1493.

Fallatah, H.I., Akbar, H.O., 2011. Autoimmune liver disease—are there spectra that we do not know? Comp. Hepatol. 10, 9.

Fickert, P., Fuchsbichler, A., Wagner, M., Zollner, G., Kaser, A., Tilg, H., Krause, R., Lammert, F., Langner, C., Zatloukal, K., Marschall, H.U., Denk, H., Trauner, M., 2004. Regurgitation of bile acids from leaky bile ducts causes sclerosing cholangitis in Mdr2 (Abcb4) knockout mice. Gastroenterology 127 (1), 261–274.

Fickert, P., Pollheimer, M.J., Beuers, U., Lackner, C., Hirschfield, G., Housset, C., Keitel, V., Schramm, C., Marschall, H.U., Karlsen, T.H., Melum, E., Kaser, A., Eksteen, B., Strazzabosco, M., Manns, M., Trauner, M., International PSC Study Group (IPSCSG), 2014. Characterization of animal models for primary sclerosing cholangitis (PSC). J. Hepatol. 60 (6), 1290–1303.

Fickert, P., Stoger, U., Fucksbichler, A., Moustafa, T., Marschall, H.U., Weiglein, A.H., Tsybrovskyy, O., Jaeschke, H., Zatloukal, K., Denk, H., Trauner, M., 2007. A new xenobiotic-induced mouse model of sclerosing cholangitis and biliary fibrosis. Am. J. Pathol. 171 (2), 525–536.

Fickert, P., Trauner, M., Fuchsbichler, A., Stumptner, C., Zatloukal, K., Denk, H., 2002. Bile acid-induced Mallory body formation in drug-primed mouse liver. Am. J. Pathol. 161 (6), 2019–2026.

Frelin, L., Brenndorfer, E.D., Ahlen, G., Weiland, M., Hultgren, C., Alheim, M., Glaumann, H., Rozell, B., Milich, D.R., Bode, J.G., Sallberg, M., 2006. The hepatitis C virus and immune evasion: non-structural 3/4A transgenic mice are resistant to lethal tumour necrosis factor alpha mediated liver disease. Gut 55 (10), 1475–1483.

French, S.W., Miyamoto, K., Tsukamoto, H., 1986. Ethanol-induced hepatic fibrosis in the rat: role of the amount of dietary fat. Alcohol Clin. Exp. Res. 10 (6 Suppl.), 13S–19S.

Frezza, E.E., Gerunda, G.E., Farinati, F., DeMaria, N., Galligioni, A., Plebani, F., Giacomin, A., Van Thiel, D.H., 1994. CCl4-induced liver cirrhosis and hepatocellular carcinoma in rats: relationship to plasma zinc, copper and estradiol levels. Hepatogastroenterology 41 (4), 367–369.

Fujii, M., Shibazaki, Y., Wakamatsu, K., Honda, Y., Kawauchi, Y., Suzuki, K., Arumugam, S., Watanabe, K., Ichida, T., Asakura, H., Yoneyama, H., 2013. A murine model for non-alcoholic steatohepatitis showing evidence of association between diabetes and hepatocellular carcinoma. Med. Mol. Morphol. 46 (3), 141–152.

Gantner, F., Leist, M., Lohse, A.W., Germann, P.G., Tiegs, G., 1995. Concanavalin A-induced T-cell-mediated hepatic injury in mice: the role of tumor necrosis factor. Hepatology 21 (1), 190–198.

Geerts, A.M., Vanheule, E., Praet, M., Van Vlierberghe, H., De Vos, M., Colle, I., 2008. Comparison of three research models of portal hypertension in mice: macroscopic, histological and portal pressure evaluation. Int. J. Exp. Pathol. 89 (4), 251–263.

Gorham, J.D., Lin, J.T., Sung, J.L., Rudner, L.A., French, M.A., 2001. Genetic regulation of autoimmune disease: BALB/c background TGF-beta 1-deficient mice develop necroinflammatory IFN-gamma-dependent hepatitis. J. Immunol. 166 (10), 6413–6422.

Grompe, M., al-Dhalimy, M., Finegold, M., Ou, C.N., Burlingame, T., Kennaway, N.G., Soriano, P., 1993. Loss of fumarylacetoacetate hydrolase is responsible for the neonatal hepatic dysfunction phenotype of lethal albino mice. Genes Dev. 7 (12A), 2298–2307.

Guidotti, L.G., Matzke, B., Schaller, H., Chisari, F.V., 1995. High-level hepatitis B virus replication in transgenic mice. J. Virol. 69 (10), 6158–6169.

Gupte, A.A., Liu, J.Z., Ren, Y., Minze, L.J., Wiles, J.R., Collins, A.R., Lyon, C.J., Pratico, D., Finegold, M.J., Wong, S.T., Webb, P., Baxter, J.D., Moore, D.D., Hsueh, W.A., 2010. Rosiglitazone attenuates age- and diet-associated nonalcoholic steatohepatitis in male low-density lipoprotein receptor knockout mice. Hepatology 52 (6), 2001–2011.

Halilbasic, E., Fiorotto, R., Fickert, P., Marschall, H.U., Moustafa, T., Spirli, C., Fuchsbichler, A., Gumhold, J., Silbert, D., Zatloukal, K., Langner, C., Maitra, U., Denk, H., Hofmann, A.F., Strazzabosco, M., Trauner, M., 2009. Side chain structure determines unique physiologic and therapeutic properties of norursodeoxycholic acid in Mdr2−/− mice. Hepatology 49 (6), 1972–1981.

Harrison, S.A., Torgerson, S., Hayashi, P.H., 2003. The natural history of nonalcoholic fatty liver disease: a clinical histopathological study. Am. J. Gastroenterol. 98 (9), 2042–2047.

Henckaerts, L., Jaspers, M., Van Steenbergen, W., Vliegen, L., Fevery, J., Nuytten, H., Roskams, T., Rutgeerts, P., Cassiman, J.J., Vermeire, S., Cuppens, H., 2009. Cystic fibrosis transmembrane conductance regulator gene polymorphisms in patients with primary sclerosing cholangitis. J. Hepatol. 50 (1), 150–157.

Hillebrandt, S., Goos, C., Matern, S., Lammert, F., 2002. Genome-wide analysis of hepatic fibrosis in inbred mice identifies the susceptibility locus Hfib1 on chromosome 15. Gastroenterology 123 (6), 2041–2051.

Holdener, M., Hintermann, E., Bayer, M., Rhode, A., Rodrigo, E., Hintereder, G., Johnson, E.F., Gonzalez, F.J., Pfeilschifter, J., Manns, M.P., Herrath, M.v., Christen, U., 2008. Breaking tolerance to the natural human liver autoantigen cytochrome P450 2D6 by virus infection. J. Exp. Med. 205 (6), 1409–1422.

Honda, H., Ikejima, K., Hirose, M., Yoshikawa, M., Lang, T., Enomoto, N., Kitamura, T., Takei, Y., Sato, N., 2002. Leptin is required for fibrogenic responses induced by thioacetamide in the murine liver. Hepatology 36 (1), 12–21.

Hooijmans, C.R., Leenaars, M., Ritskes-Hoitinga, M., 2010. A gold standard publication checklist to improve the quality of animal studies, to fully integrate the Three Rs, and to make systematic reviews more feasible. Altern. Lab. Anim. 38 (2), 167–182.

Horie, Y., Sukuki, A., Kataoka, E., Sasaki, T., Hamada, K., Sasaki, J., Mizuno, K., Hasegawa, G., Kishimoto, H., Iizuka, M., Naito, M., Enomoto, K., Watanabe, S., Mak, T.W., Nakano, T., 2004. Hepatocyte-specific Pten deficiency results in steatohepatitis and hepatocellular carcinomas. J. Clin. Invest. 113 (12), 1774–1783.

Ikejima, K., Okumura, K., Kon, K., Takei, Y., Sato, N., 2007. Role of adipocytokines in hepatic fibrogenesis. J. Gastroenterol. Hepatol. 22 (Suppl. 1), S87–S92.

Ilan, E., Arazi, J., Nussbaum, O., Zauberman, A., Eren, R., Lubin, I., Neville, L., Ben-Moshe, O., Kischitzky, A., Litchi, A., Margalit, I., Gopher, J., Mounir, S., Cai, W., Daudi, N., Eid, A., Jurim, O., Czerniak, A., Galun, E., Dagan, S., 2002. The hepatitis C virus (HCV)-Trimera mouse: a model for evaluation of agents against HCV. J. Infect. Dis. 185 (2), 153–161.

Ilan, E., Burakova, T., Dagan, S., Nussbaum, O., Lubin, I., Eren, R., Ben-Moshe, O., Arazi, J., Berr, S., Neville, L., Yuen, L., Mansour, T.S., Gillard, J., Eid, A., Jurim, O., Shouval, D., Reisner, Y., Galun, E., 1999. The hepatitis B virus-trimera mouse: a model for human HBV infection and evaluation of anti-HBV therapeutic agents. Hepatology 29 (2), 553–562.

Ip, E., Farrell, G.C., Robertson, G., Hall, P., Kirsch, R., Leclercq, I., 2003. Central role of PPARalpha-dependent hepatic lipid turnover in dietary steatohepatitis in mice. Hepatology 38 (1), 123–132.

Iredale, J.P., Benyon, R.C., Pickering, J., McCullen, M., Northrop, M., Pawley, S., Hovell, C., Arthur, M.J., 1998. Mechanisms of spontaneous resolution of rat liver fibrosis. Hepatic stellate cell apoptosis and reduced hepatic expression of metalloproteinase inhibitors. J. Clin. Invest. 102 (3), 538–549.

Irie, J., Wu, Y., Wicker, L.S., Rainbow, D., Nalesnik, M.A., Hirsch, R., Peterson, L.B., Leung, P.S., Cheng, C., Mackay, I.R., Gershwin, M.E., Ridgway, W.M., 2006. NOD.c3c4 congenic mice develop autoimmune biliary disease that serologically and pathogenetically models human primary biliary cirrhosis. J. Exp. Med. 203 (5), 1209–1219.

Issa, R., Williams, E., Trim, N., Kendall, T., Arthur, M.J., Reichen, J., Benyon, R.C., Iredale, J.P., 2001. Apoptosis of hepatic stellate cells: involvement in resolution of biliary fibrosis and regulation by soluble growth factors. Gut 48 (4), 548–557.

Ito, M., Suzuki, J., Tsujioka, S., Sasaki, M., Gomori, A., Shirakura, T., Hirose, H., Ito, M., Ishihara, A., Iwaasa, H., Kanatani, A., 2007. Longitudinal analysis of murine steatohepatitis model induced by chronic exposure to high-fat diet. Hepatol. Res. 37 (1), 50–57.

Jenkins, S.A., Grandison, A., Baxter, J.N., Day, D.W., Taylor, I., Shields, R., 1985. A dimethylnitrosamine-induced model of cirrhosis and portal hypertension in the rat. J. Hepatol. 1 (5), 489–499.

Jeong, W.I., Jeong, D.H., Do, S.H., Kim, Y.K., Park, H.Y., Kwon, O.D., Kim, T.H., Jeong, K.S., 2005. Mild hepatic fibrosis in cholesterol and sodium cholate diet-fed rats. J. Vet. Med. Sci. 67 (3), 235–242.

Kamegaya, Y., Hiasa, Y., Zukerberg, L., Fowler, N., Blackard, J.T., Lin, W., Choe, W.H., Schmidt, E.V., Chung, R.T., 2005. Hepatitis C virus acts as a tumor accelerator by blocking apoptosis in a mouse model of hepatocarcinogenesis. Hepatology 41 (3), 660–667.

Kasama, Y., Sekiguchi, S., Saito, M., Tanaka, K., Satoh, M., Kuwahara, K., Sakaguchi, N., Takeya, M., Hiasa, Y., Kohara, M., Tsukiyama-Kohara, K., 2010. Persistent expression of the full genome of hepatitis C virus in B cells induces spontaneous development of B-cell lymphomas in vivo. Blood 116 (23), 4926–4933.

Kashireddy, P.V., Rao, M.S., 2004. Lack of peroxisome proliferator-activated receptor alpha in mice enhances methionine and choline deficient diet-induced steatohepatitis. Hepatol. Res. 30 (2), 104–110.

Kawamura, T., Furusaka, A., Koziel, M.J., Chung, R.T., Wang, T.C., Schmidt, E.V., Liang, T.J., 1997. Transgenic expression of hepatitis C virus structural proteins in the mouse. Hepatology 25 (4), 1014–1021.

Kawasaki, T., Igarashi, K., Koeda, T., Sugimoto, K., Nakagawa, K., Hayashi, S., Yamaji, R., Inui, H., Fukusato, T., Yamanouchi, T., 2009. Rats fed fructose-enriched diets have characteristics of nonalcoholic hapatic steatosis. J. Nutr. 139 (11), 2067–2071.

Kersten, S., Seydoux, J., Peters, J.M., Gonzalez, F.J., Desvergne, B., Wahli, W., 1999. Peroxisome proliferator-activated receptor alpha mediates the adaptive response to fasting. J. Clin. Invest. 103 (11), 1489–1498.

Kido, M., Watanabe, N., Okazaki, T., Akamatsu, T., Tanaka, J., Saga, K., Nishio, A., Honjo, T., Chiba, T., 2008. Fatal autoimmune hepatitis induced by concurrent loss of naturally arising regulatory T cells and PD-1-mediated signaling. Gastroenterology 135 (4), 1333–1343.

Kirsch, R., Clarkson, V., Shephard, E.G., Marais, D.A., Jaffer, M.A., Woodburne, V.E., Kirsch, R.E., Hall Pde, L., 2003. Rodent nutritional model of non-alcoholic steatohepatitis: species, strain and sex difference studies. J. Gastroenterol. Hepatol. 18 (11), 1272–1282.

Kohli, R., Kirby, M., Xanthakos, S.A., Softic, S., Feldstein, A.E., Saxena, V., Tang, P.H., Miles, L., Miles, M.V., Balistreri, W.F., Woods, S.C., Seeley, R.J., 2010. High-fructose, medium chain trans fat diet induces liver fibrosis and elevates plasma coenzyme Q9 in a novel murine model of obesity and nonalcoholic steatohepatitis. Hepatology 52 (3), 934–944.

Koike, K., Moriya, K., Iino, S., Yotsuyanagi, H., Endo, Y., Miyamura, T., Kurokawa, K., 1994. High-level expression of hepatitis B virus HBx gene and hepatocarcinogenesis in transgenic mice. Hepatology 19 (4), 810–819.

Koike, K., Moriya, K., Ishibashi, K., Matsuura, Y., Suzuki, T., Saito, I., Iino, S., Kurokawa, K., Miyamura, T., 1995. Expression of hepatitis C virus envelope proteins in transgenic mice. J. Gen. Virol. 76 (Pt. 12), 3031–3038.

Kono, H., Bradford, B.U., Rusyn, I., Fujii, H., Matsumoto, Y., Yin, M., Thurman, R.G., 2000. Development of an intragastric enteral model in the mouse: studies of alcohol-induced liver disease using knockout technology. J. Hepatobiliary Pancreat. Surg. 7 (4), 395–400.

Korba, B.E., Cote, P.J., Menne, S., Toshkov, I., Baldwin, B.H., Wells, F.V., Tennant, B.C., Gerin, J.L., 2004. Clevudine therapy with vaccine inhibits progression of chronic hepatitis and delays onset of hepatocellular carcinoma in chronic woodchuck hepatitis virus infection. Antivir. Ther. 9 (6), 937–952.

Kosaka, K., Hiraga, N., Imamura, M., Yoshimi, S., Murakami, E., Nakahara, T., Honda, Y., Ono, A., Kawaoka, T., Tsuge, M., Abe, H., Hayes, C.N., Miki, D., Aikata, H., Ochi, H., Ishida, Y., Tateno, C., Yoshizato, K., Sasaki, T., Chayama, K., 2013. A novel TK-NOG based humanized mouse model for the study of HBV and HCV infections. Biochem. Biophys. Res. Commun. 441 (1), 230–235.

Kountouras, J., Billing, B.H., Scheuer, P.J., 1984. Prolonged bile duct obstruction: a new experimental model for cirrhosis in the rat. Br. J. Exp. Pathol. 65 (3), 305–311.

Krawczynski, K., Meng, X.J., Rybczynska, J., 2011. Pathogenetic elements of hepatitis E and animal models of HEV infection. Virus Res. 161 (1), 78–83.

Kulkarni, A.B., Huh, C.G., Becker, D., Geiser, A., Lyght, M., Flanders, K.C., Roberts, A.B., Sporn, M.B., Ward, J.M., Karlsson, S., 1993. Transforming growth factor beta 1 null mutation in mice causes excessive inflammatory response and early death. Proc. Natl. Acad. Sci. USA 90 (2), 770–774.

Kusters, S., Gantner, F., Kunstle, G., Tiegs, G., 1996. Interferon gamma plays a critical role in T cell-dependent liver injury in mice initiated by concanavalin A. Gastroenterology 111 (2), 462–471.

Larter, C.Z., Yeh, M.M., Williams, J., Bell-Anderson, K.S., Farrell, G.C., 2008. MCD-induced steatohepatitis is associated with hepatic adiponectin resistance and adipogenic transformation of hepatocytes. J. Hepatol. 49 (3), 407–416.

Leclercq, I.A., Farrell, G.C., Field, J., Bell, D.R., Gonzalez, F.J., Robertson, G.R., 2000. CYP2E1 and CYP4A as microsomal catalysts of lipid peroxides in murine nonalcoholic steatohepatitis. J. Clin. Invest. 105 (8), 1067–1075.

Leclercq, I.A., Farrell, G.C., Schriemer, R., Robertson, G.R., 2002. Leptin is essential for the hepatic fibrogenic response to chronic liver injury. J. Hepatol. 37 (2), 206–213.

Leclercq, I.A., Lebrun, V.A., Starkel, P., Horsmans, Y.J., 2007. Intrahepatic insulin resistance in a murine model of steatohepatitis: effect of PPARgamma agonist pioglitazone. Lab. Invest. 87 (1), 56–65.

Leo, M.A., Lieber, C.S., 1983. Hepatic fibrosis after long-term administration of ethanol and moderate vitamin A supplementation in the rat. Hepatology 3 (1), 1–11.

Lieber, C.S., DeCarli, L.M., 1982. The feeding of alcohol in liquid diets: two decades of applications and 1982 update. Alcohol Clin. Exp. Res. 6 (4), 523–531.

Lieber, C.S., DeCarli, L.M., 1986. The feeding of ethanol in liquid diets. Alcohol Clin. Exp. Res. 10 (5), 550–553.

Lieber, C.S., Leo, M.A., Mak, K.M., Xu, Y., Cao, Q., Ren, C., Ponomarenko, A., DeCarli, L.M., 2004. Model of nonalcoholic steatohepatitis. Am. J. Clin. Nutr. 79 (3), 502–509.

Lindstrom, P., 2007. The physiology of obese-hyperglycemic mice [ob/ob mice]. Sci. World J. 7, 666–685.

Liu, Y., Meyer, C., Xu, C., Weng, H., Hellerbrand, C., ten Dijke, P., Dooley, S., 2013. Animal models of chronic liver diseases. Am. J. Physiol. Gastrointest. Liver Physiol. 304 (5), G449–G468.

London, R.M., George, J., 2007. Pathogenesis of NASH: animal models. Clin. Liver Dis. 11 (1), 55–74.

Louis, H., Le Moine, O., Peny, M.O., Quertinmont, E., Fokan, D., Goldman, M., Deviere, J., 1997. Production and role of interleukin-10 in concanavalin A-induced hepatitis in mice. Hepatology 25 (6), 1382–1389.

Lu, S.C., Alvarez, L., Huang, Z.Z., Chen, L., An, W., Corrales, F.J., Avila, M.A., Kanel, G., Mato, J.M., 2001. Methionine adenosyltransferase 1A knockout mice are predisposed to liver injury and exhibit increased expression of genes involved in proliferation. Proc. Natl. Acad. Sci. USA 98 (10), 5560–5565.

Machida, K., Tsukiyama-Kohara, K., Seike, E., Tone, S., Shibasaki, F., Shimizu, M., Takahashi, H., Hayashi, Y., Funata, N., Taya, C., Yonekawa, H., Kohara, M., 2001. Inhibition of cytochrome c release in Fas-mediated signaling pathway in transgenic mice induced to express hepatitis C viral proteins. J. Biol. Chem. 276 (15), 12140–12146.

Mailly, L., Robinet, E., Meuleman, P., Baumert, T.F., Zeisel, M.B., 2013. Hepatitis C virus infection and related liver disease: the quest for the best animal model. Front. Microbiol. 4, 213.

Martinez-Chantar, M.L., Corrales, F.J., Martinez-Cruz, L.A., Garcia-Trevijano, E.R., Huang, Z.Z., Chen, L., Kanel, G., Avila, M.A., Mato, J.M., Lu, S.C., 2002. Spontaneous oxidative stress and liver tumors in mice lacking methionine adenosyltransferase 1A. FASEB J. 16 (10), 1292–1294.

Mathews, S., Xu, M., Wang, H., Bertola, A., Gao, B., 2014. Animals models of gastrointestinal and liver diseases. Animal models of alcohol-induced liver disease: pathophysiology, translational relevance, and challenges. Am. J. Physiol. Gastointest. Liver Physiol. 306 (10), G819–G823.

Matsuzawa, N., Takamura, T., Kurita, S., Misu, H., Ota, T., Ando, H., Yokoyama, M., Honda, M., Zen, Y., Nakanuma, Y., Miyamoto, K., Kaneko, S., 2007. Lipid-induced oxidative stress causes steatohepatitis in mice fed an atherogenic diet. Hepatology 46 (5), 1392–1403.

Mauad, T.H., van Nieuwkerk, C.M., Dingemans, K.P., Smit, J.J., Schinkel, A.H., Notenboom, R.G., van den Bergh Weerman, M.A., Verkruisen, R.P., Groen, A.K., Oude Elferink, R.P., et al., 1994. Mice with homozygous disruption of the mdr2 P-glycoprotein gene. A novel animal model for studies of nonsuppurative inflammatory cholangitis and hepatocarcinogenesis. Am. J. Pathol. 145 (5), 1237–1245.

Maziere, C., Meignotte, A., Dantin, F., Conte, M.A., Maziere, J.C., 2000. Oxidized LDL induces an oxidative stress and activates the tumor suppressor p53 in MRC5 human fibroblasts. Biochem. Biophys. Res. Commun. 276 (2), 718–723.

McLean, E.K., McLean, A.E., Sutton, P.M., 1969. Instant cirrhosis. An improved method for producing cirrhosis of the liver in rats by simultaneous administration of carbon tetrachloride and phenobarbitone. Br. J. Exp. Pathol. 50 (5), 502–506.

Medina, J.F., Martinez-Anso, Vazquez, J.J., Prieto, J., 1997. Decreased anion exchanger 2 imunoreactivity in the liver of patients with primary biliary cirrhosis. Hepatology 25 (1), 12–17.

Melero, S., Spirli, C., Zsembery, A., Medina, J.F., Joplin, R.E., Duner, E., Zuin, M., Neuberger, J.M., Prieto, J., Strazzabosco, M., 2002. Defective regulation of cholangiocyte Cl−/HCO3(−) and Na+/H+ exchanger activities in primary biliary cirrhosis. Hepatology 35 (6), 1513–1521.

Mercer, D.F., Schiller, D.E., Elliott, J.F., Douglas, D.N., Hao, C., Rinfret, A., Addison, W.R., Fischer, K.P., Churchill, T.A., Lakey, J.R., Tyrrell, D.L., Kneteman, N.M., 2001. Hepatitis C virus replication in mice with chimeric human livers. Nat. Med. 7 (8), 927–933.

Meuleman, P., Hesselgesser, J., Paulson, M., Vanwolleghem, T., Desombere, I., Reiser, H., Leroux-Roels, G., 2008. Anti-CD81 antibodies can prevent a hepatitis C virus infection in vivo. Hepatology 48 (6), 1761–1768.

Meuleman, P., Libbrecht, L., De Vos, R., de Hemptinne, B., Gevaert, K., Vandekerckhove, J., Roskams, T., Leroux-Roels, G., 2005. Morphological and biochemical characterization of a human liver in a uPA-SCID mouse chimera. Hepatology 41 (4), 847–856.

Moradpour, D., Penin, F., Rice, C.M., 2007. Replication of hepatitis C virus. Nat. Rev. Microbiol. 5 (6), 453–463.

Moritoki, Y., Tsuda, M., Tsuneyama, K., Zhang, W., Yoshida, K., Lian, Z.X., Yang, G.X., Ridgway, W.M., Wicker, L.S., Ansari, A.A., Gershwin, M.E., 2011. B cells promote hepatic inflammation, biliary cyst formation, and salivary gland inflammation in the NOD. c3c4 model of autoimmune cholangitis. Cell. Immunol. 268 (1), 16–23.

Moriya, K., Fujie, H., Shintani, Y., Yotsuyanagi, H., Tsutsumi, T., Ishibashi, K., Matsuura, Y., Kimura, S., Miyamura, T., Koike, K., 1998. The core protein of hepatitis C virus induces hepatocellular carcinoma in transgenic mice. Nat. Med. 4 (9), 1065–1067.

Moriya, K., Yotsuyanagi, H., Shintani, Y., Fujie, H., Ishibashi, K., Matsuura, Y., Miyamura, T., Koike, K., 1997. Hepatitis C virus core protein induces hepatic steatosis in transgenic mice. J. Gen. Virol. 78 (Pt. 7), 1527–1531.

Muller, A., Machnik, F., Zimmermann, T., Schubert, H., 1988. Thioacetamide-induced cirrhosis-like liver lesions in rats—usefulness and reliability of this animal model. Exp. Pathol. 34 (4), 229–236.

Murotomi, K., Arai, S., Uchida, S., Endo, S., Mitsuzumi, H., Tabei, Y., Yoshida, Y., Nakajima, Y., 2016. Involvement of splenic iron accumulation in the development of nonalcoholic steatohepatitis in Tsumura Suzuki Obese Diabetes mice. Sci. Rep. 6, 22476.

Nakagome, Y., Ueno, Y., Kogure, T., Fukushima, K., Moritoki, Y., Ridgway, W.M., Eric Gershwin, M., Shimosegawa, T., 2007. Autoimmune cholangitis in NOD.c3c4 mice is associated with cholangiocyte-specific Fas antigen deficiency. J. Autoimmun. 29 (1), 20–29.

Nakayama, H., Otabe, S., Ueno, T., Hirota, N., Yuan, X., Fukutani, T., Hashinaga, T., Wada, N., Yamada, K., 2007. Transgenic mice expressing nuclear sterol regulatory element-binding protein 1c in adipose tissue exhibit liver histology similar to nonalcoholic steatohepatitis. Metabolism 56 (4), 470–475.

Nelson, B.H., 2004. IL-2, regulatory T cells, and tolerance. J. Immunol. 172 (7), 3983–3988.

Newell, P., Villanueva, A., Friedman, S.L., Koike, K., Llovet, J.M., 2008. Experimental models of hepatocellular carcinoma. J. Hepatol. 48 (5), 858–879.

Nishida, T., Tsuneyama, K., Fujimoto, M., Nomoto, K., Hayashi, S., Miwa, S., Nakajima, T., Nakanishi, Y., Sasaki, Y., Suzuki, W., Iizuka, S., Nagata, M., Shimada, T., Aburada, M., Shimada, Y., Imura, J., 2013. Spontaneous onset of nonalcoholic steatohepatitis and hepatocellular carcinoma in a mouse model of metabolic syndrome. Lab. Invest. 93 (2), 230–241.

Nishikawa, S., Yasoshima, A., Doi, K., Nakayama, H., Uetsuka, K., 2007. Involvement of sex, strain and age factors in high fat diet-induced obesity in C57BL/6J and BALB/cA mice. Exp. Anim. 56 (4), 263–272.

Oertelt, S., Lian, Z.X., Cheng, C.M., Chuang, Y.H., Padgett, K.A., He, X.S., Ridgway, W.M., Ansari, A.A., Coppel, R.L., Li, M.O., Flavell, R.A., Kronenberg, M., Mackay, I.R., Gershwin, M.E., 2006. Antimitochondrial antibodies and primary biliary cirrhosis in TGF-beta receptor II dominant-negative mice. J. Immunol. 177 (3), 1655–1660.

Ogasawara, M., Hirose, A., Ono, M., Aritake, K., Nozaki, Y., Takahashi, M., Okamoto, N., Sakamoto, S., Iwasaki, S., Asanuma, T., Taniguchi, T., Urade, Y., Onishi, S., Saibara, T., Oben, J.A., 2011. A novel and comprehensive mouse model of human non-alcoholic steatohepatitis with the full range of dysmetabolic and histological abnormalities induced by gold thioglucose and a high-fat diet. Liver Int. 31 (4), 542–551.

Ohba, K., Omagari, K., Murase, K., Hazama, H., Masuda, J., Kinoshita, H., Isomoto, H., Mizuta, Y., Miyazaki, M., Murata, I., Kohno, S., 2002. A possible mouse model for spontaneous cholangitis: serological and histological characteristics of MRL/lpr mice. Pathology 34 (3), 250–256.

Okumura, K., Ikejima, K., Kon, K., Abe, W., Yamashina, S., Enomoto, N., Takei, Y., Sato, N., 2006. Exacerbation of dietary steatohepatitis and fibrosis in obese, diabetic KK-A(y) mice. Hepatol. Res. 36 (3), 217–228.

Ouyang, X., Cirillo, P., Sautin, Y., McCall, S., Bruchette, J.L., Diehl, A.M., Johnson, R.J., Abdelmalek, M.F., 2008. Fructose consumption as a risk factor for non-alcoholic fatty liver disease. J. Hepatol. 48 (6), 993–999.

Ouyang, E.C., Wu, C.H., Walton, C., Promrat, K., Wu, G.Y., 2001. Transplantation of human hepatocytes into tolerized genetically immunocompetent rats. World J. Gastroenterol. 7 (3), 324–330.

Ozeki, T., Funakoshi, K., Iwaki, K., 1985. Rapid induction of cirrhosis by administration of carbon tetrachloride plus phospholipase D. Br. J. Exp. Pathol. 66 (4), 385–390.

Pasquinelli, C., Shoenberger, J.M., Chung, J., Chang, K.M., Guidotti, L.G., Selby, M., Berger, K., Lesniewski, R., Houghton, M., Chisari, F.V., 1997. Hepatitis C virus core and E2 protein expression in transgenic mice. Hepatology 25 (3), 719–727.

Ploss, A., Evans, M.J., Gaysinskaya, V.A., Panis, M., You, H., de Jong, Y.P., Rice, C.M., 2009. Human occludin is a hepatitis C virus entry factor required for infection of mouse cells. Nature 457 (7231), 882–886.

Poirier, L.A., 1975. Hepatocarcinogenesis by diethylnitrosamine in rats fed high dietary levels of lipotropes. J. Natl. Cancer Inst. 54 (1), 137–140.

Pollheimer, M.J., Fickert, P., 2015. Animal models in primary biliary cirrhosis and primary sclerosing cholangitis. Clin. Rev. Allergy Immunol. 48 (2–3), 207–217.

Pollheimer, M.J., Trauner, M., Fickert, P., 2011. Will we ever model PSC?—"it's hard to be a PSC model!". Clin. Res. Hepatol. Gastroenterol. 35 (12), 792–804.

Popov, Y., Sverdlov, D.Y., Bhaskar, K.R., Sharma, A.K., Millonig, G., Patsenker, E., Krahenbuhl, S., Krahenbuhl, L., Schuppan, D., 2010. Macrophage-mediated phagocytosis of apoptotic cholangiocytes contributes to reversal of experimental biliary fibrosis. Am. J. Physiol. Gastrointest. Liver Physiol. 298 (3), G323–G334.

Powell, E.E., Cooksley, W.G., Hanson, R., Searle, J., Halliday, J.W., Powell, L.W., 1990. The natural history of nonalcoholic steatohepatitis: a follow-up study of forty-two patients for up to 21 years. Hepatology 11 (1), 74–80.

Purcell, R.H., Emerson, S.U., 2001. Animal models of hepatitis A and E. ILAR J. 42 (2), 161–177.

Reddy, J.K., 2001. Nonalcoholic steatosis and steatohepatitis. III. Peroxisomal beta-oxidation, PPAR alpha, and steatohepatitis. Am. J. Physiol. Gastrointest. Liver Physiol. 281 (6), G1333–G1339.

Reif, S., Aeed, H., Shilo, Y., Reich, R., Kloog, Y., Kweon, Y.O., Bruck, R., 2004. Treatment of thioacetamide-induced liver cirrhosis by the Ras antagonist, farnesylthiosalicylic acid. J. Hepatol. 41 (2), 235–241.

Rinella, M.E., Green, R.M., 2004. The methionine-choline deficient dietary model of steatohepatitis does not exhibit insulin resistance. J. Hepatol. 40 (1), 47–51.

Romestaing, C., Piquet, M.A., Bedu, E., Rouleau, V., Dautresme, M., Hourmand-Ollivier, I., Filippi, C., Duchamp, C., Sibille, B., 2007. Long term high saturated fat diet does not induce NASH in Wistar rats. Nutr. Metab. 4, 4.

Rosenheck, R., 2008. Fast food consumption and increased caloric intake: a systematic review of a trajectory towards weight gain and obesity risk. Obes. Rev. 9 (6), 535–547.

Sahai, A., Malladi, P., Pan, X., Paul, R., Melin-Aldana, H., Green, R.M., Whitington, P.F., 2004. Obese and diabetic db/db mice develop marked liver fibrosis in a model of nonalcoholic steatohepatitis: role of short-form leptin receptors and osteopontin. Am. J. Physiol. Gastrointest. Liver Physiol. 287 (5), G1035–G1043.

Salas, J.T., Banales, J.M., Sarvide, S., Recalde, S., Ferrer, A., Uriarte, I., Oude Elferink, R.P., Prieto, J., Medina, J.F., 2008. Ae2a,b-deficient mice develop antimitochondrial antibodies and other features resembling primary biliary cirrhosis. Gastroenterology 134 (5), 1482–1493.

Salguero Palacios, R., Roderfeld, M., Hemmann, S., Rath, T., Atanasova, S., Tschuschner, A., Gressner, O.A., Weiskirchen, R., Graf, J., Roeb, E., 2008. Activation of hepatic stellate cells is associated with cytokine expression in thioacetamide-induced hepatic fibrosis in mice. Lab. Invest. 88 (11), 1192–1203.

Sandgren, E.P., Palmiter, R.D., Heckel, J.L., Daugherty, C.C., Brinster, R.L., Degen, J.L., 1991. Complete hepatic regeneration after somatic deletion of an albumin-plasminogen activator transgene. Cell 66 (2), 245–256.

Shimomura, I., Hammer, R.E., Richardson, J.A., Ikemoto, S., Bashmakov, Y., Goldstein, J.L., Brown, M.S., 1998. Insulin resistance and diabetes mellitus in transgenic mice expressing nuclear SREBP-1c in adipose tissue: model for congenital generalized lipodystrophy. Genes Dev. 12 (20), 3182–3194.

Shukla, S.D., Pruett, S.B., Szabo, G., Arteel, G.E., 2013. Binge ethanol and liver: new molecular developments. Alcohol Clin. Exp. Res. 37 (4), 550–557.

Shull, M.M., Ormsby, I., Kier, A.B., Pawlowski, S., Diebold, R.J., Yin, M., Allen, R., Sidman, C., Proetzel, G., Calvin, D., et al., 1992. Targeted disruption of the mouse transforming growth factor-beta 1 gene results in multifocal inflammatory disease. Nature 359 (6397), 693–699.

Singaravelu, R., Chen, R., Lyn, R.K., Jones, D.M., O'Hara, S., Rouleau, Y., Cheng, J., Srinivasan, P., Nasheri, N., Russell, R.S., Tyrrell, D.L., Pezacki, J.P., 2014. Hepatitis C virus induced up-regulation of mi-

croRNA-27: a novel mechanism for hepatic steatosis. Hepatology 59 (1), 98–108.

Sprinzl, M.F., Oberwinkler, H., Schaller, H., Protzer, U., 2001. Transfer of hepatitis B virus genome by adenovirus vectors into cultured cells and mice: crossing the species barrier. J. Virol. 75 (11), 5108–5118.

Spruss, A., Kanuri, G., Wagnerberger, S., Haub, S., Bischoff, S.C., Bergheim, I., 2009. Toll-like receptor 4 is involved in the development of fructose-induced hepatic steatosis in mice. Hepatology 504, 1094–1104.

Starkel, P., Leclercq, I.A., 2011. Animal models for the study of hepatic fibrosis. Best Pract. Res. Clin. Gastroenterol. 25 (2), 319–333.

Svegliati-Baroni, G., Candelaresi, C., Saccomanno, S., Ferretti, G., Bachetti, T., Marzioni, M., De Minicis, S., Nobili, L., Salzano, R., Omenetti, A., Pacetti, D., Sigmund, S., Benedetti, A., Casini, A., 2006. A model of insulin resistance and nonalcoholic steatohepatitis in rats: role of peroxisome proliferator-activated receptor-alpha and n–3 polyunsaturated fatty acid treatment on liver injury. Am. J. Pathol. 169 (3), 846–860.

Takahashi, Y., Fukusato, T., 2014. Histopathology of nonalcoholic fatty liver disease/nonalcoholic steatohepatitis. World J. Gastroenterol. 20 (42), 15539–15548.

Takahashi, Y., Soejima, Y., Fukusato, T., 2012. Animal models of nonalcoholic fatty liver disease/nonalcoholic steatohepatitis. World J. Gastroenterol. 18 (19), 2300–2308.

Takahashi, Y., Soejima, Y., Kumagai, A., Watanabe, M., Uozaki, H., Fukusato, T., 2014. Japanese herbal medicines shosaikoto, inchinkoto, and juzentaihoto inhibit high-fat diet-induced nonalcoholic steatohepatitis in db/db mice. Pathol. Int. 64 (10), 490–498.

Tateno, C., Yoshizane, Y., Saito, N., Kataoka, M., Utoh, R., Yamasaki, C., Tachibana, A., Soeno, Y., Asahina, K., Hino, H., Asahara, T., Yokoi, T., Furukawa, T., Yoshizato, K., 2004. Near completely humanized liver in mice shows human-type metabolic responses to drugs. Am. J. Pathol. 165 (3), 901–912.

Tesfaye, A., Stift, J., Maric, D., Cui, Q., Dienes, H.P., Feinstone, S.M., 2013. Chimeric mouse model for the infection of hepatitis B and C viruses. PLoS One 8 (10), e77298.

Tetri, L.H., Basaranoglu, M., Brunt, E.M., Yerian, L.M., Neuschwander-Tetri, B.A., 2008. Severe NAFLD with hepatic necroinflammatory changes in mice fed trans fats and a high-fructose corn syrup equivalent. Am. J. Physiol. Gastrointest. Liver Physiol. 295 (5), G987–G995.

Tiegs, G., Hentschel, J., Wendel, A., 1992. A T cell-dependent experimental liver injury in mice inducible by concanavalin A. J. Clin. Invest. 90 (1), 196–203.

Tsuge, M., Hiraga, N., Takaishi, H., Noguchi, C., Oda, H., Imamura, M., Takahashi, S., Iwao, E., Fujimoto, Y., Ochi, H., Chayama, K., Tateno, C., Yoshizato, K., 2005. Infection of human hepatocyte chimeric mouse with genetically engineered hepatitis B virus. Hepatology 42 (5), 1046–1054.

Tsukamoto, H., French, S.W., Benson, N., Delgado, G., Rao, G.A., Larkin, E.C., Largman, C., 1985. Severe and progressive steatosis and focal necrosis in rat liver induced by continuous intragastric infusion of ethanol and low fat diet. Hepatology 5 (2), 224–232.

Tsukamoto, H., Horne, W., Kamimura, S., Niemela, O., Parkkila, S., Yla-Herttuala, S., Brittenham, G.M., 1995. Experimental liver cirrhosis induced by alcohol and iron. J. Clin. Invest. 96 (1), 620–630.

Tsukamoto, H., Matsuoka, M., French, S.W., 1990. Experimental models of hepatic fibrosis: a review. Semin. Liver Dis. 10 (1), 56–65.

Tsuneyama, K., Moritoki, Y., Kikuchi, K., Nakanuma, Y., 2012. Pathological features of new animal models for primary biliary cirrhosis. Int. J. Hepatol. 2012, 403954.

Turrini, P., Sasso, R., Germoni, S., Marcucci, I., Celluci, A., Di Marco, A., Marra, E., Paonessa, G., Eutropi, A., Laufer, R., Migliaccio, G., Padron, J., 2006. Development of humanized mice for the study of hepatitis C virus infection. Transplant. Proc. 38 (4), 1181–1184.

Vercauteren, K., de Jong, Y.P., Meuleman, P., 2014. HCV animal models and liver disease. J. Hepatol. 61 (1 Suppl.), S26–S33.

Vergnes, L., Phan, J., Strauss, M., Tafuri, S., Reue, K., 2003. Cholesterol and cholate components of an atherogenic diet induce distinct stages of hepatic inflammatory gene expression. J. Biol. Chem. 278 (44), 42774–42784.

Vierling, J.M., 2001. Animal models for primary sclerosing cholangitis. Best Pract. Res. Clin. Gastroenterol. 15 (4), 591–610.

Wakabayashi, K., Lian, Z.X., Leung, P.S., Moritoki, Y., Tsuneyama, K., Kurth, M.J., Lam, K.S., Yoshida, K., Yang, G.X., Hibi, T., Ansari, A.A., Ridgway, W.M., Coppel, R.L., Mackay, I.R., Gershwin, M.E., 2008. Loss of tolerance in C57BL/6 mice to the autoantigen E2 subunit of pyruvate dehydrogenase by a xenobiotic with eusuing biliary ductular disease. Hepatology 48 (2), 531–540.

Wakabayashi, K., Lian, Z.X., Moritoki, Y., Lan, R.Y., Tsuneyama, K., Chuang, Y.H., Yang, G.X., Ridgway, W., Ueno, Y., Ansari, A.A., Coppel, R.L., Mackay, I.R., Gershwin, M.E., 2006. IL-2 receptor alpha(−/−) mice and the development of primary biliary cirrhosis. Hepatology 44 (5), 1240–1249.

Wakabayashi, K., Yoshida, K., Leung, P.S., Moritoki, Y., Yang, G.X., Tsuneyama, K., Lian, Z.X., Hibi, T., Ansari, A.A., Wicker, L.S., Ridgway, W.M., Coppel, R.L., Mackay, I.R., Gershwin, M.E., 2009. Induction of autoimmune cholangitis in non-obese diabetic (NOD). 1101 mice following a chemical xenobiotic immunization. Clin. Exp. Immunol. 155 (3), 577–586.

Wakita, T., Taya, C., Katsume, A., Kato, J., Yonekawa, H., Kanegae, Y., Saito, I., Hayashi, Y., Koike, M., Kohara, M., 1998. Efficient conditional transgene expression in hepatitis C virus cDNA transgenic mice mediated by the Cre/loxP system. J. Biol. Chem. 273 (15), 9001–9006.

Wang, H.X., Liu, M., Weng, S.Y., Li, J.J., Xie, C., He, H.L., Guan, W., Yuan, Y.S., Gao, J., 2012. Immune mechanisms of concanavalin A model of autoimmune hepatitis. World J. Gastroenterol. 18 (2), 119–125.

Washburn, M.L., Bility, M.T., Zhang, L., Kovalev, G.I., Buntzman, A., Frelinger, J.A., Barry, W., Ploss, A., Rice, C.M., Su, L., 2011. A humanized mouse model to study hepatitis C virus infection, immune response, and liver disease. Gastroenterology 140 (4), 1334–1344.

Wu, G.Y., Konishi, M., Walton, C.M., Olive, D., Hayashi, K., Wu, C.H., 2005. A novel immunocompetent rat model of HCV infection and hepatitis. Gastroenterology 128 (5), 1416–1423.

Wu, J., Norton, P.A., 1996. Animal models of liver fibrosis. Scand. J. Gastroenterol. 31 (12), 1137–1143.

Wu, S.J., Yang, Y.H., Tsuneyama, K., Leung, P.S., Illarionov, P., Gershwin, M.E., Chuang, Y.H., 2011. Innate immunity and primary biliary cirrhosis: activated invariant natural killer T cells exacerbate murine autoimmune cholangitis and fibrosis. Hepatology 53 (3), 915–925.

Yang, P.L., Althage, A., Chung, J., Chisari, F.V., 2002. Hydrodynamic injection of viral DNA: a mouse model of acute hepatitis B virus infection. Proc. Natl. Acad. Sci. USA 99 (21), 13825–13830.

Yang, J.M., Han, D.W., Xie, C.M., Liang, Q.C., Zhao, Y.C., Ma, X.H., 1998. Endotoxins enhance hepatocarcinogenesis induced by oral intake of thioacetamide in rats. World J. Gastroenterol. 4 (2), 128–132.

Yeh, C.N., Maitra, A., Lee, K.F., Jan, Y.Y., Chen, M.F., 2004. Thioacetamide-induced intestinal-type cholangiocarcinoma in rat: an animal model recapitulating the multi-stage progression of human cholangiocarcinoma. Carcinogenesis 25 (4), 631–636.

Yimin, Furumaki, H., Matsuoka, S., Sakurai, T., Kohanawa, M., Zhao, S., Kuge, Y., Tamaki, N., Chiba, H., 2012. A novel murine model for non-alcoholic steatohepatitis developed by combination of a high-fat diet and oxidized low-density lipoprotein. Lab. Invest. 92 (2), 265–281.

Yugo, D.M., Cossaboom, C.M., Meng, X.J., 2014. Naturally occurring animal models of human hepatitis E virus infection. ILAR J. 55 (1), 187–199.

Zhang, W., Sharma, R., Ju, S.T., He, X.S., Tao, Y., Tsuneyama, K., Tian, Z., Lian, Z.X., Fu, S.M., Gershwin, M.E., 2009. Deficiency in regulatory T cells results in development of antimitochondrial antibodies and autoimmune cholangitis. Hepatology 49 (2), 545–552.

Zierden, M., Kuhnen, E., Odenthal, M., Dienes, H.P., 2010. Effects and regulation of autoreactive CD8+ T cells in a transgenic mouse model of autoimmune hepatitis. Gastroenterology 139 (3), 975–986.

Zimmermann, H., Fellay, M., Zimmermann, A., 1997. Hepatic stellate cells (Ito cells) but not collagen IV may partly be responsible for lower portal pressure after reversing secondary biliary cirrhosis in the rat. J. Hepatol. 26 (1), 158–166.

Zimmermann, T., Muller, A., Machnik, G., Franke, H., Schubert, H., Dargel, R., 1987. Biochemical and morphological studies on production and regression of experimental liver cirrhosis induced by thioacetamide in Uje: WIST rats. Z. Versuchstierkd. 30 (5–6), 165–180.

Zou, Y., Li, J., Lu, C., Wang, J., Ge, J., Huang, Y., Zhang, L., Wang, Y., 2006. High-fat emulsion-induced rat model of nonalcoholic steatohepatitis. Life Sci. 79 (11), 1100–1107.

Page left intentionally blank

PART E

SKIN

Page left intentionally blank

14

Animal Models of Skin Regeneration

Barbara Gawronska-Kozak, Joanna Bukowska

Institute of Animal Reproduction and Food Research, Polish Academy of Sciences, Olsztyn, Poland

1 INTRODUCTION

Damaged, lost, or injured animal organs can be reconciled through regeneration or repair. While regeneration results in the original architecture and functionality, repair leads to fibrotic tissue accumulation that forms a scar. Although scar tissues allow for the recovery of the integrity of injured tissues, the postinjured organ never regains its full functionality. Regeneration, a phenomenon common for invertebrates, is limited to lower vertebrate classes, such as fish and amphibians. It seems that vertebrate regenerative capacity has decreased during phylogenetic development and is almost lost in birds and mammals.

Regeneration mechanisms in animals fall into two categories: morphallaxis and epimorphosis. Morphallaxis, characteristic for invertebrates (i.e., hydra) is considered to be dependent on the presence of a neoblast, the group of totipotent stem cells persisting in adult tissues that replace lost organs (Ogawa et al., 2002). Epimorphosis, characteristic for vertebrates, relies on the proliferative capacity of reprogrammed/dedifferentiated cells in the place of injury that form the blastema structure.

During the regeneration process, blastema cells differentiate into cells that restore missing tissues to fully recover lost or amputated organs (Kragl et al., 2009). The blastema structure has been examined during zebrafish fin regeneration (Poss et al., 2003), axolotl limb regeneration (Endo et al., 2004; Kragl et al., 2009), and even sporadically in mammals (Clark et al., 1998; Goss and Grimes, 1975; Seifert et al., 2012a). Through-and-through punch wounds made in the ears of rabbits (Goss and Grimes, 1975) and MRL/MpJ (Clark et al., 1998), nude (Gawronska-Kozak, 2004), and spiny mice (Seifert et al., 2012a) regenerate with the presence of blastema structures. Similarly, their presence has been analyzed during amputated digit tip regeneration in mice (Fernando et al., 2011).

There is another form of epimorphic regeneration that is blastemal-independent, which includes vertebrate skin regeneration (Seifert and Maden, 2014).

Skin is the largest organ and fulfills multiple key functions, acting as an environmental protection barrier, an immunological response system, and a neuroendocrine organ (Slominski et al., 2012). Mammalian skin is composed of two layers: the epidermis and dermis, which

are separated by a basement membrane. Stratified epidermis, the superficial part of the skin, is mainly composed from keratinocytes and forms basal, spinous, granular, and stratum corneum layers (Visscher and Narendran, 2014). Cellular components of the dermal part of the skin consist mainly of dermal fibroblasts, macrophages, and mast cells. Dermal fibroblasts are the predominant cells responsible for extracellular matrix (ECM) composition through the synthesis of collagen, elastin, glycoproteins, proteoglycans, and enzymes, such as matrix metalloproteinases (MMPs), which participate in its turnover during skin homeostasis and wound healing (Clark, 1996).

As the most outer barrier, skin is the organ most frequently exposed to external insults. During physiological maintenance, the epithelial layer undergoes continuous renovation in the process of regeneration similar to other mammalian tissues including cells in the gut epithelium, blood cells, and the annual replacement of antlers. Pathological events (i.e., injury) evoke a wound healing process that can take two directions: reparative (scar-forming) and regenerative (scar-free). In the skin, the spectrum of scar formation depends of trauma severity. Whereas injury that affects the epidermal layer of the skin heals in a scar-free way, full-thickness excisional wounds comprising the epidermis, dermis, and hypodermis heal with scarring. However, this is only true when epidermal injury is not associated with underlying metabolic disorders, such as diabetes.

Reparative skin wound healing consists of overlapping phases: inflammation, proliferation, and remodeling (Clark, 1996; Werner and Grose, 2003). Inflammation, preceded by hemostasis achieved through provisional matrix formation in the form of fibrin cloth, is characterized by the attraction of inflammatory cells, such as neutrophils and monocytes that subsequently differentiate into macrophages to the wound. Inflammatory cells fulfill their function through bacteria elimination (neutrophils) and phagocytosis of necrotic tissues and neutrophils (macrophages). Macrophages release cytokines [e.g., transforming growth factor β (TGFβ) and platelet-derived growth factor (PDGF)] that stimulate epithelial cell and fibroblast movement into the wound area beginning the next stage of the wound healing process (Table 14.1) (Bryan et al., 2005; Couper et al., 2008; Cowin et al., 1998; Hubner et al., 1996; Liechty et al., 2000; Satish and Kathju, 2010). Proliferation begins as migration and proliferation followed by differentiation of epidermal cells to reepithelialize the wound area to restore skin barrier function. Attracted dermal fibroblasts migrate to the wounded dermis, and together with invading through the process of angiogenesis the network of blood capillaries generates granulation tissues to reestablish dermal integrity (Clark, 1996). Initially, dermal fibroblasts synthesize and release the components of so-called

"embryonic" extracellular matrix, such as collagen III and extra-domain A (EDA) fibronectin followed by collagen type I, which is characteristic of adult skin (Bielefeld et al., 2013). A sufficient amount of ECM deposition, replacement of collagen III by collagen type I, and the presence of myofibroblasts in the postwounded bed initiate the remodeling phase (Table 14.1) (Cass et al., 1997; Hinz, 2007). Dermal fibroblasts acquire a myofibroblast phenotype to contract the wound bed, which is followed by scar formation. ECM remodeling is controlled by MMPs that degrade wound collagen (Table 14.1) (Madlener et al., 1998; Soo et al., 2000). The product of wound repair is a mature scar; however, the repaired tissues lack epidermal appendages, such as hair follicles and sweat and sebaceous glands, meaning they never regain the functional properties of uninjured tissues. Scar tissues are considered to block the regeneration process; therefore recognizing molecular signals and pathways that direct scarring versus regeneration is a prerequisite for understanding organ regeneration. Animal models for skin regeneration are an essential foundation for research in this area.

With the enormous increase in the understanding of stem cells, regenerative medicine is currently focused on the benefits from embryonic, adult, and induced pluripotent stem cell (iPS) usage (Takagi et al., 2016). In vitro and in vivo data indicate that there is a reciprocal bond/relationship between stem cells and the niches in which they exist. To fulfill the regenerative task, both the niche and stem cells have to cooperate. Since the regenerative phenomenon undoubtedly involving stem cells and their niche has been solved in nature, study of the naturally existing and genetically modified examples of regeneration will shed light on the molecular and cellular mechanisms that control the process (Hu et al., 2014b).

Here we will focus on animal models to study skin regeneration, with an emphasis on vertebrates.

2 SKIN HEALING IN LOWER VERTEBRATE (ANAMNIOTES) MODEL ORGANISMS

2.1 Fish

Cutaneous diseases and wounding are relatively more frequent among fish compared to terrestrial vertebrates due to their intimate contact with an aquatic environment (Groff, 2001). Both aquatic and terrestrial vertebrates share a similar pattern of the basic cellular organization of full-thickness skin. Striking differences between fish and mammalian skin include (1) greater average thickness of epidermis, (2) a lack of stratum corneum, (Guerra et al., 2006), and (3) reduced dermal layer in fish. Furthermore, mucus secretion is a specific

TABLE 14.1 Comparative Summary of the Differences in Skin Wound Healing Process Between Reparative (Scar-Forming) and Regenerative (Scar-Free) Mammalian Models

Skin wound healing stages	Skin wound healing in mammals			
	Reparative (scar forming)	Regenerative (scar-free)		
			Adults	
	Adults	Fetuses	*Acomys*	Nude
Inflammation	Massive inflammation; cytokines excess (Bryan et al., 2005; Cowin et al., 1998; Hubner et al., 1996), increased number of monocytes and macrophages, overexpression of IL-1 and IL-8, decrease of IL-10 (Couper et al., 2008; Liechty et al., 2000; Satish and Kathju, 2010)	Minimal inflammation, reduced cytokines response, low levels of PDGF, TGFβ1, TGFβ2, high levels of TGFβ3 (Barrientos et al., 2008; Hsu et al., 2001; Olutoye et al., 1996), reduced levels of neutrophils and macrophages (Adzick and Lorenz, 1994; Cowin et al., 1998), downregulation of IL-1 and IL-8, overexpression of IL-10 (Couper et al., 2008; Satish and Kathju, 2010)	Lack of F4/80 macrophages, reduced cytokines levels, neutropenic, high amount of mast cells (Brant et al., 2016)	Lack of T lymphocytes, low levels of PDGF and TGFβ1 (Gawronska-Kozak et al., 2006)
	Rapid overexpression of MMP-1, -2, -3, -8, -9, -10, -12, -13, -14, and TIMP-1, -2 at the initial phase of healing and then their gradual downregulation (Madlener et al., 1998; Soo et al., 2000)	Higher levels of MMPs and reduced expression of their inhibitors (TIMPs) (Dang et al., 2003a)	High levels of MMP-2 and MMP-9 and low of TIMP-1 (Brant et al., 2015, 2016)	Bimodal pattern of MMP-9 and MMP-13 high expression detected at inflammatory and remodeling phases of healing (Gawronska-Kozak, 2011; Gawronska-Kozak et al., 2006)
Proliferation	Reepithelialization of 4 mm wounds extended to 5–7 days after injury (Soo et al., 2000)	Accelerated reepithelialization of 2 mm excisional wounds completed 72 h after injury (Dang et al., 2003a)	Rapid reepithelialization of 4 mm wounds within 3 days postinjury (Hubner et al., 1996)	Complete wound closure observed between days 1 and 3 (Gawronska-Kozak, 2011)
	High levels of collagen I; densely arranged, parallel collagen fibers, oriented perpendicular to the wound surface; lower ratio of collagen type III to type I (Lo et al., 2012); delayed collagen deposition and fibroblasts migration at the wound site (Larson et al., 2010); granulation tissue formation starts at days 4–7 (Clark, 1996; Gawronska-Kozak, 2011)	High levels of collagen III; fine, well-organized reticular collagen bundles; higher ratio of collagen type III to type I (Lo et al., 2012); faster migration of fibroblasts, synchronous fibroblasts proliferation and collagen production (Larson et al., 2010)	Slow ECM deposition, domination of type III collagen, low levels of collagen type I, extended cell proliferation in the wound bed (Brant et al., 2016; Seifert et al., 2012a)	Granulation tissue formation starts at day 3; rapid collagen turnover (Gawronska-Kozak, 2011)
	Low levels of hyaluronic acid (HA) (Longaker et al., 1991)	Abundance of HA, rapid HA deposition and its maintenance during healing (Larson et al., 2010)	High levels of fibronectin and tenascin C (Seifert et al., 2012a)	High levels of HA in wound bed (Gawronska-Kozak et al., 2006)
	Increasement in decorin levels (Beanes et al., 2001); low synthesis of fibromodulin (Soo et al., 2000)	Decorin downregulation (Beanes et al., 2001), fibromodulin increment (Soo et al., 2000)		
	Slow synthesis of cell adhesion molecules after injury (Whitby and Ferguson, 1991)	Early expression of cell adhesion molecules (fibronectin, tenascin C) after injury (Whitby and Ferguson, 1991)		
	Presence of myofibroblasts (Clark, 1996; Hinz, 2007)	Controversial presence of myofibroblasts in the wound bed (Cass et al., 1997)	Lack of myofibroblasts (detected as αSMA positive cells) (Seifert et al., 2012a)	

E. SKIN

(Continued)

TABLE 14.1   Comparative Summary of the Differences in Skin Wound Healing Process Between Reparative (Scar-Forming) and Regenerative (Scar-Free) Mammalian Models (*cont.*)

	Skin wound healing in mammals			
Skin wound healing stages	Reparative (scar forming)	Regenerative (scar-free)		
			Adults	
	Adults	Fetuses	*Acomys*	Nude
Remodeling	Slow collagen deposition; collagen content in postinjured skin at day 36 does not regain levels observed in noninjured tissue (Gawronska-Kozak, 2011)	Reticular pattern of deposited collagen, indistinguishable from the surrounding uninjured tissue (Cuttle et al., 2005)	Collagen's porous architecture (Seifert et al., 2012a)	Accelerated stabilization of collagen content (day 21 after injury) (Gawronska-Kozak, 2011)
				Second wave of upregulated MMP-9 and MMP-13 expression localized to dermis (Gawronska-Kozak, 2011)

feature of fish skin. Among many different functions, epidermal mucus plays a protective role in the initial stage of wound healing, possibly favoring regeneration and acting as an antibacterial agent because of its hydrolytic activity.

Skin wound healing in both scaled and nonscaled fish occurs rapidly, and the skin is dynamically covered by mucus along with a reepithelialization process initiated from the wound margin within a few hours after injury (Quilhac and Sire, 1999). In scaled fishes, skin lesions are covered several hours after the injury by a thin layer of epithelial cells that overlie the dermis. In the scaleless carp *Cyprinus carpio* L. and African catfish *Clarias gariepinus*, complete wound closing occurs within 24 h (Guerra et al., 2008). Healing of African catfish skin first involves hemostatic and inflammatory responses that are activated shortly after injury (Guerra et al., 2008). In this species hemorrhagic clots are observed 3 h of skin excision, but the numbers of clots gradually decrease within 12 h. Next, sliding of the epidermal layer over the wound is observed, and regenerated epidermis is formed within 24 h. Thickness of the newly established epidermis on the third day is equal to that observed in normal skin. During healing, fusion of the migratory fronts is accompanied by inflammation that remains until day 3 of injury. Finally, the original wound borders are undetectable and perfectly mimic intact skin. Within a few weeks, a new scale with the size and characteristics of a mature scale is completely regrown (Ohira et al., 2007).

Zebrafish (*Danio rerio*) have been established as a central model organism for studying regeneration due to their ability to regenerate various organs (e.g., fin, jaw, heart) and the wide availability of molecular genetics tools. Only a few years ago, Richardson et al. (2013) demonstrated that skin wound healing in zebrafish involves regeneration rather than repair with absent or minimal scar forming. Laser-induced full-thickness skin wounds made on the flank of adult zebrafish healed without scars. Major steps of cutaneous wound healing are conserved between adult zebrafish and adult mammals (Richardson et al., 2013). Apart from external fibrin clot formation, all crucial steps of wound healing in mammalian skin also occur in adult zebrafish. In contrast to mammalian systems, zebrafish wound repair involves minimal or a lack of scarring for both superficial and deep partial-thickness wounds, indicating regeneration (Richardson et al., 2013). In contrast to mammals, reepithelialization precedes inflammation in zebrafish despite a massive inflammatory response. This sequence of events suggests that reepithelialization is independent of chemotactic signals released by macrophages. However, similarly to mammals, macrophages and neutrophils are present in the healing wound, so inflammation occurs earlier than granulation tissue formation and vascularization (Richardson et al., 2013).

Skin wound healing depends on several internal (i.e., blood and nerve supply) and external (i.e., environment temperature and contamination) factors. Based on studies carried out on scaleless fishes (*Rita rita*), there is relationship between skin thickness and wound reepithelialization, indicating that thinner skin regenerates slower (Mittal and Munshi, 1974). Scale regeneration in the goldfish *Carassius auratus* L. occurs most rapidly during the first 5 days after injury, then new tissue formation gradually decreases, and continuous linear growth occurs over 5–28 days (Ohira et al., 2007). Another relevant factor influencing wound healing in fish is water temperature. In *C. gariepinus*, rapid and effective wound healing is associated with high water temperature (30°C) that is close to its natural environment (35°C) (Guerra

et al., 2008). In contrast, an Antarctic fish, *Notothenia coriceps*, maintained at 0°C delays reepithelization process over the period of 7–14 days. The wound is completely closed after 23–30 days, but wounding scale formation is not observed even after 90 days and, intriguingly, scars composed of fibroblasts and collagen fibers are observed suggesting that low temperature discourages skin regeneration (Cunha da Silva et al., 2005). Studies by Vieira et al. (2011) on the sea bream *Sparus auratus* indicated the effect of food deprivation on scale regeneration. Microarray data revealed that in fasted animals, scale removal resulted in upregulation of genes involved in cell division/mitosis, cell growth, and metabolism (e.g., interleukin enhancer binding factor, phosphoserine aminotransferase, D-3-phosphoglycerate dehydrogenase), cell proliferation (e.g., macrophage-stimulating 1, hepatocyte growth factor-like), and cell signaling (e.g., inositol monophosphatase). Upregulation of GINS complex subunit 1 (PSF1 homolog) was observed both 3 and 7 days after scale removal (Vieira et al., 2011). This complex is involved in hematopoietic stem cell proliferation during bone regeneration in mammals (Ueno et al., 2009). The upregulation of its transcripts might indicate that in teleosts, the GINS complex regulates the process of skin regeneration by activating cell proliferation.

2.2 Amphibians

2.2.1 Urodele Amphibians: Ambystomatidae (Mole Salamanders) Axolotls

Axolotls are pioneering and exemplary animal to study limb regeneration (Kragl et al., 2009). After limb amputation, keratinocytes surrounding the wound migrate to cover wounded tissues during the first 24 h. Later on, the neoepidermis forms an apical epidermal cap (AEC); disrupting or preventing AEC formation abrogates limb regeneration (McCusker and Gardiner, 2011). This observation brought attention to the neoepidermis as a source of factors that direct cascade of followed events and turn attention into scar-free skin wound healing/regeneration study.

Detailed studies on amphibian skin response to wounding showed that excisional (1.5-mm diameter) wounds made on the tail skin of axolotl (*Ambystoma mexicanum*) reepithelialized over 8 h. Interestingly, the partial basement membrane regeneration was detected as late as 12–18 days postinjury, with full development at day 90 (Levesque et al., 2010). Completely regenerated skin tissues at day 90 were undistinguishable from normal, unwounded skin. The skin regeneration process in axolotl was accompanied by a low inflammatory response measured as the number of neutrophils in wounded skin and a small number of cells expressing α-smooth muscle actin (SMA) as a myofibroblast indicator. Low levels of αSMA-expressing cells were associated with low and transient

(days 1–4) expression of the profibrotic cytokine TGFβ1. However, the study showed that axolotls are capable of making fibrous tissues in both uninjured and injured skin after bleomycin injection. This indicates that axolotl tissues possess all of the factors required for the fibrous response. Nonetheless, the regenerative, nonfibrous pathway of skin injury resolution was activated (Levesque et al., 2010).

Other studies have examined skin wound healing in both aquatic (paedomorphs) and metamorphose-induced terrestrial axolotls (Seifert et al., 2012b). Although both forms of axolotls were able to regenerate skin wounds, a significant delay in the process was observed for metamorphs. Skin wounds (4-mm diameter) completely reepithelialized during 24 and 72 h for paedomorphs and metamorphs, respectively. Injury caused blood flow into the area, but scabs never formed. The relatively long delay in new extracellular matrix production/remodeling was detected with low levels of fibronectin and high levels of tenascin-C, indicating the formation of an antiscarring matrix. Analysis of MMP expression patterns (MMP3/10a, MMP3/10b, MMP9, MMP19, MMP28) showed strong upregulation during the first postwounded days; however, the surge of expression was higher for metamorphs. The authors suggest that sustained MMP activity during skin regeneration may control the timing of ECM deposition (Seifert et al., 2012b).

2.2.2 Anura Amphibians: Xenopus laevis

Unlike urodele amphibians, anurans' regenerative capacity depends on the life stage. To study the adult skin wound healing process, postmetamorphosed (8- and 15-month-old) *X. laevis* were selected (Bertolotti et al., 2013). Incisional wounds were made on the dorsal skin of the hind legs. Histological examination demonstrated typical overlapping phases for wound healing: inflammation, new tissue formation, and remodeling. The skin wound healing process in postmetamorphosed *X. laevis* revealed the occurrence of two healing processes: regeneration of the epidermis and repair of the dermis. The healed epidermis in both 8- and 15-month-old animals showed morphological appearances similar to the unwounded surroundings. Moreover, epidermal regeneration was associated with the restoration of exocrine glands (Bertolotti et al., 2013). However, differences were detected in the timing of wound closure (reepithelialization). A single layer of epithelial cells covered the wound at 1 and 3 days for younger (8-month-old) and older (15-month-old) animals, respectively. Dermis reparative healing involved granulation tissue formation characterized by intense angiogenesis and the presence of inflammatory cells (neutrophils, macrophages, lymphocytes), fibroblasts, and myofibroblasts. Granulation tissues were eventually replaced by dense, fibrous tissues forming scar-like tissues that were distinguishable from the surrounding uninjured dermis even after

several months (Bertolotti et al., 2013). On the contrary, excisional skin wounds in *Xenopus* froglets (very young adults) healed without scars (Yokoyama et al., 2011). Neoepidermis covered the postwounded area at 24 h, and the presence of exocrine glands within newly formed epidermis was detected at day 10.

Collectively these data indicate that skin regenerative capacity in anuran amphibians depends on the stage of development. It occurs before metamorphosis and in young adults (froglets), while older animals (8–15 months) only regenerate the epidermis (Bertolotti et al., 2013; Yokoyama et al., 2011).

3 SKIN HEALING IN HIGHER VERTEBRATE (AMNIOTES) MODEL ORGANISMS

3.1 Reptiles

The higher vertebrates reptiles, birds, and mammals share structural skin characteristics that enable their success in a terrestrial environment. Moreover, shelled eggs protected by amniotic membranes allow them to develop outside an aquatic environment. Unlike amphibians, they do not have an aquatic larval stage. Among amniotes, the most remarkable regenerative features are displayed by some lizards followed by autotomy or amputation of the tail (Delorme et al., 2012). Tail regeneration is preceded by scar-free skin healing, which seems to be essential for regeneration (Delorme et al., 2012). Lizard skin/integument consists of the epidermis, dermis, and hypodermis. The epidermis is divided into horizontal layers of stratum basale, stratum spinosum, stratum granulosum, and the outermost stratum corneum (Delorme et al., 2012). Immunohistochemical analysis of postamputated tail tissues revealed increased expression of PCNA (proliferating cell nuclear antigen) and WE6 (wound keratin marker) in proliferating wound epithelium, more MMP9-positive cells and fibroblasts in the blastema structure, and the presence of TGFβ3 in fibroblasts and chondrocytes (Delorme et al., 2012). Skin wound healing studies in reptiles (lizards) showed regionally different responses to injury (Wu et al., 2014). Complete skin restoration was detected at the amputated/regenerated tail as a process preceding tail regeneration but not at the wounded tail or trunk skin. Molecular data suggest that β-catenin and tenascin-C are involved in epidermal differentiation and regeneration, respectively (Wu et al., 2014).

3.2 Mammals

Generally, mammals heal skin injuries in a reparative (scar-forming) manner. There are only two natural and unique models of true postinjured skin regeneration among mammals: mammalian fetuses and *Acomys* (spiny mice).

3.2.1 Mammalian Fetuses

Mammalian fetal skin integrity after injury is restored through a process that preserves the architecture and function of injured skin and is characterized by an absence of scar formation as seen in adult wounds. This regenerative capacity seems to be limited to fetal skin since other organs, such as the fetal stomach and intestines heal with scarring. The phenomenon of postinjured skin regeneration in mammalian fetuses occurs up to the third trimester of gestation in sheep (Longaker et al., 1990), monkey (Lorenz et al., 1993), mouse (Whitby and Ferguson, 1991), rat (Ihara et al., 1990), rabbit (Somasundaram and Prathap, 1970), and human (Lorenz et al., 1992). Thereafter, skin incisions cause scar formation. The transition from scarless fetal-type repair to adult-type repair with scar occurs between days 16.5 and 18.5 of gestation for rats (Ihara et al., 1990), 100–120 days for sheep (Longaker et al., 1990), 100–107 days for Rhesus monkeys (Lorenz et al., 1993), and 24 weeks for humans (Lorenz et al., 1992). Initially regenerative skin healing in fetuses was attributed to the womb environment, but experiments showed that it is an intrinsic feature of fetal skin rather than the uterine environment. Injuries made in adult sheepskin that had been grafted onto fetal lambs and perfused with fetal blood healed with scars. Conversely, fetal marsupials that developed outside the uterine environment heal wounds scarlessly (Armstrong and Ferguson, 1995).

Postinjured fetal skin ECM composition differs significantly from that of adult skin ECM (Colwell et al., 2005). Fetal skin regenerative healing shows rapid and greater collagen accumulation compared to newborns and adults (Table 14.1) (Adzick et al., 1985). Although hypoxia generally leads to decreased hydroxyproline accumulation and fetuses are hypoxemic during normal development, more rapid collagen deposition has been observed during fetal skin wound healing (Larson et al., 2010; Lo et al., 2012; Longaker et al., 1990). Furthermore, the ratio between collagen III and I deposition are higher for fetuses than postinjured adult tissues. Moreover, collagen fiber deposition in postinjured fetal skin are formed in a reticular patter characteristic for uninjured tissues (Table 14.1) (Colwell et al., 2005; Cuttle et al., 2005). The ECM of fetal wounds is rich in hyaluronic acid (HA), which sustains longer than in adult wounds. MMPs and their tissue inhibitors (TIMPs) modulate the ECM during skin wound repair. The higher ratio of MMP to TIMP expression in regenerating mammalian fetus skin suggests rapid collagen degradation over collagen accumulation processes to prevent scar formation (Dang et al., 2003a). Specifically, increased expression of MMP9, the marker of limb regeneration in amphibians, has been detected during fetal skin regeneration (Table 14.1) (Peled et al., 2002).

The regenerative ability of fetal skin has been attributed to differences in the expression of growth factors (e.g., TGFβ, PDGF, VEGF, FGF) (Table 14.1). Among them, the TGFβ family shows substantial differences

in expression between fetal and adult skin (Walraven et al., 2014). Embryonic wounds are characterized by high levels of TGFβ3 (antiscarring) and low levels of TGFβ1 and TGFβ2 (proscarring) (Table 14.1) (Ferguson and O'Kane, 2004; Ferguson et al., 2009).

There are convincing data that the capacity for skin regeneration is probably inherent to fetal skin. Comparisons between uninjured adult and fetal skin revealed several differences (Table 14.1) (Beanes et al., 2001; Coolen et al., 2010). The expression profiles of keratin 17 (K17), involucrin, dermal Ki-67, fibronectin, and chondroitin sulfate were higher in human fetal than adult skin (Coolen et al., 2010). Microarray analysis of gene profile expression in cultured keratinocytes and dermal fibroblasts collected before and after scarless/scarring transition revealed 546 differently expressed genes (Hu et al., 2014a). Among 60 signaling pathways that are differently regulated, β-catenin-dependent Wnt pathways appear to be key regulators of embryonic wound healing (Hu et al., 2014a).

Although, the mechanisms that underline the scarless skin repair in fetuses are unknown, the phenomenon has been linked to the low or absent inflammatory response (Table 14.1) (Adzick and Lorenz, 1994; Barrientos et al., 2008; Hsu et al., 2001; Olutoye et al., 1996). For example, the introduction of inflammation into normally scarless wounds produces scars (Dang et al., 2003b). On the phylogenetic ladder, immune system complexity appears to relate reciprocally to the regenerative capacities in vertebrate species (Harty et al., 2003). High regenerative capacities in fish and amphibians are reduced in reptiles and nearly absent in birds and mammals (Brockes et al., 2001). This relationship seems to be repeated in mammalian ontogeny according to the recapitulation rule that ontogeny is a shortened version of phylogeny. Mammalian fetuses can regenerate/scarlessly heal skin incisions up to the third trimester of gestation, the time when mature, single-positive T lymphocytes appear. For example, in rats, CD4-/CD8+ and CD4+/CD8- cells are observed on fetal days 18–19 and 20–21, respectively (Vicente et al., 1998). Additionally, it has been demonstrated that diminished inflammation is a key feature of the privileged repair of oral mucosa (scarless) (Szpaderska et al., 2003).

Since fetal regenerative ability is common for all mammals, the spectrum for experimental choices seems great. However, short gestation periods, together with very short postoperative/experimental time for small animals and technically challenging surgical manipulation, impose some limitations. Large animals, such as pigs or sheep with longer intrauterine periods, are more approachable; however, fewer molecular tools and higher housing cost are limitations of these species. Besides fetal skin changes dramatically with development, making it is difficult to distinguish between ongoing developmental changes and skin wound healing processes.

3.2.2 Acomys

Although adult mammalian skin generally possesses very limited regenerative ability, some representatives of this class are not completely without regenerative talents. African spiny mice (Acomys) represent a unique example of skin regeneration in large full-thickness wounds and demonstrate a unique ability for skin autotomy in the class Mammalia (Seifert et al., 2012a).

Acomys species belong to the subfamily Deomynae, not Murinae, and while there are many phenotypic similarities between them and Mus musculus, phylogenetically this genus is more related to gerbils (Gerbillinae) than true mice (Chevret et al., 1993). The genus Acomys includes at least eight species of small rodents found exclusively in Africa (Chevret et al., 1993). Two recently intensively studied species Acomys percivali and Acomys kempi (Seifert et al., 2012a), are reported to be capable of skin autotomy due to weak skin that easily tears from the body, which is presumably an antipredator behavior.

Recent studies carried out by Seifert et al. (2012a) revealed that African spiny mouse skin is 20 times weaker than the skin of lab mice, and 77 times less energy is required to break it. Interestingly, cellular features of Acomys skin is anatomically comparable to that observed in other rodents and there is no sign of evidence of a fracture plane attributed to skin autotomy in some lizards (Bauer and Lamb, 2005; Sanggaard et al., 2012). Moreover, the abundance of elastin fibers responsible for skin elasticity is reported to be similar among M. musculus, A. percivali, and A. kempi. Apparently, the main difference in skin morphology between these rodents concerns the size of hair follicles, which is greater in spiny mice (55.61 ± 4.28%) compared to lab mice (43.65 ± 4.62%). Large hair follicles in Acomys reduce the total content of connective tissue, probably contributing to lower skin flexibility and reduced resistance to mechanical tension.

The regenerative responses of spiny mouse to 4-mm, 15-mm (Seifert et al., 2012a), and 8-mm (Brant et al., 2016) full-thickness skin wounds significantly differs from that of scarring M. musculus. In wounds of all investigated sizes made for spiny mice, scab formation and shedding was rapid and completed several days before lab mice. Large (15-mm) wounds reduced the area by 64 ± 3.1% within 24 h after injury, whereas small ones (4-mm) reepithelialized completely by day 3 after wounding, at a rate not observed in M. musculus. By day 10, Acomys wounds had looser vasculature networks and far fewer cells with the matrix (Brant et al., 2016). Moreover, the ECM was dominated by collagen type III, whereas collagen type I was more abundant in M. musculus. Collagen fibers were also less densely packed and contained more porous structures in Acomys (Table 14.1) (Seifert et al., 2012a), a finding that could explain the regenerative fashion of healing in this genus. Interestingly, newly regenerated hair follicles were observed in uncontracted areas of the wound bed (Seifert et al., 2012a; Brant et al., 2016), and

they expressed embryonic cytokeratins, Wnt, and BMP signaling pathway elements (Seifert et al., 2012a). By the end of third week, the wound beds in *Acomys* were deeply penetrated with new hair follicles and developing sebaceous glands (Brant et al., 2016). In addition, unlike *M. musculus*, the third spiny mice species *Acomys cahrinus* also demonstrated a remarkable capacity to repair full-thickness 4-mm circular punches in the ear; Santos et al. (2016) reported that these were completely closed within 2 months. Ear tissue regeneration involved, not only skin (epidermis, dermis) but also cartilage, adipose tissue, hair follicles, and sebaceous glands. Histological studies of dorsal skin and ear pinna regeneration in *Acomys* revealed similar features with blastemal formation, suggesting that enormous regenerative ability of skin might be associated with blastemal-like tissue formation (Seifert et al., 2012a).

Brant et al. (2016) reported that several fundamental immune differences distinguish wound healing of African spiny mice from *M. musculus*. First, *Acomys* are neutropenic, and there is vast decrease in the number of neutrophils (6.7%) in the blood compared to lab mice (32%). Second, in normal (unwounded) *Acomys* skin there was a 3.5-fold increase in mast cells per unit area compared to *Mus* skin (Table 14.1). Similar up regulation of mast cells was reported following wounding in spiny mice. Third, mature macrophages (detected by F4/80 antibody) were not detected in *Acomys* wounds, whereas in *Mus* they were present at all stages of healing. However, MOMA-2, another marker of monocytes/macrophages, exhibited similar distributions in both *Acomys* and *Mus*. The lack of macrophages in the wound bed reflects reduced levels (or even absence) of many cytokines typically present in skin wounds. As many as 18 cytokines present in *Mus* were undetectable in *Acomys* (e.g., GM-CSF, G-CSF, CXCL10-11, IL-2, -4, -6, TIMP), 5 were present at similar levels in both rodents (e.g., IL-1α, -1β), and only 1 chemokine (C–C motif) ligand 5 (RANTES) (Table 14.1) was upregulated in spiny mice (Brant et al., 2016). Both the immunodeficiency of selected cell types and the absence of proinflammatory factors favor regeneration over fibrosis, improve wound healing, and guide this process toward the regenerative route. Proteomic data (Brant et al., 2015) and microarray analysis (Brant et al., 2015) carried out on *Acomys* and *Mus* skin 3, 5, 7, and 14 days after wounding indicated a moderated immune response in spiny mice, low cytokine (e.g., IL-1β, IL-4) and chemokine gene expression, and significant upregulation of collagen types III and V (COL3a1, COL5a1, COL5a2) (Table 14.1) (Brant et al., 2015). Similar to fetal wounds, spiny mice had significantly higher levels of MMP2 and MMP9 and lower expression of TIMP1 compared to *Mus* (Table 14.1) (Brant et al., 2015). These data indicate that a low immune reaction together with peculiar ECM composition underlie scarless wound healing in *Acomys*, and there are many similarities to the process in mammal fetuses.

4 GENETIC MOUSE MODELS FOR REGENERATIVE SKIN WOUND HEALING (TRANSCRIPTION FACTORS IN SKIN DEVELOPMENT AND REGENERATION)

A growing number of studies based on genome-wide analysis of gene expression aims to disseminate group of transcription factors that are crucial in regulating/redirecting reparative versus regenerative skin healing. Followed studies conducted on genetically modified mice systematically uncover the signaling pathways that are differentially regulated during scarless and scar-forming skin healing. Particularly transcription factors that belong to the large families of *Fox* (forkhead box), *Hox* (homeobox), and *Ovol* genes appear to be involved in regenerative versus reparative skin healing regulation.

4.1 Fox (Forkhead Box) Transcription Factor Family

4.1.1 Foxn1-Deficient (Nude) Mice

The unusual ability of skin healing in nude mice, described as a "plastic surgeon's dream" was observed by Barbul et al. (1989) during their study of the role of T lymphocytes in wound healing. Nude mice owe their name due to a lack of visible hair. They are immunodeficient as a result of thymus and T-cell deficiencies. Nehls et al. (1994) showed that this pleiotropic phenotype is the result of a point mutation in the transcription factor Foxn1, which is expressed in epithelial cells both in the thymus and skin. The initial evidence that nude mice exhibit a unique regenerative capacity was determined based on their ability to display scarless healing following ear hole—punches injuries (Gawronska-Kozak, 2004). Subsequent studies showed that skin wound healing in nude mice display characteristic features of regeneration, namely a lack of scar tissue formation, significantly different from control mice (Gawronska-Kozak et al., 2006). The skin wound healing process is also accelerated in nude mice. Rapid reepithelialization in nude postinjured skin is followed by faster granulation tissue formation/resolution compared with control mice (Gawronska-Kozak, 2011). The collagen content in nude mouse skin at postinjured day 21 had recovered to levels measured before injury, whereas control mice did not regain collagen content until day 36 (Fig. 14.1; Table 14.1; Gawronska-Kozak, 2011). The hypothesis that collagen turnover is accelerated in nude mice was further supported by the unusual expression patterns of MMPs, particularly MMP-9 and MMP-13, and their tissue inhibitor, TIMP1
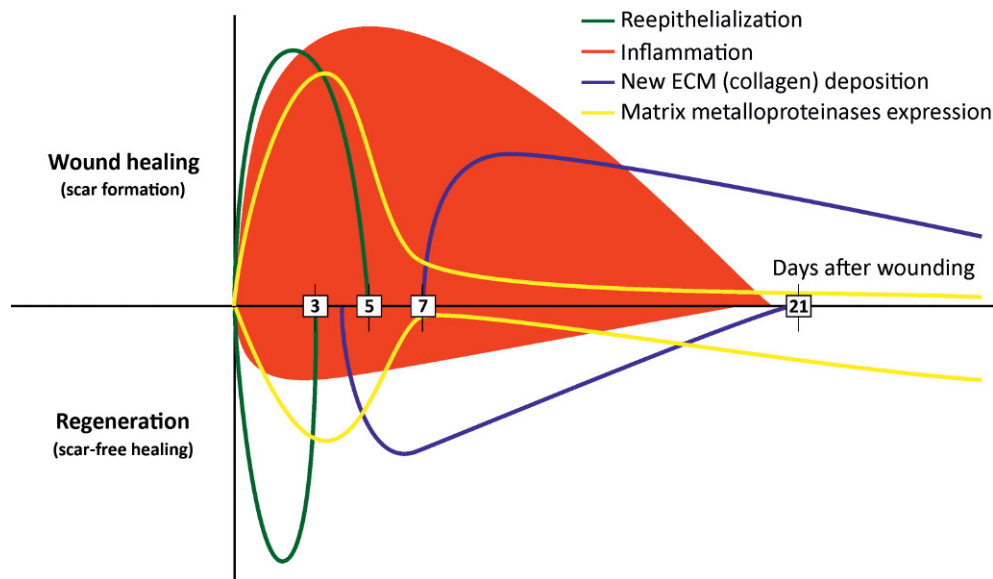
FIGURE 14.1 **Comparison of the magnitude and time span of wound healing phases between wild-type (scar-forming) and nude (scar-free) mice.** *ECM, Extracellular matrix. Source: Redrawn from Gawronska-Kozak, B., Grabowska, A., Kopcewicz, M., Kur, A., 2014. Animal models of skin regeneration. Reproduct. Biol. 14 (1), 61–67.*

(Gawronska-Kozak, 2011; Manuel and Gawronska-Kozak, 2006). The bimodal pattern of MMP-9 and MMP-13 in nude mice detected in the early and late (remodeling) healing phases was accompanied by low TIMP1 levels during the remodeling phase (Fig. 14.1, Table 14.1). Interestingly, MMP-9 expression during the first stage of wound healing is localized to the epidermis, whereas it was detected in dermal layer, particularly dermal fibroblasts, during the remodeling stage. A similar, bimodal array of MMPs expression was detected during limb regeneration in amphibians, and the authors associated it with antiscarring functionality (Vinarsky et al., 2005). The ECM of nude postinjured skin showed similarities with postinjured mammalian fetus skin with respect to high levels of HA and low levels of proscarring cytokines (TGFβ1 and PDGF), further supporting the regenerative ability of nude skin (Fig. 14.1, Table 14.1). Subsequent in vitro studies backed up in vivo data showing high expression of MMP-9 and MMP-13, as well as collagen types I and III, in nude mouse dermal fibroblasts, but not in controls fibroblasts (Gawronska-Kozak and Kirk-Ballard, 2013). Moreover, flow cytometric analysis of freshly isolated dermal fibroblasts showed that nude dermal fibroblasts express the stem cell markers CD117 and Oct3/4 (Gawronska-Kozak and Kirk-Ballard, 2013). To determine whether the regeneration phenotype of nude mice was associated with T-cell deficiency and/or lack of thymus, experiments were performed on several murine models of immunodeficiency: thymectomized young and adult mice, mice that lack T and B lymphocytes (SCID and Rag), and immunosuppressant-treated

mice (Gawronska-Kozak et al., 2006). The analysis of postinjured skin tissues showed an absence of scar tissue exclusively in nude mice. The study revealed that neither lack of the thymus nor T lymphocytes explains the regenerative phenotype in nude mice; although they do not exclude that an inflammatory response modulates skin wound healing. The nude phenotype in mice, rats, and humans is the consequence of Foxn1 inactivity. In the skin, Foxn1 expression was detected in the hair follicles and interfollicular epidermal cells where it localized to the first layer of supra-basal cells and to a few basal cells in the epidermis (Lee et al., 1999). In uninjured skin, Foxn1 appears to govern the balance between proliferation and differentiation, promoting keratinocyte differentiation; it stimulates signal transduction between melanocytes and keratinocytes and participates in hair follicle development (Lee et al., 1999; Weiner et al., 2014). Recent data showed that Foxn1-bearing cells participate in the wound healing process through engagement in reepithelialization and possible involvement in scar formation due to Foxn1 activity during the epithelial-to-mesenchymal transition (EMT) (Gawronska-Kozak et al., 2016). Collectively, the data point to Foxn1 as a regulator of the skin's regenerative capacity.

Next-generation high-throughput DNA sequencing analysis showed similarities in skin gene signatures between mice fetuses and adult Foxn1-deficient mice (unpublished data). Moreover, the data revealed that Foxn1-deficient skin shows changes in the expression of other transcription factors associated with skin wound healing including the Hox family, Foxo, and Ovol.

4.1.2 FOXO Transcription Factor Subfamily

The mammalian forkhead box O (FOXO) subfamily belongs to a large family of transcription factors characterized by a conserved DNA binding domain and consists of FOXO1, FOXO3A, FOXO4, and FOXO6 (Huang and Tindall, 2007). These proteins can regulate a huge variety of cellular processes (Accili and Arden, 2004; Barthel et al., 2005) including tissue repair (Lara-Pezzi et al., 2007; Snijders et al., 2009) and skin homeostasis (Roupe et al., 2010; Ponugoti et al., 2013; Mori et al., 2014; Zhang et al., 2015). Mori et al. (2014) indicated that in mice skin, both *Foxo1* and *Foxo3*a genes were up regulated days 3–7 after wounding, which is in agreement with a study carried out in a diabetic mice model (Siqueira et al., 2010). Moreover, Foxo1$^{+/-}$ mice exhibited many morphological and functional features indicating improving healing, including accelerated wound closure with enhanced keratinocyte migration, decreased granulation tissue formation, reduced densities of collagen types I and III, and reduced inflammatory responses at wound sites (Mori et al., 2014). In contrast, there are some reports that deletion of FOXO1 in keratinocytes significantly reduces the wound-healing rate (Ponugoti et al., 2013). Similarly, Zhang et al. (2015) demonstrated that normoglycemic transgenic mice with keratinocyte-specific Foxo1 deletion delays wound healing, whereas diabetic littermates exhibit improved skin repair. An in vitro study revealed reduced reepithelialization of "scratch" wounds under low glucose conditions in FOXO1-silenced cells, indicating that metabolic status is one of multiple factors contributing to wound healing. One of the primary mechanisms through which FOXO1 could enhance healing is upregulation of TGFβ1 and protection of keratinocytes from oxidative stress by regulating the expression of antioxidant genes and DNA repair enzymes (Ponugoti et al., 2013). In contrast, TNFα activates FOXO1 to impair the healing process in diabetic mice (Siqueira et al., 2010).

4.2 Homeobox Genes

Candidates for skin regenerative capacity include the homeobox genes, which can be divided into two large Hox and non-Hox families (Krumlauf, 1994). Homeodomain proteins are transcription factors that regulate tissue growth and development; they are involved in pattern formation during embryonic morphogenesis and organogenesis (Kessel and Gruss, 1990; Krumlauf, 1994) including skin development (Detmer et al., 1993; Stelnicki et al., 1997, 1998b). The various expression patterns of homeobox gene families define the regional identity of the skin (Yamaguchi et al., 2005).

4.2.1 Hox Gene Family

The *Hox* genes are arrayed in four genomic loci (A, B, C, D) and a variety of transcripts from each cluster have been reported in the epidermis of fetal (Detmer et al., 1993) and adult mouse (Bieberich et al., 1991) and human (Svingen and Tonissen, 2003) skin. Interestingly, higher Hox gene expression was observed in fetal versus adult skin and tended to be restricted to keratinocytes rather than dermal fibroblasts where they participate in both cell proliferation (Komuves et al., 2002) and differentiation (Tkatchenko et al., 2001). In human fetal skin downregulation of HoxB13 may affect scarless wound healing (Potter et al., 2011). This observation was supported by the HoxB13 KO mice wound model that exhibited several cellular (e.g., faster closure) and biochemical (e.g., higher HA levels) features of early gestational wounds (Mack et al., 2003). Different genetic approaches have documented that Hoxd3 (Uyeno et al., 2001) and Hoxd8 (Jain et al., 2008) are able to modulate cellular behavior during wound healing. Recent data revealed that Hoxc13-null mice and Foxn1 (nude)-deficient mice have similar defects of skin appendages. Furthermore, downregulation of *Foxn1* in the skin of Hoxc13-null mice accompanied by reduced keratin gene levels suggests the existence of a Hoxc13 regulatory network of hair shaft differentiation (Potter et al., 2011).

4.2.2 Non-Hox Gene Family

Studies carried out on adult human skin revealed that non-Hox genes (MSX-1, MSX-2, MOX-1) are dominant regulators of dermal layer functional features (Stelnicki et al., 1997). Similarly to Hox genes, such as Hox b13, the non-Hox representative Prx2 was shown to be highly expressed in fetal dermal fibroblasts and were further induced during fetal wounding, whereas this response was not observed in adult skin (Stelnicki et al., 1998a). Cultured fibroblasts derived from Prx2$^{-/-}$ mice revealed substantial changes in pro-MMP2 expression, increased HA production, and ECM reorganization in three-dimensional collagen discs (White et al., 2003).

The non-Hox genes Msx1 and Msx2 play key roles in the development of both skin (Stelnicki et al., 1997) and hair shafts (Cai et al., 2009; Ma et al., 2003) and are suggested to be strong regulators of tissue capacity to heal wounds (Carlson et al., 1998) and regenerate digit tips in mice (Han et al., 2003; Muneoka et al., 2008). A study by Yeh et al. (2009) of genetically modified mice revealed several features indicating that Msx2 regulates cellular competence during wound repair. Msx2 null mice exhibited faster reepithelialization and wound closure, earlier appearance of cell differentiation-related keratins (K10, K14), and increased expression of αSMA and tenascin-T in granulation tissue. Additionally, in vitro studies revealed faster migratory ability and enhanced collagen matrix contraction by Msx2 null keratinocytes compared to wild-type controls. Furthermore Msx2 mutation reduced the expression of Foxn1 and its target gene acidic

keratin mHa3 (Ma et al., 2003), and both transcription factors are required to maintain Notch1 expression in the hair follicle matrix (Cai et al., 2009).

4.3 Ovol Transcription Factor Family

The Ovol family constitutes evolutionarily conserved zinc-finger transcription factors among which two members Ovol1 and Ovol2 are reported to act downstream of key developmental pathways, such as Wnt, EGF, and BMP (Dai et al., 1998). Both factors are expressed in multiple somatic epithelial tissues, including skin and hair follicles. Ovol2 mRNA level increased from embryonic day E13.5 to 16.5 in mice (Lee et al., 2014). Ovol1- and Ovol2-null mouse models exhibit epithelial abnormalities, such as hyperproliferative epidermis, expansion of K1-positive cells (Nair et al., 2006), and death during midgestation (E10.5) (Mackay et al., 2006). Interestingly, genetic approaches revealed that Ovol2 provides a compensatory function for the loss of Ovol1 (Teng et al., 2007; Lee et al., 2014). Ovol1/Ovol2 epidermal-deficient mice lack proper cytoskeletal reestablishment, resulting in and defective terminal differentiation and alterations indicating EMT (Lee et al., 2014). Furthermore, the same study revealed that Ovol2 overexpression in the epidermal basal layer and outer root sheath reduces stem/progenitor cells in mice embryo skin.

5 CONCLUSIONS

This chapter provides an overview on vertebrate models for skin regeneration, showing that among all classes, there are wild-type examples of regenerative skin healing. For more than 30 years, only mammalian fetuses were thought to be capable of regenerative skin healing. Detailed studies yielded a great amount of knowledge of fetal wound repair/regeneration involving growth factors, cytokines, ECM, and other factors. Recent discoveries that *Acomys* and Foxn1-deficient mice are capable of skin scar-free healing indicate that adult mammals also possess the molecular machinery for regeneration. The skin scar-free healing characteristic of wild-living *Acomys* permits the study of naturally occurring regenerative susceptibilities. Foxn1, Ovol, and Foxo transgenic mice have focused attention onto transcription factors that may be modulated to redirect repair into regeneration. The comparison of global gene expression between reparative and regenerative models consistently shows that the greater number of down- versus upregulated genes in regenerative skin tissues supports the concept proposed by Mercer and coworkers; that is, the large number of downregulated genes suggests that the loss of their activity is involved in regeneration induction

and maintenance (Mercer et al., 2012). Moreover, comparison of the genetic profile of skin between mouse fetuses at the scar-free healing period to Foxn1 deficient mice showed similarities in transcriptional factor genes expression. Potentially, these transcription factors may be involved in directional skin wound healing resolution (Gawronska-Kozak, unpublished data). Determining whether fetal skin immaturity has an absence of particular transcriptional factors expression as observed for Foxn1- (Gawronska-Kozak, 2004, 2011; Gawronska-Kozak et al., 2006), Ovol1- (Teng et al., 2007), Msx2- (Yeh et al., 2009), and Foxo- (Mori et al., 2014) deficient mice is one of the road maps for creating an environment suitable for regeneration.

References

Accili, D., Arden, K.C., 2004. FoxOs at the crossroads of cellular metabolism, differentiation, and transformation. Cell 117 (4), 421–426.

Adzick, N.S., Harrison, M.R., Glick, P.L., Beckstead, J.H., Villa, R.L., Scheuenstuhl, H., et al., 1985. Comparison of fetal, newborn, and adult wound healing by histologic, enzyme-histochemical, and hydroxyproline determinations. J. Pediatr. Surg. 20 (4), 315–319.

Adzick, N.S., Lorenz, H.P., 1994. Cells, matrix, growth factors, and the surgeon. The biology of scarless fetal wound repair. Ann. Surg. 220 (1), 10–18.

Armstrong, J.R., Ferguson, M.W., 1995. Ontogeny of the skin and the transition from scar-free to scarring phenotype during wound healing in the pouch young of a marsupial, *Monodelphis domestica*. Dev. Biol. 169 (1), 242–260.

Barbul, A., Shawe, T., Rotter, S.M., Efron, J.E., Wasserkrug, H.L., Badawy, S.B., 1989. Wound healing in nude mice: a study on the regulatory role of lymphocytes in fibroplasia. Surgery 105 (6), 764–769.

Barrientos, S., Stojadinovic, O., Golinko, M.S., Brem, H., Tomic-Canic, M., 2008. Growth factors and cytokines in wound healing. Wound Repair Regen. 16 (5), 585–601.

Barthel, A., Schmoll, D., Unterman, T.G., 2005. FoxO proteins in insulin action and metabolism. Trends Endocrinol. Metab. 16 (4), 183–189.

Bauer, A.M., Lamb, T., 2005. Phylogenetic relationships of southern African geckos in the Pachydactylus group (Squamata : Gekkonidae). Afr. J. Herpetol. 54 (2), 105–129.

Beanes, S.R., Dang, C., Soo, C., Wang, Y., Urata, M., Ting, K., et al., 2001. Down-regulation of decorin, a transforming growth factor-beta modulator, is associated with scarless fetal wound healing. J. Pediatr. Surg. 36 (11), 1666–1671.

Bertolotti, E., Malagoli, D., Franchini, A., 2013. Skin wound healing in different aged *Xenopus laevis*. J. Morphol. 274 (8), 956–964.

Bieberich, C.J., Ruddle, F.H., Stenn, K.S., 1991. Differential expression of the Hox 3.1 gene in adult mouse skin. Ann. NY Acad. Sci. 642, 346–353, discussion 353.

Bielefeld, K.A., Amini-Nik, S., Alman, B.A., 2013. Cutaneous wound healing: recruiting developmental pathways for regeneration. Cell. Mol. Life Sci. 70 (12), 2059–2081.

Brant, J.O., Lopez, M.C., Baker, H.V., Barbazuk, W.B., Maden, M., 2015. A Comparative analysis of gene expression profiles during skin regeneration in mus and acomys. PLoS One 10 (11), e0142931.

Brant, J.O., Yoon, J.H., Polvadore, T., Barbazuk, W.B., Maden, M., 2016. Cellular events during scar-free skin regeneration in the spiny mouse, Acomys. Wound Repair Regen. 24 (1), 75–88.

Brockes, J.P., Kumar, A., Velloso, C.P., 2001. Regeneration as an evolutionary variable. J. Anat. 199 (Pt. 1–2), 3–11.

Bryan, D., Walker, K.B., Ferguson, M., Thorpe, R., 2005. Cytokine gene expression in a murine wound healing model. Cytokine 31 (6), 429–438.

Cai, J., Lee, J., Kopan, R., Ma, L., 2009. Genetic interplays between Msx2 and Foxn1 are required for Notch1 expression and hair shaft differentiation. Dev. Biol. 326 (2), 420–430.

Carlson, M.R., Bryant, S.V., Gardiner, D.M., 1998. Expression of Msx-2 during development, regeneration, and wound healing in axolotl limbs. J. Exp. Zool. 282 (6), 715–723.

Cass, D.L., Sylvester, K.G., Yang, E.Y., Crombleholme, T.M., Adzick, N.S., 1997. Myofibroblast persistence in fetal sheep wounds is associated with scar formation. J. Pediatr. Surg. 32 (7), 1017–1021, discussion 1021.

Chevret, P., Denys, C., Jaeger, J.J., Michaux, J., Catzeflis, F.M., 1993. Molecular evidence that the spiny mouse (Acomys) is more closely related to gerbils (Gerbillinae) than to true mice (Murinae). Proc. Natl. Acad. Sci. USA 90 (8), 3433–3436.

Clark, R., 1996. The Molecular and Cellular Biology of Wound Repair. Plenum Press, New York.

Clark, L.D., Clark, R.K., Heber-Katz, E., 1998. A new murine model for mammalian wound repair and regeneration. Clin. Immunol. Immunopathol. 88 (1), 35–45.

Colwell, A.S., Longaker, M.T., Lorenz, H.P., 2005. Mammalian fetal organ regeneration. Adv. Biochem. Eng. Biotechnol. 93, 83–100.

Coolen, N.A., Schouten, K.C., Middelkoop, E., Ulrich, M.M., 2010. Comparison between human fetal and adult skin. Arch. Dermatol. Res. 302 (1), 47–55.

Couper, K.N., Blount, D.G., Riley, E.M., 2008. IL-10: the master regulator of immunity to infection. J. Immunol. 180 (9), 5771–5777.

Cowin, A.J., Brosnan, M.P., Holmes, T.M., Ferguson, M.W., 1998. Endogenous inflammatory response to dermal wound healing in the fetal and adult mouse. Dev. Dyn. 212 (3), 385–393.

Cunha da Silva, J.R., Cooper, E.L., Sinhorini, I.L., Borges, J.C., Jensch-Junior, B.E., Porto-Neto, L.R., et al., 2005. Microscopical study of experimental wound healing in Notothenia coriiceps (Cabecuda) at 0 degrees C. Cell Tissue Res. 321 (3), 401–410.

Cuttle, L., Nataatmadja, M., Fraser, J.F., Kempf, M., Kimble, R.M., Hayes, M.T., 2005. Collagen in the scarless fetal skin wound: detection with picrosirius-polarization. Wound Repair Regen. 13 (2), 198–204.

Dai, X., Schonbaum, C., Degenstein, L., Bai, W., Mahowald, A., Fuchs, E., 1998. The ovo gene required for cuticle formation and oogenesis in flies is involved in hair formation and spermatogenesis in mice. Genes Dev. 12 (21), 3452–3463.

Dang, C.M., Beanes, S.R., Lee, H., Zhang, X., Soo, C., Ting, K., 2003a. Scarless fetal wounds are associated with an increased matrix metalloproteinase-to-tissue-derived inhibitor of metalloproteinase ratio. Plast. Reconstr. Surg. 111 (7), 2273–2285.

Dang, C., Ting, K., Soo, C., Longaker, M.T., Lorenz, H.P., 2003b. Fetal wound healing current perspectives. Clin. Plast. Surg. 30 (1), 13–23.

Delorme, S.L., Lungu, I.M., Vickaryous, M.K., 2012. Scar-free wound healing and regeneration following tail loss in the leopard gecko, Eublepharis macularius. Anat. Rec. (Hoboken) 295 (10), 1575–1595.

Detmer, K., Lawrence, H.J., Largman, C., 1993. Expression of class I homeobox genes in fetal and adult murine skin. J. Invest. Dermatol. 101 (4), 517–522.

Endo, T., Bryant, S.V., Gardiner, D.M., 2004. A stepwise model system for limb regeneration. Dev. Biol. 270 (1), 135–145.

Ferguson, M.W., Duncan, J., Bond, J., Bush, J., Durani, P., So, K., et al., 2009. Prophylactic administration of avotermin for improvement of skin scarring: three double-blind, placebo-controlled, phase I/II studies. Lancet 373 (9671), 1264–1274.

Ferguson, M.W., O'Kane, S., 2004. Scar-free healing: from embryonic mechanisms to adult therapeutic intervention. Philos. Trans. R. Soc. Lond. B Biol. Sci. 359 (1445), 839–850.

Fernando, W.A., Leininger, E., Simkin, J., Li, N., Malcom, C.A., Sathyamoorthi, S., et al., 2011. Wound healing and blastema formation in regenerating digit tips of adult mice. Dev. Biol. 350 (2), 301–310.

Gawronska-Kozak, B., 2004. Regeneration in the ears of immunodeficient mice: identification and lineage analysis of mesenchymal stem cells. Tissue Eng. 10 (7–8), 1251–1265.

Gawronska-Kozak, B., 2011. Scarless skin wound healing in FOXN1 deficient (nude) mice is associated with distinctive matrix metalloproteinase expression. Matrix Biol. 30 (4), 290–300.

Gawronska-Kozak, B., Bogacki, M., Rim, J.S., Monroe, W.T., Manuel, J.A., 2006. Scarless skin repair in immunodeficient mice. Wound Repair Regen. 14, 265–276.

Gawronska-Kozak, B., Grabowska, A., Kur-Piotrowska, A., Kopcewicz, M., 2016. Foxn1 transcription factor regulates wound healing of skin through promoting epithelial-mesenchymal transition. PLoS One 11 (3), e0150635.

Gawronska-Kozak, B., Kirk-Ballard, H., 2013. Cyclosporin A reduces matrix metalloproteinases and collagen expression in dermal fibroblasts from regenerative FOXN1 deficient (nude) mice. Fibrogen. Tissue Repair 6 (1), 7.

Goss, R.J., Grimes, L.N., 1975. Epidermal downgrowths in regenerating rabbit ear holes. J. Morphol. 146 (4), 533–542.

Groff, J.M., 2001. Cutaneous biology and diseases of fish. Vet. Clin. North Am. Exot. Anim. Pract. 4 (2), 321–411, v–vi.

Guerra, R.R., Santos, N.P., Cecarelli, P., Mangetti, A.J., Silva, J.R., Hernandez-Blazquez, F.J., 2006. Stratum adiposum, a special structure of the African Catfish skin (Clarias gariepinus, Burchell 1822). Anat. Histol. Embryol. 35 (3), 144–146.

Guerra, R.R., Santos, N.P., Cecarelli, P., Silva, J.R.M.C., Hernandez-Blazquez, F.J., 2008. Healing of skin wounds in the African catfish Clarias gariepinus. J. Fish Biol. 73 (3), 572–583.

Han, M., Yang, X., Farrington, J.E., Muneoka, K., 2003. Digit regeneration is regulated by Msx1 and BMP4 in fetal mice. Development 130 (21), 5123–5132.

Harty, M., Neff, A.W., King, M.W., Mescher, A.L., 2003. Regeneration or scarring: an immunologic perspective. Dev. Dyn. 226 (2), 268–279.

Hinz, B., 2007. Formation and function of the myofibroblast during tissue repair. J. Invest. Dermatol. 127 (3), 526–537.

Hsu, M., Peled, Z.M., Chin, G.S., Liu, W., Longaker, M.T., 2001. Ontogeny of expression of transforming growth factor-beta 1 (TGF-beta 1), TGF-beta 3, and TGF-beta receptors I and II in fetal rat fibroblasts and skin. Plast. Reconstr. Surg. 107 (7), 1787–1794, discussion 1795.

Hu, M.S., Januszyk, M., Hong, W.X., Walmsley, G.G., Zielins, E.R., Atashroo, D.A., et al., 2014a. Gene expression in fetal murine keratinocytes and fibroblasts. J. Surg. Res. 190 (1), 344–357.

Hu, M.S., Rennert, R.C., McArdle, A., Chung, M.T., Walmsley, G.G., Longaker, M.T., et al., 2014b. The role of stem cells during scarless skin wound healing. Adv. Wound Care (New Rochelle) 3 (4), 304–314.

Huang, H., Tindall, D.J., 2007. Dynamic FoxO transcription factors. J. Cell Sci. 120 (Pt. 15), 2479–2487.

Hubner, G., Brauchle, M., Smola, H., Madlener, M., Fassler, R., Werner, S., 1996. Differential regulation of pro-inflammatory cytokines during wound healing in normal and glucocorticoid-treated mice. Cytokine 8 (7), 548–556.

Ihara, S., Motobayashi, Y., Nagao, E., Kistler, A., 1990. Ontogenetic transition of wound healing pattern in rat skin occurring at the fetal stage. Development 110 (3), 671–680.

Jain, K., Sykes, V., Kordula, T., Lanning, D., 2008. Homeobox genes Hoxd3 and Hoxd8 are differentially expressed in fetal mouse excisional wounds. J. Surg. Res. 148 (1), 45–48.

Kessel, M., Gruss, P., 1990. Murine developmental control genes. Science 249 (4967), 374–379.

Komuves, L.G., Michael, E., Arbeit, J.M., Ma, X.K., Kwong, A., Stelnicki, E., et al., 2002. HOXB4 homeodomain protein is expressed in

developing epidermis and skin disorders and modulates keratino-cyte proliferation. Dev. Dyn. 224 (1), 58–68.

Kragl, M., Knapp, D., Nacu, E., Khattak, S., Maden, M., Epperlein, H.H., et al., 2009. Cells keep a memory of their tissue origin during axolotl limb regeneration. Nature 460 (7251), 60–65.

Krumlauf, R., 1994. Hox genes in vertebrate development. Cell 78 (2), 191–201.

Lara-Pezzi, E., Winn, N., Paul, A., McCullagh, K., Slominsky, E., Santini, M.P., et al., 2007. A naturally occurring calcineurin variant inhibits FoxO activity and enhances skeletal muscle regeneration. J. Cell Biol. 179 (6), 1205–1218.

Larson, B.J., Longaker, M.T., Lorenz, H.P., 2010. Scarless fetal wound healing: a basic science review. Plast. Reconstr. Surg. 126 (4), 1172–1180.

Lee, D., Prowse, D.M., Brissette, J.L., 1999. Association between mouse nude gene expression and the initiation of epithelial terminal differentiation. Dev. Biol. 208 (2), 362–374.

Lee, B., Villarreal-Ponce, A., Fallahi, M., Ovadia, J., Sun, P., Yu, Q.C., et al., 2014. Transcriptional mechanisms link epithelial plasticity to adhesion and differentiation of epidermal progenitor cells. Dev. Cell. 29 (1), 47–58.

Levesque, M., Villiard, E., Roy, S., 2010. Skin wound healing in axolotls: a scarless process. J. Exp. Zool. B Mol. Dev. Evol. 314 (8), 684–697.

Liechty, K.W., Adzick, N.S., Crombleholme, T.M., 2000. Diminished interleukin 6 (IL-6) production during scarless human fetal wound repair. Cytokine 12 (6), 671–676.

Lo, D.D., Zimmermann, A.S., Nauta, A., Longaker, M.T., Lorenz, H.P., 2012. Scarless fetal skin wound healing update. Birth Def. Res. C 96 (3), 237–247.

Longaker, M.T., Whitby, D.J., Adzick, N.S., Crombleholme, T.M., Langer, J.C., Duncan, B.W., et al., 1990. Studies in fetal wound healing, VI. Second and early third trimester fetal wounds demonstrate rapid collagen deposition without scar formation. J. Pediatr. Surg. 25 (1), 63–68, discussion 69.

Longaker, M.T., Chiu, E.S., Adzick, N.S., Stern, M., Harrison, M.R., Stern, R., 1991. Studies in fetal wound healing. V. A prolonged presence of hyaluronic acid characterizes fetal wound fluid. Ann. Surg. 213 (4), 292–296.

Lorenz, H.P., Longaker, M.T., Perkocha, L.A., Jennings, R.W., Harrison, M.R., Adzick, N.S., 1992. Scarless wound repair: a human fetal skin model. Development 114 (1), 253–259.

Lorenz, H.P., Whitby, D.J., Longaker, M.T., Adzick, N.S., 1993. Fetal wound healing. The ontogeny of scar formation in the non-human primate. Ann. Surg. 217 (4), 391–396.

Ma, L., Liu, J., Wu, T., Plikus, M., Jiang, T.X., Bi, Q., et al., 2003. 'Cyclic alopecia' in Msx2 mutants: defects in hair cycling and hair shaft differentiation. Development 130 (2), 379–389.

Mack, J.A., Abramson, S.R., Ben, Y., Coffin, J.C., Rothrock, J.K., Maytin, E.V., et al., 2003. Hoxb13 knockout adult skin exhibits high levels of hyaluronan and enhanced wound healing. FASEB J. 17 (10), 1352–1354.

Mackay, D.R., Hu, M., Li, B., Rheaume, C., Dai, X., 2006. The mouse Ovol2 gene is required for cranial neural tube development. Dev. Biol. 291 (1), 38–52.

Madlener, M., Parks, W.C., Werner, S., 1998. Matrix metalloproteinases (MMPs) and their physiological inhibitors (TIMPs) are differentially expressed during excisional skin wound repair. Exp. Cell Res. 242 (1), 201–210.

Manuel, J.A., Gawronska-Kozak, B., 2006. Matrix metalloproteinase 9 (MMP-9) is upregulated during scarless wound healing in athymic nude mice. Matrix Biol. 25, 505–514.

McCusker, C., Gardiner, D.M., 2011. The axolotl model for regeneration and aging research: a mini-review. Gerontology 57 (6), 565–571.

Mercer, S.E., Cheng, C.H., Atkinson, D.L., Krcmery, J., Guzman, C.E., Kent, D.T., et al., 2012. Multi-tissue microarray analysis identifies a molecular signature of regeneration. PLoS One 7 (12), e52375.

Mittal, A.K., Munshi, J.S., 1974. On the regeneration and repair of superficial wounds in the skin of *Rita rita* (Ham.) (Bagridae, Pisces). Acta Anat. (Basel) 88 (3), 424–442.

Mori, R., Tanaka, K., de Kerckhove, M., Okamoto, M., Kashiyama, K., Kim, S., et al., 2014. Reduced FOXO1 expression accelerates skin wound healing and attenuates scarring. Am. J. Pathol. 184 (9), 2465–2479.

Muneoka, K., Han, M., Gardiner, D.M., 2008. Regrowing human limbs. Sci. Am. 298 (4), 56–63.

Nair, M., Teng, A., Bilanchone, V., Agrawal, A., Li, B., Dai, X., 2006. Ovol1 regulates the growth arrest of embryonic epidermal progenitor cells and represses c-myc transcription. J. Cell Biol. 173 (2), 253–264.

Nehls, M., Pfeifer, D., Schorpp, M., Hedrich, H., Boehm, T., 1994. New member of the winged-helix protein family disrupted in mouse and rat nude mutations. Nature 372 (6501), 103–107.

Ogawa, K., Kobayashi, C., Hayashi, T., Orii, H., Watanabe, K., Agata, K., 2002. Planarian fibroblast growth factor receptor homologs expressed in stem cells and cephalic ganglions. Dev. Growth Differ. 44 (3), 191–204.

Ohira, Y., Shimizu, M., Ura, K., Takagi, Y., 2007. Scale regeneration and calcification in goldfish *Carassius auratus*: quantitative and morphological processes. Fish. Sci. 73 (1), 46–54.

Olutoye, O.O., Yager, D.R., Cohen, I.K., Diegelmann, R.F., 1996. Lower cytokine release by fetal porcine platelets: a possible explanation for reduced inflammation after fetal wounding. J. Pediatr. Surg. 31 (1), 91–95.

Peled, Z.M., Phelps, E.D., Updike, D.L., Chang, J., Krummel, T.M., Howard, E.W., et al., 2002. Matrix metalloproteinases and the ontogeny of scarless repair: the other side of the wound healing balance. Plast. Reconstr. Surg. 110 (3), 801–811.

Ponugoti, B., Xu, F., Zhang, C., Tian, C., Pacios, S., Graves, D.T., 2013. FOXO1 promotes wound healing through the up-regulation of TGF-beta1 and prevention of oxidative stress. J. Cell Biol. 203 (2), 327–343.

Poss, K.D., Keating, M.T., Nechiporuk, A., 2003. Tales of regeneration in zebrafish. Dev. Dyn. 226 (2), 202–210.

Potter, C.S., Pruett, N.D., Kern, M.J., Baybo, M.A., Godwin, A.R., Potter, K.A., et al., 2011. The nude mutant gene Foxn1 is a HOXC13 regulatory target during hair follicle and nail differentiation. J. Invest. Dermatol. 131 (4), 828–837.

Quilhac, A., Sire, J.Y., 1999. Spreading, proliferation, and differentiation of the epidermis after wounding a cichlid fish, *Hemichromis bimaculatus*. Anat. Rec. 254 (3), 435–451.

Richardson, R., Slanchev, K., Kraus, C., Knyphausen, P., Eming, S., Hammerschmidt, M., 2013. Adult zebrafish as a model system for cutaneous wound-healing research. J. Invest. Dermatol. 133 (6), 1655–1665.

Roupe, K.M., Alberius, P., Schmidtchen, A., Sorensen, O.E., 2010. Gene expression demonstrates increased resilience toward harmful inflammatory stimuli in the proliferating epidermis of human skin wounds. Exp. Dermatol. 19 (8), e329–332.

Sanggaard, K.W., Danielsen, C.C., Wogensen, L., Vinding, M.S., Rydtoft, L.M., Mortensen, M.B., et al., 2012. Unique structural features facilitate lizard tail autotomy. PLoS One 7 (12), e51803.

Santos, D.M., Rita, A.M., Casanellas, I., Brito Ova, A., Araújo, I.M., Power, D., Tiscornia, G., 2016. Ear wound regeneration in the African spiny mouse *Acomys cahirinus*. Regeneration 3, 52–61.

Satish, L., Kathju, S., 2010. Cellular and molecular characteristics of scarless versus fibrotic wound healing. Dermatol. Res. Pract. 2010, 790234.

Seifert, A.W., Kiama, S.G., Seifert, M.G., Goheen, J.R., Palmer, T.M., Maden, M., 2012a. Skin shedding and tissue regeneration in African spiny mice (Acomys). Nature 489 (7417), 561–565.

Seifert, A.W., Maden, M., 2014. New insights into vertebrate skin regeneration. Int. Rev. Cell Mol. Biol. 310, 129–169.

Seifert, A.W., Monaghan, J.R., Voss, S.R., Maden, M., 2012b. Skin regeneration in adult axolotls: a blueprint for scar-free healing in vertebrates. PLoS One 7 (4), e32875.

Siqueira, M.F., Li, J., Chehab, L., Desta, T., Chino, T., Krothpali, N., et al., 2010. Impaired wound healing in mouse models of diabetes is mediated by TNF-alpha dysregulation and associated with enhanced activation of forkhead box O1 (FOXO1). Diabetology 53 (2), 378–388.

Slominski, A.T., Zmijewski, M.A., Skobowiat, C., Zbytek, B., Slominski, R.M., Steketee, J.D., 2012. Sensing the environment: regulation of local and global homeostasis by the skin's neuroendocrine system. Adv. Anat. Embryol. Cell Biol. 212, 1–115, v, vii.

Snijders, T., Verdijk, L.B., van Loon, L.J., 2009. The impact of sarcopenia and exercise training on skeletal muscle satellite cells. Ageing Res. Rev. 8 (4), 328–338.

Somasundaram, K., Prathap, K., 1970. Intra-uterine healing of skin wounds in rabbit foetuses. J. Pathol. 100 (2), 81–86.

Soo, C., Shaw, W.W., Zhang, X., Longaker, M.T., Howard, E.W., Ting, K., 2000. Differential expression of matrix metalloproteinases and their tissue-derived inhibitors in cutaneous wound repair. Plast. Reconstr. Surg. 105 (2), 638–647.

Stelnicki, E.J., Komuves, L.G., Holmes, D., Clavin, W., Harrison, M.R., Adzick, N.S., et al., 1997. The human homeobox genes MSX-1, MSX-2, and MOX-1 are differentially expressed in the dermis and epidermis in fetal and adult skin. Differentiation 62 (1), 33–41.

Stelnicki, E.J., Komuves, L.G., Kwong, A.O., Holmes, D., Klein, P., Rozenfeld, S., et al., 1998b. HOX homeobox genes exhibit spatial and temporal changes in expression during human skin development. J. Invest. Dermatol. 110 (2), 110–115.

Stelnicki, E.J., Arbeit, J., Cass, D.L., Saner, C., Harrison, M., Largman, C., 1998a. Modulation of the human homeobox genes PRX-2 and HOXB13 in scarless fetal wounds. J. Invest. Dermatol. 111 (1), 57–63.

Svingen, T., Tonissen, K.F., 2003. Altered HOX gene expression in human skin and breast cancer cells. Cancer. Biol. Ther. 2 (5), 518–523.

Szpaderska, A.M., Zuckerman, J.D., DiPietro, L.A., 2003. Differential injury responses in oral mucosal and cutaneous wounds. J. Dent. Res. 82 (8), 621–626.

Takagi, R., Ishimaru, J., Sugawara, A., Toyoshima, K.E., Ishida, K., Ogawa, M., et al., 2016. Bioengineering a 3D integumentary organ system from iPS cells using an in vivo transplantation model. Sci. Adv. 2 (4), e1500887.

Teng, A., Nair, M., Wells, J., Segre, J.A., Dai, X., 2007. Strain-dependent perinatal lethality of Ovol1-deficient mice and identification of Ovol2 as a downstream target of Ovol1 in skin epidermis. Biochimica et Biophysica Acta 1772 (1), 89–95.

Tkatchenko, A.V., Visconti, R.P., Shang, L., Papenbrock, T., Pruett, N.D., Ito, T., et al., 2001. Overexpression of Hoxc13 in differentiating keratinocytes results in downregulation of a novel hair keratin gene cluster and alopecia. Development 128 (9), 1547–1558.

Ueno, M., Itoh, M., Sugihara, K., Asano, M., Takakura, N., 2009. Both alleles of PSF1 are required for maintenance of pool size of immature hematopoietic cells and acute bone marrow regeneration. Blood 113 (3), 555–562.

Uyeno, L.A., Newman-Keagle, J.A., Cheung, I., Hunt, T.K., Young, D.M., Boudreau, N., 2001. Hox D3 expression in normal and impaired wound healing. J. Surg. Res. 100 (1), 46–56.

Vicente, A., Varas, A., Acedon, R.S., Jimenez, E., Munoz, J.J., Zapata, A.G., 1998. Appearance and maturation of T-cell subsets during rat thymus ontogeny. Dev. Immunol. 5 (4), 319–331.

Vieira, F.A., Gregorio, S.F., Ferraresso, S., Thorne, M.A., Costa, R., Milan, M., et al., 2011. Skin healing and scale regeneration in fed and unfed sea bream *Sparus auratus*. BMC Genom. 12, 490.

Vinarsky, V., Atkinson, D.L., Stevenson, T.J., Keating, M.T., Odelberg, S.J., 2005. Normal newt limb regeneration requires matrix metalloproteinase function. Dev. Biol. 279 (1), 86–98.

Visscher, M., Narendran, V., 2014. The ontogeny of skin. Adv. Wound Care (New Rochelle) 3 (4), 291–303.

Walraven, M., Gouverneur, M., Middelkoop, E., Beelen, R.H., Ulrich, M.M., 2014. Altered TGF-beta signaling in fetal fibroblasts: what is known about the underlying mechanisms? Wound Repair Regen. 22 (1), 3–13.

Weiner, L., Fu, W., Chirico, W.J., Brissette, J.L., 2014. Skin as a living coloring book: how epithelial cells create patterns of pigmentation. Pigment Cell Melanoma Res. 27 (6), 1014–1031.

Werner, S., Grose, R., 2003. Regulation of wound healing by growth factors and cytokines. Physiol. Rev. 83 (3), 835–870.

Whitby, D.J., Ferguson, M.W., 1991. The extracellular matrix of lip wounds in fetal, neonatal and adult mice. Development 112 (2), 651–668.

White, P., Thomas, D.W., Fong, S., Stelnicki, E., Meijlink, F., Largman, C., et al., 2003. Deletion of the homeobox gene PRX-2 affects fetal but not adult fibroblast wound healing responses. J. Invest. Dermatol. 120 (1), 135–144.

Wu, P., Alibardi, L., Chuong, C.M., 2014. Regeneration of reptilian scales after wounding: neogenesis, regional difference, and molecular modules. Regeneration (Oxford) 1 (1), 15–26.

Yamaguchi, Y., Hearing, V.J., Itami, S., Yoshikawa, K., Katayama, I., 2005. Mesenchymal-epithelial interactions in the skin: aiming for site-specific tissue regeneration. J Dermatol. Sci. 40 (1), 1–9.

Yeh, J., Green, L.M., Jiang, T.X., Plikus, M., Huang, E., Chang, R.N., et al., 2009. Accelerated closure of skin wounds in mice deficient in the homeobox gene Msx2. Wound Repair Regen. 17 (5), 639–648.

Yokoyama, H., Maruoka, T., Aruga, A., Amano, T., Ohgo, S., Shiroishi, T., et al., 2011. Prx-1 expression in *Xenopus laevis* scarless skin-wound healing and its resemblance to epimorphic regeneration. J. Invest. Dermatol. 131 (12), 2477–2485.

Zhang, C., Ponugoti, B., Tian, C., Xu, F., Tarapore, R., Batres, A., et al., 2015. FOXO1 differentially regulates both normal and diabetic wound healing. J. Cell Biol. 209 (2), 289–303.

15

Animal Models of Skin Disorders

Jennifer Y. Zhang

Duke University Medical Center, Durham, NC, United States

1 INTRODUCTION

Skin covers an area of 1.5–2 m² and approximately 15% of body weight. It functions as an environmental sensor and the largest biological barrier that protects from dehydration and mechanical injury, excludes toxins and microbes, and participates in immune responses. The skin epidermis and its appendages, including hair and sebaceous and sweat glands, develop from a single layer of multipotent progenitor keratinocytes (Fuchs, 2007). The normal epidermis is comprised of multilayered and stratified epithelial cells that are organized in a polarized fashion through an integrated network of cytoskeletal elements and cellular junctions (Simpson et al., 2011). Yet, the epidermis ranks among the body's most dynamic tissues, undergoing life-long self-renewal through a tightly regulated balance of cell proliferation and terminal differentiation. Disruption of this balance, along with barrier defects, represents a central process of a myriad of skin diseases.

The outer most cornified layer of the epidermis is comprised of terminally differentiated keratinocytes also known as corneocytes, which lack a plasma membrane and are encased in a cornified envelope (CE) (Rice and Green, 1977). CE consists of keratins and a mixture of insoluble proteins, such as filaggrin (*fil*ament *aggre*gating prote*in)* and involucrin that are cross-linked by transglutaminases and surrounded by a lipid envelope. The lipid envelope, along with the natural moisturizing factors (NMFs) derived mostly from degradation products of filaggrin, is responsible for water retention by the skin (Imokawa et al., 1989; Rawlings and Harding, 2004). Defects in the cornification processes compromise the mechanical integrity and skin barrier function, and lead to increased sensitivity to environmental toxins and inflammation.

Human and animal skins exhibit substantial species-specific differences in tissue architect, spatial distribution of appendages and frequency of hair cycling, as well as immune responses and percutaneous drug penetration (Bartek et al., 1972; Porter, 2003). Relative to human skin, mouse skin has a dense distribution of hair follicles, thin epidermis, and an underlying cutaneous
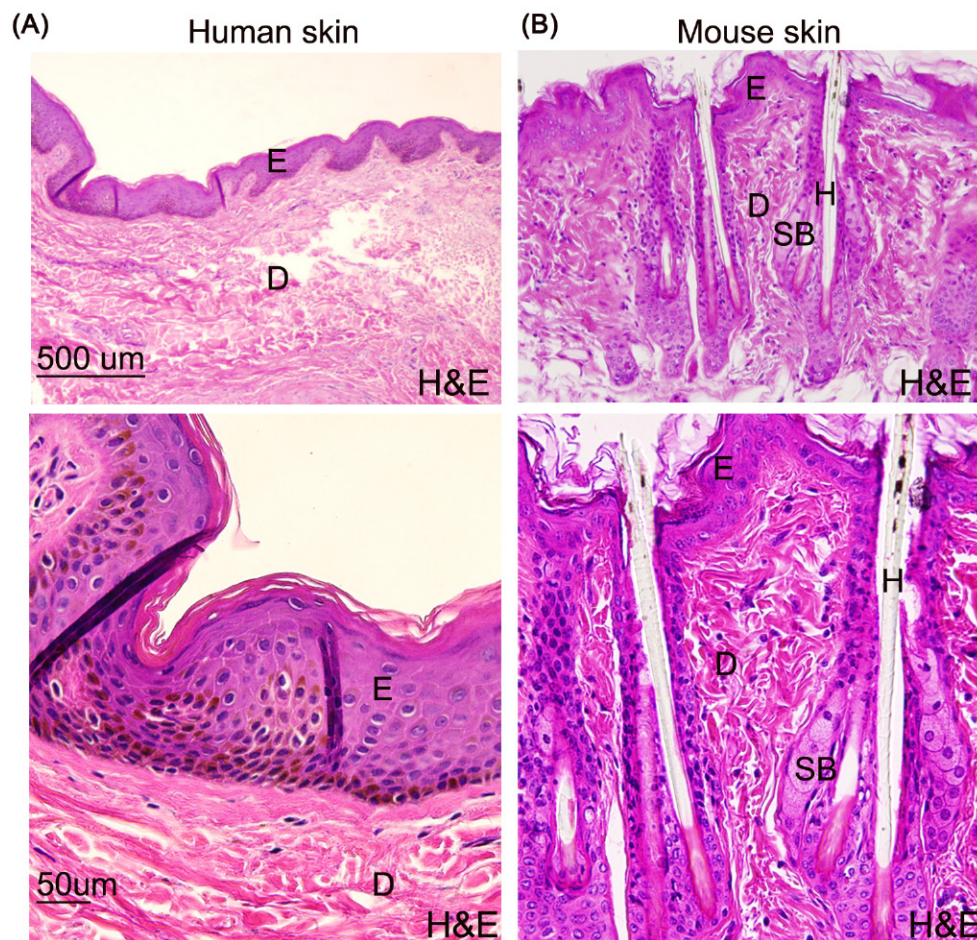
FIGURE 15.1 **Histology of human and mouse skin sections.** (A) Adult human abdominal skin. (B) Three-month-old mouse back skin. The epidermis *(E)* is comprised of stratified epithelial cells, namely keratinocytes. The skin pigment cells (melanocytes) are located in the epidermis and hair follicle of human and mouse skins, respectively. The dermis *(D)* houses hair follicles *(H)*, blood vessels, nerve fibers, and various immune cells. Human body skin is populated with sweat glands, whereas mouse body skin is devoid of sweat glands and enriched with hair follicles. Human and mouse skin tissues are obtained in accordance to institutionally approved IRB and IACUC protocols, respectively.

muscle layer that is generally absent in humans (Fig. 15.1). Thus, it is important to keep in mind that no animal model can completely recapitulate all aspects of human dermatological diseases. Nonetheless, those that can partially recap varying aspects of human diseases are instrumental for mechanistic understanding and drug development. In recent years, there has been an exponential increase of a wide range of animal models reported in the literature spanning from mice, rats, rabbits, dogs, monkeys, and fishes (Avci et al., 2013). Murine models are by far the most commonly reported model system owing to a multitude of favorable properties, such as facile husbandry requirements, rapid breeding (19 days of gestation) and inbred capability. These traits together with the modern gene targeting tools enable the generation of strains with inheritable, spatially and temporally inducible gene mutations (Paigen, 2003). With the whole genome data available for mouse and human (Consortium, 2012; Yue et al., 2014),

the similarities and the differences between the two species are ever more clear, and should be carefully considered during data interpretation.

Environmental insults and genetic defects are the primary root causes of skin diseases. As such, animal models of human skin diseases generally involve one or more of the following techniques: (1) induction with environmental allergens, (2) epidermal tissue-targeted genetic engineering, which includes transgene expression driven by gene promoters specifically expressed in the skin, such as cytokeratin promoters (K5, K14, or K15), and Cre-loxP-mediated gene deletion or mutation facilitated by Cre or Cre-ER transgenes expressed under epidermal cytokeratin promoters (Vasioukhin et al., 1999), and (3) xenografting, including subcutaneous tumor inoculation and de novo skin regeneration with genetically modified human keratinocytes on immunodeficient mice. This chapter covers a few examples of numerous animal models that have been reported to

show a remarkable resemblance to human inflammatory skin diseases, genetic diseases, and cancer. Not surprisingly, some of these models show partial resemblance to multiple skin diseases.

2 INFLAMMATORY SKIN DISEASE ANIMAL MODELS

Atopic dermatitis (AD) and psoriasis are the two most common inflammatory skin diseases. Both AD and psoriasis are characterized with keratinocyte hyperproliferation and elevated infiltration of various immune cells. While there is no doubt that immune cells play critical roles during disease progression and culmination, keratinocytes, the forefront barrier cells, can function as potent disease instigators. As the chicken-or-egg debate unfolds, evidence from an increasing number of animal models supports unequivocal roles of both immune cells and keratinocytes in the pathogenesis.

2.1 Atopic Dermatitis

Atopic dermatitis (AD, OMIM 603165) is a chronic or relapsing inflammatory skin disease that affects 15%–30% of children and 2%–10% adults worldwide with a strong correlation with industrialization (Bieber, 2008). The typical features of AD include chronic inflammation, pruritic allergy, disruption of epidermal barrier function, increased immunoglobulin E (IgE) levels, and a dysregulated Th2-biased peripheral immune response (Akdis et al., 2003; Bieber, 2008; Boguniewicz and Leung, 2011; Hamid et al., 1996). The etiology of AD is rather complex involving environmental and genetic factors (Bieber, 2008). Accordingly, AD animal models frequently involve sensitization with environmental allergens, microorganisms, and targeted gene mutations.

2.1.1 Epicutaneous Sensitization and Elicitation With Allergens

Allergens exist in the environment and food in many different forms including chemicals and peptides. Allergen entry through a defective skin barrier is the basis of AD-mouse models induced by epicutaneous (EC) sensitization and elicitation. Some of the frequently used experimental allergens are 2,4-dinitrochlorobenzene (DNCB), ovalbumin (OVA), and house dust mite (HDM) extracts.

2.1.1.1 2,4-DINITROCHLOROBENZENE

DNCB is an organic compound with the formula $(O_2N)_2C_6H_3Cl$. It is an important intermediate for many other industrial products. Exposure to DNCB was initially found to induce AD-like symptoms in humans in the 1980s (White et al., 1986). It has since been reported in over 1000 articles for the induction of AD-like responses in animals for drug development and phenotypic analyses of genetic animal models. For AD-focused pharmacological studies, Nc/Nga mice are particularly favored as they are prone to the development spontaneous of AD-like lesions upon aging and exposure to environmental factors when compared to other strains, such as Balb/c (Suto et al., 1999). To do this, mice are treated with topical doses of 0.1%–1% DNCB on the ear, footpads, the shaved abdominal or back skins (Garrigue et al., 1994). Tape stripping is sometimes applied to the shaved skin to enhance local skin barrier defects. Pharmacological compounds may be delivered topically, systemically via injection or oral consumption before or during DNCB treatment. The principal readouts include: (1) clinical signs of dermatitis, including severity of edema, erosion, dryness, hemorrhage, and alopecia; (2) serum IgE titers; (3) ear or footpad thickness measurements; (4) histological analysis of the challenged skin samples; (5) profiling of immune cells isolated from the lymph nodes or skin samples; and (6) epidermal barrier function analyses, such as measurement of transepidermal water loss (TEWL). These data are often collected at 12, 24, 36, 48, and 72-h time-points after sensitization. Results may be compared between drug treated versus untreated animals or wild-type versus mutant mice.

2.1.1.2 HOUSE DUST MITES

HDM refers to a large number of dust dwelling mites including the American HDM, *Dermatophagoides farinae* Hughes, and the European HDM, *Dermatophagoides pteronyssinus*. HDM is a common household aeroallergen known to cause asthma, allergic rhinitis and AD. The indoor level of HDM is associated with the severity of skin lesions (Kim et al., 2013). The bioreactive molecules of HDM consist of proteins and endotoxins derived from the body and feces. Various HDM extracts have been used for diagnostic tests, immunotherapy, and the induction of AD-like lesions in mice (Thomas, 2012). Recently, several recombinant proteins including Derp 11, a protein highly homologous to paramyosins of mites, ticks, and other invertebrates, have been tested for the sensitization of AD-lesions. Interestingly, Derp 11 is characterized as a major allergen for AD patients, but a minor one for those suffering from respiratory forms of HDM allergy (Banerjee et al., 2015). To induce murine AD-like skin lesions, HDM whole body extracts (in mg ranges) or a recombinant protein solution (e.g., Derp 11, in microgram ranges) may be topically applied to the ears and upper back skins twice a week for several weeks. AD lesions are analyzed at the macroscopic, microscopic, and molecular levels using the same sets of readouts as described for DNCB (Moniaga et al., 2010).

2.1.1.3 OVALBUMIN

OVA is a chicken protein allergen mainly found in egg white. It is commonly used to sensitize immune reactions. Prolonged EC exposure to OVA leads to the development of an AD-like dermatitis characterized by markedly increased expressions of total and OVA-specific serum IgE levels and infiltration of CD3(+) T-cells, eosinophils and neutrophils, as well as increased mRNA levels of interleukin (IL)-4, IL-5, and IFNγ (Spergel et al., 1998). This treatment generally consists of up to 3 courses of 1-week-long bandage of an OVA-soaked gauze (100 μg in 100 μL saline) to the back skins of mice. Each course is followed by 2-week-long breaks. Alternatively, mice may be sensitized via systemic administration of OVA (1 μg in 1 μL saline plus 1 μL adjuvant Imject Alum) prior to local challenges with EC OVA, which is shown to augment local sensitization of Balb/c mice to an acute Th2-polarized AD-like phenotype (Yoo et al., 2014).

2.1.1.4 *Staphylococcus aureus*

Human skin is colonized by vast numbers of bacterial communities that are distributed over the entire body with spatial and temporal specificities (Grice et al., 2009). Temporal microbial shifts (or dysbiosis) are associated with human diseases. Specifically, AD skin is disproportionally colonized with *S. aureus* (Leyden et al., 1974), and such a reduction of microbial diversity correlates with AD severity (Kong et al., 2012). Inhibition of *S. aureus* growth with antibiotics and sodium hypochlorite (bleach) baths improves eczema severity (Huang et al., 2009), implicating a contributing role of *S. aureus in disease progression.* Dysbiosis is also detected in mice that develop spontaneous AD-like lesions, as recently reported in an animal model generated to model ADAM metallopeptidase domain 17 (ADAM17)-deficiency in human, namely *Adam17(fl/fl).Sox9-Cre* mice (Kobayashi et al., 2015). ADAM17, also called TACE [tumor necrosis factor-α (TNFα)-converting enzyme], is induced by *S. aureus* protein A, and is important for the activation of TNFα and EGFR family ligands (Gomez et al., 2007). During the onset of on eczematous dermatitis, different strains of bacteria, including *Corynebacterium mastitides, S. aureus, and Corynebacterium bovis*, sequentially dominated the skin of *Adam17(fl/fl).Sox9-Cre* mice. Administration of antibiotics specific for these bacterial species reversed dysbiosis and eliminated skin inflammation. Further analysis showed that, while *S. aureus* prominently drove eczema formation, *C. bovis* induced robust T-helper 2 cell responses, indicating that dysbiotic flora have differential contributions to eczema formation (Kobayashi et al., 2015).

While the debate as to whether dysbiosis is a cause or a consequence of AD in patients unfolds; a causal effect is further supported by the evidence that *S. aureus* can enter epidermis of human skin equivalents and mice skin.

Bacteria entry past the epidermis is markedly increased in mice with epidermal barrier defects (e.g., *Cathelicidin* knockout and OVA-sensitized *filaggrin* mutant mice), and triggers increased expression of IL-4, IL-13, IL-22, thymic stromal lymphopoietin (TSLP), and other cytokines associated with AD (Nakatsuji et al., 2016). Taken together, *S. aureus*-induced AD-like lesions have clinical relevance in both human and mice. To induce AD-like lesions on mice with *S. aureus*, the dorsal skins of mice are typically shaved and disinfected with alcohol swaps. An agar disk (6 mm) containing *S. aureus* (ATCC35556 or MRSA USA300 LAC strains, 1×10^6 CFU) is then applied on the shaved area and kept in place with wound dressing film for 20 h.

2.1.2 *Genetic AD Animal Models*

Genetic linkage and protein expression studies have implicated over 100 genes with AD association (Boguniewicz and Leung, 2011). About 20% of them have been verified to show AD association by independent studies (Barnes, 2010). These genes encode proteins involved in (1) skin barrier function, (2) cell death and inflammatory responses, (3) lipid metabolism, and (4) innate and adaptive immune responses. As such, genetic AD mouse models reported so far generally involve epidermis-targeted loss-of-function mutation of genes important for skin barrier function or skin-specific keratin 5 or 14 promoter (K5 or K14)-driven transgene expression of inflammatory molecules.

2.1.2.1 FLAKY TAIL MICE

Filaggrin (*FLG)* encodes a filament-aggregating protein that promotes condensation of the keratin cytoskeleton and consequently the cell compaction process essential for squame biogenesis and epidermal barrier formation (Sandilands et al., 2009). It is by far the most well-characterized and prevalent AD susceptibility gene whose loss-of-function mutations are carried by up to 10% of the population worldwide (Palmer et al., 2006; Sandilands et al., 2007; Smith et al., 2006). These mutations represent a strong genetic predisposing factor for AD, asthma and allergies, as well as ichthyosis vulgaris, a common skin condition characterized by dry, scaly skin (Sandilands et al., 2007). The spontaneous flaky tail mouse contains a homozygous frameshift mutation in the murine *Flg* gene, resulting in expression of a truncated filaggrin protein (Fallon et al., 2009; Presland et al., 2000). These mutant mice exhibit a dry and flaky skin with annular tail and paw constrictions in the neonatal period. Topical application of the allergen OVA to the shaved abdominal skin of the flaky mice results in increased TEWL, cutaneous inflammatory infiltrates, and the development of allergen-specific IgG and IgE responses that resemble human AD.

2.1.2.2 INVOLUCRIN, ENVOPLAKIN, AND PERIPLAKIN KNOCKOUT MICE

Involucrin, a terminal differentiation marker, along with the plakin family desmosomal protein envoplakin and periplakin (Jefferson et al., 2004), forms the protein scaffold on which the CE assembles. Remarkably, mice with single or double knockouts (KO) of these genes are viable and fertile with no overt phenotypic abnormalities (Aho et al., 2004; Djian et al., 2000; Maatta et al., 2001; Sevilla et al., 2007). However, the triple KO mice develop a striking phenotype of dry and flaky skin over the entire body surface by a few days after birth. Their skins show delayed embryonic barrier formation and postnatal hyperkeratosis (abnormal accumulation of cornified cells) resulting from impaired desquamation. Their CEs are ultrastructurally abnormal, with reduced lipid content and defective filaggrin processing and degradation of desmoglein 1 and corneodesmosin. There is an elevated infiltration of CD4+ T-cells and a reduction in resident γδ+T-cells, reminiscent of AD. Thus, combined loss of the CE proteins impairs the epidermal barrier, and induces AD-like lesions (Sevilla et al., 2007).

2.1.2.3 CLAUDIN-1 MUTANT MICE

Claudins are adhesion molecules critical for the formation of tight junctions (TJ) and the barrier function of both simple and stratified epithelia. Claudin-1 (CLDN1) is commonly reduced in AD skin. Claudin-1-null ($Cldn1^{-/-}$) mice displayed postnatal lethality with wrinkled skin accompanied by excessive TEWL (Furuse et al., 2002). The lethality problem was eliminated in mice engineered to express varying levels of Claudin-1, which was achieved via insertion of a Neomycin selection maker in front of exon 1 (Δ) and crossbreeding of ($Cldn1^{Δ/+}$) mice with $Cldn1^{+/-}$ mice. The $Cldn1^{Δ/-}$ mice have a normal life expectancy, but exhibit morphological features of AD and an innate immune response characterized by neutrophil and macrophage recruitment to the skin (Tokumasu et al., 2016). These phenotypes were especially apparent in the infant stages. Adult mice showed an enhanced phenotype to DNCB-induced contact hypersensitivity response compared with WT mice. These results demonstrate that insufficient Claudin-1 expression not only compromises epidermal barrier defects, but also promotes AD pathogenesis and disease progression (Tokumasu et al., 2016).

2.1.2.4 CASPASE MUTANT MICE

Caspases are evolutionarily conserved family of cysteinyl aspartate-specific proteinases. Mammalian caspases play diverse functions in regulating programmed cell death (PCD), inflammation, immunity, and tissue morphogenesis (Man and Kanneganti, 2016). Dysregulation of caspases can contribute to skin inflammation through distinct mechanisms.

2.1.2.5 CASPASE-8

PCD is a key process underlying the terminal differentiation of keratinocytes and the formation of the stratum corneum (Candi et al., 2005). As a proximal caspase, activated by TNF/NGF family receptors, caspase-8 represents a major regulator of epidermal PCD. Humans with an inherited inactive caspase-8 (Arg248Trp) mutation display immunodeficiency due to pleiotropic defects that involve the functions of T-cells, natural killer cells, and B-cells (Chun et al., 2002). These patients suffer from a number of clinical symptoms including failure to thrive, lymphadenopathy, splenomegaly reactive airway disease, HSV labialis, and skin eczema. $aspase-8C^{-/-}$ mice are lethal. In contrast, K14-Cre-medaited deletion of $caspase-8$ in the mouse epidermis (C8cKO) elicits many clinical hallmarks of AD: epidermal thickening (acanthosis), scaling, elevated serum immunoglobulins, a biphasic T-helper cell response, mast cell infiltration, and spongiosis (Kovalenko et al., 2009; Lee et al., 2009; Li et al., 2010). These inflammatory skin lesions are associated with increased signaling of IL-1α (Lee et al., 2009), _matrix metalloproteinase-2-mediated cleavage of the cell–cell adhesion molecule E-cadherin (Li et al., 2010), and increased activities of interferon regulatory factor 3 and TANK-binding kinase (Kovalenko et al., 2009). Results from these animal model studies reveal that epidermal loss of $caspase 8$ not only affects PCD, but also alters the local microenvironment and elicits processes common to wound repair and skin inflammation.

2.1.2.6 CASPASE-1

Caspase-1, originally designated as IL-1β-converting enzyme (Keller et al., 2008), along with NLRP3 and the adaptor protein ASC, constitutes the inflammasome protein complex that plays a critical role in mounting an inflammatory response against a harmful stimulus. In an inflammatory microenvironment, such as the C8cKO skin, caspase-1 is induced by NF-κB, and stimulates proliferation of cutaneous epithelial stem cells (Lee et al., 2015). Transgenic mice generated with K14-driven expression of human Pro-Caspase-1 spontaneously developed recalcitrant dermatitis and skin ulcers, characterized by the presence of massive keratinocyte apoptosis (Yamanaka et al., 2000). The skin of these mice expressed increased levels of human caspase-1 and caspase-activated DNase, an effector endonuclease responsible for DNA fragmentation. In addition, their skin and sera showed elevated levels of mature IL-18 and IL-1β, but not of IFNγ. The plasma from these animals induced IFNγ production by IL-18-responsive NK cells. Administration of heat-killed *Propionibacterium acnes*, a potent in vivo type 1 T-cell inducer, caused IFNγ-mediated lethal liver injury in the transgenic mice, which was completely inhibited by treatment with neutralizing anti-IL-18 antibody. These results indicated that in vivo

overexpression of human caspase-1 caused spontaneous apoptotic tissue injury and rendered mice highly susceptible to exogenous type 1 T-cell-inducing condition in collaboration with endogenously accumulated proinflammatory cytokines.

2.1.2.7 CASPASE-14

Unlike most other caspases that are ubiquitously expressed, caspase-14 is selectively expressed and activated in the differentiating and cornifying layers of the epidermis and the hair follicles. It plays a crucial role in epidermal barrier formation, though not through direct regulation of the apoptotic process. Instead, caspase-14 is required for the proteolytic processing of filaggrin into the natural moisturizing factors (NMFs), such as urocanic acid and pyrrolidone carboxylic acid (Hoste et al., 2011). It is induced in epidermal keratinocytes by green tea polyphenol via MAPK pathways, and correlates with reductions of inflammatory skin lesions in the flaky tail mouse model (Hsu et al., 2007). In addition, elevated levels of caspase-14 were shown to protect skin from UVB irradiation (Bergeron et al., 2012). Conversely, caspase-14$^{-/-}$ mice display reduced epidermal barrier function and increased sensitivity to UVB radiation. In these mice, filaggrin is normally processed from precursor profilaggrin proteins, but fail to undergo terminal degradation, resulting in substantial reduction in the amount of NMFs and incomplete cornification (Hoste et al., 2011). In addition, caspase-14$^{-/-}$ mice are prone to the development of parakeratotic plaques following challenges of epidermal permeability barrier function by repetitive acetone treatment or induction of psoriasis-like dermatitis by imiquimod treatment (Hoste et al., 2013). Moreover, when challenged with bacteria, caspase-14$^{-/-}$ mice show an enhanced antibacterial response compared to wild-type mice and an imbalance of the skin-resident bacterial communities (Kubica et al., 2014).

2.1.2.8 K5-THYMIC STROMAL LYMPHOPOIETIN

TSLP, an IL-7 like cytokine, is highly expressed by keratinocytes of AD and correlated with Langerhans cell activation in AD lesional skin. TSLP can directly activate human CD11+ dendritic cells (DC) and DC-mediated Th2 response in cell culture (Soumelis et al., 2002). The role of keratinocyte-derived TSLP in skin inflammation was nicely demonstrated in K5-TSLP transgenic mice generated by crossing tetO-TSLP mice with K5-rtTA mice, which contains K5-driven expression of the reverse tetracycline transactivator. Two weeks after TSLP transgene induction via dietary doxycycline, K5-TSLP mice developed a spontaneous AD-like phenotype, with the development of eczematous lesions containing inflammatory dermal cellular infiltrates, including a dramatic increase of Th2 CD4+ T-cells and elevated serum levels of IgE (Yoo et al., 2005). In addition, these animals showed an influx of immature B-cells into the periphery cells with population expansion of follicular mature B-cells and a near-complete loss of marginal zone and marginal zone precursor B-cells. Thus, keratinocyte-derived TSLP modulates systemic B- cell development and promote humoral autoimmunity (Astrakhan et al., 2007). Similarly, keratinocyte-derived TSLP levels are correlated with skin sensitization strength and asthma severity, as demonstrated in mice in which TSLP expression was induced by topical application of MC903 (a vitamin D3 analog) (Leyva-Castillo et al., 2013). Conversely, TSLP oblation in epidermal keratinocytes reduces skin inflammation, and blocked the so-called atopic march, the progression from AD to asthma in animals with keratinocyte-specific deletion of RBP-j (the DNA-binding partner of Notch) (Demehri et al., 2009). Together, these evidence indicate that TSLP is a systemic driver of AD and atopic march, and that selective inhibition of systemic TSLP may block the development of asthma, a common allergic lung disease frequently affecting individuals with a prior history of eczema/AD (Demehri et al., 2009).

2.1.2.9 APOLIPOPROTEIN C1 (APOC1)

APOC1, along with several other plasma lipid transport genes [APOC2, APOCE, glucose-6-phosphate isomerase, the low-density lipoprotein receptor, complement component 3 (C3), and peptidase D], is mapped on human chromosome 19 (Lusis et al., 1986). APOC1 is linked to metabolic syndrome and skin inflammation. Consistently, transgenic mice engineered to overexpression APOC1 in liver and skin suffer from hyperlipidemia with strongly elevated serum levels of cholesterol, triglycerides, and FFA mainly to an accumulation of VLDL particles in the circulation (Jong et al., 1998). In addition, these mice spontaneously develop both gross and histologic features of human AD, including hyperkeratosis and parakeratosis, scaling, lichenification, dermal infiltration of inflammatory cells, and pruritus. These symptoms are accompanied with severe atrophy of sebaceous glands, the meibomian glands and subcutaneous fat tissues, and colitis. The AD symptoms of this model respond to topical treatment with corticosteroids. Moreover, oral treatment with probiotic Lactobacillus plantarum NCIMB8826 not only ameliorated colitis, but also improved skin barrier integrity and reduced epidermal thickening and inflammation (Mariman et al., 2016), which indicate that modulation of intestinal immune homeostasis may contribute to AD suppression. In this regard, AD is often linked to other atopic disorders, such as asthma, allergic rhinitis and food allergies (Bieber, 2008), and skin exposure to allergens is associated with food allergies later in life (Tordesillas et al., 2014). It is still unclear whether APOC1 is involved in these disease complications.

APOC1 displays genetic linkage to multiple other human diseases, including metabolic syndrome (Avery et al., 2011), cognitive disorder, memory impairment, and Alzheimer's disease (AD) (Ki et al., 2002; Zhou et al., 2014a,b), as well as cancer (Ko et al., 2014). These human data, along with the results of the APOC1 transgenic model, imply that regulators of lipid metabolism and lipid barrier formation of the epidermis represent a unique class of susceptibility genes that link multiple different diseases.

There are many more animal models that have been reported to show spontaneous or inducible AD-like lesions. These models are clearly instrumental for understanding molecular mechanisms underlying AD pathogenesis, the development of new AD therapeutics, and possibly elucidating other related disorders, such as asthma and metabolic syndromes.

2.2 Psoriasis

Psoriasis (OMIM 177900) is an ancient and universal inflammatory disease, initially described at the beginning of medicine in the *Corpus Hippocraticum* (460–377 BCE) as *psora*, meaning "to itch." Psoriasis affects 0.5%– 4.6% of the population with a highest prevalence among Caucasians (Lebwohl, 2003). Like AD, psoriasis involves a combination of genetic and environmental factors, and is frequently inherited, but not following a classical autosomal Mendelian profile (Lowes et al., 2007). The disease complexity and severity are heterogeneous and variable longitudinally. Genetic linkage studies performed during the past decade have identified a number of psoriatic susceptible loci, including PSORS1 (chromosome 6p21), PSORS2 (17q25), PSORS3 (4q), PSORS4 (1q21, S100A8, and S100A9), PSORS5 (3q21), PSORS6 (19p13), PSORS7 (1p), PSORS9 (4q31-34), and PSORAS1 (16q12) (Bowcock, 2004, 2005; Bowcock and Krueger, 2005; Krueger and Bowcock, 2005; Lebwohl, 2003). Nevertheless, definitive linkage of a single gene to psoriasis is made possible by recent RNA-sequencing technology which, for example, has identified association of TNFα promoter polymorphisms with psoriasis vulgaris and psoriatic arthritis (Mossner et al., 2005).

An ideal animal model for psoriasis would recapitulate all aspects of the clinical features of the disease. These include a marked hyperproliferation, thickening and altered differentiation of the epidermis, an increased T-cell infiltration and an altered vascularity, as well as a responsiveness to current antipsoriatic therapies. To date, hundreds of psoriasis mouse models have been reported with each recapitulating partial features of the human disease (Danilenko, 2008; Gudjonsson et al., 2007). Despite such limitations, data obtained from these animal models have shed light to specific aspects of disease pathophysiology, elucidating

dominant roles for both keratinocytes and T-cells (Danilenko, 2008; Gudjonsson et al., 2007; Nickoloff and Nestle, 2004). Due to the complexity of the disease etiology and manifestation, it is challenging to establish standardized validation criteria for psoriasis mouse models. However, with the technical versatility in obtaining and analyzing vast amount of genomic and gene expression data, quantitative parameters have emerged and become standardized. One such example is a recent study focused on the comparison of whole-genome transcriptional profiles of human psoriatic skin lesions with those of five different psoriasis mouse models (Imiquimod, K5-Tie2 (Wolfram et al., 2009), K14-AREG (Cook et al., 1997), K5-Stat3C (Sano et al., 2005) and K5-TGFβ1 (Fitch et al., 2009). These models show both similarities with respect to expression of genes involved in epidermal development and keratinization and variations in immune and inflammation-associated genes, as compared to the human disease (Swindell et al., 2011). Likewise, comparisons among psoriatic lesions from different anatomical sites reveal that scalp and skin psoriasis show strong similarities in immune responses. However, the scalp lesions show markedly higher magnitude of dysregulation and enrichment of the psoriatic genomic fingerprint than those of skin lesions. In addition, skin lesions are mainly associated with activation of TNFα/IL-17/IL-22-induced keratinocyte response, whereas the scalp lesions show increased modulation of IFNγ (Ruano et al., 2016).

The imiquimod-induced psoriasis model is most frequently utilized for drug development and gene function analysis in genetic animal models. Spontaneous development of psoriasis-like lesions is observed in many genetically altered animal models encompassing K5- or K14-promter-deriven epidermis-targeted transgene expression and less frequently epidermis-targeted gene knockout.

2.2.1 Imiquimod Induction of Psoriasis

Imiquimod (IMQ) is a nucleoside analog of the imidazoquinoline family, and is a potent agonist for the toll-like receptors (TLR)-7 and TLR-8. As a potent immune modulator, IMQ is initially used for topical treatment of genital and perianal warts caused by human papilloma virus, and later expanded for other skin abnormalities, such as actinic keratosis and superficial basal cell carcinomas (BCC) (Burns and Brown, 2005; Zitelli, 2005). At least two distinct mechanisms contribute to IMQ's antitumor effect. First, it activates TLR-7 and TLR-8 on DC and consequently NF-κB-dependent secretion of a multitude of proinflammatory cytokines and chemokines, leading to activation of antigen-presenting cells and other components of innate immunity and, eventually, the mounting of a profound T-helper 1 (Th1)-mediated antitumor immune response. Second, IMQ interferes with

adenosine receptor signaling pathways independent of TLR-7 and TLR-8, leading to augmentation of the pro-inflammatory activity (Schon and Schon, 2007). It was inadvertently discovered that, during topical treatment of actinic keratoses and BCC, patients with a well-controlled psoriasis developed exacerbated psoriatic lesions well beyond the treated area (Fanti et al., 2006; Gilliet et al., 2004; Patel et al., 2011; Wu et al., 2004). These lesions were marked by the infiltration of plasmacytoid DC and type I interferon activity (Gilliet et al., 2004).

Application of IMQ to mice induces inflamed scaly skin lesions that show hallmarks of plaque type psoriasis, including increased epidermal proliferation, abnormal differentiation and accumulation of neutrophils in microabesses, neoangiogenesis, and lymphocyte infiltrates consisting of CD4(+) T-cells, CD11c(+), and plasmacytoid DC (Palamara et al., 2004; van der Fits et al., 2009). Such lesions are apparent after 5–6 consecutive days of daily topical dose of 62.5 mg of IMQ cream on the shaved back and the right ear of mice. The IMQ-induced psoriasis model has been widely used to assess effects of nutrients, such as resveratrol and curcumin on disease initiation and progression (Kjaer et al., 2015; Sun et al., 2013). It has also been applied to genetically modified animal models to determine the role of specific genes, such as IL-23R and IL-17R, CXCR3, and Traf3ip2 (an NF-κB activator and an obligate adaptor for IL-17 receptor signaling), in the elicitation of skin inflammation (Ha et al., 2014; Morimura et al., 2016; van der Fits et al., 2009).

2.2.2 Psoriasis Models With Keratinocyte-Targeted Gene Alteration

2.2.2.1 TNFα AND TNFα-CONVERTING ENZYMES

Aberrant expression of TNFα and other cytokines, such as IL-1, IL-17, IL-22, IL-23, IL-36, and IFNγ, is a central element underlying the pathogenesis of psoriasis. These molecules induce both distinct and synergistic/additive effects on gene expression and development of psoriasis (Chiricozzi et al., 2011; Nakajima et al., 2011). In particular, TNFα is by far the most commonly utilized biomarker for assessment of inflammation, and TNF inhibition represents a gold standard for the treatment of psoriasis.

At low levels, TNFα orchestrates an important protective role in stimulating chemotaxis and antimicrobial activity of neutrophils, macrophages, and eosinophils. At high levels, it induces inflammation, cachexia, hemorrhage, necrosis and, ultimately, death. In skin, TNFα is produced by keratinocytes and skin resident CD11c(+)-DC (Cheng et al., 1992; Lowes et al., 2005). The detrimental effects of TNFα are revealed in transgenic mice with K14-driven expression of TNFα. These mice often die within 1 week after birth, and those survive after 1 week exhibit retarded growth with profoundly reduced adipose production, epidermal necrosis, and other features characteristic of cachexia (Cheng et al., 1992). In psoriasis, aberrant TNFα activity has been linked to genetic polymorphisms of the cis-regulatory domain or molecules involved in TNFα regulation, such as the TACE (also known as ADAM17), a member of the ADAM (a disintegrin and metalloprotease) family membrane-anchored metalloproteases.

ADAM17 processes and sheds the ectodomains of membrane-bound pro-TNFα and other membrane-anchored growth factors [e.g., heparin-binding EGF-like growth factor (HB-EGF), amphiregulin and transforming growth factor TGFα], cytokines, and receptors (Black et al., 1997; Blobel, 2005). $ADAM17^{-/-}$ mice die at birth with heart defects (Peschon et al., 1998). Mice with K14-Cre-mediated epidermal deletion of ADAM17 ($A17^{ΔKC}$) have normal skin architecture at birth, but develop pronounced defects in epidermal barrier integrity 2 days after birth (P2) followed by a spectrum of other skin defects (Franzke et al., 2012). These include curly whiskers, delayed hair outgrowth, shortened and disorganized hair follicles, dry scaly skin, and finally chronic dermatitis in adults. EGFR activation is significantly reduced in $A17^{ΔKC}$ skin, and topical treatment of these mice with recombinant TGFα significantly improved epidermal barrier function and decreased skin inflammation. Interestingly, $A17^{ΔKC}$ mice skin phenotypes are similar to those of mice lacking EGFR in keratinocytes ($Egfr^{ΔKC}$), and also overlap with those of mice with $TGFα$ deletion or mutation (such as waved 1) (Singh and Coffey, 2014). The ADAM17 substrates, including TNFα, amphiregulin, HB-EGF, and TGFα, are significantly upregulated in the TPA-induced psoriasis-like lesions in K5.Stat3C transgenic mice. Treatment of K5.Stat3C mice with TNFα or EGFR inhibitors attenuated the skin lesions (Sato et al., 2014). Overall, ADAM17 contributes to the development of psoriatic lesions through releasing of TNFα and EGFR ligands.

2.2.2.2 JUNB$^{EPI-/-}$ MICE

NF-κB and AP-1 family transcription factors are evolutionally conserved and functionally important for a wide range of cellular processes, including cell proliferation, cell survival, tissue homeostasis, and inflammation (Angel et al., 2001; Baldwin, 1996; Dixit and Mak, 2002; Eferl and Wagner, 2003; Hess et al., 2004; Jochum et al., 2001). These gene regulators play distinct functions in the skin. NF-κB controls epidermal cell proliferation and prevents premature cell death during differentiation (Seitz et al., 2000; Zhang et al., 2004). NF-κB plays key roles in inflammatory responses (Baker et al., 2011; Wullaert et al., 2011). Likewise, AP-1 proteins including JunB and c-Jun are dominant regulators of epidermal homeostasis and abnormalities (Angel et al., 2001; Eckert et al., 1997; Eferl and Wagner, 2003; Jochum et al., 2001). In human, JunB is encoded by a

gene previously mapped to human *PSOR6* (ch19p13), though the functional relevance of JunB to this locus is unclear. In addition, JunB mRNA level is increased (Park et al., 2010; Zenz et al., 2005), while its protein level is significantly reduced in the epidermal cells of psoriatic lesions as compared to uninvolved or healthy skin (Haider et al., 2006; Johansen et al., 2004; Kulski et al., 2005).

A pathogenic effect of JunB loss-of-function is validated in mice with epidermis-targeted deletion of *JunB* (*JunB^{Epi−/−}*) alone or together with *c-Jun. JunB^{Epi−/−}* mice develop joint and skin inflammation with histological and molecular hallmarks of psoriasis and psoriatic arthritis (Meixner et al., 2008; Zenz et al., 2005). These inflammatory skin lesions are further attributed to the decreased expression of the tissue inhibitor of metalloproteinase-3 (TIMP-3), an inhibitor of the TACE, and consequently uncontrolled TNFα shedding in the epidermis (Guinea-Viniegra et al., 2009). TNFR1-deletion or epidermal reexpression of TIMP-3 alleviates skin inflammation and TNFα-induced cachectic-like phenotype (Guinea-Viniegra et al., 2009). Using this *JunB^{Epi−/−}* mouse model, further studies show that systemic anti-VEGF treatment markedly reduces skin inflammation (Schonthaler et al., 2009), nicely supporting a major role of angiogenesis in psoriasis and the potential of VEGF-targeted therapies for this disease.

Consistent with these mice data, JunB-interference through siRNA-mediated gene silencing or expression of a dominant negative mutant in human keratinocytes leads to an increased cell proliferation and a decreased barrier function (Zhang et al., 2015), as well as promotion to Ras-driven tumorigenesis (Jin et al., 2011). Further ChIP-seq and RNA-seq analyses reveal that JunB regulates expression of an array of psoriasis-relevant proinflammatory molecules, such as TNFα, CXCL10, and CXCL11, through NF-κB.

2.2.2.3 IKK2^{EPI−/−} MICE

The IκB kinase (IKK) complex consists of two catalytic subunits (IKK1 and IKK2) and a regulatory subunit (IKKγ, also known as NEMO). Upon phosphorylation by the IKK complex, IκB proteins undergo proteosomal degradation, allowing the release and activation of activation of NF-κB family transcription factors (Israel, 2000; Karin and Ben-Neriah, 2000). IKK proteins play essential roles in embryonic development and tissue morphogenesis. IKK1 controls epidermal differentiation through RelB/p52, a noncanonical NF-κB signaling axis (Hu et al., 1999, 2001; Li et al., 1999a; Takeda et al., 1999). Deficiency in the X-linked NEMO gene causes incontinentia pigmenti (IP) (OMIM 308300) in both mice and human. IP is an inherited neurocutaneous disorder characterized by strips of hypopigmented skin and abnormalities of the teeth, skeletal system, eyes, and central nervous system (Makris et al., 2000; Schmidt-Supprian

et al., 2000). Germline deletion of IKK2 results in embryonic lethality with liver degeneration (Li et al., 1999b; Tanaka et al., 1999). Mice with K14-Cre-mediated epidermis-specific deletion of IKK2 (*IKK2^{epi−/−}*) develop a severe inflammatory skin disease which is attenuated by deletion of the TNFα receptor 1 (*TNFR1*) or elimination of skin macrophages by subcutaneous injection of clodronate liposomes (Pasparakis et al., 2002). However, this skin phenotype is irresponsive to deletion of CD18 (granulocytes) or T-cell antigen receptor (*TCRα*, αβT-cells) and the receptor for IFNγ (Pasparakis et al., 2002; Stratis et al., 2006). Thus, *IKK2*-deletion initiates IFNγ-independent psoriasis-like skin disease whose development requires macrophages but not granulocytes or αβT-lymphocytes.

Taken together, studies of various animal models demonstrate that keratinocyte-targeted gene alteration can initiate psoriasis and even arthritis-like lesions. Presumably, each relevant gene controls specific aspects of the disease.

2.2.3 Psoriasis Models Induced by Intradermal Injection of Cytokines

Psoriatic lesions are enriched with polarized subsets of T-cells, including T-helper 1 (Th1; CD4+), T-cytotoxic (TC1; CD8+), and T-helper 17 (Th17; CD4+) cells, as well as effector cells of innate immunity, such as neutrophils, plasmacytoid DCs, and CD11c+ DCs (Lowes et al., 2007). These immune cells are recruited and activated by different cytokines through a chain reaction.

As expected, different cytokines elicit varying aspect of the disease. Intradermal injection of IL-23, a cytokine responsible for the induction of IL-17 production by γδT-cells (Cai et al., 2011), induces skin inflammation that shares many characteristics with human psoriasis, including erythematosus, hyperplasia of the epidermis (acanthosis), parakeratosis, and leukocyte infiltration (Chan et al., 2006). The development of these lesions are dependent on TNF, IL-20R2, and IL-17 signaling (Chan et al., 2006).

IL-17 drives psoriatic inflammation via distinct and target cell-specific mechanisms. IL-17/Trafip2 signaling in keratinocytes is essential for neutrophilic microabscess formation and keratinocyte hyperproliferation. IL-17/Trafip2 signaling in dermal fibroblasts promotes cellular infiltration and accumulation of IL-17-producing γδT-cells cells in skin, forming a positive feed-forward mechanism (Ha et al., 2014). Interestingly, IL-17 is subject to regulation by adiponectin, a metabolic mediator of insulin sensitivity (Shibata et al., 2015). Adiponectin suppresses IL-17 synthesis via direct binding to AdipoR1 on γδ-T cells. Mice with adiponectin deficiency show severe psoriasiform skin inflammation with enhanced infiltration of IL-17-producing dermal γδ-T cells. Adiponectin is decreased in serum, skin, and fat tissues of psoriasis

patients. Thus, adiponectin deficiency may provide a mechanism underlying the relationship between psoriasis and metabolic disorders.

Treatment of antibiotics in adult mice ameliorates imiquimod-induced psoriasiform dermatitis, with decreasing numbers of IL-17 and IL-22 producing T-cells. Surprisingly, animals treated with antibiotics at neonatal stage show markedly exacerbated inflammatory responses when challenged with topical imiquimod and intradermal injection of recombinant IL-23 during adulthood. Using 16S rRNA gene compositional analysis, it is found that neonatal antibiotic treatment can lead to a dysregulation of gut and skin microbiota later in life and potentially an increased susceptibility to psoriasis during adulthood (Zanvit et al., 2015).

In summary, each of these animal models addresses specific aspects of human psoriasis. In spite of the enormous heterogeneity of human psoriasis, data obtained from animal model studies provide mechanistic insights, and are instrumental for drug development. At present, systemic therapies with TNF inhibitors, including adalimumab, etanercept, and infliximab, represent the mainstream treatment options for psoriasis. These agents are currently approved by the US Food and Drug Administration for the treatment of moderate to severe psoriasis (Kerdel, 2015). Nevertheless, systemic biological agents are inevitably associated risks of immune reactions and infection. Thus, local and keratinocyte-targeted therapies are highly desired, and maybe developed based on the findings obtained with animal models that address the role of keratinocytes in disease pathogenesis.

3 GENETIC SKIN DISEASE ANIMAL MODELS

3.1 Ichthyosis Vulgaris

Ichthyosis vulgaris (OMIM#146700) is characterized by dry, scaly skin, and propensity to the development of AD (eczema) and allergic responses, such as asthma. It is caused by loss-of-function mutations in the gene encoding filaggrin (Sandilands et al., 2007, 2009; Smith et al., 2006), and mainly treated with moisturizing agents (Hoppe et al., 2015).

The flaky tail mice which carry a spontaneous mutation in the filaggrin gene nicely recapitulate the human skin phenotype. This mutation resulted in the expression of a lower molecular weight form of profilaggrin (220 kDa instead of 500 kDa) that is resistant to proteolytic processing into filaggrin intermediates necessary for the production of moisturizing factors. Thus, the flaky tail mice are useful for both AD and ichthyosis vulgaris studies.

3.2 Netherton Syndrome

Netherton syndrome (NS) (OMIM 256500) is a rare and severe autosomal recessive congenital ichthyosiform dermatosis characterized by extensive skin desquamation, inflammation, multiple allergies, atopic manifestations, and hair shaft defects. Currently, there is no satisfactory treatment for NS, which can be life-threatening in infants, and palliative treatments are applied for management of skin infections, itching, and pain. NS is caused by truncated loss-of-function mutations of the serine protease inhibitor Kazal-type 5 (*SPINK5*), a gene that encodes LEKTI (lymphoepithelial Kazal-type inhibitor). Specifically, LETKI is an inhibitor specific for KLK serine protease family members (KLK5, KLK7, and KLK14) (Chavanas et al., 2000). KLK5 is characterized as an initiator upstream of KLK7 and elastase-2 (ELA2). The current state-of-hypothesis is that Pro-KLKs are synthesized and activated by matriptase in the *stratum granulosum*, but rapidly inactivated by LEKTI, thus preventing premature degradation of desmosomes. The acidic microenvironment of *stratum corneum* causes the release of active KLKs from LEKTI, and subsequent cleavage of corneodesmosomal proteins in the most superficial layers of the *stratum corneum*, ensuring finely balanced regulation of the desquamation process (Ovaere et al., 2009). LEKTI loss-of-function results in unopposed protease activities and over digestion of epidermal structural and barrier proteins.

As expected, $Spink5^{-/-}$ mice recapitulate cutaneous and inflammatory aspects of the NS disease including neonatal lethality (Descargues et al., 2005; Yang et al., 2004), which is associated abnormal degradation of the desmosomal cadherins, such as Desmoglein 1 (Dsg1) and Desmocollin-1 (Dsc1) desmoglein 1, due to unopposed KLK5 and KLK7 protease activities (Descargues et al., 2005). The uncontrolled KLK5 activity in NS epidermis appears to trigger AD-like lesions through PAR2-mediated TSLP expression, independently of the environment and the adaptive immune system (Briot et al., 2009).

Like $Spink5^{-/-}$ mice, transgenic mice engineered to overexpress human KLK5 in the granular layer of the epidermis via involucrin promoter display increased proteolytic activity of KLK5 and its downstream KLK7, KLK14, and ELA2. Similar to $Spink5^{-/-}$, KLK5 transgenic mice develop an exfoliative erythroderma with scaling, growth delay, and hair abnormalities, as well as cutaneous and systemic hallmarks of severe inflammation and allergy with pruritus. The skin shows increased expressions of inflammatory cytokines and chemokines, infiltrations of immune cells, and markers of Th2/Th17/Th22 T-cell responses along with elevated levels of IgE and TSLP in serum (Furio et al., 2014).

Conversely, deletion of *Klk5* rescues the neonatal lethality of in *Spink5*$^{-/-}$ newborn mice, and reverses cutaneous hallmarks of NS, including skin barrier defect, disordered epidermal structure, and skin inflammation (Furio et al., 2015). Notably, Klk5 loss results in reduced epidermal proteolytic activity, particularly KLK7, KLK14 and ELA2, and restoration of structural integrity of desmosomes and corneodesmosomes and normal epidermal differentiation as well as normalized expressions of Il-1β, Il17A, and TSLP.

Further supporting a role of KLK5 in NS, ablation of matriptase, a protease involved in processing of Pro-KLKs to active KLK, dampened inflammation, prevents detachment of the stratum corneum, and improves the barrier function of the epidermis of *Spink5*$^{-/-}$ mice (Sales et al., 2010). Results of this study indicate a crucial role of matriptase in NS pathogenesis and imply a role of the matriptase-pro-KLK pathway in other human skin and inflammatory diseases.

In addition to animal models, the epidermal defects is observed in organotypic 3D cultures generated with normal human keratinocytes transfected with SPINK5-targeted small interfering RNA (siRNA) and fibroblast-populated collagen gels (Wang et al., 2014). Gene silencing of KLK5 or KLK7 markedly ameliorates the epidermal architecture compromised by reduced SPINK5 expression. Together, these studies confirm a major role of KLK5 and its upstream and downstream regulators in NS.

4 ANIMAL MODELS OF SKIN CANCER

Skin cancer is by far the most common type of cancer of human body (Eisemann et al., 2014), accounting for more cases than the combined incidences of breast, prostate, lung, and colon cancers (American Cancer Society, 2016). BCC and squamous cell carcinoma (SCC) constitute the majority of nonmelanoma skin cancers, accounting for an annual incidence of approximately 4 and 1 million new cases, respectively, in the United States alone. These cancers, especially BCC, rarely spread to other parts of the body, and most of them can be effectively treated by surgery. Among the rare types of nonmelanoma skin tumors are cylindorma, tricoepithelioma, and sebaceous adenoma. These adnexal tumors are often observed as a mixed population in Brook-spiegler syndrome, an autosomal recessive disorder. Although mostly benign, they are difficult to treat due to the high multiplicity and the frequent recurrence after surgical removal. Melanoma incidence accounts for nearly 85% of skin cancer death.

The primary risk factor for skin cancer is UV radiation which induces DNA mutations through cyclobutane pyrimidine dimers and pyrimidine [6-4] pyrimidone photoproducts ([6-4]PPs) (de Gruijl, 1999; Freeman et al., 1989; Pleasance et al., 2010). Among the most well-characterized driver mutations are (1) gain-of-functions of oncogenes, such as those of the Ras-MAPK pathway (HRas, KRas, NRas, BRAF, and MEK) and cell cycle regulators (CDK4 and cyclinD1), and (2) loss-of-function mutations of tumor suppressors, such as p53, PTEN and PTCH, and cell cycle inhibitors, such as p16. The prevalence of a specific gene mutation differs among different skin tumors.

4.1 DMBA/TPA Two-Stage Chemical Carcinogenesis

4.1.1 Nonmelanoma Skin Cancer Induced by Chemicals

The two-stage chemical carcinogenesis protocol is initially developed based on anecdotal findings made in the 1920s that wounding of mouse skin that had previously been treated with carcinogenic tar were prone to skin tumor development. This protocol has since been optimized and widely used to study skin carcinogenesis of mice with different genetic backgrounds or targeted gene engineering (Abel et al., 2009; Neagu et al., 2016). In essence, it requires two stages (Fig. 15.2). In the initiation stage, one dose of a chemical carcinogen most frequently 7,12-dimethylbenz[*a*]anthracene (DMBA), a polycyclic aromatic hydrocarbon, is applied topically to the shaved or hairless skin. DMBA is metabolized by epidermal Langerhans cells to DMBA-*trans*-3,4-diol, an intermediate inductive of DNA mutations (Modi et al., 2012). *HRas is* a primary target gene of DMBA in most cases with a few exceptions, such as *Pten*$^{+/-}$ mice, in which *HRas* mutation appear to be exclusive of *Pten* loss (Mao et al., 2004). Activating *HRas* mutation, typically A to T (182) transversion in codon 61, is detectable 3–4 weeks after DMBA-treatment, and is characterized as critical event in skin carcinogenesis. In agreement with this, transgenic mice that express a constitutively active HRas^{V12} mutant under the control of the zeta-globin develop tumors without the requirement of DMBA initiation (Spalding et al., 1993). Similarity, mice with K14 promoter-driven expression of a 4-hydroxytamoxifen (4OHT)-regulated HRas-ER fusion develop papillomas following induction with 4OHT (Ortiz-Urda et al., 2005).

By the 6–10th weeks after TPA promotion, elevated growth of begin papillomas is readily visible. Papillomas may then progress to invasive SCC as early as 20 weeks after treatment with the promoting agent. Further progression can lead to formation of spindle cell carcinomas and even metastasis to lymph nodes, as observed in the
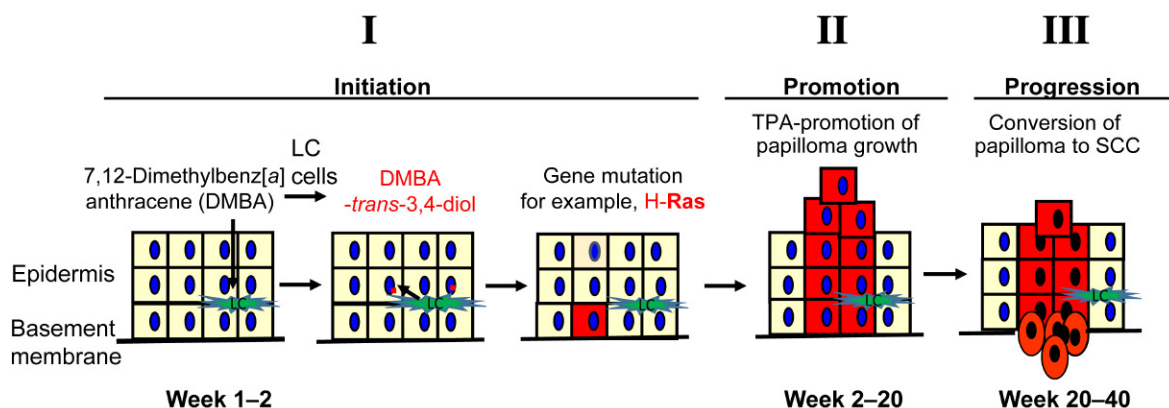
FIGURE 15.2   DMBA/TPA two-stage carcinogenesis. For initiation, one subcarcinogenic dose of 7,12-dimethylbenz[*a*] anthracene *(DMBA)* is applied to neonatal (50 μg in 50 μL acetone) or shaved adult skin (ranging from 2.5 to 100 μg in 200 μL acetone). DMBA is metabolized by skin resident Langerhans cells *(LC)* into DMBA-*trans*-3,4-diol which then induces gene mutations in keratinocytes. Two weeks after initiation, a promoting agent, such as 12-O-tetradecanoylphorbol-13-acetate *(TPA)* is applied (2–4 μg in 200 μL) biweekly and continues for the duration of the study, typically for 20 weeks. During promotion stage, TPA stimulates cell signaling, increases production of growth factors, and generates oxidative stress and tissue inflammation, which together create an environment that favors clonal expansion of cells with certain gene mutations, such as Ras (DiGiovanni, 1992).

transgenic mice with K14-driven expression of a catalytically deficient mutant of CYLD tumor suppressor (Miliani de Marval et al., 2011).

The rate and multiplicity of papilloma development and the frequency of malignant conversion are dependent on genetic background and the dosage of carcinogen and promotion agents used. In general, FVB and SENCAR mice are more sensitive to tumor induction than BALB/c mice. In order to minimize genetic background-dependent variations, multigeneration backcrossing is highly recommended when comparing tumorigenesis between WT and transgenic or knockout mice.

4.1.2 Melanoma Induced by Chemical Carcinogenesis

The DMBA/TPA protocol has been recently modified to induce melanocytic nevi and melanoma (Nasti et al., 2016). For this, the shaved back skin of C3H/HeN mice was painted with 50–100 μg of DMBA in 200 μL of acetone, and then treated twice weekly with topical doses of 6.25–12.5 μg TPA for 20 weeks. Dysplastic pigmented skin lesions appear with 100% penetrance around 7–9 weeks after TPA. It is believed that the low dose TPA results in the development of fewer and delayed appearance of epithelial papillomas (14–15 weeks after TPA). In addition, withdraw of TPA leads to regression of papillomas without affecting the development of pigmented lesions. By the 25th week, nests of melanocytic cells are detected in a subset of skin draining lymph nodes. Approximately 50% of the derived melanoma cell lines contain *HRas* mutations and *p16^{Ink4a}* loss. While the feasibility of this melanoma model is yet to be tested in other mouse strains, it might be useful for screening

therapeutics and identifying novel pathways associated with nevus formation (Nasti et al., 2016).

4.2 Modeling Skin Cancer With Genetically Engineered Animal Models

Numerous genetically engineered animal models have been used to study various skin cancers, including BCC, SCC, and melanoma (Gober et al., 2013), as well as other less common adnexal skin tumors, such as cylindroma (Jin et al., 2016).

4.2.1 BCC

BCC is primarily caused by the activation of the *Sonic hedgehog* (SHH) signaling pathway, most frequently, due to loss-of-function mutation of the tumor suppressor Patched 1 gene (*PTCH1*), and, less frequently, activating mutations of Smoothened (SMO) and the downstream Gli1 and Gli2 transcript factors (Hahn et al., 1996; Johnson et al., 1996). Recapitulating human BCC, *Ptch^{+/−}* mice and transgenic mice with K14- or K5-driven overexpression of SHH, an active SMO-mutant (SMO-M2), Gli1 or Gli2 all develop spontaneous BCC (Aszterbaum et al., 1999; Grachtchouk et al., 2000; Nilsson et al., 2000; Oro et al., 1997; Xie et al., 1998). Further studies with K15-driven expression of SMO-M2 in hair follicle bulge stem cells demonstrate that hair follicle stem cells can be mobilized by wounding to the interfollicular epithelium where they are capable of triggering BCC tumor formation (Wong and Reiter, 2011).

4.2.2 SCC

The Ras/MEK/MAPK signaling pathway is frequently activated in human cutaneous SCC, with *HRas* mutation

detected in about 20% of human SCC samples (Bamford et al., 2004; Pierceall et al., 1991). Transgenic mice with K14-driven expression of a tamoxifen-inducible mutant Ras (H-Ras^{V12}) or activated MEK1 develop skin tumors with features consistent with SCC (Pierceall et al., 1991; Scholl et al., 2004). p53 loss, frequently induced by UV-irradiation (Brash et al., 1991), represents another common feature of SCC. p53 is a potent tumor suppressor required for maintenance of genomic stability and cell cycle control (Hoeijmakers, 2001). $p53^{-/-}$ mice are sensitive to UV-induced skin carcinogenesis (Jiang et al., 1999). In addition to direct gene mutation, Ras/MAPK activation and p53 loss-of-function also function as important SCC-drivers in several other mouse models including transgenic mice with K14-driven expression of a constitutively active Fyn (K14-Fyn Y528F) (Zhao et al., 2009).

Nucleotide excision repair is a key process for the maintenance of DNA integrity. Patients with Xeroderma pigmentosum (XP), a rare autosomal recessive disease caused by XP loss of-function mutation, is in part characterized by extreme skin sensitivity to sunlight and by 1000-fold increased risk of developing cancer at sun-exposed areas of the skin. Consistently, $Xpa^{-/-}$ mice develop skin tumors at high frequency when exposed to UV light, and $Xpa/p53^{+/-}$ double KO mice develop tumors earlier and with higher incidences upon exposure to carcinogens as compared to their single knockout counterparts (van Steeg et al., 2001).

4.2.3 Melanoma

Mutational activation of BRAF is the earliest and most common genetic alteration in human melanoma. However, BRAF mutation is not sufficient to induce melanoma progression. In line with this, mice engineered with melanocyte-targeted Braf^{V600E} mutation via *tyrosinase* promoter-driven expression of the tamoxifen-regulated Cre-ER (*Tyr-CreER*) develop benign melanocytic hyperplasias that undergo senescence and fail to progress to melanoma (Dhomen et al., 2009). By contrast, expression of BRaf^{V600E} combined with *Pten* gene deletion in melanocytes elicits aggressive melanoma growth with 100% penetrance, short latency, and metastases to lymph nodes and lungs (Dankort et al., 2009). The *Tyr-CreER.Braf^{V600E}.Pten$^{-/-}$* mice have been extensively used to characterized mechanisms of chemoresistance (Holderfield et al., 2014; Shtivelman et al., 2014). It is also used to demonstrate that copper is required for Braf-driven melanoma tumorigenesis (Brady et al., 2014).

4.3 Modeling Skin Cancer With Human Cells

4.3.1 De Novo Human Skin Regeneration on Immunodeficient Mice

A key aspect of skin research is to utilize skin tissue models that have a human specific tissue architecture, an intact epidermal permeability barrier and physiologic connections to the systemic circulation. For this purpose, the de novo human skin regeneration technique has been proven very useful. It involves isolation of primary human keratinocytes, melanocytes, and dermal fibroblasts, multiplex gene transduction and subsequent seeding of the primary skin cells onto devitalized or synthetic human dermis, followed by skin grafting on mice with severe combined immunodeficiency (*SCID*) (Fig. 15.3A). A few weeks after grafting, the regenerated tissues develop a multilayered skin architecture that is indistinguishable from normal human skin or various skin tumors. For example, grafts regenerated with human keratinocytes transduced to express Ras and active c-Jun develop histological features of human SCC including an apparent dermal invasion and a high rate of cell proliferation as indicated by abundance of Ki-67-positive cells (Fig. 15.3B–C). In contrast, grafts expressing Ras and JunB display near normal clinical and histological appearances as manifested by the clear tissue boundaries between epidermis and dermis, and the basal cell restricted cell proliferation (Jin et al., 2011). This model has been successfully used to demonstrate that exogenous expression of CDK4, IκBα mutant (the super repressor of NF-κB), and the active mutants of MKK7 and JNK2 each is sufficient to couple with oncogenic Ras to transform normal keratinocytes into SCC (Dajee et al., 2002; Ke et al., 2010; Lazarov et al., 2002).

Consistent with SHH signaling pathway being a primary driver of BCC, skin grafts generated with keratinocytes transduced to express SHH develop into BCC within 1 month after the surgery (Fan et al., 1997). The regenerated skin tissue model has also been used to study melanoma development. This involves gene transduction of primary human melanocytes for expression of melanoma relevant genes, such as NRas, hTERT, CDK4, and dominant negative p53 mutant (p53^{DN}). The gene-transduced melanocytes are then mixed with human keratinocytes at 1:10 ratio for skin grafting. Pigmented lesions emerge and quickly develop into malignant melanoma within a few weeks after grafting on SCID mice (Chudnovsky et al., 2005).

4.3.2 Three-Dimensional Organotypic Human Skin Culture

The 3D organotypic skin culture system has been proven valuable in understanding the epidermal-cell intrinsic effects and the epidermal–dermal crosstalk, as well as genetic and pharmacological impacts on epidermal growth, differentiation, barrier formation, and carcinogenesis (El Ghalbzouri et al., 2002; Maas-Szabowski et al., 2001; Margulis et al., 2005a; Szabowski et al., 2000). As depicted in Fig. 15.4A, a basic 3D skin culture system is composed of an upper chamber and lower chamber that are separated by collagen gel or dermal matrices, such as split thickness human dermis
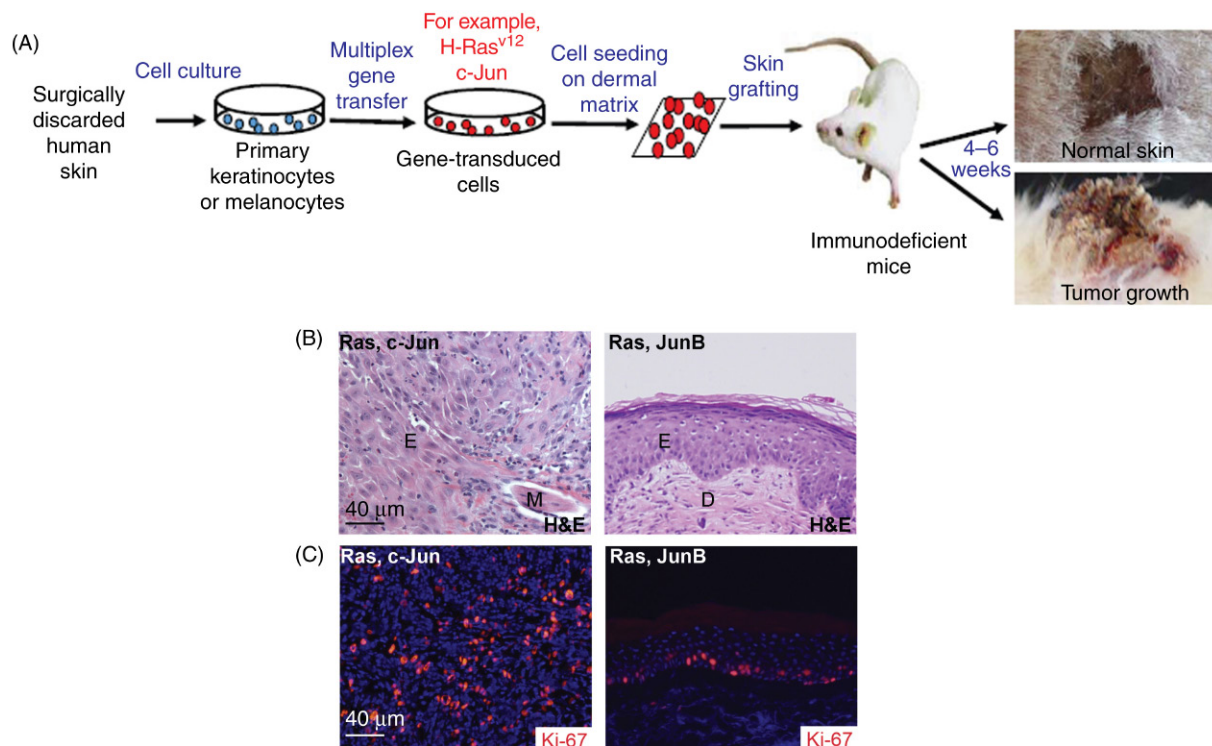
FIGURE 15.3 **De novo regeneration of human skin tissues with defined genetic changes.** (A) Diagram of de novo human skin regeneration. (B) Histological appearance of 6-week-old skin grafts generated on immunodeficient SCID mice with primary human keratinocytes transduced to express Ras and c-Jun or JunB. E, Epidermal tissue; D,dermis; M,muscle. Grafts (n = 3–5) displayed 100% phenotypic penetrance. (C) Immunoflorescent staining for Ki-67, nuclei (*blue*, Hoechst 3342), magnification. *Source: Part B and C: Reprinted from Jin, J.Y., Ke, H., Hall, R.P., Zhang, J.Y., 2011. c-Jun promotes whereas JunB inhibits epidermal neoplasia. J. Invest. Dermatol. 131 (5), 1149–1158.*

derived from cadaver or surgically discarded skin. Human keratinocytes are seeded on the top of the dermal matrices placed in the top chamber. Dermal fibroblasts and other dermal cells are seeded in the bottom chamber either as monolayer culture or with collagen gel. For gene function studies, cells may be infected with retro or lentiviruses for targeted gene expression or silencing. Once cells are settled in their respective compartment, the media on the top chamber is removed, creating an air–liquid interface which is critical for epidermal stratification. The bottom chamber will be replenished with fresh media every 2–3 days. Skin rafts may be maintained in culture for up to 1 month, and collected at various time-points for histological analyses(Margulis et al., 2005a,b). Depending on the project needs, melanocytes or melanoma cells may be seeded together with keratinocytes. Skin grafts may be subject to pharmacological treatments during the incubation. By using this 3D culture system, we have found that tissues generated with cells transduced for expression of JunB display epidermal hypoplasia as indicated by the reduced epidermal thickness and number of Ki-67(+) cells as compared to the control tissues (Fig. 15.4B). A similar 3D setting was used to demonstrate that p63, ZNF750

and methyltransferase 1 (DNMT1) are critical for the maintenance of progenitor cells in the epidermis (Sen et al., 2010, 2012; Truong et al., 2006).

The 3D skin raft system is also nicely used to identify a key role for the extracellular matrix interaction network facilitated by the β1-integrin in cancer progression (Reuter et al., 2009). Moreover, this model can be extended to epithelial cells from other tissues, such as oropharynx, esophagus, and cervix, and investigate how genetic changes affect cancer transformation and tissue invasion (Ridky et al., 2010).

5 CONCLUSIONS

Animal models are instrumental in understanding various dermatological diseases. They will continue to be utilized for future studies with the incorporation of cutting edge technologies, such as CRISPR or lentivirus-mediated gene targeting of embryonic skin (Beronja et al., 2010; Yang et al., 2013). Meantime, the 3D organotypic tissue culture systems are expected to emerge and to be optimized for more frequent use as animal free skin equivalents.
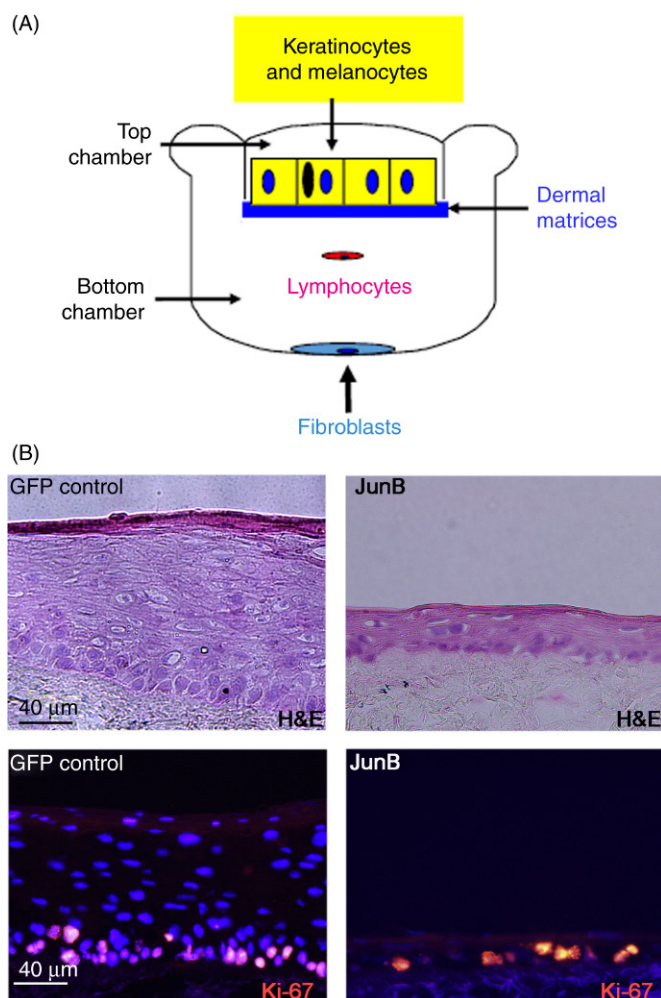
FIGURE 15.4 **Three-dimensional (3D) skin raft culture system.** (A) A schematic diagram depicting components of a 3D culture system. (B) Tissues generated by 3D culture with primary human keratinocytes transduced for expression for GFP control or JunB. Skin rafts were collected on day 4 for H&E and immunoflorescent staining with an antibody against Ki-67 *(orange)*, a cell proliferation marker. Nuclei (*blue*, Hoechst 3342).

Acknowledgment

References

Abel, E.L., Angel, J.M., Kiguchi, K., DiGiovanni, J., 2009. Multi-stage chemical carcinogenesis in mouse skin: fundamentals and applications. Nat. Protoc. 4, 1350–1362.

Aho, S., et al., 2004. Periplakin gene targeting reveals a constituent of the cornified cell envelope dispensable for normal mouse development. Mol. Cell. Biol. 24, 6410–6418.

Akdis, M., et al., 2003. T helper (Th) 2 predominance in atopic diseases is due to preferential apoptosis of circulating memory/effector Th1 cells. FASEB J. 17, 1026–1035.

Angel, P., Szabowski, A., Schorpp-Kistner, M., 2001. Function and regulation of AP-1 subunits in skin physiology and pathology. Oncogene 20, 2413–2423.

American Cancer Society, 2016. Cancer facts and figures. Available from: http://www.cancer.org/acs/groups/content/@research/documents/document/acspc-047079.pdf

Astrakhan, A., et al., 2007. Local increase in thymic stromal lymphopoietin induces systemic alterations in B cell development. Nat. Immunol. 8, 522–531.

Aszterbaum, M., et al., 1999. Ultraviolet and ionizing radiation enhance the growth of BCCs and trichoblastomas in patched heterozygous knockout mice. Nat. Med. 5, 1285–1291.

Avci, P., et al., 2013. Animal models of skin disease for drug discovery. Expert Opin. Drug Discov. 8, 331–355.

Avery, C.L., et al., 2011. A phenomics-based strategy identifies loci on APOC1, BRAP, and PLCG1 associated with metabolic syndrome phenotype domains. PLoS Genet. 7, e1002322.

Baker, R.G., Hayden, M.S., Ghosh, S., 2011. NF-kappaB, inflammation, and metabolic disease. Cell Metab. 13, 11–22.

Baldwin, Jr., A.S., 1996. The NF-kappa B and I kappa B proteins: new discoveries and insights. Annu. Rev. Immunol. 14, 649–683.

Bamford, S., et al., 2004. The COSMIC (Catalogue of Somatic Mutations in Cancer) database and website. Br. J. Cancer 91, 355–358.

Banerjee, S., et al., 2015. Der 11 is a major allergen for house dust miteallergic patients suffering from atopic dermatitis. J. Invest. Dermatol. 135, 102–109.

Barnes, K.C., 2010. An update on the genetics of atopic dermatitis: scratching the surface in 2009. J. Allergy Clin. Immunol. 125, 16–29, e1-16-29.e11.

Bartek, M.J., LaBudde, J.A., Maibach, H.I., 1972. Skin permeability in vivo: comparison in rat, rabbit, pig and man. J. Invest. Dermatol. 58, 114–123.

Bergeron, L., et al., 2012. Skin presenting a higher level of caspase-14 is better protected from UVB irradiation according to in vitro and in vivo studies. J. Cosmet. Dermatol. 11, 111–121.

Beronja, S., Livshits, G., Williams, S., Fuchs, E., 2010. Rapid functional dissection of genetic networks via tissue-specific transduction and RNAi in mouse embryos. Nat. Med. 16, 821–827.

Bieber, T., 2008. Atopic dermatitis. N. Engl. J. Med. 358, 1483–1494.

Black, R.A., et al., 1997. A metalloproteinase disintegrin that releases tumour-necrosis factor-alpha from cells. Nature 385, 729–733.

Blobel, C.P., 2005. ADAMs: key components in EGFR signalling and development. Nat. Rev. Mol. Cell Biol. 6, 32–43.

Boguniewicz, M., Leung, D.Y.M., 2011. Atopic dermatitis: a disease of altered skin barrier and immune dysregulation. Immunol. Rev. 242, 233–246.

Bowcock, A.M., 2004. Psoriasis genetics: the way forward. J. Invest. Dermatol. 122, xv–xv10.

Bowcock, A.M., 2005. The genetics of psoriasis and autoimmunity. Annu. Rev. Genomics Hum. Genet. 6, 93–122.

Bowcock, A.M., Krueger, J.G., 2005. Getting under the skin: the immunogenetics of psoriasis. Nat. Rev. Immunol. 5, 699–711.

Brady, D.C., et al., 2014. Copper is required for oncogenic BRAF signalling and tumorigenesis. Nature 509, 492–496.

Brash, D.E., et al., 1991. A role for sunlight in skin cancer: UV-induced p53 mutations in squamous cell carcinoma. Proc. Natl. Acad. Sci. USA 88, 10124–10128.

Briot, A., et al., 2009. Kallikrein 5 induces atopic dermatitis-like lesions through PAR2-mediated thymic stromal lymphopoietin expression in Netherton syndrome. J. Exp. Med. 206, 1135–1147.

Burns, C.A., Brown, M.D., 2005. Imiquimod for the treatment of skin cancer. Dermatol. Clin. 23, 151–164.

Cai, Y., et al., 2011. Pivotal role of dermal IL-17-producing gammadelta T cells in skin inflammation. Immunity 35, 596–610.

Candi, E., Schmidt, R., Melino, G., 2005. The cornified envelope: a model of cell death in the skin. Nat. Rev. Mol. Cell Biol. 6, 328–340.

Chan, J.R., et al., 2006. IL-23 stimulates epidermal hyperplasia via TNF and IL-20R2-dependent mechanisms with implications for psoriasis pathogenesis. J. Exp. Med. 203, 2577–2587.

Chavanas, S., et al., 2000. Mutations in SPINK5, encoding a serine protease inhibitor, cause Netherton syndrome. Nat. Genet. 25, 141–142.

Cheng, J., et al., 1992. Cachexia and graft-vs.-host-disease-type skin changes in keratin promoter-driven TNF alpha transgenic mice. Genes Dev. 6, 1444–1456.

Chiricozzi, A., et al., 2011. Integrative responses to IL-17 and TNF-alpha in human keratinocytes account for key inflammatory pathogenic circuits in psoriasis. J. Invest. Dermatol. 131, 677–687.

Chudnovsky, Y., Adams, A.E., Robbins, P.B., Lin, Q., Khavari, P.A., 2005. Use of human tissue to assess the oncogenic activity of melanoma-associated mutations. Nat. Genet. 37, 745–749.

Chun, H.J., et al., 2002. Pleiotropic defects in lymphocyte activation caused by caspase-8 mutations lead to human immunodeficiency. Nature 419, 395–399.

Consortium, E.P., 2012. An integrated encyclopedia of DNA elements in the human genome. Nature 489, 57–74.

Cook, P.W., et al., 1997. Transgenic expression of the human amphiregulin gene induces a psoriasis-like phenotype. J. Clin. Invest. 100, 2286–2294.

Dajee, M., Tarutani, M., Deng, H., Cai, T., Khavari, P.A., 2002. Epidermal Ras blockade demonstrates spatially localized Ras promotion of proliferation and inhibition of differentiation. Oncogene 21, 1527–1538.

Danilenko, D.M., 2008. Review paper: preclinical models of psoriasis. Vet. Pathol. 45, 563–575.

Dankort, D., et al., 2009. Braf(V600E) cooperates with Pten loss to induce metastatic melanoma. Nat. Genet. 41, 544–552.

de Gruijl, F.R., 1999. Skin cancer and solar UV radiation. Eur. J. Cancer 35, 2003–2009.

Demehri, S., Morimoto, M., Holtzman, M.J., Kopan, R., 2009. Skin-derived TSLP triggers progression from epidermal-barrier defects to asthma. PLoS Biol. 7, e1000067.

Descargues, P., et al., 2005. Spink5-deficient mice mimic Netherton syndrome through degradation of desmoglein 1 by epidermal protease hyperactivity. Nat. Genet. 37, 56–65.

Dhomen, N., et al., 2009. Oncogenic Braf induces melanocyte senescence and melanoma in mice. Cancer Cell 15, 294–303.

DiGiovanni, J., 1992. Multistage carcinogenesis in mouse skin. Pharmacol. Ther. 54, 63–128.

Dixit, V., Mak, T.W., 2002. NF-kappaB signaling. Many roads lead to madrid. Cell 111, 615–619.

Djian, P., Easley, K., Green, H., 2000. Targeted ablation of the murine involucrin gene. J. Cell Biol. 151, 381–388.

Eckert, R.L., Crish, J.F., Banks, E.B., Welter, J.F., 1997. The epidermis: genes on—genes off. J. Invest. Dermatol. 109, 501–509.

Eferl, R., Wagner, E.F., 2003. AP-1: a double-edged sword in tumorigenesis. Nat. Rev. Cancer 3, 859–868.

Eisemann, N., et al., 2014. Non-melanoma skin cancer incidence and impact of skin cancer screening on incidence. J. Invest. Dermatol. 134, 43–50.

El Ghalbzouri, A., Lamme, E., Ponec, M., 2002. Crucial role of fibroblasts in regulating epidermal morphogenesis. Cell Tissue Res. 310, 189–199.

Fallon, P.G., et al., 2009. A homozygous frameshift mutation in the mouse Flg gene facilitates enhanced percutaneous allergen priming. Nat. Genet. 41, 602–608.

Fan, H., Oro, A.E., Scott, M.P., Khavari, P.A., 1997. Induction of basal cell carcinoma features in transgenic human skin expressing Sonic hedgehog. Nat. Med. 3, 788–792.

Fanti, P.A., Dika, E., Vaccari, S., Miscial, C., Varotti, C., 2006. Generalized psoriasis induced by topical treatment of actinic keratosis with imiquimod. Int. J. Dermatol. 45, 1464–1465.

Fitch, E.L., et al., 2009. Inflammatory skin disease in K5.hTGF-beta1 transgenic mice is not dependent on the IL-23/Th17 inflammatory pathway. J. Invest. Dermatol. 129, 2443–2450.

Franzke, C.-W., et al., 2012. Epidermal ADAM17 maintains the skin barrier by regulating EGFR ligand-dependent terminal keratinocyte differentiation. J. Exp. Med. 209, 1105–1119.

Freeman, S.E., et al., 1989. Wavelength dependence of pyrimidine dimer formation in DNA of human skin irradiated in situ with ultraviolet light. Proc. Natl. Acad. Sci. USA 86, 5605–5609.

Fuchs, E., 2007. Scratching the surface of skin development. Nature 445, 834–842.

Furio, L., et al., 2014. Transgenic kallikrein 5 mice reproduce major cutaneous and systemic hallmarks of Netherton syndrome. J. Exp. Med. 211, 499–513.

Furio, L., et al., 2015. KLK5 inactivation reverses cutaneous hallmarks of Netherton syndrome. PLoS Genet. 11, e1005389.

Furuse, M., et al., 2002. Claudin-based tight junctions are crucial for the mammalian epidermal barrier: a lesson from claudin-1-deficient mice. J. Cell Biol. 156, 1099–1111.

Garrigue, J.L., et al., 1994. Optimization of the mouse ear swelling test for in vivo and in vitro studies of weak contact sensitizers. Contact Dermatitis 30, 231–237.

Gilliet, M., et al., 2004. Psoriasis triggered by toll-like receptor 7 agonist imiquimod in the presence of dermal plasmacytoid dendritic cell precursors. Arch. Dermatol. 140, 1490–1495.

Gober, M.D., Bashir, H.M., Seykora, J.T., 2013. Reconstructing skin cancers using animal models. Cancer Metastasis Rev. 32, 123–128.

Gomez, M.I., Seaghdha, M.O., Prince, A.S., 2007. *Staphylococcus aureus* protein A activates TACE through EGFR-dependent signaling. EMBO J. 26, 701–709.

Grachtchouk, M., et al., 2000. Basal cell carcinomas in mice overexpressing Gli2 in skin. Nat. Genet. 24, 216–217.

Grice, E.A., et al., 2009. Topographical and temporal diversity of the human skin microbiome. Science 324, 1190–1192.

Gudjonsson, J.E., Johnston, A., Dyson, M., Valdimarsson, H., Elder, J.T., 2007. Mouse models of psoriasis. J. Invest. Dermatol. 127, 1292–1308.

Guinea-Viniegra, J., et al., 2009. TNFalpha shedding and epidermal inflammation are controlled by Jun proteins. Genes Dev. 23, 2663–2674.

Ha, H.-L., et al., 2014. IL-17 drives psoriatic inflammation via distinct, target cell-specific mechanisms. Proc. Natl. Acad. Sci. USA 111, E3422–E3431.

Hahn, H., et al., 1996. Mutations of the human homolog of *Drosophila* patched in the nevoid basal cell carcinoma syndrome. Cell 85, 841–851.

Haider, A.S., Duculan, J., Whynot, J.A., Krueger, J.G., 2006. Increased JunB mRNA and protein expression in psoriasis vulgaris lesions. J. Invest. Dermatol. 126, 912–914.

Hamid, Q., et al., 1996. In vivo expression of IL-12 and IL-13 in atopic dermatitis. J. Allergy Clin. Immunol. 98, 225–231.

Hess, J., Angel, P., Schorpp-Kistner, M., 2004. AP-1 subunits: quarrel and harmony among siblings. J. Cell Sci. 117, 5965–5973.

Hoeijmakers, J.H., 2001. Genome maintenance mechanisms for preventing cancer. Nature 411, 366–374.

Holderfield, M., Deuker, M.M., McCormick, F., McMahon, M., 2014. Targeting RAF kinases for cancer therapy: BRAF-mutated melanoma and beyond. Nat. Rev. Cancer 14, 455–467.

Hoppe, T., et al., 2013. Moisturizing treatment of patients with atopic dermatitis and ichthyosis vulgaris improves dry skin, but has a modest effect on gene expression regardless of FLG genotype. J. Eur. Acad. Dermatol. Venereol. 29, 174–177.

Hoste, E., et al., 2011. Caspase-14 is required for filaggrin degradation to natural moisturizing factors in the skin. J. Invest. Dermatol. 131, 2233–2241.

Hoste, E., et al., 2013. Caspase-14-deficient mice are more prone to the development of parakeratosis. J. Invest. Dermatol. 133, 742–750.

Hsu, S., et al., 2007. Green tea polyphenol induces caspase 14 in epidermal keratinocytes via MAPK pathways and reduces psoriasiform lesions in the flaky skin mouse model. Exp. Dermatol. 16, 678–684.

Hu, Y., et al., 1999. Abnormal morphogenesis but intact IKK activation in mice lacking the IKKalpha subunit of IkappaB kinase. Science 284, 316–320.

Hu, Y., et al., 2001. IKKalpha controls formation of the epidermis independently of NF-kappaB. Nature 410, 710–714.

Huang, J.T., Abrams, M., Tlougan, B., Rademaker, A., Paller, A.S., 2009. Treatment of *Staphylococcus aureus* colonization in atopic dermatitis decreases disease severity. Pediatrics 123, e808–e814.

Imokawa, G., Akasaki, S., Minematsu, Y., Kawai, M., 1989. Importance of intercellular lipids in water-retention properties of the stratum corneum: induction and recovery study of surfactant dry skin. Arch. Dermatol. Res. 281, 45–51.

Israel, A., 2000. The IKK complex: an integrator of all signals that activate NF-kappaB? Trends Cell Biol. 10, 129–133.

Jefferson, J.J., Leung, C.L., Liem, R.K.H., 2004. Plakins: goliaths that link cell junctions and the cytoskeleton. Nat. Rev. Mol. Cell Biol. 5, 542–553.

Jiang, W., Ananthaswamy, H.N., Muller, H.K., Kripke, M.L., 1999. p53 protects against skin cancer induction by UV-B radiation. Oncogene 18, 4247–4253.

Jin, J.Y., Ke, H., Hall, R.P., Zhang, J.Y., 2011. c-Jun promotes whereas JunB inhibits epidermal neoplasia. J. Invest. Dermatol. 131, 1149–1158.

Jin, Y.J., et al., 2016. Epidermal CYLD inactivation sensitizes mice to the development of sebaceous and basaloid skin tumors. JCI Insight 1 (11), e86548.

Jochum, W., Passegue, E., Wagner, E.F., 2001. AP-1 in mouse development and tumorigenesis. Oncogene 20, 2401–2412.

Johansen, C., Kragballe, K., Rasmussen, M., Dam, T.N., Iversen, L., 2004. Activator protein 1 DNA binding activity is decreased in lesional psoriatic skin compared with nonlesional psoriatic skin. Br. J. Dermatol. 151, 600–607.

Johnson, R.L., et al., 1996. Human homolog of patched, a candidate gene for the basal cell nevus syndrome. Science 272, 1668–1671.

Jong, M.C., et al., 1998. Hyperlipidemia and cutaneous abnormalities in transgenic mice overexpressing human apolipoprotein C1. J. Clin. Invest. 101, 145–152.

Karin, M., Ben-Neriah, Y., 2000. Phosphorylation meets ubiquitination: the control of NF-[kappa]B activity. Ann. Rev. Immunol. 18, 621–663.

Ke, H., et al., 2010. The c-Jun NH2-terminal kinase 2 plays a dominant role in human epidermal neoplasia. Cancer Res. 70, 3080–3088.

Keller, M., Ruegg, A., Werner, S., Beer, H.-D., 2008. Active caspase-1 is a regulator of unconventional protein secretion. Cell 132, 818–831.

Kerdel, F.A.B.M., 2015. TNF inhibitors in psoriasis: a review. Semin. Cutan. Med. Surg. 34, S37–S39.

Ki, C.S., Na, D.L., Kim, D.K., Kim, H.J., Kim, J.W., 2002. Genetic association of an apolipoprotein C-I (APOC1) gene polymorphism with late-onset Alzheimer's disease. Neurosci. Lett. 319, 75–78.

Kim, J., et al., 2013. The indoor level of house dust mite allergen is associated with severity of atopic dermatitis in children. J. Korean Med. Sci. 28, 74–79.

Kjaer, T.N., Thorsen, K., Jessen, N., Stenderup, K., Pedersen, S.B., 2015. Resveratrol ameliorates imiquimod-induced psoriasis-like skin inflammation in mice. PLoS One 10, e0126599.

Ko, H.L., et al., 2014. Apolipoprotein C1 (APOC1) as a novel diagnostic and prognostic biomarker for lung cancer: a marker phase I trial. Thorac. Cancer 5, 500–508.

Kobayashi, T., et al., 2015. Dysbiosis and *Staphylococcus aureus* colonization drives inflammation in atopic dermatitis. Immunity 42, 756–766.

Kong, H.H., et al., 2012. Temporal shifts in the skin microbiome associated with disease flares and treatment in children with atopic dermatitis. Genome Res. 22, 850–859.

Kovalenko, A., et al., 2009. Caspase-8 deficiency in epidermal keratinocytes triggers an inflammatory skin disease. J. Exp. Med. 206, 2161–2177.

Krueger, J.G., Bowcock, A., 2005. Psoriasis pathophysiology: current concepts of pathogenesis. Ann. Rheum. Dis. 64 (Suppl. 2), ii30–ii36.

Kubica, M., et al., 2014. The skin microbiome of caspase-14-deficient mice shows mild dysbiosis. Exp. Dermatol. 23, 561–567.

Kulski, J.K., et al., 2005. Gene expression profiling of Japanese psoriatic skin reveals an increased activity in molecular stress and immune response signals. J. Mol. Med. (Berl.) 83, 964–975.

Lazarov, M., et al., 2002. CDK4 coexpression with Ras generates malignant human epidermal tumorigenesis. Nat. Med. 8, 1105–1114.

Lebwohl, M., 2003. Psoriasis. Lancet 361, 1197–1204.

Lee, P., et al., 2009. Dynamic expression of epidermal caspase 8 simulates a wound healing response. Nature 458, 519–523.

Lee, D.J., et al., 2015. Regulation and function of the caspase-1 in an inflammatory microenvironment. J. Invest. Dermatol. 135, 2012–2020.

Leyden, J.J., Marples, R.R., Kligman, A.M., 1974. *Staphylococcus aureus* in the lesions of atopic dermatitis. Br. J. Dermatol. 90, 525–530.

Leyva-Castillo, J.M., Hener, P., Jiang, H., Li, M., 2013. TSLP produced by keratinocytes promotes allergen sensitization through skin and thereby triggers atopic march in mice. J. Invest. Dermatol. 133, 154–163.

Li, Q., et al., 1999a. IKK1-deficient mice exhibit abnormal development of skin and skeleton. Genes Dev. 13, 1322–1328.

Li, Q., Van Antwerp, D., Mercurio, F., Lee, K.F., Verma, I.M., 1999b. Severe liver degeneration in mice lacking the IkappaB kinase 2 gene. Science 284, 321–325.

Li, C., et al., 2010. Development of atopic dermatitis-like skin disease from the chronic loss of epidermal caspase-8. Proc. Natl. Acad. Sci. USA 107, 22249–22254.

Lowes, M.A., et al., 2005. Increase in TNF-alpha and inducible nitric oxide synthase-expressing dendritic cells in psoriasis and reduction with efalizumab (anti-CD11a). Proc. Natl. Acad. Sci. USA 102, 19057–19062.

Lowes, M.A., Bowcock, A.M., Krueger, J.G., 2007. Pathogenesis and therapy of psoriasis. Nature 445, 866–873.

Lusis, A.J., et al., 1986. Regional mapping of human chromosome 19: organization of genes for plasma lipid transport (APOC1, -C2, and -E and LDLR) and the genes C3, PEPD, and GPI. Proc. Natl. Acad. Sci. USA 83, 3929–3933.

Maas-Szabowski, N., et al., 2001. Organotypic cocultures with genetically modified mouse fibroblasts as a tool to dissect molecular mechanisms regulating keratinocyte growth and differentiation. J. Invest. Dermatol. 116, 816–820.

Maatta, A., DiColandrea, T., Groot, K., Watt, F.M., 2001. Gene targeting of envoplakin, a cytoskeletal linker protein and precursor of the epidermal cornified envelope. Mol. Cell. Biol. 21, 7047–7053.

Makris, C., et al., 2000. Female mice heterozygous for IKK gamma/NEMO deficiencies develop a dermatopathy similar to the human X-linked disorder incontinentia pigmenti. Mol. Cell 5, 969–979.

Man, S.M., Kanneganti, T.D., 2016. Converging roles of caspases in inflammasome activation, cell death and innate immunity. Nat. Rev. Immunol. 16, 7–21.

Mao, J.H., et al., 2004. Mutually exclusive mutations of the Pten and ras pathways in skin tumor progression. Genes Dev. 18, 1800–1805.

Margulis, A., Zhang, W., Garlick, J.A., 2005a. In vitro fabrication of engineered human skin. Methods Mol. Biol. 289, 61–70.

Margulis, A., et al., 2005b. E-cadherin suppression accelerates squamous cell carcinoma progression in three-dimensional, human tissue constructs. Cancer Res. 65, 1783–1791.

Mariman, R., et al., 2016. *Lactobacillus plantarum* NCIMB8826 ameliorates inflammation of colon and skin in human APOC1 transgenic mice. Benef. Microbes 7, 215–225.

Meixner, A., et al., 2008. Epidermal JunB represses G-CSF transcription and affects haematopoiesis and bone formation. Nat. Cell Biol. 10, 1003–1011.

Miliani de Marval, P., et al., 2011. CYLD inhibits tumorigenesis and metastasis by blocking JNK/AP1 signaling at multiple levels. Cancer Prev. Res. (Phila) 4, 851–859.

Modi, B.G., et al., 2012. Langerhans cells facilitate epithelial DNA damage and squamous cell carcinoma. Science 335, 104–108.

Moniaga, C.S., et al., 2010. Flaky tail mouse denotes human atopic dermatitis in the steady state and by topical application with *Dermatophagoides pteronyssinus* extract. Am. J. Pathol. 176, 2385–2393.

Morimura, S., Oka, T., Sugaya, M., Sato, S., 2016. CX3CR1 deficiency attenuates imiquimod-induced psoriasis-like skin inflammation with decreased M1 macrophages. J. Dermatol. Sci. 82, 175–188.

Mossner, R., et al., 2005. Association of TNF-238 and -308 promoter polymorphisms with psoriasis vulgaris and psoriatic arthritis but not with pustulosis palmoplantaris. J. Invest. Dermatol. 124, 282–284.

Nakajima, K., et al., 2011. Distinct roles of IL-23 and IL-17 in the development of psoriasis-like lesions in a mouse model. J. Immunol. 186, 4481–4489.

Nakatsuji, T., et al., 2016. *Staphylococcus aureus* exploits epidermal barrier defects in atopic dermatitis to trigger cytokine expression. J. Invest. Dermatol. 136, 2192–2200.

Nasti, T.H., et al., 2016. A murine model for the development of melanocytic nevi and their progression to melanoma. Mol. Carcinog. 55, 646–658.

Neagu, M., et al., 2016. Chemically induced skin carcinogenesis: updates in experimental models (review). Oncol. Rep. 35, 2516–2528.

Nickoloff, B.J., Nestle, F.O., 2004. Recent insights into the immunopathogenesis of psoriasis provide new therapeutic opportunities. J. Clin. Invest. 113, 1664–1675.

Nilsson, M., et al., 2000. Induction of basal cell carcinomas and trichoepitheliomas in mice overexpressing GLI-1. Proc. Natl. Acad. Sci. USA 97, 3438–3443.

Oro, A.E., et al., 1997. Basal cell carcinomas in mice overexpressing sonic hedgehog. Science 276, 817–821.

Ortiz-Urda, S., et al., 2005. Type VII collagen is required for Ras-driven human epidermal tumorigenesis. Science 307, 1773–1776.

Ovaere, P., Lippens, S., Vandenabeele, P., Declercq, W., 2009. The emerging roles of serine protease cascades in the epidermis. Trends Biochem. Sci. 34, 453–463.

Paigen, K., 2003. One hundred years of mouse genetics: an intellectual history. II. The molecular revolution (1981-2002). Genetics 163, 1227–1235.

Palamara, F., et al., 2004. Identification and characterization of pDC-like cells in normal mouse skin and melanomas treated with imiquimod. J. Immunol. 173, 3051–3061.

Palmer, C.N., et al., 2006. Common loss-of-function variants of the epidermal barrier protein filaggrin are a major predisposing factor for atopic dermatitis. Nat. Genet. 38, 441–446.

Park, C.C., Choe, Y.B., Song, H.J., Choi, J.H., Kim, N.I., 2010. Comparison of the expression profile of junb, c-jun, and s100a8 (calgranulin a) in psoriasis vulgaris and guttate psoriasis. J. Eur. Acad. Dermatol. 24, 69.

Pasparakis, M., et al., 2002. TNF-mediated inflammatory skin disease in mice with epidermis-specific deletion of IKK2. Nature 417, 861–866.

Patel, U., Mark, N.M., Machler, B.C., Levine, V.J., 2011. Imiquimod 5% cream induced psoriasis: a case report, summary of the literature and mechanism. Br. J. Dermatol. 164, 670–672.

Peschon, J.J., et al., 1998. An essential role for ectodomain shedding in mammalian development. Science 282, 1281–1284.

Pierceall, W.E., Goldberg, L.H., Tainsky, M.A., Mukhopadhyay, T., Ananthaswamy, H.N., 1991. Ras gene mutation and amplification in human nonmelanoma skin cancers. Mol. Carcinog 4, 196–202.

Pleasance, E.D., et al., 2010. A comprehensive catalogue of somatic mutations from a human cancer genome. Nature 463, 191–196.

Porter, R.M., 2003. Mouse models for human hair loss disorders. J. Anat. 202, 125–131.

Presland, R.B., et al., 2000. Loss of normal profilaggrin and filaggrin in flaky tail (ft/ft) mice: an animal model for the filaggrin-deficient skin disease ichthyosis vulgaris. J. Invest. Dermatol. 115, 1072–1081.

Rawlings, A.V., Harding, C.R., 2004. Moisturization and skin barrier function. Dermatol. Ther. 17 (Suppl. 1), 43–48.

Reuter, J.A., et al., 2009. Modeling inducible human tissue neoplasia identifies an extracellular matrix interaction network involved in cancer progression. Cancer Cell 15, 477–488.

Rice, R.H., Green, H., 1977. The cornified envelope of terminally differentiated human epidermal keratinocytes consists of cross-linked protein. Cell 11, 417–422.

Ridky, T.W., Chow, J.M., Wong, D.J., Khavari, P.A., 2010. Invasive three-dimensional organotypic neoplasia from multiple normal human epithelia. Nat. Med. 16, 1450–1455.

Ruano, J., et al., 2016. Molecular and cellular profiling of scalp psoriasis reveals differences and similarities compared to skin psoriasis. PLoS One 11, e0148450.

Sales, K.U., et al., 2010. Matriptase initiates activation of epidermal pro-kallikrein and disease onset in a mouse model of Netherton syndrome. Nat. Genet. 42, 676–683.

Sandilands, A., et al., 2007. Comprehensive analysis of the gene encoding filaggrin uncovers prevalent and rare mutations in ichthyosis vulgaris and atopic eczema. Nat. Genet. 39, 650–654.

Sandilands, A., Sutherland, C., Irvine, A.D., McLean, W.H., 2009. Filaggrin in the frontline: role in skin barrier function and disease. J. Cell Sci. 122, 1285–1294.

Sano, S., et al., 2005. Stat3 links activated keratinocytes and immunocytes required for development of psoriasis in a novel transgenic mouse model. Nat. Med. 11, 43–49.

Sato, K., Takaishi, M., Tokuoka, S., Sano, S., 2014. Involvement of TNF-alpha converting enzyme in the development of psoriasis-like lesions in a mouse model. PLoS One 9, e112408.

Schmidt-Supprian, M., et al., 2000. NEMO/IKK gamma-deficient mice model incontinentia pigmenti. Mol. Cell 5, 981–992.

Scholl, F.A., Dumesic, P.A., Khavari, P.A., 2004. Mek1 alters epidermal growth and differentiation. Cancer Res. 64, 6035–6040.

Schon, M.P., Schon, M., 2007. Imiquimod: mode of action. Br. J. Dermatol. 157 (Suppl. 2), 8–13.

Schonthaler, H.B., Huggenberger, R., Wculek, S.K., Detmar, M., Wagner, E.F., 2009. Systemic anti-VEGF treatment strongly reduces skin inflammation in a mouse model of psoriasis. Proc. Natl. Acad. Sci. USA 106, 21264–21269.

Seitz, C.S., Freiberg, R.A., Hinata, K., Khavari, P.A., 2000. NF-kappaB determines localization and features of cell death in epidermis. J. Clin. Invest. 105, 253–260.

Sen, G.L., Reuter, J.A., Webster, D.E., Zhu, L., Khavari, P.A., 2010. DNMT1 maintains progenitor function in self-renewing somatic tissue. Nature 463, 563–567.

Sen, G.L., et al., 2012. ZNF750 is a p63 target gene that induces KLF4 to drive terminal epidermal differentiation. Dev. Cell 22, 669–677.

Sevilla, L.M., et al., 2007. Mice deficient in involucrin, envoplakin, and periplakin have a defective epidermal barrier. J. Cell Biol. 179, 1599–1612.

Shibata, S., et al., 2015. Adiponectin regulates psoriasiform skin inflammation by suppressing IL-17 production from gammadelta-T cells. Nat. Commun. 6, 7687.

Shtivelman, E., et al., 2014. Pathways and therapeutic targets in melanoma. Oncotarget 5, 1701–1752.

Simpson, C.L., Patel, D.M., Green, K.J., 2011. Deconstructing the skin: cytoarchitectural determinants of epidermal morphogenesis. Nat. Rev. Mol. Cell Biol. 12, 565–580.

Singh, B., Coffey, R.J., 2014. From wavy hair to naked proteins: the role of transforming growth factor alpha in health and disease. Semin. Cell Dev. Biol. 28, 12–21.

Smith, F.J., et al., 2006. Loss-of-function mutations in the gene encoding filaggrin cause ichthyosis vulgaris. Nat. Genet. 38, 337–342.

Soumelis, V., et al., 2002. Human epithelial cells trigger dendritic cell mediated allergic inflammation by producing TSLP. Nat. Immunol. 3, 673–680.

Spalding, J.W., Momma, J., Elwell, M.R., Tennant, R.W., 1993. Chemically induced skin carcinogenesis in a transgenic mouse line (TG. AC) carrying a v-Ha-ras gene. Carcinogenesis 14, 1335–1341.

Spergel, J.M., et al., 1998. Epicutaneous sensitization with protein antigen induces localized allergic dermatitis and hyperresponsiveness to methacholine after single exposure to aerosolized antigen in mice. J. Clin. Invest. 101, 1614–1622.

Stratis, A., et al., 2006. Pathogenic role for skin macrophages in a mouse model of keratinocyte-induced psoriasis-like skin inflammation. J. Clin. Invest. 116, 2094–2104.

Sun, J., Zhao, Y., Hu, J., 2013. Curcumin inhibits imiquimod-induced psoriasis-like inflammation by inhibiting IL-1beta and IL-6 production in mice. PLoS One 8, e67078.

Suto, H., et al., 1999. NC/Nga mice: a mouse model for atopic dermatitis. Int. Arch. Allergy Immunol. 120 (Suppl. 1), 70–75.

Swindell, W.R., et al., 2011. Genome-wide expression profiling of five mouse models identifies similarities and differences with human psoriasis. PLoS One 6, e18266.

Szabowski, A., et al., 2000. c-Jun and JunB antagonistically control cytokine-regulated mesenchymal-epidermal interaction in skin. Cell 103, 745–755.

Takeda, K., et al., 1999. Limb and skin abnormalities in mice lacking IKKalpha. Science 284, 313–316.

Tanaka, M., et al., 1999. Embryonic lethality, liver degeneration, and impaired NF-kappa B activation in IKK-beta-deficient mice. Immunity 10, 421–429.

Thomas, W.R., 2012. House dust allergy and immunotherapy. Hum. Vaccin. Immunother. 8, 1469–1478.

Tokumasu, R., et al., 2016. Dose-dependent role of claudin-1 in vivo in orchestrating features of atopic dermatitis. Proc. Natl. Acad. Sci. USA 113, E4061–E4068.

Tordesillas, L., et al., 2014. Skin exposure promotes a Th2-dependent sensitization to peanut allergens. J. Clin. Invest. 124, 4965–4975.

Truong, A.B., Kretz, M., Ridky, T.W., Kimmel, R., Khavari, P.A., 2006. p63 regulates proliferation and differentiation of developmentally mature keratinocytes. Gene Dev. 20, 3185–3197.

van der Fits, L., et al., 2009. Imiquimod-induced psoriasis-like skin inflammation in mice is mediated via the IL-23/IL-17 axis. J. Immunol. 182, 5836–5845.

van Steeg, H., et al., 2001. DNA repair-deficient Xpa and Xpa/p53+/− knock-out mice: nature of the models. Toxicol. Pathol. 29 (Suppl.), 109–116.

Vasioukhin, V., Degenstein, L., Wise, B., Fuchs, E., 1999. The magical touch: genome targeting in epidermal stem cells induced by tamoxifen application to mouse skin. Proc. Natl. Acad. Sci. USA 96, 8551–8556.

Wang, S., et al., 2014. SPINK5 knockdown in organotypic human skin culture as a model system for Netherton syndrome: effect of genetic inhibition of serine proteases kallikrein 5 and kallikrein 7. Exp. Dermatol. 23, 524–526.

White, S.I., Friedmann, P.S., Moss, C., Simpson, J.M., 1986. The effect of altering area of application and dose per unit area on sensitization by DNCB. Br. J. Dermatol. 115, 663–668.

Wolfram, J.A., et al., 2009. Keratinocyte but not endothelial cell-specific overexpression of Tie2 leads to the development of psoriasis. Am. J. Pathol. 174, 1443–1458.

Wong, S.Y., Reiter, J.F., 2011. Wounding mobilizes hair follicle stem cells to form tumors. Proc. Natl. Acad. Sci. USA 108, 4093–4098.

Wu, J.K., Siller, G., Strutton, G., 2004. Psoriasis induced by topical imiquimod. Australas. J. Dermatol. 45, 47–50.

Wullaert, A., Bonnet, M.C., Pasparakis, M., 2011. NF-kappaB in the regulation of epithelial homeostasis and inflammation. Cell Res 21, 146–158.

Xie, J., et al., 1998. Activating Smoothened mutations in sporadic basal-cell carcinoma. Nature 391, 90–92.

Yamanaka, K., et al., 2000. Skin-specific caspase-1-transgenic mice show cutaneous apoptosis and pre-endotoxin shock condition with a high serum level of IL-18. J. Immunol. 165, 997–1003.

Yang, T., et al., 2004. Epidermal detachment, desmosomal dissociation, and destabilization of corneodesmosin in Spink5−/− mice. Gene Dev 18, 2354–2358.

Yang, H., et al., 2013. One-step generation of mice carrying reporter and conditional alleles by CRISPR/Cas-mediated genome engineering. Cell 154, 1370–1379.

Yoo, J., et al., 2005. Spontaneous atopic dermatitis in mice expressing an inducible thymic stromal lymphopoietin transgene specifically in the skin. J. Exp. Med. 202, 541–549.

Yoo, J., Manicone, A.M., McGuire, J.K., Wang, Y., Parks, W.C., 2014. Systemic sensitization with the protein allergen ovalbumin augments local sensitization in atopic dermatitis. J. Inflamm. Res. 7, 29–38.

Yue, F., et al., 2014. A comparative encyclopedia of DNA elements in the mouse genome. Nature 515, 355–364.

Zanvit, P., et al., 2015. Antibiotics in neonatal life increase murine susceptibility to experimental psoriasis. Nat. commun. 6, 8424.

Zenz, R., et al., 2005. Psoriasis-like skin disease and arthritis caused by inducible epidermal deletion of Jun proteins. Nature 437, 369–375.

Zhang, J.Y., Green, C.L., Tao, S., Khavari, P.A., 2004. NF-kappaB RelA opposes epidermal proliferation driven by TNFR1 and JNK. Genes Dev. 18, 17–22.

Zhang, X., et al., 2015. RNA-Seq and ChIP-Seq Reveal SQSTM1/p62 as a key mediator of JunB suppression of NF-kappaB-dependent inflammation. J. Invest. Dermatol. 135, 1016–1024.

Zhao, L., et al., 2009. Srcasm inhibits Fyn-induced cutaneous carcinogenesis with modulation of Notch1 and p53. Cancer Res. 69, 9439–9447.

Zhou, Q., et al., 2014a. APOE and APOC1 gene polymorphisms are associated with cognitive impairment progression in Chinese patients with late-onset Alzheimer's disease. Neural Regen. Res. 9, 653–660.

Zhou, Q., et al., 2014b. Association between APOC1 polymorphism and Alzheimer's disease: a case-control study and meta-analysis. PLoS One 9, e87017.

Zitelli, J.A., 2005. Use of imiquimod for treating skin cancer. J. Am. Acad. Dermatol. 52, 177.

Page left intentionally blank

URINARY TRACT, KIDNEY, AND BOWEL

Page left intentionally blank

16

Animal Models of Kidney Disease

Zahraa Mohammed-Ali, Rachel E. Carlisle, Samera Nademi,
Jeffrey G. Dickhout

McMaster University and St. Joseph's Healthcare Hamilton, Hamilton, ON, Canada

1 INTRODUCTION

In this chapter, we detail numerous popular models of kidney disease. To organize the work, we have divided kidney disease into its acute and chronic manifestation and detail models of either form of kidney disease separately. The need for reliable models of both acute and chronic kidney disease is apparent from the increasing prevalence of these diseases in the population and the lack of effective therapies of these disease states to prevent progression to renal failure. Animal models allow the analysis of these complex disease states in terms of pathophysiology and the testing of new therapeutics to determine if they may interfere with disease progression and prevent renal failure. These preclinical studies of novel therapeutics can only be as accurate as the disease model systems they use to represent human disease. In recognition of this fact, models are discussed in terms of their similarities to human disease and shortcomings are indicated. It is our hope that this work will guide researchers in their choice of preclinical models and increase our collective ability to find solutions to progressive kidney disease.

2 ACUTE KIDNEY DISEASE

Acute kidney injury (AKI) is a form of acute kidney disease. AKI is defined by the Acute Kidney Injury Network (AKIN) as a sudden loss of renal function indicated by an increase in serum creatinine of 26.4 µmol/L (0.3 mg/dL) or more; a 50% increase in serum creatinine from baseline; or a reduction in urine output, oliguria (<0.5 mL/kg hourly for >6 h) (Farooqi and Dickhout, 2016). AKI is of critical importance in disease outcome, as its occurrence results in increased length of hospital stay and mortality (Silver et al., 2015). It also imparts a persistent increased risk of chronic kidney disease (CKD): 10-fold, end stage renal disease (ESRD): 3-fold, and premature death: 2-fold (Silver et al., 2015). Therapy for AKI is mainly supportive, with initiation of dialysis upon acute renal failure. As such, AKI represents a class of renal disease where exploration into effective therapies may take place. As AKI is difficult to diagnosis until after renal injury has occurred and serum creatinine is a trailing biomarker of AKI, animal models of AKI offer hope of developing effective interventions into AKI. These interventions then may be tested in a

human population at high risk of AKI, prophylactically. AKI can be classified by cause into three categories, prerenal, intrinsic, and postrenal AKI.

2.1 Prerenal Acute Kidney Injury

Prerenal AKI is caused by hypoperfusion of the kidney, either absent blood flow [renal ischemia/reperfusion injury (IRI)] or reduced blood flow (renal artery stenosis). In humans, prerenal AKI is typically caused by constriction or obstruction of the blood vessels supplying the kidney (Devarajan, 2006). Animal models mimic this effect by surgically clamping or clipping renal arteries to prevent/reduce renal blood flow (Al-Suraih and Grande, 2014; Wei and Dong, 2012) or inserting a copper stent to induce stenosis (Lerman et al., 1999). These animal models of prerenal AKI develop reduced renal function, as well as increased endoplasmic reticulum (ER) stress, apoptosis, inflammation, and fibrosis.

2.1.1 Renal Ischemia/Reperfusion

Renal IRI is caused by hypoperfusion of the kidney due to decreased cardiac output or constriction or obstruction of the blood vessels supplying the kidney (Devarajan, 2006). Risk factors for renal ischemia in humans include being over 50 years old, smoking, hypertension, diabetes, hypercholesterolemia, having a family history of coronary artery disease, bilateral renal artery stenosis, having only one kidney, and having one damaged kidney. The damage seen in animal models of renal ischemia is typically worse than human kidneys that have undergone ischemia.

This animal model of renal IRI restricts blood flow to the kidney, preventing oxygen from reaching the cells. However, this does not happen uniformly throughout the kidney, and blood flow is mainly reduced in the outer medulla (Devarajan, 2006; Venkatachalam et al., 1978). The medullary thick ascending limb and the S3 segment of the proximal tubules require high oxygen consumption; therefore, ischemia tends to result in damage primarily occurring in the corticomedullary region of the kidney (Venkatachalam et al., 1978), outer medulla (OM) (Fig. 16.1). However, with an increased ischemic time, the damage extends to the inner medulla (IM) (Fig. 16.1). Under ischemic conditions, glomerular filtration rate (GFR) is reduced and solute transport to the thick ascending limb is decreased to maintain oxygen levels. This increases production of reactive oxygen species (ROS), which work to further reduce GFR and increase activity, and therefore oxygen consumption, of the thick ascending limb (Venkatachalam et al., 1978). Renal ischemia increases serum creatinine levels and blood urea nitrogen levels.

Renal ischemia/reperfusion surgery is performed in an anaesthetized animal by clamping off the renal artery (or arteries) with an atraumatic microvascular clamp for a predetermined amount of time. The clamps are then removed, and the kidneys reperfuse (Wei and Dong, 2012). There are three methods of performing renal ischemia/reperfusion surgery: (1) bilateral renal ischemia, where both renal arteries are clamped and both kidneys undergo ischemia and subsequent reperfusion (Wei and Dong, 2012) (Fig. 16.1); (2) unilateral renal ischemia, where only one renal artery is clamped and one kidney undergoes ischemia and reperfusion (Le Clef et al., 2016); and (3) uninephrectomy (UNX) with unilateral renal ischemia, where one kidney is removed from the animal and the remaining kidney undergoes ischemia/reperfusion via renal artery clamping (Skrypnyk et al., 2013). After removal of the artery clamp(s), the animal is allowed to recover and is sacrificed at a time point determined by experimental end point. Earlier time points (hours to days) allow analysis of ER stress, inflammation, and apoptosis. Longer time points (days to weeks) allow examination of the fibrotic response. Renal injury in this model tends to be correlated to nephron mass. That is, in the UNX/unilateral IRI model, the animals develop significantly more chronic damage than the bilateral or unilateral IRI models, as they have reduced nephron mass caused by UNX (Cau et al., 2009).

Bilateral IRI is the model most similar to human renal ischemic injury, where both kidneys receive reduced blood supply. Renal function and functional recovery can be measured in this model (via serum creatinine analysis), unlike in the unilateral renal ischemia model. Serum creatinine levels should be elevated by 24 h, and depending on the severity of the model, will decrease or continue to increase until sacrifice/death (Wei and Dong, 2012). Unilateral renal IRI (without UNX) does not allow for measurement of renal function, as the remaining nonischemic kidney will compensate for reduced function of the injured kidney. Interestingly, the unilateral renal ischemia model develops more severe fibrosis than the bilateral model. As such, it is often used as a model of post-AKI fibrosis. UNX with unilateral renal ischemia reduces variability in results, when compared with bilateral renal ischemia (Skrypnyk et al., 2013). It also reduces surgery times, as it takes less ischemic time to cause similar levels of damage, when one kidney has been removed. However, fewer animals actually develop renal insufficiency in this model (Skrypnyk et al., 2013). Typically mice are used for IRI studies due to the availability of numerous transgenic strains; however, mice tend to demonstrate inconsistent results with regards to injury severity. Alternatively, rats, rabbits, and dogs have also been used to study renal IRI. While the molecular and cellular responses to IRI are complicated and not fully understood, it is known that this model causes ER stress, apoptosis, inflammation, and fibrosis.

AKI: Prerenal, IR
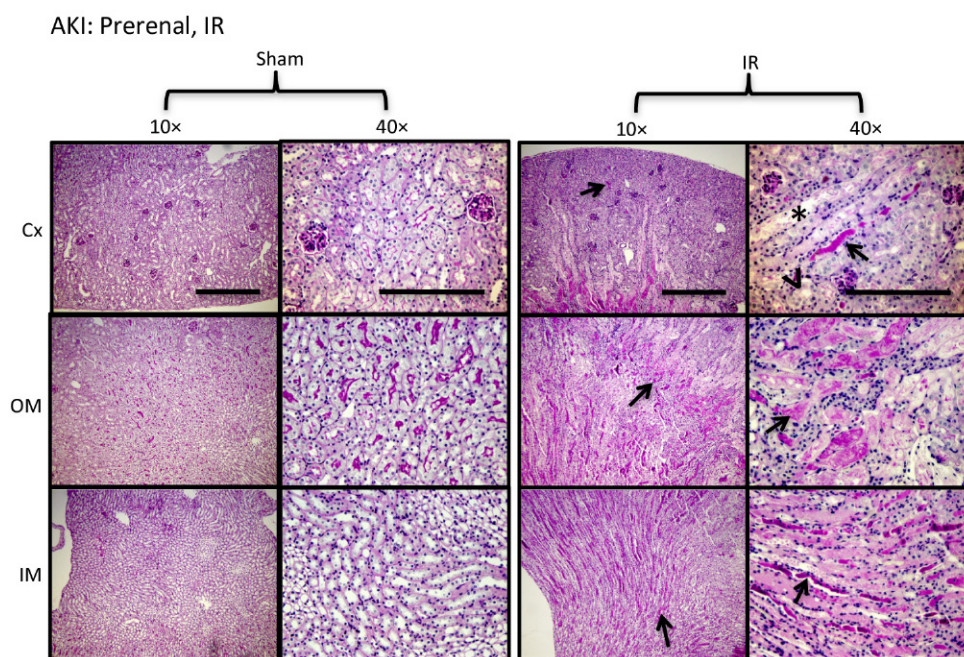
FIGURE 16.1 **Bilateral ischemia/reperfusion (IR)–induced acute kidney injury (AKI) in cortex (Cx), outer medulla (OM), and inner medulla (*IM*) compared to sham.** To induce ischemia, the right and left renal arteries of C57BL/6 male mice were clamped for 55 min. Blood flow was then allowed to recover for 48 h before sacrificing the animals. Periodic acid-Schiff staining shows IR-induced nephropathy depicted in the figure by cellular casts *(arrows)* in Cx, OM, and IM; loss of brush borders in proximal tubular cells *(arrow head)* in Cx; tubular dilation *(asterisk)* in Cx. Images were taken with an Olympus BX41 microscope using 10× (scale bar: 500 μm) and 40× (scale bar: 200 μm) objectives.

Protein folding in the ER is inhibited by prolonged lack of oxygen, ischemia, resulting in ER stress and activation of the unfolded protein response (UPR). It has been suggested that UPR activation is actually upregulated via the reperfusion stage of IRI, not ischemia (Montie et al., 2005). The UPR is activated within minutes of reperfusion, with increased expression of the molecular chaperone, GRP78; the proapoptotic protein, CHOP; and phospho-eIF2α (Montie et al., 2005; Yang et al., 2014). As with structural damage, the primary location for ER stress marker expression is the corticomedullary junction (Montie et al., 2005). Within 24 h of reperfusion, ER stress marker expression is typically decreased (Yang et al., 2014). Preventing ER stress by enhancing protein folding with a small molecular chemical chaperone prevents tubular injury, tubular necrosis, and tubular apoptosis (Gao et al., 2012). Further, knockout of CHOP protects the kidney from decreased renal function, structural damage, and apoptosis (Noh et al., 2015). Induction of ER stress and activation of the UPR can lead to various forms of cell death, such as necrosis, apoptosis, and pyroptosis (inflammatory apoptosis) (Yang et al., 2014).

Pyroptosis is characterized by activation of caspase-1. Caspase-1 activates proinflammatory cytokines, such as IL-1β and IL-18 (Yang et al., 2014). Preventing ER stress, specifically the upregulation of CHOP, can prevent the initiation of pyroptosis, indicating this inflammatory cell death is induced by ER stress. However, bone marrow transplants between wild-type and CHOP knockout mice demonstrate that the lack of CHOP in inflammatory cells is not protective against IRI (Yang et al., 2014).

ER stress and apoptosis are intertwined in renal ischemic injury. ER stress activates signaling pathways that lead to increased expression or activation of proapoptotic proteins (Yang et al., 2014). The proapoptotic family of caspases plays a significant role in IRI-mediated apoptosis, though the roles and pathways of each individual protein are still being determined. Caspase-11 activation is induced by CHOP, as is activation of its effector, caspase-1 (Yang et al., 2014), while GSK3β upregulates Bax expression, causing caspase-3 activation (Wang et al., 2010). Interestingly, melatonin inhibits caspase-3 activation in IRI, preventing apoptosis (Kunduzova et al., 2003). NGAL has also been shown to inhibit caspase-3 activation, as well as Bax expression (Zang et al., 2014). Using IGF-1 and a caspase inactivator, researchers were able to demonstrate that inhibiting apoptosis can prevent IRI-induced inflammation. Administering the apoptosis inhibitors prior to the onset of apoptosis prevented inflammation, while administration after the onset of apoptosis did not (Daemen et al., 1999).

The inflammatory response initiated by IRI is caused by endothelial and tubular cell dysfunction. Tubular atrophy and decreased cellular adhesion occurs with renal ischemic injury. β1-Integrin is a transmembrane protein found on the basal surface of renal tubular

epithelial cells. It acts as a cellular receptor for extracellular matrix (ECM) proteins, such as type IV collagen, and works to protect cell adhesion and epithelium integrity (Molina et al., 2005). Activated β1-integrin promotes adhesion, while decreased levels of β1-integrin contribute to renal tubular epithelial cell detachment into the tubule lumen. Mice treated with HUTS-21, which promotes activation of β1-integrin, prevented IRI, TNF-α activation, macrophage and T-lymphocyte infiltration, and intratubular protein cast formation caused by epithelial cell detachment (Molina et al., 2005). Directly inhibiting TNF-α activation protects renal function and prevents tubular necrosis, cell loss, intratubular debris, fibrosis, and tubular atrophy. Further, it prevents infiltration of CD3+ cells, as well as activation of p38 and MAPK (Cau et al., 2009). Toll-like receptors (TLR) activate the innate immune response, with TLR4 playing a key role in ischemia-induced IL-6 production. TLR4 knockout mice are protected from renal ischemic injury, as well as leukocyte infiltration into renal tissue (Chen et al., 2011). TLR2 is also increased in renal tubular epithelial cells after ischemia. Further, inactivation of TLR2 protected mice from IRI-mediated structural injury, as well as reduced neutrophil infiltration and expression of monocyte chemoattractant protein (MCP)-1, TNF-α, IL-6, and IL-1 (Leemans et al., 2005).

IRI-induced inflammation involves many types of inflammatory cells, such as neutrophils, macrophages, natural killer (NK) cells, and T cells (Akcay et al., 2009). The role of neutrophils in the IRI-induced inflammatory response is controversial. They are the first cells to infiltrate the reperfused kidney, but they do not appear to have much clinical significance (Patschan et al., 2012). Inhibiting macrophage production protects the kidney from IRI; similarly, a lack of T cells, as exemplified in nu/nu-mice and Rag-1 knockout mice, also protects from ischemic damage (Burne et al., 2001; Mombaerts et al., 1992). However, it has been suggested that CD4+ T cells can be protective or injurious, depending on the balance of IFN-γ and IL-4 production (Patschan et al., 2012). NK cells are essential in the innate immune response, as they are responsible for mediating neutrophil infiltration and IFN-γ production; recruitment of NK cells from the spleen can protect the kidney from ischemic injury (Zhang et al., 2014). Rapamycin, an immunosuppressant that increases NK cell infiltration in the kidney, was found to be renoprotective shortly after ischemic injury, preventing increased serum creatinine and blood urea nitrogen levels; however, rapamycin proved to aggravate renal injury long term (7 days after reperfusion) (Zhang et al., 2014).

As mentioned, fibrosis is an irreversible chronic result of IRI, and is aggravated by reduced nephron mass. IRI induces production of fibronectin and deposition of collagen, as well as increases renal expression of TGF-β1 (Chuang et al., 2014). Fibrosis occurs at a late stage, as it is caused by aberrant repair of the injured kidney. Activated macrophages remain present as the kidney is repaired; however, these macrophages produce profibrotic cytokines, increasing the rate and severity of fibrosis (Bonventre and Yang, 2011). Further, renal tubular epithelial cells undergo changes in proliferation, resulting in a secretory phenotype that increases production of profibrotic growth factors, such as TGF-β1 (Bonventre and Yang, 2011). TGF-β1 is responsible for activating supplementary profibrotic mechanisms through the induction of profibrotic gene expression. After binding with TGF-β1, the TGF-β1 receptor interacts with Smad2/3, which enters the nucleus to regulate transcription of target profibrotic genes (Chuang et al., 2014).

Ischemic preconditioning is a mechanism used to protect against further ischemia or nephrotoxic insults. IRI preconditioning has been shown to protect the kidney from further ischemic damage from 15 min to 8 days after the initial ischemic injury (Joo et al., 2006; Park et al., 2001). Typically, the preconditioning insult causes the normal response seen with renal ischemia. However, the secondary ischemic insult is protected from decreased renal function and renal structural injury, including tubular dilation, tubular swelling and necrosis, medullary luminal congestion, and hemorrhage (Joo et al., 2006; Park et al., 2001). Inflammatory markers, such as activated JNK, p38, and MAPK, are reduced (Park et al., 2001), as are ER stress markers, such as GRP78, phospho-PERK, ATF4, and sXBP-1 (Joo et al., 2006), and apoptotic markers, caspase-12 and cytochrome-c (Wu et al., 2009). While ischemic preconditioning proves to be renoprotective in rodents, its clinical significance is still being studied.

2.1.2 Renal Artery Stenosis

Renal artery stenosis is the narrowing of arteries transporting blood to the kidney(s). It is primarily caused by atherosclerosis in humans, and increases risk of developing hypertension, CKD, as well as cardiac morbidity and mortality (Al-Suraih and Grande, 2014). Much of the tissue injury caused by renal artery stenosis is due to ischemia, as the narrow arteries cause renal hypoperfusion. Risk factors for developing renal artery stenosis include age; being female; having hypertension or other vascular diseases, CKD, or diabetes; smoking; and high cholesterol. Animal models of renal artery stenosis develop characteristics found in human renal artery stenosis, such as renovascular hypertension, decreases in cortical and whole kidney volume, decreases in cortical and whole kidney blood flow, and impaired renal function. The decreases in renal volume and blood flow correlate to the severity of the stenosis, similar to human disease (Lerman et al., 1999). Unilateral renal artery stenosis produces a significant difference between the sizes of the kidneys; however, reduced renal size is not necessarily found in bilateral renal artery stenosis (Lerman

et al., 1999). Animals with atherosclerosis, as well as renal artery stenosis, develop more severe disease. They have reduced intrarenal microvascular density, as well as increased fibrosis, tubular damage, ROS, and renal microvascular media-to-lumen ratio (Sun et al., 2016). Histologically, animal models also develop vacuolization of tubular epithelial cells, crescent-shaped structures (mainly composed of podocytes) in the glomeruli, and additional podocytic injury; further, small renal arteries develop concentric intimal hyperplasia.

Porcine models of renal artery stenosis are commonly used due to comparable renal anatomy and physiology between pigs and humans. Due to this, the pathophysiology resulting from artificially induced renal artery stenosis is similar to naturally occurring renal artery stenosis in humans. For example, the intravascular copper stent model includes development of a vascular lesion (Lerman et al., 1999). This model is also noninvasive, which puts less stress on the animals involved. It involves percutaneously using a balloon to embed a copper wire in the renal artery, which causes stenosis. Invasive models of renal artery stenosis include the two-kidney/two-clip model, the two-kidney/one-clip model, and the one-kidney/one-clip model, and can be performed in mice, rats, dogs, and pigs (Al-Suraih and Grande, 2014). These models are comparable to the IRI models (bilateral, unilateral, and unilateral with UNX), though with reduced renal blood flow instead of absent renal blood flow. These models are sensitive to antagonists of the renin–angiotensin (Ang) system, as well as changes in sodium intake (Grossman, 2010). Animals are typically sacrificed 4–12 weeks after initiation of the model.

Limited research has been conducted examining the mechanisms and roles of ER stress, apoptosis, and inflammation in renal artery stenosis. As much of the damage in renal artery stenosis models is caused by reduced, but not absent, blood flow to the kidney(s), it is likely that much of the damage found is caused by similar mechanisms as those found in IRI models. ER stress is upregulated in this model, and therefore it is likely to play a role in the development of renal damage, as well as induction of apoptosis and inflammation (Yang et al., 2014). ER stress markers, such as CHOP and GRP94, have been found to be upregulated in endothelial and proximal tubular cells of kidneys that undergo this model, but not in distal tubular cells (Zhu et al., 2013).

As mentioned, little research has been conducted to examine apoptosis in depth; researchers tend to simply note the presence or absence of apoptosis (TUNEL staining) (Chade et al., 2003; Favreau et al., 2010; Zhu et al., 2013), but not examine the mechanism(s) from which it develops. Increased levels of the proapoptotic protein, CHOP, may play a role in the increased apoptosis found in this renal artery stenosis model (Zhu et al., 2013); however, it has also been suggested that

apoptosis is induced by ROS (Lerman et al., 2009). Apoptotic markers, such as increased cleaved caspase-3 and reduced Bcl-2, are found in the kidney of this model. Interestingly, mesenchymal stem cells, which have vascular repair qualities, reduce both ER stress and apoptosis in this model (Zhu et al., 2013).

In the copper stent model, inflammatory cell infiltration occurs in the renal artery near the location of the stent; this is primarily comprised of neutrophils, which are bordered by lymphocytes and macrophages. Occasional mononuclear cells can be found in the interstitium of the kidney of this model (Lerman et al., 1999). Inflammatory markers TNF-α and IL-1β are also increased in a model of unilateral renal artery stenosis; their expression was reduced by infusion of mesenchymal stem cells (Zhu et al., 2013). NF-κB, which is involved in a proinflammatory signaling pathway as well as a fibrotic pathway, was found to be significantly increased in a model of atherosclerotic renal artery stenosis, but not in a model without atherosclerosis (Sun et al., 2016). As mentioned, inhibiting apoptosis can prevent inflammation in IRI kidneys (Daemen et al., 1999). While this mechanism has not been studied in renal artery stenosis, it is possible that a similar system exists, whereby apoptosis leads to inflammation.

Renal artery stenosis causes renal fibrosis, which is worsened with atherosclerosis (Sun et al., 2016) or hypercholesterolemia (Chade et al., 2003), an atherosclerotic simulator. As mentioned, NF-κB, which activates profibrotic cytokines, is increased in tubular, interstitial, and glomerular cells. TGF-β is also increased in the renal tubules and glomeruli. Hypercholesterolemia increased levels of fibrosis, NF-κB, but not TGF-β in this model (Chade et al., 2003). When Smad3, which is downstream of TGF-β, is genetically knocked out of a mouse, the animal is almost entirely protected from renal artery stenosis. The kidneys developed less tubular atrophy, interstitial inflammation, and interstitial fibrosis (Warner et al., 2012).

2.2 Intrinsic Acute Kidney Injury

Intrinsic AKI is caused by structural damage to the kidney, specifically the glomeruli, renal tubules, and interstitium. Damage to these structures results in acute tubular necrosis, typically caused by nephrotoxic sources or ischemia. Damage is primarily found in the proximal tubules, though severe cases can also damage the distal tubules. Causes of intrinsic AKI include toxins and drugs, damage to the striated muscle, and sepsis.

2.2.1 Antibiotics

2.2.1.1 AMINOGLYCOSIDES

The effect of aminoglycosides on the kidney is most commonly studied using gentamicin. Gentamicin is frequently used to combat severe infections caused by

Gram-negative bacteria (Singh et al., 2012). It induces AKI by binding to phospholipids on the brush border, then translocating to the transmembrane protein, megalin. It is then endocytosed into the cell, where it binds to phospholipids in the lipid bilayer, reducing phospholipase activity and phospholipid metabolite production (Singh et al., 2012). Gentamicin alters other factors that may play a role in nephrotoxicity as well, such as superoxide anion and hydroxyl radical generation, antioxidant defense systems, and the renin–Ang system (Singh et al., 2012). Gentamicin accumulates in proximal tubular cells, altering the function of organelles. This results in tubular necrosis, proximal tubular cell vacuolization, mesangial hypercellularity, glomerular endothelial cell proliferation, cortical interstitial edema, and dilation and congestion of intertubular capillaries.

Typically, AKI is induced in animal models via intraperitoneal injection at a dose of 100 mg/kg for 5 days (Erdem et al., 2000), though other doses and end points have been used as well (40–200 mg/kg twice a day, for up to 14 days) (Bledsoe et al., 2008; Ortega et al., 2005; Volpini et al., 2006). While subcutaneous (Bledsoe et al., 2008) and intramuscular (Volpini et al., 2006) injections are also used, the intraperitoneal injection is the most similar to aminoglycoside-induced AKI in a clinical setting. The gentamicin model of AKI is typically performed on rats, as they are most similar to human gentamicin-induced nephrotoxicity (Suzuki et al., 1995), but other species are also used, such as mice (Whiting et al., 1981), dogs (Kai et al., 2013), and minipigs (Cui et al., 2015).

Gentamicin, once endocytosed, is reallocated into organelles via retrograde endosomal trafficking, including the ER and lysosomes (Sandoval et al., 2000). This absorption into the ER may be what initiates ER stress, which is exemplified by increased GRP78 and GRP94 expression and XBP1 splicing. Additionally, gentamicin treatment slightly increases renal expression of caspase-12 (Peyrou et al., 2007), as well as other apoptotic markers, such as caspase-3 (Bledsoe et al., 2008; Cui et al., 2015), cytochrome-c, and Bax (Suh et al., 2013). In vitro work demonstrates that apoptosis is dependent on the amount of drug accumulation in the cells (El Mouedden et al., 2000), though gentamicin-mediated lysosomal rupture also contributes to activation of proapoptotic pathways via protease release (Schnellmann and Williams, 1998). Further, it has been suggested that storage of gentamicin in lysosomes and other organelles is protective; however, gentamicin damages the lysosomal membrane (Servais et al., 2005), resulting in its release from the lysosome into the cytosol (Servais et al., 2006). Once in the cytosol, it activates the mitochondrial apoptosis pathway, induces oxidative stress, and decreases ATP stores (Morales et al., 2010; Simmons et al., 1980). Gentamicin induces upregulation of proinflammatory markers, such as NF-κB (Cui et al., 2015), TNF-α, MCP-1, and ICAM-1, and

infiltration of monocytes/macrophages and neutrophils (Bledsoe et al., 2008). It is believed that oxidative stress is responsible for the activation and nuclear translocation of NF-κB, which then regulates activation of the proinflammatory cytokines, chemokines, and adhesion molecules (Bae et al., 2014). After 10 days of gentamicin treatment, myofibroblasts are found in the renal interstitium, though fibrosis has yet to develop; several weeks after cessation of gentamicin treatment, fibrosis can be found in the kidney. This suggests that the interstitial myofibroblasts, which secrete ECM proteins and TGF-β, may encourage the development of gentamicin-induced fibrosis (Bledsoe et al., 2008).

2.2.1.2 NUCLEOSIDES

Tunicamycin is the most common agent used to study the effects of nucleoside antibiotics on the kidney. It is also commonly used in vitro to study the effects of ER stress in various cell types (Bassik and Kampmann, 2011). Tunicamycin inhibits protein glycosylation, resulting in vacuolization of the renal tubular epithelium and acute tubular necrosis (Carlisle et al., 2014). Tunicamycin is typically administered intraperitoneally at a dose of 0.5–1.0 mg/kg for 3 days (Carlisle et al., 2014; Marciniak et al., 2004). The principal area of renal damage caused by tunicamycin occurs in the corticomedullary region of the kidney (Carlisle et al., 2014) (Fig. 16.2).

By inhibiting N-linked glycosylation, tunicamycin induces ER stress, such as increased GRP78, and the proapoptotic protein, CHOP. CHOP is upregulated specifically in proximal tubular cells (Carlisle et al., 2014). CHOP knockout mice and mice with mutant GADD34 are resistant to tunicamycin-mediated renal damage (Carlisle et al., 2014; Marciniak et al., 2004), suggesting ER stress-mediated apoptosis is the primary mechanism of renal damage. Male and female mice actually have different responses to tunicamycin; female mice are more susceptible to damage in the S3 segment of the proximal tubule (Fig. 16.2, female), while male mice, and female mice pretreated with testosterone, are more susceptible to damage in the outer cortex (S1 and S2 segments). Female mice also demonstrate reduced expression of ER stress markers and proapoptotic markers (Hodeify et al., 2013). While limited studies have been performed on tunicamycin and renal inflammation, it has been noted that knockout of the inflammatory cytokine TNF-α or its receptor TNF-α-R1 results in increased sensitivity to tunicamycin-mediated ER stress and renal injury (Huang et al., 2011). While it is unknown if tunicamycin induces a fibrotic response, it is a likely outcome, as ER stress tends to facilitate the development of fibrosis (Tanjore et al., 2013).

2.2.1.3 CALCINEURIN INHIBITORS

Calcineurin inhibitors are administered to transplant patients because of their immunosuppressive properties.

AKI: Intrinsic, TM
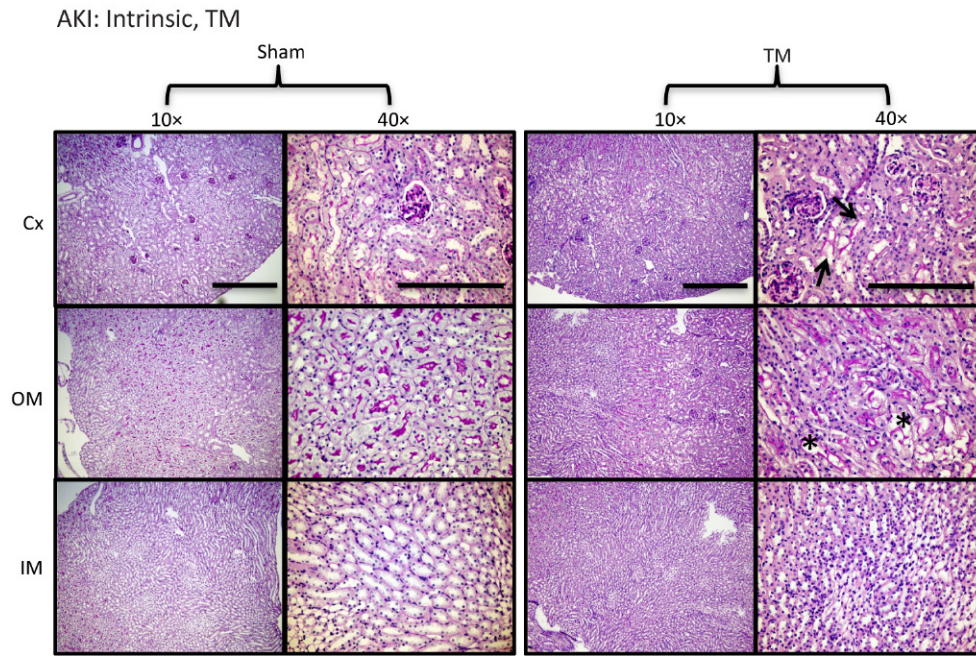
FIGURE 16.2 **Tunicamycin (TM)-induced acute kidney injury (AKI in cortex (Cx), outer medulla (OM), and inner medulla (IM) compared to sham.** Female mice were treated with saline (sham) or TM (single-bolus injection, 0.5 mg/kg) and sacrificed 3 days later. Periodic acid-Schiff staining revealed TM-induced damage to proximal convoluted tubules in Cx *(arrows)* and pars recta in OM *(asterisks)*. Images were taken with an Olympus BX41 microscope using 10× (scale bar: 500 μm) and 40× (scale bar: 200 μm) objectives.

The most common calcineurin inhibitors are cyclosporine and tacrolimus, which have both been used for decades (Naesens et al., 2009). Cyclosporine and tacrolimus competitively bind to molecules causing inhibition of the phosphatase activity of calcineurin. This alters the translocation of the nuclear factor of activated T cells (NFAT), and reduces T-cell activation (Naesens et al., 2009). It has been hypothesized that the immunosuppressive action of calcineurin inhibitors is correlated with their nephrotoxicity, suggesting that inhibition of calcineurin causes renal damage (Sigal et al., 1991). Apart from their immunosuppressive properties, calcineurin inhibitors also cause endothelial cell function impairment, resulting in vasoconstriction of glomerular arterioles and reduced blood flow. This leads to necrosis, hyalinosis of cells in afferent arterioles, and vacuolization of proximal tubular cells. These outcomes are consistent in both humans and animals, indicating translatability between species (Naesens et al., 2009).

In animals, cyclosporine is administered intraperitoneally or subcutaneously at a dose of 7.5–15.0 mg/kg/day (Islam et al., 2001; Pallet et al., 2008; Thomas et al., 1998). Tacrolimus is administered to the animal via ingestion or oral gavage (0.1–12 mg/kg/day) (Hoskova et al., 2014; Malinowski et al., 2010), intravenously at a dose of 0.5 mg/kg (McLaughlin et al., 2003), or intraperitoneally at 2 mg/kg/day (Al-Harbi et al., 2014).

ER stress is induced in the kidney, as demonstrated with increased GRP78 expression in rats (Pallet et al., 2008) and humans (Lhotak et al., 2012). It has been suggested that calcineurin inhibitors do not directly induce ER stress, but that vascular dysfunction causes hypoxia, which causes ER stress. As calcineurin inhibitors induce hypoxia (Zhong et al., 1998), it is likely that apoptosis occurs via the same mechanism as in IRI. Calcineurin inhibition may also directly induce proapoptotic genes, thereby increasing apoptosis in proximal tubular and interstitial cells (Servais et al., 2008). Calcineurin inhibitors are used as immunosuppressants and antiinflammatories; nonetheless, subclinical inflammation, with macrophage infiltration, is associated with calcineurin inhibition (Thomas et al., 1998). Cyclosporine induces fibrosis and fibrotic markers are increased, such as vimentin, fibronectin, type III collagen (Pallet et al., 2008), type I collagen, type IV collagen, and TGF-β1 (Islam et al., 2001). Interestingly, fibrosis and expression of fibrotic markers were prevented with ER stress inhibition (Pallet et al., 2008). Further, inhibiting TGF-β1 expression prevents renal function decline, arteriolar hyalinosis, and collagen expression; however, interstitial damage is worsened with TGF-β1 inhibition (Islam et al., 2001). In vitro work indicates that cyclosporine acts directly on tubulointerstitial fibroblasts and proximal tubular cells to increase collagen (Wolf et al., 1990). Acute renal damage caused by calcineurin inhibitors can progress to CKD, and can also cause hypertension (Naesens et al., 2009).

2.2.1.4 CHEMOTHERAPEUTICS

Chemotherapeutics, such as cisplatin, can cause AKI in up to one-third of patients. Cisplatin is a nephrotoxic antineoplastic drug used to treat solid-organ cancers (Miller et al., 2010). Cisplatin is freely filtered by the glomerulus, and becomes trapped in the renal cortex (Ozkok and Edelstein, 2014), causing acute tubular necrosis, dilation of proximal convoluted tubules, and sloughing of the epithelium, particularly in the corticomedullary region. Animals treated with cisplatin also display adverse clinical signs, such as altered behavior, anorexia, and dehydration (Peyrou et al., 2007).

Cisplatin is typically administered to mice or rats at a single intraperitoneal dose of 5–40 mg/kg; however, studies have used doses up to 100 mg/kg (Singh et al., 2012) or daily injections (Peyrou et al., 2007). Renal failure is induced within 72 h (Singh et al., 2012). The single-dose model is not directly translatable to human disease, as the animals are often administered a high dose of the drug, and then sacrificed days later. Low-dose/single-injection studies are somewhat relevant, as human patients often develop AKI after a single cisplatin treatment. A study providing mice with high-dose/single-injection or low-dose/weekly treatments of cisplatin, similar to what would be performed in human disease, revealed differences in renal function, renal injury, apoptosis, necrosis, inflammation, and fibrosis between the two treatments (Sharp et al., 2016).

Cisplatin has been shown to induce expression of ER stress markers in kidney cells both in vitro (Liu and Baliga, 2005) and in vivo (Peyrou et al., 2007). However, the UPR pathways do not appear to play a role in cisplatin-mediated apoptosis. ER stress–induced activation of caspase-12 appears to be responsible for cisplatin-induced cell death. Caspase-12 is induced by ER stress, but not by the pathways of the UPR (Mandic et al., 2003); thus, it is likely that caspase-12 is activated by protein aggregation and inhibiting protein misfolding could prevent cisplatin-induced acute tubular necrosis. Interestingly, inhibiting caspase activity, and thus preventing cellular autophagy, worsens renal damage and function in cisplatin-treated C57BL/6 mice (Herzog et al., 2012), though knockout of caspase-1 alone reduces injury (Faubel et al., 2004). The proinflammatory response induced by cisplatin results in infiltration of T cells, neutrophils, macrophages, and mast cells (Ozkok and Edelstein, 2014), as well as activation of cytokines, such as IL-1β, IL-6, NF-κB (Sung et al., 2008), TGF-β (Faubel et al., 2007), and TNF-α (Ramesh and Reeves, 2002). Inhibiting TNF-α expression, by pharmacological or genetic means, reduces cisplatin-mediated injury (Ramesh and Reeves, 2002), suggesting TNF-α is pivotal to cisplatin-mediated AKI. TLRs on renal parenchymal cells also play a significant role in cisplatin-mediated inflammation, activating the p38–MAPK

pathways (Zhang et al., 2008). Fibrosis can occur with single-dose (Yamate et al., 2005) or repeated-injection (Sharp et al., 2016) cisplatin treatment. Fibrosis occurs primarily in the corticomedullary region, and kidneys demonstrate increased TGF-β, fibronectin, collagen, and α-smooth muscle actin.

2.2.2 Heavy Metals

2.2.2.1 MERCURY

The nephrotoxic effects of mercury have been recognized for many years. However, the location of renal damage and physiological symptoms are dependent on the structure of the compound (Fowler, 1993). The inorganic mercuric chloride or organometallic methyl mercury are the compounds typically used in animal models, and induce damage in the S3 segment of the proximal tubule. Methyl mercury can also cause damage to the S2 segment of the proximal tubule, depending on the sex of the animal and dose and duration of exposure (Fowler, 1993). Mice and rats are given a subcutaneous injection of the mercuric compound, in doses ranging from 0.34 (Sanchez et al., 2001) to 10 mg/kg (Ahn et al., 2002), intraperitoneal injection of 6 mg/kg (Ewald and Calabrese, 2001), or 25 ppm in the drinking water daily (Abdel-Salam et al., 2010). Animals injected with 25 mg/kg mercuric chloride died within 2–4 min (Cunha et al., 2003). Animals are sacrificed at various time points, from 24 h (Stacchiotti et al., 2009) to 6 weeks (Abdel-Salam et al., 2010).

Mercury has a high bonding affinity with sulfur, specifically in the sulfhydryl groups in albumin, metallothionein, glutathione, and cysteine (Zalups, 2000). This leads to fragmentation of the plasma membrane (Kempson et al., 1977), mitochondrial swelling (Southard and Nitisewojo, 1973), and disruption of organelles (Fowler et al., 1975) in proximal tubular cells. Blebbing and sloughing of the brush border of proximal tubules (primarily the S3 segment) is also seen (Kempson et al., 1977).

It is unknown if heavy metal nephrotoxicity induces ER stress. While ER stress has not been examined in animals treated with mercury, rat renal epithelial cells treated with mercuric chloride have demonstrated increased GRP78 levels in vitro (Stacchiotti et al., 2009); this suggests that ER stress may be induced in the kidneys of treated animals. Apoptosis is present in the cortical proximal tubules, as demonstrated by transmission electron microscopy and TUNEL staining; severity of apoptosis is dependent on the dose and duration of treatment (Nava et al., 2000; Stacchiotti et al., 2009). Mercury sulfide, or cinnabar, a traditional Chinese medicine, has been studied as a source of mercurial nephrotoxicity. After daily ingestion, it increased inflammatory markers in rats, such as chemokines, selectins, ILs, and TIMPs. Further,

it causes renal tubulointerstitial fibrosis by 8 weeks of treatment (Wang et al., 2015b).

2.2.2.2 CHROMIUM

Acute exposure to chromium can cause many symptoms, such as gastrointestinal distress, fever, muscle cramps, liver damage, and renal failure. Hexavalent and trivalent chromium are used in many industrial and chemical processes, such as leather tanning, printing, and steel manufacturing (Singh et al., 2012). Hexavalent chromium is absorbed more readily than trivalent chromium, which must be reduced by glutathione, ascorbate, and hydrogen peroxide (Aiyar et al., 1991). Nephrotoxic effects of chromium are typically studied using mice, rats, or rabbits treated with potassium dichromate. Potassium dichromate is subcutaneously injected into the animal at a dose of 15 mg/kg (Appel et al., 1981), and the animal is typically sacrificed within 48 h (Khan et al., 2010). In humans, acute chromium exposure is normally due to ingestion, which differs from the animal model using subcutaneous injection.

The mechanisms by which chromium causes renal damage are largely unknown; damage includes tubular degeneration in the outer cortex, DNA damage, areas of interstitial inflammation, and intratubular protein cast formation (Sahu et al., 2014). Proapoptotic markers are increased, such as Bax and cleaved caspase-3, at 48 h postinjection. Levels of inflammatory markers, such as TNF-α and nuclear NF-κB, are also upregulated at this time point (Sahu et al., 2014). Research examining the fibrotic effects of chromium is lacking.

2.2.2.3 URANIUM

Acute uranium poisoning is studied in animal models involving uranyl nitrate or uranyl acetate (Singh et al., 2012). These animals develop reduced renal function, proteinuria, glucosuria, and tubular damage (Blantz, 1975). Uranyl-mediated damage occurs primarily in the S3 region of the proximal tubule (Bulger, 1986), causing a reduction in proximal tubular reabsorption of amino acids and low–molecular weight proteins. This leads to tubular necrosis, hyaline cast formation, vacuolization of tubules, and widening of the Bowman's capsule (Martinez et al., 2003). Animal models for uranium nephrotoxicity are typically performed in rats or mice, but vary with regards to dose of uranyl nitrate or uranyl acetate, as well as delivery method. Some studies reported using intravascular injection (5–25 mg/kg) (Avasthi et al., 1980; Kim et al., 1998), whereas others report intraperitoneal administration (0.5–10 mg/kg) (Priyamvada et al., 2010; Tolson et al., 2005) or subcutaneous injection (5 mg/kg) (Domingo et al., 1997). Each of these models develops renal failure within 3–5 days. Martinez et al. (2003) employed an oral gavage method, using 350 mg/kg uranyl nitrate in BALB/c mice, which developed AKI within 48 h.

As mentioned, renal damage, and thus apoptosis, occurs primarily in renal proximal tubular cells; electron microscopy demonstrates condensed chromatin and relatively intact cell organelles at 5 days posturanyl administration. Proximal tubules also demonstrate high expression levels of Bax and reduced levels of Bcl-2 (Sano et al., 2000). In vitro work demonstrates that uranium causes mitochondrial damage, decreasing MMPs, which produces ROS. Increased ROS ultimately leads to the activation of caspase-9 and caspase-3 (Thiebault et al., 2007). This pathway has yet to be confirmed in vivo. Inflammation occurs, with decreased innate and cellular immune function, and abnormal humoral immune function. Zheng et al. (2015) suggest that increased ROS activate the TNF-α pathway, leading to inflammation. Gene expression of other proinflammatory marks is also increased after acute exposure to uranium (Taulan et al., 2006). Uranium has been shown to cause renal interstitial fibrosis after chronic exposure (Zhu et al., 2009), but data on acute exposure are incomplete.

2.2.2.4 NONSTEROIDAL ANTIINFLAMMATORY DRUGS

Acetaminophen is an analgesic and antipyretic drug that is safe to use within the recommended doses; however, it can cause hepatic necrosis and renal failure in overdoses (Singh et al., 2012). Nonsteroidal antiinflammatory drugs (NSAIDs) typically cause damage through ischemia- or immune-related mechanisms. NSAIDs can cause reduced renal function, acute tubular necrosis, and acute interstitial nephritis, especially in the corticomedullary region (Choudhury and Ahmed, 2006). Animal models use a variety of NSAIDs, such as acetaminophen (Singh et al., 2012), indomethacin (Nagappan et al., 2015), and the NSAID metabolite p-aminophenol (Peyrou et al., 2007). Acetaminophen is typically used in a dose range of 375–13000 mg/kg via intraperitoneal injection (Singh et al., 2012), though occasionally ingestion is used as the delivery method (Kadowaki et al., 2012). Indomethacin is administered via oral gavage at a dose of 20 mg/kg (Nagappan et al., 2015), and p-aminophenol is administered by a single intraperitoneal injection at a dose of 225 mg/kg. Renal function is reduced in rodents within 6–24 h of NSAID treatment (Cekmen et al., 2009; Peyrou et al., 2007).

Information on the induction of ER stress by NSAID overdose is somewhat lacking. Treatment with the acetaminophen metabolite, p-aminophenol, resulted in increased expression of select ER stress markers (GRP94 and XBP1), but not others (GRP78) (Peyrou et al., 2007). Conversely, low-dose acetaminophen (30 mg/kg/day) was shown to reduce ER stress markers in obese kidneys (Wang et al., 2014a), suggesting more research on this topic is required. Indomethacin was shown to induce ER stress, but not apoptosis in the kidney (Nagappan et al., 2015). However, acetaminophen and

p-aminophenol promote apoptosis, as demonstrated by pyknotic nuclei (Ortiz, 2000) and increased cleaved caspase-12 (Peyrou et al., 2007). Proinflammatory cytokines, such as TNF-α and IL-6, are increased in rats overdosed with acetaminophen (Cermik et al., 2013), and a chronic inflammatory reaction is seen in response to a single dose of *p*-aminophenol (Green et al., 1969). In vitro data demonstrate that renal epithelial tubular cell death and fibroblast proliferation occur in response to acetaminophen (Yu et al., 2014). Further, chronic high doses of NSAIDs can cause medullary fibrosis (Choudhury and Ahmed, 2006), though it is unclear if acute overdose causes similar results.

2.2.2.5 RADIOCONTRAST MEDIA

Iodinated radiocontrast media are used in radiological imaging and cause AKI. Patients with volume depletion, congestive heart failure, preexisting renal failure, or diabetes mellitus (DM) are more likely to develop impaired renal function and renal damage (Singh et al., 2012). Radiocontrast medium is more viscous and has a higher osmolality than blood. As radiocontrast media travels through the kidney, water is reabsorbed, while the radiocontrast media is not. This increases the tubular fluid viscosity significantly, reducing perfusion and causing hypoxia (Seeliger et al., 2014). Radiocontrast medium causes renal damage by reducing blood flow and GFR, causing vasoconstriction of the vasa recta, and direct tubular toxicity, such as acute tubular necrosis, interstitial inflammation, and tubular cytoplasmic vacuolization (Deray, 1999). Risk of AKI increases with increasing dose volume and repeated administrations. Larger volumes are used for coronary angiography compared with other imaging studies; thus, AKI is more likely to develop in patients undergoing coronary angiography (Andreucci et al., 2014). Animal models involve intravascular iodinated contrast media of varying types, such as diatrizoate, ioxaglate, iohexol, and sodium iothalamate.

Similar to human studies, radiocontrast agents are administered to animals intravascularly, typically via aortic or jugular injection. Varying doses are used, depending on the specific agent; diatrizoate is used at 2–10 mL/kg for 2–5 min (Colbay et al., 2010; Erley et al., 1997; Yen et al., 2007), ioxaglate is used at 1 mL/min for 3 min (Touati et al., 1993), iohexol is used at 1.5–3 g/kg (Lee et al., 2006), and sodium iothalamate is used at 6 mL/kg for 2–3 min (Agmon et al., 1994). Renal failure can be induced within 1 h of administration (Agmon et al., 1994), though 24–48 h is more common.

Radiocontrast media induces ER stress, activating the PERK pathway, in rat renal proximal tubular cells in vitro (Wu et al., 2010a), but it is yet unknown if results are similar in vivo. As mentioned, radiocontrast agents induce apoptosis due to their hyperosmolality (Hizoh and Haller, 2002) and viscosity (Andreucci et al., 2014).

Radiocontrast media induce significant apoptosis within 24 h, particularly in the corticomedullary region, as demonstrated by caspase-3 and -9 upregulation (Ko et al., 2016) and decreased Bcl-2 expression (Wang et al., 2014b). Inhibiting autophagy, with 3-methyladenine, exacerbates apoptotic cell death (Ko et al., 2016), suggesting autophagy is renoprotective. Further, erythropoietin administration provides renoprotective effects, maintains renal function, and prevents apoptosis (Yokomaku et al., 2008). Interstitial inflammation is induced by contrast media, as demonstrated by macrophage infiltration (Ko et al., 2016) and increased proinflammatory cytokines IL-6 and TNF-α (Deng et al., 2015). Much like the apoptotic response, inflammatory response is worsened by inhibiting autophagy (Ko et al., 2016). Typically, radiocontrast agents do not cause renal fibrosis; however, gadolinium-based contrast agents, such as those used for MRI imaging, are associated with renal fibrosis, as well as fibrosis in other organs (Kallen et al., 2008). Radiocontrast medium–induced AKI does not develop into CKD, though it can increase the rate of progression if the patient already has CKD (Singh et al., 2012).

2.2.2.6 RHABDOMYOLYSIS

Rhabdomyolysis is a condition involving the breakdown of striated muscle fibers and release of myoglobin into the bloodstream. Myoglobin is typically filtered in the kidneys, but excessive levels can cause kidney damage. In humans, rhabdomyolysis is often caused by intrinsic muscle dysfunction, such as physical trauma, burns, disease, or excessive physical exertion; however, it can also be the result of certain metabolic disorders, hypoxia, drugs, toxins, infections, or temperature extremes.

Animal models of rhabdomyolysis include intramuscular injection of glycerol. Standard protocol calls for 50% glycerol–saline at a dose of 8 mL/kg (Savic et al., 2002), though 10 mL/kg has also been used (Vlahovic et al., 2007). The intramuscular injection is administered equally between both hind legs. Animals are usually, but not always, deprived of food and water 18–24 h prior to injection and sacrificed 24–48 h after injection (Sauriyal et al., 2012; Vlahovic et al., 2007), though longer time points are also observed (Korrapati et al., 2012). It has been suggested that models of sucrose injection or hemorrhage be performed, instead of dehydration, as this bears a more similar resemblance to clinical cases where humans are not chronically dehydrated prior to rhabdomyolysis (Zurovsky, 1993). Typically, animals used in rhabdomyolysis experiments are restricted to mice, rats, and rabbits (Singh et al., 2012).

While the mechanisms of glycerol's pathogenic effect on muscle are incompletely understood, it is known that the excessive myoglobin in the kidney causes tubular nephrotoxicity. Acute tubular necrosis develops

as excessive levels of myoglobin form intratubular protein casts, obstructing tubules (Vanholder et al., 2000). Further, there appears to be ischemic injury, possibly caused by intrarenal vasoconstriction, and the kidney undergoes ER stress, apoptosis, inflammation (Korrapati et al., 2012), and eventual fibrosis. While it is known that GRP78 levels are increased in the corticomedullary region of the kidney (Zhao et al., 2016), very little research has been performed on ER stress and rhabdomyolysis. Unfortunately, research demonstrating which of the three UPR pathways are activated has not been completed. Apoptosis occurs primarily in the renal tubular epithelial cells in this model of AKI (Komada et al., 2015; Singh et al., 2012). Increased expression of apoptotic markers, such as caspase-1 and -12, are found in the kidney (Komada et al., 2015; Zhao et al., 2016). Inflammatory markers include neutrophil and monocyte infiltration into the corticomedullary region and increased IL-1β, IL-6, and NF-κB activation (Komada et al., 2015; Korrapati et al., 2012). Komada et al. (2015) suggest that NLRP3 inflammasomes play a crucial role in the initial inflammation and injury caused by the glycerol injection, demonstrating that the inflammatory response, tubular apoptosis, and tubular injury precede leukocyte infiltration into the kidney. After 48 and 72 h of glycerol injection, TGF-β1 expression is increased, suggesting profibrotic activity (Korrapati et al., 2012). Mice injected with glycerol demonstrate fibrosis predominantly found in the interstitium and perivascular regions of the kidney; increased ECM deposition is made up of fibronectin, type IV collagen, and α-actin smooth muscle (Rubio-Navarro et al., 2015). Interestingly, macrophage depletion reduces renal fibrosis for up to 7 months after rhabdomyolysis initiation (Belliere et al., 2015).

2.2.2.7 SEPSIS

In humans, sepsis involves two stages that occasionally overlap, a proinflammatory stage that causes hypotension and organ dysfunction, and an antiinflammatory stage that leads to immunosuppression through reduced lymphocyte proliferation and increased lymphocyte apoptosis (Doi et al., 2009). The mechanism of renal damage is not completely elucidated; proposed mechanisms include endothelial dysfunction-mediated glomerular hypoperfusion, intraglomerular thrombosis, intrarenal hemodynamic changes, inflammatory response induced by systemic or local cytokines, and tubular dysfunction causing obstruction (Doi et al., 2009).

Animal models include endogenous toxin [lipopolysaccharide (LPS) injection], dysfunction of endogenous protective barrier (cecal ligation and puncture or colon ascendens stent peritonitis), or infusion of exogenous bacteria (Doi et al., 2009). LPS is typically administered intraperitoneally at a dose of 0.075–60 mg/kg (Cunningham et al., 2002; Szabo et al., 1994). The cecal ligation and puncture model involves ligating the cecum, below the iliocecal valve, and then puncturing the cecum with a needle. A small amount of feces is gently forced from the cecum through the perforation sites, and the animal is sutured and resuscitated (Toscano et al., 2011). This model is often touted as the "gold standard" sepsis model, as it is most similar to the complex response seen in humans (Dejager et al., 2011). The colon ascendens stent peritonitis method is performed by inserting a cannula into the ascending colon, and gently squeezing the colon to force feces into the cannula. This allows a continuous flow of intestinal bacteria into the peritoneum (Traeger et al., 2010). The infusion of exogenous bacteria model is not often used, as it is requires large animals, is labor intensive, and is less translatable than other methods (Doi et al., 2009). Septic AKI is usually induced in rodents, though sheep, pigs, and nonhuman primates have also been used. Results from these models may be variable due to different strains, species, and age (Zarjou and Agarwal, 2011).

ER stress appears to be induced with LPS-mediated septic AKI. GRP78, GRP94, spliced XBP1, and CHOP levels are upregulated 6 h after LPS injection. ER stress may play a protective role, as knockout of CHOP exacerbated LPS-mediated apoptosis, proinflammatory cytokine production, and inflammatory cell infiltration (Esposito et al., 2013). LPS injection induces proinflammatory cytokines, such as IL-1 and TNF-α (Okusawa et al., 1988; Tracey et al., 1986). Inhibiting either of these cytokines provides protection against renal damage (McNamara et al., 1993; Tracey et al., 1987). Further, genetic knockout of TNF-α-R1 protects against LPS-induced apoptosis and inflammation (Cunningham et al., 2002). Endotoxin-induced septic AKI induces interstitial and glomerular fibrosis within 9 h of treatment. Renal endothelial cells exhibit myofibroblast markers (Castellano et al., 2014), indicating that intrarenal vascular dysfunction may contribute to renal fibrosis.

2.3 Postrenal Acute Kidney Injury

Postrenal AKI is caused by an obstruction in the urinary tract, which increases intratubular pressure, reducing GFR. It also can reduce renal blood flow and activate inflammatory pathways that exacerbate the reduced GFR. Postrenal AKI can be caused by many factors, such as prostate cancer, gynecologic cancers, and renal or ureteral stones. Studies indicate that postrenal AKI accounts for less than 5% of all AKI cases (Basile et al., 2012).

2.3.1 Kidney Stones

Nephrolithiasis, or kidney stones, cause renal damage by acting as an obstruction in the kidney, which allows filtrate to build up and stretch the proximal ureter and collecting ducts. Kidney stones are derived from

crystal-forming substances, typically calcium, oxalate, and uric acid, and can form in the interstitium or in tubules (Khan, 2010). Crystals tend to aggregate at the corticomedullary region, papillary tips, and fornices, as these areas have reduced luminal diameter and crystal movement is blocked. The most common type of stone in humans is composed of calcium oxalate, though stones can also be composed of struvite or cystine (Khan, 2010). Formation of stones results in desquamation of epithelial cells in collecting ducts, aggregation of desquamated cells in the tubular lumen, degenerative alterations in the epithelium (Khan et al., 2006), and pyknosis of nuclei.

There are a number of animal models of kidney stone–mediated AKI, which are usually performed in rats (Oh et al., 2011), though mice (Okada et al., 2007), rabbits (Sarica et al., 2001), and pigs (Mandel et al., 2004) are also used. Hyperoxaluria can develop into calcium oxalate stones, and can be induced in animals by treatment with sodium oxalate, ammonium oxalate, hydroxyl-L-proline, ethylene glycol, glycolic acid, or glyoxalate (Khan, 2010). The features of calcium oxalate kidney stones are incredibly similar between human and rat subjects. Kidney stones develop acutely when animals are administered treatment via intraperitoneal injection (Khan, 1997), while ingestion leads to chronic development of stones (McMartin, 2009). Supplementing the animals with vitamin D or calcium chloride produces more acute results (Asplin et al., 1996). There are also a number of genetic models of nephrolithiasis and hyperoxaluria, though they simulate chronic renal damage and are inferior to the inducible models (Khan, 2010).

It is yet undiscovered if kidney stones induce ER stress in the kidney; however, levels of free radicals are increased (Thamilselvan et al., 1997) and oxidative stress is induced (Bas et al., 2009) in the early stages of kidney stone development. While crystals originally develop in renal tubules, they translocate to the interstitium; this movement is associated with an inflammatory response, characterized by leukocytes, monocytes, and macrophages (de Water et al., 1999). Renal fibrosis is present in human patients with kidney stones (Boonla et al., 2011), though it has yet to be thoroughly examined in animal models. In vitro studies suggest that the fibrotic response may be TGF-β dependent (Kanlaya et al., 2013).

2.3.2 Ureteral Obstruction

Ureteral obstruction is studied in animals using the unilateral ureteral obstruction (UUO) model, which involves obstructing one ureter. Ureteral obstruction induces TGF-β signaling, causing increased activation of Smad2/3 (Fu et al., 2006). The kidney develops tubular dilatation, flattening, and atrophy, as well as infiltration of inflammatory cells, and expansion of the interstitial area with ECM proteins (Yang et al., 2010). Originally, this model was performed in rabbits and dogs, though it has become more common to use rats and mice (Chevalier et al., 2009).

The UUO model can be used to study acute or chronic obstruction. Acute obstruction, where the insult is removed, can prevent or reverse renal injury, while chronic obstruction results in irreversible renal injury (Chevalier et al., 2009). UUO is an excellent model to use when studying the fibrotic response in the kidney, as exogenous toxins that can have additional effects on the kidney are not involved. Renal function cannot be measured in the UUO model, unless contralateral nephrectomy is performed. The UUO model is most commonly performed by ureteral ligation; in models of acute obstruction, where the insult is removed, tissue expansion around the ligation site can make removing the obstruction difficult (Chevalier et al., 2009). Alternatively, this model can be performed using microvascular clamps placed around the ureter (Puri et al., 2010). If used incorrectly, the microvascular clamps can injure the ureter or only partially obstruct the ureter. Partial UUO models are also sometimes studied, using silastic tubing (Hesketh et al., 2014) or partially ligating the ureter of a neonatal mouse (Thornhill et al., 2005). Loss of renal function typically occurs within 24 h, with fibrosis developing by 1–2 weeks of obstruction (Chevalier et al., 2009).

UUO induces ER stress in the kidney, particularly in the renal tubular cells, as demonstrated by increased GRP78 and CHOP expression (Fan et al., 2015; Liu et al., 2015). UUO-mediated renal tubular epithelial cell injury is partially caused by ischemia (Chevalier et al., 2009), which may contribute to the induction of ER stress. ER stress–dependent apoptosis is subsequently induced in the renal tubules (Liu et al., 2015; Yoneda et al., 2001). Genetic knockout of MKK3, which can be activated by ER stress (Darling and Cook, 2014), prevents UUO-mediated apoptosis and an early inflammatory response, but not fibrosis (Ma et al., 2007). Further, genetic knockout of Smad3 [which is also activated by ER stress (Tanjore et al., 2013)] prevented apoptosis, inflammation, and fibrosis mediated by UUO. It was suggested that apoptosis is induced indirectly of Smad signaling, while inflammation and fibrosis are directly caused by Smad3 activation (Inazaki et al., 2004). Apoptosis and inflammation can lead to a profibrotic response in this model. Apoptosis leads to atubular glomeruli and tubular atrophy, while cytokines that induce fibroblast proliferation and activation are released from macrophages in the interstitium (Chevalier et al., 2009). It has also been suggested that cells undergo cellular plasticity, with tubular epithelial cells, vascular endothelial cells, and pericytes differentiating into a myofibroblast phenotype (Chevalier et al., 2009).

3 CHRONIC KIDNEY DISEASE: ANIMAL MODELS

CKD is an important degenerative disease of the organs with an increasing prevalence and incidence (Jha et al., 2013). CKD is more likely to occur in older individuals, and the demographic shift in many societies toward a more aged population may, in part, explain its increasing prevalence (Jha et al., 2013). The prevalence of CKD on a global basis is about 10%–15% (Jha et al., 2013). The disease is not curable; although, interventions to slow its progression to ESRD are prevalent. Unlike AKI, the damage that occurs in the kidney is permanent, thus preventing disease progression and preserving organ function is of great importance. Strategies to prevent CKD progression, according to the 2013 KDIGO guidelines, include blood pressure control and renin/angiotensin/aldosterone system (RAAS) blockade, tight glycemic control in the case of diabetic nephropathy (DN) (target A1C of 7%), lowering of salt intake below 2 g of sodium in adults unless contraindicated, and lifestyle modification with physical activity, BMI (20–25), and smoking cessation. However, animal models are leading to an increasingly detailed understanding of the pathophysiology of CKD progression. This in turn offers real opportunities to specifically target the aspects of CKD pathology that leads to progression, including the activation of the immune system, renal interstitial fibrosis, and proteinuria/albuminuria as key mediators of progression. As such, animal models of CKD offer appropriate preclinical test systems for novel therapeutics aimed at preventing CKD progression.

3.1 Hypertensive CKD

Hypertension has been reported to occur in 85%–95% of patients with CKD (stages 3–5) (Rao et al., 2008). Hypertension has been considered a cause for CKD development and is an independent risk factor for CKD progression to ESRD, as well as cardiovascular events in CKD patients, such as myocardial infarction and stroke (Barri, 2008). In the RENAAL study, every 10-mmHg rise in systolic blood pressure increased the risk for ESRD or death by 11% (Bakris et al., 2003). Further, antihypertensive drugs, such as β-blockers and dihydropiridine calcium channel blockers, are widely used in the treatment of CKD patients. Along with increased blood pressure, hypertensive CKD in humans is characterized by proteinuria and glomerulosclerosis, resulting in declining GFR (Rao et al., 2008). Renal histological analysis shows interstitial fibrosis and associated renal inflammation, where T cells and macrophages have been implicated in the pathogenesis and progression of CKD (Silverstein, 2009). The accumulation of unfolded proteins in the ER has been reported in human CKD (Wu et al., 2010c), and results in the activation of the UPR. The UPR results in the dissociation of GRP78, an important regulatory chaperone protein, from three ER transmembrane proteins: PKR (double-stranded RNA-dependent protein kinase)–like ER protein kinase (PERK), inositol-requiring enzyme 1 (IRE1), and activating transcription factor 6 (ATF6) (Cybulsky, 2010; Dickhout and Krepinsky, 2009; Inagi, 2010). These three pathways are important in determining the fate of renal glomerular and tubular cells during CKD. The IRE1α and PERK pathway activate important apoptosis, autophagy, and inflammatory pathways that have been implicated in CKD pathogenesis (Mohammed-Ali et al., 2015a; Sano and Reed, 2013). Animal models of hypertensive CKD discussed here display most of the features of human hypertensive CKD and its associated comorbidities, particularly cardiovascular disease.

3.1.1 Spontaneously Hypertensive Rat Model

The spontaneously hypertensive rat (SHR) is the most commonly used model of hypertension and cardiovascular disease. The SHR strain was produced by Okamoto and Aoki (1963) by selective inbreeding of Wistar–Kyoto (WKY) rats with high blood pressure. Therefore, normotensive WKY rats are employed as normotensive controls in studies on SHRs. Hypertension starts to develop in these rats at 5–6 weeks of age, and blood pressure plateaus at approximately 50–60 days of age to remain stable or slightly decrease thereafter (Bianchi et al., 1974; Dickhout and Lee, 1997). In the early stages of hypertension, SHRs experience increased cardiac output and normal total peripheral resistance; however, as the hypertensive state stabilizes, cardiac output returns to normal and hypertrophied blood vessels produce a higher total peripheral resistance (Dickhout and Lee, 1997; Smith and Hutchins, 1979). Proteinuria, glomerulosclerosis, and interstitial fibrosis along with characteristics of cardiovascular disease, such as cardiac hypertrophy, begin to develop between the initiation of hypertension and its plateau phase at 40 weeks (Conrad et al., 1995; Feld et al., 1981; Ofstad and Iversen, 2005). Between 14 and 15 weeks, renal pathology begins to appear and may be exacerbated by a high-salt diet (HSD); however, this animal model is mostly salt resistant (Fig. 16.3). Between 30 and 32 weeks, male SHRs exhibit a 20%–30% decrease in GFR (Reckelhoff et al., 1997) as renal pathology progresses. Age-related GFR decrease is absent in female SHRs. Female SHRs also have approximately sixfold lower proteinuria (Reckelhoff et al., 1997). Some level of protein cast formation can be seen at 40 weeks and this increases with time (Ofstad and Iversen, 2005). Inflammation in the form of lymphocyte and macrophage infiltrates, as well as the increased expression of cytokines and chemokines has been observed at the prehypertensive stage (3 weeks) in renal tissue of SHRs (Biswas and de Faria, 2007; Rodriguez-Iturbe et al., 2004). Treatment
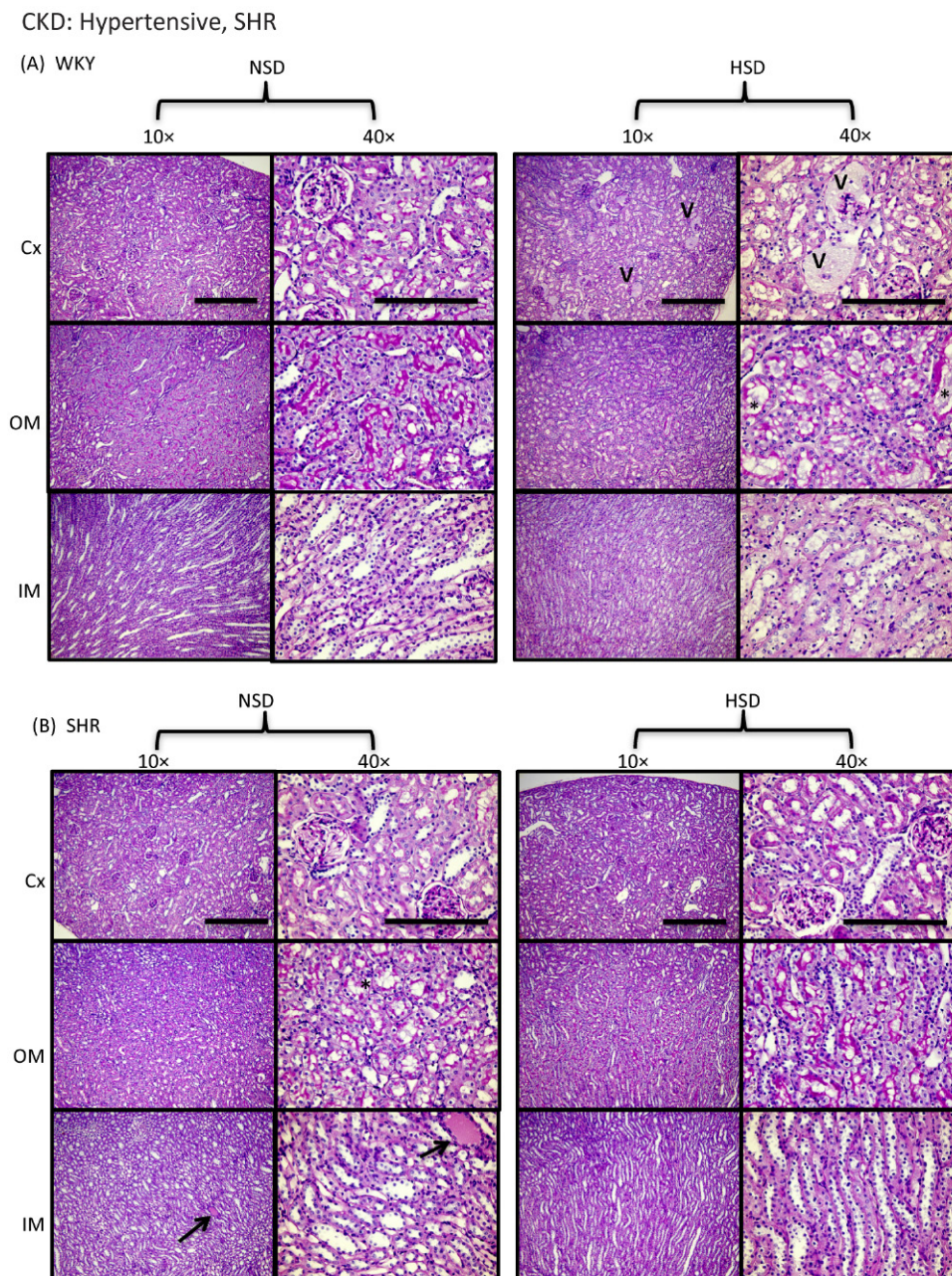
FIGURE 16.3   The effects of high- or normal-salt diet (HSD and NSD) on spontaneously hypertensive rats (SHR) compared to normotensive Wistar Kyoto (WKY) control rats. (A) Control WKY rats and (B) SHRs were given NSD (0.4% NaCl) or HSD (8% NaCl) for 4 weeks from 12 weeks of age. WKY rats fed NSD demonstrated normal renal histology, but WKY rats that were given HSD showed nephropathology, such as glomerular alterations in Bowman's space in the Cx *(arrow head)* and tubular dilation *(asterisk)* in the OM. SHRs that were given NSD suffered from minor protein cast nephropathy *(arrows)* in IM, and tubular dilation *(asterisk)* in OM. SHRs that were fed HSD showed similar pathology. Images were taken with an Olympus BX41 microscope using 10× (scale bar: 500 µm) and 40× (scale: bar 200 µm) objectives. CKD, chronic kidney disease.

with antiinflammatory agents leads to a reduction in blood pressure and inflammation in adult SHRs (Rodriguez-Iturbe et al., 2002, 2005). Oxidative stress precedes inflammation (occurs at 2 weeks) in SHR kidneys (Biswas and de Faria, 2007). Inflammatory and ER stress marker expression have been reported in the blood vessels and cardiac tissue of SHRs (Carlisle et al., 2016;

Guo and Yang, 2015; Miguel-Carrasco et al., 2010; Sanz-Rosa et al., 2005; Spitler et al., 2013; Sun et al., 2015). Compared to other models of hypertensive CKD, such as the Dahl S model, SHRs develop a much lower level of renal injury. The absence of progressive renal damage has been attributed to enhanced preglomerular vasoconstriction, which prevents systemic hypertension from

being transmitted to the glomeruli (Arendshorst and Beierwaltes, 1979; Kimura and Brenner, 1997). Combining UNX with the SHR model intensifies and accelerates glomerulosclerosis, urinary protein excretion, and fibrosis (Dworkin and Feiner, 1986; Kinuno et al., 2005). These changes have been reported due to inhibition of vascular narrowing of the preglomerular resistance vessels by UNX. Adaptations to UNX, such as glomerular enlargement are also impaired in the SHR (Kinuno et al., 2005). Alternatively, placing SHRs on high salt accelerates the development of hypertension and cardiac remodeling (Yu et al., 1998). Further, HSD–fed SHRs have higher urinary protein excretion and glomerular damage than those fed low-salt diets (Blizard et al., 1991). The SHR has become the model of choice to test antihypertensive drugs. Another valuable contribution of the SHR is in mapping and identification of genes responsible for the development of hypertension. Although, just like humans, the SHR model experiences a progression starting with a prehypertensive, developing, and sustained hypertensive phase, the life spans of SHRs (1.5–2.5 years) and their normotensive controls (2.5–3 years) are short. This makes the SHR convenient for the study of hypertension and aging. Furthermore, the SHR model is also suited for the study of gender in hypertension. Moreover, SHR has been crossed with other strains to create new models, such as the SHR heart failure (SHHF) rat to model congestive heart failure secondary to essential hypertension and the stroke-prone SHR (SHRSP), a unique model of severe hypertension and hemorrhagic stroke.

3.1.2 Dahl Salt-Sensitive Rat

The Dahl salt-sensitive (DSS) rat is another model of hypertensive CKD and develops hypertension when fed an HSD (Dahl et al., 1962, 1963). In experiments with this strain, low-salt diet generally involves 0.1%–0.4% NaCl, whereas high salt refers to 4%–8% NaCl diet (De Miguel et al., 2010; Hayakawa et al., 1997; Rapp and Dene, 1985; Yu et al., 1998). Upon high-salt feeding, these rats rapidly develop significant hypertension, mesangial expansion, and glomerulosclerosis (Raij et al., 1984). Salt-resistant Brown–Norway (BN) and consomic rats (SS. BN13) in which chromosome 13 from the BN has been introgressed into the Dahl S genetic background are included as salt-resistant controls in experiments with the Dahl S (Cowley et al., 2001; Hoagland et al., 2004). The increase in mean arterial pressure is attributed to sodium retention, and can be prevented through the use of diuretics (Greene et al., 1990; Tobian et al., 1979). Along with hypertension, Dahl S rats experience endothelial dysfunction and cardiac hypertrophy and fibrosis (Hayakawa et al., 1997; Yu et al., 2003). Cardiac hypertrophy is comparable to that seen in the SHR, but cardiac failure occurs much earlier in the Dahl S than in the SHR (Hasenfuss, 1998). Urinary excretion of protein, albumin,

and nephrin has been shown in Dahl S rats on high salt (Hye Khan et al., 2013). Protein cast formation has been reported in the medulla (Hye Khan et al., 2013; Rapp and Dene, 1985; Yu et al., 2003) and can also be observed in the cortex (Fig. 16.4). Renal interstitial fibrosis and inflammation in the form of T-cell and macrophage infiltrates has been documented in the cortex and medulla associated with renal damage in this model (De Miguel et al., 2010; Hye Khan et al., 2013; Mattson et al., 2006). High-salt Dahl S rats also show an increased renal expression of ER stress genes (Hye Khan et al., 2013). As with most rat models, the DSS model is cost effective, easily manageable, time efficient, and noninvasive. Salt sensitivity makes the Dahl S clinically relevant. Renal injury in this model is similar to that seen in patients with DN (O'Bryan and Hostetter, 1997; Ritz and Orth, 1999) and in hypertensive black Americans (Campese, 1994; Cowley and Roman, 1996), who are 5 times more likely to progress to ESRD than white Americans (Hsu et al., 2003; Norris et al., 2006).

3.1.3 Renal Mass Reduction: 5/6 Nephrectomy

The 5/6 nephrectomy model entails reducing the total mass of the kidney by 5/6th. The most common technique involves a two-step procedure. A full UNX is performed on one kidney. Two-thirds of the remnant kidney is then ablated either by anterior (Al Banchaabouchi et al., 1998) or posterior (Ma and Fogo, 2003) renal artery branch ligation or by kidney pole resection (Kren and Hostetter, 1999; Leelahavanichkul et al., 2010). The ligation method is not feasible in the mouse due to limited artery branching; however, the polar excision method can be used in both rats and mice (Yang et al., 2010). Various mouse and rat strains are differentially responsive to renal mass reduction in terms of CKD progression (Fleck et al., 2006; Ortiz et al., 2015). Both mice and rats experience hypertension, glomerular and tubulointerstitial damage, and proteinuria as a result of this model, but CKD progression is accelerated in some strains. The CD-1 strain of mice has shown progressive increase in albuminuria, severe glomerulosclerosis, hypertension, and renal interstitial and cardiac fibrosis by 4 weeks in the model (Leelahavanichkul et al., 2010). Swiss–webster mice, the 129/Sv strain and its inbred substrain (129S3) develop disease in 9–12 weeks (Leelahavanichkul et al., 2010; Ma and Fogo, 2003). The C57BL/6 strain, however, is the most resistant strain to this model, showing increased albuminuria at 16 weeks without the development of hypertension, progressive CKD, or cardiac fibrosis (Leelahavanichkul et al., 2010; Ortiz et al., 2015; Yang et al., 2010). Rats generally show more susceptibility to CKD induced by renal mass reduction. However, a report by Fleck et al. (2006) showed that Sprague–Dawley rats were less susceptible than Wistar rats. Rats show the development of hypertension and proteinuria
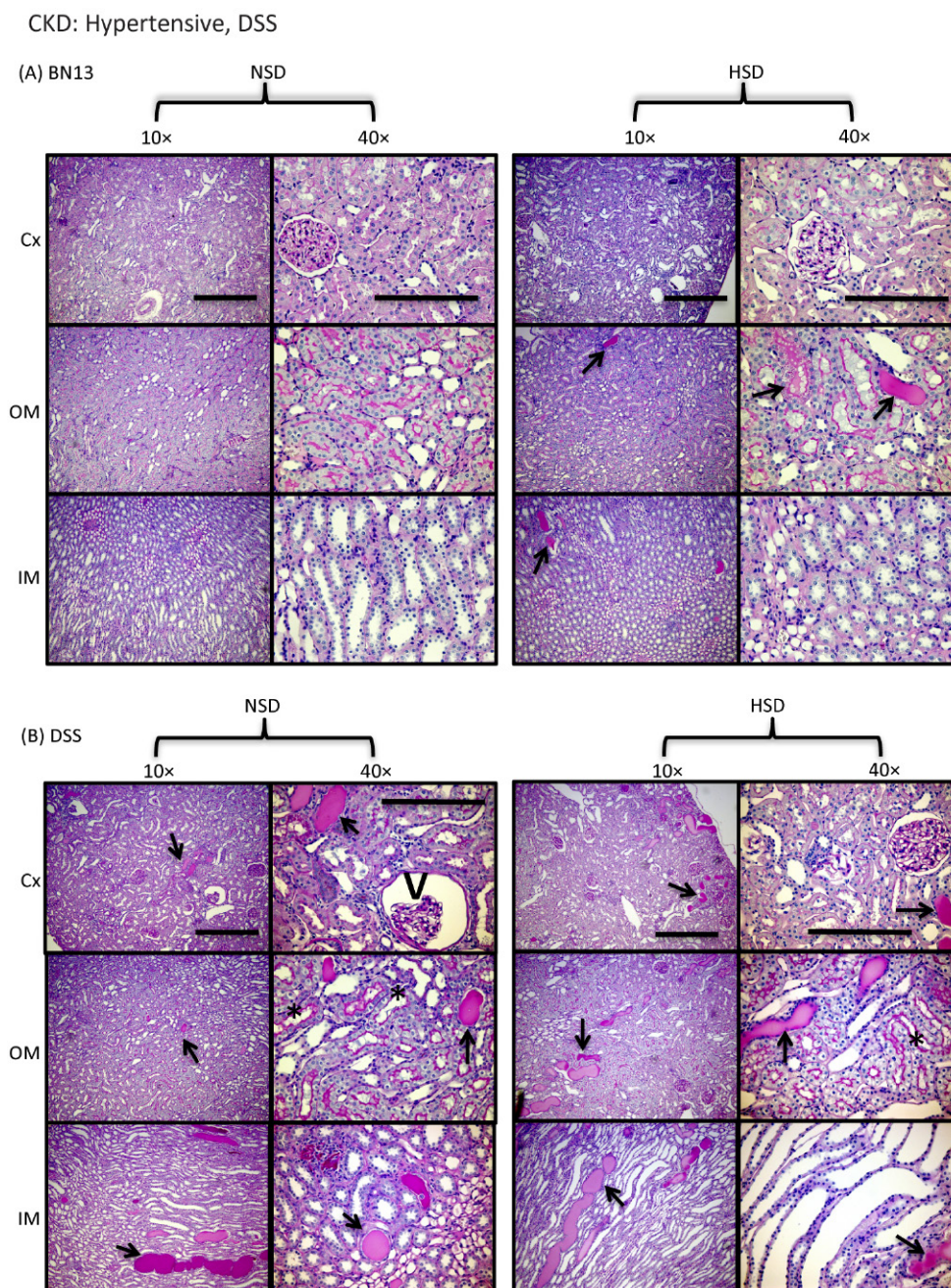
FIGURE 16.4 **Introgression of Brown Norway chromosome 13 (BN13) into Dahl salt-sensitive (DSS) rat improves its nephropathy.** (A) BN13 and (B) DSS rats were fed either normal-salt diet (NSD, 0.4% NaCl) or high-salt diet (HSD, 8% NaCl) for 4 weeks from 12 weeks of age. BN13 rats fed NSD showed normal renal histology, but BN13 rats that were fed HSD demonstrated minor protein cast nephropathy *(arrows)* in OM and IM. DSS rats that were fed either NSD or HSD showed nephropathy such as protein casts *(arrows)* in Cx, OM, and IM; shrinkage of glomerular capillaries in Cx *(arrow head)*; and tubular dilation *(asterisk)* in OM. Images were taken with an Olympus BX41 microscope using 10× (scale bar: 500 μm) and 40× (scale bar: 200 μm) objectives. CKD, chronic kidney disease.

at 4 weeks and glomerulosclerosis, renal fibrosis, and mesangial expansion by 8 weeks (Fleck et al., 2006; Ma et al., 2005; Zhao et al., 2012). Progressive CKD is also denoted by tubular protein cast formation (Li et al., 2012; Zhao et al., 2012), as well as renal inflammation and oxidative stress (Ghosh et al., 2009; Kim and Vaziri, 2010; Romero et al., 1999). ER stress inhibition has been shown to ameliorate renal injury, heart dysfunction, myocardial fibrosis, and apoptosis (Ding et al., 2016). Immune suppression has also been shown to significantly reduce fibrosis and inflammation in this model (Romero et al., 1999). Renal mass reduction is a reliable model for

the induction of CKD in rodents, as it provides robust readouts in terms of glomerulosclerosis, proteinuria, and hypertension. It is ideal to model decline in renal function in humans through loss of nephron number. The main limitation of the 5/6 nephrectomy is the need for two surgical interventions requiring technical expertise for successful surgeries. Additionally, the remnant kidney is small and, especially in the mouse, provides very little renal tissue for analysis. Another disadvantage is the variability in responses from different strains and the variability, which may be created in the model itself. As the surgery is technically demanding, and their is a direct correlation between disease severity and the amount of renal mass removed or infracted, variation in surgical technique or renal anatomy between animals will cause wide variability in disease severity requiring a large sample size to adequately power statistical tests.

3.1.4 Deoxycorticosterone Acetate Salt

This model entails the administration of deoxycorticosterone acetate (DOCA), an aldosterone precursor, combined with a unilateral UNX and an HSD. DOCA is administered through subcutaneous injection or implanted as a pellet, while salt loading involves 1% NaCl in drinking water (Dobrzynski et al., 2000; Hartner et al., 2003; Jadhav et al., 2009; Xia et al., 2005). This model exhibits a suppressed renin–Ang system with decreased plasma renin concentrations. The increased aldosterone results in increased sodium and water reabsorption from epithelial cells in the distal nephron of the kidney, thereby increasing blood pressures. Clinically, primary aldosteronism or a decrease in renin-to-aldosterone ratio is an important cause of hypertension (Drenjancevic-Peric et al., 2011; Iyer et al., 2010; Tomaschitz et al., 2010). This model has been performed in both mice and rats, and hypertension and renal damage is more severe in males than in females (Bubb et al., 2012; Karatas et al., 2008). The response to DOCA salt is strain dependent in mice, where the 129/Sv strain has shown more susceptibility to progressive renal damage and hypertension than C57BL/6 mice (Hartner et al., 2003). This model produces hypertension, proteinuria, luminal protein cast formation, and glomerulosclerosis (Hartner et al., 2003; Jadhav et al., 2009; Xia et al., 2005). Renal interstitial fibrosis and inflammation are indicated by the increase in TGF-β and collagen deposition, as well as the upregulation of proinflammatory transcription factors: NF-κB and AP-1, and immune cell infiltrates (Elmarakby et al., 2008; Jadhav et al., 2009). DOCA salt administration also results in oxidative stress through superoxide formation in the vasculature and the kidney. The mineralocorticoid receptor that aldosterone binds to is not only present on renal epithelia, but is also found on vascular smooth muscle cells, cardiac fibroblasts, and the brain. Therefore, the DOCA salt model also manifests chronic cardiovascular

remodeling, such as cardiac hypertrophy and fibrosis in both the left and right ventricles, resulting in inflammatory cell infiltration into the cardiac tissue and upregulation of hypertrophy markers ANP and BNP (Dobrzynski et al., 2000; Karatas et al., 2008). Morphological changes are accompanied by function changes that include an increase in action potential duration at 20, 50, and 90% of repolarization (Loch et al., 2006). This model is known to cause smooth muscle and endothelial dysfunction and vascular hypertrophy in small and large arteries (Cordellini, 1999; Deng and Schiffrin, 1992; Iyer et al., 2010). The DOCA salt model is a model of human primary aldosteronism and volume-dependent hypertension. The technical requirements of this model are somewhat invasive and two surgeries would be required if a DOCA pellet is implanted subcutaneously instead of injections. However, this model has a lower risk of mortality due to procedures alone in comparison to the 5/6 nephrectomy model. This model generally lasts for no more than 8–12 weeks and is, therefore, not a good model to study the effects of aging on aldosterone-induced hypertension. However, the DOCA salt model is a popular choice in the study of the effect of high–dietary salt intake on CKD progression.

3.1.5 Angiotensin II Infusion

Chronic Ang II infusion, usually through the implantation of Ang II osmotic minipumps, has been used as a model of progressive CKD in mice and rats. Sustained elevations in circulating levels of Ang II result in renal dysfunction, proteinuria, and focal tubulointerstitial and vascular damage (Ortiz et al., 2015). The pleiotropic actions of Ang II encompass Ang II-mediated vasoconstriction and hypertension, as well as stimulation of aldosterone secretion, superoxide production, TGF-β–mediated fibrosis, and inflammation via NF-κB activation (Agarwal et al., 2004; Muller et al., 2000; Ozawa et al., 2007; Ruiz-Ortega et al., 2006). Moreover, ER stress genes have been reported to be upregulated in the kidney and cardiac tissue with Ang II infusion in mice (Kassan et al., 2012; Wang et al., 2015a). In fact, ER stress inhibition has been shown to attenuate cardiac hypertrophy, cell death, and fibrosis (Kassan et al., 2012). Ang II infusion has also been combined with models of reduced renal mass and with the DOCA salt model. Ang II administration has been shown to overcome the resistance of C57BL/6 mice to CKD induction and results in hypertension, albuminuria, and severe glomerulosclerosis by 4 weeks instead of 16 weeks (Leelahavanichkul et al., 2010). The Ang II/DOCA salt model that involves a UNX following by Ang II infusion through an osmotic minipump, a DOCA pellet implantation and high salt were also designed to overcome the resistance of C57BL/6 mice to CKD development (Kirchhoff et al., 2008; Mohammed-Ali et al., 2015b) (Fig. 16.5).

CKD: Hypertensive, AngII/DOCA salt
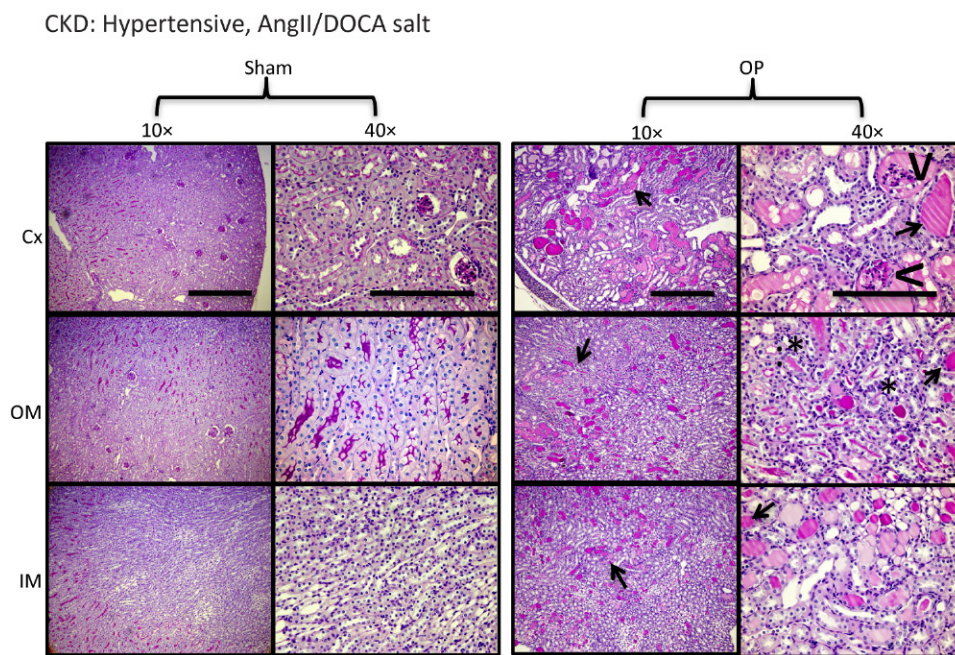
FIGURE 16.5 **Anatomical structures affected by angiotensin (Ang) II/deoxycorticosterone acetate (DOCA) salt treatment compared to sham.** Mice had an Ang II-infused osmotic mini-pump and DOCA pellet subcutaneously implanted and were given 1% salt water (operated, OP), or had sham surgeries and provided with sterile water (sham). OP mice suffered from severe nephropathy depicted in the micrograph by protein cast area density *(arrows)* in Cx, OM, and IM; shrinkage of glomerular capillaries in Cx *(arrow head)*; and tubular dilation *(asterisk)* in OM. Kidney sections were periodic acid-Schiff stained and images were taken with an Olympus BX41 microscope using 10× (scale bar: 500 μm) and 40× (scale bar: 200 μm) objectives. CKD, chronic kidney disease.

Female mice experience less severe CKD in this model compared to male mice (Mohammed-Ali et al., 2015b). Increases in systolic blood pressure and proteinuria are seen after the first week on the Ang II/DOCA salt model (Kirchhoff et al., 2008; Mohammed-Ali et al., 2015b). Renal damage involves protein cast formation, glomerulosclerosis, apoptosis, and renal interstitial fibrosis and inflammation. Inflammation resultes in both T cell and macrophage infiltration and upregulation of inflammatory mediators: MCP-1 and IP-10 (Kirchhoff et al., 2008; Mohammed-Ali et al., 2015b). Cardiac hypertrophy and fibrosis, as well as pulmonary edema also manifest in this model (Kirchhoff et al., 2008; Mohammed-Ali et al., 2015b). The intrarenal renin–Ang system is important in the pathophysiology of hypertension and hypertensive nephropathy. CKD management guidelines emphasize Ang-converting enzyme inhibitors or Ang II type 1 receptor blockers as antiproteinuric and renoprotective therapy, regardless of their effect on hypertension (Griffin and Bidani, 2009). Therefore, models of Ang II–driven CKD are clinically relevant. The C57BL/6 mouse serves as a genetic background for several transgenic and gene knockout models. However, this strain is highly resistant to CKD development. Therefore, the development of a model with stable CKD development in this strain would widen the scope of experiments focused on CKD progression.

3.2 Diabetic Nephropathy

DM is a growing worldwide epidemic and DN is one of the most important DM complications, as it is a major cause of ESRD (Martinez-Castelao et al., 2015). In humans, DN is characterized by albuminuria and progressively declining GFR. DN is primarily considered a glomerular disease based on structural abnormalities observed in patient biopsy material. Mesangial matrix accumulation affects all segments of the glomeruli (global) and all glomeruli within the cortex (diffuse) (Alpers and Hudkins, 2011; Breyer et al., 2005). This process is referred to as diffuse mesangial sclerosis (DMS) or diffuse intercapillary glomerulosclerosis and is a hallmark lesion of diabetic glomerulopathy. A reduction in podocyte number, as well as glomerular basement membrane (GBM) thickening, resulting in the loss of charge and permselectivity of the glomerular filtration barrier, which is a feature of DN (Alpers and Hudkins, 2011). Along with tubulointerstitial fibrosis, DN in animal models and in humans has been shown to induce the UPR, oxidative stress, key inflammatory mediators NFκB, MCP-1, adhesion molecules, and chemokines that aid in leukocyte migration and infiltration (Navarro-Gonzalez et al., 2011; Zhuang and Forbes, 2014). The National Institutes of Health-supported Animal Models of Diabetic Complications Consortium (AMDCC) has proposed a

list of criteria for an ideal DN mouse model. These criteria include: (1) progressive renal insufficiency in the setting of hyperglycemia; (2) greater than 50% decline in GFR over the lifetime of the animal; (3) greater than 10-fold increase in albuminuria compared with controls for that strain at the same age and gender; and (4) pathologic changes in kidneys, such as advanced mesangial matrix expansion with or without nodular sclerosis and mesangiolysis, any degree of arteriolar hyalinosis, GBM thickening by >50% over baseline, and tubulointerstitial fibrosis (Alpers and Hudkins, 2011). These criteria were aimed at standardizing the phenotyping methodology to allow better comparison of results obtained by different groups and ensure that future studies will increasingly adopt models that reliably model human disease. These criteria, however, represent goals and not absolute standards and should be used to address limitations of current models and identify models of DN that meet most of these criteria as useful research tools.

3.2.1 Streptozotocin-Induced Diabetes

Streptozotocin (STZ)-induced pancreatic injury is commonly used as a rodent model of type I diabetes mellitus (T1DM) and generally presents similar features to those found in human diabetic nephropathy. STZ, originally identified as an antibiotic, is an analog of *N*-acetylglucosamine, which is transported into pancreatic β-cells by GLUT-2 and causes β-cell toxicity, resulting in insulin deficiency (Tesch and Allen, 2007). Animal models of STZ-induced DN are usually performed in mice, Sprague–Dawley, WKY, and SHR rats. STZ is usually administered intraperitoneally in mice and intravenously (IV) in rats (Tesch and Allen, 2007). The two main type of STZ administration include multiple low-dose and moderate-to-high dose. The moderate-to-high dose model was designed to overcome the resistance of certain mouse strains to STZ-induced injury. This model involves using a single high dose of STZ (≥200 mg/kg) or a two-dose regimen of STZ (2 × 100–125 mg/kg) given on two consecutive days (Fujimoto et al., 2003; Itagaki et al., 1995). Increasing the STZ dose translates to greater cytotoxicity and a more rapid destruction of pancreatic β-cells and more severe diabetes. However at high doses, STZ has been shown to cause acute kidney damage in animals due to its non-specific cytotoxicity. This aspect also makes it difficult to differentiate between the direct toxic effect of STZ and lesions caused by hyperglycemia (Breyer et al., 2005). Thus, the low-dose STZ model was created to reduce the nonspecific nephrotoxic effects of STZ. This model involves the administration of a low dose of STZ, 40–60 mg/kg, for 5 consecutive days (Leiter, 1982, 1985; Qi et al., 2005). Inbred strains of mice have been reported to exhibit varying susceptibilities to diabetes induced by low-dose STZ and an order has been identified: DBA/2 > C57BL/6 > MRL/MP > 129/

SvEv > BALB/c (Gurley et al., 2006). Whereas in high dose–induced diabetes where increased urinary albumin excretion and GBM thickening occurs at 4 weeks postdiabetes induction (Fujimoto et al., 2003), the low-dose model requires months to induce these changes (Qi et al., 2005). In the rat models of STZ-induced diabetes, male rats at 8 weeks of age (200–250 g) are starved for 16 h and injected once into the tail vein with STZ (SD = 55 mg/kg, WKY = 60 mg/kg, SHR = 45 mg/kg) in sodium citrate buffer (1 mL/kg) (Cooper et al., 1988; Ma et al., 2004). The development of renal injury is more severe in SHR compared to normotensive (WKY) rats, and urine albumin excretion has been shown to be three-fold higher in diabetic SHR (149 ± 1 mg/24 h) compared with control SHR (49 ± 1 mg/24 h) at 32 weeks post-STZ administration (Davis et al., 2003). Vascular hypertension that occurs alters renal hemodynamics and causes GBM thickening along with inflammation and fibrosis (Allen et al., 1997). Alongside the renal damage induced in all types of STZ-induced DN, ER stress markers (GRP78 and CHOP) display an increase and are associated with apoptosis and inflammation (Liu et al., 2008; Luo et al., 2010; Wu et al., 2010b). With all types of STZ-induced diabetes, 1 week after STZ administration, rodents are assessed for hyperglycemia and those with fasting blood glucose over 15 mmol/L (280 mg/dL), which is generally the majority of them, should be included in studies of DN (Tesch and Allen, 2007). Diabetic animals in rat models of STZ-induced DN and the high-dose STZ model in mice are given insulin injections to maintain blood glucose levels in a desirable range (16–33 mmol/L) (Tesch and Allen, 2007). The STZ model in both mice and rats is sometimes performed following a UNX to accelerate the progression of renal injury (Tesch and Allen, 2007). However, it becomes difficult to interpret results from this model as one has to distinguish the effects of STZ-induced hyperglycemia from the changes induced by UNX and each of their relative contributions to renal injury.

3.2.2 Insulin 2 Akita Mouse

Akita mice develop T1DM due to a mutation in the insulin 2 (Ins2) gene that results in the abnormal folding of insulin protein, toxic injury to pancreatic β-cells, and, therefore, a decreased capacity to secrete insulin (Kong et al., 2013). The Akita mouse was originally generated on the C57BL/6 background in Akita, Japan, but is currently available commercially on various genetic backgrounds. Mice homozygous for this mutation die in the perinatal period (within 1–2 months). The heterozygous mutant mice develop hyperglycemia, hypoinsulinemia, polydipsia, and polyuria at approximately 3–4 weeks of age (Kong et al., 2013). Hyperglycemia in Ins2 Akita mice is sexually dimorphic, where males develop substantially worse hyperglycemia than females (Gurley et al., 2006).

Ins2 Akita mice develop modest levels of albuminuria and mild-to-moderate glomerular mesangial expansion; however, renal phenotype is largely dependent on their genetic background strains. C57BL/6, DBA/2, and 129/SvEv mice with the mutation develop similar degrees of hyperglycemia, but differ in their manifestation of nephropathy (Gurley et al., 2010). DBA/2 mice exhibit higher albuminuria, but only C57BL/6 and 129/SvEv strains show mesangial matrix expansion. Nevertheless, Ins2 Akita mice experience higher levels of hyperglycemia, albuminuria, blood pressure, and more consistent structural changes of the kidney compared with STZ-induced DN (Gurley et al., 2006).

3.2.3 Nonobese Diabetic Mice

The nonobese diabetic (NOD) genetic mouse model is one of the most thoroughly studied models of T1DM. The induction of diabetes in this model is due to the spontaneous autoimmune destruction of β-cells, which begins with the infiltration of innate immune cells into the pancreas as early as 3 weeks of age (Pearson et al., 2016). These cells include dendritic cells, macrophages, and neutrophils that attract CD4 and CD8 T cell subsets into the islets at 4–6 weeks of age. Studies have shown a delay in diabetes induction in this model with the depletion of dendritic cells, monocytes, and macrophages. Moreover, CD4 and CD8 T cells are required for diabetes development (Pearson et al., 2016). Overt diabetes arises at the age of 24–30 weeks and insulin is required to maintain NOD mice for any extended period of time after the onset of hyperglycemia. As opposed to enhanced susceptibility to STZ-induced DN in male mice, female NOD mice experience 4 times higher incidence of diabetes than male NOD mice (Breyer et al., 2005). Albuminuria develops in hyperglycemic NOD animals and albuminuria is sevenfold higher than in NOD mice before the development of hyperglycemia (Doi et al., 1990). Islets isolated from NOD mice display an increase in ER stress markers: XBP1s and CHOP, as well as NFκB; these results show similarity to human T1DM (Tersey et al., 2012). The involvement of TGF-β and advanced glycosylation end products has been shown to mediate the pathogenesis of mesangial proliferation and sclerosis in NOD mice (Doi et al., 1990; He et al., 2000; Pankewycz et al., 1994; Sharma and Ziyadeh, 1994). This model shares key similarities with human T1DM, such as the inheritance of specific MHC class II alleles and many non-MHC loci as polygenic susceptibility loci, transmission of disease by hematopoietic stem cells, the development of insulitis, and a strict dependence on T cells (Breyer et al., 2005).

3.2.4 OVE26 Mice

The OVE26 mouse on the FVB inbred strain is a transgenic mouse model of severe early-onset T1DM characterized by transgenic overexpression of calmodulin in pancreatic β-cells, leading to deficiency in the production of insulin (Alpers and Hudkins, 2011). These mice exhibit severe hyperglycemia 2–3 weeks after birth. Progressively increasing albuminuria has been reported to be 305 μg/24 h by 2 months to 15,000 μg/24 h by 9 months of age (Kong et al., 2013; Zheng et al., 2004). GFR decreases between 5 and 9 months, and the development of hypertension in this model coincides with albuminuria. Renal nephropathy in OVE26 mice includes enlarged glomeruli, mesangial matrix expansion, GBM thickening, global glomerulosclerosis, tubular atrophy, mononuclear cell infiltration, and tubulointerstitial fibrosis (Kong et al., 2013). The degree of renal injury is highly influenced by the mutation being expressed on the FBV mouse strain. The introduction of the transgene into the C57BL/6 or the DBA/2 mouse strains significantly diminishes albuminuria and increases mesangial matrix and fibrosis, which are key features of this model (Xu et al., 2010). Therefore, there is a limitation, as genetic mutations from a variety of backgrounds cannot be used in this model.

3.2.5 Db/db Mice

The db/db mouse model of leptin deficiency is currently the most widely used mouse model of type 2 diabetes mellitus (T2DM). This mouse has a mutation in the gene encoding the leptin receptor, and leptin deficiency confers susceptibility to obesity, insulin resistance, and T2DM (Alpers and Hudkins, 2011). Experiments using db/db mice are more widely conducted with the C57BLKS/J strain, as C57BL/6 mice do not develop significant nephropathy (Kong et al., 2013). Db/db mice in the C57BLKS/J strain display hyperinsulinemia at 10 days of age and significant hyperglycemia is reported at 8 weeks (Susztak et al., 2004). Albuminuria is detected as early as 3–4 weeks after the onset of hyperglycemia (Susztak et al., 2003). DN develops slowly, where remarkable GBM thickening, podocyte loss, and mesangial matrix expansion is observed by 18–20 months (Susztak et al., 2004). These mice do not develop mesangiolysis or nodular mesangial sclerosis, and do not experience progressive renal insufficiency. Therefore, they are good models of early changes in human DN, but fail to manifest advanced features of DN (Alpers and Hudkins, 2011). To address advanced DN experimentally, db/db mice are uninephrectomized to accelerate the development of DN. UNX at a young age was associated with increased albuminuria and severe glomerulosclerosis in 37% of glomeruli at 24 weeks of age, as compared to sham-operated db/db mice (Ninichuk et al., 2007). Additionally, uninephrectomized db/db mice displayed significant tubular atrophy and tubulointerstitial fibrosis (Ninichuk et al., 2007). Db/db mice have also been crossed with endothelial nitric oxide synthase (eNOS)–deficient mice to create eNOS$^{-/-}$/db/db mice (Kong et al., 2013).

Research has shown an association between decreased eNOS expression via endothelial dysfunction and the development of DN in T1DM and T2DM (Neugebauer et al. 2000; Zanchi et al., 2000). Along with hyperglycemia, hyperinsulinemia, hypertension, albuminuria, and decreased GFR, eNOS$^{-/-}$/db/db mice develop features of advanced DN, such as mesangiolysis, focal segmental and nodular glomerulosclerosis, striking fibronectin accumulation in glomeruli, and tubulointerstitial fibrosis (Alpers and Hudkins, 2011; Kong et al., 2013).

3.2.6 BTBR ob/ob Mice

Ob/ob mice possess a recessive mutation in leptin, the ligand for the leptin receptor, and exist in the C57BL/6J, DBA2/J, and FVB stains (Kong et al., 2013). The T2DM induced by the ob/ob mice displays only mild functional and morphological changes in the C57BL/6J strains and are, therefore, not widely used as models of DN. However, when the ob/ob mutation is generated in the BTBR strain, the resultant BTBR ob/ob mice are insulin resistant, hyperinsulinemic, severely hyperglycemic, obese, and uniformly develop features of DN (Hudkins et al., 2010). Progressive proteinuria develops by 4 weeks of age, whereas early characteristics of DN, such as glomerular hypertrophy, mesangial matrix expansion, podocyte loss, and mesangiolysis, can be detected by 8 weeks (Hudkins et al., 2010). More advanced DN is seen by 22 weeks, where there is a 20% increase in GBM thickness, 50% increase in mesangial matrix, DMS, focal arteriolar hyalinosis, and mild focal fibrosis (Hudkins et al., 2010). The relatively rapid onset and progressive nature of DN in these mice is a major advantage of this model. Moreover, the BTBR ob/ob mice allow the investigation of the therapeutic effect of leptin administration in DN as opposed to db/db mice, which are deficient in the leptin receptor. However, limitations of this model include high cost and infertility of the BTBR ob/ob mice (Kong et al., 2013).

3.2.7 New Zealand Obese Mice

The New Zealand obese (NZO) mouse was created by the selective inbreeding from polygenic mice displaying obesity and T2DM in New Zealand. These mice are hyperleptinemic by 9–12 weeks of age due to leptin resistance and have been reported to be hyperphagic and obese (Leiter and Reifsnyder, 2004). These mice are also hyperinsulinemic as a result of hepatic insulin resistance from an early age. High blood glucose levels indicate impaired glucose tolerance that worsens with age and approximately 50% of males develop diabetes by 24 weeks (Haskell et al., 2002). NZO mice are prone to autoimmune disease and develop circulating antibodies to native and single-stranded DNA (Melez et al., 1980). Renal injury in these mice exhibits features seen in both lupus nephritis (LN) and DN, such as glomerular proliferation, mesangial deposits, mild GBM thickening, and glomerulosclerosis. Eosinophilic nodules in some glomeruli are observed with occasional hyalinization of the glomerular arterioles and healing arteriolar inflammation (Melez et al., 1980). This model is a good choice for the study of the relationships between obesity and T2DM.

3.2.8 KK-Ay Mouse

The KK mouse is a polygenic mouse model of T2DM. These mice exhibit mild insulin resistance, hyperglycemia, glucose intolerance, hyperinsulinemia, mild obesity, and albuminuria (Tomino, 2012). The severity of hyperglycemia and insulin resistance is exacerbated by the introduction of the agouti (Ay) allele into the KK background (Suto et al., 1998). The Ay gene is expressed during the hair growth cycle in neonatal skin, where it functions as a paracrine regulator of pigmentation. Further, an Ay-related protein is a potent and selective antagonist of melanocortin receptors 3 and 4 that are expressed in the hypothalamus and implicated in weight regulation (Ollmann et al., 1997). Mice homozygous for the Ay mutation die before implantation or shortly after, however, heterozygous mice are viable. KK-Ay mice exhibit obesity and hyperglycemia, as well as albuminuria (Breyer et al., 2005). Renal histological changes, such as podocyte loss, diffuse mesangial expansion with mesangial cell proliferation, and segmental sclerosis in KK-Ay mice, are more severe than those that develop in KK mice (Tomino, 2012). Another manipulation of this model includes UNX of KK-Ay mice and supplementation with a HSD, resulting in a more severe decline in renal function and accelerated DN (O'Brien et al., 2013).

3.2.9 Goto Kakizaki Rat

The Goto Kakizaki (GK) rat is a spontaneously polygenic model of T2DM and has been created by repeated inbreeding of glucose-intolerant Wistar rats over many generations (Janssen et al., 2004). Characteristics of this model include moderate hyperglycemia, peripheral insulin resistance, and nonhyperlipidemic and nonobese phenotype (Kong et al., 2013). T2DM in this model is primarily caused by β-cell deficit, where there is a decrease in pancreatic cell proliferation and pancreatic cell apoptosis at the embryo stage (Kong et al., 2013). Early renal morphological changes are similar to those observed in early stages of human DN, such as glomerular hypertrophy and GBM thickening (Phillips et al., 2001). At 24 months of age, GK rats have been reported to display albuminuria, segmental glomerulosclerosis, and tubulointerstitial fibrosis, and thus the late stage of this model resembles progressive human DN (Sato et al., 2003).

3.2.10 Zucker Diabetic Fatty Rat

The Zucker diabetic fatty (ZDF) rat has a missense mutation in the gene coding the leptin receptor (fa/fa)

(Phillips et al., 1996) and spontaneously develops insulin resistance, T2DM, hyperlipidemia, moderate hypertension, and obesity, as well as progressive renal injury (Kong et al., 2013). Hyperglycemia can be detected at 12 weeks (Chen and Wang, 2005), whereas albuminuria is seen at 14 weeks (Figarola et al., 2008) followed by focal segmental glomerulosclerosis (FSGS) at 18–20 weeks of age (Coimbra et al., 2000; Hoshi et al., 2002). Additionally, renal pathology also involves mesangial expansion, macrophage infiltration, and interstitial fibrosis (Kong et al., 2013). ZDF male rats are more widely used as models of T2DM and DN because, although ZDF female rats display insulin resistance and obesity comparable to male rats, they only develop hyperglycemia when placed on a diabetogenic diet (Corsetti et al., 2000). A cross between a ZDF female and a SHHF male rat has been carried out to create the Zucker fatty/spontaneously hypertensive heart failure F1 hybrid (ZSF-1) rat (Ortiz et al., 2015). The ZSF-1 rat combines the most common contributors to the current epidemic of CKD, hypertension, obesity, T2DM, and hyperlipidemia. The high cost and large size of the animals added to their slow progression to CKD are barriers to the wider use of this model (Ortiz et al., 2015).

3.2.11 Otsuka Long-Evans Tokushima Fatty Rat

The Otsuka Long-Evans Tokushima fatty (OLETF) rat is a spontaneously diabetic rat with polyuria, polydipsia, mild obesity, hypertension, dyslipidemia, and advanced DN (Kawano et al., 1999; Kong et al., 2013). Between 12 and 20 weeks, OLETF rats exhibit mild obesity and hyperinsulinemia with a late onset of hyperglycemia at 18 weeks of age (Choi et al., 2011). Overt albuminuria occurs at 22 weeks, while at 40 weeks, proliferation of the mesangial matrix, GBM thickening, and diffuse glomerulosclerosis were observed (Kawano et al., 1994). By 70 weeks of age, nodular lesions can be seen expanded to the proliferated mesangial matrix along with tubular atrophy and associated mononuclear cell infiltration and fibrosis (Kawano et al., 1992). Just as in human disease, the progression of T2DM in OLETF rats can be prevented by exercise and caloric restriction (Kong et al., 2013). Multiple recessive genes are associated with the induction of diabetes, such as the odb-1 on X-chromosome of OLETF rats. Moreover, a major quantitative trait locus colocalizing with cholecystokinin type A receptor gene influences poor pancreatic proliferation in OLETF rats (Moralejo et al., 1998).

3.3 Glomerular Disease

3.3.1 Focal Segmental Glomerulosclerosis

FSGS can be defined as the sclerosis of some "focal" but not all glomeruli. Obliteration of the glomerular capillaries by ECM, often accompanied by hyalinosis, only affects a "segment" of the glomerular tuft. With progression, more global glomerulosclerosis occurs (Ichikawa and Fogo, 1996). In 20% of children and 40% of adults, FSGS is the underlying cause of nephrotic syndrome (D'Agati et al., 2011). Nephrotic syndrome is defined by urinary protein levels exceeding 3.5 g/1.73 m^2 of body surface area per day, hypoalbuminemia, and hyperlipidemia in the absence of systemic disease (Orth and Ritz, 1998). Proteinuria is a defining feature of FSGS with the main cellular target of disease onset being the podocyte, resulting in a compromised glomerular filtration barrier. Moreover, 80% of FSGS is idiopathic. The remaining 20% occurs secondary to other underlying diseases that cause mechanical stress on the podocytes, such as hypertension, diabetes, and obesity that increases glomerular hypertension (de Mik et al., 2013; Ichikawa and Fogo, 1996). Podocytes are terminally differentiated cells; therefore, their depletion through detachment, apoptosis, or necrosis is critical to the development of glomerulosclerosis. Experimental models have shown that a 20% decrease in podocyte number causes FSGS and low-level sustained proteinuria, whereas a 40% decrease results in high-level sustained proteinuria and a decrease in renal function (de Mik et al., 2013; Wharram et al., 2005). The ECM deposition associated with sclerosis is influenced by numerous growth factors, cytokines, and chemokines. Local stress, heightened levels of ROS, and abnormal homeostasis can modulate these factors. As such, podocyte injury has been associated with the induction of ER stress genes: GRP78, GRP94, ORP150, and CHOP (Cybulsky et al., 2011). FSGS causes TGF-β activation that results in the recruitment of monocytes, macrophages, and T cells; upregulation of other proinflammatory mediators, such as TNF-α and IL-1; and fibrosis (Imig and Ryan, 2013; Kim et al., 2003; Noel, 1999). An ideal model for human FSGS would be one where glomerular scarring develops spontaneously and has a slow chronic progression.

3.3.2 Minimal Change Disease

Minimal change disease (MCD) is the most common cause for nephrotic syndrome in children and 15%–20% of cases in adults (Fogo, 2001). MCD is characterized by explosive edema, selective proteinuria, and clinical response to glucocorticoid therapy, as T cell–related mechanisms are implicated in pathogenesis (Saleem and Kobayashi, 2016). The majority of MCD cases are idiopathic; however, the development of edema and proteinuria are preceded by upper respiratory tract infections, allergic reactions, and the use of certain drugs, such as NSAIDs (Glassock, 2003). MCD shows normal appearance of glomeruli on light microscopy, but nevertheless extensive effacement of foot processes of the podocytes

on electron microscopy. Another important feature of MCD involves lack of tubulointerstitial fibrosis despite heavy proteinuria (Saha and Singh, 2006; Saleem and Kobayashi, 2016).

3.3.3 Animal Models of FSGS and MCD

3.3.3.1 HYPERTENSIVE CKD MODELS TO STUDY FSGS

The remnant kidney model in the rat is the most commonly used animal model for FSGS. Most studies use 5/6 nephrectomy, which is also a model for hypertensive CKD. However, the 4/6 renal mass reduction is also used, as it is milder and does not induce hypertension, but only moderate renal dysfunction and glomerulosclerosis (de Mik et al., 2013). Glomerular sclerosis is seen by week 4, postrenal ablation by ligation with segmental sclerosis in about 20% of the glomeruli and by week 8, tubulointerstitial fibrosis (Hostetter et al., 1981; Yoshida et al., 1988). Renal mass reduction decreases the number of glomeruli available to filter the same amount of serum. Glomerular growth through both cellular hypertrophy (increase in cell size) and hyperplasia (increase in cell number) occurs in FSGS. Age is a contributing factor in glomerular hypertrophy, where it determines the relative contributions of hypertrophy and hyperplasia. Hyperplasia is predominant in young animals showing more severe sclerosis after renal ablation than adults (Fogo, 2003). Glomerular enlargement due to injury results in epithelial cell detachment where denuded areas are associated with hyalinosis and cause progressive scarring through the hyperfiltration of plasma proteins. Other hypertensive CKD models, such as the Dahl S rat, SHR, and chronic Ang II infusion combined with renal mass reduction have also been reported to cause FSGS. However in these models, damage to the glomerular vessels occurs secondary to hypertension. FSGS induced by renal hypertension has been detected in Sabra hypertension-prone rats; they are salt-sensitive rats that develop hypertension when chow diet and drinking water is loaded with 8% NaCl (Yagil et al., 2002). The remnant kidney model provides a limited representation of human FSGS, as glomerular damage is induced via an acute procedure, whereas in humans, FSGS onset is much slower. As only 20% of FSGS occurs due to underlying secondary causes, the FSGS seen in hypertensive CKD model can only represent a small segment of FSGS in the human population.

3.3.3.2 DRUG-INDUCED FSGS AND MCD

Adriamycin is an anthracycline, a class of antitumor drugs widely used to treat human cancers. Adriamycin induces direct toxic damage to the glomerulus, where it alters the glomerular filtration barrier; charge selectivity is reduced and podocyte cell foot processes are fused. Slit diaphragm abnormalities are critical and early events in the pathogenesis of adriamycin-induced FSGS, where the expression patterns of slit diaphragm proteins, nephrin, podocin, and NEPH1 are altered (Lee and Harris, 2011). Adriamycin is administered intravascularly in most studies; however, other routes include substernal, intracardiac, and intrarenal administration. Adriamycin doses range from 1.5 to 5 mg/kg in rats and from 10 to 15 mg/kg in mice (de Mik et al., 2013). Male rats are more susceptible than females, and BALB/c mice are used in mouse experiments, as C57BL/6 mice are the most resistant to adriamycin-induced FSGS (de Mik et al., 2013). Intravascular administration of Adriamycin at 2 mg/kg results in early phase proteinuria with focal foot process effacement after the second injection. Segmental glomerulosclerosis occurs after 16 weeks with global glomerulosclerosis and tubulointerstitial fibrosis at 24 weeks and some animals dying of uremia at 28 weeks (Fogo et al., 1988; Okuda et al., 1986). Adriamycin given in a single dose intravascularly (5 mg/kg) resulted in sclerosis in 50% of rats by 6 months (Bertani et al., 1986). Puromycin aminonucleoside (PAN) is an antibiotic that inhibits protein synthesis and has been administered subcutaneously, intravenously, and intraperitoneally to induce both MCD and FSGS (de Mik et al., 2013; Pippin et al., 2009). The degree of renal injury and onset of proteinuria are influenced by the rat strain, PAN dose, and route of administration; however, it is the cumulative exposure to PAN that determines whether rats develop MCD or FSGS (Pippin et al., 2009). The administration of five subcutaneous injections of PAN (1.5 mg/100 g body weight) produced glomerular damage and apoptosis resembling human MCD; the administration of five additional doses of PAN led to the development of irreversible sclerotic lesions characteristic of FSGS (Shiiki et al., 1998). A single dose of 50 mg/kg of PAN in the rat produces early phase proteinuria peaking at 10 days that is similar to MCD with complete effacement of foot processes. Proteinuria in this model almost resolves after this early phase followed by a progressive, lower-level proteinuria between week 10 and 13 that is associated with early segmental sclerotic lesions (Diamond and Karnovsky, 1986). The tubulointerstitial fibrosis that occurs with the progression of adriamycin- and PAN-induced nephropathy is correlated with the severity of proteinuria, and associated with macrophage and T cell infiltration and the release of chemokines: MCP-1 and -3 and RANTES (Fogo, 2003). These drugs exert direct toxicity to podocytes through the production of ROS (Fogo, 2003). The strengths of drug-induced glomerular disease models include their high reproducibility with robust degree of tissue injury and relatively low mortality and morbidity. Structural and functional injury in these models greatly resembles human FSGS and MCD,

and the administration of the drugs, albeit requiring a certain level of skill, is much less demanding than the surgery involved in remnant kidney models. The duration of these models is short, where proteinuria onset is early and glomerulosclerosis occurs within weeks. The limitations of these models include batch variability with regards to the drugs, whereby certain brands or batches of drug will produce different severity in disease. Another source of variability involves differences in susceptibility across strains of rodents. Further, the issue of drug toxicity might require the optimization of doses for experimental use, particularly in the case of adriamycin where doses as little as 0.5 mg/kg lower or higher than the optimum may lead to either lack of renal injury or toxicity leading to death, respectively (Lee and Harris, 2011).

3.3.3.3 VIRUS-INDUCED FSGS

Virus-induced FSGS occurs due to the direct infection of the podocyte or through the release of inflammatory cytokines from infected cells. HIV-associated nephropathy (HIVAN) is the most common animal model used to induce FSGS via viral infection. This transgenic model was produced using a replication-deficient version of HIV as the integrated transgene. These mice, referred to as the transgenic 26 (Tg26) mice (Dickie et al., 1991), develop proteinuria at 24 days of age with 18% of mice dying between 2 and 6 months with heavy proteinuria, elevated blood urea nitrogen, edema, and hypoalbuminemia. Focal changes were limited and described as mild to severe in animals under 2 months of age. Tg26 mice over 2 months of age had diffuse segmental and global glomerulosclerosis, as well as lymphocytic infiltrates. The severity of renal damage in Tg26 mice depends on the animals' genetic background, with the FVB/N strain being the most susceptible. Various HIVAN models have been produced, such as transgenic mice that express HIV-1 accessory genes, such as Vpr and nef, which synergistically damage podocytes, resulting in glomerulosclerosis (Rosenstiel et al., 2009). The glomerular pathology seen in HIVAN models resembles human HIVAN; however, HIVAN is a secondary cause of FSGS, therefore these models do not widen our understanding of primary FSGS, which is the most common.

3.3.3.4 GENETIC MODELS

3.3.3.4.1 PODOCYTE-SPECIFIC GENE DISRUPTION Both human and mouse studies show that FSGS is initiated by podocyte dysfunction. Mutations in nephrin (NPHS1) and podocin (NPHS2), key components of the podocyte slit diaphragm, have been shown to result in congenital nephrotic syndrome of the Finnish type and steroid-resistant nephrotic syndrome of the podocin

type, respectively in humans (Boute et al., 2000; Putaala et al., 2001). NPHS1 knockout mice die within 24 h after birth due to edema and massive proteinuria with the absence of the slit diaphragm and effacement of podocyte foot processes (Putaala et al., 2001). Similarly, humans with NPHS1 mutations are diagnosed with nephrotic syndrome at birth and albuminuria starts in utero (Patrakka et al., 2000). NPHS2 knockout mice are massively proteinuric at birth and die within the first 5 weeks of life with ESRD. NPHS2$^{-/-}$ mice do not show FSGS lesions, but exhibit DMS characterized by mesangial accumulation of ECM proteins without mesangial cell proliferation (Roselli et al., 2004). In contrast, humans with NPHS2 mutations are not proteinuric at birth, and progress slowly to ESRD through progressive FSGS (Roselli et al., 2004). Podocin inactivation in the adult mouse kidney using Cre-LoxP technology, however, presents FSGS within 4 weeks followed by diffuse glomerulosclerosis and tubulointerstitial injury (Mollet et al., 2009). Mutations in α-actinin-4 (ACTN4) have been shown to cause an autosomal dominant form of human FSGS, and decreased ACTN4 expression is seen in humans with primary glomerulopathies, such as sporadic FSGS and MCD (Feng et al., 2015; Yao et al., 2004). The ACTN4 gene encodes the production of an actin cross-linking protein and is widely expressed in the kidney. In addition to bundling F-actin, ACTN4 interacts with various proteins to modulate focal adhesion and links the cytoskeleton to the ECM, and is part of the nephrin multiprotein complex that maintains glomerular structure integrity (Feng et al., 2015). A significant percentage of ACTN4 knockout mice suffer perinatal death; however, survivors develop albuminuria and FSGS at about 10 weeks of age (Kos et al., 2003). In an effort to model human disease, certain research groups have generated transgenic mice with ACTN4 mutations. Particularly, transgenic mice with the K256E mutation (homologous to human K255E mutation) had higher expression of mutant ACTN4 and exhibited significant albuminuria, glomerulosclerosis, and foot process effacement at 10 weeks (Michaud et al., 2010).

3.3.3.4.2 INDUCIBLE FSGS USING TRANSGENIC ANIMALS As Thy1.1 cell surface antigen is not expressed on normal mouse podocytes, transgenic mice have been generated by injecting hybrid human–mouse Thy1.1 into the pronuclei of zygotes of Thy1.2 CBA + C57BI/10 parents. The injection of anti-Thy1.1 monoclonal antibodies into these mice results in rapid onset of albuminuria within 10 min to 24 h, and is strongly correlated with FSGS lesion formation. FSGS lesions developed within 3 weeks in a dose-dependent manner (Assmann et al., 2002; Smeets et al., 2004). Another model of FSGS induction includes transgenic rats with the human diph-

theria toxin (DT) receptor (hDTR) specifically expressed in podocytes (Wharram et al., 2005). Fisher 344 rats were used for these experiments and the hDTR rats were injected with DT (1 mg/10 g) when they reached 100 g body weight. This setup allows the transport of DT into podocyte cytoplasm, thereby causing podocyte depletion. Over 40% podocyte depletion in this model translated to FSGS and global glomerulosclerosis, high-grade proteinuria, and reduced renal function. Increasing the dose of DT to >50 ng/kg causes proteinuria within 7 days of toxin administration, where the mice progress to ESRD within 10 days to 3 weeks.

3.3.3.4.3 SPONTANEOUS FSGS IN THE BUFFALO/MNA RAT The Buffalo/mna rats spontaneously develop FSGS by 2 months of age in addition to proteinuria, with epithelial cell alterations with foot process flattening and vacuolization at the ultrastructural level. Lesion formation has been attributed to a circulating factor, as kidneys from other rat strains transplanted into the Buffalo/mna rats also develop proteinuria within 10 days, progressing to FSGS (Le Berre et al., 2002). However, Buffalo/mna kidneys show regression of lesions when transplanted into healthy Lewis rats. At 6 months, these rats exhibit FSGS similar to that found in humans. Early lesions have been characterized as "tip lesions," as they occur at the glomerular junction with the proximal tubule; sclerosis extends to all parts of the glomerulus later (Nakamura et al., 1986). The rats are normotensive and nonuremic and are particularly relevant in modeling the recurrence of FSGS after transplantation in humans (Nakamura et al., 1986).

3.3.3.4.4 NPHS2-ANGPTL4 TRANSGENIC RATS TO MODEL MCD Increased expression of angiopoietin-like-4 (ANGPTL4), a secreted glycoprotein, has been noted in the glomeruli, urine, and serum in patients with MCD. Whereas ANGPTL4 is normally expressed in podocytes at relatively low levels, it is highly upregulated in MCD (Chugh et al., 2012). NPHS2-ANGPTL4 transgenic rats overproduce ANGPTL4 specifically from the podocyte and exhibit several features of human MCD (Clement et al., 2011). These rats develop selective proteinuria where albumin is the dominant protein in urine and albuminuria develops at 1 month of age. Effacement of podocytes is first noted at 3 months, and increases to an extensive degree by 5 months of age. Similar to human MCD, these rats do not show tubulointerstitial fibrosis despite early and severe onset of proteinuria (Chugh et al., 2012). Studies have shown that the NPHS2-ANGPTL4 rat is the most accurate model for human MCD. However, this model shows gradual progression in renal injury, which is in contrast to the explosive onset of MCD seen in adults.

3.4 Autoimmune Kidney Diseases

3.4.1 Heymann Nephritis Model of Membranous Nephropathy

Membranous nephropathy (MN) is the leading cause of idiopathic nephrotic syndrome in adults, with approximately 40% of patients developing progressive renal insufficiency resulting in ESRD (Fervenza et al., 2008). MN is initiated by immunoglobulin G (IgG) antibodies (mostly of the IgG4 subclass) produced against autoantigens expressed by podocytes (e.g., human PLA2R, rat megalin) or antigens planted in the subepithelial space, such as cationic proteins (cBSA and α3NC1) (Jefferson et al., 2010). Upon antigen binding, the antibodies form immune complexes that deposit subepithelially, on the outer side of the GBM, resulting in complement activation that causes podocyte injury, foot process effacement, and GBM thickening. The glomerular filtration barrier is, therefore, compromised in MN, resulting in proteinuria and progression to nephrotic syndrome (Borza et al., 2013). The rat Heymann nephritis (HN) model has been established as the best model to study MN disease mechanisms, as it recapitulates the clinical and pathological aspects of human MN (Borza et al., 2013). The model is based on the use of antibodies targeted against HN antigenic complex consisting of two proteins: megalin and receptor-associated protein (RAP). Megalin forms a heterodimeric complex with RAP, and several epitopes on this complex are involved in the formation of immune deposits (Farquhar et al., 1995). There are two types of HN, active HN, where the animal's own immune system produces antibodies usually in response to an injection of kidney extracts with adjuvant, and passive HN, where rats are injected with antiserum generated in another animal to elicit immune complex formation. Although it more closely resembles human MN, active HN is rarely used, as it takes substantially longer to induce disease and MN development is very variable (Jefferson et al., 2010). In passive HN, antibodies are generated against the pelleted renal tubular epithelial fraction (Fx1A). Adult rats from various strains, Sprague Dawley, Wistar, Munich Wistar, Lewis, and Piebold Viral Glaxo, are used. The rats receive a single dose of anti-Fx1A antibody and doses range from 2 to 7 mL/kg for serum and 20–240 mg/kg for isolated IgG. UNX and multiple injections followed by sensitization with rabbit IgG have been used to accelerate passive HN (Jefferson et al., 2010). The formation of immune deposits occurs in the subepithelial space upon anti-Fx1A administration. This process obstructs the slit diaphragm and activates complement. Deposition of terminal components of complement C5b–9 is seen in both passive HN (Cybulsky et al., 1986) and in human MN (Cosyns et al., 1986). The onset of severe proteinuria manifests 4–7 days after

the injection and ranges between 100 and 500 mg/day (Nakatsue et al., 2005). The main histological changes include GBM thickening and foot process effacement progressing to glomerular and tubulointerstitial sclerosis, features resembling human MN (Beck and Salant, 2014). Limitations of this model include the fact that megalin is not expressed on human podocytes and so it not a pathogenic human antigen. Further, this model shows tubular immune deposits that do not reflect pathology in human MN. Dipeptidyl peptidase IV (DDPIV) is another major antigen that has been used in a model of MN. Administration of rabbit anti-DPPIV antibody into 6-week-old Lewis rats led to proteinuria on day 1, peaking at day 2, followed by a gradual decline. In this model, however, the immune deposits are transient and disappear within 5 days (Natori et al., 1994; Ronco et al., 1984).

3.4.2 IgA Nephropathy

IgA nephropathy (IgAN) is one of the most common forms of glomerulonephritis in the world, representing 25%–50% of patients with primary glomerulonephritis (Suzuki et al., 2014). Characteristic features of IgAN include mesangial cell proliferation, matrix expansion accompanied with granular mesangial immunodeposits of IgA, comprised of polymeric IgA1, complement 3, with variable IgG and/or IgM codeposits (Barratt and Feehally, 2005). With disease progression, crescentic changes can be superimposed on diffuse mesangial proliferative glomerulonephritis. Patients may develop nephrotic-range proteinuria at different stages of the disease from mild glomerular injury to advanced glomerulosclerosis (Barratt and Feehally, 2005; Suzuki et al., 2014). The ddY mouse strain is a well-characterized model of spontaneous IgAN, which develops glomerulonephritis and a remarkable deposition of IgA in the mesangium accompanied with codeposits of IgG, IgM, and C3 (Imai et al., 1985). However, the high degree of variability in the age of onset and severity of disease in this model presents a disadvantage. Interbreeding ddY strains with high serum levels of IgA produced the high-IgA (HIGA) mouse strain (Muso et al., 1996). However, it was observed that although HIGA mice have high IgA levels, serum IgA levels are not associated with severity of glomerular injury and incidence of disease (Suzuki et al., 2005). Another method used to overcome the high variability in ddY mice involves the selective intercrossing of early IgAN onset ddY mice for over 20 generations. This strategy established a novel 100% early-onset ddY mouse (Okazaki et al., 2012). Electron-dense deposits in these mice are manifested in the paramesangial area, similar to those found in humans. Further, glomerular deposits of IgA with IgG and C3 codeposits also occur in this model. All early-onset ddY mice develop proteinuria within 8 weeks of birth, which is higher than urinary protein excretion in HIGA mice at 8 weeks. These mice exhibit severe glomerular and tubulointerstitial lesions characterized by mesangial proliferation, mesangial matrix expansion, and tubulointerstitial infiltrations (Okazaki et al., 2012).

3.4.3 Thy-1 Nephritis

Thy-1 nephritis is an experimental rat model of membranoproliferative glomerulonephritis (MPGN). MPGN is characterized by glomerular mesangial expansion due to increased matrix and increased cellularity, thickening of peripheral capillary walls, and GBM with accumulation of subendothelial and intramembranous immune deposits (Alchi and Jayne, 2010; Smith and Alpers, 2005; Yang et al., 2010). Antigen-triggered immune MPGN in humans occurs in IgAN and Henoch–Schönlein purpura nephritis and can be modeled using the Thy-1 nephritis rat model (Alchi and Jayne, 2010). In Thy-1 nephritis, MPGN is induced by a single injection of rabbit anti-thymocyte serum or mouse anti-Thy1 monoclonal antibody through a tail vein (Ishizaki et al., 1986). The Thy-1 antigen is found on thymocytes and also is present on rat glomerular mesangial cells; therefore, an immune attack is induced. Monocyte/macrophage infiltration manifests 2 days postinjection along with mesangiolysis due to necrosis and fibrin deposition. Mesangial cell proliferation peaks at about 1 week, where mesangial matrix and small crescent formation can also be seen (Liu et al., 2004). Proteinuria and hematuria are seen but without hypertension development. The nephritis in this model repairs after 3 weeks; however, repeated injections of Thy-1 can result in chronic sclerosis and proliferative lesions with interstitial fibrosis and progressive CKD (Yabuki et al., 2006).

3.4.4 Anti-GBM Models

Anti-GBM glomerulonephritis is a category of crescentic glomerulonephritis, a morphological expression of severe glomerular injury. Crescent formation is caused mainly by rupture of glomerular capillaries, which allows cellular and humoral inflammatory mediators to spill into Bowman's space (Jennette and Thomas, 2001). Anti-GBM glomerulonephritis is caused by autoantibodies directed against the α3 chain of type IV collagen. Clinically, Goodpasture's Syndrome is an autoimmune disease where autoantibodies to the GBM and alveoli basement membrane result in pulmonary hemorrhage and anti-GBM glomerulonephritis (Jennette and Thomas, 2001). To produce a rat model of anti-GBM nephritis, anti-GBM antiserum is produced by immunizing rabbits with rat GBM. Nephritis is then induced by intravascular injection of rabbit anti-GBM IgG (Isome et al., 2004; Kim et al., 2004). Mesangial proliferation, severe necrotizing lesions, crescent formation, increased urinary protein excretion, and interstitial fibrosis are all features observed within 1–2 weeks after anti-GBM injection (Isome et al.,

2004; Kim et al., 2004; Reynolds et al., 1998). Macrophage infiltration (Isome et al., 2004) and inflammatory and fibrogenic activities of NFκB and TGF-β1 have been implicated in anti-GBM nephritis pathology (Kim et al., 2004). This model can be induced in both mice and rats; however, there is a significant variation in susceptibility among different strains. The WKY rat is highly susceptible to the development of crescentic glomerulonephritis, whereas the Lewis rat is resistant (Reynolds et al., 2006). In mice, BUB/BnJ, DBA/ 1J, and 129/svJ mice are more susceptible than A/J, AKR/J, C3H/HeJ, DBA/2J, MRL/MpJ, NOD/LtJ, P/J, SJL/J, and SWR/J mice (Xie et al., 2004).

3.4.5 Lupus Nephritis

Lupus nephritis (LN) is a form of glomerulonephritis that is clinically observed in 50%–80% of patients with systemic lupus erythematosus (SLE) and results in ESRD in 10%–20% of patients (Cameron, 1999; Ginzler et al., 1982; Peutz-Kootstra et al., 2001). SLE is an autoimmune disease affecting multiple organs and affects 1 of 750 people in Northern Europe and North America, with 80% of cases occurring in women during their childbearing years (Mills, 1994). LN is characterized by the presence of Igs of almost all isotypes in the glomerulus, as well as activation of complement components. A spectrum of glomerular lesions manifests, ranging from a complete absence of abnormalities or mild mesangial proliferation to proliferative and crescentic glomerulonephritis (McGaha and Madaio, 2014; Peutz-Kootstra et al., 2001). There are three widely used mouse models of LN: (1) (NZB × NZW) F1 hybrid (called the NZB/W F1 mice), (2) MRL/lpr, and (3) BXSB strains. NZB/W F1 mice are produced by crossing New Zealand white (NZW) mice with New Zealand black (NZB) mice (Knight and Adams, 1978). Both the NZB and the NZW strain have elevated levels of anti-DNA antibodies; however, on their own these strains develop mild pathology. The NZB/W F1 hybrid mice experience severe LN with mesangial proliferation, thickening of the glomerular capillary wall, glomerulosclerosis, tubular atrophy, and interstitial inflammation (Andrews et al., 1978; Lambert and Dixon, 1968; Peutz-Kootstra et al., 2001). Mice die of ESRD with proteinuria and azotemia between 6 and 12 months of age and females are more severely affected by the disease (McGaha and Madaio, 2014). The MRL/lpr mice show a broad spectrum of SLE features, such as arthritis, inflammatory skin lesions, and glomerulonephritis. MRL/lpr mouse pathology involves endothelial and mesangial cell proliferation; GBM thickening; macrophage, neutrophil, and T cell infiltration at 6 months of age (Andrews et al., 1978; Hahn, 1993). Glomerular Ig deposits begin to appear at 2 months accompanied with significant complement C3 deposits (Bao et al., 2011). These mice, however, have a lower incidence of glomerular crescent formation than the other models of LN (McGaha

and Madaio, 2014). MRL/lpr mice die within a year due to massive proteinuria and azotemia resulting in ESRD (Hahn, 1993; Peutz-Kootstra et al., 2001). Although both males and females are affected by the lymphoproliferation (lpr) mutation, the disease is more severe in females (Andrews et al., 1978). In contrast, the BXSB strain show a weaker disease phenotype where female mice have 50% mortality at 15 months compared to male mice, which have 50% mortality at 5 months (Andrews et al., 1978; McGaha et al., 2005; Theofilopoulos and Dixon, 1981). This effect is attributed to the presence of the Y-linked autoimmune accelerator (Yaa) driving autoimmunity (Hudgins et al., 1985; Murphy and Roths, 1979). Nevertheless, both male and female mice die due to glomerulonephritis and ESRD (McGaha and Madaio, 2014).

3.5 Hereditary/Genetic Diseases

3.5.1 Alport Syndrome

Alport syndrome is an inherited disorder due to the mutations of the α3, α4, or α5 chains of type IV collagen (COL4A3, COL4A4, and COL4A5). Characteristics include progressive glomerulosclerosis, patchy thickening and thinning of the GBM, splitting of the lamina densa, as well as deafness and retinal abnormalities (Barker et al., 1990; Kashtan, 2002). Alport mice are genetically deficient in the α3 (IV) collagen chain on a 129Sv background and are commercially available. These mice exhibit irregular thickening and splitting of GBM by 4 weeks, and experience proteinuria with mild hematuria by 5 weeks (LeBleu et al., 2009; Sugimoto et al., 2006; Yang et al., 2010). Severe glomerular sclerotic lesions and tubulointerstitial fibrosis have been seen at 10 weeks. There is a rapid decline of renal function after 14 weeks and only 5% of mice survive past 4 months (Cosgrove et al., 1996; Miner and Sanes, 1996). While highly representative of the renal pathology found in human Alport syndrome, the murine model progresses very rapidly. This aspect is not representative of the slow progression of the disease in humans between late childhood and age 40 (Pierides et al., 2009). In addition, these mice also show extracapillary crescentic proliferation in the first 4 weeks, a feature not seen in typical human Alport syndrome (LeBleu et al., 2009).

3.5.2 Polycystic Kidney Disease

Polycystic kidney disease (PKD) is a group of disorders inherited in an autosomal dominant (ADPKD) or recessive (ARPKD) fashion; however, ADPKD occurs more frequently and is in fact one of the most common genetic diseases in humans (Happe and Peters, 2014; Nagao et al., 2012). Further, 50% of patients with ADPKD develop ESRD by age 60 (Nagao et al., 2012). About 85% of ADPKD cases occur as a result of mutations in the PKD1 gene, whereas 15% occur as a result

of mutations in PKD2. ARPKD with a lower incidence is caused by a mutation in the polycystic kidney and hepatic disease 1 (PKHD1) gene, which encodes fibrocystin/polyductin (Harris, 2002; Turkbey et al., 2009). PKD is characterized by abnormal cellular proliferation, fluid accumulation in numerous cysts, remodeling of ECM, inflammation, and fibrosis in the kidney and liver. Overt proteinuria is uncommon in ADPKD with only 27% demonstrating 300 mg/day and proteinuria >2 g/day is unusual and is suggestive of the presence of another kidney disease (Chapman, 2007). There are two main types of PKD animal models: spontaneous hereditary models identified by manifestations of PKD and modified models generated by mutation of human orthologous genes (Nagao et al., 2012). Established, spontaneous hereditary models include PCK rats, Pcy mice, and juvenile cystic kidney (Jck) mice. The gene responsible for PKD in the PCK rat is orthologous to human Pkhd1. The life span of PCK rats is approximately 1.5 years, and numerous cysts are observed on the kidney and liver surface at 1 year of age. The initial cysts originate from the collecting duct and the growing cysts diffusely affect whole nephron segments with disease progression (Nagao et al., 2012). In Pcy mice, the gene target is orthologous to human Nphp3-encoding nephrocystin-3, a protein expressed in primary cilia of epithelial cells in the kidney, pancreas, heart, and liver. Numerous cysts are observed at 30 weeks of age and this is associated with the occurrence of ESRD (Nagao et al., 2012). These mice have a life span of 30 weeks on the DBA/2 or ICR strain background, but 2 years on the C57BL/6 background. Jck mice have a mutated Nek8 or Nphp9 gene, where the mutated gene product is found on primary cilia and affects the normal expression of PKD1 and PKD2 gene products: PC1 and PC2. The life span of Jck mice is 20–25 weeks and initial cysts are observed at 4 weeks (Nagao et al., 2012).

4 CONCLUSIONS

As illustrated in this work, kidney disease represents a wide range of human pathologies affecting this organ and its function. The ultimate adverse consequence for patients with kidney disease is renal failure. In this work, we have described numerous animal models and illustrated their main pathophysiological features. We have also attempted to detail the similarities, from a pathophysiological perspective, that these models share with human diseases. The goal of modeling kidney disease in animals is to better understand its underlying mechanisms of initiation and progression, thereby allowing intervention strategies to be developed that ultimately prevent renal failure. It is our hope that this work contributes to that goal.

References

Abdel-Salam, A.M., Al-Dekheil, A., Babkr, A., Farahna, M., Mousa, H.M., 2010. High fiber probiotic fermented mare's milk reduces the toxic effects of mercury in rats. N. Am. J. Med. Sci. 2 (12), 569–575.

Agarwal, R., Campbell, R.C., Warnock, D.G., 2004. Oxidative stress in hypertension and chronic kidney disease: role of angiotensin II. Semin. Nephrol. 24 (2), 101–114.

Agmon, Y., Peleg, H., Greenfeld, Z., Rosen, S., Brezis, M., 1994. Nitric oxide and prostanoids protect the renal outer medulla from radiocontrast toxicity in the rat. J. Clin. Invest. 94 (3), 1069–1075.

Ahn, C.B., Song, C.H., Kim, W.H., Kim, Y.K., 2002. Effects of *Juglans sinensis* Dode extract and antioxidant on mercury chloride-induced acute renal failure in rabbits. J. Ethnopharmacol. 82 (1), 45–49.

Aiyar, J., Berkovits, H.J., Floyd, R.A., Wetterhahn, K.E., 1991. Reaction of chromium(VI) with glutathione or with hydrogen peroxide: identification of reactive intermediates and their role in chromium(VI)-induced DNA damage. Environ. Health Perspect. 92, 53–62.

Akcay, A., Nguyen, Q., Edelstein, C.L., 2009. Mediators of inflammation in acute kidney injury. Mediators Inflamm. 2009, 137072.

Al Banchaabouchi, M., Marescau, B., D'Hooge, R., Van Marck, E., Van Daele, A., Levillain, O., et al., 1998. Biochemical and histopathological changes in nephrectomized mice. Metabolism 47 (3), 355–361.

Alchi, B., Jayne, D., 2010. Membranoproliferative glomerulonephritis. Pediatr. Nephrol. 25 (8), 1409–1418.

Al-Harbi, N.O., Imam, F., Al-Harbi, M.M., Iqbal, M., Nadeem, A., Sayed-Ahmed, M.M., et al., 2014. Olmesartan attenuates tacrolimus-induced biochemical and ultrastructural changes in rat kidney tissue. BioMed Res. Int. 2014, 607246.

Allen, T.J., Cao, Z., Youssef, S., Hulthen, U.L., Cooper, M.E., 1997. Role of angiotensin II and bradykinin in experimental diabetic nephropathy. Functional and structural studies. Diabetes 46 (10), 1612–1618.

Alpers, C.E., Hudkins, K.L., 2011. Mouse models of diabetic nephropathy. Curr. Opin. Nephrol. Hypertens. 20 (3), 278–284.

Al-Suraih, M., Grande, J.P., 2014. Management of renal artery stenosis: what does the experimental evidence tell us? World J. Cardiol. 6 (8), 855–860.

Andreucci, M., Faga, T., Pisani, A., Sabbatini, M., Michael, A., 2014. Acute kidney injury by radiographic contrast media: pathogenesis and prevention. BioMed Res. Int. 2014, 362725.

Andrews, B.S., Eisenberg, R.A., Theofilopoulos, A.N., Izui, S., Wilson, C.B., McConahey, P.J., et al., 1978. Spontaneous murine lupus-like syndromes. Clinical and immunopathological manifestations in several strains. J. Exp. Med. 148 (5), 1198–1215.

Appel, G.B., Siegel, N.J., Appel, A.S., Hayslett, J.P., 1981. Studies on the mechanism of non-oliguric experimental acute renal failure. Yale J. Biol. Med. 54 (4), 273–281.

Arendshorst, W.J., Beierwaltes, W.H., 1979. Renal and nephron hemodynamics in spontaneously hypertensive rats. Am. J. Physiol. 236 (3), F246–F251.

Asplin, J.R., Mandel, N.S., Coe, F.L., 1996. Evidence of calcium phosphate supersaturation in the loop of Henle. Am. J. Physiol. 270 (4 Pt. 2), F604–F613.

Assmann, K.J., van Son, J.P., Dijkman, H.B., Mentzel, S., Wetzels, J.F., 2002. Antibody-induced albuminuria and accelerated focal glomerulosclerosis in the Thy-1.1 transgenic mouse. Kidney Int. 62 (1), 116–126.

Avasthi, P.S., Evan, A.P., Hay, D., 1980. Glomerular endothelial cells in uranyl nitrate-induced acute renal failure in rats. J. Clin. Invest. 65 (1), 121–127.

Bae, E.H., Kim, I.J., Joo, S.Y., Kim, E.Y., Choi, J.S., Kim, C.S., et al., 2014. Renoprotective effects of the direct renin inhibitor aliskiren on gentamicin-induced nephrotoxicity in rats. J. Renin Angiotensin Aldosterone Syst. 15 (4), 348–361.

Bakris, G.L., Weir, M.R., Shanifar, S., Zhang, Z., Douglas, J., van Dijk, D.J., et al., 2003. Effects of blood pressure level on progression of

diabetic nephropathy: results from the RENAAL study. Arch. Intern. Med. 163 (13), 1555–1565.

Bao, L., Haas, M., Quigg, R.J., 2011. Complement factor H deficiency accelerates development of lupus nephritis. J. Am. Soc. Nephrol. 22 (2), 285–295.

Barker, D.F., Hostikka, S.L., Zhou, J., Chow, L.T., Oliphant, A.R., Gerken, S.C., et al., 1990. Identification of mutations in the COL4A5 collagen gene in Alport syndrome. Science 248 (4960), 1224–1227.

Barratt, J., Feehally, J., 2005. IgA nephropathy. J. Am. Soc. Nephrol. 16 (7), 2088–2097.

Barri, Y.M., 2008. Hypertension and kidney disease: a deadly connection. Curr. Hypertens. Rep. 10 (1), 39–45.

Bas, M., Tugcu, V., Kemahli, E., Ozbek, E., Uhri, M., Altug, T., et al., 2009. Curcumin prevents shock-wave lithotripsy-induced renal injury through inhibition of nuclear factor kappa-B and inducible nitric oxide synthase activity in rats. Urol. Res. 37 (3), 159–164.

Basile, D.P., Anderson, M.D., Sutton, T.A., 2012. Pathophysiology of acute kidney injury. Compr. Physiol. 2 (2), 1303–1353.

Bassik, M.C., Kampmann, M., 2011. Knocking out the door to tunicamycin entry. Proc. Natl. Acad. Sci. USA 108 (29), 11731–11732.

Beck, Jr., L.H., Salant, D.J., 2014. Membranous nephropathy: from models to man. J. Clin. Invest. 124 (6), 2307–2314.

Belliere, J., Casemayou, A., Ducasse, L., Zakaroff-Girard, A., Martins, F., Iacovoni, J.S., et al., 2015. Specific macrophage subtypes influence the progression of rhabdomyolysis-induced kidney injury. J. Am. Soc. Nephrol. 26 (6), 1363–1377.

Bertani, T., Rocchi, G., Sacchi, G., Mecca, G., Remuzzi, G., 1986. Adriamycin-induced glomerulosclerosis in the rat. Am. J. Kidney. Dis. 7 (1), 12–19.

Bianchi, G., Fox, U., Di Francesco, G.F., Giovanetti, A.M., Pagetti, D., 1974. Blood pressure changes produced by kidney cross-transplantation between spontaneously hypertensive rats and normotensive rats. Clin. Sci. Mol. Med. 47 (5), 435–448.

Biswas, S.K., de Faria, J.B., 2007. Which comes first: renal inflammation or oxidative stress in spontaneously hypertensive rats? Free Radic. Res. 41 (2), 216–224.

Blantz, R.C., 1975. The mechanism of acute renal failure after uranyl nitrate. J. Clin. Invest. 55 (3), 621–635.

Bledsoe, G., Shen, B., Yao, Y.Y., Hagiwara, M., Mizell, B., Teuton, M., et al., 2008. Role of tissue kallikrein in prevention and recovery of gentamicin-induced renal injury. Toxicol. Sci. 102 (2), 433–443.

Blizard, D.A., Peterson, W.N., Iskandar, S.S., Shihabi, Z.K., Adams, N., 1991. The effect of a high salt diet and gender on blood pressure, urinary protein excretion and renal pathology in SHR rats. Clin. Exp. Hypertens. A 13 (5), 687–697.

Bonventre, J.V., Yang, L., 2011. Cellular pathophysiology of ischemic acute kidney injury. J. Clin. Invest. 121 (11), 4210–4221.

Boonla, C., Krieglstein, K., Bovornpadungkitti, S., Strutz, F., Spittau, B., Predanon, C., et al., 2011. Fibrosis and evidence for epithelial-mesenchymal transition in the kidneys of patients with staghorn calculi. BJU Int. 108 (8), 1336–1345.

Borza, D.B., Zhang, J.J., Beck, Jr., L.H., Meyer-Schwesinger, C., Luo, W., 2013. Mouse models of membranous nephropathy: the road less travelled by. Am. J. Clin. Exp. Immunol. 2 (2), 135–145.

Boute, N., Gribouval, O., Roselli, S., Benessy, F., Lee, H., Fuchshuber, A., et al., 2000. NPHS2, encoding the glomerular protein podocin, is mutated in autosomal recessive steroid-resistant nephrotic syndrome. Nat. Genet. 24 (4), 349–354.

Breyer, M.D., Bottinger, E., Brosius, 3rd, F.C., Coffman, T.M., Harris, R.C., Heilig, C.W., et al., 2005. Mouse models of diabetic nephropathy. J. Am. Soc. Nephrol. 16 (1), 27–45.

Bubb, K.J., Khambata, R.S., Ahluwalia, A., 2012. Sexual dimorphism in rodent models of hypertension and atherosclerosis. Br. J. Pharmacol. 167 (2), 298–312.

Bulger, R.E., 1986. Renal damage caused by heavy metals. Toxicol. Pathol. 14 (1), 58–65.

Burne, M.J., Daniels, F., El Ghandour, A., Mauiyyedi, S., Colvin, R.B., O'Donnell, M.P., et al., 2001. Identification of the CD4(+) T cell as a major pathogenic factor in ischemic acute renal failure. J. Clin. Invest. 108 (9), 1283–1290.

Cameron, J.S., 1999. Lupus nephritis. J. Am. Soc. Nephrol. 10 (2), 413–424.

Campese, V.M., 1994. Salt sensitivity in hypertension. Renal and cardiovascular implications. Hypertension 23 (4), 531–550.

Carlisle, R.E., Brimble, E., Werner, K.E., Cruz, G.L., Ask, K., Ingram, A.J., et al., 2014. 4-Phenylbutyrate inhibits tunicamycin-induced acute kidney injury via CHOP/GADD153 repression. PLoS One 9 (1), e84663.

Carlisle, R.E., Werner, K.E., Yum, V., Lu, C., Tat, V., Memon, M., et al., 2016. Endoplasmic reticulum stress inhibition reduces hypertension through the preservation of resistance blood vessel structure and function. J. Hypertens. 34 (8), 1556–1569.

Castellano, G., Stasi, A., Intini, A., Gigante, M., Di Palma, A.M., Divella, C., et al., 2014. Endothelial dysfunction and renal fibrosis in endotoxemia-induced oliguric kidney injury: possible role of LPS-binding protein. Crit. Care 18 (5), 520.

Cau, J., Favreau, F., Zhang, K., Febrer, G., de la Motte, G.R., Ricco, J.B., et al., 2009. FR167653 improves renal recovery and decreases inflammation and fibrosis after renal ischemia reperfusion injury. J. Vasc. Surg. 49 (3), 728–740.

Cekmen, M., Ilbey, Y.O., Ozbek, E., Simsek, A., Somay, A., Ersoz, C., 2009. Curcumin prevents oxidative renal damage induced by acetaminophen in rats. Food Chem. Toxicol. 47 (7), 1480–1484.

Cermik, H., Taslipinar, M.Y., Aydin, I., Agilli, M., Aydin, F.N., Ucar, F., et al., 2013. The relationship between N-acetylcysteine, hyperbaric oxygen, and inflammation in a rat model of acetaminophen-induced nephrotoxicity. Inflammation 36 (5), 1145–1152.

Chade, A.R., Rodriguez-Porcel, M., Grande, J.P., Zhu, X., Sica, V., Napoli, C., et al., 2003. Mechanisms of renal structural alterations in combined hypercholesterolemia and renal artery stenosis. Arterioscler. Thromb. Vasc. Biol. 23 (7), 1295–1301.

Chapman, A.B., 2007. Autosomal dominant polycystic kidney disease: time for a change? J. Am. Soc. Nephrol. 18 (5), 1399–1407.

Chen, J., Hartono, J.R., John, R., Bennett, M., Zhou, X.J., Wang, Y., et al., 2011. Early interleukin 6 production by leukocytes during ischemic acute kidney injury is regulated by TLR4. Kidney Int. 80 (5), 504–515.

Chen, D., Wang, M.W., 2005. Development and application of rodent models for type 2 diabetes. Diabetes Obes. Metab. 7 (4), 307–317.

Chevalier, R.L., Forbes, M.S., Thornhill, B.A., 2009. Ureteral obstruction as a model of renal interstitial fibrosis and obstructive nephropathy. Kidney Int. 75 (11), 1145–1152.

Choi, R., Kim, B.H., Naowaboot, J., Lee, M.Y., Hyun, M.R., Cho, E.J., et al., 2011. Effects of ferulic acid on diabetic nephropathy in a rat model of type 2 diabetes. Exp. Mol. Med. 43 (12), 676–683.

Choudhury, D., Ahmed, Z., 2006. Drug-associated renal dysfunction and injury. Nat. Clin. Pract. Nephrol. 2 (2), 80–91.

Chuang, S.T., Kuo, Y.H., Su, M.J., 2014. Antifibrotic effects of KS370G, a caffeamide derivative, in renal ischemia-reperfusion injured mice and renal tubular epithelial cells. Sci. Rep. 4, 5814.

Chugh, S.S., Clement, L.C., Mace, C., 2012. New insights into human minimal change disease: lessons from animal models. Am. J. Kidney. Dis. 59 (2), 284–292.

Clement, L.C., Avila-Casado, C., Mace, C., Soria, E., Bakker, W.W., Kersten, S., et al., 2011. Podocyte-secreted angiopoietin-like-4 mediates proteinuria in glucocorticoid-sensitive nephrotic syndrome. Nat. Med. 17 (1), 117–122.

Coimbra, T.M., Janssen, U., Grone, H.J., Ostendorf, T., Kunter, U., Schmidt, H., et al., 2000. Early events leading to renal injury in obese Zucker (fatty) rats with type II diabetes. Kidney Int. 57 (1), 167–182.

Colbay, M., Yuksel, S., Uslan, I., Acarturk, G., Karaman, O., Bas, O., et al., 2010. Novel approach for the prevention of contrast nephropathy. Exp. Toxicol. Pathol. 62 (1), 81–89.

Conrad, C.H., Brooks, W.W., Hayes, J.A., Sen, S., Robinson, K.G., Bing, O.H., 1995. Myocardial fibrosis and stiffness with hypertrophy and heart failure in the spontaneously hypertensive rat. Circulation 91 (1), 161–170.

Cooper, M.E., Allen, T.J., Macmillan, P., Bach, L., Jerums, G., Doyle, A.E., 1988. Genetic hypertension accelerates nephropathy in the streptozotocin diabetic rat. Am. J. Hypertens. 1 (1), 5–10.

Cordellini, S., 1999. Endothelial dysfunction in DOCA-salt hypertension: possible involvement of prostaglandin endoperoxides. Gen. Pharmacol. 32 (3), 315–320.

Corsetti, J.P., Sparks, J.D., Peterson, R.G., Smith, R.L., Sparks, C.E., 2000. Effect of dietary fat on the development of non-insulin dependent diabetes mellitus in obese Zucker diabetic fatty male and female rats. Atherosclerosis 148 (2), 231–241.

Cosgrove, D., Meehan, D.T., Grunkemeyer, J.A., Kornak, J.M., Sayers, R., Hunter, W.J., et al., 1996. Collagen COL4A3 knockout: a mouse model for autosomal Alport syndrome. Genes Dev 10 (23), 2981–2992.

Cosyns, J.P., Kazatchkine, M.D., Bhakdi, S., Mandet, C., Grossetete, J., Hinglais, N., et al., 1986. Immunohistochemical analysis of C3 cleavage fragments, factor H, and the C5b-9 terminal complex of complement in de novo membranous glomerulonephritis occurring in patients with renal transplant. Clin. Nephrol. 26 (4), 203–208.

Cowley, Jr., A.W., Roman, R.J., 1996. The role of the kidney in hypertension. JAMA 275 (20), 1581–1589.

Cowley, Jr., A.W., Roman, R.J., Kaldunski, M.L., Dumas, P., Dickhout, J.G., Greene, A.S., et al., 2001. Brown Norway chromosome 13 confers protection from high salt to consomic Dahl S rat. Hypertension 37 (2 Pt. 2), 456–461.

Cui, J., Bai, X.Y., Sun, X., Cai, G., Hong, Q., Ding, R., et al., 2015. Rapamycin protects against gentamicin-induced acute kidney injury via autophagy in mini-pig models. Sci. Rep. 5, 11256.

Cunha, E.M., Silva, D.P., Aguas, A.P., 2003. High-resolution identification of mercury in particles in mouse kidney after acute lethal exposure. Biometals 16 (4), 583–590.

Cunningham, P.N., Dyanov, H.M., Park, P., Wang, J., Newell, K.A., Quigg, R.J., 2002. Acute renal failure in endotoxemia is caused by TNF acting directly on TNF receptor-1 in kidney. J. Immunol. 168 (11), 5817–5823.

Cybulsky, A.V., 2010. Endoplasmic reticulum stress in proteinuric kidney disease. Kidney Int. 77 (3), 187–193.

Cybulsky, A.V., Rennke, H.G., Feintzeig, I.D., Salant, D.J., 1986. Complement-induced glomerular epithelial cell injury. Role of the membrane attack complex in rat membranous nephropathy. J. Clin. Invest. 77 (4), 1096–1107.

Cybulsky, A.V., Takano, T., Papillon, J., Kitzler, T.M., Bijian, K., 2011. Endoplasmic reticulum stress in glomerular epithelial cell injury. Am. J. Physiol. Renal Physiol. 301 (3), F496–F508.

Daemen, M.A., van't Veer, C., Denecker, G., Heemskerk, V.H., Wolfs, T.G., Clauss, M., et al., 1999. Inhibition of apoptosis induced by ischemia-reperfusion prevents inflammation. J. Clin. Invest. 104 (5), 541–549.

D'Agati, V.D., Kaskel, F.J., Falk, R.J., 2011. Focal segmental glomerulosclerosis. N. Engl. J. Med. 365 (25), 2398–2411.

Dahl, L.K., Heine, M., Tassinari, L., 1962. Role of genetic factors in susceptibility to experimental hypertension due to chronic excess salt ingestion. Nature 194, 480–482.

Dahl, L.K., Heine, M., Tassinari, L., 1963. Effects of chronic excess salt ingestion. Role of Genetic factors in both DOCA-salt and renal hypertension. J. Exp. Med. 118, 605–617.

Darling, N.J., Cook, S.J., 2014. The role of MAPK signalling pathways in the response to endoplasmic reticulum stress. Biochim. Biophys. Acta 1843 (10), 2150–2163.

Davis, B.J., Johnston, C.I., Burrell, L.M., Burns, W.C., Kubota, E., Cao, Z., et al., 2003. Renoprotective effects of vasopeptidase inhibition in an experimental model of diabetic nephropathy. Diabetologia 46 (7), 961–971.

De Miguel, C., Das, S., Lund, H., Mattson, D.L., 2010. T lymphocytes mediate hypertension and kidney damage in Dahl salt-sensitive rats. Am. J .Physiol. Regul. Integr. Comp. Physiol. 298 (4), R1136–R1142.

de Mik, S.M., Hoogduijn, M.J., de Bruin, R.W., Dor, F.J., 2013. Pathophysiology and treatment of focal segmental glomerulosclerosis: the role of animal models. BMC Nephrol. 14, 74.

de Water, R., Noordermeer, C., van der Kwast, T.H., Nizze, H., Boeve, E.R., Kok, D.J., et al., 1999. Calcium oxalate nephrolithiasis: effect of renal crystal deposition on the cellular composition of the renal interstitium. Am. J. Kidney. Dis. 33 (4), 761–771.

Dejager, L., Pinheiro, I., Dejonckheere, E., Libert, C., 2011. Cecal ligation and puncture: the gold standard model for polymicrobial sepsis? Trends Microbiol. 19 (4), 198–208.

Deng, L.Y., Schiffrin, E.L., 1992. Effects of endothelin on resistance arteries of DOCA-salt hypertensive rats. Am. J. Physiol. 262 (6 Pt. 2), H1782–H1787.

Deng, J., Wu, G., Yang, C., Li, Y., Jing, Q., Han, Y., 2015. Rosuvastatin attenuates contrast-induced nephropathy through modulation of nitric oxide, inflammatory responses, oxidative stress and apoptosis in diabetic male rats. J. Transl. Med. 13, 53.

Deray, G., 1999. Nephrotoxicity of contrast media. Nephrol. Dial. Transplant. 14 (11), 2602–2606.

Devarajan, P., 2006. Update on mechanisms of ischemic acute kidney injury. J. Am. Soc. Nephrol. 17 (6), 1503–1520.

Diamond, J.R., Karnovsky, M.J., 1986. Focal and segmental glomerulosclerosis following a single intravenous dose of puromycin aminonucleoside. Am. J. Pathol. 122 (3), 481–487.

Dickhout, J.G., Krepinsky, J.C., 2009. Endoplasmic reticulum stress and renal disease. Antioxid. Redox Signal. 11 (9), 2341–2352.

Dickhout, J.G., Lee, R.M., 1997. Structural and functional analysis of small arteries from young spontaneously hypertensive rats. Hypertension 29 (3), 781–789.

Dickie, P., Felser, J., Eckhaus, M., Bryant, J., Silver, J., Marinos, N., et al., 1991. HIV-associated nephropathy in transgenic mice expressing HIV-1 genes. Virology 185 (1), 109–119.

Ding, W., Wang, B., Zhang, M., Gu, Y., 2016. Involvement of endoplasmic reticulum stress in uremic cardiomyopathy: protective effects of tauroursodeoxycholic acid. Cell Physiol. Biochem. 38 (1), 141–152.

Dobrzynski, E., Wang, C., Chao, J., Chao, L., 2000. Adrenomedullin gene delivery attenuates hypertension, cardiac remodeling, and renal injury in deoxycorticosterone acetate-salt hypertensive rats. Hypertension 36 (6), 995–1001.

Doi, T., Hattori, M., Agodoa, L.Y., Sato, T., Yoshida, H., Striker, L.J., et al., 1990. Glomerular lesions in nonobese diabetic mouse: before and after the onset of hyperglycemia. Lab. Invest. 63 (2), 204–212.

Doi, K., Leelahavanichkul, A., Yuen, P.S., Star, R.A., 2009. Animal models of sepsis and sepsis-induced kidney injury. J. Clin. Invest. 119 (10), 2868–2878.

Domingo, J.L., de la Torre, A., Belles, M., Mayayo, E., Llobet, J.M., Corbella, J., 1997. Comparative effects of the chelators sodium 4,5-dihydroxybenzene-1,3-disulfonate (Tiron) and diethylenetriaminepentaacetic acid (DTPA) on acute uranium nephrotoxicity in rats. Toxicology 118 (1), 49–59.

Drenjancevic-Peric, I., Jelakovic, B., Lombard, J.H., Kunert, M.P., Kibel, A., Gros, M., 2011. High-salt diet and hypertension: focus on the renin-angiotensin system. Kidney Blood Press. Res. 34 (1), 1–11.

Dworkin, L.D., Feiner, H.D., 1986. Glomerular injury in uninephrectomized spontaneously hypertensive rats. A consequence of glomerular capillary hypertension. J. Clin. Invest. 77 (3), 797–809.

El Mouedden, M., Laurent, G., Mingeot-Leclercq, M.P., Tulkens, P.M., 2000. Gentamicin-induced apoptosis in renal cell lines and embryonic rat fibroblasts. Toxicol. Sci. 56 (1), 229–239.

Elmarakby, A.A., Quigley, J.E., Imig, J.D., Pollock, J.S., Pollock, D.M., 2008. TNF-alpha inhibition reduces renal injury in DOCA-salt hypertensive rats. Am. J. Physiol. Regul. Integr. Comp. Physiol. 294 (1), R76–R83.

Erdem, A., Gundogan, N.U., Usubutun, A., Kilinc, K., Erdem, S.R., Kara, A., et al., 2000. The protective effect of taurine against gentamicin-induced acute tubular necrosis in rats. Nephrol. Dial. Transplant. 15 (8), 1175–1182.

Erley, C.M., Heyne, N., Burgert, K., Langanke, J., Risler, T., Osswald, H., 1997. Prevention of radiocontrast-induced nephropathy by adenosine antagonists in rats with chronic nitric oxide deficiency. J. Am. Soc. Nephrol. 8 (7), 1125–1132.

Esposito, V., Grosjean, F., Tan, J., Huang, L., Zhu, L., Chen, J., et al., 2013. CHOP deficiency results in elevated lipopolysaccharide-induced inflammation and kidney injury. Am. J. Physiol. Renal Physiol. 304 (4), F440–F450.

Ewald, K.A., Calabrese, E.J., 2001. Lead reduces the nephrotoxicity of mercuric chloride. Ecotoxicol. Environ. Saf. 48 (2), 215–218.

Fan, Y., Xiao, W., Li, Z., Li, X., Chuang, P.Y., Jim, B., et al., 2015. RTN1 mediates progression of kidney disease by inducing ER stress. Nat. Commun. 6, 7841.

Farooqi, S., Dickhout, J.G., 2016. Major comorbid disease processes associated with increased incidence of acute kidney injury. World J. Nephrol. 52, 139–146.

Farquhar, M.G., Saito, A., Kerjaschki, D., Orlando, R.A., 1995. The Heymann nephritis antigenic complex: megalin (gp330) and RAP. J. Am. Soc. Nephrol. 6 (1), 35–47.

Faubel, S., Lewis, E.C., Reznikov, L., Ljubanovic, D., Hoke, T.S., Somerset, H., et al., 2007. Cisplatin-induced acute renal failure is associated with an increase in the cytokines interleukin (IL)-1beta, IL-18, IL-6, and neutrophil infiltration in the kidney. J. Pharmacol. Exp. Ther. 322 (1), 8–15.

Faubel, S., Ljubanovic, D., Reznikov, L., Somerset, H., Dinarello, C.A., Edelstein, C.L., 2004. Caspase-1-deficient mice are protected against cisplatin-induced apoptosis and acute tubular necrosis. Kidney Int. 66 (6), 2202–2213.

Favreau, F., Zhu, X.Y., Krier, J.D., Lin, J., Warner, L., Textor, S.C., et al., 2010. Revascularization of swine renal artery stenosis improves renal function but not the changes in vascular structure. Kidney Int. 78 (11), 1110–1118.

Feld, L.G., Van Liew, J.B., Brentjens, J.R., Boylan, J.W., 1981. Renal lesions and proteinuria in the spontaneously hypertensive rat made normotensive by treatment. Kidney Int. 20 (5), 606–614.

Feng, D., DuMontier, C., Pollak, M.R., 2015. The role of alpha-actinin-4 in human kidney disease. Cell Biosci. 5, 44.

Fervenza, F.C., Sethi, S., Specks, U., 2008. Idiopathic membranous nephropathy: diagnosis and treatment. Clin J. Am. Soc. Nephrol. 3 (3), 905–919.

Figarola, J.L., Loera, S., Weng, Y., Shanmugam, N., Natarajan, R., Rahbar, S., 2008. LR-90 prevents dyslipidaemia and diabetic nephropathy in the Zucker diabetic fatty rat. Diabetologia 51 (5), 882–891.

Fleck, C., Appenroth, D., Jonas, P., Koch, M., Kundt, G., Nizze, H., et al., 2006. Suitability of 5/6 nephrectomy (5/6NX) for the induction of interstitial renal fibrosis in rats—influence of sex, strain, and surgical procedure. Exp. Toxicol. Pathol. 57 (3), 195–205.

Fogo, A.B., 2001. Minimal change disease and focal segmental glomerulosclerosis. Nephrol. Dial. Transplant. 16 (Suppl. 6), 74–76.

Fogo, A.B., 2003. Animal models of FSGS: lessons for pathogenesis and treatment. Semin. Nephrol. 23 (2), 161–171.

Fogo, A., Yoshida, Y., Glick, A.D., Homma, T., Ichikawa, I., 1988. Serial micropuncture analysis of glomerular function in two rat models of glomerular sclerosis. J. Clin. Invest. 82 (1), 322–330.

Fowler, B.A., 1993. Mechanisms of kidney cell injury from metals. Environ. Health Perspect. 100, 57–63.

Fowler, B.A., Brown, H.W., Lucier, G.W., Krigman, M.R., 1975. The effects of chronic oral methyl mercury exposure on the lysosome system of rat kidney. Morphometric and biochemical studies. Lab. Invest. 32 (3), 313–322.

Fu, P., Liu, F., Su, S., Wang, W., Huang, X.R., Entman, M.L., et al., 2006. Signaling mechanism of renal fibrosis in unilateral ureteral obstructive kidney disease in ROCK1 knockout mice. J. Am. Soc. Nephrol. 17 (11), 3105–3114.

Fujimoto, M., Maezawa, Y., Yokote, K., Joh, K., Kobayashi, K., Kawamura, H., et al., 2003. Mice lacking Smad3 are protected against streptozotocin-induced diabetic glomerulopathy. Biochem. Biophys. Res. Commun. 305 (4), 1002–1007.

Gao, X., Fu, L., Xiao, M., Xu, C., Sun, L., Zhang, T., et al., 2012. The nephroprotective effect of tauroursodeoxycholic acid on ischaemia/reperfusion-induced acute kidney injury by inhibiting endoplasmic reticulum stress. Basic Clin. Pharmacol. Toxicol. 111 (1), 14–23.

Ghosh, S.S., Massey, H.D., Krieg, R., Fazelbhoy, Z.A., Ghosh, S., Sica, D.A., et al., 2009. Curcumin ameliorates renal failure in 5/6 nephrectomized rats: role of inflammation. Am. J. Physiol. Renal Physiol. 296 (5), F1146–F1157.

Ginzler, E.M., Diamond, H.S., Weiner, M., Schlesinger, M., Fries, J.F., Wasner, C., et al., 1982. A multicenter study of outcome in systemic lupus erythematosus. I. Entry variables as predictors of prognosis. Arthritis Rheum. 25 (6), 601–611.

Glassock, R.J., 2003. Secondary minimal change disease. Nephrol. Dial. Transplant. 18 (Suppl. 6), vi52–vi58.

Green, C.R., Ham, K.N., Tange, J.D., 1969. Kidney lesions induced in rats by p-aminophenol. Br. Med. J. 1 (5637), 162–164.

Greene, A.S., Yu, Z.Y., Roman, R.J., Cowley, Jr., A.W., 1990. Role of blood volume expansion in Dahl rat model of hypertension. Am. J. Physiol. 258 (2 Pt. 2), H508–H514.

Griffin, K.A., Bidani, A.K., 2009. Angiotensin II type 2 receptor in chronic kidney disease: the good side of angiotensin II? Kidney Int. 75 (10), 1006–1008.

Grossman, R.C., 2010. Experimental models of renal disease and the cardiovascular system. Open Cardiovasc. Med. J. 4, 257–264.

Guo, X.F., Yang, X.J., 2015. Endoplasmic reticulum stress response in spontaneously hypertensive rats is affected by myocardial ischemia reperfusion injury. Exp. Ther. Med. 9 (2), 319–326.

Gurley, S.B., Clare, S.E., Snow, K.P., Hu, A., Meyer, T.W., Coffman, T.M., 2006. Impact of genetic background on nephropathy in diabetic mice. Am. J. Physiol. Renal Physiol. 290 (1), F214–F222.

Gurley, S.B., Mach, C.L., Stegbauer, J., Yang, J., Snow, K.P., Hu, A., et al., 2010. Influence of genetic background on albuminuria and kidney injury in Ins2(+/C96Y) (Akita) mice. Am. J. Physiol. Renal Physiol. 298 (3), F788–F795.

Hahn, B.H., 1993. Animal models of systemic lupus erythematosus. In: Wallace, D.J., Hahn, B.H. (Eds.), Duboi's lupus erythematosus. Lea and Ebiger, Philadelphia, pp. 157–177.

Happe, H., Peters, D.J., 2014. Translational research in ADPKD: lessons from animal models. Nat. Rev. Nephrol. 10 (10), 587–601.

Harris, P.C., 2002. Molecular basis of polycystic kidney disease: PKD1, PKD2 and PKHD1. Curr. Opin. Nephrol. Hypertens. 11 (3), 309–314.

Hartner, A., Cordasic, N., Klanke, B., Veelken, R., Hilgers, K.F., 2003. Strain differences in the development of hypertension and glomerular lesions induced by deoxycorticosterone acetate salt in mice. Nephrol. Dial. Transplant. 18 (10), 1999–2004.

Hasenfuss, G., 1998. Animal models of human cardiovascular disease, heart failure and hypertrophy. Cardiovasc. Res. 39 (1), 60–76.

Haskell, B.D., Flurkey, K., Duffy, T.M., Sargent, E.E., Leiter, E.H., 2002. The diabetes-prone NZO/HlLt strain. I. Immunophenotypic comparison to the related NZB/BlNJ and NZW/LacJ strains. Lab. Invest. 82 (7), 833–842.

Hayakawa, H., Coffee, K., Raij, L., 1997. Endothelial dysfunction and cardiorenal injury in experimental salt-sensitive hypertension: effects of antihypertensive therapy. Circulation 96 (7), 2407–2413.

He, C.J., Zheng, F., Stitt, A., Striker, L., Hattori, M., Vlassara, H., 2000. Differential expression of renal AGE-receptor genes in NOD mice: possible role in nonobese diabetic renal disease. Kidney Int. 58 (5), 1931–1940.

Herzog, C., Yang, C., Holmes, A., Kaushal, G.P., 2012. zVAD-fmk prevents cisplatin-induced cleavage of autophagy proteins but impairs autophagic flux and worsens renal function. Am. J. Physiol. Renal Physiol. 303 (8), F1239–F1250.

Hesketh, E.E., Vernon, M.A., Ding, P., Clay, S., Borthwick, G., Conway, B., et al., 2014. A murine model of irreversible and reversible unilateral ureteric obstruction. J. Vis. Exp. (94), e52559.

Hizoh, I., Haller, C., 2002. Radiocontrast-induced renal tubular cell apoptosis: hypertonic versus oxidative stress. Invest. Radiol. 37 (8), 428–434.

Hoagland, K.M., Flasch, A.K., Dahly-Vernon, A.J., dos Santos, E.A., Knepper, M.A., Roman, R.J., 2004. Elevated BSC-1 and ROMK expression in Dahl salt-sensitive rat kidneys. Hypertension 43 (4), 860–865.

Hodeify, R., Megyesi, J., Tarcsafalvi, A., Mustafa, H.I., Hti Lar Seng, N.S., Price, P.M., 2013. Gender differences control the susceptibility to ER stress-induced acute kidney injury. Am. J. Physiol. Renal Physiol. 304 (7), F875–F882.

Hoshi, S., Shu, Y., Yoshida, F., Inagaki, T., Sonoda, J., Watanabe, T., et al., 2002. Podocyte injury promotes progressive nephropathy in zucker diabetic fatty rats. Lab. Invest. 82 (1), 25–35.

Hoskova, L., Malek, I., Kautzner, J., Honsova, E., van Dokkum, R.P., Huskova, Z., et al., 2014. Tacrolimus-induced hypertension and nephrotoxicity in Fawn-Hooded rats are attenuated by dual inhibition of renin-angiotensin system. Hypertens. Res. 37 (8), 724–732.

Hostetter, T.H., Olson, J.L., Rennke, H.G., Venkatachalam, M.A., Brenner, B.M., 1981. Hyperfiltration in remnant nephrons: a potentially adverse response to renal ablation. Am. J. Physiol. 241 (1), F85–F93.

Hsu, C.Y., Lin, F., Vittinghoff, E., Shlipak, M.G., 2003. Racial differences in the progression from chronic renal insufficiency to end-stage renal disease in the United States. J. Am. Soc. Nephrol. 14 (11), 2902–2907.

Huang, L., Zhang, R., Wu, J., Chen, J., Grosjean, F., Satlin, L.H., et al., 2011. Increased susceptibility to acute kidney injury due to endoplasmic reticulum stress in mice lacking tumor necrosis factor-alpha and its receptor 1. Kidney Int. 79 (6), 613–623.

Hudgins, C.C., Steinberg, R.T., Klinman, D.M., Reeves, M.J., Steinberg, A.D., 1985. Studies of consomic mice bearing the Y chromosome of the BXSB mouse. J. Immunol. 134 (6), 3849–3854.

Hudkins, K.L., Pichaiwong, W., Wietecha, T., Kowalewska, J., Banas, M.C., Spencer, M.W., et al., 2010. BTBR Ob/Ob mutant mice model progressive diabetic nephropathy. J. Am. Soc. Nephrol. 21 (9), 1533–1542.

Hye Khan, M.A., Neckar, J., Manthati, V., Errabelli, R., Pavlov, T.S., Staruschenko, A., et al., 2013. Orally active epoxyeicosatrienoic acid analog attenuates kidney injury in hypertensive Dahl salt-sensitive rat. Hypertension 62 (5), 905–913.

Ichikawa, I., Fogo, A., 1996. Focal segmental glomerulosclerosis. Pediatr. Nephrol. 10 (3), 374–391.

Imai, H., Nakamoto, Y., Asakura, K., Miki, K., Yasuda, T., Miura, A.B., 1985. Spontaneous glomerular IgA deposition in ddY mice: an animal model of IgA nephritis. Kidney Int. 27 (5), 756–761.

Imig, J.D., Ryan, M.J., 2013. Immune and inflammatory role in renal disease. Compr. Physiol. 3 (2), 957–976.

Inagi, R., 2010. Endoplasmic reticulum stress as a progression factor for kidney injury. Curr. Opin. Pharmacol. 10 (2), 156–165.

Inazaki, K., Kanamaru, Y., Kojima, Y., Sueyoshi, N., Okumura, K., Kaneko, K., et al., 2004. Smad3 deficiency attenuates renal fibrosis, inflammation, and apoptosis after unilateral ureteral obstruction. Kidney Int. 66 (2), 597–604.

Ishizaki, M., Masuda, Y., Fukuda, Y., Sugisaki, Y., Yamanaka, N., Masugi, Y., 1986. Experimental mesangioproliferative glomerulonephritis in rats induced by intravenous administration of anti-thymocyte serum. Acta Pathol. Jpn. 36 (8), 1191–1203.

Isome, M., Fujinaka, H., Adhikary, L.P., Kovalenko, P., El-Shemi, A.G., Yoshida, Y., et al., 2004. Important role for macrophages in induction of crescentic anti-GBM glomerulonephritis in WKY rats. Nephrol. Dial. Transplant. 19 (12), 2997–3004.

Islam, M., Burke, Jr., J.F., McGowan, T.A., Zhu, Y., Dunn, S.R., McCue, P., et al., 2001. Effect of anti-transforming growth factor-beta antibodies in cyclosporine-induced renal dysfunction. Kidney Int. 59 (2), 498–506.

Itagaki, S., Nishida, E., Lee, M.J., Doi, K., 1995. Histopathology of sub-acute renal lesions in mice induced by streptozotocin. Exp. Toxicol. Pathol. 47 (6), 485–491.

Iyer, A., Chan, V., Brown, L., 2010. The DOCA-salt hypertensive rat as a model of cardiovascular oxidative and inflammatory stress. Curr. Cardiol. Rev. 6 (4), 291–297.

Jadhav, A., Torlakovic, E., Ndisang, J.F., 2009. Hemin therapy attenuates kidney injury in deoxycorticosterone acetate-salt hypertensive rats. Am. J. Physiol. Renal Physiol. 296 (3), F521–F534.

Janssen, U., Vassiliadou, A., Riley, S.G., Phillips, A.O., Floege, J., 2004. The quest for a model of type II diabetes with nephropathy: the Goto Kakizaki rat. J. Nephrol. 17 (6), 769–773.

Jefferson, J.A., Pippin, J.W., Shankland, S.J., 2010. Experimental models of membranous nephropathy. Drug Discov. Today Dis. Models 7 (1–2), 27–33.

Jennette, J.C., Thomas, D.B., 2001. Crescentic glomerulonephritis. Nephrol. Dial. Transplant. 16 (Suppl. 6), 80–82.

Jha, V., Garcia-Garcia, G., Iseki, K., Li, Z., Naicker, S., Plattner, B., et al., 2013. Chronic kidney disease: global dimension and perspectives. Lancet 382 (9888), 260–272.

Joo, J.D., Kim, M., D'Agati, V.D., Lee, H.T., 2006. Ischemic preconditioning provides both acute and delayed protection against renal ischemia and reperfusion injury in mice. J. Am. Soc. Nephrol. 17 (11), 3115–3123.

Kadowaki, D., Sumikawa, S., Arimizu, K., Taguchi, K., Kitamura, K., Ishitsuka, Y., et al., 2012. Effect of acetaminophen on the progression of renal damage in adenine induced renal failure model rats. Life Sci. 91 (25–26), 1304–1308.

Kai, K., Yamaguchi, T., Yoshimatsu, Y., Kinoshita, J., Teranishi, M., Takasaki, W., 2013. Neutrophil gelatinase-associated lipocalin, a sensitive urinary biomarker of acute kidney injury in dogs receiving gentamicin. J. Toxicol. Sci. 38 (2), 269–277.

Kallen, A.J., Jhung, M.A., Cheng, S., Hess, T., Turabelidze, G., Abramova, L., et al., 2008. Gadolinium-containing magnetic resonance imaging contrast and nephrogenic systemic fibrosis: a case-control study. Am. J. Kidney. Dis. 51 (6), 966–975.

Kanlaya, R., Sintiprungrat, K., Thongboonkerd, V., 2013. Secreted products of macrophages exposed to calcium oxalate crystals induce epithelial mesenchymal transition of renal tubular cells via RhoA-dependent TGF-beta1 pathway. Cell Biochem. Biophys. 67 (3), 1207–1215.

Karatas, A., Hegner, B., de Windt, L.J., Luft, F.C., Schubert, C., Gross, V., et al., 2008. Deoxycorticosterone acetate-salt mice exhibit blood pressure-independent sexual dimorphism. Hypertension 51 (4), 1177–1183.

Kashtan, C.E., 2002. Animal models of Alport syndrome. Nephrol. Dial. Transplant 17 (8), 1359–1362.

Kassan, M., Galan, M., Partyka, M., Saifudeen, Z., Henrion, D., Trebak, M., et al., 2012. Endoplasmic reticulum stress is involved in cardiac damage and vascular endothelial dysfunction in hypertensive mice. Arterioscler. Thromb. Vasc. Biol. 32 (7), 1652–1661.

Kawano, K., Hirashima, T., Mori, S., Natori, T., 1994. OLETF (Otsuka Long-Evans Tokushima Fatty) rat: a new NIDDM rat strain. Diabetes Res. Clin. Pract. 24 (Suppl.), S317–S320.

Kawano, K., Hirashima, T., Mori, S., Saitoh, Y., Kurosumi, M., Natori, T., 1992. Spontaneous long-term hyperglycemic rat with diabetic complications. Otsuka Long-Evans Tokushima Fatty (OLETF) strain. Diabetes 41 (11), 1422–1428.

Kawano, K., Mori, S., Hirashima, T., Man, Z.W., Natori, T., 1999. Examination of the pathogenesis of diabetic nephropathy in OLETF rats. J. Vet. Med. Sci. 61 (11), 1219–1228.

Kempson, S.A., Ellis, B.G., Price, R.G., 1977. Changes in rat renal cortex, isolated plasma membranes and urinary enzymes following the injection of mercuric chloride. Chem. Biol. Interact. 18 (2), 217–234.

Khan, S.R., 1997. Animal models of kidney stone formation: an analysis. World J. Urol. 15 (4), 236–243.

Khan, S.R., 2010. Nephrocalcinosis in animal models with and without stones. Urol. Res. 38 (6), 429–438.

Khan, S.R., Glenton, P.A., Byer, K.J., 2006. Modeling of hyperoxaluric calcium oxalate nephrolithiasis: experimental induction of hyperoxaluria by hydroxy-L-proline. Kidney Int. 70 (5), 914–923.

Khan, M.R., Siddiqui, S., Parveen, K., Javed, S., Diwakar, S., Siddiqui, W.A., 2010. Nephroprotective action of tocotrienol-rich fraction (TRF) from palm oil against potassium dichromate ($K_2Cr_2O_7$)-induced acute renal injury in rats. Chem. Biol. Interact. 186 (2), 228–238.

Kim, J.H., Ha, I.S., Hwang, C.I., Lee, Y.J., Kim, J., Yang, S.H., et al., 2004. Gene expression profiling of anti-GBM glomerulonephritis model: the role of NF-kappaB in immune complex kidney disease. Kidney Int. 66 (5), 1826–1837.

Kim, H.J., Vaziri, N.D., 2010. Contribution of impaired Nrf2-Keap1 pathway to oxidative stress and inflammation in chronic renal failure. Am. J. Physiol. Renal Physiol. 298 (3), F662–F671.

Kim, J.H., Kim, B.K., Moon, K.C., Hong, H.K., Lee, H.S., 2003. Activation of the TGF-beta/Smad signaling pathway in focal segmental glomerulosclerosis. Kidney Int. 64 (5), 1715–1721.

Kim, S.H., Shim, H.J., Kim, W.B., Lee, M.G., 1998. Pharmacokinetics of a new carbapenem, DA-1131, after intravenous administration to rats with uranyl nitrate-induced acute renal failure. Antimicrob. Agents Chemother. 42 (5), 1217–1221.

Kimura, G., Brenner, B.M., 1997. Implications of the linear pressure-natriuresis relationship and importance of sodium sensitivity in hypertension. J. Hypertens. 15 (10), 1055–1061.

Kinuno, H., Tomoda, F., Koike, T., Takata, M., Inoue, H., 2005. Effects of uninephrectomy on renal structural properties in spontaneously hypertensive rats. Clin. Exp. Pharmacol. Physiol. 32 (3), 173–178.

Kirchhoff, F., Krebs, C., Abdulhag, U.N., Meyer-Schwesinger, C., Maas, R., Helmchen, U., et al., 2008. Rapid development of severe end-organ damage in C57BL/6 mice by combining DOCA salt and angiotensin II. Kidney Int. 73 (5), 643–650.

Knight, J.G., Adams, D.D., 1978. Three genes for lupus nephritis in NZB × NZW mice. J. Exp. Med. 147 (6), 1653–1660.

Ko, G.J., Bae, S.Y., Hong, Y.A., Pyo, H.J., Kwon, Y.J., 2016. Radiocontrast-induced nephropathy is attenuated by autophagy through regulation of apoptosis and inflammation. Hum. Exp. Toxicol. 35 (7), 724–736.

Komada, T., Usui, F., Kawashima, A., Kimura, H., Karasawa, T., Inoue, Y., et al., 2015. Role of NLRP3 inflammasomes for rhabdomyolysis-induced acute kidney injury. Sci. Rep. 5, 10901.

Kong, L.L., Wu, H., Cui, W.P., Zhou, W.H., Luo, P., Sun, J., et al., 2013. Advances in murine models of diabetic nephropathy. J. Diabetes. Res. 2013, 797548.

Korrapati, M.C., Shaner, B.E., Schnellmann, R.G., 2012. Recovery from glycerol-induced acute kidney injury is accelerated by suramin. J. Pharmacol. Exp. Ther. 341 (1), 126–136.

Kos, C.H., Le, T.C., Sinha, S., Henderson, J.M., Kim, S.H., Sugimoto, H., et al., 2003. Mice deficient in alpha-actinin-4 have severe glomerular disease. J. Clin. Invest. 111 (11), 1683–1690.

Kren, S., Hostetter, T.H., 1999. The course of the remnant kidney model in mice. Kidney Int. 56 (1), 333–337.

Kunduzova, O.R., Escourrou, G., Seguelas, M.H., Delagrange, P., De La Farge, F., Cambon, C., et al., 2003. Prevention of apoptotic and necrotic cell death, caspase-3 activation, and renal dysfunction by melatonin after ischemia/reperfusion. FASEB J. 17 (8), 872–874.

Lambert, P.H., Dixon, F.J., 1968. Pathogenesis of the glomerulonephritis of NZB/W mice. J. Exp. Med. 127 (3), 507–522.

Le Berre, L., Godfrin, Y., Gunther, E., Buzelin, F., Perretto, S., Smit, H., et al., 2002. Extrarenal effects on the pathogenesis and relapse of idiopathic nephrotic syndrome in Buffalo/Mna rats. J. Clin. Invest. 109 (4), 491–498.

LeBleu, V., Sugimoto, H., Mundel, T.M., Gerami-Naini, B., Finan, E., Miller, C.A., et al., 2009. Stem cell therapies benefit Alport syndrome. J. Am. Soc. Nephrol. 20 (11), 2359–2370.

Le Clef, N., Verhulst, A., D'Haese, P.C., Vervaet, B.A., 2016. Unilateral renal ischemia-reperfusion as a robust model for acute to chronic kidney injury in mice. PLoS One 11, e0152153.

Lee, V.W., Harris, D.C., 2011. Adriamycin nephropathy: a model of focal segmental glomerulosclerosis. Nephrology 16 (1), 30–38.

Lee, H.T., Jan, M., Bae, S.C., Joo, J.D., Goubaeva, F.R., Yang, J., et al., 2006. A1 adenosine receptor knockout mice are protected against acute radiocontrast nephropathy in vivo. Am. J. Physiol. Renal Physiol. 290 (6), F1367–F1375.

Leelahavanichkul, A., Yan, Q., Hu, X., Eisner, C., Huang, Y., Chen, R., et al., 2010. Angiotensin II overcomes strain-dependent resistance of rapid CKD progression in a new remnant kidney mouse model. Kidney Int. 78 (11), 1136–1153.

Leemans, J.C., Stokman, G., Claessen, N., Rouschop, K.M., Teske, G.J., Kirschning, C.J., et al., 2005. Renal-associated TLR2 mediates ischemia/reperfusion injury in the kidney. J. Clin. Invest. 115 (10), 2894–2903.

Leiter, E.H., 1982. Multiple low-dose streptozotocin-induced hyperglycemia and insulitis in C57BL mice: influence of inbred background, sex, and thymus. Proc. Natl. Acad. Sci. USA 79 (2), 630–634.

Leiter, E.H., 1985. Differential susceptibility of BALB/c sublines to diabetes induction by multi-dose streptozotocin treatment. Curr. Top. Microbiol. Immunol. 122, 78–85.

Leiter, E.H., Reifsnyder, P.C., 2004. Differential levels of diabetogenic stress in two new mouse models of obesity and type 2 diabetes. Diabetes 53 (Suppl. 1), S4–S11.

Lerman, L.O., Schwartz, R.S., Grande, J.P., Sheedy, P.F., Romero, J.C., 1999. Noninvasive evaluation of a novel swine model of renal artery stenosis. J. Am. Soc. Nephrol. 10 (7), 1455–1465.

Lerman, L.O., Textor, S.C., Grande, J.P., 2009. Mechanisms of tissue injury in renal artery stenosis: ischemia and beyond. Prog. Cardiovasc. Dis. 52 (3), 196–203.

Lhotak, S., Sood, S., Brimble, E., Carlisle, R.E., Colgan, S.M., Mazzetti, A., et al., 2012. ER stress contributes to renal proximal tubule injury by increasing SREBP-2-mediated lipid accumulation and apoptotic cell death. Am. J. Physiol. Renal Physiol. 303 (2), F266–F278.

Li, P., Ma, L.L., Xie, R.J., Xie, Y.S., Wei, R.B., Yin, M., et al., 2012. Treatment of 5/6 nephrectomy rats with sulodexide: a novel therapy for chronic renal failure. Acta Pharmacol. Sin. 33 (5), 644–651.

Liu, H., Baliga, R., 2005. Endoplasmic reticulum stress-associated caspase 12 mediates cisplatin-induced LLC-PK1 cell apoptosis. J. Am. Soc. Nephrol. 16 (7), 1985–1992.

Liu, Q.F., Ye, J.M., Deng, Z.Y., Yu, L.X., Sun, Q., Li, S.S., 2015. Ameliorating effect of Klotho on endoplasmic reticulum stress and renal fibrosis induced by unilateral ureteral obstruction. Iran. J. Kidney Dis. 9 (4), 291–297.

Liu, N., Makino, T., Nogaki, F., Kusano, H., Suyama, K., Muso, E., et al., 2004. Coagulation in the mesangial area promotes ECM accumula-

tion through factor V expression in MsPGN in rats. Am. J. Physiol. Renal Physiol. 287 (4), F612–F620.

Liu, G., Sun, Y., Li, Z., Song, T., Wang, H., Zhang, Y., et al., 2008. Apoptosis induced by endoplasmic reticulum stress involved in diabetic kidney disease. Biochem. Biophys. Res. Commun. 370 (4), 651–656.

Loch, D., Hoey, A., Brown, L., 2006. Attenuation of cardiovascular remodeling in DOCA-salt rats by the vasopeptidase inhibitor, omapatrilat. Clin. Exp. Hypertens. 28 (5), 475–488.

Luo, Z.F., Feng, B., Mu, J., Qi, W., Zeng, W., Guo, Y.H., et al., 2010. Effects of 4-phenylbutyric acid on the process and development of diabetic nephropathy induced in rats by streptozotocin: regulation of endoplasmic reticulum stress-oxidative activation. Toxicol. Appl. Pharmacol. 246 (1–2), 49–57.

Ma, L.J., Fogo, A.B., 2003. Model of robust induction of glomerulosclerosis in mice: importance of genetic background. Kidney Int. 64 (1), 350–355.

Ma, G., Allen, T.J., Cooper, M.E., Cao, Z., 2004. Calcium channel blockers, either amlodipine or mibefradil, ameliorate renal injury in experimental diabetes. Kidney Int. 66 (3), 1090–1098.

Ma, L.J., Nakamura, S., Aldigier, J.C., Rossini, M., Yang, H., Liang, X., et al., 2005. Regression of glomerulosclerosis with high-dose angiotensin inhibition is linked to decreased plasminogen activator inhibitor-1. J. Am. Soc. Nephrol. 16 (4), 966–976.

Ma, F.Y., Tesch, G.H., Flavell, R.A., Davis, R.J., Nikolic-Paterson, D.J., 2007. MKK3-p38 signaling promotes apoptosis and the early inflammatory response in the obstructed mouse kidney. Am. J. Physiol. Renal Physiol. 293 (5), F1556–F1563.

Malinowski, M., Pratschke, J., Lock, J., Neuhaus, P., Stockmann, M., 2010. Effect of tacrolimus dosing on glucose metabolism in an experimental rat model. Ann. Transplant. 15 (3), 60–65.

Mandel, N.S., Henderson, Jr., J.D., Hung, L.Y., Wille, D.F., Wiessner, J.H., 2004. A porcine model of calcium oxalate kidney stone disease. J. Urol. 171 (3), 1301–1303.

Mandic, A., Hansson, J., Linder, S., Shoshan, M.C., 2003. Cisplatin induces endoplasmic reticulum stress and nucleus-independent apoptotic signaling. J. Biol. Chem. 278 (11), 9100–9106.

Marciniak, S.J., Yun, C.Y., Oyadomari, S., Novoa, I., Zhang, Y., Jungreis, R., et al., 2004. CHOP induces death by promoting protein synthesis and oxidation in the stressed endoplasmic reticulum. Genes Dev. 18 (24), 3066–3077.

Martinez, A.B., Mandalunis, P.M., Bozal, C.B., Cabrini, R.L., Ubios, A.M., 2003. Renal function in mice poisoned with oral uranium and treated with ethane-1-hydroxy-1,1-bisphosphonate (EHBP). Health Phys. 85 (3), 343–347.

Martinez-Castelao, A., Navarro-Gonzalez, J.F., Gorriz, J.L., de Alvaro, F., 2015. The concept and the epidemiology of diabetic nephropathy have changed in recent years. J. Clin. Med. 4 (6), 1207–1216.

Mattson, D.L., James, L., Berdan, E.A., Meister, C.J., 2006. Immune suppression attenuates hypertension and renal disease in the Dahl salt-sensitive rat. Hypertension 48 (1), 149–156.

Melez, K.A., Harrison, L.C., Gilliam, J.N., Steinberg, A.D., 1980. Diabetes is associated with autoimmunity in the New Zealand obese (NZO) mouse. Diabetes 29 (10), 835–840.

McGaha, T.L., Madaio, M.P., 2014. Lupus nephritis: animal modeling of a complex disease syndrome pathology. Drug Discov. Today Dis. Models 11, 13–18.

McGaha, T.L., Sorrentino, B., Ravetch, J.V., 2005. Restoration of tolerance in lupus by targeted inhibitory receptor expression. Science 307 (5709), 590–593.

McLaughlin, G.E., Kashimawo, L.A., Steele, B.W., Kuluz, J.W., 2003. Reversal of acute tacrolimus-induced renal vasoconstriction by theophylline in rats. Pediatr. Crit. Care Med. 4 (3), 358–362.

McMartin, K., 2009. Are calcium oxalate crystals involved in the mechanism of acute renal failure in ethylene glycol poisoning? Clin. Toxicol. 47 (9), 859–869.

McNamara, M.J., Norton, J.A., Nauta, R.J., Alexander, H.R., 1993. Interleukin-1 receptor antibody (IL-1rab) protection and treatment against lethal endotoxemia in mice. J. Surg. Res. 54 (4), 316–321.

Michaud, J.L., Stitt-Cavanaugh, E., Endlich, N., Endlich, K., De Repentigny, Y., Kothary, R., et al., 2010. Mice with podocyte-specific overexpression of wild type alpha-actinin-4 are healthy controls for K256E-alpha-actinin-4 mutant transgenic mice. Transgenic Res. 19 (2), 285–289.

Miguel-Carrasco, J.L., Zambrano, S., Blanca, A.J., Mate, A., Vazquez, C.M., 2010. Captopril reduces cardiac inflammatory markers in spontaneously hypertensive rats by inactivation of NF-kB. J. Inflamm. 7, 21.

Miller, R.P., Tadagavadi, R.K., Ramesh, G., Reeves, W.B., 2010. Mechanisms of cisplatin nephrotoxicity. Toxins 2 (11), 2490–2518.

Mills, J.A., 1994. Systemic lupus erythematosus. N. Engl. J. Med. 330 (26), 1871–1879.

Miner, J.H., Sanes, J.R., 1996. Molecular and functional defects in kidneys of mice lacking collagen alpha 3(IV): implications for Alport syndrome. J. Cell. Biol. 135 (5), 1403–1413.

Mohammed-Ali, Z., Cruz, G.L., Dickhout, J.G., 2015a. Crosstalk between the unfolded protein response and NF-kappaB-mediated inflammation in the progression of chronic kidney disease. J. Immunol. Res. 2015, 428508.

Mohammed-Ali, Z., Cruz, G.L., Lu, C., Carlisle, R.E., Werner, K.E., Ask, K., Dickhout, J.G., 2015b. Development of a model of chronic kidney disease in the C57BL/6 mouse with properties of progressive human CKD. BioMed Res. Int. 2015, (Article ID 172302).

Molina, A., Ubeda, M., Escribese, M.M., Garcia-Bermejo, L., Sancho, D., Perez de Lema, G., et al., 2005. Renal ischemia/reperfusion injury: functional tissue preservation by anti-activated (beta)1 integrin therapy. J. Am. Soc. Nephrol. 16 (2), 374–382.

Mollet, G., Ratelade, J., Boyer, O., Muda, A.O., Morisset, L., Lavin, T.A., et al., 2009. Podocin inactivation in mature kidneys causes focal segmental glomerulosclerosis and nephrotic syndrome. J. Am. Soc. Nephrol. 20 (10), 2181–2189.

Mombaerts, P., Iacomini, J., Johnson, R.S., Herrup, K., Tonegawa, S., Papaioannou, V.E., 1992. RAG-1-deficient mice have no mature B and T lymphocytes. Cell 68 (5), 869–877.

Montie, H.L., Kayali, F., Haezebrouck, A.J., Rossi, N.F., Degracia, D.J., 2005. Renal ischemia and reperfusion activates the eIF 2 alpha kinase PERK. Biochim. Biophys. Acta 1741 (3), 314–324.

Moralejo, D.H., Ogino, T., Zhu, M., Toide, K., Wei, S., Wei, K., et al., 1998. A major quantitative trait locus co-localizing with cholecystokinin type A receptor gene influences poor pancreatic proliferation in a spontaneously diabetogenic rat. Mamm. Genome. 9 (10), 794–798.

Morales, A.I., Detaille, D., Prieto, M., Puente, A., Briones, E., Arevalo, M., et al., 2010. Metformin prevents experimental gentamicin-induced nephropathy by a mitochondria-dependent pathway. Kidney Int. 77 (10), 861–869.

Muller, D.N., Dechend, R., Mervaala, E.M., Park, J.K., Schmidt, F., Fiebeler, A., et al., 2000. NF-kappaB inhibition ameliorates angiotensin II-induced inflammatory damage in rats. Hypertension 35 (1 Pt. 2), 193–201.

Murphy, E.D., Roths, J.B., 1979. A Y chromosome associated factor in strain BXSB producing accelerated autoimmunity and lymphoproliferation. Arthritis Rheum. 22 (11), 1188–1194.

Muso, E., Yoshida, H., Takeuchi, E., Yashiro, M., Matsushima, H., Oyama, A., et al., 1996. Enhanced production of glomerular extracellular matrix in a new mouse strain of high serum IgA ddY mice. Kidney Int. 50 (6), 1946–1957.

Naesens, M., Kuypers, D.R., Sarwal, M., 2009. Calcineurin inhibitor nephrotoxicity. Clin J. Am. Soc. Nephrol. 4 (2), 481–508.

Nagao, S., Kugita, M., Yoshihara, D., Yamaguchi, T., 2012. Animal models for human polycystic kidney disease. Exp. Anim. 61 (5), 477–488.

Nagappan, A.S., Varghese, J., James, J.V., Jacob, M., 2015. Indomethacin induces endoplasmic reticulum stress, but not apoptosis, in the rat kidney. Eur. J. Pharmacol. 761, 199–205.

Nakamura, T., Oite, T., Shimizu, F., Matsuyama, M., Kazama, T., Koda, Y., et al., 1986. Sclerotic lesions in the glomeruli of Buffalo/Mna rats. Nephron 43 (1), 50–55.

Nakatsue, T., Koike, H., Han, G.D., Suzuki, K., Miyauchi, N., Yuan, H., et al., 2005. Nephrin and podocin dissociate at the onset of proteinuria in experimental membranous nephropathy. Kidney Int. 67 (6), 2239–2253.

Natori, Y., Shindo, N., Natori, Y., 1994. Proteinuria induced by anti-dipeptidyl peptidase IV (gp108); role of circulating and glomerular antigen. Clin. Exp. Immunol. 95 (2), 327–332.

Nava, M., Romero, F., Quiroz, Y., Parra, G., Bonet, L., Rodriguez-Iturbe, B., 2000. Melatonin attenuates acute renal failure and oxidative stress induced by mercuric chloride in rats. Am. J. Physiol. Renal Physiol. 279 (5), F910–F918.

Navarro-Gonzalez, J.F., Mora-Fernandez, C., Muros de Fuentes, M., Garcia-Perez, J., 2011. Inflammatory molecules and pathways in the pathogenesis of diabetic nephropathy. Nat. Rev. Nephrol. 7 (6), 327–340.

Neugebauer, S., Baba, T., Watanabe, T., 2000. Association of the nitric oxide synthase gene polymorphism with an increased risk for progression to diabetic nephropathy in type 2 diabetes. Diabetes 49 (3), 500–503.

Ninichuk, V., Kulkarni, O., Clauss, S., Anders, H., 2007. Tubular atrophy, interstitial fibrosis, and inflammation in type 2 diabetic db/db mice. An accelerated model of advanced diabetic nephropathy. Eur. J. Med. Res. 12 (8), 351–355.

Noel, L.H., 1999. Morphological features of primary focal and segmental glomerulosclerosis. Nephrol. Dial. Transplant. 14 (Suppl. 3), 53–57.

Noh, M.R., Kim, J.I., Han, S.J., Lee, T.J., Park, K.M., 2015. C/EBP homologous protein (CHOP) gene deficiency attenuates renal ischemia/reperfusion injury in mice. Biochim. Biophys. Acta 1852 (9), 1895–1901.

Norris, K.C., Greene, T., Kopple, J., Lea, J., Lewis, J., Lipkowitz, M., et al., 2006. Baseline predictors of renal disease progression in the African American Study of Hypertension and Kidney Disease. J. Am. Soc. Nephrol. 17 (10), 2928–2936.

O'Brien, S.P., Smith, M., Ling, H., Phillips, L., Weber, W., Lydon, J., et al., 2013. Glomerulopathy in the KK.Cg-A(y)/J mouse reflects the pathology of diabetic nephropathy. J. Diabetes Res. 2013, 498925.

O'Bryan, G.T., Hostetter, T.H., 1997. The renal hemodynamic basis of diabetic nephropathy. Semin. Nephrol. 17 (2), 93–100.

Ofstad, J., Iversen, B.M., 2005. Glomerular and tubular damage in normotensive and hypertensive rats. Am. J. Physiol. Renal Physiol. 288 (4), F665–F672.

Oh, S.Y., Kwon, J.K., Lee, S.Y., Ha, M.S., Kwon, Y.W., Moon, Y.T., 2011. A comparative study of experimental rat models of renal calcium oxalate stone formation. J. Endourol. 25 (6), 1057–1061.

Okada, A., Nomura, S., Higashibata, Y., Hirose, M., Gao, B., Yoshimura, M., et al., 2007. Successful formation of calcium oxalate crystal deposition in mouse kidney by intraabdominal glyoxylate injection. Urol. Res. 35 (2), 89–99.

Okamoto, K., Aoki, K., 1963. Development of a strain of spontaneously hypertensive rats. Jpn. Circ. J. 27, 282–293.

Okazaki, K., Suzuki, Y., Otsuji, M., Suzuki, H., Kihara, M., Kajiyama, T., et al., 2012. Development of a model of early-onset IgA nephropathy. J. Am. Soc. Nephrol. 23 (8), 1364–1374.

Okuda, S., Oh, Y., Tsuruda, H., Onoyama, K., Fujimi, S., Fujishima, M., 1986. Adriamycin-induced nephropathy as a model of chronic progressive glomerular disease. Kidney Int. 29 (2), 502–510.

Okusawa, S., Gelfand, J.A., Ikejima, T., Connolly, R.J., Dinarello, C.A., 1988. Interleukin 1 induces a shock-like state in rabbits. Synergism with tumor necrosis factor and the effect of cyclooxygenase inhibition. J. Clin. Invest. 81 (4), 1162–1172.

Ollmann, M.M., Wilson, B.D., Yang, Y.K., Kerns, J.A., Chen, Y., Gantz, I., et al., 1997. Antagonism of central melanocortin receptors in vitro and in vivo by agouti-related protein. Science 278 (5335), 135–138.

Ortega, A., Ramila, D., Izquierdo, A., Gonzalez, L., Barat, A., Gazapo, R., et al., 2005. Role of the renin-angiotensin system on the parathyroid hormone-related protein overexpression induced by nephrotoxic acute renal failure in the rat. J. Am. Soc. Nephrol. 16 (4), 939–949.

Orth, S.R., Ritz, E., 1998. The nephrotic syndrome. N. Engl. J. Med. 338 (17), 1202–1211.

Ortiz, A., 2000. Nephrology forum: apoptotic regulatory proteins in renal injury. Kidney Int. 58 (1), 467–485.

Ortiz, A., Sanchez-Nino, M.D., Izquierdo, M.C., Martin-Cleary, C., Garcia-Bermejo, L., Moreno, J.A., et al., 2015. Translational value of animal models of kidney failure. Eur. J. Pharmacol. 759, 205–220.

Ozawa, Y., Kobori, H., Suzaki, Y., Navar, L.G., 2007. Sustained renal interstitial macrophage infiltration following chronic angiotensin II infusions. Am. J. Physiol. Renal Physiol. 292 (1), F330–F339.

Ozkok, A., Edelstein, C.L., 2014. Pathophysiology of cisplatin-induced acute kidney injury. BioMed Res. Int. 2014, 967826.

Pallet, N., Bouvier, N., Bendjallabah, A., Rabant, M., Flinois, J.P., Hertig, A., et al., 2008. Cyclosporine-induced endoplasmic reticulum stress triggers tubular phenotypic changes and death. Am. J. Transplant. 8 (11), 2283–2296.

Pankewycz, O.G., Guan, J.X., Bolton, W.K., Gomez, A., Benedict, J.F., 1994. Renal TGF-beta regulation in spontaneously diabetic NOD mice with correlations in mesangial cells. Kidney Int. 46 (3), 748–758.

Park, K.M., Chen, A., Bonventre, J.V., 2001. Prevention of kidney ischemia/reperfusion-induced functional injury and JNK, p38, and MAPK kinase activation by remote ischemic pretreatment. J. Biol. Chem. 276 (15), 11870–11876.

Patrakka, J., Kestila, M., Wartiovaara, J., Ruotsalainen, V., Tissari, P., Lenkkeri, U., et al., 2000. Congenital nephrotic syndrome (NPHS1): features resulting from different mutations in Finnish patients. Kidney Int. 58 (3), 972–980.

Patschan, D., Patschan, S., Muller, G.A., 2012. Inflammation and microvasculopathy in renal ischemia reperfusion injury. J. Transplant. 2012, 764154.

Pearson, J.A., Wong, F.S., Wen, L., 2016. The importance of the non obese diabetic (NOD) mouse model in autoimmune diabetes. J. Autoimmun. 66, 76–88.

Peutz-Kootstra, C.J., de Heer, E., Hoedemaeker, P.J., Abrass, C.K., Bruijn, J.A., 2001. Lupus nephritis: lessons from experimental animal models. J. Lab. Clin. Med. 137 (4), 244–260.

Peyrou, M., Hanna, P.E., Cribb, A.E., 2007. Cisplatin, gentamicin, and p-aminophenol induce markers of endoplasmic reticulum stress in the rat kidneys. Toxicol. Sci. 99 (1), 346–353.

Phillips, A.O., Baboolal, K., Riley, S., Grone, H., Janssen, U., Steadman, R., et al., 2001. Association of prolonged hyperglycemia with glomerular hypertrophy and renal basement membrane thickening in the Goto Kakizaki model of non-insulin-dependent diabetes mellitus. Am. J. Kidney Dis. 37 (2), 400–410.

Phillips, M.S., Liu, Q., Hammond, H.A., Dugan, V., Hey, P.J., Caskey, C.J., et al., 1996. Leptin receptor missense mutation in the fatty Zucker rat. Nat. Genet. 13 (1), 18–19.

Pierides, A., Voskarides, K., Athanasiou, Y., Ioannou, K., Damianou, L., Arsali, M., et al., 2009. Clinico-pathological correlations in 127 patients in 11 large pedigrees, segregating one of three heterozygous mutations in the COL4A3/COL4A4 genes associated with familial haematuria and significant late progression to proteinuria and chronic kidney disease from focal segmental glomerulosclerosis. Nephrol. Dial. Transplant 24 (9), 2721–2729.

Pippin, J.W., Brinkkoetter, P.T., Cormack-Aboud, F.C., Durvasula, R.V., Hauser, P.V., Kowalewska, J., et al., 2009. Inducible rodent models of acquired podocyte diseases. Am. J. Physiol. Renal Physiol. 296 (2), F213–F229.

Priyamvada, S., Khan, S.A., Khan, M.W., Khan, S., Farooq, N., Khan, F., et al., 2010. Studies on the protective effect of dietary fish oil on uranyl-nitrate-induced nephrotoxicity and oxidative damage in rat kidney. Prostaglandins Leukot. Essent. Fatty Acids 82 (1), 35–44.

Puri, T.S., Shakaib, M.I., Chang, A., Mathew, L., Olayinka, O., Minto, A.W., et al., 2010. Chronic kidney disease induced in mice by reversible unilateral ureteral obstruction is dependent on genetic background. Am. J. Physiol. Renal Physiol. 298 (4), F1024–F1032.

Putaala, H., Soininen, R., Kilpelainen, P., Wartiovaara, J., Tryggvason, K., 2001. The murine nephrin gene is specifically expressed in kidney, brain and pancreas: inactivation of the gene leads to massive proteinuria and neonatal death. Hum. Mol. Genet. 10 (1), 1–8.

Qi, Z., Fujita, H., Jin, J., Davis, L.S., Wang, Y., Fogo, A.B., et al., 2005. Characterization of susceptibility of inbred mouse strains to diabetic nephropathy. Diabetes 54 (9), 2628–2637.

Raij, L., Azar, S., Keane, W., 1984. Mesangial immune injury, hypertension, and progressive glomerular damage in Dahl rats. Kidney Int. 26 (2), 137–143.

Ramesh, G., Reeves, W.B., 2002. TNF-alpha mediates chemokine and cytokine expression and renal injury in cisplatin nephrotoxicity. J. Clin. Invest. 110 (6), 835–842.

Rao, M.V., Qiu, Y., Wang, C., Bakris, G., 2008. Hypertension and CKD: Kidney Early Evaluation Program (KEEP) and National Health and Nutrition Examination Survey (NHANES), 1999-2004. Am. J. Kidney. Dis. 51 (4 Suppl. 2), S30–S37.

Rapp, J.P., Dene, H., 1985. Development and characteristics of inbred strains of Dahl salt-sensitive and salt-resistant rats. Hypertension 7 (3 Pt. 1), 340–349.

Reckelhoff, J.F., Zhang, H., Granger, J.P., 1997. Decline in renal hemodynamic function in aging SHR: role of androgens. Hypertension 30 (3 Pt. 2), 677–681.

Reynolds, J., Albouainain, A., Duda, M.A., Evans, D.J., Pusey, C.D., 2006. Strain susceptibility to active induction and passive transfer of experimental autoimmune glomerulonephritis in the rat. Nephrol. Dial. Transplant 21 (12), 3398–3408.

Reynolds, J., Mavromatidis, K., Cashman, S.J., Evans, D.J., Pusey, C.D., 1998. Experimental autoimmune glomerulonephritis (EAG) induced by homologous and heterologous glomerular basement membrane in two substrains of Wistar-Kyoto rat. Nephrol. Dial. Transplant 13 (1), 44–52.

Ritz, E., Orth, S.R., 1999. Nephropathy in patients with type 2 diabetes mellitus. N. Engl. J. Med. 341 (15), 1127–1133.

Rodriguez-Iturbe, B., Ferrebuz, A., Vanegas, V., Quiroz, Y., Mezzano, S., Vaziri, N.D., 2005. Early and sustained inhibition of nuclear factor-kappaB prevents hypertension in spontaneously hypertensive rats. J. Pharmacol. Exp. Ther. 315 (1), 51–57.

Rodriguez-Iturbe, B., Quiroz, Y., Ferrebuz, A., Parra, G., Vaziri, N.D., 2004. Evolution of renal interstitial inflammation and NF-kappaB activation in spontaneously hypertensive rats. Am. J. Nephrol. 24 (6), 587–594.

Rodriguez-Iturbe, B., Quiroz, Y., Nava, M., Bonet, L., Chavez, M., Herrera-Acosta, J., et al., 2002. Reduction of renal immune cell infiltration results in blood pressure control in genetically hypertensive rats. Am. J. Physiol. Renal Physiol. 282 (2), F191–F201.

Romero, F., Rodriguez-Iturbe, B., Parra, G., Gonzalez, L., Herrera-Acosta, J., Tapia, E., 1999. Mycophenolate mofetil prevents the progressive renal failure induced by 5/6 renal ablation in rats. Kidney Int. 55 (3), 945–955.

Ronco, P., Allegri, L., Melcion, C., Pirotsky, E., Appay, M.D., Bariety, J., et al., 1984. A monoclonal antibody to brush border and passive Heymann nephritis. Clin. Exp. Immunol. 55 (2), 319–332.

Roselli, S., Heidet, L., Sich, M., Henger, A., Kretzler, M., Gubler, M.C., et al., 2004. Early glomerular filtration defect and severe renal disease in podocin-deficient mice. Mol. Cell Biol. 24 (2), 550–560.

Rosenstiel, P., Gharavi, A., D'Agati, V., Klotman, P., 2009. Transgenic and infectious animal models of HIV-associated nephropathy. J. Am. Soc. Nephrol. 20 (11), 2296–2304.

Rubio-Navarro, A., Amaro Villalobos, J.M., Lindholt, J.S., Buendia, I., Egido, J., Blanco-Colio, L.M., et al., 2015. Hemoglobin induces monocyte recruitment and CD163-macrophage polarization in abdominal aortic aneurysm. Int. J. Cardiol. 201, 66–78.

Ruiz-Ortega, M., Ruperez, M., Esteban, V., Rodriguez-Vita, J., Sanchez-Lopez, E., Carvajal, G., et al., 2006. Angiotensin II: a key factor in the inflammatory and fibrotic response in kidney diseases. Nephrol. Dial. Transplant. 21 (1), 16–20.

Saha, T.C., Singh, H., 2006. Minimal change disease: a review. South Med. J. 99 (11), 1264–1270.

Sahu, B.D., Koneru, M., Bijargi, S.R., Kota, A., Sistla, R., 2014. Chromium-induced nephrotoxicity and ameliorative effect of carvedilol in rats: involvement of oxidative stress, apoptosis and inflammation. Chem. Biol. Interact. 223, 69–79.

Saleem, M.A., Kobayashi, Y., 2016. Cell biology and genetics of minimal change disease. F1000Res., 5.

Sanchez, D.J., Belles, M., Albina, M.L., Sirvent, J.J., Domingo, J.L., 2001. Nephrotoxicity of simultaneous exposure to mercury and uranium in comparison to individual effects of these metals in rats. Biol. Trace Elem. Res. 84 (1–3), 139–154.

Sandoval, R.M., Dunn, K.W., Molitoris, B.A., 2000. Gentamicin traffics rapidly and directly to the Golgi complex in LLC-PK(1) cells. Am. J. Physiol. Renal Physiol. 279 (5), F884–F890.

Sano, R., Reed, J.C., 2013. ER stress-induced cell death mechanisms. Biochim. Biophys. Acta 1833 (12), 3460–3470.

Sano, K., Fujigaki, Y., Miyaji, T., Ikegaya, N., Ohishi, K., Yonemura, K., et al., 2000. Role of apoptosis in uranyl acetate-induced acute renal failure and acquired resistance to uranyl acetate. Kidney Int. 57 (4), 1560–1570.

Sanz-Rosa, D., Oubina, M.P., Cediel, E., de Las Heras, N., Vegazo, O., Jimenez, J., et al., 2005. Effect of AT1 receptor antagonism on vascular and circulating inflammatory mediators in SHR: role of NF-kappaB/IkappaB system. Am. J. Physiol. Heart Circ. Physiol. 288 (1), H111–H115.

Sarica, K., Yagci, F., Bakir, K., Erbagci, A., Erturhan, S., Ucak, R., 2001. Renal tubular injury induced by hyperoxaluria: evaluation of apoptotic changes. Urol. Res. 29 (1), 34–37.

Sato, N., Komatsu, K., Kurumatani, H., 2003. Late onset of diabetic nephropathy in spontaneously diabetic GK rats. Am. J. Nephrol. 23 (5), 334–342.

Sauriyal, D.S., Jaggi, A.S., Singh, N., Muthuraman, A., 2012. Investigating the role of endogenous opioids and KATP channels in glycerol-induced acute renal failure. Fundam. Clin. Pharmacol. 26 (3), 347–355.

Savic, V., Vlahovic, P., Djordjevic, V., Mitic-Zlatkovic, M., Avramovic, V., Stefanovic, V., 2002. Nephroprotective effects of pentoxifylline in experimental myoglobinuric acute renal failure. Pathol. Biol. 50 (10), 599–607.

Schnellmann, R.G., Williams, S.W., 1998. Proteases in renal cell death: calpains mediate cell death produced by diverse toxicants. Renal Fail. 20 (5), 679–686.

Seeliger, E., Lenhard, D.C., Persson, P.B., 2014. Contrast media viscosity versus osmolality in kidney injury: lessons from animal studies. BioMed Res. Int. 2014, 358136.

Servais, H., Jossin, Y., Van Bambeke, F., Tulkens, P.M., Mingeot-Leclercq, M.P., 2006. Gentamicin causes apoptosis at low concentrations in renal LLC-PK1 cells subjected to electroporation. Antimicrob. Agents Chemother. 50 (4), 1213–1221.

Servais, H., Ortiz, A., Devuyst, O., Denamur, S., Tulkens, P.M., Mingeot-Leclercq, M.P., 2008. Renal cell apoptosis induced by nephro-

toxic drugs: cellular and molecular mechanisms and potential approaches to modulation. Apoptosis 13 (1), 11–32.

Servais, H., Van Der Smissen, P., Thirion, G., Van der Essen, G., Van Bambeke, F., Tulkens, P.M., et al., 2005. Gentamicin-induced apoptosis in LLC-PK1 cells: involvement of lysosomes and mitochondria. Toxicol. Appl. Pharmacol. 206 (3), 321–333.

Sharma, K., Ziyadeh, F.N., 1994. Renal hypertrophy is associated with upregulation of TGF-beta 1 gene expression in diabetic BB rat and NOD mouse. Am. J. Physiol. 267 (6 Pt. 2), F1094–F1101.

Sharp, C.N., Doll, M.A., Dupre, T.V., Shah, P.P., Subathra, M., Siow, D., et al., 2016. Repeated administration of low-dose cisplatin in mice induces fibrosis. Am. J. Physiol. Renal Physiol. 310 (6), F560–F568.

Shiiki, H., Sasaki, Y., Nishino, T., Kimura, T., Kurioka, H., Fujimoto, S., et al., 1998. Cell proliferation and apoptosis of the glomerular epithelial cells in rats with puromycin aminonucleoside nephrosis. Pathobiology 66 (5), 221–229.

Sigal, N.H., Dumont, F., Durette, P., Siekierka, J.J., Peterson, L., Rich, D.H., et al., 1991. Is cyclophilin involved in the immunosuppressive and nephrotoxic mechanism of action of cyclosporin A? J. Exp. Med. 173 (3), 619–628.

Silver, S.A., Cardinal, H., Colwell, K., Burger, D., Dickhout, J.G., 2015. Acute kidney injury: preclinical innovations, challenges, and opportunities for translation. Can. J. Kidney Health Dis. 2, 30.

Silverstein, D.M., 2009. Inflammation in chronic kidney disease: role in the progression of renal and cardiovascular disease. Pediatr. Nephrol. 24 (8), 1445–1452.

Simmons, Jr., C.F., Bogusky, R.T., Humes, H.D., 1980. Inhibitory effects of gentamicin on renal mitochondrial oxidative phosphorylation. J. Pharmacol. Exp. Ther. 214 (3), 709–715.

Singh, A.P., Junemann, A., Muthuraman, A., Jaggi, A.S., Singh, N., Grover, K., et al., 2012. Animal models of acute renal failure. Pharmacol. Rep. 64 (1), 31–44.

Skrypnyk, N.I., Harris, R.C., de Caestecker, M.P., 2013. Ischemia-reperfusion model of acute kidney injury and post injury fibrosis in mice. J. Vis. Exp. 78, e50495.

Smeets, B., Te Loeke, N.A., Dijkman, H.B., Steenbergen, M.L., Lensen, J.F., Begieneman, M.P., et al., 2004. The parietal epithelial cell: a key player in the pathogenesis of focal segmental glomerulosclerosis in Thy-1.1 transgenic mice. J. Am. Soc. Nephrol. 15 (4), 928–939.

Smith, K.D., Alpers, C.E., 2005. Pathogenic mechanisms in membrano-proliferative glomerulonephritis. Curr. Opin. Nephrol. Hypertens. 14 (4), 396–403.

Smith, T.L., Hutchins, P.M., 1979. Central hemodynamics in the developmental stage of spontaneous hypertension in the unanesthetized rat. Hypertension 1 (5), 508–517.

Southard, J.H., Nitisewojo, P., 1973. Loss of oxidative phosphorylation in mitochondria isolated from kidneys of mercury poisoned rats. Biochem. Biophys. Res. Commun. 52 (3), 921–927.

Spitler, K.M., Matsumoto, T., Webb, R.C., 2013. Suppression of endoplasmic reticulum stress improves endothelium-dependent contractile responses in aorta of the spontaneously hypertensive rat. Am. J. Physiol. Heart Circ. Physiol. 305 (3), H344–H353.

Stacchiotti, A., Morandini, F., Bettoni, F., Schena, I., Lavazza, A., Grigolato, P.G., et al., 2009. Stress proteins and oxidative damage in a renal derived cell line exposed to inorganic mercury and lead. Toxicology 264 (3), 215–224.

Sugimoto, H., Mundel, T.M., Sund, M., Xie, L., Cosgrove, D., Kalluri, R., 2006. Bone-marrow-derived stem cells repair basement membrane collagen defects and reverse genetic kidney disease. Proc. Natl. Acad. Sci. USA 103 (19), 7321–7326.

Suh, S.H., Lee, K.E., Park, J.W., Kim, I.J., Kim, O., Kim, C.S., et al., 2013. Antiapoptotic effect of paricalcitol in gentamicin-induced kidney injury. Korean J. Physiol. Pharmacol. 17 (5), 435–440.

Sun, D., Eirin, A., Ebrahimi, B., Textor, S.C., Lerman, A., Lerman, L.O., 2016. Early atherosclerosis aggravates renal microvascular loss and fibrosis in swine renal artery stenosis. J. Am. Soc. Hypertens. 10 (4), 325–335.

Sun, Y., Zhang, T., Li, L., Wang, J., 2015. Induction of apoptosis by hypertension via endoplasmic reticulum stress. Kidney Blood Press. Res. 40 (1), 41–51.

Sung, M.J., Kim, D.H., Jung, Y.J., Kang, K.P., Lee, A.S., Lee, S., et al., 2008. Genistein protects the kidney from cisplatin-induced injury. Kidney Int. 74 (12), 1538–1547.

Susztak, K., Sharma, K., Schiffer, M., McCue, P., Ciccone, E., Bottinger, E.P., 2003. Genomic strategies for diabetic nephropathy. J. Am. Soc. Nephrol. 14 (8 Suppl. 3), S271–S278.

Susztak, K., Bottinger, E., Novetsky, A., Liang, D., Zhu, Y., Ciccone, E., et al., 2004. Molecular profiling of diabetic mouse kidney reveals novel genes linked to glomerular disease. Diabetes 53 (3), 784–794.

Suto, J., Matsuura, S., Imamura, K., Yamanaka, H., Sekikawa, K., 1998. Genetic analysis of non-insulin-dependent diabetes mellitus in KK and KK-Ay mice. Eur. J. Endocrinol. 139 (6), 654–661.

Suzuki, H., Suzuki, Y., Novak, J., Tomino, Y., 2014. Development of animal models of human IgA nephropathy. Drug Discov. Today Dis. Models 11, 5–11.

Suzuki, H., Suzuki, Y., Yamanaka, T., Hirose, S., Nishimura, H., Toei, J., et al., 2005. Genome-wide scan in a novel IgA nephropathy model identifies a susceptibility locus on murine chromosome 10, in a region syntenic to human IGAN1 on chromosome 6q22-23. J. Am. Soc. Nephrol. 16 (5), 1289–1299.

Suzuki, S., Takamura, S., Yoshida, J., Shinzawa, Y., Niwa, O., Tamatani, R., 1995. Comparison of gentamicin nephrotoxicity between rats and mice. Comp. Biochem. Physiol. C 112 (1), 15–28.

Szabo, C., Southan, G.J., Thiemermann, C., 1994. Beneficial effects and improved survival in rodent models of septic shock with S-methylisothiourea sulfate, a potent and selective inhibitor of inducible nitric oxide synthase. Proc. Natl. Acad. Sci. USA 91 (26), 12472–12476.

Tanjore, H., Lawson, W.E., Blackwell, T.S., 2013. Endoplasmic reticulum stress as a pro-fibrotic stimulus. Biochim. Biophys. Acta 1832 (7), 940–947.

Taulan, M., Paquet, F., Argiles, A., Demaille, J., Romey, M.C., 2006. Comprehensive analysis of the renal transcriptional response to acute uranyl nitrate exposure. BMC Genomics 7, 2.

Tersey, S.A., Nishiki, Y., Templin, A.T., Cabrera, S.M., Stull, N.D., Colvin, S.C., et al., 2012. Islet beta-cell endoplasmic reticulum stress precedes the onset of type 1 diabetes in the nonobese diabetic mouse model. Diabetes 61 (4), 818–827.

Tesch, G.H., Allen, T.J., 2007. Rodent models of streptozotocin-induced diabetic nephropathy. Nephrology 12 (3), 261–266.

Thamilselvan, S., Hackett, R.L., Khan, S.R., 1997. Lipid peroxidation in ethylene glycol induced hyperoxaluria and calcium oxalate nephrolithiasis. J. Urol. 157 (3), 1059–1063.

Theofilopoulos, A.N., Dixon, F.J., 1981. Etiopathogenesis of murine SLE. Immunol. Rev. 55, 179–216.

Thiebault, C., Carriere, M., Milgram, S., Simon, A., Avoscan, L., Gouget, B., 2007. Uranium induces apoptosis and is genotoxic to normal rat kidney (NRK-52E) proximal cells. Toxicol. Sci. 98 (2), 479–487.

Thomas, S.E., Andoh, T.F., Pichler, R.H., Shankland, S.J., Couser, W.G., Bennett, W.M., et al., 1998. Accelerated apoptosis characterizes cyclosporine-associated interstitial fibrosis. Kidney Int. 53 (4), 897–908.

Thornhill, B.A., Burt, L.E., Chen, C., Forbes, M.S., Chevalier, R.L., 2005. Variable chronic partial ureteral obstruction in the neonatal rat: a new model of ureteropelvic junction obstruction. Kidney Int. 67 (1), 42–52.

Tobian, L., Lange, J., Iwai, J., Hiller, K., Johnson, M.A., Goossens, P., 1979. Prevention with thiazide of NaCl-induced hypertension in Dahl "S" rats. Evidence for a Na-retaining humoral agent in "S" rats. Hypertension 1 (3), 316–323.

Tolson, J.K., Roberts, S.M., Jortner, B., Pomeroy, M., Barber, D.S., 2005. Heat shock proteins and acquired resistance to uranium nephrotoxicity. Toxicology 206 (1), 59–73.

Tomaschitz, A., Pilz, S., Ritz, E., Obermayer-Pietsch, B., Pieber, T.R., 2010. Aldosterone and arterial hypertension. Nat. Rev. Endocrinol. 6 (2), 83–93.

Tomino, Y., 2012. Lessons From the KK-Ay Mouse, a Spontaneous Animal Model for the Treatment of Human Type 2 Diabetic Nephropathy. Nephrourol. Mon. 4 (3), 524–529.

Toscano, M.G., Ganea, D., Gamero, A.M., 2011. Cecal ligation puncture procedure. J. Vis. Exp. (51), e2860.

Touati, C., Idee, J.M., Deray, G., Santus, R., Balut, C., Beaufils, H., et al., 1993. Modulation of the renal effects of contrast media by endothelium-derived nitric oxide in the rat. Invest. Radiol. 28 (9), 814–820.

Tracey, K.J., Beutler, B., Lowry, S.F., Merryweather, J., Wolpe, S., Milsark, I.W., et al., 1986. Shock and tissue injury induced by recombinant human cachectin. Science 234 (4775), 470–474.

Tracey, K.J., Fong, Y., Hesse, D.G., Manogue, K.R., Lee, A.T., Kuo, G.C., et al., 1987. Anti-cachectin/TNF monoclonal antibodies prevent septic shock during lethal bacteraemia. Nature 330 (6149), 662–664.

Traeger, T., Koerner, P., Kessler, W., Cziupka, K., Diedrich, S., Busemann, A., et al., 2010. Colon ascendens stent peritonitis (CASP)—a standardized model for polymicrobial abdominal sepsis. J. Vis. Exp. (46), e2299.

Turkbey, B., Ocak, I., Daryanani, K., Font-Montgomery, E., Lukose, L., Bryant, J., et al., 2009. Autosomal recessive polycystic kidney disease and congenital hepatic fibrosis (ARPKD/CHF). Pediatr. Radiol. 39 (2), 100–111.

Vanholder, R., Sever, M.S., Erek, E., Lameire, N., 2000. Rhabdomyolysis. J. Am. Soc. Nephrol. 11 (8), 1553–1561.

Venkatachalam, M.A., Bernard, D.B., Donohoe, J.F., Levinsky, N.G., 1978. Ischemic damage and repair in the rat proximal tubule: differences among the S1, S2, and S3 segments. Kidney Int. 14 (1), 31–49.

Vlahovic, P., Cvetkovic, T., Savic, V., Stefanovic, V., 2007. Dietary curcumin does not protect kidney in glycerol-induced acute renal failure. Food Chem. Toxicol. 45 (9), 1777–1782.

Volpini, R.A., Balbi, A.P., Costa, R.S., Coimbra, T.M., 2006. Increased expression of p38 mitogen-activated protein kinase is related to the acute renal lesions induced by gentamicin. Braz. J. Med. Biol. Res. 39 (6), 817–823.

Wang, T.N., Chen, X., Li, R., Gao, B., Mohammed-Ali, Z., Lu, C., et al., 2015a. SREBP-1 mediates angiotensin II-induced TGF-beta1 upregulation and glomerular fibrosis. J. Am. Soc. Nephrol. 26 (8), 1839–1854.

Wang, Z., Havasi, A., Gall, J., Bonegio, R., Li, Z., Mao, H., et al., 2010. GSK3beta promotes apoptosis after renal ischemic injury. J. Am. Soc. Nephrol. 21 (2), 284–294.

Wang, Y., Wang, D., Wu, J., Wang, B., Wang, L., Gao, X., et al., 2015b. Cinnabar induces renal inflammation and fibrogenesis in rats. BioMed Res. Int. 2015, 280958.

Wang, C., Wu, M., Arvapalli, R., Dai, X., Mahmood, M., Driscoll, H., et al., 2014a. Acetaminophen attenuates obesity-related renal injury through ER-mediated stress mechanisms. Cell Physiol. Biochem. 33 (4), 1139–1148.

Wang, F., Zhang, G., Zhou, Y., Gui, D., Li, J., Xing, T., et al., 2014b. Magnolin protects against contrast-induced nephropathy in rats via antioxidation and antiapoptosis. Oxid. Med. Cell Longev. 2014, 203458.

Warner, G.M., Cheng, J., Knudsen, B.E., Gray, C.E., Deibel, A., Juskewitch, J.E., et al., 2012. Genetic deficiency of Smad3 protects the kidneys from atrophy and interstitial fibrosis in 2K1C hypertension. Am. J. Physiol. Renal Physiol. 302 (11), F1455–F1464.

Wei, Q., Dong, Z., 2012. Mouse model of ischemic acute kidney injury: technical notes and tricks. Am. J. Physiol. Renal Physiol. 303 (11), F1487–F1494.

Wharram, B.L., Goyal, M., Wiggins, J.E., Sanden, S.K., Hussain, S., Filipiak, W.E., et al., 2005. Podocyte depletion causes glomerulosclerosis: diphtheria toxin-induced podocyte depletion in rats expressing human diphtheria toxin receptor transgene. J. Am. Soc. Nephrol. 16 (10), 2941–2952.

Whiting, P.H., Petersen, J., Simpson, J.G., 1981. Gentamicin-induced nephrotoxicity in mice: protection by loop diuretics. Br. J. Exp. Pathol. 62 (2), 200–206.

Wolf, G., Killen, P.D., Neilson, E.G., 1990. Cyclosporin A stimulates transcription and procollagen secretion in tubulointerstitial fibroblasts and proximal tubular cells. J. Am. Soc. Nephrol. 1 (6), 918–922.

Wu, X., He, Y., Jing, Y., Li, K., Zhang, J., 2010a. Albumin overload induces apoptosis in renal tubular epithelial cells through a CHOP-dependent pathway. OMICS 14 (1), 61–73.

Wu, H.H., Hsiao, T.Y., Chien, C.T., Lai, M.K., 2009. Ischemic conditioning by short periods of reperfusion attenuates renal ischemia/reperfusion induced apoptosis and autophagy in the rat. J. Biomed. Sci. 16, 19.

Wu, C.T., Sheu, M.L., Tsai, K.S., Weng, T.I., Chiang, C.K., Liu, S.H., 2010b. The role of endoplasmic reticulum stress-related unfolded protein response in the radiocontrast medium-induced renal tubular cell injury. Toxicol. Sci. 114 (2), 295–301.

Wu, J., Zhang, R., Torreggiani, M., Ting, A., Xiong, H., Striker, G.E., et al., 2010c. Induction of diabetes in aged C57B6 mice results in severe nephropathy: an association with oxidative stress, endoplasmic reticulum stress, and inflammation. Am. J. Pathol. 176 (5), 2163–2176.

Xia, C.F., Bledsoe, G., Chao, L., Chao, J., 2005. Kallikrein gene transfer reduces renal fibrosis, hypertrophy, and proliferation in DOCA-salt hypertensive rats. Am. J. Physiol. Renal Physiol. 289 (3), F622–F631.

Xie, C., Sharma, R., Wang, H., Zhou, X.J., Mohan, C., 2004. Strain distribution pattern of susceptibility to immune-mediated nephritis. J. Immunol. 172 (8), 5047–5055.

Xu, J., Huang, Y., Li, F., Zheng, S., Epstein, P.N., 2010. FVB mouse genotype confers susceptibility to OVE26 diabetic albuminuria. Am. J. Physiol. Renal Physiol. 299 (3), F487–F494.

Yabuki, A., Tanaka, S., Matsumoto, M., Suzuki, S., 2006. Morphometric study of gender differences with regard to age-related changes in the C57BL/6 mouse kidney. Exp. Anim. 55 (4), 399–404.

Yagil, C., Sapojnikov, M., Katni, G., Ilan, Z., Zangen, S.W., Rosenmann, E., et al., 2002. Proteinuria and glomerulosclerosis in the Sabra genetic rat model of salt susceptibility. Physiol. Genomics 9 (3), 167–178.

Yamate, J., Machida, Y., Ide, M., Kuwamura, M., Kotani, T., Sawamoto, O., et al., 2005. Cisplatin-induced renal interstitial fibrosis in neonatal rats, developing as solitary nephron unit lesions. Toxicol. Pathol. 33 (2), 207–217.

Yang, J.R., Yao, F.H., Zhang, J.G., Ji, Z.Y., Li, K.L., Zhan, J., et al., 2014. Ischemia-reperfusion induces renal tubule pyroptosis via the CHOP-caspase-11 pathway. Am. J. Physiol. Renal Physiol. 306 (1), F75–F84.

Yang, H.C., Zuo, Y., Fogo, A.B., 2010. Models of chronic kidney disease. Drug Discov. Today Dis. Models 7 (1–2), 13–19.

Yao, J., Le, T.C., Kos, C.H., Henderson, J.M., Allen, P.G., Denker, B.M., et al., 2004. Alpha-actinin-4-mediated FSGS: an inherited kidney disease caused by an aggregated and rapidly degraded cytoskeletal protein. PLoS Biol. 2 (6), e167.

Yen, H.W., Lee, H.C., Lai, W.T., Sheu, S.H., 2007. Effects of acetylcysteine and probucol on contrast medium-induced depression of intrinsic renal glutathione peroxidase activity in diabetic rats. Arch. Med. Res. 38 (3), 291–296.

Yokomaku, Y., Sugimoto, T., Kume, S., Araki, S., Isshiki, K., Chin-Kanasaki, M., et al., 2008. Asialoerythropoietin prevents contrast-induced nephropathy. J. Am. Soc. Nephrol. 19 (2), 321–328.

Yoneda, T., Imaizumi, K., Oono, K., Yui, D., Gomi, F., Katayama, T., et al., 2001. Activation of caspase-12, an endoplastic reticulum (ER) resident caspase, through tumor necrosis factor receptor-associated factor 2-dependent mechanism in response to the ER stress. J. Biol. Chem. 276 (17), 13935–13940.

Yoshida, Y., Fogo, A., Shiraga, H., Glick, A.D., Ichikawa, I., 1988. Serial micropuncture analysis of single nephron function in subtotal renal ablation. Kidney Int. 33 (4), 855–867.

Yu, H.C., Burrell, L.M., Black, M.J., Wu, L.L., Dilley, R.J., Cooper, M.E., et al., 1998. Salt induces myocardial and renal fibrosis in normotensive and hypertensive rats. Circulation 98 (23), 2621–2628.

Yu, M., Moreno, C., Hoagland, K.M., Dahly, A., Ditter, K., Mistry, M., et al., 2003. Antihypertensive effect of glucagon-like peptide 1 in Dahl salt-sensitive rats. J. Hypertens. 21 (6), 1125–1135.

Yu, Y.L., Yiang, G.T., Chou, P.L., Tseng, H.H., Wu, T.K., Hung, Y.T., et al., 2014. Dual role of acetaminophen in promoting hepatoma cell apoptosis and kidney fibroblast proliferation. Mol. Med. Rep. 9 (6), 2077–2084.

Zalups, R.K., 2000. Molecular interactions with mercury in the kidney. Pharmacol. Rev. 52 (1), 113–143.

Zanchi, A., Moczulski, D.K., Hanna, L.S., Wantman, M., Warram, J.H., Krolewski, A.S., 2000. Risk of advanced diabetic nephropathy in type 1 diabetes is associated with endothelial nitric oxide synthase gene polymorphism. Kidney Int. 57 (2), 405–413.

Zang, X.J., An, S.X., Feng, Z., Xia, Y.P., Song, Y., Yu, Q., 2014. In vivo mechanism study of NGAL in rat renal ischemia-reperfusion injury. Genet. Mol. Res. 13 (4), 8740–8748.

Zarjou, A., Agarwal, A., 2011. Sepsis and acute kidney injury. J. Am. Soc. Nephrol. 22 (6), 999–1006.

Zhang, B., Ramesh, G., Uematsu, S., Akira, S., Reeves, W.B., 2008. TLR4 signaling mediates inflammation and tissue injury in nephrotoxicity. J. Am. Soc. Nephrol. 19 (5), 923–932.

Zhang, C., Zheng, L., Li, L., Wang, L., Li, L., Huang, S., et al., 2014. Rapamycin protects kidney against ischemia reperfusion injury through recruitment of NKT cells. J. Transl. Med. 12, 224.

Zhao, W., Huang, X., Zhang, L., Yang, X., Wang, L., Chen, Y., et al., 2016. Penehyclidine hydrochloride pretreatment ameliorates rhabdomyolysis-induced AKI by activating the Nrf2/HO-1 pathway and alleviating endoplasmic reticulum stress in rats. PLoS One 11 (3), e0151158.

Zhao, G., Tu, L., Li, X., Yang, S., Chen, C., Xu, X., et al., 2012. Delivery of AAV2-CYP2J2 protects remnant kidney in the 5/6-nephrectomized rat via inhibition of apoptosis and fibrosis. Hum. Gene Ther. 23 (7), 688–699.

Zheng, S., Noonan, W.T., Metreveli, N.S., Coventry, S., Kralik, P.M., Carlson, E.C., et al., 2004. Development of late-stage diabetic nephropathy in OVE26 diabetic mice. Diabetes 53 (12), 3248–3257.

Zheng, J., Zhao, T., Yuan, Y., Hu, N., Tang, X., 2015. Hydrogen sulfide (H2S) attenuates uranium-induced acute nephrotoxicity through oxidative stress and inflammatory response via Nrf2-NF-kappaB pathways. Chem. Biol. Interact. 242, 353–362.

Zhong, Z., Arteel, G.E., Connor, H.D., Yin, M., Frankenberg, M.V., Stachlewitz, R.F., et al., 1998. Cyclosporin A increases hypoxia and free radical production in rat kidneys: prevention by dietary glycine. Am. J. Physiol. 275 (4 Pt. 2), F595–F604.

Zhu, X.Y., Urbieta-Caceres, V., Krier, J.D., Textor, S.C., Lerman, A., Lerman, L.O., 2013. Mesenchymal stem cells and endothelial progenitor cells decrease renal injury in experimental swine renal artery stenosis through different mechanisms. Stem Cells 31 (1), 117–125.

Zhu, G., Xiang, X., Chen, X., Wang, L., Hu, H., Weng, S., 2009. Renal dysfunction induced by long-term exposure to depleted uranium in rats. Arch. Toxicol. 83 (1), 37–46.

Zhuang, A., Forbes, J.M., 2014. Stress in the kidney is the road to pERdition: is endoplasmic reticulum stress a pathogenic mediator of diabetic nephropathy? J. Endocrinol. 222 (3), R97–R111.

Zurovsky, Y., 1993. Models of glycerol-induced acute renal failure in rats. J. Basic Clin. Physiol. Pharmacol. 4 (3.), 213–228.

Page left intentionally blank

Animal Models to Study Urolithiasis

David T. Tzou*, Kazumi Taguchi*,**, Thomas Chi*,
Marshall L. Stoller*

*University of California, San Francisco, CA, United States
**Nagoya City University Graduate School of Medical Sciences, Nagoya, Japan

1 INTRODUCTION

Why do stones form in human kidneys? The answer to this basic question remains elusive as currently we still do not fully understand the fundamental pathophysiology of urinary stone formation. In 1937, when Alexander Randall postulated that papillary "plaques" composed of calcium phosphate represented the nidus for future stone formation, he described such plaques to be "invading and replacing interstitial tissue." (Randall, 1937, 1940) While currently we know that Randall's plaques are present in the majority of calcium kidney stone formers, there is still more to understand with regard to the cascade of events leading to kidney stone formation. It is theorized that ectopic biomineralization in the proximal medullo-papillary complex precedes interstitial Randall

plaque in the distal papilla that ultimately culminates in urinary stone formation. We still have a limited understanding of the genetic and environmental reasons that lead to the early ectopic biomineralization process. The only way to fully understand the temporal evolution/process by which stones form will be to develop reliable animal models. There is a great need for *standardized* nephrolithiasis animal models to better understand the temporal sequence of stone growth and thus allow researchers around the world to share data from similar animal models. It is with this goal in mind that the current animal models to study urolithiasis are reviewed.

Urinary stone disease remains a prevalent disease with approximately 1 of 11 people affected in the United States (Scales et al., 2012). Multiple studies have shown that up to 50% of patients who develop a kidney stone will experience another stone episode within 5 years (Ljunghall, 1987). Acute renal colic associated with passage of a urinary stone is a major source of patient morbidity and mortality, with over 50% of these patients requiring surgical intervention and an average estimated 19 productive work hours lost each year (Pearle et al., 2005; Saigal et al., 2005). Previously an estimated $2.1 billion annual cost was linked to urolithiasis in the year 2000 (Pearle et al., 2005). The associated health costs of urolithiasis continue to rise and recently this number has risen to an estimated $10 billion annually (Scales et al., 2016). While major advancements in technique and technology have been made in the surgical treatment of kidney stones, our understanding of the fundamental mechanisms of stone formation remain limited.

A reliable and reproducible animal model for urinary stone disease is not widely accepted or used, and as such researchers frequently have resorted to studying stone specimens at the extreme ends of the spectrum (from early papillary Randall plaques, to deep sampling of the medullo-papillary complex at time of nephrectomy, and surgically excised calculi). Endoscopic papillary biopsies limit study to the tip of the renal papilla while excised medullo-papillary complexes from surgically removed kidneys reveal potential upstream development of biomineralization. Many surgically removed kidneys are removed due to infection or chronic obstruction and may not represent pristine specimens to study early elements of stone formation. As a community of clinicians and basic scientists trying to unfold the mysteries of biomineralization, there is an urgent need to develop a reliable animal model to study the pathogenesis of urinary stone disease.

Reflecting back on the last 50 years, there have been relatively few breakthroughs with respect to stone prevention. The lack of a reliable animal model has limited innovations in medicinal prophylaxis. Most urologists perform a metabolic evaluation that consists of laboratory testing including targeted 24-h urine collections and blood chemistries to try to identify risk factors for future stone formation. This metabolic evaluation has remained the same for nearly half a century, yet both the incidence and recurrence of stones continue to rise. An animal model is needed to better understand the mechanisms by which stones form to allow us to decrease future stone formation and provide a roadmap to develop new prophylactic regimens.

Currently no single animal model system can be thought of as perfect, yet valuable insight can be gained from reviewing those animals that have been utilized thus far. For each animal, the anatomic similarities and differences compared to humans will be highlighted. The methods by which investigators induce stone formation will be summarized, focusing on the advantages and disadvantages researchers have encountered to date. Each model has limitations and these will also be highlighted within each section. It is with these concepts in mind that hopefully the reader will gain an appreciation of the importance of animal models for urinary stone disease.

2 RAT MODEL

Similar to other fields in medicine, urinary stone disease has utilized the rat to attempt to systematically study the pathogenesis of urinary stone disease. Rats represent a well-established, relatively economical model that scientists have utilized since the 19th century. At the beginning of the 21st century, rats and mice accounted for over 90% of animals used in research (CCPA, 2000). For urinary stone disease, studies utilizing the rat have predominantly focused on reproducing both hypercalciuria and hyperoxaluria, two of the most common pathophysiologic changes associated with urinary stone disease.

2.1 Anatomic/Physiologic Comparison Between Rat and Humans

There are inherent differences between the kidneys of the rat and those of humans, the biggest of which is that rat kidneys are unipapillary compared to the multipapillary kidneys of humans. Average rat kidney measurements are $1.6 \times 1.0 \times 0.9$ cm, and their usual weight is 0.75–1.2 g (Khan, 2013). Despite having fewer urinary tubules and an overall smaller collecting system, rat kidneys have a similar cortex-medulla ratio (2:1) compared with humans. In general, rat kidneys are usually comprised of approximately 30,000 nephrons, compared to nearly 1,000,000 in humans (Khan, 2013). The rat bladder is different from humans in that it is considered to be more of an abdominal organ given that the shape of the rat pelvis lacks a true (lesser) cavity (DeSesso, 1995). Rat bladders generally have a pear-shape and have been

noted to have a maximum volume of 2.5 mL, with average urine output ranging between 10 and 25 mL/day (DeSesso, 1995).

2.2 Hypercalciuria

2.2.1 Cross-Breeding Model

Hypercalciuria has been established as one of the most common risk factors for the development of urinary stone disease (Bushinsky et al., 1995; Coe et al., 1992). For the rat, researchers have established a strain of multigeneration inbred Sprague-Dawley rats to produce hypercalciuric progeny (Bushinsky and Favus, 1988). While initially thought to be solely secondary to increased calcium absorption in the gut, multiple studies have since established that an increased number of vitamin D receptors in the GI tract, kidneys, and bone lead to increased calcium absorption in these genetically hypercalciuric stone-forming (GHS) rats (Krieger et al., 1996; Li et al., 1993; Yao et al., 1998). With each successive generation, these GHS rats have been shown to excrete multiple-fold times the amount of calcium compared to controls (Evan et al., 2004). While most of these studies have utilized female rats, male GHS rats have been shown to excrete a higher daily oxalate content compared to their female counterparts (Bushinsky et al., 1994).

2.2.1.1 SUPERSATURATION

While these GHS rats have been used to investigate multiple aspects of stone formation pathophysiology, one of their most important contributions has been related to stone formation and urine supersaturation. Since the development and use of the EQUIL2 equation, researchers have had a reliable program for calculating the urinary supersaturation of common stone components (Werness et al., 1985). Classic work has shown that supersaturation by itself does not necessarily equate to crystallization; compared to simple solutions, human urine contains an upper limit of metastability due to inhibitors of stone growth (Pak and Holt, 1976).

Asplin et al. (1997) demonstrated that compared to controls, GHS rats had higher calcium oxalate (CaOx) and calcium phosphate (CaP) supersaturation values, regardless of whether they were fed a low- or high-calcium diet. These increases in supersaturation were accompanied by a higher upper limit of metastability for CaOx but not so for brushite (CaP), reflecting that urine can have higher concentrations of CaOx without precipitating when under certain conditions. Meanwhile, the supersaturation level of CaP is elevated and near its upper limit of metastability, which is thought to be the main reason this GHS rat model results in CaP crystals instead of CaOx. Bushinsky et al. (2000) subsequently demonstrated that lowering dietary phosphorous in these GHS

rats resulted in decreased urinary phosphorous excretion and reduced supersaturation of calcium phosphate, with none of these rats producing CaP crystals.

As will be discussed later, Bushinsky et al. (2002) also demonstrated the ability to have these GHS rats produce calcium oxalate crystals through the addition of hydroxyl-L-proline.

2.2.1.2 APPLICABILITY

The GHS model has provided important contributions to the overall understanding of hypercalciuria and the role of supersaturation in the formation of urinary stones. Yet it remains unclear how this hypercalciuria model fits in translation to what is known regarding human hypercalciuria and stone formation. Our current classification of human hypercalciuria is not homogeneous. Classically, humans have been thought to have hypercalciuria etiologies ranging from absorptive—diet independent (type 1), diet dependent (type 2), renal urinary phosphate leak (type 3), to primary hyperparathyroidism (Stoller and Meng, 2007). All of these conditions result in large amounts of calcium present in the urine, similar to what has been created in the GHS rat model. Yet the question remains, which type of human hypercalciuria does this GHS rat model represent? Most patients with primary hyperparathyroidism should theoretically develop urinary stones, yet only about 10% of these patients will actually develop one. There must be critical factors other than serum and urinary calcium that contribute to stone formation. Therefore, this GHS rat model remains limited as it does not account for the heterogeneity that is found in clinical practice.

2.3 Hyperoxaluria

2.3.1 Exogenous Induction

A number of rat models for hyperoxaluria have relied on exogenous administration of lithogenic materials including sodium oxalate, glycolic acid, ethylene glycol (EG), and hydroxy-L-proline (HLP) (Khan, 1991; Khan and Hackett, 1993b; Khan et al., 1979a, 1982, 1992; Ogawa et al., 1990). The methods by which these materials have been delivered to the rat range from enriched chow, drinking water modification, gavage instillation, intraperitoneal injection, and even subcutaneous implantation of oxalate-containing osmotic minipumps (Khan, 2013). This section reviews how each lithogenic agent has been studied in the rat and shown to culminate in stone induction. For a summary of hyperoxaluria induction, see Table 17.1.

2.3.1.1 SODIUM OXALATE

As Khan et al. (1979a) illustrated, predictable calcium oxalate crystal formation in different areas of the nephron depends on elapsed time after intraperitoneal

TABLE 17.1　Rat Models Related to Hyperoxaluria

Type of approach	Lithogenic agent (references)	Diet/administration	Effects
Cross-breeding	Inbreeding hypercalciuric progeny (Asplin et al., 1997; Bushinsky and Favus, 1988; Bushinsky et al., 1994, 2000, 2002; Evan et al., 2004; Krieger et al., 1996; Li et al., 1993; Yao et al., 1998)	• Multiple-generation inbred • Multiple diets/agents applied	• Hypercalciuria • Hyperoxaluria • CaOx crystals • CaP crystals
Exogenous induction	Sodium oxalate (Khan and Hackett, 1993b; Khan et al., 1979a, 1982, 1991, 1992)	• Intraperitoneal injection of 10 mg/kg sodium oxalate	• Prompt CaOx crystal deposits • Crystal aggregation in the ducts of Bellini
	Glycolic acid (Ogawa et al., 1990)	• Free drinking of water with powdered 3% glycolic acid	• Hyperoxaluria • Hypocitraturia • CaOx crystal deposits
	Ethylene glycol (EG) (de Bruijn et al., 1994; de Water et al., 1996; Eder et al., 1998; Green et al., 2005; Huang et al., 2002; Khan et al., 1992, 2002a; Robinson et al., 1990; Thamilselvan et al., 1997; Yamaguchi et al., 2005)	• 0.75% EG in water with/without ammonium chloride, vitamin D, calcium chloride	• Hyperoxaluria • CaOx crystalluria • CaOx crystal deposits • Renal toxicity
	Hydroxy-L-proline (HLP) (Khan et al., 1989, 2006; Tawashi et al., 1980)	• Intraperitoneal injection of 2.5 kg/kg HLP • Mixed in chow of 5% HLP	• Hyperoxaluria • CaOx crystal deposits • Less toxic compared to other agents
Dietary manipulation	Potassium oxalate supplement (Wiessner et al., 2011)	• 5% level of potassium oxalate	• CaOx crystal deposits
	Magnesium (Mg) deficiency (Li et al., 1985; Rushton and Spector, 1982)	• Dietary Mg deprivation	• Increase of CaP crystal deposits
	Vitamin B6 (pyridoxine) deficiency (Andrus et al., 1960; Gershoff and Andrus, 1961; Gershoff and Faragalla, 1959)	• Dietary intentional deficiency of pyridoxine	• Hyperoxaluria • Hypocitraturia • CaOx crystal deposits
Surgery	Intestinal resection (O'Connor et al., 2005; Smith et al., 1972; Worcester et al., 2005)	• Resection of distal 40–45 cm of the terminal ileum • Combination diet of high oxalate/low calcium/high lipid fat	• Hyperoxaluria • Hypocitraturia • CaOx, CaP, CaCO$_3$ crystal deposits
	Gastric bypass surgery (Canales et al., 2013)	• Roux-en-Y gastric bypass • 40% fat and 1.5% sodium oxalate diet	• Hyperoxaluria • CaOx crystal deposits

injection of sodium oxalate. Male Sprague-Dawley rats receiving varied doses (3, 5, 7, 9, and 10 mg/kg) of sodium oxalate demonstrated persistent hyperoxaluria and crystals in a dose-dependent fashion (Khan, 1991; Khan and Hackett, 1993b; Khan et al., 1992). Rats receiving the highest dose of 10 mg/kg had over 500% more oxalate excreted compared to controls. Moreover, these rats demonstrated persistent crystals that remained present up to 7 days after injection. These studies also demonstrated how quickly crystals could be detected within the rat kidney, as investigators identified calcium oxalate crystals within 15 min of injection. By 6 h there was noticeable crystal aggregation in the ducts of Bellini (Khan et al., 1982). While this demonstrated the ability to induce urinary crystalluria relatively quickly, one should keep in mind that this does not necessarily equate to urinary stone development.

2.3.1.2 GLYCOLIC ACID

Through the administration of powdered 3% glycolic acid dissolved in drinking water, Ogawa et al. (1990) demonstrated the ability of male Wistar-strain rats to produce high levels of 24-h urinary oxalate and subsequent calcium oxalate calculi. Interestingly, this study also demonstrated how adding certain magnesium (Mg) salts to a diet high in glycolic acid resulted in increased urinary citrate levels despite relatively high levels of urinary oxalate excretion. Specific magnesium agents (Mg hydroxide, Mg silicate, and Mg citrate) were associated with significantly lower mean

renal tissue urinary oxalate concentrations (Ogawa et al., 1990). When compared with rats on a strict glycolic acid diet, rats who received additional Mg salt supplementation had decreased evidence of stone formation.

2.3.1.3 ETHYLENE GLYCOL

The administration of EG in drinking water has been shown to result in consistent induction of hyperoxaluria, crystalluria, and calcium oxalate nephrolithiasis (Khan et al., 2002a). Studies have shown that administering solely 0.75% EG to male rats eventually gave rise to persistent crystalluria at 12 days and renal crystal deposits at approximately 3 weeks (de Bruijn et al., 1994). To enhance the development of crystal deposition, EG often has been combined with other agents, such as ammonium chloride (AC) to reduce urinary pH, as well as vitamin D or calcium chloride to result in subsequent hypercalcemia and hypercalciuria (de Bruijn et al., 1994; de Water et al., 1996; Khan et al., 1992). The amount of calcium oxalate deposition in kidneys was found to be dependent on the concentration of both EG and AC. This lithogenic combination decreased the time for crystalluria from 12 to 3 days, and detectable calcium oxalate nephrolithiasis from 3 weeks down to 1 week (Khan et al., 1992).

A major limitation with the administration of EG is that it has been shown to be a toxic agent that can cause multiorgan failure (Eder et al., 1998). Multiple studies have shown it causes renal toxicity. Yamaguchi et al. (2005) demonstrated that the combination of EG and AC can have a significant detriment on rat health—as shown by those rats who received higher EG concentrations subsequently had increased urinary N-acetyl-β-D-glucosaminidase (NAG), an indicator of renal toxicity. These rats were found to have lower weights and worsening renal function as estimated by creatinine clearance. Other studies have also found that lipid peroxidation, increased free radicals, and metabolic acidosis also take place as a result of EG (Eder et al., 1998; Huang et al., 2002; Robinson et al., 1990; Thamilselvan et al., 1997). Even with evidence that a limited (<0.75%) dose of EG can bypass the usual resultant metabolic acidosis (Green et al., 2005), recognition of EG's toxic effects has since led to studies utilizing alternative, less toxic lithogenic agents.

2.3.1.4 HYDROXY-L-PROLINE

Hydroxy-L-proline (HLP) is a common ingredient in Western diets and has been shown to be less toxic than other lithogenic agents. It is derived from the amino acid proline and is a component of collagen that is metabolized to both pyruvate and glyoxalate, primarily in the renal proximal tubule and hepatocyte mitochondria (Knight and Holmes, 2005).

Earlier studies used intraperitoneal injection of HLP to successfully demonstrate the presence of calcium oxalate crystals within the rat kidney (Tawashi et al., 1980). This study utilized a large dose of 4-HLP (2.5 g/kg) and subsequently found a doubling of kidney volume and weight compared to controls. Using scanning electron microscopy, both calcium oxalate dihydrate (Weddellite) and calcium oxalate monohydrate (Whewellite) crystals were identified.

Initial attempts at administering HLP in chow at a dose of 5.2% for 10 days failed to produce calcium oxalate crystals despite demonstrating hyperoxaluria (Khan et al., 1989). Eventually Khan et al. (2006) provided 5% HLP (weight/weight HLP/chow) to male Sprague-Dawley rats and compared treated versus controls at 4, 6, and 9 weeks. At 4 weeks, all treated rats were found to have CaOx crystals throughout the regions of the kidney, with a majority present in the tubular lumens of the distal tubules and collecting ducts. Interestingly by 9 weeks these crystals were mainly located at the tips of the renal papillae.

2.3.1.5 DIETARY MANIPULATION

Investigators have also examined dietary administration of potassium oxalate as an alternative method compared to HLP. Wiessner et al. (2011) found that a 5% level of potassium oxalate was required to produce calcium oxalate crystals in both Dahl salt-sensitive and Brown Norway male rats. Furthermore, 2% supplemental dietary oxalate was all that was needed to result in an increased urine oxalate in control rats.

Magnesium (Mg), classically, was thought to be an inhibitor of calcium oxalate stone formation. Previous in vitro studies demonstrated the ability of Mg to decrease both calcium oxalate and calcium phosphate growth and nucleation (Li et al., 1985). Subsequently, investigators examined the effect of dietary Mg deprivation in hyperoxaluric rats, demonstrating the increased production of calcium phosphate (apatite) stones (Rushton and Spector, 1982).

Meanwhile, endogenous oxalate excretion has been shown to be inversely related to the amount of dietary vitamin B6 (pyridoxine) (Gershoff and Faragalla, 1959). The intentional deficiency of vitamin B6 can be employed in rats to enhance hyperoxaluria, hypocitraturia, and subsequent calcium oxalate crystal formation (Andrus et al., 1960). Studies exposing these pyridoxine deficient rats to supplemental Mg demonstrated the ability to counteract the hypocitraturia and effectively prevent calcium oxalate crystal formation (Gershoff and Andrus, 1961). This occurred despite these rats displaying persistent hyperoxaluria, confirming that the solvent characteristics had changed and that simply having high urinary oxalate was not the sole reason for the calcium oxalate stone formation.

2.3.2 *Intestinal Resection*

Small bowel resection has historically been associated with an increased risk of nephrolithiasis dating back to Smith et al. (1972). O'Connor et al. (2005) developed a rat model in which the distal 40–45 cm of the terminal ileum was resected and these rats were compared to sham controls that underwent transection of the distal ileum followed by reanastamosis without any intestine removal. After surgery these rats were then given either a normal versus a combination high oxalate (1% sodium oxalate)/low calcium (0.02%)/high lipids (18%) fat diet, before eventually being euthanized at 4, 5, 6, and 7 months postsurgery; 24-h urine samples demonstrated that those resected rats on the high oxalate/low calcium diet, developed hyperoxaluria, hypocitraturia, and crystals throughout the cortex, medulla, and renal papilla (Worcester et al., 2005). These crystals were comprised of a mixture of calcium oxalate, hydroxyapatite (calcium phosphate), and calcium carbonate. Meanwhile, none of the sham animals subsequently developed crystals, even those on the high oxalate diet, highlighting the importance of the bowel resection on crystal formation.

2.3.3 *Gastric Bypass Surgery*

Multiple previous studies have suggested an association between gastric-bypass surgery and an increased risk of kidney stone development (Duffey et al., 2010; Maalouf et al., 2010; Matlaga et al., 2009; Park et al., 2009; Patel et al., 2009). Patients undergoing Roux-en-Y gastric bypass (RYGB) have been shown to have significant hyperoxaluria and hypocitraturia (Maalouf et al., 2010; Patel et al., 2009). Epidemiologic studies have shown that patients post-RYGB have a increase in stone development: a twofold increase in nonstone formers and a fourfold increase in previous stone formers (Chen et al., 2013).

The pathophysiologic mechanism for this increased urinary oxalate is thought to be from a saponification process with excess fatty acids and bile salts binding to calcium, thereby leaving excess unbound oxalate free to be more easily absorbed by the enteric system (Canales and Hatch, 2014; Hofmann et al., 1983). Prospective studies have shown this hyperoxaluria to be a predictor of developing stones after RYGB, with an 8% incidence at 1-year postop reported, as well as a higher likelihood of stone formation as more time elapsed after surgery (Duffey et al., 2010; Valezi et al., 2013). Recent innovative work has delved into this process further by utilizing the rat as a successful animal model.

To investigate the mechanism by which post-RYGB hyperoxaluria takes place, Canales et al. (2013) utilized a diet-induced obesity (DIO) model in male Sprague-Dawley rats followed by subsequent intervention randomized to either sham surgery (controls) or RYGB. As shown in Fig. 17.1, this study examined stool and urine for respective fecal fat content and 24-h urine volume,

pH, oxalate and calcium levels. Results demonstrated that post-RYGB rats on a high (40%) fat and supplemental potassium oxalate had significantly less dietary fat absorption and excreted an eightfold higher amount of fecal fat compared to controls. Moreover, those post-RYGB rats with oxalate supplementation had a fivefold increase in urinary oxalate excretion, while those without supplemental oxalate had a twofold increase in urine calcium excretion.

Interestingly, this study also found that all RYGB rats had a significant 250% increase in water consumption and a twofold increase in urine volume excretion, regardless of dietary oxalate or fat content. While this finding has been postulated to be due to altered thirst mechanisms (Canales et al., 2013), it highlights a major difference compared to results from previous human studies that have shown significant decreases in urine volume post-RYGB (Agrawal et al., 2013; Hofmann et al., 1983; Wu et al., 2013). No doubt future studies will look to further elucidate the impact of RYGB and urinary volume production.

2.4 Predominant Stone Type

As mentioned previously, the GHS rat model has consistently demonstrated that those rats consuming a standard (1.2% Ca) diet for 18 weeks produce solely calcium phosphate calculi (Bushinsky et al., 1995). Bushinsky et al. (2002) examined how the addition of 1, 3, and 5% *trans*-4-HLP to GHS rats altered urine calcium and stone type. This study demonstrated that those rats receiving 5% HLP had decreased urine calcium excretion and also had consistent calcium oxalate calculi composition.

Given that the vast majority of rat studies utilizing exogenous induction have relied on oxalate precursors as the lithogenic agent, the resulting stones have been composed of calcium oxalate. There remains a void of studies that have been able to reproduce uric acid stones in the rat. Moreover, the potential role of heavy metals within rat models is an area of future research.

2.5 Limitations

While the rat model has been the most studied of all animal models for urinary stone disease, it does have some limitations. Like other vertebrates it requires formal approval for animal experimentation and lately the costs of rats has been increasing (CCPA, 2000). Rats are also corphagic (they eat their own stool) therefore they can consume elements that are not necessarily accounted for in their routine diets.

The majority of these models have focused on producing hyperoxaluria. It should be noted that the majority of human kidney stone patients do not suffer from hyperoxaluria, therefore, this modeling as limited
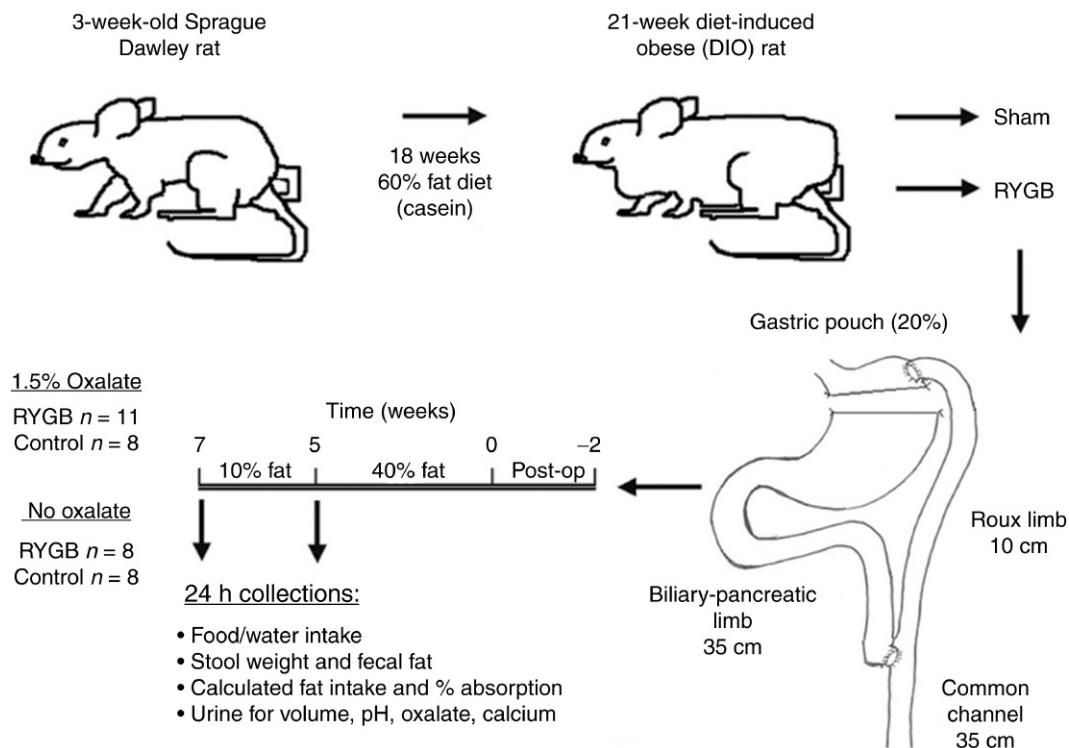
FIGURE 17.1 Diet-induced obesity *(DIO)* rat model followed by either sham or RYGB surgery. Following surgery, rats were randomized to high (40%) fat chow or 1.5% potassium oxalate for 5 weeks, followed by 2 weeks of a normal (10%) fat diet with or without 1.5% potassium oxalate. *Source: Reprinted with permission from Canales, B.K., Ellen, J., Khan, S.R., Hatch, M., 2013. Steatorrhea and hyperoxaluria occur after gastric bypass surgery in obese rats regardless of dietary fat or oxalate. J. Urol. 190, 1102–1109.*

applicability. As will be discussed later, modified gene expression studies have mainly been performed in other animal models besides the rat. While there are resources available for rat transgenic studies (Rat Genome Database, http://rgd.mcw.edu), comparatively there are considerably fewer for this application, which represents a limitation in the future use of this animal model.

3 MOUSE MODEL

Since the completion of the human genome project in 2003 (Collins et al., 2003), the mouse has been the most studied of all animals with respect to transgenic and gene-targeting research. Investigators have used the mouse model as a vehicle for genetic modification to examine both physiological and genomic features that are similar to humans. Applying molecular and genomic science to the mouse has helped unveil some of the intricacies involved in the pathogenesis of urinary stone disease.

3.1 Anatomic/Physiologic/Genomic Comparison Between Mice and Humans

The respective genomes of mice and humans are comparably similar as both genomes contain approximately 3.1 billion base pairs. Mice and human genomes are ~85% identical on an average; with some greater than 95% identical. Only about 5% of the sequence consists of protein-coding regions.

Mice generally weigh between 25 and 35 g, which is approximately 1/2500 the size of humans (Liebelt, 1998). Yet as the mean weight of an individual mouse kidney generally comprises 0.5%–0.8% of their body weight, mice kidneys are relatively denser compared to the average human kidney that comprises only 0.2% of a person's body weight (Meneton et al., 2000). Meanwhile, the maximal urine concentration (mice 4000 mOsm/kg H_2O vs. human 1200 mOsm/kg H_2O) is higher in mice than in humans (Meneton et al., 2000; Molina and DiMaio, 2012; Sands and Layton, 2009).

Like rats, the main difference in mice kidneys compared to humans is that they are unipapillary, therefore each kidney has a single papilla surrounded by the pelvis. Microscopic features show similar cortex and medullary components including a glomerular unit, tubule structures, and vascular framework (Liebelt, 1998).

3.2 Hyperoxaluria

3.2.1 Exogenous Induction

Similar to what has been performed in the rat, multiple researchers have experimented with inducing hyperoxaluria in mice by administering lithogenic agents,

such as ethylene glycol, hydroxyl-L-proline, and glyoxylate (Khan and Glenton, 2010; Okada et al., 2007). Despite successfully inducing hyperoxaluria, exogenous administration of these agents alone has demonstrated only a short duration of relatively few CaOx crystals in mice (Khan and Glenton, 2010; Okada et al., 2007). Okada et al. treated male C57BL/6 mice with either free drinking or daily intraperitoneal injections of EG, glycolate, and glyoxylate and observed crystal formation. Only the 80 mg/kg administration of glyoxalate produced detectable renal CaOx crystals after 3 days, with a peak on day 6 (Okada et al., 2007). However, a subsequent significant decline in stone presence ensued such that by day 15 hardly any stones remained. Meanwhile, Khan et al. also demonstrated that glyoxalate could produce crystalluria, however, there were significantly increased levels of lactate dehydrogenase (LDH), which has been shown to reflect renal toxicity (Khan and Glenton, 2010).

3.2.2 Genetic Modification

Given that dispensing solely lithogenic agents yielded minimal stone formation in mice, researchers have instead focused on utilizing genomic engineering using transgenic mice to help with inducing stone formation. Historically, in vitro studies demonstrated the importance of macromolecules, such as osteopontin (OPN) and Tamm–Horsfall protein (THP) as potential inhibitors of stone formation (Shiraga et al., 1992; Worcester, 1994). Employing the mouse to perform selective knockout (KO) of OPN and THP, investigators have established their critical role as inhibitors of stone formation.

OPN is an acid-rich phosphoglycoprotein that is expressed in inflammatory and wound-healing cascades, mineralized tissue like bone and teeth, as well as vascular and renal tubular cells (Giachelli and Steitz, 2000). It has also been shown to modulate ectopic calcification and bone mineralization, with OPN binding tightly to the calcium phosphate mineral, hydroxyapatite (Hunter et al., 1996). Wesson et al. (2003) were the first to demonstrate that an in vivo model of OPN KO mice could produce CaOx crystals. This study induced hyperoxaluria in both wild-type and KO mice by adding 1% ethylene glycol (EG) to drinking water for 4 weeks. Hyperoxaluric KO mice demonstrated renal tubular deposits of exclusively CaOx crystals. Wild-type hyperoxaluric mice also experienced a two- to four-fold upregulation of renal OPN expression, suggesting evidence of the renoprotective effects of this macromolecule (Wesson et al., 2003).

Meanwhile, THP, also known as uromodulin, is the most abundant urinary protein among all placental animals (Serafini-Cessi et al., 2003). Similar to OPN, THP is expressed by renal epithelial cells; however, unlike OPN, THP is kidney-specific as it is expressed only in the thick ascending loop of Henle (Kumar and Muchmore, 1990). Mo et al. (2004) compared wild-type versus THP KO

mice receiving 4 weeks of drinking water containing both 1% EG and 4 IU/mL vitamin D3. Results showed that 76% of THP KO mice produced calcium crystals while none were observed in wild-type mice.

Comparing these studies in which either THP or OPN was knocked out (Mo et al., 2004; Wesson et al., 2003), once these mice were given a hyperoxaluric load there was a compensatory increased expression of the remaining macromolecule. Yet this response was not enough to prevent crystallization, suggesting that the potential renoprotective effects of each might be based on a synergistic relationship. A subsequent study demonstrated this nicely, as a higher percentage (~39%) of double-null mice spontaneously developed renal papillary calcium deposits compared to 14% of THP–null and 10% OPN–null mice (Mo et al., 2007).

3.2.3 Metabolic Syndrome

A recent investigation looked at mice with *Leptin* gene deficiencies and metabolic syndrome (Ob/Ob) compared to wild-type (lean) mice, and how a high-fat diet in combination with hyperoxaluria induction impacted crystal production (Taguchi et al., 2015). The lithogenic agent was 1% EG in drinking water and diets consisted of either standard fat (10%) or high fat (62%). Results demonstrated those Ob/Ob mice on both EG and a high-fat diet demonstrated not only hypercalciuria and hyperoxaluria, but diffuse CaOx renal crystal deposits in the intratubular spaces of the renal cortex-medulla (Taguchi et al., 2015). This study also found a higher number of macrophages associated with these Ob/Ob mice, reinforcing findings of previous studies that found renal macrophages associated with crystal formation in the mouse (Okada et al., 2009). The true nature of this relationship between macrophages and crystal formation remains an area of future study.

3.3 Transporter Knockout Model

In addition to exogenous induction of hyperoxaluria, researchers have also performed solely transporter knockout in the mouse to induce hyperoxaluria, hypercalciuria, hyperuricosuria, and cystinuria.

3.3.1 Oxalate Transporter

Sulfate anion transporter-1 (Sat1) also known as Slc26a1, and Slc26a6 are both anion exchangers expressed on the apical membrane in renal epithelial cells that help mediate oxalate exchange (Dawson et al., 2010; Jiang et al., 2006). Both Sat1-null and Slc26a6-null mice have demonstrated abnormal oxalate homeostasis. Compared to wild-type mice, knockout mice demonstrated 2–3.5 times and 1.5–2 times higher oxalate concentrations in urine and plasma, respectively (Dawson et al., 2010; Jiang et al., 2006). Comparing Slc26a1and Slc26a6 knockout mice, 26 and 88%,

respectively had visibly detectable bladder stones, as well as CaOx crystal deposits in renal tubules and collecting ducts (Dawson et al., 2010; Jiang et al., 2006).

3.3.2 Na⁺-Phosphate Transporter

The sodium-hydrogen exchanger regulator factor-1 (NHERF-1) binds renal tubular transporters including the Na⁺-phosphate cotransporter 2a (Npt2a). NHERF-1 knockout mice have shown increased urinary calcium, phosphate, and uric acid excretion, resulting in tubulo-interstitial crystal deposits in the kidney (Weinman et al., 2006). Similar to NHEFR-1 mice, Npt2a knockout mice demonstrated hypercalciuria and renal crystal deposits in the kidney (Khan and Glenton, 2010). Both NHERF-1 and Npt2a knockout mice had calcium phosphate crystals in their kidney.

3.3.3 Cystine Transporter

A knockout transporter model has also been demonstrated for cystinuria, an autosomal-recessive disease of proximal tubular reabsorption of cystine and dibasic amino acids that results in cystine stones. Currently, there are two cystinuria phenotypes that are described, based on the heterozygosity of cystine and dibasic amino aciduria. Type I refers to the first cystinuria gene, *SLC3A1*, that is located on chromosome 2 (2p21) and encodes the rBAT transporter in both intestinal and renal epithelial cells (Biyani and Cartledge, 2006). Nontype I involves a second cystinuria gene, *SLC7A9*, that has been found on chromosome 19 (19q13) and encodes the light chain $b^{0,+}AT$ protein (Dello Strologo et al., 2002). Investigators have demonstrated that *Slc7a9* knockout mice experienced cystinuria, cystine crystalluria, and cystine urolithiasis (Fig. 17.2) (Feliubadaló et al., 2003).

Previous work by Peters et al. (2003) established a reliable *Slc3a1* murine knockout model that produces cystine stones. Recently a study by Zee et al. (2017) demonstrated the remarkable finding that oral administration of alpha-lipoic acid (ALA) significantly reduced or eliminated cystine stone development in $Slc3a1^{-/-}$ mice. ALA also dramatically reduced stone growth in those KO mice with existing stone burden. Interestingly ALA did not change the urinary pH or reduce quantitative urinary cystine levels. Furthermore, ALA tested in-vitro did not change crystallization, suggesting that it is likely one of its metabolites that alters crystal structure and thereby interferes with cystine stone pathogenesis. Future work on this exciting new pharmacologic intervention is currently underway.

3.4 Histology/Pathology/Stone Composition

CaOx crystals in hyperoxaluric mice have been shown with the use of von Kossa, Yasue, and Pizzolato stains (Mo et al., 2004, 2007; Taguchi et al., 2015; Wesson
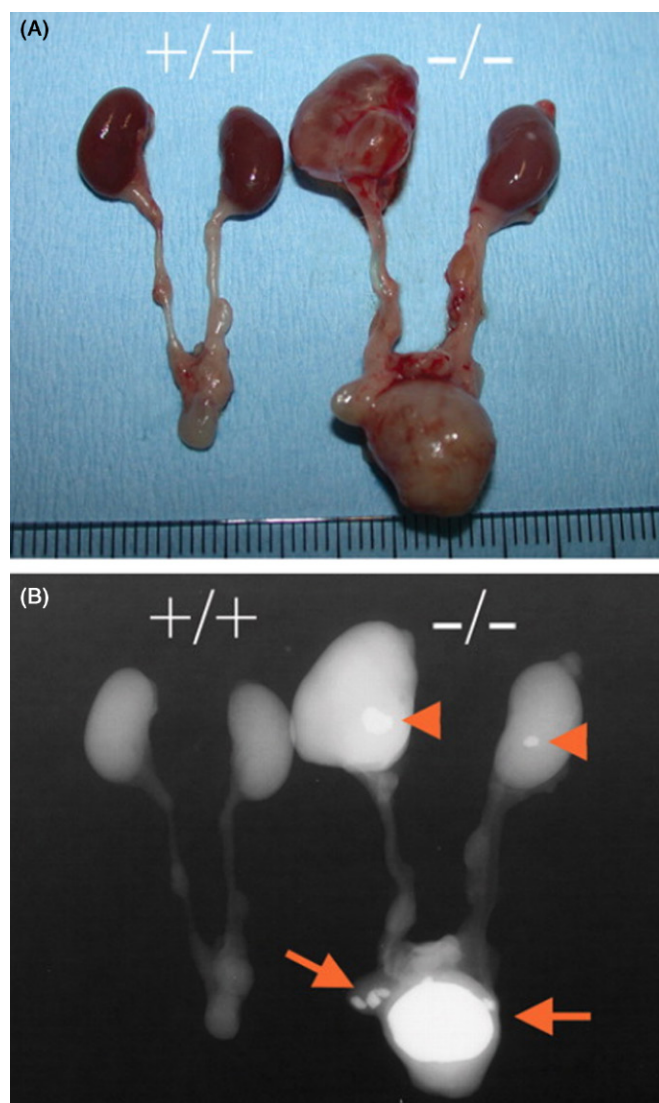
FIGURE 17.2 Cystine stones of urinary tract in *Slc7a9* knockout mice. (A) Comparison between urinary tract anatomy of a normal mouse (Slc7a9⁺/⁺) versus nontype I knockout (Slc7a9⁻/⁻) mouse. (B) Radiograph view of the same mice urinary systems—wild type (+/+, left) and homozygous (−/−, right). *Arrowheads*, kidney stones; *arrows*, bladder stones. *Source: Reproduced with permission from Feliubadaló, L., Arbonés, M.L., Mañas, S., et al., 2003. Slc7a9-deficient mice develop cystinuria non-I and cystine urolithiasis. Hum. Mol. Genet. 12, 2097–2108.*

et al., 2003). In those mice who received intraperitoneal glyoxalate injections, X-ray diffraction analysis demonstrated that crystals were composed of calcium, phosphate, and oxalate (Okada et al., 2007). This same analysis was performed in OPN null mice, finding that the predominant crystal type was composed exclusively of calcium oxalate monohydrate (Wesson et al., 2003).

OPN and NHERF-1 knockout mice mainly developed interstitial crystals in the papilla whereas Slc26a6, Npt2a knockout mice, and normal mice with intraperitoneal glyoxylate injection showed impacted crystals in dilated papillary tubular lumens (Jiang et al., 2006; Khan and

TABLE 17.2 Summary of Mice Models of Nephrocalcinosis

Author (references)	Mouse	Exogenous method	Urinary features	Nephrocalcinosis
Feliubadaló et al. (2003)	Slc7a9 KO	Normal diet	Cystinuria, cystine crystalluria	Cystine stone in pelvis and bladder
Wesson et al. (2003)	OPN KO	Four weeks administration of 1% EG in drinking water	Hyperoxaluria, COD/COM crystalluria	Intratubular COM crystals
Mo et al. (2004, 2007)	THP KO	Normal diet or 4 weeks administration of 1% EG and 4 IU/mL vit. D3 in drinking water	Not described	Intratubular and interstitial CaOx crystals
Weinman et al. (2006)	NHERF-1 KO	Normal diet	Hypercalciuria, hyperphosphosuria, hyperuricosuria	Interstitial CaOx crystals
Jiang et al. (2006)	Slc26a6	Normal diet	Hyperoxaluria, CaO_x crystalluria	Intratubular COD/COM crystals
Okada et al. (2007)	C57BL/6	Daily 80 mg/kg GOX intraperitoneal injection	Hyperoxaluria, high CaO_x index	Intratubular COM crystals
Khan and Glenton (2010)	Npt2a KO	Four weeks administration of 1.5% GOX or 5% HLP in chow	COD/COM crystalluria	Intratubular/interstitial CaOx crystals and interstitial CaP crystals
Dawson et al. (2010)	Sat1 (Slc26a1) KO	Normal diet	Hyperoxaluria	Intratubular CaOx crystals and bladder stone
Taguchi et al. (2015)	MetS model	Two weeks administration of 1% EG in drinking water and high-fat diet	Hyperoxaluria, hypercalciuria	Intratubular CaOx crystals

CaOx, Calcium Oxalate; CaP, Calcium phosphate; COD, calcium oxalate dihydrate; COM, calcium oxalate monohydrate; EG, ethylene glycol; GOX, glyoxalate; HLP, hydroxy-L-proline; KO, knockout; MetS, metabolic syndrome; THP, Tamm–Horsfall protein.

Glenton, 2010; Okada et al., 2007; Weinman et al., 2006; Wesson et al., 2003; Wu, 2015).

In comparison to the hyperoxaluria-induced mice model, CaO_x stones of Slc26a6 knockout mice and cystine stones of Slc7a9 knockout mice were actual stones found in the renal pelvis and bladder (Feliubadaló et al., 2003; Jiang et al., 2006). These urinary stones were clinically consistent with human kidney stones, not just nephrocalcinosis as in other mice models (Table 17.2).

Inflammation and renal tubular cell damage were shown in intraperitoneal glyoxylate injected mice, metabolic syndrome model mice, and Slc7a9 knockout cystinuria mice kidneys. As described earlier, intraperitoneal glyoxylate injected mice develop intratubular CaOx crystals in 6 days; however, this acute crystal formation is accompanied with severe tubular cell damage caused by oxidative stress and immune cell infiltration (Okada et al., 2009). These inflammatory changes were facilitated by immune and/or metabolic disorders, such as obesity, hyperlipidemia, and antiinflammation disorders (Taguchi et al., 2014, 2015).

3.5 Limitations

Based on its similar anatomical, physiological, and genomic features, mice theoretically would be an ideal model for nephrolithiasis. Given its history with genomic engineering, the mouse has a clear advantage over other animal models. Yet despite several transgenic tools, its accuracy and consistency in relation to human kidney stone disease remain controversial among researchers.

An important point is that the pathogenesis of crystal formation in mice is different compared to humans. Human kidney stones are believed to originate from interstitial calcifications—Randall's plaque (Randall, 1940; Stoller and Meng, 2007). While some mice models have similar interstitial calcifications; these are gradually ingested and removed by inflammatory cells, eventually appearing as intratubular crystals. These crystals were not consistent with Randall's plaque (Khan and Canales, 2011). Furthermore, the presence of severe inflammation and cellular damage in many mice models represents significant renal injury, which is significantly different from most human kidneys with urolithiasis.

Similar to other animal models that focus on hyperoxaluria, the majority of mice models rely on induction of hyperoxaluria. Except for primary hyperoxaluria patients, relatively few human kidney stone patients have hyperoxaluria. In addition, the prevalence of cystinuria is rare (less than 1% of urolithiasis patients), therefore these mice models are not representative of the majority of humans who suffer from urinary stone disease.

4 FLY MODEL

Drosophila melanogaster has been studied as a research model across multiple organ systems for over a century (Jennings, 2011). It was through his work with *Drosophila*

in the 1920s that Dr. Herman Muller won the Nobel prize for discovering the impact of radiation on gene mutation (Muller, 1928). Since then, investigators have looked to the fruit fly as a model given that it has numerous advantages over other vertebrate animal models.

As an invertebrate, the fly requires no formal animal experimentation review to initiate a research protocol. Compared to other animal models, the lack of ethical and safety concerns makes it much easier to obtain and implement a study protocol. Meanwhile, with a short life cycle under standard laboratory conditions (typically <60 days), researchers can not only observe a disease process over the animal's entire lifespan, but also screen the effectiveness of medical drugs much more rapidly. Additionally, female flies are capable of producing hundreds of offspring in a matter of days, thereby studies can have large numbers of specimens prepared in a short amount of time. As their use is associated with relatively low-cost dietary and lab spatial requirements, it is dramatically less expensive to start and maintain a fly lab (Stocker and Gallant, 2008).

From a genetic standpoint, *Drosophila* have a fewer number of chromosome pairs—only 4—compared to 23 in humans (Chien et al., 2002). The fly genome has been completely sequenced and there is a well-established, free fly database—FlyBase (http://flybase.org)—dedicated to cataloging homology between human and fly genes (Tweedie et al., 2009). Approximately 75% of human disease genes have correlates in *D. melanogaster*, with nearly 80% of human renal transporters found in the fly Malpighian tubule (Reiter et al., 2001). With such an abundance of *Drosophila* resources available, targeted

animal gene manipulation has become a much more feasible endeavor. As a result, researchers have started applying this powerful translational model in the study of urinary stone disease.

4.1 Anatomic/Physiologic Comparison Between Fly and Humans

Initially one would not necessarily think of *Drosophila* as a model for stone disease given the inherent differences between human and fly anatomy. As an invertebrate, flies lack a bony skeleton. They also go through four distinct phases of life—starting first as an egg, then larva, pupa, and finally an adult fly. Instead of a mammalian vascular system, flies have a fluid-filled hemocoel cavity. This open circulatory system uses hemolymph in a similar fashion to how human blood vessels carry blood. This cavity contains two sets of free-floating Malpighian renal tubules, as well as an aglomerular renal system (Dow and Romero, 2010). The Malpighian tubule is homologous to human renal tubules and function to filter the fly hemolymph in a manner similar to how human tubules filter blood. Recent work has elucidated that these remarkable similarities between human and fly systems suggest an evolutionary relationship (Fig. 17.3) (Weavers et al., 2009).

Drosophila have two anatomically separate organs that comprise their renal system—nephrocytes and Malpighian tubules. Nephrocytes filter the hemolymph and remove waste in a manner similar to podocytes in the human glomerulus (Weavers et al., 2009). Meanwhile, the anterior and posterior pairs of Malpighian tubules represent the functional equivalent of a human nephron.
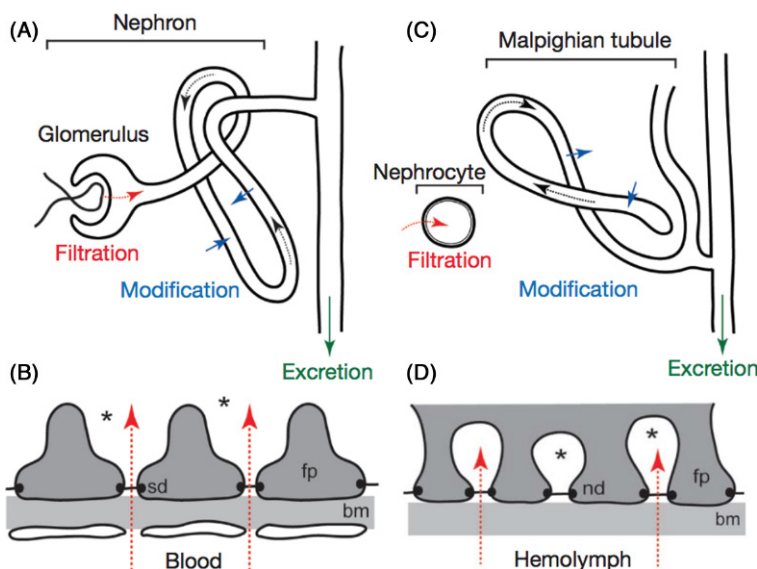
FIGURE 17.3 **Comparison of glomerular and insect renal systems.** The human glomerular (A) and podocyte slit diaphragm (B) are similar to that of insect nephrocyte renal systems (C) and their basal labyrinth (D). *bm*, Basement membrane; *fp*, foot process; *nd*, nephrocyte diaphragm. *Source: Reprinted with permission from Weavers, H., Prieto-Sanchez, S., Grawe, F., et al., 2009. The insect nephrocyte is a podocyte-like cell with a filtration slit diaphragm. Nature 457, 322–326.*
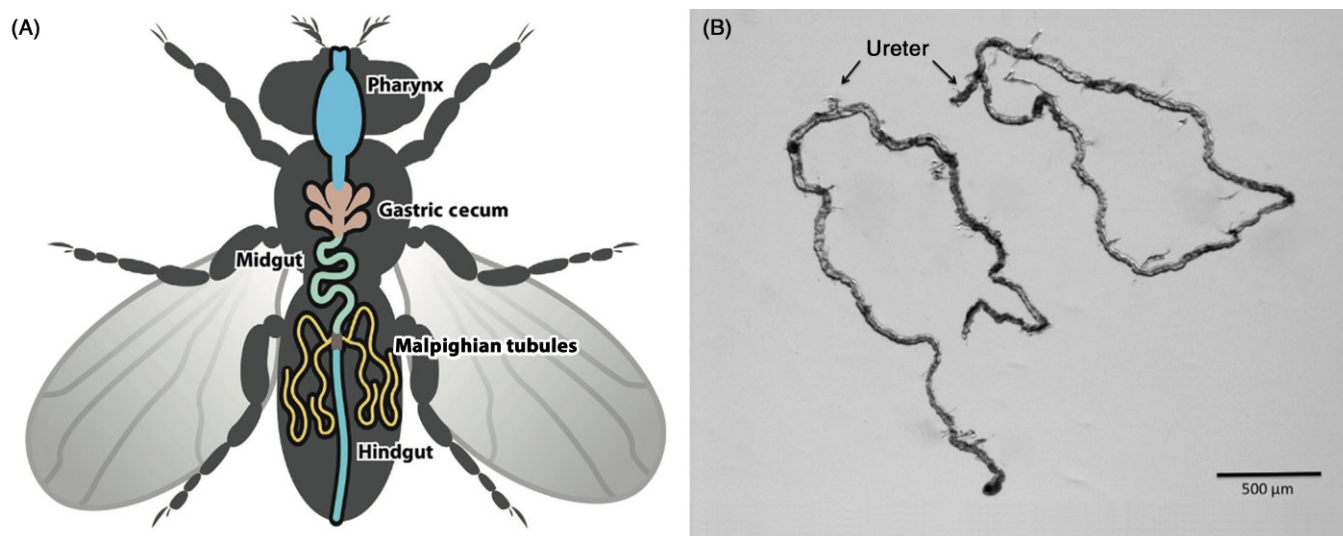
FIGURE 17.4 **Anatomy of *D. melanogaster*.** (A) Schematic of *D. melanogaster* excretory tract: two pairs of Malpighian tubules, one anterior and one posterior, each combine into a short common ureter that then joins the hindgut. (B) Example of anterior and posterior pairs of Malpighian tubules dissected free from adult *D. melanogaster*. *Arrows* represent common ureter. *Source: Reprinted with permission from Miller J., Chi T., Kapahi P., et al., 2013.* Drosophila melanogaster *as an emerging translational model of human nephrolithiasis*, J. Urol. *190, 1648–1656.*

The anterior Malpighian tubules consist of four distinct domains: the initial (distal), transitional, main and lower (proximal) segments (Rheault and O'Donnell, 2004; Sözen et al., 1997). The posterior Malpighian tubules do not possess the initial segment. The main domain segment is comprised of two main cell types—principal cells and stellate cells—both of which help control the active transport and excretion of solutes including calcium, uric acid, and phosphorous (Weavers et al., 2009). The anterior and posterior tubule pairs combine to form a common ureter (Fig. 17.4), that then joins the gastrointestinal tract at the junction of the midgut and hindgut.

Previous work has shown that *Drosophila* physiology involves the production of two types of luminal concretions (Wessing et al., 1992). Type I is composed of mainly calcium, magnesium, and a matrix of proteoglycans in the anterior Malpighian tubules. Type II is composed predominantly of potassium and phosphorous and is located in both the anterior and posterior Malpighian tubules. While these concretions appear to be a normal means by which the fly eliminates urine waste, studies have since shown that these concretions can be likened to human kidney stones (Chen et al., 2011; Chi et al., 2015; Dube et al., 2000; Hirata et al., 2012a). As a result, these concretions in *Drosophila* Malpighian tubules have been used as a functional in vivo model of kidney stones.

4.2 Diet-Induced Model

4.2.1 Hyperoxaluria

Similar to what has been done in rodent models, induction of hyperoxaluria in the fly can be accomplished with the administration of ethylene glycol or oxalate. Chen et al. (2011) found that supplementing adult *Drosophila*

with ethylene glycol produced calcium oxalate (CaOx) concretions in as little as 6 h. Feeding *Drosophila* larvae with a diet of sodium oxalate dissolved in standard growth media resulted in CaOx microliths within 2 days (Hirata et al., 2012a). As seen in Fig. 17.5, polarized light applied to dissected Malpighian tubules demonstrates the characteristic birefringence of CaOx crystals. These CaOx crystals have also been clearly visualized on microcomputed tomography (CT) (Fig. 17.6).

4.3 Genetic Models of Stone Disease

With the previously established GAL4 driver/UAS (upstream activation sequence) transgenic system (Brand and Perrimon, 1993), researchers are equipped with the ability to perform targeted gene expression in *Drosophila* and specifically knockdown those genes believed to play a role in stone formation. With the resources available for *Drosophila*, investigators can simply order their desired driver to express or silence specific
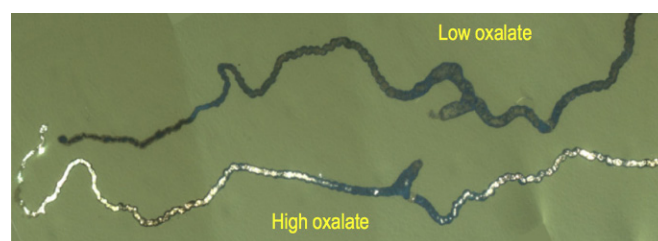
FIGURE 17.5 **Comparison of Malpighian tubules of *D. melanogaster* fed high oxalate versus control low oxalate diet.** Polarized light demonstrates birefringence of calcium oxalate concretions in high oxalate tubules. *Source: Reprinted with permission from Hirata, T., Cabrero, P., Berkholz, D.S., et al., 2012. In vivo* Drosophila *genetic model for calcium oxalate nephrolithiasis. Am. J. Physiol. Renal Physiol. 303, F1555–F1562.*
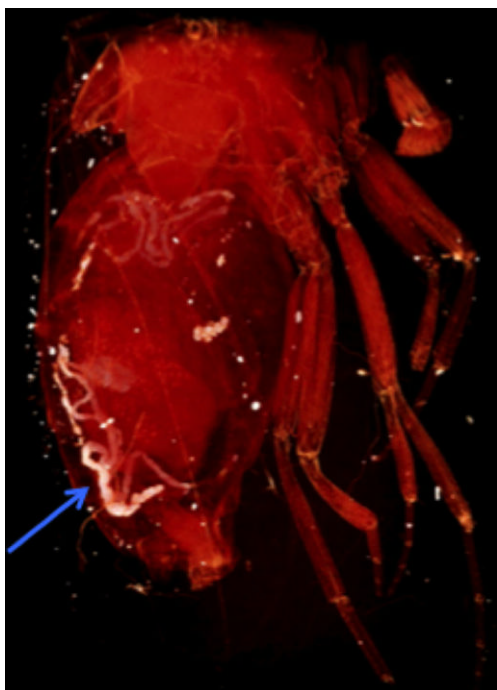
FIGURE 17.6 **3D computed tomography reconstruction of *D. melanogaster*.** *Arrow* represents calcium oxalate concretions present in *Drosophila* Malpighian tubules. Note the *white* biominerals/stones *(blue arrow)* developing in the Malpighian tubules in this invertebrate animal model.

gene end-products. This allows for studies to examine the effects of individual genes very quickly. What would take a minimum of 3–6 months to accomplish for genetic manipulation in the mouse model can take 2–3 weeks in the fly model (Dow and Romero, 2010).

4.3.1 Hyperoxaluria

As discussed previously in the mouse section, the anion exchanger SlC26A6 has been shown to be important in oxalate transport in both mice and humans (Jiang et al., 2006; Monico et al., 2008). Experiments have since shown that the *D. melanogaster* genome contains 9 homologs of the 11 human Slc26 transporters (Hirata et al., 2012b). A SLc26a5 homolog, *dPrestin*, can be considered the *Drosophila* equivalent of SLC26A6 (Hirata et al., 2009).

After administering a dietary load of sodium oxalate, researchers have demonstrated the ability to visualize real-time nucleation and growth of oxalate crystals within the relatively transparent dissected Malpighian tubules (Hirata et al., 2010). Hirata et al. (2012a) subsequently performed knockdown of *dPrestin*, and decreased mRNA levels by 50%–70%. This knockdown took place mainly in the principal cells of the initial and main segments of the Anterior Malpighian tubules, producing markedly reduced CaOx concretions (Hirata et al., 2012a). This study illustrates how the genetic capabilities of the *Drosophila* model can further our understanding of kidney stone formation.

4.3.2 Xanthinuria

Another genetically based kidney stone model mimics one of the human-inherited errors of metabolism, xanthinuria. Xanthinuria types I and II are secondary to an autosomal recessive defect in purine metabolism, resulting in increased total body levels and subsequent excretion of xanthine (Ichida et al., 2001; Levartovsky et al., 2000). Xanthine dehydrogenase (XDH) is the enzyme that normally converts hypoxanthine to xanthine as well as xanthine to uric acid. XDH is deficient in xanthinuria type Iand the responsible gene for type I has been localized to chromosome 2p22-23 (Ichida et al., 1997).

Utilizing a GAL4/UAS, Chi et al. performed *Drosophila* gene silencing of *Xdh*, the fly equivalent gene producing xanthine dehydrogenase. This resulted in the formation of large, obstructing stones in the Malphighian tubules (Fig. 17.7) (Chi et al., 2015). This study also found that pharmacologic inhibition of XDH with allopurinol demonstrated similar tubule concretions. Moreover, when these *Xdh* silenced flies were fed a high yeast diet, their survival plummeted down to a median lifespan of 3 days, compared to controls which averaged 60 days.

4.4 Stone Composition

4.4.1 Calcium oxalate

Similar to what has been shown in the rat model, the administration of lithogenic agents such as ethylene glycol and hydroxyl-L-apatite also results in reproducible calcium oxalate crystals within the *D. melanogaster* Malpighian tubules (Chen et al., 2011; Hirata et al., 2012a). Studies have utilized both scanning electron microscopy (SEM) and energy-dispersive X-ray spectroscopy (EDS) to identify crystal deposition and composition, respectively.
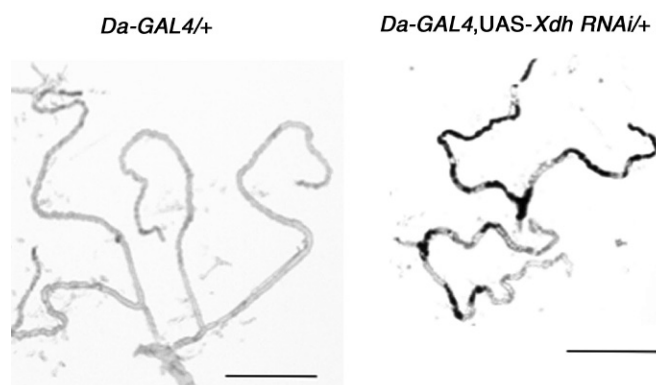
FIGURE 17.7 **Comparison of Malpighian tubules in *D. melanogaster*.** (A) Control flies. (B) *Xdh* knockdown flies. *Source: Courtesy of Chi, T., Kim, M.S., Lang, S., et al., 2015. A* Drosophila *model identifies a critical role for zinc in mineralization for kidney stone disease. PLoS One 10 (5), e0124150.*

4.4.2 Hydroxyapatite

Fourier Transform Infrared Spectroscopy (FTIR), the conventional method to determine stone composition, demonstrated that the *Xdh* knockdown fly stones indeed contained xanthine (Chi et al., 2015). However, using targeted metabolomics, these stones were also found to contain hypoxanthine. Micro X-ray absorption near edge spectroscopy (µXANES), a technique that allows for interrogation of the chemical environment within a sample point of interest with submicron resolution, confirmed the presence of hydroxyapatite. Given that noncalcium based human stone formation may still be generated from a hydroxyapatite nidus (Evan, 2010), this finding highlights potential similarities between *Drosophila* fly stone concretions and human stones.

4.4.3 Zinc

The fly model has also enabled investigators to unearth the role of other minerals in the formation of stones. While the majority of stones are still comprised of calcium oxalate, other minerals have been shown to be part of the stone composition. Zinc, an essential mineral, has been identified to play a role in the formation of both human stones and *Drosophila* Malpighian tubule concretions (Chi et al., 2015). An analysis of the mineral components of these fly concretions, human Randall's plaques, and human xanthine stones demonstrated that calcium (Ca), magnesium (Mg), and zinc (Zn) were the major metal components within each specimen (Fig. 17.8). This was determined by using inductively coupled plasma optical emission spectroscopy (ICP-OES), which showed that the relative amount of each of these metals was consistent across stone source (Fig. 17.8).

This study also found that the concentration of zinc was dependent on the amount of yeast present in a standard *Drosophila* diet (Fig. 17.9) (Chi et al., 2015). A high yeast diet—the equivalent of a high protein diet in humans—caused a high rate of stone formation, while a low yeast diet resulted in limited stone formation. Supplementing flies on a low yeast diet with zinc increased the amount of concretions present, to a level close to those flies on the high yeast diet. The importance of zinc was further shown when it was inhibited with a known zinc chelator, TPEN, resulting in a decreased amount of concretions (Chi et al., 2015). These findings reinforce the importance of an animal model for stone disease, as without this discovery one might not have recognized the presence and importance of heavy metals in urinary stones.

These two previously mentioned examples represent the first genetically based invertebrate models of kidney stones. Given the number of genetic homologs related to
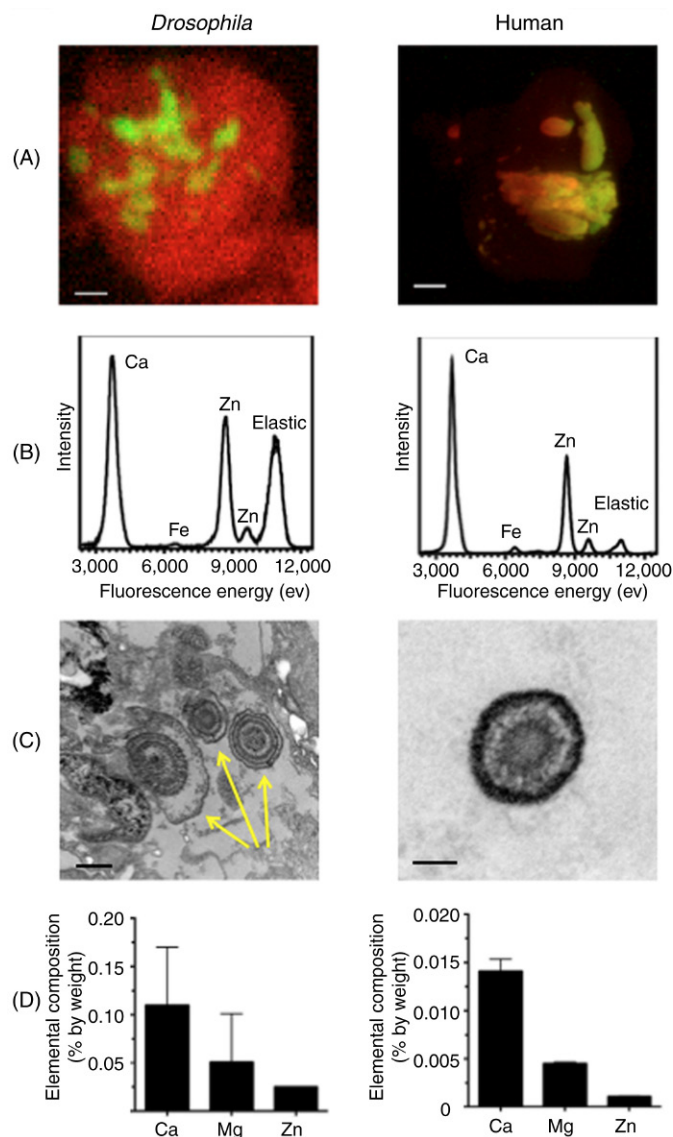
FIGURE 17.8 **Comparison of zinc in *D. Melanogaster* concretions, human Randall plaques, and human kidney stones.** (A) Micro-X-ray fluorescence *(µXRF)* maps of knockdown *Da-GAL4, UAS-Xdh RNAi/+* concretions (left panel, scale bar: 10 µm) versus human Randall's plaques (right panel, scale bar: 100 µm). Zinc shown in *red* and calcium in *green*. (B) µXRF elemental analysis demonstrates similar elemental composition for both *Da-GAL4, UAS-Xdh RNAi/+* concretions (left panel) and human Randall's plaques (right panel), including the presence of calcium *(Ca)*, iron *(Fe)*, and zinc *(Zn)*. (C) Transmission electron microscopy of concretions in the lumen of the Malpighian tubule shows the presence of ring-like structures, as indicated by the *yellow arrows* (left panel, scale bar: 500 µm). Ring structures with homologous appearance are seen in Randall's plaques taken from a human renal papilla biopsy material (right panel, scale bar: 100 µm) when imaged in a similar fashion. (D) ICP-OES analysis of fly concretion samples (left) versus human xanthine stone samples (right) shows the presence of calcium (Ca), magnesium *(Mg)*, and zinc (Zn). Data shown are the mean ± SEM. *Source: Courtesy of Chi, T., Kim, M.S., Lang, S., et al., 2015. A* Drosophila *model identifies a critical role for zinc in mineralization for kidney stone disease. PLoS One 10 (5), e0124150.*
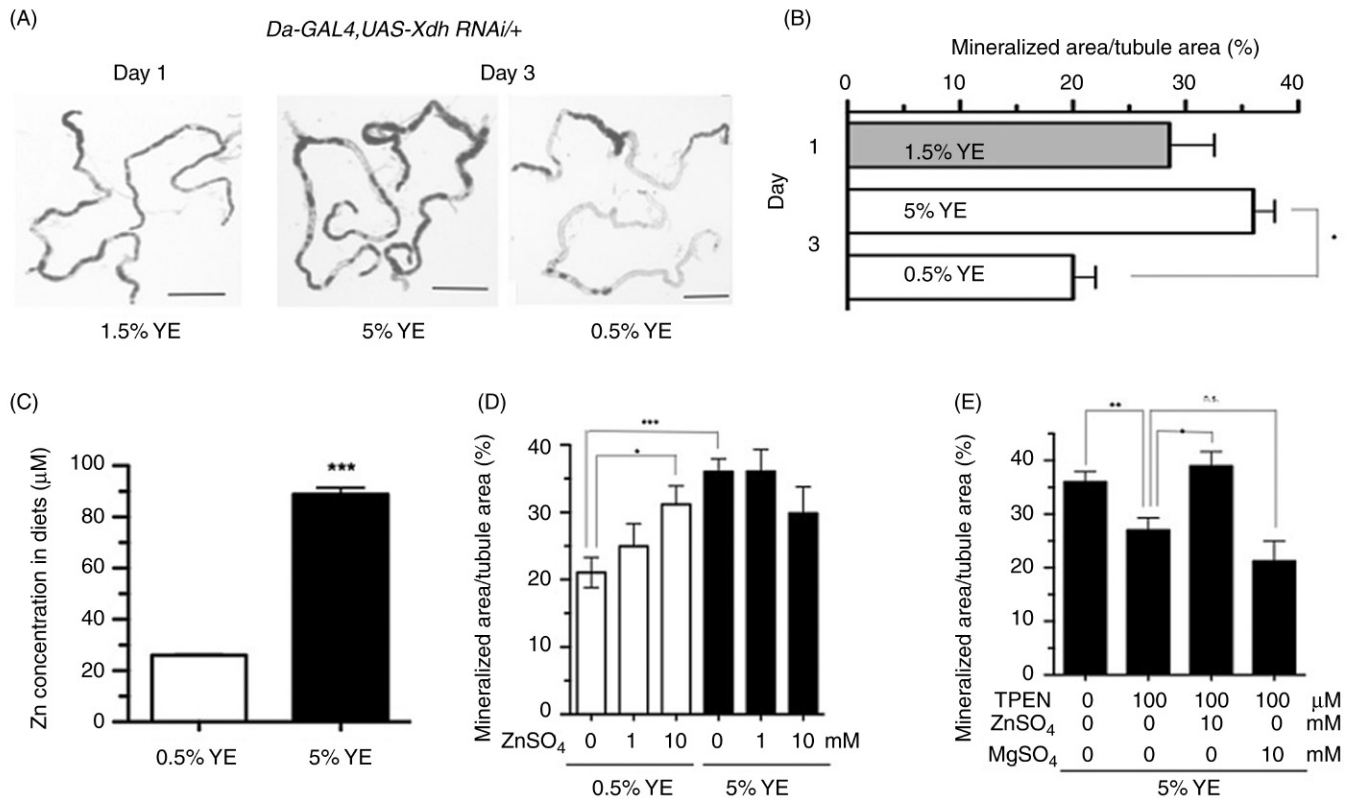
FIGURE 17.9 (A) Tubule images of Da-GAL4, UAS-Xdh-RNAi/+ flies: Day 1, 1.5% YE and after 2 days on high yeast (Day 3, 5% YE) or low yeast (Day 3, 0.5% YE) diets. (B) The mean percentage of the tubule lumen occupied by mineralized material (*$P < 0.001$, Student's t-test, $n = 14$–48). Scale bars: 500 µm. (C) The amount of Zinc (Zn) in the components of a standard *Drosophila* diet (corn meal, yeast, sugar, and agar) was measured with ICP-OES for both 0.5% YE and 5% YE diets. 0.5% YE is comprised of corn meal 8.5 g, yeast 0.5 g, sugar 5 g, and agar 0.46 g in 100 mL deionized distilled water. 5% YE is composed of the same components as 0.5% YE with the exception of 5 g yeast added instead of 0.5 g yeast (***$P < 0.001$, student t-test, $n = 3$). (D) Da-GAL4, UAS-Xdh RNAi/+ flies fed on 0.5% YE and 5% YE diets were supplemented with different doses of Zn. This led to a dose-dependent increase in accumulation of concretions on 0.5% YE feeding (*$P < 0.05$, ***$P < 0.001$, one way ANOVA with Bonferroni posthoc test, $n = 10$–48). Zn supplementation had no effect on altering concretion formation in 5% YE-fed animals, which may reflect a saturation of the calcification process under these conditions. (E) Supplementation of 5% YE diet with the zinc chelator TPEN reduced concretion formation. This effect could be reversed with the addition of 10 mM Zn but not 10 mM Mg (*$P < 0.05$, **$P < 0.01$, one way ANOVA with Bonferroni posthoc test, $n = 10$–43). Data shown are the mean ± SEM. *Source: Courtesy of Chi, T., Kim, M.S., Lang, S., et al., 2015. A* Drosophila *model identifies a critical role for zinc in mineralization for kidney stone disease. PLoS One 10 (5), e0124150.*

other stone types in flies, more model development may be expected in the future.

4.5 Limitations

While *Drosophila* represents a reliable, fast, cost-effective model system, there are some limitations to its use and applicability. First and foremost the fly is an invertebrate. Lacking a bony skeleton, it has no bone reservoir and its calcium metabolism may be fundamentally different compared to vertebrates. Next, the fly is not an ambulatory model and relies on a different feeding cycle compared to humans.

Another limitation is that it can be difficult to measure how much food and medication that *Drosophila* ingest.

Moreover, while direct injection of medication into the fly is possible, this requires specialized equipment that can be cumbersome.

Classically cited anatomic differences were addressed previously and instead should be considered more as an opportunity to study single tissue modeling of diseases that affect analogous vertebrate structures (Miller et al., 2013). Another cited limitation is that since the fly's Malpighian tubules drain into the hindgut, there is a combination of waste products in a single elimination chamber and the GI tract can contribute to the elimination of electrolyte and water waste (Assimos, 2012). Current dissection techniques allow for the Malpighian tubules and ureters to be isolated prior to their junction with the GI tract. These dissected tubules can then be

mounted and submerged in a desired medium, where they will continue to secrete fluid for several hours (Dow and Romero, 2010). Subsequent collection of this fluid can then be examined in a fashion similar to a 24-h urine analysis.

5 PORCINE MODEL

The oretically the porcine model would be an excellent model from both an anatomic structure and physiologic standpoint, as pig kidneys resemble those in humans. This has led multiple investigators to test new endourologic surgical modalities by placing human kidney stones within porcine kidneys. Moreover, in general there is not as much emotional attachment to the pig as compared to other animals that are used as domestic pets. The studies conducted thus far in the porcine model demonstrate a promising, reproducible model for inducing hyperoxaluria and calcium oxalate nephrolithiasis.

5.1 Anatomic/Physiologic Comparison Between Pigs and Humans

Comparing porcine and human kidneys, anatomic similarities include an undivided renal cortex, multiple medullary pyramids that each form a separate papilla or occasionally a complex papilla, especially in the upper pole (Thomsen et al., 1983). Pigs in general have 8–12 papillae compared to humans who usually have 4–18 (Cullen-McEwen et al., 2015). Moreover, as Kirkman showed, porcine renal physiology parallels that of humans with respect to maximal urine concentration (porcine 1080 vs. human 1160 mOsm/L), glomerular filtration rate (porcine 130 vs. human 126–175 mL/min

per 70 kg), and total renal blood flow (porcine 4.0 vs. human 3.0–4.4 mL/min·g) (Sachs, 1994). Meanwhile, other studies have noticed anatomic differences, centering around the pig kidney containing very little perinephric fat, being hypermobile, having a more spacious renal pelvis, and also tortuous, large diameter ureters (Paterson et al., 2002).

5.2 Induction of Hyperoxaluria

To date, previous porcine models have focused on replicating a hyperoxaluric state by administering hydroxyproline (HP) (Kaplon et al., 2010; Knight and Holmes, 2005; Mandel et al., 2004; Patel et al., 2012). As stated previously, hydroxyproline is derived from the amino acid proline and is a component of collagen that gets metabolized to both pyruvate and glyoxalate, primarily in the renal proximal tubule and hepatocyte mitochondria (Knight and Holmes, 2005) (Table 17.3).

As Mandel et al. (2004) showed in young pigs, delivering 10% weight per weight of *trans*-4-hydroxy-L-proline/food resulted in a maximum increased urinary oxalate concentration by day 6 in all HP-fed pigs. While the urinary oxalate levels in these young pigs did not decline until HP was removed from their diet, a noteworthy finding was that increasing the HP/food concentration up to 20% failed to result in an increased level of hyperoxaluria. This study demonstrated calcium oxalate monohydrate and dihydrate crystalline deposits in the papillary tips of the longitudinally sectioned kidneys.

Meanwhile, Kaplon et al. (2010) demonstrated that gravid sows in either a traditional or acidified diet experienced hyperoxaluria and hyperglycoluria when fed 10% HP. This study utilized 24-h urine collections via a 20-French Foley catheter attached to Tygon tubing that

TABLE 17.3   Porcine Models Related to Hyperoxaluria

Study references (year)	Porcine animal selected	Diet/intervention	Effects
Mandel et al. (2004)	Young male Yorkshire-Durox pigs	• Enriched diet: 10% HP days 1–5; 15% HP days 6–13; 20% HP days 14–21	• Hyperoxaluria • CaOx crystalluria • CaOx crystal deposition in collecting ducts nephrolithiasias at papillary tips
Kaplon et al. (2010)	Multiparous adult gestating sows	• Acidogenic diet versus control diet × 5 days • All fed diet with 10% HP for days 3–5	• Hyperoxaluria • Hyperglycoluria
Patel et al. (2012)	Gravid crossbred sows	• 5% HP diet • 10% HP diet • gelatin (12% HP + 20% glycine)	• 10% HP and gelatin diets induce hyperoxaluria • Gelatin more cost effective
Sivalingam et al. (2013)	Gravid and nongravid sows	• 5% HP diet	• Hyperoxaluria • CaOx crystals present in proximal tubule and collecting ducts • Lack of Randall plaques

FIGURE 17.10 **Photograph of porcine model arrangement.** Gravid sows with indwelling 20-French Foley catheters attached to Tygon tubing that then drains into a 20 L collection pail. *Source: Reprinted with permission from Patel, S.R., Penniston, K.L., Iwicki, L., et al., 2012. Dietary induction of long-term hyperoxaluria in the porcine model. J. Endourol. 26, 433–438.*

drained into the cap of a 20 L collection pail (Fig. 17.10). Results showed that the level of hyperoxaluria and hyperglycoluria peaked on the first day of feeding and subsequently declined despite continued HP administration. Likely this was the result of the pigs acquiring an aversion to the HP diets, as the study noted sows consuming less of their meals on days when HP was added.

Expanding on the model of the gravid sow, Patel et al. (2012) compared the effectiveness of different diet compositions of HP. The study provided pigs with a baseline 2 kg basal diet before subjecting to either 100 g L-HP (5% HP), 200 g L-HP (10% HP), or 1000 g of gelatin that consisted of high HP (12%) and glycine (20%) content. Results demonstrated that both HP and gelatin induced similar short-term (5 days) and long-term (21 days) hyperoxaluria effects (Patel et al., 2012). Interestingly, this study also highlighted some of the financial concerns associated with a HP-induced hyperoxaluria model, as they found that gelatin was significantly more cost effective than HP; $7.32 per kg for 150 Bloom gelatin versus $185.00 per kg for hydroxy-L-proline (Patel et al., 2012).

In humans, hydroxyproline ingestion can occur via either animal protein containing collagen or gelatin containing foods. Similar to these experiments in the porcine model, a study investigated whether hydroxyproline has similar effects in humans. Comparing the ingestion of different gelatin loads to whey protein, researchers found that 5 and 10 g gelatin loads were associated with significant changes in plasma hydroxyproline, urinary oxalate and glycolate (Knight and Holmes, 2005). From these results, it was inferred that the metabolism of hydroxyproline provides approximately 20%–50% of urine glycolate excretion, with a subsequent 5%–20% of urinary oxalate derived from endogenous synthesis (Knight and Holmes, 2005).

5.3 Histology/Pathology/Stone Composition

Mandel et al. (2004) demonstrated calcium oxalate monohydrate and dihydrate crystalline deposits in the papillary tips of longitudinally sectioned kidneys in young male Yorkshire-Durox pigs. Meanwhile, Sivalingam et al. (2013) demonstrated the presence of crystals in proximal tubules and at the renal papillary tips, with concomitant crystals that appeared to be embedded within the interstitium. There was widening of the interstitial spaces, presence of giant multinucleated cells surrounding these crystals, and noticeable inflammation with surrounding fibrotic changes (Fig. 17.11).

5.4 Treatment Simulation in Porcine Model

Given its similarities to human kidneys, many researchers have chosen porcine kidneys to test and evaluate new surgical techniques for the treatment of nephrolithiasis. This has centered on placing artificial or human kidney stones within swine kidneys, via ureteroscopic and percutaneous approaches, and then studying the effectiveness of these treatments in both in vivo and ex vivo models. To establish the effectiveness of different settings for shock wave lithotripsy (SWL), studies like Paterson et al. (2002) have used upper pole percutaneous access to place gypsum model stones into mainly the lower pole of female pigs, followed by treatment with extracorporeal SWL. This demonstrated superior breakup of stones treated with a slower rate (30 shocks/min) compared to a faster rate (120 shocks/min), which has helped guide practice for performing SWL at a slower, more effective rate in humans. This porcine model has been replicated to investigate the differences in focal width among shock wave lithotripter machines and their corresponding damaging effects on porcine kidneys (Connors et al., 2009, 2012).

Meanwhile, others have obtained porcine urinary tracts from slaughterhouses and used these as a model for teaching ureteroscopy (Hu et al., 2015; Strohmaier and Giese, 2001). Using mini-pigs given that they repre-
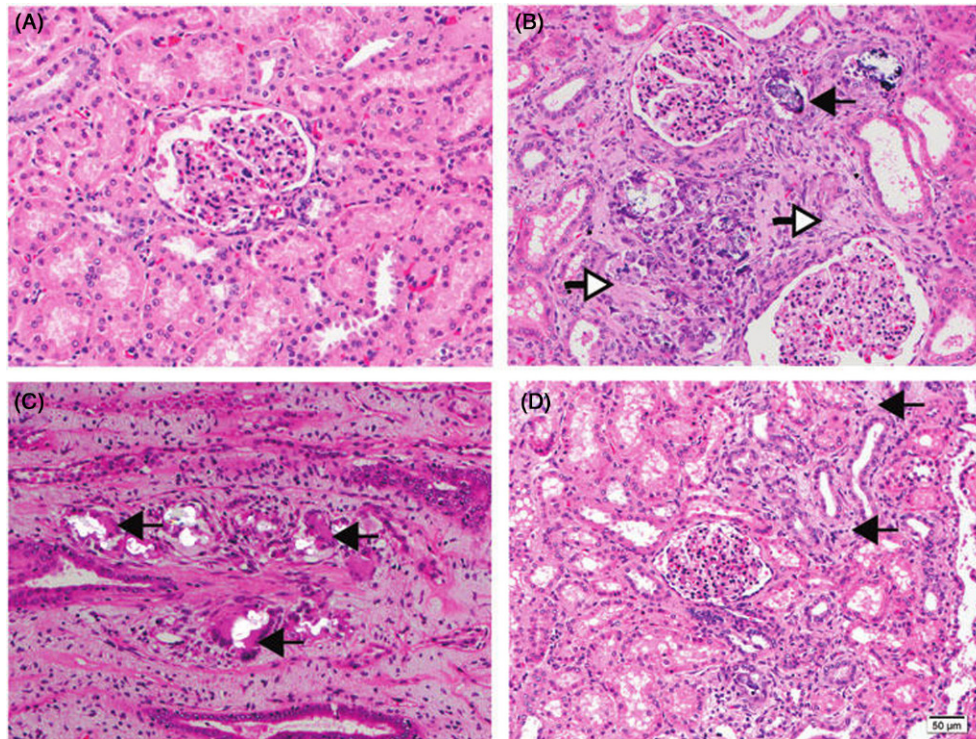
FIGURE 17.11 **Histopathology of crystal formation in porcine kidney.** (Cortical section, 21 days, H and E 20.) (A) Control kidney with normal glomerulus. (B) Inflammation with fibrotic changes *(white arrows)* surrounding glomerulus, with crystal in proximal tubule *(black arrow)*. (C) multinucleated giant cells *(arrows)* surrounding tubules; (D) 10× magnification in renal cortex regions. Notice widening of interstitium with extracellular matrix *(arrows)* considered as fibrotic changes. *Source: Reproduced with permission from Sivalingam, S., Nakada, S.Y., Sehgal, P.D., et al., 2013. Dietary hydroxyproline induced calcium oxalate lithiasis and associated renal injury in the porcine model. J. Endourol. 27, 1493–1498.*

sent a more manageable sized model compared to large adult pigs, Sorensen et al. (2010) tested the performance of a novel ultrasound probe in porcine kidneys to test the effectiveness of estimating stone size during ureteroscopy.

5.5 Limitations

With anatomy and physiology resembling humans, it is unfortunate that limitations of the porcine model reduce its ability to be widely adopted. First and foremost, adult pigs generally require a lot of space and eat substantial amounts of costly food. As previously seen in Fig. 17.10, a large facility is required to maintain a porcine model and this by itself limits its reproducibility. Meanwhile similar to all vertebrate animals, experimentation with pigs requires formal animal study review. In particular to pigs however, is that their eventual sacrifice must adhere to very specific US Department of Agriculture methods.

These limitations explain the relatively low numbers that have been seen in the porcine studies performed thus far. In addition, it also appears that obtaining urine and accurately measuring urine output can be a challenge in this animal model. An important aspect of their

initial study, Kaplon et al. (2010) noted that only 50% of the pigs were ultimately included as 6 of the 12 pigs did not make it to day 6 of the study due to infection or catheter-related problems. Nearly 1/3 of the pigs in another study also had to be excluded due to urinary tract infection or catheter-related problems (Patel et al., 2012). These results highlight the challenges associated with obtaining multiple 24-h urine collections from the pig model over an extended study duration.

Similar to other models that focus on hyperoxaluria, there is a relatively narrow application of this model given that it relates mainly to human primary hyperoxaluria. As the majority of humans with nephrolithiasis suffer from some aspect of hypercalciuria, a model in pigs replicating this physiologic state has yet to be developed.

6 OTHER ANIMAL MODELS

One should not forget that urinary stone disease remains a problem in veterinary medicine. Urinary stone disease has been shown to affect a wide variety of animals, ranging from land mammals like dogs, cats, horses, raccoons, goats, sheep, and kangaroos, to

water-based mammals, such as whales, seals, dolphins, otters, and even reptiles, such as turtles and fish like the zebrafish (Elizondo et al., 2005; Robinson et al., 2008). Of note, these animals are all protected under the Animal Welfare Act of 1966 and its subsequent provisions (US Department of Agriculture, https://www.nal.usda.gov/awic/animal-welfare-act). Therefore, the vast majority of research in these animals has been observational and epidemiologic in nature. While most studies have investigated canines and felines, there is value to reviewing the literature to help gain insight into the pathophysiology of stones in other animals and humans.

7 CANINE MODEL

7.1 Types of Stones

The dog has generated research interest because it spontaneously forms urinary stones that physically and chemically resemble those found in humans. In an effort to characterize the types of calculi formed by canines, large databases have been compiled of uroliths submitted by veterinarians in the United States since 1985 and in Canada since 1998 (Houston and Moore, 2009; Low et al., 2010). In the United States, through 2006, over 25,000 uroliths have been collected from both the upper and lower urinary tract, providing an incredible resource for research. Analysis revealed that the most common stone compositions were 53% struvite (magnesium ammonium phosphate) and 42% calcium oxalate (CaOx), with CaOx being the leading stone type collected since 1997 (Ling et al., 2003). A similar trend was noted in over 40,000 canine uroliths submitted in Canada, with ~85% of submissions being either struvite or CaOx (Houston and Moore, 2009). Meanwhile apatite, urate, silica, and cysteine were other common minerals identified in these uroliths, and over 73% of these samples contained a combination of two or more minerals (Low et al., 2010).

Interestingly, this study also found that a significantly higher proportion of CaOx-containing calculi were found in males compared to females, 69% vs. 31%, respectively (Low et al., 2010). Both cysteine and silica stones were also found more often in male dogs, while a higher percentage of struvite and apatite calculi were found for female dogs. Urate stones have been reported in a much higher percentage in male (93%) versus female (7%) Dalmatians (Houston and Moore, 2009).

7.2 Stone Risk Association With Breed

Historically, canine breeds have been associated with specific disease and stone types, such as the UK Cava-

lier King Charles Spaniels who were noted to experience xanthinuria and experience xanthine stones (Jacinto et al., 2013). Meanwhile, the Keeshond breed has been shown to be predisposed to primary hyperparathyroidism, resulting in hypercalciuria and higher risk of forming calcium oxalate calculi (Goldstein et al., 2007). Given that over the years, many canine species have been created for phenotypic characteristics—this has resulted in some breeds being more predisposed to developing stones compared to others. Based on Low et al. (2010), specific breeds have been associated with a higher and lower risk for specific types of urinary stones (Table 17.4).

In examining those breeds associated with a higher risk of forming stones, overall smaller dogs tended to be the ones associated with higher risk. While this could be secondary to a variety of reasons, investigators have suggested lower urine volumes, potential changes in diet composition, and rising obesity as possible etiologies (Low et al., 2010; Speakman et al., 2008). These smaller dogs are popular breeds with over half of the 9 breeds predisposed to CaOx-containing uroliths (Miniature Schnauzer, Shih Tzu, Pomeranian, Yorkshire Terrier, and Maltese) ranked in the top 20 of the most common dog breeds in the United States (American Kennel Club, 2009; Low et al., 2010). Intuitively, smaller dogs tend to be more popular in metropolitan areas and potentially could have less ability to exercise, contributing to rising obesity rates (Speakman et al., 2008). Further investigations are needed to establish this as a potential etiology for these breeds' increased risk of stone disease.

The Dalmatian represents a unique example of breed-specific calculi. Besides human and great apes, Dalmatians are the only other example of a mammal that excretes uric acid instead of allantoin (Kuster et al., 1972). In humans, high levels of uric acid can accumulate in blood and urine, leading to diseases such as gout. Meanwhile in Dalmatians, recent work involving interbreed backcrossing has shown that Dalmatians have a defect of the SLC2A9 gene, resulting in defective uric acid transport in the kidneys and liver (Bannasch and Henthorn, 2009; Bannasch et al., 2008; Giesecke and Tiemeyer, 1984). These dogs are homozygous for this autosomal recessive trait, with the end result being hyperuricosuria and hyperuricemia (Bannasch and Henthorn, 2009). This hyperuricosuria can be easily identified as Dalmatian urine forms a precipitate when cooled (Fig. 17.12) (Bannasch et al., 2008). Therefore, this breed is at high risk for urate stone development, as shown in the study by Low et al. (2010) where 80% of Dalmatian urate containing uroliths contained 100% urate. Interestingly, this study also found that nearly 69% of English Bulldog urate containing uroliths contained 100% urate, suggesting this breed may have a similar pathophysiologic condition.

TABLE 17.4 Canine Stone Risk Association With Breed—Based on Results Reported in Low et al. (2010)

Stone type (%)	Breeds at higher risk	Breeds at lower risk	Comments
Struvite (53.4%)	• Bichon Frise • Miniature Schnauzer • Shih Tzu • Pekingese	• Australian Cattle Dog • Rottweiler • Boxer • Border Collie • Standard Poodle	• Most commonly in bladder • Decreasing incidence • More in younger dogs • Female versus male: 76% versus 22%
Calcium oxalate (42.0%)	• Bichon Frise • Miniature Schnauzer • Shih Tzu • Lhasa Apso • Pomeranian • Cairn Terrier • Yorkshire Terrier • Maltese • Keeshond	• German Shorthair Pointer • Great Dane • Rottweiler • Australian Cattle Dog • Labrador Retriever • Boxer • German Shepherd Dog • Border Collie • Bull Mastiff	• Most commonly in bladder • Most common type of upper urinary tract stone • More often found in older dogs
Apatite (38.0%)	• Bichon Frise • Miniature Schnauzer • Shih Tzu • Pekingese • Lhasa Apso	• Rottweiler • Dalmatian • Great Dane • Boxer • German Shorthair Pointer • Golden Retriever	• 78% female versus 22% male • No changes in trends over time
Urate (23.8%)	• Dalmatian • Miniature Schnauzer • English Bulldog • Bichon Frise • Pekingese • Scottish Terrier	• Australian Cattle Dog • German Shorthair Pointer • Great Dane • Border Collie • Doberman Pinscher	• 80% of Dalmatian urate containing uroliths were 100% urate • More often in younger dogs
Silica (6.7%)	• Miniature Schnauzer • Lhasa Apso • Samoyed • Bichon Frise • Pekingese	• Australian Cattle Dog • German Shorthair Pointer • Great Dane	• Distribution: 89% male versus 11% female
Cysteine (1.3%)	• English Bulldog • Newfoundland • Dachshund • Chihuahua • Miniature Pinscher • Welsh Corgi	• Labrador Retriever • Cocker Spaniel	• 97.8% male versus 2.2% female • 77% in dogs <7 years old

7.3 Effect of Diet on Stone Risk

In 2004, there was an outbreak in Asia where over 6000 dogs and some cats experienced pet-food associated renal failure (Brown et al., 2007; Jeong et al., 2006). Reviewing the pathology demonstrated that these dogs experienced renal tubular necrosis, calcification, and green–yellow calculi (Jeong et al., 2006). Further investigation revealed that certain brands of commercial pet food were the culprit, stemming back to contamination of raw materials at a pet-food manufacturing plant in Thailand (Honnold, 2005; Thompson et al., 2008).

History repeated itself in North America in 2007, when a Canadian manufacturer of pet food issued a large-scale recall due to multiple reported deaths of both dogs and cats. The pathologic features were similar, acute renal failure with green–yellow calculi reported (Jeong et al., 2006). An analysis of the crystals associated with both outbreaks revealed predominantly birefringent melamine–cyanuric acid complexes, as well as a lesser number of calcium oxalate monohydrate crystals (Thompson et al., 2008). The FDA eventually announced that cyanuric acid and melamine had contaminated ingredients from China that subsequently entered the pet food (Thompson et al., 2008).

The knowledge gained from these canine intoxications helped with the identification of infant formula being contaminated with melamine in 2008. Ultimately there were 6 deaths, over 50,000 children hospitalized, and several hundred thousand affected (Gossner et al., 2009). Subsequent research has shown that melamine exposure measured by urinary melamine levels has an association
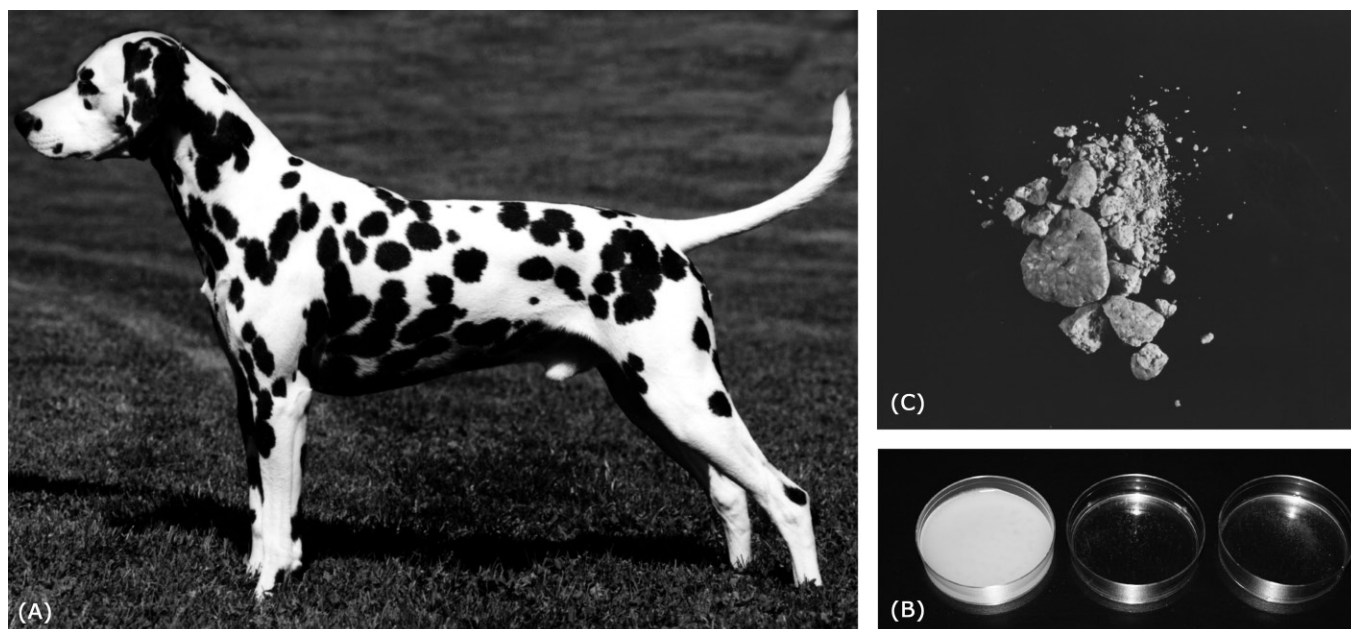
FIGURE 17.12 (A) Classic phenotype of Dalmatian with spotting. (B) Example of Dalmatian urine in crystallized precipitate (far left), compared to heterozygous backcross dog (middle) and dog from an unaffected breed (right). (C) Urinary urate calculi. *Source: Courtesy of Bannasch, D., Safra, N., Young, A., et al., 2008. Mutations in the SLC2A9 gene cause hyperuricosuria and hyperuricemia in the dog. PLoS Genet. 4, e1000246.*

with increased calcium-based stone formation in adults (Lu et al., 2011). These events provide a reminder of how veterinary medicine can help further the understanding of urinary stone disease.

8 FELINE MODEL

8.1 Types of Stones

For the other animal models presented thus far, the predominant discussion has focused on upper-tract stone formation. Yet for the sake of completeness, a discussion on bladder stones should be mentioned, as this brings attention to how environment contributes to and plays a role in stone formation. The bladder represents another environment where stone formation takes place that could be helpful to compare to the medullo-papillary complex, thought to be the main location of kidney stones.

Cats represent an example of an animal model where the vast majority of stones (98%) submitted for analysis are lower urinary tract (bladder) stones (Cannon et al., 2007). While recent reports have cited that the number of ureteral stone submissions has increased over the past 15 years (Cannon et al., 2007; Kyles et al., 2005a; Palm and Westropp, 2011), upper urinary tract stones still represent a minority of stones found in cats. Male cats are also anatomically set up for urethral obstruction given their narrow distal urethra (Cooper et al., 2010). Previous studies have cited that almost all (98%) of feline upper urinary tract calculi are calcium oxalate (Kyles et al., 1998, 2005b).

Similar to the dog, centers have collected large numbers of feline uroliths and been able to analyze trends in stone types. The same centers in the United States and Canada that collected the large number of dog uroliths have also collected over 5,200 and 11,000 feline bladder calculi, respectively (Cannon et al., 2007; Houston and Moore, 2009). As in dogs, the vast majority of feline urinary stones are composed of calcium oxalate and struvite, and there has been a significantly lower amount of struvite calculi since the late 1990s (Cannon et al., 2007; Lekcharoensuk et al., 2000).

8.2 Stone Risk Association With Breed

Similar to the dog, specific breeds of cats have been reported to have increased risks of certain types of uroliths. Persian and Himalayan (Colourpoint Persian) cats were found to have significantly increased risk for CaOx calculi, while Birman, Abyssinian, and Siamese were found to be at lower risk (Cannon et al., 2007). Compared to humans where studies have shown >50% patients have a stone recurrence within 5 years (Ljunghall, 1987), a similar figure has been reported for CaOx producing cats with 6.8% having another stone submitted within 2 years (Albasan et al., 2009).

9 CONCLUSIONS

The sequence of events that leads to urinary stone formation remains unclear. As discussed here, there are multiple animal models that have been used to date in an

effort to better understand the pathophysiologic chain of events that ultimately leads to the formation of a urinary calculus.

When one assesses most of these animal models, the surrogate endpoints used were the development of crystals seen either in the urine or with histologic examination of the renal papilla rather than documentation of a true stone. As appreciated in our clinical practices, crystalluria does not necessarily equate with future stone formation. Crystals may be an early form of eventual aggregation and stone fragmentation; or they may reflect a process of nucleation that may or may not be critical to stone formation. Future research is needed to determine whether the process of crystallization is independent of stone formation.

The eventual goal of these animal models is to help understand the temporal development of urinary stone formation. Translating these animal models to humans, one needs to appreciate the subtle differences in renal anatomy (unipapillary versus multiple renal papilla), as well as potential pathophysiologic differences between quadrupeds versus bipeds. Ultimately, it would be ideal for the urology and nephrology communities to agree on a few selected animal models such that results could be complimentary and comparable. It is only with such animal models that novel new interventions can be undertaken to help reduce the incidence and recurrence of urinary stone disease.

References

Agrawal, V., Liu, X.J., Campfield, T., Romanelli, J., Enrique Silva, J., Braden, G.L., 2013. Calcium oxalate supersaturation increases early after Roux-en-Y gastric bypass. Surg. Obes. Relat. Dis. 10, 88–94.

Albasan, H., Osborne, C.A., Lulich, J.P., et al., 2009. Rate and frequency of recurrence of uroliths after an initial ammonium urate, calcium oxalate, or struvite urolith in cats. J. Am. Vet. Med. Assoc. 235, 1450–1455.

American Kennel Club Website, 2009. Available from: www.akc.org/reg/dogreg_stats.cfm

Andrus, S.B., Gershoff, S.N., Faragalla, F.F., et al., 1960. Production of calcium oxalate renal calculi in vitamin B-6-deficient rats; study of the influence of urine pH. Lab. Invest. 9, 7–27.

Asplin, J.R., Bushinsky, D.A., Singharetnam, W., et al., 1997. Relationship between supersaturation and crystal inhibition in hypercalciuric rats. Kidney Int. 51, 640–645.

Assimos, D., 2012. Ethylene glycol induces calcium oxalate crystal deposition in Malpighian tubules: a *Drosophila* model for nephrolithiasis/urolithiasis. J. Urol. 187, 1299.

Bannasch, D., Henthorn, P.S., 2009. Changing paradigms in diagnosis of inherited defects associated with urolithiasis. Vet. Clin. North Am. Small Anim. Pract. 39, 111–125.

Bannasch, D., Safra, N., Young, A., et al., 2008. Mutations in the SLC2A9 gene cause hyperuricosuria and hyperuricemia in the dog. PLoS Genet. 4, e1000246.

Biyani, C.S., Cartledge, J.J., 2006. Cystinuria—diagnosis and management. EAU-EBU Update Series 4, 175–183.

Brand, A.H., Perrimon, N., 1993. Targeted gene expression as a means of altering cell fates and generating dominant phenotypes. Development 118, 401–415.

Brown, C.A., Jeong, K., Poppenga, R.H., et al., 2007. Outbreaks of renal failure associated with melamine and cyanuric acid in dogs and cats in 2004 and 2007. J. Vet. Diagn. Invest. 19, 525–531.

Bushinsky, D.A., Asplin, J.R., Grynpas, M.D., et al., 2002. Calcium oxalate stone formation in genetic hypercalciuric stone-forming rats. Kidney Int. 61, 975–987.

Bushinsky, D.A., Favus, M.J., 1988. Mechanism of hypercalciuria in genetic hypercalciuric rats. Inherited defect in intestinal calcium transport. J. Clin. Invest. 82, 1585–1591.

Bushinsky, D.A., Grynpas, M.D., Nilsson, E.L., et al., 1995. Stone formation in genetic hypercalciuric rats. Kidney Int. 48, 1705–1713.

Bushinsky, D.A., Kim, M., Sessler, N.E., et al., 1994. Increased urinary saturation and kidney calcium content in genetic hypercalciuric rats. Kidney Int. 45, 58–65.

Bushinsky, D.A., Parker, W.R., Asplin, J.R., 2000. Calcium phosphate supersaturation regulates stone formation in genetic hypercalciuric stone-forming rats. Kidney Int. 57, 550–560.

Canales, B.K., Ellen, J., Khan, S.R., Hatch, M., 2013. Steatorrhea and hyperoxaluria occur after gastric bypass surgery in obese rats regardless of dietary fat or oxalate. J. Urol. 190, 1102–1109.

Canales, B.K., Hatch, M., 2014. Kidney stone incidence and metabolic urinary changes after modern bariatric surgery: review of clinical studies, experimental models, and prevention strategies. Surg. Obes. Rel. Dis. 10, 734–742.

Cannon, A.B., Westropp, J.L., Ruby, A.L., et al., 2007. Evaluation of trends in urolith composition in cats; 5,230 cases (1985–2004). J. Am. Vet. Med. Assoc. 231, 570–576.

Chen, T., Godebu, E., Horgan, S., Mirheydar, H.S., Sur, R.L., 2013. The effect of restrictive bariatric surgery on urolithiasis. J. Endourol. 27, 242–244.

Chen, Y.H., Liu, H.P., Chen, H.Y., et al., 2011. Ethylene glycol induces calcium oxalate crystal deposition in Malpighian tubules: a *Drosophila* model for nephrolithiasis/urolithiasis. Kidney Int. 80, 369–377.

Chi, T., Kim, M.S., Lang, S., et al., 2015. A *Drosophila* model identifies a critical role for zinc in mineralization for kidney stone disease. PLoS One 10 (5), e0124150.

Chien, S., Reiter, L.T., Bier, E., et al., 2002. Homophila: human disease gene cognates in *Drosophila*. Nucl. Acids Res. 30, 149.

Coe, F.L., Parks, J.H., Asplin, J.R., 1992. The pathogenesis and treatment of kidney stones. N. Engl. J. Med. 327, 1141–1152.

Committee on Cost of Payment for Animal Research Institute for Laboratory Animal Research National Research Council, 2000. Future directions in research animal use: infrastructure, cost, and productivity. Strategies That Influence Cost Containment in Animal Research Facilities. National Academy Press, Washington, DC, USA, pp. 53–59.

Collins, F.S., Morgan, M., Patrinos, A., et al., 2003. The human genome project: lessons from large-scale biology. Science 300, 286–290.

Connors, B.A., Evan, A.P., Blomgren, P.M., et al., 2009. Extracorporeal shock wave lithotripsy at 60 shock waves/min reduces renal injury in a porcine model. BJU Int. 104, 1004–1008.

Connors, B.A., McAteer, J.A., Evan, A.P., et al., 2012. Evaluation of shock wave lithotripsy injury in the pig using a narrow focal zone lithotriptor. BJU Int. 110, 1376–1385.

Cooper, E.S., Owens, T.J., Chew, D.J., et al., 2010. A protocol for managing urethral obstruction in male cats without ureteral catheterization. J. Am. Vet. Med. Assoc. 237, 1261–1266.

Cullen-McEwen, L., Sutherland, M.R., Black, M.J., 2015. The human kidney: parallels in structure, spatial development, and timing of nephrogenesis. Kidney Development, Disease, Repair and Regeneration. Elsevier, Amsterdam, Netherlands, pp. 27–40.

Dawson, P.A., Russell, C.S., Lee, S., et al., 2010. Urolithiasis and hepatotoxicity are linked to the anion transporter Sat1 in mice. J. Clin. Invest. 120, 706–712.

de Bruijn, W.C., Boeve, E.R., van Run, P.R., et al., 1994. Etiology of experimental calcium oxalate monohydrate nephrolithiasis in rats. Scan. Microsc. 8, 541–549.

de Water, R., Boeve, E.R., van Miert, P.P., et al., 1996. Experimental nephrolithiasis in rats: the effect of ethylene glycol and vitamin D3 on the induction of renal calcium oxalate crystals. Scan. Microsc. 10, 591–601.

Dello Strologo, L., Pras, E., Pontesilli, C., et al., 2002. Comparison between SLC3A1 and SLC7A9 cystinuria patients and carriers: a need for a new classification. J. Am. Soc. Nephrol. 13, 2547–2553.

DeSesso, J.M., 1995. Anatomical relationships of urinary bladders compared: their potential role in the development of bladder tumours in humans and rats. Food Chem. Toxic. 33, 705–714.

Dow, J.A.T., Romero, M.F., 2010b. *Drosophila* provides rapid modeling of renal development, function and disease. Am. J. Physiol. Renal. Physiol. 299, F1237–F1244.

Dube, K.A., McDonald, D.G., O'Donnell, M.J., 2000. Calcium homeostasis in larval and adult *Drosophila melanogaster*. Arch. Insect. Biochem. Physiol. 44, 27–39, 2000.

Duffey, B.G., Alanee, S., Pedro, R.N., et al., 2010b. Hyperoxaluria is a long-term consequence of Roux-en-Y gastric bypass: a 2-year prospective longitudinal study. J. Am. Coll. Surg. 211, 8–15.

Eder, A.F., McGrath, C.M., Dowdy, Y.G., et al., 1998. Ethylene glycol poisoning: toxicokinetic and analytical factors affecting laboratory diagnosis. Clin. Chem. 44, 168–177.

Elizondo, M.R., Arduini, B.L., Paulsen, J., et al., 2005. Defective skeletogenesis with kidney stone formation in dwarf zebrafish mutant for trpm7. Curr. Biol. 15, 667–671.

Evan, A.P., 2010. Physiopathology and etiology of stone formation in the kidney and the urinary tract. Pediatr. Nephrol. 25, 831–841.

Evan, A.P., Bledsoe, S.B., Smith, S.B., et al., 2004. Calcium oxalate crystal localization and osteopontin immunostaining in genetic hypercalciuric stone-forming rats. Kidney Int. 65, 154–161.

Feliubadaló, L., Arbonés, M.L., Mañas, S., et al., 2003. Slc7a9-deficient mice develop cystinuria non-I and cystine urolithiasis. Hum. Mol. Genet. 12, 2097–2108.

Gershoff, S.N., Andrus, S.B., 1961. Dietary magnesium, calcium, and vitamin B$_6$ and experimental nephropathies in rats: calcium oxalate calculi, apatite nephrocalcinosis. J. Nutr. 73, 308–316.

Gershoff, S.N., Faragalla, F.F., 1959. Endogenous oxalate synthesis and glycine, serine, deoxypyridoxine interrelationships in vitamin B6-deficient rats. J. Biol. Chem. 234, 2391.

Giachelli, C.M., Steitz, S., 2000. Osteopontin: a versatile regulator of inflammation and biomineralization. Matrix Biol. 19, 615–622.

Giesecke, D., Tiemeyer, W., 1984. Defect of uric acid uptake in Dalmatian dog liver. Experientia 40, 1415–1416.

Goldstein, R.E., Atwater, D.Z., Cazolli, D.M., et al., 2007. Inheritance, mode of inheritance, and candidate genes for primary hyperparathyroidism in Keeshonden. J. Vet. Intern. Med. 21, 199–203.

Gossner, C.M., Schlundt, J., Ben Embarek, P., et al., 2009. The melamine incident: implications for international food and feed safety. Environ. Health Perspect. 117, 1803–1808.

Green, M.L., Hatch, M., Freel, R.W., 2005. Ethylene glycol induces hyperoxaluria without metabolic acidosis in rats. Am. J. Physiol. Renal Physiol. 289, F536–F543.

Hirata, T., Cabrero, P., Berkholz, D.S., et al., 2012a. In vivo *Drosophila* genetic model for calcium oxalate nephrolithiasis. Am. J. Physiol. Renal. Physiol. 303, F1555–F1562.

Hirata, T., Cabrero, P., Dow, J.A.T., et al., 2010. *Drosophila* Prestin provides an in vivo model for oxalate kidney stone formation. J. Am. Soc. Nephrol 21, 486A.

Hirata, T., Czapar, A., Brin, L., et al., 2012b. Ion and solute transport by Prestin in *Drosophila* and Anopheles. J. Insect. Physiol. 58, 563–569.

Hirata, T., Kato, A., Cabrero, P., et al., 2009. *Drosophila* Slc26a5 functions as a Cl/oxalate exchanger similar to mammalian Slc26a6. J. Am. Soc. Nephrol. 20, 385A.

Hofmann, A.F., Laker, M.F., Dharmsathaphorn, K., et al., 1983. Complex pathogenesis of hyperoxaluria after jejunoileal bypass surgery. Oxalogenic substances in diet contribute to urinary oxalate. Gastroenterology 84, 293.

Honnold SP, 2005. Proceedings Department of Veterinary Pathology Wednesday Slide Conference, Armed Forces Institute of Pathology, Washington DC. pp. 147–150.

Houston, D.M., Moore, A.E.P., 2009. Canine and feline urolithiasis: examination of over 50,000 urolith submissions to the Canadian Veterinary Urolith Centre from 1998 to 2008. Can. Vet. J. 50, 1263–1268.

Hu, D., Liu, T., Wang, X., 2015. Flexible ureteroscopy training for surgeons using isolated porcine kidneys in vitro. BMC Urol. 15, 71.

Huang, H.-S., Ma, M.-C., Chen, J., Chen, C.-F., 2002. Changes in the oxidant–antioxidant balance in the kidneys of rats with nephrolithiasis induced by ethylene glycol. J. Urol. 167, 2584–2593.

Hunter, G.K., Hauschka, P.V., Poole, A.R., et al., 1996. Nucleation and inhibition of hydroxyapatite formation by mineralized tissue proteins. Biochem. J. 317, 59–64.

Ichida, K., Amaya, Y., Kamatani, N., et al., 1997. Identification of two mutations in human xanthine dehydrogenase gene responsible for classical type I xanthinuria. J. Clin. Invest. 99, 2391.

Ichida, K., Matsumura, T., Sakuma, R., et al., 2001. Mutation of human molybdenum cofactor sulfurase gene is responsible for classical xanthinuria type II. Biochem. Biophys. Res. Commun. 282, 1194–1200.

Jacinto, A.M.L., Mellanby, R.J., Chandler, M., et al., 2013. Urine concentrations of xanthine, hypoxanthine and uric acid in UK Cavalier King Charles spaniels. J. Small Anim. Pract. 54, 395–398.

Jennings, B.H., 2011. *Drosophila*—a versatile model in biology and medicine. Mater. Today 14, 190–195.

Jeong, W., Do, S.H., Jeong, D., et al., 2006. Canine renal failure syndrome in three dogs. J. Vet. Sci. 7, 299–301.

Jiang, Z., Asplin, J.R., Evan, A.P., et al., 2006. Calcium oxalate urolithiasis in mice lacking anion transporter Slc26a6. Nat. Genet. 38, 474–478.

Kaplon, D.M., Penniston, K.L., Darriet, C., et al., 2010. Hydroxyproline-induced hyperoxaluria using acidified and traditional diets in the porcine model. J. Endourol. 24, 355–359.

Khan, S.R., 1991. Pathogenesis of oxalate urolithiasis: lessons from experimental studies with rats. Am. J. Kidney Dis. 17, 398–401.

Khan, S.R., 2013. Animal Models of Calcium Oxalate Kidney Stone Formation. Animal Models for the Study of Human Disease. Elsevier, Amsterdam, Netherlands, pp. 483–498.

Khan, S.R., Canales, B.K., 2011. Ultrastructural investigation of crystal deposits in Npt2a knockout mice: are they similar to human Randall's plaques? J. Urol. 186, 1107–1113.

Khan, S.R., Finlayson, B., Hackett, R.L., 1979a. Histologic study of the early events in oxalate induced intranephronic calculosis. Invest. Urol. 17, 199–202.

Khan, S.R., Finlayson, B., Hackett, R.L., 1982. Experimental calcium oxalate nephrolithiasis in the rat: role of the renal papilla. Am. J. Pathol. 107, 59–69.

Khan, S.R., Glenton, P.A., 2010. Experimental induction of calcium oxalate nephrolithiasis in mice. J. Urol. 184, 1189–1196.

Khan, S.R., Glenton, P.A., Byer, K.J., 2006. Modeling of hyperoxaluric calcium oxalate nephrolithiasis: experimental induction of hyperoxaluria by hydroxy-L-proline. Kidney Int. 70, 914–923.

Khan, S.R., Hackett, R.L., 1993b. Hyperoxaluria, enzymuria and nephrolithiasis. Contrib. Nephrol. 101, 190–193.

Khan, S.R., Johnson, J.M., Peck, A.B., et al., 2002a. Expression of osteopontin in rat kidneys: induction during ethylene-glycol-induced calcium oxalate nephrolithiasis. J. Urol. 168, 1173–1181.

Khan, S.R., Shevock, P.N., Hackett, R., 1989. Urinary enzymes and CaO$_x$ urolithiasis. J. Urol. 142, 846–849.

Khan, S.R., Shevock, P.N., Hackett, R.L., 1992. Acute hyperoxaluria, renal injury and calcium oxalate urolithiasis. J. Urol. 147, 226–230.

Knight, J., Holmes, R.P., 2005. Mitochondrial hydroxyproline metabolism: implications for primary hyperoxaluria. Am. J. Nephrol. 25, 171–175.

Krieger, N.S., Stathopoulos, V.M., Bushinsky, D.A., 1996. Increased sensitivity to 1,25(OH)$_2$D$_3$ in bone from genetic hypercalciuric rats. Am. J. Physiol. 271 (1 Pt 1), C130–C135.

Kumar, S., Muchmore, A., 1990. Tamm–Horsfall protein—uromodulin (1950–1990). Kidney Int. 37, 1395–1401.

Kuster, G., Shorter, R.G., Dawson, B., et al., 1972. Uric acid metabolism in dalmatians and other dogs. Role of the liver. Arch. Intern. Med. 129, 492–496.

Kyles, A.E., Hardie, E.M., Wooden, B.G., Adin, C.A., Stone, E.A., Gregory, C.R., et al., 2005a. Management and outcome of cats with ureteral calculi: 153 cases (1984–2002). J. Am. Vet. Med. Assoc. 226, 937.

Kyles, A.E., Hardie, E.M., Wooden, B.G., Adin, C.A., Stone, E.A., Gregory, C.R., et al., 2005b. Clinical, clinicopathologic, radiographic, and ultrasonographic abnormalities in cats with ureteral calculi: 163 cases (1984–2002). J. Am. Vet. Med. Assoc. 226, 932.

Kyles, A.E., Stone, E.A., Gookin, J.L., et al., 1998. Diagnosis and surgical management of obstructive ureteral cacluli in cats: 11 cases (1993–1996). J. Am. Vet. Med. Assoc. 213, 1150–1156.

Lekcharoensuk, C., Lulich, J.P., Osborne, C.A., et al., 2000. Association between patient-related factors and risk of calcium oxalate and magnesium ammonium phosphate urolithiasis in cats. J. Am. Vet. Med. Assoc. 217, 520–525.

Levartovsky, D., Lagziel, A., Sperling, O., et al., 2000. XDH gene mutation is the underlying cause of classical xanthinuria: a second report. Kidney Int. 57, 2215–2220.

Li, M.K., Blacklock, N.J., Garside, J., 1985. Effects of magnesium on calcium oxalate crystallization. J. Urol. 133, 123–125.

Li, X.Q., Tembe, V., Horwitz, G.M., Bushinsky, D.A., Favus, M.J., 1993. Increased intestinal vitamin D receptor in genetic hypercalciuric rats: a cause of intestinal calcium hyperabsorption. J. Clin. Invest. 91, 661–667.

Liebelt, A.G., 1998. Unique Features of Anatomy, Histology, and Ultrastructure Kidney, Mouse. Springer, Berlin, Heidelberg, New York, Tokyo.

Ling, G.V., Thurmond, M.C., Choi, Y.K., et al., 2003. Changes in proportion of canine urinary calculi composed of calcium oxalate or struvite in specimens analyzed from 1981 through 2001. J. Vet. Intern. Med. 17, 817–823.

Ljunghall, S., 1987. Incidence of upper urinary tract stones. Miner. Electrolyte Metab. 13, 220–227.

Low, W.W., Uhl, J.M., Kass, P.H., et al., 2010. Evaluation of trends in urolith composition and characteristics of dogs with urolithiasis: 25,499 cases (1985–2006). J. Am. Vet. Med. Assoc. 236, 193–200.

Lu, C.C., Wu, C.F., Chen, B.H., et al., 2011. Low exposure to melamine increases the risk of urolithiasis in adults. Kidney Int. 80, 746–752.

Maalouf, N.M., Tondapu, P., Guth, E.S., et al., 2010. Hypocitraturia and hyperoxaluria after Roux-en-Y gastric bypass surgery. J. Urol. 183, 1026–1030.

Mandel, N.S., Henderson, J.D., Hung, L.Y., et al., 2004. A porcine model of calcium oxalate kidney stone disease. J. Urol. 171, 1301–1303.

Matlaga, B.R., Shore, A.D., Magnuson, T., et al., 2009. Effect of gastric bypass surgery on kidney stone disease. J. Urol. 181, 2573.

Meneton, P., Ichikawa, I., Inagami, T., et al., 2000. Renal physiology of the mouse. Am. J. Physiol. Renal. Physiol. 278, F339–F351.

Miller, J., Chi, T., Kapahi, P., et al., 2013. Drosophila melanogaster as an emerging translational model of human nephrolithiasis. J. Urol. 190, 1648–1656.

Mo, L., Huang, H.Y., Zhu, X.H., et al., 2004. Tamm–Horsfall protein is a critical renal defense factor protecting against calcium oxalate crystal formation. Kidney Int. 66, 1159–1166.

Mo, L., Liaw, L., Evan, A.P., et al., 2007. Renal calcinosis and stone formation in mice lacking osteopontin, Tamm–Horsfall protein, or both. Am. J. Physiol. Renal Physiol. 293, F1935–F1943.

Molina, D.K., DiMaio, V.J.M., 2012. Normal Organ Weights in Men. Am. J. Forensic Med. Pathol. 33, 368–372.

Monico, C.G., Weinstein, A., Jiang, Z., et al., 2008. Phenotypic and functional analysis of human SLC26A6 variants in patients with familial hyperoxaluria and calcium oxalate nephrolithiasis. Am. J. Kidney Dis. 52, 1096–1103.

Muller, H.J., 1928. The production of mutations by X-rays. Proc. Natl. Acad. Sci. 14, 714–726.

O'Connor, R.C., Worcester, E.M., Evan, A.P., et al., 2005. Nephrolithiasis and nephrocalcinosis in rats with small bowel resection. Urol. Res. 33, 105–115.

Ogawa, Y., Yamaguchi, K., Morozumi, M., 1990. Effects of magnesium salts in preventing experimental oxalate urolithiasis in rats. J. Urol. 144, 385–389.

Okada, A., Nomura, S., Higashibata, Y., et al., 2007. Successful formation of calcium oxalate crystal deposition in mouse kidney by intraabdominal glyoxylate injection. Urol. Res. 35, 89–99.

Okada, A., Yasui, T., Hamamoto, S., et al., 2009. Genome-wide analysis of genes related to kidney stone formation and elimination in the calcium oxalate nephrolithiasis model mouse: detection of stone-preventive factors and involvement of macrophage activity. J. Bone Miner. Res. 24, 908–924.

Pak, C.Y.C., Holt, K., 1976. Nucleation and growth of brushite and calcium oxalate in urine stone formers. Metabolism 25, 665–673.

Palm, C., Westropp, J., 2011. Cats and calcium oxalate: Strategies for managing lower and upper tract stone disease. J. Feline Med. Surg. 13, 651–660.

Park, A.M., Storm, D.W., Fulmer, B.R., et al., 2009. A prospective study of risk factors for nephrolithiasis after Roux-en-Y gastric bypass surgery. J. Urol. 182, 2334.

Patel, B.N., Passman, C.M., Fernandez, A., et al., 2009. Prevalence of hyperoxaluria after bariatric surgery. J. Urol. 181, 161.

Patel, S.R., Penniston, K.L., Iwicki, L., et al., 2012. Dietary induction of long-term hyperoxaluria in the porcine model. J. Endourol. 26, 433–438.

Paterson, R.F., Lifshitz, D.A., Lingeman, J.E., Evan, A.P., et al., 2002. Stone fragmentation during shock wave lithotripsy is improved by slowing the shock wave rate: studies with a new animal model. J. Urol. 168, 2211–2215.

Pearle, M.S., Calhoun, E.A., Curhan, G.C., 2005. Urologic diseases in America project: urolithiasis. J. Urol. 173, 848–857.

Peters, T., Thaete, C., Wolf, S., et al., 2003. A mouse model for cystinuria type 1. Hum. Mol. Genet. 12, 2109–2120.

Randall, A., 1937. The origin and growth of renal calculi. Ann. Surg. 105, 1009–1027.

Randall, A., 1940. Papillary pathology as a precursor of primary renal calculus. J. Urol. 44, 580.

Reiter, L.T., Potocki, L., Chien, S., et al., 2001. A systemic analysis of human disease-associated gene sequences in Drosophila melanogaster. Genome Res. 11, 1114–1125.

Rheault, M.R., O'Donnell, M.J., 2004. Organic cation transport by Malpighian tubules of Drosophila melanogaster: application of two novel electrophysiological methods. J. Exp. Biol. 207, 2173–2184.

Robinson, M., Pond, C.L., Laurie, R.D., et al., 1990. Subacute and subchronic toxicity of ethylene glycol administered in drinking water to Sprague–Dawley rats. Drug Chem. Toxic. 13, 43–47.

Robinson, M.R., Norris, R.D., Sur, R.L., et al., 2008. Urolithiasis: not just a 2-legged animal disease. J. Urol. 179, 46–52.

Rushton, H.G., Spector, M., 1982. Effects of magnesium deficiency on intratubular calcium oxalate formation and crystalluria in hyperoxaluric rats. J. Urol. 127 (3), 598–604.

Sachs, D.H., 1994. The pig as potential xenograft donor. Vet. Immunol. Immunopathol. 43, 185–191.

Saigal, C.S., Joyce, G., Timilsina, A.R., et al., 2005. Urologic diseases in America Project. Direct and indirect costs of nephrolithiasis in an

employed population: opportunity for disease management? Kidney Int. 68, 1808–1814.

Sands, J.M., Layton, H.E., 2009. The physiology of urinary concentration: an update. Semin. Nephrol. 29, 178–195.

Scales, C.D., Smith, A.C., Hanley, J.M., et al., 2012. Prevalence of kidney stones in the United States. Eur. Urol. 62, 160–165.

Scales, C.D., Tasian, G.E., Schwaderer, A.L., et al., 2016. Urinary stone disease: advancing knowledge, patient care, and population health. Clin. J. Am. Soc. Nephrol. 11, 1305–1312.

Serafini-Cessi, F., Malagolini, N., Cavallone, D., 2003. Tamm–Horsfall glycoprotein: biology and clinical relevance. Am. J. Kidney Dis. 42, 658–676.

Shiraga, H., Min, W., VanDuse, W.J., et al., 1992. Inhibition of calcium oxalate crystal growth in vitro by uropontin: another member of the aspartic acid-rich protein superfamily. Proc. Natl. Acad. Sci. 89, 426–430.

Sivalingam, S., Nakada, S.Y., Sehgal, P.D., et al., 2013. Dietary hydroxyproline induced calcium oxalate lithiasis and associated renal injury in the porcine model. J. Endourol. 27, 1493–1498.

Smith, L.H., Fromm, H., Hofmann, A.F., 1972. Acquired hyperoxaluria, nephrolithiasis, and intestinal disease. Description of a syndrome. N. Engl. J. Med. 286, 1371.

Sorensen, M.D., Shah, A.R., Canney, M.S., et al., 2010. Ureteroscopic ultrasound technology to size kidney stone fragments: proof of principle using a miniaturized probe in a porcine model. J. Endourol. 24, 939–942.

Sözen, M.A., Armstrong, J.D., Yang, M., et al., 1997. Functional domains are specified to single-cell resolution in a *Drosophila* epithelium. Proc. Natl. Acad. Sci. 94, 5207–5212.

Speakman, J., Hambly, C., Mitchell, S., et al., 2008. The contribution of animal models to the study of obesity. Lab. Anim. 42, 413–432.

Stocker, H., Gallant, P., 2008. Getting started: an overview on raising and handling *Drosophila*. Methods Mol. Biol. 420, 27–42.

Stoller, M.L., Meng, M., 2007. Urinary Stone Disease: The Practical Guide to Medical and Surgical Management. Humana Press, New York, NY, USA.

Strohmaier, W.L., Giese, A., 2001. Porcine urinary tract as a training model for ureteroscopy. Urol. Int. 66, 30–32.

Taguchi, K., Okada, A., Kitamura, H., et al., 2014. Colony-stimulating factor-1 signaling suppresses renal crystal formation. J. Am. Soc. Nephrol. 25, 1680–1697.

Taguchi, K., Okada, A., Hamamoto, S., et al., 2015. Proinflammatory and metabolic changes facilitate renal crystal deposition in an obese mouse model of metabolic syndrome. J. Urol. 194, 1787–1796.

Tawashi, R., Cousineau, M., Sharkawi, M., 1980. Calcium oxalate crystal formation in the kidneys of rats injected with 4-hydroxy-L-proline. Urol. Res. 8, 121–127.

Thamilselvan, S., Hackett, R.L., Khan, S.R., 1997b. Lipid peroxidation in ethylene glycol induced hyperoxaluria and calcium oxalate nephrolithiasis. J. Urol. 157, 1059–1063.

Thompson, M.E., Lewin-Smith, M.R., Kalasinsky, V.F., et al., 2008. Characterization of melamine-containing and calcium oxalate crystals in three dogs with suspected pet food-induced nephrotoxicosis. Vet. Pathol. 45, 417.

Thomsen, H.S., Larsen, S., Talner, L.B., 1983. Papillary morphology in adult human kidneys and in baby and adult pig kidneys. Eur. Urol. 9, 170–180.

Tweedie, S., Ashburner, M., Falls, K., et al., 2009. FlyBase: enhancing *Drosophila* gene ontology annotations. Nucl. Acids Res. 37 (Suppl. 1), D555–D559.

Valezi, A.C., Fuganti, P.E., Junior, J.M., Delfino, V.D., 2013. Urinary evaluation after RYGBP: a lithogenic profile with early postoperative increase in the incidence of urolithiasis. Obes. Surg. 23, 1575–1580.

Weavers, H., Prieto-Sanchez, S., Grawe, F., et al., 2009. The insect nephrocyte is a podocyte-like cell with a filtration slit diaphragm. Nature 457, 322–326.

Weinman, E.J., Mohanlal, V., Stoycheff, N., et al., 2006. Longitudinal study of urinary excretion of phosphate, calcium, and uric acid in mutant NHERF-1 null mice. Am. J. Physiol. Renal. Physiol. 290, F838–F843.

Werness, P.G., Brown, C.M., Smith, L.H., et al., 1985. EQUIL2: a BASIC computer program for the calculation of urinary saturation. J. Urol. 134, 1242–1244.

Wessing, A., Zierold, K., Hevert, F., 1992. Two types of concretions in *Drosophila* Malpighian tubules as revealed by X-ray microanalysis: a study on urine formation. J. Insect. Physiol. 38, 543–554.

Wesson, J.A., Johnson, R.J., Mazzali, M., et al., 2003. Osteopontin is a critical inhibitor of calcium oxalate crystal formation and retention in renal tubules. J. Am. Soc. Nephrol. 14, 139–147.

Wiessner, J.H., Garrett, M.R., Hung, L.Y., et al., 2011. Improved methodology to induce hyperoxaluria without treatment using hydroxyproline. Urol. Res. 39, 373–377.

Worcester, E.M., 1994. Urinary calcium oxalate crystal growth inhibitors. J. Am. Soc. Nephrol. 5, S46–S53.

Worcester, E.M., Chuang, M., Laven, B., et al., 2005. A new animal model of hyperoxaluria and nephrolithiasis in rats with small bowel resection. Urol. Res. 33, 380–382.

Wu, X.-R., 2015. Interstitial calcinosis in renal papillae of genetically engineered mouse models: relation to Randall's plaques. Urolithiasis 43 (Suppl.), 65–76.

Wu, J.N., Craig, J., Chamie, K., Asplin, J., Ali, M.R., Low, R.K., 2013. Urolithiasis risk factors in the bariatric population undergoing gastric bypass surgery. Surg. Obes. Relat. Dis. 9, 83–87.

Yamaguchi, S., Wiessner, J.H., Hasegawa, A.T., et al., 2005. Study of a rat model for calcium oxalate crystal formation without severe renal damage in selected conditions. Int. J. Urol. 12, 290–298.

Yao, J., Kathpalia, P., Bushinsky, D.A., Favus, M.J., 1998. Hyperresponsiveness of vitamin D receptor gene expression to 1,25-dihydroxyvitamin D3. J. Clin. Invest. 101, 2223–2232.

Zee, T., Bose, N., Zee, J., et al., 2017. α-Lipoic acid treatment prevents cystine urolithiasis in a mouse model of cystinuria. Nat. Med. 23, 288–290.

Page left intentionally blank

18

Animals Models for Healing Studies After Partial Nephrectomy

Diogo B. de Souza*, Marco A. Pereira-Sampaio*,**, Francisco J.B. Sampaio*

*State University of Rio de Janeiro, Rio de Janeiro, RJ, Brazil
**Fluminense Federal University, Niteroi, RJ, Brazil

1 INTRODUCTION

Renal tumors account for 3.9% of the new cancer diagnosis in the United States, which represents more than 57,000 new cases and more than 12,000 deaths, being on the 10 more common tumors in humans (Jemal et al., 2009). According to Russo, the patients with renal tumors can be divided in two groups. In the first group are symptomatic patients, with large tumors which require radical nephrectomy. In the second group, representing 70% of the cases, are patients who had an incidental diagnosis. The tumors of these patients are discovered during abdominal ultrasound, computed tomography, or nuclear magnetic resonance, with indication not related to the renal tumor (e.g., spinal column diseases) (Russo and Huang, 2008). Frequently, in these patients, small tumors are found and radical nephrectomy may not be necessary for most cases.

Conservative renal surgery (partial nephrectomy) is indicated for patients with bilateral tumors, compromised renal function, or single kidney (Lane and Novick, 2007). It has been recently included as primary indication for patients with T1a tumors (masses smaller than 4 cm, restrained to the kidney) and electively indicated for T1b tumors (masses larger than 4 cm but smaller than 7 cm, restrained to the kidney) (Campbell et al., 2009; Ljungberg et al., 2015).

Partial nephrectomy is still considered a challenging procedure, and underutilized. Only 8% of surgeries for treating renal tumors in the United States, between 1988 and 2002, were partial nephrectomies (Hollenbeck et al., 2006). In the United Kingdom, only 4% of renal surgeries were partial nephrectomies in the year 2002 (Nuttall et al., 2005).

It is thought that this surgery involves technically difficult aspects, especially when performed with laparoscopic or robotic access, the use of radical nephrectomy is favored despite the size of the tumor. It has been reported that patients treated in large hospitals, university hospitals, or urban centers are more commonly submitted to partial surgery than in other medical institutions (Hollenbeck et al., 2006).

Clearly, partial nephrectomy has been underutilized because of its technical difficulties. One of the most

difficult aspects of this surgery is the closure of the collecting system. This step involves suturing the renal calices and/or pelvis, which is considered an advanced skill, especially when performing laparoscopically. It has already been shown that the intracorporeal collecting system closure increases the surgical time and requires longer warm ischemia time (Zorn et al., 2007), which is associated with postoperative renal function prejudice (de Souza et al., 2012). Therefore, there have been research efforts for simplifying and accelerating this step (Bishoff et al., 2003; Hacker et al., 2007; Kouba et al., 2004; Orvieto et al., 2007; Shikanov et al., 2009).

Several types of surgical glues or hemostatic agents (Bernie et al., 2005; Bishoff et al., 2003; Johnston et al., 2006; Kouba et al., 2004; L'Esperance et al., 2005; Margulis et al., 2005a; Murat et al., 2004, 2006b; Rouach et al., 2009), surgical bolsters (Abou-Elela et al., 2009; Johnston et al., 2006; Sabino et al., 2007; Xie et al., 2008a,b), lasers (and other types of energy) (Anderson et al., 2007; Bui et al., 2007; Collyer et al., 2002; Eret et al., 2009; Hindley et al., 2006; Honeck et al., 2008; Lafon et al., 2007; Lucioni et al., 2008; Murat et al., 2005, 2006a; Ogan et al., 2002; Sprunger and Herrell, 2005; Zeltser et al., 2008), and suturing methods (Orvieto et al., 2007; Shikanov et al., 2009) have been studied for developing an easier technique for the collecting system closure. Moreover, models simulating a renal tumor have been proposed for training purposes (Eun et al., 2008; Hidalgo et al., 2005; Taylor and Cadeddu, 2006; Taylor et al., 2004; Yang et al., 2009), which is associated with a reduction on the learning curve for performing partial nephrectomy (Rouach et al., 2008).

As the number of training programs for partial nephrectomy (both for open and minimally invasive access) increases, the utilization of conservative renal surgery would increase. Furthermore, the advent of the techniques for renal closure, which makes the procedure easier, would favor the utilization of partial nephrectomy, with potential benefits for several patients.

In this regard, the utilization of a good animal model is of great importance, both for the development and testing of new techniques and equipments, and for surgical training programs. This animal model should reproduce not only human renal anatomy (size, shape, and internal anatomy), but also the healing after the surgical aggression.

Other aspects, such as handling characteristics, cost, and necessary infrastructure should be also taken into account for deciding which animals would be the most adequate for experimentation and/or training.

For a long time, the pig was considered the best animal model for studying renal procedures due to its anatomical and physiological resemblances to human kidneys. Unlike the kidneys of dogs, rabbits, and rats, the swine kidneys are multipyramidal, and have length, weight, and shape similar to human kidneys (Sampaio et al., 1998).

Vascular intrarenal anatomy is very similar between humans and pigs, although some differences exist in the dorsal arteries (Pereira-Sampaio et al., 2004a), the proportional area of the arterial segments (Pereira-Sampaio et al., 2007), and the venous arrangement on dorsal renal surface has been described (Bagetti Filho et al., 2008).

For all these reasons, the pig has been largely used for the development and improvement of surgical methods applicable to conventional, laparoscopic, and robotic partial nephrectomy. However, we will observe that this species has some important differences from humans concerning renal healing after partial nephrectomy.

Thus, the present chapter presents the characteristics of some species that has been investigated as models for healing studies after partial nephrectomy.

2 THE PIG AS ANIMAL MODEL

As previously stated, the pig kidney has been largely used as animal model for studying renal surgery and other urological procedures. In the early 1990s, there was a considerable increase in the use of swine kidneys as models for different surgical purposes. Not only partial nephrectomy (McDougall et al., 1993; Valdivia Uria et al., 1992) was studied in this animal model, but also renal transplant (Yanaga et al., 1991), lithotripsy (Evan et al., 1991; van Dongen et al., 1993), and hidronephrosis (Kelleher et al., 1992) were investigated using the pig as an experimental model. More recently, this species remained in use for the development of new surgical technologies, such as ureterorenoscopy (Ptashnyk et al., 2002), use of biologic glues (Hick et al., 2005), cryoablation (Collyer et al., 2004; Janzen et al., 2005), and radiofrequency ablation (Janzen et al., 2005; Margulis et al., 2005b). Furthermore, the pig kidney also plays an important role as a training model, being the most used animal in hands-on courses for surgical procedures and training with new surgical equipment and instruments (Earp, 2003; Hammond et al., 2004; Katz et al., 2003; Rassweiler et al., 1993; Strohmaier and Giese, 2005).

The pig kidney is considered the best animal model for studying human surgical procedures due to its anatomical resemblance to the human kidney (Bagetti Filho et al., 2008; Pereira-Sampaio et al., 2004a,b; Sampaio et al., 1998, 2001). As in humans, the swine kidney is a bean-shaped bilateral organ, localized in the retroperitoneal space. Notably, unlike what is seen in humans, the pig kidney is not involved by a renal fascia (called Gerota's fascia). Furthermore, for most animals, a small amount of whitish fatty tissue is found in the retroperitoneal space, instead of the yellowish and abundant fatty tissue found in the human's retroperitoneum. Despite these differences, the pig kidney has a mean length of 11.79 cm and mean weight of 98 g (Sampaio et al., 1998),
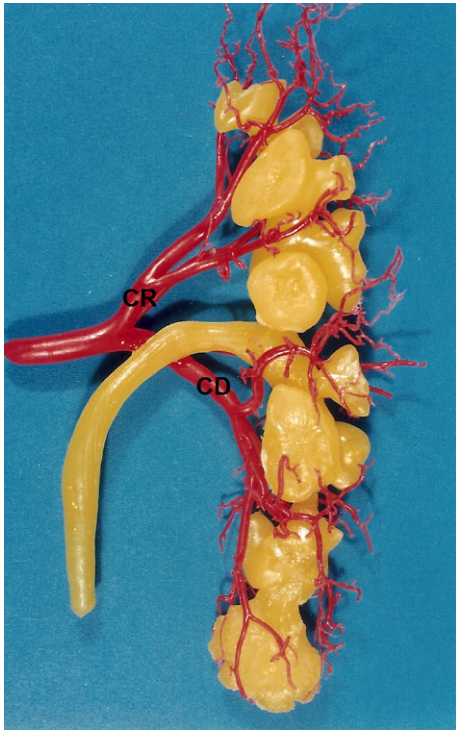
FIGURE 18.1 **Dorsal view of endocast (pelvicaliceal system and arteries) of pig right kidney, showing the primary division of the renal artery into cranial *(CR)* and caudal *(CD)* segmental arteries.**

FIGURE 18.2 **Dorsal view of pig kidney with two arterial segments.** Cranial segment *(red)* and caudal segment *(yellow). Source: Obtained from Pereira-Sampaio, M., Favorito, L.A., Henry, R., Sampaio, F.J., 2007. Proportional analysis of pig kidney arterial segments: differences from the human kidney. J. Endourol. 21 (7), 784–788.*

which is very similar to human kidneys (Sampaio and Mandarim-de-Lacerda, 1989). As in human kidneys, the mean width of the cranial renal pole is slightly superior to the caudal pole (Sampaio and Mandarim-de-Lacerda, 1989; Sampaio et al., 1998).

Internally, the renal collecting system of pigs is especially similar to the corresponding human system. The swine is one of the few animals that have a complex collecting system, with major and minor calyces. All kidneys of pigs show two major calyces (one cranial and one caudal), with 4–19 minor calyces (9 in mean). Thus, despite a great variation in the number of minor calyces, this is very similar to what is observed in human kidneys, in 62% of organs 5–14 minor calyces and 2 major calyces are found (38% of human kidneys show 3 major calyces) (Sampaio, 1993; Sampaio and Mandarim-de-Lacerda, 1988). Thus, pig's kidneys have the most similar collecting system to what is found in humans.

In 93% of kidneys, the renal artery of pigs is always single and divides into two branches (one cranial and one caudal) (Fig. 18.1). Only in 7% of kidneys, the renal artery gives a dorsal and a ventral branch (as seen in humans) (Pereira-Sampaio et al., 2004a). As in human kidneys, the swine renal artery splits into segmental arteries. However, instead of what is seen in humans where most kidneys have five segments, the most common division in swine kidneys (accounting for 42% of organs) is two segments, one cranial and another caudal (Fig. 18.2),

while three, four, or five segments can be found in 24%, 23%, and 3%, respectively (Pereira-Sampaio et al., 2007). The renal venous system of pigs is quite similar to that found in humans. Common to those species, and of surgical importance, is the occurrence of free venous anastomosis on different levels (Bagetti Filho et al., 2008; Sampaio and Aragao, 1990) (Fig. 18.3).

Despite these anatomical similarities and differences, we must say that the pig kidney is the most useful model when anatomical aspects are of interest. However, this is not what is observed when we desire to study the kidney healing after laparoscopic partial nephrectomy.

Several authors used the pig for studying novel techniques and technologies for hemostasis and collecting system closure during laparoscopic partial nephrectomy. However, this was performed without validating this model for this purpose. Moreover, most studies did not use control groups. Ames et al. (2005) published a study that investigated if the porcine kidney would be an appropriate model for experimental evaluation of renal collecting system closure during laparoscopic partial nephrectomy. In this experiment, eight pigs were submitted to heminephrectomy, exposing the collecting system, which was left opened. The authors visualized the opened collecting system by transoperatory retrograde ureteropyelogram, and performed renal hemostasis with a monopolar energy source, applied only on renal parenchyma, and taking care to avoid the collecting system. Contrary to what was expected, none of the animals
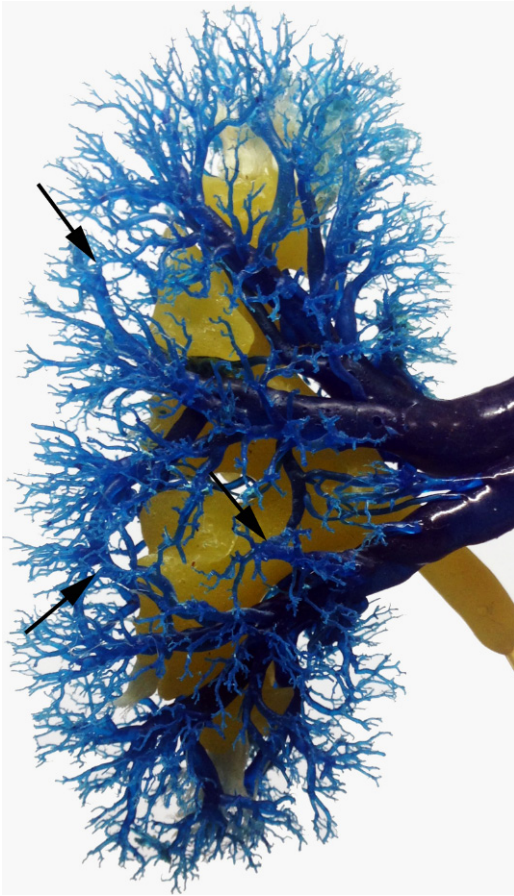
FIGURE 18.3   **Ventral view of endocast (pelvicaliceal system and renal veins) of pig right kidney, showing transverse anastomoses (arrows).**

showed urinary leakage after 1 or 3 weeks. Furthermore, these authors operated six pigs, which were also submitted to partial nephrectomy without collecting system closure, but their ureters were dissected, and after placement of an 8-french catheter in its lumen, a suture ligature was tied around it and left postoperatively. This intended to create a high-pressure renal collecting system porcine model, which was more prone to develop urinary leakage. All these six high-pressure renal collecting system animals had moderate hydronephrosis to the level of the tie obstruction, as documented by visual inspection on autopsy, on the eighth postoperative day. Even so, only one pig showed an urinoma. The conclusion of this study was that the porcine model (both with normal and high-pressure renal collecting system) is inadequate for evaluating the renal collecting system closure after partial nephrectomy.

After the publication of this study, our group decided to further investigate the subject. We performed a similar experiment in which 14 male domestic pigs were submitted to left partial laparoscopic nephrectomy, with the removal of 25% of the kidney total length at the caudal pole ($n = 7$) or at the cranial pole ($n = 7$) (de Souza et al., 2011). According to previous anatomical literature (Pereira-Sampaio et al., 2007), this would expose the caudal or the cranial major calices in all animals. During the surgery, the collecting system entering was determined when the surgeon felt a more dense structure to incise, and after complete removal of the renal pole region, the opening of the collecting system was confirmed by direct visualization (Fig. 18.4). In the same manner as
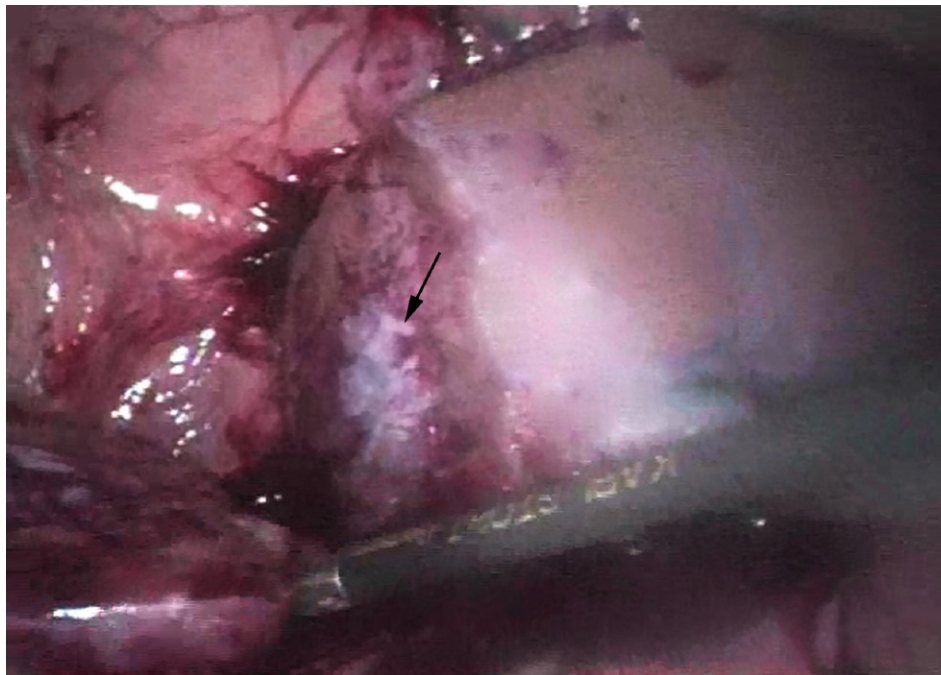
FIGURE 18.4   **Intraoperatory view of the opened collecting system (arrow) after the cranial pole resection of a pig kidney.**
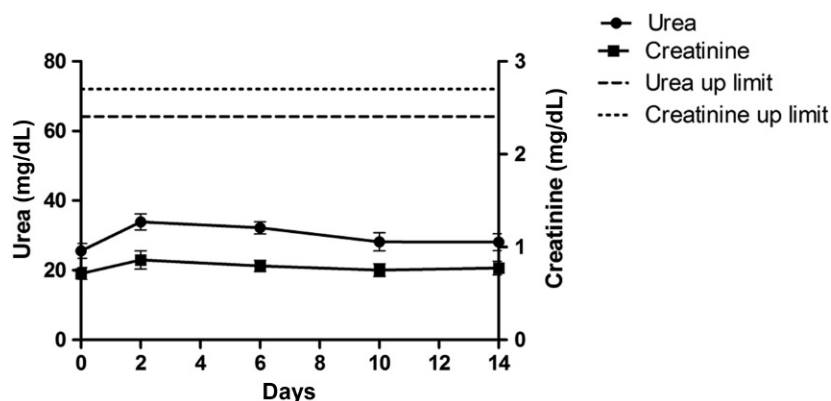
FIGURE 18.5 **Serum levels of urea and creatinine during the postoperative period of the experiment with pigs.** *Source: Obtained from de Souza, D.B., Abilio, E.J., Costa, W.S., Sampaio, M.A., Sampaio, F.J., 2011. Kidney healing after laparoscopic partial nephrectomy without collecting system closure in pigs. Urology 77 (2), 508.e5–508.e9.*

performed by Ames et al. (2005), monopolar energy was applied for hemostasis only in the parenchyma, avoiding coagulation near the collecting system. Once again, after complete hemostasis, the collecting system opening was verified and no internal collecting system drainage catheter was inserted. The animals were clinically evaluated during 14 days after surgery, and afterward, they were submitted to euthanasia by anesthetic overdose. At the 13th postoperative day, the animals were transferred to individual stalls. Methylene blue was diluted in the drinking water for staining the urine to demonstrate any urinary leakage, which would stain the tissue around the kidney. Furthermore, serum levels of urea and creatinine were assessed prior to surgery and at postoperative days 2, 6, 10, and 14, to assess the renal function and any possible peritoneal absorption due to intracavitary urinary leakage.

We observed that all animals recovered well after surgery, presenting normal functions (ambulation, food and water intake, urination, and defecation) within the first 24 postoperative hours. Although serum levels of urea and creatinine showed a slight increase in the second postoperative day, these levels gradually decreased to preoperative levels until the end of the experiment period. Even so, these levels remained far below the upper limit of reference levels for pigs. At necropsy, the abdominal cavity was normal, with normal quantity and aspect of peritoneal liquid. Moreover, the peritoneal fluid levels of urea and creatinine were similar to the normal serum levels (Fig. 18.5).

During necropsy, the peritoneal fluid was collected for urea and creatinine analysis. The abdominal cavity and retroperitonium were evaluated for any evidence of urinary leakage around the operated kidney. Special attention was paid for identification of urinomas, urinary fistulae, peritonitis, and methylene blue extravasation. The operated kidney was removed, and the ureter was catheterized for performing an ex vivo retrograde

pyelogram, to evaluate any leakage of the contrast medium. Then, the organ was fixed in 4% formaldehyde, and the operated pole was cleaved to obtain a fragment of renal tissue together with adhered adjacent tissues. This fragment was processed for histological analyses.

In all animals, the operated pole was completely covered by fibrous tissue, which hindered the identification of the collecting system (Fig. 18.6). We also observed several adherences of the operated pole to adjacent organs (spleen, colon, and pancreas). The urinary bladder was filled with blue-colored urine; nevertheless, no blue stained tissue was observed around the kidney. No
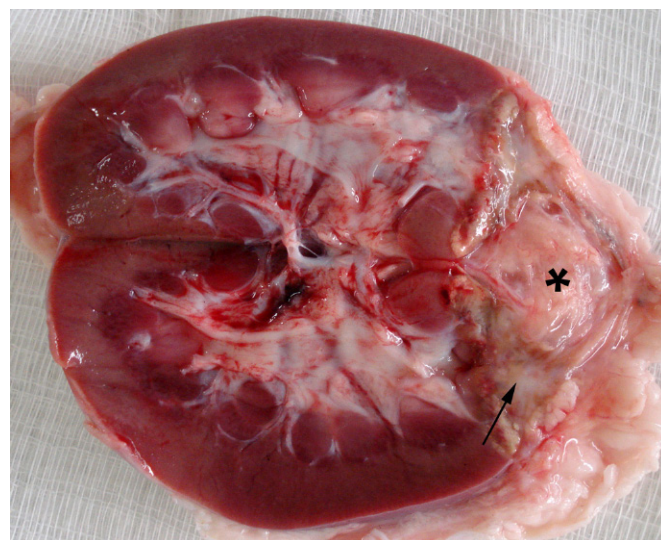
FIGURE 18.6 **Longitudinal section of a left pig kidney submitted to a caudal pole partial nephrectomy.** It is noted a fibrosis in the operated renal pole sealing the collecting system that was sectioned *(arrow)*. It is also depicted the presence of fat firmly adhered to the fibrotic tissue *(asterisk)*. *Source: Obtained from de Souza, D.B., Abilio, E.J., Costa, W.S., Sampaio, M.A., Sampaio, F.J., 2011. Kidney healing after laparoscopic partial nephrectomy without collecting system closure in pigs. Urology 77 (2), 508.e5–508.e9.*
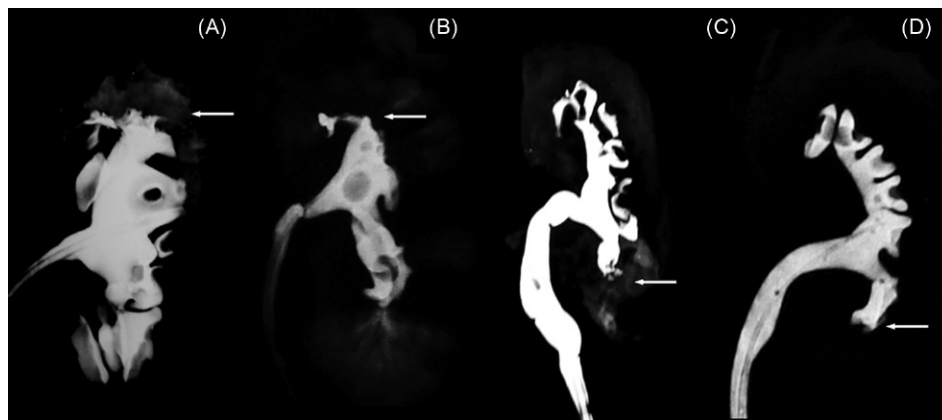
FIGURE 18.7   Ex vivo swine retrograde pyelograms performed 14 days after left kidney laparoscopic partial nephrectomy without closure of the collecting system in the cranial pole (A–B) and in the caudal pole (C–D) show the absence of contrast medium leakage at the operated poles *(arrows). Source: Obtained from de Souza, D.B., Abilio, E.J., Costa, W.S., Sampaio, M.A., Sampaio, F.J., 2011. Kidney healing after laparoscopic partial nephrectomy without collecting system closure in pigs. Urology 77 (2), 508.e5–508.e9.*

urinomas, fistulae, or any other signs of urine leakage were found in any animal; moreover, no abnormalities were found in the nonoperated (right) kidney.

The retrograde pyelograms depicted the collecting system anatomy without evidence of any contrast medium extravasation. In some kidneys, submitted to pyelograms with injection under high pressure, the contrast medium penetrated the renal parenchyma (collecting ducts) and still did not present any leakage in the operated pole (Fig. 18.7). Interestingly, we have some cases of high pressure pyelograms, in which we observed a rupture of collecting ducts and extravasation in the nonoperated pole, while the operated pole remained without leakage.

As observed in the histological analysis, the operated pole healed with a connective fibrotic tissue completely covering the renal tissue in all analyzed fields. Several adherences between the operated pole and adjacent organs were also observed under microscopy. The connective tissue presented great density of fibroblasts, which were more commonly seen around the blood vessels. As depicted by Sirius red staining method, observed under polarized light, the connective tissue covering the operated pole was bright red, indicating a predominance of type I collagen (Fig. 18.8).

Therefore, this study showed that the pig collecting system healing is quite different from that of humans. Although in pigs, the kidney heals after partial nephrectomy without any attempt for collecting system closure or internal drainage, with great deposition of collagen and firm adherences to adjacent organs; in humans, urinary leakage after this kind of surgery is considered a common and major complication (Breda et al., 2009), and is observed in 1.9%–5.5% of patients, even after suturing of the collecting system and applying sealant agents (Stephenson et al., 2004; Zorn et al., 2007).

Ames et al. (2005), in their study, postulated that the absence of Gerota's fascia and diminished renal adipose capsule in pigs would allow urine to flow into the peritoneal cavity and be absorbed. Nevertheless, the findings of our study (de Souza et al., 2011) are not in agreement with this theory because our analysis showed no significant alterations in the levels of urea and creatinine both in serum and peritoneal fluid.

The deposit of firm connective tissue over operated kidney is a common finding in several studies, which applied different methods of hemostasis and collecting system repair after partial nephrectomies in pigs (Anderson et al., 2007; Eret et al., 2009; Sabino et al., 2007; Sprunger and Herrell, 2005), although local adherences, as seen in our study, were not reported. The great amount of fibroblasts in tissue examined 14 days after surgery, especially around blood vessels, indicates that synthesis and degradation of collagen may still be occurring.

At the time of the publication of our study, although it was not exactly known how the swine collecting system spontaneously heals after partial nephrectomy, we suggested that the swine has an abundant muscular coat on its renal pelvis and calyces, as noted on our gross examinations. Thus, this musculature would contract and temporarily close the opened collecting system until connective tissue is deposited over the kidney wound. Then, we further investigated, and objectively compared, the human and pig's histological aspects of the collecting system by using histomorphometric methods (Simoes et al., 2016).

For this purpose, ten control kidneys from each species were obtained and fixed in 4% formaldehyde. Fragments containing the renal collecting system were collected from each kidney, routinely processed for paraffin embedding, and used for the histomorphometric analysis.
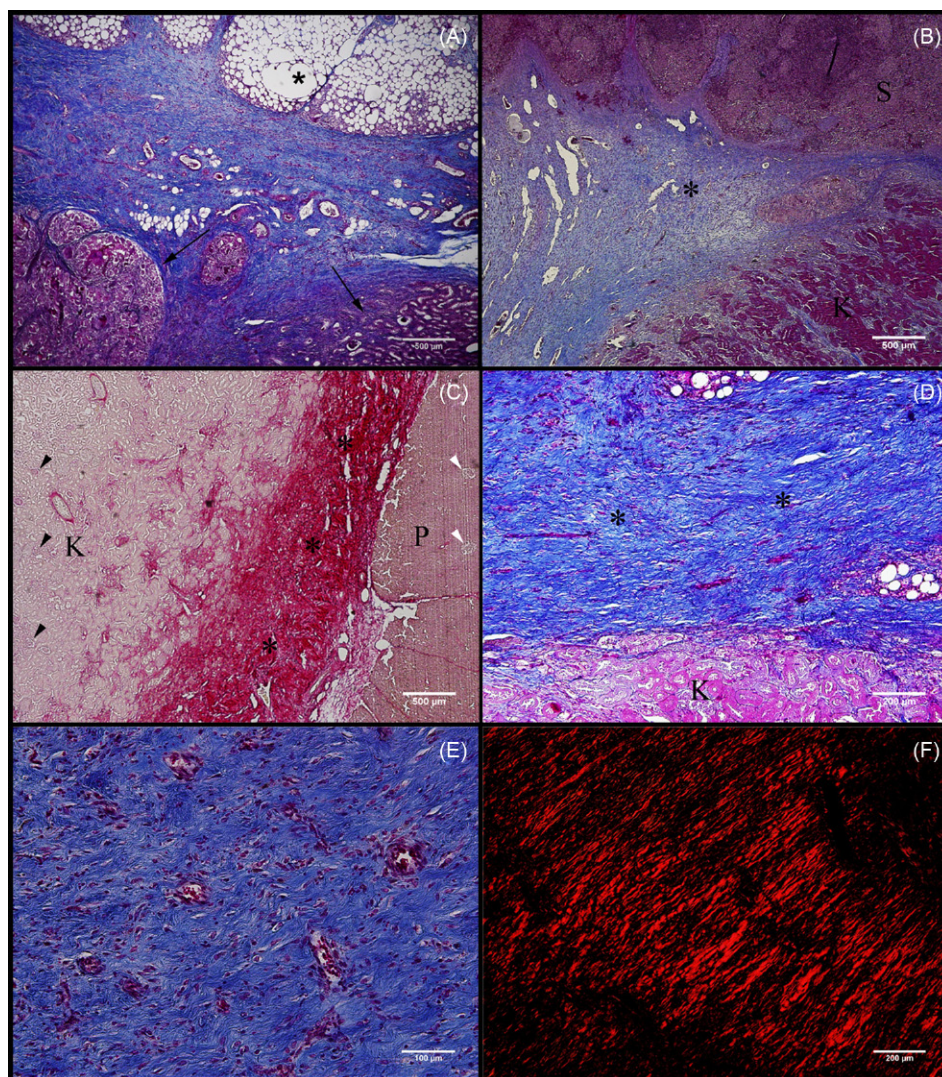
FIGURE 18.8 **Histological images of the operated region in left swine kidneys submitted to partial nephrectomy, in the 14th postoperative day.** (A) Image shows connective tissue between the renal parenchyma *(arrows)* and the adipose renal capsule *(asterisk)*. Masson's trichrome, ×40. (B) Image demonstrating adherence *(asterisk)* between splenic tissue *(S)* and kidney parenchyma *(K)*. Masson's trichrome, ×40. (C) Image depicted the pancreas *(P)* attached to the kidney parenchya *(K)* by collagen *(asterisks)*. Note islets of Langerhans *(white arrowheads)* and glomeruli *(black arrowheads)*. Picrosirius red, ×40. (D) Image shows the kidney parenchyma at the operated pole *(K)* covered by connective tissue *(asterisks)*. Masson's trichrome, ×100. (E) Image shows a strong presence of fibroblasts in the conective tissue. Masson trichrome, ×200. (F) Image demonstrates a predominance of type-I collagen covering the operated renal pole. Picrosirius red under polarization, ×100. *Source: Obtained from de Souza, D.B., Abilio, E.J., Costa, W.S., Sampaio, M.A., Sampaio, F.J., 2011. Kidney healing after laparoscopic partial nephrectomy without collecting system closure in pigs. Urology 77 (2), 508.e5–508.e9.*

Gosling et al. (1983) described the collecting system wall, including renal calyces and pelvis, with three distinct subepithelial layers: a mucosal connective tissue (which we referred as superficial layer), a submucosal muscular layer (which we referred as middle layer), and an adventitial connective tissue (which we referred as inner layer). In our study, we analyzed the thickness and the surface density of smooth muscle fibers, elastic system fibers, and cellular density of each of the three layers. We also analyzed the blood vessel surface density in the inner layer, where there is a higher concentration of blood vessels.

In both species, as described by Gosling et al. (1983), the superficial layer was found immediately under the urothelium and was composed mainly of connective tissue. Under this layer, there was a middle layer, where an aggregation of smooth muscle fibers was observed. Finally, the inner layer connective tissue with a high concentration of blood vessels was observed.

We found that the swine kidney superficial layer was 43% thinner than that in humans; the thickness of the middle layer was similar in human and swine samples; and the thickness of the inner layer of swine was 53% higher than those of the human samples (Fig. 18.9).
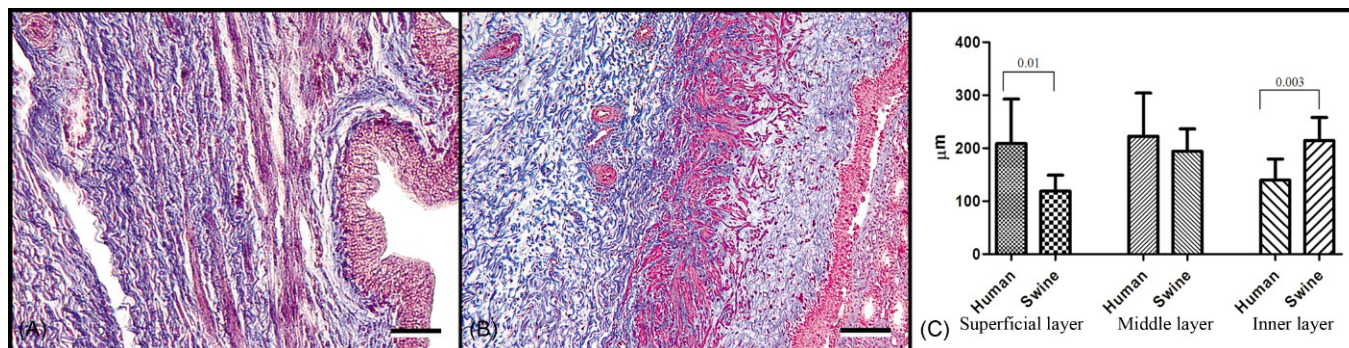
FIGURE 18.9 Photomicrographs (of sections stained with Masson's trichrome and captured under 100× magnification) illustrating the three different layers observed under the urothelium: (A) human and (B) swine. Image (C) shows the differences in layer thickness between the species. Scale bar represents 200 μm. *Source: Modified from Simoes, M., de Souza, D.B., Gallo, C.B., Pereira-Sampaio, M.A., Costa, W.S., Sampaio, F.J., 2016. Histomorphometric comparison of the human, swine, and ovine collecting systems. Anat. Rec. (Hoboken) 299 (7), 967–972.*
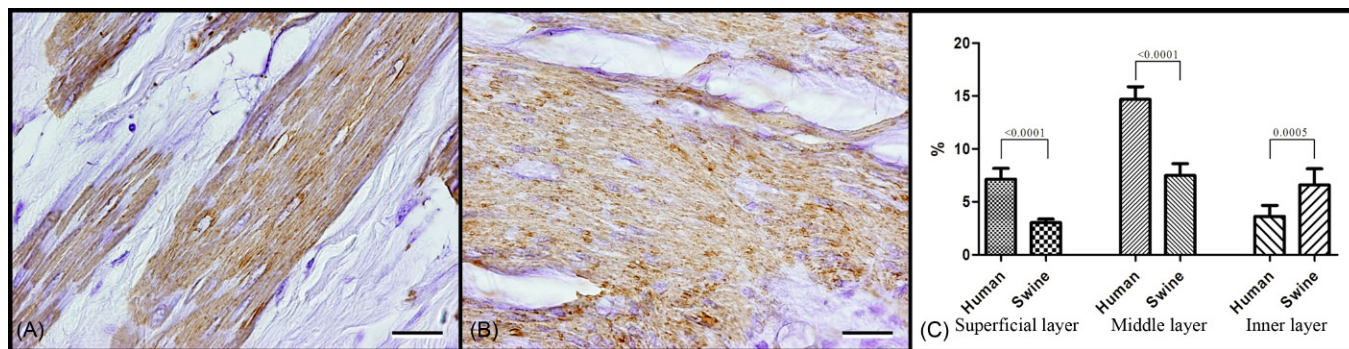
FIGURE 18.10 Photomicrographs (of sections immunolabeled with anti alpha-actin antibodies and captured under 1000× magnification) illustrating the smooth muscle fibers (seen in *brown*) in the inner layer of (A) human kidneys and (B) swine kidneys. The swine sections have a much higher density of muscle fibers than do sections from humans. Image (C) shows the differences in muscle fiber densities in the three layers among the species. Scale bar represents 20 μm. *Source: Modified from Simoes, M., de Souza, D.B., Gallo, C.B., Pereira-Sampaio, M.A., Costa, W.S., Sampaio, F.J., 2016. Histomorphometric comparison of the human, swine, and ovine collecting systems. Anat. Rec. (Hoboken) 299 (7), 967–972.*

With regard to the surface density of the smooth muscle fibers, in the superficial layer, swine samples had 58% less muscle than humans; in the middle layer, swine samples showed 49% less density than human tissue; however, as for the inner layer, swine samples had values 82% higher than those observed in the human samples (Fig. 18.10).

No difference was observed on the surface density of elastic fibers in the superficial layer between human and swine samples; however, in the middle layer, pig kidney had values 87% higher than those of the human samples; a 15% lower density of elastic fibers in the inner layer was also present in human samples, as compared with swine samples.

The surface density of blood vessels in swine samples (which was analyzed only in the inner layer) was 59% higher than that in the human samples (Fig. 18.11).

The cellular density of the superficial layer in human samples was 19% lower than those of the swine; in the middle layer, the human samples had 46% lower density than the swine; and in the inner layer human samples was 59% higher than that in the swine samples.

With these results we demonstrated that the swine collecting system has a rich vasculature in its inner layer, which is also thicker than that in humans. Thus, it is possible that after the surgical opening, the blood vessels of the inner layer of the swine kidney deposit a clot that covers the collecting system (Fogelson and Neeves, 2015). This would temporarily seal the opening until the collagen that was reported on our previous study (de Souza et al., 2011) is deposited. In addition, this rich vascularization can facilitate chemotaxis, improving the inflammatory response and fibroblast migration to the local area.

A higher density of elastic fibers in the middle layer of the swine collecting system was also observed. It is well known that these elastic fibers are the source of elasticity in the tissue, increasing its resistance to mechanical pressures (Gallo et al., 2012). Therefore, the large amount of elastic fibers found in the swine kidney could cause contraction of the injured collecting system, contributing to its temporary sealing. Furthermore, in the thicker inner layer, swine have a massive density of smooth muscle. Contraction of the smooth muscle could help
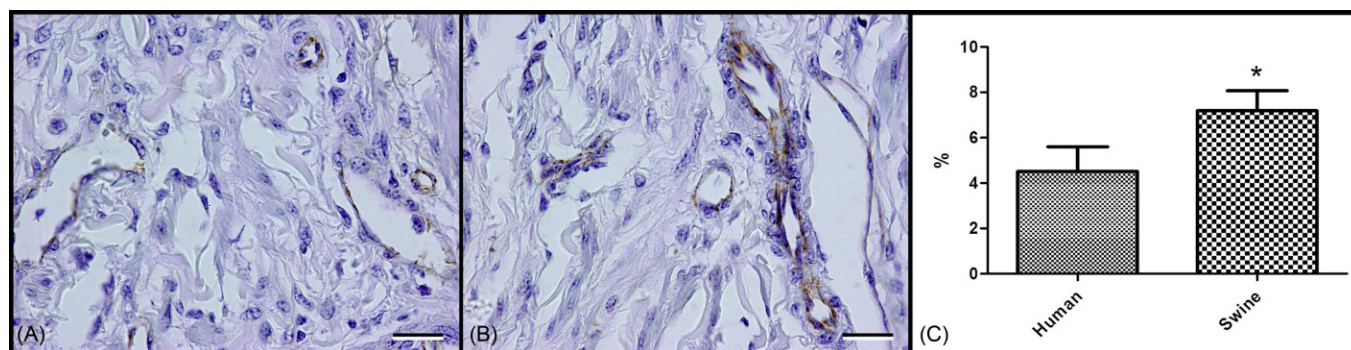
FIGURE 18.11 Photomicrographs (of sections immunolabeled with anti-CD31 antibodies and captured under 1000× magnification) illustrating the blood vessels (seen in *brown*) in the inner layer of (A) human kidneys and (B) swine kidneys. Image (C) shows the differences in blood vessels density in the inner layer among the species. Scale bar represents 20 μm.

in temporarily sealing the collecting system, which may explain the absence of urinary leakage in swine.

The results of this study suggested some links between the histology of the collecting system and its healing. Even so, other mechanisms must be involved. As we previously hypothesized (de Souza et al., 2011), the anatomical differences may play a role in the unusual kidney healing mechanism observed in swine. As the collecting system of this animal is narrower than that of humans, it could be sealed more easily. We also suggested that the swine kidney may have a more muscular collecting system than does the human kidney. However, the histological study of the collecting system showed that only the inner layer of the swine collecting system is more muscular than that of humans.

Other possible involved aspect that may explain the differences on collecting system healing after partial nephrectomy is the absence of renal fascia (Gerota's fascia) and the low amount of perinephric fat observed in swine. According to Ames et al. (2005), these structures could contribute to the closure of the collecting system in pigs. Future studies are still necessary to fully understand the differences and similarities among kidney healing processes in these species. It is possible that these differences and similarities may relate not only to the histological characteristics, but also to anatomical, physiological, and molecular aspects.

Even so, the morphological features of the human and swine collecting systems may partially explain the different healing processes following partial nephrectomy. The highly vascular, thicker, and more muscular inner layer (adventitial connective tissue) of the swine kidney, as well as the higher density of elastic fibers in the middle layer (submucosal muscular), may be important factors in elucidating the unique collecting system healing process seen in this animal. This reinforces our previous conclusion that the pig kidney is not an adequate experimental model for research on which collecting system healing is an important aspect to be considered.

3 THE SHEEP AS ANIMAL MODEL

After reporting the pig as an inadequate model for research on collecting system healing after partial nephrectomy, one major concern arose. Which other animal should be used for this purpose, instead of the traditional swine model? Until early 2016 no other animal has been suggested to be a more suitable model for research on collecting system repair (de Souza et al., 2016). Therefore, even knowing that the pig model shows major limitations, this species continued to be used for this purpose (Duchene, 2011; Shikanov et al., 2009). We started then to investigate an alternative animal model that may show a collecting system healing more similar to that seen in human clinical settings.

The sheep has been used as a model for healing studies since 1960 (Lascelles and Claringbold, 1960), and is currently widely used for studying bone healing (Christou et al., 2014; James et al., 2016; Liu et al., 2016; Malhotra et al., 2014; Martini et al., 2001). It was shown that ovine show a comparable bone healing rate to that of humans and have been previously established as a useful model for human bone turnover and remodeling activity (Malhotra et al., 2014; Martini et al., 2001; Pearce et al., 2007). Thus, we supposed that as this species shows similar aspects on bone healing, it may also be a suitable model for studying kidney healing. Sheep have been used for some studies on renal denervation, radiofrequency, and hydronephrosis (Alexander et al., 2014; Booth et al., 2015; Haghighi et al., 2006; Springer et al., 2015; Tanaka et al., 2014); however, the kidney healing after laparoscopic partial resection was not reported. With the objective of investigating the kidney healing in sheep after laparoscopic partial nephrectomy without closure of the collecting system, we performed a study very similar to that previously done in pigs (de Souza et al., 2011).

Eight adult female domestic sheep were subjected to laparoscopic partial nephrectomy. The caudal pole of the left kidney was removed, and the renal pelvis was

purposefully left open to assess the animal's spontaneous healing. As in pigs, a more dense structure was felt during the incision of the collecting system. After completely removing the renal pole region, the opened collecting system was confirmed by direct visualization, and monopolar cautery was applied for hemostasis only in the parenchyma. The opened collecting system was once again verified after hemostasis, and no internal collecting system drainage catheter was inserted.

The animals were evaluated daily for 14 days after surgery and, after this period, were euthanized by anesthetic overdose. Serum levels of urea and creatinine were drawn before surgery and on postoperative days 2, 6, 10, and 14, to assess renal function and any possible peritoneal absorption due to intracavital urinary leakage.

During necropsy, peritoneal fluid was collected for urea and creatinine analysis. The peritoneal cavity and retroperitoneal space were evaluated for evidence of urinary leakage around the operated kidney. Special attention was given to identifying any urinomas, urinary fistulae, or peritonitis and visceral adhesions.

The operated kidney was removed, and the ureter was catheterized. To evaluate any leakage of contrast medium, an ex vivo retrograde pyelogram was performed, and after the pyelogram, the kidney was injected with methylene blue ink through the ureter to directly distinguish the area of urinary leakage onto the kidney. The kidneys were then fixed in 4% formaldehyde, and the operated pole was sectioned to obtain renal tissue together with adhered adjacent tissues for histological analyses.

As in the experiment with pigs, all animals had a normal postoperative recovery with a return to normal functioning (ambulation, food and water intake, urination, and defecation) within the first 24 h. Serum levels of urea and creatinine increased on postoperative day 2, but both levels gradually decreased from their early postoperative levels on the following days (Fig. 18.12).

FIGURE 18.13 Urea and creatinine levels in serum samples collected preoperatively (A) and postmortem (B) and in peritoneal fluid samples (C) of sheep subjected to laparoscopic partial nephrectomy without collecting system closure, indicating some urine leakage to the peritoneal cavity. †, Different from A; ‡, different from B. *Source: Obtained from de Souza, D.B., Abilio, E.J., Costa, W.S., Sampaio, M.A., Sampaio, F.J., 2011. Kidney healing after laparoscopic partial nephrectomy without collecting system closure in pigs. Urology 77 (2), 508.e5–508.e9.*

Peritoneal fluid collected during necropsy contained higher urea levels than serum samples collected both preoperatively and postoperatively. Necropsy-obtained creatinine peritoneal fluid levels were also higher than preoperative serum levels (Fig. 18.13).

During the postmortem gross examination, it was possible to note an urinoma surrounding the caudal pole in one animal. In this animal, the levels of urea and creatinine in the peritoneal liquid were 7.6 and 18.9 times higher, respectively, than its previous serum levels. No other macroscopic signs of urine leakage were found in the other animals. Moreover, several adhesions were observed connecting the operated pole with adjacent organs (rumen, omentum, and colon) and perirenal adipose tissue.

The retrograde pyelograms demonstrated contrast-medium extravasation through the operated pole in all kidneys. Usually, the contrast medium was observed in sinus tracts in the perirenal tissue. Injection of methylene blue ink through the ureter also confirmed that the collecting system was still open, as the contrast was easily observed extravasating into the perirenal area (Fig. 18.14).

Histological analysis confirmed the adhesions to adjacent organs in which connective tissue with fibroblasts covered the operated pole. The analysis of Sirius red–stained slides under polarized light indicated that this connective tissue had areas with different amounts of collagen fibers, which were characterized as types I and III (Fig. 18.15).

The deposit of firm connective tissue over the operated kidney has been a common finding after partial nephrectomies in pigs (Anderson et al., 2007; Eret et al., 2009; Sabino et al., 2007; Sprunger and Herrell, 2005), and we have also reported and described the histological aspects of this connective tissue (de Souza et al., 2011).

FIGURE 18.12 **Serum creatinine and urea levels of sheep submitted to laparoscopic partial nephrectomy without collecting-system closure.** Both creatinine and urea levels increased on day 2 postoperatively, followed by a gradual decrease to preoperative levels. *Source: Obtained from de Souza, D.B., Abilio, E.J., Costa, W.S., Sampaio, M.A., Sampaio, F.J., 2011. Kidney healing after laparoscopic partial nephrectomy without collecting system closure in pigs. Urology 77 (2), 508.e5–508.e9.*

FIGURE 18.14 Ex vivo retrograde pyelograms (A–B) and methylene blue–injected operated sheep kidney (C) removed 14 days after laparoscopic partial nephrectomy without collecting system closure. (A–B) Ex vivo retrograde pyelograms demonstrated leakage of the opened collecting system *(arrows)* and sinus tracts forming *(arrowheads)*. (C) Retrograde injection of methylene blue ink showed leakage from the collecting system into the perirenal tissue. *Source: Obtained from de Souza, D.B., Abilio, E.J., Costa, W.S., Sampaio, M.A., Sampaio, F.J., 2011. Kidney healing after laparoscopic partial nephrectomy without collecting system closure in pigs. Urology 77 (2), 508.e5–508.e9.*
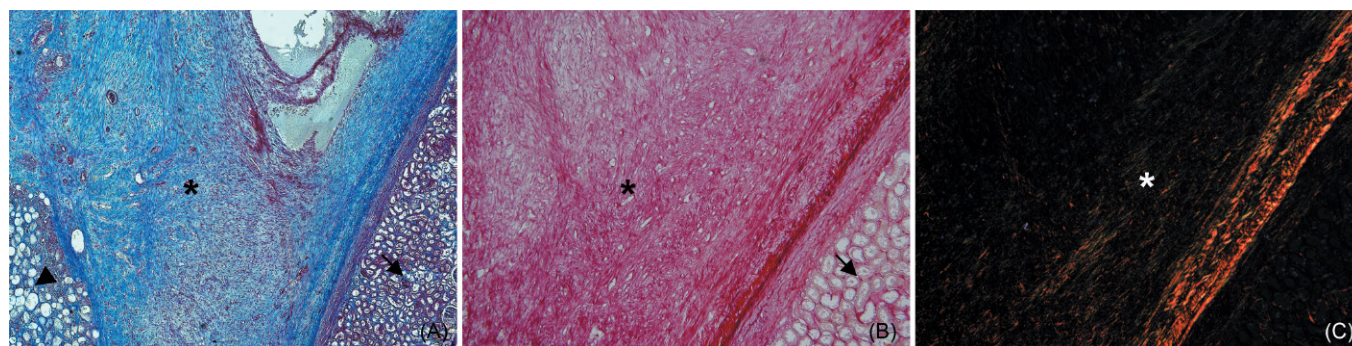
FIGURE 18.15 **Photomicrographs of ovine operated kidneys covered by connective tissue *(asterisk)*.** (A) Masson's trichrome stain shows an adhesion of connective tissue between the renal cortex *(arrow)* and adipose tissue *(arrowhead)*. (B–C) The same histological field observed under bright (B) and polarized light (C). Outside the renal capsule, Sirius red stain highlights loose connective tissue with types I and III collagen fibers. *Source: Obtained from de Souza, D.B., Abilio, E.J., Costa, W.S., Sampaio, M.A., Sampaio, F.J., 2011. Kidney healing after laparoscopic partial nephrectomy without collecting system closure in pigs. Urology 77 (2), 508.e5–508.e9.*

This tissue is mainly composed by type I collagen in pigs, while in sheep, type III collagen was also present in the connective tissue deposited over the resection area. This indicates that the healing process is histologically different between pigs and sheep, and may help to understand why urinary leakage occurs in one but not in other species.

With these results, we figured out that the sheep's collecting system does not heal as it does in pigs (de Souza et al., 2011), rather behaves similarly to what is seen clinically in humans in which urinary leakage is a common complication after partial nephrectomies (Breda et al., 2009; Zorn et al., 2007). Thus, we concluded that the sheep, instead of the pig, should be considered as an adequate experimental model for research on collecting system healing after partial nephrectomy.

Furthermore, many studies advocating different methods for collecting system closure were performed in pigs (Bishoff et al., 2003; Ogan et al., 2003; Orvieto et al., 2007; Shikanov et al., 2009), which is an inadequate model for studying kidney healing (closing spontaneously within 14 days). These methods should be evaluated in the sheep model before clinical usage.

Ames et al. (2005), in their study, postulated one possible explanation for the absence of urinoma formation in pigs as the inexistence of Gerota's fascia, and that the diminished renal adipose capsule in pigs would allow urine to flow into the peritoneal cavity and be absorbed. Although we refuted this theory in our study performed in pigs (de Souza et al., 2011), we reevaluated this hypothesis after the sheep experiment. Interestingly, some sheep specimens showed extravasation running around the kidney toward the cranial pole during retrograde pyelogram and methylene blue injection, suggesting the presence of a renal fascia similar to Gerota's fascia in humans. If confirmed, this anatomical feature might
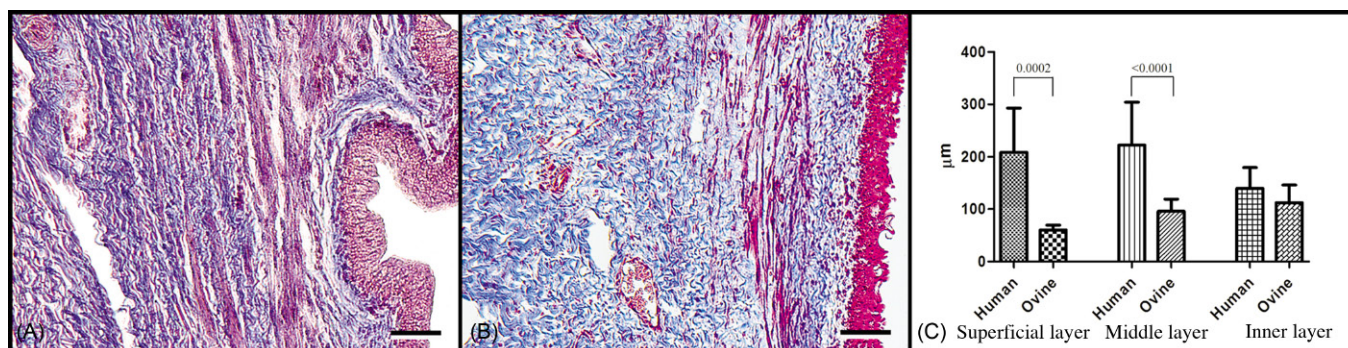
FIGURE 18.16 Photomicrographs (of sections stained with Masson's trichrome and captured under 100× magnification) illustrating the three different layers observed under the urothelium: (A) human and (B) ovine. Image (C) shows the differences in layer thickness between the species. Scale bar represents 200 μm. *Source: Modified from Simoes, M., de Souza, D.B., Gallo, C.B., Pereira-Sampaio, M.A., Costa, W.S., Sampaio, F.J., 2016. Histomorphometric comparison of the human, swine, and ovine collecting systems. Anat. Rec. (Hoboken) 299 (7), 967–972.*

help explain the similarity between kidney healing in sheep and humans. This question highlights the importance of knowing the anatomy of the experimental model used. After reviewing the literature regarding the theme, we realized that the anatomy of the sheep kidney and retroperitoneum has been little described, specially referring to renal surgery. Thus, we decided to deeply study and describe the renal anatomy of sheep (Buys-Goncalves et al., 2016).

The sheep kidneys are retroperitoneal and bean-shaped, but unlike the human and pig kidneys, they are asymmetric. The right kidney is most cranial and extends from the first to the third lumbar vertebrae, while the left kidney extends from the second to the fourth lumbar vertebrae. Concerning the volume, sheep kidney is smaller than the human and porcine kidney. The kidney length in an adult animal ranges from 5.5 to 7 cm, while the renal weight ranges from 100 to 160 g (Nickel et al., 1979). The lower kidney volume can interfere with healing and injury caused by less invasive procedures, such as cryoablation and radiofrequency ablation. Thus, sheep kidney does not seem to be a good model for renal

procedures in which the volume and position of the kidneys are relevant points to be considered.

We have also studied the sheep collecting system normal histology, and compared it with human and pigs' samples (Simoes et al., 2016). As we hypothesized, the collecting system of sheep is much more similar to that in humans than the pig's is, although differences are still present.

The superficial and middle layer of the ovine collecting system is 43% and 57% thinner than humans, respectively. However, the inner layer thickness of human and ovine is similar (Fig. 18.16).

The surface density of the smooth muscle fibers in superficial and middle layers also showed differences between humans and sheep. In the superficial layer, sheep had 36% less smooth muscle fibers than humans, and in the middle layer, ovine samples were 18% lower than that in human samples. However, in the inner layer, ovine samples had 39% less smooth muscle than that in human samples (Fig. 18.17).

With regard to the surface density of elastic fibers in the superficial layer, no difference was observed between
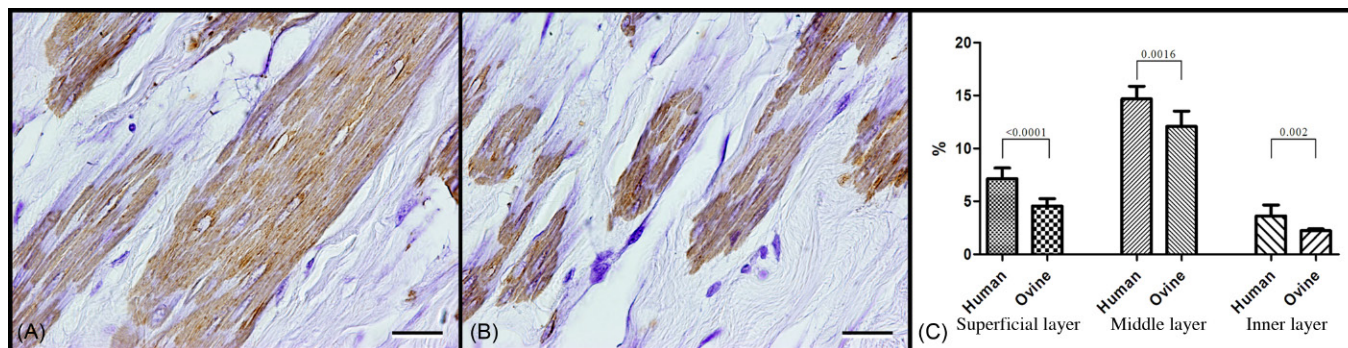
FIGURE 18.17 Photomicrographs (of sections immunolabeled with anti alpha-actin antibodies and captured under 1000× magnification) illustrating the smooth muscle fibers (seen in *brown*) in the inner layer of (A) human kidneys and (B) ovine kidneys. Image (C) shows the differences in muscle fiber densities in the three layers among the species. Scale bar represents 20 μm. *Source: Modified from Simoes, M., de Souza, D.B., Gallo, C.B., Pereira-Sampaio, M.A., Costa, W.S., Sampaio, F.J., 2016. Histomorphometric comparison of the human, swine, and ovine collecting systems. Anat. Rec. (Hoboken) 299 (7), 967–972.*
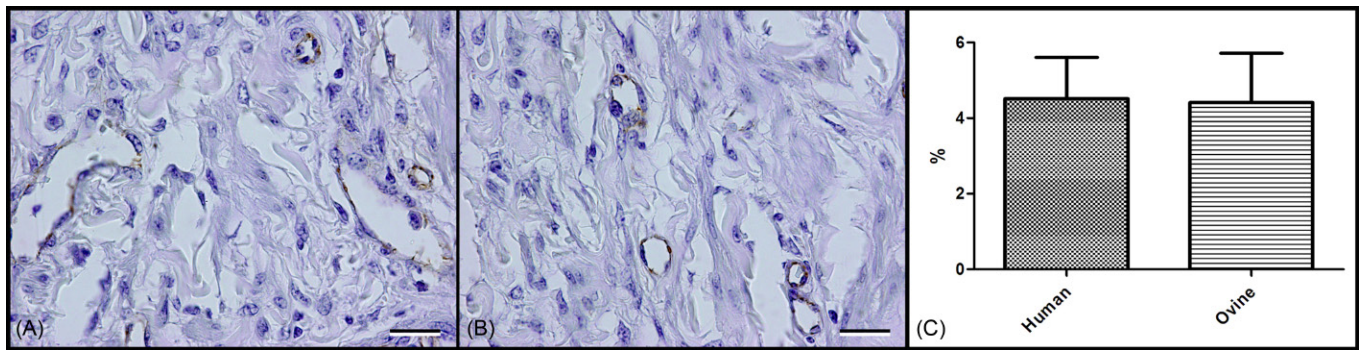
FIGURE 18.18 Photomicrographs (of sections immunolabeled with anti-CD31 antibodies and captured under 1000× magnification) illustrating the blood vessels (seen in *brown*) in the inner layer of (A) human kidneys and (B) ovine kidneys. Image (C) shows the differences in blood vessels density in the inner layer among the species. Scale bar represents 20 μm.

humans and sheep. As for the middle and inner layers, ovine samples had 46% and 15% more fibers than humans samples, respectively. However, the surface density of blood vessels (which was analyzed only in the inner layer) was statistically similar among these species (Fig. 18.18).

The cellular density of human superficial layer was 18% lower than those of ovine values. With regard to the middle and inner layers, no difference was observed between the human and ovine sample cellular densities.

This histological study depicted similarities between the ovine and human collecting systems, which supports our previous findings that the sheep's collecting system heals more similarly to what is seen clinically in humans, and this species should be considered an adequate experimental model for research on collecting system healing after partial nephrectomy. Specifically, it seems that the densities of blood vessels and elastic fibers are quite similar between these two species. Furthermore, the muscle fibers and cellular densities in the middle and inner layers of ovine samples resemble those of humans.

We then concluded that the comparable vascular and elastic fiber densities observed in all layers of the human and ovine kidneys, as well as the similar cellular and muscular densities of the middle and inner layers, may be the reasons for the similarities observed between human and ovine kidney healing (Simoes et al., 2016).

In addition to the histology, detailed anatomical study was recently published on the kidney collecting system and the branching pattern of the renal artery in ovine (Buys-Goncalves et al., 2016). We analyzed 38 ovine kidneys using three-dimensional endocasts of the collecting system together with the intrarenal arteries. The endocasts were prepared injecting a yellow and red polyester resin into the ureter and renal artery, respectively, and further digesting all tissue by immersion in hydrochloric acid baths.

The casts of the renal collecting system demonstrated a renal pelvis with several recesses. Thus, instead of a calyceal system as in human and pig kidneys (Barcellos

Sampaio and Mandarim-de-Lacerda, 1988; Sampaio et al., 1998), the collecting system consists only of a renal pelvis with several recesses on its edge. The recesses of the renal pelvis are expansions of the renal pelvis cavity, surrounding the renal pyramids. Researchers, who are familiar with the human calyceal system, may confuse the recesses of the renal pelvis with the minor calyces in urograms. Recesses were observed on both dorsal and ventral surfaces of the renal pelvis, varying from 11 to 19 (mean of 16) in each kidney. Due to lack of renal calices, the sheep kidney is not considered an adequate model for humans if the collecting system anatomy is the main point. Nevertheless, understanding its anatomy is important because we demonstrated that sheep could be a better model than pig for studies on collecting system healing.

In all endocasts, the renal artery was singular and divided into dorsal and ventral primary branches. These branches of the renal artery gave rise to different segmental branches that ran along the dorsal and ventral surface of the renal pelvis, which passed into the space between the recesses of the renal pelvis as interlobar arteries to reach the renal cortex (Fig. 18.19). This primary division of the renal artery is similar to humans (Sampaio and Aragao, 1990).

The cranial pole of all casts was supplied by two segmental arteries originating from the cranial segmental arteries from both dorsal and ventral branches of the renal artery. Interlobar arteries originated from these cranial segmental arteries and passed throughout the grooves between the recesses of the renal pelvis to reach the cortex (Fig. 18.20). This relationship between the arteries and the collecting system at the cranial pole is very similar to that of human (Sampaio and Aragao, 1990). However, the sheep does not have the retropelvic artery related to the upper infundibulum as humans. This artery, when present in humans (57% of cases), irrigates the posterior region of the kidney and, when injured during partial nephrectomy of the upper pole, can promote important bleeding and a large damage of the remaining
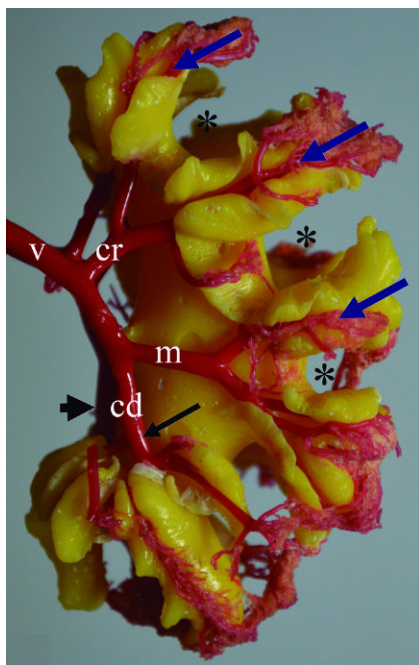
FIGURE 18.19 **Ventral view of endocast of sheep left kidney, showing ventral branch *(v)* of the renal artery divided into cranial *(cr)* middle *(m)*, and caudal *(cd)* segmental arteries.** Ventral mid zone is supplied only by the middle segmental artery. The caudal pole is supplied by the ventral *(black long arrow)* and dorsal *(black short arrow)* caudal segmental arteries. The interlobar arteries *(blue arrows)* run between the recesses of the renal pelvis *(asterisk)*. *Source: Obtained from Buys-Goncalves, G.F., De Souza, D.B., Sampaio, F.J., Pereira-Sampaio, M.A., 2016. Anatomical relationship between the kidney collecting system and the intrarenal arteries in the sheep: contribution for a new urological model. Anat. Rec. 299 (4), 405–411.*

FIGURE 18.20 **Ventral view of endocast of sheep left kidney, showing ventral branch *(v)* of the renal artery divided into cranial *(cr)*, and caudal *(cd)* segmental arteries.** Ventral mid zone is supplied by the cranial and caudal segmental arteries *(asterisk)*. Cranial pole is supplied by the ventral *(long arrow)* and dorsal *(short arrow)* cranial segmental arteries. *Source: Obtained from Buys-Goncalves, G.F., De Souza, D.B., Sampaio, F.J., Pereira-Sampaio, M.A., 2016. Anatomical relationship between the kidney collecting system and the intrarenal arteries in the sheep: contribution for a new urological model. Anat. Rec. 299 (4), 405–411.*

parenchyma (Sampaio, 1992). Consequently, the cranial pole of the sheep kidney should not be considered as an adequate model for experimental procedures in which the retropelvic artery is the main point to be considered. In this case, the damage of the remaining parenchyma could form a fistula, which can cause an impairment in the kidney healing.

In 71% of the kidneys, the caudal segmental artery from the dorsal branch of the renal artery supplied the entire or part of the dorsal mid zone (Fig. 18.21). This relationship between the arterial branching pattern and the collecting system is different from humans, where the dorsal mid zone is irrigated by the posterior segmental artery (Sampaio and Aragao, 1990).

The ventral mid zone of the sheep kidney was also mostly supplied by the caudal segmental artery from the ventral branch of the renal artery. In 71% of the kidneys, the blood supply of the ventral mid zone was partial or entirely provided by the caudal segmental artery. This is different from humans, where the ventral mid zone is vascularized by horizontal branches from the anterior segmental artery (Sampaio and Aragao, 1990).

The caudal pole of the sheep kidney was supplied by the interlobar branches from the caudal segmental arteries of the dorsal and ventral primary branches of the renal artery in all cases. In humans (62%), the caudal pole is vascularized by inferior segmental arteries, which divide into anterior and posterior branches, sending interlobar arteries on both ventral and dorsal surfaces of the caudal pole (Sampaio and Aragao, 1990). Although the branching pattern of the intrarenal arteries into the caudal pole of the sheep kidney is not exactly the same, the relationship between the intrarenal arteries and the collecting system in the caudal pole is similar to humans, showing one artery on each side, which originated in the interlobar branches. Therefore, the sheep kidney can be considered a good model for urological procedures when the caudal pole arterial branching pattern is an important topic to be considered.

Despite the different anatomy of the sheep kidney collecting system from the human kidney, without a calyceal system, it does not preclude its use as a model for urologic procedures in which the anatomy of the collecting system is not the main point. Due to the similarities of the arterial branching pattern in the caudal renal pole between human and sheep, the sheep kidney could serve as an experimental model. However, the lack of a retropelvic artery discourages the use of the cranial renal pole in experiments in which arterial branches are an important aspect to be considered.
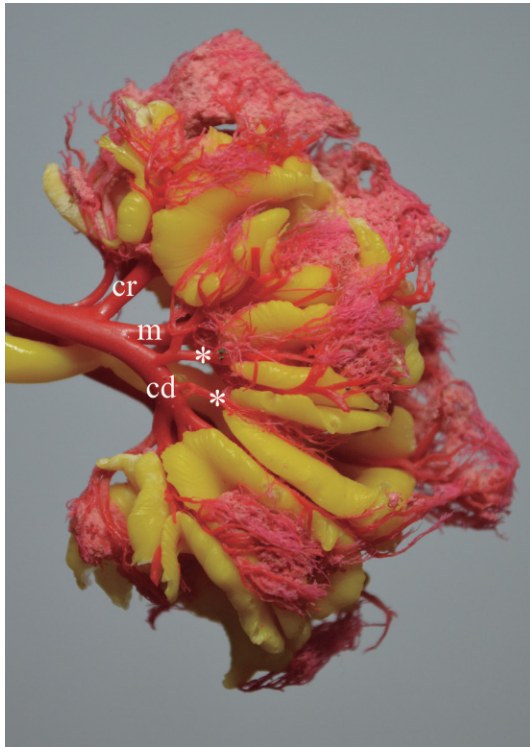
FIGURE 18.21 **Dorsal view of endocast of sheep right kidney, showing the dorsal mid zone irrigated only by branches (asterisk) from the caudal segmental artery (cd).** The cranial pole is supplied by the cranial (cr) and the middle (m) segmental arteries. *Source: Obtained from Buys-Goncalves, G.F., De Souza, D.B., Sampaio, F.J., Pereira-Sampaio, M.A., 2016. Anatomical relationship between the kidney collecting system and the intrarenal arteries in the sheep: contribution for a new urological model. Anat. Rec. 299 (4), 405–411.*

The sheep has other advantages as an experimental model over a pig. Sheep are very docile animals. Handling these animals is much easier than handling pigs; they offer a very calibrous external jugular vein for blood retrieval. Other beneficial aspects that should be pointed out are the more hygienic ovine stall, instead of the (almost always) malodorous swine facility, and the quietness ambient during restraint (instead of the screaming pigs). These factors make sheep handling for experimental purposes much less stressful than handling pigs, and this should also be considered when choosing the experimental model to be used.

4 THE RABBIT AS ANIMAL MODEL

Simultaneous to the experiment performed in sheep, we investigated the rabbit as a model for kidney healing studies after partial nephrectomy. Rabbits are widely used as animal models for studying different surgical and nonsurgical conditions (Abdullahi et al., 2014; Deponti et al., 2015; Kim et al., 2015; Lossi et al., 2016). This species is especially important as a kidney transplantation
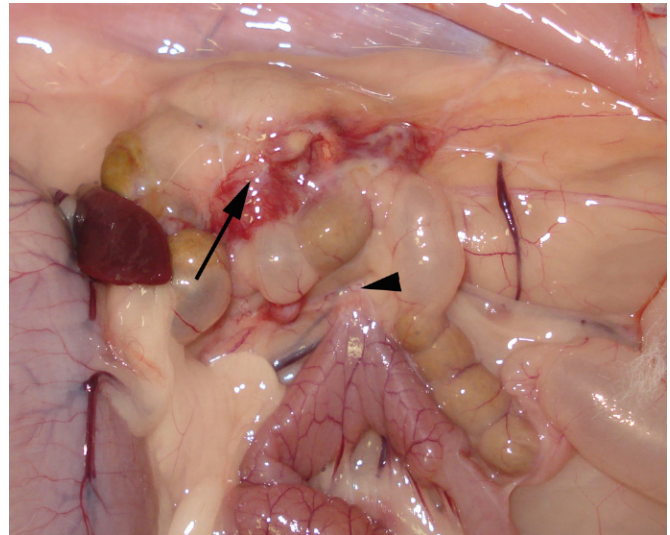
FIGURE 18.22 **Appearance of the abdominal cavity (dorsal region) of a rabbit, 14 days after laparoscopic partial nephrectomy without collecting system closure.** Note the adherence of a intestinal loop (arrowhead) to the renal adipose capsule (arrow).

model (He et al., 2015; Vera-Donoso et al., 2015; Yazici et al., 2015). Thus, we performed a similar experiment, as conducted in pigs and sheep, to evaluate if the rabbit would be an adequate model for kidney healing studies.

We studied eight rabbits that were submitted to left partial nephrectomy under laparoscopic access. The collecting system was left opened and the animals were submitted to euthanasia after 14 days. Kidneys were collected, and the same evaluation performed in sheep (necropsy, retrograde pyelogram, and retrograde injection of methylene blue ink) was conducted in rabbits.

During gross necroscopic examination, no evidence of urinary leakage or urinoma was observed, but adhesions of the operated pole to surrounding organs (mainly intestinal loops) were present (Fig. 18.22). The retrograde pyelogram depicted contrast-medium extravasation through the operated pole in six kidneys (75% of the eight operated) (Fig. 18.23). The other two kidneys did not present any extravasation, even after the collecting system being fulfilled with the contrast medium. In addition, the injection of methylene blue through the ureter confirmed that the collecting system was opened in 75% of the kidneys after 14 days from partial nephrectomy.

As seen in humans, the collecting system of rabbits does not heal spontaneously after being left opened in a partial nephrectomy. Thus, based only on these findings, we may conclude that the rabbit could be a good model for studying kidney healing after partial nephrectomy. However, other factors should be taken into account.

The kidney of an adult rabbit has a length of 3.5 cm (right kidney) and 3.9 cm (left kidney), a width of 2.5 cm (right kidney) and 2.6 cm (left kidney), and a thickness of 1.8 cm (right kidney) and 1.7 cm (left kidney) (Dimitrov
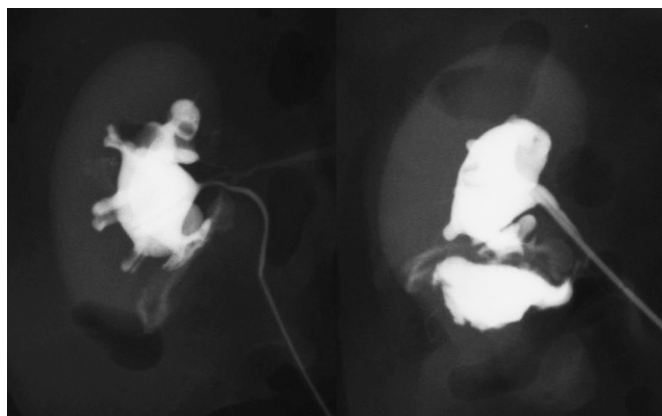
FIGURE 18.23 **Ex vivo retrograde pyelograms of rabbit kidneys removed 14 days after laparoscopic partial nephrectomy without collecting system closure.** The images demonstrated leakage of the opened collecting system.

et al., 2012). This is much inferior to the human kidney, which has a mean length of 10.97 cm (Sampaio and Mandarim-de-Lacerda, 1989), and this is an important aspect to be considered when considering a surgical model.

The size of the kidney is not the only embarrassment for considering it as an adequate model for studying partial nephrectomy healing. We must consider the small size and weight of rabbits (somehow) as a negative factor. These animals have small abdominal cavities that make it difficult for laparoscopic manipulation, as the instruments hit each other inside the cavity. Furthermore, as they have a high superficial area (in proportion to their weight), they easily develop hypothermia during surgical procedures. This is especially important when performing longer surgical procedures (such as partial nephrectomy) and when using cold carbon dioxide for intraabdominal insufflation during laparoscopic procedures. On the contrary, the small size of rabbits makes the handling and housing of these animals much easier than the other studied species (sheep or pigs).

With regard to the intrarenal anatomy, the rabbit kidney collecting system is very similar to those of sheep. It consists of a renal pelvis with 8–12 recesses on its edge, with more recesses on the dorsal surface than in the ventral surface (Shalgum et al., 2012). This demonstrates that as sheep, the rabbit is not a good model for experiments anatomy being an important factor to be considered.

The renal artery of rabbits divides into one dorsal and one ventral branch (Shalgum et al., 2012). This division of the renal artery is similar to what is found in humans (Sampaio et al., 1993) and in sheep (Buys-Goncalves et al., 2016), but different to that of swine (Pereira-Sampaio et al., 2007). This is an important aspect to be considered in favor of rabbits. However, there is a report of a dorsal and a ventral polar branch in 42% of the kidneys (Sindel et al., 1990).
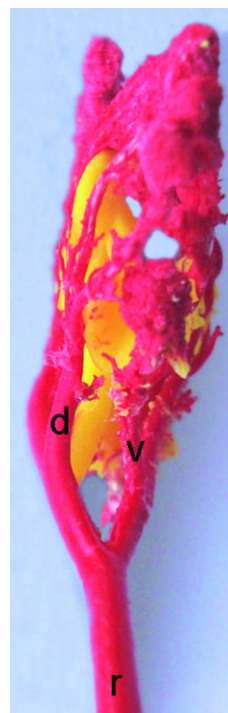
FIGURE 18.24 **Cranial view of endocast of rabbit left kidney showing the collecting system involved by a dorsal (d) and ventral (v) division of the renal artery (r).** *Source: Obtained from Shalgum, A., Marques-Sampaio, B.P., Dafalla, A., Pereira-Sampaio, M.A., 2012. Anatomical relationship between the collecting system and the intrarenal arteries in the rabbit: contribution for an experimental model. Anat. Histol. Embryol. 41 (2), 130–138.*

Two main arteries, cranial branches of the dorsal and ventral division of the renal artery, involve the rabbit kidney cranial pole in 56% of cases (Fig. 18.24). This relationship between intrarenal arteries and the collecting system of the cranial pole is similar to that in human, sheep, and pig (Buys-Goncalves et al., 2016; Pereira-Sampaio et al., 2004a; Sampaio and Aragao, 1990). Therefore, this similarity supports the use of the rabbit as an animal model for urologic procedures in the cranial pole.

The caudal pole receives caudal branches from both dorsal and ventral divisions of the renal artery in all cases (100%), and the collecting system of the caudal pole was supplied by branches of these two arteries (Fig. 18.25). This differs from man, where the inferior pole is irrigated only by the inferior segmental artery of the ventral division of renal artery in 62% of kidneys (Sampaio and Aragao, 1990).

Overall, we feel that rabbits can be used as an alternative animal model to sheep when studying the collecting system healing after partial nephrectomy. As sheep and humans, they are prone to urinary extravasation if no attempt of closing the collecting system is performed. Rabbits present advantages on handling and housing; as it is a more commonly used experimental model, most
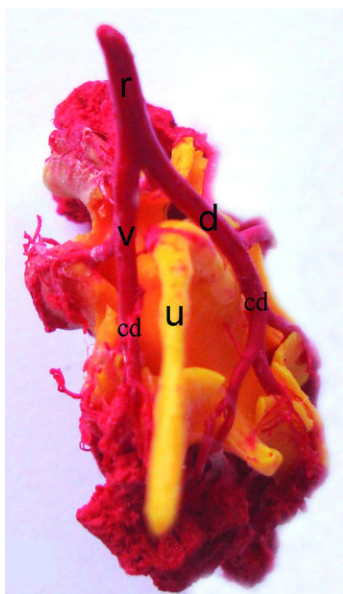
FIGURE 18.25   **Caudal view of endocast of rabbit right kidney showing the collecting system involved by caudal branches *(cd)* of the dorsal *(d)*, and ventral *(v)* division of the renal artery *(r)*** . *Source: Obtained from Shalgum, A., Marques-Sampaio, B.P., Dafalla, A., Pereira-Sampaio, M.A., 2012. Anatomical relationship between the collecting system and the intrarenal arteries in the rabbit: contribution for an experimental model. Anat. Histol. Embryol. 41 (2), 130–138.*

FIGURE 18.26   **Dorsal view of a dog kidney's collecting system endocast, showing the ureter *(u)* and the renal pelvis *(p).*** *Arrows point to the recesses of the renal pelvis. Source: Obtained from Pereira-Sampaio, M.A., Marques-Sampaio, B.P., Henry, R.W., Favorito, L.A., Sampaio, F.J., 2009. The dog kidney as experimental model in endourology: anatomic contribution. J. Endourol. 23 (6), 989–993.*

research centers have animal facilities for providing rabbits. Furthermore, most experimental surgical units should be adequate for operating rabbits (while operating pigs or sheep implies having special facilities). On the contrary, rabbits have an important disadvantage in comparison to sheep, as their body and kidneys are much smaller than humans.

5 THE DOG AS ANIMAL MODEL

Although there is little information regarding the use of dogs as model for studying kidney healing after partial nephrectomy, we should briefly comment on this species. First of all, we must note that scientists have made great efforts to replace dogs with other models to the extent possible. Even so, this species is still used in experimental surgical studies (Davari et al., 2016; Goudie et al., 2016; Yamada et al., 2016; Zou et al., 2016).

In 2005, when Ames et al. published their experiments with pigs, they also reported a small study with two beagle dogs. In these animals, they performed laparoscopic heminephrectomy (in the superior pole in one animal and in the inferior pole in the other). The hemostasis was achieved by a wet monopolar cautery with meticulous care to avoid the collecting system (Ames et al., 2005).

They found, after 1 week from surgery, that none of the animals developed urinoma, sepsis, or renal failure. Instead, an intense fibrotic response was observed around the site of heminephrectomy, similar to what had been observed in their swine (Ames et al., 2005), and in all species that we studied (pigs, sheep, and rabbits). Thus, they concluded that canine models cannot be used to evaluate collecting system closure because they do not manifest the same propensity for leakage as is seen clinically.

We further studied the canine renal anatomy in 110 kidneys from mongrel dogs (Pereira-Sampaio et al., 2009). The canine kidney has a great variance in size as a dog's size is significantly variable too. The smaller kidney length was of 4 cm, from a dog with 4.6 kg body weight and 41.5 cm height (measured at the withers, i.e., from the forehand to the highest point of the vertebral column of the thoracic segment), while the higher kidney length was of 9 cm, from a dog with 32.7 kg body weight and 73 cm height. This high variation should be taken into account when thinking of using a dog as an animal model. Dogs taller than 70 cm had a renal length of 9 cm, which is similar to adult human data (Sampaio and Mandarim-de-Lacerda, 1989). Therefore, kidneys from this size dog (which is not very common) might be useful as a model in experimental studies in which renal volume is an important aspect.

Furthermore, similar to sheep and rabbits (and different from pigs and humans), the dog's kidney does not present renal calices. The collecting system has only a renal pelvis with 9–17 (median 14) recesses in its margin (Figs. 18.26 and 18.27) (Pereira-Sampaio et al., 2009).

Thus, the dog kidney is not a good model for studying renal healing after partial nephrectomy, and to any

FIGURE 18.27 **Lateral view of a dog kidney's collecting system endocast, showing the ureter (u).** *Arrow* points to the groove made by the renal crest in the renal pelvis cast. *Source: Obtained from Pereira-Sampaio, M.A., Marques-Sampaio, B.P., Henry, R.W., Favorito, L.A., Sampaio, F.J., 2009. The dog kidney as experimental model in endourology: anatomic contribution. J. Endourol. 23 (6), 989–993.*

experimental studies in which collecting system morphology is an important factor to be considered. Kidneys of dogs that are taller than 70 cm at the withers might be useful as a model in experimental studies in which renal volume is an important aspect. However, other species that present renal volume similar to humans' should be preferred because of ethical considerations.

6 CONCLUDING REMARKS

After studying pigs, sheep, dogs, and rabbits, and comparing the results obtained in these species with the literature of humans in clinical conditions, several lessons were learned. The pig has the most similar renal anatomy with humans, especially in regards to renal size and collecting system anatomy. However, the pig kidney collecting system healed well without any kind of suture or internal drainage after partial nephrectomy. As this is much different from human kidney healing, we must say that the pig kidney is not an adequate experimental model for research on which collecting system healing is an important aspect to be considered.

Although limited data are disponible regarding the use of dogs as models for studying kidney healing. This species, as well as pigs, did not present the expected urinary leakage after partial nephrectomy. Furthermore, collecting system anatomy, and ethical considerations regarding the experimental use of dogs, precludes its indication as model for studying kidney healing after partial nephrectomy.

Sheep and rabbits showed signs that their kidneys' collecting system does not heal without surgical maneuvers for its closure. This is more similar to what is found in human clinical settings, and thus these animals should be preferred when studying the collecting system healing after partial nephrectomy. It should be considered that the collecting system anatomy of these species, without minor renal calices, is very different from humans. Thus, the pig should be preferred for studies in which the collecting system anatomy is important. On the contrary, the division of the renal artery of sheep and rabbits, in one anterior and one posterior branch, is more similar to humans; therefore for studies in which this vascularization is of importance, these species should be preferred.

It should be considered that sheep are animals with a renal size more similar to humans than rabbits. Moreover, the abdominal cavity's limited volume of rabbits sometimes makes it difficult for the execution of surgical maneuvers; this is especially important when performing laparoscopic surgery. Thus, sheep should be considered the best animal model for studying kidney healing after partial nephrectomy. Rabbits may be considered as an alternative when the experimental facility does not permit studies with sheep.

Acknowledgments

References

Abdullahi, A., Amini-Nik, S., Jeschke, M.G., 2014. Animal models in burn research. Cell. Mol. Life Sci. 71 (17), 3241–3255.

Abou-Elela, A., Morsy, A., Badawy, H., Fathy, M., 2009. Use of oxidized cellulose hemostats (surgicel) to support parenchymal closure and achieve hemostasis following partial nephrectomy. Surg. Technol. Int. 18, 75–79.

Alexander, V.V., Shi, Z., Iftekher, F., Welsh, M.J., Gurm, H.S., Rising, G., 2014. Renal denervation using focused infrared fiber lasers: a potential treatment for hypertension. Lasers Surg. Med. 46 (9), 689–702.

Ames, C.D., Vanlangendonck, R., Morrissey, K., Venkatesh, R., Landman, J., 2005. Evaluation of surgical models for renal collecting system closure during laparoscopic partial nephrectomy. Urology 66 (2), 451–454.

Anderson, J.K., Baker, M.R., Lindberg, G., Cadeddu, J.A., 2007. Large-volume laparoscopic partial nephrectomy using the potassium-titanyl-phosphate (KTP) laser in a survival porcine model. Eur. Urol. 51 (3), 749–754.

Bagetti Filho, H.J., Pereira-Sampaio, M.A., Favorito, L.A., Sampaio, F.J., 2008. Pig kidney: anatomical relationships between the renal venous arrangement and the kidney collecting system. J. Urol. 179 (4), 1627–1630.

Barcellos Sampaio, F.J., Mandarim-de-Lacerda, C.A., 1988. 3-Dimensional and radiological pelviocaliceal anatomy for endourology. J. Urol. 140 (6), 1352–1355.

Bernie, J.E., Ng, J., Bargman, V., Gardner, T., Cheng, L., Sundaram, C.P., 2005. Evaluation of hydrogel tissue sealant in porcine laparoscopic partial-nephrectomy model. J. Endourol. 19 (9), 1122–1126.

Bishoff, J.T., Cornum, R.L., Perahia, B., Seay, T., Eliason, S., Katus, M., 2003. Laparoscopic heminephrectomy using a new fibrin sealant powder. Urology 62 (6), 1139–1143.

Booth, L.C., Nishi, E.E., Yao, S.T., Ramchandra, R., Lambert, G.W., Schlaich, M.P., 2015. Reinnervation of renal afferent and efferent nerves at 5.5 and 11 months after catheter-based radiofrequency renal denervation in sheep. Hypertension 65 (2), 393–400.

Breda, A., Finelli, A., Janetschek, G., Porpiglia, F., Montorsi, F., 2009. Complications of laparoscopic surgery for renal masses: prevention, management, and comparison with the open experience. Eur. Urol. 55 (4), 836–850.

Bui, M.H., Breda, A., Gui, D., Said, J., Schulam, P., 2007. Less smoke and minimal tissue carbonization using a thulium laser for laparoscopic partial nephrectomy without hilar clamping in a porcine model. J. Endourol. 21 (9), 1107–1111.

Buys-Goncalves, G.F., de Souza, D.B., Sampaio, F.J., Pereira-Sampaio, M.A., 2016. Anatomical relationship between the kidney collecting system and the intrarenal arteries in the sheep: contribution for a new urological model. Anat. Rec. (Hoboken) 299 (4), 405–411.

Campbell, S.C., Novick, A.C., Belldegrun, A., Blute, M.L., Chow, G.K., Derweesh, I.H., 2009. Guideline for management of the clinical T1 renal mass. J. Urol. 182 (4), 1271–1279.

Christou, C., Oliver, R.A., Pelletier, M.H., Walsh, W.R., 2014. Ovine model for critical-size tibial segmental defects. Comp. Med. 64 (5), 377–385.

Collyer, W.C., Landman, J., Olweny, E.O., Andreoni, C., Kibel, A., Andriole, G.L., 2002. Laparoscopic partial nephrectomy with a novel electrosurgical snare in a porcine model. J. Endourol. 16 (9), 673–679.

Collyer, W., Venkatesh, R., Vanlangendonck, R., Morissey, K., Humphrey, P., Yan, Y., 2004. Enhanced renal cryoablation with hilar clamping and intrarenal cooling in a porcine model. Urology 63 (6), 1209–1212.

Davari, H.R., Rahim, M.B., Tanideh, N., Sani, M., Tavakoli, H.R., Rasekhi, A.R., 2016. Partial replacement of left hemidiaphragm in dogs by either cryopreserved or decellularized heterograft patch. Interact. Cardiovasc. Thorac. Surg. 23 (4), 623–629.

de Souza, D.B., Abilio, E.J., Costa, W.S., Sampaio, M.A., Sampaio, F.J., 2011. Kidney healing after laparoscopic partial nephrectomy without collecting system closure in pigs. Urology 77 (2), 508.e5–508.e9.

de Souza, D.B., Costa, W.S., Damasceno-Ferreira, J.A., Nascimento Junior, A., Ascoli, F.O., Pereira-Sampaio, M.A., 2016. The sheep as a model for healing studies after partial nephrectomy. J. Surg. Res. 200 (1), 387–391.

de Souza, D.B., de Oliveira, L.L., da Cruz, M.C., Abilio, E.J., Costa, W.S., Pereira-Sampaio, M.A., 2012. Laparoscopic partial nephrectomy under warm ischemia reduces the glomerular density in a pig model. J. Endourol. 26 (6), 706–710.

Deponti, D., Di Giancamillo, A., Scotti, C., Peretti, G.M., Martin, I., 2015. Animal models for meniscus repair and regeneration. J. Tissue Eng. Regen. Med. 9 (5), 512–527.

Dimitrov, M., Kostov, D., Stamatova, K., Yordanova, V., 2012. Anatomotopographical and morphological analysis of normal kidneys of rabbit (Oryctolaguscuniculus). Trakia J. Sci. 10 (2), 79–84.

Duchene, D.A., 2011. Sprayed fibrin sealant as the sole hemostatic agent for porcine laparoscopic partial nephrectomy—commentary. J. Endourol. 25 (1), 906–907.

Earp, P.P., 2003. Percutaneous renal surgery—new model for learning and training. Int. Braz. J. Urol. 29 (2), 151–154.

Eret, V., Hora, M., Sykora, R., Hes, O., Urge, T., Klecka, J., 2009. GreenLight (532 nm) laser partial nephrectomy followed by suturing of collecting system without renal hilar clamping in porcine model. Urology 73 (5), 1115–1118.

Eun, D., Bhandari, A., Boris, R., Lyall, K., Bhandari, M., Menon, M., 2008. A novel technique for creating solid renal pseudotumors and renal vein-inferior vena caval pseudothrombus in a porcine and cadaveric model. J. Urol. 180 (4), 1510–1514.

Evan, A.P., Willis, L.R., Connors, B., Reed, G., McAteer, J.A., Lingeman, J.E., 1991. Shock wave lithotripsy-induced renal injury. Am. J. Kidney Dis. 17 (4), 445–450.

Fogelson, A.L., Neeves, K.B., 2015. Fluid mechanics of blood clot formation. Annu. Rev. Fluid Mech. 47, 377–403.

Gallo, C.B., Miranda, A.F., Felix-Patricio, B., Ramos, C.F., Cardoso, L.E., Costa, W.S., 2012. Effects of castration and hormone replacement in the urinary bladder of rats: structural, ultrastructural, and biochemical analysis. J. Androl. 33 (4), 684–690.

Gosling, J.A., Dixon, J.S., Humpherson, J.R., 1983. Functional Anatomy of the Urinary Tract: An Integrated Text and Colour Atlas. Churchill Livingstone, Edinburgh.

Goudie, E., Khereba, M., Tahiri, M., Hegde, P., Thiffault, V., Hadjeres, R., 2016. Pulmonary artery sealing with an ultrasonic energy device in video-assisted thoracoscopic surgery lobectomy: an animal survival study. Ann. Thorac. Surg. 102 (4), 1088–1094.

Hacker, A., Albadour, A., Jauker, W., Ziegerhofer, J., Albquami, N., Jeschke, S., 2007. Nephron-sparing surgery for renal tumours: acceleration and facilitation of the laparoscopic technique. Eur. Urol. 51 (2), 358–365.

Haghighi, K.S., Steinke, K., Hazratwala, K., Kam, P.C., Daniel, S., Morris, D.L., 2006. Controlled study of Inline radiofrequency coagulation-assisted partial nephrectomy in sheep. J. Surg. Res. 133 (2), 215–218.

Hammond, L., Ketchum, J., Schwartz, B.F., 2004. A new approach to urology training: a laboratory model for percutaneous nephrolithotomy. J. Urol. 172 (5 Pt. 1), 1950–1952.

He, Y., Zhou, S., Liu, H., Shen, B., Zhao, H., Peng, K., 2015. Indoleamine 2,3-dioxgenase transfected mesenchymal stem cells induce kidney allograft tolerance by increasing the production and function of regulatory T cells. Transplantation 99 (9), 1829–1838.

Hick, E.J., Morey, A.F., Harris, R.A., Morris, M.S., 2005. Gelatin matrix treatment of complex renal injuries in a porcine model. J. Urol. 173 (5), 1801–1804.

Hidalgo, J., Belani, J., Maxwell, K., Lieber, D., Talcott, M., Baron, P., 2005. Development of exophytic tumor model for laparoscopic partial nephrectomy: technique and initial experience. Urology 65 (5), 872–876.

Hindley, R.G., Barber, N.J., Walsh, K., Petersen, A., Poulsen, J., Muir, G.H., 2006. Laparoscopic partial nephrectomy using the potassium titanyl phosphate laser in a porcine model. Urology 67 (5), 1079–1083.

Hollenbeck, B.K., Taub, D.A., Miller, D.C., Dunn, R.L., Wei, J.T., 2006. National utilization trends of partial nephrectomy for renal cell carcinoma: a case of underutilization? Urology 67 (2), 254–259.

Honeck, P., Wendt-Nordahl, G., Bolenz, C., Peters, T., Weiss, C., Alken, P., 2008. Hemostatic properties of four devices for partial nephrectomy: a comparative ex vivo study. J. Endourol. 22 (5), 1071–1076.

James, A.W., Chiang, M., Asatrian, G., Shen, J., Goyal, R., Chung, C.G., 2016. Vertebral implantation of NELL-1 enhances bone formation in an osteoporotic sheep model. Tissue Eng. Part A 22 (11–12), 840–849.

Janzen, N.K., Perry, K.T., Han, K.R., Kristo, B., Raman, S., Said, J.W., 2005. The effects of intentional cryoablation and radio frequency ablation of renal tissue involving the collecting system in a porcine model. J. Urol. 173 (4), 1368–1374.

Jemal, A., Siegel, R., Ward, E., Hao, Y., Xu, J., Thun, M.J., 2009. Cancer statistics, 2009. CA Cancer J. Clin. 59 (4), 225–249.

Johnston, 3rd, W.K., Kelel, K.M., Hollenbeck, B.K., Daignault, S., Wolf, Jr., J.S., 2006. Acute integrity of closure for partial nephrectomy: comparison of 7 agents in a hypertensive porcine model. J. Urol. 175 (6), 2307–2311.

Katz, R., Hoznek, A., Antiphon, P., Van Velthoven, R., Delmas, V., Abbou, C.C., 2003. Cadaveric versus porcine models in urological laparoscopic training. Urol Int 71 (3), 310–315.

Kelleher, J.P., Shah, V., Godley, M.L., Wakefield, A.J., Gordon, I., Ransley, P.G., 1992. Urinary endothelin (ET1) in complete ureteric obstruction in the miniature pig. Urol. Res. 20 (1), 63–65.

Kim, D.J., Mustoe, T., Clark, R.A., 2015. Cutaneous wound healing in aging small mammals: a systematic review. Wound Repair Regen. 23 (3), 318–339.

Kouba, E., Tornehl, C., Lavelle, J., Wallen, E., Pruthi, R.S., 2004. Partial nephrectomy with fibrin glue repair: measurement of vascular and pelvicaliceal hydrodynamic bond integrity in a live and abbatoir porcine model. J. Urol. 172 (1), 326–330.

Lafon, C., Bouchoux, G., Murat, F.J., Birer, A., Theillere, Y., Chapelon, J.Y., 2007. High intensity ultrasound clamp for bloodless partial nephrectomy: in vitro and in vivo experiments. Ultrasound Med. Biol. 33 (1), 105–112.

Lane, B.R., Novick, A.C., 2007. Nephron-sparing surgery. BJU Int. 99 (5 Pt. B), 1245–1250.

Lascelles, A.K., Claringbold, P.J., 1960. The effects of suture materials and suture techniques on the healing of wounds in the skin of the sheep. Aust. J. Exp. Biol. Med. Sci. 38, 111–115.

L'Esperance, J.O., Sung, J.C., Marguet, C.G., Maloney, M.E., Springhart, W.P., Preminger, G.M., 2005. Controlled survival study of the effects of Tisseel or a combination of FloSeal and Tisseel on major vascular injury and major collecting-system injury during partial nephrectomy in a porcine model. J. Endourol. 19 (9), 1114–1121.

Liu, J., Schmidlin, P.R., Philipp, A., Hild, N., Tawse-Smith, A., Duncan, W., 2016. Novel bone substitute material in alveolar bone healing following tooth extraction: an experimental study in sheep. Clin. Oral Implants Res. 27 (7), 762–770.

Ljungberg, B., Bensalah, K., Canfield, S., Dabestani, S., Hofmann, F., Hora, M., 2015. EAU guidelines on renal cell carcinoma: 2014 update. Eur. Urol. 67 (5), 913–924.

Lossi, L., D'Angelo, L., De Girolamo, P., Merighi, A., 2016. Anatomical features for an adequate choice of experimental animal model in biomedicine: II. Small laboratory rodents, rabbit, and pig. Ann. Anat. 204, 11–28.

Lucioni, A., Orvieto, M.A., Zorn, K.C., Lotan, T., Gong, E.M., Steinberg, G.D., 2008. Efficacy of the argon beam coagulator alone in obtaining hemostasis after laparoscopic porcine heminephrectomy: a pilot study. Can. J. Urol. 15 (3), 4091–4096.

Malhotra, A., Pelletier, M.H., Yu, Y., Christou, C., Walsh, W.R., 2014. A sheep model for cancellous bone healing. Front. Surg. 1, 37.

Margulis, V., Matsumoto, E.D., Svatek, R., Kabbani, W., Cadeddu, J.A., Lotan, Y., 2005a. Application of novel hemostatic agent during laparoscopic partial nephrectomy. J. Urol. 174 (2), 761–764.

Margulis, V., Matsumoto, E.D., Taylor, G., Shaffer, S., Kabbani, W., Cadeddu, J.A., 2005b. Retrograde renal cooling during radio frequency ablation to protect from renal collecting system injury. J. Urol. 174 (1), 350–352.

Martini, L., Fini, M., Giavaresi, G., Giardino, R., 2001. Sheep model in orthopedic research: a literature review. Comp. Med. 51 (4), 292–299.

McDougall, E.M., Clayman, R.V., Chandhoke, P.S., Kerbl, K., Stone, A.M., Wick, M.R., 1993. Laparoscopic partial nephrectomy in the pig model. J. Urol. 149 (6), 1633–1636.

Murat, F.J., Ereth, M.H., Dong, Y., Piedra, M.P., Gettman, M.T., 2004. Evaluation of microporous polysaccharide hemospheres as a novel hemostatic agent in open partial nephrectomy: favorable experimental results in the porcine model. J. Urol. 172 (3), 1119–1122.

Murat, F.J., Lafon, C., Cathignol, D., Theillere, Y., Gelet, A., Chapelon, J.Y., 2005. [Haemostatic efficacy of a high intensity focused ultrasound applicator in lower pole partial nephrectomy in the pig]. Prog. Urol. 15 (4), 684–688.

Murat, F.J., Lafon, C., Cathignol, D., Theillere, Y., Gelet, A., Chapelon, J.Y., 2006a. Bloodless partial nephrectomy with a new high-intensity collimated ultrasonic coagulating applicator in the porcine model. Urology 68 (1), 226–230.

Murat, F.J., Le, C.Q., Ereth, M.H., Piedra, M.P., Dong, Y., Gettman, M.T., 2006b. Evaluation of microporous polysaccharide hemospheres for parenchymal hemostasis during laparoscopic partial nephrectomy in the porcine model. JSLS 10 (3), 302–306.

Nickel, R., Schummer, A., Sack, W.O., 1979. The Viscera of the Domestic Animals. Springer-Verlag, New York.

Nuttall, M., Cathcart, P., van der Meulen, J., Gillatt, D., McIntosh, G., Emberton, M., 2005. A description of radical nephrectomy practice and outcomes in England: 1995–2002. BJU Int. 96 (1), 58–61.

Ogan, K., Jacomides, L., Saboorian, H., Koeneman, K., Li, Y., Napper, C., 2003. Sutureless laparoscopic heminephrectomy using laser tissue soldering. J. Endourol. 17 (5), 295–300.

Ogan, K., Wilhelm, D., Lindberg, G., Lotan, Y., Napper, C., Hoopman, J., 2002. Laparoscopic partial nephrectomy with a diode laser: porcine results. J. Endourol. 16 (10), 749–753.

Orvieto, M.A., Lotan, T., Lyon, M.B., Zorn, K.C., Mikhail, A.A., Rapp, D.E., 2007. Assessment of the LapraTy clip for facilitating reconstructive laparoscopic surgery in a porcine model. Urology 69 (3), 582–585.

Pearce, A.I., Richards, R.G., Milz, S., Schneider, E., Pearce, S.G., 2007. Animal models for implant biomaterial research in bone: a review. Eur. Cell Mater. 13, 1–10.

Pereira-Sampaio, M., Favorito, L.A., Henry, R., Sampaio, F.J., 2007. Proportional analysis of pig kidney arterial segments: differences from the human kidney. J. Endourol. 21 (7), 784–788.

Pereira-Sampaio, M.A., Favorito, L.A., Sampaio, F.J., 2004a. Pig kidney: anatomical relationships between the intrarenal arteries and the kidney collecting system. Applied study for urological research and surgical training. J. Urol. 172 (5 Pt. 1), 2077–2081.

Pereira-Sampaio, M.A., Favorito, L.A., Sampaio, F.J., 2004b. Pig kidney: precise anatomic study for laparoscopic trainning. J. Endourol. 18, 21A.

Pereira-Sampaio, M.A., Marques-Sampaio, B.P., Henry, R.W., Favorito, L.A., Sampaio, F.J., 2009. The dog kidney as experimental model in endourology: anatomic contribution. J. Endourol. 23 (6), 989–993.

Ptashnyk, T., Cueva-Martinez, A., Michel, M.S., Alken, P., Kohrmann, K.U., 2002. Comparative investigations on the retrieval capabilities of various baskets and graspers in four ex vivo models. Eur. Urol. 41 (4), 406–410.

Rassweiler, J.J., Henkel, T.O., Potempa, D.M., Frede, T., Stock, C., Gunther, M., 1993. Laparoscopic training in urology. An essential principle of laparoscopic interventions in the retroperitoneum. Urologe A 32 (5), 393–402.

Rouach, Y., Delongchamps, N.B., Patey, N., Fontaine, E., Timsit, M.O., Thiounn, N., 2009. Suture or hemostatic agent during laparoscopic partial nephrectomy? A randomized study using a hypertensive porcine model. Urology 73 (1), 172–177.

Rouach, Y., Timsit, M.O., Delongchamps, N.B., Fontaine, E., Peyromaure, M., Thiounn, N., 2008. Laparoscopic partial nephrectomy: urology resident learning curve on a porcine model. Prog. Urol. 18 (6), 344–350.

Russo, P., Huang, W., 2008. The medical and oncological rationale for partial nephrectomy for the treatment of T1 renal cortical tumors. Urol. Clin. North Am. 35 (4), 635–643.

Sabino, L., Andreoni, C., Faria, E.F., Ferreira, P.S., Paz, A.R., Kalil, W., 2007. Evaluation of renal defect healing, hemostasis, and urinary fistula after laparoscopic partial nephrectomy with oxidized cellulose. J. Endourol. 21 (5), 551–556.

Sampaio, F.J., 1992. Anatomical background for nephron-sparing surgery in renal cell carcinoma. J. Urol. 147 (4), 999–1005.

Sampaio, F.J.B., 1993. Anatomic classification of the pelviocaliceal system. Urologic and radiologic implications. In: Sampaio, F.J.B., Uflacker, R. (Eds.), Renal Anatomy Applied to Urology, Endourology, and Interventional Radiology. Thieme Medical Publishers, New York, pp. 1–6.

Sampaio, F.J., Aragao, A.H., 1990. Anatomical relationship between the renal venous arrangement and the kidney collecting system. J. Urol. 144 (5), 1089–1093.

Sampaio, F.J.B., Mandarim-de-Lacerda, C.A., 1988. Anatomic classification of the kidney collecting system for endourologic procedures. J. Endourol. 2 (3), 247–251.

Sampaio, F.J., Mandarim-de-Lacerda, C.A., 1989. Morphometry of the kidney. Applied study in urology and imaging. J. Urol. (Paris) 95 (2), 77–80.

Sampaio, F.J., Pereira-Sampaio, M.A., Favorito, L.A., 1998. The pig kidney as an endourologic model: anatomic contribution. J. Endourol. 12 (1), 45–50.

Sampaio, F.J., Pereira-Sampaio, M.A., Marques, B.P.S., Favorito, L.A., 2001. Laparoscopic partial nephrectomy. Is the pig a good animal model? Eur. Urol. 39, 168.

Sampaio, F.J., Schiavini, J.L., Favorito, L.A., 1993. Proportional analysis of the kidney arterial segments. Urol. Res. 21 (6), 371–374.

Shalgum, A., Marques-Sampaio, B.P., Dafalla, A., Pereira-Sampaio, M.A., 2012. Anatomical relationship between the collecting system and the intrarenal arteries in the rabbit: contribution for an experimental model. Anat. Histol. Embryol. 41 (2), 130–138.

Shikanov, S., Wille, M., Large, M., Lifshitz, D.A., Zorn, K.C., Shalhav, A.L., 2009. Knotless closure of the collecting system and renal parenchyma with a novel barbed suture during laparoscopic porcine partial nephrectomy. J. Endourol. 23 (7), 1157–1160.

Simoes, M., de Souza, D.B., Gallo, C.B., Pereira-Sampaio, M.A., Costa, W.S., Sampaio, F.J., 2016. Histomorphometric comparison of the human, swine, and ovine collecting systems. Anat. Rec. (Hoboken) 299 (7), 967–972.

Sindel, M., Ucar, Y., Ozkan, O., 1990. Renal arterial system of the domestic rabbits (oryctolagus cuniculus): corrosion cast study. J. Anat. Soc. India 39 (1), 31–40.

Springer, A., Kratochwill, K., Bergmeister, H., Csaicsich, D., Huber, J., Mayer, B., 2015. A fetal sheep model for studying compensatory mechanisms in the healthy contralateral kidney after unilateral ureteral obstruction. J. Pediatr. Urol. 11 (6), 352.e1–352.e7.

Sprunger, J., Herrell, S.D., 2005. Partial laparoscopic nephrectomy using monopolar saline-coupled radiofrequency device: animal model and tissue effect characterization. J. Endourol. 19 (4), 513–519.

Stephenson, A.J., Hakimi, A.A., Snyder, M.E., Russo, P., 2004. Complications of radical and partial nephrectomy in a large contemporary cohort. J. Urol. 171 (1), 130–134.

Strohmaier, W.L., Giese, A., 2005. Ex vivo training model for percutaneous renal surgery. Urol. Res. 33 (3), 191–193.

Tanaka, K., Manabe, S., Ooyama, K., Seki, Y., Nagae, H., Takagi, M., 2014. Can a pressure-limited V-A shunt for obstructive uropathy really protect the kidney? J. Pediatr. Surg. 49 (12), 1831–1834.

Taylor, G.D., Cadeddu, J.A., 2006. Training for renal ablative technique using an agarose-based renal tumour-mimic model. BJU Int. 97 (1), 179–181.

Taylor, G.D., Johnson, D.B., Hogg, D.C., Cadeddu, J.A., 2004. Development of a renal tumor mimic model for learning minimally invasive nephron sparing surgical techniques. J. Urol. 172 (1), 382–385.

Valdivia Uria, J.G., Viloria Gonzalez, A., Rodriguez Gomez, J., Martinez Sanudo, M.J., Whyte Orozco, A., Valle Gerhold, J., 1992. Laparoscopic nephrectomy: experimental surgical model. Actas Urol. Esp. 16 (2), 169–174.

van Dongen, J.J., Grossi, F.S., Bosman, F.T., Schroder, F.H., 1993. Quantitative and qualitative evaluation of renal injury induced by shock waves delivered with the Siemens C generator. J. Endourol. 7 (5), 379–381.

Vera-Donoso, C.D., Garcia-Dominguez, X., Jimenez-Trigos, E., Garcia-Valero, L., Vicente, J.S., Marco-Jimenez, F., 2015. Laparoscopic transplantation of metanephroi: a first step to kidney xenotransplantation. Actas Urol. Esp. 39 (9), 527–534.

Xie, H., Khajanchee, Y.S., Shaffer, B.S., 2008a. Chitosan hemostatic dressing for renal parenchymal wound sealing in a porcine model: implications for laparoscopic partial nephrectomy technique. JSLS 12 (1), 18–24.

Xie, H., Khajanchee, Y.S., Teach, J.S., Shaffer, B.S., 2008b. Use of a chitosan-based hemostatic dressing in laparoscopic partial nephrectomy. J. Biomed. Mater. Res. B Appl. Biomater. 85 (1), 267–271.

Yamada, T., Sowa, T., Bando, T., Date, H., 2016. Experimental study in pulmonary artery sealing with a vessel-sealing device. Asian Cardiovasc. Thorac. Ann. 24 (6), 562–567.

Yanaga, K., Makowka, L., Shimada, M., Lebeau, G., Kahn, D., Mieles, L.A., 1991. Improved method of porcine renal allografting for transplantation research. J. Invest. Surg. 4 (2), 231–236.

Yang, B., Zeng, Q., Yinghao, S., Wang, H., Wang, L., Xu, C., 2009. A novel training model for laparoscopic partial nephrectomy using porcine kidney. J. Endourol. 23 (12), 2029–2033.

Yazici, M., Celebi, S., Kuzdan, O., Kocan, H., Ayyildiz, H.S., Bayrak, I.K., 2015. Current radiological techniques used to evaluate unilateral partial ureteral obstruction: an experimental rabbit study. Int. Urol. Nephrol. 47 (7), 1045–1050.

Zeltser, I.S., Gupta, A., Bensalah, K., Kabbani, W., Jenkins, A., Park, S., 2008. Focal radiofrequency coagulation-assisted laparoscopic partial nephrectomy: a novel nonischemic technique. J. Endourol. 22 (6), 1269–1273.

Zorn, K.C., Gong, E.M., Orvieto, M.A., Gofrit, O.N., Mikhail, A.A., Shalhav, A.L., 2007. Impact of collecting-system repair during laparoscopic partial nephrectomy. J. Endourol. 21 (3), 315–320.

Zou, L., Mao, S., Liu, S., Zhang, L., Xu, H., Yang, T., 2016. Unilateral long-segment ureteral reconstruction using a bilateral Boari flap bridge: an experimental model in dogs. Scand. J. Urol. 50 (5), 401–404.

Page left intentionally blank

Animal Models of Inflammatory Bowel Disease

Sumit Jamwal, Puneet Kumar

I.S.F College of Pharmacy, Moga, Punjab, India

1 INTRODUCTION

Inflammatory bowel disease (IBD) is a group of idiopathic, chronic, and relapsing inflammatory conditions mainly affecting colon and small intestine and characterized by severe abdominal pain and diarrhea. IBD mainly covers Crohn's disease (CD) and ulcerative colitis (UC). CD and UC are chronic and progressive inflammatory conditions that may affect the entire GI tract and the colonic mucosa and might be associated with an increased risk for colon cancer (Arthur et al., 2010). Most of the pathological and clinical characteristics of CD and UC are similar, but they differ in some features, that is, regions of the GI tract affected and depth of inflammation. The GI tract is responsible for digestion of food, absorption of nutrients, and elimination of waste. Chronic inflammation impairs the ability of GI organs to function properly, leading to symptoms, such as persistent diarrhea, abdominal pain, rectal bleeding, weight loss and fatigue. It may result in significant morbidity and mortality, with compromised quality of life and life expectancy (Goyal et al., 2014).

CD may affect any part of the GI tract from mouth to anus most but commonly affects the end of the small intestine (the ileum) near the beginning of the colon. It mainly causes abdominal pain, diarrhea, vomiting, and weight loss. CD may appear in "patches," affecting some areas of the GI tract while leaving other sections completely untouched. In CD, the inflammation may extend through the entire thickness of the bowel wall. On the other hand, UC is mainly confined to the colon, and may involve the rectum. The inflammation occurs only in the innermost layer of the lining of the intestine and usually starts from lower colon, but may involve the entire colon. It is primarily manifested as continuous areas of inflammation, ulceration, edema, and hemorrhage along

the length of the colon. The most observational feature of UC is the presence of blood in stool and is associated with lower abdominal cramping during the bowel movements (Ordas et al., 2012).

In Western Europe and USA, CD and UC have an incidence of approximately 6–8 cases per 100,000 populations and an estimated prevalence of approximately 70–150 per 100,000 populations. The peak occurrence is between ages 15 and 35. Both sexes are equally affected in case of these diseases (Burisch, 2014).

The pathophysiology is not fully understood but is thought to be caused by a complex interplay between gut microbiota, dysregulation of the host's immune system, genetic susceptibility, and environmental factors. To study these different etiological factors, various experimental models are available in the scientific research, which includes chemical-induced, spontaneous, genetically engineered and transgenic models. These models represent a major source of information about biological systems and pathogenesis of the disease and are clinically relevant to both human UC, as well as CD. Though there is less information available in literature about all the models, in this chapter we have collected and presented systematically arranged data on pathophysiology involved in the disease and various types of animal models of IBD and other disease-related complications.

2 HISTORICAL PERSPECTIVES

UC was first described by two English physicians, Wilks and Moxon in 1875, who distinguished it from diarrheal diseases caused by bacterial and viral agents. There are reports of a disease with similar symptoms to UC in 16th and 17th century but it was not named as a distinct disease until 1875. CD was first described in 1932 by three doctors—Burrill Crohn, Leon Ginzberg, and Gordon D. Oppenheimer. During that period, any disease affecting small intestine was thought to be intestinal tuberculosis. These doctors collected data with symptoms of abdominal cramps, diarrhea, fever, and weight loss from 14 patients and revealed that the symptoms were not due to intestinal tuberculosis or any other known disease. Therefore, they described a new disease entity, which was first called regional ileitis and later on CD.

3 PATHOPHYSIOLOGY OF IBD

Although the exact cause of IBD remains unclear it but molecular assessment during IBD progression shows alteration in immune system, gut microbiota, disruption in mucosal barrier, increase in level of proinflammatory cytokines and oxidative stress.

3.1 Innate and Adaptive Immunity

The immune system is the collection of cells and macromolecules that protects the body from numerous pathogenic microbes and toxins in our environment. This defense against microbes involves two types of reactions: reactions of innate immunity and reactions of adaptive immunity. Innate and adaptive immunity are two equally important aspects of the immune system in which innate immune response acts as a first line of defense and provides nonspecific protection whereas adaptive immune response is highly specific in nature and gets activated by the innate immunity.

Innate immunity is formed by epithelial barrier, neutrophils, macrophages, dendritic cells, natural killer cells (NK cells) and others. It is activated by the toxin and microbial agents which are recognized by the specific recognition receptors, such as toll-like receptors (TLRs) and NOD-like receptors. Neutrophils along with other cells start the process of inflammation by releasing proinflammatory cytokines, such as TNF-α, IL-1, IL-6, and IL-8, which further activate the adaptive immune response (Wallace et al. 2014).

Adaptive immune system is composed of T-lymphocytes and B-cells, which on activation releases cytokines and antibodies. T cells have been reported to be the main contributor to IBD due to the increased production and release of proinflammatory cytokines and interferons (IFNs) in lower GI tract. IL-12 activates Th1 cells to produce large amount of IFNs and mainly responsible for inflammation in CD patients. Th2 cells increase the production and release of IL-4, IL-5, and IL-13 and are responsible for inflammation in UC patients. Recently, a third type of T-helper cell has been reported to involved in IBD pathogenesis, that is, Th17 cells. These cells cause the release of IL-17 and IL-22 and play role in destruction of local tissue (Siegmund and Zeitz, 2011). Further, reports are available that proinflammatory cytokines disrupts epithelial barrier and increases gut permeability; thereby accounts for an uncontrolled inflammation.

3.2 Gut Microbiota

The impairment in gut bacterial flora is well implicated in the pathophysiology of IBD. Alteration in the intestinal mucosa layer in IBD results in increased association of gut bacteria to innermost lining of mucosa. This association of bacteria is recognized as hapten and results in activation of the inflammatory process by binding on antigen-presenting cells (APC) and ultimately causing damage to mucosal layer (Wallace et al., 2014). Though the clear role of gut bacterial flora in the pathogenesis of IBD is unclear, but some of investigators have showed that some bacterial species like *Bacteroides* or *Clostridium* spp. and aerobic E. increases in IBD mucosa (Beisner et al., 2010).

3.3 Disruption of Mucosal Barrier

Mucosal surfaces are composed of epithelial cells and these cells form a barrier between hostile external environments and the internal milieu. Mucosal surfaces have selective permeability barrier and are responsible for nutrient absorption and waste secretion. Variations of the intestinal mucus layer concerning its thickness, continuity and composition, as well as the mucin-structure have been reported in IBD patients, especially in UC. These changes are thought to adversely affect the protective properties of the gel layer and consequently might cause an increased vulnerability of the epithelium to bacterial invasion. Disruption of this barrier results in dysregulated gut epithelial permeability, which can induce an overactive mucosal immune response and chronic intestinal inflammation. The exact mechanism of the loss of barrier is not known, but several studies have reported that cytokines, TNF-α, interleukins, etc. involved in the pathogenesis of UC and CD may attribute to the increased epithelial permeability and alteration of tight junctions resulting into barrier disruption (McGuckin et al., 2009).

3.4 Inflammatory Mediators

IBD is a chronic inflammatory condition in which several genetic, environmental, and biological factors trigger inappropriate immune responses, that is, overproduction of different proinflammatory mediators, such as TNF-α, ILs, cytokines, and chemokines. The concentration of these mediators is highly elevated in blood, stool, and intestinal mucosa of IBD patients. Inflammatory mediator profile of CD and UC is different, such as IL-2 and IFN-γ are responsible for the inflammation in CD whereas IL-4, IL-5, and IL-10 are involved in UC pathogenesis. The release of these inflammatory cells is regulated by different pathways involved in inflammation, that is, nuclear factor-κB (NF-κB) and mitogen-activated protein kinases (MAPK) and JAK/STAT pathway. NF-κB and MAPK are activated by the TLR-4 which further stimulates the release of TNF-α, IL-6, and IL-12 through macrophages, and thereby exacerbating the inflammatory response (Goyal et al., 2014). In addition to this, cytokines exert their signaling by activating JAK/STAT pathway and involved in the production of a number of interleukins. The proinflammatory mediators release is major factor involved in the progression of IBD.

3.5 Oxidative Stress

Oxidative stress has been well documented in IBD patients with increased ROS levels and decreased antioxidant levels in the inflamed mucosal layer, which ultimately contribute to tissue damage. A significant infiltration by neutrophils and increase in MPO levels was observed in the inflamed lamina propria of humans with UC. In IBD patients, an imbalance has been reported between oxidative species, such as superoxide ions, peroxynitrite ions, and hydrogen peroxide, and endogenous antioxidant levels, such as glutathione (GSH), catalase, and superoxide dismutase (SOD), resulting in the oxidative stress. These ROS are generated by the activated neutrophils and macrophages, and can be assessed by examining the amount of 8-hydroxy-20-deoxyguanosine (8-OHdG) in blood or malondialdehyde (MDA) in colonic biopsies, which are well-established biomarker for oxidative damage. These various factors are interlinked and functions in a viscous cycle, which contributes to the progression of disease leading to uncontrolled inflammation (Goyal et al., 2014). Various pathways involve in the pathogenesis of IBD as shown in Fig. 19.1.

4 ANIMAL MODELS OF INFLAMMATORY BOWEL DISEASES

Over the past 2–3 decades, several animal models of IBD have been developed which helped out in identification of novel drug targets and drug treatments, as well as helped to clarify a mechanism for abortive and prophylactic drugs. These animal models have provided translational knowledge and a framework to think about the impact of hormones, genes, and various environmental factors like sound, light, and so forth, on IBD pathophysiology. Although most of researchers have suggested that these animal models have lot of shortcomings but still some promising new drugs have been developed by utilization of these preclinical models. IBD has recently become of one of major interest to researchers. Various models for studying IBD mechanisms have been developed and exploited efficiently, leading to better understanding of the pathophysiology of the disorder. Since the exact etiology of IBD is not known yet, a number of animal models have been developed over past decades to study the possible mechanism involved in pathogenesis of disease and new therapeutic targets. The different types of animal models are developed for the study of IBD, which are discussed here, emphasizing on their clinical and histological features showing relevance to human IBD (Fig. 19.2).

4.1 Chemically Induced Model

4.1.1 Dinitrobenzene Sulfonic Acid

Dinitrobenzene sulfonic acid (DNBS) is a hapten, which induces the colonic inflammation and features of colitis. DNBS consist of additional active nitro group and binds more readily at lower concentrations. DNBS binds to the e-amino group of lysine is more selectively
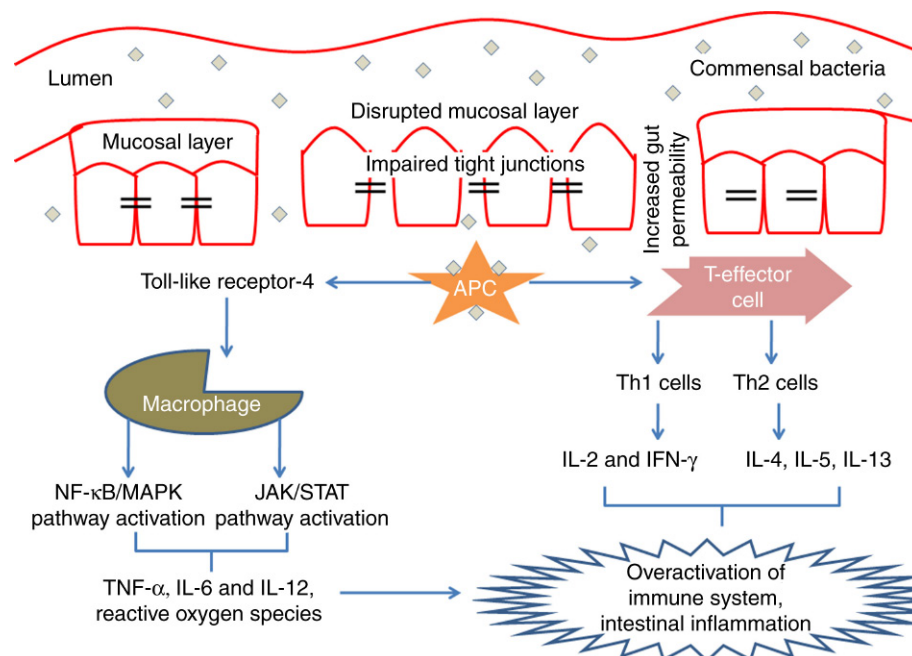
FIGURE 19.1   **Various pathways involved in the pathophysiology of inflammatory bowel disease.** *APC*, Antigen-presenting cell; *JAK/STAT*, Janus kinase/signal transducers and activators of transcription; *IFN-γ*, interferon-gamma; *IL-2*, interleukin-2; *IL-4*, interleukin-4; *IL-5*, interleukin-5; *IL-6*, interleukin-6; *IL-12*, interleukin-12; *IL-13*, interleukin-13; *NF-κB*, nuclear factor-kappa B; *Th1*, T-helper cells type 1; *Th2*, T-helper cells type 2.
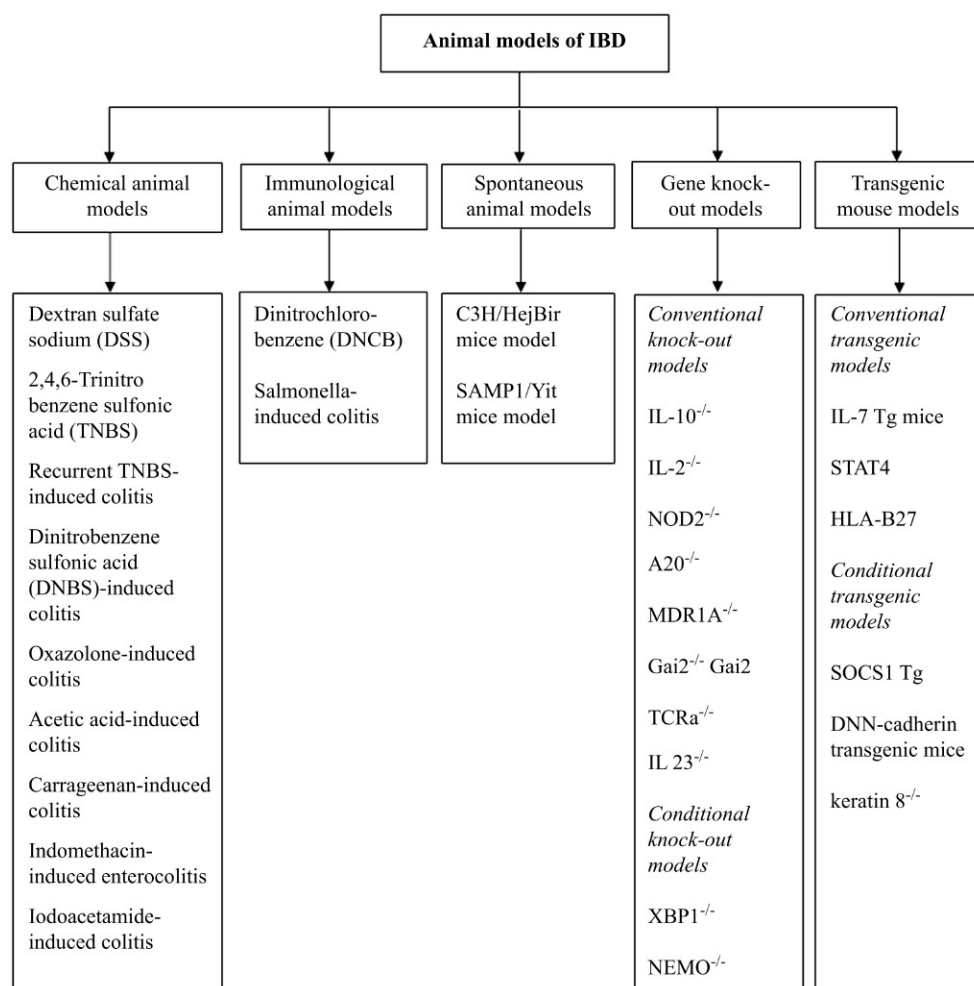
FIGURE 19.2   **Classification of animal models of inflammatory bowel disease.**

and used to induce colonic inflammation. The clinical features of colitis are presented in this model with bloody diarrhea and significant loss of body weight. DNBS administration (intrarectally) results in decreased food intake, increased colon weight, and changed stool consistency. DNBS causes overproduction of nitric oxide (NO) due to induction of inducible nitric oxide synthase (iNOS) and contribute to inflammatory processes. This model features transmural necrosis along with extensive morphological disorientation, edema, and immune cell infiltration in the submucosa of colon section.

4.1.1.1 PROCEDURE

Animals are on fasting overnight and on next day fasted rats are lightly anesthetized with ether. DNBS (3 mg in 100 mL of 50% ethanol) is administered to lightly anesthetized mice by an intrarectal injection with the help of a polyethylene catheter. Thereafter, animals were kept in trendelenburg position for 15 min to avoid reflux.

4.1.1.2 CLINICAL FEATURES

Decreased food intake, body weight, increased colon weight, and changed stool consistency are the common symptoms.

4.1.1.3 MOLECULAR CHANGES

- Overproduction of NO due to induction of iNOS
- Significant increase in myeloperoxidase (MPO) activity
- Elevated levels of MDA and decreased levels of SOD and GSH

4.1.1.4 HISTOLOGICAL FEATURES

- Transmural necrosis along with extensive morphological disorientation, edema and a diffuse leukocyte cellular infiltrate, as well as lymphocyte in the submucosa of colon section (Joshi et al., 2011)

4.1.2 Dextran Sulfate Sodium

Dextran sulfate sodium (DSS) is a synthetic sulfated polysaccharide composed of dextran and sulfated anhydroglucose unit and has highly water solubility. The colitogenic potential of DSS depends on its molecular weight. In general laboratory practice, a molecular weight of 36–50 kDa is used for inducing colitis. The low molecular weight DSS (5 kDa) results in milder colitis while higher weight DSS (500 kDa) does not cause colonic injury. DSS has high negative charge due to presence of sulfate group and is toxic to colonic epithelia and induces erosions that ultimately compromise barrier integrity resulting in increased colonic epithelial permeability. The anticoagulant property also aggravates intestinal bleeding. The mechanism by which DSS entry into mucosa remains unclear, but it has been suggested

that DSS forms nanolipocomplexes with medium-chain-length fatty acids in the colon.

4.1.2.1 PROCEDURE

DSS is commonly administered in a dose range of 3%–10% for 7–10 days to induce an acute inflammation depending on the type of the species used (Balb/c mice are more susceptible) or the molecular weight of DSS. For chronic colitis, DSS can be administered in three to five cycles with a 1- to 2-week rest between cycles (Mitrovic et al., 2010).

4.1.2.2 CLINICAL FEATURES

Weight loss, diarrhea and occult blood in stools, piloerection, anemia, and eventually death whereas in chronic phase of colitis usually do not reflect severity of inflammation or histological features found in large bowel

4.1.2.3 MOLECULAR CHANGES

1. Upregulation of cytokines, chemokines, NO, and iNOS levels
2. Increased activation of NF-κB
3. Increased expression of inflammatory cytokines genes (IL-1, TNF-α, IL-6, and IL-8), and some adhesion molecules genes [endothelial leukocyte adhesion molecule-1 (ELAM-1) and ICAM-1]

4.1.2.4 HISTOLOGICAL FEATURE

- Mucin depletion, epithelial degeneration, and necrosis leading to disappearance of epithelial cells which further leads to the formation of cryptitis and crypt abscesses.
- Chronic phase includes mononuclear leukocytes infiltration, crypt architectural disarray, increasing the distance (widening of the gap) between crypt bases and muscularis mucosa, deep mucosal lymphocytosis, and transmural inflammation.
- Increased apoptosis and decreased proliferation of epithelium that takes place in the acute phase of DSS further causing relevant leaks in the epithelial barrier.

4.1.3 2,4,6-Trinitrobenzene Sulfonic Acid

2,4,6-Trinitrobenzene sulfonic acid (TNBS) is a hapten, which when binds to tissue protein turns into an antigen and elicits number of immunologic responses. TNBS-induced colitis is a delayed-type hypersensitivity reaction to haptenized proteins, whereas DSS colitis is the result of a disruption in epithelial barrier. The major inflammatory mediators involved in this TNBS-induced colitis are leukotriene B4 (LTB4) and the monhydroxyl fatty acids 5-HETE, 12-HETE and 15-HETE. Ethanol is used in high concentration as a vehicle for the TNBS administration. Ethanol acts as a mucosal barrier breaker so

that TNBS can enter the mucosa to induce colitis where it binds to the amino group of lysine and modify cell surface proteins.

4.1.3.1 PROCEDURE

TNBS is administered using a trocar needle along with rubber catheter via the anus. TNBS is used in dose range of 0.5–4.0 mg in 45%–50% ethanol intrarectally. The dose varies between different mouse strains, such as SJL and BALB/c mice are highly susceptible, whereas C57Bl/6 and 10 mice are resistant (Kawada et al., 2007).

4.1.3.2 CLINICAL FEATURES

This model showed features, such as progressive weight loss, bloody diarrhea, rectal prolaspe, and large bowel wall thickening.

4.1.3.3 MOLECULAR CHANGES

- Increased level of various inflammatory mediators, such as prostaglandin E_2, thromboxane B_2, leukotriene B_4, 6-keto-prostaglandin F_{1a}, leukotriene C_4
- Increased colonic MPO activity and level of PAF

4.1.3.4 HISTOLOGICAL EXAMINATIONS

- Severe and intense transmural inflammation and/or necrosis, inflammatory granulomas, and submucosal neutrophils infiltration in mucosal and submucosal layers
- Cryptitis and architectural distortion are seen in endoscopic biopsies

4.1.3.5 ADVANTAGES AND DISADVANTAGES

This model has many advantages, which include (1) simple protocol, (2) reproducible colonic injury, (3) short length of the experiment, and (4) chronic damage accompanied by inflammatory cell infiltration and ulcers as seen clinically.

This model also suffers from some disadvantages like the absence of spontaneous relapse, which is the hallmark of human IBD. Also, ethanol itself causes severe inflammation in the intestinal mucosa, which makes it difficult to distinguish between the ethanol-induced inflammation and hapten-induced inflammation.

4.1.4 Recurrent TNBS-Induced Colitis

In this model, colitis is induced by repeated intrarectal administration of TNBS leading to the development of chronic intestinal inflammation. The inflamed colon shows increased weight and increased thickness, especially in the distal part. Histopathologically, it is associated with increased inflammatory cellular infiltration, which consists of $CD4^+$ and $CD8^+$ T cells, macrophages, granulocytes and mast cells, irregular crypts, and loss of Goblet cells (Goyal et al., 2014).

4.1.5 Oxazolone

Oxazolone when administered intrarectally with ethanol induces Th2-mediated acute colitis. Unlike TNBS-induced colitis, this model resembles only UC and is limited to the distal part of the colon only. Oxazolone-induced colitis has been suggested to be dependent on the presence of IL-13 producing invariant NK-T cells.

4.1.5.1 PROCEDURE

Colitis can be induced by applying 1% oxazolone (100 mL) dissolved in a mixture of four parts acetone and one part olive oil to the shaved abdominal skin of male C57BL/6CrSlc mice under pentobarbital anesthesia. Then, 1 week later, 100 mL of 50% ethanol solution with 1% oxazolone is administered intra rectally under pentobarbital and atropine anesthesia. Recently, oxazolone-induced colitis is used as a chronic model in Balb/c mice via repeated intrarectal administration of oxazolone in ethanol (Goyal et al., 2014).

4.1.5.2 CLINICAL FEATURES

The clinical manifestations of this model are weight loss, thin stool with pus and blood, bowel wall thickening, erosion, edema, and small patches of ulcer on colon.

4.1.5.3 MOLECULAR CHANGES

- Increased production of IL-4 and IL-5
- Rapid increase in the production of IL-13 in the lamina propria and the appearance of NK-T cells, both of which are immunologic features of acute oxazolone-induced colitis

4.1.5.4 HISTOLOGICAL FEATURES

- Neutrophil infiltration, fibrin deposition, submucosal neutrophil migration, submucosal edema, epithelial necrosis, and epithelial ulceration with loss of epithelial villi in the colon section
- Increase in MPO activity and decrease in number of goblet cells (Patel et al., 2012)

4.1.6 Acetic Acid

Acetic acid induces acute inflammation confined to the colon and produces characteristic features of UC. The colonic injury depends on the concentrations and length of exposure of acetic acid and is related to the necrosis and edema in epithelial cells mainly confined to the gastric mucosal layers. Mucosa and submucosal inflammation in this model is associated with activation of NF-κB and other inflammatory mediators. The transient local ischemia might contribute to the acute injury in this model.

4.1.6.1 PROCEDURE

Colitis is induced by intrarectal administration of 0.5 mL of 10%–50% acetic acid diluted with water in male Wistar rats. After 10 s of surface contact, the

acidic solution was withdrawn, and the lumen is flushed 3 times with 0.5 mL saline (Low et al., 2013).

Recently, this method is modified in which 1.5 mL of 4% acetic acid (pH 2.3) was slowly infused 8 cm into the colon through anus with a rubber cannula of a lightly anesthetized rat. After a 30-s exposure, excess fluid was withdrawn, and the colon was flushed with 1.5 mL PBS (Sotnikova et al., 2013).

Moreover, number of modifications has been made and now most of study used intrarectal administration of 2 mL of 4% acetic acid solution with the help of 2.7-mm soft pediatric catheter under light ether anesthesia. Animal is to be held horizontally for 2 min to avoid AA solution leakage because higher concentrations induced frequent perforations.

4.1.6.2 CLINICAL FEATURES

Weight loss, decreased mucous production, and increased colonic weight are the common manifestations of this model. Extensive hemorrhage, occasional ulceration, and bowel wall thickening were also observed in some studies.

4.1.6.3 MOLECULAR CHANGES

- Massive intracellular acidification resulting in massive epithelial damage
- Influx of acute inflammatory cells

4.1.6.4 HISTOLOGICAL FEATURES

- Eroded mucosa with ulceration and necrosis
- Edema, goblet cell depletion, lymphoid follicular hyperplasia, and heavy infiltration of inflammatory cells

4.1.6.5 ADVANTAGES AND DISADVANTAGES

The advantages of acetic acid-induced colitis are its low cost and the ease of administration.

The disadvantage of this model is that the epithelial injury observed within the first 24 h of acetic acid induction is not immunologic in nature. Thus, designing drugs that target immune responses should be tested at a time point after 24 h postinduction.

4.1.7 Carrageenan

Carrageenan is a proinflammatory agent and high molecular weight sulfated polygalactan, derived from several species of red seaweeds (Rhodophyceae), including *Gigartina*, *Chondrus*, and *Eucheuma*. Carrageenan triggers innate immune pathways of inflammation that resembles UC in which TLR-4 and BCL10 play critical role (Bhattacharyya et al., 2011).

4.1.7.1 PROCEDURE

The administration of 10% carrageen for 10 days in the drinking water of CF1 mice induces colitis exhibiting similar macro- and microscopic features as seen in UC.

4.1.7.2 CLINICAL FEATURES

Bloody diarrhea, colon length shortening, and pericryptal inflammation, with marked dilatation of the cecum and ascending colon, are the clinical features observed in this model (Tran et al., 2012).

4.1.7.3 MOLECULAR CHANGES

- Activation of NF-κB in the intestinal cells following carrageenan exposure
- Increase in Bcl-10 and TLR-4

4.1.7.4 HISTOLOGICAL FEATURES

- Mucosal ulceration with distorted crypt architecture, inflammatory infiltration of the lamina propria and hyperplastic epithelium, conditions are more pronounced in the proximal colon but also present in the distal colon.

4.1.8 Indomethacin-Induced Enterocolitis

Indomethacin is NSAID and induces small intestinal and colonic ulceration in a dose-dependent manner in rodents. Although small bowel ulceration and transmural inflammation have some similarity to CD, the chronic ulcerations are located in the mid-small intestine rather than the ileum. It involves small and large intestines and is associated with extraintestinal lesions (Stadnicki and Colman 2003).

4.1.8.1 PROCEDURE

Indomethacin is subcutaneously administered at dose of 7.5 mg/kg solubilized in 100% alcohol to fasted male Wistar rats, resulting in an acute inflammation. This acute response reaches its maximum intensity at 24 h and reversed within 7 days, whereas two daily subcutaneous injections of indomethacin induce a chronic inflammation that lasts for at least 2 weeks.

4.1.8.2 CLINICAL FEATURES

Acute intestinal inflammation, characterized by a thickening of the bowel wall, mesenteric hemorrhage, mesentery adhesion, and multiple mucosal ulcers of small intestine and colon.

4.1.8.3 MOLECULAR CHANGES

- Synthesis inhibition of the protective prostaglandins PGE1, PGE2, and prostacyclin
- Luminal bacteria and bacterial products contribute to the exacerbation and perpetuation of the chronic phase of indomethacin-induced inflammation

4.1.8.4 HISTOLOGICAL FEATURES

- Lymphoid hyperplasia, neutrophilic infiltration, crypt damage, and submucosal inflammation

4.1.9 Iodoacetamide

Iodoacetamide is a blocker of enzymes that contain SH-group (sulfhydryl) in the colon area. GSH contains SH-group and plays an important role in the protection of gastric mucosa; blockade of GSH by the iodoacetamide induces UC and produces injury to the mucosa by decreasing the amount of defensive SH compounds (Jurjus et al., 2004).

4.1.9.1 PROCEDURE

Single dose intrarectal (7 cm from anus) administration of 0.1 mL of 6% iodoacetamide dissolved in 1% methylcellulose via a rubber catheter induces reproducible colonic lesions in female Sprague Dawley rats after 1–2 h, leading to erosions and ulcers formation at 6–12 h. This is followed by extensive acute and chronic inflammation on 7–14 days.

4.1.9.2 CLINICAL FEATURES

The different clinical alterations in this model include diarrhea, dilatation, adhesion, mucosal damage, increased colon wet weight, and inhibition of body weight gain.

4.1.9.3 HISTOLOGICAL EXAMINATION

- Deep mucosal and submucosal ulcerations associated with an inflammatory infiltrate consisting mainly of lymphocytes and macrophages

4.2 Immunologic Model of Colitis

4.2.1 Dinitrochlorobenzene

Dinitrochlorobenzene (DNCB) is a hapten and is capable of inducing a cell-mediated (T-lymphocyte dependent) immune response with significant elevation in levels of CD4$^+$ and CD29$^+$ cells. First, animals are made sensitive to DNCB by placing it on their skin. Then, reapplication of DNCB induces an immune response at the same site.

Clinical and histological features of DNCB:
- crypt abscesses, superficial mucosal ulcerations, and depletion of mucus in the cells lining the crypts;
- edema in mucosa and submucosa, and infiltration of the lamina propria with plasma cells, lymphocytes and polymorphonuclear leukocytes, including eosinophils.

However, due to self-limited course of 2 weeks of DNCB, it is too short to be utilized as an ideal model for UC. To overcome these shortcomings, a new chronic UC model was established, that is, by using DNCB and AA in combination because of the following advantages: (1) like human UC, it manifests mucus in stools, bloody diarrhea, and weight loss; (2) it reflects the pathologic characteristics of UC, such as continuous superficial colonic inflammation. Microscopically, there exist mucosal edema and congestion, infiltration of lymphocytes, plasma cells and polymorphonuclear cells, crypt abscesses and ulceration; (3) also, it is an immune response model; immunology is well studied in UC (Goyal et al., 2014).

4.2.2 Bacterial Induction of Colitis (Salmonella-Induced Colitis)

The Gram-negative *Salmonella typhimurium* and *Salmonella dublin* are bacterial pathogens that can cause systemic infection and intestinal inflammation. The inflammation is very similar to human UC, including epithelial crypt loss, erosion, and neutrophilic infiltration. The colitis is induced by these pathogenic microbes usually after 5–7 days of systemic infection in C57BL/6 mice. Therefore, it is apparent that *S. typhimurium* infection is a important tool to study the acute phase of colitis (Low et al., 2013).

4.3 Spontaneous Model

Spontaneous models are one of the most effective, efficient, and attractive animal model systems for studying pathogenesis of IBD because they develop similar clinical features to human disease, intestinal inflammation without any apparent exogenous manipulations. Spontaneous models are broadly classified into two subcategories: (1) animals that spontaneously develop intestinal inflammation and (2) models in which a gene knockout results in an inappropriate mucosal immune response. For example, C3H/HeJBir murine model of colitis is characterized by spontaneous and chronic focal inflammation localized to the right colon and cecal region.

4.3.1 C3H/HejBir Mice Model

C3H/HejBir mice are produced by selective breeding of C3H/Hej mice with colitis known to develop ulcers and colitis. The intestinal inflammation in this model is limited to ileum and the right side of the colon and occurs spontaneously at age of 1 month of life and then completely disappears after 1 year of age. This model is also used in combination with other inducible colitis models and has proven to be effective tool for studying and identifying genetic factors underlying pathophysiology of IBD (Jurjus et al., 2004).

4.3.1.1 HISTOLOGICAL CHANGES

- Crypt abscesses and regeneration of epithelium
- Thickening of the intestinal wall and granulomas is not observed

4.3.1.2 MOLECULAR CHANGES

- Increased levels of IFN-c and IL-2 in the lamina propria lymphocyte, which shows that colitis in this model is a Th type-1 response, and thus represents CD.

4.3.2 SAMP1/Yit Mice Model

This model system develops spontaneously and presents itself as one of best is experimental system to study disease mechanisms of CD. It is characterized by severe inflammation in the last part of ileum, the primary location of CD lesions. The mucosal injury in this model system is characterized by presence by transmural inflammation, granuloma formation, and alterations in epithelial morphology. Increased epithelial permeability precedes the onset of inflammation, and epithelial cell dysfunction is primarily responsible for the disease progression. Ileitis develops at 10 weeks of age and the incidence of skin lesions inversely correlated with the occurrence of intestinal inflammation (Rivera-Nieves et al., 2003).

4.4 Conventional Gene Knockout Models

4.4.1 IL-10^{−/−}

IL-10 are proinflammatory cytokine and play important role in the pathophysiology of IBD. IL-10-deficient mice spontaneously develop a transmural pancolitis and cecal inflammation at the age of 2–4 months and symptoms completely resembles CD in humans. The inflammation is confined the whole intestine, mainly in the duodenum, proximal jejunum, and ascending colon (Modi, 2012).

4.4.2 TGF-β^{−/−}

TGF-$\beta^{-/-}$ is mainly produced by number macrophages and develops multiorgan dysfunction due to macrophage hyperactivation and reduced regulatory T cell activity, including severe colitis. These mice die within 4–5 weeks. The exact role of TGF-β in the intestine remains unclear, but it has been suggested to increase the production and release of IL-10 and downregulates the receptor expression of IL-12 (Boismenu and Chen, 2000).

4.4.3 IL-2^{−/−}

IL-2 is a four-bundled a-helical regulatory cytokine mainly produced by activated T lymphocytes, and its synthesis is highly regulated at the mRNA level by signals from the TCR and CD28^{+}. The small intestine of IL-2$^{-/-}$ mice remains intact, whereas the colon (from rectum to cecum) was severely affected with ulcers and wall thickening (Modi, 2012). Mice deficient in the cytokine IL-2 develop a chronic inflammation of the colonic mucosa/submucosa at 8–9 weeks of age that resembles UC.

4.4.4 NOD2^{−/−}

Nucleotide-binding oligomerization domain 2 (NOD2) that is also known as caspase recruitment domain-containing protein 15 (CARD15) has been shown to be expressed in myeloid cell line, including macrophages, monocytes, Paneth cells, and dendritic cells, and is induced by the proinflammatory cytokines, such as TNF-α and IFN-γ, exhibiting features of CD. Mutations of NOD2 result in an alteration in the ability of NOD2 to activate NF-kB (Rosenstiel et al., 2003).

4.4.5 A20^{−/−}

A20 is an ubiquitin-modifying enzyme in mice induced by TNF R, IL-1 R, and even NOD2. A20 is an inducible and broadly expressed cytoplasmic protein that inhibits TNF-induced NF-κB activity. A20-deficient mice develop spontaneous inflammation, cachexia, and premature death due to failure of A20 deficient cells to terminate TNF-α induced NF-κB responses. Thus, mice deficient in A20 develop spontaneous colitis indicating that NOD2 signaling alone is not sufficient to cause colitis (Hammer et al., 2011).

4.4.6 MDR1A^{−/−}

MDR1A gene is an ATP-binding transporter limited to intestinal epithelial cells and mucosal lymphocytes. Knockout of this gene induces a severe spontaneous colitis via Th1-type inflammation. MDR1A$^{-/-}$ knockout mice are devoid of the proper ability to dispose off the bacterial breakdown products in epithelial cells which increases abnormal antigen presentation to T cells, leads to a marked T cell activation and inflammation. Histology includes pancolitis with enlarged crypts, immune cell infiltration, crypt abscesses, and ulceration similar to the pathology of UC in humans (Wilk et al., 2005).

4.4.7 Gai2^{−/−}

Gai2 protein is a member of signal transduction molecules mainly expressed in intestinal epithelial cells, myofibroblasts, and intestinal T and B lymphocytes. Knockout of Gai2 in mice results in a development of spontaneous colitis at 8–12 weeks of age. Gai2-deficient colitis resembles UC, with the most severe inflammation occurring in the distal colon. The clinical and histopathological features include colonic thickening, lymphocyte and neutrophilic infiltrations, crypt and goblet loss, and crypt abscesses (Goyal et al., 2014).

4.4.8 TCRa^{−/−}

T-cell receptor a (TCRa) chain knockout mice spontaneously developed chronic colitis, mediated by Th2-type immune response. It closely resembles the human UC with an inflammatory pattern restricted mainly confined to the colonic mucosa. TCRa$^{-/-}$ mice develop colitis at the age of 12–16 weeks of age. It is characterized with soft stools, associated with loss of goblet cells, and a mixed cellular infiltration mainly consisting of lymphocytes and neutrophils (Nagatani et al., 2012).

4.4.9 IL 23⁻/⁻

IL-23 belongs to IL-12 family of heterodimeric cytokines and is specific to mucosal inflammation rather than systemic inflammation. IL-23 is an important cytokine required for the initiation, generation, and development of Th17 cytokines, such as IL-17 (Lees et al., 2011).

4.5 Conditional Knockout Models (Cell Type-Specific Gene Alteration)

4.5.1 XBP1⁻/⁻

Xbp1 is a protein essential for the development of secretory cells, such as goblet and Paneth cells which are involved in mucus secretion in the gut. Deletion of this protein from small intestinal epithelium results in total loss of Paneth cells and reduced size and number of goblet cells, which make it susceptible to UC (Kaser et al., 2008).

4.5.2 NEMO⁻/⁻

NEMO (IKKc) is a regulatory unit of the IKK complex. NEMO⁻/⁻ model exhibits T cell-mediated immune response. Targeted deletion of this gene leads to the intestinal epithelial integrity. The characteristic histopathological features of this model are severe transmural pancolitis with enlargement of crypts, goblet cell ablation, and mononuclear cell infiltration into the mucosa, similar to that observed in IBD (Nenci et al., 2007).

4.6 Transgenic Mouse Models of Colitis

Unlike knockout mice, transgenic mouse models of colitis express one or more copies of the gene of interest resulting in over expression of that particular gene. However, similar to genetically engineered mice, the transgenic mice can be either conventional or cell-specific targeted conditional transgenic animals.

4.7 Conventional Transgenic Mouse Models

4.7.1 IL-7 Tg Mice

IL-7 is synthesized in intestinal epithelial cells and regulates the proliferation and differentiation of lymphocytes within the mucosal layers. IL-7 has been found to be upregulated in case of patients with UC. The overexpression of IL-7 in the colonic mucosa of IL-7 transgenic mice is associated with chronic colitis caused by infiltration of CD4⁺ T cells with overexpression of IL-7 mRNA. An IL-7 Tg mouse model is valuable tool to understand T cell-mediated pathogenesis of colitis for therapeutic interventions targeting mainly T cell functions. Therefore, this is a chronic colitis model that closely resembles human UC (Watanabe et al., 1998).

4.7.2 STAT4

STAT4 is an important transcription factor involved in the development and regulation of Th1 cells that regulates the IL-12 pathway, which in turn is responsible for the regulation of Th1 cytokines, such as the proinflammatory interferon gamma (IFN-γ). STAT4 transgenic mice develop weight loss, diarrhea, and severe colitis resembling human CD.

4.7.3 HLA-B27

Human MHC class I allele HLA-B27 overexpression in both mice and rats results in intestinal inflammation. Rats transgenic for human HLA-B27 develops a spontaneous IBD which affects the stomach, ileum, and in particular the entire colon. Crypt hyperplasia and mucosal infiltration of mostly mononuclear inflammatory cells are characteristic features of the disease. This model has been used extensively to study the effect of resident intestinal bacteria for acute and chronic stages of gastrointestinal inflammation (Rath et al., 1999).

4.8 Conditional (Cell-Specific) Transgenic Mouse Models

4.8.1 SOCS1 Tg Mice

Transgenic (Tg) mouse models of intestinal significance with cell-specific deletions include T cell-specific SOCS1 Tg in which CTLA-4 mediated control of T cell proliferation resulted in spontaneous colitis (Inagaki-Ohara et al., 2006).

4.8.2 DNN-Cadherin Transgenic Mice/Keratin 8⁻/⁻ Mice

Keratin 8 is one of the major intermediate filament proteins present in intestinal enterocytes of patients with IBD. So, mice deficient for Keratin 8 develop colonic hyperplasia and colitis due to a primary epithelial rather than immune cell defect. This model provides direct evidence for the importance of an intact epithelial barrier for mucosal homeostasis, expressing a dominant negative mutation of the cell adhesion molecule N-cadherin in intestinal epithelial cells along the crypt villus axis (Owens et al., 2004).

5 CONCLUSIONS

IBD is a chronic inflammatory disorder of unknown etiology and characterized by chronic intestinal mucosal inflammation. Different drugs are available to treat IBD but need for novel effective therapy is insistent. Different animal models described in this chapter can be used to explore the pathophysiology of IBD and to test novel drugs. Every model described reflects some particular

pathological features of the IBD like chronic inflammation, mucosal layer disruption, increased gut permeability, and immune system overactivation. A specific model can be picked to induce the disease on the basis of expected mechanism of action of new drug.

References

Arthur, K., Zeissig, S., Blumberg, R.S., 2010. Inflammatory bowel disease. Annu. Rev. Immunol. 28, 573–621.

Beisner, J., Stange, E.F., Wehkamp, J., 2010. Innate antimicrobial immunity in inflammatory bowel diseases. Expert Rev. Clin. Immunol. 6 (5), 809–818.

Bhattacharyya, S., Borthakur, A., Anbazhagan, A.N., Katyal, S., Dudeja, P.K., Tobacman, J.K., 2011. Specific effects of BCL10 serine mutations on phosphorylations in canonical and noncanonical pathways of NF-κB activation following carrageenan. Am. J. Physiol. Gastrointest. Liver Physiol. 301 (3), G475–G486.

Boismenu, R., Chen, Y., 2000. Insights from mouse models of colitis. J. Leukoc. Biol. 67 (3), 267–278.

Burisch, J., 2014. Crohn's disease and ulcerative colitis. Occurrence, course and prognosis during the first year of disease in a European population-based inception cohort. Dan. Med. J. 61 (1), B4778–B14778.

Goyal, N., Rana, A., Ahlawat, A., Bijjem, K.R.V., Kumar, P., 2014. Animal models of inflammatory bowel disease: a review. Inflammopharmacology 22 (4), 219–233.

Hammer, G.E., Turer, E.E., Taylor, K.E., Fang, C.J., Advincula, R., Oshima, S., et al., 2011. Expression of A20 by dendritic cells preserves immune homeostasis and prevents colitis and spondyloarthritis. Nat. Immunol. 12 (12), 1184–1193.

Inagaki-Ohara, K., Sasaki, A., Matsuzaki, G., Ikeda, T., Hotokezaka, M., Chijiiwa, K., et al., 2006. Suppressor of cytokine signalling 1 in lymphocytes regulates the development of intestinal inflammation in mice. Gut 55 (2), 212–219.

Joshi, S.V., Vyas, B.A., Shah, P.D., Shah, D.R., Shah, S.A., Gandhi, T.R., 2011. Protective effect of aqueous extract of Oroxylum indicum Linn. (root bark) against DNBS-induced colitis in rats. Indian J. Pharmacol. 43 (6), 656.

Jurjus, A.R., Khoury, N.N., Reimund, J.M., 2004. Animal models of inflammatory bowel disease. J. Pharmacol. Toxicol. Methods 50 (2), 81–92.

Kaser, A., Lee, A.H., Franke, A., Glickman, J.N., Zeissig, S., Tilg, H., et al., 2008. XBP1 links ER stress to intestinal inflammation and confers genetic risk for human inflammatory bowel disease. Cell 134 (5), 743–756.

Kawada, M., Arihiro, A., Mizoguchi, E., 2007. Insights from advances in research of chemically induced experimental models of human inflammatory bowel disease. World J. Gastroenterol. 13 (42), 5581.

Lees, C.W., Barrett, J.C., Parkes, M., Satsangi, J., 2011. New IBD genetics: common pathways with other diseases. Gut 60 (12), 1739–1753.

Low, D., Nguyen, D.D., Mizoguchi, E., 2013. Animal models of ulcerative colitis and their application in drug research. Drug Des. Devel. Ther 7, 1341–1357.

McGuckin, M.A., Eri, R., Simms, L.A., Florin, T.H., Radford-Smith, G., 2009. Intestinal barrier dysfunction in inflammatory bowel diseases. Inflamm. Bowel Dis. 15 (1), 100–113.

Mitrovic, M., Shahbazian, A., Bock, E., Pabst, M.A., Holzer, P., 2010. Chemo-nociceptive signalling from the colon is enhanced by mild colitis and blocked by inhibition of transient receptor potential ankyrin 1 channels. Br. J. Pharmacol. 160 (6), 1430–1442.

Modi, H.K., 2012. A review on: screening models of inflammatory bowel disease. J. Global Pharm. Technol. 4 (7), 01–09.

Nagatani, K., Wang, S., Llado, V., Lau, C.W., Li, Z., Mizoguchi, A., et al., 2012. Chitin microparticles for the control of intestinal inflammation. Inflamm. Bowel Dis. 18 (9), 1698–1710.

Nenci, A., Becker, C., Wullaert, A., Gareus, R., Van Loo, G., Danese, S., et al., 2007. Epithelial NEMO links innate immunity to chronic intestinal inflammation. Nature 446 (7135), 557–561.

Ordas, I., Eckmann, L., Talamini, M., Baumgart, D.C., Sandborn, W.J., 2012. Ulcerative colitis. Lancet 380 (9853), 1606–1619.

Owens, D.W., Wilson, N.J., Hill, A.J.M., Rugg, E.L., Porter, R.M., Hutcheson, A.M., et al., 2004. Human keratin 8 mutations that disturb filament assembly observed in inflammatory bowel disease patients. J. Cell Sci. 117 (10), 1989–1999.

Patel, S.H., Rachchh, M.A., Jadav, P.D., 2012. Evaluation of anti-inflammatory effect of anti-platelet agent-clopidogrel in experimentally induced inflammatory bowel disease. Indian J. Pharmacol. 44 (6), 744.

Rath, H.C., Wilson, K.H., Sartor, R.B., 1999. Differential induction of colitis and gastritis in HLA-B27 transgenic rats selectively colonized with Bacteroides vulgatus or Escherichia coli. Infect. Immun. 67 (6), 2969–2974.

Rivera-Nieves, J., Bamias, G., Vidrich, A., Marini, M., Pizarro, T.T., McDuffie, M.J., et al., 2003. Emergence of perianal fistulizing disease in the SAMP1/YitFc mouse, a spontaneous model of chronic ileitis. Gastroenterology 124 (4), 972–982.

Rosenstiel, P., Fantini, M., Bräutigam, K., Kühbacher, T., Waetzig, G.H., Seegert, D., Schreiber, S., 2003. TNF-α and IFN-γ regulate the expression of the NOD2 (CARD15) gene in human intestinal epithelial cells. Gastroenterology 124 (4), 1001–1009.

Siegmund, B., Zeitz, M., 2011. Innate and adaptive immunity in inflammatory bowel disease. World J. Gastroenterol. 17 (27), 3178–3183.

Stadnicki, A., Colman, R.W., 2003. Experimental models of inflammatory bowel disease. Arch. Immunol. Ther. Exp. (Warsz) 51 (3), 149–156.

Tran, C.D., Katsikeros, R., Abimosleh, S.M., 2012. Current and novel treatments for ulcerative colitis. In: Shennak, M. (Ed.), Ulcerative Colitis From Genetics to Complications. InTech.

Wallace, K.L., Zheng, L.B., Kanazawa, Y., Shih, D.Q., 2014. Immunopathology of inflammatory bowel disease. World J. Gastroenterol. 20 (1), 6–21.

Watanabe, M., Ueno, Y., Yajima, T., Okamoto, S., Hayashi, T., Yamazaki, M., et al., 1998. Interleukin 7 transgenic mice develop chronic colitis with decreased interleukin 7 protein accumulation in the colonic mucosa. J. Exp. Med. 187 (3), 389–402.

Wilk, J.N., Bilsborough, J., Viney, J.L., 2005. The mdr1a$^{-/-}$ mouse model of spontaneous colitis. Immunol. Res. 31 (2), 151–159.

Further Reading

Wirtz, S., Neurath, M.F., 2007. Mouse models of inflammatory bowel disease. Adv. Drug Deliv. Rev. 59 (11), 1073–1083.

Page left intentionally blank

STROKE AND NEUROMUSCULAR

Page left intentionally blank

Animal Models of Ischemic Stroke Versus Clinical Stroke: Comparison of Infarct Size, Cause, Location, Study Design, and Efficacy of Experimental Therapies

Victoria E. O'Collins*, Geoffrey A. Donnan*, Malcolm R. Macleod**, David W. Howells*,†

*Florey Neuroscience Institutes, Melbourne Brain Centre, University of Melbourne, Heidelberg, VIC, Australia
**University of Edinburgh, Edinburgh, United Kingdom
†University of Tasmania, Hobart, TAS, Australia

OUTLINE

1 INTRODUCTION

The drug development paradigm postulates that treatments are tested for safety and efficacy in animal disease models, and then carried through to clinical trial. Results from the clinical trial then generate hypotheses, which are used to guide and inform subsequent animal testing. The reality for stroke medicine is quite different.

Clinical evidence currently supports the use of five acute stroke therapies (Donnan et al., 2008): hemicraniectomy (Vahedi et al., 2007); aspirin (CAST, 1997; ISTC, 1997); specialist care in hospital stroke units (Langhorne et al., 1993, 1995; Seenan et al., 2007), and the reestablishment of blood flow to the ischemic brain using tissue plasminogen activator (tPA) (NIND, 1995; Hacke et al., 2004) or by mechanical clot removal (Goyal et al., 2016). Of these treatments, only tPA has a legacy in experimental medicine, and this has largely been grounded in the field of cardiology.

Critiques of the merits or otherwise of animal models of stroke have been made in a number of comprehensive, lucid and insightful essays (Alonso de Lecinana et al., 2001; Carmichael, 2005; Dirnagl, 2006; Dirnagl et al., 1999; Durukan and Tatlisumak, 2007; Fukuda and del Zoppo, 2003; Ginsberg and Busto, 1989; Green et al., 2003; Hainsworth and Markus, 2008; Hossmann, 1998; Hossmann and Traystman, 2008; Hunter et al., 1998; Karpiak et al., 1989; Small and Buchan, 2000; Traystman, 2003). We sought to extend this work by directly comparing animal models of cerebral ischemia with the clinical disease they purport to model. By explicitly contrasting animal models with the clinical manifestation of stroke, we hoped to bridge the gap between the experimental and the clinical, and to examine the contribution of animal models to the understanding and management of stroke.

To this end, we undertook a wide ranging and detailed systematic review and metaanalysis of studies reporting—in clinical trials or animal experiments—the effect of acute stroke treatments. The analysis was restricted to those studies reporting infarct size—the amount of brain damage following stroke—as an outcome measure (endpoint). Although clinical outcomes, such as death, disability, and quality of life are the most important measures in the appraisal of a patient's health, infarct size has several advantages as an outcome measure: it is relatively free from bias (NINDS, 2000), it is routinely used in animal research and has been used more frequently in clinical trials in recent years. Consequently, measures of brain damage are useful for translational medicine research and enable a quantitative comparison of two key parameters, the size of a stroke and the efficacy of a treatment. The flipside of the focus on the amount of brain damage rather than behavioral or neurological scales is that it is still largely used as a surrogate or secondary outcome measure in clinical trials, so the relevance of infarct size to patient outcomes has yet to be fully established, a factor which will be discussed in further detail later.

After reporting on the methods of systematic review and analysis used herein, the results of the review are presented commencing with the general characteristics of the animal experiments and clinical trials, including: reasons for exclusion; sample size, quality of experimental design and reporting, comorbidities and species tested. Following this, results relating to infarct size in human trials and animal experiments are presented, together with analyses of factors moderating infarct size. Factors considered included a comparison of the cause, location, timing, and treatment of stroke in animal models and in clinical trials. The analysis of clinical trials is very much biased toward the perspective of the animal experimental paradigm and the underlying pathophysiology of stroke.

2 SYSTEMATIC REVIEW AND METAANALYSIS METHOD

2.1 Definitions and Scope

Stroke is a heterogeneous group of cerebrovascular conditions caused by the interruption of blood supply to the brain, usually due to the blockage of a vessel by a clot or due to a burst blood vessel. The World Health Organization defined stroke as "rapidly developing clinical signs of focal (or global) disturbance of cerebral function lasting more than 24 h (unless interrupted by surgery or death) with no apparent cause other than a vascular origin" (WHO-MONICA, 1988). While this definition is commonly acknowledged, it is not without controversy (Saver, 2008) as it excludes shorter ischemic episodes (transient ischemic attacks), subarachnoid hemorrhages, and the diagnosis of stroke using modern imaging methods.

Stroke is typically accompanied by impairment in movement, sensation, or cognition as measured against various clinical and neurological scales. The amount of brain damage caused by the stroke may also be quantified with brain imaging or after death (histologically) as the volume of infarction. For smaller mammals, brain damage is usually in the order of 10s–100s mm^3, while in humans it is typically in the order of 10s–100s cm^3.

The term neuroprotection is used to denote the average percentage reduction in infarct size in the treatment group compared to the control group. A negative level of neuroprotection would suggest that the treatment is damaging as it increases infarct size. The terms neuroprotection and efficacy are used interchangeably here, as are infarct size, stroke size, and infarct volume (unless

otherwise specified). Reperfusion refers to the reestablishment of perfusion to the ischemic area in the brain. Similarly, recanalization refers to the reestablishment of the patency of the blood vessels. Comorbidities are other diseases, such as hypertension that a patient may have in conjunction with stroke.

The scope of this review is limited to controlled studies. A controlled animal experiment or clinical trial is one which measures the effect of a treatment by comparing the outcome in one cohort given the experimental treatment, to another cohort which does not receive the intervention, the control group. Selection was not limited to studies where subjects were randomly allocated to treatment groups; however, this was taken into account in the analysis and interpretation of results.

Animal experiments included in this review are restricted to those employing focal models of cerebral ischemia. Focal models purport to induce a circumscribed region of damage in the brain, as occurs when the middle cerebral artery (MCA) is occluded. Focal models are typically distinguished from global models of ischemia which induce a reduction of blood flow to the whole brain, such as via the occlusion of both common carotid and vertebral arteries Focal models of cerebral ischemia are believed to be more relevant to stroke than global models (Molinari, 1979), while global models may be more representative of cardiac arrest.

2.2 Search Strategy

2.2.1 Animal Search Strategy

Animal data was collected prior to the clinical data and was initially collected for the purpose of identifying potential neuroprotective agents (O'Collins et al., 2006). Drugs or treatments used in experimental stroke were identified by: (1) PubMed search for "neuroprotection"; (2) PubMed search for "cerebral ischemia" from 1960 to 1980 (to capture agents tested prior to the use of the keyword "neuroprotection"); (3) from the reference lists of articles identified by (1) and (2). For each drug identified, a separate PubMed search was undertaken using the criteria "(drug name) AND (cerebral ischemia OR stroke OR neuroprotection)." Where no results were found, the search was repeated using only the drug name as the search term.

Since the initial identification of animal experiments was performed prior to the search for clinical trials (date: December 2004), additional searches were again undertaken for the therapies also tested in acute stroke clinical trials. A PubMed search (date: December 2007) using the criteria "(drug name) AND (cerebral ischemia OR stroke OR neuroprotection)" was again carried out, and if no results were found, the search was repeated using only the drug name.

2.2.2 Clinical Search Strategy

Clinical data was collected using a top-down and bottom-up search strategy (search date: December 2007). The top-down strategy involved searching clinical trial databases for trials listing infarction or brain imaging as an endpoint. The databases searched included the Washington University Stroke Trials Registry (Goldberg, 2007), the Cochrane Controlled Trials Register (Cochrane, 2007), and the National Institute of Health Trials Database (NIH, 2007). Once candidate trials were identified, the original papers documenting the results were sought using the reference provided in the trial database or by searching PubMed or Web of Science under the trial or drug name.

The bottom-up search strategy involved a PubMed scan using the search terms: (1) [(infarct volume OR infarct size OR lesion volume OR lesion size) AND (randomized controlled trial OR randomized controlled trial) AND (human)]; (2) (acute stroke AND human) cross-referenced with the terms (imaging OR infarct volume) and (neuroprotection OR thrombolysis). An additional search was undertaken in the Cochrane Controlled Trials Register and Review databases using the search terms [(infarct volume AND acute stroke) OR (imaging AND acute stroke) OR (infarct volume AND randomized controlled trial AND human)].

2.3 Study Selection and Data Extraction

2.3.1 Animal Data

Controlled focal cerebral ischemia experiments measuring the effect of treatment on the infarct size, and reporting this effect as the mean and standard error or deviation, as well as the sample size for each group, were retained for further analysis. Gene-knockout technology was not deemed a "treatment" for the purpose of the analysis. Where available, the following type of information was extracted for each experiment: animal characteristics (species, strain, sex, age, comorbidities), stroke model (method of induction, vessels occluded, hemisphere damaged), intervention (mode of delivery, control condition), outcome (imaging/histology method, percentage/absolute measure of infarct), and study quality (randomization and blinded assessment of outcome).

2.3.2 Clinical Data

Controlled clinical trials reporting the effect of an acute stroke therapy infarct size were included. Data were extracted for the sample size, the average outcome, and the standard deviation or error in the control and treatment groups. In a subset of trials, the results were presented as medians and ranges, usually without reporting whether the data was normally distributed. The method of metaanalysis applied here assumes the use

of a normally distributed population, so the presence of median data raises a conundrum. The approach adopted here was based on the methods canvassed by Hozo et al. (2005): (1) exclude trials reporting data only as medians, (2) include trials with median data as reported, and (3) use an estimate of the mean and variance values. For estimates of overall effect size, all three methods were used to gain a better insight into how data reporting may affect outcome.

Estimates of the mean value derived from the median were calculated using formulas (1) and (2). Using sample data-sets with known median and mean values, these formulas yielded estimated means within 3%–4.5% of the true value. Interquartile range was substituted if the range was not available.

1   Mean = Median

$$+ \sqrt{(\text{Maximum} - \text{Median}) - (\text{Median} - \text{Minimum})} :$$
Positively skewed data

2   Mean = Median

$$- \sqrt{(\text{Median} - \text{Minimum}) - (\text{Maximum} - \text{Median})} :$$
Negatively skewed data

Where standard deviation or error data was not available it was estimated as one quarter of the range. For sample sizes of 15–70 (the typical size of clinical trial groups), Hozo reports that this formula for standard deviation is a good approximation to the variance (Hozo et al., 2005).

Where available, information about the following variables was also extracted: pretreatment infarct volumes, patient characteristics (age, sex, comorbidities), cause of stroke, location of stroke, reperfusion/recanalization (proportion of patients), treatment (treatment type, control condition), method of evaluation of outcome, and quality of study.

The quality of the clinical trials was calculated using a scale adapted from previous preclinical analyses (Macleod et al., 2005a). One point was assigned for each of the following criterion met by the trial: (1) publication in a peer reviewed journal; (2) inclusion of a conflict of interest statement; (3) testing in aged, hypertensive, or diabetic patients; (4) inclusion of an ethics statement; (5) measurement of temperature; (6) patients blinded to the treatment; (7) outcome assessed by a person blinded to the treatment group; (8) patients randomly assigned to different treatment groups; (9) sample size calculations performed before trial commencement, and (10) placebo or vehicle administered to the patients in the control group.

2.4 Data Analysis of Infarct Size and Treatment Effects

Metaanalysis is the statistical method for combining the results of different studies to obtain an overall measure of the effect of the treatment. Different weights are accorded to each study based on the sample size and the amount of variance in the outcome. Data were analyzed to yield two main parameters: (1) treatment efficacy (neuroprotection) and (2) infarct size. Stratified analyses were also conducted to investigate whether the characteristics of the subject, the study or the treatment had an effect on the level of therapeutic efficacy and the infarct size.

2.5 Metaanalysis of Treatment Effects

Within each study, the average size of the infarct in the control group was designated as equal to 100%. The average infarct volume in the treatment group and the standard deviations were then expressed as a percentage of the control infarct volume. The treatment effect size for each study was then estimated as the difference between control and treatment groups:

$$\% \text{ Treatment effect} = \frac{\text{Mean control infarct volume} - \text{Mean treatment infarct volume}}{\text{Mean control infarct volume}} \times 100$$

Across all studies, an overall estimate of treatment effect was calculated using the random effects metaanalysis method of DerSimonian and Laird (1986) as described in other publications (Macleod et al., 2004, 2005a,b). To account for median data, the analysis of clinical trials was repeated 3 times: first, with only those trials reporting the mean and standard deviation. second, using both the means and the medians as reported, and last, using the means and an estimated mean value derived from the median as described previously.

Studies were then partitioned into categories based on factors, such as the cause of stroke to determine whether the treatment differentially affected subjects in those categories. Since the number of clinical trials using infarct volume as an endpoint is small, stratified analyses were based on the full data-set including those results with means estimated from median values.

2.6 Infarct size

Reported results were also used to obtain the estimated infarct size or infarct volume in the untreated patients or animals. The mean infarct size across studies was weighted according to the number of subjects in the control group, adjusting for the number of treatment arms. To facilitate the comparison of strokes across species differing by up to three orders of magnitude in their brain size, mean infarct size was expressed as a percentage of brain volume. Where values were reported as an absolute volumetric level, they were converted to a

TABLE 20.1   Hemispheric Volumes Used to Convert Results from Absolute to Percentage Values

Species	Hemispheric volume (mm³)	Sources
Mice	173	Sampei et al. (2000a,b)
Rat: Sprague Dawley	675	Marinov et al. (1996), Modo et al. (2002), Rewell et al. (2008)
Rat: Wistar and other strains	487	Rewell et al. (2008), Sahin et al. (2001)
Rat: spontaneous hypertensive	483	Rewell et al. (2008)
Gerbil	555	Chalfin et al. (2007)
Hamster[a]	481	Chalfin et al. (2007)
Guinea pig	533	Kowianski et al. (1999)
Rabbit[a]	1,843	Kawano et al. (2000)
Cat	9,020	Rathjen et al. (2003)
Primate	29,370	Dorph-Petersen et al. (2005)
Dog[a]	34,749	Chalfin et al. (2007)
Human[a]	591,500	Brott et al. (1989), Ho et al. (2005), Janssen et al. (2007), Lyden et al. (1994), Tupler et al. (2007), van der Worp et al. (2001)

[a]Hemispheric volumes were taken as half the value of total brain volumes. Where edematous effects are large, this may underestimate hemispheric volume.

percentage of the hemisphere infarcted using the brain volumes given in Table 20.1. Where results were given only as areas, these values were taken into account in calculating the putative level of neuroprotection, but not in estimating the infarct size. Infarct size estimation was derived only from volumetric measurements. Partitioned analyses were also conducted to investigate the effects of subject characteristics, the stroke model or subtype, the intervention, and the outcome measurement on the infarct size.

2.7 Comparison of Human and Experimental Data

Results from the metaanalyses were then used to compare the human and the experimental findings. Regression analysis was used to evaluate the extent to which animal experimental results predicted clinical trial findings. The proportion of variance in clinical trial results predicted by the experimental results can be estimated using the adjusted R^2 statistic.

Cohen's Kappa was used measure of concordance between the results of the metaanalyses for each drug tested in animals and taken to clinical trial, and the results of each clinical outcome themselves ($N_T = 39$). In particular, Cohen's Kappa was used to measure the concordance between the direction (positive/negative) of efficacy for each drug in animal experiments and the direction prespecified hypothesis outcome in the clinical trial and the direction of the infarct size outcome in the treated versus control group. This measure takes into account agreement, which may occur due to random chance.

2.8 Effect of Pretreatment Infarct Size on Final Outcome

Those studies, which recorded pretreatment infarct size (in addition to final infarct outcome) were identified and selected for further analysis. Regression modeling was used to determine the extent to which pretreatment infarct size could predict the final infarct volume.

Unless otherwise stated, values are reported as means and standard errors. N_T refers to the number of animal experiments or clinical trials and N_P refers to the number of patients or animals. Mean is abbreviated to M, and standard deviation and standard error to SD and SE, respectively. CI denotes 95% confidence intervals.

3 RESULTS

3.1 Inclusions and Exclusions

Three-hundred and ninety-six acute stroke clinical trials were identified, 330 of which had been completed at the time of analysis. Although many trials ($N_T = 204$, 52%) reported using imaging as part of their inclusion/exclusion criteria or some other part of the protocol, only 13% ($N_T = 44$) of all completed trials used imaging parameters as an endpoint. In ongoing trials, the proportion was higher, with 21% ($N_T = 14$) of ongoing trials expecting to report infarct volume measures derived from brain imaging.

The top-down search of clinical trials databases was combined with a bottom-up search strategy of using prespecified criteria to yield a total of 177 clinical papers containing 188 controlled trials of experiential

TABLE 20.2   Included and Excluded Clinical Trials

Features	Clinical trials
CLINICAL TRIALS IDENTIFIED	
Number of trials	396
Ongoing trials	66
Completed	330
Number of trials with imaging as an inclusion/exclusion	204
Ongoing trials with imaging as an endpoint	14 (21% of all ongoing trials)
Completed/halted trials with imaging as an endpoint	44 (13% of completed trials)
CLINICAL TRIALS REVIEWED	
Number of clinical papers	177
Clinical trial controlled comparisons[a]	184
REASONS FOR EXCLUSION	
Review paper	17 (9%)
Not acute stroke	7 (4%)
No treatment	15 (8%)
No control group	29 (15%)
No separate analysis of treatment versus control groups	23 (9%)
No imaging outcome	22 (12%)
No infarct size measurement	34 (9%)
Unable to source paper	2 (1%)
CLINICAL TRIALS INCLUDED	
Number of clinical papers	30
Controlled trial comparisons[b]	35

[a]*A single paper sometimes contained a comparison between a control group and more than one treatment group, hence the number of papers is less than the number of comparisons.*
[b]*This value refers to 35 unique treatment-control group comparisons coming from 30 papers.*

treatments potentially relevant to the review. Of these, 155 trials were excluded for the reasons detailed in Table 20.2. Thus, 35 controlled comparisons from 30 papers met the criteria for inclusion in the meta-analysis (Table 20.3) (ASSI, 1994; RANTTAS, 1996; Berrouschot et al., 2000; Blanco et al., 2007; Clark et al., 2000, 2001; Emsley et al., 2005; Fiehler et al., 2002; Fogelholm et al., 2000; Hillis et al., 2003; Horstmann et al., 2003; Infeld et al., 1996, 1999; Loh et al., 2005; Martin et al., 1985; Molina et al., 2001; Obrig et al., 2000; Ogawa et al., 1999; Parsons et al., 2002; Roberts et al., 2002; Rother et al., 2002; Seitz et al., 2004, 2005; Selim et al., 2005; Shi et al., 2000; Thomalla et al., 2003; van der Worp et al., 2002; Warach et al., 2000, 2006; Wu et al., 2006; Yasaka et al., 1998).

Fourteen unique treatments were tested in these 35 trial comparisons, with a large proportion testing the efficacy of tPA (N_T = 14 trials and 16 comparisons). Several studies also reported results for a combination of treatment types.

The initial search for animal experiments identified 8516 results extracted from approximately 3500 papers (O'Collins et al., 2006). Of these, 3867 experimental results were conducted in the focal ischemia model. A follow-up search for testing in animal experiments of treatments identified as having been tested in clinical trial yielded an additional 110 experimental results. Studies were excluded if there was not sufficient information regarding means, variance, and sample size to warrant inclusion (N_T = 832). Included in the final analysis were a total of 3145 experimental results testing 492 different treatment types in animal models of focal cerebral ischemia published between 1978 and 2007.

3.2 Sample Size

One reason frequently given for the apparent failure of neuroprotection studies is that their small size leaves them without the statistical power to detect any real changes in outcome. On average, we found that clinical

TABLE 20.3 Clinical Trials Reporting Infarct Volume Measurements

	Year	Trial name	Sample size	Treatment started (min)	Control infusion	Outcome Time	Positive outcome	Blind: patient	Blinding: outcome	Randomization	References
ACE inhibitors	2005		126		Historical: retrospective	Upon presentation	No	1	0	0	Selim et al. (2005)
Ancrod	1994	Ancrod Stroke Study Investigators	132	296	Saline	Day 8	Yes	1	1	1	ASSI (1994)
Atorvastatin	2007		89	300	Statin withdrawal		Yes	0	1	1	Blanco et al. (2007)
Citicoline	2001	Citicoline Stroke Study Group	899	792	Placebo	3 Months	No	1	1	1	Clark et al. (2001)
Citicoline	2000	Citicoline 010 Investigators	81	690	Placebo	12 weeks	Yes	1	1	1	Warach et al. (2006)
Aspirin, phenylephrine, midodrine fludrocortisone, sodium chloride	2003		15		Aspirin, saline		Yes	1	0	1	Hillis et al. (2003)
Ebselen	1999		99	528	Mixed: channel blockers, antiplatelet, anticoagulants, glycerol, thrombolytics	Day 7	No	1	1	1	Ogawa et al. (1999)
Gavestinel	2006	GAIN MRI	75	342	Placebo	Day 90	No	1	1	1	Warach et al. (2006)
Hypothermia	2003		100	720	Heparin control	Day 4	NA	0	1	0	Horstmann et al. (2003)
IL 1 receptor antagonist	2005		34	216	No thrombolytics	Day 6	No	1	1	1	Emsley et al. (2005)
Nimodipine	2000		153	2880	Placebo	Day 26	No	1	1	1	Fogelholm et al. (2000)
Nimodipine	1999		26	492	Placebo	Day 90	No	1	1	1	Infeld et al. (1999)
Prostacyclin	1985		31	1800	Placebo	Day 14	No	1	1	1	Martin et al. (1985)
r-proUK and heparin	2002	PROACT II	162	139	Heparin	Day 1, 7	NA	0	1	1	Roberts et al. (2002)
Streptokinase	1996	ASK	24	240	Placebo	Day 24	No	1	1	1	Infeld et al. (1996)
Streptokinase	1996	ASK	11	282	Placebo	Day 24	No	1	1	1	Infeld et al. (1996)
Streptokinase	1998	Australian Streptokinase Trial Study Group	37	21			No	1	1	1	Yasaka et al. (1998)

(Continued)

TABLE 20.3   Clinical Trials Reporting Infarct Volume Measurements *(cont.)*

	Year	Trial name	Sample size	Treatment started (min)	Control infusion	Outcome Time	Positive outcome	Blind: patient	Blinding: outcome	Randomization	References
Tirilazad mesylate	1996	RANTAAS	556	252	Vehicle: heparin, aspirin, surgery, and rehabilitation	Days 7–10	No	1	1	1	RANTTAS (1996)
Tirilazad mesylate	2002	TESS I and 2	368	360	Vehicle	Day 8	No	1	1	1	van der Worp et al. (2001)
tPA	2000		142	267	Placebo	Day 30	No	1	1	1	Clark et al. (2000)
tPA	2002	Kompetenz-netzwerk Schlaganfall Study Group	139	180	Conservative management	Day 7	No	0	0	0	Rother et al. (2002)
tPA	2005		26	360	Historical control: conservatively management	Day 90	Yes	0	0	0	Loh et al. (2005)
tPA	2003		100	720	Heparin	Day 4	NA[a]	0	1	0	Horstmann et al. (2003)
tPA	2005		47	153	Heparin and magnesium	Day 8	No	0	1	0	Seitz et al. (2005)
tPA	2000	NINDS rt-PA Stroke Study	606	180	Placebo	Day 1, 7, 90	Yes and no	1	1	1	NINDS (2000)
tPA	2004		47	121	Heparin and magnesium	Day 8	Yes	1	1	0	Seitz et al. (2004)
tPA	2002		40		Historical controls	Day 3	Yes	1	1	0	Parsons et al. (2002)
tPA	2002		15		Not stated	Day 7	NA	1	0	0	Fiehler et al. (2002)
tPA	2006		37	180	Noninterventional standard medical treatment (i.e., no thrombolysis)	At least 5 Days poststroke	Yes[b]	1	0	0	Wu et al. (2006)
tPA	2001		72	67.5	Historical controls	Day 7	Yes	1	1	0	Molina et al. (2001)
tPA	2000	ECASS II	52	239	Placebo	Day 1 and 7	No	1	1	1	Berrouschot et al. (2000)
tPA and tirofiban	2004		47	153	Heparin and magnesium	Day 8	Yes	1	1	0	Seitz et al. (2004)
tPA and tirofiban	2005		47	121	Heparin and magnesium	Day 8	Yes	0	1	0	Seitz et al. (2005)
tPA, hemicraniectomy	2003		37	360	Hemicraniectomy		Yes	1	1	0	Thomalla et al. (2003)
Urokinase	2000		31	360		Day 21	Yes				Shi et al. (2000)

Treatment time started—median time of commencement of drug administration.

[a]*NA, No priori hypotheses.*

[b]*Rescued tissue at higher infarction risk.*

study group sizes were 10 times larger than experimental groups. The 39 clinical trial comparisons of infarct volume included comparisons in 5532 patients, an average of 142 patients per clinical trial or $N_P = 71$ patients per treatment group. In contrast, the 3,145 experimental studies were undertaken on 45,476 animals, yielding an average of 14 animals per comparison or 7 animals per treatment group.

While sample sizes were larger in the clinical trials, so was the variance. In the 26 clinical trial results stating raw variance data as a standard deviation, the average standard deviation per trial equalled 99% in the control group and 105% in the treatment group (normalized with the mean control group infarct volume as 100%). In contrast, the animal studies showed an average standard deviation per experiment of 30% in the control group and 29% in the treatment group.

Overall, both animal and clinical studies tended to be underpowered. Estimates of sample size for a planned comparison of two independent means using a two-tailed test was undertaken using an online calculator (Brant, 2008) and in STATA v.10. To detect a 25% reduction in infarct volume in animals receiving treatment relative to animals in the control group and assuming a standard deviation of 30% of the control infarct volume (the average experimental variance reported previously), then the recommended sample size is 23 per group (powered at 80%, $\alpha = 0.05$, two-sided test). Based on these estimates, animal experiments were only 30% of the size needed to detect this level of difference. There is a prevailing dogma in animal research because animal experiments are controlled; there is less variance, so sample sizes can be small. Variance is indeed less than found in clinical trials, and sample sizes can be smaller, but not quite so small.

A similar calculation performed on the clinical data using a standard deviation of 99% yields a recommended sample size of 247 patients per treatment group (powered at 80%, $\alpha = 0.05$, two-sided test to detect a 25% difference in infarct size). Thus, on average, clinical trials were about only 28% of the size needed to detect a difference in infarct size. By clinical standards an effect size of 25% is large, so the degree to which clinical trials are underpowered would be much larger when trying to detect a smaller difference in independent groups.

The preceding analysis is of course just an estimate: Different animals, strains, models of stroke induction, and laboratories are associated with different degrees of variance, hence different required sample sizes. Similarly, using different types of analyses yields different estimates of group sizes, so smaller sample sizes may be required when looking at the effect of the treatments effect on the proportion of patients with expanding infarcts within each group (Phan et al., 2006), rather than comparing the treatment and control groups as two independent means (as is typically done in animal studies). Nevertheless, these rough estimates suggest both clinical trials and animal experiments were powered—or underpowered—to about the same extent.

3.3 Subject Characteristics

A frequent criticism of laboratory work is that animal studies are largely conducted in young, healthy male rats (Millikan, 1992). This criticism is supported by the findings of this review (Table 20.4): the vast majority of animal experiments were conducted in male animals ($N_T = 94\%$) while the clinical studies were undertaken in mixed sex patient groups ($N_T = 64\%$), or the sex was not specified ($N_T = 36\%$). Similarly, hypertension was the only risk factor for stroke that was represented in any sizable proportion of the animal experiments ($N_T = 14\%$), although still less than the prevalence in patients (66% of patients). Diabetes was underrepresented in animals (1.3% of animals vs. 26% of patients), and despite heart disease being major comorbidity in the clinical cohort (57% of patients), it was not modeled in animal experiments. Atherosclerotic animal models have been developed using modified genotypes or atherogenic diets (Moghadasian, 2002); however, these too are rarely used in neuroprotection research.

Animal experiments were almost exclusively conducted in the rat. Eighty percent of experiments employed rats ($N_T = 2506$), with 32% of all experiments ($N_T = 1016$) being undertaken in the Sprague Dawley strain. Previous meetings of the Stroke Therapy Academic and Industry Roundtable (STAIR) recommended that neuroprotection be explored in larger species, notably primates (STAIR, 1999). Only a handful of experiments in this data-set were conducted in primates ($N_T = 22$ experiments).

3.4 Study Quality

Clinical stroke medicine has been setting the pace for experimental stroke medicine in terms of its understanding of the need to maintain adequate standards of reporting results (Bath et al., 1998) and to minimize the potential for bias in experimental design through measures, such as blinding and randomization (Kidwell, 2001). While these issues are now more widely considered in animal experimentation (Fisher et al., 2009; Macleod et al., 2008), it was not surprising to find that clinical trial standards tend to surpass experimental standards, when assessed on the same scale.

The average quality score in the clinical trials was 6.2 points out of 10 (Table 20.5). Clinical quality was not related to the level of efficacy, as measured by a lower level of infarction in the treatment group ($r = 0.1$, $P > .05$, $N_T = 38$). Blinding of patients to treatment condition was

TABLE 20.4　Animal and Patient Comorbidities and Characteristics

Features	Clinical	Animal
SAMPLE SIZE		
Total number of experiments	35	3,145
Total number of animals or patients	5,532	45,476
Average treatment group size	142 per trial	14 per experiment
	71 per treatment arm	7 per treatment arm
SEX		
Male	—	94%
Female	—	2.5%
Both	64%	1.0%
Not stated	36%	2.5%
RISK FACTORS[a]		
Diabetes[c,d]	$26\% \left(N_P = \dfrac{552}{2152}, N_T = 11 \right)$	$1.3\% \left(N_T = \dfrac{31}{2364} \right)$
Hypertension	$66\% \left(N_P = \dfrac{1634}{2484}, N_T = 14 \right)$	$14\% \left(N_T = \dfrac{332}{2364} \right)$
Cardiovascular disease	$57\% \left(N_P = \dfrac{583}{1029}, N_T = 6 \right)$	Not reported
Atrial fibrillation	$24\% \left(N_P = \dfrac{118}{495}, N_T = 6 \right)$	Not reported
Age[b]	66 Years	0.6% middle aged/old $\left(N_T = \dfrac{19}{3145} \right)$

[a]Information not available for all studies, hence the percentage values are only calculated for the numbers reported.
[b]Weight, not age, is generally reported for animal studies. If age was not reported, it was assumed that young adult animals were used in the experiment.
[c]N_P, Number of patients or animals (as appropriate).
[d]N_T, Number of experimental contrasts.

undertaken in 50% of trials and in 84% of trials the outcome assessment was undertaken blind to the treatment condition. Sixty-three percent of trials randomized patients to treatment groups and in 16% temperature was monitored. The level of blinding and randomization in clinical trials was somewhat lower than that reported by Kidwell and coworkers (71% double-blinded and 93% randomized) (Kidwell, 2001), which may be due to the high proportion of thrombolytic reports in this data-set which were not yet complete at the time of Kidwell's analysis.

Study quality data was recorded in 80% of the animal experiment data. On average, about 38% of animal experimentation was randomized and in 32% the outcome was measured blind to the treatment group. These values are comparable to what has been found in earlier metaanalyses for individual drugs and are consistently below the levels of blinding and randomization for clinical trials (Table 20.5).

Over 10 years ago, quality in the design and implementation of animal studies was addressed by a consortium of researchers under the banner of the STAIR (STAIR, 1999). Since the initial STAIR recommendations were made, reporting standards have improved but there is still room for further gains. In the subset of animal experiments for which quality data was available, randomization was undertaken in 33% of studies published after STAIR (2000 onward) as opposed to 31% of studies published prior to STAIR, a 2% improvement. Blinded assessment of outcome has been raised from 34% pre-STAIR to 41% post-STAIR.

3.5 Infarct size

3.5.1 Background

Being a vascular disease, hemodynamic factors critically influence stroke size: blood pressure (Castillo et al., 2004), collateral flow (Toni et al., 1994), the

TABLE 20.5 Quality of Reporting in Acute Stroke Studies

Study	Quality (mean)	N_T	Randomization (%)	Blind: patient or induction of ischemia (%)	Blind: outcome assessment (%)	References
This review						
Clinical data[a]	6.2	35	63	50	84	Current publication
Animal data	—	2610	38	—	32	Current publication
Past animal reviews						
FK506	3.3	29	21	3	7	Macleod et al. (2005a)
Melatonin[a]	4.2	13	31	15	31	Macleod et al. (2005b)
Nimodipine[b]	—	20	10	—	30	Horn et al. (2001)
Nicotinamide	3.6	14	21	14	21	Macleod et al. (2004)
Thrombolysis	—	113	38	20	21	Perel et al. (2007)
Tirilazad	—	12	67	6	72	Perel et al. (2007)
Tirilazad	4.9	18	67	6	72	Sena et al. (2007)
Average[c]			36	15	29	

"—", Animal data was captured prior to clinical data and included only a subset of the quality data, consequently, an overall mean quality rating was not calculated for the animal data in the present review. Overall quality ratings were also not available for several other analyses reported here. Maximum quality score—10.

N_T—number of experimental contrasts.

[a]Calculated on the number of papers, not experiments or trials.

[b]Used an eight point scoring system for quality.

[c]Average number of experiments from past metaanalyses fulfilling these criteria and weighted for the number of experiments in the metaanalyses.

duration of occlusion (Arenillas et al., 2002), and the time to reperfusion (Molina et al., 2001) are all documented correlates or predictors of infarct development. Physiological factors, such as temperature (Leira et al., 2006; Reith et al., 1996), glycemic levels (Toni et al., 1994), and acidification (Smith et al., 1990; Wagner et al., 1992) have also been demonstrated to have a significant impact on infarct size.

Defining the volume of infarction is no trivial matter. Early computed tomography (CT) technology did not readily lend itself to infarct delineation, and the issue of what measure to use and where to threshold it remains open. Conventions in infarct measurement, analysis, and reporting also differ between the clinical and animal literature, hindering translational work. Clinical trial outcomes are often summarized using medians and ranges by virtue of having skewed data-sets and hence requiring different tests, such as the Wilcoxon rank sum test or Kruskal–Wallis test (Roberts et al., 2002). In contrast, animal findings are almost exclusively reported as a mean and standard deviation or error without regard to skewing of the data.

While clinical symptoms remain the gold standard in terms of patient assessment, imaging data is taking on a more prominent role in the management of the disease (Cramer et al., 2007; Selim et al., 2002). For instance, in order to minimize the risk of hemorrhagic transformation after thrombolytic therapy, imaging has been used to identify target patients with infarcts occupying less than one third of their MCA territory (Hacke et al., 1995; Pexman et al., 2001; Selim et al., 2002).

The size of a stroke is also of some importance in prognosis (Derex et al., 2004a). CT lesion volumes of less than 10 cm^3 have been associated with a favorable outcome (Saver et al., 1999), and clinical outcome has been shown to be better where diffusion weighted imaging (DWI) lesion size falls below 70 cm^3 (Sanak et al., 2006). DWI lesions larger than 89 cm^3 have been shown to predict early neurological deterioration (Arenillas et al., 2002). Similarly, CT lesions greater than 100 cm^3 have also predicted unfavorable outcomes (Saver et al., 1999). Malignant infarcts (massive hemispheric infarcts with a high mortality rate) were predicted by DWI volumes of greater than 145 cm^3 (Oppenheim et al., 2000), and patients with malignant infarcts occupying greater than 39% of the hemisphere are said to have little chance of responding to treatment (Carmichael, 2005) (Fig. 20.1).

3.5.2 Infarct Size in Different Species

The average infarct size in the control group of patients across all clinical trials included in this review was found to be 47.4 ± 28.3 cm^3, equivalent to 8.0% of one hemisphere (note, variance represents standard

Clinical outcome associated with infarct size

	Good outcome	CT < 10 cm^3	Saver et al. (1999)
	Fair outcome	DWI < 70 cm^3	Sanak (2006)
	Early neurological deterioration	DWI > 89 cm^3	Arenillas et al. (2002)
	Unfavorable	CT < 100 cm^3	Saver et al. (1999)
	Malignant infarct	DWI < 145 cm^3	Oppenheim et al. (2000)
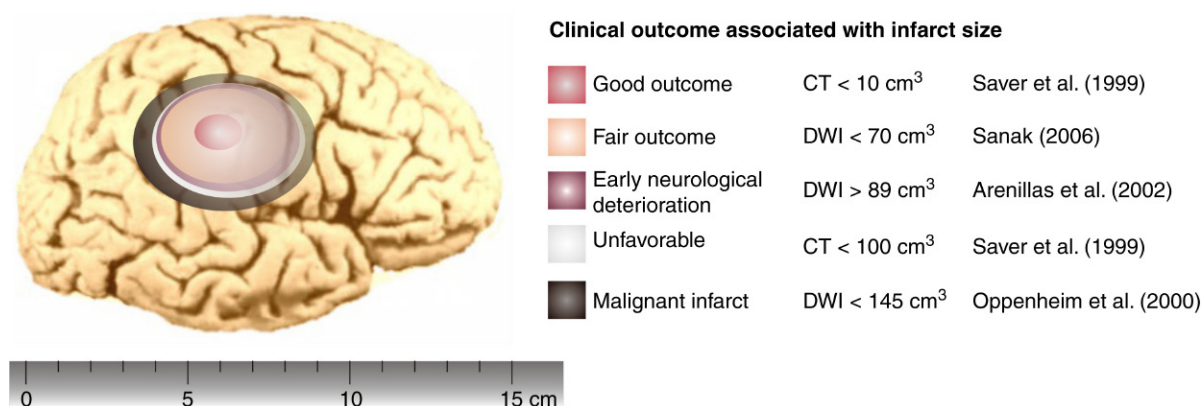
FIGURE 20.1   **Infarct size and clinical outcome.** Note: infarct volumes are presented roughly to scale assuming they may be modeled as prolate spheroids.

deviation of mean outcomes). The mean stroke volumes from individual clinical trials ranged from 5.3 (0.9% of the hemisphere) to 124.8 cm^3 (21.1% of the hemisphere), with a median of 51.4 cm^3 (IQR: 34.0–70.0 cm^3, 5.7%–11.8% of the hemisphere). This is comparable with the findings of Brott et al. (1989) where infarct size averaged 55 cm^3 at 1 week using CT, though smaller than the volumes reported by Caviness et al. (2002) where infarct volumes ranged from 3.1 to 256 cm^3 with a mean of 103.3 cm^3.

The average infarct size in control animals across all studies was 30.7% ± 16.3% of the hemisphere (median: 29.6%, IQR: 19.0%–40.6%, note, variance represents standard deviation of mean outcomes). When the weighting is adjusted for the number of animals in the control group of each study and the number of treatment groups compared to the control, the mean size of animal stroke averaged 26.6% of the hemisphere. Relative to brain volume, the brain damage caused by animal strokes was on average about 4 times larger than for human strokes. While clinical cases have been reported with infarcts of up to 47% of the brain volume (Brott et al., 1989), strokes occupying most of the MCA territory in humans are a minority of about 7%–10% of all strokes (Caviness et al., 2002; Heinsius et al., 1998).

In the subset of studies which presented infarct size as an absolute volume rather than percentages, average stroke size ranged across species from 53.6 mm^3 in the mouse to 47.4 cm^3 in the human (Table 20.6). Within different rat strains, stroke size ranged from an average of 112.5 mm^3 in Long Evans rats to 197.6 mm^3 in Hooded Listar rats (Fig. 20.2). The pattern of differences shifted somewhat when looking at relative (percentage) stroke sizes, due to different brain volumes. Note, diabetic rats are not a strain as diabetes has been induced in a number of different strains but they are included for sake of comparison.
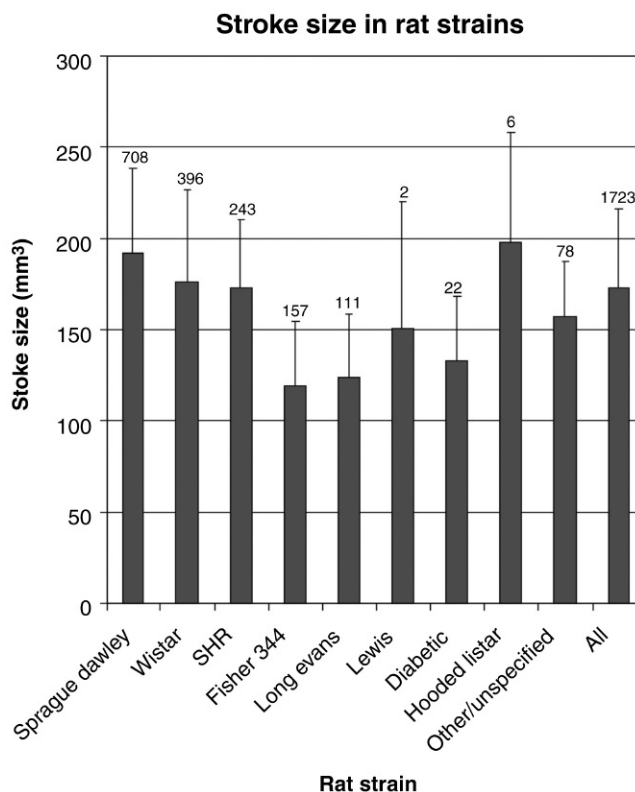
FIGURE 20.2   **Absolute infarct sizes in different rat strains or groups.** Consistent with the findings of Brint et al. (1988), stroke in the SHR rat was the tightest model in terms of having the lowest variance (average SD per experiment = 19%). In contrast to the results of Duverger and MacKenzie (1988), the Fisher produced the most variable infarct size models (average SD per experiment = 35%). Other rats tended to have experimental standard deviations averaging around 30%: Sprague Dawley (29%), Wistar (31%), Long Evans (27%), Lewis (30%), and diabetic (33%).

TABLE 20.6   Absolute Infarct Size in Control Cohorts

Species (strain)	N_{Trials}	Infarct size (mm³)[a]
Mouse	332	53.6 ± 12.9
Gerbil	3	57.9.1 ± 10.3
Rat	1,723	172.4 ± 43.7
Sprague Dawley	708	192.3 ± 46.1
Wistar	396	176.2 ± 50.6
SHR	243	173.0 ± 37.5
Fisher 344	157	119.4 ± 35.5
Long Evans	111	112.5 ± 35.2
Lewis	2	150.5 ± 69.7
Diabetic	22	132.8 ± 35.8
Hooded Lister	6	197.6 ± 60.1
Other/uncategorized	76	157.4 ± 30.1
Hamster	14	14.4 ± 5.9
Rabbit	24	525.7 ± 384.5
Cat	23	2,394 ± 4,047
Dog	—	—
Primate	9	3,760 ± 1220
Human	35	47,366 ± 5,231

SHR, Spontaneous hypertensive rat.
[a]*Variance reflects average standard deviation per experiment.*

Relative infarct size across species ranged from an average of 4% to 28% of the hemisphere (Table 20.7 and Fig. 20.3A). (Note: estimates were derived from data reported as percentages of hemisphere infarct, together with absolute volume data converted to a percentage using brain volumes). Of all the animal models, the rat (28%) and cat (27%) gave the largest average stroke volume and the hamster (4%), gerbil (8%), and primate (9%) the smallest. Within the rat genus, the spontaneous hypertensive rat (SHR) had the largest volume of damage (35%). This was expected on the basis of strain comparison data from individual studies (Brint et al., 1988; Duverger and MacKenzie, 1988; Gratton et al., 1998). In contrast, Lewis rats had comparatively small strokes (17% of the hemisphere), while Fischer 344 rats (23%), Long Evans (26%), Sprague Dawley (26%), diabetic rats (27%), and Wistar rats (32%) had intermediate infarct volumes (Fig. 20.3B).

The greatest variability in infarct size was seen in the human population, where the average standard deviation per trial was 99% of the infarct volume in the control group (Table 20.7 and Fig. 20.4). Among the stroke models, the greatest variability in infarct size (average SD per experiment) was seen in the cat (48%), the guinea pig (52%), and the rabbit models (58%), perhaps owing to greater variability in collateral flow in the embolic and proximal MCA occlusion models typically used in the rabbit and cat, respectively. The least variable stroke was seen in the gerbil (20%), while mice and rats had an average experimental standard deviation of 24% and 29%, respectively.

Consistent with the findings of Brint (Brint et al., 1988), stroke in the SHR rat was the tightest model in terms of having the lowest variance (average SD per experiment = 20%). In contrast to the results of Duverger (Duverger and MacKenzie, 1988), the Fisher produced the most variable infarct size models (average SD per experiment = 35%). Other rats tended to have experimental standard deviations averaging around 30%: Sprague Dawley (29%), Wistar (32%), Long Evans (27%), Lewis (30%), and diabetic (33%).

3.5.3 Acute Stroke Treatment Effects and Reporting Standards

Overall, both animal and human studies suggest that acute stroke treatment reduces infarct size when the comparison is based upon the treatment group relative to an untreated control cohort. Using the Der Simonian and Laird metaanalytic method, animals receiving treatment had infarct volumes 25.5% smaller than those in the control group (M ± SE: 25.5 ± 0.2%, 95% CI = 25.2–25.8, N_P = 45, 476, N_T = 3145). A similar level of benefit was
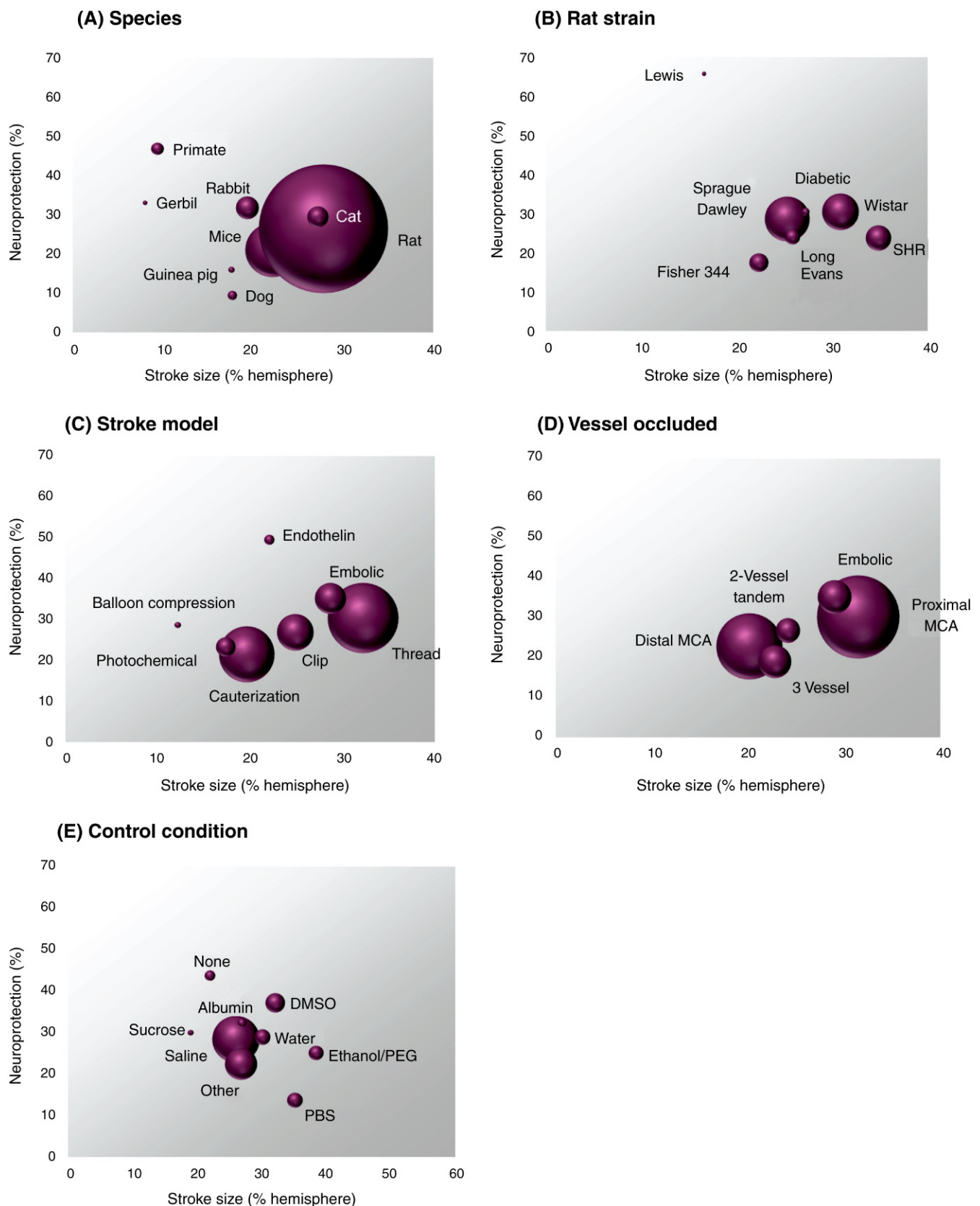
FIGURE 20.3 **Infarct size and neuroprotection in animal models of stroke.** Size of the bubble is proportional to the number of subjects in each category. The infarct size represents an average infarct volume, expressed as a percentage of the hemisphere, for each category. Where the data was not reported as a percentage, then the absolute value was transformed into an average using the values described in the methods section. Panels A–E display the results for species, rat strain, stroke model type, the vessels occluded, and different control conditions, respectively. So for instance, in subplot (A) species, the size of the bubbles indicates that the greatest number of experiments by far was conducted in the rat. Further, the plotting along the *x*-axis indicates that infarct size as a percentage of the hemisphere was greatest in the rat, closely followed by the cat, while along the *y*-axis, the treated primates tended to show the greatest level of recovery compared with the control group, while guinea pigs did not respond greatly to treatment. The percentage neuroprotection represents the difference in infarct volume between the control group and the treatment group, with values above 100% suggesting that the treatment is damaging and values below 100% suggesting that the treatment is able to reduce the amount of brain damage. Data relating to rat strains also includes diabetic rats, not technically a strain, but a disease state usually induced in Wistar rats.

TABLE 20.7   Relative Infarct Size, Variability, Sample Size, and Neuroprotection

Features	N_T	Variability (SD) (%)[a]	Suggested sample size[b]	Infarct size (hemisphere %)	Neuroprotection (M ± SE%)
OVERALL					
Clinical	35	99	247	8	27 ± 1.9
Animal	3145	30	23	31	26 ± 0.2
SPECIES COMPARISON					
Mice	439	24	15	22	21 ± 0.4
Gerbil	3	20	11	8	33 ± 8
Rat	2506	29	22	28	26 ± 0.2
Guinea pig	5	52	68	18	16 ± 0.4
Hamster	15	42	45	4	−83 ± 11
Rabbit	76	58	85	19	32 ± 2
Cat	66	48	58	27	29 ± 2
Dog	13	35	31	18	10 ± 4
Primate	22	34	30	9	47 ± 3
Human	35	99	247	8	27 ± 1.9
RAT STRAIN COMPARISON					
Sprague Dawley	1016	29	22	26	28 ± 0.3
Wistar	681	32	26	32	30 ± 0.4
SHR	332	20	11	35	23 ± 0.5
Fisher 344	180	35	31	23	18 ± 0.6
Long Evans	115	27	19	26	24 ± 0.7
Lewis	9	30	23	17	66 ± 5
Diabetic	31	33	28	27	31 ± 3
Hooded Lister	6	34	30	44	60 ± 4
Other/ uncategorized	136	27	19	24	
METHOD OF STROKE INDUCTION					
Thread occlusion	1325	29	22	32	30 ± 0.3
Electrocoagulation	797	25	16	20	21 ± 0.2
Clip or ligation	343	34	30	25	27 ± 1
Balloon cuff	10	61	94	12	29 ± 13
Photochemical	97	25	16	17	23 ± 1
Embolic	253	44	49	29	35 ± 1
Endothelin-1	25	34	30	22	50 ± 2
HEMISPHERE OCCLUDED					
Left	1128	26	17	25	24 ± 0.3
Right	1202	32	33	29	29 ± 0.3
VESSEL OCCLUDED					
Distal MCA	936	25	16	20	23 ± 0.2
Proximal MCA	1497	29	20	32	29 ± 0.3

(Continued)

TABLE 20.7　Relative Infarct Size, Variability, Sample Size, and Neuroprotection *(cont.)*

Features	N_T	Variability (SD) (%)[a]	Suggested sample size[b]	Infarct size (hemisphere %)	Neuroprotection (M ± SE%)
2-Vessel: MCA + CCA	130	36	33	24	26 ± 0.8
3-Vessel: MCA + CCAs	236	30	25	23	19 ± 0.7
Embolic/ unclassified	250	44	47	29	35 ± 0.8
SEX					
Male	2658	26	17	27	26 ± 0.2
Female	73	34	30	34	31 ± 1.4
Both	30	69	120	29	41 ± 2.9
Not stated	73	47	14	22	26 ± 1.5

N_T, Number of experimental contrasts; N_P, number of patients or animals.

[a]*SD is the average standard deviation, normalized to the control group infarct volume at 100%.*

[b]*Recommended sample size per treatment arm to detect a treatment effect of 25%, using a two-tailed test powered at 80% . Infarct size—average % hemisphere infarcted in the control group. Neuroprotection—average reduction in infarct volume (M ± SE). MCA + CCA—middle cerebral artery and common carotid artery.*
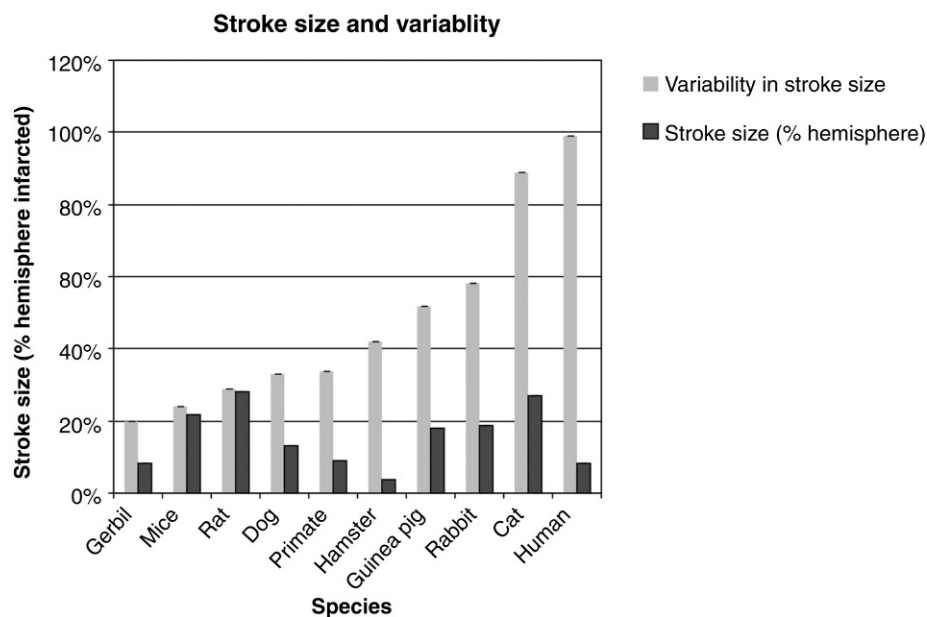
FIGURE 20.4　Relative stroke size and variability per experiment in different species. Each point on the graph represents the mean infarct volume in the treated group, expressed as a percentage of the control group. Ratios of baseline (pretreatment) infarct volume are depicted on the *x*-axis and final infarct volumes on the *y*-axis.

found for patients receiving treatment, with the treatment group having a stroke volume of 18%–29% smaller than the control group, depending on the method of reporting results (Table 20.8).

Where the effect size in clinical trials was based on the pooled estimate of data reported as means and raw or untransformed medians, the putative effect size was 31% (M ± SE: 30.7 ± 2.1%, 95% CI = 26.5%–34.9%, N_P = 5532 patients, N_T = 39 trial comparisons). For the effect size based on means and means estimated from median values, the effect size was 27% (M ± SE: 27.0 ± 1.9%, 95% CI = 23.3%–30.8%, N_P = 5532, N_T = 39). Looking at the subgroups, in those trials where the outcome was given as a mean (M ± SE: 18.3 ± 4.4%, N_P = 3432, N_T = 26) the estimated reduction was smaller than where it was given as a median and transformed into a mean (M ± SE: 29.1 ± 2.1%, 95% CI = 9.7%–26.9%, N_P = 2100, N_T = 13). There was significant statistical heterogeneity in the trial results based

TABLE 20.8   Method of Reporting and Outcome Measures

Reporting	Infarct volume (hemisphere %)	Neuroprotection ($M \pm SE$%)	Number of experimental contrasts
ANIMAL			
Absolute volume	30	25 ± 0.2	2107
Percentage of hemisphere	29	30 ± 0.4	755
Area of infarction	—	19 ± 0.7	145
Other/not known	—	30 ± 0.9	138
CLINICAL			
Mean	10	18 ± 4	26
Median	7	29 ± 2	13

Note: Infarct size—mean hemispheric volume in the control group. Neuroprotection—the percentage reduction in infarct volume in the treated group versus the control group.

on means and estimated means [$\chi^2(38) = 156$, $P < 3E^{-16}$] and means and medians [$\chi^2(38) = 155$, $P < 5E^{-16}$], though the heterogeneity was reduced when only the studies reporting means were included [$\chi^2(25) = 59$, $P < .0005$].

The effect of reporting method on the pooled estimate of efficacy may be a consequence of distortion of the data, with the conversion to a mean overstating the effect of the treatment. However, clinical trials reporting a median value tended to have smaller infarcts (*median*: 7.0% of hemisphere, *mean*: 9.8% of hemisphere) and thus their higher associated level of neuroprotection may have occurred as a consequence of the smaller infarct, irrespective of the reporting method.

Animal experiments also differed in their method of reporting results. Sixty-seven percent of experimental comparisons reported findings with an absolute value of brain damage, 24% as a percentage of hemispheric volume, with 9% of experiments recording damage as percentage hemispheric area, another geometric measure or measure unknown. Reports stating animal infarct volumes as an absolute value were associated with lower levels of neuroprotection than where volumes were reported as a percentage of the hemisphere (Table 20.8). However, the estimates of infarct size were similar, suggesting that some of the effect may be attributable to their effect on edema. A correlation of 0.97 has been found between edema volume and infarct volume in a tandem MCA model in rats (Kaplan et al., 1991), so a proportion of what is detected in the stroke neuroprotection literature may be due to the effect on the fluid balance in the brain and the molecules regulating it, such as aquaporins (Chen et al., 2007). Though not investigated here, treatment and postfixation tissue shrinkage may also differentially affect fluid balance within the ischemic and nonischemic brain tissues.

Of all the animals, the primate was associated with the highest level of neuroprotection ($M \pm SE$: 46.9 ± 3.0%, 95% CI = 40.9%–52.9%, N_P = 229 primates, N_T = 22 experiments). This was in spite of having the smallest infarct size. Conversely, the rat studies yielded a similar estimate of neuroprotection to that produced in clinical trials using the Der Simonian and Laird method ($M \pm SE$: 26.3 ± 0.2%, 95% CI = 26.1%–26.8%, N_P = 35,751 rats, N_T = 2,506 animal experiments), but their infarct size was much larger than seen in patients (when expressed relative to brain volume). The lowest level of neuroprotection was found in the hamster (Table 20.7), but this was found in a small sample ($M \pm SE$: 82.7 ± 11.42%, 95% CI = −104.9% to −60.4%, N_P = 128 hamsters, N_T = 2 papers and 15 experimental comparisons).

The more common strains of rats were associated with levels of neuroprotection in the order of 18%–31%. Neuroprotection was hardest to establish in the Fisher 344 strain ($M = 17.5\%$) and was most readily demonstrated in the Lewis rat ($M = 65.9\%$) (Table 20.7). This difference is of interest as the Lewis and Fisher strains are closely related, and it may have arisen due to differences in their corticosterone and hypothalamic–pituitary–adrenal axis mediated immune responses. Evidence indicates that the Lewis rat does not produce normal corticosterone responses (Sternberg et al., 1989a,b), and is highly susceptible to arthritis, while the Fisher is highly resistant and will withstand many attempts at inducing an inflammatory response (Lovallo, 2005). This suggests that the immune response greatly influences neuroprotective response. An alternate explanation might be found in differences in the vasculature. For instance, Dittmar has stated that the F344 rats are unsuitable for MCA occlusion due to vascular anatomy of their internal carotid artery (ICA), the ICA being heavily kinked (Dittmar et al., 2006), hence it
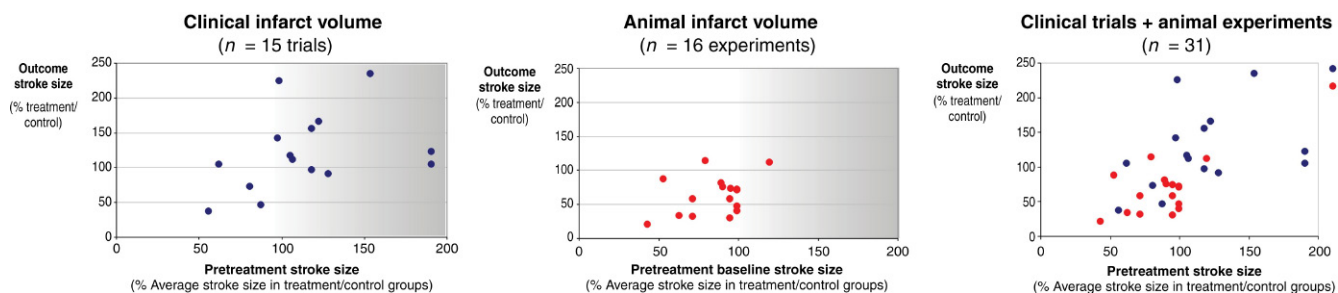
FIGURE 20.5   Pretreatment and final infarct size in treated patients and animals.

is conceivable that the F344 rat is less able to reperfuse and drugs which assist reperfusion might be associated with a lower associated level of efficacy.

3.5.4 Pretreatment Infarct Size and Relationship With Stroke Treatment

Early last century, Garrison wrote "Primitive man... tried to treat the disease rather than the patient, not realizing... that the dynamic effect of a drug upon the patients' body depends as much upon the delicate chemical adjustments of that body as upon the composition of the drug itself (Garrison, 1929)." The importance of individual variability of patients has been studied in a number of clinical trials, with the finding that pretreatment characteristics including site of arterial lesion, hypoperfusion volume, and clinical scores are predictive of therapeutic response (Adams et al., 1999; NINDS, 2000; Saqqur et al., 2007; Seitz et al., 2004; Warach et al., 2000).

Previous work has demonstrated that clinical outcome in stroke patients may be related to various pretreatment factors, including brain image characteristics (von Kummer et al., 1997), fibrinolytic profile (Ribo et al., 2004), and NIHSS scores (Adams et al., 1999; Uchino et al., 2001). Pretreatment measurement of infarct volume does not typically form part of the protocol in animal studies. This data is much more readily available clinically, as early imaging data is needed for diagnosis and treatment selection. But the issue is an important one, for if the treatment and control groups are not balanced—if they have different infarct sizes prior to treatment—it may affect the interpretation of results.

In the data collected for this review, pre- and posttreatment infarct volumes were available for 15 of the animal experiments (out of 3145 experiments) and 16 of 35 clinical trials (Fig. 20.5). The average infarct volume in the groups receiving treatment were expressed as a percentage of the control, with 100% indicating that on average the groups had the same size lesion, and values less than 100% expressing that the mean infarct volume in the treatment group was smaller than the control group. For each study, the ratios of treatment to control group were calculated pretreatment and at the final outcome assessment. A linear regression was then undertaken us-

ing the ratio of pretreatment stroke volume ratio as the independent variable and the outcome infarct size ratio as the dependent variable. Overall, pretreatment stroke volume significantly predicted outcome size ($b = 0.559$, $t(31) = 3.7$, $P < .01$). Pretreatment stroke volumes also explained a significant amount of variance in the outcome size ($R^2 = 0.312$, $F(1, 31) = 13.6$, $P < .0124$). Thus, pretreatment infarct sizes explained 31% of the heterogeneity in the model.

Interestingly, in two thirds of the clinical trials, the treatment groups had larger pretreatment stroke volumes, while in only 1 of the 16 animal studies was infarct volume larger in the treatment group prior to therapy (Fig. 20.5). Consequently, adding a variable to explain whether the results came from a clinical trial or animal experiment explained a greater amount of the variance in the outcome, and the cohort type (human or animal) was a significant predator of outcome (*adjusted $R^2 = 0.39$*, $b = 55.8$, $t(31) = 4.4$, $P < .001$). Given that pretreatment infarct size is an important predictor of outcome, an imbalance in infarct size at the outset may introduce bias into the results, with an underestimation of treatment effects in the case of clinical trials, and an overstatement of the effect of treatments in animal experiments. However, only a small subset of animal experiments acquired data on pretreatment lesion size so this may not be representative of the general experimental results. On the other hand, pretreatment conditions in animals are typically measured using a neurological score and/or the level of change in blood flow measured over a single point of the brain. Perhaps these measures are not sensitive enough to establish the equivalence of control and treatment groups prior to treatment administration and should be supplemented with subtler measures?

3.6 Temporal Factors in Stroke

3.6.1 Length of Occlusion

The criticality of reestablishing blood flow to ischemic tissue has been known at least since Harvey (Harvey, 2001). Through experimentation, Harvey demonstrated that ligation of a vessel may "induce sloughing and more extensive mortification in extremities" and

that upon reperfusion "all things immediately return to their natural state." Skip forward 380 years, and extensive clinical evidence has been furnished to support this point: where recanalization occurs, patients generally fare better (Rha and Saver, 2007). This is so even if some of the influx of blood is "nonnutritional" or "luxury" perfusion, that is, blood flow in excess of what is required to meet the metabolic demands of the surviving tissue (Barber et al., 1998). Reperfusion may be induced mechanically with specially crafted clot retrieval devices (Goyal et al., 2016), with antithrombolytic drugs, such as tPA, or it may occur spontaneously. Spontaneous reperfusion may lead to an improvement in clinical function (Barber et al., 1998), but evidence suggests that it must occur early to benefit a patient (Lees et al., 2010).

The perspective of experimentalists and clinicians diverge when looking at the duration of ischemia. Instead of asking how early the reperfusion must occur to benefit patients, experimentalists tend to emphasize the duration of ischemia needed to produce a reproducible infarct. To achieve this, Durukan recommended a minimum of 90–120 min of ischemia (Durukan and Tatlisumak, 2007). Prolonged periods of ischemia and reperfusion have been found to influence infarct volume, with both increasing it (Vosko et al., 2006).

The duration of occlusion in animals (N_P = 45,512) commonly spanned less than 6 h (N_P = 45%) or 1–3 days (N_P = 27%) and stroke of 6–24 h tended to be underrepresented compared with the clinical prevalence of stroke (N_P = 2% vs. 46%, respectively: Table 20.9). This comparison is limited by the paucity of included clinical trials in the review reporting this information, N_T = 1 (Molina et al., 2001). This trial, in particular, has relatively high levels of 24 h recanalization: 90% in the treated group and 61% in the untreated group. By way of contrast, Rha and Saver's metaanalysis of 53 studies placed the esti-

mated rate of recanalization at 55.1% after revascularization therapy, and 24.1% without treatment, measured at 24 h (Rha and Saver, 2007).

Trials documenting recanalization time, typically using transcranial Doppler, are bedeviled by considerable variability: failure to reperfuse occurs in untreated patients at a rate of 29%–88% (Molina et al., 2004; Poncyljusz et al., 2007; Vang et al., 1999); in treated populations, the range is lower at 8%–35% (Molina et al., 2004; Poncyljusz et al., 2007; Ringelstein et al., 1992). The juxtaposition of clinical and animal data is further hampered by the inability to accurately record of the number of patients who reperfuse before the first scan, typically in the first 6 h after onset of symptoms.

Data on the time of recanalization and infarct size was shown in only one clinical study reviewed here (Molina et al., 2001). This study demonstrated a clear positive relationship between time of recanalization after stroke onset and the subsequent size of the stroke: with recanalization earlier than 6 h, infarct size averaged around 25 cm³. Where recanalization took place at 6–12 h strokes were larger at around 90 cm³, and where blood flow restoration occurred at 12–24 h or 24–48 h patients had the largest infarcts of around 150 cm³. Failure to reperfuse leads to infarct volumes reaching almost 240 cm³.

Postponing reperfusion has a considerable impact on the progression of ischemia in animal models. The largest deficit was seen in animals with durations of ischemia of 90 min to 2 h (Table 20.10). Somewhat paradoxically, temporary ischemia of both under 30 min and over 3 h yielded smaller strokes, although this finding makes more sense when examining the trend within a single type of model. The inflatable balloon cuff model with its smaller lesion size was frequently conducted for over 3 h. Both thread occlusion models and models involving the placement of an external clip or ligature,

TABLE 20.9 Time of Recanalization

Length of occlusion	Number of animals	Number of tPA-treated patients	Number of untreated patients
0 up to 6 h	20,405 (45%)	16 (66%)	7 (15%)
6 and <12 h	587 (1%)	5 (20%)	15 (31%)
12 to <24 h	412 (1%)	1 (4%)	7 (15%)
24 to <48 h	7,877 (17%)	—	5 (10%)
48 to <72 h	4,662 (10%)	—	—
72 to <1 week	849 (2%)	—	—
>1 week/no reperfusion	1,743 (4%)	2 (8%)	14 (29%)
Undefined[a]	5,273 (12%)	—	—
Not known	3,705 (8%)	—	—
Total	45,512 (100%)	24 (100%)	48 (100%)

tPA, Tissue plasminogen activator.
[a]Occlusion induced using the embolic, endothelin-1 and photochemical models do not result in a controlled period of occlusion.

TABLE 20.10   Duration of Ischemia and Infarct Size in Animal Models

Duration	All models		Thread models		Clip/ligation models	
	Infarct size (%)	N_T	Infarct size (%)	N_T	Infarct size (%)	N_T
0–30 min	20.0	70	23.4	34	18.9	29
>30–60 min	31.2	247	36.4	190	19.9	34
>60–90 min	30.0	244	31.4	177	26.5	45
>90–120 min	34.6	554	36.2	472	31.7	58
>2–3 h	26.1	176	30.8	71	26.2	78
>3 h temporary	18.7	32	48.5	15	28.5	7
>3 h permanent	23.8	1023	42.3	203	28.4	58

N_T, Number of trials. Infarct size represents infarct size in the control group as a percentage of the hemisphere. Duration—duration of ischemia.

generally exhibited larger infarct sizes with longer occlusion times, but with exceptions. For the thread occlusion model, the largest occlusion time was seen with temporary occlusions greater than 3 h, compared with 90–120 min for the clip models. This time point is not without physiological significance: After 90 min of ischemia, edema increases and its imaging correlate—the ADC lesion volume on MRI imaging—eclipses the CBF lesion (Dzialowski et al., 2007; Meng et al., 2004). This length occlusion has also been associated with a peak in pCO_2, blood glucose and scalp temperature, and with the nadir in blood pressure (Memezawa et al., 1992).

At what time point is it no longer beneficial to restore blood flow, and can it be harmful? The injury said to arise from late restitution of blood flow, reperfusion injury, is typically imputed in animal studies when the infarct volume caused by temporary ischemia exceeds that in permanent ischemia. Supporting the idea of reperfusion injury, the thread occlusion models tended to show larger damage in the temporary models (48% of the hemisphere) than the permanent models with occlusion lengths greater than 3 h (42% of the hemisphere) (Table 20.10). Curiously, this pattern was not demonstrated in the clip and ligature models, with both occlusion lengths demonstrating stroke volumes of around 28%. This suggests that reperfusion injury may be more likely to arise in the filament models, perhaps due to greater damage to the endothelium or perhaps as a consequence of the larger infarct size.

These findings are generally concordant with individual studies looking at the outcome with different lengths of occlusion. Studies supporting the notion of reperfusion injury tend to come from filament or thread occlusion models (Yang and Betz, 1994) but not always (Memezawa et al., 1992). Those studies using microvascular clips or ligatures tend to refute the notion of reperfusion (Kaplan et al., 1991; Slivka et al., 1995; Young et al., 1997), but not always (Crowell et al., 1981).

A number of factors could account for a possible difference in susceptibility to reperfusion injury in different models. The discrepancy may have occurred by chance, but there also exist plausible physiological explanations, including edema, vessel damage, locus of occlusion, and differential effects of temperature, and anesthesia. Reperfusion after long periods in the thread occlusion model is associated with vasogenic edema (Neumann-Haefelin et al., 2000). Edema may have a reduced effect on some extravascular clip or ligature models because these models frequently involve removal of a small portion of the skull or the drilling of a hole—in order to reach distal MCA branches. This may mimic some of the effects of decompressive craniectomy, a procedure which has been found clinically to be useful in the treatment of malignant infarcts where edema and intracranial pressure management is critical (Vahedi et al., 2007).

Removal of the intravascular filament to allow reperfusion may also cause damage to the inner lining of the vessel, the endothelial cells and pericytes, instigating a pernicious response, a response exacerbated by the tendency of the filament model toward spontaneous hyperthermia associated with hypothalamic damage (Li et al., 1999). A complex interaction exists between the locus of occlusion and length of anesthesia (Hashimoto et al., 2008). A differential susceptibility of basal ganglia and cortical tissue to damage (Neumann-Haefelin et al., 2000) may also play a role. The basal ganglia may be more sensitive to ischemic damage than in the clip models, especially where the clip or ligature is placed prior to the origin of the lenticulostriate arteries. But this brings us back to the problem of experimental design; it is insufficient to imply reperfusion injury without first having established that blood flow did indeed return. Laser Doppler probes placed on the cortical surface measure only blood velocity in the surrounding 1 mm^3 and it would be insufficient to impute the return of blood flow to subcortical regions. The question of reperfusion injury therefore remains open.

Blood perfusion status is also an important mediator and indicator of treatment efficacy. The metaanalysis of Rha and Saver suggests that active revascularization

treatment raises the level of reperfusion to 55.1%, compared 24.1% with patients who receive no treatment (Rha and Saver, 2007). They found that the degree of reperfusion is moderated by stroke type, with occlusions of the ICA having the lowest rate of recanalization (49.1%) compared with the MCA/ACA occlusion (61%) and the vertebral and basilar arteries (66.2%) (Bamford et al., 1988).

The timing and effect of recanalization was reported in only two clinical studies, but there was greater neuroprotection ($M \pm SE$: $59.8 \pm 5.0\%$, $N_T = 1$) where the median reperfusion time was 3–6 h, compared with 6–12 h, where there was a 12% increase in damage ($M \pm SE$: $-11.8 \pm 35.4\%$, $N_T = 1$).

3.6.2 Time of Treatment Administration

Much effort over the preceding decades has been directed toward promoting the recognition of stroke as a medical emergency requiring immediate action. This urgency has been underwritten by several large thrombolysis trials finding benefit when treatment has been administered within the first four and half hours following stroke.

About one third of clinical trials included in this review involved the administration of drugs within 3 h or less ($N_T = 12$, 31%) and two thirds within 6 h or less ($N_T = 26$, 67%). This is exceptionally early, by standards of clinical trials, and accounts for the relatively early mean time of drug administration of 7 h after stroke onset ($M \pm SD$: 7.0 ± 9.0 h, median = 4.1 h, range: 1.1–48 h, $N_T = 34$, $N_P = 5299$). By contrast, in Kidwell's review of clinical trials before 2000, the median time to treatment was 24 h (range 3–360 h) (Molina et al., 2001). Treatment time is nevertheless protracted in clinical trials compared with the experimental counterparts. In experiments, the mean time of drug delivery is 10 h prior to stroke onset, with a median of 5 min poststroke ($M \pm SD$: -10.0 ± 67.2 h, median = 5.0 min poststroke, range: -84 to -15 days, $N_T = 3,048$, $N_P = 44,028$).

3.6.3 Time of Measurement

Study of the infarction as it develops over time is often referred to as the natural history of stroke. As time progresses after stroke onset, the amount of brain damage increases to reach a maximum at about day 2–3 poststroke (Lansberg et al., 2001; Schwamm et al., 1998), after which some patients plateau and some decline (Brott et al., 1989; Schwamm et al., 1998) contingent upon the recanalization status (Schellinger et al., 2001).

This pattern of infarct development is consistent with the findings in this study, with clinical trials tending to show a declining stroke volume in the control group as the time after stroke onset increased. For those studies looking in the acute phase, infarct size tended to be larger, perhaps reflecting the effect of edema or different types of measurands. The average infarct size occupied 11.6% of the hemisphere on day 1 ($N_T = 2$) and 9.3% at day 3–7 ($N_T = 3$). Most clinical trials ($N_T = 15$) measured infarct volume between week 1 and week 2, and at this time point, the average infarct size was 8.6%. After week 2, average size measured 7.8% of the hemisphere ($N_T = 13$).

Animal studies also followed this pattern. When measured less than 24 h after stroke induction, infarct volume in animals averaged 23.8% of the hemisphere ($N_T = 330$) and reached a maximum at 24–48 h, occupying 30.8% of the hemisphere ($N_T = 1353$). After 2–3 days, the stroke volume was 25.4% ($N_T = 513$), and at 3–7 days 24.4% ($N_T = 383$). During week 1–2 the infarct size was 23.7% ($N_T = 340$) and was smallest when measured after 14 days (19.8%, $N_T = 107$).

A frequent criticism leveled at animal studies is that outcome measurement is somewhat myopic, and that given enough time any differences between treatment groups may resolve. The median time of measurement was 8 days after stroke onset for patients and 1 day for animals (clinical: median = 8 days, range = 1–82 days; animal: median = 1 day, range: 20 min to 120 days). Twenty-six percent of clinical trials ($N_T = 10$) were measured at 4 weeks or beyond, compared to 1.7% of animal experiments ($N_T = 52$).

3.7 Cause of Stroke

3.7.1 Clinical Etiology of Stroke

The etiology of clinical stroke is commonly assigned using the TOAST classification system (Adams et al., 1993). According to this system, stroke is attributable to one of five conditions: (1) large vessel atherosclerosis, (2) cardioembolism, (3) small vessel occlusion/lacunar stroke, (4) stroke of other determined etiology, and (5) stroke of unknown etiology. In this review, 12 clinical trials with 2219 patients reported the cause of stroke (ASSI, 1994; Blanco et al., 2007; Clark et al., 2001; Fogelholm et al., 2000; Hillis et al., 2003; Obrig et al., 2000; Roberts et al., 2002; Selim et al., 2005; Shi et al., 2000; Thomalla et al., 2003; Yasaka et al., 1998). The most common attributable causes of stroke were large vessel disease ($N_P = 39\%$ of patients) and cardioembolism ($N_P = 39\%$ of patients). Small vessel disease was reported in 13% of patients, and 9% of patients had a stroke of unknown or some other etiology (Fig. 20.6). This population is less representative of small vessel stroke than has been found in other stroke studies (Salerno et al., 1996), perhaps because lacunar stroke patients are less likely to be included in imaging trials or receive thrombolytic therapy.
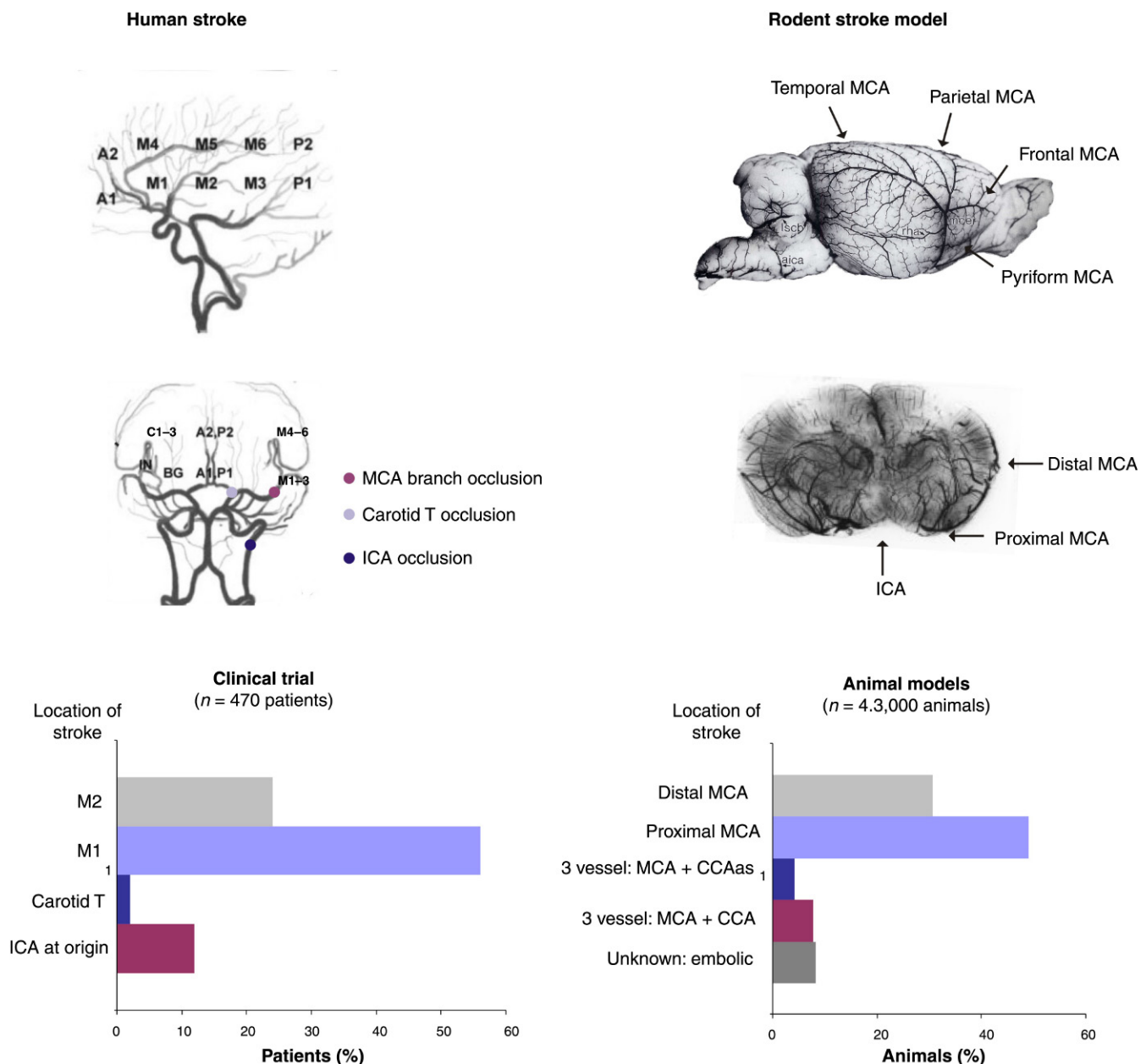
FIGURE 20.6   Location of occlusion in treated patients and animals. *Source: Human pictures adapted from Kim, J.J., Fischbein, N.J., Lu, Y., Pham, D., Dillon, W.P., 2004. Regional angiographic grading system for collateral flow: correlation with cerebral infarction in patients with middle cerebral artery occlusion. Stroke 35 (6), 1340–1344. Animal pictures adapted from Scremin, O.U., 2004. Cerebral vascular system. In: Paxinos, G. (Ed.), The Rat Nervous System. Elsevier, London, pp. 1167–1202.*

3.7.2 Method of Stroke Induction in Animals

The most common mechanism of stroke induction in animals involved the insertion of a filament into the common carotid artery, and threaded up to the point of origin of the MCA (N_T = 47%). This model has been variously called the thread occlusion model, the filament occlusion model, and the suture model. Ischemia by cauterization or thermocoagulation of the MCA was also popular (N_T = 28% of experiments). Occlusion of a vessel with a clip or by ligation was less common

(N_T = 12% of experiments), as were embolic models of stroke (N_T = 9% of experiments), and infarction induced by the laser activation of a photosensitive dye (N_T = 3% of experiments) or by application the vasoconstrictor endothelin-1 (N_T = 1% of experiments).

Methods of experimental stroke induction do not easily find parity with their clinical counterparts; nevertheless, it could be argued that the majority of animal models represent a nonatherosclerotic form of large vessel occlusion or a noncardiac form of cardioembolic stroke.

Although, the photochemical model of stroke may also mimic features of lacunae (Futrell et al., 1989), it is thought that no specific model captures all aspects of small vessel disease (Hainsworth and Markus, 2008): chronic models of hypertension have been suggested to be the best approximation (Hainsworth and Markus, 2008). Nevertheless, small vessel disease has been underrepresented in experimental stroke compared with its clinical prevalence.

Previous work has found that stroke of different etiologies may be associated with different sized infarcts (Brott et al., 1989). In the present review, the infarct occupied 15% of the hemisphere in control patients from trials only including cardioembolic strokes (N_T = 5). In trials of patients with stroke of mixed etiology, infarct size amounted to 6.5% of the hemisphere (N_T = 10), and where the cause was not reported, to 9.5% of the hemisphere (N_T = 24). Only one trial reported infarct volumes for the control patients grouped by causation, the NINDS tPA trial (Obrig et al., 2000). In this trial, the median CT volumes at 1 week were 40 cm^3 for cardioembolic, 32 cm^3 for large vessel stroke, and 4 cm^3 for small vessel stroke.

In animal experiments, establishing a relationship between infarct size and cause is aided by the fact that stroke may be tied to a single causal factor (Fig. 20.3C). The filament model induced the largest stroke (32% of the hemisphere), and the inflatable balloon cuff model the smallest (12% of the hemisphere). However, the balloon cuff model was also applied in larger species, perhaps accounting for the small infarct size. Similarly, the extensive nature of the damage caused by the filament occlusion model may be due to the location of the vessel involved—the origin of the MCA, a factor explored in the next section.

3.7.3 Cause of Stroke and Neuroprotection

Different stroke types may require different treatments and show different degrees of recovery (Murat Sumer and Erturk, 2002). For instance, Molina found that treatment efficacy depends on the cause of stroke with superior outcomes in cardioembolic strokes versus large artery disease, or other etiologies (Molina et al., 2004).

Establishing a relationship between stroke subtype and therapeutic efficacy in this review was hampered by the fact that clinical trials tend to include patients of multiple stroke typologies. In the five trial results including only cardioembolic strokes, the level of efficacy tended to be smaller (M ± SE: 4.4 ± 5.3%, N_T = 5) than where the cause of stroke was mixed (M ± SE: 32.8 ± 2.5%, N_T = 10) or not stated (M ± SE: 25.0 ± 4.0%, N_T = 24). However, the infarct sizes in these cardioembolic groups also tended to be larger occupying 14.5% of the hemisphere.

For animals, the relationship between the features of the stroke and level of neuroprotection was easier to ascertain, as the populations tend to be more homogenous

by design. In general, the relationship between type of stroke model and level of treatment efficacy may be explained by reperfusion. Models which permit reperfusion, such as the endothelin model (M ± SE: 49.6 ± 2.4%, 95% CI = 44.8%–54.3%, N_T = 25) and the embolic model (M ± SE: 35.3 ± 0.8%, 95% CI = 33.7%–26.9%, N_T = 253) tend to be associated with a higher level of efficacy. Models which permanently stop blood flow, such as the cauterization models tend to be associated with the lowest level of efficacy (M ± SE: 21.4 ± 0.2%, 95% CI = 21.0%–21.9%, N_T = 797). Clip and thread occlusion models which sometimes temporarily and sometimes permanently occlude the vessels had levels of efficacy in between. The relationship between treatment efficacy and infarct size for each type of model is depicted in Fig. 20.3C.

3.8 Location of Stroke

3.8.1 Background

In humans, the principal sources of arterial blood supply to the brain are the vertebrobasilar system or the carotid system (Fig. 20.6). The common carotid artery bifurcates or divides into the external carotid artery (supplying the external parts of the head), and the ICA (supplying the brain). The point of intracranial bifurcation of the internal carotid is often called the carotid T intersection, and beyond the carotid T, blood flows through to the MCA or anterior cerebral artery (if it has not already been diverted along one of the many other branches off the carotid arteries).

The branches of the MCA have been labeled M1 (the horizontal segment supplying the anterior MCA cortex), M2 (the sylvian segment supplying the cortex lateral to the insular ribbon), M3 (the cortical segment supplying the posterior MCA cortex), and M4–6 (the anterior, lateral, and posterior cortical segments supplying the anterior, lateral, and posterior cortical territories 2 cm superior to M1–3) (Kim et al., 2004; Pexman et al., 2001).

The rat brain is also supplied by the carotid and vertebrobasilar systems, but a different nomenclature is used to describe the vessels (Fig. 20.6). The major cortical branches of the MCA fan out across the cortical surface and have been called the frontal, parietal, temporal, and pyriform branches (from the frontal to posterior orientation, respectively) (Fox et al., 1993; Rubino and Young, 1988; Yamori et al., 1976). The lenticulostriate branches originate along the MCA and turn inward to supply the subcortical regions of the brain, notably, the basal ganglia.

An adjunctive classification of the MCA describes the proximal MCA as the portion of the MCA as it branches off the Circle of Willis and transcends anteriorly giving off the lateral and medial lenticulostriate arteries, up to the point of the olfactory tract (Fox et al., 1993; Yamori

et al., 1976). The distal MCA is then the portion of the MCA as it proceeds dorsally and traverses the inferior cerebral vein (ICV), the vein running with the rhinal fissure (Fox et al., 1993).

Differences in brain vasculature have been found both within and across species. Major variations have been found in the branching pattern of the Sprague Dawley, the most commonly used animal in stroke experiments (Fox et al., 1993; Niiro et al., 1996). Other species may exhibit features of the vasculature not found in people, notably, the carotid rete mirabilis, a fine web of vessels found in the neck of birds, ox, cats, sheep, swine, and to some extent in dogs (Daniel et al., 1953; Jewell, 1952; Scremin, 2004). Dogs may also have extensive intraextra cranial anastomoses (Jewell, 1952), as discovered in the 19th century by Astley Cooper. In his seminal ischemia experiments, Cooper and others who replicated his experiments were surprised to find that many dogs survived the occlusion of all carotid and vertebral arteries (Whisnant et al., 1956), a feat probably achieved by the diversion of extracranial blood supply to the brain regions critical for survival.

The location of a stroke may be defined either by the vessel occluded or by the territory affected. Each vessel is said to supply blood to a certain amount of brain tissue, its vascular territory. Estimates place the MCA territory at about 280 cm^3 or about 50% of the hemisphere (van der Zwan et al., 1993). By contrast, the anterior cerebral artery supplies about 138 cm^3 (23%) and the posterior about 119 cm^3 (20% of the hemisphere) (van der Zwan et al., 1993). However, the vascular territories of major vessels may be quite variable (van der Zwan and Hillen, 1991; van der Zwan et al., 1992, 1993), and the territory normally perfused by a certain vessel may not match the territory vulnerable to ischemia by occlusion of the same vessel (Phan et al., 2005). For instance, collateral blood supply from vertebrobasilar arteries may flow into the territory normally supplied by the MCA (van Laar et al., 2007). Thus, the effective area of the MCA territory may vary 34%–64% of the hemisphere (Provenzale et al., 2003).

The locus of the occlusion prejudices the final infarct size and the rate of recanalization of blood flow. Occlusions of larger vessels closer to the heart are frequently termed proximal lesions, while infarcts in smaller vessels further from the heart may be termed distal lesions. Distal MCA lesions tend to be smaller than proximal MCA lesions because they are less likely to involve the subcortical blood supply, the lenticulostriate arteries (Fig. 20.7 for the occlusion sites in the rat). However, distal lesions may also be smaller in size because they reperfuse more readily after stroke or respond better to thrombolytic therapy or because they receive more cortical collateral flow (Christoforidis et al., 2005; Rother et al., 2002). Collateral flow may alter this pattern, with occlusion of M1

resulting in more damage than an ICA occlusion where the ICA occlusion is accompanied by collateral flow to M1 (Liu et al., 2004).

Multifocal infarcts occur in 15% of patients with MCA territory lesions (Caviness et al., 2002) and in 10% of posterior territory lesions (Bernasconi et al., 1996). Multifocal lesions may occur in more proximal occlusions or where there are multiple embolic sources (Fiehler et al., 2005). Lesions may also occur bilaterally in patients, with around 10%–20% of patients showing signs of damage spanning both hemispheres (Arakawa et al., 2003; Castaigne et al., 1970). This is mirrored in rat embolic models, where Kaneko found that one third of rats (N_T = 12) had exhibited signs of a contralateral lesion (Kaneko et al., 1985). Multihemispheric infarcts may suggest a hemodynamic origin of stroke, but may also be due to the MCA or ACA vessels supplying both hemispheres, as occurs in a sizeable minority of patients (Provenzale et al., 2003).

3.8.2 Location of Stroke in Patients

Identifying the location of an infarct prior to the availability of brain imaging was the high-art of stroke diagnosis; careful clinicians, such as C. Miller Fisher wrote extensively on the subject (Miller Fisher, 1975). He listed the sites of predilection of large vessel or atherosclerotic stroke as the origin of the internal carotid in the neck, at the lower basilar and upper vertebral arteries at or near their junction and at the MCA stem (Miller Fisher, 1975). This description does not include embolic stroke or lacunar stroke, but with the exception of vertebral basilar artery territory stroke, this description largely characterizes the findings of the six trials in this review which documented the location of the stroke according to site of arterial obstruction (Fiehler et al., 2002; Hillis et al., 2003; Ogawa et al., 1999; Parsons et al., 2002; Roberts et al., 2002; Rother et al., 2002).

In the data from 470 patients included in these trials, 13% of strokes were located at the origin of the ICA, 2% were at the carotid T, 56% involved occlusion of M1 or M1 and extensions and 24% were occlusions of the M2 or distal branches of the MCA (Fig. 20.6). These findings are similar to those of Brott who found occlusion of the MCA in 82% of patients and of the ICA in 8% of patients (Brott et al., 1989). They are also congruent with the findings of Arnold, who found that the site of occlusion was more common in the larger M1 segment of the MCA (57 patients), compared with the smaller MCA branches (M2: 21 patients; M3 or M4 22 patients) (Arnold et al., 2002). In sum, the occlusion may occur anywhere along the carotid pathway, but it was most commonly found near the M1 segment of the MCA.

An alternate clinical stroke classification system is the Bamford or Oxford Classification System (IST Trial) (Bamford et al., 1988). Using this schema, clinical

Lateral surface of rat brain

1. Photothrombotic
Inferior cerebral vein (rhinal fissure)
2. Distal MCA model
Brain stem
Middle cerebral artery

Basal surface of rat brain

Middle cerebral artery
Inferior cerebral vein
2. ← Distal MCA model
Olfactory tract →
3. Proximal MCA model
Endothelin 4. 5. 6. Filament (koizumi)
Filament (longa)
Pons-isthmus Brain stem
Circle of willis
7. Embolic
Lenticulostriate arteries →
← Internal cerebral artery
← Middle cerebral artery

FIGURE 20.7 **Location of occlusion in rat models of stroke.** (1) The photothrombotic model may be applied by shining a laser on the MCA above the rhinal fissure (Yao et al., 1996). The actual location of the point of occlusion may vary (Cai et al., 1998). (2) Distal MCA occlusions have been induced by thermocoagulation, electrocauterization, or with a clip (Bederson et al., 1986; Coert et al., 1999). It has also been achieved in tandem with occlusion of the ipsilateral CCA or both CCA (Aronowski et al., 1996, 1997). The success of the model depends on the both the location of the occlusion and the length of vessel occluded (Bederson et al., 1986). (3) The proximal MCA model typically involves cauterizing or clipping the MCA proximal to the lenticulostriate arteries yields a model of cortical and caudate damage (Davis et al., 1995; Tamura et al., 1986). (4) Endothelin-1 is commonly applied close to the origin of the MCA to obtain drops in blood flow to the caudate nucleus and cortex. However, it may also be applied more distally, or on the cortical surface to obtain smaller lesions (Sharkey et al., 1993; Windle et al., 2006; Macrae et al., 1993). (5) The filament or thread occlusion model of Zea Longa uses a heat-blunted filament inserted up to the base of the MCA (Longa et al., 1989). (6) The thread or filament model of Koizumi uses a silicon-coated thread (Koizumi et al., 1986). Depending on the length of the silicon tip on the thread, this has the potential to also occlude other branches off the internal carotid, including the hypothalamic arteries. (7) Embolic models involve injecting a material (typically an autologous clot, macrospheres, or microspheres) into the circulation near the origin of the MCA. *Source: Modified from Bremer, A.M., Yamada, K., West, C.R., 1978. Experimental regional cerebral ischemia in the middle cerebral artery territory in primates. Part 3: effects on brain water and electrolytes in the late phase of acute MCA stroke. Stroke 9(4), 387–391; Busch, E., Kruger, K., Hossmann, K.A., 1997. Improved model of thromboembolic stroke and rt-PA induced reperfusion in the rat. Brain Res. 778(1), 16–24; Gerriets, T., Li, F., Silva, M.D., et al., 2003. The macrosphere model: evaluation of a new stroke model for permanent middle cerebral artery occlusion in rats. J. Neurosci. Methods 122(2), 201–211; Kudo, M., Aoyama, A., Ichimori, S., Fukunaga, N., 1982. An animal model of cerebral infarction. Homologous blood clot emboli in rats. Stroke 13(4), 505–508; Zivin, J.A., DeGirolami, U., Kochhar, A., et al., 1987. A model for quantitative evaluation of embolic stroke therapy. Brain Res. 435(1–2), 305–309.*

G. STROKE AND NEUROMUSCULAR

symptoms define the stroke type as a total anterior circulation syndrome (TACS), a partial anterior circulation syndrome (PACS), a posterior circulation syndrome (POCS), or a lacunar syndrome (LACS). This classification system was reported in only one clinical trial paper included in this review (Emsley et al., 2005) and the patients were overwhelmingly of the anterior or partial anterior type (71%, N_P = 24 of 34).

The location of an infarct may prejudice the ability of blood flow to return to the dying tissue, and as a general rule, the more proximal the stroke the poorer the reperfusion. In the recanalization metaanalysis of Rha and Saver (2007), occlusion of the ICA had lower rates of recanalization (49.1%) compared with the MCA/ACA (61%) and the vertebral and basilar arteries (66.2%). Similar results were found here, with the four studies reporting data on the rate of recanalization and occlusion location (Derex et al., 2004b; Fiehler et al., 2005; Poncyljusz et al., 2007; Rother et al., 2002). Those patients with occlusion of the MCA segment M2 recanalized on average more readily (N_P = 69%) than M1 (N_P = 57%), which in turn fared better than occlusions at the carotid T (N_P = 22%) or origin of the ICA (N_P = 24%) (Table 20.11).

Infarct location influences not only recanalization, but also the size of the stroke. Clinical trials including only MCA infarcts had an average infarct size of 10.5%

of the hemisphere (N_T = 15), larger than where strokes were of mixed loci (6.6%, N_T = 4) or where the site of occlusion was not stated (6.8%, N_T = 20). Where infarct data was broken down by occlusion location, patients with M2 or smaller MCA branch lesions had stroke volumes of 56.6 cm^3 (9.6% of the hemisphere, N_P = 79); lesions of the M1 segment, M1 and extensions, or the MCA trunk were larger (89.3 cm^3, 15.1% of the hemisphere, N_P = 97) and those blocking the carotid T, ICA, or both ICA and MCA spanned an average of 113.7 cm^3 (19.2% of the hemisphere, N_P = 42). Predictably, the larger the vessel occluded, the larger the resulting infarct.

3.8.3 Location of Stroke in Animals

Information about the infarct in animal models is typically given as a total volume, sometimes supplemented with data on cortical and subcortical volumes. It is rare to find more detailed delineations of the location of damage, except in the early experimental work, or in papers establishing the methodology. Excellent and extensive descriptions of the locus of damage caused by different stroke models have been given by Ginsberg and Busto (1989) and Carmichael (2005). A précis of their work, together with descriptions from the original papers is given next in Table 20.12 (Fig. 20.8).

TABLE 20.11   Recanalization With Different Stroke Loci

Time	N_P	Drug	ICA origin	Carotid T	M1/proximal	M2/distal	Overall	References
NO TREATMENT								
24 h	63	Conservative treatment	0/9 (0%)	2/14 (14%)	4/17 (24%)	11/21 (52%)	17/63 (27%)	Rother et al. (2002)
7 Days	16	Control	—	—	1/3 (33%)	12/14 (86%)	2/16 (12.5%)	Poncyljusz et al. (2007)[a,b]
TREATMENT								
24 h	76	i.v. tPA	0/5 (0%)	5/12 (42%)	23/30 (77%)	16/23 (70%)	47/76 (62%)	Rother et al. (2002)
24 h	65	i.v. tPA	5/11 (45%)	1/12 (8%)	12/24 (50%)	12/17 (71%)	30/65 (46%)	Fiehler et al. (2005)
24 h	47	i.v. tPA	4/12 (33%)	—	12/19 (63%)	12/16 (75%)	28/47 (60%)	Derex et al. (2004b)[b]
7 Days	16	i.a. tPA	—	—	—	12/14 (86%)	12/16 (75%)	Poncyljusz et al. (2007)[a,b]
	32	Both			1/3 (33%)	12/14 (86%)	14/32 (44%)	Poncyljusz et al. (2007)[a,b]
Overall	283		24%	22%	57%	69%	48%	

Time—time measured. N_P, number of patients. Numbers indicate the percentage of patients recanalized in relation to the total number of patients in each group.
[a]Not all results reported in paper.
[b]Identified in the search, but excluded from the metaanalysis because no infarct data or no control group. M1—M1 branch of the MCA. M2—M2 branch of the MCA. Proximal—proximal MCA. Distal—distal MCA. Rother—partial or full recanalization. Fiehler—reported as reperfusion or no reperfusion. Derex—reported as no recanalization or recanalization.

Animal experiments versus clinical trials

Ranking of individual drugs
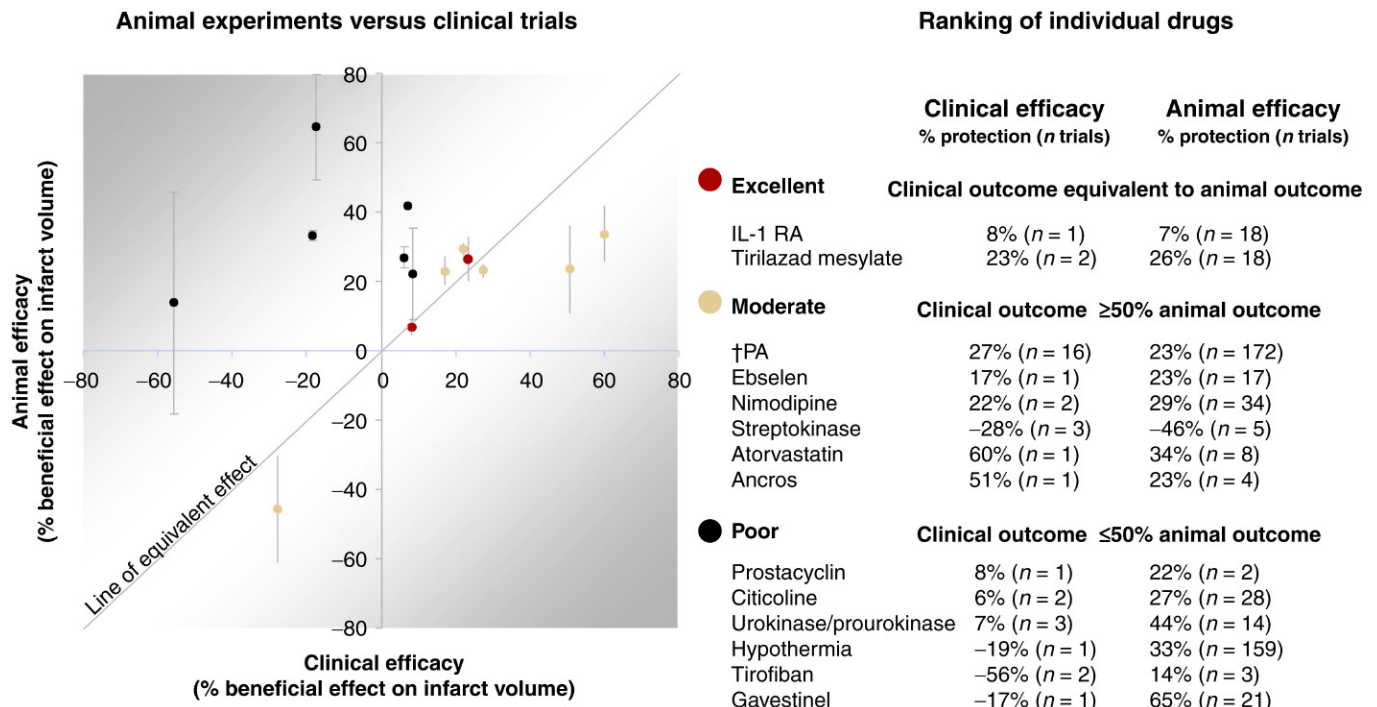
FIGURE 20.8   **Treatment efficacy in animal versus clinical trials.** Each point on the graph represents the effect size for a single intervention in clinical trials *(horizontal axis)* versus animal experiments *(vertical axis)*. Efficacy estimates are derived from metaanalyses of differences in infarct volume in control versus treated groups. Higher estimates in efficacy represent a smaller infarct volume in the treated group. The correspondence between animal and clinical efficacy ratings for the same intervention were described as excellent if the confidence intervals overlapped; moderate, if the clinical outcome was at least half as effective as animal estimates predicted (on this scale); poor, if the clinical estimate of efficacy was less than 50% of the animal estimate.

In the analysis of animal data, the location of stroke was approximated by virtue of the model used. Experiments were deemed to fall into one of five categories: (1) MCA branch occlusions—occlusion of a branch of the MCA via cauterization, clips, ligation, endothelin-1, or a photochemical dye; (2) MCA origin occlusions—occlusion of origin of the MCA with a filament; (3) tandem occlusions—occlusion of the MCA and CCA; (4) three-vessel occlusion—occlusion of both common carotid arteries and the MCA, and (5) undefined—embolic models where the final place of lodgment of the clot or clot substitute is not controlled.

The largest strokes were induced by occlusion at the origin of the MCA with 32% of the hemisphere damaged ($N_T = 1497$) (Fig. 20.3D). The smallest strokes were found in the MCA branch occlusions, with 20% of the hemisphere damaged ($N_T = 936$). In spite of having the larger common carotid artery occluded, tandem and three-vessel occlusions were only slightly larger on average than the distal MCA models (24% $N_T = 130$ vs. 23% $N_T = 236$, respectively).

The relationship between the location of occlusion and the degree of neuroprotection is given in Table 20.7. The greatest neuroprotection was seen where the location of the infarct was not specified (embolic models: $M \pm SE = 35.9 \pm 0.8\%$, 95% CI = 33.7%–36.9%,

$N_T = 250$) and the smallest with the occlusion of both common carotid arteries and the MCA (3-vessel occlusion: $M \pm SE = 18.9 \pm 0.7\%$, 95% CI = 17.7%–20.3%, $N_T = 236$). Occlusions at the origin of the MCA ($M \pm SE = 29.5 \pm 0.3\%$, 95% CI = 29.0%–30.0%, $N_T = 1497$) showed greater neuroprotection than in an MCA branch occlusion ($M \pm SE = 22.9 \pm 0.2\%$, 95% CI = 22.5%–23.4%, $N_T = 936$).

Thus while animal models tend to correctly represent the proportion of different types of carotid pathway lesions, they tend to show a different pattern of protection to the clinical disease. In animal models, distal occlusions are linked with lower neuroprotection while clinically they are more likely to be associated with a positive outcome. This difference is probably due to an interaction of the type of model and the location of the occlusion, with occlusions of an MCA branch more likely to be induced by thermocoagulation or cauterization and hence more likely to permanently prevent the return of blood flow.

3.9 Study Design

3.9.1 Outcome Measures

The choice of outcome measure has a profound effect on the findings, as pointedly illustrated by a recent

TABLE 20.12 Location of Damage in Stroke Models

Models	Location of damage	Figure ID	References
Photothrombotic	Variable, as it can be manipulated stereotaxically. Typically confined to the cortex.	1	Cai et al. (1998), Futrell (1991)
Distal MCA	Cortex, hippocampus, caudoputamen. Depends both on the size and location of the segment occluded.	2	Bederson et al. (1986), Brint et al. (1988), Flaumenhaft and Lo (2006)
Proximal MCA	Sensorimotor and auditory cortex (75% of rats), occipital (25%), lateral caudate nucleus (100%), medial caudate nucleus (38%). No damage to hypothalamus, globus pallidus, thalamus, hippocampus, subthalamic nuclei, cerebellum, or pons. Sometimes undertaken in tandem with CCA occlusion to reduce variability of infarction.	3	Aronowski et al. (1996), Davis et al. (1995), Tamura et al. (1981)
3-Vessel MCA and CCA	Frontal and parietal cortex, temporal, and cingulate cortex. Dorsolateral striatum.	NS	Aronowski et al. (1997)
Endothelin-1	Variable as it can be manipulated stereotaxically. Typically cortical or cortical and striatal.	4	Macrae et al. (1993), Sharkey et al. (1993), Windle et al. (2006)
Filament (thread occlusion)	Cortex (frontal, parietal, temporal, occipital) and striatum. May also occlude the thalamus, cervicomedullary junction, substantia nigra and hypothalamus, typically with a longer thread and a longer occlusion.	5 + 6	Koizumi et al. (1986), Longa et al. (1989)
Embolic/clot[a]	Clot dependent. Large clots induce widespread cortical and subcortical damage. Microspheres produce smaller, distal, multifocal infarcts.	7	Bremer et al. (1978), Busch et al. (1997), Gerriets et al. (2003), Kudo et al. (1982), Zivin et al. (1987)

Figure ID refers to the numbers used in Fig. 20.7. Proximal and distal MCA occlusions are grouped together as MCA branch occlusions.

[a]Clot may be composed of blood from a different animal [homologous (Kudo et al., 1982)], from the same animal (Busch et al., 1997), or of nonbiological material (macrospheres or microspheres). NS—not shown [typically involves occlusion at distal MCA (location 2)] + CCA (not shown on diagram).

comparison of 10 different MRI perfusion measures (Kane et al., 2007). In this study, the smallest and largest measures differed in their estimation of the volume of perfusion volume deficit by a factor of 13 (Kane et al., 2007).

In animal studies, the histological damage delineated with the hematoxylin and eosin (H + E) is a common outcome measure following the focal ischemia mode. However, immunohistochemical markers may be more sensitive to postischemic changes. Carmichael found that histological damage was only a fraction of the metabolic deficit in a model of distal MCA occlusion (Carmichael et al., 2004). While metabolic and histological markers may vary in their delineation of the lesion, histology, and MR imaging used in animal experiments have been found to have good correlations at the same time point (Bochelen et al., 1999; Sauer et al., 1995).

In clinical trials, the most commonly used measure of outcome was CT imaging (N_T = 15). This gave a mean infarct size of 6.2% of the hemisphere and was associated with neuroprotection of 18 ± 3% ($M ± SE$). The second most common measure was T2-weighted magnetic resonance imaging (N_T = 10). T2-weighted imaging was associated with a mean infarct size of 12.5% of the hemisphere, and a higher but more variable level of neuroprotection 31 ± 9%. DWI weighted imaging yielded an average infarct size of 5% (N_T = 2) probably reflecting the use of this modality in the acute or early phase of stroke. DWI imaging was similarly associated with a more variable level of neuroprotection ($M ± SE$: 12 ± 17%). Stroke volumes were 17.8% for clinical trials reporting ADC measures (N_T = 1), and the putative level of neuroprotection was high ($M ± SE$: 67 ± 17%). The average stroke volume for a SPECT study was 7% and the treatment group fared worse than the control patients ($M ± SE$: −36% ± 50%, N_T = 1).

In the animal experiments for which data on the endpoint was available, 55% of animal infarcts were measured with the mitochondrial stain TTC. TTC was associated with a 28% level of neuroprotection ($M ± SE$ = 28.1 ± 0.2%, 95% CI = 27.7–28.6, N_T = 1609) and a stroke covering on average 33% of the hemisphere. This value was very similar to that found for MRI measures of infarction, with an infarct size of 34% and a

level of neuroprotection of 31% ($M \pm SE = 31.3 \pm 0.7\%$, 95% CI = 33.1%–73.0%, $N_T = 199$). Hematoxylin and eosin (H&E) was used in 612 experiments and yielded a slightly smaller infarct size (27% of the hemisphere), probably reflecting the fact that H&E would be used as later time points than TTC (TTC: median time of use 24 h, IQR = 24–48 h. H&E: median time of use 72 h, mean time, IQR = 24–168 h). Nevertheless, the estimates of neuroprotection with H&E were similar to those obtained with TTC ($M \pm SE = 28.0 \pm 0.4\%$, 95% CI = 27.3%–28.8%, $N_T = 612$). Smaller estimates of infarct size and neuroprotection were found with the stain neutral red ($M \pm SE = 11.3 \pm 0.9\%$, 95% CI = 9.6%–13.0%, $N_T = 51$), but these were undertaken almost exclusively in a single model of permanent occlusion in a mouse. Unusual results were also found with the ballistic light method of measuring output: the infarct size was comparable at 32% of the hemisphere, but the level of neuroprotection was high ($M \pm SE = 53.1 \pm 10.1\%$, 95% CI = 33.1%–73.0%, $N_T = 4$).

3.9.2 Control Conditions

Just over one third of the clinical trials were placebo controlled (31%, $N_T = 11$), a number administered heparin to all of the control patients (20%, $N_T = 7$), several reported giving aspirin (6%, $N_T = 2$) or saline (3%, $N_T = 1$), and several used an historical control group (11%, $N_T = 4$). In a number of trials, the control condition was not stated (29%, $N_T = 10$). The nature of the placebo treatment, whether it was a drug vehicle or some other substance, was rarely reported.

Due to small number of clinical trials, interpreting the effect of the control group on outcome must proceed with caution. However, where the control group received a drug known to have some effect, then neuroprotection was less readily demonstrated, as occurred with heparin ($M \pm SE$: $-12.2 \pm 5.8\%$, $N_T = 8$) and aspirin ($M \pm SE$: -8.4%, $N_T = 2$). Where the control group received saline ($M \pm SE$: $50.8 \pm 26.2\%$, $N_T = 1$), a historical control ($M \pm SE$: $49.3 \pm 7.6\%$, $N_T = 4$), placebo ($M \pm SE$: $24.5 \pm 3\%$, $N_T = 14$) or the control was not stated ($M \pm SE$: $45.2 \pm 4\%$, $N_T = 9$), then the level of neuroprotection was much higher.

The control condition in animals was related to both infarct size and the estimated outcome effect (Fig. 20.3E). Animal experiments most commonly used saline as a control, with an average effect size of 28% ($M \pm SE = 28.3 \pm 0.3\%$, 95% CI = 27.8%–28.9%, $N_T = 1091$) and an infarct size of 25.9%. Greater neuroprotection was found when treatment was combined with DMSO (($M \pm SE = 37.2 \pm 0.75\%$, 95% CI = 35.7%–38.7%, $N_T = 185$) and was reduced when using PBS ($M \pm SE$: $13.7 \pm 0.9\%$, 95% CI = 11.9%–15.5%, $N_T = 110$). With DMSO, the infarct volume was also much greater in the

control group (32.7% of the hemisphere), as it was with PBS (35% of the hemisphere). Where sucrose was used, the infarct size was smaller (14.5% of the hemisphere), but this was used in only a small number of animals ($N_T = 10$, $N_P = 46$).

Intriguingly, where animals were fasted the night before the experiment, neuroprotection was 10% higher (fasted: $M \pm SE$: $29.1 \pm 1.3\%$, 95% CI = 26.5–31.8, $N_T = 72$) than where they were not given free access to food or it was not stated if food was restricted (nonfasted: $M \pm SE$: $18.1 \pm 0.57\%$, 95% CI = 17.0–19.2, $N_T = 178$). Infarct size was also slightly smaller in the nonfasted control group (nonfasted: 25.1%, fasted 22.7%). This factor was only included in latter studies, but these initial findings suggest a possible benefit of fasting on stroke outcome, perhaps attributable to an upregulation of the ketogenic metabolism.

3.10 Translation of Animal Results to Clinical Trial

Fourteen interventions were tested individually in clinical trial. The direction of outcome in the trial was assessed using both animal experiment criteria (difference in infarct size between treatment groups) and using the hypothesis relating to imaging outcome prespecified in the study. Where a positive effect was reported in clinical trials, it was frequently on a measure of a reduction in infarct volume expansion, as opposed to an absolute overall difference between treatment groups. Where a hypothesis was tested, 44% of tPA results ($N_T = 7$) were positive and 30% of non-tPA results ($N_T = 7$) provided a significant improvement in the specified hypothesis. The overall number of clinical results demonstrating an improvement in the specified hypothesis was 14 trials, 36% of all results or 41% of all results specifying hypotheses. Applying the criteria used to assess animal studies (i.e., difference in infarct size between treatment groups) the putative positive outcomes in clinical trials was marginally higher (Table 20.13).

To gauge how well the results of the animal metaanalyses predicted the overall outcome in clinical trial metaanalyses results for each drug, the partitioned effect sizes of these interventions on the infarct volume in clinical trial were mapped against their partitioned effect size in animal stroke studies (Fig. 20.8). The overall effect for 11 of the 14 interventions was congruent (in the same direction in both animal and clinical trials). The exceptions were the antiplatelet tirofiban, the glycine antagonist gavestinel and hypothermia, where for each of these treatments infarct volume in animals was reduced, whereas in human trials it was increased. Apart from streptokinase, the mean efficacy of animal experiments was positive for all drugs taken to clinical

TABLE 20.13 Clinical and Animal Outcomes With Different Therapies

Features	tPA therapy	Other therapy (clinically tested)	Other therapy (not tested clinically)	All therapies
Clinical trials				
Improvement in specified hypothesis[a]				
Yes	7 (44%)	7 (30%)	—	14 (36%)
No	7 (44%)	13 (57%)	—	20 (51%)
No hypothesis testing	2	3 (13%)	—	5 (13%)
Total	16 (100%)	23 (100%)		39 (100%)
Improvement in infarct size[b]				
Yes	9 (56%)	12 (52%)	—	21 (54%)
No	7 (44%)	11 (48%)	—	18 (46%)
Total	16 (100%)	23 (100%)		39 (100%)
Animal experiments				
Improvement in infarct size[b]				
Yes	122 (71%)	328 (91%)	2244 (86%)	2694 (86%)
No	50 (29%)	33 (9%)	368 (14%)	451 (14%)
Total	172 (100%)	361 (100%)	2612 (100%)	3145 (100%)
Infarct volume average reduction				
Animal—overall reduction in meta-analysis	22.8 ± 1.0%	26.5 ± 0.5%	25.5 ± 0.1%	25.5 ± 0.2%
Clinical—overall reduction in meta-analysis	27.4 ± 2.7%	26.3 ± 2.7%	—	27.0 ± 1.9%
Difference—average difference in volume per drug as determined by partitioned analysis for each drug	−4.7%	8.1%	—	7.2%
Animal versus clinical outcomes				
Infarct volume in same direction[a]	N_T = 9/16 (56%)	N_T = 15/23 (65%)	—	N_T = 24/39 (62%)
Outcome in same direction[c]	N_T = 7/14 (50%)	N_T = 10/20 (50%)		N_T = 17/34 (50%)

tPA therapy group includes trials which administered tPA as well as other drugs. Clinical trials single time point—number of trials with a single endpoint. Multiple time points—number of clinical endpoints including multiple time-points form a single trial. N_T—number of experimental contrasts.

[a]*Refers to the infarct volume in the control group versus the treatment group. When outcome was measured multiple times, the latest time point was taken (Berrouschot et al., 2000; NINDS, 2000; Roberts et al., 2002).*

[b]*Reduction in infarct volume refers to a smaller infarct volume in the treatment group compared with the control group measured after treatment.*

[c]*Outcome in animal experiments refers to the control group versus the treatment group, but in clinical trials may differ. Some defined a positive result as less growth in infarct volume in the treatment group versus the control group. Five comparisons not included because no hypothesis was tested, and three were not included because tested at multiple time points. Percentages are calculated not on the total number of clinical trials or animal experiments but as a percentage of the numbers where tested.*

trial, as opposed to human trials, which showed both positive and negative effects. The performance of only two drugs (IL-1 receptor antagonist and tirilizad mesylate) had equivalent levels of neuroprotection in that the confidence intervals of the effect sizes in animals and humans overlapped. On average, the effect size as determined by the partitioned analyses for each drug were 7% higher in animal studies than in clinical trials, although for tPA the putative effect size was 4.7% higher in clinical trials.

Statistically, the extent to which the effect of drugs in animal experiments was related to the effect of the same drugs in clinical trial (as estimated by portioned effect sizes) was assessed in four ways: (1) simple linear correlation, and (2) simple linear regression models based on the average effect sizes from the metaanalyses of clinical and animal data, (3) hierarchical linear regression models, and (4) measures of agreement using Cohen's Kappa. While the overall pooled response to any treatment was similar between animal and humans (25.5% vs. 27.0%),

using simple linear correlation the response to individual treatments did not correlate well between animal and human studies ($r = 0.25$, $P > .05$, $N_{Drugs} = 14$). Similarly, the results from the regression analyses suggest that the average levels of neuroprotection from animal studies did not predict the average drug response in stroke trials [$b = 0.20$, $t(1,13) = 1.1$, $P > .05$]. Animal results failed to explain any significant amount of variance in the outcome [$R^2 = .02$, $F(1, 12) = 1.3$, $P > .05$]. A hierarchical regression was then conducted to determine whether animal experimental data predicted outcome, after taking into account the average time to treatment in the clinical trials, and whether clinical trials were placebo controlled. After controlling for these factors, the estimated treatment efficacy in animal models explained an additional 9.4% of the variance in clinical trials results, but this result was not significant. The measure of agreement between partitioned analyses of animal experiments for each drug and the partitioned analyses for each drug used in clinical trial results (with infarct volume between control and treated group as the outcome measure) was assessed using Cohen's Kappa. There was fair agreement between the direction of the effect sizes for each drug derived from animal studies and from clinical trial ($\kappa = 0.32$, $N_{Drugs} = 14$).

The measure of agreement between metaanalyses of animal experiments for each drug and the individual clinical trial results (with infarct volume between control and treated group as the outcome measure) was assessed using Cohen's Kappa. There was agreement between the direction of the trial result and the animal metaanalysis result for that drug in 24 out of 39 clinical trial results (62%). Taking into account the probability of random agreement using Cohen's Kappa, there was only a slight agreement between animal metaanalysis results and clinical trial outcomes ($\kappa = 0.18$, $N_T = 39$). For the 21 clinical trial results, which showed a smaller infarct volume in the treated group, the animal metaanalyses also yielded a positive effect size in all cases (100%). For the 15 negative clinical trial outcomes in which there was a larger infarct volume in the treated group, the animal metaanalyses yielded a negative effect size in only three of these cases (17%).

Where there was a prespecified hypothesis in the clinical trial, there was agreement between the direction of the trial result and the animal metaanalysis result for that drug in 17 out of 34 clinical trial results (50%). For the 14 positive clinical trial outcomes, the animal metaanalyses also yielded a positive effect size (100%). For the 17 negative clinical trial outcomes, the animal metaanalyses yielded a negative effect size in only three of these cases (18%). Taking into account the probability of random agreement using Cohen's Kappa, there was found to be none or only slight agreement between animal metaanalyses and clinical trial results ($\kappa = 0.00$, $N_T = 34$).

In general, the portioned estimates of treatment effect from metaanalyses were 7.2% higher in animal studies compared with clinical trial results for the same drugs. For treatments other than tPA, outcome in animal experiments was 8.1% higher than in clinical trials; for tPA studies outcome was better in humans by 4.7%.

4 DISCUSSION

4.1 What is the Legacy of Stroke Models?

How do you gauge the success or failure of a model? A successful animal model of stroke might be one that enables insights into the disease process or which predicts the therapeutic response to experimental treatments. How much have animal models contributed to stroke research, according to these criteria?

Experiments in cerebral ischemia have been integral in defining the mechanics of blood flow, especially circulation. Circulation is a cornerstone of modern medicine. Many aspects of stroke medicine from hypertension to intravenous drug delivery presuppose the existence of a closed circulatory system. The existence of such a system was articulated in the *Nei Jing* attributed to Huang Ti, the Yellow Emperor of China (2697 BC) but probably written during the Warring States Period (475–221 BC) (Fung, 1997). In the *Nei Jing*, it was written that blood "circulate(s) without stopping. In 50 steps they return to the starting point…like a circle without end" (p. 15) (Fung, 1997). Claims to the historical precedence of the discovery of circulation have also been made by Islamic and Italian historians on account of the work of Ibn An-Nafîs (1210–88) and Andrea Cesalpino (1524–1603) (Garrison, 1929; Meyerhof, 1935), but it was the ischemia experiments of William Harvey, which really embedded the concept of circulation in the scientific consciousness.

And what of the role of animal experiments in the development of acute stroke treatments? Generally speaking, animal models have helped define the rationale for therapeutic intervention, so that the choice of treatments is taken out of the realm of folklore, custom, and guess work. The thrombolysis story is a good case in point (and arguably the only solid case to date). Thrombolysis therapy with tPA did not begin with the NINDS trial in 1995 (NIND, 1995): its genesis can be traced back over the centuries to the work of John Hunter and Taag Astrup (Jaques, 1988) and the many less-lauded individuals who nevertheless played important roles in elucidating the details of the coagulation process without passing into the footnotes of history.

The success of stroke models for the evaluation of treatment efficacy (rather than safety or mechanism) is less clear. On the one hand, metaanalysis of data from animals and patients has yielded similar pooled levels of efficacy for acute stroke treatments measured in terms of infarct volumes in the control versus the treatment groups. On the other hand, the considerable heterogeneity in the findings suggest a need for exercising caution before extrapolating from pooled estimates of treatment effects (Thompson, 2001). A number of ongoing clinical trials have included volumetric measures as endpoints, and will be of considerable help in fleshing out this analysis when published. However, on the data analyzed here (summarized in Table 20.14), doubt remains over the role of animal models of stroke—in their present form—as tools for anticipating the effect of drugs in clinical trial, except perhaps at the most general level (agreement between the general direction of overall estimates of clinical and animal results for each drug). This challenge in translation is not unique to stroke research. Important work by Hackam and Redelmeier found that where drugs tested or developed in animal disease models were taken to clinical trial (57% of treatments in trial), only two thirds of those trials replicated the findings of animal studies (Hackam and Redelmeier, 2006).

4.2 Scope and Limitations of this Review

Recent critiques of animal models have highlighted the shortcomings of laboratory experiments when judged by clinical trial standards (STAIR, 1999). The purpose of this review was instead to evaluate clinical stroke from the perspective of the laboratory bench in order to evaluate the concordance of animal and human stroke. As most animal experiments tend to rely heavily on histological outcomes for assessment, the principle comparator used in this review was infarct size. However, when judged from a clinical perspective, there are several shortcomings to this approach: imaging outcomes are included in only a minority of clinical trials and where they are included they tend to be a surrogate outcome rather than a primary endpoint (although this is beginning to change).

By virtue of being imaging trials, the clinical trials included here also tend to be recent, to have short time windows and to be more likely to deploy thrombolytics compared with earlier trials (Kidwell, 2001). For instance, compared with the excellent review of pre-2000 clinical trials, tended to use thrombolytics (N = 13) compared with agents targeting excitotoxicity, calcium influx, oxidative stress, and other mechanisms which formed the basis of trials in the 1980s and 1990s (Kidwell, 2001). Imaging trials may also differ in design from stroke trials in general: By definition, imaging outcome studies would tend to be either Phase II trials or substudies of Phase III trials. Although an attempt was made to peer behind the "clinical trial veil" to investigate not the intent of the trial but the outcomes, the intentions of the investigators are paramount to both the design of the trial and the interpretation of the results.

A further suggestion that the clinical trials included here may not be representative of trials in general comes from the high proportion of positive findings: here, using the surrogate marker of infarct size, with 54% showing a smaller infarct size in the treated group compared with the control group and with 41% showing an improvement in the researchers' prespecified imaging hypothesis. Nevertheless, a similar finding was reported by Kidwell in the review of pre-2000 clinical stroke trials. Kidwell reported that 23% of trials had a beneficial outcome as defined by the authors, with 50% showing a beneficial trend or subgroup benefit. This was in spite of less than 2% of trials meeting strict criteria for a positive outcome.

Using outcome measures common in animal experiments may introduce bias from the clinical perspective. Clinical trials may use other imaging endpoints than absolute infarct volume (e.g., lesion growth). To some extent, investigators' trial design and hypotheses were acknowledged here when comparisons were made about whether the stated clinical imaging hypotheses were substantiated. But even if there is agreement between different types of imaging outcomes, the use of imaging outcomes may not show a uniformly high level of concordance with clinical outcome. If functional measures show no treatment effect in patients where an improvement in infarct size or growth has been observed, then it would suggest that volumetric analyses are flawed and the design of animal and human studies needs to be reassessed.

Adapting the metaanalysis to accommodate the many different endpoints in this comparison is the next logical step in this analysis. A broader and more balanced picture about the equivalence of animal and human trials will be achieved by extending this analysis to incorporate not only heterogeneity in imaging endpoints, but also the functional clinical scales and the primary clinical hypotheses. This project is currently underway and will enable questions to be addressed, which escaped the scope of the present review. For instance, is the variability the same with the NIHSS and infarct volume? How robust are the effect sizes? What was the primary clinical outcome and how did this change in outcome relate to changes in infarct volume? Is the variability the same with the NIHSS and infarct volume and how robust are the effect sizes? It seems logical that outcomes combining volume and measures of damaged tissue function will ultimately be required.

TABLE 20.14 Summary of Key Findings

Features		Findings
Studies	Exclusions	Clinical trials that lacked a control group (15%, N_T = 29/188 trials), lacked volumetric analysis of imaging data (18%, N_T = 34/188 trials), or failed to report treatment effects (12%, N_T = 23/188 trials) were excluded.
	Sample size	Clinical trials were 10 times the size of animal studies (N_P = 71 per clinical treatment cohort versus N_P = 7 per animal treatment group) but variance was substantially greater in clinical trials (average SD = 99% vs. 30%), so both were underpowered to the same extent.
	Quality	Random allocation to groups was done in 63% of clinical trials and 38% of animal experiments. Outcome was blinded in 84% of clinical trials and 32% of animal experiments. Mean quality in trials was 6.2/10 and ranged from 3.3 to 4.9/10 in past estimates of study quality in experimental metaanalyses.
Subjects	Sex	Ninety-four percent of animal studies were undertaken in male animals while clinical trials were conducted in both sexes (64% mixed, 26% sex not stated).
	Diabetes	Diabetes was 19 times more common in the clinical population than the animal population (26% vs. 1.3%).
	Hypertension	Hypertension was present in 66% of patients and 14% of animals.
	Age	Average age of patients was 66 years. Less than 1% of experiments (0.6%) used middle-aged or old animals.
	Species	Eighty percent of animal experiments were conducted in the rat, and of these 41% were in Sprague Dawley rats (32% of all experiments).
Infarct Size	Human stroke	The average infarct size was 47.4 cm³ (range: 5.3 cm³ (0.9% of the hemisphere) to 124.8 cm³ (21.1% of the hemisphere). *Median*: 51.4 cm³ (IQR: 34.0–70.0 cm³, 5.7%–11.8% of the hemisphere).
	Animal stroke	The average infarct size was 31% of the hemisphere (*median*: 29%, IQR: 19%–41% of the hemisphere).
	Comparative size	Animal strokes were on average 4 times larger than human stroke, measured as a percentage of the hemisphere (31% vs. 8%).
	Variability	Humans produced a more variable stroke (average SD = 99%) compared with animals (average SD = 30%). Of the animals, the rabbit (SD = 59%), guinea pig (SD = 52%), and cat (SD = 48%) produced the most variable infarct size and the gerbil (SD = 20%) and mice (SD = 24%) the least. Rats produced an average variability of 29%, with the SHR having the tightest model (average SD = 19%) and the Fisher 344 the most variable (average SD = 35%).
	Species	The rat (28%) and cat (27%) gave the largest average infarct volume and the hamster (4%), gerbil (8%), and primate (9%) the smallest. Where infarct sizes were reported in absolute terms, the infarcts were: mouse (M ± SD: 53.6 ± 12.9 mm³, N_T = 332), Gerbil (M ± SD: 57.9.1 ± 10.3 mm³, N_T = 3), rat (M ± SD: 172.4 ± 43.7 mm³, N_T = 1716), hamster (M ± SD: 14.4 ± 5.9 mm³, N_T = 14), rabbit (M ± SD: 525.7 ± 384.5 mm³, N_T = 24), cat (M ± SD: 2394 ± 4047 mm³, N_T = 23), primate (M ± SD: 3.76 ± 1.2 cm³ N_T = 9), and human (M ± SD: 47.36 ± 12.9 cm³, N_T = 39).
	Strain	The Hooded Listar (44%) and the SHR had the largest stroke (35%), and the Lewis the smallest (17%). Sprague Dawley rats (26%), diabetic rats (27%), and Wistar rats (32%) had intermediate volumes.
Cause of stroke	Animals	Forty-seven percent of animal experiments used the thread occlusion model (suture model) and 28% the cauterization model. Embolic models were less common (N_T = 9). Filament occlusion resulted in the largest infarct size expressed as a proportion of the hemisphere (32%) and the balloon or compression model the smallest (12%). Photochemical models (17%), endothelin-1 (22%), coagulation (20%), clip/ligation (25%), and embolic models (29%) had intermediate stroke sizes. Greatest protection was in the endothelin model (50% neuroprotection) and the embolic model (35% neuroprotection), and the lowest was observed in the permanent cauterization model (21% neuroprotection).
	Clinical	Etiology (TOAST criteria) was reported in 12 trials, with large vessel disease (N_P= 29%) and cardioembolism the most common (N_P 39%) and small vessel disease less common (N_P = 13%).
Location	Animals	Infarct volume was largest with occlusions of the MCA origin (32% hemispheric damage) versus MCA branch occlusions (20% hemispheric damage) or two-vessel (24%) or three-vessel occlusion models (23%). The three-vessel occlusion model (30% variability per experiment) and the two-vessel occlusion model MCA/CCA (36% variability) were no less variable than the distal MCA occlusions (25% variability) or proximal MCA occlusions (29% variability).

(Continued)

TABLE 20.14   Summary of Key Findings (*cont.*)

Features		Findings
	Clinical	Occlusion was most common at the M1 branch or M1 and extensions (N_P = 56%) and 24% at M2 or distal branches (N_P = 56%), with 13% at the ICA origin and 2% at the carotid T (N_T = 6, N_P = 470).
	Recanalization	Recanalization rates for clinical trials were (N_T = 4, N_P = 283): ICA origin occlusion (24%), carotid T occlusion (22%), M1 or proximal MCA occlusion (57%), and M2 or distal MCA/ACA occlusion (69%) with an overall rate of 48%.
	Reperfusion	Reperfusion injury is suggested in the thread models but not the clip/ligation models, possibly due to differences in basal ganglia and cortical susceptibility to this injury type (via edema, FRS, or collateral flow effects).
Temporal	Duration of occlusion	In animals, 45% of occlusions lasted less than 6 h, while 27% of animals had occlusions of 24 to 72 h. Durations of 6–24 h were conducted in 2% of animals, but may arise more frequently clinically. Infarct size in control animals reached a maximum value with occlusions of 1.5–2 h in the clip/ligation model and in temporary occlusions of greater than 3 h using the thread model. Permanent occlusion in the thread model leads to an infarct size 6% smaller than temporary ischemia, while there was no difference in the clip/ligation model.
	Treatment time	Treatment was administered within 3 h in 31% of trials and in 84% of animal experiments (where recorded N_T = 2982). Average time to treatment was 7 h (median = 4.1 h post stroke) for clinical trials, and 10 h prior to stroke onset (median = 5 min poststroke) for animal experiments.
	Outcome	The median time of outcome assessment was 1 day for animals and 8 days for patients. Average stroke volume for patients was 11.6% (day 1), 9.3% (day 3–7), 8.6% (week 1–2), and 7.8% (after week 2). Infarct volume for animals was 23.8% (<day 1), 30.8% day 1–2, 25.4% (day 2–3), 24.4% (day 3–7), 23.7% (week 1–2), 19.8% (after week 2).
Treatment	Animal versus clinical	Acute stroke interventions were associated with a 26% smaller infarct volume in animals receiving treatment, and an 18%–31% smaller volume in humans receiving treatment compared to the control group. However, there was no correlation between the overall performance of individual drugs in animal experiments and clinical trials. There was no agreement between the general direction of the estimated effect sizes of drugs from portioned metaanalyses of animal studies and individual trial results using the same drugs. However, there was fair agreement between the direction of the overall estimates from animal experiments and the overall estimates from clinical trials using the same drugs. Animal experiments underestimated the effect of tPA by 4.7% and overestimated the effect of other treatments on infarct volume by 8.13% (average 7.2%).
	Reporting method	Animal experiments were associated with a 25% reduction in infarct where reported as an absolute level, and a 30% reduction where reported as a percentage of the hemisphere (stroke volume did not differ). When results where reported as areas, the average reduction was 19%. Clinical trials were associated with a 29% reduction where reported as a mean and 18% reduction where reported as a median value.
	Species	The greatest level of neuroprotection was seen in the nonhuman primate (47%, N_T = 22 experiments) and the least in the hamster (−83%, N_T = 15 experiments).
	Strain	Efficacy was lowest in the F344 (18%) and highest in the Lewis rat (66%) and Hooded Listar (60%) perhaps because of differences in the inflammatory response.
	Pretreatment effect	Pretreatment differences in infarct volumes explained 31% of the variance in the final outcome (N_T = 31). Animal studies rarely had smaller infarcts in the control group prior to treatment, suggesting a selection bias for the treatment groups may be operating.
	Positive results	Animal experiments were more likely to show a reduction in infarct volume (86% experiments) than clinical trials (54% trials). Improvement in the prespecified imaging hypothesis was 41% in clinical trials.
	tPA versus other	Where a hypothesis was tested, 50% of tPA clinical trials were beneficial and 56% showed a reduction in infarct volume in the treated group compared with control. In animal experiments this was 71%. In drugs other than tPA tested in clinical trial, 35% met the prespecified imaging hypotheses and 52% showed a reduction in infarct volume (compared with 91% of animal experiments using the same drugs).

In addition to the theoretical validity of the review process, other prominent limitations of this review pertain to the search strategy and the method of analysis. The search strategy was limited, restricted only to PubMed, trial databases, cross-referencing and hand searching. Calculations of stroke size (as a percentage of hemisphere) relied upon assumptions—in many cases—about hemispheric volumes. Estimates of infarct size were also adjusted for the number of animals in each group, but not for the variance. Further, there was no easy method of how to deal with data presented as medians. We tried to get around this by presenting the pooled estimate of drug efficacy using three different methods, but in the future, the investigation of nonparametric metaanalysis methods may assist. Further, any hypotheses generated about factors relevant to clinical outcomes are hampered by the small number of clinical trials reporting subject and stroke characteristics or by the homogeneity of these populations. To obtain this kind of information, analysis of data from individual patients pooled across a number of trials would be more appropriate. Alternatively, clinical trials might provide more meaningful data if restricted to patients with similar characteristics—such as angiographic criteria—as suggested 20 years ago by Molinari (1988).

At the broadest level the adequacy of the statistical approach in drug trials is open to question, particularly with its neglect of individual differences (Hildebrandt, 2004). "Drug testing, as legally required today, has only arisen in modem times and is the result of an exchange between rational physiological medicine with its long-standing empirical therapeutics and the traditional natural historical school of the seventeenth and nineteenth centuries" (p. 847). Individual differences may be overlooked when gathering the information to generate information about efficacy, but this neglect may be replicated if these results are then reapplied to new patient groups without taking into account differences in this population.

It is also difficult to place a value on the contribution of animal models to something, which cannot be readily quantified—an idea, a theory, and an inspiration—something, such as circulation. Qualitative criteria—as largely used here—are not the only ones that matter. Nevertheless, they might provide some insight into factors important to experimental design, such as the choice of animal species in experiments and how to improve the translation of experimental results—factors discussed in the final part of this paper.

4.3 Findings From This Review

4.3.1 Mouse or Monkey

The choice of animal species is often influenced by practical considerations, such as the cost and availability of animals, access to appropriate housing, and what species can be squeezed into a brain-imaging scanner. Though these concerns are important, they are subordinate to the issue of ethics and concordance of the models with the human disease.

Primate research has been favored by some researchers because of the apparent face validity of these models. Although the infarct size generated in the primate model was similar to the humans (about 8% of the hemisphere), the level of neuroprotection was substantially higher ($M \pm SE$: primates: $47 \pm 3\%$, humans: $27 \pm 1.9\%$). By contrast, infarction in the rat occupies a larger proportion of the hemisphere than in patients (28% vs. 8%), but exhibits a similar level of neuroprotection ($M \pm SE$: rats: $26 \pm 0.2\%$, humans: $27 \pm 1.9\%$).

If rats are to be used to model stroke, and if the choice is determined by the need to obtain the most consistent infarct, then this study supports the use of SHRs. On the basis of similarity in infarct size to humans (as a percentage of the brain infarcted), then the results favor the use of the Lewis rat, as it has the smallest size stroke. However, on the basis of an equivalent level of neuroprotection to clinical findings, results would support the use of either the Sprague Dawley or the SHR. Other factors will, of course, guide decisions determining strain choice—especially genetics—as researchers attempt to model subtypes of patients and comorbidities and other individual differences.

4.3.2 Individual Characteristics and Initial Differences

Early last century, Garrison wrote "Primitive man... tried to treat the disease rather than the patient, not realizing... that the dynamic effect of a drug upon the patient's body depends as much upon the delicate chemical adjustments of that body as upon the composition of the drug itself (Garrison, 1929)." The importance of individual variability of patients has been studied in a number of clinical trials, with the finding that baseline characteristics including site of arterial lesion, hypoperfusion volume and clinical scores are predictive of therapeutic response (Adams et al., 1999; NINDS, 2000; Saqqur et al., 2007; Warach et al., 2000). For instance, in the citicoline trial smaller pretreatment lesions in the treatment group were associated with a positive outcome (Warach et al., 2000), while the converse was found in a tPA combination therapy trial (Seitz et al., 2004). Other researchers have focused on the interactions of preexisting inflammatory conditions and hyperglycemia (Kent et al., 2001).

Due to comparatively small sample size in animal experiments, initial differences have the potential to skew experimental results. In this review, in the few studies, which measured pretreatment stroke size, baseline

infarction explained a large portion of the variance in outcome. Characterization of pretreatment stroke size and use of outcome measures which reflect pretreatment stroke size—such as infarct growth—may reduce the possibility for this bias. More sensitive tools than neurological score or a laser Doppler reading may be necessary to rate the size of strokes in animals prior to treatment administration.

4.3.3 Mechanisms of Ischemic Damage

Can anything be adumbrated from this analysis regarding the mechanisms of stroke damage? All aspects of stroke models allude to the importance of blood flow in determining the outcome of ischemia. All factors that reduce blood flow tend to increase brain damage, including permanent occlusion in animals, failure to reperfuse in patients, and delayed reperfusion in animals.

A role for edema is also imputed by the differences between percentage and absolute measures of infarct volume in the animals. The importance of metabolic factors is suggested by data demonstrating that fasted animals have a smaller infarct volume and by the utility of hypothermia as a protective treatment in animals. Additionally, the influence of the choice of vehicle and the different response of those given glucose or cellulose-loaded vehicles also attest to the impact of metabolism on outcome.

A potential role for the inflammatory response comes from an observation about stroke volumes. Interestingly, there is a suggestion that brain volumes from stroke patients tended to be larger than brain volumes from cohorts of a similar age and sex but without a history of stroke (Janssen et al., 2007; Tupler et al., 2007). These differences persisted even after several months. Edematous changes are believed to resolve within the 1st week or so after stroke, suggesting that a persistent residual level of brain inflammation may contribute to the larger size of stroke brains. A recent study of brain sizes has found that of the inflammatory markers tested, only the CD40 ligand was associated—albeit nonsignificantly—with increasing brain size (Jefferson et al., 2007). Interestingly, the plasma CD40 ligand has been linked to stroke (Duygu et al., 2008; Ferro et al., 2007). Given the incidence of asymptomatic stroke in the population, brain volume may be a useful marker for identification of patients at risk of stroke.

4.3.4 Framework for Translational Research

Much effort has been directed toward trying to explain the failure of animal models to predict clinical trial results (Green et al., 2003; Millikan, 1992; Molinari, 1988; Zivin and Grotta, 1990; Wiebers et al., 1990). The most easily remedied outcome would be if the failure was attributable to insufficient rigor in experimental design,

both on the part of scientists through a failure to tame potential sources of bias with blinding, randomization and adjustments for pretreatment levels of damage, and on the part of the clinical personnel, in attempting to apply treatments to heterogeneous populations in time frames beyond which they have been shown to be effective and without using comparable control groups.

Failing that, the next best outcome would be if the experimental parameters and endpoints themselves require modification. The validity of animal models may be compromised by experimental factors, such as the control of respiration, the use of anesthesia, the artificiality of the occlusion device and the failure to provide adequate social and environmental stimulation for normal neuronal network development. Such a scenario would require adaptation of existing models.

A more challenging scenario would be if the failure were attributable to a lack of resemblance in the physiological processes of different species, perhaps due to scaling and vascular dissimilarities. Smaller brains have different patterns of fluid and heat transport, and network connectivity: the importance of these factors has not yet been fully evaluated. Qualitatively different types of tissue might also be destroyed in brains of a different scale. For instance, the hypothalamus is commonly damaged in longer occlusions using the suture model in rodents (Li et al., 1999). This may result in disturbances in temperature homeostasis, osmotic regulation, and the hypothalamic–pituitary axis stress response. This type of damage might not be evident if the results are given as a total infarct volume or if hypothalamic damage is subsumed as "subcortical" damage. Similarly, amygdaloid nuclei are sometimes demarcated as "cortical" tissue in rat models. Standardized terminology and the development of software for automated morphing of images into brain atlases may overcome some of these problems.

A new challenge to the relevance of animal models comes from the intriguing work of Garosi and coworkers documenting the imaging of spontaneous strokes in dogs. Dogs are one of the few species where strokes have been documented to occur spontaneously in nature (or at least, to occur in urban areas near veterinary surgeons with animal MRI equipment). A remarkable thing about the location of infarcts in these dogs is that it differs markedly from that induced in animal models of stroke. The location of the infarct typically occurs more posteriorly, with a greater preponderance of occlusion in the rostral cerebellar artery (15 of 33 dogs) (Garosi et al., 2006). Few dogs had MCA occlusions (4 of 33 dogs) (Garosi et al., 2006). The dog does have some peculiar vascular features, which may prevent MCA occlusions, such as a well-developed set of extraintracranial arterial anastomoses, which would facilitate blood flow to the brain in the event of occlusion (Daniel et al., 1953;

TABLE 20.15 Recommendations

Features	Finding
Reporting	All studies report mean, SD, median and range
	Report statistics for individual drugs, even if not statistically significant and even if the focus of the paper is not the treatment but some other factors, such as imaging algorithms
Pretreatment	Evaluate measures of brain damage before treatment (whether imaging or blood flow)
Control group	Use historical controls with caution
	Report drugs given in the human control group
	Consider the use of a tPA, best medical care, or other positive control in animal experiments
Endpoints	Develop scale independent endpoints or methods to assist in translation of results between animal and clinical fields

Jewell, 1952). Even so, surgically inducing a stroke in tissue not usually the target of stroke in humans does raise the issue of the realism and generalizability of such an animal model.

"Natural" stroke has also been studied in rats, in the genetically modified strain stroke-prone spontaneous hypertensive rat (SPSHR) model. In this model, infarcts tend to occur in the medial cortex (in regions sometimes called "border zones") (Yamori et al., 1976), rather than laterally as it does when stroke is surgically induced. One third of occlusions occur occipitally, again somewhat differently from the typical MCA lesion pattern in animal models

Establishing the equivalence in the progression of the infarct in animals and humans, and a methodology to scale and transform the experimental results to accurately predict clinical outcomes is a necessary prerequisite for the use of animals as drug-screening tools. Failure to establish equivalence in physiology may sound the death knell for use of existing animal models for efficacy testing, though not necessarily for generating and testing hypotheses about the pathophysiology of ischemia. Nevertheless, more studies are needed to assess the vascular, neuronal, and genetic differences in humans and animals used in stroke research if we are to determine their relevance.

For the purpose of evaluating translational research, it would be useful if both animal and clinical trials reported data for all relevant summary statistics (including means and medians), together with inclusion and exclusion criteria (Table 20.15). This is especially so in the case of clinical trials where data may be archived, as was the case for several clinical trials in this review. The development of novel, reproducible, and scale-independent endpoints will also assist with the measurements of treatment effects. Algorithms for the adjustment of endpoints for scale and pretreatment characteristics, and alternative measures, such as combined efficacy and safety data may also be useful (Dawson et al., 2001). Animal

experimentalists might consider also using best medical care as a positive control group. All such factors are easily remedied by exercising adequate control over the experimental design phase.

5 CONCLUSIONS

"Whenever many different remedies are proposed for a disease, it usually means that we know very little about treating the disease, which is also true of a drug when it is vaunted as a panacea or cure-all for many disease" Garrison (1929), p. 25. And so it is for stroke: many drugs have been tested in animal models of stroke, and by and large we've been short changed. But is it reasonable to expect that libraries of compounds or treatments imported from other areas of medicine will serendipitously toss up the next "penicillin" for stroke? May be, may be not. Adherence to this course of action is more than likely fuelled by underfunding of stroke research than by the belief that this is the optimal course of action. But the risk of second-hand science is the prospect of second-class results. Arguably, it is not the animal models, which have failed, but the neuroprotection research strategy.

The future landscape of stroke medicine may be very different. Effective primary prevention strategies may reduce the need for acute stroke treatments or change the nature of the disease itself, as might the aging of the population. Human imaging and genetics promise to reduce the historical reliance on animal models. Nevertheless, current costs provide hurdles to wholesale introduction of these technologies in the immediate future, so in the interim, treatments should ideally be tailored to fit the disease, not the disease-model or the budget. This may necessitate a return to first principles and greater emphasis on understanding the fundamentals of stroke pathophysiology (Dirnagl et al., 1999; Lo et al., 2003).

ACRONYMS

M	Mean
SD	Standard deviation
N_T	Number of clinical trials or experiments
N_P	Number of patients or animals
IV	Infarct volume
MCA	Middle cerebral artery
ECA	External carotid artery
ICA	Internal carotid artery
M1-6	Categorization of the branches of the MCA used for the description of the human cerebrovasculature
STAIR	Stroke Therapy Academic and Industry Roundtable

Acknowledgments

References

Adams, Jr., H.P., Bendixen, B.H., Kappelle, L.J., et al., 1993. Classification of subtype of acute ischemic stroke. Definitions for use in a multicenter clinical trial. TOAST. Trial of Org 10172 in Acute Stroke Treatment. Stroke 24 (1), 35–41.

Adams, H.P., Davis, P.H., Leira, E.C., et al., 1999. Baseline NIH stroke scale score strongly predicts outcome after stroke. A report of the Trial of Org 10172 in Acute Stroke Treatment (TOAST). Neurology 53, 126–131.

Alonso de Lecinana, M., Diez-Tejedor, E., Carceller, F., Roda, J.M., 2001. Cerebral ischemia: from animal studies to clinical practice. Should the methods be reviewed? Cerebrovasc. Dis. 11 (Suppl. 1), 20–30.

Ancrod Stroke Study Investigators (ASSI), 1994. Ancrod for the treatment of acute ischemic brain infarction. Stroke 25 (9), 1755–1759.

Arakawa, S., Minematsu, K., Hirano, T., et al., 2003. Topographic distribution of misery perfusion in relation to internal and superficial borderzones. AJNR 24 (3), 427–435.

Arenillas, J.F., Rovira, A., Molina, C.A., Grive, E., Montaner, J., Alvarez-Sabin, J., 2002. Prediction of early neurological deterioration using diffusion- and perfusion-weighted imaging in hyperacute middle cerebral artery ischemic stroke. Stroke 33 (9), 2197–2203.

Arnold, M., Schroth, G., Nedeltchev, K., et al., 2002. Intra-arterial thrombolysis in 100 patients with acute stroke due to middle cerebral artery occlusion. Stroke 33 (7), 1828–1833.

Aronowski, J., Samways, E., Strong, R., Rhoades, H.M., Grotta, J.C., 1996. An alternative method for the quantitation of neuronal damage after experimental middle cerebral artery occlusion in rats: analysis of behavioral deficit. J. Cereb. Blood Flow Metab. 16 (4), 705–713.

Aronowski, J., Strong, R., Grotta, J.C., 1997. Reperfusion injury: demonstration of brain damage produced by reperfusion after transient focal ischemia in rats. J. Cereb. Blood Flow Metab. 17 (10), 1048–1056.

Bamford, J., Sandercock, P., Dennis, M., et al., 1988. A prospective study of acute cerebrovascular disease in the community: the Oxfordshire Community Stroke Project 1981-86. 1. Methodology, demography and incident cases of first-ever stroke. J. Neurol. Neurosurg. Psychiatry 51 (11), 1373–1380.

Barber, P.A., Davis, S.M., Infeld, B., et al., 1998. Spontaneous reperfusion after ischemic stroke is associated with improved outcome. Stroke 29 (12), 2522–2528.

Bath, F.J., Owen, V.E., Bath, P.M., 1998. Quality of full and final publications reporting acute stroke trials: a systematic review. Stroke 29 (10), 2203–2210.

Bederson, J.B., Pitts, L.H., Germano, S.M., Nishimura, M.C., Davis, R.L., Bartkowski, H.M., 1986. Evaluation of 2,3,5-triphenyltetrazolium chloride as a stain for detection and quantification of experimental cerebral infarction in rats. Stroke 17 (6), 1304–1308.

Bernasconi, A., Bogousslavsky, J., Bassetti, C., Regli, F., 1996. Multiple acute infarcts in the posterior circulation. J. Neurol. Neurosurg. Psychiatry 60 (3), 289–296.

Berrouschot, J., Barthel, H., Hesse, S., Knapp, W.H., Schneider, D., von Kummer, R., 2000. Reperfusion and metabolic recovery of brain tissue and clinical outcome after ischemic stroke and thrombolytic therapy. Stroke 31 (7), 1545–1551.

Blanco, M., Nombela, F., Castellanos, M., et al., 2007. Statin treatment withdrawal in ischemic stroke: a controlled randomized study. Neurology 69 (9), 904–910.

Bochelen, D., Rudin, M., Sauter, A., 1999. Calcineurin inhibitors FK506 and S DZ ASM 981 alleviate the outcome of focal cerebral ischemic/reperfusion injury. J. Pharmacol. Exp. Ther. 288 (2), 653–659.

Brant, R., 2008. Inference for means: comparing two independent samples. Available from: http://stat.ubc.ca/~rollin/stats/ssize/n2.html

Bremer, A.M., Yamada, K., West, C.R., 1978. Experimental regional cerebral ischemia in the middle cerebral artery territory in primates. Part 3: effects on brain water and electrolytes in the late phase of acute MCA stroke. Stroke 9 (4), 387–391.

Brint, S., Jacewicz, M., Kiessling, M., Tanabe, J., Pulsinelli, W., 1988. Focal brain ischemia in the rat: methods for reproducible neocortical infarction using tandem occlusion of the distal middle cerebral and ipsilateral common carotid arteries. J. Cereb. Blood Flow Metab. 8 (4), 474–485.

Brott, T., Marler, J.R., Olinger, C.P., et al., 1989. Measurements of acute cerebral infarction: lesion size by computed tomography. Stroke 20 (7), 871–875.

Busch, E., Kruger, K., Hossmann, K.A., 1997. Improved model of thromboembolic stroke and rt-PA induced reperfusion in the rat. Brain Res. 778 (1), 16–24.

Cai, H., Yao, H., Ibayashi, S., Uchimura, H., Fujishima, M., 1998. Photothrombotic middle cerebral artery occlusion in spontaneously hypertensive rats: influence of substrain, gender, and distal middle cerebral artery patterns on infarct size. Stroke 29 (9), 1982–1986.

Carmichael, S.T., 2005. Rodent models of focal stroke: size, mechanism, and purpose. NeuroRx 2 (3), 396–409.

Carmichael, S.T., Tatsukawa, K., Katsman, D., Tsuyuguchi, N., Kornblum, H.I., 2004. Evolution of diaschisis in a focal stroke model. Stroke 35 (3), 758–763.

CAST (Chinese Acute Stroke Trial) Collaborative Group, 1997. CAST: randomised placebo-controlled trial of early aspirin use in 20,000 patients with acute ischaemic stroke. Lancet 349 (9066), 1641–1649.

Castaigne, P., Lhermitte, F., Gautier, J.C., Escourolle, R., Derouesne, C., 1970. Internal carotid artery occlusion. A study of 61 instances in 50 patients with post-mortem data. Brain 93 (2), 231–258.

Castillo, J., Leira, R., Garcia, M.M., Serena, J., Blanco, M., Davalos, A., 2004. Blood pressure decrease during the acute phase of ischemic stroke is associated with brain injury and poor stroke outcome. Stroke 35 (2), 520–526.

Caviness, V.S., Makris, N., Montinaro, E., et al., 2002. Anatomy of stroke, Part I: an MRI-based topographic and volumetric system of analysis. Stroke 33 (11), 2549–2556.

Chalfin, B.P., Cheung, D.T., Muniz, J.A., de Lima Silveira, L.C., Finlay, B.L., 2007. Scaling of neuron number and volume of the pulvinar complex in New World primates: comparisons with humans, other primates, and mammals. J. Comp. Neurol. 504 (3), 265–274.

Chen, C.H., Xue, R., Zhang, J., Li, X., Mori, S., Bhardwaj, A., 2007. Effect of osmotherapy with hypertonic saline on regional cerebral edema following experimental stroke: a study utilizing magnetic resonance imaging. Neurocrit. Care 7 (1), 92–100.

Christoforidis, G.A., Mohammad, Y., Kehagias, D., Avutu, B., Slivka, A.P., 2005. Angiographic assessment of pial collaterals as a prognostic indicator following intra-arterial thrombolysis for acute ischemic stroke. AJNR 26 (7), 1789–1797.

Clark, W.M., Albers, G.W., Madden, K.P., Hamilton, S., 2000. The rtPA (alteplase) 0- to 6-hour acute stroke trial, part A (A0276g): results of a double-blind, placebo-controlled, multicenter study. Thrombolytic therapy in acute ischemic stroke study investigators. Stroke 31 (4), 811–816.

Clark, W.M., Wechsler, L.R., Sabounjian, L.A., Schwiderski, U.E., 2001. A phase III randomized efficacy trial of 2000 mg citicoline in acute ischemic stroke patients. Neurology 57 (9), 1595–1602.

Cochrane, 2007. Cochrane central register of controlled trials (CENTRAL). Available from: http://www.cochrane.org

Coert, B.A., Anderson, R.E., Meyer, F.B., 1999. Reproducibility of cerebral cortical infarction in the Wistar rat after middle cerebral artery occlusion. J. Stroke Cerebrovasc. Dis. 8 (6), 380–387.

Cramer, S.C., Parrish, T.B., Levy, R.M., et al., 2007. Predicting functional gains in a stroke trial. Stroke 38 (7), 2108–2114.

Crowell, R.M., Marcoux, F.W., DeGirolami, U., 1981. Variability and reversibility of focal cerebral ischemia in unanesthetized monkeys. Neurology 31 (10), 1295–1302.

Daniel, P.M., Dawes, J.D.K., Prichard, M.M.L., 1953. Studies of the carotid rete and its associated arteries. Philos. Trans. R. Soc. Lond. B Biol. Sci. 237 (645), 173–208.

Davis, M., Mendelow, A.D., Perry, R.H., Chambers, I.R., James, O.F., 1995. Experimental stroke and neuroprotection in the aging rat brain. Stroke 26 (6), 1072–1078.

Dawson, D.A., Wadsworth, G., Palmer, A.M., 2001. A comparative assessment of the efficacy and side-effect liability of neuroprotective compounds in experimental stroke. Brain Res. 892 (2), 344–350.

Derex, L., Nighoghossian, N., Hermier, M., et al., 2004a. Influence of pretreatment MRI parameters on clinical outcome, recanalization and infarct size in 49 stroke patients treated by intravenous tissue plasminogen activator. J. Neurol. Sci. 225 (1–2), 3–9.

Derex, L., Hermier, M., Adeleine, P., et al., 2004b. Influence of the site of arterial occlusion on multiple baseline hemodynamic MRI parameters and post-thrombolytic recanalization in acute stroke. Neuroradiology 46 (11), 883–887.

DerSimonian, R., Laird, N., 1986. Meta-analysis in clinical trials. Control. Clin. Trials 7 (3), 177–188.

Dirnagl, U., 2006. Bench to bedside: the quest for quality in experimental stroke research. J. Cereb. Blood Flow Metab. 26 (12), 1465–1478.

Dirnagl, U., Iadecola, C., Moskowitz, M.A., 1999. Pathobiology of ischaemic stroke: an integrated view. Trends Neurosci. 22 (9), 391–397.

Dittmar, M.S., Vatankhah, B., Fehm, N.P., et al., 2006. Fischer-344 rats are unsuitable for the MCAO filament model due to their cerebrovascular anatomy. J. Neurosci. Methods 156 (1–2), 50–54.

Donnan, G.A., Fisher, M., Macleod, M., Davis, M., 2008. Stroke. Lancet 371 (9624), 1612–1623.

Dorph-Petersen, K.A., Pierri, J.N., Perel, J.M., Sun, Z., Sampson, A.R., Lewis, D.A., 2005. The influence of chronic exposure to antipsychotic medications on brain size before and after tissue fixation: a comparison of haloperidol and olanzapine in macaque monkeys. Neuropsychopharmacology 30 (9), 1649–1661.

Durukan, A., Tatlisumak, T., 2007. Acute ischemic stroke: overview of major experimental rodent models, pathophysiology, and therapy of focal cerebral ischemia. Pharmacol. Biochem. Behav. 87 (1), 179–197.

Duverger, D., MacKenzie, E.T., 1988. The quantification of cerebral infarction following focal ischemia in the rat: influence of strain, arterial pressure, blood glucose concentration, and age. J. Cereb. Blood Flow Metab. 8 (4), 449–461.

Duygu, H., Barisik, V., Kurt, H., Turk, U., Ercan, E., Kose, S., 2008. Prognostic value of plasma soluble CD40 ligand in patients with chronic non-valvular atrial fibrillation. Europace 10 (2), 210–214.

Dzialowski, I., Klotz, E., Goericke, S., Doerfler, A., Forsting, M., von Kummer, R., 2007. Ischemic brain tissue water content: CT monitoring during middle cerebral artery occlusion and reperfusion in rats. Radiology 243 (3), 720–726.

Emsley, H.C., Smith, C.J., Georgiou, R.F., et al., 2005. A randomised phase II study of interleukin-1 receptor antagonist in acute stroke patients. J. Neurol. Neurosurg. Psychiatry 76 (10), 1366–1372.

Ferro, D., Loffredo, L., Polimeni, L., et al., 2007. Soluble CD40 ligand predicts ischemic stroke and myocardial infarction in patients with nonvalvular atrial fibrillation. Arterioscler. Thromb. Vasc. Biol. 27 (12), 2763–2768.

Fiehler, J., Foth, M., Kucinski, T., et al., 2002. Severe ADC decreases do not predict irreversible tissue damage in humans. Stroke 33 (1), 79–86.

Fiehler, J., Knudsen, K., Thomalla, G., et al., 2005. Vascular occlusion sites determine differences in lesion growth from early apparent diffusion coefficient lesion to final infarct. Ajnr 26 (5), 1056–1061.

Fisher, M., Feuerstein, G., Howells, D.W., et al., 2009. Update of the stroke therapy academic industry round table preclinical recommendations. Stroke 40 (6), 2244–2250.

Flaumenhaft, R., Lo, E.H., 2006. Different strokes for rodent folks. Nat. Methods 3 (2), 79–80.

Fogelholm, R., Erila, T., Palomaki, H., Murros, K., Kaste, M., 2000. Effect of nimodipine on final infarct volume after acute ischemic stroke. Cerebrovasc. Dis. 10 (3), 189–193.

Fox, G., Gallacher, D., Shevde, S., Loftus, J., Swayne, G., 1993. Anatomic variation of the middle cerebral artery in the Sprague-Dawley rat. Stroke 24 (12), 2087–2092.

Fukuda, S., del Zoppo, G.J., 2003. Models of focal cerebral ischemia in the nonhuman primate. ILAR J. 44 (2), 96–104.

Fung, Y.C., 1997. Biomechanics: Circulation, second ed. Springer-Verlag, New York.

Futrell, N., 1991. An improved photochemical model of embolic cerebral infarction in rats. Stroke 22 (2), 225–232.

Futrell, N., Millikan, C., Watson, B.D., Dietrich, W.D., Ginsberg, M.D., 1989. Embolic stroke from a carotid arterial source in the rat: pathology and clinical implications. Neurology 39 (8), 1050–1056.

Garosi, L., McConnell, J.F., Platt, S.R., et al., 2006. Clinical and topographic magnetic resonance characteristics of suspected brain infarction in 40 dogs. J. Vet. Inter. Med. 20 (2), 311–321.

Garrison, F.H., 1929. History of Medicine. W.B. Saunders, Philadelphia, PHL.

Gerriets, T., Li, F., Silva, M.D., et al., 2003. The macrosphere model: evaluation of a new stroke model for permanent middle cerebral artery occlusion in rats. J. Neurosci. Methods 122 (2), 201–211.

Ginsberg, M.D., Busto, R., 1989. Rodent models of cerebral ischemia. Stroke 20 (12), 1627–1642.

Goldberg, M.P., 2007. Stroke trials registry. Internet Stroke Center. Available from: www.strokecenter.org

Goyal, M., Menon, B.K., van Zwam, W.H., et al., 2016. Endovascular thrombectomy after large-vessel ischaemic stroke: a meta-analysis of individual patient data from five randomised trials. Lancet 387 (10029), 1723–1731.

Gratton, J.A., Sauter, A., Rudin, M., et al., 1998. Susceptibility to cerebral infarction in the stroke-prone spontaneously hypertensive rat is inherited as a dominant trait. Stroke 29 (3), 690–694.

Green, A.R., Odergren, T., Ashwood, T., 2003. Animal models of stroke: do they have value for discovering neuroprotective agents? Trends Pharmacol. Sci. 24 (8), 402–408.

Hackam, D.G., Redelmeier, D.A., 2006. Translation of research evidence from animals to humans. JAMA 296 (14), 1731–1732.

Hacke, W., Kaste, M., Fieschi, C., et al., 1995. Intravenous thrombolysis with recombinant tissue plasminogen activator for acute hemispheric stroke. The European Cooperative Acute Stroke Study (ECASS). JAMA 274 (13), 1017–1025.

Hacke, W., Donnan, G., Fieschi, C., et al., 2004. Association of outcome with early stroke treatment: pooled analysis of ATLANTIS, ECASS, and NINDS rt-PA stroke trials. Lancet 363 (9411), 768–774.

Hainsworth, A.H., Markus, H.S., 2008. Do in vivo experimental models reflect human cerebral small vessel disease? A systematic review. J. Cereb. Blood Flow Metab. 28, 1877–1891.

Harvey, W., 2001. On the Motion of the Heart and Blood in Animals. P.F. Collier & Son Company, New York, NY.

Hashimoto, M., Zhao, L., Nowak, Jr., T.S., 2008. Temporal thresholds for infarction and hypothermic protection in Long-Evans rats: factors affecting apparent 'reperfusion injury' after transient focal ischemia. Stroke 39 (2), 421–426.

Heinsius, T., Bogousslavsky, J., Van Melle, G., 1998. Large infarcts in the middle cerebral artery territory. Etiology and outcome patterns. Neurology 50 (2), 341–350.

Hildebrandt, A.G., 2004. Pharmacology, drug efficacy, and the individual. Drug Metab. Rev. 36 (3–4), 845–852.

Hillis, A.E., Ulatowski, J.A., Barker, P.B., et al., 2003. A pilot randomized trial of induced blood pressure elevation: effects on function and focal perfusion in acute and subacute stroke. Cerebrovasc. Dis. 16 (3), 236–246.

Ho, P.W., Reutens, D.C., Phan, T.G., et al., 2005. Is white matter involved in patients entered into typical trials of neuroprotection? Stroke 36 (12), 2742–2744.

Horn, J., de Haan, R.J., Vermeulen, M., Luiten, P.G., Limburg, M., 2001. Nimodipine in animal model experiments of focal cerebral ischemia: a systematic review. Stroke 32 (10), 2433–2438.

Horstmann, S., Kalb, P., Koziol, J., Gardner, H., Wagner, S., 2003. Profiles of matrix metalloproteinases, their inhibitors, and laminin in stroke patients: influence of different therapies. Stroke 34 (9), 2165–2170.

Hossmann, K.A., 1998. Experimental models for the investigation of brain ischemia. Cardiovasc. Res. 39 (1), 106–120.

Hossmann, K.A., Traystman, R.J., 2008. Cerebral blood flow and the ischemic penumbra. Vinken, P.J. (Ed.), Handbook of Clinical Neurology, vol. 92, Elsevier, pp. 67–92, (Chapter 4).

Hozo, S.P., Djulbegovic, B., Hozo, I., 2005. Estimating the mean and variance from the median, range, and the size of a sample. BMC Med. Res. Methodol. 5 (1), 13.

Hunter, A.J., Mackay, K.B., Rogers, D.C., 1998. To what extent have functional studies of ischaemia in animals been useful in the assessment of potential neuroprotective agents? Trends Pharmacol. Sci. 19 (2), 59–66.

Infeld, B., Davis, S.M., Donnan, G.A., et al., 1996. Streptokinase increases luxury perfusion after stroke. Stroke 27 (9), 1524–1529.

Infeld, B., Davis, S.M., Donnan, G.A., et al., 1999. Nimodipine and perfusion changes after stroke. Stroke 30 (7), 1417–1423.

International Stroke Trial Collaborative (ISTC) Group, 1997. The International Stroke Trial (IST): a randomised trial of aspirin, subcutaneous heparin, both, or neither among 19435 patients with acute ischaemic stroke. Lancet 349 (9065), 1569–1581.

Janssen, J., Pol, H.E., Schnack, H.G., et al., 2007. Cerebral volume measurements and subcortical white matter lesions and short-term treatment response in late life depression. Int. J. Geriatr. Psychiatry 22 (5), 468–474.

Jaques, L.B., 1988. The Howell theory of blood coagulation: a record of the pernicious effects of a false theory. Can. Bull. Med. Hist. 5 (2), 143–165.

Jefferson, A.L., Massaro, J.M., Wolf, P.A., et al., 2007. Inflammatory biomarkers are associated with total brain volume: the Framingham Heart Study. Neurology 68 (13), 1032–1038.

Jewell, P.A., 1952. The anastomoses between internal and external carotid circulations in the dog. J. Anat. 86 (2), 83–94.

Kane, I., Carpenter, T., Chappell, F., et al., 2007. Comparison of 10 different magnetic resonance perfusion imaging processing methods in acute ischemic stroke: effect on lesion size, proportion of patients with diffusion/perfusion mismatch, clinical scores, and radiologic outcomes. Stroke 38 (12), 3158–3164.

Kaneko, D., Nakamura, N., Ogawa, T., 1985. Cerebral infarction in rats using homologous blood emboli: development of a new experimental model. Stroke 16 (1), 76–84.

Kaplan, B., Brint, S., Tanabe, J., Jacewicz, M., Wang, X.J., Pulsinelli, W., 1991. Temporal thresholds for neocortical infarction in rats subjected to reversible focal cerebral ischemia. Stroke 22 (8), 1032–1039.

Karpiak, S.E., Tagliavia, A., Wakade, C.G., 1989. Animal models for the study of drugs in ischemic stroke. Annu. Rev. Pharmacol. Toxicol. 29, 403–414.

Kawano, K.I., Fujishima, K., Ikeda, Y., Kondo, K., Umemura, K., 2000. ME3277, a GPIIb/IIIa antagonist reduces cerebral infarction without enhancing intracranial hemorrhage in photothrombotic occlusion of rabbit middle cerebral artery. J. Cereb. Blood Flow Metab. 20 (6), 988–997.

Kent, T.A., Soukup, V.M., Fabian, R.H., 2001. Heterogeneity affecting outcome from acute stroke therapy: making reperfusion worse. Stroke 32 (10), 2318–2327.

Kidwell, C.S., 2001. Trends in acute ischemic stroke trials through the 20th century. Stroke 32, 1349–1359.

Kim, J.J., Fischbein, N.J., Lu, Y., Pham, D., Dillon, W.P., 2004. Regional angiographic grading system for collateral flow: correlation with cerebral infarction in patients with middle cerebral artery occlusion. Stroke 35 (6), 1340–1344.

Koizumi, J., Yoshida, Y., Nakazawa, T., Ooneda, G., 1986. Experimental studies of ischemic brain edema, I: a new experimental model of cerebral embolism in rats in which recirculation can be introduced in the ischemic area [reference unverified]. Jnp. J. Stroke 8, 1–8.

Kowianski, P., Dziewiatkowski, J., Kowianska, J., Morys, J., 1999. Comparative anatomy of the claustrum in selected species: a morphometric analysis. Brain Behav. Evol. 53 (1), 44–54.

Kudo, M., Aoyama, A., Ichimori, S., Fukunaga, N., 1982. An animal model of cerebral infarction. Homologous blood clot emboli in rats. Stroke 13 (4), 505–508.

Langhorne, P., Williams, B.O., Gilchrist, W., Howie, K., 1993. Do stroke units save lives? Lancet 342 (8868), 395–398.

Langhorne, P., Williams, B.O., Gilchrist, W., Dennis, M.S., Slattery, J., 1995. A formal overview of stroke unit trials. Revista de neurologia 23 (120), 394–398.

Lansberg, M.G., O'Brien, M.W., Tong, D.C., Moseley, M.E., Albers, G.W., 2001. Evolution of cerebral infarct volume assessed by diffusion-weighted magnetic resonance imaging. Arch. Neurol. 58 (4), 613–617.

Lees, K.R., Bluhmki, E., von Kummer, R., et al., 2010. Time to treatment with intravenous alteplase and outcome in stroke: an updated pooled analysis of ECASS, ATLANTIS, NINDS, and EPITHET trials. Lancet 375 (9727), 1695–1703.

Leira, R., Rodriguez-Yanez, M., Castellanos, M., et al., 2006. Hyperthermia is a surrogate marker of inflammation-mediated cause of brain damage in acute ischaemic stroke. J. Inter. Med. 260 (4), 343–349.

Li, F., Omae, T., Fisher, M., 1999. Spontaneous hyperthermia and its mechanism in the intraluminal suture middle cerebral artery occlusion model of rats. Stroke 30 (11), 2464–2470.

Liu, Y., Karonen, J.O., Vanninen, R.L., et al., 2004. Acute ischemic stroke: predictive value of 2D phase-contrast MR angiography—serial study with combined diffusion and perfusion MR imaging. Radiology 231 (2), 517–527.

Lo, E.H., Dalkara, T., Moskowitz, M.A., 2003. Mechanisms, challenges and opportunities in stroke. Nat. Rev. Neurosci. 4 (5), 399–415.

Loh, P.S., Butcher, K.S., Parsons, M.W., et al., 2005. Apparent diffusion coefficient thresholds do not predict the response to acute stroke thrombolysis. Stroke 36 (12), 2626–2631.

Longa, E.Z., Weinstein, P.R., Carlson, S., Cummins, R., 1989. Reversible middle cerebral artery occlusion without craniectomy in rats. Stroke 20 (1), 84–91.

Lovallo, W.R., 2005. Stress and Health: Biological and Psychological Interactions. Sage, California, CA, United States.

Lyden, P.D., Zweifler, R., Mahdavi, Z., Lonzo, L., 1994. A rapid, reliable, and valid method for measuring infarct and brain compartment volumes from computed tomographic scans. Stroke 25 (12), 2421–2428.

Macleod, M.R., O'Collins, T., Howells, D.W., Donnan, G.A., 2004. Pooling of animal experimental data reveals influence of study design and publication bias. Stroke 35 (5), 1203–1208.

Macleod, M.R., O'Collins, T., Horky, L.L., Howells, D.W., Donnan, G.A., 2005a. Systematic review and metaanalysis of the efficacy of FK506 in experimental stroke. J. Cereb. Blood Flow Metab. 25 (6), 713–721.

Macleod, M.R., O'Collins, T., Horky, L.L., Howells, D.W., Donnan, G.A., 2005b. Systematic review and meta-analysis of the efficacy of melatonin in experimental stroke. J. Pineal Res. 38 (1), 35–41.

Macleod, M.M., Fisher, M., O'Collins, V., et al., 2008. Good laboratory practice. preventing introduction of bias at the bench. Stroke 40, e50–e52.

Macrae, I.M., Robinson, M.J., Graham, D.I., Reid, J.L., McCulloch, J., 1993. Endothelin-1-induced reductions in cerebral blood flow: dose dependency, time course, and neuropathological consequences. J. Cereb. Blood Flow Metab. 13 (2), 276–284.

Marinov, M.B., Harbaugh, K.S., Hoopes, P.J., Pikus, H.J., Harbaugh, R.E., 1996. Neuroprotective effects of preischemia intraarterial magnesium sulfate in reversible focal cerebral ischemia. J. Neurosurg. 85 (1), 117–124.

Martin, J.F., Hamdy, N., Nicholl, J., et al., 1985. Double-blind controlled trial of prostacyclin in cerebral infarction. Stroke 16 (3), 386–390.

Memezawa, H., Smith, M.L., Siesjo, B.K., 1992. Penumbral tissues salvaged by reperfusion following middle cerebral artery occlusion in rats. Stroke 23 (4), 552–559.

Meng, X., Fisher, M., Shen, Q., Sotak, C.H., Duong, T.Q., 2004. Characterizing the diffusion/perfusion mismatch in experimental focal cerebral ischemia. Ann. Neurol. 55 (2), 207–212.

Meyerhof, M., 1935. Ibn An-Nafis (XIIIth Cent) and his theory of the lesser circulation. Isis 23 (1), 100–120.

Miller Fisher, C., 1975. The anatomy and pathology of the cerebral vasculature. In: Meyer, J.S. (Ed.), Modern Concepts of Cerebovascular Disese. Spectrum Publications, New York, NY, pp. 63–86.

Millikan, C., 1992. Animal stroke models. Stroke 23 (6), 795–797.

Modo, M., Stroemer, R.P., Tang, E., Patel, S., Hodges, H., 2002. Effects of implantation site of stem cell grafts on behavioral recovery from stroke damage. Stroke 33 (9), 2270–2278.

Moghadasian, M.H., 2002. Experimental atherosclerosis: a historical overview. Life Sci. 70 (8), 855–865.

Molina, C.A., Montaner, J., Abilleira, S., et al., 2001. Time course of tissue plasminogen activator-induced recanalization in acute cardioembolic stroke: a case-control study. Stroke 32 (12), 2821–2827.

Molina, C.A., Montaner, J., Arenillas, J.F., Ribo, M., Rubiera, M., Alvarez-Sabin, J., 2004. Differential pattern of tissue plasminogen activator-induced proximal middle cerebral artery recanalization among stroke subtypes. Stroke 35 (2), 486–490.

Molinari, G.F., 1979. Clinical Relevance of Experimental Stroke Models. Raven Press, New York, NY.

Molinari, G.F., 1988. Why model strokes? Stroke 19 (10), 1195–1197.

Murat Sumer, M., Erturk, O., 2002. Ischemic stroke subtypes: risk factors, functional outcome and recurrence. Neurol. Sci. 22 (6), 449–454.

National Institute of Neurological Disorders and Stroke rt-PA Stroke Study Group (NIND), 1995. Tissue plasminogen activator for acute ischemic stroke. N. Engl. J. Med. 33 (24), 1581–2157.

NIH, 2007. National Institute of Health Clinical Trials Registry. Available from: www.clinicaltrials.org

Neumann-Haefelin, T., Kastrup, A., de Crespigny, A., et al., 2000. Serial MRI after transient focal cerebral ischemia in rats: dynamics of tissue injury, blood-brain barrier damage, and edema formation. Stroke 31 (8), 1965–1972.

Niiro, M., Simon, R.P., Kadota, K., Asakura, T., 1996. Proximal branching patterns of middle cerebral artery (MCA) in rats and their influence on the infarct size produced by MCA occlusion. J. Neurosci. Methods 64 (1), 19–23.

NINDS, 2000. Effect of intravenous recombinant tissue plasminogen activator on ischemic stroke lesion size measured by computed tomography. NINDS; The National Institute of Neurological Disorders and Stroke (NINDS) rt-PA Stroke Study Group. Stroke 31 (12), 2912–2919.

Obrig, H., Neufang, M., Wenzel, R., et al., 2000. Spontaneous low frequency oscillations of cerebral hemodynamics and metabolism in human adults. Neuroimage 12, 623–639.

O'Collins, V.E., Macleod, M.R., Donnan, G.A., Horky, L.L., van der Worp, B.H., Howells, D.W., 2006. 1,026 experimental treatments in acute stroke. Ann. Neurol. 59 (3), 467–477.

Ogawa, A., Yoshimoto, T., Kikuchi, H., et al., 1999. Ebselen in acute middle cerebral artery occlusion: a placebo-controlled, double-blind clinical trial. Cerebrovasc. Dis. 9 (2), 112–118.

Oppenheim, C., Samson, Y., Manai, R., et al., 2000. Prediction of malignant middle cerebral artery infarction by diffusion-weighted imaging. Stroke 31 (9), 2175–2181.

Parsons, M.W., Barber, P.A., Chalk, J., et al., 2002. Diffusion- and perfusion-weighted MRI response to thrombolysis in stroke. Ann. Neurol. 51 (1), 28–37.

Perel, P., Roberts, I., Sena, E., et al., 2007. Comparison of treatment effects between animal experiments and clinical trials: systematic review. Br. Med. J. 334 (7586), 197–200.

Pexman, J.H., Barber, P.A., Hill, M.D., et al., 2001. Use of the Alberta Stroke Program Early CT Score (ASPECTS) for assessing CT scans in patients with acute stroke. AJNR 22 (8), 1534–1542.

Phan, T.G., Donnan, G.A., Wright, P.M., Reutens, D.C., 2005. A digital map of middle cerebral artery infarcts associated with middle cerebral artery trunk and branch occlusion. Stroke 36 (5), 986–991.

Phan, T.G., Donnan, G.A., Davis, S.M., Byrnes, G., 2006. Proof-of-principle phase II MRI studies in stroke: sample size estimates from dichotomous and continuous data. Stroke 37 (10), 2521–2525.

Poncyljusz, W., Falkowski, A., Kojder, I., et al., 2007. Treatment of acute ischemic brain infarction with the assistance of local intraarterial thrombolysis with recombinant tissue-type plasminogen activator. Acta Radiol. 48 (7), 774–780.

Provenzale, J.M., Jahan, R., Naidich, T.P., Fox, A.J., 2003. Assessment of the patient with hyperacute stroke: imaging and therapy. Radiology 229 (2), 347–359.

RANTTAS Investigators, 1996. A randomized trial of tirilazad mesylate in patients with acute stroke (RANTTAS). Stroke 27 (9), 1453–1458.

Rathjen, S., Engelmann, R., Struif, S., Kaulisch, T., Stiller, D., Lowel, S., 2003. The growth of cat cerebral cortex in postnatal life: a magnetic resonance imaging study. Eur. J. Neurosci. 18 (7), 1797–1806.

Reith, J., Jorgensen, H.S., Pedersen, P.M., et al., 1996. Body temperature in acute stroke: relation to stroke severity, infarct size, mortality, and outcome. Lancet 347 (8999), 422–425.

Rewell, S., Cox, S.F., Howells, D.W., 2008. Personal Communication. 2008.

Rha, J.H., Saver, J.L., 2007. The impact of recanalization on ischemic stroke outcome: a meta-analysis. Stroke 38 (3), 967–973.

Ribo, M., Montaner, J., Molina, C.A., Arenillas, J.F., Santamarina, E., Alvarez-Sabin, J., 2004. Admission fibrinolytic profile predicts clot lysis resistance in stroke patients treated with tissue plasminogen activator. Thromb. Haemost. 91 (6), 1146–1151.

Ringelstein, E.B., Biniek, R., Weiller, C., Ammeling, B., Nolte, P.N., Thron, A., 1992. Type and extent of hemispheric brain infarctions and clinical outcome in early and delayed middle cerebral artery recanalization. Neurology 42 (2), 289–298.

Roberts, H.C., Dillon, W.P., Furlan, A.J., et al., 2002. Computed tomographic findings in patients undergoing intra-arterial thrombolysis for acute ischemic stroke due to middle cerebral artery occlusion: results from the PROACT II trial. Stroke 33 (6), 1557–1565.

Rother, J., Schellinger, P.D., Gass, A., et al., 2002. Effect of intravenous thrombolysis on MRI parameters and functional outcome in acute stroke <6 hours. Stroke 33 (10), 2438–2445.

Rubino, G.J., Young, W., 1988. Ischemic cortical lesions after permanent occlusion of individual middle cerebral artery branches in rats. Stroke 19 (7), 870–877.

Sahin, B., Aslan, H., Unal, B., et al., 2001. Brain volumes of the lamb, rat and bird do not show hemispheric asymmetry: a stereological study. Image Anal. Stereo. 20, 9–13.

Salerno, S.M., Landry, F.J., Schick, J.D., Schoomaker, E.B., 1996. The effect of multiple neuroimaging studies on classification, treatment, and outcome of acute ischemic stroke. Ann. Inter. Med. 124 (1 Pt 1), 21–26.

Sampei, K., Mandir, A.S., Asano, Y., et al., 2000a. Stroke outcome in double-mutant antioxidant transgenic mice. Stroke 31 (11), 2685–2691.

Sampei, K., Goto, S., Alkayed, N.J., et al., 2000b. Stroke in estrogen receptor-alpha-deficient mice. Stroke 31 (3), 738–743.

Sanak, D., Nosal, V., Horak, D., et al., 2006. Impact of diffusion-weighted MRI-measured initial cerebral infarction volume on clinical outcome in acute stroke patients with middle cerebral artery occlusion treated by thrombolysis. Neuroradiology 48 (9), 632–639.

Saqqur, M., Uchino, K., Demchuk, A.M., et al., 2007. Site of arterial occlusion identified by transcranial Doppler predicts the response to intravenous thrombolysis for stroke. Stroke 38 (3), 948–954.

Sauer, D., Weber, E., Luond, G., Da Silva, F., Allegrini, P.R., 1995. The competitive NMDA antagonist CGP 40116 permanently reduces brain damage after middle cerebral artery occlusion in rats. J. Cereb. Blood Flow Metab. 15 (4), 602–610.

Saver, J.L., 2008. Proposal for a universal definition of cerebral infarction. Stroke 39 (11), 3110–3115.

Saver, J.L., Johnston, K.C., Homer, D., et al., 1999. Infarct volume as a surrogate or auxiliary outcome measure in ischemic stroke clinical trials. The RANTTAS Investigators. Stroke 30 (2), 293–298.

Schellinger, P.D., Fiebach, J.B., Jansen, O., et al., 2001. Stroke magnetic resonance imaging within 6 hours after onset of hyperacute cerebral ischemia. Ann. Neurol. 49 (4), 460–469.

Schwamm, L.H., Koroshetz, W.J., Sorensen, A.G., et al., 1998. Time course of lesion development in patients with acute stroke: serial diffusion- and hemodynamic-weighted magnetic resonance imaging. Stroke 29 (11), 2268–2276.

Scremin, O.U., 2004. Cerebral vascular system. In: Paxinos, G. (Ed.), The Rat Nervous, System. Elsevier, London, pp. 1167–1202.

Seenan, P., Long, M., Langhorne, P., 2007. Stroke units in their natural habitat: systematic review of observational studies. Stroke 38 (6), 1886–1892.

Seitz, R.J., Meisel, S., Moll, M., Wittsack, H.J., Junghans, U., Siebler, M., 2004. The effect of combined thrombolysis with rtPA and tirofiban on ischemic brain lesions. Neurology 62 (11), 2110–2112.

Seitz, R.J., Meisel, S., Moll, M., Wittsack, H.J., Junghans, U., Siebler, M., 2005. Partial rescue of the perfusion deficit area by thrombolysis. J. Magn. Reson. Imaging 22 (2), 199–205.

Selim, M., Fink, J.N., Kumar, S., et al., 2002. Predictors of hemorrhagic transformation after intravenous recombinant tissue plasminogen activator: prognostic value of the initial apparent diffusion coefficient and diffusion-weighted lesion volume. Stroke 33 (8), 2047–2052.

Selim, M., Savitz, S., Linfante, I., Caplan, L., Schlaug, G., 2005. Effect of pre-stroke use of ACE inhibitors on ischemic stroke severity. BMC Neurol. 5 (1), 10.

Sena, E., Wheble, P., Sandercock, P., Macleod, M., 2007. Systematic review and meta-analysis of the efficacy of tirilazad in experimental stroke. Stroke 38 (2), 388–394.

Sharkey, J., Ritchie, I.M., Kelly, P.A., 1993. Perivascular microapplication of endothelin-1: a new model of focal cerebral ischaemia in the rat. J. Cereb. Blood Flow Metab. 13 (5), 865–871.

Shi, Y., Li, D., Zhao, Y., 2000. [Clinical study on ultra-early intravenous thrombolysis with high-dose urokinase in treatment of acute cerebral infarction]. Zhonghua yi xue za zhi 80 (2), 101–103.

Slivka, A., Murphy, E., Horrocks, L., 1995. Cerebral edema after temporary and permanent middle cerebral artery occlusion in the rat. Stroke 26 (6), 1061–1065.

Small, D.L., Buchan, A.M., 2000. Animal models. Br. Med. Bull. 56 (2), 307–317.

Smith, C.D., Thomas, G.S., Kryscio, R.J., Markesbery, W.R., 1990. 31P spectroscopy in experimental embolic stroke: correlation with infarct size. NMR Biomed. 3 (6), 259–264.

STAIR, 1999. Recommendations for standards regarding preclinical neuroprotective and restorative drug development. Stroke 30 (12), 2752–2758.

Sternberg, E.M., Young, 3rd, W.S., Bernardini, R., et al., 1989a. A central nervous system defect in biosynthesis of corticotropin-releasing hormone is associated with susceptibility to streptococcal cell wall-induced arthritis in Lewis rats. Proc. Natl. Acad. Sci. USA 86 (12), 4771–4775.

Sternberg, E.M., Hill, J.M., Chrousos, G.P., et al., 1989b. Inflammatory mediator-induced hypothalamic-pituitary-adrenal axis activation is defective in streptococcal cell wall arthritis-susceptible Lewis rats. Proc. Natl. Acad. Sci. USA 86 (7), 2374–2378.

Tamura, A., Graham, D.I., McCulloch, J., Teasdale, G.M., 1981. Focal cerebral ischaemia in the rat: 1. Description of technique and early neuropathological consequences following middle cerebral artery occlusion. J. Cereb. Blood Flow Metab. 1 (1), 53–60.

Tamura, A., Gotoh, O., Sano, K., 1986. [Focal cerebral infarction in the rat: I. Operative technique and physiological monitorings for chronic model]. No To Shinkei 38 (8), 747–751.

Thomalla, G.J., Kucinski, T., Schoder, V., et al., 2003. Prediction of malignant middle cerebral artery infarction by early perfusion- and diffusion-weighted magnetic resonance imaging. Stroke 34 (8), 1892–1899.

Thompson, S.G., 2001. Why and how sources of heterogeneity should be investigated. In: Egger, M., Smith, G.D., Altman, D.G. (Eds.), Systematic Reviews in Health Care Meta-Analysis in Context. BMJ Books, London, pp. 157–175.

Toni, D., De Michele, M., Fiorelli, M., et al., 1994. Influence of hyperglycaemia on infarct size and clinical outcome of acute ischemic stroke patients with intracranial arterial occlusion. J. Neurol. Sci. 123 (1–2), 129–133.

Traystman, R.J., 2003. Animal models of focal and global cerebral ischemia. ILAR J. 44 (2), 85–95.

Tupler, L.A., Krishnan, K.R., Greenberg, D.L., et al., 2007. Predicting memory decline in normal elderly: genetics, MRI, and cognitive reserve. Neurobiol. Aging 28 (11), 1644–1656.

Uchino, K., Billheimer, D., Cramer, S.C., 2001. Entry criteria and baseline characteristics predict outcome in acute stroke trials. Stroke 32 (4), 909–916.

Vahedi, K., Hofmeijer, J., Juettler, E., et al., 2007. Early decompressive surgery in malignant infarction of the middle cerebral artery: a pooled analysis of three randomised controlled trials. Lancet Neurol. 6 (3), 215–222.

van der Worp, H.B., Claus, S.P., Bar, P.R., et al., 2001. Reproducibility of measurements of cerebral infarct volume on CT scans. Stroke 32 (2), 424–430.

van der Worp, H.B., Kappelle, L.J., Algra, A., et al., 2002. The effect of tirilazad mesylate on infarct volume of patients with acute ischemic stroke. Neurology 58 (1), 133–135.

van der Zwan, A., Hillen, B., 1991. Review of the variability of the territories of the major cerebral arteries. Stroke 22 (8), 1078–1084.

van der Zwan, A., Hillen, B., Tulleken, C.A., Dujovny, M., Dragovic, L., 1992. Variability of the territories of the major cerebral arteries. J. Neurosurg. 77 (6), 927–940.

van der Zwan, A., Hillen, B., Tulleken, C.A., Dujovny, M., 1993. A quantitative investigation of the variability of the major cerebral arterial territories. Stroke 24 (12), 1951–1959.

van Laar, P.J., Hendrikse, J., Klijn, C.J., Kappelle, L.J., van Osch, M.J., van der Grond, J., 2007. Symptomatic carotid artery occlusion: flow territories of major brain-feeding arteries. Radiology 242 (2), 526–534.

Vang, C., Dunbabin, D., Kilpatrick, D., 1999. Effects of spontaneous recanalization on functional and electrophysiological recovery in acute ischemic stroke. Stroke 30 (10), 2119–2125.

von Kummer, R., Allen, K.L., Holle, R., et al., 1997. Acute stroke: usefulness of early CT findings before thrombolytic therapy. Radiology 205 (2), 327–333.

Vosko, M.R., Burggraf, D., Liebetrau, M., et al., 2006. Influence of the duration of ischemia and reperfusion on infarct volume and microvascular damage in mice. Neurol. Res. 28 (2), 200–205.

Wagner, K.R., Kleinholz, M., de Courten-Myers, G.M., Myers, R.E., 1992. Hyperglycemic versus normoglycemic stroke: topography of brain metabolites, intracellular pH, and infarct size. J. Cereb. Blood Flow Metab. 12 (2), 213–222.

Warach, S., Pettigrew, L.C., Dashe, J.F., et al., 2000. Effect of citicoline on ischemic lesions as measured by diffusion-weighted magnetic resonance imaging. Citicoline 010 Investigators. Ann. Neurol. 48 (5), 713–722.

Warach, S., Kaufman, D., Chiu, D., et al., 2006. Effect of the Glycine Antagonist Gavestinel on cerebral infarcts in acute stroke patients, a randomized placebo-controlled trial: The GAIN MRI Substudy. Cerebrovasc. Dis. 21 (1–2), 106–111.

Whisnant, J.P., Millikan, C.H., Wakim, K.H., Sayre, G.P., 1956. Collateral circulation to the brain of the dog following bilateral ligation of the carotid and vertebral arteries. Am. J. Physiol. 186 (2), 275–277.

WHO MONICA Project Principal Investigators (WHO-MONICA), 1988. The World Health Organization MONICA Project (monitoring trends and determinants in cardiovascular disease): a major international collaboration. J. Clin. Epidemiol. 41 (2), 105–114.

Wiebers, D.O., Adams, Jr., H.P., Whisnant, J.P., 1990. Animal models of stroke: are they relevant to human disease? Stroke 21 (1), 1–3.

Windle, V., Szymanska, A., Granter-Button, S., et al., 2006. An analysis of four different methods of producing focal cerebral ischemia with endothelin-1 in the rat. Exp. Neurol. 201 (2), 324–334.

Wu, O., Christensen, S., Hjort, N., et al., 2006. Characterizing physiological heterogeneity of infarction risk in acute human ischaemic stroke using MRI. Brain 129 (Pt 9), 2384–2393.

Yamori, Y., Horie, R., Handa, H., Sato, M., Fukase, M., 1976. Pathogenic similarity of strokes in stroke-prone spontaneously hypertensive rats and humans. Stroke 7, 46–53.

Yang, G.Y., Betz, A.L., 1994. Reperfusion-induced injury to the blood-brain barrier after middle cerebral artery occlusion in rats. Stroke 25 (8), 1658–1664.

Yao, H., Ibayashi, S., Sugimori, H., Fujii, K., Fujishima, M., 1996. Simplified model of krypton laser-induced thrombotic distal middle cerebral artery occlusion in spontaneously hypertensive rats. Stroke 27 (2), 333–336.

Yasaka, M., O'Keefe, G.J., Chambers, B.R., et al., 1998. Streptokinase in acute stroke: effect on reperfusion and recanalization. Australian Streptokinase Trial Study Group. Neurology 50 (3), 626–632.

Young, A.R., Touzani, O., Derlon, J.M., Sette, G., MacKenzie, E.T., Baron, J.C., 1997. Early reperfusion in the anesthetized baboon reduces brain damage following middle cerebral artery occlusion: a quantitative analysis of infarction volume. Stroke 28 (3), 632–637.

Zivin, J.A., Grotta, J.C., 1990. Animal stroke models. They are relevant to human disease. Stroke 21, 981–983.

Zivin, J.A., DeGirolami, U., Kochhar, A., et al., 1987. A model for quantitative evaluation of embolic stroke therapy. Brain Res. 435 (1–2), 305–309.

Page left intentionally blank

21

The Importance of Olfactory and Motor Endpoints for Zebrafish Models of Neurodegenerative Disease

Angela L. Shamchuk, W. Ted Allison, Keith B. Tierney

University of Alberta, Edmonton, AB, Canada

1 INTRODUCTION

1.1 The Function and Importance of Olfaction

Olfaction or the sense of smell is the process of odorant reception and interpretation by neuronal tissue. This aspect of the sensory system is important to animal survival because odorants provide cues for essential behaviors such as foraging, mating, and predator evasion. Outwardly, humans do not have the same dependence on the olfactory system for survival; however, they do retain similar capabilities. Although often overlooked, the sense of smell has a significant effect on human behavior and emotions (Stevenson, 2010). Not only can we recognize certain odors and interpret them accordingly, but we also learn to associate certain odors with memories and positive or negative experiences (Table 21.1).

Due to the emotional associations with certain odors, the olfactory system is considered important for quality of psychological life and its impairment has thus been associated with cases of depression (Pause et al., 2001). The decrease in quality of life associated with individuals who have olfactory deficits is largely due to paralleled impairments in eating, safety, personal hygiene, and sex life (Hummel and Nordin, 2005).

Deficits in olfaction also represent accessible symptoms to aid in clinical diagnosis of neurodegenerative disease. Diagnosis of neurodegenerative disease is a key challenge because discriminating between similar diseases is critical to proper disease management, early diagnosis is believed to be central to effective intervention, and accurate measures of disease progression remain a fundamental challenge in assessing treatments in experimental trials.

TABLE 21.1   Human Olfactory Ability

Odors	Associated abilities	References
Food	Edibility recognition, taste–odor association, dietary management	Aschenbrenner et al. (2008); Bonfils et al. (2008); Fallon and Rozin (1983); Stevenson et al. (1995)
Environmental hazards (e.g., fire, gas leaks)	Danger identification	Aschenbrenner et al. (2008)
Microbial hazards (e.g., waste, illness)	Disgust/aversion, immune response	Moscavitch et al. (2009); Rubio-Godoy et al. (2007); Stevenson et al. (2010)
Other humans	Kin recognition, mate selection, anxiety/fear recognition	Ackerl et al. (2002); Olsson et al. (2006); Prehn et al. (2006); Thornhill et al. (2003); Weisfeld et al. (2003)

Adapted from Stevenson, R.J., 2010. An initial evaluation of the functions of human olfaction. Chem. Senses 35 (1), 3–20.

Although chemosensation is not essential to survival, specific odors will stimulate behaviors that can be considered attractive or aversive. The same is true for animals, and while sensitivity thresholds, specific odorants, and behaviors vary across vertebrates, the major anatomical and neurophysiological components that make up the olfactory system are conserved across many species (Ache and Young, 2005; Tierney, 2015). In general, the process of olfaction involves three stages: (1) odorant binding to a specific receptor on an olfactory sensory neuron (OSN); (2) a cascade of intracellular events leading to neuron depolarization; and (3) signal relay to the olfactory bulb for interpretation via comparison of OSN depolarizations. To facilitate odorant–receptor interaction, OSNs are exposed to the external environment, typically as part olfactory epithelia in the nasal pit or cavity. Odorants are believed to bind or otherwise interact with OSN receptors in a manner ranging from the specific (lock and key) to the general (Amoore, 1964; Brookes, 2011; Doty, 2010). Some receptors are believed to exhibit steric interaction with multiple odorants that are structurally similar, but bind to them with different affinities. Following this theory, receptors on OSNs are odorant specific to varying degrees and receptor expression is variable across species. Most commonly, the receptors in question are G-protein coupled, and upon odorant binding, G-protein activation results in one of two known signaling cascades (adenylyl cyclase/cyclic-AMP or phosphoinositide/IP_3) resulting in a neuron depolarization. If the signal from the activated neuron is sufficiently strong, an action potential may be conducted along an axon to the olfactory bulb in the brain. At the level of the brain, the odorant is interpreted and physiological or behavioral responses may ensue. A more detailed explanation of anatomy and neuronal process is beyond the scope of this chapter, but is reviewed in Ache and Young (2005) and Firestein (2001).

1.2 Olfactory Dysfunction

Deficits in olfactory function can occur at several levels of the olfactory system and to varying degrees. Typically, olfactory distortions present in one of three ways (Leopold, 2002). The first type refers to a decreased ability to perceive odors from partial (hyposmic) to complete (anosmic) loss of olfactory sensitivity. The two remaining types of dysfunction involve a change in odorant perception (dysosmia). The two known types of change refer to either odorant perception in an odorless environment (phantosmia) or a change in odorant perception, that is, odors are perceived incorrectly (troposmia). These conditions represent the main problems associated with olfactory dysfunction in general: detection, identification, and distinction. The etiologies for each dysfunction are variable, and documented cases suggest potential malformation, damage, or degeneration of the chemosensory tissues (Table 21.2). To investigate the relative frequencies of causes, a study examined 278 patients with olfactory dysfunction and found the proportions of causes to be posttraumatic (17%), postviral (39%) sinonasal disease (21%), congenital (3%), sporadic (18%), and other (3%) (Temmel et al., 2002). Congenital olfactory disorders (a relatively small proportion of cases) are unique in that they are typically the result of genetic defects that prevent either partial or entire olfactory tract or bulb development (Yousem et al., 1996). These disorders are usually part of congenital syndromes and thus accompany other major physiological abnormalities such as hypogonadism in Kallmann's and Bardet-Biedl syndromes (Hummel et al., 1991; Iannaccone et al., 2005). The other potential causes are related to damage inflicted upon the olfactory system. For example, case studies have demonstrated associations between exposure to metals, industrial agents, and pesticides and morphological and functional damage

TABLE 21.2 Olfactory Dysfunction Etiologies

Route	Example		References
Genetic	Kallmann's	Mutations resulting in aplasia or hypoplasia of olfactory bulb or neuronal tracts	Hummel et al. (1991); Karstensen and Tommerup (2012); Schwanzel-Fukuda et al. (1989)
Toxins	Industrial agents, metals	Morphological damage to either exposed olfactory epithelium and metal transport to olfactory bulb	Smith et al. (2009); Sunderman (2001); Upadhyay and Holbrook (2004)
Post viral	Rhinovirus	Direct attack on olfactory epithelium	Jafek et al. (2002); Seiden (2004); Suzuki et al. (2007)
Autoimmune diseases	Multiple sclerosis	Plaque formation in olfactory-related brain regions	Doty et al. (1998); Moscavitch et al. (2009); Zivadinov et al. (1999)
Neurodegenerative diseases	Alzheimer's	Nonfibrillar amyloid-β deposition and taupathies in the olfactory bulb	Wesson et al. (2010)

Adapted from Gaines, A.D., 2010. Anosmia and hyposmia. Allergy Asthma Proc. 31, 185–189; Harris, R., Davidson, T.M., Murphy, C., Gilbert, P.E., Chen, M., 2006. Clinical evaluation and symptoms of chemosensory impairment: One thousand consecutive cases from the Nasal Dysfunction Clinic in San Diego. Am. Journal Rhinol. 20, 101–108 .

(Smith et al., 2009; Sunderman, 2001; Upadhyay and Holbrook, 2004). Despite the rarity, it is important to note the permanence of damage-induced olfactory loss in cases where the tissue cannot fully recover. As an example, there is a case study of a head trauma patient who experienced anosmia following injury with an eventual shift to dysosmia (phantosmia) and reported the consistent detection of a "rotting garbage" odor (Kern et al., 2000). Tissue samples from this case indicated incomplete regeneration of the olfactory tissue following damage. There are also anecdotes that a change in smell or perception of "burning toast" indicates a stroke or heart attack, although this is not substantiated, but is not without some logic.

Natural aging and degeneration of sensory tissue is also a common source of olfactory loss. Whether or not increased damage over time or decreased ability to repair damage is the route of olfactory senescence has not been determined. Nevertheless, it has been documented that with increased age there is a higher incidence of olfactory dysfunction which supports a natural loss of sensory skill with an aging brain (Robinson et al., 2002; Wong et al., 2010). Functionally, elderly people show a reduction in abilities related to odor identification, memory, and sensitivity (Lehrner et al., 1999). In terms of pathological changes, little is known about neuronal modifications in healthy human aging and even less that is specific to the olfactory system (Dickstein et al., 2007). However, it is well known that older cohorts of individuals are more likely to be diagnosed with several neurodegenerative diseases that are also associated with, and likely causative of, olfactory dysfunction. Pervasive challenges in early diagnosis of neurodegenerative disease make it difficult to discriminate whether olfactory dysfunction in elderly populations represents healthy aging versus undetected early stage neurodegeneration.

1.3 Neurodegenerative Diseases and Loss of Olfaction

Prior to association with neurodegenerative diseases, little was published concerning olfactory inconsistency and disease. Investigations began in the industrial world as early as 1947 in relation to olfactory loss in varnishing industry workers, and following this work, subsequent industry related studies followed (Joyner, 1963). Along the same lines as chemical disturbances and olfaction, smoking and effects on olfactory deficit were also investigated (Joyner, 1964). Surprisingly, the first published association between olfactory dysfunction and neurodegenerative disease did not appear until 1975, and it described the symptom in patients suffering from Parkinson's disease (PD) (Ansari and Johnson, 1975). Since then, researchers have shown many cases of correlation between olfactory deficiency and neurodegenerative disease with varying severity (Table 21.3).

Olfaction–disease associations have resulted in a multitude of theories concerning not only the route and targets in the pathogenesis, but also the validity in identifying hyposmia and anosmia as disease precursors. Alzheimer's disease (AD), PD, Huntington's disease (HD), multiple system atrophy (MSA), and amyotrophic lateral sclerosis (ALS) all have associated olfactory loss in conjunction with cognitive symptoms and neuropathological markers. Interestingly, the diseases in question, perhaps excluding AD, also exhibit varying degrees and types of defective motor skills. The diseases also have specific cognitive and neuropathological markers (Table 21.4). Each condition is associated with the development of unique neuronal protein aggregates as well selective neuron loss. By investigating both the similarities and differences between these diseases, researchers are beginning to provide insight into their acquisition and progression (Leighton and Allison, 2016).

TABLE 21.3   Olfactory Impairment in Neurodegenerative Disease

Disease	Degree of olfactory impairment	References
Alzheimer's disease	severe	Devanand et al. (2000); Djordjevic et al. (2008); Doty et al. (1987)
Parkinson's disease	severe	Ponsen et al. (2009); Ross et al. (2008); Tissingh et al. (2001)
Huntington's disease	moderate	Barrios et al. (2007); Lazic et al. (2007)
Multiple system atrophy	moderate	Abele et al. (2003); Kovács et al. (2003)
Amyotrophic lateral sclerosis/motor neuron disease	mild	Hawkes et al. (1998); Sajjadian et al. (1994)
Amyotrophic lateral sclerosis – parkinsonism dementia complex of Guam	severe	Ahlskog et al. (1998)

Adapted from Hawkes, C.H., Shephard, B.C., 1998. Olfactory evoked responses and identification tests in neurological disease. Ann. N. Y. Acad. Sci. 855 (1), 608–615.

1.4 Disease Models and Olfactory Focus

Despite all the challenges, uncertainty and complexity of assessing patients for externally manifested symptoms such as cognitive, olfactory, and motor performance, such tests are relatively simple in contrast to those that define causality of disease progression and etiology, which is limited to biomarkers, noninvasive imaging, and postmortem histological analysis. As a result, researchers rely heavily on simulating these diseases in animal models to gain an understanding of pathogenesis, as well as to establish platforms for testing of potential treatments. Classically, studies have relied heavily on rodents due to their genetic and physiological similarities to humans. However, recent developments in zebrafish (*Danio rerio*) have allowed them to emerge as a viable complementary model of human neurodegenerative diseases. The zebrafish genome has been fully sequenced, being the most thoroughly annotated genome available after human and mouse. Many methods of genetic modifications are evolving quickly in zebrafish. Despite being nonmammalian, zebrafish have general vertebrate anatomical structures and many human genes have high sequence similarity and are functionally conserved. In addition, their relatively modest cost, high fecundity, and ability to breed throughout the year enable high throughput in vivo screening of phenotypes, which is invaluable to forward genetic and pharmaceutical studies. To facilitate their application, the scientific community has developed resources such as ZFIN: The Zebrafish Model Organism Database and

TABLE 21.4   Markers for Select Neurodegenerative Diseases With Olfactory Dysfunction

Disease	Neuropathological markers	Motor defects	Cognitive/psychological symptoms	References
Parkinson's	Lewy bodies; loss of dopaminergic neurons	Tremor; dyskinesia	Depression, apathy, anxiety	Poletti et al. (2012)
Alzheimer's	Amyloidβ plaques; neurofibrillary tangles; neuron loss	—	Dementia, memory loss, confusion paranoia, loss of language	Helmes and Østbye (2002)
Multiple system atrophy	Glial cytoplasmic inclusions; neuronal cytoplasmic inclusions; neuronal nuclear inclusions; regional neuron loss/atrophy	Dystonia, ataxia	Depression; visuospatial, constructional, verbal fluency and executive functional deficits	Balas et al. (2010); Boesch et al. (2002); Burn and Jaros (2001); Kawai et al. (2008); Nakazato and Suzuki (1996)
Huntington's	Atrophy and neuron loss; aggregates	Chorea, rigidity, dystonia	Visuospatial, memory, and prefrontal associated tasks dysfunction	Gómez-Tortosa et al. (1998); Gutekunst et al. (1999); Halliday et al. (1998); Walker (2007)
Amyotrophic lateral sclerosis	Bunina bodies, ubiquinated and Lewy body-like inclusions; motor neuron degeneration	Muscle atrophy and loss of movement; parkinsonian tremor associated with some subsets	Dementia associated with some disease subsets	He and Hays (2004); Ikemoto et al. (2000); Okamoto et al. (2008); Wilson et al. (2004)

Zebrafish International Resource Center for information sharing concerning zebrafish research to enhance knowledge and future discovery. For these reasons, zebrafish represent an alternative for fast and economical investigatory and therapeutic studies of neurodegenerative disease. The use of zebrafish continues to grow, with expanding examples of neurodegenerative disease models (Benedetti et al., 2016; Das and Rajanikant, 2014; Lattante et al., 2015; Li et al., 2015; Liu et al., 2015; Newman et al. 2014a; Sarath Babu et al., 2016; Schmid et al., 2013; Veldman et al., 2015; Yu et al., 2015). Through studies applying "omics" and systems biology approaches, rich information can be produced about how treatments of interest impact upon the diseases in question, allowing zebrafish studies to contribute to future modeling and serve as an effective comparator to mouse models.

Intriguingly, for the zebrafish models that exist, behavioral and physiological assays using olfaction are rare. However, this can also be said of rodent models; despite the prevalence of loss of olfaction in neurodegenerative diseases (Table 21.3), olfactory endpoints are also rare (Glasl et al., 2012; Ubhi et al., 2010). The techniques established for sensory assessment therefore hold a great deal of unexplored potential. This chapter describes the current methods used to model certain neurodegenerative characteristics in zebrafish and suggests novel applications for established techniques to enhance future studies.

2 BUILDING RELEVANT MODELS

In modeling human disease in animal models, the goal is to create a condition that recapitulates the symptoms, pathology, and/or molecular events of the disease as closely as possible. Techniques typically used in zebrafish exist in two distinct categories: genetic and nongenetic.

2.1 Genetic

As defects in genes or gene products are common contributors to the development of disease, studying the phenotypes that result from induced gain and loss of function can help elucidate normal gene activity and pathogenic events. Typically, genetic engineering to create animal models of disease has a necessary focus on familial forms of disease that are the minority of patient cases; the so-called "sporadic" forms of disease, that is, those with no clear genetic link or insult to begin the disease progress, are prominent in patients and remain very challenging to model in any animal system because they cannot (almost by definition) be predictably induced.

Here we describe methods for gene knockdown and overexpression in zebrafish, allowing tractable in vivo

assessment of disease-related outcomes. In the diseases of interest herein, the causal mutations typically lead to misfolding and aggregation of proteins, and animal modeling has focused on overexpression of aggregating disease-related gene variants. However, such protein misfolding also results in at least partial loss or subversion of protein function (Leighton and Allison, 2016), such that gene knockdown and mutagenesis approaches can inform disease etiology. We begin by discussing methods of transient gene knockdown and overexpression in zebrafish that are suitable for assessing embryos and larvae, and subsequently review methods enabling long-term and progressive genetic impacts.

Although many tools are currently available to zebrafish, not all of them have been applied to modeling the diseases in question, but in future will serve as novel approaches to existing problems [Skromne and Prince (2008) provides a review of genetic manipulation tools in zebrafish]. It is also noteworthy that the diseases in question are generally associated with aging, and are late-onset progressive diseases, whereas much of the technological innovation surrounding zebrafish genetics and drug screening has centered on early development as a natural consequence to zebrafish being originally introduced as a model of vertebrate development rather than degeneration. Thus, disease modeling in zebrafish may, in some instances, be most powerful when it is designed to represent in vivo modeling of physiological or molecular aspects of disease etiology, rather than end-stage degeneration and process that generally occur only in aged patients. Despite this history of zebrafish technologies having a focus on early development, several instances of modeling and measuring disease progression exist (DuVal et al., 2014; McGown et al., 2013; Ramesh et al., 2010), enabled by transgenesis and adapting the techniques from comparative fish physiology used to asses adults of other fish species.

2.1.1 Morpholinos

The use of antisense morpholino oligonucleotides (morpholinos) in embryonic zebrafish was first demonstrated to be an effective method of transient loss-of-function in 2000 (Nasevicius and Ekker, 2000). Morpholinos, as modified oligonucleotides, bind target mRNA and block translation, thereby knocking down gene expression; alternatively, morpholinos can induce abnormal intron inclusion or skipping and thus modify (abrogate) protein production. Embryos are injected at the one cell to four stage, and efficacy can last for up to 5 days but may vary with dose or transcript and/or protein kinetics (Bill et al., 2009). Along with established controls for efficacy, microinjection of synthetic target mRNA is coinjected to show phenotype rescue and control for morpholino specificity (Bedell et al., 2011; Bill et al., 2009), whereas delivery of null mutant mRNA should fail to

rescue the same phenotypes (Bedell and Ekker, 2015a). With the recent advent of practical targeted mutagenesis (see later), additional controls may be advisable such as demonstrating that the morpholino has no effect in zebrafish carrying null mutations in the target gene. However, this latter control requires fulfilling the rarely met assumption that phenotypes resulting from acute partial loss of function (via morpholino) will be similar to phenotypes resulting from long-term loss of function; in the latter, breeding strategies to recover mutants are obliged to select for individuals that compensate for lack of the gene product (Rossi et al., 2015). The temporary nature of this microinjection knockdown typically limits observations to early life stages, which can be challenging when attempting to model an adult-onset disease. Furthermore, genes of interest often have multiple roles in development, resulting in off-target effects presenting as lethality or physical abnormalities. Nevertheless, morpholinos provide insight into gene function through temporary deficiency. Studies discussed further on in this chapter have already used morpholinos to target certain genes related to neurodegenerative diseases and have been able to induce the desired phenotypes in zebrafish. However, a recent advancement in this method called a photomorpholino or photo-caging remains rarely applied to disease target genes. Photomorpholinos (sense and antisense) are a novel technique that allows gene function to be manipulated when desired through ultraviolet light exposure (Deiters et al., 2010; Tallafuss et al., 2012). Photomorpholinos can be controlled temporally and spatially and be as specific as single-cell activation (Shestopalov et al., 2007; Tallafuss et al., 2012). The targeting and temporal control available with a photomorpholino could provide interesting results if applied to specific brain structures such as the olfactory bulb. Another recent way to control spatial and temporal morpholino action is through electroporation (Cerda et al., 2006; Thummel et al., 2006). With this technique, targeted electrical current temporarily changed the permeability of cells, which allowed for the entrance of morpholinos into the organism. Although photo-caging and electroporation have not yet been widely applied to disease modeling, they have potential for future application. Until then morpholino-mediated knockdown in general is the most common approach of initiating loss-of-function in zebrafish.

An alternative to morpholinos that is on the horizon for gene knockdown in zebrafish is CRISPRi (CRISPR Interference). This requires delivery of guide RNA designed to bind the transcript of interest, along with CRISPR/Cas9 as per emerging methods targeted mutagenesis (see later), except that the Cas9 is catalytically inactive and instead of cutting DNA remains bound and represses translation (Larson et al., 2013; Long et al., 2015). This approach has potential to be an effective complement to morpholinos, as it will be an independent method to assess the effects of acute gene knockdown, though it will certainly require the thorough controls for efficacy and specificity that have come to be expected for assessing outcomes of morpholino delivery in zebrafish (Long et al., 2015).

2.1.2 mRNA Injection

In addition to being used as a rescue control for morpholino work, mRNA can be injected into embryos to investigate the transient effects of overexpression (Kelly et al., 1995). Gain-of-function is an effective approach for studying gene function by inducing expression spatially and/or temporally where it would otherwise not be present or be present at lower levels. Methods remain limited to microinjection, and as with morpholinos, the use of photo-caging and electroporation may be applied to enhance the spatiotemproal specificity of expression (Ando et al., 2001; Cerda et al., 2006; Skromne and Prince, 2008). This technique may also be used to investigate loss-of-function by comparing results of wild-type versus mutant or nonfunctional mRNA, or can be used to overwhelm endogenous gene expression via production of a dominant-negative protein (Koos and Ho, 1998). Both types of construct injection have been integral in the existing studies of neurodegenerative disease.

2.1.3 Transgenics

Animal modeling in neurodegenerative disease has frequently utilized overexpression of human disease-related gene variants. Transgenic zebrafish can be used in this fashion, and have essentially had exogenous genes added to their genome, and as such can be used for many different experimental applications such stable overexpression, dominant-negative mutation expression, and general analysis of gene regulation. Another common use is the expression of fluorescent proteins in cells of interest to allow monitoring of the health of specific cells or tissues following genetic or chemical treatment. Fluorescent reporters deployed in zebrafish can report a myriad of gene functions and cell states, such as abundance of intracellular signaling [retinoic acid abundance (Schilling et al., 2016) or Wnt signalling (Dorsky et al., 2002)], cell death (McCutcheon et al., 2016; van Ham et al., 2010), or genetically encoded calcium imaging to reveal neuronal activity (Fosque et al., 2015; Kim et al., 2014). Transgenesis can be induced in a variety of ways and manipulated for temporal and tissue specific expression; however, this chapter will not go into the specific mechanisms of action (Skromne and Prince, 2008). The three established methods for transgenic generation in zebrafish use microinjection or electroporation of either linearized DNA, meganuclease, or a transposon into single-cell embryos (Sager et al., 2010). The most commonly used method in zebrafish involves

microinjection of embryos with a plasmid DNA (construct) composed of the transposase mRNA and transposon (often Tol2) (Clark et al., 2011; Kawakami, 2004; Kawakami et al., 2004). The insertion can then be passed on to approximately 50% of the progeny. In the last few years, transposon-mediated transgenesis has allowed for effective use of Cre/lox constructs which is a critical technique in mice (Hans et al., 2009). Transgenesis has become a common method for disease model creation and several models currently exist pertaining to neurodegenerative conditions (Sager et al., 2010).

2.1.4 Zinc-Finger Nucleases and TALENs to Induce Mutations

Zinc-finger nuclease (ZFN)-mutagenesis is currently one of the few methods to create a genetic knockout or permanent mutation in zebrafish. The lack of an effective method is a significant disadvantage in comparison to rodent models, especially in relation to disease modeling where long-term mutation is relevant; however, ZFN is a potential technique in development. Embryos are injected mRNA which encodes DNA-binding proteins fused to endonucleases that cut DNA (Bandmann and Burton, 2010; Fleisch et al., 2013; Gupta et al., 2011; Meng et al., 2008). The proteins then create double strain breaks in the gene of interest to which they have been targeted. Cellular repair of the induced break is prone to error leading to a stable mutation (often a small insertion or deletion that causes a frame shift and truncated protein) in the appropriate gene. An alternative to ZFNs in zebrafish is TALENs (transcription activator-like effector nucleases) that work on a similar principle of creating DNA-binding domains to target a gene of interest, fused to endonuclease domains to cut the target DNA (Sun and Zhao, 2013). Both ZFNs and TALENs require substantial expertise and time to construct prior to delivery to zebrafish. Researchers worked to perfect and enhance the success rate of these costly method to expand its use (Foley et al., 2009; McCammon et al., 2011; Pillay et al., 2013); however, the technology has been supplanted by CRISPR/Cas9 which is easier to deploy and more efficient.

2.1.5 CRISPR/Cas9 to Induce Mutations

The approach to targeted mutagenesis in zebrafish using CRISPR/Cas9 can be very similar clustered regularly interspaced short palindromic repeats (CRISPR)/ CRISPR.

CRISPR-associated protein 9 type II (Cas9) system (Armstrong et al., 2016) can be very similar to that described earlier using ZFN or TALENs. In each instance one can target a gene of interest to induce a cut in that DNA sequence, and repair of said cut is error-prone, thus leading to frame shifts and nonfunctional protein products. The CRISPR/Cas9 protein complex is directed to the target DNA by a guide RNA (gRNA) that is complementary to the DNA of interest, enabling cutting of the target DNA. The appeal of CRISPR/Cas9 is that, once operational in a laboratory, it is rather straightforward to generate gRNAs designed to cut the target DNA, and several sites can simultaneously be targeted within many genes to increase success rates and/or produce larger mutations such as exon deletions and clear null alleles. Although producing gRNAs is straightforward for molecular biologists accustomed to such work, it should be noted that the effort to generate a stable mutant line remains resource-intensive with respect to time, husbandry space, and technical work. Regardless, the CRISPR/Cas9 system has already produced intriguing mutants in zebrafish (Hruscha et al., 2013; Hwang et al., 2013; Jao et al., 2013). Caution is warranted with respect to whether mutations produced are null alleles, as in some instances insertions or deletions created in the target gene may not disrupt the gene in a straightforward manner; downstream translational start sites, phantom exons, and copy number variants all have the potential to confound the approach. Furthermore, specificity of the mutagenesis methods must be assumed to be imperfect and creating other mutations throughout the genome, such that any phenotypes observed must be proven to be causally linked to the engineered mutation of interest. Finally, genetic compensation for mutations may be substantial in zebrafish (Bedell and Ekker, 2015b), wherein acute gene knockdown produces phenotypes that are demonstrably specific, yet mutations in the same gene produce no overt phenotype and confound analysis.

2.1.6 Zebrafish Knock-In

Until recently a major limitation to disease modeling in zebrafish was the inability to edit DNA as is done to successfully model disease genetics in other model systems. The introduction of targeted mutagenesis to zebrafish, especially the efficient CRISPR/Cas9 system, promises to enable genome editing in zebrafish. Briefly, one delivers CRISPR/Cas9 with targeted gRNA as described earlier to induce cuts in a target gene; alongside this one delivers a synthetic section of DNA with high percent identity to the region being altered, to serve as a template that is used to repair the DNA. The synthetic donor DNA template can be manipulated to encode various disease-related mutations or other genetic elements, promising great flexibility in how diseases are modeling in zebrafish. The approach has already allowed engineering of several unique zebrafish strains (Armstrong et al., 2016; Auer et al., 2014; Bedell and Ekker, 2015b; Irion et al., 2014; Kimura et al., 2014).

2.1.7 Gene Targeting

Due to the current limitations of morpholinos and ZFNs, another method has been developed in an attempt to obtain a stable genetic knockout in zebrafish. A strategy

called TILLING (Targeting Induced Local Lesions in Genomes) combines chemical mutagenesis (e.g., N-ethyl-N-nitrosourea) with high throughput genetic screening to identify animals with the mutations of interest (Wienholds et al., 2003). This protocol has successfully created genetic knockouts in zebrafish modeling fragile X-syndrome and its success hints at application to neurodegenerative genes of interest (den Broeder et al., 2009). TILLING provides an attractive knockout alternative to ZFNs.

2.2 Nongenetic

Although genetic manipulation is very effective at inducing the appropriate defects, there are certain compounds that mimic the neurological loss and the locomotion phenotypes specific to the diseases in question. Further merit to this method is supported by reported instances of neurodegenerative disease correlated with toxic exposure (Gorell et al., 1998; Li et al., 2014; Smith et al., 2009). Treatments that evoke responses can be carried out via environmental contact (aqueous solution), ingestion, or injection. The methods of treatment can potentially yield different or off-target results, and therefore the likely mode of exposure for humans as well as the most relevant induced phenotype must be taken into consideration when evaluating these models. The neurological disorders discussed in this chapter are commonly modeled in this fashion and successfully express appropriate disease characteristics (Anichtchik et al., 2004; Bretaud et al., 2004; Lee and Freeman, 2016; McKinley et al., 2005; Pinho et al., 2016). Even so, there are some compounds that have been tested in rodents that have yet to be tested on zebrafish (Beal et al., 1991).

2.3 Genetic and Nongenetic Summary

By attempting both genetic and chemical types of models separately or in concert, researchers gain not only more information about pathogenesis, but also potential therapeutic and preventative measures. The methods described here have been applied in some capacity to investigate zebrafish olfactory and neuromuscular systems. For example, transgenic expression of fluorescent proteins has been used to visualize motor and olfactory neurons (Higashijima et al., 2000; Yanicostas et al., 2009). Direct modification of these systems helps elucidate functional and developmental aspects that may be relevant to disease pathogenesis. However, in terms of modeling neurodegenerative diseases, studies tend to target already suspected genetic and chemical links to replicate the symptoms observed in humans. As motor and olfactory deficits are characteristic symptoms of the diseases discussed here, it is important to examine related endpoints in animal models.

3 OLFACTORY–NEUROMUSCULAR DISEASES

3.1 Parkinson's Disease

The first official documented study on PD was described as a shaking palsy and is accredited to James Parkinson's essay in 1817, which described several case studies (Parkinson, 2002). Over time, closer examination of symptomatic and postmortem patients led to an array of recognizable disease characteristics. PD is now classified as a progressive disease largely affecting the motor system with generally middle-age onset, although incidence increases with age (Dauer and Przedborski, 2003). Currently, PD is the second most common neurodegenerative disease.

The hallmark physical manifestation of PD is tremor or shaking palsy. Although it is easy to identify when present, clinical expression between patients is variable and may or may not appear in conjunction with bradykinesia (slowness of movement), rigidity, and postural difficulties. As a result, a PD-specific tremor is classified as such only when associated with a positive neurologically based diagnosis (Dauer and Przedborski, 2003; Deuschl et al., 1998). The neurological traits primarily involve loss of nigrostriatal dopaminergic (DA) neurons in the substantia nigra leading to dopamine depletion in the striatum and the development Lewy bodies (abnormal intraneuronal protein aggregates). Although DA neuron loss is considered the hallmark of PD, neurodegeneration and Lewy bodies affect other parts of the brain including the amygdala and the olfactory tract and bulb (Braak et al., 2003). Mitochondrial dysfunction, with respect to complex I in particular, in the affected neuronal areas has also been linked to PD and may be linked to both sporadic and familial causes of PD (Büeler, 2009).

Olfactory impairment in PD patients was first noted in 1975, and it has been shown repeatedly that defects in sense of smell can be severe, stable, and may occur in PD cases as frequently as tremor (Ansari and Johnson, 1975). Those affected have impairments in odor detection (thresholds), discrimination, and identification, although it is important to note that with reduced detection ability, discrimination and identification also prove more challenging (Boesveldt et al., 2008; Tissingh et al., 2001). Since discovering the link between compromised olfaction and PD, impaired smell has been used as an early indicator of PD, and has been suggested as a valuable screening tool because it can predate clinical PD by approximately 4 years in men (Ross et al., 2008, 2012). First-degree relatives of individuals with PD that had idiopathic olfactory dysfunction had 10% increased chance of developing the disease (Ponsen et al., 2004, 2009). Postmortem studies of olfactory bulb and tract in patients showed Lewy bodies to be most numerous in the anterior olfactory nucleus (AON), which is an essential brain structure for odor processing (Hawkes et al., 1997).

PD patients may also have an olfactory bulb volume ~70% of normal (Brodoehl et al., 2012). Lewy bodies localized to olfactory tissue in presymptomatic cases of PD further support olfactory function as a preliminary test for diagnosis (Dickson et al., 2008; Ross et al., 2006).

The etiology of PD can be case specific, and as with most diseases, there are idiopathic and familial examples (Dauer and Przedborski, 2003). Numerous genetic mutations have been found in PD patients, which have led to focused genetic investigation. Furthermore, certain pesticides such as 1-methyl-4-phenyl-1,2,3,6-tetrahydropyridine (MPTP), paraquat, and rotenone have been shown to induce PD-like phenotypes in humans and animal models, although evidence is insufficient to conclude that exposure is the definitive cause of sporadic PD. Even so, several studies suggest that people living in rural environments with increased exposures to such chemicals have a greater chance of developing PD (Gorell et al., 1998; Priyadarshi et al., 2001). The suspected etiologies have led to studies pertaining to disease-related genes, toxins, and these routes in combination (Table 21.5).

TABLE 21.5 Zebrafish Models of Parkinson's

Target	Method	Phenotype	References
PARKIN	Morpholino/gripNA™ knockdown	Increased cell death post proteotoxic stress (heat shock) Conflicting evidence concerning mitochondrial dysfunction and DA neuron loss	Fett et al. (2010); Flinn et al. (2009)
	Transgenic	Human Parkin overexpression increases resistance to proteotoxic stress (heat shock)	Fett et al. (2010)
	Morpholino knockdown and MPP+ treatment	Increased damage/susceptibility to MPP+	Flinn et al. (2009)
PINK1	Morpholino knockdown	Changes in DA neuron axonal projections and expression in ventral diencephalon; TH positive (DA) diencephalic neuron loss; reduced locomotion behavior; mitochondrial dysfunction and increased ROS	Anichtchik et al. (2008); Sallinen et al. (2010); Xi et al. (2010)
	Morpholino knockdown and MPTP treatment	Increased damage/susceptibility to MPTP neurologically and behaviorally	Sallinen et al. (2010)
PARLa	Morpholino knockdown	Decreased survival; altered DA neurons	Noble et al. (2012)
PARLb	Morpholino knockdown	Decreased survival; altered DA neurons	Noble et al. (2012)
DJ-1	Morpholino knockdown	DA neuron loss with cellular stress (H_2O_2 and MG132)	Bretaud et al. (2007)
LRRK2	Morpholino knockdown	Conflicting evidence for DA neuron loss and reduced locomotion response	Ren et al. (2011); Sheng et al. (2010)
UCH-L1	Transgenesis	UCH-L1 promoter driven GFP expression	Son et al. (2003)
SNCA	Transgenesis	Overexpression of human α-syn induces deformity, lethality, and aggregates	Prabhudesai et al. (2012)
DA neurons	MPTP	Loss of DAT positive cells; reduced DA neurons; decreased locomotion behavior; increased ventilation; increased pigmentation	Bretaud et al. (2004)
	MPTP with DAT morpholino knockdown	Reduced toxin induced damage	McKinley et al. (2005)
	MPTP with DAT inhibitors	Reduced toxin induced damage	McKinley et al. (2005)
	MPP+	Loss of DAT positive cells	Lam et al. (2005)
	Paraquat	No effect	Bretaud et al. (2004)
	Rotenone	No effect (low dose); increased morphological changes and lethality (high dose)	Bretaud et al. (2004)
	Paraquat and rotenone	No effect (low dose); increased morphological changes and cardiovascular defects (high dose)	Bretaud et al. (2004)
	6-ODHA	Decreased DA and noradrenaline concentrations in brain; decreased locomotion	Anichtchik et al. (2004)

3.1.1 PD Genetic Models

Attempts to create a genetic PD model have been centered on functional investigations of mutations found in patients. The genes of interest include Parkin, phosphatase and tensin homolog-induced kinase1 (PINK1), presenilins-associated rhomboid-like (PARL), DJ-1, leucine-rich repeat kinase 2 (LRRK2), Ubiquitin C-Terminal Hydrolase-L1 (UCH-L1), and α-synuclein (SNCA/α-syn). There have been several attempts to modify expression of these genes in an effort to induce classical PD symptoms such as DA neuronal loss, formation of Lewy bodies, mitochondrial dysfunction, and locomotion abnormalities. Olfactory function has not yet been tested in the existing zebrafish models, but may serve as an important endpoint in future experiments.

3.1.1.1 PARKIN

Parkin mutations have been linked to both early and late-stage onset of PD with greater frequency in young cases (approximately 20 years of age) (Lücking et al., 2000). In vitro, Parkin functions as an E3 ubiquitin protein ligase contributing to protein degradation and when mutated is potentially involved in protein aggregation (Büeler, 2009; Periquet et al., 2005; Shimura et al., 2000). The current model predicts disruption of Parkin-mediated protein degradation either by genetic mutation or cellular stress, which leads to accumulation of Parkin substrates, impaired presynaptic function in DA neurons, increased dopamine levels and subsequent neurodegeneration (Imai and Takahashi, 2004). Parkin has also been shown to play a role in mitochondrial protection from oxidative stress and Parkin-deficient mice have had decreased expression of mitochondrial Complex I and reduced mitochondrial function (Büeler, 2009; Palacino et al., 2004). The three studies involving modification of *Parkin* expression in zebrafish have provided conflicting results. Zebrafish express a *Parkin* ortholog which has 62% sequence identity to human *Parkin* and up to 87% identity in functional domains (Fett et al., 2010; Flinn et al., 2009). One study reported that morpholino-induced blockage of *Parkin* in zebrafish was not associated with any effect on gross morphology, number of DA neurons, tyrosine hydroxylase positive (TH+) cells (a conversion enzyme for the dopamine precursor) or mitochondrial integrity (morphology or membrane potential). Despite the lack of physical change, embryos were more susceptible to cell death induced by proteotoxic stress (heat shock). In support of this finding, it was also observed that when heat shock was applied to transgenic zebrafish expressing human *Parkin*, embryos showed greater resistance to cellular stress (Fett et al., 2010). A separate morpholino investigation conflicted with the aforementioned study and found Parkin knockdown decreased mitochondrial Complex I activity and potentially causing

loss of diencephalic DA neurons. Differences between the studies may be attributed to morpholino specificity and effectiveness because the experiment with negative results used gripNAs antisense oligonucleotides as opposed to classical morpholinos (Fett et al., 2010). Further studies will need to be conducted to clarify Parkin deficiency in zebrafish.

3.1.1.2 PINK1

PINK1 encodes a mitochondrial serine/threonine protein kinase expressed not only in many brain regions, including the substantia nigra, but other tissue as well (Gandhi et al., 2006). Mutations in this gene have been associated with early-onset parkinsonism in humans (Bonifati et al., 2005). PINK1 has an established link with mitochondrial function, and its deficiency in both drosophila and mice has led to mitochondrial dysfunction and specific reduction of Complex I activity (Morais et al., 2009). In addition, in mouse cell cultures, PINK1 deficiency affects mitochondrial membrane potential and fragmentation, and increases the reactive oxygen species (ROS) in substantia nigra DA neurons (Wang et al., 2011). A study in PINK1 knockout did not yield the expected deficiencies in mitochondria and DA neurons; however, mice did exhibit classical PD precursor symptoms including impaired olfaction (Glasl et al., 2012). In zebrafish PINK1 protein has only 57.8% identity with humans, but the known functional domains are highly conserved (Sallinen et al., 2010). Morpholino knockdown of PINK1 in zebrafish was associated with alterations in DA neuron axonal projections and expression patterns in the ventral diencephalon paired with reduction in locomotion behavior and response (Xi et al., 2010). Other PINK1 knockdown studies also showed reduced number of DA TH+ neurons in the diencephalon (Anichtchik et al., 2008; Sallinen et al., 2010). Partial phenotypic rescue in knockdown fish with human PINK1 mRNA further validates zebrafish as an appropriate model by way of functional overlap between species (Anichtchik et al., 2008). Transient PINK1 knockdown caused a decrease in mitochondrial potential and increased ROS levels. Successful induction of DA neuron loss, locomotion deficits, and mitochondrial dysfunction supports the use of zebrafish models of PINK1-deficient PD. Nevertheless, the model can be improved by additional testing particularly by assessing olfactory function due to its importance as a symptom and marked impairment in the mouse model.

3.1.1.3 PARL

The PARL gene is more recently associated with PD and therefore less commonly studied to date (Shi et al., 2011). Whole organism experiments with PARL have been limited, but the use of cell lines has established a link between PARL, PINK1, and Parkin. It is

proposed that PARL is required for proper localization of PINK1 which, in turn, is necessary for Parkin recruitment for mitophagy (Shi et al., 2011). If true, it implies that PARL silencing may result in PINK1- and Parkin-related dysfunction in PD. Zebrafish have two PARL orthologs, Parla and Parlb, with 67 and 55% amino acid sequence identity compared to humans (Noble et al., 2012). When blocked with morpholinos, Parla- and Parlb-deficient larvae have reduced survival, increased cell death, and altered DA neuron phenotypes. Of note is that this study made effective use of a dopamine transporter (DAT)-driven green fluorescent protein transgenic line Tg(dat:EGFP) to mark DA neurons and effectively observe induced phenotypes. Both neuronal and lethality effects were rescued by coinjection of human PARL and zebrafish PINK1 mRNA separately. These results support functional overlap between human and zebrafish PARL and also the projected associations between PINK1 and PARL (Noble et al., 2012).

3.1.1.4 DJ-1

DJ-1 mutations and downregulation of DJ-1 mRNA and protein have been found in brain tissue from several PD cases (Bonifati et al., 2003; Kumaran et al., 2009). The normal function of the DJ-1 gene is not well. It was originally found as an oncogene, but in PD it is suspected to be critical to oxidative stress response (Kumaran et al., 2009). DJ-1 knockout mice showed progressive hypoactivity and gait abnormalities with age but no DA abnormalities (Chandran et al., 2008). Zebrafish DJ-1 is 83% identical and 89% similar to humans and colocalizes with TH+ neurons (Bai et al., 2006). A single study concerning DJ-1 deficiency in zebrafish showed that morpholino knockdown does not affect DA neuron numbers, but does cause upregulation of apoptosis regulator genes and increased embryo sensitivity to oxidative stress (H_2O_2 exposure and proteasome inhibition). With oxidative stress, there was an observed DA neuronal loss. Despite positive results, these studies have yet to be replicated and future studies should endeavor to include motor and olfactory assays to evaluate this model.

3.1.1.5 LRRK2

Since 2004, studies have found PD patients with mutations in the LRRK2 gene, with mutation frequencies ranging from 1.6% to 40%, depending on the type of mutation and the demographic analyzed (Gilks et al., 2005; Sharma et al., 2011). LRRK2 function is not fully understood; however, it has ubiquitous neuronal expression and known associations with cellular stress and neuronal maintenance by regulating neurite growth (Iaccarino et al., 2007; MacLeod et al., 2006; Sharma et al., 2011). In vivo models for these mutations are limited; however, in the few mouse studies conducted, there have been no DA neuron loss or protein aggregation (Yue, 2009). There

is reasonable amino acid sequence identity between zebrafish and humans with the highest conservation in the kinase domain (71%). Studies in zebrafish conflict as to whether LRRK2 knockdown results in loss of DA neurons and movement deficits (Ren et al., 2011; Sheng et al., 2010). One study demonstrated loss of TH+ neurons and severe defects with LRRK2 morpholino knockdown (Sheng et al., 2010). In addition, when morpholinos targeted the WD40 domain of LRRK2 specifically, survival was improved and larvae showed DA neuron loss, disorganization of axonal tracts, and locomotion irregularities. Functional overlap was suggested to be conserved due to phenotypic rescue by human LRRK2. Despite these promising results, another more recent study used the same methods and failed to replicate the neurological and behavioral phenotypes (Ren et al., 2011). Nevertheless, the potential for the creation of PD-like characteristics encourages further investigation.

3.1.1.6 UCH-L1

UCH-L1, another source of PD mutations, is involved in the ubiquitin-dependent proteolytic pathway and has been identified as a component of Lewy bodies in PD patients (Leroy et al., 1998). Its role in pathogenesis is proposed to be improper function of protein processing and degradation as well as suspected interaction with α-synuclein, another major component of neuronal aggregates (Leroy et al., 1998; Yasuda et al., 2009), and Parkin (McKeon et al., 2015). The function of UCH-L1 is not fully understood in vivo, but is a neuronal deubiquitinating enzyme (McKeon et al., 2015). Mice lacking UCH-L1 have demonstrated loss of DA neurons and have movement defects reminiscent of PD (Setsuie et al., 2007). There is a UCH-L1 homolog in zebrafish which encodes a protein that has 79% similarity with humans and is coexpressed with TH+ cells in the ventral diencephalon during embryonic development (Son et al., 2003). Experiments on gain or loss of function in zebrafish have not yet been performed, but they have been able to confirm expression and have developed a tool for future studies. Researchers have isolated a promoter containing region of UCH-L1 and combined it with a transgene encoding GFP (Son et al., 2003). The result was fluorescent marking of UCH-L1's neuron-specific expression. Effective transgenesis with this tissue-specific promoter will be of benefit for investigation of UCH-L1 and other coexpressed PD genes.

3.1.1.7 α-SYN

The α-syn gene (SNCA) encodes for a presynaptic protein involved in synaptic plasticity and has found to be mutated in some PD cases (Polymeropoulos et al., 1997). As previously mentioned, α-syn protein is a major component of Lewy bodies in PD patients (Spillantini et al., 1998). Transgenic mice overexpressing

human α-syn had α-syn containing inclusions along with DA neuron loss and motor defects, which indicates α-syn is an important target in modeling and therapeutics (Masliah et al., 2000). Investigations of the protein in zebrafish have been limited. Zebrafish express their own family of synucleins *sncga*, *sncgb*, and *sncb*, which each have different embryonic spatial and temporal expression (Sun and Gitler, 2008). To date these synucleins have not been investigated further. Instead, fish have been modeled to overexpress human α-syn resulting in high frequencies of mortality and deformity (Prabhudesai et al., 2012). Gain and loss of function of α-syn in zebrafish is needed to fully evaluate this organism to model this gene. Modification of endogenous synucleins may prove more effective.

3.1.2 PD Toxin-Induced Models

There are several toxins that due to their correlation between exposure and development of PD have been used in attempts to mimic PD characteristics. The most common ones are as follows: rotenone, paraquat, 1-methyl-4-phenyl-1,2,3,6-tetrahydropyridine (MPTP), and 6-hydroxydopamine (6-ODHA). These compounds are used to induce DA neuronal loss and their efficacy has been demonstrated in rodent models. Application of these toxins to zebrafish is relatively novel; however, there have been some published results.

Rotenone, commonly used as a pesticide, is toxic to humans and animals by way of mitochondrial disruption. In rats and mice, it has been shown to selectively bind mitochondrial Complex I and induce nigrostriatal DA neuron loss and neuronal cytoplasmic inclusions (NCIs) (Alam and Schmidt, 2002; Betarbet et al., 2000; Sherer et al., 2003). Treated animals also developed poor posture, rigidity, and demonstrated hypokinetic behavior paw shaking resembling a tremor, akin to PD patients. Unfortunately, in adult zebrafish a 4-week exposure to rotenone did not replicate these neurological and behavioral defects (Bretaud et al., 2004). Negative results were also seen in larval fish raised in rotenone solutions although higher doses (50 μg/L) did increase morphological abnormalities and lethality (Bretaud et al., 2004). Increased exposure length in future investigations may successfully induce PD-like symptoms. Alternately, perhaps fish will need to be exposed using a different route such as via intraperitoneal injections.

Similar to rotenone, paraquat acts via inducing oxidative to stress and is normally used as a herbicide. In mice paraquat treatment has caused nigral DA neuron loss as well as upregulation and aggregation of α-synuclein (Manning-Bog et al., 2002; McCormack et al., 2002). Despite the effective modeling in mice, in both adult and larval zebrafish paraquat exposures have not resulted in any locomotion or DA neuron loss (Bretaud et al., 2004). However, this investigation did

not examine α-synuclein expression levels or protein aggregation, so some effects may have been overlooked. The joint exposure of larval fish to high concentrations of paraquat and rotenone did increase incidence of morphological abnormalities and cardiovascular defects (Bretaud et al., 2004).

MPTP is a neurotoxin that when converted to MPP+ via monoamine oxidase B (MAO-B) has direct toxic effects on mitochondria that leads to cell death. In zebrafish MAO activity has been observed in general in the telencephalon and the diencephalon with weak action in the olfactory bulb (Anichtchik et al., 2006). MPTP exposure in adult zebrafish was able to reduce locomotion and cause increases in both ventilation and pigmentation; however, DA neurons were unaffected which is potentially due to the length of exposure (Bretaud et al., 2004). In contrast, larval fish, however, with exposure both during and after DA neuron development showed DA-specific neuron loss, decreased mobility, and diminished touch response (Bretaud et al., 2004; Lam et al., 2005). In adult zebrafish, exposure was associated with decreased movement and changes in a suite of genes and proteins (Sarath Babu et al., 2016). MPTP damage was prevented in the presence of a MAO-B inhibitor, while MPP+ effectively reduced DA neurons, suggesting that the precursor is metabolized to MPP+ in zebrafish by a mechanism similar to mammals (Lam et al., 2005). Recently, it was shown that melatonin can also counteract the effects of MPTP in the olfactory bulb (Díaz-Casado et al., 2016). The confirmed reduction of DA neurons in the olfactory bulb supports investigation into olfactory dysfunction in this model. MPTP uptake via DAT as in mammals was confirmed in zebrafish with reduced MPTP neurotoxicity when paired with DAT pharmaceutical inhibition or morpholino-mediated knockdown (McKinley et al., 2005). MPTP is currently the most effective method of inducing DA neuron loss in zebrafish and consequently it has been paired with genetic models to test for increased susceptibility to the toxin. Morpholino knockdown of both Parkin and PINK1 paired with MPTP exposure demonstrated enhanced neuronal loss and decreased movement behavior (Flinn et al., 2009; Sallinen et al., 2010).

6-ODHA is a neurotoxin that accumulates in neuron terminals after being taken up by DATs or noradrenaline transporters and causes DA and noradrenergic neuronal damage. Compared to MPTP, 6-ODHA causes less specific damage and is not used as frequently in models. Nevertheless, it has been tested in zebrafish. Intramuscular injections of the compound cause decrease in DA and noradrenaline concentrations in the brain, but no changes in TH levels or patterning of TH+ cells. 6-ODHA was also correlated with changes in locomotion activity, including decreased swimming distance and increased turn angle (Anichtchik et al., 2004).

Overall, genetic, toxic, and combination of zebrafish models are arguably still in the early stages for PD; however, results are promising. In most cases researchers have effectively analyzed neuron condition and locomotion defects. There remains a great deal of potential in future studies for electrophysiology and olfactory response. For example, a study may examine changes in odorant activation of neurons at the levels of the olfactory epithelium and bulb following exposure to chemical compounds. In the same respect, if olfactory tissue is found to be functional, behavioral analysis of odorant responses can determine whether fish have impaired capacities for odor identification and interpretation.

3.2 Amyotrophic Lateral Sclerosis

ALS, also known as Lou Gehrig's disease, involves progressive loss of both upper and lower motor neurons, and manifests as a subsequent impaired capacity to move and perform basic functions such as swallowing and breathing. The disease was first described in scientific literature by Jean-Martin Charcot in 1869. ALS is a devastating disease that limits survival to 5 years for 80% of diagnosed patients; 90% of classical ALS cases can be attributed to sporadic acquisition (Kiernan et al., 2011). Diagnosis can be a challenge, not only due to the variation between individual patients, but also due to the subtypes of ALS. ALS not only exhibits in its classical form, but also exists with dementia (ALS-D) and as a Guam-specific ALS-Parkinsonism-Dementia Complex (ALS-PDC). The latter subtype involves Parkinsonian tremors and Alzheimer's-like cognitive dysfunction along with the motor neuron degeneration (Ikemoto et al., 2000).

Pathologically, there are several types of inclusions linked to ALS, but the most specific is known as the Bunina body (small eosinophilic granular inclusions) found within cytoplasm or dendrites (Kato, 2008; Okamoto et al., 2008). Skein- and Lewy body-like inclusions that stain positively for ubiquitin have also been identified in some ALS patients that had severe neuronal loss in the spine and medulla (Ikemoto et al., 2000; Shibata et al., 1994; van Welsem et al., 2002). Other neuronal aggregates of basophilic and hyaline bodies have also been observed, but these are less specific to ALS (Ikemoto et al., 2000; Kato, 2008; Wood et al., 2003). In some cases, neurofibrillary tangles (NFTs) have been noted in patients with ALS-PDC (Ikemoto et al., 2000).

There is some controversy over symptomatic olfactory loss in ALS. Although ALS-PDC has confirmed association with olfactory impairment, the link to classical ALS patients is an area of contention (Doty, 1995). Although there have been studies that find no correlation, many studies argue that chemosensory function is affected; however, it is mild in comparison to other neurodegenerative diseases (Ahlskog et al., 1998; Doty, 1995;

Elian, 1991; Hawkes and Shephard, 1998; Sajjadian et al., 1994). The variation in results could be due to variation between cases in terms of severity and perhaps even the type of ALS. Few studies have endeavored to investigate it as a disease marker of the symptom in terms of disease time course. Long-term case studies in conjunction with postmortem olfactory structure analysis and testing in ALS models will need to be conducted to confirm associations.

The animal models for ALS to date have attempted to replicate ALS phenotypes by manipulating genes found to be mutated in diseased patients. Specific mutations in ALS2, the gene encoding aslin, led to juvenile onset of ALS, which will not be discussed in this chapter (Chandran et al., 2007). Within adult cases of ALS, three main genes have been identified: superoxide dismutase (SOD1), TAR DNA-binding protein (TARDBP), and fused in sarcoma (FUS) (Rosen et al., 1993). C9orf72 is a gene more recently found to be causal of ALS (DeJesus-Hernandez et al., 2011; Renton et al., 2011), and bone morphogenetic protein (bmp) signaling pathway genes may act as modifiers on disease severity (DuVal et al., 2014). There is little evidence to suggest that exposure to chemicals enhances the risk of developing ALS and therefore it is not generally used in modeling (Weisskopf et al., 2009). However in ALS-PDC, there is a dominating theory that neurotoxin beta-methylamino-L-alanine (BMAA), from the local cycad seed, induces the disease (Cheng and Banack, 2009; Wilson et al., 2004). As a result there have been specific models that use it to induce disease-like symptoms (Ahlskog et al., 1998; Wilson et al., 2002, 2004).

3.2.1 SOD1

Many different missense mutations in SOD1 occur in ALS patients (Gamez et al., 2006; Rosen et al., 1993). SOD1 has also been found within Lewy body-like inclusions of ALS patients (Shibata et al., 1994). In transgenic mice expressing mutations in SOD1, it was shown that SOD1 was crucial to mitochondrial function and that ubiquitous but not neuron specific dysfunction leads to ALS-like phenotypes (Mattiazzi et al., 2002). Zebrafish SOD1 has a 77% sequence identity to humans and has already been examined in several models. Overexpression of mutant SOD1 in zebrafish through construct injection can induce abnormal motor neuron axonal branching and length (Lemmens et al., 2007; Pramatarova et al., 2001). Another study generated fish that expressed mutant zebrafish SOD1 along with fluorescent protein DsRed driven by heat shock protein 70 (to show transgene expression) (Ramesh et al., 2010). Both larval and adult fish from this transgenic line had abnormal neuromuscular junctions and spinal cord motor neuron loss in adults (Ramesh et al., 2010. This study is of particular interest because of its use of a swimming tunnel to test motor abilities at several different ages

in transgenic fish. Swim tunnels are used to assess the physical endurance of a fish by monitoring its capacity to swim against applied water currents (Brett, 1964; Gilbert et al., 2014; Tierney, 2011). Remarkably, these fish showed progressive decline in swim performance with increased age. Mutant models also displayed serious decreases in movement and some instances of paralysis in late stages, with overall exhibiting a shorter lifespan. In this model, the worsened performance correlative with aging best replicates the progressive trait of ALS. Additional models of ALS have identified SOD1 mutants using the TILLING strategy or transient transgenesis, and they also assessed swimming though using less traditional measures of fish swim physiology (Da Costa et al., 2014; Sakowski et al., 2012). Other models of neuromuscular degeneration would benefit from following this example of longitudinal testing of motor endurance.

3.2.2 TARDBP and FUS

Both the TDP-43 protein, encoded by TARDBP, and FUS mutations have been reported in ALS patients (Kabashi et al., 2008; Kwiatkowski et al., 2009; Neumann et al., 2006; Vance et al., 2009). These proteins have also been identified as components of ALS aggregates (Arai et al., 2006; Deng et al., 2010). Overexpression of mutant human TDP-43 in rats led to motor neuron loss and reduced movement capacity; however, TDP-43 inclusions were not observed, which indicates the aggregates are not essential for neuron death (Huang et al., 2012). Similar to TDP-43 mutants, rats overexpressing mutant human FUS had motor neuron degeneration accompanied by progressive paralysis and ubiquitin accumulation (Huang et al., 2011). In terms of modeling in zebrafish, there are already several examples of successful functional disruption. Overexpression of several different mutant human TARDBP (and therefore TP-43) in larvae resulted in deficits in swimming response as well as decreased motor neuron length and increased branching (Kabashi et al., 2010). Morpholino-induced knockdown of TARDBP resulted in the same motor neuron phenotype and defective swim response which suggests potential pathogenesis via toxic gain of function and as TARDBP deficiency (Kabashi et al., 2010). Knockdown of FUS also resulted in abnormal motor behavior and reduced outgrowth of motor neuron axons (Kabashi et al., 2011). Both FUS-deficient phenotypes were rescued by human FUS mRNA (Armstrong and Drapeau, 2013). Targeted mutagenesis to induce FUS or TARDBP mutations have exhibited some ALS-related phenotypes (Armstrong et al., 2016). CRISPR/Cas9 knockins into zebrafish SOD1 have been remarkably effective in modeling disease-related mutations and will be intriguing models for determining what phenotypes, if any, these mutations cause in zebrafish (Armstrong et al., 2016).

To investigate the potential interactions between SOD1, TARDBP, and FUS, a study used zebrafish to conduct a multigenetic analysis (Kabashi et al., 2011). FUS mRNA coinjection rescued TARDBP knockdown; however, the inverse rescue was not observed, indicating an in vivo interaction in which FUS is the downstream effector. A particularly intriguing finding was the enhanced neurological phenotypes and locomotion deficits observed in both double mutant mRNA expression and double knockdown experiments with SOD1 and either FUS or TARDBP. Although ALS-like symptoms were worsened by doubled genetic defects, it was suggested that SOD1 acts independently from FUS and TARDBP through lack of phenotypic rescue.

Although SOD1, TARDBP, and FUS remain the main focus for investigations, a study on mutations in elongator protein 3 (ELP3) in ALS patients and subsequent examination of EPL3 knockdown zebrafish had unique findings (Simpson et al., 2009). EPL3 has a 91.3% identity to humans, which strongly supports the model validity for investigation of this protein. Morpholino injection resulted in abnormal branching and length of motor axons reminiscent of the SOD1-, TARDBP-, and FUS-deficient phenotypes. Future EPL3 studies may find it has an important if not multigene interactive role in ALS pathogenesis.

Genetic ALS modeling in zebrafish thus far has been exploratory out of necessity, but has effectively used the tools available to zebrafish. Not only have they used overexpression, transgenic and transient knockdown, but they have performed multigenetic experiments to elucidate pathogenic interactions. Zebrafish models were also routinely tested for motion defects, and a swim tunnel provided an appropriate measure for muscle strength and endurance.

The lack of olfactory-based endpoints in ALS models may be in part due to the dispute on sensory loss association with the disease. In terms of rodent studies, only one particular study examined olfactory structure, but not function, in a cycad ingestion-induced ALS-PDC-specific model. Notably, these mice demonstrated reduced size in PD-related structures such as the striatum, substantia nigra, and the olfactory bulb (Wilson et al., 2004). BMAA, the putative toxic element in cycad seeds, has been tested in larval zebrafish where exposure during development caused pericardial and spinal defects, increased mortality, and convulsions (Purdie et al., 2009). Further investigations including exposure from ingestion may cause appropriate ALS-PDC phenotypes to complement mammalian models.

3.3 Alzheimer's Disease

The behavioral symptoms and basic neuropathology of a single affected patient with AD was first described in 1906 by Alois Alzheimer (Small and Cappai, 2006).

Today, AD is the most commonly acquired neurodegenerative disease in the elderly and is notorious for the devastating effects on cognition and memory (Selkoe, 2001). As noted in the original patient, AD cases involve not only the progressive loss of memory, but also changes in behavior that may cause episodic paranoia, delusion, and social inappropriateness (Galton et al., 2000; Selkoe, 2001; Stopford et al., 2007). Although AD is associated with extensive cognitive decline, there is no evidence to support major motor dysfunction excepting perhaps the increased risk of seizures (Born, 2015). Conversely, severe olfactory impairment has been reported in AD patients and is considered a potential preclinical marker (Albers et al., 2015; Devanand et al., 2000; Wang et al., 2010). AD subjects have demonstrated a correlation between impaired sense of smell and decreased volume of the olfactory bulb and tract (Thomann et al., 2009).

Pathologically, there are two markers for AD: amyloid-β (Aβ) plaques and NFTs. Aβ plaques are named after the Aβ protein which comprises the majority of the deposit (Masters et al., 1985). In terms of areas of the brain affected, most AD brains show amyloid deposits in the cerebral cortex and subcortical regions, particularly in the isocortex (Braak and Braak, 1991). One of the primary theories for Alzheimer's pathogenesis called the "Amyloid Hypothesis" is based on the formation of these plaques (Hardy and Selkoe, 2002). Essentially, the theory details missense mutations in known disease-related genes that result in increased or aberrant production and accumulation of Aβ. Aβ proteins then oligomerize and deposit as plaques in certain regions of the brain (Della Bianca et al., 1999; Takahashi et al., 2004). These plaques may either cause direct damage to neurons and synaptic function or indirect destruction through microglia activation (Della Bianca et al., 1999), although the causality of plaques in AD has been scrutinized often in recent years (Albers et al., 2015), and it may be that oligomeric forms of Aβ (presumed to be a precursor of plaque formation) are causal of disease. There is also evidence to suggest that misfolded proteins such as α-syn and tau can propagate aggregation within a diseased subject (Polymenidou and Cleveland, 2012; Sydow and Mandelkow, 2010). Aβ oligomers, or its parent protein APP, may effect some of their action through binding to the prion protein (Kaiser et al., 2012; Nelson et al., 2012), which is known to be critical for neuroprotection. Ultimately, Aβ presence is proposed to cause neuronal damage leading to cell death and eventual cognitive impairment. There is evidence to suggest that plaque deposition is involved in the development of the second AD neurological marker, NFTs. NFTs are bundles of abnormal fibers composed of hyperphosphorylated tau proteins (Grundke-Iqbal et al., 1986; Selkoe, 2001). Many kinases may be capable of initiating development; however, whether it is one or a combination of many has yet to be established. NFTs

are also found in the isocortex and are most identifiable in the later stages of the disease, particularly in the entorhinal and transentorhinal regions of the brain. Most studies identify a typical trend of degeneration beginning in the transentorhinal (or perirhinal) region before spreading to the temporal lobe (particularly the hippocampus complex) and the basal forebrain; however, there have been documented cases of patients who vary from this pattern (Galton et al., 2000). Notably, while Aβ aggregates are less frequently observed in the olfactory system, tau pathology has been seen to severely affect the olfactory bulb and nerves in *postmortem* analysis of AD patients (Attems et al., 2005; Kovacs et al., 1999).

Although causes and potential therapies for AD are heavily researched areas, the underlying causes for the disease remain unknown. The observed pathological changes are often believed to be secondary to changes in gene expression. The genetics behind AD are difficult to interpret and model because there is no singular mutation behind the syndrome. The complexity stems from the variety of genetic mutations linked to early-onset familial cases versus those related to late onset. Pathways and interacting components continue to be investigated, but there are several genes that seem to play a significant role and consequently have been the focus in most animal models. Mutations in amyloid β-protein precursor (APP), presenilin 1 (Psen1), presenilin 2 (Psen2), tau, and Apolipoprotein E4 (ApoE) have been reported in AD patients and correlated with one of the two cerebral pathological markers.

3.3.1 APP

The amyloid hypothesis has made APP, the precursor protein to Aβ, a focal point in AD research. APP has several suspected roles in vivo, but perhaps the most relevant to AD is the production of the Aβ protein upon cleavage (see APP functions review in Zheng and Koo, 2011). Mutations in APP have been found in AD patients and shown to enhance Aβ production, thereby contributing to its aggregation and cerebral plaque deposition (Goate et al., 1991; Scheuner et al., 1996). There have been many variations of APP transgenic mutation models in mice, but the overall endpoints and observed phenotypes are generally conserved (Ashe, 2001; Dodart et al., 2002; Lalonde et al., 2012). Mice with defective APP function show progressive increases in plaque formation, plasma β-amyloid levels, and deficits in learning and memory, but generally fail to recapitulate the hallmark neuronal death (Moechars et al., 1999; Rustay et al., 2010). Importantly, transgenic mice with increased Aβ deposition have shown a variety of olfactory deficits such as atypical odor responses, failure to habituate to repetitive odorant exposure, and reduced ability to discriminate between odors (Wesson et al., 2010).

Zebrafish have two APP orthologs, APPa and APPb, each showing developmental expression in the nervous system and relatively high (63%–66%) sequence identity to mice and humans (Joshi et al., 2009; Liao et al., 2012; Musa et al., 2001). It has been suggested that morpholino knockdown of APPa and APPb together and APPb alone results in shortened body, curly tail, and convergent-extension defects (Joshi et al., 2009), though further controls for MO specificity are warranted. Larvae lacking APPb also had impaired motor neuron axonal outgrowth providing another clue in its role during embryonic development. Although typical AD model endpoints were not examined, human APP695 was shown in rescue of the APPb-deficient phenotypes, which does suggest some functional conservation across species (Joshi et al., 2009; Song and Pimplikar, 2012). Combinations of morpholino knockdown and concerted recovery using mRNA variants demonstrated that human APP interacts with human prion protein (Kaiser et al., 2012), in a niche interaction required for neuroprotection. Early studies using targeted mutagenesis in zebrafish support a role for prion protein in neurodevelopment, neuroprotection, and regulation of NMDA receptors, further supporting a role in AD (Huc-Brandt et al., 2014). A few studies involving APP and zebrafish focused on the creation of transgenic lines for future investigations. These studies exemplify the typical approach to transgenic models by inducing RFP or GFP expression under the control of APPa and APPb, respectively, to locate secreted soluble forms of the proteins (Lee and Cole, 2007; Liao et al., 2012). The use of the transgenic models will be critical to future AD investigations.

3.3.2 Presenilins

Presenilins are transmembrane proteins that encode the catalytic component of the γ-secretase complex (GSC) suspected to play a role in proteolysis regulation of APP. Mutations in Psen1 and Psen2 have both been identified in early-onset familial cases of AD (Janssen et al., 2003; Sherrington et al., 1995; Żekanowski et al., 2003). Through studies in mice it has been established that mutations in Psen1 and Psen 2 can result in characteristic loss of learning and memory functions, NFT-like structure, tau pathology, Aβ deposition, and neuron degeneration (Chen et al., 2008; Elder et al., 2010). Compared with human presenilin, zebrafish express orthologs of Psen1 and Psen2 (Groth et al., 2002) that are highly similar. Investigations into presenilin dysfunction in zebrafish thus far have been limited, and did not examine the expected AD-like phenotypes (Moussavi Nik et al., 2015; Newman et al., 2014a,b). Overexpression of Psen2 in zebrafish through mRNA construct injection does not affect transcription or protein levels of Psen1 perhaps indicating differential regulation (Nornes et al., 2003). In addition, overexpression of a truncated form of Psen2 led to an increased number of dorsal longitudinal ascending (DoLA)

interneurons (Nornes et al., 2009). However, there remains some interaction between the two presenilins, as loss of Psen1 reduces the DoLA phenotype, that is, Psen1 and Psen2 may regulate each other. Basic morphology and development were also observed for separate morpholino knockdown of Psen1 and Psen2, with each leading to impaired somite formation, reduced melanocytes, and hydrocephalus, suggesting functional overlaps (Nornes et al., 2003, 2009). More related to AD, one of these studies also examined morpholino knockdown of presenilin enhancer 2 (PEN-2), which is another component of the GSC. PEN-2 deficiency resulted in reduced Notch signaling and caused a loss of islet-1 positive neurons through what was proposed to be increased apoptosis (Campbell et al., 2006). Caution must be used in interpreting the various studies applying GSC inhibitors as models of AD because GSC has at least several dozens of substrates, including those fundamental to neuron development and maintenance such as Notch (Jurisch-Yaksi et al., 2013). Although Notch's direct role in AD pathogenesis has not been elucidated, Notch may be an influencing factor because of its role in memory deficits and associated neuronal degeneration (Woo et al., 2009). Verification of a relationship between PEN-2 and Notch in zebrafish in conjunction with observation for other AD markers is of potential interest and disease relevance.

3.3.3 ApoE

ApoE was identified in the 1990s as associated with plaques found in AD patients (Dickson et al., 1997). Since then it has become an important area of investigation for sporadic AD cases due to its proposed roles in amyloid deposition and neurodegeneration (DeMattos, 2004; Holtzman et al., 2000). A point of particular interest is that mice deficient in ApoE demonstrated deficits in olfactory functionality (Nathan et al., 2004). A gene homologous to mammalian ApoE with low amino acid sequence identity (27.5%) has been identified in zebrafish (Babin et al., 1997; Durliat et al., 2000). Functionally, there has been an observed expression in the yolk syncytial layer, brain, and eyes during development (Babin et al., 1997). There has also been marked expression during morphogenesis and regeneration of fins (Monnot et al., 1999). Future investigations will need to determine functional overlap with humans if zebrafish are to be used as model for ApoE-related AD.

3.3.4 MAPT/tau

Impaired function of microtubule-associated protein tau (MAPT) is another hallmark of AD. As previously mentioned, NFTs are composed of altered MAPT that have formed aggregates similar to Aβ plaques. The steps that lead to the modification of tau via hyperphosphorylation are not wholly understood, but several kinases, including GSK3β, have been implicated

(Grundke-Iqbal et al., 1986; Hanger et al., 1992). Transgenic mouse models overexpressing or expressing mutant tau have displayed phenotypes reflective of AD, including NFTs, memory deficits, neuronal degeneration, and, importantly, olfactory deficits (Lewis et al., 2000; Macknin et al., 2004; Tatebayashi et al., 2002). Within zebrafish, two orthologous candidates to human MAPT, MAPTa and MAPTb, have been identified, but they have not been examined for loss or gain of function (Chen et al., 2009). Instead, taupathies in zebrafish have been replicated using a transgenic approach. A study used a Tol2 transposon and Gal4/UAS system to generate a transgenic model expressing mutant human tau. This model has proven extremely effective as fish develop hyperphosphorylized tau aggregates or NFTs, and show increased cell death and neuron motor neuron disruption in the spinal cord. Neuronal defects were paired with reduced movement and defective touch response. Interestingly, the application of GSK3β inhibitors can reduce the hyperphosphorylation seen in this model (Paquet et al., 2009). Another transgenic model used an enolase-2 (*eno2*) to drive overexpression of human tau in the CNS (Bai et al., 2007). Antibody staining for tau revealed dense labeling resembling possible deposition of NFTs in the adult brains. Zebrafish models of tauopathy have been used to examine the contribution of autophagy to pathogenesis (Moreau et al., 2014). Replication of human histology for AD in these transgenic models is encouraging and should now be paired with the testing of cognitive and olfactory capacities.

3.3.5 Chemical Modeling of AD

There is some evidence to suggest that nitrosamine-related compounds typically found in foods are related to sporadic cases of AD, as cognitive impairment and neuronal degeneration postexposure have been found in several rodent studies (de la Monte et al., 2009). Chemical modeling in AD in zebrafish largely pertains to the impairment of memory or learning through the use pharmaceuticals. For example, scopolamine, a muscarinic receptor inhibitor that reduces memory function in zebrafish, permits testing of pharmaceuticals for attempted recovery or improvement (Kim et al., 2010; Lester-Coll et al., 2006; Richetti et al., 2011) The mechanisms and methods behind memory and learning testing are not within the focus of this chapter; however, these endpoints may be invaluable for modeling neurodegenerative diseases and could be applied to genetically modified models (Table 21.6).

3.4 Multiple System Atrophy

The disease now referred to as MSA was documented as early as the 1891, but due to overlapping pathologies with PD, the current name was not suggested until 1969 by Graham and Oppenheimer (Burn and Jaros, 2001;

TABLE 21.6 Examples of Zebrafish Alzheimer's Disease Models

Target	Method	Phenotype	References
APPa	Transgenic-RFP	Fluorescent localization of proteins in embryonic vasculature	Liao et al. (2012)
APPa and APPb	Morpholino knockdown	Shortened axis, curly tail, convergent-extension defects	Joshi et al. (2009)
APPb	Morpholino knockdown	Shortened axis, curly tail, convergent-extension defects; impaired motor neuron axonal outgrowth	Joshi et al. (2009); Song and Pimplikar (2012)
	Transgenic-GFP	Fluorescent localization of proteins in embryonic and young adult CNS and vasculature	Lee and Cole (2007)
Psen-2	Morpholino knockdown	Disrupted somitogenesis; increased apoptosis; loss of islet-1 positive cells	Campbell et al. (2006)
Psen1	Morpholino knockdown	Disrupted somitogenesis; hydrocephalus; reduced melanocytes	Campbell et al. (2006); Nornes et al. (2003); Nornes et al. (2009)
Psen 2	Morpholino knockdown	Increased DoLA interneurons; reduced melanocytes; hydrocephalus; disrupted somitogenesis	Nornes et al. (2003); Nornes et al. (2009)
tau	Transgenic expressing mutant human tau via Tol_2 Gal_4/UAS; transgenic overexpressing human tau via *eno2*	Rapid tau aggregation; increased cell death; altered motor neuron morphology and stimulus response; tau aggregates	Bai et al. (2007); Paquet et al. (2009)
Muscarinic receptors	Scopolamine	Learning and memory deficits	Kim et al. (2010)

Rehman, 2001; Ubhi et al., 2011). MSA has sporadic onset in adults aged 50 and older and is pathologically associated with neuron loss and neuronal inclusions. Generally, the areas of the brain that suffer from neurodegeneration vary in severity between MSA patients; however, they have included the cerebellum, basal ganglia, pons, and inferior olivary nuclei (Ubhi et al., 2011). Symptoms can manifest as any combination of ataxia, parkinsonism, or autonomic dysfunction, which typically can be designated as one of the specific MSA subtypes: parkinsonian (MSA-P) or the less common cerebellar (MSA-C). MSA-P is usually associated with the striatonigral (basal ganglia) region, and MSA-C cases refer to olivopontocerebellar regions (Rockenstein et al., 2007). The observed symptoms of the two subtypes do differ slightly. In terms of cognitive impairment, MSA-P tends to involve deficiencies in visuospatial, construction, verbal fluency (retrieval), and executive functions, whereas MSA-C patients have difficulties with attention, learning verbal information, as well as visuospatial and constructional functions, but to a lesser degree (Balas et al., 2010; Kawai et al., 2008). Some studies of MSA patients indicate differences in specific autonomic subsystem dysfunctions; however, results are variable (Schmidt et al., 2008). Although it may present with degeneration and movement akin to PD, MSA is distinguished by several features including irresponsiveness to levodopa treatment, autonomic failure, and cerebellar signs (Rehman, 2001).

In addition to neuron loss, MSA is accompanied by several types of inclusions: glial cytoplasmic inclusions (GCIs), glial nuclear inclusions (GNIs), NCIs, and neuronal nuclear inclusions (NNIs). The most commonly identified aggregates in MSA patients are the GCIs found in oligodendrocytes (Ubhi et al., 2011). The mechanisms underlying inclusion formation in MSA have yet to be determined; however, α-syn protein has been identified as a major component of these aggregates, which draws yet another interesting parallel to PD (Burn and Jaros, 2001; Nakazato and Suzuki, 1996; Wakabayashi et al., 1998).

In terms of olfactory dysfunction, postmortem examinations of MSA patients showed positive α-syn stained GCIs in olfactory bulbs and tracts. Within the olfactory bulb, GCIs were mainly in the superficial layers and rarely in AON (Kovács et al., 2003). Despite a lack of inclusions, the number of AON neurons in MSA cases was significantly reduced (Kovács et al., 2003). Considering this pathology, it is not surprising that MSA patients have difficulties processing odor-related information (Abele et al., 2003).

MSA cases suggest the disease to be sporadic and therefore underlying causes are not well known. There are is little evidence supporting certain genetic polymorphisms and mutations are associated with the condition. Candidates found in MSA patients include ApoE allele, α-syn, and ZNF231 (Cairns et al., 1997; Hashida et al., 1998). In terms of specific MSA modeling, there has been no

further research on ApoE4 or ZNF31. The sporadic nature of this disease has spurred investigation of environmental toxins as a potential cause. A study in humans documented a strong correlation between toxic exposure and MSA development, and toxic modeling in animals has had some success (Hanna et al., 1999). Interestingly, the use of zebrafish in establishing an MSA-specific model has yet to be achieved. However, due to the symptomatic and pathogenic overlap with PD, some basic genetic investigations carried out on both mice and zebrafish have potential application for zebrafish MDA models.

Genetic studies have focused mainly on α-syn overexpression due to its association with GCIs. As previously described, the overexpression of α-syn in zebrafish leads to increased lethality and deformity, and the endogenous synucleins have yet to be modified (Prabhudesai et al., 2012; Sun and Gitler, 2008). To best model the disease, targeted α-syn upregulation is ideal and could be achieved by using transgenesis and tissue-specific promoters. Mouse models have taken advantage of this strategy to overexpress α-syn using the oligodendrocytic-specific promoters myelin basic protein (MBP) and proteolipid protein (PLP). The MBP model had the desired α-syn accumulations in oligodendrocytes and decreased motor capacity (Shults et al., 2005). Of particular interest was a potential olfactory deficit, as transgenic mice took longer to find their food source (Ubhi et al., 2010). A PLP-α syn model was used to investigate the hypothesis that microglial activation (glial CNS macrophage) has a prominent role in MSA neurodegeneration (Ishizawa et al., 2004; Stefanova et al., 2007). The results showed oligodendroglial α-syn accumulation was paralleled with progressive and regional microglial build-up. Several neuronal structures including the MSA targets of the substantia nigra and striatum in particular were affected, which provides another avenue for future MSA research. Although these models have not yet been attempted in zebrafish, there have been transgenic lines developed that utilize zebrafish P0, MBP, and mouse PLP promoters to drive oligodendrocyte-specific enhanced GFP expression (Jung et al., 2010; Yoshida and Macklin, 2005). Using these tools, MSA α-synucleinopathy could be replicated in zebrafish.

Rodent studies have also attempted to model MSA with toxin exposure such as MPTP, ODHA, quinolinic acid (QA), and 3-nitropropionic acid (3NP) (Fernagut and Tison, 2012; Ubhi et al., 2011). 3NP and QA have yet to be applied to zebrafish, but they have been successfully modeled in certain mice phenotypes. For example, 3NP enhanced the motor function and neuronal loss seen in the α-syn transgenic models (Stefanova et al., 2005). MPTP and ODHA have already been used in zebrafish PD models without compromising lethality or deformity, and therefore future studies could be adapted to look for MSA-specific degeneration.

MSA modeling remains relatively new and will expand as associated mutations and toxins continue to be discovered. Although an MSA model in zebrafish has not yet been published, the genetic and toxic experiments performed in mice can be theoretically be applied to zebrafish in the future.

3.5 Huntington's Disease

HD is another example of a neurodegenerative disease associated with olfactory loss and motor dysfunction. The trademark symptom of HD involves a condition of irregular involuntary movements called chorea. Since its original description from the observation of a patient by George Huntington in 1872, HD diagnosis and research have uncovered not only unique neuropathology but also a genetic link. Presently, HD is known as an autosomal dominant largely identified by the trinucleotide (CAG) repeat expansion in the *hd* gene (IT15) that translates as an abnormally long polyglutamine (polyQ) insertion in the huntingtin protein (Htt). The mutation results subsequent dysfunction and degeneration (Walker, 2007).

Interestingly, HD patients can develop symptoms at any life stage, but there is a proposed inverse relationship between the length of polyQ insertions and age of onset (Duyao et al., 1993). Apart from chorea, HD patients have exhibited degeneration of executive functions including planning and organising as and may have certain psychiatric symptoms such as depression, anxiety, and ideas of suicidal thoughts (Gómez-Tortosa et al., 1998; Lemiere et al., 2004; Montoya et al., 2006). In terms of neuropathology, HD is marked by severe neuron loss and atrophy in the neostriatum (caudate nucleus and putamen) and cortex. Htt neuronal inclusions have also been reported in these affected brain regions (DiFiglia et al., 1997; Gómez-Tortosa et al., 1998; Gutekunst et al., 1999). Olfactory dysfunction was recognized early in the disease history as a marker prior to the onset of motor and cognitive symptoms, as patients have difficulties in odorant detection, identification, and discrimination (Hamilton et al., 1999; Nordin et al., 1995).

Despite the strong correlation between dysfunction and disease, the neuronal reasons underlying observed olfactory dysfunction are not fully understood. There are, however, reported correlates of degeneration of cerebral regions involved in olfaction such as the entorhinal cortex, the thalamus, the parahippocampal gyrus, and the caudate nucleus with olfactory loss (Barrios et al., 2007).

3.5.1 Htt

Wild-type Htt function is not fully understood; however, the protein has been demonstrated to have ubiquitous tissue expression with highest levels in the brain. Expression in the brain is not restricted to HD-affected striatum, but is also apparent in the cerebellar cortex, hippocampus, and neocortex. At the cellular level, Htt may associate with proteins in the cytosol and nucleus, which suggests roles in cell signaling, transport, and gene transcription (Borrell-Pagès et al., 2006; Harjes and Wanker, 2003; Kegel et al., 2002). It is accepted that both wild-type and mutant Htt undergo caspase-mediated cleavage; however, mutated Htt fragments are neurotoxic and form aggregates in striatal neurons, neurites, and axonal terminals (Li et al., 2000; Wellington et al., 2002). The formation of these intranuclear inclusions was not correlated with mutant Htt's induction of neurodegeneration through apoptotic pathways (Saudou et al., 1998).

The established genetic link between HD and Htt has led to research on the creation of animal models to elucidate the mechanism by which mutant Htt results in neurodegeneration. Many experiments have been executed in mice, while zebrafish models are just beginning to emerge and their use has tended to focus on testing potential therapies. Zebrafish have a homolog for the HD gene that has 70% amino acid identity with humans (Karlovich et al., 1998). Several genetics techniques have been used to replicate HD symptoms in zebrafish (Table 21.7).

One study conducted morpholino knockdown of *hd* and found it may play a role in iron uptake; researchers did not test for neuron loss and motor defects (Lumsden et al., 2007). Building on this study, a more recent

TABLE 21.7 Examples of Current Zebrafish Models of Huntington's Disease

Target	Method	Phenotype	References
hd	Morpholino knockdown	Small eye, lower jaw and swim bladder defects; symptoms of cellular iron deficiency; increased cell death in midbrain, hindbrain; reduced cell death in the olfactory placode and lateral line neuromasts; upregulated caspase activity; reduced BDNF	Diekmann et al. (2009); Henshall et al. (2009); Lumsden et al. (2007)
BDNF	Morpholino knockdown	Small eye, lower jaw and swim bladder defects; increased cell death in midbrain and hindbrain; upregulated caspase activity	Diekmann et al. (2009)
PolyQ proteins	Overexpression construct injection	Inclusion formation; morphological abnormalities; cell death	Miller et al. (2005)

investigation showed that Htt knockdown resulted in minor morphological abnormalities and desired neuronal loss in the midbrain and hindbrain (Diekmann et al., 2009). Htt-deficient larvae also had elevated caspase and decreased levels of brain-derived neurotrophic factor (BDNF), which have both been previously implicated in HD (Hermel et al., 2004; Zuccato et al., 2001). To determine BDNF's role in the observed phenotype, fish were injected with a BDNF morpholino. BDNF-deficient fish expressed the same phenotypes as the Htt knockdowns. In addition, BDNF treatment rescued Htt knockdown fish further supporting the idea that BDNF is a contributing factor in HD pathology. Transient knockdown has also shown that Htt is required for the development of the olfactory and lateral line systems in zebrafish. Specifically, knockdown showed reduced apoptosis at the within lateral line neuromasts and olfactory placode along with the absence of mature OSNs (Henshall et al., 2009). The phenotypes noted of the olfactory tissue suggest a link between Htt dysfunction and olfactory impairment in humans.

Zebrafish models for HD have also been created by injecting embryos with plasmids that encoded normal or expanded polyQ tracts fused with GFP. Plasmids that encoded longer polyQ repeats were correlated with the formation of insoluble polyQ inclusions as well as increased morphological abnormalities and cell death (Henshall et al., 2009). Ideally, a zebrafish model for HD should not only replicate the polyQ inclusions and isolated neurodegeneration, but also display motor and olfactory defects. The abnormalities observed in zebrafish and mouse olfactory tissue within HD models merit investigation of sensory function (Kohl et al., 2010; Menalled et al., 2003; Petrasch-Parwez et al., 2007). Adding olfactory and movement endpoints to model evaluation will strengthen any results obtained from therapeutic testing.

Toxin-induced HD models have not yet been published with zebrafish subjects; however, there are existing rodent models that have used QA to induce lesions and cell loss in the striatum of the brain (Beal et al., 1991; Tattersfield et al., 2004). Furthermore, chronic treatment with 3NP mimics the striatal damage and similar movement abnormalities observed in HD (Guyot et al., 1997). Toxic exposures conducted in mice could easily be applied to zebrafish to complement current genetic investigations.

4 CONCLUSIONS

4.1 Therapeutic Potential

For the diseases discussed in this chapter, the majority of therapeutic investigations have involved pharmaceutical application to genetic or toxin-induced models in an attempt to recover the disease-like phenotypes. Although many potential drugs prove effective in vitro, it is necessary to test these compounds in vivo, not only

to confirm functionality, but also to rule out any unforeseen toxicity. Zebrafish have been shown to be excellent models for identifying potential neuroprotectants, antioxidants, and drug screens in vivo (Parng et al., 2006; Zon and Peterson, 2005). They are the optimal choice for early chemical screens for several reasons. First, treatment or exposure is simple and fast compared to other vertebrate tests, at least partly because zebrafish can absorb the compound in question from the aqueous environment through their skin and gills. Second, compared to rodent studies, zebrafish can be tested faster and in higher volumes. This owes to their high fecundity, small size, and low cost. Even the creation of genetic models prior to testing can be completed comparatively quickly because of their short life cycle. Third, despite being a nonmammalian vertebrate, disease-related targets are often functionally conserved.

4.2 Future Motion and Olfactory Endpoints

It is important to note that the enthusiasm concerning the use of zebrafish in genetic modeling is not meant to suggest substitution for mammalian models. On the contrary, zebrafish should be used for complementation, comparison, and prescreening of results in relation to mammalian studies. In terms of the diseases discussed in this chapter, many of the existing models are still in the development phase. With the advancement of effective knockout methods and continued creation of transgenic lines, the amount of information gained from zebrafish is expected to increase dramatically. For the models described in this chapter, applied endpoints encompass neuronal abnormalities, cell death, and basic touch response. Monitoring of activity has been applied to some disease models discussed such as PD and ALS, but it has not been given the same level of importance as it is in mammalian studies (Table 21.8). High throughput automated analysis of larval and adult fish motion is currently available through video tracking software (Cachat et al., 2011; Cario et al., 2011; Kane et al., 2004). Not only can basal movement be assessed, but behavioral responses can also be evaluated (Bhinder and Tierney, 2012; Shamchuk and Tierney, 2012). As mentioned in AD models, the testing of fish in a T-maze provides a learning and memory-based assay for the measurement of dementia. In the case of ALS, testing motors skills using a swim tunnel was uniquely applied (DuVal et al., 2014; McGown et al., 2013; Ramesh et al., 2010), providing novel information in longitudinal study design that increased the relevance of the model to human study and created another point of measure for therapeutic analysis. Similar longitudinal observations of neuromuscular deficits during normal aging have also been reported in zebrafish (Gilbert et al., 2014), providing context for endpoints in these disease models.

TABLE 21.8 Motion Endpoints Applied to Zebrafish Models of Neurodegenerative Disease

Disease	Endpoints applied	Potential endpoints[a]	References
Parkinson's disease	Larval touch response; larval and adult basal activity	Adult escape response; swimming performance	Anichtchik et al. (2008); Anichtchik et al. (2004); Bretaud et al. (2004); Ren et al. (2011); Sallinen et al. (2010); Sheng et al. (2010); Xi et al. (2010)
Alzheimer's disease	Larval touch response	Larval and adult basal activity[b]	Paquet et al. (2009)
Huntington's disease	—	Larval touch response; adult escape response; larval and adult basal activity; swimming performance	—
Multiple system atrophy	—	Larval touch response; adult escape response; larval and adult basal activity; swimming performance	—
Amyotrophic lateral sclerosis	Swimming performance; larval touch response	Adult escape response; larval and adult basal activity	DuVal et al. (2014); Kabashi et al. (2011); Kabashi et al. (2010); McGown et al. (2013); Ramesh et al. (2010)

[a] Olfactory endpoints pertaining to odor evoked behavior, tissue analysis, and electrophysiology can be applied to larval and adult zebrafish models of these diseases.
[b] AD is not considered a neuromuscular disease; however, measuring basal activity will contribute to assessments of overall heath.

Although the study of movement is making its way into zebrafish disease models, there has been no indication that olfactory testing will gain popularity. It is interesting that the olfactory symptoms so frequently remarked upon in diseased humans are rarely applied to animal models. Zebrafish olfaction can be tested in several different capacities. Electrophysiological recordings can be taken at the level of the olfactory bulb and epithelium to detect neuronal activity following odorant exposure (Friedrich et al., 2004; Michel et al., 2003). Using electrophysiology, the impairments in olfaction can be isolated to a particular structure, or olfactory neuron class. The characterization of odor-evoked activities in zebrafish could also provide an interesting parameter of analysis (Lindsay and Vogt, 2004; Speedie and Gerlai, 2008; Vitebsky et al., 2005). By combining the results of behavior with electrophysiology, it could help elucidate whether olfactory loss is due to physical damage or the inability to interpret the odor. With the latter result also comes the prospect of inappropriate responses to established odors, thereby replicating cases of dysosmia. Loss of odorant sensitivity can also be tested using various odorant concentrations. As support for using olfaction assays in neurodegenerative studies with zebrafish grows, there is an interesting theory on disease acquisition called the "Olfactory Vector Hypothesis" (OVH) (Prediger et al., 2012). The general principle of the theory concerns the transfer of exogenous agents, be they metals, toxins, or viruses, across the olfactory epithelium and through the olfactory nerve to the brain (Doty, 2008; Prediger et al., 2012). In his review, Doty (2008) also discusses the idea of an "olfactory damage hypothesis" that suggests damage to the olfactory system may in fact enhance the risk factor for genetically susceptible patients for developing AD and PD. In other words, individuals that have a genetic or physiological predisposition for neurodegenerative disease may have such conditions arise after olfactory damage. There has yet to be a substantial amount of evidence to support the OVH; however, zebrafish could be an effective model to test isolated olfactory exposures and damage. In sum, increased integration of motor and olfactory systems toward understanding neurodegenerative etiology and early diagnosis is warranted, and the promise of such approaches is gaining recognition (Albers et al., 2015). Overall, the inclusion of olfactory endpoints in future zebrafish studies of neurodegenerative diseases should increase both study relevance and the potential to elucidate characteristics of dysfunction and causation.

References

Abele, M., Riet, A., Hummel, T., Klockgether, T., Wullner, U., 2003. Olfactory dysfunction in cerebellar ataxia and multiple system atrophy. J. Neurol. 250 (12), 1453–1455.

Ache, B.W., Young, J.M., 2005. Olfaction: diverse species, conserved principles. Neuron 48 (3), 417–430.

Ackerl, K., Atzmueller, M., Grammer, K., 2002. The scent of fear. Neuro Endocrinol. Lett. 23 (2), 79–84.

Ahlskog, J.E., Waring, S.C., Petersen, R.C., Esteban-Santillan, C., Craig, U.K., O'Brien, P.C., et al., 1998. Olfactory dysfunction in Guamanian ALS, parkinsonism, and dementia. Neurology 51 (6), 1672–1677.

Alam, M., Schmidt, W.J., 2002. Rotenone destroys dopaminergic neurons and induces parkinsonian symptoms in rats. Behav. Brain Res. 136 (1), 317–324.

Albers, M.W., Gilmore, G.C., Kaye, J., Murphy, C., Wingfield, A., Bennett, D.A., et al., 2015. At the interface of sensory and motor dysfunctions and Alzheimer's Disease. Alzheimers Dement. 11 (1), 70–98.

Amoore, J.E., 1964. Current status of steric theory of odor. Ann. N. Y. Acad. Sci. 116 (A2), 457.

Ando, H., Furuta, T., Tsien, R.Y., Okamoto, H., 2001. Photo-mediated gene activation using caged RNA/DNA in zebrafish embryos. Nat. Genet. 28 (4), 317–325.

Anichtchik, O., Diekmann, H., Fleming, A., Roach, A., Goldsmith, P., Rubinsztein, D.C., 2008. Loss of PINK1 function affects development and results in neurodegeneration in zebrafish. J. Neurosci. 28 (33), 8199–8207.

Anichtchik, O.V., Kaslin, J., Peitsaro, N., Scheinin, M., Panula, P., 2004. Neurochemical and behavioural changes in zebrafish Danio rerio after systemic administration of 6-hydroxydopamine and 1-methyl-4-phenyl-1,2,3,6-tetrahydropyridine. J. Neurochem. 88 (2), 443–453.

Anichtchik, O., Sallinen, V., Peitsaro, N., Panula, P., 2006. Distinct structure and activity of monoamine oxidase in the brain of zebrafish (Danio rerio). J. Comp. Neurol. 498 (5), 593–610.

Ansari, K.A., Johnson, A., 1975. Olfactory function in patients with Parkinson's disease. J. Chronic Dis. 28 (9), 493–497.

Arai, T., Hasegawa, M., Akiyama, H., Ikeda, K., Nonaka, T., Mori, H., et al., 2006. TDP-43 is a component of ubiquitin-positive tau-negative inclusions in frontotemporal lobar degeneration and amyotrophic lateral sclerosis. Biochem. Biophys. Res. Commun. 351 (3), 602–611.

Armstrong, G.A., Drapeau, P., 2013. Loss and gain of FUS function impair neuromuscular synaptic transmission in a genetic model of ALS. Hum. Mol. Genet. 22 (21), 4282–4292.

Armstrong, G.A.B., Liao, M., You, Z., Lissouba, A., Chen, B.E., Drapeau, P., 2016. Homology directed knockin of point mutations in the zebrafish *tardbp* and *fus* genes in ALS using the CRISPR/Cas9 system. PLoS One 11 (3), e0150188.

Aschenbrenner, K., Hummel, C., Teszmer, K., Krone, F., Ishimaru, T., Seo, H.-S., Hummel, T., 2008. The influence of olfactory loss on dietary behaviors. Laryngoscope 118 (1), 135–144.

Ashe, K.H., 2001. Learning and memory in transgenic mice modeling Alzheimer's disease. Learn. Mem. 8 (6), 301–308.

Attems, J., Lintner, F., Jellinger, K.A., 2005. Olfactory involvement in aging and Alzheimer's disease: an autopsy study. J. Alzheimers Dis. 7 (2), 149–157.

Auer, T.O., Duroure, K., Concordet, J.-P., Del Bene, F., 2014. CRISPR/Cas9-mediated conversion of eGFP- into Gal4-transgenic lines in zebrafish. Nat. Protocols 9 (12), 2823–2840.

Babin, P.J., Thisse, C., Durliat, M., Andre, M., Akimenko, M.A., Thisse, B., 1997. Both apolipoprotein E and A-I genes are present in a non-mammalian vertebrate and are highly expressed during embryonic development. Proc. Natl. Acad. Sci. USA 94 (16), 8622–8627.

Bai, Q., Garver, J.A., Hukriede, N.A., Burton, E.A., 2007. Generation of a transgenic zebrafish model of Tauopathy using a novel promoter element derived from the zebrafish eno2 gene. Nucleic Acids Res. 35 (19), 6501–6516.

Bai, Q., Mullett, S.J., Garver, J.A., Hinkle, D.A., Burton, E.A., 2006. Zebrafish DJ-1 is evolutionarily conserved and expressed in dopaminergic neurons. Brain Res. 1113 (1), 33–44.

Balas, M., Balash, Y., Giladi, N., Gurevich, T., 2010. Cognition in multiple system atrophy: neuropsychological profile and interaction with mood. J. Neural Transm. 117 (3), 369–375.

Bandmann, O., Burton, E.A., 2010. Genetic zebrafish models of neurodegenerative diseases. Neurobiol. Dis. 40 (1), 58–65.

Barrios, F.A., Gonzalez, L., Favila, R., Alonso, M.E., Salgado, P.M., Diaz, R., Fernandez-Ruiz, J., 2007. Olfaction and neurodegeneration in HD. Neuroreport 18 (1), 73–76.

Beal, M., Ferrante, R., Swartz, K., Kowall, N., 1991. Chronic quinolinic acid lesions in rats closely resemble Huntington's disease. J. Neurosci. 11 (6), 1649–1659.

Bedell, V.M., Ekker, S.C., 2015a. Using engineered endonucleases to create knockout and knockin zebrafish models. In: Pruett-Miller, M.S. (Ed.), Chromosomal Mutagenesis. Springer New York, New York, NY, pp. 291–305.

Bedell, V.M., Ekker, S.C., 2015b. Using engineered endonucleases to create knockout and knockin zebrafish models. Methods Mol. Biol. 1239, 291–305.

Bedell, V.M., Westcot, S.E., Ekker, S.C., 2011. Lessons from morpholino-based screening in zebrafish. Brief. Funct. Genomics 10 (4), 181–188.

Benedetti, L., Ghilardi, A., Rottoli, E., De Maglie, M., Prosperi, L., Perego, C., et al., 2016. INaP selective inhibition reverts precocious inter- and motorneurons hyperexcitability in the Sod1-G93R zebrafish ALS model. Sci. Rep. 6, 24515.

Betarbet, R., Sherer, T.B., MacKenzie, G., Garcia-Osuna, M., Panov, A.V., Greenamyre, J.T., 2000. Chronic systemic pesticide exposure reproduces features of Parkinson's disease. Nat. Neurosci. 3 (12), 1301–1306.

Bhinder, G., Tierney, K.B., 2012. Olfactory-evoked activity assay for larval zebrafish. Zebrafish Protocols for Neurobehavioral Research. Neuromethods, vol. 66. Springer, pp 71–84.

Bill, B.R., Petzold, A.M., Clark, K.J., Schimmenti, L.A., Ekker, S.C., 2009. A primer for morpholino use in zebrafish. Zebrafish 6 (1), 69–77.

Boesch, S.M., Wenning, G.K., Ransmayr, G., Poewe, W., 2002. Dystonia in multiple system atrophy. J. Neurol. Neurosurg. Psychiatry 72 (3), 300–303.

Boesveldt, S., Verbaan, D., Knol, D.L., Visser, M., van Rooden, S.M., van Hilten, J.J., Berendse, H.W., 2008. A comparative study of odor identification and odor discrimination deficits in Parkinson's disease. Mov. Disord. 23 (14), 1984–1990.

Bonfils, P., Faulcon, P., Tavernier, L., Bonfils, N.A., Malinvaud, D., 2008. Accidents domestiques chez 57 patients ayant une perte sévère de l'odorat. La Presse Médicale 37 (5, Pt. 1), 742–745.

Bonifati, V., Rizzu, P., van Baren, M.J., Schaap, O., Breedveld, G.J., Krieger, E., et al., 2003. Mutations in the DJ-1 gene associated with autosomal recessive early-onset parkinsonism. Science 299 (5604), 256–259.

Bonifati, V., Rohé, C.F., Breedveld, G.J., Fabrizio, E., De Mari, M., Tassorelli, C., et al., 2005. Early-onset parkinsonism associated with PINK1 mutations. Neurology 65 (1), 87–95.

Born, H.A., 2015. Seizures in Alzheimer's disease. Neuroscience 286, 251–263.

Borrell-Pagès, M., Zala, D., Humbert, S., Saudou, F., 2006. Huntington's disease: from huntingtin function and dysfunction to therapeutic strategies. Cell. Mol. Life Sci. 63 (22), 2642–2660.

Braak, H., Braak, E., 1991. Neuropathological stageing of Alzheimer-related changes. Acta Neuropathol. 82 (4), 239–259.

Braak, H., Tredici, K.D., Rüb, U., de Vos, R.A.I., Jansen Steur, E.N.H., Braak, E., 2003. Staging of brain pathology related to sporadic Parkinson's disease. Neurobiol. Aging 24 (2), 197–211.

Bretaud, S., Allen, C., Ingham, P.W., Bandmann, O., 2007. p53-dependent neuronal cell death in a DJ-1-deficient zebrafish model of Parkinson's disease. J. Neurochem. 100 (6), 1626–1635.

Bretaud, S., Lee, S., Guo, S., 2004. Sensitivity of zebrafish to environmental toxins implicated in Parkinson's disease. Neurotoxicol. Teratol. 26 (6), 857–864.

Brett, J.R., 1964. The respiratory metabolism and swimming performance of young sockeye salmon. J. Fish Res. Board Can. 21 (5), 1183–1226.

Brodoehl, S., Klingner, C., Volk, G.F., Bitter, T., Witte, O.W., Redecker, C., 2012. Decreased olfactory bulb volume in idiopathic Parkinson's disease detected by 3.0-Tesla magnetic resonance imaging. Mov. Disord. 27 (8), 1019–1025.

Brookes, J.C., 2011. Olfaction: the physics of how smell works? Contemp. Phys. 52 (5), 385–402.

Büeler, H., 2009. Impaired mitochondrial dynamics and function in the pathogenesis of Parkinson's disease. Exp. Neurol. 218 (2), 235–246.

Burn, D.J., Jaros, E., 2001. Multiple system atrophy: cellular and molecular pathology. Mol. Pathol. 54 (6), 419–426.

Cachat, J.M., Stewart, A., Utterback, E., Kyzar, E., Hart, P.C., Carlos, D., et al., 2011. Deconstructing adult zebrafish behavior with swim trace visualizations. In: Kalueff, A.V., Cachat, J.M. (Eds.), Zebrafish Neurobehavioral Protocols, vol. 51, Humana Press Inc, Totowa, pp. 191–201.

Cairns, N.J., Atkinson, P.F., Kovács, T., Lees, A.J., Daniel, S.E., Lantos, P.L., 1997. Apolipoprotein E e4 allele frequency in patients with multiple system atrophy. Neurosci. Lett. 221 (2-3), 161–164.

Campbell, W.A., Yang, H., Zetterberg, H., Baulac, S., Sears, J.A., Liu, T., et al., 2006. Zebrafish lacking Alzheimer presenilin enhancer 2 (Pen-2) demonstrate excessive p53-dependent apoptosis and neuronal loss. J. Neurochem. 96 (5), 1423–1440.

Cario, C.L., Farrell, T.C., Milanese, C., Burton, E.A., 2011. Automated measurement of zebrafish larval movement. J. Physiol. 589 (15), 3703–3708.

Cerda, G.A., Thomas, J.E., Allende, M.L., Karlstrom, R.O., Palma, V., 2006. Electroporation of DNA, RNA, and morpholinos into zebrafish embryos. Methods 39 (3), 207–211.

Chandran, J., Ding, J., Cai, H., 2007. Alsin and the molecular pathways of amyotrophic lateral sclerosis. Mol. Neurobiol. 36 (3), 224–231.

Chandran, J.S., Lin, X., Zapata, A., Höke, A., Shimoji, M., Moore, S.O.L., et al., 2008. Progressive behavioral deficits in DJ-1-deficient mice are associated with normal nigrostriatal function. Neurobiol. Dis. 29 (3), 505–514.

Chen, M.Q., Martins, R.N., Lardelli, M., 2009. Complex splicing and neural expression of duplicated tau genes in zebrafish embryos. J. Alzheimers Dis. 18 (2), 305–317.

Chen, Q., Nakajima, A., Choi, S.H., Xiong, X., Tang, Y.-P., 2008. Loss of presenilin function causes Alzheimer's disease-like neurodegeneration in the mouse. J. Neurosci. Res. 86 (7), 1615–1625.

Cheng, R., Banack, S.A., 2009. Previous studies underestimate BMAA concentrations in cycad flour. Amyotroph. Lateral Scler. 10 (s2), 41–43.

Clark, K.J., Urban, M.D., Skuster, K.J., Ekker, S.C., 2011. Transgenic zebrafish using transposable elements. Methods Cell Biol. 104, 137–149.

Da Costa, M.M.J., Allen, C.E., Higginbottom, A., Ramesh, T., Shaw, P.J., McDermott, C.J., 2014. A new zebrafish model produced by TILLING of SOD1-related amyotrophic lateral sclerosis replicates key features of the disease and represents a tool for in vivo therapeutic screening. Dis. Model Mech. 7 (1), 73–81.

Das, S., Rajanikant, G.K., 2014. Huntington disease: can a zebrafish trail leave more than a ripple? Neurosci. Biobehav. Rev. 45, 258–261.

Dauer, W., Przedborski, S., 2003. Parkinson's disease: mechanisms and models. Neuron 39 (6), 889–909.

de la Monte, S.M., Neusner, A., Chu, J., Lawton, M., 2009. Epidemiological trends strongly suggest exposures as etiologic agents in the pathogenesis of sporadic Alzheimer's disease, diabetes mellitus, and non-alcoholic steatohepatitis. J. Alzheimers Dis. 17 (3), 519–529.

Deiters, A., Garner, R.A., Lusic, H., Govan, J.M., Dush, M., Nascone-Yoder, N.M., Yoder, J.A., 2010. Photocaged morpholino oligomers for the light-regulation of gene function in zebrafish and Xenopus embryos. J. Am. Chem. Soc. 132 (44), 15644–15650.

DeJesus-Hernandez, M., Mackenzie, I.R., Boeve, B.F., Boxer, A.L., Baker, M., Rutherford, N.J., et al., 2011. Expanded GGGGCC hexanucleotide repeat in non-coding region of C9ORF72 causes chromosome 9p-linked frontotemporal dementia and amyotrophic lateral sclerosis. Neuron 72 (2), 245–256.

Della Bianca, V., Dusi, S., Bianchini, E., Dal Prà, I., Rossi, F., 1999. β-Amyloid activates the O_2 forming NADPH oxidase in microglia, monocytes, and neutrophils. J. Biol. Chem. 274 (22), 15493–15499.

DeMattos, R., 2004. Apolipoprotein E dose-dependent modulation of β-amyloid deposition in a transgenic mouse model of Alzheimer's disease. J. Mol. Neurosci. 23 (3), 255–262.

den Broeder, M.J., van der Linde, H., Brouwer, J.R., Oostra, B.A., Willemsen, R., Ketting, R.F., 2009. Generation and Characterization of Fmr1 knockout zebrafish. PLoS One 4 (11), e7910.

Deng, H.-X., Zhai, H., Bigio, E.H., Yan, J., Fecto, F., Ajroud, K., et al., 2010. FUS-immunoreactive inclusions are a common feature in sporadic and non-SOD1 familial amyotrophic lateral sclerosis. Ann. Neurol. 67 (6), 739–748.

Deuschl, G., Bain, P., Brin, M., Ad Hoc Sci, C., 1998. Consensus statement of the movement disorder society on tremor. Mov. Disord. 13, 2–23.

Devanand, D.P., Michaels-Marston, K.S., Liu, X.H., Pelton, G.H., Padilla, M., Marder, K., et al., 2000. Olfactory deficits in patients with mild cognitive impairment predict Alzheimer's disease at follow-up. Am. J. Psychiatry 157 (9), 1399–1405.

Díaz-Casado, M.E., Lima, E., García, J.A., Doerrier, C., Aranda, P., Sayed, R.K.A., et al., 2016. Melatonin rescues zebrafish embryos from the parkinsonian phenotype restoring the parkin/PINK1/DJ-1/MUL1 network. J. Pineal Res. 61 (1), 96–107.

Dickson, D., Fujishiro, H., DelleDonne, A., Menke, J., Ahmed, Z., Klos, K., et al., 2008. Evidence that incidental Lewy body disease is presymptomatic Parkinson's disease. Acta Neuropathol. 115 (4), 437–444.

Dickson, T.C., Saunders, H.L., Vickers, J.C., 1997. Relationship between apolipoprotein E and the amyloid deposits and dystrophic neurites of Alzheimer's disease. Neuropathol. Appl. Neurobiol. 23 (6), 483–491.

Dickstein, D.L., Kabaso, D., Rocher, A.B., Luebke, J.I., Wearne, S.L., Hof, P.R., 2007. Changes in the structural complexity of the aged brain. Aging Cell 6 (3), 275–284.

Diekmann, H., Anichtchik, O., Fleming, A., Futter, M., Goldsmith, P., Roach, A., Rubinsztein, D.C., 2009. Decreased BDNF levels are a major contributor to the embryonic phenotype of huntingtin knockdown zebrafish. J. Neurosci. 29 (5), 1343–1349.

DiFiglia, M., Sapp, E., Chase, K.O., Davies, S.W., Bates, G.P., Vonsattel, J.P., Aronin, N., 1997. Aggregation of huntingtin in neuronal intranuclear inclusions and dystrophic neurites in Brain. Science 277 (5334), 1990–1993.

Djordjevic, J., Jones-Gotman, M., De Sousa, K., Chertkow, H., 2008. Olfaction in patients with mild cognitive impairment and Alzheimer's disease. Neurobiol. Aging 29 (5), 693–706.

Dodart, J.C., Mathis, C., Bales, K.R., Paul, S.M., 2002. Does my mouse have Alzheimer's disease? Genes Brain Behav. 1 (3), 142–155.

Dorsky, R.I., Sheldahl, L.C., Moon, R.T., 2002. A transgenic Lef1/β-catenin-dependent reporter is expressed in spatially restricted domains throughout zebrafish development. Dev. Biol. 241 (2), 229–237.

Doty, R.L., 1995. Studies of olfactory dysfunction in major neurological disorders. Apfelbach, R., MullerSchwarze, D., Reutter, K., Weiler, E. (Eds.), Chemical Signals in Vertebrates Vii, vol. 93, Pergamon Press, Oxford, pp. 593–602.

Doty, R.L., 2008. The olfactory vector hypothesis of neurodegenerative disease: is it viable? Ann. Neurol. 63 (1), 7–15.

Doty, R.L., 2010. The great Pheromone Myth. JHU Press, Baltimore, MD.

Doty, R.L., Li, C., Mannon, L.J., Yousem, D.M., 1998. Olfactory dysfunction in multiple sclerosis: relation to plaque load in inferior frontal and temporal lobesa. Ann. N. Y. Acad. Sci. 855 (1), 781–786.

Doty, R.L., Reyes, P.F., Gregor, T., 1987. Presence of both odor identification and detection deficits in Alzheimer's disease. Brain Res. Bull. 18 (5), 597–600.

Durliat, M., Andre, M., Babin, P.J., 2000. Conserved protein motifs and structural organization of a fish gene homologous to mammalian apolipoprotein E. Eur. J. Biochem. 267 (2), 549–559.

DuVal, M.G., Gilbert, M.J., Watson, D.E., Zerulla, T.C., Tierney, K.B., Allison, W.T., 2014. Growth differentiation factor 6 as a putative risk factor in neuromuscular degeneration. PLoS One 9 (2), e89183.

Duyao, M., Ambrose, C., Myers, R., Novelletto, A., Persichetti, F., Frontali, M., et al., 1993. Trinucleotide repeat length instability and age-of-onset in huntingtons-disease. Nat. Genet. 4 (4), 387–392.

Elder, G.A., Sosa, M.A.G., De Gasperi, R., Dickstein, D.L., Hof, P.R., 2010. Presenilin transgenic mice as models of Alzheimer's disease. Brain Struct. Funct. 214 (2-3), 127–143.

Elian, M., 1991. Olfactory impairment in motor-neuron disease—a pilot-study. J. Neurol. Neurosurg. Psychiatry 54 (10), 927–928.

Fallon, A.E., Rozin, P., 1983. The psychological bases of food rejections by humans. Ecol. Food Nutr. 13 (1), 15–26.

Fernagut, P.O., Tison, F., 2012. Animal models of multiple system atrophy. Neuroscience 211 (0), 77–82.

Fett, M.E., Pilsl, A., Paquet, D., van Bebber, F., Haass, C., Tatzelt, J., et al., 2010. Parkin is protective against proteotoxic stress in a transgenic zebrafish model. PLoS One 5 (7), e11783.

Firestein, S., 2001. How the olfactory system makes sense of scents. Nature 413 (6852), 211–218.

Fleisch, V.C., Leighton, P.L., Wang, H., Pillay, L.M., Ritzel, R.G., Bhinder, G., et al., 2013. Targeted mutation of the gene encoding prion protein in zebrafish reveals a conserved role in neuron excitability. Neurobiol. Dis. 55, 11–25.

Flinn, L., Mortiboys, H., Volkmann, K., Koester, R.W., Ingham, P.W., Bandmann, O., 2009. Complex I deficiency and dopaminergic neuronal cell loss in parkin-deficient zebrafish (Danio rerio). Brain 132, 1613–1623.

Foley, J.E., Yeh, J.-R.J., Maeder, M.L., Reyon, D., Sander, J.D., Peterson, R.T., Joung, J.K., 2009. Rapid mutation of endogenous zebrafish genes using zinc finger nucleases made by Oligomerized Pool ENgineering (OPEN). PLoS One 4 (2), e4348.

Fosque, B.F., Sun, Y., Dana, H., Yang, C.-T., Ohyama, T., Tadross, M.R., et al., 2015. Labeling of active neural circuits in vivo with designed calcium integrators. Science 347 (6223), 755–760.

Friedrich, R.W., Habermann, C.J., Laurent, G., 2004. Multiplexing using synchrony in the zebrafish olfactory bulb. Nat. Neurosci. 7 (8), 862–871.

Galton, C.J., Patterson, K., Xuereb, J.H., Hodges, J.R., 2000. Atypical and typical presentations of Alzheimer's disease: a clinical, neuropsychological, neuroimaging and pathological study of 13 cases. Brain 123 (3), 484–498.

Gamez, J., Corbera-Bellalta, M., Nogales, G., Raguer, N., García-Arumí, E., Badia-Canto, M., et al., 2006. Mutational analysis of the Cu/Zn superoxide dismutase gene in a Catalan ALS population: should all sporadic ALS cases also be screened for SOD1? J. Neurol. Sci. 247 (1), 21–28.

Gandhi, S., Muqit, M.M.K., Stanyer, L., Healy, D.G., Abou-Sleiman, P.M., Hargreaves, I., et al., 2006. PINK1 protein in normal human brain and Parkinson's disease. Brain 129 (7), 1720–1731.

Gilbert, M.J.H., Zerulla, T.C., Tierney, K.B., 2014. Zebrafish (Danio rerio) as a model for the study of aging and exercise: physical ability and trainability decrease with age. Exp. Gerontol. 50, 106–113.

Gilks, W.P., Abou-Sleiman, P.M., Gandhi, S., Jain, S., Singleton, A., Lees, A.J., et al., 2005. A common LRRK2 mutation in idiopathic Parkinson's disease. Lancet 365 (9457), 415–416.

Glasl, L., Kloos, K., Giesert, F., Roethig, A., Di Benedetto, B., Kühn, R., et al., 2012. Pink1-deficiency in mice impairs gait, olfaction and serotonergic innervation of the olfactory bulb. Exp. Neurol. 235 (1), 214–227.

Goate, A., Chartierharlin, M.C., Mullan, M., Brown, J., Crawford, F., Fidani, L., et al., 1991. Segregation of a missense mutation in the amyloid precursor protein gene with familial alzheimers-disease. Nature 349 (6311), 704–706.

Gómez-Tortosa, E., del Barrio, A., García Ruiz, P.J., et al., 1998. Severity of cognitive impairment in juvenile and late-onset huntington disease. Arch. Neurol. 55 (6), 835–843.

Gorell, J.M., Johnson, C.C., Rybicki, B.A., Peterson, E.L., Richardson, R.J., 1998. The risk of Parkinson's disease with exposure to pesticides, farming, well water, and rural living. Neurology 50 (5), 1346–1350.

Groth, C., Nornes, S., McCarty, R., Tamme, R., Lardelli, M., 2002. Identification of a second presenilin gene in zebrafish with similarity to the human Alzheimer's disease gene presenilin2. Dev. Genes Evol. 212 (10), 486–490.

Grundke-Iqbal, I., Iqbal, K., Tung, Y.-C., Quinlan, M., Wisniewski, H.M., Binder, L.I., 1986. Abnormal phosphorylation of the microtubule-associated protein τ (tau) in Alzheimer cytoskeletal pathology. Proc. Natl. Acad. Sci. USA 83 (13), 4913–4917.

Gupta, A., Meng, X., Zhu, L.J., Lawson, N.D., Wolfe, S.A., 2011. Zinc finger protein-dependent and -independent contributions to the in vivo off-target activity of zinc finger nucleases. Nucleic Acids Res. 39 (1), 381–392.

Gutekunst, C.-A., Li, S.-H., Yi, H., Mulroy, J.S., Kuemmerle, S., Jones, R., et al., 1999. Nuclear and neuropil aggregates in Huntington's disease: relationship to neuropathology. J. Neurosci. 19 (7), 2522–2534.

Guyot, M.C., Hantraye, P., Dolan, R., Palfi, S., Maziére, M., Brouillet, E., 1997. Quantifiable bradykinesia, gait abnormalities and Huntington's disease-like striatal lesions in rats chronically treated with 3-nitropropionic acid. Neuroscience 79 (1), 45–56.

Halliday, G.M., McRitchie, D.A., Macdonald, V., Double, K.L., Trent, R.J., McCusker, E., 1998. Regional specificity of brain atrophy in Huntington's disease. Exp. Neurol. 154 (2), 663–672.

Hamilton, J.M., Murphy, C., Paulsen, J.S., 1999. Odor detection, learning, and memory in Huntington's disease. J. Int. Neuropsychol. Soc. 5 (7), 609–615.

Hanger, D.P., Hughes, K., Woodgett, J.R., Brion, J.P., Anderton, B.H., 1992. Glycogen-synthase kinase-3 induces alzheimers disease-like phosphorylation of tau—generation of paired helical filament epitopes and neuronal localization of the kinase. Neurosci. Lett. 147 (1), 58–62.

Hanna, P.A., Jankovic, J., Kirkpatrik, J.B., 1999. Multiple system atrophy: the putative causative role of environmental toxins. Arch. Neurol. 56 (1), 90–94.

Hans, S., Kaslin, J., Freudenreich, D., Brand, M., 2009. Temporally-controlled site-specific recombination in zebrafish. PLoS One 4 (2), e4640.

Hardy, J., Selkoe, D.J., 2002. The amyloid hypothesis of Alzheimer's disease: progress and problems on the road to therapeutics. Science 297 (5580), 353–356.

Harjes, P., Wanker, E.E., 2003. The hunt for huntingtin function: interaction partners tell many different stories. Trends Biochem. Sci. 28 (8), 425–433.

Hashida, H., Goto, J., Zhao, N., Takahashi, N., Hirai, M., Kanazawa, I., Sakaki, Y., 1998. Cloning and mapping of ZNF231, a novel brain-specific gene encoding neuronal double zinc finger protein whose expression is enhanced in a neurodegenerative disorder, multiple system atrophy (MSA). Genomics 54 (1), 50–58.

Hawkes, C.H., Shephard, B.C., 1998. Olfactory evoked responses and identification tests in neurological disease. Ann. N. Y. Acad. Sci. 855 (1), 608–615.

Hawkes, C.H., Shephard, B.C., Daniel, S.E., 1997. Olfactory dysfunction in Parkinson's disease. J. Neurol. Neurosurg. Psychiatry 62 (5), 436–446.

Hawkes, C.H., Shephard, B.C., Geddes, J.F., Body, G.D., Martin, J.E., 1998. Olfactory disorder in motor neuron disease. Exp. Neurol. 150 (2), 248–253.

He, C.Z., Hays, A.P., 2004. Expression of peripherin in ubiquinated inclusions of amyotrophic lateral sclerosis. J. Neurol. Sci. 217 (1), 47–54.

Helmes, E., Østbye, T., 2002. Beyond memory impairment: cognitive changes in Alzheimer's disease. Arch. Clin. Neuropsychol. 17 (2), 179–193.

Henshall, T.L., Tucker, B., Lumsden, A.L., Nornes, S., Lardelli, M.T., Richards, R.I., 2009. Selective neuronal requirement for huntingtin in the developing zebrafish. Hum. Mol. Genet. 18 (24), 4830–4842.

Hermel, E., Gafni, J., Propp, S.S., Leavitt, B.R., Wellington, C.L., Young, J.E., et al., 2004. Specific caspase interactions and amplification are involved in selective neuronal vulnerability in Huntington's disease. Cell Death Differ. 11 (4), 424–438.

Higashijima, S., Hotta, Y., Okamoto, H., 2000. Visualization of cranial motor neurons in live transgenic zebrafish expressing green fluorescent protein under the control of the Islet-1 promoter/enhancer. J. Neurosci. 20 (1), 206–218.

Holtzman, D.M., Bales, K.R., Tenkova, T., Fagan, A.M., Parsadanian, M., Sartorius, L.J., et al., 2000. Apolipoprotein E isoform-dependent

amyloid deposition and neuritic degeneration in a mouse model of Alzheimer's disease. Proc. Natl. Acad. Sci. USA 97 (6), 2892–2897.

Hruscha, A., Krawitz, P., Rechenberg, A., Heinrich, V., Hecht, J., Haass, C., Schmid, B., 2013. Efficient CRISPR/Cas9 genome editing with low off-target effects in zebrafish. Development 140 (24), 4982–4987.

Huang, C., Tong, J.B., Bi, F.F., Zhou, H.X., Xia, X.G., 2012. Mutant TDP-43 in motor neurons promotes the onset and progression of ALS in rats. J. Clin. Invest. 122 (1), 107–118.

Huang, C., Zhou, H.X., Tong, J.B., Chen, H., Liu, Y.J., Wang, D.A., et al., 2011. FUS transgenic rats develop the phenotypes of amyotrophic lateral sclerosis and frontotemporal lobar degeneration. PLoS Genet. 7 (3.), e1002011.

Huc-Brandt, S., Hieu, N., Imberdis, T., Cubedo, N., Silhol, M., Leighton, P.L.A., et al., 2014. Zebrafish prion protein PrP2 controls collective migration process during lateral line sensory system development. PLoS One 9 (12), e113331.

Hummel, T., Nordin, S., 2005. Olfactory disorders and their consequences for quality of life. Acta Otolaryngol. 125 (2), 116–121.

Hummel, T., Pietsch, H., Kobal, G., 1991. Kallmann's syndrome and chemosensory evoked potentials. Eur. Arch. Otorhinolaryngol. 248 (5), 311–312.

Hwang, W.Y., Fu, Y., Reyon, D., Maeder, M.L., Tsai, S.Q., Sander, J.D., et al., 2013. Efficient in vivo genome editing using RNA-guided nucleases. Nat. Biotechnol. 31 (3), 227–229.

Iaccarino, C., Crosio, C., Vitale, C., Sanna, G., Carrri, M.T., Barone, P., 2007. Apoptotic mechanisms in mutant LRRK2-mediated cell death. Hum. Mol. Genet. 16 (11), 1319–1326.

Iannaccone, A., Mykytyn, K., Persico, A.M., Searby, C.C., Baldi, A., Jablonski, M.M., Sheffield, V.C., 2005. Clinical evidence of decreased olfaction in Bardet–Biedl syndrome caused by a deletion in the BBS4 gene. Am. J. Med. Genet. A 132A (4), 343–346.

Ikemoto, A., Hirano, A., Akiguchi, I., 2000. Neuropathology of amyotrophic lateral sclerosis with extra-motor system degeneration: characteristics and differences in the molecular pathology between ALS with dementia and Guamanian ALS. Amyotroph. Lateral Scler. 1 (2), 97–104.

Imai, Y., Takahashi, R., 2004. How do Parkin mutations result in neurodegeneration? Curr. Opin. Neurobiol. 14 (3), 384–389.

Irion, U., Krauss, J., Nüsslein-Volhard, C., 2014. Precise and efficient genome editing in zebrafish using the CRISPR/Cas9 system. Development 141 (24), 4827–4830.

Ishizawa, K., Komori, T., Sasaki, S., Arai, N., Mizutani, T., Hirose, T., 2004. Microglial activation parallels system degeneration in multiple system atrophy. J. Neuropathol. Exp. Neurol. 63 (1), 43–52.

Jafek, B.W., Murrow, B., Michaels, R., Restrepo, D., Linschoten, M., 2002. Biopsies of human olfactory epithelium. Chem. Senses 27 (7), 623–628.

Janssen, J.C., Beck, J.A., Campbell, T.A., Dickinson, A., Fox, N.C., Harvey, R.J., et al., 2003. Early onset familial Alzheimer's disease—mutation frequency in 31 families. Neurology 60 (2), 235–239.

Jao, L.-E., Wente, S.R., Chen, W., 2013. Efficient multiplex biallelic zebrafish genome editing using a CRISPR nuclease system. Proc. Natl. Acad. Sci. USA 110 (34), 13904–13909.

Joshi, P., Liang, J.O., DiMonte, K., Sullivan, J., Pimplikar, S.W., 2009. Amyloid precursor protein is required for convergent-extension movements during Zebrafish development. Dev. Biol. 335 (1), 1–11.

Joyner, R.E., 1963. Olfactory acuity in an industrial population. J. Occup. Med. 5 (1), 37–42.

Joyner, R.E., 1964. Effect of cigarette smoking on olfactory acuity. Arch. Otolaryngol. 80, 576–579.

Jung, S.-H., Kim, S., Chung, A.-Y., Kim, H.-T., So, J.-H., Ryu, J., et al., 2010. Visualization of myelination in GFP-transgenic zebrafish. Dev. Dyn. 239 (2), 592–597.

Jurisch-Yaksi, N., Sannerud, R., Annaert, W., 2013. A fast growing spectrum of biological functions of gamma-secretase in development and disease. Biochim. Biophys. Acta 1828 (12), 2815–2827.

Kabashi, E., Bercier, V., Lissouba, A., Liao, M.J., Brustein, E., Rouleau, G.A., Drapeau, P., 2011. FUS and TARDBP but not SOD1 interact in genetic models of amyotrophic lateral sclerosis. PLoS Genet. 7 (8), e1002214.

Kabashi, E., Lin, L., Tradewell, M.L., Dion, P.A., Bercier, V., Bourgouin, P., et al., 2010. Gain and loss of function of ALS-related mutations of TARDBP (TDP-43) cause motor deficits in vivo. Hum. Mol. Genet. 19 (4), 671–683.

Kabashi, E., Valdmanis, P.N., Dion, P., Spiegelman, D., McConkey, B.J., Velde, C.V., et al., 2008. TARDBP mutations in individuals with sporadic and familial amyotrophic lateral sclerosis. Nat. Genet. 40 (5), 572–574.

Kaiser, D.M., Acharya, M., Leighton, P.L.A., Wang, H., Daude, N., Wohlgemuth, S., et al., 2012. Amyloid beta precursor protein and prion protein have a conserved interaction affecting cell adhesion and CNS development. PLoS One 7 (12), e51305.

Kane, A.S., Salierno, J.D., Gipson, G.T., Molteno, T.C.A., Hunter, C., 2004. A video-based movement analysis system to quantify behavioral stress responses of fish. Water Res. 38 (18), 3993–4001.

Karlovich, C.A., John, R.M., Ramirez, L., Stainier, D.Y.R., Myers, R.M., 1998. Characterization of the Huntington's disease (HD) gene homolog in the zebrafish Danio rerio. Gene 217 (1-2), 117–125.

Karstensen, H.G., Tommerup, N., 2012. Isolated and syndromic forms of congenital anosmia. Clin. Genet. 81 (3), 210–215.

Kato, S., 2008. Amyotrophic lateral sclerosis models and human neuropathology: similarities and differences. Acta Neuropathol. 115 (1), 97–114.

Kawai, Y., Suenaga, M., Takeda, A., Ito, M., Watanabe, H., Tanaka, F., et al., 2008. Cognitive impairments in multiple system atrophy—MSA-C vs MSA-P. Neurology 70 (16), 1390–1396.

Kawakami, K., 2004. Transgenesis and gene trap methods in zebrafish by using the Tol2 transposable element. William Detrich, I.I.I.M.W.H., Leonard, I.Z. (Eds.), Methods in Cell Biology, vol. 77, Academic Press, Cambridge, MA, pp. 201–222.

Kawakami, K., Takeda, H., Kawakami, N., Kobayashi, M., Matsuda, N., Mishina, M., 2004. A transposon-mediated gene trap approach identifies developmentally regulated genes in zebrafish. Dev. Cell 7 (1), 133–144.

Kegel, K.B., Meloni, A.R., Yi, Y., Kim, Y.J., Doyle, E., Cuiffo, B.G., et al., 2002. Huntingtin Is present in the nucleus, interacts with the transcriptional corepressor C-terminal binding protein, and represses transcription. J. Biol. Chem. 277 (9), 7466–7476.

Kelly, G.M., Erezyilmaz, D.F., Moon, R.T., 1995. Induction of a secondary embryonic axis in zebrafish occurs following the overexpression of β-catenin. Mech. Dev. 53 (2), 261–273.

Kern, R.C., Quinn, B., Rosseau, G., Farbman, A.I., 2000. Posttraumatic olfactory dysfunction. Laryngoscope 110 (12), 2106–2109.

Kiernan, M.C., Vucic, S., Cheah, B.C., Turner, M.R., Eisen, A., Hardiman, O., et al., 2011. Amyotrophic lateral sclerosis. Lancet 377 (9769), 942–955.

Kim, Y.-H., Lee, Y., Kim, D., Jung, M.W., Lee, C.-J., 2010. Scopolamine-induced learning impairment reversed by physostigmine in zebrafish. Neurosci. Res. 67 (2), 156–161.

Kim, C.K., Miri, A., Leung, L.C., Berndt, A., Mourrain, P., Tank, D.W., Burdine, R.D., 2014. Prolonged, brain-wide expression of nuclear-localized GCaMP3 for functional circuit mapping. Front. Neural Circuits 8, 138.

Kimura, Y., Hisano, Y., Kawahara, A., Higashijima, S.-i., 2014. Efficient generation of knock-in transgenic zebrafish carrying reporter/driver genes by CRISPR/Cas9-mediated genome engineering. Sci. Rep. 4, 6545.

Kohl, Z., Regensburger, M., Aigner, R., Kandasamy, M., Winner, B., Aigner, L., Winkler, J., 2010. Impaired adult olfactory bulb

neurogenesis in the R6/2 mouse model of Huntington's disease. BMC Neurosci. 11, 114.

Koos, D.S., Ho, R.K., 1998. The nieuwkoid gene characterizes and mediates a Nieuwkoop-center-like activity in the zebrafish. Curr. Biol. 8 (22), 1199–1206.

Kovacs, T., Cairns, N.J., Lantos, P.L., 1999. beta-amyloid deposition and neurofibrillary tangle formation in the olfactory bulb in ageing and Alzheimer's disease. Neuropathol. Appl. Neurobiol. 25 (6), 481–491.

Kovács, T., Papp, M.I., Cairns, N.J., Khan, M.N., Lantos, P.L., 2003. Olfactory bulb in multiple system atrophy. Mov. Disord. 18 (8), 938–942.

Kumaran, R., Vandrovcova, J., Luk, C., Sharma, S., Renton, A., Wood, N.W., et al., 2009. Differential DJ-1 gene expression in Parkinson's disease. Neurobiol. Dis. 36 (2), 393–400.

Kwiatkowski, T.J., Bosco, D.A., LeClerc, A.L., Tamrazian, E., Vanderburg, C.R., Russ, C., et al., 2009. Mutations in the FUS/TLS gene on chromosome 16 cause familial amyotrophic lateral sclerosis. Science 323 (5918), 1205–1208.

Lalonde, R., Fukuchi, K., Strazielle, C., 2012. APP transgenic mice for modelling behavioural and psychological symptoms of dementia (BPSD). Neurosci. Biobehav. Rev. 36 (5), 1357–1375.

Lam, C.S., Korzh, V., Strahle, U., 2005. Zebrafish embryos are susceptible to the dopaminergic neurotoxin MPTP. Eur. J. Neurosci. 21 (6), 1758–1762.

Larson, M.H., Gilbert, L.A., Wang, X., Lim, W.A., Weissman, J.S., Qi, L.S., 2013. CRISPR interference (CRISPRi) for sequence-specific control of gene expression. Nat. Protoc. 8 (11), 2180–2196.

Lattante, S., de Calbiac, H., Le Ber, I., Brice, A., Ciura, S., Kabashi, E., 2015. Sqstm1 knock-down causes a locomotor phenotype ameliorated by rapamycin in a zebrafish model of ALS/FTLD. Hum. Mol. Genet. 24 (6), 1682–1690.

Lazic, S.E., Goodman, A.O.G., Grote, H.E., Blakemore, C., Morton, A.J., Hannan, A.J., et al., 2007. Olfactory abnormalities in Huntington's disease: decreased plasticity in the primary olfactory cortex of R6/1 transgenic mice and reduced olfactory discrimination in patients. Brain Res. 1151 (0), 219–226.

Lee, J.A., Cole, G.J., 2007. Generation of transgenic zebrafish expressing green fluorescent protein under control of zebrafish amyloid precursor protein gene regulatory elements. Zebrafish 4 (4), 277–286.

Lee, J., Freeman, J.L., 2016. Embryonic exposure to 10 μg L-1 lead results in female-specific expression changes in genes associated with nervous system development and function and Alzheimer's disease in aged adult zebrafish brain. Metallomics 8 (6), 589–596.

Lehrner, J.P., Glück, J., Laska, M., 1999. Odor identification, consistency of label use, olfactory threshold and their relationships to odor memory over the human lifespan. Chem. Senses 24 (3), 337–346.

Leighton, P.L., Allison, W.T., 2016. Protein misfolding in prion and prion-like diseases: reconsidering a required role for protein loss-of-function. J. Alzheimers Dis. 54 (1), 3–29.

Lemiere, J., Decruyenaere, M., Evers-Kiebooms, G., Vandenbussche, E., Dom, R., 2004. Cognitive changes in patients with Huntington's disease (HD) and asymptomatic carriers of the HD mutation. J. Neurol. 251 (8), 935–942.

Lemmens, R., Van Hoecke, A., Hersmus, N., Geelen, V., D'Hollander, I., Thijs, V., et al., 2007. Overexpression of mutant superoxide dismutase 1 causes a motor axonopathy in the zebrafish. Hum. Mol. Genet. 16 (19), 2359–2365.

Leopold, D., 2002. Distortion of olfactory perception: diagnosis and treatment. Chem. Senses 27 (7), 611–615.

Leroy, E., Boyer, R., Auburger, G., Leube, B., Ulm, G., Mezey, E., et al., 1998. The ubiquitin pathway in Parkinson's disease. Nature 395 (6701), 451–452.

Lester-Coll, N., Rivera, E.J., Soscia, S.J., Doiron, K., Wands, J.R., De la Monte, S.M., 2006. Intracerebral streptozotocin model of type 3

diabetes: relevance to sporadic Alzheimer's disease. J. Alzheimers Dis. 9 (1), 13–33.

Lewis, J., McGowan, E., Rockwood, J., Melrose, H., Nacharaju, P., Van Slegtenhorst, M., et al., 2000. Neurofibrillary tangles, amyotrophy and progressive motor disturbance in mice expressing mutant (P301L) tau protein. Nat. Genet. 25 (4), 402–405.

Li, H., Li, S.H., Johnston, H., Shelbourne, P.F., Li, X.J., 2000. Amino-terminal fragments of mutant huntingtin show selective accumulation in striatal neurons and synaptic toxicity. Nat. Genet. 25 (4), 385–389.

Li, X., Li, X., Li, Y.-X., Zhang, Y., Chen, D., Sun, M.-Z., et al., 2015. The difference between anxiolytic and anxiogenic effects induced by acute and chronic alcohol exposure and changes in associative learning and memory based on color preference and the cause of parkinson-like behaviors in zebrafish. PLoS One 10 (11), e0141134.

Li, X., Liu, B., Li, X.-L., Li, Y.-X., Sun, M.-Z., Chen, D.-Y., et al., 2014. SiO2 nanoparticles change colour preference and cause Parkinson's-like behaviour in zebrafish. Sci. Rep. 4, 3810.

Liao, H.-K., Wang, Y., Noack Watt, K.E., Wen, Q., Breitbach, J., Kemmet, C.K., et al., 2012. Tol2 gene trap integrations in the zebrafish amyloid precursor protein genes appa and aplp2 reveal accumulation of secreted APP at the embryonic veins. Dev. Dyn. 241 (2), 415–425.

Lindsay, S.M., Vogt, R.G., 2004. Behavioral responses of newly hatched zebrafish (Danio rerio) to amino acid chemostimulants. Chem. Senses 29 (2), 93–100.

Liu, J.-C., Koppula, S., Huh, S.-J., Park, P.-J., Kim, C.-G., Lee, C.-J., Kim, C.-G., 2015. Necrosis inhibitor-5 (NecroX-5), attenuates MPTP-induced motor deficits in a zebrafish model of Parkinson's disease. Genes Genom. 37 (12), 1073–1079.

Long, L., Guo, H., Yao, D., Xiong, K., Li, Y., Liu, P., et al., 2015. Regulation of transcriptionally active genes via the catalytically inactive Cas9 in C. elegans and D. rerio. Cell Res. 25 (5), 638–641.

Lücking, C.B., Dürr, A., Bonifati, V., Vaughan, J., De Michele, G., Gasser, T., et al., 2000. Association between early-onset Parkinson's disease and mutations in the parkin gene. N. Engl. J. Med. 342 (21), 1560–1567.

Lumsden, A.L., Henshall, T.L., Dayan, S., Lardelli, M.T., Richards, R.I., 2007. Huntingtin-deficient zebrafish exhibit defects in iron utilization and development. Hum. Mol. Genet. 16 (16), 1905–1920.

Macknin, J.B., Higuchi, M., Lee, V.M.Y., Trojanowski, J.Q., Doty, R.L., 2004. Olfactory dysfunction occurs in transgenic mice overexpressing human tau protein. Brain Res. 1000 (1-2), 174–178.

MacLeod, D., Dowman, J., Hammond, R., Leete, T., Inoue, K., Abeliovich, A., 2006. The familial parkinsonism gene LRRK2 regulates neurite process morphology. Neuron 52 (4), 587–593.

Manning-Bog, A.B., McCormack, A.L., Li, J., Uversky, V.N., Fink, A.L., Di Monte, D.A., 2002. The herbicide paraquat causes up-regulation and aggregation of α-synuclein in mice. J. Biol. Chem. 277 (3), 1641–1644.

Masliah, E., Rockenstein, E., Veinbergs, I., Mallory, M., Hashimoto, M., Takeda, A., et al., 2000. Dopaminergic loss and inclusion body formation in alpha-synuclein mice: implications for neurodegenerative disorders. Science 287 (5456), 1265–1269.

Masters, C.L., Simms, G., Weinman, N.A., Multhaup, G., McDonald, B.L., Beyreuther, K., 1985. Amyloid plaque core protein in Alzheimer disease and down syndrome. Proc. Natl. Acad. Sci. USA 82 (12), 4245–4249.

Mattiazzi, M., D'Aurelio, M., Gajewski, C.D., Martushova, K., Kiaei, M., Beal, M.F., Manfredi, G., 2002. Mutated human SOD1 causes dysfunction of oxidative phosphorylation in mitochondria of transgenic mice. J. Biol. Chem. 277 (33), 29626–29633.

McCammon, J.M., Doyon, Y., Amacher, S.L., 2011. Inducing high rates of targeted mutagenesis in zebrafish using zinc finger nucleases (ZFNs). Pelegri, F.J. (Ed.), Vertebrate Embryogenesis: Embryological, Cellular and Genetic Methods, vol. 770, Humana Press, Totowa, pp. 505–527.

McCormack, A.L., Thiruchelvam, M., Manning-Bog, A.B., Thiffault, C., Langston, J.W., Cory-Slechta, D.A., Di Monte, D.A., 2002. Environmental risk factors and Parkinson's disease: selective degeneration of nigral dopaminergic neurons caused by the herbicide paraquat. Neurobiol. Dis. 10 (2), 119–127.

McCutcheon, V., Park, E., Liu, E., Wang, Y., Wen, X.Y., Baker, A.J., 2016. A model of excitotoxic brain injury in larval zebrafish: potential application for high-throughput drug evaluation to treat traumatic brain injury. Zebrafish 13 (3), 161–169.

McGown, A., McDearmid, J.R., Panagiotaki, N., Tong, H., Al Mashhadi, S., Redhead, N., et al., 2013. Early interneuron dysfunction in ALS: insights from a mutant sod1 zebrafish model. Ann. Neurol. 73 (2), 246–258.

McKeon, J.E., Sha, D., Li, L., Chin, L.-S., 2015. Parkin-mediated K63-polyubiquitination targets ubiquitin C-terminal hydrolase L1 for degradation by the autophagy-lysosome system. Cell. Mol. Life Sci. 72 (9), 1811–1824.

McKinley, E.T., Baranowski, T.C., Blavo, D.O., Cato, C., Doan, T.N., Rubinstein, A.L., 2005. Neuroprotection of MPTP-induced toxicity in zebrafish dopaminergic neurons. Mol. Brain Res. 141 (2), 128–137.

Menalled, L.B., Sison, J.D., Dragatsis, I., Zeitlin, S., Chesselet, M.-F., 2003. Time course of early motor and neuropathological anomalies in a knock-in mouse model of Huntington's disease with 140 CAG repeats. J. Comp. Neurol. 465 (1), 11–26.

Meng, X., Noyes, M.B., Zhu, L.J., Lawson, N.D., Wolfe, S.A., 2008. Targeted gene inactivation in zebrafish using engineered zinc-finger nucleases. Nat. Biotechnol. 26 (6), 695–701.

Michel, W.C., Sanderson, M.J., Olson, J.K., Lipschitz, D.L., 2003. Evidence of a novel transduction pathway mediating detection of polyamines by the zebrafish olfactory system. J. Exp. Biol. 206 (10), 1697–1706.

Miller, V.M., Nelson, R.F., Gouvion, C.M., Williams, A., Rodriguez-Lebron, E., Harper, S.Q., et al., 2005. CHIP suppresses polyglutamine aggregation and toxicity in vitro and in vivo. J. Neurosci. 25 (40), 9152–9161.

Moechars, D., Dewachter, I., Lorent, K., Reversé, D., Baekelandt, V., Naidu, A., et al., 1999. Early phenotypic changes in transgenic mice that overexpress different mutants of amyloid precursor protein in brain. J. Biol. Chem. 274 (10), 6483–6492.

Monnot, M.J., Babin, P.J., Pole, G., Andre, M., Laforest, L., Ballagny, C., Akimenko, M.A., 1999. Epidermal expression of apolipoprotein E gene during fin and scale development and fin regeneration in zebrafish. Dev. Dyn. 214 (3), 207–215.

Montoya, A., Price, B.H., Menear, M., Lepage, M., 2006. Brain imaging and cognitive dysfunctions in Huntington's disease. J. Psychiatry Neurosci. 31 (1), 21–29.

Morais, V.A., Verstreken, P., Roethig, A., Smet, J., Snellinx, A., Vanbrabant, M., et al., 2009. Parkinson's disease mutations in PINK1 result in decreased Complex I activity and deficient synaptic function. EMBO Mol. Med. 1 (2), 99–111.

Moreau, K., Fleming, A., Imarisio, S., Lopez Ramirez, A., Mercer, J.L., Jimenez-Sanchez, M., et al., 2014. PICALM modulates autophagy activity and tau accumulation. Nat. Commun. 5, 4998.

Moscavitch, S.-D., Szyper-Kravitz, M., Shoenfeld, Y., 2009. Autoimmune pathology accounts for common manifestations in a wide range of neuro-psychiatric disorders: the olfactory and immune system interrelationship. Clin. Immunol. 130 (3), 235–243.

Moussavi Nik, S.H., Newman, M., Wilson, L., Ebrahimie, E., Wells, S., Musgrave, I., et al., 2015. Alzheimer's disease-related peptide PS2V plays ancient, conserved roles in suppression of the unfolded protein response under hypoxia and stimulation of γ-secretase activity. Hum. Mol. Genet. 24 (13), 3662–3678.

Musa, A., Lehrach, H., Russo, V.E.A., 2001. Distinct expression patterns of two zebrafish homologues of the human APP gene during embryonic development. Dev. Genes Evol. 211 (11), 563–567.

Nakazato, Y., Suzuki, S., 1996. Oligodendroglial microtubular tangles in multiple system atrophy. Neuropathology 16 (2), 145–150.

Nasevicius, A., Ekker, S.C., 2000. Effective targeted gene 'knockdown' in zebrafish. Nat. Genet. 26 (2), 216–220.

Nathan, B.P., Yost, J., Litherland, M.T., Struble, R.G., Switzer, P.V., 2004. Olfactory function in apoE knockout mice. Behav. Brain Res. 150 (1–2), 1–7.

Nelson, P.T., Alafuzoff, I., Bigio, E.H., Bouras, C., Braak, H., Cairns, N.J., et al., 2012. Correlation of Alzheimer disease neuropathologic changes with cognitive status: a review of the literature. J. Neuropathol. Exp. Neurol. 71 (5), 362–381.

Neumann, M., Sampathu, D.M., Kwong, L.K., Truax, A.C., Micsenyi, M.C., Chou, T.T., et al., 2006. Ubiquitinated TDP-43 in frontotemporal lobar degeneration and amyotrophic lateral sclerosis. Science 314 (5796), 130–133.

Newman, M., Ebrahimie, E., Lardelli, M., 2014a. Using the zebrafish model for Alzheimer's disease research. Front. Genet. 5, 189.

Newman, M., Wilson, L., Verdile, G., Lim, A., Khan, I., Moussavi Nik, S.H., et al., 2014b. Differential, dominant activation and inhibition of Notch signalling and APP cleavage by truncations of Psen1 in human disease. Hum. Mol. Genet. 23 (3), 602–617.

Noble, S., Ismail, A., Godoy, R., Xi, Y., Ekker, M., 2012. Zebrafish Parla- and Parlb-deficiency affects dopaminergic neuron patterning and embryonic survival. J. Neurochem. 122 (1), 196–207.

Nordin, S., Paulsen, J.S., Murphy, C., 1995. Sensory- and memory-mediated olfactory dysfunction in Huntington's disease. J. Int. Neuropsychol. Soc. 1 (03), 281–290.

Nornes, S., Groth, C., Camp, E., Ey, P., Lardelli, M., 2003. Developmental control of Presenilin1 expression, endoproteolysis, and interaction in zebrafish embryos. Exp. Cell Res. 289 (1), 124–132.

Nornes, S., Newman, M., Wells, S., Verdile, G., Martins, R.N., Lardelli, M., 2009. Independent and cooperative action of Psen2 with Psen1 in zebrafish embryos. Exp. Cell Res. 315 (16), 2791–2801.

Okamoto, K., Mizuno, Y., Fujita, Y., 2008. Bunina bodies in amyotrophic lateral sclerosis. Neuropathology 28 (2), 109–115.

Olsson, S., Barnard, J., Turri, L., 2006. Olfaction and identification of unrelated individuals: examination of the mysteries of human odor recognition. J. Chem. Ecol. 32 (8), 1635–1645.

Palacino, J.J., Sagi, D., Goldberg, M.S., Krauss, S., Motz, C., Wacker, M., et al., 2004. Mitochondrial dysfunction and oxidative damage in parkin-deficient mice. J. Biol. Chem. 279 (18), 18614–18622.

Paquet, D., Bhat, R., Sydow, A., Mandelkow, E.M., Berg, S., Hellberg, S., et al., 2009. A zebrafish model of tauopathy allows in vivo imaging of neuronal cell death and drug evaluation. J. Clin. Invest. 119 (5), 1382–1395.

Parkinson, J., 2002. An essay on the shaking palsy (reprinted). J. Neuropsychiatry Clin. Neurosci. 14 (2), 223–236.

Parng, C., Ton, C., Lin, Y.-X., Roy, N.M., McGrath, P., 2006. A zebrafish assay for identifying neuroprotectants in vivo. Neurotoxicol. Teratol. 28 (4), 509–516.

Pause, B.M., Miranda, A., Göder, R., Aldenhoff, J.B., Ferstl, R., 2001. Reduced olfactory performance in patients with major depression. J. Psychiatric Res. 35 (5), 271–277.

Periquet, M., Corti, O., Jacquier, S., Brice, A., 2005. Proteomic analysis of parkin knockout mice: alterations in energy metabolism, protein handling and synaptic function. J. Neurochem. 95 (5), 1259–1276.

Petrasch-Parwez, E., Nguyen, H.-P., Löbbecke-Schumacher, M., Habbes, H.-W., Wieczorek, S., Riess, O., et al., 2007. Cellular and subcellular localization of Huntington aggregates in the brain of a rat transgenic for Huntington disease. J. Comp. Neurol. 501 (5), 716–730.

Pillay, L.M., Selland, L.G., Fleisch, V.C., Leighton, P.L., Cheng, C.S., Famulski, J.K., et al., 2013. Evaluating the mutagenic activity of targeted endonucleases containing a Sharkey FokI cleavage domain variant in zebrafish. Zebrafish 10 (3), 353–364.

Pinho, B.R., Reis, S.D., Guedes-Dias, P., Leitão-Rocha, A., Quintas, C., Valentão, P., et al., 2016. Pharmacological modulation of HDAC1 and HDAC6 in vivo in a zebrafish model: therapeutic implications for Parkinson's disease. Pharmacol. Res. 103, 328–339.

Poletti, M., De Rosa, A., Bonuccelli, U., 2012. Affective symptoms and cognitive functions in Parkinson's disease. J. Neurol. Sci. 317 (1-2), 97–102.

Polymenidou, M., Cleveland, D.W., 2012. Prion-like spread of protein aggregates in neurodegeneration. J. Exp. Med. 209 (5), 889–893.

Polymeropoulos, M.H., Lavedan, C., Leroy, E., Ide, S.E., Dehejia, A., Dutra, A., et al., 1997. Mutation in the alpha-synuclein gene identified in families with Parkinson's disease. Science 276 (5321), 2045–2047.

Ponsen, M.M., Stoffers, D., Booij, J., van Eck-Smit, B.L.F., Wolters, E.C., Berendse, H.W., 2004. Idiopathic hyposmia as a preclinical sign of Parkinson's disease. Ann. Neurol. 56 (2), 173–181.

Ponsen, M.M., Stoffers, D., Twisk, J.W.R., Wolters, E.C., Berendse, H.W., 2009. Hyposmia and executive dysfunction as predictors of future Parkinson's disease: A prospective study. Mov. Disord. 24 (7), 1060–1065.

Prabhudesai, S., Sinha, S., Attar, A., Kotagiri, A., Fitzmaurice, A.G., Lakshmanan, R., et al., 2012. A novel "molecular tweezer" inhibitor of alpha-synuclein neurotoxicity in vitro and in vivo. Neurotherapeutics 9 (2), 464–476.

Pramatarova, A., Laganière, J., Roussel, J., Brisebois, K., Rouleau, G.A., 2001. Neuron-specific expression of mutant superoxide dismutase 1 in transgenic mice does not lead to motor impairment. J. Neurosci. 21 (10), 3369–3374.

Prediger, R.D.S., Aguiar, A.S., Matheus, F.C., Walz, R., Antoury, L., Raisman-Vozari, R., Doty, R.L., 2012. Intranasal administration of neurotoxicants in animals: support for the olfactory vector hypothesis of Parkinson's Disease. Neurotox. Res. 21 (1), 90–116.

Prehn, A., Ohrt, A., Sojka, B., Ferstl, R., Pause, B.M., 2006. Chemosensory anxiety signals augment the startle reflex in humans. Neurosci. Lett. 394 (2), 127–130.

Priyadarshi, A., Khuder, S.A., Schaub, E.A., Priyadarshi, S.S., 2001. Environmental risk factors and Parkinson's disease: a metaanalysis. Environ. Res. 86 (2), 122–127.

Purdie, E.L., Samsudin, S., Eddy, F.B., Codd, G.A., 2009. Effects of the cyanobacterial neurotoxin β-N-methylamino-L-alanine on the early-life stage development of zebrafish (Danio rerio). Aquat. Toxicol. 95 (4), 279–284.

Ramesh, T., Lyon, A.N., Pineda, R.H., Wang, C., Janssen, P.M., Canan, B.D., et al., 2010. A genetic model of amyotrophic lateral sclerosis in zebrafish displays phenotypic hallmarks of motoneuron disease. Dis. Model Mech. 3 (9-10), 652–662.

Rehman, H.U., 2001. Multiple system atrophy. Postgrad. Med. J. 77 (908), 379–382.

Ren, G.Q., Xin, S.C., Li, S., Zhong, H.B., Lin, S., 2011. Disruption of LRRK2 does not cause specific loss of dopaminergic neurons in zebrafish. PLoS One 6 (6), e20630.

Renton, A.E., Majounie, E., Waite, A., Simón-Sánchez, J., Rollinson, S., Gibbs, J.R., et al., 2011. A hexanucleotide repeat expansion in C9ORF72 is the cause of chromosome 9p21-linked ALS-FTD. Neuron 72 (2), 257–268.

Richetti, S.K., Blank, M., Capiotti, K.M., Piato, A.L., Bogo, M.R., Vianna, M.R., Bonan, C.D., 2011. Quercetin and rutin prevent scopolamine-induced memory impairment in zebrafish. Behav. Brain Res. 217 (1), 10–15.

Robinson, A.M., Conley, D.B., Shinners, M.J., Kern, R.C., 2002. Apoptosis in the aging olfactory epithelium. Laryngoscope 112 (8), 1431–1435.

Rockenstein, E., Crews, L., Masliah, E., 2007. Transgenic animal models of neurodegenerative diseases and their application to treatment development. Adv. Drug Deliv. Rev. 59 (11), 1093–1102.

Rosen, D.R., Siddique, T., Patterson, D., Figlewicz, D.A., Sapp, P., Hentati, A., et al., 1993. Mutations in Cu/Zn superoxide dismutase gene are associated with familial amyotrophic lateral sclerosis. Nature 362 (6415), 59–62.

Ross, G.W., Abbott, R.D., Petrovitch, H., Tanner, C.M., Davis, D.G., Nelson, J., et al., 2006. Association of olfactory dysfunction with incidental Lewy bodies. Mov. Disord. 21 (12), 2062–2067.

Ross, G.W., Abbott, R.D., Petrovitch, H., Tanner, C.M., White, L.R., 2012. Pre-motor features of Parkinson's disease: the Honolulu-Asia Aging Study experience. Parkinsonism Relat. Disord. 18 (Suppl. 1), S199–S202.

Ross, G.W., Petrovitch, H., Abbott, R.D., Tanner, C.M., Popper, J., Masaki, K., et al., 2008. Association of olfactory dysfunction with risk for future Parkinson's disease. Ann. Neurol. 63 (2), 167–173.

Rossi, A., Kontarakis, Z., Gerri, C., Nolte, H., Holper, S., Kruger, M., Stainier, D.Y.R., 2015. Genetic compensation induced by deleterious mutations but not gene knockdowns. Nature 524 (7564), 230–233.

Rubio-Godoy, M., Aunger, R., Curtis, V., 2007. Serotonin—a link between disgust and immunity? Med. Hypotheses 68 (1), 61–66.

Rustay, N.R., Cronin, E.A., Curzon, P., Markosyan, S., Bitner, R.S., Ellis, T.A., et al., 2010. Mice expressing the Swedish APP mutation on a 129 genetic background demonstrate consistent behavioral deficits and pathological markers of Alzheimer's disease. Brain Res. 1311 (0), 136–147.

Sager, J., Bai, Q., Burton, E., 2010. Transgenic zebrafish models of neurodegenerative diseases. Brain Struct. Funct. 214 (2), 285–302.

Sajjadian, A., Doty, R.L., Gutnick, D.N., Chirurgi, R.J., Sivak, M., Perl, D., 1994. Olfactory dysfunction in amyotrophic-lateral-sclerosis. Neurodegeneration 3 (2), 153–157.

Sakowski, S.A., Lunn, J.S., Busta, A.S., Oh, S.S., Zamora-Berridi, G., Palmer, M., et al. 2012. Neuromuscular effects of G93A-SOD1 expression in zebrafish. Mol. Neurodegener. 7, 44–144.

Sallinen, V., Kolehmainen, J., Priyadarshini, M., Toleikyte, G., Chen, Y.-C., Panula, P., 2010. Dopaminergic cell damage and vulnerability to MPTP in Pink1 knockdown zebrafish. Neurobiol. Dis. 40 (1), 93–101.

Sarath Babu, N., Murthy, C.L.N., Kakara, S., Sharma, R., Brahmendra Swamy, C.V., Idris, M.M., 2016. 1-Methyl-4-phenyl-1,2,3,6-tetrahydropyridine induced Parkinson's disease in zebrafish. Proteomics 16 (9), 1407–1420.

Saudou, F., Finkbeiner, S., Devys, D., Greenberg, M.E., 1998. Huntingtin acts in the nucleus to induce apoptosis but death does not correlate with the formation of intranuclear inclusions. Cell 95 (1), 55–66.

Scheuner, D., Eckman, C., Jensen, M., Song, X., Citron, M., Suzuki, N., et al., 1996. Secreted amyloid beta-protein similar to that in the senile plaques of Alzheimer's disease is increased in vivo by the presenilin 1 and 2 and APP mutations linked to familial Alzheimer's disease. Nat. Med. 2 (8), 864–870.

Schilling, T.F., Sosnik, J., Nie, Q., 2016. Visualizing retinoic acid morphogen gradients. William Detrich, M.W.H., Leonard, I.Z. (Eds.), Methods in Cell Biology, vol. 133, Academic Press, Cambridge, MA, pp. 139–163, Chapter 7.

Schmidt, C., Herting, B., Prieur, S., Junghanns, S., Schweitzer, K., Globas, C., et al., 2008. Autonomic dysfunction in different subtypes of multiple system atrophy. Mov. Disord. 23 (12), 1766–1772.

Schmid, B., Hruscha, A., Hogl, S., Banzhaf-Strathmann, J., Strecker, K., van der Zee, J., et al., 2013. Loss of ALS-associated TDP-43 in zebrafish causes muscle degeneration, vascular dysfunction, and reduced motor neuron axon outgrowth. Proc. Natl. Acad. Sci. USA 110 (13), 4986–4991.

Schwanzel-Fukuda, M., Bick, D., Pfaff, D.W., 1989. Luteinizing hormone-releasing hormone (LHRH)-expressing cells do not migrate normally in an inherited hypogonadal (Kallmann) syndrome. Mol. Brain Res. 6 (4), 311–326.

Seiden, A.M., 2004. Postviral olfactory loss. Otolaryngol. Clin. North Am. 37 (6), 1159–1166.

Selkoe, D.J., 2001. Alzheimer's disease: genes, proteins, and therapy. Physiol. Rev. 81 (2), 741–766.

Setsuie, R., Wang, Y.-L., Mochizuki, H., Osaka, H., Hayakawa, H., Ichihara, N., et al., 2007. Dopaminergic neuronal loss in transgenic mice expressing the Parkinson's disease-associated UCH-L1 I93M mutant. Neurochem. Int. 50 (1), 119–129.

Shamchuk, A.L., Tierney, K.B., 2012. Phenotyping stimulus evoked responses in larval zebrafish. Behaviour 149 (10-12), 1177–1203.

Sharma, S., Bandopadhyay, R., Lashley, T., Renton, A.E.M., Kingsbury, A.E., Kumaran, R., et al., 2011. LRRK2 expression in idiopathic and G2019S positive Parkinson's disease subjects: a morphological and quantitative study. Neuropathol. Appl. Neurobiol. 37 (7), 777–790.

Sheng, D., Qu, D., Kwok, K.H.H., Ng, S.S., Lim, A.Y.M., Aw, S.S., et al., 2010. Deletion of the WD40 domain of LRRK2 in zebrafish causes parkinsonism-like loss of neurons and locomotive defect. PLoS Genet. 6 (4), e1000914.

Sherer, T.B., Kim, J.-H., Betarbet, R., Greenamyre, J.T., 2003. Subcutaneous rotenone exposure causes highly selective dopaminergic degeneration and α-synuclein aggregation. Exp. Neurol. 179 (1), 9–16.

Sherrington, R., Rogaev, E.I., Liang, Y., Rogaeva, E.A., Levesque, G., Ikeda, M., et al., 1995. Cloning of a gene bearing missense mutations in early-onset familial Alzheimer's disease. Nature 375 (6534), 754–760.

Shestopalov, I.A., Sinha, S., Chen, J.K., 2007. Light-controlled gene silencing in zebrafish embryos. Nat. Chem. Biol. 3 (10), 650–651.

Shi, G., Lee, J.R., Grimes, D.A., Racacho, L., Ye, D., Yang, H., et al., 2011. Functional alteration of PARL contributes to mitochondrial dysregulation in Parkinson's disease. Hum. Mol. Genet. 20 (10), 1966–1974.

Shibata, N., Hirano, A., Kobayashi, M., Sasaki, S., Takeo, K., Matsumoto, S., et al., 1994. CuZn superoxide dismutase-like immunoreactivity in Lewy body-like inclusions of sporadic amyotrophic lateral sclerosis. Neurosci. Lett. 179 (1-2), 149–152.

Shimura, H., Hattori, N., Kubo, S.I., Mizuno, Y., Asakawa, S., Minoshima, S., et al., 2000. Familial Parkinson disease gene product, parkin, is a ubiquitin-protein ligase. Nat. Genet. 25 (3), 302–305.

Shults, C.W., Rockenstein, E., Crews, L., Adame, A., Mante, M., Larrea, G., et al., 2005. Neurological and neurodegenerative alterations in a transgenic mouse model expressing human α-synuclein under oligodendrocyte promoter: implications for multiple system atrophy. J. Neurosci. 25 (46), 10689–10699.

Simpson, C.L., Lemmens, R., Miskiewicz, K., Broom, W.J., Hansen, V.K., van Vught, P.W.J., et al., 2009. Variants of the elongator protein 3 (ELP3) gene are associated with motor neuron degeneration. Hum. Mol. Genet. 18 (3), 472–481.

Skromne, I., Prince, V.E., 2008. Current perspectives in zebrafish reverse genetics: moving forward. Dev. Dyn. 237 (4), 861–882.

Small, D.H., Cappai, R., 2006. Alois Alzheimer and Alzheimer's disease: a centennial perspective. J. Neurochem. 99 (3), 708–710.

Smith, W.M., Davidson, T.M., Murphy, C., 2009. Toxin-induced chemosensory dysfunction: a case series and review. Am. J. Rhinol. Allergy 23 (6), 578–581.

Son, O.-L., Kim, H.-T., Ji, M.-H., Yoo, K.-W., Rhee, M., Kim, C.-H., 2003. Cloning and expression analysis of a Parkinson's disease gene, uch-L1, and its promoter in zebrafish. Biochem. Biophys. Res. Commun. 312 (3), 601–607.

Song, P., Pimplikar, S.W., 2012. Knockdown of amyloid precursor protein in zebrafish causes defects in motor axon outgrowth. PLoS One 7 (4), e34209.

Speedie, N., Gerlai, R., 2008. Alarm substance induced behavioral responses in zebrafish (Danio rerio). Behav. Brain Res. 188 (1), 168–177.

Spillantini, M.G., Crowther, R.A., Jakes, R., Hasegawa, M., Goedert, M., 1998. alpha-synuclein in filamentous inclusions of Lewy bodies from Parkinson's disease and dementia with Lewy bodies. Proc. Natl. Acad. Sci. USA 95 (11), 6469–6473.

Stefanova, N., Reindl, M., Neumann, M., Haass, C., Poewe, W., Kahle, P.J., Wenning, G.K., 2005. Oxidative stress in transgenic mice with oligodendroglial α-synuclein overexpression replicates the characteristic neuropathology of multiple system atrophy. Am. J. Pathol. 166 (3), 869–876.

Stefanova, N., Reindl, M., Neumann, M., Kahle, P.J., Poewe, W., Wenning, G.K., 2007. Microglial activation mediates neurodegeneration related to oligodendroglial α-synucleinopathy: Implications for multiple system atrophy. Mov. Disord. 22 (15), 2196–2203.

Stevenson, R.J., 2010. An initial evaluation of the functions of human olfaction. Chem. Senses 35 (1), 3–20.

Stevenson, R.J., Oaten, M.J., Case, T.I., Repacholi, B.M., Wagland, P., 2010. Children's response to adult disgust elicitors: development and acquisition. Dev. Psychol. 46 (1), 165–177.

Stevenson, R.J., Prescott, J., Boakes, R.A., 1995. The acquisition of taste properties by odors. Learn. Motiv. 26 (4), 433–455.

Stopford, C.L., Snowden, J.S., Thompson, J.C., Neary, D., 2007. Distinct memory profiles in Alzheimer's disease. Cortex 43 (7), 846–857.

Sun, Z., Gitler, A.D., 2008. Discovery and characterization of three novel synuclein genes in zebrafish. Dev. Dyn. 237 (9), 2490–2495.

Sun, N., Zhao, H., 2013. Transcription activator-like effector nucleases (TALENs): a highly efficient and versatile tool for genome editing. Biotechnol. Bioeng. 110 (7), 1811–1821.

Sunderman, F.W., 2001. Nasal toxicity, carcinogenicity, and olfactory uptake of metals. Ann. Clin. Lab. Sci. 31 (1), 3–24.

Suzuki, M., Saito, K., Min, W.-P., Vladau, C., Toida, K., Itoh, H., Murakami, S., 2007. Identification of viruses in patients with postviral olfactory dysfunction. Laryngoscope 117 (2), 272–277.

Sydow, A., Mandelkow, E.M., 2010. 'Prion-like' propagation of mouse and human tau aggregates in an inducible mouse model of tauopathy. Neurodegener. Dis. 7 (1-3), 28–31.

Takahashi, R.H., Almeida, C.G., Kearney, P.F., Yu, F., Lin, M.T., Milner, T.A., Gouras, G.K., 2004. Oligomerization of Alzheimer's β-amyloid within processes and synapses of cultured neurons and brain. J. Neurosci. 24 (14), 3592–3599.

Tallafuss, A., Gibson, D., Morcos, P., Li, Y., Seredick, S., Eisen, J., Washbourne, P., 2012. Turning gene function ON and OFF using sense and antisense photo-morpholinos in zebrafish. Development 139 (9), 1691–1699.

Tatebayashi, Y., Miyasaka, T., Chui, D.H., Akagi, T., Mishima, K., Iwasaki, K., et al., 2002. Tau filament formation and associative memory deficit in aged mice expressing mutant (R406W) human tau. Proc. Natl. Acad. Sci. USA 99 (21), 13896–13901.

Tattersfield, A.S., Croon, R.J., Liu, Y.W., Kells, A.P., Faull, R.L.M., Connor, B., 2004. Neurogenesis in the striatum of the quinolinic acid lesion model of Huntington's disease. Neuroscience 127 (2), 319–332.

Temmel, A.F., Quint, C., Schickinger-Fischer, B., Klimek, L., Stoller, E., Hummel, T., 2002. Characteristics of olfactory disorders in relation to major causes of olfactory loss. Arch. Otolaryngol. Head Neck Surg. 128 (6), 635–641.

Thomann, P.A., Dos Santos, V., Toro, P., Schönknecht, P., Essig, M., Schröder, J., 2009. Reduced olfactory bulb and tract volume in early Alzheimer's disease—a MRI study. Neurobiol. Aging 30 (5), 838–841.

Thornhill, R., Gangestad, S.W., Miller, R., Scheyd, G., McCollough, J.K., Franklin, M., 2003. Major histocompatibility complex genes, symmetry, and body scent attractiveness in men and women. Behav. Ecol. 14 (5), 668–678.

Thummel, R., Bai, S., Sarras, M.P., Song, P., McDermott, J., Brewer, J., et al., 2006. Inhibition of zebrafish fin regeneration using in vivo electroporation of morpholinos against fgfr1 and msxb. Dev. Dyn. 235 (2), 336–346.

Tierney, K.B., 2011. Swimming performance assessment in fishes. J. Vis. Exp. (51), 1–4.

Tierney, K.B., 2015. Olfaction in Aquatic Vertebrates. Handbook of Olfaction and Gustation. John Wiley & Sons, Hoboken, NJ, pp. 547–564.

Tissingh, G., Berendse, H.W., Bergmans, P., DeWaard, R., Drukarch, B., Stoof, J.C., Wolters, E.C., 2001. Loss of olfaction in de novo and treated Parkinson's disease: possible implications for early diagnosis. Mov. Disord. 16 (1), 41–46.

Ubhi, K., Low, P., Masliah, E., 2011. Multiple system atrophy: a clinical and neuropathological perspective. Trends Neurosci. 34 (11), 581–590.

Ubhi, K., Rockenstein, E., Mante, M., Inglis, C., Adame, A., Patrick, C., et al., 2010. Neurodegeneration in a transgenic mouse model of multiple system atrophy is associated with altered expression of oligodendroglial-derived neurotrophic factors. J. Neurosci. 30 (18), 6236–6246.

Upadhyay, U.D., Holbrook, E.H., 2004. Olfactory loss as a result of toxic exposure. Otolaryngol. Clin. North Am. 37 (6), 1185–1207.

van Ham, T.J., Mapes, J., Kokel, D., Peterson, R.T., 2010. Live imaging of apoptotic cells in zebrafish. FASEB J. 24 (11), 4336–4342.

van Welsem, M.v.W., Hogenhuis, J.H., Meininger, V.M., Metsaars, W.M., Hauw, J.J.H., Seilhean, D.S., 2002. The relationship between Bunina bodies, skein-like inclusions and neuronal loss in amyotrophic lateral sclerosis. Acta Neuropathol. 103 (6), 583–589.

Vance, C., Rogelj, B., Hortobágyi, T., De Vos, K.J., Nishimura, A.L., Sreedharan, J., et al., 2009. Mutations in FUS, an RNA processing protein, cause familial amyotrophic lateral sclerosis type 6. Science 323 (5918), 1208–1211.

Veldman, M.B., Rios-Galdamez, Y., Lu, X.-H., Gu, X., Qin, W., Li, S., et al., 2015. The N17 domain mitigates nuclear toxicity in a novel zebrafish Huntington's disease model. Mol. Neurodegener. 10 (1), 1–16.

Vitebsky, A., Reyes, R., Sanderson, M.J., Michel, W.C., Whitlock, K.E., 2005. Isolation and characterization of the laure olfactory behavioral mutant in the zebrafish, Danio rerio. Dev. Dyn. 234 (1), 229–242.

Wakabayashi, K., Yoshimoto, M., Tsuji, S., Takahashi, H., 1998. α-Synuclein immunoreactivity in glial cytoplasmic inclusions in multiple system atrophy. Neurosci. Lett. 249 (2-3), 180–182.

Walker, F.O., 2007. Huntington's disease. Lancet 369 (9557), 218–228.

Wang, H.-L., Chou, A.-H., Wu, A.-S., Chen, S.-Y., Weng, Y.-H., Kao, Y.-C., et al., 2011. PARK6 PINK1 mutants are defective in maintaining mitochondrial membrane potential and inhibiting ROS formation of substantia nigra dopaminergic neurons. Biochim. Biophys. Acta 1812 (6), 674–684.

Wang, J.L., Eslinger, P.J., Doty, R.L., Zimmerman, E.K., Grunfeld, R., Sun, X.Y., et al., 2010. Olfactory deficit detected by fMRI in early Alzheimer's disease. Brain Res. 1357, 184–194.

Weisfeld, G.E., Czilli, T., Phillips, K.A., Gall, J.A., Lichtman, C.M., 2003. Possible olfaction-based mechanisms in human kin recognition and inbreeding avoidance. J. Exp. Child Psychol. 85 (3), 279–295.

Weisskopf, M.G., Morozova, N., O'Reilly, E.J., McCullough, M.L., Calle, E.E., Thun, M.J., Ascherio, A., 2009. Prospective study of chemical exposures and amyotrophic lateral sclerosis. J. Neurol. Neurosurg. Psychiatry 80 (5), 558–561.

Wellington, C.L., Ellerby, L.M., Gutekunst, C.-A., Rogers, D., Warby, S., Graham, R.K., et al., 2002. Caspase cleavage of mutant huntingtin precedes neurodegeneration in Huntington's disease. J. Neurosci. 22 (18), 7862–7872.

Wesson, D.W., Levy, E., Nixon, R.A., Wilson, D.A., 2010. Olfactory dysfunction correlates with amyloid-β burden in an Alzheimer's disease mouse model. J. Neurosci. 30 (2), 505–514.

Wienholds, E., van Eeden, F., Kosters, M., Mudde, J., Plasterk, R.H.A., Cuppen, E., 2003. Efficient target-selected mutagenesis in zebrafish. Genome Res. 13 (12), 2700–2707.

Wilson, J.M.B., Khabazian, I., Wong, M.C., Seyedalikhani, A., Bains, J.S., Pasqualotto, B.A., et al., 2002. Behavioral and neurological correlates of ALS-parkinsonism dementia complex in adult mice fed washed cycad flour. Neuromolecular Med. 1 (3), 207–221.

Wilson, J.M.B., Petrik, M.S., Grant, S.C., Blackband, S.J., Lai, J., Shaw, C.A., 2004. Quantitative measurement of neurodegeneration in an ALS–PDC model using MR microscopy. NeuroImage 23 (1), 336–343.

Wong, K.K., Muller, M.L.T.M., Kuwabara, H., Studenski, S.A., Bohnen, N.I., 2010. Olfactory loss and nigrostriatal dopaminergic denervation in the elderly. Neurosci. Lett. 484 (3), 163–167.

Woo, H.-N., Park, J.-S., Gwon, A.R., Arumugam, T.V., Jo, D.-G., 2009. Alzheimer's disease and Notch signaling. Biochem. Biophys. Res. Commun. 390 (4), 1093–1097.

Wood, J.D., Beaujeux, T.P., Shaw, P.J., 2003. Protein aggregation in motor neurone disorders. Neuropathol. Appl. Neurobiol. 29 (6), 529–545.

Xi, Y., Ryan, J., Noble, S., Yu, M., Yilbas, A.E., Ekker, M., 2010. Impaired dopaminergic neuron development and locomotor function in zebrafish with loss of pink1 function. Eur. J. Neurosci. 31 (4), 623–633.

Yanicostas, C., Herbomel, E., Dipietromaria, A., Soussi-Yanicostas, N., 2009. Anosmin-1a is required for fasciculation and terminal targeting of olfactory sensory neuron axons in the zebrafish olfactory system. Mol. Cell. Endocrinol. 312 (1-2), 53–60.

Yasuda, T., Nihira, T., Ren, Y.R., Cao, X.Q., Wada, K., Setsuie, R., et al., 2009. Effects of UCH-L1 on alpha-synuclein over-expression mouse model of Parkinson's disease. J. Neurochem. 108 (4), 932–944.

Yoshida, M., Macklin, W.B., 2005. Oligodendrocyte development and myelination in GFP-transgenic zebrafish. J. Neurosci. Res. 81 (1), 1–8.

Yousem, D.M., Geckle, R.J., Bilker, W., McKeown, D.A., Doty, R.L., 1996. MR evaluation of patients with congenital hyposmia or anosmia. Am. J. Roentgenol. 166 (2), 439–443.

Yu, Y., Chi, B., Xia, W., Gangopadhyay, J., Yamazaki, T., Winkelbauer-Hurt, M.E., et al., 2015. U1 snRNP is mislocalized in ALS patient fibroblasts bearing NLS mutations in FUS and is required for motor neuron outgrowth in zebrafish. Nucleic Acids Res..

Yue, Z., 2009. LRRK2 in Parkinson's disease: in vivo models and approaches for understanding pathogenic roles. FEBS J. 276 (22), 6445–6454.

Żekanowski, C., Styczyńska, M., Pepłońska, B., Gabryelewicz, T., Religa, D., Ilkowski, J., et al., 2003. Mutations in presenilin 1, presenilin 2 and amyloid precursor protein genes in patients with early-onset Alzheimer's disease in Poland. Exp. Neurol. 184 (2), 991–996.

Zheng, H., Koo, E.H., 2011. Biology and pathophysiology of the amyloid precursor protein. Mol. Neurodegener. 6 (1), 27.

Zivadinov, R., Zorzon, M., Monti Bragadin, L., Pagliaro, G., Cazzato, G., 1999. Olfactory loss in multiple sclerosis. J. Neurol. Sci. 168 (2), 127–130.

Zon, L.I., Peterson, R.T., 2005. In vivo drug discovery in the zebrafish. Nat. Rev. Drug Discov. 4 (1), 35–44.

Zuccato, C., Ciammola, A., Rigamonti, D., Leavitt, B.R., Goffredo, D., Conti, L., et al., 2001. Loss of huntingtin-mediated BDNF gene transcription in Huntington's disease. Science 293 (5529), 493–498.

PART H

BEHAVIOR

Page left intentionally blank

22

Animal Models for Studying Substance Use Disorder: Place and Taste Conditioning

Catherine M. Davis

Johns Hopkins University School of Medicine, Baltimore, MD, United States

1 WHAT IS SUBSTANCE USE DISORDER AND WHY SHOULD WE STUDY IT?

With the release of the *Diagnostic and Statistical Manual*, Version 5 (DSM-5, 2013), the terminology and criteria for additive disorders underwent a substantial revision. Terms commonly used in the literature, including "abuse" and "dependence," were replaced by the phrase "substance use disorder." Substance use disorder (SUD) is now subdivided into mild, moderate, or severe forms of the disease. While many of the features that previously defined "drug addiction" are still included, tolerance and withdrawal in the DSM-5 are specific to nonprescription drug use, and these effects when associated with the cessation of prescribed medications, no longer fall into the SUD category. The most severe form of SUD, however, is often still referred to as addiction and is still considered a chronically relapsing disorder, characterized by the compulsion to seek out and take the drug and a loss of control in limiting drug intake, despite a desire to stop using the drug (Koob and Volkow, 2010; Volkow et al., 2016). Use of licit (e.g., alcohol, nicotine) and illicit (e.g., marijuana, cocaine, heroin) substances are pervasive societal problems resulting in severe emotional, financial, and physical cost to the substance abusing individual, the individual's family, and the community (Nicholson and Ator, 2011). The economic cost (e.g., healthcare costs, crime-related costs, loss of productivity) of SUD in the United States exceeds $700 billion annually, with approximately 70% of these costs associated with abuse of alcohol and tobacco (CDC, 2014; US Department of Health and Human Services, 2014; US Department of Justice, 2011). Substance use and abuse is also associated with other

public health issues, including the spread of infectious diseases (e.g., HIV, hepatitis C) and impaired driving (CDC, 2005a,b). Despite the myriad costs to individuals and society, justifying the need for animal models of SUD can be a difficult task for researchers given that drug addiction is perceived by a large portion of the general public to result from moral weakness, a lack of will power, and/or self-discipline (Leshner, 1997; Nicholson and Ator, 2011).

In the scientific community, however, SUD is viewed as a disease of the brain that warrants the same type of investments in research and treatment strategies as those given to diseases, such as autism, schizophrenia, and Alzheimer's and Parkinson's disease (Leshner, 1997). Further, researchers studying SUD employ the same strategies as researchers investigating these other diseases: animal models are developed to represent some characteristic of the disorder and then studied, with the understanding that every detail of the disorder is most often not completely reproducible in a laboratory animal, but that a better understanding of the factors that contribute to the disease-process can be gained. For example, "schizophrenic" or "autistic" rats and mice do not exist (Baker, 2011), although there are rats and mice that exhibit behaviors characteristic of schizophrenia, autism, or even obsessive-compulsive disorder (Peca et al., 2011; Welch et al., 2007); these animal models are used to further our understanding of the molecular, cellular, and genetic components of a specific disorder and how these deficiencies translate into quantifiable behavioral symptoms.

Similar to many of these other human disease states, SUD is a uniquely human phenomenon, thus any attempt to study it in the laboratory inevitably constrains it reproducibility. Investigators must keep this in mind when designing and employing animal models of drug addiction. Some models have very good face validity, such as the drug self-administration procedure in which an animal emits a response (e.g., lever press) to receive a drug injection reinforcer. Elegant experiments using the self-administration procedure to study in rats the diagnostic criteria of addiction (outlined in a previous version of the *Diagnostic and Statistical Manual of Mental Disorders*; DSM-IV-TR) have been reported and arguably provide new approaches to study the neurobiology of addiction (Belin et al., 2008; Deroche-Gamonet et al., 2004; Robinson, 2004; Vanderschuren and Everitt, 2004). For other methods, the connection to the human drug user is not as evident, but the procedure nonetheless allows researchers to examine some aspect of addiction that is important to its overall etiology. Thus, the specific question under investigation influences the methodology and procedure employed. Great care must be taken to understand each procedure's strengths and limitations and how these factors impact

the interpretation of the results of the study. Even with these caveats, preclinical animal models have been instrumental in furthering our understanding of the neurobiological and behavioral characteristics of addiction, including drug-taking, physical dependence, tolerance, drug craving, and the factors that might increase the likelihood of relapse; however there is still much to learn and numerous reasons to continue refining our current models, in addition to developing new models as various techniques become even more sophisticated (Lobo et al., 2010; Tsai et al., 2009).

In the current review, two popular methods used to study SUD, place conditioning (primarily focused on conditioned place preference or CPP) and conditioned taste aversion (CTA) will be discussed. Both procedures have been used extensively to study the rewarding and aversive effects associated with drug exposure. With each of these procedures comes a rather large literature base that includes, but is not limited to, variations in procedural details, equipment, and study design, debates on data analysis and interpretation, and excellent reviews commenting on the strengths, weaknesses, and controversies surrounding each procedure. Although many of these factors will be discussed in the current review, readers are encouraged to access these resources for additional information (Bardo and Bevins, 2000; Bardo et al., 1995; Huston et al., 2013; Liu et al., 2008; Mueller and de Wit, 2011; Riley et al., 2012; Schechter and Calcagnetti, 1993, 1998; Tzschentke, 1998, 2007; van der Kooy, 1987).

2 REWARD AND REINFORCEMENT

When beginning any discussion of animal models of drug addiction, the distinction between reward and reinforcement should be made and include what these terms mean in the context of drug addiction research. Drugs of abuse are considered reinforcers and, in a Skinnerian view, are received as a consequence of an instrumental response and influence the probability of that response occurring in future. Regardless of the valence (i.e., positive or negative), reinforcement will increase the probability of behavioral output in an organism, in order for the organism to earn an appetitive reinforcer or to avoid experiencing an aversive one. At different stages in the addiction process, drugs of abuse are thought to differently reinforce drug-taking behavior with positive reinforcement occurring in the early stages of drug use (i.e., binge and intoxication, Volkow et al., 2016), and negative reinforcement involved predominantly following more chronic drug taking (e.g., to decrease or obtain relief from a dysphoric state). Sanchis-Segura and Spanagel (2006) argue that in this context drugs of abuse serve as reinforcers

in three distinct ways: (1) Drugs serve as primary motivators (i.e, positive reinforcement) where behavioral contingencies are positively reinforced, that is, they serve as appetitive stimuli that increase the emission of the instrumental response; stimuli associated with drug intake in these situations can also become "conditioned reinforcers," a process by which they acquire incentive-motivational properties (which are considered to become pathological in addiction), and when these stimuli are presented in the absence of drug, elicit "wanting" or craving responses (Robinson and Berridge, 1993, 2000, 2001, 2008). (2) Drugs acting as reinforcers increase the associative strength of specific stimulus-response contingencies, which results in an increased probability of the instrumental response occurring; reinforcers thus serve to enhance information storage about the situations in which they occur, a process that can bias response choice when those situations occur in the future. (3) Acting as a negative reinforcer, drugs can reduce specific needs/drives or eliminate/prevent the occurrence of a negative state; this process is most important after prolonged drug taking when abstinence can result in withdrawal symptoms that are alleviated following drug intake (Koob and Le Moal, 2006; Sanchis-Segura and Spanagel, 2006).

Although negative reinforcement by drugs of abuse is an important aspect of the addiction process (Koob and Le Moal, 2006), drugs have traditionally been viewed as appetitive stimuli, for which responding is thought to be due to positive reinforcement. Another common term used to describe positive reinforcement in this regard is reward. This term is often mistakenly used as a synonym for reinforcement, without any distinction between the valences used to distinguish the type of reinforcement. When describing positive reinforcement, rewards are those appetitive reinforcers that increase the probability of emission of the instrumental response. Reward is also used to describe hedonia, which is defined as a hypothetical internal state of pleasure associated with acquiring, using, and/or consuming appetitive stimuli (Everitt and Robbins, 2005; Sanchis-Segura and Spanagel, 2006). Given these definitions of reward, it is clear that this term can be used to describe positive reinforcement contingencies or appetitive stimuli, but is distinct from that of the broader concept of reinforcement.

3 AVERSIVE DRUG EFFECTS

Although drugs of abuse are typically viewed as appetitive stimuli, it is argued that these compounds have multiple behavioral effects, including aversive properties that might impact the overall acceptability of a drug and its subsequent self-administration (Davis

and Riley, 2010; Hunt and Amit, 1987; Riley, 2011; Stolerman and D'Mello, 1981; Verendeev and Riley, 2012, 2013; White et al., 1977; Wise et al., 1976). For example, Riley (2011) argues that the "overall hedonic effect of a drug" and the likelihood of its use and abuse, is dependent on the balance of a drug's rewarding and aversive effects. When examining patterns of self-administration an inverted U-shaped function typically emerges, such that drug intake increases with dose until some asymptotic level is achieved; as the dose continues to increase, self-administration begins to decrease.

A drug's rewarding effects are hypothesized to increase with dose until some maximal level is achieved, where fewer self-injections are needed to attain the desired effect, in addition to possible receptor saturation (Lynch and Carroll, 2001). As the drug dose is increasing, a drug's aversive effects are also hypothesized to be increasing and the overall balance of these effects presumably results in the observed pattern of drug intake (Riley, 2011; Verendeev and Riley, 2013). Describing use and abuse as a balance of these affective properties suggests that reward and aversion are on a continuum where a drug with robust rewarding effects must also be weakly aversive (or the opposite, an aversive drug must be weakly rewarding). It is more likely, however, that each of these effects is mediated independently, such that a drug has some level of rewarding and/or aversive effects (Verendeev and Riley, 2011). The perceived balance of these effects then dictates drug intake, where a drug perceived as "more aversive" is theoretically self-administered less than a drug that is perceived as "more rewarding." Importantly, these aversive drug effects are considered distinct from those that negatively reinforce drug-taking following withdrawal; aversive drug effects in this context are experienced following acute administration and could serve a protective function by limiting (or eliminating) future intake. Thus, aversive drug effects could decrease the likelihood that drug use would lead to misuse of that drug. Interestingly, the two procedures reviewed in this chapter have been used independently and in combination to demonstrate that a drug's rewarding and aversive effects are measurable simultaneously in individual subjects following a single drug administration. Further, these procedures have shown that not all manipulations and subject variables, including drug history, strain, and other genetic differences, sex, and stress, alter these effects in the same manner (e.g., decreased aversion and increased reward), which makes these procedures useful for continued investigations focused on understanding the factors that impact substance use disorder (Bahi et al., 2013; Cunningham, 2014; Davis and Riley, 2010; Riley, 2011; Riley et al., 2009).

4 THE PLACE CONDITIONING PROCEDURE

4.1 What are Conditioned Place Preferences?

Place conditioning is a simple procedure used to assess the positive (rewarding) or negative (aversive) motivational effects of exposure to various stimuli, including, but not limited to, drugs of abuse, food, sexual behavior, novel environments, social reward, music, or footshock, and in many species, including rodents, zebrafish, birds, and humans (Astur et al., 2014, 2016; Childs and de Wit, 2009; Collier and Echevarria, 2013; Cunningham et al., 2006; Dixon et al., 2013; Lahvis et al., 2015; Molet et al., 2013). Conditioned place preference or CPP is a procedure commonly used to assess the rewarding effects of a stimulus by measuring increased approach and contact behaviors to a certain location or place, whereas conditioned place aversion (CPA) measures increased avoidance and/or escape behaviors indicative of the aversive effects of a specific stimulus. Although these procedures are simple and effective methods for assessing the motivational effects of various stimuli in different species, the CPP procedure is most commonly used in rodents (rats and mice) as an indirect assessment of the rewarding effects of various classes of drugs, especially drugs of abuse. In a standard CPP experiment, subjects undergo conditioning sessions, in which a drug injection is paired with specific cues (e.g., tactile, visual, olfactory) while the subject is confined to one compartment of a conditioning apparatus, typically a shuttle box-like apparatus (Fig. 22.2); subjects experience different cues paired with a saline injection while confined to the opposite compartment. After several drug-environment and saline-environment pairings (i.e., conditioning trials), subjects are tested for the expression of a CPP during a drug-free test session in which subjects are given access to the entire apparatus and can move freely between the conditioning compartments for a specified timeperiod (typically 15–30 min). Subjects that spend significantly more time in the compartment paired with drug administration are said to express a conditioned preference. In contrast, avoidance of the drug-paired compartment, by spending more time in the saline-paired side, is often interpreted as a CPA (Cunningham et al., 2006; Mueller and de Wit, 2011).

This procedure is based on principles of Pavlovian classical conditioning, where the drug administered serves as the unconditioned stimulus (US) and is paired with the initially neutral environmental cues of the shuttle box compartment—after several pairings as stated earlier, these neutral environmental cues become associated with the rewarding effects of the drug and acquire secondary motivational properties. The drug-paired compartment then becomes the positive conditioned stimulus (CS+) that evokes a conditioned motivational response and elicits approach and contact behavior during the subsequent drug-free test session. The other shuttle box compartment, which is usually paired with saline injections (or no injection at all), contains different cues from those of the CS+. These environmental cues remain neutral in that they do not become associated with the drug's effects (US) and thus become the negative conditioned stimulus (CS−). The fact that an animal will approach and/or contact stimuli that have been previously paired with rewarding drug effects is fundamental to the CPP procedure. When an animal receives these drug-environment pairings and subsequently approaches and spends time in contact with the drug-paired side of the conditioning apparatus, it is inferred that the drug administered had rewarding effects and these effects have become associated with the specific compartment in which the conditioning trials occurred. In a similar manner, avoidance and/or escape behaviors elicited by a CS+ paired with an aversive stimulus are essential to the CPA procedure as well. Although most drugs of abuse result in conditioned preferences for the CS+, these same drugs can result in a CPA in different strains of rodents or following variations in the route of drug administration or temporal parameters used when pairing the drug's effects with the environmental cues available in the conditioning apparatus (see later). An understanding of the procedure and careful selection of the parameters used will help to reduce many of these confounding factors and provide for an easier, more straightforward interpretation of the results.

While place preference is most often described in terms of Pavlovian conditioning as detailed earlier, Huston et al. (2013) have argued that this interpretation of CPP might oversimplify a procedure that includes multiple learning processes, memory retrieval, and various neurobiological mechanisms. In an operant conditioning account of place conditioning, for example, drug effects that are typically perceived and expressed during and after place conditioning sessions could elicit behaviors that are inadvertently reinforced by drug exposure. In this context, the cues (e.g., floor texture, wall pattern, etc.) in the drug-paired chamber would arguably serve as discriminative stimuli (SD); thus, the behavior(s) previously reinforced in this compartment would then be under stimulus control and increase the probability that the subject would remain in the presence of the SD upon subsequent encounters. These behaviors are argued to be similar to "superstitious behaviors" in pigeons previously reported by Skinner (1948) (Staddon, 1992), where spontaneous behaviors were inadvertently reinforced by delivery of a food reinforcer.

Huston et al. (2013) argue that conditioned treatment effects induced by the pharmacological agent used during CPP conditioning are a third theoretical explanation

of preference for the drug-paired chamber. Given that the various behavioral effects induced by psychoactive drug administration can be conditioned to environmental cues (Banasikowski and Beninger, 2010), these effects could increase or decrease the probability that a subject will remain in the chamber associated with drug administration. For example, conditioned drug effects that prevent a subject from leaving the drug-paired chamber would increase the likelihood of a CPP and would arguably be independent of the rewarding effects of the drug. Thus, CPP induced by some classes of psychoactive drugs could simply indicate that due to the conditioned drug effects, the subject was less likely to leave the drug-paired chamber and explore the entire apparatus (Meyer et al., 2012). In this context, a false positive CPP could result from a psychoactive drug that is due to these conditioned drug effects and not rewarding drug effects per se; this interpretation is especially important for assessing the rewarding effects of novel therapeutic compounds. In a similar vein, psychoactive drugs that increase movement or activity during conditioning sessions could result in conditioned hyperactivity. During the CPP test session, the conditioned hyperactivity would be elicited by exposure to the drug-paired chamber, which could weaken the overall "preference" for the drug-paired cues because the subject is moving around the entire conditioning apparatus; Huston et al. (2013) argue that these effects could impact cocaine-induced CPP (Bardo et al., 1995). Empirical evaluation of these alternative interpretations is needed and could be accomplished by altering the place conditioning apparatus (White et al., 2005) and comparing spontaneous behaviors during the CPP test to the CPP pretest, although this second suggestion requires recording and scoring the various behaviors emitted by each subject during all phases of the CPP procedure, including (and arguably most importantly) during the CPP conditioning sessions (Cunningham, 2014).

4.2 A Brief History of Place Conditioning

Garcia et al. (1957) first used the place conditioning procedure to assess the motivational effects of whole-body gamma (γ) or X-ray irradiation in male rats. A two-compartment apparatus was employed, which included one compartment that was painted black and contained a grid floor; the opposite compartment was painted white and contained a wire mesh floor. Rats experienced four irradiation-compartment pairings in either the black or the white compartment; the radiation-paired compartment (or sham-irradiation) was divided across subjects such that baseline preference for the black compartment was used to divide rats into groups with comparable baselines (i.e., time spent in the black compartment). Half of the rats were irradiated in the

black compartment and half received the exposures in the white compartment. Following conditioning, all animals displayed significant *decreases* in the amount of time spent in the compartment paired with irradiation, indicating a *conditioned place aversion*. Although the groups conditioned with γ irradiation in the black compartment initially spent more time there during the pretest session compared to rats conditioned in the white compartment, there were no significant differences in the radiation-induced conditioned place aversion between the groups.

Although this initial study was assessing aversion induced by irradiation, Garcia et al. (1957) employed several techniques that are currently used in place conditioning studies with drugs of abuse. For instance, the baseline preference for each conditioning compartment was determined on the day prior to the first conditioning session during a pretest session, which consisted of a test period (150-min) where the rats could freely explore both the black and white compartments. This study was one of the first to use the pretest session in order to determine each subject's baseline preference for the compartment subsequently paired with the US (in this case, irradiation). In this way, these investigators compared the shift in the amount of time spent in this compartment during the pretest to the amount of time spent in the same compartment following the conditioning sessions for each subject. Although the rats conditioned with irradiation in the black or white compartment were treated as separate experimental groups, a procedure similar to this is commonly used in place conditioning with drugs of abuse to specifically assign the CS-US pairings across the experimental groups (see Section 4.5). Garcia et al. (1957) conditioned some rats to their naturally preferred sides (i.e., groups receiving γ irradiation-black compartment pairings) and others to their naturally less-preferred side (i.e., groups receiving γ irradiation-white compartment pairings); the former procedure is more common in place aversion work in order to avoid a floor effect, that is, an aversive stimulus is paired with the naturally preferred side of the conditioning apparatus because subjects are most likely to decrease the amount of time spent in the compartment paired with an aversive stimulus. Both groups conditioned with X-ray irradiation paired with the white or black compartment were conditioned to their naturally preferred side (e.g., the group of rats receiving irradiation-black compartment pairings preferred the black compartment during the pretest and the group of rats receiving irradiation-white compartment pairings preferred the white compartment during the pretest). Interestingly, the irradiation-induced aversions were similar in strength regardless of what compartment the animals received the exposures. This is not always the case when assessing drugs of abuse in the CPP design and the choice of the drug-paired compartment is an important one (Bardo et al., 1995).

While Garcia and colleagues were interested in examining the effects of irradiation in the place conditioning procedure, Beach (1957) published the first paper assessing a drug-induced CPP in rats. Beach hypothesized that rats would associate a specific place with the drug's effects, if they were confined to this place *after* each drug administration and remained in this place long enough to adequately experience the drug's effects. This work was to demonstrate that rats could learn to associate a specific environment with a drug's effects and would subsequently prefer this environment when tested while "needing" morphine (tested 2–4 h following saline administration) or while morphine "sated" (tested 2–4 h after being injected with morphine; Beach, 1957). Rats were chosen as subjects for this study to determine if this species could learn drug effect-environment associations in a manner similar to the morphine-environment associations displayed by morphine-dependent chimpanzees in an earlier report by Spragg (1940). Beach successfully demonstrated that morphine-dependent and nondependent rats both learned to associate the effects of morphine administration with a specific environment and subsequently preferred this environment to the one in which the rats received saline injections (or no injection at all).

This study is not only the first report of a drug-induced CPP, but also is an example of simple changes to the place conditioning procedure and apparatus from those reported by Garcia and colleagues. For example, Beach employed a Y-shaped discrimination box in which two distinct arms connected a starting box to two separate "goal boxes" (i.e., conditioning compartments) (Fig. 22.1).

The start box, left goal box, and right goal box were each painted a different color and each contained additional visual and tactile cues. The left goal box had grey walls with square black insets and a flyscreen-covered floor. The right goal box had black walls with circular white insets and a wood floor. Additionally, the Y-shaped discrimination box had four doors that could be used to close off the start box or either of the goal boxes. In 16 pretest choice sessions, rats were placed in the start box and allowed to access either of the goal boxes. Once the rats reached a goal box, a choice for that goal box was recorded; after 5 s in the chosen goal box, rats were removed to prevent them from moving back down the arm and into the start box and/or the other goal box. From these pretest choice sessions, preferred and nonpreferred goal boxes were determined for each rat. Rats were subsequently conditioned to their nonpreferred goal box, that is, rats were injected with morphine, placed in the start box, and run to the goal box that was chosen *less* during the pretest sessions. In this way, some of the rats experienced morphine in the gray goal box and others experienced morphine in the black goal box, but all rats
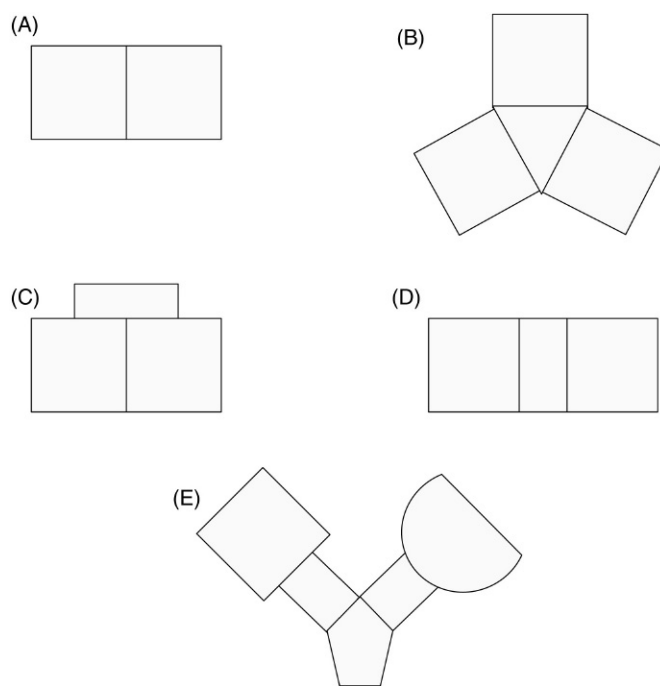
FIGURE 22.1   **Various place conditioning apparatuses have been reported in the literature, including two- and three-compartment designs with additional alleys and/or goal boxes.** (A) Barr et al., 1985; Garcia et al., 1957; Cunningham et al., 2006; (B) Mucha and Iversen, 1984; Parker, 1992; (C) Carr and White, 1983; (D) Davis et al., 2007; Mueller and de Wit, 2011; Roma and Riley, 2005; Spyraki et al., 1982; (E) Beach, 1957. *Source: Some examples have been redrawn from Carr, G.D., Fibiger, H.C., Phillips, A.G., 1989. Conditioned place preference as a measure of drug reward. In: Liebman, J.M., Cooper, S.J. (Eds.), The Neuropharmacological Basis of Reward. New York, Oxford, pp. 264–319.*

were conditioned to the nonpreferred goal box. This study can be considered the first use of the "biased" design in place conditioning with drugs of abuse, a technique where subjects are conditioned to their initially nonpreferred side. A significant change in the amount of time subjects spend in the nonpreferred side following conditioning with morphine, for example, indicates a preference for the drug-paired side. This is in contrast with the "unbiased" design in which the drug-paired compartment is counterbalanced across subjects regardless of initial compartment preference (see later for more details on biased vs. unbiased designs).

Following Beach's report of morphine CPP in morphine-dependent and nondependent rats, Kumar reported conditioned preferences for morphine-paired environments in morphine-dependent rats tested during withdrawal (i.e., 48 h after the last morphine injection) using a two-compartment apparatus. Further, two additional studies included interesting changes to the CPP procedure that have since received considerable attention in the CPP literature (Reicher and Holman, 1977; Rossi and Reid, 1976). More specifically, Rossi and Reid reported "acquisition" of a morphine CPP by conditioning and testing rats over a 4-day cycle where

rats received morphine- or saline-environment pairings over 3 days and were then tested for CPP on the 4th day of the cycle; four conditioning cycles were completed which allowed for analysis of the CPP after additional morphine-environment pairings. Although initial side preferences influenced the results, morphine did condition a significant CPP, however a clear increase in the conditioned preference over test trials was not evident (for a more recent study of morphine CPP acquisition, Davis et al., 2007). In the study by Reicher and Holman (1977), CPP procedures were combined with the conditioned taste aversion (CTA) procedure to simultaneously test the rewarding and aversive effects of amphetamine administration. In this combined CTA/CPP procedure, Reicher and Holman reported amphetamine-induced taste aversions and place preferences conditioned in rats that consumed a distinctively flavored solution in one shuttle box compartment and a different flavored solution on the other side (Simpson and Riley, 2005; Verendeev and Riley, 2011).

Since these initial studies, the use of the place conditioning procedure has become widespread in the field of SUD research and has amassed an extensive literature containing the use of different species, classes of drug, procedures, and methodologies. For example, drug-induced place conditioning has been reported in rats and mice, hamsters, birds, zebrafish, nonhuman primates, and humans (Borges et al., 2015; Childs and de Wit, 2009; Collier and Echevarria, 2013; Cunningham et al., 2006). These studies have also demonstrated that most drugs serving as reinforcers in self-administration procedures also condition place preferences, including cocaine, amphetamine, nicotine, morphine, and ethanol. Numerous variations in the place conditioning procedure exist in literature, including the experimental design used, shape and layout of the conditioning apparatus, and environmental cues employed; further, the procedure has evolved considerably since these early studies. Thus, it is not surprising that no single method for conducting place-conditioning studies exists. Nonetheless, generalities among most studies are apparent, but substantial variability still exists in these items throughout the place conditioning literature. While many of these variations impact the interpretation of the results of place conditioning studies, others have demonstrated interesting interactions between route and timing of drug administration, strain of animals employed, and strength of preference or aversion conditioning (Bardo et al., 1995; Cunningham et al., 2002). For example, intraperitoneal or intravenous injection of ethanol in mice results in a CPP, whereas a 5-min delay following drug administration and prior to placement into the ethanol-paired compartment is needed for intragastric ethanol administration to condition a place preference. Intraperitoneal or intragastric ethanol administration interestingly results

in place *aversions* when exposure to the conditioning compartment (i.e., CS+) occurs immediately prior to or immediately following ethanol administration, respectively (Cunningham et al., 2002).

Recently, the CPP procedure has been used in the pain field to investigate motivated behaviors associated with analgesic administration and pain relief (Gerber et al., 2014; Navratilova and Porreca, 2014). Pain relief in humans is rewarding (Leknes et al., 2008, 2011) and recent work employing CPP has demonstrated this effect in laboratory animals (Andreatta et al., 2012; Becerra et al., 2013; Gerber et al., 2014; Navratilova et al., 2012). In most of these studies, relief of ongoing pain is paired with one compartment of the CPP apparatus (CS+). In the subsequent test session, subjects prefer this context over the CS− that was paired with vehicle administration (i.e., no pain relief). Significant preferences for the pain-relief paired context have been shown in rodents following postsurgical pain, neuropathic pain, inflammation, osteoarthritic pain, cephalic pain, and bladder and bone cancer pain models (Davoody et al., 2011; De Felice et al., 2013; Hung et al., 2015; Navratilova et al., 2012, 2015; Okun et al., 2012; Park et al., 2013, 2016; Qu et al., 2011; Remeniuk et al., 2015; Roughan et al., 2014; Sufka, 1994; Wei et al., 2013). Further, many of these studies demonstrate pain relief-induced CPPs with analgesic agents that are not rewarding in the absence of pain. For example, intrathecal clonidine administration conditions a significant CPP only in rats with spinal nerve ligation, but not sham-operated rats (King et al., 2009), further supporting the hypothesis that pain relief is rewarding and when paired with distinct contextual cues, will elicit approach behaviors following conditioning. While the positive reinforcing effects of other analgesic compounds (e.g., opioids) can confound interpretation of pain relief-induced CPPs, these effects appear to be dose-dependent, given that morphine doses that do not condition a CPP in control or sham-operated subjects, condition significant pain relief-induced CPPs in certain animal models (Hung et al., 2015; Navratilova et al., 2015; Roughan et al., 2014).

4.3 Advantages of the Place Conditioning Procedure

Place conditioning is a methodologically simple and relatively inexpensive procedure: Place conditioning is a popular method in the drug addiction field because it provides numerous advantages compared to other methods used to assess the conditioned motivational effects of drugs. First, the procedure is methodologically simple in terms of (1) experimenter training and (2) expensiveness of the necessary experimental equipment. More specifically, extensive training in survival surgery, jugular catheter implantation, and proper anesthesia/analgesia

procedures needed for intravenous self-administration protocols are not required for a general place conditioning study. Indeed, intraperitoneal (i.p.) or subcutaneous (s.c.) drug injections are the most widely used methods to administer drug in the place conditioning procedure, although oral gavage and intragastric cannulas have been used for ethanol administrations (Ciccocioppo et al., 1999; Cunningham et al., 2002). While intravenous (i.v.) drug administration via indwelling jugular catheters is not a requirement for a standard place conditioning study, this drug administration technique has been used in the CPP procedure for several different drugs of abuse, including amphetamine, morphine, and ethanol (Bardo and Neisewander, 1986; Bardo et al., 1999; Kelley et al., 1997; Mucha et al., 1982).

In terms of the equipment needed for a place conditioning study, the conditioning apparatus can be purchased from a commercial vendor (e.g., Med Associates, Harvard Apparatus, San Diego Instruments) or hand-made with some common materials found at home improvement stores, for example. While commercially available place conditioning systems commonly require the added expense of a computer and software package for data acquisition and analysis, these systems are fully automated in terms of data collection and result in immediate access to each animal's data once the test session has ended. For example, the rodents' movements are typically tracked by a series of infrared light sources and detectors (i.e., photobeams) located on opposite sides of the apparatus that form a grid to monitor body positions in each chamber. Beam breaks that occur when an animal traverses the apparatus are recorded by a computer software package and are easily transformed into "time spent in compartment" measures. That is, the breaking of specific photobeams is used to determine the animal's position in the apparatus and to determine in what compartment the animal is located. Further, a break in one or several photobeams, in addition to photobeams in another area being released, is used to determine when the animal has entered a specific compartment. Some systems also monitor vertical movements (rearing) in addition to horizontal movement throughout the apparatus. Test sessions in an automated apparatus can be video recorded for later analysis, but this is not necessary for data acquisition like it is in a system without photobeams.

Although the commercially available systems confer many advantages in terms of ease of data collection, purchasing an expensive system is not required to do place conditioning studies because the place conditioning apparatus can be constructed of readily available materials, such as wood or Plexiglas sheets. Size measurements for rat or mouse place conditioning chambers are easily acquired through a brief literature search (Fig. 22.2), in addition to examples of visual and tactile cues used in
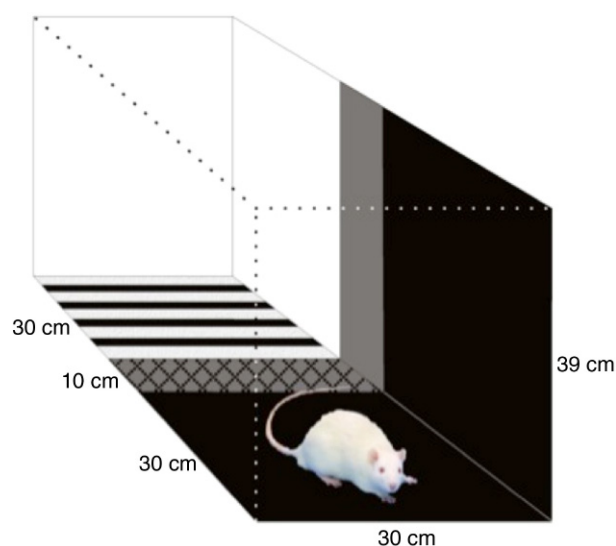
FIGURE 22.2　Illustration of a three-compartment apparatus used for place conditioning studies with rats. Each individual conditioning compartment measures 30 cm × 30 cm × 39 cm and the center compartment measures 10 cm × 30 cm × 39 cm (total size: 70 cm × 30 cm × 39 cm). The "white" compartment consists of a black-and-white striped floor and solid white walls (in addition to a textured floor surface, see Davis et al., 2007). The "black" compartment contains a solid-colored floor and walls (in addition to a smooth floor surface). During the pretest or the posttest, rats have free access to all three compartments. During the conditioning trials, however, guillotine doors are inserted at the border of the white and center compartments and at the border of the black and center compartments. *Source: Picture courtesy of Peter G. Roma.*

each compartment and variations in lighting schemes that can help to reduce bias for one compartment over another in experimental subjects.

When constructing an apparatus out of materials like wood, it is imperative that the apparatus can be sanitized easily so painting of the wood surface is necessary; this is not the case for materials, such as Plexiglas which will not absorb liquids on their surfaces (e.g., urine). Custom-made conditioning chambers allow the experimenter to fully control the appearance of each compartment of the apparatus and the ease with which a compartment's appearance can be altered, if necessary. In this way, an experimenter can design an apparatus with floor textures and/or wall patterns that are easily interchangeable (Cunningham et al., 2006; Roma and Riley, 2005). The advantage of an easily alterable apparatus is that the cues within each compartment of the apparatus can be changed to manipulate the initial side preference that is typically found in rodents. For example, one strain of rats or mice might show no bias when a wire mesh floor, grid floor, or different lighting conditions are used in the opposing compartments (Roma and Riley, 2005); however, this might not be the case for a different strain of rodent or for the opposite sex of the same strain of rodent.

In a handmade place conditioning apparatus, the infrared light sensors and detectors can be added to automate data collection during the test session(s) in a manner similar to that described earlier; this will require electronic circuits and computer software that can be made in the laboratory. If constructing these types of circuits and software is not possible, other methods are available for collecting data in this type of apparatus, and although they can be labor-intensive, most only require a video camera (or cameras depending on the number and/or placement of the apparatus in the laboratory), a stopwatch (or some other way to keep track of the time spent in each compartment), and an experimenter/technician (or several); additionally, experimenters can use computer-based event logging software (free software is available: JWatcher: http://www.jwatcher.ucla.edu/; Observational Data Recorder (Beta version): http://www.samuelpean.com/odrec/). When "scoring" place conditioning test sessions (e.g., pretest, posttest) in this manner, each shuttle box apparatus needs to be in full view of a video camera so that the entire apparatus can be seen easily on playback (Myers et al., 2012). To achieve this, the camera needs to be positioned above the apparatus, looking down at the conditioning compartments such that an animal's body position is easily discerned above the border for each compartment. Experimenters must consider rodent coat color and its contrast with the floor material/color in order to adequately determine each subject's movement during the test sessions (Myers et al., 2012). Further, all experimenters responsible for scoring the data need to be adequately trained on what criteria will be used to determine when an animal is one compartment of the shuttle box and what criteria will be used to determine when that animal is no longer considered to be in that specific compartment. These criteria should be determined ahead of time and reliability testing between experimenters should be conducted; use of an event logging software with experimenter training sessions and reliability testing can easily overcome any issues between experimenters (e.g., The Observer software by Noldus; http://www.noldus.com/animal-behavior-research/products/the-observer-xt). With reliably trained experimenters and consistent methodology in the laboratory, scoring video recorded place conditioning test sessions provides an inexpensive alternative to purchasing a fully automated system from a commercial vendor. Additionally, with a video recording set up in place, experimenters can easily record all sessions of the CPP procedure (e.g., conditioning sessions) for detailed behavioral analyses (Huston et al., 2013).

Place conditioning studies are short in duration and have the potential for high throughput of subjects: Another advantage to the standard place conditioning procedure is the large number of animals that can be conditioned and tested in a relatively short period of time. If no other experimental manipulations are required, a standard place conditioning study can run anywhere from 8–14 days. More specifically, the standard place conditioning procedure usually consists of a pretest session or a habituation day (day 1), four drug and four vehicle conditioning trials (days 2–9), and a test session (day 10). If all sessions occur on consecutive days, including on the weekends, then the procedure requires 10 days; if weekends are excluded, the procedure takes two 5-day weeks (or 12 total days), where week 1 would include days 1–5 (days 6–7 would be the weekend days where no sessions would occur) and week 2 would include days 8–12. Some investigators recommend inserting a 2-day break between the end of the conditioning trials and the place conditioning test (Mueller and de Wit, 2011) given that they have acquired a greater drug-induced CPP following this protocol compared to testing immediately after conditioning (i.e., the day following the last conditioning trial).

It should be noted that when conditioning with different drugs or routes of administration, only one or two CS+ drug trials are sometimes necessary to condition a preference, which subsequently results in a shorter experimental period. For example, Bardo et al. (1999) used a one-trial (a single exposure to the CS+ and CS−) place conditioning procedure in which rats received a single IV injection of amphetamine during one CS+ conditioning session; doses of 1 or 3 mg/kg amphetamine induced a significant CPP in this design (Bardo and Neisewander, 1986; Bardo et al., 1999; Mucha et al., 1982). Ethanol-induced place conditioning studies with a reduced number of conditioning sessions (i.e., two CS+ trials and two CS− trials) have been reported as well (Cunningham et al., 2002). While these shorter conditioning periods have been reported in other laboratories, adhering to a more common conditioning approach is beneficial to a laboratory that lacks substantial experience with the place conditioning procedure. Once the parameters within the laboratory are established and place conditioning produced with known drug(s) and doses, then alterations to this standard timeline can be made; these changes however, could require additional control groups to demonstrate reliability of the findings.

In a standard place conditioning experiment, a period of at least 24 h commonly separates the conditioning trials, and this results in either one CS+ or one CS− trial being run per day in each animal. The studies mentioned earlier decreased the total number of conditioning trials, but still maintained this 24-h interval (i.e., intertrial interval). Several investigators have reported place conditioning following two conditioning trials in 1 day (e.g., a drug trial in the AM followed by the vehicle trial in the PM). Use of an intertrial interval less than 24 h should be carefully considered (Bevins and Cunningham, 2006, for

a discussion of the advantages and disadvantages of this procedure).

Other advantages of the place conditioning procedure: In addition to the advantages discussed earlier, there are several additional items that make the place conditioning procedure an excellent preparation with which to study the conditioned motivational effects of drugs of abuse. First, test sessions in this procedure are drug-free, which eliminates the confounding effects of drug-induced motor and/or sensory impairments (or enhancements) that occur in other procedures where subjects are tested shortly following drug administration. Second, this procedure is sensitive to the effects of low drug doses and when a variety of doses are tested in separate groups of subjects within the procedure, monophasic dose-response curves have been reported. It is important to note that this is not always the case and a common criticism of the CPP design is the difficulty in obtaining well-defined dose-dependent responses (Ahsan et al., 2014; Bardo et al., 1995; Durazzo et al., 1994; Spyraki et al., 1985). Further, many studies report an "all-or-none" effect where after achieving a threshold dose and inducing CPP, no further increase in CPP occurs at higher doses (for discussions of this effect, see Carr et al., 1989; Mueller and de Wit, 2011).

The use of drug-naïve subjects is an additional advantage to the place conditioning procedure. Several different drugs of abuse induce CPP in a variety of drug-naïve subjects, which provides a reliable method to study the rewarding effects of a specific drug without the added effects of tolerance (or sensitization) from previous drug exposures (Cunningham, 2014; Meyer et al., 2012). Generally speaking, the fact that a lengthy drug history is not necessary to induce place conditioning and, as mentioned earlier, specific routes of administration can reduce the number of conditioning trials needed to induce CPP all add to this procedure's flexibility and adaptability. Although a drug history is most often not needed for drug-induced CPP, there are examples of rats needing previous drug exposures (with the US or a different drug) or stressful experiences to induce an ethanol CPP (Marglin et al., 1988; Matsuzawa et al., 1998, 2000). Thus experimenters should research extensively the specific species and/or strain to be used in the place conditioning procedure, understand these differences, and adapt the general procedure and/or interpretation of the results to account for these factors.

Finally, the neurobiological underpinnings of drug reward can be investigated in the place conditioning procedure and recent work in the SUD field demonstrates the utility of this procedure for these types of studies. This procedure has been used extensively to investigate differences in drug-induced reward among genetically modified rodents, different rodent strains, and even different animal species with the goal of understanding the neurobiological mechanisms responsible for the rewarding effects of abused drugs and how these effects are altered following chronic drug exposure or withdrawal. For instance, inhibition of the IRS2-Akt (protein kinase B) pathway, which is thought to mediate opiate-induced changes in dopaminergic neurons of the ventral tegmental area, results in a diminished morphine-induced CPP (Russo et al., 2007). Morphine CPP is dependent on certain brain regions (e.g., nucleus accumbens, amygdala), but only in the presence of certain conditioning cues or apparatus configurations (White et al., 2005). Cocaine CPP, interestingly, is apparent at a lower dose in fosB mutant mice compared to wildtype mice (Hiroi et al., 1997), which demonstrates the sensitivity of the place conditioning procedure to molecular changes related to chronic cocaine use as well.

4.4 Place Conditioning: Experimental Protocol and Conditioning Apparatus

Although the characteristics of a place conditioning study were mentioned briefly in the preceding text, the current section aims to describe the place conditioning study in detail, including a discussion of some general parameters and characteristics of the experimental design that should be taken into consideration when designing and executing a place conditioning experiment.

Phases of a place conditioning study: There are several general phases to a place conditioning study and these will be discussed here. These phases are included because they are commonly reported in place conditioning studies however, some can be altered or eliminated depending on the goals of the experiment and the extent to which the laboratory has experience with the procedure and/or apparatus.

The pretest: The pretest or preconditioning test is performed at least 1 day prior to the start of the place conditioning trials and consists of a drug-free test period (typically 15-min) where subjects are allowed to freely explore all parts of the apparatus. During this test, the amount of time spent in the to-be-conditioned compartments is recorded. This test is used to accomplish several important experimental goals, including (1) to determine whether the subjects have an inherent bias for one set of cues within one chamber over another, (2) to give the subjects a brief exposure to the novel environment of the place conditioning apparatus, and (3) provide a data point to which posttest changes in preference are compared. Following the pretest, the baseline preference score for each compartment for each individual animal is used to assign drug- and vehicle-paired environments. If an unconditioned preference for one of the compartments exists (i.e., an inherent or natural bias or side-preference), subjects then receive drug injections in their least-preferred compartment (i.e., the compartment

in which they spent the least amount of time) and this is termed a "biased procedure."

If no inherent side preferences exist, the drug-paired compartment is counterbalanced across animals, where half of the subjects receive drug in one compartment and the other half receive drug in the opposite compartment; this is termed the "unbiased procedure."

The pretest is not always necessary, and in laboratories where the place conditioning parameters have been optimized (Cunningham, 2014; Cunningham et al., 2006) for a specific procedure, drug, and/or rodent strain(s), the pretest is not regularly used. In these cases, a short (e.g., 5-min) habituation session is used to reduce the effect of novelty and stress. However, the pretest is recommended if the apparatus (or cues within either compartment) or rodent strain is new to the laboratory. In addition, acquiring the pretest data allows experimenters the opportunity to alter the cues within each compartment in order to eliminate any inherent side preferences and use the "unbiased procedure" (described later; see also Roma and Riley, 2005) and to compare activity or other behaviors across the conditioning and testing phases to this first exposure to the apparatus.

Conditioning trials: In a standard place conditioning study, there are typically four conditioning trials in which the drug is administered prior to placement into the CS+ compartment and four additional trials where vehicle (or no injection) is administered prior to placement into the CS− compartment (for a vehicle-only control group, vehicle injections are administered prior to placement into both the CS+ or CS− compartments). More specifically, for each drug conditioning trial, animals are removed from their home cages, injected with the appropriate dose of drug (or vehicle), and immediately placed into the CS+ compartment (or the CS− compartment if receiving vehicle). In order to counterbalance the drug and vehicle pairings across subjects on each conditioning trial, half of the experimental animals are injected with drug and the other half are injected with vehicle; this arrangement is reversed on the next conditioning trial. A vehicle-only control group is injected with vehicle prior to placement in either the CS+ or CS− compartments; these vehicle-compartment pairings should also be counterbalanced, such that half of the control group receives vehicle paired with the CS+ and the other received vehicle paired with the CS− on each conditioning trial.

Conditioning trials typically occur once every 24-h, with the same type of trial occurring at 48-h intervals, that is, a conditioning trial in which drug was administered is followed 24-h later by a conditioning trial in which vehicle is administered, for example. Thus, the conditioning period typically requires 8 days of altering drug and vehicle trials. As mentioned earlier, changes in route of drug administration or other parameters provide a means by which the number of conditioning trials is reduced or otherwise altered from this common arrangement (e.g., i.v. administration and one-trial conditioning, see earlier). Further, greater CPP has been reported for the same drug with an increasing number of conditioning trials, a finding that encourages the use of more than one or two conditioning trials. For example, morphine CPP increases with the number of conditioning trials and a significant CPP is apparent after three or four conditioning trials, but not after one or two (Mucha and Iversen, 1984; but see Parker, 1992). However, in strains that show differential sensitivity to opioids, a significant morphine-induced CPP is apparent after only two conditioning trials for a 1 mg/kg dose of morphine, but is not apparent after four conditioning trials with a higher 10 mg/kg dose (Davis et al., 2007; Grakalic et al., 2006).

While the duration of the conditioning trials is commonly 30 min, this parameter varies considerably across studies with reports of conditioning trials as short as 4 min and as long as 120 min (Cunningham et al., 2006; Parker et al., 1994; Reid et al., 1985). One of the most important factors used to determine the length of the conditioning sessions is the duration of the drug effect, such that longer conditioning trials are typically used for drugs with longer half-lives. For example, studies assessing cocaine-induced CPP in rats commonly report 20–30 min conditioning trials (Guitart et al., 1992; Isaac et al., 1989; Kosten et al., 1994; Mucha et al., 1982; Spyraki et al., 1982), whereas morphine conditioning trials are usually 30 min or longer (see also Bardo et al., 1995; up to 120 min, see Parker et al., 1994). Conditioning trial duration is also dependent on the strain of rodent used as subjects. More specifically, 60-min cocaine conditioning trials are most effective when DBA/2J mice are used as subjects, but in C57BL/6J inbred mice, cocaine-induced CPP occurs following conditioning trials between 15–60 min in length (Cunningham et al., 1999). Additionally, ethanol is most effective in the CPP procedure in various strains of mice when 5-min conditioning trials are used (Cunningham and Prather, 1992). These differences emphasize the importance of selecting the appropriate trial duration for the drug of interest and subjects used.

The posttest: Following the conditioning period, a CPP test is run to determine if subjects spend more time in the drug-paired compartment. The posttest is identical to the pretest: in a drug-free state, subjects are allowed to move through all compartments of the apparatus for a specific amount of time (usually 15-min). The amount of time spent in each compartment is recorded. A drug-induced CPP is apparent when a subject spends more time in the drug-paired compartment compared to the time spent in that same compartment during the pretest or compared to the time spent in the CS− compartment. Thus CPP data is expressed as either an increase in preference for the CS+ compartment from pretest to posttest

or as an increase in preference for the CS+ compartment compared to the CS− compartment (Carr et al., 1989). As mentioned previously, the posttest occurs at some point following the final conditioning trial, where some studies assess CPP 24 h following the last conditioning trial and others asses CPP 2 days following the last conditioning trial. In the latter instance, no drug injections and/or exposure to the compartments are given during these 2 "rest" days (Mueller and de Wit, 2011).

The place conditioning apparatus: The most common apparatus used in place conditioning studies is a two- or three-compartment shuttle box, but several different arrangements have been reported and are shown in Fig. 22.1 (Carr et al., 1989). While these shuttle boxes vary in size, lighting conditions, and environmental cues, there are several characteristics common to the experimental apparatuses of most place conditioning studies with rodents. For mice, a standard size conditioning apparatus is approximately 30 cm long, 15 cm high, and 15 cm deep (Cunningham et al., 2006); for rats, a commercially available apparatus from San Diego Instruments, for example, is approximately 68.5 cm long, 34.5 cm high, and 21 cm deep (Fig. 22.2); these sizes can vary slightly with the addition of a third compartment. Importantly, each compartment is distinct from the other, regardless of whether a two- or three-compartment apparatus is used. The differences most often include the type and texture of flooring material and the color and appearance of the walls of each compartment. The floors are typically made of various materials including wire mesh, steel panels with holes or rods, textured or smooth Plexiglas, textured or smooth Kydex plastic, or rodent bedding. If the floor cues (i.e., tactile cues) are the to-be-conditioned cues associated with the CS+ compartment, the walls of the apparatus do not necessarily need to include any visual cues. However, if visual cues, in addition to the tactile cues, are to be used, a common practice is for one compartment to be a solid color (e.g., black) and another compartment to contain some type of pattern (e.g., black and white stripes) or for both compartments to be solid colors (e.g., black or white) with different texture and/or colored floors (Davis et al., 2007). While most studies use opaque barriers between the conditioning chambers during training and no barriers during testing, White et al. (2005) used clear barriers and a tunnel to allow subjects to see the visual cues in the adjacent chamber during testing, which unmasked differential effects of brain lesions on morphine CPP. Regardless of the floor and/or wall materials chosen, it is imperative that all surfaces of the apparatus are constructed of materials that are easy to sanitize (in accordance with institutional animal care guidelines) during a place conditioning study in order to eliminate olfactory cues from each subject (Fig. 22.3).

The use of a two- or three-compartment apparatus has received some attention in the place conditioning literature as an important design characteristic that provides an advantage in terms of a control for novelty, but has been shown to impact the strength of conditioning with certain drugs. More specifically, a third compartment in the conditioning apparatus is typically situated in between each conditioning compartment and is only available for exploration during the test trials (e.g., pretest, posttest); since this compartment is not accessed during conditioning, it is considered a novel environment compared to the other compartments. However, the number of pretest sessions where subjects have access to this third compartment can impact the novelty of this area and the amount of time spent in this area during a test session (Myers et al., 2012; Parker, 1992) (Fig. 22.4).

Rats, for example, exhibit preferences for novel environments (Bardo et al., 1989; Carr et al., 1988; Hughes, 1968; Parker, 1992; Scoles and Siegel, 1986) and it has been argued that drug-induced place conditioning actually represents avoidance of the saline-paired compartment (Scoles and Siegel, 1986), since the effects of the drug could interfere with habituation to the drug-paired compartment and is perceived as the more novel compartment during the drug-free test session. In a series of studies, however, Parker (1992) demonstrated that for several drugs, including apomorphine, amphetamine, and morphine, rats displayed significant preferences for the drug-paired compartment compared to both the saline-paired and novel compartments of a three-compartment, Y-shaped apparatus. Interestingly, rats' preferences for the novel compartment were intermediate to those of the drug- and saline-paired compartments, with rats preferring the novel compartment more than the saline-paired compartment, but less than the drug-paired one (Parker, 1992). Further, in a meta-analysis by Bardo et al. (1995), a three-compartment apparatus was associated with a larger effect size in heroin and cocaine place conditioning studies, but no association was found when morphine or amphetamine was used. These authors argue further that drug-induced CPP might be enhanced in the three-compartment apparatus because the availability of the novel compartment during the test session reduces the amount of time spent in the saline-paired chamber (Bardo et al., 1995). Thus these data demonstrate that the choice of using a two- or three-compartment apparatus is an important one that can impact the results of the study and should only be made after careful consideration of these issues and the benefits (or limitations) associated with the use of each type of apparatus (Fig. 22.5).

General rodent place conditioning procedure:

Pretest session (day 1)

1. Clean all conditioning chambers thoroughly with soap and water; allow to air dry before beginning the pretest. If changing of floor materials is required, make certain that the appropriate
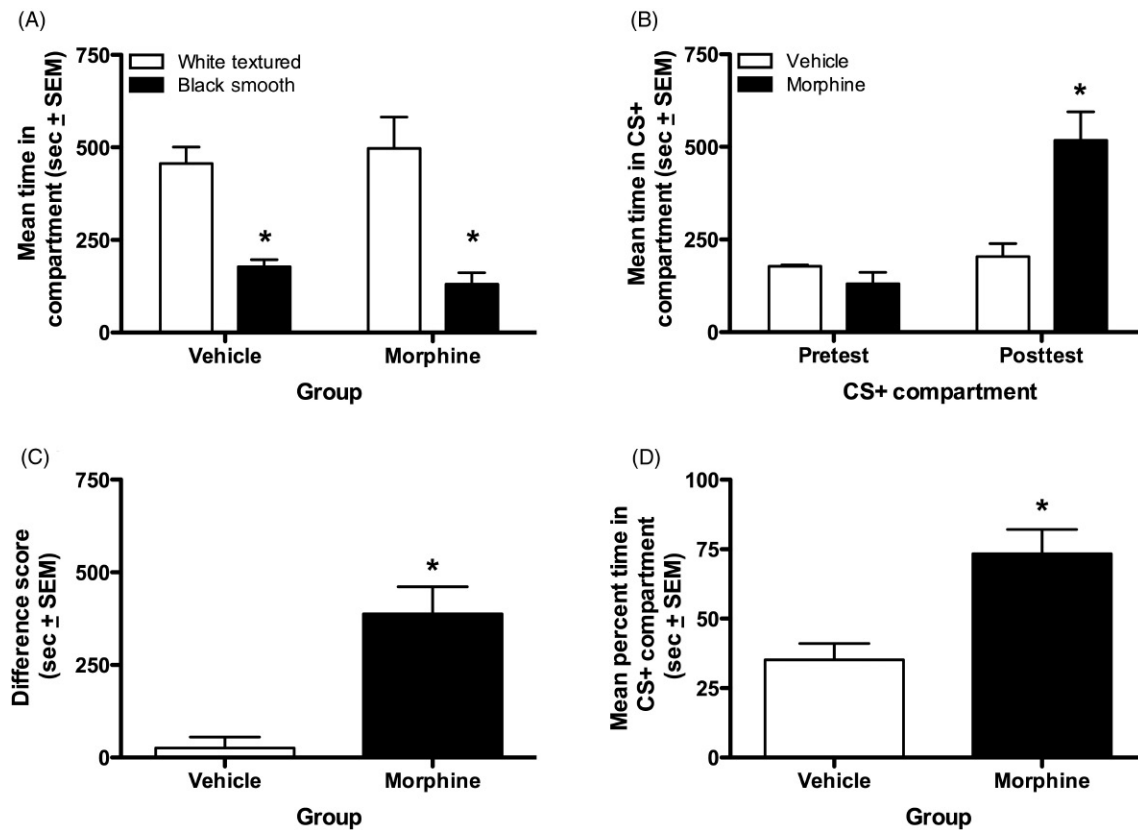
FIGURE 22.3 **Morphine-induced place preference in adult male Fisher 344 inbred rats.** (A) All rats received one 15-min pretest on the day prior to the start of the conditioning phase. There was a significant preference for the white textured side of the apparatus, thus a "biased-design" was used and rats were conditioned with morphine in the black smooth side (i.e., the least-preferred compartment was the CS+). Rats then received four morphine (5 mg/kg, SC)-CS+ pairings and four vehicle-CS− pairings. The control group received vehicle paired with both compartments. (B) Mean time in seconds spent in the CS+ compartment on the pretest and posttest by the vehicle-conditioned and morphine-conditioned rats. Morphine-conditioned rats displayed a significant preference for the CS+ compartment compared to rats conditioned with vehicle. (C) This figure presents the same data as a difference score (i.e., posttest seconds in CS+ minus pretest seconds in CS+) to demonstrate the significant morphine-induced CPP. (D) The same CPP data presented as mean percentage time spent in the CS+ compartment (i.e., CS+ compartment seconds divided by total time spent in both the CS+ and CS− compartments times 100). Although there was a pretest in this study, there are numerous ways to present the data and not all require a comparison to the pretest performance. *Source: Data redrawn from Davis, C.M., Riley, A.L., 2006. Drug preexposure in Fischer (F344) and Lewis (LEW) rats: effects on place and taste conditioning. Paper presented at the College on the Problems of Drug Dependence (CPDD) Annual Meeting, Scottsdale, AZ.*

conditioning floors/cues are inserted into the appropriate chambers. These cues will be the same ones used during conditioning and on the posttest.

2. Weigh rodents. Place each subject into the middle of the two-compartment apparatus and record movements for 15 min. If the apparatus has a third (middle) compartment, place the rodent into the middle compartment, remove the barriers, and allow the animal to freely explore all compartments for 15-min while recording the animal's movements.

    Note: If the home cage area and the conditioning apparatus are not located in the same location, some investigators recommend moving all

animals to a quiet area closer to the conditioning location for an hour prior to the start of the pretest (or conditioning sessions, posttest).

3. Using the pretest data, determine each subject's initial side preferences. If an unconditioned preference exists, the least-preferred compartment is the drug-paired compartment (CS+) and a biased procedure should be used. If there is no unconditioned preference, drug- and vehicle-paired compartments are counterbalanced across subjects, such that half receive drug (or vehicle) in one compartment and half receive drug (or vehicle) in the other compartment (i.e., an unbiased procedure). Once subjects are assigned a drug-paired compartment, the presentation of
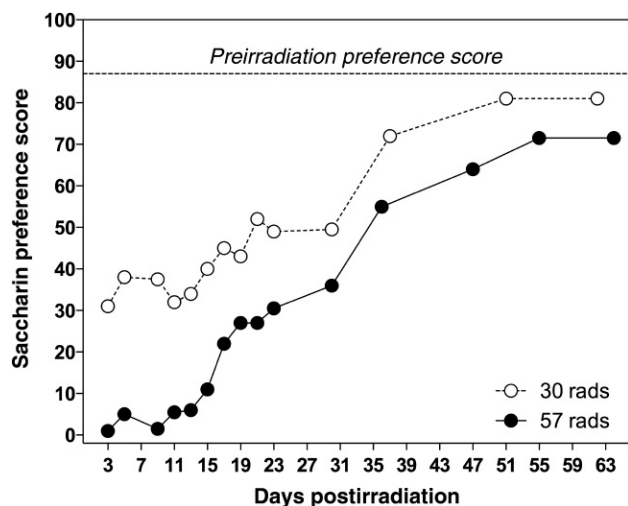
FIGURE 22.4 **Median saccharin preference in rats conditioned with a single exposure to gamma irradiation at 30 or 57 rads.** The irradiation-induced CTA was apparent for approximately 30 days postirradiation and after that time, some extinction of the aversion was apparent. *Source: Redrawn from Garcia, J., Kimeldorf, D.J., Koelling, R.A., 1955. Conditioned aversion to saccharin resulting from exposure to gamma radiation. Science 122(3160), 157–158.*

CS+ and CS− trials must be counterbalanced as well. That is, half of the subjects receive drug-compartment pairings (or CS+ trials) on odd-numbered conditioning trials (i.e., drug on days 3, 5, 7, and 9) and half receive these pairings on even-numbered conditioning trials (i.e., drug on days 2, 4, 6, and 8).

4. Thoroughly clean all compartments between animals and at the end of the day.

Conditioning trials (days 2–9)

5. Twenty-four hours following the pretest, the conditioning trials commence. Begin by cleaning each compartment and placing the appropriate floor materials/cues in each conditioning compartment; insert barriers to keep animals confined to a specific compartment.
Note: Some laboratories use the entire conditioning apparatus during each conditioning trial, such that the floor material for the CS+ or CS− trial covers the entire apparatus. Others insert barriers between the two compartments such that the apparatus is split into its conditioning compartments and the barrier is present throughout the entire conditioning phase. Regardless of what option is used, the conditioning apparatus must contain both conditioning floors/cues during the posttest session.

6. Weigh each subject, inject with the appropriate solution (i.e., drug or vehicle), and immediately place the subject into the assigned compartment for a specified time period—a general duration is 30 min, however this parameter varies with different drug USs and should be chosen for the specific drug being studied. Subjects' activity can be recorded during the conditioning trials
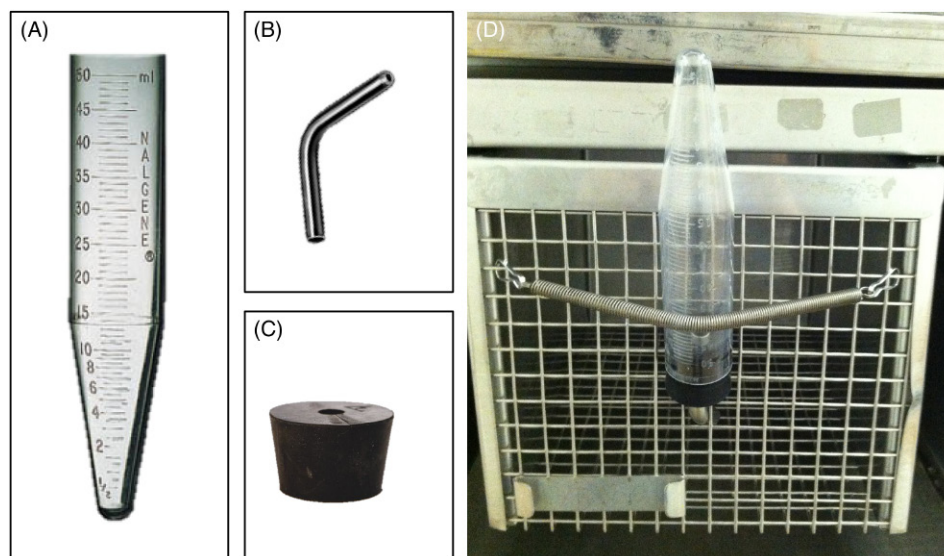
FIGURE 22.5 (A) 50-mL Nalgene tube for fluid access during taste aversion conditioning. This volume of fluid is adequate for a 20–30 min fluid access period. The tube is inverted when it is attached to the rat's cage. (B) Curved steel sipper tube. If rats are housed in wire mesh cages, these curved sipper tubes are needed for fluid access. If rats are housed in polycarbonate cages with a wire top, curved or straight sipper tubes can be used. (C) Size #7 rubber stopper. This size fits snugly in the 50-mL Nalgene tube. When putting the stoppers into the tubes, wet the stopper and twist it once it has been inserted. This provides tight seal so that the stoppers are not easily knocked out of the tube. (D) The tube, with inserted stopper, inverted, and attached to a wire mesh rat cage.

for a more detailed behavioral analysis (Huston et al., 2013), but it is not required.

Note: Subjects should be run at the same time each day throughout the entire procedure (i.e., from pretest through conditioning and the posttest). Thus, drug solutions should be made in advance to allow enough time for the equipment set-up and syringe preparation each day. It is recommended that drug solutions are made fresh daily.

7. Once the trial is complete, remove the animal and return it to its home cage. Clean each compartment and prepare the equipment for conditioning trials with additional subjects, if necessary.

8. Twenty-four hours after the first conditioning trial, steps 5–7 are repeated. Animals receive an injection of the opposite solution, followed by confinement to the other compartment. More specifically, an animal that received a drug-compartment pairing (or CS+ trial) on day 2, now receives a vehicle-compartment pairing (or CS− trial) on day 3. This process is reversed for animals that received CS− trials on day 2. Conditioning trials continue in alternating manner every 24 h until day 9, which results in 4 CS+ trials and 4 CS− trials.

Posttest (preference test; day 10)

9. Twenty-four hours after the final conditioning trial, clean all compartments. Prepare each conditioning apparatus with the appropriate floor materials/cues. If using a two-compartment apparatus, remove the barrier between the compartments and place the animal in the middle of the apparatus. Record activity. If using a three-compartment apparatus, place the animal in the middle compartment of the apparatus; remove the barriers and record activity. Other barrier configurations can be used, such that clear or opaque barriers with a tunnel remain in place during the test session (White et al., 2005).

10. Once the test is complete, remove the animal from the conditioning apparatus and return it to its home cage. Clean each compartment thoroughly and prepare for additional animals, if necessary.

5 THE FLAVOR CONDITIONING PROCEDURE

5.1 What are Conditioned Taste Aversions?

Flavor conditioning is a simple procedure most commonly used to assess the positive (appetitive) or negative (aversive) effects of numerous compounds, including various nutrients, food sources, toxins, poisons, ionizing radiation, and drugs of abuse (Freeman and Riley, 2009). Conditioned flavor preference (CFP) is a procedure used to assess the positive effects of a stimulus by measuring increased consumption of a solution, whereas conditioned taste aversion (CTA) is used to assess the aversive effects of different stimuli by measuring decreases in consumption of a palatable solution. While CFP is a common procedure used to assess the positive effects of oral and postoral associations (Sclafani, 2004; Touzani et al., 2010), the current review will focus on the use of the taste aversion procedure in measuring the aversive effects of drugs of abuse. In a standard CTA experiment, subjects undergo conditioning trials in which consumption of a novel, palatable solution (typically saccharin) is paired with the injection of a drug. Interspersed between conditioning trials are water recovery days where subjects receive water (or a solution with another distinct flavor) to drink, but do not receive any drug injections. After several saccharin-drug pairings, subjects are tested for the expression of the CTA during a final test trial in which subjects are given access to the saccharin solution and consumption is recorded; no injections follow saccharin access on this test trial. Subjects that decrease consumption of the saccharin solution following the saccharin-drug pairings are said to express a conditioned taste aversion. While the methodology is slightly different, procedures similar to this that result in greater consumption of the novel fluid are indicative of conditioned flavor preferences.

Similar to the CPP procedure discussed earlier, the CTA procedure is also based on principles of Pavlovian classical conditioning, where the drug administered serves as the US and is subsequently paired with the novel saccharin solution—after several saccharin-drug pairings, decreases in consumption or avoidance (CR) of the saccharin solution (CS) are evident, due to its association with the aversive effects of drug administration. Interestingly, most drugs that serve as reinforcers in the self-administration procedure and that condition place preferences also induce taste aversions, which suggests that reinforcing drugs of abuse have both rewarding and aversive effects, and that the balance of these effects (i.e., reward and aversion; see earlier) could impact overall acceptability, which could influence subsequent misuse of these compounds (Davis and Riley, 2010; Verendeev and Riley, 2013).

5.2 A Brief History of Taste Aversion Learning

One of the first demonstrations of taste aversion learning was in 1951 when John Garcia and colleagues observed that rats decreased consumption of water from bottles that had been present during the irradiation (for a review of the history of CTA, see Davidson and Riley, 2015; Freeman and Riley, 2009; Verendeev

and Riley, 2012). Garcia argued that the decrease in consumption following exposure to radiation was due to the acquired association of the taste (imparted on the water from the plastic bottles in which it was contained) with the aversive effects of gamma irradiation. This explanation appeared to be valid, given that the same rats would ingest water from glass bottles in their home cage. In 1955, Garcia et al. (1955) sought to systematically test this hypothesis by pairing a novel saccharin solution with gamma irradiation. Consistent with his earlier findings, rats receiving saccharin-irradiation pairings decreased consumption of this palatable solution, whereas rats receiving saccharin paired with sham-irradiation displayed no change in saccharin consumption. Thus the effects of gamma radiation were causing a decrease in consumption of the novel fluid, demonstrating that radiation exposure had identifiable effects that could be readily associated with other stimuli, such as taste. Importantly, this effect was not simply a direct effect of radiation-induced damage impairing the ability of these animals to consume the sweetened solution, given that rats receiving exposure to gamma radiation that was not explicitly paired with the saccharin solution continued to consume the saccharin solution at control levels (Garcia et al., 1955, 1968). The effects of gamma irradiation were thus associated with the novel tasting saccharin solution, and this association created the decrease in consumption on successive saccharin presentations. Garcia and colleagues determined that irradiation could condition a decrease in saccharin consumption indicative of a taste aversion.

Following these initial studies, numerous reports from Garcia and his colleagues and other investigators detailed several important findings that now characterize the phenomenon of taste aversion learning as a "specialized form of learning." In their initial study, Garcia et al. (1955) demonstrated that radiation-induced taste aversion were evident following only one saccharin-radiation pairing. Further, these aversions were still evident at 30-days postirradiation (Garcia et al., 1955). Shortly following this report of one-trial learning of CTA, it was shown that taste aversions could be acquired over long time delays between consumption of the saccharin CS and presentation of the US, which in these early studies was ionizing radiation (McLaurin and Scarborough, 1963; Revusky, 1968; Smith and Roll, 1967), but has since been shown to occur with other compounds serving as the US, such as lithium chloride, an emetic, and cocaine, a drug of abuse (Etscorn and Stephens, 1973; Freeman and Riley, 2005; Nachman, 1963; Riley and Mastropaolo, 1989). Lastly, Garcia and Koelling (1966) reported that taste aversions appeared to be selectively acquired to gustatory stimuli, whereas stimuli like audiovisual cues did not serve as a CS in this design because they were not readily associated with the X-ray or lithium chloride USs

(see also Garcia and Ervin, 1968; McGowan et al., 1972). Taken together, one-trial learning, long-delay learning, and the selective associations of this procedure took aversion learning beyond an interesting radiation-induced effect to a learning example that was somewhat at odds with the traditional views of associative learning. More specifically, traditional associative models generally assumed that control could only be established after many conditioning trials with short-delay and/or trace conditioning techniques and that conditioning could be achieved equally well with most CS-US combinations (Klosterhalfen and Klosterhalfen, 1985; Rescorla and Wagner, 1972). Conditioned taste aversion learning was thus described as a specialized form of learning that facilitated specific associations imperative to an animal's survival, such as those between taste and the postingestive consequences of consumption (e.g., illness). These associations are argued to be highly adaptive because they provide an animal a means by which rapid acquisition of taste-illness associations can occur following consumption of natural toxins in the environment (e.g., those most likely found in food sources) followed sometime later (e.g., after the natural delay imposed by digestion) by illness.

After these initial assessments in which radiation and lithium chloride induced taste aversions to palatable saccharin solutions, investigations began to assess what other compounds could induce a CTA. Given that aversion learning is viewed as a unique form of learning that enables an animal to learn about and subsequently avoid food sources containing poisons or toxins, many of these early studies focused on assessing taste aversion learning induced by compounds or substances with known aversive effects, including poisons, classical toxins, and common emetics. One of the first emetic compounds examined in this context was apomorphine, a nonselective dopamine agonist. Apomorphine-induced aversions were robust, readily acquired after only one CS-US pairing, and could withstand long-delays during conditioning, much like the taste aversions reported earlier following irradiation (Brackbill et al., 1971; Garcia et al., 1966; Stolerman and D'Mello, 1979). Further, lithium chloride gained popularity as a tool to investigate how manipulations to the standard taste aversion procedure would impact acquisition of a taste aversion (Nachman and Ashe, 1973; Nachman et al., 1970). Work assessing other aversive compounds in the CTA design steadily increased throughout the 1970s and into the 1980s: various well-known toxins, including strychnine sulfate, acetaldehyde, sodium fluoride, paraquat, and physostigmine sulfate, all reportedly induced CTAs (for a review, see Riley and Tuck, 1985). Clearly taste aversion learning and the conditions under which it is acquired are not simply an effect of exposure to irradiation, but are common characteristics of a procedure that has general utility as a measure of drug toxicity; more specifically, the fact that

toxin- and poison-induced CTAs are acquired at doses much lower than those needed to adversely impact other behaviors, including food and water consumption, demonstrates the sensitivity of this procedure for measuring the aversive effects of various compounds.

While toxins, poisons, and emetics are common USs in the CTA procedure, drugs of abuse have received considerable attention in taste aversion experiments as well. Further, the taste aversion procedure was viewed as a sensitive assay with which to investigate the potential aversive effects of these drugs, given that these compounds were viewed as stimuli with numerous behavioral effects because they were reinforcers in self-administration and discriminative stimuli in drug discrimination studies and could alter learning and memory in other procedures (Colpaert et al., 1975; D'Mello and Stolerman, 1977; Schuster and Thompson, 1969). One of the first reports of drug-induced taste aversion learning was published in 1971, in which Cappell and LeBlanc assessed the aversive effects of amphetamine or mescaline in rats (Cappell and LeBlanc, 1971). In this study, both compounds induced dose-dependent aversions to the saccharin solution following one conditioning trial in which a drug administration was paired with saccharin to drink. These authors argued that the amphetamine- and mescaline-induced CTAs support the idea that these two drugs, at the doses used, had aversive effects that resulted in significant decreases in saccharin consumption of the test day. They argued further that the CTA results also support the lack of self-administration of mescaline in monkeys (Deneau et al., 1969) and the decrease in amphetamine self-administration in rats at 1 and 2 mg/kg (doses that conditioned a taste aversion; see Pickens and Harris, 1968; see also, Verendeev and Riley, 2011).

In a relatively short period of time, most major drugs of abuse were shown to induce CTAs, including alcohol, morphine, cocaine, Δ9-tetrahydrocannabinol (THC), and 3,4-methylenedioxypyrovaleron (MDPV), under the same parametric conditions as irradiation, emetics, and toxins, for example, one-trial learning, long-delay learning (Freeman and Riley, 2005; King et al., 2015). The fact that drugs of abuse were found to have aversive effects is not surprising since drug effects are generally dose-dependent, with toxicity occurring at greater drug doses. Yet the fact that these effects are evident at the same drug dose is less intuitive. In a combined CPP-CTA study, Reicher and Holman (1977) presented data demonstrating that the same injection of amphetamine could condition a taste aversion while conditioning a place preference to the environment in which the saccharin was consumed. More specifically, rats received an injection of amphetamine prior to placement into one compartment of a place conditioning apparatus. Within in this amphetamine-paired (CS+) compartment, rats had access to a distinctly flavored solution (almond or banana flavor). In the CS− compartment, rats had access to a different solution; if almond was the flavor used in the CS+ compartment, banana was the flavor used in the CS− compartment. Interestingly, amphetamine administration in this design conditioned a significant place preference while also conditioning a significant taste aversion. Further, these same results were evident after a 20-min delay between amphetamine administration and placement into the CS+ compartment. Reicher and Holman argued that amphetamine had rewarding and aversive effects that occurred simultaneously in the same animal and that each of these effects could condition different behaviors (i.e., approach and avoidance).

Since these initials studies with drugs of abuse in the taste aversion procedure, a wealth of literature has accumulated investigating drug-induced CTAs and factors that influence drug taking, including drug history, genetic manipulations (e.g., inbred rats and mice, genetically-modified animals), stress, age, and the maternal environment. In addition, the taste aversion procedure is used in behavioral pharmacology studies aimed at determining what receptor systems are responsible for drug-induced CTAs (Freeman et al., 2005; Serafine and Riley, 2010) and has been adapted for use as a procedure to assess the discriminative stimulus effects of various drugs, especially low doses of opioid antagonists in drug-naïve rats (Riley, 1997). Thus the CTA procedure is commonly used to assess the aversive effects of drugs of abuse and once the general procedure is instituted, adaptations to the procedure can be made to enable subsequent investigations in a manner similar to those mentioned earlier.

5.3 Advantages of the Conditioned Taste Aversion Procedure

The advantages of the CTA procedure are similar to those listed earlier for the CPP procedure; nonetheless, this section will outline these advantages and focus on specific equipment and techniques that are useful for taste aversion studies.

The conditioned taste aversion procedure is methodologically simple and does not require special and/or expensive equipment. The taste aversion procedure is a popular method to study the aversive effects of drugs of abuse for several reasons including (1) the procedure's simplicity in terms of experimenter training and (2) the fact that little specialized equipment is needed; most CTA studies are conducted in an animal's home cage environment. Much like that described earlier for the place conditioning procedure, taste aversion conditioning does not require any specialized training like jugular catheter surgery for self-administration studies. For the CTA procedure, drug is most commonly administered via the intraperitoneal (IP) or subcutaneous (SC) route. While these drug administrations are relatively simple, the route of

administration used in taste aversion conditioning is an important factor and has been shown to differentially impact CTAs induced by different drugs of abuse. Cocaine-induced aversions, for instance, are weaker when drug administrations are IP compared to aversions induced by subcutaneously administered cocaine. Ferrari et al. (1991) demonstrated that IP cocaine induced weak dose-independent aversions, such that all three dose groups (18, 32, and 50 mg/kg) significantly decreased saccharin consumption on the final test trial when compared to consumption of the vehicle control group. In contrast, rats injected SC with cocaine exhibited robust taste aversions at 32 and 50 mg/kg doses; decreases in saccharin consumption in these two groups were evident on the second conditioning trial (Busse et al., 2005; Ferrari et al., 1991; Grigson et al., 2001; Mayer and Parker, 1993). In addition, intracerebroventricular (ICV) drug administrations are also used in taste aversion learning, primarily in studies interested in determining whether a drug's aversive effects are centrally- or peripherally-mediated or what brain areas are involved in a drug-induced CTA (Amit et al., 1977; Clegg et al., 2002; Greenshaw and Buresova, 1982; Liu and Sue Grigson, 2005).

The equipment needed for a taste aversion study is relatively simple and typically includes two different sets of water bottles with rubber stoppers and sipper tubes, in addition to some type of sweetener, which will be prepared as a solution in tap-water and paired with drug administrations. Two sets of water bottles are needed because one set is used to provide the animals with plain tap water (or plain filtered water) and the other set is used for the saccharin solution during the conditioning trials. The use of different water and saccharin water bottles helps to ensure that the taste of the saccharin remains novel and prohibits subjects' exposure to this taste on habituation and/or water recovery days. For this reason, two sets of rubber stoppers with sipper tubes are needed as well. Different types of drinking tubes are used in taste aversion studies and the type of tube chosen usually determines how fluid consumption is measured.

For example, graduated 50-mL Nalgene drinking tubes are commonly used for taste aversion studies with rats and fluid consumption is easily recorded in 0.5 mL increments. Fluid measurements are taken prior to placement of the drinking tube onto each subject's cage and are taken again after the drinking period has ended. Given that movement of the drinking tubes can lead to some fluid loss, care must be taken to place drinking tubes on the cages while minimizing dripping or spilling. To determine the amount of fluid loss that occurs during placement of the drinking tube, a full drinking tube can be placed on an empty cage and pre- and postfluid access measurements can be recorded. Nongraduated drinking bottles are commonly used as well, however, bottles are weighed prior to each subject's fluid access period and then weighed again immediately following the end of the drinking period.

A review of the taste aversion literature demonstrates the variety of gustatory stimuli that have been used in taste aversion studies. For example, numerous studies have used condensed milk or other flavored solutions, including Kool-aid, flavor extracts (e.g., almond, banana, coconut, orange), vanilla, sucrose, or polycose. One of the most common gustatory stimuli is a 0.1% sodium saccharin solution, a relatively inexpensive noncaloric sweetener dissolved in tap water. Noncaloric sweeteners are typically used to decrease the likelihood that changes in consumption result from the high caloric value of a solution, such as sucrose, glucose, or polycose (Gomez and Grigson, 1999); nonetheless, caloric sweeteners are used in drug-induced aversion learning (Grigson et al., 2001; McDonald et al., 1997; Parker and Brosseau, 1990) and to examine the specificity of the tastant-CS association (Nissenbaum and Sclafani, 1987). In addition, strain differences in preference for various gustatory stimuli exist, with most rats and mice displaying a preference for saccharin solutions over water; however, the amount of saccharin (or other flavored solution) consumed does differ between many of these strains and this can impact the results of a taste aversion study. For example, Tordoff et al. (2008) examined two-bottle choices tests (i.e., water vs. solutions containing sucrose, NaCl, saccharin, etc.) in 14 common laboratory rat strains that included 3 outbred and 11 inbred strains. All of these strains displayed a preference for various concentrations of saccharin, but the amount of saccharin consumed did differ among rat strains (Tordoff et al., 2008). Similar results have been reported for numerous strains of inbred mice as well, and most strains display a preference for at least one concentration of saccharin in solution (Bachmanov et al., 2001; Fuller, 1974; Kotlus and Blizard, 1998; Reed et al., 2004). Selection of the appropriate gustatory stimuli for aversion learning can depend up on the strain of rodent(s) used in the study, thus experimenters should be aware of any possible strain differences in tastant preferences prior to the start of conditioning. If strain differences are a focus of the aversion study, the US tastant chosen should be equally preferred between the strains. Finally, while drinking tubes/bottles and a novel tastant, such as saccharin are required for an aversion study, a specific conditioning apparatus is not necessary and most CTA studies condition subjects in their home cages when animals are housed individually; a conditioning apparatus, such as a test cage, has been used when taste aversion conditioning is done in animals that are group housed (Smith et al., 1998).

The conditioned taste aversion procedure is relatively short in duration and has the potential for high throughput of subjects. Another advantage to the conditioned taste

aversion procedure is the fact that large numbers of subjects can be conditioned in a relatively short period of time. For example, taste aversion studies commonly employ 4-day conditioning cycles that begin with a conditioning trial where 20-min access to saccharin is followed by an injection of a drug of abuse; 3 water recovery days follow in which subjects only have access to plain water during the 20-min fluid access period and do not receive postconsumption drug injections. This 4-day conditioning cycle is typically repeated 4 times and is then followed by a test day in which subjects receive access to saccharin, but do not receive any injections following the consumption period. When a taste aversion study is conducted using these common parameters, the entire conditioning period requires only 17 consecutive days (including weekends). The conditioning cycles are however preceded by a habituation phase in which subjects are given 20-min access to plain tap water at the same time each day. The length of this habituation phase is determined by the variability in water consumption: once subjects display stability in the amount of water consumed each day (e.g., for rats, amount consumed not differing by more than 2 mL for 3 consecutive days; Davis et al., 2010) and are approaching and drinking from the water bottle almost immediately after its placement on the cage (i.e., within 2 s of its presentation), the conditioning phase begins. While there is no standard method for determining stability, these criteria result in relatively stable levels of water consumption in approximately 7–14 days, depending on the strain of rodent (Fig. 22.6; see Davis et al., 2009). If no other manipulations are included, a taste aversion study requires a little more than a month (i.e., 31 consecutive days) to complete, assuming a 2-week habituation phase. Obviously, additional manipulations, such as a drug preexposure phase, increase the number of days needed to complete the taste aversion study (Berman and Cannon, 1974; Davis et al., 2010; Risinger and Cunningham, 1995).

Although the 4-day conditioning cycle is common in the taste aversion literature, shorter conditioning cycles have been reported, and depending on the manipulation, are necessary for the specific experimental protocol. For instance, in the combined conditioned taste aversion/conditioned place preference procedure (King et al., 2015; Pomfrey et al., 2015; Roma et al., 2006; Simpson and Riley, 2005; Verendeev and Riley, 2011; Wakeford et al., 2016), the taste aversion procedure is adapted to fit the conditioning phase of the CPP procedure, such that saccharin access occurs on the same day as the drug injection and placement into the CS+ compartment. Water access occurs on the intervening days when vehicle injections precede placement into the CS− compartment. In this combined design, the taste aversion conditioning cycles are 2 days and include a conditioning trial followed by 1 water recovery day, instead of the 3 water
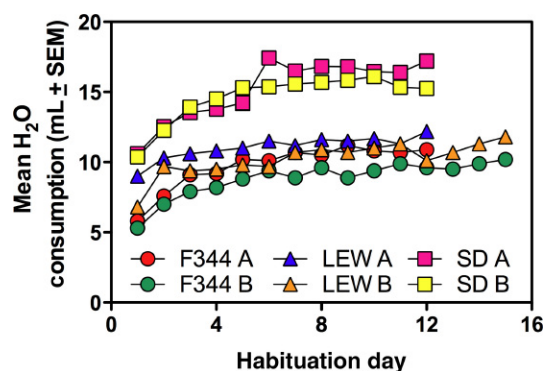
FIGURE 22.6 Mean water consumption in three different rat strains during the habituation phase of six different taste aversion studies (A or B). Although some rat strains consume more water compared to others, all strains display the same pattern of water consumption during the habituation phase. More specifically, water consumption increases over the habituation period to an asymptotic volume from which most rats do not vary (note the errors bars are within the symbol for each point on the graph). The SD rats *(pink and yellow squares)* only needed a 12-day habituation phase, whereas the F344 and LEW rats required 12–15 days, depending on the study (A or B, respectively). *F344*, inbred Fischer 344; *inbred LEW*, Lewis; *SD*, outbred Sprague Dawley. *Source: Data redrawn from Davis, C.M., Riley, A.L., 2006. Drug preexposure in Fischer (F344) and Lewis (LEW) rats: effects on place and taste conditioning. Paper presented at the College on the Problems of Drug Dependence (CPDD) Annual Meeting, Scottsdale, AZ; Davis, C.M., Riley, A.L., 2007. The effects of cocaine preexposure on cocaine-induced taste aversion learning in Fischer and Lewis rat strains. Pharmacol. Biochem. Behav. 87(1), 198–202; and Davis, C.M., de Brugada, I., Riley, A.L., 2010. The role of injection cues in the production of the morphine preexposure effect in taste aversion learning. Learn. Behav. 38(2), 103–110.*

recovery days described earlier. The concern with this procedure is that subjects displaying a conditioned taste aversion will not be adequately rehydrated during the one water recovery day, which could negatively impact the subsequent conditioning trial. Using this combined design however Roma et al. (2006) demonstrated that inbred Fischer and Lewis rats both maintained relatively stable levels of fluid consumption on each water recovery day separating each saccharin-IP ethanol-CS+ conditioning trial, regardless of the strength of the ethanol-induced aversion. Further, body weights of both strains remained stable over the 13-day habituation phase and the 8-day CTA/CPP conditioning phase (Roma et al., 2006) in all rats, including those subjects displaying robust ethanol-induced aversions, that is, subjects that were only consuming water every other day due the to the aversion to the saccharin solution (for similar conditioning cycles with cocaine, see Davis and Riley, 2007). Regardless of the length of the conditioning phase, almost all drug-induced taste aversion studies report dose-response assessments in which different groups of subjects (8–10 per dose group) receive saccharin paired with a specific dose of the drug of interest, in addition to a control group that receives saccharin-vehicle injection pairings. Dose-response assessments typically include

two or more drug doses with separate groups of animals for each dose used; in this way, large numbers of animals can be conditioned in a relatively short period of time in a single taste aversion study.

Other advantages of the taste aversion procedure: In addition to the advantages described earlier, there are several additional advantages of the taste aversion procedure that add its utility and ease with which it can be performed in the laboratory. First, consumption of the fluid CS is always done under drug-free conditions. More specifically, subjects receive the fluid CS to drink for a specified amount of time (e.g., 20-min); once this period is over, subjects are then injected with the drug US. Any changes in consumption then are not simply a function of drug-induced motor impairments for example, because the subjects receive drug only after the fluid access period has ended. Similar to the drug-free posttest in the place conditioning procedure described earlier, the taste aversion test day (i.e., the day after the final conditioning cycle) is a drug-free test as well.

A second additional advantage is the fact that taste aversion studies routinely report dose-response functions where conditioning day saccharin consumption decreases over trials, such that increasing drug doses are typically associated with a more robust decrease in saccharin consumption. While these functions are common in taste aversion learning, floor effects (i.e., no saccharin consumption on subsequent conditioning days) do occur and are not only influenced by the conditioning dose, but also by other factors including baseline consumption of the novel fluid US and strain of rodent used as subjects. For this reason, choosing a novel fluid US that is readily consumed by the strain of rodent serving as subjects in a taste aversion study is important. Nonetheless, most drug-induced CTAs are conditioned at relatively low doses where toxicity is not an issue and conditioning of other behaviors is supported. For example, morphine CTAs are readily acquired at 5 mg/kg, a dose that also conditions a significant place preference in the same animals (Martin et al., 1988; Simpson and Riley, 2005; Verendeev and Riley, 2011). These findings are true for most drugs of abuse, such that the range of drug doses supporting taste aversion learning also support conditioned place preferences.

5.4 Conditioned Taste Aversion: Experimental Protocol and Conditioning Apparatus

Although the characteristics of a taste aversion study were mentioned briefly in the preceding text, the current section aims to describe taste aversion conditioning in detail, including a discussion of some general parameters and characteristics of the experimental design that should be taken into consideration when designing and executing a conditioned taste aversion experiment.

Phases of a conditioned taste aversion study: There are several general phases to a conditioned taste aversion study and these will be discussed in detail here. These phases are included because they are commonly reported in taste aversion studies however some can be altered depending on the goals of the experiment.

The habituation phase: When beginning a taste aversion study, subjects are typically water-restricted and habituated to drinking during a specified period (i.e., the fluid access period) each day. In order to achieve reliable drinking during this period, rats are presented with plain tap water following 23.5 h of water deprivation. More specifically, rats are maintained on *ad libitum* access to water up to the day prior to the start of the habituation phase. On this day, *ad libitum* water bottles are removed from the rats' home cages at a specified time (e.g., 1000 h). On the following day, which is the start of the habituation phase, subjects receive water bottles containing plain water to drink at this same time; rats are given 20-min access to these water bottles and consumption is recorded. If presentation of the drinking bottles occurs earlier or later than the predetermined fluid access period, the amount of water consumed can vary substantially between individual subjects. For this reason, the water bottles must be presented at the same time each day to maintain the subjects' level of fluid restriction throughout the study.

It is common for subjects to increase water consumption throughout the habituation period, thus this phase continues until all subjects display stable day-to-day consumption levels.

Using each subject's mean water consumption, stability is commonly defined as a subject consuming within 2 mL of its mean fluid consumption over 3 consecutive days (Davis et al., 2010). Beginning the conditioning phase after subjects' habituation water consumption has stabilized helps to ensure that changes in consumption are a function of conditioning and are not due to continued habituation to the fluid restriction procedure. Further, subjects should be weighed each day prior to the fluid access period and weights should be closely monitored throughout this phase and the conditioning phase described later.

Although a single, daily fluid access period is commonly used in taste aversion conditioning, some investigators also include an additional drinking period during which subjects only have access to water. For example, Grigson and Freet (2000) employed a 5-min fluid access period in the morning followed by an hour-long fluid access period in the afternoon (Grigson et al., 2001; Liu and Sue Grigson, 2005). During the habituation phase, rats had access to distilled water during the 5-min and 1-hour fluid access periods, but on conditioning trials saccharin was available during the 5-min period only; distilled water was always available during the 1-hour

afternoon fluid access period. This additional fluid access period is included because subjects were only given 5-min access to water or saccharin during conditioning and needed the afternoon period to rehydrate; conditioning trials in this study occurred every other day, instead of every 4th day (see later).

The conditioning phase: Once subjects are maintaining stable levels of fluid consumption during the habituation phase (approximately 10–14 days), the conditioning phase begins. On the conditioning days of this phase, subjects receive saccharin during their 20-min fluid access period and consumption is recorded. Following the fluid access period, subjects are removed from the home cage, injected with the appropriate drug dose or vehicle, and returned to the home cage. The water recovery days of this phase however are identical to the habituation phase: subjects receive plain water during the 20-min fluid access period and consumption is recorded. No drug injections occur on these days. Taken together, one conditioning cycle consists of a saccharin-conditioning day, in which saccharin consumption precedes an injection of drug or vehicle, followed by 3 water recovery days. This 4-day conditioning cycle is then repeated 4 times for a total of 4 conditioning days and 12 water recovery days.

The first day of the conditioning cycle is important for two reasons: (1) subjects are assigned to an experimental or control group based on their saccharin consumption and (2) the CS-US interval is determined at this time. While subjects can be grouped by mean water consumption on the 3–5 days prior to the 1st conditioning day, it is common for subjects to be assigned to a group based on total saccharin consumed on the 1st day of conditioning. More specifically, once the fluid access period is over, the consumption values are ranked from largest to smallest and subjects are assigned to an experimental or control group such that mean consumption is comparable across groups. By using this pseudorandom assignment technique, saccharin consumption on the first conditioning day is not significantly different between the various experimental (and control) groups, which provide a good baseline for subsequent saccharin consumption day comparisons. This comparable baseline also increases the likelihood that data can be presented as total milliliters consumed instead of having to be transformed to a percentage shift from or percentage of control consumption.

In addition to grouping subjects on this day, the CS-US interval is determined as well and this interval needs to be maintained on subsequent conditioning days. For example, each subject receives 20-min access to saccharin followed by an injection sometime after fluid consumption. The time between fluid consumption and the subsequent drug injection should be carefully timed on the 1st conditioning day and this CS-US interval should be maintained throughout the conditioning phase. Thus, if subjects are injected 5-min after saccharin consumption on the 1st conditioning day, subsequent injections should also occur 5-min after saccharin access as well.

The one-bottle final aversion test: Following the final water recovery day of the last conditioning cycle, the final aversion test is typically administered. This test consists of 20-min access to saccharin during the fluid access period following which no injections are administered. When done in this manner, this test is also referred to as a one-bottle aversion test. If the drug-induced taste aversions are robust—subjects are consuming little to no saccharin on this test—the one-bottle aversion test is typically the final day of a conditioned taste aversion study.

The two-bottle final aversion test: If the conditioned taste aversion is not robust, does not differ by dose, or is relatively weak, etc., a more sensitive two-bottle test is usually administered. This test is considered to be more sensitive than the one-bottle test described earlier because subjects have access to saccharin and water concurrently during the 20-min access period and can choose to drink the saccharin or water during this time. If a taste aversion has been conditioned, subjects consume a greater percentage of water compared to saccharin during this period, with similar levels of total fluid consumption (i.e., saccharin + water consumption) between experimental and control groups. If the two-bottle test will be run following the one-bottle aversion test, it is important to consider injecting the subjects following the one-bottle test and giving the subjects 3 water recovery days (i.e., running a 5th conditioning cycle). In this way, the subjects have always experienced saccharin paired with the drug effects and no extinction effects will be evident on the results of the two-bottle test.

In a recent paper examining taste aversions induced by opioid receptor agonists, Davis et al. (2009) demonstrated the sensitivity of the two-bottle aversion test following what appeared to be weak aversions induced by (-)-U50.488H, SNC80, kappa and delta opioid receptor agonists, respectively (Fig. 22.7).

Saccharin consumption in the experimental groups conditioned with either drug did not differ much from their control group's saccharin consumption over five conditioning trials. More specifically, only the subjects conditioned with the highest dose of the kappa agonist displayed significant decreases in saccharin consumption compared to control subjects; subjects conditioned with SNC80 displayed similar levels of saccharin consumption throughout conditioning that did not differ between the conditioning doses. However, robust and dose-dependent (for the kappa agonist only) drug-induced aversions were apparent in the two-bottle aversion test, which was administered following the one-bottle test and 3 water recovery days (i.e., a 5th conditioning cycle; Fig. 22.8). These results demonstrate the
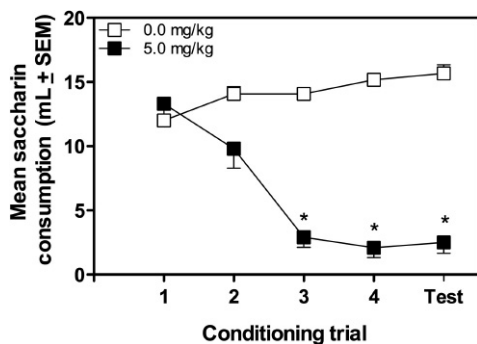
FIGURE 22.7 **Morphine-induced conditioned taste aversion in adult male Fischer 344 rats.** Following the habituation phase on conditioning day 1, all rats received 20-min access to saccharin followed by an injection of morphine (5 mg/kg, SC) or vehicle. Consumption on this day is equivalent between the groups because group assignments were made based on the ranking procedure described in the text. Over the three subsequent Conditioning Days, rats receiving morphine display a significant decrease in saccharin consumption compared to vehicle-treated control rats, in addition to a significant decrease in saccharin intake on the one-bottle final aversion test. *Source: Redrawn from Davis, C.M., Riley, A.L., 2006. Drug preexposure in Fischer (F344) and Lewis (LEW) rats: effects on place and taste conditioning. Paper presented at the College on the Problems of Drug Dependence (CPDD) Annual Meeting, Scottsdale, AZ.*

usefulness of the two-bottle aversion test and while it is not required, administering this test is highly recommended, especially when aversions are weak over consecutive conditioning trials.

General rat taste aversion conditioning procedure:

Prehabituation (day 0):

1. Weigh rats. Remove *ad libitum* water bottles to provide 23.5 h of water deprivation prior to the start of the habituation phase on the following day.

Habituation phase (days 1–14):

2. Fill one set of 50-mL Nalgene tubes with plain water (e.g., distilled, filtered, tap) and allow the water to come to room temperature.
3. Weigh rats.
4. Once water has reached room temperature, invert the first Nalgene tube. Allow the air bubbles to escape and record the preconsumption volume. Attach this bottle to the cage of the first rat. Start

(-)-U50,488H one- and two-bottle aversion tests
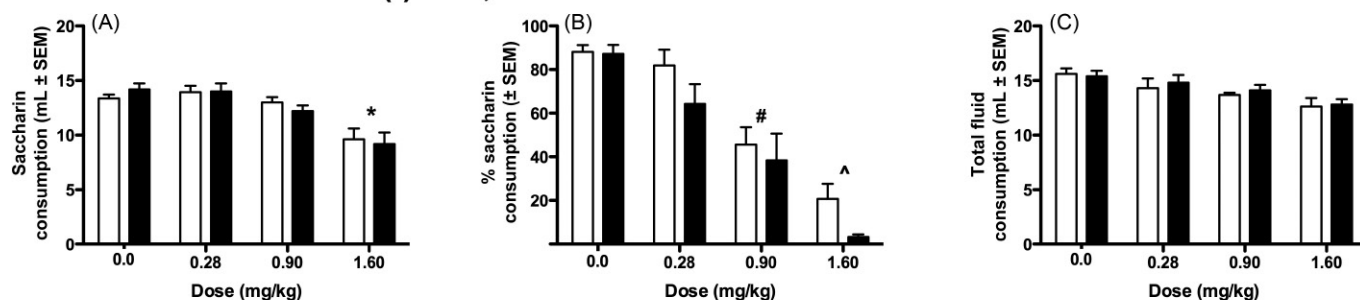
SNC80 one- and two-bottle aversion tests
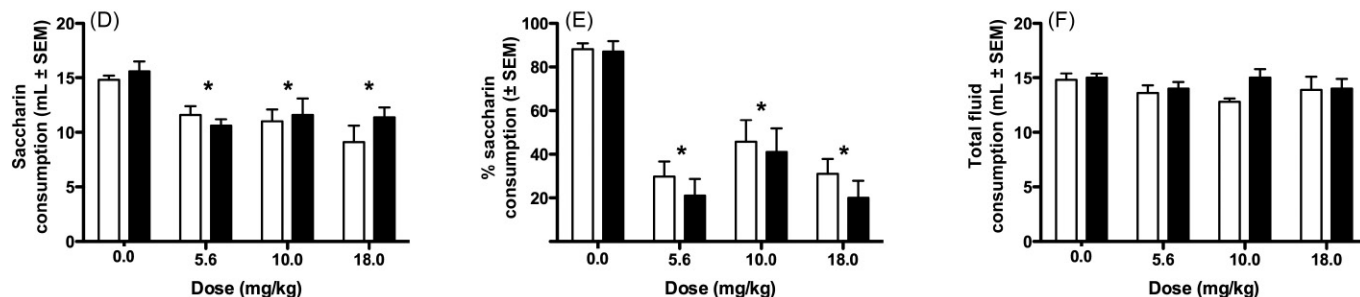
FIGURE 22.8 **Mean consumption during one- and two-bottle final aversion tests for Fischer 344 and Lewis conditioned with (-)-U50,488H, a kappa opioid receptor agonist, or SNC80, a delta opioid receptor agonist.** All rats received 4 saccharin-drug pairings and then received a one-bottle final aversion test (panels A and D). The drug-induced decreases in saccharin consumption were weak and did not differ by dose, thus a two-bottle aversion test followed a fifth conditioning cycle. On the two-bottle test, taste aversions following conditioning with (-)-U50,488H were robust and differed by dose but not by strain (panel B). Rats conditioned with 0.90 (#) or 1.6 mg/kg (^) consumed significantly less saccharin than rats receiving 0.0 or 0.28 mg/kg. For SNC80 conditioned rats, the two-bottle test revealed a more robust decrease in saccharin consumption that remained dose-independent (*denotes all groups consuming significantly less saccharin than rats receiving 0.0 mg/kg; panel E). Panels C and F depict total fluid consumption on the two-bottle test for both strains; no differences were evident in overall fluid consumption, even though significant aversions to the saccharin solution were apparent. *Source: Redrawn from Davis, C.M., Rice, K.C., Riley, A.L., 2009. Opiate-agonist induced taste aversion learning in the Fischer 344 and Lewis inbred rat strains: evidence for differential mu opioid receptor activation. Pharmacol. Biochem. Behav. 93(4), 397–405.*

stopwatch or timer. Invert the next Nalgene tube; allow air bubbles to escape, and record preconsumption volume.

5. Once 10–15 s has passed, attach the second water bottle to the second rat's cage. Continue in this manner until all rats have water bottles. Exit the drinking area with the stopwatch or timer.
Note: A standard time interval should occur between the placements of each water bottle, such that each subject receives a full 20-min consumption period. This is easily done by placing water bottles on individual cages at 10–15 s intervals. Depending on the number of subjects, the total experimental time could exceed 20 min due to the staggered drinking periods, however this technique ensures that each subject receives the full time to drink regardless of when the water bottle is placed on the cage.

6. Once 20 min has elapsed, return to the drinking area and gently remove the first Nalgene tube from the first rat's cage; avoid spilling/ dripping any saccharin from the tube. Record the postconsumption volume. Wait 10–15 s and remove the next bottle; record postconsumption volume. Repeat until all bottles have been removed.

7. Empty bottles and rinse with fresh tap water. Store bottles inverted and allow to air dry.

8. Repeat steps 2–7 on each day of the habituation phase. Monitor body weights and daily water intake.
Note: If any subject is not adapting to the habituation schedule and is showing signs of distress and/or illness, the animal should be removed from the study and given *ad libitum* access to water, in addition to softened food and any other necessary veterinary care.

9. After approximately 7 days, water consumption by most subjects will begin to stabilize. Acquire 3-day averages for each subject and compare them to that day's consumption values. When average daily consumption does not vary by more than ±2 mL, water consumption is stable.

Conditioning phase:

Conditioning cycle day 1 (day 15):

10. On the morning of the 1st conditioning day, dissolve saccharin in plain water—use the same type of water that was used during habituation, for example, distilled, filtered, tap. Fill the second set of Nalgene tubes with the saccharin; let the bottles sit to warm to room temperature.
Note: A different set of bottles and stoppers must be used for saccharin access to avoid exposing the subjects to the saccharin flavor on water

recovery days (or habituation days in a future study). Labeling the saccharin bottles prior to the start of conditioning should be done to avoid any cross-contamination. Further, once the saccharin bottles/stoppers have been used for saccharin access, they should never be used for plain tap water and should not be stored with the water-only bottles/stoppers.

11. Weigh rats; prepare drugs and syringes.

12. Similar to the habituation phase, invert the first Nalgene tube, allow the air bubbles to escape, record preconsumption volume, and place the bottle on the cage of the first rat. Start the stopwatch or timer.

13. Invert the second Nalgene tube and repeat, placing the second bottle on the next rat's cage 10–15 s after placement of the first bottle.

14. Continue until all rats have saccharin bottles on their cages. Exit the drinking area with the stopwatch or timer.

15. Return to the drinking area after 20 min and remove the first rat's saccharin bottle. Record the postconsumption volume. Wait 10–15 s and remove the next rat's saccharin bottle and record postconsumption volume. Repeat every 10–15 s to remove all bottles.

16. Rank subjects by saccharin consumption from greatest to least. Denoting each dose group by a different letter (e.g., high dose = 1, control = 0), assign each subject a dose value in ascending order (i.e., 0, 1, 2); after the last dose value, repeat the values in descending order (i.e., 2, 1, 0). In this way, average saccharin consumption across all groups on the first conditioning day will be similar.
Note: This ranking procedure typically takes about 3–5 min; use of a computer with Microsoft Excel is highly recommended. If an experimenter allots 5 min to this ranking procedure, drug injections will not begin until 5-min after the saccharin access period. It is important that this time interval be maintained on subsequent conditioning days when the ranking procedure is not completed (because group assignment has been completed), such that the CS-US interval is consistent across conditioning days. If an experimenter does not allot a specified period of time to ranking, it is recommended that the stopwatch or timer be used to time the ranking procedure and determine precisely when the first injection was administered following saccharin access.

17. After the last injection, dispose of needles/ syringes. Empty saccharin bottles, rinse with warm tap water, and invert to dry. Soap should *not* be used to clean the saccharin

bottles because this could impart a taste on the bottle and/or stopper that could influence conditioning.

Conditioning cycle 1 days 2–4 (days 16–18):

18. During the water recovery days, no saccharin is consumed and no injections are administered. Similar to the habituation phase, fill Nalgene tubes with plain water and let sit out to warm to room temperature.
19. Weigh rats.
20. Place Nalgene bottles on cages as described earlier; record pre- and postconsumption volumes. Empty and rinse bottles.

Conditioning cycles 2–4 (days 19–30):

21. The 2nd conditioning day is similar to the 1st in all respects except that there is no ranking procedure.
22. Prepare saccharin as stated earlier. Prepare drug and syringes.
23. Place saccharin on cages and record preconsumption volumes.
24. After 20 min, return to drinking area and remove saccharin.
25. Maintaining the same CS-US interval employed on conditioning day 1, inject subjects after the saccharin access period.
26. On the following 3 water recovery days, prepare Nalgene tubes with plain water, weigh rats, and record water consumption.

One-bottle final aversion test (day 31):

27. On the day following the last water recovery day of the final conditioning cycle, prepare saccharin in the morning and fill the Nalgene tubes.
28. Similar to the conditioning days, place saccharin bottles on the rats' cages at 10–15 s intervals. Record pre-and postconsumption volumes. If no two-bottle test will not be run, no injections are necessary and this is the last day of the taste aversion study.
29. If a two-bottle aversion test will be run, prepare drug and syringes. Inject subjects after saccharin access. Provide plain water during the fluid access period on the following 3 days—this constitutes a fifth conditioning cycle (days 31–34).

Two-bottle final aversion test (day 35):

30. Twenty-four hours following the last water recovery day dissolve saccharin in plain water and fill the Nalgene tubes. Additionally, fill the other set of Nalgene tubes with plain water. Let water in both sets of tubes warm to room temperature.

31. Invert the first saccharin Nalgene tube, allow bubbles to escape, and record preconsumption volume. Invert the first plain water Nalgene tube, allow bubbles to escape, and record preconsumption volume. Holding one bottle in each hand, present both sipper tubes to the first rat simultaneously. Attach both tubes to the first cage.
32. For the second rat, place the saccharin tube on the opposite side of the cage compared to the first rat. More specifically, if the saccharin tube is on the right side of the first rat's cage, place the saccharin tube on the left side of the second rat's cage. Repeat at 10–15 s intervals for the remaining subjects; continue to alter the location of the saccharin bottle from left to right. Exit the drinking area.
   Note: The two-bottle test is easier to administer if there are two experiments—one to invert and place the bottles on the cages and another person to record the consumption values and monitor the stopwatch or timer.
33. After 20 min, return to the drinking area and remove each rat's bottles at the same time. Record postconsumption volume for both bottles.
34. Rinse both sets of bottles and invert to air dry.

6 CONCLUSIONS

The conditioned place preference and conditioned taste aversion procedures are two common methods for assessing the rewarding and aversive, respectively, effects of drugs of abuse. Both of these procedures have numerous advantages, including the ease with which the procedures can be performed and the fact that both procedures require relatively inexpensive equipment. Further, the popularity of these procedures in the drug addiction field gives investigators a wealth of data that can be examined when designing new CPP and/or CTA studies to aid in the selection of parameters, methodology, and other important experimental variables. While these procedures might not represent every aspect of SUD or addiction, these procedures are valuable tools to enable researchers to gain a greater understanding of the effects of drugs on the brain and behavior and to enable discovery of pharmacotherapeutic strategies to treat SUD.

Acknowledgment

References

Ahsan, H.M., de la Pena, J.B., Botanas, C.J., Kim, H.J., Yu, G.Y., Cheong, J.H., 2014. Conditioned place preference and self-administration induced by nicotine in adolescent and adult rats. Biomol. Ther. 22 (5), 460–466.

Amit, Z., Levitan, D.E., Brown, Z.W., Rogan, F., 1977. Possible involvement of central factors in the mediation of conditioned taste aversion. Neuropharmacology 16 (2), 121–124.

Andreatta, M., Fendt, M., Muhlberger, A., Wieser, M.J., Imobersteg, S., Yarali, A., et al., 2012. Onset and offset of aversive events establish distinct memories requiring fear and reward networks. Learn. Mem. 19 (11), 518–526.

Astur, R.S., Carew, A.W., Deaton, B.E., 2014. Conditioned place preferences in humans using virtual reality. Behav. Brain Res. 267, 173–177.

Astur, R.S., Palmisano, A.N., Carew, A.W., Deaton, B.E., Kuhney, F.S., Niezrecki, R.N., et al., 2016. Conditioned place preferences in humans using secondary reinforcers. Behav. Brain Res. 297, 15–19.

Bachmanov, A.A., Tordoff, M.G., Beauchamp, G.K., 2001. Sweetener preference of C57BL/6ByJ and 129P3/J mice. Chem. Senses 26 (7), 905–913.

Bahi, A., Tolle, V., Fehrentz, J.A., Brunel, L., Martinez, J., Tomasetto, C.L., Karam, S.M., 2013. Ghrelin knockout mice show decreased voluntary alcohol consumption and reduced ethanol-induced conditioned place preference. Peptides 43, 48–55.

Baker, M., 2011. Animal models: inside the minds of mice and men. Nature 475 (7354), 123–128.

Banasikowski, T.J., Beninger, R.J., 2010. Conditioned drug effects. In: Stolerman, P.I., Price, H.L. (Eds.), Encyclopedia of Psychopharmacology. Springer Berlin Heidelberg, Berlin, Heidelberg, pp. 1–8.

Bardo, M.T., Bevins, R.A., 2000. Conditioned place preference: what does it add to our preclinical understanding of drug reward? Psychopharmacology (Berl.) 153 (1), 31–43.

Bardo, M.T., Neisewander, J.L., 1986. Single-trial conditioned place preference using intravenous morphine. Pharmacol. Biochem. Behav. 25 (5), 1101–1105.

Bardo, M.T., Neisewander, J.L., Pierce, R.C., 1989. Novelty-induced place preference behavior in rats: effects of opiate and dopaminergic drugs. Pharmacol. Biochem. Behav. 32 (3), 683–689.

Bardo, M.T., Rowlett, J.K., Harris, M.J., 1995. Conditioned place preference using opiate and stimulant drugs: a meta-analysis. Neurosci. Biobehav. Rev. 19 (1), 39–51.

Bardo, M.T., Valone, J.M., Bevins, R.A., 1999. Locomotion and conditioned place preference produced by acute intravenous amphetamine: role of dopamine receptors and individual differences in amphetamine self-administration. Psychopharmacology (Berl.) 143 (1), 39–46.

Barr, G.A., Paredes, W., Bridger, W.H., 1985. Place conditioning with morphine and phencyclidine: dose dependent effects. Life Sci 36, 363–368.

Beach, H.D., 1957. Morphine addiction in rats. Can. J. Psychol. 11 (2), 104–112.

Becerra, L., Navratilova, E., Porreca, F., Borsook, D., 2013. Analogous responses in the nucleus accumbens and cingulate cortex to pain onset (aversion) and offset (relief) in rats and humans. J. Neurophysiol. 110 (5), 1221–1226.

Belin, D., Mar, A.C., Dalley, J.W., Robbins, T.W., Everitt, B.J., 2008. High impulsivity predicts the switch to compulsive cocaine-taking. Science 320 (5881), 1352–1355.

Berman, R.F., Cannon, D.S., 1974. The effect of prior ethanol experience on ethanol-induced saccharin aversions. Physiol. Behav. 12 (6), 1041–1044.

Bevins, R.A., Cunningham, C.L., 2006. Place conditioning: a methodological analysis. In: Anderson, M.J. (Ed.), Tasks and Techniques: A Sampling of the Methodologies for the Investigation of Animal Learning, Behavior, & Cognition. Nove Science Publishers, Inc, Hauppauge, NY, pp. 99–110.

Borges, A.C., Duarte, R.B., Nogueira, L., Barros, M., 2015. Temporal and dose-dependent differences in simultaneously-induced cocaine hypervigilance and conditioned-place-preference in marmoset monkeys. Drug Alcohol Depend. 148, 188–194.

Brackbill, R.M., Rosenbush, S.N., Brookshire, K.H., 1971. Acquisition and retention of conditioned taste aversion as a function of the taste quality of the CS. Learn. Motiv. 2 (4), 341–350.

Busse, G.D., Freeman, K.B., Riley, A.L., 2005. The interaction of sex and route of drug administration in cocaine-induced conditioned taste aversions. Pharmacol. Biochem. Behav. 81 (4), 814–820.

Cappell, H., LeBlanc, A.E., 1971. Conditioned aversion to saccharin by single administrations of mescaline and d-amphetamine. Psychopharmacologia 22 (4), 352–356.

Carr, G.D., Phillips, A.G., Fibiger, H.C., 1988. Independence of amphetamine reward from locomotor stimulation demonstrated by conditioned place preference. Psychopharmacology 94 (2), 221–226.

Carr, G.D., Fibiger, H.C., Phillips, A.G., 1989. Conditioned place preference as a measure of drug reward. In: Liebman, J.M., Cooper, S.J. (Eds.), The Neuropharmacological Basis of Reward. Oxford, New York, pp. 264–319.

Carr, G.D., White, N.M., 1983. Conditioned place preference from intraaccumbens but not intra-caudate amphetamine injections. Life Sci 33, 2551–2557.

CDC, 2005a. AIDS Surveilance—General Epidemiology L178 Slide Series (slide 9). Atlanta: CDC Division of HIV/AIDS Prevention, National Center for HIV, STD, and TB Prevention.

CDC, 2005b. Targeting Tobacco Use: The Nation's Leading Cause of Death. Atlanta: CDC National Center for Chronic Disease Prevention and Health Promotion.

CDC, 2014. Excessive drinking costs U.S. $223.5 billion. Available from: http://www.cdc.gov/features/alcoholconsumption/

Childs, E., de Wit, H., 2009. Amphetamine-induced place preference in humans. Biol. Psychiatry 65 (10), 900–904.

Ciccocioppo, R., Panocka, I., Froldi, R., Quitadamo, E., Massi, M., 1999. Ethanol induces conditioned place preference in genetically selected alcohol-preferring rats. Psychopharmacology (Berl.) 141 (3), 235–241.

Clegg, D.J., Wortman, M.D., Benoit, S.C., McOsker, C.C., Seeley, R.J., 2002. Comparison of central and peripheral administration of C75 on food intake, body weight, and conditioned taste aversion. Diabetes 51 (11), 3196–3201.

Collier, A.D., Echevarria, D.J., 2013. The utility of the zebrafish model in conditioned place preference to assess the rewarding effects of drugs. Behav. Pharmacol. 24 (5–6), 375–383.

Colpaert, F.C., Niemegeers, C.J., Kuyps, J.J., Janssen, P.A., 1975. Apomorphine as a discriminative stimulus, and its antagonism by haloperidol. Eur. J. Pharmacol. 32 (02), 383–386.

Cunningham, C.L., 2014. Genetic relationship between ethanol-induced conditioned place preference and other ethanol phenotypes in 15 inbred mouse strains. Behav. Neurosci. 128 (4), 430–445.

Cunningham, C.L., Prather, L.K., 1992. Conditioning trial duration affects ethanol-induced conditioned place preference in mice. Anim. Learn. Behav. 20 (2), 187–194.

Cunningham, C.L., Dickinson, S.D., Grahame, N.J., Okorn, D.M., McMullin, C.S., 1999. Genetic differences in cocaine-induced conditioned place preference in mice depend on conditioning trial duration. Psychopharmacology 146 (1), 73–80.

Cunningham, C.L., Clemans, J.M., Fidler, T.L., 2002. Injection timing determines whether intragastric ethanol produces conditioned place preference or aversion in mice. Pharmacol. Biochem. Behav. 72 (3), 659–668.

Cunningham, C.L., Gremel, C.M., Groblewski, P.A., 2006. Drug-induced conditioned place preference and aversion in mice. Nat. Protoc. 1 (4), 1662–1670.

Davidson, T.L., Riley, A.L., 2015. Tast, sickness, and learning. Am. Sci. 103 (3), 204.

Davis, C.M., Riley, A.L., 2007. The effects of cocaine preexposure on cocaine-induced taste aversion learning in Fischer and Lewis rat strains. Pharmacol. Biochem. Behav. 87 (1), 198–202.

Davis, C.M., Riley, A.L., 2010. Conditioned taste aversion learning: implications for animal models of drug abuse. Ann. N Y Acad. Sci. 1187, 247–275.

Davis, C.M., Roma, P.G., Dominguez, J.M., Riley, A.L., 2007. Morphine-induced place conditioning in Fischer and Lewis rats: acquisition and dose-response in a fully biased procedure. Pharmacol. Biochem. Behav. 86 (3), 516–523.

Davis, C.M., Rice, K.C., Riley, A.L., 2009. Opiate-agonist induced taste aversion learning in the Fischer 344 and Lewis inbred rat strains: evidence for differential mu opioid receptor activation. Pharmacol. Biochem. Behav. 93 (4), 397–405.

Davis, C.M., de Brugada, I., Riley, A.L., 2010. The role of injection cues in the production of the morphine preexposure effect in taste aversion learning. Learn. Behav. 38 (2), 103–110.

Davoody, L., Quiton, R.L., Lucas, J.M., Ji, Y., Keller, A., Masri, R., 2011. Conditioned place preference reveals tonic pain in an animal model of central pain. J. Pain 12 (8), 868–874.

De Felice, M., Eyde, N., Dodick, D., Dussor, G.O., Ossipov, M.H., Fields, H.L., Porreca, F., 2013. Capturing the aversive state of cephalic pain preclinically. Ann. Neurol. 74 (2), 257–265.

Deneau, G., Yanagita, T., Seevers, M.H., 1969. Self-administration of psychoactive substances by the monkey. Psychopharmacologia 16 (1), 30–48.

US Department of Health and Human Services, C.D.C., 2014. The health consequences of smoking—50 years of progress. A report of the Surgeion General. Atlanta, GA: U.S. Department of Health and Human Services. Available from: http://www.surgeongeneral.gov/library/reports/50-years-of-progress/full-report.pdf

US Department of Justice, N.D. I. C., 2011. National drug threat assessment. (2011-Q0317-001). Johnstown, PA: National Drug Intelligence Center. Available from: https://www.justice.gov/archive/ndic/pubs44/44849/44849p.pdf

Deroche-Gamonet, V., Belin, D., Piazza, P.V., 2004. Evidence for addiction-like behavior in the rat. Science 305 (5686), 1014–1017.

Dixon, L.M., Sandilands, V., Bateson, M., Brockelhurst, S., Tolkamp, B.J., D'Eath, R.B., 2013. Conditioned place preference or aversion as animal welfare assessment tools: Limitations to their application. App. Anim. Behav. Sci. 148, 13.

D'Mello, G.D., Stolerman, I.P., 1977. Comparison of the discriminative stimulus properties of cocaine and amphetamine in rats. Br. J. Pharmacol. 61 (3), 415–422.

Durazzo, T.C., Gauvin, D.V., Goulden, K.L., Briscoe, R.J., Holloway, F.A., 1994. Cocaine-induced conditioned place approach in rats: the role of dose and route of administration. Pharmacol. Biochem. Behav. 49 (4), 1001–1005.

Etscorn, F., Stephens, R., 1973. Establishment of conditioned taste aversion with a 24-hour CS-UCS interval. Physiol. Psychol. 1 (3), 251–253.

Everitt, B.J., Robbins, T.W., 2005. Neural systems of reinforcement for drug addiction: from actions to habits to compulsion. Nat. Neurosci. 8 (11), 1481–1489.

Ferrari, C.M., O'Connor, D.A., Riley, A.L., 1991. Cocaine-induced taste aversions: effect of route of administration. Pharmacol. Biochem. Behav. 38 (2), 267–271.

Freeman, K.B., Riley, A.L., 2005. Cocaine-induced conditioned taste avoidance over extended conditioned stimulus-unconditioned stimulus intervals. Behav. Pharmacol. 16 (7), 591–595.

Freeman, K.B., Riley, A.L., 2009. The origins of conditioned taste aversion learning: a historical analysis. In: Reilly, S., Schachtman, T.R.

(Eds.), Conditioned Taste Aversion: Behavioral and Neural Processes. Oxford University Press, New York, pp. 9–36.

Freeman, K.B., Konaklieva, M.I., Riley, A.L., 2005. Assessment of the contributions of Na+ channel inhibition and general peripheral action in cocaine-induced conditioned taste aversion. Pharmacol. Biochem. Behav. 80 (2), 281–288.

Fuller, J.L., 1974. Single-locus control of saccharin preference in mice. J. Hered. 65 (1), 33–36.

Garcia, J., Ervin, F.R., 1968. Gustatory-visceral and telereceptor-cutaneous conditioning--adapation in internal and external milieus. Commun. Behav. Biol. 1, 389–415.

Garcia, J., Koelling, R.A., 1966. Relation of cue to consequence in avoidance learning. Psychonomic Sci. 4, 2.

Garcia, J., Kimeldorf, D.J., Koelling, R.A., 1955. Conditioned aversion to saccharin resulting from exposure to gamma radiation. Science 122 (3160), 157–158.

Garcia, J., Kimeldorf, D.J., Hunt, E.L., 1957. Spatial avoidance in the rat as a result of exposure to ionizing radiation. Br. J. Radiol. 30 (354), 318–321.

Garcia, J., Ervin, F.R., Koelling, R.A., 1966. Learning with prolonged delay of reinforcement. Psychonomic Sci. 5 (3), 121–122.

Garcia, J., McGowan, B.K., Ervin, F.R., Koelling, R.A., 1968. Cues: their relative effectiveness as a function of the reinforcer. Science 160 (3829), 794–795.

Gerber, B., Yarali, A., Diegelmann, S., Wotjak, C.T., Pauli, P., Fendt, M., 2014. Pain-relief learning in flies, rats, and man: basic research and applied perspectives. Learn. Mem. 21 (4), 232–252.

Gomez, F., Grigson, P.S., 1999. The suppressive effects of LiCl, sucrose, and drugs of abuse are modulated by sucrose concentration in food-deprived rats. Physiol. Behav. 67 (3), 351–357.

Grakalic, I., Schindler, C.W., Baumann, M.H., Rice, K.C., Riley, A.L., 2006. Effects of stress modulation on morphine-induced conditioned place preferences and plasma corticosterone levels in Fischer, Lewis, and Sprague-Dawley rat strains. Psychopharmacology 189 (3), 277–286.

Greenshaw, A.J., Buresova, O., 1982. Learned taste aversion to saccharin following intraventricular or intraperitoneal administration of D,L-amphetamine. Pharmacol. Biochem. Behav. 17 (6), 1129–1133.

Grigson, P.S., Freet, C.S., 2000. The suppressive effects of sucrose and cocaine, but not lithium chloride, are greater in Lewis than in Fischer rats: evidence for the reward comparison hypothesis. Behav. Neurosci. 114 (2), 353–363.

Grigson, P.S., Cornelius, K., Wheeler, D.S., 2001. The suppressive effects of intraperitoneal cocaine are augmented when evaluated in nondeprived rats. Pharmacol. Biochem. Behav. 69 (1–2), 117–123.

Guitart, X., Beitner-Johnson, D., Marby, D.W., Kosten, T.A., Nestler, E.J., 1992. Fischer and Lewis rat strains differ in basal levels of neurofilament proteins and their regulation by chronic morphine in the mesolimbic dopamine system. Synapse 12 (3), 242–253.

Hiroi, N., Brown, J.R., Haile, C.N., Ye, H., Greenberg, M.E., Nestler, E.J., 1997. FosB mutant mice: loss of chronic cocaine induction of Fos-related proteins and heightened sensitivity to cocaine's psychomotor and rewarding effects. Proc. Natl. Acad. Sci. USA 94 (19), 10397–10402.

Hughes, R.N., 1968. Behaviour of male and female rats with free choice of two environments differing in novelty. Anim. Behav. 16 (1), 92–96.

Hung, C.H., Wang, J.C., Strichartz, G.R., 2015. Spontaneous chronic pain after experimental thoracotomy revealed by conditioned place preference: morphine differentiates tactile evoked pain from spontaneous pain. J. Pain 16 (9), 903–912.

Hunt, T., Amit, Z., 1987. Conditioned taste aversion induced by self-administered drugs: paradox revisited. Neurosci. Biobehav. Rev. 11 (1), 107–130.

Huston, J.P., Silva, M.A., Topic, B., Muller, C.P., 2013. What's conditioned in conditioned place preference? Trends Pharmacol. Sci. 34 (3), 162–166.

Isaac, W.L., Nonneman, A.J., Neisewander, J., Landers, T., Bardo, M.T., 1989. Prefrontal cortex lesions differentially disrupt cocaine-reinforced conditioned place preference but not conditioned taste aversion. Behav. Neurosci. 103 (2), 345–355.

Kelley, B.M., Bandy, A.L., Middaugh, L.D., 1997. A study examining intravenous ethanol-conditioned place preference in C57BL/6J mice. Alcohol Clin. Exp. Res. 21 (9), 1661–1666.

King, T., Vera-Portocarrero, L., Gutierrez, T., Vanderah, T.W., Dussor, G., Lai, J., et al., 2009. Unmasking the tonic-aversive state in neuropathic pain. Nat. Neurosci. 12 (11), 1364–1366.

King, H.E., Wakeford, A., Taylor, W., Wetzell, B., Rice, K.C., Riley, A.L., 2015. Sex differences in 3,4-methylenedioxypyrovalerone (MDPV)-induced taste avoidance and place preferences. Pharmacol. Biochem. Behav. 137, 16–22.

Klosterhalfen, S., Klosterhalfen, W., 1985. Conditioned taste aversion and traditional learning. Psychol. Res. 47 (2), 71–94.

Koob, G.F., Le Moal, M., 2006. Neurobiology of Addiction. Academic Press, New York.

Koob, G.F., Volkow, N.D., 2010. Neurocircuitry of addiction. Neuropsychopharmacology 35 (1), 217–238.

Kosten, T.A., Miserendino, M.J., Chi, S., Nestler, E.J., 1994. Fischer and Lewis rat strains show differential cocaine effects in conditioned place preference and behavioral sensitization but not in locomotor activity or conditioned taste aversion. J. Pharmacol. Exp. Ther. 269 (1), 137–144.

Kotlus, B.S., Blizard, D.A., 1998. Measuring gustatory variation in mice: a short-term fluid-intake test. Physiol. Behav. 64 (1), 37–47.

Lahvis, G.P., Panksepp, J.B., Kennedy, B.C., Wilson, C.R., Merriman, D.K., 2015. Social conditioned place preference in the captive ground squirrel (Ictidomys tridecemlineatus): social reward as a natural phenotype. J. Comp. Psychol. 129 (3), 291–303.

Leknes, S., Brooks, J.C., Wiech, K., Tracey, I., 2008. Pain relief as an opponent process: a psychophysical investigation. Eur. J. Neurosci. 28 (4), 794–801.

Leknes, S., Lee, M., Berna, C., Andersson, J., Tracey, I., 2011. Relief as a reward: hedonic and neural responses to safety from pain. PLoS One 6 (4), e17870.

Leshner, A.I., 1997. Addiction is a brain disease, and it matters. Science 278 (5335), 45–47.

Liu, C., Sue Grigson, P., 2005. Mu opioid receptor agonist DAMGO-induced suppression of saccharin intake in Lewis and Fischer rats. Brain Res. 1064 (1–2), 155–160.

Liu, Y., Le Foll, B., Wang, X., Lu, L., 2008. Conditioned place preference induced by licit drugs: establishment, extinction, and reinstatement. Sci. World J. 8, 1228–1245.

Lobo, M.K., Covington, 3rd, H.E., Chaudhury, D., Friedman, A.K., Sun, H., Damez-Werno, D., et al., 2010. Cell type-specific loss of BDNF signaling mimics optogenetic control of cocaine reward. Science 330 (6002), 385–390.

Lynch, W.J., Carroll, M.E., 2001. Regulation of drug intake. Exp. Clin. Psychopharmacol. 9 (2), 131–143.

Marglin, S.H., MacKechnie, D.K., Mattie, M.E., Hui, Y.H., Reid, L.D., 1988. Ethanol with small doses of morphine establishes a conditioned place preference. Alcohol 5 (4), 309–313.

Martin, G.M., Bechara, A., van der Kooy, D., 1988. Morphine preexposure attenuates the aversive properties of opiates without preexposure to the aversive properties. Pharmacol. Biochem. Behav. 30 (3), 687–692.

Matsuzawa, S., Suzuki, T., Misawa, M., 1998. Conditioned fear stress induces ethanol-associated place preference in rats. Eur. J. Pharmacol. 341 (2–3), 127–130.

Matsuzawa, S., Suzuki, T., Misawa, M., 2000. Ethanol, but not the anxiolytic drugs buspirone and diazepam, produces a conditioned place preference in rats exposed to conditioned fear stress. Pharmacol. Biochem. Behav. 65 (2), 281–288.

Mayer, L.A., Parker, L.A., 1993. Rewarding and aversive properties of IP and SC cocaine: assessment by place and taste conditioning. Psychopharmacology (Berl.) 112 (2–3), 189–194.

McDonald, R.V., Parker, L.A., Siegel, S., 1997. Conditioned sucrose aversions produced by naloxone-precipitated withdrawal from acutely administered morphine. Pharmacol. Biochem. Behav. 58 (4), 1003–1008.

McGowan, B.K., Hankins, W.G., Garcia, J., 1972. Limbic lesions and control of the internal and external environment. Behav. Biol. 7 (6), 841–852.

McLaurin, W.A., Scarborough, B.B., 1963. Extension of the interstimulus interval in saccharin avoidance conditioning. Radiat. Res. 20, 317–324.

Meyer, P.J., Ma, S.T., Robinson, T.E., 2012. A cocaine cue is more preferred and evokes more frequency-modulated 50-kHz ultrasonic vocalizations in rats prone to attribute incentive salience to a food cue. Psychopharmacology (Berl.) 219 (4), 999–1009.

Molet, M., Billiet, G., Bardo, M.T., 2013. Conditioned place preference and aversion for music in a virtual reality environment. Behav. Process. 92, 31–35.

Mucha, R.F., Iversen, S.D., 1984. Reinforcing properties of morphine and naloxone revealed by conditioned place preferences: a procedural examination. Psychopharmacology 82 (3), 241–247.

Mucha, R.F., van der Kooy, D., O'Shaughnessy, M., Bucenieks, P., 1982. Drug reinforcement studied by the use of place conditioning in rat. Brain Res. 243 (1), 91–105.

Mueller, D., de Wit, H., 2011. Conditioned place preference in rodents and humans. Raber, J. (Ed.), Animal Models of Behavioral Analysis, Neuromethods 50, vol. 50, Springer, New Jersey, pp. 133–152.

Myers, K.M., Bechtholt-Gompf, A.J., Coleman, B.R., Carlezon, Jr., W.A., 2012. Extinction of conditioned opiate withdrawal in rats in a two-chambered place conditioning apparatus. Nat. Protoc. 7 (3), 517–526.

Nachman, M., 1963. Learned aversion to the taste of lithium chloride and generalization to other salts. J. Comp. Physiol. Psychol. 56, 343–349.

Nachman, M., Ashe, J.H., 1973. Learned taste aversions in rats as a function of dosage, concentration, and route of administration of LiCl. Physiol. Behav. 10 (1), 73–78.

Nachman, M., Lester, D., Le Magnen, J., 1970. Alcohol aversion in the rat: behavioral assessment of noxious drug effects. Science 168 (3936), 1244–1246.

Navratilova, E., Porreca, F., 2014. Reward and motivation in pain and pain relief. Nat. Neurosci. 17 (10), 1304–1312.

Navratilova, E., Xie, J.Y., Okun, A., Qu, C., Eyde, N., Ci, S., et al., 2012. Pain relief produces negative reinforcement through activation of mesolimbic reward-valuation circuitry. Proc. Natl. Acad. Sci. USA 109 (50), 20709–20713.

Navratilova, E., Xie, J.Y., Meske, D., Qu, C., Morimura, K., Okun, A., et al., 2015. Endogenous opioid activity in the anterior cingulate cortex is required for relief of pain. J. Neurosci. 35 (18), 7264–7271.

Nicholson, K.L., Ator, N.A., 2011. IACUC perspective on drug addiction research. ILAR J. 52 (3), 7.

Nissenbaum, J.W., Sclafani, A., 1987. Qualitative differences in polysaccharide and sugar tastes in the rat: a two-carbohydrate taste model. Neurosci. Biobehav. Rev. 11 (2), 187–196.

Okun, A., Liu, P., Davis, P., Ren, J., Remeniuk, B., Brion, T., et al., 2012. Afferent drive elicits ongoing pain in a model of advanced osteoarthritis. Pain 153 (4), 924–933.

Park, H.J., Stokes, J.A., Pirie, E., Skahen, J., Shtaerman, Y., Yaksh, T.L., 2013. Persistent hyperalgesia in the cisplatin-treated mouse as defined by threshold measures, the conditioned place preference paradigm, and changes in dorsal root ganglia activated transcription factor 3: the effects of gabapentin, ketorolac, and etanercept. Anesth. Analg. 116 (1), 224–231.

Park, H.J., Sandor, K., McQueen, J., Woller, S.A., Svensson, C.I., Corr, M., Yaksh, T.L., 2016. The effect of gabapentin and ketorolac on allodynia and conditioned place preference in antibody-induced inflammation. Eur. J. Pain 20 (6), 917–925.

Parker, L.A., 1992. Place conditioning in a three- or four-choice apparatus: role of stimulus novelty in drug-induced place conditioning. Behav. Neurosci. 106 (2), 294–306.

Parker, L.A., Brosseau, L., 1990. Apomorphine-induced flavor-drug associations: a dose-response analysis by the taste reactivity test and the conditioned taste avoidance test. Pharmacol. Biochem. Behav. 35 (3), 583–587.

Parker, L.A., Tomlinson, T., Horn, D., Erb, S.M., 1994. Relative strength of place conditioning produced by cocaine and morphine assessed in a three-choice paradigm. Learn. Motiv. 25, 83–94.

Peca, J., Feliciano, C., Ting, J.T., Wang, W., Wells, M.F., Venkatraman, T.N., et al., 2011. Shank3 mutant mice display autistic-like behaviours and striatal dysfunction. Nature 472 (7344), 437–442.

Pickens, R., Harris, W.C., 1968. Self-administration of d-amphetamine by rats. Psychopharmacologia 12 (2), 158–163.

Pomfrey, R.L., Bostwick, T.A., Wetzell, B.B., Riley, A.L., 2015. Adolescent nicotine exposure fails to impact cocaine reward, aversion and self-administration in adult male rats. Pharmacol. Biochem. Behav. 137, 30–37.

Qu, C., King, T., Okun, A., Lai, J., Fields, H.L., Porreca, F., 2011. Lesion of the rostral anterior cingulate cortex eliminates the aversiveness of spontaneous neuropathic pain following partial or complete axotomy. Pain 152 (7), 1641–1648.

Reed, D.R., Li, S., Li, X., Huang, L., Tordoff, M.G., Starling-Roney, R., et al., 2004. Polymorphisms in the taste receptor gene (Tas1r3) region are associated with saccharin preference in 30 mouse strains. J. Neurosci. 24 (4), 938–946.

Reicher, M.A., Holman, E.W., 1977. Location preference and flavor aversion reinforced by amphetamine in rats. Anim. Learn. Behav. 5 (4), 4.

Reid, L.D., Hunter, G.A., Beaman, C.M., Hubbell, C.L., 1985. Toward understanding ethanol's capacity to be reinforcing: a conditioned place preference following injections of ethanol. Pharmacol. Biochem. Behav. 22 (3), 483–487.

Remeniuk, B., Sukhtankar, D., Okun, A., Navratilova, E., Xie, J.Y., King, T., Porreca, F., 2015. Behavioral and neurochemical analysis of ongoing bone cancer pain in rats. Pain 156 (10), 1864–1873.

Rescorla, R.A., Wagner, A.R., 1972. A theory of Pavlovian conditioing: variations in the effectiveness of reinforcement and nonreinforcement. In: Black, A.H., Prokasy, W.F. (Eds.), Classical Conditioning II: Current Research and Theory. Appleton Century Crofts, New York, pp. 64–99.

Revusky, S.H., 1968. Aversion to sucrose produced by contingent x-irradiation: temporal and dosage parameters. J. Comp. Physiol. Psychol. 65 (1), 17–22.

Riley, A.L., 1997. Drug discrimination learning: assessment of opioid receptor pharmacology. In: Bouton, M.E., Fanselow, M.S. (Eds.), Learning, Motivation, and Cognition: The Functional Behaviorism of Robert C. Bolles. American Psychological Association, Wasington, DC, pp. 225–254.

Riley, A.L., 2011. The paradox of drug taking: the role of the aversive effects of drugs. Physiol. Behav. 103 (1), 69–78.

Riley, A.L., Mastropaolo, J.P., 1989. Long-delay taste aversion learning: effects of repeated trials and two-bottle testing. Bull. Psychonomic Soc. 27 (2), 145–148.

Riley, A.L., Tuck, D.L., 1985. Conditioned taste aversions: a behavioral index of toxicity. Ann. N Y Acad. Sci. 443, 272–292.

Riley, A.L., Davis, C.M., Roma, P.G., 2009. Strain differences in taste aversion learning: implications for animal models of drug abuse. In: Reilly, S., Schachtman, T.R. (Eds.), Conditioned Taste Aversion: Behavioral and Neural Processes. Oxford University Press, New York, pp. 226–261.

Riley, A.L., King, H.E., Hurwitz, Z.E., 2012. Conditioned Taste Aversion: An Annotated Bibliography. Available from: http://ctalearning.com/

Risinger, F.O., Cunningham, C.L., 1995. Genetic differences in ethanol-induced conditioned taste aversion after ethanol preexposure. Alcohol 12 (6), 535–539.

Robinson, T.E., 2004. Neuroscience. Addicted rats. Science 305 (5686), 951–953.

Robinson, T.E., Berridge, K.C., 1993. The neural basis of drug craving: an incentive-sensitization theory of addiction. Brain Res. Brain Res. Rev. 18 (3), 247–291.

Robinson, T.E., Berridge, K.C., 2000. The psychology and neurobiology of addiction: an incentive-sensitization view. Addiction 95 (Suppl. 2), S91–S117.

Robinson, T.E., Berridge, K.C., 2001. Incentive-sensitization and addiction. Addiction 96 (1), 103–114.

Robinson, T.E., Berridge, K.C., 2008. Review. The incentive sensitization theory of addiction: some current issues. Philos. Trans. R Soc. Lond. B Biol. Sci. 363 (1507), 3137–3146.

Roma, P.G., Riley, A.L., 2005. Apparatus bias and the use of light and texture in place conditioning. Pharmacol. Biochem. Behav. 82 (1), 163–169.

Roma, P.G., Flint, W.W., Higley, J.D., Riley, A.L., 2006. Assessment of the aversive and rewarding effects of alcohol in Fischer and Lewis rats. Psychopharmacology (Berl.) 189 (2), 187–199.

Rossi, N.A., Reid, L.D., 1976. Affective states associated with morphine injections. Physiol. Psychol. 4 (3), 5.

Roughan, J.V., Coulter, C.A., Flecknell, P.A., Thomas, H.D., Sufka, K.J., 2014. The conditioned place preference test for assessing welfare consequences and potential refinements in a mouse bladder cancer model. PLoS One 9 (8), e103362.

Russo, S.J., Bolanos, C.A., Theobald, D.E., DeCarolis, N.A., Renthal, W., Kumar, A., et al., 2007. IRS2-Akt pathway in midbrain dopamine neurons regulates behavioral and cellular responses to opiates. Nat. Neurosci. 10 (1), 93–99.

Sanchis-Segura, C., Spanagel, R., 2006. Behavioural assessment of drug reinforcement and addictive features in rodents: an overview. Addict. Biol. 11 (1), 2–38.

Schechter, M.D., Calcagnetti, D.J., 1993. Trends in place preference conditioning with a cross-indexed bibliography; 1957–1991. Neurosci. Biobehav. Rev. 17 (1), 21–41.

Schechter, M.D., Calcagnetti, D.J., 1998. Continued trends in the conditioned place preference literature from 1992 to 1996, inclusive, with a cross-indexed bibliography. Neurosci. Biobehav. Rev. 22 (6), 827–846.

Schuster, C.R., Thompson, T., 1969. Self administration of and behavioral dependence on drugs. Annu. Rev. Pharmacol. 9, 483–502.

Sclafani, A., 2004. Oral and postoral determinants of food reward. Physiol. Behav. 81 (5), 773–779.

Scoles, M.T., Siegel, S., 1986. A potential role of saline trials in morphine-induced place-preference conditioning. Pharmacol. Biochem. Behav. 25 (6), 1169–1173.

Serafine, K.M., Riley, A.L., 2010. Preexposure to cocaine attenuates aversions induced by both cocaine and fluoxetine: implications for the basis of cocaine-induced conditioned taste aversions. Pharmacol. Biochem. Behav. 95 (2), 230–234.

Simpson, G.R., Riley, A.L., 2005. Morphine preexposure facilitates morphine place preference and attenuates morphine taste aversion. Pharmacol. Biochem. Behav. 80 (3), 471–479.

Skinner, B.F., 1948. Superstition in the pigeon. J. Exp. Psychol. 38 (2), 168–172.

Smith, J.C., Roll, D.L., 1967. Trace conditioning with X-rays as an aversive stimulus. Psychonomic Sci. 9 (1), 11–12.

Smith, J.K., Neill, J.C., Costall, B., 1998. The influence of postweaning housing conditions on drug-induced conditioned taste aversion. Pharmacol. Biochem. Behav. 59 (2), 379–386.

Spragg, S.D.S., 1940. Morphine addiction in chimpanzees. Comp. Psychol. Monogr. 15, 1–132.

Spyraki, C., Fibiger, H.C., Phillips, A.G., 1982. Cocaine-induced place preference conditioning: lack of effects of neuroleptics and 6-hydroxydopamine lesions. Brain Res. 253 (1–2), 195–203.

Spyraki, C., Kazandjian, A., Varonos, D., 1985. Diazepam-induced place preference conditioning: appetitive and antiaversive properties. Psychopharmacology (Berl.) 87 (2), 225–232.

Staddon, J.E., 1992. The 'superstition' experiment: a reversible figure. J. Exp. Psychol. Gen. 121 (3), 270–272.

Stolerman, I.P., D'Mello, G.D., 1979. Conditioned taste aversions induced with apomorphine and apomorphine analogue in rats. Exp. Brain Res. 36, R22–R23.

Stolerman, I.P., D'Mello, G.D., 1981. Oral self-administration and the relevance of conditioned taste aversions. In: Thompson, T., Dews, P.B., McKim, W.A. (Eds.), Advances in Behavioral Pharmacology. Lawrence Erlbaum, HIllsdale, NJ, pp. 169–214.

Sufka, K.J., 1994. Conditioned place preference paradigm: a novel approach for analgesic drug assessment against chronic pain. Pain 58 (3), 355–366.

Tordoff, M.G., Alarcon, L.K., Lawler, M.P., 2008. Preferences of 14 rat strains for 17 taste compounds. Physiol. Behav. 95 (3), 308–332.

Touzani, K., Bodnar, R.J., Sclafani, A., 2010. Neuropharmacology of learned flavor preferences. Pharmacol. Biochem. Behav. 97 (1), 55–62.

Tsai, H.C., Zhang, F., Adamantidis, A., Stuber, G.D., Bonci, A., de Lecea, L., Deisseroth, K., 2009. Phasic firing in dopaminergic neurons is sufficient for behavioral conditioning. Science 324 (5930), 1080–1084.

Tzschentke, T.M., 1998. Measuring reward with the conditioned place preference paradigm: a comprehensive review of drug effects, recent progress and new issues. Progress Neurobiol. 56 (6), 613–672.

Tzschentke, T.M., 2007. Measuring reward with the conditioned place preference (CPP) paradigm: update of the last decade. Addict. Biol. 12 (3–4), 227–462.

van der Kooy, D., 1987. Place conditioning: a simple and effective method for assessing the motivational properties of drugs. In: Bozarth, M.A. (Ed.), Methods of Assessing the Reinforcing Properties of Abused Drugs. Springer-Verlag, New York, pp. 229–240.

Vanderschuren, L.J., Everitt, B.J., 2004. Drug seeking becomes compulsive after prolonged cocaine self-administration. Science 305 (5686), 1017–1019.

Verendeev, A., Riley, A.L., 2011. Relationship between the rewarding and aversive effects of morphine and amphetamine in individual subjects. Learn. Behav. 39 (4), 399–408.

Verendeev, A., Riley, A.L., 2012. Conditioned taste aversion and drugs of abuse: history and interpretation. Neurosci. Biobehav. Rev. 36 (10), 2193–2205.

Verendeev, A., Riley, A.L., 2013. The role of the aversive effects of drugs in self-administration: assessing the balance of reward and aversion in drug-taking behavior. Behav. Pharmacol. 24 (5–6), 363–374.

Volkow, N.D., Koob, G.F., McLellan, A.T., 2016. Neurobiologic advances from the brain disease model of addiction. N. Engl. J. Med. 374 (4), 363–371.

Wakeford, A.G., Flax, S.M., Pomfrey, R.L., Riley, A.L., 2016. Adolescent delta-9-tetrahydrocannabinol (THC) exposure fails to affect THC-induced place and taste conditioning in adult male rats. Pharmacol. Biochem. Behav. 140, 75–81.

Wei, H., Viisanen, H., Amorim, D., Koivisto, A., Pertovaara, A., 2013. Dissociated modulation of conditioned place-preference and mechanical hypersensitivity by a TRPA1 channel antagonist in peripheral neuropathy. Pharmacol. Biochem. Behav. 104, 90–96.

Welch, J.M., Lu, J., Rodriguiz, R.M., Trotta, N.C., Peca, J., Ding, J.D., et al., 2007. Cortico-striatal synaptic defects and OCD-like behaviours in Sapap3-mutant mice. Nature 448 (7156), 894–900.

White, N., Sklar, L., Amit, Z., 1977. The reinforcing action of morphine and its paradoxical side effect. Psychopharmacology (Berl.) 52 (1), 63–66.

White, N.M., Chai, S.C., Hamdani, S., 2005. Learning the morphine conditioned cue preference: cue configuration determines effects of lesions. Pharmacol. Biochem. Behav. 81 (4), 786–796.

Wise, R.A., Yokel, R.A., DeWit, H., 1976. Both positive reinforcement and conditioned aversion from amphetamine and from apomorphine in rats. Science 191 (4233), 1273–1275.

Further Reading

American Psychiatric Association, 2013. Diagnostic and Statistical Manual of Mental Disorders: DSM-5. American Psychiatric Association, Washington, DC.

Kumar, R., 1972. Morphine dependence in rats: secondary reinforcement from environmental stimuli. Psychopharmacologia 25 (4), 332–338.

Page left intentionally blank

23

Modeling Schizophrenia in Animals

David Feifel, Paul D. Shilling

University of California, San Diego, La Jolla, CA, United States

1 OVERVIEW OF SCHIZOPHRENIA

1.1 Clinical Presentation

Schizophrenia is a chronic, debilitating disorder, which affects approximately 1% of the world's population. While there is a fair degree of heterogeneity in the clinical presentation of schizophrenia, the unifying thread among individuals stricken with this condition is psychosis, a profound disorder of perception and thinking that robs a person of the capability of reaching a culturally normative interpretation of the external world and thereby prevents him or her from participating in the collective perceptions of reality.

The first overt manifestations of schizophrenia typically emerge in late adolescence to early adulthood. Although men and women are affected in equal proportion, the emergence of symptoms occurs several years later, on average, in women (Sham et al., 1994). There is often a "prodromal" period, characterized by various subclinical features that precedes the first frank psychotic break that heralds the unequivocal onset of the disorder (Cadenhead, 2011; Hafner et al., 2004).

The current version of the *Diagnostic and Statistical Manual for Mental Disorders* (DSM-V) (American Psychiatric Association, 2013), the most widely accepted source for diagnostic criteria of mental disorders, delineates five potential clinical features of schizophrenia. It requires that, within a period of at least 6 months of continuous disturbance in function (that may include the prodromal period), an individual exhibit at least two of these features concurrently for at least 1 month without a remittance of symptoms Under certain circumstances, only one symptom need to be present (vide infra). Moreover, the symptoms also must not be better accounted for by another cause, such as substance use or a medical condition, such as Huntington's disease or a severe endocrine abnormality, such as thyrotoxicosis.

The first four diagnostic features listed in DSM-V, delusional thinking, hallucinations, disorganized speech, and disorganized behavior, are collectively referred to as "positive" symptoms. DSM-V recognizes the *sine-qua-non*

nature of these positive symptoms is that it is not possible to achieve the diagnostic criteria without at least the presence of two of them. The disorganized speech and behavior of schizophrenia are not the type that might be observed in a person suffering from a neurological disorder affecting speech output, such as a receptive aphasia, or motor output, such as the choreoathetotic movement associated with advanced Huntington's disease. Rather, the disorganized speech and behavior seen in schizophrenia are outward manifestations of disordered thinking and perception occurring internally. Qualified clinician's familiar with schizophrenia's clinical presentation are able to recognize its distinct disturbances of speech and behavior.

The fifth feature listed in DSM-V is, in fact, a collection of behavioral deficits collectively referred to as "negative" symptoms. Negative symptoms include poverty of speech (alogia), reduced or absent outward expression of emotions and reduced volitional, goal-directed behavior. As DSM-V acknowledges, negative symptoms are less characteristic in nature than positive symptoms and can, *prima facie*, be hard to distinguish from symptoms of other conditions, such as clinical depression or certain neurological disorders. For this reason, negative symptoms cannot, by themselves, warrant a schizophrenia diagnosis no matter how severe or pervasive they may be. Furthermore, genuine primary negative symptoms can be hard to distinguish clinically from the secondary effects of severe and overwhelming positive symptoms (e.g., a catatonic manifestation) or from side effects of some antipsychotic drugs used to treat them.

In addition to the positive and negative symptoms, people with schizophrenia typically exhibit broad impairments in formal cognitive functions. Several discrete and measurable domains of cognition have been identified as commonly deficient among people diagnosed with schizophrenia. These domains include: attention, learning and memory (including visual, verbal, and working memory), information processing speed, reasoning and problem solving, and social cognition. Although commonalities exist within these specific cognitive domains, the severity and extent (i.e., number of domains) of cognitive impairment vary substantially among individuals with schizophrenia. Furthermore, like negative symptoms, they do not appear to have a characteristic nature in schizophrenia, which would distinguish them from cognitive impairments occurring in other disorders. Also, like negative symptoms, impairments in cognitive performance can be secondary to the presence of strong positive symptoms or side effects of medication, making it hard to distinguish such secondary impairments from primary cognitive deficits emanating from the schizophrenia. Nevertheless, cognitive impairments are widely regarded as an additional core feature of schizophrenia even though they are not part of the formal DSM-V diagnostic criteria.

1.2 Etiology

The current consensus is that the etiology of schizophrenia is multifactorial, resulting from a combination of genetic and environmental factors. Genetic inheritance is believed to account for 50%–80% of the incidence of schizophrenia as evidenced by substantially higher concordance rates in monozygotic versus dizygotic twins (Lewis and Lieberman, 2000). It is manifestly clear that the genetic contribution, albeit a strong one, is complex. No single mutation or genetic variant has been found to be sufficient to cause this disorder. Although genome-wide and single-gene association studies have implicated a long list of candidate genes (Allen et al., 2008), only a small number among these candidate genes have shown to be associated with schizophrenia in many studies and/or to play a biological role that is likely to contribute to the development of this disorder. Genes on that short candidate list include DISC1, neuregulin, ErbB4, reelin, and dysbindin. In addition, recent evidence suggests the association of a small proportion of schizophrenia cases (5%–8%) with de novo copy number variants (CNVs) (Sebat et al., 2009). The lack of a strong association of identified gene candidates with the incidence of schizophrenia may suggest that multiple genes acting in combination through epistasis or synergistically with epigenetic effects may underlie manifestations of this disorder. Some investigators have suggested that the causative gene variants have not been identified at this time because this disease may be caused by rare variants with high penetrance having a large effect (Walsh et al., 2008). Discussion of the studies aimed at gaining a better understanding of the function of schizophrenia candidate genes and how they may contribute to this disorder have been published elsewhere (Jones et al., 2011; Powell et al., 2009).

A "two-hit" developmental model has been proposed in which a combination of environmental and genetic factors affecting early development is responsible for the emergence of the schizophrenia in adolescence/early adulthood (Lewis and Levitt, 2002). Among environmental contributors that have been implicated in the development of schizophrenia, those associated with the neonatal or perinatal period have the strongest scientific support. Prenatal risk factors for schizophrenia include maternal malnutrition and maternal infection. Risk factors associated with the perinatal period have been reported in the medical histories of approximately 20% of patients who suffer from schizophrenia include complication during labor and delivery (e.g., hypoxia) (Lewis and Levitt, 2002; Powell, 2010). Childhood abuse and psychological trauma have also been found to be

associated with the development of schizophrenia later in life and, therefore, may constitute risk factors for this disorder (Sideli et al., 2012).

Finally, there is compelling evidence that the use of certain drugs can trigger the onset of schizophrenia or a relapse. Drugs that have been strongly associated with this include stimulants, such as amphetamines, cannabis, and hallucinogens, such as lysergic acid diethylamide (LSD) or phencyclidine (PCP). However, it has been hard to establish a clear causal connection between drug use and schizophrenia as well as the extent that drug use can trigger schizophrenia because it is likely to occur only in people with an underlying biological predisposition for the disorder (Hermens et al., 2009; Yui et al., 1999).

1.3 Pathophysiology

Despite intense investigation for decades using the best available tools of neuroscience, the fundamental pathophysiological abnormality that underlies the clinical presentation of schizophrenia remains elusive. That is not to say that structural and functional abnormalities have not been found, but rather there does not appear to be a single set of consistent findings. This may be due to the fact that the clinical presentation that satisfies the diagnostic criteria for schizophrenia may not result from a single brain dysfunction but, rather, a large number of potential CNS malfunctions. Indeed many have suggested that schizophrenia is not a unitary disorder, even when taking into account its descriptive subtypes, but instead a heterogeneous collection of disorders with overlapping clinical manifestations (Lewis and Lieberman, 2000; Young et al., 2010). Adding to the challenge of parsing out the etiology of schizophrenia is that it has been hard to disentangle abnormalities that are causative or contributory to the symptoms from those that are a result of or perhaps an epiphenomenon of this chronic disorder (e.g., social isolation) and from the effects of medications used to treat it.

Originally proposed in the 1960s, the dopamine hypothesis (Carlsson, 1977), which posits that schizophrenia is the result of excess dopamine neurotransmission, still dominates the thinking regarding pathophysiology of schizophrenia. This hypothesis was primarily based on two observations. The first observation was that drugs that enhanced dopamine neurotransmission in the brain had a proclivity to transiently replicate the psychosis of schizophrenia in people that did not have this condition and to exacerbate it in people who did (Byne et al., 1999). The second observation was that all efficacious antipsychotics at the time inhibited dopamine transmission by binding and blocking activation of the dopamine-2 (D2) receptor. The potency of antipsychotics was correlated with their affinity for that receptor (Seeman, 1992, 1995). Over time the dopamine hypothesis has become more

nuanced, positing that excess dopamine transmission in subcortical limbic areas (mesolimbic pathway) produces positive symptoms (Howes and Kapur, 2009; Szekeres et al., 2002; Walter et al., 2009), while concurrent dopamine deficiency in the prefrontal cortical areas (mesocortical pathway) predisposes one to negative symptoms and cognitive deficits (Fusar-Poli et al., 2011; Szekeres et al., 2002).

Although the dopamine hypothesis remains the dominant pathophysiological theory of schizophrenia, direct evidence to support it has been surprisingly difficult to obtain and examination of the brains of people with schizophrenia have yielded inconsistent results. However, there currently exists reasonably good evidence for increased density of D2 receptors (Klaning et al., 2002; Onstad et al., 1991), increased presynaptic dopaminergic function (Howes et al., 2012) in the striatal regions, and decreased activation and dopamine tone in the prefrontal cortex in people with schizophrenia compared to controls (Fusar-Poli et al., 2011; Szekeres et al., 2002).

More recently the search for neurochemical perturbations underlying schizophrenia has shifted from an exclusive focus on dopamine to include other neurotransmitters. In this respect, dysregulation of the glutamate and gamma aminobutyric acid (GABA) neurotransmitter systems have been detected in people with schizophrenia (Kantrowitz and Javitt, 2010). For example, the loss of excitatory glutamatergic synapses leading to decreased dendritic density and reduced functional activity of GABAergic interneurons have been a consistent finding in people with schizophrenia (Beneyto et al., 2011). Expression of glutamate decarboxylase (GAD) 67, an enzyme that metabolizes glutamate into GABA, has been consistently found to be reduced in the brains of people afflicted with schizophrenia compared to people without any mental illness (Bullock et al., 2008).

Some of the more consistent alterations in brain structure associated with schizophrenia include lateral ventricle enlargement, decreased hippocampus volume, and decreased gray matter in a number of brain regions that modulate cognition, including the prefrontal, medial, temporal, and inferior parietal cortex (Nasrallah et al., 2011; Yeganeh-Doost et al., 2011). Although these differences in brain structure have been noted in relation to schizophrenia, it is not entirely clear if these pathophysiological abnormalities contribute to the development of the disorder or are the result of mechanisms associated with the underlying etiology.

1.4 Treatment

The mainstays of treatments for schizophrenia are medications and psychosocial interventions. The first member of today's antipsychotic drug family, chlorpromazine, was discovered by serendipity in the early

1950s. Between 1955 and 1990, approximately one dozen "typical" or first generation antipsychotics (FGAs) were approved in the United States for the treatment of schizophrenia. In the 1970s, investigators elucidated that all FGAs had a common mechanism of action, which was pharmacological antagonism of the dopamine-2 (D2) receptors in the brain. Later research localized the therapeutic mechanism to D2 blockade in the mesolimbic areas (Seeman, 1992, 1995). FGAs are generally efficacious in reducing positive symptoms when taken regularly. However, their efficacy against negative symptoms and cognitive deficits is poor. Furthermore, FGAs have a propensity to produce side effects related to their pharmacological actions at other brain receptor sites, such as histamine-1 (sedation, weight gain), acetylcholine-muscarinic (dry mouth, blurry vision, constipation, cognitive impairments), and alpha-1 (orthostatic dizziness, hypotension). They also have a tendency to antagonize D2 receptors in brain pathways, other than the mesolimbic pathway, which often causes muscle and movement abnormalities (extrapyramidal symptoms) as well as changes in libido and menstrual cycle due to increased release of the reproductive hormone prolactin (Tamminga, 2003).

The entry of the drug clozapine into the US marketplace in 1990 after a protracted FDA approval process, due to serious safety risks, marked the beginning of the atypical or second generation antipsychotics (SGAs). The FDA agreed to approve clozapine because of evidence that it benefited schizophrenia patients who did not respond to FGAs. Despite its efficacy, clozapine does not have a propensity to produce the extrapyramidal side effects or raise prolactin blood levels, which is something that had previously been considered inextricably connected with clinical efficacy (Tamminga, 1997).

It was not immediately clear why clozapine had these unique clinical benefits but the fact that it has a wider profile of receptor affinities than most FGAs was thought to underlie this clinical benefit. Clozapine's success spurred development of a family of SGAs with multireceptor affinities (Tamminga, 1997). SGAs are considered to generally produce less side effects related to blockade of D2 receptors and to have some therapeutic advantages over FGAs, namely with regards to negative symptoms and cognitive deficits. However, there is a substantial degree of controversy regarding the magnitude of their efficacy advantage over FGAs and clozapine remains the only SGA with strong evidence for a superior efficacy profile. Unfortunately, clozapine's prodigious side effect and safety burden limit its use. Furthermore, the precise mechanism responsible for clozapine's superior efficacy remains unknown.

To date all SGAs, like FGA, have clinically relevant affinity for D2 receptors and all, except for aripiprazole, act as D2 antagonists. Aripiprazole is a partial agonist at the D2 receptor. In addition to D2 affinity, SGAs have affinity for serotonin 2A (5-HT2A) receptors that is comparable and usually greater than their affinity for D2 receptors. It is this pharmacological property, which generally distinguishes SGAs from FGAs and which is considered by many investigators to underlie their clinical differences from the FGAs (Tamminga, 2003).

Despite the reasonable success of both FGAs and SGAs in attenuating positive symptoms, the lack of effective treatments for the cognitive deficits and negative symptoms has substantially contributed to the poor functional outcomes and long-term morbidity of this disorder. The long-term prognosis for schizophrenia has shown little if any improvement (Carpenter and Koenig, 2008) during the past nearly 60 years of drug development. Therefore, there remains a strong need for antipsychotic drugs with novel mechanisms that can deliver more efficacious benefits.

2 APPROACHES TO CREATE ANIMAL MODELS WITH RELEVANCE TO SCHIZOPHRENIA

Developing animal models that have validity for schizophrenia presents formidable challenges since the biological mechanisms underlying the clinical features of this disorder have thus far eluded discovery despite the identification of numerous neurobiological abnormalities associated with schizophrenia. Additionally, the most characteristic features of schizophrenia, auditory hallucinations and delusional thinking cannot be directly modeled in animals. We have reviewed these and other challenges encountered in developing animal models of schizophrenia in greater depth elsewhere (Feifel and Shilling, 2010). Despite these challenges animal models with relevance to schizophrenia continue to be developed and to play an important role in the effort to understand this disease and identify new treatments.

Several general approaches are available to investigators who are interested in using animals to study a disease related abnormality. The majority of well-characterized animal models considered to have relevance to schizophrenia involve manipulations that induce, usually in rodents, a homolog, or, if that is not achievable, a presumed analog of one or more of the abnormal features associated with the disorder. Table 23.1 displays examples of some of the more common approaches used to model schizophrenia in rodents. Commonly induced schizophrenia-like abnormalities in rodents are deficits in information gating, such as prepulse inhibition, latent inhibition, deficits in social interaction, and tasks that are thought to model human cognitive functions, such as working memory.

Model	Schizophrenia-like features		Effects of antipsychotics and other drugs	Strengths and limitations
	Behavioral	Pathophysiology		
Pharmacological Acute PCP injections Rodents are administered one-time dose of PCP, an antagonist of NMDA subtype, glutamate receptor	Increased locomotion analogous to positive symptoms of SCZ (Jentsch and Roth, 1999; Neill et al., 2016) Reduced social interaction homologous with negative symptoms (Neill et al., 2016; Mouri et al., 2007) PPI deficits homologous with PPI deficits in SCZ (Geyer et al., 2001) Reduced performance on animal cognitive tasks that are thought to be analogous to human cognitive tasks that SCZ patients perform poorly on (Mouri et al., 2007; Rajagopal et al., 2014)	Some evidence exists for glutamate hypofunction in brains of patients with SCZ, which is transiently induced by PCP in animal (Mouri et al., 2007)	Acute: SGAs but not HAL attenuate PPI deficits (Geyer et al., 2001; Barros et al., 2009; Fejgin et al., 2007; Pouzet et al., 2005) SGAs and HAL attenuate cognitive deficits (Neill et al., 2016; Mouri et al., 2007; Rajagopal et al., 2014; Grayson et al., 2007; Nagai et al., 2009; Snigdha et al., 2011; Didriksen et al., 2006; Terranova et al., 2005) Non-APDs: Citalopram, bupropion, and desipramine have no effect on PPI deficits (Pouzet et al., 2005). Diazepam, citalopram, methadone and naloxone have no effect on social interaction deficits (Sams-Dodd, 1998a) (3 days) Other: modafinil, and erythropoietin attenuate cognitive deficits (Goetghebeur and Dias, 2009; Goetghebeur et al., 2010) Subchronic (3 days): CLOZ but not HAL, reverse social and cognitive deficits (Jentsch and Roth, 1999; Mouri et al., 2007; Sams-Dodd, 1998a; Sams-Dodd, 1999; He et al., 2006) Chronic (21 days): Neither CLOZ, nor HAL, reverse social interaction deficits (Sams-Dodd, 1998b)	Strengths: Displays features relevant to positive and negative symptoms and cognitive deficits of SCZ Limitations: Induction of SCZ-like features is transient Acute administration of FGAs and SGAs reverse social interaction and cognitive deficits but these drugs produce, at best, a partial improvement in negative symptoms and cognitive deficits when given chronically to SCZ patients does not seem to model the therapeutic time course of APDs as chronic administration less efficacious than acute

(Continued)

TABLE 23.1 Comparison of Three Rodent Models Representing Different Inducing Strategies: Pharmacologic, Developmental and Genetic *(cont.)*

Model	Schizophrenia-like features		Effects of antipsychotics and other drugs	Strengths and limitations
	Behavioral	**Pathophysiology**		
Developmental Neonatal hippocampal lesions Rats are administered neurotoxin into the hippocampus during the neonatal period	Cognitive deficits and social deficits appear prior to puberty (Tseng et al., 2009) PPI deficits may appear after puberty (Tseng et al., 2009) or before it (Swerdlow et al., 2012)	Consistent with evidence of hippocampal atrophy in SCZ Consistent with theory that brain abnormalities exist long before people develop SCZ, as early as in utero or early childhood (Tandon et al., 2008)	Acute APDs: PPI deficits reversed by CLOZ, but not HAL (Le Pen and Moreau, 2002) Chronic APDs: CLOZ attenuates PPI deficits similar to acute administration but does not reverse cognitive or social deficits (Rueter et al., 2004; Levin and Christopher, 2006; Sams-Dodd et al., 1997) Chronic CLOZ reverses locomotor activation (Bringas et al., 2012) Non-APDs: No Reports	Strengths: Models the construct of an early brain pathology that remains latent until adolescence/early adulthood Limitations: No strong evidence yet that PPI deficits emerge late in development versus congenital Specificity for APD effects not reported
Genetic: Natural Vasopressin-deficient Brattleboro rat The result of a mutation in the vasopressin gene	Spontaneous hyperlocomotion—thought to be an analog of positive symptoms (van den Buuse, 2010) PPI (Demeter et al., 2016), LI and habituation deficits homologous with same deficits in SCZ patients (Feifel and Priebe, 2001) Cognitive deficits relevant to SCZ (Demeter et al., 2016; Laycock et al., 1983; Feifel et al., 2009) Polydipsia/polyuria similar to polydipsia seen in significant proportion of SCZ patients (de Leon, 2003)	Strong genetic component as in SCZ (Feifel and Priebe, 2007) Increased dopamine (Feenstra et al., 1990; Dawson et al., 1990) and D2 receptor brain density in striatum similar to several findings of postmortem SCZ (Shilling et al., 2006) Consistent with vasopressin system dysfunction reported in SCZ (Linkowski et al., 1984; Frederiksen et al., 1991; Krishnamurthy et al., 2012) H3 acetylation changes in prefrontal region and hippocampus (Demeter et al., 2016) Reduced brain GAD 67 consistent findings of reduced brain GAD 67 in SCZ (Akbarian and Huang, 2006)	Acute: SGAs and FGAs reverse PPI deficits (Feifel et al., 2007; Feifel et al., 2004) CLOZ reverses social recognition deficits (Feifel et al., 2009) Valproate, diazepam and imipramine had no effect on PPI (Feifel et al., 2011a) Putative APD, neurotensin-1 agonist produces effects similar to APDs (Feifel et al., 2004) Chronic: FGAs and SGAs produce stronger effect after chronic administration than after acute (Feifel et al., 2007)	Strengths: Does not require manipulation to induce SCZ-like features Good sensitivity and good specificity regarding responding only to drugs with known or putative APD efficacy Models therapeutic time course of APDs in which therapeutic effect begins after acute administration but grows stronger with repeat administration (Feifel et al., 2007) Limitation: No evidence for gene based vasopressin dysfunction in SCZ

APD, antipsychotic drug; CLOZ, clozapine; FGA, first generation antipsychotic; GAD67, glutamate decarboxylase isom; HAL, haloperidol; LI, latent inhibition; NMDA, *N*-methyl-D-aspartate; PCP, phencyclidine; PPI, prepulse inhibition; SGA, second generation antipsychotic; SCZ, schizophrenia; AVP, vasopressin

Some of these models are based on transient induction of schizophrenia-relevant features. Classic examples of these features are abnormalities produced by acute administration of psychotomimetic drugs (e.g., amphetamine, PCP), such as hyperactivity and reduced prepulse inhibition of the startle response. The duration of the induced changes is correlated with the pharmacokinetic properties of the administered psychotomimetic. Other experimental approaches produce more enduring abnormalities consistent with the chronic nature of schizophrenia. An example of enduring, induced, schizophrenia-like features are those produced by genetic engineering or by manipulations to the nervous system applied during the developmental period. Even among enduring abnormalities induced in rodents, there may be differences in the degree of robustness. For example, prepulse inhibition deficits produced in adult rats by chemical lesions of the hippocampus during the neonatal period are robust, whereas prepulse inhibition deficits induced by social isolation rearing of rats during early development can dissipate due to handling or changes in the home cage (Lipska et al., 1995; Powell et al., 2002).

Another approach has been to identify animals that spontaneously exhibit relevant abnormal features that are germane to schizophrenia. This is typically achieved by screening different strains of rats or mice, or by selecting individual animals that exhibit a certain schizophrenia-relevant feature from a normal colony (Ellenbroek et al., 1995). The selected individuals may then be interbred to produce a man-made strain of animals that spontaneously exhibit schizophrenia-relevant behaviors, for example, (Ellenbroek et al., 1995; Hitzemann et al., 2008; Schwabe et al., 2009).

Yet another approach foregoes both inducing schizophrenia-like abnormalities and identifying spontaneous abnormalities in favor of studying normal expression of an animal phenotype that is assumed to have some relevance to schizophrenia. These approaches are usually used for drug discovery rather than for identifying mechanisms underlying the disease, and are based on the concept that an abnormal behavior or physiological function exists on a continuum with normal levels of that behavior or function and share the same underlying biological mechanisms. It follows therefore that treatments that alter normal levels of a phenotype in a certain direction (e.g., enhance it) are likely to do the same thing to abnormal levels of that phenotype in people with schizophrenia. For example, enhancement of normal latent inhibition in rodents or their performance on animal tasks modeling human cognition have been used as a putative predictive test of drugs with efficacy for schizophrenia (Feldon and Weiner, 1991). Though these models may have reduced validity for the abnormal features in schizophrenia, they have the advantage of not requiring unique expensive animal strains or time-consuming special preparations to induce deficits. Other examples of normal behavior used as models to screen for antipsychotics include catalepsy (Greenblatt et al., 1980) and conditioned avoidance response (Wadenberg, 2010).

3 FEATURES OF SCHIZOPHRENIA THAT CAN BE MODELED IN ANIMALS

3.1 Clinical Time Course and Response to Treatment

Before describing the symptoms, biological perturbations, and other specific clinically-relevant features of schizophrenia that are able to be modeled in animals, it should be noted that there are secondary features related to these, namely the developmental timing and the response to antipsychotic medication, that can also be modeled in principal and when done so successfully, further enhance the animal model's validity.

With regards to developmental timing, the emergence of a clinically relevant phenotype sometime after puberty in an animal model is considered validity enhancing because it is viewed to reflect the typical temporal emergence of the core clinical features of schizophrenia in early adulthood. In reality, the onset of schizophrenia is clinically identified by the emergence of positive symptoms, with or without negative symptoms, and at present we do not know whether or not the emergence of other clinically relevant features, such as cognitive or information gating deficits, coincide with the emergence of positive and negative symptoms. Therefore, strictly speaking, until the timing of those other clinically relevant features is well established, only the postpubertal emergence of phenotypes directly relevant to positive and negative symptoms should be considered to enhance the validity of an animal model.

An animal model that measurably responds to treatments for the disease being modeled is said to have predictive validity. Predictive validity is most strongly demonstrated when an animal model of schizophrenia responds to all antipsychotic drugs with established efficacy for the symptoms of schizophrenia, but not does respond to drugs that lack efficacy for schizophrenia but are efficacious for other related disorders. For example, an animal model that responds consistently to all antipsychotics but not to any mood stabilizer or antidepressant would be considered to have very strong predictive validity. The predictive validity of an animal model is considered a major determinant

of its utility in identifying potential new treatments for the modeled disease. However, beyond that, predictive validity is often thought to enhance the overall validity of an animal model for the disease, especially, if the effect of antipsychotic medication is to normalize or ameliorate a clinically relevant, abnormal phenotype. Some have argued that predictive validity is the most important feature in assessing the validity of an animal model (Geyer and Markou, 1995). However, there are some vexing dilemmas related to the predictive validity of animal models of schizophrenia since antipsychotics display unequivocal efficacy only against positive symptoms but, as will be discussed later, there are no animal homologs for positive symptoms, only presumed analogs, such as motor hyperactivity. Additional challenges are presented by the fact that antipsychotic drugs are not highly efficacious against cognitive deficits or negative symptoms of schizophrenia and it is controversial whether they are completely without efficacy or have moderate efficacy against these clinical components of schizophrenia (Blin, 1999). As such, it is unclear whether the validity of a phenotypic abnormality in an animal that is proposed to represent negative symptoms, is enhanced or compromised, by the amelioration of the abnormality by antipsychotic drugs. The same applies to animal phenotypes that are proposed to represent schizophrenia's cognitive deficits. Despite these conceptual challenges, most animal models are evaluated for the effect of antipsychotic drugs on one or more of their clinically relevant phenotypes.

3.2 Positive Symptoms and Hyperdopaminergia

Though positive symptoms are the most characteristic clinical feature of schizophrenia and a requirement for making the diagnosis, they are the most challenging to model in humans. Clinicians ascertain the presence of hallucinations and delusional thinking in a schizophrenia candidate through his or her language, whether it is in response to directed questions or spontaneously generated speech. This approach is obviously not possible with animals and there is no reliable way for researchers to probe the internal mental state of animals. As such, there are no animal models, to date, that credibly replicate the phenomenology of positive symptoms although chronic administration of PCP, a psychogenic drug, in monkeys will cause them to exhibit behaviors suggestive of humans experiencing positive symptoms (see Section 4). The dopamine theory of schizophrenia, which is based upon strong but indirect evidence, posits that increased dopamine transmission in the subcortical mesolimbic brain pathway mediates positive symptoms. Despite limited direct evidence for increased dopamine transmission in the brains of people with schizophrenia,

the dopamine theory remains the dominant theory regarding the underlying pathophysiology of schizophrenia and, in particular, it's positive symptoms. It is not, therefore, surprising that much of the effort toward developing animal models of this disorder has historically been guided by this theory. Indeed, inducing hyperdopaminergia in rodents has been the basis of the earliest and most ubiquitous attempts to model schizophrenia and study antipsychotic drugs in animals. In the absence of the ability to replicate the phenomenology of positive symptoms, animal models of hyperdopaminergia have been largely considered to be animal models of positive symptoms.

The simplest and most common approach used to model hyperdopaminergia in animals has been to administrator prodopamine drugs to rodents. Apomorphine, a direct agonist at the D2/D3 dopamine receptors, and amphetamine, an indirect agonist that enhances synaptic levels of dopamine, are the most commonly used drugs for this purpose. Animals given systemic injections of these drugs display characteristic acute effects that can be measured quantitatively. The most apparent effect is increased locomotor behavior, however, increased cage climbing, stereotypic movements, and reduced PPI and latent inhibition are also induced. All of the established antipsychotics that have been tested are able to block these effects and therefore blockade of apomorphine- or amphetamine-induced behaviors is the most common preclinical screening test for putative antipsychotics and is considered predictive of efficacy to treat positive symptoms of psychosis.

While reduced PPI is an established feature of schizophrenia, increased motor activity is not considered one of its prominent features. Therefore, measuring the PPI effects of prodopamine drugs is preferable to measure their locomotor effects when using the hyperdopaminergia model.

People with schizophrenia have increased sensitivity to the psychosis inducing effects of prodopamine psychostimulants, such as amphetamine. This is thought to be due to an upregulation of their dopamine system. Increased sensitivity to the prodopamine drugs has been proposed as a validating feature of an animal model for schizophrenia. The APO-SUS rat (Wistar) strain was developed by selecting the individual rats from among a colony of rats that exhibited the strongest stereotypy response to apomorphine. These APO-SUS rats were then interbred to produce a strain of rats with a genetic sensitivity to apomorphine (Ellenbroek et al., 1995).

Similarly, there exists evidence for increased striatal presynaptic dopamine function (increased synthesis and release) and increased dopamine receptor density (Howes et al., 2012). Therefore the existence of similar findings occurring naturally in animals, or as a result

of specific preparations, is considered a validating feature for their relevance to schizophrenia. In this regard, rats raised in social isolation have been reported to exhibit elevated presynaptic DA levels (Powell, 2010) and Brattleboro rats, a strain of rats with deficient vasopressin, have increased striatal D2 receptor levels (Shilling et al., 2006). The presence of certain dopamine-regulated behaviors has also served as the presumed behavioral marker for increased brain dopamine "tone" and increased spontaneous hyperactivity has been suggested to be a schizophrenia-validating feature for an animal model despite the fact that people with schizophrenia do not exhibit prominent hyperactivity (Minassian et al., 2010). One study showed that rats exhibiting the lowest PPI among a colony were more sensitive to further reduction of their PPI by apomorphine than rats with naturally high PPI, suggesting that the low PPI exhibited by people with schizophrenia may be due to the increased central dopamine tone, which also makes them more sensitive to prodopamine drugs (Feifel, 1999).

3.3 Negative Symptoms

As mentioned previously, negative symptoms are one of the core features of schizophrenia and it is included in the DSM list of symptoms of schizophrenia that are included in the diagnostic criteria. There have been several attempts to model negative symptoms in animals. While some specifics manifestations of negative symptom, such as alogia (reduced speech) and affective flattening are difficult to model in animals, modeling reduced social interaction, one manifestation of negative symptoms is viable and a widely accepted paradigm. This is accomplished with the social interaction test, which measures the social interaction between individual members of species placed together in a test arena (Neill et al., 2016; Sams-Dodd, 1998b). Unlike control animals who freely explore the environment and interact frequently with the other members of their species, rodents that are treated with the NMDA receptor antagonist PCP for 3 consecutive days typically ambulate along the periphery of the arena and avoid contact with the other members of their species. This PCP-induced phenotype is considered to be analogous to the social avoidance displayed at times by some schizophrenia patients. FGA's and SGA's reverse the effects of PCP in the social interaction test when administered for 3 or 21 days in combination with PCP. However, the antipsychotics also increase social interaction in animals that did not receive PCP (Sams-Dodd, 1998b). Given the equivocal nature of the benefit of antipsychotics in treating negative symptoms, their distinct efficacy in the social interaction test may, arguably, weaken the predictive validity of this animal model of negative symptoms.

3.4 Information Processing Abnormalities Associated with Schizophrenia

Substantial evidence suggests that people with schizophrenia have deficiencies in processing information including a reduction in normal automatic filtering, or gating, of irrelevant internal and external stimuli, resulting in a greater intrusion of irrelevant stimuli on the conscious awareness in people with schizophrenia (Braff and Geyer, 1990; McGhie and Chapman, 1961). This abnormality may be fundamental to the disturbances of thought associated with schizophrenia (Braff and Geyer, 1990). Several cross-species operational measures of sensory and sensorimotor gating have been characterized and used to develop animal models of the gating deficits observed in schizophrenia. The abnormalities in these gating measures are considered "endophenotypes" of schizophrenia—phenotypic features that are not symptoms of the disorder but are likely to reflect the underlying neuropathology that contributes to the core symptoms. The endophenotypes of schizophrenia described later can be modeled in rodents in a manner homologous to their manifestation in people with schizophrenia.

3.4.1 Prepulse Inhibition (PPI)

The most researched schizophrenia endophenotype related to information gating is PPI. PPI refers the normal suppression of the reflexive startle response to a brief intense startling stimulus (pulse) when it is preceded by a barely detectable, nonstartling, lead stimulus (prepulse) that is presented 30–500 ms before the pulse (Swerdlow and Geyer, 1998). PPI is an operational measure of a phenomenon referred to as sensorimotor gating, which is an early stage (preattentional) perceptual filtering mechanism that allows some stimuli to proceed through for further processing while filtering out other stimuli. Weak sensorimotor gating can, in theory, allow higher order processing centers to become overwhelmed by irrelevant information. This can reduce the efficiency of cognitive processing and produce disordered thinking. The startle reflex is mediated by a monosynaptic circuit that transfers information from sensory receptors to motor neurons. PPI is mediated by a multisynaptic circuitry that modulates the startle circuit and overlaps substantially with circuits implicated in schizophrenia (Swerdlow and Geyer, 1998; Swerdlow et al., 1986, 2001). The suppression of the motor response to the startling stimulus occurs because the processing of the prepulse creates a time limited gating mechanism that inhibits processing of other stimuli (Fig. 23.1).

People with schizophrenia have decreased PPI compared to matched control subjects (Braff and Geyer, 1990). Though the precise clinical correlation of low PPI in schizophrenia has not been established,

(A)
Stimulus pulse

NO PPI →

Startle

(B)
Stimulus pulse

PPI →

PPI
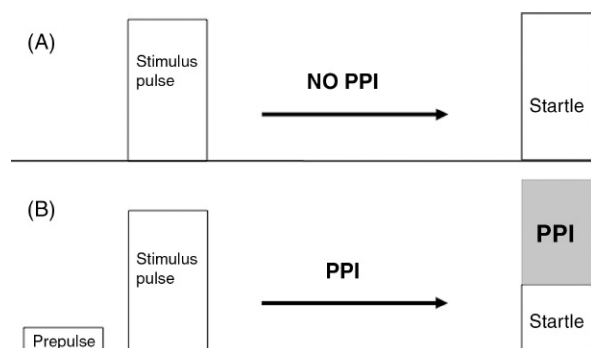
Startle

Prepulse

FIGURE 23.1 **Diagram is representative of prepulse inhibition.** (A) The presentation of Stimulus A (pulse) results in a large startle response. (B) When a subthreshold prepulse is presented 50–500 ms prior to Stimulus B (pulse), the startle response is decreased. Prepulse inhibition is represented by the *grayed box* (Startle A–Startle B).

schizophrenia patients with maximal PPI deficits have been shown to have the greatest thought disorder (Perry and Braff, 1994). Several lines of evidence suggest that these PPI deficits represent a vulnerability trait. For example, first degree relatives of schizophrenia patients not afflicted with the disorder and people with schizotypal personality, a condition associated with milder forms of psychosis than schizophrenia, have been shown to have PPI that is intermediate between people with schizophrenia and healthy people who do not have first degree relatives with schizophrenia (Cadenhead et al., 1993). There is also evidence that low PPI may represent somewhat of a state marker for psychosis, as hospitalized bipolar patients in the midst of an acute manic episode with psychosis displayed reduced PPI whereas stable outpatient bipolar patients did not (Perry et al., 2001a).

PPI can also be measured in animals under parametric conditions similar to those used to measure it in humans. Some common parameters used to elicit PPI in both rodents and humans include a startling auditory stimulus (pulse) of approximately 120 dB, preceded by a much weaker stimuli (prepulse) ranging from 4–16 dB that is presented 50–500 ms before the pulse. A test session includes presentation of both startling pulses alone and prepulse-pulse pairs. In humans, the startling acoustic pulse and nonstartling stimulus are delivered through headphones and the startle response is measured by the strength of the involuntary eye blink, which is measured electromyographically via electrodes positioned below one eye on the ocular blink muscle (orbicularis oculi). To measure the startle response in rodents, mice or rats are placed in cylindrical enclosures housed within soundproof boxes. Acoustic stimuli are delivered via speakers and startle response is measured by mechanical transducers, which detect the downward displacement of the cylinders produced by the rodent's involuntary limb extension in response to the startling stimulus.

PPI is commonly calculated in each human or animal subject by comparing the average magnitude of the startle responses to the startling pulses presented alone with the magnitude of the startle response to the prepulse-pulse presentations. The most common way to report the attenuation in startle produced by the prepulses is as the average percentage reduction of the unmodified startle response.

$$[(1 - (\text{Startle}_{\text{prepulse}} - \text{Startle}_{\text{noprepulse}}) / \text{Startle}_{\text{noprepulse}})) \times 100)]$$

PPI deficits can be induced in animals by a variety of interventions. Psychostimulant drugs that have a proclivity to temporarily induce psychotic symptoms in humans, such as amphetamine, PCP, and LSD, produce transient PPI deficits in rodents. Nonpharmacological interventions can also produce PPI deficits in rodents and are often more enduring than those deficits produced by drugs. Examples of these interventions include lesions induced in the ventral hippocampus during the neonatal period, rearing rodents in social isolation, in-utero viral infections and certain genetic manipulations. In addition, some rodent strains, such as the Brattleboro rat and C57BL/6j mice exhibit naturally low PPI. Antipsychotic drugs, specifically SGAs, tend to reverse PPI deficits in people with schizophrenia (Braff, 2010). PPI deficits in rats and mice have been widely used as predictive test for drugs with therapeutic potential for schizophrenia (Braff, 2010; Geyer et al., 2001).

A limitation of PPI deficiency as a basis for modeling features of schizophrenia in animals is that PPI deficits are not specific to schizophrenia as people with other neuropsychiatric disorders have been shown to exhibit PPI deficits, including Huntington's disease (Swerdlow et al., 1995), obsessive compulsive disorder (Swerdlow et al., 1993), Tourette's disorder (Castellanos et al., 1996), and bipolar mania with psychosis (Perry et al., 2001a). These findings raise questions regarding the fundamental nature of the PPI deficiency in schizophrenia.

One of the advantages of using PPI as the basis for an animal model of relevance to schizophrenia is that the PPI measurement itself is highly automated and provides an objective quantitative output. Moreover, it does not require any physical preparation or training of animals.

3.4.2 P50/N40 Gating

Electroencephalographic (EEG) monitoring following presentation of a stimulus reveals electrical potentials that are generated at highly predictable times following the stimulus presentation. Evoked responses to auditory stimuli, termed auditory event related potentials (AERP), have been well studied in humans and animals. One well-characterized AERP occurs 50 ms after an auditory stimulus is presented and is called the P50 wave.
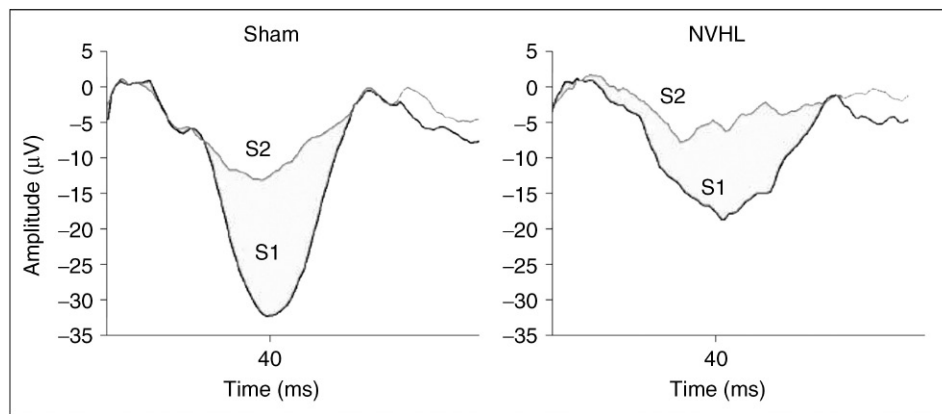
FIGURE 23.2   **N40 gating in sham and NVHL rats.** Grand average auditory ERPs in sham and lesion (NVHL) groups showing prominent reduction in S1 magnitude among NVHL group rats. *Source: Reprinted with Permissions from S. Karger, A.G., Basel; adapted from Swerdlow, N.R., Light, G.A., Breier, M.R. et al., 2012. Sensory and sensorimotor gating deficits after neonatal ventral hippocampal lesions in rats. Dev. Neurosci. 34(2–3), 240–249.*

When two auditory clicks are presented in sequence with an interstimulus interval of 0.5 ms or less, there is a marked attenuation of the P50 invoked by the second click (S2), compared to the one evoked by the first click (S1). This is thought to be an operational measure of sensory gating (versus sensorimotor gating, since P50 gating involves no motor response), which is a process by which the brain filters the flow of sensory information that is allowed to pass through to higher processing centers. It is presumed that sensory gating helps avoid flooding of those systems. In the paired click paradigm an inhibitory mechanism or sensory gate is activated by the first click (Swerdlow et al., 2006).

P50 gating is usually measured as a ratio of the amplitude of the P50 response to the second click to that of the first click (S2/S1) or as a percentage reduction similar to the formula for percentage PPI $(1-(S2/S1) \times 100)$ (Swerdlow et al., 2006). People with schizophrenia exhibit much smaller P50 gating compared to nonclinical control subjects. It has been suggested that PPI and P50 suppression measure complementary aspects of inhibitory neural circuitry (Braff et al., 2007) and are not correlated in patients with schizophrenia.

This abnormality in the P50 gating, which is genetically linked to the α-7 nicotinic receptor, can be transiently reversed in people with schizophrenia through acute nicotine administration (Martin and Freedman, 2007). However, investigations into the ability of antipsychotics to reverse P50 deficits have been inconsistent (Adler et al., 2005; Su et al., 2012) (Fig. 23.2).

Rodents do not exhibit a P50, but they exhibit a similar AERP, the N40. The N40 and its attenuation by a preceding auditory event are considered to be analogous to human P50 and P50 gating, respectively (Stevens et al., 1991). Similar to PPI, N40 gating deficits in rodents can be induced by psychotomimetic drugs including apomorphine and amphetamine (Swerdlow et al., 2006)

as well as NMDA receptor antagonists, such as PCP (Miller et al., 1992). Social isolation rearing (Stevens et al., 1997) and neurotoxic-induced lesions of the CNS (Stevens et al., 1998) also disrupt N40 gating in rodents. Measuring N40 gating requires implanting and securing electrodes in the brains of rodents, making this paradigm much less practical than PPI testing. Furthermore, studies have not yet found a strong association with the P50 deficits in schizophrenia and any of the clinical features of that disorder (Potter et al., 2006). Additionally, unlike the case with PPI deficits, P50 gating deficits are not remediated by antipsychotic medication. Studies of the antipsychotic effect on N40 gating deficits in rodents have produced mixed results. For example, haloperidol reverses N40 gating deficits in rats that are induced by neurotoxins (Stevens et al., 1998). However, social isolation induced N40 gating deficits are reversed by nicotine, which is consistent with findings in schizophrenia patients (Bickford-Wimer et al., 1990; Stevens et al., 1997, 1998). In DBA/2 mice, SGAs, but not FGAs improve, N40 gating (Simosky et al., 2003, 2008).

3.4.3 Habituation

Another measure of information processing plasticity based upon the startle response is habituation, which refers to the normal decrement in startle response when the startling stimulus is repeatedly presented. Habituation is considered the simplest form of learning and is considered essential for selective attention. Habituation is deficient in schizophrenia [see (Geyer et al., 1990; Hammer et al., 2011) for review] but was not found to be abnormal in patients with obsessive compulsive disorder (Swerdlow et al., 1993), Huntington's disease (Swerdlow et al., 1995), or autism (Perry et al., 2007) conditions that are associated with PPI deficits. These findings suggest that habituation and PPI are independent measures of startle plasticity and that habituation

deficits may be more specific to schizophrenia than PPI deficits.

Habituation can easily be measured concurrently with PPI testing in the same session by presenting a short series of consecutive pulse-alone stimuli at the very beginning of the startle session and at the end of the session. The average startle response to both series is calculated and the percentage decrease from the first to second series represents habituation. The clinical correlates of habituation have not been well studied.

Concerning modeling habituation deficits in rodents, the DBA/2 mouse (Brooks et al., 2004), the Maudsley Nonreactive rat (Commissaris et al., 1988) and the Brattleboro rat (Feifel and Priebe, 2001) show innate startle habituation deficits.

In regards to drug effects on habituation deficits in patients with schizophrenia, Perry et al. (2002) reported no difference in habituation deficits in acutely ill patients who were being treated with antipsychotics and those who were medication free.

3.4.4 Latent Inhibition

Latent inhibition is a normal modulation of associative learning. Specifically, latent inhibition refers to the reduced ability to learn the relevance of a stimulus that is paired with an aversive or positive condition through classic conditioning if there has been a previous exposure to the stimulus in a neutral context (Lubow, 1965; Swerdlow et al., 1996). In humans, associative learning is typically measured in a laboratory setting by pairing an initially neutral stimulus (e.g., image of a blue circle) with an aversive one, such as a mild shock to the hand until the previously neutral stimulus elicits a similar physiological response as the shock. For example, this learned association can be measured by the ability of the once neutral stimulus to potentiate the subject's startle response to a startling stimulus, such as a sudden brief sound. To measure latent inhibition, some subjects are exposed to the neutral stimulus on its own before the first pairing with mild shock. The preexposure to the neutral stimulus normally inhibits its ability to become associated with the shock as measured by a reduced ability to potentiate startle compared to a neutral stimulus that is not preexposed.

Both PPI and latent inhibition are considered measures of information gating and their underlying neural circuitry overlap (Bakshi et al., 1995). However, whereas PPI assesses early attentional or "preattentional" gating mechanisms, latent inhibition assesses later stages of information processing gating (Leumann et al., 2002). The degree to which PPI and latent inhibition are related within individual animals or humans is not well established. Latent inhibition, like PPI, is deficient in schizophrenia patients (Bakshi et al., 1995; Baruch et al., 1988; Gray et al., 1995) although there is some degree of

controversy (Swerdlow et al., 1996; Rascle et al., 2001). Latent inhibition is also deficient in a subgroup of Parkinson's patients (Lubow et al., 1999). However, in contrast to PPI deficits, latent inhibition deficits, like startle habituation deficits, are not found in patients with obsessive compulsive disorder (Swerdlow et al., 1999).

Latent inhibition can be measured in rodents using paradigms similar to those in humans. For example, a colored light can be used as the conditioned stimulus and an electric shock delivered through a grid in a cage floor can be used as the unconditioned stimulus (Weiner et al., 1996). Another approach to study latent inhibition has been to use a conditioned taste aversion paradigm (Simonyi et al., 2009) where a distinct gustatory stimulus, such as saccharin-sweetened water is presented to rodents just prior to administration of a substance, such as lithium chloride that induces malaise. Animals who are presented with the colored light or saccharin flavored water not paired with shock or malaise, respectively, will develop weaker potentiation of startle or aversion to drinking saccharin flavored water when those stimuli are later paired with the shock or lithium (Fig. 23.3).

In humans and rats, the indirect dopamine agonist amphetamine produces latent inhibition deficits (Russig et al., 2002; Thornton et al., 1996; Weiner et al., 1988). In addition, an injection of interleukin-6 (IL-6), which stimulates the immune system, in pregnant mice causes latent inhibition deficits in their adult offspring (Smith et al., 2007).

In rodents, antipsychotic drugs, such as haloperidol and clozapine reverse amphetamine-induced latent inhibition deficits (Thornton et al., 1996; Williams et al., 1996) and facilitate latent inhibition that is above baseline levels when given alone (Bethus et al., 2006; Feldon and Weiner, 1991). Additionally, compounds that lack antipsychotic activity are usually not active in this model (Moser et al., 2000). Based upon these findings, enhancement of baseline latent inhibition or reversal of amphetamine-induced reduction of latent inhibition, have been proposed as predictive tests of antipsychotic activity (Moser et al., 2000). In addition, some strains of rodents, such as the Brown Norway (Conti et al., 2001) and Brattleboro rat (Feifel et al., unpublished), as well as 29/SvJ, CBA, A/J, and C3H/Ibg mice (Gould and Wehner, 1999) exhibit spontaneous deficits in latent inhibition. In this regard, Feifel et al. (2015, 2016) recently reported that both oxytocin and a brain penetrating neurotensin-1 agonist, PD149163, modulate latent inhibition in a manner consistent with antipsychotic drugs in Brown Norway rats.

3.4.5 Other Cognitive Deficits

Cognitive deficits are highly prevalent in schizophrenia and are considered by many schizophrenia investigators to be a core feature of the disorder, despite

	Stage 1 (preexposure)	Stage 2 (conditioning)	Stage 3 (test)
Control group	Normal water +++ imbibed	Flavored water and saline +++ imbibed	Flavored water +++ imbibed (no conditioned taste aversion)
Non-preexposed group	Normal water +++ imbibed	Flavored water and LiCl* +++ imbibed	Flavored water + imbibed (conditioned taste aversion)
Preexposed group	Flavored water +++ imbibed	Flavored water and LiCl +++ imbibed	Flavored water ++ imbibed (latent inhibition of conditioned taste aversion)

FIGURE 23.3 **The three stages of the latent inhibition paradigm using a conditioned taste aversion procedure.** In stage 1, water-restricted animals are given a drinking session with either flavored water (e.g., 1% saccharin) (preexposed group) or regular drinking water (nonpreexposed group and control group). In the second stage, all animals are given a drinking session with flavored water. The nonpreexposed and preexposed groups are then injected immediately with LiCl, which induces malaise. The controls are injected with saline instead of LiCl. In the third stage (Test), conditioned taste aversion and latent inhibition are tested by exposing all animals to the flavored water (CS) alone. All animals except the controls exhibit conditioned taste aversion. Furthermore, the group that had experience with flavored water before it was paired with lithium-inducing malaise demonstrates less aversion to the flavored water on the test day, indicating that the preexposure to the flavored water produced a latent inhibition of the conditioned taste aversion. Thanks to Dr. Robert Lubow for assistance in preparing this figure. *LiCl is administered in doses that produce a rapid, but transient sensation of malaise in rodents.

that they are not counted among the DSM criteria for making the diagnosis of schizophrenia. The cognitive deficits experienced by people with schizophrenia are responsible for a substantial amount of the functional disabilities associated with this disorder. Moreover, as with negative symptoms, the beneficial effects of antipsychotic drugs on the cognitive deficits of schizophrenia are, at best, modest (Woodward et al., 2005). Due to these modest effects, there has been much effort recently to develop drugs that specifically address the cognitive deficits of schizophrenia (Young and Geyer, 2015). This has, in turn, energized efforts to develop and optimize animal models and animal tests that have validity for the cognitive deficits of schizophrenia. Several distinct domains of cognitive function have been identified to be perturbed in people with schizophrenia including attention, memory and learning (visual, verbal and working), reasoning and problem solving, processing speed, and social cognition (Hagan and Jones, 2005). There are established tests to assess each of these cognitive domains in humans and tests have also been developed to measure analogous cognitive functions in rodents and other animals. Researchers interested in studying the cognitive dysfunction associated with schizophrenia in animals have generally utilized those preclinical tests. Pharmacological, neuroanatomical lesion, neurodevelopmental intervention, and genetic approaches have been used to induce deficient performance in these animal tasks in order to create animal models for these cognitive deficits. For example, PCP, a noncompetitive NMDA antagonist, induces reduced performance in rats and mice on tests of

animal attention (Jentsch and Anzivino, 2004), working memory (Marrs et al., 2005), problem solving (Egerton et al., 2005), social cognition (Terranova et al., 2005), and novel object recognition (Neill et al., 2016).

Investigators have attempted to improve animal performance on cognitive tasks with a variety of compounds in the hope of identifying therapeutic treatments for the cognitive deficits exhibited by patients with schizophrenia. A major barrier to this effort is the lack of positive controls for establishing predictive validity for animal models of cognitive dysfunction since, at this time, there are no known drugs that have good efficacy against these cognitive abnormalities exhibited by people with schizophrenia. The human clinical batteries and their corresponding preclinical cognitive tests, for which performance is assumed to be analogous, are displayed in Table 23.2.

3.4.6 Genetic Abnormalities

A large number of genetic variants have been identified from various studies comparing the genome of people with schizophrenia to the general population, suggesting multiple susceptibility loci for schizophrenia (Allen et al., 2008) (Also see SZGene URL http://www.szgene.org/). For example, specific single nucleotide polymorphisms (SNP) variants have been detected significantly more often in people with schizophrenia in association studies. In addition, family studies have detected linkage to an array of chromosomal regions. Several knockout and transgenic approaches have been used to model some of these genetic abnormalities in animals.

TABLE 23.2   Cognitive Domains Impaired in Schizophrenia, Tests Used to Measure These Behaviors in Humans Animal Tests That Measure Analogous Cognitive Domains in Animals

Cognitive domain	Clinical battery	Animal tests
Working Memory	BACS, Spatial delayed response task, WMS-III spatial span WAIS-III letter-number sequence, UoM letter-number span	Operant or T-maze, delayed nonmatch to position/sample Radial arm maze
Attention/vigilance (preattentive processing)	3-7 CPT, Identical pairs CPT	Latent inhibition, 5-choice serial reaction time task
Visual learning and memory	NAB—Shape learning, BVMT—Revised	Novel object recognition, Social recognition
Speed of processing	5-choice serial reaction time task, simple reaction time tasks	Category fluency, Trail making A, WAIS-III digit symbol coding, BACS—Symbol coding
Reasoning and problem solving	WAIS-III Block design, BACS—Tower of London, NAB—Mazes	Attentional set-shifting, maze tasks
Social cognition	MSCEIT—Managing emotions, MSCEIT—Perceiving emotions	Social interaction, social recognition
Verbal learning and memory	NAB—Daily Living Memory, HVLT—Revised	Not applicable to animals

BACS, Brief assessment of cognition in Schizophrenia; BVMT, Brief Visuospatial Memory Test–Revised; CPT, Continuous Performance Test; HVLT, Hopkins Verbal Learning Test–Revised; MSCEIT, Mayer-Salovey-Caruso Emotional Intelligence Test; NAB, Neuropsychological Assessment Battery; UoM, University of Maryland; WMS-III, Wechsler Memory Scale–III; WAIS-III, Wechsler Adult Intelligence Scale

Adapted from Hagan, J.J., Jones, D.N., 2005. Predicting drug efficacy for cognitive deficits in schizophrenia. Schizophr. Bull. 31(4), 830–853.

Characterization of these genetically engineered animal models has revealed inconsistent findings regarding the manifestation of schizophrenia relevant phenotypes, endophenotypes, or pathophysiological abnormalities. The effects of a single gene abnormality are not likely to be sufficient to cause schizophrenia and environmental risk factors also play an important role. Therefore, creating animal models that combine two or more candidate genetic abnormalities, or combine a candidate genetic abnormality with environmental factors in a "two-hit" model, may produce more valid animal models.

Table 23.3 displays examples of genetically engineered mouse models of the genetic alterations that have been found to be associated with schizophrenia in many studies.

4 SPECIFIC ANIMAL MODELS

4.1 Pharmacological Approaches

Animal models have primarily used psychotomimetics, such as dopamine agonists and noncompetitive NMDA (glutamate) receptor antagonists to produce deficits in behaviors that are analogous to phenotypes exhibited by people with schizophrenia, such as deficits in PPI, latent inhibition, cognitive task performance, and social interaction.

4.1.1 Administration of Prodopamine Drugs

Early efforts at modeling schizophrenia in animals relied on acute administration of indirect dopamine agonists, such as amphetamine or direct dopamine receptor

agonists, such as apomorphine to induce a transient central hyperdopaminergia. This approach remains highly utilized and it is driven by the prominence of the dopamine hypothesis of schizophrenia (Carlsson, 1977; Luchins, 1975; Willner, 1997) and the strong corpus of evidence linking hyperdopaminergia in the mesolimbic pathway to positive symptoms. The dependent measures usually studied are the well-known effects produced in rodents by prodopamine drugs, namely hyperlocomotion, stereotypy, and the disruption of PPI and latent inhibition (Geyer et al., 2001; Swerdlow et al., 1994). Typically, a single administration of 0.5–1.0 mg/kg of amphetamine is used to produce hyperlocomotion in rats, whereas higher doses (2.0–5.0 mg/kg) induce stereotypy and deficits in latent inhibition and PPI. Disrupted PPI is a well-established feature of schizophrenia and the evidence for a latent inhibition deficit in schizophrenia is also strong, with some inconsistent findings, but there is no strong evidence supporting increased locomotion in people with schizophrenia (Minassian et al., 2010) and stereotypy is exhibited by only a small percentage of them. As such, the rationale for studying hyperlocomotion and stereotypy induced by prodopamine drugs is that they are considered animal analogs of positive symptoms because they are reliably produced by increasing mesolimbic dopamine transmission. However, the ability to induce and measure a phenomenon that is actually associated with schizophrenia enhances the validity of the prodopamine pharmacological animal models and, not surprisingly, PPI has become the output of choice to measure in these hyperdopaminergia-based animal models as well as other animal models of relevance to schizophrenia. Unlike its deficit inducing

TABLE 23.3   Mouse Models Based on Some of the Most Promising Susceptibility Genes for Schizophrenia

Candidate gene and it's known function	Animal models	Schizophrenia-like features		Effects of antipsychotics (APDs)
		Phenotype	Pathophysiology	
Neuregulin 1 Growth factor involved in neuronal migration, synaptogenesis, and neuron glial interactions in brain development. (Harrison and Law, 2006)	Neuregulin 1 Knockout/hypomorph (Chen et al., 2008; Stefansson et al., 2002; O'Tuathaigh et al., 2008; Zhang et al., 2016)	PPI Deficits (Chen et al., 2008; Stefansson et al., 2002) Impaired performance on delayed alternation memory tasks, (Chen et al., 2008) Social Interaction deficits (O'Tuathaigh et al., 2008) Hyperactive in open field (O'Tuathaigh et al., 2008)	Larger lateral ventricles, decreased spine density (Chen et al., 2008) Reduced NMDA receptor activity (Stefansson et al., 2002)	Acute CLOZ reversed hyper-activity but not PPI deficits (Stefansson et al., 2002) Acute olanzapine prevented PCP-induced effects in normal neurons but not in neurons from KOs (Zhang et al., 2016) Non-APDs: Chronic Nicotine attenuated PPI deficits in HETs (Chen et al., 2008)
ERBB4 Neuregulin receptor	ERBB4 knockout (Barros et al., 2009; Golub et al., 2004; Roy et al., 2007) Specific to KO in excitatory pyramidal neurons (Cooper and Koleske, 2014)	PPI Deficits (Barros et al., 2009) HETS: Deficit in spatial learning (Golub et al., 2004) Hypoactive, social interaction deficits, enhanced AMPH sensitization (Roy et al., 2007)	Reduced spine density in hippocampus (Barros et al., 2009) Oligodendrocyte abnormalities (Roy et al., 2007)	Acute CLOZ reverses PPI deficits (Barros et al., 2009)
DISC1 Scaffolding protein critical role in neuron development, to cellular proliferation, intracellular signaling, migration and transport (Jaaro-Peled, 2009)	DISC1 L100P mutant (2nd exon) (Lipina et al., 2010)	Spontaneous hyperactivity and deficits in PPI and LI (Lipina et al., 2010) Facilitation of AMPH effect on locomotor activity and PPI (Lipina et al., 2010)	None reported	Acute HAL blocked hyper-activity, deficits in PPI and LI and blocked enhanced sensitivity to AMPH (Lipina et al., 2010)
	DISC1 KO/Knockdown (Clapcote et al., 2007; Niwa et al., 2010; Hikida et al., 2007; Umeda et al., 2016)	Deficits in PPI, working memory and LI (Clapcote et al., 2007) PPI and novel object recognition deficits after but not before puberty (Niwa et al., 2010) Increased sensitivity to MethAMPH induced disruption of PPI vs. WT (Niwa et al., 2010)	Less cortical parvalbumin containing cells (Hikida et al., 2007)	PPI deficits reversed by acute CLOZ and HAL (Clapcote et al., 2007; Niwa et al., 2010) Bupropion had no effect on PPI (Clapcote et al., 2007) LI deficits reversed by acute CLOZ (Clapcote et al., 2007)
	DISC1 (Truncated) (Shen et al., 2008)	Deficit in LI and social interaction (Shen et al., 2008)	Enlarged ventricles (Shen et al., 2008) Decreased paralbumin neurons in mPFC and hippocampus (Shen et al., 2008)	None reported
	DISC1 129S6/SvEv Naturally occurring mutant (termination codon at exon 7, abolishes production of the full-length protein) (Koike et al., 2006)	Working memory deficit (Koike et al., 2006)	Naturally occurring DISC1 truncated protein (Koike et al., 2006)	None reported

(Continued)

TABLE 23.3   Mouse Models Based on Some of the Most Promising Susceptibility Genes for Schizophrenia (cont.)

Candidate gene and it's known function	Animal models	Schizophrenia-like features		Effects of antipsychotics (APDs)
		Phenotype	Pathophysiology	
Dysbindin 1 Synaptic protein, regulates exocytosis and receptor trafficking in excitatory neurotransmission (Karlsgodt et al., 2011)	Sandy (sdy) Mouse Spontaneous mutation in dysbindin (Bhardwaj et al., 2009; Takao et al., 2008; Feng et al., 2008; Hattori et al., 2008; Murotani et al., 2007; Chen et al., 2017)	Working memory deficits (Takao et al., 2008) Social interaction deficits (Feng et al., 2008) Decreased basal locomotor (Hattori et al., 2008) Lack of locomotor habituation (Bhardwaj et al., 2009) Enhanced AMPH sensitization (Bhardwaj et al., 2009)	Decreased DA levels in cortex, HPC, hypothalamus (Hattori et al., 2008) DA turnover increased in specific regions of brain (Murotani et al., 2007)	None reported
Reelin Extracellular matrix protein essential for cell positioning and neuronal migration during development implicated in synaptic formation and cellular plasticity. (Cassidy et al., 2010)	Reeler Mouse, Heterozygous (Barr et al., 2008; Costa et al., 2002; Howell and Pillai, 2016)	Habituation and PPI deficits (Barr et al., 2008)	Reduced GAD 67 expression (Costa et al., 2002) Dendritic spine defects (Costa et al., 2002)	None reported

AMPH, amphetamine; APD, antipsychotic drug; CLOZ, clozapine; DA, dopamine; GAD, glutamate decarboxylase; HPC, hippocampus; HAL, haloperidol; PPI, prepulse inhibition; NMDA, N-methyl D-aspartate

effects on PPI and latent inhibition, acute administration of prodopamine drugs in animals does not consistently produce impairments in their performance on cognitive tasks that are considered analogs of those that people with schizophrenia perform poorly on. In fact, these drugs often enhance performance on these tasks (Menesses, 2011). Similarly, impairments in social interaction or other behaviors relevant to negative symptoms are not induced by acute administration of prodopamine drugs. Therefore, the acute administration of prodopamine drugs does not seem useful as an animal model of the cognitive deficits or negative symptoms associated with schizophrenia.

In addition to having some degree of validity based upon sharing the pathophysiological feature presumed to be an important mechanism underlying its clinical features (hyperdopaminergia) with schizophrenia and exhibiting a homolog of the information gating deficits (PPI and latent inhibition) exhibited in schizophrenia, the acute prodopamine pharmacological model also appears to exhibit predictive validity based upon its response to acute administration of antipsychotic drugs. FGAs and SGAs block the PPI effects of dopamine agonists and a strong correlation has been found between the potency of antipsychotics to block apomorphine-induced disruption of PPI in rodents and their clinical potency as well as their D2 receptor affinity (Swerdlow et al., 1994). Nevertheless, this finding is not surprising,

as it seems to reflect a "pharmacological tautology" since apomorphine acts as an agonist at D2 receptors and all antipsychotics tested have been D2 receptor antagonists. However, the efficacy of clozapine in the prodopamine drug animal model has been inconsistent, reducing the model's predictive validity, although strain differences across these studies may have contributed to this discrepancy (Swerdlow et al., 1998). Nonetheless, the predictive validity of this animal model is also reduced somewhat by an apparent lack of specificity for antipsychotic drugs. For example, the antidepressant desipramine, a noradrenergic reuptake inhibitor (Pouzet et al., 2005), the mood stabilizer lithium (Ong et al., 2005), and the anticonvulsant topiramate (Frau et al., 2007), none of which have any known antipsychotic efficacy, block amphetamine- or apomorphine-induced PPI deficits.

The prodopamine drug animal model also does not appear to be well suited for modeling the efficacy time course associated with antipsychotic drugs in schizophrenia. Whereas the therapeutic efficacy of antipsychotic drugs in schizophrenia patients reaches optimal levels after several weeks of continuous administration, the efficacy of single doses of antipsychotics to attenuate prodopamine drug-induced PPI deficits in rodents has been shown to weaken (Martinez et al., 2000) or disappear altogether (Andersen and Pouzet, 2001) after chronic administration.

However, the amphetamine model seems to have exhibited true predictive validity (i.e., to predict an aspect of schizophrenia not yet known) with at least one novel drug for schizophrenia. Oxytocin, a neuropeptide with no affinity for dopamine receptors, blocked amphetamine-induced PPI disruption in rats suggesting that it would be efficacious in schizophrenia before oxytocin had been systematically tested. Subsequently, oxytocin was found to be efficacious in reducing symptoms of schizophrenia (Feifel et al., 2010; Pedersen et al., 2011).

A single administration of a prodopamine drug produces only a short-lived hyperdopaminergia and related behavioral effects. In this respect, acute pharmacological animal models do not replicate the chronic hyperdopaminergia and chronic phenomenology associated with schizophrenia. Furthermore, the emergence of psychosis in people who do not have schizophrenia and take prodopamine drugs recreationally is typically exhibited after repetitive use over an extended period (Segal et al., 1981). Therefore many investigators have attempted to model psychosis in animals using chronic administration of prodopamine drugs. Some paradigms employ repeated administration of the same dose whereas others employ an escalating doses administered in binges to replicate the pattern of use in many amphetamine and cocaine addicts, which can lead to the development of stimulant-induced psychosis (Kreek et al., 2009; Segal and Kuczenski, 1999). This approach typically involves administering escalating doses of amphetamine over the course of several days (1.0–8.0 mg/kg), followed by 4 binges/day of a very high dose (8.0 mg/kg) for a variable number of days (Segal and Kuczenski, 1997). Both the steady dose and escalating dose paradigms of chronic administration induce a persistent sensitization in which rodents exhibit an amplified response to acute administration of the same drug or another pro-dopamine agent (Kalivas and Duffy, 1993a,b; Kuczenski and Segal, 1999; Segal and Kuczenski, 1992, 2006). This sensitization emulates the increased sensitivity that people with schizophrenia demonstrate to the psychotogenic effects of prodopamine drugs. Of particular interest, non-human primates administered a repeated single dose of amphetamine or an intermittent escalating dose regimen of amphetamine exhibited behaviors similar to people experiencing hallucinations including picking at imaginary parasites, orienting to nonexistent stimuli, swatting at imaginary objects and staring into empty space (Featherstone et al., 2007). Sensitized animals display persistent deficits in some cognitive tasks relevant to schizophrenia whereas others are not affected (Featherstone et al., 2007). In addition, chronic administration of prodopamine drugs seems no better than acute administration at inducing behaviors in animals that are reminiscent of the negative symptoms of schizophrenia. The findings regarding the PPI and latent inhibition effects of chronic regimens of amphetamine administration in rodents are inconsistent, as some studies have reported PPI and latent inhibition deficits in amphetamine-sensitized rodents (Featherstone et al., 2007). Although not well studied, PPI and latent inhibition deficits in sensitized rats have been reversed by FGAs and SGAs (Abekawa et al., 2008; Russig et al., 2002). Biochemical and structural changes are induced in the brain by chronic administration of amphetamine in animals, which may account for the persistent changes observed in behavioral and cognitive measures.

In conclusion, pharmacological induction of hyperdopaminergia by acute or chronic administration of prodopamine drugs in animals seems to have reasonable validity and utility as models to study positive symptoms of schizophrenia. The acute models have limitations as a valid predictive assay for efficacious treatments and the chronic model has not been studied sufficiently in this regard. Both acute and chronic models lack validity for the negative symptoms or cognitive deficits associated with schizophrenia.

4.1.2 NMDA Receptor Antagonists

Converging evidence supports the notion that, in addition to the dopamine system, dysfunction of the glutamate system contributes to the manifestation of schizophrenia (Geyer and Moghaddam, 2002; Tsai and Coyle, 2002). This evidence includes the observation that PCP and ketamine, drugs that block the N-methyl d-aspartate (NMDA) subtype of the glutamate receptor, can produce a transient psychosis similar to that experienced by people with schizophrenia. However, unlike the transient psychosis produced by prodopamine drugs, such as cocaine or amphetamine, these NMDA antagonists can induce a phenomenon that emulates both the negative and positive symptoms, as well as the cognitive deficits of schizophrenia (Krystal et al., 1994; Tamminga et al., 1995). PCP and ketamine can also exacerbate positive and negative symptoms in people with schizophrenia. Studies have provided support for reduced NMDA receptor function in the brains of people with schizophrenia (Coyle et al., 2003; Pilowsky et al., 2006). This body of converging evidence has led to the development of the glutamate hypothesis of schizophrenia, which posits that in addition to subcortical hyperdopaminergia, hypofunction of glutamate transmission through NMDA receptors, and possibly other glutamate receptor subtypes, contributes to clinical features of schizophrenia, especially the negative symptoms and cognitive deficits (Javitt, 2010).

In response to increasing recognition of the potential role of glutamate perturbation in schizophrenia, NMDA antagonists, such as PCP, ketamine, and dizocilpine (MK801) have been used to create pharmacological

animal models of schizophrenia in an attempt to better understand the role of glutamate hypofunction in this disorder and to screen for new treatments (Brown et al., 2014; Geyer et al., 2001; Jentsch and Roth, 1999; Mouri et al., 2007). A single administration of noncompetitive NMDA antagonists, such as PCP (0.1–10 mg/kg) produces a wide array of schizophrenia-relevant behaviors in rodents, such as hyperlocomotion, deficits in PPI and latent inhibition (Gaisler-Salomon and Weiner, 2003; Jentsch and Roth, 1999; Mansbach and Geyer, 1989; Neill et al., 2016), social withdrawal (Sams-Dodd et al., 1997) and impairment in performance on several animal cognition tasks including set shifting (Goetghebeur and Dias, 2009; Goetghebeur et al., 2010), novel object recognition (Grayson et al., 2007; Nagai et al., 2009; Neill et al., 2016; Rajagopal et al., 2014), spatial learning (Beraki et al., 2008), 5-choice serial reaction time tasks (Baviera et al., 2008), and latent visuospatial learning and memory (Wang et al., 2007).

Acute administration of FGAs and SGAs reverse the hyperlocomotion induced by acute administration of NMDA antagonists, whereas NMDA antagonist-induced disruption of PPI is blocked by acute administration of SGAs but not FGAs (Geyer et al., 2001; Jentsch and Roth, 1999). Several studies, however, have found that chronic administration of the FGA haloperidol is able to block the NMDA antagonist-induced PPI deficits (Feifel and Priebe, 1999; Martinez et al., 2000). NMDA antagonist-induced hypoglutamatergic models do not seem to be sensitive to drugs with no antipsychotic efficacy and, therefore, they seem to have greater specificity for drugs with antipsychotic efficacy than the animal models that utilize prodopamine drug administration (Pouzet et al., 2005). The neuropeptide oxytocin attenuated PPI deficits induced by an NMDA antagonist in rats as it did with PPI deficits induced by amphetamine (Feifel and Reza, 1999). Oxytocin was later found to improve positive and negative symptoms and cognitive performance in people with schizophrenia (Feifel, 2012; Feifel et al., 2010).

As with animal models based upon prodopamine drug administration, the desire to replicate the chronic nature of the hypoglutamatergia in schizophrenia has motivated the development of pharmacological animal models based upon chronic administration of NMDA antagonists (Mouri et al., 2007). Chronic PCP treatment results in sensitization to the locomotor-activating effects of a challenge dose of PCP (Jentsch and Roth, 1999) analogous to the effects of chronic amphetamine treatment. In some studies, chronic PCP administration produced more enduring social withdrawal and impairments in cognitive performance than single doses of PCP (Mouri et al., 2007). On the other hand, the duration of PPI deficits induced by acute and chronic PCP treatment seem to be comparable (Martinez et al., 1999).

Few studies have investigated effects of antipsychotics on repeated administration of NMDA antagonists, however, acute clozapine administration was found to potentiate PPI deficits induced by 12-days of PCP treatment (Schwabe et al., 2005). Repeated clozapine, seroquel and risperidone, but not haloperidol or olanzapine, blocked PPI deficits in mice subchronically treated with PCP (Li et al., 2011). Neither risperidone nor haloperidol reversed set shifting deficits induced by subchronic PCP (Goetghebeur and Dias, 2009). Both clozapine and risperidone, but not haloperidol, reversed PCP-induced visual learning and memory deficits (Grayson et al., 2007). SGAs were also superior to FGAs at improving social withdrawal behaviors reminiscent of negative symptoms that are induced by repeated injections of PCP in rats, (Sams-Dodd, 1997; Sams-Dodd et al., 1997) while nonantipsychotic drugs were without effect (Sams-Dodd, 1998a).

In conclusion, hypoglutamatergia induced in animals by acute and chronic administration of NMDA antagonists seem to model a wider spectrum of the clinical features of schizophrenia compared to models that induce hyperdopaminergia. Most notably, they induce features that are similar to negative symptoms and cognitive deficits. This model seems to be sensitive to the effects of drugs that have effects beyond D2 antagonism.

4.2 Neurodevelopmental Approach

The neurodevelopment hypothesis of schizophrenia posits that critical pathological perturbations in the brains of people with schizophrenia start well before the clinical onset of the disorder, beginning as early as in-utero or early childhood. For reasons not yet understood, these brain abnormalities give rise to characteristic symptoms in adolescence or early adulthood when brain areas underlying cognitive processing, such as the dorsal lateral prefrontal cortex, are not fully mature (Goldman-Rakic, 1994; Weinberger, 1987). In this regard, exposure to environmental insults during gestation and the perinatal period, including maternal malnutrition, infection and perinatal hypoxia, have been reported to increase the risk for developing schizophrenia (Lewis and Levitt, 2002).

Several efforts have been made to develop animal models of this neurodevelopmental hypothesis. These efforts typically involve inducing a deleterious biological effect, relevant to the known risk factors or pathophysiology of schizophrenia, during an animal's prenatal or perinatal period. Validity for these models is based upon the emergence of schizophrenia-relevant features after the rat reaches puberty. However, the timing of the emergence of many schizophrenia-relevant features, aside from positive and negative symptoms, that are commonly modeled in animals, such as gating deficits,

are not well known and may be congenital. Therefore, developmental models that rely heavily on the latent emergence of these features for validity may in fact lack validity.

4.2.1 The Social Isolation Rearing Model

Rats that are housed in cages by themselves immediately after weaning exhibit abnormalities in behavior relevant to schizophrenia when they are tested as adults (Geyer et al., 1993; Powell et al., 2002; Varty and Higgins, 1995). These abnormalities include locomotor hyperactivity, PPI deficits, and reduced performance on cognitive tasks, such as an object recognition task, T-maze (Li et al., 2007; Millan and Brocco, 2008), reversal (Powell et al., 2015), and probabilistic learning (Amitai et al., 2014). Single injections of both FGAs and SGAs reverse social isolation rearing-induced PPI deficits (Bakshi et al., 1998; Cilia et al., 2001; Geyer et al., 1993; Powell et al., 2002; Varty and Higgins, 1995), whereas several psychotropics that are devoid of antipsychotic efficacy, including the anxiolytics chlordiazepoxide and diazepam as well as the antidepressant amitriptyline, have no effect on PPI deficits (Powell, 2010; Powell et al., 2002) suggesting this animal model responds with good sensitivity and specificity to drugs with antipsychotic efficacy. Chronic administration of clozapine reverses learning deficits in a T-maze in social isolation reared rats (Li et al., 2007). A potential limitation of this model is related to the robustness of the induced deficits. Some studies have found that handing of social isolation reared rats or changes in the bedding of their home cages can eliminate the PPI deficits (Lipska et al., 1995; Powell et al., 2002).

4.2.2 The Methylazoxymethanol Acetate Model

Methylazoxymethanol acetate (MAM) is an antimitotic and proliferative compound toxin that targets neuroblast development (Moore et al., 2006; Penschuck et al., 2006). In the MAM developmental animal model, MAM is administered intraperitoneally to pregnant rats, either during midgestation (embryonic day 9–12) or late gestation (embryonic day 17–18), and through selective disturbance of proliferation and migration of neuronal precursor cells, MAM induces brain morphology and cytology changes in specific brain areas of their offspring (e.g., entorhinal cortices, frontal cortex, and hippocampus) that are similar to those observed in some patients with schizophrenia (Lodge and Grace, 2009). During adolescence, these offspring exhibit some features of schizophrenia including PPI deficits, increased sensitivity to prodopamine and NMDA inhibitory drugs (Moore et al., 2006; Le Pen et al., 2006), as well as schizophrenia-like glutamate transmission abnormalities in the hippocampus (Hradetzky et al., 2012). These offspring also exhibit social interaction deficits and cognitive

impairments including deficits in reversal learning (Le Pen et al., 2006; Moore et al., 2006) and spatial recognition memory (Le Pen et al., 2006). The most robust behavioral effects have been reported after late gestational MAM administration. To date, predictive validity has not been examined in this model.

4.2.3 The Neonatal Ventral Hippocampus Lesion Model

The neonatal ventral hippocampus lesion (NVHL) model is based on the convergent findings of disrupted hippocampus function in many people with schizophrenia (Jaaro-Peled et al., 2010; Whitworth et al., 1998) and is the best characterized neurodevelopmental animal model of schizophrenia (Lipska and Weinberger, 1993, 1994; Lipska et al., 1992, 1993). In this model, ibotenic acid is infused bilaterally into the hippocampus of 7-day old neonatal rats to disrupt hippocampal circuits. Rats prepared this way exhibit many schizophrenia-like features, which emerge during the rats' peripuberty period of development. Specifically, in the prepubertal period, NVHL rats begin to exhibit deficits in social interaction and grooming as well as impaired performance on cognitive tasks, such as those that measure working and spatial memory (Lipska and Weinberger, 2002; Lipska et al., 1993). These deficits are considered analogous to the emergence of negative symptoms and cognitive impairments that are part of a prodromal period before the presentation of full-blown positive symptoms. (Levin and Christopher, 2006; Sams-Dodd et al., 1997). The NVHL rat also exhibits behavioral changes believed to be associated with positive symptoms including locomotor hyperactivity and exaggerated behavioral response to amphetamine and NMDA antagonists as well as deficits in PPI and N40 gating (Lipska and Weinberger, 2000; Swerdlow et al., 2012; Tseng et al., 2009). NVHL rats also have reduced expression of glutamate decarboxylase-67 (GAD67) mRNA consist with reduced GAD67 in the brains of people with schizophrenia (Lipska and Weinberger, 2000).

Single doses of clozapine, risperidone, and olanzapine, but not haloperidol, reverse the hyperlocomotion and PPI deficits in the NVHL model (Le Pen and Moreau, 2002). Chronic (21 days) administration of clozapine and haloperidol reverses the hyperlocomotion, PPI deficits but not the social interaction deficit (Rueter et al., 2004; Sams-Dodd et al., 1997).

Unfortunately, there do not appear to be any reports on testing nonantipsychotic drugs to determine the specificity of this model for drugs with antipsychotic efficacy.

4.3 Genetic Models

Given the strong genetic contribution to schizophrenia and the many genetic variations identified in

people with schizophrenia, there is a strong impetus for developing genetically based animals models of this disorder. Two approaches have been used in the development of genetic animal models of schizophrenia. The first approach has employed genetic engineering to induce abnormalities in the expression of the mouse version of genes that are associated with patients with schizophrenia or that regulate neurotransmitter or other systems that are implicated in the pathophysiology of schizophrenia. The second approach involves identifying strains of rodents or individual rodents among the rodent population who exhibit schizophrenia-like abnormalities.

4.3.1 Models Created by Genetic Engineering

An abundance of genetically engineered mice have been created with the intention of modeling schizophrenia (Powell et al., 2009). Genetic manipulation models fall into two categories: those developed based on pathophysiological hypotheses of schizophrenia and those developed based upon empirically identified candidate genes for the disorder.

An example of the pathophysiology approach based on the dopamine hypothesis of schizophrenia is one in which mice are genetically engineered to lack dopamine transporters. The primary function of this protein is the transport of dopamine from the synaptic cleft back into presynaptic neuron. Reducing the dopamine transporter function increases dopamine in the synaptic cleft and thereby increases dopamine transmission. Mice that have been engineered to lack dopamine transporters (i.e., dopamine transporter knockout mice) exhibit disrupted PPI and increased locomotor activity (Rodriguiz et al., 2004). However, abnormalities in the dopamine transporter have not been identified in schizophrenia patients (Mazzoncini et al., 2009). Furthermore, the PPI deficits in the dopamine transporter mice are reversed by cocaine, methylphenidate, and amphetamine (Yamashita et al., 2006), greatly reducing the validity of this model for schizophrenia.

Of relevance to the glutamate hypothesis of schizophrenia, mice lacking the mGluR5 subtype of glutamate receptors exhibit deficits in PPI and short-term spatial memory. Single dose administration of antipsychotics, raclopride, and clozapine do not attenuate these deficits, whereas chronic clozapine administration mitigates them (Brody et al., 2003; Gray et al., 2009; Kinney et al., 2003). Because these mice seem more sensitive to chronic effects of antipsychotics than to acute effects, they may have the ability to model the time course of the therapeutic effects of antipsychotics. Testing single versus repeated administration of other antipsychotics will be necessary to determine if this notion is correct.

Over the past two decades, linkage and association studies comparing people with schizophrenia and schizophrenia-free people have identified a number of candidate genes (see SCZGENE website http://www.szgene.org/). To better understand the function of these candidate genes and their potential relevance to schizophrenia, investigators have used genetic engineering techniques in mice, which have resulted in either a loss or gain of function of the targeted protein, to assess whether these mice exhibit features associated with schizophrenia. Table 23.3 displays animal models based on some of the most promising susceptibility genes for schizophrenia.

This short list of candidate genes includes disrupted in schizophrenia 1 (DISC1) (Devon et al., 2001; Millar et al., 2001), neuregulin 1 (Stefansson et al., 2002), ERBB4 (Silberberg et al., 2006), dysbindin (Bhardwaj et al., 2009), and reelin (Chen et al., 2002). At this time, genetically engineered mouse models for these candidate genes have not been characterized well enough to determine if any of them would be useful to screen for novel antipsychotics. It will be necessary to test a wider array of antipsychotics for sensitivity and non-antipsychotic psychotropics for selectivity in these models.

While mice exhibiting abnormalities in the expression of schizophrenia candidate genes provide useful tools to better understand the biological role of those genes, including previously unknown roles in regulating specific animal behaviors, such as PPI, locomotor activity, latent inhibition, and social affiliation, they have limitations in regards to their validity as genetic models for schizophrenia since the perturbation of a schizophrenia candidate gene in mice is not likely to replicate the genetic perturbation of the gene that occurs in schizophrenia. The biological impact of any given candidate gene variation identified in schizophrenia is usually not well-known. For example, it is often not known whether the function of a schizophrenia-associated gene is enhanced or reduced (Mazzoncini et al., 2009). Therefore, knocking out a candidate gene in mice, one of the more common genetic engineering approaches used to study candidate genes, will not induce the same biological perturbation that is produced in a person with schizophrenia due to a function-reducing alteration in that candidate gene. For that matter, a knockout of a candidate gene may produce a qualitatively distinct biological impact than the impact of an alteration that reduces, but does not shut-off, the function of that gene in people with schizophrenia. Furthermore, it is almost certain that no single genetic perturbation is responsible for schizophrenia and thus, animal models based on alterations in the expression of a single gene, even if the functional change of that gene in schizophrenia is replicated, are unlikely to reliably model this disorder. Models based on interactions between multiple genetic variations or combinations of genetic and environmental alterations ("two-hit" models)

are potentially a more promising approach to modeling schizophrenia.

4.3.2 Models Based on Inherent Genetic Variation

Animal models have been developed by identifying certain strains of rodents that exhibit schizophrenia-relevant phenotypes or by generating new strains with these characteristics through selective breeding of selected animals from a larger population. The schizophrenia-like phenotypes in these models result from underlying genetic differences between strains, although the specific genetic differences responsible may not have been identified. One of the major strengths of these models is that they obviate the necessity to use an intervention, such as a drug, virus, lesion, or gene knockout to induce the deficits of interest. The complexity of models where a manipulation is required to induce impairments that are then reversed by antipsychotics produce additional variance that can be avoided by using rodents with natural deficits (Crawley et al., 1997). For example, mice strains exhibit a wide range of baseline PPI levels. In this respect, C57BL/6J (Chang et al., 2010; Lipina et al., 2005; Ouagazzal et al., 2001) and DBA/2 mice (Browman et al., 2004; Flood et al., 2011; Zhang et al., 2006) exhibit naturally low levels of PPI compared to other mice strains. These strains have undergone testing with antipsychotic drugs to varying degrees and those that have been tested display varying degrees of predictive validity. C57BL/6j and DBA/2 mice, for example, appear to have reasonably good predictive validity (Olivier et al., 2001; Ouagazzal et al., 2001).

Regarding other phenotypes relevant to modeling schizophrenia, while both C57BL/6j and DBA/2 mice exhibit low PPI, DBA/2 mice exhibit latent inhibition deficits compared to C57BL/6j mice (Singer et al., 2009). The effects of antipsychotics on latent inhibition deficits in DBA/2 mice have not been well-studied.

Strain differences in PPI and latent inhibition have also been reported in rats. Palmer et al. (2000) and Feifel and Priebe (2001) were the first to report naturally occurring PPI deficits in Brown Norway rats and Brattleboro rats, respectively. Furthermore, Brown Norway (Conti et al., 2001; Feifel et al., 2016) and Brattleboro HET rats (Feifel et al., 2015) also exhibit deficits in latent inhibition. The Brattleboro rat has been well-characterized and the behavioral phenotypes exhibited by this rat model, as well as the effects of antipsychotics and nonantipsychotic psychotropics on these impaired behaviors, are discussed in the following section of this chapter. There have been several reports on the effects of antipsychotics in Brown Norway rats. The earliest study found that neither haloperidol nor clozapine attenuated PPI deficits in Brown Norway rats (Conti et al., 2005), whereas a more recent study indicated that PPI in Brown Norway rats was increased by clozapine but not

haloperidol (Feifel et al., 2011b). Furthermore, oxytocin, a neuropeptide that has demonstrated clinical efficacy in patients with schizophrenia (Feifel et al., 2010; Pedersen et al., 2011), increased PPI in Brown Norway rats (Feifel et al., 2012). PD149163, an agonist of the neurotensin-1 receptor and a putative antipsychotic has also increased PPI in this rat strain (Feifel et al., 2011b).

Examples of models based upon selecting individual animals from a large population include apomorphine susceptible (APO-SUS) (Ellenbroek et al., 1995) and low-PPI rats (Schwabe et al., 2007) and mice (Hitzemann et al., 2008). In regards to the APO-SUS model, rats were selected for their response to apomorphine. High responders were used to create a colony of apomorphine susceptible (APO-SUS) rats and low responders were used to create a colony of apomorphine unsusceptible (APO-UNSUS) rats. Compared to APO-UNSUS, APO-SUS rats exhibited deficits in PPI and latent inhibition similar to those exhibited by patients with schizophrenia (Ellenbroek et al., 1995). Unfortunately, it does not appear that predictive validity of this model has been investigated.

Schwabe and coworkers were the first group to report that outbred rats could be selectively bred for PPI differences. PPI deficits in the PPI low group were reversed by haloperidol but not clozapine (Hadamitzky et al., 2007), which is not consistent with the predictive validity of this model. The effects of nonantipsychotic psychotropic drugs on this model have not been reported. Hitzemann et al. (2008) selectively bred low/high PPI mice and found that haloperidol increased PPI in a similar manner in low and high PPI mice. However, they did not test these mice in paradigms relevant to the cognitive or negative deficits seen in schizophrenia.

4.4 The Brattleboro Rat

The Brattleboro (BRAT) rat is a strain of rat derived from a single litter of Long Evans rats born in 1961 in a colony maintained by Dr. Henry Schroeder, a physiologist associated with Dartmouth medical school. It was observed that several pups among a litter displayed severe polydipsia and polyuria. Breeding of those pups produced a colony of rats exhibiting this phenotype and subsequent analysis revealed that the underlying cause of the polydipsia and polyuria was a lack of circulating vasopressin or antidiuretic hormone, due to a frameshift mutation in a single gene that resulted in deficient secretion of vasopressin in response to physiological stimulation (Birkett and Pickering, 1988; Valtin and Schroeder, 1964). The Brattleboro rat is the first natural knockout model in medical research and the forerunner of genetically engineered knockout animals that are widely studied today. As knockouts are almost exclusively created in mice, the Brattleboro rat

is unique in that it is a well-characterized, single gene deficient knockout rat. The Brattleboro rat has become a highly studied animal model for diabetes insipidus, which is the first such animal model for that condition. The polydipsia and polyuria in the Brattleboro rat is due to a lack of activation of the vasopressin-2 (V2) receptors located on the kidney, which stimulates concentration of urine (Bouby et al., 1999). Moreover, vasopressin acts as a neurotransmitter on the other two vasopressin receptor subtypes, V1a and V1b, which are primarily located in the brain (Hurbin et al., 1998), and also has a high affinity for the oxytocin receptor (Tahara et al., 2000). Vasopressin has been found to play an important role in a number of cognitive, emotional, and social functions (Bohus and de Wied, 1998; Reghunandanan et al., 1998) and, not surprisingly, the Brattleboro rat displays abnormalities in several of these domains including memory (Laycock et al., 1983), emotional reactivity (Williams et al., 1985), and social recognition (Engelmann and Landgraf, 1994). Additionally, Jentsch et al. (2003) found that Brattleboro rats displayed a complex pattern of abnormal attention.

Our laboratory has been investigating the Brattleboro rat specifically for potential to serve as a model for psychiatric disorders. We have found that these rats exhibit several features that are homologous or analogous to features observed in schizophrenia and some other neuropsychiatric disorders. For example, Brattleboro rats exhibit baseline PPI that is significantly lower than most strains including the Long Evans rat, their parental strain (Demeter et al., 2016; Feifel and Priebe, 2001; Feifel et al., 2004). This is a finding homologous with PPI deficits in schizophrenia. This is a highly robust and consistent finding that does not dissipate with repeat testing, which facilitates the use of this animal for experiments involving repeated testing on PPI (Feifel et al., 2007), such as investigating the chronic effects of drugs on PPI.

The PPI deficits in the Brattleboro rat appear to be related to their genetic abnormality rather than possible abnormalities in early development since Brattleboro pups removed from their mothers after weaning and raised by Long Evans foster mothers exhibit PPI deficits of similar magnitude to those raised by their biological Brattleboro mothers (Feifel and Priebe, 2007). Similarly, Long Evans pups raised by Brattleboro foster mothers exhibit intact PPI, ruling out the maternal behavior of Brattleboro mothers as a possible contributor to the PPI deficit in their offspring (Feifel and Priebe, 2007). This is consistent with the evidence for a strong genetic contribution and relatively inconsequential contribution of parenting factors to the manifestation of schizophrenia in individuals (Seeman, 2009; Neill, 1990). The onset of PPI deficits in Brattleboro rats can be seen early in

development, prior to puberty, which is consistent with some evidence that low PPI is a feature of schizophrenia that is expressed in childhood well before the manifestation of the overt symptoms of this disorder in early adulthood (Sobin et al., 2005) and thus may represent a vulnerability trait marker. Interestingly, separate lines of V1a and V1b knockout mice have been created and both lines exhibit PPI deficits (Egashira et al., 2009) compared to wild type mice suggesting that a lack of vasopressin activation of both receptors may contribute to the PPI deficits seen in Brattleboro rats.

Brattleboro rats have been shown to display reduced startle habituation (Feifel and Priebe, 2001) and Het-Brattleboro exhibit latent inhibition deficits (Feifel et al., 2015) compared to Long Evans rats, which are two additional features observed in schizophrenia. Brattleboro rats also exhibit increased spontaneous locomotor hyperactivity, which is considered to reflect central hyperdopaminergia and is a rodent analog of positive psychotic symptoms (van den Buuse, 2010); while they also exhibit cognitive-like deficits in novel object recognition (Demeter et al., 2016) and social recognition tasks (Demeter et al., 2016; Feifel et al., 2009), and attention as detected by the five-choice serial reaction time task (Berquist Ii et al., 2013).

Juvenile Brattleboro rats display social deficits as well as stereotypic movements causing some authors to suggest that, in addition to schizophrenia, they may be a valuable model of autism and autism spectrum disorders (Schank, 2009). In this regard, it is noteworthy that recent studies suggest autism spectrum disorders and schizophrenia may have an underlying relationship, which is in sharp contrast to the traditional view that they are distinct (Bevan Jones et al., 2012; Pelletier and Mittal, 2012).

Testing of Brattleboro rats in animal paradigms proposed to have validity for human anxiety and mood disorders, such as the elevated plus maze and the forced swim test, have not revealed evidence that Brattleboro rats have anxiety- and depression-like behaviors. In some cases, lower levels of these behaviors in Brattleboro rats have been found (Mlynarik et al., 2007; Williams et al., 1985). These findings indicate that although Brattleboro rats have a general psychopathology phenotype consistent with multiple psychiatric disorders, they may also represent an animal model with some specificity for schizophrenia and autism.

Brattleboro rats also exhibit certain pathophysiological similarities with schizophrenia. While abnormal VP function has not garnered as much attention as a possible biological mechanism underlying schizophrenia, such as the neurotransmitters dopamine or glutamate, abnormal central VP function has, nevertheless, been a consistent finding among studies that have investigated

this neurochemical system in people with schizophrenia. Several groups have found significantly lower peripheral (Elman et al., 2003; Kishimoto et al., 1989; Legros and Ansseau, 1992) and central (Frederiksen et al., 1991; Linkowski et al., 1984) levels of vasopressin or the vasopressin precursor peptide (Krishnamurthy et al., 2012) in people with schizophrenia. Furthermore, normal stimulation of vasopressin by the direct dopamine agonist, apomorphine, is significantly blunted in people with schizophrenia (Legros et al., 1992). Thus, downregulation of the vasopressin system appears to be a robust physiological abnormality associated with this disorder. Given the well-established role that it plays in cognitive, emotional, and social regulation (Engelmann and Landgraf, 1994; Laycock et al., 1983; Reghunandanan et al., 1998; Williams et al., 1983, 1985), vasopressin dysfunction is a viable mechanistic candidate for at least a subgroup of people with schizophrenia.

The polydipsia and polyuria exhibited by the Brattleboro rat is also analogous to observations of similar behavior in some people with schizophrenia. The association between disturbances in water balance and schizophrenia has been recognized for almost a century (Rowntree, 1973). Disordered water homeostasis is a well-recognized complication of schizophrenia and its prevalence is estimated to be 20% of chronic psychiatric inpatients (de Leon, 2003; de Leon et al., 1994).

In regards to other pathophysiological similarities with schizophrenia, Brattleboro rats have increased density of striatal D2 receptors (Shilling et al., 2006) and dopamine content in the ventral striatal region (Dawson et al., 1990; Feenstra et al., 1990) [but see (Cilia et al., 2010)], which is consistent with findings from several studies of people with schizophrenia (Keshavan et al., 2008). A highly consistent finding in postmortem studies of the brains of people with schizophrenia is reduced levels of GAD67 (Akbarian and Huang, 2006; Akbarian et al., 1995; Volk et al., 2000), an enzyme that catalyzes the decarboxylation of glutamate to GABA. Using a real time reverse polymerase chain reaction (RT-PCR), we have found similar reductions of GAD67 mRNA in the brains of Brattleboro rats (unpublished data). Although there are several brain regions of Brattleboro rats that exhibit abnormal development, the cerebellum is the most prominent (Boer et al., 1982). Cerebellum abnormalities have been reported in people with schizophrenia, including reduced overall volumes and correlations of psychopathological subscores with their cerebellar volume reduction. Evidence from positron emission tomography (PET) and functional magnetic resonance imaging (fMRI) studies has shown decreased activation of the cerebellar subregions at rest and during certain cognitive tasks [see (Yeganeh-Doost et al., 2011) for review].

4.4.1 Heterozygous Brattleboro Rats

Most of the research in Brattleboro rats has focused on rats homozygous for the mutated VP allele. Our laboratory has recently begun to investigate Brattleboro rats that are heterozygous for the mutated allele (Het-Brattleboro). These animals have one normal allele and one mutated allele. Importantly, het-Brattleboros have normal peripheral levels of VP and do not display the polydipsia and polyuria that are seen in homozygous Brattleboro rats (Bohus and de Wied, 1998). Nevertheless, Het-Brattleboro rats have a robust deficiency of PPI (Feifel and Priebe, 2001) and latent inhibition (unpublished results), as do their homozygous counterparts. Het-Brattleboros have also been found to exhibit deficits in tasks modeling working memory in rodents (Aarde and Jentsch, 2004), which is highly relevant for schizophrenia as working memory deficits are a consistent finding among people with this disorder (Goldman-Rakic, 1994; Perry et al., 2001b). The finding that Het-Brattleboros display many of the schizophrenia-like features exhibited by homozygous Brattleboro rats indicates that these schizophrenia-like deficits are not secondary to possible CNS dysfunction caused by wide shifts in tissue hydration due to the abnormal fluid regulation occurring in homozygous Brattleboro rats.

4.4.2 Drug Effects on Brattleboro Rats

Several studies have tested the predictive validity of BRAT rats and most have focused on the effects of antipsychotic drugs on their PPI deficits. Single doses of peripherally (subcutaneous or intraperitoneally) administered FGAs and SGAs reverse the PPI deficits in Brattleboro rats, although there have been some inconsistent findings with single doses of haloperidol (Cilia et al., 2010; Feifel and Priebe, 2001). Repeated administration of FGAs and SGAs produce a greater increase in BRAT rat PPI (Feifel et al., 2007) than a single administration (Feifel et al., 2004, 2007), which indicates that the Brattleboro rat is able to model the efficacy time course of antipsychotic drugs in schizophrenia. Brattleboro rat PPI has also been increased by both single and chronic administration of putative antipsychotics that work via novel mechanisms, such as neurotensin receptor agonists (Feifel et al., 2004, 2007). In contrast, Brattleboro PPI was not significantly affected by a single injection of an antidepressant, an anticonvulsant mood stabilizer or a benzodiazepine (Feifel et al., 2011a), indicating that amelioration of Brattleboro PPI deficits is selective for drugs with antipsychotic efficacy. We have recently begun testing the predictive validity of het-Brattleboro rats and the preliminary results indicate that, like homozygous Brattleboro rats, their PPI deficits are reversed by single and repeated administration of antipsychotics but not psychotropic drugs devoid of antipsychotic efficacy (unpublished results).

References

Aarde, S., Jentsch, J.D., 2004. Heterozygosity for the Brattleboro allele (null mutation of the vasopressin gene) is associated with poor spatial working memory. Soc. Neurosci. Abstr. 35, 911–912.

Abekawa, T., Ito, K., Nakagawa, S., Nakato, Y., Koyama, T., 2008. Olanzapine and risperidone block a high dose of methamphetamine-induced schizophrenia-like behavioral abnormalities and accompanied apoptosis in the medial prefrontal cortex. Schizophr. Res. 101 (1–3), 84–94.

Adler, L.E., Cawthra, E.M., Donovan, K.A., et al., 2005. Improved p50 auditory gating with ondansetron in medicated schizophrenia patients. Am. J. Psychiatry 162 (2), 386–388.

Akbarian, S., Huang, H.S., 2006. Molecular and cellular mechanisms of altered GAD1/GAD67 expression in schizophrenia and related disorders. Brain Res. Rev. 52 (2), 293–304.

Akbarian, S., Kim, J.J., Potkin, S.G., et al., 1995. Gene expression for glutamic acid decarboxylase is reduced without loss of neurons in prefrontal cortex of schizophrenics. Arch. Gen. Psychiatry 52 (4), 258–266.

Allen, N.C., Bagade, S., McQueen, M.B., et al., 2008. Systematic meta-analyses and field synopsis of genetic association studies in schizophrenia: the SzGene database. Nat. Genet. 40 (7), 827–834.

American Psychiatric Association, 2013. Diagnostic and Statistical Manual of Mental Disorders, fifth ed., DSM-5. Washington, DC, American Psychiatric Association.

Amitai, N., Young, J.W., Higa, K., Sharp, R.F., Geyer, M.A., Powell, S.B., 2014. Isolation rearing effects on probabilistic learning and cognitive flexibility in rats. Cogn. Affect Behav. Neurosci. 14 (1), 388–406.

Andersen, M.P., Pouzet, B., 2001. Effects of acute versus chronic treatment with typical or atypical antipsychotics on D-amphetamine-induced sensorimotor gating deficits in rats. Psychopharmacology (Berl.) 156 (2–3), 291–304.

Bakshi, V.P., Geyer, M.A., Taaid, N., Swerdlow, N.R., 1995. A comparison of the effects of amphetamine, strychnine and caffeine on prepulse inhibition and latent inhibition. Behav. Pharmacol. 6 (8), 801–809.

Bakshi, V.P., Swerdlow, N.R., Braff, D.L., Geyer, M.A., 1998. Reversal of isolation rearing-induced deficits in prepulse inhibition by Seroquel and olanzapine. Biol. Psychiatry 43 (6), 436–445.

Barr, A.M., Fish, K.N., Markou, A., Honer, W.G., 2008. Heterozygous reeler mice exhibit alterations in sensorimotor gating but not presynaptic proteins. Eur. J. Neurosci. 27 (10), 2568–2574.

Barros, C.S., Calabrese, B., Chamero, P., et al., 2009. Impaired maturation of dendritic spines without disorganization of cortical cell layers in mice lacking NRG1/ErbB signaling in the central nervous system. Proc. Natl. Acad. Sci. USA 106 (11), 4507–4512.

Baruch, I., Hemsley, D.R., Gray, J.A., 1988. Differential performance of acute and chronic schizophrenics in a latent inhibition task. J. Nerv. Ment. Dis. 176 (10), 598–606.

Baviera, M., Invernizzi, R.W., Carli, M., 2008. Haloperidol and clozapine have dissociable effects in a model of attentional performance deficits induced by blockade of NMDA receptors in the mPFC. Psychopharmacology (Berl.) 196 (2), 269–280.

Beneyto, M., Abbott, A., Hashimoto, T., Lewis, D.A., 2011. Lamina-specific alterations in cortical GABA(A) receptor subunit expression in schizophrenia. Cereb. Cortex 21 (5), 999–1011.

Beraki, S., Kuzmin, A., Tai, F., Ogren, S.O., 2008. Repeated low dose of phencyclidine administration impairs spatial learning in mice: blockade by clozapine but not by haloperidol. Eur. Neuropsychopharmacol. 18 (7), 486–497.

Berquist Ii, M.D., Mooney-Leber, S.M., Feifel, D., Prus, A.J., 2013. Assessment of attention in male and female Brattleboro rats using a self-paced five-choice serial reaction time task. Brain Res. 1537, 174–179.

Bethus, I., Muscat, R., Goodall, G., 2006. Dopamine manipulations limited to preexposure are sufficient to modulate latent inhibition. Behav. Neurosci. 120 (3), 554–562.

Bevan Jones, R., Thapar, A., Lewis, G., Zammit, S., 2012. The association between early autistic traits and psychotic experiences in adolescence. Schizophr. Res. 135 (1–3), 164–169.

Bhardwaj, S.K., Baharnoori, M., Sharif-Askari, B., Kamath, A., Williams, S., Srivastava, L.K., 2009. Behavioral characterization of dysbindin-1 deficient sandy mice. Behav. Brain Res. 197 (2), 435–441.

Bickford-Wimer, P.C., Nagamoto, H., Johnson, R., et al., 1990. Auditory sensory gating in hippocampal neurons: a model system in the rat. Biol. Psychiatry 27 (2), 183–192.

Birkett, S.D., Pickering, B.T., 1988. The vasopressin precursor in the Brattleboro (di/di) rat. Int. J. Pept. Protein Res. 32 (6), 565–572.

Blin, O., 1999. A comparative review of new antipsychotics. Can. J. Psychiatry 44 (3), 235–244.

Boer, G.J., Van Rheenen-Verberg, C.M., Uylings, H.B., 1982. Impaired brain development of the in the diabetes insipidus Brattleboro rat. Brain Res. 255 (4), 557–575.

Bohus, B., de Wied, D., 1998. The vasopressin deficient Brattleboro rats: a natural knockout model used in the search for CNS effects of vasopressin. Prog. Brain Res. 119, 555–573.

Bouby, N., Hassler, C., Bankir, L., 1999. Contribution of vasopressin to progression of chronic renal failure: study in Brattleboro rats. Life Sci. 65 (10), 991–1004.

Braff, D.L., 2010. Prepulse inhibition of the startle reflex: a window on the brain in schizophrenia. Curr. Top Behav. Neurosci. 4, 349–371.

Braff, D.L., Geyer, M.A., 1990. Sensorimotor gating and schizophrenia. Human and animal model studies [see comments]. Arch. Gen. Psychiatry 47 (2), 181–188.

Braff, D.L., Light, G.A., Swerdlow, N.R., 2007. Prepulse inhibition and P50 suppression are both deficient but not correlated in schizophrenia patients. Biol. Psychiatry 61 (10), 1204–1207.

Bringas, M.E., Morales-Medina, J.C., Flores-Vivaldo, Y., et al., 2012. Clozapine administration reverses behavioral, neuronal, and nitric oxide disturbances in the neonatal ventral hippocampus rat. Neuropharmacology 62 (4), 1848–1857.

Brody, S.A., Conquet, F., Geyer, M.A., 2003. Effect of antipsychotic treatment on the prepulse inhibition deficit of mGluR5 knockout mice. Psychopharmacology (Berl.) 172 (2), 187–195.

Brooks, S.P., Pask, T., Jones, L., Dunnett, S.B., 2004. Behavioural profiles of inbred mouse strains used as transgenic backgrounds. I: motor tests. Genes Brain Behav. 3 (4), 206–215.

Browman, K.E., Komater, V.A., Curzon, P., et al., 2004. Enhancement of prepulse inhibition of startle in mice by the H3 receptor antagonists thioperamide and ciproxifan. Behav. Brain Res. 153 (1), 69–76.

Brown, J.W., Rueter, L.E., Zhang, M., 2014. Predictive validity of a MK-801-induced cognitive impairment model in mice: implications on the potential limitations and challenges of modeling cognitive impairment associated with schizophrenia preclinically. Prog. Neuropsychopharmacol. Biol. Psychiatry 49, 53–62.

Bullock, W.M., Cardon, K., Bustillo, J., Roberts, R.C., Perrone-Bizzozero, N.I., 2008. Altered expression of genes involved in GABAergic transmission and neuromodulation of granule cell activity in the cerebellum of schizophrenia patients. Am. J. Psychiatry 165 (12), 1594–1603.

Byne, W., Kemether, E., Jones, L., Haroutunian, V., Davis, K.L., 1999. The neurochemistry of schizophrenia. In: Charney, D.S., Nestler, E.J., Bunney, B.S. (Eds.), Neurobiology of Mental Illness. Oxford University Press, New York, pp. 236–245.

Cadenhead, K.S., 2011. Startle reactivity and prepulse inhibition in prodromal and early psychosis: effects of age, antipsychotics, tobacco and cannabis in a vulnerable population. Psychiatry Res. 188 (2), 208–216.

Cadenhead, K.S., Geyer, M.A., Braff, D.L., 1993. Impaired startle prepulse inhibition and habituation in patients with schizotypal personality disorder. Am. J. Psychiatry 150 (12), 1862–1867.

Carlsson, A., 1977. Does dopamine play a role in schizophrenia? Psychol. Med. 7 (4), 583–597.

Carpenter, W.T., Koenig, J.I., 2008. The evolution of drug development in schizophrenia: past issues and future opportunities. Neuropsychopharmacology 33 (9), 2061–2079.

Cassidy, A.W., Mulvany, S.K., Pangalos, M.N., Murphy, K.J., Regan, C.M., 2010. Developmental emergence of reelin deficits in the prefrontal cortex of Wistar rats reared in social isolation. Neuroscience 166 (2), 377–385.

Castellanos, F.X., Fine, E.J., Kaysen, D., Marsh, W.L., Rapoport, J.L., Hallett, M., 1996. Sensorimotor gating in boys with Tourette's syndrome and ADHD: preliminary results. Biol. Psychiatry 39 (1), 33–41.

Chang, W.L., Geyer, M.A., Buell, M.R., Weber, M., Swerdlow, N.R., 2010. The effects of pramipexole on prepulse inhibition and locomotor activity in C57BL/6J mice. Behav. Pharmacol. 21 (2), 135–143.

Chen, M.L., Chen, S.Y., Huang, C.H., Chen, C.H., 2002. Identification of a single nucleotide polymorphism at the 5' promoter region of human reelin gene and association study with schizophrenia. Mol. Psychiatry 7 (5), 447–448.

Chen, Y.J., Johnson, M.A., Lieberman, M.D., et al., 2008. Type III neuregulin-1 is required for normal sensorimotor gating, memory-related behaviors, and corticostriatal circuit components. J. Neurosci. 28 (27), 6872–6883.

Chen, Y., Bang, S., McMullen, M.F., et al., 2017. Neuronal activity-induced sterol regulatory element binding protein-1 (SREBP1) is disrupted in dysbindin-null mice-potential link to cognitive impairment in schizophrenia. Mol. Neurobiol 54 (3), 1699–1709.

Cilia, J., Reavill, C., Hagan, J.J., Jones, D.N., 2001. Long-term evaluation of isolation-rearing induced prepulse inhibition deficits in rats. Psychopharmacology (Berl.) 156 (2–3), 327–337.

Cilia, J., Gartlon, J.E., Shilliam, C., Dawson, L.A., Moore, S.H., Jones, D.N., 2010. Further neurochemical and behavioural investigation of Brattleboro rats as a putative model of schizophrenia. J. Psychopharmacol. 24 (3), 407–419.

Clapcote, S.J., Lipina, T.V., Millar, J.K., et al., 2007. Behavioral phenotypes of Disc1 missense mutations in mice. Neuron 54 (3), 387–402.

Commissaris, R.L., Harrington, G.M., Baginski, T.J., Altman, H.J., 1988. MR/Har and MNRA/Har Maudsley rat strains: differences in acoustic startle habituation. Behav. Genet. 18 (6), 663–669.

Conti, L.H., Palmer, A.A., Vanella, J.J., Printz, M.P., 2001. Latent inhibition and conditioning in rat strains which show differential prepulse inhibition. Behav. Genet. 31 (3), 325–333.

Conti, L.H., Costill, J.E., Flynn, S., Tayler, J.E., 2005. Effects of a typical and an atypical antipsychotic on the disruption of prepulse inhibition caused by corticotropin-releasing factor and by rat strain. Behav. Neurosci. 119 (4), 1052–1060.

Cooper, M.A., Koleske, A.J., 2014. Ablation of ErbB4 from excitatory neurons leads to reduced dendritic spine density in mouse prefrontal cortex. J. Comp. Neurol. 522 (14), 3351–3362.

Costa, E., Davis, J., Pesold, C., Tueting, P., Guidotti, A., 2002. The heterozygote reeler mouse as a model for the development of a new generation of antipsychotics. Curr. Opin. Pharmacol. 2 (1), 56–62.

Coyle, J.T., Tsai, G., Goff, D., 2003. Converging evidence of NMDA receptor hypofunction in the pathophysiology of schizophrenia. Ann. NY Acad. Sci. 1003, 318–327.

Crawley, J.N., Belknap, J.K., Collins, A., et al., 1997. Behavioral phenotypes of inbred mouse strains: implications and recommendations for molecular studies. Psychopharmacology 132 (2), 107–124.

Dawson, Jr., R., Wallace, D.R., King, M.J., 1990. Monoamine and amino acid content in brain regions of Brattleboro rats. Neurochem. Res. 15 (7), 755–761.

de Leon, J., 2003. Polydipsia—a study in a long-term psychiatric unit. Eur. Arch. Psychiatry Clin. Neurosci. 253 (1), 37–39.

de Leon, J., Verghese, C., Tracy, J.I., Josiassen, R.C., Simpson, G.M., 1994. Polydipsia and water intoxication in psychiatric patients: a review of the epidemiological literature. Biol. Psychiatry 35 (6), 408–419.

Demeter, K., Torok, B., Fodor, A., et al., 2016. Possible contribution of epigenetic changes in the development of schizophrenia-like behavior in vasopressin-deficient Brattleboro rats. Behav. Brain Res. 300, 123–134.

Devon, R.S., Anderson, S., Teague, P.W., et al., 2001. Identification of polymorphisms within Disrupted in Schizophrenia 1 and Disrupted in Schizophrenia 2, and an investigation of their association with schizophrenia and bipolar affective disorder. Psychiatr. Genet. 11 (2), 71–78.

Didriksen, M., Kreilgaard, M., Arnt, J., 2006. Sertindole, in contrast to clozapine and olanzapine, does not disrupt water maze performance after acute or chronic treatment. Eur. J. Pharmacol. 542 (1–3), 108–115.

Egashira, N., Mishima, K., Iwasaki, K., Oishi, R., Fujiwara, M., 2009. New topics in vasopressin receptors and approach to novel drugs: role of the vasopressin receptor in psychological and cognitive functions. J. Pharmacol. Sci. 109 (1), 44–49.

Egerton, A., Reid, L., McKerchar, C.E., Morris, B.J., Pratt, J.A., 2005. Impairment in perceptual attentional set-shifting following PCP administration: a rodent model of set-shifting deficits in schizophrenia. Psychopharmacology (Berl.) 179 (1), 77–84.

Ellenbroek, B.A., Geyer, M.A., Cools, A.R., 1995. The behavior of APO-SUS rats in animal models with construct validity for schizophrenia. J. Neurosci. 15 (11), 7604–7611.

Elman, I., Lukas, S., Shoaf, S.E., Rott, D., Adler, C., Breier, A., 2003. Effects of acute metabolic stress on the peripheral vasopressinergic system in schizophrenia. J. Psychopharmacol. 17 (3), 317–323.

Engelmann, M., Landgraf, R., 1994. Microdialysis administration of vasopressin into the septum improves social recognition in Brattleboro rats. Physiol. Behav. 55 (1), 145–149.

Featherstone, R.E., Kapur, S., Fletcher, P.J., 2007. The amphetamine-induced sensitized state as a model of schizophrenia. Prog. Neuropsychopharmacol. Biol. Psychiatry 31 (8), 1556–1571.

Feenstra, M.G., Snijdewint, F.G., Van Galen, H., Boer, G.J., 1990. Widespread alterations in central noradrenaline, dopamine, and serotonin systems in the Brattleboro rat not related to the local absence of vasopressin. Neurochem. Res. 15 (3), 283–288.

Feifel, D., 1999. Individual differences in prepulse inhibition of startle as a measure of individual dopamine function. Behav. Neurosci. 113 (5), 1020–1029.

Feifel, D., 2012. Oxytocin as a potential therapeutic target for schizophrenia and other neuropsychiatric conditions. Neuropsychopharmacology 37 (1), 304–305.

Feifel, D., Priebe, K., 1999. The effects of subchronic haloperidol on intact and dizocilpine-disrupted sensorimotor gating. Psychopharmacology 146 (2), 175–179.

Feifel, D., Priebe, K., 2001. Vasopressin-deficient rats exhibit sensorimotor gating deficits that are reversed by subchronic haloperidol. Biol. Psychiatry 50 (6), 425–433.

Feifel, D., Priebe, K., 2007. The effects of cross-fostering on inherent sensorimotor gating deficits exhibited by Brattleboro rats. J. Gen. Psychol. 134 (2), 173–182.

Feifel, D., Reza, T., 1999. Oxytocin modulates psychotomimetic-induced deficits in sensorimotor gating. Psychopharmacology 141 (1), 93–98.

Feifel, D., Shilling, P.D., 2010. Promise and pitfalls of animal models of schizophrenia. Curr. Psychiatry Rep. 12 (4), 327–334.

Feifel, D., Melendez, G., Shilling, P.D., 2004. Reversal of sensorimotor gating deficits in Brattleboro rats by acute administration of clozapine and a neurotensin agonist, but not haloperidol: a potential predictive model for novel antipsychotic effects. Neuropsychopharmacology 29 (4), 731–738.

Feifel, D., Melendez, G., Priebe, K., Shilling, P.D., 2007. The effects of chronic administration of established and putative antipsychotics on natural prepulse inhibition deficits in Brattleboro rats. Behav. Brain Res. 181 (2), 278–286.

Feifel, D., Mexal, S., Melendez, G., Liu, P.Y., Goldenberg, J.R., Shilling, P.D., 2009. The brattleboro rat displays a natural deficit in social discrimination that is restored by clozapine and a neurotensin analog. Neuropsychopharmacology 34 (8), 2011–2018.

Feifel, D., Macdonald, K., Nguyen, A., et al., 2010. Adjunctive intranasal oxytocin reduces symptoms in schizophrenia patients. Biol. Psychiatry 68 (7), 678–680.

Feifel, D., Shilling, P.D., Melendez, G., 2011a. Further characterization of the predictive validity of the Brattleboro rat model for antipsychotic efficacy. J. Psychopharmacol. 25 (6), 836–841.

Feifel, D., Shilling, P.D., Melendez, G., 2011b. Clozapine and PD149163 elevate prepulse inhibition in Brown Norway rats. Behav. Neurosci. 125 (2), 268–272.

Feifel, D., Shilling, P.D., Belcher, A.M., 2012. The effects of oxytocin and its analog, carbetocin, on genetic deficits in sensorimotor gating. Eur. Neuropsychopharmacol. 22 (5), 374–378.

Feifel, D., Shilling, P.D., Hillman, J., Maisel, M., Winfield, J., Melendez, G., 2015. Peripherally administered oxytocin modulates latent inhibition in a manner consistent with antipsychotic drugs. Behav. Brain Res. 278, 424–428.

Feifel, D., Shilling, P.D., Fazlinejad, A.A., Melendez, G., 2016. Antipsychotic drug-like facilitation of latent inhibition by a brain-penetrating neurotensin-1 receptor agonist. J. Psychopharmacol. 30 (3), 312–317.

Fejgin, K., Safonov, S., Palsson, E., et al., 2007. The atypical antipsychotic, aripiprazole, blocks phencyclidine-induced disruption of prepulse inhibition in mice. Psychopharmacology (Berl.) 191 (2), 377–385.

Feldon, J., Weiner, I., 1991. The latent inhibition model of schizophrenic attention disorder. Haloperidol and sulpiride enhance rats' ability to ignore irrelevant stimuli. Biol. Psychiatry 29 (7), 635–646.

Feng, Y.Q., Zhou, Z.Y., He, X., et al., 2008. Dysbindin deficiency in sandy mice causes reduction of snapin and displays behaviors related to schizophrenia. Schizophr. Res. 106 (2–3), 218–228.

Flood, D.G., Zuvich, E., Marino, M.J., Gasior, M., 2011. Prepulse inhibition of the startle reflex and response to antipsychotic treatments in two outbred mouse strains in comparison to the inbred DBA/2 mouse. Psychopharmacology (Berl.) 215 (3), 441–454.

Frau, R., Orru, M., Fa, M., et al., 2007. Effects of topiramate on the prepulse inhibition of the acoustic startle in rats. Neuropsychopharmacology 32 (2), 320–331.

Frederiksen, S.O., Ekman, R., Gottfries, C.G., Widerlov, E., Jonsson, S., 1991. Reduced concentrations of galanin, arginine vasopressin, neuropeptide Y and peptide YY in the temporal cortex but not in the hypothalamus of brains from schizophrenics. Acta Psychiatr. Scand. 83 (4), 273–277.

Fusar-Poli, P., Howes, O.D., Allen, P., et al., 2011. Abnormal prefrontal activation directly related to pre-synaptic striatal dopamine dysfunction in people at clinical high risk for psychosis. Mol. Psychiatry 16 (1), 67–75.

Gaisler-Salomon, I., Weiner, I., 2003. Systemic administration of MK-801 produces an abnormally persistent latent inhibition which is reversed by clozapine but not haloperidol. Psychopharmacology (Berl.) 166 (4), 333–342.

Geyer, M.A., Markou, A., 1995. Animal models of psychiatric disorders. In: Bloom, F.E., Kupfer, D.J. (Eds.), Psychopharmacology: The Fourth Generation of Progress. Raven Press, New York, pp. 787–798.

Geyer, M.A., Moghaddam, B., 2002. Animal models relevant to schizophrenia disorders. In: Davis, K.L., Charney, D., Coyle, J.T., Nemeroff, C. (Eds.), Neuropsychopharmacology: The Fifth Generation of Progress: American College of Neuropsychopharmacology. Lippincott Williams & Wilkins, Philadelphia, PA, pp. 689–701.

Geyer, M.A., Swerdlow, N.R., Mansbach, R.S., Braff, D.L., 1990. Startle response models of sensorimotor gating and habituation deficits in schizophrenia. Brain Res. Bull. 25 (3), 485–498.

Geyer, M.A., Wilkinson, L.S., Humby, T., Robbins, T.W., 1993. Isolation rearing of rats produces a deficit in prepulse inhibition of acoustic startle similar to that in schizophrenia. Biol. Psychiatry 34 (6), 361–372.

Geyer, M.A., Krebs-Thomson, K., Braff, D.L., Swerdlow, N.R., 2001. Pharmacological studies of prepulse inhibition models of sensorimotor gating deficits in schizophrenia: a decade in review. Psychopharmacology (Berl.) 156 (2–3), 117–154.

Goetghebeur, P., Dias, R., 2009. Comparison of haloperidol, risperidone, sertindole, and modafinil to reverse an attentional set-shifting impairment following subchronic PCP administration in the rat—a back translational study. Psychopharmacology (Berl.) 202 (1–3), 287–293.

Goetghebeur, P.J., Lerdrup, L., Sylvest, A., Dias, R., 2010. Erythropoietin reverses the attentional set-shifting impairment in a rodent schizophrenia disease-like model. Psychopharmacology (Berl.) 212 (4), 635–642.

Goldman-Rakic, P.S., 1994. Working memory dysfunction in schizophrenia. J. Neuropsychiatry Clin. Neurosci. 6 (4), 348–357.

Golub, M.S., Germann, S.L., Lloyd, K.C., 2004. Behavioral characteristics of a nervous system-specific erbB4 knock-out mouse. Behav. Brain Res. 153 (1), 159–170.

Gould, T.J., Wehner, J.M., 1999. Genetic influences on latent inhibition. Behav. Neurosci. 113 (6), 1291–1296.

Gray, N.S., Pilowsky, L.S., Gray, J.A., Kerwin, R.W., 1995. Latent inhibition in drug naive schizophrenics: relationship to duration of illness and dopamine D2 binding using SPET. Schizophr. Res. 17 (1), 95–107.

Gray, L., van den Buuse, M., Scarr, E., Dean, B., Hannan, A.J., 2009. Clozapine reverses schizophrenia-related behaviours in the metabotropic glutamate receptor 5 knockout mouse: association with N-methyl-D-aspartic acid receptor up-regulation. Int. J. Neuropsychopharmacol. 12 (1), 45–60.

Grayson, B., Idris, N.F., Neill, J.C., 2007. Atypical antipsychotics attenuate a sub-chronic PCP-induced cognitive deficit in the novel object recognition task in the rat. Behav. Brain Res. 184 (1), 31–38.

Greenblatt, E.N., Coupet, J., Rauh, E., Szucs-Myers, V.A., 1980. Is dopamine antagonism a requisite of neuroleptic activity? Arch. Int. Pharmacodyn. Ther. 248 (1), 105–119.

Hadamitzky, M., Harich, S., Koch, M., Schwabe, K., 2007. Deficient prepulse inhibition induced by selective breeding of rats can be restored by the dopamine D2 antagonist haloperidol. Behav. Brain Res. 177 (2), 364–367.

Hafner, H., Maurer, K., Ruhrmann, S., et al., 2004. Early detection and secondary prevention of psychosis: facts and visions. Eur. Arch. Psychiatry Clin. Neurosci. 254 (2), 117–128.

Hagan, J.J., Jones, D.N., 2005. Predicting drug efficacy for cognitive deficits in schizophrenia. Schizophr. Bull. 31 (4), 830–853.

Hammer, T.B., Oranje, B., Fagerlund, B., Bro, H., Glenthoj, B.Y., 2011. Stability of prepulse inhibition and habituation of the startle reflex in schizophrenia: a 6-year follow-up study of initially antipsychotic-naive, first-episode schizophrenia patients. Int. J. Neuropsychopharmacol. 14 (7), 913–925.

Harrison, P.J., Law, A.J., 2006. Neuregulin 1 and schizophrenia: genetics, gene expression, and neurobiology. Biol. Psychiatry 60 (2), 132–140.

Hattori, S., Murotani, T., Matsuzaki, S., et al., 2008. Behavioral abnormalities and dopamine reductions in sdy mutant mice with a deletion in Dtnbp1, a susceptibility gene for schizophrenia. Biochem. Biophys. Res. Commun. 373 (2), 298–302.

He, J., Xu, H., Yang, Y., Rajakumar, D., Li, X., Li, X.M., 2006. The effects of chronic administration of quetiapine on the phencyclidine-induced reference memory impairment and decrease of Bcl-XL/Bax ratio in the posterior cingulate cortex in rats. Behav. Brain Res. 168 (2), 236–242.

Hermens, D.F., Lubman, D.I., Ward, P.B., Naismith, S.L., Hickie, I.B., 2009. Amphetamine psychosis: a model for studying the onset and course of psychosis. Med. J. Aust. 190 (4 Suppl.), S22–S25.

Hikida, T., Jaaro-Peled, H., Seshadri, S., et al., 2007. Dominant-negative DISC1 transgenic mice display schizophrenia-associated phenotypes detected by measures translatable to humans. Proc. Natl. Acad. Sci. USA 104 (36), 14501–14506.

Hitzemann, R., Malmanger, B., Belknap, J., Darakjian, P., McWeeney, S., 2008. Short-term selective breeding for high and low prepulse inhibition of the acoustic startle response; pharmacological characterization and QTL mapping in the selected lines. Pharmacol. Biochem. Behav. 90 (4), 525–533.

Howell, K.R., Pillai, A., 2016. Long-term effects of prenatal hypoxia on schizophrenia-like phenotype in heterozygous Reeler mice. Mol. Neurobiol. 53 (5), 3267–3276.

Howes, O.D., Kapur, S., 2009. The dopamine hypothesis of schizophrenia: version III—the final common pathway. Schizophr. Bull. 35 (3), 549–562.

Howes, O.D., Kambeitz, J., Kim, E., et al., 2012. The nature of dopamine dysfunction in schizophrenia and what this means for treatment: meta-analysis of imaging studies. Arch. Gen. Psychiatry.

Hradetzky, E., Sanderson, T.M., Tsang, T.M., et al., 2012. The methylazoxymethanol acetate (MAM-E17) rat model: molecular and functional effects in the hippocampus. Neuropsychopharmacology 37 (2), 364–377.

Hurbin, A., Boissin-Agasse, L., Orcel, H., et al., 1998. The V1a and V1b, but not V2, vasopressin receptor genes are expressed in the supraoptic nucleus of the rat hypothalamus, and the transcripts are essentially colocalized in the vasopressinergic magnocellular neurons. Endocrinology 139 (11), 4701–4707.

Jaaro-Peled, H., 2009. Gene models of schizophrenia: DISC1 mouse models. Prog. Brain Res. 179, 75–86.

Jaaro-Peled, H., Ayhan, Y., Pletnikov, M.V., Sawa, A., 2010. Review of pathological hallmarks of schizophrenia: comparison of genetic models with patients and nongenetic models. Schizophr. Bull. 36 (2), 301–313.

Javitt, D.C., 2010. Glutamatergic theories of schizophrenia. Isr. J. Psychiatry Relat. Sci. 47 (1), 4–16.

Jentsch, J.D., Anzivino, L.A., 2004. A low dose of the alpha2 agonist clonidine ameliorates the visual attention and spatial working memory deficits produced by phencyclidine administration to rats. Psychopharmacology (Berl.) 175 (1), 76–83.

Jentsch, J.D., Roth, R.H., 1999. The neuropsychopharmacology of phencyclidine: from NMDA receptor hypofunction to the dopamine hypothesis of schizophrenia. Neuropsychopharmacology 20 (3), 201–225.

Jentsch, J.D., Arguello, P.A., Anzivino, L.A., 2003. Null mutation of the arginine-vasopressin gene in rats slows attentional engagement and facilitates response accuracy in a lateralized reaction time task. Neuropsychopharmacology 28 (9), 1597–1605.

Jones, C.A., Watson, D.J., Fone, K.C., 2011. Animal models of schizophrenia. Br. J. Pharmacol. 164 (4), 1162–1194.

Kalivas, P.W., Duffy, P., 1993a. Time course of extracellular dopamine and behavioral sensitization to cocaine. I. Dopamine axon terminals. J. Neurosci. 13 (1), 266–275.

Kalivas, P.W., Duffy, P., 1993b. Time course of extracellular dopamine and behavioral sensitization to cocaine. II. Dopamine perikarya. J. Neurosci. 13 (1), 276–284.

Kantrowitz, J.T., Javitt, D.C., 2010. N-methyl-d-aspartate (NMDA) receptor dysfunction or dysregulation: the final common pathway on the road to schizophrenia? Brain Res. Bull. 83 (3–4), 108–121.

Karlsgodt, K.H., Robleto, K., Trantham-Davidson, H., et al., 2011. Reduced dysbindin expression mediates N-methyl-D-aspartate receptor hypofunction and impaired working memory performance. Biol. Psychiatry 69 (1), 28–34.

Keshavan, M.S., Tandon, R., Boutros, N.N., Nasrallah, H.A., 2008. Schizophrenia, "just the facts": what we know in 2008 Part 3: neurobiology. Schizophr. Res. 106 (2–3), 89–107.

Kinney, G.G., Burno, M., Campbell, U.C., et al., 2003. Metabotropic glutamate subtype 5 receptors modulate locomotor activity and sensorimotor gating in rodents. J. Pharmacol. Exp. Ther. 306 (1), 116–123.

Kishimoto, T., Hirai, M., Ohsawa, H., Terada, M., Matsuoka, I., Ikawa, G., 1989. Manners of arginine vasopressin secretion in schizophrenic patients--with reference to the mechanism of water intoxication. Jpn. J. Psychiatry Neurol. 43 (2), 161–169.

Klaning, U., Pedersen, C.B., Mortensen, P.B., Kyvik, K.O., Skytthe, A., 2002. A possible association between the genetic predisposition for dizygotic twinning and schizophrenia. Schizophr. Res. 58 (1), 31–35.

Koike, H., Arguello, P.A., Kvajo, M., Karayiorgou, M., Gogos, J.A., 2006. Disc1 is mutated in the 129S6/SvEv strain and modulates working memory in mice. Proc. Natl. Acad. Sci. USA 103 (10), 3693–3697.

Kreek, M.J., Schlussman, S.D., Reed, B., et al., 2009. Bidirectional translational research: progress in understanding addictive diseases. Neuropharmacology 56 (Suppl. 1), 32–43.

Krishnamurthy, D., Harris, L.W., Levin, Y., et al., 2012. Metabolic, hormonal and stress-related molecular changes in post-mortem pituitary glands from schizophrenia subjects. World J. Biol. Psychiatry 14 (7), 478–479.

Krystal, J.H., Karper, L.P., Seibyl, J.P., et al., 1994. Subanesthetic effects of the noncompetitive NMDA antagonist, ketamine, in humans. Psychotomimetic, perceptual, cognitive, and neuroendocrine responses. Arch. Gen. Psychiatry 51 (3), 199–214.

Kuczenski, R., Segal, D.S., 1999. Sensitization of amphetamine-induced stereotyped behaviors during the acute response. J. Pharmacol. Exp. Ther. 288 (2), 699–709.

Laycock, J.F., Gartside, I.B., Chapman, J.T., 1983. A comparison of the learning abilities of Brattleboro rats with hereditary diabetes insipidus and Long-Evans rats using positively reinforced operant conditioning. Prog. Brain Res. 60, 183–187.

Le Pen, G., Moreau, J.L., 2002. Disruption of prepulse inhibition of startle reflex in a neurodevelopmental model of schizophrenia: reversal by clozapine, olanzapine and risperidone but not by haloperidol. Neuropsychopharmacology 27 (1), 1–11.

Le Pen, G., Gourevitch, R., Hazane, F., Hoareau, C., Jay, T.M., Krebs, M.O., 2006. Peri-pubertal maturation after developmental disturbance: a model for psychosis onset in the rat. Neuroscience 143 (2), 395–405.

Legros, J.J., Ansseau, M., 1992. Neurohypophyseal peptides and psychopathology. Prog. Brain Res. 93, 455–460.

Legros, J.J., Gazzotti, C., Carvelli, T., et al., 1992. Apomorphine stimulation of vasopressin- and oxytocin-neurophysins. Evidence for increased oxytocinergic and decreased vasopressinergic function in schizophrenics. Psychoneuroendocrinology 17 (6), 611–617.

Leumann, L., Feldon, J., Vollenweider, F.X., Ludewig, K., 2002. Effects of typical and atypical antipsychotics on prepulse inhibition and latent inhibition in chronic schizophrenia. Biol. Psychiatry 52 (7), 729–739.

Levin, E.D., Christopher, N.C., 2006. Effects of clozapine on memory function in the rat neonatal hippocampal lesion model of schizophrenia. Prog. Neuropsychopharmacol. Biol. Psychiatry 30 (2), 223–229.

Lewis, D.A., Levitt, P., 2002. Schizophrenia as a disorder of neurodevelopment. Annu. Rev. Neurosci. 25, 409–432.

Lewis, D.A., Lieberman, J.A., 2000. Catching up on schizophrenia: natural history and neurobiology. Neuron 28 (2), 325–334.

Li, N., Wu, X., Li, L., 2007. Chronic administration of clozapine alleviates reversal-learning impairment in isolation-reared rats. Behav. Pharmacol. 18 (2), 135–145.

Li, M., He, E., Volf, N., 2011. Time course of the attenuation effect of repeated antipsychotic treatment on prepulse inhibition disruption induced by repeated phencyclidine treatment. Pharmacol. Biochem. Behav. 98 (4), 559–569.

Linkowski, P., Geenen, V., Kerkhofs, M., Mendlewicz, J., Legros, J.J., 1984. Cerebrospinal fluid neurophysins in affective illness and in schizophrenia. Eur. Arch. Psychiatry Neurol. Sci. 234 (3), 162–165.

Lipina, T., Labrie, V., Weiner, I., Roder, J., 2005. Modulators of the glycine site on NMDA receptors, D-serine and ALX 5407, display

similar beneficial effects to clozapine in mouse models of schizophrenia. Psychopharmacology (Berl.) 179 (1), 54–567.

Lipina, T.V., Niwa, M., Jaaro-Peled, H., et al., 2010. Enhanced dopamine function in DISC1-L100P mutant mice: implications for schizophrenia. Genes Brain Behav. 9 (7), 777–789.

Lipska, B.K., Weinberger, D.R., 1993. Delayed effects of neonatal hippocampal damage on haloperidol-induced catalepsy and apomorphine-induced stereotypic behaviors in the rat. Brain Res. Dev. Brain Res. 75 (2), 213–222.

Lipska, B.K., Weinberger, D.R., 1994. Subchronic treatment with haloperidol and clozapine in rats with neonatal excitotoxic hippocampal damage. Neuropsychopharmacology 10 (3), 199–205.

Lipska, B.K., Weinberger, D.R., 2000. To model a psychiatric disorder in animals: schizophrenia as a reality test. Neuropsychopharmacology 23 (3), 223–239.

Lipska, B.K., Weinberger, D.R., 2002. A neurodevelopmental model of schizophrenia: neonatal disconnection of the hippocampus. Neurotox. Res. 4 (5–6), 469–475.

Lipska, B.K., Jaskiw, G.E., Chrapusta, S., Karoum, F., Weinberger, D.R., 1992. Ibotenic acid lesion of the ventral hippocampus differentially affects dopamine and its metabolites in the nucleus accumbens and prefrontal cortex in the rat. Brain Res. 585 (1–2), 1–6.

Lipska, B.K., Jaskiw, G.E., Weinberger, D.R., 1993. Postpubertal emergence of hyperresponsiveness to stress and to amphetamine after neonatal excitotoxic hippocampal damage: a potential animal model of schizophrenia. Neuropsychopharmacology 9 (1), 67–75.

Lipska, B.K., Swerdlow, N.R., Geyer, M.A., Jaskiw, G.E., Braff, D.L., Weinberger, D.R., 1995. Neonatal excitotoxic hippocampal damage in rats causes post-pubertal changes in prepulse inhibition of startle and its disruption by apomorphine. Psychopharmacology 122 (1), 35–43.

Lodge, D.J., Grace, A.A., 2009. Gestational methylazoxymethanol acetate administration: a developmental disruption model of schizophrenia. Behav. Brain Res. 204 (2), 306–312.

Lubow, R.E., 1965. Latent inhibition: effects of frequency of nonreinforced preexposure of the CS. J. Comp. Physiol. Psychol. 60 (3), 454–457.

Lubow, R.E., Dressler, R., Kaplan, O., 1999. The effects of target and distractor familiarity on visual search in de novo Parkinson's disease patients: latent inhibition and novel pop-out. Neuropsychology 13 (3), 415–423.

Luchins, D., 1975. The dopamine hypothesis of schizophrenia. A critical analysis. Neuropsychobiology 1 (6), 365–378.

Mansbach, R.S., Geyer, M.A., 1989. Effects of phencyclidine and phencyclidine biologs on sensorimotor gating in the rat. Neuropsychopharmacology 2 (4), 299–308.

Marrs, W., Kuperman, J., Avedian, T., Roth, R.H., Jentsch, J.D., 2005. Alpha-2 adrenoceptor activation inhibits phencyclidine-induced deficits of spatial working memory in rats. Neuropsychopharmacology 30 (8), 1500–1510.

Martin, L.F., Freedman, R., 2007. Schizophrenia and the alpha7 nicotinic acetylcholine receptor. Int. Rev. Neurobiol. 78, 225–246.

Martinez, Z.A., Ellison, G.D., Geyer, M.A., Swerdlow, N.R., 1999. Effects of sustained phencyclidine exposure on sensorimotor gating of startle in rats. Neuropsychopharmacology 21 (1), 28–39.

Martinez, Z.A., Oostwegel, J., Geyer, M.A., Ellison, G.D., Swerdlow, N.R., 2000. Early" and "late" effects of sustained haloperidol on apomorphine- and phencyclidine-induced sensorimotor gating deficits. Neuropsychopharmacology 23 (5), 517–527.

Mazzoncini, R., Zoli, M., Tosato, S., Lasalvia, A., Ruggeri, M., 2009. Can the role of genetic factors in schizophrenia be enlightened by studies of candidate gene mutant mice behaviour? World J. Biol. Psychiatry 10 (4 Pt. 3), 778–797.

McGhie, A., Chapman, J., 1961. Disorders of attention and perception in early schizophrenia. Br. J. Med. Psychol. 34, 102–116.

Menesses, A., 2011. Effects of D-amphetamine on short- and long-term memory in spontaneously hypertensive, Wistar-Kyoto and Sprague-Dawley rats. Behav. Brain Res. 216 (1), 472–476.

Millan, M.J., Brocco, M., 2008. Cognitive impairment in schizophrenia: a review of developmental and genetic models, and pro-cognitive profile of the optimised D(3) > D(2) antagonist, S33138. Therapie 63 (3), 187–229.

Millar, J.K., Christie, S., Anderson, S., et al., 2001. Genomic structure and localization within a linkage hotspot of Disrupted in Schizophrenia 1, a gene disrupted by a translocation segregating with schizophrenia. Mol. Psychiatry 6 (2), 173–178.

Miller, C.L., Bickford, P.C., Luntz-Leybman, V., Adler, L.E., Gerhardt, G.A., Freedman, R., 1992. Phencyclidine and auditory sensory gating in the hippocampus of the rat. Neuropharmacology 31 (10), 1041–1048.

Minassian, A., Henry, B.L., Geyer, M.A., Paulus, M.P., Young, J.W., Perry, W., 2010. The quantitative assessment of motor activity in mania and schizophrenia. J. Affect Disord. 120 (1–3), 200–206.

Mlynarik, M., Zelena, D., Bagdy, G., Makara, G.B., Jezova, D., 2007. Signs of attenuated depression-like behavior in vasopressin deficient Brattleboro rats. Horm. Behav. 51 (3), 395–405.

Moore, H., Jentsch, J.D., Ghajarnia, M., Geyer, M.A., Grace, A.A., 2006. A neurobehavioral systems analysis of adult rats exposed to methylazoxymethanol acetate on E17: implications for the neuropathology of schizophrenia. Biol. Psychiatry 60 (3), 253–264.

Moser, P.C., Hitchcock, J.M., Lister, S., Moran, P.M., 2000. The pharmacology of latent inhibition as an animal model of schizophrenia. Brain Res. Brain Res. Rev. 33 (2–3), 275–307.

Mouri, A., Noda, Y., Enomoto, T., Nabeshima, T., 2007. Phencyclidine animal models of schizophrenia: approaches from abnormality of glutamatergic neurotransmission and neurodevelopment. Neurochem. Int. 51 (2–4), 173–184.

Murotani, T., Ishizuka, T., Hattori, S., Hashimoto, R., Matsuzaki, S., Yamatodani, A., 2007. High dopamine turnover in the brains of Sandy mice. Neurosci. Lett. 421 (1), 47–51.

Nagai, T., Murai, R., Matsui, K., et al., 2009. Aripiprazole ameliorates phencyclidine-induced impairment of recognition memory through dopamine D1 and serotonin 5-HT1A receptors. Psychopharmacology (Berl.) 202 (1–3), 315–328.

Nasrallah, H., Tandon, R., Keshavan, M., 2011. Beyond the facts in schizophrenia: closing the gaps in diagnosis, pathophysiology, and treatment. Epidemiol. Psychiatr. Sci. 20 (4), 317–327.

Neill, J., 1990. Whatever became of the schizophrenogenic mother? Am. J. Psychother. 44 (4), 499–505.

Neill, J.C., Grayson, B., Kiss, B., Gyertyan, I., Ferguson, P., Adham, N., 2016. Effects of cariprazine, a novel antipsychotic, on cognitive deficit and negative symptoms in a rodent model of schizophrenia symptomatology. Eur. Neuropsychopharmacol. 26 (1), 3–14.

Niwa, M., Kamiya, A., Murai, R., et al., 2010. Knockdown of DISC1 by in utero gene transfer disturbs postnatal dopaminergic maturation in the frontal cortex and leads to adult behavioral deficits. Neuron 65 (4), 480–489.

Olivier, B., Leahy, C., Mullen, T., et al., 2001. The DBA/2J strain and prepulse inhibition of startle: a model system to test antipsychotics? Psychopharmacology (Berl.) 156 (2–3), 284–290.

Ong, J.C., Brody, S.A., Large, C.H., Geyer, M.A., 2005. An investigation of the efficacy of mood stabilizers in rodent models of prepulse inhibition. J. Pharmacol. Exp. Ther. 315 (3), 1163–1171.

Onstad, S., Skre, I., Torgersen, S., Kringlen, E., 1991. Twin concordance for DSM-III-R schizophrenia. Acta Psychiatr. Scand. 83 (5), 395–401.

O'Tuathaigh, C.M., O'Connor, A.M., O'Sullivan, G.J., et al., 2008. Disruption to social dyadic interactions but not emotional/anxiety-related behaviour in mice with heterozygous 'knockout' of the schizophrenia risk gene neuregulin-1. Prog. Neuropsychopharmacol. Biol. Psychiatry 32 (2), 462–466.

Ouagazzal, A.M., Jenck, F., Moreau, J.L., 2001. Drug-induced potentiation of prepulse inhibition of acoustic startle reflex in mice: a model for detecting antipsychotic activity? Psychopharmacology (Berl.) 156 (2–3), 273–283.

Palmer, A.A., Dulawa, S.C., Mottiwala, A.A., Conti, L.H., Geyer, M.A., Printz, M.P., 2000. Prepulse startle deficit in the brown norway rat: a potential genetic model. Behav. Neurosci. 11 (2), 374–388.

Pedersen, C.A., Gibson, C.M., Rau, S.W., et al., 2011. Intranasal oxytocin reduces psychotic symptoms and improves Theory of Mind and social perception in schizophrenia. Schizophr. Res. 132 (1), 50–53.

Pelletier, A.L., Mittal, V.A., 2012. An autism dimension for schizophrenia in the next Diagnostic and Statistical Manual? Schizophr. Res. 137 (1–3), 269–270.

Penschuck, S., Flagstad, P., Didriksen, M., Leist, M., Michael-Titus, A.T., 2006. Decrease in parvalbumin-expressing neurons in the hippocampus and increased phencyclidine-induced locomotor activity in the rat methylazoxymethanol (MAM) model of schizophrenia. Eur. J. Neurosci. 23 (1), 279–284.

Perry, W., Braff, D.L., 1994. Information-processing deficits and thought disorder in schizophrenia. Am. J. Psychiatry 151 (3), 363–367.

Perry, W., Minassian, A., Feifel, D., Braff, D.L., 2001a. Sensorimotor gating deficits in bipolar disorder patients with acute psychotic mania. Biol. Psychiatry 50 (6), 418–424.

Perry, W., Heaton, R.K., Potterat, E., Roebuck, T., Minassian, A., Braff, D.L., 2001b. Working memory in schizophrenia: transient "online" storage versus executive functioning. Schizophr. Bull. 27 (1), 157–176.

Perry, W., Feifel, D., Minassian, A., Bhattacharjie, I., Braff, D.L., 2002. Information processing deficits in acutely psychotic schizophrenia patients medicated and unmedicated at the time of admission. Am. J. Psychiatry 159 (8), 1375–1381.

Perry, W., Minassian, A., Lopez, B., Maron, L., Lincoln, A., 2007. Sensorimotor gating deficits in adults with autism. Biol. Psychiatry 61 (4), 482–486.

Pilowsky, L.S., Bressan, R.A., Stone, J.M., et al., 2006. First in vivo evidence of an NMDA receptor deficit in medication-free schizophrenic patients. Mol. Psychiatry 11 (2), 118–119.

Potter, D., Summerfelt, A., Gold, J., Buchanan, R.W., 2006. Review of clinical correlates of P50 sensory gating abnormalities in patients with schizophrenia. Schizophr. Bull. 32 (4), 692–700.

Pouzet, B., Andersen, M.P., Hogg, S., 2005. Effects of acute treatment with antidepressant drugs on sensorimotor gating deficits in rats. Psychopharmacology (Berl.) 178 (1), 9–16.

Powell, S.B., 2010. Models of neurodevelopmental abnormalities in schizophrenia. Curr. Top Behav. Neurosci. 4, 435–481.

Powell, S.B., Swerdlow, N.R., Pitcher, L.K., Geyer, M.A., 2002. Isolation rearing-induced deficits in prepulse inhibition and locomotor habituation are not potentiated by water deprivation. Physiol. Behav. 77 (1), 55–64.

Powell, S.B., Zhou, X., Geyer, M.A., 2009. Prepulse inhibition and genetic mouse models of schizophrenia. Behav. Brain Res. 204 (2), 282–294.

Powell, S.B., Khan, A., Young, J.W., et al., 2015. Early adolescent emergence of reversal learning impairments in isolation-reared rats. Dev. Neurosci. 37 (3), 253–262.

Rajagopal, L., Massey, B.W., Huang, M., Oyamada, Y., Meltzer, H.Y., 2014. The novel object recognition test in rodents in relation to cognitive impairment in schizophrenia. Curr. Pharm. Des. 20 (31), 5104–5114.

Rascle, C., Mazas, O., Vaiva, G., et al., 2001. Clinical features of latent inhibition in schizophrenia. Schizophr. Res. 51 (2–3), 149–161.

Reghunandanan, V., Reghunandanan, R., Mahajan, K.K., 1998. Arginine vasopressin as a neurotransmitter in brain. Indian J. Exp. Biol. 36 (7), 635–643.

Rodriguiz, R.M., Chu, R., Caron, M.G., Wetsel, W.C., 2004. Aberrant responses in social interaction of dopamine transporter knockout mice. Behav. Brain Res. 148 (1–2), 185–198.

Rowntree, D.W., 1973. Significance of metabolic disorders in schizophrenia. Lancet 2 (7821), 151.

Roy, K., Murtie, J.C., El-Khodor, B.F., et al., 2007. Loss of erbB signaling in oligodendrocytes alters myelin and dopaminergic function, a potential mechanism for neuropsychiatric disorders. Proc. Natl. Acad. Sci. USA 104 (19), 8131–8136.

Rueter, L.E., Ballard, M.E., Gallagher, K.B., Basso, A.M., Curzon, P., Kohlhaas, K.L., 2004. Chronic low dose risperidone and clozapine alleviate positive but not negative symptoms in the rat neonatal ventral hippocampal lesion model of schizophrenia. Psychopharmacology (Berl.) 176 (3–4), 312–319.

Russig, H., Murphy, C.A., Feldon, J., 2002. Clozapine and haloperidol reinstate latent inhibition following its disruption during amphetamine withdrawal. Neuropsychopharmacology 26 (6), 765–777.

Sams-Dodd, F., 1997. Effect of novel antipsychotic drugs on phencyclidine-induced stereotyped behaviour and social isolation in the rat social interaction test. Behav. Pharmacol. 8 (2–3), 196–215.

Sams-Dodd, F., 1998a. Effects of diazepam, citalopram, methadone, and naloxone on PCP-induced stereotyped behaviour and social isolation in the rat social interaction test. Neurosci. Biobehav. Rev. 23 (2), 287–293.

Sams-Dodd, F., 1998b. A test of the predictive validity of animal models of schizophrenia based on phencyclidine and D-amphetamine. Neuropsychopharmacology 18 (4), 293–304.

Sams-Dodd, F., 1999. Phencyclidine in the social interaction test: an animal model of schizophrenia with face and predictive validity. Rev. Neurosci. 10 (1), 59–90.

Sams-Dodd, F., Lipska, B.K., Weinberger, D.R., 1997. Neonatal lesions of the rat ventral hippocampus result in hyperlocomotion and deficits in social behaviour in adulthood. Psychopharmacology (Berl.) 132 (3), 303–310.

Schank, J.C., 2009. Early locomotor and social effects in vasopressin deficient neonatal rats. Behav. Brain Res. 197 (1), 166–177.

Schwabe, K., Brosda, J., Wegener, N., Koch, M., 2005. Clozapine enhances disruption of prepulse inhibition after sub-chronic dizocilpine- or phencyclidine-treatment in Wistar rats. Pharmacol. Biochem. Behav. 80 (2), 213–219.

Schwabe, K., Freudenberg, F., Koch, M., 2007. Selective breeding of reduced sensorimotor gating in Wistar rats. Behav. Genet. 37 (5), 706–712.

Schwabe, K., Polikashvili, N., Krauss, J.K., 2009. Deficient sensorimotor gating induced by selective breeding in rats is improved by entopeduncular nucleus lesions. Neurobiol. Dis. 34 (2), 351–356.

Sebat, J., Levy, D.L., McCarthy, S.E., 2009. Rare structural variants in schizophrenia: one disorder, multiple mutations; one mutation, multiple disorders. Trends Genet. 25 (12), 528–535.

Seeman, P., 1992. Dopamine receptor sequences. Therapeutic levels of neuroleptics occupy D2 receptors, clozapine occupies D4. Neuropsychopharmacology 7 (4), 261–284.

Seeman, P., 1995. Dopamine receptors: clinical correlates. In: Bloom, F.E., Kupfer, D.J. (Eds.), Psychopharmacology: The Fourth Generation of Progress. Raven Press, NY, NY, pp. 295–302.

Seeman, M.V., 2009. The changing role of mother of the mentally ill: from schizophrenogenic mother to multigenerational caregiver. Psychiatry 72 (3), 284–294.

Segal, D.S., Kuczenski, R., 1992. Repeated cocaine administration induces behavioral sensitization and corresponding decreased extracellular dopamine responses in caudate and accumbens. Brain Res. 577 (2), 351–355.

Segal, D.S., Kuczenski, R., 1997. An escalating dose "binge" model of amphetamine psychosis: behavioral and neurochemical characteristics. J. Neurosci. 17 (7), 2551–2566.

Segal, D.S., Kuczenski, R., 1999. Escalating dose-binge stimulant exposure: relationship between emergent behavioral profile and differential caudate-putamen and nucleus accumbens dopamine responses. Psychopharmacology(Berl.) 142, 182–192.

Segal, D.S., Kuczenski, R., 2006. Human methamphetamine pharmacokinetics simulated in the rat: single daily intravenous administration reveals elements of sensitization and tolerance. Neuropsychopharmacology 31 (5), 941–955.

Segal, D.S., Geyer, M.A., Schuckit, M.A., 1981. Stimulant-induced psychosis: an evaluation of animal methods. Essays Neurochem. Neuropharmacol. 5, 95–129.

Sham, P.C., MacLean, C.J., Kendler, K.S., 1994. A typological model of schizophrenia based on age at onset, sex and familial morbidity. Acta Psychiatr. Scand. 89 (2), 135–141.

Shen, S., Lang, B., Nakamoto, C., et al., 2008. Schizophrenia-related neural and behavioral phenotypes in transgenic mice expressing truncated Disc1. J. Neurosci. 28 (43), 10893–10904.

Shilling, P.D., Kinkead, B., Murray, T., Melendez, G., Nemeroff, C.B., Feifel, D., 2006. Upregulation of striatal dopamine-2 receptors in Brattleboro rats with prepulse inhibition deficits. Biol. Psychiatry 60 (11), 1278–1281.

Sideli, L., Mule, A., La Barbera, D., Murray, R.M., 2012. Do child abuse and maltreatment increase risk of schizophrenia? Psychiatry Investig. 9 (2), 87–99.

Silberberg, G., Darvasi, A., Pinkas-Kramarski, R., Navon, R., 2006. The involvement of ErbB4 with schizophrenia: association and expression studies. Am. J. Med. Genet. B Neuropsychiatr. Genet. 141B (2), 142–148.

Simonyi, A., Serfozo, P., Parker, K.E., Ramsey, A.K., Schachtman, T.R., 2009. Metabotropic glutamate receptor 5 in conditioned taste aversion learning. Neurobiol. Learn. Mem. 92 (3), 460–463.

Simosky, J.K., Stevens, K.E., Adler, L.E., Freedman, R., 2003. Clozapine improves deficient inhibitory auditory processing in DBA/2 mice, via a nicotinic cholinergic mechanism. Psychopharmacology (Berl.) 165 (4), 386–396.

Simosky, J.K., Freedman, R., Stevens, K.E., 2008. Olanzapine improves deficient sensory inhibition in DBA/2 mice. Brain Res. 1233, 129–136.

Singer, P., Feldon, J., Yee, B.K., 2009. Are DBA/2 mice associated with schizophrenia-like endophenotypes? A behavioural contrast with C57BL/6 mice. Psychopharmacology (Berl.) 206 (4), 677–698.

Smith, S.E., Li, J., Garbett, K., Mirnics, K., Patterson, P.H., 2007. Maternal immune activation alters fetal brain development through interleukin-6. J. Neurosci. 27 (40), 10695–10702.

Snigdha, S., Idris, N., Grayson, B., Shahid, M., Neill, J.C., 2011. Asenapine improves phencyclidine-induced object recognition deficits in the rat: evidence for engagement of a dopamine D1 receptor mechanism. Psychopharmacology (Berl.) 214 (4), 843–853.

Sobin, C., Kiley-Brabeck, K., Karayiorgou, M., 2005. Lower prepulse inhibition in children with the 22q11 deletion syndrome. Am. J. Psychiatry 162 (6), 1090–1099.

Stefansson, H., Sigurdsson, E., Steinthorsdottir, V., et al., 2002. Neuregulin 1 and susceptibility to schizophrenia. Am. J. Hum. Genet. 71 (4), 877–892.

Stevens, K.E., Fuller, L.L., Rose, G.M., 1991. Dopaminergic and noradrenergic modulation of amphetamine-induced changes in auditory gating. Brain Res. 555 (1), 91–98.

Stevens, K.E., Johnson, R.G., Rose, G.M., 1997. Rats reared in social isolation show schizophrenia-like changes in auditory gating. Pharmacol. Biochem. Behav. 58 (4), 1031–1036.

Stevens, K.E., Nagamoto, H., Johnson, R.G., Adams, C.E., Rose, G.M., 1998. Kainic acid lesions in adult rats as a model of schizophrenia: changes in auditory information processing. Neuroscience 82 (3), 701–708.

Su, L., Cai, Y., Wang, L., Shi, S., 2012. Various effects of antipsychotics on p50 sensory gating in Chinese schizophrenia patients: a meta-analysis. Psychiatr. Danub. 24 (1), 44–50.

Swerdlow, N.R., Geyer, M.A., 1998. Using an animal model of deficient sensorimotor gating to study the pathophysiology and new treatments of schizophrenia. Schizophr. Bull. 24 (2), 285–301.

Swerdlow, N.R., Braff, D.L., Geyer, M.A., Koob, G.F., 1986. Central dopamine hyperactivity in rats mimics abnormal acoustic startle response in schizophrenics. Biol. Psychiatry 21 (1), 23–33.

Swerdlow, N.R., Benbow, C.H., Zisook, S., Geyer, M.A., Braff, D.L., 1993. A preliminary assessment of sensorimotor gating in patients with obsessive compulsive disorder. Biol. Psychiatry 33 (4), 298–301.

Swerdlow, N.R., Braff, D.L., Taaid, N., Geyer, M.A., 1994. Assessing the validity of an animal model of deficient sensorimotor gating in schizophrenic patients. Arch. Gen. Psychiatry 51 (2), 139–154.

Swerdlow, N.R., Paulsen, J., Braff, D.L., Butters, N., Geyer, M.A., Swenson, M.R., 1995. Impaired prepulse inhibition of acoustic and tactile startle response in patients with Huntington's disease. J. Neurol. Neurosurg. Psychiatry 58 (2), 192–200.

Swerdlow, N.R., Braff, D.L., Hartston, H., Perry, W., Geyer, M.A., 1996. Latent inhibition in schizophrenia. Schizophr. Res. 20 (1–2), 91–103.

Swerdlow, N.R., Varty, G.B., Geyer, M.A., 1998. Discrepant findings of clozapine effects on prepulse inhibition of startle: is it the route or the rat? Neuropsychopharmacology 18 (1), 50–56.

Swerdlow, N.R., Hartston, H.J., Hartman, P.L., 1999. Enhanced visual latent inhibition in obsessive-compulsive disorder. Biol. Psychiatry 45 (4), 482–488.

Swerdlow, N.R., Geyer, M.A., Braff, D.L., 2001. Neural circuit regulation of prepulse inhibition of startle in the rat: current knowledge and future challenges. Psychopharmacology (Berl.) 156 (2–3), 194–215.

Swerdlow, N.R., Geyer, M.A., Shoemaker, J.M., et al., 2006. Convergence and divergence in the neurochemical regulation of prepulse inhibition of startle and N40 suppression in rats. Neuropsychopharmacology 31 (3), 506–515.

Swerdlow, N.R., Light, G.A., Breier, M.R., et al., 2012. Sensory and sensorimotor gating deficits after neonatal ventral hippocampal lesions in rats. Dev. Neurosci. 34 (2–3), 240–249.

Szekeres, G., Pavics, L., Janka, Z., 2002. [Investigation of the dopamine dysregulation hypothesis of schizophrenia with neuroimaging techniques]. Ideggyogy. Sz. 55 (7–8), 226–232.

Tahara, A., Tsukada, J., Tomura, Y., et al., 2000. Pharmacologic characterization of the oxytocin receptor in human uterine smooth muscle cells. Br. J. Pharmacol. 129 (1), 131–139.

Takao, K., Toyama, K., Nakanishi, K., et al., 2008. Impaired long-term memory retention and working memory in sdy mutant mice with a deletion in Dtnbp1, a susceptibility gene for schizophrenia. Mol. Brain 1, 11.

Tamminga, C.A., 1997. The promise of new drugs for schizophrenia treatment [see comments]. Can. J. Psychiatry 42 (3), 265–273.

Tamminga, C.A., 2003. The science of antipsychotics: mechanistic insight. CNS Spectr. 8 (11 Suppl. 2), 5–9.

Tamminga, C.A., Holcomb, H.H., Gao, X.M., Lahti, A.C., 1995. Glutamate pharmacology and the treatment of schizophrenia: current status and future directions. Int. Clin. Psychopharmacol. 10 (4), 29–37.

Tandon, R., Keshavan, M.S., Nasrallah, H.A., 2008. Schizophrenia, "Just the Facts": what we know in 2008 part 1: overview. Schizophr. Res. 100 (1–3), 4–19.

Terranova, J.P., Chabot, C., Barnouin, M.C., et al., 2005. SSR181507, a dopamine D(2) receptor antagonist and 5-HT(1A) receptor agonist, alleviates disturbances of novelty discrimination in a social context in rats, a putative model of selective attention deficit. Psychopharmacology (Berl.) 181 (1), 134–144.

Thornton, J.C., Dawe, S., Lee, C., et al., 1996. Effects of nicotine and amphetamine on latent inhibition in human subjects. Psychopharmacology (Berl.) 127 (2), 164–173.

Tsai, G., Coyle, J.T., 2002. Glutamatergic mechanisms in schizophrenia. Annu. Rev. Pharmacol. Toxicol. 42, 165–179.

Tseng, K.Y., Chambers, R.A., Lipska, B.K., 2009. The neonatal ventral hippocampal lesion as a heuristic neurodevelopmental model of schizophrenia. Behav. Brain Res. 204 (2), 295–305.

Umeda, K., Iritani, S., Fujishiro, H., et al., 2016. Immunohistochemical evaluation of the GABAergic neuronal system in the prefrontal cortex of a DISC1 knockout mouse model of schizophrenia. Synapse 70 (12), 508–518.

Valtin, H., Schroeder, H.A., 1964. Familial hypothalamic diabetes insipidus in rats (Brattleboro strain). Am. J. Physiol. 206, 425–430.

van den Buuse, M., 2010. Modeling the positive symptoms of schizophrenia in genetically modified mice: pharmacology and methodology aspects. Schizophr. Bull. 36 (2), 246–270.

Varty, G.B., Higgins, G.A., 1995. Examination of drug-induced and isolation-induced disruptions of prepulse inhibition as models to screen antipsychotic drugs. Psychopharmacology 122 (1), 15–26.

Volk, D.W., Austin, M.C., Pierri, J.N., Sampson, A.R., Lewis, D.A., 2000. Decreased glutamic acid decarboxylase67 messenger RNA expression in a subset of prefrontal cortical gamma-aminobutyric acid neurons in subjects with schizophrenia. Arch. Gen. Psychiatry 57 (3), 237–245.

Wadenberg, M.L., 2010. Conditioned avoidance response in the development of new antipsychotics. Curr. Pharm. Des. 16 (3), 358–370.

Walsh, T., McClellan, J.M., McCarthy, S.E., et al., 2008. Rare structural variants disrupt multiple genes in neurodevelopmental pathways in schizophrenia. Science 320 (5875), 539–543.

Walter, H., Kammerer, H., Frasch, K., Spitzer, M., Abler, B., 2009. Altered reward functions in patients on atypical antipsychotic medication in line with the revised dopamine hypothesis of schizophrenia. Psychopharmacology (Berl.) 206 (1), 121–132.

Wang, D., Noda, Y., Zhou, Y., Nitta, A., Furukawa, H., Nabeshima, T., 2007. Synergistic effect of combined treatment with risperidone and galantamine on phencyclidine-induced impairment of latent visuospatial learning and memory: role of nAChR activation-dependent increase of dopamine D1 receptor-mediated neurotransmission. Neuropharmacology 53 (3), 379–389.

Weinberger, D.R., 1987. Implications of normal brain development for the pathogenesis of schizophrenia. Arch. Gen. Psychiatry 44 (7), 660–669.

Weiner, I., Lubow, R.E., Feldon, J., 1988. Disruption of latent inhibition by acute administration of low doses of amphetamine. Pharmacol. Biochem. Behav. 30 (4), 871–878.

Weiner, I., Shadach, E., Tarrasch, R., Kidron, R., Feldon, J., 1996. The latent inhibition model of schizophrenia: further validation using the atypical neuroleptic, clozapine. Biol. Psychiatry 40 (9), 834–843.

Whitworth, A.B., Honeder, M., Kremser, C., et al., 1998. Hippocampal volume reduction in male schizophrenic patients. Schizophr. Res. 31 (2–3), 73–81.

Williams, A.R., Carey, R.J., Miller, M., 1983. Behavioral differences between vasopressin-deficient (Brattleboro) and normal Long-Evans rats. Peptides 4 (5), 711–716.

Williams, A.R., Carey, R.J., Miller, M., 1985. Altered emotionality of the vasopressin-deficient Brattleboro rat. Peptides 6 (Suppl. 1), 69–76.

Williams, J.H., Wellman, N.A., Geaney, D.P., Cowen, P.J., Feldon, J., Rawlins, J.N., 1996. Antipsychotic drug effects in a model of schizophrenic attentional disorder: a randomized controlled trial of the effects of haloperidol on latent inhibition in healthy people. Biol. Psychiatry 40 (11), 1135–1143.

Willner, P., 1997. The dopamine hypothesis of schizophrenia: current status, future prospects. Int. Clin. Psychopharmacol. 12 (6), 297–308.

Woodward, N.D., Purdon, S.E., Meltzer, H.Y., Zald, D.H., 2005. A meta-analysis of neuropsychological change to clozapine, olanzapine, quetiapine, and risperidone in schizophrenia. Int. J. Neuropsychopharmacol. 8 (3), 457–472.

Yamashita, M., Fukushima, S., Shen, H.W., et al., 2006. Norepinephrine transporter blockade can normalize the prepulse inhibition deficits found in dopamine transporter knockout mice. Neuropsychopharmacology 31 (10), 2132–2139.

Yeganeh-Doost, P., Gruber, O., Falkai, P., Schmitt, A., 2011. The role of the cerebellum in schizophrenia: from cognition to molecular pathways. Clinics (Sao Paulo) 66 (Suppl. 1), 71–77.

Young, J., Geyer, M., 2015. Developing treatments for cognitive deficits in schizophrenia: The challenge of translation. J. Psychopharmacol. 29 (2), 178–196.

Young, J.W., Zhou, X., Geyer, M.A., 2010. Animal models of schizophrenia. Curr. Top Behav. Neurosci. 4, 391–433.

Yui, K., Goto, K., Ikemoto, S., et al., 1999. Neurobiological basis of relapse prediction in stimulant-induced psychosis and schizophrenia: the role of sensitization. Mol. Psychiatry 4 (6), 512–523.

Zhang, M., Ballard, M.E., Kohlhaas, K.L., et al., 2006. Effect of dopamine D3 antagonists on PPI in DBA/2J mice or PPI deficit induced by neonatal ventral hippocampal lesions in rats. Neuropsychopharmacology 31 (7), 1382–1392.

Zhang, Q., Yu, Y., Huang, X.F., 2016. Olanzapine Prevents the PCP-induced Reduction in the Neurite Outgrowth of Prefrontal Cortical Neurons via NRG1. Sci. Rep. 6, 19581.

Page left intentionally blank

PART I

GENETICS

Page left intentionally blank

Mouse Models for the Exploration of Klinefelter's Syndrome

Joachim Wistuba*, Cristin Brand*, Steffi Werler*,
Lars Lewejohann**, Oliver S. Damm*

***Institute of Reproductive and Regenerative Biology, Centre of Reproductive Medicine and Andrology,
University Clinics, Münster, Germany**
**University of Münster, Münster, Germany

1 INTRODUCTORY REMARKS

In 1942, a publication appeared reporting on a thus far unknown male disorder in which the patients revealed a combination of small firm testes, azoospermia, gynecomastia, low androgen levels, and elevated FSH. This pathology was described in a cohort of only nine patients. Nevertheless, it was the first definition of the clinical features of the most prevalent male chromosomal disorder, Klinefelter's syndrome (KS), named after the main author of the publication, Harry F. Klinefelter (Klinefelter et al., 1942). Seventeen years later, Jacobs and Strong (1959) revealed an extra X chromosome to be the underlying cause of this syndrome, hence exhibiting a karyotype of 47,XXY. This nonlethal chromosomal aberration, results from meiotic nondisjunction of the sex chromosomes, a segregation failure occurring during the differentiation of the gametes (Lanfranco et al., 2004). The 47,XXY karyotype is the most frequently seen in Klinefelter patients (9 out of 10 cases). The pure lineage is the classical variant, however there are other chromosomal aberrations that are also designated to KS which are either mosaic (e.g., 47,XXY/46,XY or 47,XXY/46,XY/45,X) or men with more than one supernumerary X chromosome (48,XXXY, 49,XXXXY, or 49,XXYY) that generally show more severe phenotypes (Bojesen et al., 2003; Pacenza et al., 2012).

Reviewing the literature of the past 7 decades, almost 4000 articles have been published on KS, a tremendous amount of clinical research describing the endocrine, genetic, metabolic, epidemiological, and behavioral aspects of the disorder (Nieschlag et al., 2014; Sokol, 2012). However, some of the most important questions, in particular the regulatory molecular mechanisms underlying the condition, remain unresolved (Nieschlag et al., 2016). To obtain this crucial knowledge, experimental access and manipulation is required, prerequisites which are practically and ethically impossible when dealing with patients. Understanding germ cell loss, endocrine disturbances or defects in cognitive function on a cellular or even molecular level, therefore needs the availability of animal models (Wistuba, 2010). Sporadically occurring in some mammalian species, males with a supernumerary X chromosome are naturally infertile. Consequently, they are unable to fulfil the most important requirement for an experimental model: the standardized production of a sufficient amount of subjects which would allow experiments to be designed that ensure statistical relevance. Almost 50 years after the discovery of KS, a mutated mouse line, the B6Ei.Lt-Y* strain, was described in which the Y chromosome acquired a new centromere. Following a complex breeding scheme, this strain regularly produces male mice with a supernumerary X chromosome (Eicher et al., 1991) which constitute the basis for the current mouse models of KS. To date, two such mouse models have been successfully established, both mimic human KS and can be expected by an animal model (Wistuba, 2010). In the approximately 25 articles that have appeared which make use of these KS mouse models, many open questions concerning the pathophysiology have been addressed. Apart from the two classical models, others with aberrant sex-chromosomal composition have been used to address more generally the impact of sex-chromosomes and sex-specificity on metabolic aspects (Chen et al., 2013a,b; Link et al., 2015; Ngun et al., 2014). Also these findings were of importance for our understanding of the effects of a supernumerary X-chromosome in the male. As a consequence mechanisms, which were previously only suggested have now been confirmed as regards X-inactivation, Leydig cell hyperplasia, and the putative contribution of X-linked genes on the phenotype (Poplinski et al., 2010; Swerdloff et al., 2011; Werler et al., 2011; Wistuba, 2010; Wistuba et al., 2010). Interestingly, findings from the mouse models, as the surprising fact that intratesticular testosterone (ITT) levels were found normal in 41,XX^{Y*} mice, were confirmed in the meantime in patients (Tüttelmann et al., 2014) as well as the different expression of X-linked genes escaping from silencing (escapees) observed in mice hold also true in patients (Zitzmann et al., 2015). Furthermore, these models have provided

the means to examine features of the KS not possible in a clinical setting, facets, such as the very early onset of germ cell loss, the general cognitive dysfunctions which are linked to the karyotype, and not to social or learning problems as well as the general disturbance in bone metabolism (Lewejohann et al., 2009a; Liu et al., 2010; Lue et al., 2010a; Mroz et al., 1998). "Retranslation" of the design and findings of the investigations utilizing the mouse models was performed that indicated the cognitive phenotype observed in the mice's memory recognition (Lewejohann et al., 2009a) paralleled the learning behavior seen in KS boys. The lessons garnered by this approach were not only useful in providing some understanding of the cognitive failure of young KS patients (Bruining et al., 2011) but also demonstrated how well designed investigations using the mouse models can examine and provide explanations for the clinically observed manifestations of the condition.

The following chapter summarizes the state of the art on animal models for KS and provides some perspectives for further research on the disorder.

2 KLINEFELTER'S SYNDROME—AN UNDERESTIMATED DISEASE

Klinefelter's syndrome consists of a broad spectrum of traits with no homogeneous phenotype or even a subset of features that occurs in every patient. As mentioned in the introductory remarks, KS is the most frequent male chromosomal disorder affecting approximately 0.2% of the male population (an incidence of 1 in 600–1000 new born boys (Aksglaede et al., 2006; Bojesen and Gravholt, 2011a; Bojesen et al., 2011b; Pacenza et al., 2012; Wikström and Dunkel, 2008). Despite this, screening studies indicate that only a quarter of all KS individuals are diagnosed during their lifetime (Bojesen and Gravholt, 2011a; Bojesen et al., 2003). As the main features associated with the syndrome are concealed, the disorder is often diagnosed only late in life, mostly after puberty. Although some aspects are visible in childhood, for example, Klinefelter boys have been found to be taller than matched healthy boys (Aksglaede et al., 2011), due to the heterogeneity and the diversity of the phenotype, a certain proportion of the men with milder forms of the symptoms are not diagnosed at all.

Interestingly, of all the features that are associated with KS, only two are found in almost every adult patient, namely infertility (due to azoospermia and small testes) and the endocrine disturbance of elevated gonadotropins (Aksglaede et al., 2011; Pacenza et al., 2012). In addition, other conditions, such as diabetes, osteoporosis, and various types of cancer (Aguirre et al., 2006; Aizenstein et al., 1997; Sokol, 2012; Swerdlow et al., 2005) have been associated with KS. It is not surprising therefore that the

morbidity and mortality risk for Klinefelter men is increased (Bojesen and Gravholt, 2011a).

Of equal importance are the varying degrees of cognitive impairment which affect language skills and learning behavior. As the condition is normally only diagnosed after puberty, this delay places the boys at a disadvantage as the opportunity to provide effective means of counteracting the impairments is usually missed. Additionally, due to the altered testicular and endocrine conditions, KS boys often suffer from delayed puberty, a factor which might further impair their mental development and can result in social isolation. Because of the socioeconomic trajectories that have been described to be associated with the disorder, a proper diagnosis of KS to the earliest time point possible would be in particular important. There are very few epidemiological studies on KS, almost all are from Denmark due to the excellent health registries which have been set up some decades ago (Aksglaede et al., 2011; Bojesen et al., 2003; Bojesen and Gravholt, 2011a). Significantly, these reports reveal that beyond the repercussions of the syndrome on the individual, the frequency and consequences of KS are greatly underestimated. Bojesen and coworkers evaluated data from more than 1000 KS patients which they matched with more than 100,000 control men. Among other parameters, they examined traits, such as partnership, educational level, income, and age at retirement as well as at mortality. They found that beyond infertility, endocrine and metabolic disturbances, which affected each individual, collectively KS patients presented with a poorer socioeconomic status compared to the control population (Bojesen et al., 2011b). KS men had significantly fewer partnerships, the time point when they entered a relationship was clearly later in life, and they possessed lower educational level, hence received lower income and retired earlier. More importantly, mortality risk in these men was significantly increased. These findings are consistent with those of Stochholm et al. (2012), who examined criminality in KS patients, specifically, the incidence of convictions for various criminal activities (e.g., arson, burglary sexual abuse, and drug related offenses). They found that KS patients did indeed have a higher proportion of convictions significantly though when the data was corrected for socioeconomic state, the differences disappeared indicating that the higher incidence for criminality was related to the poorer socioeconomic conditions the patients face (Stochholm et al., 2012). Such epidemiological analyses are important as they provide insights that cannot be obtained in experimental settings, by the animal models, or clinical reviews of patients. They expose the hitherto hidden effects of KS, which extend beyond the physical features of the condition and contribute to the lower quality of life experienced by these men. Taking into account the importance of early intervention for the circumvention

of many of the consequences identified by the epidemiological studies, the need for screening approaches capable of early diagnosis is obvious and there are ongoing attempts to provide simple, cheap, and—if possible—noninvasive tests (Hager et al., 2012; Mehta et al., 2012, 2014; Werler and Wistuba, 2014). If successfully implemented, these screenings may provide some therapeutic interventions and opportunities; however, for the development of novel and effective therapeutic options, which tackle the root consequences of the condition, a deeper understanding of the specific mechanisms by which the sex chromosomal imbalance instigates the detrimental milieu is needed.

In the following sections, we will examine what the X chromosome does in the male, what a supernumerary X chromosome means, and what clinical features associated with the disorder are caused in individual patients and the corollary of these features which animal models can help us to understand and to ideally solve.

3 THE X CHROMOSOME IN THE MALE

3.1 Sex Chromosomal Balance and Gender

In most animal species, sex is determined by an X chromosome to autosome ratio (X:autosome) usually of 0.5. In mammals, however, it is the presence of a Y chromosome that is the primary signal for male sexual determination, making mammalian sexual development more complex. For example, X0 containing fruit flies become male whereas mammals with the same X0 chromosomal complement are females. In mammals, sexual development is regulated by a cascade of gene expression beginning with the fetal activation of the *sry* (sex-determining region on the Y chromosome) gene which in turn causes the differentiation of the embryonic genital into a testis. The male gonad consists of two compartments: the seminiferous tubules where the somatic Sertoli cells provide nutritive and regulatory support for the spermatogonial stem cells, which constantly renew themselves while giving rise to daughter cells which undergo meiosis and differentiate to mature spermatozoa, and the interstitium responsible for blood supply, immunological responses, and containing the steroidogenic Leydig cells, which produce testosterone needed for normal androgenization and hence the formation of the male endocrine milieu.

Unlike all other chromosomes, only a small section of the Y chromosome (the pseudoautosomal region or PAR), undergoes recombination. Because of this, it has undergone evolutionary degeneration resulting in the loss of most of its functional genes (Hughes et al., 2012). In contrast, due to recombination events during cell division, the X chromosome has acquired new active genes in the course of evolution. Therefore, the heterosomes are

divergent with regard to the number of genes they carry; compared to the X chromosome, the Y chromosome bears only a few genes. As males possess only one copy for numerous X chromosomal genes (Hughes et al., 2012), but gene expression levels are strongly correlated in both males and females, a dosage-compensation has to occur to account for this sex-chromosomal divergence and the loss of genes on the Y chromosome (Dupont and Gribnau, 2013; Gribnau and Grootegoed, 2012). This compensation is achieved via the phenomenon of X chromosome inactivation (XCI) in females, a process which realigns the effective gene dosage and equilibrates the transcription rate in the two sexes.

In order to explain the remarkable impact of the instigation of X-inactivation must have had on the X:autosome ratio in females during chromosomal evolution, Ohno (1967) proposed a two-step process for the evolution of XCI and the dosage-compensation mechanism.

First, the global expression of the X chromosome genes must have doubled in both sexes, hence solving the X:autosome imbalance in males, then the XCI evolved resulting in the reduced output of X-linked genes back to the ancestral levels in females. Some credence to this meaning that the gene dosage X:AA was compensated (i.e. expression from one X chromosome vs expression from two autosomes is balanced to an approximately equal ratio, has been provided by microarray data which revealed the gene expression on the X-chromosome in mammals to be comparable with that expression from the autosomes (Gupta et al., 2006; Lin et al., 2007) and by RNA sequencing, which demonstrated that the expression level from both sex-chromosomes is only half that of the autosomes (Xiong et al., 2010). However, as the possibility cannot be excluded that the expression of testis-specific genes linked to the X chromosome affected these results, even though the purported combination still did not reach the expression level of the autosomes (Deng et al., 2011; Kharchenko et al., 2011), the origins of XCI and the dosage compensation mechanism remain contentious and the focus of ongoing debate (Casci, 2011). What is awaited are technical developments allowing more molecular explorations of the mechanisms of chromosomal regulation which can provide deeper insights into the dosage compensation between heterosomes.

The following section summarizes the current state of our understanding on the process of XCI.

3.2 X-Inactivation

Thus far, all available data indicates that in female cells, one of the two X-chromosomes is inactivated to achieve dosage equilibrium between the sexes (Lyon, 1961). This silencing is established in the early embryo and remains stable throughout life. The process of X-inactivation comprises several distinct steps:

X chromosome counting, the choice which copy is to be inactivated and finally, the initiation and maintenance of the chromosome silencing. An important player in the process is the noncoding RNA of the *Xist* gene. In early embryonic life, this RNA is only expressed from the X-chromosome that will later become inactive (Xi). Once transcribed, *Xist* RNA spreads over the entire chromosome exclusively *in cis*, that is, on the same chromosome on which *Xist* is transcribed. This leads to heterochromatization, the suppression of gene expression and thus chromosomal inactivation. Located within the X chromosome inactivation center (Xic), the *Xist* gene is in close proximity to several of its regulators, required for the initiation of silencing of the X chromosome, but not for the maintenance of the repression of other genes in differentiated cells (Brown and Willard, 1994; Csankovszki et al., 1999). Once *Xist* RNA is spread across the Xi, the transcription machinery becomes excluded from the *Xist* domain forming a repressive compartment (Brown and Willard, 1994; Csankovszki et al., 1999). The recruitment of the so called polycomb repressive complexes PRC1 and PRC2 induces chromosome wide histone modifications on the Xi, which together with other changes affecting the Xi result in a stable inactivation of genes which is subsequently maintained in differentiated cells independent of *Xist* (Plath et al., 2002).

Most but not all genes on the Xi are silenced; some "escape" inactivation and are responsible for the differing expression patterns found in males and females. In humans, approximately 15% of the X-chromosomal genes bypass inactivation, most of which are clustered together, and the majority is located in the pseudoautosomal region 1 of the long arm of the X chromosome (PAR 1 Xq; Carrel and Willard, 2005). Because of their relative high number, analysis of these so called X chromosomal "escapee" genes is highly complex in the human. In contrast, in the mouse only about 3% of the X-linked genes escape inactivation indicating that although inactivation is a general mechanism among mammals, it varies in a species-specific manner with mouse X-inactivation being more stringent than that of humans. Interestingly there is some overlap between species, in that most of the mouse escapee genes are also active in women. However, this is not all embracing as three mouse escapee genes are silent in humans (Yang et al., 2010). Furthermore, in contrast to the human, murine escapee genes are not clustered together and the manner of their escape from X-inactivation may be controlled on the level of individual genes. Recently, it was reported that, although most murine "escapee genes" are distributed along the entire X chromosome, four escapees (*Ddx3x*, *Eif2s3*, *Kdm5c*, and *Cxorf26)* are clustered in small domains with noncoding RNAs (ncRNA) which also escape inactivation. It seems plausible that these ncRNAs either directly or indirectly regulate the activation status of their

surrounding genes (Lopes et al., 2011). In combination, these attributes make the study of murine escapee genes easier than their human counterparts and enables genotype-phenotype correlations to be made which are not possible in the human.

Important factors enabling the escape from silencing are the LINE (long interspersed nuclear elements) repeat elements. On the X chromosome, LINE-1 repeats are overrepresented where it is suggested that they recruit and anchor *Xist* RNA (Chow et al., 2010; Lyon, 1998). As genes escaping from silencing contain fewer LINE-1 repeats than silenced ones (Carrel et al., 2006; Ross et al., 2006), it is likely that LINE-1 repeats are involved in the process.

Histone modifications are also thought to contribute to the silencing mechanisms. Transcriptional repressive marks, such as trimethylation of Lysine 27 on Histone 3 (H3K27me3) and trimethylation of Lysine 9 on histone (H3K9me3) are enriched on the Xi, while the histone variant macroH2A, which renders transcription factors unable to bind DNA sites, is depleted in escapee genes (Changolkar et al., 2010; Goto and Kimura, 2009). H3K4me3 and acetylated H3 and H4 which mark active chromatin portions are lost in the silenced parts of the X chromosome but remain in the escape gene sites (Goto and Kimura, 2009; Jeppesen and Turner, 1993; Khalil and Driscoll, 2007; Marks et al., 2009). It has been also suggested that the insulator protein CTCF, which blocks interactions between enhancers and promoters, may also act as a chromatin barrier, which prevents the spread of heterochromatin structures, thus prevents their spread to the genes that escape inactivation (Filippova, 2008; Goto and Kimura, 2009).

The relative expression of escapee genes from the inactive X-allele has been shown to be lower than their counterparts on the active allele (Carrel and Willard, 2005; Yang et al., 2010). This "partial" silencing may be due to RNA spreading over portions, but not all, of the gene domains thus hampering full expression. Interestingly, there appears to be some sort of "differential escape" mechanism that only functions during certain developmental phases. For example, the murine escapee gene *Kdm5c* escapes X-inactivation in adult tissue but is silenced in embryonic cells (Lingenfelter et al., 1998).

3.3 X-Inactivation in Klinefelter Patients

Whether the clinical features of KS result from the altered endocrine milieu, genetic effects due to altered X-linked gene expression or a combination of both is still a matter of contention. An indicator of whether altered X-chromosomal gene expression could be due to incorrect X-inactivation is the epigenetic status of the affected genes. If the cytosine-guanine rich regions (CpG islands) located in the promoter are methylated to totality (i.e.,

100%), the gene is silenced. In the case of *XIST*, such a methylation profile would show that expression of the gene is lacking and hence the X chromosome remains active. This is the situation observed in healthy males. In healthy females, where one of the two X chromosome remains active, the corresponding profile shows 50% methylation of the *XIST* promoter region. Examining blood samples in KS patients, Poplinski et al. (2010) found the *XIST* methylation pattern to be approximately 50% and comparable to healthy females and correct X-inactivation. In addition, the results also suggest the possible involvement of the Xi escapee genes in the KS phenotype. It is plausible that the enhanced expression of these genes is a normal component of the female cellular environment; however, in the male they constitute an aberration which has detrimental consequences (Nieschlag et al., 2014; Poplinski et al., 2010; Stabile et al., 2008; Zitzmann et al., 2015). Some credence to this proposition is the dosage effect on the extent of cognitive deficit in KS patients where the sequelae of the condition become more severe with increasing numbers of X chromosomes (i.e., 48,XXXY and 49,XXXY; Tüttelmann and Gromoll, 2010).

A further example of the influence of an Xi escapee is the *SHOX* (short stature homeobox) gene, whose increased expression is accommodated in females while in Klinefelter patients it results in increased height. This might be due to the escape of the *SHOX* gene in Klinefelter patients and an increased gene dosage compared to healthy male controls. To truly gauge the influence of genetic factors on KS, more sophisticated and comprehensive investigations need to be undertaken. The breadth of these studies and the amount of material required is only possible with the availability of suitable animal models.

4 CLINICAL FEATURES OF KLINEFELTER'S SYNDROME

The symptoms of this complex condition are so varied that only a fraction of sufferers are actually diagnosed; those with a mild phenotype may go through life never knowing they have the syndrome. The majority of patients that are diagnosed are identified either when they attend an infertility clinic seeking help to fulfil their wish for a child or when asking for the treatment of endocrine or psychological problems (often a combination of both). On rarer occasions, some KS prepubertal or pubertal boys are identified due to the development of social or learning problems. Nevertheless, underdiagnoses remains an issue due to the known increased mortality and morbidity and concerns the clinical community. Therefore, pros and cons of a neonatal screening program are currently intensively debated (Nieschlag et al., 2016).

KS was acknowledged as a disease of sexual development during the International Consensus Conference in 2006 (Hughes et al., 2006; Lee et al., 2006; Pacenza et al., 2012), a recognition that infertility is the feature of KS which is most ubiquitously exhibited. The reason for the infertility of KS patients is the massive loss of germ cells manifesting after puberty. However, beyond its association with disturbed karyotype and sex chromosomal imbalance, little is known about the causative mechanism responsible for the germ cells disappearance.

The presence of a supernumerary X chromosome is the most frequent genetic reason for male infertility, affecting 1 in 600–1000 men (Lanfranco et al., 2004). The detrimental influence of an additional copy(ies) of the X chromosome on male reproductive function is not unexpected when it is taken into account that approximately 10% of this chromosome's genes exhibit testis specific expression (Ross et al., 2006). Some of which are only expressed in spermatogonia, the undifferentiated germ cell type that is most severely affected by the syndrome and the one which is central for the maintenance of a residual germ cell population (Wang et al., 2001).

When the KS testicular phenotype is fully established after puberty, it is manifest not only in the loss of germ cells, but also in serious perturbations of the seminiferous tubules structure. First in the form of hyalinization which with time leads to tubules populated only by Sertoli cells (Sertoli cell only syndrome, SCO) and then finally the testes are composed of "ghost tubules" comprising of extracellular matrix components and Leydig cell hyperplasia (Aksglaede et al., 2006). As most of these features are not pronounced before the onset of puberty, the presence of KS is cloaked until later in life. Unfortunately, in terms of fertility, the time of diagnosis may already be too late, as most, if not all of the germ cells may already be gone (Wikström et al., 2006a).

Despite being the most common feature of KS, it is not uniform in its manifestation, in that, in a proportion of patients a few germ cells survive and differentiate for periods beyond puberty. Microscopic examination of testicular biopsies of KS men have found that in approximately 40% of patient's focal spermatogenesis can be detected (Fullerton et al., 2010). Although overall it is highly unlikely that these small areas with spermatogenic activity would be able to produce sufficient postmeiotic cells needed for a naturally derived pregnancy (Lanfranco et al., 2004), there have been two case reports demonstrating spontaneous paternity in KS (Laron et al., 1982; Terzoli et al., 1992). However, these successes are so few that until recently the perspective for KS patients to father a child seemed hopeless. However, novel methods of assisted reproductive techniques (ART), such as micro testicular sperm extraction (mTESE), revealed a substantial percentage of KS men to exhibit small foci of intact spermatogenesis from which testicular sperm could be harvested in approximately 50% of patients and used to father children by intracytoplasmatic sperm injection (ICSI). The adoption of this combination of techniques: TESE followed by ICSI, then normal IVF culture and finally embryo transfer has resulted in over 100 pregnancies and live births worldwide being reported for KS fathers (Fullerton et al., 2010; Lanfranco et al., 2004).

The second major group of KS patients who by seeking medical attention diagnosed with the syndrome are those with various metabolic or psychological conditions that are determined as being provoked by a disturbed male endocrine milieu. Considering KS's actions on the composition and structure of the testis, it is not surprising that it also detrimentally influences its function as a major endocrine organ. As a consequence, the majority of the adult Klinefelter men are described as having "hypergonadotropic hypogonadism" (Christiansen et al., 2003; De Braekeleer and Dao, 1991; Kamischke et al., 2003; Lanfranco et al., 2004; Nielsen and Wohlert, 1991; Simpson et al., 2003; Yoshida et al., 1997).

When the hypothalamic-pituitary-gonadal (HPG) axis works normally, the levels of androgens (i.e., testosterone) and gonadotropins [luteinizing hormone (LH) and follicle stimulating hormone (FSH)] are highly synchronized by a finely tuned feedback loop. Driven by the hypothalamic pulse generator, gonadotropin releasing hormone (GnRH), the pituitary produces LH and FSH which in turn induce the steroidogenic Leydig cells to produce T in the testis. FSH is necessary for the maintenance of the supportive functions of the Sertoli cells while T and FSH are required for full and complete spermatogenesis to occur. Beyond its testicular function, T is also pivotal for the maintenance of many aspects of the male phenotype, among others: muscle strength, deep voice, hair growth, and bone metabolism.

Hypergonadotropic hypogonadism is defined by lowered androgen levels (although serum T concentrations might be above the lower limit of the normal range) and significantly elevated levels of LH and FSH. To date, it is still contentious whether the endocrine phenotype is cause or consequence of the disturbed testicular situation, that is, whether it is a secondary effect of a dysfunctional gonad, due to sex chromosomal genetics, or a mixture of both. What is not debated is that the endocrine situation in KS influences metabolism and is associated with decreased life expectancy (Bojesen and Gravholt, 2011a; Bojesen et al., 2004, 2006; Swerdlow et al., 2005) due to altered insulin resistance, gynecomastia, and dyslipidemia. Additionally, also the risk for some types of cancer is elevated in 47,XXY patients, for example, non-Hodgkin lymphoma, some extragonadal germ cell tumors, and male breast cancer (Aizenstein et al., 1997; Aguirre et al., 2006; Sokol, 2012; Swerdlow et al., 2005).

Reduced diameters of arteries, cardiovascular problems, such as pulmonary embolism, peripheral vascular diseases, and altered QTc times have also been directly associated with the condition in a substantial proportion of KS men, contributing substantially to the increased morbidity and mortality (Foresta et al., 2012; Jørgensen et al., 2015; Nieschlag et al., 2014; Pasquali et al., 2013). Additionally, very recently, an association between an increased risk for thromboembolism was reported in a Swedish registry study (Zöller et al., 2016). We could recently demonstrate that KS men have increased insulin resistance, enhanced inflammatory, and procoagulatory status, higher waist circumference, clinical dyshomeostasis, and dyslipidemia (Zitzmann et al., 2015). As they possess more active *SHOX* gene copies due to the supernumerary X chromosome, the body proportions of KS men are altered. Specifically, they are taller in stature and as early as the prepubertal period, they have increased fat mass and a negative fat to muscle ratio, which may result in the aforementioned metabolic disturbances (Aksglaede et al., 2006; Kamischke et al., 2003; Lanfranco et al., 2004). These disturbances may in turn provoke lower bone mineral density and the increased risk for osteoporosis (Aksglaede et al., 2008) seen in KS men. However, these complications may also be linked to the enhanced expression of specific genes found on the X chromosome. These features are not present in all KS men; they rather affect only certain proportions of the patient population (Lanfranco et al., 2004; Sokol, 2012). Another novel aspect of KS has been recently reported by Foresta et al., 2012, who found morphological differences in the blood vessels, specifically nonmosaic Klinefelter men had arterial diameters significantly smaller than non-KS men but similar to those found in females. Although these alterations are yet to be verified, they do raise questions as to the possible consequences on the circulation of these patients (Foresta et al., 2012).

The third and only set of clinical indications that lead to the early diagnosis of KS are altered cognitive skills and behavior. Usually identified due the normal mild phenotype becoming manifest in learning problems or mild linguistic impairments around puberty, the severity of these sequelae is increased, up to complete retardation, depending upon the number of additional X chromosomes present (Bruining et al., 2011). X-chromosomal imbalance is known to affect brain function however it remains to be shown whether the cognitive deficits in KS are due to gene expression changes only or are induced or at least enhanced by the disturbed endocrine milieu (Itti et al., 2006; Temple and Sanfilippo, 2003; van Rijn et al., 2006). More details of the cognitive phenotype are discussed later.

5 SEX CHROMOSOMAL ABERRATIONS IN MALE MAMMALS

As mentioned earlier, in mammals, male gender is generally determined by the presence of two activated and different sex chromosomes, a Y and X, which together with the autosomes comprise the normal karyotype. During meiotic division errors, such as disturbed separation can occur which result in chromosomal aberrations forming in the gametes. When these malformed gametes fuse with their counterparts during fertilization, the zygotes formed contain aberrant karyotypes, most of which cause severe damage impairing developmental progression and result in embryonic lethality. Only the few, "mild" perturbations survive into adulthood. In humans the most prominent are trisomy 21 (Down syndrome) and the sex chromosomal aberrations, Turner Syndrome (45,X0), KS in its various forms (i.e., the pure lineage or the more severe variants with more than one supernumerary X chromosome), 46,XX men (where the decisive part of the Y chromosome is translocated to one of the X or an autosome), and 47,XYY syndrome (de la Chapelle, 1972; Hager et al., 2012; Lanfranco et al., 2004; Stochholm et al., 2010; Vorona et al., 2007; Yencilek and Baykal, 2005).

The XXY karyotype is not exclusive to KS humans, in some mammalian species similar sex chromosomal conditions have been reported and all have been found in a variety of animals, for example, experimental animals (e.g., monkeys), domestic pets (dogs, cats), zoo species (tiger), and farm animals (horse, cattle, pig, goat). All of which showed varying degrees of a disturbed male phenotype (Wistuba, 2010).

XXY tomcats were found to have testicular changes similar to the gonadal pathology of humans and also displayed reduced body and facial hair (Centerwall and Benirschke, 1975) and also a "canine Klinefelter syndrome" (karyotype 79,XXY, Nie et al., 1998) has been described. For the latter, mainly the mosaic form of the sex chromosomal aberration was observed; however, there have also been some reports of animals exhibiting the pure lineage. These dogs displayed several features associated with their chromosomal disorder, some of which resembled human KS. In all cases, testicular phenotype was altered and the testes were small, in one animal there was eunuchoidal stature, lowered T and a Sertoli cell tumor, another was found to have a congenital heart disease while a dog with 79,XXY/78XY mosaicism was cryptorchid (Clough et al., 1970; Goldschmidt et al., 2001; Meyers-Wallen, 1993; Reimann-Berg et al., 2008).

The 39,XXY karyotype in boars has been associated with azoospermia, small testes, and a complete loss of germ cells resulting in SCO syndrome. No data on the endocrine state of these animals is available, so it is impossible to discern whether they were also

hypogonadal. However, their testicular interstitium appeared to be normal (Hancock and Daker, 1981; Mäkinen et al., 1998). The first bovine counterpart of KS was described over 30 years ago, a Hereford bull with 61,XXY karyotype who had markedly reduced testes (approximately 10% of the normal size), degenerating tubules containing Sertoli cells only, and Leydig cell hyperplasia (Dunn et al., 1980). Two other bulls (Chianina) with the same karyotype showed similar features: testicular degeneration which was complete at 5 months of age, SCO syndrome, hyalinized tubular walls, and Leydig cell hyperplasia (Molteni et al., 1999). As animals related to these calves were found to be karyotypically and phenotypically normal, the origin of the disorder was attributed to de novo meiotic disjunction failure.

Also for cattle, apart from the classic cytogenetic Giemsa staining methods, more sophisticated sex chromosome painting methods have been developed (Słota et al., 2003) and a Klinefelter bull was one of the first azoospermic animals in which germ cell transplantation was applied in an attempt to experimentally rescue its fertility and determine the feasibility and utility of the technique (Joerg et al., 2003). However, all donor cells transferred into this bull were rejected after a few months and hence no donor-derived spermatogenesis could be induced.

Sex chromosomal abnormalities appear to be more frequent and better tolerated by horses as they comprised more than 90% of all chromosomal disorders (Chowdhary and Raudsepp, 2000). To date there have been at least three published cases of stallions with a pure lineage "KS"-like karyotype of 65,XXY (Iannuzzi et al., 2004; Kubień et al., 1993; Mäkinen et al., 2000). In one, the parental origin was examined but no chromosomal aberrations were found, thus suggesting that a de novo nondisjunction event caused the aberrant karyotype. All stallions were found to be infertile due to azoospermia and in those analyzed histologically, the testes were found to have a disturbed phenotype with Sertoli cells only and degenerating tubules. Two animals were taller than comparative breed and one was reported to have a relatively small penis (Iannuzzi et al., 2004; Mäkinen et al., 2000); features that have been well chronicled in human KS.

Of all the animals identified, one outstanding exotic case deserves mention, namely that of a 13-year-old "Klinefelter" Siberian tiger exhibiting a karyotype of 39,XXY. The chromosomal aberration was detected during a routine health check prior to the animals' registration in a breeding program. When the tiger had to be killed later due to an acute disease, the testicular histology revealed azoospermia and hyalinization typical for the presence of a supernumerary X chromosome (Suedmeyer et al., 2003).

As in humans, in other mammals, mosaic individuals occur presenting a mixture of cell lines containing different karyotypes. Generally, in mosaic humans, the sequelae are less severe. Interestingly, this is not the case in other species. For example, a case report on a male baboon (*Papio hamadryas*) with a 43,XXY/42,XY mosaic karyotype, found no spermatogonia in the testes despite the animal being examined at an early age, that is, 175 days of gestation, the late fetal stage. This is in contrast to human mosaic patients who are those with the best chances of possessing surviving germ cells beyond puberty (Lanfranco et al., 2004; Dudley et al., 2006) and suggests that unlike humans where mosaicism ameliorates the effects of the syndrome, no such action is present in other animals. This becomes particularly clear when examining the effects of sex chromosomal mosaicism in farm animals. Apart from pure XXY karyotypes, mosaic males (XX/XXY or XY/XXY, respectively) have been found in pigs, horses, and cattle, all of whom have exhibited phenotypes akin to pronounced "feminization" (Breeuwsma, 1968; Dain and Bridge, 1978; Iannuzzi et al., 2004; Pinton et al., 2011). Intersexuality and true hermaphroditism have been reported in sex chromosomal mosaic animals, for example, rams (XY/XXY mosaic with ovotestes but male like behavior; Bunch et al., 1991) and goats (XX/XY mosaic with male and female parts of the reproductive tract, a testis and an ovary; Bongso et al., 1982).

Considering the history and importance of domesticated and captive animals to humanity, it is not surprising that they have been studied more intensely and hence provide the bulk of our knowledge regarding the incidence and consequences of male sex chromosomal disorders, which are similar to human KS. The existence and prevalence of the syndrome however is not restricted to these species but a wide spread throughout the animal kingdom. Although admittedly few, there is evidence of these aberrations also in wild species. "KS" like rodents and insectivores have been described (Searle and Jones, 2002). In the shrew family (*Soricidae*), XXY males from two species (*Sorex araneus*, Searle, 1984; *Scuncus murinus*, Rogatcheva et al., 1998) have been found. Interestingly they possessed small testes, absence of germ cells and increased numbers of interstitial cells similar to the testicular phenotype present in other XXY male animals as well as to the features described for the human KS.

Hauffe et al., 2010 characterized wild house mouse populations in which they found two XXY males, who were phenotypically similar to the male mice generated experimentally (see later) and who had small testes devoid of all germ cells. Based on their findings and the data available from the literature, the authors calculated that the XXY karyotype in mice occurs with an incidence that is 5 times lower (0.04%) than that in humans.

Comparing the clinical features of human KS and manifestations seen in the various animal species where a similar sex chromosomal aberration has been found, it is obvious that the condition produces common sequelae. Specifically, a perturbed testicular structure, frequently with Leydig cell hyperplasia (and thus endocrine changes and hampered androgenization), massively impaired spermatogenesis, germ cell loss, and as a consequence, infertility is observed. The impact of supernumerary X chromosome genes that escape X-inactivation thus seem to have the same effect regardless of which male environment they are found.

Because of this commonality in cause and consequence, it is not surprising that most of the publications and case reports mentioned in the preceding section, suggested that the animal they describe could/should serve as the experimental model to study the principles and mechanisms underlying human KS. An experimental model is desperately needed to understand the complexities and difficulties of areas, such as the molecular underpinnings of the condition. However, despite the similarities, none of the cited examples can realistically fulfil the requirements of an experimental animal model for the following reasons:

- All animals reported were infertile.
- In such cases in which the parental generation was examined, the abnormalities were de novo in origin.
- XXY males occurred irregularly and only sporadically in the breedings.

In contrast, an animal model that can be useful for research has to fulfil certain criteria:

- The model animals and their matching controls have to be available (i.e., reproduce) in numbers that are sufficient for the design of experiments which are statistically robust.
- Animals with the target karyotype must be accessible on a regular basis in order to allow experimental designs and endpoints to being planned beforehand.
- Animals have to resemble not only the karyotype but also mirror as many features of the human phenotype as possible.

The main obstacle for the use of the animals previously described as experimental models for human KS is that they were "random" occurrences. Although the observations, descriptions, and analyses of these animals are helpful and interesting, they cannot form the basis for the types of investigation needed to truly understand and elucidate the human syndrome. As the condition is accompanied by infertility, generation of similar animals is unlikely, so the identification of similarly affected animal would depend upon happenstance. It is for this reason that the published information has been limited to descriptive studies of the condition, more systematic investigations of the mechanisms underlying the syndrome using the available examples have been impossible.

6 MOUSE MODELS FOR KLINEFELTER'S SYNDROME

Based on the observation that in many mammalian species, males carrying a supernumerary X chromosome occur and possess similar phenotypes, particularly anomalous testicular structure and function, as human KS, the possibility existed to obtain an animal model. The availability of such an animal would circumvent the limitations of experiments involving patients (e.g., ethical concerns, availability of material) and would provide the chance to investigate in detail pathophysiological consequences of the additional X chromosome.

When techniques for chromosomal manipulation became available, it was a logical extension to use the technique for the generation of chimeric mice for KS research. The concept being that by injecting embryonic stem cells with an extra X-chromosome into mouse blastocysts, the resultant male progeny would have an XXY karyotype. The approach proved to be of limited value, as the male animals born with a supernumerary X chromosome were difficult to obtain and few in number. The "KS"-like males did resemble the desired phenotype (Lue et al., 2001); however, the line could not be maintained as a permanent strain necessitating the constant generation of chimeric females. The XXY males derived from these approaches therefore only constituted a "transient" model, which, for the reasons mentioned previously, were unsuitable for involvement in complex experimental designs.

Twenty-five years ago, a fortuitous and remarkable breakthrough occurred, when male mice from the B6Ei. Lt-Y* strain were found to carry a spontaneous mutation of the Y chromosome (Y* which lost the normal centromere but acquired a new centromere distally; see later). These mice acted as progenitors in a complex, staggered, multigeneration breeding scheme that resulted in offspring with a karyotype containing a supernumerary X and a male phenotype (Eicher et al., 1991; Hunt and Eicher, 1991; Lue et al., 2005). The availability of this mouse line made possible the design and undertaking of more sophisticated experimental approaches, which promised to broaden the scope of investigations into the mechanisms of KS. It is not surprising that, to date, the only two mouse models that have been successfully utilized for animal research on KS have been derived from breedings of this certain strain.

In order to understand the rationale behind the development and research in the mouse models reported in the following paragraphs, one has to keep in mind

the major question arising from translational research, which uses animals to gain insights into human disease. Namely, what does an animal model have to provide in order to serve as an experimental surrogate of KS? For this condition, first of all, males with a supernumerary X chromosome but a full male phenotype must be obtainable on a regular base by a breeding protocol. Second, as we learnt from the clinical appearance of the disorder, such mice must present the whole gamut of features that we know from KS to be associated with the actions of a supernumerary X chromosome in a male environment. This is of importance, because the phenotype observed in patients is complex and reflects the effects of the sex chromosomal imbalance on different systemic levels in the organism. For example, T treatment on a KS adolescent patient might result in improved cognitive performance and may well treat their hypogonadism, but it will concurrently kill the few remaining testicular germ cells that the patient might have.

If such pathophysiological relationships are to be addressed experimentally, the animal model must resemble as many features of the human phenotype as possible so that the metabolic interactions and reactions of the entire organism due to experimental manipulation can be deciphered. So the question posed is which key features should an animal model for KS mimic? From the previously detailed descriptions we know that altered body proportions, an endocrinology of hypergonadotropic hypogonadism, infertility due to azoospermia, small firm testes in which all germ cells are lost after puberty at the latest, the presence of Leydig cell hyperplasia, cognitive deficits, disturbed bone, and/or carbohydrate metabolism are characteristic traits of the syndrome. In addition, considering the recent findings that KS patients have normal X-inactivation, thus raising suspicions that the expression of escapee genes could play a role in the induction of the pathophysiology, the candidate model should have a similar X-inactivation profile.

B6Ei.Lt-Y* males with the mutated Y* chromosome present a completely normal male phenotype (Wistuba, 2010). However, when these mice are mated to normal (40,XX) females, genetically aberrant offspring with a wide variety of differing karyotypes were obtained during subsequent generations. In the progeny, the sex chromosomal content was altered most probably due to the mutated Y* chromosome inducing meiotic non-disjunction because of its structural alterations (Eicher et al., 1991; Hunt and Eicher, 1991; Lue et al., 2005). This Y* chromosome exhibits a rearrangement at the distal part of the short arm and in the pseudoautosomal region where a functional centromere has been newly acquired and the entire region inverted in wide parts. Sex chromosomal recombination, albeit in an aberrant way, was successful in producing offspring that are able to survive. Resulting from the recombination processes,

an X^{Y*} chromosome, in which the X and substantial parts of the Y* are linked in close attachment or a Y^{*X} chromosome is transmitted to the next generation. Female 41 XY^{*X} are fertile while males with the X^{Y*} (41,XX^{Y*}) are sterile. The fertile 41,XY^{*X} females are used as founders for subsequent generations in which, by the fourth generation, the male offspring have a 41,XXY karyotype (Eicher et al., 1991; Wistuba, 2010). Karyotypes regularly derived from the various generations during the staggered breeding of this mouse strain include XXY, XX^{Y*}, XXY^{*Y}, XY^{*Y}, XYY^{*X}, XY^{Y*}, XY^{*X} (Wistuba, 2010).

When this phenomenon was reported in 1991, the importance of these 41,XXY male mice was immediately recognized due to their potential worth for the in depth exploration of KS. Although time consuming, expensive, and difficult via this strategy, for the first time it became possible to obtain sufficient numbers of 41,XXY male mice and matched controls on a regular basis which would enable complex experimental designs. Unfortunately, in these early animal experiments, karyotype could be only determined cytogenetically from dead males, thus making manipulative or behavioral experiments impossible and limiting studies to a descriptive level. Nevertheless, two key criteria for a true animal model were fulfilled: regular production and the access to numbers allowing robust statistical evaluation.

The first investigation showed that physiologically, histologically, and morphologically, the XXY mice had features that resembled the pathophysiology seen in KS patients, giving credence to the idea that a mouse model was now truly available. More specifically, early testis differentiation in XXY male mice followed the normal time course, testicular architecture is morphologically normal containing spermatogonia and showing intact migration, and colonization of the genital ridge by primordial germ cells. These germ cells follow the normal male developmental pathway in the testicular environment. They do not enter a stage of meiotic arrest which would be assumed if X chromosomal reactivation was independent of sex differentiation (Hunt et al., 1998; Mroz et al., 1998, 1999). From postcoital day 12.5, there is a progressive loss of germ cells (Hunt et al., 1998), indicating defects that impair early proliferation driving the mitotic spread (Hunt et al., 1998). Subsequently, germ cell loss continues in the postnatal period of life, resulting in aspermatogenic testis in adulthood with testicular tubules showing predominantly the SCO phenotype (Hunt et al., 1998). Interestingly, when cultured, these testicular cells could not only be maintained and propagated in vitro but also retained their normal morphology. Therefore, it has been suggested that a disturbed interaction between the somatic Sertoli cells and the undifferentiated germ cells might be the cause or at least enhance germ cell depletion in vivo (Hunt et al., 1998; Wang et al., 2001). The spermatogonial stem cells of XXY mice were found

to undergo apoptosis, while stem cells from mosaics (XXY/XY) survived but produced an increased number of aneuploid daughter cells. This indicates that XY germ cells exposed to a XXY testicular environment are subverted to a certain extent, that is, they are at higher risk of meiotic aberrations. This phenomenon suggests meiotic errors may not to be due to the XXY testicular environment alone, but may represent a more general mechanism in testes with reduced germ cell content. Against this background, the role of the Sertoli cells in the synchronous regulatory support was shown to be of equal importance for the germ cell fate in the disturbed testicular phenotype (Mroz et al., 1998). Our recently published data also indicate an early, intrauterine starting point of the germ cell loss. However, at least postnatally we could not confirm an apoptotic cause in vivo but rather found a lack of proliferation of the germ cells (Werler et al., 2014). As a consequence of these results, many questions have been posed and investigative paths opened, all of which rely on this animal model, for example, the elucidation of the interaction between the germ line and the somatic testicular environment by transplantation approaches (Mroz et al., 1999). However, as stated, the limitation posed by the inability to karyotype living animals made it impossible to conduct such studies. Thus, the development and availability of novel methods and tools, which were able to remove this impediment were of tantamount importance. This breakthrough was achieved when Lue et al., 2005, 2010b) developed a fluorescence in situ hybridization (FISH) method for their 41,XXY mouse model of detecting metaphase sex chromosomes from fibroblast cultures derived from tail tip biopsies, while Lewejohann et al. (2009a) used a similar approach utilizing interphase nuclei obtained from peripheral blood samples in the 41,XX^{Y*} mouse.

These methods allowed for the first time, the possibility to identify the "target" animal and thus opening the way for hitherto impossible experimental designs, for example, evaluation of the cognitive functions of the males with a supernumerary X-chromosome (Lewejohann et al., 2009a; Lue et al., 2005). Not surprisingly, this opportunity was readily accepted and a number of new studies were immediately undertaken.

From the earliest investigation of the 41,XXY males, it was recognized that during the breeding scheme another variant male karyotype occurred regularly even in the first generation, the 41,XX^{Y*}. Other than being reported as sterile (Eicher et al., 1991), little attention was paid to these animals. While searching for an animal model for XX male syndrome, these animals were reexamined due to their sex chromosomal constitution of two X and a part of the Y chromosome. As mentioned previously, in the rare 46,XX testicular disorder of sex development, the vast majority (>90%) of patients have two X chromosomes, which contain some Y chromosomal material,

harboring the *SRY* gene, which is essential for male sexual determination and induces the gonadal development during the embryonic life (de la Chapelle, 1972; de la Chapelle et al., 1964, 1990; Hughes et al., 2006; Kashimada and Koopman, 2010; Vorona et al., 2007).

Compared to KS patients, these XX men exhibit some similarity but also differ in certain phenotypical features, such as clinical appearance and epigenetics (Vorona et al., 2007). For example, while KS patients are in general tall, XX men are smaller than average and exhibit a higher incidence of gynecomastia and maldescended testes. The detailed analysis of the 41,XX^{Y*} males found them not to resemble the features of the XX males but rather they had characteristics that were almost identical to those of the 41,XXY mice and symptoms similar to human KS.

These two models (male 41,XXY and the 41,XX^{Y*}) have formed the basis for numerous investigations into the underlying mechanisms that provoke the disturbance of the male phenotype, for example, the endocrine, cognitive, gonadal, and metabolic changes. In the next part, we discuss the findings of these studies in detail and reveal why the male mice with a supernumerary X chromosome from the B6Ei.Lt-Y* strain are the most valid animal models available for KS (Wistuba, 2010).

7 LESSONS FROM ANIMAL EXPERIMENTS

With the availability of the earlier mentioned mice, the initial set of experiments that was conducted set out to establish their bonafides as true models for KS. Therefore, a complete characterization of the animals was the essential first step, before the design or performance of any novel approaches could be considered. Without these investigations research on the animal model would have been restricted to descriptive studies and no deeper insights into cellular and molecular mechanisms of the sex chromosomal imbalance due to the supernumerary X chromosome in a male environment could be gained.

7.1 X-Inactivation in the 41,XX^{Y*} Mouse Model

As noted previously, there are differences in the X-inactivation process between mice and humans. However, the relatively few genes which escape X-inactivation in the mouse make it an interesting model for providing some insights into the genotype-phenotype relation of KS. The caveat being that the X-inactivation process seen in the model reflects the findings obtained from patients, healthy men and women (Poplinski et al., 2010). Only then meaningful conclusions could be derived that would have relevance to the more complex human situation.

In line with the study previously conducted on human Klinefelter patients (Poplinski et al., 2010), the X-inactivation profile in the 41,XX^{Y*} mice was determined in peripheral blood samples by assessing the *Xist* promoter region methylation profile. As expected, female mice were found to possess a *Xist* methylation status of approximately 55% indicating that one of the two X chromosomes was inactive, while male 40,XY* mice had approximately 100% *Xist* methylation, indicative of a silenced *Xist* gene and hence an active X-chromosome. The 41,XX^{Y*} mice were found to possess 57% *Xist* methylation, significantly different from the male controls but consistent with the pattern seen in the healthy female mice (Wistuba et al., 2010). These results confirmed that in the 41,XX^{Y*} mouse, the *Xist* methylation pattern and as a consequence the X chromosomal inactivation status mimicked that seen in human KS patients. Hence, beyond the hormonal, phenotypic, and behavioral, these male mice could also provide comparable insights into the genetic underpinnings of the human condition.

In follow up experiments, genes escaping X-inactivation were analyzed in the animal model. It has been reported that in contrast to the approximately 15% of X-linked genes escaping silencing in the human, only about 13 genes do so in the mouse (Carrel and Willard, 2005). As only four, *Kdm6a*, *Kdm5c*, *Ddx3x*, and *Eif2s3*, are known to escape X-inactivation in both species, these were the most interesting to gauge the suitability of the 41,XX^{Y*} model. *Kdm6a* is a H3K27-demethylase, whose overexpression results in the decreased levels of di-and trimethylation of Lysine 27 on Histone 3 (Hong et al., 2007; Hosey et al., 2010). *Ddx3x*, ubiquitously expressed by all cells of the testis, has an autosomal homolog which has been suggested to play a role in spermatogenesis (Vong et al., 2006). *Eif2s3x* encodes a subunit of eukaryotic translation initiation factor 2. Its expression is coupled to brain function and has a Y-homolog which plays a role in spermatogonial proliferation (Mazeyrat et al., 2001; Xu et al., 2006). Finally, *Kdm5c*, a H3K4 demethylase, is ubiquitously expressed and has been associated with mental retardation (Iwase et al., 2007).

As it has been previously reported that the expression of "escapee genes" can vary among individuals as well as between tissues (Carrel and Willard, 2005), the expression pattern of the four genes was determined in various organs, namely in liver, kidney, and brain tissue.

In the liver and kidney, the mRNA transcript expression pattern in the 41,XX^{Y*} mice resembled that of the female mice and differed from that seen in the healthy males, proving that in both females and the KS model, the genes do escape X-inactivation while in the healthy males they do not (Werler et al., 2011). These findings have been recently corroborated in a study of sex differences in adiposity, which demonstrated that the number of X chromosomes and escapee gene expression may play a role (Chen et al., 2012).

In contrast, the expression pattern in the brains of healthy male (40,XY*) and female (40,XX) animals was similar—indicating that the gene expression in the brain is differently regulated compared to the other tissues—while, in the 41,XX^{Y*} mice, the "escapee genes" were found to be upregulated (Werler et al., 2011). This finding is of particular interest when considering the cognitive deficits observed in the 41,XX^{Y*} and 41,XXY mice and in Klinefelter patients (Bruining et al., 2011; Lewejohann et al., 2009a,b; Lue et al., 2005). So far, there has been no explanation as to whether or how X-linked gene expression in KS can be related to the cognitive phenotype. If, as previously shown, the X-inactivation pattern of KS males is similar to that of normal females yet healthy women do not exhibit cognitive changes. Why should this be the case in KS patients? For the first time, the gene expression data obtained from the 41,XX^{Y*} mouse model sheds some light on a possible mechanism explaining this phenomenon. The upregulation (or the missing downregulation) of these particular genes suggests their possible involvement or even direct contribution to the altered cognitive phenotype observed. For example, variation in the expression of *Kdm5*c has been shown to influence either directly or obliquely the regulation of other genes involved in brain development (Iwase et al., 2007).

We also examined the expression pattern of six more escapee genes (i.e., *Bgn*, *Cxorf26*, *Car5b*, *Mid1*, *Shroom4*, and *1810030O07Rik)* in the liver and brain of the 41,XX^{Y*} mouse. In humans, *Bgn* expression levels are reduced in patients with 45,X Turner Syndrome and elevated in patients with additional sex-chromosomes, such as KS. Interestingly this gene is subject to X-inactivation in humans, and only the murine form escapes inactivation (Geerkens et al., 1995). *Cxorf26* is expressed in most adult brain structures, most prominently in the cerebellum (Lopes et al., 2011). Like *Bgn*, the human ortholog does not escape X-inactivation (Carrel and Willard, 2005). Similarly, the *Mid1* gene, which encodes a protein that forms homodimers which associate with microtubules in the cytoplasm (Cainarca et al., 1999; Dal Zotto et al., 1998; Schweiger et al., 1999). *Shroom4*, a regulator of the cytoskeletal architecture, is associated with Stoco dos Santos like X-linked mental retardation (XLMR), where affected males have severe mental retardation (Hagens et al., 2006; Yoder and Hildebrand, 2007). The functions of *Car5b* and *1810030O07Rik* are thus far not completely assessed.

We found that for all six genes, the mRNA expression in the liver of 41,XX^{Y*} males to be akin to the four escapees previously reported, namely similar to that of the females and higher than in their healthy male littermates (Werler et al., 2011). Interestingly, unlike *Kdm6a*, *Kdm5c*, *Ddx3x*, and *Eif2s3x* for which increased mRNA expression was found in the brain (Werler et al., 2011), *Bgn*, *Cxorf26*, *Car5b*, *Mid1*, *Shroom4*, and *1810030O07Rik*
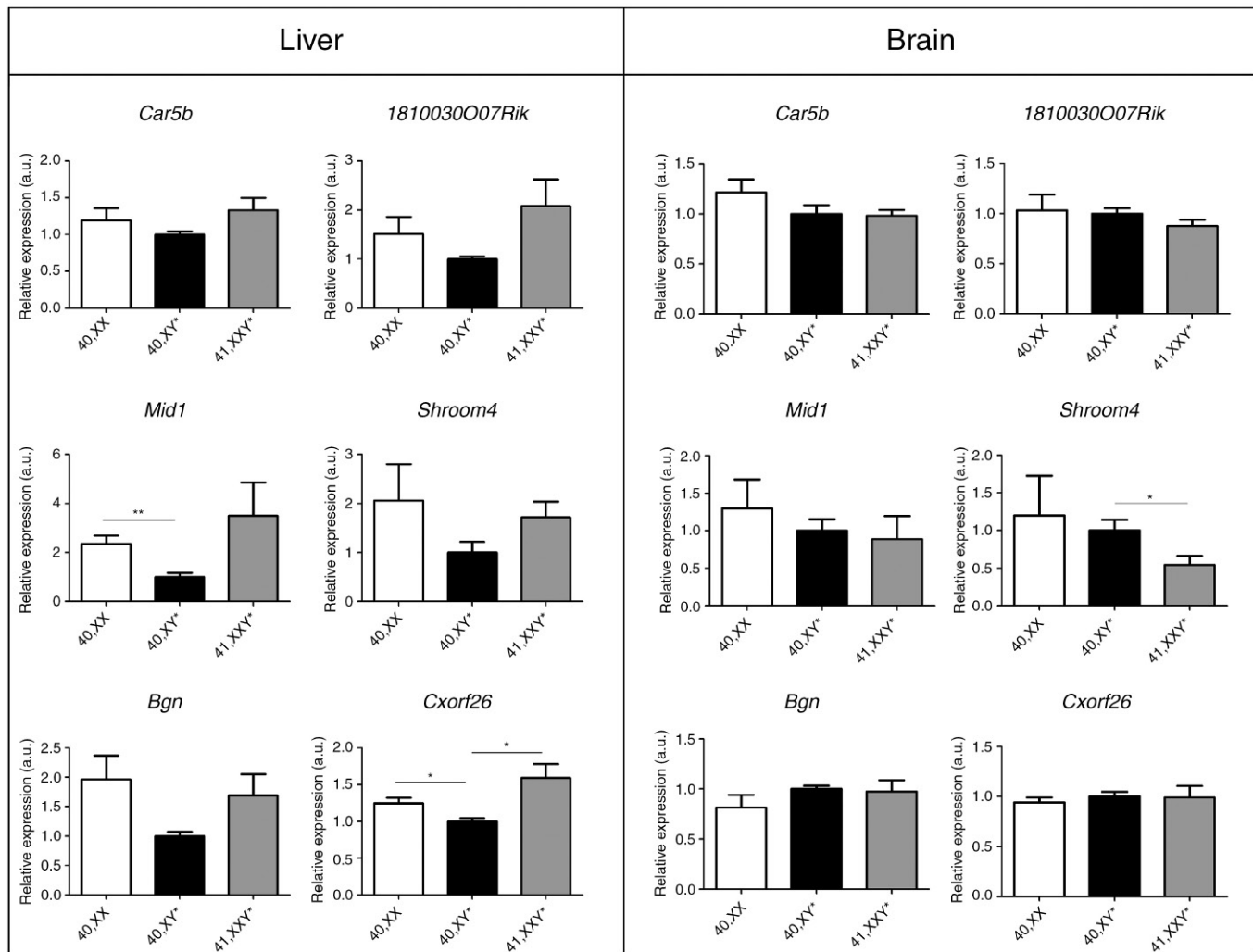
FIGURE 24.1 Relative expression of the genes *Car5b, 1810030O07Rik, Mid1, Shroom4, Bgn,* and *Cxorf26* in liver and brain of 40,XX (*n* = 3); 40,XY* (*n* = 6); and 41,XX^{Y*} (*n* = 6) mice; * *P* < 0.05, ** *P* < 0.001.

expression levels in the 41,XX^{Y*}, healthy males and female littermate controls were similar (Fig. 24.1). These new findings confirm the tissue and gene specificity of the escapee genes and show that the expression pattern is independent of the tissue environment in which the genes are transcribed, that is, in the brain some are over expressed and some are not. When taken overall, the results of the mouse model experiments show that although escapee genes probably contribute to the phenotypical alterations, a general mechanism, such as a simple over expression in the male cellular environment does not exist. In contrast every gene has to be examined independently and with regard to the target organ. These first findings on the genetic background of KS provide tantalizing clues as to the mechanisms causing the manifestations of the condition. Thus far the information available is restricted to the transcription level. To what extent the regulation of these genes' translation into the proteins is affected and if/how this is involved in the

sequelae of the syndrome remains to be clarified. The quest for answers to these questions will be aided by the mouse model which—unlike its human counterparts—presents a more homogeneous population where only 13 genes are affected.

7.2 Testicular Architecture

Lue et al. (2005, 2010a) reported that adult 41,XXY mice had small, firm testes containing SCO tubules of decreased diameter with increased numbers of Leydig cells in the interstitium. These findings are identical to those for the alternative KS model, the 41,XX^{Y*} mouse (Lewejohann et al., 2009a; Wistuba et al., 2010, Fig. 24.2) and resemble perfectly the testicular phenotype seen in the vast majority of adult KS men (Fig. 24.3). Additionally 41,XXY mice displayed an aberrant pattern of androgen receptor (AR) expression, not observed thus far in KS (Lue et al., 2005).
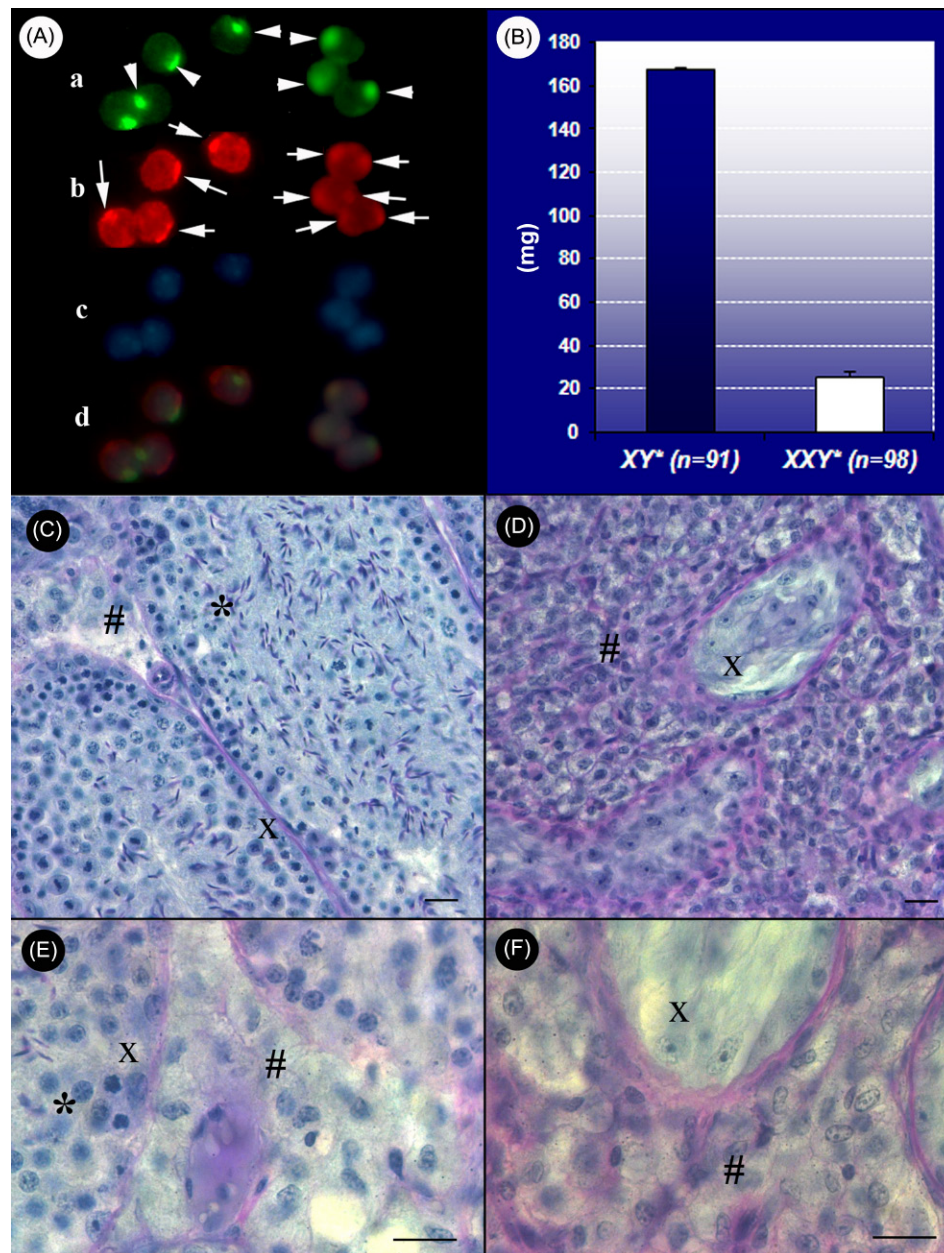
FIGURE 24.2   **Testicular phenotype of the 41,XX^{Y*} mouse model of KS.** (A) Fluorescence in situ hybridization (FISH) of sex chromosomes in interphase nuclei obtained from peripheral blood samples of male mice of the strain B6Ei.Lt-Y*. *Left side*: leucocyte nuclei from 40,XY*, *right side*: leucocyte nuclei from 41,XX^{Y*} male mice. (a) Y* chromosomes *(arrowheads)* detected by green fluorescent mouse specific probe; (b) X chromosome *(arrows)* detected by red fluorescent mouse specific probe; (c) DAPI nuclear stain; (d) overlay of a–c. Note the two X chromosome signals in 41,XX^{Y*} leucocytes. One X chromosome is always situated in close association to the Y* signal. Partial overlap of these chromosomes can be detected by the yellowish color. (B) Comparison of bitesticular weights between adult 41,XX^{Y*} males ($n = 98$) and their 40,XY* littermate controls ($n = 91$). The germ cell loss in males with a supernumerary X chromosome resulted in significantly reduced testis size. Values are mean ± SEM. (C and D) Representative micrographs of testicular histology of the seminiferous epithelium. (C) 40,XY* control mouse exhibiting full spermatogenesis. (D) 41,XX^{Y*} mouse testis. All germ cells were depleted from the seminiferous epithelium leaving Sertoli cell only syndrome. Sertoli cells show the beginning of vacuolization. (E and F) Representative micrographs of testicular histology of the interstitial space. (E) In the 40,XY* control mice Leydig cells are normally arranged in the interstitial spaces between the tubular walls. (F) In contrast in the 41,XX^{Y*} mice, Leydig Cell number is increased, forming a hyperplasia. Bars represents 20 μm. Symbols: *X*, Sertoli cells; *, differentiating germ cells; #, Leydig cells. Staining: Hematoxylin-Eosin.
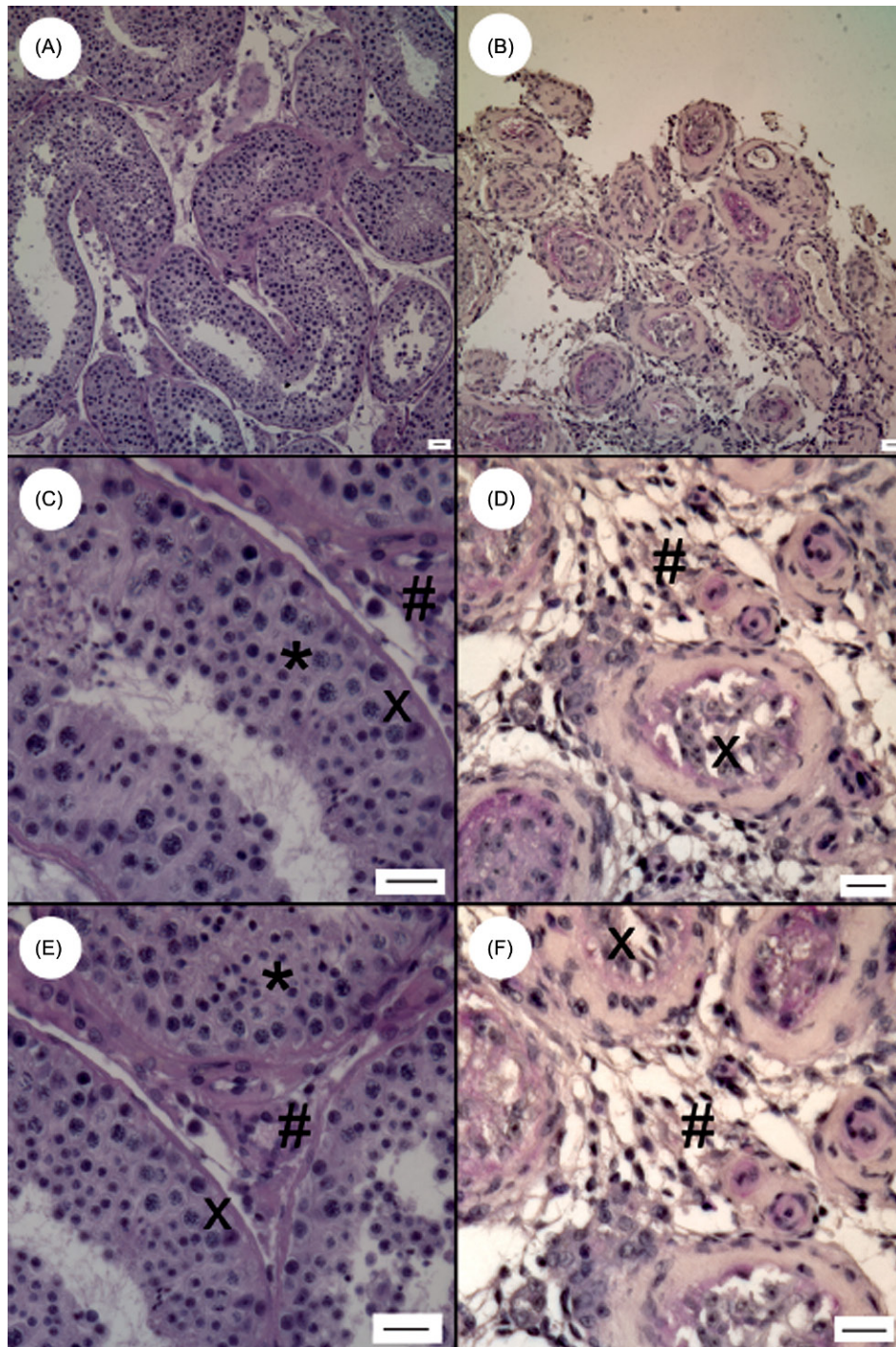
FIGURE 24.3 **Histology of human testicular tissue: Comparison of normal spermatogenesis and SCO syndrome typically observed in Klinefelter patients.** (A, C, and E) Representative micrographs of the normal human testicular histology exhibiting full spermatogenesis. (B, D, and F) Representative micrographs of the testicular histology of a KS patient with SCO syndrome. (A and B) overview of tubular cross sections: while the control tissue shows normal distribution of interstitial and tubular areas, the SCO situation exhibits complete loss of germ cells and hyalinized tubular walls. The seminiferous tubules only contain Sertoli cells. (C and D) Detail of the seminiferous epithelium: In the control, all germ cell stages up to mature spermatozoa are present. Typically for adult KS men, all germ cells are lacking. Sertoli cells show the beginning of vacuolization. (E and F) Detail of the interstitial space. In the control testis, Leydig cells are normally arranged in the interstitial spaces between the tubular walls. In contrast in the tissue obtained from a KS patient, Leydig cell number is elevated showing typical hyperplasia. Bars represents 20 µm. Symbols: *X*, Sertoli cells; *, differentiating germ cells; #, Leydig cells. Staining: Hematoxylin-Eosin.

Sertoli cells are situated in the seminiferous tubules where they support spermatogenic differentiation by providing nourishment and mediation of endocrine signalling (Wistuba et al., 2007). As such any alterations in these essential cells profoundly influence testicular function. Evidence has been found for early apoptosis of Sertoli cells in KS, leading to the proposition that loss of support and communication between Sertoli cells and germ cells might be related to the germ cell depletion seen in the syndrome (Aksglaede et al., 2006; Wistuba et al., 2010). Sertoli cells express the androgen receptor (AR) and produce androgen binding protein and inhibin. Any perturbation of the cells therefore, might influence the amount of ITT in the interstitial spaces and, as a consequence, affect the endocrine feedback along the hypothalamic—pituitary gonadal axis. No empirically robust evidence on altered Sertoli cell presence, development, and/or function could be obtained until the first systematic findings from the experimental models became available. The findings of the first studies (Lue et al., 2005) were of particular interest and importance as they showed AR was expressed in the Sertoli cells of adult XY control mice but not in the XXY mice. This is despite both animals having a similar pattern up until day 20 postpartum (pp), indicating that the loss of AR expression in the XXY mice occurs around puberty and suggests that in these animals, the maturation of Sertoli cells may be altered indicating that they may influence or be influenced by abnormal germ cell development. Some credence to this notion was provided by a histological evaluation of the testes of the 41,XX^{Y*} model, which found the number of Sertoli cells to be decreased compared to controls.

The investigations performed thus far provide sufficient evidence to surmise that Sertoli cells are altered in males with a supernumerary X chromosome. To understand the underpinnings of Sertoli cell germ cell interaction, Sertoli cell apoptosis, maturation, and differentiation, more in depth evaluations are needed; studies that require substantial amounts of material and the chronicling of proliferation, differentiation, and maturation over an extensive timeperiod. These investigations are impossible to perform in humans. Only with the aid of the mouse models can any meaningful exploration of the changes in this crucial somatic testicular cell be undertaken.

It was reported that during testicular degeneration observed in KS also Sertoli cells degenerate over time (Aksglaede and Juul, 2013; Aksglaede et al., 2006), an observation which is in line with data in our mouse model demonstrating that Sertoli cell numbers are altered during postnatal development (Werler et al., 2014). Taken together, the altered Sertoli cell physiology needs more detailed analyses of this somatic cell type already during prenatal development. Germ line propagation

and differentiation is in particular affected by the consequences of the chromosomal aberration. Thus, major checkpoints and consequently processes occurring specifically in the germ line might be altered by the chromosomal imbalance, that is, the development of the primordial and the spermatogonial stem cell (PGC, SSC) system. As mentioned earlier, in vitro studies have shown that aneuploid undifferentiated germ cells died when isolated from embryonic gonads and only those with a randomly corrected karyotype survived in culture (Hunt et al., 1998; Mroz et al., 1999). Thus, SSCs with an aberrant karyotype must have entered a default pathway during the intrauterine phase but latest in the perinatal period. When only germ cells with a corrected karyotype survive in vitro after they were isolated from the embryonic gonad, while aberrant germ cells died over time, the question arises, why—in vivo—the germ cell loss progresses postnatally as shown recently (Werler et al., 2014). Even if a few aberrant germ cells are still present in the perinatal testis, a certain proportion of those present at the time point of birth should be of correct karyotype and the population of spermatogonial cells should at least stay stable if not propagating. From this in part contradictory observation and accepting the most plausible assumption that correction by random propulsion explains the survival of a reduced population of primordial germ cells (PGCs; Mroz et al., 1999; Sciurano et al., 2009) and subsequently gonocytes into the postnatal period, some of those survivors might lose their stem cell properties already before birth. Apparently they get lost during peripubertal differentiation while very few can occasionally survive, express all relevant markers correctly and drive foci of spermatogenesis. Systematic evaluation of the phenotypic changes during development in utero is per se only possible in a mouse model.

The disturbance of the HPG axis, which causes the hypergonadotropic hypogonadism commonly seen in KS patients together with the suggested increased numbers of Leydig cell in testicular biopsies has led to the hypothesis that Leydig cell function and/or maturation might be affected by the sex chromosomal imbalance. Leydig cells are steroidogenic being the source of testosterone which is essential for the development of the healthy male phenotype and crucial for the continuance and completion of normal spermatogenesis.

As with the other facets of KS, the restrictive factor for any in depth investigation is the limited access to testicular tissue. With the availability of the 41,XX^{Y*} male mice, studies on Leydig cells from males with a supernumerary X chromosome became feasible to investigate. Using this model we confirmed the presence of Leydig cell hyperplasia as determined by stereological microscopy and also found that ITT levels were similar to those in the control mice (Wistuba et al., 2010). This was surprising

considering the low serum T levels seen in KS patients and 41,XX^{Y*} mice alike (Lanfranco et al., 2004; Smyth and Bremner, 1998; Wistuba, 2010). In line with low circulating T levels was the finding that once Leydig cells from the KS model were taken out of the testicular environment, grown in vitro and normalized for cell number, their function was indeed altered. However, it was not impaired, as would first be thought, but hyperactivated. When the mRNA expression profiles of the marker genes *Tsp2* (thrombospondin 2: a matricellular protein of fetal origin which is predominantly expressed in juvenile Leydig cells), *Rlf* (relaxin-like factor: marker of mature Leydig cells), *Est* (estrogen sulfotransferase: marker of mature Leydig cells), and *LHR* (LH receptor: investigated for correlation with Leydig cell stimulation experiments, see later) were determined, the isolated XX^{Y*} Leydig cells showed a mature mRNA expression profile and significantly higher transcriptional activity compared to controls (Wistuba et al., 2010; O'Shaughnessy et al., 2002). The gene expression analysis revealed an overall increase in expression of XX^{Y*} Leydig cell specific genes with *Est* expressed approximately 20-fold, *Rlf* 8-fold, *Tsp2* 5-fold, and *LHR* 3-fold higher than wild-type Leydig cells. Stimulation of the XX^{Y*} Leydig cells in vitro indicated a mature LH receptor which responded even stronger to human Chorionic Gonadotropin (hCG, a surrogate for LH) stimulation than cells from controls. Furthermore, the steroidogenic activity of the XX^{Y*} Leydig cells was elevated, in that more T per cell was produced in response to hCG.

These exciting results not only lead to a new concept on the origin of hypergonadotropic hypogonadism but also demonstrate the validity of the KS mouse model, with its direct translational consequences for our understanding of KS patients. The results from the mouse model indicate that Leydig cell function is not impaired per se, hinting that other factors in the testicular environment are responsible for the disturbed androgen endocrinology seen in KS patients. In particular, as we could confirm also in patients that ITT values were not different from controls (Tüttelmann et al., 2014). Possibly the altered testicular architecture associated with the disorder may hamper endocrine transport into the circulation, a proposition which was supported by the findings that KS patients also have diminished blood vessel diameter (Foresta et al., 2012). Taking this into account, we set out to find a possible "vascular" explanation for the lack of T release into the testicular blood stream. In testis biopsies from patients, reliable analysis of the vessels is, however, not possible because of the bias resulting from the dissection technique requiring avoidance of larger blood vessels to prevent bleeding. Consequently, the blood vessel constitution was evaluated in whole testis sections from adult male 41,XX^{Y*} and 40,XY* mice. Indeed, the blood vessel/testes surface ratio correcting for the smaller

testes of XX^{Y*} mice was significantly lower in these mice compared with XY* controls. In conclusion, testicular T production does not seem to be impaired in men with KS. The data from the mouse model let us speculate that a reduced vascular supply might be involved in lower release of T into the bloodstream.

7.3 Infertility in KS—A Stem Cell Disease?

Beside hypergonadotropic hypogonadism, the clinical feature that is consistently present in KS is infertility. Caused by the degeneration of germ cells, their depletion from the seminiferous epithelium occurs in a process most likely beginning prenatally and progressing during infancy (Coerdt et al., 1985; Murken et al., 1974). The number of germ cells dramatically decreases by the onset of puberty and is often accompanied by a massive hyalinization of the seminiferous tubules (Aksglaede et al., 2006). As already mentioned, although the germ cell degeneration in patients, in general, leads to complete azoospermia, small foci of full spermatogenesis in the testicular tissue can be found in some Klinefelter men (Foresta et al., 1999; Schiff et al., 2005), which with the aid of assisted reproductive techniques make paternity possible (Denschlag et al., 2004; Kyono et al., 2007).

In patients with focal spermatogenesis, FISH evaluation has shown that the premeiotic and meiotic germ cells still undergoing differentiation and forming normal haploid gametes, possess a 46,XY karyotype while the nurturing somatic Sertoli cells have the aberrant 47,XXY karyotype (Sciurano et al., 2009). These results provide two useful pieces of information: First, germ cells that survive in the KS testis are karyotypically corrected and second, the somatic testicular environment despite being composed of aberrant cell types is able to support germ cell differentiation to some extent. Taken together, this indicates that the germ cell communication is able to overcome and/or to compensate the disturbances in the somatic testicular components (Sciurano et al., 2009).

Focal spermatogenesis is present in a substantial proportion of KS patients but was also observed to some extent in KS mice (Werler et al., 2014). Some 41,XX^{Y*} animals exhibited few tubules with differentiating germ cells up to late meiotic stages were observed (Fig. 24.4).

Again, the 41,XXY mouse model played an important role in the elucidation of these observations as it provided the experimental means which made the proof of principle possible. Specifically, transplantation assays in the mice allowed for the separate analysis of the germ cell line and the somatic testicular components by permitting the transplantation of germ cells from KS mice into healthy hosts and vice versa (Brinster, 2007; Wistuba and Schlatt, 2002). Lue et al. (2010a,b) transplanted healthy spermatogonial cells from donor mice into the germ cell depleted testes of 41,XXY recipient mice and
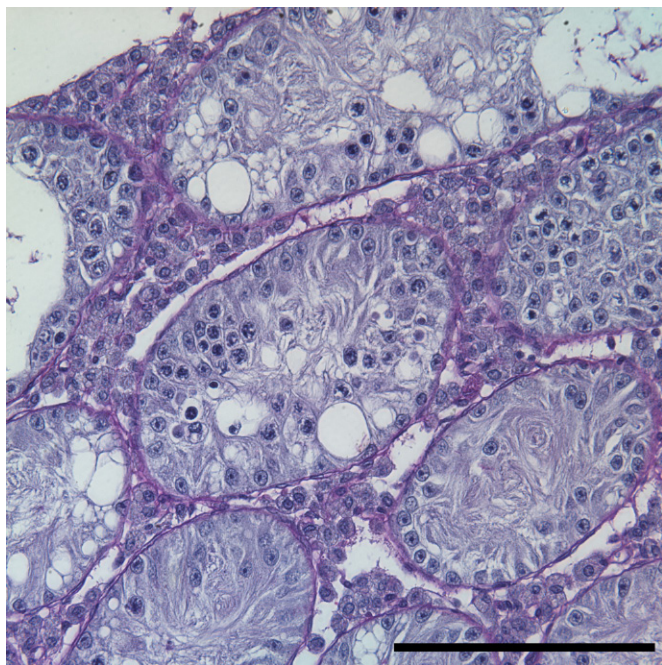
FIGURE 24.4 **Focal spermatogenesis in a testis obtained from a 41,XX^{Y*} male mouse.** Histology rarely exhibits foci of spermatogenic differentiation. In this testis of a 3-week-old 41, XX^{Y*} mouse a few tubular cross sections show differentiation of germ cells up to meiotic pachytene spermatocytes. Staining: Periodic Acid Schiff (PAS), the bar equals 100 μm.

found that normal mature spermatozoa could be derived. An experimental finding that supports the focal spermatogenesis observed in patients. In humans and mice alike, it appears that germ cells with an XXY karyotype are lost with only those that are corrected, very likely by random expulsion of one X chromosome, able to survive (Sciurano et al., 2009). Furthermore, despite the surrounding environment being altered, it is still capable of providing sufficient support to nurture the few surviving germ cells throughout the entire differentiating process and culminating in the successful production of mature gametes.

As material from immature and pubertal boys is extremely rare, the mouse models offer the only realistic means for studying the processes associated with the germ cell loss in KS in detail. In the 41,XXY mice, it was noted that at the early stages of testicular differentiation, when germ cell proliferation is underway, fewer germ cells are present compared to littermate controls. Chronicling testicular formation, development and content from day 10.5 postcoitum (pc) to day 6 pp, Hunt et al. (1998) noted that the numbers of germ cells present in the genital ridges of both XXY and XY animals were similar. However, perinatally, around the period when testicular differentiation begins a marked reduction in the quantity of germ cells in the tubular cross sections of XXY animals was found. It has been suggested, that the cause of this impaired proliferation might be the

reactivation of the inactivated X chromosome when the XXY germ cells enter the genital ridge (Mroz et al., 1999). If the XXY cells are removed from their somatic environment they proliferate similarly to normal XY germ cells. This ability in vitro is suggestive of an error in germ cell-somatic cell communication (Hunt et al., 1998), a disturbance that afflicts spermatogonia at a very early undifferentiated stem cell level, possibly by interfering with the colonization of the stem cell niches. At present, the topic of germ cell loss is a matter of contention and debate. Hampered by the technical difficulties inherent in the handling of prenatal and neonatal experimental animals, together with the small quantity of tissue obtained from such young mice, only a few studies have been performed. Lue et al. (2005) found decreased germ cell numbers as early as day 3 pp but no differences in the number of gonocytes at day 1 pp; findings which are contrary to those of Hunt et al. (1998) who assessed the same mouse model. We have performed a systematic study by the postnatal time course of germ cell loss in vivo. When utilizing the 41,XX^{Y*} mice, we found the number of undifferentiated germ cells to be reduced already from the time point of birth onward and could link this to altered protein expression of spermatogonial stem cell markers: Lin28 and Pgp9.5 expression were not detected after day 3 pp and day 5 pp, respectively. Lin28 regulation implements a network of several miRNAs of which we analyzed miR-125b and miR-let7g. Both miRNAs are normally expressed in a complementary pattern in the healthy developing testis, in 41,XX^{Y*} mice we found this pattern to be completely disturbed (Werler et al., 2014). In tubules with germ cells, the expression of Lin28 and Pgp9.5 was corrected. Based on these findings, we developed a model for prenatal germ cell loss in our KS mouse model (Fig. 24.5). Preliminary evidence suggests that also in the human the germ cell loss starts earlier than thought so far (Davis et al., 2015). We hypothesize that a first wave of germ cell death occurs already in the early embryonic phase during colonization of the developing gonad, a second phase, when gonocytes propagate followed by a third phase, when germ cells that survived enter meiosis but fail to complete this process except of a few germ cells which eventually can undergo full spermatogenesis (Fig. 24.5, Werler et al., 2014). Apart from the evidence provided by our group that the only parameter correlating with the success of testicular sperm retrieval by mTESE in young KS patients is age (Rohayem et al., 2015), the scenario currently discussed in the clinical and scientific community is to offer a fertility preservation option already in infantile KS boys by cryopreservation and -storage of immature testicular tissue for later maturation of the spermatogonia in vitro by methods which however, are currently still on the experimental level (Stukenborg et al., 2009; Van Saen et al., 2012; Kossack et al., 2013).
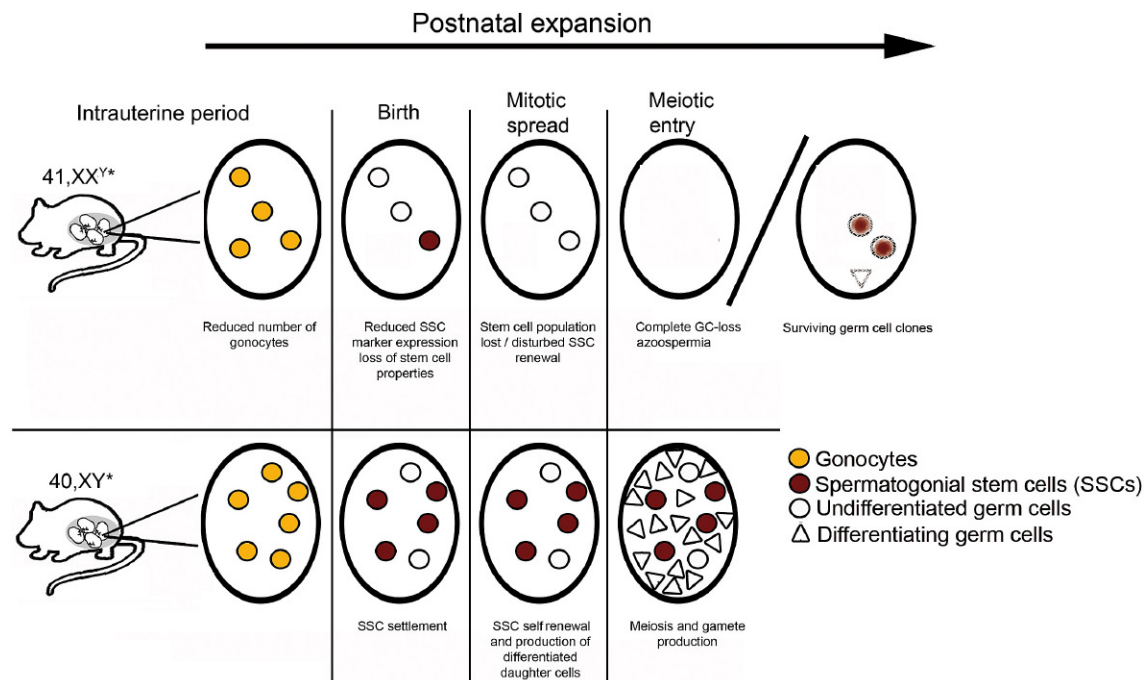
FIGURE 24.5 **A revised model of germ cell loss in mouse models for Klinefelter Syndrome.** A reduced number of gonocytes is proposed already during the intrauterine period. Consequently, at birth, a reduced number of germ cells (GC) expressing SSC markers is present and the stem cell potential is lost during the mitotic propagation after birth. When the germ cells afterwards enter meiosis, they are finally depleted in the 41,XX^{Y}* testis whereas in normal 40,XY* control mice spermatogenic differentiation starts. The exception of the rule is seen in focal spermatogenesis were single germ cell clones can survive (dotted lines). *Source: Modified from Werler, S., Demond, H., Ehmcke, J., Damm, O.S., Middendorff, R., Gromoll, J., Wistuba, J., 2014. Early loss of germ cells is associated with fading expression of Lin28, a spermatogonial stem cell marker in the 41,XX^{Y}* mouse model for Klinefelter Syndrome. Reproduction 147, 253–264.*

Consequently, in the light of the most prominent features of KS, the testis has to be seen as the most severely affected organ, thus reflecting the genotype-phenotype relation of this condition most strongly. Both testicular functions, the maintenance of the male endocrine milieu as well as the production of gametes are the features of KS which are consistently affected. Therefore, the logical target for the exploration of gene dosage effects is the analysis of gene expression and the functional response of testicular cell types. The availability of mouse models, the option to analyze gene expression patterns and somatic cell responses offers the privileged situation not only to study aspects of the mechanisms by which, for example, escapee genes provoke a complex phenotype but also to directly translate those findings into a clinical context (Nieschlag et al., 2014; Rohayem et al., 2015; Tüttelmann et al., 2014; Zitzmann et al., 2015).

7.4 Behavior and Cognition

New technologies in molecular biology which allow for the selective manipulation of genomic sequences have dramatically reshaped biomedical research during the last decades. The extensive utilization of these techniques in mice together with the animals' high reproduction rate, small size, and low maintenance costs, have made it the most widely used mammalian model organism.

The rapid rise in the number of different mouse models available now has greatly outpaced the behavioral characterization of these animals as these analyses are complex and time-consuming. The KS mice are indicative of the situation as only a minority of publications deal with detailed investigation of this murine model and report any behavioral data.

The first examination of cognitive ability of XXY mice was undertaken by Lue et al. (2005) in order to determine if their murine model exhibits cognitive deficits comparable to those found in human Klinefelter patients. To test cognitive functions, they used a Pavlovian conditioning box located in a sound-attenuating chamber. The mice were trained to acquire a tone-food association by providing food rewards only while a 20-kHz tone was presented for 20 s. Pavlovian or classical conditioning is based on the famous experiments conducted by Ivan Petrovich Pavlov where food was presented to dogs and the amount of saliva they produced measured. Before presenting the food, he rang a bell (although it has been questioned whether or not it was a bell or some other sound in the original experiment) as a

conditioning stimulus. After several repetitions the dogs associated the sound of the bell with food and started salivating regardless of whether food was present or not (Pavlov, 1906).

In the experiments by Lue et al. (2005), in lieu of saliva, the latency to pick up a food pellet after a 20-kHz tone was measured. In this study a relatively low number of seven XXY and seven XY mice were tested owing to the experiments being designated as preliminary. The mice were adult but of varying ages ranging from 4 to 12 months. The tone-food association was repeated 10 times a day for 4 consecutive days. Pellets were presented in a magazine that automatically recorded head dips by means of an infrared beam. Prior to testing the mice were provided with 90% of the food that they would freely consume for 3 days in order to increase motivation for a food reward. Both, XY and XXY mice learned the association of the tone with the food reward, but the XY controls proved to be faster learners. On the first day XY mice obtained the reward on average 6 s after the tone was presented. XXY mice took 9 s on average—significantly longer—to pick up the pellets on day 1. The latencies of picking up the reward by the XXY mice were also significantly longer on day 2 and 3 but equilibrium was reached on day 4. The authors speculated that the delayed latency might be due to either decreased plasma T levels, a defect of the androgen receptor or increased X-linked gene expression in specific brain regions, such as the medial temporal lobe. We ourselves conducted similar experiments testing conditional learning in a pavlonian setting under the administration of testosterone enanthate (TE). Mice of both karyotypes (41,XX^{Y}* and 40,XY* littermates) were placed individually into cages which allowed for applying stimulants (acoustical signals) and rewards (food) in an automatized way. An animal with normal learning abilities should be able to respond the signal within a small timeframe and the more sessions applied; the better the animal should respond until habituation sets in. Animals with reduced learning abilities should respond worse, that is, the duration until the task has been successfully fulfilled should be longer. We aimed at investigating whether a T supplementation of 2 µg/g bodyweight prior to the experiments would improve the outcome of conditional learning. However, we found no change under TE treatment for both groups, neither for XY* nor for XX^{Y}* males. While the wild types show normal learning behavior with and without TE, XX^{Y}* mice did not benefit from the T administration, which was unable to compensate the worse performance of these animals in the setting chosen (Fig. 24.6). Thus learning behavior might be unaffected from rising androgen levels and thus rather due to genetic reasons, however other reasons as altered androgen receptor functionality has still to be fully excluded.
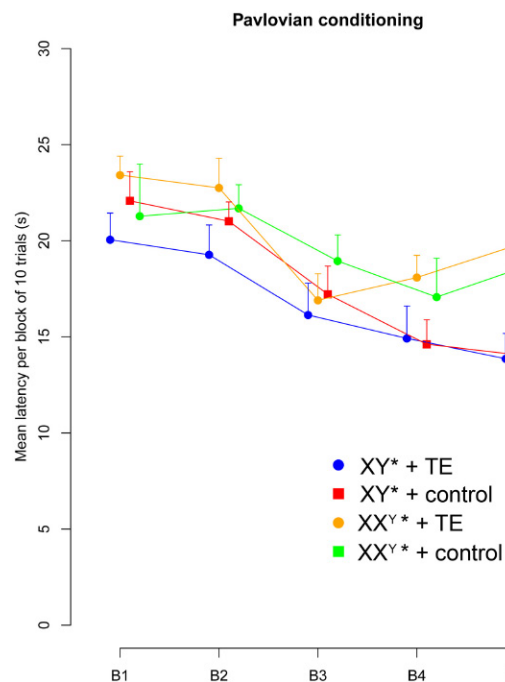
FIGURE 24.6   **Conditional learning after T supplementation.** Data points summarize ten trials each. TE administration does not improve conditional learning in 41,XX^{Y}* mice which are slower than their 40, XY* littermates. Response times of all groups remained stable under T supplementation indicating an underlying genetic mechanism likely not affected by androgen increase. *B*, Behavioral testing.

In another study (Liu et al., 2010) the social behavior and sex preference of the XXY mouse model was explored to determine if they mimicked the known peculiarities of KS patients' social skills. A series of tests was conducted using a "choice" apparatus which comprised three chambers, the mice could explore. Entrance into the apparatus was either from a left or right compartment where social partners or inanimate objects were presented. The preference was measured by the relative amount of time spent in the compartments. XXY mice preferred ovariectomized female mice or male mice over the inanimate objects. A finding that may appear inconspicuous until it is compared with that from the XY mice in this study (in contrast to the observations made by Ryan et al. (2008) who did not show such a preference). This test gauges whether the preference was based on social or sexual interest. When given the choice between an unknown male and an unknown ovariectomized female, XXY mice did not prefer the male. Furthermore, similar to XY mice, the XXY mice preferred the odor of intact females in oestrus over the odor of male conspecifics indicating that the preference for males over inanimate objects was socially rather than sexually motivated. In a second step, the authors investigated whether or not the observed differences in social preference were related to T. In order to match androgen exposure, castrated animals of both groups were tested before and after

T substitution. Neither castrated nor T substituted males of either group showed a specific preference for unknown males over an inanimate object. Castrated XXY mice preferred unknown males over unknown ovariectomized females in contrast to castrated XY mice that did not show any preference. When substituted with T neither group showed any partiality for unknown males or unknown ovariectomized females. Overall, the XXY mice exhibited increased rather than decreased social interest in these tests which is contradictory to the initial hypothesis derived from observations of disturbed social skills in KS patients. Nevertheless, the fact that differences in social behavior could be related to karyotypic differences is noteworthy and awaits further analysis.

The study by Lewejohann et al. (2009a) investigated the 41,XX^{Y*} mouse model with the intension of clarifying whether these mice can be used as an easier to obtain model to analyze the linkage between sex chromosomal imbalance and cognition processes. In contrast to the XXY model, the KS like mice were compared to XY* littermates, a group of animals that was deemed suitable to

act as controls based on their physiological and morphological similarities to XY mice.

The evaluations were based on a nonconditional test of recognition memory which uses an object recognition paradigm and measures the exploration of known versus unknown objects based on the tendency of mice to prefer novel objects over familiar objects. As it has been suggested that anxiety related behavior can bias the exploration in this test (Görtz et al., 2008), it was important to ensure that the preconditions for recognition memory were identical for both groups. Preceding the tests, a general health check and analysis of exploration and anxiety like behavior was conducted. The results of testing the preconditions could only be briefly presented in the paper. For the preparation of this chapter, we revisited the data in order to provide a more detailed picture of the XX^{Y*} model. The health check comprised the inspection of physical appearance and neurological testing including acoustic startle, visual placing, grip strength, and reflex functions. Mice of both groups appeared healthy and no differences were found (Fig. 24.7A). Spontaneous
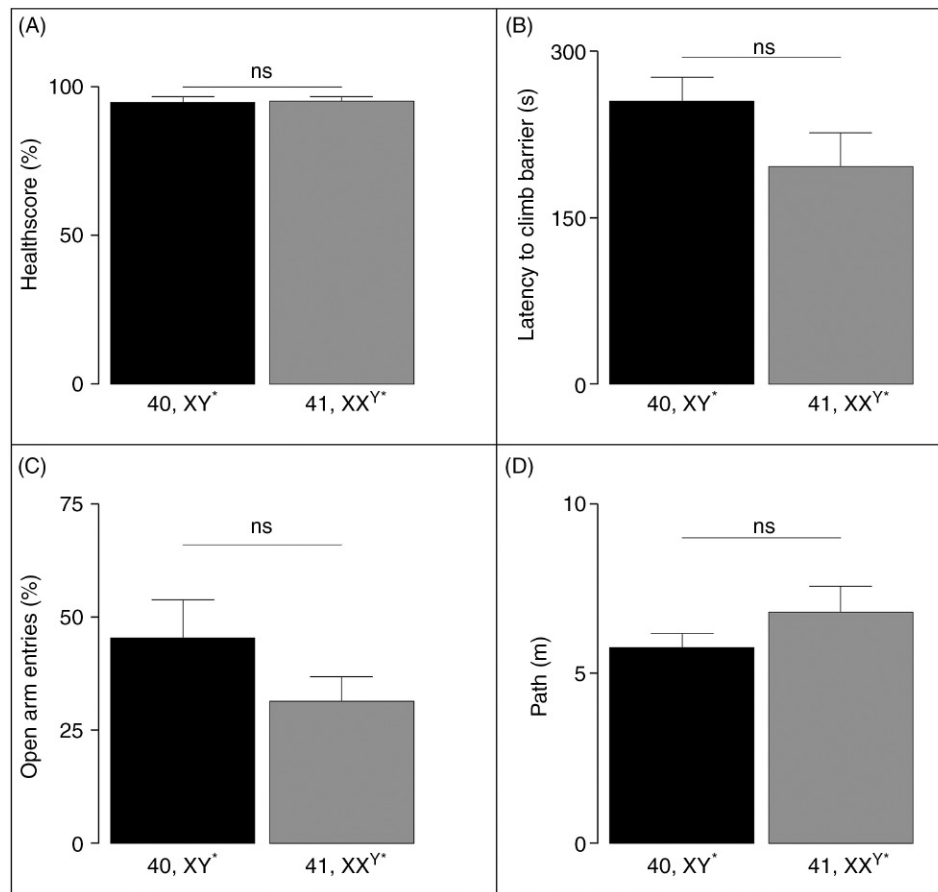
FIGURE 24.7 **Behavioral phenotyping of 41,XX^{Y*} mice.** (A) Mice were subjected to a general health check including visual inspection of fur and whiskers as well as tests for eye sight, hearing, reflex functions, and basic motor skills. The maximal test score of 14 points was assigned as 100%. (B) Spontaneous exploration was measured as the latency to climb over a barrier of 3 cm height dividing the test cage into two compartments. (C) Percentage of arm entries into open arms of an elevated plus maze to measure anxiety related behavior. (D) Locomotor activity in a 30 by 30 cm open field box was measured using a video based animal tracking software.

exploratory behavior was measured by the barrier test using a standard cage, which was divided by a 3 cm high barrier into two equally sized compartments. Spontaneous exploration was measured for 5 min by the latency to climb over the barrier into the other compartment. No statistical difference was detectable between XX^{Y*} and XY* mice, indicating no difference in spontaneous exploratory behavior (Fig. 24.7B). There is evidence of a reduced volume of the amygdala of KS patients (Patwardhan et al., 2002; Shen et al., 2004). Since this region of the brain is strongly involved in emotional processing, it is tempting to speculate that there might also be differences regarding anxiety related behavior. We measured this aspect by calculating the proportion of open versus shielded arm entries in an elevated plus-maze test. This test is pharmacologically validated, showing that less anxious mice explore open arms more frequently (Lister, 1987). Mice of both groups explored the open arms similarly and often indicating no difference between the animals nor severe anxiety related disturbances (Fig. 24.7C). In the open field test, the mice were allowed to explore a 30×30 cm^2 arena for 3 min. This test assesses locomotor behavior by means of a video-based automated tracking system that calculates the path length travelled. The test was also included to habituate the mice to the arena where the object recognition task would be performed. Again both groups explored the arena to a similar extent and no significant differences were detectable (Fig. 24.7D). However, when the objects were provided, the XY* male mice significantly preferred the novel object indicating that they remembered the object that was presented 1 h before. In contrast, the XX^{Y*} males did not show a preference indicating poor recognition memory or less interest in novelty. For each mouse a recognition index was calculated by dividing the time spent exploring a novel object by the total time spent exploring objects. XY* male mice had significantly higher recognition indices than the XX^{Y*} males. Interestingly, T concentrations correlated significantly with object recognition memory in XY* mice but not in XX^{Y*}. These correlations are consistent with the findings that T substitution in human KS patients failed to bring about an increase in memory performance (DeLisi et al., 2005). We therefore propose that the T driven organizing effects which occur during adolescence play a vital role for memory performance later in life. Adolescence is not only a period where secondary and tertiary sexual characters develop but is also the period where the behavioral responses of individuals changes from the juvenile to the adult phenotype. This phenomenon is highly conserved in mammals and has been found in just about all species studied (Spear and Kulbok, 2004). The obvious changes in behavior are driven by processes of brain development and reorganization that are unique to the periadolescent phase of development. For example, the maturation of

brain regions with high numbers of androgen receptors has been shown to be dependent upon testosterone-by-sex interactions in humans (Bramen et al., 2012).

Determining the validity of the animal models for KS, 34 human KS patients were assessed for visual object memory (Bruining et al., 2011), a task directly comparable to tests undertaken in the study by Lewejohann et al. (2009a). Indeed, the human KS subjects were found to have difficulties in processing visual objects as well as visual pattern information especially when temporal information needed to be processed and reproduced. Seven of the participating patients were treated with androgens during the time of testing, although the treatment did not appear to improve cognitive performance, due to the low number of patients receiving androgens, an affect cannot be entirely excluded. Overall, the cross-species comparison of cognitive behavior in KS is an important step in understanding the full spectrum of KS sequelae.

The behavioral studies of the KS mouse models provide a valuable tool for understanding social as well as cognitive aspects of the syndrome. There is no doubt that we are still at the very beginning, and a plethora of questions remain to be solved. In most studies analyzing behavioral phenotypes of mice, the animals are housed in small standard sized cages, preventing them from showing a variety of species specific behavior (Lewejohann et al., 2010). For example, anxiety-related behavior is usually characterized outside the home-cage using artificial apparatuses which investigate the motivational differences between fear and exploration by subjecting the mice to a challenging situation. Although it is acknowledged that such tests are fundamental for the characterization of animal models, for these behavioral traits to be more comparable to the human condition, an in-depth characterization of how the day-to-day life of these mice is affected in their home environment is also needed. For example, considering the association of supernumerary X chromosome and social interactions, it would be interesting to see, whether or not, the social day-to-day behavior of these mice is affected including an analysis of social dominance hierarchies (Lewejohann et al., 2009b, 2010). The cognitive phenotyping of the murine KS models which also awaits further in depth analysis would possibly benefit from a similar approach namely tests conducted in the home cages of the mice (de Visser et al., 2006).

As with the previously detailed physical and physiological consequences of KS, the influence of the disturbed endocrine milieu, differential gene expression and/or the mixture of both on brain function need to be clarified. The murine models allow for the systematic study of the effect of T treatment on behavioral and cognitive skills, not only in adulthood, but just as importantly during the early stages of life when androgens play a significant role in the organization of the brain.

In addition, the behavioral phenotypes of individual mice are known to be affected by environmental factors as well as gene-environment interactions (Lewejohann et al., 2011). For example, cognitively stimulating environments may help to ameliorate observed cognitive deficits. Translational research which relates human phenotypes with the behavioral data obtained from the murine models will help to further facilitate the value of these models by increasing their face validity (Bruining et al., 2011).

7.5 Endocrinology and Metabolism

Beyond infertility, hypergonadotropic hypogonadism is the condition present in almost all KS patients. The disturbed hormonal milieu is supposed to cause, or at least is involved in, many of the metabolic features that can accompany KS (e.g., gynecomastia, disturbed bone metabolism, increased diabetic risk) (Lanfranco et al., 2004). Cognitive deficits are also influenced by endocrine alterations, although experimental work using the mouse KS models has revealed that the hormonal influence on brain function is complex and multifaceted and that altered gene expression may play an important role despite the lack of T.

The most common therapeutic strategy to deal with the hypergonadotropic hypogonadism of Klinefelter patients is by the administration of exogenous T. Beyond redressing the androgen imbalance, T administration has been reported to have other beneficial effects, such as treating delayed puberty (Richmond and Rogol, 2007), enhancing bone metabolism (KS patients have a significantly higher risk of developing osteoporosis), and circumventing the development of metabolic syndrome (Bojesen et al., 2010; Gravholt et al., 2011). At present one of the treatments suggested for KS boys suffering from behavioral deficits is to administer T, a strategy that is claimed to aid a portion of patients; however, the purported beneficial attributes of this approach have yet to be proven unequivocally. T treatment is not without risks; its use has been linked to psychiatric consequences (Rogol and Tartaglia, 2010) and it undermines the small foci of spermatogenesis that may persist in KS patients, in particular for pubertal boys that may have sperm, this treatment effectively subverts their fertility potential, as exogenous T administration results in lowered ITT levels and thereby jeopardizes spermatogenic progress, which requires sufficient levels of T in the surrounding testicular environment (Wistuba et al., 2007).

As both mouse models exhibit hypergonadotropic hypogonadism with low plasma T and high gonadotropin levels, they closely mimic the endocrine profile of patients. This makes them ideal to the study of the true worth and consequences of T treatment which in turn may open routes for the development of novel therapeutic strategies.

Two examples of such investigations illustrate the potential of this approach. First, the study by Liu et al. (2010) on androgen action and effect on adult 41,XXY mice where they analyzed the impact of T on the bone metabolism in order to separate endocrine from genetic effects. In an elegant experimental design they used castrated 40,XY males as hypogonadal controls to assess solely the influence androgens on the bone phenotype. They treated these animals with T via silastic implants and monitored bone volume, trabecular thickness, and trabecular separation, all of which are deficient in 41,XXY mice. Following castration the controls' bone metabolism was to such an extent altered that it was indistinguishable from condition seen in the 41,XXY animals, demonstrating the importance of normal androgenization for the maintenance of a normal bone metabolism. Interestingly, although treatment did return serum T to values similar to the controls, the bone volume in males with a supernumerary X chromosome remained reduced. Thus, the authors suggested that as well as disturbed endocrine regulation, genetic causes must contribute to the bone volume loss in 41,XXY mice. Meaning, that like disturbances in brain function, bone metabolism is also adversely affected by a combination of altered gene expression and endocrine changes. The clinical corollary of these findings is that although T replacement therapy can be helpful for dealing with some of the sequelae it is not a panacea for KS, as it is unable to overcome the contribution of the genetic component.

In a second study (Wistuba et al., 2010, described in detail earlier), our group demonstrated that Leydig cells from 41,XX[Y*] mice are not impaired but rather hyperactivated probably in a compensatory response to the hypergonadotropic hypogonadism. Taken together with the normal ITT values in these animals, we proposed that it is not the production of T but rather its transport to/in the circulation that is hampered, perhaps due to the altered testicular architecture. By supplementing these findings with an observation from a study of KS patients from the 1970s, we suggested a new hypothesis. Smals et al. (1974) proposed the presence of a so-called "steroidogenic reserve" in Klinefelter men in an attempt to explain their finding that these patients responded with increasing serum T levels after treatment with CG. At the first glance, such a treatment seems to be absurd, treating hypergonadotropic patients with a gonadotropin, and the response paradoxical. However, our recent experimental findings that the Leydig cells in the 41,XX[Y*] mouse are functionally normal provides a possible explanation for Smals et al. (1974) conundrum, in that rather than a "reserve" increasing gonadotropin levels might further enhance steroidogenic activity and hence result in the noted rise of serum androgen levels. This might open a new route for therapy, in that instead of treating—in particular boys—with exogenous T and placing

their remaining spermatogenesis at risk, CG administration might be considered as it also increases serum T but more importantly it does so via the production of the patient's own testis. This is the crucial aspect as endogenous T is not harmful to spermatogenic progression. By this tack, the patients still achieve the androgenization state that is desired but no longer risk the loss of their small fertility reserve. Experimental and clinical testing of this hypothesis is still to be performed.

8 PERSPECTIVES—WHAT CAN BE EXPECTED FROM FUTURE ANIMAL EXPERIMENTS AND HOW TO RETRANSLATE EXPERIMENTAL FINDINGS INTO CLINICAL ROUTINE—CONCLUSIVE REMARKS

The generation and availability of mouse models of KS have led to some remarkable progress in our knowledge of the molecular and cellular mechanisms that form the aberrant male phenotype associated with this chromosomal disorder. On the genetic level, research on the mouse model has shown that X-inactivation is seemingly normal providing credence to the hypothesis that it is the expression of "escapee" genes that differentiates the normal condition from that seen in male mice with a supernumerary X chromosome. The use of these animal models has allowed for the identification of this very basic molecular mechanism along which the affected phenotype may become manifest namely, female expression patterns of X chromosomal genes that escape silencing, when present in a male cellular environment, act either directly or along regulatory pathways to undermine fertility, endocrine status cognition, and bone metabolism (Nieschlag et al., 2014; Wistuba, 2010; Zitzmann et al., 2015).

Some studies have already been undertaken to investigate this hypothesis and although the findings broadly support the proposition (Werler et al., 2011; Zitzmann et al., 2015), it is equally apparent that the situation is far more complex than first thought as some of the candidate genes are expressed in a tissue and gene-specific way and also autosomal gene expression appears to be affected by the disorder, likely downstream of the escapee action (Zitzmann et al., 2015). Therefore, more information is needed before the idea of developing novel therapies targeting on the human homologs of these genes can become a reality. Such deeper insights can only be made possible with the use of the animal model as they require experimental manipulation and functional studies.

As mentioned earlier, infertility due to the SCO phenotype is one of the major problems caused by KS. Unfortunately, primarily due to the late diagnosis of the syndrome, other than the cases where TESE/ICSI can

be performed, there is little that can be done to treat or preserve the fertility of KS patients and as a consequence, the majority of these men will never have the chance to father a child. In the 41,XX^{Y*} mice, the time course of germ cell loss was shown to occur earlier than thought and some studies in patients confirm at least partly that this is also true in human (Davis et al., 2015; Rohayem et al., 2015). Thus germ cell loss has likely to be encountered early, be it during puberty or even during childhood. The mouse models might provide an experimental basis for the development of innovative approaches to rescue the germ line and by these possibly open new routes for fertility preservation. Already the mouse models have shown that the aberrant somatic cells of the testis are able to support spermatogenesis. The transplantation experiments performed by Lue et al. (2010b) demonstrated that germ cells can differentiate, as long as they have a corrected karyotype; an observation confirmed in patients with focal spermatogenesis by Sciurano et al. (2009).

Therefore, the target for novel approaches may well be the germ line. If it becomes possible to harvest germ cells and to provoke the expulsion of one X chromosome from the cells (e.g., by certain culture conditions) it might become possible to either differentiate the cells in some novel in vitro system or to retransplant them. At present, these suggestions remain speculative. However, in vitro differentiation of mouse germ cells in three-dimensional matrices has recently been shown to be able to produce morphologically mature spermatozoa in a culture dish (Abu Elhija et al., 2012; Stukenborg et al., 2008, 2009). For further proof of principle studies, the KS mouse models are the perfect model. As the in vitro differentiation protocols are available for murine germ cells, immature mice of the 41,XXY and 41,XX^{Y*} karyotype may provide undifferentiated spermatogonia which could be sorted for to identify those that by random expulsion have already corrected their karyotype or could be cultured under certain conditions that force high mitotic activity which provokes the loss of the supernumerary X chromosome. These corrected germ cells could then be brought together with somatic testicular cells and undergo in vitro differentiation. Once the proof of principle has been provided under such an experimental design, then protocols might be developed for future fertility preservation attempts in human patients.

Male mice with a supernumerary X chromosome will also be useful to improve endocrine treatments for hypergonadotropic hypogonadism. As both mouse models possess endocrine phenotypes which are regulated along the HPG axis similar to humans, experiments can be designed that aim at improving routine T treatment and as such provide greater choice, safety, and efficacy in the protocols devised at overcoming the hypogonadal state and impaired androgenization. However, as mentioned

earlier, T treatment also bears some risks, that is, for the maintenance of remaining spermatogenesis. As the analysis of the Leydig cell physiology of 41,XX^{Y}* mice has shown, there might be alternative treatments, that is, the administration of gonadotropins to improve the endocrine milieu in patients without augmenting some of the adverse features of KS further. The availability of the mouse models permits the systematic testing of such novel and alternative treatments.

Acknowledgments

References

Abu Elhija, M., Lunenfeld, E., Schlatt, S., Huleihel, M., 2012. Differentiation of murine male germ cells to spermatozoa in a soft agar culture system. Asian J. Androl. 14, 285–293.

Aguirre, D., Nieto, K., Lazos, M., Pena, Y.R., Palma, I., Kofman-Alfaro, S., Queipo, G., 2006. Extragonadal germ cell tumours are often associated with Klinefelter syndrome. Hum. Pathol. 37, 477–480.

Aizenstein, R.I., Hibbeln, J.F., Sagireddy, B., Wilbur, A.C., O'Neill, H.K., 1997. Klinefelter's syndrome associated with testicular microlithiasis and mediastenal germ cell neoplasm. J. Clin. Ultrasound 9, 508–510.

Aksglaede, L., Juul, A., 2013. Testicular function and fertility in men with Klinefelter syndrome: a review. Eur. J. Endocrinol. 168, R67–R76.

Aksglaede, L., Wikström, A.M., Rajpert-De Meyts, E., Dunkel, L., Skakkebaek, N.E., Juul, A., 2006. Natural history of seminiferous tubule degeneration in Klinefelter syndrome. Hum. Reprod. Update 12, 39–48.

Aksglaede, L., Skakkebaek, N.E., Almstrup, K., Juul, A., 2011. Clinical and biological parameters in 166 boys, adolescents and adults with nonmosaic Klinefelter syndrome: a Copenhagen experience. Acta Paediatr. 100, 793–806.

Aksglaede, L., Moolgard, C., Skakkebaek, N.E., Juul, A., 2008. Normal bone mineral content but unfavourable muscle/fat ratio in Klinefelter Syndrome. Arch. Dis. Child 93, 30–34.

Bojesen, A., Gravholt, C.H., 2011a. Morbidity and mortality in Klinefelter Syndrome. Acta Paediatr. 100, 807–813.

Bojesen, A., Juul, S., Gravholt, C.H., 2003. Prenatal and postnatal prevalence of Klinefelter Syndrome: a national registry study. J. Clin. Endocrinol. Metab. 88, 622–626.

Bojesen, A., Juul, S., Birkebaek, N., Gravholt, C.H., 2004. Increased mortality in Klinefelter syndrome. J. Clin. Endocrinol. Metab. 89, 3830–3834.

Bojesen, A., Juul, S., Birkebaek, N.H., Gravholt, C.H., 2006. Morbidity in Klinefelter syndrome: a Danish register study based on hospital discharge diagnoses. J. Clin. Endocrinol. Metab. 91, 1254–1260.

Bojesen, A., Høst, C., Gravholt, C.H., 2010. Klinefelter's syndrome, type 2 diabetes and the metabolic syndrome: the impact of body composition. Mol. Hum. Reprod. 16, 396–401.

Bojesen, A., Stochholm, K., Juul, S., Gravholt, C.H., 2011b. Socioeconomic trajectories affect mortality in Klinefelter Syndrome. J. Clin. Endocrinol. Metab. 96, 2098–2104.

Bongso, T.A., Thavalingam, M., Mukherjee, T.K., 1982. Intersexuality associated with XX/XY mosaicism in a horned goat. Cytogenet. Cell Genet. 34, 315–319.

Bramen, J.E., Hranilovich, J.A., Dahl, R.E., Chen, J., Rosso, C., Forbes, E.E., Dinov, I.D., Worthman, C.M., Sowell, E.R., 2012. Sex matters during adolescence: testosterone-related cortical thickness maturation differs between boys and girls. PLoS One 7 (3), e33850.

Breeuwsma, A.J., 1968. A case of XXY sex chromosome constitution in an intersex pig. J. Reprod. Fertil. 16 (1), 119–120.

Brinster, R.L., 2007. Male germline stem cells: from mice to men. Science 316, 404–405.

Brown, C.J., Willard, H.F., 1994. The human X-inactivation centre is not required for maintenance of X-chromosome inactivation. Nature 368 (6467), 154–156.

Bruining, H., Swaab, H., de Sonneville, L.M., van Rijn, S., van Engeland, H., Kas, M.J., 2011. In search for significant cognitive features in Klinefelter syndrome through cross-species comparison of a supernumerary X chromosome. Genes Brain Behav. 10, 658–662.

Bunch, T.D., Callan, R.J., Maciulis, A., Dalton, J.C., Figueroa, M.R., Kunzler, R., Olson, R.E., 1991. True hermaphroditism in a wild sheep: a clinical report. Theriogenology 36, 185–190.

Cainarca, S., Messali, S., Ballabio, A., Meroni, G., 1999. Functional characterization of the Opitz syndrome gene product (midin): evidence for homodimerization and association with microtubules throughout the cell cycle. Hum. Mol. Genet. 8, 1387–1396.

Carrel, L., Willard, H.F., 2005. X-inactivation profile reveals extensive variability in X-linked gene expression in females. Nature 434, 400–404.

Carrel, L., Park, C., Tyekucheva, S., Dunn, J., Chiaromonte, F., Makova, K.D., 2006. Genomic environment predicts expression patterns on the human inactive X chromosome. PLoS Genet. 29 (2), e151.

Casci, T., 2011. What dosage compensation? Nat. Rev. Genet. 12, 2.

Centerwall, W.R., Benirschke, K., 1975. An animal model for the XXY Klinefelter's syndrome in man: tortoiseshell and calico male cats. Am. J. Vet. Res. 36, 1275–1280.

Changolkar, L.N., Singh, G., Cui, K., Berletch, J.B., Zhao, K., Disteche, C.M., Pehrson, J.R., 2010. Genome-wide distribution of macroH2A1 histone variants in mouse liver chromatin. Mol. Cell Biol. 30 (23), 5473–5483.

Chen, X., McClusky, R., Chen, J., Beaven, S.W., Tontonoz, P., Arnold, A.P., Reue, K., 2012. The number of x chromosomes causes sex differences in adiposity in mice. PLoS Genet. 8, e1002709.

Chen, X., McClusky, R., Itoh, Y., Reue, K., Arnold AP, 2013a. X and Y chromosome complement influence adiposity and metabolism in mice. Endocrinology 154, 1092–1104.

Chen, X., Williams-Burris, S.M., McClusky, R., Ngun, T.C., Ghahramani, N., Barseghyan, H., Reue, K., Vilain, E., Arnold, A.P., 2013b. The sex chromosome trisomy mouse model of XXY and XYY: metabolism and motor performance. Biol. Sex. Differ. 4, 15.

Chow, J.C., Ciaudo, C., Fazzari, M.J., Mise, N., Servant, N., Glass, J.L., Attreed, M., Avner, P., Wutz, A., Barillot, E., Greally, J.M., Voinnet, O., Heard, E., 2010. LINE-1 activity in facultative heterochromatin formation during X chromosome inactivation. Cell 141 (6), 956–969.

Chowdhary, B.P., Raudsepp, T., 2000. Cytogenetics and physical gene map. In: Bowling, A.T., Ruvinsky, A. (Eds.), The Genetics of the Horse. CAB International Publishing, Cambridge, MA, USA, pp. 171–242.

Christiansen, P., Andersson, A.M., Skakkebaek, N.E., 2003. Longitudinal studies of inhibin B levels in boys and young adults with Klinefelter syndrome. J. Clin. Endocrinol. Metab. 88, 888–891.

Clough, E., Pyle, R.L., Hare, W.C., Kelly, D.F., Patterson, D.F., 1970. An XXY sex-chromosome constitution in a dog with testicular hypoplasia and congenital heart disease. Cytogenetics 9, 71–77.

Coerdt, W., Rehder, H., Gausmann, I., Johannisson, R., Gropp, A., 1985. Quantitative histology of human fetal testes in chromosomal disease. Pediatr. Pathol. 3, 245–259.

Csankovszki, G., Panning, B., Bates, B., Pehrson, J.R., Jaenisch, R., 1999. Conditional deletion of Xist disrupts histone macroH2A localization but not maintenance of X inactivation. Nat. Genet. 22 (4), 323–324.

Dain, A.R., Bridge, P.S., 1978. A chimaeric calf with XY/XXY mosaicism and intersexuality. J. Reprod. Fertil. 54 (1), 197–201.

Dal Zotto, L., Quaderi, N.A., Elliott, R., Lingerfelter, P.A., Carrel, L., Valsecchi, V., Montini, E., Yen, C.-H., Chapman, V., Kalcheva, I., Arrigo, G., Zuffardi, O., Thomas, S., Willard, H.F., Ballabio, A., Disteche, C.M., Rugarli, E.I., 1998. The mouse Mid1 gene: implications for the pathogenesis of Opitz syndrome and the evolution of the mammalian pseudoautosomal region. Hum. Molec. Genet. 7, 489–499.

Davis, S.M., Rogol, A.D., Ross, J.L., 2015. Testis development and fertility potential in boys with Klinefelter Syndrome. Endocrinol. Metab. Clin. North Am. 44, 843–865.

De Braekeleer, M., Dao, T.N., 1991. Cytogenetic studies in male infertility: a review. Hum. Reprod. 6, 245–250.

de la Chapelle, A., 1972. Analytic review: nature and origin of males with XX sex chromosomes. Am. J. Hum. Genet. 24, 71–105.

de la Chapelle, A., Hortling, H., Niemi, M., Wennstroem, J., 1964. XX sex chromosomes in a human male. First case. Acta Med. Scand. 175, 25–28.

de la Chapelle, A., Hästbacka, J., Korhonen, T., Mäenpää, J., 1990. The etiology of XX sex reversal. Reprod. Nutr. Dev. 1 (Suppl.), 39s–49s.

de Visser, L., van den Bos, R., Kuurman, W.W., Kas, M.J., Spruijt, B.M., 2006. Novel approach to the behavioural characterization of inbred mice: automated home cage observations. Genes Brain Behav. 5, 458–466.

DeLisi, L.E., Maurizio, A.M., Svetina, C., Ardekani, B., Szulc, K., Nierenberg, J., Leonard, J., Harvey, P.D., 2005. Klinefelter's syndrome (XXY) as a genetic model for psychotic disorders. Am. J. Med. Genet. B Neuropsychiatric Genet. 135B, 15–23.

Deng, X., Hiatt, J.B., Nguyen, D.K., Ercan, S., Sturgill, D., Hillier, L.W., Schlesinger, F., Davis, C.A., Reinke, V.J., Gingeras, T.R., Shendure, J., Waterston, R.H., Oliver, B., Lieb, J.D., Disteche, C.M., 2011. Evidence for compensatory upregulation of expressed X-linked genes in mammals, *Caenorhabditis elegans* and *Drosophila melanogaster*. Nat. Genet. 43, 1179–1185.

Denschlag, D., Tempfer, C., Kunze, M., Wolff, G., Keck, C., 2004. Assisted reproductive techniques in patients with Klinefelter syndrome: a critical review. Fertil. Steril. 82, 775–779.

Dudley, C.J., Hubbard, G.B., Moore, C.M., Dunn, B.G., Raveendran, M., Rogers, J., Nathanielsz, P.W., McCarrey, J.R., Schlabritz-Loutsevitch, N.E., 2006. A male baboon (Papio hamadryas) with a mosaic 43,XXY/42,XY karyotype. Am. J. Med. Genet. A 140, 94–97.

Dunn, H.O., Lein, D.H., McEntee, K., 1980. Testicular hypoplasia in a Hereford bull with 61,XXY karyotype: the bovine counterpart of human Klinefelter's syndrome. Cornell Vet. 70, 137–146.

Dupont, C., Gribnau, J., 2013. Different flavors of X-chromosome inactivation in mammals. Curr. Opin. Cell. Biol. 25 (3), 314–321.

Eicher, E.M., Hale, D.W., Hunt, P.A., Lee, B.K., Tucker, P.K., King, T.R., Eppig, J.T., Washburn, L.L., 1991. The mouse Y* chromosome involves a complex rearrangement, including interstitial positioning of the pseudoautosomal region. Cytogenet. Cell Genet. 57, 221–230.

Filippova, G.N., 2008. Genetics and Epigenetics of the multifunctional protein CTCF. Curr. Top. Dev. Biol. 80, 337–360.

Foresta, C., Galeazzi, C., Bettella, A., Marin, P., Rossato, M., Garolla, A., Ferlin, A., 1999. Analysis of meiosis in intratesticular germ cells from subjects affected by classic Klinefelter's syndrome. J. Clin. Endocrinol. Metab. 84, 3807–3810.

Foresta, C., Caretta, N., Palego, P., Ferlin, A., Zuccarello, D., Lenzi, A., Selice, R., 2012. Reduced artery diameters in Klinefelter syndrome. Int. J. Androl. 35 (5), 720–725.

Fullerton, G., Hamilton, M., Maheshwari, A., 2010. Should non-mosaic Klinefelter syndrome men be labelled as infertile in 2009? Hum. Reprod. 25, 588–597.

Geerkens, C., Vetter, U., Just, W., Fedarko, N.S., Fisher, L.W., Young, M.F., Termine, J.D., Robey, P.G., Wöhrle, D., Vogel, W., 1995. The X-chromosomal human biglycan gene BGN is subject to X inactivation but is transcribed like an X-Y homologous gene. Hum. Genet. 96, 44–52.

Goldschmidt, B., El-Jaick, K.B., Souza, L.M., Carvalho, E.C.Q., Moura, V.L.S., Benevides Filho, I.M., 2001. Cryptorchidism associated with 78,XY/79,XXY mosaicism in dog. Israel J. Vet. Med. 56, 56–58.

Görtz, N., Lewejohann, L., Tomm, M., Ambrée, O., Keyvani, K., Paulus, W., Schwarze-Eicker, K., Sachser, N., 2008. Effects of environmental enrichment on exploration, anxiety, and memory in female TgCRND8 alzheimer mice. Behav. Brain Res. 191, 43–48.

Goto, Y., Kimura, H., 2009. Inactive X chromosome-specific histone H3 modifications and CpG hypomethylation flank a chromatin boundary between an X-inactivated and an escape gene. Nucleic Acids Res. 37, 7416–7428.

Gravholt, C.H., Jensen, A.S., Høst, C., Bojesen, A., 2011. Body composition, metabolic syndrome and type 2 diabetes in Klinefelter syndrome. Acta Paediatr. 100, 871–877.

Gribnau, J., Grootegoed, J.A., 2012. Origin and evolution of X chromosome inactivation. Curr. Opin. Cell Biol. 24 (3), 397–404.

Gupta, V., Parisi, M., Sturgill, D., Nuttall, R., Doctolero, M., Dudko, O.K., Malley, J.D., Eastman, P.S., Oliver, B., 2006. Global analysis of X-chromosome dosage compensation. J. Biol. 5, 3.

Hagens, O., Dubos, A., Abidi, F., Barbi, G., Van Zutven, L., Hoeltzenbein, M., Tommerup, N., Moraine, C., Fryns, J.P., Chelly, J., van Bokhoven, H., Gecz, J., Dollfus, H., Ropers, H.-H., Schwartz, C.E., Stocco dos Santos, R.C., Kalscheuer, V., Hanauer, A., 2006. Disruptions of the novel KIAA1202 gene are associated with X-linked mental retardation. Hum. Genet. 118, 578–590.

Hager, K., Jennings, K., Hososno, S., Howell, S., Gruen, J.R., Scott, A.R., Tartaglia, N.R., Rinder, H.M., 2012. Molecular diagnostic testing for Klinefelter syndrome and other male sex chromosome aneuploidies. Int. J. Pediatr. Endocrinol. 2012 (1), 8.

Hancock, J.L., Daker, M.G., 1981. Testicular hypoplasia in a boar with abnormal sex chromosome constitution (39 XXY). J. Reprod. Fertil. 61, 395–397.

Hauffe, H.C., Giménez, M.D., Garagna, S., Searle, J.B., 2010. First wild XXY house mice. Chromosome Res. 18, 599–604.

Hong, S., Cho, Y.W., Yu, L.R., Yu, H., Veenstra, T.D., Ge, K., 2007. Identification of JmjC domain-containing UTX and JMJD3 as histone H3 lysine 27 demethylases. Pro. Natl. Acad. Sci. USA. 104, 18439–18444.

Hosey, A.M., Chaturvedi, C.P., Brand, M., 2010. Crosstalk between histone modifications maintains the developmental pattern of gene expression on a tissue-specific locus. Epigenetics 5, 273–281.

Hughes, I.A., Houk, C., Ahmed, S.F., Lee, P.A., LWPES Consensus group, ESPE Consensus Group, 2006. Consensus statement on management of intersex disorders. Arch. Dis. Child. 91, 554–563.

Hughes, J.F., Skaletsky, H., Brown, L.G., Pyntikova, T., Graves, T., Fulton, R.S., Dugan, S., Ding, Y., Buhay, C.J., Kremitzki, C., Wang, Q., Shen, H., Holder, M., Villasana, D., Nazareth, L.V., Cree, A., Courtney, L., Veizer, J., Kotkiewicz, H., Cho, T.J., Koutseva, N., Rozen, S., Muzny, D.M., Warren, W.C., Gibbs, R.A., Wilson, R.K., Page, D.C., 2012. Strict evolutionary conservation followed rapid gene loss on human and rhesus Y chromosomes. Nature 483, 82–86.

Hunt, P., Eicher, E., 1991. Fertile male mice with three sex chromosomes: evidence that infertility in XYY mice is an effect of two Y chromosomes. Chromosoma 100, 293.

Hunt, P.A., Worthman, C., Levinson, H., Stallings, J., LeMaire, R., Mroz, K., Park, C., Handel, M.A., 1998. Germ cell loss in the XXY male mouse: altered X-chromosome dosage affects prenatal development. Mol. Reprod. Dev. 49, 101–111.

Iannuzzi, L., Di Meo, G.P., Perucatti, A., Spadetta, M., Incarnato, D., Parma, P., Iannuzzi, A., Ciotola, F., Peretti, V., Perrotta, G., Di Palo, R., 2004. Clinical, cytogenetic and molecular studies on sterile stallion and mare affected by XXY and sex reversal syndromes, respectively. Caryologia 57, 400–404.

Itti, E., Gaw Gonzalo, I.T., Pawlikowska-Haddal, A., Boone, K.B., Mlikotic, A., Itti, L., Mishkin, F.S., Swerdloff, R.S., 2006. The structural brain correlates of cognitive deficits in adults with Klinefelter's syndrome. J. Clin. Endocrinol. Metab. 91, 1423–1427.

Iwase, S., Lan, F., Bayliss, P., de la Torre-Ubieta, L., Huarte, M., Qi, H.H., et al., 2007. The X-linked mental retardation gene SMCX/JARID1C defines a family of histone H3 lysine 4 demethylases. Cell 128, 1077–1088.

Jacobs, P.A., Strong, J.A., 1959. A case of human intersexuality having a possible XXY sex-determining mechanism. Nature 183, 302–303.

Jeppesen, P., Turner, B.M., 1993. The inactive X chromosome in female mammals is distinguished by a lack of histone H4 acetylation, a cytogenetic marker for gene expression. Cell 74, 281–289.

Joerg, H., Janett, F., Schlatt, S., Mueller, S., Graphodatskaya, D., Suwattana, D., Asai, M., Stranzinger, G., 2003. Germ cell transplantation in an azoospermic Klinefelter bull. Biol. Reprod. 69, 1940–1944.

Jørgensen, I.N., Skakkebaek, A., Andersen, N.H., Pedersen, L.N., Hougaard, D.M., Bojesen, A., Trolle, C., Gravholt, C.H., 2015. Short QTc interval in males with Klinefelter Syndrome-Influence of CAG repeat length, body composition, and testosterone replacement therapy. Pacing Clin. Electrophysiol. 38 (4), 472–482.

Kamischke, A., Baumgardt, A., Horst, J., Nieschlag, E., 2003. Clinical and diagnostic features of patients with suspected Klinefelter syndrome. J. Androl. 24, 41–48.

Kashimada, K., Koopman, P., 2010. Sry: the master switch in mammalian sex determination. Development 137, 3921–3930.

Khalil, A.M., Driscoll, D.J., 2007. Trimethylation of histone H3 lysine 4 is an epigenetic mark at regions escaping mammalian X inactivation. Epigenetics 2, 114–118.

Kharchenko, P.V., Xi, R., Park, P.J., 2011. Evidence for dosage compensation between the X chromosome and autosomes in mammals. Nat. Genet. 43, 1167–1169.

Klinefelter, H.F., Reifenstein, E.C., Albright, F., 1942. Syndrome characterized by gynecomastia, aspermatogenesis without a Leydigism and increased excretion of Follicle-stimulating hormone. J. Clin. Endocrinol. Metab. 2, 615–627.

Kossack, N., Terwort, N., Wistuba, J., Ehmcke, J., Schlatt, S., Schöler, H., Kliesch, S., Gromoll, J., 2013. A combined approach facilitates the reliable detection of human spermatogonia in vitro. Hum. Reprod. 28 (11), 3012–3025.

Kubień, E.M., Pozor, M.A., Tischner, M., 1993. Clinical, cytogenetic and endocrine evaluation of a horse with a 65,XXY karyotype. Equine Vet. J. 25, 333–335.

Kyono, K., Uto, H., Nakajo, Y., Kumagai, S., Araki, Y., Kanto, S., 2007. Seven pregnancies and deliveries from non-mosaic Klinefelter syndrome patients using fresh and frozen testicular sperm. J. Assist. Reprod. Genet. 24, 47–51.

Lanfranco, F., Kamischke, A., Zitzmann, M., Nieschlag, E., 2004. Klinefelter's syndrome. Lancet 364, 273–283.

Laron, Z., Dickerman, Z., Zamir, R., Galatzer, A., 1982. Paternity in Klinefelter's syndrome—a case report. Arch. Androl. 8, 149–151.

Lee, P.A., Houk, C.P., Ahmed, S.F., Hughes, I.A., International Consensus Conference on Intersex organized by the Lawson Wilkins Pediatric Endocrine Society and the European Society for Paediatric Endocrinology., 2006. Consensus statement on management of intersex disorders. International Consensus Conference on Intersex. Pediatrics 118, e488–e500.

Lewejohann, L., Damm, O., Luetjens, C.M., Hämäläinen, T., Simoni, M., Nieschlag, E., Gromoll, J., Wistuba, J., 2009a. Impaired recognition memory in male mice with a supernumerary X chromosome. Physiol. Behav. 96, 23–29.

Lewejohann, L., Reefmann, N., Widmann, P., Ambrée, O., Herring, A., Keyvani, K., Paulus, W., Sachser, N., 2009b. Transgenic alzheimer mice in a semi-naturalistic environment: more plaques, yet not compromised in daily life. Behav. Brain Res. 201, 99–102.

Lewejohann, L., Kloke, V., Heiming, R.S., Jansen, F., Kaiser, S., Schmitt, A., Lesch, K.P., Sachser, N., 2010. Social status and day-to-day behaviour of male serotonin transporter knockout mice. Behav. Brain Res. 211, 220–228.

Lewejohann, L., Zipser, B., Sachser, N., 2011. 'Personality' in laboratory mice used for biomedical research: a way of understanding variability? Dev. Psychobiol. 53, 631–640.

Lin, H., Gupta, V., Vermilyea, M.D., Falciani, F., Lee, J.T., O'Neill, L.P., Turner, B.M., 2007. Dosage compensation in the mouse balances up-regulation and silencing of X-linked genes. PLoS Biol. 5, e326.

Lingenfelter, P.A., Adler, D.A., Poslinski, D., Thomas, S., Elliott, R.W., Chapman, V.M., Disteche, C.M., 1998. Escape from X inactivation of Smcx is preceded by silencing during mouse development. Nat. Genet. 18, 212–213.

Link, J.C., Chen, X., Prien, C., Borja, M.S., Hammerson, B., Oda, M.N., Arnold, A.P., Reue, K., 2015. Increased high-density lipoprotein cholesterol levels in mice with XX versus XY sex chromosomes. Arterioscler. Thromb. Vasc. Biol. 35, 1778–1786.

Lister, R.G., 1987. The use of a plus-maze to measure anxiety in the mouse. Psychopharmacology 92, 180–185.

Liu, P.Y., Kalak, R., Lue, Y., Jia, Y., Erkkila, K., Zhou, H., Seibel, M.J., Wang, C., Swerdloff, R.S., Dunstan, C.R., 2010. Genetic and hormonal control of bone volume, architecture and remodelling in XXY mice. J. Bone Miner. Res. 25, 2148–2154.

Lopes, A.M., Arnold-Croop, S.E., Amorim, A., Carrel, L., 2011. Clustered transcripts that escape X inactivation at mouse XqD. Mamm. Genome 22, 572–582.

Lue, Y., Rao, P.N., Sinha Hikim, A.P., Im, M., Salameh, W.A., Yen, P.H., Wang, C., Swerdloff, R.S., 2001. XXY male mice: an experimental model for Klinefelter syndrome. Endocrinology 142, 1461–1470.

Lue, Y., Jentsch, J.D., Wang, C., Rao, P.N., Sinha Hikim, A.P., Salameh, W., Swerdloff, R.S., 2005. XXY mice exhibit gonadal and behavioral phenotypes similar to Klinefelter syndrome. Endocrinology 146, 4148–4154.

Lue, Y.H., Wang, C., Liu, P.Y., Erkilla, K., Swerdloff, R.S., 2010a. Insights into the pathogenesis of XXY phenotype from comparison of the clinical syndrome with an experimental XXY mouse model. Pediatr. Endocrinol. Rev. 8, 140–144.

Lue, Y., Liu, P.Y., Erkkila, K., Ma, K., Schwarcz, M., Wang, C., Swerdloff, R.S., Transplanted XY, 2010b. germ cells produce spermatozoa in testes of XXY mice. Int. J. Androl. 33, 581–587.

Lyon, M.F., 1961. Gene action in the X-chromosome of the mouse (*Mus musculus* L.). Nature 190, 372–373.

Lyon, M.F., 1998. X-chromosome inactivation: a repeat hypothesis. Cytogenet. Cell Genet. 80, 133–137.

Mäkinen, A., Andersson, M., Nikunen, S., 1998. Detection of the X-chromosomes in a Klinefelter boar using a whole human X-chromosome painting probe. Anim. Reprod. Sci. 52, 317–323.

Mäkinen, A., Katila, T., Andersson, M., Gustavsson, I., 2000. Two sterile stallions with XXY-syndrome. Equine Vet. J. 32, 358–360.

Marks, H., Chow, J.C., Denissov, S., Françoijs, K.J., Brockdorff, N., Heard, E., Stunnenberg, H.G., 2009. High-resolution analysis of epigenetic changes associated with X inactivation. Genome Res. 19, 1361–1373.

Mazeyrat, S., Saut, N., Grigoriev, V., Mahadevaiah, S.K., Ojarikre, O.A., Rattigan, A., et al., 2001. A Y-encoded subunit of the translation initiation factor Eif2 is essential for mouse spermatogenesis. Nat. Genet. 29, 49–53.

Mehta, A., Malek-Jones, M., Bolyakov, A., Mielnik, A., Schlegel, P.N., Paduch, D.A., 2012. Methylation-specific PCR allows for fast diagnosis of X chromosome disomy and reveals skewed inactivation of the X chromosome in men with Klinefelter syndrome. J. Androl. 33 (5), 955–962.

Mehta, A., Mielnik, A., Schlegel, P.N., Paduch, D.A., 2014. Novel methylation specific real-time PCR test for the diagnosis of Klinefelter syndrome. Asian J. Androl. 16 (5), 684–688.

Meyers-Wallen, V.N., 1993. Genetics of sexual differentiation and anomalies in dogs and cats. J. Reprod. Fertil. Suppl. 47, 441–452.

Molteni, L., De Giovanni Macchi, A., Meggiolaro, D., Sironi, G., Enice, F., Popescu, P., 1999. New cases of XXY constitution in cattle. Anim. Reprod. Sci. 55, 107–113.

Mroz, K., Carrel, L., Hunt, P.A., 1998. Germ cell development in the XXY mouse: evidence that a compromised testicular environment increases the incidence of meiotic errors. Hum. Reprod. 14, 1151–1156.

Mroz, K., Hassold, T.J., Hunt, P.A., 1999. Meiotic aneuploidy in the XXY mouse: evidence that X chromosome reactivation is independent of sexual differentiation. Dev. Biol. 207, 229–238.

Murken, J.D., Stengel-Rutkowski, S., Walther, J.U., Westenfelder, S.R., Remberger, K.H., Zimmer F, 1974. Letter: Klinefelter's syndrome in a fetus. Lancet 2, 171.

Ngun, T.C., Ghahramani, N.M., Creek, M.M., Williams-Burris, S.M., Barseghyan, H., Itoh, Y., Sánchez, F.J., McClusky, R., Sinsheimer, J.S., Arnold, A.P., Vilain, E., 2014. Feminized behavior and brain gene expression in a novel mouse model of Klinefelter Syndrome. Arch. Sex. Behav. 43, 1043–1057.

Nie, G.J., Johnston, S.D., Hayden, D.W., Buoen, L.C., Stephens, M., 1998. Theriogenology question of the month. Azoospermia associated with 79,XXY chromosome complement (canine Klinefelter's syndrome). J. Am. Vet. Med. Assoc. 212, 1545–1547.

Nielsen, J., Wohlert, M., 1991. Chromosome abnormalities found among 34,910 newborn children: results from a 13-year incidence study in Arhus, Denmark. Hum. Genet. 87, 81–83.

Nieschlag, E., Werler, S., Wistuba, J., Zitzmann, M., 2014. New approaches to the Klinefelter Syndrome. Ann. Endocrinol. (Paris) 75 (2), 88–97.

Nieschlag, E., Ferlin, A., Gravholt, C.H., Gromoll, J., Köhler, B., Lejeune, H., Rogol, A.D., Wistuba, J., 2016. The Klinefelter syndrome: current management and research challenges. Andrology 4 (3), 545–549.

Ohno, S., 1967. Sex Chromosomes and Sex-Linked Genes. Springer, Berlin, pp. 1–140.

O'Shaughnessy, P.J., Johnston, H., Willerton, L., Baker, P.J., 2002. Failure of normal adult Leydig cell development in androgen-receptor-deficient mice. J. Cell Sci. 115, 3491–3496.

Pacenza, N., Pasqualini, T., Gottlieb, S., Knoblovits, P., Costanzo, P.R., Usher, J.S., Rey, R.A., Martinez, M.P., Aszpis, S., 2012. Clinical presentation of Klinefelter's Syndrome: differences according to age. Internat. J. Endocrinol. 2012, 6.

Pasquali, D., Arcopinto, M., Renzullo, A., Rotondi, M., Accardo, G., Salzano, A., Esposito, D., Saldamarco, L., Isidori, A.M., Marra, A.M., Ruvolo, A., Napoli, R., Bossone, E., Lenzi, A., Baliga, R.R., Saccà, L., Cittadini, A., 2013. Cardiovascular abnormalities in Klinefelter syndrome. Int. J. Cardiol. 168 (2), 754–759.

Patwardhan, A.J., Brown, W.E., Bender, B.G., Linden, M.G., Eliez, S., Reiss, A.L., 2002. Reduced size of the amygdala in individuals with 47,XXY and 47,XXX karyotypes. Am. J. Med. Genet. 114, 93–98.

Pavlov, I.P., 1906. The scientific investigation of the psychical faculties or processes in higher animals. Science 24, 613–619.

Pinton, A., Barasc, H., Raymond Letron, I., Bordedebat, M., Mary, N., Massip, K., Bonnet, N., Calgaro, A., Dudez, A.M., Feve, K., Riquet, J., Yerle, M., Ducos, A., 2011. Meiotic studies of a 38,XY/39,XXY mosaic boar. Cytogenet. Genome Res. 133, 202–208.

Plath, K., Mlynarczyk-Evans, S., Nusinow, D.A., Panning, B., 2002. Xist RNA and the mechanism of X chromosome inactivation. Annu. Rev. Genet. 36, 233–278.

Poplinski, A., Wieacker, P., Kliesch, S., Gromoll, J., 2010. Severe XIST hypomethylation clearly distinguishes (SRY +) 46,XX-maleness from Klinefelter syndrome. Eur. J. Endocrinol. 162, 169–175.

Reimann-Berg, N., Murua Escobar, H., Nolte, I., Bullerdiek, J., 2008. Testicular tumor in an XXY dog. Cancer Genet. Cytogenet. 183, 114–116.

Richmond, E.J., Rogol, A.D., 2007. Male pubertal development and the role of androgen therapy. Nat. Clin. Pract. Endocrinol. Metab. 3, 338–344.

Rogatcheva, M.B., Oda, S.I., Zhelezova, A.I., Borodin, P.M., 1998. An XXY sex chromosome constitution in a house musk shrew (*Suncus murinus L.*) with testicular hypoplasia. J. Reprod. Fertil. 113, 91–93.

Rogol, A.D., Tartaglia, N., 2010. Considerations for androgen therapy in children and adolescents with Klinefelter syndrome (47XXY). Pediatr. Endocrinol. Rev. 8, 145–150.

Rohayem, J., Bongers, R., Czeloth, K., Mallidis, C., Wistuba, J., Krallmann, C., Zitzmann, M., Kliesch, S., 2015. Age and markers of Leydig cell function, but not of Sertoli cell function predict the success of sperm retrieval in adolescents and adults with Klinefelter's syndrome. Andrology 3 (5), 868–875.

Ross, N.L., Wadekar, R., Lopes, A., Dagnall, A., Close, J., Delisi, L.E., Crow, T.J., 2006. Methylation of two Homo sapiens-specific X-Y homologous genes in Klinefelter's syndrome (XXY). Am. J. Med. Genet. B Neuropsychiatr. Genet. 141B, 544–548.

Ryan, B.C., Young, N.B., Moy, S.S., Crawley, J.N., 2008. Olfactory cues are sufficient to elicit social approach behaviors but not social transmission of food preference in C57BL/6J mice. Behav. Brain Res. 193, 235–242.

Schiff, J.D., Palermo, G.D., Veeck, L.L., Goldstein, M., Rosenwaks, Z., Schlegel, P.N., 2005. Success of testicular sperm injection and intracytoplasmic sperm injection in men with Klinefelter syndrome. J. Clin. Endocrinol. Metab. 90, 6263–6267.

Schweiger, S., Foerster, J., Lehmann, T., Suckow, V., Muller, Y.A., Walter, G., Davies, T., Porter, H., van Bokhoven, H., Lunt, P.W., Traub, P., Ropers, H.H., 1999. The Opitz syndrome gene product, MID1, associates with microtubules. Proc. Nat. Acad. Sci. USA 96, 2794–2799.

Sciurano, R.B., Luna Hisano, C.V., Rahn, M.I., Brugo Olmedo, S., Rey Valzacchi, G., Coco, R., Solari, A.J., 2009. Focal spermatogenesis originates in euploid germ cells in classical Klinefelter patients. Hum. Reprod. 24, 2353–2360.

Searle, J.B., 1984. A wild common shrew (*Sorex araneus*) with an XXY sex chromosome constitution. J. Reprod. Fertil. 70, 353–356.

Searle, J.B., Jones, R.M., 2002. Sex chromosome aneuploidy in wild small mammals. Cytogenet. Genome Res. 96, 239–243.

Shen, D., Liu, D., Liu, H., Clasen, L., Giedd, J., Davatzikos, C., 2004. Automated morphometric study of brain variation in XXY males. NeuroImage 23, 648–653.

Simpson, J.L., de la Cruz, F., Swerdloff, R.S., Samango-Sprouse, C., Skakkebaek, N.E., Graham, Jr., J.M., Hassold, T., Aylstock, M., Meyer-Bahlburg, H.F., Willard, H.F., Hall, J.G., Salameh, W., Boone, K., Staessen, C., Geschwind, D., Giedd, J., Dobs, A.S., Rogol, A., Brinton, B., Paulsen, C.A., 2003. Klinefelter syndrome: expanding the phenotype and identifying new research directions. Genet. Med. 5, 460–468.

Słota, E., Kozubska-Sobocińska, A., Kościelny, M., Danielak-Czech, B., Rejduch, B., 2003. Detection of the XXY trisomy in a bull by using sex chromosome painting probes. J. Appl. Genet. 44, 379–382.

Smals, A.G., Kloppenborg, P.W., Benraad, T.J., 1974. 1974 The effect of short and long term human chorionic gonadotrophin (HCG) administration on plasma testosterone levels in Klinefelter's syndrome. Acta Endocrinol. 77, 753–764.

Smyth, C.M., Bremner, W.J., 1998. Klinefelter syndrome. Arch. Intern. Med. 158, 1309–1314.

Sokol, R.Z., 2012. It's not all about the testes: medical issues in Klinefelter patients. Fertil. Steril. 98 (2), 261–265.

Spear, H.J., Kulbok, P., 2004. Autonomy and adolescence: a concept analysis. Public Health Nurs. 21 (2), 144–152.

Stabile, M., Angelino, T., Caiazzo, F., Olivieri, P., De Marchi, N., De Petrocellis, L., Orlando, P., 2008. Fertility in a i(Xq) Klinefelter patient: importance of XIST expression level determined by qRT-PCR in ruling out Klinefelter cryptic mosaicism as cause of oligozoospermia. Mol. Hum. Reprod. 14, 635–640.

Stochholm, K., Juul, S., Gravholt, C.H., 2010. Diagnosis and mortality in 47,XYY persons: a registry study. Orphanet. J. Rare Dis. 5, 15.

Stochholm, K., Bojesen, A., Skakkebaek Jensen, Q., Juul, S., Hojberg Gravholt, C., 2012. Criminality in men with Klinefelter's syndrome and XYY syndrome: a cohort study. BMJ Open 2, e000650.

Stukenborg, J.B., Wistuba, J., Luetjens, C.M., Elhija, M.A., Huleihel, M., Lunenfeld, E., Gromoll, J., Nieschlag, E., Schlatt, S., 2008. Coculture of spermatogonia with somatic cells in a novel three-dimensional soft-agar-culture-system. J. Androl. 29, 312–329.

Stukenborg, J.B., Schlatt, S., Simoni, M., Yeung, C.H., Elhija, M.A., Luetjens, C.M., Huleihel, M., Wistuba, J., 2009. New horizons for in vitro spermatogenesis? An update on novel three-dimensional culture systems as tools for meiotic and post-meiotic differentiation of testicular germ cells. Mol. Hum. Reprod. 15, 521–529.

Suedmeyer, W.K., Houck, M.L., Kreeger, J., 2003. Klinefelter syndrome (39 XXY) in an adult Siberian tiger (*Panthera tigris altaica*). J. Zoo Wildl. Med. 34, 96–99.

Swerdloff, R.S., Lue, Y., Liu, P.Y., Erkkilä, K., Wang, C., 2011. Mouse model for men with Klinefelter syndrome: a multifaceted fit for a complex disorder. Acta Paediatr. 100, 892–899.

Swerdlow, A.J., Schoemaker, M.J., Higgins, C.D., Wright, A.F., Jacobs, P.A., UK Clinical Cytogenetics Group, 2005. Cancer incidence and mortality in men with Kilnefelter syndrome: a cohort study. J. Natl. Cancer Inst. 97, 1204–1210.

Temple, C.M., Sanfilippo, P.M., 2003. Executive skills in Klinefelter's syndrome. Neuropsychologia 41, 1547–1559.

Terzoli, G., Lalatta, F., Lobbiani, A., Simoni, G., Colucci, G., 1992. Fertility in a 47,XXY patient: assessment of biological paternity by deoxyribonucleic acid fingerprinting. Fertil. Steril. 58, 821–822.

Tüttelmann, F., Gromoll, J., 2010. Novel genetic aspects of Klinefelter's syndrome. Mol. Hum. Reprod. 16, 386–395.

Tüttelmann, F., Damm, O.S., Luetjens, C.M., Baldi, M., Zitzmann, M., Kliesch, S., Nieschlag, E., Gromoll, J., Wistuba, J., Simoni, M., 2014. Intratesticular testosterone is increased in men with Klinefelter syndrome and may not be released into the bloodstream owing to altered testicular vascularization—a preliminary report. Andrology 2, 275–281.

van Rijn, S., Aleman, A., Swaab, H., Kahn, R., 2006. Klinefelter's syndrome (karyotype 47,XXY) and schizophrenia-spectrum pathology. Br. J. Psychiatry 189, 459–460.

Van Saen, D., Gies, I., De Schepper, J., Tournaye, H., Goossens, E., 2012. Can pubertal boys with Klinefelter syndrome benefit from spermatogonial stem cell banking? Hum. Reprod. 27 (2), 323–330.

Vong, Q.P., Li, Y., Lau, Y.F., Dym, M., Rennert, O.M., Chan, W.Y., 2006. Structural characterization and expression studies of Dby and its homologs in the mouse. J. Androl. 27, 653–661.

Vorona, E., Zitzmann, M., Gromoll, J., Schüring, A.N., Nieschlag, E., 2007. Clinical, endocrinological, and epigenetic features of the 46,XX male syndrome, compared with 47,XXY Klinefelter patients. J. Clin. Endocrinol. Metab. 92, 3458–3465.

Wang, P.J., McCarrey, J.R., Yang, F., Page, D.C., 2001. An abundance of X-linked genes expressed in spermatogonia. Nat. Genet. 27, 422–426.

Werler, S., Wistuba, J., 2014. A possible means of countering the under diagnosis of Klinefelter Syndrome. Asian J. Androl. 16 (5), 785.

Werler, S., Poplinski, A., Gromoll, J., Wistuba, J., 2011. Expression of Genes escaping from X inactivation in the 41, XX^{Y*} mouse model for Klinefelter's Syndrome. Acta Paediatr. 100, 885–891.

Werler, S., Demond, H., Ehmcke, J., Damm, O.S., Middendorff, R., Gromoll, J., Wistuba, J., 2014. Early loss of germ cells is associated with

fading expression of Lin28, a spermatogonial stem cell marker in the 41,XXY* mouse model for Klinefelter Syndrome. Reproduction 147, 253–264.

Wikström, A.M., Dunkel, L., 2008. Testicular function in Klinefelter syndrome. Horm. Res. 69, 317–326.

Wikström, A.M., Painter, J.N., Raivio, T., Aittomäki, K., Dunkel, L., 2006a. Genetic features of the X chromosome affect pubertal development and testicular degeneration in adolescent boys with Klinefelter syndrome. Clin. Endocrinol. 65, 92–97.

Wistuba, J., 2010. Animal models for Klinefelter's Syndrome and their relevance for the clinic. Mol. Hum. Reprod. 16, 375–385.

Wistuba, J., Schlatt, S., 2002. Transgenic mouse models and germ cell transplantation: two excellent tools for the analysis of genes regulating male fertility. Mol. Genet. Metab. 77, 61–67.

Wistuba, J., Stukenborg, J.M., Luetjens, C.M., 2007. Mammalian Spermatogenesis. Funct. Dev. Embryol. 1, 99–117.

Wistuba, J., Luetjens, C.M., Dittmann, M., Werler, S., Poplinski, A., Damm, O., Stukenborg, J.B., Hämäläinen, T., Simoni, M., Gromoll, J., 2010. Male 41, XX^{Y*} mice as a model for Klinefelter syndrome: hyperactivation of Leydig cells. Endocrinology 151, 2898–2910.

Xiong, Y., Chen, X., Chen, Z., Wang, X., Shi, S., Wang, X., Zhang, J., He, X., 2010. RNA sequencing shows no dosage compensation of the active X-chromosome. Nat. Genet. 42, 1043–1047.

Xu, J., Watkins, R., Arnold, A.P., 2006. Sexually dimorphic expression of the X-linked gene Eif2s3x mRNA but not protein in mouse brain. Gene Expr. Patterns. 6, 146–155.

Yang, F., Babak, T., Shendure, J., Disteche, C.M., 2010. Global survey of escape from X inactivation by RNA-sequencing in mouse. Genome Res. 20, 614–622.

Yencilek, F., Baykal, C., 2005. 46 XX male syndrome: a case report. Clin. Exp. Obst. Gyn. 32, 263–264.

Yoder, M., Hildebrand, J.D., 2007. Shroom4 (Kiaa1202) is an actin-associated protein implicated in cytoskeletal organization. Cell Motil. Cytoskeleton 64, 49–63.

Yoshida, A., Miura, K., Nagao, K., Hara, H., Ishii, N., Shirai, M., 1997. Sexual function and clinical features of patients with Klinefelter's syndrome with the chief complaint of male infertility. Int. J. Androl. 20, 80–85.

Zitzmann, M., Bongers, R., Werler, S., Bogdanova, N., Wistuba, J., Kliesch, S., Gromoll, J., Tüttelmann, F., 2015. Gene expression patterns in relation to the clinical phenotype in Klinefelter syndrome. J. Clin. Endocrinol. Metab. 100, E518–E523.

Zöller, B., Ji, J., Sundquist, J., Sundquist, K., 2016. High risk of venous thromboembolism in Klinefelter Syndrome. J. Am. Heart Assoc. 20:5(5), e003567.

Further Reading

Liu, P.Y., Erkkila, K., Lue, Y., Jentsch, J.D., Schwarcz, M.D., Abuyounes, D., Hikim, A.S., Wang, C., Lee, P.W., Swerdloffm, R.S., 2010. Genetic, hormonal and metabolomic influences on social behaviour and gender preference of XXY mice. Am. J. Physiol. Endocrinol. Metab. 299, E446–E455.

Lopes, A.M., Burgoyne, P.S., Ojarikre, A., Bauer, J., Sargent, C.A., Amorim, A., et al., 2010. Transcriptional changes in response to X chromosome dosage in the mouse: implications for X inactivation and the molecular basis of turner syndrome. BMC Genomics 11, 82.

Page left intentionally blank

25

Zebrafish: A Model System to Study the Architecture of Human Genetic Disease

Erica E. Davis, Nicholas Katsanis

Center for Human Disease Modeling, Duke University Medical Center, Durham, NC, United States

1 INTRODUCTION

The past decade has heralded an exponential growth in the number of human genomes and exomes, in large part due to the combination of improved technology and turnaround time with concomitant erosion in cost. For rare disorders, genes underlying >4000 Mendelian phenotypes have now been characterized, and account for the causal basis of as many as 50% of such conditions (Chong et al., 2015). Furthermore, genome-wide association studies (GWAS) have associated >2000 genomic loci with as many as 300 different complex traits (Manolio, 2013). For rare or common phenotypes, population-based evidence has been a consistent first-line argument supporting the implication of a locus in disease: rarity of a mutation in the general population supports the candidacy of novel Mendelian alleles (Bamshad et al., 2011), while replicated association of a locus with a measurable trait in well-powered

populations suggests a possible role in complex phenotype determinism (Altshuler et al., 2008). Although the community has excelled at increasing the size and ethnic diversity of human populations enrolled in genetic studies (Fu et al., 2013; Lek et al., 2016; Tennessen et al., 2012), such population genetic arguments often remain insufficient to explain causality. Furthermore, in silico tools that—in addition to population frequency—consider evolutionary constraint, protein structure, and other biochemical properties have only improved partially the predictive power of the genotype (Cooper and Shendure, 2011). Still, these computational approaches remain limited in their sensitivity and specificity (Castellana and Mazza, 2013), and provide a paucity of information about cellular and molecular basis of disease.

The overarching goals for genetic studies pertaining to human health can be subdivided into the following bench-to-bedside themes: (1) discover loci that underscore

TABLE 25.1   General Attributes and Similarities of Laboratory Organisms Used to Model Human Genetic Disease

	C. elegans	*D. melanogaster*	*D. rerio*	*M. musculus*
Percent identity with H. sapiens	43%	61%	70%	80%
Genome size	9.7×10^7 bp	1.3×10^8 bp	1.4×10^9 bp	2.5×10^9 bp
Exome size	28.1 Mb	30.9 Mb	96 Mb	49.6 Mb
Practical attributes				
Husbandry demands	$	$	$	$$$
Cost per animal	$	$	$	$$$
Characterized inbred strains	+	+	+	++ + +
Outbred laboratory strains	+	+	+++	++
Germline/embryonic cryopreservation	Yes	No	Yes	Yes
Lifespan	2 weeks	0.3 years	2–3 years	1.3–3 years
Generation interval	5.5 days	2 weeks	3 months	6–8 weeks
Number of offspring	300 larva	10–20 eggs	>200 embryos/clutch	10–12 pups/litter
Embryonic development	Ex vivo	Ex vivo	Ex vivo	In utero
Molecular biology tools				
Transgenesis[a]	++ + +	+++	++ + +	+++
Gene targeting[a]	++ + +	+++	+	++ + +
Conditional gene targeting	+	++	+	++ + +
Transient in vivo assays[a]	+++	++	++ + +	+
Allelic series from TILLING[a]	+++	+++	++ + +	++
Affordability of large scale screens[b]	++ + +	++ + +	+++	+
Cell biology tools				
Cell lines and tissue culture	+	++	+	++ + +
Antibody reagents	+	++	+	++ + +
In situ probes	+	+++	++ + +	+++
Disease process				
Birth defects	+	++	++ + +	++ + +
Adult-onset	++	+	+	++ + +
Behavioral	++	++	++	++
Aging	+++	++	++	++
Metabolic	++	++	+++	+++

[a] *Reverse genetics*
[b] *Forward genetics*
Table adapted with permission from Lieschke, G.J., Currie, P.D., 2007. Nat Rev Genet 8, 353–367; Davis, E.E., Katsanis, N., 2014. Biochim. Biophys. Acta 1842, 1960–1970.

pathology; (2) investigate the mechanistic basis of such genes or genomic regions as they pertain to disease; and (3) develop therapeutics to delay or ameliorate symptoms. Historically, animal studies have enhanced gene discovery, and have served critical roles in mechanistic investigation and therapeutic avenue development (Aitman et al., 2011). Gene modulation in animal models, either through knockout approaches or knock-in of human alleles, have improved our understanding of disease manifestation by offering a physiologically relevant system in which to study recapitulation of the human phenotype. Numerous laboratory models have been employed to understand the causal link between genotype and phenotypic trait. Each model system has its advantages and disadvantages including genomic conservation; anatomical and physiological similarity to humans; generation interval; versatility of the molecular toolkit; and operational cost (Table 25.1).

Although in vitro cell culture systems or biochemical assays have proven utility to inform human genetic disease (James and Parkinson, 2015; Tiscornia et al., 2011), a broad array of laboratory animal systems have been harnessed to diversify and expand the spatiotemporal study of novel disease genes and alleles. Mammalian models, such as the mouse (*Mus musculus*) or rat (*Rattus norvegicus*) traditionally have been attractive disease modeling platforms due to their high degree of genomic orthology with human [>80%; (Gibbs et al., 2004; Mouse Genome Sequencing et al., 2002)]; conserved organ structure and function; and a broad array of gene targeting or transgenesis approaches to induce disease phenotypes (for scholarly reviews see Capecchi, 2005; Devoy et al., 2012). However, in the context of modeling human genetic findings—especially for rapid clinical use—time, cost, and footprint represent major drawbacks for rodents and most other mammalian models. By contrast, invertebrate models, such as the fruit fly (*Drosophila melanogaster*) or nematode worm (*Caenorhabditis elegans*) are tractable and inexpensive alternatives. Through strong community efforts, these laboratory species have extensive availability of RNAi resources, transgenic reporters, and mutant lines (Antoshechkin and Sternberg, 2007; Ugur et al., 2016). Nevertheless, the obvious advantages of fly and worm systems are accompanied by diminished

homology with human genes [61 and 43% for fly and worm genomes, respectively; (Lander et al., 2001)]; and disparate anatomical features and molecular or cellular processes. The zebrafish (*Danio rerio*), however, is a compromise between mammals and invertebrates, and has emerged as a model system that is employed increasingly to model human disease.

Here, we will provide a comprehensive overview of zebrafish as a model of human disease phenotypes (Table 25.2). Although not the panacea to the continually compounded challenge of interpreting human genetic variation, we will discuss how in vivo complementation studies in zebrafish have accelerated gene discovery in rare and complex traits (Niederriter et al., 2013); and we will highlight successes in modeling multigene phenomena, such as copy number variants (CNVs) and oligogenic interactions. We will also summarize the current stateofthe art in terms of zebrafish model resources, molecular technologies, and phenotyping approaches. Driven by a dedicated community whose efforts have built substantial zebrafish resources over the past decades, the zebrafish has been adapted not only for research on human genetic disease, but also to toxicology (Garcia et al., 2016), aquatic physiology (Alestrom et al., 2006), and tissue regeneration studies (Gemberling et al., 2013).

TABLE 25.2 Anatomical Comparisons Between Zebrafish and Humans

Anatomy	Key similarities	Key differences
Embryology	• Cleavage, early patterning, gastrulation, somitogenesis, organogenesis are all represented	• Rapid • Influence of maternal transcripts • Nonplacental, involves hatching
Skeletal system	• Ossified skeleton comprising cartilage and bone	• Lack long bone, cancellous bone, and bone marrow • Joints are not weight-bearing
Muscle	• Axial and appendicular muscle groups • Skeletal, cardiac, and smooth muscle cell types, with similar cellular architecture and machinery • Fast and slow skeletal muscle fibers	• Fast- and slow-twitch muscle topographically separate • Tail-driven locomotion depends on alternating contraction of myotomal muscle • Appendicular muscle bulk is proportionately small
Nervous system and behavior	• Central nervous system anatomy: fore-, mid-, and hindbrain, including diencephalon, telencephalon, and cerebellum • Peripheral nervous system has motor and sensory components • Enteric and autonomic nervous systems • Specialized sensory organs, eye, olfactory system, and vestibular system, are well conserved • Complex behaviors and integrated neural function: memory, conditioned responses, and social behaviors (e.g., schooling)	• Telencephalon has only a rudimentary cortex • Fish-specific sensory organs, such as the lateral line • Fish behaviors and cognitive function are simplified compared with human behavior • Significant difference in population of dopaminergic neurons (telencephalic vs. midbrain) • Some immediate early genes and neuropeptides not conserved in zebrafish

(Continued)

TABLE 25.2　Anatomical Comparisons Between Zebrafish and Humans (*cont.*)

Anatomy	Key similarities	Key differences
Hematopoietic and lymphoid/immune systems	• Multiple hematopoietic cell types: erythrocytes, myeloid cells (neutrophils, eosinophils, monocytes, and macrophages), T- and B-lymphocytes • Coagulation cascade for hemostasis • Innate and adaptive humoral and cellular immunity	• Erythrocytes are nucleated • Possess thrombocytes rather than platelets • Kidney interstitium is the hematopoietic site
Cardiovascular system	• Multichamber heart with an atrium and ventricle • Circulation within arteries and veins • Separate lymphatic circulation • Cardiac differentiation occurs through similar signaling pathways (e.g., *nkx2.5*, *bmp2b*) • Similar electrical properties and conduction patterns (SA node, slow atrial conductance, AV node, fast ventricular conductance)	• Has left–right distinctions in cardiac anatomy, but does not have separate left–right circulations, that is, the heart has only two chambers • So far no evidence for secondary heart field derivatives • Lymph nodes have not been described • Embryos are not dependent on functioning CV system for larval development • Atria and ventricles express different myosin heavy chains during development (human hearts only later differentiate between atrial and ventricular mhc) • Heart has high regenerative capacity, even in adult animals
Respiratory system	• Cellular gas exchange • Oxygenation is dependent on circulation and hemoglobin carriage	• Respiration occurs in gills, not lungs • No pulmonary circulation • Endoderm-derived swim bladder (functioning as a variable buoyancy device), which corresponds embryologically but not functionally to the lungs
Gastrointestinal system	• Major organs: liver, exocrine and endocrine pancreas, gall bladder • Zonal specializations along the length of the absorptive alimentary tract • Immune cells in lamina propria	• Lack an acidified digestive organ • Have an intestinal bulb rather than stomach • Intestinal Paneth cell not present
Renal and urinary systems	• Glomerular anatomy and function	• Filtration occurs in anterior and posterior kidneys • Mesonephric rather than metanephric adult kidney • No bladder or prostate gland • No structure in zebrafish homologous to descending or ascending thin limb of nephron in mammals
Reproductive system	• Molecular and embryological biology of germ-cell development • Cellular anatomy of germ-cell organs, the testis and ovary	• No sex chromosomes; • Mechanism of sex determination is uncertain • Fertilization is ex vivo (no uterus or the related internal female reproductive organs) • Oocytes are surrounded by a chorion, not the zona pellucida, which must be penetrated by sperm • Nonlactating; no breast equivalent
Endocrine system	• Most endocrine systems represented, including hypothalamic/hypophyseal axis (glucocorticoids, growth hormone, thyroid hormone, prolactin), parathyroid hormone, insulin, and rennin	• Differences in anatomical distribution of glands, for example, discrete parathyroid glands do not seem to be present • Prolactin has a primary role in osmoregulation
Skin and appendages	• Ectodermal derivative • Pigmentation pattern is due to neural-crest-derived pigment cells including melanocytes	• Structures unique to fish that are specialized for the aquatic environment (including elasmoid scales, mucous cells) • Lack appendages (hair follicles, sebaceous glands) • Additional pigment cell types: xanthophores and iridophores

Table adapted with permission from Lieschke, G.J., Currie, P.D., 2007; Davis, E.E., Katsanis, N., 2014. Biochim. Biophys. Acta 1842, 1960–1970.

2 ZEBRAFISH IN THE LABORATORY: A HISTORICAL OVERVIEW

The zebrafish is a tropical teleost that has found its way from the freshwater rivers and streams of southeast Asia, to pet stores and home aquaria worldwide, and eventually to hundreds of research laboratories over the course of the past ~50 years (Fig. 25.1). One common zebrafish strain, AB, actually originates from a mating of strain A and strain B purchased on two different occasions from a pet store in Albany, Oregon (Chakrabarti et al., 1983; Streisinger et al., 1981; Wilson et al., 2014). Led in large part by University of Oregon researcher George Streisinger in the 1960s and 1970s, zebrafish transitioned from a household pet to a preeminent model of embryonic development because of a unique blend of attributes. First, one pair of zebrafish adults can produce several hundred embryos in a single mating, and can be mated repeatedly every 10–14 days for a sustained period of several months. Second, embryos develop synchronously ex vivo, enabling uninhibited visualization during early development; early organ formation is rapid, with major organ systems formed within the first few days postfertilization; and importantly, zebrafish embryos are optically transparent (Kimmel et al., 1995; Streisinger et al., 1981). Finally, zebrafish have modest diet, space, and water-quality requirements, and the emergence of husbandry standards has improved consistency and ease of care in the laboratory setting (Lawrence, 2016).

The zebrafish has a diploid genome for which the sequence is publicly available, and ~70% of human genes have at least one zebrafish ortholog (Howe et al., 2013b). The most notable structural difference of the zebrafish genome, and a major cause for the challenges of initial genome assembly, stems from the teleost specific duplication event (Amores et al., 1998; Meyer and Schartl, 1999; Postlethwait et al., 1998), which has resulted in an average of 2.28 zebrafish genes per human ortholog (Howe et al., 2013b). As a result of the genomic duplication, certain zebrafish gene pairs have acquired one of four different functional classifications: (1) redundant function; (2) neofunctionalization; (3) subfunctionalization; or (4) pseudogenization. The zebrafish orthologs of *NF1*, the genetic cause of neurofibromatosis in humans (Cawthon et al., 1990; Viskochil et al., 1990; Wallace et al., 1990), are an example of redundant function; loss of both orthologs is required to recapitulate *Ras* signaling defects
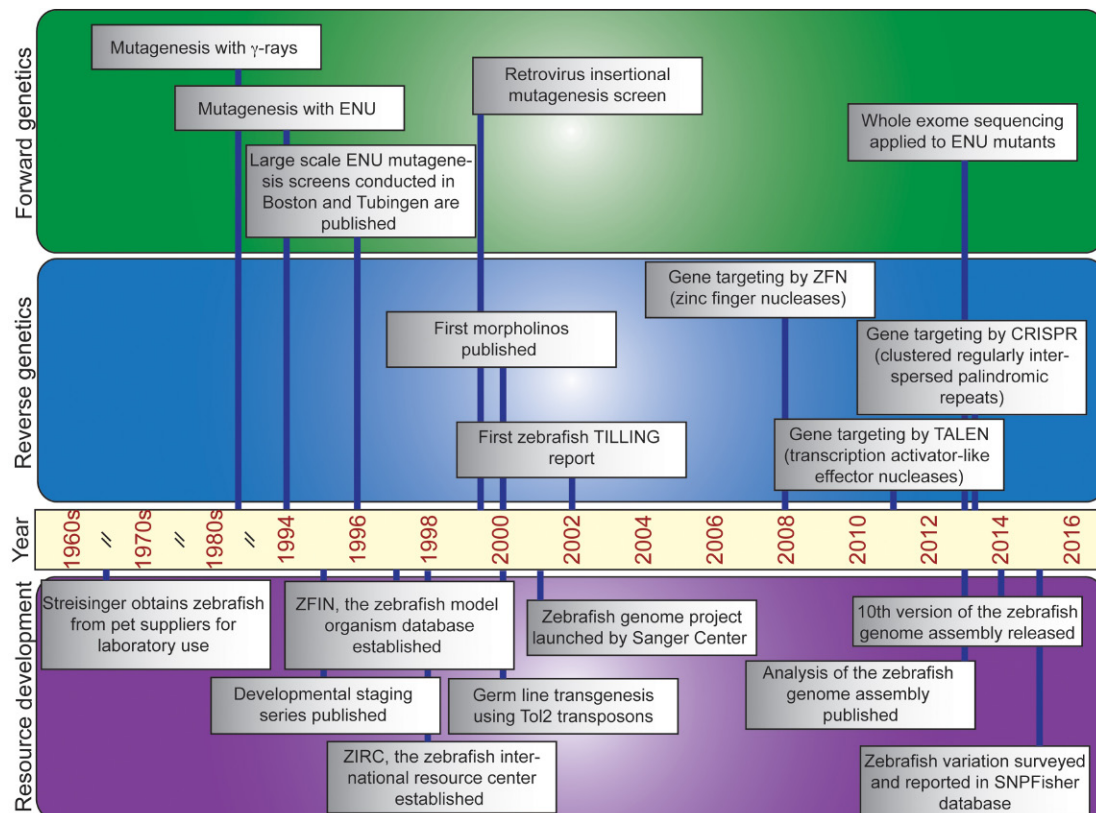
FIGURE 25.1 **Timeline summarizing landmarks in zebrafish model organism research.** Over the past ~50 years, numerous landmarks in resource development (bottom; *purple box*), forward genetic screening (top; *green box*), and reverse genetics approaches (middle; *blue box*) have improved our knowledge of vertebrate animal development, as well as human genetic disease through the use of zebrafish studies. *ENU*, *N*-ethyl-*N*-nitrosourea; *TILLING*, targeting-induced local lesions in genomes.

and relevant neuronal and tumorigenesis phenotypes observed in humans (Shin et al., 2012). Subfunctionalization is the phenomenon in which orthologous pairs of genes have the same function, but in discrete contexts. One example of subfunctionalization is the expression of the transcription factors *pax6a* and *pax6b* [orthologous to *PAX6*, the cause of multiple ocular disorders in humans (Jordan et al., 1992)]; the former is expressed primarily in the brain, and the latter has predominant expression in the pancreas (Kleinjan et al., 2008). Neofunctionalization, less frequently documented, is the phenomenon in which one of the two orthologs has acquired a distinct function from its cognate partner. However, in some instances, there is only one functional ortholog of the zebrafish pair of genes, termed pseudogenization (Force et al., 1999). In sum, the accurate characterization of the zebrafish genome has been critical to inform the development of models to mimic human phenotypes.

The zebrafish genome harbors extensive variation, and recent application of whole genome sequencing (WGS) and whole exome sequencing (WES) approaches have elucidated the differences within and across wild-type zebrafish strains (Leshchiner et al., 2012; Obholzer et al., 2012; Ryan et al., 2013). A recent WGS study comparing natural genetic variation across three laboratory-reared strains (Tupfel long fin [TL]; Wild India Kolkata [WIK]; and EkkWill [EK]) identified an average of 5.04 million single nucleotide polymorphisms (SNPs) per strain in comparison to the Zv9 reference genome, and uncovered population isolates that had arisen in the same strain maintained in independent laboratories. The SNP density in zebrafish, ~7 SNPs per 1 kb of unique sequence, is higher than that of any human population surveyed to date using WGS [2.6–4.4 SNPs per 1 kb; (Genomes Project et al., 2010)], and is publicly accessible through the SNPfisher website (Butler et al., 2015). This initial characterization of genetic variability and drift is not only a starting point toward understanding the buffering capacity of the zebrafish genome, but is also a valuable resource that will assist with the precise development of tools that depend on base complementarity to target the genome.

Extensive genomic characterization, in addition to systematic expression studies using primarily RNA in situ hybridization (Thisse and Thisse, 2008), have motivated the generation of a repertoire of zebrafish mutants and transgenic reporter lines. These data are curated in ZFIN (the Zebrafish Model Organism Database; www.zfin.org), a publicly available, searchable database (Howe et al., 2013a). Furthermore, zebrafish reagents have been centralized by ZFIN's sister organization, ZIRC (Zebrafish International Resource Center; www.zirc.org), a US-government supported center that maintains zebrafish lines, frozen sperm, and reagents for redistribution to the scientific community (Carmichael et al., 2009; Varga, 2011).

3 FORWARD GENETICS: PHENOTYPE-DRIVEN STUDIES OF VERTEBRATE DEVELOPMENT

Long before widespread access to databases or curated genomic sequencing data, zebrafish research was motivated primarily to answer questions about vertebrate embryonic development (Fig. 25.1). Initial genetic screens in any model organism were predated by the practice of enthusiasts to collect animals with unusual traits that likely arose spontaneously. This was a well-known practice for mice, and a series of spontaneous mutants with peculiar phenotypes were collected at major facilities, such as the Jackson Laboratory; however, a major drawback was the investigator's inability to generate a predetermined phenotype of interest for further genetic mapping (Kile and Hilton, 2005). Random mutagenesis revolutionized the ability to create mutant animals; although zebrafish became a laboratory model later than the mouse, the employment of mutagens to conduct efficient forward genetic screening occurred in parallel for both species. Reviewed extensively elsewhere (Lawson and Wolfe, 2011), this "phenotype-first" approach involves the following steps: (1) random, and evenly dispersed introduction of mutations throughout the genome; (2) generation of progeny who harbor recessive mutations using informative breeding schemes; (3) assessment of animals for measurable phenotypic readouts; and (4) identification of the gene and mutation underlying the phenotype. This approach involves significant time, space, and personnel but has served as an important platform to expand our understanding of embryonic development.

The first zebrafish screens were reported in the 1980s and used gamma rays to introduce recessive lethal mutations. However, this resulted in substantial chromosomal breaks and rendered the mapping to a single causal locus challenging (Chakrabarti et al., 1983; Streisinger, 1983). This approach was replaced with a more refined method, treatment of alkylating reagents including *N*-ethyl-*N*-nitrosourea (ENU), resulting in less severe genomic lesions than that of its predecessor through introduction of point mutations at the rate of approximately one mutation per genome (Mullins et al., 1994; Solnica-Krezel et al., 1994). The success of this approach motivated two large scale forward screening efforts in the 1990s; laboratories in Tübingen and Boston applied ENU to zebrafish, and within 2 years, their combined efforts led to the characterization of ~4000 embryonic lethal phenotypes affecting early patterning [e.g., gastrulation (Hammerschmidt et al., 1996; Solnica-Krezel et al., 1996); somitogenesis (van Eeden et al., 1996); notochord formation (Odenthal et al., 1996)]; organogenesis [e.g., brain (Brand et al., 1996; Jiang et al., 1996; Schier et al., 1996); cardiovascular system (Stainier et al., 1996)]; and the

craniofacial skeleton (Neuhauss et al., 1996; Piotrowski et al., 1996; Schilling et al., 1996).

How did the products of forward genetic screens inform genetic findings from humans? The initial torrent of zebrafish ENU screen publications from the December 1996 issue of *Development* (Driever et al., 1996; Haffter et al., 1996), and the ensuing characterization of such mutants contributed significantly to our knowledge of vertebrate development. However, the direct contribution as models of human disease was more modest. There are four primary reasons for this: First, because most forward screen mutants display embryonic lethal phenotypes, many postnatal or adult phenotypes would likely have been missed. Second, the breeding strategy of forward genetics paradigms mandates a recessive mode of inheritance and a loss-of-function effect, excluding the possibility of capturing dominant negative or gain-of-function alleles. Third, the randomness of chemical mutagens means that the chance of recapitulating human variants of interest, especially recurrent point mutations present in human cohorts, is low. Finally, the unique structure of the partially duplicated zebrafish genome is such that a null mutation in a zebrafish locus corresponding to an orthologous human disease gene may produce a negative phenotype. Among the genes for which there is an identifiable human ortholog, 47% have a reciprocal relationship with a human counterpart while the remainder of zebrafish genes have complex one-to-many or many-to-one orthology in comparison to the human gene (Howe et al., 2013b). Especially problematic are zebrafish genes with redundant function; the wild-type duplicate might mask the effects of a null mutation present in only one of the two orthologs. Furthermore, mutation in one of the two orthologous gene partners that have undergone neo- or subfunctionalization would have imperfect recapitulation of the human disease phenotype, thereby confounding mechanistic studies of genes underscoring such human pathologies.

Nonetheless, there are notable examples in which ENU mutants have been successful in drawing anatomical correlates for genes implicated in human disorders with anatomical defects. For instance, the *crusher*[m299] mutant was identified in a craniofacial phenotyping forward screen, and the causal nonsense mutation was mapped to *sec23a* (Lang et al., 2006). Coincident with this discovery, *SEC23A* mutations in humans were shown to cause a clinically relevant craniofacial dysmorphology, craniolenticulo-sutural dysplasia, bolstering the evidence of causality in both species (Boyadjiev et al., 2006). Importantly, the application of WGS (Obholzer et al., 2012) and WES (Ryan et al., 2013), and improved mapping strategies (Leshchiner et al., 2012) to zebrafish ENU mutants has accelerated the speed of gene discovery. As an example, this approach has also generated mechanistic hypotheses for complex traits, such as inflammatory bowel

disease (IBD). In a recent screen to identify mutants with defects in gut epithelium integrity (Ryan et al., 2013), WES of two different mutant larval progeny identified disruption of *uhrf1* and *dnmt1*, both of which have been associated previously in GWAS for IBD risk of onset in humans (Franke et al., 2010). Although infrequent, the intersection of a zebrafish mutant with a human disease locus provides functional information justifying the continued use of forward genetics approaches. Furthermore, forward screen models will maintain an important role in the context human genetics by generating hypotheses to test in human cohorts.

4 REVERSE GENETICS: TESTING CANDIDATE GENES IN ZEBRAFISH MODELS

Forward genetic screening is a powerful method that involves the grouping of phenotypic anomalies and subsequent dissection of the underlying gene and variant to inform aberrant development. However, this approach produces a random distribution of mutations and there is no certainty that targeting will occur in a specific locus of interest. To overcome this limitation, and to circumvent the cumbersome breeding strategy hallmarked by the approach, precise targeting of candidate genes and alleles can be achieved through several methods that have been developed (Fig. 25.1).

For early patterning and organogenesis phenotypes, transient gene manipulation can be achieved through the injection of either morpholino (MO) antisense oligonucleotides (gene suppression) or capped in vitro transcribed mRNA (ectopic expression) into zebrafish embryos. MOs are stable molecules that consist of a large, nonribose morpholine backbone with the four DNA bases pairing stably with mRNA at either the translation start site (to disrupt protein translation), or at exon–intron boundaries (to inhibit mRNA splicing) (Summerton and Weller, 1997). In 2000, Nasevicius and Ekker showed the first effective gene knockdown in zebrafish embryos; they injected MOs targeting five different genes shown previously through forward genetics to cause embryonic lethal phenotypes, and reproduced the mutant defects. Further, they suppressed *urod* and *shh* as a proof of concept to model the human genetic disorders hepatoerythropoietic porphyria and holoprosencephaly, respectively (Nasevicius and Ekker, 2000). Since this report, thousands of studies have used this technology to expand our knowledge of vertebrate developmental mechanisms and to mimic human pathologies. Additionally, in vivo complementation approaches—coinjection of MO and capped human mRNA harboring either wild-type or human mutant versions of a gene followed by statistical comparisons of rescue efficiency
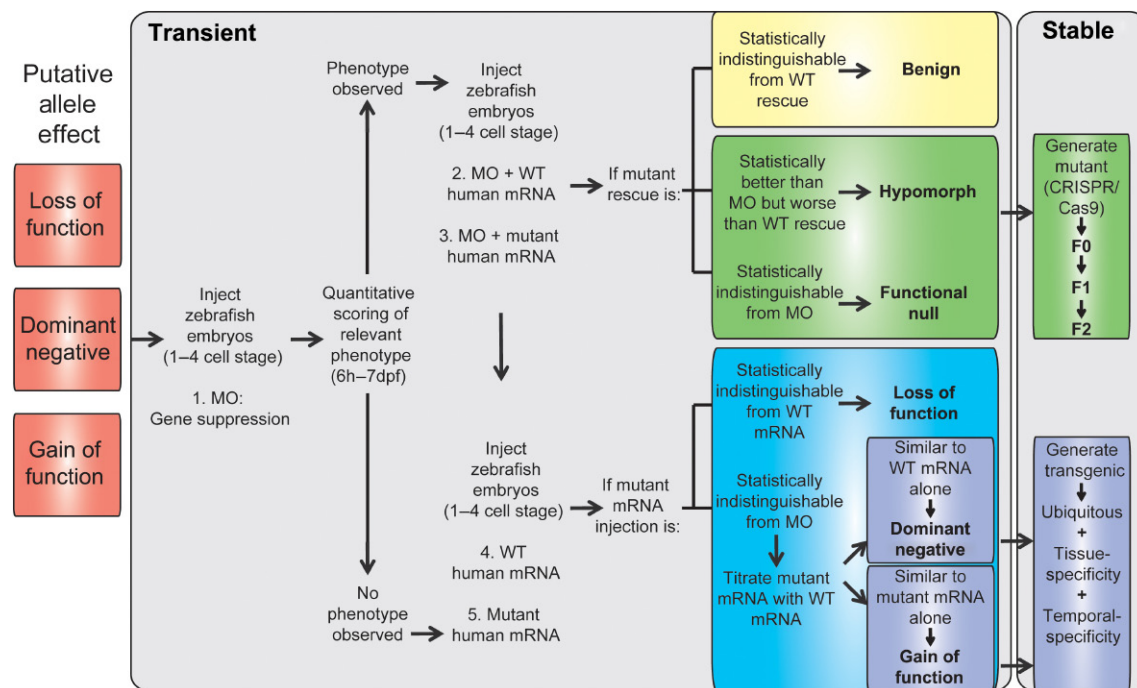
FIGURE 25.2   **In vivo complementation assay to test variants of uncertain significance.** Nonsynonymous variants, in-frame insertion/deletions, or truncating mutations that are not subject to nonsense-mediated decay can be assessed in zebrafish using the following approach. Briefly, the assay begins with (1) suppression of a gene of interest using MOs, and subsequent quantitative scoring of a phenotype relevant to the human pathology. If a phenotype is observed, the assay proceeds to loss-of-function tests. If the knockdown results in a phenotype that can be rescued similarly with (2) wild type *(WT)* and with (3) mutant mRNA, the allele is likely a benign variant *(yellow box)*. If the mutant rescue is statistically improved from MO, but worse than WT, the allele is a hypomorph *(green box)*; and if the MO and mutant rescue are indistinguishable, the variant is a functional null *(green box)*. To recapitulate transient phenotypes, a genome-editing technology, such as CRISPR/Cas9 should be employed to generate founder (F0) and subsequent stable mutants (F1 and F2). For dominant tests, if the injection of (4) WT mRNA or (5) mutant mRNA do not yield a phenotype, this indicates that the variant is a loss-of-function or the assay may have failed *(blue box)*. If the mutant mRNA alone results in a phenotype that can be titrated with increasing doses of WT mRNA to rescue the phenotype, it is likely to be a dominant negative *(lavender box)*; if the titration of mutant mRNA with WT mRNA is indistinguishable from mutant mRNA alone, the allele is scored as a gain-of-function variant *(lavender box)*. Stable transgenesis can be used to induce ectopic expression of human genes harboring dominant negative or gain-of-function variants; if ubiquitous expression results in embryonic lethality, tissue-specific or temporal-specific approaches can be used to study variant effects. *Source: Figure adapted from Niederriter, A.R., Davis, E.E., Golzio, C., Oh, E.C., Tsai, I.C., Katsanis, N., 2013. In vivo modeling of the morbid human genome using* Danio rerio. *J. Vis. Exp. 78, e50338.*

(Fig. 25.2)—have been used to test variant pathogenicity (Niederriter et al., 2013); to determine direction of allele effect (loss-of-function, dominant negative, or gain-of-function) (Niederriter et al., 2013); to dissect isoform-specific effects on variant pathogenicity (Borck et al., 2015; Sarparanta et al., 2012; Schulte et al., 2014); to test evolutionary genomic hypotheses, such as *cis* compensation (Jordan et al., 2015); and to test whether pathway-specific modulation with small molecule compounds can ameliorate zebrafish phenotypes analogous to human pathologies (Bogershausen et al., 2015).

Some 15 years of broad MO use has propelled multiple discoveries, but it is not a panacea. There are multiple drawbacks to this reagent that include: (1) limited efficacy to the first 3–5 days postfertilization (Nasevicius and Ekker, 2000); (2) with few exceptions, injected MOs and mRNAs do not confer spatial or temporal specific activity (Shestopalov et al., 2007); and (3) MOs can produce nonspecific developmental phenotypes due to

off-target effects (Eisen and Smith, 2008). Still, for transient studies of early developmental phenotypes, the MO remains a valuable reagent that can enhance human genetic studies, provided that appropriate experimental controls are employed. Such controls include: (1) direct demonstration of efficient gene-specific knockdown; this can be accomplished through either immunoblot for translation blocking MOs (dependent upon antibody availability), or RT-PCR studies for splice-blocking MOs; (2) significant and reproducible rescue of MO phenotypes with coinjection of orthologous wild-type RNA; (3) observation of similar phenotypic outcomes when two or more MOs targeting different sites of the gene are injected independently; (4) phenotypic similarities with a stable mutant; and (5) when possible, demonstration that injection of MO into embryos harboring a null allele in the same target gene do not induce additional phenotypes (Eisen and Smith, 2008; Kok et al., 2015; Rossi et al., 2015).

Independently of MOs, the molecular techniques to develop germline zebrafish mutants for a gene of interest have evolved substantially. Iterative refinement of zebrafish mutant approaches have been motivated, in part, by some key limitations of MOs, including phenotypic variability and the restriction to anatomical assessment in early larval stages. Targeting-Induced Local Lesions in Genomes (TILLING) was the first reverse genetic approach to produce germline mutations (Wienholds et al., 2002). Similar to forward screens, TILLING harnesses the mutagenic properties of ENU to introduce mutations into male zebrafish sperm, and then generate F1 families. Sperm from F1 males is cryopreserved while genomic lesions are screened in target genes. This was accomplished initially by PCR amplicon screening in early exons or critical protein domains, and is now carried out by WES to augment mutant discovery rates; at the initial time of publication, TILLING mutants were reported for ~38% of all known zebrafish protein coding genes (Kettleborough et al., 2013). This corresponds to ~60% of orthologous genes associated with a human phenotype in the Online Mendelian Inheritance in Man (OMIM; http://www.omim.org) database and has expanded to >36,000 mutant alleles (www.sanger.ac.uk/Projects/D_rerio/zmp), although it is not clear how many of these are genuinely recoverable to propagate mutant lines. While the TILLING efforts have generated a comprehensive resource of putative loss-of-function or hypomorphic models of human genetic disorders, there is the possibility that ENU may have introduced lesions at multiple sites in the genome. Therefore, it remains critical to obtain multiple mutant alleles in a gene of interest for phenotypic characterization to ensure specificity of the pathology. These guidelines also apply to transposon (Sivasubbu et al., 2007) or retrovirus (Wang et al., 2007) insertional mutants developed using similar reverse genetics approaches.

Neither forward ENU screens nor reverse TILLING approaches are experimentally tractable; fortunately genome-editing techniques have propelled the utility of zebrafish further by enabling precise and germline transmittable gene targeting that does not require excessive downstream screening to identify mutations (Wijshake et al., 2014). One approach, zinc finger nucleases (ZFN), employs a zinc finger array to target specific genomic regions (usually in the early exon of a gene), and *FokI* endonuclease guides cleavage and repair at a target cleavage site (Urnov et al., 2010); this approach was first used to generate proof-of-principle models that altered pigment formation (*gol* locus); disrupted early embryogenesis (*ntl*), or resulted in aberrant vascular endothelial growth (*kdr*) (Doyon et al., 2008; Meng et al., 2008). Second, transcription activator-like TAL effector nucleases (TALEN) emerged as a locus-specific genome editing approach that has demonstrated improved

specificity and superior germline efficacy than that of ZFN, accompanied by reduced technical costs (Bedell et al., 2012). The most recently developed genome-editing technology involves clustered, regularly interspaced, short palindromic repeats (CRISPR), which are bacterial type II systems that guide RNAs unique to a target site in the genome to drive DNA cleavage by the Cas9 endonuclease (Hwang et al., 2013). Subsequent repair of this event will either induce small insertions or deletions, or accomplish knock-in of sequence with a repair template. In a short period of time, multiple human genetic studies have reported the use of MO alongside CRISPR/Cas9 models to support human-driven WES/WGS studies. Notable examples include CRISPR/Cas9 mutagenesis of the *gata5* locus mimicking the *faut^{m236a}* zebrafish mutant and humans with congenital heart defects (Chang et al., 2013; Reiter et al., 1999); recapitulation of the human macrocephaly and gut phenotypes in humans with *CHD8* mutations that were reproduced in one CRISPR/Cas9 founder mutant (F0) model and four different *chd8* MO models (Bernier et al., 2014); modeling of *mmp21* in a rare human laterality disorder with morphant and CRISPR/Cas9 F0s (Perles et al., 2015) (Fig. 25.3); and modeling of the vertebrate hedgehog effector *PTCH1* as a candidate microphthalmia locus in which two MO and one CRISPR/Cas9 F0 zebrafish models displayed eye size phenotypes reminiscent of the *leprechaun* mutant (Bibliowicz and Gross, 2009; Chassaing et al., 2016).

Although a multitude of studies have now shown that MOs and CRISPR/Cas9 often produce equivalent, or at least overlapping phenotypes, there have also been reports of discordance. Two publications in 2015 highlighted an absence of phenotype in mutant models of vascular development, which disagreed with clear phenotypes in MO-induced zebrafish models. First, Kok et al. (2015) selected more than 20 genes with previously published morphant phenotypes, and used ZFN, TALEN, or CRISPR/Cas9 to generate null mutations in each gene; they observed mutant phenotypes in only a minority of genes assessed and concluded that MOs produce a high false-positive rate. However, an independent study that probed the discrepant phenotypes of endothelial extracellular matrix gene morphants and mutants corresponding to *egfl7* and *vegfaa*, showed that compensatory networks can be activated in mutants (but not morphants) to buffer against phenotype-inducing thresholds (Rossi et al., 2015). While these studies have motivated the zebrafish community to assess critically the best practices for transient gene suppression approaches, they have also opened the tantalizing possibility that genetic compensation can account for phenotypic differences across different strains or species in the context of loss of orthologous gene function. Assessment of additional genes with diverse functions will
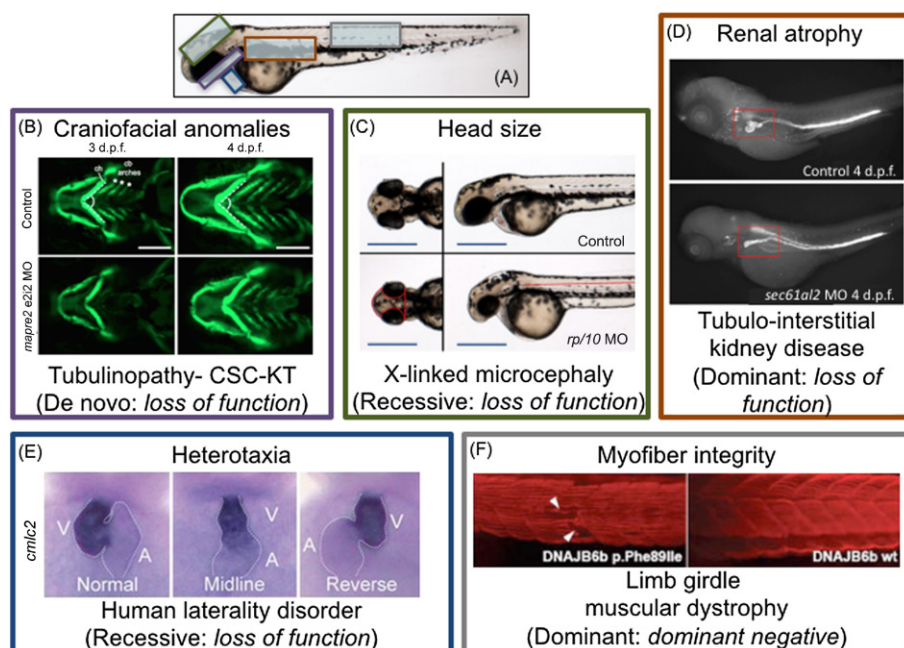
FIGURE 25.3 **Zebrafish models of human genetic disease.** In vivo assays in zebrafish can be applied to determine the physiological relevance of a candidate gene in various organ systems; these models can then be used to determine the direction of allele effect (i.e., loss-of-function or dominant negative) underlying diverse inheritance patterns. (A) Representative bright field lateral view of a 2 day postfertilization (dpf) wild-type embryo with anatomical features highlighted with colors corresponding to each example. (B) Craniofacial anomalies (top, left): ventral view of cartilage structures as demarcated by automated live imaging of *-1.4col1a1:egfp* transgenic larvae at 3 and 4 dpf using Vertebrate Automated Screening Technology *(VAST)* as a model of a tubulinopathy caused by mutations in *MAPRE2*. CSC-KT, Circumferential skin crease—Kunze type. (C) Head size (top, center): ventral and lateral views of 2 dpf larvae; *rpl10* suppression mimics the head size defect of a pedigree with X-linked microcephaly. (D) Renal atrophy (top, right): lateral view of 4 dpf controls and *sec61al2* morphants immunostained with antiNa + /K + -ATPase antibody to assess renal tubular structure in a model of autosomal dominant tubululo-interstitial kidney disease; this defect was reproduced in CRISPR/Cas9 F0 founders. (E) Heterotaxia (bottom, left): *mmp21* mutants and morphants display left-right asymmetry defects at 2 dpf as indicated by RNA in situ hybridization with *cmlc2* to model a rare recessive heterotaxia syndrome; V, ventricle; A, atrium;. (F) Myofiber integrity (bottom, right): injection with mutant human *DNAJB6* mRNA resulted in myofiber detachment at 2 dpf as indicated by immunostaining with slow myosin antibody to model adult onset limb girdle muscular dystrophy. *Source: Image reproduced with permission from (B) Isrie, M., Breuss, M., Tian, G., Hansen, A.H., Cristofoli, F., Morandell, J., et al., 2015. Mutations in either TUBB or MAPRE2 cause circumferential skin creases Kunze type. Am. J. Hum. Genet. 97, 790–800. (C) Brooks, S.S., Wall, A.L., Golzio, C., Reid, D.W., Kondyles, A., Willer, J.R., et al., 2014. A novel ribosomopathy caused by dysfunction of RPL10 disrupts neurodevelopment and causes X-linked microcephaly in humans. Genetics 198, 723–733. (D) Bolar, N.A., Golzio, C., Zivna, M., Hayot, G., Van Hemelrijk, C., Schepers, D., et al., 2016. Heterozygous loss-of-function SEC61A1 mutations cause autosomal-dominant tubulo-interstitial and glomerulocystic kidney disease with anemia. Am. J. Hum. Genet. 99, 174–187. (E) Perles, Z., Moon, S., Ta-Shma, A., Yaacov, B., Francescatto, L., Edvardson, S., et al., 2015. A human laterality disorder caused by a homozygous deleterious mutation in MMP21. J. Med. Genet. 52, 840–847. (F) Sarparanta, J., Jonson, P.H., Golzio, C., Sandell, S., Luque, H., Screen, M., et al., 2012. Mutations affecting the cytoplasmic functions of the co-chaperone DNAJB6 cause limb-girdle muscular dystrophy. Nat. Genet. 44, 450–455, S451–452.*

be required to determine whether or not this is a widespread phenomenon.

5 HUMANIZING ZEBRAFISH TO STUDY HUMAN GENETIC VARIATION

An expanding number of reports have demonstrated the ability of zebrafish to assist with the dissection of allele causality under Mendelian paradigms, as well as more complicated phenomena including oligogenic disorders and contiguous gene syndromes. Certainly, there are some experimental limitations, including a lack of orthology for ~30% of human genes in the zebrafish genome (Howe et al., 2013b), and the technical challenges

associated with in vitro transcription of mRNA >6 kb in length (Niederriter et al., 2013). Even so, the major benefits of zebrafish—experimental tractability and cross-species structural and functional conservation—have been harnessed to establish: (1) physiological relevance of gene alteration to human pathology; (2) variant pathogenicity, especially for nonsynonymous changes; and (3) direction of allele effect for a multifarious array of human genetic conditions with diverse modes of inheritance, phenotypes, and ages of onset.

5.1 Single Gene Effects in Mendelian Disease

Zebrafish have been instrumental in modeling disorders that segregate primarily under a recessive mode

of inheritance, especially congenital or childhood onset conditions with an orthologous anatomical structure. Through different strategies, zebrafish have provided layers of evidence to support the candidacy of a gene/allele in disease. Regardless of whether the genetic evidence is strong (multiple cases harboring unambiguous loss-of-function variants in the same gene); or exemplifies an "n-of-one" (ultra-rare condition in which a single case has rare variation that is predicted to impact protein function), a starting point in modeling recessive conditions is to recapitulate the disease phenotype in a zebrafish model. For instance, zebrafish have provided mechanistic insight into primary ciliary dyskinesia (PCD), a condition observed in 1/10,000 live births that is caused by almost exclusively null changes (nonsense, frameshift, or splice-site) (Praveen et al., 2015). Transient MO-based studies have shown that proteins of a priori unknown function including *CCDC39*, *ARMC4*, and *ZMYND10* give rise to left–right asymmetry defects in zebrafish that are consistent with the situs inversus phenotypes observed in affected humans (Hjeij et al., 2013; Merveille et al., 2011; Zariwala et al., 2013). A more poignant problem in clinical genetics, however, is the challenge of supporting the candidacy of ultra-rare alleles in isolated cases or pedigrees. Community efforts to identify multiple rare cases with mutations in the same gene (Sobreira et al., 2015) can be unfruitful, necessitating the use of an animal model (Hieter and Boycott, 2014). This can be especially challenging for the clinically heterogeneous neurodevelopmental defects that encompass microcephaly, intellectual disability, autism spectrum disorders, and structural anomalies of the brain. One example is the identification of a rare missense mutation in the 60S ribosomal protein component gene *RPL10* that segregated with microcephaly in three males of a single X-linked pedigree. Suppression of the gene in zebrafish embryos resulted in a significant reduction in larval head size (Fig. 25.3), and in vivo complementation with mutant mRNA failed to rescue the phenotype indicating that the p.K78E variant shared by affected individuals was a loss-of-function allele (Brooks et al., 2014). Clinical relevance and variant pathogenicity was also determined in a similar fashion for a candidate pontocerebellar hypoplasia locus, *EXOSC3*, encoding exosome component 3. Wan et al. (2012) identified nonsynonymous changes in four affected siblings through WES, and used zebrafish assays to demonstrate that the cerebellar phenotype could be mimicked in zebrafish *exosc3* morphants, and that coinjection of human mRNA harboring these changes failed to rescue the neuroanatomical defect. Finally, the use of complementation studies have uncovered apparent isoform-specific effects in recessive neurological disease, such as the observation that candidate missense changes present in both *BRF1* transcripts, encoding B-related factor involved in RNA transcription, are only deleterious in the short protein isoform implicating it specifically in cerebellar hypoplasia and intellectual disability (Borck et al., 2015).

Differing from recessive conditions, in which the variant is more likely to result in a loss of protein function, traits that segregate in an autosomal dominant paradigm could be the result of three mechanisms: (1) loss-of-function; (2) gain-of-function; or (3) dominant negative. A heterozygous null variant in some pediatric-onset dominant diseases that segregates in multiple affected individuals in a multigenerational pedigree is often sufficient to suggest a haploinsufficiency model; this has been confirmed in zebrafish through MO-induced gene suppression. For example, dilated cardiomyopathy is caused by ablation of the gene encoding heat shock protein cochaperone BCL2-associated athanogene 3 (*BAG3*), and knockdown studies in zebrafish reproduce the human cardiac defects (Norton et al., 2011). Likewise, autosomal dominant tubule-interstitial kidney disease (ADTKD) has been modeled in zebrafish to show both phenotypic relevance and loss-of-function effects of putative causal alleles. CRISPR/Cas9 F0 mutants and morphants of *sec61a1* displayed renal tubular atrophy consistent with the human phenotypes (Fig. 25.3); and assay of two different missense changes suggested that allelism at that locus was consistent with patient severity (a functional null in the syndromic ADTKD pedigree; a hypomorphic variant in the family with renal disease and anemia) (Bolar et al., 2016).

Not all dominant conditions are the result of insufficient dose, however, and injection of human mRNA bearing a mutation can uncover dominant negative effects in developing zebrafish. One example is the transient functional study of the cochaperone DNAJB6, mutations which cause adult-onset limb girdle muscular dystrophy (Sarparanta et al., 2012). Coinjection of mutant *DNAJB6* mRNA in the presence of equivalent amounts of wild-type transcript resulted in myofiber defects in zebrafish embryos (Fig. 25.3); injection of increasing amounts of wild-type mRNA with a fixed concentration of mutant transcript resulted in a phenotypic rescue, suggesting the dominant toxicity of the mutant alleles. Given the nature of dominant mutations (pathogenic in heterozygosity), the use of zebrafish to investigate such disorders will likely remain restricted to transient MO, CRISPR/Cas9 F0, or mRNA-based studies until the refinement of more tractable gene suppression/expression techniques in zebrafish has been achieved.

In addition to recessive or dominant inheritance, variants can arise de novo; these phenomena are significant contributors to the human mutational burden (Veltman and Brunner, 2012). Similar to dominant inherited disorders, de novo variants can either cause haploinsufficiency, novel allele function, or dominant negative effects. Therefore use of an unbiased approach to discern the

direction of allele effect is critical. For example, zebrafish were employed to study de novo missense mutations in *CACNA1C*, encoding the voltage-gated calcium channel Cav$_{1.2}$, in Timothy syndrome (TS), a pediatric disorder hallmarked by cardiac arrhythmias, syndactyly, and craniofacial dysmorphisms. Expression of mutant mRNA and suppression of *cacna1c* in zebrafish larvae not only showed that the mutation confers a gain-of-function effect, but also demonstrated a novel role for Cav1.2 in the nonexcitable cells of the developing mandible (Ramachandran et al., 2013). Taken together, these Mendelian examples demonstrate the diversity of zebrafish as a tool to characterize diverse pathomechanisms.

5.2 Second-Site Modifiers and Oligogenic Effects

Dissection of second-site phenotype modification in primarily recessive human genetic disorders is a challenge, primarily due to the power limitations of small cohorts. However, multiple modifier and oligogenic hypotheses have been tested successfully in zebrafish and the ciliopathies epitomize this approach. Underscored by the structural or functional defects of the primary cilium, the ciliopathies have been causally linked with >100 different loci and can give rise to a constellation of human phenotypes (Davis and Katsanis, 2012). Dissection of the genetic architecture of Bardet–Biedl syndrome (BBS), a ciliopathy characterized by retinal degeneration, truncal obesity, postaxial polydactyly, renal abnormalities and intellectual disability, using zebrafish models demonstrated: (1) the pathogenic potential of >100 alleles identified in cases, most of which are nonsynonymous changes; (2) revealed an unexpected contribution of dominant negative variants in oligogenic pedigrees with BBS; (3) provided sensitivity (98%) and specificity (82%) metrics for the in vivo complementation assay to predict allele pathogenicity; and (4) has suggested that as many as >50% of cases have one to four additional heterozygous deleterious variants in BBS genes outside of the primary causal locus that interact either additively or synergistically to aggravate phenotype (Lindstrand et al., 2016; Zaghloul et al., 2010). Transient zebrafish in vivo complementation assays have similarly been used to support the *RPGRIP1L* p.A229T as a modulator of retinal endophenotypes in ciliopathies (Khanna et al., 2009); *TTC21B* as a common contributor to mutational burden in ciliary disease (Davis et al., 2011); *RET* as a modifier of Hirschsprung phenotypes in BBS (de Pontual et al., 2009); and trans-heterozygous interaction between *DNAH5* and *DNAH6* as a likely molecular basis for the heterotaxy phenotypes of some PCD cases (Li et al., 2016). Increased genetic resolution of oligogenic phenomena in disorders such as the ciliopathies offers a platform to test tractability thresholds in zebrafish (Lindstrand et al., 2016); it is unclear whether coinjection

of more than two or three MOs will still yield meaningful results.

Although the semiclosed organellar basis of the ciliopathies makes them a tractable model to study epistasis, the use of zebrafish modeling is not exclusive to this class of disorder. Notably, zebrafish interaction studies were used to support the candidacy of homozygous digenic mutations in *OTUD4* and *RNF216*, encoding components of the ubiquitin system, as the genetic basis of ataxia with hypogonadotropic hypogonadism (Margolin et al., 2013). Compared to exacerbative multigene effects, protective effects are even more challenging to identify in human genetics. For example, spinal muscular atrophy (SMA) is caused by mutations in *SMN1*, but mutation-bearing unaffected individuals have been shown to overexpress plastin 3 (*PLS3*). To test the putative protective effects of *PLS3* or *CORO1C*, another F-actin binding protein, in the absence of *SMN1*, these genes were overexpressed and suppressed in zebrafish larvae and phenotyped using axon length and growth measures (Hosseinibarkooie et al., 2016; Oprea et al., 2008).

5.3 Contiguous Gene Syndromes

Frequently arising de novo, CNVs account for a significant proportion of the molecular basis of human genetic disease (Carvalho and Lupski, 2016). This class of variation can range in size from a few thousand to millions of base pairs; is not identifiable by conventional chromosomal banding; and in the absence of specific depth of coverage algorithms, can also be missed by WES (Katsanis and Katsanis, 2013). Thus, the augmented use of array comparative genomic hybridization (aCGH), and SNP arrays in recent years has uncovered a plethora of CNVs, with the progressive transition to whole genome sequencing expected to enrich the catalogs of this mutational class further. Although genotype–phenotype correlations among affected individuals with either overlapping CNVs, or clinical comparisons of individuals with deleterious point mutations in genes that are encompassed by CNVs, can assist in narrowing specific genetic drivers, this class of genomic lesion has been historically intractable to functional study (Lindsay, 2001). Until recently, the majority of reports aiming to elucidate human CNVs utilized the mouse, and rather than unbiased systematic generation of mutants corresponding to each gene within the CNV, mutants are prioritized typically because of a priori biological function that could pertain to patient phenotype (Iyer and Girirajan, 2015). Some notable examples include the *Rai1* null mutant or overexpression models that recapitulate most neurological, body mass, and craniofacial aspects of the reciprocal 17p11.2 CNV (Bi et al., 2005; Walz et al., 2003); or the *Tbx1*$^{-/-}$ mouse that has demonstrated the cardiac and craniofacial anomalies associated with 22q11.2 deletion syndrome

(Lindsay et al., 2001). Because of their superior experimental tractability in comparison to mammalian counterparts, zebrafish have emerged, recently, as a robust model to dissect both recurrent and nonrecurrent CNVs. Shown previously to model CNVs in malignant tumors (Ceol et al., 2011), one of the first reported examples to dissect a germline CNV in zebrafish was the systematic assessment of 29 genes in the recurrent reciprocal 16p11.2 duplication/deletion CNV. This locus is associated with neurocognitive defects that include intellectual disability, autism spectrum disorder, and epilepsy for either the deletion or duplication, and schizophrenia that is associated primarily with the duplication CNV (McCarthy et al., 2009; Weiss et al., 2008). Using mRNA suppression and overexpression, and focusing on the mirrored macro- and microcephaly phenotypes as directly relevant and measurable readouts for the mirrored CNVs, respectively, Golzio and coworkers showed that *KCTD13* is the major driver of head size phenotypes in zebrafish. Additionally, pairwise gene modulation of *KCTD13* and every other gene in the 16p11.2 region followed by head size measurement of embryo batches revealed that mitogen-activated protein kinase 3 (*MAPK3*) and major vault protein (*MVP*) interact genetically with *KCTD13* to worsen the phenotype (Golzio et al., 2012). In another example of CNV dissection, MO-induced knockdown of three genes orthologous to the 8q24.3 nonrecurrent deletion CNV showed that the loci encoding the planar cell polarity effector *SCRIB*, and the splicing factor, *PUF60* were the major drivers of phenotype. Both genes were implicated synergistically in the neurological and short stature phenotypes; whereas *SCRIB* appeared to be the main contributor to the renal abnormalities and coloboma; and *PUF60* ablation was linked to the cardiac phenotypes observed in the five individuals harboring overlapping microdeletions in the genomic region on 8q (Dauber et al., 2013). Finally, in vivo dissection of the 17p13.1 CNV, the underlying cause of a microdeletion syndrome involving intellectual disability, poor to absent speech, dysmorphic features, and microcephaly, showed that the combinatorial effects of at least three genes likely cause the head size defects in affected individuals. Dosage perturbation of the nine genes localized to the minimal interval the 17p13.1 locus revealed that at least three transcripts (*ACADVL*, *DVL2*, and *GABARAP*) are the major drivers of neurodevelopment phenotypes (Carvalho et al., 2014). Together, these studies demonstrate how zebrafish have provided insight into penetrance and phenotypic variability of reciprocal CNVs. The single-gene tests and genetic interaction assays have helped to classify a growing number of CNVs into recently described paradigms to explain clinical manifestation in cases. The 16p11.2 CNV exemplifies the *cis*-epistasis simplex CNV model in which one or multiple genes are necessary and sufficient to cause phenotypes but epistasis interactions modulate the expressivity and penetrance of the phenotype; or the 8q24.3 CNV typifies the *cis*-epistasis complex CNV model in which multiple primary driver genes are sufficient to cause independent or similar phenotypes (Golzio and Katsanis, 2013).

5.4 From GWAS to Biology Underlying Complex Traits

Unlike penetrant Mendelian alleles or driver genes in CNVs, GWAS are more likely to detect loci of modest effect. One consequence of this is that GWAS alone have been challenged to link risk loci with genes, while poor statistical power and scant functional data hamper the identification of potential epistatic interactions. However, recent reports have indicated promise for the utility of zebrafish to dissect genes at or near loci that confer significant risk for some complex traits. Rare alleles identified after GWAS and targeted resequencing of the associated locus are reasonably straightforward to study; the experimental paradigm is similar to that of Mendelian conditions. For example, combined in vitro analysis of enzyme stability with vascular integrity studies in the larval retina demonstrated a critical role for a rare variant in *CFI*, the gene encoding complement factor I, thus providing direct evidence supporting a loss of CFI function in age-related macular degeneration (AMD) (van de Ven et al., 2013). Similarly, in vivo complementation assays were critical to show pathogenicity for a rare missense change (p.I397V) in *BBS10* shown to be associated with type 2 diabetes (T2D) in Finnish individuals (Lim et al., 2014). Importantly, this study demonstrated a phenotypic continuum in which loss of function of a gene causing a Mendelian disorder (BBS) could also contribute to a complex trait (T2D).

Zebrafish have also been employed to test the physiological relevance of novel risk loci in the absence of underlying rare variants. For example, functional testing of loci associated with platelet count in cohorts of European ancestry identified 11 novel genes implicated in *D. rerio* blood cell formation (Gieger et al., 2011). Additionally, Liu et al. conducted a GWAS to identify risk factors for chronic kidney disease in African American populations. To assess the physiological relevance of candidate loci, they suppressed orthologous zebrafish genes systematically and analyzed glomerular filtration defects in zebrafish; these efforts yielded *KCNQ1* as a functionally relevant candidate (Liu et al., 2011). In addition, zebrafish have been instrumental in dissecting the relative contribution of the chromosome 22q12 locus, encompassing *APOL1* (apolipoprotein L1), and *MYH9* (myosin heavy chain IIA), to nephropathy risk in African Americans with sickle cell disease (SCD). Suppression or CRISPR/Cas9 genome-editing of *apol1* and *myh9* in zebrafish independently give rise to proteinuria (Anderson et al., 2015;

Muller et al., 2011), and in vivo complementation with human mRNA harboring the common *APOL1* coding G1 (encoding p.S342G and p.I384M in *cis*) or G2 (encoding p.N388del:Y389del) risk alleles indicated that both changes are pathogenic. Importantly, a genetic interaction between *APOL1* and *MYH9* loci could only be detected in zebrafish renal models in the context of anemic stress, a surrogate for SCD (Anderson et al., 2015). These exemplars provided an entry point into biology. Further work remains to dissect the combinatorial effects of multiple GWAS hits; to probe the mechanistic basis for promoting disease risk; and to develop tools to assess noncoding association loci.

6 MODELING ADULT ONSET DISEASE IN EMBRYONIC OR LARVAL STAGES

With some exceptions, the majority of the applications of zebrafish to study human genetic disorders have been focused on genes and variants identified in congenital and pediatric conditions. Nevertheless, there are multiple instances in which zebrafish have been useful in the study of adult-onset disorders through either: (1) the ability to generate a directly related phenotype in zebrafish larvae that is similar/relevant to the adult-onset disorder; (2) assessment of a surrogate (indirectly or partially related) phenotype in early zebrafish development that is relevant to the gene function of the human condition; or (3) development of a stable mutant (loss-of-function) or transgenic (gain-of-function or dominant negative) zebrafish raised to adulthood. Adult-onset muscular dystrophies represent one example; most patients with *DNAJB6* mutations had an age of onset ranging from 20 to 60 years, yet myofiber detachment was detected in zebrafish larvae at 2 days postfertilization (Sarparanta et al., 2012). AMD was another adult-onset example. Although macular degeneration is not a phenotype that can be assessed in zebrafish embryos, vascular integrity is a quantitative phenotype that can be scored in larval stages and is relevant to AMD pathology (van de Ven et al., 2013). Finally, there are certain conditions in which adult zebrafish is the optimal model, particularly for adult neurodegenerative conditions, such as schizophrenia, Huntington, Parkinson, and Alzheimer disease [reviewed extensively in (Bandmann and Burton, 2010; Best and Alderton, 2008)], and have involved stable mutant or transgenic models. In one study that modeled neurodegeneration, expression of human 4-repeat Tau showed TAU accumulation within neuronal cell bodies and axons in neurons throughout the adult brain, reminiscent of neurofibrillary tangles (Bai et al., 2007). Some human phenotypes, such as the behavioral phenotypes diagnostic of psychiatric disease, are not immediately observable through anatomic or histological methods,

making it necessary to employ more sensitive methods of analysis. For this purpose, memory and learning assays (Fernandes et al., 2016) and conditioned avoidance studies (von Trotha et al., 2014) can be employed in adult fish to detect subtle behavioral abnormalities.

7 THERAPEUTIC DISCOVERY IN ZEBRAFISH MODELS OF DISEASE

An ever-increasing repertoire of human disease models has been generated in zebrafish. Not only has this resource been useful in establishing the relevance of a candidate gene to human pathology, but it has also informed the direction of effect of mutations. A natural extension of this paradigm is to use zebrafish models to identify novel therapeutic avenues. In addition to conserved genomic content and physiology, zebrafish also has documented conservation of pharmacology and drug metabolism akin to that of human (e.g., functioning livers, blood–brain barriers, and kidneys) (Jeong et al., 2008; Li et al., 2011). Furthermore, the combined experimental tractability in which embryos will uptake small molecules when bathed in media, combined with the widespread availability of well-characterized tool compounds or FDA-approved chemical libraries make zebrafish an attractive choice for high-throughput screening. Although reviewed extensively elsewhere (MacRae and Peterson, 2015; Tan and Zon, 2011; Zon and Peterson, 2005), there are several notable examples in which treatment of zebrafish disease models with small molecules have been successful. In some instances, the known function of the human disease gene is sufficient to suggest a candidate therapeutic modulator in zebrafish; this was true for the recent identification of *NANS*, the causal gene underlying an infantile-onset severe developmental delay and skeletal dysplasia disorder. *NANS* encodes the synthase for *N*-acetylneuraminic acid (NeuNAc; sialic acid). MO-induced suppression of the zebrafish ortholog *nansa* recapitulated the abnormal skeletal development and, crucially, could be rescued with exogenous treatment with sialic acid (van Karnebeek et al., 2016). In other examples, modulation of a signaling pathway with a small molecule can restore signaling output, and thus improve the disease phenotype. Mutations in *RAP1A* have been implicated as a molecular cause of Kabuki syndrome, a congenital disorder with a characteristic facial gestalt and accompanying intellectual disability, short stature, cardiac, and renal anomalies (Bogershausen et al., 2015). Suppression or CRISPR/Cas9 mutation of the zebrafish orthologs, *rap1a* and *rap1b*, reproduced the mandibular defects observed in patients and elucidated the involvement of known Kabuki syndrome genes in MEK/ERK signaling; administration of the MEK inhibitor PD184161 was shown to

improve relevant phenotypes in zebrafish (Bogershausen et al., 2015).

In addition to candidate treatment approaches, large-scale phenotypic screens have also shown promise in either uncovering repurposing opportunities for known drugs, or discovering novel compound classes. For example, disruption of *ACVR1* activates the bone morphogenetic protein (BMP) type I receptor and causes fibrodysplasia ossificans progressiva (FOP), a congenital disorder of progressive postnatal ossification of soft tissues (Shore et al., 2006). By screening a diverse chemical library of 7500 compounds, Yu et al. (2008) identified a pyrazolopyrimidine called dorsomorphin as a BMP inhibitor that could compensate for the overactive signaling induced by *ACVR1* mutations; this compound, and its derivatives, are currently in mammalian trials for FOP (MacRae and Peterson, 2015). In sum, zebrafish phenotype screens have potential to contribute to novel therapeutic development for human genetic disorders, but are contingent upon a robust and quantifiable phenotype that can be assessed in an automated fashion. Further work is required to characterize compound exposure in zebrafish, and to understand how timing and delivery in zebrafish is relevant to that of human. Nonetheless, the increasing number of phenotype screens in zebrafish is testament to its growing niche in drug development.

8 CONCLUSIONS: THE FUTURE OF ZEBRAFISH AS A HUMAN GENETIC DISEASE MODEL

Here, we have highlighted how the zebrafish has emerged as a tractable animal model system both to inform the architecture of human genetic phenomena, and also to generate hypotheses that can be tested in human cohorts. As genomic data from human cohorts continues to amass, the community will continue to grapple with variant interpretation, as well as establishment of direction of effect as a necessary preamble to understanding pathomechanism. Zebrafish represents a premier tool by offering the benefits of high genomic and physiological conservation to that of humans, while maintaining ease of use and low cost. To keep pace with human genomics, however, further refinements are essential. These include: (1) to diversify the modulation parameters of the zebrafish genome in discrete spatiotemporal contexts; (2) to improve the resolution at which phenotypes are assessed, while still maintaining speed and throughput; and (3) to improve our ability to study noncoding regions of the genome. First, much of the utility of zebrafish has come from transient models in which MO-induced gene suppression or mRNA injection has been employed to elicit short-term, and finite effects during the first few days of development. Genome-editing tools, especially

CRISPR/Cas9, have offered a rapid new reverse genetics approach; we anticipate further refinement of this method through the use of tight spatiotemporal regulation mediated by transgenic Cas9 expression driven by tissue-specific promoters (Ablain and Zon, 2016). Further, the employment of multiplexed CRISPR/Cas9 strategies (Jao et al., 2013) and knock-in approaches using repair templates (Auer et al., 2014) will accelerate our ability to model human genetic conditions while also enabling greater precision.

Our capacity to assess measurable phenotypic differences in zebrafish is dependent upon the ability to resolve the anatomical structure of interest, and the time involved to record these data for large batches of embryos. The classic methods of RNA in situ hybridization, tissue sectioning, and histological processing are cumbersome and offer a mere snapshot of a single time point or context. New technologies have emerged to catalog either normal or diseased zebrafish phenotypes with exquisite detail down to the level of individual cells with microcomputed tomography (micro-CT) (Cheng et al., 2016); however, it will likely require augmented throughput capacity before it is embraced broadly by the community. In parallel, automated imaging technologies have been developed to overcome manual orientation challenges associated with whole-mount imaging (Pardo-Martin et al., 2010). One system, the Vertebrate Automated Screening Technology (VAST) has been used to acquire images of the larval craniofacial skeleton to model a novel tubulinopathy in humans caused by mutations in *TUBB* or *MAPRE* (Fig. 25.3), which is hallmarked by dysmorphic facial features, circumferential skin creases, and intellectual disability (Isrie et al., 2015). Development of additional transgenic reporter lines that demarcate organ systems or cell types of interest will be critical to advance further the automation of live imaging, or indeed the defined transcriptomic profiling of zebrafish in specific spatiotemporal contexts (Junker et al., 2014).

Finally, as with all laboratory model organisms, it is important to be cognizant of the limitations of the zebrafish system. Although there is substantial conservation between zebrafish and human physiology, there are some organ systems that are intractable in zebrafish (e.g., pulmonary physiology). Furthermore, there are certain processes that are either divergent from human, or have not yet been elucidated fully in zebrafish. Notably, sex determination in zebrafish remains poorly understood; *D. rerio* lack heteromorphic sex chromosomes, and genetic regions on chromosomes 4, 5, and 16 have been associated but not fine-mapped to the level of the contributory genes (Nagabhushana and Mishra, 2016; Wilson et al., 2014). Further, the majority of zebrafish models of human disease have focused on coding regions of the genome that have greater sequence conservation, rather

than regulatory regions and intergenic sequences associated with disease. Whole human genomes will continue to be generated, and further GWAS predicting noncoding loci to confer risk for complex traits will be uncovered; therefore, use of the zebrafish to study intergenic regions must expand. This work is possible in some instances, but examples are still sparse, such as the testing of multiple noncoding sequences within the regulatory domain of *IRX3*, associated with obesity in humans. This approach identified transgenic expression of a reporter gene in the zebrafish pancreas; and suppression of the *irx* transcript resulted in the physiologically relevant reduction in the number of pancreatic beta cells (Ragvin et al., 2010).

In summary, *D. rerio* is a small fish that has had a large impact on informing human genetic disease. We expect that the continued expansion of the molecular toolkit; increased phenotyping throughput capacity; and improved resolution of anatomical and molecular signatures will be necessary to achieve a saturated understanding of the morbid human genome and to eventually elucidate novel therapeutic avenues.

Acknowledgments

References

Ablain, J., Zon, L.I., 2016. Tissue-specific gene targeting using CRISPR/Cas9. Methods Cell Biol. 135, 189–202.

Aitman, T.J., Boone, C., Churchill, G.A., Hengartner, M.O., Mackay, T.F., Stemple, D.L., 2011. The future of model organisms in human disease research. Nat. Rev. Genet. 12, 575–582.

Alestrom, P., Holter, J.L., Nourizadeh-Lillabadi, R., 2006. Zebrafish in functional genomics and aquatic biomedicine. Trends Biotechnol. 24, 15–21.

Altshuler, D., Daly, M.J., Lander, E.S., 2008. Genetic mapping in human disease. Science 322, 881–888.

Amores, A., Force, A., Yan, Y.L., Joly, L., Amemiya, C., Fritz, A., et al., 1998. Zebrafish hox clusters and vertebrate genome evolution. Science 282, 1711–1714.

Anderson, B.R., Howell, D.N., Soldano, K., Garrett, M.E., Katsanis, N., Telen, M.J., et al., 2015. In vivo modeling implicates APOL1 in nephropathy: evidence for dominant negative effects and epistasis under anemic stress. PLoS Genet. 11, e1005349.

Antoshechkin, I., Sternberg, P.W., 2007. The versatile worm: genetic and genomic resources for *Caenorhabditis elegans* research. Nat. Rev. Genet. 8, 518–532.

Auer, T.O., Duroure, K., De Cian, A., Concordet, J.P., Del Bene, F., 2014. Highly efficient CRISPR/Cas9-mediated knock-in in zebrafish by homology-independent DNA repair. Genome Res. 24, 142–153.

Bai, Q., Garver, J.A., Hukriede, N.A., Burton, E.A., 2007. Generation of a transgenic zebrafish model of tauopathy using a novel promoter element derived from the zebrafish eno2 gene. Nucleic Acids Res. 35, 6501–6516.

Bamshad, M.J., Ng, S.B., Bigham, A.W., Tabor, H.K., Emond, M.J., Nickerson, D.A., et al., 2011. Exome sequencing as a tool for Mendelian disease gene discovery. Nat. Rev. Genet. 12, 745–755.

Bandmann, O., Burton, E.A., 2010. Genetic zebrafish models of neurodegenerative diseases. Neurobiol. Dis. 40, 58–65.

Bedell, V.M., Wang, Y., Campbell, J.M., Poshusta, T.L., Starker, C.G., Krug, II, R.G., et al., 2012. In vivo genome editing using a high-efficiency TALEN system. Nature 491, 114–118.

Bernier, R., Golzio, C., Xiong, B., Stessman, H.A., Coe, B.P., Penn, O., et al., 2014. Disruptive CHD8 mutations define a subtype of autism early in development. Cell 158, 263–276.

Best, J.D., Alderton, W.K., 2008. Zebrafish: An in vivo model for the study of neurological diseases. Neuropsychiatr. Dis. Treat. 4, 567–576.

Bi, W., Ohyama, T., Nakamura, H., Yan, J., Visvanathan, J., Justice, M.J., et al., 2005. Inactivation of Rai1 in mice recapitulates phenotypes observed in chromosome engineered mouse models for Smith-Magenis syndrome. Hum. Mol. Genet. 14, 983–995.

Bibliowicz, J., Gross, J.M., 2009. Expanded progenitor populations, vitreo-retinal abnormalities, and Muller glial reactivity in the zebrafish leprechaun/patched2 retina. BMC Dev. Biol. 9, 52.

Bogershausen, N., Tsai, I.C., Pohl, E., Kiper, P.O., Beleggia, F., Percin, E.F., et al., 2015. RAP1-mediated MEK/ERK pathway defects in Kabuki syndrome. J. Clin. Invest. 125, 3585–3599.

Bolar, N.A., Golzio, C., Zivna, M., Hayot, G., Van Hemelrijk, C., Schepers, D., et al., 2016. Heterozygous loss-of-function SEC61A1 mutations cause autosomal-dominant tubulo-interstitial and glomerulocystic kidney disease with anemia. Am. J. Hum. Genet. 99, 174–187.

Borck, G., Hog, F., Dentici, M.L., Tan, P.L., Sowada, N., Medeira, A., et al., 2015. BRF1 mutations alter RNA polymerase III-dependent transcription and cause neurodevelopmental anomalies. Genome Res. 25, 155–166.

Boyadjiev, S.A., Fromme, J.C., Ben, J., Chong, S.S., Nauta, C., Hur, D.J., et al., 2006. Cranio-lenticulo-sutural dysplasia is caused by a SEC23A mutation leading to abnormal endoplasmic-reticulum-to-Golgi trafficking. Nat. Genet. 38, 1192–1197.

Brand, M., Heisenberg, C.P., Jiang, Y.J., Beuchle, D., Lun, K., Furutani-Seiki, M., et al., 1996. Mutations in zebrafish genes affecting the formation of the boundary between midbrain and hindbrain. Development 123, 179–190.

Brooks, S.S., Wall, A.L., Golzio, C., Reid, D.W., Kondyles, A., Willer, J.R., et al., 2014. A novel ribosomopathy caused by dysfunction of RPL10 disrupts neurodevelopment and causes X-linked microcephaly in humans. Genetics 198, 723–733.

Butler, M.G., Iben, J.R., Marsden, K.C., Epstein, J.A., Granato, M., Weinstein, B.M., 2015. SNPfisher: tools for probing genetic variation in laboratory-reared zebrafish. Development 142, 1542–1552.

Capecchi, M.R., 2005. Gene targeting in mice: functional analysis of the mammalian genome for the twenty-first century. Nat. Rev. Genet. 6, 507–512.

Carmichael, C., Westerfield, M., Varga, Z.M., 2009. Cryopreservation and in vitro fertilization at the zebrafish international resource center. Methods Mol. Biol. 546, 45–65.

Carvalho, C.M., Lupski, J.R., 2016. Mechanisms underlying structural variant formation in genomic disorders. Nat. Rev. Genet. 17, 224–238.

Carvalho, C.M., Vasanth, S., Shinawi, M., Russell, C., Ramocki, M.B., Brown, C.W., et al., 2014. Dosage changes of a segment at 17p13.1 lead to intellectual disability and microcephaly as a result of complex genetic interaction of multiple genes. Am. J. Hum. Genet. 95, 565–578.

Castellana, S., Mazza, T., 2013. Congruency in the prediction of pathogenic missense mutations: state-of-the-art web-based tools. Brief Bioinform. 14, 448–459.

Cawthon, R.M., Weiss, R., Xu, G.F., Viskochil, D., Culver, M., Stevens, J., et al., 1990. A major segment of the neurofibromatosis type 1 gene: cDNA sequence, genomic structure, and point mutations. Cell 62, 193–201.

Ceol, C.J., Houvras, Y., Jane-Valbuena, J., Bilodeau, S., Orlando, D.A., Battisti, V., et al., 2011. The histone methyltransferase SETDB1 is recurrently amplified in melanoma and accelerates its onset. Nature 471, 513–517.

Chakrabarti, S., Streisinger, G., Singer, F., Walker, C., 1983. Frequency of gamma-ray induced specific locus and recessive lethal mutations in mature germ cells of the zebrafish, *Brachydanio rerio*. Genetics 103, 109–123.

Chang, N., Sun, C., Gao, L., Zhu, D., Xu, X., Zhu, X., et al., 2013. Genome editing with RNA-guided Cas9 nuclease in zebrafish embryos. Cell Res. 23, 465–472.

Chassaing, N., Davis, E.E., McKnight, K.L., Niederriter, A.R., Causse, A., David, V., et al., 2016. Targeted resequencing identifies PTCH1 as a major contributor to ocular developmental anomalies and extends the SOX2 regulatory network. Genome Res. 26, 474–485.

Cheng, K.C., Katz, S.R., Lin, A.Y., Xin, X., Ding, Y., 2016. Whole-organism cellular pathology: a systems approach to phenomics. Adv. Genet. 95, 89–115.

Chong, J.X., Buckingham, K.J., Jhangiani, S.N., Boehm, C., Sobreira, N., Smith, J.D., et al., 2015. The genetic basis of Mendelian phenotypes: discoveries, challenges, and opportunities. Am. J. Hum. Genet. 97, 199–215.

Cooper, G.M., Shendure, J., 2011. Needles in stacks of needles: finding disease-causal variants in a wealth of genomic data. Nat. Rev. Genet. 12, 628–640.

Dauber, A., Golzio, C., Guenot, C., Jodelka, F.M., Kibaek, M., Kjaergaard, S., et al., 2013. SCRIB and PUF60 are primary drivers of the multisystemic phenotypes of the 8q24.3 copy-number variant. Am. J. Hum. Genet. 93, 798–811.

Davis, E.E., Katsanis, N., 2012. The ciliopathies: a transitional model into systems biology of human genetic disease. Curr. Opin. Genet. Dev. 22, 290–303.

Davis, E.E., Zhang, Q., Liu, Q., Diplas, B.H., Davey, L.M., Hartley, J., et al., 2011. TTC21B contributes both causal and modifying alleles across the ciliopathy spectrum. Nat. Genet. 43, 189–196.

de Pontual, L., Zaghloul, N.A., Thomas, S., Davis, E.E., McGaughey, D.M., Dollfus, H., et al., 2009. Epistasis between RET and BBS mutations modulates enteric innervation and causes syndromic Hirschsprung disease. Proc. Natl. Acad. Sci. USA 106, 13921–13926.

Devoy, A., Bunton-Stasyshyn, R.K., Tybulewicz, V.L., Smith, A.J., Fisher, E.M., 2012. Genomically humanized mice: technologies and promises. Nat. Rev. Genet. 13, 14–20.

Doyon, Y., McCammon, J.M., Miller, J.C., Faraji, F., Ngo, C., Katibah, G.E., et al., 2008. Heritable targeted gene disruption in zebrafish using designed zinc-finger nucleases. Nat. Biotechnol. 26, 702–708.

Driever, W., Solnica-Krezel, L., Schier, A.F., Neuhauss, S.C., Malicki, J., Stemple, D.L., et al., 1996. A genetic screen for mutations affecting embryogenesis in zebrafish. Development 123, 37–46.

Eisen, J.S., Smith, J.C., 2008. Controlling morpholino experiments: don't stop making antisense. Development 135, 1735–1743.

Fernandes, Y.M., Rampersad, M., Luchiari, A.C., Gerlai, R., 2016. Associative learning in the multichamber tank: a new learning paradigm for zebrafish. Behav. Brain Res. 312, 279–284.

Force, A., Lynch, M., Pickett, F.B., Amores, A., Yan, Y.L., Postlethwait, J., 1999. Preservation of duplicate genes by complementary, degenerative mutations. Genetics 151, 1531–1545.

Franke, A., McGovern, D.P., Barrett, J.C., Wang, K., Radford-Smith, G.L., Ahmad, T., et al., 2010. Genome-wide meta-analysis increases to 71 the number of confirmed Crohn's disease susceptibility loci. Nat. Genet. 42, 1118–1125.

Fu, W., O'Connor, T.D., Jun, G., Kang, H.M., Abecasis, G., Leal, S.M., et al., 2013. Analysis of 6,515 exomes reveals the recent origin of most human protein-coding variants. Nature 493, 216–220.

Garcia, G.R., Noyes, P.D., Tanguay, R.L., 2016. Advancements in zebrafish applications for 21st century toxicology. Pharmacol. Ther. 161, 11–21.

Gemberling, M., Bailey, T.J., Hyde, D.R., Poss, K.D., 2013. The zebrafish as a model for complex tissue regeneration. Trends Genet. 29, 611–620.

Genomes Project, C., Abecasis, G.R., Altshuler, D., Auton, A., Brooks, L.D., Durbin, R.M., et al., 2010. A map of human genome variation from population-scale sequencing. Nature 467, 1061–1073.

Gibbs, R.A., Weinstock, G.M., Metzker, M.L., Muzny, D.M., Sodergren, E.J., Scherer, S., et al., 2004. Genome sequence of the Brown Norway rat yields insights into mammalian evolution. Nature 428, 493–521.

Gieger, C., Radhakrishnan, A., Cvejic, A., Tang, W., Porcu, E., Pistis, G., et al., 2011. New gene functions in megakaryopoiesis and platelet formation. Nature 480, 201–208.

Golzio, C., Katsanis, N., 2013. Genetic architecture of reciprocal CNVs. Curr. Opin. Genet. Dev. 23, 240–248.

Golzio, C., Willer, J., Talkowski, M.E., Oh, E.C., Taniguchi, Y., Jacquemont, S., et al., 2012. KCTD13 is a major driver of mirrored neuroanatomical phenotypes of the 16p11.2 copy number variant. Nature 485, 363–367.

Haffter, P., Granato, M., Brand, M., Mullins, M.C., Hammerschmidt, M., Kane, D.A., et al., 1996. The identification of genes with unique and essential functions in the development of the zebrafish, *Danio rerio*. Development 123, 1–36.

Hammerschmidt, M., Pelegri, F., Mullins, M.C., Kane, D.A., Brand, M., van Eeden, F.J., et al., 1996. Mutations affecting morphogenesis during gastrulation and tail formation in the zebrafish, *Danio rerio*. Development 123, 143–151.

Hieter, P., Boycott, K.M., 2014. Understanding rare disease pathogenesis: a grand challenge for model organisms. Genetics 198, 443–445.

Hjeij, R., Lindstrand, A., Francis, R., Zariwala, M.A., Liu, X., Li, Y., et al., 2013. ARMC4 mutations cause primary ciliary dyskinesia with randomization of left/right body asymmetry. Am. J. Hum. Genet. 93, 357–367.

Hosseinibarkooie, S., Peters, M., Torres-Benito, L., Rastetter, R.H., Hupperich, K., Hoffmann, A., et al., 2016. The power of human protective modifiers: PLS3 and CORO1C unravel impaired endocytosis in spinal muscular atrophy and rescue SMA phenotype. Am. J. Hum. Genet. 99, 647–665.

Howe, D.G., Bradford, Y.M., Conlin, T., Eagle, A.E., Fashena, D., Frazer, K., et al., 2013a. ZFIN, the zebrafish model organism database: increased support for mutants and transgenics. Nucleic Acids Res. 41, D854–860.

Howe, K., Clark, M.D., Torroja, C.F., Torrance, J., Berthelot, C., Muffato, M., et al., 2013b. The zebrafish reference genome sequence and its relationship to the human genome. Nature 496, 498–503.

Hwang, W.Y., Fu, Y., Reyon, D., Maeder, M.L., Tsai, S.Q., Sander, J.D., et al., 2013. Efficient genome editing in zebrafish using a CRISPR-Cas system. Nat. Biotechnol. 31, 227–229.

Isrie, M., Breuss, M., Tian, G., Hansen, A.H., Cristofoli, F., Morandell, J., et al., 2015. Mutations in either TUBB or MAPRE2 cause circumferential skin creases kunze type. Am. J. Hum. Genet. 97, 790–800.

Iyer, J., Girirajan, S., 2015. Gene discovery and functional assessment of rare copy-number variants in neurodevelopmental disorders. Brief Funct. Genomics 14, 315–328.

James, E.L., Parkinson, E.K., 2015. Serum metabolomics in animal models and human disease. Curr. Opin. Clin. Nutr. Metab. Care 18, 478–483.

Jao, L.E., Wente, S.R., Chen, W., 2013. Efficient multiplex biallelic zebrafish genome editing using a CRISPR nuclease system. Proc. Natl. Acad. Sci. USA 110, 13904–13909.

Jeong, J.Y., Kwon, H.B., Ahn, J.C., Kang, D., Kwon, S.H., Park, J.A., et al., 2008. Functional and developmental analysis of the blood-brain barrier in zebrafish. Brain Res. Bull. 75, 619–628.

Jiang, Y.J., Brand, M., Heisenberg, C.P., Beuchle, D., Furutani-Seiki, M., Kelsh, R.N., et al., 1996. Mutations affecting neurogenesis and brain morphology in the zebrafish, *Danio rerio*. Development 123, 205–216.

Jordan, D.M., Frangakis, S.G., Golzio, C., Cassa, C.A., Kurtzberg, J., Task Force for Neonatal, G., et al., 2015. Identification of cis-suppression of human disease mutations by comparative genomics. Nature 524, 225–229.

Jordan, T., Hanson, I., Zaletayev, D., Hodgson, S., Prosser, J., Seawright, A., et al., 1992. The human PAX6 gene is mutated in two patients with aniridia. Nat. Genet. 1, 328–332.

Junker, J.P., Noel, E.S., Guryev, V., Peterson, K.A., Shah, G., Huisken, J., et al., 2014. Genome-wide RNA Tomography in the zebrafish embryo. Cell 159, 662–675.

Katsanis, S.H., Katsanis, N., 2013. Molecular genetic testing and the future of clinical genomics. Nat. Rev. Genet. 14, 415–426.

Kettleborough, R.N., Busch-Nentwich, E.M., Harvey, S.A., Dooley, C.M., de Bruijn, E., van Eeden, F., et al., 2013. A systematic genome-wide analysis of zebrafish protein-coding gene function. Nature 496, 494–497.

Khanna, H., Davis, E.E., Murga-Zamalloa, C.A., Estrada-Cuzcano, A., Lopez, I., den Hollander, A.I., et al., 2009. A common allele in RPGRIP1L is a modifier of retinal degeneration in ciliopathies. Nat. Genet. 41, 739–745.

Kile, B.T., Hilton, D.J., 2005. The art and design of genetic screens: mouse. Nat. Rev. Genet. 6, 557–567.

Kimmel, C.B., Ballard, W.W., Kimmel, S.R., Ullmann, B., Schilling, T.F., 1995. Stages of embryonic development of the zebrafish. Dev. Dyn. 203, 253–310.

Kleinjan, D.A., Bancewicz, R.M., Gautier, P., Dahm, R., Schonthaler, H.B., Damante, G., et al., 2008. Subfunctionalization of duplicated zebrafish pax6 genes by cis-regulatory divergence. PLoS Genet. 4, e29.

Kok, F.O., Shin, M., Ni, C.W., Gupta, A., Grosse, A.S., van Impel, A., et al., 2015. Reverse genetic screening reveals poor correlation between morpholino-induced and mutant phenotypes in zebrafish. Dev. Cell 32, 97–108.

Lander, E.S., Linton, L.M., Birren, B., Nusbaum, C., Zody, M.C., Baldwin, J., et al., 2001. Initial sequencing and analysis of the human genome. Nature 409, 860–921.

Lang, M.R., Lapierre, L.A., Frotscher, M., Goldenring, J.R., Knapik, E.W., 2006. Secretory COPII coat component Sec23a is essential for craniofacial chondrocyte maturation. Nat. Genet. 38, 1198–1203.

Lawrence, C., 2016. New frontiers for zebrafish management. Methods Cell Biol. 135, 483–508.

Lawson, N.D., Wolfe, S.A., 2011. Forward and reverse genetic approaches for the analysis of vertebrate development in the zebrafish. Dev. Cell 21, 48–64.

Lek, M., Karczewski, K.J., Minikel, E.V., Samocha, K.E., Banks, E., Fennell, T., et al., 2016. Analysis of protein-coding genetic variation in 60,706 humans. Nature 536, 285–291.

Leshchiner, I., Alexa, K., Kelsey, P., Adzhubei, I., Austin-Tse, C.A., Cooney, J.D., et al., 2012. Mutation mapping and identification by whole-genome sequencing. Genome Res. 22, 1541–1548.

Li, Y., Yagi, H., Onuoha, E.O., Damerla, R.R., Francis, R., Furutani, Y., et al., 2016. DNAH6 and its interactions with PCD genes in heterotaxy and primary ciliary dyskinesia. PLoS Genet. 12, e1005821.

Li, Z.H., Alex, D., Siu, S.O., Chu, I.K., Renn, J., Winkler, C., et al., 2011. Combined in vivo imaging and omics approaches reveal metabolism of icaritin and its glycosides in zebrafish larvae. Mol. Biosyst. 7, 2128–2138.

Lim, E.T., Liu, Y.P., Chan, Y., Tiinamaija, T., Karajamaki, A., Madsen, E., et al., 2014. A novel test for recessive contributions to complex diseases implicates Bardet-Biedl syndrome gene BBS10 in idiopathic type 2 diabetes and obesity. Am. J. Hum. Genet. 95, 509–520.

Lindsay, E.A., 2001. Chromosomal microdeletions: dissecting del22q11 syndrome. Nat. Rev. Genet. 2, 858–868.

Lindsay, E.A., Vitelli, F., Su, H., Morishima, M., Huynh, T., Pramparo, T., et al., 2001. Tbx1 haploinsufficieny in the DiGeorge syndrome region causes aortic arch defects in mice. Nature 410, 97–101.

Lindstrand, A., Frangakis, S., Carvalho, C.M., Richardson, E.B., McFadden, K.A., Willer, J.R., et al., 2016. Copy-number variation contributes to the mutational load of Bardet-Biedl syndrome. Am. J. Hum. Genet. 99, 318–336.

Liu, C.T., Garnaas, M.K., Tin, A., Kottgen, A., Franceschini, N., Peralta, C.A., et al., 2011. Genetic association for renal traits among participants of African ancestry reveals new loci for renal function. PLoS Genet. 7, e1002264.

MacRae, C.A., Peterson, R.T., 2015. Zebrafish as tools for drug discovery. Nat. Rev. Drug Discov. 14, 721–731.

Manolio, T.A., 2013. Bringing genome-wide association findings into clinical use. Nat. Rev. Genet. 14, 549–558.

Margolin, D.H., Kousi, M., Chan, Y.M., Lim, E.T., Schmahmann, J.D., Hadjivassiliou, M., et al., 2013. Ataxia, dementia, and hypogonadotropism caused by disordered ubiquitination. N. Engl. J. Med. 368, 1992–2003.

McCarthy, S.E., Makarov, V., Kirov, G., Addington, A.M., McClellan, J., Yoon, S., et al., 2009. Microduplications of 16p11.2 are associated with schizophrenia. Nat. Genet. 41, 1223–1227.

Meng, X., Noyes, M.B., Zhu, L.J., Lawson, N.D., Wolfe, S.A., 2008. Targeted gene inactivation in zebrafish using engineered zinc-finger nucleases. Nat. Biotechnol. 26, 695–701.

Merveille, A.C., Davis, E.E., Becker-Heck, A., Legendre, M., Amirav, I., Bataille, G., et al., 2011. CCDC39 is required for assembly of inner dynein arms and the dynein regulatory complex and for normal ciliary motility in humans and dogs. Nat. Genet. 43, 72–78.

Meyer, A., Schartl, M., 1999. Gene and genome duplications in vertebrates: the one-to-four (-to-eight in fish) rule and the evolution of novel gene functions. Curr. Opin. Cell Biol. 11, 699–704.

Mouse Genome Sequencing, C., Waterston, R.H., Lindblad-Toh, K., Birney, E., Rogers, J., Abril, J.F., et al., 2002. Initial sequencing and comparative analysis of the mouse genome. Nature 420, 520–562.

Muller, T., Rumpel, E., Hradetzky, S., Bollig, F., Wegner, H., Blumenthal, A., et al., 2011. Non-muscle myosin IIA is required for the development of the zebrafish glomerulus. Kidney Int. 80, 1055–1063.

Mullins, M.C., Hammerschmidt, M., Haffter, P., Nusslein-Volhard, C., 1994. Large-scale mutagenesis in the zebrafish: in search of genes controlling development in a vertebrate. Curr. Biol. 4, 189–202.

Nagabhushana, A., Mishra, R.K., 2016. Finding clues to the riddle of sex determination in zebrafish. J. Biosci. 41, 145–155.

Nasevicius, A., Ekker, S.C., 2000. Effective targeted gene 'knockdown' in zebrafish. Nat. Genet. 26, 216–220.

Neuhauss, S.C., Solnica-Krezel, L., Schier, A.F., Zwartkruis, F., Stemple, D.L., Malicki, J., et al., 1996. Mutations affecting craniofacial development in zebrafish. Development 123, 357–367.

Niederriter, A.R., Davis, E.E., Golzio, C., Oh, E.C., Tsai, I.C., Katsanis, N., 2013. In vivo modeling of the morbid human genome using *Danio rerio*. J. Vis. Exp. 78, e50338.

Norton, N., Li, D., Rieder, M.J., Siegfried, J.D., Rampersaud, E., Zuchner, S., et al., 2011. Genome-wide studies of copy number variation and exome sequencing identify rare variants in BAG3 as a cause of dilated cardiomyopathy. Am. J. Hum. Genet. 88, 273–282.

Obholzer, N., Swinburne, I.A., Schwab, E., Nechiporuk, A.V., Nicolson, T., Megason, S.G., 2012. Rapid positional cloning of zebrafish mutations by linkage and homozygosity mapping using whole-genome sequencing. Development 139, 4280–4290.

Odenthal, J., Haffter, P., Vogelsang, E., Brand, M., van Eeden, F.J., Furutani-Seiki, M., et al., 1996. Mutations affecting the formation of the notochord in the zebrafish, *Danio rerio*. Development 123, 103–115.

Oprea, G.E., Krober, S., McWhorter, M.L., Rossoll, W., Muller, S., Krawczak, M., et al., 2008. Plastin 3 is a protective modifier of autosomal recessive spinal muscular atrophy. Science 320, 524–527.

Pardo-Martin, C., Chang, T.Y., Koo, B.K., Gilleland, C.L., Wasserman, S.C., Yanik, M.F., 2010. High-throughput in vivo vertebrate screening. Nat. Methods 7, 634–636.

Perles, Z., Moon, S., Ta-Shma, A., Yaacov, B., Francescatto, L., Edvardson, S., et al., 2015. A human laterality disorder caused by a homozygous deleterious mutation in MMP21. J. Med. Genet. 52, 840–847.

Piotrowski, T., Schilling, T.F., Brand, M., Jiang, Y.J., Heisenberg, C.P., Beuchle, D., et al., 1996. Jaw and branchial arch mutants in zebrafish II: anterior arches and cartilage differentiation. Development 123, 345–356.

Postlethwait, J.H., Yan, Y.L., Gates, M.A., Horne, S., Amores, A., Brownlie, A., et al., 1998. Vertebrate genome evolution and the zebrafish gene map. Nat. Genet. 18, 345–349.

Praveen, K., Davis, E.E., Katsanis, N., 2015. Unique among ciliopathies: primary ciliary dyskinesia, a motile cilia disorder. F1000Prime Rep. 7, 36.

Ragvin, A., Moro, E., Fredman, D., Navratilova, P., Drivenes, O., Engstrom, P.G., et al., 2010. Long-range gene regulation links genomic type 2 diabetes and obesity risk regions to HHEX, SOX4, and IRX3. Proc. Natl. Acad. Sci. USA 107, 775–780.

Ramachandran, K.V., Hennessey, J.A., Barnett, A.S., Yin, X., Stadt, H.A., Foster, E., et al., 2013. Calcium influx through L-type CaV1.2 Ca2+ channels regulates mandibular development. J. Clin. Invest. 123, 1638–1646.

Reiter, J.F., Alexander, J., Rodaway, A., Yelon, D., Patient, R., Holder, N., et al., 1999. Gata5 is required for the development of the heart and endoderm in zebrafish. Genes Dev. 13, 2983–2995.

Rossi, A., Kontarakis, Z., Gerri, C., Nolte, H., Holper, S., Kruger, M., et al., 2015. Genetic compensation induced by deleterious mutations but not gene knockdowns. Nature 524, 230–233.

Ryan, S., Willer, J., Marjoram, L., Bagwell, J., Mankiewicz, J., Leshchiner, I., et al., 2013. Rapid identification of kidney cyst mutations by whole exome sequencing in zebrafish. Development 140, 4445–4451.

Sarparanta, J., Jonson, P.H., Golzio, C., Sandell, S., Luque, H., Screen, M., et al., 2012. Mutations affecting the cytoplasmic functions of the co-chaperone DNAJB6 cause limb-girdle muscular dystrophy. Nat. Genet. 44, 450–455, S451–452.

Schier, A.F., Neuhauss, S.C., Harvey, M., Malicki, J., Solnica-Krezel, L., Stainier, D.Y., et al., 1996. Mutations affecting the development of the embryonic zebrafish brain. Development 123, 165–178.

Schilling, T.F., Piotrowski, T., Grandel, H., Brand, M., Heisenberg, C.P., Jiang, Y.J., et al., 1996. Jaw and branchial arch mutants in zebrafish I: branchial arches. Development 123, 329–344.

Schulte, E.C., Kousi, M., Tan, P.L., Tilch, E., Knauf, F., Lichtner, P., et al., 2014. Targeted resequencing and systematic in vivo functional testing identifies rare variants in MEIS1 as significant contributors to restless legs syndrome. Am. J. Hum. Genet. 95, 85–95.

Shestopalov, I.A., Sinha, S., Chen, J.K., 2007. Light-controlled gene silencing in zebrafish embryos. Nat. Chem. Biol. 3, 650–651.

Shin, J., Padmanabhan, A., de Groh, E.D., Lee, J.S., Haidar, S., Dahlberg, S., et al., 2012. Zebrafish neurofibromatosis type 1 genes have redundant functions in tumorigenesis and embryonic development. Dis. Model Mech. 5, 881–894.

Shore, E.M., Xu, M., Feldman, G.J., Fenstermacher, D.A., Cho, T.J., Choi, I.H., et al., 2006. A recurrent mutation in the BMP type I receptor ACVR1 causes inherited and sporadic fibrodysplasia ossificans progressiva. Nat. Genet. 38, 525–527.

Sivasubbu, S., Balciunas, D., Amsterdam, A., Ekker, S.C., 2007. Insertional mutagenesis strategies in zebrafish. Genome Biol. 8 (Suppl. 1), S9.

Sobreira, N., Schiettecatte, F., Valle, D., Hamosh, A., 2015. GeneMatcher: a matching tool for connecting investigators with an interest in the same gene. Hum. Mutat. 36, 928–930.

Solnica-Krezel, L., Schier, A.F., Driever, W., 1994. Efficient recovery of ENU-induced mutations from the zebrafish germline. Genetics 136, 1401–1420.

Solnica-Krezel, L., Stemple, D.L., Mountcastle-Shah, E., Rangini, Z., Neuhauss, S.C., Malicki, J., et al., 1996. Mutations affecting cell fates and cellular rearrangements during gastrulation in zebrafish. Development 123, 67–80.

Stainier, D.Y., Fouquet, B., Chen, J.N., Warren, K.S., Weinstein, B.M., Meiler, S.E., et al., 1996. Mutations affecting the formation and function of the cardiovascular system in the zebrafish embryo. Development 123, 285–292.

Streisinger, G., 1983. Extrapolations from species to species and from various cell types in assessing risks from chemical mutagens. Mutat. Res. 114, 93–105.

Streisinger, G., Walker, C., Dower, N., Knauber, D., Singer, F., 1981. Production of clones of homozygous diploid zebra fish (*Brachydanio rerio*). Nature 291, 293–296.

Summerton, J., Weller, D., 1997. Morpholino antisense oligomers: design, preparation, and properties. Antisense Nucleic Acid Drug Dev. 7, 187–195.

Tan, J.L., Zon, L.I., 2011. Chemical screening in zebrafish for novel biological and therapeutic discovery. Methods Cell Biol. 105, 493–516.

Tennessen, J.A., Bigham, A.W., O'Connor, T.D., Fu, W., Kenny, E.E., Gravel, S., et al., 2012. Evolution and functional impact of rare coding variation from deep sequencing of human exomes. Science 337, 64–69.

Thisse, C., Thisse, B., 2008. High-resolution in situ hybridization to whole-mount zebrafish embryos. Nat. Protoc. 3, 59–69.

Tiscornia, G., Vivas, E.L., Izpisua Belmonte, J.C., 2011. Diseases in a dish: modeling human genetic disorders using induced pluripotent cells. Nat. Med. 17, 1570–1576.

Ugur, B., Chen, K., Bellen, H.J., 2016. *Drosophila* tools and assays for the study of human diseases. Dis. Model Mech. 9, 235–244.

Urnov, F.D., Rebar, E.J., Holmes, M.C., Zhang, H.S., Gregory, P.D., 2010. Genome editing with engineered zinc finger nucleases. Nat. Rev. Genet. 11, 636–646.

van de Ven, J.P., Nilsson, S.C., Tan, P.L., Buitendijk, G.H., Ristau, T., Mohlin, F.C., et al., 2013. A functional variant in the CFI gene confers a high risk of age-related macular degeneration. Nat. Genet. 45, 813–817.

van Eeden, F.J., Granato, M., Schach, U., Brand, M., Furutani-Seiki, M., Haffter, P., et al., 1996. Mutations affecting somite formation and patterning in the zebrafish, *Danio rerio*. Development 123, 153–164.

van Karnebeek, C.D., Bonafe, L., Wen, X.Y., Tarailo-Graovac, M., Balzano, S., Royer-Bertrand, B., et al., 2016. NANS-mediated synthesis of sialic acid is required for brain and skeletal development. Nat. Genet. 48, 777–784.

Varga, Z.M., 2011. Aquaculture and husbandry at the zebrafish international resource center. Methods Cell Biol. 104, 453–478.

Veltman, J.A., Brunner, H.G., 2012. De novo mutations in human genetic disease. Nat. Rev. Genet. 13, 565–575.

Viskochil, D., Buchberg, A.M., Xu, G., Cawthon, R.M., Stevens, J., Wolff, R.K., et al., 1990. Deletions and a translocation interrupt a cloned gene at the neurofibromatosis type 1 locus. Cell 62, 187–192.

von Trotha, J.W., Vernier, P., Bally-Cuif, L., 2014. Emotions and motivated behavior converge on an amygdala-like structure in the zebrafish. Eur. J. Neurosci. 40, 3302–3315.

Wallace, M.R., Marchuk, D.A., Andersen, L.B., Letcher, R., Odeh, H.M., Saulino, A.M., et al., 1990. Type 1 neurofibromatosis gene: identification of a large transcript disrupted in three NF1 patients. Science 249, 181–186.

Walz, K., Caratini-Rivera, S., Bi, W., Fonseca, P., Mansouri, D.L., Lynch, J., et al., 2003. Modeling del(17)(p11.2p11. 2) and dup(17)(p11. 2p11. 2) contiguous gene syndromes by chromosome engineering in mice: phenotypic consequences of gene dosage imbalance. Mol. Cell Biol. 23, 3646–3655.

Wan, J., Yourshaw, M., Mamsa, H., Rudnik-Schoneborn, S., Menezes, M.P., Hong, J.E., et al., 2012. Mutations in the RNA exosome component gene EXOSC3 cause pontocerebellar hypoplasia and spinal motor neuron degeneration. Nat. Genet. 44, 704–708.

Wang, D., Jao, L.E., Zheng, N., Dolan, K., Ivey, J., Zonies, S., et al., 2007. Efficient genome-wide mutagenesis of zebrafish genes by retroviral insertions. Proc. Natl. Acad. Sci. USA 104, 12428–12433.

Weiss, L.A., Shen, Y., Korn, J.M., Arking, D.E., Miller, D.T., Fossdal, R., et al., 2008. Association between microdeletion and microduplication at 16p11.2 and autism. N. Engl. J. Med. 358, 667–675.

Wienholds, E., Schulte-Merker, S., Walderich, B., Plasterk, R.H., 2002. Target-selected inactivation of the zebrafish rag1 gene. Science 297, 99–102.

Wijshake, T., Baker, D.J., van de Sluis, B., 2014. Endonucleases: new tools to edit the mouse genome. Biochim. Biophys. Acta 1842, 1942–1950.

Wilson, C.A., High, S.K., McCluskey, B.M., Amores, A., Yan, Y.L., Titus, T.A., et al., 2014. Wild sex in zebrafish: loss of the natural sex determinant in domesticated strains. Genetics 198, 1291–1308.

Yu, P.B., Hong, C.C., Sachidanandan, C., Babitt, J.L., Deng, D.Y., Hoyng, S.A., et al., 2008. Dorsomorphin inhibits BMP signals required for embryogenesis and iron metabolism. Nat. Chem. Biol. 4, 33–41.

Zaghloul, N.A., Liu, Y., Gerdes, J.M., Gascue, C., Oh, E.C., Leitch, C.C., et al., 2010. Functional analyses of variants reveal a significant role for dominant negative and common alleles in oligogenic Bardet-Biedl syndrome. Proc. Natl. Acad. Sci. USA 107, 10602–10607.

Zariwala, M.A., Gee, H.Y., Kurkowiak, M., Al-Mutairi, D.A., Leigh, M.W., Hurd, T.W., et al., 2013. ZMYND10 is mutated in primary ciliary dyskinesia and interacts with LRRC6. Am. J. Hum. Genet. 93, 336–345.

Zon, L.I., Peterson, R.T., 2005. In vivo drug discovery in the zebrafish. Nat. Rev. Drug Discov. 4, 35–44.

Genetically Tailored Pig Models for Translational Biomedical Research

Bernhard Aigner*,**, Barbara Kessler*,**, Nikolai Klymiuk*,**, Mayuko Kurome*,**, Simone Renner*,**, Annegret Wünsch*,**, Eckhard Wolf*,**,†

*Molecular Animal Breeding and Biotechnology, Ludwig-Maximilian University, Munich, Germany
**Center for Innovative Medical Models (CiMM), Ludwig-Maximilian University, Munich, Germany
†Gene Center, Ludwig-Maximilian University, Munich, Germany

O U T L I N E

1 INTRODUCTION

Laboratory rodents are most widely used as models in basic biomedical research due to their high cost effectiveness, easy handling and the availability of tools for the genetic and environmental standardization of experiments to achieve valid and reproducible results. Obviously, mammalian genome sequences show species-specific differences with regard to structure and function. Therefore, additional nonrodent mammalian species including pigs are increasingly used as appropriate animal models for specific human diseases.

Pigs are members of the artiodactyls (cloven-hoofed mammals). Domestication of pigs (*Sus scrofa domestica*) from the species *Sus scrofa* (wild boar) that is classified to a number of subspecies, started about 9000 years ago. More than 500 different breeds are described worldwide, 90% of them are local breeds. Only about 60 breeds are regional or international breeds occurring in more than one country. The five most common breeds are Large White, Duroc, Landrace, Hampshire, and Pietrain, however different breeding standards are used by the respective national breeding organizations. The efforts for improving economic performance and quality of pig production resulted in hybrid breeding programs which are based on pure-bred pigs as grandparent and great-grandparent stocks. These programs use crosses between specialized sire and dam lines which have been developed through intense within-line selection of a small number of international transboundary breeds. The commercial interest in the efficient agricultural production has also driven the scientific progress in the genetic and phenotypic characterization, as well as in the artificial genetic modification of the species (http://www.animalgenome.org/cgi-bin/QTLdb/SS/index) (Food and Agriculture Organization of the United Nations, 2007; Frantz et al., 2016). Monogenic traits and diseases of pigs are collected in the "OMIA—Online Mendelian Inheritance in Animals" database (http://omia.angis.org.au).

From a female domestic Duroc pig, a high-quality draft pig genome sequence was established using bacterial artificial chromosome and whole genome shotgun sequences. The assembly (Sscrofa10.2) comprised 2.6 Gb assigned to chromosomes, and additionally more than 200 Mb in unplaced scaffolds. Predicted porcine protein sequences were compared with their human orthologues (http://www.ensembl.org) (Groenen et al., 2012). Using four 12–16-week old male and female juvenile Landrace pigs and a porcine expression array, a genome-wide transcriptome atlas of pig tissues derived from 62 tissue/cell types was generated. The transcripts were grouped according to the location and the network with coexpressed genes (Freeman et al., 2012).

For biomedical research, miniature pig breeds with substantially decreased body size and improvement in the standardization of the genetic background were produced (Köhn, 2012). Minipig outbred stocks with full pedigree can be obtained from commercial suppliers. Göttingen minipigs are approved by regulatory authorities worldwide as nonrodent models for pharmacological and toxicological studies (http://www.minipigs.dk) (Bode et al., 2010). The appropriateness of minipigs for modeling complex physiologic systems and for presenting a preclinical platform to validate efficacy and safety of therapies and devices was compiled (Schomberg et al., 2016). Minipigs inbred for many generations are also available (Mezrich et al., 2003; Wu et al., 2004; Yu et al., 2004). Whole genome sequencing of highly inbred Wuzhishan minipigs revealed a high level of homozygosity in the diploid genome combined with genomic regions with unexpectedly high rates of heterozygosity (Fang et al., 2012).

Breeding strategies (Kaneko et al., 2011), as well as genetic engineering techniques were used for the generation of pigs with even lower adult body weight for their subsequent use as genetic background for pig models in biomedical research. For instance, growth hormone receptor (*GHR*) gene knockout Bama minipigs (Li et al., 2014a), as well as transgenic Wuzhishan minipigs expressing a dominant-negative porcine GHR (Li et al., 2015a) were established.

The reproductive performance of pigs is characterized by sexual maturity at the age of 6 months, a gestation period of less than 4 months, a generation interval of less than 1 year, parturition of about 10 piglets per litter and all season breeding. Their lifespan can be 15 years and more. In pigs, a broad spectrum of techniques necessary for biomedical research are established (McAnulty et al., 2012; Swindle and Smith, 2015). Pig cell lines from kidney and other tissues are commercially available for accompanying in vitro studies (http://www.lgcstandards-atcc.org). Environmental standardization of experimental pig housing regarding microbial health monitoring was established (Rehbinder et al., 1998; Schuurman, 2009). For carrying out qualitative and quantitative analyses with porcine biomedical models, detailed protocols for the determination of sampling locations and sampling numbers, as well as recommendations on the orientation, size, and trimming of samples from about 50 different porcine organs and tissues were provided (Albl et al., 2016).

Here, we first give a short description of the techniques which are currently used for the production of genetically engineered pigs. The subsequent chapter then summarizes the genetically engineered pig models that were established for specific human diseases.

2 TECHNIQUES USED FOR THE GENERATION OF GENETICALLY ENGINEERED PIGS

Gene transfer into the porcine genome was first carried out in 1985 via DNA microinjection into the pronuclei of fertilized oocytes (Brem et al., 1985; Hammer et al., 1985). Subsequently, sperm-mediated gene transfer, lentiviral transgenesis, somatic cell nuclear transfer from genetically modified cells, as well as gene editing techniques based on designer nucleases were used for the generation of mutant pig lines. Compared to the low efficiency of the basal DNA microinjection technique, the other methods have the potential of increased efficiency thereby leading to the use of smaller numbers of animals in the production of genetically engineered animals. Functional porcine embryonic stem (ES) cells or other pluripotent stem cells are not yet available (Soto and Ross, 2016). Chronological descriptions of the milestones in the development of techniques used for the genetic modification of pigs are published (Aigner et al., 2013; Dmochewitz and Wolf, 2015).

Genetic modification of animals is done by somatic and/or germline modification of the host genome. Somatic modifications include the production of mosaics, for example, by genetic alteration of a part of the body cells by viral vectors, and of chimeras by insertion of foreign cells into an organism (Matsunari et al., 2013). Animals with germline modifications are used for the production of stable mutant lines which make the model permanently and reproducibly available during all developmental stages. Genetically engineered animals are either transgenic animals harboring experimentally transferred DNA sequences or genetically modified animals without transfer of foreign DNA into the host genome.

Genetically engineered animals are used for the analysis of gene function and gene regulation (functional genome analysis), for the generation of disease models, as well as for the production of biologically active proteins or modified animal products (gene farming). The aim of a project involving genetic engineering may be the analysis of an additional function by over- and/or ectopic expression of a transgene (gain of function) and/or the partial or complete loss of function of host genes (loss of function). This includes the inactivation of specific genomic sequences (knockout), defined genomic modifications (knockin), specific suppression of the synthesis of gene products (knockdown, gene silencing), as well as random mutagenesis of the host genome (insertional mutagenesis). The aim of the project determines the strategy and the techniques used for the genetic modification of the respective animal models. Production of valid data in such a project generally requires the generation and analysis of several independent genetically engineered lines, as genetic and/or epigenetic alterations due to the techniques used for genetic modification may occur. If these alterations are not linked to the modified locus, they can be removed by conventional breeding.

Animal welfare issues require the systematic analysis of the genetically engineered lines for the occurrence of burden caused by the induced mutation. The international nomenclature is described in the internet (http://www.informatics.jax.org).

2.1 Sequence-Specific Nuclease-Mediated Genetic Engineering

Sequence-specific nuclease-mediated gene editing in pigs may be done either in primary cells followed by somatic cell nuclear transfer (SCNT) to generate animals, or in porcine embryos (mostly zygotes). Protein-guided zinc finger nucleases (ZFN) and transcription activator-like effector nucleases (TALEN), as well as the RNA-guided CRISPR-Cas9 (clustered regularly interspaced short palindromic repeat associated protein 9) system have been successfully used for the establishment of genetically engineered pig lines (Tan et al., 2016).

All three systems induce sequence-specific double strand breaks in a targeted region of the host genome. DNA repair via the nonhomologous end joining (NHEJ) pathway often leads to insertions and/or deletions of variable length, potentially resulting in partial or complete inactivation of the target gene. Sequence analysis of the novel alleles is carried out to predict their functional effects. Simultaneously editing two host genome loci on the same chromosome can also lead to the deletion of the DNA sequence between both loci. DNA repair via nonhomologous end joining (NHEJ) in the presence of exogenous DNA, such as an expression vector, can lead to transgenic cells via nonhomologous site-specific integration. Homology-directed repair (HDR) of a DNA double strand break can either restore the previous sequence or—in the presence of a targeting vector—facilitate targeted integration of a DNA sequence via homologous recombination. This strategy can be used for multiple purposes including additive gene transfer, partial or complete inactivation, as well as defined modification of a specific gene. Possible unspecific off-target effects of the nucleases may occur in loci with DNA sequences that are highly homologous to the target locus, and have been found in pig projects using these techniques (Yang et al., 2011). Unwanted unspecific host genome alterations not linked to the specific mutation can be removed by conventional breeding. Use of the sequence-specific nuclease-mediated systems by microinjection into zygotes may give rise to a high proportion of mutant founder offspring. Monoallelic or biallelic mutant and/or mosaic (animals harboring cells with different genotypes which arise either from onset of the first cell

division in the embryo before the induction of mutations or prolonged mutation induction activity after the one-cell stage) founder animals may appear which are analyzed to detect appropriate mutations for the subsequent breeding of mutant lines.

In pigs, the use of sequence-specific nuclease-mediated techniques started with the production of a ZFN-induced knockout of the *EGFP* transgene integrated in transgenic primary porcine somatic cells and the subsequent generation of heterozygous knockout pigs with these mutant cells by SCNT (Watanabe et al., 2010; Whyte et al., 2011a). A heterozygous knockout pig was also achieved for the *PPARG* gene by using ZFN and SCNT (Yang et al., 2011) (see Section 3.10). In addition, ZFNs were used to induce a biallelic knockout of the porcine α1,3-galactosyltransferase (*GGTA1*) gene in primary porcine fibroblasts which were subsequently used for SCNT (Hauschild et al., 2011). SCNT of TALEN-modified fetal fibroblasts with various mutant genotypes resulted in Ossabaw minipigs harboring biallelic low density lipoprotein receptor (*LDLR*) gene mutations. Piglets carried biallelic *LDLR* mutations which are expected to prematurely truncate the *LDLR* open reading frame, or are implicated in familial hypercholesterolemia in humans (Carlson et al., 2012) (see Section 3.11). The CRISPR-Cas9 system was used to establish pig models for the von Willebrand disease which is caused by von Willebrand factor (*VWF*) gene deficiencies. By editing *VWF* directly in Bama minipig zygotes, monoallelic, as well as biallelic *VWF* mutant piglets were born (Hai et al., 2014) (see Section 3.13).

2.2 Somatic Cell Nuclear Transfer

Somatic cell nuclear transfer (SCNT, cloning) in pigs (Betthauser et al., 2000; Onishi et al., 2000; Polejaeva et al., 2000) is carried out to produce mutations (knockout, -in) in defined loci of the porcine genome after using the sequence-specific nuclease-mediated techniques described above or after classical gene targeting by homologous recombination of targeting vector and host genome in the nuclear donor cells. In addition, the method is also used for additive gene transfer by random transgene integration in the nuclear donor cells. In both cases, preselection of donor cells with regard to the induced genetic modification, transgene expression and/or gender is possible. The production of genetically engineered animals by SCNT includes the transfection and selection of somatic donor cells in vitro, recovery and enucleation of recipient metaphase II oocytes, transfer of genetically modified somatic cell nuclei into the cytoplasm of the enucleated oocytes, activation of the reconstructed oocytes, and embryo transfer to recipients. In the case that genetically modified donor cells are used, 100% genetically modified founder animals

without genetic mosaicism are received. As prolonged in vitro culture periods of the nuclear donor cells negatively influences the success of SCNT, use of pools of small clones of genetically modified nuclear donor cells rather than expansion of individual cell clones to high cell numbers may improve the efficiency of SCNT (Kurome et al., 2015).

The cloning efficiency is varying within relatively low values between 0.5% and 5% offspring per transferred SCNT embryos. The successful embryonic, fetal, and neonatal development of the transferred embryos derived from SCNT depends on the correct epigenetic reprogramming of the donor cell nuclei. Insufficient epigenetic reprogramming may lead to an overall low cloning efficiency, as well as to peri- and neonatal health problems of cloned mammals. Abnormal phenotypes of cloned pigs occur less frequently than in other mammals, and they normally are not transmitted to the offspring of the affected clones (Cho et al., 2007; Shi et al., 2003; Suzuki et al., 2012). Genome-wide gene expression and DNA methylation profiling of different tissues in phenotypically normal cloned pigs and conventionally bred control pigs revealed differentially expressed genes and moderate alterations in DNA methylation (Gao et al., 2011; Park et al., 2011). Proteomic analyses of hearts of adult SCNT-derived Bama minipigs compared to controls also identified differentially expressed proteins thereby demonstrating that SCNT might result in abnormal expression of important proteins in cardiac development (Shu-Shan et al., 2014). Thus, genetically engineered founders derived from SCNT may be used in experiments only with caution with regard to the validity and reproducibility of the results.

Various somatic cell types were successfully used in the cloning procedure and numerous technical variations were established to increase the efficiency of porcine SCNT (Kurome et al., 2015). Furthermore, recombinant adeno-associated virus (rAAV) vectors (Rogers et al., 2008a), as well as modified bacterial artificial chromosomes (Klymiuk et al., 2012a) were successfully used for efficient gene targeting in porcine cells. As minipigs are suitable experimental animals for biomedical research, genetically modified cloned minipigs were produced by using minipigs as nuclear donors and common large-sized domestic farm breeds as both oocyte donors and recipients. This method combines the wide availability of domestic farm breeds with the biomedical value of minipigs (Estrada et al., 2008; Kurome et al., 2008).

2.3 Embryo Microinjection

Embryo microinjection of sequence-specific nucleases with or without foreign DNA results in the generation of either transgenic animals harboring experimentally transferred DNA sequences or genetically modified

animals without transfer of transgenes into the host genome. In addition, basal microinjection of only DNA sequences as transgenes into the pronuclei of fertilized oocytes is still carried out but generally results in low efficiency of transgene integration, random integration of multiple transgene copies including rearrangement of the host genome around the integration site and/or insertional mutagenesis, high numbers of transgenic mosaic founders, and possible genome position effects on the expression of the transgene. Porcine in vivo produced embryos, as well as embryos following in vitro fertilization (IVF) of in vitro matured (IVM) oocytes derived from ovaries of slaughtered gilts are used for the procedure.

2.4 Transposon Systems

Random enzyme-mediated gene transfer is done with DNA transposon systems derived from different species, for example, Sleeping Beauty (SB) or PiggyBac (PB). The transgene is flanked on both sides by recognition sites (inverted terminal repeats, ITR) of the enzyme transposase. Usually comicroinjection of transgene and transposase is carried out. Increased efficiency of gene transfer, integration of single copies per host genome site and multiple segregating transgene integration sites may occur. Normally only small recombinations are caused in the surrounding host genome. However, efficiency of the gene transfer in vivo decreases with increasing length of the transgene (Ivics et al., 2009). In pigs, use of the Sleeping Beauty system in vitro in fibroblasts and the subsequent use of the transgenic cells in SCNT was carried out (Carlson et al., 2011; Jakobsen et al., 2011). Single transgene copies are presumably less prone to transgene silencing than concatemeric transgene insertions. Studies with the Sleeping Beauty system suggest that Sleeping Beauty rarely targets heterochromatic chromosomal regions for insertion, and that it is unlikely that certain sequence motifs in the transposon vector are recognized by mediators of silencing in the cell. In transgenic pigs, long-term observation for more than 12 months found no changes in the transgene expression suggesting that no age-related silencing of the transgene occurred (Garrels et al., 2011; Ivics et al., 2014).

2.5 Inducible Transgene Expression

Conditional transgene expression can be achieved by using regulatory elements that can be induced or inactivated by exogenous stimuli. The most widely used systems are the tetracycline-regulated Tet-On and Tet-Off systems which consist of two parts. In mice, usually two genetically engineered lines are produced and then mated to achieve double modified offspring for the induction of the transgene expression.

Due to the relatively long generation interval in pigs, the combination of all elements of this system, for example, expression of the tetracycline-dependent transactivator and the transactivator-dependent expression of the target gene, on a single construct was tested. Transgenic pigs were produced with a construct consisting of an autoregulatory bicistronic Tet-Off-based expression cassette, where the transactivator responsive promoter (PtTA) drives the cDNA for the human complement regulatory proteins CD55 (decay-accelerating factor, DAF) or CD59 (membrane inhibitor of reactive lysis, MIRL). Via a poliovirus internal ribosomal entry site (IRES), this was linked with a Tet-Off transactivator (tTA). Minimal expression of the Tet-Off transactivator promoter results in tTA expression and binding to the transactivator responsive promoter PtTA which initiates an autoregulative loop. In the presence of exogenous doxycycline, the transactivator tTA is inactivated and transgene transcription is silenced. Using the DNA microinjection technique, these constructs were used to produce transgenic pig lines expressing CD55 or CD59. Transgene expression did not affect animal health and fertility. Mosaic transgene expression restricted to muscle was observed in the transgenic lines. After crossbreeding, animals double transgenic for *CD55* and *CD59* were obtained with tissue-independent expression of CD59, but not CD55. The asymmetric expression pattern correlated with differences in methylation patterns of the integrated transgenes. Feeding transgenic animals with doxycycline for 6 days eliminated the transgene expression within 2–6 days. Doxycycline levels in porcine plasma rapidly declined after termination of the application; however, transgene reexpression did not resume earlier than 8 weeks later (Kues et al., 2006).

As only the use of the Tet-Off system has been published for pigs, we established a model for the induction of the expression of transgenes on the genetic background of the Swabian-Hall breed. The Tet-On strategy was based on a similar principle but used the modified rtTA transactivator that binds to the PtTA only in the presence of tetracycline or derivates, such as doxycycline. Binding of the doxycycline-rtTA product to PtTA causes transcriptional activation and, thus, expression of a desired gene of interest. The switch-on principle may reflect the requirements of transgene regulation in biomedical research more closely. As the Tet-On system requires the expression of two independent transcripts, and the transgene vector needs a positive selection cassette for generating transgenic pigs by SCNT, we decided to place the constitutive rtTA construct and the gene of interest on different vectors to avoid negative influences of closely adjacent transgenes on the transcription. In addition, transgenic pigs with a suitable expression level and pattern of rtTA can be used as genetic basis for any PtTA-controlled expression cassette. In a first step,

founder pigs expressing rtTA under a ubiquitous cytomegalovirus enhancer/chicken β-actin (CAG) promoter were generated and characterized for rtTA expression by RT-PCR. Primary cells were prepared from all transgenic animals and transfected with constructs carrying the genes of interest, porcine soluble receptor activator of NF-κB ligand (*RANKL*) or cytotoxic T-lymphocyte associated antigen 4-Fc domain of immunoglobulin G1 (*CTLA4-Ig*). In the absence of doxycycline, the levels of both proteins were below the detection limit. The induction upon administration of various concentrations of doxycycline was measured at protein level by ELISA for both regulated transgenes. The induction potential for RANKL and CTLA4-Ig in the cell lines grossly correlated to the transcriptional level of rtTA expression and identified several of the rtTA transgenic pigs as appropriate founder animals. Primary cells of these pigs were used to establish double transgenic animals carrying the constitutive rtTA construct, as well as the regulated gene of interest, in a second round of SCNT. For both regulated genes, *RANKL* or *CTLA4-Ig*, the potential of the Tet-On system to drive transgene expression in vivo was evaluated after oral administration of doxycycline (Klymiuk et al., 2012b).

The in vivo induction of CTLA4-Ig expression was limited to a 6-day feeding protocol with 25 mg/kg/day doxycycline to avoid impairment of the immune status. This was sufficient to yield detectable levels of CTLA4-Ig in blood serum. The serum was able to inhibit T-cell proliferation in a standard in vitro assay and confirmed the biological function of the induced transgene product. Thus, the induced expression of a transgene was successfully carried out in pigs (Klymiuk et al., 2012b). The induction of the expression of RANKL was carried out in order to produce large animal models for osteoporosis (see Section 3.19). Successful use of the Tet-On system in transgenic pigs established by SCNT was also demonstrated for inducible expression of enhanced green fluorescent protein (Jin et al., 2014) or porcine growth hormone (Ju et al., 2015).

Further refinements of the transgene technology in pigs include the *Cre/loxP* system for conditional transgenic modifications where parts of the system were analyzed in initial studies of transgenic pig lines (Li et al., 2009; Chen et al., 2010). The *Cre/loxP* system was recently used for the generation of conditional porcine cancer models (see Section 3.23).

2.6 Further Technical Improvements

In transgene projects, often multiple genes are required to be simultaneously modified in the animals to achieve the desired phenotype. This can be done by the production of transgenic lines harboring one transgene each that are subsequently used in complex breeding programs. On the other hand, expression of several proteins from a single vector has been done by using internal ribosomal entry site (IRES) placed between the coding sequences for the respective proteins. However, in vectors containing the IRES sequence, the gene placed downstream is often expressed at a much lower level than the gene located upstream. The viral 2A peptide is used as alternative. It is about 19 amino acids long and contains a conserved and functional motif. Separation of the sequences upstream and downstream of this site is done through ribosomal skipping during protein translation between the last two amino acids at its C terminus resulting in the expression of two independent proteins from a single transcription event. By SCNT, transgenic pigs were produced uniformly coexpressing four fluorescent proteins in various tissues using a single 2A peptide-based double-promoter vector. Ribosomal skipping during protein translation results in small peptides of the 2A peptide site fused to the upstream and downstream proteins. As this may interfere with intracellular localization and function of the transgene-encoded proteins, modification of the 2A sequence has been described to greatly circumvent this problem (Deng et al., 2011).

The aim of standardized expression of transgenes from defined host genome loci was addressed in projects targeting the ROSA26 locus (Kong et al., 2014; Li et al., 2014b) or the H11 locus (Ruan et al., 2015) of the pig genome.

Additional transgenic pigs with the ubiquitous or tissue-specific expression of reporter genes, such as the green fluorescent protein (GFP) were established for the use in further fine tuning the techniques for precise genetic modification of pigs, as well as tools in basic biological research (Matsunari and Nagashima, 2009).

3 GENETICALLY ENGINEERED PIGS AS MODELS FOR HUMAN DISEASES

Beneath the identification of spontaneously arosen mutations leading to interesting phenotypes (http://omia.angis.org.au), transgenic pigs initially have been predominantly established to examine traits of livestock performance (growth, reproduction, disease resistance, product quality and safety, environmental pollution) and to establish bioreactors for the production of human proteins related to biomedical applications in various body fluids or tissues (Martin and Pinkert, 2002; Pursel and Rexroad, 1993; Whyte and Prather, 2011). Recently, the development of transgenic pig models for biomedical research strongly increased (Tan et al., 2016; Rogers, 2016). The current state of the establishment and analysis of genetically engineered pigs for biomedical research is reviewed here (Table 26.1). This does not include the transgenic animals generated for the purpose

TABLE 26.1   Genetically Engineered Pigs as Disease Models

Disorder	Disease	Transgene/induced mutation	References
Neurodegenerative	Alzheimer's disease	Expression of mutant human APP^{sw} in the brain	Kragh et al. (2009)
		Ubiquitous expression of mutant human $PSEN1^{M146I}$	Jakobsen et al. (2013)
	Huntington's disease	Neuronal expression of mutant pig HTT (75Q)	Uchida et al. (2001)
		Ubiquitous expression of mutant human HTT (N208-105Q)	Yang et al. (2010)
		Expression of mutant human HTT (N548-124Q)	Baxa et al. (2013)
	Parkinson's disease	Biallelic $PARK7$ knockout	Yao et al. (2014)
		Biallelic $PARK2$ and $PINK1$ knockout	Zhou et al. (2015), Wang et al. (2016)
	Spinal muscular atrophy	Heterozygous SMN knockout and expression of human $SMN2$	Lorson et al. (2011), Prather et al. (2013)
	Amyotrophic lateral sclerosis	Ubiquitous expression of mutant human $SOD1^{G93A}$	Chieppa et al. (2014), Yang et al. (2014)
		Ubiquitous expression of mutant human $TDP43^{M337V}$ (TARDBP ^{M337V})	Wang et al. (2015a)
	Ataxia–telangiectasia	ATM knockout	Kim et al. (2014), Beraldi et al. (2015)
Retinal	Retinitis pigmentosa	Retinal expression of mutant pig RHO^{P347L} or RHO^{P347S}, or mutant human RHO^{P23H}	Petters et al. (1997), Kraft et al. (2005), Ross et al. (2012)
	Macular dystrophy	Photoreceptor-specific expression of mutant human $ELOVL4$	Sommer et al. (2011b)
	Cone dystrophy	Cone-specific expression of mutant human $GUCY2D^{E837D/R838S}$	Kostic et al. (2013)
Cardiovascular	Vascular	Endothelial overexpression of pig $NOS3$ ($eNOS$)	Hao et al. (2006)
		Expression of a modified pig $NOS3$ ($eNOS$)	Whyte and Laughlin (2010)
		Endothelial-specific expression of human CAT	Whyte et al. (2011b)
		Heterozygous $PPARG$ knockout	Yang et al. (2011)
	Atherosclerosis	Expression of human $APOC3$	Wei et al. (2012)
		Ubiquitous expression of human LPA ($Apo(a)$)	Ozawa et al. (2015), Shimatsu et al. (2016)
		Biallelic $LDLR$ mutations, $LDLR$ knockout	Carlson et al. (2012), Davis et al. (2014), Li et al. (2016)
		Liver-specific expression of mutant human $PCSK9^{D374Y}$	Al-Mashhadi et al. (2013)
		Ubiquitous overexpression of pig $PLA2G7$	Tang et al. (2015)
		Biallelic $NPC1L1$ knockout	Wang et al. (2015b)
	Cardiomyopathy	Expression of human $ENTPD1$ ($CD39$)	Wheeler et al. (2012)
		Ubiquitous expression of $TMSB4X$ ($T\beta4$)	Hinkel et al. (2014)
		Heterozygous mutant $SCN5A^{E558X}$	Park et al. (2015b)
Blood	Hemophilia A	Heterozygous $F8$ knockout	Kashiwakura et al. (2012)
	Von Willebrand disease	Biallellic VWF knockout	Hai et al. (2014)

(Continued)

TABLE 26.1   Genetically Engineered Pigs as Disease Models (*cont.*)

Disorder	Disease	Transgene/induced mutation	References
Respiratory	Cystic fibrosis	*CFTR* knockout (disruption of exon 10) or mutant pig *CFTR*$^{\Delta F508}$ knockin	Rogers et al. (2008a), Rogers et al. (2008b)
		CFTR knockout (STOP box downstream of the start codon in exon 1)	Klymiuk et al. (2012a)
		Intestinal CFTR expression in *CFTR* knockouts	Stoltz et al. (2013)
Muscle	Duchenne muscular dystrophy	*DMD* knockout	Klymiuk et al. (2013)
		In-frame exon deletion in the rod domain of *DMD*	Selsby et al. (2015)
β-cells	Type 2 diabetes mellitus	β-cell expression of mutant dominant-negative human *GIPR*^{dn}	Renner et al. (2010), Cheng et al. (2015)
		β-cell expression of mutant pig *INS*^{C94Y}	Renner et al. (2013)
	Type 3 of maturity-onset diabetes of the young	β-cell expression of mutant dominant-negative human *HNF1A*^{P291fsinsC}	Umeyama et al. (2009)
Liver	Liver disease	*FAH* knockout	Hickey et al. (2014)
Kidney	Polycystic kidney disease	Ubiquitous overexpression of pig *PKD2*	He et al. (2013)
		Heterozygous *PKD1* knockout	He et al. (2015)
		Overexpression of pig *MYC* in kidney	Ye et al. (2013)
Bone	Osteoporosis	Inducible expression of porcine soluble *RANKL* (*TNFSF11*)	Klymiuk et al. (2012b)
	Marfan syndrome	*FBN1* knockout	Umeyama et al. (2016)
Skin		Cutaneous expression of mutant human *GLI2*	McCalla-Martin et al. (2010)
		Cutaneous expression of human *ITGB1* or *ITGA2*	Staunstrup et al. (2012)
		Biallelic *MITF* knockout	Wang et al. (2015c)
		Biallelic *TYR* knockout	Zhou et al. (2015)
Circadian rhythm		Ubiquitous expression of mutant human *CRY1*^{C414A}	Liu et al. (2013)
Cancer		Expression of MMTV/v-Ha-ras	Yamakawa et al. (1999)
		Heterozygous *BRCA1* knockout	Luo et al. (2011)
		Heterozygous mutant *APC*^{1061Stop} or *APC*^{1311Stop}	Flisikowska et al. (2012)
		Monoallelic and biallelic *APC* knockout	Tan et al. (2013)
		Heterozygous mutant *TP53*^{R167H}	Leuchs et al. (2012), Saalfrank et al. (2016)
		Homozygous mutant *TP53*^{R167H}	Sieren et al. (2014)
		Latent mutant *KRAS*^{G12D}	Li et al. (2015b)
		Ubiquitous expression of *Cre* inducible mutant pig *KRAS*^{G12D} and *TP53*^{R167H}	Schook et al. (2015)
Immune system	Infectious diseases	Homozygous disruption of the J-region gene segment of the heavy chain locus	Mendicino et al. (2011), Chen et al. (2015)
		Homozygous disruption of the immunoglobulin κ light chain locus	Ramsoondar et al. (2011)
	Immunodeficiency	*IL2RG* knockout	Suzuki et al. (2012), Watanabe et al. (2013)
		Biallelic *RAG1* or *RAG2* knockout, *RAG1* knockout	Huang et al. (2014), Lee et al. (2014), Ito et al. (2014)
		Class I MHC knockout	Reyes et al. (2014)
		CD1D knockout	Whitworth et al. (2014)

of xenotransplantation that have been reviewed elsewhere (Cooper et al., 2016; Ekser et al., 2015; Klymiuk et al., 2010).

At least some of the genetically modified pigs established for xenotransplantation research are also used for basic biomedical research. One example is transgenic pigs ubiquitously expressing human heme oxygenase 1 (HMOX1, HO-1) which is an inducible protein capable of cytoprotection by scavenging reactive oxygen species and preventing apoptosis caused by cellular stress during inflammatory processes. The transgenic pigs exhibited lower body weights and lower subcutaneous fat tissue compared to controls. Further analyses revealed that HMOX1 overexpression reduced adipogenesis both in vivo and in vitro, which makes them an interesting model in the research of obesity and related metabolic diseases (Park et al., 2015a).

In basic research, production of valid data in a project involving genetic modification generally requires the production and analysis of several independent lines, as nontransgene-specific genetic and/or epigenetic alterations may appear in all techniques used for the generation of genetically engineered animals. In addition, different alleles of the examined gene may cause different phenotypes. For the establishment of an appropriate animal model showing specific pathophysiological characteristics of a human disease in question, selection, and analysis of one particular transgenic line exhibiting the desired phenotype stably over several generations may be practicable.

3.1 Alzheimer's Disease

Several inherited neurological diseases in humans are caused by misfolded proteins that accumulate in neuronal cells of the brain and lead to apoptosis. Transgenic mouse models of these diseases often fail to replicate apoptosis and overt neurodegeneration in the brain. Establishment of porcine models for human late-onset neurodegenerative disorders, such as Alzheimer's disease, Huntington's disease, or Parkinson's disease may solve the practical issue of ageing as a crucial pathogenic factor of these diseases. Specific disease phenotypes might eventually evolve in these pig models in 10–15 years which is theoretically possible, but practically and economically impossible for scientific research and preclinical investigation (Holm et al., 2016).

Alzheimer's disease is a multifactorial neurodegenerative disease. Aberrant processing and clearance of amyloid β-precursor protein (APP) from the brain is central to the pathogenesis of Alzheimer's disease. The onset of the disease appears after 40 years or more. In some families, *APP* mutations were identified to cause an autosomal dominant disorder where the mutant *APP* leads to the increased production of distinct protein fragments

which in turn results in neuropathy. The development of a pig model for Alzheimer's disease was attempted by producing transgenic pigs using the human dominant mutant allele *APP^sw* harboring two amino acid exchanges due to two neighboring nucleotide exchanges (K670N and M671L) which was found to cause Alzheimer's disease. The 7.5-kb transgene was the same as already used in previous transgenic mouse studies. It comprises a 1-kb platelet-derived growth factor-β (PDGFβ) promoter, intronic and exonic sequences of the β-globin gene, the cDNA encoding the mutant allele *APP^sw* and SV40 polyadenylation sequences. After stable transfection of fibroblasts of the Göttingen minipig breed, one transgenic cell clone was used for SCNT to produce seven healthy transgenic cloned pigs with normal weight gain. The transgenic pigs harbored a single full-length copy of the transgene in their genome and showed strong, promoter-specific expression of the transgene-encoded protein in brain tissues. Accumulation of the pathogenic protein and subsequent appearance of clinical consequences were estimated to develop with increasing age (Kragh et al., 2009).

As memory impairment is the most striking and consistent feature in human patients of Alzheimer's disease, the memory of the transgenic pigs was analyzed at the age of 1 and 2 years using the spontaneous object recognition test which has been established for minipigs and is based on behavioral discrimination of familiar and novel objects. High interindividual variability and no significant difference between transgenic animals and controls were revealed. Positron emission tomography (PET) scans, as well as neuropathological analysis of a 2-year old transgenic animal showed normal histology without deposition of the pathogenic protein (Sondergaard et al., 2012). In further analyses, the transgene was shown to be expressed in relevant brain regions at a fairly constant level during the 5-year examination period, but no pathological changes were revealed (Holm et al., 2016).

Further cleavage of APP is dependent on the function of the transmembrane protein presenilin 1 (PSEN1). Mutations in *PSEN1* are known to cause autosomal dominant early-onset Alzheimer's disease. Using recombinase-mediated cassette exchange (RMCE) in Göttingen minipig cells and SCNT, the same group produced transgenic animals harboring a single transgene copy consisting of the cDNA of the Alzheimer's disease-causing mutation *PSEN1^M146I* driven by a promoter allowing ubiquitous expression (Jakobsen et al., 2013). The mutant human PSEN1 protein was expressed in the porcine neurons, but no Alzheimer's disease-like pathological changes were revealed over a period of 3 years. Currently, double transgenic Göttingen minipigs exhibiting the combined expression of mutant human *APP* and *PSEN1* genes are under study (Holm et al., 2016).

3.2 Huntington's Disease

Huntington's disease is an autosomal dominant, progressive neurodegenerative disorder leading to the premature loss of specific neurons. It is associated with an expansion of a CAG trinucleotide repeat in the 5' region of the huntingtin (*HTT*) gene that results in a elongated polyglutamine (polyQ) tract of the protein. The CAG repeat number is polymorphic and ranges from 6 and 35 units in normal alleles and from 36 and 120 units in alleles associated with Huntington's disease. Several mouse models of Huntington's disease were extensively studied, but none of them showed robust neurodegeneration as observed in the brains of patients of Huntington's disease.

The 12.8-kb *HTT* transcript of Göttingen minipigs codes for a 345-kDa protein (3139 amino acids) (Matsuyama et al., 2000). A transgenic pig model was generated by DNA microinjection of an 8.2-kb transgene into minipig embryos consisting of the 4-kb rat neuron specific enolase (*Nse*) promoter, a 3.3-kb 5' minipig huntingtin cDNA which was mutated by insertion of 75 CAG repeats into the triplet region of exon 1, and a 0.9-kb SV40 polyadenylation signal. Five transgenic founder pigs were produced each harboring 1–3 different integration sites with variable copy numbers and indication of genetic mosaicism (Uchida et al., 2001). To date, no follow-up publication describing mutant phenotypes appeared.

Another transgenic pig model for Huntington's disease was established with Tibetan minipigs as genetic background. As transgenic mouse models showed that N-terminal huntingtin fragments with expanded polyglutamine tracts cause more severe neurological symptoms than full-length mutant huntingtin (3144 amino acids), two expression vectors were constructed. They included the cytomegalovirus enhancer and chicken β-actin (CAG) promoter and human N-terminal (208 amino acids) mutant *HTT* with two different expanded polyglutamine tracts (105Q or 160Q). Transfected cell clones were used for SCNT. The transfer of about 2000 reconstructed embryos for each transgene yielded the birth of five pigs transgenic for mutant *HTT* N208-105Q, but none was born that was transgenic for mutant *HTT* N208-160Q. It was concluded that the transgene with the longer polyQ repeat is more toxic and did not allow the early development of transgenic pigs. The *HTT* N208-105Q transgenic pigs were derived from different transgenic cell clones showing multicopy transgene loci with the insertion in estimated 3–4 sites. The five piglets appeared normal at birth, but three were weak and died within the first 3 days after birth. A fourth piglet died within the first month, and the fifth pig showed no obvious symptoms after 4 months after birth. Expression analysis of the transgene-derived protein and its degraded product showed that the fifth animal showed the lowest expression, and the fourth animal also showed lower expression compared to the three animals which died very early. Thus, the expression level of mutant *HTT* may negatively contribute to the life span of the transgenic pigs. For comparison purposes, two transgenic FVB mouse lines were generated with the same transgene which also expressed the transgene in the brain. Typical apoptotic neurons with nuclear DNA fragmentation were found in the brains of the four dead transgenic pigs whereas transgenic mice showed no apoptotic neurons. Compared to the transgenic mouse brains, a higher number of neurons with activated caspase-3 was found in transgenic pig brains resulting from caspase activation and reflecting early apoptotic events (Yang et al., 2010).

A further transgenic pig model for Huntington's disease was generated by using lentiviral-based transgenes carrying a human minimal *HTT* gene promoter driving either a 548-amino acid or full length (3144 amino acids) human *HTT* cDNA containing 145 repeats of a mixed CAG/CAA sequence. Transgenic founder pigs harboring one copy of the human *HTT* transgene encoding 124 glutamines due to polyglutamine contraction (N548-124Q) were born and bred for three generations. Mutant *HTT* mRNA and protein fragments were detected in brain and peripheral tissues. No aggregate formation in brain up to 16 months was seen. No developmental or gross motor deficits were observed up to 40 months of age. Compared to controls, 1-year old transgenic boars showed reduced fertility including reduced spermatozoa and oocyte penetration (Baxa et al., 2013). In addition, work is described to be underway at Exemplar Genetics (Sioux City, IA) to generate a knockin model of Huntington's disease in minipigs (Morton and Howland, 2013).

3.3 Parkinson's Disease

Parkinson's disease is a progressive neurodegenerative movement disorder that is characterized by the degeneration of dopamine neurons in the substantia nigra and the intracytoplasmic inclusion of Lewy bodies. By far the most cases are sporadic, but several causative mutations have been identified in patients of familial Parkinson's disease, including mutated *PARK7* (*DJ-1*). In Large White pig fibroblast cells, TALEN-mediated editing of *PARK7* resulted in monoallelic and biallelic mutations of *PARK7*. Use of mixed *PARK7* mutant colonies for SCNT obtained one monoallelic and two biallelic live-born *PARK7* knockout piglets. All three piglets died in the first days after birth presumably due to cloning defects. Western blot analysis confirmed the absence of PARK7 in these pigs (Yao et al., 2014).

Mutations of *PARK2*—encoding parkin, a component of the multiprotein E3 ubiquitin ligase complex—and

PINK1 (*PARK6*)—encoding PTEN induced putative kinase 1, a mitochondrial serine/threonine-protein kinase—are also known to cause autosomal recessive early-onset Parkinson's disease in humans. Using the CRISPR-Cas9 system, combined *PARK2* and *PINK1* homozygous knockout cell clones of Banna minipigs and Bama minipigs were produced by editing the first exon region following the start codon of each gene, and further used for SCNT. Viable, normally developing, combined *PARK2* and *PINK1* homozygous knockout pigs were generated harboring various types of mutations at both target loci corresponding to the respective donor cells. Expression of *PARK2* and *PINK1* in brain cortex sections was undetectable in these animals. No typical Parkinson symptoms were detected up to 7 months of age (Zhou et al., 2015).

In addition, one homozygous triple biallelic knockout piglet affecting the genes *PARK2*, *PARK7* and *PINK1* was produced using the CRISPR-Cas9 system by simultaneous coinjection of two adjacent single guide RNAs targeting one locus for each gene in Bama minipig one-cell stage embryos. A second piglet showed biallelic modifications of the genes *PARK7* and *PINK1* and a monoallelic mutation of the *PARK2* gene. Absence of PARK7 protein and highly decreased mRNA levels of *PARK2* and *PINK1* were found in the triple biallelic knockout pig. Whole-genome sequencing of the parents and the triple biallelic knockout pig was carried out to assess the degree of mutagenesis across the entire genome. No significant off-target cleavage of the CRISPR-Cas9 system was found. The two piglets remained healthy with a normal growth rate. Typical symptoms of Parkinson's disease were not observed in the study period up of 10 months p.p. (Wang et al., 2016).

3.4 Spinal Muscular Atrophy

Spinal muscular atrophy (SMA) is an autosomal recessive neurodegenerative disease that is characterized by the progressive degeneration of spinal motor neurons and muscle atrophy leading to various clinical severities. It is caused by mutations of the survival motor neuron 1 (*SMN1*) gene. The nearly identical gene *SMN2* is present only in humans and works as a disease modifier as increasing *SMN2* copy number decreases the severity of the disease. Mutations in *SMN2* have no clinical consequence if *SMN1* is functional. Several mouse models have been developed to study SMN function and SMA disease pathology, but they show limitations in testing the efficacy of therapeutics. Deletion of *Smn* in mice, as in all mammals but humans, results in embryonic lethality; however, the lethality can be rescued by transgenic expression of the human SMN2. Analogously, the prerequisite for the successful production of genetically engineered pigs with functional knockout of SMA is that

human SMA2 is functional as a transgene in porcine cells. Therefore, it was shown in vitro that splicing of human *SMN1* and *SMN2* as transgenes in porcine cells is consistent with splicing in human cells. Next, gene targeting of porcine *SMN* (Lorson et al., 2008) was carried out via homologous recombination in fetal fibroblast cells of Large White pigs leading to the deletion of essential functional domains of SMN encoded by the exons 2b, 3, and part of exon 4, and to a further disruption of the reading frame. Cells harboring the heterozygous *SMN* knockout were used for SCNT. Phenotypically normal, healthy pigs heterozygous for the *SMN* knockout were produced. No significant reduction in *SMN* RNA between heterozygous mutant and control animals was detected which is consistent with the results in humans and transgenic mice (Lorson et al., 2011). For the second step of the production of a genetically engineered pig model of SMA, heterozygous *SMN* knockout primary cells were used for transfection of a 35.5-kb fragment carrying the human *SMN2* gene and its promoter sequence. Multiple positive clones expressing SMN from *SMN2* were obtained and used for SCNT (Prather et al., 2013).

3.5 Amyotrophic Lateral Sclerosis

Amyotrophic lateral sclerosis (ALS) is a fatal neurodegenerative disease which is characterized by progressive selective degeneration of motor neurons, leading to muscle weakness and atrophy and evolving to complete paralysis. It occurs in two clinically indistinguishable forms, the sporadic and the familial form. The familial form is linked to several gene mutations, mostly heritable in a dominant manner. One of the mutant genes is the Cu/Zn superoxide dismutase 1 (*SOD1*) gene. A transgene consisting of the cDNA of the mutant human $SOD1^{G93A}$ sequence, a mutation found in human ALS patients, driven by the ubiquitous pCAGGS promoter (CMV-IE enhancer and chicken β-actin promoter) was transfected into Yucatan minipig cells, and different transgenic cell clones showing high expression were used for SCNT. Five transgenic pigs derived from various transgenic cell clones survived and developed normally reaching adulthood. Since Yucatan minipigs live up to 13–15 years, pigs with high expression of human $SOD1^{G93A}$ are expected to show ALS symptoms in 3–4 years (Chieppa et al., 2014).

Another group also generated transgenic pigs expressing mutant human $SOD1^{G93A}$ using the cytomegalovirus promoter in the genetic background of Tibetan minipigs. The transgenic pigs derived from various transgenic cell clones grew normally and did not show obvious body weight differences compared to controls. Different transgenic lines were produced from the founders. The oldest transgenic pigs were studied for about 2 years. The transgenic pigs developed movement disorders by showing hind limb motor defects, skeletal muscle atrophy and

motor neuron degeneration in a transgene expression level- and age-dependent manner. In addition, transgenic pigs showed neuronal intranuclear inclusions, which were not found in brains of corresponding transgenic ALS mouse models. The findings indicated that higher expression or rapid accumulation of mutant *SOD1* in motor neurons of the spinal cord usually induced a more severe disease phenotype (Yang et al., 2014).

The same workgroup analogously generated transgenic pigs expressing mutant human *TDP43*^{M337V}. TAR DNA binding protein 43 (TARDBP, TDP43) is a multifunctional nuclear protein that binds RNA to regulate RNA processing. Mutant TDP43^{M337V} is redistributed in the neuronal cytoplasm in human patients of both amyotrophic lateral sclerosis (ALS) and frontotemporal lobar degeneration (FTLD). In both diseases, the key pathological change is accumulation of pathogenic TDP43 in the cytoplasm and formation of cytoplasmic aggregates. In mutant human *TDP43*^{M337V} transgenic Tibetan minipigs, TDP43^{M337V} was also distributed in the cytoplasm of neuronal cells in the spinal cord and brain. Histological analysis revealed neurodegeneration in transgenic pig brains. Newborn transgenic pigs appeared normal. Compared to *SOD1*^{G93A} transgenic pigs, the transgenic pigs expressing human *TDP43*^{M337V} showed a more severe phenotype. This included reduced body weight gain from 3 months after birth, a loose and wrinkled appearance of the skin, progressive weakness, and limb movement defects associated with markedly reduced muscle fiber size, and early death starting at the age of 4–5 months. A high number of the transgenic pigs died within 1 year. Further analyses aimed at the examination of the interaction of TDP43 and further factors of RNA processing (Wang et al., 2015a).

3.6 Ataxia Telangiectasia

Ataxia telangiectasia is a recessive autosomal disorder associated with pleiotropic phenotypes, including progressive cerebellar degeneration leading to motor impairment. It is caused by mutations in the Ataxia telangiectasia mutated (*ATM*) gene (65 exons, 350-kDa protein). ATM is a ubiquitously expressed protein involved with many cell cycle checkpoints and functions as a DNA damage response protein. The *Atm* mutant mouse models did not fully reproduce the hallmark neuropathological phenotype of Purkinje cell loss. A targeting vector was used in Minnesota minipig cells to disrupt exon 59 where the kinase activity is encoded. Using SCNT, five heterozygous *ATM* knockout founders were produced. Studies of the phenotype were not described. In addition, heterozygous *ATM* mutations are suggested to predispose to breast cancer in human patients. Thus, disruption of exon 59 which is suggested to result in a truncated ATM protein, may also model this disease (Kim et al., 2014).

Another workgroup developed homozygous *ATM* knockout pigs with a targeting vector disrupting exon 57 of *ATM* which encodes a significant portion of the ATP binding region within the kinase domain, and subsequent SCNT. Homozygous *ATM* knockout Yucatan minipigs were born with the expected Mendelian inheritance ratio after mating heterozygous mutants. ATM kinase domain, kinase activity, as well as truncated proteins were not detectable in the homozygous mutants. Unlike in the mouse models, the homozygous *ATM* knockout pigs showed early cerebellar lesions including loss of Purkinje cells and altered Purkinje cell architecture, as well as growth retardation and gait/motor coordination deficits. In addition, an increased number of chromosomal breaks were found in fibroblasts derived from the homozygous mutants when compared to controls (Beraldi et al., 2015).

3.7 Retinitis Pigmentosa

Retinitis pigmentosa comprises a group of inherited retinal diseases leading to the most frequent cause of hereditary visual loss in humans. It causes night blindness early in life due to loss of rod photoreceptors. The remaining cone photoreceptors slowly degenerate leading ultimately to blindness. Over 200 mutations in 45 genes have been identified as causative in various monogenic forms of retinitis pigmentosa. Both transgenic and knockout rodent models of retinal dystrophy contributed to the analysis of disease mechanisms. Compared to humans, rodent models are limited by two disadvantages, the small number and different distribution of photoreceptors in the retina and the small eyes (Gregory-Evans and Weleber, 1997).

Mutations in the rhodopsin (*RHO*) gene are known causes for retinitis pigmentosa in humans. Transgenic pigs expressing mutant porcine rhodopsin (RHO^{P347L} or RHO^{P347S}) were produced by additive gene transfer. A 12.5-kb porcine genomic DNA containing 4-kb 5′ flanking sequences, the coding sequences for the 348 amino acid protein and 2.9-kb 3′ flanking sequences of the porcine *RHO* gene was used including the mutation CCA (Pro) to CTA (Leu) or TCA (Ser) at codon 347. DNA microinjection of the expression vectors for mutant rhodopsin resulted in the generation of transgenic lines. Retinal mRNA expression of the mutant transgene exceeded the expression of the wild-type endogenous gene. Like human patients with the same mutation, the transgenic pigs showed early and severe loss of rod photoreceptors, and the surviving cone photoreceptors slowly degenerated. The phenotypes of mutant *RHO* transgenic pigs and of patients of retinitis pigmentosa are comparable. Therefore, this pig model is intensely used for studying the pathogenesis of retinitis pigmentosa and for preclinical treatment trials (Petters et al., 1997; Kraft et al., 2005).

The stability of the mutant phenotype in the RHO^{P347L} transgenic pigs was analyzed after maintaining the model for nine generations on a heterogeneous genetic background. In each generation, hemizygous transgenic boars were mated to unrelated nontransgenic sows. The sows used were composites of the Yorkshire, Landrace, and Large White breeds to minimize inbreeding and the negative consequences thereof in the transgenic line. Assessment of the photoreceptor degeneration in transgenic animals after nine generations showed a phenotype similar to that of the first description of the transgenic animals. Thus, the RHO^{P347L} transgenic pigs exhibited a stable phenotype after multiple generations of outcrossing (Sommer et al., 2011a).

The rhodopsin mutation RHO^{P23H} underlies the most common form of human autosomal dominant retinitis pigmentosa. Therefore, in another project transgenic pigs were produced on the genetic background of NIH inbred minipigs with a 17.5-kb human genomic RHO^{P23H} sequence including 4.2 and 8.4 kb of 5′ and 3′ sequences, respectively. After SCNT, the retinal function of transgenic founders was analyzed from 3 months up to 2 years after birth. The transgenic animals showed progressive rod and cone photoreceptor dysfunction and degeneration. The animals were classified to a moderately and a severely affected group. mRNA analysis in a severely affected line found that 80% of total RHO mRNA was mutant RHO^{P23H} mRNA (Ross et al., 2012). The pathogenesis of the disease in this pig model was analyzed in detail in further prenatal and early postnatal studies using hybrid progeny of a cross of the transgenic NIH inbred minipigs and domestic pigs (Fernandez de Castro et al., 2014; Scott et al., 2014).

3.8 Macular Dystrophy

The macula is the central region of the retina and includes the fovea centralis which is essential for sharp vision in conditions of bright light. Stargardt-like macular dystrophy type 3 (STGD3) is an autosomal dominant disease leading to macular degeneration. Three different mutations in the photoreceptor-specific gene elongation of very long chain fatty acids, such as 4 ($ELOVL4$) were found to cause the disease. $ELOVL4$ encodes a 314-amino acid protein that harbors an endoplasmic reticulum retention sequence at the C terminus which is eliminated in all three STGD3 mutations. ELOVL4 belongs to the elongase family of enzymes and catalyzes the synthesis of very long chain fatty acids. The disease-associated C-terminally truncated proteins mislocalize to nonendoplasmic reticulum juxtanuclear aggregates and exert a dominant-negative effect on the wild-type protein. In addition to transgenic mice which develop rapid retinal degeneration due to the expression of human truncated $ELOVL4$ sequences, transgenic pigs were produced

as further disease models. Two transgenes were used harboring human truncated $ELOVL4$ sequences driven by the $Rho4.4$ photoreceptor-specific promoter. For DNA microinjection into zygotes (breed not stated), an $ELOVL4$ coding sequence with a 5-bp deletion, resulting in a protein lacking the last 51 amino acids, was used. For transfection of cells to be used for SCNT, an expression vector with an $ELOVL4$ 270 stop mutation and an N-terminal EYFP fusion was used. Transgenic pig lines were produced with both transgenes. Transgene expression and mislocalization in the retina, as well as abnormal retinal morphology were found for both mutations. Thus, new disease models for STGD3 were established (Sommer et al., 2011b).

3.9 Cone Dystrophy

Cone(-rod) dystrophy (CORD) is caused in some patients by dominant-negative mutations of the guanylate cyclase 2D ($GUCY2D$) gene which is involved in the regulation of calcium influx in rods and cones. Thus, a lentiviral vector was constructed with 0.7 kb of the cone-specific pig arrestin 3 ($ARR3$) promoter and the human cDNA coding for the double mutant allele $GUCY2D^{E837D/R838S}$. Using microinjection into zygotes of Large White pigs, a number of transgenic founders were produced harboring 1–6 copies of the transgene and expressing the transgene in the retina. On a gross level, transgenic founders were indistinguishable from controls both physiologically and behaviorally. Functional analysis of the retina by electrophysiological and behavioral tests, as well as histological analysis of the retina at different ages revealed a range in the severity of retinal alteration in the transgenic founders (Kostic et al., 2013).

3.10 Cardiovascular Diseases

Endothelial cell nitric oxide synthase 3 (NOS3, eNOS) regulates vascular function by releasing nitric oxide (NO) (Huang, 2009). Transgenic pigs were produced for the analysis of the cardiovascular function by eNOS. The 7.3-kb transgene consisted of the 3.6-kb Yucatan pig $eNOS$ cDNA and a V5 epitope and polyhistidine tag (V5-His tag) to discriminate between endogenous and transgenic eNOS. Endothelial cell-specific expression of the transgene was driven by 2-kb $TIE2$ promoter sequences and 1.7-kb $TIE2$ intron/enhancer elements. After additive gene transfer into Yucatan pig fetal fibroblasts, SCNT of transgene-positive cells resulted in four cloned transgenic pigs. They expressed the fusion protein which was localized to the endothelial cells of placental vasculature from the conceptuses. The same localization was shown for the endogenous eNOS. Compared to the size of endogenous eNOS (133 kDa, 1205 amino acids), the predicted size of the recombinant eNOS (1242 amino acids)

was 138 kDa. Localization of endogenous and transgenic eNOS revealed the expression in the endothelium. The transgenic pigs are further used to analyze the function of eNOS in the regulation of muscle metabolism and in the cardiorespiratory system (Hao et al., 2006). In addition, the expression of a modified porcine *eNOS* in cloned fetuses was described as a valuable tool for understanding the relationship between placental growth, vascular nutrient exchange and cloning efficiency (Whyte and Laughlin, 2010).

Endothelial hydrogen peroxide (H_2O_2) plays a key role in vasomotor control mechanisms and stimulates the upregulation of eNOS. Enzymes including catalase (CAT) tightly regulate H_2O_2 levels in vascular tissue. Therefore, transgenic pigs were produced using a 15-kb human *CAT* transgene whose expression was driven to endothelial cells by *TIE2* regulatory sequences. Earlier, transgenic mice have been produced with the same transgene. In pigs, one clone of transgenic NIH Yucatan minipig cells was used for SCNT and yielded transgenic offspring. Expression of human catalase mRNA and overall elevated catalase protein were found in isolated umbilical endothelial cells, and the endothelial localization of the protein was confirmed. In vitro tests of transgenic endothelial cells also revealed significantly reduced levels of H_2O_2 suggesting increased enzymatic activity of catalase (Whyte et al., 2011b).

The peroxisome proliferator activated receptor γ (PPARG, PPARγ) is another factor that plays an important role in cardiovascular diseases. Selective ligands of PPARG, such as thiazolidinediones (TZDs) may be analyzed for their function as insulin sensitizers for the treatment of type 2 diabetes. To establish a large animal model for these purposes, ZFN editing of the *PPARG* gene was done in fibroblast cells of Tibetan minipigs. *PPARG* mutant cell clones were isolated and genotyped, and a cell clone with a premature stop codon in exon 1 was further used for SCNT. This resulted in pigs harboring a heterozygous knockout of the *PPARG* gene. PPARG protein expression seemed to be decreased in the heterozygous knockouts. Analysis of ZFN off-target cleavage sites was done using bioinformatics tools. Sequencing of the most likely off-target sites revealed two unspecific mutation events in segregating, noncoding genomic regions of the genetically modified pigs (Yang et al., 2011).

The purposes for the generation of transgenic pig models are not strictly separated. One example is the modification of the fatty acid composition of meat products beneficial to human health by additive gene transfer of the fatty acid desaturation 2 gene for a Δ12 fatty acid desaturase from spinach (Saeki et al., 2004), by expressing a humanized *Caenorhabditis elegans* gene, Fat-1, encoding a *n*-3 fatty acid desaturase (Lai et al., 2006) or by expression of omega-3 fatty acid desaturase (s*Fat*-1) from *Caenorhabditis briggsae* (Pan et al., 2010) in transgenic pigs.

The transgenic animals may also provide large animal models for studying the role of unsaturated fatty acids in the prevention and treatment of clinical conditions, such as cardiovascular disease and immune-mediated disorders or cancer.

3.11 Atherosclerosis

Hypertriglyceridemia is an independent risk factor for cardiovascular disease, and high levels of apolipoprotein CIII (APOC3) are often correlated with hypertriglyceridemia. APOC3 acts as an inhibitor of lipoprotein lipase activity and interferes with the receptor-mediated endocytosis of lipoprotein particles. Mature APOC3 is a 79-amino acid glycoprotein which is found in chylomicrons, very low-density lipoproteins, and high-density lipoproteins. Mutant APOC3 has been found to directly affect plasma lipid profiles, whereby people with deficiencies in APOC3 generally show lower plasma triglyceride levels. *Apoc3* knockout mice have reduced levels of plasma triglyceride-containing lipoproteins, and overexpression of human APOC3 in transgenic mice leads to hypertriglyceridemia. As the lipoprotein metabolism and the functional consequences thereof in mice differ greatly from those in humans, transgenic minipigs were produced which express human APOC3. A 10-kb human genomic *APOC3* sequence including 5′ and 3′ sequences was used as transgene, and one positive cell clone was used for SCNT. Transgenic founders were born, part of them showed early postnatal death, and from the remaining five healthy grown transgenic pigs, all but one died at various ages up to 4 months p.p. The cause for this was not identified. The transgenic pigs showed expression of human APOC3 in the liver and intestine, and increased plasma triglyceride levels, but normal total cholesterol and high-density lipoprotein levels. They had delayed triglyceride absorbance and clearance. The plasma lipoprotein lipase amount was increased but the activity was significantly reduced. Thus, hypertriglyceridemic human *APOC3* transgenic minipigs were established. For comparative analyses, the same transgenic model was generated in rabbits which also showed hypertriglyceridemia (Wei et al., 2012).

High lipoprotein a levels of more than 50 mg/dL in humans are a major risk factor for the development of atherosclerosis. Apolipoprotein a [LPA, Apo(a)], the unique component of lipoprotein a, is described to be found only in Old World monkeys and humans. Analogous to human *Apo(a)* transgenic mice and rabbits, human *Apo(a)* transgenic pigs were generated using a transgene with the cDNA of human *Apo(a)* under the control of the β-actin promoter and cytomegalovirus enhancer (CAG promoter). Clawn minipig cells stably expressing and secreting human Apo(a) into the culture medium were used for SCNT. The transgenic offspring

expressed human Apo(a) in all tissues examined including blood plasma. Compared to the low plasma concentrations of lipoprotein a in *Apo(a)* transgenic mice and rabbits (<10 mg/dL), the human *Apo(a)* transgenic pig line showed high plasma levels (>400 mg/dL) of lipoprotein a without a significant change in plasma total cholesterol, low-density lipoprotein cholesterol (LDL-C), high-density lipoprotein cholesterol (HDL-C) or triglyceride levels. Studies of spontaneous or induced atherosclerosis in this novel animal model were not yet done (Ozawa et al., 2015). Using the same transgene, human *Apo(a)* transgenic pigs were also generated in the genetic background of NIBS (Nippon Institute for Biological Science) minipigs (Shimatsu et al., 2016).

In humans, loss-of-function mutations in the low-density lipoprotein receptor (*LDLR*) gene lead to familial hypercholesterolemia. The heterozygous mutant patients typically show twice the normal plasma LDL levels and a significantly increased risk for atherosclerosis. Individuals with both *LDLR* alleles defective face early-onset atherosclerosis. Pigs with spontaneous familial hypercholesterolemia have been described harboring the mutation $LDLR^{R84C}$ that reduces receptor binding (Hasler-Rapacz et al., 1998). As a model of familial hypercholesterolemia, Ossabaw minipigs harboring biallelic *LDLR* mutations were produced by SCNT of TALEN-modified fetal fibroblasts with various mutant genotypes. Piglets carried biallelic *LDLR* mutations which are expected to prematurely truncate the *LDLR* open reading frame, or are implicated in familial hypercholesterolemia (Carlson et al., 2012).

Another workgroup used gene targeting by homologous recombination to disrupt the porcine *LDLR* gene and SCNT to produce Yucatan minipigs with the mutation $LDLR^{C128X}$. Homozygous $LDLR^{C128X}$ mutants produced no functional LDLR protein. Breeding of heterozygous mutants resulted in the expected Mendelian ratio of homozygous mutant, heterozygous mutant and wild-type offspring. When fed a standard swine diet (low fat, no cholesterol), heterozygous mutant $LDLR^{C128X}$ pigs exhibited increased total and low-density lipoprotein cholesterol levels, whereas homozygous mutant $LDLR^{C128X}$ pigs showed highly elevated levels. The severe hypercholesterolemia in homozygous mutant animals resulted in atherosclerotic lesions. When fed a diet containing high fat and high cholesterol, hypercholesterolemia and atherosclerosis developed faster and more severe in the mutant pigs (Davis et al., 2014). The $LDLR^{C128X}$ mutant pig model was subsequently used to analyze the effects of statins on the hypercholesterolemia and atherosclerosis phenotype (Amuzie et al., 2016).

The same strategy (gene targeting by homologous recombination to disrupt exon 4 of the porcine *LDLR* gene and subsequent SCNT) was used in the genetic background of Landrace × Large White crossbred pigs,

and homozygous mutant *LDLR* pigs were produced by mating heterozygous mutant *LDLR* pigs. The mutant pig model was also used to analyze the effects of statins on the hypercholesterolemia and atherosclerosis phenotype (Li et al., 2016).

Atherosclerosis is a low-grade inflammatory disease of the arterial wall caused primarily by cholesterol-containing low-density lipoprotein particles in the blood. Mouse models are missing central features of human atherosclerosis. Proprotein convertase subtilisin/kexin type 9 (PCSK9) is an important regulator of low-density lipoprotein cholesterol by binding hepatic low-density lipoprotein receptors and targeting them to lysosomal degradation. The human gain-of-function mutation $PCSK9^{D374Y}$ increases affinity of this binding, which causes a severe form of autosomal dominant familial hypercholesterolemia. Using Sleeping Beauty DNA transposition and SCNT, transgenic Yucatan minipigs were created to express mutant human $PCSK9^{D374Y}$ under the control of the liver-specific human α1 antitrypsin promoter and a hepatocyte control region from the apolipoprotein E gene. Transgenic pigs with high transgene expression fed on a low-fat diet showed higher plasma low-density lipoprotein cholesterol levels compared to controls. A high-fat, high-cholesterol diet induced severe hypercholesterolemia in these animals, as well as accelerated development of atherosclerosis that has human-like lesions (Al-Mashhadi et al., 2013). Diabetes is associated with an increased risk of atherosclerotic cardiovascular disease. Mutant human $PCSK9^{D374Y}$ expressing Yucatan minipigs were fed a cholesterol-enriched, high-fat diet and injected with streptozotocin to generate a model of diabetes. Stable hyperglycemia was achieved in the diabetic minipigs, while the plasma total cholesterol, low-density lipoprotein cholesterol and creatinine levels were unaffected. Diabetes failed to increase atherosclerosis in any of the vessels examined (Al-Mashhadi et al., 2015).

Lipoprotein-associated phospholipase A2 (PLA2G7), also known as platelet-activating factor acetylhydrolase (PAFAH) circulates in human blood predominantly in association with low-density lipoprotein cholesterol and hydrolyses oxidized phospholipids into proinflammatory products. Increased circulating levels or elevated activity of PLA2G7 are associated with the risk of vascular disease. However, in the mouse circulation, it predominantly binds to high-density lipoprotein cholesterol and exhibits antiinflammatory properties. Therefore, transgenic Beijing minipigs ubiquitously overexpressing pig PLA2G7 were generated using a transgene with the pig *PLA2G7* cDNA driven by the translation elongation factor 1a promoter. Three transgenic founders derived by SCNT were examined and showed a more than fivefold *PLA2G7* RNA expression and an around twofold increased enzymatic activity in the blood compared to controls. The body weight of transgenic pigs did not differ at

birth or at 6 months of age compared to controls. The activity of PLA2G7 did not interfere with the feeding state. Inflammatory gene mRNA levels in the peripheral blood mononuclear cells of transgenic pigs were significantly elevated. Transgenic pigs did not exhibit increased total cholesterol, low-density lipoprotein cholesterol or high-density lipoprotein cholesterol levels. Triglyceride levels during the fasting state also were not different between transgenic pigs and controls. However, in the fed state, the triglyceride levels of transgenic pigs were significantly elevated compared to the fasting state which was not seen in the controls (Tang et al., 2015).

NPC1L1 (Niemann Pick C1 Like 1) is highly expressed in small intestine and plays a critical role in both dietary cholesterol absorption and biliary cholesterol reabsorption thereby influencing cardiovascular and metabolic pathways. Using the CRISPR-Cas9 system by directly editing exon 2 of *NPC1L1* in zygotes, live biallelic *NPC1L1* knockout Bama minipigs exhibiting different kinds of indels in *NPC1L1* were generated. The sequence data revealed more than two different knockout genotypes in some pigs, suggesting that cleavage had occurred multiple times and resulted in mosaicism of the modification. Analysis of the mutant phenotype was not described (Wang et al., 2015b).

3.12 Cardiomyopathy

Myocardial infarction and heart failure are severe causes for death in humans. Extracellular nucleotides (ATP and ADP) released at the site of myocardial damage induce thrombosis, apoptosis and necrosis. ENTPD1 (ectonucleoside triphosphate diphosphohydrolase 1, CD39) rapidly hydrolyzes ATP and ADP to AMP. An in vivo myocardial ischemia/reperfusion injury test in transgenic mice expressing human CD39 resulted in a decrease of the infarct size. The same transgene including the human *CD39* cDNA driven by the murine MHC class I gene H-$2K^b$ promoter was used for the generation of transgenic pigs via SCNT. Expression of human CD39 was detected on circulating blood cells and in myocardial tissue of the transgenic animals. After in vivo induction of myocardial ischemia/reperfusion injury, a reduction of the myocardial injury analogous to the results in the transgenic mice was found (Wheeler et al., 2012).

Thymosin β4 (TMSB4X, Tβ4) is the most abundant G-actin binding peptide of the cytosol and is a potent proangiogenic factor. The role of myocardin-related transcription factors (MRTF) and serum response factor (SRF) for this function was examined in experimentally induced prolonged ischemic myocardium areas of transgenic pigs ubiquitously and constitutively overexpressing Tβ4 driven by the cytomegalovirus promoter. Upon induction of a reversible loss of cardiomyocyte function which is amenable to therapeutic neovascularization,

transgenic pigs did not experience a significant loss of perfusion nor myocardial function at rest or under rapid pacing. Functional vascular regeneration by induced capillary growth and maturation was found in the transgenic pigs (Hinkel et al., 2014).

The pore-forming subunit of the cardiac sodium channel Nav1.5 encoded by *SCN5A* is a critical determinant of myocardial excitability and conduction. Loss-of-function mutations in *SCN5A* can clinically manifest as progressive cardiac conduction disorders or as arrhythmic syndromes, such as Brugada syndrome. In addition to electrophysiological dysfunction, *SCN5A* mutations are also associated with myocardial fibrosis manifesting as global cardiomyopathy. In a 10-year old child exhibiting Brugada syndrome, the mutation $SCN5A^{E555X}$ was discovered. Therefore, cardiac sodium channelopathy pig models were generated by homologous recombination in the genetic background of outbred Yucatan minipigs via SCNT exhibiting the orthologous porcine heterozygous mutation $SCN5A^{E558X}$. The heterozygous mutant animals were viable and fertile, and showed no sudden death over a 2-year monitoring period. They showed reduced SCN5A protein expression, which resulted in diminished total sodium conductance. The heterozygous mutant hearts showed slowed conduction and increased susceptibility for ventricular arrhythmias in the absence of structural defects of the myocardium or specialized conduction system. In total, a novel animal model was established for understanding the mechanisms linking sodium channel dysfunction to cardiac pathophysiology (Park et al., 2015b).

3.13 Blood Disorders

Human hemophilia A is a common X chromosome-linked genetic bleeding disorder caused by abnormalities in the coagulation factor VIII (*F8*) gene. F8 works as heterodimer of a heavy and light chain processed from the 2351-amino acid precursor (256 kDa). Hemophilia A patients suffer from bleeding diathesis. Using a targeting vector for the disruption of exon 16 of *F8*, thereby referring to the targeting vector used to generate hemophilia A mice, and two rounds of SCNT, four heterozygous *F8* knockout Large White pigs were born exhibiting severely decreased F8 levels to less than 1% compared to controls. The hemophilia A pigs showed a severe bleeding tendency upon birth leading to the early loss of the animals (Kashiwakura et al., 2012). Already some years before, transgenic pigs were established as bioreactors which produced human F8 in the milk (Paleyanda et al., 1997).

Von Willebrand factor (*VWF*) gene deficiency in human causes severe von Willebrand disease. Using the CRISPR-Cas9 system for editing exon 5 of *VWF*, which encodes the first trypsin inhibitory-like domain, directly in Bama minipig zygotes, monoallelic, as well as biallelic

VWF mutant piglets were born. Plasma VWF protein expression was largely reduced in monoallelic mutant pigs, and was nearly undetectable in biallelic mutant pigs. As in human patients, homozygous *VWF* knockout pigs showed a severe bleeding tendency and a decreased plasma level of coagulation factor VIII, but no significant differences in other parameters of the hematological analysis compared to controls (Hai et al., 2014). Already some years before, transgenic pigs were established as bioreactors which produced recombinant human von Willebrand factor in the milk (Lee et al., 2009).

3.14 Cystic Fibrosis

Alterations of the cystic fibrosis transmembrane conductance regulator (CFTR, 1480 amino acids) were identified to cause the autosomal recessive cystic fibrosis (CF) which still remains incurable. Loss of CFTR function causes pancreatic insufficiency, focal biliary cirrhosis, infertility, and chronic airway infections. In addition, up to 20% of babies with CF are born with meconium ileus. Mutant mice have been established harboring a disrupted *Cftr* gene, but they failed to develop the lung and pancreatic disease causing most of the morbidity and mortality in human patients (Cohen and Prince, 2012). Mutant pigs were produced using SCNT and fetal fibroblasts with the *CFTR* gene either disrupted or containing the most common cystic fibrosis-associated mutation (ΔF508). Therefore, recombinant adeno-associated virus (rAAV) vectors were used to target *CFTR* in male fetal fibroblasts of outbred domestic pigs. The 4.5-kb knockout gene construct disrupted exon 10 encoding a portion of nucleotide-binding domain 1 with a stop codon at position 508 (F508X) followed by a floxed neomycin resistance gene driven by the phosphoglycerate kinase (*PGK*) promoter, whereas the ΔF508 knockin gene construct harbors the 3-bp deletion in exon 10 leading to ΔF508 followed by a floxed neomycin resistance gene driven by the *PGK* promoter in the downstream intronic region. Using successfully targeted cells without viral vector sequences for SCNT, heterozygous mutant male piglets were generated with each mutation. Newborn piglets with a targeted disruption of both *CFTR* alleles exhibited similar defects as seen in newborn human patients, that is, meconium ileus, exocrine pancreatic destruction, and focal biliary cirrhosis (Rogers et al., 2008a; Rogers et al., 2008b). The analysis of the CF pigs provided detailed insights into the pathology of affected organ systems, such as the respiratory tract and the gastrointestinal organs (Cohen and Prince, 2012).

We produced an independent CF pig model on the genetic background of the Landrace breed by sequential BAC targeting of the *CFTR* locus. CH242-248P18, a BAC containing parts of the *CFTR* gene was modified by placing a STOP box adjacent to the *CFTR* start codon to suppress *CFTR* mRNA translation. Using two rounds of targeting by homologous recombination and SCNT, homozygous knockout piglets were produced. In general, the observed CF phenotype closely reflects the human situation, as well as that of the previously published CF piglets (Rogers et al., 2008b). Most prominent and in accordance to the previously published CF piglets (Rogers et al., 2008b), our homozygous knockout piglets showed 100% penetrance of a severe meconium ileus. Efforts to overcome this fatal complication by surgical or conservative treatment were not successful leading to the death or euthanasia of the animals within the first days after birth (Klymiuk et al., 2012a).

To overcome the appearance of the severe meconium ileus, *CFTR* knockout pigs were produced with the intestinal expression of wild-type *CFTR*. In analogy to experiments in rats, pig *CFTR* knockout cells were transfected with a transgene harboring 1.8 kb of the rat intestinal fatty acid binding protein (*iFABP*) promoter and the porcine *CFTR* cDNA. Using five different cell clones for SCNT, different pig lines with various intestinal expression levels of *CFTR* were produced. In three transgenic lines, intestinal *CFTR* expression improved the intestinal phenotype. In all transgenic lines, a similar degree of pancreatic destruction, microgallbladder, and focal biliary cirrhosis as previously reported in newborn *CFTR* knockout pigs was observed. They also showed reduced weight gain and lung disease (Stoltz et al., 2013).

3.15 Duchenne Muscular Dystrophy

Duchenne muscular dystrophy (DMD) is caused by loss-of-function mutations in the X-linked dystrophin (*DMD*) gene leading to progressive muscle weakness and wasting. *DMD* is among the largest genes in the mammalian genome with a length of more than 2 Mb. DMD is mostly caused by deletions in the *DMD* gene, but point mutations and duplications also appear. Pigs with the spontaneous mutation *DMD^{R1958W}* in exon 41 were identified and phenotypically characterized as a natural porcine model of DMD insufficiency (Nonneman et al., 2012).

Using SCNT, pigs with a deletion of exon 52 of the *DMD* gene which is a frequent mutation in human DMD, were produced resulting in a frame shift in the transcript. *DMD* mutant pigs exhibited absence of DMD in skeletal muscles, increased serum creatine kinase levels, progressive dystrophic changes of skeletal muscles, impaired mobility, muscle weakness, and a maximum life span of 3 months due to respiratory impairment. Unlike human DMD patients, some *DMD* knockout pigs died shortly after birth. The development of muscular dystrophy in *DMD* knockout pigs appears in an accelerated manner when compared with human patients, and was further analyzed in genome-wide transcriptome studies of muscle tissue (Klymiuk et al., 2013, 2016).

Another workgroup announced the development of a DMD minipig model harboring an in-frame exon deletion in the rod domain of DMD and their subsequent phenotypic characterization (Selsby et al., 2015). Information regarding a third porcine DMD model is available through a patent of Exemplar Genetics. The minipigs possess a deletion of exon 52 and show pathological alterations consistent with the human DMD phenotype (Selsby et al., 2015).

3.16 Diabetes Mellitus

Diabetes mellitus is a group of chronic metabolic disorders characterized by hyperglycemia resulting from defects in insulin secretion, insulin action or a combination of both. In the majority of cases diabetes mellitus is diagnosed too late, namely when considerable pathological alterations of the pancreatic β-cells are manifest. Changes in insulin secretion, glucose homeostasis, and insulin sensitivity occur many years before clinical manifestation of diabetes. Therefore biomarkers indicating early stages of β-cell dysfunction and mass reduction would allow early therapeutic intervention. For the search of biomarkers animal models resembling β-cell dysfunction in the prediabetic state are needed (reviewed in Renner et al., 2016a).

Transgenic pigs expressing a dominant-negative receptor for the incretin hormone glucose-dependent insulinotropic polypeptide (*GIPR^dn*) were established by our group (Renner et al., 2010). The incretin hormones glucose-dependent insulinotropic polypeptide (GIP) and glucagon-like peptide-1 (GLP-1) are secreted by enteroendocrine cells and are responsible for the so-called incretin effect, the phenomenon that an oral glucose load elicits a higher insulin response compared with an isoglycemic intravenous glucose infusion. Inactivation of incretins takes place via enzymatic cleavage by the enzyme dipeptidyl peptidase–4 (DPP-4). In type 2 diabetic patients the incretin effect was found to be highly diminished which is related to a reduced insulinotropic action of GIP. Nearly sustained insulinotropic action of GLP-1 in type 2 diabetic patients revealed its therapeutic potential and initiated the ongoing development of GLP-1 receptor agonists, as well as DPP-4 inhibitors. Variation in the *GIPR* gene, desensitization of the GIP/GIPR axis or downregulation of the GIPR on the β-cell have been discussed as possible reasons for the reduced insulinotropic action of GIP (reviewed in Renner et al., 2016b).

GIPR^dn transgenic pigs were generated by lentiviral gene transfer to mimic the reduced insulinotropic effect of GIP. The dominant-negative GIPR has an 8-amino acid deletion (amino acid position 319–326, nucleotide position 955–978), and two additional point mutations (amino acid position 340, nucleotide position 1018–1020) leading to an amino acid exchange from alanine to glutamic acid (Ala → Glu) in the third intracellular loop which is known to be essential for further signal transduction. The ligand GIP can bind the GIPR^dn with nearly the same binding affinity compared with the endogenous GIPR, albeit binding the GIPR^dn does not lead to any further signal transduction. As a result, competition of the GIPR^dn and endogenous GIPR for the ligand GIP leads to a reduced insulinotropic action of GIP (Herbach et al., 2005).

GIPR^dn transcription was detected in isolated islets of Langerhans. *GIPR^dn* transgenic pigs developed normally and did not show any difference in body weight gain compared to littermate controls. Young, 11-week old *GIPR^dn* transgenic pigs exhibited reduced oral glucose tolerance due to delayed insulin secretion. However, the overall insulin secretion considering the complete duration of the oral glucose tolerance test (120 min following oral glucose load), as well as the intravenous glucose tolerance was found to be unaltered compared to controls. Also, both groups showed similar β-cell mass at this age. With increasing age glucose control deteriorated so that 5-month old *GIPR^dn* transgenic pigs showed reduced oral glucose tolerance due to reduced insulin secretion. At the age of 11 months, intravenous glucose tolerance was also impaired and insulin secretion diminished. Quantitative-stereological analyses of the pancreas of 5-month old transgenic and control pigs revealed a reduction of 35% of the total β-cell volume in *GIPR^dn* transgenic pigs while an even more pronounced reduction of 58% of the total β-cell volume was detected in 1–1.4-year old *GIPR^dn* transgenic pigs compared to controls (Renner et al., 2010).

GIPR^dn transgenic pigs show progressive deterioration of glucose control and reduction of β-cell mass, but fasting normoglycemia, thus providing a unique opportunity to study metabolic changes during the prediabetic period. We used plasma samples from intravenous glucose tolerance tests of 2.5- and 5-month old *GIPR^dn* transgenic pigs for a targeted metabolomics approach. Additionally, a holistic transcriptome analysis of liver samples from 5-month old *GIPR^dn* transgenic pigs and controls was performed to evaluate if plasma metabolite alterations are accompanied by expression changes of targets within corresponding pathways (Renner et al., 2012).

GLP1R agonists represent a promising group of incretin-based therapeutics for type 2 diabetes. Liraglutide is approved for the use in adult type 2 diabetic patients and was shown to reduce body weight and improve glycemic control. Therefore, we studied the effects of liraglutide in adolescent 2-month old *GIPR^dn* transgenic pigs exhibiting a prediabetic condition including disturbed glucose tolerance, reduced insulin secretion, and progressive reduction of functional β-cell mass, by daily injections for 90 days. Although plasma liraglutide levels of adolescent transgenic pigs treated in our study were higher compared to human trials, proproliferative effects on the endocrine or exocrine pancreas were not observed (Streckel et al., 2015).

Another workgroup also generated mutant human $GIPR^{dn}$ transgenic pigs exhibiting human GIPR that is modified in the region of the third intracellular loop by a single amino acid exchange (A340E) and a deletion of eight amino acids (residues 319–326) essential for signal transduction. In the transgenic pigs established by SCNT, $GIPR^{dn}$ was expressed under the control of rat *Ins2* promoter in the pancreas. In summary, $GIPR^{dn}$ transgenic pigs exhibited impaired glucose metabolism and β-cell function (Cheng et al., 2015).

Heterozygous missense mutations in the insulin (*INS*) gene have been identified to cause permanent neonatal diabetes mellitus in humans. To establish a large animal model of permanent neonatal diabetes mellitus, we generated INS^{C94Y} transgenic pigs which correspond to the human INS^{C96Y} mutation and the $Ins2^{C96Y}$ mutation of the Akita mouse. INS^{C96Y} disrupts one of the two interchain disulfide bonds of INS. The mutant insulin leads to impaired trafficking of normal proinsulin, accumulation of misfolded insulin in the endoplasmic reticulum (ER), and ER stress which finally triggers β-cell apoptosis. The transgene harboring porcine INS^{C94Y} with its essential regulatory elements was transduced in pig cells, and SCNT was used to generate transgenic founder pigs. A line expressing high levels of INS^{C94Y} mRNA (70–86% of the wild-type *INS* transcript level) exhibited elevated blood glucose soon after birth but unaltered β-cell mass at the age of 8 days. At 4.5 months, INS^{C94Y} transgenic pigs exhibited 41% reduced body weight, 72% decreased β-cell mass, and 60% lower fasting insulin levels compared with littermate controls. β-cells of INS^{C94Y} transgenic pigs showed a marked reduction of insulin secretory granules and severe dilation of the endoplasmic reticulum. Cataract development was already visible in 8-day old INS^{C94Y} transgenic pigs and became more severe with increasing age. Diabetes-associated pathological alterations of kidney and nervous tissue were not detected during the observation period of 1 year. INS^{C94Y} transgenic pigs can be propagated by conventional breeding when treated with insulin. However, the costs for maintenance of diabetic pigs are high (Renner et al., 2013).

Effects of maternal diabetes mellitus on embryos, fetuses, and offspring are another attractive research topic which can be addressed using this model. In a preliminary study we observed that both transgenic and wild-type offspring of diabetic INS^{C94Y} transgenic sows mated to a wild-type boar exhibited reduced absolute and relative weights of most organs when compared to the offspring of matings with INS^{C94Y} transgenic boars and wild-type sows, which emphasizes potential developmental effects of maternal diabetes in this model (Wolf et al., 2014).

In addition, we previously established a mutant mouse line showing diabetes which was caused by a point mutation in the insulin 2 (*Ins2*) gene. The point mutation leads to the amino acid exchange C95S and the loss of the A6-A11 intrachain disulfide bond of the insulin. Male heterozygous $Ins2^{C95S}$ mutant mice develop progressive diabetes mellitus with strong reduction of the total pancreatic islet volume and the total β-cell volume together with severe alterations of the β-cell structure (Herbach et al., 2007). Therefore, we established a transgenic pig model expressing mutant porcine insulin analogous to the mutant mouse insulin by additive gene transfer for the subsequent study of β-cell dysfunction in diabetes mellitus. Using SCNT, transgenic founder pigs were established with normal development and unaltered fasting blood glucose levels, but disturbed intravenous glucose tolerance and reduced insulin secretion (unpublished own data).

Another transgenic porcine diabetes model was produced for type 3 of maturity-onset diabetes of the young (MODY3) which is caused by dominant mutations of the hepatocyte nuclear factor 1α (*HNF1A*) gene. The effect of the dominant-negative mutation used was previously verified in transgenic mice. The transgene consisted of the 1.2-kb chicken β-globin insulator, the 0.4-kb enhancer for the immediate-early gene of the cytomegalovirus followed by the 0.7-kb porcine insulin promoter, a 2.3-kb mutant human hepatocyte nuclear factor 1α cDNA with the most common mutation (P291fsinsC), the 0.1-kb SV40 polyadenylation signal, and the 1.2-kb chicken β-globin insulator. A transgenic cell clone with ten copies of the transgene was used for SCNT. Twenty two live transgenic cloned pigs were produced. Most of them died within 2 weeks after birth. The transgene-derived protein was detected in pancreas, heart and kidney. Persistent diabetes with nonfasting blood glucose levels over 200 mg/dL was observed in four transgenic pigs with longer living time. Histological analysis revealed abnormal pancreatic islet morphogenesis and pathological alterations of the kidneys, such as glomerular hypertrophy and sclerosis (Umeyama et al., 2009). Transgenic pigs were continuously treated with insulin to allow for normal growth to sexual maturity. Sperm quality of transgenic boars in in vitro fertilization experiments was lower compared to controls but live transgenic offspring were produced by in vitro fertilization with cryopreserved sperm (Umeyama et al., 2013).

3.17 Liver Disease

Hereditary tyrosinemia type I is a severe, autosomal recessive disease caused by a deficiency in the enzyme fumarylacetoacetate hydrolase (FAH) that catalyzes the last step of tyrosine metabolism. The absence of FAH causes accumulation of the toxic metabolite fumarylacetoacetate in hepatocytes and renal proximal tubules, the two major cell types that express FAH. This results in hepatic failure, cirrhosis, and hepatocellular carcinoma

early in childhood. For targeting porcine *FAH*, a similar approach as for the generation of *Fah* knockout mice was used. An in-frame stop codon and a neomycin resistance cassette were inserted into exon 5 of the porcine *FAH* gene, and the knockout construct was delivered to fetal pig fibroblasts with a recombinant adeno-associated virus (rAAV) vector. Heterozygous knockout cells were used for SCNT, and viable and healthy heterozygous *FAH* knockout pigs were generated. The heterozygous knockouts were phenotypically normal, showed normal tyrosine metabolism and histologically normal livers. Compared to controls, transcript, and protein expression of *FAH*, as well as the enzyme activity were reduced (Hickey et al., 2011). After mating heterozygous *FAH* knockout Large White and Landrace pigs, no homozygous *FAH* knockout piglets were born. FAH deficiency in mice does not produce an in utero lethal defect and mice are born, albeit with severe liver damage. Further analyses indicated robust FAH protein expression in wild-type pigs at day 30 of gestation and in utero lethality of the homozygous *FAH* knockouts prior to day 35 of gestation. As human patients are successfully treated with a low-tyrosine diet combined with the administration of the potent inhibitor of 4-hydroxyphenylpyruvate dioxygenase NTBC, heterozygous *FAH* knockout females were treated with NTBC prior to conception with heterozygous *FAH* knockout boars and for the duration of the pregnancy. This treatment rescued the in utero lethality of FAH deficiency as healthy homozygous *FAH* knockout piglets were born within the predicted Mendelian ratio. Animals treated with NTBC were phenotypically normal at birth, however, withdrawal of NTBC resulted in rapid clinical decline including multiple biochemical abnormalities, dysmorphic kidney morphology and death due to progressive liver injury without showing other major abnormalities (Hickey et al., 2014).

3.18 Kidney Disease

Autosomal dominant polycystic kidney disease (ADPKD) is a common human chronic genetic disease. It is characterized by the progressive formation of cysts in bilateral kidneys and numerous extrarenal manifestations including hepatic and pancreatic cysts, intracranial aneurysms, and abnormalities in cardiovascular systems. The progressive growth of cysts in kidneys eventually leads to renal failure in 50% of patients, and there is currently no effective treatment. Mutations in *PKD1* and *PKD2* are responsible for autosomal dominant polycystic kidney disease, which represent about 85% and 15% of patient cases, respectively. Polycystin 2 encoded by *PKD2* is a calcium-permeable cation channel that plays a role in many aspects of cell function. Transgenic mice or rats overexpressing cDNA or genomic sequences of PKD1 and PKD2 show typical cystic kidneys, and the severity of the disease is positively correlated with the copy number and the expression level of the transgenes. Porcine PKD1 and PKD2 are highly similar to the human orthologs. Using full-length porcine *PKD2* cDNA driven by a ubiquitous cytomegalovirus enhancer/promoter, four transgenic Chinese experimental minipigs (CEMP) were generated by SCNT. The transgenic pigs showed approximately 10 insertion events and PKD2 was more highly expressed in transgenic pigs than in wild-type controls. Blood urea nitrogen and serum creatinine levels were continuously measured up to 1 year of age to assess the pig kidney function. The transgenic pigs showed no significant alteration in kidney function, and there were no cystic manifestations by 1 year of age in this model. It is estimated that more than 2 years may be required for manifestation of renal cystogenesis in these pigs (He et al., 2013).

Subsequently, the same workgroup produced heterozygous *PKD1* knockout Chinese experimental minipigs (CEMP) by editing exon 5 of *PKD1* in porcine cells by ZFN. *PKD1* is ubiquitously expressed in various organs. Using various edited cell clones in SCNT, pigs with various monoallelic indels in *PKD1* were achieved and showed a lower *PKD1* expression at both the transcriptional and translational level. Breeding to wild-type pigs revealed the germline transmission of the mutant alleles according to the Mendelian ratio. In the heterozygous *PKD1* knockouts, no macroscopic or microscopic cysts appeared in the kidneys 48 h p.p., but renal cysts appeared as early as 3 months after birth without affecting the whole kidney in the early stage of the disease. Most renal cysts were derived from the proximal tubules and collecting ducts and grew progressively. In addition, renal fibrosis was associated with disease progression, and liver cysts were found (He et al., 2015).

The protooncogene c-Myc is overexpressed in cystic kidneys, and transgenic mouse models of autosomal dominant polycystic kidney disease overexpressing c-Myc in kidney tissue exist. Therefore, the same workgroup generated transgenic Chinese experimental minipigs (CEMP) by SCNT using the porcine *MYC-b* cDNA driven by the cytomegalovirus enhancer and the mouse cadherin 16 promoter. The transgenic founders each had multiple integrated copies of the transgene vector and exhibited overexpression of *MYC* in kidney tissues. Blood urea nitrogen and serum creatinine levels were measured up to 6 months of age, but no obvious abnormalities were detected (Ye et al., 2013).

3.19 Osteoporosis

Transgenic mice overexpressing the soluble receptor activator of NF-κB ligand (RANKL, TNFSF11) in the liver after birth showed hyperactivation of osteoclasts resulting in resorptive osteoporosis. In humans, inhibition of RANKL by monoclonal antibodies is a current approach

in osteoporosis therapy. For generating a large animal model with osteoporosis, the spatio-temporally regulated or inducible expression of RANKL is required, since mice overexpressing RANKL ubiquitously from the early developmental stage died at the late fetal stage. Therefore, the Tet-On system was used and double transgenic pigs were generated by SCNT for the inducible expression of RANKL by administration of doxycycline (Klymiuk et al., 2012b) (see Section 2.5). One living double transgenic founder pig and a double transgenic offspring on the genetic background of the Swabian-Hall breed were analyzed. In the absence of doxycycline, the RANKL protein level was below the detection limit. The oral administration of increasing concentrations of doxycycline revealed a minimal dose of 25 mg/kg/day to detect significantly increased RANKL levels after 6 days. The RANKL levels were further increased with higher doses of doxycycline, but induction with 25 mg/kg/day was sufficient not only to induce RANKL but also to increase the levels of endogenous cathepsin K, a marker for activation of osteoclasts. This confirmed the biological function of the induced transgene expression for osteoporosis. Future studies will clarify whether induced overexpression of RANKL in the pig results in osteoporosis (Klymiuk et al., 2012b).

3.20 Marfan Syndrome

Fibrillin 1 (FBN1) is the principal structural component of extracellular microfibrils in the connective-tissue matrix of the body. Heterozygous mutations resulting in the abnormal formation of the extracellular matrix cause the Marfan syndrome. Human patients experience poor quality of life caused by skeletal disorders and cardiovascular impairment. Using the ZFN system in porcine Large White/Landrace × Duroc fetal fibroblasts, a heterozygous *FBN1* mutant cell clone (Glu433AsnfsX98) was established encoding a truncated FBN1 protein caused by a new stop codon at amino acid residue 531. By SCNT, heterozygous *FBN1* mutant founder pigs were generated from one single line of nuclear donor cells but showed no homogenous phenotype, as Marfan-like skeletal symptoms occurred in only a part of the heterozygous mutant founders. Various expression of the pathological phenotype due to differences in genetic and epigenetic factors has been also observed both in human patients and heterozygous *Fbn1* mutant mouse models. Generation of heterozygous G1 mutants by mating founder animals to wild-type pigs resulted in the appearance of the similar pathological phenotype in the founder and their progeny. After mating heterozygous mutants, homozygous mutants appeared showing typical symptoms of the Marfan syndrome and a survival time up to 28 days of age. Neonatal lethality has been also described in homozygous *Fbn1* mutant mouse models (Umeyama et al., 2016).

3.21 Skin Disease

In the Sonic hedgehog signaling pathway (SHH-GLI), the soluble protein SHH activates the transmembrane protein smoothened (SMO) allowing the subsequent activation of the transcriptional regulators GLI1, GLI2, and GLI3. Normal hair follicle and sebaceous gland development is tightly regulated by SHH-GLI signaling. GLI2 has both repressor and activator functions including in the oncogenic hedgehog signaling. *Gli2* knockout mice show multiple developmental abnormalities in the skin. Basal cell carcinoma is associated with constitutive signaling of the Shh-Gli pathway. In contrast to mice, the skin of pigs is very similar to that of humans.

Transgenic pigs (breed not specified) were produced to analyze the constitutive expression of the hedgehog transcriptional activator GLI2 in porcine skin. The transgene K5-hGLI2ΔN consists of the 5.3-kb bovine keratin 5 (*K5*) promoter and a *c-Myc* tagged N-terminal truncated form of the human *GLI2* gene, which has only activator function and shows 30-fold more activity than endogenous GLI2 in vitro. After transfection of fibroblasts, four different transgenic cell clones were used for SCNT to produce transgenic animals. Nontransgenic controls were produced in the same litters by using nontransgenic fibroblasts. The transgenic animals showed the keratinocyte-specific expression of the transgene in the stratum basale and the outer follicular root sheath of the skin at different levels. SHH-GLI target genes and endogenous *c-Myc*, as well as the immature keratinocyte markers K5, K14, and K17 were upregulated. This resulted in the development of a hyperproliferative and immature epidermis. Expression of genes associated with differentiation, adhesion, and signal transduction was normal. Histological analysis showed generalized epidermal abnormalities including epidermal hyperplasia and hyperkeratosis, as well as sebaceous gland hyperplasia. The transgenic animals developed skin infections soon after birth progressing to deep alterations at exposed skin areas. The animals died or were euthanized within few weeks after birth. The transgenic animal with the lowest expression of the transgene was alive for 6 months of age. The same transgene has been used to produce transgenic mice. The mice showed epithelial alterations resembling basal cell carcinomas and advanced neoplastic development (Roessler et al., 2005). In contrast to the transgenic mice, the transgenic pigs showed no gross signs of cutaneous tumors 2 weeks after birth, but diffuse epidermal changes and susceptibility to cutaneous infections were observed. The phenotype resembled those described for some forms of human psoriasis. Association between psoriasis and activated hedgehog signaling is discussed (McCalla-Martin et al., 2010).

The development of transgenic pigs as a model for cutaneous inflammation was the aim of another project.

Integrins are transmembrane signaling receptors that are important for cell growth and differentiation, as well as inflammatory responses in the skin. Transgenic mice showing the subrasal expression of the human integrins α2 (*ITGA2*) and/or β1 (*ITGB1*) in the epidermis developed hyperproliferation and aberrant differentiation of keratinocytes and a phenotype resembling psoriasis. Using SCNT and the transposon system, transgenic Göttingen minipigs were produced with transgenes analogous to the mouse project. The subrasal expression in keratinocytes was driven by the involucrin promoter, followed by the first intron of the involucrin gene and the coding sequences of human β1 or α2 integrin. For human β1 integrin, six transgenic pigs living more than 2 weeks were produced. All of them arose from different donor cell clones, and most of them showed several transgene integration sites. The transgene-derived protein was found to be correctly processed after translation in in vitro cultured transgenic porcine keratinocytes. No apparent differences in skin morphology between the transgenic pigs and controls were visible over an examination period of 14 months. For human α2 integrin, three living transgenic pigs were produced. The transgene-derived integrin was observed in the plasma membrane of transgenic keratinocytes. In addition, lower amounts of transgenic mRNA were also detected in all other tissues analyzed. Again, no visible epidermal abnormalities or psoriasis-like phenotypes were detected. However, markers of perturbed skin homeostasis in keratinocytes and of chronic inflammatory phenotype in the skin were identified (Staunstrup et al., 2012).

Microphthalmia-associated transcription factor (MITF) is a master regulator of melanocyte development and an important oncogene in melanoma. Mutations in the human *MITF* gene have been found in patients of the Waardenburg syndrome showing hypopigmentation and deafness. Cytoplasmic injections of the CRISPR-Cas9 system into zygotes editing exon 8 of the porcine *MITF*, which encodes part of the basic helix-loop-helix leucine zipper domain and is essential for MITF DNA-binding, achieved two live-born piglets showing no pigmentation over its entire body. RFLP and sequence analysis found biallelic mutations in both piglets, and Western blot analysis of tail skin tissues showed that MITF was completely absent in the two mutant piglets (Wang et al., 2015c).

In addition, using the CRISPR-Cas9 system and SCNT, biallelic tyrosinase (*TYR*) knockout pigs in the genetic background of Banna minipigs and Bama minipigs were produced. They harbored various types of mutations in the first exon region following the start codon corresponding to the respective donor cells. The *TYR* knockouts showed typical albinism with complete absence of melanin production in skin and eyes (Zhou et al., 2015).

3.22 Circadian Rhythm Disorder

The homeostasis of circadian rhythms in both central and peripheral tissues is pivotal for numerous biological processes. Transgenic mice expressing the mutant human cryptochrome 1 (*CRY1^{C414A}*) revealed disturbance of the circadian rhythm, as well as signs of type 2 diabetes, such as hyperglycemia and polydipsia. Therefore, an analogous Bama minipig model was produced with a transgene harboring the mutant human *CRY1^{C414A}* cDNA driven by the cytomegalovirus early enhancer and chicken β-actin (CAG) promoter and SCNT. Twenty-one transgenic founder piglets originating from two different donor cell clones and expressing the transgene remained healthy and gained normal weight under controlled external factors (light, food). Core circadian clock and proinflammatory cytokine gene expression were analyzed in ex vivo derived, cultured fibroblasts, and altered expression patterns were found compared to controls (Liu et al., 2013).

3.23 Cancer

For the development of an animal model for the study of human tumors, transgenic pigs were generated with a 4.8-kb fragment containing the long terminal repeat (LTR) of mouse mammary tumor virus (MMTV) and the activated v-Ha-ras sequence. The carcinogenic effect of the transgene has been proven in transgenic mice. DNA microinjection of fertilized oocytes was carried out on the mixed genetic background of the Landrace, Large White, and Duroc breeds. One female transgenic founder was produced which gave rise to hemizygous transgenic offspring. The expression analysis detected transgene-specific RNA in various tissues of the founder. Tumor development was not found in the transgenic founder and its transgenic offspring during the observation period for 30 months and 1–8 months, respectively. Breeding of G1 transgenic pigs to nontransgenic pigs confirmed their fertility. Reasons for the absence of tumor development might be low transgene expression levels, the lack of cofactors for the tumorigenesis, and/or tumor development in older ages which were not included in this study (Yamakawa et al., 1999).

Inactivating mutations of the breast cancer 1 (*BRCA1*) gene predispose to breast cancer and are often correlated to familiar breast and/or ovarian cancer. More than 1200 BRCA1 variants have been found, often leading to functional inactivation and predisposition to cancer. The *BRCA1* gene contains 22 coding exons encoding a nuclear protein of 1863 amino acids in humans and pigs, and 1812 amino acids in mice. Compared to the human BRCA1 protein, porcine BRCA1 showed 74% identity, and mouse BRCA1 showed 58% identity. Transgenic mouse models carrying targeted disruptions of *Brca1* revealed

the crucial role of the gene in embryonic development and cell proliferation regulation. Homozygous knockout mice lacking exon 11 died during the second half of the gestation. Developing tumors in the *Brca1* transgenic mouse models showed varying degrees of similarity to their human counterparts. Heterozygous *Brca1* knockout mice are developmentally and reproductively normal. Without exogenous stress factors, they showed no predisposition to breast cancer at an advanced age whereas heterozygosity for *BRCA1* mutations in humans strongly increase the risk of developing breast cancer at an older age. Somatic loss of heterozygosity (LOH) of the remaining wild-type allele is frequently found in human breast cancer cells but not in mice.

Most of the disease-related mutations have been found in exon 11, therefore this exon was used for gene targeting via homologous recombination by using recombinant adeno-associated virus (rAAV)-mediated gene targeting. Heterozygous *BRCA1* knockout cells of Yucatan minipigs with the deletion of large parts of exon 11 were used for SCNT giving rise to the birth of eight piglets, and seven of them were identified as heterozygous *BRCA1* mutants. Compared to control animals, the heterozygous *BRCA1* mutants showed decreased *BRCA1* mRNA in isolated fibroblasts, but no significant differences were observed with respect to the BRCA1 protein levels. Unexpectedly, all heterozygous *BRCA1* knockout piglets died within 18 days after birth while the wild-type littermate was still alive after half a year. The causes for the perinatal mortality remained unclear but may be the result of the SCNT technique used. Viability problems of other transgenic or nontransgenic Yucatan minipigs cloned by SCNT were frequently observed. To examine the role of the genetic background for the phenotype, the same knockout is intended to be produced with Göttingen minipigs where both the pregnancy rate and the number of piglets referring to the number of transferred embryos are higher in SCNT. Also the creation of a conditional pig model harboring a mammary-specific *BRCA1* knockout is intended. In addition, high efficiencies in gene targeting by using recombinant adeno-associated virus (rAAV) vectors were obtained in this project. This might allow the correct design of mutant cells without selection procedures based on drug resistance in the future (Luo et al., 2011).

Familial adenomatous polyposis (FAP) is characterized by foci of dysplastic growth in the colon and rectum that develop to adenomatous polyps and adenocarcinoma. Germline mutations in the adenomatous polyposis coli (*APC*) tumor-suppressor gene are responsible for familial adenomatous polyposis, and somatic *APC* mutations are found in most sporadic colorectal tumors at the earliest stages. Using mesenchymal stem cells of Landrace/Pietrain or Landrace pigs for SCNT, gene-targeted pigs carrying translational stop signals in the

APC gene at codons 1061 and 1311, that is orthologous to common germline mutations (*APC1061* and *APC1309*) in human familial adenomatous polyposis, were generated. Mutation at human codon 1309 is associated with a particularly severe phenotype with early onset and prolific polyposis when compared to mutation at codon 1061 which causes less severe polyposis. A 1-year old heterozygous *APC1061Stop* mutant pig showed no evidence of polyposis, whereas a heterozygous *APC1311Stop* mutant pig of the same age showed aberrant crypt foci, as well as low-grade and high-grade dysplastic adenomas in the large intestine, which is similar to the precancerous lesions that develop in patients with familial adenomatous polyposis. Thus, the mutant pig exhibited the well-characterized precancer phenotypic sequence leading to adenomas in the large intestine, replicating early-stage human familial adenomatous polyposis which is not the case for *Apc* mutant mice (Flisikowska et al., 2012).

Another workgroup used TALEN-stimulated mutagenesis to generate knockout alleles of the *APC* gene by short indels in Ossabaw pig fibroblasts which were used to produce monoallelic and biallelic *APC* mutant pigs by SCNT to model colon cancer. Phenotypic data were not yet published (Tan et al., 2013).

The tumor suppressor gene *TP53* encoding p53 is the most commonly inactivated gene in sporadic human cancers. Most of the *TP53* somatic mutations occur between codons 125 and 300 including the DNA binding region. The dominant-negative mutation *TP53R175H* is the most frequent missense mutation in many sporadic human cancers. Using porcine mesenchymal stem cells of Landrace pigs, a latent oncogenic mutant porcine *TP53* gene was constructed by insertion of a floxed transcriptional termination signal (LSL cassette) in the first intron and a point mutation encoding the oncogenic activation mutation R167H (that is equivalent to human R175H) in exon 5. The allele *TP53LSL-R167H* was predicted to lack TP53 expression, whereas *Cre* recombinase-mediated removal of the LSL cassette generates the allele designated *TP53L-R167H*. Fifteen viable heterozygous mutant *TP53LSL-R167H* piglets were produced by SCNT, all of them were free of any apparent abnormality (Leuchs et al., 2012). To determine whether pigs carrying the latent *TP53LSL-R167H* mutation in heterozygous or homozygous form would spontaneously develop tumors, animals were regularly analyzed for alterations in health and well-being. Nine heterozygous knockout pigs with an age up to 32 months were examined by necropsy. There was no evidence of tumors or other abnormalities in animals up to 16 months. Of the five older animals, four had tumors, and one animal had disseminated calcifying, ossifying lesions but no identifiable primary tumor. Lesions from three pigs were determined by histology as osteoblastic osteosarcomas. Osteosarcoma is a relatively rare solid tumor but the most common primary bone cancer, and is highly malignant

with bad prognosis. In addition, two G2 generation homozygous *TP53^{LSL-R167H}* knockout pigs were examined. Both animals grew more slowly than wild-type and heterozygous mutant controls, and revealed multiple large osteosarcomas at the age of 7–8 months which indicates accelerated tumor development in the homozygous p53 mutants (Saalfrank et al., 2016).

The human mutation *TP53^{R175H}* (corresponding to R167H in pigs) is also found in the germline of Li-Fraumeni patients who are strongly predisposed to developing multiple types of cancers. Gene targeting via homologous recombination in Yucatan minipig fibroblasts and subsequent SCNT obtained heterozygous *TP53^{R167H}* mutant founders. Mating of the heterozygous mutants revealed the expected ratio of Mendelian inheritance in the offspring. No tumors were detected via in vivo imaging or necropsy in the heterozygous *TP53^{R167H}* mutant pigs over 30 months of observation. All homozygous *TP53^{R167H}* mutant pigs that reached sexual maturity developed neoplastic lesions, including lymphomas and osteogenic tumors, thereby recapitulating the tumor types observed in mice and humans expressing orthologous *TP53* mutant alleles (Sieren et al., 2014).

Activating mutations in the protooncogene KRAS initiate pancreatic adenocarcinoma and nonsmall-cell lung cancer and occur in many other human cancers with *KRAS^{G12D}* as the most common mutation. Using mesenchymal stem cells of Landrace pigs, a latent oncogenic mutant porcine *KRAS* gene was constructed by insertion of a floxed transcriptional termination signal (LSL cassette) and a point mutation encoding the oncogenic activation mutation *KRAS^{G12D}*. In the intact form, the mutant allele does not express mutant KRAS. Expression can be induced by *Cre*-mediated excision of the LSL cassette, generating the allele designated *KRAS^{L-G12D}*. By SCNT, viable gene-targeted pigs carrying a latent mutant *KRAS^{G12D}* allele were produced that can be activated by *Cre* recombination (Li et al., 2015b).

Analogously, a *Cre* recombinase inducible porcine transgene ubiquitously expressing both *KRAS^{G12D}* and *TP53^{R167H}* was constructed, and transgenic pigs were generated with Minnesota minipig fibroblasts cells and SCNT. A transgenic pig line harboring a single copy of the transgene was further analyzed. Local expression of *Cre* by adenoviral administration of *Cre* at different sites in three transgenic pigs (intramuscularly in the legs, intratesticularly, or subcutaneously in the ear, neck, or abdomen) inevitably resulted in the development of tumors at the injection sites (Schook et al., 2015).

3.24 Infectious Diseases

Multiple lines of B-cell and T-cell deficient mice have been used for the study of B-cell (humoral) and T-cell (cellular) responses for many diseases. Compared to humans, pigs are often infected by closely-related viral and bacterial pathogens. They can serve as zoonotic reservoirs for human pathogens. For major enteropathogens, mouse models do not reproduce the tropism and immunopathology of the corresponding human infections. Thus, experiments in pigs may contribute to the study of the basic immune response to a pathogenic challenge, as well as to discriminate cellular and humoral protective immunity to infectious agents.

Rodents and humans can utilize 4–6 functional joining gene segments (J_H) of the heavy chain locus, whereas pigs only possess one functional J_H locus. Targeting the single functional joining region (J_H) of the heavy chain locus in porcine fibroblasts of the Large White breed was carried out by homologous recombination with a knockout vector removing the single functional J_H sequences. SCNT using one targeted cell clone produced heterozygous knockout animals which were mated to produce homozygous knockout piglets. The homozygous knockouts appeared in the litters with the expected Mendelian ratio. mRNA analysis in spleen and mesenteric lymph nodes, as well as protein analysis by flow cytometry detected that homozygous knockout piglets did not show mature B cells and antibodies of any isotype. No circulating IgM^+ B cells were observed in the homozygous knockouts, showing that VDJ rearrangement is impaired. Functional VDJ rearrangement at the heavy chain locus has been shown to be required for B-cell development. No transcription or secretion of immunoglobulin isotypes were observed in blood and secondary lymphoid tissues. No lymph node follicles were found. The findings were consistent to published results in B-cell deficient mice and humans. Heterozygous knockouts showed IgM^+ B cells of more than half of the amount of wild-type controls. In contrast, T-cell receptor $(Tcr)_\beta$ transcription and T cells appeared largely unaffected in homozygous knockouts.

The homozygous knockout pigs were conventionally reared by allowing them to suckle until weaning 4 weeks after birth. In the suckling period they remained healthy, however, thereafter they were severely susceptible to bacterial infections leading to a wasting-like syndrome and the impossibility to conventionally maintaining them longer than a few weeks after weaning. Thus, gnotobiotic facilities have to be used for maintaining the homozygous knockouts. These antibody- and B-cell deficient pigs may be used as the first step in the generation of heavy chain knockout pigs for the subsequent complete replacement of the porcine immunoglobulin loci with the human homologous genomic sites. These genetically engineered animals in the future might also serve as a source of pathogen-specific human polyclonal antibodies thereby alleviating both the supply and specificity issues as polyclonal antibodies harvested from

human donors by plasmapheresis are of broad specificity and the supply is limited (Mendicino et al., 2011).

Therefore, the next step for this aim was carried out. The porcine κ light chain immunoglobulin locus is in the megabase range and comprises multiple families of variable (Vκ) genes, five joining (Jκ) regions and—as found for most common mammals including the mouse—a single constant (Cκ) gene. To inactivate the pig κ locus, the single Cκ gene offered the best option, as this strategy has been proven successful in the mouse. Therefore, targeted deletion of the most part of the porcine κ light chain constant (Cκ) region was carried out in pig primary fetal fibroblasts. By SCNT, heterozygous knockouts were produced with one mutant cell clone. Heterozygous knockouts were bred together to generate homozygous knockouts at a ratio close to that expected by the Mendelian inheritance. Peripheral blood mononuclear cells as circulating B cells and secondary lymphoid organs, such as mesenteric lymph nodes—which contain follicles that consist of a dense population of B cells—from homozygous knockouts were devoid of κ-containing immunoglobulins. Furthermore, there was an increase in λ light chain expression when compared to that of wild-type littermates. Tcr$_\beta$ rearranged gene transcription was not altered.

Even though there are two light chain loci (κ and λ), usage is unequal among mammals. In mice >95% of the light chain used by mature B cells are κ while >90% of immunoglobulins in ungulates, such as sheep, horses, and cattle use λ. In contrast, κ:λ usage in the pig is almost equal and corresponds to what is found in humans. The phenomenon of allelic exclusion, whereby any given mature B cell can express only one Ig heavy chain and one Ig light chain allele even though there are two alleles at each of the three Ig loci, is also true for the pig (Ramsoondar et al., 2011).

After the homozygous disruption of the J-region gene segment of the heavy chain locus (Mendicino et al., 2011) and of the porcine κ light chain (Ramsoondar et al., 2011), the targeted disruption of λ light chains was described to be underway (Mendicino et al., 2011).

Subsequently, another workgroup edited the functional JH region of the IgM heavy chain locus in porcine fibroblasts using the CRISPR-Cas9 system. Piglets with biallelic IgM heavy chain gene mutation were produced after SCNT. The piglets also showed no antibody-producing B cells which resulted in a B-cell deficient phenotype (Chen et al., 2015).

3.25 Immunodeficiency

Techniques for the production of genetically engineered animals were used to establish porcine models of severe combined immunodeficiency (SCID) primarily not to further examine analogous human SCID diseases,

but mainly to use these immune deficient pigs as tools for reconstitution experiments related to the immune system, human cancer studies, allograft and xenograft transplantation studies, regenerative medicine, and the evaluation of stem cells for clinical therapy.

X-linked interleukin-2 receptor γ chain gene (IL2RG) was disrupted in fetal fibroblasts by removing exon 6, which were used for SCNT to generate IL2RG mutant pigs on the genetic background of Landrace × Large White animals. Heterozygous IL2RG mutant females were healthy, whereas IL2RG mutant males were athymic and exhibited markedly impaired immunoglobulin and T- and NK-cell production, mirroring the situation in human SCID. Further, the model was validated by engraftment of allogeneic bone marrow transplants (Suzuki et al., 2012).

Another workgroup also generated male IL2RG knockout pigs which lacked thymus and were deficient in T and NK cells. The ZFN-mediated mutation in exon 1 consisted of both a 3-bp substitution and an 86-bp deletion spanning the major transcription start point and the start codon (ATG) of IL2RG which leads to the lack of IL2RG protein expression (Watanabe et al., 2013).

In addition, the recombination activating genes 1 (RAG1) and 2 (RAG2) were disrupted to produce immune deficient pigs. RAG1 and RAG2 are two adjacent genes, and their encoded enzymes function synergistically as a protein complex. If either of the two genes is disrupted, VDJ recombination is compromised and the B- and T-cell development is arrested in an immature status. In humans, mutations in RAG1 or RAG2 result in the complete absence of both B and T cells. TALEN were constructed to edit either RAG1 or RAG2 in Bama minipig cells. Using SCNT, live piglets with monoallelic or biallelic frameshift mutations in either RAG1 or RAG2 were generated therefore producing a nonfunctional RAG1 or RAG2 enzyme. Piglets with biallelic mutations in either RAG1 or RAG2 exhibited hypoplasia of immune organs, failed to perform VDJ rearrangement, and lacked mature B and T cells. RAG1 or RAG2 biallelic knockout pigs showed slower weight gain than controls and did not survive for more than 1 month under conventional housing conditions because of the deficient immune function. Heterozygous RAG1 or RAG2 mutants were healthy and grew normally under the same conditions (Huang et al., 2014).

Another workgroup also produced biallelic RAG2 knockout pigs. Using the TALEN system editing a functionally essential domain in exon 2 and subsequent SCNT, biallelic knockout Minnesota minipigs were established with a SCID phenotype lacking mature B and T cells but possessing NK cells and macrophages. They showed normal birth weight, but lower weight gain, and all either died or were euthanized before reaching 1 month of age under standard housing

environment. Pigs raised in a clean environment were healthier. The biallelic *RAG2* knockout pigs had no or an underdeveloped thymus, and the spleen was also smaller with a markedly hypoplastic white pulp compared to controls. Injection of human induced pluripotent stem cells (iPSC) resulted in efficient teratoma formation in biallelic *RAG2* knockout pigs. They also tolerated grafts of allogeneic porcine stem cells (Lee et al., 2014). In addition, another workgroup produced *RAG1* knockout Duroc pigs using SCNT after successfully targeting exon 2 (Ito et al., 2014). Two homozygous *RAG1* knockout neonatal piglets were established and showed phenotypical defects which are comparable to those described in the reports of Huang et al. (2014) and Lee et al. (2014).

Recently, direct injection of the CRISPR-Cas9 system into in vitro fertilization-derived Yorkshire cross breed zygotes and subsequent embryo transfer resulted in the generation of biallelic double knockout founder pigs for both *IL2RG* and *RAG2* exhibiting a SCID phenotype. Near-term founder pigs were derived via hysterectomy and maintained under germ-free condition in isolators. Various gnotobiotic double knockout founders were used for the evaluation of the infection with human norovirus (Lei et al., 2016).

The major histocompatibility complex (MHC) is pivotal to the function of the immune system in health and disease. As the function of human class I MHC in infection is already understood in great detail, the development of class I MHC deficient pigs will more aid to the species-specific response to infectious diseases in the agricultural industry, as well as allograft and xenograft rejection studies. The class I region of swine MHC contains the three classical class I swine leukocyte antigen (*SLA*) 1, 2, and 3 genes. Exon 4 has limited genetic variability in these genes and, therefore, was edited using CRISPR-Cas9 in porcine cells with known class I *SLA* alleles. After two rounds of SCNT, viable pigs were produced which were negative for class I SLA cell surface expression due to frameshifts arising from indels in the class I *SLA* genes. The SLA deficient animals showed a significant reduction in CD3$^+$/CD8$^+$ mature T lymphocytes and an increase in CD3$^+$/CD4$^+$ T cells. The class I MHC knockout pigs were observed to be healthy and grow well up to sexual maturity (Reyes et al., 2014).

CD1 molecules are a family of highly conserved antigen presenting glycoproteins. In humans, the CD1 family comprises five members encoded by *CD1A* to *CD1E*. CD1D is predominantly found on hematopoietic cell types, is considered a nonclassical major histocompatibility complex protein and is involved in presentation of lipid antigens to invariant natural killer T cells. Large White crossbred pigs deficient in this gene were produced with the CRISPR-Cas9 system. SCNT of edited

pig cells resulted in piglets containing either the biallelic or homozygous mutation of *CD1D*. In addition, embryo transfer of CRISPR-Cas9 injected in vitro-derived zygotes also led to the production of pigs with mutations in *CD1D* (Whitworth et al., 2014). *CD1D* knockout pigs failed to develop invariant natural killer T cells, whereas other leukocyte populations remained intact. In analogous mouse models, CD1d and NKT cells have been shown to be involved in shaping the composition of the commensal microbiota. However, no such effects were observed in *CD1D* knockout pigs (Yang et al., 2015).

4 CONCLUSIONS

Biomedical research requires nonrodent model organisms for the confirmation and translation of novel results for the pathogenesis and therapy of human diseases that have been found in classical rodent models. Genetically modified and/or transgenic pigs were produced and analyzed for their potential as appropriate animal models for specific human diseases. Some published projects up to now only showed the first steps in the development of the final disease model and/or only included the analysis of founder animals and/or few genetically modified animals. Apart from intrinsic problems in the use of large animals where the number of individuals and the use of aged animals in the experimental groups is practically limited, the outcome to date varies between the different projects. Some genetically modified pigs covered pathophysiological characteristics of the respective human disease which were not seen in the analogous genetically modified mouse models. In particular genetically modified pig projects, no pathologic phenotypes occurred that are similar to those seen in the respective human disease. This may be caused by project-specific parameters, as well as by species-specific differences in the respective pathway between humans and pigs. Analogous to rodent species, attempts for increasing the genetic, environmental, and experimental standardization of the studies may further increase the success in the work with genetically modified pigs.

Acknowledgments

References

Aigner, B., Kessler, B., Klymiuk, N., Kurome, M., Renner, S., Wünsch, A., et al., 2013. Genetically tailored pig models for translational biomedical research. In: Conn, P.M. (Ed.), Animal Models for the Study of Human Disease. Academic Press, London, pp. 785–809, first ed.

Albl, B., Haesner, S., Braun-Reichhart, C., Streckel, E., Renner, S., Seeliger, F., et al., 2016. Tissue sampling guides for porcine biomedical models. Toxicol. Pathol. 44, 414–420.

Al-Mashhadi, R.H., Sorensen, C.B., Kragh, P.M., Christoffersen, C., Mortensen, M.B., Tolbod, L.P., et al., 2013. Familial hypercholesterolemia and atherosclerosis in cloned minipigs created by DNA transposition of a human PCSK9 gain-of-function mutant. Sci. Transl. Med. 5, 166ra1.

Al-Mashhadi, R.H., Bjorklund, M.M., Mortensen, M.B., Christoffersen, C., Larsen, T., Falk, E., et al., 2015. Diabetes with poor glycaemic control does not promote atherosclerosis in genetically modified hypercholesterolaemic minipigs. Diabetologia 58, 1926–1936.

Amuzie, C., Swart, J.R., Rogers, C.S., Vihtelic, T., Denham, S., Mais, D.E., 2016. A translational model for diet-related atherosclerosis: effect of statins on hypercholesterolemia and atherosclerosis in a minipig. Toxicol. Pathol. 44, 442–449.

Baxa, M., Hruska-Plochan, M., Juhas, S., Vodicka, P., Pavlok, A., Juhasova, J., et al., 2013. A transgenic minipig model of Huntington's Disease. J. Huntingtons Dis. 2, 47–68.

Beraldi, R., Chan, C.H., Rogers, C.S., Kovacs, A.D., Meyerholz, D.K., Trantzas, C., et al., 2015. A novel porcine model of ataxia telangiectasia reproduces neurological features and motor deficits of human disease. Hum. Mol. Genet. 24, 6473–6484.

Betthauser, J., Forsberg, E., Augenstein, M., Childs, L., Eilertsen, K., Enos, J., et al., 2000. Production of cloned pigs from in vitro systems. Nat. Biotechnol. 18, 1055–1059.

Bode, G., Clausing, P., Gervais, F., Loegsted, J., Luft, J., Nogues, V., et al., 2010. The utility of the minipig as an animal model in regulatory toxicology. J. Pharmacol. Toxicol. Methods 62, 196–220.

Brem, G., Brenig, B., Goodman, H.M., Selden, R.C., Graf, F., Kruff, B., et al., 1985. Production of transgenic mice, rabbits and pigs by microinjection into pronuclei. Zuchthygiene 20, 251–252.

Carlson, D.F., Garbe, J.R., Tan, W., Martin, M.J., Dobrinsky, J.R., Hackett, P.B., et al., 2011. Strategies for selection marker-free swine transgenesis using the Sleeping Beauty transposon system. Transgenic Res. 20, 1125–1137.

Carlson, D.F., Tan, W., Lillico, S.G., Stverakova, D., Proudfoot, C., Christian, M., et al., 2012. Efficient TALEN-mediated gene knockout in livestock. Proc. Natl. Acad. Sci. USA 109, 17382–17387.

Chen, L., Li, L., Pang, D., Li, Z., Wang, T., Zhang, M., et al., 2010. Construction of transgenic swine with induced expression of Cre recombinase. Animal 4, 767–771.

Chen, F., Wang, Y., Yuan, Y., Zhang, W., Ren, Z., Jin, Y., et al., 2015. Generation of B cell-deficient pigs by highly efficient CRISPR/Cas9-mediated gene targeting. J. Genet. Genomics 42, 437–444.

Cheng, J., Wang, Y., Zhang, Z., Jin, Y., Li, Q., Want, R., et al., 2015. Dominant-negative inhibition of glucose-dependent insulinotropic polypeptide impairs function of beta cells in transgenic pigs. J. Biomed. Res. 29, 512–514.

Chieppa, M.N., Perota, A., Corona, C., Grindatto, A., Lagutina, I., Vallino Costassa, E., et al., 2014. Modeling amyotrophic lateral sclerosis in hSOD1 transgenic swine. Neurodegener. Dis. 13, 246–254.

Cho, S.K., Kim, J.H., Park, J.Y., Choi, Y.J., Bang, J.I., Hwang, K.C., et al., 2007. Serial cloning of pigs by somatic cell nuclear transfer: restoration of phenotypic normality during serial cloning. Dev. Dyn. 236, 3369–3382.

Cohen, T.S., Prince, A., 2012. Cystic fibrosis: a mucosal immunodeficiency syndrome. Nat. Med. 18, 509–519.

Cooper, D.K., Ekser, B., Ramsoondar, J., Phelps, C., Ayares, D., 2016. The role of genetically engineered pigs in xenotransplantation research. J. Pathol. 238, 288–299.

Davis, B.T., Wang, X.J., Rohret, J.A., Struzynski, J.T., Merricks, E.P., Bellinger, D.A., et al., 2014. Targeted disruption of LDLR causes hypercholesterolemia and atherosclerosis in Yucatan miniature pigs. PLoS One 9, e93457.

Deng, W., Yang, D., Zhao, B., Ouyang, Z., Song, J., Fan, N., et al., 2011. Use of the 2A peptide for generation of multi-transgenic pigs through a single round of nuclear transfer. PLoS One 6, e19986.

Dmochewitz, M., Wolf, E., 2015. Genetic engineering of pigs for the creation of translational models of human pathologies. Anim. Front. 5, 50–56.

Ekser, B., Tector, A.J., Cooper, D.K.C., 2015. Special Issue: Xenotransplantation. Int. J. Surg. 32 (Part B), 197–326.

Estrada, J.L., Collins, B., York, A., Bischoff, S., Sommer, J., Tsai, S., et al., 2008. Successful cloning of the Yucatan minipig using commercial/occidental breeds as oocyte donors and embryo recipients. Cloning Stem Cells 10, 287–296.

Fang, X., Mou, Y., Huang, Z., Li, Y., Han, L., Zhang, Y., et al., 2012. The sequence and analysis of a Chinese pig genome. Gigascience 1, 16.

Fernandez de Castro, J.P., Scott, P.A., Fransen, J.W., Demas, J., DeMarco, P.J., Kaplan, H.J., et al., 2014. Cone photoreceptors develop normally in the absence of functional rod photoreceptors in a transgenic swine model of retinitis pigmentosa. Invest. Ophthalmol. Vis. Sci. 55, 2460–2468.

Flisikowska, T., Merkl, C., Landmann, M., Eser, S., Rezaei, N., Cui, X., et al., 2012. A porcine model of familial adenomatous polyposis. Gastroenterology 143, 1173–1175.

Food and Agriculture Organization of the United Nations, 2007. The state of the world's animal genetic resources for food and agriculture. FAO, Rome.

Frantz, L., Meijaard, E., Gongora, J., Haile, J., Groenen, M.A., Larson, G., 2016. The evolution of suidae. Annu. Rev. Anim. Biosci. 4, 61–85.

Freeman, T.C., Ivens, A., Baillie, J.K., Beraldi, D., Barnett, M.W., Dorward, D., et al., 2012. A gene expression atlas of the domestic pig. BMC Biol. 10, 90.

Gao, F., Luo, Y., Li, S., Li, J., Lin, L., Nielsen, A.L., et al., 2011. Comparison of gene expression and genome-wide DNA methylation profiling between phenotypically normal cloned pigs and conventionally bred controls. PLoS One 6, e25901.

Garrels, W., Mates, L., Holler, S., Dalda, A., Taylor, U., Petersen, B., et al., 2011. Germline transgenic pigs by Sleeping Beauty transposition in porcine zygotes and targeted integration in the pig genome. PLoS One 6, e23573.

Gregory-Evans, K., Weleber, R.G., 1997. An eye for an eye: new models of genetic ocular disease. Nat. Biotechnol. 15, 947–948.

Groenen, M.A., Archibald, A.L., Uenishi, H., Tuggle, C.K., Takeuchi, Y., Rothschild, M.F., et al., 2012. Analyses of pig genomes provide insight into porcine demography and evolution. Nature 491, 393–398.

Hai, T., Teng, F., Guo, R., Li, W., Zhou, Q., 2014. One-step generation of knockout pigs by zygote injection of CRISPR/Cas system. Cell Res. 24, 372–375.

Hammer, R.E., Pursel, V.G., Rexroad, Jr., C.E., Wall, R.J., Bolt, D.J., Ebert, K.M., et al., 1985. Production of transgenic rabbits, sheep and pigs by microinjection. Nature 315, 680–683.

Hao, Y.H., Yong, H.Y., Murphy, C.N., Wax, D., Samuel, M., Rieke, A., et al., 2006. Production of endothelial nitric oxide synthase (eNOS) over-expressing piglets. Transgenic Res. 15, 739–750.

Hasler-Rapacz, J., Ellegren, H., Fridolfsson, A.K., Kirkpatrick, B., Kirk, S., Andersson, L., et al., 1998. Identification of a mutation in the low density lipoprotein receptor gene associated with recessive familial hypercholesterolemia in swine. Am. J. Med. Genet. 76, 379–386.

Hauschild, J., Petersen, B., Santiago, Y., Queisser, A.L., Carnwath, J.W., Lucas-Hahn, A., et al., 2011. Efficient generation of a biallelic knockout in pigs using zinc-finger nucleases. Proc. Natl. Acad. Sci. USA 108, 12013–12017.

He, J., Ye, J., Li, Q., Feng, Y., Bai, X., Chen, X., et al., 2013. Construction of a transgenic pig model overexpressing polycystic kidney disease 2 (PKD2) gene. Transgenic Res. 22, 861–867.

He, J., Li, Q., Fang, S., Guo, Y., Liu, T., Ye, J., et al., 2015. PKD1 mono-allelic knockout is sufficient to trigger renal cystogenesis in a mini-pig model. Int. J. Biol. Sci. 11, 361–369.

Herbach, N., Goeke, B., Schneider, M., Hermanns, W., Wolf, E., Wanke, R., 2005. Overexpression of a dominant negative GIP receptor in transgenic mice results in disturbed postnatal pancreatic islet and beta-cell development. Regul. Pept. 125, 103–117.

Herbach, N., Rathkolb, B., Kemter, E., Pichl, L., Klaften, M., Hrabé de Angelis, M., et al., 2007. Dominant-negative effects of a novel mutated Ins2 allele causes early-onset diabetes and severe beta-cell loss in Munich Ins2C95S mutant mice. Diabetes 56, 1268–1276.

Hickey, R.D., Lillegard, J.B., Fisher, J.E., McKenzie, T.J., Hofherr, S.E., Finegold, M.J., et al., 2011. Efficient production of Fah-null heterozygote pigs by chimeric adeno-associated virus-mediated gene knockout and somatic cell nuclear transfer. Hepatology 54, 1351–1359.

Hickey, R.D., Mao, S.A., Glorioso, J., Lillegard, J.B., Fisher, J.E., Amiot, B., et al., 2014. Fumarylacetoacetate hydrolase deficient pigs are a novel large animal model of metabolic liver disease. Stem Cell Res. 13, 144–153.

Hinkel, R., Trenkwalder, T., Petersen, B., Husada, W., Gesenhues, F., Lee, S., et al., 2014. MRTF-A controls vessel growth and maturation by increasing the expression of CCN1 and CCN2. Nat. Commun. 5, 3970.

Holm, I.E., Alstrup, A.K., Luo, Y., 2016. Genetically modified pig models for neurodegenerative disorders. J. Pathol. 238, 267–287.

Huang, P.L., 2009. eNOS, metabolic syndrome and cardiovascular disease. Trends Endocrinol. Metab. 20, 295–302.

Huang, J., Guo, X., Fan, N., Song, J., Zhao, B., Ouyang, Z., et al., 2014. RAG1/2 knockout pigs with severe combined immunodeficiency. J. Immunol. 193, 1496–1503.

Ito, T., Sendai, Y., Yamazaki, S., Seki-Soma, M., Hirose, K., Watanabe, M., et al., 2014. Generation of recombination activating gene-1-deficient neonatal piglets: a model of T and B cell deficient severe combined immune deficiency. PLoS One 9, e113833.

Ivics, Z., Li, M.A., Mates, L., Boeke, J.D., Nagy, A., Bradley, A., et al., 2009. Transposon-mediated genome manipulation in vertebrates. Nat. Methods 6, 415–422.

Ivics, Z., Garrels, W., Mates, L., Yau, T.Y., Bashir, S., Zidek, V., et al., 2014. Germline transgenesis in pigs by cytoplasmic microinjection of Sleeping Beauty transposons. Nat. Protoc. 9, 810–827.

Jakobsen, J.E., Li, J., Kragh, P.M., Moldt, B., Lin, L., Liu, Y., et al., 2011. Pig transgenesis by Sleeping Beauty DNA transposition. Transgenic Res. 20, 533–545.

Jakobsen, J.E., Johansen, M.G., Schmidt, M., Dagnaes-Hansen, F., Dam, K., Gunnarsson, A., et al., 2013. Generation of minipigs with targeted transgene insertion by recombinase-mediated cassette exchange (RMCE) and somatic cell nuclear transfer (SCNT). Transgenic Res. 22, 709–723.

Jin, Y.X., Jeon, Y., Lee, S.H., Kwon, M.S., Kim, T., Cui, X.S., et al., 2014. Production of pigs expressing a transgene under the control of a tetracycline-inducible system. PLoS One 9, e86146.

Ju, H., Zhang, J., Bai, L., Mu, Y., Du, Y., Yang, W., et al., 2015. The transgenic cloned pig population with integrated and controllable GH expression that has higher feed efficiency and meat production. Sci. Rep. 5, 10152.

Kaneko, N., Itoh, K., Sugiyama, A., Izumi, Y., 2011. Microminipig, a non-rodent experimental animal optimized for life science research: preface. J. Pharmacol. Sci. 115, 112–114.

Kashiwakura, Y., Mimuro, J., Onishi, A., Iwamoto, M., Madoiwa, S., Fuchimoto, D., et al., 2012. Porcine model of hemophilia A. PLoS One 7, e49450.

Kim, Y.J., Ahn, K.S., Kim, M., Kim, M.J., Park, S.M., Ryu, J., et al., 2014. Targeted disruption of Ataxia-telangiectasia mutated gene in miniature pigs by somatic cell nuclear transfer. Biochem. Biophys. Res. Commun. 452, 901–905.

Klymiuk, N., Aigner, B., Brem, G., Wolf, E., 2010. Genetic modification of pigs as organ donors for xenotransplantation. Mol. Reprod. Dev. 77, 209–221.

Klymiuk, N., Mundhenk, L., Kraehe, K., Wuensch, A., Plog, S., Emrich, D., et al., 2012a. Sequential targeting of CFTR by BAC vectors generates a novel pig model of cystic fibrosis. J. Mol. Med. 90, 597–608.

Klymiuk, N., Bocker, W., Schonitzer, V., Bahr, A., Radic, T., Frohlich, T., et al., 2012b. First inducible transgene expression in porcine large animal models. FASEB J. 26, 1086–1099.

Klymiuk, N., Blutke, A., Graf, A., Krause, S., Burkhardt, K., Wuensch, A., et al., 2013. Dystrophin-deficient pigs provide new insights into the hierarchy of physiological derangements of dystrophic muscle. Hum. Mol. Genet. 22, 4368–4382.

Klymiuk, N., Seeliger, F., Bohlooly, Y.M., Blutke, A., Rudmann, D.G., Wolf, E., 2016. Tailored pig models for preclinical efficacy and safety testing of targeted therapies. Toxicol. Pathol. 44, 346–357.

Köhn, F., 2012. History and development of miniature, micro- and minipigs. In: McAnulty, P.A., Dayan, A.D., Ganderup, N.C., Hastings, K.L. (Eds.), The Minipig in Biomedical Research. Taylor & Francis, Boca Raton, FL, pp. 3–15.

Kong, Q., Hai, T., Ma, J., Huang, T., Jiang, D., Xie, B., et al., 2014. Rosa26 locus supports tissue-specific promoter driving transgene expression specifically in pig. PLoS One 9, e107945.

Kostic, C., Lillico, S.G., Crippa, S.V., Grandchamp, N., Pilet, H., Philippe, S., et al., 2013. Rapid cohort generation and analysis of disease spectrum of large animal model of cone dystrophy. PLoS One 8, e71363.

Kraft, T.W., Allen, D., Petters, R.M., Hao, Y., Peng, Y.W., Wong, F., 2005. Altered light responses of single rod photoreceptors in transgenic pigs expressing P347L or P347S rhodopsin. Mol. Vis. 11, 1246–1256.

Kragh, P.M., Nielsen, A.L., Li, J., Du, Y., Lin, L., Schmidt, M., et al., 2009. Hemizygous minipigs produced by random gene insertion and handmade cloning express the Alzheimer's disease-causing dominant mutation APPsw. Transgenic Res. 18, 545–558.

Kues, W.A., Schwinzer, R., Wirth, D., Verhoeyen, E., Lemme, E., Herrmann, D., et al., 2006. Epigenetic silencing and tissue independent expression of a novel tetracycline inducible system in double-transgenic pigs. FASEB J. 20, 1200–1202.

Kurome, M., Ishikawa, T., Tomii, R., Ueno, S., Shimada, A., Yazawa, H., et al., 2008. Production of transgenic and non-transgenic clones in miniature pigs by somatic cell nuclear transfer. J. Reprod. Dev. 54, 156–163.

Kurome, M., Kessler, B., Wuensch, A., Nagashima, H., Wolf, E., 2015. Nuclear transfer and transgenesis in the pig. Methods Mol. Biol. 1222, 37–59.

Lai, L., Kang, J.X., Li, R., Wang, J., Witt, W.T., Yong, H.Y., et al., 2006. Generation of cloned transgenic pigs rich in omega-3 fatty acids. Nat. Biotechnol. 24, 435–436.

Lee, H.G., Lee, H.C., Kim, S.W., Lee, P., Chung, H.J., Lee, Y.K., et al., 2009. Production of recombinant human von Willebrand factor in the milk of transgenic pigs. J. Reprod. Dev. 55, 484–490.

Lee, K., Kwon, D.N., Ezashi, T., Choi, Y.J., Park, C., Ericsson, A.C., et al., 2014. Engraftment of human iPS cells and allogeneic porcine cells into pigs with inactivated RAG2 and accompanying severe combined immunodeficiency. Proc. Natl. Acad. Sci. USA 111, 7260–7265.

Lei, S., Ryu, J., Wen, K., Twitchell, E., Bui, T., Ramesh, A., et al., 2016. Increased and prolonged human norovirus infection in RAG2/IL2RG deficient gnotobiotic pigs with severe combined immunodeficiency. Sci. Rep. 6, 25222.

Leuchs, S., Saalfrank, A., Merkl, C., Flisikowska, T., Edlinger, M., Durkovic, M., et al., 2012. Inactivation and inducible oncogenic mutation of p53 in gene targeted pigs. PLoS One 7, e43323.

Li, L., Pang, D., Wang, T., Li, Z., Chen, L., Zhang, M., et al., 2009. Production of a reporter transgenic pig for monitoring Cre recombinase activity. Biochem. Biophys. Res. Commun. 382, 232–235.

Li, F., Li, Y., Liu, H., Zhang, H., Liu, C., Zhang, X., et al., 2014a. Production of GHR double-allelic knockout Bama pig by TALENs and handmade cloning. Yi Chuan 36, 903–911.

Li, X., Yang, Y., Bu, L., Guo, X., Tang, C., Song, J., et al., 2014b. Rosa26-targeted swine models for stable gene over-expression and Cre-mediated lineage tracing. Cell Res. 24, 501–504.

Li, F., Li, Y., Liu, H., Zhang, X., Liu, C., Tian, K., et al., 2015a. Transgenic Wuzhishan minipigs designed to express a dominant-negative porcine growth hormone receptor display small stature and a perturbed insulin/IGF-1 pathway. Transgenic Res. 24, 1029–1042.

Li, S., Edlinger, M., Saalfrank, A., Flisikowski, K., Tschukes, A., Kurome, M., et al., 2015b. Viable pigs with a conditionally-activated oncogenic KRAS mutation. Transgenic Res. 24, 509–517.

Li, Y., Fuchimoto, D., Sudo, M., Haruta, H., Lin, Q.F., Takayama, T., et al., 2016. Development of human-like advanced coronary plaques in low-density lipoprotein receptor knockout pigs and justification for statin treatment before formation of atherosclerotic plaques. J. Am. Heart Assoc. 5, e002779.

Liu, H., Li, Y., Wei, Q., Liu, C., Bolund, L., Vajta, G., et al., 2013. Development of transgenic minipigs with expression of antimorphic human cryptochrome 1. PLoS One 8, e76098.

Lorson, M.A., Spate, L.D., Prather, R.S., Lorson, C.L., 2008. Identification and characterization of the porcine (Sus scrofa) survival motor neuron (SMN1) gene: an animal model for therapeutic studies. Dev. Dyn. 237, 2268–2278.

Lorson, M.A., Spate, L.D., Samuel, M.S., Murphy, C.N., Lorson, C.L., Prather, R.S., et al., 2011. Disruption of the Survival Motor Neuron (SMN) gene in pigs using ssDNA. Transgenic Res. 20, 1293–1304.

Luo, Y., Li, J., Liu, Y., Lin, L., Du, Y., Li, S., et al., 2011. High efficiency of BRCA1 knockout using rAAV-mediated gene targeting: developing a pig model for breast cancer. Transgenic Res. 20, 975–988.

Martin, M.J., Pinkert, C.A., 2002. Production of transgenic swine by DNA microinjection. In: Pinkert, C.A. (Ed.), Transgenic Animal Technology—a Laboratory Handbook. Academic Press, Burlington, MA, pp. 307–336.

Matsunari, H., Nagashima, H., 2009. Application of genetically modified and cloned pigs in translational research. J. Reprod. Dev. 55, 225–230.

Matsunari, H., Nagashima, H., Watanabe, M., Umeyama, K., Nakano, K., Nagaya, M., et al., 2013. Blastocyst complementation generates exogenic pancreas in vivo in apancreatic cloned pigs. Proc. Natl. Acad. Sci. USA 110, 4557–4562.

Matsuyama, N., Hadano, S., Onoe, K., Osuga, H., Showguchi-Miyata, J., Gondo, Y., et al., 2000. Identification and characterization of the miniature pig Huntington's disease gene homolog: evidence for conservation and polymorphism in the CAG triplet repeat. Genomics 69, 72–85.

McAnulty, P.A., Dayan, A.D., Ganderup, N.C., Hastings, K.L., 2012. The Minipig in Biomedical Research. Taylor & Francis, Boca Raton, FL.

McCalla-Martin, A.C., Chen, X., Linder, K.E., Estrada, J.L., Piedrahita, J.A., 2010. Varying phenotypes in swine versus murine transgenic models constitutively expressing the same human Sonic hedgehog transcriptional activator, K5-HGLI2 Delta N. Transgenic Res. 19, 869–887.

Mendicino, M., Ramsoondar, J., Phelps, C., Vaught, T., Ball, S., LeRoith, T., et al., 2011. Generation of antibody- and B cell-deficient pigs by targeted disruption of the J-region gene segment of the heavy chain locus. Transgenic Res. 20, 625–641.

Mezrich, J.D., Haller, G.W., Arn, J.S., Houser, S.L., Madsen, J.C., Sachs, D.H., 2003. Histocompatible miniature swine: an inbred large-animal model. Transplantation 75, 904–907.

Morton, A.J., Howland, D.S., 2013. Large genetic animal models of Huntington's Disease. J. Huntingtons Dis. 2, 3–19.

Nonneman, D.J., Brown-Brandl, T., Jones, S.A., Wiedmann, R.T., Rohrer, G.A., 2012. A defect in dystrophin causes a novel porcine stress syndrome. BMC Genomics 13, 233.

Onishi, A., Iwamoto, M., Akita, T., Mikawa, S., Takeda, K., Awata, T., et al., 2000. Pig cloning by microinjection of fetal fibroblast nuclei. Science 289, 1188–1190.

Ozawa, M., Himaki, T., Ookutsu, S., Mizobe, Y., Ogawa, J., Miyoshi, K., et al., 2015. Production of cloned miniature pigs expressing high levels of human apolipoprotein(a) in plasma. PLoS One 10, e0132155.

Paleyanda, R.K., Velander, W.H., Lee, T.K., Scandella, D.H., Gwazdauskas, F.C., Knight, J.W., et al., 1997. Transgenic pigs produce functional human factor VIII in milk. Nat. Biotechnol. 15, 971–975.

Pan, D., Zhang, L., Zhou, Y., Feng, C., Long, C., Liu, X., et al., 2010. Efficient production of omega-3 fatty acid desaturase (sFat-1)-transgenic pigs by somatic cell nuclear transfer. Sci. China Life Sci. 53, 517–523.

Park, J., Lai, L., Samuel, M., Wax, D., Bruno, R.S., French, R., et al., 2011. Altered gene expression profiles in the brain, kidney, and lung of one-month-old cloned pigs. Cell Reprogram 13, 215–223.

Park, E.J., Koo, O.J., Lee, B.C., 2015a. Overexpressed human heme Oxygenase-1 decreases adipogenesis in pigs and porcine adipose-derived stem cells. Biochem. Biophys. Res. Commun. 467, 935–940.

Park, D.S., Cerrone, M., Morley, G., Vasquez, C., Fowler, S., Liu, N., et al., 2015b. Genetically engineered SCN5A mutant pig hearts exhibit conduction defects and arrhythmias. J. Clin. Invest. 125, 403–412.

Petters, R.M., Alexander, C.A., Wells, K.D., Collins, E.B., Sommer, J.R., Blanton, M.R., et al., 1997. Genetically engineered large animal model for studying cone photoreceptor survival and degeneration in retinitis pigmentosa. Nat. Biotechnol. 15, 965–970.

Polejaeva, I.A., Chen, S.H., Vaught, T.D., Page, R.L., Mullins, J., Ball, S., et al., 2000. Cloned pigs produced by nuclear transfer from adult somatic cells. Nature 407, 86–90.

Prather, R.S., Lorson, M., Ross, J.W., Whyte, J.J., Walters, E., 2013. Genetically engineered pig models for human diseases. Annu. Rev. Anim. Biosci. 1, 203–219.

Pursel, V.G., Rexroad, C.E., 1993. Status of research with transgenic farm animals. J. Anim. Sci. 71 (Suppl), 10–19.

Ramsoondar, J., Mendicino, M., Phelps, C., Vaught, T., Ball, S., Monahan, J., et al., 2011. Targeted disruption of the porcine immunoglobulin kappa light chain locus. Transgenic Res. 20, 643–653.

Rehbinder, C., Baneux, P., Forbes, D., van Herck, H., Nicklas, W., Rugaya, Z., et al., 1998. FELASA recommendations for the health monitoring of breeding colonies and experimental units of cats, dogs and pigs. Lab Anim. 32, 1–17.

Renner, S., Fehlings, C., Herbach, N., Hofmann, A., von Waldthausen, D.C., Kessler, B., et al., 2010. Glucose intolerance and reduced proliferation of pancreatic beta-cells in transgenic pigs with impaired glucose-dependent insulinotropic polypeptide function. Diabetes 59, 1228–1238.

Renner, S., Romisch-Margl, W., Prehn, C., Krebs, S., Adamski, J., Goke, B., et al., 2012. Changing metabolic signatures of amino acids and lipids during the prediabetic period in a pig model with impaired incretin function and reduced beta-cell mass. Diabetes, 2166–2175.

Renner, S., Braun-Reichhart, C., Blutke, A., Herbach, N., Emrich, D., Streckel, E., et al., 2013. Permanent neonatal diabetes in INS(C94Y) transgenic pigs. Diabetes 62, 1505–1511.

Renner, S., Dobenecker, B., Blutke, A., Zols, S., Wanke, R., Ritzmann, M., et al., 2016a. Comparative aspects of rodent and nonrodent animal models for mechanistic and translational diabetes research. Theriogenology 86, 406–421.

Renner, S., Blutke, A., Streckel, E., Wanke, R., Wolf, E., 2016b. Incretin actions and consequences of incretin-based therapies: lessons from complementary animal models. J. Pathol. 238, 345–358.

Reyes, L.M., Estrada, J.L., Wang, Z.Y., Blosser, R.J., Smith, R.F., Sidner, R.A., et al., 2014. Creating class I MHC-null pigs using guide RNA and the Cas9 endonuclease. J. Immunol. 193, 5751–5757.

Roessler, E., Ermilov, A.N., Grange, D.K., Wang, A., Grachtchouk, M., Dlugosz, A.A., et al., 2005. A previously unidentified amino-terminal domain regulates transcriptional activity of wild-type and disease-associated human GLI2. Hum. Mol. Genet. 14, 2181–2188.

Rogers, C.S., 2016. Genetically engineered livestock for biomedical models. Transgenic Res. 25, 345–359.

Rogers, C.S., Hao, Y., Rokhlina, T., Samuel, M., Stoltz, D.A., Li, Y., et al., 2008a. Production of CFTR-null and CFTR-DeltaF508 heterozygous pigs by adeno-associated virus-mediated gene targeting and somatic cell nuclear transfer. J. Clin. Invest. 118, 1571–1577.

Rogers, C.S., Stoltz, D.A., Meyerholz, D.K., Ostedgaard, L.S., Rokhlina, T., Taft, P.J., et al., 2008b. Disruption of the CFTR gene produces a model of cystic fibrosis in newborn pigs. Science 321, 1837–1841.

Ross, J.W., Fernandez de Castro, J.P., Zhao, J., Samuel, M., Walters, E., Rios, C., et al., 2012. Generation of an inbred miniature pig model of retinitis pigmentosa. Invest. Ophthalmol. Vis. Sci. 53, 501–507.

Ruan, J., Li, H., Xu, K., Wu, T., Wei, J., Zhou, R., et al., 2015. Highly efficient CRISPR/Cas9-mediated transgene knockin at the H11 locus in pigs. Sci. Rep. 5, 14253.

Saalfrank, A., Janssen, K.P., Ravon, M., Flisikowski, K., Eser, S., Steiger, K., et al., 2016. A porcine model of osteosarcoma. Oncogenesis 5, e210.

Saeki, K., Matsumoto, K., Kinoshita, M., Suzuki, I., Tasaka, Y., Kano, K., et al., 2004. Functional expression of a Delta12 fatty acid desaturase gene from spinach in transgenic pigs. Proc. Natl. Acad. Sci. USA 101, 6361–6366.

Schomberg, D.T., Tellez, A., Meudt, J.J., Brady, D.A., Dillon, K.N., Arowolo, F.K., et al., 2016. Miniature swine for preclinical modeling of complexities of human disease for translational scientific discovery and accelerated development of therapies and medical devices. Toxicol. Pathol. 44, 299–314.

Schook, L.B., Collares, T.V., Hu, W., Liang, Y., Rodrigues, F.M., Rund, L.A., et al., 2015. A genetic porcine model of cancer. PLoS One 10, e0128864.

Schuurman, H.J., 2009. The International Xenotransplantation Association consensus statement on conditions for undertaking clinical trials of porcine islet products in type 1 diabetes-chapter 2: source pigs. Xenotransplantation 16, 215–222.

Scott, P.A., Fernandez de Castro, J.P., Kaplan, H.J., McCall, M.A., 2014. A Pro23His mutation alters prenatal rod photoreceptor morphology in a transgenic swine model of retinitis pigmentosa. Invest. Ophthalmol. Vis. Sci. 55, 2452–2459.

Selsby, J.T., Ross, J.W., Nonneman, D., Hollinger, K., 2015. Porcine models of muscular dystrophy. ILAR J. 56, 116–126.

Shi, W., Zakhartchenko, V., Wolf, E., 2003. Epigenetic reprogramming in mammalian nuclear transfer. Differentiation 71, 91–113.

Shimatsu, Y., Horii, W., Nunoya, T., Iwata, A., Fan, J., Ozawa, M., 2016. Production of human apolipoprotein(a) transgenic NIBS miniature pigs by somatic cell nuclear transfer. Exp. Anim. 65, 37–43.

Shu-Shan, Z., Jian-Jun, D., Cai-Feng, W., Ting-Yu, Z., De-Fu, Z., 2014. Comparative proteomic analysis of hearts of adult SCNT Bama miniature pigs (Sus scrofa). Theriogenology 81, 901–905.

Sieren, J.C., Meyerholz, D.K., Wang, X.J., Davis, B.T., Newell, Jr., J.D., Hammond, E., et al., 2014. Development and translational imaging of a TP53 porcine tumorigenesis model. J. Clin. Invest. 124, 4052–4066.

Sommer, J.R., Wong, F., Petters, R.M., 2011a. Phenotypic stability of Pro347Leu rhodopsin transgenic pigs as indicated by photoreceptor cell degeneration. Transgenic Res. 20, 1391–1395.

Sommer, J.R., Estrada, J.L., Collins, E.B., Bedell, M., Alexander, C.A., Yang, Z., et al., 2011b. Production of ELOVL4 transgenic pigs: a large animal model for Stargardt-like macular degeneration. Br. J. Ophthalmol. 95, 1749–1754.

Sondergaard, L.V., Ladewig, J., Dagnaes-Hansen, F., Herskin, M.S., Holm, I.E., 2012. Object recognition as a measure of memory in 1–2 years old transgenic minipigs carrying the APPsw mutation for Alzheimer's disease. Transgenic Res. 21, 1341–1348.

Soto, D.A., Ross, P.J., 2016. Pluripotent stem cells and livestock genetic engineering. Transgenic Res. 25, 289–306.

Staunstrup, N.H., Madsen, J., Primo, M.N., Li, J., Liu, Y., Kragh, P.M., et al., 2012. Development of transgenic cloned pig models of skin inflammation by DNA transposon-directed ectopic expression of human beta1 and alpha2 integrin. PLoS One 7, e36658.

Stoltz, D.A., Rokhlina, T., Ernst, S.E., Pezzulo, A.A., Ostedgaard, L.S., Karp, P.H., et al., 2013. Intestinal CFTR expression alleviates meconium ileus in cystic fibrosis pigs. J. Clin. Invest. 123, 2685–2693.

Streckel, E., Braun-Reichhart, C., Herbach, N., Dahlhoff, M., Kessler, B., Blutke, A., et al., 2015. Effects of the glucagon-like peptide-1 receptor agonist liraglutide in juvenile transgenic pigs modeling a prediabetic condition. J. Transl. Med. 13, 73.

Suzuki, S., Iwamoto, M., Saito, Y., Fuchimoto, D., Sembon, S., Suzuki, M., et al., 2012. Il2rg gene-targeted severe combined immunodeficiency pigs. Cell Stem Cell 10, 753–758.

Swindle, M.M., Smith, A.C., 2015. Swine in the Laboratory—Surgery, Anesthesia, Imaging, and Experimental Techniques. CRC Press, Boca Raton, FL.

Tan, W., Carlson, D.F., Lancto, C.A., Garbe, J.R., Webster, D.A., Hackett, P.B., et al., 2013. Efficient nonmeiotic allele introgression in livestock using custom endonucleases. Proc. Natl. Acad. Sci. USA 110, 16526–16531.

Tan, W., Proudfoot, C., Lillico, S.G., Whitelaw, C.B., 2016. Gene targeting, genome editing: from Dolly to editors. Transgenic Res. 25, 273–287.

Tang, X., Wang, G., Liu, X., Han, X., Li, Z., Ran, G., et al., 2015. Over-expression of porcine lipoprotein-associated phospholipase A2 in swine. Biochem. Biophys. Res. Commun. 465, 507–511.

Uchida, M., Shimatsu, Y., Onoe, K., Matsuyama, N., Niki, R., Ikeda, J.E., et al., 2001. Production of transgenic miniature pigs by pronuclear microinjection. Transgenic Res. 10, 577–582.

Umeyama, K., Watanabe, M., Saito, H., Kurome, M., Tohi, S., Matsunari, H., et al., 2009. Dominant-negative mutant hepatocyte nuclear factor 1alpha induces diabetes in transgenic-cloned pigs. Transgenic Res. 18, 697–706.

Umeyama, K., Honda, K., Matsunari, H., Nakano, K., Hidaka, T., Sekiguchi, K., et al., 2013. Production of diabetic offspring using cryopreserved epididymal sperm by in vitro fertilization and intrafallopian insemination techniques in transgenic pigs. J. Reprod. Dev. 59, 599–603.

Umeyama, K., Watanabe, K., Watanabe, M., Horiuchi, K., Nakano, K., Kitashiro, M., et al., 2016. Generation of heterozygous fibrillin-1 mutant cloned pigs from genome-edited foetal fibroblasts. Sci. Rep. 6, 24413.

Wang, G., Yang, H., Yan, S., Wang, C.E., Liu, X., Zhao, B., et al., 2015a. Cytoplasmic mislocalization of RNA splicing factors and aberrant neuronal gene splicing in TDP-43 transgenic pig brain. Mol. Neurodegener. 10, 42.

Wang, Y., Du, Y., Shen, B., Zhou, X., Li, J., Liu, Y., et al., 2015b. Efficient generation of gene-modified pigs via injection of zygote with Cas9/sgRNA. Sci. Rep. 5, 8256.

Wang, X., Zhou, J., Cao, C., Huang, J., Hai, T., Wang, Y., et al., 2015c. Efficient CRISPR/Cas9-mediated biallelic gene disruption and site-specific knockin after rapid selection of highly active sgRNAs in pigs. Sci. Rep. 5, 13348.

Wang, X., Cao, C., Huang, J., Yao, J., Hai, T., Zheng, Q., et al., 2016. One-step generation of triple gene-targeted pigs using CRISPR/Cas9 system. Sci. Rep. 6, 20620.

Watanabe, M., Umeyama, K., Matsunari, H., Takayanagi, S., Haruyama, E., Nakano, K., et al., 2010. Knockout of exogenous EGFP gene in porcine somatic cells using zinc-finger nucleases. Biochem. Biophys. Res. Commun. 402, 14–18.

Watanabe, M., Nakano, K., Matsunari, H., Matsuda, T., Maehara, M., Kanai, T., et al., 2013. Generation of interleukin-2 receptor gamma gene knockout pigs from somatic cells genetically modified by zinc finger nuclease-encoding mRNA. PLoS One 8, e76478.

Wei, J., Ouyang, H., Wang, Y., Pang, D., Cong, N.X., Wang, T., et al., 2012. Characterization of a hypertriglyceridemic transgenic miniature pig model expressing human apolipoprotein CIII. FEBS J. 279, 91–99.

Wheeler, D.G., Joseph, M.E., Mahamud, S.D., Aurand, W.L., Mohler, P.J., Pompili, V.J., et al., 2012. Transgenic swine: expression of human CD39 protects against myocardial injury. J. Mol. Cell. Cardiol. 52, 958–961.

Whitworth, K.M., Lee, K., Benne, J.A., Beaton, B.P., Spate, L.D., Murphy, S.L., et al., 2014. Use of the CRISPR/Cas9 system to produce genetically engineered pigs from in vitro-derived oocytes and embryos. Biol. Reprod. 91, 78.

Whyte, J., Laughlin, M.H., 2010. Placentation in the pig visualized by eGFP fluorescence in eNOS over-expressing cloned transgenic swine. Mol. Reprod. Dev. 77, 565.

Whyte, J.J., Prather, R.S., 2011. Genetic modifications of pigs for medicine and agriculture. Mol. Reprod. Dev. 78, 879–891.

Whyte, J.J., Zhao, J., Wells, K.D., Samuel, M.S., Whitworth, K.M., Walters, E.M., et al., 2011a. Gene targeting with zinc finger nucleases to produce cloned eGFP knockout pigs. Mol. Reprod. Dev. 78, 2.

Whyte, J.J., Samuel, M., Mahan, E., Padilla, J., Simmons, G.H., Arce-Esquivel, A.A., et al., 2011b. Vascular endothelium-specific overexpression of human catalase in cloned pigs. Transgenic Res. 20, 989–1001.

Wolf, E., Braun-Reichhart, C., Streckel, E., Renner, S., 2014. Genetically engineered pig models for diabetes research. Transgenic Res. 23, 27–38.

Wu, Q., Xiong, P., Liu, J.Y., Feng, S.T., Gong, F.L., Chen, S., 2004. The study of new SLA classical molecules in inbreeding Chinese Wuzhishan pig. Transplant Proc. 36, 2483–2484.

Yamakawa, H., Nagai, T., Harasawa, R., Yamagami, T., Takahashi, J., Ishikawa, K., et al., 1999. Production of transgenic pig carrying MMTV/v-Ha-*ras*. J. Reprod. Dev. 45, 111–118.

Yang, D., Wang, C.E., Zhao, B., Li, W., Ouyang, Z., Liu, Z., et al., 2010. Expression of Huntington's disease protein results in apoptotic neurons in the brains of cloned transgenic pigs. Hum. Mol. Genet. 19, 3983–3994.

Yang, D., Yang, H., Li, W., Zhao, B., Ouyang, Z., Liu, Z., et al., 2011. Generation of PPARgamma mono-allelic knockout pigs via zinc-finger nucleases and nuclear transfer cloning. Cell Res. 21, 979–982.

Yang, H., Wang, G., Sun, H., Shu, R., Liu, T., Wang, C.E., et al., 2014. Species-dependent neuropathology in transgenic SOD1 pigs. Cell Res. 24, 464–481.

Yang, G., Artiaga, B.L., Hackmann, T.J., Samuel, M.S., Walters, E.M., Salek-Ardakani, S., et al., 2015. Targeted disruption of CD1d prevents NKT cell development in pigs. Mamm. Genome 26, 264–270.

Yao, J., Huang, J., Hai, T., Wang, X., Qin, G., Zhang, H., et al., 2014. Efficient bi-allelic gene knockout and site-specific knock-in mediated by TALENs in pigs. Sci. Rep. 4, 6926.

Ye, J., He, J., Li, Q., Feng, Y., Bai, X., Chen, X., et al., 2013. Generation of c-Myc transgenic pigs for autosomal dominant polycystic kidney disease. Transgenic Res. 22, 1231–1239.

Yu, P., Zhang, L., Li, S., Li, Y., Cheng, J., Lu, Y., et al., 2004. Screening and analysis of porcine endogenous retrovirus in Chinese Banna minipig inbred line. Transplant Proc. 36, 2485–2487.

Zhou, X., Xin, J., Fan, N., Zou, Q., Huang, J., Ouyang, Z., et al., 2015. Generation of CRISPR/Cas9-mediated gene-targeted pigs via somatic cell nuclear transfer. Cell. Mol. Life Sci. 72, 1175–1184.

Page left intentionally blank

Genetically Modified Animal Models

Lucas M. Chaible, Denise Kinoshita**, Marcus A. Finzi Corat[†],
Maria L. Zaidan Dagli[‡]*

*Meyerhofstr, Heidelberg, Germany
**Ibirapuera University, Interlagos, São Paulo, Brazil
[†]University of Campinas, Campinas, São Paulo, Brazil
[‡]School of Veterinary Medicine and Animal Science, University of São Paulo, São Paulo, Brazil

1 INTRODUCTION

Science has advanced through observation and experimentation. So has the evolution of biotechnology. The emergence of animal models through genetic manipulation has greatly helped the development of scientific and biomedical knowledge. To speak of genetically modified animals is to focus on very important chapters in the history of the science of laboratory animals, in which the function of genes was first identified in living individuals. Based on this knowledge, new ideas for treatment of genetic diseases and other diseases have emerged; these tend to revolutionize classic medicine, bringing benefits not only to man, but to all living things. Here we give a brief history of biotechnology and the production of genetically modified animals, as well as the types of

Chromosomal location of mouse genes associated with human disease
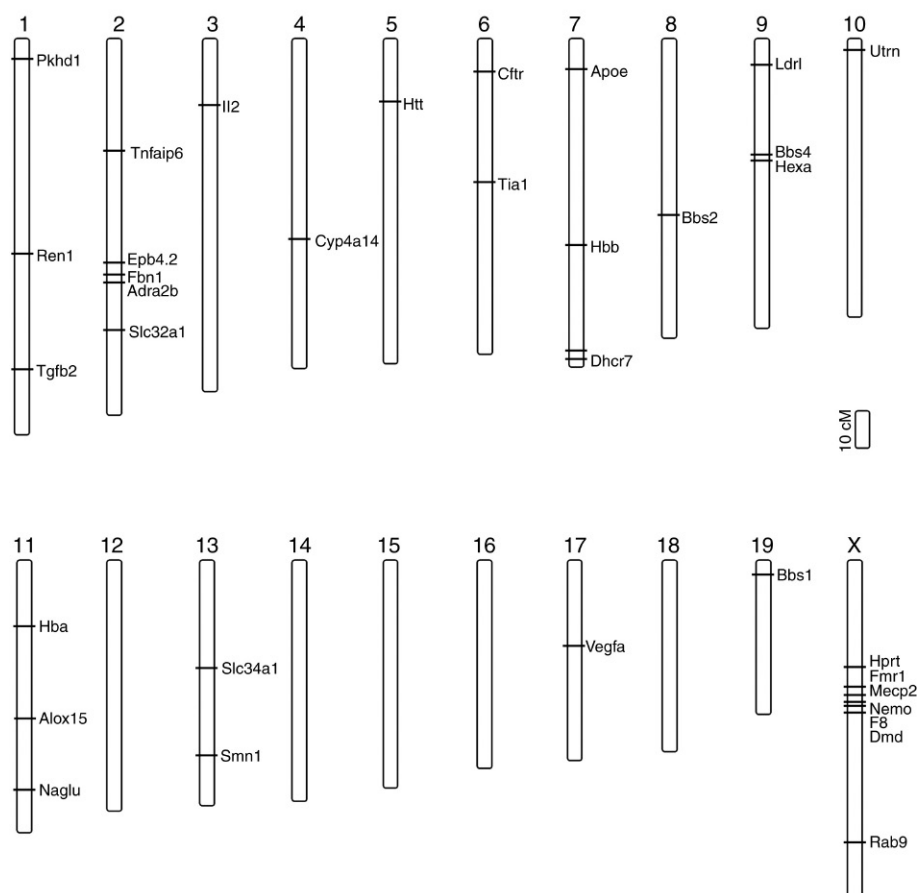
FIGURE 27.1　**Illustration of mouse chromosomes showing some genes location.** The genes cited in image are associated with human diseases and were used to produce transgenic models. The distance of genes are proportional and indicated a probability of recombination during meiosis. Scale 10 cM.

animals that can be created, and findings derived from recombinant DNA technology, gene targeting and, more recently, gene editing.

2 SOME HISTORICAL ASPECTS

After more than 150 years of research, science has progressed from uncovering the principles of heredity to mimicking biological events in the laboratory. This information has provided significant advances in medicine over the last century, creating a new branch of industry, the billion-dollar biotechnology industry. Since the initial genetic studies of Gregor Mendel in 1865, numerous researchers have contributed to the understanding and consolidation of his idea, which until then was only promising. In the last century, important events took place, such as the discovery of the relationship of DNA with the transmission of genetic traits, the characterization of its chemical structure and of its

three-dimensional structure, methodology to produce recombinant DNA, DNA cloning, and sequencing, new animal models with random and, later, directed mutations, allowing the production of the first transgenic mice (Fig. 27.1)

3 TECHNIQUES FOR THE CREATION OF GENETICALLY MODIFIED ANIMALS

3.1 Techniques Based on Recombinant DNA

In order to create embryos in which the genome is permanently altered and the transfected DNA is permanently and irreversibly incorporated into the genetic material of the host cells, there are at least three important steps to be surmounted:

1. to produce an in vitro gene construct that is functional in accordance with the hypothesis of the proposed study.
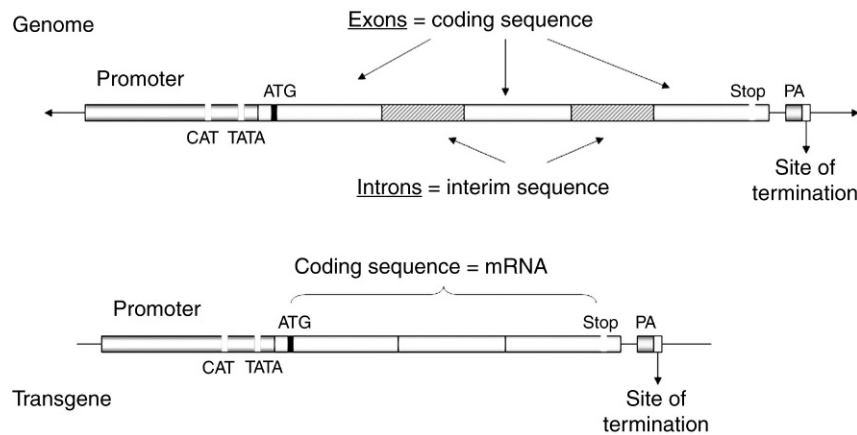
FIGURE 27.2   **Design of basic transgenic vector carrying a single interest gene.** The interest gene has not introns to facilitate the transcription process and must have important sequences like a promoter to drive gene expression, a start and stop codon and a polyA signal called site of termination.

2. to cause the required DNA to cross the plasma membrane, the cytoplasm and reach the nucleus.
3. to make the exogenous DNA integrate into the genome of the host cell and to be transmitted to the following generations.

3.1.1 Gene Construct

A gene construct can vary in complexity according to the approach and the insertion of interest. The construct can be inserted randomly into the genome of the animal, which is called transgenesis by addition, or can be inserted into the genome at a specific targeted site, into the correct position of a determined chromosome, which is called transgenesis by homologous recombination. In both cases, the construct must be impeccable, with structures to control gene expression, such as: a promoter, a site of transcription initiation, a site of polyadenylation, a site of transcription termination, and accessories regions, for example, Intronic regions, UTR sites, tags, and polyadenylation sequence.

That means that the information that is being inserted into the receptor genome has a beginning, middle, and end, thus avoiding problems of uncontrolled expression in the host cell. In order to accomplish the objectives of the proposed genetic modification studies, a large variety of machinery is available today to control the expression of transgenes in a ubiquitous or conditional manner (Fig. 27.2).

3.1.2 Insertion of the DNA of Interest Into Cells

A variety of strategies can be used to cause exogenous DNA to penetrate the host cell.

3.1.2.1 MICROINJECTION

This is the most widely used method in transgenesis for gene addition. In this method, the DNA in solution is physically injected into the cell nucleus. This method is considered efficient to carry the DNA into the nucleus of somatic cells, but it has some disadvantages; it requires specialized equipment and highly skilled individuals, trained to perform the microinjection. This technique is widely used for insertion of gene vectors into fertilized oocytes, and it has a success rate of 4%–8% of animals born with the transgene integrated into the genome (Capecchi, 1980) (Fig. 27.3).

3.1.3 Integration

Integration of exogenic DNA into the host genome occurs with extremely low efficiency. It is believed that the integration of exogenic DNA into the genome of the host cell occurs during the mitosis, as a consequence of errors made when the DNA repair machinery of the host cell accidentally incorporates the exogenous molecule in an attempt to repair breaks in the double-stranded DNA that occasionally occur in cells (Capecchi, 1980). Due to the random nature of DNA breakage, integration of
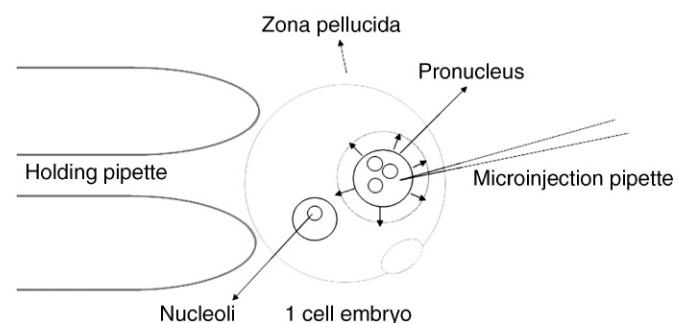
FIGURE 27.3   **Microinjection is a process of using a glass micropipette to insert DNA into egg cell.** It is a simple mechanical process in which a needle roughly 0.5–5 µm in diameter penetrates the cell membrane. The DNA content is injected inside pronucleus and the needle is removed.

transfected DNA typically also occurs in random locations in the genome. Incorporated exogenous DNA could potentially disrupt, prevent or impede the expression of a gene of the host, although this probability is also rare.

3.2 Double-Strand Break as a Genome Editing Tool to Generate Genetically Modified Animals

Although the genome editing by DNA homologous recombination employed in embryonic stem cell has been feasible in mice, recent reports found that the double strand break (DSB), caused by endonucleases, is a powerful strategy to accomplish and boost genome engineering and generate genetically modified animals more efficiently (Carbery et al., 2010; Geurts et al., 2009; Li et al., 2014; Shen et al., 2013; Sung et al., 2013; Tesson et al., 2011; Wang et al., 2013; Yang et al., 2013). Genome editing methodologies, that target the genome in a sequence-specific site and generate DSBs, have arisen and improved in the last decade. The DSBs activate the endogenous DNA repair machinery, resulting in either nonhomologous end joining (NHEJ) characterized by recombination mediating insertions, deletions and mutations (indels), or homology directed repair (HDR) with replacement of the genomic sequence with donor DNA carrying homology arms to broken DNA sequence, that introduces or corrects mutation into genome (Fig. 27.4). The production of genetically modified mice and rats has been greatly accelerated by novel approaches using direct injection of DNA or mRNA of site-specific nucleases into the one-cell-stage embryo, generating DNA double-strand breaks (DSB) at specified sequences leading to targeted mutations (Carbery et al., 2010; Geurts et al., 2009; Li et al., 2014; Shen et al., 2013; Sung et al., 2013; Tesson et al., 2011; Wang et al., 2013).

Methodologies that combine a sequence-specific DNA binding domain with engineered FokI endonuclease in a single molecule; as zinc finger nucleases (ZFN) or as transcription activator-like effector nuclease (TALEN); were the first approaches that allowed gene editing by DSBs. Those techniques, besides showing good results in generating knockout animals, have a limited use, since the generation of the ZFN, in special, is quite expensive and with huge effort in troubleshooting during the vector design. The real propagation of gene editing occurred in 2012 in the first reporter regarding the clustered regulatory interspaced short palindromic repeats (CRISPR) associated with the nuclease Cas9 (Jinek et al., 2012) and in January of 2013 it was reported for the first time a successfully adaptation of CRISPR-Cas9 for genome editing in eukaryotic cells (Cong et al., 2013). Basically, the system designed by Jennifer Doudna and Emmanuelle Charpentier in 2012 (Jinek et al., 2012) consists in a gRNA (guide-RNA) and the tracrRNA that can be fused together to create a single, synthetic guide, which drives

the nuclease Cas9 into a specific site of action. The system will be described in details ahead.

All these techniques have shown a potential to generate knockout and knockin animals, not only mice, but also others as rats, pigs, fishes and monkey (Geurts et al., 2009; Li et al., 2014; Liu et al., 2014; Niu et al., 2014; Sung et al., 2013; Wang et al., 2013). The DSBs approaches may be launched by microinjection of the complete system (DNA, RNA, or protein) into the one cell embryo or embryonic stem cells, and generate transgenic models efficiently (Fig. 27.4).

3.3 ZFNs

Zinc finger protein (ZFP) is a common DNA binding domain found in many transcription factors. It consists of ~30 amino acids that may recognize three base pairs of DNA. Combining 3–6 ZFP in a molecule, it can recognize and bind to a specific DNA into the genome. The ZFN approach mix the features of ZFP specificity and add to this molecule a modified restriction enzyme FokI, with endonuclease feature; that is, as much the ZFP bind the specific region of DNA the FokI cleaves one strain of this DNA. To get the complete DSB is necessary two ZFNs design close to each other as exemplified in Fig. 27.4. Its use is not spread due to complex design and the high cost to develop the vectors, but is considered the best choice in gene therapy in animals and humans, since this methodology has low off-target rate.

3.4 TALENs

Similar to ZFNs, TALEN uses DNA biding motifs to get specific region of DNA to cut by FokI. The binding motifs are made with repeat domains named transcription activator-like effectors (TALEs), each domain presents 33–35 amino acids, and recognize one specific base pare. Hence it combines ~18 repeats and FokI endonuclease we may cut one strain of the specific region at the genomic DNA, addressed by the TALEs combination. TALENs also need to be applied with two designs to get DSBs. (Fig. 27.4). Genetically modified mice (Sung et al., 2013) and rats (Tesson et al., 2011) were created by this technique.

3.5 CRISPR/Cas9

Clustered regularly interspaced short palindromic repeats (CRISPR)/CRISPR-associated (Cas) adaptive immune systems are found in bacteria and other microorganisms, and their function is to protect the hosts against the invasion of viruses and plasmids. They were described by Jinek et al. (2012). Three types (I-III) of CRISPR systems with different features have been identified. The CRISPR-associated protein Cas9, that belongs
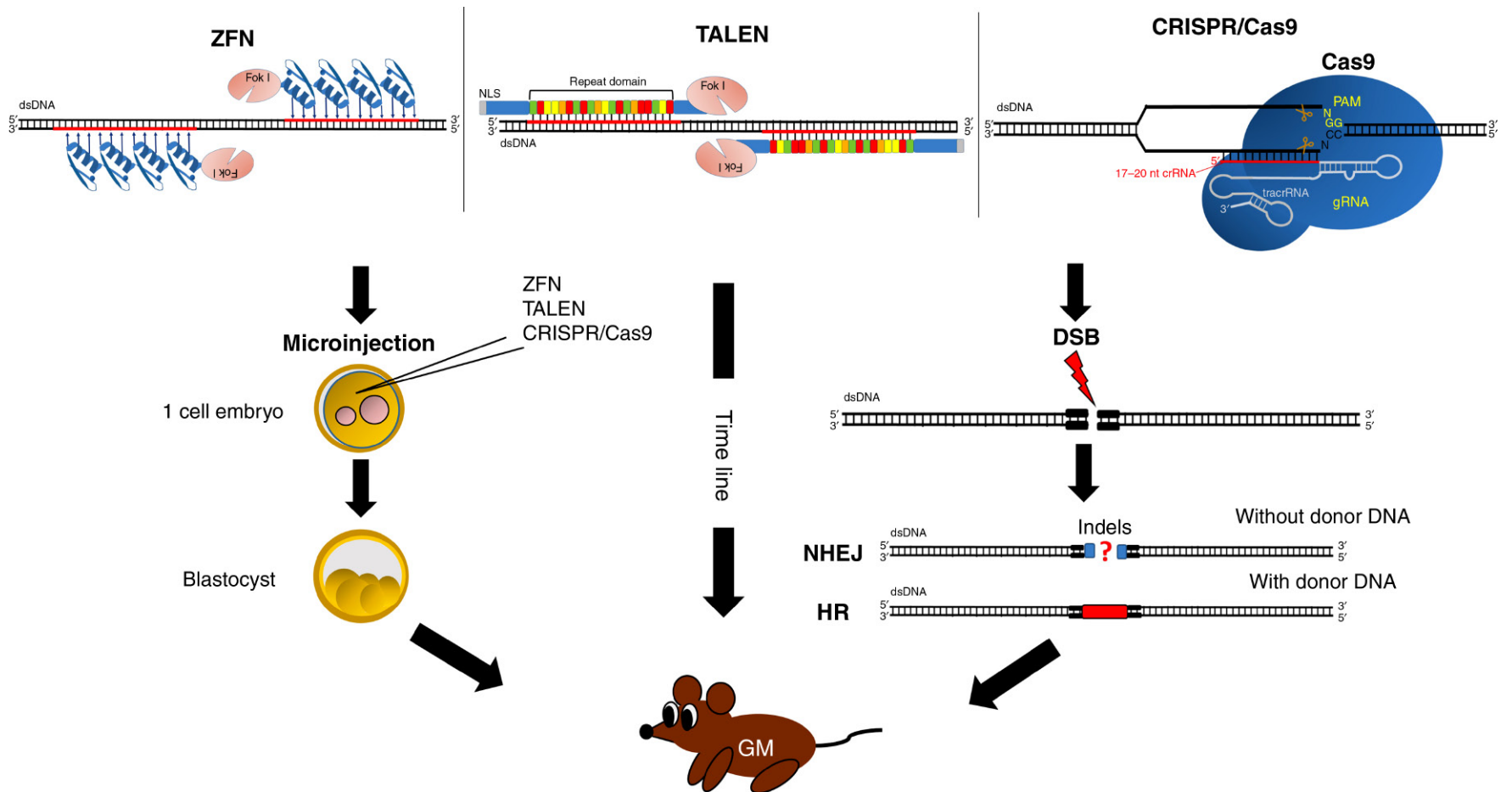
FIGURE 27.4 Genome editing techniques for generation of genetically modified animals.

to the type II CRISPR/Cas system, has attracted much attention due to its potential use in genomic engineering. This is the most recent and exciting system for genome editing to date. That is because of the easy design and specificity for DSB with only one guide. The Cas9 from *Streptococcus pyogenes* is the most widely used endonuclease used to CRISPR/Cas9 system. It consists of endonuclease Cas9 and a single guide RNA (gRNA) that is a chimera of tracrRNA; that is, *trans*-encoded RNA interacts with Cas9 protein, and crRNA; that is, RNA that specifies the region for cut. The guide RNA complexed with Cas9 targets a specific DNA sequence, and generates DSBs in the genomic DNA.

The gRNA, which drives the Cas9 to the region of cut, has around 20 nucleotides and, as a PCR primer, it must have a unique homology region. One very important characteristic during the gRNA design is the identification of the protospacer adjacent motif (PAM). The gRNA must be designed immediately upstream of this region (PAM), in the complementary strand of PAM site. This site will provide a binding site for the nuclease, for the Cas9 the PAM is the NGG sequence; it is absolutely necessary for the Cas9 activity and must not be included in the gRNA design. The DSB will occur 3 nucleotides upstream of the PAM (Garneau et al., 2010).

That is the newest technology and many improvements have been proposed to allow different features of Cas9 activity. Different Cas9 were designed to cut in just one strain as "nickase" Cas9 and dCas9 (nuclease-deficient Cas9), which is catalytically inactive. Because of dCas9 features of specific-sequence binding in genome and no cut it has been used for different propose as combining the dCas9 with some activator or repressor targeting to a promoter region in the genome then promoting gene activation or gene repression respectively (Shalem et al., 2015), or also can be associated with the FokI nuclease providing more specificity of the DSB, and decreasing the number of off-targets. Multiplex genome engineering with multiple guide RNAs has been tested to successfully target more than one region in the genome (Cong et al., 2013; Kabadi et al., 2014; Sakuma et al., 2014). Other origins of Cas9 and others groups of endonuclease has been tested and advances in this field is coming up quickly to next generation.

3.6 Knockout Mouse Lines Created by CRISPR/Cas9 Technique

Shen et al. (2013) created the first knockout animals with CRISPR/Cas9 genome editing technique. Firstly, they modified a zebrafish, and then a mouse line. Initially, the authors used the Pouf5-IRES-EGFP knockin mouse line, that carries one copy of the *EGFP* gene incorporated into the mouse genome. Twenty nanograms per microliter of NLS-flag-linker-Cas9 mRNA and 20 ng/µL preannealed EGFP-A chimeric RNA were coinjected into one-cell mouse embryos obtained from the crosses between male homozygous Pouf5-IRES-EGFP knockin mice and superovulated C57BL/6J female mice. The Pouf5-IRES-EGFP male mice were homozygous for the knockin gene, and then they were genotyped as heterozygous, as indicated by PCR amplification of a knockin fragment using genomic DNA extracted from the tails of the founders 5 days after birth. Their findings demonstrated that Cas9/RNA could site-specifically cut DNA in zebrafish and mouse embryos, "paving the way for its use in the generation of gene-disrupted animals".

Mou et al. (2015) described a series of CRISPR-generated animal models for the study of cancer and other chronic diseases (Mou et al., 2015). Among them, Xue et al. (2014) presented a CRISPR-mediated direct mutation of cancer genes in mouse liver (Xue et al., 2014).

Recently, Tu et al. (2015) proposed that CRISPR/Cas9 could be a powerful genetic engineering tool for creating animal models for neurodegenerative diseases. Among these animals, they propose that transgenic approach and CRISPR/Cas9 can be used to generate large animal models of diseases, such as nonhuman primate models.

3.7 Knockin Mouse Lines Created by CRISPR/Cas9 Technique

As the knockout animals, knockin animals can be generated using the CRISPR/Cas9 methodology. Taking advantage of DBS repair, we can drive the process of HDR to be used to generate specific nucleotide changes, changing from a single nucleotide to large insertions (e.g., addition of a fluorophore, tag, or gene replacement).

In order to drive the HDR for gene editing, a DNA repair template must be delivered at the same time of gRNA and Cas9 sequences directly into cell of interest, zygote, or ES cells. This template is called DNA donor, and can be used since single or double-stranded oligonucleotides or plasmids.

The traditional methodology of HDR was used during 20 years to produce knockout and knockin animals, however, the majority of those animal were mice models. However, the CRISPR/Cas9 approach provided a new tool, with good efficiency and low cost to create knockin in any species of interest. Yoshimi et al. (2016) showed the high efficiency to produce a rat model to KI-GFP-Rosa26 using ssODN coinjected with gRNA and Cas9 messenger RNA, the authors got 41.9% of positive animals (13 positives in 31 offspring).

4 TYPES OF GENETICALLY MODIFIED ANIMALS AND HOW THEY ARE PRODUCED

4.1 Transgenic Animals

Transgenic animals are those in which an exogenous gene was artificially inserted and stably incorporated into the genome of every cell of the organism and that can be transmitted to their descendants. The first transgenic mouse had the genome sequence of the Maloney leukemia virus inserted into its genome (Jaenisch, 1976). The best way to get all the cells that compose the organism to express the exogenous gene is to insert it into cells that give rise to other cell types, that is, the fertilized egg cell. In simple terms, the creation of transgenic animals begins with proper construction of the gene of interest and its transfection to the fertilized egg cell.

In most mammals, the exogenous DNA is inserted by pronuclear microinjection. In mice, the most commonly used model, the frequency with which the exogenous DNA is incorporated into the genome is satisfactory in the case of the egg cell, a totipotent cell with a high capacity for cell division. Certain strains possess egg cells with larger pronuclei, providing a greater ease of microinjection. An example is the use of oocytes derived from FVB animals.

The animal generated from this egg cell, known as a transgenic founder, is heterozygous for the transgene, that is, one of the chromosomes has incorporated the transgenic DNA, but not the homologous chromosome. Consequently, only half of the animals obtained from the F1 mating will also be heterozygous. Transgenic models have diverse functions in research, in which the inserted gene may have its effects evaluated in vivo during the developmental stages, as in the evolution of diseases, in studies of mutations, in the search for therapies, and other parameters that necessitate an animal model for study. Industrially, the transgenic model can be used to obtain commercial productivity characteristics, and disease resistance, and can be used as a bioreactor in the production of biopharmaceuticals.

4.2 Knockout Animals

The great contribution of these models was in the study of gene function through the phenotype presented due to the effect of allelic deletion. Until very recently, the only way to do this was to look for animals or humans suffering from hereditary diseases. In the case of animals, the incidence of such diseases could be increased by using mutagenic chemicals or irradiation, then the location of the mutation was mapped and the defective gene cloned. Unlike the transgenic model produced by the addition of random exogenous DNA, the knockout model is obtained by targeted insertion. This targeted integration is performed through the mechanism of homologous recombination and has an extremely low success rate (Gama Sosa et al., 2010).

Homologous recombination is a separate chapter in the methodology for obtaining knockout animals. This technique allows the insertion of a determined transgene into a specific locus, causing it to locate exactly in the desired portion of the chromosome. The most common way to delete exons is through the creation of a targeted construct, also called "targeted". In this case, the plasmid must contain a homologous portion of the start of the gene, known as "left arm" and a portion obtained along the gene, or even the final portion, called the "right arm" (Capecchi, 1980). Between these portions, an exon must be situated that is important for the functionality of the protein.

These homologous regions will pair with the corresponding sequences in the gene of interest. The longer the arms, the greater probability that pairing will occur. In practice, the combined length of both arms is between 6 and 10 kb (Joyner and Sedivy, 2000). As a result of this pairing and a double recombination, one in each arm, the original gene, or "wild type" is replaced by the transgene contained between the two arms of the construct. The gene sequence to be introduced may contain another gene, usually a reference sequence of a positive selection gene, thus generating substitution of expression of the original gene for NeoR.

Due to the low efficiency of the occurrence of two recombinations so close together, the strategy of performing this process in cell culture is used; but for these cells to give rise in the future to a complete organism they need to be pluripotent cells. The ideal cells are known as ES cells (embryonic stem) (Notarianni and Evans, 2006; Smithies et al., 1985). It was found that these cells called "germ lines" were perfectly suited for targeted insertion and could be identified through mechanisms of positive and negative selection. Currently, protocols for the cultivation and maintenance of these cells exist for only a few species (Grivennikov, 2008). ES cells can be transferred by micromanipulation into the interior of murine embryos at about 3–4 days of age, during the blastocyst preimplantation phase (Fig. 27.5).

4.3 Conditional Knockout Animals

Deletion of genes essential for development can result in embryonic lethality, due to lack of influence of this gene in the embryogenesis of the animal; thus mice die in the uterus, making it difficult to study events that occur after birth, and impossible to study the function of these genes in adult animals. Fortunately there are strategies, which are now becoming prevalent, to circumvent this problem, aiming to avoid problems with embryonic
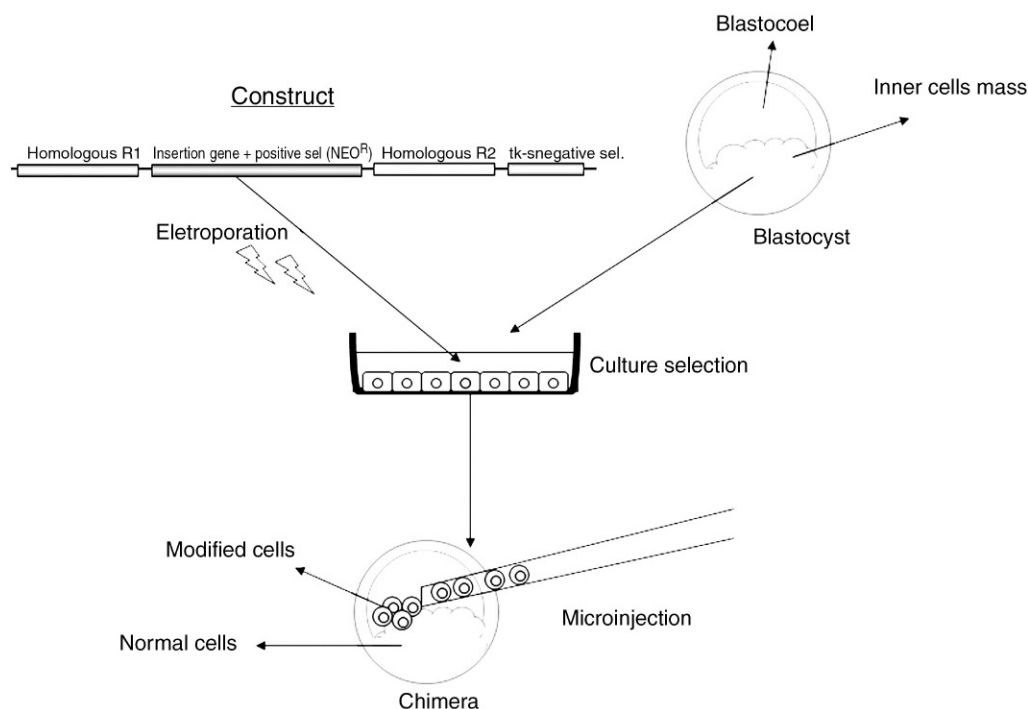
FIGURE 27.5 **Microinjection of ES Cells is a process of using a glass micropipette to insert embryonic stem cells transformed by transgenic vector, theses cells are selected and cultured in vitro and microinjected inside blastocyst.** After birth the animals are called chimeras and are selected by fenotype to more analysis and verification of germline.

lethality (Gama Sosa et al., 2010). One possible strategy is the use of the conditional deletion system, which involves gene deletion under specific conditions. The main strategy is known as the Cre-Lox system.

The Cre enzyme is a 38-kDa recombinase, present in the P1 bacteriophage, which mediates recombination of DNA regions flanked by sequences, such as loxP (Hamilton and Abremski, 1984). The loxP sequence has 34 bp with a defined orientation. When the loxP flanks are in consensus, the region contained between them is excised, leaving a single loxP sequence. When the flanking sites are in opposite positions, the Cre enzyme recombines the contained region, reversing it. That is, animals with a targeted insertion in the same position as the loxP flanks are obtained by means of homologous recombination in ES cells.

This insertion gene may be the same gene present in the locus, but now flanked by the loxP sequence. The situation that will permit its normally conditional expression is expression of Cre recombinase, which may be ubiquitous or conditioned to a determined organ or cell type, and eliminates the flanked gene. This Cre recombinase gene can be inherited from another transgenic animal and will allow conditional expression of this protein. This conditional control is based on the Cre enzyme, which may have its expression controlled through the promoter related to it. The promoter that regulates the expression of the Cre gene will control the pattern of deletion of the target gene. This promoter may be specific to cell types, the physiological state of the animal or inducible by drugs.

1. Cell-specific promoter. The regulatory region of the Cre gene is important in determining the cell or group of cells that express the recombinase. Using the aP2 promoter, it is possible to delete the gene of interest only in adipocytes, the αMHC promoter for deletion in cardiomyocytes, the ALB promoter for hepatic cells, the Nestin promoter for neurons, the K5 promoter for epithelial cells of the skin, the CD19 promoter for B lymphocytes, and the Cola1 promoter for osteoblasts.
2. Temporal promoters. Regulatory sequences that promote gene expression at specific periods or physiological states. The CaMKII promoter can be used for gene deletion in neurons only after birth.
3. Inducible promoters. Regulatory sequences that are activated or deactivated by exogenous molecules. The TET system of induction, based on the TET operon system of *Escherichia coli*, is the most widely used (Sun et al., 2007). With this strategy, the Cre enzyme can be expressed, and consequently delete the gene at a specific time according to the research objective. To accomplish this, tet-Cre animals are crossed with loxP animals, and after mating of homozygous flanked animals, tetracycline or its analogue, doxycycline, is administered, excising the gene of interest and obtaining the desired knockout at the targeted systemic site, at the determined time of development of the animal.

4.4 Knockin Animals

As described, these techniques are most frequently used to introduce genes into random locations (transgenics) or to delete specific portions of genes (targeted knockout). The same techniques can be used to introduce new genetic elements into specific sites, known as knock-in (Haruyama et al., 2009). One application of this technique is to study the expression of molecules, identifying cells that express and modulate expression, using reporter molecules for this. The most commonly used reporter is the enzyme β-galactosidase, which can be detected with a variety of colored substrates, and the "green fluorescent protein", also known as GFP (Welsh and Kay, 1997).

A very interesting technical use of knock-in is the insertion of a target gene into the locus of another gene, substituting it. Some genes belong to a large family, but the members display individual characteristics, which often preclude compensation. Zheng-Fischhöfer et al. (2006), in an attempt to avoid embryonic lethality in knockout animals for the Cx43 gene, substituted the loci deleted with the Cx31 gene, producing the knock-in animal Cx43[31/31]. The authors perceived that despite the relative gene homology, the restoration of cell communication via Cx31 was not sufficient for normal development of the heart, showing selectivity of size and electrical charge between proteins Cx43 and Cx31.

Some knockin models intending the introduction of the new gene, but avoiding any problem with gene disruption, and for this proposal, the transgene must be inserted in a safe harbor locus, the most famous locus is the ROSA26 also known as ROSAβgeo26. This locus in mice genome was first found in chromosome 6 in one particular strain of mice and expresses one coding transcript and two noncoding transcripts, but only the noncoding transcripts are disrupted by the insertion. After transgene insertion that causes no apparent adverse effects on fitness, and permits stable gene expression.

ROSA26-specific TALENs or CRISPR-Cas9 system can generate a DNA DSB in ROSA26 in mouse genome, stimulating natural DNA repair mechanism. In the presence of ROSA26 ORF knockin clones, homologous recombination HR happens and integrantes DNA fragment from ORF knockin clone into the safe harbor locus.

5 GENETICALLY MODIFIED MICE AS MODELS OF HUMAN DISEASES

5.1 Genetic Disorders

Genetic disorders are changes in the communication of genes inserted into a genetic background present in the genome of living organisms that may cause disease. Diseases caused by genetic disorders are generally very common in humans and major economic partner in our community. Therefore, the development of animal models that match these diseases, or that may help unravel its mysteries and possible treatments is a major challenge to the scientific community. The use of genetic modification by insertion of foreign genetic material into the genome of an animal is a methodology widely used today to accelerate the process of mutation of animals by directed way and so favor the accumulation of scientific knowledge about living organisms and its disorders.

The disorder is hereditary or not depends largely on the type of genetic change or mutation occurred and the behavior of this information. Some disorders are caused only by changes in a particular gene, called disorder autosomal or X-linked, when this is the affected chromosome. They can be either dominant or recessive according to their power of penetration of information generated from this disorder and thus showing very typical and obvious phenotypes. Other features may be more complex, polygenic traits, where alterations can generate phenotypes depending on the genetic background of the individual. That is, there may be a phenotypic variability according to genetic susceptibility and behavior of the individual, reacting to stimuli and responses often not fully understood and clarified.

Changes in particular gene makes autosomal much simpler to interfere or manipulate through directed genetic manipulation in a living organism. Thus, soon after the advent of transgenesis methodology in the 80s, in the beginning of 90s until the early turn of the century, there was a significant increase in the development of genetically modified animal models with genetic disorders caused by the change in a single gene, as can be seen in Table 27.1.

6 MULTIFACTORIAL AND POLYGENIC (COMPLEX) DISORDERS

In general, the multifactorial disorders, as hypertension, diabetes, autoimmune diseases, heart failure, obesity among others, are more difficult to obtain genetically engineered animal models, once the phenotypes are produced by a large number of genes and so they are often not totally clear which. Therefore, it may happen the features of genetically modified animal models that are showed their phenotypes with some characteristics for complex diseases and may therefore to be utilized as this disease model, although not specific to a given disease, sometimes the models worth to better understand the disorder and much of the times it is not totally similar to human disorders. However, there are models that contribute to disorder clarifying.

Typically, because of its particular characteristics, models of complex diseases are best produced by spon-

TABLE 27.1　Genetically Modified Animal Models With Genetic Disorders

Human disease	Gene symbol	Model	Phenotype	References
Autossomal Dominant				
Familial hypercholesterolemia	*Ldlr*	B6; 129S7-*Ldlr*^{tm1Her}	*Increased circulating cholesterol level*	Ishibashi et al. (1993a)
Polycystic kidney disease	*Pkhd1*	B6.129S6-*Pkhd1*^{tm1Cjwa}	*Progressive fibrocystic liver disease and cystic dilation of the kidney*	Woollard et al. (2007)
Hereditary spherocytosis	*Epb4.2*	B6.129P2-*Epb4.2*^{tm1Llp}	*Abnormal erythrocyte morphology, decreased erythrocyte cell number*	Peters et al. (1999)
Marfan syndrome	*Fbn1*	B6.129-*Fbn1*^{tm1Hcd}	*Abnormal heart morphology, abnormal skeleton morphology*	Judge et al. (2004)
Huntington's disease	*Htt*	B6.129-*Htt*^{tm5Mem}	*Abnormal striatum and cerebral cortex morphology, abnormal behavior*	Wheeler et al. (1999)
Peters anomaly	*Tgfb2*	STOCK *Tgfb2*^{tm1Doe}	*Wide range of developmental defects including cardiac, lung, craniofacial, limb, spinal column, eye, inner, and urogenital defects*	Sanford et al. (1997)
Autossomal Recessive				
Sickle cell anemia	*Hba, Hbb*	STOCK *Hba*^{tm1Paz} *Hbb*^{tm1Tow} Tg(HBA-HBBs)41Paz	*Irreversibly sickled red blood cells, anemia, and multiorgan pathology*	Paszty et al. (1997)
Cystic fibrosis	*Cftr*	B6.129P2-*Cftr*^{tm1Unc}	*Abnormal pancreatic acinus and intestine morphology, abnormal respiratory system physiology*	Snouwaert et al. (1992)
Tay-Sachs disease	*Hexa*	B6;129S4-*Hexa*^{tm1Rlp}	*Abnormal brain and neuron morphology*	Yamanaka et al. (1994)
Mucopolysaccharidoses	*Naglu*	B6.129S6-*Naglu*^{tm1Efn}	*Abnormal locomotor behavior, abnormal nervous system, accumulation of heparan sulfate*	Gografe et al. (2003)
Spinal muscular atrophy	*Smn1*	FVB.Cg-Tg(SMN2)2Hung *Smn1*^{tm1Hung}	*Abnormal skeletal muscle fiber and Motor neuron morphology*	Hsieh-Li et al. (2000)
Smith-Lemli-Opitz syndrome	*Dhcr7*	B6.129P2(Cg)-*Dhcr7*^{tm1Gst}	*Lack of spontaneous movement in newborns, fetal growth retardation, abnormal cholesterol homeostasis.*	Fitzky et al. (2001)
Hypophosphatemic rickets	*Slc34a1*	B6.129S2-*Slc34a1*^{tm1Hten}	*Hypophosphatemia, hypercalcemia*	Beck et al. (1998)
X-Linked dominant				
Rett syndrome	*Mecp2*	B6.129P2(C)-*Mecp2*^{tm1.1Bird}	*Weight loss, shivering, continued mobility problems*	Guy et al. (2001)
Incontinentia pigmenti	*Nemo*	—	*Develop patchy skin lesions with massive granulocyte infiltration and hyperproliferation and increased apoptosis of keratinocytes*	Schmidt-Supprian et al. (2000)
Fragile X mental retardation syndrome	*Fmr1*	FVB; 129P-*Fmr1*^{tm1Cgr}	*Audiogenic seizures, hyperactivity, decreased startle reflex*	Bakker et al. (1994)
X-Linked recessive				
Lesch–Nyhan syndrome	*Hprt*	B6; 129-*Hprt*^{tm1Detl}	*Abnormal motor capabilities/coordination/ movement*	Ordway et al. (1997); Grady et al. (1997b)
Duchenne muscular dystrophy	*Dmd, Utrn*	STOCK *Utrn*^{tm1Jrs} *Dmd*^{mdx}	*Exhibit skeletal muscle dystrophy, skeletal muscle degeneration, necrosis and interstitial fibrosis*	Grady et al. (1997a)
Hemophilia	*F8*	B6; 129S-*F8*^{tm1Kaz}	*Deficient of endogenous Factor 8, abnormal blood coagulation*	Bi et al. (1995)
Nielmann-Pick disease	*Rab9*	STOCK Tg(CAG-RAB9A)500Repa	*RAB9 expression is approximately 30-fold higher than endogenous protein in the liver*	Kaptzan et al. (2009)

TABLE 27.2   Genetically Modified Animal Models for the Study of Protein Signaling Disorders

Human disease	Gene symbol	Model	Phenotype	References
Cleft palate	*Slc32a1*	B6.129X1(Cg)-*Slc32a1*$^{tm1.1Bgc}$	*Cleft secondary palate*	Oh et al. (2010)
Hypertension (hormonal matters)	*Cyp4a14*	129S-*Cyp4a14*^{tm1Jhc}	*Abnormal renal vascular resistance, increased systemic arterial blood pressure*	Holla et al. (2001)
Hypertension	*Ren1*	129S/SvEv-Tg(Alb1-Ren2)2Unc	*Increased systemic arterial blood pressure, cardiac hypertrophy*	Caron et al. (2002)
Hypertension	*Adra2b*	FVB-Tg(PDGFB-Adra2b)13Hag	*Increased systemic arterial systolic blood pressure*	Kintsurashvili et al. (2009)
Bardet-Biedl Syndrome	*Bbs1*	129S.129-*Bbs1*^{tm1Vcs}	*Photoreceptor degeneration, severe obesity, hyperphagia and are hyperleptinemic with reduced locomotor activity*	Davis et al. (2007)
Bardet-Biedl Syndrome	*Bbs2*	129S.129-*Bbs2*^{tm1Vcs}	*Obesity, decreased startle reflex, disorganized photoreceptor*	Nishimura et al. (2004)
Bardet-Biedl Syndrome	*Bbs4*	129S.129-*Bbs4*^{tm1Vcs}	*Obesity, retinal degeneration, hyporesponsive to tactile stimuli*	Mykytyn et al. (2004)
Infertility	*Hspa2*	B6.129P2-*Hspa2*^{tm1Dix}	*Male infertile, reduced number of postmeitotic spermatids*	Dix et al. (1996)
Infertility	*Tnfaip6*	C.129S6-*Tnfaip6*^{tm1Cful}	*Female infertility, absent cumulus expansion, decreased ovulation rate*	Fulop et al. (2003)

taneous mutation, by induction by physical or chemical mutagenic agents, as well as for genome rearrangement among different inbred strains with possible genetic trait control. Some phenotype products of genetically modified models for complex diseases may be unintended consequences for the model, except those that have a well established signaling pathway, which modification of an involved gene can cause a rupture in a cascade of signaling proteins and cause disease. This is exemplified in Table 27.2 for Bardet–Biedl syndrome.

7 INFLAMMATORY DISEASES

Inflammatory diseases with genetic susceptibility are not very uncommon in humanity, as well as autoimmune diseases, rheumatoid arthritis, atherosclerosis, colitis, dermatitis, among others. They are mostly complex and multifactorial diseases that often depend on genetic susceptibility linked to individual behavior to their development. All these factors make the development of genetically modified animal models difficult to be constructed through the use of manipulation of specific genes. Even why, many diseases are not yet fully understood and known causes.

Many models are generated from spontaneous and induced mutations in addition to handling the environmental stress and diet to induce inflammations, always considering the animal's susceptible genetic backgrounds. Table 27.3 shows some models of genetically engineered animals that have been bred to develop

similar phenotypes to human inflammatory diseases, in order to allow interventions to treat these disorders and facilitate their understanding.

8 NEURODEGENERATIVE DISEASES

Neurodegenerative diseases are chronic, progressive disorders, with variable symptoms and outcomes. Clinical signs are usually related to the topography of the lesions, which usually involve neuronal degeneration and loss of function. Although the most common forms of these diseases are sporadic (with the exception of Huntington's disease), development of genetically modified animal models are mainly based on inherited, familial forms (Gama Sosa et al., 2012; Harvey et al., 2011; Van Den Bosch, 2011). Sporadic and familial forms do not share the same causes, but pathogenesis and neurodegenerative process are very similar in both forms (Gama Sosa et al., 2012; Selkoe, 2001). Therefore, animal models based on deletion or overexpression of genes linked to familial forms are important tools for the research of neurodegenerative diseases (Table 27.4).

Most used genetically modified mouse models of Alzheimer's disease (AD) (Duyckaerts et al., 2008; Gurney, 2000; Hall and Roberson, 2012; Hock and Lamb, 2001; Kokjohn and Roher, 2009; Price et al., 1998; Theuring et al., 1997; Wisniewski and Sigurdsson, 2010) Parkinson's disease (PD) (Bezard and Przedborski, 2011; Chesselet, 2008; Dawson et al., 2010; Dehay and Bezard, 2011; Gupta et al., 2008; Hall and Roberson, 2012;

TABLE 27.3   Genetically Modified Animal Models for Human Inflammatory Diseases

Human disease	Gene symbol	Model	Phenotype	References
Asthma	*Tbx21*	B6.129S6-*Tbx21*^{tm1Glm}	*Abnormal CD4-positive T cell differentiation*	Finotto et al. (2002)
Asthma, allergic inflammation	*F2rl1*	B6.Cg-F2rl1^{tm1Mslb}	*Decreased inflammatory response*	Schmidlin et al. (2002)
Multiple sclerosis	*Prf1*	C57BL/6-*Prf1*^{tm1Sdz}	*CNS inflammation, demyelization*	Kagi et al. (1994)
Systemic lupus erythematosus	*C3, Man2a1*	B6;129-C3^{tm1Crr} Man2a1^{tm1Jxm}	*Rise in antinuclear antibody (ANA) titers, abnormal hematology characterized as dyserythropoietic anemia, and nephritis.*	Green et al. (2007)
Arthritis	*Tia1*	B6.129S2(C)-*Tia1*^{tm1Andp}	*Develop mild arthritis and are more susceptible to endotoxin shock*	Piecyk et al. (2000)
Psoriasis	*Vegfa*	FVB-Tg(KRT14-Vegfa)3Dtm	*Develop severe psoriasis-like lesions*	Detmar et al. (1998)
Atherosclerosis	*Alox15*	C57BL/6J-Tg(Alox15)41FChed	*Atherosclerosis, develop spontaneous aortic fatty streak lesions*	Reilly et al. (2004)
Diabetes, atherosclerosis	*Apoe, Ins2*	B6.Cg-*Apoe*^{tm1Unc} Ins2^{Akita}	*Atherosclerosis, hypercholesterolemia, hyperglycemia*	Piedrahita et al. (1992); Mathews et al. (2002)
Diabetes, atherosclerosis	*Ldlr, Lep*	B6.Cg-Lep^{ob} Ldlr^{tm1Her}	*Atherosclerosis, hypercholesterolemia, hyperglycemia*	Ishibashi et al. (1993b); Ingalls et al. (1950)
Crohn's disease	*Tnf*	TNF(DeltaARE/+)^{tm}	*Development of chronic inflammatory arthritis and inflammatory bowel disease*	Kontoyiannis et al. (1999)
Ulcerative Colitis	*Il2*	C.129P2(B6)-*Il2*^{tm1Hor}	*Develop inflammatory bowel disease, intestinal ulcer*	Schorle et al. (1991)

Price et al., 1998; Selkoe, 2001; Theuring et al., 1997; Wisniewski and Sigurdsson, 2010), Huntington's disease (HD) (Gurney, 2000; Heng et al., 2008; Imarisio et al., 2008; Kumar et al., 2012; Price et al., 1998; Theuring et al., 1997) and amyotrophic lateral sclerosis (ALS) (Gurney, 2000; Harvey et al., 2011; Price et al., 1998; Selkoe, 2001; Theuring et al., 1997; Turner and Talbot, 2008; Van Den Bosch, 2011) are presented. The genes used in the development of the described mouse models, and the probable relevance of their encoded protein to the disease, are listed here:

1. AD:
   a. Amyloid precursor protein (APP) gene—AD1; amyloid-β (Aβ) precursor, the main constituent of amyloid plaques (Hall and Roberson, 2012; Harvey et al., 2011; Hock and Lamb, 2001).
   b. Presenilin 1 and 2 (PSEN1 and PSEN2) genes—AD3 and AD4; involved in APP processing and Aβ production (Hall and Roberson, 2012; Harvey et al., 2011; Hock and Lamb, 2001).
   c. Microtubule-associated protein tau gene—MAPT; main constituent of neurofibrillary tangles (Hall and Roberson, 2012; Harvey et al., 2011; Hock and Lamb, 2001)
2. PD:
   a. α-synuclein (α-syn) gene—PARK1 and PARK4; synaptic protein, main constituent of Lewy bodies (Blandini and Armentero, 2012; Harvey et al., 2011; Gupta et al., 2008).
   b. Parkin gene—PARK2; ubiquitin ligase activity (Hall and Roberson, 2012; Harvey et al., 2011; Hock and Lamb, 2001).
   c. DJ-1 gene—PARK7; anti oxidative-stress properties (Hall and Roberson, 2012; Harvey et al., 2011; Hock and Lamb, 2001).
   d. PTEN-induced kinase 1 (PINK1) gene—PARK6; antioxidative-stress properties, protection against mitochondrial dysfunction (Hall and Roberson, 2012; Harvey et al., 2011; Hock and Lamb, 2001).
   e. Ubiquitin carboxy-terminal hydrolase-L1 (UCH-L1) gene—PARK5; ubiquitin ligase activity (Harvey et al., 2011)
   f. Leucine-rich repeat kinase 2 (LRRK2) gene—PARK8; kinase and GTPase activity (Hall and Roberson, 2012; Harvey et al., 2011; Hock and Lamb, 2001).
3. HD:
   a. Huntingtin (htt) gene—IT15; expansions of GAC repeats lead to its aggregation in neuronal intranuclear inclusions. Mutations in htt are causative of HD (Games et al., 1995; Harvey et al., 2011; Hsiao et al., 1996).
4. ALS:
   a. Superoxide dismutase (SOD1) gene—ALS1; inactivates superoxide radicals (Harvey et al., 2011; Turner and Talbot, 2008; Van Den Bosch, 2011).

TABLE 27.4 Genetically Modified Animal Models for the Study of Neurodegenerative Diseases

Human disease	Gene symbol	Model	Phenotype	References
Alzheimer's disease	AD1	Tg(APPV717F)109Ili or PDAPP Background: not specified	Extracellular Aá deposits in hippocampus, corpus callosum and cerebral cortex (6-9 months). Cognitive deficits (6 months).	Games et al. (1995)
	AD1	Tg(APPSWE)2576Kha or Tg2576 Background: C57BL/6 x SJL	Aá deposits (9-11 months). Cognitive impairments and behavioral disorders (10 months).	Hsiao et al. (1996)
	AD1	Tg(Thy1-APP)3Somm or APP23 Background: C57BL/6 x DBA/2	Aá deposits in hippocampus and cortex, thalamus and olfactory nucleus (6 months). Cognitive deficits (3 months). Cerebrovascular amyloid. Subtle neuronal loss.	Sturchler-Pierrat et al. (1997)
	AD1	Tg(PRNP-APPSweInd)8Dwst or Tg CRND8 Background: C3H/ HeJx C57BL/6	Aá deposits in subiculum, frontal cortex, hippocampus, thalamus, striatum, and cerebral vasculature (3 months). Cognitive deficits (3 months).	Chishti et al. (2001)
		Tg(Thy1-AppDutch)#Jckr Background: C57BL/6	Congophilic amyloid angiopathy.	Herzig et al. (2004)
	PSEN1	Tg(PDGFB-PSEN1)1Jhd Background: SW x (C57BL/6 x DBA/2)	Enhanced Aá42 production.	Duff et al. (1996)
	AD1 and PSEN1	B6C3-Tg(APPswe, PSEN1dE9)85Dbo	Aá depostis (4-5 months). Behavioral alterations (6-7 months).	Jankowsky et al. (2001)
	AD1 and PSEN1	B6.Cg-Tg(APPSwFILon,PSEN1*M146L*L286V)6 799Vas	Accelerated Aá deposition: intracellular Aá42 (1.5 months), and Aá deposits starting at 2 months. Cognitive deficits (4 months). Neuronal loss.	Oakley et al. (2006)
	AD1, PSEN1 and MAPT	B6; 129-Psen1 tm 1 MpmTg(APPSwe, tauP301L)1Lfa	Intracellular Aá peptide accumulation (3-4 months). Aá extracellular deposits (at 6 months old). Neurofibrillary tangles (12 months). Cognitive deficits (starting at 4.5 months)	Oddo et al. (2003)
Parkinson's disease	PARK2	FVB/NJ-Tg(Slc6a3-PARK2*Q311X)AXwy	Progressive hypokinetic motor deficits. Reduction in striatal dopaminergic levels. Loss of dopaminergic neurons in substantia nigra.	Goldberg et al. (2005)
	PARK7	B6.Cg-Park7tm1Shn or DJ-1-	Mitochondrial dysfunction. Abnormal dopamine neurotransmission in nigrostriatal pathway.	Gispert et al. (2009)
	PARK6	B6;129-Pink1tm1Aub	Mitochondrial dysfunction. Weight loss. Impaired spontaneous locomotor activity. Dopamine reduction in striatum.	Setsuie et al. (2007)
	PARK5	Tg(PDGFB-UCHL1*I93M)HWada or H-hI93M Background: C57BL/6	Dopaminergic neuron reduction in substantia nigra. Dopamine reduction in striatum.	Li et al. (2007)
	PARK8	B6.Cg-Tg(Lrrk2*G2019S)2Yue	Dopamine levels reduction in striatum (12 months).	Li et al. (2009)
	PARK8	FVB/N-Tg(LRRK2*R1441G)135Cjli	Dopamine levels reduction in striatum. Progressive locomotor alterations, leading to immobility, which is responsive to levodopa and apomorphine treatment.	Mangiarini et al. (1996)

(*Continued*)

TABLE 27.4   Genetically Modified Animal Models for the Study of Neurodegenerative Diseases (*cont.*)

Human disease	Gene symbol	Model	Phenotype	References
Huntington's disease	IT15	B6CBA-Tg(HDexon1)62Gpb	Transgene is ubiquitously expressed. Behavioral deficits (5 weeks), choreiform-like movements, stereotypic movements, tremor, cognitive deficits (5 weeks), premature death (12-15 weeks). Decreased brain and striatal volume (12 weeks), loss of striatal neurons (12 weeks), reduced D1 and D2 receptors in striatum (8-12 weeks), Htt aggregates in c¢rtex, neostriatum and hippocampus. Widespread NIIs (12 weeks).	Slow et al. (2003)
	IT15	FVB-Tg(YAC128)53Hay	Motor abnormalities (starting from 3 months). Progressive behavioral and cognitive alterations. Striatal (9 months) and cortical atrophy (12 months) and subtle striatal neuronal loss (12 months). Httimmunoreactivity in striatal (2-3 months), cortical (3 months), hippocampal (3 months), cerebellar (3 months) neurons, spreading to many neurons (6 months). Normal striatal neurotransmitter expression.	Lin et al. (2001)
	IT5	B6.129P2-Htttm2Detl	Nuclear immunoreactivity for htt in striatum (27-29 weeks), NIIs in striatum (37 or 40 weeks; homozygotes and heterozygotes, respectively), locomotory abnormalities (70 or 100 weeks; homozygotes and heterozygotes, respectively), loss of D1 and D2 receptors in striatum (70 weeks).	Gurney et al. (1994)
Amyotrophic lateral sclerosis	ALS1	B6SJL-Tg(SOD1)2Gur	Motor neuron loss within spinal cord. Progressive hind limb weakness, leading to paralysis. Death (5-6 months).	Wong et al. (1995)
	ALS1	B6.Cg-Tg(SOD1*G37R)42Dpr	Motor neuron loss within spinal cord, Paralysis in one or more limbs.	Ripps et al. (1995)
	ALS1	FVB-Tg(Sod1*G86R)M1Jwg	Motor neuron degeneration within spinal cord, brain stem, and neocortex. Progressive decline of motor function (beginning at 3-4 months). Death (4 months)	Ripps et al. (1995)

9 CANCER

Despite the enormous numbers of studies involving cancer, it is still considered a challenging disease. One of the major challenges facing cancer research is the necessity to find suitable models to the human diseases. These needs include validating/determining the contribution of a gene to cancer, establishing systems for drug discovery and validation, and discovering factors that modify the oncogenic process.

A number of mouse strains that develop cancers spontaneously are available; in general they develop neoplastic diseases at late ages. Transplantable tumors of several types (melanomas, sarcomas, lymphomas, mammary carcinomas, and others) have been extensively used during the 20th century to answer specific questions in cancer research, including their susceptibility to antineoplastic new agents. Currently, the standard anticancer drug development pipeline uses xenograft and/or orthotopic implantation of human tumor cell lines in immunocompromised mice as the primary in vivo models for investigating drug candidate efficacy and mechanism(s) of action. Although these models provide valuable information and somewhat greater predictability than cell/tissue cultures in vitro, their prognostic usefulness for human clinical trials has been limited. Genetically engineered mouse models of cancer are becoming useful systems for understanding the molecular and cellular determinants of tumorigenesis and for refining anticancer agents targeted to various facets of carcinogenesis in vivo

There are many advantages of using genetically engineered mice in cancer research. Researchers in academia and industry, as well as clinicians are all using mice extensively in their work. What makes the mouse so special is how similar its genome is to the human genome (99% of human genes are conserved in the mouse), the availability of a unique battery of sophisticated molecular and genetic tools, and the animal's small size, all of which facilitate large scale/high throughput studies and make it a cost-efficient model providing functional information on human genes in health and disease. In fact, the potential of mouse models to make medical research, and in particular drug development, more efficient could be increased by solving a series of research, intellectual property rights (IPR), communication, training, and regulatory bottlenecks.

Although there are species (such as dogs, pigs, and nonhuman primates) that are even more closely related to us than mice, working with these large animals is extremely expensive and is fraught with ethical concerns. With their small size and short generation times, breeding, and keeping mice is comparatively simple and inexpensive. In addition, because they have been widely used in research for decades, researchers have built up a detailed understanding of mouse biology and genetics and developed large numbers of tools and techniques to study them. These powerful genetics tools are not yet available for larger mammals. Recent years have seen a rise in the use of genetically engineered mice in research and preclinical studies. Some of these models can mimic a wide range of human diseases and health problems, such as cancer and diabetes. In addition, the mouse is so far the only mammalian model in which it is technically possible to generate an organism in which a particular mouse gene has been replaced by its human counterpart. This "humanized" mouse will produce and live with the human version of the protein. "Humanized" mice can be created bearing a mutated version of a human gene known to be associated with a specific human disease. Such a mouse can be used to test the possible efficacy of a drug designed to bind to the relevant human protein.

Some strains of genetically modified mice can be used in preclinical tests in order to provide information on the carcinogenic potential of a compound, as alternative models for the conventional 2 years carcinogenicity assay. The three most extensively studied of these mice are Trp53$^{+/-}$, Tg/AC, and RasH2. Recently, a study compared their performance with the traditional 2-year rodent bioassay, and the individual transgenic models made the "correct" determinations (positive for carcinogens; negative for noncarcinogens) for 74%–81% of the chemicals, with an increase to as much as 83% using combined strategies (e.g., Trp53$^{+/-}$ for genotoxic chemicals for all chemicals). For comparison, identical analysis of chemicals in this data set that were tested in the 2-year, two-species rodent bioassay yielded correct determinations for 69% of the chemicals. RasH2 one example is the rasH2 mice.

Here we present some genetically modified mouse models for the study of human cancers (Table 27.5).

TABLE 27.5 Genetically Modified Animal Models for the Study of Human Cancers

Human disease	Gene symbol	Model	References
Breast cancer	Cre	WAP-Cre	Wagner et al. (1997)
	Cre	MMTV-Cre	Robinson and Hennighausen (2011)
	Brca2	Brca2 floxed	Jonkers et al. (2001)
	Brca1	Brca1 null, Brca1 KO	Shen et al. (1998)
	Brca2	SWR Brca2 exon 27 deletion	Unpublished
	rtTA	WAP-rtTA-Cre	Utomo et al. (1999)
	Trp53	Tg p53 R172H	Li et al. (1998)
	MYC	MMTV/c-myc	Sinn et al. (1987)
	TAg	WAP-Tag	Tzeng et al. (1993)
Lung cancer	Kras	K-rasLA1	Johnson et al. (2001)
	Kras	K-rasLA2	Johnson et al. (2001)
	Kras	LSL K-ras G12D	Jackson et al. (2001)
	EGFR-L858R	EGFR-L858R	Politi et al. (2006)
Prostate cancer	Nkx3-1	Nkx3.1 null (B6;129)	Bhatia-Gaur et al. (1999)
	Nkx3-1	Nkx3.1-Cre	Lin et al. (2007)
	Nkx3-1	Nkx3.1-CreERT2	Wang et al. (2009)
	Nkx3-1	Nkx3.1 null (B6)	Kim et al. (2002)
	Nkx3-1	Nkx3.1 null (FVB)	Kim et al. (2002)
	c-Myc	Hi-Myc	Ellwood-Yen et al. (2003)
	c-Myc	Lo-Myc	Ellwood-Yen et al. (2003)
	TAg	12T-7f	Kasper et al. (1998)
	TAg	12T-10	Masumori et al. (2001)
	Fgf8b	PB-FGF8b-line 3	Song et al. (2002)
	Cre	PB-Cre4	Wu et al. (2001)
	Akt1	Akt1, MPAKT	Majumder et al. (2003)

(Continued)

TABLE 27.5   Genetically Modified Animal Models for the Study of Human Cancers (*cont.*)

Human disease	Gene symbol	Model	References
Hematopoietic cancer	PML/RARA	PML-RARa	Grisolano et al. (1997)
	RARa-PML	RARa-PML	Pollock et al. (1999)
	MYC	Lambda-MYC	Kovalchuk et al. (2000)
	Gadd45a	Gadd45a null	Hollander et al. (1999)
	Nras	N-ras null, Nras KO	Umanoff et al. (1995)
	Tgfbr2	C57BL/6 DNTGFRII	Lucas et al. (2000)
	LANA	LANA	Fakhari et al. (2006)
	Cdkn2a	p16(Ink4a) null	Sharpless et al. (2001)
	BCR/ABL	P190 BCR-ABL	Voncken et al. (1992)
	PML	PML null	Wang et al. (1998)
	Igh-Myc	iMycEu	Park et al. (2005)
	TAg	Tdn/11, LST1135, dl1135	Symonds et al. (1993)
Brain tumors	ires-CreER	Pax7(CreERp)	Nishijo et al. (2009)
	TAg	SV11	Chen and Van Dyke (1991)
	TAg	LPV-TAg, T121, LST1137, dl1137	Saenz-Robles et al. (1994)
	hCDK4	GFAP-hCDK4	Huang et al. (2002)
	Nf1	Nf1 flox	Zhu et al. (2001)
	CreLacZ	BLBP-cre	Unpublished
	Cre	hGFAP-Cre	Bajenaru et al. (2002)
	MYCN	TH-MYCN	Weiss et al. (1997)
Gastrointestinal tumors	Ahr	Ahr null	Fernandez-Salguero et al. (1995)
	Apc	Apc1638	Fodde et al. (1994)
	Apc	Apc Delta 580	Smits et al. (2000)
	Mlh1	Mlh1 null	Edelmann et al. (1996)
	Msh3	Msh3 null	Edelmann et al. (2000)
	Msh6	Msh6 null	Edelmann et al. (1997)
	Msh2	Msh2 null	Temme et al. (1997)
	TAg	RIP1-Tag5	Hanahan (1985)
	TAg	RIP1-Tag2 (B6)	Adams et al. (1987); Hanahan (1985)
	TAg	RIP1-Tag2 (C3)	Hanahan (1985)
	Cre	Fabp1-Cre	Wong and Gordon (2000)
	Cre	Villin-Cre, vil-Cre Fo20	el Marjou et al. (2004)
	Cre	ED-L2/Cre	Tetreault et al. (2010)
	Cre	Pdx-1-cre	Hingorani et al. (2003)
	Tgfb1	Tgfb1 Rag2 null	Engle et al. (1999)
	Fen1	Fen1	Kucherlapati et al. (2002)
	Stk11	Lkb1 flox	Bardeesy et al. (2002)
	Connexin 32	Cx 32 KO mouse	Temme et al. (1997)
Ovarian tumors	Brca1	Brca1 floxed (FVB;129)	Unpublished

TABLE 27.5   Genetically Modified Animal Models for the Study of Human Cancers (*cont.*)

Human disease	Gene symbol	Model	References
Thyroid tumors	HPV16	TG-E6/E7	Souders et al. (2007)
Skin tumors	iCre	Langerin-Cre	Kaplan et al. (2007)
	HRAS	Tyr-HRAS	Chin et al. (1999a)
	rtTA	Tyr-rtTA	Chin et al. (1999a)
	Ahr	Ahr null	Fernandez-Salguero et al. (1995)
	HPV16	HPV16-E6	Chin et al. (1999b)
	Polh	XPV knockout	Lin et al. (2006)
	HPV16	K14-HPV16	Arbeit et al. (1994)
Multiple tumors	Rb1	Rb1 null	Jacks et al. (1992)
	Rb1	Rbfloxed	Marino et al. (2000)
	Apc	Apc CKO	Kuraguchi et al. (2006)
	EGFRvIII	CAG-LSL-EGFRvIII	Zhu et al. (2009)
	ROSA26	RosaSB	Dupuy et al. (2005)
	Gt(ROSA)26Sor	ROSA-CreER	Ventura et al. (2007)
	Gt(ROSA)26Sor	ROSA26-pCAGGs-LSL-Luciferase	Unpublished
	Cdkn2a	Ink4a/Arf null (B6)	Serrano et al. (1996)
	Cdkn2a	Ink4a/Arf null (FVB)	Serrano et al. (1996)
	Cdkn2a	p19(Arf) null (FVB)	Sharpless et al. (2004)
	Cdkn2a	ArfGFP	Zindy et al. (2003)
	Cdkn2a	p19(Arf) null (B6;129)	Kamijo et al. (1997)
	HRAS	TetO-HRAS	Chin et al. (1999b)
	T2/Onc2	TG6113	Dupuy et al. (2005)
	T2/Onc2	TG6070	Dupuy et al. (2005)
	sb	Rosa LSL SBase/TG6113	Starr et al. (2009)
	sb	Rosa LSL SBase/TG12740	Dupuy et al. (2009)
	sb	Rosa LSL SBase/TG12775	Dupuy et al. (2009)
	sb	76 T2/Onc	Collier et al. (2005)
	sb	68 T2/Onc	Collier et al. (2005)
	sb	Rosa LSL SBase/TG6070	Starr et al. (2009)
	Dmtf1	DMP-1 null	Inoue et al. (2000)
	PTEN	PTEN	Podsypanina et al. (1999)
	Men1	Men1 null, Men1deltaN3-8	Crabtree et al. (2001)
	Aprt	Aprt	Shao et al. (1999)
	Pax3	Pax3:Fkhr knock-in	Keller et al. (2010)
	Trp53	p53 R172H	Olive et al. (2004)
	Trp53	p53 R270H	Olive et al. (2004)
	KRT5	K5/tTA	Diamond et al. (2000)
	SB10	CAGGS-SB10	Dupuy et al. (2001)
	Tgfbr2	Tgfbr2 flox (FVB)	Chytil et al. (2002)

References

Adams, T.E., Alpert, S., Hanahan, D., 1987. Nono-tolerance and auto-antibodies to a grangenic self antigen expressed in pancreatic beta cells. Nature 325, 223–228.

Arbeit, J.M., Munger, K., Howley, P.M., Hanahan, D., 1994. Progressive squamous epithelial neoplasia in K14-human papillomavirus type 16 transgenic mice. J. Virol. 68, 4358–4368.

Bajenaru, M.L., Zhu, Y., Hedrick, N.M., Donahoe, J., Parada, L.F., Gutmann, D.H., 2002. Astrocyte-specific inactivation of the neurofibromatosis 1 Gene (Nf1) is insufficient for astrocytoma formation. Mol. Cell. Biol. 22, 5100–5113.

Bakker, C.E., Verheij, C., Willemsen, R., Vanderhelm, R., Oerlemans, F., Vermey, M., Bygrave, A., Hoogeveen, A.T., Oostra, B.A., Reyniers, E., Deboulle, K., Dhooge, R., Cras, P., Vanvelzen, D., Nagels, G., Martin, J.J., Dedyn, P.P., Darby, J.K., Willems, P.J., The Dutch-Belgium Fragile X Consortium., 1994. Fmr1 knockout mice: a model to study fragile x mental retardation. Dutch-Belgium Fragile X Consortium Cell 78 (1), 23–33.

Bardeesy, N., Sinha, M., Hezel, A.F., Signoretti, S., Hathaway, N.A., Sharpless, N.E., Loda, M., Carrasco, D.R., DePinho, R.A., 2002. Loss of the Lkb1 tumour suppressor provokes intestinal polyposis but resistance to transformation. Nature 419, 162–167.

Beck, L., Karaplis, A.C., Amizuka, N., Hewson, A.S., Ozawa, H., Tenenhouse, H.S., 1998. Targeted inactivation of Npt2 in mice leads to severe renal phosphate wasting, hypercalciuria, and skeletal abnormalities. Proc. Natl. Acad. Sci. USA 95 (9), 5372–5377.

Bezard, E., Przedborski, S., 2011. A tale on animal models of Parkinson's disease. Mov. Disord. 26 (6), 993–1002.

Bhatia-Gaur, R., Donjacour, A.A., Sciavolino, P.J., Kim, M., Desai, N., Young, P., Norton, C.R., Gridley, T., Cardiff, R.D., Cunha, G.R., Abate-Shen, C., Shen, M.M., 1999. Roles for Nkx3.1 in prostate development and cancer. Genes. Dev. 13, 966–977.

Bi, L., Lawler, A.M., Antonarakis, S.E., High, K.A., Gearhart, J.D., Kazazian, Jr., H.H., 1995. Targeted disruption of the mouse factor VIII gene produces a model of haemophilia A [letter]. Nat. Genet. 10 (1), 119–121.

Blandini, F., Armentero, M.T., 2012. Animal models of Parkinson's disease. FEBS J. 279 (7), 1156–1166.

Capecchi, M.R., 1980. High efficiency transformation by direct microinjection of DNA into cultured mammalian cells. Cell 22, 479–488.

Carbery, I.D., Ji, D., Harrington, A., Brown, V., Weinstein, E.J., Liaw, L., Cui, X., 2010. Targeted genome modification in mice using zinc-finger nucleases. Genetics 186, 451–459.

Caron, K.M., James, L.R., Kim, H.S., Morham, S.G., Sequeira Lopez, M.L., Gomez, R.A., Reudelhuber, T.L., Smithies, O., 2002. A genetically clamped renin transgene for the induction of hypertension. Proc. Natl. Acad. Sci. USA 99 (12), 8248–8252.

Chen, J.D., Van Dyke, T., 1991. Uniform cell-autonomous tumorigenesis of the choroid plexus by papovavirus large T antigens. Mol. Cell. Biol. 11, 5968–5976.

Chesselet, M.F., 2008. In vivo alpha-synuclein overexpression in rodents: a useful model of Parkinson's disease? Exp. Neurol. 209 (1), 22–27.

Chin, L., Tam, A., Pomerantz, J., Wong, M., Holash, J., Bardeesy, N., Shen, Q., O'Hagan, R., Pantginis, J., Zhou, H., Horner, II, J.W., Cordon-Cardo, C., Yancopoulos, G.D., DePinho, R.A., 1999a. Essential role for oncogenic Ras in tumour maintenance. Nature 400, 468–472.

Chin, L., Tam, A., Pomerantz, J., Wong, M., Holash, J., Bardeesy, N., Shen, Q., et al., 1999b. Essential role for oncogenic Ras in tumour maintenance. Nature 400, 468–472.

Chishti, M.A., Yang, D.S., Janus, C., Phinney, A.L., Horne, P., Pearson, J., Strome, R., Zuker, N., Loukides, J., French, J., Turner, S., Lozza, G., Grilli, M., Kunicki, S., Morissette, C., Paquette, J., Gervais, F., Bergeron, C., Fraser, P.E., Carlson, G.A., St George-Hyslop, P., Westaway, D., 2001. Early-onset amyloid deposition and cognitive deficits in transgenic mice expressing a double mutant form of amyloid precursor protein 695. J. Biol. Chem. 276, 21562–21570.

Chytil, A., Magnuson, M.A., Wright, C.V.E., Moses, H.L., 2002. Conditional inactivation of the TGF-beta type II receptor using Cre:Lox. Genesis 32, 73–75.

Collier, L.A., Carlson, C.M., Ravimohan, S., Dupuy, A.J., Largaespada, D.A., 2005. Cancer gene discovery in solid tumours using transposon-based somatic mutagenesis in the mouse. Nature 436, 272–276.

Cong, L., Ran, F.A., Cox, D., Lin, S., Barretto, R., Habib, N., Hsu, P.D., Wu, X., Jiang, W., Marraffini, L.A., Zhang, F., 2013. Multiplex genome engineering using CRISPR/Cas systems. Science 339, 819–823.

Crabtree, J.S., Scacheri, P.C., Ward, J.M., Garrett-Beal, L., Emmert-Buck, M.R., Edgemon, K.A., Lorang, D., Libutti, S.K., Chandrasekharappa, S.C., Marx, S.J., Spiegel, A.M., Collins, F.S., 2001. A mouse model of multiple endocrine neoplasia, type 1, develops multiple endocrine tumors. Proc. Natl. Acad. Sci. USA 98, 1118–1123.

Davis, R.E., Swiderski, R.E., Rahmouni, K., Nishimura, D.Y., Mullins, R.F., Agassandian, K., Philp, A.R., Searby, C.C., Andrews, M.P., Thompson, S., Berry, C.J., Thedens, D.R., Yang, B., Weiss, R.M., Cassell, M.D., Stone, E.M., Sheffield, V.C., 2007. A knockin mouse model of the Bardet-Biedl syndrome 1 M390R mutation has cilia defects, ventriculomegaly, retinopathy, and obesity. Proc. Natl. Acad. Sci. U S A 104 (49), 19422–19427.

Dawson, T.M., Ko, H.S., Dawson, V.L., 2010. Genetic animal models of Parkinson's disease. Neuron 66 (5), 646–661.

Dehay, B., Bezard, E., 2011. New animal models of Parkinson's disease. Mov. Disord. 26 (7), 1198–1205.

Detmar, M., Brown, L.F., Schon, M.P., Elicker, B.M., Velasco, P., Richard, L., Fukumura, D., Monsky, W., Claffey, K.P., Jain, R.K., 1998. Increased microvascular density and enhanced leukocyte rolling and adhesion in the skin of VEGF transgenic mice. J. Invest. Dermatol. 111 (1), 1–6.

Diamond, I., Owolabi, T., Marco, M., Lam, C., Glick, A., 2000. Conditional gene expression in the epidermis of transgenic mice using the tetracyclin-regulated transactivators tTA and rTA linked to the keratin 5 promoter. J. Invest. Dermatol. 115, 788–794.

Dix, D.J., Allen, J.W., Collins, B.W., Mori, C., Nakamura, N., Poorman-Allen, P., Goulding, E.H., Eddy, E.M., 1996. Targeted gene disruption of Hsp70-2 results in failed meiosis, germ cell apoptosis, and male infertility. Proc. Natl. Acad. Sci. USA 93 (8), 3264–3268.

Duff, K., Eckman, C., Zehr, C., Yu, X., Prada, C.M., Perez-Tur, J., Hutton, M., Buee, L., Harigaya, Y., Yager, D., Morgan, D., Gordon, M.N., Holcomb, L., Refolo, L., Zenk, B., Hardy, J., Younkin, S., 1996. Increased amyloid-beta42(43) in brains of mice expressing mutant presenilin 1. Nature 383, 710–713.

Dupuy, A.J., Fritz, S., Largaespada, D.A., 2001. Transposition and gene disruption in the male germline of the mouse. Genesis 30, 82–88.

Dupuy, A.J., Akagi, K., Largaespada, D.A., Copeland, N.G., Jenkins, N.A., 2005. Mammalian mutagenesis using a highly mobile somatic Sleeping Beauty transposon system. Nature 436, 221–226.

Dupuy, A.J., Rogers, L.M., Kim, J., Nannapaneni, K., Starr, T.K., Liu, P., Largaespada, D.A., Scheetz, T.E., Jenkins, N.A., Copeland, N.G., 2009. A modified sleeping beauty transposon system that can be used to model a wide variety of human cancers in mice. Cancer Res. 69 (20), 8150–8156.

Duyckaerts, C., Potier, M.C., Delatour, B., 2008. Alzheimer disease models and human neuropathology: similarities and differences. Acta Neuropathol. 115 (1), 5–38.

Edelmann, W., Cohen, P.E., Kane, M., Lau, K., Morrow, B., Bennett, S., Umar, A., Kunkel, T., Cattoretti, G., Chaganti, R., Pollard, J.W., Kolodner, R.D., Kucherlapati, R., 1996. Meiotic pachytene arrest in MLH1-deficient mice. Cell 85, 1125–1134.

Edelmann, W., Yang, K., Umar, A., Heyer, J., Lau, K., Fan, K., Liedtke, W., Cohen, P.E., Kane, M.F., Lipford, J.R., Yu, N., Crouse, G.F., Pollard, J.W., Kunkel, T., Lipkin, M., Kolodner, R., Kucherlapati, R.,

1997. Mutation in the mismatch repair gene Msh6 causes cancer susceptibility. Cell 91, 467–477.

Edelmann, W., Umar, A., Yang, K., Heyer, J., Kucherlapati, M., Lia, M., Kneitz, B., Avdievich, E., Fan, K., Wong, E., Crouse, G., Kunkel, T., Lipkin, M., Kolodner, R.D., Kucherlapati, R., 2000. The DNA mismatch repair genes Msh3 and Msh6 cooperate in intestinal tumor suppression. Cancer Res. 60 (4), 803–807.

el Marjou, F., Janssen, K.P., Chang, B.H., Li, M., Hindie, V., Chan, L., Louvard, D., Chambon, P., Metzger, D., Robine, S., 2004. Tissue-specific and inducible Cre-mediated recombination in the gut epithelium. Genesis 39 (3), 186–193.

Ellwood-Yen, K., Graeber, T.G., Wongvipat, J., Iruela-Arispe, M.L., Zhang, J., Matusik, R., Thomas, G.V., Sawyers, C.L., 2003. Myc-driven murine prostate cancer shares molecular features with human prostate tumors. Cancer Cell 4, 223–238.

Engle, S.J., Hoying, J.B., Boivin, G.P., Ormsby, I., Gartside, P.S., Doetschman, T., 1999. Transforming growth factor beta1 suppresses nonmetastatic colon cancer at an early stage of tumorigenesis. Cancer Res. 59, 3379–3386.

Fakhari, F.D., Jeong, J.H., Kanan, Y., Dittmer, D.P., 2006. The latency-associated nuclear antigen of Kaposis sarcoma-associated herpesvirus induces B cell hyperplasia and lymphoma. J. Clin. Invest. 3, 735–742.

Fernandez-Salguero, P., Pineau, T., Hilbert, D.M., McPhail, T., Lee, S.S., Kimura, S., Nebert, D.W., Rudikoff, S., Ward, J.M., Gonzalez, F.J., 1995. Immune system impairment and hepatic fibrosis in mice lacking the dioxin-binding Ah receptor. Science 268, 722–726.

Finotto, S., Neurath, M.F., Glickman, J.N., Qin, S., Lehr, H.A., Green, F.H., Ackerman, K., Haley, K., Galle, P.R., Szabo, S.J., Drazen, J.M., De Sanctis, G.T., Glimcher, L.H., 2002. Development of spontaneous airway changes consistent with human asthma in mice lacking T-bet. Science 295 (5553), 336–338.

Fitzky, B.U., Moebius, F.F., Asaoka, H., Waage-Baudet, H., Xu, L., Xu, G., Maeda, N., Kluckman, K., Hiller, S., Yu, H., Batta, A.K., Shefer, S., Chen, T., Salen, G., Sulik, K., Simoni, R.D., Ness, G.C., Glossmann, H., Patel, S.B., Tint, G.S., 2001. 7-Dehydrocholesterol-dependent proteolysis of HMG-CoA reductase suppresses sterol biosynthesis in a mouse model of Smith-Lemli-Opitz/RSH syndrome. J. Clin. Invest. 108 (6), 905–915.

Fodde, R., Edelmann, W., Yang, K., van Leeuwen, C., Carlson, C., Renault, B., Breukel, C., Alt, E., Lipkin, M., Khan, P.M., Kucherlapati, R., 1994. A targeted chain-termination mutation in the mouse Apc gene results in multiple intestinal tumors. Proc. Natl. Acad. Sci. USA 13, 8969–8973.

Fulop, C., Szanto, S., Mukhopadhyay, D., Bardos, T., Kamath, R.V., Rugg, M.S., Day, A.J., Salustri, A., Hascall, V.C., Glant, T.T., Mikecz, K., 2003. Impaired cumulus mucification and female sterility in tumor necrosis factor-induced protein-6 deficient mice. Development 130 (10), 2253–2261.

Gama Sosa, M.A., De Gasperi, R., Elder, G.A., 2010. Animal transgenesis: an overview. Brain Struct. Funct. 214, 91–109.

Gama Sosa, M.A., Gasperi, R., Elder, G.A., 2012. Modeling human neurodegenerative diseases in transgenic systems. Hum. Genet. 131, 535–563.

Games, D., Adamas, D., Alessandrini, R., Barbour, R., Berthelette, P., Blackwell, C., Carr, T., Clemens, J., Donaldson, T., Gillespie, F., Guido, T., Hagoplan, S., Johnson-Wood, K., Kan, K., Lee, M., Leibowitz, P., Lieberburg, I., Little, S., Masliah, E., McConlogue, L., Montoya-Zavala, M., Mucke, L., Paganini, L., Penniman, E., Ppower, M., Shenk, D., Seubert, P., Snyder, F., Soriano, F., Tan, H., Vitale, J., Wadsworth, S., Wolozin, B., Zhao, J., 1995. Alzheimer-type neuropathology in transgenic mice overexpressing V717F β-amyloid precursor protein. Nature 373, 523–527.

Garneau, J.E., Dupuis, M.E., Villion, M., Romero, D.A., Barrangou, R., Boyaval, P., Fremaux, C., Horvath, P., Magadan, A.H., Moineau, S., 2010. The CRISPR/Cas bacterial immune system cleaves bacteriophage and plasmid DNA. Nature 468, 67–71.

Geurts, A.M., Cost, G.J., Freyvert, Y., Zeitler, B., Miller, J.C., Choi, V.M., Jenkins, S.S., Wood, A., Cui, X., Meng, X., Vincent, A., Lam, S., Michalkiewicz, M., Schilling, R., Foeckler, J., Kalloway, S., Weiler, H., Menoret, S., Anegon, I., Davis, G.D., Zhang, L., Rebar, E.J., Gregory, P.D., Urnov, F.D., Jacob, H.J., Buelow, R., 2009. Knockout rats via embryo microinjection of zinc-finger nucleases. Science 325, 433.

Gispert, S., Ricciardi, F., Kurz, A., Azizov, M., Hoepken, H.H., Becker, D., Voos, W., Leuner, K., Muller, W.E., Kudin, A.P., Kunz, W.S., Zimmermann, A., Roeper, J., Wenzel, D., Jendrach, M., Garcia-Arencibia, M., Fernandez-Ruiz, J., Huber, L., Rohrer, H., Barrera, M., Reichert, A.S., Rub, U., Chen, A., Nussbaum, R.L., Auburger, G., 2009. Parkinson phenotype in aged PINK1-deficient mice isaccompanied by progressive mitochondrial dysfunction inabsence of neurodegeneration. PLoS One 4 (6), 5777.

Gografe, S.I., Garbuzova-Davis, S., Willing, A.E., Haas, K., Chamizo, W., Sanberg, P.R., 2003. Mouse model of Sanfilippo syndrome type B: relation of phenotypic features to background strain. Comp. Med. 53 (6), 622–632.

Goldberg, M.S., Pisani, A., Haburcak, M., Vortherms, T.A., Kitada, T., Costa, C., Tong, Y., Martella, G., Tscherter, A., Martins, A., Bernardi, G., Roth, B.L., Pothos, E.N., Calabresi, P., Shen, J., 2005. Nigrostriatal dopaminergic deficits and hypokinesia caused by inactivation of the familial Parkinsonism-linked gene DJ-1. Neuron 45, 486–489.

Grady, R.M., Merlie, J.P., Sanes, J.R., 1997a. Subtle neuromuscular defects in utrophin-deficient mice. J. Cell Biol. 136, 871–882.

Grady, R.M., Teng, H., Nichol, M.C., Cunningham, J.C., Wilkinson, R.S., Sanes, J.R., 1997b. Skeletal and cardiac myopathies in mice lacking utrophin and dystrophin: a model for Duchenne muscular dystrophy. Cell 90, 729–738.

Green, R.S., Stone, E.L., Tenno, M., Lehtonen, E., Farquhar, M.G., Marth, J.D., 2007. Mammalian N-glycan branching protects against innate immune self-recognition and inflammation in autoimmune disease pathogenesis. Immunity 27 (2), 308–320.

Grisolano, J.L., Wesselschmidt, R.L., Pelicci, P.G., Ley, T.J., 1997. Altered myeloid development and acute leukemia in transgenic mice expressing PML-RARa under control of cathepsin G regulatory sequences. Blood 89, 376–387.

Grivennikov, I.A., 2008. Embryonic stem cells and the problem of directed differentiation. Biochemistry 73, 1438–1452.

Gupta, A., Dawson, V.L., Dawson, T.M., 2008. What causes cell death in Parkinson's disease? Ann. Neurol. 64, S3–S15.

Gurney, M.E., 2000. What transgenic mice tell us about neurodegenerative disease. Bioessays 22 (3), 297–304.

Gurney, M.E., Pu, H., Chiu, A.Y., Dal Canto, M.C., Polchow, C.Y., Alexander, D.D., Caliendo, J., Hentati, A., Kwon, Y.W., Deng, H.X., Chen, W., Zhai, P., Sufit, R.L., Siddique, T., 1994. Motor neuron degeneration in mice that express a human Cu, Zn superoxide dismutase mutation. Science 264 (5166), 1772–1775.

Guy, J., Hendrich, B., Holmes, M., Martin, J.E., Bird, A., 2001. A mouse Mecp2-null mutation causes neurological symptoms that mimic Rett syndrome. Nat. Genet. 27 (3), 322–326.

Hall, A.M., Roberson, E.D., 2012. Mouse models of Alzheimer's disease. Brain Res. Bull. 88 (1), 3–12.

Hamilton, D.L., Abremski, K, 1984. Site-specific recombination by the bacteriophage P1 lox-Cre system. Cre-mediated synapsis of two lox sites. J. Mol. Biol. 178, 481–486.

Hanahan, D., 1985. Heritable formation of pancreatic beta-cell tumors in transgenic mice expressing recombinant insulin/simian virus 40 oncogenes. Nature 315, 115–122.

Haruyama, N., Cho, A., Kulkarni, AB, 2009. Overview: engineering transgenic constructs and mice. Curr. Protoc. Cell Biol., (Chapter 19): Unit: 19.

Harvey, B.K., Richie, C.T., Hoffer, B.J., Airavaara, M., 2011. Transgenic animal models of neurodegeneration based on human genetic studies. J. Neural. Transm. 118, 27–45.

Heng, M.Y., Detloff, P.J., Albin, R.L., 2008. Rodent genetic models of Huntington disease. Neurobiol. Dis. 32 (1), 1–9.

Herzig, M.C., Winkler, D.T., Burgermeister, P., Pfeifer, M., Kohler, E., Schmidt, S.D., Danner, S., Abramowski, D., Sturchler-Pierrat, C., Burki, K., van Duinen, S.G., Maat-Schieman, M.L., Staufenbiel, M., Mathews, P.M., Jucker, M., 2004. Abeta is targeted to the vasculature in a mouse model of hereditary cerebral hemorrhage with amyloidosis. Nat. Neurosci. 7, 954–960.

Hingorani, S.R., Petricoin, E.F., Maitra, A., Rajapakse, V., King, C., Jacobetz, M.A., Ross, S., Conrads, T.P., Veenstra, T.D., Hitt, B.A., Kawaguchi, Y., Johann, D., Liotta, L.A., Crawford, H.C., Putt, M.E., Jacks, T., Wright, C.V., Hruban, R.H., Lowy, A.M., Tuveson, D.A., 2003. Preinvasive and invasive ductal pancreatic cancer and its early detection in the mouse. Cancer Cell 4, 437–450.

Hock, Jr., B.J., Lamb, B.T., 2001. Transgenic mouse models of Alzheimer's disease. Trends Genet. 17 (10), S7–S12.

Holla, V.R., Adas, F., Imig, J.D., Zhao, X., Price, Jr, E., Olsen, N., Kovacs, W.J., Magnuson, M.A., Keeney, D.S., Breyer, M.D., Falck, J.R., Waterman, M.R., Capdevila, J.H., 2001. Alterations in the regulation of androgen-sensitive Cyp 4a monooxygenases cause hypertension. Proc. Natl. Acad. Sci. USA 98 (9), 5211–5216.

Hollander, M.C., Sheikh, M.S., Bulavin, D.V., Lundgren, K., Augeri-Henmueller, L., Shehee, R., Molinaro, T.A., Kim, K.E., Tolosa, E., Ashwell, J.D., Rosenberg, M.P., Zhan, Q., Fernandez-Salguero, P.M., Morgan, W.F., Deng, C.X., Fornace, Jr., A.J., 1999. Genomic instability in Gadd45a-deficient mice. Nat. Genet. 23, 176–184.

Hsiao, K., Chapman, P., Nilsen, S., Eckman, C., Harigaya, Y., YounKin, S., Yang, F., Cole, G., 1996. Correlative memory deficits, Abeta elevation, and amyloid plaques in trangenic mice. Science 274, 99–102.

Hsieh-Li, H.M., Chang, J.G., Jong, Y.J., Wu, M.H., Wang, N.M., Tsai, C.H., Li, H., 2000. A mouse model for spinal muscular atrophy. Nat. Genet. 24 (1), 66–70.

Huang, Z., Baldwin, R.L., Hedrick, N.M., Gutmann, D.H., 2002. Astrocyte-specific expression of CDK4 is not sufficient for tumor formation, but cooperates with p53 heterozygosity to provide a growth advantage for astrocytes in vivo. Oncogene 21, 1325–1334.

Imarisio, S., Carmichael, J., Korolchuk, V., Chen, C.W., Saiki, S., Rose, C., Krishna, G., Davies, J.E., Ttofi, E., Underwood, B.R., Rubinsztein, D.C., 2008. Huntington's disease: from pathology and genetics to potential therapies. Biochem. J. 412 (2), 191–209.

Ingalls, A.M., Dickie, M.M., Snell, G.D., 1950. Obese, a new mutation in the house mouse. J. Hered. 41, 317–318.

Inoue, K., Wen, R., Rehg, J.E., Adachi, M., Cleveland, J.L., Roussel, M.F., Sherr, C.J., 2000. Disruption of the ARF transcriptional activator DMP1 facilitates cell immortalization, Ras transformation, and tumorigenesis. Genes Dev. 14, 1797–1809.

Ishibashi, S., Brown, M.S., Goldstein, J.L., Gerard, R.D., Hammer, R.E., Herz, J., 1993a. Hypercholesterolemia in low density lipoprotein receptor knockout mice and its reversal by adenovirus-mediated gene delivery. J. Clin. Invest. 92 (2), 883–893.

Ishibashi, S., Brown, M.S., Goldstein, J.L., Gerard, R.D., Hammer, R.E., et al., 1993b. Hypercholesterolemia in low density lipoprotein receptor knockout mice and its reversal by adenovirus-mediated gene delivery. J. Clin. Invest. 92, 883–893.

Jacks, T., Fazeli, A., Schmitt, E.M., Bronson, R.T., Goodell, M.A., Weinberg, R.A., 1992. Effects of an Rb mutation in the mouse. Nature 359, 295–300.

Jackson, E.L., Willis, N., Mercer, K., Bronson, R.T., Crowley, D., Montoya, R., Jacks, T., Tuveson, D.A., 2001. Analysis of lung tumor initiation and progression using conditional expression of K-ras. Genes Dev. 15, 3243–3248.

Jaenisch, R., 1976. Germ line integration and Mendelian transmission of the exogenous Moloney leukemia virus. Proc. Natl. Acad. Sci. USA 73, 1260–1264.

Jankowsky, J.L., Slunt, H.H., Ratovitski, T., Jenkins, N.A., Copeland, N.G., Borchelt, D.R., 2001. Co-expression of multiple transgenes in mouse CNS: acomparison of strategies. Biomol. Eng. 17 (6), 157–165.

Jinek, M., Chylinski, K., Fonfara, I., Hauer, M., Doudna, J.A., Charpentier, E., 2012. A programmable dual-RNA-guided DNA endonuclease in adaptive bacterial immunity. Science 337, 816–821.

Johnson, L., Mercer, K., Greenbaum, D., Bronson, R.T., Crowley, D., Tuveson, D.A., Jacks, T, 2001. Somatic activation of the K-ras oncogene causes early onset lung cancer in mice. Nature 410, 1111–1116.

Jonkers, J., Meuwissen, R., van der Gulden, H., Peterse, H., van der Valk, M., Berns, A., 2001. Synergistic tumor suppressor activity of BRCA2 and p53 in a conditional mouse model for breast cancer. Nat. Genet. 29, 418–425.

Joyner, A.L., Sedivy, J.M., 2000. Gene targeting: a practical approach. Oxford University Press, Oxford.

Judge, D.P., Biery, N.J., Keene, D.R., Geubtner, J., Myers, L., Huso, D.L., Sakai, L.Y., Dietz, H.C., 2004. Evidence for a critical contribution of haploinsufficiency in the complex pathogenesis of Marfan syndrome. J. Clin. Invest. 114 (2), 172–181.

Kabadi, A.M., Ousterout, D.G., Hilton, I.B., Gersbach, C.A., 2014. Multiplex CRISPR/Cas9-based genome engineering from a single lentiviral vector. Nucleic Acids Res. 42, e147.

Kagi, D., Ledermann, B., Burki, K., Seiler, P., Odermatt, B., Olsen, K.J., Podack, E.R., Zinkernagel, R.M., Hengartner, H., 1994. Cytotoxicity mediated by T cells and natural killer cells is greatly impaired in perforin-deficient mice [see comments]. Nature 369 (6475), 31–37.

Kamijo, T., Zindy, F., Roussel, M.F., Quelle, D.E., Downing, J.R., Ashmun, R.A., Grosveld, G., Sherr, C.J., 1997. Tumor suppression at the mouse INK4a locus mediated by alternative reading frame product p19(Arf). Cell 91, 649–659.

Kaplan, D.H., et al., 2007. Autocrine/paracrine TGFbeta1 is required for the development of epidermal Langerhans cells. J. Exp. Med. 204 (11), 2545–2552.

Kaptzan, T., West, S.A., Holicky, E.L., Wheatley, C.L., Marks, D.L., Wang, T., Peake, K.B., Vance, J., Walkley, S.U., Pagano, R.E., 2009. Development of a Rab9 transgenic mouse and its ability to increase the lifespan of a murine model of Niemann-Pick type C disease. Am. J. Pathol. 174 (1), 14–20.

Kasper, S., Sheppard, P.C., Yan, Y., Pettigrew, N., Borowsky, A.D., Prins, G.S., Dodd, J.G., Duckworth, M.L., Matusik, R.J., 1998. Development, progression, and androgen-dependence of prostate tumors in probasin-large T antigen transgenic mice: a model for prostate cancer. Lab. Invest. 78, 319–333.

Keller, C., Hansen, M.S., Coffin, C.M., Capecchi, M.R., 2010. Division of Pediatric Hematology-Oncology, Department of Pediatrics, University of Utah, Salt Lake City, UtahUSA.

Kim, M.J., Bhatia-Gaur, R., Banach-Petrosky, W.A., Desai, N., Wang, Y., Hayward, S.W., Cunha, G.R., Cardiff, R.D., Shen, M.M., Abate-Shen, C., 2002. Nkx3.1 mutant mice recapitulate early stages of prostate carcinogenesis. Cancer Res. 62, 2999–3004.

Kintsurashvili, E., Shenouda, S., Ona, D., Ona, L., Ahmad, S., Ravid, K., Gavras, I., Gavras, H., 2009. Hypertension in transgenic mice with brain-selective overexpression of the alpha(2B)-adrenoceptor. Am. J. Hypertens. 22 (1), 41–45.

Kokjohn, T.A., Roher, A.E., 2009. Amyloid precursor protein transgenic mouse models and Alzheimer's disease: understanding the paradigms, limitations and contributions. Alzheimers Dement. 5 (4), 340–347.

Kontoyiannis, D., Pasparakis, M., Pizarro, T.T., et al., 1999. Impaired on/off regulation of TNF biosynthesis in mice lacking TNF AU-rich elements: implications for joint and gut-associated immunopathologies. Immunity 10, 387–398.

Kovalchuk, A.L., Qi, C.F., Torrey, T.A., Taddesse-Heath, L., Feigenbaum, L., Park, S.S., Gerbitrz, A., Klobeck, G., Hoertnagel, K., Polack, A., Bornkamm, G.W., Janz, S., Morse, III, H.C., 2000. Burkitt lymphoma in the mouse. J. Exp. Med. 192, 1183–1190.

Kucherlapati, M., Yang, K., Kuraguchi, M., Zhao, J., Lia, M., Heyer, J., et al., 2002. Haploinsufficiency of Flap endonuclease (Fen 1) leads to rapid tumor progression. Proc. Natl. Acad. Sci. USA 99 (15), 9924–9929.

Kumar, K.R., Lohmann, K., Klein, C., 2012. Genetics of Parkinson disease and other movement disorders. Curr. Opin. Neurol. 25 (4), 466–474.

Kuraguchi, M., Wang, X.P., Bronson, R.T., Rothenberg, R., Ohene-Baah, N.Y., Lund, J.J., Kucherlapati, M., Maas, R.L., Kucherlapati, R., 2006. Adenomatous polyposis coli (Apc) is required for normal development of skin and thymus. PLoS Genetics 2, 1362–1374.

Li, B., Murphy, K.L., Laucirica, R., Kittrell, F., Medina, D., Rosen, J.M., 1998. A transgenic mouse model for mammary carcinogenesis. Oncogene 16, 997–1007.

Li, X., Tan, Y.C., Poulose, S., Olanow, C.W., Huang, X.Y., Yue, Z., 2007. Leucine rich repeat kinase 2 (LRRK2)/PARK8 possesses GTPase-activity that is altered in familial Parkinson's disease R1441C/Gmutants. J Neurochem. 103 (1), 238–247.

Li, Y., Liu, W., Oo, T.F., Wang, L., Tang, Y., Jackson-Lewis, V., Zhou, C., Geghman, K., Bogdanov, M., Przedborski, S., Beal, M.F., Burke, R.E., Li, C., 2009. Mutant LRRK2(R1441G) BAC transgenic mice recapitulate cardinal features of Parkinson's disease. Nat. Neurosci. 12, 826–828.

Li, M., Yang, H., Zhao, J., Fang, L., Shi, H., Li, M., Sun, Y., Zhang, X., Jiang, D., Zhou, L., Wang, D., 2014. Efficient and heritable gene targeting in tilapia by CRISPR/Cas9. Genetics 197, 591–599.

Lin, C.H., Tallaksen-Greene, S., Chien, W.M., Cearley, J.A., Jackson, W.S., Crouse, A.B., Ren, S., Li, X.J., Albin, R.L., Detloff, P.J., 2001. Neurological abnormalities in a knock-in mouse model of Huntington's disease. Hum. Mol. Genet. 10 (2), 137–144.

Lin, Q., Clark, A.B., McCulloch, S.D., Yuan, T., Bronson, R.T., Kunkel, T.A., Kucherlapati, R., 2006. Increased susceptibility to UV-induced skin carcinogenesis in polymerase eta-deficient mice. Cancer Res. 66, 87–94.

Lin, Y., Lui, G., Zhang, Y., Hu, Y.-P., Yu, K., Lin, C., McKeehan, K., Xuan, J.W., Ornitz, D., Shen, M.M., Greenberg, N., McKeehan, W.L., Wang, F., 2007. Fibroblast growth factor receptor 2 tyrosine kinase is required for prostatic morphogenesis and acquisition of strict androgen dependency for adult tissue homeostasis. Development 134, 723–734.

Liu, H., Chen, Y., Niu, Y., Zhang, K., Kang, Y., Ge, W., Liu, X., Zhao, E., Wang, C., Lin, S., Jing, B., Si, C., Lin, Q., Chen, X., Lin, H., Pu, X., Wang, Y., Qin, B., Wang, F., Wang, H., Si, W., Zhou, J., Tan, T., Li, T., Ji, S., Xue, Z., Luo, Y., Cheng, L., Zhou, Q., Li, S., Sun, Y.E., Ji, W., 2014. TALEN-mediated gene mutagenesis in rhesus and cynomolgus monkeys. Cell Stem Cell 14, 323–328.

Lucas, P.J., Kim, S.-J., Melby, S.J., Gress, R.E., 2000. Disruption of T-cell homeostasis in mice expressing a T cell-specific dominant negative transforming growth factor beta II receptor. J. Exp. Med. 191, 1187–1196.

Majumder, P.K., Yeh, J.J., George, D.J., Febbo, P.G., Kum, J., Xue, Q., Bikoff, R., Ma, H., Kantoff, P.W., Golub, T.R., Loda, M., Sellers, W.A., 2003. Prostate intraepithelial neoplasia induced by prostate restricted Akt activation: the MPAKT model. Proc. Natl. Acad. Sci. USA 100, 7841–7846.

Mangiarini, L., Sathasivam, K., Seller, M., Cozens, B., Harper, A., Hetherington, C., Lawton, M., Trottier, Y., Lehrach, H., Davies, S.W., Bates, G.P., 1996. Exon 1 of the HD gene with an expanded CAG repeat is sufficient to cause a progressive neurological phenotype in transgenic mice. Cell 87 (3), 493–506.

Marino, S., Vooijs, M., van Der Gulden, H., Jonkers, J., Berns, A., 2000. Induction of medulloblastomas in p53-null mutant mice by somatic inactivation of Rb in the external granular layer cells of the cerebellum. Genes Dev. 14, 994–1004.

Masumori, N., Thomas, T.Z., Chaurand, P., Case, T., Paul, M., Kasper, S., Caprioli, R.M., Tsukamoto, T., Shappell, S.B., Matusik, R.J., 2001. A probasin-large T antigen transgenic mouse line develops prostate adenocarcinoma and neuroendocrine carcinoma with metastatic potential. Cancer Res. 61 (5), 2239–2249.

Mathews, C.E., Langley, S.H., Leiter, E.H., 2002. New mouse model to study islet transplantation in insulin-dependent diabetes mellitus. Transplantation 73 (8), 1333–1336.

Mou, H., Kennedy, Z., Anderson, D.G., Yin, H., Xue, W., 2015. Precision cancer mouse models through genome editing with CRISPR-Cas9. Genome Med. 7, 53.

Mykytyn, K., Mullins, R.F., Andrews, M., Chiang, A.P., Swiderski, R.E., Yang, B., Braun, T., Casavant, T., Stone, E.M., Sheffield, V.C., 2004. Bardet-Biedl syndrome type 4 (BBS4)-null mice implicate Bbs4 in flagella formation but not global cilia assembly. Proc. Natl. Acad. Sci. USA 101 (23), 8664–8669.

Nishijo, K., Hosoyama, T., Bjornson, C.R.R., Schaffer, B., Bahadur, A.N., Hansen, M.S., Blandford, M.C., McCleish, A.T., Rubin, B.P., Epstein, J.A., Rando, T.A., Capecchi, M.R., Keller, C., 2009. Biomarker System for studying muscle, stem cells and cancer in vivo. FASEB J. 23 (8), 2681–2690.

Nishimura, D.Y., Fath, M., Mullins, R.F., Searby, C., Andrews, M., Davis, R., Andorf, J.L., Mykytyn, K., Swiderski, R.E., Yang, B., Carmi, R., Stone, E.M., Sheffield, V.C., 2004. Bbs2-null mice have neurosensory deficits, a defect in social dominance, and retinopathy associated with mislocalization of rhodopsin. Proc. Natl. Acad. Sci. USA 101 (47), 16588–16593.

Niu, Y., Shen, B., Cui, Y., Chen, Y., Wang, J., Wang, L., Kang, Y., Zhao, X., Si, W., Li, W., Xiang, A.P., Zhou, J., Guo, X., Bi, Y., Si, C., Hu, B., Dong, G., Wang, H., Zhou, Z., Li, T., Tan, T., Pu, X., Wang, F., Ji, S., Zhou, Q., Huang, X., Ji, W., Sha, J., 2014. Generation of gene-modified cynomolgus monkey via Cas9/RNA-mediated gene targeting in one-cell embryos. Cell 156, 836–843.

Notarianni, E., Evans, M.J., 2006. Embryonic Stem Cells: A Practical Approach. Oxford University Press, Oxford.

Oakley, H., Cole, S.L., Logan, S., Maus, E., Shao, P., Craft, J., Guillozet-Bongaarts, A., Ohno, M., Disterhoft, J., van Eldik, L., Berry, R., Vassar, R., 2006. Intraneuronal beta-amyloid aggregates, neurodegeneration, and neuron loss in transgenic mice with five familial Alzheimer's disease mutations: potential factors in amyloid plaque formation. J. Neurosci. 26 (40), 10129–10140.

Oddo, S., Caccamo, A., Shepherd, J.D., Murphy, M.P., Golde, T.E., Kayed, R., Metherate, R., Mattson, M.P., Akbari, Y., LaFerla, F.M., 2003. Triple-transgenic model of Alzheimer's disease with plaque-sand tangles: intracellular Abeta and synaptic dysfunction. Neuron 39 (3), 409–421.

Oh, W.J., Westmoreland, J.J., Summers, R., Condie, B.G., 2010. Cleft palate is caused by CNS dysfunction in Gad1 and Viaat knockout mice. PLoS One 5 (3), e9758.

Olive, K.P., Tuveson, D.A., Ruhe, Z.C., Yin, B., Willis, N.A., Bronson, R.T., Crowley, D., Jacks, T., 2004. Mutant p53 gain of function in two mouse models of Li-Fraumeni syndrome. Cell 119 (6), 847–860.

Ordway, J.M., Tallaksen-Greene, S., Gutekunst, C.A., Bernstein, E.M., Cearley, J.A., Wiener, H.W., Dure, 4th, L.S., Lindsey, R., Hersch, S.M., Jope, R.S., Albin, R.L., Detloff, P.J., 1997. Ectopically expressed CAG repeats cause intranuclear inclusions and a progressive late onset neurological phenotype in the mouse. Cell 91 (6), 753–763.

Park, S.S., Kim, J.S., Tessarollo, L., Owens, J.D., Peng, L., Han, S.S., Tae Chung, S., Torrey, T.A., Cheung, W.C., Polakiewicz, R.D., McNeil, N., Ried, T., Mushinski, J.F., Morse, III, H.C., Janz, S., 2005. Insertion of c-Myc into Igh induces B-cell and plasma-cell neoplasms in mice. Cancer Res. 65 (4), 1306–1315.

Paszty, C., Brion, C.M., Manci, E., Witkowska, H.E., Stevens, M.E., Mohandas, N., Rubin, E.M., 1997. Transgenic knockout mice with exclusively human sickle hemoglobin and sickle cell disease. Science 278 (5339), 876–878.

Peters, L.L., Jindel, H.K., Gwynn, B., Korsgren, C., John, K.M., Lux, S.E., Mohandas, N., Cohen, C.M., Cho, M.R., Golan, D.E., Brugnara,

C., 1999. Mild spherocytosis and altered red cell ion transport in protein 4. 2-null mice. J. Clin. Invest. 103 (11), 1527–1537.

Piecyk, M., Wax, S., Beck, A.R., Kedersha, N., Gupta, M., Maritim, B., Chen, S., Gueydan, C., Kruys, V., Streuli, M., Anderson, P., 2000. TIA-1 is a translational silencer that selectively regulates the expression of TNF-alpha. EMBO J. 19 (15), 4154–4163.

Piedrahita, J.A., Zhang, S.H., Hagaman, J.R., Oliver, P.M., Maeda, N., 1992. Generation of mice carrying a mutant apolipoprotein E gene inactivated by gene targeting in embryonic stem cells. Proc. Natl. Acad. Sci. USA 89 (10), 4471–4475.

Podsypanina, K., Ellenson, L.H., Nemes, A., Gu, J., Tamura, M., Yamada, K.M., Cardo, C.C., Catoretti, G., Fisher, P.E., Parsons, R., 1999. Mutation of Pten/Mmac1 in mice causes neoplasia in multiple organ systems. Proc. Natl. Acad. Sci. USA 96, 1563–1568.

Politi, K., Zakowski, M.F., Fan, P.D., Schonfeld, E.A., Pao, W., Varmus, H.E., 2006. Lung adenocarcinomas induced in mice by mutant EGFR receptors found in human lung cancers respond to a tyrosine kinase inhibitor or to down-regulation of the receptors. Genes Dev. 20, 1496–1510.

Pollock, J.L., Westervelt, P., Kurichety, A.K., Pelicci, P.G., Grisolano, J.L., Ley, T.J., 1999. A bcr-3 isoform of RARa-PML potentiates the development of PML-RARa-driven acute promyelocytic leukemia. PNAS 96, 15103–15108.

Price, D.L., Sangram, S.S., Borchelt, D.R., 1998. Genetic neurodegenerative diseases: the human illness and transgenic models. Science 282 (5391), 1079–1083.

Reilly, K.B., Srinivasan, S., Hatley, M.E., Patricia, M.K., Lannigan, J., Bolick, D.T., Vandenhoff, G., Pei, H., Natarajan, R., Nadler, J.L., Hedrick, C.C., 2004. 12/15-Lipoxygenase activity mediates inflammatory monocyte/endothelial interactions and atherosclerosis in vivo. J. Biol. Chem. 279 (10), 9440–9450.

Ripps, M.E., Huntley, G.W., Hof, P.R., Morrison, J.H., Gordon, J.W., 1995. Transgenic mice expressing an altered murine superoxidedismutase gene provide an animal model of amyotrophic lateralsclerosis. Proc. Natl. Acad. Sci. USA 92 (3), 689–693.

Robinson, G.W., Hennighausen, L., 2011. MMTV-Cre transgenes can adversely affect lactation: considerations for conditional gene deletion in mammary tissue. Anal. Biochem. 412 (1), 92–95.

Saenz-Robles, M.T., Symonds, H., Chen, J., Van Dyke, T., 1994. Induction versus progression of brain tumor development: differential functions for the pRB- and p53-targeting domains of simian virus 40 T antigen. Mol. Cell Biol. 14, 2686–2698.

Sakuma, T., Nishikawa, A., Kume, S., Chayama, K., Yamamoto, T., 2014. Multiplex genome engineering in human cells using all-in-one CRISPR/Cas9 vector system. Sci. Rep. 4, 5400.

Sanford, L.P., Ormsby, I., Gittenberger-de Groot, A.C., Sariola, H., Friedman, R., Boivin, G.P., Cardell, E.L., Doetschman, T., 1997. TGF-beta2 knockout mice have multiple developmental defects that are non-overlapping with other TGFbeta knockout phenotypes. Development 124 (13), 2659–2670.

Schmidlin, F., Amadesi, S., Dabbagh, K., Lewis, D.E., Knott, P., Bunnett, N.W., Gater, P.R., Geppetti, P., Bertrand, C., Stevens, M.E., 2002. Protease-activated receptor 2 mediates eosinophil infiltration and hyperreactivity in allergic inflammation of the airway. J. Immunol. 169 (9), 5315–5321.

Schmidt-Supprian, M., Bloch, W., Courtois, G., Addicks, K., Israel, A., Rajewsky, K., Pasparakis, M., 2000. NEMO/IKK gamma-deficient mice model incontinentia pigmenti. Mol. Cell 5, 981–992.

Schorle, H., Holtschke, T., Hunig, T., Schimpl, A., Horak, I., 1991. Development and function of T cells in mice rendered interleukin-2 deficient by gene targeting. Nature 352 (6336), 621–624.

Selkoe, D.J., 2001. Alzheimer's disease: genes, proteins, and therapy. Physiol. Rev. 81 (2), 741–766.

Serrano, M., Lee, H.-W., Chin, L., Cordon-Cardo, C., Beach, D., DePinho, R.A., 1996. Role of the INK4a locus in tumor suppression and cell mortality. Cell 85, 27.

Setsuie, R., Wang, Y.L., Mochizuki, H., Osaka, H., Hayakawa, H., Ichihara, N., Li, H., Furuta, A., Sano, Y., Sun, Y.J., Kwon, J., Kabuta, T., Yoshimi, K., Aoki, S., Mizuno, Y., Noda, M., Wada, K., 2007. Dopaminergic neuronal loss in transgenic mice expressing the Parkinson's diseaseassociated UCH-L1 I93M mutant. Neurochem. Int. 50, 119–129.

Shalem, O., Sanjana, N.E., Zhang, F., 2015. High-throughput functional genomics using CRISPR-Cas9. Nat. Rev. Genet. 16, 299–311.

Shao, C., Deng, L., Henegariu, O., Liang, L., Raikwar, N., Sahota, A., Stambrook, P.J., Tischfield, J.A., 1999. Mitotic recombination produces the majority of recessive fibroblast variants in heterozygous mice. Proc. Natl. Acad. Sci. USA 96, 9230–9235.

Sharpless, M.E., Bardeesy, N., Lee, K.H., Carrasco, D., Castrillon, D.H., Aguirre, A.J., Wu, E.A., Horner, J.W., DePinho, R.A., 2001. Loss of p16(Ink4a) with retention of p19(Arf) predisposes mice to tumorigenesis. Nature 413, 86–91.

Sharpless, N.E., Ramsey, M.R., Balasubramanian, P., Castrillon, D.H., DePinho, R.A., 2004. The differential impact of p16(INK4a) or p19(ARF) deficiency on cell growth and tumorigenesis. Oncogene 23, 379–385.

Shen, S.X., Weaver, Z., Xu, X., Li, C., Weinstein, M., Chen, L., Guan, X.Y., Ried, T., Deng, C.X., 1998. A targeted disruption of the murine Brca1 gene causes gamma-irradiation hypersensitivity and genetic instability. Oncogene 17, 3115–3124.

Shen, B., Zhang, J., Wu, H., Wang, J., Ma, K., Li, Z., Zhang, X., Zhang, P., Huang, X., 2013. Generation of gene-modified mice via Cas9/RNA-mediated gene targeting. Cell ResV 23, 720–723.

Sinn, E., Muller, W., Pattengale, P., Tepler, I., Wallace, R., Leder, P., 1987. Coexpression of MMTV/v-Ha-ras and MMTV/c-myc genes in transgenic mice: synergistic action of oncogenes in vivo. Cell 49, 465–475.

Slow, E.J., van Raamsdonk, J., Rogers, D., Coleman, S.H., Graham, R.K., Deng, Y., Oh, R., Bissada, N., Hossain, S.M., Yang, Y.Z., Li, X.J., Simpson, E.M., Gutekunst, C.A., Leavitt, B.R., Hayden, M.R., 2003. Selective striatal neuronal loss in a YAC128 mouse model of Huntington disease. Hum. Mol. Genet. 12, 1555–1567.

Smithies, O., Gregg, R.G., Boggs, S.S., Koralewski, M.A., et al., 1985. Insertion of DNA sequences into the human chromosomal beta-globin locus by homologous recombination. Nature 317, 230–234.

Smits, R., Hofland, N., Edelmann, W., Geugien, M., Jagmohan-Changur, S., Albuquerque, C., Breukel, C., Kucherlapati, R., Kielman, M.F., Fodde, R., 2000. Somatic Apc mutations are selected upon their capacity to inactivate the beta-catenin downregulating activity. Genes Chromosomes Cancer 23, 223–229.

Snouwaert, J.N., Brigman, K.K., Latour, A.M., Malouf, N.N., Boucher, R.C., Smithies, O., Koller, B.H., 1992. An animal model for cystic fibrosis made by gene targeting. Science 257 (5073), 1083–1088.

Song, Z., Wu, X., Powell, W.C., Cardiff, R.D., Cohen, M.B., Tin, R.T., Matusik, R.J., Miller, G.J., Roy-Burman, P., 2002. Fibroblast growth factor 8 isoform B overexpression in prostate epithelium: a new mouse model for prostatic intraepithelial neoplasia. Cancer Res. 62 (17), 5096–5105.

Souders, N.C., Sewell, D.A., Pan, Z.-K., Hussain, S.F., Rodriguez, A., Wallecha, A., Paterson, Y., 2007. Listeria-based vaccines can overcome tolerance by expanding low avidity CD8+ T cells capable of eradicating a solid tumor in a transgenic mouse model of cancer. Cancer Immun. 7, 2–14.

Starr, T.K., Allaei, R., Silverstein, K.A., Staggs, R.A., Sarver, A.L., Bergemann, T.L., Gupta, M., O'Sullivan, M.G., Matise, I., Dupuy, A.J., Collier, L.S., Powers, S., Oberg, A.L., Asmann, Y.W., Thibodeau, S.N., Tessarollo, L., Copeland, N.G., Jenkins, N.A., Cormier, R.T., Largaespada, D.A., 2009. A transposon-based genetic screen in mice identifies genes altered in colorectal cancer. Science 323 (5922), 1747–1750.

Sturchler-Pierrat, C., Abramowski, D., Duke, M., Wiederhold, K.H., Mistl, C., Rothacher, S., Ledermann, B., Burki, K., Frey, P., Paganetti, P.A., Waridel, C., Calhoun, M.E., Jucker, M., Probst, A., Staufenbiel, M., Sommer, B., 1997. Two amyloid precursor protein transgenic mouse modelswith Alzheimer disease-like pathology. Proc. Natl. Acad. Sci. USA 94 (24), 13287–13292.

Sun, Y., Chen, X., Xiao, D., 2007. Tetracycline-inducible expression systems: new strategies and practices in the transgenic mouse modeling. Acta Biochim. Biophys. Sin. 39, 235–246.

Sung, Y.H., Baek, I.J., Kim, D.H., Jeon, J., Lee, J., Lee, K., Jeong, D., Kim, J.S., Lee, H.W., 2013. Knockout mice created by TALEN-mediated gene targeting. Nat. Biotechnol. 31, 23–24.

Symonds, H.S., McCarthy, S.A., Chen, J., Pipas, J.M., Van Dyke, T., 1993. Use of transgenic mice reveals cell-specific transformation by a simian virus 40 T-antigen amino-tenal mutant. Mol. Cell Biol. 13 (6), 3255–3265.

Temme, A., Buchmann, A., Gabriel, H.D., Nelles, E., Schwarz, M., Willecke, K., 1997. High incidence of spontaneous and chemically induced liver tumors in mice deficient for connexin32. Curr. Biol. 7 (9), 713–716.

Tesson, L., Usal, C., Menoret, S., Leung, E., Niles, B.J., Remy, S., Santiago, Y., Vincent, A.I., Meng, X., Zhang, L., Gregory, P.D., Anegon, I., Cost, G.J., 2011. Knockout rats generated by embryo microinjection of TALENs. Nat. Biotechnol. 29, 695–696.

Tetreault, M.P., Yang, Y., Travis, J., Yu, Q.C., Klein-Szanto, A., Tobias, J.W., Katz, J.P., 2010. Esophageal squamous cell dysplasia and delayed differentiation with deletion of krüppel-like factor 4 in murine esophagus. Gastroenterology 139, 171–181.

Theuring, F., Thunecke, M., Kosciessa, U., Turner, J.D., 1997. Transgenic animals as models of neurodegenerative diseases in humans. Trends Biotechnol. 15 (8), 320–325.

Tu, Z., Yang, W., Yan, S., Guo, X., Li, X.-J., 2015. CRISPR/Cas9: a powerful genetic engineering tool for establishing large animal models of neurodegenerative diseases. Mol. Neurodegen. 10, 35.

Turner, B.J., Talbot, K., 2008. Trasgenics, toxicity and therapeutics in rodent models of mutant SOD1- mediated familial ALS. Prog. Neurobiol. 85 (1), 94–134.

Tzeng, Y.J., Guhl, E., Graessmann, M., Graessmann, A., 1993. Breast cancer formation in transgenic animals induced by the whey acidic protein SV40 T antigen (WAP-SV-T) hybrid gene. Oncogene 8, 1965–1971.

Umanoff, H., Edelmann, W., Pellicer, A., Kucherlapati, R., 1995. The murine N-ras gene is not essential for growth and development. Proc. Natl. Acad. Sci. USA 92, 1709–1713.

Utomo, A.R.H., Kikitin, A.Y., Lee, W.H., 1999. Temporal, spatial, and cell type-specific control of Cre-mediated DNA recombination in transgenic mice. Nat. Biotechnol. 17, 1091–1096.

Van Den Bosch, L., 2011. Genetic rodent models of amyotrophic lateral sclerosis. J. Biomed. Biotechnol. 2011, 348765.

Ventura, A., Kirsch, D.G., McLaughlin, M.E., Tuveson, D.A., Grimm, J., Lintault, L., Newman, J., Reczek, E.E., Weissleder, R., Jacks, T., 2007. Restoration of p53 function leads to tumor regression in vivo. Nature. 445 (7128), 606–607.

Voncken, J.W., Griffiths, S., Greaves, M.F., Pattengale, P.K., Heisterkamp, N., Groffen, J., 1992. Restricted oncogenicity of BCR/ABL p190 in transgenic mice. Cancer Res. 52, 4534–4539.

Wagner, K.U., Wall, R.J., St-Onge, L., Gruss, P., Wynshaw-Boris, A., Garrett, L., Li, M., Furth, P.A., Hennighausen, L., 1997. Cre-mediated gene deletion in the mammary gland. Nucleic Acids Res. 25 (21), 4323–4330.

Wang, Z.G., Delva, L., Gaboli, M., Rivi, R., Giorgio, M., Cordon-Cardo, C., Grosveld, F., Pandolfi, P.P., 1998. Role of PML in cell growth and the retinoic acid pathway. Science 279, 1547–1551.

Wang, X., Kruithof-de Julio, M., Economides, K.D., Walker, D., Yu, H., Halili, M.V., Hu, Y.-P., Price, S.M., Abate-Shen, C., Shen, M.M., 2009. A luminal epithelial stem cell that is a cell of origin for prostate cancer. Nature 461, 495–500.

Wang, H., Yang, H., Shivalila, C.S., Dawlaty, M.M., Cheng, A.W., Zhang, F., Jaenisch, R., 2013. One-step generation of mice carrying mutations in multiple genes by CRISPR/Cas-mediated genome engineering. Cell 153, 910–918.

Weiss, W.A., Aldape, K., Mohapatra, G., Feuerstein, B.G., Bishop, J.M., 1997. Targeted expression of MYCN causes neuroblastoma in transgenic mice. EMBO J. 16, 2985–2995.

Welsh, S., Kay, S.A., 1997. Reporter gene expression for monitoring gene transfer. Curr. Opin. Biotechnol. 8, 617–622.

Wheeler, V.C., Auerbach, W., White, J.K., Srinidhi, J., Auerbach, A., Ryan, A., Duyao, M.P., Vrbanac, V., Weaver, M., Gusella, J.F., Joyner, A.L., MacDonald, M.E., 1999. Length-dependent gametic CAG repeat instability in the Huntington's disease knock-in mouse. Hum. Mol. Genet. 8 (1), 115–122.

Wisniewski, T., Sigurdsson, E.M., 2010. Murine models of Alzheimer's disease and their use in developing immunotherapies. Biochim. Biophys. Acta 1802 (10), 847–859.

Wong, M.H., Gordon, J.I., 2000. Genetic mosaic analysis based on Cre recombinase and navigated laser capture microdissection. Proc. Natl. Acad. Sci. USA 97, 12601–12606.

Wong, P.C., Pardo, C.A., Borchelt, D.R., Lee, M.K., Copeland, N.G., Jenkins, N.A., Sisodia, S.S., Cleveland, D.W., Price, D.L., 1995. An adverse property of a familial ALS-linked SOD1 mutationcauses motor neuron disease characterized by vacuolardegeneration of mitochondria. Neuron 14 (6), 1105–1116.

Woollard, J.R., Punyashtiti, R., Richardson, S., Masyuk, T.V., Whelan, S., Huang, B.Q., Lager, D.J., vanDeursen, J., Torres, V.E., Gattone, V.H., LaRusso, N.F., Harris, P.C., Ward, C.J., 2007. A mouse model of autosomal recessive polycystic kidney disease with biliary duct and proximal tubule dilatation. Kidney Int. 72 (3), 328–336.

Wu, X., Wu, J., Huang, J., Powell, W.C., Zhang, J., Matusik, R.J., Sangiorgi, F.O., Maxson, R.E., Sucov, H.M., Roy-Burman, P., 2001. Generation of a prostate epithelial cell-specific Cre transgenic mouse model for tissue-specific gene ablation. Mech. Dev. 101, 61–69.

Xue, W., Chen, S., Yin, H., Tammela, T., Papagiannakopoulos, T., Joshi, N.S., Cai, W., Yang, G., Bronson, R., Crowley, D.G., Zhang, F., Anderson, D.G., Sharp, P.A., Jacks, T., 2014. CRISPR-mediated direct mutation of cancer genes in the mouse liver. Nature 514, 380–384.

Yamanaka, S., Johnson, M.D., Grinberg, A., Westphal, H., Crawley, J.N., Taniike, M., Suzuki, K., Proia, R.L., 1994. Targeted disruption of the Hexa gene results in mice with biochemical and pathologic features of Tay-Sachs disease. Proc. Natl. Acad. Sci. USA 91 (21), 9975–9979.

Yang, H., Wang, H., Shivalila, C.S., Cheng, A.W., Shi, L., Jaenisch, R., 2013. One-step generation of mice carrying reporter and conditional alleles by CRISPR/Cas-mediated genome engineering. Cell 154, 1370–1379.

Yoshimi, Kazuto, Kunihiro, Yayoi, Kaneko, Takehito, Nagahora, Hitoshi, Voigt, Birger, Mashimo, Tomoji, 2016. ssODN-mediated knock-in with CRISPR-Cas for large genomic regions in zygotes. Nat. Commun. 7, Article number: 10431.

Zheng-Fischhöfer, Q., Ghanem, A., Kim, J.S., Kibschull, M., et al., 2006. Connexin31 cannot functionally replace connexin43 during cardiac morphogenesis in mice. J. Cell Sci. 119, 693–701.

Zhu, Y., Romero, M.I., Ghosh, P., Ye, Z., Charnay, P., Rushing, E.J., Marth, J.D., Parada, L.F., 2001. Ablation of NF1 function in neurons induces abnormal development of cerebral cortex and reactive gliosis in the brain. Genes Dev. 15, 859–876.

Zhuu, et al., 2009. Proc. Natl. Acad. Sci. USA 106 (8), 2712–2716.

Zindy, F., Williams, R.T., Baudino, T.A., Rehg, J.E., Skapek, S.X., Cleveland, J.L., Roussel, M.F., Sherr, C.J., 2003. Arf tumor suppressor promoter monitors latent oncogenic signals in vivo. Proc. Natl. Acad. Sci. USA 100, 2003.

Further Reading

Chin, L, Pomerantz, J., Polsky, D., Jacobson, M., Cohen, C., Cordon-Cardo, C., Horner, II, J.W., DePinho, R.A., 1997. Cooperative effects of INK4a and Ras in melanoma susceptibility in vivo. Genes Dev. 11, 2822–2834.

Giasson, B.I., Duda, J.E., Quinn, S.M., Zhang, B., Trojanowski, J.Q., Lee, V.M., 2002. Neuronal alpha-synucleinopathy with severe movement disorder in mice expressing A53T human alpha-synuclein. Neuron 34, 521–533.

Kahle, P., Neumann, M., Ozmen, L., Muller, V., Jacobsen, H., Schindzielorz, A., Okochi, M., Leimer, U., van Der Putten, H., Probst, A., Kremmer, E., Kretzschmar, H.A., Haass, C., 2000. Subcellularlocalization of wild-type and Parkinson's disease-associated mutant alpha-synuclein in human and transgenic mouse brain. J. Neurosci. 20, 6365–6373.

Lu, X.H., Fleming, S.M., Meurers, B., Ackerson, L.C., Mortazavi, F., Lo, V., Hernandez, D., Sulzer, D., Jackson, G.R., Maidment, N.T., Chesselet, M.F., Yang, X.W., 2009. Bacterial artificial chromosome transgenic mice expressing atruncated mutant parkin exhibit age-dependent hypokineticmotor deficits, dopaminergic neuron degeneration, andaccumulation of proteinase K-resistant alpha-synuclein. J. Neurosci. 29 (7), 1962–1976.

Matsuoka, Y., Vila, M., Lincoln, S., McCormack, A., Picciano, M., LaFrancois, J., Yu, X., Dickson, D., Langston, W.J., McGowan, E., Farrer, M., Hardy, J., Duff, K., Przedborski, S., Di Monte, D.A., 2001. Lack of nigral pathology in transgenic mice expressing human alpha-synuclein driven by the tyrosine hydroxylase promoter. Neurobiol. Dis. 8, 535–539.

Richfield, E.K., Thiruchelvam, M.J., Cory-Slechta, D.A., Wuertzer, C., Gainetdinov, R.R., Caron, M.G., Di Monte, D.A., Federoff, H.J., 2002. Behavioral and neurochemical effects of wild-type and mutated human alpha-synuclein in transgenic mice. Exp. Neurol. 175, 35–48.

van der Putten, H., Wiederhold, K.H., Probst, A., Barbieri, S., Mistl, C., Danner, S., Kauffmann, S., Hofele, K., Spooren, W.P., Ruegg, M.A., Lin, S., Caroni, P., Sommer, B., Tolnay, M., Bilbe, G., 2000. Neuropathology in mice expressing human alpha-synuclein. J. Neurosci. 20, 6021–6029.

28

Forward and Reverse Genetics to Model Human Diseases in the Mouse

Yoichi Gondo, Shigeru Makino, Ryutaro Fukumura

RIKEN BioResource Center, Tsukuba, Ibaraki, Japan

OUTLINE

In this Chapter, we summarize development and establishment of mutant mouse strains focusing on modeling human diseases. Around the year 2000, the human disease modeling showed a striking breakthrough due to the accomplishment of the Human and Mouse Genome Projects (International Human Genome Sequencing, 2001, 2004; Mouse Genome Sequencing et al., 2002). Multidisciplinary efforts then advanced various next-generation technologies, databases, and bioinformatics. The key of modeling human diseases is the newly established mutagenesis technologies, often called "forward" and "reverse" genetics (reviewed by Gondo, 2008). Starting from the establishment of disease models for Mendelian disorders, namely, monogenic traits, modeling of quantitative and polygenic traits (classically, one of non-Mendelian traits) are also anticipated, since most of human diseases are complex traits.

1 GENETIC OR ENVIRONMENTAL

Most of human diseases are developed by a combination of genetic and environmental factors. When the genetic factor is a single exclusive element, it is easily observed the inheritance in a Mendelian fashion. A typical example is the Huntington's disease. The patients carrying the expanded CAG triplet repeats on their *Huntingtin* gene, they develop the disease in their midage irrespective of their environmental history and conditions (The Huntington's Disease Collaborative Research Group, 1993).

When the number of the genetic factors for the disease becomes more multigenic with a lower penetrance, it becomes harder to conclude the existence of genetic contributions to the disease. The key to distinguish the genetic factors is to identify the causative genes and mutations. Prominent evidences of Mendelian inheritance in a defined pedigree(s) often lead to such identification of major causative genes and responsible mutations among many genetic factors. For instance, inherited mutations of the *glucokinase* (Froguel et al., 1993; Vionnet et al., 1992) and *Apc* (Groden et al., 1991; Ichii et al., 1993; Joslyn et al., 1991; Nishisho et al., 1991) genes were independently discovered concordance with the patients of

diabetes (type 2) and colon cancers (familial adenomatous polyposis; FAP) in the pedigrees, respectively. The carriers of identified mutations mostly develop the corresponding diseases; thus, the penetrance is very high. However, many diabetic and colon cancer patients do not carry any mutations in the *glucokinase* and *Apc* genes, respectively. Other responsible genes and genetic factors have been anticipated and indeed identified affecting the diabetes (Lambrinoudaki et al., 2010; Vaxillaire and Froguel, 2008) and colon cancers (Hassen et al., 2012; Pineda et al., 2010; Plotz et al., 2012).

Most of human diseases including common diseases are caused by a combination of mutations on several major (and minor) genes with various environmental factors. It is noteworthy that the minor genetic factors, often called "modifiers," are extremely difficult to identify. The population studies, for instance, with identical twins, are also revealing that some psychiatric diseases have high heritability (reviewed by Burmeister et al., 2008). For instance, the heritability of schizophrenia, bipolar disorders, and autism is often estimated to be ~80%, indicating that the genetic influence is much higher than environmental conditions in the studied populations. Nevertheless, no major genes to cause these mental illnesses have yet been identified, although many candidate mutations and genes have been nominated. No major but many minor genes with fewer effects of environmental factors are, therefore considered to govern such psychiatric diseases that exhibit higher heritability.

2 GENOME PROJECT AND HUMAN DISEASES

The primary driving force of the Human Genome Project in 1990 was to systematically identify all the responsible genes for genetic diseases (Watson, 1990). The Huntington's disease, for instance, was identified as a dominant Mendelian monogenic disease and the responsible gene, *Huntingtin*, was mapped on chromosome 4q16.3 in human genome. The *Huntingtin* gene was then molecularly cloned, sequenced, and the causative mutation, CAG triplet expansion, was discovered (The Huntington's Disease Collaborative Research Group, 1993).

These findings gave rise to a concrete method to diagnose patients. Similar forward genetics to identify the genetic cause of various diseases and traits have been conducted. Duchenne muscular dystrophy (Monaco et al., 1985), Retinoblastoma (Friend et al., 1986), cystic fibrosis (Riordan et al., 1989), and familial adenomatous polyposis (Groden et al., 1991; Joslyn et al., 1991; Kinzler et al., 1991) were successful examples.

Considering the total cost, manpower, and time, a systematic and collaborative international effort to sequence whole human genome seemed to be much more effective (Cantor, 1990; Watson, 1990). The sequencing of the whole human genome should also contribute primarily for the detection and diagnosis and ultimately for the cure and prevention of all the human diseases and disorders.

In addition, the knowledge of the human genome should accelerate the study of basic and general biology, in particular, genetics, evolution, and developmental biology. Thus, it was recognized that the completion of the whole human genomic DNA sequence was not the ultimate goal but just the first step to conduct functional and comparative genomics to understand basic biology and to apply for the prevention and therapeutics of human diseases.

In this context, Helmholtz Zentrum München (HZM; formally, GSF) in Germany (Hrabe de Angelis and Balling, 1998; Hrabe de Angelis et al., 2000) and Medical Research Council (MRC), UK (Brown and Nolan, 1998; Nolan et al., 2000) have started the large-scale ENU mouse mutagenesis projects in 1997 to model human diseases in the mouse. The research community also proposed the necessity of the Mouse Genome Project to sequence the whole genome of the standard laboratory strain, C57BL/6J (Nadeau et al., 2001). Following to the progress of the Human Genome Project, thus, the Mouse Genome Project has been conducted and completed (Mouse Genome Sequencing et al., 2002) in parallel aiming the functional and comparative genomics between the human and mouse.

3 BASIC GENETICS TO DEVELOP AND USE MODEL MICE

In this section, basic genetics is summarized focusing on the key genetic terminology, the concept of which is useful to design and to experimentally develop new mutant mice as models for diseases. The fundamental knowledge of the genetics also promotes the better practical use of the established mutant mice as well.

3.1 Locus (pl. Loci)

The both terms of "locus" and "allele" are often collectively called as "gene." To explain the Mendelian inheritance, locus and allele are distinctively used. The gene is coded in a particular location of the genome to give rise to certain function or "trait." To define the unique location coding for the gene in the genome, the term "locus" is used. Thus, the number of loci and the sequence of each locus are predetermined specific to each species. Not only the location but also the DNA sequence of each locus is unique and distinctive from those of the other loci. The key rationale of the mutant mouse to be a model for the human disease is the high similarity of entire genome between human and mouse. Classically, the size of the genome and the number of the genes in the human and mouse genomes had been estimated to be very similar values of 3×10^9 bp and 100,000–150,000 genes (Chikaraishi et al., 1978), respectively. The completion of the Human and Mouse Genome Projects gave rise to better estimates to confirm the total size of the genome to be $\sim 3 \times 10^9$ bp but the number of the coded genes, or loci, to be 30,000 or less in both the species (International Human Genome Sequencing, 2001, 2004; Mouse Genome Sequencing et al., 2002). Not only the total number of loci, the locus order of local locations, called "synteny," but also the sequences of the corresponding loci, called "orthologs," are very similar, indicating the good conservation of the gene function between human and mouse.

3.2 Allele

Even within a species, polymorphisms exist producing various phenotypes and genetic variability in natural populations. Most of the unique sequences of a particular locus have some minor differences, giving rise to different subtypes of the locus. The subtype is called "allele." Mutations are the origin of new alleles in a particular locus (Fig. 28.1). In theory, many subtypes may exist per locus.

The Human Genome Project (International Human Genome Sequencing, 2001; International SNP Map Working Group, 2001) actually detected more than 1.4 million single nucleotide polymorphisms (SNPs) in the human population; thus, approximately 0.1% of human genomic sequences are polymorphic.

At the molecular level, the whole consensus genomic DNA sequence ultimately defines the species. The number of the alleles in one species defines the degree of the genetic variability of the species. Any subpopulations of a particular species must have the same set of the loci, namely, the same consensus DNA sequences in the genome. On the other hand, each subpopulation may have a distinct set of alleles. Thus, even in the same species, the genetic variability and diversities may be different from the other depending on each subpopulation. One extreme case is that all the loci have only one allele in a subpopulation, which is called an "inbred" subpopulation (described in details later).
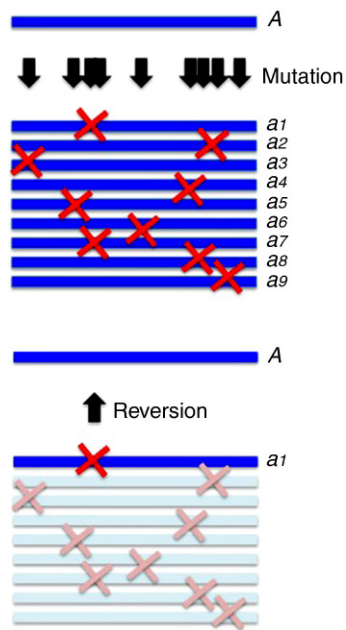
FIGURE 28.1   **Molecular view of mutations to create new alleles.** In general, a gene is coded ~1000 bp or more of protein-coding sequences called open reading frame (ORF) in addition to introns and regulatory elements. Subtle mutations randomly change a small number of or a single base pair of genomic DNA sequences of the gene. The random nature of the mutation usually disrupts the normal function of the gene. Therefore, the mutant allele is usually a loss-of-function type mutation. In one wild-type locus as shown in the *upper panel*, there are many base pairs to disrupt the wild-type functional sequence. On the other hand, there is only one way to reverse a particular mutant allele to the wild type allele. It is the base of the molecular view that the mutation rate ($\sim 10^{-5}$/locus/gamete) of the gene is usually three orders of magnitude higher than the reversion rate ($\sim 10^{-8}$/locus/gamete) of any mutant allele. The reversion is a gain-of-function type event to restore the normal function of the gene. Loss-of-function type mutations are usually recessive to the wild type allele as shown in Fig. 2. Inversely, the gain-of-function type mutant allele tends to become dominant. In analogy to the reversion, the mutation rate to change the normal gene to more or additional functional gene, namely, to gain-of-function type allele, is similar to the reversion rate of $\sim 10^{-8}$/locus/gamete. Based on this molecular view, recessive mutations are usually loss-of-function types with three orders of magnitude higher mutation rate to dominant gain-of-function types mutations.

Some SNPs show no functional differences form the wild-type allele. Such functionally identical SNPs may be collectively called the wild-type alleles. Some other SNPs may be evolutionarily neutral but the function of each allele may be different from the other. For instance, in the ABO blood type locus, the three well-known alleles of A, B, and O exist. The A and B alleles produce the same enzyme, glycosyltransferase, with a subtle difference that makes distinctive glycosilation to a precursor substance, the H antigen, on the red blood cells. The O allele has no function to make such glycosilation by a single deletion of the glycosyltransferase gene (Yamamoto et al., 1990). Thus, all the three alleles of the ABO blood-type locus are functionally different but

may be evolutionarily neutral. Even in each allele, many differences of genomic sequences have been identified, indicating the practical existence of silent alleles in collectively called A, B, or O allele (Yip, 2002).

The SNPs responsible for genetic factors of human diseases have also been identified. The Haplotype Mapping (HapMap) Project (International HapMap Consortium, 2003), the Genome-Wide Association Studies (GWAS) (Wellcome Trust Case Control, 2007), and the 1000 Genomes Project (Via et al., 2010) are to primarily identify such SNPs responsible for human diseases. The scale has been expanded to the order of million based on new technologies (reviewed by Auffray et al., 2016). One of the major goals of the mouse mutagenesis is to produce mutant alleles analogous to human SNPs as a model.

4 DIPLOID AND GENOTYPE

Both human and mouse are diploid organisms, each of which has two sets of the genome. Namely, one individual has the two whole sets of loci with two alleles on each locus. When an individual carries the same and different two alleles in a locus, it is called a "homozygote" and "heterozygote," respectively, with respect to the locus. The combination of the two alleles in a particular locus is called genotype.

In the example of the ABO-blood type, three distinctive alleles exist. Accordingly, the six different genotypes, three of which are *AA*, *BB*, and *OO* homozygotes and the other three of which are *AB*, *AO*, and *BO* heterozygotes, appear in human population.

The alleles exhibiting and concealing their phenotypes in the heterozygotes are called "dominant" and "recessive," respectively. Thus, the dominant-recessive relations are defined for a set of two alleles in one locus and the effect of the relation is only observed in the heterozygotes (Fig. 28.2).

In the example of the *ABO* blood type in the previous section, the *ABO*-blood-type locus has three alleles, *A*, *B*, and *O*; thus, the dominant-recessive relations are defined for all the three possible heterozygotes, *AB*, *AO*, and *BO*. The phenotype, namely blood type, of *AO* and *BO* heterozygotes are [A] and [B], respectively. In genetics, the phenotypes are often shown in brackets like [A] in order to distinguish from the allele of *A*. *A* and *B* alleles are thus dominant to *O* allele. The *AB* heterozygotes show [AB] blood type. In this case, the relation between *A* and *B* alleles are called "codominant." As described before, the *O* allele produces no functional glycosyltransferase enzyme. Such allele, like the *O* allele, is called a "loss of function" type or a null allele. In general, the gene product of the loss-of-function allele does not hamper the functional counterpart. The functional allele, such as the
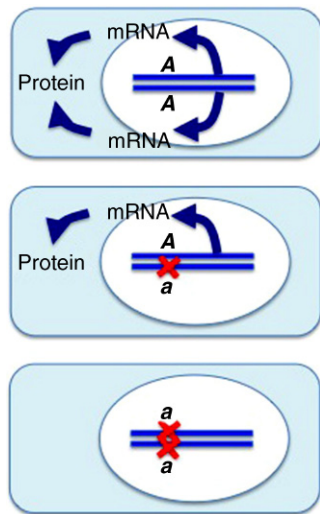
FIGURE 28.2 **Molecular and cellular view of dominant versus recessive alleles.** *Top panel*: Hypothetical locus *A* encodes mRNA that is translated to protein in the cell. Mutant allele *a* changed a part of the functional sequence of the locus so that no functional proteins translated from the *a* allele. *Bottom panel*: Due to the lack of the functional protein, *aa* mutant homozygotes, exhibit the mutant phenotype different from the *AA* wild-type homozygotes. *Middle panel*: The *Aa* heterozygotes usually exhibit indistinguishable phenotype to the *AA* wild types. It is because the one allele of *A* produces enough active proteins and the mutant allele *a* produce nothing (null) or no functional proteins (amorph) that do not hamper the normal function of the *A* protein, making the *A* allele is dominant to the *a* allele.

A and *B* alleles, is usually produces an enough amount of the active enzyme to exhibit the corresponding phenotypes. Mutations usually occur randomly by disturbing the functional sequence of the locus; thus, the mutant allele tends to become a loss-of-function type, namely, recessive. It is the basic molecular-biological-view of the Mendel's dominant versus recessive relation. It is, however, noteworthy that many exceptions have been identified. For instance, the loss-of-function mutations exhibited dominant phenotypes in *glucokinase* and *Apc* mutations in diabetes and colon cancer by haploinsufficiency and dominant negative effects, respectively.

When an allele is only observed in heterozygotes but never in homozygotes, the allele is considered to be recessive lethal. If the product of the gene function is necessary and indispensable for the organisms, the loss-of-function mutation tends to make a recessive lethal allele. Thus, the gene coded by the locus that potentially has a recessive lethal allele is considered as an essential gene.

In the previously demonstrated "inbred" subpopulations, all the loci have only the same pair of one allele, namely, all the loci are homozygous. When a female is mated to any male of an inbred subpopulation, all the offspring again have the same homozygous inbred genetic background called "isogenic." Such inbred subpopulations have hardly been found in natural population but are possible to establish in the laboratory by consecutive

mating a pair of a sister and a brother in the same litter, or sib mating, more than 20 generations. The previously mentioned C57BL/6J mouse, which is subjected to the Mouse Genome Project, is one of the many inbred laboratory strains.

5 COISOGENIC AND CONGENIC STRAINS

In mutagenesis studies, various phenotypes of the mutant mice are compared to those of the wild types to study the gene function. Since mouse is diploid, the comparison may be made between the wild-type homozygotes, heterozygotes, and mutant homozygotes. In this phenotype assessment, all the mice not only have the two alleles in the locus but also have the pairs of alleles in all the other loci in entire genome. Various allelic differences in the genetic background may disturb the phenotype assessment for the particular allelic difference of the objective locus. It is therefore ideal to make an isogenic background except for the objective locus to distinctively elucidate the function of the objective locus.

When two strains have a difference only on the objective locus but all the other loci are completely identical, they are called "coisogenic" each other. The coisogenic strains may be obtained by a spontaneously arisen mutation in an inbred strain because the mutation is a very rare event and occurs only once at most in one animal. The availability of the coisogenic strains have been, thus, very limited due to the extremely rate event of spontaneous mutations. Recently, however, the genome editing method has become available to systematically construct coisogenic strains in any loci in almost any species as described later in this Chapter.

In order to establish a coisogenic-like strain, so-called congenic strain, for any mutations in any genetic background, an objective mouse is backcrossed to an isogenic inbred strain. After six generations of backcrosses, 99% of the genome becomes the inbred isogenic background except the linked loci. The alleles in the closely linked loci may still remain the same as in the original founder mouse due to the linkage disequilibrium. The degree of the linkage disequilibrium is dependent on the probability of the recombination; thus, more backcrossing conducted, narrower down to only the objective allele from the founder. The backcrossing more than 20 generations is conventionally considered to be congenic.

Both coisogenic and congenic strains are useful to conduct the analysis of the monogenic trait of the objective locus. One of the historical landmarks using congenic strains was the discovery of the *histocompatibility-2* (*H-2*) locus in the mouse, one of the histocompatibility loci mapped by the tumor rejection and congenic technology (Snell and Higgins, 1951). The further analyses

revealed that the H-2 "locus" encompassed many loci and renamed to H-2 complex (reviewed by Klein, 1979). The discovery of the H-2 complex in the mouse led to the identification of the major histocompatibility complex (MHC) class I, II, and III that is common in the mammalian species including human, namely, HLA complex.

6 DOUBLE STRANDED DNA, LINKAGE, AND HAPLOTYPE

One chromosome consists of one double-stranded helix DNA molecule. Human and mouse has 22 and 19 pairs of autosomes, respectively, in addition to XX in female and XY in male. As mentioned earlier, the genotype is defined as a set of two alleles at a single locus. Haplotype is, on the other hand, defined a set of alleles found in a haploid gamete, namely either in a mature oocyte or sperm. The largest haplotype is, thus, the whole set of alleles in one oocyte or sperm. The haplotype is usually used, however, to describe a set of alleles in closely linked loci on one double-stranded DNA. Such alleles do not segregate independently. Rather, inherited together until a recombination disrupts the linkage on the same DNA strand. The schematic view of the haplotype with genotype is depicted in Fig. 28.3.

On five pairs of autosomal homologs, eight loci, *A, B, C, … and H* are shown. The locus names are conventionally designated as the names of the wild-type dominant alleles. The genotypes are defined on each locus, for instance, *A*, *B*, and *C* loci are all heterozygote of *Aa*, *Bb*, and *Cc*. On the other hand, from the particular three loci of A, B, and C may give rise to one of the eight different combinations of haplotypes to a given gamete, *A-B-C, A-B-c, A-b-C, A-b-b, a-B-C, a-B-c, a-b-C,* and *a-b-c*. The three loci are on independent autosomes so that the probabilities to have any one of the eight haplotypes in one gamete are all equal. On the other hand, when three loci are on a pair of autosomal homo-

logs, the set of three alleles of the three loci on the same homolog, namely, on the same double-stranded DNA, is cotransmitted to the gamete unless a recombination occurs between the three loci during the meiosis. For instance, only the two haplotypes of *C-f-g* and *c-F-G* among the eight possible ones may be transmitted to gamete without recombination in the case for Fig. 28.3. Snell and Higgins (1951) considered the *H-2* complex as a single locus at first. Later on, they identified that the *H-2* region of about 2-cM encompassed many loci; therefore the haplotypes were conventionally used to specify a particular set of alleles on one DNA strand or one homolog in the MHC complex. A particular haplotype of alleles of closely linked loci shows linkage disequilibrium in a few generations. Meantime, DNA recombinations occur in meiosis and shuffle the haplotype and gradually the linkage disequilibrium disappears. Therefore, the degree of the linkage disequilibrium of a haplotype is dependent on the genetic distances of the loci in the haplotype and the number of the generations since the haplotype was formed. It is noteworthy that the natural selection often disturbs the hypothetical situation of the established strains. For instance, twenty generations of the sib mating are theoretically enough to establish an inbred strain with more than 99% homozygosity. When detrimental alleles exist in the original mouse, however, the heterozygosity may be kept much longer generations. In the Fig. 28.3, when the *d* and *h* alleles are recessive lethal in the tightly linked loci *D* and *H*, both the haplotypes of *D-h* and *d-H* always transmitted to the next generation as *D/d, h/H* mice, because other possible mice carrying *D/D, h/h,* and *d/d, H/H* die due to the recessive lethality of *h* and *d*, respectively.

7 MUTANT MICE AS DISEASE MODELS

The spontaneous mutation rate is very low; for instance, roughly three orders of magnitude lower than that induced by the most potent mutagen, ethylnitrosourea (ENU) in the mouse (Russell et al., 1981). Thus, the development and establishment of mutant strains are often laborious and take time. Once mutant strains are established and maintained, however, any researchers may access to the strains as a research resource.

Mutations usually occur randomly in the genome. Most of the mutations are a loss-of-function type due to the disturbance or disruption of the functional DNA sequences (Figs. 28.1 and 28.2). Thereby, a biological effect(s) of most of the mutations is a detrimental to the organisms. Namely, mutations are likely to induce some disorders modeling many diseases and deficiencies in human.
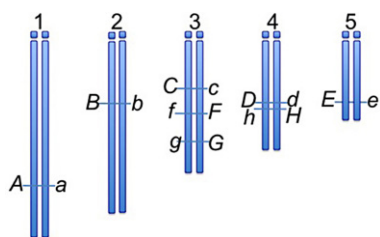
FIGURE 28.3   Linkage and haplotype on the chromosome. Five pairs of autosomes with the genotypes of eight loci are schematically shown. The alleles on the different chromosomes are segregated to gamete with 50:50 chances according to the Mendel's second law. The linked alleles on the same chromosomes are cotransmitted to gamete unless a recombination occurs between the linked loci. For instance, C-f-g, c-F-G, d-H, and D-g are cotransmitted without recombination.

8 FANCY MICE

Even before the establishment of Mendelian genetics, many mutant mice in *Mus musculus*, had been isolated, established, and accumulated, called "fancy mice," by collectors, often called mouse fanciers, as pets (Rader, 2004). To make them easier to handle, smaller, gentler more fertile and less aggressive mice were usually selected in addition to some peculiar phenotypes of eye and coat colors, coat patterns, morphological anomalies, strange behaviors, and other traits. Thus, many of the mutations in fancy mice are monogenic visible mutations with high penetrance.

When the Mendel's inheritance laws were rediscovered in 1900, fancy mice immediately bacame a good resource for the experimental studies. The mutant alleles, *a*, *b*, *c*, *d*, and *e* in the *nonagouti*, *brown*, *albino*, *dilute*, and *pink-eyed dilution* loci, respectively, were established from fancy mice in this early period of the 20th century. In the classic genetics, the names of wild-type alleles, as well as the names of loci for *a*, *b*, *c*, *d*, and *e* mutant alleles were both designated to *A*, *B*, *C*, *D*, and *E*. The first linkage of any mammalian species was indeed discovered between the *C* and *E* loci by (Haldane et al., 1915). Namely, it was the first gene mapping in the mammalian species. The nomenclature of these mutant alleles is still actively used even now except for *e* of the *pink-eyed dilution* locus. At present, this classic allele of the pink-eyed dilution locus is renamed to *p*.

In the field of the mutagenesis of the mouse, Russell (1951) developed a test strain called **T** for the specific locus test (SLT) by adding two more loci to the five loci as shown in Fig. 28.4. Russell and his coworkers have extensively used the **T** strain for the various mutagenesis studies (Russell et al., 1979).

9 LABORATORY MOUSE STRAINS

Since early 20th century, various laboratory mouse strains have been developed (reviewed by Lyon et al., 1996; Rader, 2004). Updated list and information of available mutant mice and strains are also found in the Mouse Genome Informatics (MGI; http://www.informatics.jax.org/) at the Jackson Laboratory and the International Mouse Strain Resources (IMSR) (http://www.findmice.org/). The mouse and strains are directly available from a member of the Federation of International Mouse Resources (FIMRe; http://www.fimre.org/); for instance, the Jackson Laboratory (http://www.jax.org/), European Mutant Mouse Archives (EMMA; http://www.emmanet.org/) and RIKEN BioResource Center (http://www.brc.riken.jp/lab/animal/en/).
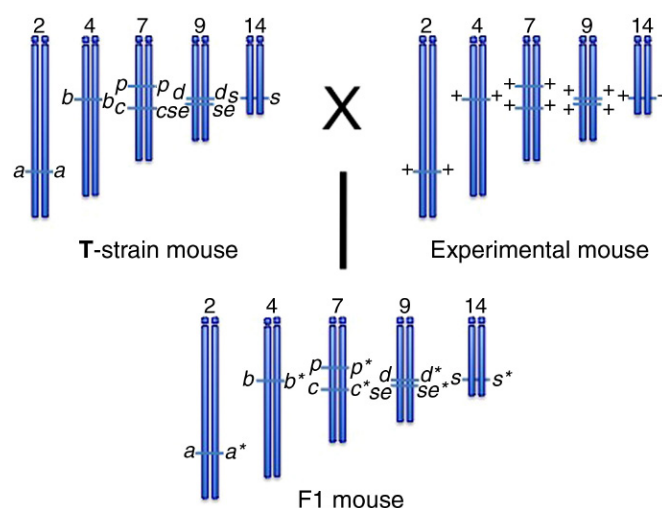
FIGURE 28.4 **Basic scheme of the Specific Locus Test (SLT).** T strain homozygously carries recessive visible mutant alleles, nonagouti *(a)*, brown *(b)*, albino *(c)*, pink-eyed dilution *(p)*, dilute *(d)*, short ear *(se)*, and piebald *(s)*, on the seven loci. In this scheme, only the five pairs of autosomes carrying the seven loci are depicted. A **T** mouse is mated with an experimental mouse that homozygously has wild-type alleles *(+)* on the seven loci with or without prior treatment by a mutagen. The produced F1 mice are subjected to the phenotype assessment for the corresponding seven visible traits. Only when a de novo mutation occurs on any of the seven visible marker loci shown by alleles with asterisks, F1 exhibits the corresponding visible phenotype of the locus. The detection is easy because the expected seven mutant phenotypes are known. The mutation rate is also quantitatively assessed by ratio of the mutant mice to the totally produced F1 mice.

10 REDUNDANCY OF GENES: OCULOCUTANEOUS ALBINISM

In human, eye and coat color anomalies have been well recognized as oculocutaneous albinisms (OCAs). The coat color mutations found in fancy mice have been contributed to identify the causative genes of human OCAs. The well-known albino locus (*c*) was mapped on chromosome 11 and 7 in human and mouse, respectively. The key enzyme in the melanin synthesis is tyrosinase that catalyzes the rate-limiting step of tyrosine to dihydroxyphenylananine (DOPA) as well as DOPA to DOPA-quinone. Shibahara et al. (1986) reported a cDNA clone, pMT4, encoding mouse tyrosinase. Later, Kwon et al. (1987) and Yamamoto et al. (1987) also reported cDNA clones for human and mouse tyrosinase, respectively, both of which were similar to pMT4. In spite of a good functional and sequence similarity to tyrosinase, the whole sequences of pMT4 were identified not of the *c* locus but of the *b* locus on mouse chromosome 4 (Jackson, 1988). This is a good lesson to note that even if a DNA clone is obtained with enough functional and sequence similarity, it might be a paralog rather than the orthologs of the objective locus. Based on these cloning and analyses, the *c* and *b* loci were revealed to encode tyrosinase and tyrosinase-related protein-1, respectively.

In human OCAs, four linkage groups have been identified; OCA1, 2, 3, and 4. OCA1 and 3 are caused by mutations of the tyrosinase (*c*) and tyrosine-related protein-1 (*b*) genes, respectively. The OCA2 (*p*) and SLC45A2 (*uw*) mutations are responsible for OCA2 and 4, respectively. The OCA2 and SLC45A2 genes are totally different from each other with respect to the sequences and their gene functions. Neither OCA2 nor SLC45A2 has any similarity to tyrosinase or tyrosinase-related protein-1. Thus, similar phenotypes may also derive from a distinct gene as well.

As shown in the cases for OCAs, the responsible genes are often redundantly coded in the genome, although mutations of each gene act as monogenic trait or Mendelian inheritance. Lyon et al. (1996) listed 81 loci in which eye and coat color mutations had been found.

It is noteworthy here that historically the locus names used to origin from the identified mutations. The locus names of brown (*b*), albino (*c*) and dilute (*d*) are typical examples. At present, HUGO Gene Nomenclature Committee and International Committee on Standardized Genetic Nomenclature for Mice currently determine the official gene names and symbols mostly based on the functionality of the gene, usually, protein product. Thus, official gene names for *b*, *c*, and *d* now are tyrosinase (*Tyr*), tyrosinase-related protein-1 (*Tyrp1*) and myosin VA (*Myo5a*), respectively.

11 BODY WEIGHT AND BRAIN FUNCTION: PLEIOTROPY OF *ob* AND *db*

Obese (*ob*) and diabetes (*db*) mutant mice spontaneously arose in laboratory stocks, both of which also exhibit very similar phenotype, the increase in body weight and infertilities in homozygotes. Zhang et al. (1994) positionally cloned and identified the mouse *ob* gene and human homolog. The *ob* gene encodes for a secretary protein, leptin.

Tartaglia et al. (1995) then cloned the leptin receptor (*db*) gene from a mouse choroid plexus cDNA library. They first found the candidate sequence mapped to the *db* locus on mouse chromosome 4; however, they could not detect causative mutations in the cDNA sequences of the *db* mice. The leptin receptor was found to be transcribed to many alternatively spliced variants. Ghilardi et al. (1996) identified a long isoform of the leptin receptor transcripts that was preferentially expressed in the hypothalamus. They further discovered a point mutation in the leptin receptor gene of the *db* mice. As a consequence, a point mutation in the leptin receptor gene of the *db* mice caused an alternative splicing only producing a short form of the leptin receptor.

Both mutant mice, *ob* and *db*, exhibit two distinct phenotypes, obesity and infertility. When one mutation affects two or more of phenotypes, it is called pleiotropic. The identification of responsive genes with causative mutations has led to the molecular and physiological understanding of the pleiotropy. The circulating adipocyte-derived endocrine hormone, leptin, is recognized by leptin receptor at the hypothalamus. The neuroendocrine system then seems to trigger the subsequent gene networks for the appetite, feeding behaviors, circadian rhythm, puberty, sexual maturation, and maintenance of the reproductive cycles. Mouse models are now revealing that the brain acts a key role in the *db* and *ob* pleiotropy (reviewed by Donato et al., 2011).

12 CONVENTIONAL POSITIONAL CLONING AND FORWARD GENETICS

In the aforementioned examples, classic mutations and de novo mutations arose in laboratory stocks have been identified by their peculiar phenotypes first. Based on the phenotype segregation in the pedigree, responsible loci have been mapped using backcross and other linkage mapping technologies. The power of the mapping is usually dependent on the recombination events. The genetic maps of human and mouse genomes are about 3000 and 1500 cM, respectively in the 3×10^9 bp genomic sequences. It implies that one gamete has ~30 and ~15 recombinations, respectively, on average. Thus, 1 cM corresponds to 1 and 2 Mbp in human and mouse genomic DNA sequences, respectively. In order to identify the responsible gene and causative mutation of the mutant, the mapping of the mutation in the genome is the first key to narrow the candidate genomic region down to about centimorgan or 1–2 Mbps. Assuming that mammalian genome encodes 30,000 genes and that 0.1% of the genome has SNPs as described earlier, the candidate region of 1–2 Mbps thus still has 10–20 genes with 1000–2000 SNPs on average. The next step to identify responsible gene is to search mutations in ORF sequences or splicing donor/acceptor dinucleotide consensus sequences. Nowadays, whole human, as well as mouse genome reference sequences with SNP information are available so that it is much simpler and quicker to nominate such candidate mutations than the time of period before the Genomic Sequencing Project. Nevertheless, The final proof from a few centimorgan to the molecular identification of the mutation and gene is not always straightforward but still laborious and times taking even now as previously shown in the case for the *db* positional cloning by Tartaglia et al. (1995).

13 UNIQUE POSITIONAL CLONING: HIGH REVERSION RATES OF d^v AND p^{un} MUTATIONS

13.1 Positional Cloning of d

Many mutant alleles have been identified exhibiting pleiotropic effect of not only the coat color reduction but also some alleles with neurological anomalies and/or lethalities. In addition to the pleiotropy, very rare event of reversion of d mutation has also been recognized. Jenkins et al., (1981, 1982) and Mercer et al., (1991) conducted the positional cloning of d depending on these unique features of the d mutation and ultimately revealed the molecular mechanism of the pleiotropic phenotypes and high reversion rate.

An endogenous ecotropic murine leukemia virus (MuLV) DNA was found in many laboratory strains with various copy numbers. One of MuLV sequences called Emv3 was 100% concordant with the d mutation in various recombinant inbred (RI) strains as described later. This particular allele was thus renamed as d^v (Jenkins et al., 1981, 1982). They also found that a spontaneously obtained revertant allele d^{+2J} had no MuLV sequence. As shown in Fig. 28.1, conventional loss-of-function type mutations hardly revert back to restore the wild-type sequence and phenotype. They interpreted the mechanism of the reversion that the MuLV had been lost by a homologous recombination between the long terminal repeats at both ends of the MuLV.

The consequent molecular identification of the interrupted gene by MuLV was myosine VA encoded by dilute (d) locus (Mercer et al., 1991). The *Myo5a* mutation interferes the formation of dendritic processes in the melanocyte, causing the melanin granules to clump around the nucleus of the melanocyte and give rise to the coat color reduction. In particular, Huang et al. (1998) found that the most of mutations with neurological anomalies existed in the C-terminal "tail" region of MyoVA, indicating some significant C-terminal function for neuron and neuron development. Their study is a good example to conduct the functional analysis of the gene by using various allelic series of mutations. Just studying with only one mutant allele, it may overlook and dismiss other significant functions of the gene.

In human, the *Myo5a* mutations have been identified for the cause of Griscelli syndrome, a rare autosomal recessive disorder characterized by hypopigmentation and either central nervous system (Griscelli syndrome type 1, or GS1) or immunologic (GS2) defects (OMIM 160777).

13.2 Positional Cloning of p

The positional cloning of another classic eye and coat color locus of pink-eyed dilution (p) was conducted in this case "without positioning/mapping" (Brilliant et al., 1991). Many de novo mutations have been identified in the p locus and one of them, pink-eyed unstable (p^{un}) had a unique feature of the highest reversion rates in mammals. Thus, some structural mutations were anticipated like retroviral integration or transposon. Brilliant et al. (1991) conducted southern hybridization analysis of p^{un} and coisogenic wild type and revertant genomic DNAs with a part of intracisternal particle A (IAP) DNA sequence as a probe. The IAP fragment had ~1,000 copies in the mouse genome; thus, if any large DNA structural change, for example, deletions and duplications, occurred, such repetitive probe may directly reveal the site of mutation without mapping or positioning (Gondo and Brilliant, 1995). In addition, IAP per se might have been the cause of mutation and high incidence of the reversion, in which case the IAP probe might have detected the mutated gene as in the case for the d^v mutation shown earlier.

The IAP probe detected 2.9-kb enhanced signal only in the p^{un} but neither in coisogenic wild type nor revertant genomic DNAs. The 2.9-kb enhanced DNA fragment was indeed mapped to the p locus (Brilliant et al., 1991). Further molecular analysis revealed that the p^{un} mutation is caused by a large direct head-to-tail duplication of an internal ~70-kb fragment of the p locus encompassing the 2.9-kb enhanced fragment (Gondo et al., 1993). All the tested revertant genomes had only one copy of the large 70-kb sequence that was indistinguishable to the wild-type genome due to an unequal homologous recombination between the duplicated fragments to revert the duplicated structure back to one single copy as in the wild-type genome (Gondo et al., 1993).

14 RECOMBINANT INBRED STRAINS FOR QUICK GENETIC MAPPING

Similar to the inbred and congenic strains described earlier, many recombinant inbred (RI) strains have also been developed as shown in Fig. 28.5 by conducting a series of sib mating of more than 20 generations starting from two established inbred strains.

The RI strains have an immediate power to map the polymorphic loci between the two inbred strains, as well as the quantitative trait locus (QTL) analyses of the complex traits. Some examples are shown in the positional cloning of dilute (d) and pink-eyed dilution (p) loci.

The d^v mutation allele described earlier was originated from DBA/2J inbred strain. Jenkins et al. (1981) vindicated the d^v cloning by the RI strain (Fig. 28.5) as follows. DBA/2J exhibited the reduced pigmentation of the coat color due to the homozygosity of d^v allele. Likewise, other established inbred strains, as well as any RI strains were easily distinguished whether they carry wild type or mutant d allele. The coat color of AKR/J
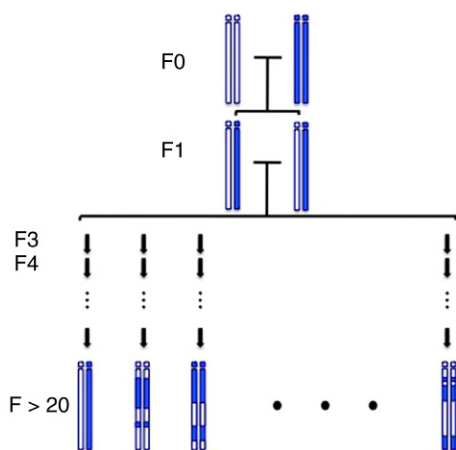
FIGURE 28.5 **Establishment of recombinant inbred strains.** The basic scheme to establish inbred strain is the continuous sister–brother (sib) mating in the same litter for more than 20 generations. The original pair of F0 mice may carry two each alleles thus a total of 4 different alleles at most on any loci. Locus *A* may have *A1/A2* in one F0 and *A3/A4* in the other F0. By chance, during the 20 consecutive sib matings, any loci may be fixed to have only one type of alleles homozygously. Once a locus is fixed to one allele, namely, A1/A1 sister and A1/A1 brother mating pair, thereafter the locus is maintained as A1/A1 homozygote forever. In theory, more than 99% of loci become homozygous. In order to establish RI strains, a pair of different inbred strains is chosen for F0 as shown in this figure. In the F1 generation, all the genome becomes heterozygous for the two strains (white and blue). Then, many pairs of F1 are intercrossed and the sib matings are conducted to establish independent RI strains as many as possible. After 20 generations of sib matings, all the loci become homozygous with mosaic components of the two original inbred strains depending on the event of recombinations.

and C57BL/5J inbred strains were indeed apparently different from that of DBA/2J and many RI strains had been established between them with the easy identification of the strain distribution pattern (SDP) of the *d* phenotypes. Thus, they used 26 and 27 RI strains of C57BL/6JXDBA2/J (BXD) and AKR/JXDBA/2J (AXD), respectively, for the mapping of the candidate DNA fragment, a part of MuLV sequence. Using the unique signals on Southern hybridization with the MuLV sequence as a probe, they found that the SDP of all the 53 phenotypes in the total of 53 RI strains were 100% concordance with the segregation of the coat the MuLV signals.

Nakatsu et al. (1992) also used the RI mapping system to indicate that the *p* locus is closely linked to the Prader-Willi chromosomal region (PWCR). First, Brilliant et al. (1991) found a 13.6-kb Southern hybridization signal with a 394-bp of genomic DNA from p^{un} duplication as a probe in DBA/2J inbred strain. On the other hand, both C57BL/6J and AKR/J inbred strains exhibited a 4.8-kb signal with the 394-bp p^{un} probe. They analyzed the SDPs of the identified Southern signals in 26 and 24 RI strains of BXD and AXD, respectively. The SDPs of the 394 bp p^{un} probe was also 100% concordant with those of the D7Nic1, the mouse homolog of the human gene in the PWCR.

RI strains have strong mapping power because neither mating nor mouse productions are needed when molecular markers in the RI genomic DNA are analyzed. Southern restriction fragment length polymorphisms (RFLPs), simple size length polymorphisms (SSLPs) and single nucleotide polymorphisms (SNPs) may be quickly assessed for the mapping. Once the SDPs are identified in a particular set of the RI strains, it is directly applicable when the same set of the RI strains are used as shown by Nakatsu et al. (1992); thus, the SDPs are cumulatively enhance the strength of the RI mapping power.

15 MUTAGENESIS FOR FORWARD GENETICS

15.1 Mutagenesis

Little and Bagg (1923) reported for the first time the possibility of X-ray induced mutations in the mouse. While taking time to prove the Mendelian inheritance of X-ray induced variation to the offspring in the mouse, the transmission of the X-ray induced phenotype was first proved in *Drosophila melanogaster* (Muller, 1927).

15.2 X-ray Induced Mutations

Since the discovery of X-ray as a strong mutagen, the risk assessment studies of radiation have been conducted in various organisms including mice (Russell et al., 1958). At the same time, obtained and established mutants contributed to accelerate the pace of genetics by providing many useful mutants compared to the very rare event of spontaneous mutations. For instance, Medical Council Research (MRC) in UK and National Oak Ledge National Laboratory (OLNR) in USA produced many mutant mice by X-ray irradiations shown by the super script numeric series of "*H*" and "*R*" alleles, respectively, in many loci (Lyon et al., 1996).

15.3 Allelic Series of *Pink-Eyed Dilution* Locus

As shown in Fig. 28.4, new *p* mutation alleles have been easily identified and established by X-ray irradiations. Among many *p* mutation alleles, variety of pleiotropic phenotypes has also been recognized in addition to the OCA2 phenotype of reduced eumelanin. For instance, neurological/behavioral anomalies (p^{6H}, p^{25H}, p^{bs}, and p^{cp}), cleft palate (p^{cp}), sterility (p^{6H}, p^{25H}, p^{bs}), lethality (p^{81H}, p^{82H}, p^{87H}) and genetic instability (p^{un}) have been reported (Lyon et al., 1992; Lyon et al., 1996). Lyon et al. (1992) analyzed X-ray induced mutant alleles by Southern hybridization and found large deletions encompassing whole or a part of the *p* locus. Based on the deletion mapping with the complementation analyses for the

pleiotropy of X-ray induced *p* allelic series, Lyon et al. (1992) implicated that the new neurological gene(s), essential gene(s), sterility-related gene(s) and cleft palate-responsible gene(s) were located closed to the *p* locus. Thus, they considered that the pleiotropy was not caused by the *p* mutations per se but a large deletion of concomitant nearby gene(s) by the X-ray. Indeed, Nakatsu et al. (1993) isolated a new neurological gene cluster of three $GABA_A$ receptor subunit genes in the p^{cp} deletion allele.

The deletion mutations, as well as previously described RI mappings are a good tool to molecularly analyze the conserved homologous region in two different species. Analysis of the *p* region on mouse chromosome 7 contributed to the molecular analysis of the syntenic region on human chromosome 15 including OCA2 and PWCR (Gardner et al., 1992; Nakatsu et al., 1992).

15.4 ENU: The Most Potent Mutagen in the Mouse

Mustard gas was first identified as a chemical mutagen in *D. melanogaster* (Auerbach and Robson, 1946) followed by many other chemicals. For instance, Russell et al. (1979) found that the ENU was the most potent mutagen in the mouse. With a fractionated dose of 100 mg/kg at weekly interval for a total of 300 and 400 mg/kg gave rise to the mutation rates of 125 and 153×10^{-5}/locus/gamete, respectively (Hitotsumachi et al., 1985). The ENU mutagenesis scheme based on their extensive studies for ENU mutagenesis in the mouse by Russell and his coworkers was adapted to the large-scale ENU mouse project started from 1997.

15.5 Forward Genetics With ENU

ENU exclusively induces base substitutions (Noveroske et al., 2000). Thus, one of the key steps of forward genetics with ENU by phenotype-driven approach is the positional cloning to identify the mutated single base pair in 3×10^9 bp of the genome that often carries many background SNPs and unrelated mutations. Around 1990, the advancement of the positional cloning technologies has made it possible to identify and isolate the causative base substitutions and responsible genes in the established mutant strains by phenotype-driven mutagenesis. In this section, two pioneering positional cloning of ENU-induced mutations are demonstrated.

15.5.1 Multiple Intestinal Neoplasia (Apc^Min)

Moser et al. (1990) conducted ENU mutagenesis to directly obtain model mice for human diseases. The basic scheme of ENU mutagenesis is shown in Fig. 28.6. Their approach is a phenotype-driven forward genetics to establish dominant mutant mouse strain. In the dominant mutation screening, larger number of G1 mice

(Fig. 28.6) gives more chance to have mutant mice. It also depends on what kind of phenotypes to focus on for the screening. An anemic G1 was found and its inheritance was confirmed in G2 (Moser et al., 1990). The anemic mice were always found in 50:50 ratios in G2 or from equivalent mating, were passed bloody feces, and had numerous adenomas in intestine with 100% penetrance. They considered that the anemic trait is secondary to the development of multiple adenomas, naming the mutant allele multiple intestinal neoplasia (*Min*).

Based on the similarity of *Min* mice to the human FAP patient, Su et al. (1992) postulated that *Min* was an allele of *Apc* locus. They conducted candidate approach to clone a mouse homolog cDNA with human APC probe just after the human *APC* cloning (Kinzler et al., 1991). Su et al. (1992) found that the isolated cDNA, as well as corresponding genomic DNA had significant homologies to human *APC* gene and identified that the *Min* mice carry a nonsense mutation of codon 850 from Leu (TTG) to Stop (TAG) in the *Apc* gene. Thus, Su et al. (1992) renamed the mutation Apc^{Min} allele.

The homozygotes for the Apc^{Min} allele were never observed (Moser et al., 1995), indicating the *Apc* gene as an essential gene. As found in the human tumorigenesis with *Apc* mutations, Luongo et al. (1994) also showed
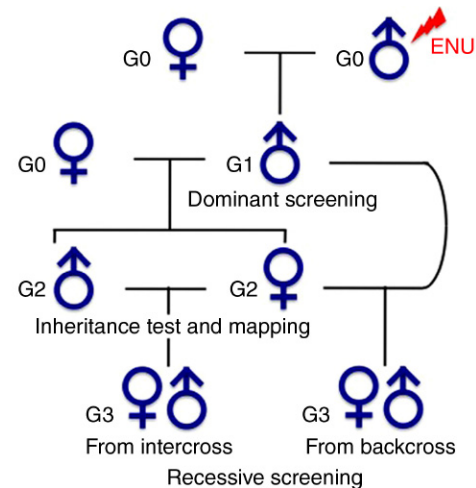
FIGURE 28.6 Typical scheme of phenotype-driven ENU mutagenesis in the mouse. ENU-treated G0 males are mated with untreated G0 females to produce G1 offspring. Each sperm in G0 males has thousands of independent ENU-induced base substitutions and each G1 mouse clonally inherits the thousands of the germline mutations in the sperm. Many G1 mice are then subjected to comprehensive phenotyping to detect dominant mutations. Each candidate G1 is then mated to a female or a male of the same inbred strain of G0 female to confirm the germline transmission in G2 population. For the recessive screening, on the other hand, the phenotype first appears in the G3 mice. Mating a G2 mouse to the parental G1 mouse may produce G3 mice. Intercrosses between G2 pairs also generate G3 mice for the recessive phenotype screening. For both dominant and recessive screening of mutant mice, all the key germline mutations exist in the G1 mice; thus, the G1 mouse preservation is the primary resource for the ENU mouse mutagenesis project.

that adenomas in Apc^{Min} mice also had loss of hetero-zygosities (LOH), indicating the effectiveness of Apc^{Min} mouse as a model for tumorigenesis due to the loss-of-function mutations of tumor suppressor genes. Further-more, Moser et al. (1992) mated the congenic B6-Min mice to several different inbred strains. They observed the effects of F1 genetic background with respect to the longevities or survival rates, number of adenomas, and development of invasive tumors, implicating the existence of modifiers and gene-to-gene interactions between *Apc* and other genetic networks.

15.5.2 Circadian Locomotor Output Cycles Kaput (Clock)

Vitaterna et al. (1994) considered that mutations for circadian-related genes might be obtained by domi-nant G1 screening, because the majority of circadian rhythm-related mutations in other species had been semidominant. Based on this assumption, they con-ducted a phenotype-driven forward genetics with ENU to establish mutant mouse models for circadian rhythm. They focused on the mutant phenotypes by using wheel-running activity in a light-dark cycle and constant dark environments. Among the tested 304 G1 mice generated from C57BL/6J G0 parents (Fig. 28.6), one G1 exhib-ited an extended clock of 24.8 h circadian rhythm in a constant dark condition. Wild-type mice usually have 23.3–23.8 h circadian rhythm. They mated this G1 mouse to C57BL/6J and obtained 23 G2 mice, of which 13 and 10 G2 had 23.3–24.0 h and 24.5–24.8 h circadian periods, respectively, indicating the Mendelian monogenic domi-nant inheritance.

Vitaterna et al. (1994) named the mutated locus and allele "*circadian locomotor output cycles kaput*" (*Clock*). The heterozygotes of *Clock*/+ were intercrossed to examine the phenotype of homozygotes of *Clock*/*Clock*. At this point they did not have any markers to distin-guish the genotypes. Nevertheless, the 1:2:1 Mendelian segregation was observed in the tested population cor-responding to short (~23.3 h) wild-type homozygotes, long (~24.4 h) heterozygotes, and very long (~27.3 h) *Clock*/*Clock* homozygotes. Therefore, the mutant allele of *Clock* had additive codominant effects. In addition, the very long circadian rhythm in *Clock*/*Clock* was only sus-tained for the beginning two weeks followed by a total loss of the rhythmicity, which had not been observe in *Clock*/ + heterozygotes and thus was a recessive trait.

Based on the monogenic inheritance of the Clock phenotype, King et al. (1997) isolated the Clock gene by positional cloning. They intensively screened cDNA libraries from suprachiasmatic nuclei (SCN) of the hypo-thalamus, because SCN had been proposed to be a cen-ter of the mammalian circadian rhythm regulation. The identified *Clock* gene encoded a novel transcription fac-tor with a basic helix-loop-helix (bHLH)-PAS domain.

The northern hybridization primarily revealed the ubiq-uitous expression of *Clock* in most tissues. In situ hybrid-ization in the mouse brain further indicated apparent expression of *Clock* mRNA in SCN and hippocampus and low-level expressions in the rest of brain. In the *Clock* mutant mice, the causative A to T transversion was found in a splice donor dinucleotide sequence caused exon skipping and deletion of 51 residues in the Clock protein. The PAS domains of the *Clock* gene as probes, the evolutionary conservation was also revealed in not only mammalian species but also in reptile, amphibian, and fish (King et al., 1997).

16 LARGE-SCALE ENU MOUSE MUTAGENESIS PROJECT

The Human Genome Project started 1990 as an inter-national collaborative effort with public funds. The next challenge foreseeing the completion of the human genome sequencing is the functional annotation to decode the sequences. As shown in previous section, mutant mice are good models to analyze the function of the gene with mutagenesis. Prior to the completion of the Genome Project, only a small part of entire gene set in the genome was known. In this context, the forward genetics was the best approach with random genome-wide mutagenesis in a large scale, in which no prior knowledge of the target genes was required at all.

ENU was chosen because it is the most potent known mutagen in the mouse as shown earlier. ENU exclu-sively induced base substitutions (Justice et al., 1999; Noveroske et al., 2000); thus, many allelic series of muta-tions were also expected for each gene with variety of effects, dominant, recessive, null, hypomorph, and so on for the fine functional analysis of the gene. The nature of base substitutions should also provide good models for the diseases due to SNPs in human populations. Finally, the success of the identification of *Apc* and *Clock* by for-ward genetics with ENU mutagenesis described in the previous section made the last push to initiate the large-scale comprehensive ENU mouse mutagenesis projects in a worldwide manner (reviewed by Gondo, 2008).

16.1 Dominant Forward Genetics With ENU

ENU randomly induces somatic base substitutions most of the tissues in the injected mouse. When muta-tions occur in germ cells, they transmitted to the next generation and may be established as mutant strains. ENU induces mutations much less effectively in oogonia than sparmatogonia; thus, only males are used as G0 for the ENU mutagenesis (Fig. 28.6). In order to avoid any genetic background effects, an isogenic inbred strain may be used for the entire ENU mutagenesis scheme except

for genetic mapping. Dominant germline mutations may be primarily detected in G1 screening by intensive and comprehensive phenotyping.

The identified dominant mutation exists only in the G1 mouse at this time point; thus, the G1 candidate is immediately mated to propagate the mutant allele. G1 males are usually much easier to propagate and preserve the induced mutations than G1 females. Males may be mated to several females consecutively or even at the same time in the same cage. On the other hand, females may produce only one litter of less than 20 pups per several months. The robust technologies are also established for the cryopreservation of mouse sperm in liquid nitrogen semipermanently and for the reviving mice from frozen sperm (Nakagata, 1993, 2000) with the in vitro fertilization and embryo transfer (Whittingham et al., 1972). No reliable ovary cryopreservation and implantation technologies, on the other hand, have been established yet.

The identified dominant-candidate character may not be due to a mutation but just a deviation by chance and/or by an environmental effect(s). With respect to this possibility, all the candidate G1 mice are also necessary to produce G2 in order to confirm the Mendelian inheritance as a dominant trait. Only one allele in G1 candidates carries the dominant mutation; therefore a 50% appearance is expected in the G2 population assuming it is a monogenic dominant trait with 100% penetrance. Any detrimental effect(s) of the dominant trait may reduce the number of the heterozygous mutation carriers in the G2 population distorting the 1:1 segregation. Considering these possibilities, we usually produced, at least, 20 G2 mice to make a decision if each G1 candidate carry a dominant mutation or not at the RINE ENU forward mouse mutagenesis. Based on this criterion, about 2%–4% in all of the produced G1 mice carried an ENU-induced dominant mutation (reviewed by Gondo, 2008; Gondo et al., 2010).

The next step is the mapping of the confirmed dominant mutations toward the positional cloning. In the aforementioned coisogenic scheme that uses a single inbred mouse strain, no genetic markers for the mapping are yet available. In this case, one heterozygous carrier is first mated to another inbred strain to use the genomewide strain polymorphisms (e.g., SNPs and SSLPs) as genetic markers. It is one option to use G0 females of another inbred strain that are different from the G0 males' strain to begin with, as in the scheme of Fig. 28.6. In this optional scheme, all the G1 have the uniform F1 genetic background between the two inbred strains, carrying the ENU-induced mutations on the paternal chromosomes. The candidate G1 is then mated to a mouse of the same inbred strain of G0 females. In this optional case, the G2 mice directly provide the materials for the genetic mapping of the candidate dominant mutation when the inheritance of the candidate domi-

nant mutation is confirmed in the same G2 population. This optional scheme significantly reduces the necessary time period from the mutagenesis to the mapping and identification of the causative mutation, although the heterogeneity of the genetic background might disturb the interpretation of experimental data.

With the dominant screening of G1 mice, RIKEN phenotype-driven mutagenesis project per se has established various human disease models; diabetes type 2 with *glucokinase* mutations (Inoue et al., 2004), amelogenesis imperfecta (AI) with *enamelin* mutations (Masuya et al., 2005), osteoarthritis with a *Gdf5* mutation (Masuya et al., 2007a), retinal degeneration with a *Rom1* mutation (Sato et al., 2010), and attention deficit hyperactivity deficit with a *Grin1* mutation (Furuse et al., 2010).

16.2 Recessive Forward Genetics With ENU

Based on the SLT, ENU induced recessive mutation at a frequency up to one in 700/locus/gamete (Moser et al., 1990; Vitaterna et al., 1994). Taking a conservative frequency of at least one in 1000/locus/gamete, any single G1 mouse may carry ~30 recessive mutations in the total of 30,000 loci. On the other hand, each G1 carried ~0.03 dominant mutations as shown in the previous section, namely 2%–4% of G1 inherited its dominant trait to G2. The ENU induced dominant mutation, thus, was at a frequency of one in million/locus/gamete. The number of recessive mutations is 1000-fold more than that of dominant mutations in the produced G1 mice (Supplementary Information in Gondo, 2008). Most of the human genetic diseases are based on the inactivation of the gene or gene network; thus, large numbers of G1 mice are a good resource for modeling such recessive human diseases.

Any recessive traits, however, cannot be recognized in G1 mice, since all the G1 mice carry the ENU-induced mutations heterozygously on only the paternal chromosome in the scheme of Fig. 28.6. The conventional mating scheme to produce homozygotes for the ENU-induced mutations is either by intercross of arbitrary chosen G2 pairs or by backcross any G2 to its G1 parent as shown in Fig. 28.6. Each G2 randomly inherits half of ~30 recessive mutations in G1. An arbitrary chosen G2 pair has 7–8 (=30 divided by 2 twice) recessive mutations in common by chance. Each of commonly inherited 7–8 recessive mutations in a G2 pair then gives rise to the 1:2:1 Mendelian segregation of wild type homozygotes:heterozygotes:recessive homozygotes in G3. In other words, any single G2 intercross pair should provide the recessive mutant homozygotes for the 7–8 loci if enough numbers of G3 are produced. The detection efficiency of ~30 and ~15 recessive mutations of G1 and G2, respectively, in the G3 population as homozygotes may be furthermore improved by the backcross scheme in Fig. 28.6.

The G1–G2 backcross pair shares all the ~15 recessive mutations in common, since the ~15 mutations are inherited from the G1 parent. The number of observable recessive phenotypes by the backcross scheme, thus, is for ~15 loci in the enough number of their G3 population, which is twofold more than that by the intercross scheme in Fig. 28.6.

In spite of the theoretical feasibility and efficacy of the recessive forward genetics with ENU described earlier, the practical identification of recessive mutant mice has been hampered with several reasons. (1) In the G3 population, 7–8 mutations from independent loci overlaid the corresponding multiple phenotypes to each G3 depending on the 3:1 ratio for each locus, exhibiting multilocus compound phenotypes. Multilocus segregation was often too complex to extract the single locus effects of each recessive mutation. In order to reduce the complexity of G3 segregation as low as possible, all the recessive forward genetics at RIKEN were conducted in the C57BL/6J background. (2) Recessive lethal mutations also segregated according to the Mendelian law but were impossible to observe other than the reduction of the litter size. The average litter size of the G3 production was indeed smaller than that of the G1 or G2 production. The litter size of G3 from the backcross scheme was also smaller than that from the intercross scheme, supporting the significant number of recessive lethal mutations or detrimental mutations in the original ~30 recessive mutations in each G1. (3) Even if a Mendelian inheritance for a recessive mutation was confirmed and the strain was established, the genetic mapping became often impossible because the identified phenotype disappeared in the F1 genetic background, which is the necessary first step of the mapping. These difficulties of the recessive forward genetics with ENU, however, strongly vindicate the value of the G1 mice as a resource for the elucidation of gene-to-gene interactions and genetic network. The further details will be discussed in Section 23.

17 MUTAGENESIS FOR REVERSE GENETICS

In 1980's, various advanced technologies for genetic and embryonic engineering were established in the mouse, which subsequently has made it possible to conduct reverse genetics in the mouse. The "giant" transgenic mouse was constructed by injecting DNA fragments encompassing the human growth hormone gene under the metallothionein promoter to fertilized oocyte (Palmiter et al., 1982), providing a new tool to introduce exogenous DNA into mouse genome and to make gain-of-function mutant mice. The embryonic stem (ES) cell technology was also established to make mice

from the pluripotent ES cells developed by Evans and Kaufman (1981). The genes and genome in the ES cells were transmitted to germline chimeric mice by injecting manipulated ES cells into blastocyst-stage embryos (Gossler et al., 1986; Robertson et al., 1986).

18 GENE TARGETING AND KNOCKOUT MOUSE

Smithies et al. (1985) and Thomas et al. (1986) independently showed the feasibility of the site-directed mutagenesis in the mouse by the somatic–homologous–recombination method, which had been a useful tool to disrupt or manipulate target genes in bacteria and lower eukaryotes. The site-directed mutagenesis in the mouse has become a practical technology in the mouse cells by using selectable marker genes (Doetschman et al., 1988; Mansour et al., 1988). These technologies were then integrated to a powerful reverse genetics tool, for the first time, in the mouse, which is gene targeting or knockout mouse (reviewed by Capecchi, 1989). It is noteworthy that in the broad sense the transgenic mouse stands for the genetically engineered mouse inheriting a modified genome by the random insertion, as well as by targeted integration using homologous recombination; however, it is often defined as the former, namely, the genome-manipulated mouse with a randomly integrated DNA fragment in a narrow sense. This manuscript uses the narrow definition in order to distinguish between the engineered mice by random and targeted integrations.

19 TRANSGENIC MICE AS DISEASE MODELS

By using transgenic mice carrying an exogenous DNA, it is possible to analyze the gain of function due to the exogenous DNA. Transgenic mice, thus, may model dominant genetic diseases in human. For instance, Mangiarini et al. (1996) constructed transgenic mice carrying an expanded CAG repeats in exon 1 of the human *Huntingtin* gene to model Huntington's disease. They found that only the small fraction of human *Huntingtin* gene with ~130 repeats of CAG was sufficient to cause various neurological anomalies that exhibited many of the characteristics of Huntington's disease. On the other hand, the homozygous and heterozygous knockout mice for the *Huntingtin* gene exhibited early embryonic lethality and no obvious phenotypes, respectively (Duyao et al., 1995; Nasir et al., 1995; Zeitlin et al., 1995). Thus, the knockout mice vindicated the essentiality of the *Huntingtin* gene but provided no models for Huntington's disease (reviewed by Menalled and Chesselet, 2002).

Another application of transgenic mice is to rescue the mutant phenotype by introducing the wild type DNA fragment to the mutant mice. It is useful for the recessive phenotypes due to loss-of-function type mutations. The transgenic rescues also provide feasibility studies toward the application for the gene therapies of recessive human genetic diseases.

20 KNOCKOUT MICE AS DISEASE MODELS

Knockout mice have been contributing for the elucidation of the biological function of target genes at the live mouse level. In particular, this new reverse genetics tool in the mouse immediately applied to the gene-driven elucidation of candidate genes for human diseases. The knockout mice for the mouse homologs of human *glucokinase* (Bali et al., 1995; Grupe et al., 1995; Postic et al., 1999; Terauchi et al., 1995 and reviewed by Osbak et al., 2009) and *Apc* genes (Fodde et al., 1994; Oshima et al., 1995) clearly vindicated the direct causality for the diabetes and colon cancer, respectively.

Another good example is p53 knockout mice. p53 was identified abundantly in various mouse tumors and originally considered to be protooncogene later hypothesized as a tumor suppressor gene (reviewed by Donehower et al., 1992). Zakut-Houri et al. (1983) identified a single p53 gene in the mouse based on the cDNA cloning. Li and Fraumeni (1969) had previously identified four human pedigrees susceptible to various types of tumors. Malkin et al. (1990) identified a strong association of p53 mutations in Li-Fraumeni tumors in human. Donehower et al. (1992) and Gondo et al. (1994) constructed p53 knockout mice and found that heterozygous p53 knockout mice were predisposed to develop thymic lymphoma and various other tumors.

Intriguingly, the homozygous p53 knockout mice were also born normally except the earlier onset for various tumors than the wild type control mice. p53 homozygous knockout mice even produced offspring normally before the tumor development. Thus, p53 was considered to simply act a gatekeeper for the cell cycle and to trigger the programmed cell death in transformed cells, consequently suppressing the tumor development (reviewed by Vousden and Lane, 2007). Norimura et al. (1996), however, found a pleiotropic function of p53. They irradiated the pregnant mice carrying p53 homozygous knockout fetuses, as well as homozygous wild type fetuses as controls with 2 Gy of X-ray on day 3.5 and 9.5 of gestation. They found no tumor development but significant increase and decrease in teratogenesis and embryonic death, respectively, in the p53 homozygous knockout fetuses.

21 CONDITIONAL TARGETING

The homozygous knockout mice for the *Huntingtin* gene were embryonic lethal, vindicating it is essential for the early development of the mouse. Such essential genes are often dispensable in adults. In order to investigate essential genes in a specific tissue and/or developmental time, conditional knockout system has been developed, for instance, by using Cre-loxP site-specific recombination in bacteriophage P1 (Sauer and Henderson, 1988). Cre enzyme efficiently recognizes and causes homologous recombination between a pair of short 34-bp sequence of loxP even in eukaryotic cells including the mouse. Placing two loxP sequences in the same and opposite orientation in a double helix DNA strand, the intervened sequence is looped out and inverted, respectively, by the site-specific recombination. Lakso et al. (1992) indeed succeeded in the conditional expression of the SV40 large tumor antigens (Tags) under the αA-crystallin (αA) promoter in the transgenic mice. The original transgene had a 1.3-kb intervening sequence flanked by a pair of loxP between the αA promoter and Tags. As a consequence, the 1.3-kb insertion hampered the expression of Tags under the control of the αA promoter. Thus, transgenic mice with the transgene was constructed and established without any tumor formation. Then, the transgenic mice were mated to the Cre-expressing transgenic mice to loop the 1.3-kb intervening sequence out from the transgenic genome, and developed lens tumors due to the expression of Tags in lens cells.

By adopting the Cre-loxP system in the targeting vector, the target gene may be conditionally knocked down based on the Cre expression under the control of tissue-specific and/or developmental time-specific promoters. Cre expression transgenic mice may be constructed independently from the conditional targeting mice. Cre transgenic mouse strains, therefore, have been a versatile tool for the conditional knockout mouse analyses. For instance, Shibata et al. (1997) constructed *Apc* conditional knockout mice based on the Cre-loxP system.

22 INTERNATIONAL KNOCKOUT MOUSE CONSORTIUM

Based on the drastic reduction of the number of encoded gene in the human genome, as well as in the mouse genome to be 30,000 or less, the mouse research communities proposed to conduct the knockout mouse project to make a full set of knockout ES cell lines for every gene in the mouse genome (Austin et al., 2004; Auwerx et al., 2004). With the core of the three public domains of KOMP, EUCOMM, and NorCOMM, the International Knockout Mouse Consortium (IKMC) was organized and the 5-year project was launched in 2007 (Editorial, 2007;

International Mouse Knockout Consortium, 2007). The accumulated technologies and knowledge of the International Gene Trap Consortium (Skarnes et al., 2004) was also integrated to the IKMC (Hansen et al., 2008). The gene trapping was originally developed as a tool for the forward genetics (Gossler et al., 1989). Then, the trapping vector has been modified to the conditional targeting vector for the reverse genetics (Hansen et al., 2008; International Mouse Knockout Consortium, 2007). Thus, the basic scheme of the IKMC was to establish "knockout first and conditional ready" ES cell lines in a C57BL/6N coisogenic background (Hansen et al., 2008; International Mouse Knockout Consortium, 2007).

The 5 years of the IKMC efforts was summarized in 2011 and availability of the developed ES cell lines and resources were reported (Skarnes et al., 2011). Many knockout alleles have been established in the C57BL/6N coisogenic background and the International Mouse Phenotyping Consortium (IMPC) has also started (Brown and Moore, 2012a,b).

23 ENU-BASED REVERSE GENETICS IN THE MOUSE

ENU may have not been considered for the reverse genetics because ENU randomly induces thousands of genomewide base substitutions. The construction of large-enough ENU mutant mouse library, however, may provide many allelic series of base substitutions in any given gene in the mouse genome. Having the large-scale ENU mutant mouse library and the high-throughput mutation discovery system, it has become possible to provide allelic series of point mutations in any target gene. (Beier, 2000; Coghill et al., 2002) suggested the feasibility of such ENU-based reverse genetics in the mouse in a small test scale.

23.1 ENU Mutant Mouse Library

During the course of the phenotype-driven forward genetics with ENU, the preservation of G1 mice were indispensable as discussed before. Thus, many ENU mouse mutagenesis projects cryopreserved the sperm of G1 males (Augustin et al., 2005; Michaud et al., 2005; Quwailid et al., 2004; Sakuraba et al., 2005). At time of their publications, the total size of the archived G1 mice in the four projects was ~40,000 G1 (reviewed by Gondo, 2008). Considering the ENU-induced mutation rate to be at least one in every megabase (Concepcion et al., 2004; Gondo et al., 2009), each G1 carries more than 3000 ENU-induced base substitution in the 3000-Mb genome. Thus, the total number of the archived ENU-induced mutations is $>1 \times 10^8$ in 40,000 G1 mice. Namely, it is possible to find one ENU-induced mutation every 25 bp in the 40,000 worldwide ENU mutant mouse library.

The best estimate of the average size of the coding sequences per gene is 1,437 bp in the mouse (MGC Project Team, 2004); therefore the average number of allelic series of ENU-induced mutations per gene in the 40,000 G1 mouse library is ~60. The worldwide ENU mutant mouse library has, therefore 60-fold coverage per protein-coding gene. When ENU-induced mutations occur in the protein coding sequences plus splicing acceptor/donor dinucleotide consensus sequence, ~70, 10, and 20% were missense, KO-equivalent and synonymous mutations, respectively (Gondo, 2008, 2010; Gondo and Fukumura, 2009).

With respect to the functional mutations, each G1 has ~30 recessive mutations that exhibit some biological changes in homozygotes as discussed before in this Chapter. The worldwide 40,000 G1 archive thus encompasses 1.2×10^6 functional mutations in ~30,000 genes or 40 functional mutations per gene, which is a consistent estimate with the expected ~60 base substitutions per gene with ~42 missense (70%) and ~6 KO-equivalent mutations (10%) as discussed in the previous paragraph.

23.2 High Throughput De Novo Mutation Discovery

The ENU mutant mouse library is an enormous resource for the reverse genetics if the mutations in target genes are effectively identified. The Sanger sequencing is a straightforward method to detect base substitutions but it is neither cost effective nor high throughput. Various PCR-based heteroduplex detection systems, therefore, have been used as a primary screening for the ENU-induced mutations on target genes. Among tested heteroduplex detection systems of denaturing high-performance liquid chromatography (Gross et al., 1999; Xiao and Oefner, 2001), temperature gradient capillary electrophoresis (Gao and Yeung, 2000; Li et al., 2002; Murphy et al., 2003), TILLING/Cel1 digestion (Oleykowski et al., 1998; Till et al., 2003), and high resolution melting (Bennett et al., 2003; Wittwer et al., 2003), we have been succeeded in identifying ENU-induced mutations effectively on target genes (Gondo and Fukumura, 2009; Gondo et al., 2009; Sakuraba et al., 2005). The RIKEN ENU mutant mouse library has been open to the research community since 2002 (reviewed by Gondo, 2008; Gondo et al., 2010; http://www.brc.riken.jp/lab/mutants/RGDMSavailability.htm).

23.3 Examples of Reverse Genetics With ENU Mutagenesis

Targeting the *disrupted in schizophrenia 1* (*Disc1*) gene in the mouse, (Clapcote et al., 2007) established two independent psychiatric disease models, schizophrenic and major depression disorder strains, from RIKEN ENU mutant mouse library. Schizophrenic mice were also established with a *serine racemase* nonsense mutation

(Labrie et al., 2009). Various behavioral mutant mice were established in the *reticulon-4* (Lazar et al., 2011), *Ncs-1* (Mun et al., 2015), and *STEP* (Kim et al., 2016) genes. Rivkin et al. (2013) discovered a novel function of the *gumby* (*Fam105b*) gene for angiogenesis with detailed molecular mechanism. Katsuragi et al. (2013) and Hirose et al. (2015) identified pleiotropic phenotypes of the S826G substitution of the *Bcl11b* gene. Shibata et al. (2015) reported abnormal hepatocyte apoptosis in the *cFLIP* mutant mice. Murata et al. (2014) found that the C429S missense mutation of the *β-catenin* gene caused sterility in both female and male in spite of their normal production of ova and sperm, respectively. Makino et al. (2015) identified that the T396 residue in the *Sufu* gene was critical for the Gli3 regulation in the Hh signaling.

The reverse genetics with ENU mutant mouse library has also been effectively identified functional noncoding mutations, since ENU induced base substitutions in noncoding sequences with equal frequencies to coding sequences in the mouse genome (Sakuraba et al., 2005). Masuya et al. (2007b) targeted ~1 kb of the MFCS1 sequence and identified six independent base substitutions in MFCS1. One strain indeed exhibited the preaxial polydactyly with an ectopic expression of sonic hedgehog gene in limb buds as expected. The MFCS1 had previously identified as a cis-regulatory noncoding sequence about 1 Mb upstream to the sonic hedgehog gene (Sagai et al., 2004).

24 FURTHER ADVANCEMENT OF GENOME TECHNOLOGIES

24.1 High-Throughput DNA Sequencing

The advancement of the next-generation sequencing (NGS) should also make the ENU mutant mouse library much more useful resource to model human diseases and for the functional genomics. The comprehensive identification of all the ENU-induced mutations in the worldwide ~40,000 G1 mouse library is very doable with comparable or even less cost and manpower compared to any large-scale Genome Projects so far conducted.

The NGS technology should also enhance the detection of causative mutations in the forward genetics. Conventional and NGS sequencing systems are summarized in Table 28.1.

Using these NGS systems, large-scale population sequencing studies in human has also been being conducted around the world (Genomes Project Consortium et al., 2010; Genomes Project Consortium et al., 2012) to primarily identify the responsible genes for Mendelian diseases (Rabbani et al., 2012; Tennessen et al., 2012) by the forward genetics.

24.2 Whole Exome Sequencing

Although the NGS has much higher throughput than ABI3730 sequencer (Table 28.1), mammalian genome including human has been too large to read entire genomic sequences. Considering only 1%–2% of human genome code proteins, various methods have been developed to focusing the sequencing on the coding regions, for example, the PCR amplification for targeted exons of interesting genes (Dahl et al., 2007; Porreca et al., 2007; Tewhey et al., 2009) and the enrichment by probe hybridization to capture targeted exons (Albert et al., 2007; Gnirke et al., 2009). In human, the methods to capture cancer or hereditary disorder-related genes have been also developed (Onoufriadis et al., 2014; Summerer et al., 2010). The whole exome sequencing (WES), by which all coding sequences were targeted, has also been developed for human, mouse, and other species (Choi et al., 2009; Hedges et al., 2009; Ng et al., 2009). The causative genes

TABLE 28.1 Example of Next-Generation Sequencing System

Sequencing system	Read length (fragment, bp)	Gigabase per run	Method
ABI 3730xl	900	0.00009	Fluorecence dye-terminator
Roche GS20	100	0.02	emPCR, pyrosequencing
Roche FLX	250	0.25	emPCR, pyrosequencing
IlluminaGAII	35	5	Bridge PCR, SBS chemistry
Illumina HiSeq2000	100	170	Bridge PCR, SBS chemistry
Illumina HiSeqX10	150	1,800	Bridge PCR, SBS chemistry
LifeTech SOLiD3	50	6	emPCR, sequence by oligo ligation
LifeTech IonProton	100	10	emPCR, hydorogen ion detection
PacBio RSII	10,000	1	Non-PCR, long single molecule sequencing

emPCR, Emulsion PCR; SBS, sequencing by synthesis.

for many Mendelian diseases and traits in human (Choi et al., 2009; Ng et al., 2009; Rabbani et al., 2012) as well as in the mouse (Andrews et al., 2012; Fairfield et al., 2011; Fairfield et al., 2015) have been identified by WES.

24.3 Whole Genome Sequencing

The further advancement of the NGS technologies have also made plausible to conduct whole genome sequencing (WGS) even in human. WGS has identified causative genes for several hereditary diseases and character of human. In addition to base substitutions and small indel, WGS has also efficiently detected structural variations, such as copy number variations, large indels, and translocations than WES (Alkan et al., 2011; Mills et al., 2011). The detection rate of the causative genes for Mendelian diseases in human by WES was ~50% (Beaulieu et al., 2014; Gilissen et al., 2012). It may have indicated that structural variations and/or noncoding mutations may, which are difficult to detect by WES, may be a significant fraction of the causative mutations. Similarly, the detection rate of Mendelian traits in the mouse was also reported to be 53% (Fairfield et al., 2015). Among such Mendelian mutant mouse strains, WGS succeeded in identifying causative mutations in four out of five strains in which WES could not identify (Fairfield et al., 2015).

PacBio RS II (Pacific Biosciences) has enabled ultralong one-molecule sequencing of more than 10-kb read path. The basecall precision of the PacBio system is somewhat lower than that of, for example, Illumina but effective in de novo assembly of microbial genomes (Eid et al., 2009; Fang et al., 2012) as well as the human genome (Chaisson et al., 2015; Pendleton et al., 2015). It may be also effective to de novo assemble and/or update reference genome sequences of any model organisms including various mouse strains.

24.4 High-Throughput Genotyping

Many SNPs have been registered in the genome of several inbred mouse strains as genetic markers for the mapping and the maintenance of strains (Petkov et al., 2004). For the genotyping of strain-specific SNPs, several high-throughput systems have also been developed by using NGS, for example, RAD-Seq and multiplexed shotgun genotyping (MSG) (Andolfatto et al., 2011; Davey et al., 2011; Etter et al., 2011) encompassing unknown SNPs or amplicon-sequencing (Campbell et al., 2015) for known SNPs. By using these methods, it is possible to genotype more than 100 markers from numbers of samples at once.

24.5 Additional NGS Applications

Not only for genotyping but also for molecular phenotyping is feasible with NGS technologies, for example,

RNA-seq, DNA methylation-seq and chromatin-immunoprecipitation (ChIP)-seq. RNA-seq determines whole transcripts comprehensively, which detects not only the expression level of the entire transcripts but also the alternative splicing products and/or chimeric transcripts (Ameur et al., 2010; Cloonan et al., 2008; Mortazavi et al., 2008). Therefore, RNA-seq provides big digital data with comprehensive coverage while the microarray gives analog data for only the known transcripts.

Whole-genome bisulfite sequencing (WGBS) is a popular method for DNA methylation sequencing using NGS (Cokus et al., 2008; Miura and Ito, 2015; Taylor et al., 2007). The bisulfite treatments in genomic DNA convert only nonmethylated cytosine residues into uracil residues while methylated cytosine intact. Therefore, cytosine residues in sequencing data from bisulfite treated DNA are a position of methylated cytosine residues in genome.

ChIP-seq uncovers the histone modifications or the binding sites of DNA-associated proteins on the genome (Barski et al., 2007; Blecher-Gonen et al., 2013; Johnson et al., 2007; Mikkelsen et al., 2007; Robertson et al., 2007). After the crosslinking DNA-binding proteins to DNA, target binding protein(s) are immunoprecipitated by the specific antibody. The recovered DNA is then subjected to NGS to reveal what kind of genomic sequences are enriched by the specific bindings.

24.6 Coming New Technologies

In addition to the PacBio one-molecule long sequencing, some other systems may become available for the forward genetics, as well as for the molecular phenotyping. Oxford Nanopore technology (Ashton et al., 2015; Sovic et al., 2016) gives rise to a median read length of more than 5,000 bp with a maximum length of over 60,000 bp. Both PacBio and Oxford Nanopore technologies exhibit a lower basecall precision of up to 85% accuracy; however, the error calls occur randomly so that 10–20 reading depth gives rise to accurate basecalls by these one-molecule long sequencing systems. Recently, another one-molecule long reading system, GemCode (10XGenomics) becomes available (Narasimhan et al., 2016; Zheng et al., 2016). This system allows constructing barcoded libraries for Illumina sequencing in a huge number of emulsion droplet each has only a few molecule of several hundred kilo base DNA fragments. As a consequence, it is possible to obtain N50 phase block length over 100 kb with the basecall precision of Illumina sequencing (Zheng et al., 2016).

25 GENOME EDITING TECHNOLOGIES

Genome-editing technologies have widely used to modify target genome sequences with high efficiency and specificity (Carroll, 2014; Kim and Kim, 2014; Maggio

and Goncalves, 2015) as a reverse genetic tool. These techniques enable us to directly introduce virtually any types of mutations, for example, small insertion/deletion (indel) mutations, base substitutions, large insertions/deletions, and chromosomal rearrangement, to any cells and whole organisms. Available genome editing systems include zinc-finger nucleases (ZFNs) (Carroll, 2011; Urnov et al., 2010) (Fig. 28.7A), transcription activator-like effector nucleases (TALENs) (Cermak et al., 2011; Joung and Sander, 2013) (Fig. 28.7B), and clustered regulatory interspaced short palindromic repeat (CRISPR)-associated Cas9 (Barrangou and Marraffini, 2014; Doudna and Charpentier, 2014; Hsu et al., 2014; Sander and Joung, 2014) (Fig. 28.7C).

All the three genome-editing vectors share the same two steps to modify the target genome sequence (Kim and Kim, 2014; Maggio and Goncalves, 2015). The first step is to deliver endonuclease to the target sequence to introduce a double-strand break (DSB) to the target site. The second step is the nonhomologous end joining (NHEJ) driven by cell autonomously. The NHEJ is error prone and often introduces a small insertion/deletion (indel) mutation to the DSB point (Jasin and Rothstein, 2013). Some "homologous" DNA may be codelivered with the

endonuclease to drive homology-directed repair (HDR) between the targeted DSB site and the homologous donor DNA at the second step (Jasin and Rothstein, 2013). By designing an insertion, deletion, point mutation, or chromosomal rearrangement in the homologous donor DNA fragment, the genome editing is also able to introduce the designed mutations to the target site. Thus, not only the knockout alleles but also any designed mutations may be created in cultured cells or animals.

25.1 Mechanism of CRISPR-Cas9 System

The CRISPR-Cas9 system is developed from a bacterial adaptive immune system against invading virus and plasmids and has been widely used since 2013 as a genome-editing tool (Barrangou and Marraffini, 2014; Doudna and Charpentier, 2014; Hsu et al., 2014; Sander and Joung, 2014). In natural type II CRISPR system, only the three components are required to introduce DSB at the target site; CRISPR RNAs (crRNAs), transactivating CRISPR RNA (tracrRNA), and Cas9 nuclease. crRNAs carry various sequences derived from invading DNA, which is known as "protospacer." crRNAs hybridizes with tracrRNA, and the hybrid generates a complex with the Cas9 nuclease.

In order to enhance the utility of CRISPR-Cas9 system as a genome-editing tool, crRNA and tracrRNA are fused to single-guide RNA (sgRNA) to simplify the components (Cong et al., 2013; Mali et al., 2013b). The expression of both sgRNA and Cas9 causes the DSB to the target genomic DNA site that is complementary to the guide sequence in the sgRNA (Fig. 28.7C).

The target sequence of the CRISPR-Cas9 system must locate immediately 5′ to a 5′-NGG-3′ sequences known as the protospacer adjacent motif (PAM), which is necessary to induce Cas9-directed DSBs (Jiang et al., 2013; Jinek et al., 2012). Cas9 specifically generates a blunt-ended DSB at 3 bp upstream to PAM through two nuclease domains, RuvC near the N-terminus and HNH at the middle part of Cas9 (Gasiunas et al., 2012; Jinek et al., 2012). HNH domain cleaves the complementary strand of the sgRNA, whereas RuvC domain cleaves the noncomplementary strand.

The CRISPR-Cas9 vector is simpler to design and conduct than the ZFN and TALEN vectors. sgRNA is produced either in vitro or in vivo. Plasmid encoding sgRNA is constructed by cloning of 20 bp guide sequences (Ran et al., 2013b). Double-stranded oligonucleotides may be used as a template to obtain sgRNA by in vitro transcription (Cho et al., 2013).

FIGURE 28.7 **A schematic representation of widely used genome editing systems.** (A) ZFNs consist of ZFPs at the N-terminal and the FokI nuclease domain at the C-terminal. Single ZFP contains typically three to six zinc fingers, each of which recognizes a 3-bp DNA sequence. Thus, DNA sequences of 18–36 bp are recognized by a pair of ZPNs. (B) TALENs contain TALEs at the N-terminal and the FokI nuclease domain at the C-terminal. Single TALE repeat consists of 33–35 amino acids and recognizes a single base pair of DNA. Individual TALEN is composed of typically up to 20 TALE repeats. Thus, a TALEN pair recognizes ~40 bp DNA sequences as a target sequence. (C) CRISPR-Cas9 system requires sgRNA and the Cas9 nuclease. The 20 bp target sequence needs to locate immediate upstream of the 5′-NGG-3′ sequences known as PAM *(blue)*. The expression of both sgRNA and Cas9 causes the DSB 3 bp upstream of PAM *(red arrow)*.

25.2 Efficiency and Specificity of CRISPR-Cas9 System

Among the three genome editing systems, the CRISPR-Cas9 has shown the high targeting rate enough to conduct multiplex simultaneous editing up to five

loci in mouse ES cells (Yang et al., 2013). In addition, the biallelic targeting rate was ~80% so that it is possible to directly obtain homozygous knockout cells without breeding (Wang et al., 2013). The high biallelic target efficiency may become a problem in some cases; for instance, live cells or animals may not be alive due to the homozygous lethality of the target gene.

Due to the efficiency and specificity of the CRISPR-Cas9 system, the genome editing may be anticipated to become a future tool for the gene therapy. Then, all the effects must be carefully examined including the off-target effects that genome sequence is modified at the sites other than desired site (Hendel et al., 2015; Peng et al., 2015). Cas9 target recognition is determined by Watson-Crick base-pairing interaction of an sgRNA, and off-target effect can be evaluated at potential Cas9 recognition sites that are similar to the guide sequence. Many studies indeed reported that substantial amount of off-target effect by CRISPR-Cas9 was observed in cultured cells (Fu et al., 2013; Hsu et al., 2013; Mali et al., 2013a; Pattanayak et al., 2013).

To minimize off-target effects, programmable Cas9 nickases that carry a mutation in one of the nuclease domains of either RuvC or HNH (Ran et al., 2013a; Shen et al., 2014) have been developed (Kim and Kim, 2014). Single strand break introduced by a Cas9 nickase is repaired through high-fidelity base excision repair pathway (Dianov and Hubscher, 2013). On the other hands, when Cas9 nickase very closely introduces a pair of nicks on the opposite strand, double strand break with 5′ or 3′ overhangs is created and is repaired by error-prone NHEJ. Double nicking strategy using two independent sgRNAs on the close position increases specificity without reducing on-target cleavage (Ran et al., 2013a; Shen et al., 2014). Thus, Cas9 nickase is expected to induce little off-target effects.

Even if the designed on-target editing is achieved, especially in the case for the design to construct knockout null alleles, any protein product from the manipulated allele may also be carefully examined, since exon skipping to produce a part of the target genes has sometimes observed (Uddin et al., 2015).

In general, the target site selection is another critical step for the successful genome editing. Designing of ZFNs, TALENs, and sgRNA requires various considerations in many criteria. The success rate and activity differ depending on the nuclease system, cell line/organism, target gene/sequence, and delivery method. Available programs to design ZFNs, TALENs, and sgRNA are summarized in review articles (Kim and Kim, 2014; Peng et al., 2015).

25.3 Additional Genome-Editing Applications

The targeting efficiency of CRISPR-Cas9 system is also applied for other uses (Hsu et al., 2014; Kim and Kim, 2014; Wang et al., 2016). For instance, nuclease deactivated Cas9 (dCas9) was fused to transcriptional repressor domain, for example, KRAB effector, and was used to inhibit transcription of the target gene, termed CRISPR interference (CRISPRi) (Gilbert et al., 2013). CRISPR activation (CRISPRa) was also reported, in which dCas9 was fused to transcriptional activator domain, such as VP16 /VP64 activation domains, and was used to activate transcription of particular endogenous genes (Gilbert et al., 2013; Mali et al., 2013a; Perez-Pinera et al., 2013). Site-specific epigenetic control by engineering of ZFNs (Keung et al., 2014; Rivenbark et al., 2012), TALENs (Konermann et al., 2013; Maeder et al., 2013; Mendenhall et al., 2013), and dCas9 (Hilton et al., 2015; Kearns et al., 2015; Thakore et al., 2015) was another example of the application.

To visualize genome organization and dynamics in live cells, programmable DNA binding modules are applied for the imaging of specific loci (Chen et al., 2016; Wang et al., 2016). Chen et al. (2013) visualized telomeres and coding genes in living human cells using EGFP tagged dCas9, showing that CRISPR imaging tool improves studies in the spatiotemporal organization and dynamics of native chromosomes. Multicolor genomic imaging was developed to determine relative distance of several loci in a living cell (Ma et al., 2015). dCas9 from three bacterial orthologs were fused to BFP, GFP, and RFP, and sgRNA cognate with each Cas9 ortholog was designed to target locus. Using three pairs of colored dCas9-sgRNA, relative distance of three loci can be determined.

26 CONCLUDING REMARKS

The knockout mouse resources and phenotyping by IKMC/IMPC now provide powerful tool to reveal the monogenic traits of most of coding sequence in the coisogenic mouse strains to C57BL/6N genetic background. The ENU mutant mouse libraries of ~40,000 G1 mice should shed light on the analyses of multigenic traits, since each G1 mouse carry thousands of base substitutions in a defined genetic background in any genomic sequences not only of coding sequences but also of noncoding sequences. Furthermore, by establishing a large-scale recombinant inbred strains between eight inbred mouse strains by Collaborative Cross (Churchill et al., 2004), the elucidation for the genetic interactions and gene networks should be systematically challenged. These three different phases of mutant mouse resources from monogenic to polygenic traits will orchestrated to the understanding of functional genomics modeling human diseases and complex traits with various environmental factors.

Acknowledgments

References

Albert, T.J., Molla, M.N., Muzny, D.M., Nazareth, L., Wheeler, D., Song, X., et al., 2007. Direct selection of human genomic loci by microarray hybridization. Nat. Methods 4 (11), 903–905.

Alkan, C., Coe, B.P., Eichler, E.E., 2011. Genome structural variation discovery and genotyping. Nat. Rev. Genet. 12 (5), 363–376.

Ameur, A., Wetterbom, A., Feuk, L., Gyllensten, U., 2010. Global and unbiased detection of splice junctions from RNA-seq data. Genome Biol. 11 (3), R34.

Andolfatto, P., Davison, D., Erezyilmaz, D., Hu, T.T., Mast, J., Sunayama-Morita, T., Stern, D.L., 2011. Multiplexed shotgun genotyping for rapid and efficient genetic mapping. Genome Res. 21 (4), 610–617.

Andrews, T.D., Whittle, B., Field, M.A., Balakishnan, B., Zhang, Y., Shao, Y., et al., 2012. Massively parallel sequencing of the mouse exome to accurately identify rare, induced mutations: an immediate source for thousands of new mouse models. Open Biol. 2 (5), 120061.

Ashton, P.M., Nair, S., Dallman, T., Rubino, S., Rabsch, W., Mwaigwisya, S., et al., 2015. MinION nanopore sequencing identifies the position and structure of a bacterial antibiotic resistance island. Nat. Biotechnol. 33 (3), 296–300.

Auerbach, C., Robson, J.M., 1946. Chemical production of mutations. Nature 157, 302.

Auffray, C., Balling, R., Barroso, I., Bencze, L., Benson, M., Bergeron, J., et al., 2016. Making sense of big data in health research: Towards an EU action plan. Genome Med. 8 (1), 71.

Augustin, M., Sedlmeier, R., Peters, T., Huffstadt, U., Kochmann, E., Simon, D., et al., 2005. Efficient and fast targeted production of murine models based on ENU mutagenesis. Mamm. Genome 16 (6), 405–413.

Austin, C.P., Battey, J.F., Bradley, A., Bucan, M., Capecchi, M., Collins, F.S., et al., 2004. The knockout mouse project. Nat. Genet. 36 (9), 921–924.

Auwerx, J., Avner, P., Baldock, R., Ballabio, A., Balling, R., Barbacid, M., et al., 2004. The European dimension for the mouse genome mutagenesis program. Nat. Genet. 36 (9), 925–927.

Bali, D., Svetlanov, A., Lee, H.W., Fusco-DeMane, D., Leiser, M., Li, B., et al., 1995. Animal model for maturity-onset diabetes of the young generated by disruption of the mouse glucokinase gene. J. Biol. Chem. 270 (37), 21464–21467.

Barrangou, R., Marraffini, L.A., 2014. CRISPR-Cas systems: Prokaryotes upgrade to adaptive immunity. Mol. Cell 54 (2), 234–244.

Barski, A., Cuddapah, S., Cui, K., Roh, T.Y., Schones, D.E., Wang, Z., et al., 2007. High-resolution profiling of histone methylations in the human genome. Cell 129 (4), 823–837.

Beaulieu, C.L., Majewski, J., Schwartzentruber, J., Samuels, M.E., Fernandez, B.A., Bernier, F.P., et al., 2014. FORGE Canada Consortium: outcomes of a 2-year national rare-disease gene-discovery project. Am. J. Hum. Genet. 94 (6), 809–817.

Beier, D.R., 2000. Sequence-based analysis of mutagenized mice. Mamm. Genome 11 (7), 594–597.

Bennett, C.D., Campbell, M.N., Cook, C.J., Eyre, D.J., Nay, L.M., Nielsen, D.R., et al., 2003. The LightTyper: high-throughput genotyping using fluorescent melting curve analysis. Biotechniques 34 (6), 1288–1292, 1294-1285.

Blecher-Gonen, R., Barnett-Itzhaki, Z., Jaitin, D., Amann-Zalcenstein, D., Lara-Astiaso, D., Amit, I., 2013. High-throughput chromatin immunoprecipitation for genome-wide mapping of in vivo protein-DNA interactions and epigenomic states. Nat. Protoc. 8 (3), 539–554.

Brilliant, M.H., Gondo, Y., Eicher, E.M., 1991. Direct molecular identification of the mouse pink-eyed unstable mutation by genome scanning. Science 252 (5005), 566–569.

Brown, S.D., Moore, M.W., 2012a. The International Mouse Phenotyping Consortium: past and future perspectives on mouse phenotyping. Mamm. Genome 23 (9–10), 632–640.

Brown, S.D., Moore, M.W., 2012b. Towards an encyclopaedia of mammalian gene function: the International Mouse Phenotyping Consortium. Dis. Model Mech. 5 (3), 289–292.

Brown, S.D., Nolan, P.M., 1998. Mouse mutagenesis-systematic studies of mammalian gene function. Hum. Mol. Genet. 7 (10), 1627–1633.

Burmeister, M., McInnis, M.G., Zollner, S., 2008. Psychiatric genetics: progress amid controversy. Nat. Rev. Genet. 9 (7), 527–540.

Campbell, N.R., Harmon, S.A., Narum, S.R., 2015. Genotyping-in-Thousands by sequencing (GT-seq): A cost effective SNP genotyping method based on custom amplicon sequencing. Mol. Ecol. Resour. 15 (4), 855–867.

Cantor, C.R., 1990. Orchestrating the Human Genome Project. Science 248 (4951), 49–51.

Capecchi, M.R., 1989. Altering the genome by homologous recombination. Science 244 (4910), 1288–1292.

Carroll, D., 2011. Genome engineering with zinc-finger nucleases. Genetics 188 (4), 773–782.

Carroll, D., 2014. Genome engineering with targetable nucleases. Annu. Rev. Biochem. 83, 409–439.

Cermak, T., Doyle, E.L., Christian, M., Wang, L., Zhang, Y., Schmidt, C., et al., 2011. Efficient design and assembly of custom TALEN and other TAL effector-based constructs for DNA targeting. Nucleic Acids Res. 39 (12), e82.

Chaisson, M.J., Huddleston, J., Dennis, M.Y., Sudmant, P.H., Malig, M., Hormozdiari, F., et al., 2015. Resolving the complexity of the human genome using single-molecule sequencing. Nature 517 (7536), 608–611.

Chen, B., Gilbert, L.A., Cimini, B.A., Schnitzbauer, J., Zhang, W., Li, G.W., et al., 2013. Dynamic imaging of genomic loci in living human cells by an optimized CRISPR/Cas system. Cell 155 (7), 1479–1491.

Chen, B., Guan, J., Huang, B., 2016. Imaging Specific Genomic DNA in Living Cells. Annu. Rev. Biophys. 45, 1–23.

Chikaraishi, D.M., Deeb, S.S., Sueoka, N., 1978. Sequence complexity of nuclear RNAs in adult rat tissues. Cell 13 (1), 111–120.

Cho, S.W., Kim, S., Kim, J.M., Kim, J.S., 2013. Targeted genome engineering in human cells with the Cas9 RNA-guided endonuclease. Nat. Biotechnol. 31 (3), 230–232.

Choi, M., Scholl, U.I., Ji, W., Liu, T., Tikhonova, I.R., Zumbo, P., et al., 2009. Genetic diagnosis by whole exome capture and massively parallel DNA sequencing. Proc. Natl. Acad. Sci. USA 106 (45), 19096–19101.

Churchill, G.A., Airey, D.C., Allayee, H., Angel, J.M., Attie, A.D., Beatty, J., et al., 2004. The Collaborative Cross, a community resource for the genetic analysis of complex traits. Nat. Genet. 36 (11), 1133–1137.

Clapcote, S.J., Lipina, T.V., Millar, J.K., Mackie, S., Christie, S., Ogawa, F., et al., 2007. Behavioral phenotypes of Disc1 missense mutations in mice. Neuron 54 (3), 387–402.

Cloonan, N., Forrest, A.R., Kolle, G., Gardiner, B.B., Faulkner, G.J., Brown, M.K., et al., 2008. Stem cell transcriptome profiling via massive-scale mRNA sequencing. Nat. Methods 5 (7), 613–619.

Coghill, E.L., Hugill, A., Parkinson, N., Davison, C., Glenister, P., Clements, S., et al., 2002. A gene-driven approach to the identification of ENU mutants in the mouse. Nat. Genet. 30 (3), 255–256.

Cokus, S.J., Feng, S., Zhang, X., Chen, Z., Merriman, B., Haudenschild, C.D., et al., 2008. Shotgun bisulphite sequencing of the Arabidopsis genome reveals DNA methylation patterning. Nature 452 (7184), 215–219.

Concepcion, D., Seburn, K.L., Wen, G., Frankel, W.N., Hamilton, B.A., 2004. Mutation rate and predicted phenotypic target sizes in ethylnitrosourea-treated mice. Genetics 168 (2), 953–959.

Cong, L., Ran, F.A., Cox, D., Lin, S., Barretto, R., Habib, N., et al., 2013. Multiplex genome engineering using CRISPR/Cas systems. Science 339 (6121), 819–823.

Dahl, F., Stenberg, J., Fredriksson, S., Welch, K., Zhang, M., Nilsson, M., et al., 2007. Multigene amplification and massively parallel sequencing for cancer mutation discovery. Proc. Natl. Acad. Sci. USA 104 (22), 9387–9392.

Davey, J.W., Hohenlohe, P.A., Etter, P.D., Boone, J.Q., Catchen, J.M., Blaxter, M.L., 2011. Genome-wide genetic marker discovery and genotyping using next-generation sequencing. Nat. Rev. Genet. 12 (7), 499–510.

Dianov, G.L., Hubscher, U., 2013. Mammalian base excision repair: the forgotten archangel. Nucleic Acids Res. 41 (6), 3483–3490.

Doetschman, T., Maeda, N., Smithies, O., 1988. Targeted mutation of the Hprt gene in mouse embryonic stem cells. Proc. Natl. Acad. Sci. USA 85 (22), 8583–8587.

Donato, Jr., J., Cravo, R.M., Frazao, R., Elias, C.F., 2011. Hypothalamic sites of leptin action linking metabolism and reproduction. Neuroendocrinology 93 (1), 9–18.

Donehower, L.A., Harvey, M., Slagle, B.L., McArthur, M.J., Montgomery, Jr., C.A., Butel, J.S., Bradley, A., 1992. Mice deficient for p53 are developmentally normal but susceptible to spontaneous tumours. Nature 356 (6366), 215–221.

Doudna, J.A., Charpentier, E., 2014. Genome editing. The new frontier of genome engineering with CRISPR-Cas9. Science 346 (6213), 1258096.

Duyao, M.P., Auerbach, A.B., Ryan, A., Persichetti, F., Barnes, G.T., McNeil, S.M., et al., 1995. Inactivation of the mouse Huntington's disease gene homolog Hdh. Science 269 (5222), 407–410.

Editorial, 2007. Mutant mice galore. Nature 446 (7135), 469–470.

Eid, J., Fehr, A., Gray, J., Luong, K., Lyle, J., Otto, G., et al., 2009. Real-time DNA sequencing from single polymerase molecules. Science 323 (5910), 133–138.

Etter, P.D., Bassham, S., Hohenlohe, P.A., Johnson, E.A., Cresko, W.A., 2011. SNP discovery and genotyping for evolutionary genetics using RAD sequencing. Methods Mol. Biol. 772, 157–178.

Evans, M.J., Kaufman, M.H., 1981. Establishment in culture of pluripotential cells from mouse embryos. Nature 292 (5819), 154–156.

Fairfield, H., Gilbert, G.J., Barter, M., Corrigan, R.R., Curtain, M., Ding, Y., et al., 2011. Mutation discovery in mice by whole exome sequencing. Genome Biol. 12 (9), R86.

Fairfield, H., Srivastava, A., Ananda, G., Liu, R., Kircher, M., Lakshminarayana, A., et al., 2015. Exome sequencing reveals pathogenic mutations in 91 strains of mice with Mendelian disorders. Genome Res. 25 (7), 948–957.

Fang, G., Munera, D., Friedman, D.I., Mandlik, A., Chao, M.C., Banerjee, O., et al., 2012. Genome-wide mapping of methylated adenine residues in pathogenic Escherichia coli using single-molecule real-time sequencing. Nat. Biotechnol. 30 (12), 1232–1239.

Fodde, R., Edelmann, W., Yang, K., van Leeuwen, C., Carlson, C., Renault, B., et al., 1994. A targeted chain-termination mutation in the mouse Apc gene results in multiple intestinal tumors. Proc. Natl. Acad. Sci. USA 91 (19), 8969–8973.

Friend, S.H., Bernards, R., Rogelj, S., Weinberg, R.A., Rapaport, J.M., Albert, D.M., Dryja, T.P., 1986. A human DNA segment with properties of the gene that predisposes to retinoblastoma and osteosarcoma. Nature 323 (6089), 643–646.

Froguel, P., Zouali, H., Vionnet, N., Velho, G., Vaxillaire, M., Sun, F., et al., 1993. Familial hyperglycemia due to mutations in glucokinase. Definition of a subtype of diabetes mellitus. N. Engl. J. Med. 328 (10), 697–702.

Fu, Y., Foden, J.A., Khayter, C., Maeder, M.L., Reyon, D., Joung, J.K., Sander, J.D., 2013. High-frequency off-target mutagenesis induced by CRISPR-Cas nucleases in human cells. Nat. Biotechnol. 31 (9), 822–826.

Furuse, T., Wada, Y., Hattori, K., Yamada, I., Kushida, T., Shibukawa, Y., et al., 2010. Phenotypic characterization of a new Grin1 mutant mouse generated by ENU mutagenesis. Eur. J. Neurosci. 31 (7), 1281–1291.

Gao, Q., Yeung, E.S., 2000. High-throughput detection of unknown mutations by using multiplexed capillary electrophoresis with poly(vinylpyrrolidone) solution. Anal. Chem. 72 (11), 2499–2506.

Gardner, J.M., Nakatsu, Y., Gondo, Y., Lee, S., Lyon, M.F., King, R.A., Brilliant, M.H., 1992. The mouse pink-eyed dilution gene: association with human Prader-Willi and Angelman syndromes. Science 257 (5073), 1121–1124.

Gasiunas, G., Barrangou, R., Horvath, P., Siksnys, V., 2012. Cas9-crRNA ribonucleoprotein complex mediates specific DNA cleavage for adaptive immunity in bacteria. Proc. Natl. Acad. Sci. USA 109 (39), E2579–E2586.

Genomes Project Consortium, Abecasis, G.R., Altshuler, D., Auton, A., Brooks, L.D., Durbin, R.M., et al., 2010. A map of human genome variation from population-scale sequencing. Nature 467 (7319), 1061–1073.

Genomes Project Consortium, Abecasis, G.R., Auton, A., Brooks, L.D., DePristo, M.A., Durbin, R.M., et al., 2012. An integrated map of genetic variation from 1,092 human genomes. Nature 491 (7422), 56–65.

Ghilardi, N., Ziegler, S., Wiestner, A., Stoffel, R., Heim, M.H., Skoda, R.C., 1996. Defective STAT signaling by the leptin receptor in diabetic mice. Proc. Natl. Acad. Sci. USA 93 (13), 6231–6235.

Gilbert, L.A., Larson, M.H., Morsut, L., Liu, Z., Brar, G.A., Torres, S.E., et al., 2013. CRISPR-mediated modular RNA-guided regulation of transcription in eukaryotes. Cell 154 (2), 442–451.

Gilissen, C., Hoischen, A., Brunner, H.G., Veltman, J.A., 2012. Disease gene identification strategies for exome sequencing. Eur. J. Hum. Genet. 20 (5), 490–497.

Gnirke, A., Melnikov, A., Maguire, J., Rogov, P., LeProust, E.M., Brockman, W., et al., 2009. Solution hybrid selection with ultra-long oligonucleotides for massively parallel targeted sequencing. Nat. Biotechnol. 27 (2), 182–189.

Gondo, Y., 2008. Trends in large-scale mouse mutagenesis: from genetics to functional genomics. Nat. Rev. Genet. 9 (10), 803–810.

Gondo, Y., 2010. Now and future of mouse mutagenesis for human disease models. J. Genet. Genomics 37 (9), 559–572.

Gondo, Y., Brilliant, M.H., 1995. Theoretical basis of one-dimensional genome scanning: a direct method to identify the site of a mutation. Electrophoresis 16 (2), 174–178.

Gondo, Y., Fukumura, R., 2009. ENU-induced mutant mice for a next-generation gene-targeting system. Prog. Brain Res. 179, 29–34.

Gondo, Y., Gardner, J.M., Nakatsu, Y., Durham-Pierre, D., Deveau, S.A., Kuper, C., Brilliant, M.H., 1993. High-frequency genetic reversion mediated by a DNA duplication: the mouse pink-eyed unstable mutation. Proc. Natl. Acad. Sci. USA 90 (1), 297–301.

Gondo, Y., Nakamura, K., Nakao, K., Sasaoka, T., Ito, K., Kimura, M., Katsuki, M., 1994. Gene replacement of the p53 gene with the lacZ gene in mouse embryonic stem cells and mice by using two steps of homologous recombination. Biochem. Biophys. Res. Commun. 202 (2), 830–837.

Gondo, Y., Fukumura, R., Murata, T., Makino, S., 2009. Next-generation gene targeting in the mouse for functional genomics. BMB Rep. 42 (6), 315–323.

Gondo, Y., Fukumura, R., Murata, T., Makino, S., 2010. ENU-based gene-driven mutagenesis in the mouse: a next-generation gene-targeting system. Exp. Anim. 59 (5), 537–548.

Gossler, A., Doetschman, T., Korn, R., Serfling, E., Kemler, R., 1986. Transgenesis by means of blastocyst-derived embryonic stem cell lines. Proc. Natl. Acad. Sci. USA 83 (23), 9065–9069.

Gossler, A., Joyner, A.L., Rossant, J., Skarnes, W.C., 1989. Mouse embryonic stem cells and reporter constructs to detect developmentally regulated genes. Science 244 (4903), 463–465.

Groden, J., Thliveris, A., Samowitz, W., Carlson, M., Gelbert, L., Albertsen, H., et al., 1991. Identification and characterization of the familial adenomatous polyposis coli gene. Cell 66 (3), 589–600.

Gross, E., Arnold, N., Goette, J., Schwarz-Boeger, U., Kiechle, M., 1999. A comparison of BRCA1 mutation analysis by direct sequencing, SSCP and DHPLC. Hum. Genet. 105 (1–2), 72–78.

Grupe, A., Hultgren, B., Ryan, A., Ma, Y.H., Bauer, M., Stewart, T.A., 1995. Transgenic knockouts reveal a critical requirement for pancreatic beta cell glucokinase in maintaining glucose homeostasis. Cell 83 (1), 69–78.

Haldane, J.B.S., Sprunt, A.D., Haldane, N.M., 1915. Reduplication in mice. J. Genet. 5, 133–135.

Hansen, G.M., Markesich, D.C., Burnett, M.B., Zhu, Q., Dionne, K.M., Richter, L.J., et al., 2008. Large-scale gene trapping in C57BL/6N mouse embryonic stem cells. Genome Res. 18 (10), 1670–1679.

Hassen, S., Ali, N., Chowdhury, P., 2012. Molecular signaling mechanisms of apoptosis in hereditary non-polyposis colorectal cancer. World J. Gastrointest. Pathophysiol. 3 (3), 71–79.

Hedges, D.J., Burges, D., Powell, E., Almonte, C., Huang, J., Young, S., et al., 2009. Exome sequencing of a multigenerational human pedigree. PLoS One 4 (12), e8232.

Hendel, A., Fine, E.J., Bao, G., Porteus, M.H., 2015. Quantifying on- and off-target genome editing. Trends Biotechnol. 33 (2), 132–140.

Hilton, I.B., D'Ippolito, A.M., Vockley, C.M., Thakore, P.I., Crawford, G.E., Reddy, T.E., Gersbach, C.A., 2015. Epigenome editing by a CRISPR-Cas9-based acetyltransferase activates genes from promoters and enhancers. Nat. Biotechnol. 33 (5), 510–517.

Hirose, S., Touma, M., Go, R., Katsuragi, Y., Sakuraba, Y., Gondo, Y., et al., 2015. Bcl11b prevents the intrathymic development of innate CD8 T cells in a cell intrinsic manner. Int. Immunol. 27 (4), 205–215.

Hitotsumachi, S., Carpenter, D.A., Russell, W.L., 1985. Dose-repetition increases the mutagenic effectiveness of N-ethyl-N-nitrosourea in mouse spermatogonia. Proc. Natl. Acad. Sci. USA 82 (19), 6619–6621.

Hrabe de Angelis, M., Balling, R., 1998. Large scale ENU screens in the mouse: genetics meets genomics. Mutat. Res. 400 (1–2), 25–32.

Hrabe de Angelis, M.H., Flaswinkel, H., Fuchs, H., Rathkolb, B., Soewarto, D., Marschall, S., et al., 2000. Genome-wide, large-scale production of mutant mice by ENU mutagenesis. Nat. Genet. 25 (4), 444–447.

Hsu, P.D., Scott, D.A., Weinstein, J.A., Ran, F.A., Konermann, S., Agarwala, V., et al., 2013. DNA targeting specificity of RNA-guided Cas9 nucleases. Nat. Biotechnol. 31 (9), 827–832.

Hsu, P.D., Lander, E.S., Zhang, F., 2014. Development and Applications of CRISPR-Cas9 for Genome Engineering. Cell 157 (6), 1262–1278.

Huang, J.D., Mermall, V., Strobel, M.C., Russell, L.B., Mooseker, M.S., Copeland, N.G., Jenkins, N.A., 1998. Molecular genetic dissection of mouse unconventional myosin-VA: tail region mutations. Genetics 148 (4), 1963–1972.

Ichii, S., Takeda, S., Horii, A., Nakatsuru, S., Miyoshi, Y., Emi, M., et al., 1993. Detailed analysis of genetic alterations in colorectal tumors from patients with and without familial adenomatous polyposis (FAP). Oncogene 8 (9), 2399–2405.

Inoue, M., Sakuraba, Y., Motegi, H., Kubota, N., Toki, H., Matsui, J., et al., 2004. A series of maturity onset diabetes of the young, type 2 (MODY2) mouse models generated by a large-scale ENU mutagenesis program. Hum. Mol. Genet. 13 (11), 1147–1157.

International HapMap Consortium, 2003. The International HapMap Project. Nature 426 (6968), 789–796.

International Human Genome Sequencing Consortium, 2001. Initial sequencing and analysis of the human genome. Nature 409 (6822), 860–921.

International Human Genome Sequencing Consortium, 2004. Finishing the euchromatic sequence of the human genome. Nature 431 (7011), 931–945.

Collins, F.S., Rossant, J., Wurst, W., International Mouse Knockout Consortium, 2007. A mouse for all reasons. Cell 128 (1), 9–13.

International SNP Map Working Group, 2001. A map of human genome sequence variation containing 1.42 million single nucleotide polymorphisms. Nature 409 (6822), 928–933.

Jackson, I.J., 1988. A cDNA encoding tyrosinase-related protein maps to the brown locus in mouse. Proc. Natl. Acad. Sci. USA 85 (12), 4392–4396.

Jasin, M., Rothstein, R., 2013. Repair of strand breaks by homologous recombination. Cold Spring Harb. Perspect. Biol. 5 (11), a012740.

Jenkins, N.A., Copeland, N.G., Taylor, B.A., Lee, B.K., 1981. Dilute (d) coat colour mutation of DBA/2J mice is associated with the site of integration of an ecotropic MuLV genome. Nature 293 (5831), 370–374.

Jenkins, N.A., Copeland, N.G., Taylor, B.A., Lee, B.K., 1982. Organization, distribution, and stability of endogenous ecotropic murine leukemia virus DNA sequences in chromosomes of Mus musculus. J. Virol. 43 (1), 26–36.

Jiang, W., Bikard, D., Cox, D., Zhang, F., Marraffini, L.A., 2013. RNA-guided editing of bacterial genomes using CRISPR-Cas systems. Nat. Biotechnol. 31 (3), 233–239.

Jinek, M., Chylinski, K., Fonfara, I., Hauer, M., Doudna, J.A., Charpentier, E., 2012. A programmable dual-RNA-guided DNA endonuclease in adaptive bacterial immunity. Science 337 (6096), 816–821.

Johnson, D.S., Mortazavi, A., Myers, R.M., Wold, B., 2007. Genome-wide mapping of in vivo protein-DNA interactions. Science 316 (5830), 1497–1502.

Joslyn, G., Carlson, M., Thliveris, A., Albertsen, H., Gelbert, L., Samowitz, W., et al., 1991. Identification of deletion mutations and three new genes at the familial polyposis locus. Cell 66 (3), 601–613.

Joung, J.K., Sander, J.D., 2013. TALENs: a widely applicable technology for targeted genome editing. Nat. Rev. Mol. Cell Biol. 14 (1), 49–55.

Justice, M.J., Noveroske, J.K., Weber, J.S., Zheng, B., Bradley, A., 1999. Mouse ENU mutagenesis. Hum. Mol. Genet. 8 (10), 1955–1963.

Katsuragi, Y., Anraku, J., Nakatomi, M., Ida-Yonemochi, H., Obata, M., Mishima, Y., et al., 2013. Bcl11b transcription factor plays a role in the maintenance of the ameloblast-progenitors in mouse adult maxillary incisors. Mech. Dev. 130 (9–10), 482–492.

Kearns, N.A., Pham, H., Tabak, B., Genga, R.M., Silverstein, N.J., Garber, M., Maehr, R., 2015. Functional annotation of native enhancers with a Cas9-histone demethylase fusion. Nat. Methods 12 (5), 401–403.

Keung, A.J., Bashor, C.J., Kiriakov, S., Collins, J.J., Khalil, A.S., 2014. Using targeted chromatin regulators to engineer combinatorial and spatial transcriptional regulation. Cell 158 (1), 110–120.

Kim, H., Kim, J.S., 2014. A guide to genome engineering with programmable nucleases. Nat. Rev. Genet. 15 (5), 321–334.

Kim, Y.J., Kang, Y., Park, H.Y., Lee, J.R., Yu, D.Y., Murata, T., et al., 2016. STEP signaling pathway mediates psychomotor stimulation and morphine withdrawal symptoms, but not for reward, analgesia and tolerance. Exp. Mol. Med. 48, e212.

King, D.P., Zhao, Y., Sangoram, A.M., Wilsbacher, L.D., Tanaka, M., Antoch, M.P., et al., 1997. Positional cloning of the mouse circadian clock gene. Cell 89 (4), 641–653.

Kinzler, K.W., Nilbert, M.C., Su, L.K., Vogelstein, B., Bryan, T.M., Levy, D.B., et al., 1991. Identification of FAP locus genes from chromosome 5q21. Science 253 (5020), 661–665.

Klein, J., 1979. The major histocompatibility complex of the mouse. Science 203 (4380), 516–521.

Konermann, S., Brigham, M.D., Trevino, A.E., Hsu, P.D., Heidenreich, M., Cong, L., et al., 2013. Optical control of mammalian endogenous transcription and epigenetic states. Nature 500 (7463), 472–476.

Kwon, B.S., Haq, A.K., Pomerantz, S.H., Halaban, R., 1987. Isolation and sequence of a cDNA clone for human tyrosinase that maps at the mouse c-albino locus. Proc. Natl. Acad. Sci. USA 84 (21), 7473–7477.

Labrie, V., Fukumura, R., Rastogi, A., Fick, L.J., Wang, W., Boutros, P.C., et al., 2009. Serine racemase is associated with schizophrenia susceptibility in humans and in a mouse model. Hum. Mol. Genet. 18 (17), 3227–3243.

Lakso, M., Sauer, B., Mosinger, Jr., B., Lee, E.J., Manning, R.W., Yu, S.H., et al., 1992. Targeted oncogene activation by site-specific recombination in transgenic mice. Proc. Natl. Acad. Sci. USA 89 (14), 6232–6236.

Lambrinoudaki, I., Vlachou, S.A., Creatsas, G., 2010. Genetics in gestational diabetes mellitus: association with incidence, severity, pregnancy outcome and response to treatment. Curr. Diabetes Rev. 6 (6), 393–399.

Lazar, N.L., Singh, S., Paton, T., Clapcote, S.J., Gondo, Y., Fukumura, R., et al., 2011. Missense mutation of the reticulon-4 receptor alters spatial memory and social interaction in mice. Behav. Brain Res. 224 (1), 73–79.

Li, F.P., Fraumeni, Jr., J.F., 1969. Rhabdomyosarcoma in children: epidemiologic study and identification of a familial cancer syndrome. J. Natl. Cancer Inst. 43 (6), 1365–1373.

Li, Q., Liu, Z., Monroe, H., Culiat, C.T., 2002. Integrated platform for detection of DNA sequence variants using capillary array electrophoresis. Electrophoresis 23 (10), 1499–1511.

Little, C.C., Bagg, H.J., 1923. The occurrence of two heritable types of abnormality among the descendants of X-rayed mice. Am. J. Roentgenol. Radiat. Therap. 10, 975–989.

Luongo, C., Moser, A.R., Gledhill, S., Dove, W.F., 1994. Loss of Apc+ in intestinal adenomas from Min mice. Cancer Res. 54 (22), 5947–5952.

Lyon, M.F., King, T.R., Gondo, Y., Gardner, J.M., Nakatsu, Y., Eicher, E.M., Brilliant, M.H., 1992. Genetic and molecular analysis of recessive alleles at the pink-eyed dilution (p) locus of the mouse. Proc. Natl. Acad. Sci. USA 89 (15), 6968–6972.

Lyon, M.F., Rastan, S., Brown, S.D.M. (Eds.), 1996. Genetic Variants and Strains of the Laboratory Mouse, third ed. Oxford University Press, Oxford, UK.

Ma, H., Naseri, A., Reyes-Gutierrez, P., Wolfe, S.A., Zhang, S., Pederson, T., 2015. Multicolor CRISPR labeling of chromosomal loci in human cells. Proc. Natl. Acad. Sci. USA 112 (10), 3002–3007.

Maeder, M.L., Angstman, J.F., Richardson, M.E., Linder, S.J., Cascio, V.M., Tsai, S.Q., et al., 2013. Targeted DNA demethylation and activation of endogenous genes using programmable TALE-TET1 fusion proteins. Nat. Biotechnol. 31 (12), 1137–1142.

Maggio, I., Goncalves, M.A., 2015. Genome editing at the crossroads of delivery, specificity, and fidelity. Trends Biotechnol. 33 (5), 280–291.

Makino, S., Zhulyn, O., Mo, R., Puviindran, V., Zhang, X., Murata, T., et al., 2015. T396I mutation of mouse Sufu reduces the stability and activity of Gli3 repressor. PLoS One 10 (3), e0119455.

Mali, P., Aach, J., Stranges, P.B., Esvelt, K.M., Moosburner, M., Kosuri, S., et al., 2013a. CAS9 transcriptional activators for target specificity screening and paired nickases for cooperative genome engineering. Nat. Biotechnol. 31 (9), 833–838.

Mali, P., Yang, L., Esvelt, K.M., Aach, J., Guell, M., DiCarlo, J.E., et al., 2013b. RNA-guided human genome engineering via Cas9. Science 339 (6121), 823–826.

Malkin, D., Li, F.P., Strong, L.C., Fraumeni, Jr., J.F., Nelson, C.E., Kim, D.H., et al., 1990. Germ line p53 mutations in a familial syndrome of breast cancer, sarcomas, and other neoplasms. Science 250 (4985), 1233–1238.

Mangiarini, L., Sathasivam, K., Seller, M., Cozens, B., Harper, A., Hetherington, C., et al., 1996. Exon 1 of the HD gene with an expanded CAG repeat is sufficient to cause a progressive neurological phenotype in transgenic mice. Cell 87 (3), 493–506.

Mansour, S.L., Thomas, K.R., Capecchi, M.R., 1988. Disruption of the proto-oncogene int-2 in mouse embryo-derived stem cells: a general strategy for targeting mutations to non-selectable genes. Nature 336 (6197), 348–352.

Masuya, H., Shimizu, K., Sezutsu, H., Sakuraba, Y., Nagano, J., Shimizu, A., et al., 2005. Enamelin (Enam) is essential for amelogenesis: ENU-induced mouse mutants as models for different clinical subtypes of human amelogenesis imperfecta (AI). Hum. Mol. Genet. 14 (5), 575–583.

Masuya, H., Nishida, K., Furuichi, T., Toki, H., Nishimura, G., Kawabata, H., et al., 2007a. A novel dominant-negative mutation in Gdf5 generated by ENU mutagenesis impairs joint formation and causes osteoarthritis in mice. Hum. Mol. Genet. 16 (19), 2366–2375.

Masuya, H., Sezutsu, H., Sakuraba, Y., Sagai, T., Hosoya, M., Kaneda, H., et al., 2007b. A series of ENU-induced single-base substitutions in a long-range cis-element altering Sonic hedgehog expression in the developing mouse limb bud. Genomics 89 (2), 207–214.

Menalled, L.B., Chesselet, M.F., 2002. Mouse models of Huntington's disease. Trends Pharmacol. Sci. 23 (1), 32–39.

Mendenhall, E.M., Williamson, K.E., Reyon, D., Zou, J.Y., Ram, O., Joung, J.K., Bernstein, B.E., 2013. Locus-specific editing of histone modifications at endogenous enhancers. Nat. Biotechnol. 31 (12), 1133–1136.

Mercer, J.A., Seperack, P.K., Strobel, M.C., Copeland, N.G., Jenkins, N.A., 1991. Novel myosin heavy chain encoded by murine dilute coat colour locus. Nature 349 (6311), 709–713.

MGC Project Team, 2004. The status, quality, and expansion of the NIH full-length cDNA project: the Mammalian Gene Collection (MGC). Genome Res. 14 (10B), 2121–2127.

Michaud, E.J., Culiat, C.T., Klebig, M.L., Barker, P.E., Cain, K.T., Carpenter, D.J., et al., 2005. Efficient gene-driven germ-line point mutagenesis of C57BL/6J mice. BMC Genomics 6, 164.

Mikkelsen, T.S., Ku, M., Jaffe, D.B., Issac, B., Lieberman, E., Giannoukos, G., et al., 2007. Genome-wide maps of chromatin state in pluripotent and lineage-committed cells. Nature 448 (7153), 553–560.

Mills, R.E., Walter, K., Stewart, C., Handsaker, R.E., Chen, K., Alkan, C., et al., 2011. Mapping copy number variation by population-scale genome sequencing. Nature 470 (7332), 59–65.

Miura, F., Ito, T., 2015. Highly sensitive targeted methylome sequencing by post-bisulfite adaptor tagging. DNA Res. 22 (1), 13–18.

Monaco, A.P., Bertelson, C.J., Middlesworth, W., Colletti, C.A., Aldridge, J., Fischbeck, K.H., et al., 1985. Detection of deletions spanning the Duchenne muscular dystrophy locus using a tightly linked DNA segment. Nature 316 (6031), 842–845.

Mortazavi, A., Williams, B.A., McCue, K., Schaeffer, L., Wold, B., 2008. Mapping and quantifying mammalian transcriptomes by RNA-Seq. Nat. Methods 5 (7), 621–628.

Moser, A.R., Pitot, H.C., Dove, W.F., 1990. A dominant mutation that predisposes to multiple intestinal neoplasia in the mouse. Science 247 (4940), 322–324.

Moser, A.R., Dove, W.F., Roth, K.A., Gordon, J.I., 1992. The Min (multiple intestinal neoplasia) mutation: its effect on gut epithelial cell differentiation and interaction with a modifier system. J. Cell Biol. 116 (6), 1517–1526.

Moser, A.R., Shoemaker, A.R., Connelly, C.S., Clipson, L., Gould, K.A., Luongo, C., et al., 1995. Homozygosity for the Min allele of Apc results in disruption of mouse development prior to gastrulation. Dev. Dyn. 203 (4), 422–433.

Mouse Genome Sequencing, C., Waterston, R.H., Lindblad-Toh, K., Birney, E., Rogers, J., Abril, J.F., et al., 2002. Initial sequencing and comparative analysis of the mouse genome. Nature 420 (6915), 520–562.

Muller, H.J., 1927. Artificial Transmutation of the Gene. Science 66 (1699), 84–87.

Mun, H.S., Saab, B.J., Ng, E., McGirr, A., Lipina, T.V., Gondo, Y., et al., 2015. Self-directed exploration provides a Ncs1-dependent learning bonus. Sci. Rep. 5, 17697.

Murata, T., Ishitsuka, Y., Karouji, K., Kaneda, H., Toki, H., Nakai, Y., et al., 2014. beta-CateninC429S mice exhibit sterility consequent to spatiotemporally sustained Wnt signalling in the internal genitalia. Sci. Rep. 4, 6959.

Murphy, K., Hafez, M., Philips, J., Yarnell, K., Gutshall, K., Berg, K., 2003. Evaluation of temperature gradient capillary electrophoresis for detection of the Factor V Leiden mutation: coincident identification of a novel polymorphism in Factor V. Mol. Diagn. 7 (1), 35–40.

Nadeau, J.H., Balling, R., Barsh, G., Beier, D., Brown, S.D., Bucan, M., et al., 2001. Sequence interpretation. Functional annotation of mouse genome sequences. Science 291 (5507), 1251–1255.

Nakagata, N., 1993. Production of normal young following transfer of mouse embryos obtained by in vitro fertilization between cryopreserved gametes. J. Reprod. Fertil. 99 (1), 77–80.

Nakagata, N., 2000. Cryopreservation of mouse spermatozoa. Mamm. Genome 11 (7), 572–576.

Nakatsu, Y., Gondo, Y., Brilliant, M.H., 1992. The p locus is closely linked to the mouse homolog of a gene from the Prader-Willi chromosomal region. Mamm. Genome 2 (1), 69–71.

Nakatsu, Y., Tyndale, R.F., DeLorey, T.M., Durham-Pierre, D., Gardner, J.M., McDanel, H.J., et al., 1993. A cluster of three GABAA receptor subunit genes is deleted in a neurological mutant of the mouse p locus. Nature 364 (6436), 448–450.

Narasimhan, V.M., Hunt, K.A., Mason, D., Baker, C.L., Karczewski, K.J., Barnes, M.R., et al., 2016. Health and population effects of rare gene knockouts in adult humans with related parents. Science 352 (6284), 474–477.

Nasir, J., Floresco, S.B., O'Kusky, J.R., Diewert, V.M., Richman, J.M., Zeisler, J., et al., 1995. Targeted disruption of the Huntington's disease gene results in embryonic lethality and behavioral and morphological changes in heterozygotes. Cell 81 (5), 811–823.

Ng, S.B., Turner, E.H., Robertson, P.D., Flygare, S.D., Bigham, A.W., Lee, C., et al., 2009. Targeted capture and massively parallel sequencing of 12 human exomes. Nature 461 (7261), 272–276.

Nishisho, I., Nakamura, Y., Miyoshi, Y., Miki, Y., Ando, H., Horii, A., et al., 1991. Mutations of chromosome 5q21 genes in FAP and colorectal cancer patients. Science 253 (5020), 665–669.

Nolan, P.M., Peters, J., Strivens, M., Rogers, D., Hagan, J., Spurr, N., et al., 2000. A systematic, genome-wide, phenotype-driven mutagenesis programme for gene function studies in the mouse. Nat. Genet. 25 (4), 440–443.

Norimura, T., Nomoto, S., Katsuki, M., Gondo, Y., Kondo, S., 1996. p53-dependent apoptosis suppresses radiation-induced teratogenesis. Nat. Med. 2 (5), 577–580.

Noveroske, J.K., Weber, J.S., Justice, M.J., 2000. The mutagenic action of N-ethyl-N-nitrosourea in the mouse. Mamm. Genome 11 (7), 478–483.

Oleykowski, C.A., Bronson Mullins, C.R., Godwin, A.K., Yeung, A.T., 1998. Mutation detection using a novel plant endonuclease. Nucleic Acids Res. 26 (20), 4597–4602.

Onoufriadis, A., Shoemark, A., Schmidts, M., Patel, M., Jimenez, G., Liu, H., et al., 2014. Targeted NGS gene panel identifies mutations in RSPH1 causing primary ciliary dyskinesia and a common mechanism for ciliary central pair agenesis due to radial spoke defects. Hum. Mol. Genet. 23 (13), 3362–3374.

Osbak, K.K., Colclough, K., Saint-Martin, C., Beer, N.L., Bellanne-Chantelot, C., Ellard, S., Gloyn, A.L., 2009. Update on mutations in glucokinase (GCK), which cause maturity-onset diabetes of the young, permanent neonatal diabetes, and hyperinsulinemic hypoglycemia. Hum. Mutat. 30 (11), 1512–1526.

Oshima, M., Oshima, H., Kitagawa, K., Kobayashi, M., Itakura, C., Taketo, M., 1995. Loss of Apc heterozygosity and abnormal tissue building in nascent intestinal polyps in mice carrying a truncated Apc gene. Proc. Natl. Acad. Sci. USA 92 (10), 4482–4486.

Palmiter, R.D., Brinster, R.L., Hammer, R.E., Trumbauer, M.E., Rosenfeld, M.G., Birnberg, N.C., Evans, R.M., 1982. Dramatic growth of mice that develop from eggs microinjected with metallothionein-growth hormone fusion genes. Nature 300 (5893), 611–615.

Pattanayak, V., Lin, S., Guilinger, J.P., Ma, E., Doudna, J.A., Liu, D.R., 2013. High-throughput profiling of off-target DNA cleavage reveals RNA-programmed Cas9 nuclease specificity. Nat. Biotechnol. 31 (9), 839–843.

Pendleton, M., Sebra, R., Pang, A.W., Ummat, A., Franzen, O., Rausch, T., et al., 2015. Assembly and diploid architecture of an individual human genome via single-molecule technologies. Nat. Methods 12 (8), 780–786.

Peng, R., Lin, G., Li, J., 2015. Potential pitfalls of CRISPR/Cas9-mediated genome editing. FEBS J. 283, 1218–1231.

Perez-Pinera, P., Kocak, D.D., Vockley, C.M., Adler, A.F., Kabadi, A.M., Polstein, L.R., et al., 2013. RNA-guided gene activation by CRISPR-Cas9-based transcription factors. Nat. Methods 10 (10), 973–976.

Petkov, P.M., Cassell, M.A., Sargent, E.E., Donnelly, C.J., Robinson, P., Crew, V., et al., 2004. Development of a SNP genotyping panel for genetic monitoring of the laboratory mouse. Genomics 83 (5), 902–911.

Pineda, M., Gonzalez, S., Lazaro, C., Blanco, I., Capella, G., 2010. Detection of genetic alterations in hereditary colorectal cancer screening. Mutat. Res. 693 (1–2), 19–31.

Plotz, G., Casper, M., Raedle, J., Hinrichsen, I., Heckel, V., Brieger, A., et al., 2012. MUTYH gene expression and alternative splicing in controls and polyposis patients. Hum. Mutat. 33 (7), 1067–1074.

Porreca, G.J., Zhang, K., Li, J.B., Xie, B., Austin, D., Vassallo, S.L., et al., 2007. Multiplex amplification of large sets of human exons. Nat. Methods 4 (11), 931–936.

Postic, C., Shiota, M., Niswender, K.D., Jetton, T.L., Chen, Y., Moates, J.M., et al., 1999. Dual roles for glucokinase in glucose homeostasis as determined by liver and pancreatic beta cell-specific gene knockouts using Cre recombinase. J. Biol. Chem. 274 (1), 305–315.

Quwailid, M.M., Hugill, A., Dear, N., Vizor, L., Wells, S., Horner, E., et al., 2004. A gene-driven ENU-based approach to generating an allelic series in any gene. Mamm. Genome 15 (8), 585–591.

Rabbani, B., Mahdieh, N., Hosomichi, K., Nakaoka, H., Inoue, I., 2012. Next-generation sequencing: impact of exome sequencing in characterizing Mendelian disorders. J. Hum. Genet. 57 (10), 621–632.

Rader, K.A., 2004. Making Mice. Princeton University Press, Princeton, NJ.

Ran, F.A., Hsu, P.D., Lin, C.Y., Gootenberg, J.S., Konermann, S., Trevino, A.E., et al., 2013a. Double nicking by RNA-guided CRISPR Cas9 for enhanced genome editing specificity. Cell 154 (6), 1380–1389.

Ran, F.A., Hsu, P.D., Wright, J., Agarwala, V., Scott, D.A., Zhang, F., 2013b. Genome engineering using the CRISPR-Cas9 system. Nat. Protoc. 8 (11), 2281–2308.

Riordan, J.R., Rommens, J.M., Kerem, B., Alon, N., Rozmahel, R., Grzelczak, Z., et al., 1989. Identification of the cystic fibrosis gene: cloning and characterization of complementary DNA. Science 245 (4922), 1066–1073.

Rivenbark, A.G., Stolzenburg, S., Beltran, A.S., Yuan, X., Rots, M.G., Strahl, B.D., Blancafort, P., 2012. Epigenetic reprogramming of cancer cells via targeted DNA methylation. Epigenetics 7 (4), 350–360.

Rivkin, E., Almeida, S.M., Ceccarelli, D.F., Juang, Y.C., MacLean, T.A., Srikumar, T., et al., 2013. The linear ubiquitin-specific deubiquitinase gumby regulates angiogenesis. Nature 498 (7454), 318–324.

Robertson, E., Bradley, A., Kuehn, M., Evans, M., 1986. Germ-line transmission of genes introduced into cultured pluripotential cells by retroviral vector. Nature 323 (6087), 445–448.

Robertson, G., Hirst, M., Bainbridge, M., Bilenky, M., Zhao, Y., Zeng, T., et al., 2007. Genome-wide profiles of STAT1 DNA association using chromatin immunoprecipitation and massively parallel sequencing. Nat. Methods 4 (8), 651–657.

Russell, W.L., 1951. X-ray-induced mutations in mice. Cold Spring Harb. Symp. Quant. Biol. 16, 327–336.

Russell, W.L., Russell, L.B., Kelly, E.M., 1958. Radiation dose rate and mutation frequency. Science 128 (3338), 1546–1550.

Russell, W.L., Kelly, E.M., Hunsicker, P.R., Bangham, J.W., Maddux, S.C., Phipps, E.L., 1979. Specific-locus test shows ethylnitrosourea to be the most potent mutagen in the mouse. Proc. Natl. Acad. Sci. USA 76 (11), 5818–5819.

Russell, L.B., Selby, P.B., von Halle, E., Sheridan, W., Valcovic, L., 1981. The mouse specific-locus test with agents other than radiations: interpretation of data and recommendations for future work. Mutat. Res. 86 (3), 329–354.

Sagai, T., Masuya, H., Tamura, M., Shimizu, K., Yada, Y., Wakana, S., et al., 2004. Phylogenetic conservation of a limb-specific, cis-acting regulator of Sonic hedgehog (Shh). Mamm. Genome 15 (1), 23–34.

Sakuraba, Y., Sezutsu, H., Takahasi, K.R., Tsuchihashi, K., Ichikawa, R., Fujimoto, N., et al., 2005. Molecular characterization of ENU mouse mutagenesis and archives. Biochem. Biophys. Res. Commun. 336 (2), 609–616.

Sander, J.D., Joung, J.K., 2014. CRISPR-Cas systems for editing, regulating and targeting genomes. Nat. Biotechnol. 32 (4), 347–355.

Sato, H., Suzuki, T., Ikeda, K., Masuya, H., Sezutsu, H., Kaneda, H., et al., 2010. A monogenic dominant mutation in Rom1 generated by N-ethyl-N-nitrosourea mutagenesis causes retinal degeneration in mice. Mol. Vis. 16, 378–391.

Sauer, B., Henderson, N., 1988. Site-specific DNA recombination in mammalian cells by the Cre recombinase of bacteriophage P1. Proc. Natl. Acad. Sci. USA 85 (14), 5166–5170.

Shen, B., Zhang, W., Zhang, J., Zhou, J., Wang, J., Chen, L., et al., 2014. Efficient genome modification by CRISPR-Cas9 nickase with minimal off-target effects. Nat. Methods 11 (4), 399–402.

Shibahara, S., Tomita, Y., Sakakura, T., Nager, C., Chaudhuri, B., Muller, R., 1986. Cloning and expression of cDNA encoding mouse tyrosinase. Nucleic Acids Res. 14 (6), 2413–2427.

Shibata, H., Toyama, K., Shioya, H., Ito, M., Hirota, M., Hasegawa, S., et al., 1997. Rapid colorectal adenoma formation initiated by conditional targeting of the Apc gene. Science 278 (5335), 120–123.

Shibata, N., Ohoka, N., Sugaki, Y., Onodera, C., Inoue, M., Sakuraba, Y., et al., 2015. Degradation of stop codon read-through mutant proteins via the ubiquitin-proteasome system causes hereditary disorders. J. Biol. Chem. 290 (47), 28428–28437.

Skarnes, W.C., von Melchner, H., Wurst, W., Hicks, G., Nord, A.S., Cox, T., et al., 2004. A public gene trap resource for mouse functional genomics. Nat. Genet. 36 (6), 543–544.

Skarnes, W.C., Rosen, B., West, A.P., Koutsourakis, M., Bushell, W., Iyer, V., et al., 2011. A conditional knockout resource for the genome-wide study of mouse gene function. Nature 474 (7351), 337–342.

Smithies, O., Gregg, R.G., Boggs, S.S., Koralewski, M.A., Kucherlapati, R.S., 1985. Insertion of DNA sequences into the human chromosomal beta-globin locus by homologous recombination. Nature 317 (6034), 230–234.

Snell, G.D., Higgins, G.F., 1951. Alleles at the histocompatibility-2 locus in the mouse as determined by tumor transplantation. Genetics 36 (3), 303–310.

Sovic, I., Sikic, M., Wilm, A., Fenlon, S.N., Chen, S., Nagarajan, N., 2016. Fast and sensitive mapping of nanopore sequencing reads with GraphMap. Nat. Commun. 7, 11307.

Su, L.K., Kinzler, K.W., Vogelstein, B., Preisinger, A.C., Moser, A.R., Luongo, C., et al., 1992. Multiple intestinal neoplasia caused by a mutation in the murine homolog of the APC gene. Science 256 (5057), 668–670.

Summerer, D., Schracke, N., Wu, H., Cheng, Y., Bau, S., Stahler, C.F., et al., 2010. Targeted high throughput sequencing of a cancer-related exome subset by specific sequence capture with a fully automated microarray platform. Genomics 95 (4), 241–246.

Tartaglia, L.A., Dembski, M., Weng, X., Deng, N., Culpepper, J., Devos, R., et al., 1995. Identification and expression cloning of a leptin receptor. OB-R Cell 83 (7), 1263–1271.

Taylor, K.H., Kramer, R.S., Davis, J.W., Guo, J., Duff, D.J., Xu, D., et al., 2007. Ultradeep bisulfite sequencing analysis of DNA methylation patterns in multiple gene promoters by 454 sequencing. Cancer Res. 67 (18), 8511–8518.

Tennessen, J.A., Bigham, A.W., O'Connor, T.D., Fu, W., Kenny, E.E., Gravel, S., et al., 2012. Evolution and functional impact of rare coding variation from deep sequencing of human exomes. Science 337 (6090), 64–69.

Terauchi, Y., Sakura, H., Yasuda, K., Iwamoto, K., Takahashi, N., Ito, K., et al., 1995. Pancreatic beta-cell-specific targeted disruption of glucokinase gene. Diabetes mellitus due to defective insulin secretion to glucose. J. Biol. Chem. 270 (51), 30253–30256.

Tewhey, R., Warner, J.B., Nakano, M., Libby, B., Medkova, M., David, P.H., et al., 2009. Microdroplet-based PCR enrichment for large-scale targeted sequencing. Nat. Biotechnol. 27 (11), 1025–1031.

Thakore, P.I., D'Ippolito, A.M., Song, L., Safi, A., Shivakumar, N.K., Kabadi, A.M., et al., 2015. Highly specific epigenome editing by CRISPR-Cas9 repressors for silencing of distal regulatory elements. Nat. Methods 12 (12), 1143–1149.

The Huntington's Disease Collaborative Research Group, 1993. A novel gene containing a trinucleotide repeat that is expanded and unstable on Huntington's disease chromosomes. Cell 72 (6), 971–983.

Thomas, K.R., Folger, K.R., Capecchi, M.R., 1986. High frequency targeting of genes to specific sites in the mammalian genome. Cell 44 (3), 419–428.

Till, B.J., Reynolds, S.H., Greene, E.A., Codomo, C.A., Enns, L.C., Johnson, J.E., et al., 2003. Large-scale discovery of induced point mutations with high-throughput TILLING. Genome Res. 13 (3), 524–530.

Uddin, B., Chen, N.P., Panic, M., Schiebel, E., 2015. Genome editing through large insertion leads to the skipping of targeted exon. BMC Genomics 16, 1082.

Urnov, F.D., Rebar, E.J., Holmes, M.C., Zhang, H.S., Gregory, P.D., 2010. Genome editing with engineered zinc finger nucleases. Nat. Rev. Genet. 11 (9), 636–646.

Vaxillaire, M., Froguel, P., 2008. Monogenic diabetes in the young, pharmacogenetics and relevance to multifactorial forms of type 2 diabetes. Endocr. Rev. 29 (3), 254–264.

Via, M., Gignoux, C., Burchard, E.G., 2010. The 1000 Genomes Project: new opportunities for research and social challenges. Genome Med. 2 (1), 3.

Vionnet, N., Stoffel, M., Takeda, J., Yasuda, K., Bell, G.I., Zouali, H., et al., 1992. Nonsense mutation in the glucokinase gene causes early-onset non-insulin-dependent diabetes mellitus. Nature 356 (6371), 721–722.

Vitaterna, M.H., King, D.P., Chang, A.M., Kornhauser, J.M., Lowrey, P.L., McDonald, J.D., et al., 1994. Mutagenesis and mapping of a mouse gene, Clock, essential for circadian behavior. Science 264 (5159), 719–725.

Vousden, K.H., Lane, D.P., 2007. p53 in health and disease. Nat. Rev. Mol. Cell Biol. 8 (4), 275–283.

Wang, H., Yang, H., Shivalila, C.S., Dawlaty, M.M., Cheng, A.W., Zhang, F., Jaenisch, R., 2013. One-step generation of mice carrying mutations in multiple genes by CRISPR/Cas-mediated genome engineering. Cell 153 (4), 910–918.

Wang, H., La Russa, M., Qi, L.S., 2016. CRISPR/Cas9 in genome editing and beyond. Annu. Rev. Biochem. 85, 227–264.

Watson, J.D., 1990. The human genome project: past, present, and future. Science 248 (4951), 44–49.

Wellcome Trust Case Control Consortium, 2007. Genome-wide association study of 14,000 cases of seven common diseases and 3,000 shared controls. Nature 447 (7145), 661–678.

Whittingham, D.G., Leibo, S.P., Mazur, P., 1972. Survival of mouse embryos frozen to -196 degrees and -269 degrees C. Science 178 (4059), 411–414.

Wittwer, C.T., Reed, G.H., Gundry, C.N., Vandersteen, J.G., Pryor, R.J., 2003. High-resolution genotyping by amplicon melting analysis using LCGreen. Clin. Chem. 49 (6 Pt 1), 853–860.

Xiao, W., Oefner, P.J., 2001. Denaturing high-performance liquid chromatography: a review. Hum. Mutat. 17 (6), 439–474.

Yamamoto, H., Takeuchi, S., Kudo, T., Makino, K., Nakata, A., Shinoda, T., Takeuchi, T., 1987. Cloning and sequencing of mouse Tyrosinase cDNA. Jpn. J. Genet. 62 (3), 271–274.

Yamamoto, F., Marken, J., Tsuji, T., White, T., Clausen, H., Hakomori, S., 1990. Cloning and characterization of DNA complementary to human UDP-GalNAc: Fuc alpha 1----2Gal alpha 1----3GalNAc transferase (histo-blood group A transferase) mRNA. J. Biol. Chem. 265 (2), 1146–1151.

Yang, H., Wang, H., Shivalila, C.S., Cheng, A.W., Shi, L., Jaenisch, R., 2013. One-step generation of mice carrying reporter and conditional alleles by CRISPR/Cas-mediated genome engineering. Cell 154 (6), 1370–1379.

Yip, S.P., 2002. Sequence variation at the human ABO locus. Ann. Hum. Genet. 66 (Pt 1), 1–27.

Zakut-Houri, R., Oren, M., Bienz, B., Lavie, V., Hazum, S., Givol, D., 1983. A single gene and a pseudogene for the cellular tumour antigen p53. Nature 306 (5943), 594–597.

Zeitlin, S., Liu, J.P., Chapman, D.L., Papaioannou, V.E., Efstratiadis, A., 1995. Increased apoptosis and early embryonic lethality in mice nullizygous for the Huntington's disease gene homologue. Nat. Genet. 11 (2), 155–163.

Zhang, Y., Proenca, R., Maffei, M., Barone, M., Leopold, L., Friedman, J.M., 1994. Positional cloning of the mouse obese gene and its human homologue. Nature 372 (6505), 425–432.

Zheng, G.X., Lau, B.T., Schnall-Levin, M., Jarosz, M., Bell, J.M., Hindson, C.M., et al., 2016. Haplotyping germline and cancer genomes with high-throughput linked-read sequencing. Nat. Biotechnol. 34 (3), 303–311.

PART J

EARLY LIFE

Page left intentionally blank

29

Experimental Febrile Seizures in Rodents

Ryuta Koyama

Graduate School of Pharmaceutical Sciences, The University of Tokyo, Tokyo, Japan

1 INTRODUCTION

The proper formation of neural circuits during early development is fundamental to brain function in adulthood. Thus, it is important to determine whether environmental factors affect neural circuit formation and characterize the mechanisms involved in this process. The results of studies on the association of febrile seizures with adult epilepsy provide insights into these underlying mechanisms. A link between complex febrile seizures and temporal lobe epilepsy has been suggested; however, the cellular and molecular mechanisms involved in this association remain unclear. The limitations of human studies on epilepsy, in which tissue samples are only available from adult patients in the advanced and drug-resistant stages of the disease, mask the underlying etiology. Thus, researchers have utilized well-established animal models of febrile seizures to examine the cellular and molecular mechanisms underlying the relationship between febrile seizures and the development of epilepsy. Here, accumulating evidence from studies that have utilized animal models to investigate the mechanisms underlying the causes and consequences of febrile seizures will be discussed. This chapter is based on a previous review article on animal models of febrile seizures from our laboratory (Koyama and Matsuki, 2010) and will include recent and more detailed information.

2 FEBRILE SEIZURES IN HUMANS AND THEIR RELATIONSHIP TO EPILEPSY

Febrile seizures associated with fevers typically greater than 38°C are the most common convulsive event in infancy and childhood. Febrile seizures usually occur between 3 months and 5 years of age, peaking at 16–18 months (Annegers et al., 1987; Hauser, 1994; Offringa et al., 1991; Vestergaard and Christensen, 2009). The worldwide incidence of febrile seizures is approximately 2%–5% of the population (Hauser, 1994; Nelson and Ellenberg, 1976, 1978; Verity et al., 1985; Verity and Golding, 1991; Vestergaard and Christensen, 2009); however, higher incidences of approximately 6%–9% in Japan (Bird, 1987; Tsuboi, 1984) and 14% in the Pacific islands (Stanhope et al., 1972) have been reported.

Febrile seizures can be classified as "simple" febrile seizures, which are generalized, isolated, brief single events that occur during febrile illness, or as "complex" febrile seizures, which are focal, multiple (more than one seizure per febrile illness), or prolonged. Approximately 60%–70% of febrile seizures are "simple," and 30%–40% are "complex" (Berg and Shinnar, 1996a; Nelson and Ellenberg, 1976). Simple febrile seizures are generalized tonic-clonic seizures without focal neurological features lasting less than 10 min (Annegers et al., 1987; Berg et al., 1997) or 15 min (Nelson and Ellenberg, 1978) without recurrence within 24 h. In most cases, simple febrile seizures are not followed by epilepsy or by the development of cognitive deficits (Annegers et al., 1987; Berg and Shinnar, 1996b; Verity et al., 1985, 1998). It was reported that only 2% of children with simple febrile seizures develop epilepsy (Annegers et al., 1987) and that these children's risk of developing epilepsy was not significantly different from that of the general population. Complex febrile seizures are prolonged, lasting longer than 10 min (Annegers et al., 1987, 1979, 1990; Berg et al., 1997) or 15 min (Berg and Shinnar, 1996a; Nelson and Ellenberg, 1976, 1978), and display focal neurological features and/or seizure recurrence within 24 h or within the same febrile illness. In a prospective cohort study of 428 children with first febrile seizures, 35% experienced complex febrile seizures (Berg and Shinnar, 1996a). Importantly, febrile status epilepticus, which is defined as the presence of febrile seizures lasting 30 min or longer, was observed in 5% of the children in the group (Berg and Shinnar, 1996a). Notably, febrile status epilepticus, which represents 5% of febrile seizures, accounts for approximately 25% of all episodes of childhood status epilepticus, and more than 60% of the status epilepticus cases occur during the second year of life (Berg and Shinnar, 1996a), as noted by Shinnar and Glauser (2002).

Whereas simple febrile seizures are typically not followed by epilepsy, it is debatable whether complex febrile seizures result in long-term sequelae (Annegers

et al., 1987; Berg and Shinnar, 1996a). Prospective epidemiological studies have generally failed to show a strong association between the occurrence of complex febrile seizures and the development of epilepsy (Berg and Shinnar, 1996b; Nelson and Ellenberg, 1976, 1978; Shinnar et al., 2001; Verity and Golding, 1991); however, according to a follow-up study that took place over more than 20 years (Annegers et al., 1987), the cumulative risk of unprovoked convulsions after complex febrile seizures increased to 49% (16%–93%). Furthermore, retrospective studies have reported an association between a history of complex febrile seizures and subsequent temporal lobe epilepsy in as many as 40% of adult patients (Cendes et al., 1993; French et al., 1993; Hamati-Haddad and Abou-Khalil, 1998; Theodore et al., 1999). In a study of 43 patients with temporal lobe epilepsy not controlled by optimal drug treatment, 15 patients (35%) had a history of complex febrile seizures (Cendes et al., 1993). In another study of 67 patients with temporal lobe epilepsy, at least 33 individuals (50%) for whom a detailed description of febrile seizure history was obtained had experienced complex febrile seizures (French et al., 1993). Importantly, patients with temporal lobe epilepsy with a history of complex febrile seizures exhibited more severe mesial temporal sclerosis than patients without a history of prolonged febrile seizures (Cendes et al., 1993). A smaller volume of the hippocampal formation was reported in patients with temporal lobe epilepsy (Cendes et al., 1993) and a history of complex febrile seizures in early childhood; a significant relationship between the volume of the hippocampus and epilepsy duration has also been shown (Theodore et al., 1999). A large-scale study of 1005 patients with epilepsy at a clinic in the United States revealed that temporal lobe epilepsy (78/310, 25%) is more likely to be preceded by febrile seizures than extratemporal epilepsy (12/216, 6%) (Hamati-Haddad and Abou-Khalil, 1998). In this study, 63 of the 78 patients with temporal lobe epilepsy had a history of complex febrile seizures. Febrile status epilepticus, in which febrile seizures last for 30 min or more, was observed in 5% of 428 children (Berg and Shinnar, 1996a).

In patients with mesial temporal lobe epilepsy, the hippocampus displays characteristic pathological changes, including dispersion of dentate granule cells (Houser, 1990; Thom et al., 2005), sprouting of hippocampal mossy fibers (Isokawa et al., 1993; Sutula et al., 1989), and hippocampal sclerosis, including selective neuronal loss and reactive gliosis in Ammon's horn (Fisher et al., 1998). Each of these features has been suggested to play a role in the initiation and propagation of epileptic activity in hippocampal neurons. The relationship between the development of these pathological changes and early life febrile seizures has been a topic of discussion. Evidence of hippocampal injury has been reported after febrile status epilepticus, particularly in

cases in which the febrile seizures lasted longer than 90 min (VanLandingham et al., 1998). More recently, a prospective multicenter study was performed by the FEBSTAT Study Team to further investigate the consequences of febrile status epilepticus (FEBSTAT study) in children between 1 month and 6 years of age (Hesdorffer et al., 2012; Lewis et al., 2014; Seinfeld et al., 2014; Shinnar et al., 2008). However, to directly dissect this relationship, cellular and molecular approaches are necessary, and these approaches cannot be adequately applied to respected and fixed human tissues.

The biological basis of febrile seizures also remains largely unclear. Although the existence of a genetic predisposition to febrile seizures has been widely suggested, both sporadic and familial cases of febrile seizures have been reported (Berg et al., 1999), indicating a considerable contribution of environmental factors to the induction of febrile seizures. Of these environmental factors, immature brain development (age specificity) and fever are indispensable contributing factors. However, the limitations of human studies have made it difficult to clarify the mechanisms involved.

To counteract these limitations, several animal models of febrile seizures have been developed through which the potential mechanisms underlying the generation and consequences of febrile seizures can be directly examined. The information obtained from these febrile seizure models has attracted the attention of clinicians and neurobiologists with a wide range of backgrounds.

3 ANIMAL MODELS OF FEBRILE SEIZURES (EXPERIMENTAL FEBRILE SEIZURES)

Several hyperthermia-induced rodent models of complex febrile seizures have been developed and used to study the mechanisms and consequences of febrile seizures (Koyama and Matsuki, 2010). These include the hair dryer model (Baram et al., 1997; Chen et al., 2001; Dube et al., 2000; Koyama et al., 2012; van Gassen et al., 2008), the heated chamber model (Holtzman et al., 1981; Schuchmann et al., 2006), the hot water model, which might also be categorized as a model for hotwater epilepsy (Jiang et al., 1999; Kim et al., 2001; Ullal et al., 1996), the microwave model (Hjeresen et al., 1983), and the lipopolysaccharide model (Heida et al., 2004).

This chapter will include a discussion of two of the most widely used models for the induction of febrile seizures in which the ambient temperature is elevated to elicit an increase in the body (rectal) temperature, the hair dryer model and the heated chamber model. Reports that refer to the hair dryer model in the methods section, as well as those that use other terms, such as "a regulated stream of moderately heated air" to describe

the heat delivery method are categorized as studies that utilized the hair dryer model and are discussed in this chapter.

3.1 Hair Dryer Model

Baram and coworkers originally developed and refined the hair dryer model (Bender et al., 2004; Dubé and Baram, 2006). We primarily use this model in our laboratory because of its relative ease of use, its low setup cost, and most importantly, the reproducibility and reliability of the behaviors observed during the process of febrile seizures induced using this method. Sprague-Dawley rats at postnatal day 10–11 (P10–11) or 129/Sv or C57BL mice at postnatal day 11–15 (P11–15) are typically used because the developmental stage of the hippocampal formation at these ages likely corresponds to that during human infancy and early childhood, when human individuals are most susceptible to febrile seizures (Avishai-Eliner et al., 2002). In addition, the threshold temperature required to evoke seizures is lowest at these ages (P10–13) in the rat (Hjeresen and Diaz, 1988) and is comparable to that observed for human complex febrile seizures (Berg et al., 1992). Considering the development of this animal model, it is also important to note that the behavioral seizures induced in rats and mice at these ages are highly reproducible (Dubé and Baram, 2006; our own observations in our laboratory). Although gender is not reported in all studies, a single sex is used in most cases. Notably, no significant gender difference in average seizure duration has been reported in this model (males, 7.86 ± 0.81 min; females, 10 ± 1.54 min) (Lemmens et al., 2005).

The description of the protocol for the hair dryer model in rats is primarily based on the procedures used in our laboratory, which have been slightly modified from the established protocol (Bender et al., 2004; Dubé and Baram, 2006). The animals are placed in individual glass jars and heated with a commercial hair dryer. A hair dryer is placed 30–50 cm above the rats, and an adjustable stream of heated air (40–45°C recorded at 2 cm above the bottom of the cylinder) is directed into the cylinder (Fig. 29.1A). The glass cylinder should be carefully selected to maintain ambient temperature. We use 20-cm-high, 10-cm-diameter glass cylinders with approximately 0.5-cm-thick walls. We also place a piece of filter paper on the bottom of the glass cylinder so that the animals are not directly heated by the glass. It is important to preheat and maintain the ambient temperature in the glass jar between 40–45°C prior to the induction of seizures. The position of the hair dryer should be adjusted depending on the height and diameter of the glass cylinder. The animal's rectal temperature is recorded digitally every 2 min starting 10 min prior to treatment and during hyperthermia treatment using a digital rectal
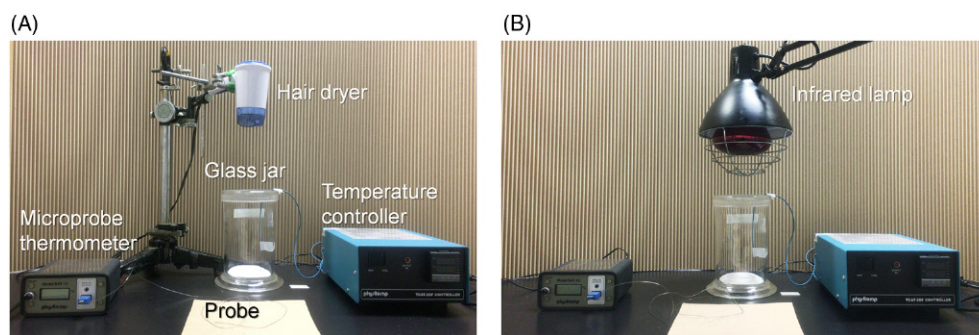
FIGURE 29.1   **Basic setups for the experimental induction of febrile seizures in rodents using a hair dryer.** (A) or an infrared lamp, (B). In our laboratory, a BAT12 microprobe thermometer (Physitemp Instruments, Inc., Clifton, NJ, USA) equipped with a RET4 rectal probe (Physitemp) is used to measure the rectal temperatures of neonatal rodents. To measure and maintain the temperature of the air within a glass jar, a TCAT-2DF temperature controller (Physitemp) is used. The lamp (HL-1, Physitemp) consists of a 250-W (infrared) heat lamp bulb and a reflector.

probe. Alternatively, the temperature can be recorded every 3 min if the maintenance of rectal temperature is difficult. When the core temperature reaches 39.5°C, which typically occurs after 8–12 min, the temperature and volume of the air are adjusted to maintain the animal's core temperature at 39.5–42.5°C for 30 min to induce prolonged experimental febrile seizures that typically last for approximately 24 min in total. Correlation of core temperature with brain temperature at the onset of hyperthermic seizures (core temperature, 40.7 ± 0.2°C; brain temperature 40.88 ± 0.3°C) suggests that measurements of core temperature provide an adequate approximation of brain threshold temperatures for experimental febrile seizures (Dube et al., 2005a). Urination is occasionally observed, particularly during the early stages of the hyperthermia process. Urine should be immediately wiped from the bottom of the cylinder if a piece of filter paper has not been placed on the floor of the jar. If the core temperature exceeds 42.5°C, the animal is removed from the cylinder and transferred to a cool metal surface until its core temperature decreases to 39.5–42.5°C. Immediately following the 30-min hyperthermia treatment, the animals are cooled on a cool metal surface to room temperature and subsequently returned to their mothers. In some studies, the rat pups were injected with saline to prevent dehydration during the hyperthermia procedure (Lemmens et al., 2008, 2005). We observed that the injection of saline prior to the hyperthermia process assists in the animals' recovery from hyperthermia, particularly in the case of mice (unpublished data). Oral hydration (approximately 0.1 mL water) following hyperthermia has also been reported (Dubé and Baram, 2006). If the recovery process is not properly conducted, the dams often do not take care of their pups (including a lack of lactation) and may even kill the pups.

Both normothermic controls and hyperthermic controls are included in the procedure. For the normothermic control group, rats are exposed to the same conditions as the hyperthermic group, but a stream of air is used to maintain normal core temperature (Lemmens et al., 2008).

Although it has been suggested that fever per se does not cause febrile seizures because antipyretics do not reduce the risk of febrile seizures (Bethune et al., 1993; Camfield et al., 1980), it is always important to examine the direct effects of fever on the cellular, molecular, and behavioral changes that occur after experimental febrile seizures. For this purpose, hyperthermic controls are generated via the intraperitoneal injection of a short-acting barbiturate (pentobarbital) prior to the induction of hyperthermia (Brewster et al., 2002; Dube et al., 2000, 2006) to distinguish whether the observed experimental febrile seizures are a consequence of the hyperthermia.

The onset of experimental typical febrile seizures of limbic origin typically consists of an acute sudden arrest of hyperthermia-induced hyperactivity, such as running followed by oral automatism (biting and chewing). Electroencephalographic (EEG) recordings from the basal amygdala, dorsal hippocampus, and frontoparietal cortex of freely moving rat and mouse pups suggest that the onset of hippocampal and amygdaloid EEG spike waves and trains coincides with behavioral arrest and oral automatism and precedes events recorded in the cortex (Baram et al., 1992, 1997; Brewster et al., 2002; Dube et al., 2000). Forelimb clonic movements typically follow oral automatism. Later during the seizure, tonic body flexion is frequently observed in rats, but this occurs only sometimes in mice. Strain-dependent differences in susceptibility to warm air stream-induced experimental febrile seizures have been reported in mice (van Gassen et al., 2008) but not in rats. Using a similar experimental febrile seizure induction model in mice in which a temperature-regulated laminar stream of warm air (41–48°C) is used, Jongbloets et al. (2015) reported short- and longer-term gene expression profiles after experimental febrile seizures.

In the hair dryer model, the duration of febrile seizures can be controlled. A recent study utilized this characteristic to induce febrile status epilepticus-like seizures in rat pups by increasing the duration of hyperthermia (body temperature of 39.5–41°C) to 70 min (Dube et al., 2010).

It remains unclear whether the duration of seizures is related to the development of epilepsy. Thus, a comparison of this model with the typical hair dryer model in which hyperthermia duration of 30 min is used would provide information that would contribute to our understanding of how seizure duration in febrile seizures might serve as a biomarker for the future development of epilepsy.

3.2 Heated Chamber Model

Holtzman et al. (1981) developed another reliable seizure model, the heated chamber model; a modification of this model has been used in several studies (Schuchmann et al., 2006, 2009). In the original study (Holtzman et al., 1981), Sprague-Dawley rat pups (P2–10) were placed on the paper towel-covered floor of a Lucite chamber. The body temperature of the rat pups was elevated using a 250-W infrared lamp mounted 10 cm above the chamber. In this study, the seizure threshold temperature, that is, the rectal temperature, at the onset of seizure activity was approximately 37°C at P2, 40–41°C at P5, and 43°C at P7 and P10. The age-dependent increase in rectal temperature at the seizure threshold was correlated with an increase in brain temperature. It was reported that all P2 animals immediately resumed normal nursing behavior when the temperature was reduced and that all the P5–7 animals survived and behaved normally after the procedure, whereas only half of the P10 animals survived. The onset of generalized seizure activity in P5–10 animals at a body temperature of 40–41°C was manifested by loss of upright posture, tonic extension of the trunk, and rapid synchronous clonic movements of the extremities and mouth, followed by limp and unreactive behavior for 2–3 min. It was also shown that animals older than P10 did not experience seizures until the body temperature reached 44–45°C; none of these animals survived after the procedure. Simultaneous recordings of rectal temperature and EEG have confirmed that hyperthermia induces electrocortical paroxysmal discharges in P6 and P10 rats. In our laboratory, we also used a heated chamber model with an infrared lamp placed 25–30 cm above mice (Fig. 29.1B). We found that clonic seizures can be induced in C57BL mouse pups between P10–14.

Schuchmann et al. (2006, 2008, 2009) utilized a modified heated chamber model in P8–11 Wistar rat pups. The animals were placed in a chamber at an ambient temperature of 48 ± 0.3°C (Schuchmann et al., 2006). The latency to onset of hyperthermia-induced seizures was 31.2 ± 3.7 min, and the duration of the seizures was 24.6 ± 1.7 min. Behavioral seizures began with a sudden interruption of movement, followed by oral automatism. The behavioral arrest was followed by clonic movements of the limbs and head, chewing of extremities and tonic flexion of the body, often associated with a loss of postural control.

Compared with the hair dryer model, the increase in body temperature is much slower, and the latency to the onset of hyperthermia-induced seizures is longer in the heated chamber model. However, Schuchmann et al. (2009) proposed that the rate of fever increase does not affect the likelihood of the occurrence of human febrile seizures (Berg, 1993). These authors also suggested that the possible effects of pain and inflammation are reduced in the heated chamber model, whereas in the hair dryer model, in which heat transfer is heavily dependent on convection and the increase in body temperature is rapid, activation of thermal nociceptors, as well as inflammatory responses occur, as demonstrated by examination of the ears and paws of the animals (Schuchmann et al., 2009). From our own experience with the hair dryer model, we have observed that mounting the hair dryer 50–60 cm above the animals (instead of approximately 30 cm above the animals as described in some protocols) can reduce the inflammatory responses in the ears and paws. It should be noted that the body temperature of the animals should be raised by the use of heated air in a glass cylinder but not directly by the use of heating instruments.

4 OTHER ANIMAL MODELS OF EARLY LIFE SEIZURES

Depending on their experimental purposes, researchers have also used other animal models of febrile seizure. Several examples of animal models for early life seizures will be discussed, and interested readers are encouraged to refer to the articles cited herein. The models are as follows: hypoxia-induced seizures induced using low inhaled oxygen concentrations (Jensen et al., 1991, 1992; Owens et al., 1997), recurrent generalized tonic-clonic seizures induced by flurothyl inhalation (Holmes et al., 1998; Huang et al., 1999; Sogawa et al., 2001), absent and generalized tonic-clonic seizures induced by pentylenetetrazol injection (Holmes et al., 1999; Huang et al., 2002a, b), status epilepticus induced by the injection of kainic acid (Santos et al., 2000; Sarkisian et al., 1997; Stafstrom et al., 1992) or pilocarpine (Cilio et al., 2003; Hirsch et al., 1992), and recurrent generalized tonic-clonic seizures induced by electroshock (Dwyer and Wasterlain, 1982; Jorgensen et al., 1980).

5 MECHANISMS UNDERLYING HYPERTHERMIA-INDUCED EXPERIMENTAL FEBRILE SEIZURES

5.1 Interleukin-1β (IL-1β)

Animal models of febrile seizures have revealed that several molecules are associated with fever and seizures.

Among these, the role of IL-1β, a proinflammatory cytokine, has been well documented using animal models of febrile seizures. Although it is still controversial whether IL-1β levels are increased in the brains of individuals with febrile seizures (Haspolat et al., 2002; Lahat et al., 1997), inflammation has been associated with epileptogenesis, and the involvement of inflammatory mediators in febrile seizures has also been proposed. In the hair dryer model, the threshold temperature for the generation of experimental febrile seizures was significantly higher in transgenic mice deficient in the type I receptor for IL-1β (IL-1R1$^{-/-}$ mice; 42.4 ± 0.3°C) than in wild-type 129/Sv (41.3 ± 0.2°C) and C57BL mice (39.7 ± 0.2°C) (Dube et al., 2005b). The seizure threshold of wild-type 129/Sv mice, but not that of IL-1R1$^{-/-}$ mice, decreased after intracerebroventricular (i.c.v.) infusion of IL-1β (5 ng). Furthermore, the infusion of a high dose of IL-1β (116 ng) resulted in limbic behavioral seizures that were confirmed by simultaneous hippocampal EEG recordings that showed prolonged spike trains in normothermic wild-type 129/Sv mice but not in IL-1R1$^{-/-}$ mice. These data suggest that activation of IL-1R by endogenous IL-1β underlies the fever-induced neuronal hyperexcitability that leads to the generation of experimental febrile seizures; however, it remains unclear whether seizures induce IL-1β expression and, if so, whether IL-1β contributes to the epileptogenic process that occurs after febrile seizures. The same group addressed this question using the hair dryer model with longer seizure duration (febrile status epilepticus-like seizures) (Dube et al., 2010). In that study, western blot analyses of hippocampal homogenates harvested 24, 48, and 72 h after 64-min-long febrile seizures revealed that IL-1β levels in the experimental group were significantly increased compared to the levels in control animals at 24 h and that IL-1β expression gradually returned to control levels at 48–72 h. The authors further determined that the IL-1β-secreting cells were reactive astrocytes in the hippocampus that express glial fibrillary acidic protein (GFAP). They also observed that these astrocytes were more abundant at 6 and 24 h after seizures in animals with febrile seizures than in controls. In the same study, OX-42-expressing reactive microglias were more commonly observed in the hippocampi of rats with febrile seizures compared with controls. The activation state of these microglias in rats with febrile seizures is unclear, although their morphology (they possess moderate hypertrophic processes) suggests that they are slightly more active than microglias in control rats.

5.2 Respiratory Alkalosis

Using a heated chamber model, Schuchmann et al. (2006) examined whether a hyperthermia-induced increase in the rate of breathing, which is observed in young children (O'Dempsey et al., 1993; Gadomski et al., 1994; Taylor et al., 1995), plays a role in inducing febrile seizures. These authors demonstrated that hyperthermia-induced respiratory alkalosis precipitates experimental febrile seizures. In P8–11 rats, behavioral seizures occurred approximately 30–40 min after the induction of hyperthermia, a time when breathing frequency had increased from a control level of 163 ± 14 breaths/min to an elevated level of 254 ± 44 breaths/min. The hyperthermia-induced increase in the breathing rate was also reproduced in the hair dryer model; there, the animals showed a slightly higher breathing rate at the onset of seizures than in the heated chamber model (Schuchmann et al., 2008). The thermal tachypnea observed in the heated chamber closely paralleled the observed increase in intracortical pH, which increased by a maximum of 0.27 ± 0.04 units from its control level of 7.22 ± 0.096. An increase in cortical pH of 0.29 ± 0.05 units was elicited through intraperitoneal (i.p.) injection of bicarbonate; this also caused seizures with behavioral characteristics resembling those induced by hyperthermia, suggesting that hyperthermia-induced brain alkalosis triggers experimental febrile seizures. Importantly, it has been shown that hippocampal and cortical electrographic ictal activity and the associated behavioral activity are blocked in rats exposed to 5% CO_2. Electrographic ictal activity was abolished within approximately 15–25 s without affecting the body temperature during hyperthermia. Thus, the administration of CO_2-enriched air could be a novel therapeutic strategy for the treatment of febrile seizures (Schuchmann et al., 2009).

5.3 Findings From In Vitro Analyses

In vitro studies were conducted to directly examine the effects of hyperthermia on neuronal excitability. In hippocampal slices from P2–38 rats, the effect of temperature elevation on stimulation-evoked extracellular field potentials in the CA1 region was investigated. When the temperature of the recording chamber was elevated from the control level of 35–36°C to > 38°C, an increase in the amplitude and duration of the field response was observed; this increase persisted for more than 15 min, even after the temperature was returned to the control level (Tancredi et al., 1992). In addition, the temperature elevation induced epileptiform activity such as spontaneous multiple population spikes and long-lasting ictal-like discharges in neurons. These effects were most frequently observed in slices from P13–20 rats and were not observed in slices from <P4 or >P28 rats, suggesting that age-dependent factors are responsible for the differential neuronal responses to hyperthermia observed in these rats. Age dependency of hyperthermia-induced hippocampal excitability was also observed in electrophysiological studies in vivo in which hyperthermia induced

using a heating pad resulted in a decrease of paired-pulse inhibition in CA1 that was more prominent in P15–17 rat pups than in adult rats (Liebregts et al., 2002). Applying functional multineuron calcium imaging (fMCI) techniques, Ishikawa et al. (2015) found that the epileptic activity of CA3 neurons during heating to 40.5°C was suppressed by the non-NMDA receptor antagonist CNQX in slice cultures prepared from P7 rat pups.

The involvement of $GABA_A$ receptor-governed gamma oscillations in temperature elevation-induced population spikes has been demonstrated using P17–29 rat slices (Wu et al., 2001). Hyperthermia-induced attenuation of inhibitory neurotransmission in CA1 pyramidal neurons in P11–17 rat brain slices has been reported. Specifically, both reduction of GABA release from presynaptic terminals and decreased postsynaptic function of $GABA_A$ receptors have been suggested as potential mechanisms (Qu and Leung, 2008; Qu et al., 2007). Reduced GABAergic transmission could rapidly contribute to hippocampal hyperexcitability after hyperthermia. However, it should be noted that at 2–6 h after ultrared-light-induced experimental febrile seizures in P16 rats, GABA content was significantly increased in several regions of the brain, including the hippocampus, and it returned to control levels within 24 h after the onset of the seizures (Nagaki et al., 1996).

6 NEUROANATOMICAL CHANGES AFTER EXPERIMENTAL FEBRILE SEIZURES

Conclusions concerning the causal relationship between childhood febrile seizures and subsequent hippocampal atrophy or sclerosis in temporal lobe epilepsy patients have been controversial. Several retrospective studies have reported relationships between a history of febrile seizures and increased incidence of sclerosis (Falconer, 1974; Falconer et al., 1964; Sagar and Oxbury, 1987) or reductions in hippocampal and amygdala volume (Cendes et al., 1993), whereas prospective studies, including recent magnetic resonance imaging (MRI) studies, have failed to confirm these observations (Berg and Shinnar, 1991; Shinnar, 1998; Tarkka et al., 2003). These inconsistencies may partially result from the fact that human studies inevitably involve diversity in the frequency of seizures (both febrile and afebrile), in the history of medication in retrospective studies, and in the length of the follow-up period in prospective studies.

Many of the difficulties associated with human studies can be controlled using experimental models of febrile seizures. These models have yielded reliable evidence regarding cell loss, neurogenesis, and alterations in dendritic and axonal morphogenesis that occur after experimental febrile seizures.

6.1 Cell Loss

Cell loss in the hippocampus is one of the structural hallmarks of patients with mesial temporal lobe epilepsy, but it is unclear whether febrile seizures cause the cell loss. No significant loss of pyramidal cells in the CA1 or CA3 regions, GluR2/3-immunoreactive mossy cells in the hilus, or GAD67 mRNA-positive interneurons in these regions was observed in histological studies at 3 months after induction of experimental febrile seizures in the hair dryer model, indicating that febrile seizures do not induce delayed, chronic hippocampal cell loss (Bender et al., 2003). Importantly, significant neuronal loss was not observed in adult rats that became epileptic after experimental febrile seizures induced using the hair dryer model (Dube et al., 2006), indicating that cell loss is not necessary for the development of epilepsy after febrile seizures. However, another study reported a reduced density of parvalbumin-immunopositive interneurons in the hilus at 5, 7, and 11 weeks after mercury-vapor-lamp-induced experimental febrile seizures at P11 (Kwak et al., 2008).

6.2 Neurogenesis

To examine the effects of experimental febrile seizures on granule cell neurogenesis, Bender et al. (2003) injected a single dose of the S-phase marker 5-bromo-2′-deoxyuridine (BrdU) into rat pups at 3, 7, or 28 days after experimental febrile seizures (hair dryer model, P10–11) and perfused the pups 48 h later. The number of BrdU-positive nuclei in the granule cell layer was not significantly different from that in control animals (Bender et al., 2003). However, Lemmens et al. (2005) reported that in the dentate gyrus of male (but not female) P66 animals with experimental febrile seizures (hair dryer model, P10) in which BrdU was injected twice daily from P11–16, 25% more BrdU-positive cells existed than in age-matched normothermic controls. The authors reported that gender also affected the survival of newborn cells in the dentate gyrus; the survival of BrdU-positive cells at P66 (percentage of P17) was significantly higher in female rats (control: 44% vs. experimental febrile seizures: 53%, $P < 0.05$) than in male rats (control: 20% vs. experimental febrile seizures: 23%, not significant). The factors that regulate the effects of gender on these phenomena remain unknown.

A recent study reported that experimental febrile seizures (hair dryer model, P10) decreased the percentage of cells born at P11–16 that survive and differentiate into excitatory amino acid transporter 3-positive neurons in the granule cell layer at P66 from the control level of 23%–14% ($P < 0.01$). Since the amino acid transporter eliminates glutamate from the synaptic cleft, these results suggest that experimental febrile seizures influence

the excitability of the regional network (Lemmens et al., 2008).

Altogether, the results described above suggest that experimental febrile seizures affect the survival (with gender differences) and differentiation, but not the proliferation, of newborn cells in the dentate gyrus. More specific markers for granule cells, such as prospero-related homeobox 1 (Prox1), should be used to further determine whether these "newborn" cells are indeed dentate granule cells (Koyama et al., 2012).

6.3 Ectopic Granule Cells

Both human and animal studies have indicated that febrile seizures do not result in severe loss of primary neurons in Ammon's horn or the dentate gyrus; however, it remains largely unknown whether the surviving dentate granule cells possess normal morphological, anatomical, and functional properties. Considering that the dentate gyrus prevents cortex-derived epileptiform discharges from invading the hippocampus, it is important to investigate whether the properties of the dentate gyrus are modulated by early life febrile seizures. Thus, utilizing several techniques, including time-lapse imaging of cultured neurons prepared from rats subjected to experimental febrile seizures (hair dryer model, P11), we examined whether such seizures induce hilar ectopic granule cells that persist into adulthood (Koyama et al., 2012). Ectopic granule cells of this type create abnormal neural circuits in the hippocampus that induce synchronous epileptiform bursting in other hippocampal neurons (Scharfman et al., 2007). As we have previously demonstrated, an overwhelming majority of the dentate granule cells in the adult rat brain are generated during the 2 weeks after birth and migrate toward the granule cell layer (Muramatsu et al., 2007). Therefore, we hypothesized that induction of experimental febrile seizures during this period would disturb this developmental process and result in the emergence of ectopic granule cells. This hypothesis is supported by evidence from our previous study showing that granule cells born at P0–2 become ectopic granule cells at 6 months if the animals are subjected to pilocarpine-induced status epilepticus at P14 (Muramatsu et al., 2008). We found that experimental febrile seizures induced at P11 using the hair dryer model increased the surface expression of GABA$_A$ receptors on migrating granule cells during development, resulting in increased excitatory GABAergic input to these cells (Koyama et al., 2012). The enhanced excitatory GABAergic signaling caused a reversal in the direction of newborn granule cell migration via calcium influx, resulting in an ectopic localization of these cells that persisted into adulthood. Furthermore, there was a significant correlation between the number of ectopic granule cells and the occurrence of limbic seizures in

adulthood. Importantly, these phenomena were blocked by inhibition of the Na$^+$K$^+$2Cl$^-$ cotransporter (NKCC1), which regulates the excitatory action of GABA. Furthermore, inhibition of NKCC1 by the diuretic bumetanide after febrile seizures prevented granule cell ectopia, susceptibility to limbic seizures, and the development of epilepsy. Thus, this work identifies a novel pathogenic role of excitatory GABA$_A$ receptor signaling and highlights NKCC1 as a potential therapeutic target for preventing granule cell ectopia and the development of epilepsy after febrile seizures.

6.4 Dendritic Morphogenesis

Silver staining revealed that experimental febrile seizures (hair dryer model, P10) resulted in a number of neurons with shrunken dendrites in the central nucleus of the amygdala and in the hippocampal CA1 and CA3 pyramidal cell layers within 24 h. These "injured" neurons survived for at least two weeks (Toth et al., 1998). These alterations were not followed by significant DNA fragmentation, and no significant neuronal cell loss was observed in these regions 4 weeks after seizure induction. The presence of surviving neurons with malformed dendrites could potentially disrupt the balance between excitatory and inhibitory inputs to these neurons, resulting in hyperexcitability of the focal networks. However, in another study, biocytin-mediated tracing after whole-cell recording at 1 week following experimental febrile seizures (hair dryer model, P10) did not reveal any differences in the dendritic arborization of CA1 pyramidal cells in animals subjected to experimental febrile seizures (Chen et al., 2001). Interestingly, it has been reported that the dentate granule cells born 1 day after induction of experimental febrile seizures by a regulated heated air stream at P10 had dendrites that were 66% longer than those of the corresponding cells in normothermic controls (Raijmakers et al., 2016). The authors also found an increase in the number of mushroom-type spines 8 weeks after experimental febrile seizures. These data indicate that the timing of febrile seizures with respect to neuronal differentiation affects whether febrile seizures induce changes in dendritic and spine morphologies.

6.5 Axonal Morphogenesis (Mossy Fiber Sprouting)

The contribution of experimental febrile seizures to the sprouting of hippocampal mossy fibers has also been examined. Mossy fiber sprouting is an important pathology that is frequently observed in the hippocampi of individuals with temporal lobe epilepsy, and a relationship of this sprouting to the hyperexcitability of the dentate gyrus has been suggested (Koyama

and Ikegaya, 2004). Significantly increased numbers of Timm-positive puncta, which represent the zinc-containing presynaptic terminals of mossy fibers, were observed in the granule cell and molecular layers of the hippocampus in 3-month-old rats subjected to experimental febrile seizures at P10–11 (hair dryer model) (Bender et al., 2003). Increased hippocampal activity was detected in these experimental animals, although its relationship to mossy fiber sprouting is unclear. Bundled dense sprouting in the molecular layer has also been observed at 11 weeks after mercury-vapor lamp-induced experimental febrile seizures at P11 (heated chamber model) that were later followed by spontaneous recurrent seizures (Kwak et al., 2008). Although the cellular mechanisms underlying experimental febrile seizure-induced sprouting remain unknown, brain-derived neurotrophic factor (BDNF), which is sufficient and necessary to induce sprouting in vitro (Koyama et al., 2004), is a strong candidate because BDNF mRNA has been shown to increase after hot-water-induced febrile seizures at P21 (Kim et al., 2001). BDNF has also been shown to mediate a febrile seizure (P11 and P14 mice, hair dryer model)-induced increase in the density of mossy fiber synapses in CA3 (Tao et al., 2016).

7 NEUROPHYSIOLOGICAL CHANGES AFTER EXPERIMENTAL FEBRILE SEIZURES

Long-lasting modulation of neuronal network functions after induction of experimental febrile seizures using the hair dryer model has been reported. At 1 week after the induction of experimental febrile seizures at P10, whole-cell patch clamp recordings from CA1 pyramidal cells in brain slices revealed that the amplitude of evoked inhibitory postsynaptic currents (IPSCs) was significantly increased compared with controls (Chen et al., 2001). The authors further showed that the frequency of miniature IPSCs (mIPSCs) in experimental febrile seizure-induced rats was nearly doubled and that there was no change in mIPSC amplitude or kinetics, indicating that the observed potentiation of inhibitory transmission had a presynaptic locus. Finally, it was pharmacologically shown that activation of protein kinase A (PKA) underlies the potentiation of the inhibitory responses.

Altogether, these results suggest that long-lasting potentiation of inhibitory transmission decreases susceptibility to seizures. However, increased inhibition has been associated with a persistent decrease in the seizure threshold after experimental febrile seizures (hair dryer model); one example is the observed reduction in seizure threshold in response to chemical convulsants in vivo and electrical stimulation in vitro (Dube et al., 2000).

As a mechanism underlying this paradox, the contribution of the "molecular inhibition excitation converter" has been clearly demonstrated (Chen et al., 2001). The hyperpolarization-activated depolarizing current I_h generated by hyperpolarization-activated cyclic nucleotide-gated (HCN) channels acts as a converter. In CA1 pyramidal cells in brain slices, the membrane potential for the half-maximal activation (V_{50}) of I_h was significantly shifted in the depolarizing direction by 3.3 and 5.9 mV at 1 and 9 weeks, respectively, after induction of experimental febrile seizures at P10 using the hair dryer model. A significantly larger I_h in cells from rats subjected to experimental febrile seizures compared with those from control rats has also been shown. Importantly, in pyramidal cells of rats subjected to experimental febrile seizures, a short train of inhibitory postsynaptic potentials (IPSPs; 6 IPSPs at 50 Hz) resembling those that occur spontaneously during the θ rhythm in vivo, but not single IPSPs, were shown to trigger postinhibitory rebound depolarization and firing. This phenomenon was inhibited by application of the selective HCN blocker ZD-7288. Using both whole-cell dendritic recordings and computer models of CA1 pyramidal cells, Dyhrfjeld-Johnsen et al. (2008) further confirmed the upregulation of dendritic I_h in rats with experimental febrile seizures and showed that it leads to persistent dendritic hyperexcitability as a consequence of increased I_h-induced depolarization of the resting membrane potential. Thus, it is likely that a combination of the potentiation of inhibitory input and frequency-dependent modified I_h-mediated events generates persistent hyperexcitable foci in the hippocampus following febrile seizures.

Another solution to the above paradox is suggested by the demonstration of persistent potentiation of the depolarization-induced suppression of inhibition (DSI) in CA1 pyramidal cells 1–5 weeks after the induction of experimental febrile seizures at P10 (hair dryer model) (Chen et al., 2003). In this study, depolarization of CA1 pyramidal cells resulted in a transient depression of spontaneous IPSCs (sIPSCs), or DSI; in slices from rats that had experienced experimental febrile seizures, this DSI was significantly increased both in magnitude and in duration. In both control and experimental febrile seizure slices, DSI was abolished in the presence of SR141716A, a cannabinoid type 1 (CB1) receptor antagonist, indicating the involvement of endocannabinoid signaling. Further pharmacological manipulation of the evoked IPSCs (eIPSCs) suggested the activation of presynaptic CB1 receptors by the retrograde release of endocannabinoids from pyramidal cells. Potentiation of endocannabinoid-mediated retrograde signaling after experimental febrile seizures was demonstrated using several qualitative and quantitative methods that showed an increased number of CB1 receptors in the presynaptic terminals of cholecystokinin (CCK)-positive interneurons without any

significant change in the concentration of endocannabinoids in the hippocampi of animals that had undergone experimental febrile seizures.

Thereafter, the same group succeeded in preventing both the potentiation of DSI and the increase in CB1 receptor number by i.p. injection of SR141716A 1 h prior to experimental febrile seizure induction (P10, hair dryer model) (Chen et al., 2007). By blocking CB1 receptors in vivo, the authors further prevented experimental febrile seizure-induced long-lasting hippocampal excitability in vitro and in vivo as follows: both the electrical-stimulation-induced, self-sustaining population activity of neurons in vitro (1 week after experimental febrile seizures) and the decreased seizure threshold in response to the injection of kainate in vivo (6 weeks after experimental febrile seizures) were blocked.

Notably, dentate granule cells, which do not normally show DSI in control rats, exhibited DSI via CB1 receptor activation after the induction of experimental febrile seizures (Chen et al., 2003). The dentate gyrus has been implicated as a highly resistant gate that blocks the transmission of epileptiform activity from the entorhinal cortex to the hippocampus (Heinemann et al., 1992; Hsu, 2007; Lothman et al., 1992) via the static characteristics of the dentate granule cells, including strong tonic, and phasic GABA inhibition by surrounding inhibitory interneurons (Nadler, 2003). Thus, it is possible that dentate DSI, in combination with the mossy fiber sprouting that occurs following experimental febrile seizures, induces the malfunction of this gate, leading to hyperexcitability of the hippocampus. This idea is supported by EEG recordings that show synchronized spiking and long-lasting abnormal discharges in the dentate gyrus 11 weeks after mercury vapor lamp-induced experimental febrile seizures at P11 (Kwak et al., 2008).

8 NEURONAL HYPERACTIVITY AFTER EXPERIMENTAL FEBRILE SEIZURES

Long-term hyperexcitability of the hippocampal network following the induction of experimental febrile seizures using the hair dryer model has been confirmed in both in vitro and in vivo experiments (Dube et al., 2000). In adult rats subjected to induce experimental febrile seizures, the administration of a low dose of kainate (5 mg/kg, i.p.) 10–11 weeks after the experimental febrile seizures induced hippocampal EEG seizures and associated behavioral seizures, most of which (8 of 11 rats) progressed to status epilepticus. In contrast, only 25% (2 of 8) of normothermic controls and 16.6% (1 of 6) of hyperthermic controls exhibited EEG or behavioral seizures, and none of the control animals developed status epilepticus. These in vivo data were further supported by in vitro electrophysiological experiments. In hippocampal-entorhinal cortical slices prepared 1 week after the induction of experimental febrile seizures, recurrent, spontaneous, self-sustaining field discharges of progressively increasing amplitude and frequency were recorded in the CA1 pyramidal cell layer in response to the stimulation of Schaffer collaterals. These phenomena were not observed in slices from control animals. These results indicate that induction of experimental febrile seizures in early life reduces the seizure threshold to convulsant challenge in adulthood.

In addition, chronic video monitoring of spontaneous behavioral seizures and measurement of concurrent hippocampal and cortical EEGs revealed the development of limbic epilepsy in a significant proportion of rats approximately 3 months after the occurrence of experimental febrile seizures (hair dryer model) (Dube et al., 2006).

9 BEHAVIORAL CHANGES AFTER EXPERIMENTAL FEBRILE SEIZURES

Epidemiologic studies of the outcome of febrile seizures in humans have reported no association between early life febrile seizures and global cognitive dysfunction in later life. A febrile seizure cohort in the United States demonstrated that the intelligence and school performance of 7-year-old children with febrile seizures were not different from those of their unaffected siblings (Ellenberg and Nelson, 1978). In addition, a cohort study in the United Kingdom (Verity et al., 1998) reported that 10-year-old children who experienced febrile seizures did not differ in academic progress, intellect, or behavior from children without febrile seizures.

The studies cited previously did not specifically investigate whether febrile seizures affect memory function. In another population-based study that examined the effects of febrile seizures on working memory, Chang et al. (2001) found that 87 school-aged children with febrile seizures performed significantly better than 87 age-matched control children in learning, consolidation, memory retrieval, and delayed recognition; however, children that had experienced febrile seizures prior to 1 year of age showed deficits in these skills, suggesting an age-dependent vulnerability to febrile seizures. Using a mouse model of febrile seizures (hair dryer, P11, or P14), we investigated the cellular mechanisms underlying the age-dependent effects of febrile seizures on memory (Tao et al., 2016). We found that adult mice that had been subjected to experimental febrile seizures at P14 performed better in a cognitive task that requires dentate granule cells. The enhanced memory performance of these animals correlated with an increase in the density of the large mossy fiber terminals of granule cells that was partly mediated by BDNF-TrkB signaling. In contrast, memory enhancement was

not observed in mice subjected to experimental febrile seizures at P11; these animals exhibited ectopic granule cells in addition to an increased density of large mossy fiber terminals. Importantly, the ectopic granule cells in these animals were abolished by administration of the diuretic bumetanide, which unveiled the masked memory enhancement. Our finding that experimental febrile seizures at P14 but not at P11 enhanced adult memory performance is apparently consistent with the results obtained in the human studies; the first postnatal week in rodents roughly corresponds to the first 2–3 postnatal months in humans, and the next 2 postnatal weeks in rodents correspond to postnatal years 4–5 in humans in terms of the developmental stage of the hippocampus and its role in learning and memory (Avishai-Eliner et al., 2002).

Several animal studies have investigated the molecular mechanisms underlying the relationship between early life febrile seizures and later hippocampal-dependent memory dysfunction. In an infrared-lamp-induced experimental febrile seizure model, it was shown that single experimental febrile seizures at P10, 15, or 20, but not at P5, resulted in impaired inhibitory avoidance responses at P50–60 (McCaughran et al., 1982). Seizures induced by repeated episodes of brief hyperthermia (10 min at a rectal temperature of 40–43°C) at P10–12 resulted in long-term memory deficits in both the Morris water maze (starting at P36) and an inhibitory avoidance task at P45; however, this study modeled brief, recurrent febrile seizures, not prolonged febrile seizures (Chang et al., 2003). Western blotting showed that the phosphorylation of cAMP response-element binding (CREB) protein was significantly reduced in the hippocampi of rats that had been subjected to repeated experimental febrile seizures. Moreover, the authors showed that administration of rolipram, which activates the cAMP-CREB signaling pathway, reversed long-term memory deficits via enhanced CREB phosphorylation. Repeated febrile seizures also induced long-lasting deficits in synaptic plasticity in CA1 pyramidal cells and reduced the tyrosine phosphorylation of the NMDA receptor subunit NR2A (Chang et al., 2005). Recently, abnormal firing rates of hippocampal CA1 cells and poor stability of their activity have been proposed as a basis for deficits in hippocampal-dependent memory in animals subjected to experimental febrile seizures (hair dryer model) (Dube et al., 2009).

To understand the effect of febrile seizures on later memory dysfunction, large-scale human, and animal studies targeting the age-dependent effects of febrile seizures and the cellular and molecular mechanisms underlying these effects are necessary. Moreover, the use of noninvasive methods, such as MRI (Dube et al., 2009) to detect the later effects of febrile seizures on hippocampal function is required.

10 CONCLUSIONS

Animal models of febrile seizures have provided us with extensive evidence regarding the effects of early life seizures on the formation of neural circuits and on later behavior, including the development of epilepsy, which has been difficult to assess using human tissue samples alone. Studies using these models have also identified novel therapeutic strategies, such as increased ambient CO_2 (Schuchmann et al., 2006) and the inhibition of NKCC1 (Koyama et al., 2012) that might be used to prevent the induction of febrile seizures and the later development of epilepsy, respectively. As performed in our laboratory (Koyama et al., 2012), experiments involving cultured brain slices and neurons from rat pups that experienced febrile seizures will help to further clarify the cellular and molecular mechanisms underlying febrile seizure-induced changes in neural circuit formation. It is also important to examine the role of glial cells in febrile seizures and the subsequent development of epilepsy.

Although one must be cautious when extrapolating results obtained from experimental febrile seizure models to human febrile seizures, the residual effects of a single episode of early life experimental febrile seizures have been observed in the adult brain. Future studies using these well-established experimental animal models will provide invaluable information concerning the causes and consequences of early life seizures and their relationship to epileptogenesis and will contribute both to the clarification of the mechanisms underlying neural circuit formation and to the development of therapeutic strategies to prevent epilepsy development.

References

Annegers, J.F., Blakley, S.A., Hauser, W.A., Kurland, L.T., 1990. Recurrence of febrile convulsions in a population-based cohort. Epilepsy Res. 5, 209–216.

Annegers, J.F., Hauser, W.A., Elveback, L.R., Kurland, L.T., 1979. The risk of epilepsy following febrile convulsions. Neurology 29, 297–303.

Annegers, J.F., Hauser, W.A., Shirts, S.B., Kurland, L.T., 1987. Factors prognostic of unprovoked seizures after febrile convulsions. N. Engl. J. Med. 316, 493–498.

Avishai-Eliner, S., Brunson, K.L., Sandman, C.A., Baram, T.Z., 2002. Stressed-out, or in (utero)? Trends Neurosci. 25, 518–524.

Baram, T.Z., Hirsch, E., Snead, III, O.C., Schultz, L., 1992. Corticotropin-releasing hormone-induced seizures in infant rats originate in the amygdala. Ann. Neurol. 31, 488–494.

Baram, T.Z., Gerth, A., Schultz, L., 1997. Febrile seizures: an appropriate-aged model suitable for long-term studies. Brain Res. Dev. Brain Res. 98, 265–270.

Bender, R.A., Dube, C., Gonzalez-Vega, R., Mina, E.W., Baram, T.Z., 2003. Mossy fiber plasticity and enhanced hippocampal excitability, without hippocampal cell loss or altered neurogenesis, in an animal model of prolonged febrile seizures. Hippocampus 13, 399–412.

Bender, R.A., Dube, C., Baram, T.Z., 2004. Febrile seizures and mechanisms of epileptogenesis: insights from an animal model. Adv. Exp. Med. Biol. 548, 213–225.

Berg, A.T., 1993. Are febrile seizures provoked by a rapid rise in temperature? Am J. Dis. Child 147, 1101–1103.

Berg, A.T., Shinnar, S., 1991. The risk of seizure recurrence following a first unprovoked seizure: a quantitative review. Neurology 41, 965–972.

Berg, A.T., Shinnar, S., 1996a. Complex febrile seizures. Epilepsia 37, 126–133.

Berg, A.T., Shinnar, S., 1996b. Unprovoked seizures in children with febrile seizures: short-term outcome. Neurology 47, 562–568.

Berg, A.T., Shinnar, S., Hauser, W.A., Alemany, M., Shapiro, E.D., Salomon, M.E., et al., 1992. A prospective study of recurrent febrile seizures. N. Engl. J. Med. 327, 1122–1127.

Berg, A.T., Shinnar, S., Darefsky, A.S., Holford, T.R., Shapiro, E.D., Salomon, M.E., et al., 1997. Predictors of recurrent febrile seizures. A prospective cohort study. Arch. Pediatr. Adolesc. Med. 151, 371–378.

Berg, A.T., Shinnar, S., Levy, S.R., Testa, F.M., 1999. Childhood-onset epilepsy with and without preceding febrile seizures. Neurology 53, 1742–1748.

Bethune, P., Gordon, K., Dooley, J., Camfield, C., Camfield, P., 1993. Which child will have a febrile seizure? Am. J. Dis. Child 147, 35–39.

Bird, T.D., 1987. Genetic considerations in childhood epilepsy. Epilepsia 28 (Suppl 1), S71–S81.

Brewster, A., Bender, R.A., Chen, Y., Dube, C., Eghbal-Ahmadi, M., Baram, T.Z., 2002. Developmental febrile seizures modulate hippocampal gene expression of hyperpolarization-activated channels in an isoform- and cell-specific manner. J. Neurosci. 22, 4591–4599.

Camfield, P.R., Camfield, C.S., Shapiro, S.H., Cummings, C., 1980. The first febrile seizure—antipyretic instruction plus either phenobarbital or placebo to prevent recurrence. J. Pediatr. 97, 16–21.

Cendes, F., Andermann, F., Dubeau, F., Gloor, P., Evans, A., Jones-Gotman, M., et al., 1993. Early childhood prolonged febrile convulsions, atrophy and sclerosis of mesial structures, and temporal lobe epilepsy: an MRI volumetric study. Neurology 43, 1083–1087.

Chang, Y.C., Guo, N.W., Wang, S.T., Huang, C.C., Tsai, J.J., 2001. Working memory of school-aged children with a history of febrile convulsions: a population study. Neurology 57, 37–42.

Chang, Y.C., Huang, A.M., Kuo, Y.M., Wang, S.T., Chang, Y.Y., Huang, C.C., 2003. Febrile seizures impair memory and cAMP response-element binding protein activation. Ann. Neurol. 54, 706–718.

Chang, Y.C., Kuo, Y.M., Huang, A.M., Huang, C.C., 2005. Repetitive febrile seizures in rat pups cause long-lasting deficits in synaptic plasticity and NR2A tyrosine phosphorylation. Neurobiol. Dis. 18, 466–475.

Chen, K., Aradi, I., Thon, N., Eghbal-Ahmadi, M., Baram, T.Z., Soltesz, I., 2001. Persistently modified h-channels after complex febrile seizures convert the seizure-induced enhancement of inhibition to hyperexcitability. Nat. Med. 7, 331–337.

Chen, K., Ratzliff, A., Hilgenberg, L., Gulyas, A., Freund, T.F., Smith, M., et al., 2003. Long-term plasticity of endocannabinoid signaling induced by developmental febrile seizures. Neuron 39, 599–611.

Chen, K., Neu, A., Howard, A.L., Foldy, C., Echegoyen, J., Hilgenberg, L., et al., 2007. Prevention of plasticity of endocannabinoid signaling inhibits persistent limbic hyperexcitability caused by developmental seizures. J. Neurosci. 27, 46–58.

Cilio, M.R., Sogawa, Y., Cha, B.H., Liu, X., Huang, L.T., Holmes, G.L., 2003. Long-term effects of status epilepticus in the immature brain are specific for age and model. Epilepsia 44, 518–528.

Dubé, C., Baram, T.Z., 2006. Complex febrile seizures-an experimental model in immature rodents. In: Pitkänen, A., Schwartzkroin, P.A., Moshé, S.L. (Eds.), Models of Seizures and Epilepsy. Academic Press, San Diego, pp. 333–340.

Dube, C., Chen, K., Eghbal-Ahmadi, M., Brunson, K., Soltesz, I., Baram, T.Z., 2000. Prolonged febrile seizures in the immature rat model enhance hippocampal excitability long term. Ann. Neurol. 47, 336–344.

Dube, C., Brunson, K.L., Eghbal-Ahmadi, M., Gonzalez-Vega, R., Baram, T.Z., 2005a. Endogenous neuropeptide Y prevents recurrence of experimental febrile seizures by increasing seizure threshold. J. Mol. Neurosci. 25, 275–284.

Dube, C., Vezzani, A., Behrens, M., Bartfai, T., Baram, T.Z., 2005b. Interleukin-1beta contributes to the generation of experimental febrile seizures. Ann. Neurol. 57, 152–155.

Dube, C., Richichi, C., Bender, R.A., Chung, G., Litt, B., Baram, T.Z., 2006. Temporal lobe epilepsy after experimental prolonged febrile seizures: prospective analysis. Brain 129, 911–922.

Dube, C.M., Zhou, J.L., Hamamura, M., Zhao, Q., Ring, A., Abrahams, J., et al., 2009. Cognitive dysfunction after experimental febrile seizures. Exp. Neurol. 215, 167–177.

Dube, C.M., Ravizza, T., Hamamura, M., Zha, Q., Keebaugh, A., Fok, K., et al., 2010. Epileptogenesis provoked by prolonged experimental febrile seizures: mechanisms and biomarkers. J. Neurosci. 30, 7484–7494.

Dwyer, B.E., Wasterlain, C.G., 1982. Electroconvulsive seizures in the immature rat adversely affect myelin accumulation. Exp. Neurol. 78, 616–628.

Dyhrfjeld-Johnsen, J., Morgan, R.J., Foldy, C., Soltesz, I., 2008. Upregulated H-current in hyperexcitable CA1 dendrites after febrile seizures. Front. Cell Neurosci. 2, 2.

Ellenberg, J.H., Nelson, K.B., 1978. Febrile seizures and later intellectual performance. Arch. Neurol. 35, 17–21.

Falconer, M.A., 1974. Mesial temporal (Ammon's horn) sclerosis as a common cause of epilepsy. Aetiology, treatment, and prevention. Lancet 2, 767–770.

Falconer, M.A., Serafetinides, E.A., Corsellis, J.A., 1964. Etiology and pathogenesis of temporal lobe epilepsy. Arch. Neurol. 10, 233–248.

Fisher, P.D., Sperber, E.F., Moshe, S.L., 1998. Hippocampal sclerosis revisited. Brain Dev. 20, 563–573.

French, J.A., Williamson, P.D., Thadani, V.M., Darcey, T.M., Mattson, R.H., Spencer, S.S., et al., 1993. Characteristics of medial temporal lobe epilepsy: I. Results of history and physical examination. Ann. Neurol. 34, 774–780.

Gadomski, A.M., Permutt, T., Stanton, B., 1994. Correcting respiratory rate for the presence of fever. J. Clin. Epidemiol. 47, 1043–1049.

Hamati-Haddad, A., Abou-Khalil, B., 1998. Epilepsy diagnosis and localization in patients with antecedent childhood febrile convulsions. Neurology 50, 917–922.

Haspolat, S., Mihci, E., Coskun, M., Gumuslu, S., Ozben, T., Yegin, O., 2002. Interleukin-1beta, tumor necrosis factor-alpha, and nitrite levels in febrile seizures. J. Child Neurol. 17, 749–751.

Hauser, W.A., 1994. The prevalence and incidence of convulsive disorders in children. Epilepsia 35 (Suppl 2), S1–S6.

Heida, J.G., Boisse, L., Pittman, Q.J., 2004. Lipopolysaccharide-induced febrile convulsions in the rat: short-term sequelae. Epilepsia 45, 1317–1329.

Heinemann, U., Beck, H., Dreier, J.P., Ficker, E., Stabel, J., Zhang, C.L., 1992. The dentate gyrus as a regulated gate for the propagation of epileptiform activity. Epilepsy Res. Suppl. 7, 273–280.

Hesdorffer, D.C., Shinnar, S., Lewis, D.V., Moshé, S.L., Nordli, Jr., D.R., Pellock, J.M., et al., 2012. Design and phenomenology of the FEBSTAT study. Epilepsia 53, 1471–1480.

Hirsch, E., Baram, T.Z., Snead, III, O.C., 1992. Ontogenic study of lithium-pilocarpine-induced status epilepticus in rats. Brain Res. 583, 120–126.

Hjeresen, D.L., Diaz, J., 1988. Ontogeny of susceptibility to experimental febrile seizures in rats. Dev. Psychobiol. 21, 261–275.

Hjeresen, D.L., Guy, A.W., Petracca, F.M., Diaz, J., 1983. A microwave-hyperthermia model of febrile convulsions. Bioelectromagnetics 4, 341–355.

Holmes, G.L., Gairsa, J.L., Chevassus-Au-Louis, N., Ben Ari, Y., 1998. Consequences of neonatal seizures in the rat: morphological and behavioral effects. Ann. Neurol. 44, 845–857.

Holmes, G.L., Sarkisian, M., Ben Ari, Y., Chevassus-Au-Louis, N., 1999. Mossy fiber sprouting after recurrent seizures during early development in rats. J. Comp. Neurol. 404, 537–553.

Holtzman, D., Obana, K., Olson, J., 1981. Hyperthermia-induced seizures in the rat pup: a model for febrile convulsions in children. Science 213, 1034–1036.

Houser, C.R., 1990. Granule cell dispersion in the dentate gyrus of humans with temporal lobe epilepsy. Brain Res. 535, 195–204.

Hsu, D., 2007. The dentate gyrus as a filter or gate: a look back and a look ahead. Prog. Brain Res. 163, 601–613.

Huang, L., Cilio, M.R., Silveira, D.C., McCabe, B.K., Sogawa, Y., Stafstrom, C.E., et al., 1999. Long-term effects of neonatal seizures: a behavioral, electrophysiological, and histological study. Brain Res. Dev. Brain Res. 118, 99–107.

Huang, L.T., Holmes, G.L., Lai, M.C., Hung, P.L., Wang, C.L., Wang, T.J., et al., 2002a. Maternal deprivation stress exacerbates cognitive deficits in immature rats with recurrent seizures. Epilepsia 43, 1141–1148.

Huang, L.T., Yang, S.N., Liou, C.W., Hung, P.L., Lai, M.C., Wang, C.L., et al., 2002b. Pentylenetetrazol-induced recurrent seizures in rat pups: time course on spatial learning and long-term effects. Epilepsia 43, 567–573.

Ishikawa, T., Okamoto, K., Ikegaya, Y., 2015. Homeostatic hippocampal activity against reduced glutamatergic neurotransmission. Int. J. Pharmacol. 11, 318–326.

Isokawa, M., Levesque, M.F., Babb, T.L., Engel, Jr., J., 1993. Single mossy fiber axonal systems of human dentate granule cells studied in hippocampal slices from patients with temporal lobe epilepsy. J. Neurosci. 13, 1511–1522.

Jensen, F.E., Applegate, C.D., Holtzman, D., Belin, T.R., Burchfiel, J.L., 1991. Epileptogenic effect of hypoxia in the immature rodent brain. Ann. Neurol. 29, 629–637.

Jensen, F.E., Holmes, G.L., Lombroso, C.T., Blume, H.K., Firkusny, I.R., 1992. Age-dependent changes in long-term seizure susceptibility and behavior after hypoxia in rats. Epilepsia 33, 971–980.

Jiang, W., Duong, T.M., de Lanerolle, N.C., 1999. The neuropathology of hyperthermic seizures in the rat. Epilepsia 40, 5–19.

Jongbloets, B.C., van Gassen, K.L., Kan, A.A., Olde Engberink, A.H., de Wit, M., Wolterink-Donselaar, I.G., Groot Koerkamp, M.J., van Nieuwenhuizen, O., Holstege, F.C., de Graan, P.N., 2015. Expression profiling after prolonged experimental febrile seizures in mice suggests structural remodeling in the hippocampus. PLoS One 10, e0145247.

Jorgensen, O.S., Dwyer, B., Wasterlain, C.G., 1980. Synaptic proteins after electroconvulsive seizures in immature rats. J. Neurochem. 35, 1235–1237.

Kim, Y.H., Rhyu, I.J., Park, K.W., Eun, B.L., Kim, Y.I., Rha, H.K., et al., 2001. The induction of BDNF and c-fos mRNA in the hippocampal formation after febrile seizures. Neuroreport 12, 3243–3246.

Koyama, R., Ikegaya, Y., 2004. Mossy fiber sprouting as a potential therapeutic target for epilepsy. Curr. Neurovasc. Res. 1, 3–10.

Koyama, R., Matsuki, N., 2010. Novel etiological and therapeutic strategies for neurodiseases: mechanisms and consequences of febrile seizures: lessons from animal models. J. Pharmacol. Sci. 113, 14–22.

Koyama, R., Yamada, M.K., Fujisawa, S., Katoh-Semba, R., Matsuki, N., Ikegaya, Y., 2004. Brain-derived neurotrophic factor induces hyperexcitable reentrant circuits in the dentate gyrus. J. Neurosci. 24, 7215–7224.

Koyama, R., Tao, K., Sasaki, T., Ichikawa, J., Miyamoto, D., Muramatsu, R., Matsuki, N., Ikegaya, Y., 2012. GABAergic excitation after febrile seizures induces ectopic granule cells and adult epilepsy. Nat. Med. 18, 1271–1278.

Kwak, S.E., Kim, J.E., Kim, S.C., Kwon, O.S., Choi, S.Y., Kang, T.C., 2008. Hyperthermic seizure induces persistent alteration in excitability of the dentate gyrus in immature rats. Brain Res. 1216, 1–15.

Lahat, E., Livne, M., Barr, J., Katz, Y., 1997. Interleukin-1beta levels in serum and cerebrospinal fluid of children with febrile seizures. Pediatr. Neurol. 17, 34–36.

Lemmens, E.M., Lubbers, T., Schijns, O.E., Beuls, E.A., Hoogland, G., 2005. Gender differences in febrile seizure-induced proliferation and survival in the rat dentate gyrus. Epilepsia 46, 1603–1612.

Lemmens, E.M., Schijns, O.E., Beuls, E.A., Hoogland, G., 2008. Cytogenesis in the dentate gyrus after neonatal hyperthermia-induced seizures: what becomes of surviving cells? Epilepsia 49, 853–860.

Lewis, D.V., Shinnar, S., Hesdorffer, D.C., Bagiella, E., Bello, J.A., Chan, S., et al., 2014. Hippocampal sclerosis after febrile status epilepticus: the FEBSTAT study. Ann. Neurol. 75, 178–185.

Liebregts, M.T., McLachlan, R.S., Leung, L.S., 2002. Hyperthermia induces age-dependent changes in rat hippocampal excitability. Ann. Neurol. 52, 318–326.

Lothman, E.W., Stringer, J.L., Bertram, E.H., 1992. The dentate gyrus as a control point for seizures in the hippocampus and beyond. Epilepsy Res. Suppl. 7, 301–313.

McCaughran, J.A., Manetto, C., Schechter, N., 1982. Long-term deficits in passive avoidance responding following experimental febrile convulsions during infancy. Behav. Brain Res. 5, 73–79.

Muramatsu, R., Ikegaya, Y., Matsuki, N., Koyama, R., 2007. Neonatally born granule cells numerically dominate adult mice dentate gyrus. Neuroscience 148, 593–598.

Muramatsu, R., Ikegaya, Y., Matsuki, N., Koyama, R., 2008. Early-life status epilepticus induces ectopic granule cells in adult mice dentate gyrus. Exp. Neurol. 211, 503–510.

Nadler, J.V., 2003. The recurrent mossy fiber pathway of the epileptic brain. Neurochem. Res. 28, 1649–1658.

Nagaki, S., Nagaki, S., Minatogawa, Y., Sadamatsu, M., Kato, N., Osawa, M., et al., 1996. The role of vasopressin, somatostatin and GABA in febrile convulsion in rat pups. Life Sci. 58, 2233–2242.

Nelson, K.B., Ellenberg, J.H., 1976. Predictors of epilepsy in children who have experienced febrile seizures. N. Engl. J. Med. 295, 1029–1033.

Nelson, K.B., Ellenberg, J.H., 1978. Prognosis in children with febrile seizures. Pediatrics 61, 720–727.

O'Dempsey, T.J., Laurence, B.E., McArdle, T.F., Todd, J.E., Lamont, A.C., Greenwood, B.M., 1993. The effect of temperature reduction on respiratory rate in febrile illnesses. Arch. Dis. Child 68, 492–495.

Offringa, M., Hazebroek-Kampschreur, A.A., Derksen-Lubsen, G., 1991. Prevalence of febrile seizures in Dutch schoolchildren. Paediatr. Perinat. Epidemiol. 5, 181–188.

Owens, Jr., J., Robbins, C.A., Wenzel, H.J., Schwartzkroin, P.A., 1997. Acute and chronic effects of hypoxia on the developing hippocampus. Ann. Neurol. 41, 187–199.

Qu, L., Leung, L.S., 2008. Mechanisms of hyperthermia-induced depression of GABAergic synaptic transmission in the immature rat hippocampus. J. Neurochem. 106, 2158–2169.

Qu, L., Liu, X., Wu, C., Leung, L.S., 2007. Hyperthermia decreases GABAergic synaptic transmission in hippocampal neurons of immature rats. Neurobiol. Dis. 27, 320–327.

Raijmakers, M., Clynen, E., Smisdom, N., Nelissen, S., Brône, B., Rigo, J.M., Hoogland, G., Swijsen, A., 2016. Experimental febrile seizures increase dendritic complexity of newborn dentate granule cells. Epilepsia 57, 717–726.

Sagar, H.J., Oxbury, J.M., 1987. Hippocampal neuron loss in temporal lobe epilepsy: correlation with early childhood convulsions. Ann. Neurol. 22, 334–340.

Santos, N.F., Marques, R.H., Correia, L., Sinigaglia-Coimbra, R., Calderazzo, L., Sanabria, E.R., et al., 2000. Multiple pilocarpine-induced status epilepticus in developing rats: a long-term behavioral and electrophysiological study. Epilepsia 41 (Suppl 6), S57–S63.

Sarkisian, M.R., Tandon, P., Liu, Z., Yang, Y., Hori, A., Holmes, G.L., et al., 1997. Multiple kainic acid seizures in the immature and adult brain: ictal manifestations and long-term effects on learning and memory. Epilepsia 38, 1157–1166.

Scharfman, H., Goodman, J., McCloskey, D., 2007. Ectopic granule cells of the rat dentate gyrus. Dev. Neurosci. 29, 14–27.

Schuchmann, S., Schmitz, D., Rivera, C., Vanhatalo, S., Salmen, B., Mackie, K., et al., 2006. Experimental febrile seizures are precipitated by a hyperthermia-induced respiratory alkalosis. Nat. Med. 12, 817–823.

Schuchmann, S., Tolner, E.A., Marshall, P., Vanhatalo, S., Kaila, K., 2008. Pronounced increase in breathing rate in the "hair dryer model" of experimental febrile seizures. Epilepsia 49, 926–928.

Schuchmann, S., Vanhatalo, S., Kaila, K., 2009. Neurobiological and physiological mechanisms of fever-related epileptiform syndromes. Brain Dev. 31, 378–382.

Seinfeld, S., Shinnar, S., Sun, S., Hesdorffer, D.C., Deng, X., Shinnar, R.C., et al., 2014. Emergency management of febrile status epilepticus: results of the FEBSTAT study. Epilepsia 55, 388–395.

Shinnar, S., 1998. Prolonged febrile seizures and mesial temporal sclerosis. Ann. Neurol. 43, 411–412.

Shinnar, S., Berg, A.T., Moshe, S.L., Shinnar, R., 2001. How long do new-onset seizures in children last? Ann Neurol. 49, 659–664.

Shinnar, S., Glauser, T.A., 2002. Febrile seizures. J. Child. Neurol. 17 (Suppl 1), S44–S52.

Shinnar, S., Hesdorffer, D.C., Nordli, Jr., D.R., Pellock, J.M., O'Dell, C., Lewis, D.V., et al., 2008. Phenomenology of prolonged febrile seizures: results of the FEBSTAT study. Neurology 71, 170–176.

Sogawa, Y., Monokoshi, M., Silveira, D.C., Cha, B.H., Cilio, M.R., McCabe, B.K., et al., 2001. Timing of cognitive deficits following neonatal seizures: relationship to histological changes in the hippocampus. Brain Res. Dev. Brain Res. 131, 73–83.

Stafstrom, C.E., Thompson, J.L., Holmes, G.L., 1992. Kainic acid seizures in the developing brain: status epilepticus and spontaneous recurrent seizures. Brain Res. Dev. 65, 227–236.

Stanhope, J.M., Brody, J.A., Brink, E., Morris, C.E., 1972. Convulsions among the Chamorro people of Guam, Mariana islands. II. Febrile convulsions. Am. J. Epidemiol. 95, 299–304.

Sutula, T., Cascino, G., Cavazos, J., Parada, I., Ramirez, L., 1989. Mossy fiber synaptic reorganization in the epileptic human temporal lobe. Ann. Neurol. 26, 321–330.

Tancredi, V., D'Arcangelo, G., Zona, C., Siniscalchi, A., Avoli, M., 1992. Induction of epileptiform activity by temperature elevation in hippocampal slices from young rats: an in vitro model for febrile seizures? Epilepsia 33, 228–234.

Tao, K., Ichikawa, J., Matsuki, N., Ikegaya, Y., Koyama, R., 2016. Experimental febrile seizures induce age-dependent structural plasticity and improve memory in mice. Neuroscience 318, 34–44.

Tarkka, R., Paakko, E., Pyhtinen, J., Uhari, M., Rantala, H., 2003. Febrile seizures and mesial temporal sclerosis: no association in a long-term follow-up study. Neurology 60, 215–218.

Taylor, J.A., Del Beccaro, M., Done, S., Winters, W., 1995. Establishing clinically relevant standards for tachypnea in febrile children younger than 2 years. Arch. Pediatr. Adolesc. Med. 149, 283–287.

Theodore, W.H., Bhatia, S., Hatta, J., Fazilat, S., DeCarli, C., Bookheimer, S.Y., et al., 1999. Hippocampal atrophy, epilepsy duration, and febrile seizures in patients with partial seizures. Neurology 52, 132–136.

Thom, M., Martinian, L., Williams, G., Stoeber, K., Sisodiya, S.M., 2005. Cell proliferation and granule cell dispersion in human hippocampal sclerosis. J. Neuropathol. Exp. Neurol. 64, 194–201.

Toth, Z., Yan, X.X., Haftoglou, S., Ribak, C.E., Baram, T.Z., 1998. Seizure-induced neuronal injury: vulnerability to febrile seizures in an immature rat model. J. Neurosci. 18, 4285–4294.

Tsuboi, T., 1984. Epidemiology of febrile and afebrile convulsions in children in Japan. Neurology 34, 175–181.

Ullal, G.R., Satishchandra, P., Shankar, S.K., 1996. Hyperthermic seizures: an animal model for hot-water epilepsy. Seizure 5, 221–228.

van Gassen, K.L., Hessel, E.V., Ramakers, G.M., Notenboom, R.G., Wolterink-Donselaar, I.G., Brakkee, J.H., et al., 2008. Characterization of febrile seizures and febrile seizure susceptibility in mouse inbred strains. Genes Brain Behav. 7, 578–586.

VanLandingham, K.E., Heinz, E.R., Cavazos, J.E., Lewis, D.V., 1998. Magnetic resonance imaging evidence of hippocampal injury after prolonged focal febrile convulsions. Ann. Neurol. 43, 413–426.

Verity, C.M., Golding, J., 1991. Risk of epilepsy after febrile convulsions: a national cohort study. BMJ 303, 1373–1376.

Verity, C.M., Butler, N.R., Golding, J., 1985. Febrile convulsions in a national cohort followed up from birth. II—medical history and intellectual ability at 5 years of age. Br. Med. J. (Clin. Res. Ed.) 290, 1311–1315.

Verity, C.M., Greenwood, R., Golding, J., 1998. Long-term intellectual and behavioral outcomes of children with febrile convulsions. N. Engl. J. Med. 338, 1723–1728.

Vestergaard, M., Christensen, J., 2009. Register-based studies on febrile seizures in Denmark. Brain Dev. 31, 372–377.

Wu, J., Javedan, S.P., Ellsworth, K., Smith, K., Fisher, R.S., 2001. Gamma oscillation underlies hyperthermia-induced epileptiform-like spikes in immature rat hippocampal slices. BMC Neurosci. 2, 18.

Further Reading

Consensus Statement, 1980. Febrile seizures: long-term management of children with fever-associated seizures. Pediatrics 66, 1009–1012.

30

Infection-Associated Preterm Birth: Advances From the Use of Animal Models

Matthew W. Kemp*,**, Gabrielle C. Musk†,
Haruo Usuda*,**, Masatoshi Saito*,**

*The University of Western Australia, Perth, Australia
**Tohoku University Hospital, Sendai, Japan
†Animal Care Services, The University of Western Australia, Perth, Australia

1 INTRODUCTION

It is increasingly apparent that preterm birth (PTB) is a complex, multifactorial syndrome wherein both the risk of both preterm delivery and resultant perinatal outcomes for the infant are predicated on the actions of a network of intractable (e.g., genetic background, family history) and modifiable (e.g., maternal stress, environmental exposures, sterile inflammation, infection) factors (Nadeau et al., 2016; Romero et al., 2014). The classical World Health Organisation (WHO) definition of PTB is live delivery prior to 37 weeks' gestation (Blencowe et al., 2012). PTBs are further subclassified as extremely preterm (occurring before 28 weeks' gestation), very preterm (occurring between 28 and 32 weeks' gestation), and moderate to late preterm (occurring from

32 to 36 weeks' gestation) (Goldenberg et al., 2008b). Although a range of factors including a history of preterm delivery or a cervix of less than 25 mm in length at 18-week pregnancy assessment are indicators of elevated risk of preterm delivery, no definitive diagnostic test for PTB exists, and there are limited effective treatment options (Goldenberg et al., 2008a).

Highlighting comparatively recent evidence demonstrating an increased risk of perinatal death and adverse neurodevelopmental outcomes in babies delivered at 37 and 38 weeks gestation (Tita et al., 2009; Zhang and Kramer, 2009), a number of investigators have called for a reassessment of the definition of PTB, proposing a new cutoff gestation of 39 weeks (Goldenberg et al., 2012). Citing etiological similarities between spontaneous deliveries between 16 and 24 weeks' gestation, the same group has also called for the adoption of a standardized, empirically based definition of the lower limit of prematurity, including, perhaps, deliveries as early as 16 weeks' gestation (Goldenberg et al., 2012).

Currently, preterm deliveries are phenotypically classified as either: spontaneous (sPTB; 45% of preterm deliveries); preterm premature rupture of membranes (pPROM; 25% of preterm deliveries); or indicated delivery due to the identification of risk factors including fetal growth restriction or preeclampsia (30% of preterm deliveries) (Goldenberg et al., 2008b). Villar et al. (2012) have advocated for the adoption of a more granular phenotypic classification system that excludes risk factors to focus on five components of PTB: prelabor maternal conditions; prelabor fetal conditions, placental pathology, signs of the initiation of parturition, and the pathway to delivery. Given the substantial geographical variations that exist in how PTB is defined (especially with regards the lower limit of prematurity and the techniques used to estimate the date of conception), the adoption of a standardized, empirically defined definition of PTB supported by a more granular phenotypic classification system may benefit both our understanding of the PTB syndrome and allow more accurate assessment of global PTB trends.

The socioeconomic burden caused by PTB is profound. The estimates of 2010 suggest that, worldwide, 11.1% of all babies are born preterm (Harrison and Goldenberg, 2016). It is estimated that there are 15 million preterm deliveries each year; 965,000 neonatal deaths, and a further 125,000 deaths among children aged 1–5 years are attributable to PTB (Harrison and Goldenberg, 2016). Approximately 50% of chronic childhood neurological deficit is a result of preterm delivery (Harrison and Goldenberg, 2016). Preterm infants are at elevated risk of respiratory, cardiovascular, and metabolic diseases and the risk of death and developmental disability increases markedly with the degree of prematurity at birth (Harrison and Goldenberg, 2016). Data released by the

WHO reveals that, despite significant improvements in reducing total under-five deaths, there has been little or no progress in reducing the rate of early neonatal death (Lawn et al., 2005).

A 2005 report by the Institute of Medicine estimated the annual societal cost of PTB to the USA at $26 billion (Institute of Medicine Committee on Understanding Premature Books and Assuring Healthy Outcomes, 2007). A subsequent report assessing PTB-associated costs in England and Wales during 2006 reported an attributable cost of £2.946 billion, 92% of which related to in-patient hospital costs after birth (Mangham et al., 2009). The treatment-to-discharge cost for a moderately preterm infant in the United Kingdom is approximately £11,629, some 6.3 times more than the treatment-to-discharge cost of infant delivered at term (Khan et al., 2016). Treatment costs escalate markedly in proportion to the degree of prematurity; the cost of treating an extremely preterm infant has been estimated to be as high as $US 195,245 (Khan et al., 2016). The majority of PTBs occur between 32 and 36 weeks of gestation; for example, 75% of UK PTBs (6%–7% of total live births) fall in this moderate-late PTB range (Khan et al., 2016). In contrast, 2013 data from the USA show that extremely preterm (<28 weeks' gestation; 0.75% of total live births) and very preterm (28–32 weeks' gestation; 1.2% of total live births) account for a comparatively small percentage of live births (Frey and Klebanoff, 2016).

Rates of PTB demonstrate marked geographic and socioeconomic variation. Broadly speaking, the rates of PTB are lowest among Caucasian populations living in high-resource environments. The overall rate of PTB in northern Europe is around 5%; in contrast, the rate of PTB in low-resource, sub-Saharan countries is around 18%. In the USA, the overall rate of birth in 2013 was 11.4%, down from a 2006 peak of 12.8%, potentially as a consequence of fewer early inductions (Behnia et al., 2016). Interestingly, the rate of early PTB has not changed over the same period. A clear discrepancy in PTB rates exists between ethnic groups in the USA; 2013 data show, for example, that 16.3% of pregnant non-Hispanic black, 10.2% pregnant non-Hispanic white, and 11.3% of pregnant Hispanic women had a preterm delivery (Harrison and Goldenberg, 2016). Interestingly, data from migrating Chinese populations suggest that differences in PTB rates between ethnicities may be geographically modifiable (Newnham et al., 2011). A disparate range of candidate factors (e.g., stress, socioeconomic disadvantage, genetic background, lifestyle factors) make unpacking the origin of these differences in the interracial PTB rate a difficult task.

Of the factors hypothesized to induce PTB, a significant body of clinical and experimental data now exists to highlight the importance of intrauterine infection as a causal agent, especially in preterm infants who are

born at or before 32 weeks' completed gestation (Kemp et al., 2010; Menon et al., 2009; Viscardi, 2010). The development of this evidence, with specific reference to the use of animals in clarifying the role of infection and inflammation (both infectious and sterile in origin) in PTB, will constitute the focus of the present chapter.

2 INFECTION, INFLAMMATION, AND PRETERM BIRTH

Inflammation is tightly regulated process mounted by the body in response to tissue injury or microbial invasion. A properly regulated inflammatory response acts to protect the body by limiting tissue damage, preventing further dissemination of infection, and initiating tissue repair. The presence of an active inflammatory response may, depending upon the stage of inflammation and the tissue in question, be determined by clinical signs (redness, swelling, loss of function, heat), a molecular signature (elevated expression of proinflammatory cytokines and chemokines), or histological analyses (with regard to PTB, histological chorioamnionitis neutrophils, lymphocytes, and macrophages). With regard to PTB, histological chorioamnionitis [neutrophil invasion of the chorionic and amniotic membranes, with severity and additional pathology described a grading system, such as that proposed by Redline et al. (2003)], and funisitis (inflammatory involvement of the umbilical cord) are hallmarks of the presence of an intrauterine infection (Goldenberg et al., 2002; Grigsby et al., 2010; Kim et al., 2009; Lahra et al., 2007).

There is some debate, however, as to whether the infiltration of immune cells into the fetal membranes in response to infection initiates or amplifies the induction of PTB, or is merely an associated phenomenon. A recent microarray analysis of laboring and nonlaboring myometrial samples identified a pattern of molecular inflammatory signaling consistent with neutrophil activity (Sharp et al., 2016). However inflammation of uterine tissues is characteristic of uninfected pregnancies delivering at term, although the magnitude of the inflammation is considered to be lower than in cases of preterm delivery with demonstrated uterine infection (Dudley et al., 1996; Keelan et al., 2003; Liggins, 1981). Moreover, acute chorioamnionitis has also been detected in the absence of intrauterine infection (Kim et al., 2015). Perhaps even more intriguing is data generated in an elegant study by Rinaldi et al. (2014), who showed that neutrophil-depleted mice had a reduction in LPS-driven uterine and placental IL-1β expression, but no change in LPS-driven PTB. These findings were subsequently corroborated by work in a rabbit model or prematurity; again, neutrophil-depleted animals stimulated with killed *Escherichia coli* relative had negligible signs of uterine or placental neutrophil invasion relative to control, but maintained high relative expression of inflammatory cytokines (including IL-1β) and increased rates of PTB (Filipovich et al., 2015).

The strongest association between intrauterine infection and preterm delivery is in cases of early PTB (prior to 32 weeks' gestation). The long-held view of the etiology of intrauterine infection in cases of PTB was that microorganisms ascended from the genital tract, invaded the fetal membranes [either generally (Goldenberg et al., 2008b) or as proposed more recently via a discrete focal region (Kim et al., 2009)] before accessing the amniotic fluid and fetus. Recent data also suggests a role for hematogenously (Prince et al., 2014) spread oral microorganisms in PTB (Vanterpool et al., 2016) in support of earlier work by Offenbacher et al. (1996, 1998). It is tempting to speculate that the means by which a particular microorganism gains access to the gestational tissues is dependent on both host (i.e., pregnancy related) and microbial factors. For example, the *Ureaplasma* spp. are exquisitely sensitive to inactivation by complement (Kemp, 2014). Accordingly, they are unlikely to disseminate to the fetus effectively by hematogenous spread unless the mother is severely complement deficient.

The application of metagenomics technologies to the question of PTB etiology has led to the generation of data suggesting that dysbiosis of the vaginal, gastrointestinal, and perhaps even placental microbiome may play an important role or at least be predictive of PTB (Vinturache et al., 2016). Vaginal microbiome diversity has been shown to decrease and population stability to increase, as pregnancy progresses (Vinturache et al., 2016). One particularly interesting hypothesis is that dysregulation of the cervical microbiome (which appears to show some homology to the oral microbiome) is associated with microbially induced shortening of the cervix, itself a known risk factor for PTB (Vinturache et al., 2016). Complicating the interpretation of these data are observations that tissue sites once thought to be sterile, such as the placenta, do possess a native, low-biomass microbiome (Aagaard et al., 2014), and that the microbial population (most notably species diversity) of the vagina differs between ethnicities (Hyman et al., 2014), proximity to the cervix, and with gestation (Aagaard et al., 2012). Although much remains to be understood with regard to the role of the microbiome in PTB, these observations raise the question as to whether disruption of a yet-to-be defined "normal placental or intrauterine" microbiome may increase the risk of a preterm delivery.

What is apparent is data from clinical studies demonstrating that the frequency of intrauterine infection and histological chorioamnionitis correlates inversely with gestational age at birth (Bastek et al., 2011; Goldenberg et al., 2000; Romero et al., 2005, 2007). Bacterial colonization of the amniotic fluid is detected in <1% of women

not in labor at term; seminal research (now replicated by numerous investigators) demonstrated that in very low-birth weight infants (<1500 g), the extraplacental membranes had bacteria in 80% and chorioamnionitis in 60% of cases (Hillier et al., 1988). Before moving to discuss data from animal-based studies that support a role for infection and inflammation in PTB, it is useful to review some of the key microorganisms clinically associated with PTB.

2.1 Bacteria

An increasingly wide range of bacteria are identified from clinical samples in association with PTB, with some suggestion that the spread and diversity of microorganisms identified alters with gestational age at delivery (Jones et al., 2009). Both genital tract and oropharyngeal microorganisms are implicated in the etiology of PTB, and will be introduced briefly in this section.

Members of the *Ureaplasma* spp. are present in the urogenital tract of up to 40%–80% of healthy women (Viscardi, 2014). Recent work by Sweeney et al. (2016) showed that the presence of *Ureaplasma* spp. in mid-late preterm and term placental samples was associated with chorioamnionitis, elevated cord blood granulocyte colony stimulating factor [but not IL-6, IL-8, or monocyte chemoattractant protein-1 (MCP-1)], and increased postnatal oxygen use (>6 h). Interestingly, there was no difference in gestational age at delivery between the infected and noninfected groups, and the term delivery cohort (*n* = 92) had a higher total proportion of mild or severe chorioamnionitis than the mid-late preterm cohort (*n* = 443) (Sweeney et al., 2016). Chorioamnionitis and funisitis at term has also been reported due to intrauterine infection by *Fusobacterium nucleatum* (Bohrer et al., 2012). One interpretation of these data is that although chorioamnionitis and *Ureaplasma* spp. infection in mid-late pregnancy or at term is associated with modest adverse fetal outcomes (i.e., increased oxygen use), it does not correlate with an increased risk of preterm delivery, in contrast to findings at earlier gestations. This interpretation may not be true for all infecting microorganisms; however, as term still birth has been reported in association with *F. nucleatum* infection (Han et al., 2010). Further interpreting these data from a pregnancy risk perspective is difficult given the problems inherent in determining when the *Ureaplasma* spp. infection became established. That said, these data do suggest that the identification of particular factors (in this cause *Ureaplasma* spp. and chorioamnionitis) may equate with a different risk assessment at different stages of pregnancy.

In this, and numerous subsequent studies, *Ureaplasma* spp. were the microorganisms most commonly isolated in PTB, although studies by several groups have demonstrated the potential importance of polymicrobial infection of the uterus in prematurity (DiGiulio, 2012; DiGiulio et al., 2010; Jones et al., 2009). Ureaplasmas are small free-living bacteria that lack a cell wall and have been shown to activate the innate immune system via Toll-like receptors (TLRs)-1, -2, and -6 (Shimizu et al., 2008). The original 14 serovars and 2 biovars of *Ureaplasma urealyticum* have now been reclassified into two species, *Ureaplasma parvum* (serovars 1, 3, 6, and 14) and *U. urealyticum* (serovars 2, 4, 5, 7–13) (Robertson et al., 2002). This taxonomy has been inconsistently employed by investigators and *U. urealyticum* is often still used to describe all 14 serovars.

The presence of *Ureaplasma* spp. in clinical specimens can be confirmed by culture or PCR assays, with more recent assays allowing for discrimination to serovar level (Payne et al., 2014a). A substantial body of data exists to suggest an important role of *Ureaplasma* spp. in early PTB; analysis of women with preterm labor or preterm prelabor rupture of membranes at 23–34 weeks gestation demonstrated *Ureaplasma* spp. in 43.9% of cases, compared with 2.7% at this age where the indication for Cesarean section did not include preterm labor or ruptured membranes (Witt et al., 2005). In a study of umbilical cord blood at birth, positive cultures for *Ureaplasma* spp. were observed in 34.7% of spontaneous PTB at 23–32 weeks gestation, compared with 3.2% for PTB at this age where the indication for delivery was for other reasons (Goldenberg et al., 2006, 2008a). *Ureaplasma* spp. are detected in respiratory tract samples of 20%–45% of very low (<1501 g) infants (Viscardi, 2014); data from a recent US cohort study demonstrated a statistically significant association between *Ureaplasma* spp. colonization of the respiratory tract and decreased gestational age; 65% of babies born before 26 weeks' gestation tested culture or PCR positive for *Ureaplasma* spp. during the first month of life—more than double the rate of detected for preterm infants born between 26 and 33 weeks' gestation (Sung et al., 2011). *Ureaplasma* spp. are 3 times more prevalent in the chorioamnion of early PTB deliveries than in preterm deliveries at later gestational ages (Kundsin et al., 1984), with serovars 3 and 6 being the most commonly detected (Sung et al., 2011).

A multitude of studies over the past 20 years have demonstrated strong associations between *Ureaplasma* colonization of the upper genital tract (causing histological chorioamnionitis) and PTB in addition to spontaneous abortion, neonatal pneumonia, meningitis, and stillbirth (Cassell et al., 1993; Colaizy et al., 2007; Garland and Murton, 1987). Ureaplasmas are microaerophiles and demonstrate a marked affinity for epithelial surfaces (Cassell et al., 1993), and are phenotypically distinguished from Mycoplasmas by their ability to hydrolyze urea as their sole energy source, resulting in production of ammonia, an increase in proton electrochemical potential, and de novo ATP synthesis (Volgmann et al., 2005). Interestingly, despite possessing a minimal

genome, *Ureaplasma* spp. widely express an IgA protease (Paralanov et al., 2012), which may act as a virulence factor in establishing mucosal infections. More recently, mycoplasmas, which are also implicated in infection-associated PTB, have been shown to possess a two-component IgG binding and protease system (Arfi et al., 2016). Such a system may not only act as a means of circumventing host defense, it may also activate an innate immune system-drive inflammatory response; recent data have suggested that leukocyte immunoglobulin-like receptor (LILR) A2, which is expressed on human myeloid cells, has the ability to bind with variable affinity IgM, IgG1, IgG2, IgG3, IgG4 fragments produced by microbial proteases (Hirayasu et al., 2016).

There is ongoing debate regarding the role of periodontitis and oral microorganisms in the etiology of PTB. Species including *F. nucleatum* (Gardella et al., 2004), *Streptococcus agalactiae* (Feikin et al., 2001), and *Porphyromonas gingivalis* (León et al., 2007) are among the oral microorganisms most commonly identified in either chorioamnion or amniotic fluid samples from cases of PTB. The most likely means by which oral microorganisms are able to gain access to the uterine environment is predicted to be by hematogenous distribution (DiGiulio, 2012). Han et al. (2010), for example, isolated the same clonal type of *F. nucleatum* from the lung of a stillborn term infant and the mother's gingival crevice, but did not identify the same isolate in the mother's vagina, suggesting hematogenous spread. Adding weight to the argument for periodontitis having a causal role in PTB are a number of studies linking periodontitis with PTB, low-birth weight, and adverse pregnancy outcomes (Ide and Papapanou, 2013; Offenbacher et al., 2006). In addition to directly impacting pregnancy, a review of periodontitis in adverse pregnancy outcomes by Madianos et al. (2013) proposes that periodontitis may indirectly impact pregnancy well-being via cytokines/chemokines or proinflammatory bacterial products that may interfere with the immunological balance at the maternal/fetal interface. Studies performed in the pig-tailed macaque (*Macaca nemestrina)* provide further support for the importance of systemic inflammation in adverse pregnancy outcomes. Employing a chronically catheterized model, Adams Waldorf et al. (2008) established an infection of the uterus with a clinical isolate of Group B *Streptococcus* and investigated changes in fetal development and intraamniotic inflammation. Despite being unable to isolate the infecting microorganism from the amniotic fluid, maternal blood and fetal blood, the investigators demonstrated marked lung injury and significant elevation of IL-6 and IL-8 in the amniotic fluid (Waldorf et al., 2011). Increased IL-8 levels were also reported in the fetal plasma. These findings indicate that the direct induction of inflammation may not be necessary for the initiation of intrauterine inflammation or fetal injury.

Arguing against a role for periodontitis in PTB are data from two large trials, the Obstetric and Periodontal Therapy Study (Michalowicz et al., 2006) (823 women randomized to receive scaling and root planing either before 21 weeks' gestation or after delivery) and the Smile Study (1078 women with periodontitis randomized to receive periodontal treatment in midpregnancy or after delivery). Both studies noted an improvement in oral health as a result of treatment and there were no adverse side effects resulting from treatment. However, both studies also reported that periodontal treatment did not prevent PTB. Interestingly, the findings of these two studies are supported by data from a rat study of periodontitis. Observing that many previous studies used models of oral pathogen challenge, rather than periodontitis per se, Fogacci et al. (2016) showed that periodontitis in Wistar rats did not alter cytokine levels in gestational tissues and, furthermore, that there was no difference in adverse pregnancy outcomes. One difference that was identified, however, was that fertility rates were reduced in rats with periodontitis. If and how periodontitis is related to PTB remains uncertain, and several authors have concluded that differences in how periodontitis is categorized may contribute to conflicting study findings (Ide and Papapanou, 2013). With a recent appreciation that the placenta possesses its own microbiome-bearing similarities to that of the oral cavity, Aagaard et al. (2014) have assessed this apparent paradox from a microbiome perspective. They hypothesize that the apparent contradiction in the literature over the role of periodontitis in PTB may derive from the hematogenous spread of pathogenic periodontal bacteria to the placenta during early pregnancy (Aagaard et al., 2014). In such a scenario, although mid-trimester periodontal treatment may improve clinical signs of active periodontitis, it is unlikely to impact the microbial population of the placenta, or any inflammatory response potentially predisposing the pregnancy to early delivery or adverse outcome. Some support for this theory comes from work in baboons (*Papio anubis*) undertaken by Ebersole et al. (2014). Using a ligature model of periodontitis, they demonstrated significant increases in low-birth weight, spontaneous abortion, and a decrease in gestational age among animals with periodontitis, relative to control. Interestingly, the authors concluded that the animals at greatest risk of adverse pregnancy outcomes were also those that had the most severe/extensive periodontal disease in the first half of pregnancy.

2.2 Viruses

The body of literature describing the role of viral pathogens in the etiology of PTB is, relative to that describing bacterial infection, comparatively small. Accordingly, much remains to be understood about the role of

viral infection in adverse pregnancy outcomes and PTB. At an epidemiological level, maternal infection caused by a range of viruses including: influenza virus (Meijer et al., 2015; Nakai et al., 2012), human immunodeficiency virus (Montgomery-Taylor and Hemelaar, 2015; Xiao et al., 2015), dengue virus (Hanf et al., 2014), adenovirus (Tsekoura et al., 2010), hepatitis B (Sirilert et al., 2014), and hepatitis C virus (Huang et al., 2015; Money et al., 2014) are associated with variably increased rates of PTB. Using newborn screening cards, Gibson and coworkers reported that the presence of cytomegalovirus was associated with a statistically significant increase in PTB (OR 1.61, 95% CI 1.14–2.27). Of some comfort, however, are studies demonstrating that vaccination against a number of these pathogens (i.e., influenza, hepatitis) during pregnancy poses virtually no risk to the fetus (Moro et al., 2013, 2014). A number of viruses have been detected in mid-trimester amniotic fluid samples using molecular methods; two studies, by Wenstrom et al. (1998) and Baschat et al. (2003) have identified (among others) the presence of adenovirus and cytomegalovirus in amniotic fluid, but both studies concluded that there was no association between the presence of virus and pregnancy loss or adverse pregnancy outcome, respectively. In contrast, Srinivas et al. (2006) reported that the presence of histologic chorioamnionitis and any viral infection was independently associated with second trimester pregnancy loss. More recently, Gervasi et al. (2012) examined the potential association between the presence of specific viral nucleic acids (adenoviruses, herpes simplex virus, varicella zoster virus, human herpesvirus 6, human cytomegalovirus, Epstein–Barr virus, parvovirus B19, and enteroviruses) in 729 mid-trimester amniotic fluid samples and pregnancy outcomes. The authors reported identifying viral nucleic acid in 2.2% of samples, with human herpes virus 6 (seven cases), human cytomegalovirus (six cases) being the most commonly pathogens identified. Interestingly, although the study did identify an association between maternal plasma and amniotic fluid interferon-γ-inducible protein 10 and human cytomegalovirus copy number (but not human herpes virus 6 copy number), the authors concluded that their data did not support a causal association between the presence of viral nucleic acid in the amniotic fluid at mid-trimester screening and adverse pregnancy outcomes (Gervasi et al., 2012).

2.3 Fungi

Traditionally, fungi have not been considered important in the etiology of PTB. Members of the genus *Candida*, including *Candida albicans* (Romero et al., 1985), *Candida glabrata* have been identified from amniotic fluid samples, with *C. albicans* being the species most commonly isolated (DiGiulio, 2012). There is some debate surrounding the role of *Candida* spp. in the etiology of PTB. As many as 40%

of pregnant women may have vaginal colonization by *Candida* spp.—a significantly higher rate than in nonpregnant women (DiGiulio, 2012; DiGiulio et al., 2010; Jones et al., 2009). The presence of *C. albicans* has been identified in amniotic fluid samples from women with spontaneous PTB with intact membranes (Andrew Combs et al., 2014). Although congenital candidiasis is a comparatively rare finding, intraamniotic *C. albicans* infection has been linked to fetal demise and adverse pregnancy outcomes (Chaim et al., 1992; DiGiulio, 2012; DiGiulio et al., 2008, 2010). Work by DiGuilio and coworkers indicate that *C. albicans* may be present in the intrauterine environment more frequently than has been suggested by studies employing culture-based techniques.

3 INNATE IMMUNE RESPONSES

Before moving to review a selection of the studies providing evidence for the role of infection-driven inflammation in PTB, it is useful to touch briefly on the innate immune system and, more specifically, the pattern recognition receptors (PRRs) that play a key role in the recognition of microbial agonist.

Comprised of pathogen and damage-recognizing cellular [i.e., natural killer cells, macrophages, eosinophils, neutrophils (Alberts et al., 2002)] and humoral [(i.e., natural IgM, IgG3, and IgA antibodies (Cao, 2016), complement (Dunkelberger and Song, 2009), defensins (Hazlett and Wu, 2011)] elements, the innate arm of the immune system plays a pivotal role in defending the body from infection due to its ability to recognize and respond to de novo microorganisms. In addition to mounting an initial antimicrobial defense, the innate immune system also acts to recruit an adaptive immune response (Agrawal and Hirsch, 2012). Innate immune cell receptors are known as pattern recognition receptors (PRRs). PRRs are transmembrane and intracellular proteins with the ability to recognize a wide range of conserved pathogen-associated molecular patterns [PAMPs; including lipopolysaccharide, lipoproteins, peptidoglycans, and nucleic acids (i.e., unmethylated CpG motifs) (Kawai and Akira, 2011)] and danger-associated molecular patterns [DAMPs; cellular molecules generated in response to trauma, ischemia, cancer, etc., including heat shock proteins, high mobility-group box 1 (HMGB1), nucleic acids, ATP, and hyaluronic acid (Tang et al., 2012)]. Activation of PRRs leads to the induction of an intracellular signaling cascade, resulting in the production of cytokines and chemokines. Today, major classes of PRRs are known to include the TLRs (De Nardo, 2015; Kawai and Akira, 2011), C-type lectin receptors (CLRs) (Dambuza and Brown, 2015), retinoic acid-inducible gene I (RIG-I)-like receptors (RLRs) (Matsumiya and Stafforini, 2010), Nod-like receptors (NLRs) (Franchi et al., 2009), and LILRs

(Hirayasu et al., 2016; Sloane et al., 2004). In addition to acting individually, a number of investigators have suggested that PRR systems have the ability to interact; for example, Chaput et al. (2013) have suggested that the stimulation of TLRs may facilitate the internalization of muramyl dipeptide, which is necessary for the activation of NOD-2 signaling. LILRs, which demonstrate inhibitory effects on antigen presenting cell activity, may also act to downregulate TLR-driven proinflammatory signaling (Anderson and Allen, 2009).

3.1 Toll-like Receptors

TLRs were the first class of pf PRRs to be discovered. Ten TLRs in have been identified in humans (TLRs1–10) and twelve (TLRs1–9, 11, 12, 13) in mice, each recognizing a range of specific agonists (De Nardo, 2015). Plasma membrane expressed TLRs include: TLR1 (triacyl lipopeptides), TLR2 (lipopeptides, peptidoglycan, lipoteichoic acid), TLR4 (lipopolysaccharide; note TLR4 also has endosomal activity), TLR5 (flagellin), and TLR6 (diacyl lipopeptides, lipoteichoic acid). These TLRs interact with microbial wall or membrane proteins and their activation results in the upregulation of proinflammatory signaling cascades (Hess et al., 2016). TLR3 (dsRNA), TLR7 (ssRNA), TLR8 (ssRNA), and TLR9 (CpG-containing DNA) are sequestered within endosomes and mainly respond to nucleic acids, resulting in the increased expression of type-I interferons (De Nardo, 2015). TLR10 remains an orphan receptor; the activating ligand(s) and effector signaling pathways remain unresolved for this TLR. Interestingly, recent work by Jiang et al. (2016) showed TLR-10 suppression of IL-6 and tumor necrosis factor (TNF)-α expression in vitro, suggesting a potential role as a generalized negative regulator of proinflammatory TLR signaling.

TLRs have been identified in a range of human and animal fetal tissues [including lung (Petrikin et al., 2010; Sow et al., 2012), skin (Iram et al., 2012), spleen (Nalubamba et al., 2008), and CNS (Vontell et al., 2013)] from a very early gestational age. PAMP recognition by a TLR leads to the recruitment of adaptor protein(s) to the intracellular TIR domain and proinflammatory signaling via myeloid differentiation primary response 88 (MyD88)-dependent or TIR domain-containing adapter-inducing interferon-β (TRIF)-dependant pathways—TLR-4 being the only receptor to utilize both signaling pathways. Initiation of the MyD88-dependant pathway leads to early activation of NF-κβ and MAP kinases, resulting (in conjunction with TRIF signaling) in the elaboration of inflammatory cytokines including interleukin (IL)-1β, IL-6, TNF-α, and chemokines including IL-8 and MCP-1. Activation of the TRIF-dependant pathway induces TNF receptor-associated factor 3 activation of interferon regulatory factor 3 and the elaboration of type-I interferons

(Akira and Takeda, 2004; Kawai and Akira, 2011). Additionally, TRIF signaling can also promote RIP-1 kinase interaction with TRAF6, leading to NF-κB-driven proinflammatory cytokine expression (De Nardo, 2015).

3.2 C-type Lectin Receptors

Historically, CLRs have been of interest due to their involvement in host defense from fungal infection; more recently, CLRs have been shown to play a role in defense against bacterial infection (notably the mycobacteria) and tissue homeostasis (Dambuza and Brown, 2015; Sancho and Reis e Sousa, 2012). CLRs are members of a superfamily of around 1000 proteins that are subclassified into 17 groups on the basis of phylogenetic analysis and the protein domain organization. The ability to bind carbohydrate in a calcium-dependent manner is a common characteristic of CLRs, although not all CLRs possess this functionality, and many exhibit specificity for different agonists, including proteins and lipids (Dambuza and Brown, 2015; Sancho and Reis e Sousa, 2012). Dectin-1 and Dectin-2 are among the best characterized members of the CLR superfamily. Dectin-1 (alternatively named CLEC7A) is expressed by human monocytes, macrophages, dendritic cells, neutrophils, and B cells (Dambuza and Brown, 2015; Sancho and Reis e Sousa, 2012). It is activated by β-1,3 glucans from a range of fungi including *Mycobacteria* spp.—*Pneumocystis carinii, C. albicans, Aspergillus fumigatus, Penicillium marneffei, Coccidioides posadasii,* and *Histoplasma capsulatum,* which it binds with an a-typical carbohydrate-binding motif in a calcium-independent fashion (Dambuza and Brown, 2015; Sancho and Reis e Sousa, 2012). Dectin-1 signals via the recruitment and activation of Syk kinase-dependent and -independent pathways to regulate a range of cellular responses including phagocytosis, respiratory burst, enhanced production of IL-2, IL-6, IL-10, IL-23, and also the production of type-I interferons in response to stimulation by *C. albicans.* Dectin-2 (alternatively termed CLEC6A) is expressed in macrophages, monocytes, and some classes of dendritic cells (Dambuza and Brown, 2015; Sancho and Reis e Sousa, 2012). Dectin-2 is primarily activated by fungal α-mannans and in mice plays a greater role than Dectin-1 in driving dendritic cell responses to *C. albicans* (Sancho and Reis e Sousa, 2012).

3.3 RIG-I-like Receptors

RLRs are helicase proteins that respond to the presence of cytoplasmic RNA (Matsumiya and Stafforini, 2010), making them an important defense against viral infection due to their ability to induce the expression of type-I interferons (Loo and Gale, 2011; Matsumiya and Stafforini, 2010). Members of the RLR family include retinoic acid inducible gene-I (RIG-I), melanoma

differentiation-associated gene 5 (MDA5), and laboratory of genetics and physiology 2 (LGP2) (Loo and Gale, 2011; Matsumiya and Stafforini, 2010). As is the case with TLRs, RLRs each respond to a range of viruses; RIG-I has been shown to respond to viruses including Paramyxoviridae (e.g., measles and respiratory syncytial virus), Orthomyxoviridae (e.g., influenza A and B), and the Flavivirus Hepatitis C. MDA5 has a been shown to respond to a smaller range of viruses, including members of the Picornaviridae and the DNA virus vaccinia (Loo and Gale, 2011). The role of LGP2 in antiviral signaling is somewhat unclear; LGP2 differs structurally from both RIG-I and MDA5 due to the lack of two N-terminal caspase recruitment domains (CARDs), which are implicated in interacting with downstream effector molecules to drive upregulation of antiviral gene expression (Bruns et al., 2013). Studies to date have shown that LGP2 has the ability to inhibit RIG-I-driven signaling activation; conversely, LGP2 has been shown to be a critical element of MDA5-driven signaling (Zhu et al., 2014). One potential role for LGP2 may, however, lie in controlling antigen-specific CD8^{+} T cell survival during population expansion in response to viral infection. Elegant work in *Dhx58* (the gene encoding LGP2)-null mice by Suthar et al. (2012) demonstrated elevated expression of death receptors in antigen-specific CD8^{+} T cells. This observation led the authors to conclude that LGP2 may function as a molecular switch to control death receptor signaling during the early stages of T cell activation (Suthar et al., 2012).

3.4 NOD-Like Receptors

NLRs are a large family of cytosolic sensors primarily involved in the detection of bacteria. Human NLRs are subclassified into one of five groups based on the nature of their N-terminal effector domain homology. Of the NLRs, members of the NLRC family NOD-1 (which possesses one N-terminal CARD) and NOD-2 (two N-terminal CARDs) are among the best characterized (Moreira and Zamboni, 2012). NOD-1 is widely expressed, whereas NOD-2 expression is believed to be more restricted; NOD-2 expression has been detected in macrophages, dendritic cells, keratinocytes, epithelial cells, and osteoblasts (Franchi et al., 2009). NOD-1 and -2 expression can be induced by a range of stimuli including TNF-α, IFN-γ, and bacterial agonist (Chaput et al., 2013). NOD-1 and NOD-2 respond to products of Gram-positive and Gram-negative peptidoglycan synthesis and degradation, including *meso*-diaminopimelic acid and muramyl dipeptide, respectively. NOD-1 signaling has been shown to be induced by respiratory pathogens including *Chlamydophila pneumoniae, Legionella pneumophila, Klebsiella pneumoniae, Haemophilus influenzae*, and *Pseudomonas aeruginosa*. Similarly, NOD-2

responds to stimulation by *Streptococcus pneumoniae, Staphylococcus aureus, E. coli, C. pneumoniae*, and *Mycobacterium tuberculosis* (Chaput et al., 2013). Activation of NOD-signaling results in the NF-κB and mitogen-activated protein kinase-driven expression of numerous antimicrobial peptides, cytokines, and chemokines including human β-defensin 2, IL-6, IL-8, CCL2, and CCL5 (Chaput et al., 2013; Voss et al., 2006).

4 INFLAMMATION AND LABOR

The net upregulation of proinflammatory mediators during pregnancy has the ability to shift the uterus from a quiescent state into one primed for labor by inducing remodeling and opening the cervix (otherwise known as cervical ripening), weakening, and eventually rupturing the fetal membranes, and inducing coordinated uterine contractions.

Increased cytokine/chemokine levels in the amniotic fluid and fetal membranes elicit proparturition changes via tissue remodeling of the membranes and cervix as a result of altered matrix metalloproteinase (MMP) and tissue inhibitors of matrix metalloproteinases in conjunction with alterations in uterine contractility via alterations in prostaglandin synthesis and metabolism. MMPs comprise a group of some 20 endopeptidases whose proteolytic remodeling of the extracellular matrix plays an important role in a host of normal and pathological processes (Cockle et al., 2007). Each MMP possesses a range of substrate specificities, which results in considerable heterogeneity in their activities. A number of inducible factors including cytokines, hormones (including prostaglandins), and reactive oxygen species (especially nitric oxide) can induce MMP transcription. MMP activity is suggested to play a role in both membrane rupture and cervical ripening. Elevated levels of MMP-9, a gelatinase, which degrades basement membrane proteins, have been described in the placenta, membranes, and amniotic fluid in term and PTB studies performed in rhesus macaques (Cockle et al., 2007).

Uterine activity during pregnancy and labor can be divided into four phases (0, quiescence; 1, activation; 2, stimulation; 3, involution) during quiescent pregnancy and the eventual transformation to parturition. During phase 0, a host of endocrine mediators including corticotrophin-releasing hormone (CRH), progesterone, prostacyclin (PGI_2), relaxin, and nitric oxide act to maintain quiescence by limiting intracellular Ca^{2+} release (and thus myofilament shortening via reduced myosin light chain kinase activity) in response to elevated intracellular levels of cyclic adenosine monophosphate (cAMP) and/or cyclic guanosine monophosphate (cGMP) (Challis et al., 2000; Lye et al., 1998). In phase 1, the uterus is primed for activation (either by mechanostimulation or

uterotrophic priming) resulting in increased expression of procontractility proteins including the gap-junction protein connexion 43 and prostaglandin and oxytocin agonist receptors. The generation of prostaglandin H_2 from arachidonic acid is under the control of prostaglandin cyclooxygenase endoperoxidase synthase 1 (PTGS1) and 2 (PTGS2). PTGS1 is a constitutively expressed enzyme, whereas increases in *Ptgs*2 expression is closely associated with inflammation or injury. With regards the role of infection in PTB, of interest is work by Timmons et al. (2014) demonstrating that in mice neither the level of prostaglandins nor the expression of prostaglandin synthase enzymes are altered in term cervices; however and in contrast, LPS exposure induced significant increases in prostaglandin synthesis and tissue levels, mediated by increased activity of PTGS2. In phase 2, uterine contractility is stimulated by prostaglandins, oxytocin, and CRH. The third phase of parturition is characterized by involution of the uterus following delivery of the fetus and placenta, primarily under the control of oxytocin (Challis et al., 2000; Lye et al., 1998).

5 THE USE OF ANIMALS IN THE STUDY OF PRETERM BIRTH—JUSTIFICATION AND VALIDITY

The use of animals in the study of human PTB is, quite rightly, a contentious undertaking requiring careful consideration of pragmatic and ethical aspects. In this regard, the work of Russell and Burch (1959), a lucid, rigorous, and compassionate treatment of humane experimental technique remains a landmark text in the field of animal experimentation. It should be considered essential reading for all individuals contemplating the use of animals in scientific research (Russell and Burch, 1959).

At a pragmatic level, much of the progress made in our understanding of human PTB is, as with many areas of biomedical science, derived from the use of animal experimentation. One of the most important questions facing the investigator thus relates to the "best" animal in which to model human PTB. We, and others, have suggested that there is no "best" animal system with which to model human PTB; a particular animal model, due to the nature and regulation of fetal development, may be well suited to one area of investigation (Bastek et al., 2011; Kemp et al., 2010). Alveolar development in rats and mice, for example, occurs predominantly in the postnatal period; in contrast, alveolar development in sheep, guinea pigs, and humans is well advanced at the time of birth (Warburton et al., 2000). As such, investigating the impact of antenatal steroids, such as betamethasone phosphate or dexamethasone phosphate on antenatal alveolar development and surfactant production is likely better undertaken in the fetal sheep than in

a rodent. Similarly, demonstrating that infection of the amniotic cavity induces preterm labor is likely better undertaken in a rodent model than in a sheep, due to the sheep's resistance to preterm labor in response to florid uterine inflammation (Kemp et al., 2010). As a means of framing our subsequent discussion, we will draw briefly on mice, sheep, and nonhuman primates, three experimental models that will form the bulk of our subsequent discussion on the study of animal models of human PTB.

Rats (commonly derived from the brown or Norwegian rat, *Rattus norvegicus*) and mice (*Mus musculus*) are commonly employed as models of infection-derived PTB. Their use confers numerous advantages due to their small size, ease of housing, and that they may be cheaply and easily obtained from defined, commercial breeding lines. Rats and mice have a brief gestation (21–23 days for rats and 19–21 days for mice), produce large litters (6–12 pups for rats and 4–15 pups for mice), and rapidly reach sexual maturity (puberty occurs at 50–60 days for rats and 6–7 weeks of age in mice) meaning that colonies can rapidly be expanded to meet experimental needs and precise age/gender matching is generally achievable (Wolfenson and Lloyd, 2003). Mice in particular are especially amenable to genetic modification and both rats and mice have well-characterized genomes. Studies involving rats and mice also benefit from the wide range of array platforms, multiplex protein assays, and siRNA probes that are commercially available (Kemp et al., 2010).

There are also a number of potential drawbacks to the use of rodents to model human PTB that need to be considered in experimental design. Rats and mice have a greatly shortened gestation when compared with humans and large litters, which limits the usefulness of this model when studying chronic infections/standardized fetal drug exposures or performing longitudinal analyses. There are significant variations in responsiveness to inflammatory compounds (e.g., LPS) exhibited between strains of mice, which necessitates caution in designing and comparing experiments. Additionally, their small anatomical size and elevated litter size makes maternal and fetal instrumentation, surgical interventions, perinatal ventilation, and amniotic fluid sampling difficult.

Primates are the closest animal model to humans in terms of pregnancy and labor, and marmosets and macaques are among the most commonly used primates in research (Wolfenson and Lloyd, 2003). Primate genomes are well studied and a host of molecular tools and commercially available antibody/probe/array tools exist to support analytical work. Despite possessing a host of attractive attributes, their use in PTB research remains comparatively limited. Primates possess elevated sentience, resulting in their use in experimental studies constituting an ethically difficult question. They are expensive, require substantial environmental enrichment,

are at times aggressive and are also a potential source of zoonotic disease, all of which necessitate specialized housing and care and dedicated, experienced technical staff (Wolfenson and Lloyd, 2003). Although amenable to chronic instrumentation and surgical interventions, they require significant suppression of labor postoperatively and extended postoperative recovery times which may introduce a potential source of experimental confounding in addition to posing additional cost to the investigators (Gravett et al., 2007).

Sheep have traditionally proved a valuable model in which to study fetal physiology, respiratory development and the development of neonatal ventilation techniques. More recently, sheep have been employed in the study of the infectious and inflammatory origins of PTB and in the development of antibiotic therapies for PTB. Sheep can be selectively bred for single pregnancies by adaptation of the ewe's nutritional plane and have a gestational length of 144–150 days (the average is 147 days) (Wolfenson and Lloyd, 2003) which enables longitudinal sampling and the analysis of the effects of chronic fetal exposure to pharmaceutical compounds and infectious agents. Both the ewe and fetus are well suited to a range of surgical interventions, ultrasound-guided injections, and studies requiring long-term catheterization (Meschia et al., 1969; Newnham et al., 1989). Sheep are easy to handle once an appreciation of flock behavior is gained and show a remarkable resilience to surgical interventions. The disadvantages of using sheep as an experimental model relate primarily to their size and their historical status as a production rather than laboratory animal. Sheep require large landholdings to breed, specialized housing facilities and are, relative to rodent models, expensive to purchase and slow to reach sexual maturity (ewes may be mated at 6 months of age assuming 70% of adult body weight has been achieved) (Wolfenson and Lloyd, 2003) and breed. From a postoperative care perspective, sheep are adept at disguising pain, making assessment of pain difficult. Sheep are well characterized from a physiological and parturition perspective but their immunology and genome is much less well understood. The pronounced lack of commercially available molecular and protein-based tools available to perform analyses on sheep tissues constitutes an additional drawback.

6 ANIMAL MODELS OF INFECTION-ASSOCIATED INFLAMMATION

As will be discussed, animal studies addressing the form and origins of PTB-associated inflammation have utilized nonviable microbial agonist (i.e., *E. coli* lipopolysaccharides or synthetic TLR3 agonist poly I:C), viable microorganisms (i.e., *Ureaplasma* spp., *C. albicans*,

F. nucleatum, Group B streptococci), or inflammatory cytokines and chemokines (i.e., IL-1, IL-8, TNF-α) to directly and indirectly induce inflammatory changes in gestational tissues (the fetus, uterus, and placenta) with a view to investigating fetal injury responses, patterns of uterine activation and perinatal outcomes. The use of purified bacterial or synthetic TLR agonist allows for assessment of the inflammatory response derived from the activation of a discrete set of PRRs (such as TLR-4 activation by *E. coli* LPS or TLR-3 activation by poly I:C) but is artificial in the sense that in utero inflammation is likely caused by more than one microbial agonist. The use of intact heat-killed bacteria (including *E. coli* and Group B Streptococci) may, on the basis that many PRRs act synergistically, provide a more translatable response and controls for growth-related variation in bacterial stimulation; however, the presence of multiple potential agonists may complicate investigations into pathway-specific signaling in the induction of subsequent inflammation.

The use of viable microorganisms including *F. nucleatum, U. parvum,* or *C. albicans* may provide the most translatable model of fetomaternal inflammation, and is certainly appropriate when antimicrobial and antiinflammatory interventions are being tested. However, there are a number of potential complications to be controlled for in the study design, as host-dependent variations in microbial growth and tissue colonization in utero may greatly increase the variability of experimental data. As with the choice of a particular animal model with which to assess inflammation, we suggest that the choice of agonist employed needs to be selected with reference to the specific objectives of the experimental model. Purified agonist is likely of most use when investigating specific inflammatory responses to identify potential signaling control points for therapeutic intervention, and live microorganism is an appropriate choice when seeking to assess the therapeutic efficacy of a combined antibiotic and antiinflammatory intervention.

6.1 Cytokine and Chemokine-Based Models of Intrauterine Inflammation

The elevated expression of proinflammatory mediators in gestational tissues, amniotic fluid, and cord blood is associated with both preterm labor and adverse perinatal outcomes (Gomez et al., 1998; Gotsch et al., 2007). Accordingly, a number of investigators have focused on specific cytokines and chemokines as the basis of in vivo experiments to investigate the role played by individual proteins in the induction of these two processes. Of these, IL-1 (Kallapur et al., 2009, 2013; Leitner et al., 2014; Romero and Tartakovsky, 1992; Romero et al., 1991; Sadowsky et al., 2006; Wang et al., 2006), IL-6 (Robertson et al., 2010; Sadowsky et al., 2006; Wakabayashi et al., 2013), IL-8

(Cheah et al., 2009; Sadowsky et al., 2006), and TNF-α (Ikegami et al., 2003; Sadowsky et al., 2006) have received particular attention.

There is good evidence to suggest an important role for IL-1 in PTB. Expression of precursor IL-1β is induced following PRR signaling induction. Precursor IL-1β then undergoes caspase-1-mediated proteolytic cleavage before being secreted as mature IL-1β. In human cord blood monocytes, overexpression of IL-1β is controlled by inhibition of precursor IL-1β production and the downregulation of TLR-mediated NLRP3 expression, of which caspase-1 is a component (Sharma et al., 2015). The mature forms of both IL-1α and IL-1β bind to the widely expressed IL-1 receptor 1 (IL-1R1). IL-1R2, which has a more restricted pattern of expression (neutrophils, monocytes, and B cells), acts as a signal transduction-deficient decoy due to the absence of a cytoplasmic tail (Nadeau-Vallée et al., 2016). Binding of ligand to IL-1R1 induces accessory protein recruitment leading to the translocation of signaling pathway intermediates including MyD88, TRAF6, and IL-1 receptor-associated kinase 4, resulting in MAPK and or NF-κB activation (Sims and Smith, 2010).

Unlike IL-1β, IL-1α is primarily an intracellular mediator and is seldom released to the extracellular environment unless cell damage occurs (Werman et al., 2004). IL-1α is constitutively expressed in a wide variety of cell types and functions as an early responder to an inflammatory stimulus, acting before IL-1β to initiate an immune response (Idan et al., 2015). IL-1α also differs from IL-1β in that it is biologically active in its precursor form. Work by Werman et al. (2004) demonstrated that TLR stimulation induces translocation of precursor IL-1α to the nucleus where it has the ability to activate NF-κB and AP-1. Subsequent studies have demonstrated that IL-1α is an important early responder to DNA damage, hypoxia, or heat shock (Idan et al., 2015).

Increases in amniotic fluid IL-1β concentrations have been identified in women in labor at term and in infection-associated PTB (Nadeau-Vallée et al., 2016; Romero et al., 1989). Studies in several population groups have concluded that IL-1, IL-1R1, IL-1R2 polymorphisms modify the risk for PTB (Cui et al., 2015; Kayar et al., 2015; Langmia et al., 2015; Pandey and Awasthi, 2016; Schmid et al., 2012). Accordingly, IL-1 is of interest in terms of both PTB etiology and as a potential therapeutic intervention point. However, whether IL-1 plays a role in all PTB phenotypes, or only those induced by infection, remains unclear. Wei et al. (2010), for example, performed a metaanalysis of the association between common inflammatory cytokines and spontaneous PTB as an outcome in asymptomatic women. Their findings demonstrated an association between IL-6 and C-reactive protein (CRP), but did not identify a PTB association for a number of common inflammatory mediators including IL-1, IL-2, IL-8, IL-10, and TNF-α. It

is important to note, however, that this conclusion may be due to the small number of studies involving these mediators that were included in the metaanalysis (Wei et al., 2010). In contrast, cervical concentrations of IL-1β were shown to be elevated in a cohort of symptomatic women (22–33 weeks' gestation) with intact membranes who delivered preterm (Edwards et al., 2006). A metaanalysis of IL-1β gene variants in four ethnicities (Caucasian, African American, Hispanic, Asian) from the USA, China, and Chile revealed an association between IL-1 genotype pattern and moderate to severe periodontitis (itself associated with an increased risk of PTB) with an odds ratio of 1.95 ($P < 0.001$) (Wu et al., 2015). Additional work in a Turkish population has reported a potential association between IL-1 receptor antagonist (IL-1ra) allele 2, periodontal disease, and previous PTB, or low-birth weight delivery (Kayar et al., 2015).

In addition to investigations based on human clinical samples, animal studies have made a substantial contribution to our understanding of the role of individual cytokines and chemokines in PTB and fetal injury. Work by Romero et al. (1991) describing the systemic administration of IL-1 to pregnant, C3H/HeJ LPS resistant mice revealed that IL-1 induces preterm delivery in pregnant mice via interaction with the IL-1 receptor (Romero and Tartakovsky, 1992). Interestingly, studies undertaken by Hirsch et al. (2002) demonstrated that IL-1β is not an essential regulator of preterm labor induction in the mouse; mice lacking a functional IL-1 receptor were as equally susceptible to LPS-induced preterm labor as their wild-type counterparts (Hirsch et al., 2002). Genetically modified mouse models allow detailed studies of the molecular pathways underlying inflammation and PTB. An excellent example of this is work by Hirsch et al. (2002, 2006), who utilized a double knockout (Il1r1/Tnfrsf1a) mouse model to demonstrate marked reductions in the rate of PTB even at high (1.4×10^8) doses of intraamniotic heat-killed *E. coli*. This study is of particular interest as it serves both to highlight the importance of multisystem signaling in infection-derived inflammation and PTB and also suggests that cytokine signaling (in this case IL-1 and TNF-α) constitutes an appropriate therapeutic target for pharmacological intervention. Interestingly, at the highest dose delivered (7×10^8–1.4×10^9 heat-killed *E. coli*) there was no difference in the rate of preterm delivery between wild-type and double-knockout groups. Although this may be attributable to confounding following the exclusion of most of the double knockout group on the basis of maternal shock, it may also suggest that targeting cytokine pathways may only be efficacious up until a certain infectious or inflammatory load has been reached.

Reznikov et al. (1999) employed a IL-1β knockout mouse model to study the mechanistic role of IL-1β signaling in the induction of preterm labor. Intracervical

E. coli or LPS was administered to C57BL/6J wild-type and IL-1β knockout mice at 70% of term gestation. PTB was initiated within 36 h of inoculation in 90%–100% of both groups of animals studied. Control animals treated with saline did not exhibit preterm delivery of pups. Interestingly, although analysis of infected IL-1β knockout mice demonstrated lower levels of cytokine expression, pregnancy loss rates were not reduced (Reznikov et al., 1999). These data suggest that an intervention for infection-derived preterm labor may require the control of IL-1 family signaling (in addition to the control of other proinflammatory cytokines/chemokines) as opposed to controlling the expression of an individual cytokine.

In a study of chronically instrumented rhesus monkeys (*Macaca mulatta*), Sadowsky et al. (2006) demonstrated that infusions of IL-1β resulted in significant increases in amniotic fluid concentrations of IL-6, IL-8, TNF-α, prostaglandins, MMP9, histologic chorioamnionitis, coordinated uterine contractions, and preterm delivery. TNF-α infusions generated a similar response pattern, but with smaller increases in amniotic fluid prostaglandin concentrations and preterm delivery in only two of five animals. Interestingly, although both IL-6 and IL-8 were upregulated in response to IL-1β and TNF-α, infusion of these mediators alone (albeit in only two animals per group) was insufficient to provoke the induction of preterm labor, but did induce histologic chorioamnionitis (Sadowsky et al., 2006). In earlier work employing in a sheep model of pregnancy, Ikegami et al. (2003) demonstrated that preterm fetal sheep exhibit only a minor inflammatory response to TNF-α, but a comparatively pronounced response to IL-1α. Subsequent work, again in the sheep, demonstrated that IL-1α signaling was involved in intestinal injury and caused disruption to the maturation of the fetal gut (Nikiforou et al., 2016). More recent work by Kallapur et al. (2013) demonstrated a similarly strong proinflammatory response in rhesus monkeys given intraamniotic injections of IL-1β. The investigators reported substantial increases in histologic chorioamnionitis, neutrophil infiltration of the fetal airways, and increased pulmonary surfactant and cytokine mRNA expression. Of interest in this study was the observation that IL-1β administration was associated with a perturbation of the frequency of CD4⁺FOXP3⁺ cells in the CD4⁺CD3⁺ cell population (predicted to be T-regulatory cells) in the mediastinal and mesenteric lymph nodes and the spleen at 24 h post-IL-1β administration. A transient increase in the frequency of IL-17⁺ T cells was also identified (Kallapur et al., 2013). These data are in keeping with clinical observations demonstrating that CD4⁺ T cells collected from extremely preterm infants have a strong IL-17 bias (Black et al., 2012). The importance of these findings relates to an appreciation for the importance of CD4⁺ T cell polarization during pregnancy.

An increasing body of data exists to suggest that the balance of Th1 (CD4⁺ T cells polarized by IL-12 and characterized by prodigious interferon-γ production), Th2 (CD4⁺ T cells polarized by IL-4 and characterized by the expression of several cytokines including IL-4, -5, and -6 and IL-13), T-regulatory (CD4⁺CD25⁺FOXP3⁺ T cells) and Th17 (CD4⁺ T cells polarized under the control of transforming growth factor β, IL-6, IL-21, and IL-23 that express IL-17a and IL-17f) is critical to the maintenance of pregnancy (Polese et al., 2014). For example, a decrease in T-regulatory cells has been linked with abortion in human pregnancy and that Th17 cells may promote inflammation at the fetomaternal interface in PTB (Polese et al., 2014). For a comprehensive review of T cell regulation in pregnancy see Polese et al. (2014).

In a sheep model of pregnancy, use of recombinant IL-1ra in combination with LPS-driven TLR-4 stimulation showed the importance of IL-1 signaling chorioamnionitis and lung maturation; the use of IL-1ra significantly inhibited, but did not entirely resolve fetal lung and systemic inflammation (Kallapur et al., 2009). Arguing for a central role for IL-1 in the induction of infection-associated PTB, Nadeau-Vallée et al. (2016) have developed a noncompetitive peptide termed rytvela which functions to selectively inhibit IL-1β signaling in an NF-κB-independent fashion. Data from a number of elegant in vitro and murine studies suggested that rytvela acts by inhibiting the p38, JNK, c-jun, and the Rho/ROCK pathways (Nadeau-Vallée et al., 2015). Rytvela has shown promise for prolonging labor and reducing the magnitude of intrauterine inflammation. When administered to mice in combination with bacterial agonists TLR2 and TLR4 or recombinant IL-1β it has exhibited strong inhibitory effects; however, as with other inhibitors tested to date, it does not entirely resolve inflammatory activation or completely prevent preterm labor.

Wakabayashi et al. (2013) reported a similar pattern of findings in murine experiments with the anti-IL-6 receptor antibody MR16-1; administration of this inhibitor prior to LPS treatment lowered, but did not inhibit preterm delivery. Studies undertaken in C57BL/6 *IL6* knockout mice by Robertson et al. (2010) demonstrated that IL-6 is likely an important, but nonessential factor in the induction of labor either at term or preterm. These experiments demonstrated a significant delay in term labor in *IL6⁻/⁻* mice of around 24 h, a reduction in the ability of LPS to induce preterm labor, and a reduction in the number pups that died in response to LPS exposure (Robertson et al., 2010). Given changes in genes involved in uterine activation (e.g., oxytocin receptor) relative to wild-type animals, combined with an absence of change in serum progesterone levels in *IL6⁻/⁻* mice, the authors concluded that IL-6 acts within the uterus to regulate genes important to uterine activation (Robertson et al., 2010). In addition to suggesting the importance of

specific inflammatory mediators, such as IL-1β and IL-6 in the induction of preterm labor, these data from animal studies also suggest that any potential intervention will likely have to account for the action of multiple cytokines and redundancy in cytokine signaling to prevent fetal injury and PTB.

6.2 Microbial Agonist

A number of animal models based around the intravenous, intraamniotic, intraperitoneal, or intracervical administration of LPS from *E. coli* or *P. gingivalis* have been employed to explore the causal relationship between infection, inflammation, and PTB. Each model is useful for unpacking slightly different elements of the PTB-infection paradigm. Intraamniotic models allow the analysis of direct exposure of agonist to the gestational tissues and fetus; cervical models are useful in studying inflammatory signaling arising from vaginal dysbiosis or ascending infection; intravenous and intraperitoneal studies allow the assessment of the impact of systemic maternal inflammation and, in the cause of intravenous systems, hematogenous spread on pregnancy well-being.

Studies undertaken in the early 1990s by Collins et al. (1994a,b) demonstrated that the intravenous administration of LPS isolated from *E. coli* or *P. gingivalis* caused a dose-dependent inflammatory response and negatively affected fetal well-being in hamster models of pregnancy. In a series of elegant experiments performed by Hirsch et al., high doses of attenuated *E. coli* were injected into a ligated uterine horn of pregnant mice, resulting in localized induction of IL-1α, IL-1β, and IL-6 expression. The unligated horn, which did not receive *E. coli*, was subsequently induced to labor (Hirsch et al., 2002).

Studies in mice revealed that repeated, low doses of LPS [which does not readily cross cell–cell barriers (Romero et al., 1987)] administered via intraperitoneal injection resulted in preterm delivery and uterine inflammation in a cohort of 60 C3H/HeN × B6D2F1 mice. Together, these studies suggest that labor may be induced by systemic mediators, and even when the primary site of infection is at a distance from the gestational tissues. The scenario of "remote inflammatory activation" is supported by work undertaken in rhesus monkeys by Adams Waldorf et al. (2008). With the use of chronically catheterized animals, a Group B streptococci infection of the uterus was initiated, with subsequent analyses focusing on alterations to fetal development and the presence of intraamniotic inflammation (Waldorf et al., 2011). Of additional interest with regards the potentially infection-specific nature of PTB is subsequent work demonstrating, again in mice, that different isolates of *E. coli* LPS exert markedly different effects on inflammatory signaling, and fetal well-being (Migale et al., 2015).

The impact of direct exposure of the fetomaternal tissues has also received a significant amount of attention from investigators. Work undertaken in the 1990s by several groups demonstrated the induction of uterine inflammation and preterm delivery in a rabbit model following intrauterine administration of *E. coli* to does at 21 days (70% of term) gestation (Dombroski et al., 1990; Heddleston et al., 1993; McDuffie et al. 1991). Compounding the complexity introduced by apparent species-derived differences in LPS response is a recent appreciation of the differences in inflammatory response conveyed by alterations in the structure of LPS itself. Chang et al. (2010) employed a macaque explant model to investigate changes in cytokine, chemokine, prostaglandin, and TLR expression in response to LPS structural variants. First demonstrating consistency in TLR expression, they demonstrated the macaque amniochorion could distinguish between LPS variants—suggesting that some strains of a particular microorganism may be more adept at inducing an inflammatory response, fetal injury, and PTB than others (Chang et al., 2010).

Identifying the tissues responsible for driving intrauterine inflammation is an important step in efforts to develop interventions for PTB and fetal injury. Applying the observation that MyD88 is a critical mediator in TLR signaling; Filipovich et al. (2009) demonstrated an absence of preterm labor in MyD88 knockout mice following LPS challenge, whereas wild-type and TRIF knockout animals remained susceptible to LPS-induced preterm labor. Using rhesus macaques, the pretreatment of pregnant animals with a TLR-4 antagonist reduced proinflammatory cytokine expression and uterine contractility following LPS administration, relative to animals that received LPS alone (Adams Waldorf et al., 2008).

In sheep, selective exposure of *E. coli* LPS to the lung, gut, or oropharyngeal cavity has been demonstrated to induce a systemic fetal immune response characterized by changes in liver enzymes associated with injury, changes in LPS-isolated tissues, and alterations in cord blood immunocyte populations (Kemp et al., 2013; Maneenil et al., 2015a; Nikiforou et al., 2016; Wolfs et al., 2014). More recently, Kemp et al. (2016) demonstrated that in a sheep model of early pregnancy, acute systemic fetal inflammation is rapidly initiated by *E. coli* LPS stimulating amniotic fluid-exposed tissues (most notably the fetal lung), and that this acute response is not derived from cells in the fetal blood. A rabbit model has also been used to study the temporal relationship between histological inflammation and intraamniotic infection, illustrating that inflammation was present in the placenta and uterus 8 h after infection, and inflammation in the fetal lung 30 h after infection.

A similar pattern has been identified in a sheep model of pregnancy; intraamniotic injection of *E. coli* LPS

resulted in immunocyte infiltration of the chorioamnion by within 5 h, and increases in chorioamnion cytokine/chemokine mRNA by 15 h. Cytokine mRNA was increased in the fetal lung at 2 days postexposure, and evidence of lung maturation was apparent after 7 days (Kallapur et al., 2001). These studies suggest that inflammation and fetal injury is an evolving process rather than a "single strike" phenomenon. This observation may be of importance as it suggests that timely diagnosis of infection and treatment may allow for the prevention of preterm delivery and fetal injury. This phenomenon has been assessed in rhesus macaques by Grigsby et al. (2010), who concluded that choriodecidual inflammation occurs before premature ripening of the cervix, fetal membranes rupture, and eventual preterm labor.

One of the most interesting contemporary areas of study involving animal models involves assessment of the impact of subclinical intrauterine inflammation, partly in response to the identification of an association between intrauterine inflammation and an increased risk of developing cerebral palsy or other neurodevelopmental disorders in infancy. Burd et al. used RU486 (a progesterone antagonist) and LPS in a PTB mouse model to investigate the effect of PTB per se on the fetal brain. When administered individually at embryonic day 15, both agents induced PTB, however, only the LPS-induced animals demonstrated increases in neuronal damage and cytokine expression (Burd et al., 2010).

The impact of subclinical inflammation in term and preterm fetuses was then elegantly demonstrated by employing a low dose LPS (50 μg) model of intraamniotic inflammation in CD-1 mice. In this study, 30% of animals exposed to LPS at embryonic day 15 delivered preterm, compared with no preterm deliveries in animals exposed to LPS at embryonic day 18. At both gestational ages, 50 μg LPS exposure elicited an increase in IL-1β and TNF-α expression in the fetal brain, but no increase in IL-6. White matter injury was induced at both time points although the expression of glial fibrillary acid protein (GFAP, a 432 residue type III intermediate filament protein expressed in astrocytes and used as a marker of astrocytosis) was unchanged (Elovitz et al., 2011). A further study in term CD-1 mouse fetuses demonstrated aberrations in in vitro dendrite arborization and growth following in utero exposure to LPS (Burd et al., 2011). These studies suggest that although PTB may not occur, exposing the fetus to even relatively low levels of uterine inflammation early in gestation and, perhaps most surprisingly, close to term can lead to alterations in fetal neurological development and neurological injury. As such these recent findings highlight the need to control both the preterm induction of labor and uterine inflammation in an attempt to improve pregnancy outcomes.

Data from several studies suggest a potential role for virus-driven TLR3 signaling (agonized by ds-RNA) in PTB. Ilievski et al. (2007) used intraamniotic injections of the synthetic TLR3 agonist, polyinosinic:cytidylic acid (poly[I:C]) to demonstrate increased expression of interferon-β and PTB in one-third of mice treated intraamniotically at 75% gestation. Similar findings were reported by Koga et al. in a series of experiments involving wild-type (C57B/6) and TLR-3 knockout mice (Koga et al., 2009); maternal administration (intraperitoneal) of poly[I:C] had no effect in knockout animals, but induced preterm delivery in wild-type mice in a dose-dependent fashion (Koga et al., 2009). Interestingly, more recent work involving TLR-3 has suggested the existence of a synergistic, "double hit" mechanism wherein the simultaneous administration of peptidoglycan (a TLR-2 agonist) and poly[I:C] resulted in enhanced expression of proinflammatory mediators (IL-1β, TNF-α, CCL5) relative to the response elicited by either agonist in isolation (Ilievski and Hirsch, 2010).

Two subsequent papers by Racicot et al. have provided additional and important insights into the potential role of viruses in PTB. First, using a mouse model, maternal infection with murine γ-herpesvirus 68 (MHV-68) was shown to downregulate cervical TLR expression and cytokine/chemokine expression, relative to uninfected control. Interestingly, this observation correlated with both reduced cytokine/chemokine expression and increased ascending (intrauterine) infection when MHV-68-infected animals were challenged with *E. coli* or *U. urealyticum*. The authors concluded by proposing a role for viral infections in making the female reproductive tract more permissible for the transcervical passage of PTB-associated bacteria (Racicot et al., 2013). Second, the authors demonstrated that inhibition of the interferon-β signaling pathway results in impaired control of LPS-driven proinflammatory changes. In trophoblast cells, MHV-68 downregulated two transcription factors, STAT3 and Twist1—changes consistent with increased expression of inflammatory mediators when combined with TLR-4 activation by LPS (Racicot et al., 2016). Based on these data, a viral infection may play multiple roles in predisposing a pregnancy to preterm labor; by making the cervix more permissible to the passage of invading bacteria, and by increasing the subsequent proinflammatory response at the maternal–fetal interface.

6.3 Viable Infection

As discussed, the use of viable, PTB-associated microorganisms to study fetal injury and inflammatory activation of the uterus presents a number of challenges. It also affords the opportunity to investigate the role

of infection in PTB and the efficacy of potential anti-microbial and antiinflammatory interventions. Model systems describing the use of viable *Ureaplasma* spp., oral microbes, and *Candida* spp. will be covered in the present section.

Some of the earliest studies into the effects *Ureaplasma* spp. on pregnancy well-being were undertaken in early gestation sheep by Ball et al. (1985). *Ureaplasma* spp. infection and intraamniotic inflammation has also been demonstrated in a baboon model (Yoder et al., 2003). We have developed a sheep model of intraamniotic *Ureaplasma* spp. infection wherein chronic (70 day) and acute (1, 3, and 7) day exposures can be initiated and then sequentially sampled using ultrasound-guided injections. Using this model, we have demonstrated that intraamniotic injection of *Ureaplasma* spp. in early pregnancy induced statistically significant increases in fetal lung IL-1β mRNA expression 6 and 10 weeks after administration (Moss et al., 2005). We have also demonstrated that *Ureaplasma* spp. elicits a robust inflammatory response in the fetal skin characterized by increases in TNF-α and MCP-1 expression, but no changes in IL-1β or IL-8 expression as recorded in response to LPS exposure (Kemp et al., 2011). These data indicate that *Ureaplasma* spp. induces a far more variable and subtle inflammatory response than purified LPS, an observation in agreement with data obtained from studies of PTB in humans. Lending weight to the association of *Ureaplasma* spp. with PTB, work Novy et al. (2009) in a macaque model demonstrated increases in cytokine, MMP, and prostaglandin expression along with enhanced uterine activity in response to intraamniotic administration of *U. parvum*.

As noted previously, *Ureaplasma* spp. are the microorganisms most commonly isolated from cases of PTB. Novy et al. (2009) employed a macaque model to investigate the fetomaternal responses to intrauterine infection with *U. parvum* and *Mycoplasma hominum* infection. They demonstrated a correlation between amniotic infection and elevated MMP-9 activity, increased amniotic fluid cytokines, prostaglandins (E2 and F2a), and chorioamnionitis (Novy et al., 2009). We have previously demonstrated similar findings including lung inflammation, chorioamnionitis, and inflammation of the fetal skin in response to intrauterine *U. parvum* infection in sheep (Kemp et al., 2011; Moss et al., 2005, 2008). These data are in agreement with clinical findings and support the hypothesis that *Ureaplasma* spp. and *Mycoplasma* spp. are key microorganisms in PTB.

Maternal treatment with the macrolide antibiotic erythromycin is a standard clinical intervention for *Ureaplasma* spp. infection. Attempts to prevent PTB with maternally administered antibiotics during the third trimester of pregnancy have proven largely ineffective.

Inappropriate antibiotic use, antibiotic resistance, and a lack of maternal–fetal transfer, and continued inflammatory activation by nonviable microbial agonist are all potential reasons for these disappointing results to date. The ORACLE II trial, for example, compared perinatal outcomes in 6295 women (in spontaneous preterm labor with intact membranes and no evidence of clinical infection) randomly assigned to maternal amoxicillin clavulanate (coamoxiclav) or erythromycin, or both, or placebo, 4 times daily, orally for up to 10 days. Approximately 90% of participants were enrolled in the third trimester of pregnancy. No improvement in primary outcome measure (a composite of neonatal death, chronic lung disease, or major cerebral abnormality) was associated with antibiotic use compared to placebo (Kenyon et al., 2001). In contrast, recent metaanalyses demonstrated a statistically significant reduction in the risk of early PTB and increased average gestational age at delivery when macrolide antibiotics were administered to women with bacterial vaginosis before 22 weeks' completed gestation (Lamont et al., 2011).

We hypothesized that the inability of maternally administered antibiotics to resolve PTB may be derived from a lack of placental transfer, rather than microbial resistance to the antimicrobial agents used. Using a chronically catheterized sheep model, we generated data in third trimester sheep pregnancies to demonstrate that maternally administered erythromycin failed to reach therapeutic levels in utero due to poor placental transfer. Maternal administration of erythromycin achieved therapeutic maternal plasma macrolide concentrations (<0.5 μg/mL) with low concentrations in amniotic fluid equivalent to less than 7% transfer; fetal plasma levels were even lower (<1.5% transfer). In contrast, maternal administration of azithromycin during the second trimester of pregnancy has been demonstrated to result in significant fetal tissue accumulation and plasma levels in the sheep model (Kemp et al., 2014). These data are in keeping with additional studies demonstrating the efficacy of macrolide antibiotics azithromycin and solithromycin in eradicating amniotic fluid *U. parvum* infection in a sheep model of pregnancy (Kemp et al., 2014). Grigsby et al. employed a chronically catheterized macaque model to similarly address the question of placental transfer of maternally administered azithromycin and the clearance of *U. parvum* serovar 1 from the amniotic sphere. *U. parvum* serovar 1-infected macaques received maternal intravenous azithromycin (12.5 mg/kg) twice daily for 10 days. Repeated dosing yielded amniotic fluid azithromycin levels similar to that of maternal plasma and effective clearance of *U. parvum* serovar 1 from the amniotic environment (Grigsby et al., 2009).

A number of investigators have used a mouse model of pregnancy to study the impact of *F. nucleatum* on

pregnancy outcomes (Han et al., 2004; Liu et al., 2007; Stockham et al., 2015). Han et al. used a CF-1 mouse model of pregnancy to induce a transient bacteremia by intravenously administering *F. nucleatum*, resulting in PTB, and fetal demise. The authors demonstrated that *F. nucleatum* preferentially colonized the uterus by invading blood vessel endothelial cells in the placenta, proliferating in the surrounding tissues, and subsequently gaining access to the amniotic cavity (Han et al., 2004). Subsequent work in TLR4$^{-/-}$ knockout mice suggested that TLR-4 plays a primary role in *F. nucleatum*-driven inflammation signaling, and that inflammation, rather than the microbe itself was likely the primary cause of fetal demise (Liu et al., 2007). *P. gingivalis* is also implicated as a PTB-associated pathogen of oral origin. Miyoshi et al. used a mouse model to generate a chronic (6 weeks) odontogenic *P. gingivalis* infection, and then mated the animals to assess the impact of infection on inflammation, contractile apparatus, and pregnancy outcomes. Having previously demonstrated an association between shortened gestation and *P. gingivalis* infection relative to control (18.3 ± 0.9 days vs. 20.5 ± 0.5 days, respectively) (Ao et al., 2015), *P. gingivalis* colonies were identified in villus cells and amniotic epithelial cells in association with two- to threefold increases in serum IL-1β and TNF-α, and significant increases in myometrial oxytocin receptor and connexion 43 mRNA (Miyoshi et al., 2016) at 18 days gestational age.

A small number of studies have also investigated the impact of intrauterine *C. albicans* infection on fetal well-being in a sheep model of pregnancy (Maneenil et al., 2015b; Ophelders et al., 2016; Payne et al., 2014b; Stock et al., 2016). In these studies, infection with *C. albicans* was accompanied by marked fetal inflammatory responses, increased amniotic fluid cytokines, fetal cardiac dysfunction, but a lack of chorioamnionitis in both mid-late and early gestation pregnancies, highlighting the highly nuanced and organism-specific nature of responses to intrauterine infection.

Studies in macaques have demonstrated the potential for using combined immunomodulating and antibacterial agents to simultaneously prevent preterm labor and downregulate in utero inflammation. Gravett and Sadowsky demonstrated that an intraamniotic infusion of the nonsteroidal antiinflammatory drug (NSAID) indomethancin suppressed uterine contractility (ostensibly via reduced prostaglandin expression in utero) in chronically catheterized macaques exposed to intraamniotic IL-1β. Interestingly, indomethacin did not resolve the amniotic fluid leukocytosis or levels of proinflammatory cytokines IL-1β, IL-8, or TNF-α (Sadowsky et al., 2000). Similar findings were derived from a subsequent study employing dexamethasone and IL-10 to control uterine contractility following IL-1β infusion in chronically

catheterized macaques (Sadowsky et al., 2003). More recently, the same investigators used ampicillin in conjunction with dexamethasone and indomethacin to successfully resolve Group B *Streptococcus* infection and limit the expression of IL-1β, TNF-α, prostaglandin E2 and F2α (Gravett et al., 2007). Despite this, chorioamnionitis was unresolved and the expression of MM-9 (a key agent in cervical remodeling and fetal membrane degradation) remained elevated.

7 SUMMARY

Animal models, including rodents, nonhuman primates, and sheep have played a key role over the past 2 decades in allowing the advancement our understanding of the pathophysiological mechanisms underlying PTB. These studies have: (1) demonstrated the proinflammatory role of microorganisms in human preterm labor, (2) provided clarification on the route(s) by which uterine infection may occur, (3) identified the innate immune signaling pathways involved in the induction of preterm labor via modulation of prostaglandin metabolism and structural alteration of the fetal membranes and the cervix, (4) demonstrated the importance of controlling fetomaternal inflammation, not just as a means of preventing PTB but also to protect the fetus, and (5) offered insight into how antibiotics and antiinflammatory agents may be used in combination to develop interventions for PTB.

8 PRACTICAL STUDY—FETAL SURGERY IN THE SHEEP

The sheep is a uniquely versatile model organism; its size, resistance to labor following surgery and inflammatory agonist exposure allows for the surgical isolation of maternal and fetal tissues and the chronic catheterization of maternal and fetal circulations and the amniotic cavity. The remainder of this chapter will focus on providing an introduction to a number of the key issues relating to performing aseptic, recovery surgery in pregnant sheep. This section will begin with a discussion of the perioperative management of sheep, and provide an introduction to the anesthetic and analgesic management of animals. An important point to note at this juncture is that rigorous perioperative management of pregnant sheep is as *absolutely critical* to the success of a surgical study as is the conduct of the surgery itself. In this regard, we cannot overemphasize the importance of gaining an appreciation for sheep behavior (both in flock and pen environments) to accurately assess animal welfare and analgesic requirements in the postoperative phase of a study.

8.1 Anesthesia of Pregnant Sheep

8.1.1 Planning

Preparation of pregnant sheep for general anesthesia and surgery begins well before the day of surgery: transport from the farm of origin and acclimatization to the research facility must be carefully planned to minimize the stress associated with a change in feed, climate, company, and daylight hours. Transport from the farm of origin or the field should be no later than 100 days gestation and pregnant sheep should not be starved prior to transport. The veterinary inspection prior to transport must include assessment of body condition score as underweight pregnant sheep are more prone to pregnancy toxemia.

8.1.1.1 INTRODUCTION TO THE ANIMAL FACILITY

The institutional procedures for introduction of sheep to the facility should be adhered to with particular emphasis on low stress handling of pregnant sheep. Communal pens will maintain the dynamics of the sheep group so they should be housed as such until the day prior to surgery. This acclimatization period should be at least 7 days. On the day prior to surgery the ewes should be introduced to single pens, which are large enough for them to turn around in. They should always have at least one other ewe adjacent to them. A sudden change of available feed may decrease caloric intake and this may be detrimental to the pregnant ewe and the fetus. Introducing the feed that will be available in the research facility at the farm of origin may help familiarize the sheep with the different substrate. The ration should be carefully calculated to ensure it meets the requirements of pregnancy and decreases the risk of metabolic disorders.

8.1.1.2 PREGNANCY TOXEMIA

Pregnancy toxemia is a potentially fatal metabolic disorder of glucose and fat metabolism in sheep, which usually occurs spontaneously in the last 3 weeks before parturition (Schlumbohm and Harmeyer, 2008). While ewes with multiple fetuses are more commonly affected, the disease can occur in singleton pregnancies as well. The clinical signs of the disease may take a few days to develop and include weakness, drowsiness, sluggish behavior, and apparent blindness. These signs may deteriorate to recumbency, tremors, spasms, and death. A combination of low plasma glucose concentration and increased plasma concentration of ketone bodies characterize the disease (Van Saun, 2000) and occur as a result of inadequate energy intake in the face of growing energy demands of the developing fetus(es). The pathophysiology, however, is complex and several preventative measures must be taken to reduce the risk of this disease. Preventative measures include: avoid interruptions to feed intake (e.g., transport-associated stress), ensure a suitable body condition score prior to transport, utilize singleton ewes where possible, and monitor food intake during the acclimatization period. Treatment is more likely to be successful if a timely diagnosis is made and an energy source is administered to sick animals (Brozos et al., 2011). Oral or injectable glucose solutions can be administered in the short term but veterinary advice should be sought urgently.

8.1.1.3 HYPOCALCEMIA

An increase in calcium demand by a fetus may overwhelm the ewe's calcium homeostasis mechanisms and cause a drop in plasma calcium concentration (Larsen et al., 1986). Late pregnant ewes are particularly susceptible to this metabolic disorder and prompt and aggressive treatment may be required. The clinical signs of hypocalcemia usually develop relatively rapidly and include tremors, a stilted gait and generalized weakness. Death may ensue within hours. Preventative measures should always be considered when working with pregnant sheep: avoid interruptions to feed intake (e.g., transport-associated stress) and supplement calcium, especially if the diet is low in calcium. Oral administration of a calcium solution, such as Unimix (The Mackinnon Project, Werribee, Victoria, Australia) prior to transport or as part of the introduction to the facility has been incorporated into the standard operating procedures of the authors' institution to decrease the risk of hypocalcemia. The pathophysiology of this metabolic disorder is complex and treatment should be administered promptly and in accordance with veterinary advice. Hypocalcemia is potentially fatal and as it often occurs as a result of nutritional stress, it is commonly associated with pregnancy toxemia. Preventative measures taken for one disease, invariably apply to both.

8.1.1.4 LAMINITIS

As sheep transition from a farm environment to a research facility their diet changes from a cellulose-based diet to a more readily digestible starch-based diet. If this change is abrupt ruminal acidosis may develop. Ruminal acidosis may manifest as laminitis, which is a painful condition of the hooves. Laminitis refers to inflammation of the laminae of the hoof wall and presents with reluctance to stand or move. The hooves may feel warm and the animal may overreact to pressure applied to this area. The condition is painful so, while the underlying cause should be addressed, the administration of analgesia is essential. Treatment of

the underlying cause is focused on modification of the diet to increase the intake of lucerne hay and chaff (at least matchstick length) and limit the intake of grain or pelleted feed. Oral sodium bicarbonate may be administered under veterinary direction to alter the pH of the rumen. For analgesia buprenorphine is suitable and a single dose of a nonsteroidal antiinflammatory may be appropriate. Analgesia should be administered under veterinary direction.

8.1.2 Anesthetic Considerations for Pregnant Sheep

General anesthesia causes a range of major physiological alterations and in combination with pregnancy there are a number of specific considerations, which require attention when planning anesthesia for pregnant animals. These considerations relate to the global increase in oxygen consumption and decreased functional residual capacity of the lung during pregnancy. Furthermore, during pregnancy, the mean arterial blood pressure (ABP) is lower and the heart rate and cardiac output are higher than during the nonpregnant state. Pregnant animals also have an increased blood volume and a dilutional anemia. These changes contribute to an increased risk of hypotension, hypercapnia, and hypoxemia during general anesthesia. It is important that these physiological parameters are monitored and managed for the well-being of both the ewe and the fetus.

8.1.3 Preanesthetic Preparation, Assessment, and Premedication

Preanesthetic fasting is routine for ruminants but during pregnancy it is preferable to maintain caloric intake prior to anesthesia and allow access to food and water up until the administration of preanesthetic medication. This approach will minimize the risk of perioperative pregnancy toxemia and hypocalcemia, and will contribute to an uneventful recovery from anesthesia and surgery. However, the anesthetic complications associated with a full rumen include: regurgitation of rumen contents and the risk of aspiration; rumen bloat; a decrease in functional residual capacity as a result of the weight of the rumen on the diaphragm, especially in dorsal recumbency; hypoventilation; and decreased cardiac output due to decreased venous return. These potential complications can be managed by ensuring placement of an appropriately sized cuffed endotracheal tube promptly after induction of anesthesia, monitoring, and management of rumen bloat, intermittent positive pressure ventilation during anesthesia and appropriate cardiovascular support during anesthesia (e.g., intravenous fluid therapy).

On the morning of anesthesia and surgery, the ewe should be examined. This preanesthetic assessment should include observation of the ewe from a distance to subjectively assess demeanor, comfort, and gait. Objective measurements of rectal body temperature, heart rate, respiratory rate, and character should also be made. If the preanesthetic assessment is satisfactory a tranquilizing combination of drugs should be administered as a "premed." This preanesthetic medication provides anxiolysis, mild tranquilization, and preemptive analgesia and will facilitate a smoother induction of and recovery from anesthesia. Premedication should also make physical restraint for placement of an intravenous catheter less stressful for both the ewe and personnel. The premedication combination of drugs should be administered by intramuscular (IM) injection 30–40 min prior to induction of anesthesia unless α_2 adrenoreceptor agonist drugs are being used. In this case the premed can be given just 10–15 min prior to induction of anesthesia. It is best to leave the ewe in the same room as other ewes until the latest possible moment. Isolating her will cause significant stress. The induction of anesthesia should occur a short distance from the housing area to minimize the stress of being alone. Table 30.1 includes drugs that can be used for premedication. The dose of drugs should be calculated according to lean body mass. If the sheep have significant wool growth then this should be considered when estimating their actual weight from the weight given by reliable scales.

8.1.4 Induction of Anesthesia

Following premedication, the ewe should be tranquilized or sedated, and can be transported to the anesthetic induction area. The ewe should be restrained in the "shearing position" (Fig. 30.1A). The wool over the cephalic vein should be clipped and the site prepared for aseptic placement of an intravenous catheter. The person restraining the ewe will occlude the vein by placing pressure over it as it traverses the radius and ulna, close to the elbow joint (Fig. 30.1B). This occlusion will "raise" the vein to facilitate identification and catheterization. An 18 gauge catheter can be placed in most pregnant ewes (Fig. 30.1C). The catheter should be secured in place with adhesive tape and flushed with 3–5 mL of heparinized saline (5 IU/mL heparin in 0.9% NaCl).

Once the catheter is placed, secured and flushed intravenous anesthetic induction drugs can be administered. Drugs that can be used for induction of anesthesia are listed in Table 30.2. Immediately after induction of anesthesia, an oral endotracheal tube is placed. The positioning of the ewe is important to ensure that saliva or regurgitated rumen contents are not aspirated. The neck should be extended and the tongue must be withdrawn (Fig. 30.2A). A laryngoscope is used to facilitate placement of the endotracheal tube by optimizing the view of the larynx. A long straight laryngoscope blade is used

TABLE 30.1 Premedicant Drugs for Use in Pregnant Sheep Prior to General Anesthesia

Drugs	Dose	Comments
Acetylpromazine (phenothiazine tranquilizer)	0.01–0.04 mg/kg SC or IM	Mild tranquilizer when used alone, moderate tranquilizer when used in combination with an opioid
		Causes a dose-dependent decrease in arterial blood pressure due to vasodilation
		Long duration of action (~6 h)
Buprenorphine (partial μ agonist opioid)	0.01–0.02 mg/kg IM	Moderate tranquilization occurs when combined with acepromazine
		Provides preemptive analgesia
		Long duration of action (~6–8 h)
Morphine (pure μ agonist opioid)	0.1–0.3 mg/kg IM	Moderate tranquilization occurs when combined with acepromazine
		Provides preemptive analgesia
		Moderate duration of action (~2–4 h).
Xylazine (α₂ adrenoreceptor agonist)	0.1–0.3 mg/kg IM	Heavy sedation, especially when combined with an opioid
		Provides some analgesia.
		May cause pulmonary edema in sheep
		Short duration of action (~1 h).
		Side effects include hyperglycemia, hypotension, hypoxemia, and cardiac arrhythmias
		Can be reversed with yohimbine or atipamezole
Medetomidine (α₂ adrenoreceptor agonist)	10–30 μg/kg IM	Heavy sedation, especially when combined with an opioid
		Provides some analgesia
		May cause pulmonary edema in sheep
		Short duration of action (~1 h).
		Side effects include hyperglycemia, hypotension, hypoxemia, and cardiac arrhythmias
		Can be reversed with yohimbine or atipamezole

IM, Intramuscular; SC, subcutaneous.

and the tip of the blade is positioned to depress the base of the tongue and allow a good view of the arytenoid cartilages. The endotracheal tube must have an inflatable cuff to create a seal within the lumen of the trachea. An 8–8.5 mm cuffed endotracheal tube is appropriate for a 50–60 kg ewe.

To confirm correct placement of the endotracheal tube in the trachea, there are a few tests which should be performed: visualize the passage of the endotracheal tube over the epiglottis and between the arytenoid cartilages, attach a capnograph to ensure carbon dioxide is detected during expiration, observe condensation on the inside of the tube, observe the displacement of wool fibers held at the end of the tube during inspiration and expiration. Once correct placement is confirmed, secure the tube in place with a gauze tie and inflate the cuff. Do not move the animal until the tube is secured and the cuff has been inflated.

To optimize conditions for successful tracheal intubation, the animal must be adequately anesthetized. Trauma to the larynx, laryngospasm, and laryngeal edema are all more likely if the patient is inadequately anesthetized. Consider giving more of the intravenous induction agent or, in the instance of using midazolam or diazepam and ketamine, wait another 15–30 s to allow the drugs to have their full effect. A long straight blade laryngoscope with a light is also essential in this species. The position of the neck has been discussed but subtle changes can alter the view of the larynx considerably so instruct the person restraining the animal accordingly. Suction may also be helpful as saliva can accumulate around the larynx if there is a delay to intubation. Regurgitated rumen material can also present a risk of aspiration, but the potential for active regurgitation is less if the depth of anesthesia is adequate.

8.1.5 Maintenance of Anesthesia

The best option for maintenance of anesthesia in pregnant sheep is delivery of an inhalational anesthetic agent, such as isoflurane or sevoflurane in 100% oxygen. An anesthetic machine with a circle breathing system and a mechanical ventilator is required and this should be assembled and leak tested prior to induction of anesthesia.
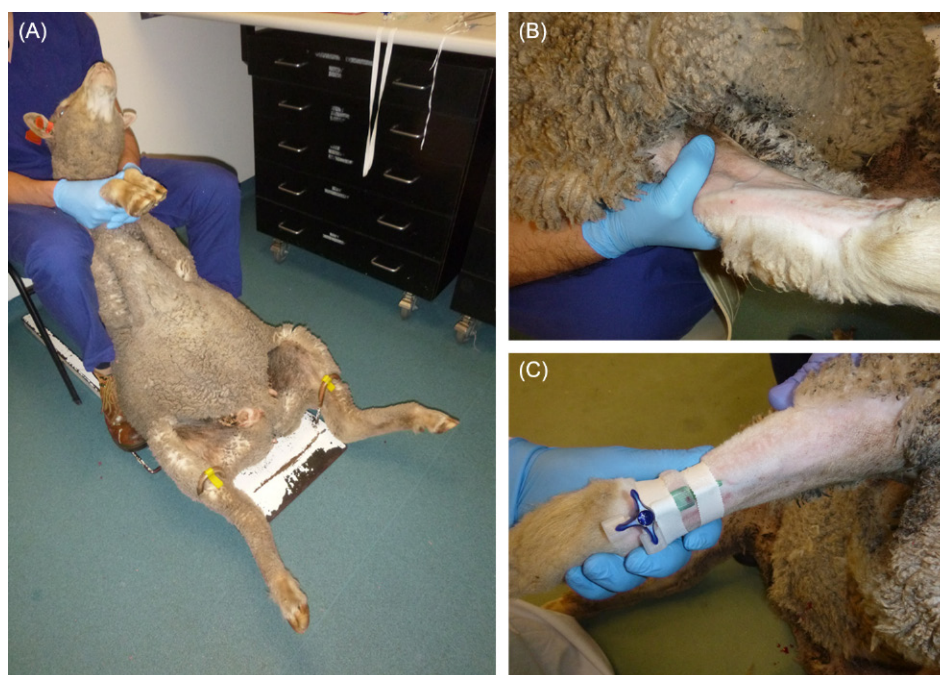
FIGURE 30.1   (A) Restraint in the "shearing position." (B) An assistant occludes the cephalic vein to facilitate identification of the vessel and placement of the intravenous catheter. (C) An intravenous catheter placed in a cephalic vein for administration of anesthetic induction drugs and intraoperative fluid therapy.

The breathing system is connected to the endotracheal tube and an initial fresh gas flow of 2 L/min and an appropriate vaporizer setting should be set. The vaporizer setting should then be adjusted according to clinical assessment of anesthetic depth with an understanding of the physicochemical properties of the agent being used (Table 30.3). Maintenance of anesthesia at 1.5 x MAC is standard.

The use of nitrous oxide as part of the carrier gas for sheep is controversial. Nitrous oxide has a very low blood:gas partition coefficient so rapidly moves from the blood to gas filled cavities in the body, including the

TABLE 30.2   Anesthetic Induction Drugs for Use in Pregnant Sheep. The Authors' Preference is Midazolam or Diazepam and Ketamine

Drugs	Dose	Comments
Propofol (phenol)	4–6 mg/kg IV	No analgesia
		Rapid onset and short duration of action
		Postinduction apnea may occur for 3–5 min
		May cause a decrease in blood pressure due to vasodilation
Alfaxalone (steroid anaesthetic)	1–2 mg/kg IV	No analgesia
		Rapid onset and short duration of action
		Postinduction apnea may occur for 3–5 min
		May cause a decrease in blood pressure due to vasodilation.
Midazolam or diazepam and ketamine (benzodiazepine and a dissociative anaesthetic)	0.25 and 5 mg/kg IV	Delayed onset of action (~30–60 s)
		Ketamine has analgesic properties
		Maintenance of heart rate and blood pressure
Thiopentone (barbiturate)	6–10 mg/kg IV	No analgesia
		Rapid onset of action
		May cause a decrease in blood pressure due to vasodilation
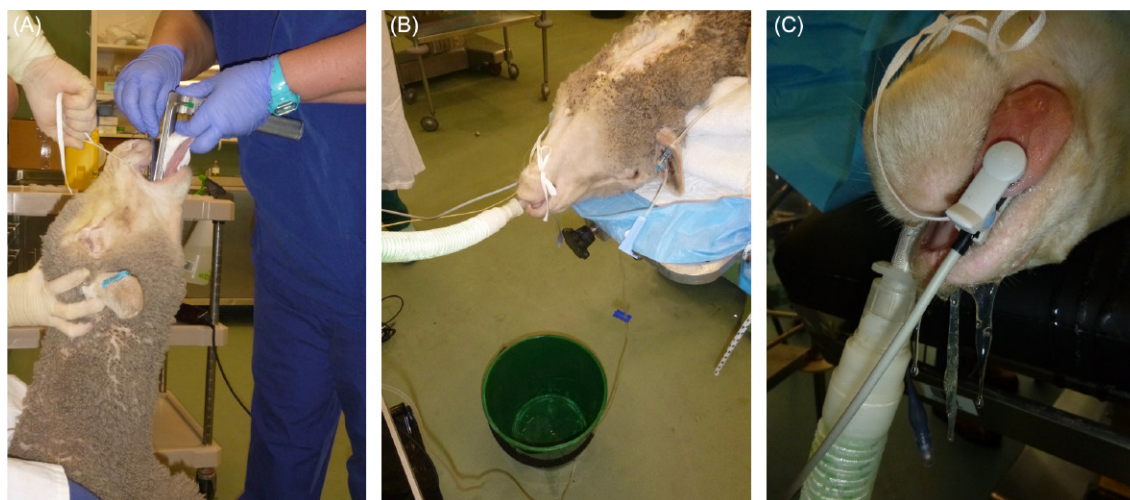
FIGURE 30.2   (A) Placement of an endotracheal tube after induction of anesthesia. The neck is extended and the tongue is withdrawn. A long straight bladed laryngoscope is used to help visualize the larynx. (B) Positioning of the head and neck during general anesthesia is essential to facilitate drainage of saliva and regurgitated material away from the larynx. A bucket is used to collect this fluid, which may be a significant volume after 2 h of anesthesia. (C) Profuse salivation is normal for sheep.

rumen. Given this property of nitrous oxide there is a theoretical concern, at least, that the inclusion of nitrous oxide in the carrier gas will exacerbate rumen bloat and compromise both venous return to the heart and therefore cardiac output, and decrease the functional residual capacity of the lungs. The argument for using nitrous oxide is that through the second gas effect it will increase the speed of uptake of other inhalant anesthetic drugs, such as isoflurane, and it may have analgesic properties. If nitrous oxide is included in the carrier gas, it should be no more than 70% and no less than 50% of the fresh gas flow. Hypoxemia is a common complication of general anesthesia in pregnant sheep so 100% oxygen as the carrier gas is often required, precluding the use of nitrous oxide.

8.1.5.1 MECHANICAL VENTILATION

Intermittent positive pressure ventilation during general anesthesia of pregnant sheep will achieve a stable plane of anesthesia, adequate oxygenation, and ventilation and

TABLE 30.3   Physical and Chemical Properties of Isoflurane and Sevoflurane in Pregnant Sheep

Physicochemical property	Isoflurane	Sevoflurane
MAC (%) in pregnant sheep (Okutomi et al., 2009)	1.02 ± 0.19	1.52 ± 0.15
Blood:Gas partition coefficient	1.46	0.68
Boiling point (°C)	49	59
Saturated vapor pressure at 20°C (mmHg)	240	160

may help prevent lung collapse associated with positioning (Dugdale, 2007). It is routine to use a mechanical ventilator throughout anesthesia to achieve normocapnia and prevent hypoxemia. Ventilator settings will vary between models but delivering a tidal volume between 10 and 15 mL/kg to a peak inspiratory pressure no greater than 20–25 cmH$_2$O at a rate to achieve normocapnia (end-tidal CO$_2$ of 35–45 or ~4.6–5.8 kPa) should be appropriate for the majority of animals (Davis and Musk, 2014). Monitoring the adequacy of ventilation is covered in Section 9.13.

Efficient mechanical ventilation will only be possible if the animal is adequately anesthetized. If resistance to breaths is observed (bucking the ventilator), the depth of anesthesia should be assessed carefully and adjusted accordingly. Neuromuscular blockade may be required, but in this species it is not usually necessary. Atracurium and pancuronium are nondepolarizing neuromuscular blocking agents that could be used for this purpose. These drugs should only be administered by personnel familiar with their clinical effects, when adequate monitoring of the depth of anesthesia can be performed, and when intermittent positive pressure ventilation can be provided.

8.1.5.2 INTRAVENOUS FLUID THERAPY

Fluids are administered during general anesthesia to expand the blood volume and offset drug-mediated vasodilation, replace losses associated with surgery or exposure of body cavities, and provide maintenance needs. A balanced electrolyte crystalloid solution is usually sufficient (e.g., Hartmann's or lactated Ringer's solution) when delivered at 10 mL/kg/h during anesthesia. If the animal is hypotensive or there is significant hemorrhage

associated with the surgical procedure, a higher infusion rate of the crystalloid should be administered and a colloid solution may be indicated. Colloids are starch, gelatin, or dextrans in origin and have the advantage of more prolonged plasma volume expansion when compared to crystalloids. The infusion rate of a colloid is lower than that of a crystalloid (2–5 mL/kg/h). Crystalloids and colloids can be given concurrently but if large volumes are required a second intravenous catheter may be useful. Consider catheterizing the other cephalic vein or the jugular vein. Blood pressure should be monitored throughout anesthesia and the infusion rate of fluids adjusted accordingly.

8.1.5.3 POSITIONING

The surgical procedure will usually dictate the position in which the animal is placed for the majority of the anesthetic. Invariably dorsal recumbency is required but this position predisposes the animal to hypotension and a decrease in the functional residual capacity of the lungs. Monitoring and managing blood pressure and ventilation is important during anesthesia, but especially during positioning in dorsal recumbency. Given the propensity for ruminants to salivate it is important to position the animal to prevent saliva entering the larynx by lowering the head or creating an uphill gradient to the pharynx to prevent accumulation of fluids around the cuff of the endotracheal tube (Fig. 30.2B). Creating a passage for drainage of these secretions and any regurgitated material is essential (Fig. 30.2C). It is also important to avoid hyperextension of the hips and shoulders during positioning on the surgery table.

8.1.5.4 MONITORING ANESTHESIA

The ultimate aims during anesthesia are to ensure an adequate depth of anesthesia, the provision of appropriate analgesia and maintenance of oxygen delivery to ensure cells and tissues can continue functioning normally. This approach can be considered as monitoring the central nervous system, the cardiovascular system (delivering blood to the tissues) and the respiratory system (adding oxygen and removing carbon dioxide from the circulation). Analgesia will be discussed in the next section.

8.1.5.5 ASSESSMENT OF DEPTH OF ANESTHESIA

Monitoring central nervous system depression is essential during anesthesia. Electroencephalography (EEG) may be one of the most extensively utilized methods for objective evaluation of the state of responsiveness of the central nervous system and is considered the most direct indicator of central nervous system depression (Serfontein, 2010). There is, however, considerable variation between species and the EEG changes associated with different drugs may also complicate interpretation. Recent work suggests that the EEG can be relied upon in sheep to determine depth of anesthesia (Otto et al., 2012) but in the majority of environments assessing the depth of anesthesia will be a subjective exercise.

There are a number of observations to make when undertaking subjective assessment of anesthetic depth in sheep: palpebral (blink) reflex, muscle tone, eye position, and tongue withdrawal. At an adequate depth of anesthesia, there should be a sluggish palpebral reflex when the medial commissure of the eyelids is gently stimulated. The muscles should be relaxed without any resistance to manipulation. During a laparotomy an anesthetist has access to the head so testing jaw tone is helpful to determine the muscle tone of the masseter muscles. The position of the eye will change during anesthesia and although it can be difficult to interpret when an animal is in dorsal recumbency the basic pattern is that the eye is in a central position initially and rotates ventrally during anesthesia. It will return to the central position if the depth of anesthesia is too deep or if the animal is waking up. Lastly, tongue withdrawal can easily be checked regularly. The tongue should be relaxed at an adequate depth of anesthesia. When assessing depth of anesthesia by these subjective techniques, it is essential to evaluate more than one parameter before deciding whether the depth of anesthesia is adequate.

8.1.5.6 CARDIOVASCULAR PERFORMANCE

The overall aim of monitoring and managing the cardiovascular and respiratory systems during anesthesia is to ensure that the oxygen supply to the tissues exceeds the oxygen demand of the tissues. If oxygen delivery (DO_2) is a product of the cardiac output (CO) and the oxygen content of arterial blood (CaO_2) then maintaining these two parameters is essential. Measuring the cardiac output is not routinely performed during anesthesia as it is a technically challenging technique that is relatively invasive and expensive. As a surrogate for cardiac output, ABP is measured. If CO = heart rate × stroke volume and ABP = CO × total peripheral resistance, we can see that measuring the heart rate and ABP during anesthesia can indirectly indicate the adequacy of cardiac output. During anesthesia pregnant ewes may be anemic so CaO_2 may be lower than normal (Musk and Kemp, 2016). Low CaO_2 will compromise DO_2 so it is especially important that CO is monitored and managed.

The heart rate can be measured with an electrocardiograph (ECG) and the pulse rate can be measured with a pulse oximeter. The ECG displays the electrical activity of the heart and is used to assess heart rate and rhythm. The pulse oximeter measures oxyhemoglobin saturation and pulse rate. The normal heart rate of a pregnant sheep during anesthesia will vary according to anesthetic and

TABLE 30.4 Factors Affecting the Heart Rate During Anesthesia

Change in heart rate	Cause	Management
Increase	Inadequate depth of anesthesia: "too light"	Assess depth of anesthesia and deliver more anesthetic agent (intravenous or inhalant drugs) if appropriate. Check endotracheal tube position and cuff
	Inadequate analgesia	Assess depth of anesthesia and if adequately anesthetized, administer more analgesia
	Hypotension	Isotonic crystalloids: initiate intravenous fluid therapy (10 mL/kg/h) or deliver a bolus of (40–80 mL/kg/h) for 10–15 min
		Colloids: deliver 2–10 mL/kg/h of gel or starch-based colloid
	Hypovolemia	Isotonic crystalloids: initiate intravenous fluid therapy (10 mL/kg/h) or deliver a bolus of (40–80 mL/kg/h) for 10–15 min
		Colloids: deliver 2–10 mL/kg/h of gel or starch-based colloid
	Hypercapnia	Initiate mechanical ventilation or adjust ventilation parameters to achieve normocapnia
	Hypoxemia (early)	Mechanical ventilation with 100% oxygen and positive end-expiratory pressure (PEEP)
	Drugs	Ketamine may cause a transient tachycardia after induction of anesthesia
Decrease	Excessive depth of anesthesia: "too deep"	Assess depth of anesthesia and adjust delivery of anaesthetic drugs accordingly
	Overdose of analgesic drugs (especially opioids)	Administer atropine (0.02 mg/kg) or glycopyrrolate (0.01 mg/kg) IV
	Hypertension	Stop IV fluids
	Hypervolemia	Stop IV fluids
	Hypoxemia (advanced)	Mechanical ventilation with 100% oxygen and PEEP
	Hypothermia	Check core body temperature and provide insulation, circulating warm air blankets, hot water bottles, heat pads, heat lamps, warm IV fluids
	Overdose of alpha 2 adrenoreceptor agonist drugs (e.g., xylazine)	Administer atipamezole (5 µg/kg) IM

analgesic protocol employed but should be between 70 and 100 beats/min. Alterations in the heart rate can be caused by a number of different factors (Table 30.4).

ABP can be measured noninvasively with either an oscillometric technique or a Doppler technique. The former measures systolic, mean, and diastolic ABP while the latter measures systolic ABP only. The aim is to maintain mean ABP over 60 mmHg or the systolic ABP over 90 mmHg. It is important to familiarize yourself with your equipment to ensure accurate measurements are made and appropriate therapy is instituted. The gold standard of ABP measurement is an invasive technique where a catheter is placed in a peripheral artery, connected by a fluid filled tube to a transducer, and converted to an electrical signal. Invasive ABP measurement is the most accurate method for the measurement of ABP and should be considered if the duration of anesthesia is likely to be greater than 1 h.

The most common alteration to ABP is hypotension and in turn, the most common cause of hypotension is vasodilation induced by inhalant anesthetics (especially isoflurane). Decreasing inhalant anesthetic requirements can be achieved with premedication, as discussed previously and appropriate analgesia. The management of hypotension is usually most successful with IV fluid therapy. Isotonic crystalloids should be delivered at 10 mL/kg/h during anesthesia but the rate of administration can be increased up to 80 mL/kg/h for a brief period if required. Colloid infusions can be given concurrently (2–5 mL/kg/h). The most common causes of hypotension are presented in Table 30.5.

8.1.6 Respiratory Performance

The adequacy of ventilation is best assessed by measuring the partial pressure of CO_2 in arterial blood ($PaCO_2$). Alternatively, end-tidal CO_2 can be measured as a noninvasive estimate of $PaCO_2$. In the absence of significant lung collapse or compromise to pulmonary perfusion, the measurement of end-tidal CO_2 by capnography gives a good indication of the adequacy of

TABLE 30.5   Factors Affecting Blood Pressure During Anesthesia

Change in blood pressure	Cause	Management
Increase	Inadequate depth of anesthesia: "too light"	Assess depth of anesthesia and deliver more anesthetic agent (intravenous or inhalant drugs) if appropriate. Check endotracheal tube position and cuff
	Inadequate analgesia	Assess depth of anesthesia and if adequately anesthetized, administer more analgesia
	Hypervolemia	Stop IV fluid therapy
	Hypercapnia	Initiate mechanical ventilation or adjust ventilation parameters to achieve normocapnia
Decrease	Excessive depth of anesthesia: "too deep"	Assess depth of anesthesia and adjust delivery of anesthetic drugs accordingly
	Bradycardia	Check heart rate and/or pulse rate and administer atropine (0.02 mg/kg) IV or glycopyrrolate (0.01 mg/kg) IV if the heart rate is below 50 beats/min
	Overdose of alpha 2 adrenoreceptor agonist drugs (e.g., xylazine)	Administer atipamezole (5 μg/kg) IM
	Hypovolemia	Isotonic crystalloids: initiate intravenous fluid therapy (10 mL/kg/h) or deliver a bolus of (40–80 mL/kg/h) for 10–15 min
		Colloids: deliver 2–5 mL/kg/h of gel- or starch-based colloid

ventilation (Bilbrough, 2006). End-tidal CO_2 should be between 35 and 45 mmHg (~4.6–5.8 kPa). If the $PaCO_2$ increases ventilation is inadequate and if it decreases ventilation is excessive (Table 30.6).

Oxygenation should also be monitored during anesthesia. Pulse oximetry is a noninvasive method for assessing oxyhemoglobin saturation (Quinn et al., 2013) and is useful as an indicator of peripheral perfusion and oxygenation. The normal oxyhemoglobin saturation (SpO_2) is above 95% and if it decreases it is essential to determine if the reading is accurate. To obtain a reliable reading, the pulse oximeter must be positioned on a nonpigmented and hairless tissue. The tongue is an ideal site. Factors that interfere with the accuracy of the reading include: vasoconstriction, pigment, theatre lights, movement, and hypotension. If the carrier gas for inhalant anesthesia is 100% oxygen, a decrease in SpO_2 will be a late indicator of respiratory compromise. Pulse oximetry is, in fact, best used to monitor peripheral perfusion.

Arterial blood gas analyses are the best method for assessing the physiological status of the ewe. These analyses provide information about the acid base status of the ewe and the blood gases carbon dioxide and oxygen. This information is invaluable for guiding the management of ventilation and fluid therapy during anesthesia. These data will also help in determinations about fetal health

TABLE 30.6   Alterations in Ventilation May Occur During General Anesthesia and Should be Managed Appropriately

Change in end-tidal CO_2	Cause	Management
Increase due to hypoventilation (decreased minute volume)	Excessive depth of anesthesia: "too deep"	Assess anesthetic depth and decrease anesthetic drug delivery if possible
	Dorsal recumbency	Mechanical ventilation. Minimize the duration of time in this position
	Pressure of the gravid uterus on the diaphragm	Mechanical ventilation. Tilt the table to decrease pressure on the diaphragm.
Decrease due to hyperventilation (increased minute volume)	Inadequate depth of anesthesia: "too light"	Assess anesthetic depth and administer more anesthetic drugs
	Inadequate analgesia	If depth of anesthesia is appropriate, more analgesia may be required
	Hypoxemia	Mechanical ventilation with 100% oxygen and PEEP

(Musk and Kemp, 2016). Arterial blood samples can be collected from the radial artery of the ewe through a pre-placed catheter or from a single needle-stick sample.

8.1.6.1 RECOVERY FROM ANESTHESIA

Ruminants present a number of challenges during the recovery phase of anesthesia. Their propensity for regurgitation and salivation becomes particularly problematic when the endotracheal tube is removed and the airway is no longer protected. The primary challenge during this time is to prevent aspiration of such fluids. Returning the animal to a more physiologically normal position is important to facilitate eructation and the expulsion of gas from the rumen. Positioning in "sternal recumbency" will also support spontaneous ventilation. The endotracheal tube should be removed when the animal is observed to swallow. The return of this reflex indicates the animal is able to protect the airway and aspiration is less likely. It is worth having equipment on hand to reintubate a sheep if they develop an upper respiratory tract obstruction following extubation. This equipment should be kept in the area where sheep are recovered from anesthesia and surgery, and be readily available in the event of a crisis. Anesthetic drugs for induction of anesthesia, heparinized saline, a laryngoscope, and endotracheal tube are the basic necessities. An ambu bag will enable ventilation on room air if required. A syringe to inflate the cuff of the endotracheal tube and a gauze tie to secure it in place will also be useful. Food and water should be offered as soon as possible and in the author's experience sheep that have received appropriate analgesia will eat within 30 min of recovery from anesthesia.

8.1.7 Analgesia

Sheep have evolved to hide signs of pain. Pain assessment is difficult in any species, but this instinctive behavior to conceal pain makes the provision of analgesia particularly challenging. Nevertheless, analgesia must be provided if an animal has undergone a surgical procedure. There are important ethical and moral obligations, which ensure the administration of analgesic drugs and techniques that are appropriate to the species, the procedure that has been performed and the circumstances in which it has been performed (Australian Government, 2013). This remit is difficult to achieve in sheep as there is not an extensive scientific database from which to draw sound conclusion. Furthermore, there are no validated pain scoring systems, which reliably indicate the severity of pain a sheep may be experiencing. With these limitations in mind a multi-modal analgesic approach is prudent. In the perioperative period, analgesia can be provided by administering drugs from the following drug classes: opioids; NSAIDs; local or regional anesthetic drugs; alpha 2 adrenoreceptor agonist

drugs; and other miscellaneous drugs, such as ketamine and tramadol. The efficacy of opioids in sheep is controversial and while there is little convincing data to support or refute their use for acute surgical pain, the author includes these drugs in perioperative analgesic protocols as part of the premed and for postoperative analgesia (Musk et al., 2014). Transdermal fentanyl delivery in pregnant sheep has been described and is part of the author's multimodal analgesia regime for pregnant sheep undergoing anesthesia and surgery (Heikkinen et al., 2015; Musk et al., 2014). There is a significant body of evidence regarding the danger of NSAID use in a range of species, during pregnancy, as theoretically these drugs may cause premature closure of the ductus arteriosus (Baragatti et al., 2003; Van Overmeire and Chemtob, 2005). This side effect may be fatal for the fetus and the author therefore excludes this class of drug from perioperative analgesia protocols for pregnant sheep. Local anesthetic drugs are commonly used in sheep for regional anesthesia and analgesia (Harris, 1991; Hodgkinson and Dawson, 2007) and should always be considered as part of a multimodal analgesic regime. Local anesthetic drugs should be administered preemptively to optimize their effects. Alpha 2 adrenoreceptor agonists are commonly used in sheep (Grant and Upton, 2001, 2004; Grant et al., 2001; Kastner et al., 2003; Murdoch et al., 2013). They are perhaps the most extensively studied class of analgesic drugs in sheep but have significant side effects, which must be understood. These side effects are dose dependent and include peripheral vasoconstriction, bradycardia, hypoxemia, and uterine muscle contraction. Ketamine is a drug with analgesic properties that may be used as part of the anesthetic induction protocol and/or infused during surgery for both analgesia and anesthetic sparing effects. The cardiovascular and respiratory side effects of ketamine are unlikely to have detrimental effects on uterine blood flow (Strumper et al., 2004). Finally, tramadol has also been used in sheep for its opioid analgesic effects and could be considered an option for chronic pain management.

Combining analgesic drugs from different classes (multimodal analgesia) will decrease the dose of each individual drug, thus enhance the effects, and decrease the potential for adverse side effects of the drugs. Furthermore, multimodal analgesia targets the pain pathway at multiple sites and mitigates pain more effectively than using an analgesic drug from a single class. As more research is conducted in sheep, valuable data about pain assessment and efficacy of analgesic drugs data will enable more evidence-based decision-making in this species. Until then the pharmacokinetic and pharmacodynamic data of a drug should form the basis of analgesia regimes. Table 30.7 includes some analgesic drugs for consideration in pregnant sheep.

Pain assessment must form part of any analgesic protocol. Ideally, pain should be assessed before and after the administration of analgesic drugs to determine the

TABLE 30.7   Analgesic Drugs for Use in Pregnant Sheep

Drug	Dose and route of administration	Side effects
Buprenorphine (partial μ agonist opioid)	0.01–0.02 mg/kg IM	Moderate tranquilization occurs when combined with acepromazine
	Long duration of action (~6–8 h)	Bradycardia at high doses
Morphine (pure μ agonist opioid)	0.1–0.3 mg/kg IM	Moderate tranquilization occurs when combined with acepromazine
	Moderate duration of action (~2–4 h)	Bradycardia at high doses
Fentanyl (pure μ agonist opioid)	0.1–0.3 μg/kg/min IV	Bradycardia and respiratory depression
	1–2 μg/kg/h transdermal (allow 12–24 h to achieve therapeutic plasma concentrations)	
Lidocaine (local anesthetic)	Up to 5 mg/kg infiltration at the surgical site	Rare unless given IV
	Short duration of action (~1 h)	Hypotension, tachycardia, cardiac arrhythmias, seizures
Bupivacaine (local anaesthetic)	Up to 2 mg/kg infiltration at the surgical site	Rare unless given IV
	Long duration of action (~6 h)	Cardiac arrhythmias, seizures, death.
Xylazine (alpha 2 adrenoreceptor agonist)	0.1 mg/kg then 0.04 mg/kg/h IV (Grant et al., 2001)	Dose-dependent sedation, hyperglycemia, hypotension, hypoxemia, cardiac arrhythmias
		Can be reversed with yohimbine or atipamezole
Medetomidine (α_2 adrenoreceptor agonist)	1–3 μg/kg/h IV	Dose-dependent sedation, hyperglycemia, hypotension, hypoxemia, cardiac arrhythmias
		Can be reversed with yohimbine or atipamezole
Ketamine (N-methyl-D-aspartate antagonist)	2–5 μg/kg/min IV	Tachycardia and hypertension

analgesic requirements and response to therapy. Objective assessments of pain include changes in physiology (e.g., alterations in the heart rate and circulating plasma cortisol) and nociceptive threshold testing (Musk et al., 2014) while subjective assessments rely upon observations of behavior. Understanding the normal behavior of sheep (in a specific environment) is essential for the identification and interpretation of abnormal behaviors. A composite pain score assessing a combination of physiological and behavioral parameters should be developed for the environment in which the sheep will be kept. An intervention score should also be set to ensure that optimal analgesia is achieved. Pain assessment tools for sheep require further development and investigation to determine the most accurate method.

8.2 Preoperative Preparation for Aseptic Surgery

Surgical preparation of the skin may commence once anesthesia has been induced and stabilized. The ewe should be placed in dorsal recumbency, allowing exposure of the abdomen (Fig. 30.3A). The wool should be wetted with 70% ethanol in H_2O and clipped to the skin between the groin and the sternum (Fig. 30.3B) to create a surgical field. Special care should be taken not to abrade or cut the skin during clipping (especially around the groin flaps)—placing tension on the skin will assist in ensuring a clean, trauma-free clip. Once the abdomen has been carefully shorn, use a damp sponge and chlorhexidine (4%) surgical skin disinfectant to thoroughly remove all feces and lanolin from the clipped area. Wetting down the wool at the periphery of clipped surface helps to prevent loose strands of wool falling back onto the surgical field during cleaning and subsequent draping.

Once all obvious contaminants have been removed from the surgical field, the skin may be disinfected with a chlorhexidine surgical scrub (4%) as follows: take a clean, fist-sized wad of cotton wool, and soak liberally in chlorhexidine surgical scrub. Starting on the abdominal midline, scrub a 15 cm × 5 cm (length × width) zone moving in a straight line up and down the abdomen. Then scrub the skin in a circular pattern, moving outward from the abdominal midline until you reach the periphery of the surgical field. Clean the surgical site with 70% ethanol. Then discard the used wad of cotton wool for a new one, soak in chlorhexidine surgical scrub,
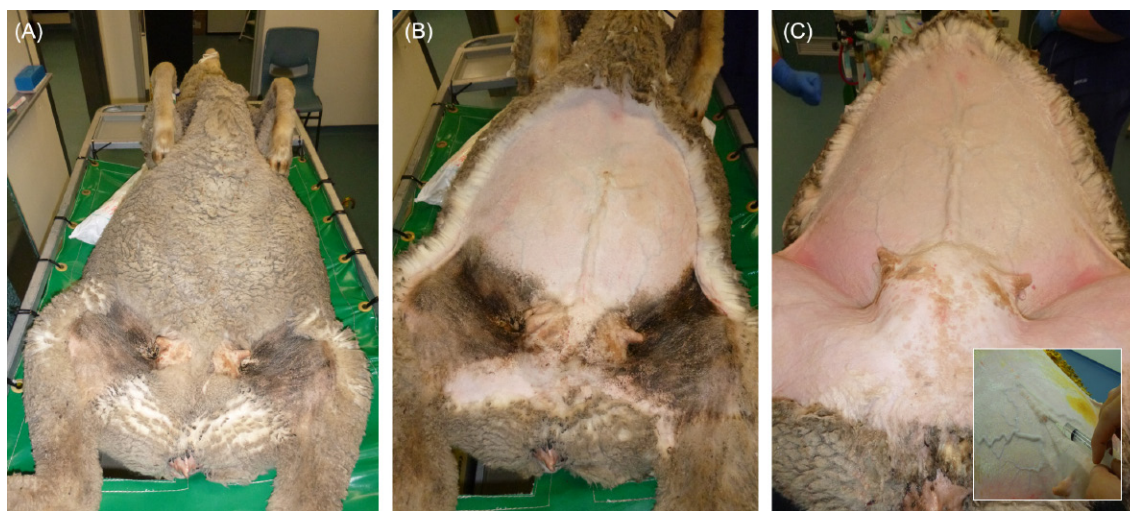
FIGURE 30.3 (A) Ewe abdomen clipped for presurgical preparation. (B) Ewe abdomen following preoperative scrub. (C) Ewe abdomen prepared for surgical draping. Inset demonstrates subcutaneous administration of local anesthetic to the incision site.

and repeat the previous process 3 times. This process should take no less than 5 min to complete, leaving the abdomen resembling the image shown in Fig. 30.3C.

Once preparation of the skin is complete, the ewe should be transferred to the operating theatre and positioned for surgery on a surgical table. Care should be taken not to contaminate the surgical field during the transfer. Furthermore, care should be taken not to hyperextend the ewe's hips or shoulders during positioning. Prior to draping the animal, the surgical team should select an incision site (approximately 8 cm in length) just large enough to allow exteriorization of the fetal head and neck. A number of large, superficial veins populate the abdomen in a pregnant ewe and the incision site should be selected to avoid cutting these. Using a 21-gauge needle, introduce 10 mL of 1% ropivacaine hydrochloride (or similarly long-acting local anesthetic) subcutaneously along the incision site (Fig. 30.3C Inset).

Once the animal has been covered with a fenestrated surgical drape and an anesthetist has confirmed that the ewe is adequately anesthetized, the surgical team (at least two skilled surgeons) can proceed to scrub and gown prior to commencing surgery. We cannot overemphasize that rigorous aseptic technique from the initiation of scrubbing through to the closure of the abdominal incision is *absolutely critical* to the success of surgical studies of this nature. All surgical equipment should be sterilized by high temperature autoclave and all sterile consumables opened by a surgical assistant proficient in theater technique.

8.3 Surgical Protocol—Isolation of the Fetal Lung and Gut

The following protocol provides a guide to surgically isolating the fetal lung and gut from the amniotic environment. We have performed this protocol on fetuses at 118–122 days gestation. Following exteriorization of the fetal head, the fetal esophagus and trachea are sequentially exposed and ligated. In addition, a tracheal catheter attached to a fluid collection bag (1.5 L total volume) is installed, with the collection bag sited in the amniotic cavity. This apparatus allows for collection of fetal lung fluid preventing overdistension and injury to the fetal lung. This basic protocol may be readily adapted to allow for the selective exposure of the fetal lung or gut to an agent of interest by inserting a fine catheter attached to a subcutaneously sited osmotic pump. Additionally, the fetal skin and membranes can be selectively isolated and exposed to intervention compounds by the installation of an additional surgical seal around the fetal snout. Interventions may be administered for between 24 h and 6 days following surgery. Suggested surgical consumables and equipment are detailed in Table 30.8 and 30.9, respectively.

8.3.1 Surgery Phase 1—Abdominal Incision (Laparotomy) to Exteriorization of the Fetal Head via Hysterotomy

Surgery should only commence once an anesthetist has confirmed that anesthesia is stable. The following protocol assumes a good level of surgical proficiency and as such does not detail fundamental techniques, such as those necessary for maintaining hemostasis, suturing tissue, and general instrument handling. This protocol also assumes that a veterinary anesthetist (or similarly experienced person) is continually monitoring the animal throughout surgery to ensure the maintenance of an adequate plane of anesthesia.

1. Using a disposable size 20 scalpel blade, make a superficial, 8 cm long incision along the incision site

TABLE 30.8 Sterile Surgical Consumables

Number	Item
1	0–0 Sofsilk (Medtronic, Australia)
1	1–0 Polysorb braided suture with 26 mm taper needle (Medtronic, Australia)
1	1–0 Maxon monofilament suture with 65 mm taper needle (Medtronic, Australia)
1	Bag of large laparotomy sponges
1	Catheter bag and circuit for lung fluid collection
1	Transdermal fentanyl patch

TABLE 30.9 Sterile Surgical Equipment

Number	Item
1	Size (20) scalpel blade (maternal)
1	Size (10) scalpel blade (fetal)
1	Size (4) scalpel handle (maternal)
1	Size (3) scalpel handle (fetal)
1	Metzenbaum (14 cm) curved tissue scissors (maternal)
1	Vessel scissors (fetal)
1	Suture scissors
2	Curved needles—curved triangular cutting size 10
2	Straight needles—straight triangular cutting size 6
4	Atraumatic (Babcock) clamps
4	Medium traumatic (Kelly) clamps
4	Small (14 cm) hemostat (curved nose)
4	Medium (16 cm) hemostat (curved nose)
1	Small (14 cm) needle driver
1	Large (18 cm) needle driver
1	Medium Steinhauser forceps
1	Medium Allis clamps

where local anesthetic has been injected, taking care to stay lateral to the superficial mammary vein. The surgical pack should contain a number of precut lengths of size 0 Sofsilk that can be rapidly deployed to control any bleeding.

2. Using 2–3 surgical swabs in each hand, a-traumatically dissect the subcutaneous tissue to expose the *linea alba*.
3. Using a size 20 scalpel blade, make a superficial 1 cm long incision in the *linea alba*.
4. Using an index finger rotating in a circular motion about the incision site, ensure that *linea alba* is separated from the tissue below.

5. Elevating/tensioning the *linea alba* with the index and forefinger, use pair of 14 cm curved Metzenbaum tissue scissors to enlarge the *linea alba* incision to a final length of 8 cm.
6. Retract the omentum and palpate the uterus to identify the fetal head. Careful pressure may be used to reorient the fetal head within the uterus, allowing for exteriorization of the head.
7. Using both hands, gently exteriorize the fetal head within the uterus and stabilize with laterally placed laparotomy sponges (Fig. 30.4A).
8. The surgical assistant now places the uterine wall under tension. Taking care to avoid uterine vasculature, use a disposable size 10 scalpel blade to make a 5 cm long incision in the uterine wall and fetal membranes (Fig. 30.4B).
9. Use 4×20 cm atraumatic Babcock tissue clamps to secure the incision site and exteriorize the fetal snout by gently pushing down on the fetal skull while simultaneously squeezing the snout forward and up through the uterine incision. It is important to minimize the loss of amniotic fluid and to exteriorize as little of the fetus as possible (Fig. 30.4C).
10. The fetal head and neck are extended and rested on a sterile laparotomy sponge. Each Babcock clamp used in (9) should be relocated to clamp the uterine wall to the fetal neck, creating a seal, and preventing the loss of amniotic fluid during the subsequent fetal surgery (Fig. 30.5A).

8.3.2 Surgery Phase 2—Installation of Fetal Esophageal and Tracheal Ligations

1. Palpate the cricoid cartilage on the fetal neck to identify the trachea. Use forceps to raise the skin above the cricoid cartilage and make a small lateral incision with the fetal vessel scissors. Keeping tension on the skin flap, use the Metzenbaum tissue scissors to make a 3 cm long incision, parallel to the trachea.
2. Blunt dissect the connective tissue from around the trachea using a small hemostat. Introduce two lengths of size 0 Sofsilk around the trachea, laterally relocate and clamp in place (Fig. 30.5B).
3. Blunt dissect the connective tissue from around the esophagus using a small hemostat. Introduce two lengths of size 0 Sofsilk around the esophagus and ligate.
4. Using a size 10 scalpel blade, make a transverse incision around one of the cartilage rings in the fetal trachea, taking care not to cut completely through the trachea.
5. Using traumatic forceps to hold the tracheal incision open, insert the tracheal catheter into the incision site to a depth of 2 cm.
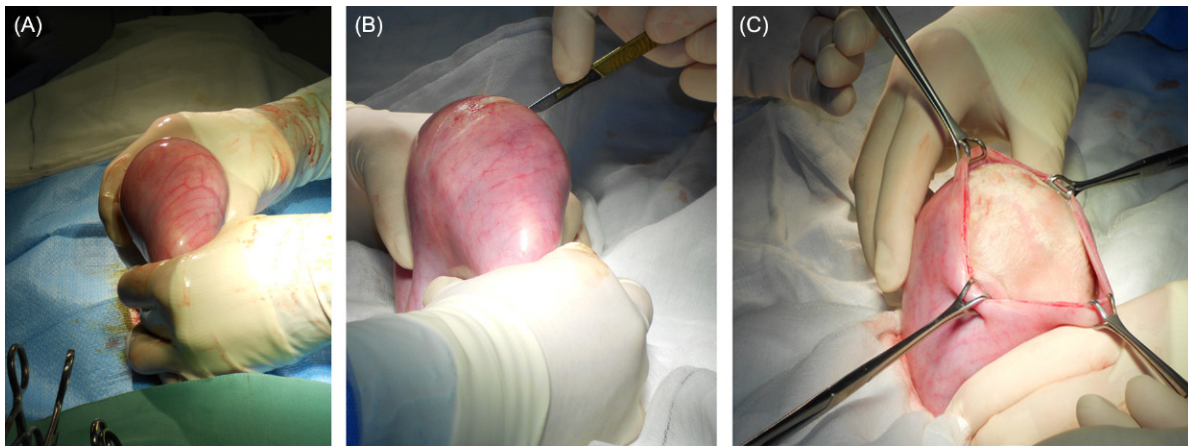
FIGURE 30.4 (A) Exposure of the fetal head within the uterus. (B) Lateral incision of the uterine wall and fetal membranes. (C) Atraumatic Babcock clamps are used to secure the fetal membranes and uterine wall in preparation for exteriorization of the fetal head.
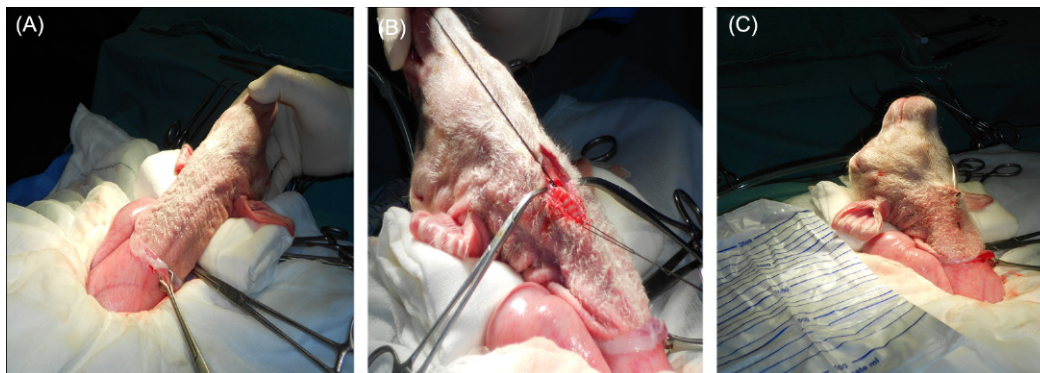
FIGURE 30.5 (A) The fetal head is secured in place, exposing the trachea. (B) Surgical silk is introduced underneath the trachea (following blunt dissection) to assist in manipulation and to allow occlusion superior to the tracheal cannula. (C) The fetal head with surgical implants installed, prior to reintroduction to the uterus.

6. Introduce two additional lengths of size 0 Sofsilk around the tracheal catheter site and ligate firmly in place. Pull gently on the ligated catheter to confirm sound installation.
7. Use the two lengths of Sofsilk introduced around the esophagus in (3) to ligate the esophagus superior to the tracheal catheter insertion site and to tether the extension of the catheter line.
8. Holding the catheter line flat to the fetal neck, use an additional length of size 0 Sofsilk to close the incision site made in the fetal skin (Fig. 30.5C).

8.3.3 Surgery Phase 3—Closure of Uterine and Abdominal Incisions

1. Elevate the fetal head and release the Babcock clamps from the fetal neck. Reattach Babcock clamps to the uterine wall and elevate to prevent the loss of amniotic fluid and to make room to return the fetal head to the uterus.

2. Gently slide the connection bag attached to the tracheal catheter along the fetal spine and into the uterus. Administer an appropriate dose of prophylactic antibiotic to the fetus via subcutaneous injection.
3. Keeping the uterine incision elevated by tensioning the attached Babcock clamps, tilt the fetal snout forward and down. Using gentle downward pressure, reintroduce the fetal head into the uterus, taking care to return the head and neck to the same preoperative orientation.
4. Use size 2.0 Polysorb in a purse-string oversuture pattern to close the uterine incision. Take particular care to suture the fetal membranes to the internal aspect of the uterus during closure of the first layer (Fig. 30.6A–B).
5. Use size 1.0 Maxon in a running suture pattern to close the *linea alba* incision. Take particular care the suture through the fascia on the internal aspect of the *linea alba* incision (Fig. 30.6C).
6. Pause briefly to ensure that incision hemostasis has been achieved. Use size 2.0 Polysorb to close the

FIGURE 30.6　(A) Closure of the uterine wall (first suture layer). (B) Closure of the uterine wall (overlapping suture layer). (C) Closure of the *linea alba.*

superficial incision made in (1). Spray the incision site with Opsite (or similar spray dressing)

7. If the provision of postoperative analgesia is from a transdermal fentanyl patch, clean and dry the skin in the groin and apply the patch to this site. Judicious use of surgical adhesive may assist in keeping the patch in place.

8.4 Euthanasia

The most common method of euthanasia is intravenous injection of pentobarbitone (Leary et al., 2013). In an adult sheep, intravenous access is possible at a number of sites. If a catheter has been placed for use during surgery then ensure the catheter is kept patent with continuous delivery of IV fluids or intermittent flushing with heparinized saline. The cephalic or jugular veins are usually easily accessible. If euthanasia of the fetus is required during surgery an intravenous injection can be given into the umbilical vein. Death must be confirmed before tissues are harvested or the carcass is disposed of. Three checks must be made: ensure absence of a heart beat by auscultating the chest, ensure absence of spontaneous ventilation by observing the chest wall, and ensure absence of a corneal reflex by stimulating the cornea with light digital pressure.

Acknowledgments

References

Aagaard, K., Riehle, K., Ma, J., Segata, N., Mistretta, T.-A., Coarfa, C., Versalovic, J., et al., 2012. A metagenomic approach to characterization of the vaginal microbiome signature in pregnancy. PLoS One 7 (6), e36466.

Aagaard, K., Ma, J., Antony, K.M., Ganu, R., Petrosino, J., Versalovic, J., 2014. The placenta harbors a unique microbiome. Sci. Transl. Med. 6 (237).

Adams Waldorf, K.M., Persing, D., Novy, M.J., Sadowsky, D.W., Gravett, M.G., 2008. Pretreatment with toll-like receptor 4 antagonist inhibits lipopolysaccharide-induced preterm uterine contractility, cytokines, and prostaglandins in rhesus monkeys. Reprod. Sci. 15 (2), 121–127.

Agrawal, V., Hirsch, E., 2012. Intrauterine infection and preterm labor. Semin. Fetal Neonatal Med. 17 (1), 12–19.

Akira, S., Takeda, K., 2004. Toll-like receptor signalling. Nat. Rev. Immunol. 4 (7), 499–511.

Alberts, B., Johnson, A., Lewis, J., Raff, M., Roberts, K., Walter, P., 2002. Molecular Biology of the Cell, forth ed. Garland Science, New York, NY.

Anderson, K.J., Allen, R.L., 2009. Regulation of T-cell immunity by leucocyte immunoglobulin-like receptors: innate immune receptors for self on antigen-presenting cells. Immunology 127 (1), 8–17.

Andrew Combs, C., Gravett, M., Garite, T.J., Hickok, D.E., Lapidus, J., Porreco, R., et al., 2014. Amniotic fluid infection, inflammation, and colonization in preterm labor with intact membranes. Am. J. Obstet. Gynecol. 210 (2), 125.e1–125.e15.

Ao, M., Miyauchi, M., Furusho, H., Inubushi, T., Kitagawa, M., Nagasaki, A., et al., 2015. Dental infection of *Porphyromonas gingivalis* induces preterm birth in mice. PLoS One 10 (8).

Arfi, Y., Minder, L., Di Primo, C., Roy, A.L., Ebel, C., Coquetk, L., et al., 2016. MIB-MIP is a mycoplasma system that captures and cleaves immunoglobulin G. Proc. Natl. Acad. Sci. USA 113 (19), 5406–5411.

Australian Government, 2013. Australian code of practice for the care and use of animals for scientific purposes 8th edition. NHMRC.

Ball, H.J., McCaughey, W.J., Kennedy, S., McLoughlin, M., 1985. Experimental intrauterine inoculation of pregnant ewes with ureaplasmas. Vet. Res. Commun. 9 (1), 35–43.

Baragatti, B., Brizzi, F., Ackerley, C., Barogi, S., Ballou, L.R., Coceani, F., 2003. Cyclooxygenase-1 and cyclooxygenase-2 in the mouse ductus arteriosus: individual activity and functional coupling with nitric oxide synthase. Br. J. Pharmacol. 139 (8), 1505–1515.

Baschat, A.A., Towbin, J., Bowles, N.E., Harman, C.R., Weiner, C.P., 2003. Prevalence of viral DNA in amniotic fluid of low-risk pregnancies in the second trimester. J. Matern. Fetal Neonatal Med. 13 (6), 381–384.

Bastek, J.A., Gomez, L.M., Elovitz, M.A., 2011. The role of inflammation and infection in preterm birth. Clin. Perinatol. 38 (3), 385–406.

Behnia, F., Sheller, S., Menon, R., 2016. Mechanistic differences leading to infectious and sterile inflammation. Am. J. Reprod. Immunol. 75 (5), 505–518.

Bilbrough, G., 2006. A practical guide to capnography. InPractice 28 (6), 312–319.

Black, A., Bhaumik, S., Kirkman, R.L., Weaver, C.T., Randolph, D.A., 2012. Developmental regulation of Th17-cell capacity in human neonates. Eur. J. Immunol. 42 (2), 311–319.

Blencowe, H., Cousens, S., Oestergaard, M.Z., Chou, D., Moller, A.-B., Narwal, R., et al., 2012. National, regional, and worldwide estimates of preterm birth rates in the year 2010 with time trends since 1990 for selected countries: a systematic analysis and implications. The Lancet 379 (9832), 2162–2172.

Bohrer, J.C., Kamemoto, L.E., Almeida, P.G., Ogasawara, K.K., 2012. Acute chorioamnionitis at term caused by the oral pathogen *Fusobacterium nucleatum*. Hawai J. Med. Health 71 (10), 280–281.

Brozos, C., Mavrogianni, V.S., Fthenakis, G.C., 2011. Treatment and control of peri-parturient metabolic diseases: pregnancy toxemia, hypocalcemia, hypomagnesemia. Vet. Clin. North Am. Food Anim. Pract. 27 (1), 105–113.

Bruns, A.M., Pollpeter, D., Hadizadeh, N., Myong, S., Marko, J.F., Horvath, C.M., 2013. ATP hydrolysis enhances RNA recognition and antiviral signal transduction by the innate immune sensor, laboratory of genetics and physiology 2 (LGP2). J. Biol. Chem. 288 (2), 938–946.

Burd, I., Bentz, A.I., Chai, J., Gonzalez, J., Monnerie, H., Le Roux, P.D., et al., 2010. Inflammation-induced preterm birth alters neuronal morphology in the mouse fetal brain. J. Neurosci. Res. 88 (9), 1872–1881.

Burd, I., Brown, A., Gonzalez, J.M., Chai, J., Elovitz, M.A., 2011. A mouse model of term chorioamnionitis: unraveling causes of adverse neurological outcomes. Reprod. Sci. 18 (9), 900–907.

Cao, X., 2016. Self-regulation and cross-regulation of pattern-recognition receptor signalling in health and disease. Nat. Rev. Immunol. 16 (1), 35–50.

Cassell, G.H., Waites, K.B., Watson, H.L., Crouse, D.T., Harasawa, R., 1993. *Ureaplasma urealyticum* intrauterine infection: role in prematurity and disease in newborns. Clin. Microbiol. Rev. 6 (1), 69–87.

Chaim, W., Mazor, M., Wiznitzer, A., 1992. The prevalence and clinical significance of intraamniotic infection with *Candida* species in women with preterm labor. Arch. Gynecol. Obstet. 251 (1), 9–15.

Challis, J.R.G., Matthews, S.G., Gibb, W., Lye, S.J., 2000. Endocrine and paracrine regulation of birth at term and preterm. Endocr. Rev. 21 (5), 514–550.

Chang, J., Jain, S., Carl, D.J., Paolella, L., Darveau, R.P., Gravett, M.G., Adams Waldorf, K.M., 2010. Differential host response to LPS variants in amniochorion and the TLR4/MD-2 system in *Macaca nemestrina*. Placenta 31 (9), 811–817.

Chaput, C., Sander, L.E., Suttorp, N., Opitz, B., 2013. NOD-like receptors in lung diseases. Front. Immunol. 4, 393.

Cheah, F.C., Pillow, J.J., Kramer, B.W., Polglase, G.R., Nitsos, I., Newnham, J.P., et al., 2009. Airway inflammatory cell responses to intra-amniotic lipopolysaccharide in a sheep model of chorioamnionitis. Am. J. Physiol. Lung Cell. Mol. Physiol. 296 (3), L384–L393.

Cockle, J.V., Gopichandran, N., Walker, J.J., Levene, M.I., Orsi, N.M., 2007. Matrix metalloproteinases and their tissue inhibitors in preterm perinatal complications. Reprod. Sci. 14 (7), 629–645.

Colaizy, T.T., Morris, C.D., Lapidus, J., Sklar, R.S., Pillers, D.A.M., 2007. Detection of ureaplasma DNA in endotracheal samples is associated with bronchopulmonary dysplasia after adjustment for multiple risk factors. Pediatr. Res. 61 (5 Pt 1), 578–583.

Collins, J.G., Smith, M.A., Arnold, R.R., Offenbacher, S., 1994a. Effects of *Escherichia coli* and *Porphyromonas gingivalis* lipopolysaccharide on pregnancy outcome in the golden hamster. Infect. Immun. 62 (10), 4652–4655.

Collins, J.G., Windley Iii, H.W., Arnold, R.R., Offenbacher, S., 1994b. Effects of a *Porphyromonas gingivalis* infection on inflammatory mediator response and pregnancy outcome in hamsters. Infect. Immun. 62 (10), 4356–4361.

Cui, J., Wang, F., Zhang, X., Liu, L., 2015. Maternal and fetal IL1RN polymorphisms and the risk of preterm delivery: a meta-analysis. J. Matern. Fetal Neonatal Med. 28 (1), 100–105.

Dambuza, I.M., Brown, G.D., 2015. C-type lectins in immunity: recent developments. Curr. Opin. Immunol. 32, 21–27.

Davis, J., Musk, G., 2014. Pressure and volume controlled mechanical ventilation in anaesthetized pregnant sheep. Labor. Anim. 48 (4), 321–327.

De Nardo, D., 2015. Toll-like receptors: activation, signalling and transcriptional modulation. Cytokine 74 (2), 181–189.

DiGiulio, D.B., 2012. Diversity of microbes in amniotic fluid. Semin. Fetal Neonatal Med. 17 (1), 2–11.

DiGiulio, D.B., Romero, R., Amogan, H.P., Kusanovic, J.P., Bik, E.M., Gotsch, F., et al., 2008. Microbial prevalence, diversity and abundance in amniotic fluid during preterm labor: a molecular and culture-based investigation. PLoS One 3 (8), e3056.

DiGiulio, D.B., Romero, R., Kusanovic, J.P., Gomez, R., Kim, C.J., Seok, K.S., et al., 2010. Prevalence and diversity of microbes in the amniotic fluid, the fetal inflammatory response, and pregnancy outcome in women with preterm pre-labor rupture of membranes. Am. J. Reprod. Immunol. 64 (1), 38–57.

Dombroski, R.A., Woodard, D.S., Harper, M.J.K., Gibbs, R.S., 1990. A rabbit model for bacteria-induced preterm pregnancy loss. Am. J. Obstet. Gynecol. 163 (6 I), 1938–1943.

Dudley, D.J., Collmer, D., Mitchell, M.D., Trautman, M.S., 1996. Inflammatory cytokine mRNA in human gestational tissues: implications for term and preterm labor. J. Soc. Gynecol. Invest. 3 (6), 328–335.

Dugdale, A., 2007. The ins and outs of ventilation 1. Basic principles. InPractice 29 (4), 186–193.

Dunkelberger, J.R., Song, W.-C., 2009. Complement and its role in innate and adaptive immune responses. Cell Res. 20 (1), 34–50.

Ebersole, J.L., Holt, S.C., Cappelli, D., 2014. Periodontitis in pregnant baboons: systemic inflammation and adaptive immune responses and pregnancy outcomes in a baboon model. J. Periodontal Res. 49 (2), 226–236.

Edwards, R.K., Ferguson, R.J., Duff, P., 2006. The interleukin-1β +3953 single nucleotide polymorphism: cervical protein concentration and preterm delivery risk. Am. J. Reprod. Immunol. 55 (4), 259–264.

Elovitz, M.A., Brown, A.G., Breen, K., Anton, L., Maubert, M., Burd, I., 2011. Intrauterine inflammation, insufficient to induce parturition, still evokes fetal and neonatal brain injury. Int. J. Dev. Neurosci. 29 (6), 663–671.

Feikin, D.R., Thorsen, P., Zywicki, S., Arpi, M., Westergaard, J.G., Schuchat, A., 2001. Association between colonization with group B streptococci during pregnancy and preterm delivery among Danish women. Am. J. Obstet. Gynecol. 184 (3), 427–433.

Filipovich, Y., Lu, S.J., Akira, S., Hirsch, E., 2009. The adaptor protein MyD88 is essential for *E. coli*-induced preterm delivery in mice. Am. J. Obstet. Gynecol. 200 (1), 93.e1–93.e8.

Filipovich, Y., Agrawal, V., Crawford, S.E., Fitchev, P., Qu, X., Klein, J., Hirsch, E., 2015. Depletion of polymorphonuclear leukocytes has no effect on preterm delivery in a mouse model of *Escherichia coli*-induced labor. Am. J. Obstet. Gynecol. 213 (5), 697.e1–697.e10.

Fogacci, M.F., Da Silva Barbirato, D., Da Silva Furtado Amaral, C., Da Silva, P.G., De Oliveira Coelho, M., Bertozi, G., et al., 2016. No association between periodontitis, preterm birth, or intrauterine growth restriction: experimental study in Wistar rats. Am. J. Obstet. Gynecol. 214 (6), 749.e1–749.e11.

Franchi, L., Warner, N., Viani, K., Nuñez, G., 2009. Function of Nod-like receptors in microbial recognition and host defense. Immunol. Rev. 227 (1), 106–128.

Frey, H.A., Klebanoff, M.A., 2016. The epidemiology, etiology, and costs of preterm birth. Semin. Fetal Neonatal Med. 21 (2), 68–73.

Gardella, C., Riley, D.E., Hitti, J., Agnew, K., Krieger, J.N., Eschenbach, D., 2004. Identification and sequencing of bacterial rDNAs

in culture-negative amniotic fluid from women in premature labor. Am. J. Perinatol. 21 (6), 319–323.

Garland, S.M., Murton, L.J., 1987. Neonatal meningitis caused by *Ureaplasma urealyticum*. Pediatr. Infect. Dis. J. 6 (9), 868–870.

Gervasi, M.T., Romero, R., Bracalente, G., Chaiworapongsa, T., Erez, O., Dong, Z., et al., 2012. Viral invasion of the amniotic cavity (VIAC) in the midtrimester of pregnancy. J. Matern. Fetal Neonatal Med. 25 (10), 2002–2013.

Goldenberg, R.L., Hauth, J.C., Andrews, W.W., 2000. Intrauterine infection and preterm delivery. N. Engl. J. Med. 342 (20), 1500–1507.

Goldenberg, R.L., Andrews, W.W., Hauth, J.C., 2002. Choriodecidual infection and preterm birth. Nutr. Rev. 60 (5 Pt 2), S19–S25.

Goldenberg, R.L., Andrews, W.W., Faye-Petersen, O.M., Goepfert, A.R., Cliver, S.P., Hauth, J.C., 2006. The Alabama Preterm Birth Study: intrauterine infection and placental histologic findings in preterm births of males and females less than 32 weeks. Am. J. Obstet. Gynecol. 195 (6), 1533–1537.

Goldenberg, R.L., Andrews, W.W., Goepfert, A.R., Faye-Petersen, O., Cliver, S.P., Carlo, W.A., Hauth, J.C., 2008a. The Alabama Preterm Birth Study: umbilical cord blood *Ureaplasma urealyticum* and *Mycoplasma hominis* cultures in very preterm newborn infants. Am. J. Obstet. Gynecol. 198 (1), 43.e1–43.e5.

Goldenberg, R.L., Culhane, J.F., Iams, J.D., Romero, R., 2008b. Epidemiology and causes of preterm birth. Lancet 371 (9606), 75–84.

Goldenberg, R.L., Gravett, M.G., Iams, J., Papageorghiou, A.T., Waller, S.A., Kramer, M., et al., 2012. The preterm birth syndrome: Issues to consider in creating a classification system. Am. J. Obstet. Gynecol. 206 (2), 113–118.

Gomez, R., Romero, R., Ghezzi, F., Yoon, B.H., Mazor, M., Berry, S.M., 1998. The fetal inflammatory response syndrome. Am. J. Obstet. Gynecol. 179 (1), 194–202.

Gotsch, F., Romero, R., Kusanovic, J.P., Mazaki-Tovi, S., Pineles, B.L., Erez, O., et al., 2007. The fetal inflammatory response syndrome. Clin. Obstet. Gynecol. 50 (3), 652–683.

Grant, C., Upton, R.N., 2001. The anti-nociceptive efficacy of low dose intramuscular xylazine in lambs. Res. Vet. Sci. 70 (1), 47–50.

Grant, C., Upton, R.N., 2004. Comparison of the analgesic effects of xylazine in sheep via three different administration routes. Aust. Vet. J. 82 (5), 304–307.

Grant, C., Summersides, G.E., Kuchel, T.R., 2001. A xylazine infusion regimen to provide analgesia in sheep. Lab. Anim. 35 (3), 277–281.

Gravett, M.G., Adams, K.M., Sadowsky, D.W., Grosvenor, A.R., Witkin, S.S., Axthelm, M.K., Novy, M.J., 2007. Immunomodulators plus antibiotics delay preterm delivery after experimental intraamniotic infection in a nonhuman primate model. Am. J. Obstet. Gynecol. 197 (5), 518e1–518e8.

Grigsby, P.L., Long, M., Novy, M.J., Sadowsky, D.W., Duffy, L.B., Waites, K.B., Acosta, E.P., 2009. Transplacental pharmacokinetics (PK) and pharmacodynamics (PD) of azithromycin (AZI) treatment for intraamniotic *Ureaplasma* infection. Am. J. Obstet. Gynecol. 201, S179.

Grigsby, P.L., Novy, M.J., Waldorf, K.M., Sadowsky, D.W., Gravett, M.G., 2010. Choriodecidual inflammation: a harbinger of the preterm labor syndrome. Reprod. Sci. 17 (1), 85–94.

Han, Y.W., Redline, R.W., Li, M., Yin, L., Hill, G.B., McCormick, T.S., 2004. *Fusobacterium nucleatum* induces premature and term stillbirths in pregnant mice: implication of oral bacteria in preterm birth. Infect. Immun. 72 (4), 2272–2279.

Han, Y.W., Fardini, Y., Chen, C., Iacampo, K.G., Peraino, V.A., Shamonki, J.M., Redline, R.W., 2010. Term stillbirth caused by oral *Fusobacterium nucleatum*. Obstet. Gynecol. 115 (2 Pt 2), 442–445.

Hanf, M., Friedman, E., Basurko, C., Roger, A., Bruncher, P., Dussart, P., et al., 2014. Dengue epidemics and adverse obstetrical outcomes in French guiana: a semi-ecological study. Trop. Med. Int. Health 19 (2), 153–158.

Harris, T., 1991. Caudal epidural anaesthesia in the ewe. InPractice 13 (6), 234–235.

Harrison, M.S., Goldenberg, R.L., 2016. Global burden of prematurity. Semin. Fetal Neonatal Med. 21 (2), 74–79.

Hazlett, L., Wu, M., 2011. Defensins in innate immunity. Cell Tissue Res. 343 (1), 175–188.

Heddleston, L., McDuffie, Jr., R.S., Gibbs, R.S., 1993. A rabbit model for ascending infection in pregnancy: intervention with indomethacin and delayed ampicillin-sulbactam therapy. Am. J. Obstet. Gynecol. 169 (3), 708–712.

Heikkinen, E.M., Voipio, H.-M., Laaksonen, S., Haapala, L., Räsänen, J., Acharya, G., et al., 2015. Fentanyl pharmacokinetics in pregnant sheep after intravenous and transdermal administration to the ewe. Basic Clin. Pharmacol. Toxicol. 117 (3), 156–163.

Hess, N.J., Felicelli, C., Grage, J., Mercado, R., Tapping, R.I., 2016. TLR10 is a negative regulator of human monocyte innate immune responses. J. Immunol. 196 (1 Suppl.), 126.123.

Hillier, S.L., Martius, J., Krohn, M., Kiviat, N., Holmes, K.K., Eschenbach, D.A., 1988. A case-control study of chorioamniotic infection and histologic chorioamnionitis in prematurity. N. Engl. J. Med. 319 (15), 972–978.

Hirayasu, K., Saito, F., Suenaga, T., Shida, K., Arase, N., Oikawa, K., et al., 2016. Microbially cleaved immunoglobulins are sensed by the innate immune receptor LILRA2. Nat. Microbiol. 1, 16054.

Hirsch, E., Muhle, R.A., Mussalli, G.M., Blanchard, R., 2002. Bacterially induced preterm labor in the mouse does not require maternal interleukin-1 signaling. Am. J. Obstet. Gynecol. 186 (3), 523–530.

Hirsch, E., Filipovich, Y., Mahendroo, M., 2006. Signaling via the type I IL-1 and TNF receptors is necessary for bacterially induced preterm labor in a murine model. Am. J. Obstet. Gynecol. 194 (5), 1334–1340.

Hodgkinson, O., Dawson, L., 2007. Practical anaesthesia and analgesia in sheep, goats and calves. InPractice 29 (10), 596–603.

Huang, Q.T., Huang, Q., Zhong, M., Wei, S.S., Luo, W., Li, F., Yu, Y.H., 2015. Chronic hepatitis C virus infection is associated with increased risk of preterm birth: a meta-analysis of observational studies. J. Viral Hepat. 22 (12), 1033–1042.

Hyman, R.W., Fukushima, M., Jiang, H., Fung, E., Rand, L., Johnson, B., et al., 2014. Diversity of the vaginal microbiome correlates with preterm birth. Rep. Sci. 21 (1), 32–40.

Idan, C., Peleg, R., Elena, V., Martin, T., Cicerone, T., Mareike, W., et al., 2015. IL-1α is a DNA damage sensor linking genotoxic stress signaling to sterile inflammation and innate immunity. Sci. Rep. 5, 14756.

Ide, M., Papapanou, P.N., 2013. Epidemiology of association between maternal periodontal disease and adverse pregnancy outcomes—systematic review. J. Clin. Periodontol. 40 (Suppl. 14), S181–S194.

Ikegami, M., Moss, T.J.M., Kallapur, S.G., Mulrooney, N., Kramer, B.W., Nitsos, I., et al., 2003. Minimal lung and systemic responses to TNF-α in preterm sheep. Am. J. Physiol. Lung Cell. Mol. Physiol. 285, L121–L129.

Ilievski, V., Hirsch, E., 2010. Synergy between viral and bacterial toll-like receptors leads to amplification of inflammatory responses and preterm labor in the mouse. Biol. Reprod. 83 (5), 767–773.

Ilievski, V., Lu, S.J., Hirsch, E., 2007. Activation of toll-like receptors 2 or 3 and preterm delivery in the mouse. Reprod. Sci. 14 (4), 315–320.

Institute of Medicine Committee on Understanding Premature Books and Assuring Healthy Outcomes, 2007. The National Academies Collection: Reports funded by National Institutes of Health. In: Behrman, R.E., Butler, A.S. (Eds.), Preterm Birth: Causes, Consequences, and Prevention. National Academies Press, Washington (DC), United States.

Iram, N., Mildner, M., Prior, M., Petzelbauer, P., Fiala, C., Hacker, S., et al., 2012. Age-related changes in expression and function of toll-like receptors in human skin. Development 139 (22), 4210–4219.

Jiang, S., Li, X., Hess, N.J., Guan, Y., Tapping, R.I., 2016. TLR10 is a negative regulator of both MyD88-dependent and -independent TLR signaling. J. Immunol. 196 (9), 3834–3841.

Jones, H.E., Harris, K.A., Azizia, M., Bank, L., Carpenter, B., Hartley, J.C., et al., 2009. Differing prevalence and diversity of bacterial species in fetal membranes from very preterm and term labor. PLoS One 4 (12), e8205.

Kallapur, S.G., Willet, K.E., Jobe, A.H., Ikegami, M., Bachurski, C.J., 2001. Intra-amniotic endotoxin: chorioamnionitis precedes lung maturation in preterm lambs. Am. J. Physiol. Lung Cell. Mol. Physiol. 280 (3), L527–L536.

Kallapur, S.G., Nitsos, I., Moss, T.J.M., Polglase, G.R., Pillow, J.J., Cheah, F.C., et al., 2009. IL-1 mediates pulmonary and systemic inflammatory responses to chorioamnionitis induced by lipopolysaccharide. Am. J. Respir. Crit. Care Med. 179 (10), 955–961.

Kallapur, S.G., Presicce, P., Senthamaraikannan, P., Alvarez, M., Tarantal, A.F., Miller, L.M., et al., 2013. Intra-Amniotic IL-1b induces fetal inflammation in rhesus monkeys and alters the regulatory t Cell/IL-17 balance. J. Immunol. 191 (3), 1102–1109.

Kastner, S.B.R., Wapf, P., Feige, K., Demuth, D., Bettschart-Wolfensberger, R., Akens, M.K., Huhtinen, M., 2003. Pharmacokinetics and sedative effects of intramuscular medetomidine in domestic sheep. J. Vet. Pharmacol. Ther. 26, 271–276.

Kawai, T., Akira, S., 2011. Toll-like receptors and their crosstalk with other innate receptors in infection and immunity. Immunity 34 (5), 637–650.

Kayar, N.A., Alptekin, N.Ö., Erdal, M.E., 2015. Interleukin-1 receptor antagonist gene polymorphism, adverse pregnancy outcome and periodontitis in Turkish women. Arch. Oral Biol. 60 (12), 1777–1783.

Keelan, J.A., Blumenstein, M., Helliwell, R.J.A., Sato, T.A., Marvin, K.W., Mitchell, M.D., 2003. Cytokines, prostaglandins and parturition—a review. Placenta 24 (Suppl. A), S33–S46.

Kemp, M.W., 2014. Preterm birth, intrauterine infection, and fetal inflammation. Front. Immunol. 5, 574.

Kemp, M.W., Saito, M., Newnham, J.P., Nitsos, I., Okamura, K., Kallapur, S.G., 2010. Preterm birth, infection, and inflammation advances from the study of animal models. Reprod. Sci. 17 (7), 619–628.

Kemp, M.W., Saito, M., Kallapur, S., Jobe, A., Keelan, J.A., Li, S., et al., 2011. Inflammation of the fetal ovine skin following in utero exposure to Ureaplasma parvum. Reprod. Sci. 18, 1128–1137.

Kemp, M.W., Kannan, P.S., Saito, M., Newnham, J.P., Cox, T., Jobe, A.H., et al., 2013. Selective exposure of the fetal lung and skin/amnion (but not gastro-intestinal tract) to LPS elicits acute systemic inflammation in fetal sheep. PLoS One 8. (5), e63355.

Kemp, M.W., Miura, Y., Payne, M.S., Jobe, A.H., Kallapur, S.G., Saito, M., et al., 2014. Maternal intravenous administration of azithromycin results in significant fetal uptake in a sheep model of second trimester pregnancy. Antimicrob. Agents Chemother. 58 (11), 6581–6591.

Kemp, M.W., Molloy, T.J., Usuda, H., Woodward, E., Miura, Y., Payne, M.S., et al., 2016. Outside-in? Acute fetal systemic inflammation in very preterm chronically catheterized sheep fetuses is not driven by cells in the fetal blood. Am. J. Obstet. Gynecol. 214 (2), 281.e1–281. e10.

Kenyon, S.L., Taylor, D.J., Tarnow-Mordi, W., 2001. Broad-spectrum antibiotics for spontaneous preterm labour: the ORACLE II randomised trial. Lancet 357 (9261), 989–994.

Khan, K.A., Petrou, S., Dritsaki, M., Johnson, S.J., Manktelow, B., Draper, E.S., et al., 2016. Economic costs associated with moderate and late preterm birth: a prospective population-based study. BJOG 122 (11), 1495–1505.

Kim, M.J., Romero, R., Gervasi, M.T., Kim, J.S., Yoo, W., Lee, D.C., et al., 2009. Widespread microbial invasion of the chorioamniotic membranes is a consequence and not a cause of intra-amniotic infection. Lab. Invest. 89 (8), 924–936.

Kim, C.J., Romero, R., Chaemsaithong, P., Chaiyasit, N., Yoon, B.H., Kim, Y.M., 2015. Acute chorioamnionitis and funisitis: definition, pathologic features, and clinical significance. Am. J. Obstet. Gynecol. 213 (4 Suppl.), S29–S52.

Koga, K., Cardenas, I., Aldo, P., Abrahams, V.M., Peng, B., Fill, S., et al., 2009. Activation of TLR3 in the trophoblast is associated with preterm delivery. Am. J. Reprod. Immunol. 61 (3), 196–212.

Kundsin, R.B., Driscoll, S.G., Monson, R.R., 1984. Association of Ureaplasma urealyticum in the placenta with perinatal morbidity and mortality. N. Engl. J. Med. 310 (15), 941–945.

Lahra, M.M., Gordon, A., Jeffery, H.E., 2007. Chorioamnionitis and fetal response in stillbirth. Am. J. Obstet. Gynecol. 196 (3), 229.

Lamont, R.F., Nhan-Chang, C.L., Sobel, J.D., Workowski, K., Conde-Agudelo, A., Romero, R., 2011. Treatment of abnormal vaginal flora in early pregnancy with clindamycin for the prevention of spontaneous preterm birth: a systematic review and metaanalysis. Am. J. Obstet. Gynecol. 205 (3), 177–190.

Langmia, I.M., Apalasamy, Y.D., Omar, S.Z., Mohamed, Z., 2015. Interleukin 1 receptor type 2 gene polymorphism is associated with reduced risk of preterm birth. J. Matern. Fetal. Neonatal Med. 29, 3347–3350.

Larsen, J.W.A., Constable, P.D., Napthine, D.V., 1986. Hypocalcaemia in ewes after a drought. Aust. Vet. J. 63 (1), 25–26.

Lawn, J.E., Cousens, S., Zupan, J., 2005. 4 Million neonatal deaths: when? where? why? Lancet 365 (9462), 891–900.

Leary, S., Underwood, W., Anthony, R., Cartner, S., Corey, D., Grandin, T., Yanong, R., 2013. AVMA guidelines for the euthanasia of animals: 2014 edition. Am. Vet. Med. Assoc.

Leitner, K., Al Shammary, M., McLane, M., Johnston, M.V., Elovitz, M.A., Burd, I., 2014. IL-1 receptor blockade prevents fetal cortical brain injury but not preterm birth in a mouse model of inflammation-induced preterm birth and perinatal brain injury. Am. J. Reprod. Immunol. 71 (5), 418–426.

León, R., Silva, N., Ovalle, A., Chaparro, A., Ahumada, A., Gajardo, M., et al., 2007. Detection of Porphyromonas gingivalis in the amniotic fluid in pregnant women with a diagnosis of threatened premature labor. J. Periodontol. 78 (7), 1249–1255.

Liggins, G.C., 1981. Cervical ripening as an inflammatory reaction. In: Ellwood, D.A., Anderson, A.B.M. (Eds.), The Cervix in Pregnancy and Labour, Clinical and Biochemical Investigations. Churchill Livingstone, Edinburgh, pp. 1–9.

Liu, H., Redline, R.W., Han, Y.W., 2007. Fusobacterium nucleatum induces fetal death in mice via stimulation of TLR4-mediated placental inflammatory response. J. Immunol. 179 (4), 2501–2508.

Loo, Y.-M., Gale, M., 2011. Immune signaling by RIG-I-like receptors. Immunity 34 (5), 680–692.

Lye, S.J., Ou, C.W., Teoh, T.G., Erb, G., Stevens, Y., Casper, R., et al., 1998. The molecular basis of labour and tocolysis. Fetal Matern. Med. Rev. 10 (3), 121–136.

Madianos, P.N., Bobetsis, Y.A., Offenbacher, S., 2013. Adverse pregnancy outcomes (APOs) and periodontal disease: pathogenic mechanisms. J. Clin. Periodontol. 40 (Suppl. 14), S170–S180.

Maneenil, G., Kemp, M.W., Kannan, P.S., Kramer, B.W., Saito, M., Newnham, J.P., et al., 2015a. Oral, nasal and pharyngeal exposure to lipopolysaccharide causes a fetal inflammatory response in sheep. PLoS One 10 (3).

Maneenil, G., Payne, M.S., Kannan, P.S., Kallapur, S.G., Kramer, B.W., Newnham, J.P., et al., 2015b. Fluconazole treatment of intrauterine Candida albicans infection in fetal sheep. Pediatr. Res. 77 (6), 740–748.

Mangham, L.J., Petrou, S., Doyle, L.W., Draper, E.S., Marlow, N., 2009. The cost of preterm birth throughout childhood in England and Wales. Pediatrics 123 (2), e312–e327.

Matsumiya, T., Stafforini, D.M., 2010. Function and regulation of retinoic acid-inducible gene-I. Crit. Rev. Immunol. 30 (6), 489–513.

McDuffie, Jr., R.S., Blanton, S.J., Shikes, R.H., Gibbs, R.S., 1991. A rabbit model for bacterially induced preterm pregnancy loss: Intervention studies with ampicillin-sulbactam. Am. J. Obstet. Gynecol. 165 (5 I), 1568–1574.

Meijer, W.J., Van Noortwijk, A.G.A., Bruinse, H.W., Wensing, A.M.J., 2015. Influenza virus infection in pregnancy: a review. Acta Obstet. Gynecol. Scand. 94 (8), 797–819.

Menon, R., Peltier, M.R., Eckardt, J., Fortunato, S.J., 2009. Diversity in cytokine response to bacteria associated with preterm birth by fetal membranes. Am. J. Obstet. Gynecol. 201 (3), 306.e1–306.e6.

Meschia, G., Makowski, E.L., Battaglia, F.C., 1969. The use of indwelling catheters in the uterine and umbilical veins of sheep for a description of fetal acid-base balance and oxygenation. Yale J. Biol. Med. 42 (3–4), 154–165.

Michalowicz, B.S., Hodges, J.S., DiAngelis, A.J., Lupo, V.R., Novak, M.J., Ferguson, J.E., et al., 2006. Treatment of periodontal disease and the risk of preterm birth. N. Engl. J. Med. 355 (18), 1885–1894.

Migale, R., Herbert, B.R., Lee, Y.S., Sykes, L., Waddington, S.N., Peebles, D., et al., 2015. Specific lipopolysaccharide serotypes induce differential maternal and neonatal inflammatory responses in a murine model of preterm labor. Am. J. Pathol. 185 (9), 2390–2401.

Miyoshi, H., Konishi, H., Teraoka, Y., Urabe, S., Furusho, H., Miyauchi, M., et al., 2016. Enhanced expression of contractile-associated proteins and ion channels in preterm delivery model mice with chronic odontogenic *Porphyromonas gingivalis* infection. Reprod. Sci. 23, 838–846.

Money, D., Boucoiran, I., Wagner, E., Dobson, S., Kennedy, A., Lohn, Z., et al., 2014. Obstetrical and neonatal outcomes among women infected with hepatitis C and their infants. J. Obstet. Gynaecol. Can. 36 (9), 785–794.

Montgomery-Taylor, S., Hemelaar, J., 2015. Management and outcomes of pregnancies among women with HIV in Oxford, UK, in 2008-2012. Int. J. Gynecol. Obstet. 130 (1), 59–63.

Moreira, L.O., Zamboni, D.S., 2012. NOD1 and NOD2 signaling in infection and inflammation. Front. Immunol. 3, 328.

Moro, P.L., Museru, O.I., Broder, K., Cragan, J., Zheteyeva, Y., Tepper, N., et al., 2013. Safety of influenza a (H1N1) 2009 live attenuated monovalent vaccine in pregnant women. Obstet. Gynecol. 122 (6), 1271–1278.

Moro, P.L., Museru, O.I., Niu, M., Lewis, P., Broder, K., 2014. Reports to the vaccine adverse event reporting system after hepatitis a and hepatitis AB vaccines in pregnant women. Am. J. Obstet. Gynecol. 210 (6), e1–e6.

Moss, T.J.M., Nitsos, I., Ikegami, M., Jobe, A.H., Newnham, J.P., 2005. Experimental intrauterine *Ureaplasma* infection in sheep. Am. J. Obstet. Gynecol. 192 (4), 1179–1186.

Moss, T.J.M., Knox, C.L., Kallapur, S.G., Nitsos, I., Theodoropoulos, C., Newnham, J.P., et al., 2008. Experimental amniotic fluid infection in sheep: effects of *Ureaplasma parvum* serovars 3 and 6 on preterm or term fetal sheep. Am. J. Obstet. Gynecol. 198 (1), e121–e128.

Murdoch, F.R., Maker, G.L., Nitsos, I., Polglase, G.R., Musk, G.C., 2013. Intraperitoneal medetomidine: a novel analgesic strategy for postoperative pain management in pregnant sheep. Lab. Anim. 47 (1), 66–70.

Musk, G.C., Kemp, M.W., 2016. Maternal and fetal arterial blood gas data during general anaesthesia for caesarean delivery of preterm twin lambs. Lab. Anim. 50 (3), 198–203.

Musk, G.C., Murdoch, F.R., Tuke, J., Kemp, M.W., Dixon, M.J., Taylor, P.M., 2014. Thermal and mechanical nociceptive threshold testing in pregnant sheep. Vet. Anaesth. Analg. 41 (3), 305–311.

Nadeau, H.C.G., Subramaniam, A., Andrews, W.W., 2016. Infection and preterm birth. Semin. Fetal Neonatal Med. 21 (2), 100–105.

Nadeau-Vallée, M., Quiniou, C., Palacios, J., Hou, X., Erfani, A., Madaan, A., et al., 2015. Novel noncompetitive IL-1 receptor-biased ligand prevents infection- and inflammation-induced preterm birth. J. Immunol. 195 (7), 3402–3415.

Nadeau-Vallée, M., Obari, D., Quiniou, C., Lubell, W.D., Olson, D.M., Girard, S., Chemtob, S., 2016. A critical role of interleukin-1 in preterm labor. Cytokine Growth Factor Rev. 28, 37–51.

Nakai, A., Saito, S., Unno, N., Kubo, T., Minakami, H., 2012. Review of the pandemic (H1N1) 2009 among pregnant Japanese women. J. Obstet. Gynaecol. Res. 38 (5), 757–762.

Nalubamba, K.S., Gossner, A.G., Dalziel, R.G., Hopkins, J., 2008. Differential expression of pattern recognition receptors during the development of foetal sheep. Dev. Comp. Immunol. 32 (7), 869–874.

Newnham, J.P., Kelly, R.W., Boyne, P., Reid, S.E., 1989. Ultrasound guided blood sampling form fetal sheep. Aust. J. Agric. Res. 40, 401–407.

Newnham, J.P., Sahota, D.S., Zhang, C.Y., Xu, B., Zheng, M., Doherty, D.A., et al., 2011. Preterm birth rates in Chinese women in China, Hong Kong and Australia—the price of Westernisation. Aust. N. Z. J. Obstet. Gynaecol. 51 (5), 426–431.

Nikiforou, M., Kemp, M.W., Van Gorp, R.H., Saito, M., Newnham, J.P., Reynaert, N.L., et al., 2016. Selective IL-1α exposure to the fetal gut, lung, and chorioamnion/skin causes intestinal inflammatory and developmental changes in fetal sheep. Lab. Invest. 96 (1), 69–80.

Novy, M.J., Duffy, L., Axthelm, M.K., Sadowsky, D.W., Witkin, S.S., Gravett, M.G., et al., 2009. *Ureaplasma parvum* or *Mycoplasma hominis* as sole pathogens cause chorioamnionitis, preterm delivery, and fetal pneumonia in rhesus macaques. Reprod. Sci. 16 (1), 56–70.

Offenbacher, S., Katz, V., Fertik, G., Collins, J., Boyd, D., Maynor, G., et al., 1996. Periodontal infection as a possible risk factor for preterm low birth weight. J. Periodontol. 67 (10 Suppl.), 1103–1113.

Offenbacher, S., Jared, H.L., O'Reilly, P.G., Wells, S.R., Salvi, G.E., Lawrence, H.P., et al., 1998. Potential pathogenic mechanisms of periodontitis associated pregnancy complications. Ann. Periodontol. 3 (1), 233–250.

Offenbacher, S., Boggess, K.A., Murtha, A.P., Jared, H.L., Lieff, S., McKaig, R.G., et al., 2006. Progressive periodontal disease and risk of very preterm delivery. Obstet. Gynecol. 107 (1), 29–36.

Okutomi, T., Whittington, R., Stein, D., Morishima, H., 2009. Comparison of the effects of sevoflurane and isoflurane anesthesia on the maternal-fetal unit in sheep. J. Anesth. 23 (3), 392–398.

Ophelders, D.R., Gussenhoven, R., Lammens, M., Küsters, B., Kemp, M.W., Newnham, J.P., et al., 2016. Neuroinflammation and structural injury of the fetal ovine brain following intra-amniotic *Candida albicans* exposure. J. Neuroinflammation 13 (1), 1.

Otto, K.A., Cebotari, S., Höffler, H.-K., Tudorache, I., 2012. Electroencephalographic Narcotrend index, spectral edge frequency and median power frequency as guide to anaesthetic depth for cardiac surgery in laboratory sheep. Vet. J. 191, 354–359.

Pandey, M., Awasthi, S., 2016. Prognostic role of Interluekin-1 α and β gene polymorphisms in preterm birth. Gene Rep. 4, 112–117.

Paralanov, V., Lu, J., Duffy, L.B., Crabb, D.M., Shrivastava, S., Methé, B.A., et al., 2012. Comparative genome analysis of 19 *Ureaplasma urealyticum* and *Ureaplasma parvum* strains. BMC Microbiol. 12, 88.

Payne, M.S., Kemp, M.W., Kallapur, S.G., Kannan, P.S., Saito, M., Miura, Y., et al., 2014a. Intrauterine *Candida albicans* infection elicits severe inflammation in fetal sheep. Pediatr. Res. 75 (6), 716.

Payne, M.S., Tabone, T., Kemp, M.W., Keelan, J.A., Spiller, O.B., Newnham, J.P., 2014b. High-resolution melt PCR analysis for genotyping of *Ureaplasma parvum* isolates directly from clinical samples. J. Clin. Microbiol. 52 (2), 599–606.

Petrikin, J.E., Gaedigk, R., Leeder, J.S., Truog, W.E., 2010. Selective toll-like receptor expression in human fetal lung. Pediatr. Res. 68 (4), 335–338.

Polese, B., Gridelet, V., Araklioti, E., Martens, H., d'Hauterive, S.P., Geenen, V., 2014. The endocrine milieu and CD4 T-lymphocyte polarization during pregnancy. Front. Endocrinol. 5, 106.

Prince, A.L., Antony, K.M., Chu, D.M., Aagaard, K.M., 2014. The microbiome, parturition, and timing of birth: more questions than answers. J. Reprod. Immunol. 104–105 (1), 12–19.

Quinn, C., Raisis, A., Musk, G., 2013. Evaluation of Masimo signal extraction technology pulse oximetry. Vet. Anaesth. Analg. 40 (2), 149–156.

Racicot, K., Cardenas, I., Wünsche, V., Aldo, P., Guller, S., Means, R.E., et al., 2013. Viral infection of the pregnant cervix predisposes to ascending bacterial infection. J. Immunol. 191 (2), 934–941.

Racicot, K., Kwon, J.Y., Aldo, P., Abrahams, V., El-Guindy, A., Romero, R., Mor, G., 2016. Type I interferon regulates the placental inflammatory response to bacteria and is targeted by virus: mechanism of polymicrobial infection-induced preterm birth. Am. J. Reprod. Immunol. 75 (4), 451–460.

Redline, R.W., Faye-Petersen, O., Heller, D., Qureshi, F., Savell, V., Vogler, C., 2003. Amniotic infection syndrome: nosology and reproducibility of placental reaction patterns. Pediatr. Dev. Pathol. 6 (5), 435–448.

Reznikov, L.L., Fantuzzi, G., Selzman, C.H., Shames, B.D., Barton, H.A., Bell, H., et al., 1999. Utilization of endoscopic inoculation in a mouse model of intrauterine infection-induced preterm birth: role of interleukin 1? Biol. Reprod. 60 (5), 1231–1238.

Rinaldi, S.F., Catalano, R.D., Wade, J., Rossi, A.G., Norman, J.E., 2014. Decidual neutrophil infiltration is not required for preterm birth in a mouse model of infection-induced preterm labor. J. Immunol. 192 (5), 2315–2325.

Robertson, J.A., Stemke, G.W., Davis, Jr., J.W., Harasawa, R., Thirkell, D., Kong, F., et al., 2002. Proposal of Ureaplasma parvum sp. nov. and emended description of Ureaplasma urealyticum (Shepard et al. 1974) Robertson et al. 2001. Int. J. Syst. Evol. Microbiol. 52 (2), 587–597.

Robertson, S.A., Christiaens, I., Dorian, C.L., Zaragoza, D.B., Care, A.S., Banks, A.M., Olson, D.M., 2010. Interleukin-6 is an essential determinant of on-time parturition in the mouse. Endocrinology 151 (8), 3996–4006.

Romero, R., Tartakovsky, B., 1992. The natural interleukin-1 receptor antagonist prevents interleukin-1-induced preterm delivery in mice. Am. J. Obstet. Gynecol. 167 (4 I), 1041–1045.

Romero, R., Reece, E.A., Duff, G.W., Coultrip, L., Hobbins, J.C., 1985. Prenatal diagnosis of Candida albicans chorioamnionitis. Am. J. Perinatol. 2 (2), 121–122.

Romero, R., Lafreniere, D., Duff, G.W., Kadar, N., Durum, S., Hobbins, J.C., 1987. Failure of endotoxin to cross the chorioamniotic membranes in vitro. Am. J. Perinatol. 4 (4), 360–362.

Romero, R., Brody, D.T., Oyarzun, E., Mazor, M., Wu, Y.K., Hobbins, J.C., Durum, S.K., 1989. Infection and labor. III. Interleukin-1: a signal for the onset of parturition. Am. J. Obstet. Gynecol. 160 (5 Pt 1), 1117–1123.

Romero, R., Mazor, M., Tartakovsky, B., 1991. Systemic administration of interleukin-1 induces preterm parturition in mice. Am. J. Obstet. Gynecol. 165 (4 I), 969–971.

Romero, R., Erez, O., Espinoza, J., 2005. Intrauterine infection, preterm labor, and cytokines. J. Soc. Gynecol. Investig. 12 (7), 463–465.

Romero, R., Espinoza, J., Goncalves, L.F., Kusanovic, J.P., Friel, L., Hassan, S., 2007. The role of inflammation and infection in preterm birth. Semin. Reprod. Med. 25 (1), 21–39.

Romero, R., Dey, S.K., Fisher, S.J., 2014. Preterm labor: one syndrome, many causes. Science 345 (6198), 760–765.

Russell, W.M.A., Burch, R.L., 1959. The Principles of Human Experimental Technique. Methuen & Co Ltd, London.

Sadowsky, D.W., Haluska, G.J., Gravett, M.G., Witkin, S.S., Novy, M.J., 2000. Indomethacin blocks interleukin 1beta-induced myometrial contractions in pregnant rhesus monkeys. Am. J. Obstet. Gynecol. 183 (1), 173–180.

Sadowsky, D.W., Novy, M.J., Witkin, S.S., Gravett, M.G., 2003. Dexamethasone or interleukin-10 blocks interleukin-1beta-induced uterine contractions in pregnant rhesus monkeys. Am. J. Obstet. Gynecol. 188 (1), 252–263.

Sadowsky, D.W., Adams, K.M., Gravett, M.G., Witkin, S.S., Novy, M.J., 2006. Preterm labor is induced by intraamniotic infusions of interleukin-1β and tumor necrosis factor-α but not by interleukin-6 or interleukin-8 in a nonhuman primate model. Am. J. Obstet. Gynecol. 195 (6), 1578–1589.

Sancho, D., Reis e Sousa, C., 2012. Signaling by myeloid C-type lectin receptors in immunity and homeostasis. Annu. Rev. Immunol. 30, 491–529.

Schlumbohm, C., Harmeyer, J., 2008. Twin-pregnancy increases susceptibility of ewes to hypoglycaemic stress and pregnancy toxaemia. Res. Vet. Sci. 84 (2), 286–299.

Schmid, M., Haslinger, P., Stary, S., Leipold, H., Egarter, C., Grimm, C., 2012. Interleukin-1 beta gene polymorphisms and preterm birth. Eur. J. Obstet. Gynecol. Reprod. Biol. 165 (1), 33–36.

Serfontein, L., 2010. Awareness in cardiac anesthesia. Curr. Opin. Anaesthesiol. 23 (1), 103–108.

Sharma, A.A., Jen, R., Kan, B., Sharma, A., Marchant, E., Tang, A., et al., 2015. Impaired NLRP3 inflammasome activity during fetal development regulates IL-1β production in human monocytes. Eur. J. Immunol. 45 (1), 238–249.

Sharp, G.C., Hutchinson, J.L., Hibbert, N., Freeman, T.C., Saunders, P.T.K., Norman, J.E., 2016. Transcription analysis of the myometrium of labouring and non-labouring women. PLoS One 11 (5).

Shimizu, T., Kida, Y., Kuwano, K., 2008. Ureaplasma parvum lipoproteins, including MB antigen, activate NF-κB through TLR1, TLR2 and TLR6. Microbiology 154 (5), 1318–1325.

Sims, J.E., Smith, D.E., 2010. The IL-1 family: regulators of immunity. Nat. Rev. Immunol. 10 (2), 89–102.

Sirilert, S., Traisrisilp, K., Sirivatanapa, P., Tongsong, T., 2014. Pregnancy outcomes among chronic carriers of hepatitis B virus. Int. J. Gynecol. Obstet. 126 (2), 106–110.

Sloane, D.E., Tedla, N., Awoniyi, M., MacGlashan, Jr., D.W., Borges, L., Austen, K.F., Arm, J.P., 2004. Leukocyte immunoglobulin-like receptors: novel innate receptors for human basophil activation and inhibition. Blood 104 (9), 2832–2839.

Sow, F.B., Gallup, J.M., Derscheid, R., Krishnan, S., Ackermann, M.R., 2012. Ontogeny of the immune response in the ovine lung. Immunol. Investigat. 41 (3), 304–316.

Srinivas, S.K., Ma, Y., Sammel, M.D., Chou, D., McGrath, C., Parry, S., Elovitz, M.A., 2006. Placental inflammation and viral infection are implicated in second trimester pregnancy loss. Am. J. Obstet. Gynecol. 195 (3), 797–802.

Stock, S.J., Patey, O., Thilaganathan, B., White, S., Furfaro, L.L., Payne, M.S., Carter, S., 2016. Intrauterine Candida albicans infection causes systemic fetal Candidiasis with progressive cardiac dysfunction in a sheep model of early pregnancy. Reprod. Sci. 24 (1), 77–84.

Stockham, S., Stamford, J.E., Roberts, C.T., Fitzsimmons, T.R., Marchant, C., Bartold, P.M., Zilm, P.S., 2015. Abnormal pregnancy outcomes in mice using an induced periodontitis model and the haematogenous migration of Fusobacterium nucleatum sub-species to the murine placenta. PLoS One 10 (3), e0120050.

Strumper, D., Gogarten, W., Durieux, M.E., Hartleb, K., Van Aken, H., Marcus, M.A.E., 2004. The effects of S(+)-ketamine and racemic ketamine on uterine blood flow in chronically instrumented pregnant sheep. Anesth. Analg. 98 (2), 497–502.

Sung, T.J., Xiao, L., Duffy, L., Waites, K.B., Chesko, K.L., Viscardi, R.M., 2011. Frequency of ureaplasma serovars in respiratory secretions of preterm infants at risk for bronchopulmonary dysplasia. Pediatr. Infect. Dis. J. 30 (5), 379–383.

Suthar, M.S., Ramos, H.J., Brassil, M.M., Netland, J., Chappell, C.P., Blahnik, G., et al., 2012. The RIG-I like receptor LGP2 controls CD8(+) T cell survival and fitness. Immunity 37 (2), 235–248.

Sweeney, E.L., Kallapur, S.G., Gisslen, T., Lambers, D.S., Chougnet, C.A., Stephenson, S.A., et al., 2016. Placental infection with Ureaplasma species is associated with histologic chorioamnionitis and adverse outcomes in moderately preterm and late-preterm infants. J. Infect. Dis. 213 (8), 1340–1347.

Tang, D., Kang, R., Coyne, C.B., Zeh, H.J., Lotze, M.T., 2012. PAMPs and DAMPs: signal 0s that spur autophagy and immunity. Immunol. Rev. 249 (1), 158–175.

Timmons, B.C., Reese, J., Socrate, S., Ehinger, N., Paria, B.C., Milne, G.L., et al., 2014. Prostaglandins are essential for cervical ripening in LPS-Mediated preterm birth but not term or antiprogestin-driven preterm ripening. Endocrinology 155 (1), 287–298.

Tita, A.T.N., Landon, M.B., Spong, C.Y., Lai, Y., Leveno, K.J., Varner, M.W., et al., 2009. Timing of elective repeat cesarean delivery at term and neonatal outcomes. N. Engl. J. Med. 360 (2), 111–120.

Tsekoura, E.A., Konstantinidou, A., Papadopoulou, S., Athanasiou, S., Spanakis, N., Kafetzis, D., et al., 2010. Adenovirus genome in the placenta: association with histological chorioamnionitis and preterm birth. J. Med. Virol. 82 (8), 1379–1383.

Van Overmeire, B., Chemtob, S., 2005. The pharmacologic closure of the patent ductus arteriosus. Semin. Fetal Neonatal Med. 10 (2), 177–184.

Van Saun, R.J., 2000. Pregnancy toxemia in a flock of sheep. J. Am. Vet. Med. Assoc. 217 (10), 1536–1539.

Vanterpool, S.F., Been, J.V., Houben, M.L., Nikkels, P.G.J., De Krijger, R.R., Zimmermann, L.J.I., et al., 2016. *Porphyromonas gingivalis* within placental villous mesenchyme and umbilical cord stroma is associated with adverse pregnancy outcome. PLoS One 11 (1), e0146157.

Villar, J., Papageorghiou, A.T., Knight, H.E., Gravett, M.G., Iams, J., Waller, S.A., et al., 2012. The preterm birth syndrome: a prototype phenotypic classification. Am. J. Obstet. Gynecol. 206 (2), 119–123.

Vinturache, A.E., Gyamfi-Bannerman, C., Hwang, J., Mysorekar, I.U., Jacobsson, B., 2016. Maternal microbiome—a pathway to preterm birth. Semin. Fetal Neonatal Med. 21 (2), 94–99.

Viscardi, R.M., 2010. *Ureaplasma* species: role in diseases of prematurity. Clin. Perinatol. 37 (2), 393–409.

Viscardi, R.M., 2014. *Ureaplasma* species: role in neonatal morbidities and outcomes. Arch. Dis. Childhood Fetal Neonatal Ed. 99 (1), F87–F92.

Volgmann, T., Ohlinger, R., Panzig, B., 2005. *Ureaplasma urealyticum*-harmless commensal or underestimated enemy of human reproduction? A review. Arch. Gynecol. Obstet. 273 (3), 133–139.

Vontell, R., Supramaniam, V., Thornton, C., Wyatt-Ashmead, J., Mallard, C., Gressens, P., et al., 2013. Toll-like receptor 3 expression in Glia and neurons alters in response to white matter injury in preterm infants. Dev. Neurosci. 35 (2–3), 130–139.

Voss, E., Wehkamp, J., Wehkamp, K., Stange, E.F., Schröder, J.M., Harder, J., 2006. NOD2/CARD15 mediates induction of the antimicrobial peptide human beta-defensin-2. J. Biol. Chem. 281 (4), 2005–2011.

Wakabayashi, A., Sawada, K., Nakayama, M., Toda, A., Kimoto, A., Mabuchi, S., et al., 2013. Targeting interleukin-6 receptor inhibits preterm delivery induced by inflammation. Mol. Hum. Reprod. 19 (11), 718–726.

Waldorf, K.M.A., Gravett, M.G., McAdams, R.M., Paolella, L.J., Gough, G.M., Carl, D.J., et al., 2011. Choriodecidual group B streptococcal inoculation induces fetal lung injury without intra-amniotic infection and preterm labor in *Macaca nemestrina*. PLoS One 6 (12), e28972.

Wang, X., Hagberg, H., Mallard, C., Zhu, C., Hedtjärn, M., Tiger, C.F., et al., 2006. Disruption of interleukin-18, but not interleukin-1, increases vulnerability to preterm delivery and fetal mortality after intrauterine inflammation. Am. J. Pathol. 169 (3), 967–976.

Warburton, D., Schwarz, M., Tefft, D., Flores-Delgado, G., Anderson, K.D., Cardoso, W.V., 2000. The molecular basis of lung morphogenesis. Mech. Dev. 92 (1), 55–81.

Wei, S.Q., Fraser, W., Luo, Z.C., 2010. Inflammatory cytokines and spontaneous preterm birth in asymptomatic women: a systematic review. Obstet. Gynecol. 116 (2 Pt 1), 393–401.

Wenstrom, K.D., Andrews, W.W., Bowles, N.E., Towbin, J.A., Hauth, J.C., Goldenberg, R.L., 1998. Intrauterine viral infection at the time of second trimester genetic amniocentesis. Obstet. Gynecol. 92 (3), 420–424.

Werman, A., Werman-Venkert, R., White, R., Lee, J.K., Werman, B., Krelin, Y., et al., 2004. The precursor form of IL-1α is an intracrine proinflammatory activator of transcription. Proc. Natl. Acad. Sci. USA 101 (8), 2434–2439.

Witt, A., Berger, A., Gruber, C.J., Petricevic, L., Apfalter, P., Worda, C., Husslein, P., 2005. Increased intrauterine frequency of *Ureaplasma urealyticum* in women with preterm labor and preterm premature rupture of the membranes and subsequent cesarean delivery. Am. J. Obstet. Gynecol. 193 (5), 1663–1669.

Wolfenson, S., Lloyd, M., 2003. Handbook of Laboratory Animal Management and Welfare, third ed. Blackwell Publishing Limited, Oxford, United Kingdom.

Wolfs, T.G.A.M., Kramer, B.W., Thuijls, G., Kemp, M.W., Saito, M., Willems, M.G.M., et al., 2014. Chorioamnionitis-induced fetal gut injury is mediated by direct gut exposure of inflammatory mediators or by lung inflammation. Am. J. Physiol. Gastrointest. Liver Physiol. 306 (5), G382–G393.

Wu, X., Offenbacher, S., López, N.J., Chen, D., Wang, H.Y., Rogus, J., et al., 2015. Association of interleukin-1 gene variations with moderate to severe chronic periodontitis in multiple ethnicities. J. Periodontal Res. 50 (1), 52–61.

Xiao, P.L., Zhou, Y.B., Chen, Y., Yang, M.X., Song, X.X., Shi, Y., Jiang, Q.W., 2015. Association between maternal HIV infection and low birth weight and prematurity: a meta-analysis of cohort studies. BMC Pregnancy Childbirth 15 (1), 246.

Yoder, B.A., Coalson, J.J., Winter, V.T., Siler-Khodr, T., Duffy, L.B., Cassell, G.H., 2003. Effects of antenatal colonization with *Ureaplasma urealyticum* on pulmonary disease in the immature Baboon. Pediatr. Res. 54 (6), 797–807.

Zhang, X., Kramer, M.S., 2009. Variations in mortality and morbidity by gestational age among infants born at term. J. Pediatr. 154 (3), 358–362.

Zhu, Z., Zhang, X., Wang, G., Zheng, H., 2014. The laboratory of genetics and physiology 2: emerging insights into the controversial functions of this RIG-I-like receptor. BioMed Res. Int. 2014, 960190.

31

Animal Models for the Study of Neonatal Disease

Jean-Paul Praud*, Yuichiro Miura**, Martin G. Frasch†

*Université de Sherbrooke, Sherbrooke, QC, Canada
**The University of Western Australia, Perth, Australia
†University of Washington, Seattle, WA, United States

O U T L I N E

NEONATAL RESPIRATION

A thorough review of the literature on the animal models used to study neonatal breathing is clearly beyond the scope of this short review. A biased choice of a few items in this area is proposed in the following paragraphs. We have attempted to illustrate the variety of animal models that have been used to unravel the normal establishment of successful breathing at birth and its maintenance in the early postnatal period, as well as a number of abnormal conditions that can interfere with those processes.

1 ESTABLISHMENT OF AIR BREATHING AT BIRTH

At birth, an immediate adaptation to air breathing is a vital requirement for the newborn. This adaptation includes lung aeration as well as maintenance of regular and efficient respiratory efforts.

1.1 Transition From a Liquid-Filled Lung to Air Breathing at Birth

1.1.1 Normal Lung Aeration at Birth

Rapid aeration of liquid-filled lungs at birth is mandatory for a successful transition from the fetal to the newborn state. Forceful inspiratory efforts create a pressure gradient within the airways, which moves air into the lungs. This in turn opens the distal airways and moves the liquid across the epithelial alveoli into the parenchyma. At the same time, lung inflation decreases the pulmonary vascular resistance and increases pulmonary blood flow, creating an optimal situation for gas exchange. Air stacking in the lungs initially depends not only on inspiratory efforts, but also on active expiratory laryngeal closure to keep a sufficient amount of air into the lung at the end of expiration, namely the functional residual capacity. The presence of surfactant is crucial in this process; by decreasing the surface tension of the distal airways, the surfactant decreases the elastic recoil of the lung, hence decreasing expiratory emptying of the lung.

Studies in spontaneously breathing newborn rabbits have shown that lung aeration is predominantly achieved by inspiratory efforts, while expiratory efforts are involved in maintaining functional residual capacity (Siew et al., 2009). Further studies in newborn rabbits have shown that lung aeration is not homogeneous at birth (Hooper et al., 2007), and that monitoring of expired CO_2 in lambs and rabbits is a useful indicator of the degree of lung aeration (Hooper et al., 2013).

1.1.2 Influence of Premature Birth and Resuscitative Maneuvers to Aerate the Lung at Birth

While the transition to air breathing occurs smoothly at birth in the vast majority of full-term newborns, a number of premature neonates, especially the very low birth weight, are not capable to successfully transition to air breathing at birth. Inadequate command from the respiratory centers to initiate breathing, weak inspiratory muscles, absence of functional surfactant, extremely pliable rib cage, persistence of a high pulmonary vascular resistance are among the factors that negatively impact respiration onset at birth.

Most very preterm infants at birth hence require the use of some form of positive pressure respiratory support, such as positive end-expiratory pressure, sustained lung inflation, or mechanical ventilation at fixed tidal volumes. This can, however, have highly deleterious effects on the immature lungs. For instance, studies in preterm lambs have shown that the use of large tidal volumes (35 mL/kg) for only six breaths to aerate the lungs at birth is sufficient to induce lung inflammation, initiate ventilator-induced lung injury (VILI), setting the stage for chronic lung disease, namely bronchopulmonary dysplasia (Bjorklund et al., 1997). In addition, very high pressures (40 cmH_2O) are needed in the preterm lamb to open the airways filled of liquid and assure a tidal volume of 6–8 mL/kg at 5 min of life (Wada et al., 1997). Convincing evidence on the proinflammatory effect of positive pressure ventilation at the onset of breathing

at birth has now been collected in a number of preclinical studies, using the preterm lamb model (Hillman et al., 2011a,b; Hillman et al., 2012b; Tingay et al., 2015a). Long-lasting consequences of this lung inflammation will be further reviewed in the section on bronchopulmonary dysplasia (see Section 2.3).

1.1.3 The Quest for the Optimal Ventilator Strategy to Support Lung Aeration at Birth in Very Preterm Newborns

Given the deleterious effect of positive pressure ventilation at birth in preterm lungs, a number of studies have been conducted in animal models, mainly in preterm lambs, with the aim to find out which ventilator strategy could minimize lung injury and reduce the development of bronchopulmonary dysplasia. Unfortunately, as reviewed later, the results do not allow to draw a clear picture of the optimal ventilator strategy to use to aerate the lung at birth (Jobe, 2015).

Endotracheal respiratory support. Lung inflammation induced at birth by endotracheal positive pressure mechanical ventilation was not prevented by using a low tidal volume (8 mL/kg) and a PEEP in lambs (Polglase et al., 2008). Moreover, other studies found that the inflammatory response and lung injury were lessened with surfactant treatment prior to ventilation (Hillman et al., 2011a; Wada et al., 1997), with antenatal corticosteroid treatment (Hillman et al., 2009) or with the use of PEEP (Hillman et al., 2011a; Ingimarsson et al., 2004). The latter was especially shown in lambs supported with higher levels of PEEP during high-frequency jet ventilation (Pillow et al., 2011).

On the other hand, variable ventilation improves ventilation efficiency and in vivo lung compliance (Pillow et al., 2011). While the use of a sustained inflation with a fixed duration was reported not to prevent lung inflammation (Hillman et al., 2013; Polglase et al., 2014), a further study suggested that a sustained inflation with an individualized duration is a better approach (Tingay et al., 2015a). However, this team also demonstrated that an incremental tidal volume strategy resulted in worse oxygenation and gravity-dependent heterogeneity of aeration in 131 days preterm lambs resuscitated at birth (Tingay et al., 2015b).

Noninvasive respiratory support. Given the deleterious effects of aerating the lungs at birth using endotracheal mechanical ventilation, noninvasive respiratory support from birth is an attracting modality. Studies using preterm experimental animal models (mainly lambs, but also piglets or mice) have revealed that the early use of noninvasive respiratory support is associated with better respiratory outcomes (Dargaville et al., 2015; Null et al., 2014; Reyburn et al., 2008; Thomson et al., 2004, 2006; Yoder et al., 2016). However, the optimal noninvasive support modality for preventing lung injury remains unclear. An animal model of nasal CPAP applied from birth has been designed, using short binasal prongs in newborn preterm lambs at 136 days of gestation (Rahmel et al., 2012). Also, nonintubated preterm lambs were effectively transitioned from nasal intermittent positive pressure ventilation + respiratory stimulants to nasal CPAP soon after birth (Dargaville et al., 2015). However, premature lambs with significant respiratory distress showed a progressive deterioration of respiratory gas exchanges after 3–4 h, while supported with bubble CPAP through nasal prongs or a nasopharyngeal tube (Reyburn et al., 2008).

1.2 Establishment and Maintenance of Regular Breathing Movements in the Newborn

Besides successful lung aeration at birth, regular breathing movements are vital for the newborn. Animal studies have allowed to show that breathing movements are present in the fetus before birth, and have helped to understand the normal perinatal control of breathing and its alterations in disease states.

1.2.1 Fetal Breathing Movements

Fetal breathing movements have been observed in utero either by chronic instrumentation or via ultrasound in a number of mammal species, including the horse, goat, rat, guinea pig, dog, rabbit, and baboon [reviewed in Jansen and Chernick (1983), Teppema and Dahan (2010)]. The vast majority of our knowledge on fetal breathing movements comes, however, from studies in the chronically instrumented lamb in utero initiated by Barcroft's team in the 1930s in Cambridge. Numerous experiments since then have shown the presence of fetal breathing movements, which can be observed as early as 40 days in the fetal lamb (versus 110 days in the human fetus). While continuous in early gestation, they follow the differentiation of electrocorticogram between states so that they are linked to low voltage electrocorticogram (REM sleep-like state) in the third trimester. This modulatory role of sleep states is demonstrated by the observation in the fetal lamb of almost continuous fetal breathing movements following brainstem transection at the upper pontine level [close to the principal trigeminal nuclei; reviewed in Teppema and Dahan (2010)]. Beyond being evidence of the early maturation of respiratory control, fetal breathing movements are crucial for prenatal lung growth [reviewed in Jansen and Chernick (1983), Teppema and Dahan (2010)]. During fetal breathing movements, diaphragmatic contractions are already well coordinated with contraction of the upper airway muscles, so that laryngeal constrictor muscles are tonically active when phasic diaphragm activity is absent, but silent when the diaphragm contracts (Kianicka et al., 1998a). Together with continuous lung liquid secretion, this tonic closure of the larynx allows to build

up positive pressure in the lung, in turn promoting lung growth. Fetal breathing movements have been shown to be the major stimulus for lung growth and maturation via mechanical stretch of the lung (Kitterman, 1996) and, at least partly, via stimulation of the epidermal growth factor receptor (Huang et al., 2012). Mechanical stretch of the lung occurs both with fetal breathing movements, which change the shape of the thorax, and during the prolonged phases without FBM, when active tonic closure of the larynx prevents the egress of lung liquid into the amniotic cavity, in turn distending the lungs.

1.2.2 Control of Breathing in the Perinatal Period

Establishment of respiratory efforts at birth. The process underlying the dramatic change from intermittent breathing in the fetus to continuous breathing in the newborn is far from being completely understood. Most of the information comes from studies in the fetal and newborn lamb. A number of stimuli are likely involved in the process, including the increased arterial pressure in CO_2 (Kuipers et al., 1992; Praud et al., 1997) and decreased arterial pressure in O_2 (not if severe hypoxia is present), the surge in catecholamines, the state of wakefulness, body cooling, and sensorial stimulations (Hillman et al., 2012a). In addition, controversial results have been reported on the crucial importance of a breathing inhibitory factor from placental origin, which would be prostaglandin E_2, and whose effect is suddenly stopped at birth with section of the umbilical cord (Alvaro et al., 1993; Kuipers et al., 1992).

Maturation of the hypoxic ventilatory response in the newborn. The importance and frequency of hypoxic conditions in the newborn has led to numerous experiments conducted in various animal species, including newborn lambs, kittens, piglets, monkeys, guinea pigs, rats, and mice, to study the hypoxic ventilatory response in the neonatal period [see reviews by Darnall (2013), Teppema and Dahan (2010)]. Prenatally, results have shown that hypoxia in the fetal lamb as well as in rhesus monkeys and rats is responsible for a decrease in ventilation. This inhibitory effect of hypoxia on fetal breathing movements' response is likely due to stimulation of the upper pons, as shown by the conversion to a stimulatory effect after lesions in the region of the upper pons, in the region of the parabrachial, and Kolliker-Fuse nuclei [reviewed in Teppema and Dahan (2010)]. Postnatally, the hypoxic ventilatory response is biphasic in the newborn mammals studied to date. Following a rapid increase in minute ventilation for 1–2 min due to carotid body stimulation, various central mechanisms, such as adenosine, GABA and endogenous opioids, as well as decreased metabolism are responsible for a roll-off of the hypoxic ventilatory response (Darnall, 2013; Teppema and Dahan, 2010). In newborn rats and mice, as well as in the preterm human, minute ventilation in the second phase of

the hypoxic response can even decrease below baseline level, with a significant decrease in body temperature (Gallego and Matrot, 2010). In the preterm lamb, the decreased hypoxic ventilatory response is related to the absence of the normal increase in tidal volume (as well as in heart rate) seen in full-term lambs (Pladys et al., 2008).

Postnatal maturation of the carotid body response to hypoxia has also been the subject of numerous studies in animals (Canet et al., 1996). Overall, these studies have established that following birth, carotid body sensitivity to O_2 is reset in a few days, from 3 days in lambs to 2–3 weeks in rodents and 4 weeks in the kitten [reviewed in Carroll and Kim (2013)]. Carotid body resetting is related to the increase in PaO_2 occurring with the transition to air breathing at birth (PaO_2 rapidly increases from 25 to 80 mmHg), as demonstrated by the fact that rising PaO_2 in the fetal lamb in utero by mechanical ventilation during 27 h is responsible for increased carotid body sensitivity at birth (=carotid body resetting had occurred prenatally) (Blanco et al., 1987).

Ventilatory response to CO_2 in the newborn. The ventilatory response to CO_2 in the newborn is very different from the hypoxic ventilatory response. Hypercapnia was shown to stimulate fetal breathing movement in lambs (Jansen and Chernick, 1983). Several studies have been conducted in animals (piglets, puppies, newborn rats, and mice) on the postnatal maturation of the ventilatory response to CO_2 [reviewed by Putnam et al. (2005)]. Depending on the species and the experimental conditions, the response at birth appeared as vigorous or sometimes less than the adult response. In all species, the CO_2 response was low between the 1st and 2nd postnatal week and then increased toward the adult level. The relative importance of breathing frequency or tidal volume in the response to CO_2 during maturation was variable among studies. Intriguingly, a prolongation of expiration was shown during the response to CO_2 in piglets, suggesting that postinspiratory laryngeal braking of the expiratory flow served to reduce the large variations in functional residual capacity, in turn optimizing gas exchange (Dreshaj et al., 2001).

Importance of vagal afferences for neonatal breathing. By constantly monitoring the mechanical status of the lungs throughout the breathing cycle, continuous vagal afferent information from bronchopulmonary receptors has a major influence on respiratory center output. Among other roles, slowly adapting receptors are responsible for the Hering–Breuer reflex that tightly controls tidal volume in newborn mammals, rapidly adapting receptors induce augmented breaths (=sighs), and C fibers participate with slowly adapting receptors in dynamically maintaining a high end-expiratory lung volume (Diaz et al., 1999). The vital importance of such information in the immediate postnatal period has been demonstrated in vagotomized newborn lambs, which die

from respiratory failure in a few hours, likely from at-electasis and hypoxia secondary to the loss of both the active maintenance of a high end-expiratory lung volume and the augmented breaths (Lalani et al., 2001). Though not so crucial a few days after birth, vagal afferent information is still of major importance for normal breathing in the 1st month of life. Indeed, the role of the Hering–Breuer reflex in exerting a tight control at this period is well established in newborn mammals (Trippenbach, 1994), underlying the important role of slowly adapting bronchopulmonary receptors. Experiments in lambs have shown that preterm birth does not alter maturation of the Hering–Breuer reflex. In addition, reflexes originating from C fibers are also present at birth in preterm lambs, though less potent than after full-term birth (Arsenault et al., 2003).

1.2.3 Apnea of Prematurity

Apnea of prematurity continues to be a daily, very important problem in neonatology. It is clearly related to the overall neural immaturity of the preterm newborn, so that the incidence is proportional to the degree of prematurity. Given that virtually all preterm infants born before 28 weeks of gestation suffer from clinically significant apnea of prematurity, and that the number of extreme preterm newborns (22–26 weeks) has been on the rise in neonatal intensive care units (NICUs) within the last years, the incidence of severe apnea of prematurity has similarly increased.

Apnea of prematurity is defined by the occurrence of repetitive, acute, and symptomatic cardiorespiratory events manifesting in a preterm infant as apneas longer than 20 s or shorter if accompanied with bradycardias and/or desaturations. Various mechanisms can be responsible for apnea of prematurity. For instance, the event can be primarily due to immaturity of the brainstem centers responsible for the basal respiratory rhythm, manifesting either as periodic breathing with intermittent hypoxia or as an isolated prolonged apnea + bradycardia + desaturation. In addition, other events can represent a reflex response, for example, originating from laryngeal or esophageal receptor stimulation during a gastric reflux.

A number of studies on apnea of prematurity have been conducted directly in preterm human infants. Animal models, however, have been also frequently used, when there was a need either for invasive instrumentation (e.g., in studies on upper airway muscle activity) or for experimental conditions unacceptable in human infants (e.g., repeated stimulation of the laryngeal mucosa, use of drugs). The following paragraphs summarize a few studies performed in that area. It begins by highlighting the preterm lamb model, which constitutes a unique and real asset for studying apnea of prematurity.

Preterm animal models to study apnea of prematurity. Apart from human newborn infants, most of the studies on spontaneous breathing reported in unanesthetized preterm animals have been performed in lambs, rabbits, monkeys, and in the very immature newborn opossum (Davey et al., 1996; Farber, 1972; Guthrie et al., 1980; Hedner et al., 1984; Marchal et al., 1982). To our knowledge, however, the only reports of *prolonged* recordings during sleep of cardiorespiratory variables in nonsedated, spontaneously breathing preterm mammals are in lambs. The preterm lamb constitutes a unique model of neonatal spontaneous respiratory instability, in which extensive chronic instrumentation and prolonged polysomnographic recordings are possible.

Personal experience (JPP) in prolonged recordings of spontaneously breathing, nonsedated preterm lambs dates from about 20 years. Our preterm lamb model has a postconceptional age of 131 ± 2 days (normal gestation 147 days). Over the years, many improvements have been made in order to increase survival rate and health outcomes of the animals. Following several protocols comparing cesarean section versus vaginal delivery, different methods to induce delivery, more or less postnatal intensive care (Arsenault et al., 2003; Reix et al., 2003, 2004; Renolleau et al., 1999; St-Hilaire et al., 2007), we are now using the following protocol, which ensures a mean survival of ~75% after 5–7 days of life, when we can perform surgical instrumentation followed by polysomnographic recordings. Premature labor is induced by mifepristone in ewes with dated gestation, after antenatal lung maturation by two betamethasone injections. Vaginal delivery occurs under continuous surveillance, in order to intervene in case of dystocia. At birth, lambs are cared by their mother, under strict and continuous supervision by an observer present for 48 h. Vital signs, including body temperature, heart and respiratory rate, oxygen saturation, blood glucose level, and weight are regularly monitored. Lambs need to be bottle-fed (preferably with mother's milk) in the first 24–48 h until they are strong enough to feed by themselves from the ewe. Apart from severe dystocia, the problems often encountered in the first 24–48 h include hypoglycemia, slight hypoxemia and hypothermia, which are immediately corrected. No exogenous surfactant is administered and no endotracheal support is given (Boudaa et al., 2013). The most recent addition is the successful use of high-frequency nasal cannula as a primary respiratory support in lambs with mild to moderate respiratory distress syndrome, which parallels recent results from randomized controlled trials in preterm infants with a gestational age (GA) greater than 28 weeks (Lavizzari et al., 2016). About 20% of the preterm lambs must be euthanized within the first 24 h due to severe respiratory distress syndrome. General anesthesia for chronic surgical instrumentation can be given

without problem after 5 days; local anesthesia is preferable when the research protocol necessitates earlier surgical instrumentation.

Availability of both the preterm and full-term lamb model constitute a truly unique asset to assess the effect of preterm birth both during physiological studies and in experiments mimicking pathological conditions encountered in the NICU and beyond. We have taken advantage of this comparison especially to perform studies on the control of breathing and apneas of prematurity, as reported in the following sections.

Active glottal closure during neonatal central apneas. Current knowledge ascribes an essential role to the larynx in perinatal respiration. Accordingly, the larynx helps the newborn in its transition from intrauterine to extra uterine environment by promotion of fetal lung growth, establishment of functional residual capacity, reabsorption of lung water (Praud et al., 1995), and maintenance of a high functional residual capacity in the early postnatal life (Harding, 1984). Moreover, several studies suggest an important role of the larynx in neonatal central apneas. In 1980, Milner speculated that glottal closure was frequently present during central apneas in preterm newborns (Milner et al., 1980). Since then, several observations in the newborn lamb have supported Milner's speculation [reviewed in Dorion and Praud (2003)]. In a first series of experiments on artificially induced central apneas, continuous electrical activity (EMG) of the thyroarytenoid muscle (TA, a glottal constrictor muscle) was observed throughout central apneas, irrespective of arterial oxygenation (from hypoxemia to hyperoxemia) and arterial pressure in CO_2 (from hypocapnia to hypercapnia) (Kianicka et al., 1998b; Praud et al., 1992, 1996). Moreover, direct endoscopic observation showed complete glottal closure, associated with positive subglottal and translaryngeal pressure and with a high apneic lung volume well above the end-expiratory volume during these central apneas (Fortier et al., 2003; Lemaire et al., 1999). Overall, results showed that central apneas in the lambs were alike inspiratory breath holdings due to active glottal closure. The latter was also shown to be present between the gasps observed during anoxic gasping in lambs. This was interpreted as allowing the lamb to keep more air within its lungs to promote more efficient oxygenation between the low-frequency gasps (Thuot et al., 2001).

However, all of the aforementioned results were obtained during artificially induced apneas, as very few spontaneous apneas are actually observed in full-term lambs. Thus, laryngeal dynamics were also studied and characterized during spontaneously occurring apneas in preterm lambs (Renolleau et al., 1999). Results from preterm lambs born between 129 and 132 days of gestation showed that continuous TA EMG was observed throughout 88% of all apneas, including periodic

breathing epochs and regardless of the sleep state (Diaz et al., 1999). This glottal constrictor activity was also associated with positive subglottal pressure and maintenance of a high apneic lung volume well over the passive functional residual capacity, consequently limiting the decrease in hemoglobin desaturation secondary to the central apnea (Reix et al., 2003).

Apneas triggered by the stimulation of laryngeal chemoreceptors. Laryngeal chemoreflexes (LCR) are a set of reflexes triggered by the contact between a liquid, especially acid or liquid with low chloride content, and the laryngeal mucosa. LCR trigger highly protective lung reflexes in the mature organism, consisting primarily of swallowing, coughing and arousal, aimed at limiting contact duration with the laryngeal mucosa and at preventing subglottal aspiration (Thach, 2001). However, in immature organisms, LCR are rather characterized by a vagal efferent component that includes laryngospasms, central or mixed/obstructive apneas, oxygen desaturation and bradycardia, and can be life-threatening; LCR also comprehend a sympathetic efferent component, which includes systemic hypertension and redistribution of blood flow to vital organs (Thach, 2001). Clinical relevance of LCR stems from common observations that LCR can be triggered by laryngopharyngeal refluxes or during oral feeding, or intake of medications (e.g., vitamins or iron) and even by upper airway secretions in preterm neonates (Thach, 2001). In addition, LCR can be responsible in a few infants, even when born after full-term gestation, for apparent life-threatening events and probably some cases of sudden infant death syndrome (Page and Jeffery, 2000; Thach, 2001).

Since the first observation by Johnson et al. (1972) in the anesthetized lamb, several studies have assessed LCR in response to various liquids in newborn mammals (Marchal et al., 1982, 1986; Page et al., 1995; St-Hilaire et al., 2005, 2007) or in human infants (Davies et al., 1988; Page and Jeffery, 1998; Pickens et al., 1988). In full-term lambs, LCR induced during non-REM sleep are mainly characterized by lower airway protective responses, such as swallowing, cough and arousal, with mild cardiorespiratory responses (St-Hilaire et al., 2005); results similar to those obtained in nonsedated piglets (Page et al., 1995). Identical observations have been made in healthy human neonates in whom the onset of apnea-bradycardia is rare after a term birth, apart from the unexpected apparent life-threatening events described in ~1% of infants in their 1st weeks of life (Thach, 2010). Conversely to full-term lambs, studies in the preterm lamb strongly suggest that prematurity is responsible for fetal-type LCR, with prominent apnea, bradycardia and hemoglobin desaturation, which can at times be life-threatening (St-Hilaire et al., 2007). A similar enhancing effect of prematurity on reflex apnea from laryngeal origin had been previously reported in the monkey (Sutton

et al., 1978). This enhanced LCR-related cardiorespiratory inhibition in preterm lambs largely decreases with postnatal maturation (St-Hilaire et al., 2007). In addition, while application of nasal continuous positive airway pressure was consistently found to blunt the LCR-related cardiorespiratory inhibition in preterm lambs, the overall effect of caffeine was nonsignificant, which is in accordance to the well-reported observation in preterm human infants that some apneic–bradycardic events, especially those related to oral intake, are not prevented by caffeine (Boudaa et al., 2013).

Apart from preterm birth, other neonatal conditions have been reported to enhance the cardiorespiratory inhibition during LCR. These conditions include reflux laryngitis artificially induced in rabbits (Ludemann et al., 1998) or full-term lambs (Carreau et al., 2011), respiratory syncytial virus infection in newborn lambs (Lindgren et al., 1992), hyperthermia in piglets, (Xia et al., 2008), sedation in piglets (Donnelly and Haddad, 1986), hypoxia in newborn lambs (Sladek et al., 1993) or piglets (Lanier et al., 1983), and acidosis in piglets (Heman-Ackah et al., 2009).

Apneas triggered by the stimulation of esophageal receptors. The involvement of gastroesophageal refluxes (GERs) in apnea–bradycardia of prematurity remains controversial (Abu Jawdeh and Martin, 2013). While a few physiological studies have shown that the stimulation of esophageal receptors leads to cardiorespiratory reflexes (Jadcherla et al., 2005; Lang et al., 2008; Ramet et al., 1990), the later remain largely unknown in the neonatal period, especially after premature birth. Recent results in nonsedated preterm lambs revealed that, compared to full-term lambs, esophageal stimulations (balloon distension and/or HCl injection) can induce forceful, clinically relevant apneas and bradycardias, especially when mimicking a proximal GER (unpublished results).

Neonatal apneas and sepsis. Late-onset sepsis in the preterm newborn is a life-threatening condition, occurring in about 35% of preterms born before 28 weeks of gestation in the NICU. Mortality is as high as 15% (Dong and Speer, 2015). The first sign of sepsis is often repetitive, severe bouts of apneas and/or bradycardias (Fairchild, 2013). Studies in newborn rats have shown that apneas are related to systemic inflammation via the inhibiting action of prostaglandin E_2 on the respiratory centers; during sepsis, interleukin 1-beta binds to receptors on the vascular endothelial cells of the blood brain barrier, which in turn induces microsomal prostaglandin E synthase-1 (mPGES-1) activity and the secretion of prostaglandin E_2 (Hofstetter et al., 2007). Though this hypothesis has received some confirmation in preterm humans, the severe bradycardias that are often prominent in late onset sepsis do not seem to be fully explained by the action of PGE_2 (Siljehav et al., 2015).

2 NEONATAL LUNG DISEASES

2.1 Congenital Diaphragmatic Hernia

Congenital diaphragmatic hernia is an anatomical defect of the diaphragm, most often located on the left side posteriorly. Its prevalence is between 1000 and 4000 live births. It is secondary to various genetic mutations as well as poorly known environmental factors. It is a life-threatening condition, resulting from the lung hypoplasia directly related to the volume of the abdominal viscera herniating through the diaphragmatic hole into the thorax. Congenital diaphragmatic hernia can be diagnosed prenatally by ultrasound; the latter can measure the extent of lung hypoplasia, which is directly related to postnatal clinical outcomes. When isolated, congenital diaphragmatic hernia is lethal in about 30% of the cases (Deprest et al., 2014). Randomized control trials have shown that surgical repair of the hernia in utero does not increase survival. Following in utero transfer in a specialized tertiary center as soon as the diagnosis is made by prenatal ultrasound, current management at birth consists in "gentle" ventilation with permissive hypercapnia and minimal sedation to prevent VILI, the surgical closure of the diaphragmatic defect being delayed until clinical stabilization. In addition, nitric oxide inhalation, high-frequency ventilation and extracorporeal oxygenation are used as needed. However, despite in utero transfer and optimized postnatal care, about 30% of newborns with congenital diaphragmatic hernia still do not survive the neonatal period in tertiary centers. The problem is that postnatal care cannot be sufficient in the most severe cases with major lung hypoplasia and persistent pulmonary hypertension of the newborn, so that treatment of lung hypoplasia must be addressed prenatally.

Animal models of congenital diaphragmatic hernia have greatly contributed to the understanding of the pathogenesis and to the design of treatment options, especially in the fetal period. The two main animal models are the nitrofen-induced congenital diaphragmatic hernia in the rat and the surgically induced congenital diaphragmatic hernia in the fetal lamb or rabbit (van Loenhout et al., 2009). These models are well established and reproduce not only the diaphragmatic defect, but also the accompanying bilateral pulmonary hypoplasia. The fetal lamb model has been the most useful for preclinical studies on in utero surgical procedures to alleviate prenatal lung hypoplasia, due to its size similar to a human fetus. Conversely, the nitrofen rat model can be used to understand the pathogenesis of congenital diaphragmatic hernia. More recently, transgenic models have also been designed by ablation of the retinoic acid receptor signaling (Mendelsohn et al., 1994).

Numerous preclinical studies have focused on the prenatal treatment of congenital diaphragmatic hernia, with the aim to reverse lung hypoplasia. Fetal endoscopic tracheal occlusion consists in the placement of a balloon in the trachea to prevent the efflux of lung fluid, increase the pressure into the lung and promote lung growth via pulmonary stretch (Deprest et al., 2014). Preclinical studies in lambs, rats, rabbits, and mice have indeed shown that tracheal obstruction at the late canalicular–early saccular stage efficiently stimulates lung growth and maturation [reviewed in Khan et al. (2007)]. Consequent lung hyperplasia was shown to be associated to decreased pulmonary hypertension resulting from decreased muscularization of the distal pulmonary vessels. More recently, a further translational model of percutaneous fetoscopic tracheal occlusion has been reported in baboons, in order to obtain the closest possible model to humans (Mari et al., 2014). Translation of those preclinical studies is currently culminating in the still ongoing international TOTAL trial (Tracheal Occlusion To Accelerate Lung growth trial) (Deprest et al., 2014). Previous studies with historical controls suggest that this randomized control trial will confirm a decrease in mortality with percutaneous fetal endoscopic tracheal occlusion in congenital diaphragmatic hernia patients with moderate to severe lung hypoplasia. However, given that survival should reach 50% at best in the most severe cases after fetal tracheal occlusion, studies on complementary medical treatments given prenatally have been also conducted in animal models of congenital diaphragmatic hernia.

Medical treatment, consisting mainly of vitamins (A, C, or E) and corticoids (betamethasone, dexamethasone, or prednisolone), was given either to the mother (rats, rabbits, or lambs) or directly into the amniotic cavity (rats, rabbits, or lambs) or the trachea (lambs) [reviewed in Eastwood et al. (2015)]. While some positive effect was shown, the overall conclusion is that at the moment no medical treatment can be considered effective for use in humans.

2.2 Meconium Aspiration Syndrome

Meconium aspiration syndrome is a respiratory disorder of the term and near-term newborns. It is defined by inhalation of the meconium present in the amniotic fluid during or before delivery, secondary to anoxic gasping in utero. Meconium aspiration syndrome induces: (1) mechanical obstruction of airways, (2) chemical alveolitis and epithelial damage, (3 and 4) inhibition of surfactant pulmonary artery hypertension (Dargaville and Mills, 2005; Davey et al., 1993; Moses et al., 1991; Park et al., 1996). A variety of animal models of meconium aspiration syndrome have allowed to test various therapeutic options, such as high-frequency ventilation in mongrel puppies (Keszler et al., 1986) or piglets (Wiswell et al., 1994), pulmonary lavage with diluted surfactant in adult rabbits and newborn rhesus monkeys (Cochrane et al., 1998), piglets (Dargaville et al., 2003), newborn rabbits (Lyra et al., 2004) and lambs (Avoine et al., 2011), and liquid ventilation in lambs (Avoine et al., 2011; Foust et al., 1996; Gastiasoro-Cuesta et al., 2001) or piglets (Barrington et al., 1999; Jeng et al., 2006; Kuo et al., 1998; Onasanya et al., 2001).

2.3 Bronchopulmonary Dysplasia

Bronchopulmonary dysplasia, or chronic lung disease of infancy, occurs most frequently in the premature newborn. Bronchopulmonary dysplasia is usually defined by the need for oxygen supplementation at 28 days of life, its severity being further characterized by the level of inspiratory oxygen fraction needed at 36 weeks corrected age (Jobe and Bancalari, 2001). Despite continuing improvements in the overall perinatal care of preterm infants and, more specifically, in the treatment of neonatal respiratory distress syndrome, the increase in the number of extreme premature newborns (22–26 weeks GA) explains that the incidence and severity of bronchopulmonary dysplasia is still very high. Bronchopulmonary dysplasia is diagnosed in 30,000 infants every year in North America and increases the risk of respiratory problems in the 1st year of life, hospital admission being necessary in more than 50% of the infants (Smith et al., 2004). In addition, bronchopulmonary dysplasia has long-term consequences, the incidence of asthma and chronic obstructive pulmonary disease being increased at adult age (Hadchouel, 2016; Landry, 2016).

Numerous studies conducted in animal models have attempted to gain a better understanding of the pathogenesis as well as the prevention of this dramatic disease.

2.3.1 Pathogenesis of Bronchopulmonary Dysplasia

Bronchopulmonary dysplasia is due to both genetic factors and environmental factors. While genetic factors have been studied in humans (Lavoie, 2016), studies in animal models have contributed to give a better understanding of how the environment contributes to the disease. Environmental factors include mechanical ventilation, oxygen exposure, as well as pre- and postnatal infections. They are responsible for an important inflammatory response of the lung. The later ultimately leads to a decrease in alveolarization and pulmonary microvascular development, that is, characteristics of the bronchopulmonary dysplasia occurring in very preterm infants nowadays.

Effects of hyperoxia on the newborn lung. Though its effects are difficult to distinguish from those of mechanical ventilation, hyperoxia is undoubtedly involved in the pathogenesis of bronchopulmonary dysplasia [reviewed

in Harijith (2016)]. The transition from the intrauterine environment to ambient air at birth in itself constitutes a hyperoxic stress that is especially deleterious in the very preterm newborn. Reactive oxygen and nitrogen species released by alveolar epithelial cells and inflammatory cells promote death of the endothelial and epithelial cells. Ultimately, hyperoxia largely contributes to decreased alveolarization and microvascular pulmonary development.

Newborn mice and rats have been extensively used to study the effect of hyperoxia. Mice and rats, which are normally born at the saccular stage of lung development but with a mature lung surfactant and antioxidant system, are studied after term or near-term birth (Berger and Bhandari, 2014; O'Reilly and Thebaud, 2014). Their low price, the ability to study many newborn pups at a time, together with the availability of transgenic animals and numerous molecular biology tools, make them especially attractive. These models are, however, not adapted to the study of prolonged mechanical ventilation, and their size limits instrumentation and in vivo blood sampling.

Newborn rabbits have been used in hyperoxia research since the mid-20th century [reviewed in D'Angio and Ryan (2014)]. Like newborn mice and rats, and conversely to their adult counterparts, they can withstand exposure to 95% oxygen for several days. Like the human newborn, they are normally born at the alveolar stage of lung development. Their size permits some more instrumentation than in newborn mice and rats, and their cost is relatively low. Both term and preterm rabbit models have been used to study the effect of hyperoxia exposure, sometimes with additional neonatal infection/inflammation or postnatal malnutrition. While some studies on mechanical ventilation have been performed in newborn rabbits, their low size relative to the human preterm newborn does not offer the possibility to mimic the conditions encountered in the NICU as well as with the sheep or nonhuman primate model.

Effect of mechanical ventilation on the preterm lung. VILI has been shown to be a major factor in the pathogenesis of bronchopulmonary dysplasia, mainly via volutrauma and atelectrauma that are responsible for shear stress and stretch lesions of the lung cells [reviewed in Ramos (2016)]. These mechanical factors can very rapidly induce extensive inflammation and death of the resident lung cells and augment alveolar–capillary permeability in a few minutes. The latter leads to an influx of neutrophils and macrophages that release proinflammatory cytokines and chemokines, and amplify the inflammatory response initiated by resident lung cells. Consequences of the extensive VILI include decreased alveoralization and microvascular pulmonary development. Reduced alveolarization proceeds from alterations of the normal extracellular matrix remodeling and elastin deposition

in the developing secondary septae, which are crucially involved in alveolarization at the saccular stage. Decreased microvascular pulmonary development is caused by a decrease in vascular endothelial growth factor (VEGF) secondary to the hyperoxia associated to mechanical ventilation.

The preterm lamb and the preterm nonhuman primate newborn have been frequently used for studying the effects of mechanical ventilation. They offer several distinct advantages over the other smaller models. Lambs and nonhuman primates are normally born at term at the same early/middle alveolar stage of lung development than human newborns. While many studies have been performed on the effects of mechanical ventilation in the preterm lamb, the majority lasted only a few hours. With proper around-the-clock intensive care, however, preterm lambs and nonhuman primates born at the saccular stage of lung development and with immature surfactant, and antioxidant lung systems have a prolonged viability that allows to study them during several weeks under mechanical ventilation (Albertine, 2015). Their large size close to that of a preterm human newborn allows to mimic the conditions encountered in the NICU, with extensive instrumentation and possibility of repetitive blood sampling. They have the downside to be expensive and to necessitate special animal facilities. In addition, while the preterm nonhuman primate model is the closest to the human preterm, its price and ethical considerations severely restrict its use.

2.3.2 Prevention and Treatment of Bronchopulmonary Dysplasia

Apart from preventing premature delivery, which is the focus of many ongoing clinical studies, prevention of bronchopulmonary dysplasia begins by the prevention of respiratory distress syndrome via antenatal administration of glucocorticoids to the mother. At birth, as already summarized (see Section 1.1.3; "The quest for the optimal ventilator strategy to support lung aeration at birth in very preterm newborns"), studies are ongoing to find the optimal positive pressure ventilatory support technique to aerate the lung when needed. Thereafter, early surfactant administration, closure of the ductus arteriosus, optimization of nutritional intake, prevention of late onset sepsis, prudent use of systemic or intratracheal glucocorticoids, and the use of the less invasive form of ventilatory support are all important aspects of the care of newborns with bronchopulmonary dysplasia. While many of the studies dealing with the prevention and treatment of bronchopulmonary dysplasia have been performed in the newborn infant, animal models have greatly contributed to some important aspects, as summarized subsequently.

Antenatal glucocorticoids administration. Since the work by Liggins and Howie (1972), antenatal glucocorticoids

administration is now a standard care for the prevention of respiratory distress syndrome when preterm delivery. An elegant review of the scientific literature on the usage of glucocorticoids in pregnancy was recently performed (Kemp et al., 2016). Studies in the rhesus macaque (Bunton and Plopper, 1984), the preterm lamb (Jobe et al., 2003; Polglase et al., 2007), and in knockout mice models (Bird et al., 2015) have clearly demonstrated that antenatal corticosteroid exposure induces fetal lung maturation and largely prevents the occurrence and the severity of respiratory distress syndrome in preterm newborns. Results in these preterm models suggested that improvement in lung function was most likely mediated by surfactant production (Bolt et al., 2001; Garbrecht et al., 2006), structural lung modifications (Bird et al., 2015; Bunton and Plopper, 1984; Polglase et al., 2007), and alveolar fluid clearance (Whitsett and Matsuzaki, 2006).

Noninvasive ventilatory support. Apart from the use of noninvasive ventilatory support for ensuring lung aeration at birth, noninvasive ventilatory support has gained popularity in recent years in neonatal care, either for primary use from birth, for weaning from endotracheal ventilation, or for treating apneas of prematurity in infants with bronchopulmonary dysplasia (DiBlasi, 2011; Flanagan, 2016; Garg and Sinha, 2013; Ramanathan, 2010). The bulk of knowledge in this area comes from clinical studies. Nevertheless, some studies conducted primarily in newborn lambs have brought unique information.

The use of long-term high-frequency nasal ventilation during several weeks from birth has been shown in preterm lambs to provide adequate gas exchange at lower inspired O_2 level and respiratory pressures compared to endotracheal intermittent mandatory ventilation. Simultaneously, alveolarization was promoted (Null et al., 2014; Reyburn et al., 2008).

A series of experiments in term newborn lambs brought clinically relevant information on nasal ventilation. A major difference when using a nasal interface as opposed to an endotracheal tube for respiratory support is the interposition of the larynx between the ventilator and the lungs. Studies in newborn lambs have shown that some modes of nasal positive pressure ventilation, such as nasal pressure support, elicit an active inspiratory laryngeal closure, which impedes ventilator insufflations and limits lung ventilation in proportion to the inspiratory positive pressure (Moreau-Bussiere et al., 2007). On the contrary, neurally adjusted ventilatory assist (Hadj-Ahmed et al., 2012) and nasal high-frequency oscillatory ventilation (Hadj-Ahmed et al., 2015), did not induce active inspiratory laryngeal narrowing. The reflex inspiratory closure of the larynx in nasal pressure support ventilation was shown to originate from bronchopulmonary mechanoreceptors (Roy et al., 2008; Samson et al., 2014), and to be prevented by permitting moderate hypercapnia (Carriere et al., 2015).

Besides limiting lung ventilation, inspiratory closure of the larynx may be responsible for deviation of the insufflated gas into the digestive system, leading, in turn, to gastric distension and GERs (DiBlasi, 2011; Lagarde et al., 2010; Shepherd et al., 2013). Importance of the latter stems from their potential deleterious effects, as reviewed previously (see Section 1.2.3). Further experiments in the newborn lamb, however, have recently shown that both nasal pressure support and neurally adjusted ventilatory assist inhibit GERs at positive pressures of 15/4 cmH$_2$O (Cantin et al., 2016). An important inhibition had also been shown previously with the application of nCPAP at 6 cmH$_2$O, the mechanism being seemingly related to the decrease of the duration and depth of transient relaxation of the lower esophageal sphincter (Djeddi et al., 2014).

Stem cells and bronchopulmonary dysplasia. Stem cells are promising for preventing and treating bronchopulmonary dysplasia. The newborn mouse, rat, and sheep models of bronchopulmonary dysplasia have been used to show the beneficial effects of stem cell therapy. Stem cells, including those derived from the amnion or umbilical cord blood, were shown to induce a reduction of VILI, improved alveolarization, increased survival, and better lung function (Fung and Thebaud, 2014; Hodges et al., 2012; O'Reilly and Thebaud, 2015).

PATENT DUCTUS ARTERIOSUS

1 INTRODUCTION

The ductus arteriosus is an essential component of fetal circulation allowing for communication between the pulmonary artery and the aorta (Hermes-DeSantis and Clyman, 2006). It functions to keep blood away from lungs filled with amniotic fluid toward a descending aorta and a placenta in utero. After birth, the direction of the blood flow through the ductus arteriosus reverses as the pulmonary blood pressure drops. Then, the ductus arteriosus constricts and functionally closes spontaneously by 72 h of age in more than 95% of term infants (Lim et al., 1992). A patent ductus arteriosus (PDA) is a left-to-right shunt disease caused by the failure of the closing process. PDA is associated with several neonatal morbidities, and the severity of clinical symptoms depends on the magnitude of the left-to-right shunt and on the cardiac and pulmonary responses to the shunt (Clyman, 2013).

First, the left-to-right shunt flow causes increased pulmonary blood flow that leads to increased preload of the left ventricle. Combined with the prematurity of ventricle, namely, less distensible compared to that at term, the shunt causes high left ventricular end-diastolic pressure and increased pulmonary venous pressure. This high pulmonary venous pressure leads to pulmonary

congestion (Clyman, 2013), resulted in increased needs for respiratory support. It has been suggested this pulmonary congestion/edema contributes to develop and exacerbate bronchopulmonary dysplasia, however, there is little evidence from controlled, clinical trials to support this hypothesis (Clyman, 2013).

Second, the shunt causes the decreased blood flow to the pressure passive organs like the intestines, skin, muscle, and kidneys. This redistribution may result in several adverse outcomes including feeding intolerance, necrotizing enterocolitis (NEC), metabolic acidosis, and renal dysfunction (Dice and Bhatia, 2007; Hermes-DeSantis and Clyman, 2006).

2 NORMAL PHYSIOLOGICAL COURSE OF DUCTUS ARTERIOSUS

During fetal life, low fetal systemic PaO_2 and circulating prostaglandin keep the lumen of the ductus arteriosus open. As fetuses do not breathe but depend on the placental circulation with gas exchange in utero, the maintenance of fetal circulation is literally vital. On the other hand, failure to close the ductus arteriosus after birth leads to the morbidity described previously. The closure of the ductus arteriosus in full-term infants occurs in two steps below. First, increased arterial PaO_2 and decreased circulating prostaglandins allow the smooth muscle media of the ductus to constrict within the first few hours (functional closure). Second, the inner muscle wall of the ductus arteriosus develops profound ischemic hypoxia which leads to the anatomic remodeling that transforms the ductus into a noncontractile ligament (structural closure) (Clyman et al., 1999; Hermes-DeSantis and Clyman, 2006).

3 PATHOPHYSIOLOGY OF PATENT DUCTUS ARTERIOSUS

Contrary to full-term ductus arteriosus, premature ductus arteriosus often fails to close due to several reasons.

First, the premature ductus is less likely to constrict and is easy to reopen. The premature ductus is less sensitive to elevated PaO_2 due to immature oxygen sensitive K^+ channel (Thebaud, 2004). And it loses its ability to respond to vasoconstrictive stimulants with increasing postnatal age owing to depletion of oxygen and ATP (Levin et al., 2006). While, the premature ductus is more sensitive to the effects of prostaglandins (Clyman et al., 1985) that are produced in inflammation (Ricciotti and FitzGerald, 2011). This characteristic contributes to easy reopening of the ductus. Thus, the premature ductus is less likely to achieve the functional closure.

Second, the premature ductus is less likely to develop profound hypoxia that leads to the structural closure, because the diameter of the lumen is larger compared to that of full-term ductus (Hermes-DeSantis and Clyman, 2006), due to lack of intimal cushion formation (Gittenberger-de Groot et al., 1985; Tada et al., 1985). This anatomical characteristic makes it difficult to develop complete luminal obliteration and complete elimination of nutrient flow to its wall (Hermes-DeSantis and Clyman, 2006). As a result, the premature ductus is less likely to achieve the structural closure.

4 TREATMENT FOR PATENT DUCTUS ARTERIOSUS

Indomethacin is a cyclooxygenase inhibitor that has been used for the closure of PDA by lowering circulating prostaglandin levels since the late 1970s (Friedman et al., 1976; Heymann et al., 1976). Although the efficacy of indomethacin has been well established, paradoxically, prenatal indomethacin as a tocolytic agent increases both the incidence and clinical severity of postnatal PDA (Hammerman et al., 1998), suggesting a more complex role for prostaglandins in the developmentally regulated process of maturation and postnatal closure of ductus arteriosus. An alternative treatment strategy for PDA is a surgical ligation. It was reported that no significant difference between indomethacin treatment and surgical closure was found for in-hospital mortality, chronic lung disease, NEC, sepsis, creatinine level, or intraventricular hemorrhage (IVH) (Malviya et al., 2013).

5 ANIMAL MODELS OF PATENT DUCTUS ARTERIOSUS

Bergwerff et al. (1999) reviewed the anatomy and physiological ductal closure in various vertebrates from lungfish to mammals, and showed anatomical similarities in all mammals and differences between mammals and other vertebrates. In all mammals, including human, it is the left aortic arch that persists and only the left ductus arteriosus is maintained throughout fetal life. Most of previous studies employed mammal models, and several mammal models have been used depending on the purpose. Meanwhile, the potential utility of chicken embryo models was reported recently (Agren et al., 2007; Sutendra and Michelakis, 2007).

5.1 Large Mammal Models

Large mammals including dog, sheep, and nonhuman primates have been employed mainly in the anatomical and physiological studies.

PDA is the most common cardiac anomaly observed in dogs (Patterson, 1968). Histological features of the normal ductus arteriosus and PDA in dogs resemble those of the normal ductus arteriosus and PDA in humans, suggesting a similar pathogenesis in both species (Bökenkamp et al., 2010). Using dog models, it is reported that the aortic end of the ductus is the least advanced toward closure, and the pulmonary end the most advanced (Gittenberger-de Groot et al., 1985).

Other large mammal models, such as premature lamb or primate models have been mainly used when exploring the physiological effects of PDA including changes in ventilation and cardiac function (Pérez Fontán et al., 1987; Shimada et al., 1989). Their large body sizes allow to employ several intensive care strategies including intratracheal intubation, mechanical ventilation, and central catheterization, then enable us to reproduce the clinical setting. The premature baboon [delivered at 125 days of GA, term = 185 days] has a similar neonatal course including a spontaneous closure with premature human infants delivered between 25 and 26 weeks of GA (Clyman et al., 1999, 2012).

Although anatomically similar, there are some differences in the process of ductal closure between humans and large mammals, that is, the timing of the intimal cushion formation. Ductal closure is accompanied by intimal cushion formation as described previously, which starts during fetal life. Humans show the earliest onset of intimal thickening and, by far, the most extensive cushion formation (Bökenkamp et al., 2010; Groot and van Ertbruggen, 1980).

5.2 Small Mammal Models

In contrast to large mammal models, small mammal models including rodents have been mainly employed to explore the mechanism of ductal closure on the molecular level. Gene-targeted mouse models have been created to elucidate mechanisms by which known effectors affect ductus development, prenatal patency, and postnatal ductal closure (Bökenkamp et al., 2010). Using mouse models, it has been revealed that genetic disruption of the prostaglandin E specific receptor EP4 paradoxically results in fatal PDA (Nguyen et al., 1997; Segi et al., 1998). The deficiency in both COX-1 and COX-2 also resulted in fatal PDA (Loftin et al., 2001). Yokoyama et al. (2006) revealed the mechanism of this mystery using mouse models as well, that is, persistent prostaglandin E stimulation via EP4 plays a role of vascular remodeling of the ductus arteriosus to promote the intimal cushion formation and structural closure of the vascular lumen.

5.3 Chicken Models

Although most of current available data are derived from mammals, there is the limitation in mammal models when it comes to explore the developmental physiology of ductus in utero, since (1) the fetal/placental circulation has to be exposed to intervention only through complex surgery and (2) manipulation of the ambient oxygen levels affects both the mother and the fetus (Sutendra and Michelakis, 2007). The chicken embryo models solve these problems and represent an excellent model to investigate developmental physiology of the cardiovascular system. Birds have completely septated hearts and arterial outflows, in contrast to reptiles (except for crocodilians) and lower vertebrates (Bergwerff et al., 1999). Chicken ductus has been shown its sensitivity to a wide range of vasoactive agonists including oxygen, prostaglandin, and NO as with mammals (Agren et al., 2009). Thus, the chicken embryo appears as another good model for the study of ductus arteriosus. However, there are also limitations in these models, namely, birds maintain bilaterally developed ductus arteriosus, that is contrast to mammals but similar in anatomy and physiology to reptiles. In addition, all birds close their ductus arteriosus permanently from the time of hatching without exception (Bergwerff et al., 1999).

RETINOPATHY OF PREMATURITY

1 INTRODUCTION

Retinopathy of prematurity (ROP) is an eye disease of developing blood vessels that affects preterm babies. It was reported that the incidence of ROP was 68% among infants whose birth weights were less than 1251 g (Good et al., 2005). Although the severity decreased as the mechanism of this disease has been revealed and then the management of oxygen therapy has been refined, it becomes the leading cause of childhood blindness due to progressive increasing the number of preterm birth all over the world (Hartnett and Penn, 2012).

This disease was first described as the "retrolental fibrodysplasia" by Terry more than 70 years ago (Terry, 1942), followed by numerous studies, in which animal models including kittens, mice, and rats were mainly employed to reveal the underlying mechanism and to explore the efficient treatment strategy.

2 NORMAL VASCULARIZATION OF HUMAN RETINA

In humans, normal vascularization of the retina and vitreous body begins at approximately 16 weeks of GA (Flynn, 1992). The process starts with the most superficial (or inner) retinal layers at the optic nerve head, and radiates outward or anteriorly from this central point (Gariano and Gardner, 2004). During the early stages,

vascular supply to the eye is partially provided by the hyaloid vasculature originating from the optic nerve and traversing the primitive vitreous toward the anterior segment. The hyaloid vasculature is a transient existing network of capillaries, and is regressed and removed when ocular development proceeds (Mitchell et al., 1998). Hyaloid regression is usually completed before 34 weeks of GA in humans. By this time, development of the intraretinal vasculature is already well advanced. The nasal retina becomes fully vascularized at approximately 36 weeks of GA, and the temporal vessels reach the ora serrata at approximately 40 weeks of GA. Thus, a human term infant is born with fully developed retinal vessels and with regressed hyaloid vasculature (Stahl et al., 2010).

3 PATHOPHYSIOLOGY OF RETINOPATHY OF PREMATURITY

ROP consists of following two phases. The first phase is delayed or attenuated retinal vascular development. This occurs when the premature infant is born into a hyperoxic postnatal environment, and is worsened by supplemental oxygen therapy. The second phase is neovascularization stimulated by the oxygen-related factors, such as erythropoietin and VEGF (Hellström et al., 2013). This neovascularization potentially leads to intravitreal hemorrhages, retinal detachment, and ultimately, vision loss because these vessels are often disorganized and leaky due to a lack of the normal developmental regulatory mechanisms (Dorrell and Friedlander, 2006). The transition between first phase and second phase seems to depend on the postmenstrual age of the infant rather than the postnatal age (Hellström et al., 2013). It is reported that ROP begins at roughly 30 weeks of GA and peaked at 36–38 weeks of GA, irrespective of GA at birth (Palmer et al., 1991).

As it was reported in early 1950s that high oxygen level is strongly associated with the development of ROP (Campbell, 1951); most of the studies after that have employed oxygen-induced retinopathy models. On the other hand, the association between the ROP and the inflammatory response, which plays an important role in several diseases that affect premature infants including bronchopulmonary dysplasia and white matter injury, had not been explored for a long period. However, the evidence of association between the inflammation and the ROP has been emerged recently (Chen et al., 2011b; Dammann et al., 2009; Hong et al., 2014; Sood et al., 2010). The extreme prematurity plus multiple hits of perinatal inflammation, such as clinical chorioamnionitis and neonatal systemic inflammatory response syndrome, are associated with an increased risk of ROP (Chen et al., 2011a; Dammann et al., 2009). Of note, the three risk factors, (1) neonatal sepsis, (2) oxygen exposure, and (3) low GA, increase the risk of ROP not additively but multiplicatively (Dammann, 2010).

4 TREATMENT OF RETINOPATHY OF PREMATURITY

Cryotherapy, ablation of the peripheral nonvascularized retina in order to stop the progression of ROP by decreasing VEGF level and other angiogenic factors from the hypoxic retina, was induced in 1980s. The multicenter trial of cryotherapy revealed that this treatment had significantly reduced total retinal detachments by 19.8% at 10 years of age (Cryotherapy for Retinopathy of Prematurity Cooperative Group, 2001). This has been confirmed over time, and cryotherapy has become established as standard care for threshold ROP (Palmer et al., 2005). Laser photocoagulation has taken over the role as a standard treatment for ROP in developed countries (Cuthbertson and Newsom, 2006), owing to its advantages including easier administration, lower rates of complications, and efficacy that is at least equivalent to cryotherapy, although no randomized clinical trial that compared cryotherapy with laser photocoagulation directly has been conducted yet (Simpson et al., 2012).

5 ANIMAL MODELS OF RETINOPATHY OF PREMATURITY

Despite the severity with regards to the quality of life for affected infants, ROP is not life-threating disease. It is relatively and ethically difficult to obtain samples from human infants suffering from this disease in timely manner. Therefore, animal models have been quite important to reveal the mechanism of ROP. While, unlike humans, the retinal vascularization occurs postnatally in many mammals, which made it easy to establish animal models for exploring the underlying mechanism of ROP due to availability of administering exogenous materials, such as molecular agonists or antagonists, directly, eliminating many of the difficulties associated with studying embryonic vascular development (Dorrell and Friedlander, 2006). Meanwhile, this fact can be a potential limitation when the findings are adapted to human infants. Although no animal model is perfect, several species have been tested as appropriate animal models of ROP. An ideal animal model should reproduce the two phases of ROP. Besides, it should display revascularization of the avascular area with functional intraretinal vasculature and regression of pathologic neovascularization during the later disease stages (Stahl et al., 2010).

5.1 Kitten Models

Kitten models were historically one of the first animal models to be used to imitate the ROP (Ashton et al., 1954; Patz, 1968), as the neonatal cat retina is at a stage of development equivalent to that of the human retina at the beginning of the third trimester (Chan-Ling et al., 1990). At birth, most of the cat retina is covered by spindle cells, the inner vasculature has formed over 30%–40% of the retina, and the outer vasculature has not begun to form (Chan-Ling et al., 1990). They well mimic biphasic response of retinal vasculature to oxygen, thus, the kitten retina may provide an accurate model of the critical early and middle stages of ROP (Chan-Ling et al., 1990). However, kitten models never develop cicatricial retinal disease seen in human premature infants. In addition, major drawback to these models is high cost and poor availability of reagents (Connor et al., 2009). Thus, kitten models are no longer as popular models of ROP as they used to be.

5.2 Rat Models

Meanwhile, rat models have been proved to be alternative good models of ROP because of several reasons. First, the rat retina develops in a way similar to that of the human as follows: (1) the retina is one of the last tissues to be vascularized, (2) the retinal vasculature derives from mesenchymal precursor cells of the hyaloid artery, and (3) vascularization proceeds in a wave-like fashion, beginning at the optic disk and growing outward until the vessels reach the retinal periphery (Barnett et al., 2010). Second, the pattern of neovascularization induced by hyperoxia is quite similar to that seen in the human retina with ROP. Third, the rat models are relatively cheap compared to kitten models (Barnett et al., 2010).

Despite the utility described previously, these models were once abandoned as Ashton and Blach (1961) casted doubt on the validity of the achievements using these models before them, although Patz reported the retinal vascularization in the rat models as early as 1954 (Patz, 1954). The reason why Ashton and Blach failed to reproduce ROP in the rat models was unclear, however, it was possibly due to strain differences of susceptibility described later. The interest in these models reemerged in late 1980s. Many studies have been conducted using these models, and these models have contributed much of what is currently known regarding the growth of physiological and pathological blood vessels in the retina (Barnett et al., 2010). Rat models are useful in therapeutic drug screening or in exploring the mechanisms of angiogenesis (Lai and Lo, 2013). On the other hand, the demerits of rat models are: (1) susceptibility to hyperoxia differs among strains, and (2) the production of specific mutations, conditional mutations, and marker manipulations has been problematic (Iannaccone and Jacob, 2009).

5.3 Mouse Models

The mouse retina is quite similar with the rat retina, and therefore mouse models also have a number of reasons to be another good animal model of ROP. First, the normal development of the mouse retinal vasculature occurs within 2 weeks of birth, that allows to observe the full spectrum of vascular development. Second, the developmental stage of retinal vessels in the newborn mouse retina approximates that of premature human infants of 4–5 months of GA. Third, the retinal development of mouse is initiated by spindle-cell precursors that form a superficial layer, followed by the development of a deep retinal vascular layer, same with that of human (Smith et al., 1994). However, historically, trials to develop mouse models of oxygen-induced retinopathy had a variable success owing to its inconsistency of the neovascular response to hyperoxia and the lack of quantification of that response. This inconsistency was considered to be derived from the incomplete regression of hyaloid vessels. And in 1994, Smith and coworkers reported that the mouse retina of postnatal day 7 most closely resembled that of premature infants with optimization of maximal hyaloid vascular regression and minimal retinal vascular development. They demonstrated that exposure of postnatal day 7 mice to 5 days of 75% oxygen followed by return to room air resulted in reproducible and quantifiable retinal neovascularization without hypertrophy or dilation of the hyaloid vessels (Smith et al., 1994). Their model has become the protocol of choice (Connor et al., 2009; Scott and Fruttiger, 2010), and followed by more than 15,000 publications within only 15 years (Stahl et al., 2010).

Mouse pups also have an immature retinal vasculature and persistent hyaloid vessels at birth same with the rat models. The highly organized pruning of hyaloid vessels in the postnatal mouse eye has been a very useful tool in the study of mechanisms of physiological vessel regression (Stahl et al., 2010). Parallel to hyaloid regression, mouse retinal developmental vascularization occurs postnatally when well-defined vascular plexuses form in a highly reproducible temporal and spatial pattern (Dorrell and Friedlander, 2006; Stahl et al., 2010). Although the time course of vascularization in wildtype mice varies considerably among the strains like rat models (Stahl et al., 2010), mouse models provide a solution with regards to the difference among strains due to their availability of transgenic strains. Using the mouse models also enable access to a wide range of recombinant proteins and antibodies. Despite the merits described earlier, mouse models are not suitable for the therapeutic

drug research owing to the spontaneous regression of the neovascularization within a week (Lai and Lo, 2013).

5.4 Zebrafish Models

Zebrafish models have been emerged more recently compared to other animal models described earlier. Zebrafish and human retinal vasculatures share some common features (Alvarez et al., 2007). The genetic techniques, such as cloning, mutagenesis, transgenesis, and mapping approaches have already been established in this model (Lieschke and Currie, 2007). Besides, these models have a superiority to other animal models, namely, transparency that facilitates in vivo and in real time observation (Lieschke and Currie, 2007; Wu et al., 2015). Exposure of either embryo or adult zebrafish to hypoxia leads to neovascularization response, thus these are good models to explore the mechanism of angiogenesis (Cao et al., 2008; Wu et al., 2015). In addition, Zebrafish models cost less compared to even rodent models, and has high fecundity (Lieschke and Currie, 2007).

On the other hand, zebrafish models also have several drawbacks. First, although zebrafish and human retinal vasculatures share some common features as mentioned previously, the similarities are less compared to rodent models (Lieschke and Currie, 2007). For example, the coupled hyaloid regression and retinal angiogenesis described earlier is not observed in zebrafish (Alvarez et al., 2007). Second, skillful techniques and a large quantity of eyeballs are required in dissection and for molecular analysis due to the limited supply of tissue from a single animal (Lai and Lo, 2013).

INTRAVENTRICULAR HEMORRHAGE

1 INTRODUCTION

Intraventricular hemorrhage (IVH) is a major neurological complication of prematurity. Although it is reported that the overall percentage of infants with severe IVH decreased in past 2 decades, it is still as high as 13% in preterm infants born between 22 and 28 weeks of GA. In addition, the incidence in infants born between 22 and 25 weeks of GA demonstrated no change (Stoll et al., 2015).

A majority of these infants are asymptomatic and the diagnosis is based on screening cranial ultrasound, while some infants manifest with subtle abnormalities in the level of consciousness, movement, tone, respiration, and eye movement. Although uncommon, some demonstrate catastrophic deterioration presenting with stupor, coma, decerebrate posture, generalized tonic seizure, and quadriparesis (Ballabh, 2010).

IVH strongly correlates with neonatal morbidity and mortality. More than 60% of preterm survivors with IVH demonstrate some neurosensory impairments, including abnormal neurologic examination, cerebral palsy (CP), posthemorrhagic ventricular dilation, and seizure (Luu et al., 2009).

2 PATHOPHYSIOLOGY OF INTRAVENTRICULAR HEMORRHAGE

Pathophysiology of IVH is multifactorial, complex, and heterogeneous. IVH usually initiates in the periventricular germinal matrix and progresses to IVH upon the rupture of the underlying ependyma. Germinal matrix hemorrhage is primarily venous in origin (Ghazi-Birry et al., 1997). The inherent fragility of the germinal matrix vasculature is supposed to underlie as a basis (Ballabh, 2014), however, the trigger for the hemorrhage remains unclear although the fluctuation in the cerebral blood flow is a convincing candidate.

First, IVH mainly occurs in the germinal matrix, which consists of neuronal and glial precursor cells. The subependymal germinal matrix is highly vascular and is selectively vulnerable to hemorrhage. The thickness of the germinal matrix decreases after 24 weeks of GA, and it almost disappears by 36–37 weeks of GA (Ballabh, 2014). The vulnerability to hemorrhage derives from (1) the paucity of pericytes (Braun et al., 2007), (2) the reduced expression of fibronectin (Xu et al., 2008), and (3) the less degree of glial fibrillary acidic protein expression in astrocyte end feet (El-Khoury et al., 2006).

Second, fluctuating pattern of cerebral blood flow velocity during the 1st day of life strongly correlates with the development of IVH (Perlman et al., 1983). However, surprisingly, a correlation between the impaired autoregulation and IVH has not been demonstrated (Soul et al., 2007; Wong et al., 2008), although it is logical that cerebral autoregulation is impaired when the IVH occurs because autoregulation is the capability of the blood vessels in the brain to retain a constant blood flow in spite of fluctuation. Thus, the role of impaired autoregulation in the development of IVH needs further evaluation (Ballabh, 2014).

Other conceivable contributing factors include coagulation/clotting disorder. A number of studies have suggested the correlation between coagulopathy and IVH, although there is no significant correlation between the degree of coagulopathy and that of IVH (Lupton et al., 1988; Van de Bor et al., 1986). Therefore, Ballabh (2014) concluded that "coagulopathy does not seem to play a key role in pathogenesis of IVH, but can modify the risk and severity of IVH."

3 PREVENTION OF INTRAVENTRICULAR HEMORRHAGE

The two main strategies to prevent IVH are (1) to strengthen the germinal matrix vasculature and (2) to stabilize the cerebral blood flow (Ballabh, 2014).

First, germinal matrix is highly vascular and is selectively vulnerable to hemorrhage as described previously. The levels of VEGF and angiopoietin-2 are high in the germinal matrix than in the cerebral cortex or white matter in both humans and rabbits, and the decreased level of them resulted in the suppressed incidence of germinal matrix hemorrhage (Ballabh et al., 2007). It has been demonstrated that prenatal glucocorticoids (1) suppress VEGF expression, (2) elevate transforming growth factor-β, and (3) enhance pericyte coverage, in the germinal matrix (Vinukonda et al., 2010). Indeed, a number of studies have demonstrated that glucocorticoids reduce the incidence of IVH (Roberts and Dalziel, 2006).

Second, several trials to reduce the fluctuation of cerebral blood flow have been conducted to prevent IVH. Phenobarbital has failed to show its efficacy to reduce IVH (Smit et al., 2013). While pancuronium demonstrated a significant reduction in IVH, uncertainty remains regarding the long-term neurologic effects. Thus, the routine use of pancuronium in ventilated premature infants is not recommended at present (Cools and Offringa, 2005).

4 ANIMAL MODELS OF INTRAVENTRICULAR HEMORRHAGE

In 1980s, studies to explore the underlying mechanism of IVH were conducted using mainly rabbit and beagle models. They have played important roles in understanding the physiologic factors that predispose to IVH.

4.1 Rabbit Models

Rabbit models have been shown to be appropriate models for the study of IVH because (1) the maximal growth of the brain occurs perinatally, (2) there is an abundant germinal matrix near term, and this is substantially reduced by birth, (3) there is no *rete mirabile* that is not observed in human but observed in sheep and dog models, (4) the blood flow to the brain is via internal carotid and vertebral arteries and the proportion of brain perfused by each of these vessels is similar to that in the human, (5) the maturation of the lungs is completed just before term, (6) the rabbit pup can maintain a separate existence from the dam when delivered prematurely, and (7) although quite small, monitoring of several physiological variables can be carried out

(Lorenzo et al., 1982). In addition, IVH occurs even spontaneously in rabbit models (Lorenzo et al., 1982). Rabbit models have been used to clarify whether the physiological insult, such as intracranial hypotension, causes IVH or not (Conner et al., 1983). Although, Coulter et al. (1984) directed questions at the reproducibility of these models based on their failure to demonstrate IVH using 225 premature pups; these models are employed even nowadays and achieved long survival that enables us to observe the consequences of IVH (Chua et al., 2009).

4.2 Beagle Models

Beagle models were quite popular among researchers who explored the mechanisms of IVH in 1980s due to their reproducibility of IVH. Etiologically, IVH occurs in beagle models in a similar way with human premature infants. IVH can be produced in these animal models by several insults including hypercarbia (Goddard et al., 1980a) and hypertension (Goddard et al., 1980b). Besides, the pathologic findings in these models, namely, periventricular and intraventricular hemorrhages including hemorrhages in subependymal regions in and near the germinal matrix, in the tela choroidea, and in the choroid plexus, are similar to that in human preterm brains (Goddard-Finegold and Armstrong, 1987). Additionally, beagle models also demonstrate spontaneous IVH (Ment et al., 1982).

4.3 Other Models

There are a few more animal models to explore the posthemorrhagic ventricular dilation. Rat models (Cherian et al., 2004; Xin et al., 2010) and piglet models (Aquilina et al., 2007, 2012) have been developed to reveal the mechanisms and long-term consequences of posthemorrhagic ventricular dilation. However, in these models, IVH is not caused by some insults but is mimicked by intraventricular injection of their own blood.

CEREBRAL PALSY

The definition of CP includes five key elements: (1) it is an "umbrella term"; (2) it is permanent but not unchanging; (3) it involves a disorder of movement and/or posture and of motor function; (4) it is due to a non-progressive interference, lesion, or abnormality; (5) the interference, lesion, or abnormality arose in the developing or immature brain (Shepherd et al., 2016).

CP represents the most common physical disability in childhood. In a recent metaanalysis, including 19 studies, the global pooled prevalence was 2.11 per 1000 live births (95% confidence interval 1.98–2.25). Sadly, the

progress in reducing the numbers of individuals affected by CP has been slow; a cumulative metaanalysis demonstrated stability in the prevalence over the past 10 years (Oskoui et al., 2013). The prevalence expressed by GA was highest in children weighing 1000–1499 g at birth (59.18 per 1000 live births) and for children born before 28 weeks of gestation (111.80 per 1000 live births).

1 EPIDEMIOLOGY, ETIOLOGY, AND ANIMAL MODELS

Approximately 6% of children with CP are due to a cerebrovascular or cardiac event after the 1st month of life and before 2nd–5th year of life (Shepherd et al., 2016; Smithers-Sheedy et al., 2016). The overwhelming majority of individuals with CP (94%) will have suffered the insult antenatally or perinatally, including the first 28 days of life. Of those, ~80%–90% are due to antenatal events, rather than the labor process per se. Factors, precipitating CP include, aside of genetics, preterm birth, infection, and intrapartum acidemia (Oskoui et al., 2013). The influence of these factors is further potentiated by the chronic fetal hypoxia or inflammation, at least in part via cardiogenic insults that affect cerebral perfusion, which usually are clinically asymptomatic and thus go currently unnoticed (Frasch et al., 2011; Herry et al., 2016; Wibbens et al., 2007). Over 40% of individuals with CP are born preterm, compared with approximately 8% of the general population. Overall, however, most individuals with CP (50%–60%) are born at term (Shepherd et al., 2016; Smithers-Sheedy et al., 2016). CP and the underlying brain injury lead to life-long disabilities including motor difficulties as well as problems with hearing, sight, speech, seizures, and cognition, but with hardly diminished life expectancy for the ~90% of the individuals with CP who reach 20 years of life. The combined burden of life-long individual suffering and health-economic impact is considerable.

As evidenced by these data, the etiology of CP and the underlying brain injury are complex and so is the spread of the animal models required to mimic the causative mechanisms, which represents the first step in defining the therapeutic options. Factors to consider are the presumed timing of the insult and the key organ contributing to the insult. For example, as is the case with the impact of preterm birth, an immature brain injury manifests typically with white matter pathology due to immaturity of oligodendroglia at the time of the insult, while mature fetus will present with grey matter injury and underlying neuronal insult pattern (Dean et al., 2011; Mallard and Vexler, 2015).

The animal models mimicking various stages of CP etiology aim at understanding the molecular steps involved, biomarkers for early identification of fetuses or neonates at risk of developing CP, and early therapeutic intervention.

The selection of the animal models depends on the physiological maturity comparable to the human situation at the given GA. Consequently, mice have emerged as potent models of fetal inflammation, prematurity, and ensuing brain injury (Burd et al., 2009, 2011); guinea pigs have been used as models of intrauterine growth restriction, a condition associated with chronic fetal hypoxia, allowing studies in the offspring (Dong et al., 2011; Elias et al., 2016). Rabbits have been used to test novel promising CP treatments using nanoparticles (Kannan et al., 2012). Fetal sheep models of acute (De Haan et al., 1997; Drury et al., 2014; Frasch et al., 2016) and chronic (Keen et al., 2011) brain injury represent the most commonly used large animal model of mechanisms underlying CP and the only animal model so far that resulted in bedside translation of the research findings to mitigate CP development: the therapeutic hypothermia in neonates (Davidson et al., 2015; Gunn et al., 1997). These references represent but a snap shot of the rich experimental literature in the field.

Current methods to diagnose fetal inflammation or acidemia are inadequate as they are imprecise (indirect biomarkers measured from the mother), invasive (amniocentesis), and "noncontinuous" (sample obtained at a time point may become "out-of-date") (Fahey, 2008; Garite, 2001). They are also insensitive to subtle inflammation caused by ischemia, hypoxic acidemia, or infection. Even subtle inflammation is consequential because it "programs" myeloid cells, such as microglia in the brain to be hyperresponsive to future insults, potentially enlarging the zones of tissue damage (Cao et al., 2014; Xu et al., 2014). An urgent need exists to identify early signs of the septic or acidotic fetus and neonate at risk of adverse outcome in order to intervene therapeutically (Fahey, 2008; Garite, 2001). Early detection of incipient brain injury is urgently needed, as, currently, the diagnosis of CP is often made years after the insult.

In the subsequent sections, we focus on two select and important causes of CP, fetal inflammation and acidemia, and the animal model of fetal sheep used to mimic the condition and identify potential early biomarkers of these pathophysiological processes to reduce the disease burden. The basic experimental design of the fetal sheep model is reported in Burns et al. (2015) and many other original research articles.

2 FETAL INFLAMMATION

The main manifestation of pathologic inflammation in the fetoplacental unit, chorioamnionitis, affects 20% of term pregnancies and up to 60% of preterm pregnancies (preterm birth occurs in 8%–13% of pregnancies

in Canada). It remains often undiagnosed (Gotsch et al., 2007; Lahra and Jeffery, 2004). Even asymptomatic inflammation may inhibit placental angiogenesis, impede delivery of nutrients, and alter the fetus' hormonal/cytokine environment, leading to deranged inflammatory and metabolic responses (Dowling and Levy, 2014; Garnier et al., 2008). Both symptomatic and asymptomatic, histologically detected chorioamnionitis are associated with a ~ninefold increased risk of CP (Grether and Nelson, 1997). Similarly, chorioamnionitis is strongly associated with NEC, a frequent life-threatening complication in NICUs with 20%–40% mortality (Garzoni et al., 2013). NEC predisposes to functional impairment and confers increased risk for worse neurodevelopmental outcomes in the long term than prematurity alone (Pike et al., 2012; Rees et al., 2007; Sharma and Hudak, 2013).

Since CP is likely a result of multiple insults of various types (e.g., inflammation, hypoxia, or acidemia) intensity and duration, several labs developed multihit paradigms to mimic the human situation more closely (Cao et al., 2015; Dean et al., 2015; van den Heuij et al., 2014). Fetal sheep model provides an excellent possibility to induce and monitor fetal insult in vivo and then create primary pure brain cultures to further study molecular mechanisms involved in memory of in utero inflammatory insult, a likely contributor to the increased susceptibility to perinatal or early postnatal brain injury, especially under conditions of prematurity and during stay in a NICU (Cao et al., 2015). Fetal sheep model of lipopolysaccharide (LPS)-induced inflammatory response has further contributed to development of novel monitoring technologies to detect early fetuses at risk of brain injury due to infection, systemically, in the gut or in the brain (Durosier et al., 2015; Liu et al., 2016).

Advances have also been made using septic neonatal rat model to develop heart rate algorithms for early sepsis detection in neonates (Fairchild et al., 2011). Together, these findings in animal models point to the diagnostic potential of fetal heart rate (FHR) variability monitoring in fetuses and neonates to detect early onset of sepsis on systemic and organ-specific scales. This approach is based on the notion of the fetal cholinergic antiinflammatory pathway and the "vagus code" (Frasch et al., 2016; Herry et al., 2016; Kwan et al., 2016). Together, animal models have been instrumental in developing means to identify babies requiring neuroprotective intervention.

3 FETAL ACIDEMIA

Human clinical studies with umbilical cord blood gas and pH assessment at birth indicate an increasing risk for neonatal adverse outcome and longer-term sequelae including CP with pH values <7.00 (Liston et al., 2002a,b, 2007). Additionally, growth-restricted infants with chronic hypoxemia due to placental dysfunction are at greater risk for concerning acidemia at birth and thereby subsequent adverse neurological outcomes due to superimposed acute hypoxemia during labor (Frasch et al., 2009a, 2010, 2011; Kaneko et al., 2003). This is supported by studies in the ovine fetus showing that preexisting hypoxia alters cerebral and cardiovascular responses to labor-like umbilical cord occlusions (UCOs) (Wassink et al., 2013).

The absence of FHR decelerations along with presence of FHR variability is highly predictive for normal fetal blood gas/pH at birth (Liston et al., 2002a,b, 2007). However, clinical FHR monitoring has a low positive predictive value for concerning acidemia at birth (~50%), so there is continued need for improving existing technologies for the detection of fetal hypoxic acidemia during labor (Liston et al., 2002a,b, 2007).

Fetal sheep model of human labor allows to study patterns of electrocortical activity (ECOG) and FHR in response to repetitive UCOs insults to delineate the time-course and correlation of ECOG change with worsening acidemia (Frasch et al., 2011). Fetal ECOG responds to labor-like UCOs with amplitude suppression and frequency increase during FHR decelerations in association with pathological decreases in fetal arterial blood pressure. These changes in ECOG suggest an "adaptive brain shutdown" and occur on average 50 min prior to attaining a severe degree of acidemia with fetal arterial pH < 7.00. Translational implications are that fetal ECOG monitoring can improve the positive predictive value of FHR monitoring for worsening acidemia at birth, which should contribute to early detection of babies at risk of developing CP.

Fetal acidemia is required to produce neuroinflammation as evidenced by the findings in fetal sheep near term where chronic hypoxia does not lead to microglial activation, but acidemia does (Prout et al., 2009, 2012). Moreover, isolated systemic hypoxia without ischemia does not cause neuronal necrosis as shown in middle cerebral artery occlusion model of stroke in adult rats; however, it will exacerbate ischemic necrosis (Miyamoto and Auer, 2000). In line with these findings, pediatric patients less than 9 months old with proven hypoxic or hypotensive episodes due to perinatal asphyxia, congenital heart defects, or chronic pulmonary dysfunction were found to often show a dense infiltrate of microglial cells in the dentate gyrus making this neuroinflammation a neuropathological marker of mild hypoxic–ischemic brain injury (Del Bigio and Becker, 1994). That is, neuroinflammation, preceding brain necrosis, plays a pivotal role in mediating brain injury induced by neonatal hypoxic ischemic encephalopathy, the neuropathological

substrate of CP (Liu and McCullough, 2013). Meanwhile, suspending neuronal activity is known to result in prolonged preservation of viability in adults and neonates (Glass and Ferriero, 2007; Safar et al., 2002). It is hence plausible that fetal or perinatal neuroinflammation are mitigated by an early adaptive neuronal shutdown in response to repetitive intermittent hypoxic episodes with cumulative acidemia. These findings in rat and sheep models underscore the intricate interaction between inflammation and acidemia resulting in brain injury.

Consequently, fetal sheep studies of human labor indicate that EEG–FHR monitoring during labor, as a novel ancillary modality of intrapartum monitoring, may not only identify fetuses at risk of developing severe acidemia, but it may also provide information to the neonatologist as to which babies may be at higher risk of brain injury resulting in conditions, such as CP due to developing neuroinflammation. FHR monitoring may guide this diagnostic process by helping to distinguish chronically hypoxic fetuses prior to labor onset from the normoxic fetuses. The therapeutic implication is that neuroprotective drug treatments need to target the postnatal 24 h time window to benefit from the anti-neuroinflammatory effect the adaptive brain shutdown may have in the chronically hypoxic fetuses when they are born.

Another finding from fetal sheep model was the role of FHR sampling rate in clinical setting to enable early detection of fetal acidemia (Durosier et al., 2014). Currently, this sampling rate is inadequate explaining poor positive predictive value of FHR monitoring for detection of acidemia.

It should be noted, that animal models, such as fetal sheep model not only informed clinically testable algorithms for detection of acidemia and inflammation, but also provided a unique foundation for creation of a novel generation of "animal" models, namely *in silico* models of human labor (Wang et al., 2015). *In silico* or computer models allow, naturally, more exhaustive testing of various labor scenarios than animal models. This approach already led to new predictions for FHR-derived biomarkers of fetal acidemia (Wang et al., 2015).

NECROTIZING ENTEROCOLITIS

1 ETIOLOGY

NEC is an acute inflammatory disease that affects the intestine of neonates resulting in intestinal necrosis, systemic sepsis and multisystem organ failure (Garzoni et al., 2013). NEC is extremely frequent and affects 5%–10% of all infants born at 1500 g or less birth weight or less than 30 weeks GA (Lin and Stoll, 2006). The incidence of NEC varies from 0.3 to 2.4 infants per 1000 live births, with nearly 90% of cases occurring in infants born at less than 36 weeks of gestation. NEC affects 2%–5% of all premature infants and accounts for up to 8% of all NICU admissions. Actually, the incidence of NEC has increased despite surfactant replacement therapy because of increased survival of very premature infants (born at 800 g or less) (Lin et al., 2008). NEC is the leading cause of death and long-term disability from gastrointestinal disease in preterm infants. The overall mortality for NEC ranges from 10% to 50% but approaches 100% for infants with the most severe form of the disease, characterized by full-thickness destruction of the intestine leading to intestinal perforation, peritonitis, bacterial invasion, sepsis, and multiorgan failure.

NEC is not only one of the most serious clinical problems to affect neonates, but also one of the most challenging to treat. Since the etiology and the mechanisms leading to NEC are unknown, the treatment is symptomatic. Minor cases and early stage of NEC are managed by antibiotics and cessation of oral feeding, advanced cases, in which intestinal necrosis is present, may require surgery with intestinal resection.

Despite several decades of work into the pathogenesis of NEC (Hunter et al., 2008), the overall mortality rate remains high and our overall understanding of its causes remains low. Clearly, a more complete understanding of the causes of NEC is required to more effectively design preventive and therapeutic strategies (Bisquera et al., 2002; Ganapathy et al., 2012).

2 CHORIOAMNIONITIS: PATHOLOGICAL FETAL INFLAMMATION IS A RISK FACTOR

The events leading to NEC are complex and multifactorial, including preterm birth, complicated early neonatal trajectory, adverse intrauterine environment, and poor perinatal transition. The most important ones are preterm birth and a history of enteral feeding (Lin and Stoll, 2006). A significant number of fetuses are exposed to various degrees of inflammation, which impacts on their intestinal development.

Chorioamnionitis associated with maternal infection has been strongly implicated in fetal intracerebral hemorrhage (Andrews et al., 2006, 2008; Aziz et al., 2009). However, an increased incidence of NEC has also been reported in neonates of mothers presenting with chorioamnionitis, in several independent studies (Andrews et al., 2006; Aziz et al., 2009; Been et al., 2009) as well as a recent metaanalysis. The role of prenatal infection in the development of NEC is most significant in very preterm infants (24–26 weeks' GA) (Aziz et al., 2009), but

is also apparent in preterm births <32 weeks (Andrews et al., 2006; Been et al., 2009) and in full-term births (Martinez-Tallo et al., 1997).

3 TIGHT JUNCTIONS: INTESTINAL PERMEABILITY AND INTEGRITY

After birth, the intestinal lumen is subject to external environmental influences, including bacterial colonization of the gastrointestinal tract (Gronlund et al., 1999). Cells that cover the intestinal surface must form a barrier to protect the "*milieu intérieur*" from the external world and prevent unrestricted exchange of materials. The intestinal epithelial barrier needs to allow the passage of water and nutrients but prevent microbial contamination and the invasion of interstitial tissues by foreign antigens (Turner, 2009). Tight junctions, essential to the paracellular pathway, are the primary determinants of barrier function. Tight junctions are situated at the apical pole of epithelial cells, and comprise over 50 associated proteins. The first group includes claudins (a family of at least 24 members) and occludin. These proteins span the plasma membrane and are attached to a second group of proteins including zonula occludens (ZO)-1, -2 and -3, which link them to actin and myosin in the cytoskeleton (Turner, 2009).

The properties of tight junctions differ from one tissue to another, as evidenced by the 1000-fold variation in electrical resistance between different epithelia. Barrier properties are not fixed: they can be modulated and regulated on a short- or long-term basis. Short-term regulation is achieved by deformation of the cytoskeleton: myosin light chain phosphorylation permits interaction with actin and contraction of the actin filaments in the perijunctional ring. Contraction of the actin filaments favors the passage of macromolecules by opening the pores. Myosin light chain kinase-1 (MLCK-1) controls the phosphorylation/dephosphorylation of the myosin light chains in the villus enterocytes and surface colonocytes (Clayburgh et al., 2004). Further downstream, during alterations of the tight junction permeability, the transmembrane protein occludin is subject to endocytosis (Schwarz et al., 2007; Turner, 2009). Long-term regulation of intestinal permeability depends on the synthesis and trafficking of claudin-2, a molecule that is overexpressed in intestinal cells of animal models of colitis and in human ulcerative colitis specimens (Heller et al., 2005).

It has been suggested that abnormalities in intestinal permeability may be key to the facilitation of intestinal inflammation leading to NEC (Petrosyan et al., 2009). Intestinal barrier integrity and its appropriate regulation are essential to the prevention of antigen diffusion and bacterial contamination into the lamina propria and interstitial tissue.

4 INTESTINAL PERMEABILITY IS INFLUENCED BY PATHOGENS AND INFLAMMATION

Intestinal barrier dysfunction in newborns may be triggered by exogenous agents. Such enteric pathogens trigger local inflammatory responses through specific receptors [e.g., toll-like receptor 4 (TLR4) for LPS recognition] or by proinflammatory cytokines [e.g., tumor necrosis factor alpha (TNF-α)] (Clayburgh et al., 2005), interferon-γ (Wang et al., 2005), interleukin 1-beta (Al-Sadi et al., 2008), and high-mobility group box 1 (HMGB1) protein (Liu et al., 2006; Raman et al., 2006; Sappington et al., 2002). TNF-α-induced barrier loss is associated with increased transcription and translation of MLCK (Clayburgh et al., 2005). In vivo, intestinal epithelial MLCK is induced by TNF-α. In the rat model of sepsis, an intraperitoneal injection of LPS demonstrably resulted in a rapid rise of TNF-α in the colonic mucosa followed by an increase in myosin light chain phosphorylation and colonic permeability (Moriez et al., 2005). Interestingly, studies in the fetal rat model of NEC have also shown that prenatal bacterial LPS exposure alters the development and permeability of intestinal epithelium (Giannone et al., 2006) and increases ileal injury (Giannone et al., 2009). Similarly, in fetal sheep, preterm intraamniotic LPS exposure induces abnormal expression of ZO-1 in the ileum (Wolfs et al., 2009).

5 ENS CONTROLS EPITHELIAL BARRIER FUNCTION

The enteric nervous system (ENS) is defined as the arrangement of neurons and supporting cells throughout the gastrointestinal tract, from the esophagus to the anus (Goyal and Hirano, 1996). The ENS is organized in ganglia that contain neurons, glial cells, and interstitial cells. Each enteric ganglion contains many different neuron types (Furness, 2000). The ENS consists of some 100 million neurons, or about one tenth of the number of neurons of the spinal cord. Glial cells in the ENS have similar properties to those in the central nervous system (Gershon et al., 1993). The numbers and types of neurotransmitters expressed by enteric neurons are comparable to those found in the central nervous system. The ENS is capable of autonomy with elicitation of reflexes (complete reflex circuitry in the intestinal wall comprises intrinsic sensory neurons, interneurons, and intrinsic motor neurons) after total extrinsic denervation of the gut (Furness et al., 1995). However, the ENS is under physiological influence of the sympathetic and vagus nerves. The ENS controls intestinal motility, modulates visceral sensation, and plays a role in the regulation of the intestinal blood supply and the secretion of digestive

hormones (Boeckxstaens, 2002; Costa and Brookes, 1994; Kunze and Furness, 1999). It also plays a major role in water and electrolyte transport. As a consequence, intestinal permeability is under neural control (Keita and Soderholm, 2010). The ENS should thus be considered, along with the microflora, immune system, and fibroblasts, as a major player in the maintenance of intestinal homeostasis and integrity. The ENS has the ability to fine-tune intestinal barrier function via the release of mediators, such as acetylcholine that enhance—via muscarinic receptors—(Cameron and Perdue, 2007) and vasoactive intestinal peptide (VIP) that constrict (Neunlist et al., 2003) intestinal permeability over short-term or long-term periods (Neunlist et al., 2013). Similarly, the ENS can modulate the proliferation and differentiation of the intestinal epithelial barrier via the secretion of distinct neuromediators, such as VIP (Neunlist et al., 2013). VIP exerts antiproliferative effects, while mediators, such as acetylcholine, glucagon-like peptide 2 (GLP-2), or substance P stimulate intestinal epithelial cell proliferation (Neunlist et al., 2013).

6 NEC: IMMATURE IMMUNE RESPONSE

Local intestinal immune response is normally tightly controlled (Su et al., 2009). The premature gastrointestinal tract has increased permeability, low levels of protective mucus and secretory immunoglobuline A, higher risk of bacterial overgrowth caused by dysmotility due to ENS immaturity, and decreased regenerative capabilities (Neu, 2007). Uncontrolled intestinal inflammation may result from immaturity of the innate immune system of the developing gut (Lin and Stoll, 2006; Lin et al., 2008). Immature regulation could lead to an exaggerated inflammatory response, leading to greater injury and increased intestinal barrier damage. Alternatively, immature regulation could result in minimal immune response due to insufficient inflammatory signaling, thus contributing to bacterial overgrowth and invasion of interstitial tissue. The uncontrolled intestinal inflammation observed in NEC may also depend on dysregulation of intestinal permeability in relation to localized immune response (Turner, 2009). In most individuals and specifically in healthy full-term newborns, a localized break in the intestinal barrier induces a localized immune response that is finely tuned and controlled to avoid overinflammation and a subsequent increase of intestinal permeability. This normal immunoregulatory response is the result of a delicate balance between proinflammatory (TNF-α, IL-1β) and antiinflammatory (IL-10) processes. If even small anomalies occurred in any of the components of the system (tight junction dysregulation, immune regulatory response), the inflammatory response would be amplified and would result in

intestinal injury. Such anomalies may occur secondary to immaturity in preterm babies.

Furthermore, immunomodulatory nutrients, such as glutamine, arginine, nucleotides, omega-3 polyunsaturated fatty acids, and lactoferrin are provided with enteral nutrition and prevent diseases, such as NEC. Difficulties with enteral feeding in the 1st week of life predispose premature infants to sepsis and NEC (Neu et al., 2013).

7 DEVELOPMENT AND MONITORING OF THE AUTONOMIC NERVOUS SYSTEM ACTIVITY

The autonomic nervous system plays a predominant role in complex coordinated control of multiple vitally important physiological subsystems in the organism and is part of the neuroimmunological response to pathogens via CAP (Fairchild et al., 2011). Since autonomic nervous system development and activity are reflected in the heart rate patterns, an appropriate analysis of the fetal heart rate variability (fHRV) may provide information regarding the individual fetal development (Hoyer et al., 2013; Van Leeuwen et al., 1999). fHRV is a noninvasively obtainable marker of changes in vagal (parasympathetic) and sympathetic activity (Frank et al., 2006). Increase in fHRV is associated with fetal growth in general and with the increase in neural integration in particular (Van Leeuwen et al., 2013). Understanding of the dynamics of fHRV in human and ovine fetuses during physiologic (e.g., sleep states) and pathophysiologic (e.g., asphyxia) conditions has evolved over the past 2 decades (Frank et al., 2006; Karin et al., 1993). FHR and fHRV are regulated by a complex interplay of the parasympathetic and sympathetic nervous systems accounting for the baseline FHR as well as short-term and long-term variability and nonlinear properties (Frasch et al., 2009b; Gieraltowski et al., 2013). Nonlinear properties of fHRV in late gestation fetuses are present and a higher vagal tone is associated with more efficient regulation of homeostasis (Groome et al., 1999).

8 CAP CONTROLS IMMUNE HOMEOSTASIS

CAP has been implicated in the regulation of the inflammatory reflex in adult organisms including humans (Cailotto et al., 2012; Olofsson et al., 2012; Tracey, 2002, 2007, 2009). CAP is a neural mechanism that influences the magnitude of the innate immune response and maintains homeostasis. As part of CAP, increased vagal activity inhibits the release of proinflammatory cytokines. Vagal nerve stimulation decreases LPS-induced

systemic TNF-α release in adult rats (Borovikova et al., 2000). Suppression of proinflammatory cytokine expression via agonistic action on the α7 subunit nicotinic acetylcholine receptor (α7nAChR) was confirmed in innate immune cells, such as macrophages [reviewed in Tracey (2007)]. Systemically via CAP, this is mediated via the spleen: Adrenergic nerve fibers in the spleen activate acetylcholine-producing T-lymphocytes, thereby inhibiting systemic cytokine production (Huston et al., 2007; Olofsson et al., 2012; Rosas-Ballina et al., 2011).

Vagal nerve activity in basal conditions provides inhibitory input that dampens innate immune response (Haensel et al., 2008; Thayer and Fischer, 2009). The CAP influences the magnitude of the innate immune response and maintains homeostasis (Tracey, 2009). Depressed vagal nerve activity is associated with an exaggerated proinflammatory response and increased morbidity and mortality in various contexts, such as acute or stable coronary heart disease, metabolic syndrome or impaired glucose tolerance and kidney failure (Haensel et al., 2008; Thayer and Fischer, 2009). The inhibitory role of CAP on innate immune function can be thought of as analogous to the inhibitory role of the vagus nerve on the resting heart rate (Tracey, 2009).

Under resting conditions, the inflammatory reflex helps establish the set point for the magnitude of the innate immune response to molecules arising from infection, injury, or ischemia. Vagus nerve output maintains homeostasis by limiting proinflammatory response to the healthy, protective, and nontoxic range. However, when vagal activity is absent or diminished, the set point increases; exposure to pathogens then results in an exaggerated proinflammatory response and eventual tissue damage as demonstrated in different experiments with murine models (Ghia et al., 2006, 2007a,b, 2008).

Numerous factors can experimentally or clinically impair the CAP, each resulting in an exaggerated innate immune response. For instance, in animal models with vagotomy or deficient in α7nAChR, the magnitude of the proinflammatory cytokine response and the extent of tissue damage increase during infection, hemorrhagic shock and stroke (Ghia et al., 2008; Guarini et al., 2003; Ottani et al., 2009; Tracey, 2009; van Westerloo et al., 2005). The observation that vagal nerve activity influences circulating TNF-α amounts and the shock response to endotoxemia has widespread implications. It is a previously unrecognized, direct, and rapid endogenous mechanism that can suppress the lethal effects of biological toxins. The CAP has much shorter response times than humoral antiinflammatory pathways. Electrical stimulation of the vagus nerve or administration of α7nAChR agonists in rat model of LPS-induced sepsis reduces the magnitude of proinflammatory cytokine production by 50%–75% but does not eliminate cytokine activity (Borovikova et al., 2000; Tracey, 2009). Activation of CAP has not been observed to cause immunosuppression because maximal suppression only reduces proinflammatory cytokine levels from the toxic to the healthy range. This concept has been studied as a potential treatment for a range of inflammatory diseases, including infection [reviewed in Tracey (2009)]. The role of CAP in the perinatal inflammatory response and the priming of subsequent innate immune response require elucidation.

Studies are needed to explore the impact of CAP activity on chorioamnionitis (Shapiro et al., 2013). Such studies could lead to the development of novel prognostic markers to better identify fetuses at risk of NEC. We hypothesize that increased CAP activity would inhibit the activation of intestinal innate immune cells, such as macrophages and thus suppress the inflammatory response to bacterial infection. Effectively, pathological inflammation and intestinal permeability as a *locus minoris resistentiae* of incipient NEC would be decreased or normalized.

9 VAGAL NERVE STIMULATION AND THE GUT INFLAMMATION

As vagal nerve stimulation stimulates CAP activity without causing immunosuppression (Borovikova et al., 2000), it has been shown to improve intestinal inflammation in murine models of experimental colitis (Ghia et al., 2006, 2007a,b, 2008) and postoperative ileus (The et al., 2007; van Bree et al., 2012). The role of intestinal macrophages seems pivotal (Costantini et al., 2010a; Rosas-Ballina et al., 2011; The et al., 2007; van Bree et al., 2012). In a murine model of dextran sodium sulfate-induced colitis, Ghia et al. demonstrated an increased inflammatory response in the colonic mucosa of the vagotomy group as compared to control animals. They showed the protective effect of vagal activity in acute colitis (Ghia et al., 2006) and in acute relapses within a background of chronic inflammation (Ghia et al., 2007b).

In a murine model of postoperative ileus, the antiinflammatory effect of intracerebroventricular injection of semapimod was abolished in the presence of vagotomy (The et al., 2011). Vagal nerve stimulation also modulates intestinal permeability and integrity. In a murine model of intestinal injury caused by severe burns, vagal nerve stimulation performed before injury improved intestinal barrier integrity through an efferent signaling pathway and was associated with improved tight junction protein expression (Costantini et al., 2010b). In the same model, stimulating the vagus nerve at the time of injury promoted enteric glial cell activation. Either method could prevent intestinal barrier injury (Costantini et al., 2010a). Activation of enteric glial cells has been reported in a rat

model of burn-induced stress and gut injury (Costantini et al., 2010a).

The optimal choice of vagal nerve stimulation parameters in order to activate the CAP for therapeutic purposes remains challenging (Kwan et al., 2016). Although the literature provides a spectrum of possibilities, further studies are needed. Huston et al. (2007) demonstrated improved survival in murine polymicrobial sepsis with transcutaneous vagal nerve stimulation, suggesting that this mode might be an effective therapy for sepsis generally and NEC specifically. Pharmacologically, cholinergic neuronal circuitry can be stimulated peripherally using α7nAChR agonists to act on macrophages; or centrally using intracerebroventricular injections of semapimod (The et al., 2011), muscarinic receptor agonist McN-A-343 (Pavlov et al., 2006), or an acetylcholinesterase inhibitor (galantamine) (Pavlov et al., 2009). Importantly, enteral feeding of lipid-rich nutrition may also be used to activate the CAP pathway (Luyer et al., 2005).

10 NEAR FUTURE: EARLY DETECTION OF NEC USING FETAL AND NEONATAL HEART RATE MONITORING?

Human and animal studies using fetal sheep indicate that heart rate monitoring can signal early onset of NEC (Liu et al., 2016; Stone et al., 2013). A unique subset of fHRV measures reflecting 1.5 days ahead of time the levels of macrophage activation and increased leakiness in terminal ileum (Liu et al., 2016). Such subset of fHRV measures may reflect the brain–gut communication via the vagus nerve. This supports the notion of a common neuroregulatory mechanism via CAP and requires further studies in animal models of NEC to hack the "vagus code" (Kwan et al., 2016).

Ultimately, such animal studies should lead to a noninvasively obtained fetal CAP response signature to help identify babies at risk of developing NEC.

Together, the potential of creating organ-specific fHRV signatures of inflammation obtainable noninvasively by hacking the brain–body communication via the vagus nerve by using multidimensional HRV analysis needs to be explored and exploited in further animal studies. Some early work in human cohorts already indicates the value of such approach for early prediction of perinatal health outcomes (Frasch et al., 2014).

Acknowledgments

References

Abu Jawdeh, E.G., Martin, R.J., 2013. Neonatal apnea and gastroesophageal reflux (GER): is there a problem? Early Hum. Dev. 89 (Suppl. 1), S14–S16.

Agren, P., Cogolludo, A.L., Kessels, C.G.A., Pérez-Vizcaíno, F., De Mey, J.G.R., Blanco, C.E., Villamor, E., 2007. Ontogeny of chicken ductus arteriosus response to oxygen and vasoconstrictors. Am. J. Physiol. Regul. Integr. Comp. Physiol. 292 (1), R485–R496.

Agren, P., Van der Sterren, S., Cogolludo, A.L., Blanco, C.E., Villamor, E., 2009. Developmental changes in the effects of prostaglandin E2 in the chicken ductus arteriosus. J. Comp. Physiol. B. 179 (2), 133–143.

Albertine, K.H., 2015. Utility of large-animal models of BPD: chronically ventilated preterm lambs. Am. J. Physiol. Lung Cell Mol. Physiol. 308 (10), L983–L1001.

Al-Sadi, R., Ye, D., Dokladny, K., Ma, T.Y., 2008. Mechanism of IL-1beta-induced increase in intestinal epithelial tight junction permeability. J. Immunol. 180 (8), 5653–5661.

Alvaro, R., de Almeida, V., al-Alaiyan, S., Robertson, M., Nowaczyk, B., Cates, D., Rigatto, H., 1993. A placental extract inhibits breathing induced by umbilical cord occlusion in fetal sheep. J. Dev. Physiol. 19 (1), 23–28.

Alvarez, Y., Cederlund, M.L., Cottell, D.C., Bill, B.R., Ekker, S.C., Torres-Vazquez, J., et al., 2007. Genetic determinants of hyaloid and retinal vasculature in zebrafish. BMC Dev. Biol. 7 (1), 114–117.

Andrews, W.W., Goldenberg, R.L., Faye-Petersen, O., Cliver, S., Goepfert, A.R., Hauth, J.C., 2006. The Alabama Preterm Birth study: polymorphonuclear and mononuclear cell placental infiltrations, other markers of inflammation, and outcomes in 23- to 32-week preterm newborn infants. Am. J. Obstet. Gynecol. 195 (3), 803–808.

Andrews, W.W., Cliver, S.P., Biasini, F., Peralta-Carcelen, A.M., Rector, R., Alriksson-Schmidt, A.I., et al., 2008. Early preterm birth: association between in utero exposure to acute inflammation and severe neurodevelopmental disability at 6 years of age. Am. J. Obstet. Gynecol. 198 (4), 466.e1–466.e11.

Aquilina, K., Chakkarapani, E., Thoresen, M., 2012. Early deterioration of cerebrospinal fluid dynamics in a neonatal piglet model of intraventricular hemorrhage and posthemorrhagic ventricular dilation. J. Neurosurg. Pediatr. 10 (6), 529–537.

Aquilina, K., Hobbs, C., Cherian, S., Tucker, A., Porter, H., Whitelaw, A., Thoresen, M., 2007. A neonatal piglet model of intraventricular hemorrhage and posthemorrhagic ventricular dilation. J. Neurosurg. 107 (2 Suppl.), 126–136.

Arsenault, J., Moreau-Bussiere, F., Reix, P., Niyonsenga, T., Praud, J.P., 2003. Postnatal maturation of vagal respiratory reflexes in preterm and full-term lambs. J. Appl. Physiol. (1985) 94 (5), 1978–1986.

Ashton, N., Blach, R., 1961. Studies on developing retinal vessels VIII. Effect of oxygen on the retinal vessels of the ratling. Br. J. Ophthalmol. 45 (5), 321–340.

Ashton, N., Ward, B., Serpell, G., 1954. Effect of oxygen on developing retinal vessels with particular reference to the problem of retrolental fibroplasia. Br. J. Ophthalmol. 38 (7), 397–432.

Avoine, O., Bosse, D., Beaudry, B., Beaulieu, A., Albadine, R., Praud, J.P., et al., 2011. Total liquid ventilation efficacy in an ovine model of severe meconium aspiration syndrome. Crit. Care Med. 39 (5), 1097–1103.

Aziz, N., Cheng, Y.W., Caughey, A.B., 2009. Neonatal outcomes in the setting of preterm premature rupture of membranes complicated by chorioamnionitis. J. Matern. Fetal Neonatal Med. 22 (9), 780–784.

Ballabh, P., 2010. Intraventricular hemorrhage in premature infants: mechanism of disease. Pediatr. Res. 67 (1), 1–8.

Ballabh, P., 2014. Pathogenesis and prevention of intraventricular hemorrhage. Clin. Perinatol. 41 (1), 47–67.

Ballabh, P., Xu, H., Hu, F., Braun, A., Smith, K., Rivera, A., et al., 2007. Angiogenic inhibition reduces germinal matrix hemorrhage. Nat. Med. 13 (4), 477–485.

Barnett, J.M., Yanni, S.E., Penn, J.S., 2010. The development of the rat model of retinopathy of prematurity. Doc. Ophthalmol. 120 (1), 3–12.

Barrington, K.J., Singh, A.J., Etches, P.C., Finer, N.N., 1999. Partial liquid ventilation with and without inhaled nitric oxide in a newborn piglet model of meconium aspiration. Am. J. Respir. Crit. Care Med. 160 (6), 1922–1927.

Been, J.V., Rours, I.G., Kornelisse, R.F., Lima Passos, V., Kramer, B.W., Schneider, T.A., et al., 2009. Histologic chorioamnionitis, fetal involvement, and antenatal steroids: effects on neonatal outcome in preterm infants. Am. J. Obstet. Gynecol. 201 (6), 587.e1–587.e8.

Berger, J., Bhandari, V., 2014. Animal models of bronchopulmonary dysplasia. The term mouse models. Am. J. Physiol. Lung Cell Mol. Physiol. 307 (12), L936–L947.

Bergwerff, M., DeRuiter, M.C., Gittenberger-de Groot, A.C., 1999. Comparative anatomy and ontogeny of the ductus arteriosus, a vascular outsider. Anat. Embryol. 200 (6), 559–571.

Bird, A.D., McDougall, A.R., Seow, B., Hooper, S.B., Cole, T.J., 2015. Glucocorticoid regulation of lung development: lessons learned from conditional GR knockout mice. Mol. Endocrinol. 29 (2), 158–171.

Bisquera, J.A., Cooper, T.R., Berseth, C.L., 2002. Impact of necrotizing enterocolitis on length of stay and hospital charges in very low birth weight infants. Pediatrics 109 (3), 423–428.

Bjorklund, L.J., Ingimarsson, J., Curstedt, T., John, J., Robertson, B., Werner, O., Vilstrup, C.T., 1997. Manual ventilation with a few large breaths at birth compromises the therapeutic effect of subsequent surfactant replacement in immature lambs. Pediatr. Res. 42 (3), 348–355.

Blanco, C.E., Martin, Jr., C.B., Hanson, M.A., McCooke, H.B., 1987. Breathing activity in fetal sheep during mechanical ventilation of the lungs in utero. Eur. J. Obstet. Gynecol. Reprod. Biol. 26 (2), 175–182.

Boeckxstaens, G.E., 2002. Understanding and controlling the enteric nervous system. Best Pract. Res. Clin. Gastroenterol. 16 (6), 1013–1023.

Bökenkamp, R., DeRuiter, M.C., van Munsteren, C., Gittenberger-de Groot, A.C., 2010. Insights into the pathogenesis and genetic background of patency of the ductus arteriosus. Neonatology 98 (1), 6–17.

Bolt, R.J., van Weissenbruch, M.M., Lafeber, H.N., Delemarre-van de Waal, H.A., 2001. Glucocorticoids and lung development in the fetus and preterm infant. Pediatr. Pulmonol. 32 (1), 76–91.

Borovikova, L.V., Ivanova, S., Zhang, M., Yang, H., Botchkina, G.I., Watkins, L.R., et al., 2000. Vagus nerve stimulation attenuates the systemic inflammatory response to endotoxin. Nature 405 (6785), 458–462.

Boudaa, N., Samson, N., Carriere, V., Germim, P.S., Pasquier, J.C., Bairam, A., Praud, J.P., 2013. Effects of caffeine and/or nasal CPAP treatment on laryngeal chemoreflexes in preterm lambs. J. Appl. Physiol. (1985) 114 (5), 637–646.

Braun, A., Xu, H., Hu, F., Kocherlakota, P., Siegel, D., Chander, P., et al., 2007. Paucity of pericytes in germinal matrix vasculature of premature infants. J. Neurosci. 27 (44), 12012–12024.

Bunton, T.E., Plopper, C.G., 1984. Triamcinolone-induced structural alterations in the development of the lung of the fetal rhesus macaque. Am. J. Obstet. Gynecol. 148 (2), 203–215.

Burd, I., Chai, J., Gonzalez, J., Ofori, E., Monnerie, H., Le Roux, P.D., Elovitz, M.A., 2009. Beyond white matter damage: fetal neuronal injury in a mouse model of preterm birth. Am. J. Obstet. Gynecol. 201 (3), 279.e1–279.e8.

Burd, I., Brown, A., Gonzalez, J.M., Chai, J., Elovitz, M.A., 2011. A mouse model of term chorioamnionitis: unraveling causes of adverse neurological outcomes. Reprod. Sci. 18 (9), 900–907.

Burns, P., Liu, H.L., Kuthiala, S., Fecteau, G., Desrochers, A., Durosier, L.D., et al., 2015. Instrumentation of near-term fetal sheep for multivariate chronic non-anesthetized recordings. J. Vis. Exp. (105), e52581.

Cailotto, C., Costes, L.M., van der Vliet, J., van Bree, S.H., van Heerikhuize, J.J., Buijs, R.M., Boeckxstaens, G.E., 2012. Neuroanatomical evidence demonstrating the existence of the vagal anti-inflammatory reflex in the intestine. Neurogastroenterol. Motil. 24 (2), e191–e193.

Cameron, H.L., Perdue, M.H., 2007. Muscarinic acetylcholine receptor activation increases transcellular transport of macromolecules across mouse and human intestinal epithelium in vitro. Neurogastroenterol. Motil. 19 (1), 47–56.

Campbell, K., 1951. Intensive oxygen therapy as a possible cause of retrolental fibroplasia; a clinical approach. Med. J. Aust. 2 (2), 48–50.

Canet, E., Kianicka, I., Praud, J.P., 1996. Postnatal maturation of peripheral chemoreceptor ventilatory response to O_2 and CO_2 in newborn lambs. J. Appl. Physiol. (1985) 80 (6), 1928–1933.

Cantin, D., Djeddi, D., Carriere, V., Samson, N., Nault, S., Jia, W.L., et al., 2016. Inhibitory effect of nasal intermittent positive pressure ventilation on gastroesophageal reflux. PLoS One 11 (1), e0146742.

Cao, M., Durosier, L.D., Burns, P., Fecteau, G., Desrochers, A., Frasch, M.G., 2014. In vitro pro-inflammatory phenotype of fetal brain microglia is potentiated by an in vivo pre-exposure to inflammation: a prospective study in ovine fetus near term. J. Dev. Neurosci, (47), 103.

Cao, M., Cortes, M., Moore, C.S., Leong, S.Y., Durosier, L.D., Burns, P., et al., 2015. Fetal microglial phenotype in vitro carries memory of prior in vivo exposure to inflammation. Front. Cell Neurosci. 9, 294.

Cao, R., Jensen, L.D.E., Söll, I., Hauptmann, G., Cao, Y., 2008. Hypoxia-induced retinal angiogenesis in zebrafish as a model to study retinopathy. PLoS One 3 (7), e2748–e2749.

Carreau, A.M., Patural, H., Samson, N., Doueik, A.A., Hamon, J., Fortier, P.H., Praud, J.P., 2011. Effects of simulated reflux laryngitis on laryngeal chemoreflexes in newborn lambs. J. Appl. Physiol. (1985) 111 (2), 400–406.

Carriere, V., Cantin, D., Nault, S., Nadeau, C., Samson, N., Beck, J., Praud, J.P., 2015. Effects of inspiratory pressure rise time and hypoxic or hypercapnic breathing on inspiratory laryngeal constrictor muscle activity during nasal pressure support ventilation. Crit. Care Med. 43 (8), e296–303.

Carroll, J.L., Kim, I., 2013. Carotid chemoreceptor "resetting" revisited. Respir. Physiol. Neurobiol. 185 (1), 30–43.

Chan-Ling, T.L., Halasz, P., Stone, J., 1990. Development of retinal vasculature in the cat: processes and mechanisms. Curr. Eye Res. 9 (5), 459–478.

Chen, M.L., Allred, E.N., Hecht, J.L., Onderdonk, A., VanderVeen, D., Wallace, D.K., et al., 2011a. Placenta microbiology and histology and the risk for severe retinopathy of prematurity. Invest. Ophthalmol. Vis. Sci. 52 (10), 7052–7058.

Chen, M., Çitil, A., McCabe, F., Leicht, K.M., Fiascone, J., Dammann, C.E.L., Dammann, O., 2011b. Infection, Oxygen, and Immaturity: Interacting Risk Factors for Retinopathy of Prematurity. Neonatology 99 (2), 125–132.

Cherian, S., Thoresen, M., Silver, I.A., Whitelaw, A., Love, S., 2004. Transforming growth factor-betas in a rat model of neonatal posthaemorrhagic hydrocephalus. Neuropathol. Appl. Neurobiol. 30 (6), 585–600.

Chua, C.O., Chahboune, H., Braun, A., Dummula, K., Chua, C.E., Yu, J., et al., 2009. Consequences of intraventricular hemorrhage in a rabbit pup model. Stroke 40 (10), 3369–3377.

Clayburgh, D.R., Barrett, T.A., Tang, Y., Meddings, J.B., Van Eldik, L.J., Watterson, D.M., et al., 2005. Epithelial myosin light chain kinase-

dependent barrier dysfunction mediates T cell activation-induced diarrhea in vivo. J. Clin. Invest. 115 (10), 2702–2715.

Clayburgh, D.R., Rosen, S., Witkowski, E.D., Wang, F., Blair, S., Dudek, S., et al., 2004. A differentiation-dependent splice variant of myosin light chain kinase, MLCK1, regulates epithelial tight junction permeability. J. Biol. Chem. 279 (53), 55506–55513.

Clyman, R.I., 2013. The role of patent ductus arteriosus and its treatments in the development of bronchopulmonary dysplasia. Semin. Perinatol. 37 (2), 102–107.

Clyman, R.I., Campbell, D., Heymann, M.A., Mauray, F., 1985. Persistent responsiveness of the neonatal ductus arteriosus in immature lambs: a possible cause for reopening of patent ductus arteriosus after indomethacin-induced closure. Circulation 71 (1), 141–145.

Clyman, R.I., Chan, C.Y., Mauray, F., Chen, Y.Q., Cox, W., Seidner, S.R., et al., 1999. Permanent anatomic closure of the ductus arteriosus in newborn baboons: the roles of postnatal constriction, hypoxia, and gestation. Pediatr. Res. 45 (1), 19–29.

Clyman, R.I., Couto, J., Murphy, G.M., 2012. Patent Ductus Arteriosus: Are Current Neonatal Treatment Options Better or Worse Than No Treatment at All? Semin. Perinatol. 36 (2), 123–129.

Cochrane, C.G., Revak, S.D., Merritt, T.A., Schraufstatter, I.U., Hoch, R.C., Henderson, C., et al., 1998. Bronchoalveolar lavage with KL4-surfactant in models of meconium aspiration syndrome. Pediatr. Res. 44 (5), 705–715.

Conner, E.S., Lorenzo, A.V., Welch, K., Dorval, B., 1983. The role of intracranial hypotension in neonatal intraventricular hemorrhage. J. Neurosurg. 58 (2), 204–209.

Connor, K.M., Krah, N.M., Dennison, R.J., Aderman, C.M., Chen, J., Guerin, K.I., et al., 2009. Quantification of oxygen-induced retinopathy in the mouse: a model of vessel loss, vessel regrowth and pathological angiogenesis. Nat. Protoc. 4 (11), 1565–1573.

Cools, F., Offringa, M., 2005. Neuromuscular paralysis for newborn infants receiving mechanical ventilation. Cochrane Database Syst. Rev. (2).

Costa, M., Brookes, S.J., 1994. The enteric nervous system. Am. J. Gastroenterol. 89 (8 Suppl), S129–S137.

Costantini, T.W., Bansal, V., Krzyzaniak, M.J., Putnam, J.G., Peterson, C.Y., Loomis, W.H., et al., 2010a. Vagal nerve stimulation protects against burn-induced intestinal injury through activation of enteric glia cells. Am. J. Physiol. Gastrointest. Liver Physiol. 299, G1308–G1318.

Costantini, T.W., Bansal, V., Peterson, C.Y., Loomis, W.H., Putnam, J.G., Rankin, F., et al., 2010b. Efferent vagal nerve stimulation attenuates gut barrier injury after burn: modulation of intestinal occludin expression. J. Trauma 68 (6), 1349–1354.

Coulter, D.M., LaPine, T., Gooch, W.M., 1984. Intraventricular hemorrhage in the premature rabbit pup. Limitations of this animal model. J. Neurosurg. 60 (6), 1243–1245.

Cryotherapy for Retinopathy of Prematurity Cooperative Group, 2001. Multicenter trial of cryotherapy for retinopathy of prematurity: ophthalmological outcomes at 10 years. Arch. Ophthalmol. 119 (8), 1110–1118.

Cuthbertson, F., Newsom, R., 2006. UK retinopathy of prematurity treatment survey. Eye 21 (2), 156–157.

Dammann, O., 2010. Inflammation and retinopathy of prematurity. Acta Paediatr. 99 (7), 975–977.

Dammann, O., Brinkhaus, M.-J., Bartels, D.B., Dördelmann, M., Dressler, F., Kerk, J., et al., 2009. Immaturity, perinatal inflammation, and retinopathy of prematurity: a multi-hit hypothesis. Early Hum. Dev. 85 (5), 325–329.

D'Angio, C.T., Ryan, R.M., 2014. Animal models of bronchopulmonary dysplasia. The preterm and term rabbit models. Am. J. Physiol. Lung Cell Mol. Physiol. 307 (12), L959–L969.

Dargaville, P.A., Mills, J.F., 2005. Surfactant therapy for meconium aspiration syndrome: current status. Drugs 65 (18), 2569–2591.

Dargaville, P.A., Mills, J.F., Headley, B.M., Chan, Y., Coleman, L., Loughnan, P.M., Morley, C.J., 2003. Therapeutic lung lavage in the piglet model of meconium aspiration syndrome. Am. J. Respir. Crit. Care Med. 168 (4), 456–463.

Dargaville, P.A., Lavizzari, A., Padoin, P., Black, D., Zonneveld, E., Perkins, E., et al., 2015. An authentic animal model of the very preterm infant on nasal continuous positive airway pressure. Intensive Care Med. Exp. 3 (1), 51.

Darnall, R.A., 2013. The carotid body and arousal in the fetus and neonate. Respir. Physiol. Neurobiol. 185 (1), 132–143.

Davey, A.M., Becker, J.D., Davis, J.M., 1993. Meconium aspiration syndrome: physiological and inflammatory changes in a newborn piglet model. Pediatr. Pulmonol. 16 (2), 101–108.

Davey, M.G., Moss, T.J., McCrabb, G.J., Harding, R., 1996. Prematurity alters hypoxic and hypercapnic ventilatory responses in developing lambs. Respir. Physiol. 105 (1–2), 57–67.

Davidson, J.O., Wassink, G., van den Heuij, L.G., Bennet, L., Gunn, A.J., 2015. Therapeutic hypothermia for neonatal hypoxic-ischemic encephalopathy—where to from here? Front. Neurol. 6, 198.

Davies, A.M., Koenig, J.S., Thach, B.T., 1988. Upper airway chemoreflex responses to saline and water in preterm infants. J. Appl. Physiol. (1985) 64 (4), 1412–1420.

De Haan, H.H., Gunn, A.J., Williams, C.E., Gluckman, P.D., 1997. Brief repeated umbilical cord occlusions cause sustained cytotoxic cerebral edema and focal infarcts in near-term fetal lambs. Pediatr. Res. 41 (1), 96–104.

Dean, J.M., van de Looij, Y., Sizonenko, S.V., Lodygensky, G.A., Lazeyras, F., Bolouri, H., et al., 2011. Delayed cortical impairment following lipopolysaccharide exposure in preterm fetal sheep. Ann. Neurol. 70 (5), 846–856.

Dean, J.M., Shi, Z., Fleiss, B., Gunn, K.C., Groenendaal, F., van Bel, F., et al., 2015. A critical review of models of perinatal infection. Dev. Neurosci. 37 (4–5), 289–304.

Del Bigio, M.R., Becker, L.E., 1994. Microglial aggregation in the dentate gyrus: a marker of mild hypoxic-ischaemic brain insult in human infants. Neuropathol. Appl. Neurobiol. 20 (2), 144–151.

Deprest, J., Brady, P., Nicolaides, K., Benachi, A., Berg, C., Vermeesch, J., et al., 2014. Prenatal management of the fetus with isolated congenital diaphragmatic hernia in the era of the TOTAL trial. Semin. Fetal Neonatal Med. 19 (6), 338–348.

Diaz, V., Dorion, D., Renolleau, S., Letourneau, P., Kianicka, I., Praud, J.P., 1999. Effects of capsaicin pretreatment on expiratory laryngeal closure during pulmonary edema in lambs. J. Appl. Physiol. (1985) 86 (5), 1570–1577.

DiBlasi, R.M., 2011. Neonatal noninvasive ventilation techniques: do we really need to intubate? Respir. Care 56 (9), 1273–1294.

Dice, J.E., Bhatia, J., 2007. Patent ductus arteriosus: an overview. J. Pediatr. Pharmacol. Ther. 12 (3), 138–146.

Djeddi, D., Cantin, D., Samson, N., Praud, J.P., 2014. Nasal continuous positive airway pressure inhibits gastroesophageal reflux in newborn lambs. PLoS One 9 (9), e107736.

Dong, Y., Speer, C.P., 2015. Late-onset neonatal sepsis: recent developments. Arch. Dis. Child Fetal Neonatal Ed. 100 (3), F257–F263.

Dong, Y., Yu, Z., Sun, Y., Zhou, H., Stites, J., Newell, K., Weiner, C.P., 2011. Chronic fetal hypoxia produces selective brain injury associated with altered nitric oxide synthases. Am. J. Obstet. Gynecol. 204 (3), 254.e16–254.e28.

Donnelly, D.F., Haddad, G.G., 1986. Effect of graded anesthesia on laryngeal-induced central apnea. Respir. Physiol. 66 (2), 235–245.

Dorion, D., Praud, J.P., 2003. The larynx and neonatal apneas. Otolaryngol. Head Neck Surg. 128 (4), 463–469.

Dorrell, M.I., Friedlander, M., 2006. Mechanisms of endothelial cell guidance and vascular patterning in the developing mouse retina. Prog. Retin. Eye Res. 25 (3), 277–295.

Dowling, D.J., Levy, O., 2014. Ontogeny of early life immunity. Trends Immunol. 35 (7), 299–310.

Dreshaj, I.A., Haxhiu, M.A., Miller, M.J., Abu-Shaweesh, J., Martin, R.J., 2001. Differential effects of hypercapnia on expiratory phases of respiration in the piglet. Respir. Physiol. 126 (1), 43–51.

Drury, P.P., Davidson, J.O., van den Heuij, L.G., Wassink, G., Gunn, E.R., Booth, L.C., et al., 2014. Status epilepticus after prolonged umbilical cord occlusion is associated with greater neural injury in [corrected] fetal sheep at term-equivalent. PLoS One 9 (5), e96530.

Durosier, L.D., Green, G., Batkin, I., Seely, A.J., Ross, M.G., Richardson, B.S., Frasch, M.G., 2014. Sampling rate of heart rate variability impacts the ability to detect acidemia in ovine fetuses near-term. Front. Pediatr. 2, 38.

Durosier, L.D., Herry, C.L., Cortes, M., Cao, M., Burns, P., Desrochers, A., et al., 2015. Does heart rate variability reflect the systemic inflammatory response in a fetal sheep model of lipopolysaccharide-induced sepsis? Physiol. Meas. 36 (10), 2089–2102.

Eastwood, M.P., Russo, F.M., Toelen, J., Deprest, J., 2015. Medical interventions to reverse pulmonary hypoplasia in the animal model of congenital diaphragmatic hernia: a systematic review. Pediatr. Pulmonol. 50 (8), 820–838.

El-Khoury, N., Braun, A., Hu, F., Pandey, M., Nedergaard, M., Lagamma, E.F., Ballabh, P., 2006. Astrocyte end-feet in germinal matrix, cerebral cortex, and white matter in developing infants. Pediatr. Res. 59 (5), 673–679.

Elias, A.A., Ghaly, A., Matushewski, B., Regnault, T.R., Richardson, B.S., 2016. Maternal nutrient restriction in guinea pigs as an animal model for inducing fetal growth restriction. Reprod. Sci. 23 (2), 219–227.

Fahey, J.O., 2008. Clinical management of intra-amniotic infection and chorioamnionitis: a review of the literature. J. Midwifery Womens Health 53 (3), 227–235.

Fairchild, K.D., 2013. Predictive monitoring for early detection of sepsis in neonatal ICU patients. Curr. Opin. Pediatr. 25 (2), 172–179.

Fairchild, K.D., Srinivasan, V., Moorman, J.R., Gaykema, R.P., Goehler, L.E., 2011. Pathogen-induced heart rate changes associated with cholinergic nervous system activation. Am. J. Physiol. Regul. Integr. Comp. Physiol. 300 (2), R330–R339.

Farber, J.P., 1972. Development of pulmonary reflexes and pattern of breathing in Virginia opossum. Respir. Physiol. 14 (3), 278–286.

Flanagan, K.A., 2016. Noninvasive ventilation in premature neonates. Adv. Neonatal Care 16 (2), 91–98.

Flynn, J.T., 1992. The premature retina: a model for the in vivo study of molecular genetics? Eye (Lond.) 6 (Pt (2)), 161–165.

Fortier, P.H., Reix, P., Arsenault, J., Dorion, D., Praud, J.P., 2003. Active upper airway closure during induced central apneas in lambs is complete at the laryngeal level only. J. Appl. Physiol. (1985) 95 (1), 97–103.

Foust, 3rd, R., Tran, N.N., Cox, C., Miller, Jr., T.F., Greenspan, J.S., Wolfson, M.R., Shaffer, T.H., 1996. Liquid assisted ventilation: an alternative ventilatory strategy for acute meconium aspiration injury. Pediatr. Pulmonol. 21 (5), 316–322.

Frank, B., Frasch, M.G., Schneider, U., Roedel, M., Schwab, M., Hoyer, D., 2006. Complexity of heart rate fluctuations in near-term sheep and human fetuses during sleep. Biomed. Tech. (Berl) 51 (4), 233–236.

Frasch, M.G., Mansano, R.Z., Gagnon, R., Richardson, B.S., Ross, M.G., 2009a. Measures of acidosis with repetitive umbilical cord occlusions leading to fetal asphyxia in the near-term ovine fetus. Am. J. Obstet. Gynecol. 200 (27), 200.e1–200.e7.

Frasch, M.G., Muller, T., Hoyer, D., Weiss, C., Schubert, H., Schwab, M., 2009b. Nonlinear properties of vagal and sympathetic modulations of heart rate variability in ovine fetus near term. Am. J. Physiol. Regul. Integr. Comp. Physiol. 296 (3), R702–R707.

Frasch, M.G, Keen, A.E., Matushewski, B., Richardson, B.S., 2010. Comparability of electroenkephalogram (EEG) versus electrocorticogram (ECOG) in the ovine fetus near term. 57th Annual Scientific Meeting of the Society for Gynecologic Investigation, vol. 17 (3 Suppl.). p. 51A.

Frasch, M.G., Keen, A.E., Gagnon, R., Ross, M.G., Richardson, B.S., 2011. Monitoring fetal electrocortical activity during labour for predicting worsening acidemia: a prospective study in the ovine fetus near term. PLoS One 6 (7), e22100.

Frasch, M.G., Xu, Y., Stampalija, T., Durosier, L.D., Herry, C., Wang, X., et al., 2014. Correlating multidimensional fetal heart rate variability analysis with acid-base balance at birth. Physiol. Meas. 35 (12), L1–L12.

Frasch, M.G., Szynkaruk, M., Prout, A.P., Nygard, K., Cao, M., Veldhuizen, R., et al., 2016. Decreased neuroinflammation correlates to higher vagus nerve activity fluctuations in near-term ovine fetuses: a case for the afferent cholinergic anti-inflammatory pathway? J. Neuroinflammation 13 (1), 103.

Friedman, W.F., Hirschklau, M.J., Printz, M.P., Pitlick, P.T., Kirkpatrick, S.E., 1976. Pharmacologic closure of patent ductus arteriosus in the premature infant. N. Engl. J. Med. 295 (10), 526–529.

Fung, M.E., Thebaud, B., 2014. Stem cell-based therapy for neonatal lung disease: it is in the juice. Pediatr. Res. 75 (1–1), 2–7.

Furness, J.B., 2000. Types of neurons in the enteric nervous system. J. Auton. Nerv. Syst. 81 (1–3), 87–96.

Furness, J.B., Johnson, P.J., Pompolo, S., Bornstein, J.C., 1995. Evidence that enteric motility reflexes can be initiated through entirely intrinsic mechanisms in the guinea-pig small intestine. Neurogastroenterol. Motil. 7 (2), 89–96.

Gallego, J., Matrot, B., 2010. Arousal response to hypoxia in newborns: insights from animal models. Biol. Psychol. 84 (1), 39–45.

Ganapathy, V., Hay, J.W., Kim, J.H., 2012. Costs of necrotizing enterocolitis and cost-effectiveness of exclusively human milk-based products in feeding extremely premature infants. Breastfeed Med. 7 (1), 29–37.

Garbrecht, M.R., Klein, J.M., Schmidt, T.J., Snyder, J.M., 2006. Glucocorticoid metabolism in the human fetal lung: implications for lung development and the pulmonary surfactant system. Biol. Neonate 89 (2), 109–119.

Garg, S., Sinha, S., 2013. Non-invasive ventilation in premature infants: based on evidence or habit. J. Clin. Neonatol. 2 (4), 155–159.

Gariano, R.F., Gardner, T.W., 2004. Retinal angiogenesis in development and disease. Nature 438 (7070), 960–966.

Garite, T.J., 2001. Management of premature rupture of membranes. Clin. Perinatol. 28 (4), 837–847.

Garnier, Y., Kadyrov, M., Gantert, M., Einig, A., Rath, W., Huppertz, B., 2008. Proliferative responses in the placenta after endotoxin exposure in preterm fetal sheep. Eur. J. Obstet. Gynecol. Reprod. Biol. 138 (2), 152–157.

Garzoni, L., Faure, C., Frasch, M.G., 2013. Fetal cholinergic anti-inflammatory pathway and necrotizing enterocolitis: the brain-gut connection begins in utero. Front. Integr. Neurosci. 7, 57.

Gastiasoro-Cuesta, E., Alvarez-Diaz, F.J., Arnaiz-Renedo, A., Fernandez-Ruanova, B., Lopez-de-Heredia, Y.G.J., Roman-Etxebarria, L., et al., 2001. The cardiovascular effects of partial liquid ventilation in newborn lambs after experimental meconium aspiration. Pediatr. Crit. Care Med. 2 (4), 334–339.

Gershon, M.D., Chalazonitis, A., Rothman, T.P., 1993. From neural crest to bowel: development of the enteric nervous system. J. Neurobiol. 24 (2), 199–214.

Ghazi-Birry, H.S., Brown, W.R., Moody, D.M., Challa, V.R., Block, S.M., Reboussin, D.M., 1997. Human germinal matrix: venous origin of hemorrhage and vascular characteristics. AJNR Am. J. Neuroradiol. 18 (2), 219–229.

Ghia, J.E., Blennerhassett, P., Kumar-Ondiveeran, H., Verdu, E.F., Collins, S.M., 2006. The vagus nerve: a tonic inhibitory influence associated with inflammatory bowel disease in a murine model. Gastroenterology 131 (4), 1122–1130.

Ghia, J.E., Blennerhassett, P., Collins, S.M., 2007a. Vagus nerve integrity and experimental colitis. Am. J. Physiol. Gastrointest. Liver Physiol. 293 (3), G560–G567.

Ghia, J.E., Blennerhassett, P., El-Sharkawy, R.T., Collins, S.M., 2007b. The protective effect of the vagus nerve in a murine model of chronic relapsing colitis. Am. J. Physiol. Gastrointest. Liver Physiol. 293 (4), G711–G718.

Ghia, J.E., Blennerhassett, P., Collins, S.M., 2008. Impaired parasympathetic function increases susceptibility to inflammatory bowel disease in a mouse model of depression. J. Clin. Invest. 118 (6), 2209–2218.

Giannone, P.J., Schanbacher, B.L., Bauer, J.A., Reber, K.M., 2006. Effects of prenatal lipopolysaccharide exposure on epithelial development and function in newborn rat intestine. J. Pediatr. Gastroenterol. Nutr. 43 (3), 284–290.

Giannone, P.J., Nankervis, C.A., Richter, J.M., Schanbacher, B.L., Reber, K.M., 2009. Prenatal lipopolysaccharide increases postnatal intestinal injury in a rat model of necrotizing enterocolitis. J. Pediatr. Gastroenterol. Nutr. 48 (3), 276–282.

Gieraltowski, J., Hoyer, D., Tetschke, F., Nowack, S., Schneider, U., Zebrowski, J., 2013. Development of multiscale complexity and multifractality of fetal heart rate variability. Auton. Neurosci. 178, 29–36.

Gittenberger-de Groot, A.C., Strengers, J.L., Mentink, M., Poelmann, R.E., Patterson, D.F., 1985. Histologic studies on normal and persistent ductus arteriosus in the dog. J. Am. Coll. Cardiol. 6 (2), 394–404.

Glass, H.C., Ferriero, D.M., 2007. Treatment of hypoxic-ischemic encephalopathy in newborns. Curr. Treat Options Neurol. 9 (6), 414–423.

Goddard, J., Lewis, R.M., Alcala, H., Zeller, R.S., 1980a. Intraventricular hemorrhage--an animal model. Biol. Neonate. 37 (1–2), 39–52.

Goddard, J., Lewis, R.M., Armstrong, D.L., Zeller, R.S., 1980b. Moderate, rapidly induced hypertension as a cause of intraventricular hemorrhage in the newborn beagle model. J. Pediatr. 96 (6), 1057–1060.

Goddard-Finegold, J., Armstrong, D.L., 1987. Reduction in incidence of periventricular, intraventricular hemorrhages in hypertensive newborn beagles pretreated with phenobarbital. Pediatrics 79 (6), 901–906.

Good, W.V., Hardy, R.J., Dobson, V., Palmer, E.A., Phelps, D.L., Quintos, M., et al., 2005. The incidence and course of retinopathy of prematurity: findings from the early treatment for retinopathy of prematurity study. Pediatrics 116 (1), 15–23.

Gotsch, F., Romero, R., Kusanovic, J.P., Mazaki-Tovi, S., Pineles, B.L., Erez, O., et al., 2007. The fetal inflammatory response syndrome. Clin. Obstet. Gynecol. 50 (3), 652–683.

Goyal, R.K., Hirano, I., 1996. The enteric nervous system. N. Engl. J. Med. 334 (17), 1106–1115.

Grether, J.K., Nelson, K.B., 1997. Maternal infection and cerebral palsy in infants of normal birth weight. JAMA 278 (3), 207–211.

Gronlund, M.M., Lehtonen, O.P., Eerola, E., Kero, P., 1999. Fecal microflora in healthy infants born by different methods of delivery: permanent changes in intestinal flora after cesarean delivery. J. Pediatr. Gastroenterol. Nutr. 28 (1), 19–25.

Groome, L.J., Loizou, P.C., Holland, S.B., Smith, L.A., Hoff, C., 1999. High vagal tone is associated with more efficient regulation of homeostasis in low-risk human fetuses. Dev. Psychobiol 35 (1), 25–34.

Groot, A.G.-D., van Ertbruggen, I., 1980. The ductus arteriosus in the preterm infant: histologic and clinical observations. J. Pediatr. 96 (1), 88–93.

Guarini, S., Altavilla, D., Cainazzo, M.M., Giuliani, D., Bigiani, A., Marini, H., et al., 2003. Efferent vagal fibre stimulation blunts nuclear factor-kappaB activation and protects against hypovolemic hemorrhagic shock. Circulation 107 (8), 1189–1194.

Gunn, A.J., Gunn, T.R., de Haan, H.H., Williams, C.E., Gluckman, P.D., 1997. Dramatic neuronal rescue with prolonged selective head cooling after ischemia in fetal lambs. J. Clin. Invest. 99 (2), 248–256.

Guthrie, R.D., Standaert, T.A., Hodson, W.A., Woodrum, D.E., 1980. Sleep and maturation of eucapnic ventilation and CO_2 sensitivity in the premature primate. J. Appl. Physiol. Respir. Environ. Exerc. Physiol. 48 (2), 347–354.

Hadchouel, A., 2016. Chronic obstructive pulmonary disease following bronchopulmonary dysplasia. In Bhandari, V., (Ed.), Bronchopulmonary Dysplasia, first ed. In: SIS Rounds (Ed.), Respiratory Medicine Series. Humana Press, pp. 93–105. Available from: http://dx.doi.org/10.1007/978-3-319-28486-6.

Hadj-Ahmed, M.A., Samson, N., Bussieres, M., Beck, J., Praud, J.P., 2012. Absence of inspiratory laryngeal constrictor muscle activity during nasal neurally adjusted ventilatory assist in newborn lambs. J. Appl. Physiol. (1985) 113 (1), 63–70.

Hadj-Ahmed, M.A., Samson, N., Nadeau, C., Boudaa, N., Praud, J.P., 2015. Laryngeal muscle activity during nasal high-frequency oscillatory ventilation in nonsedated newborn lambs. Neonatology 107 (3), 199–205.

Haensel, A., Mills, P.J., Nelesen, R.A., Ziegler, M.G., Dimsdale, J.E., 2008. The relationship between heart rate variability and inflammatory markers in cardiovascular diseases. Psychoneuroendocrinology 33 (10), 1305–1312.

Hammerman, C., Glaser, J., Kaplan, M., Schimmel, M.S., Ferber, B., Eidelman, A.I., 1998. Indomethacin tocolysis increases postnatal patent ductus arteriosus severity. Pediatrics 102 (5), E56.

Harding, R., 1984. Function of the larynx in the fetus and newborn. Annu. Rev. Physiol. 46, 645–659.

Harijith, A.K., 2016. Hyperoxia in the pathogenesis of bronchopulmonary dysplasia. In: Bhandari, V., (Ed.), Bronchopulmonary Dysplasia, first ed. In: SIS Rounds (Ed.), Respiratory Medicine Series. Humana Press, pp. 3–26. Available from: http://dx.doi.org/10.1007/978-3-319-28486-6.

Hartnett, M.E., Penn, J.S., 2012. Mechanisms and Management of Retinopathy of Prematurity. N. Engl. J. Med. 367 (26), 2515–2526.

Hedner, T., Hedner, J., Jonason, J., Wessberg, P., 1984. Effects of theophylline on adenosine-induced respiratory depression in the preterm rabbit. Eur. J. Respir. Dis. 65 (2), 153–156.

Heller, F., Florian, P., Bojarski, C., Richter, J., Christ, M., Hillenbrand, B., et al., 2005. Interleukin-13 is the key effector Th2 cytokine in ulcerative colitis that affects epithelial tight junctions, apoptosis, and cell restitution. Gastroenterology 129 (2), 550–564.

Hellström, A., Smith, L.E.H., Dammann, O., 2013. Retinopathy of prematurity. Lancet (Lond.) 382 (9902), 1445–1457.

Heman-Ackah, Y.D., Pernell, K.J., Goding, Jr., G.S., 2009. The laryngeal chemoreflex: an evaluation of the normoxic response. Laryngoscope 119 (2), 370–379.

Hermes-DeSantis, E.R., Clyman, R.I., 2006. Patent ductus arteriosus: pathophysiology and management. J. Perinatol. 26, S14–S18.

Herry, C.L., Cortes, M., Wu, H.T., Durosier, L.D., Cao, M., Burns, P., et al., 2016. Temporal patterns in sheep fetal heart rate variability correlate to systemic cytokine inflammatory response: a methodological exploration of monitoring potential using complex signals bioinformatics. PLoS One 11 (4), e0153515.

Heymann, M.A., Rudolph, A.M., Silverman, N.H., 1976. Closure of the ductus arteriosus in premature infants by inhibition of prostaglandin synthesis. N Engl J Med 295 (10), 530–533.

Hillman, N.H., Pillow, J.J., Ball, M.K., Polglase, G.R., Kallapur, S.G., Jobe, A.H., 2009. Antenatal and postnatal corticosteroid and resuscitation induced lung injury in preterm sheep. Respir. Res. 10, 124.

Hillman, N.H., Nitsos, I., Berry, C., Pillow, J.J., Kallapur, S.G., Jobe, A.H., 2011a. Positive end-expiratory pressure and surfactant decrease lung injury during initiation of ventilation in fetal sheep. Am. J. Physiol. Lung Cell Mol. Physiol. 301 (5), L712–L720.

Hillman, N.H., Polglase, G.R., Pillow, J.J., Saito, M., Kallapur, S.G., Jobe, A.H., 2011b. Inflammation and lung maturation from stretch injury in preterm fetal sheep. Am. J. Physiol. Lung Cell Mol. Physiol. 300 (2), L232–L241.

Hillman, N.H., Kallapur, S.G., Jobe, A.H., 2012a. Physiology of transition from intrauterine to extrauterine life. Clin. Perinatol. 39 (4), 769–783.

Hillman, N.H., Moss, T.J., Nitsos, I., Jobe, A.H., 2012b. Moderate tidal volumes and oxygen exposure during initiation of ventilation in preterm fetal sheep. Pediatr. Res. 72 (6), 593–599.

Hillman, N.H., Kemp, M.W., Noble, P.B., Kallapur, S.G., Jobe, A.H., 2013. Sustained inflation at birth did not protect preterm fetal sheep from lung injury. Am. J. Physiol. Lung Cell Mol. Physiol. 305 (6), L446–L453.

Hodges, R.J., Jenkin, G., Hooper, S.B., Allison, B., Lim, R., Dickinson, H., et al., 2012. Human amnion epithelial cells reduce ventilation-induced preterm lung injury in fetal sheep. Am. J. Obstet. Gynecol. 206 (5), 448.e8–448.e15.

Hofstetter, A.O., Saha, S., Siljehav, V., Jakobsson, P.J., Herlenius, E., 2007. The induced prostaglandin E2 pathway is a key regulator of the respiratory response to infection and hypoxia in neonates. Proc. Natl. Acad. Sci. USA 104 (23), 9894–9899.

Hong, H., Lee, H., Ko, J., Park, J., Park, J., Choi, C., et al., 2014. Neonatal systemic inflammation in rats alters retinal vessel development and simulates pathologic features of retinopathy of prematurity. J Neuroinflammation 11 (1), 87.

Hooper, S.B., Kitchen, M.J., Wallace, M.J., Yagi, N., Uesugi, K., Morgan, M.J., et al., 2007. Imaging lung aeration and lung liquid clearance at birth. FASEB J. 21 (12), 3329–3337.

Hooper, S.B., Fouras, A., Siew, M.L., Wallace, M.J., Kitchen, M.J., te Pas, A.B., et al., 2013. Expired CO_2 levels indicate degree of lung aeration at birth. PLoS One 8 (8), e70895.

Hoyer, D., Nowack, S., Bauer, S., Tetschke, F., Rudolph, A., Wallwitz, U., et al., 2013. Fetal development of complex autonomic control evaluated from multiscale heart rate patterns. Am. J. Physiol. Regul. Integr. Comp. Physiol. 304 (5), R383–R392.

Huang, Z., Wang, Y., Nayak, P.S., Dammann, C.E., Sanchez-Esteban, J., 2012. Stretch-induced fetal type II cell differentiation is mediated via ErbB1-ErbB4 interactions. J. Biol. Chem. 287 (22), 18091–18102.

Hunter, C.J., Upperman, J.S., Ford, H.R., Camerini, V., 2008. Understanding the susceptibility of the premature infant to necrotizing enterocolitis (NEC). Pediatr. Res. 63, 117–123.

Huston, J.M., Gallowitsch-Puerta, M., Ochani, M., Ochani, K., Yuan, R., Rosas-Ballina, M., et al., 2007. Transcutaneous vagus nerve stimulation reduces serum high mobility group box 1 levels and improves survival in murine sepsis. Crit. Care Med. 35 (12), 2762–2768.

Iannaccone, P.M., Jacob, H.J., 2009. Rats! Dis. Model Mech. 2 (5–6), 206–210.

Ingimarsson, J., Bjorklund, L.J., Curstedt, T., Gudmundsson, S., Larsson, A., Robertson, B., Werner, O., 2004. Incomplete protection by prophylactic surfactant against the adverse effects of large lung inflations at birth in immature lambs. Intensive Care Med. 30 (7), 1446–1453.

Jadcherla, S.R., Duong, H.Q., Hofmann, C., Hoffmann, R., Shaker, R., 2005. Characteristics of upper oesophageal sphincter and oesophageal body during maturation in healthy human neonates compared with adults. Neurogastroenterol. Motil. 17 (5), 663–670.

Jansen, A.H., Chernick, V., 1983. Development of respiratory control. Physiol. Rev. 63 (2), 437–483.

Jeng, M.J., Soong, W.J., Lee, Y.S., Chang, H.L., Shen, C.M., Wang, C.H., et al., 2006. Effects of therapeutic bronchoalveolar lavage and partial liquid ventilation on meconium-aspirated newborn piglets. Crit. Care Med. 34 (4), 1099–1105.

Jobe, A.H., 2015. Animal models, learning lessons to prevent and treat neonatal chronic lung disease. Front. Med. (Lausanne) 2, 49.

Jobe, A.H., Bancalari, E., 2001. Bronchopulmonary dysplasia. Am. J. Respir. Crit. Care Med. 163 (7), 1723–1729.

Jobe, A.H., Newnham, J.P., Moss, T.J., Ikegami, M., 2003. Differential effects of maternal betamethasone and cortisol on lung maturation and growth in fetal sheep. Am. J. Obstet. Gynecol. 188 (1), 22–28.

Johnson, P., Dawes, G.S., Robinson, J.S., 1972. Maintenance of breathing in newborn lamb. Arch. Dis. Child 47 (251), 151.

Kaneko, M., White, S., Homan, J., Richardson, B., 2003. Cerebral blood flow and metabolism in relation to electrocortical activity with severe umbilical cord occlusion in the near-term ovine fetus. Am. J. Obstet. Gynecol. 188 (4), 961–972.

Kannan, S., Dai, H., Navath, R.S., Balakrishnan, B., Jyoti, A., Janisse, J., et al., 2012. Dendrimer-based postnatal therapy for neuroinflammation and cerebral palsy in a rabbit model. Sci. Transl. Med. 4 (130), 130ra146.

Karin, J., Hirsch, M., Akselrod, S., 1993. An estimate of fetal autonomic state by spectral analysis of fetal heart rate fluctuations. Pediatr. Res. 34 (2), 134–138.

Keen, A.E., Frasch, M.G., Sheehan, M.A., Matushewski, B., Richardson, B.S., 2011. Maturational changes and effects of chronic hypoxemia on electrocortical activity in the ovine fetus. Brain Res. 1402, 38–45.

Keita, A.V., Soderholm, J.D., 2010. The intestinal barrier and its regulation by neuroimmune factors. Neurogastroenterol. Motil. 22 (7), 718–733.

Kemp, M.W., Newnham, J.P., Challis, J.G., Jobe, A.H., Stock, S.J., 2016. The clinical use of corticosteroids in pregnancy. Hum. Reprod. Update 22 (2), 240–259.

Keszler, M., Molina, B., Butterfield, A.B., Subramanian, K.N., 1986. Combined high-frequency jet ventilation in a meconium aspiration model. Crit. Care Med. 14 (1), 34–38.

Khan, P.A., Cloutier, M., Piedboeuf, B., 2007. Tracheal occlusion: a review of obstructing fetal lungs to make them grow and mature. Am. J. Med. Genet. C Semin. Med. Genet. 145C (2), 125–138.

Kianicka, I., Diaz, V., Dorion, D., Praud, J.P., 1998a. Coordination between glottic adductor muscle and diaphragm EMG activity in fetal lambs in utero. J. Appl. Physiol. (1985) 84 (5), 1560–1565.

Kianicka, I., Diaz, V., Renolleau, S., Canet, E., Praud, J.P., 1998b. Laryngeal and abdominal muscle electrical activity during periodic breathing in nonsedated lambs. J. Appl. Physiol. (1985) 84 (2), 669–675.

Kitterman, J.A., 1996. The effects of mechanical forces on fetal lung growth. Clin. Perinatol. 23 (4), 727–740.

Kuipers, I.M., Maertzdorf, W.J., Keunen, H., De Jong, D.S., Hanson, M.A., Blanco, C.E., 1992. Fetal breathing is not initiated after cord occlusion in the unanaesthetized fetal lamb in utero. J. Dev. Physiol. 17 (5), 233–240.

Kunze, W.A., Furness, J.B., 1999. The enteric nervous system and regulation of intestinal motility. Annu. Rev. Physiol. 61, 117–142.

Kuo, C.Y., Hsueh, C., Wang, C.R., 1998. Liquid ventilation for treatment of meconium aspiration syndrome in a piglet model. J. Formos. Med. Assoc. 97 (6), 392–399.

Kwan, H., Garzoni, L., Liu, H.L., Cao, M., Desrochers, A., Fecteau, G., et al., 2016. VNS in inflammation: systematic review of animal models and clinical studies. Bioelectron. Med, 3, 1–6.

Lagarde, S., Semjen, F., Nouette-Gaulain, K., Masson, F., Bordes, M., Meymat, Y., Cros, A.M., 2010. Facemask pressure-controlled ventilation in children: what is the pressure limit? Anesth. Analg. 110 (6), 1676–1679.

Lahra, M.M., Jeffery, H.E., 2004. A fetal response to chorioamnionitis is associated with early survival after preterm birth. Am. J. Obstet. Gynecol. 190 (1), 147–151.

Lai, A.K.W., Lo, A.C.Y., 2013. Animal models of diabetic retinopathy: summary and comparison. J. Diabetes Res. 2013 (2), 106594.

Lalani, S., Remmers, J.E., Hasan, S.U., 2001. Breathing patterns, pulmonary mechanics and gas exchange: role of vagal innervation in neonatal lamb. Exp. Physiol. 86 (6), 803–810.

Landry, J., 2016. Pulmonary function in survivors of bronchopulmonary dysplasia. In: Bhandari, V., (Ed.), Bronchopulmonary, first ed. In: SIS Rounds (Ed.), Dysplasia Respiratory Medicine Series. Humana Press, pp. 281–298. Available from: http://dx.doi.org/10.1007/978-3-319-28486-6.

Lang, I.M., Haworth, S.T., Medda, B.K., Roerig, D.L., Forster, H.V., Shaker, R., 2008. Airway responses to esophageal acidification. Am. J. Physiol. Regul. Integr. Comp. Physiol. 294 (1), R211–R219.

Lanier, B., Richardson, M.A., Cummings, C., 1983. Effect of hypoxia on laryngeal reflex apnea—implications for sudden infant death. Otolaryngol. Head Neck Surg. 91 (6), 597–604.

Lavizzari, A., Colnaghi, M., Ciuffini, F., Veneroni, C., Musumeci, S., Cortinovis, I., Mosca, F., 2016. Heated, humidified high-flow nasal cannula vs nasal continuous positive airway pressure for respiratory distress syndrome of prematurity: a randomized clinical non-inferiority trial. JAMA Pediatr. In press.

Lavoie, P., 2016. Genetics of bronchopulmonary dysplasia. In: Bhandari, V., (Ed.), Bronchopulmonary Dysplasia, first ed. In: SIS Rounds (Ed.), Respiratory Medicine Series. Humana Press, pp. 109–128. Available from: http://dx.doi.org/10.1007/978-3-319-28486-6.

Lemaire, D., Letourneau, P., Dorion, D., Praud, J.P., 1999. Complete glottic closure during central apnea in lambs. J. Otolaryngol. 28 (1), 13–19.

Levin, M., McCurnin, D., Seidner, S.R., Yoder, B., Waleh, N., Goldbarg, S., et al., 2006. Postnatal constriction, ATP depletion, and cell death in the mature and immature ductus arteriosus. Am. J. Physiol. Regul. Integr. Comp. Physiol. 290 (2), R359–R364.

Lieschke, G.J., Currie, P.D., 2007. Animal models of human disease: zebrafish swim into view. Nat. Rev. Genet. 8 (5), 353–367.

Liggins, G.C., Howie, R.N., 1972. A controlled trial of antepartum glucocorticoid treatment for prevention of the respiratory distress syndrome in premature infants. Pediatrics 50 (4), 515–525.

Lim, M.K., Hanretty, K., Houston, A.B., Lilley, S., Murtagh, E.P., 1992. Intermittent ductal patency in healthy newborn infants: demonstration by colour Doppler flow mapping. Arch. Dis. Child. 67 (10 Spec No), 1217–1218.

Lin, P.W., Stoll, B.J., 2006. Necrotising enterocolitis. Lancet 368 (9543), 1271–1283.

Lin, P.W., Nasr, T.R., Stoll, B.J., 2008. Necrotizing enterocolitis: recent scientific advances in pathophysiology and prevention. Semin. Perinatol. 32 (2), 70–82.

Lindgren, C., Jing, L., Graham, B., Grogaard, J., Sundell, H., 1992. Respiratory syncytial virus infection reinforces reflex apnea in young lambs. Pediatr. Res. 31 (4 Pt 1), 381–385.

Liston, R., Crane, J., Hamilton, E., Hughes, O., Kuling, S., MacKinnon, C., et al., 2002a. Fetal health surveillance in labour. J. Obstet. Gynaecol. Can. 24 (3), 250–276.

Liston, R., Crane, J., Hughes, O., Kuling, S., MacKinnon, C., Milne, K., et al., 2002b. Fetal health surveillance in labour. J. Obstet. Gynaecol. Can. 24 (4), 342–355.

Liston, R., Sawchuck, D., Young, D., 2007. Fetal health surveillance: antepartum and intrapartum consensus guideline. J. Obstet. Gynaecol. Can. 29 (9 Suppl. 4), S3–S56.

Liu, F., McCullough, L.D., 2013. Inflammatory responses in hypoxic ischemic encephalopathy. Acta Pharmacol. Sin. 34 (9), 1121–1130.

Liu, S., Stolz, D.B., Sappington, P.L., Macias, C.A., Killeen, M.E., Tenhunen, J.J., et al., 2006. HMGB1 is secreted by immunostimulated enterocytes and contributes to cytomix-induced hyperpermeability of Caco-2 monolayers. Am. J. Physiol. Cell Physiol. 290 (4), C990–C999.

Liu, H.L., Garzoni, L., Herry, C., Durosier, L.D., Cao, M., Burns, P., et al., 2016. Can monitoring fetal intestinal inflammation using heart rate variability analysis signal incipient necrotizing enterocolitis of the neonate? Pediatr. Crit. Care Med. 17 (4), e165–e176.

Loftin, C.D., Trivedi, D.B., Tiano, H.F., Clark, J.A., Lee, C.A., Epstein, J.A., et al., 2001. Failure of ductus arteriosus closure and remodeling in neonatal mice deficient in cyclooxygenase-1 and cyclooxygenase-2. Proc. Natl. Acad. Sci. USA 98 (3), 1059–1064.

Lorenzo, A.V., Welch, K., Conner, S., 1982. Spontaneous germinal matrix and intraventricular hemorrhage in prematurely born rabbits. J. Neurosurg. 56 (3), 404–410.

Ludemann, J.P., Manoukian, J., Shaw, K., Bernard, C., Davis, M., al-Jubab, A., 1998. Effects of simulated gastroesophageal reflux on the untraumatized rabbit larynx. J. Otolaryngol. 27 (3), 127–131.

Lupton, B.A., Hill, A., Whitfield, M.F., Carter, C.J., Wadsworth, L.D., Roland, E.H., 1988. Reduced platelet count as a risk factor for intraventricular hemorrhage. Am J Dis Child. 142 (11), 1222–1224.

Luu, T.M., Ment, L.R., Schneider, K.C., Katz, K.H., Allan, W.C., Vohr, B.R., 2009. Lasting effects of preterm birth and neonatal brain hemorrhage at 12 years of age. Pediatrics 123 (3), 1037–1044.

Luyer, M.D., Greve, J.W., Hadfoune, M., Jacobs, J.A., Dejong, C.H., Buurman, W.A., 2005. Nutritional stimulation of cholecystokinin receptors inhibits inflammation via the vagus nerve. J. Exp. Med. 202 (8), 1023–1029.

Lyra, J.C., Mascaretti, R.S., Precioso, A.R., Chang, Y.C., Costa, M.T., Vaz, F.A., et al., 2004. Different doses of exogenous surfactant for treatment of meconium aspiration syndrome in newborn rabbits. Rev. Hosp. Clin. Fac. Med. Sao. Paulo. 59 (3), 104–112.

Mallard, C., Vexler, Z.S., 2015. Modeling ischemia in the immature brain: how translational are animal models? Stroke 46 (10), 3006–3011.

Malviya, M.N., Ohlsson, A., Shah, S.S., 2013. Surgical versus medical treatment with cyclooxygenase inhibitors for symptomatic patent ductus arteriosus in preterm infants. Cochrane Database Syst. Rev. 3.

Marchal, F., Corke, B.C., Sundell, H., 1982. Reflex apnea from laryngeal chemo-stimulation in the sleeping premature newborn lamb. Pediatr. Res. 16 (8), 621–627.

Marchal, F., Crance, J.P., Arnould, P., 1986. Ventilatory and waking responses to laryngeal stimulation in sleeping mature lambs. Respir. Physiol. 63 (1), 31–41.

Mari, G., Deprest, J., Schenone, M., Jackson, S., Samson, J., Brocato, B., et al., 2014. A novel translational model of percutaneous fetoscopic endoluminal tracheal occlusion—baboons (*Papio* spp.). Fetal Diagn. Ther. 35 (2), 92–100.

Martinez-Tallo, E., Claure, N., Bancalari, E., 1997. Necrotizing enterocolitis in full-term or near-term infants: risk factors. Biol. Neonate 71 (5), 292–298.

Mendelsohn, C., Lohnes, D., Decimo, D., Lufkin, T., LeMeur, M., Chambon, P., Mark, M., 1994. Function of the retinoic acid receptors (RARs) during development (II). Multiple abnormalities at various stages of organogenesis in RAR double mutants. Development 120 (10), 2749–2771.

Ment, L.R., Stewart, W.B., Duncan, C.C., Lambrecht, R., 1982. Beagle puppy model of intraventricular hemorrhage. J. Neurosurg. 57 (2), 219–223.

Milner, A.D., Boon, A.W., Saunders, R.A., Hopkin, I.E., 1980. Upper airways obstruction and apnoea in preterm babies. Arch. Dis. Child 55 (1), 22–25.

Mitchell, C.A., Risau, W., Drexler, H.C., 1998. Regression of vessels in the tunica vasculosa lentis is initiated by coordinated endothelial apoptosis: a role for vascular endothelial growth factor as a survival factor for endothelium. Dev. Dyn. 213 (3), 322–333.

Miyamoto, O., Auer, R.N., 2000. Hypoxia, hyperoxia, ischemia, and brain necrosis. Neurology 54 (2), 362–371.

Moreau-Bussiere, F., Samson, N., St-Hilaire, M., Reix, P., Lafond, J.R., Nsegbe, E., Praud, J.P., 2007. Laryngeal response to nasal ventilation in nonsedated newborn lambs. J. Appl. Physiol. (1985) 102 (6), 2149–2157.

Moriez, R., Salvador-Cartier, C., Theodorou, V., Fioramonti, J., Eutamene, H., Bueno, L., 2005. Myosin light chain kinase is involved in lipopolysaccharide-induced disruption of colonic epithelial barrier and bacterial translocation in rats. Am. J. Pathol. 167 (4), 1071–1079.

Moses, D., Holm, B.A., Spitale, P., Liu, M.Y., Enhorning, G., 1991. Inhibition of pulmonary surfactant function by meconium. Am. J. Obstet. Gynecol. 164 (2), 477–481.

Neu, J., 2007. Gastrointestinal development and meeting the nutritional needs of premature infants. Am. J. Clin. Nutr. 85 (2), 629S–634S.

Neu, J., Mihatsch, W.A., Zegarra, J., Supapannachart, S., Ding, Z.Y., Murguia-Peniche, T., 2013. Intestinal mucosal defense system, part 1. Consensus recommendations for immunonutrients. J. Pediatr. 162 (3 Suppl.), S56–S63.

Neunlist, M., Toumi, F., Oreschkova, T., Denis, M., Leborgne, J., Laboisse, C.L., et al., 2003. Human ENS regulates the intestinal epithelial barrier permeability and a tight junction-associated protein ZO-1 via VIPergic pathways. Am. J. Physiol. Gastrointest. Liver Physiol. 285 (5), G1028–G1036.

Neunlist, M., Van Landeghem, L., Mahe, M.M., Derkinderen, P., Bruley des Varannes, S.B., Rolli-Derkinderen, M., 2013. The digestive neuronal-glial-epithelial unit: a new actor in gut health and disease. Nat. Rev. Gastroenterol. Hepatol. 10, 90–100.

Nguyen, M., Camenisch, T., Snouwaert, J.N., Hicks, E., Coffman, T.M., Anderson, P.A., et al., 1997. The prostaglandin receptor EP4 triggers remodelling of the cardiovascular system at birth. Nature 390 (6655), 78–81.

Null, D.M., Alvord, J., Leavitt, W., Wint, A., Dahl, M.J., Presson, A.P., et al., 2014. High-frequency nasal ventilation for 21 d maintains gas exchange with lower respiratory pressures and promotes alveolarization in preterm lambs. Pediatr Res 75 (4), 507–516.

Olofsson, P.S., Rosas-Ballina, M., Levine, Y.A., Tracey, K.J., 2012. Rethinking inflammation: neural circuits in the regulation of immunity. Immunol Rev 248 (1), 188–204.

Onasanya, B.I., Rais-Bahrami, K., Rivera, O., Seale, W.R., Short, B.L., 2001. The use of intratracheal pulmonary ventilation and partial liquid ventilation in newborn piglets with meconium aspiration syndrome. Pediatr. Crit. Care Med. 2 (1), 69–73.

O'Reilly, M., Thebaud, B., 2014. Animal models of bronchopulmonary dysplasia. The term rat models. Am. J. Physiol. Lung Cell Mol. Physiol. 307 (12), L948–L958.

O'Reilly, M., Thebaud, B., 2015. Stem cells for the prevention of neonatal lung disease. Neonatology 107 (4), 360–364.

Oskoui, M., Coutinho, F., Dykeman, J., Jette, N., Pringsheim, T., 2013. An update on the prevalence of cerebral palsy: a systematic review and meta-analysis. Dev. Med. Child Neurol. 55 (6), 509–519.

Ottani, A., Giuliani, D., Mioni, C., Galantucci, M., Minutoli, L., Bitto, A., et al., 2009. Vagus nerve mediates the protective effects of melanocortins against cerebral and systemic damage after ischemic stroke. J. Cereb. Blood Flow Metab. 29 (3), 512–523.

Page, M., Jeffery, H.E., 1998. Airway protection in sleeping infants in response to pharyngeal fluid stimulation in the supine position. Pediatr. Res. 44 (5), 691–698.

Page, M., Jeffery, H., 2000. The role of gastro-oesophageal reflux in the aetiology of SIDS. Early Hum. Dev. 59 (2), 127–149.

Page, M., Jeffery, H.E., Marks, V., Post, E.J., Wood, A.K., 1995. Mechanisms of airway protection after pharyngeal fluid infusion in healthy sleeping piglets. J. Appl. Physiol. (1985) 78 (5), 1942–1949.

Palmer, E.A., Flynn, J.T., Hardy, R.J., Phelps, D.L., Phillips, C.L., Schaffer, D.B., Tung, B., 1991. Incidence and early course of retinopathy of prematurity. The Cryotherapy for Retinopathy of Prematurity Cooperative Group. Ophthalmology 98 (11), 1628–1640.

Palmer, E.A., Hardy, R.J., Dobson, V., Phelps, D.L., Quinn, G.E., Summers, C.G., et al., 2005. 15-year outcomes following threshold retinopathy of prematurity: final results from the multicenter trial of cryotherapy for retinopathy of prematurity. Arch. Ophthalmol. 123 (3), 311–318.

Park, K.H., Bae, C.W., Chung, S.J., 1996. In vitro effect of meconium on the physical surface properties and morphology of exogenous pulmonary surfactant. J. Korean Med. Sci. 11 (5), 429–436.

Patterson, D.F., 1968. Epidemiologic and Genetic Studies of Congenital Heart Disease in the Dog. Circ. Res. 23 (2), 171–202.

Patz, A., 1954. Oxygen studies in retrolental fibroplasia. IV. Clinical and experimental observations. Am J Ophthalmol. 38 (3), 291–308.

Patz, A., 1968. The role of oxygen in retrolental fibroplasia. Trans. Am. Ophthalmol. Soc. 66, 940–985.

Pavlov, V.A., Ochani, M., Gallowitsch-Puerta, M., Ochani, K., Huston, J.M., Czura, C.J., et al., 2006. Central muscarinic cholinergic regulation of the systemic inflammatory response during endotoxemia. Proc. Natl. Acad. Sci. USA 103 (13), 5219–5223.

Pavlov, V.A., Parrish, W.R., Rosas-Ballina, M., Ochani, M., Puerta, M., Ochani, K., et al., 2009. Brain acetylcholinesterase activity controls systemic cytokine levels through the cholinergic anti-inflammatory pathway. Brain Behav. Immun. 23 (1), 41–45.

Perlman, J.M., McMenamin, J.B., Volpe, J.J., 1983. Fluctuating cerebral blood-flow velocity in respiratory-distress syndrome. Relation to the development of intraventricular hemorrhage. N. Engl. J. Med. 309 (4), 204–209.

Pérez Fontán, J.J., Clyman, R.I., Mauray, F., Heymann, M.A., Roman, C., 1987. Respiratory effects of a patent ductus arteriosus in premature newborn lambs. J. Appl. Physiol. 63 (6), 2315–2324.

Petrosyan, M., Guner, Y.S., Williams, M., Grishin, A., Ford, H.R., 2009. Current concepts regarding the pathogenesis of necrotizing enterocolitis. Pediatr. Surg. Int. 25 (4), 309–318.

Pickens, D.L., Schefft, G., Thach, B.T., 1988. Prolonged apnea associated with upper airway protective reflexes in apnea of prematurity. Am. Rev. Respir. Dis. 137 (1), 113–118.

Pike, K., Brocklehurst, P., Jones, D., Kenyon, S., Salt, A., Taylor, D., Marlow, N., 2012. Outcomes at 7 years for babies who developed neonatal necrotising enterocolitis: the ORACLE Children Study. Arch. Dis. Child Fetal Neonatal Ed. 97 (5), F318–F322.

Pillow, J.J., Musk, G.C., McLean, C.M., Polglase, G.R., Dalton, R.G., Jobe, A.H., Suki, B., 2011. Variable ventilation improves ventilation and lung compliance in preterm lambs. Intensive Care Med. 37 (8), 1352–1359.

Pladys, P., Arsenault, J., Reix, P., Rouillard Lafond, J., Moreau-Bussiere, F., Praud, J.P., 2008. Influence of prematurity on postnatal maturation of heart rate and arterial pressure responses to hypoxia in lambs. Neonatology 93 (3), 197–205.

Polglase, G.R., Nitsos, I., Jobe, A.H., Newnham, J.P., Moss, T.J., 2007. Maternal and intra-amniotic corticosteroid effects on lung morphometry in preterm lambs. Pediatr. Res. 62 (1), 32–36.

Polglase, G.R., Hillman, N.H., Pillow, J.J., Cheah, F.C., Nitsos, I., Moss, T.J., et al., 2008. Positive end-expiratory pressure and tidal volume during initial ventilation of preterm lambs. Pediatr. Res. 64 (5), 517–522.

Polglase, G.R., Tingay, D.G., Bhatia, R., Berry, C.A., Kopotic, R.J., Kopotic, C.P., et al., 2014. Pressure- versus volume-limited sustained inflations at resuscitation of premature newborn lambs. BMC Pediatr. 14, 43.

Praud, J.P., Canet, E., Bureau, M.A., 1992. Chemoreceptor and vagal influences on thyroarytenoid muscle activity in awake lambs during hypoxia. J. Appl. Physiol. (1985) 72 (3), 962–969.

Praud, J.P., Diaz, V., Kianicka, I., Dalle, D., 1995. Active expiratory glottic closure during permeability pulmonary edema in nonsedated lambs. Am. J. Respir. Crit. Care Med. 152 (2), 732–737.

Praud, J.P., Kianicka, I., Diaz, V., Leroux, J.F., Dalle, D., 1996. Prolonged active glottic closure after barbiturate-induced respiratory arrest in lambs. Respir. Physiol. 104 (2–3), 221–229.

Praud, J.P., Diaz, V., Kianicka, I., Chevalier, J.Y., Canet, E., Thisdale, Y., 1997. Abolition of breathing rhythmicity in lambs by CO_2 unloading in the first hours of life. Respir. Physiol. 110 (1), 1–8.

Prout, A., Frasch, M.G., Veldhuizen, R., Hammond, R., Ross, M.G., Richardson, B.S., 2009. Inflammatory response to repetitive umbilical cord occlusions with worsening acidosis in the near term ovine fetus. Am. J. Obstet. Gynecol. 202 (1), 82.e1–82.e9.

Prout, A.P., Frasch, M.G., Veldhuizen, R., Hammond, R., Matushewski, B., Richardson, B.S., 2012. The impact of intermittent umbilical cord occlusions on the inflammatory response in pre-term fetal sheep. PLoS One 7 (6), e39043.

Putnam, R.W., Conrad, S.C., Gdovin, M.J., Erlichman, J.S., Leiter, J.C., 2005. Neonatal maturation of the hypercapnic ventilatory response and central neural CO_2 chemosensitivity. Respir. Physiol. Neurobiol. 149 (1–3), 165–179.

Rahmel, D.K., Pohlmann, G., Iwatschenko, P., Volland, J., Liebisch, S., Kock, H., et al., 2012. The non-intubated, spontaneously breathing, continuous positive airway pressure (CPAP) ventilated pre-term lamb: a unique animal model. Reprod. Toxicol. 34 (2), 204–215.

Raman, K.G., Sappington, P.L., Yang, R., Levy, R.M., Prince, J.M., Liu, S., et al., 2006. The role of RAGE in the pathogenesis of intestinal barrier dysfunction after hemorrhagic shock. Am. J. Physiol. Gastrointest. Liver Physiol. 291 (4), G556–G565.

Ramanathan, R., 2010. Nasal respiratory support through the nares: its time has come. J. Perinatol. 30 (Suppl.), S67–S72.

Ramet, J., Praud, J.P., d'Allest, A.M., Dehan, M., Guilleminault, C., Gaultier, C., 1990. Cardiac and respiratory responses to esophageal dilatation during REM sleep in human infants. Biol. Neonate 58 (4), 181–187.

Ramos, L.M., 2016. Invasive mechanical ventilation in the pathogenesis of bronchopulmonary dysplasia. In: Bhandari, V. (Ed.), Bronchopulmonary Dysplasia, first ed. In: SIS Rounds (Ed.), Respiratory Medicine Series. Humana Press, pp. 27–54. Available from: http://dx.doi.org/10.1007/978-3-319-28486-6.

Rees, C.M., Pierro, A., Eaton, S., 2007. Neurodevelopmental outcomes of neonates with medically and surgically treated necrotizing enterocolitis. Arch. Dis. Child Fetal Neonatal Ed. 92 (3), F193–F198.

Reix, P., Arsenault, J., Dome, V., Fortier, P.H., Lafond, J.R., Moreau-Bussiere, F., et al., 2003. Active glottal closure during central apneas limits oxygen desaturation in premature lambs. J. Appl. Physiol. (1985) 94 (5), 1949–1954.

Reix, P., Arsenault, J., Langlois, C., Niyonsenga, T., Praud, J.P., 2004. Nonnutritive swallowing and respiration relationships in preterm lambs. J. Appl. Physiol. (1985) 97 (4), 1283–1290.

Renolleau, S., Letourneau, P., Niyonsenga, T., Praud, J.P., Gagne, B., 1999. Thyroarytenoid muscle electrical activity during spontaneous apneas in preterm lambs. Am. J. Respir. Crit. Care Med. 159 (5 Pt 1), 1396–1404.

Reyburn, B., Li, M., Metcalfe, D.B., Kroll, N.J., Alvord, J., Wint, A., et al., 2008. Nasal ventilation alters mesenchymal cell turnover and improves alveolarization in preterm lambs. Am. J. Respir. Crit. Care Med. 178 (4), 407–418.

Ricciotti, E., FitzGerald, G.A., 2011. Prostaglandins and inflammation. Arterioscler Thromb. Vasc. Biol. 31 (5), 986–1000.

Roberts, D., Dalziel, S., 2006. Antenatal corticosteroids for accelerating fetal lung maturation for women at risk of preterm birth. Cochrane Database Syst. Rev. (3).

Rosas-Ballina, M., Olofsson, P.S., Ochani, M., Valdes-Ferrer, S.I., Levine, Y.A., Reardon, C., et al., 2011. Acetylcholine-synthesizing T cells relay neural signals in a vagus nerve circuit. Science 334 (6052), 98–101.

Roy, B., Samson, N., Moreau-Bussiere, F., Ouimet, A., Dorion, D., Mayer, S., Praud, J.P., 2008. Mechanisms of active laryngeal closure during noninvasive intermittent positive pressure ventilation in nonsedated lambs. J. Appl. Physiol. (1985) 105 (5), 1406–1412.

Safar, P., Behringer, W., Bottiger, B.W., Sterz, F., 2002. Cerebral resuscitation potentials for cardiac arrest. Crit. Care Med. 30 (4 Suppl.), S140–S144.

Samson, N., Niane, L., Nault, S., Nadeau, C., Praud, J.P., 2014. Laryngeal narrowing during nasal ventilation does not originate from bronchopulmonary C-fibers. Respir. Physiol. Neurobiol. 202, 32–34.

Sappington, P.L., Yang, R., Yang, H., Tracey, K.J., Delude, R.L., Fink, M.P., 2002. HMGB1 B box increases the permeability of Caco-2 enterocytic monolayers and impairs intestinal barrier function in mice. Gastroenterology 123 (3), 790–802.

Schwarz, B.T., Wang, F., Shen, L., Clayburgh, D.R., Su, L., Wang, Y., et al., 2007. LIGHT signals directly to intestinal epithelia to cause barrier dysfunction via cytoskeletal and endocytic mechanisms. Gastroenterology 132 (7), 2383–2394.

Scott, A., Fruttiger, M., 2010. Oxygen-induced retinopathy: a model for vascular pathology in the retina. Eye (Lond.) 24 (3), 416–421.

Segi, E., Sugimoto, Y., Yamasaki, A., Aze, Y., Oida, H., Nishimura, T., et al., 1998. Patent ductus arteriosus and neonatal death in prostaglandin receptor EP4-deficient mice. Biochem. Biophys. Res. Commun. 246 (1), 7–12.

Shapiro, G., Fraser, W.D., Frasch, M.G., Seguin, J.R., 2013. Psychosocial stress in pregnancy and preterm birth: associations and mechanisms. J. Perinat. Med. 41 (6), 631–645.

Sharma, R., Hudak, M.L., 2013. A clinical perspective of necrotizing enterocolitis: past, present, and future. Clin. Perinatol. 40 (1), 27–51.

Shepherd, K., Hillman, D., Eastwood, P., 2013. Symptoms of aerophagia are common in patients on continuous positive airway pressure therapy and are related to the presence of nighttime gastroesophageal reflux. J. Clin. Sleep Med. 9 (1), 13–17.

Shepherd, E., Middleton, P., Makrides, M., McIntyre, S.J., Badawi, N., Crowther, C.A., 2016. Antenatal and intrapartum interventions for preventing cerebral palsy: an overview of Cochrane systematic reviews. Cochrane Database Syst. Revi. (2).

Shimada, S., Raju, T.N., Bhat, R., Maeta, H., Vidyasagar, D., 1989. Treatment of patent ductus arteriosus after exogenous surfactant in baboons with hyaline membrane disease. Pediatr. Res. 26 (6), 565–569.

Siew, M.L., Wallace, M.J., Kitchen, M.J., Lewis, R.A., Fouras, A., Te Pas, A.B., et al., 2009. Inspiration regulates the rate and temporal pattern of lung liquid clearance and lung aeration at birth. J. Appl. Physiol. (1985) 106 (6), 1888–1895.

Siljehav, V., Hofstetter, A.M., Leifsdottir, K., Herlenius, E., 2015. Prostaglandin E2 mediates cardiorespiratory disturbances during infection in neonates. J. Pediatr. 167 (6), 1207.e3–1213.e3.

Simpson, J.L., Melia, M., Yang, M.B., Buffenn, A.N., Chiang, M.F., Lambert, S.R., 2012. Current role of cryotherapy in retinopathy of prematurity. Ophthalmology 119 (4), 873–877.

Sladek, M., Grogaard, J.B., Parker, R.A., Sundell, H.W., 1993. Prolonged hypoxemia enhances and acute hypoxemia attenuates laryngeal reflex apnea in young lambs. Pediatr. Res. 34 (6), 813–820.

Smit, E., Odd, D., Whitelaw, A., 2013. Postnatal phenobarbital for the prevention of intraventricular haemorrhage in preterm infants. Cochrane Database Syst. Rev. (8), CD001691.

Smith, L.E., Wesolowski, E., McLellan, A., Kostyk, S.K., D'Amato, R., Sullivan, R., D'Amore, P.A., 1994. Oxygen-induced retinopathy in the mouse. Invest. Ophthalmol. Visual Sci. 35 (1), 101–111.

Smith, V.C., Zupancic, J.A., McCormick, M.C., Croen, L.A., Greene, J., Escobar, G.J., Richardson, D.K., 2004. Rehospitalization in the first year of life among infants with bronchopulmonary dysplasia. J. Pediatr. 144 (6), 799–803.

Smithers-Sheedy, H., McIntyre, S., Gibson, C., Meehan, E., Scott, H., Goldsmith, S., et al., 2016. A special supplement: findings from the Australian Cerebral Palsy Register, birth years 1993 to 2006. Dev. Med. Child Neurol. 58 (Suppl. 2), 5–10.

Sood, B.G., Madan, A., Saha, S., Schendel, D., Thorsen, P., Skogstrand, K., et al., 2010. Perinatal Systemic Inflammatory Response Syndrome and Retinopathy of Prematurity. Pediatr. Res. 67 (4), 394–400.

Soul, J.S., Hammer, P.E., Tsuji, M., Saul, J.P., Bassan, H., Limperopoulos, C., et al., 2007. Fluctuating Pressure-Passivity Is Common in the Cerebral Circulation of Sick Premature Infants. Pediatr. Res. 61 (4), 467–473.

Stahl, A., Connor, K.M., Sapieha, P., Chen, J., Dennison, R.J., Krah, N.M., et al., 2010. The mouse retina as an angiogenesis model. Invest. Ophthalmol. Visual Sci. 51 (6), 2813–2826.

St-Hilaire, M., Nsegbe, E., Gagnon-Gervais, K., Samson, N., Moreau-Bussiere, F., Fortier, P.H., Praud, J.P., 2005. Laryngeal chemoreflexes induced by acid, water, and saline in nonsedated newborn lambs during quiet sleep. J. Appl. Physiol. (1985) 98 (6), 2197–2203.

St-Hilaire, M., Samson, N., Nsegbe, E., Duvareille, C., Moreau-Bussiere, F., Micheau, P., et al., 2007. Postnatal maturation of laryngeal chemoreflexes in the preterm lamb. J. Appl. Physiol. (1985) 102 (4), 1429–1438.

Stoll, B.J., Hansen, N.I., Bell, E.F., Walsh, M.C., Carlo, W.A., Shankaran, S., et al., 2015. Trends in care practices, morbidity, and mortality of extremely preterm neonates 1993–2012. JAMA 314 (10), 1039–1051.

Stone, M.L., Tatum, P.M., Weitkamp, J.H., Mukherjee, A.B., Attridge, J., McGahren, E.D., et al., 2013. Abnormal heart rate characteristics before clinical diagnosis of necrotizing enterocolitis. J. Perinatol. 33 (11), 847–850.

Su, L., Shen, L., Clayburgh, D.R., Nalle, S.C., Sullivan, E.A., Meddings, J.B., et al., 2009. Targeted epithelial tight junction dysfunction causes immune activation and contributes to development of experimental colitis. Gastroenterology 136 (2), 551–563.

Sutendra, G., Michelakis, E.D., 2007. The chicken embryo as a model for ductus arteriosus developmental biology: cracking into new territory. Am. J. Physiol. 292 (1), R481–R484.

Sutton, D., Taylor, E.M., Lindeman, R.C., 1978. Prolonged apnea in infant monkeys resulting from stimulation of superior laryngeal nerve. Pediatrics 61 (4), 519–527.

Tada, T., Wakabayashi, T., Nakao, Y., Ueki, R., Ogawa, Y., Inagawa, A., et al., 1985. Human ductus arteriosus. A histological study on the relation between ductal maturation and gestational age. Acta. Pathol. Jpn. 35 (1), 23–34.

Teppema, L.J., Dahan, A., 2010. The ventilatory response to hypoxia in mammals: mechanisms, measurement, and analysis. Physiol. Rev. 90 (2), 675–754.

Terry, T.L., 1942. Extreme prematurity and fibroblastic overgrowth of persistent vascular sheath behind each crystalline lens: I. Preliminary report. Am. J. Ophthalmol. 25 (2), 203–204.

Thach, B.T., 2001. Maturation and transformation of reflexes that protect the laryngeal airway from liquid aspiration from fetal to adult life. Am. J. Med. 111 (Suppl. 8A), 69S–77S.

Thach, B., 2010. Laryngeal chemoreflexes and development. Paediatr. Respir. Rev. 11 (4), 213–218.

Thayer, J.F., Fischer, J.E., 2009. Heart rate variability, overnight urinary norepinephrine and C-reactive protein: evidence for the cholinergic anti-inflammatory pathway in healthy human adults. J. Intern. Med. 265 (4), 439–447.

The, F.O., Boeckxstaens, G.E., Snoek, S.A., Cash, J.L., Bennink, R., Larosa, G.J., et al., 2007. Activation of the cholinergic anti-inflammatory pathway ameliorates postoperative ileus in mice. Gastroenterology 133 (4), 1219–1228.

The, F., Cailotto, C., van der Vliet, J., de Jonge, W.J., Bennink, R.J., Buijs, R.M., Boeckxstaens, G.E., 2011. Central activation of the cholinergic anti-inflammatory pathway reduces surgical inflammation in experimental post-operative ileus. Br. J. Pharmacol. 163 (5), 1007–1016.

Thebaud, B., 2004. Oxygen-sensitive Kv channel gene transfer confers oxygen responsiveness to preterm rabbit and remodeled human ductus arteriosus: implications for infants with patent ductus arteriosus. Circulation 110 (11), 1372–1379.

Thomson, M.A., Hamburger, J., Stewart, D.G., Lewis, H.M., 2004. Treatment of erosive oral lichen planus with topical tacrolimus. J. Dermatolog. Treat 15 (5), 308–314.

Thomson, M.A., Yoder, B.A., Winter, V.T., Giavedoni, L., Chang, L.Y., Coalson, J.J., 2006. Delayed extubation to nasal continuous positive airway pressure in the immature baboon model of bronchopulmonary dysplasia: lung clinical and pathological findings. Pediatrics 118 (5), 2038–2050.

Thuot, F., Lemaire, D., Dorion, D., Letourneau, P., Praud, J.P., 2001. Active glottal closure during anoxic gasping in lambs. Respir. Physiol. 128 (2), 205–218.

Tingay, D.G., Lavizzari, A., Zonneveld, C.E., Rajapaksa, A., Zannin, E., Perkins, E., et al., 2015a. An individualized approach to sustained inflation duration at birth improves outcomes in newborn preterm

lambs. Am. J. Physiol. Lung Cell Mol. Physiol. 309 (10), L1138–L1149.

Tingay, D.G., Polglase, G.R., Bhatia, R., Berry, C.A., Kopotic, R.J., Kopotic, C.P., et al., 2015b. Pressure-limited sustained inflation vs. gradual tidal inflations for resuscitation in preterm lambs. J. Appl. Physiol. (1985) 118 (7), 890–897.

Tracey, K.J., 2002. The inflammatory reflex. Nature 420 (6917), 853–859.

Tracey, K.J., 2007. Physiology and immunology of the cholinergic anti-inflammatory pathway. J. Clin. Invest. 117 (2), 289–296.

Tracey, K.J., 2009. Reflex control of immunity. Nat. Rev. Immunol. 9 (6), 418–428.

Trippenbach, T., 1994. Pulmonary reflexes and control of breathing during development. Biol. Neonate 65 (3–4), 205–210.

Turner, J.R., 2009. Intestinal mucosal barrier function in health and disease. Nat. Rev. Immunol. 9 (11), 799–809.

van Bree, S.H., Nemethova, A., Cailotto, C., Gomez-Pinilla, P.J., Matteoli, G., Boeckxstaens, G.E., 2012. New therapeutic strategies for postoperative ileus. Nat. Rev. Gastroenterol. Hepatol. 9, 675–683.

Van de Bor, M., Briet, E., van Bel, F., Ruys, J.H., 1986. Hemostasis and periventricular-intraventricular hemorrhage of the newborn. Am. J. Dis. Children 140 (11), 1131–1134.

van den Heuij, L.G., Mathai, S., Davidson, J.O., Lear, C.A., Booth, L.C., Fraser, M., et al., 2014. Synergistic white matter protection with acute-on-chronic endotoxin and subsequent asphyxia in preterm fetal sheep. J. Neuroinflammation 11, 89.

Van Leeuwen, P., Lange, S., Bettermann, H., Gronemeyer, D., Hatzmann, W., 1999. Fetal heart rate variability and complexity in the course of pregnancy. Early Hum. Dev. 54 (3), 259–269.

Van Leeuwen, P., Cysarz, D., Edelhauser, F., Gronemeyer, D., 2013. Heart rate variability in the individual fetus. Auton. Neurosci. 178, 24–28.

van Loenhout, R.B., Tibboel, D., Post, M., Keijzer, R., 2009. Congenital diaphragmatic hernia: comparison of animal models and relevance to the human situation. Neonatology 96 (3), 137–149.

van Westerloo, D.J., Giebelen, I.A., Florquin, S., Daalhuisen, J., Bruno, M.J., de Vos, A.F., et al., 2005. The cholinergic anti-inflammatory pathway regulates the host response during septic peritonitis. J. Infect. Dis. 191 (12), 2138–2148.

Vinukonda, G., Dummula, K., Malik, S., Hu, F., Thompson, C.I., Csiszar, A., et al., 2010. Effect of prenatal glucocorticoids on cerebral vasculature of the developing brain. Stroke 41 (8), 1766–1773.

Wada, K., Jobe, A.H., Ikegami, M., 1997. Tidal volume effects on surfactant treatment responses with the initiation of ventilation in preterm lambs. J. Appl. Physiol. (1985) 83 (4), 1054–1061.

Wang, F., Graham, W.V., Wang, Y., Witkowski, E.D., Schwarz, B.T., Turner, J.R., 2005. Interferon-gamma and tumor necrosis factor-alpha synergize to induce intestinal epithelial barrier dysfunction by up-regulating myosin light chain kinase expression. Am. J. Pathol. 166 (2), 409–419.

Wang, Q., Gold, N., Frasch, M.G., Huang, H., Thiriet, M., Wang, X., 2015. Mathematical model of cardiovascular and metabolic responses to umbilical cord occlusions in fetal sheep. Bull. Math. Biol. 77 (12), 2264–2293.

Wassink, G., Bennet, L., Davidson, J.O., Westgate, J.A., Gunn, A.J., 2013. Pre-existing hypoxia is associated with greater EEG suppression and early onset of evolving seizure activity during brief repeated asphyxia in near-term fetal sheep. PLoS One 8 (8), e73895.

Whitsett, J.A., Matsuzaki, Y., 2006. Transcriptional regulation of perinatal lung maturation. Pediatr. Clin. North Am. 53 (5), 873–887.

Wibbens, B., Bennet, L., Westgate, J.A., De Haan, H.H., Wassink, G., Gunn, A.J., 2007. Preexisting hypoxia is associated with a delayed but more sustained rise in T/QRS ratio during prolonged umbilical cord occlusion in near-term fetal sheep. Am. J. Physiol. Regul. Integr. Comp. Physiol. 293 (3), R1287–R1293.

Wiswell, T.E., Peabody, S.S., Davis, J.M., Slayter, M.V., Bent, R.C., Merritt, T.A., 1994. Surfactant therapy and high-frequency jet

ventilation in the management of a piglet model of the meconium aspiration syndrome. Pediatr. Res. 36 (4), 494–500.

Wolfs, T.G., Buurman, W.A., Zoer, B., Moonen, R.M., Derikx, J.P., Thuijls, G., et al., 2009. Endotoxin induced chorioamnionitis prevents intestinal development during gestation in fetal sheep. PLoS One 4 (6), e5837.

Wong, F.Y., Leung, T.S., Austin, T., Wilkinson, M., Meek, J.H., Wyatt, J.S., Walker, A.M., 2008. Impaired Autoregulation in Preterm Infants Identified by Using Spatially Resolved Spectroscopy. Pediatrics 121 (3), e604–e611.

Wu, Y.-C., Chang, C.-Y., Kao, A., Hsi, B., Lee, S.-H., Chen, Y.-H., Wang, I.-J., 2015. Hypoxia-induced retinal neovascularization in zebrafish embryos: a potential model of retinopathy of prematurity. PLoS One 10 (5), e0126750.

Xia, L., Damon, T., Leiter, J.C., Bartlett, Jr., D., 2008. Elevated body temperature exaggerates laryngeal chemoreflex apnea in decerebrate piglets. Adv. Exp. Med. Biol. 605, 249–254.

Xin, C., Xin, H., Bin, L., Zhenyu, Z., Lei, J., Chengguang, H., Yicheng, L., 2010. Changes in neural dendrites and synapses in rat somatosensory cortex following neonatal post-hemorrhagic hydrocephalus. Brain Res. Bull. 83 (1–2), 44–48.

Xu, A., Durosier, L.D., Ross, M.G., Hammond, R., Richardson, B.S., Frasch, M.G., 2014. Adaptive brain shut-down counteracts neuroinflammation in the near-term ovine fetus. Front. Neurol. 5, 110.

Xu, H., Hu, F., Sado, Y., Ninomiya, Y., Borza, D.-B., Ungvari, Z., et al., 2008. Maturational changes in laminin, fibronectin, collagen IV, and perlecan in germinal matrix, cortex, and white matter and effect of betamethasone. J. Neurosci. Res. 86 (7), 1482–1500.

Yoder, B.A., Albertine, K.H., Null, Jr., D.M., 2016. High-frequency ventilation for non-invasive respiratory support of neonates. Semin. Fetal Neonatal Med. 21 (3), 162–173.

Yokoyama, U., Minamisawa, S., Quan, H., Ghatak, S., Akaike, T., Segi-Nishida, E., et al., 2006. Chronic activation of the prostaglandin receptor EP4 promotes hyaluronan-mediated neointimal formation in the ductus arteriosus. J. Clin. Invest. 116 (11), 3026–3034.

Page left intentionally blank

32

Animal Models of Fetal Programming: Focus on Chronic Maternal Stress During Pregnancy and Neurodevelopment

Martin G. Frasch*, Jay Schulkin*, Gerlinde A.S. Metz**, Marta Antonelli[†]

*University of Washington, Seattle, WA, United States
**Canadian Centre for Behavioural Neuroscience, University of Lethbridge, Lethbridge, Alberta, Canada
[†]Institute of Cellular Biology and Neuroscience "Prof Dr. Eduardo de Robertis", Buenos Aires University, Buenos Aires, Argentina

1 INTRODUCTION

1.1 The Concept of Fetal Programming and Overview of Animal Models

The period of intrauterine development represents a sensitive window during which disruption or modification of the environment can influence fetal development to potentially alter lifetime health trajectories (Barker and Clark, 1997; Godfrey and Barker, 2001). Depending on the time window of exposure during gestation, different physiological systems are affected by the exterior or interior milieu. Consequently, different animal models have been used to address pertinent questions about mechanisms of the programming effects and therapeutic options (Chavatte-Palmer et al., 2016; Sutton et al., 2016). Here, we focus on animal models reproducing the effects
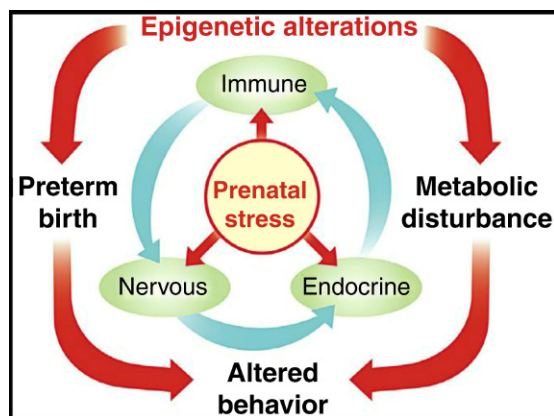
FIGURE 32.1 **Conceptual framework illustrating the interplay between prenatal stress and altered pregnancy outcomes.** Late gestation stress alters the maternal endocrine, immune and nervous system phenotypes, and expression of epigenetic markers. Epigenetic modifications may have no influence, partial influence or extensive influences on pregnancy outcomes, altered maternal and offspring behavior, and metabolic imbalances. Some or all of these outcomes may be influenced by epigenetic modifications (Metz et al., 2015).

taking place during fetal development, rather than periconceptually (Heijmans et al., 2008) or during embryonic development. We will also consider the transgenerational effects of fetal programming as they are being modeled in a number of animal systems. This is important, as it appears established now that a combination of genetic and epigenetic mechanisms can convey memory not only across a single generation, but even persist as a multigenerational memory of acute and chronic insults endured during fetal development. The potential adaptive and maladaptive physiological phenomena resulting from such programming are considered within the concept of the developmental origins of health and disease or DOHaD (Fig. 32.1) (Gluckman et al., 2010; Metz et al., 2015).

Animal models of fetal programming contribute in three synergistic ways to understanding and treating human diseases or predispositions to diseases, which emerge from in utero insults leading to fetal programming. Firstly, animal models serve to confirm observations derived in epidemiological studies. Secondly, animal models provide insights into mechanisms and render novel putative biomarkers of various effects of fetal programming that are relevant for early identification of affected individuals, children and adults. Thirdly, animal models permit testing of therapeutic interventions before they are translated into clinical intervention studies (Care et al., 2016; Leshem and Schulkin, 2012; Zucchi et al., 2014).

DOHaD have been linked to a number of modifiable and nonmodifiable factors and factors that, arguably, are settled somewhere in between, such as socioeconomic status (Borghol et al., 2012; King et al., 2015).

The modifiable risk factors include, for example, patterns of nutrition, including both chronic fetal and early postnatal under- and overnutrition (Chavatte-Palmer et al., 2016; El Hajj et al., 2014; Morrison and Regnault, 2016), drug intake, including smoking, cannabis and alcohol (Szutorisz and Hurd, 2016; Westbrook et al., 2010), intrauterine growth restriction (Regnault et al., 2013; Zhang et al., 2015), intrauterine infection (Cao et al., 2015; Cordeiro et al., 2015). To the nonmodifiable factors belong such events as wars, famines (Symonds et al., 2001) and other inescapable stress experiences that may occur before or during pregnancy (King and Laplante, 2005; Veru et al., 2014), and, notably, can be inherited in the off-spring paternally or maternally and in a sexually dimorphic manner (Petropoulos et al., 2014; Short et al., 2016). The developmental consequences of in utero exposures to these various factors, modeled in a number of animal models including rat (Care et al., 2016), guinea pig (Iqbal et al., 2012; Pappas et al., 2014), sheep (Barry and Anthony, 2008; Burns et al., 2015) and nonhuman primate (Li et al., 2007), include metabolic syndrome, obesity and diabetes in particular; cardiovascular development including susceptibility to atherosclerosis, hypertension, and coronary heart disease, but also other forms of heart disease including cardiomyopathies (Frasch, 2008; Frasch et al., 2007; Morton et al., 2016; Thornburg, 2015) and alterations in neurodevelopment, including emotional and cognitive development which have been linked to autism spectrum disorder, attention deficit hyperactivity disorder, learning disabilities, to name a few.

Enigmatically, in the domain of stress research, in utero exposure to inescapable stress appears to exert a dramatic spectrum of effects across all of the above-mentioned physiological systems (Maccari et al., 2014). Stress exposure is also probably the most common driver of fetal programming, iatrogenic via antenatal glucocorticoids (~10% of all pregnancies), or in form of life events (~25%–50% of all pregnancies) (Roosevelt and Low, 2016; Shapiro et al., 2013; Woods et al., 2010).

The literature dealing with fetal programming has undergone rapid growth over the past decade. A PubMed search in September 2016 rendered ~150,000 hits. Hence, the authors make no attempt to provide a systematic review in this chapter. Rather, we hope to demonstrate on some select examples how exactly animal models of fetal programming due to stress exposure have continued to expand our knowledge of this fascinating phenomenon with major health-economic and social impact. We will distinguish two types of stress exposure resulting in fetal programming: iatrogenic, due to administration of synthetic glucocorticoids (sGC), where key models are guinea pig and sheep and exogenous stress, also referred to as prenatal stress (PS) where key models are rat and sheep.

2 SIGNIFICANCE

By 2007, 200 million children under 5 years of age living in developing countries were not fulfilling their developmental potential, mostly due to exposure to biological and psychosocial factors that might alter brain function (Grantham-McGregor et al., 2007; Walker et al., 2007). Maternal depression was identified as a key risk factor affecting child development that requires urgent intervention (Walker et al., 2007). Early postnatal care was shown to partially reverse the effects of PS on brain reprogramming in animal models (Barros et al., 2004, 2006b; Weaver et al., 2005).

A key challenge of the animal models of fetal programming of PS is the identification of changes of the intrauterine environment represented by reliable biomarkers of stress-related epigenetic reprogramming. This is a vital step toward diagnosis and devising early interventions such as promoting mother-infant bonding and cognitive stimulation to improve developmental outcomes in PS-exposed children. This is mainly based on education and maternal support programs which are accessible in developing countries. Testing of this hypothesis has been subject of a number of animal model-based studies, primarily in pregnant rat using enrichment paradigms (Barros et al., 2004, 2006b; Weaver et al., 2005).

Among early developmental disruptors, prenatal exposure to maternal psychosocial stress, depression, and anxiety confers lifelong risk for behavioral alterations that last beyond childhood (O'Connor et al., 2003). Concern for the infant's future underlies much of the research on transgenerational transmission of maternal stress (Leshem et al., 2016). The developmental perspective that early experience is formative of long-term behavioral and cognitive patterns is reflected in the numerous studies that have demonstrated effects of PS during the prenatal, perinatal, and postnatal periods on offspring brain development, stress reactivity, and behavior regulation (Leshem et al., 2016) and cognitive development in human infants (Beydoun and Saftlas, 2008; Mulder et al., 2002). Animal studies in rat, mouse, guinea pig, and nonhuman primate show that PS leads to vulnerability to anxiety and impaired learning, memory and locomotor dysfunction (Weinstock, 2008). Moderate to severe stressful life-events, in combination with inadequate social network, are closely associated with increased child morbidity and neurological dysfunction, such as attention-deficit hyperactivity disorder (ADHD) and sleep disturbance during infancy (Weinstock, 1997) which if persistent in adulthood might result in depression and vulnerability to psychotic disorders (Cohen et al., 1983; van Os and Selten, 1998). The intrauterine period has been implicated as the most sensitive time for the establishment of epigenetic variability, "fetal programming", which in turn affects offspring development, cell- and tissue-specific gene expression, potentially altering lifetime health trajectories and risk for a range of disorders (Barker and Clark, 1997; Tobi et al., 2009). Far less is known about how fetal programming is influenced by the PS occurring *before* pregnancy. As such, studies on PS effects during pregnancy and transgenerational transfer of PS are needed to define the mechanisms, identify the biomarkers for early detection and begin to devise early therapeutic approaches. This is especially relevant now, as nongenomic and epigenetic transmission offer a conceptualization of how experience may be transferred across generations (Caldji et al., 2011; Mulligan et al., 2012; Weaver et al., 2004). The key biological systems upon which the PS-triggered epigenetic mechanisms are thought to act are hypothalamic-pituitary-adrenal (HPA) axis and the autonomic nervous system (ANS).

The HPA axis regulates homeostatic mechanisms, including the ability to respond to stressors (Van den Hove et al., 2006) and is highly sensitive to adverse early life experiences (Meaney, 2001). Exposure to PS results in increased responsiveness of the HPA axis to stress, and reductions of glucocorticoid receptor (GR) expression in the hippocampus of adult offspring (Zuena et al., 2008). In humans, PS is associated with higher rates of preterm delivery and lower birth weight (Van den Bergh et al., 2005; Wadhwa et al., 1993), elevated cortisol (Field et al., 2004), impaired subsequent working memory performance in young women (Entringer et al., 2009) and changes in the epigenetic regulation of GR expression (Mulder et al., 1997). Increased HPA stress reactivity in the offspring of low maternal care rats is associated with higher DNA methylation at the promoter of *NR3C1* (which encodes GR) (Francis et al., 1999; Liu et al., 1997; Weaver et al., 2004). Maternal prenatal depressive symptoms predict increased *NR3C1* 1F DNA methylation in buccal cells of male infants (Braithwaite et al., 2015). Moreover, PS modified the expression of several microRNAs in the hippocampus and prefrontal cortex of prepubertal and adult offspring, microRNA-133b being altered most significantly (Monteleone et al., 2014) (Fig. 32.1). In mice, levels of both OGT [O-linked-*N*-acetylglucosamine (O-GlcNAc) transferase] and its biochemical mark, O-GlcNAcylation, were significantly lower in males and further reduced by prenatal stress (Howerton et al., 2013). In humans, differential methylation is associated with prenatal exposure to maternal depression (O'Connor et al., 2003; Teh et al., 2014), PS, and birth weight (Filiberto et al., 2011; Mulligan et al., 2012; Vidal et al., 2014). Corticosteroid administration during pregnancy has shown to affect autonomic balance in utero (Dawes et al., 1994; Derks et al., 1995; Mulder et al., 1997; Senat et al., 1998).

Early adversity may elevate corticotropin-releasing hormone (CRH) gene expression in the mother's brain and (during pregnancy) placenta, stimulating fetal cortisol and adrenocorticotropic hormone (ACTH) and signaling

premature maturation of fetal tissue (Horan et al., 2000; Moog et al., 2016). Women exposed to early adversity may be more susceptible to stress during a major life event like pregnancy. This may be due in part to HPA dysregulation along with elevated CRH and cortisol levels. Pregestational stress increased the expression of corticotropin-releasing factor type 1 (CRF1) messenger RNA in the brains of mothers and offspring, suggesting an epigenetic route of transgenerational transmission (Zaidan et al., 2013). Pregestational stress to female rats two weeks prior to mating resulted in reduced anxiety, enhanced fear learning, and improved adaptive learning for second generation offspring (Zaidan and Gaisler-Salomon, 2015). In addition, levels of the stress hormone corticosterone (CORT; an indicator of HPA functioning) was altered across the three generations in a sex-dependent manner (Zaidan and Gaisler-Salomon, 2015). Maternal stress during the third, but not the second, week of gestation in rats was associated with alterations in stress reactivity behaviors and prolonged elevations in glucocorticoid levels among adult male offspring (Koenig et al., 2005). Heightened anxiety was associated with greater CRH mRNA gene expression in the amygdala, and attenuated stress responses were associated with greater glucocorticoid mRNA expression in the hippocampus and impaired feedback to the HPA (Grundwald and Brunton, 2015). The offspring of rats exposed to either a daily injection of CORT or prenatal stress during the third week of gestation all displayed decreased GR protein levels in the medial prefrontal cortex, hippocampus, and hypothalamus, as compared to controls (Bingham et al., 2013).

Higher levels of CRH during pregnancy also increase maternal vulnerability to a suppressed HPA axis after delivery and postpartum depression, for which the CRH-R1 receptor has been implicated (Engineer et al., 2013; Meltzer-Brody et al., 2011). Changes in maternal and offspring HPA function, which can be altered via stress induced changes to CRF (or CRH) expression (Zaidan et al., 2013), are often accompanied by behavioral effects. Together, CRH can impact behavior and brain function and should continue to remain in focus of animal model-based investigations of stress-mediated fetal programming effects of neurodevelopmental trajectories.

3 PRECLINICAL STUDIES OF PRENATAL STRESS IN RODENT MODELS

3.1 Single Generation PS Exposure Effects on Programming of Postnatal Brain Development

3.1.1 PS Impairs Dopamine Metabolism Throughout Development of the Male Offspring

PS can be induced in pregnant rats by restriction of movement and subsequent crossfostering. PS increases DA D2 receptors in limbic areas, decreases DA-stimulated release in cortical areas and impairs the expression of specific transcription factors during development, as well as the expression of TH and transporters. PS alters the asymmetry in D2 type receptors in the Nucleus Accumbens, an area associated with impulsivity (Adrover et al., 2007; Berger et al., 2002; Barros et al., 2004; Carboni et al., 2010; Katunar et al., 2010; Silvagni et al., 2008). Adoption at birth reverses the receptor increase, reflecting the high vulnerability of DA system to variations both in prenatal and in postnatal environment.

3.1.2 PS Impairs the Hypothalamic-Pituitary-Gonadal Axis in Male Offspring (Fig. 32.2)

PS impairments of DA metabolism were differentially affected after puberty, suggesting that perinatal events might render the DA circuitry more vulnerable to puberty variation of the hormonal circulating hormones. PS induces long-term imbalance of male sexual hormones concentrations in serum, advanced spermatogenesis development and age-dependent misbalance in oestrogen receptor alpha expression in PFC and HPC brain areas (Pallares et al., 2013a,b).

3.1.3 PS Alters Behavioral and Morphological Parameters in Offspring

Behavioral studies have shown an anxiogenic behavior that can be reversed after early adoptions. A direct relation was found between the anxiety states and levels of benzodiazepine (BDZ) receptors. At the morphological level there is a reduced dendritic arborization and astroglial hypertrophy with synaptic loss suggesting a possible alteration of glutamate metabolism. Glutamate transporters were altered in frontal cortex and hippocampus of PS offspring (Adrover et al., 2015; Barros et al., 2006a).

3.1.4 PS Exerts Epigenetic Changes in Adult Offspring

The expression of the gene gpm6a (which encodes membrane M6A glycoprotein) is increased in the hippocampus of the PS rats' brains. The pattern of methylation in a CpG island of the first intron of the gene gpm6a was altered in rats subjected to PS (Monteleone et al., 2014).

Taken together, these results suggest that PS insults are critical in the development of biochemical responses and behavior in adults, and that maternal care is crucial in the first weeks of life. It has been postulated that several psychiatric disorders that manifest themselves in the adult human, such as schizophrenia, depression, anxiety, and drug abuse, are imbalances of dopaminergic, glutamatergic, and GABAergic systems as a consequence, among other reasons, of alterations in the early development of the corticostriatal pathway. Rat models of gestational stress will provide clues to understanding
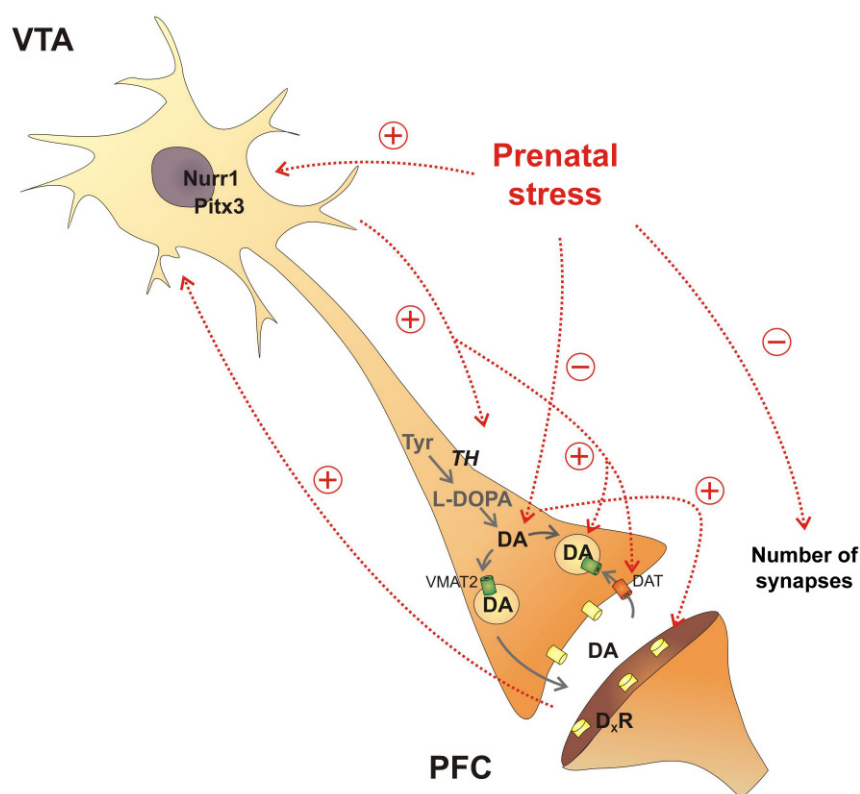
FIGURE 32.2 **Schematic representations of the effects exerted by PS on the dopaminergic function.** The data correspond to the VTA–PFC pathway of an offspring that was prenatally stressed employing a restraint protocol. The effects described occur at different stages of development. PS exerts an inhibitory effect (indicate by [−]) on DA levels at some unknown stage of DA biosynthesis. Low levels of DA produce an up-regulation (indicate by [+]) of DA D2 receptors, which in turn activates Nurr1. High levels of this transcription factor could up- regulate TH expression, and eventually DAT and VMAT2, which will increase DA levels in an attempt to compensate for the imbalance produced by PS. PS also produces synaptic loss in the brain of adult offspring (Baier et al., 2012). DA, Dopamine; DAT, dopamine transporter; Nurr-1, nuclear receptor related 1-protein; PFC, prefrontal cortex; PS, prenatal stress; TH, tyrosine hydroxylase; VMAT2, vesicular monoamine transporter 2; VTA, ventral tegmental area.

the mechanisms by which a PS insult in early life contributes to the breakdown of the balance in neurotransmission and the formation of aberrant cortical connections, which would entail the establishment of abnormal cognitive behaviors.

3.1.4.1 EXPERIMENTAL PARADIGM FOR A SINGLE-GENERATIONAL PS RAT MODEL

Virgin female Wistar rats are individually mated with a sexually experienced male Wistar rat. The day on which the vaginal plug is found is designated as the first day of pregnancy.

Prenatal stress: Pregnant dams are randomly assigned to either the control (C) or the prenatal stress (PS) group and individually housed with *ad libitum* access to standard rat chow and water. C rats are left undisturbed in the home cage, while PS dams are subjected to a restraint stress procedure, which involves rats being transferred to an experimental room where the stressor is applied. Pregnant females are individually placed into a transparent plastic restrainer fitted closely to body size for three 45 min periods per day (09:00, 12:00, and 16:00 h) between days 14 and 21 of pregnancy. The restrainer

has ventilation holes, and dimensions appropriate for a pregnant rat of 350 g: internal diameter 64 mm, and an adjustable length of 149–208 mm. This type of stressor is chosen because it has an indirect influence on the fetuses via a direct stress on the mother. The sessions are performed in a lit environment. No other subjects should be present in the experimental room during the stress exposure.

Postnatal procedures: On the day of parturition, litter characteristics are recorded and litters are culled to 10 pups, maintaining similar number of males and females, when possible. Weaning is performed at postnatal day (PND) 21. The male and female offspring are housed in separated cages, with no more than 5 rats per cage, and in standard housing conditions. To avoid litter effects, 1–2 pups from each litter (a female and a male) should be tested for each experiment. Behavioral testing is conducted at that period using the elevated plus maze and light–dark box tests for anxiety-like behaviors and sucrose anhedonia test for depressive-like behavior. Brains are collected after decapitation at the end of behavioral tests at PND 35 or other date depending on the milestones to be assessed in the given study.
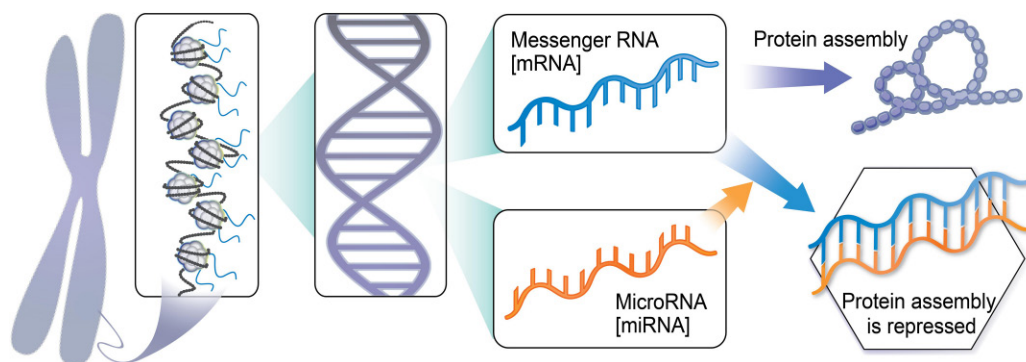
FIGURE 32.3 **Epigenetic regulation through microRNA expression.** A microRNA is a small noncoding RNA molecule containing approximately 22 nucleotides. MicroRNAs function in RNA silencing and posttranscriptional regulation of gene expression. When mRNA is translated into a protein product, a microRNA molecule can repress this process by binding to the mRNA. Each microRNA can bind to the mRNA of up to 200 gene targets. MicroRNAs can also be involved in establishing DNA methylation, and may influence chromatin structure by regulating histone modifiers (Metz et al., 2015).

3.2 Effects of Multigenerational PS on Programming of Postnatal Brain Development

The lifetime risk of mental illness is greater if an individual has family history of a similar condition. Therefore, most efforts during the past decades have focused on the identification of genetic associations, but the results were often met with disappointment, as the associations with genetic variations were weak. In the postgenomic era, the focus has shifted to identify associations between epigenetic regulators that can be modified by environmental factors, such as stress. Importantly, epigenetic marks are potentially heritable. *Trans*-generational studies are uniquely suited to reveal mechanisms of *trans*-generational programming by inheritance of epigenetic, metabolomic, and phenotypic traits. The multigenerational stress resembles human populations living in chronic stress conditions, for example, several generations exposed to residential school, war, or poverty.

Compared to single-generation PS, the multigenerational stress has somewhat different consequences: it facilitates adaptation to the recurrent maternal stress across generations, thus generating stress resilience. This causes new behavioral traits and better brain activity coherence. Based on the mismatch hypothesis, the multigenerational stress leads to better adaptation because the offspring is bred for a stressful environment and the stress is indeed occurring again when the daughters get pregnant. The *trans*-generational cohort faces the mismatch problem because they are bred for a stressful environment, but there is no more experimental stress during pregnancy or any other time.

3.2.1 PS Elevates Stress Responses and the Risk of Mental Illness

PS (F1 generation) impedes developmental milestones in rats, thus desynchronizing brain development along with epigenetic signatures of human anxiety, depression,

and adverse brain development (Zucchi et al., 2014). Interestingly, PS-induced anxiety-like and depression-like behaviors become most evident at the most vulnerable periods in life, early development and old age (Erickson et al., 2014).

3.2.2 PS programs Risk of Anxiety and Depression in Future Generations (Fig. 32.3)

In a rat model of trans- and multigenerational experience, PS induces increased risk of gestational diabetes, preterm birth, and delayed brain development across generations. These manifestations are linked to microRNA (miRNA) and mRNA signatures of preterm birth (Yao et al., 2014) and mental illness, in particular anxiety and depression-like symptoms, and altered brain connectivity in adulthood (McCreary et al., 2016). Interestingly, these studies revealed striking sex differences, with stressed females displaying partial stress resilience until the F3 generation, suggesting truly epigenetic inheritance.

3.2.3 Stress-Induced Epigenetic and Metabolic Changes Propagate Across Generations

Stress alters miRNA expression patterns in the brain (Babenko et al., 2012), thus generating potentially heritable biomarkers of disease. New miRNA pathways have been identified which are involved in neurotrophin and myelin regulation, providing a mechanistic link to mental illness REF. Furthermore, altered epigenetic regulation of gene expression is also accompanied by altered metabolic footprints, which can be assessed in animals and humans using body hair, biofluids or solid tissues using NMR spectroscopy and inductively coupled plasma mass spectroscopy (Ambeskovic et al., 2013; Kiss et al., 2016). These findings suggest that PS induces stable transgenerational specific epigenetic and metabolic alterations that can also be found in human disease.

4 EXPERIMENTAL PARADIGM FOR A TRANS- AND MULTIGENERATIONAL PS RAT MODEL

The trans- and multigenerational PS rat model allows studies of the genetic and epigenetic mechanisms on DNA and miRNA levels as well as of the down-stream metabolomics signatures in organs such as brain and blood. This may identify mechanisms of transgenerational inheritance of signatures linked to mental illness and potential predictive and diagnostic biomarkers.

Multi- and trans-generational stress: Restraint is used to induce a stress response in 100–150 day old timed-pregnant dams. Assessments are performed in the parental generation (F0), their offspring (F1), grand-offspring (F2), and great-grand-offspring (F3), for both males and females in each generation. Behavioral assessments include F4 pups. The F3 and F4 generations are central to identifying germ line epigenetic influences. *Trans*-generational Stress refers to stress in only the parental generation (S in F0, SN in F1, SNN in F2, SNNN in F3; N: no stress). F3 offspring (F4) development will also be assessed. Multigenerational Stress refers to continuous experience of maternal stress through all generations (S in F0, SS in F1, SSS in F2, SSSS in F3) and Controls will consist of nonstressed, handled animals (N, NN, NNN, NNNN). To carefully standardize conditions across generations, personal breeding colony room in a dedicated facility is advised.

Postnatal Procedures: Physiological correlates of stress are determined based on body weight, food intake, post-mortem brain and adrenal weight, and blood serum markers. Litter size and sex ratios are determined prior to culling each litter to $n = 8$ to standardize litter size effects on maternal care and offspring development. Infrared surveillance systems should monitor maternal care and behavior around the clock.

Behavior: This model is amenable for continuous cage site recordings of pre-partum maternal behavior, maternal care (nest building, grooming, stereotypy, circadian rhythm, pup retrieval; and maternal defense on lactational day (LD) 5 toward a virgin intruder female approaching the nest area. A comprehensive test battery assesses offspring development (P7 infantile, P21 juvenile) in sensorimotor and physical features (skilled walking, vestibular, and proprioceptive functions, body weight, eye opening, play). Measures of maturation at P60 (adolescence) and adult behavior (P90-18 months) can include 5 classes of behavior: (1) skilled movement (reaching, ladder rung walking); (2) sensorimotor function (adhesive removal, von-Frey-hair test); (3) learning and memory (water maze, Ziggurat task, Go-No Go decision making); (4) social behavior (play fighting, hierarchy, aggressive, defensive, and submissive behavior); (5) depression- and anxiety-like behavior (light–dark test, elevated plus maze, open field, open table exploration).

Physiology: Blood samples are collected via tail vein nick on days without behavioral tests. Measurements include blood glucose to determine hyperglycemia and dehydration, stress plasma markers CRH, CORT, ACTH, and sex hormone levels of estrogen and testosterone. Puberty, estrous cycle (weekly vaginal swabs and Shorr's staining) and number of breeding sessions further determine female stress response. Multiple complementary behavioral, physical and endocrine hallmarks reflect the complex manifestations of transgenerational stress across the lifespan. HPA axis activity is closely linked to GR and MR density in the hypothalamic paraventricular nucleus and hippocampus. In all brain tissues, immunocytochemical and stereological analysis of GR, MR, CRH, and oxytocin receptor (OXTR) density and intracellular location should be performed to assess PS effects on stress axis. General morphology (cortical thickness, volume, neuron density) should be assessed for central structures involved in stress response and affective disorders, such as prefrontal cortex, hippocampus, basolateral amygdala, and paraventricular hypothalamus.

5 LARGE ANIMAL MODELS OF FETAL DEVELOPMENT TO MODEL PS: PREGNANT SHEEP

Chronically instrumented nonanesthetized fetal sheep is an appropriate and uniquely suited animal model for studying the effects of in utero insults on fetal development, because of its recognized physiological and pathophysiological similarities to human fetal developmental profile and the unique ability to chronically instrument and monitor the fetus while manipulating the intrauterine environment. Fetal sheep and guinea pig (Iqbal et al., 2012) in particular have been used extensively for studies of effects of antenatal sGC treatment on fetal brain development. Many studies showed detrimental acute and transgenerational effects on neurodevelopment and HPA axis responsiveness to stress (Anegroaie et al., 2016; Antonow-Schlorke et al., 2009; McCallum et al., 2008; Schwab et al., 2001, 2012; Iqbal et al., 2012). It is not clear whether the postnatal brain can fully compensate for these changes. Consequently, despite the acute benefits of the antenatal sGC treatment to the fetus during labour and in the early postnatal period, further studies are needed to delineate the long-term effects of repeated sGC courses on postnatal brain development. For such fetal/postnatal experimental paradigms, the guinea pig model has been most instrumental, although it is possible to do similar work in larger mammals, such as sheep or nonhuman primate. To the extent that sGCs represent a stress stimulus to

the fetus and can be injected directly intravenously to the fetus, this experimental approach also represents a possible paradigm for mimicking human fetal stress exposure to maternal stress hormones without accounting for the interindividual and interspecies differences in the placental transfer dynamics. Taken together, as an iatrogenic stressor or a model for stress-induced fetal programming, sGC-driven studies in guinea pig and sheep have shown the potential of fetal stress exposure to alter organ development, in particular that of the brain (Moisiadis and Matthews, 2014a,b).

A more "human-like", but also technically more complex experimental paradigm involves isolation of pregnant ewes based on the fact that they are flock animals and experience such isolation as stress. Such approach, as presented below, has been shown to result in acute and chronic stress-induced adaptations and represents the most comprehensive animal experimental model of human *fetal* stress exposure (Rakers et al., 2013). Rakers et al. (2013) showed that the development of HPA axis function, which matures during late gestation, is sensitive to inappropriate levels of GCs during preceding periods of fetal life. Earlier periods of gestation are particularly vulnerable. Exposure to endogenous or synthetic GCs during late gestation has similar effects, although transfer of endogenous GCs through the placental barrier is extremely limited. Finally, GCs reset the set point of the HPA axis rather than having an effect on its maturation.

6 EXPERIMENTAL PARADIGM FOR PRENATAL STRESS MODEL IN FETAL SHEEP

A detailed anesthesia and surgical protocol for creating a chronically instrumented nonanesthetized fetal sheep model has been reported recently (Burns et al., 2015). Pregnant sheep are randomly assigned to control or maternal stress groups. Stress group follows a repeated maternal stress protocol between 105 and 135 days of gestation (dGA, term = 145 dGA) according to the protocol by Rakers et al. (2013). Maternal stress is induced by isolating pregnant ewes in a well-lit box with no visual, tactile, or auditory contact with flockmates. During isolation, ewes have no access to food or water supply. Ewes are isolated 3 h for 2 days per week (Monday to Friday) with at least 2 days recovery time between the particular isolation bouts. Isolation is performed either between 07:00 and 10:00 h, 11:00 and 14:00 h, or 15:00 and 18:00 h. Day of the week and time of isolation, as well as the isolation box are to be changed randomly within the mentioned parameters to reduce habituation. Maternal blood samples are collected from the chronically installed jugular vein catheter at 105 dGA or another day of choosing, depending on the desired stress exposure observation window, before and during isolation to estimate maternal cortisol concentrations and the degree of habituation. Maternal and fetal ECG and fetal blood and amniotic pressures are recorded continuously throughout the experiment. Pregnant control ewes are held under the same conditions as the stressed ewes, but do not undergo the isolation procedures.

7 CONCLUSIONS

In summary, the protocols discussed here provides an overview and specific examples of experimental designs using animal models to assist in DOHaD-related research. Although each of the animal models comes with inherent limitations in resembling human conditions, rodents and sheep are especially suited for obtaining first primary data about human pregnancy and early development upon which to build future hypotheses.

References

Adrover, E., Berger, M.A., Perez, A.A., Tarazi, F.I., Antonelli, M.C., 2007. Effects of prenatal stress on dopamine D2 receptor asymmetry in rat brain. Synapse 61 (6), 459–462.

Adrover, E., Pallarés, M.E., Baier, C.J., Monteleone, M.C., Giuliani, F.A., Waagepetersen, H.S., et al., 2015. Glutamate neurotransmission is affected in prenatally stressed offspring. Neurochem. Int. 88, 73–87.

Ambeskovic, M., Fuchs, E., Beaumier, P., Gerken, M., Metz, G.A., 2013. Hair trace elementary profiles in aging rodents and primates: links to altered cell homeodynamics and disease. Biogerontology 14 (5), 557–567.

Anegroaie, P., Frasch, M., Rupprecht, S., Antonow-Schlorke, I., Muller, T., Schubert, H., et al., 2016. Development of somatosensory evoked potentials in fetal sheep: effects of betamethasone. Acta Physiol. (Oxford), doi: 10.1111/apha.12795.

Antonow-Schlorke, I., Helgert, A., Gey, C., Coksaygan, T., Schubert, H., Nathanielsz, P.W., et al., 2009. Adverse effects of antenatal glucocorticoids on cerebral myelination in sheep. Obstet. Gynecol. 113 (1), 142–151.

Babenko, O., Golubov, A., Ilnytskyy, Y., Kovalchuk, I., Metz, G.A., 2012. Genomic and epigenomic responses to chronic stress involve miRNA-mediated programming. PLoS ONE 7 (1), e29441.

Baier, C.J., Katunar, M.R., Adrover, E., Pallares, M.E., Antonelli, M.C., 2012. Gestational restraint stress and the developing dopaminergic system: an overview. Neurotox. Res. 22 (1), 16–32.

Barker, D.J., Clark, P.M., 1997. Fetal undernutrition and disease in later life. Rev. Reprod. 2 (2), 105–112.

Barros, V.G., Berger, M.A., Martijena, I.D., Sarchi, M.I., Perez, A.A., Molina, V.A., et al., 2004. Early adoption modifies the effects of prenatal stress on dopamine and glutamate receptors in adult rat brain. J. Neurosci. Res. 76 (4), 488–496.

Barros, V.G., Duhalde-Vega, M., Caltana, L., Brusco, A., Antonelli, M.C., 2006a. Astrocyte-neuron vulnerability to prenatal stress in the adult rat brain. J. Neurosci. Res. 83 (5), 787–800.

Barros, V.G., Rodriguez, P., Martijena, I.D., Perez, A., Molina, V.A., Antonelli, M.C., 2006b. Prenatal stress and early adoption effects on benzodiazepine receptors and anxiogenic behavior in the adult rat brain. Synapse 60 (8), 609–618.

Barry, J.S., Anthony, R.V., 2008. The pregnant sheep as a model for human pregnancy. Theriogenology 69 (1), 55–67.

Berger, M.A., Barros, V.G., Sarchi, M.I., Tarazi, F.I., Antonelli, M.C., 2002. Long-term effects of prenatal stress on dopamine and glutamate receptors in adult rat brain. Neurochem. Res. 27 (11), 1525–1533.

Beydoun, H., Saftlas, A.F., 2008. Physical and mental health outcomes of prenatal maternal stress in human and animal studies: a review of recent evidence. Paediatr. Perinat. Epidemiol. 22 (5), 438–466.

Bingham, B.C., Sheela Rani, C.S., Frazer, A., Strong, R., Morilak, D.A., 2013. Exogenous prenatal corticosterone exposure mimics the effects of prenatal stress on adult brain stress response systems and fear extinction behavior. Psychoneuroendocrinology 38 (11), 2746–2757.

Borghol, N., Suderman, M., McArdle, W., Racine, A., Hallett, M., Pembrey, M., et al., 2012. Associations with early-life socio-economic position in adult DNA methylation. Int. J. Epidemiol. 41 (1), 62–74.

Braithwaite, E.C., Kundakovic, M., Ramchandani, P.G., Murphy, S.E., Champagne, F.A., 2015. Maternal prenatal depressive symptoms predict infant NR3C1 1F and BDNF IV DNA methylation. Epigenetics 10 (5), 408–417.

Burns, P., Liu, H.L., Kuthiala, S., Fecteau, G., Desrochers, A., Durosier, L.D., et al., 2015. Instrumentation of near-term fetal sheep for multivariate chronic non-anesthetized recordings. J. Vis. Exp. (105), e52581.

Caldji, C., Hellstrom, I.C., Zhang, T.Y., Diorio, J., Meaney, M.J., 2011. Environmental regulation of the neural epigenome. FEBS Lett. 585 (13), 2049–2058.

Cao, M., Cortes, M., Moore, C.S., Leong, S.Y., Durosier, L.D., Burns, P., et al., 2015. Fetal microglial phenotype in vitro carries memory of prior in vivo exposure to inflammation. Front. Cell Neurosci. 9, 294.

Carboni, E., Barros, V.G., Ibba, M., Silvagni, A., Mura, C., Antonelli, M.C., 2010. Prenatal restraint stress: an in vivo microdialysis study on catecholamine release in the rat prefrontal cortex. Neuroscience 168 (1), 156–166.

Care, A.S., Sung, M.M., Panahi, S., Gragasin, F.S., Dyck, J.R., Davidge, S.T., Bourque, S.L., 2016. Perinatal resveratrol supplementation to spontaneously hypertensive rat dams mitigates the development of hypertension in adult offspring. Hypertension 67 (5), 1038–1044.

Chavatte-Palmer, P., Tarrade, A., Rousseau-Ralliard, D., 2016. Diet before and during pregnancy and offspring health: the importance of animal models and what can be learned from them. Int. J. Environ. Res. Public Health 13 (6).

Cohen, S., Kamarck, T., Mermelstein, R., 1983. A global measure of perceived stress. J. Health Soc. Behav. 24 (4), 385–396.

Cordeiro, C.N., Tsimis, M., Burd, I., 2015. Infections and brain development. Obstet. Gynecol. Surv. 70 (10), 644–655.

Dawes, G.S., Serra-Serra, V., Moulden, M., Redman, C.W., 1994. Dexamethasone and fetal heart rate variation. Br. J. Obstet. Gynaecol. 101 (8), 675–679.

Derks, J.B., Mulder, E.J., Visser, G.H., 1995. The effects of maternal betamethasone administration on the fetus. Br. J. Obstet. Gynaecol. 102 (1), 40–46.

El Hajj, N., Schneider, E., Lehnen, H., Haaf, T., 2014. Epigenetics and life-long consequences of an adverse nutritional and diabetic intrauterine environment. Reproduction 148 (6), R111–120.

Engineer, N., Darwin, L., Nishigandh, D., Ngianga-Bakwin, K., Smith, S.C., Grammatopoulos, D.K., 2013. Association of glucocorticoid and type 1 corticotropin-releasing hormone receptors gene variants and risk for depression during pregnancy and post-partum. J. Psychiatr. Res. 47 (9), 1166–1173.

Entringer, S., Buss, C., Kumsta, R., Hellhammer, D.H., Wadhwa, P.D., Wust, S., 2009. Prenatal psychosocial stress exposure is associated with subsequent working memory performance in young women. Behav. Neurosci. 123 (4), 886–893.

Erickson, Z.T., Falkenberg, E.A., Metz, G.A., 2014. Lifespan psychomotor behaviour profiles of multigenerational prenatal stress and artificial food dye effects in rats. PLoS ONE 9 (6), e92132.

Field, T., Diego, M., Hernandez-Reif, M., Vera, Y., Gil, K., Schanberg, S., et al., 2004. Prenatal maternal biochemistry predicts neonatal biochemistry. Int. J. Neurosci. 114 (8), 933–945.

Filiberto, A.C., Maccani, M.A., Koestler, D., Wilhelm-Benartzi, C., Avissar-Whiting, M., Banister, C.E., et al., 2011. Birthweight is associated with DNA promoter methylation of the glucocorticoid receptor in human placenta. Epigenetics 6 (5), 566–572.

Francis, D., Diorio, J., Liu, D., Meaney, M.J., 1999. Nongenomic transmission across generations of maternal behavior and stress responses in the rat. Science 286 (5442), 1155–1158.

Frasch, M.G., 2008. The perinatal development of arterial pressure in sheep: effects of low birth weight due to twinning. Reprod. Sci. 15 (9), 863–864, author reply 865.

Frasch, M.G., Muller, T., Wicher, C., Weiss, C., Lohle, M., Schwab, K., et al., 2007. Fetal body weight and the development of the control of the cardiovascular system in fetal sheep. J. Physiol. 579 (Pt 3), 893–907.

Gluckman, P.D., Hanson, M.A., Buklijas, T., 2010. A conceptual framework for the developmental origins of health and disease. J. Dev. Orig. Health. Dis. 1 (1), 6–18.

Godfrey, K.M., Barker, D.J., 2001. Fetal programming and adult health. Public Health Nutr. 4 (2B), 611–624.

Grantham-McGregor, S., Cheung, Y.B., Cueto, S., Glewwe, P., Richter, L., Strupp, B., 2007. Developmental potential in the first 5 years for children in developing countries. Lancet 369 (9555), 60–70.

Grundwald, N.J., Brunton, P.J., 2015. Prenatal stress programs neuroendocrine stress responses and affective behaviors in second generation rats in a sex-dependent manner. Psychoneuroendocrinology 62, 204–216.

Heijmans, B.T., Tobi, E.W., Stein, A.D., Putter, H., Blauw, G.J., Susser, E.S., et al., 2008. Persistent epigenetic differences associated with prenatal exposure to famine in humans. Proc. Natl. Acad. Sci. USA 105 (44), 17046–17049.

Horan, D.L., Hill, L.D., Schulkin, J., 2000. Childhood sexual abuse and preterm labor in adulthood: an endocrinological hypothesis. Women s Health Issues 10 (1), 27–33.

Howerton, C.L., Morgan, C.P., Fischer, D.B., Bale, T.L., 2013. O-GlcNAc transferase (OGT) as a placental biomarker of maternal stress and reprogramming of CNS gene transcription in development. Proc. Natl. Acad. Sci. USA 110 (13), 5169–5174.

Iqbal, M., Moisiadis, V.G., Kostaki, A., Matthews, S.G., 2012. Transgenerational effects of prenatal synthetic glucocorticoids on hypothalamic-pituitary-adrenal function. Endocrinology 153 (7), 3295–3307.

Katunar, M.R., Saez, T., Brusco, A., Antonelli, M.C., 2010. Ontogenetic expression of dopamine-related transcription factors and tyrosine hydroxylase in prenatally stressed rats. Neurotox. Res. 18 (1), 69–81.

King, S., Laplante, D.P., 2005. The effects of prenatal maternal stress on children's cognitive development: project ice storm. Stress 8 (1), 35–45.

King, K., Murphy, S., Hoyo, C., 2015. Epigenetic regulation of newborns' imprinted genes related to gestational growth: patterning by parental race/ethnicity and maternal socioeconomic status. J. Epidemiol. Commun. Health 69 (7), 639–647.

Kiss, D., Ambeskovic, M., Montinam, T., Metz, G.A., 2016. Stress transgenerationally programs metabolic pathways linked to altered mental health. Cell Mol. Life Sci. 73 (23), 4547–4557.

Koenig, J.I., Elmer, G.I., Shepard, P.D., Lee, P.R., Mayo, C., Joy, B., et al., 2005. Prenatal exposure to a repeated variable stress paradigm elicits behavioral and neuroendocrinological changes in the adult offspring: potential relevance to schizophrenia. Behav. Brain Res. 156 (2), 251–261.

Leshem, M., Schulkin, J., 2012. Transgenerational effects of infantile adversity and enrichment in male and female rats. Dev. Psychobiol. 54 (2), 169–186.

Leshem, M., Taouk, L., Schulkin, J., 2016. Transgenerational transmission of pregestational and prenatal experience: maternal adversity, enrichment, and underlying epigenetic and environmental mechanisms. J. Dev. Orig. Health Dis. 7 (6), 588–601.

Li, C., Levitz, M., Hubbard, G.B., Jenkins, S.L., Han, V., Ferry, Jr., R.J., et al., 2007. The IGF axis in baboon pregnancy: placental and systemic responses to feeding 70% global ad libitum diet. Placenta 28 (11–12), 1200–1210.

Liu, D., Diorio, J., Tannenbaum, B., Caldji, C., Francis, D., Freedman, A., et al., 1997. Maternal care, hippocampal glucocorticoid receptors, and hypothalamic-pituitary-adrenal responses to stress. Science 277 (5332), 1659–1662.

Maccari, S., Krugers, H.J., Morley-Fletcher, S., Szyf, M., Brunton, P.J., 2014. The consequences of early-life adversity: neurobiological, behavioural and epigenetic adaptations. J. Neuroendocrinol. 26 (10), 707–723.

McCallum, J., Smith, N., Schwab, M., Coksaygan, T., Reinhardt, B., Nathanielsz, P., Richardson, B.S., 2008. Effects of antenatal glucocorticoids on cerebral substrate metabolism in the preterm ovine fetus. Am. J. Obstet. Gynecol. 198 (1), 105 e101–109.

McCreary, J.K., Truica, L.S., Friesen, B., Yao, Y., Olson, D.M., Kovalchuk, I., et al., 2016. Altered brain morphology and functional connectivity reflect a vulnerable affective state after cumulative multigenerational stress in rats. Neuroscience 330, 79–89.

Meaney, M.J., 2001. Maternal care, gene expression, and the transmission of individual differences in stress reactivity across generations. Annu. Rev. Neurosci. 24, 1161–1192.

Meltzer-Brody, S., Stuebe, A., Dole, N., Savitz, D., Rubinow, D., Thorp, J., 2011. Elevated corticotropin releasing hormone (CRH) during pregnancy and risk of postpartum depression (PPD). J. Clin. Endocrinol. Metab. 96 (1), E40–E47.

Metz, G.A., Ng, J.W., Kovalchuk, I., Olson, D.M., 2015. Ancestral experience as a game changer in stress vulnerability and disease outcomes. Bioessays 37 (6), 602–611.

Moisiadis, V.G., Matthews, S.G., 2014a. Glucocorticoids and fetal programming part 1: outcomes. Nat. Rev. Endocrinol. 10 (7), 391–402.

Moisiadis, V.G., Matthews, S.G., 2014b. Glucocorticoids and fetal programming part 2: mechanisms. Nat. Rev. Endocrinol. 10 (7), 403–411.

Monteleone, M.C., Adrover, E., Pallares, M.E., Antonelli, M.C., Frasch, A.C., Brocco, M.A., 2014. Prenatal stress changes the glycoprotein GPM6A gene expression and induces epigenetic changes in rat offspring brain. Epigenetics 9 (1), 152–160.

Moog, N.K., Buss, C., Entringer, S., Shahbaba, B., Gillen, D.L., Hobel, C.J., Wadhwa, P.D., 2016. Maternal exposure to childhood trauma is associated during pregnancy with placental-fetal stress physiology. Biol. Psychiatry 79 (10), 831–839.

Morrison, J.L., Regnault, T.R., 2016. Nutrition in pregnancy: optimising maternal diet and fetal adaptations to altered nutrient supply. Nutrients 8 (6).

Morton, J.S., Cooke, C.L., Davidge, S.T., 2016. In utero origins of hypertension: mechanisms and targets for therapy. Physiol. Rev. 96 (2), 549–603.

Mulder, E.J., Derks, J.B., Visser, G.H., 1997. Antenatal corticosteroid therapy and fetal behaviour: a randomised study of the effects of betamethasone and dexamethasone. Br. J. Obstet. Gynaecol. 104 (11), 1239–1247.

Mulder, E.J., Robles de Medina, P.G., Huizink, A.C., Van den Bergh, B.R., Buitelaar, J.K., Visser, G.H., 2002. Prenatal maternal stress: effects on pregnancy and the (unborn) child. Early Hum. Dev. 70 (1–2), 3–14.

Mulligan, C.J., D'Errico, N.C., Stees, J., Hughes, D.A., 2012. Methylation changes at NR3C1 in newborns associate with maternal prenatal stress exposure and newborn birth weight. Epigenetics 7 (8), 853–857.

O'Connor, T.G., Heron, J., Golding, J., Glover, V., 2003. Maternal antenatal anxiety and behavioural/emotional problems in children: a test of a programming hypothesis. J. Child Psychol. Psychiatry 44 (7), 1025–1036.

Pallares, M.E., Adrover, E., Baier, C.J., Bourguignon, N.S., Monteleone, M.C., Brocco, M.A., et al., 2013a. Prenatal maternal restraint stress exposure alters the reproductive hormone profile and testis development of the rat male offspring. Stress 16 (4), 429–440.

Pallares, M.E., Baier, C.J., Adrover, E., Monteleone, M.C., Brocco, M.A., Antonelli, M.C., 2013b. Age-dependent effects of prenatal stress on the corticolimbic dopaminergic system development in the rat male offspring. Neurochem. Res. 38 (11), 2323–2335.

Pappas, J.J., Petropoulos, S., Suderman, M., Iqbal, M., Moisiadis, V., Turecki, G., et al., 2014. The multidrug resistance 1 gene Abcb1 in brain and placenta: comparative analysis in human and guinea pig. PLoS ONE 9 (10), e111135.

Petropoulos, S., Matthews, S.G., Szyf, M., 2014. Adult glucocorticoid exposure leads to transcriptional and DNA methylation changes in nuclear steroid receptors in the hippocampus and kidney of mouse male offspring. Biol. Reprod. 90 (2), 43.

Rakers, F., Frauendorf, V., Rupprecht, S., Schiffner, R., Bischoff, S.J., Kiehntopf, M., et al., 2013. Effects of early- and late-gestational maternal stress and synthetic glucocorticoid on development of the fetal hypothalamus-pituitary-adrenal axis in sheep. Stress 16 (1), 122–129.

Regnault, T.R., Nijland, M.J., Budge, H., Morrison, J.L., 2013. Basic experimental and clinical advances in the mechanisms underlying abnormal pregnancy outcomes. J. Pregnancy 2013, 327638.

Roosevelt, L., Low, L.K., 2016. Exploring fear of childbirth in the united states through a qualitative assessment of the wijma delivery expectancy questionnaire. J. Obstet. Gynecol. Neonatal Nurs. 45 (1), 28–38.

Schwab, M., Schmidt, K., Roedel, M., Mueller, T., Schubert, H., Anwar, M.A., Nathaniels, P.W., 2001. Non-linear changes of electrocortical activity after antenatal betamethasone treatment in fetal sheep. J. Physiol. 531 (Pt 2), 535–543.

Schwab, M., Coksaygan, T., Rakers, F., Nathanielsz, P.W., 2012. Glucocorticoid exposure of sheep at 0.7 to 0.75 gestation augments late-gestation fetal stress responses. Am. J. Obstet. Gynecol. 206 (3), 253 e216–e222.

Senat, M.V., Minoui, S., Multon, O., Fernandez, H., Frydman, R., Ville, Y., 1998. Effect of dexamethasone and betamethasone on fetal heart rate variability in preterm labour: a randomised study. Br. J. Obstet. Gynaecol. 105 (7), 749–755.

Shapiro, G.D., Fraser, W.D., Frasch, M.G., Seguin, J.R., 2013. Psychosocial stress in pregnancy and preterm birth: associations and mechanisms. J. Perinat. Med. 41 (6), 631–645.

Short, A.K., Fennell, K.A., Perreau, V.M., Fox, A., O'Bryan, M.K., Kim, J.H., et al., 2016. Elevated paternal glucocorticoid exposure alters the small noncoding RNA profile in sperm and modifies anxiety and depressive phenotypes in the offspring. Transl. Psychiatry 6 (6), e837.

Silvagni, A., Barros, V.G., Mura, C., Antonelli, M.C., Carboni, E., 2008. Prenatal restraint stress differentially modifies basal and stimulated dopamine and noradrenaline release in the nucleus accumbens shell: an 'in vivo' microdialysis study in adolescent and young adult rats. Eur. J. Neurosci. 28 (4), 744–758.

Sutton, E.F., Gilmore, L.A., Dunger, D.B., Heijmans, B.T., Hivert, M.F., Ling, C., et al., 2016. Developmental programming: state-of-the-science and future directions-Summary from a Pennington Biomedical symposium. Obesity (Silver Spring) 24 (5), 1018–1026.

Symonds, M.E., Budge, H., Stephenson, T., McMillen, I.C., 2001. Fetal endocrinology and development—manipulation and adaptation to long-term nutritional and environmental challenges. Reproduction 121 (6), 853–862.

Szutorisz, H., Hurd, Y.L., 2016. Epigenetic effects of cannabis exposure. Biol. Psychiatry 79 (7), 586–594.

Teh, A.L., Pan, H., Chen, L., Ong, M.L., Dogra, S., Wong, J., et al., 2014. The effect of genotype and in utero environment on interindividual variation in neonate DNA methylomes. Genome Res. 24 (7), 1064–1074.

Thornburg, K.L., 2015. The programming of cardiovascular disease. J. Dev. Orig. Health Dis. 6 (5), 366–376.

Tobi, E.W., Lumey, L.H., Talens, R.P., Kremer, D., Putter, H., Stein, A.D., et al., 2009. DNA methylation differences after exposure to prenatal famine are common and timing- and sex-specific. Hum. Mol. Genet. 18 (21), 4046–4053.

Van den Bergh, B.R., Mulder, E.J., Mennes, M., Glover, V., 2005. Antenatal maternal anxiety and stress and the neurobehavioural development of the fetus and child: links and possible mechanisms. A review. Neurosci. Biobehav. Rev. 29 (2), 237–258.

Van den Hove, D.L., Steinbusch, H.W., Scheepens, A., Van de Berg, W.D., Kooiman, L.A., Boosten, B.J., et al., 2006. Prenatal stress and neonatal rat brain development. Neuroscience 137 (1), 145–155.

van Os, J., Selten, J.P., 1998. Prenatal exposure to maternal stress and subsequent schizophrenia. The May 1940 invasion of The Netherlands. Br. J. Psychiatry 172, 324–326.

Veru, F., Laplante, D.P., Luheshi, G., King, S., 2014. Prenatal maternal stress exposure and immune function in the offspring. Stress 17 (2), 133–148.

Vidal, A.C., Benjamin Neelon, S.E., Liu, Y., Tuli, A.M., Fuemmeler, B.F., Hoyo, C., et al., 2014. Maternal stress, preterm birth, and DNA methylation at imprint regulatory sequences in humans. Genet. Epigenet. 6, 37–44.

Wadhwa, P.D., Sandman, C.A., Porto, M., Dunkel-Schetter, C., Garite, T.J., 1993. The association between prenatal stress and infant birth weight and gestational age at birth: a prospective investigation. Am. J. Obstet. Gynecol. 169 (4), 858–865.

Walker, S.P., Wachs, T.D., Gardner, J.M., Lozoff, B., Wasserman, G.A., Pollitt, E., Carter, J.A., 2007. Child development: risk factors for adverse outcomes in developing countries. Lancet 369 (9556), 145–157.

Weaver, I.C., Cervoni, N., Champagne, F.A., D'Alessio, A.C., Sharma, S., Seckl, J.R., et al., 2004. Epigenetic programming by maternal behavior. Nat. Neurosci. 7 (8), 847–854.

Weaver, I.C., Champagne, F.A., Brown, S.E., Dymov, S., Sharma, S., Meaney, M.J., Szyf, M., 2005. Reversal of maternal programming of stress responses in adult offspring through methyl supplementation: altering epigenetic marking later in life. J. Neurosci. 25 (47), 11045–11054.

Weinstock, M., 1997. Does prenatal stress impair coping and regulation of hypothalamic-pituitary-adrenal axis? Neurosci. Biobehav. Rev. 21 (1), 1–10.

Weinstock, M., 2008. The long-term behavioural consequences of prenatal stress. Neurosci. Biobehav. Rev. 32 (6), 1073–1086.

Westbrook, D.G., Anderson, P.G., Pinkerton, K.E., Ballinger, S.W., 2010. Perinatal tobacco smoke exposure increases vascular oxidative stress and mitochondrial damage in non-human primates. Cardiovasc. Toxicol. 10 (3), 216–226.

Woods, S.M., Melville, J.L., Guo, Y., Fan, M.Y., Gavin, A., 2010. Psychosocial stress during pregnancy. Am. J. Obstet. Gynecol. 202 (1), 61 e61–e67.

Yao, Y., Robinson, A.M., Zucchi, F.C., Robbins, J.C., Babenko, O., Kovalchuk, O., et al., 2014. Ancestral exposure to stress epigenetically programs preterm birth risk and adverse maternal and newborn outcomes. BMC Med. 12, 121.

Zaidan, H., Gaisler-Salomon, I., 2015. Prereproductive stress in adolescent female rats affects behavior and corticosterone levels in second-generation offspring. Psychoneuroendocrinology 58, 120–129.

Zaidan, H., Leshem, M., Gaisler-Salomon, I., 2013. Prereproductive stress to female rats alters corticotropin releasing factor type 1 expression in ova and behavior and brain corticotropin releasing factor type 1 expression in offspring. Biol. Psychiatry 74 (9), 680–687.

Zhang, S., Regnault, T.R., Barker, P.L., Botting, K.J., McMillen, I.C., McMillan, C.M., et al., 2015. Placental adaptations in growth restriction. Nutrients 7 (1), 360–389.

Zucchi, F.C., Yao, Y., Ilnytskyy, Y., Robbins, J.C., Soltanpour, N., Kovalchuk, I., et al., 2014. Lifetime stress cumulatively programs brain transcriptome and impedes stroke recovery: benefit of sensory stimulation. PLoS ONE 9 (3), e92130.

Zuena, A.R., Mairesse, J., Casolini, P., Cinque, C., Alema, G.S., Morley-Fletcher, S., et al., 2008. Prenatal restraint stress generates two distinct behavioral and neurochemical profiles in male and female rats. PLoS ONE 3 (5), e2170.

Page left intentionally blank

VIRAL DISEASE

Page left intentionally blank

33

Animal Models of Human Viral Diseases

Sara I. Ruiz*, Elizabeth E. Zumbrun**, Aysegul Nalca*

*Center for Aerobiological Sciences, United States Army Institute of Infectious Diseases (USAMRIID), Fort Detrick, Frederick, MD, United States
**United States Army Institute of Infectious Diseases (USAMRIID), Fort Detrick, Frederick, MD, United States

1 INTRODUCTION

Well-developed animal models are necessary to understand disease progression, pathogenesis, and immunologic responses to viral infections in humans. Furthermore, to test vaccines and medical countermeasures, animal models are essential for preclinical studies.

Ideally, an animal model of human viral infection should mimic the host–pathogen interactions and the disease progression that is seen in the natural disease course. A good animal model of viral infection should

allow assay of many parameters of infection, including clinical signs, growth of virus, clinicopathological parameters, cellular and humoral immune responses, and virus–host interactions. Furthermore, viral replication should be accompanied by measurable clinical manifestations and pathology should resemble that of human cases such that a better understanding of the disease process in humans is attained. There is often more than one animal model that closely represents human disease for a given pathogen. Small animal models are typically used for first-line screening, and for testing the efficacy of vaccines or therapeutics. In contrast, nonhuman primate (NHP) models are often used for pivotal preclinical studies. This approach is also used for basic pathogenesis studies, with most studies in small animal models when possible, and studies in NHPs to fill in the remaining gaps in knowledge.

The advantages of using mice to develop animal models are low cost, low genetic variability in inbred strains, and abundant molecular biological and immunological reagents. Specific pathogen free (SPF), transgenic and knockout mice are also available. A major pitfall of mouse models is that the pathogenesis and protection afforded by vaccines and therapeutics cannot always be extrapolated to humans. Additionally, blood volumes for sampling are limited in small animals, and viruses often need to be adapted through serial passage in the species to induce a productive infection.

The ferret's airways are anatomically and histologically similar to that of humans, and their size enables collection of larger or more frequent blood samples, making them an ideal model for certain respiratory pathogens. Ferrets are outbred, with no standardized breeds or strains, thus greater numbers are required in studies to achieve statistical significance and overcome the resulting variable responses. Additionally, SPF and transgenic ferrets are not available, and molecular biological reagents are lacking. Other caveats making ferret models more difficult to work with are their requirement for more space than mice (rabbit-style cages), and the development of aggressive behavior with repeated procedures.

NHPs are genetically, the closest species to humans, thus disease progression and host–pathogen responses to viral infections are often the most similar to that of humans. However, ethical concerns pertaining to experimentation on NHPs along with the high cost and lack of SPF NHPs raise barriers for such studies. NHP studies should be carefully designed to ensure the fewest number of animals are used, and the studies should address the most critical questions regarding disease pathogenesis, host–pathogen responses, and protective efficacy of vaccines and therapeutics.

Well-designed experiments should carefully evaluate the choice of animal, including the strain, sex, and age.

Furthermore, depending on the pathogen, the route of exposure and the dose should mimic the route of exposure and dose of human disease. The endpoint for these studies is also an important criterion. Depending on the desired outcome, the model system should emulate the host responses in humans when infected with the same pathogen.

In summary, small animal models are helpful for the initial screening of vaccines and therapeutics, and are often beneficial in obtaining a basic understanding of the disease. NHP models should be used for a more detailed characterization of pathogenesis and for pivotal preclinical testing studies. Ultimately, an ideal animal model may not be available. In this case, a combination of different well-characterized animal models should be considered to understand the disease progression and to test medical countermeasures against the disease.

In this chapter, we will be reviewing the animal models for representative members of numerous virus families causing human diseases. We will focus on viruses for each family that are of the greatest concern for public health worldwide.

2 CALICIVIRIDAE

2.1 Norwalk Virus

Norovirus, the genus of which Norwalk is the prototypic member, is the most common cause of gastroenteritis in the United States (Hall et al., 2013). There are five distinct genogroups (GI–GV) and numerous strains of Norwalk virus, including the particularly significant human pathogens GI.1 Norwalk virus, GII.2 Snow Mountain virus, and GII.1 Hawaii virus. In developing countries, Norwalk virus, also known as "winter vomiting virus," is responsible for approximately 200,000 deaths annually (Patel et al., 2008). A typical disease course is self-limiting, but there have been incidences of necrotizing enterocolitis and seizures in infants (Chen et al., 2009; Lutgehetmann et al., 2012; Turcios-Ruiz et al., 2008). Symptoms of infection include diarrhea, vomiting, nausea, abdominal cramping, dehydration, and fever. Incubation is normally 1–3 days, with symptoms persisting for 2–3 days (Koopmans and Duizer, 2004). Viral shedding can range from 6 to 55 days in healthy individuals (Atmar et al., 2014). However, longer illness duration can be indicative of immunocompromised status, with the elderly and young having a prolonged state of shedding (Harris et al., 2008; Rockx et al., 2002). Interestingly, individuals vary greatly in susceptibility to norovirus infection depending on their fucosyl transferase 2 (FUT2) allele functionality and histoblood group antigen status, with type A and O individuals susceptible and types AB and B resistant (Hutson et al., 2005).

Transmission occurs predominately through the oral–fecal route with contaminated food and water being a major vector (Atmar and Estes, 2001; Becker et al., 2000; Koopmans and Duizer, 2004). Vomiting results in airborne dissemination of the virus with areas of 7.8 m^2 being contaminated and subsequent transmission from oral deposition of airborne particles or contact with contaminated fomites, which can remain contaminated for up to 42 days (Makison Booth, 2014; Tung-Thompson et al., 2015). Each vomiting event in a classroom setting elevates the risk of norovirus illness among elementary students with proximity correlating with attack rates (Evans et al., 2002; Marks et al., 2003). Viral titers in emesis and fecal suspensions are as high as 1.2×10^7 and 1.6×10^{11} GES (genomic equivalent copies per milliliter), respectively and the 50% infectious dose is 1320 GES (Atmar et al., 2014). Therefore, outbreaks can be extremely difficult to contain. Therapeutic intervention consists of rehydration therapy and antiemetic medication (Bucardo et al., 2008; Moe et al., 2001). No approved vaccine or therapeutic is available, and development has been challenging given that immunity is short-lived after infection, new strains rapidly evolve and the correlates of protection are not completely understood (Chen et al., 2013). However, one promising strategy utilized a virus-like particle (VLP)-based vaccine that protected or reduced infection by almost 50% in human volunteers (Aliabadi et al., 2015; Atmar et al., 2011).

Given the relatively benign disease in adults, experimental challenge has been carried out on human volunteers (Ball et al., 1999; Tacket et al., 2000). Viral titers are determined by shedding in feces and sera with histopathology changes monitored by biopsies particularly of the duodenum. The pH of emesis samples collected containing virus is consistent with viral replication in the small intestine with reflux to the stomach (Kirby et al., 2016). Additionally, Norwalk virus has been shown to bind to duodenal tissue (Chan et al., 2011). However, this type of research is technically difficult and expensive, and thus other models have been developed.

A major hindrance to basic research into this pathogen is the lack of permissive cell culture systems or animal models for Norwalk virus. NHPs including marmosets, cotton-top tamarins, and rhesus macaques infected with Norwalk virus are monitored for the extent of viral shedding; however, no clinical disease is observed in these models. Disease progression and severity is measured exclusively by assay of viral shedding (Rockx et al., 2005). Incidentally, more viruses were needed to create an infection when challenging by the oral route than by the intravenous (IV) route (Purcell et al., 2002). Chimpanzees were exposed to a clinical isolate of Norwalk virus by the IV route (Bok et al., 2011). Although none of the animals developed disease symptoms, viral shedding within the feces was observed within 2–5 days postinfection and lasted anywhere from 17 days to 6 weeks. Viremia never occurred and no histopathological changes were detected. The amount and duration of viral shedding was in-line with what is observed upon human infection. As such, chimeric chimpanzee–human anti-norovirus neutralizing antibodies have been explored as a possible therapeutic strategy (Chen et al., 2013).

A recently identified Calicivirus of rhesus origin, named Tulane virus, has been used as a surrogate model of infection. Unlike Norwalk virus, Tulane virus can be cultured in cells. Rhesus macaques exposed to Tulane virus intragastrically developed diarrhea and fever 2 days postinfection. Viral shedding was detected for 8 days. The immune system produced antibodies that dropped in concentration within 38 days postinfection, mirroring the short-lived immunity documented in humans. The intestine developed moderate blunting of the villi as seen in human disease (Sestak et al., 2012).

A murine norovirus has been identified and is closely related to human Norwalk virus (Karst et al., 2003). However, clinically the virus presents a different disease. The murine norovirus model does not include observable gastrointestinal clinical signs, possibly in part because rodents lack a vomiting reflex. Additionally, mice infected with norovirus develop a persistent infection in contrast to human disease (Hsu et al., 2006, 2007; Khan et al., 2009).

Porcine enteric caliciviruses can induce diarrheal disease in young pigs, and an asymptomatic infection in adults (Wang et al., 2006, 2007). Gnotobiotic pigs can successfully be infected with a passaged clinical norovirus isolate by the oral route. Diarrheal disease developed in 74% of the animals and virus was detected in the stool of 44% of the animals. No major histopathological changes or viral persistence was noted (Cheetham et al., 2006).

Calves are naturally infected with bovine noroviruses (Scipioni et al., 2008). Experimental challenge of calves by oral inoculation with a bovine isolate resulted in diarrheal disease 14–16 h postinfection. Recovery of virus was achieved after 53.5 and 67 h postinfection (Otto et al., 2011).

3 TOGAVIRIDAE

3.1 Eastern Equine Encephalitis Virus, Western Equine Encephalitis Virus, and Venezuelan Equine Encephalitis Virus

Eastern equine encephalitis virus (EEEV), Western equine encephalitis virus (WEEV), and Venezuelan equine encephalitis virus (VEEV) present with near synonymous symptoms. The majorities of human cases are asymptomatic, but can present as a flu-like illness progressing to central nervous system (CNS) involvement

to include seizures and paralysis. Mortality rates vary among the virus, with the highest reported for EEV at 36%–75% followed by WEEV and lastly VEEV at less than 1% (Ayers et al., 1994; Griffin, 2007; Steele and Twenhafel, 2010). There are currently no licensed vaccines or therapies but a recent Phase 1 clinical trial of a VEEV DNA vaccine resulted in VEEV-neutralizing antibody responses in 100% of the subjects (Hannaman et al., 2016).

Mouse models have been developed for numerous routes of infection including cutaneous, intranasal (IN), intracranial (IC), and aerosol. EEEV susceptibility in mouse models is correlated with age, with younger mice being more susceptible than adults. Importantly, EEEV pathogenesis is dependent on route of infection with delayed progression upon subcutaneous (subQ) exposure (Honnold et al., 2015). Newborn mice display neuronal damage with rapid disease progression, resulting in death (Murphy and Whitfield, 1970). Similarly, EEEV produces fatal encephalitis in older mice when administered via the intracerebral route, while inoculation via the subQ route causes a pantropic infection eventually resulting in encephalitis (Liu et al., 1970; Morgan, 1941). A general drawback to the usage of the mouse model is the lack of vascular involvement during the disease course (Liu et al., 1970).

After subQ inoculation with WEEV, suckling mice started to show signs of disease by 24 h and died within 48 h (Aguilar, 1970). The heart was the only organ in which pathologic changes were observed. Conversely, adult mice exhibited signs of lethargy and ruffled fur on day 4–5 postinfection. Mice were severely ill by day 8 and appeared hunched and dehydrated. Death occurred between days 7 and 14 with brain and mesodermal tissues, such as heart, lungs, liver, and kidney involvement (Aguilar, 1970; Monath et al., 1978). Intracerebral and IN routes of infection resulted in a fatal disease that was highly dependent on dose while intradermal (ID) and subQ inoculations caused only 50% fatality in mice regardless of the amount of virus (Liu et al., 1970). Comparing susceptibility of inbred and outbred strains revealed that CD-1, BALB/c, A/J, and C57BL6 mice were all highly susceptible to experimental infection via subQ inoculation when challenged prior to 10 weeks old with CNS involvement and lethality (Blakely et al., 2015). SubQ/dermal infection in the mouse model results in encephalitic disease very similar to that seen in horses and humans (MacDonald and Johnston, 2000). Virus begins to replicate in the draining lymph nodes at 4 h postinoculation. Eventually, virus enters the brain primarily via the olfactory system.

Furthermore, aerosol exposure of mice to VEEV can result in massive infection of the olfactory neuroepithelium, olfactory nerves, and olfactory bulbs and viral spread to brain, resulting in necrotizing panencephalitis (Charles et al., 1995; Steele et al., 1998). Aerosol and dermal inoculation routes cause neurological pathology in mice much faster than other routes of exposure. The clinical signs of disease in mice infected by aerosol are ruffled fur, lethargy, and hunching progressing to death (Charles et al., 1995; Steele and Twenhafel, 2010; Steele et al., 1998). IN challenge of C3H/HeN mice with high dose VEEV caused high morbidity and mortality (Julander et al., 2008b). Viral titers in brain peaked on day 4 postchallenge and remained elevated until animals succumbed on day 9–10 postchallenge. Protein cytokine array performed on brains of infected mice showed elevated IL-1a, IL-1b, IL-6, IL-12, MCP-1, IFNγ, MIP-1a, and RANTES levels. This model was used successfully to test antivirals against VEEV (Julander et al., 2008a). Additionally, a VEEV vaccine inactivated with 1,5-iodonaphthyl azide V3526 protects against both footpad and aerosol challenge with virulent VEEV in a mouse model (Gupta et al., 2016).

Guinea pigs and hamsters have also been developed as animal models for EEEV studies (Paessler et al., 2004; Roy et al., 2009). Guinea pigs developed neurological involvement with decreased activity, tremors, circling behavior, and coma. Neuronal necrosis was observed in brain lesions in the experimentally challenged animals (Roy et al., 2009). SubQ inoculation of EEEV produced lethal biphasic disease in hamsters with severe lesions of nerve cells. The early visceral phase with viremia was followed by neuroinvasion, encephalitis, and death. In addition, parenchyma necrosis were observed in the liver and lymphoid organs (Paessler et al., 2004). Harlan Sprague–Dawley hamsters develop viremia and progress to respiratory, gastrointestinal, and nervous system involvement when inoculated via subQ route. Vasculitis and encephalitis were both evident in this model, which mirrors the human disease clinical spectrum (Paessler et al., 2004).

WEEV is highly infectious to guinea pigs and has been utilized for prophylactic screening (Sidwell and Smee, 2003). Studies demonstrated that although the length of the incubation period and the disease duration varied, WEEV infection resulted in mortality in hamsters by all routes of inoculation. Progressive lack of coordination, shivering, rapid and noisy breathing, corneal opacity, and conjunctival discharge resulting in closing of the eyelids were indicative of disease in all cases (Zlotnik et al., 1972). CNS involvement was evident with intracerebral, intraperitoneal (IP), and ID inoculations (Zlotnik et al., 1972). IP inoculation of WEEV is fatal in guinea pigs regardless of amount of virus inoculum, with the animals exhibiting signs of illness on day 3–4, followed by death on day 5–9 (Nalca, unpublished results).

ID, IM, or IV inoculations of EEEV in NHPs cause disease, but does not reliably result in neurological symptoms (Dupuy and Reed, 2012). Intracerebral

infection of EEEV produces nervous system disease and fatality in monkeys (Nathanson et al., 1969). The differences in these models indicate that the initial viremia and the secondary nervous system infection do not overlap in NHPs when they are inoculated by the peripheral route (Wyckoff, 1939). IN and intralingual inoculations of EEEV also cause nervous system symptoms in monkeys, but are less drastic than intracerebral injections (Wyckoff, 1939). The aerosol route of delivery will result in uniformly lethal disease in cynomolgus macaques (Reed et al., 2007). In this model, fever was followed by elevated white blood cells and liver enzymes. Neurological signs subsequently developed and NHPs became moribund and were euthanized between 5–9 days postexposure. Meningoencephalomyelitis was the main pathology observed in the brains of these animals (Steele and Twenhafel, 2010). Similar clinical signs and pathology were observed when common marmosets were infected with EEEV by the IN route (Adams et al., 2008). Both aerosol and IN NHP models had similar disease progression and pathology as seen in human disease. Very limited studies have been performed with NHPs.

Reed et al. exposed cynomolgus macaques to low and high doses of aerosolized WEEV. The animals subsequently developed fever, increased white blood counts, and CNS involvement, demonstrating that the cynomolgus macaque model could be useful for testing of vaccines and therapeutics against WEEV (Reed et al., 2005).

VEEV infection causes a typical biphasic febrile response in NHPs. Initial fever was observed at 12–72 h after infection and lasted less than 12 h. Secondary fever generally began on day 5 and lasted 3–4 days (Gleiser et al., 1961). VEEV-infected NHPs exhibited mild symptoms, such as anorexia, irritability, diarrhea, and tremors. Leukopenia was common in animals exhibiting fever (Monath et al., 1974). Supporting the leukopenia, microscopic changes in lymphatic tissues, such as early destruction of lymphocytes in lymph nodes and spleen, a mild lymphocytic infiltrate in the hepatic triads, and focal myocardial necrosis with lymphocytic infiltration have been observed in monkeys infected with VEEV. Surprisingly, characteristic lesions of the CNS were observed histopathologically in monkeys in spite of the lack of any clinical signs of infection (Gleiser et al., 1961). The primary lesions were lymphocytic perivascular cuffing and glial proliferation and generally observed at day 6 postinfection during the secondary febrile episode. Similar to these observations, when cynomolgus macaques were exposed to aerosolized VEEV, fever, viremia, lymphopenia, and clinical signs of encephalitis were observed but the NHPs did not succumb to disease (Reed et al., 2004).

A common marmoset model was utilized for comparison studies of South America (SA) and North America (NA) strains of EEEV (Adams et al., 2008). Previous studies indicated that the SA strain is less virulent than NA strain for humans. Common marmosets were infected IN with either the NA or SA strain of EEEV. NA strain-infected animals showed signs of anorexia and neurological involvement and were euthanized 4–5 days after the challenge. Although SA strain-infected animals developed viremia, they remained asymptomatic and survived until the end of study.

3.2 Chikungunya Virus

Chikungunya virus (CHIKV) is a member of the genus *Alphaviruses*, specifically the Semliki Forest complex, and has been responsible for a multitude of epidemics centered within Africa and Southeast Asia (Griffin, 2007). The virus is transmitted by *Aedes aegypti* and *Aedes albopictus* mosquitoes. Given the widespread endemicity of *Aedes* mosquitoes, CHIKV has the potential to spread to previously unaffected areas. This is typified by the emergence of disease reported for the first time in 2005 in the islands of South-West Indian Ocean, including the French La Reunion island, and the appearance in Central Italy in 2007 (Charrel et al., 2007; Rezza et al., 2007).

The incubation period following a mosquito bite is 2–5 days, leading to a self-limiting acute phase that lasts 3–4 days. Symptoms during this period include fever, arthralgia, myalgia, and rash. Headache, weakness, nausea, vomiting, and polyarthralgia have all been reported (Powers and Logue, 2007). Individuals typically develop a stooped posture due to the pain. For approximately 12% of infected individuals, joint pain can last months after resolution of primary disease, and has the possibility to relapse. Underlying health conditions including diabetes, alcoholism, or renal disease, increase the risk of developing a severe form of disease that includes hepatitis or encephalopathy. Children between the ages of 3 and 18 years old have an increased risk of developing neurological manifestations (Arpino et al., 2009). There is currently no approved vaccine or antiviral.

Wild-type C57BL/6 adult mice are not permissive to CHIKV infection by ID inoculation. However, it was demonstrated that neonatal mice were susceptible and severity was dependent upon age at infection. Six-day-old mice developed paralysis by day 6, and all succumbed by day 12, whereas 50% of 9-day-old mice were able to recover from infection. By 12 days, mice were no longer permissive to disease. Symptomatic mice developed loss of balance, hind limb dragging, and skin lesions. Neonatal mice were also used as a model for neurological complications (Couderc et al., 2008; Ziegler et al., 2008).

An adult mouse model has been developed by injection of the ventral side of the footpad of C57BL/6J mice. Viremia lasted 4–5 days accompanied with foot swelling and noted inflammation of the musculoskeletal tissue (Gardner et al., 2010; Morrison et al., 2011). Adult

IFNα/βR knockout mice also developed mild disease with symptoms including muscle weakness and lethargy, symptoms that mirrored human infection. All adult mice died within 3 days. This model was useful in identifying the viral cellular tropism for fibroblasts (Couderc et al., 2008). ICR and CD-1 mice can also be utilized as a disease model. Neonatal mice inoculated subQ with a passaged clinical isolate of CHIKV developed lethargy, loss of balance, and difficulty walking. Mortality was low, 17 and 8% for newborn CD-1 and ICR mice, respectively. The remaining mice fully recovered within 6 weeks after infection (Ziegler et al., 2008). A drawback of both the IFNα/βR and CD-1 mice is that the disease is not a result of immunopathogenesis as occurs in human cases, given that the mice are immunocompromised (Teo et al., 2012).

A chronic infection model was developed using recombinant activating gene 1 (RAG1$^{-/-}$) knockout mice. In this study, mice inoculated via the footpad lost weight in comparison to the control group. Both footpad and subQ injected mice developed viremia 5–6 days postinfection, which was detectable up to 28 days postinfection. Inflammation was evident in the brain, liver, and lung of the subQ inoculated animals at 28–56 days postinfection. Despite minimal footpad swelling on day 2 postinfection, on day 14 there was severe muscle damage noted at necropsy, which resolved by day 28 (Seymour et al., 2015).

Golden hamsters serve as another option for small animal modeling. Although hamsters do not appear to develop overt clinical symptoms following subQ inoculation, viremia developed in the majority of animals within 1 day postinfection with clearance following from day 3 to 4. Histologically, inflammation was noted at the skeletal muscle, fascia, and tendon sheaths of numerous limbs. This study was limited in the number of animals utilized, and more work is needed to further develop the hamster model (Bosco-Lauth et al., 2015).

NHP models of disease include adult, aged, and pregnant rhesus macaques in addition to cynomolgus macaques (Broeckel et al., 2015). Differing routes of infection (subQ, IV, and IM) have been successfully administered, although there is not a clear understanding of the role that route of transmission plays in subsequent pathogenesis and clinical symptoms. Typically, viremia is observed 4–5 days postinfection with a correlation between infectious titer and time to viremia observed in cynomolgus but not rhesus (Labadie et al., 2010; Messaoudi et al., 2013). Fever began at 1–2 days postinfection and persisted for 2–7 days and 3–7 days in cynomolgus and rhesus, respectively and coincided with rash (Chen et al., 2010; Labadie et al., 2010; Messaoudi et al., 2013). Overall blood chemistries changed in conjunction with initiation of viremia, and returned to baseline 10–15 days postexposure (Chen et al., 2010). CNS involvement has been difficult to reproduce in NHP models, although it was reported that high inoculum in cynomolgus did result in meningoencephalitis (Labadie et al., 2010). The NHP models have been utilized to conduct efficacy testing on novel vaccines and therapeutics (Broeckel et al., 2015).

4 FLAVIVIRIDAE

4.1 Dengue Virus

Dengue virus (DENV) is transmitted via the mosquito vectors *A. aegypti* and *A. albopictus* (Moore and Mitchell, 1997). Given the endemicity of the vectors, it is estimated that half of the world's population is at risk for exposure to DENV. This results in approximately 50 million cases of dengue each year, with the burden of disease in the tropical and subtropical regions of Latin America, South Asia, and Southeast Asia (Gubler, 2002). It is estimated that there are 20,000 deaths each year due to dengue hemorrhagic fever (DHF) (Guzman and Kouri, 2002).

There are four distinct serotypes of DENV, numbered 1–4, which are capable of causing a wide clinical spectrum that ranges from asymptomatic to severe with the development of DHF (World Health Organization, 1997). Incubation can range from 3 to 14 days, with the average being 4–7 days. The virus targets dendritic cells and macrophages following a mosquito bite (Balsitis et al., 2009). Typical infection results in classic dengue fever (DF), which is self-limiting and has flu-like symptoms in conjunction with retroorbital pain, headache, skin rash, and bone and muscle pain. DHF can follow, with vascular leak syndrome and low platelet count, resulting in hemorrhage. In the most extreme cases, dengue shock syndrome (DSS) develops, characterized by hypotension, shock, and circulatory failure (World Health Organization, 1997). Thrombocytopenia is a hallmark clinical sign of infection, and aids in differential diagnosis (Gregory et al., 2010).

Severe disease has a higher propensity to occur upon secondary infection with a different DENV serotype (Thein et al., 1997). This is hypothesized to occur due to antibody dependent enhancement (ADE). There is no approved vaccine or drug, and hospitalized patients receive supportive care including fluid replacement. In order to further progress toward an effective drug or vaccine, small human cohort studies have taken place. However, to provide statistically relevant results, testing must progress in an animal model. In developing an animal model, it is important to note that mosquitoes typically deposit 10^4–10^6 pfu, and is considered the optimal range during experimental challenge (Chan et al., 2015).

DENV does not naturally replicate effectively in rodent cells, creating the need for mouse-adapted strains, engineered mouse lines, and a variety of inoculation routes to overcome the initial barrier. Several laboratory mouse strains including A/J, BALB/c, and C57BL/6 are permissive to dengue infection. However, the resulting disease has little resemblance to human clinical signs, and death results from paralysis (Huang et al., 2000; Paes et al., 2005; Shresta et al., 2004). A higher dose of an adapted DENV strain induced DHF symptoms in both BALB/c and C57BL/6 (Chen et al., 2007; Souza et al., 2009). This model can also yield asymptomatic infections. A mouse-adapted strain of DENV 2 introduced into AG129 mice developed vascular leak syndrome similar to the severe disease seen in humans (Shresta et al., 2006). Passive transfer of monoclonal dengue antibodies within mice leads to ADE. During the course of infection, viremia was increased and animals died due to vascular leak syndrome (Balsitis et al., 2010). Another mouse-adapted strain injected into BALB/c caused liver damage, hemorrhagic manifestations, and vascular permeability (Souza et al., 2009). IC injection of suckling mice with DENV leads to death by paralysis and encephalitis, which is rare in human infection (Lee et al., 2015; Parida et al., 2002; Zhao et al., 2014a).

Immunocompromised mice have also been used to gain an understanding of the pathogenesis of DENV. The most well-defined model is AG129 which is deficient in IFNα/β and γ receptors and can recapitulate DHF/DSS if a mouse-adapted strain is utilized (Watanabe et al., 2012; Yauch et al., 2009). SCID mice engrafted with human tumor cells develop paralysis upon infection, and thus are not useful for pathogenesis studies (Blaney et al., 2002; Lin et al., 1998). DF symptoms developed after infection in NOD/SCID/IL2RγKO mice engrafted with CD34$^+$ human progenitor cells (Mota and Rico-Hesse, 2011). RAG-hu mice developed fever, but no other symptoms upon infection with a passaged clinical isolate and lab-adapted strain of DENV 2 (Kuruvilla et al., 2007).

A passaged clinical isolate of DENV 3 was used to create a model in immunocompetent adult mice. IP injection in C57BL/6j and BALB/c caused lethality by day 6–7 postinfection in a dose dependent manner. The first indication of infection was weight loss beginning on day 4 followed by thrombocytopenia. A drop in systolic blood pressure along with noted increases in the liver enzymes, AST and ALT, were also observed. Viremia was established by day 5. This model mimicked the characteristic symptoms observed in human DHF/DSS cases (Costa et al., 2012). Vascular leakage was also observed when C57BL/6 were inoculated with DENV 2 (St John et al., 2013).

A murine model was developed that utilized infected mosquitoes as the route of transmission to hu-NSG mice. Female mosquitoes were intrathoracically inoculated with a clinical isolate of DENV 2. Infected mosquitoes then fed upon the mouse footpad to allow for transmission of the virus via the natural route. The amount of virus detected within the mouse was directly proportional to the number of mosquitoes it was exposed to, with 4–5 being optimal. Detectable viral RNA was in line with historical human infection data. Severe thrombocytopenia developed on day 14. This model is notable in that disease was enhanced with mosquito delivery of the virus in comparison to injection of the virus (Cox et al., 2012).

NHP models have used a subQ inoculation in an attempt to induce disease. Although the animals are permissive to viral replication, it is to a lower degree than that observed in human infection (Marchette et al., 1973). The immunosuppressive drug, cyclophosphamide enhances infection in rhesus macaques by allowing the virus to invade monocytes (Marchette et al., 1980). Throughout these preliminary studies, no clinical disease was detected. In order to circumvent this, a higher dose of DENV was used in an IV challenge of rhesus macaques. Hemorrhagic manifestations appeared by day 3 and resulted in petechiae, hematomas, and coagulopathy; however, no other symptoms developed (Onlamoon et al., 2010). A robust antibody response was observed in multiple studies (Marchette et al., 1973; Onlamoon et al., 2010). Marmosets also mirror human dengue infection, developing fever, leukopenia, and thrombocytopenia following subQ inoculation (Omatsu et al., 2011, 2012).

NHPs are able to produce antibodies similar to those observed during the course of human infection, making them advantageous in studying ADE. Sequential infection led to a cross-reactive antibody response which has been demonstrated in both humans and mice (Midgley et al., 2011). This phenotype can also be seen upon passive transfer of a monoclonal antibody to dengue and subsequent infection with the virus. Rhesus macaques exposed in this manner developed viremia that was 3- to 100-fold higher than previously reported, however, no clinical signs were apparent (Goncalvez et al., 2007). The lack of inducible DHF or DSS symptoms hinders further examination of pathogenesis within this model.

4.2 West Nile Virus

West Nile virus (WNV) was first isolated from the blood of a woman in the West Nile district of Uganda in 1937 (Smithburn et al., 1940). After the initial isolation of WNV, the virus was subsequently isolated from patients, birds, and mosquitoes in Egypt in the early 1950s (Melnick et al., 1951; Taylor et al., 1953) and was shown to cause encephalitis in humans and horses. WNV is recognized as the most widespread of the flaviviruses, with a geographical distribution that includes Africa, the Middle East, western Asia, Europe, and Australia

(Hayes, 1989). The virus first reached the Western Hemisphere in the summer of 1999, during an outbreak involving humans, horses, and birds in the New York City metropolitan area (Centers for Disease Control and Prevention, 1999; Lanciotti et al., 1999). Since 1999, the range of areas affected by WNV quickly extended. Older people and children are most susceptible to WNV disease. WNV generally causes asymptomatic disease or a mild undifferentiated fever (West Nile fever), which can last from 3 to 6 days (Monath and Tsai, 2002). The mortality rate following neuroinvasive disease ranges from 4% to 11% (Asnis et al., 2000; Hayes, 1989; Hubalek and Halouzka, 1999; Komar, 2000). The most severe complications are commonly seen in the elderly, with reported case fatality rates from 4% to 11%. Hepatitis, myocarditis, and pancreatitis are unusual, severe, nonneurologic manifestations of WNV infection.

Inoculation of WNV into NHPs intracerebrally resulted in the development of either encephalitis, febrile disease, or an asymptomatic infection, depending on the virus strain and dose. Viral persistence is observed in these animals regardless of the outcome of infection (i.e., asymptomatic, fever, encephalitis) (Pogodina et al., 1983). Thus, viral persistence is regarded as a typical result of NHP infection with various WNV strains. After both intracerebral and subQ inoculation, the virus localizes predominantly in the brain and may also be found in the kidneys, spleen, and lymph nodes. WNV does not result in clinical disease in NHPs although the animals show a low level of viremia (Lieberman et al., 2009; Pletnev et al., 2003). This is mirrored in New Zealand White rabbits in that they only develop fever and low levels of viremia following inoculation via footpad (Suen et al., 2015). ID inoculation of both marmosets and rhesus macaques did not yield any clinical signs of disease including fever. Viremia was detected in both NHP species, but marmosets developed a higher titer for a greater duration than rhesus (Verstrepen et al., 2014).

WNV has also been extensively studied in small animals. All classical laboratory mouse strains are susceptible to lethal infections by the intracerebral and IP routes, resulting in encephalitis and 100% mortality. ID route pathogenesis studies indicated that Langerhans dendritic cells are the initial viral replication sites in the skin (Brown et al., 2007; Johnston et al., 1996). The infected Langerhans cells then migrate to lymph nodes and the virus enters the blood through lymphatic and thoracic ducts and disseminates to peripheral tissues for secondary viral replication. Virus eventually travels to the CNS and causes pathology that is similar to human cases (Byrne et al., 2001; Cunha et al., 2000; Diamond et al., 2003; Fratkin et al., 2004). The Swiss mouse strain was inoculated IP in order to screen a variety of viral lineages to assess differences in pathogenesis (Bingham et al., 2014).

Tesh et al. developed a model for WN encephalitis using the golden hamster, *Mesocricetus auratus*. Hamsters appeared asymptomatic during the first 5 days, became lethargic at approximately day 6, and developed neurologic symptoms between days 7 and 10 (Tesh et al., 2005). Many of the severely affected animals died 7–14 days after infection. Viremia was detected in the hamsters within 24 h after infection and persisted for 5–6 days. Although there were no substantial changes in internal organs, progressive pathologic differences were seen in the brain and spinal cord of infected animals. Furthermore, similar to the previously mentioned monkey experiments by Pogodina et al. (1983), persistent WNV infection was found in the brains of hamsters.

4.3 Zika Virus

Zika virus recently came to the forefront of public health concerns with the outbreak in Brazil at the end of 2015. The clinical disease spectrum is highly variable with reports of a flu-like illness accompanied by rash, Guillan–Barre syndrome, and microcephaly in newborns (Ramos da Silva and Gao, 2016). To date, a correlation between gestational age at which exposure to the virus occurs and severity of microcephaly is not fully understood (Brasil et al., 2016). However, a recent study of pregnant women in Columbia found that infection with Zika virus during the third trimester was not associated with any obvious structural abnormalities of the fetus (Pacheco et al., 2016). Transmission of the virus occurs via the bite from an infected *A. aegypti* or *A. albopictus* (Ramos da Silva and Gao, 2016). Other reported routes of exposure include sexual transmission and blood transfusion (Cunha et al., 2016; D'Ortenzio et al., 2016; Hills et al., 2016; McCarthy, 2016). The emergence of this virus with no approved vaccine or therapy, and few diagnostic options demonstrates the utility of well-characterized animal model development.

It was first demonstrated in 1956 that experimentally infected mosquitoes could be used to transmit the virus to mice and NHPs (Boorman and Porterfield, 1956). A129 mice were susceptible to nonadapted Zika virus infection following subQ inoculation of the limbs. Mice began to lose weight 3 days postinfection and met euthanasia criteria by day 6. Microscopic lesions within the brain were noted upon necropsy. In conjunction, viral RNA was detected in the blood, brain, ovary, spleen, and liver of the infected mice. Wild-type 129Sv/Ev mice were also challenged with no observable clinical disease. However, viral RNA was detected at day 3 postinfection in the blood, ovary and spleen, and then remained at detectable levels in the ovaries and spleen on day 7 (Dowall et al., 2016). Footpad inoculation of the virus leads to a fatal disease in AG129 mice by day 7 postinoculation with significant histopathological changes in

the brain noted at necropsy (Aliota et al., 2016). AG129 mice were also observed to develop neurologic disease by day 6 postexposure (Rossi et al., 2016). Immunocompetent mice are resistant to infection via the subQ route (Rossi et al., 2016).

Recently, a mouse model was identified to verify vertical transmission of the virus. Pregnant C57 mice were injected either IP or in utero into the lateral ventricle of the fetal brain. IP inoculation induced transient viremia in the pregnant mice on day 1. Viral RNA was detected in five out of nine placentas on day 3 postinfection. The virus was able to infect the radial glia cells in the fetal brain and leads to a reduction in the cortical neural progenitors (Wu et al., 2016). Viral exposure via cerebroventricular space/lateral ventricle of the fetal brain exhibited small brain size at day 5 postexposure in addition to cortical thinning (Cugola et al., 2016; Li et al., 2016a). Ifnar1$^{-/-}$ pregnant mice exposed to the virus had nonviable fetuses. In the same study, wild-type mice were given an anti-ifnar antibody prior to and during infection resulting in detectable virus in the fetal head with mild intrauterine growth restriction (Miner et al., 2016). All of these murine studies will further study of the pathogenesis of vertical transmission and the resulting neurological disorders in conjunction with screening novel countermeasures. NHP studies are currently ongoing for animal model development.

5 CORONAVIRIDAE

Numerous viruses from the Coronavirus (CoV) family exist that infect a wide range of animals. Six species have been identified that can infect humans. Two of these are alpha coronavirues: HCoV-229E and HCoV-NL63. Four are beta coronavirueses: HCoV-OC43, HCoV-HKU1, HCoV-SARS, and MERS-CoV. HCoV-229E and HCoV-OC43 were first detected in the 1960s from the nasal passages of humans with the "common cold" (Gaunt et al., 2010). HCoV-NL63, which was first isolated in 2004, causes upper and lower respiratory infections of varying intensity and has been continuously circulating among humans (van der Hoek et al., 2006). HCoV-HKU1, first isolated in 2002, has been identified more sporadically but also causes respiratory infections (Lau et al., 2006). A significant portion of common cold infections in humans are caused by coronaviruses. In 2002 and 2012, two human coronaviruses, SARS-CoV and MERS-CoV, emerged that caused a great deal of alarm since these infections have resulted in nearly 10 and 40% fatality, respectively (Assiri et al., 2013; Peiris et al., 2004).

5.1 SARS-Coronavirus

The etiologic agent of severe acute respiratory syndrome (SARS), SARS-CoV, emerged in 2002 as it spread throughout 32 countries in a period of 6 months, with 8437 confirmed infections and 813 deaths (Roberts and Subbarao, 2006; World Health Organization, 2003). No additional cases of community acquired SARS-CoV infection have been reported since 2004. The natural reservoir of SARS-CoV is the horseshoe bat and the palm civet is an intermediate host (Lau et al., 2005). The main mechanism of transmission of SARS-CoV is through droplet spread, but it is also viable in dry form on surfaces for up to 6 days and can be detected in stool, suggesting other modes of transmission are also possible (Pearson et al., 2003; Rabenau et al., 2005; Rota et al., 2003).

SARS-CoV infection has a 10% case fatality with the majority of cases in people over the age of 15 (Peiris et al., 2003; Wang et al., 2004). After an incubation period of 2–10 days, clinical signs of SARS include general malaise, fever, chills, diarrhea, dyspnea, and cough (Drosten et al., 2003). In some SARS cases, pneumonia may develop and progress to acute respiratory distress syndrome (ARDS). Fever usually dissipates within 2 weeks and coincides with the induction of high levels of neutralizing antibodies (Tan et al., 2004).

In humans, SARS-CoV replication destroys respiratory epithelium, and a great deal of the pathogenesis is due to the subsequent immune responses (Chen and Subbarao, 2007; Perlman and Dandekar, 2005). Infiltrates persisting within the lung and diffuse alveolar damage (DAD) are common sequelae of SARS-CoV infection (Perlman and Dandekar, 2005). Virus can be isolated from secretions of the upper airways during early, but not later stages of infection as well as from other tissues (Cheng et al., 2004).

SARS-CoV can replicate in many species, including: dogs, cats, pigs, mice, rats, ferrets, foxes, and monkeys (Roper and Rehm, 2009). No model captures all aspects of human clinical disease (pyrexia and respiratory signs), mortality (~10%), viral replication, and pathology (Roberts et al., 2008). In general, the SARS-CoV disease course in the model species is much milder and of shorter duration than in humans. Viral replication in the various animal models may occur without clinical illness and/or histopathologic changes. The best-characterized models utilize mice, hamsters, ferrets, and NHPs.

Mouse models of SARS-CoV typically are inoculated by the IN route under light anesthesia (Roberts et al., 2005). Young, 6- to 8-week-old BALB/c mice exposed to SARS-CoV have viral replication detected in the lungs and nasal turbinate, with a peak on day 2 and clearance by day 5 postexposure (McAuliffe et al., 2004). There is also viral replication within the small intestines of young BALB/c mice. However, young mice have no clinical signs, aside from reduced weight gain, and have little to no inflammation within the lungs (pneumonitis) (Gillim-Ross et al., 2004). IN SARS-CoV infection of C57BL/6 (B6), also yields reduced weight gain and viral

TABLE 33.1   Coronaviridae Animal Models

Virus species	Route of exposure	Characteristics of human disease	Animal model	Route of exposure	Clinical outcome	References
SARS-CoV	Droplet	Fever, lung damage, 10% mortality	Young mouse	IN	Little to no clinical signs or lung disease	McAuliffe et al. (2004), Roberts et al. (2005)
			Old mouse	IN	Clinical signs and lung damage, mortality	Bisht et al. (2004)
			Hamster	IN	Reduced activity, lung damage, mortality	Roberts et al. (2008)
			Ferret	IT	Fever, lung damage, mortality	Skowronski et al. (2005)
			NHP	IN or IT	Little to no clinical signs, variable mild lung damage	Fouchier et al. (2003), Haagmans et al. (2004), McAuliffe et al. (2004), Rowe et al. (2004)
MERS-CoV	Droplet	Fever, lung damage, neurological symptoms, over 35% mortality (in confirmed cases)	Mice expressing hDPP4	IN	Sublethal or lethal, lung and brain involvement	Agrawal et al. (2015), Li et al. (2016b), Tao et al. (2016)
			New Zealand White Rabbits	IN and IT	Virus isolated but no clinical disease	Haagmans et al. (2015)
			Rhesus macaque	IT or combined IT, IN, oral and ocular	No lethality, mild respiratory disease, transient lung infection with pneumonia	de Wit et al. (2013), Munster et al. (2013), Yao et al. (2014)
			Common marmoset	Combined IT, IN, oral and ocular	High lethality, moderate to severe lung disease, systemic infection	Falzarano et al. (2014)

hDPP4, Human dipeptidy peptidase four; IN, intranasal; IT, intratracheal; SARS-CoV, severe acute respiratory syndrome-coronavirus.

replication in the lungs, with a peak on day 3 and clearance by day 9 (Glass et al., 2004).

In contrast, BALB/c mice 13–14 months of age show weight loss, hunched posture, dehydration, and ruffled fur on day 3–6 postexposure (Bisht et al., 2004). Interstitial pneumonitis, alveolar damage, and death also occur in old mice, resembling the age-dependent virulence observed in humans. 129S mice and B6 mice show outcomes to SARS-CoV infection similar to those observed for BALB/c mice but have lower titers and less prolonged disease. While the aged mouse model is more frequently used then young mice, it is more difficult to obtain large numbers of mice older than 1 year (Table 33.1).

A number of immunocompromised knockout mouse models of IN SARS-CoV infection have also been developed. 129SvEV mice infected with SARS-CoV by the IN route develop bronchiolitis, with peribronchiolar inflammatory infiltrates and interstitial inflammation in adjacent alveolar septae (Hogan et al., 2004). Viral replication and disease in these mice resolves by day 14 postexposure. Beige, CD1$^{-/-}$, and RAG1$^{-/-}$ mice infected with SARS-CoV have similar outcomes to infected BALB/c

mice with regard to viral replication, timing of viral clearance, and a lack of clinical signs (Glass et al., 2004). STAT1 KO mice infected IN with SARS-CoV have severe disease, with weight loss, pneumonitis, interstitial pneumonia, and some deaths (Hogan et al., 2004). The STAT1 KO mouse model is therefore useful for studies of pathogenicity, pathology, and evaluation of vaccines.

Angiotensin converting enzyme 2 (ACE2) and CD209L were identified as cellular receptors for SARS-CoV, with affinity for the spike (S) protein of the virus (Jeffers et al., 2004). The variations in the ACE2 sequence across animal species could partially explain the differences in infection severity (Li et al., 2016b; Sutton and Subbarao, 2015). Since mice in particular have a greater number of sequence differences in ACE2, transgenic mice were created that express human ACE2 (McCray et al., 2007; Netland et al., 2008; Yang et al., 2007). Unlike other murine models of SARS-CoV, mice expressing hACE2 had up to 100% mortality, with severity correlating to the level of hACE2 expression (Tseng et al., 2007). With high levels of hACE2 expression, mice developed a severe lung and brain infection. However, CNS

infection is only rarely observed in humans infected with SARS-CoV.

Syrian golden hamsters (strain LVG) are also susceptible to IN exposure of SARS-CoV. After the administration of 10^3 TCID$_{50,}$ along with a period of transient viremia, SARS-CoV replicates in nasal turbinates and lungs, resulting in pneumonitis (Roberts et al., 2005). There are no obvious signs of disease, but exercise wheels can be used to monitor decrease in nighttime activity. Limited mortality has been observed, but it was not dose dependent and could have more to do with genetic differences between animals because the strain is not inbred (Roberts et al., 2008). Damage is not observed in the liver or spleen despite detection of virus within these tissues.

Several studies have shown that intratracheal (IT) inoculation of SARS-CoV in anesthetized ferrets (*Mustela furo*) results in lethargy, fever, sneezing, and nasal discharge (Skowronski et al., 2005). Clinical disease has been observed in several studies excluding one, perhaps due to characteristics of the inoculating virus (Kobinger et al., 2007). SARS-CoV is detected in pharyngeal swabs, trachea, tracheobronchial lymph nodes, and high titers within the lungs. Mortality has been observed around day 4 postexposure as well as mild alveolar damage in 5%–10% of the lungs, occasionally accompanied by severe pathology within the lungs (Martina et al., 2003; ter Meulen et al., 2004). With fever, overt respiratory signs, lung damage, and some mortality, the ferret intratracheal model of SARS-CoV infection is perhaps most similar to human SARS, albeit with a shorter time course.

SARS-CoV infection of NHPs by intransal or IT routes generally results in a very mild infection that resolves quickly. SARS-CoV infection of old world monkeys, such as rhesus macaques, cynomolgus macaques (cynos), and African green monkeys (AGMs) have been studied with variable results, possibly due to the outbred nature of the groups studied or previous exposure to related pathogens. Clinical illness and viral loads have not been consistent; however, replication within the lungs and DAD are features of the infections for each of the primate species. Some cynos have no illness but others have rash, lethargy, and respiratory signs and pathology (Haagmans et al., 2004; Martina et al., 2003; McAuliffe et al., 2004; Rowe et al., 2004). Rhesus have little to no disease and only have mild findings upon histopathological analysis (Rowe et al., 2004). AGMs infected with SARS-CoV have no overt clinical signs but DAD and pneumonitis has been documented (McAuliffe et al., 2004). Viral replication has been detected for up to 10 days in the lungs of AGMS; however, the infection resolves, and does not progress to fatal ARDS.

Farmed Chinese masked palm civets, sold in open markets in China, were involved in the SARS-CoV outbreak. IT and IN inoculation of civets with SARS-CoV results in lethargy, decreased aggressiveness, fever, diarrhea, and conjunctivitis (Wu et al., 2005). Leucopenia, pneumonitis, and alveolar septal enlargement, with lesions similar to those observed in ferrets and NHPs, have also been observed in laboratory-infected civets. Squirrel monkeys, mustached tamarinds, and common marmosets have not been susceptible to SARS-CoV infection (Greenough et al., 2005; Roberts et al., 2008).

Vaccines have been developed for related animal CoVs in chickens, cattle, dogs, cats, and swine, and have included live-attenuated, killed, DNA and viral-vectored vaccine strategies (Cavanagh, 2003). An important issue to highlight from work on these vaccines is that CoV vaccines, such as those developed for cats, may induce a more severe disease (Perlman and Dandekar, 2005; Weiss and Scott, 1981). As such, immune mice had Th2-type immunopathology upon SARS-CoV challenge (Tseng et al., 2012). Severe hepatitis in vaccinated ferrets with antibody enhancement in liver has been reported (Weingartl et al., 2004). Additionally, rechallenge of AGMs showed limited viral replication but significant lung inflammation, including alveolitis and interstitial pneumonia, which persisted for long periods of time after viral clearance (Clay et al., 2012).

Mouse and NHP models with increased virulence may be developed by adapting the virus by repeated passage within the species of interest. Mouse-adapted SARS with uniform lethality was developed from 15 serial passages in the lungs of young BALB/c mice (McCray et al., 2007; Roberts et al., 2007; Rockx et al., 2007).

5.2 MERS-Coronavirus

Middle East respiratory syndrome (MERS-CoV) emerged in Saudi Arabia and is associated with fever, severe lower respiratory tract infection, and oftentimes renal failure (Al-Tawfiq et al., 2016; Omrani et al., 2015). MERS patients can also occasionally manifest with neurological symptoms. MERS-CoV infection has a high fatality rate. Infections in humans can also be asymptomatic. As of October 2015, there were 1589 confirmed cases and 567 deaths (Li et al., 2016b). Bats serve as the likely natural reservoir since virus with 100% nucleotide identity to the index case was isolated from Egyptian tomb bats (Memish et al., 2013). Spread to humans likely comes from infected dromedary camels (Adney et al., 2014; Azhar et al., 2014).

The host range for MERS-CoV is dependent on the binding of the viral S protein to the host receptor, which is human dipeptidyl peptidase four (hDPP4), also known as CD26 (Raj et al., 2013). The expression and distribution of DPP4 in the human respiratory tract has recently been well characterized (Meyerholz et al., 2016). Interestingly, DPP4 expression is preferentially localized to alveolar regions, perhaps explaining why MERS predominantly manifests as an infection of the lower respiratory tract.

Humans with preexisting pulmonary disease have increased DPP4 expression in alveolar epithelia.

Small animals typically used for viral disease research, such as mice, hamsters, guinea pigs, and ferrets are naturally nonpermissive to MERS-CoV infection due to a low binding efficiency of the viral S protein to the host DPP4 (Sutton and Subbarao, 2015). In contrast the rhesus macaque and common marmoset have complete homology to human DPP4, allowing productive MERS-CoV infection to occur (de Wit et al., 2013; Falzarano et al., 2014; Munster et al., 2013; Yao et al., 2014). New Zealand White Rabbits can be infected with MERS-CoV, and virus was isolated from the upper respiratory tract, but there were no clinical symptoms or significant histopathological changes (Haagmans et al., 2015).

Due to the lack of strong binding affinity of the MERS-CoV S protein to the murine DPP4 receptor, wild-type mice are not susceptible to MERS-CoV infection. As such, several approaches have been used to create susceptible murine animal models of MERS-CoV infection by inducing the expression of hDPP4. One approach utilized an adenovirus vector expressing hDPP4 to transduce mice (Zhao et al., 2014b). These mice developed pneumonia but survived MERS-CoV infection. IN MERS-CoV infection of mice with global expression of hDPP4 resulted in ID_{50} and LD_{50} values of <1 and 10 $TCID_{50}$, respectively (Tao et al., 2016). Thus, MERS-CoV infection of these transgenic mice can be either sublethal or uniformly lethal depending on the dose. Inflammatory infiltrates were found in the lungs and brain stems of mice with some focal infiltrates in the liver as well. Another strategy uses transgenic mice expressing hDPP4 under either a surfactant protein C or cytokeratin 10 promoter (Li et al., 2016b). IN MERS-CoV infection in these mice resulted in a uniformly lethal disease characterized by alveolar edema and microvascular thrombosis and mononuclear clear cell infiltration in the lungs. The brain stem was also impacted by the infection. DPP4 expression with an ubiquitously expressing promoter from cytomegalovirus also had a uniformly lethal infection with predominant lung and brain involvement, but numerous other tissues were also impacted and contained virus (Agrawal et al., 2015).

Common marmosets infected with 5.2×10^6 $TCID_{50}$ (EMC-2012) MERS-CoV by the combined IN, oral, ocular, and IT routes capitulate the severe disease in human infections (Falzarano et al., 2014). The animals manifested moderate to severe clinical disease, with interstitial infiltration of both lower lung lobes. Two of nine animals became moribund between days 4 and 6. Viral RNA was detected in nasal and throat swabs, various organs, and in the blood of some animals, indicating a systemic infection. Histologically, animals showed evidence of acute bronchial interstitial pneumonia as well as other pathological defects.

Infection of rhesus macaques with MERS-CoV results in a mild clinical disease characterized by a transient lung infection with pneumonia. Rhesus macaques were inoculated with at least 10^7 $TCID_{50}$ (EMC-2012) MERS-CoV either by the IT route or a combined IN, IT, oral, and ocular inoculation (de Wit et al., 2013). The result was a mild respiratory illness including nasal swelling and a short fever with all animals surviving. Viral RNA was recovered from nasal swab samples and replicating virus was found in lung tissue (Munster et al., 2013). Mild pathological lesions were found only in the lungs. Radiographic imaging of the lungs revealed interstitial infiltrates, which are signs of pneumonia (Yao et al., 2014).

Interestingly, MER-CoV infection is more severe in marmosets compared to rhesus macaques (Falzarano et al., 2014). This is despite the finding that both species have complete homology with humans within the DPP4 domain that interacts with the viral S protein. Other host factors influencing disease severity have not yet been identified. Transgenic mouse models expressing hDPP4 are ideal for initial development and screening of MERS-CoV countermeasures, and marmosets can be used for final selection and characterization.

6 FILOVIRIDAE

6.1 Filoviruses

Filoviridae consists of three genera, *Ebolavirus* and *Marburgvirus*, and a newly discovered group, *Cuevavirus* (Kuhn, 2008). It is thought that various species of bats are the natural host reservoir for these viruses that have lethality rates from 40% to 82% in humans. There is evidence that the Egyptian rousette bat (*Rousettus aegyptiacus*) is the natural reservoir for marburgviruses but may not be for ebolaviruses (Jones et al., 2015). Marburg virus (MARV) first emerged in 1967 in Germany when laboratory workers contracted the virus from AGMs (*Chlorocebus aerthiops*) that were shipped from Uganda. Ebolaviruses Sudan and Zaire (SUDV and EBOV) caused nearly simultaneous outbreaks in 1976 in what is now the Democratic Republic of Congo (DRC). The most recent outbreak of EBOV in West Africa was by far the largest with over 28,000 suspected, probable and confirmed cases and over 11,000 deaths. Bundibugyo virus (BDBV) first emerged in 2007 in Bundibugyo, Uganda with 56 confirmed cases (MacNeil et al., 2010). Two other ebolaviruses are known: Taï Forest (TAFV) (previously named Cote d'Ivoire) (CIEBOV) and Reston (RESTV), which have not caused major outbreaks or lethal disease in humans. Filovirus disease in humans is a characterized by aberrant innate immunity and a number of clinical symptoms: fever, nausea, vomiting,

TABLE 33.2 Filoviruses Causing Human Diseases

Genus	Species	Virus	Disease in humans
Marburgvirus	*Marburg marburgvirus*	Marburg virus (MARV)	Yes
		Ravn virus (RAVV)	Yes
Ebolavirus	*Zaire ebolavirus*	Ebola virus (EBOV)	Yes
	Sudan ebolavirus	Sudan virus (SUDV)	Yes
	Taï Forest ebolavirus	Taï Forest virus (TAFV)	Yes
	Reston ebolavirus	Reston virus (RESTV)	No
	Bundibugyo ebolavirus	Bundibugyo virus (BDBV)	Yes

arthralgia/myalgia, headaches, sore throat, diarrhea, abdominal pain, and anorexia as well as numerous others (Mehedi et al., 2011; Wauquier et al., 2010). Approximately 10% of patients develop petechia and a greater percentage, depending on the specific strain, may develop bleeding from various sites (gums, puncture sites, stools, etc.) (Table 33.2). Natural transmission in an epidemic is through direct contact or needle sticks in hospital settings. However, much of the research interest in filoviruses primarily stems from biodefense needs, particularly from aerosol biothreats. As such, IM, IP, and aerosol models have been developed in mice, hamsters, guinea pigs, and NHPs for the study of pathogenesis, correlates of immunity, and for testing countermeasures (Bradfute and Bavari, 2011; Bradfute et al., 2011). Since filoviruses have such high lethality rates in humans, scientists have looked for models that are uniformly lethal to stringently test efficacy of candidate vaccines and therapeutics. One issue to take note of in animal model development of filovirus infection is the impact of particle to plaque-forming unit (PFU) ratios on lethality, wherein it is possible that increasing the dose could actually decrease infectivity due to an immunogenic effect produced by inactive virions in the stock. Additionally, the plaque assay used to measure live virions in a stock may greatly underestimate the true quantity of infectious virions in a preparation (Alfson et al., 2015; Smither et al., 2013a).

Immunocompetent mice have not been successfully infected with wild-type filoviruses due to the control of the infection by the murine type 1 interferon response (Bray, 2001). However, wild-type inbred mice are susceptible to filovirus that has been mouse adapted (MA) by serial passage in mice (Bray et al., 1999). MARV Angola was particularly resistant to adaptation, but after 24 serial passages in SCID mice, infection caused severe disease in BALB/c and C57BL/6 mice when administered IN or IP (Qiu et al., 2014). These mice had pathology with some similarities to infection in humans including lymphopenia, thrombocytopenia, liver damage, and viremia. BALB/c mice, which are the strain of choice for

IP inoculation of MA-EBOV, are not susceptible by the aerosol route (Bray et al., 1999; Zumbrun et al., 2012a). For aerosol infection of immunocompetent mice, a panel of BXD (BALB/c x DBA) recombinant inbred strains were screened and one strain, BXD34, was particularly susceptible to airborne MA-EBOV, with 100% lethality to low or high doses (approximately 100 or 1000 pfu) (Zumbrun et al., 2012a). These mice developed weight loss of greater than 15% and succumbed to infection between days 7 and 8 postexposure. The aerosol infection model utilizes a whole-body exposure chamber to expose mice aged 6–8 weeks to MA-EBOV aerosols with a mass median aerodynamic diameter (MMAD) of approximately 1.6 μm and a geometric standard deviation (GSD) of approximately 2.0 for 10 min. Another approach uses immunodeficient mouse strains, such as SCID, STAT1 KO, IFN receptor KO, or perforin KO with a wild-type EBOV inoculum by IP or aerosol routes (Bray, 2001; Lever et al., 2012; Zumbrun et al., 2012a). Mice are typically monitored for clinical disease "scores" based on activity and appearance, weight loss, and moribund condition (survival). Coagulopathy, a hallmark of filovirus infection in humans, has been observed, with bleeding in a subset of animals and failure of blood samples to coagulate late in infection (Bray et al., 1999). Liver, kidney, spleen, and lung tissue taken from moribund mice have pathology characteristic of filovirus disease in NHPs (Zumbrun et al., 2012a). While most mouse studies have used MA-EBOV or EBOV, an IP mouse-adapted MARV model is also available (Warfield et al., 2007, 2009). MA-MARV and MA-EBOV models are particularly useful for screening novel antiviral compounds (Panchal et al., 2012).

Recently, a model was created using immunodeficient NSG [nonobese diabetic (NOD)/SCID/IL-2 receptor chain knockout] mice with transplanted human hematopoietic stem cells from umbilical cord blood. These mice were susceptible to lethal WT (nonadapted) EBOV by IP and IN exposure (Ludtke et al., 2015). The transplanted mice had all of the cellular components of a fully functional adaptive human immune system and upon EBOV

infection, had several features typical of EBOV disease. These included viremia, cellular damage, liver steatosis, and signs of hemorrhage. INFa/bR$^{-/-}$ mice infected with WT SUDV or EBOV have a partially lethal disease with weight loss and evidence of disseminated intravascular coagulation (DIC) in the liver (Brannan et al., 2015; Lever et al., 2012). Interestingly, inoculation of INFa/bR$^{-/-}$ mice with TAFV and RESTV does not result in clinical signs. Yet another strategy uses knockout mice lacking possible receptors for filovirus entry, such as Niemann-Pick C1 and C2 (NPC1 and NPC2). Npc2$^{(-/-)}$ mice were fully susceptible to infection with EBOV but Npc1$^{(-/-)}$ mice were completely resistant (Herbert et al., 2015).

Hamsters are frequently used to study cardiovascular disease, coagulation disorders, and thus serve as the basis for numerous viral hemorrhagic fever models (Gowen and Holbrook, 2008; Herbert et al., 2015). An IP MA-EBOV infection model has been developed in Syrian hamsters (Ebihara et al., 2013; Gowen and Holbrook, 2008; Herbert et al., 2015; Tsuda et al., 2011). This model, which has been used to test a vesicular stomatitis virus vectored vaccine approach, utilizes male 5- to 6-week-old Syrian hamsters which are infected with 100 LD$_{50}$ of MA-EBOV. Virus is present in tissues and blood collected on day 4 and all animals succumbed to the disease by day 6. Infected hamsters had severe coagulopathy and uncontrolled host immune responses, similar to what is observed in primates. (Ebihara et al., 2010)

Guinea pig models of filovirus infection have been developed for IP and aerosol routes using guinea pig-adapted EBOV (GP-EBOV) and MARV (GP-MARV) (Choi et al., 2012; Connolly et al., 1999; Twenhafel et al., 2015; Zumbrun et al., 2012c). Guinea pig models of filovirus infection are quite useful in that they develop fever, which can be monitored at frequent intervals by telemetry. Additionally, the animals are large enough for regular blood sampling in which measurable coagulation defects are observed as the infection progresses. A comparison of IP infection of outbred guinea pigs with guinea pig-adapted MARV Angola and MARV Ravn revealed similar pathogenesis (Cross et al., 2015). Infection with either strain resulted in features of the disease that are similar to what is seen in human and NHP infection, such as viremia, fever, coagulopathy, lymphopenia, elevated liver enzymes (ALT and AST), thrombocytopenia, and splenic, gastrointestinal and hepatic lesions. GP-MARV-Ravn had a delayed disease progression relative to GP-MARV-Ang.

Hartley guinea pigs exposed to aerosolized GP-EBOV develop lethal interstitial pneumonia. This is in contrast to subQ infection of guinea pigs, aerosol EBOV challenge of NHPs, and natural human infection (Twenhafel et al., 2015). Both subQ and aerosol exposure of guinea pigs to GP-EBOV resulted in only mild lesions in the liver and spleen. By aerosol exposure, GP-EBOV is uniformly lethal at both high and low doses (100 or 1000 pfu target doses) but lethality drops with low (less than 1000 pfu) presented doses of airborne GP-MARV and more protracted disease is seen in some animals (our unpublished observations) (Zumbrun et al., 2012c). Weight loss of between 15% and 25% is a common finding in guinea pigs exposed to GP-EBOV or GP-MARV. Fever, which becomes apparent by day 5, occurs more rapidly in GP-EBOV exposed guinea pigs than with GP-MARV exposure. Lymphocytes and neutrophils increase during the earlier part of the disease, and platelet levels steadily drop as the disease progresses. Increases in coagulation time can be seen as early as day 6 postexposure. Blood chemistries (i.e., ALT, AST, ALKP, and BUN) indicating problems with liver and kidney function are also altered late in the disease course.

Transmission of EBOV has been documented from swine to NHPs via the respiratory tract (Kobinger et al., 2011). As such, guinea pigs have been used to establish transmission models (Wong et al., 2015a,b). Nonexposed guinea pigs were placed in the cages with infected guinea pigs 1 day postexposure to GP-EBOV. Guinea pigs challenged intanasally were more likely to transmit virus to naive cagemates than those that were exposed by the IP route. NHP models of filovirus infection are the preferred models for more advanced disease characterization and testing of countermeasures because they most closely mimic the disease and immune correlates seen in humans (Dye et al., 2012). Old world primates have been primarily used for development of IP, IM, and aerosol models of filovirus infection (Twenhafel et al., 2013). Uniformly lethal filovirus models have been developed for most of the virus strains in cynomolgus macaques, rhesus macaques, and to a lesser degree, AGMs (Alves et al., 2010; Carrion et al., 2011; Davis et al., 1997; Hensley et al., 2011a; Reed et al., 2007; Zumbrun et al., 2012b).

Low-passage human isolates that have not been passaged in animals have been sought for development of NHP models to satisfy the Food and Drug Administration (FDA) Animal Rule. EBOV-Makona, the strain responsible for the recent large outbreak in West Africa, was compared to the "prototype" 1976 EBOV strain (Marzi et al., 2015). The disease in cynos was similar for both viruses, but disease progression was delayed for EBOV-Makona. This delay as well as the lower fatality rate in the 2014 epidemic compared to the 1976 outbreak suggest that EBOV-Makona is less virulent. The large number of cases in the 2014–15 EBOV outbreak brought to light previously underappreciated eye pathology and ocular viral persistence in survivors. While survivors of NHP filovirus infection are infrequent, necrotizing scleritis, conjunctivitis, and other ocular pathology has been observed in EBOV-infected animals (Alves et al., 2016).

Prominent features of the filovirus infections in NHPs are onset of fever by day 5 postexposure, viremia, lymphopenia, tachycardia, azotemia, alteration in liver function enzymes (ALT, AST, and ALKP), decrease in platelets, and increased coagulation times. Petechial rash is a common sign of filovirus disease and may be more frequently observed in cynomolgus macaques than in other NHP species (Zumbrun et al., 2012b). Immunological parameters have been evaluated and T, B, and natural killer cells are greatly diminished as the infection progresses (Fernando et al., 2015). A cytokine storm occurs with rises in IFNγ, TNF, IL-6, and CCL2 (Fernando et al., 2015). However, there is also evidence from transcriptional profiling of circulating immune cells that the early immune response is skewed toward a Th2 response (Connor et al., 2015). Strikingly, animals surviving challenge may have a delay in the production of inflammatory cytokines and chemokines (Martins et al., 2015).

Clinical disease parameters may have a slightly delayed onset in aerosol models. Dyspnea late in infection is a prominent feature of disease after aerosol exposure (Zumbrun et al., 2012b). Aerosol filovirus infection of NHPs results in early infection of respiratory lymphoid tissues, dendritic cells, alveolar macrophages, blood monocytes, and fibroblastic reticular cells followed by spread to regional lymph nodes then multiple organs (Ewers et al., 2016; Twenhafel et al., 2013). A number of pronounced pathology findings include multifocal hepatic necrosis and fibrin accumulation, particularly within the liver and the spleen. For aerosolized MARV infection of rhesus, the most significant pathology included destruction of the tracheobronchial and mediastinal lymph nodes (Ewers et al., 2016). Lymphocytolysis and lymphoid depletion are also observed (Alves et al., 2010). Multilead, surgically implanted telemetry devices are useful in continuous collection of temperature, blood pressure, heart rate, and activity levels. As such, blood pressure drops as animals become moribund and heart rate variability (standard deviation of the heart rate) is altered late in infection (Zumbrun et al., 2012b). The most recently developed telemetry devices can also aid in plethysmography to measure respiratory minute volume for accurate delivery of presented doses for aerosol exposure. Standardized filovirus-infected NHP euthanasia criteria have also been developed to enhance reproducibility for studies that evaluate therapeutic and vaccine countermeasures (Warren et al., 2014).

Filovirus infection of common marmosets (*Callithrix jacchus*) is also a viable model to study the disease course. Respiratory infection of marmosets with MARV results in a lethal infection with fever, hemorrhaging, transient rash, disseminated viral infection, increases in liver function enzymes, coagulopathy, hepatitis, and histological lesions particularly in the kidney and liver (Smither et al., 2013b). Marmosets are similarly susceptible to infection with EBOV-Kikwit (Smither et al., 2015). Thus, EBOV or MARV infection of marmosets produces features of the disease that are very similar to that of other NHPs and humans.

6.2 Hendra and Nipah Virus

Hendra and Nipah virus are unusual within the Paramyxoviridae family given that they can infect a large range of mammalian hosts. Both viruses are grouped under the genus *Henipavirus*. The natural reservoirs of the viruses are the fruit bats from the genus *Pteropus*. Hendra and Nipah have the ability to cause severe disease in humans with the potential for a high case fatality rate (Rockx et al., 2012). Outbreaks due to Nipah virus have been recognized in Malaysia, Singapore, Bangladesh, and India, while Hendra virus outbreaks have yet to be reported outside of Australia (Luby et al., 2009a,b).

Hendra was the first member of the genus identified and was initially associated with an acute respiratory disease in horses. All human cases have been linked to transmission through close contact with an infected horse. There have been no confirmed cases of direct transmission from bat to human. Nipah has the distinction of transmission among, although the exact route is unknown (Homaira et al., 2010). The virus is susceptible to pH, temperature, and desiccation, and thus close contact is hypothesized as needed for successful transmission (Fogarty et al., 2008). Both viruses have a tropism for the neurological and respiratory tracts.

The incubation period for Hendra virus is 7–17 days and is marked by a flu-like illness. Symptoms at this initial stage include myalgia, headache, lethargy, sore throat, and vomiting (Hanna et al., 2006). Disease progression can continue to pneumonitis or encephalitic manifestations, with the person succumbing to multiorgan failure (Playford et al., 2010). Nipah virus has an incubation period of 4 days to 2 weeks (Goh et al., 2000). Much like Hendra, the first signs of disease are nondescript. Severe neurological symptoms subsequently develop including encephalitis and seizures that can progress to coma within 24–48 h (Lo and Rota, 2008). Survivors of infection typically make a full recovery; however, 22% suffer permanent sequelae, including persistent convulsions (Tan and Chua, 2008). At this time, there is no approved vaccine or antiviral, and treatment is purely supportive. Animal models are being used to not only test novel vaccines and therapeutics, but also deduce the early events of disease because documentation of human cases is at terminal stages.

The best small animal model is the Syrian golden hamster due to their high susceptibility to both henipaviruses. Clinical signs upon infection recapitulate the disease course in humans including acute encephalitis

and respiratory distress. Challenged animals died within 4–17 days postinfection. The progression of disease and timeline is highly dependent on dose and route of infection. IN inoculation leads to imbalance, limb paralysis, lethargy, and breathing difficulties whereas IP resulted in tremors and paralysis within 24 h before death. Virus was detected in lung, brain, spleen, kidney, heart, spinal cords, and urine, with the brain having the highest titer. This model is used for vaccination and passive protection studies (Guillaume et al., 2009; Rockx et al., 2011; Wong et al., 2003).

The guinea pig model has not been widely used due to the lack of a respiratory disease upon challenge (Torres-Velez et al., 2008; Williamson et al., 2001). Inoculation with Hendra virus via the subQ route leads to a generalized vascular disease with 20% mortality. Clinical signs were apparent 7–16 days postinfection with death occurring within 2 days of CNS involvement. Higher inoculum has been associated with development of encephalitis and CNS lesions. ID and IN injection does not lead to disease, although the animals are able to seroconvert upon challenge. The inoculum source does not affect clinical progression. Nipah virus challenge only causes disease upon IP injection and results in weight loss and transient fever for 5–7 days. Virus was shed through urine and was present in the brain, spleen, lymph nodes, ovary, uterus, and urinary bladder (Hooper et al., 1997).

Ferrets infected with Hendra or Nipah virus display the same clinical disease as seen in the hamster model and human cases (Bossart et al., 2009; Pallister et al., 2011). Upon inoculation by the oronasal route, ferrets develop severe pulmonary and neurological disease within 6–9 days including fever, coughing, and dyspnea. Lesions do develop in the ferret's brains, but to a lesser degree than seen in humans.

Cats have also been utilized as an animal model for henipaviruses. Disease symptoms are not dependent upon the route of infection. The incubation period is 4–8 days and leads to respiratory and neurological symptoms (Mungall et al., 2007; Johnston et al., 2015; Westbury et al., 1996). This model has proven useful for vaccine efficacy studies.

Squirrel and AGMs are representative of the NHP models. For squirrel monkeys, Nipah virus is introduced by either the IN or IV route and subsequently leads to clinical signs similar to humans, although IN challenge results in milder disease. Upon challenge, only 50% of animals develop disease manifestations including anorexia, dyspnea, and acute respiratory syndrome. Neurological involvement is characterized by uncoordinated motor skills, loss of consciousness, and coma. Viral RNA can be detected in lung, brain, liver, kidney, spleen, and lymph nodes but is only found upon IV challenge (Marianneau et al., 2010). AGMs are very consistent model of both viruses. IT inoculation of the

viruses results in 100% mortality, and death within 8.5 and 9–12 days postinfection for Hendra and Nipah viruses, respectively. The animals develop severe respiratory and neurological disease with generalized vasculitis (Geisbert et al., 2010; Rockx et al., 2010).

The reservoir of the viruses, gray-headed fruit bats, has been experimentally challenged. Due to their status as the host organism for henipaviruses, the bats do not develop clinical disease. However, Hendra virus can be detected in kidneys, heart, spleen, and fetal tissue, and Nipah virus can be located in urine (Middleton et al., 2007).

Pigs develop a respiratory disease upon infection with both Nipah and Hendra viruses (Berhane et al., 2008; Li et al., 2010; Middleton et al., 2002). Oral inoculation does not produce a clinical disease, but subQ injection represents a successful route of infection. Live virus can be isolated from the oropharynx as early as 4 days postinfection. Nipah virus can also be transmitted between pigs. Nipah virus was able to induce neurological symptoms in 20% of the pigs, even though virus was present in all neurological tissues regardless of symptoms (Weingartl et al., 2005). Within the pig model, it appeared that Nipah virus had a greater tropism for the respiratory tract, while Hendra for the neurological system.

Horses are also able to develop a severe respiratory tract infection accompanied with fever and general weakness upon exposure to Nipah and Hendra viruses. Oronasal inoculation led to systemic disease with viral RNA detected in nasal swabs within 2 days (Marsh et al., 2011; Williamson et al., 1998). Animals died within 4 days postexposure and have interstitial pneumonia with necrosis of alveoli (Murray et al., 1995a,b). Virus could be detected in all major systems.

Mice, rats, rabbits, chickens, and dogs have been tested but are nonpermissive to infection (Westbury et al., 1995; Wong et al., 2003). Suckling BALB/c mice succumb to infection if the virus is inoculated intracranially (Mungall et al., 2006). IN exposure with Nipah does not induce a clinical disease; however, there is evidence of a subclinical infection in the lungs following euthanasia of the mice (Dups et al., 2014). In addition, a human lung xenograph model in NSG mice demonstrated that the human lung is highly susceptible to Nipah viral replication and damage (Valbuena et al., 2014). Embryonated chicken eggs have been inoculated with Nipah virus leading to a universally fatal disease within 4–5 days postinfection (Tanimura et al., 2006).

6.3 Respiratory Syncytial Virus

Annually, respiratory syncytial virus (RSV) is responsible for the lower respiratory tract infections of 33 million children under the age of 5, which in turn results in 3 million hospitalizations and approximately 200,000

deaths (Nair et al., 2010). Within the United States, hospital costs alone amount to over 600 million dollars per year (Paramore et al., 2004). Outbreaks are common in the winter (Yusuf et al., 2007). The virus is transmitted by large respiratory droplets that replicate initially within the nasopharynx and spreads to the lower respiratory tract. Incubation for the virus is 2–8 days. RSV is highly virulent leading to very few asymptomatic infections (Collins and Graham, 2008). Disease manifestations are highly dependent upon the age of the individual.

RSV infections in neonates produce nonspecific symptoms including overall failure to thrive, apnea, and feeding difficulties. Infants present with a mild upper respiratory tract disease that could develop into bronchiolitis and bronchopneumonia. Contracting RSV at this age results in an increased chance of developing childhood asthma (Wu et al., 2008). Young children develop recurrent wheezing while adults have exacerbation of previously existing respiratory conditions (Falsey et al., 2005). Common clinical symptoms are runny nose, sneezing, and coughing accompanied by fever.

Mortality rates from RSV in hospitalized children are 1%–3% with the greatest burden of disease seen in 3–4 month olds (Ruuskanen and Ogra, 1993). Hematopoietic stem cell transplant patients, solid organ transplant patients, and COPD patients are particularly vulnerable to RSV infection and have mortality rates between 7.3% and 13.3% upon infection (Anderson et al., 2016). Although there are almost 60 RSV vaccine candidates which are in preclinical and clinical phases, there is no licensed vaccine available and ribavirin usage is not recommended for routine treatment (American Academy of Pediatrics Subcommittee on Diagnosis and Management of Bronchiolitis, 2006; Higgins et al., 2016; Kim and Chang, 2016). Animal models of RSV were developed in the hopes of formulating an effective and safe vaccine unlike the formalin-inactivated RSV (FI-RSV) vaccine. This vaccine induced severe respiratory illness in infants whom received the vaccine and were subsequently infected with live virus (Kim et al., 1969).

Mice can be used to model RSV infection, although a very high IN inoculation is needed to achieve clinical symptoms (Jafri et al., 2004; Stark et al., 2002). Strain choice is crucial to reproducing a physiological relevant response (Stokes et al., 2011). Age does not affect primary disease manifestations (Graham et al., 1988). However, it does play a role in later sequelae showing increased airway hyperreactivity (Cormier et al., 2010). Primary RSV infection produces increased breathing with airway obstruction (Jafri et al., 2004; van Schaik et al., 1998). Virus was detected as early as day 3 and reached maximum titer at day 6 postinfection. Clinical illness is defined in the mouse by weight loss and ruffled fur as opposed to runny nose, sneezing, and coughing as seen in humans. A humanized mouse model was recently developed by

IN inoculation. The challenged mice experienced weight loss and demonstrated a humoral and cellular immune response to the infection (Sharma et al., 2016).

Cotton rats are useful given that RSV is able to replicate to high titers within the lungs and can be detected in both the upper and lower airways after IN inoculation (Boukhvalova et al., 2009; Niewiesk and Prince, 2002). Viral replication is 50- to 1000-fold greater in the cotton rat model than mouse model (Wyde et al., 1993). The cotton rats develop mild to moderate bronchiolitis or pneumonia (Grieves et al., 2015; Prince et al., 1999). Although age does not appear to factor into clinical outcome, it has been reported that older cotton rats tend to take longer to achieve viral clearance. Viral loads peak by the 5th day, dropping to below the levels of detection by day 8. The histopathology of the lungs appears similar to that of humans after infection (Piazza et al., 1993). This model has limited use in modeling the human immune response to infection as challenge with the virus induces a Th2 response in cotton rats, whereas humans tend to have a response skewed toward Th1 (Culley et al., 2002; Dakhama et al., 2005; Ripple et al., 2010). FI-RSV disease was recapitulated upon challenge with live virus after being vaccinated twice with FI-RSV.

Chinchillas have been challenged experimentally with RSV via IN inoculation. The virus was permissive within the nasopharynx and Eustachian tube. The animals displayed an acute respiratory tract infection. This model is therefore useful in studying mucosal immunity during infection (Gitiban et al., 2005). Ferrets infected by IT were found to have detectable RSV in throat swabs up to day 7 postinfection, and positive qPCR up to day 10. Immunocompromised ferrets were observed to have higher viral loads accompanied with detectable viral replication in the upper respiratory tract (Stittelaar et al., 2016).

Chimpanzees are permissive to replication and clinical symptoms of RSV including rhinorrhea, sneezing, and coughing. Adult squirrel monkeys, newborn rhesus macaques, and infant cebus monkeys were also challenged but did not exhibit any disease symptoms or high levels of viral replication (Belshe et al., 1977). Bonnet monkeys were developed an inflammatory response by day 7 with viral RNA detected in both bronchial and alveolar cells (Simoes et al., 1999). The chimpanzee model has been proven useful for vaccine studies (Hancock et al., 2000; Teng et al., 2000).

Sheep have also been challenged experimentally since they develop respiratory disease when exposed to ovine RSV (Meyerholz et al., 2004). Lambs are also susceptible to human respiratory syncytial infection (Olivier et al., 2009; Sow et al., 2011). When inoculated intratracheally, the lambs developed an upper respiratory tract infection with cough after 6 days. Some lambs went on to develop lower respiratory disease including

bronchiolitis. The pneumonia resolved itself within 14 days. RSV replication peaked at 6 days, and rapidly declined. Studying respiratory disease in sheep is beneficial given the shared structural features with humans (Plopper et al., 1983; Scheerlinck et al., 2008).

7 ORTHOMYXOVIRIDAE

7.1 Influenza Virus

The influenza viruses consist of three types: influenza A, B, and C, based on antigenic differences. Influenza A is further classified by subtypes; 16 HA and 9 NA subtypes are known. Seasonal influenza is the most common infection and usually causes a self-limited febrile illness with upper respiratory symptoms and malaise that resolves within 10 days (Taubenberger and Morens, 2008). The rate of infection is estimated at 10% in the general population and can result in billions of dollars of loss annually from medical costs and reduced work-force productivity. Approximately 40,000 people in the United States die each year from seasonal influenza (Dushoff et al., 2006). Thus, vaccines and therapeutics play a critical role in controlling infection, and development using animal models is ongoing (Braun et al., 2007b).

Influenza virus replicates in the upper and lower airways, peaking at approximately 48-h postexposure. Infection can be more severe in infants and children under the age of 22, people over the age of 65, or immunocompromised individuals where viral pneumonitis or pneumonia can develop or bacterial superinfection resulting in pneumonia or sepsis (Barnard, 2009; Glezen, 1982). Pneumonia from secondary bacterial infection, such as *Streptococcus pneumonia*, *Streptococcus pyogenes*, and *Neisseria meningitides*, and more rarely, *Staphylococcus aureus*, is more common than viral pneumonia from the influenza virus itself, accounting for ~27% of all influenza associated fatalities (Alonso et al., 2003; Ison and Lee, 2010; Speshock et al., 2007). Death, often due to ARDS can occur as early as 2 days after onset of symptoms. Lung histopathology in severe cases may include DAD, alveolar edema and damage, hemorrhage, fibrosis, and inflammation (Taubenberger and Morens, 2008).

The H5N1 avian strain of influenza, has lethality rates of around ~50% (of known cases), likely because the virus preferentially binds to the cells of the lower respiratory tract, and thus the potential for global spread is a major concern (Matrosovich et al., 2004; Wang et al., 2016). H7N9 is another avian influenza A strain that infected more than 130 people and was implicated in 37 deaths. Approximately 75% of infected people had a known exposure to birds. There is no evidence of sustained spread between humans but these viruses are of great concern for their pandemic potential (Zhang et al., 2013).

The most frequently used animal models of influenza infection include mice, ferrets, and NHPs. A very thorough guide to working with mouse, guinea pig, ferret, and cynomolgus models was published by Kroeze et al. (2012). Swine are not frequently utilized but are also a potentially useful model for influenza research since they share many similarities to human anatomy, genetics, susceptibility, and pathogenesis (Rajao and Vincent, 2015). Lethality rates can vary with virus strain used (with or without adaptation), dose, route of inoculation, age, and genetic background of the animal. The various animal models can capture differing diseases caused by influenza: benign, severe, super infection, and sepsis, severe with ARDS, and neurologic manifestations (Barnard, 2009). Also, models can utilize seasonal or avian strains and have been developed to study transmission, important for understanding the potential for more lethal strains, such as H5N1 for spreading among humans.

Mouse models of influenza infection are very predictive for antiviral activity and tissue tropism in humans, and are useful in testing and evaluating vaccines (Gilbert and McLeay, 2008; Hagenaars et al., 2008; Ortigoza et al., 2012). Inoculation is by the IN route, utilizing approximately 60 μL of inoculum in each nare of anesthetized mice. Exposure may also be to small particle aerosols containing influenza with a MMAD of <5 μL. Most inbred strains are susceptible, with particularly frequent use of BALB/c followed by C57BL/6J mice. Males and females have equivalent disease but influenza is generally more infectious in younger 2- to 4-week-old (8–10 g) mice.

Mice are of somewhat limited use in characterizing the immune response to influenza. Most inbred laboratory mice lack the MxA gene which is an important part of human innate immune response to influenza infection. The mouse homolog to MxA, Mx1 is defective in most inbred mouse strains (Staeheli and Haller, 1987). Mice with the knocked-in MX1 gene have a 1000-fold higher LD-50 for an influenza A strain (PR8) than wild-type background C57BL/6 mice (Grimm et al., 2007).

Weight loss or reduced weight gain, decreased activity, huddling, ruffled fur, and increased respiration are the most common clinical signs in influenza infected mice. For more virulent strains, mice may require euthanasia as early as 48 h postexposure, but most mortality occurs from 5 to 12 days postexposure accompanied by decreases in rectal temperature (Sidwell and Smee, 2000). Pulse oximeter readings and measurement of blood gases for oxygen saturation are also used to determine the impact of influenza infection on respiratory function (Sidwell et al., 1992). Virus can be isolated from bronchial lavage (BAL) fluids throughout the infection and from tissues after euthanasia. For influenza strains with mild to moderate pathogenicity, disease is nonlethal and virus

replication is detected within the lungs, but usually not other organs. Increases in serum alpha-1-acidglycoprotein and lung weight also frequently occur. However, mice infected with influenza do not develop fever, dyspnea, nasal exudates, sneezing, or coughing.

Mice can be experimentally infected with influenza A or B, but the virus generally requires adaptation to produce clinical signs. Mice express the receptors for influenza attachment in the respiratory tract; however, the distribution varies and SA 2,3 predominates over SA 2,6 which is why H1, H2, and H3 subtypes usually need to be adapted to mice and H5N1, H2, H6, and H7 viruses do not require adaptation (O'Donnell and Subbarao, 2011). To adapt, mice are infected intratracheally or intranasally by virus isolated from the lungs, and reinfected into mice and then the process is repeated a number of times. Once adapted, influenza strains can produce severe disease, systemic spread, and neurotropism.

H5N1 and the 1918 pandemic influenza virus can cause lethal infection in mice without adaptation (Gao et al., 1999; Taubenberger, 2006). H5N1 infection of mice results in viremia and viral replication in multiple organ systems, severe lung pathology, fulminant diffuse interstitial pneumonia, pulmonary edema, high levels of proinflammatory cytokines, and marked lymphopenia (Dybing et al., 2000; Gubareva et al., 1998; Lu et al., 1999). As in humans, the virulence of H5N1 is attributable to damage caused by an overactive host immune response. Additionally, mice infected with the 1918 H1N1 influenza virus produce severe lung pathology and oxygen saturation levels that decrease with increasing pneumonia (Barnard et al., 2007). Reassortment influenza viruses of the 2009 H1N1 virus and a low-pathogenicity avian H7N3 virus can also induce disease in mice without adaptation (Williams et al., 2016).

In superinfection models, a sublethal dose of influenza is given to mice followed 7 days later by IN inoculation of a sublethal dose of a bacterial strain, such as *S. pneumoniae* or *S. pyogenes* (Chaussee et al., 2011). Morbidity, characterized by inflammation in the lungs, but not bacteremia, begins a couple of days after superinfection and may continue for up to 2 weeks. At least one transmission model has also been developed in mice. With H2N2 influenza, transmission rates of up to 60% among cagemates can be achieved after infection by the aerosol route and cocaging after 24 h (Schulman, 1968).

Rats (F344 and SD) inoculated with rat-adapted H3N2 developed inflammatory infiltrates and cytokines in bronchoalveolar lavage fluids, but had no lethality and few histopathological changes (Daniels et al., 2003). Additionally, an influenza transmission model has been developed in guinea pigs as an alternative to ferrets (Lowen et al., 2006).

Cotton rats (*Sigmodon hispidus*) have been used to test vaccines and therapeutics in a limited number of studies (Eichelberger et al., 2004). Cotton rats have an advantage over mice in that the immune system is similar to humans (including the presence of the Mx gene) and influenza viruses do not have to be adapted (Eichelberger et al., 2006; Ottolini et al., 2005). Nasal and pulmonary tissues of cotton rats were infected with unregulated cytokines and lung viral load peaking at 24 h postexposure. Virus was cleared from the lung by day 3 and from the nares by day 66, but animals had bronchial and alveolar damage, and pneumonia for up to 3 weeks. There is also a *S. aureus* superinfection model in cotton rats (Braun et al., 2007a). Coinfection resulted in bacteremia, high bacterial load in lungs, peribronchiolitis, pneumonitis, alveolitis, hypothermia, and higher mortality.

Domestic ferrets (*Mustela putorius furo*) are frequently the animal species of choice for influenza animal studies because the susceptibility, clinical signs, peak virus shedding, kinetics of transmission, local expression of cytokine mRNAs, and pathology resemble that of humans (Lambkin et al., 2004; Maines et al., 2012; McLaren and Butchko, 1978). Like humans, ferrets exclusively express Neu5Ac, which acts as a receptor for influenza A virus, a feature likely contributing to the susceptibility of ferrets to human-adapted influenza A virus strains (Ng et al., 2014). The glycomic characterization of ferret respiratory tract tissues demonstrated some similarities and some differences to humans in terms of the potential glycan binding sites for the influenza virus (Jia et al., 2014). Ferrets also have airway morphology, respiratory cell types, and a distribution of influenza receptors (SA 2,6 and SA 2,3) within the airways similar to that of humans (van Riel et al., 2007).

Influenza was first isolated from ferrets infected IN with throat washes from humans harboring the infection and ferret models have since been used to test efficacy of vaccines and therapeutic treatments (Huber et al., 2008; Lambkin et al., 2004; Maines et al., 2012). When performing influenza studies in ferrets, animals should be serologically negative for circulating influenza viruses. Infected animals should be placed in a separate room from uninfected animals. If animals must be placed in the same room, uninfected ferrets should be handled before infected ferrets. Anesthetized ferrets are experimentally exposed to influenza by IN inoculation of 0.25–0.5 mL containing approximately 10^4–10^6 egg ID_{50} dropwise to each nostril. However, a larger inoculum volume of 1.0 mL has also been explored as being more appropriate, yielding more severe and consistent respiratory tract pathology, likely because the larger inoculum is more widely distributed in the lower respiratory tract (Moore et al., 2014). Video tracking to assign values to activity levels in ferrets can aid ferret studies, eliminating the need for collection of subjective and arbitrary clinical scores (Oh et al., 2015). Viral replication in the upper respiratory tract is typically measured by

nasal washes, but virus can also be measured in bronchoalveolar lavage fluid using a noninvasive technique (Lee et al., 2014).

Influenza types A and B naturally infect ferrets, resulting in an acute illness, which usually lasts 3–5 days for mild to moderately virulent strains (Maher and DeStefano, 2004). Ferrets are more susceptible to influenza A than influenza B strains and are also susceptible to avian influenza H5N1 strains without adaptation (Zitzow et al., 2002). However, the localized immune responses within the respiratory tract of ferrets infected with influenza A and B have been characterized and are similar (Carolan et al., 2015). Virulence and degree of pneumonitis caused by different influenza subtypes and strains vary from mild to severe and generally mirrors that seen in humans (Stark et al., 2013). Nonadapted H1N1, H2N2, and H3N2 have mild to moderate virulence in ferrets. The sequencing of the ferret genome has allowed for the characterization of the ferret host response using RNA-seq analysis (Peng et al., 2014). Distinct signatures were obtained depending on the particular influenza strain to inoculate the ferrets. Also helpful is the sequencing and characterization of the influenza ferret infectome during different stages of the infection in naïve or immune ferrets (Leon et al., 2013).

Since influenza infection is particularly devastating to the elderly population, an aged ferret model of H1N1 influenza infection was developed (Paquette et al., 2014). Features associated with increased clinical disease are weakened hemagglutinin antibody generation and attenuated Th1 responses. Pregnant and breastfeeding women and infants are also susceptible to more severe illness from influenza virus. To study this dynamic, a breastfeeding mother–infant ferret influenza infection model was created (Paquette et al., 2015). Notably, the mammary gland itself harbored virus and transcript analysis showed downregulation of milk production genes. In support of the development of therapies, the ferret influenza model for pharmacokinetic/pharmacodynamics studies of antiviral drugs as also been developed (Reddy et al., 2015). Critical to this model is ensuring pronounced clinical signs and robust viral replication upon influenza infection. Strains of low virulence have predominant replication in the nasal turbinates of ferrets. Clinical signs and other disease indicators in ferrets are similar to that of humans with mild respiratory disease, sneezing, nasal secretions containing virus, fever, weight loss, high viral titers, and inflammatory infiltrate in the airways, bronchitis, and pneumonia (Svitek et al., 2008). Replication in both the upper and lower airways is associated with more severe disease and greater mortality. Additionally, increased expression of proinflammatory mediators and reduced expression of antiinflammatory mediators in the lower respiratory tract of ferrets correlates with severe disease and lethal outcome. H5N1-infected ferrets develop severe lethargy, greater interferon response, transient lymphopenia, and replication in respiratory tract, brain, and other organs (Peng et al., 2012; Zitzow et al., 2002).

Immunocompromised humans have influenza illness of greater duration and complications. Immunocompromised ferrets infected with influenza similarly had prolonged virus shedding (van der Vries et al., 2013). Interestingly, antiviral resistance emerged in both humans and ferrets with immunocompromised status infected with influenza. Alveolar macrophage depleted of ferrets infected with 2009 pandemic H1N1 influenza also had a more severe disease with greater viral replication in the lungs and greater induction of inflammatory chemokines (Kim et al., 2013). A superinfection model resembling that of mice has been developed by IN instillation of influenza in 6- to 8-week-old ferrets followed by IN inoculation of *S. pneumonia* 5 days later (Peltola et al., 2006). This typically resulted in otitis media, sinusitis, and pneumonia.

Transmission models in ferrets have recently met with worldwide media attention and controversy with regard to the study of H5N1 (Enserink, 2013; Fouchier et al., 2012; Herfst et al., 2012; Oh et al., 2014). In general, some subtypes, such as the 2009 H1N1, can transmit easily through aerosol and respiratory droplets (Munster et al., 2009). Of concern, H7N9 isolated from humans was more pathogenic and readily transmissible between ferrets by larger respiratory droplets and smaller particle aerosols (Kreijtz et al., 2013; Richard et al., 2013; Zhang et al., 2013). H5N1 became transmissible by adopting just four mutations, spreading between ferrets in separate cages (Imai et al., 2012). Transmission occurs more readily at the height of pyrexia, but for the 2009 H1N1 in particular, can occur before fever is detected (Roberts et al., 2012). Ferret-to-ferret transmission of a mouse-adapted influenza B virus has also been demonstrated (Kim et al., 2015). Since ferrets can be expensive and cumbersome, influenza infection has been characterized and a transmission model developed in the guinea pig; however, this is a newer model with infrequent utilization thus far (Lowen et al., 2014).

Old and new world primates are susceptible to influenza infection and have an advantage over ferret and mouse models which are deficient for H5N1 vaccine studies because there is a lack of correlation with hemagglutination inhibition (Murphy et al., 1980). Of old world primates, cynomolgus macaque (*Macaca fascicularis*) is most frequently utilized for studies of vaccines and antiviral drug therapies (Stittelaar et al., 2008).

H5N1 and H1N1 1918 infection of cynos is very similar to humans (Rimmelzwaan et al., 2001). Cynos develop fever and ARDS upon IN inoculation of H5N1 with necrotizing bronchial interstitial pneumonia (Kuiken et al., 2003). NHPs are challenged by multiple routes

(ocular, nasal, and tracheal) simultaneously 1×10^6 pfu per site. Virus antigen is primarily localized to the tonsils and pulmonary tissues. Infection of cynos with H5N1 results in fever, lethargy, nasal discharge, anorexia, weight loss, nasal and tracheal washes, pathologic and histopathologic changes, and alveolar and bronchial inflammation. The 1918 H1N1 caused a very high mortality rate due to an aberrant immune response and ARDs and had more than 50% lethality (humans only had a 1%–3% lethality) (Kobasa et al., 2007).

ARDS and mortality also occur with the more pathogenic strains, but NHPs show reduced susceptibility to less virulent strains, such as H3N2 (O'Donnell and Subbarao, 2011). Influenza-infected rhesus macaques represent a mild disease model for vaccine and therapeutic efficacy studies (Baas et al., 2006). Host microarray and qRT-PCR proved useful for analysis of infected lung tissues. Other NHP models include influenza infection of pigtailed macaques as a mild disease model and infection of new world primates, such as squirrel and cebus monkeys (Baskin et al., 2009).

Domestic pig models have been developed for vaccine studies for swine flu. Pigs are susceptible in nature as natural or intermediate hosts but are not readily susceptible to H5N1 (Isoda et al., 2006; Lipatov et al., 2008). While pigs infected with influenza may have fever, anorexia, and respiratory signs, such as dyspnea and cough, mortality is rare (van der Laan et al., 2008). Size and space requirements make this animal difficult to work with, although the development of minipig models may provide an easier to use alternative.

Cat and dog influenza models have primarily been utilized to study their susceptibility to H5N1 with the thought that these animals could act as sentinels or could serve to transmit the virus to humans (Giese et al., 2008; Rimmelzwaan et al., 2006). These models are not generally used to better understand the disease in humans or for testing vaccines or antivirals.

8 BUNYAVIRIDAE

8.1 Rift Valley Fever Virus

Rift Valley fever virus (RVFV) causes epizootics and human epidemics in Africa. RVFV mainly infects livestock, such as sheep, cattle, goats, etc. After 2–4 days incubation period, animals show signs of fever, hepatitis, and abortion, which is a hallmark diagnostic sign known among farmers (Balkhy and Memish, 2003).

Mosquito vectors, unpasteurized milk, aerosols of infected animal's body fluids, or direct contact with infected animals are the important routes of transmission to humans (Abu-Elyazeed et al., 1996; Mundel and Gear, 1951). After 2- to 6-day-incubation period, RVFV causes a wide range of signs and symptoms in humans ranging from asymptomatic to severe disease with hepatitis, vision loss, encephalitis, and hemorrhagic fever (Ikegami and Makino, 2011; Laughlin et al., 1979; Peters and Linthicum, 1994). Depending on the severity of the disease when the symptoms start, 10%–20% of the hospitalized patients might die in 3–6 days or 12–17 days after the disease onset (Ikegami and Makino, 2011). Hepatic failure, renal failure or DIC, and encephalitis are demonstrated within patients during postmortem examination.

Live domestic animals especially sheep and goats were used to develop animal models of RVFV (Weingartl et al., 2014). This study indicated that goats were more resistant to the disease compared to sheep. The viremia in goats was lower and had a shorter duration with only some animals developing fever. The susceptibility is influenced by route of infection, breed of animals, the RVFV strain, and growth conditions as well as the passage history. Therefore, it might be difficult to establish an animal model with domestic ruminants.

Mice are one of the most susceptible animal species to RVFV infection. Several mouse models including BALB/c, IFNAR$^{-/-}$, MBT/PAS, 129 and C57BL/6 were exposed to RVFV via parental or aerosol routes of infection (Ross et al., 2012). SubQ or IP routes of infection cause acute hepatitis and lethal encephalitis at a late stage of the disease in mice (Mims, 1956; Smith et al., 2010). Mice start to show signs of decreased activity and ruffled fur by day 2–3 postexposure. Immediately following these signs, they become lethargic and generally die 3–6 days postexposure. Ocular disease or the hemorrhagic form of the disease has not been observed in mouse models so far (Ikegami and Makino, 2011). Increased viremia and tissue tropism were reported in mice with (Smith et al., 2010) increased liver enzymes and lymphopenia observed in sick mice. Aerosolized RVFV causes faster and more severe neuropathy in mice compared to the parental route (Dodd et al., 2014; Reed et al., 2014). The liver is a target organ following aerosol exposure and liver failure results in fatality.

Rats and gerbils are also susceptible to RVFV infection. The rat's susceptibility is dependent on the rat strain utilized for the challenge model and route of exposure. There is also noted age dependence in the susceptibility of rats. While Wistar-Furth and Brown Norway strains, and young rats are highly susceptible to RVFV infection, Fisher 344, Buffalo and Lewis strains, and old rats demonstrated resistance to infection via subQ route of infection (Findlay and Howard, 1952; Peters and Slone, 1982). Similar pathologic changes, such as liver damage and encephalopathy were observed in both rats and mice. The recent study by Bales et al. (2012) showed that aerosolized RVFV caused similar disease outcome in Wistar-Furth and ACI rats while Lewis rats developed fatal encephalitis which was much more severe than the subQ

route of infection. There was no liver involvement in the gerbil model and animals died from severe encephalitis. The mortality rate was dependent on the strain used and the dose given to gerbils (Anderson et al., 1988). Similar to the rat model, the susceptibility of gerbils was also dependent on age.

Natural history studies with Syrian hamsters indicated that the liver was the target organ with highly elevated ALT levels and viral titers (Scharton et al., 2015). Lethargy, ruffled fur, and hunched posture were observed in hamsters by day 2 post-subQ inoculation and the disease was uniformly lethal by day 2–3 postexposure. This model has been successfully used to test antivirals against RVFV (Scharton et al., 2015).

Studies thus far showed that RVFV does not cause uniform lethality in a NHP model. IP, IN, IV, and aerosol routes have been utilized to develop NHP model. Rhesus macaques, cynomolgus macaques, African monkeys, and South American monkeys were some of the NHP species used for this effort (Peters et al., 1988). Monkeys showed a variety of signs ranging from febrile disease to hemorrhagic disease and mortality. Temporal viremia, increased coagulation parameters (PT, APTT), and decreased platelets were some other signs observed in NHPs. Animals that succumbed to disease showed very similar pathogenesis to humans, such as pathological changes in the liver and hemorrhagic disease. There was no ocular involvement in this model.

Smith et al. compared IV, IN and subQ routes of infection in common marmosets and rhesus macaques (Peng et al., 2012). Marmosets were more susceptible to RVFV infection than rhesus macaques with marked viremia, acute hepatitis, and late onset of encephalitis. Increased liver enzymes were observed in both species. Necropsy results showed enlarged livers in the marmosets exposed by IV or subQ routes. Although there were no gross lesions in the brains of marmosets, histopathology showed encephalitis in the brains of IN challenged marmosets.

A recent study by Hartman et al. (2014) demonstrated that aerosolized RVFV only caused mild fever in cynomolgus macaques and rhesus macaques, while AGMs and marmosets had encephalitis and succumbed to disease between days 9 and 11 postexposure. In contrast to other lethal models, the brain was the target organ in AGMs and marmosets. Although no change was observed in AST levels, ALP levels were increased in marmosets. Little or no change was observed in hepatic enzyme levels in AGMs. Lack of information regarding human disease concerning the aerosol route of exposure makes it difficult to evaluate these animal models.

8.2 Crimean–Congo Hemorrhagic Fever Virus

Crimean–Congo hemorrhagic fever virus (CCHFV) generally circulates in nature unnoticed in an enzootic tick–vertebrate–tick cycle and similar to other zoonotic agents, appears to produce little or no disease in its natural hosts, but causes severe disease in humans.

CCHFV transmits to humans by ixodid ticks, direct contact with sick animals/humans, or body fluids of animals/humans (Ergonul and Whitehouse, 2007). Incubation, prehemorrhagic, hemorrhagic, and convalescence are the four phases of the disease seen in humans. The incubation period lasts 1–9 days. During the prehemorrhagic phase, patients show signs of nonspecific flu-like disease for approximately a week. The hemorrhagic period results in circulatory shock and DIC in some patients (Mardani and Keshtkar-Jahromi, 2007; Swanepoel et al., 1989).

Over the years, several attempts have been made to establish an animal model for CCHF in adult mice, guinea pigs, hamsters, rats, rabbits, sheep, NHPs, etc. (Fagbami et al., 1975; Nalca and Whitehouse, 2007; Shepherd et al., 1989; Smirnova, 1979). Until recently, the only animal that manifests disease is the newborn mouse. Infant mice IP infected with CCHFV resulted in fatality around day 8 postinfection (Tignor and Hanham, 1993). Pathogenesis studies showed that virus replication was first detected in the liver, with subsequent spread to the blood (serum). Virus was detected very late during the disease course in other tissues including the heart (day 6) and the brain (day 7).

The recent studies utilizing knockout adult mice were successful to develop a lethal small animal model for CCHFV infection (Bente et al., 2010; Bereczky et al., 2010). Bente et al. infected STAT1 knockout mice by the IP route. In this model, after the signs of fever, leukopenia, thrombocytopenia, viremia, elevated liver enzymes and proinflammatory cytokines, mice were moribund and succumbed to disease in 3–5 days postexposure. The second model was developed by using interferon alpha/beta (IFNα/β) receptor knockout mice (IFNAR$^{-/-}$) (Bereczky et al., 2010). Similar observations were made in this model as in the STAT1 knockout mouse model. Animals were moribund and died 2–4 days after exposure with high viremia levels in liver and spleen. Characterization studies with IFNAR$^{-/-}$ mice challenged with different routes (IP, IN, IM, and subQ) showed that CCHFV causes acute disease with high viral loads, pathology in liver and lymphoid tissues, increased proinflammatory response, severe thrombocytopenia, coagulopathy, and death, all of which are characteristics of human disease (Zivcec et al., 2013). Proinflammatory cytokines and chemokines, such as G-CSF, IFNγ, CXCL10, CCL2 increased dramatically day 3 postchallenge and GM-CSF, IL-1a, IL-1b, IL-2, IL-6, IL-12p70, IL-13, IL-17, CXCL1, CCL3, CCL5, and TNF-α concentrations were extremely elevated at the time of death/euthanasia. This model is also utilized to test therapeutics, such as ribavirin, arbidol, and T-705 (favipiravir) successfully

(Oestereich et al., 2014). Experimental vaccines developed for CCHF were evaluated in this model provided protection compare to unvaccinated mice (Buttigieg et al., 2014; Canakoglu et al., 2015, p. 725). Thus, the IFNAR$^{-/-}$ mouse model would be a good choice to test medical countermeasures against CCHFV, although they have an impaired IFN and immune response phenotype.

Other laboratory animals, including NHPs, show little or no sign of infection or disease when infected with CCHFV (Nalca and Whitehouse, 2007). Butenko et al. utilized AGMs (Cercopithecus aethiops) for experimental CCHFV infections. Except one monkey with a fever on day 4 postinfection, the animals did not show signs of disease. Antibodies to the virus were detected in three out of five monkeys, including the one with fever. Fagbami et al. (1975) infected two Patas monkeys (Erythrocebus patas) and one Guinea baboon (Papio papio) with CCHFV. Whereas all three animals had low-level viremia between days 1 and 5 after inoculation, only the baboon serum had neutralizing antibody activity on day 137 postinfection.

Similar results were obtained when horses and donkeys have been used for experimental CCHFV infections. Donkeys develop a low-level viremia (Rabinovich et al., 1972) and horses developed little or no viremia, but high levels of virus-neutralizing antibodies, which remained stable for at least 3 months. These studies suggest that horses may be useful in the laboratory to obtain serum for diagnostic and possible therapeutic purposes (Blagoveshchenskaya et al., 1975).

Shepherd et al. (1989) infected 11 species of small African wild mammals and laboratory rabbits, guinea pigs, and Syrian hamsters with CCHFV. Whereas scrub hares (Lepus saxatilis), cape ground squirrels (Xerus inauris), red veld rats (Aethomys chrysophilus), white-tailed rats (Mystromys pumilio), and guinea pigs had viremia; South African hedgehogs (Atelerix frontalis), highveld gerbils (Gerbilliscus brantsii), Namaqua gerbils (Desmodillus auricularis), two species of multimammate mouse (Mastomys natalensis and Mastomys coucha), and Syrian hamsters were negative for virus. All species regardless of viremia levels developed antibody responses against CCHFV. IV and intracranially infected animals showed onset of viremia earlier than those infected by the subQ or IP routes.

8.3 Hanta Virus

The genus Hantavirus is unique among the family Bunyaviridae in that it is not transmitted by an arthropod vector, but rather rodents (Schmaljohn and Nichol, 2007). Rodents of the family Muridae are the primary reservoir for hantaviruses. Infected host animals develop a persistent infection that is typically asymptomatic. Transmission is achieved by inhalation of infected rodent saliva, feces, and urine (Xu et al., 1985). Human infections can normally be traced to a rural setting with activities, such as farming, land development, hunting, and camping as possible sites of transmission. Rodent control is the primary route of prevention (Lednicky, 2003).

The viruses have a tropism for endothelial cells within the microvasculature of the lungs (Zaki et al., 1995). There are two distinct clinical diseases that infection can yield: hemorrhagic fever with renal syndrome (HFRS) due to infection with old world hantaviruses or hantavirus pulmonary syndrome (HPS) caused by new world hantaviruses (Nichol, 2001). HFRS is mainly seen outside of the Americas and is associated with the hantaviruses Dobrava-Belgrade (also known as Dobrava), Hantaan, Puumala, and Seoul (Lednicky, 2003). Incubation lasts 2–3 weeks and presents as flu-like in the initial stages that can further develop into hemorrhagic manifestations and ultimately renal failure. Thrombocytopenia subsequently develops which can further progress to shock in approximately 15% patients. Overall mortality rate is 7%. Infection with Dobrava and Hantaan viruses are typically linked to development of severe disease.

HPS was first diagnosed in 1993 within southwestern United States when healthy young adults became suddenly ill, progressing to severe respiratory distress and shock. The etiological agent responsible for this outbreak was identified as Sin Nombre virus (SNV) (Centers for Disease Control and Prevention, 1993). This virus is still the leading cause within North America of HPS. HPS due to other hantaviruses has been reported in Argentina, Bolivia, Brazil, Canada, Chile, French Guiana, Panama, Paraguay, and Uruguay (Padula et al., 2000; Stephen et al., 1994). The first report of HPS in Maine was recently documented (Centers for Disease Control and Prevention, 1993). Andes virus (ANDV) was first identified in outbreaks in Chile and Argentina. This hantavirus is distinct in that it can be transmitted between humans (Wells et al., 1997). The fulminant disease is more lethal than that observed of HFRS with a mortality rate of 40%.

There are four phases of disease including prodromal, pulmonary, cardiac depression, and hematologic manifestation (Peters and Khan, 2002). Incubation typically occurs 14–17 days following exposure (Young et al., 2000). Unlike HFRS, renal failure is not a major contributing factor to the disease. There is a short prodromal phase that gives way to cardiopulmonary involvement accompanied by cough and gastrointestinal symptoms. It is at this point that individuals are typically admitted to the hospital. Pulmonary function is hindered and continues to suffer within 48 h after cardiopulmonary involvement. Interstitial edema and air-space disease normally follow. In fatal cases, cardiogenic shock has been noted (Hallin et al., 1996).

Syrian golden hamsters are the most widely utilized small animal model for hantavirus infection. Hamsters

inoculated IM with a passaged Andes viral strain died within 11 days postinfection. Clinical signs did not appear until 24 h prior to death at which point the hamsters were moribund and in respiratory distress. Mortality was dose dependent, with high inoculums leading to a shorter incubation before death. During the same study, hamsters were inoculated with a passaged SNV isolate. No hamsters developed any symptoms during the course of observation. However, an antibody response to the virus that was not dose dependent was determined via ELISA. Hamsters infected with ANDV have significant histopathological changes to their lung, liver, and spleen. All had an interstitial pneumonia with intraalveolar edema. Infectious virus could be recovered from these organs. Viremia began on day 8 and lasted up to 12 days postinfection. Infection of hamsters with ANDV yielded a similar clinical disease progression as is seen in human HPS including rapid progression to death, fluid in the pleural cavity, and significant histopathological changes to the lungs and spleen. A major deviation in the hamster model is the detection of infectious virus within the liver (Hooper et al., 2001). Normally, SNV does not cause a disease in hamsters (Wahl-Jensen et al., 2007). But a recent study showed that immunosuppression with dexamethasone and cyclophosphamide in combination causes lethal disease with SNV in hamsters (Brocato et al., 2014). The disease was very similar to the disease caused by ANDV in hamsters.

Lethal disease can be induced in newborn mice, but does not recapitulate the clinical symptoms observed in human disease (Kim and McKee, 1985). The disease outcome is very much dependent on the age of the mice. Younger mice are much more susceptible to virus than the adult mice. Adult mice exposed to Hanta virus leads to a fatal disease dependent upon viral strain and route of infection. The disease progression is marked by neurological or pulmonary manifestations that do not mirror human disease (Seto et al., 2012; Wichmann et al., 2002). Knockout mice lacking IFNα/β are highly susceptible to Hanta virus infection (Muller et al., 1994). In a study of panel of laboratory strains of mice, C57BL/6 mice were most susceptible to a passaged Hanta viral strain injected IP. Animals progressed to neurological manifestation including paralyses and convulsions, and succumbed to infection within 24–36 h postinfection. Clinical disease was markedly different from that observed in human cases (Wichmann et al., 2002). In a recent study, 2-week-old ICR mice was exposed to HTNV strain AA57 via the subQ route (Seto et al., 2012). Mice started to show signs of disease by day 11 postinoculation. Piloerection, trembling, hunching, loss of body weight, labored breathing, and severe respiratory disease were observed in mice.

Studies to develop NHP models were not successful until recently. NHPs have been challenged with new world hantaviruses; however, no clinical signs were reported (Hooper et al., 2006; McElroy et al., 2002). Cynomolgus monkeys challenged with a clinical isolate of Puumala virus developed a mild disease (Klingstrom et al., 2002; Sironen et al., 2008). Challenge with ANDV to cynomolgus macaques by both IV and aerosol exposure led to no signs of disease. All animals did display a drop in total lymphocytes within 5 days postinfection. Four of six aerosol exposed monkeys and 8 of 11 IV injected monkeys developed viremia. Infectious virus could not be isolated from any of the animals. In a recent study, rhesus macaques were inoculated by the intramuscular route with SNV passaged only in deer mice (Safronetz et al., 2014). Characteristics of HPS disease including rapid onset of respiratory distress, severe pulmonary edema, thrombocytopenia, and leukocytosis were observed in this promising model. Viremia was observed 4–10 days prior to respiratory signs of the disease that were observed on days 14–16 postinoculation. With all aspects, this animal model would be very useful to test medical countermeasures against Hanta virus.

9 ARENAVIRIDAE

9.1 Lassa Fever Virus

The family Arenaviridae is composed of two serogroups: old world arenaviruses including Lassa fever virus and lymphocytic choriomeningitis virus and the new world viruses of Pichinde virus and Junin virus. All of these viruses share common clinical manifestations (McCormick and Fisher-Hoch, 2002). Lassa fever virus is endemic in parts of West Africa and outbreaks are typically seen in the dry season between January and April (Curtis, 2006). This virus is responsible for 100,000–500,000 infections per year, leading to approximately 5000 deaths (Khan et al., 2008). Outbreaks have been reported in Guinea, Sierra Leone, Liberia, Nigeria, and Central African Republic. However, cases have sprung up in Germany, Netherlands, United Kingdom, and the United States due to transmission to travelers on commercial airlines (Amorosa et al., 2010).

Transmission of this virus typically occurs via rodents, in particular the multimammate rat, *Mastomys* species complex (Curtis, 2006). Humans become infected by inhaling the aerosolized virus or eating contaminated food. There has also been noted human-to-human transmission by direct contact with infected secretions or needle-stick injuries. The majority of infections are asymptomatic; however, severe disease occurs in 20% of individuals. The incubation period is from 5 to 21 days and initial onset is characterized by flu-like illness. This is followed by diarrheal disease that can progress to hemorrhagic symptoms including encephalopathy, encephalitis, and meningitis. A third of patients develop

deafness in the early phase of disease that is permanent for a third of those affected. The overall fatality is about 1%; however, of those admitted to the hospital it is between 15% and 25%. There is no approved vaccine and besides supportive measures, ribavirin is effective only if started within 7 days (McCormick et al., 1986a,b).

The primary animal model used to study Lassa fever is the rhesus macaque (Jahrling et al., 1980). Aerosolized infection of lymphocytic choriomeningitis virus has been a useful model for Lassa fever. Both rhesus and cynomolgus monkeys exposed to the virus developed disease, but rhesus mirrored more closely the disease course and histopathology observed in human infection (Danes et al., 1963). IV or intragastric inoculation of the virus led to severe dehydration, erythematous skin, submucosal edema, necrotic foci in the buccal cavity, and respiratory distress. The liver was severely affected by the virus as depicted by measuring the liver enzymes AST and ALT (Lukashevich et al., 2003). Disease was dose dependent with IV, intramuscular, and subQ inoculation requiring the least amount of virus to induce disease. Aerosol infections and eating contaminated food could also be utilized, and mimic a more natural route of infection (Peters et al., 1987). Within this model, the NHP becomes viremic after 4–6 days. Clinical manifestations were present by day 7 and death typically occurred within 10–14 days (Lukashevich et al., 2004; Rodas et al., 2004). Intramuscular injection of Lassa virus into cynomolgus monkeys also produced a neurological disease due to lesions within the CNS (Hensley et al., 2011b). This pathogenicity is seen in select cases of human Lassa fever (Cummins et al., 1992; Gunther et al., 2001).

A marmoset model has recently been defined utilizing a subQ injection of Lassa fever virus. Virus was initially detected by day 8 and viremia achieved by day 14. Liver enzymes were elevated and an enlarged liver was noted upon autopsy. There was a gradual reduction in platelets and interstitial pneumonitis diagnosed in a minority of animals. The physiological signs were the same as seen in fatal human cases (Carrion et al., 2007).

Mice develop a fatal neurological disorder upon intracerebral inoculation with Lassa, although the outcome of infection is dependent on the MHC background, age of the animal, and inoculation route (Salvato et al., 2005). STAT1 knockout mice inoculated IP with both lethal and nonlethal Lassa virus strains develop hearing loss accompanied by damage to the inner ear hair cells and auditory nerve (Yun et al., 2015). Guinea pig inbred strain 13 was highly susceptible to Lassa virus infection. The outbred Hartley strain was less susceptible, and thus strain 13 has been the preferred model given its assured lethality. The clinical manifestations mirror those seen in humans and rhesus (Jahrling et al., 1982). Infection with Pichinde virus passaged in guinea pigs has also been used. Disease signs include fever, weight loss, vascular

collapse, and eventual death (Lucia et al., 1990; Qian et al., 1994). The guinea pig is an excellent model given that it not only results in similar disease pattern, viral distribution, histopathology, and immune response to humans (Connolly et al., 1993; Katz and Starr, 1990).

Infection of hamsters with a cotton rat isolate of Pirital virus is similar to what is characterized in humans, and the NHP and guinea pig models. The virus was injected IP resulting in lethargy and anorexia within 6–7 days. Virus was first detected at 3 days, and reached maximum titers within 5 days. Neurological symptoms began to appear at the same time, and all animals died by day 9. Pneumonitis, pulmonary hemorrhage, and edema were also present (Sbrana et al., 2006). These results were recapitulated with a nonadapted Pichinde virus (Buchmeier and Rawls, 1977; Gowen et al., 2005; Smee et al., 1993).

10 RETROVIRIDAE

10.1 Human Immunodeficiency Virus Type 1

The Lentiviruses are a subfamily of Retroviridae, which includes human immunodeficiency virus (HIV), a virus that infects 0.6% of the world's population. A greater proportion of infections and deaths occur in sub-Saharan Africa. Worldwide, there are approximately 1.8 million deaths per year with over 260,000 being children. Transmission of HIV occurs by exposure to infectious body fluids. There are two species, HIV-1 and HIV-2, with HIV-2 having lower infectivity and virulence (confined mostly to West Africa). The vast majority of cases worldwide are HIV-1 (De Cock et al., 2011).

HIV targets T-helper cells (CD4+), macrophages, dendritic cells (Fields et al., 2007). Acute infection occurs 2–4 weeks after exposure, with flu-like symptoms and viremia followed by chronic infection. Symptoms in the acute phase may include fever, body aches, nausea, vomiting, headache, lymphadenopathy, pharyngitis, rash, and sores in the mouth or esophagus. CD8+ T-cells are activated which kill HIV-infected cells, and are responsible for antibody production and seroconversion. Acquired immune deficiency syndrome (AIDS) develops when CD4+ T-cells decline to less than 200 cells/μL; thus cell-mediated immunity becomes impaired and the person is more susceptible to opportunistic infections as well as certain cancers.

HIV has a narrow host range likely because the virus is unable to antagonize and evade effector molecules of the interferon response (Thippeshappa et al., 2012). Humanized mice, created by engrafting human cells and tissues into SCID mice, have been critical for the development of mouse models for the study of HIV infection. A number of different humanized mouse models allow for the study of HIV infection in the context of an intact and

functional human innate and adaptive immune responses (Berges and Rowan, 2011). The SCIDHu HIV infection model has proven useful, particularly in screening antivirals and therapeutics (Denton et al., 2008; Melkus et al., 2006). A number of different humanized mouse models have been developed for the study of HIV, including Rag1$^{-/-}$γc$^{-/-}$, Rag2$^{-/-}$γc$^{-/-}$, NOD/SCIDγc$^{-/-}$ (hNOG), NOD/SCIDγc$^{-/-}$ (hNSG), NOD/SCID BLT, and NOD/SCIDγc$^{-/-}$ (hNSG) BLT (Karpel et al., 2015; Li et al., 2015; Shimizu et al., 2015). CD34+ human stem cells derived from umbilical cord blood or fetal liver are used for humanization (Baenziger et al., 2006; Watanabe et al., 2007). HIV-1 infection by IP injection can be successful with as little as 5% peripheral blood engraftment (Berges et al., 2006). Vaginal and rectal transmission models have been developed in BLT SCID Hu mice in which mice harbor human bone marrow, liver, and thymus tissue. HIV-1 viremia occurs within approximately 7 days postinoculation (Zhang et al., 2007). In many of these models, spleen, lymph nodes, and thymus tissues are highly positive for virus, similar to humans (Brainard et al., 2009). Importantly, depletion of human T-cells can be observed in blood and lymphoid tissues of HIV-infected humanized mice and at least some mechanisms of pathogenesis that occur in HIV-infected humans, also occur in the HIV-infected humanized mouse models (Baenziger et al., 2006; Neff et al., 2011). The advantage of these models is that these mice are susceptible to HIV infection and thus the impact of drugs on the intended viral targets can be tested. One caveat is that while mice have a "common mucosal immune system," humans do not, due to differences in the distribution of addressins (Holmgren and Czerkinsky, 2005). Thus, murine mucosal immune responses to HIV do not reflect those of humans. Another strategy uses a human CD4- and human CCR5- expressing transgenic luciferase reporter mouse to study HIV-1 pseudovirus entry (Gruell et al., 2013).

HIV-1 transgenic (Tg) rats are also used to study HIV related pathology, immunopathogenesis, and neuropathology (Lentz et al., 2014; Reid et al., 2001). The clinical signs include skin lesions, wasting, respiratory difficulty, and neurological signs. Brain volume decreases have been documented and the HIV-1 Tg rat is thus used as a model of neuropathology in particular.

There are a number of important NHP models for human HIV infection (Hessell and Haigwood, 2015). An adaptation of HIV-1 was obtained by four passages in pigtailed macaques transiently depleted of CD8(+) cells during acute infection (Hatziioannou et al., 2014). The resulting disease has several similarities to AIDS in humans, such as depletion of CD4(+) T-cells (Kimata, 2014). Simian immunodeficiency virus (SIV) infection of macaques has been widely used as a platform for modeling HIV infection of humans (Demberg and Robert-Guroff, 2015; Walker et al., 2015). Importantly, NHPs

have similar, pharmacokinetics, metabolism, mucosal T-cell homing receptors, and vascular addressins to those of humans. Thus, while the correlates of protection against HIV are still not completely known, immune responses to HIV infection and vaccination are likely comparable. These models mimic infection through use of contaminated needles (IV), sexual transmission (vaginal or rectal), and maternal transmission in utero or through breast milk (Keele et al., 2009; Miller et al., 2005; Stone et al., 2009). There are also macaque models to study the emergence and clinical implications of HIV drug resistance (Van Rompay et al., 2002).

These models most routinely utilize rhesus macaques (*Macaca mulatta*), cynomolgus macaques (*M. fasicularis*), and pigtailed macaques (*Macaca nemestrina*). All ages are used, depending on the needs of the study. For instance, use of newborn macaques may be more practical for evaluating the effect of prolonged drug therapy on disease progression; however, adult NHPs are more frequently employed. Female pigtailed macaques have been used to investigate the effect of the menstrual cycle on HIV susceptibility (Vishwanathan et al., 2015). Studies are performed in BSL-2 animal laboratories and NHPs must be Simian type-D retrovirus free and SIV seronegative. SIV infection of pigtailed macaques is a useful model for HIV peripheral nervous system pathology, wherein an axotomy is performed and regeneration of axons is studied (Ebenezer et al., 2012).

Exposure in model systems is typically through a single high-dose challenge. IV infection of rhesus macaques with 100 TCID$_{50}$ of the highly pathogenic SIV/DeltaB670 induces AIDS in most macaques within 5–17 months (mean of 11 months) (Fuller et al., 2012). Peak viremia occurs around week 4. AIDS in such models is often defined as CD4+ T-cells that have dropped to less than 50% of the baseline values. Alternatively, repeated low dose challenges are often utilized, depending on the requirements of the model (Henning et al., 2014; Moldt et al., 2012; Reynolds et al., 2012).

Since NHPs infected with HIV do not develop an infection with a clinical disease course similar to humans, SIV or SIV/HIV-1 laboratory-engineered chimeric viruses (SHIVs) are used as surrogates. NHPs infected with pathogenic SIV may develop clinical disease which progresses to AIDS, and are thus useful pathogenesis models. A disadvantage is that SIV is not identical to HIV-1 and is more closely related to HIV-2. However, the polymerase region of SIV is 60% homologous to that of HIV-1 and it is susceptible to many reverse transcriptase (RT) and protease inhibitors. SIV is generally not susceptible to nonnucleoside inhibitors, thus HIV-1 RT is usually put into SIV for such studies (Uberla et al., 1995).

SIVmac239 is similar to HIV in the polymerase region and is therefore susceptible to nucleoside, RT, or integrase inhibition (Witvrouw et al., 2004). NHPs

infected with SIVmac239 have an asymptomatic period and disease progression resembling AIDS in humans, characterized by weight loss/wasting, CD4+ T-cell depletion. Additionally, SIVmac239 utilizes the CXCR5 chemokine receptor as a coreceptor, similar to HIV, which is important for drugs that target entry (Veazey et al., 2003).

NHPs infected with SHIV strains, may not develop AIDS, but these models are useful in testing vaccine efficacy (Del Prete et al., 2014). For example, RT-SHIVs and env-SHIVs are useful for testing and evaluation of drugs that may target the envelope or RT, respectively (Uberla et al., 1995). One disadvantage of the highly virulent env-SHIV (SHIV-89.6 P), is that it uses the CXCR4 coreceptor. Of note, env-SHIVs that do use the CXCR5 coreceptor are less virulent; viremia develops then resolves without further disease progression (Humbert et al., 2008).

Simian-tropic (st) HIV-1 contains the Vif gene from SIV. Infection of pigtailed macaques with this virus results in viremia, which can be detected for 3 months, followed by clearance (Haigwood, 2009).

A number of routes are utilized for SIV or SHIV infection of NHPs, with IV inoculation the most common route. Mucosal routes include vaginal, rectal, and intracolonic. Mucosal routes require a higher one-time dose than the IV route for infection. For the vaginal route, female macaques are treated with Depo-Provera (estrogen) 1 month before infection to synchronize the menstrual cycle, thin the epithelial lining of the vagina, and increase susceptibility to infection by atraumatic vaginal instillation (Burton et al., 2011). Upon vaginal instillation of 500 $TCID_{50}$ of SHIV-162P3, peak viremia was seen around 12 days postexposure with greater than 10^7 copies/mL and dropping thereafter to a constant level of 10^4 RNA copies/mL at 60 days and beyond. In another example, in an investigation of the effect of vaccine plus vaginal microbicide on preventing infection, rhesus macaques were vaginally infected with a high dose of SIVmac251 (Barouch et al., 2012). An example of an intrarectal model utilized juvenile (2-year-old) pigtailed macaques, challenged intrarectally with 10^4 $TCID_{50s}$ of SIV_{mne027} to study the pathogenesis related to the virulence factor, Vpx (Belshan et al., 2012). Here, viremia peaked at approximately 10 days with more than 10^8 copies/mL. Viral RNA was expressed in the cells of the mesenteric lymph nodes.

The male genital tract is seen as a viral sanctuary with persistent high levels of HIV shedding even with antiretroviral therapy. To better understand the effect of HAART therapy on virus and T-cells in the male genital tract, adult (3- to 4-year-old) male cynomolgus macaques were intravenously inoculated with 50 AID50s of SIVmac251 and the male genital tract tissues were tested after euthanasia by PCR, IHC, and in situ hybridization (Moreau et al., 2012).

Pediatric models have been developed in infant rhesus macaques through the infection of SIV, allowing for the study of the impact of developmental and immunological differences on the disease course (Abel, 2009). Importantly, mother-to-infant transmission models have also been developed (Jayaraman et al., 2004). Pregnant female pigtailed macaques were infected during the second trimester with 100 MID_{50} SHIV-SF162P3 by the IV route. Four of nine infants were infected, one in utero and three either intrapartum or immediately postpartum through nursing. This model is useful for the study of factors involved in transmission as well as the underlying immunology.

NHPs infected with SIV or SHIV are routinely evaluated for weight loss, activity level, stool consistency, appetite, virus levels in blood, and T-cell populations. Cytokine and chemokine levels, antibody responses, and cytotoxic T-lymphocyte responses may also be evaluated.

The ultimate goal of an HIV vaccine is sterilizing immunity (preventing infection). However, a more realistic result may be to reduce severity of infection and permanently prevent progression. Strategies have included live attenuated, nonreplicating, and subunit vaccines. These have variable efficacy in NHPs due to the genetics of the host (MHC and TRIM alleles), differences between challenge strains, and challenge routes (Letvin et al., 2011). NHP models have led to the development of antiviral treatments that are effective at reducing viral load and indeed transmission of HIV among humans. One preferred variation on the models for testing the long-term clinical consequences of antiviral treatment is to use newborn macaques and treat from birth onward, in some cases more than a decade (Van Rompay et al., 2008). Unfortunately, however, successes in NHP studies do not always translate to success in humans, as seen with the recent STEP study which used an adenovirus-based vaccine approach (Buchbinder et al., 2008). Vaccinated humans were not protected and may have even been more susceptible to HIV, viremia was not reduced, and the infections were not attenuated as hoped. With regard to challenge route, IV exposure is more difficult to protect than mucosal exposure and is used as a "worst case scenario." However, efficacy at one mucosal route is usually comparable to other mucosal routes.

11 PAPILLOMAVIRIDAE

11.1 Papillomavirus

Human and animal papillomaviruses cause benign epithelial proliferations (warts) and malignant tumors of the various tissues that they infect (Bosch and de Sanjose, 2002). There are over 100 human

papillomaviruses, with different strains causing warts on the skin, oropharynx, nasopharynx, larynx, and anogenital tissues. Approximately one third of papillomaviruses are transmitted sexually. Of these, virulent subtypes, such as HPV-16, HPV-18, HPV-31, HPV-33, and HPV-45 place individuals at high risk for cervical and other cancers. Up to 35% of head and neck cancers are caused by HPV-16, particularly oropharyngeal cancers. Major challenges in the study of these viruses are that papillomaviruses generally do not infect any other species outside of the natural hosts and can cause a very large spectrum of severity. Thus, no wild-type animal models have been identified that are susceptible to HPV. However, a number of useful surrogate models exist which use animal papillomaviruses in their natural host or a very closely related species (Borzacchiello et al., 2009; Brandsma, 1994; Campo, 2002). These models have facilitated the recent development of useful and highly effective prophylactic HPV vaccines (Rabenau et al., 2005).

Wild-type inbred mice cannot be used to study disease caused by papillomaviruses unless they are engrafted with relevant tissue, orthotopically transplanted or transgenic, but they are often used to look at immunogenicity of vaccines (Jagu et al., 2011; Oosterhuis et al., 2011). Transgenic mice used for HPV animal modeling typically express the viral oncogenes E5, E6, E7, or the entire early region of HPV-16 from the keratin 14 promoter which is only active in the basal cells of the mouse epithelium (Chow, 2015). Cancers in these models develop upon extended estrogen exposure (Maufort et al., 2010; Ocadiz-Delgado et al., 2009; Stelzer et al., 2010; Thomas et al., 2011). Transgenic mice with constitutively active Wnt/B-catenin signaling in cervical epithelial cells expressing the HPB oncoprotein E7 develop invasive cervical squamous carcinomas (Bulut and Uren, 2015). The tumors occur within 6 months approximately 94% of the time. Another model uses C57BL/6 mice expressing the HPV16-E7 transgene which are then treated topically with 7,12-dimethylbenz(a)anthracene (DMBA) (De Azambuja et al., 2014). These mice developed benign and malignant cutaneous lesions.

Cervical cancers can also be induced in human cervical cancer xenografts transplanted onto the flanks of athymic mice and serially transplanted thereafter (Hiroshima et al., 2015; Siolas and Hannon, 2013).

A wild-type immunocompetent rodent model uses *M. coucha*, which is naturally infected with *Mastomys natalensis* papillomavirus (MnPV) (Vinzon et al., 2014). MnPV induces papillomas, keratoacanthomas, and squamous cell carcinomas and provides a means to study vaccination in an immunocompetent small animal model.

Wild cottontail rabbits (*Sylvilagus floridanus*) are the natural host for cottontail rabbit papillomavirus (CRPV), but this virus also infects domestic rabbits (*Oryctolagus cuniculus*), which is a very closely related species (Breitburd et al., 1997). In this model, papillomas can range from cutaneous squamous cell carcinomas on one end of spectrum, and spontaneous regression on the other. Lesions resulting from CRPV in domestic rabbits do not typically contain infectious virus.

Canine oral papillomavirus (COPV) causes florid warty lesions in mucosa of the oral cavity within 4–8 weeks postexposure in experimental settings (Johnston et al., 2005). The mucosatrophic nature of these viruses and the resulting oropharyngeal papillomas that are morphologically similar to human vaginal papillomas caused by HPV-6 and HPV-11 make this a useful model (Nicholls et al., 1999). These lesions typically spontaneously regress 4–8 weeks after appearing; this model is therefore useful in understanding the interplay between the host immune defense and viral pathogenesis. Male and female beagles, aged 10 weeks to 2 years, with no history of COPV, are typically used for these studies. Infection is achieved by application of a 10 μL droplet of virus extract to multiple 0.5 cm^2 scarified areas within the mucosa of the upper lip of anesthetized beagles (Nicholls et al., 2001). Some investigators have raised concerns that dogs are not a suitable model for high-risk HPV-induced oral cancer (Staff, 2015).

Bovine papillomavirus (BPV) has a wider host range than most papillomaviruses, infecting the fibroblasts cells of numerous ungulates (Campo, 2002). BPV-4 infection of cattle feeding on bracken fern, which is carcinogenic, can result in lesions of the oral and esophageal mucosa that lack detectable viral DNA. BPV infections in cattle can result in a range of diseases, such as skin warts, cancer of the upper gastrointestinal tract and urinary bladder, and papillomatosis of the penis, teats, and udder.

Finally, rhesus papillomavirus (RhPV), a sexually transmitted papillomaviruses in rhesus macaques and cynomolgus macaques is very similar to HPV-16 and is associated with the development of cervical cancer (Ostrow et al., 1990; Wood et al., 2007).

12 POXVIRIDAE

12.1 Monkeypox Virus

Monkeypox virus (MPXV) causes disease in both animals and humans. Human monkeypox, which is clinically almost identical to ordinary smallpox, occurs mostly in the rainforest of central and western Africa. The virus is maintained in nature in rodent reservoirs including

squirrels (Charatan, 2003; Khodakevich et al., 1986). MPXV was discovered during the pox-like disease outbreak among laboratory monkeys (mostly cynomolgus and rhesus macaques) in Denmark in 1958. No human cases were observed during this outbreak. The first human case was not recognized as a distinct disease until 1970 in Zaire (the present DRC) with continued occurrence of a smallpox-like illness despite eradication efforts of smallpox in this area.

During the global eradication campaign, extensive vaccination in central Africa decreased the incidence of human monkeypox, but the absence of immunity in the generation born since that time and increased dependence on bush meat have resulted in renewed emergence of the disease.

In the summer of 2003, a well-known outbreak in the Midwest was the first occurrence of monkeypox disease in the United States and Western Hemisphere. Among 72 reported cases, 37 human cases were laboratory confirmed during an outbreak (Nalca et al., 2005; Sejvar et al., 2004). It was determined that native prairie dogs (*Cynomys* sp.) housed with rodents imported from Ghana in West Africa were the primary source of outbreak.

The virus is mainly transmitted to humans while handling infected animals or by direct contact with the infected animal's body fluids, or lesions. Person-to-person spread occurs by large respiratory droplets or direct contact (Jeézek and Fenner, 1988). Most of the clinical features of human monkeypox are very similar to those of ordinary smallpox (Breman and Arita, 1980). After a 7- to 21-day-incubation period, the disease begins with fever, malaise, headache, sore throat, and cough. The main sign of the disease that distinguishes monkeypox from smallpox is swollen lymph nodes (lymphadenitis), which is observed in most of the patients before the development of rash (Di Giulio and Eckburg, 2004; Jeézek and Fenner, 1988). A typical maculopapular rash follows the prodromal period, generally lasting 1–3 days. The average size of the skin lesions are 0.5–1 cm and the progress of lesions follows the order: macules, papules, vesicles, pustules, umblication then scab, and desquamation and lasts typically 2–4 weeks. The fatality rate is 10% among the unvaccinated population and death generally occurs during the 2nd week of the disease (Jeézek and Fenner, 1988; Nalca et al., 2005).

MPXV is highly pathogenic for a variety of laboratory animals and many animal models have been developed by using different species and different routes of exposure (Table 33.3). Due to unavailability of variola virus (smallpox) to develop animal models and similar disease manifestations in humans that are similar, MPXV

TABLE 33.3 MPXV Animal Models

Animal model	Route of exposure	Clinical outcome in animals	References
Mice	IN	Weight loss, viremia, mortality	Americo et al. (2010)
	Intraperitoneal	Weight loss, viremia, mortality	Americo et al. (2010), Osorio et al. (2009)
Prairie dogs	Intraperitoneal	Rash, viremia, splenic/hepatic lesions, mortality	Xiao et al. (2005)
	IN	Rash, viremia, pulmonary edema,	Hutson et al. (2009), Xiao et al. (2005)
	Intradermal	Rash (generalized), viremia	Hutson et al. (2009)
Ground squirrels	Intraperitoneal	Anorexia, lethargy, viremia, mortality	Tesh et al. (2004)
	IN	Anorexia, lethargy, viremia, mortality	Tesh et al. (2004)
	Subcutaneous	Anorexia, lethargy, viremia, mortality	Sbrana et al. (2007)
Dormice	IN	Weight loss, viremia, hemorrhage in internal organs	Schultz et al. (2009)
	Footpad injection	Lethargy, weight loss, hemorrhage in internal organs, mortality	Schultz et al. (2009)
NHP	Aerosol	Fever, lymphadenopathy, rash (−/+), broncho-pneumonia, viremia	Nalca et al. (2010), Zaucha et al. (2001)
	Intravenous	fever, lymphadenopathy, vesiculopustular rash, viremia, mortality	Earl et al. (2015), Edghill-Smith et al. (2005)
	IN	Fever, weight loss, rash, viremia	Saijo et al. (2009)
	Intratracheal	Fever, weight loss, lymphadenopathy, rash, viremia	Goff et al. (2011), Stittelaar et al. (2006)
	Intrabronchial	Fever, rash, viremia	Johnson et al. (2011)

IN, Intranasal; MPXV, monkeypox virus.

is one of the pox viruses that are utilized very heavily to develop a number of small animal models via different routes of exposure. Wild-derived inbred mouse, STAT1-deficient C57BL/6 mouse, ICR mouse, prairie dogs, African dormice, ground squirrels, and Gambian pouched rats are highly susceptible to MPXV by different exposure routes (Americo et al., 2010; Falendysz et al., 2015; Hutson et al., 2009; Osorio et al., 2009; Sbrana et al., 2007; Schultz et al., 2009; Sergeev et al., 2016; Stabenow et al., 2010; Tesh et al., 2004; Xiao et al., 2005).

CAST/EiJ mice, one of the 38 inbred mouse strains tested for susceptibility to MPXV, showed weight loss and dose dependent mortality after IN exposure to MPXV. Studies with IP route of challenge indicated a 50-fold higher susceptibility to MPXV when compared to IN route (Americo et al., 2010).

SCID-BALB/c mice were also susceptible to the IP challenge route and the disease resulted in mortality on day 9 postinfection (Osorio et al., 2009). Similarly, C57BL/6 STAT1$^{-/-}$ mice were infected IN with MPXV and the infection resulted in weight loss and mortality 10 days postexposure. Recently Sergeev et al. (2016) showed that IN challenge of ICR mice with MPXV resulted in purulent conjunctivitis, blepharitis, and ruffled fur in these mice although there was no death. The mouse models mentioned here are very promising for screening therapeutics against poxviruses but testing in additional models will be required for advanced development.

High doses of the MPXV by IP or IN routes caused 100% mortality in 6 days postexposure and 8 days postexposure, respectively, in ground squirrels (Tesh et al., 2004). The disease progressed very quickly and most of the animals were lethargic and moribund by day 5 postexposure without any pox lesions or respiratory changes. A comparison study of USA MPXV and Central African strain of MPXV strains in ground squirrels by the subQ route resulted in systemic disease and mortality in 6–11 days postexposure. The disease resembles hemorrhagic smallpox with nosebleeds, impaired coagulation parameters, and hemorrhage in the lungs of the animals. Another study by Sergeev et al. (2017) showed that IN challenge with MPXV caused fever, lymphadenitis, and skin rash in ground squirrels 7–9 days postexposure. Mortality was observed in 40% of the animals 13–22 days postexposure (Sergeev et al., 2017).

Since MPXV was transmitted by infected prairie dogs in the US outbreak, this animal model has been more thoroughly studied and utilized to test therapeutics and vaccines compared to other small animal models (Hutson et al., 2009; Keckler et al., 2011; Smith et al., 2011; Xiao et al., 2005). Studies using IN, IP, and ID routes of exposure showed that MPXV was highly infectious to prairie dogs, IP infection with the West African MPXV strain caused a more severe disease and 100% mortality than challenge by the IN route. Anorexia and lethargy were

common signs of the disease for both exposure routes. In contrast to IP route, the IN route of exposure caused severe pulmonary edema and necrosis of lungs in prairie dogs, while splenic necrosis and hepatic lesions were observed in IP-infected animals (Xiao et al., 2005). Hutson et al. (2009) utilized IN and ID infections with West African and Congo basin strains and showed that both strains and routes caused smallpox-like disease with longer incubation periods and most importantly generalized pox lesions. Therefore, this model has the utility for testing therapeutics and vaccines against pox viruses. Furthermore, MPXV challenged prairie dogs were used to perform in vivo bioluminescent imaging (BLI) studies (Falendysz et al., 2015). BLI studies showed real time spread of virus in prairie dogs as well as potential routes for shedding and transmission.

The African dormouse is susceptible to MPXV by a footpad injection or IN routes (Schultz et al., 2009). Mice had decreased activity, hunched posture, dehydration, conjunctivitis, and weight loss. Viral doses of 200 and 2000 pfu provided 100% mortality with a mean time to death of 8 days. Upper gastrointestinal hemorrhage, hepatomegaly, lymphadenopathy, and lung hemorrhage were observed during necropsy. With the hemorrhage in several organs, this model resembles hemorrhagic smallpox.

In a recent study, comparison of the disease pathogenesis was performed by using live bioluminescence imaging in the CAST/EiJ mouse and African dormouse challenged with low dose of MPXV (Earl et al., 2015). Following IN challenge, MPXV dissemination occurred through the blood or lymphatic system in dormice compared to dissemination that was through the nasal cavity and lungs in CAST/EiJ mice. The disease course was much faster in CAST/EiJ mice (Earl et al., 2015). Considering the limited availability of prairie dogs, ground squirrels and African dormice, lack of reagents specific for these species, and not having commercial sources of these species, these small animal models are as attractive for further characterization and vaccine, and countermeasure testing studies.

NHPs were exposed to MPXV by several different routes to develop animal model for MPXV (Edghill-Smith et al., 2005; Johnson et al., 2011; Nalca et al., 2010; Stittelaar et al., 2006; Zaucha et al., 2001). During our studies using an aerosol route of exposure, we observed that macaques had mild anorexia, depression, fever, and lymphadenopathy on day 6 postexposure (Nalca et al., 2010). Complete blood count and clinical chemistries showed abnormalities similar to human monkeypox cases with leukocytosis and thrombocytopenia (Huhn et al., 2005). Whole blood and throat swabs had viral loads peak around day 10, and in survivors, gradually decrease until day 28 postexposure. Since doses of 4×10^4 pfu, 1×10^5 pfu, or 1×10^6 pfu resulted in lethality for 70% of the animals,

whereas a dose of 4×10^5 pfu resulted in 85% lethality, survival was not dose dependent. The main pitfall of this model was the lack of pox lesions. With the high dose, animals succumbed to disease before developing pox lesions. With the low challenge dose, pox lesions were observed but they were few in comparison to the IV model. A recent study also evaluated the cytokine levels in aerosol challenged animals. (Tree et al., 2015). Tree et al. (2015) showed that IFNγ, IL-1rα, and IL-6 increased dramatically on day 8 postexposure the day that death was most likely to occur, and viral DNA was detected in most of the tissues. These results support the idea of a cytokine storm causing mortality in monkeypox disease.

MPXV causes dose dependent disease in NHPs when given by the IV route (Johnson et al., 2011). Studies showed that a 1×10^7 pfu IV challenge results in systemic disease with fever, lymphadenopathy, macula-papular rash, and mortality.

An IT infection model skips the upper respiratory system and deposits virus into the trachea, delivering the virus directly to the airways without regard to particle size and the physiological deposition that occurs during the process of inhalation. Fibrinonecrotic bronchopneumonia was described in animals that received 10^7 pfu of MPXV intratracheally (Stittelaar et al., 2006). Although a similar challenge dose of IT MPXV infection resulted in a similar viremia in NHPs to the aerosol route of infection, the timing of the first peak was delayed by 5 days in intratracheally exposed macaques compared to aerosol infection, and the amount of virus detected by qPCR was approximately 100-fold lower. This suggests that local replication is more prominent after aerosol delivery compared to the IT route.

An intrabronchial route of exposure resulted in pneumonia in NHPs (Johnson et al., 2011). Delayed onset of clinical signs and viremia were observed during the disease progression. In this model, similar to aerosol and IT infection models, the number of pox lesions was much less than in the IV infection model.

A major downside of the IV, IT, and intrabronchial models is that the initial infection of respiratory tissue, incubation, and prodromal phases are circumvented with the direct inoculation of virus to the blood stream or to the lung. This is an important limitation when the utility of these models is to test possible vaccines and treatments in which the efficacy may depend on protecting the respiratory mucosa and targeting the subsequent early stages of the infection, which are not represented in these challenge models. Although the aerosol model is the natural route of transmission for human VARV infections and a secondary route for human MPXV infections, the lack of pox lesions is the main drawback of this model. Therefore, when this model is used to test medical countermeasures, the endpoints and the biomarkers to initiate treatment should be chosen carefully.

13 HEPADNAVIRIDAE

13.1 Hepatitis B

Hepatitis B virus (HBV) is one of the most common infections worldwide with over 400 million people chronically infected and 316,000 cases per year of liver cancer due to infection (Lee, 1997). The virus can naturally infect both humans and chimpanzees (Guha et al., 2004). HBV is transmitted parenterally or postnatally from infected mothers. It can also be transmitted by sexual contact, IV drug use, blood transfusion, and acupuncture (Lai et al., 2003). The age at which one is infected dictates the risk of developing chronic disease (Hyams, 1995).

Acute infection during adulthood is self-limiting and results in flu-like symptoms that can progress to hepatocellular involvement as observed with the development of jaundice. The clinical symptoms of HBV infection last for a few weeks before resolving (Ganem and Prince, 2004). After this acute phase, lifetime immunity is achieved (Wright and Lau, 1993). Of those infected, less than 5% will develop the chronic form of the disease. Chronicity is the most serious outcome of the disease as it can result in cirrhosis or liver cancer. Hepatocellular carcinoma is 100 times more likely to develop in a chronically infected individual than a noncarrier (Beasley, 1988). The viral determinant for cellular transformation has yet to be determined, although studies involving the woodchuck hepatitis virus suggest that X protein may be responsible (Spandau and Lee, 1988). Many individuals are asymptomatic until complications emerge related to chronic HBV carriage.

Chimpanzees have a unique strain that circulates within the population (Hu et al., 2000; MacDonald et al., 2000). It was found that 3%–6% of all wild-caught animals from Africa are positive for HBV antigen (Lander et al., 1972). Natural and experimental challenge with the virus follows the same course as human disease; however, this is only an acute model of disease (Prince, 1972). To date, chimpanzees are the only reliable method to ensure that plasma vaccines are free from infectious particles (Prince and Brotman, 2001). This animal model has been used to study new therapeutics and vaccines. Chimpanzees are especially ideal for these studies given that their immune response to infection directly mirrors humans (Nayersina et al., 1993). Recent regulations by the National Institute of Health (NIH) and restrictions to use great apes as animal models forced researches to find alternate models for HBV infection.

Other NHPs that have been evaluated are gibbons, orangutans, and rhesus monkeys. Although these animals can be infected with HBV, none develops hepatic lesions or liver damage as noted by monitoring of liver enzymes (Pillot, 1990).

Mice are not permissible to infection, and thus numerous transgenic and humanized lines that express HBV proteins have been created to facilitate their usage as an animal model. These include both immunocompetent and immunosuppressed hosts. The caveat to all of these mouse lines is that they reproduce only the acute form of disease (Guha et al., 2004). Recently, the entire genome of HBV was transferred to an immunocompetent mouse line via adenovirus. This provides a model for persistent infection (Huang et al., 2012).

Another model that has been developed is hydrodynamic injection of HBV genomes in the liver of mice (Liu et al., 1999; Yang et al., 2002). Although this model is very stressful to mice and has liver toxicity, it is successfully used to evaluate antivirals against HBV (McCaffrey et al., 2003). Liver chimeric mouse models are an additional set of surrogate models for HBV infection (Dandri and Lutgehetmann, 2014). In these models human hepatocytes are integrated into the murine liver parenchyma (Allweiss and Dandri, 2016). This model might be used to test antivirals as well as to study the molecular biology of HBV infection.

HBV can also be studied using surrogate viruses, naturally occurring mammalian hepadna viruses (Mason et al., 1982). The woodchuck hepatitis virus induces hepatocellular carcinoma (Summers et al., 1978). Within a population, 65%–75% of all neonatal woodchucks are susceptible to chronic infection (Cote et al., 2000). A major difference between the two hepatitis isolates is the rate at which they induce cancer; almost all chronic carriers developed hepatocellular carcinoma within 3 years of the initial infection in woodchucks, whereas human carcinogenesis takes much longer (Gerin et al., 1989). The acute infection strongly resembles what occurs during the course of human disease. There is a self-limiting acute phase resulting in a transient viremia that has the potential of chronic carriage (Tennant, 2001). Challenge with virus in neonates leads to a chronic infection while adults only develop the acute phase of disease (Buendia, 1992). A closely related species to the woodchuck is the *Marmota himalayan*. This animal is also susceptible to the woodchuck hepadna virus upon IV injection. The marmot Himalayan develops an acute hepatitis with a productive infection (Lucifora et al., 2010).

Hepatitis D virus (HDV) is dependent upon HBV to undergo replication and successful infection in its human host (Gerin, 2001). There are two modes of infection possible between the viruses: coinfection where a person is simultaneously infected or superinfection in which a chronic carrier of HBV is subsequently infected with HDV (Purcell et al., 1987). Coinfection leads to a similar disease as seen with HBV alone; however, superinfection can result in chronic HDV infection and severe liver damage (Guilhot et al., 1994). Both coinfection and superinfection can be demonstrated within the chimpanzee and woodchuck by inoculation of human hepatitis D (Ponzetto et al., 1991). A recently published report demonstrated the use of a humanized chimeric uPA mouse to study interactions between the two viruses and drug testing (Lutgehetmann et al., 2012)

14 CONCLUSIONS

New models ranging from NHPs to small animals and representing the disease characteristics in humans are necessary to study viral and host factors that drive disease pathogenesis and evaluate medical countermeasures. The ideal animal model for human viral disease should closely recapitulate the spectrum of clinical symptoms and pathogenesis observed during the course of human infection. Whenever feasible, the model should use the same virus and strain that infects humans. It is also preferable that the virus is a low passage clinical isolate thus animal passage or adaptation should be avoided if model species can be identified that are susceptible. Ideally, the experimental route of infection would mirror that occurs in natural disease. In order to understand the interplay and contribution of the immune system during infection, an immunocompetent animal should be used. The aforementioned characteristics cannot always be satisfied; however, and often virus must be adapted, knockout mice must be used, and/or the disease is not perfectly mimicked in the animal model. Well-characterized animal models are critical for licensure to satisfy FDA "Animal Rule." This rule applies to situations in which vaccine and therapeutic efficacy cannot safely or ethically be tested in humans; thus licensure will come only after preclinical tests are performed in animal models. Many fields in virology are moving toward standardized models that can be used across institutions to test vaccines and therapeutics. A current example of such an effort is within the filovirus community, where animal models, euthanasia criteria, assays, and virus strains are in the process of being standardized. The hope is that these efforts will enable results of efficacy tests on medical countermeasures compared across institutions. This chapter has summarized the best models available for each of the viruses described.

Acknowledgments

References

Abel, K., 2009. The rhesus macaque pediatric SIV infection model—a valuable tool in understanding infant HIV-1 pathogenesis and for designing pediatric HIV-1 prevention strategies. Curr. HIV Res. 7 (1), 2–11.

Abu-Elyazeed, R., el-Sharkawy, S., Olson, J., Botros, B., Soliman, A., Salib, A., et al., 1996. Prevalence of anti-Rift-Valley-fever IgM antibody in abattoir workers in the Nile delta during the 1993 outbreak in Egypt. Bull. World Health Organ. 74 (2), 155–158.

Adams, A.P., Aronson, J.F., Tardif, S.D., Patterson, J.L., Brasky, K.M., Geiger, R., et al., 2008. Common marmosets (Callithrix jacchus) as a nonhuman primate model to assess the virulence of eastern equine encephalitis virus strains. J. Virol. 82 (18), 9035–9042.

Adney, D.R., van Doremalen, N., Brown, V.R., Bushmaker, T., Scott, D., de Wit, E., et al., 2014. Replication and shedding of MERS-CoV in upper respiratory tract of inoculated dromedary camels. Emerg. Infect. Dis. 20 (12), 1999–2005.

Agrawal, A.S., Garron, T., Tao, X., Peng, B.H., Wakamiya, M., Chan, T.S., et al., 2015. Generation of a transgenic mouse model of Middle East respiratory syndrome coronavirus infection and disease. J. Virol. 89 (7), 3659–3670.

Aguilar, M.J., 1970. Pathological changes in brain and other target organs of infant and weanling mice after infection with non-neuroadapted Western equine encephalitis virus. Infect. Immun. 2 (5), 533–542.

Alfson, K.J., Avena, L.E., Beadles, M.W., Staples, H., Nunneley, J.W., Ticer, A., et al., 2015. Particle-to-PFU ratio of Ebola virus influences disease course and survival in cynomolgus macaques. J. Virol. 89 (13), 6773–6781.

Aliabadi, N., Lopman, B.A., Parashar, U.D., Hall, A.J., 2015. Progress toward norovirus vaccines: considerations for further development and implementation in potential target populations. Expert. Rev. Vaccines 14 (9), 1241–1253.

Aliota, M.T., Caine, E.A., Walker, E.C., Larkin, K.E., Camacho, E., Osorio, J.E., 2016. Characterization of lethal Zika virus infection in AG129 mice. PLoS Negl. Trop. Dis. 10 (4), e0004682.

Allweiss, L., Dandri, M., 2016. Experimental in vitro and in vivo models for the study of human hepatitis B virus infection. J. Hepatol. 64 (1 Suppl.), S17–S31.

Alonso, J.M., Guiyoule, A., Zarantonelli, M.L., Ramisse, F., Pires, R., Antignac, A., et al., 2003. A model of meningococcal bacteremia after respiratory superinfection in influenza A virus-infected mice. FEMS Microbiol. Lett. 222 (1), 99–106.

Al-Tawfiq, J.A., Omrani, A.S., Memish, Z.A., 2016. Middle East respiratory syndrome coronavirus: current situation and travel-associated concerns. Front. Med. 10 (2), 111–119.

Alves, D.A., Glynn, A.R., Steele, K.E., Lackemeyer, M.G., Garza, N.L., Buck, J.G., et al., 2010. Aerosol exposure to the Angola strain of marburg virus causes lethal viral hemorrhagic fever in cynomolgus macaques. Vet. Pathol. 47 (5), 831–851.

Alves, D.A., Honko, A.N., Kortepeter, M.G., Sun, M., Johnson, J.C., Lugo-Roman, L.A., Hensley, L.E., 2016. Necrotizing scleritis, conjunctivitis, and other pathologic findings in the left eye and brain of an Ebola Virus-Infected rhesus macaque (Macaca mulatta) with apparent recovery and a delayed time of death. J. Infect. Dis. 213 (1), 57–60.

American Academy of Pediatrics Subcommittee on Diagnosis and Management of Bronchiolitis, 2006. Diagnosis and management of bronchiolitis. Pediatrics 118 (4), 1774–1793.

Americo, J.L., Moss, B., Earl, P.L., 2010. Identification of wild-derived inbred mouse strains highly susceptible to monkeypox virus infection for use as small animal models. J. Virol. 84 (16), 8172–8180.

Amorosa, V., MacNeil, A., McConnell, R., Patel, A., Dillon, K.E., Hamilton, K., et al., 2010. Imported Lassa fever, Pennsylvania, USA, 2010. Emerg. Infect. Dis. 16 (10), 1598–1600.

Anderson, Jr., G.W., Slone, Jr., T.W., Peters, C.J., 1988. The gerbil, Meriones unguiculatus, a model for Rift Valley fever viral encephalitis. Arch. Virol. 102 (3–4), 187–196.

Anderson, N.W., Binnicker, M.J., Harris, D.M., Chirila, R.M., Brumble, L., Mandrekar, J., Hata, D.J., 2016. Morbidity and mortality among patients with respiratory syncytial virus infection: a 2-year retrospective review. Diagn. Microbiol. Infect. Dis. 85 (3), 367–371.

Arpino, C., Curatolo, P., Rezza, G., 2009. Chikungunya and the nervous system: what we do and do not know. Rev. Med. Virol. 19 (3), 121–129.

Asnis, D.S., Conetta, R., Teixeira, A.A., Waldman, G., Sampson, B.A., 2000. The West Nile virus outbreak of 1999 in New York: the Flushing Hospital experience. Clin. Infect. Dis. 30 (3), 413–418.

Assiri, A., McGeer, A., Perl, T.M., Price, C.S., Al Rabeeah, A.A., Cummings, D.A., et al., 2013. Hospital outbreak of Middle East respiratory syndrome coronavirus. N. Engl. J. Med. 369 (5), 407–416.

Atmar, R.L., Estes, M.K., 2001. Diagnosis of noncultivatable gastroenteritis viruses, the human caliciviruses. Clin. Microbiol. Rev. 14 (1), 15–37.

Atmar, R.L., Bernstein, D.I., Harro, C.D., Al-Ibrahim, M.S., Chen, W.H., Ferreira, J., et al., 2011. Norovirus vaccine against experimental human Norwalk Virus illness. N. Engl. J. Med. 365 (23), 2178–2187.

Atmar, R.L., Opekun, A.R., Gilger, M.A., Estes, M.K., Crawford, S.E., Neill, F.H., et al., 2014. Determination of the 50% human infectious dose for Norwalk virus. J. Infect. Dis. 209 (7), 1016–1022.

Ayers, J.R., Lester, T.L., Angulo, A.B., 1994. An epizootic attributable to Western equine encephalitis virus infection in emus in Texas. J. Am. Vet. Med. Assoc. 205 (4), 600–601.

Azhar, E.I., El-Kafrawy, S.A., Farraj, S.A., Hassan, A.M., Al-Saeed, M.S., Hashem, A.M., Madani, T.A., 2014. Evidence for camel-to-human transmission of MERS coronavirus. N. Engl. J. Med. 370 (26), 2499–2505.

Baas, T., Baskin, C.R., Diamond, D.L., Garcia-Sastre, A., Bielefeldt-Ohmann, H., Tumpey, T.M., et al., 2006. Integrated molecular signature of disease: analysis of influenza virus-infected macaques through functional genomics and proteomics. J. Virol. 80 (21), 10813–10828.

Baenziger, S., Tussiwand, R., Schlaepfer, E., Mazzucchelli, L., Heikenwalder, M., Kurrer, M.O., et al., 2006. Disseminated and sustained HIV infection in CD34+ cord blood cell-transplanted Rag2$^{-/-}$gamma c$^{-/-}$ mice. Proc. Natl. Acad. Sci. USA 103 (43), 15951–15956.

Bales, J.M., Powell, D.S., Bethel, L.M., Reed, D.S., Hartman, A.L., 2012. Choice of inbred rat strain impacts lethality and disease course after respiratory infection with Rift Valley fever virus. Front. Cell Infect. Microbiol. 2, 105.

Balkhy, H.H., Memish, Z.A., 2003. Rift Valley fever: an uninvited zoonosis in the Arabian peninsula. Int. J. Antimicrob. Agents 21 (2), 153–157.

Ball, J.M., Graham, D.Y., Opekun, A.R., Gilger, M.A., Guerrero, R.A., Estes, M.K., 1999. Recombinant Norwalk virus-like particles given orally to volunteers: phase I study. Gastroenterology 117 (1), 40–48.

Balsitis, S.J., Coloma, J., Castro, G., Alava, A., Flores, D., McKerrow, J.H., et al., 2009. Tropism of dengue virus in mice and humans defined by viral nonstructural protein 3-specific immunostaining. Am. J. Trop. Med. Hyg. 80 (3), 416–424.

Balsitis, S.J., Williams, K.L., Lachica, R., Flores, D., Kyle, J.L., Mehlhop, E., et al., 2010. Lethal antibody enhancement of dengue disease in mice is prevented by Fc modification. PLoS Pathog. 6 (2), e1000790.

Barnard, D.L., 2009. Animal models for the study of influenza pathogenesis and therapy. Antiviral Res. 82 (2), A110–122.

Barnard, D.L., Wong, M.H., Bailey, K., Day, C.W., Sidwell, R.W., Hickok, S.S., Hall, T.J., 2007. Effect of oral gavage treatment with ZnAL42 and other metallo-ion formulations on influenza A H5N1 and H1N1 virus infections in mice. Antivir. Chem. Chemother. 18 (3), 125–132.

Barouch, D.H., Klasse, P.J., Dufour, J., Veazey, R.S., Moore, J.P., 2012. Macaque studies of vaccine and microbicide combinations for preventing HIV-1 sexual transmission. Proc. Natl. Acad. Sci. USA 109 (22), 8694–8698.

Baskin, C.R., Bielefeldt-Ohmann, H., Tumpey, T.M., Sabourin, P.J., Long, J.P., Garcia-Sastre, A., et al., 2009. Early and sustained innate immune response defines pathology and death in nonhuman primates infected by highly pathogenic influenza virus. Proc. Natl. Acad. Sci. USA 106 (9), 3455–3460.

Beasley, R.P., 1988. Hepatitis B virus. The major etiology of hepatocellular carcinoma. Cancer 61 (10), 1942–1956.

Becker, K.M., Moe, C.L., Southwick, K.L., MacCormack, J.N., 2000. Transmission of Norwalk virus during football game. N. Engl. J. Med. 343 (17), 1223–1227.

Belshan, M., Kimata, J.T., Brown, C., Cheng, X., McCulley, A., Larsen, A., et al., 2012. Vpx is critical for SIVmne infection of pigtail macaques. Retrovirology 9, 32.

Belshe, R.B., Richardson, L.S., London, W.T., Sly, D.L., Lorfeld, J.H., Camargo, E., et al., 1977. Experimental respiratory syncytial virus infection of four species of primates. J. Med. Virol. 1 (3), 157–162.

Bente, D.A., Alimonti, J.B., Shieh, W.J., Camus, G., Stroher, U., Zaki, S., Jones, S.M., 2010. Pathogenesis and immune response of Crimean-Congo hemorrhagic fever virus in a STAT-1 knockout mouse model. J. Virol. 84 (21), 11089–11100.

Bereczky, S., Lindegren, G., Karlberg, H., Akerstrom, S., Klingstrom, J., Mirazimi, A., 2010. Crimean-Congo hemorrhagic fever virus infection is lethal for adult type I interferon receptor-knockout mice. J. Gen. Virol. 91 (Pt 6), 1473–1477.

Berges, B.K., Rowan, M.R., 2011. The utility of the new generation of humanized mice to study HIV-1 infection: transmission, prevention, pathogenesis, and treatment. Retrovirology 8, 65.

Berges, B.K., Wheat, W.H., Palmer, B.E., Connick, E., Akkina, R., 2006. HIV-1 infection and CD4 T cell depletion in the humanized Rag2$^{-/-}$ gamma c$^{-/-}$ (RAG-hu) mouse model. Retrovirology 3, 76.

Berhane, Y., Weingartl, H.M., Lopez, J., Neufeld, J., Czub, S., Embury-Hyatt, C., et al., 2008. Bacterial infections in pigs experimentally infected with Nipah virus. Transbound. Emerg. Dis. 55 (3–4), 165–174.

Bingham, J., Payne, J., Harper, J., Frazer, L., Eastwood, S., Wilson, S., et al., 2014. Evaluation of a mouse model for the West Nile virus group for the purpose of determining viral pathotypes. J. Gen. Virol. 95 (Pt 6), 1221–1232.

Bisht, H., Roberts, A., Vogel, L., Bukreyev, A., Collins, P.L., Murphy, B.R., et al., 2004. Severe acute respiratory syndrome coronavirus spike protein expressed by attenuated vaccinia virus protectively immunizes mice. Proc. Natl. Acad. Sci. USA 101 (17), 6641–6646.

Blagoveshchenskaya, N.M., Donets, M.A., Zarubina, L.V., Kondratenko, V.F., Kuchin, V.V., 1975. Study of susceptibility to Crimean hemorrhagic fever (CHF) virus in European and long-eared hedgehogs. Tezisy Konf. Vop. Med. Virus., 269–270.

Blakely, P.K., Delekta, P.C., Miller, D.J., Irani, D.N., 2015. Manipulation of host factors optimizes the pathogenesis of Western equine encephalitis virus infections in mice for antiviral drug development. J. Neurovirol. 21 (1), 43–55.

Blaney, Jr., J.E., Johnson, D.H., Manipon, G.G., Firestone, C.Y., Hanson, C.T., Murphy, B.R., Whitehead, S.S., 2002. Genetic basis of attenuation of dengue virus type 4 small plaque mutants with restricted replication in suckling mice and in SCID mice transplanted with human liver cells. Virology 300 (1), 125–139.

Bok, K., Parra, G.I., Mitra, T., Abente, E., Shaver, C.K., Boon, D., et al., 2011. Chimpanzees as an animal model for human norovirus infection and vaccine development. Proc. Natl. Acad. Sci. USA 108 (1), 325–330.

Boorman, J.P., Porterfield, J.S., 1956. A simple technique for infection of mosquitoes with viruses; transmission of Zika virus. Trans. R. Soc. Trop. Med. Hyg. 50 (3), 238–242.

Borzacchiello, G., Roperto, F., Nasir, L., Campo, M.S., 2009. Human papillomavirus research: do we still need animal models? Int. J. Cancer 125 (3), 739–740.

Bosch, F.X., de Sanjose, S., 2002. Human papillomavirus in cervical cancer. Curr. Oncol. Rep. 4 (2), 175–183.

Bosco-Lauth, A.M., Han, S., Hartwig, A., Bowen, R.A., 2015. Development of a hamster model for Chikungunya virus infection and pathogenesis. PLoS One 10 (6), e0130150.

Bossart, K.N., Zhu, Z., Middleton, D., Klippel, J., Crameri, G., Bingham, J., et al., 2009. A neutralizing human monoclonal antibody protects against lethal infection in a new ferret model of acute nipah virus infection. PLoS Pathog. 5 (10), e1000642.

Boukhvalova, M.S., Prince, G.A., Blanco, J.C., 2009. The cotton rat model of respiratory viral infections. Biologicals 37 (3), 152–159.

Bradfute, S.B., Bavari, S., 2011. Correlates of immunity to filovirus infection. Viruses 3 (7), 982–1000.

Bradfute, S.B., Dye, Jr., J.M., Bavari, S., 2011. Filovirus vaccines. Hum. Vaccin. 7 (6), 701–711.

Brainard, D.M., Seung, E., Frahm, N., Cariappa, A., Bailey, C.C., Hart, W.K., et al., 2009. Induction of robust cellular and humoral virus-specific adaptive immune responses in human immunodeficiency virus-infected humanized BLT mice. J. Virol. 83 (14), 7305–7321.

Brandsma, J.L., 1994. Animal models of human-papillomavirus-associated oncogenesis. Intervirology 37 (3–4), 189–200.

Brannan, J.M., Froude, J.W., Prugar, L.I., Bakken, R.R., Zak, S.E., Daye, S.P., et al., 2015. Interferon alpha/beta receptor-deficient mice as a model for Ebola virus disease. J. Infect. Dis. 212 (Suppl. 2), S282–S294.

Brasil, P., Calvet, G.A., Siqueira, A.M., Wakimoto, M., de Sequeira, P.C., Nobre, A., et al., 2016. Zika virus outbreak in Rio de Janeiro, Brazil: clinical characterization, epidemiological and virological aspects. PLoS Negl. Trop. Dis. 10 (4), e0004636.

Braun, L.E., Sutter, D.E., Eichelberger, M.C., Pletneva, L., Kokai-Kun, J.F., Blanco, J.C., et al., 2007a. Co-infection of the cotton rat (*Sigmodon hispidus*) with *Staphylococcus aureus* and influenza A virus results in synergistic disease. Microb. Pathog. 43 (5–6), 208–216.

Braun, M.M., Izurieta, H.S., Ball, R., 2007b. Effectiveness of influenza vaccination. N. Engl. J. Med. 357 (26), 2730, (author reply 2730–2731).

Bray, M., 2001. The role of the type I interferon response in the resistance of mice to filovirus infection. J. Gen. Virol. 82 (Pt 6), 1365–1373.

Bray, M., Davis, K., Geisbert, T., Schmaljohn, C., Huggins, J., 1999. A mouse model for evaluation of prophylaxis and therapy of Ebola hemorrhagic fever. J. Infect. Dis. 179 (Suppl. 1), S248–S258.

Breitburd, F., Salmon, J., Orth, G., 1997. The rabbit viral skin papillomas and carcinomas: a model for the immunogenetics of HPV-associated carcinogenesis. Clin. Dermatol. 15 (2), 237–247.

Breman, J.G., Arita, I., 1980. The confirmation and maintenance of smallpox eradication. N. Engl. J. Med. 303 (22), 1263–1273.

Brocato, R.L., Hammerbeck, C.D., Bell, T.M., Wells, J.B., Queen, L.A., Hooper, J.W., 2014. A lethal disease model for hantavirus pulmonary syndrome in immunosuppressed Syrian hamsters infected with Sin Nombre virus. J. Virol. 88 (2), 811–819.

Broeckel, R., Haese, N., Messaoudi, I., Streblow, D.N., 2015. Nonhuman primate models of Chikungunya virus infection and disease (CHIKV NHP model). Pathogens 4 (3), 662–681.

Brown, A.N., Kent, K.A., Bennett, C.J., Bernard, K.A., 2007. Tissue tropism and neuroinvasion of West Nile virus do not differ for two mouse strains with different survival rates. Virology 368 (2), 422–430.

Bucardo, F., Nordgren, J., Carlsson, B., Paniagua, M., Lindgren, P.E., Espinoza, F., Svensson, L., 2008. Pediatric norovirus diarrhea in Nicaragua. J. Clin. Microbiol. 46 (8), 2573–2580.

Buchbinder, S.P., Mehrotra, D.V., Duerr, A., Fitzgerald, D.W., Mogg, R., Li, D., et al., 2008. Efficacy assessment of a cell-mediated immunity HIV-1 vaccine (the Step Study): a double-blind, randomised, placebo-controlled, test-of-concept trial. Lancet 372 (9653), 1881–1893.

Buchmeier, M.J., Rawls, W.E., 1977. Variation between strains of hamsters in the lethality of Pichinde virus infections. Infect. Immun. 16 (2), 413–421.

Buendia, M.A., 1992. Hepatitis B viruses and hepatocellular carcinoma. Adv. Cancer Res. 59, 167–226.

Bulut, G., Uren, A., 2015. Generation of K14-E7/N87betacat double transgenic mice as a model of cervical cancer. Methods Mol. Biol. 1249, 393–406.

Burton, D.R., Hessell, A.J., Keele, B.F., Klasse, P.J., Ketas, T.A., Moldt, B., et al., 2011. Limited or no protection by weakly or nonneutralizing antibodies against vaginal SHIV challenge of macaques compared with a strongly neutralizing antibody. Proc. Natl. Acad. Sci. USA 108 (27), 11181–11186.

Buttigieg, K.R., Dowall, S.D., Findlay-Wilson, S., Miloszewska, A., Rayner, E., Hewson, R., Carroll, M.W., 2014. A novel vaccine against Crimean-Congo haemorrhagic fever protects 100% of animals against lethal challenge in a mouse model. PLoS One 9 (3), e91516.

Byrne, S.N., Halliday, G.M., Johnston, L.J., King, N.J., 2001. Interleukin-1beta but not tumor necrosis factor is involved in West Nile virus-induced Langerhans cell migration from the skin in C57BL/6 mice. J. Invest. Dermatol. 117 (3), 702–709.

Campo, M.S., 2002. Animal models of papillomavirus pathogenesis. Virus Res. 89 (2), 249–261.

Canakoglu, N., et al., 2015. Immunization of knock-out alpha/beta interferon receptor mice against high lethal dose of Crimean-Congo hemorrhagic fever virus with a cell culture based vaccine. PLoS Negl. Trop. Dis. 9 (3), e0003579.

Carolan, L.A., Rockman, S., Borg, K., Guarnaccia, T., Reading, P., Mosse, J., et al., 2015. Characterization of the localized immune response in the respiratory tract of ferrets following infection with influenza A and B viruses. J. Virol. 90 (6), 2838–2848.

Carrion, Jr., R., Brasky, K., Mansfield, K., Johnson, C., Gonzales, M., Ticer, A., et al., 2007. Lassa virus infection in experimentally infected marmosets: liver pathology and immunophenotypic alterations in target tissues. J. Virol. 81 (12), 6482–6490.

Carrion, Jr., R., Ro, Y., Hoosien, K, Ticer, A., Brasky, K., de la Garza, M., et al., 2011. A small nonhuman primate model for filovirus-induced disease. Virology 420, 117–124.

Cavanagh, D., 2003. Severe acute respiratory syndrome vaccine development: experiences of vaccination against avian infectious bronchitis coronavirus. Avian Pathol. 32, 567–582.

Centers for Disease Control and Prevention, 1993. Outbreak of acute illness—southwestern United States, 1993. MMWR Morb. Mortal. Wkly. Rep. 42 (22), 421–424.

Centers for Disease Control and Prevention, 1999. Outbreak of West Nile-like viral encephalitis—New York, 1999. MMWR Morb. Mortal. Wkly. Rep. 48 (38), 845–849.

Chan, M.C., Ho, W.S., Sung, J.J., 2011. In vitro whole-virus binding of a norovirus genogroup II genotype 4 strain to cells of the lamina propria and Brunner's glands in the human duodenum. J. Virol. 85 (16), 8427–8430.

Chan, K.W., Watanabe, S., Kavishna, R., Alonso, S., Vasudevan, S.G., 2015. Animal models for studying dengue pathogenesis and therapy. Antiviral Res. 123, 5–14.

Charatan, F., 2003. US doctors investigate more than 50 possible cases of monkeypox. BMJ 326 (7403), 1350.

Charles, P.C., Walters, E., Margolis, F., Johnston, R.E., 1995. Mechanism of neuroinvasion of Venezuelan equine encephalitis virus in the mouse. Virology 208 (2), 662–671.

Charrel, R.N., de Lamballerie, X., Raoult, D., 2007. Chikungunya outbreaks—the globalization of vectorborne diseases. N. Engl. J. Med. 356 (8), 769–771.

Chaussee, M.S., Sandbulte, H.R., Schuneman, M.J., Depaula, F.P., Addengast, L.A., Schlenker, E.H., Huber, V.C., 2011. Inactivated and live, attenuated influenza vaccines protect mice against influenza: *Streptococcus pyogenes* super-infections. Vaccine 29 (21), 3773–3781.

Cheetham, S., Souza, M., Meulia, T., Grimes, S., Han, M.G., Saif, L.J., 2006. Pathogenesis of a genogroup II human norovirus in gnotobiotic pigs. J. Virol. 80 (21), 10372–10381.

Chen, J., Subbarao, K., 2007. The immunobiology of SARS*. Annu. Rev. Imsmunol. 25, 443–472.

Chen, S., Yu, M., Jiang, T., Deng, Y., Qin, C., Qin, E., 2007. Induction of tetravalent protective immunity against four dengue serotypes by the tandem domain III of the envelope protein. DNA Cell Biol. 26 (6), 361–367.

Chen, S.Y., Tsai, C.N., Lai, M.W., Chen, C.Y., Lin, K.L., Lin, T.Y., Chiu, C.H., 2009. Norovirus infection as a cause of diarrhea-associated benign infantile seizures. Clin. Infect. Dis. 48 (7), 849–855.

Chen, C.I., Clark, D.C., Pesavento, P., Lerche, N.W., Luciw, P.A., Reisen, W.K., Brault, A.C., 2010. Comparative pathogenesis of epidemic and enzootic Chikungunya viruses in a pregnant Rhesus macaque model. Am. J. Trop. Med. Hyg. 83 (6), 1249–1258.

Chen, Z., Sosnovtsev, S.V., Bok, K., Parra, G.I., Makiya, M., Agulto, L., et al., 2013. Development of Norwalk virus-specific monoclonal antibodies with therapeutic potential for the treatment of Norwalk virus gastroenteritis. J. Virol. 87 (17), 9547–9557.

Cheng, P.K., Wong, D.A., Tong, L.K., Ip, S.M., Lo, A.C., Lau, C.S., et al., 2004. Viral shedding patterns of coronavirus in patients with probable severe acute respiratory syndrome. Lancet 363 (9422), 1699–1700.

Choi, J.H., Schafer, S.C., Zhang, L., Kobinger, G.P., Juelich, T., Freiberg, A.N., Croyle, M.A., 2012. A single sublingual dose of an adenovirus-based vaccine protects against lethal Ebola challenge in mice and guinea pigs. Mol. Pharm. 9 (1), 156–167.

Chow, L.T., 2015. Model systems to study the life cycle of human papillomaviruses and HPV-associated cancers. Virol. Sin. 30 (2), 92–100.

Clay, C., Donart, N., Fomukong, N., Knight, J.B., Lei, W., Price, L., et al., 2012. Primary severe acute respiratory syndrome coronavirus infection limits replication but not lung inflammation upon homologous rechallenge. J. Virol. 86 (8), 4234–4244.

Collins, P.L., Graham, B.S., 2008. Viral and host factors in human respiratory syncytial virus pathogenesis. J. Virol. 82 (5), 2040–2055.

Connolly, B.M., Jenson, A.B., Peters, C.J., Geyer, S.J., Barth, J.F., McPherson, R.A., 1993. Pathogenesis of Pichinde virus infection in strain 13 guinea pigs: an immunocytochemical, virologic, and clinical chemistry study. Am. J. Trop. Med. Hyg. 49 (1), 10–24.

Connolly, B.M., Steele, K.E., Davis, K.J., Geisbert, T.W., Kell, W.M., Jaax, N.K., Jahrling, P.B., 1999. Pathogenesis of experimental Ebola virus infection in guinea pigs. J. Infect. Dis. 179 (Suppl. 1), S203–S217.

Connor, J.H., Yen, J., Caballero, I.S., Garamszegi, S., Malhotra, S., Lin, K., et al., 2015. Transcriptional profiling of the immune response to Marburg virus infection. J. Virol. 89 (19), 9865–9874.

Cormier, S.A., You, D., Honnegowda, S., 2010. The use of a neonatal mouse model to study respiratory syncytial virus infections. Expert. Rev. Anti. Infect. Ther. 8 (12), 1371–1380.

Costa, V.V., Fagundes, C.T., Valadao, D.F., Cisalpino, D., Dias, A.C., Silveira, K.D., et al., 2012. A model of DENV-3 infection that recapitulates severe disease and highlights the importance of IFN-gamma in host resistance to infection. PLoS Negl. Trop. Dis. 6 (5), e1663.

Cote, P.J., Korba, B.E., Miller, R.H., Jacob, J.R., Baldwin, B.H., Hornbuckle, W.E., et al., 2000. Effects of age and viral determinants on chronicity as an outcome of experimental woodchuck hepatitis virus infection. Hepatology 31 (1), 190–200.

Couderc, T., Chretien, F., Schilte, C., Disson, O., Brigitte, M., Guivel-Benhassine, F., et al., 2008. A mouse model for Chikungunya: young age and inefficient type-I interferon signaling are risk factors for severe disease. PLoS Pathog. 4 (2), e29.

Cox, J., Mota, J., Sukupolvi-Petty, S., Diamond, M.S., Rico-Hesse, R., 2012. Mosquito bite delivery of dengue virus enhances immunogenicity and pathogenesis in humanized mice. J. Virol. 86 (14), 7637–7649.

Cross, R.W., Fenton, K.A., Geisbert, J.B., Ebihara, H., Mire, C.E., Geisbert, T.W., 2015. Comparison of the pathogenesis of the Angola and Ravn strains of Marburg virus in the outbred guinea pig model. J. Infect. Dis. 212 (Suppl. 2), S258–S270.

Cugola, F.R., Fernandes, I.R., Russo, F.B., Freitas, B.C., Dias, J.L.,-Guimaraes, K.P., et al., 2016. The Brazilian Zika virus strain causes birth defects in experimental models. Nature 534 (7606), 267–271.

Culley, F.J., Pollott, J., Openshaw, P.J., 2002. Age at first viral infection determines the pattern of T cell-mediated disease during reinfection in adulthood. J. Exp. Med. 196 (10), 1381–1386.

Cummins, D., Bennett, D., Fisher-Hoch, S.P., Farrar, B., Machin, S.J., McCormick, J.B., 1992. Lassa fever encephalopathy: clinical and laboratory findings. J. Trop. Med. Hyg. 95 (3), 197–201.

Cunha, B.A., Minnaganti, V., Johnson, D.H., Klein, N.C., 2000. Profound and prolonged lymphocytopenia with West Nile encephalitis. Clin. Infect. Dis. 31 (4), 1116–1117.

Cunha, M.S., Esposito, D.L., Rocco, I.M., Maeda, A.Y., Vasami, F.G., Nogueira, J.S., et al., 2016. First complete genome sequence of Zika virus (Flaviviridae, Flavivirus) from an autochthonous transmission in Brazil. Genome Announc. 4 (2), 1–2.

Curtis, N., 2006. Viral haemorrhagic fevers caused by Lassa, Ebola, and Marburg viruses. In: Pollard, A.J., Finn, A. (Eds.), Hot Topics in Infection and Immunity in Children. Springer, New York, NY, pp. 35–44.

Dakhama, A., Park, J.W., Taube, C., Joetham, A., Balhorn, A., Miyahara, N., et al., 2005. The enhancement or prevention of airway hyperresponsiveness during reinfection with respiratory syncytial virus is critically dependent on the age at first infection and IL-13 production. J. Immunol. 175 (3), 1876–1883.

Dandri, M., Lutgehetmann, M., 2014. Mouse models of hepatitis B and delta virus infection. J. Immunol. Methods 410, 39–49.

Danes, L., Benda, R., Fuchsova, M., 1963. [Experimental inhalation infection of monkeys of the *Macacus cynomolgus* and Macacus rhesus species with the virus of lymphocytic choriomeningitis (We)]. Bratisl. Lek. Listy. 2, 71–79.

Daniels, M.J., Selgrade, M.K., Doerfler, D., Gilmour, M.I., 2003. Kinetic profile of influenza virus infection in three rat strains. Comp. Med. 53 (3), 293–298.

Davis, K.J., Anderson, A.O., Geisbert, T.W., Steele, K.E., Geisbert, J.B., Vogel, P., et al., 1997. Pathology of experimental Ebola virus infection in African green monkeys. Involvement of fibroblastic reticular cells. Arch. Pathol. Lab. Med. 121 (8), 805–819.

De Azambuja, K., Barman, P., Toyama, J., Elashoff, D., Lawson, G.W., Williams, L.K., et al., 2014. Validation of an HPV16-mediated carcinogenesis mouse model. In Vivo 28 (5), 761–767.

De Cock, K.M., Jaffe, H.W., Curran, J.W., 2011. Reflections on 30 years of AIDS. Emerg. Infect. Dis 17 (6), 1044–1048.

de Wit, E., Rasmussen, A.L., Falzarano, D., Bushmaker, T., Feldmann, F., Brining, D.L., et al., 2013. Middle East respiratory syndrome coronavirus (MERS-CoV) causes transient lower respiratory tract infection in rhesus macaques. Proc. Natl. Acad. Sci. USA 110 (41), 16598–16603.

Del Prete, G.Q., Ailers, B., Moldt, B., Keele, B.F., Estes, J.D., Rodriguez, A., et al., 2014. Selection of unadapted, pathogenic SHIVs encoding newly transmitted HIV-1 envelope proteins. Cell Host Microbe 16 (3), 412–418.

Demberg, T., Robert-Guroff, M., 2015. B-cells and the use of non-human primates for evaluation of HIV vaccine candidates. Curr. HIV Res. 13 (6), 462–478.

Denton, P.W., Estes, J.D., Sun, Z., Othieno, F.A., Wei, B.L., Wege, A.K., et al., 2008. Antiretroviral pre-exposure prophylaxis prevents vaginal transmission of HIV-1 in humanized BLT mice. PLoS Med. 5 (1), e16.

Di Giulio, D.B., Eckburg, P.B., 2004. Human monkeypox. Lancet Infect. Dis. 4 (4), 199.

Diamond, M.S., Shrestha, B., Mehlhop, E., Sitati, E., Engle, M., 2003. Innate and adaptive immune responses determine protection against disseminated infection by West Nile encephalitis virus. Viral Immunol. 16 (3), 259–278.

Dodd, K.A., McElroy, A.K., Jones, T.L., Zaki, S.R., Nichol, S.T., Spiropoulou, C.F., 2014. Rift Valley fever virus encephalitis is associated with an ineffective systemic immune response and activated T cell infiltration into the CNS in an immunocompetent mouse model. PLoS Negl. Trop. Dis. 8 (6), e2874.

D'Ortenzio, E., Matheron, S., Yazdanpanah, Y., de Lamballerie, X., Hubert, B., Piorkowski, G., et al., 2016. Evidence of sexual transmission of Zika virus. N. Engl. J. Med. 374 (22), 2195–2198.

Dowall, S.D., Graham, V.A., Rayner, E., Atkinson, B., Hall, G., Watson, R.J., et al., 2016. A susceptible mouse model for Zika virus infection. PLoS Negl. Trop. Dis. 10 (5), e0004658.

Drosten, C., Gunther, S., Preiser, W., van der Werf, S., Brodt, H.R., Becker, S., et al., 2003. Identification of a novel coronavirus in patients with severe acute respiratory syndrome. N. Engl. J. Med. 348 (20), 1967–1976.

Dups, J., Middleton, D., Long, F., Arkinstall, R., Marsh, G.A., Wang, L.F., 2014. Subclinical infection without encephalitis in mice following intranasal exposure to Nipah virus-Malaysia and Nipah virus-Bangladesh. Virol. J. 11, 102.

Dupuy, L.C., Reed, D.S., 2012. Nonhuman primate models of encephalitic alphavirus infection: historical review and future perspectives. Curr. Opin. Virol. 2 (3), 363–367.

Dushoff, J., Plotkin, J.B., Viboud, C., Earn, D.J., Simonsen, L., 2006. Mortality due to influenza in the United States—an annualized regression approach using multiple-cause mortality data. Am. J. Epidemiol. 163 (2), 181–187.

Dybing, J.K., Schultz-Cherry, S., Swayne, D.E., Suarez, D.L., Perdue, M.L., 2000. Distinct pathogenesis of hong kong-origin H5N1 viruses in mice compared to that of other highly pathogenic H5 avian influenza viruses. J. Virol. 74 (3), 1443–1450.

Dye, J.M., Herbert, A.S., Kuehne, A.I., Barth, J.F., Muhammad, M.A., Zak, S.E., et al., 2012. Postexposure antibody prophylaxis protects nonhuman primates from filovirus disease. Proc. Natl. Acad. Sci. USA 109 (13), 5034–5039.

Earl, P.L., Americo, J.L., Cotter, C.A., Moss, B., 2015. Comparative live bioluminescence imaging of monkeypox virus dissemination in a wild-derived inbred mouse (*Mus musculus castaneus*) and outbred African dormouse (*Graphiurus kelleni*). Virology 475, 150–158.

Ebenezer, G.J., McArthur, J.C., Polydefkis, M., Dorsey, J.L., O'Donnell, R., Hauer, P., et al., 2012. SIV-induced impairment of neurovascular repair: a potential role for VEGF. J. Neurovirol. 18 (3), 222–230.

Ebihara, H., Kawaoka, Y., Feldmann, H., 2010. Pathogenesis of filoviruses in small animal models [abstract 2S-7]. Program and Abstracts of the 5th International Symposium of Filoviruses. Tokyo, p. 29.

Ebihara, H., Zivcec, M., Gardner, D., Falzarano, D., LaCasse, R., Rosenke, R., et al., 2013. A Syrian golden hamster model recapitulating ebola hemorrhagic fever. J. Infect. Dis. 207 (2), 306–318.

Edghill-Smith, Y., Bray, M., Whitehouse, C.A., Miller, D., Mucker, E., Manischewitz, J., et al., 2005. Smallpox vaccine does not protect macaques with AIDS from a lethal monkeypox virus challenge. J. Infect. Dis. 191 (3), 372–381.

Eichelberger, M.C., Prince, G.A., Ottolini, M.G., 2004. Influenza-induced tachypnea is prevented in immune cotton rats, but cannot be treated with an anti-inflammatory steroid or a neuraminidase inhibitor. Virology 322 (2), 300–307.

Eichelberger, M.C., Bauchiero, S., Point, D., Richter, B.W., Prince, G.A., Schuman, R., 2006. Distinct cellular immune responses following primary and secondary influenza virus challenge in cotton rats. Cell Immunol. 243 (2), 67–74.

Enserink, M., 2013. Dual-use research. Dutch H5N1 ruling raises new questions. Science 342 (6155), 178.

Ergonul, O., Whitehouse, C.A., 2007. Crimean-Congo hemorrhagic fever: a global perspective. Springer Berlin, Heidelberg.

Evans, M.R., Meldrum, R., Lane, W., Gardner, D., Ribeiro, C.D., Gallimore, C.I., Westmoreland, D., 2002. An outbreak of viral gastroenteritis following environmental contamination at a concert hall. Epidemiol. Infect. 129 (2), 355–360.

Ewers, E.C., Pratt, W.D., Twenhafel, N.A., Shamblin, J., Donnelly, G., Esham, H., et al., 2016. Natural history of aerosol exposure with Marburg virus in rhesus macaques. Viruses 8 (4.), 87.

Fagbami, A.H., Tomori, O., Fabiya, A., Isoun, T.T., 1975. Experimental Congo virus (IB-AN7620) infection in primates. Virologie 26 (1), 33–37.

Falendysz, E.A., Lopera, J.G., Lorenzsonn, F., Salzer, J.S., Hutson, C.L., Doty, J., et al., 2015. Further assessment of monkeypox virus infection in gambian pouched rats (Cricetomys gambianus) using in vivo bioluminescent imaging. PLoS Negl. Trop. Dis. 9 (10), e0004130.

Falsey, A.R., Hennessey, P.A., Formica, M.A., Cox, C., Walsh, E.E., 2005. Respiratory syncytial virus infection in elderly and high-risk adults. N. Engl. J. Med. 352 (17), 1749–1759.

Falzarano, D., de Wit, E., Feldmann, F., Rasmussen, A.L., Okumura, A., Peng, X., et al., 2014. Infection with MERS-CoV causes lethal pneumonia in the common marmoset. PLoS Pathog. 10 (8), e1004250.

Fernando, L., Qiu, X., Melito, P.L., Williams, K.J., Feldmann, F., Feldmann, H., et al., 2015. Immune response to Marburg virus Angola infection in nonhuman primates. J. Infect. Dis. 212 (Suppl. 2), S234–S241.

Fields, B.N., Knipe, D.M., Howley, P.M., 2007. Fields' Virology, fifth ed. Lippincott Williams & Wilkins, Philadelphia.

Findlay, G.M., Howard, E.M., 1952. The susceptibility of rats to Rift Valley fever in relation to age. Ann. Trop. Med. Parasitol. 46 (1), 33–37.

Fogarty, R., Halpin, K., Hyatt, A.D., Daszak, P., Mungall, B.A., 2008. Henipavirus susceptibility to environmental variables. Virus Res. 132 (1–2), 140–144.

Fouchier, R.A., Garcia-Sastre, A., Kawaoka, Y., Barclay, W.S., Bouvier, N.M., Brown, I.H., et al., 2012. Pause on avian flu transmission research. Science 335 (6067), 400–401.

Fouchier, R.A., et al., 2003. Aetiology: Koch's postulates fulfilled for SARS virus. Nature 423 (6937), 240.

Fratkin, J.D., Leis, A.A., Stokic, D.S., Slavinski, S.A., Geiss, R.W., 2004. Spinal cord neuropathology in human West Nile virus infection. Arch. Pathol. Lab. Med. 128 (5), 533–537.

Fuller, D.H., Rajakumar, P., Che, J.W., Narendran, A., Nyaundi, J., Michael, H., et al., 2012. Therapeutic DNA vaccine induces broad T cell responses in the gut and sustained protection from viral rebound and AIDS in SIV-infected rhesus macaques. PLoS One 7 (3), e33715.

Ganem, D., Prince, A.M., 2004. Hepatitis B virus infection—natural history and clinical consequences. N. Engl. J. Med. 350 (11), 1118–1129.

Gao, P., Watanabe, S., Ito, T., Goto, H., Wells, K., McGregor, M., et al., 1999. Biological heterogeneity, including systemic replication in mice, of H5N1 influenza A virus isolates from humans in Hong Kong. J. Virol. 73 (4), 3184–3189.

Gardner, J., Anraku, I., Le, T.T., Larcher, T., Major, L., Roques, P., et al., 2010. Chikungunya virus arthritis in adult wild-type mice. J. Virol. 84 (16), 8021–8032.

Gaunt, E.R., Hardie, A., Claas, E.C., Simmonds, P., Templeton, K.E., 2010. Epidemiology and clinical presentations of the four human coronaviruses 229E, HKU1, NL63, and OC43 detected over 3 years using a novel multiplex real-time PCR method. J. Clin. Microbiol. 48 (8), 2940–2947.

Geisbert, T.W., Daddario-DiCaprio, K.M., Hickey, A.C., Smith, M.A., Chan, Y.P., Wang, L.F., et al., 2010. Development of an acute and highly pathogenic nonhuman primate model of Nipah virus infection. PLoS One 5 (5), e10690.

Gerin, J.L., 2001. Animal models of hepatitis delta virus infection and disease. ILAR J. 42 (2), 103–106.

Gerin, J.L., Cote, P.J., Korba, B.E., Tennant, B.C., 1989. Hepadnavirus-induced liver cancer in woodchucks. Cancer Detect. Prev. 14 (2), 227–229.

Giese, M., Harder, T.C., Teifke, J.P., Klopfleisch, R., Breithaupt, A., Mettenleiter, T.C., Vahlenkamp, T.W., 2008. Experimental infection and natural contact exposure of dogs with avian influenza virus (H5N1). Emerg. Infect. Dis. 14 (2), 308–310.

Gilbert, B.E., McLeay, M.T., 2008. MegaRibavirin aerosol for the treatment of influenza A virus infections in mice. Antiviral Res. 78 (3), 223–229.

Gillim-Ross, L., Taylor, J., Scholl, D.R., Ridenour, J., Masters, P.S., Wentworth, D.E., 2004. Discovery of novel human and animal cells infected by the severe acute respiratory syndrome coronavirus by replication-specific multiplex reverse transcription-PCR. J. Clin. Microbiol. 42 (7), 3196–3206.

Gitiban, N., Jurcisek, J.A., Harris, R.H., Mertz, S.E., Durbin, R.K., Bakaletz, L.O., Durbin, J.E., 2005. Chinchilla and murine models of upper respiratory tract infections with respiratory syncytial virus. J. Virol. 79 (10), 6035–6042.

Glass, W.G., Subbarao, K., Murphy, B., Murphy, P.M., 2004. Mechanisms of host defense following severe acute respiratory syndrome-coronavirus (SARS-CoV) pulmonary infection of mice. J. Immunol. 173 (6), 4030–4039.

Gleiser, C.A., Gochenour, Jr., W.S., Berge, T.O., Tigertt, W.D., 1961. Studies on the virus of Venezuelan equine encephalomyelitis. I. Modification by cortisone of the response of the central nervous system of Macaca mulatta. J. Immunol. 87, 504–508.

Glezen, W.P., 1982. Serious morbidity and mortality associated with influenza epidemics. Epidemiol. Rev. 4, 25–44.

Goff, A.J., et al., 2011. A novel respiratory model of infection with monkeypox virus in cynomolgus macaques. J. Virol. 85 (10), 4898–4909.

Goh, K.J., Tan, C.T., Chew, N.K., Tan, P.S., Kamarulzaman, A., Sarji, S.A., et al., 2000. Clinical features of Nipah virus encephalitis among pig farmers in Malaysia. N. Engl. J. Med. 342 (17), 1229–1235.

Goncalvez, A.P., Engle, R.E., St Claire, M., Purcell, R.H., Lai, C.J., 2007. Monoclonal antibody-mediated enhancement of dengue virus infection in vitro and in vivo and strategies for prevention. Proc. Natl. Acad. Sci. USA 104 (22), 9422–9427.

Gowen, B.B., Holbrook, M.R., 2008. Animal models of highly pathogenic RNA viral infections: hemorrhagic fever viruses. Antiviral Res. 78 (1), 79–90.

Gowen, B.B., Barnard, D.L., Smee, D.F., Wong, M.H., Pace, A.M., Jung, K.H., et al., 2005. Interferon alfacon-1 protects hamsters from lethal Pichinde virus infection. Antimicrob. Agents Chemother. 49 (6), 2378–2386.

Graham, B.S., Perkins, M.D., Wright, P.F., Karzon, D.T., 1988. Primary respiratory syncytial virus infection in mice. J. Med. Virol. 26 (2), 153–162.

Greenough, T.C., Carville, A., Coderre, J., Somasundaran, M., Sullivan, J.L., Luzuriaga, K., Mansfield, K., 2005. Pneumonitis and multi-organ system disease in common marmosets (Callithrix jacchus) infected with the severe acute respiratory syndrome-associated coronavirus. Am. J. Pathol. 167 (2), 455–463.

Gregory, C.J., Santiago, L.M., Arguello, D.F., Hunsperger, E., Tomashek, K.M., 2010. Clinical and laboratory features that differentiate dengue from other febrile illnesses in an endemic area—Puerto Rico, 2007–2008. Am. J. Trop. Med. Hyg. 82 (5), 922–929.

Grieves, J.L., Yin, Z., Durbin, R.K., Durbin, J.E., 2015. Acute and chronic airway disease after human respiratory syncytial virus infection in cotton rats (Sigmodon hispidus). Comp. Med. 65 (4), 315–326.

Griffin, D.E., 2007. Alphaviruses. In: Knipe, D.M.a.P.M.H. (Ed.), Fields Virology. Lippincott, Williams & Wilkins, Philadelphia, pp. 1023–1068.

Grimm, D., Staeheli, P., Hufbauer, M., Koerner, I., Martinez-Sobrido, L., Solorzano, A., et al., 2007. Replication fitness determines high virulence of influenza A virus in mice carrying functional Mx1 resistance gene. Proc. Natl. Acad. Sci. USA 104 (16), 6806–6811.

Gruell, H., Bournazos, S., Ravetch, J.V., Ploss, A., Nussenzweig, M.C., Pietzsch, J., 2013. Antibody and antiretroviral preexposure prophylaxis prevent cervicovaginal HIV-1 infection in a transgenic mouse model. J. Virol. 87 (15), 8535–8544.

Gubareva, L.V., McCullers, J.A., Bethell, R.C., Webster, R.G., 1998. Characterization of influenza A/HongKong/156/97 (H5N1) virus in a mouse model and protective effect of zanamivir on H5N1 infection in mice. J. Infect. Dis. 178 (6), 1592–1596.

Gubler, D.J., 2002. Epidemic dengue/dengue hemorrhagic fever as a public health, social and economic problem in the 21st century. Trends Microbiol. 10 (2), 100–103.

Guha, C., Mohan, S., Roy-Chowdhury, N., Roy-Chowdhury, J., 2004. Cell culture and animal models of viral hepatitis. Part I: hepatitis B. Lab Anim. (NY) 33 (7), 37–46.

Guilhot, S., Huang, S.N., Xia, Y.P., La Monica, N., Lai, M.M., Chisari, F.V., 1994. Expression of the hepatitis delta virus large and small antigens in transgenic mice. J. Virol. 68 (2), 1052–1058.

Guillaume, V., Wong, K.T., Looi, R.Y., Georges-Courbot, M.C., Barrot, L., Buckland, R., et al., 2009. Acute Hendra virus infection: analysis of the pathogenesis and passive antibody protection in the hamster model. Virology 387 (2), 459–465.

Gunther, S., Weisner, B., Roth, A., Grewing, T., Asper, M., Drosten, C., et al., 2001. Lassa fever encephalopathy: Lassa virus in cerebrospinal fluid but not in serum. J. Infect. Dis. 184 (3), 345–349.

Gupta, P., Sharma, A., Spurgers, K.B., Bakken, R.R., Eccleston, L.T., Cohen, J.W., et al., 2016. 1, 5-Iodonaphthyl azide-inactivated V3526 protects against aerosol challenge with virulent Venezuelan equine encephalitis virus. Vaccine 34 (25), 2762–2765.

Guzman, M.G., Kouri, G., 2002. Dengue: an update. Lancet Infect. Dis. 2 (1), 33–42.

Haagmans, B.L., Kuiken, T., Martina, B.E., Fouchier, R.A., Rimmelzwaan, G.F., van Amerongen, G., et al., 2004. Pegylated interferon-alpha protects type 1 pneumocytes against SARS coronavirus infection in macaques. Nat. Med. 10 (3), 290–293.

Haagmans, B.L., van den Brand, J.M., Provacia, L.B., Raj, V.S., Stittelaar, K.J., Getu, S., et al., 2015. Asymptomatic Middle East respiratory syndrome coronavirus infection in rabbits. J. Virol. 89 (11), 6131–6135.

Hagenaars, N., Mastrobattista, E., Glansbeek, H., Heldens, J., van den Bosch, H., Schijns, V., et al., 2008. Head-to-head comparison of four non-adjuvanted inactivated cell culture-derived influenza vaccines: effect of composition, spatial organization and immunization route on the immunogenicity in a murine challenge model. Vaccine 26 (51), 6555–6563.

Haigwood, N.L., 2009. Update on animal models for HIV research. Eur. J. Immunol. 39 (8), 1994–1999.

Hall, A.J., Lopman, B.A., Payne, D.C., Patel, M.M., Gastanaduy, P.A., Vinje, J., Parashar, U.D., 2013. Norovirus disease in the United States. Emerg. Infect. Dis. 19 (8), 1198–1205.

Hallin, G.W., Simpson, S.Q., Crowell, R.E., James, D.S., Koster, F.T., Mertz, G.J., Levy, H., 1996. Cardiopulmonary manifestations of hantavirus pulmonary syndrome. Crit. Care Med. 24 (2), 252–258.

Hancock, G.E., Smith, J.D., Heers, K.M., 2000. Serum neutralizing antibody titers of seropositive chimpanzees immunized with vaccines coformulated with natural fusion and attachment proteins of respiratory syncytial virus. J. Infect. Dis. 181 (5), 1768–1771.

Hanna, J.N., McBride, W.J., Brookes, D.L., Shield, J., Taylor, C.T., Smith, I.L., et al., 2006. Hendra virus infection in a veterinarian. Med. J. Aust. 185 (10), 562–564.

Hannaman, D., Dupuy, L.C., Ellefsen, B., Schmaljohn, C.S., 2016. A Phase 1 clinical trial of a DNA vaccine for Venezuelan equine encephalitis delivered by intramuscular or intradermal electroporation. Vaccine 34 (31), 3607–3612.

Harris, J.P., Edmunds, W.J., Pebody, R., Brown, D.W., Lopman, B.A., 2008. Deaths from norovirus among the elderly, England and Wales. Emerg. Infect. Dis. 14 (10), 1546–1552.

Hartman, A.L., Powell, D.S., Bethel, L.M., Caroline, A.L., Schmid, R.J., Oury, T., Reed, D.S., 2014. Aerosolized Rift Valley fever virus causes fatal encephalitis in African green monkeys and common marmosets. J. Virol. 88 (4), 2235–2245.

Hatziioannou, T., Del Prete, G.Q., Keele, B.F., Estes, J.D., McNatt, M.W., Bitzegeio, J., et al., 2014. HIV-1-induced AIDS in monkeys. Science 344 (6190), 1401–1405.

Hayes, C.G., 1989. West Nile fever. Monath, T.P. (Ed.), The Arboviruses: Epidemiology and Ecology, vol. V, CRC Press, Boca Raton, pp. 59–88.

Henning, T.R., Hanson, D., Vishwanathan, S.A., Butler, K., Dobard, C., Garcia-Lerma, G., et al., 2014. Short communication: viremic control is independent of repeated low-dose SHIVSF162p3 exposures. AIDS Res. Hum. Retroviruses 30 (11), 1125–1129.

Hensley, L.E., Alves, D.A., Geisbert, J.B., Fritz, E.A., Reed, C., Larsen, T., Geisbert, T.W., 2011a. Pathogenesis of Marburg hemorrhagic fever in cynomolgus macaques. J. Infect. Dis. 204 (Suppl. 3), S1021–S1031.

Hensley, L.E., Smith, M.A., Geisbert, J.B., Fritz, E.A., Daddario-DiCaprio, K.M., Larsen, T., Geisbert, T.W., 2011b. Pathogenesis of Lassa fever in cynomolgus macaques. Virol. J. 8, 205.

Herbert, A.S., Davidson, C., Kuehne, A.I., Bakken, R., Braigen, S.Z., Gunn, K.E., et al., 2015. Niemann-pick C1 is essential for ebolavirus replication and pathogenesis in vivo. MBio 6 (3), e00565–e005615.

Herfst, S., Schrauwen, E.J., Linster, M., Chutinimitkul, S., de Wit, E., Munster, V.J., et al., 2012. Airborne transmission of influenza A/H5N1 virus between ferrets. Science 336 (6088), 1534–1541.

Hessell, A.J., Haigwood, N.L., 2015. Animal models in HIV-1 protection and therapy. Curr. Opin. HIV AIDS 10 (3), 170–176.

Higgins, D., Trujillo, C., Keech, C., 2016. Advances in RSV vaccine research and development—a global agenda. Vaccine 34 (26), 2870–2875.

Hills, S.L., Russell, K., Hennessey, M., Williams, C., Oster, A.M., Fischer, M., Mead, P., 2016. Transmission of Zika virus through sexual contact with travelers to areas of ongoing transmission—continental United States, 2016. MMWR Morb. Mortal. Wkly. Rep. 65 (8), 215–216.

Hiroshima, Y., Zhang, Y., Zhang, N., Maawy, A., Mii, S., Yamamoto, M., et al., 2015. Establishment of a patient-derived orthotopic Xenograft (PDOX) model of HER-2-positive cervical cancer expressing the clinical metastatic pattern. PLoS One 10 (2), e0117417.

Hogan, R.J., Gao, G., Rowe, T., Bell, P., Flieder, D., Paragas, J., et al., 2004. Resolution of primary severe acute respiratory syndrome-associated coronavirus infection requires Stat1. J. Virol. 78 (20), 11416–11421.

Holmgren, J., Czerkinsky, C., 2005. Mucosal immunity and vaccines. Nat. Med. 11 (4 Suppl.), S45–S53.

Homaira, N., Rahman, M., Hossain, M.J., Epstein, J.H., Sultana, R., Khan, M.S., et al., 2010. Nipah virus outbreak with person-to-person transmission in a district of Bangladesh, 2007. Epidemiol. Infect. 138 (11), 1630–1636.

Honnold, S.P., Mossel, E.C., Bakken, R.R., Fisher, D., Lind, C.M., Cohen, J.W., et al., 2015. Eastern equine encephalitis virus in mice I: clinical course and outcome are dependent on route of exposure. Virol. J. 12, 152.

Hooper, P.T., Westbury, H.A., Russell, G.M., 1997. The lesions of experimental equine morbillivirus disease in cats and guinea pigs. Vet. Pathol. 34 (4), 323–329.

Hooper, J.W., Larsen, T., Custer, D.M., Schmaljohn, C.S., 2001. A lethal disease model for hantavirus pulmonary syndrome. Virology 289 (1), 6–14.

Hooper, J.W., Custer, D.M., Smith, J., Wahl-Jensen, V., 2006. Hantaan/Andes virus DNA vaccine elicits a broadly cross-reactive neutralizing antibody response in nonhuman primates. Virology 347 (1), 208–216.

Hsu, C.C., Riley, L.K., Wills, H.M., Livingston, R.S., 2006. Persistent infection with and serologic cross-reactivity of three novel murine noroviruses. Comp. Med. 56 (4), 247–251.

Hsu, C.C., Riley, L.K., Livingston, R.S., 2007. Molecular characterization of three novel murine noroviruses. Virus Genes 34 (2), 147–155.

Hu, X., Margolis, H.S., Purcell, R.H., Ebert, J., Robertson, B.H., 2000. Identification of hepatitis B virus indigenous to chimpanzees. Proc. Natl. Acad. Sci. USA 97 (4), 1661–1664.

Huang, K.J., Li, S.Y., Chen, S.C., Liu, H.S., Lin, Y.S., Yeh, T.M., et al., 2000. Manifestation of thrombocytopenia in dengue-2-virus-infected mice. J. Gen. Virol. 81 (Pt 9), 2177–2182.

Huang, L.R., Gabel, Y.A., Graf, S., Arzberger, S., Kurts, C., Heiken-walder, M., et al., 2012. Transfer of HBV genomes using low doses of adenovirus vectors leads to persistent infection in immune competent mice. Gastroenterology 142 (7), 1447.e3-1450.e3.

Hubalek, Z., Halouzka, J., 1999. West Nile fever—a reemerging mosquito-borne viral disease in Europe. Emerg. Infect. Dis. 5 (5), 643–650.

Huber, V.C., Kleimeyer, L.H., McCullers, J.A., 2008. Live, attenuated influenza virus (LAIV) vehicles are strong inducers of immunity toward influenza B virus. Vaccine 26 (42), 5381–5388.

Huhn, G.D., Bauer, A.M., Yorita, K., Graham, M.B., Sejvar, J., Likos, A., et al., 2005. Clinical characteristics of human monkeypox, and risk factors for severe disease. Clin. Infect. Dis. 41 (12), 1742–1751.

Humbert, M., Rasmussen, R.A., Song, R., Ong, H., Sharma, P., Chenine, A.L., et al., 2008. SHIV-1157i and passaged progeny viruses encoding R5 HIV-1 clade C env cause AIDS in rhesus monkeys. Retrovirology 5, 94.

Hutson, A.M., Airaud, F., LePendu, J., Estes, M.K., Atmar, R.L., 2005. Norwalk virus infection associates with secretor status genotyped from sera. J. Med. Virol. 77 (1), 116–120.

Hutson, C.L., Olson, V.A., Carroll, D.S., Abel, J.A., Hughes, C.M., Braden, Z.H., et al., 2009. A prairie dog animal model of systemic orthopoxvirus disease using West African and Congo Basin strains of monkeypox virus. J. Gen. Virol. 90 (Pt 2), 323–333.

Hyams, K.C., 1995. Risks of chronicity following acute hepatitis B virus infection: a review. Clin. Infect. Dis. 20 (4), 992–1000.

Ikegami, T., Makino, S., 2011. The pathogenesis of Rift Valley fever. Viruses 3 (5), 493–519.

Imai, M., Watanabe, T., Hatta, M., Das, S.C., Ozawa, M., Shinya, K., et al., 2012. Experimental adaptation of an influenza H5 HA confers respiratory droplet transmission to a reassortant H5 HA/H1N1 virus in ferrets. Nature 486 (7403), 420–428.

Isoda, N., Sakoda, Y., Kishida, N., Bai, G.R., Matsuda, K., Umemura, T., Kida, H., 2006. Pathogenicity of a highly pathogenic avian influenza virus, A/chicken/Yamaguchi/7/04 (H5N1) in different species of birds and mammals. Arch. Virol. 151 (7), 1267–1279.

Ison, M.G., Lee, N., 2010. Influenza 2010-2011: lessons from the 2009 pandemic. Cleve. Clin. J. Med. 77 (11), 812–820.

Jafri, H.S., Chavez-Bueno, S., Mejias, A., Gomez, A.M., Rios, A.M., Nassi, S.S., et al., 2004. Respiratory syncytial virus induces pneumonia, cytokine response, airway obstruction, and chronic inflammatory infiltrates associated with long-term airway hyperresponsiveness in mice. J. Infect. Dis. 189 (10), 1856–1865.

Jagu, S., Malandro, N., Kwak, K., Yuan, H., Schlegel, R., Palmer, K.E., et al., 2011. A multimeric L2 vaccine for prevention of animal papillomavirus infections. Virology 420 (1), 43–50.

Jahrling, P.B., Hesse, R.A., Eddy, G.A., Johnson, K.M., Callis, R.T., Stephen, E.L., 1980. Lassa virus infection of rhesus monkeys: pathogenesis and treatment with ribavirin. J. Infect. Dis. 141 (5), 580–589.

Jahrling, P.B., Smith, S., Hesse, R.A., Rhoderick, J.B., 1982. Pathogenesis of Lassa virus infection in guinea pigs. Infect. Immun. 37 (2), 771–778.

Jayaraman, P., Mohan, D., Polacino, P., Kuller, L., Sheikh, N., Bielefeldt-Ohmann, H., et al., 2004. Perinatal transmission of SHIV-SF162P3 in Macaca nemestrina. J. Med. Primatol. 33 (5–6), 243–250.

Jeézek, Z., Fenner, F., 1988. Human Monkeypox and Other Poxvirus Infections of Man. Karger, Basel; New York, NY.

Jeffers, S.A., Tusell, S.M., Gillim-Ross, L., Hemmila, E.M., Achenbach, J.E., Babcock, G.J., et al., 2004. CD209L (L-SIGN) is a receptor for severe acute respiratory syndrome coronavirus. Proc. Natl. Acad. Sci. USA 101 (44), 15748–15753.

Jia, N., Barclay, W.S., Roberts, K., Yen, H.L., Chan, R.W., Lam, A.K., et al., 2014. Glycomic characterization of respiratory tract tissues of ferrets: implications for its use in influenza virus infection studies. J. Biol. Chem. 289 (41), 28489–28504.

Johnson, R.F., Dyall, J., Ragland, D.R., Huzella, L., Byrum, R., Jett, C., et al., 2011. Comparative analysis of monkeypox virus infection of cynomolgus macaques by the intravenous or intrabronchial inoculation route. J. Virol. 85 (5), 2112–2125.

Johnston, L.J., Halliday, G.M., King, N.J., 1996. Phenotypic changes in Langerhans' cells after infection with arboviruses: a role in the immune response to epidermally acquired viral infection? J. Virol. 70 (7), 4761–4766.

Johnston, K.B., Monteiro, J.M., Schultz, L.D., Chen, L., Wang, F., Ausensi, V.A., et al., 2005. Protection of beagle dogs from mucosal challenge with canine oral papillomavirus by immunization with recombinant adenoviruses expressing codon-optimized early genes. Virology 336 (2), 208–218.

Johnston, S.C., Briese, T., Bell, T.M., Pratt, W.D., Shamblin, J.D., Esham, H.L., et al., 2015. Detailed analysis of the African green monkey model of Nipah virus disease. PLoS One 10 (2), e0117817.

Jones, M.E., Schuh, A.J., Amman, B.R., Sealy, T.K., Zaki, S.R., Nichol, S.T., Towner, J.S., 2015. Experimental inoculation of Egyptian rousette bats (Rousettus aegyptiacus) with viruses of the Ebolavirus and Marburgvirus genera. Viruses 7 (7), 3420–3442.

Julander, J.G., Bowen, R.A., Rao, J.R., Day, C., Shafer, K., Smee, D.F., et al., 2008a. Treatment of Venezuelan equine encephalitis virus infection with (-)-carbodine. Antiviral Res. 80 (3), 309–315.

Julander, J.G., Skirpstunas, R., Siddharthan, V., Shafer, K., Hoopes, J.D., Smee, D.F., Morrey, J.D., 2008b. C3H/HeN mouse model for the evaluation of antiviral agents for the treatment of Venezuelan equine encephalitis virus infection. Antiviral Res. 78 (3), 230–241.

Karpel, M.E., Boutwell, C.L., Allen, T.M., 2015. BLT humanized mice as a small animal model of HIV infection. Curr. Opin. Virol. 13, 75–80.

Karst, S.M., Wobus, C.E., Lay, M., Davidson, J., Virgin, H.W.t., 2003. STAT1-dependent innate immunity to a Norwalk-like virus. Science 299 (5612), 1575–1578.

Katz, M.A., Starr, J.F., 1990. Pichinde virus infection in strain 13 guinea pigs reduces intestinal protein reflection coefficient with compensation. J. Infect. Dis. 162 (6), 1304–1308.

Keckler, M.S., Carroll, D.S., Gallardo-Romero, N.F., Lash, R.R., Salzer, J.S., Weiss, S.L., et al., 2011. Establishment of the black-tailed prairie dog (Cynomys ludovicianus) as a novel animal model for comparing smallpox vaccines administered preexposure in both high- and low-dose monkeypox virus challenges. J. Virol. 85 (15), 7683–7698.

Keele, B.F., Li, H., Learn, G.H., Hraber, P., Giorgi, E.E., Grayson, T., et al., 2009. Low-dose rectal inoculation of rhesus macaques by SIVsmE660 or SIVmac251 recapitulates human mucosal infection by HIV-1. J. Exp. Med. 206 (5), 1117–1134.

Khan, S.H., Goba, A., Chu, M., Roth, C., Healing, T., Marx, A., et al., 2008. New opportunities for field research on the pathogenesis and treatment of Lassa fever. Antiviral Res. 78 (1), 103–115.

Khan, R.R., Lawson, A.D., Minnich, L.L., Martin, K., Nasir, A., Emmett, M.K., et al., 2009. Gastrointestinal norovirus infection associated with exacerbation of inflammatory bowel disease. J. Pediatr. Gastroenterol. Nutr. 48 (3), 328–333.

Khodakevich, L., Jezek, Z., Kinzanzka, K., 1986. Isolation of monkeypox virus from wild squirrel infected in nature. Lancet 1 (8472), 98–99.

Kim, J.Y., Chang, J., 2016. In Hot pursuit of the first vaccine against respiratory syncytial virus. Yonsei Med. J. 57 (4), 809–816.

Kim, G.R., McKee, Jr., K.T., 1985. Pathogenesis of Hantaan virus infection in suckling mice: clinical, virologic, and serologic observations. Am. J. Trop. Med. Hyg. 34 (2), 388–395.

Kim, H.W., Canchola, J.G., Brandt, C.D., Pyles, G., Chanock, R.M., Jensen, K., Parrott, R.H., 1969. Respiratory syncytial virus disease in infants despite prior administration of antigenic inactivated vaccine. Am. J. Epidemiol. 89 (4), 422–434.

Kim, H.M., Kang, Y.M., Ku, K.B., Park, E.H., Yum, J., Kim, J.C., et al., 2013. The severe pathogenicity of alveolar macrophage-depleted ferrets infected with 2009 pandemic H1N1 influenza virus. Virology 444 (1–2), 394–403.

Kim, E.H., Park, S.J., Kwon, H.I., Kim, S.M., Kim, Y.I., Song, M.S., et al., 2015. Mouse adaptation of influenza B virus increases replication in the upper respiratory tract and results in droplet transmissibility in ferrets. Sci. Rep. 5, 15940.

Kimata, J.T., 2014. Stepping toward a macaque model of HIV-1 induced AIDS. Viruses 6 (9), 3643–3651.

Kirby, A.E., Streby, A., Moe, C.L., 2016. Vomiting as a symptom and transmission risk in Norovirus illness: evidence from Human Challenge Studies. PLoS One 11 (4), e0143759.

Klingstrom, J., Plyusnin, A., Vaheri, A., Lundkvist, A., 2002. Wild-type Puumala hantavirus infection induces cytokines, C-reactive protein, creatinine, and nitric oxide in cynomolgus macaques. J. Virol. 76 (1), 444–449.

Kobasa, D., Jones, S.M., Shinya, K., Kash, J.C., Copps, J., Ebihara, H., et al., 2007. Aberrant innate immune response in lethal infection of macaques with the 1918 influenza virus. Nature 445 (7125), 319–323.

Kobinger, G.P., Figueredo, J.M., Rowe, T., Zhi, Y., Gao, G., Sanmiguel, J.C., et al., 2007. Adenovirus-based vaccine prevents pneumonia in ferrets challenged with the SARS coronavirus and stimulates robust immune responses in macaques. Vaccine 25 (28), 5220–5231.

Kobinger, G.P., Leung, A., Neufeld, J., Richardson, J.S., Falzarano, D., Smith, G., et al., 2011. Replication, pathogenicity, shedding, and transmission of *Zaire ebolavirus* in pigs. J. Infect. Dis. 204 (2), 200–208.

Komar, N., 2000. West Nile viral encephalitis. Rev. Sci. Tech. 19 (1), 166–176.

Koopmans, M., Duizer, E., 2004. Foodborne viruses: an emerging problem. Int. J. Food Microbiol. 90 (1), 23–41.

Kreijtz, J.H., Kroeze, E.J., Stittelaar, K.J., de Waal, L., van Amerongen, G., van Trierum, S., et al., 2013. Low pathogenic avian influenza A(H7N9) virus causes high mortality in ferrets upon intratracheal challenge: a model to study intervention strategies. Vaccine 31 (43), 4995–4999.

Kroeze, E.J., Kuiken, T., Osterhaus, A.D., 2012. Animal models. Methods Mol. Biol. 865, 127–146.

Kuhn, J.H., 2008. Filoviruses: A Compendium of 40 Years of Epidemiological, Clinical, and Laboratory Studies. Arch. Virol. Suppl. 20, 13–360. Available from: http://dx.doi.org/10.1007/978-3-211-69495-4.

Kuiken, T., Rimmelzwaan, G.F., Van Amerongen, G., Osterhaus, A.D., 2003. Pathology of human influenza A (H5N1) virus infection in cynomolgus macaques (*Macaca fascicularis*). Vet. Pathol. 40 (3), 304–310.

Kuruvilla, J.G., Troyer, R.M., Devi, S., Akkina, R., 2007. Dengue virus infection and immune response in humanized RAG2(-/-)gamma(c)(-/-) (RAG-hu) mice. Virology 369 (1), 143–152.

Labadie, K., Larcher, T., Joubert, C., Mannioui, A., Delache, B., Brochard, P., et al., 2010. Chikungunya disease in nonhuman primates involves long-term viral persistence in macrophages. J. Clin. Invest. 120 (3), 894–906.

Lai, C.L., Ratziu, V., Yuen, M.F., Poynard, T., 2003. Viral hepatitis B. Lancet 362 (9401), 2089–2094.

Lambkin, R., Oxford, J.S., Bossuyt, S., Mann, A., Metcalfe, I.C., Herzog, C., et al., 2004. Strong local and systemic protective immunity induced in the ferret model by an intranasal virosome-formulated influenza subunit vaccine. Vaccine 22 (31–32), 4390–4396.

Lanciotti, R.S., Roehrig, J.T., Deubel, V., Smith, J., Parker, M., Steele, K., et al., 1999. Origin of the West Nile virus responsible for an outbreak of encephalitis in the northeastern United States. Science 286 (5448), 2333–2337.

Lander, H.J., Holland, P.V., Alter, H.J., Chanock, R.M., Purcell, R.H., 1972. Antibody to hepatitis-associated antigen. Frequency and pattern of response as detected by radioimmunoprecipitation. JAMA 220 (8), 1079–1082.

Lau, S.K., Woo, P.C., Li, K.S., Huang, Y., Tsoi, H.W., Wong, B.H., et al., 2005. Severe acute respiratory syndrome coronavirus-like virus in Chinese horseshoe bats. Proc. Natl. Acad. Sci. USA 102 (39), 14040–14045.

Lau, S.K., Woo, P.C., Yip, C.C., Tse, H., Tsoi, H.W., Cheng, V.C., et al., 2006. Coronavirus HKU1 and other coronavirus infections in Hong Kong. J. Clin. Microbiol. 44 (6), 2063–2071.

Laughlin, L.W., Meegan, J.M., Strausbaugh, L.J., Morens, D.M., Watten, R.H., 1979. Epidemic Rift Valley fever in Egypt: observations of the spectrum of human illness. Trans. R. Soc. Trop. Med. Hyg. 73 (6), 630–633.

Lednicky, J.A., 2003. Hantaviruses. a short review. Arch. Pathol. Lab. Med. 127 (1), 30–35.

Lee, W.M., 1997. Hepatitis B virus infection. N. Engl. J. Med. 337 (24), 1733–1745.

Lee, D.H., Kim, J.I., Lee, J.W., Chung, W.H., Park, J.K., Lee, Y.N., et al., 2014. Quantitative measurement of influenza virus replication using consecutive bronchoalveolar lavage in the lower respiratory tract of a ferret model. J. Vet. Sci. 15 (3), 439–442.

Lee, J.C., Tseng, C.K., Wu, Y.H., Kaushik-Basu, N., Lin, C.K., Chen, W.C., Wu, H.N., 2015. Characterization of the activity of 2′-C-methylcytidine against dengue virus replication. Antiviral Res. 116, 1–9.

Lentz, M.R., Peterson, K.L., Ibrahim, W.G., Lee, D.E., Sarlls, J., Lizak, M.J., et al., 2014. Diffusion tensor and volumetric magnetic resonance measures as biomarkers of brain damage in a small animal model of HIV. PLoS One 9 (8), e105752.

Leon, A.J., Banner, D., Xu, L., Ran, L., Peng, Z., Yi, K., et al., 2013. Sequencing, annotation, and characterization of the influenza ferret infectome. J. Virol. 87 (4), 1957–1966.

Letvin, N.L., Rao, S.S., Montefiori, D.C., Seaman, M.S., Sun, Y., Lim, S.Y., et al., 2011. Immune and genetic correlates of vaccine protection against mucosal infection by SIV in monkeys. Sci. Transl. Med. 3 (81), 81ra36.

Lever, M.S., Piercy, T.J., Steward, J.A., Eastaugh, L., Smither, S.J., Taylor, C., et al., 2012. Lethality and pathogenesis of airborne infection with filoviruses in A129 alpha/beta$^{-/-}$ interferon receptor-deficient mice. J. Med. Microbiol. 61 (Pt 1), 8–15.

Li, M., Embury-Hyatt, C., Weingartl, H.M., 2010. Experimental inoculation study indicates swine as a potential host for Hendra virus. Vet. Res. 41 (3), 33.

Li, Q., Tso, F.Y., Kang, G., Lu, W., Li, Y., Fan, W., et al., 2015. Early initiation of antiretroviral therapy can functionally control productive HIV-1 infection in humanized-BLT mice. J. Acquir. Immune Defic. Syndr. 69 (5), 519–527.

Li, C., Xu, D., Ye, Q., Hong, S., Jiang, Y., Liu, X., et al., 2016a. Zika virus disrupts neural progenitor development and leads to microcephaly in mice. Cell Stem Cell. 19, 120–126.

Li, K., Wohlford-Lenane, C., Perlman, S., Zhao, J., Jewell, A.K., Reznikov, L.R., et al., 2016b. Middle East respiratory syndrome coronavirus causes multiple organ damage and lethal disease in mice transgenic for human dipeptidyl peptidase 4. J. Infect. Dis. 213 (5), 712–722.

Lieberman, M.M., Nerurkar, V.R., Luo, H., Cropp, B., Carrion, Jr., R., de la Garza, M., et al., 2009. Immunogenicity and protective efficacy of a recombinant subunit West Nile virus vaccine in rhesus monkeys. Clin. Vaccine Immunol. 16 (9), 1332–1337.

Lin, Y.L., Liao, C.L., Chen, L.K., Yeh, C.T., Liu, C.I., Ma, S.H., et al., 1998. Study of dengue virus infection in SCID mice engrafted with human K562 cells. J. Virol. 72 (12), 9729–9737.

Lipatov, A.S., Kwon, Y.K., Sarmento, L.V., Lager, K.M., Spackman, E., Suarez, D.L., Swayne, D.E., 2008. Domestic pigs have low susceptibility to H5N1 highly pathogenic avian influenza viruses. PLoS Pathog. 4 (7), e1000102.

Liu, C., Voth, D.W., Rodina, P., Shauf, L.R., Gonzalez, G., 1970. A comparative study of the pathogenesis of western equine and eastern equine encephalomyelitis viral infections in mice by intracerebral and subcutaneous inoculations. J. Infect. Dis. 122 (1), 53–63.

Liu, F., Song, Y., Liu, D., 1999. Hydrodynamics-based transfection in animals by systemic administration of plasmid DNA. Gene Ther. 6 (7), 1258–1266.

Lo, M.K., Rota, P.A., 2008. The emergence of Nipah virus, a highly pathogenic paramyxovirus. J. Clin. Virol. 43 (4), 396–400.

Lowen, A.C., Mubareka, S., Tumpey, T.M., Garcia-Sastre, A., Palese, P., 2006. The guinea pig as a transmission model for human influenza viruses. Proc. Natl. Acad. Sci. USA 103 (26), 9988–9992.

Lowen, A.C., Bouvier, N.M., Steel, J., 2014. Transmission in the guinea pig model. Curr. Top. Microbiol. Immunol. 385, 157–183.

Lu, X., Tumpey, T.M., Morken, T., Zaki, S.R., Cox, N.J., Katz, J.M., 1999. A mouse model for the evaluation of pathogenesis and immunity to influenza A (H5N1) viruses isolated from humans. J. Virol. 73 (7), 5903–5911.

Luby, S.P., Gurley, E.S., Hossain, M.J., 2009a. Transmission of human infection with Nipah virus. Clin. Infect. Dis. 49 (11), 1743–1748.

Luby, S.P., Hossain, M.J., Gurley, E.S., Ahmed, B.N., Banu, S., Khan, S.U., et al., 2009b. Recurrent zoonotic transmission of Nipah virus into humans, Bangladesh, 2001-2007. Emerg. Infect. Dis. 15 (8), 1229–1235.

Lucia, H.L., Coppenhaver, D.H., Harrison, R.L., Baron, S., 1990. The effect of an arenavirus infection on liver morphology and function. Am. J. Trop. Med. Hyg. 43 (1), 93–98.

Lucifora, J., Vincent, I.E., Berthillon, P., Dupinay, T., Michelet, M., Protzer, U., et al., 2010. Hepatitis B virus replication in primary macaque hepatocytes: crossing the species barrier toward a new small primate model. Hepatology 51 (6), 1954–1960.

Ludtke, A., Oestereich, L., Ruibal, P., Wurr, S., Pallasch, E., Bockholt, S., et al., 2015. Ebola virus disease in mice with transplanted human hematopoietic stem cells. J. Virol. 89 (8), 4700–4704.

Lukashevich, I.S., Tikhonov, I., Rodas, J.D., Zapata, J.C., Yang, Y., Djavani, M., Salvato, M.S., 2003. Arenavirus-mediated liver pathology: acute lymphocytic choriomeningitis virus infection of rhesus macaques is characterized by high-level interleukin-6 expression and hepatocyte proliferation. J. Virol. 77 (3), 1727–1737.

Lukashevich, I.S., Rodas, J.D., Tikhonov, I.I., Zapata, J.C., Yang, Y., Djavani, M., Salvato, M.S., 2004. LCMV-mediated hepatitis in rhesus macaques: WE but not ARM strain activates hepatocytes and induces liver regeneration. Arch. Virol. 149 (12), 2319–2336.

Lutgehetmann, M., Mancke, L.V., Volz, T., Helbig, M., Allweiss, L., Bornscheuer, T., et al., 2012. Humanized chimeric uPA mouse model for the study of hepatitis B and D virus interactions and preclinical drug evaluation. Hepatology 55 (3), 685–694.

MacDonald, G.H., Johnston, R.E., 2000. Role of dendritic cell targeting in Venezuelan equine encephalitis virus pathogenesis. J. Virol. 74 (2), 914–922.

MacDonald, D.M., Holmes, E.C., Lewis, J.C., Simmonds, P., 2000. Detection of hepatitis B virus infection in wild-born chimpanzees (*Pan troglodytes verus*): phylogenetic relationships with human and other primate genotypes. J. Virol. 74 (9), 4253–4257.

MacNeil, A., Farnon, E.C., Wamala, J., Okware, S., Cannon, D.L., Reed, Z., et al., 2010. Proportion of deaths and clinical features in Bundibugyo Ebola virus infection, Uganda. Emerg. Infect. Dis. 16 (12), 1969–1972.

Maher, J.A., DeStefano, J., 2004. The ferret: an animal model to study influenza virus. Lab Anim. (NY) 33 (9), 50–53.

Maines, T.R., Belser, J.A., Gustin, K.M., van Hoeven, N., Zeng, H., Svitek, N., et al., 2012. Local innate immune responses and influenza virus transmission and virulence in ferrets. J. Infect. Dis. 205 (3), 474–485.

Makison Booth, C., 2014. Vomiting Larry: a simulated vomiting system for assessing environmental contamination from projectile vomiting related to norovirus infection. J. Infect. Prev. 15 (5), 176–180.

Marchette, N.J., Halstead, S.B., Falkler, Jr., W.A., Stenhouse, A., Nash, D., 1973. Studies on the pathogenesis of dengue infection in monkeys. 3. Sequential distribution of virus in primary and heterologous infections. J. Infect. Dis. 128 (1), 23–30.

Marchette, N.J., O'Rourke, T., Halstead, S.B., 1980. Studies on dengue 2 virus infection in cyclophosphamide-treated rhesus monkeys. Med. Microbiol. Immunol. 168 (1), 35–47.

Mardani, M., Keshtkar-Jahromi, M., 2007. Crimean-Congo hemorrhagic fever. Arch. Iran Med. 10 (2), 204–214.

Marianneau, P., Guillaume, V., Wong, T., Badmanathan, M., Looi, R.Y., Murri, S., et al., 2010. Experimental infection of squirrel monkeys with Nipah virus. Emerg. Infect. Dis. 16 (3), 507–510.

Marks, P.J., Vipond, I.B., Regan, F.M., Wedgwood, K., Fey, R.E., Caul, E.O., 2003. A school outbreak of Norwalk-like virus: evidence for airborne transmission. Epidemiol. Infect. 131 (1), 727–736.

Marsh, G.A., Haining, J., Hancock, T.J., Robinson, R., Foord, A.J., Barr, J.A., et al., 2011. Experimental infection of horses with Hendra virus/Australia/horse/2008/Redlands. Emerg. Infect. Dis. 17 (12), 2232–2238.

Martina, B.E., Haagmans, B.L., Kuiken, T., Fouchier, R.A., Rimmelzwaan, G.F., Van Amerongen, G., et al., 2003. Virology: SARS virus infection of cats and ferrets. Nature 425 (6961), 915.

Martins, K., Cooper, C., Warren, T., Wells, J., Bell, T., Raymond, J., et al., 2015. Characterization of clinical and immunological parameters during Ebola virus infection of rhesus macaques. Viral Immunol. 28 (1), 32–41.

Marzi, A., Feldmann, F., Hanley, P.W., Scott, D.P., Gunther, S., Feldmann, H., 2015. Delayed disease progression in cynomolgus macaques infected with Ebola virus Makona strain. Emerg. Infect. Dis. 21 (10), 1777–1783.

Mason, W.S., Aldrich, C., Summers, J., Taylor, J.M., 1982. Asymmetric replication of duck hepatitis B virus DNA in liver cells: free minus-strand DNA. Proc. Natl. Acad. Sci. USA 79 (13), 3997–4001.

Matrosovich, M.N., Matrosovich, T.Y., Gray, T., Roberts, N.A., Klenk, H.D., 2004. Human and avian influenza viruses target different cell types in cultures of human airway epithelium. Proc. Natl. Acad. Sci. USA 101 (13), 4620–4624.

Maufort, J.P., Shai, A., Pitot, H.C., Lambert, P.F., 2010. A role for HPV16 E5 in cervical carcinogenesis. Cancer Res. 70 (7), 2924–2931.

McAuliffe, J., Vogel, L., Roberts, A., Fahle, G., Fischer, S., Shieh, W.J., et al., 2004. Replication of SARS coronavirus administered into the respiratory tract of African Green, rhesus and cynomolgus monkeys. Virology 330 (1), 8–15.

McCaffrey, A.P., Nakai, H., Pandey, K., Huang, Z., Salazar, F.H., Xu, H., et al., 2003. Inhibition of hepatitis B virus in mice by RNA interference. Nat. Biotechnol. 21 (6), 639–644.

McCarthy, M., 2016. Zika virus was transmitted by sexual contact in Texas, health officials report. BMJ 352, i720.

McCormick, J.B., Fisher-Hoch, S.P., 2002. Lassa fever. Curr. Top. Microbiol. Immunol. 262, 75–109.

McCormick, J.B., King, I.J., Webb, P.A., Scribner, C.L., Craven, R.B., Johnson, K.M., et al., 1986a. Lassa fever. Effective therapy with ribavirin. N. Engl. J. Med. 314 (1), 20–26.

McCormick, J.B., Walker, D.H., King, I.J., Webb, P.A., Elliott, L.H., Whitfield, S.G., Johnson, K.M., 1986b. Lassa virus hepatitis: a study of fatal Lassa fever in humans. Am. J. Trop. Med. Hyg. 35 (2), 401–407.

McCray, Jr., P.B., Pewe, L., Wohlford-Lenane, C., Hickey, M., Manzel, L., Shi, L., et al., 2007. Lethal infection of K18-hACE2 mice infected with severe acute respiratory syndrome coronavirus. J. Virol. 81 (2), 813–821.

McElroy, A.K., Bray, M., Reed, D.S., Schmaljohn, C.S., 2002. Andes virus infection of cynomolgus macaques. J. Infect. Dis. 186 (12), 1706–1712.

McLaren, C., Butchko, G.M., 1978. Regional T- and B-cell responses in influenza-infected ferrets. Infect. Immun. 22 (1), 189–194.

Mehedi, M., Groseth, A., Feldmann, H., Ebihara, H., 2011. Clinical aspects of Marburg hemorrhagic fever. Future Virol. 6 (9), 1091–1106.

Melkus, M.W., Estes, J.D., Padgett-Thomas, A., Gatlin, J., Denton, P.W., Othieno, F.A., et al., 2006. Humanized mice mount specific adaptive and innate immune responses to EBV and TSST-1. Nat. Med. 12 (11), 1316–1322.

Melnick, J.L., Paul, J.R., Riordan, J.T., Barnett, V.H., Goldblum, N., Zabin, E., 1951. Isolation from human sera in Egypt of a virus apparently identical to West Nile virus. Proc. Soc. Exp. Biol. Med. 77 (4), 661–665.

Memish, Z.A., Mishra, N., Olival, K.J., Fagbo, S.F., Kapoor, V., Epstein, J.H., et al., 2013. Middle East respiratory syndrome coronavirus in bats, Saudi Arabia. Emerg. Infect. Dis. 19 (11), 1819–1823.

Messaoudi, I., Vomaske, J., Totonchy, T., Kreklywich, C.N., Haberthur, K., Springgay, L., et al., 2013. Chikungunya virus infection results in higher and persistent viral replication in aged rhesus macaques due to defects in anti-viral immunity. PLoS Negl. Trop. Dis. 7 (7), e2343.

Meyerholz, D.K., Grubor, B., Fach, S.J., Sacco, R.E., Lehmkuhl, H.D., Gallup, J.M., Ackermann, M.R., 2004. Reduced clearance of respiratory syncytial virus infection in a preterm lamb model. Microbes Infect. 6 (14), 1312–1319.

Meyerholz, D.K., Lambertz, A.M., McCray, Jr., P.B., 2016. Dipeptidyl peptidase 4 distribution in the human respiratory tract: implications for the Middle East respiratory syndrome. Am. J. Pathol. 186 (1), 78–86.

Middleton, D.J., Westbury, H.A., Morrissy, C.J., van der Heide, B.M., Russell, G.M., Braun, M.A., Hyatt, A.D., 2002. Experimental Nipah virus infection in pigs and cats. J. Comp. Pathol. 126 (2–3), 124–136.

Middleton, D.J., Morrissy, C.J., van der Heide, B.M., Russell, G.M., Braun, M.A., Westbury, H.A., et al., 2007. Experimental Nipah virus infection in pteropid bats (Pteropus poliocephalus). J. Comp. Pathol. 136 (4), 266–272.

Midgley, C.M., Bajwa-Joseph, M., Vasanawathana, S., Limpitikul, W., Wills, B., Flanagan, A., et al., 2011. An in-depth analysis of original antigenic sin in dengue virus infection. J. Virol. 85 (1), 410–421.

Miller, C.J., Li, Q., Abel, K., Kim, E.Y., Ma, Z.M., Wietgrefe, S., et al., 2005. Propagation and dissemination of infection after vaginal transmission of simian immunodeficiency virus. J. Virol. 79 (14), 9217–9227.

Mims, C.A., 1956. Rift Valley fever virus in mice. I. General features of the infection. Br. J. Exp. Pathol. 37 (2), 99–109.

Miner, J.J., Cao, B., Govero, J., Smith, A.M., Fernandez, E., Cabrera, O.H., et al., 2016. Zika virus infection during pregnancy in mice causes placental damage and fetal demise. Cell 165 (5), 1081–1091.

Moe, C.L., Christmas, W.A., Echols, L.J., Miller, S.E., 2001. Outbreaks of acute gastroenteritis associated with Norwalk-like viruses in campus settings. J. Am. Coll. Health 50 (2), 57–66.

Moldt, B., Shibata-Koyama, M., Rakasz, E.G., Schultz, N., Kanda, Y., Dunlop, D.C., et al., 2012. A nonfucosylated variant of the anti-HIV-1 monoclonal antibody b12 Has enhanced FcgammaRIIIa-mediated antiviral activity in vitro but does not improve protection against mucosal SHIV challenge in macaques. J. Virol. 86 (11), 6189–6196.

Monath, T.P., Tsai, T.F., 2002. Flaviviruses. In: Richman, D.D., Whitley, R.J., Hayden, F.G. (Eds.), Clinical Virology. second ed. ASM Press, Washington, DC, pp. 1097–1151.

Monath, T.P., Calisher, C.H., Davis, M., Bowen, G.S., White, J., 1974. Experimental studies of rhesus monkeys infected with epizootic and enzootic subtypes of Venezuelan equine encephalitis virus. J. Infect. Dis. 129 (2), 194–200.

Monath, T.P., Kemp, G.E., Cropp, C.B., Chandler, F.W., 1978. Necrotizing myocarditis in mice infected with Western equine encephalitis virus: clinical, electrocardiographic, and histopathologic correlations. J. Infect. Dis. 138 (1), 59–66.

Moore, C.G., Mitchell, C.J., 1997. Aedes albopictus in the United States: ten-year presence and public health implications. Emerg. Infect. Dis. 3 (3), 329–334.

Moore, I.N., Lamirande, E.W., Paskel, M., Donahue, D., Kenney, H., Qin, J., Subbarao, K., 2014. Severity of clinical disease and pathology in ferrets experimentally infected with influenza viruses is influenced by inoculum volume. J. Virol. 88 (23), 13879–13891.

Moreau, M., Le Tortorec, A., Deleage, C., Brown, C., Denis, H., Satie, A.P., et al., 2012. Impact of short-term HAART initiated during the chronic stage or shortly post-exposure on SIV infection of male genital organs. PLoS One 7 (5), e37348.

Morgan, I.M., 1941. Influence of age on susceptibility and on immune response of mice to eastern equine encephalomyelitis virus. J. Exp. Med. 74 (2), 115–132.

Morrison, T.E., Oko, L., Montgomery, S.A., Whitmore, A.C., Lotstein, A.R., Gunn, B.M., et al., 2011. A mouse model of chikungunya virus-induced musculoskeletal inflammatory disease: evidence of arthritis, tenosynovitis, myositis, and persistence. Am. J. Pathol. 178 (1), 32–40.

Mota, J., Rico-Hesse, R., 2011. Dengue virus tropism in humanized mice recapitulates human dengue fever. PLoS One 6 (6), e20762.

Muller, U., Steinhoff, U., Reis, L.F., Hemmi, S., Pavlovic, J., Zinkernagel, R.M., Aguet, M., 1994. Functional role of type I and type II interferons in antiviral defense. Science 264 (5167), 1918–1921.

Mundel, B., Gear, J., 1951. Rift valley fever; I. The occurrence of human cases in Johannesburg. S. Afr. Med. J. 25 (44), 797–800.

Mungall, B.A., Middleton, D., Crameri, G., Bingham, J., Halpin, K., Russell, G., et al., 2006. Feline model of acute Nipah virus infection and protection with a soluble glycoprotein-based subunit vaccine. J. Virol. 80 (24), 12293–12302.

Mungall, B.A., Middleton, D., Crameri, G., Halpin, K., Bingham, J., Eaton, B.T., Broder, C.C., 2007. Vertical transmission and fetal replication of Nipah virus in an experimentally infected cat. J. Infect. Dis. 196 (6), 812–816.

Munster, V.J., de Wit, E., van den Brand, J.M., Herfst, S., Schrauwen, E.J., Bestebroer, T.M., et al., 2009. Pathogenesis and transmission of swine-origin 2009 A(H1N1) influenza virus in ferrets. Science 325 (5939), 481–483.

Munster, V.J., de Wit, E., Feldmann, H., 2013. Pneumonia from human coronavirus in a macaque model. N. Engl. J. Med. 368 (16), 1560–1562.

Murphy, F.A., Whitfield, S.G., 1970. Eastern equine encephalitis virus infection: electron microscopic studies of mouse central nervous system. Exp. Mol. Pathol. 13 (2), 131–146.

Murphy, B.R., Sly, D.L., Hosier, N.T., London, W.T., Chanock, R.M., 1980. Evaluation of three strains of influenza A virus in humans and in owl, cebus, and squirrel monkeys. Infect. Immun. 28 (3), 688–691.

Murray, K., Rogers, R., Selvey, L., Selleck, P., Hyatt, A., Gould, A., et al., 1995a. A novel morbillivirus pneumonia of horses and its transmission to humans. Emerg. Infect. Dis. 1 (1), 31–33.

Murray, K., Selleck, P., Hooper, P., Hyatt, A., Gould, A., Gleeson, L., et al., 1995b. A morbillivirus that caused fatal disease in horses and humans. Science 268 (5207), 94–97.

Nair, H., Nokes, D.J., Gessner, B.D., Dherani, M., Madhi, S.A., Singleton, R.J., et al., 2010. Global burden of acute lower respiratory infections due to respiratory syncytial virus in young children: a systematic review and meta-analysis. Lancet 375 (9725), 1545–1555.

Nalca, A., Whitehouse, C.A., 2007. CCHF infection among animals. In: Ergonul, O., Whitehouse, C.A. (Eds.), Crimean-Congo Hemorrhagic Fever: A Global Perspective. Springer, The Netherlands.

Nalca, A., Rimoin, A.W., Bavari, S., Whitehouse, C.A., 2005. Reemergence of monkeypox: prevalence, diagnostics, and countermeasures. Clin. Infect. Dis. 41 (12), 1765–1771.

Nalca, A., Livingston, V.A., Garza, N.L., Zumbrun, E.E., Frick, O.M., Chapman, J.L., Hartings, J.M., 2010. Experimental infection of cynomolgus macaques (Macaca fascicularis) with aerosolized monkeypox virus. PLoS One 5 (9), e12880.

Nathanson, N., Stolley, P.D., Boolukos, P.J., 1969. Eastern equine encephalitis. Distribution of central nervous system lesions in man and Rhesus monkey. J. Comp. Pathol. 79 (1), 109–115.

Nayersina, R., Fowler, P., Guilhot, S., Missale, G., Cerny, A., Schlicht, H.J., et al., 1993. HLA A2 restricted cytotoxic T lymphocyte responses to multiple hepatitis B surface antigen epitopes during hepatitis B virus infection. J. Immunol. 150 (10), 4659–4671.

Neff, C.P., Zhou, J., Remling, L., Kuruvilla, J., Zhang, J., Li, H., et al., 2011. An aptamer-siRNA chimera suppresses HIV-1 viral loads and protects from helper CD4(+) T cell decline in humanized mice. Sci. Transl. Med. 3 (66), 66ra66.

Netland, J., Meyerholz, D.K., Moore, S., Cassell, M., Perlman, S., 2008. Severe acute respiratory syndrome coronavirus infection causes neuronal death in the absence of encephalitis in mice transgenic for human ACE2. J. Virol. 82 (15), 7264–7275.

Ng, P.S., Bohm, R., Hartley-Tassell, L.E., Steen, J.A., Wang, H., Lukowski, S.W., et al., 2014. Ferrets exclusively synthesize Neu5Ac and express naturally humanized influenza A virus receptors. Nat. Commun. 5, 5750.

Nichol, S.T., 2001. Bunyaviruses. Knipe, D.M., Howley, P.M. (Eds.), Field's Virology, vol. 2, forth ed. Lippincott Williams & Wilkins, Philadelphia, pp. 1603–1633.

Nicholls, P.K., Klaunberg, B.A., Moore, R.A., Santos, E.B., Parry, N.R., Gough, G.W., Stanley, M.A., 1999. Naturally occurring, nonregressing canine oral papillomavirus infection: host immunity, virus characterization, and experimental infection. Virology 265 (2), 365–374.

Nicholls, P.K., Moore, P.F., Anderson, D.M., Moore, R.A., Parry, N.R., Gough, G.W., Stanley, M.A., 2001. Regression of canine oral papillomas is associated with infiltration of CD4+ and CD8+ lymphocytes. Virology 283 (1), 31–39.

Niewiesk, S., Prince, G., 2002. Diversifying animal models: the use of hispid cotton rats (*Sigmodon hispidus*) in infectious diseases. Lab. Anim. 36 (4), 357–372.

Ocadiz-Delgado, R., Marroquin-Chavira, A., Hernandez-Mote, R., Valencia, C., Manjarrez-Zavala, M.E., Covarrubias, L., Gariglio, P., 2009. Induction of focal epithelial hyperplasia in tongue of young bk6-E6/E7 HPV16 transgenic mice. Transgenic Res. 18 (4), 513–527.

O'Donnell, C.D., Subbarao, K., 2011. The contribution of animal models to the understanding of the host range and virulence of influenza A viruses. Microbes Infect. 13 (5), 502–515.

Oestereich, L., Rieger, T., Neumann, M., Bernreuther, C., Lehmann, M., Krasemann, S., et al., 2014. Evaluation of antiviral efficacy of ribavirin, arbidol, and T-705 (favipiravir) in a mouse model for Crimean-Congo hemorrhagic fever. PLoS Negl. Trop. Dis. 8 (5), e2804.

Oh, D.Y., Lowther, S., McCaw, J.M., Sullivan, S.G., Leang, S.K., Haining, J., et al., 2014. Evaluation of oseltamivir prophylaxis regimens for reducing influenza virus infection, transmission and disease severity in a ferret model of household contact. J. Antimicrob. Chemother. 69 (9), 2458–2469.

Oh, D.Y., Barr, I.G., Hurt, A.C., 2015. A novel video tracking method to evaluate the effect of influenza infection and antiviral treatment on ferret activity. PLoS One 10 (3), e0118780.

Olivier, A., Gallup, J., de Macedo, M.M., Varga, S.M., Ackermann, M., 2009. Human respiratory syncytial virus A2 strain replicates and induces innate immune responses by respiratory epithelia of neonatal lambs. Int. J. Exp. Pathol. 90 (4), 431–438.

Omatsu, T., Moi, M.L., Hirayama, T., Takasaki, T., Nakamura, S., Tajima, S., et al., 2011. Common marmoset (*Callithrix jacchus*) as a primate model of dengue virus infection: development of high levels of viraemia and demonstration of protective immunity. J. Gen. Virol. 92 (Pt 10), 2272–2280.

Omatsu, T., Moi, M.L., Takasaki, T., Nakamura, S., Katakai, Y., Tajima, S., et al., 2012. Changes in hematological and serum biochemical parameters in common marmosets (*Callithrix jacchus*) after inoculation with dengue virus. J. Med. Primatol. 41 (5), 289–296.

Omrani, A.S., Al-Tawfiq, J.A., Memish, Z.A., 2015. Middle East respiratory syndrome coronavirus (MERS-CoV): animal to human interaction. Pathog. Glob. Health 109 (8), 354–362.

Onlamoon, N., Noisakran, S., Hsiao, H.M., Duncan, A., Villinger, F., Ansari, A.A., Perng, G.C., 2010. Dengue virus-induced hemorrhage in a nonhuman primate model. Blood 115 (9), 1823–1834.

Oosterhuis, K., Ohlschlager, P., van den Berg, J.H., Toebes, M., Gomez, R., Schumacher, T.N., et al., 2011. Preclinical development of highly effective and safe DNA vaccines directed against HPV 16 E6 and E7. Int. J. Cancer 129 (2), 397–406.

Ortigoza, M.B., Dibben, O., Maamary, J., Martinez-Gil, L., Leyva-Grado, V.H., Abreu, Jr., P., et al., 2012. A novel small molecule inhibitor of influenza A viruses that targets polymerase function and indirectly induces interferon. PLoS Pathog. 8 (4), e1002668.

Osorio, J.E., Iams, K.P., Meteyer, C.U., Rocke, T.E., 2009. Comparison of monkeypox viruses pathogenesis in mice by in vivo imaging. PLoS One 4 (8), e6592.

Ostrow, R.S., McGlennen, R.C., Shaver, M.K., Kloster, B.E., Houser, D., Faras, A.J., 1990. A rhesus monkey model for sexual transmission of a papillomavirus isolated from a squamous cell carcinoma. Proc. Natl. Acad. Sci. USA 87 (20), 8170–8174.

Otto, P.H., Clarke, I.N., Lambden, P.R., Salim, O., Reetz, J., Liebler-Tenorio, E.M., 2011. Infection of calves with bovine norovirus GIII. 1 strain Jena virus: an experimental model to study the pathogenesis of norovirus infection. J. Virol. 85 (22), 12013–12021.

Ottolini, M.G., Blanco, J.C., Eichelberger, M.C., Porter, D.D., Pletneva, L., Richardson, J.Y., Prince, G.A., 2005. The cotton rat provides a useful small-animal model for the study of influenza virus pathogenesis. J. Gen. Virol. 86 (Pt 10), 2823–2830.

Pacheco, O., Beltran, M., Nelson, C.A., Valencia, D., Tolosa, N., Farr, S.L., et al., 2016. Zika virus disease in Colombia—preliminary report. N. Engl. J. Med., 1–10.

Padula, P.J., Colavecchia, S.B., Martinez, V.P., Gonzalez Della Valle, M.O., Edelstein, A., Miguel, S.D., et al., 2000. Genetic diversity, distribution, and serological features of hantavirus infection in five countries in South America. J. Clin. Microbiol. 38 (8), 3029–3035.

Paes, M.V., Pinhao, A.T., Barreto, D.F., Costa, S.M., Oliveira, M.P., Nogueira, A.C., et al., 2005. Liver injury and viremia in mice infected with dengue-2 virus. Virology 338 (2), 236–246.

Paessler, S., Aguilar, P., Anishchenko, M., Wang, H.Q., Aronson, J., Campbell, G., et al., 2004. The hamster as an animal model for eastern equine encephalitis—and its use in studies of virus entrance into the brain. J. Infect. Dis. 189 (11), 2072–2076.

Pallister, J., Middleton, D., Wang, L.F., Klein, R., Haining, J., Robinson, R., et al., 2011. A recombinant Hendra virus G glycoprotein-based subunit vaccine protects ferrets from lethal Hendra virus challenge. Vaccine 29 (34), 5623–5630.

Panchal, R.G., Reid, S.P., Tran, J.P., Bergeron, A.A., Wells, J., Kota, K.P., et al., 2012. Identification of an antioxidant small-molecule with broad-spectrum antiviral activity. Antiviral Res. 93 (1), 23–29.

Paquette, S.G., Huang, S.S., Banner, D., Xu, L., Leomicronn, A., Kelvin, A.A., Kelvin, D.J., 2014. Impaired heterologous immunity in aged ferrets during sequential influenza A H1N1 infection. Virology 464–465, 177–183.

Paquette, S.G., Banner, D., Huang, S.S., Almansa, R., Leon, A., Xu, L., et al., 2015. Influenza transmission in the mother-infant dyad leads to severe disease, mammary gland infection, and pathogenesis by regulating host responses. PLoS Pathog. 11 (10), e1005173.

Paramore, L.C., Ciuryla, V., Ciesla, G., Liu, L., 2004. Economic impact of respiratory syncytial virus-related illness in the US: an analysis of national databases. Pharmacoeconomics 22 (5), 275–284.

Parida, M.M., Upadhyay, C., Pandya, G., Jana, A.M., 2002. Inhibitory potential of neem (*Azadirachta indica* Juss) leaves on dengue virus type-2 replication. J. Ethnopharmacol. 79 (2), 273–278.

Patel, M.M., Widdowson, M.A., Glass, R.I., Akazawa, K., Vinje, J., Parashar, U.D., 2008. Systematic literature review of role of noroviruses in sporadic gastroenteritis. Emerg. Infect. Dis. 14 (8), 1224–1231.

Pearson, H., Clarke, T., Abbott, A., Knight, J., Cyranoski, D., 2003. SARS: what have we learned? Nature 424 (6945), 121–126.

Peiris, J.S., Yuen, K.Y., Osterhaus, A.D., Stohr, K., 2003. The severe acute respiratory syndrome. N. Engl. J. Med. 349 (25), 2431–2441.

Peiris, J.S., Guan, Y., Yuen, K.Y., 2004. Severe acute respiratory syndrome. Nat. Med. 10 (12 Suppl.), S88–S97.

Peltola, V.T., Boyd, K.L., McAuley, J.L., Rehg, J.E., McCullers, J.A., 2006. Bacterial sinusitis and otitis media following influenza virus infection in ferrets. Infect. Immun. 74 (5), 2562–2567.

Peng, B.H., Yun, N., Chumakova, O., Zacks, M., Campbell, G., Smith, J., et al., 2012. Neuropathology of H5N1 virus infection in ferrets. Vet. Microbiol. 156 (3–4), 294–304.

Peng, X., Alfoldi, J., Gori, K., Eisfeld, A.J., Tyler, S.R., Tisoncik-Go, J., et al., 2014. The draft genome sequence of the ferret (*Mustela putorius furo*) facilitates study of human respiratory disease. Nat. Biotechnol. 32 (12), 1250–1255.

Perlman, S., Dandekar, A.A., 2005. Immunopathogenesis of coronavirus infections: implications for SARS. Nat. Rev. Immunol. 5 (12), 917–927.

Peters, C.J., Khan, A.S., 2002. Hantavirus pulmonary syndrome: the new American hemorrhagic fever. Clin. Infect. Dis. 34 (9), 1224–1231.

Peters, C.J., Linthicum, K.J., 1994. Rift Valley fever. In: Beran, G.W. (Ed.), CRC Handbook Series in Zoonoses. secoond ed. CRC Press Inc, Boca Raton, FL, pp. 125–138.

Peters, C.J., Slone, T.W., 1982. Inbred rat strains mimic the disparate human response to Rift Valley fever virus infection. J. Med. Virol. 10 (1), 45–54.

Peters, C.J., Jahrling, P.B., Liu, C.T., Kenyon, R.H., McKee, Jr., K.T., Barrera Oro, J.G., 1987. Experimental studies of arenaviral hemorrhagic fevers. Curr. Top. Microbiol. Immunol. 134, 5–68.

Peters, C.J., Jones, D., Trotter, R., Donaldson, J., White, J., Stephen, E., Slone, Jr., T.W., 1988. Experimental Rift Valley fever in rhesus macaques. Arch. Virol. 99 (1–2), 31–44.

Piazza, F.M., Johnson, S.A., Darnell, M.E., Porter, D.D., Hemming, V.G., Prince, G.A., 1993. Bovine respiratory syncytial virus protects cotton rats against human respiratory syncytial virus infection. J. Virol. 67 (3), 1503–1510.

Pillot, J., 1990. [Primates in the study of hepatitis viruses]. Pathol. Biol. (Paris) 38 (3), 177–181.

Playford, E.G., McCall, B., Smith, G., Slinko, V., Allen, G., Smith, I., et al., 2010. Human Hendra virus encephalitis associated with equine outbreak, Australia, 2008. Emerg. Infect. Dis. 16 (2), 219–223.

Pletnev, A.G., Claire, M.S., Elkins, R., Speicher, J., Murphy, B.R., Chanock, R.M., 2003. Molecularly engineered live-attenuated chimeric West Nile/dengue virus vaccines protect rhesus monkeys from West Nile virus. Virology 314 (1), 190–195.

Plopper, C.G., Mariassy, A.T., Lollini, L.O., 1983. Structure as revealed by airway dissection. A comparison of mammalian lungs. Am. Rev. Respir. Dis. 128 (2 Pt 2), S4–S7.

Pogodina, V.V., Frolova, M.P., Malenko, G.V., Fokina, G.I., Koreshkova, G.V., Kiseleva, L.L., et al., 1983. Study on West Nile virus persistence in monkeys. Arch. Virol. 75 (1–2), 71–86.

Ponzetto, A., Negro, F., Gerin, J.L., Purcell, R.H., 1991. Experimental hepatitis delta virus infection in the animal model. Prog. Clin. Biol. Res. 364, 147–157.

Powers, A.M., Logue, C.H., 2007. Changing patterns of chikungunya virus: re-emergence of a zoonotic arbovirus. J. Gen. Virol. 88 (Pt 9), 2363–2377.

Prince, A.M., 1972. Grune and Stratton. Hepatitis and Blood Transfusion. New York, NY.

Prince, A.M., Brotman, B., 2001. Perspectives on hepatitis B studies with chimpanzees. ILAR J. 42 (2), 85–88.

Prince, G.A., Prieels, J.P., Slaoui, M., Porter, D.D., 1999. Pulmonary lesions in primary respiratory syncytial virus infection, reinfection, and vaccine-enhanced disease in the cotton rat (*Sigmodon hispidus*). Lab. Invest. 79 (11), 1385–1392.

Purcell, R.H., Satterfield, W.C., Bergmann, K.F., Smedile, A., Ponzetto, A., Gerin, J.L., 1987. Experimental hepatitis delta virus infection in the chimpanzee. Prog. Clin. Biol. Res. 234, 27–36.

Purcell, R.H., Wong, D.C., Shapiro, M., 2002. Relative infectivity of hepatitis A virus by the oral and intravenous routes in 2 species of nonhuman primates. J. Infect. Dis. 185 (11), 1668–1671.

Qian, C., Jahrling, P.B., Peters, C.J., Liu, C.T., 1994. Cardiovascular and pulmonary responses to Pichinde virus infection in strain 13 guinea pigs. Lab. Anim. Sci. 44 (6), 600–607.

Qiu, X., Wong, G., Audet, J., Cutts, T., Niu, Y., Booth, S., Kobinger, G.P., 2014. Establishment and characterization of a lethal mouse model for the Angola strain of Marburg virus. J. Virol. 88 (21), 12703–12714.

Rabenau, H.F., Cinatl, J., Morgenstern, B., Bauer, G., Preiser, W., Doerr, H.W., 2005. Stability and inactivation of SARS coronavirus. Med. Microbiol. Immunol. 194 (1–2), 1–6.

Rabinovich, V.D., Milyutin, V.N., Artyushenko, A.A., Buryakov, B.G., Chumakov, M.P., 1972. Possibility of extracting hyperimmune gammaglobulin against CHF from doneky blood sera. Tezisy 17 Nauchn Sess Inst Posvyashch Aktual Probl Virus Profilakt Virus Zabolev, 350–351.

Raj, V.S., Mou, H., Smits, S.L., Dekkers, D.H., Muller, M.A., Dijkman, R., et al., 2013. Dipeptidyl peptidase 4 is a functional receptor for the emerging human coronavirus-EMC. Nature 495 (7440), 251–254.

Rajao, D.S., Vincent, A.L., 2015. Swine as a model for influenza A virus infection and immunity. ILAR J. 56 (1), 44–52.

Ramos da Silva, S., Gao, S.J., 2016. Zika virus: an update on epidemiology, pathology, molecular biology, and animal model. J. Med. Virol. 88 (8), 1291–1296.

Reddy, M.B., Yang, K.H., Rao, G., Rayner, C.R., Nie, J., Pamulapati, C., et al., 2015. Oseltamivir population pharmacokinetics in the ferret: model application for pharmacokinetic/pharmacodynamic study design. PLoS One 10 (10), e0138069.

Reed, D.S., Lind, C.M., Sullivan, L.J., Pratt, W.D., Parker, M.D., 2004. Aerosol infection of cynomolgus macaques with enzootic strains of Venezuelan equine encephalitis viruses. J. Infect. Dis. 189 (6), 1013–1017.

Reed, D.S., Larsen, T., Sullivan, L.J., Lind, C.M., Lackemeyer, M.G., Pratt, W.D., Parker, M.D., 2005. Aerosol exposure to Western equine encephalitis virus causes fever and encephalitis in cynomolgus macaques. J. Infect. Dis. 192 (7), 1173–1182.

Reed, D.S., Lackemeyer, M.G., Garza, N.L., Norris, S., Gamble, S., Sullivan, L.J., et al., 2007. Severe encephalitis in cynomolgus macaques exposed to aerosolized Eastern equine encephalitis virus. J. Infect. Dis. 196 (3), 441–450.

Reed, D.S., Bethel, L.M., Powell, D.S., Caroline, A.L., Hartman, A.L., 2014. Differences in aerosolization of Rift Valley fever virus resulting from choice of inhalation exposure chamber: implications for animal challenge studies. Pathog. Dis. 71 (2), 227–233.

Reid, W., Sadowska, M., Denaro, F., Rao, S., Foulke, Jr., J., Hayes, N., et al., 2001. An HIV-1 transgenic rat that develops HIV-related pathology and immunologic dysfunction. Proc. Natl. Acad. Sci USA 98 (16), 9271–9276.

Reynolds, M.R., Weiler, A.M., Piaskowski, S.M., Piatak, Jr., M., Robertson, H.T., Allison, D.B., et al., 2012. A trivalent recombinant Ad5 gag/pol/nef vaccine fails to protect rhesus macaques from infection or control virus replication after a limiting-dose heterologous SIV challenge. Vaccine 30, 4465–4475.

Rezza, G., Nicoletti, L., Angelini, R., Romi, R., Finarelli, A.C., Panning, M., et al., 2007. Infection with chikungunya virus in Italy: an outbreak in a temperate region. Lancet 370 (9602), 1840–1846.

Richard, M., Schrauwen, E.J., de Graaf, M., Bestebroer, T.M., Spronken, M.I., van Boheemen, S., et al., 2013. Limited airborne transmission of H7N9 influenza A virus between ferrets. Nature 501 (7468), 560–563.

Rimmelzwaan, G.F., Baars, M., van Amerongen, G., van Beek, R., Osterhaus, A.D., 2001. A single dose of an ISCOM influenza vaccine induces long-lasting protective immunity against homologous challenge infection but fails to protect Cynomolgus macaques against distant drift variants of influenza A (H3N2) viruses. Vaccine 20 (1–2), 158–163.

Rimmelzwaan, G.F., van Riel, D., Baars, M., Bestebroer, T.M., van Amerongen, G., Fouchier, R.A., et al., 2006. Influenza A virus (H5N1) infection in cats causes systemic disease with potential novel routes of virus spread within and between hosts. Am. J. Pathol. 168 (1), 176–183, (quiz 364).

Ripple, M.J., You, D., Honnegowda, S., Giaimo, J.D., Sewell, A.B., Becnel, D.M., Cormier, S.A., 2010. Immunomodulation with IL-4R alpha antisense oligonucleotide prevents respiratory syncytial virus-mediated pulmonary disease. J. Immunol. 185 (8), 4804–4811.

Roberts, A., Subbarao, K., 2006. Animal models for SARS. Adv Exp. Med. Biol. 581, 463–471.

Roberts, A., Paddock, C., Vogel, L., Butler, E., Zaki, S., Subbarao, K., 2005. Aged BALB/c mice as a model for increased severity of severe acute respiratory syndrome in elderly humans. J. Virol. 79 (9), 5833–5838.

Roberts, A., Deming, D., Paddock, C.D., Cheng, A., Yount, B., Vogel, L., et al., 2007. A mouse-adapted SARS-coronavirus causes disease and mortality in BALB/c mice. PLoS Pathog. 3 (1), e5.

Roberts, A., Lamirande, E.W., Vogel, L., Jackson, J.P., Paddock, C.D., Guarner, J., et al., 2008. Animal models and vaccines for SARS-CoV infection. Virus Res. 133 (1), 20–32.

Roberts, K.L., Shelton, H., Stilwell, P., Barclay, W.S., 2012. Transmission of a 2009 H1N1 pandemic influenza virus occurs before fever is detected, in the ferret model. PLoS One 7 (8), e43303.

Rockx, B., De Wit, M., Vennema, H., Vinje, J., De Bruin, E., Van Duynhoven, Y., Koopmans, M., 2002. Natural history of human calicivirus infection: a prospective cohort study. Clin. Infect. Dis. 35 (3), 246–253.

Rockx, B.H., Bogers, W.M., Heeney, J.L., van Amerongen, G., Koopmans, M.P., 2005. Experimental norovirus infections in non-human primates. J. Med. Virol. 75 (2), 313–320.

Rockx, B., Sheahan, T., Donaldson, E., Harkema, J., Sims, A., Heise, M., et al., 2007. Synthetic reconstruction of zoonotic and early human severe acute respiratory syndrome coronavirus isolates that produce fatal disease in aged mice. J. Virol. 81 (14), 7410–7423.

Rockx, B., Bossart, K.N., Feldmann, F., Geisbert, J.B., Hickey, A.C., Brining, D., et al., 2010. A novel model of lethal Hendra virus infection in African green monkeys and the effectiveness of ribavirin treatment. J. Virol. 84 (19), 9831–9839.

Rockx, B., Brining, D., Kramer, J., Callison, J., Ebihara, H., Mansfield, K., Feldmann, H., 2011. Clinical outcome of henipavirus infection in hamsters is determined by the route and dose of infection. J. Virol. 85 (15), 7658–7671.

Rockx, B., Winegar, R., Freiberg, A.N., 2012. Recent progress in henipavirus research: molecular biology, genetic diversity, animal models. Antiviral Res. 95, 135–149.

Rodas, J.D., Lukashevich, I.S., Zapata, J.C., Cairo, C., Tikhonov, I., Djavani, M., et al., 2004. Mucosal arenavirus infection of primates can protect them from lethal hemorrhagic fever. J. Med. Virol. 72 (3), 424–435.

Roper, R.L., Rehm, K.E., 2009. SARS vaccines: where are we? Expert. Rev. Vaccines 8 (7), 887–898.

Ross, T.M., Bhardwaj, N., Bissel, S.J., Hartman, A.L., Smith, D.R., 2012. Animal models of Rift Valley fever virus infection. Virus Res. 163 (2), 417–423.

Rossi, S.L., Tesh, R.B., Azar, S.R., Muruato, A.E., Hanley, K.A., Auguste, A.J., et al., 2016. Characterization of a novel murine model to study Zika virus. Am. J. Trop. Med. Hyg. 94 (6), 1362–1369.

Rota, P.A., Oberste, M.S., Monroe, S.S., Nix, W.A., Campagnoli, R., Icenogle, J.P., et al., 2003. Characterization of a novel coronavirus associated with severe acute respiratory syndrome. Science 300 (5624), 1394–1399.

Rowe, T., Gao, G., Hogan, R.J., Crystal, R.G., Voss, T.G., Grant, R.L., et al., 2004. Macaque model for severe acute respiratory syndrome. J. Virol 78 (20), 11401–11404.

Roy, C.J., Reed, D.S., Wilhelmsen, C.L., Hartings, J., Norris, S., Steele, K.E., 2009. Pathogenesis of aerosolized Eastern equine encephalitis virus infection in guinea pigs. Virol. J. 6, 170.

Ruuskanen, O., Ogra, P.L., 1993. Respiratory syncytial virus. Curr. Probl. Pediatr. 23 (2), 50–79.

Safronetz, D., Prescott, J., Feldmann, F., Haddock, E., Rosenke, R., Okumura, A., et al., 2014. Pathophysiology of hantavirus pulmonary syndrome in rhesus macaques. Proc. Natl. Acad. Sci. USA 111 (19), 7114–7119.

Saijo, M., et al., 2009. Virulence and pathophysiology of the Congo Basin and West African strains of monkeypox virus in non-human primates. J. Gen. Virol. 90 (Pt 9), 2266–2271.

Salvato, M.S., Clegg, J.C.S., Buchmeier, M.J., Charrel, R.N., Gonzales, J.P., Lukashevich, I.S., Peters, C.J., Rico-Hesse, R., Romanowski, V., 2005. Arenaviridae. Virus taxonomy, VIIIth Report of the International Committee on Taxonomy of Viruses. Elsevier Academic Press, London, pp. 725–733.

Sbrana, E., Mateo, R.I., Xiao, S.Y., Popov, V.L., Newman, P.C., Tesh, R.B., 2006. Clinical laboratory, virologic, and pathologic changes in hamsters experimentally infected with Pirital virus (Arenaviridae): a rodent model of Lassa fever. Am. J. Trop. Med. Hyg. 74 (6), 1096–1102.

Sbrana, E., Xiao, S.Y., Newman, P.C., Tesh, R.B., 2007. Comparative pathology of North American and central African strains of monkeypox virus in a ground squirrel model of the disease. Am. J. Trop. Med. Hyg. 76 (1), 155–164.

Scharton, D., Van Wettere, A.J., Bailey, K.W., Vest, Z., Westover, J.B., Siddharthan, V., Gowen, B.B., 2015. Rift Valley fever virus infection in golden Syrian hamsters. PLoS One 10 (1), e0116722.

Scheerlinck, J.P., Snibson, K.J., Bowles, V.M., Sutton, P., 2008. Biomedical applications of sheep models: from asthma to vaccines. Trends Biotechnol. 26 (5), 259–266.

Schmaljohn, C.S., Nichol, S.T., 2007. Bunyaviruses. In: Knipe, D.M., Howley, P.M. (Eds.), Field's Virology. fifth ed. Lippincott Williams & Wilkins, Philadelphia, pp. 1741–1789.

Schulman, J.L., 1968. The use of an animal model to study transmission of influenza virus infection. Am. J. Public Health Nations Health 58 (11), 2092–2096.

Schultz, D.A., Sagartz, J.E., Huso, D.L., Buller, R.M., 2009. Experimental infection of an African dormouse (*Graphiurus kelleni*) with monkeypox virus. Virology 383 (1), 86–92.

Scipioni, A., Mauroy, A., Vinje, J., Thiry, E., 2008. Animal noroviruses. Vet. J. 178 (1), 32–45.

Sejvar, J.J., Chowdary, Y., Schomogyi, M., Stevens, J., Patel, J., Karem, K., et al., 2004. Human monkeypox infection: a family cluster in the midwestern United States. J. Infect. Dis. 190 (10), 1833–1840.

Sergeev, A.A., Kabanov, A.S., Bulychev, L.E., Sergeev, A.A., Pyankov, O.V., Bodnev, S.A., et al., 2016. The possibility of using the ICR mouse as an animal model to assess Antimonkeypox drug efficacy. Transbound. Emerg. Dis. 63 (5), e419–e430.

Sergeev, A.A., Kabanov, A.S., Bulychev, L.E., Sergeev, A.A., Pyankov, O.V., Bodnev, S.A., et al., 2017. Using the ground squirrel (*Marmota bobak*) as an animal model to assess monkeypox drug efficacy. Transbound. Emerg. Dis 64 (1), 226–236.

Sestak, K., Feely, S., Fey, B., Dufour, J., Hargitt, E., Alvarez, X., et al., 2012. Experimental inoculation of juvenile rhesus macaques with primate enteric caliciviruses. PLoS One 7 (5), e37973.

Seto, T., Nagata, N., Yoshikawa, K., Ichii, O., Sanada, T., Saasa, N., et al., 2012. Infection of Hantaan virus strain AA57 leading to pulmonary disease in laboratory mice. Virus Res. 163 (1), 284–290.

Seymour, R.L., Adams, A.P., Leal, G., Alcorn, M.D., Weaver, S.C., 2015. A rodent model of Chikungunya virus infection in RAG1$^{-/-}$ mice, with features of persistence, for vaccine safety evaluation. PLoS Negl. Trop. Dis. 9 (6), e0003800.

Sharma, A., Wu, W., Sung, B., Huang, J., Tsao, T., Li, X., et al., 2016. Respiratory syncytial virus (RSV) pulmonary infection in humanized mice induces human anti-RSV Immune responses and pathology. J. Virol. 90 (10), 5068–5074.

Shepherd, A.J., Leman, P.A., Swanepoel, R., 1989. Viremia and anti-body response of small African and laboratory animals to Crimean-Congo hemorrhagic fever virus infection. Am. J. Trop. Med. Hyg. 40 (5), 541–547.

Shimizu, S., Ringpis, G.E., Marsden, M.D., Cortado, R.V., Wilhalme, H.M., Elashoff, D., et al., 2015. RNAi-mediated CCR5 knockdown provides HIV-1 resistance to memory T cells in humanized BLT mice. Mol. Ther. Nucleic Acids 4, e227.

Shresta, S., Kyle, J.L., Robert Beatty, P., Harris, E., 2004. Early activation of natural killer and B cells in response to primary dengue virus infection in A/J mice. Virology 319 (2), 262–273.

Shresta, S., Sharar, K.L., Prigozhin, D.M., Beatty, P.R., Harris, E., 2006. Murine model for dengue virus-induced lethal disease with increased vascular permeability. J. Virol. 80 (20), 10208–10217.

Sidwell, R.W., Smee, D.F., 2000. In vitro and in vivo assay systems for study of influenza virus inhibitors. Antiviral Res. 48 (1), 1–16.

Sidwell, R.W., Smee, D.F., 2003. Viruses of the Bunya- and Togaviridae families: potential as bioterrorism agents and means of control. Antiviral Res. 57 (1–2), 101–111.

Sidwell, R.W., Huffman, J.H., Smee, D.F., Gilbert, J., Gessaman, A., Pease, A., et al., 1992. Potential role of immunomodulators for treatment of phlebovirus infections of animals. Ann. NY Acad. Sci. 653, 344–355.

Simoes, E.A., Hayward, A.R., Ponnuraj, E.M., Straumanis, J.P., Stenmark, K.R., Wilson, H.L., Babu, P.G., 1999. Respiratory syncytial virus infects the Bonnet monkey, *Macaca radiata*. Pediatr. Dev. Pathol. 2 (4), 316–326.

Siolas, D., Hannon, G.J., 2013. Patient-derived tumor xenografts: transforming clinical samples into mouse models. Cancer Res. 73 (17), 5315–5319.

Sironen, T., Klingstrom, J., Vaheri, A., Andersson, L.C., Lundkvist, A., Plyusnin, A., 2008. Pathology of Puumala hantavirus infection in macaques. PLoS One 3 (8), e3035.

Skowronski, D.M., Astell, C., Brunham, R.C., Low, D.E., Petric, M., Roper, R.L., et al., 2005. Severe acute respiratory syndrome (SARS): a year in review. Annu. Rev. Med. 56, 357–381.

Smee, D.F., Gilbert, J., Leonhardt, J.A., Barnett, B.B., Huggins, J.H., Sidwell, R.W., 1993. Treatment of lethal Pichinde virus infections in weanling LVG/Lak hamsters with ribavirin, ribamidine, selenazofurin, and ampligen. Antiviral Res. 20 (1), 57–70.

Smirnova, S.E., 1979. A comparative study of the Crimean hemorrhagic fever-Congo group of viruses. Arch. Virol. 62 (2), 137–143.

Smith, D.R., Steele, K.E., Shamblin, J., Honko, A., Johnson, J., Reed, C., et al., 2010. The pathogenesis of Rift Valley fever virus in the mouse model. Virology 407 (2), 256–267.

Smith, S.K., Self, J., Weiss, S., Carroll, D., Braden, Z., Regnery, R.L., et al., 2011. Effective antiviral treatment of systemic orthopoxvirus disease: ST-246 treatment of prairie dogs infected with monkeypox virus. J. Virol. 85 (17), 9176–9187.

Smithburn, K.C., Hughes, T.P., Burke, A.W., Paul, J.H., 1940. A neurotropic virus isolated from the blood of a native Uganda. Am. J. Trop. Med. Hug. 20, 471–492.

Smither, S.J., Lear-Rooney, C., Biggins, J., Pettitt, J., Lever, M.S., Olinger, Jr., G.G., 2013a. Comparison of the plaque assay and 50% tissue culture infectious dose assay as methods for measuring filovirus infectivity. J. Virol. Methods 193 (2), 565–571.

Smither, S.J., Nelson, M., Eastaugh, L., Laws, T.R., Taylor, C., Smith, S.A., et al., 2013b. Experimental respiratory Marburg virus haemorrhagic fever infection in the common marmoset (*Callithrix jacchus*). Int. J. Exp. Pathol. 94 (2), 156–168.

Smither, S.J., Nelson, M., Eastaugh, L., Nunez, A., Salguero, F.J., Lever, M.S., 2015. Experimental respiratory infection of marmosets (*Callithrix jacchus*) with Ebola virus Kikwit. J. Infect. Dis. 212 (Suppl. 2), S336–S345.

Souza, D.G., Fagundes, C.T., Sousa, L.P., Amaral, F.A., Souza, R.S., Souza, A.L., et al., 2009. Essential role of platelet-activating factor receptor in the pathogenesis of dengue virus infection. Proc. Natl. Acad. Sci. USA 106 (33), 14138–14143.

Sow, F.B., Gallup, J.M., Olivier, A., Krishnan, S., Patera, A.C., Suzich, J., Ackermann, M.R., 2011. Respiratory syncytial virus is associated with an inflammatory response in lungs and architectural remodeling of lung-draining lymph nodes of newborn lambs. Am. J. Physiol. Lung Cell Mol. Physiol. 300 (1), L12–24.

Spandau, D.F., Lee, C.H., 1988. trans-activation of viral enhancers by the hepatitis B virus X protein. J. Virol. 62 (2), 427–434.

Speshock, J.L., Doyon-Reale, N., Rabah, R., Neely, M.N., Roberts, P.C., 2007. Filamentous influenza A virus infection predisposes mice to fatal septicemia following superinfection with *Streptococcus pneumoniae* serotype 3. Infect. Immun. 75 (6), 3102–3111.

St John, A.L., Rathore, A.P., Raghavan, B., Ng, M.L., Abraham, S.N., 2013. Contributions of mast cells and vasoactive products, leukotrienes and chymase, to dengue virus-induced vascular leakage. Elife 2, e00481.

Stabenow, J., Buller, R.M., Schriewer, J., West, C., Sagartz, J.E., Parker, S., 2010. A mouse model of lethal infection for evaluating prophylactics and therapeutics against Monkeypox virus. J. Virol. 84 (8), 3909–3920.

Staeheli, P., Haller, O., 1987. Interferon-induced Mx protein: a mediator of cellular resistance to influenza virus. Interferon 8, 1–23.

Staff, P.O., 2015. Correction: a retrospective investigation on Canine Papillomavirus 1 (CPV1) in oral oncogenesis reveals dogs are not a suitable animal model for high-risk HPV-induced oral cancer. PLoS One 10 (2), e0118051.

Stark, J.M., McDowell, S.A., Koenigsknecht, V., Prows, D.R., Leikauf, J.E., Le Vine, A.M., Leikauf, G.D., 2002. Genetic susceptibility to respiratory syncytial virus infection in inbred mice. J. Med. Virol. 67 (1), 92–100.

Stark, G.V., Long, J.P., Ortiz, D.I., Gainey, M., Carper, B.A., Feng, J., et al., 2013. Clinical profiles associated with influenza disease in the ferret model. PLoS One 8 (3), e58337.

Steele, K.E., Twenhafel, N.A., 2010. Pathology of animal models of alphavirus encephalitis. Vet. Pathol. 47 (5), 790–805.

Steele, K.E., Davis, K.J., Stephan, K., Kell, W., Vogel, P., Hart, M.K., 1998. Comparative neurovirulence and tissue tropism of wild-type and attenuated strains of Venezuelan equine encephalitis virus administered by aerosol in C3H/HeN and BALB/c mice. Vet. Pathol. 35 (5), 386–397.

Stelzer, M.K., Pitot, H.C., Liem, A., Schweizer, J., Mahoney, C., Lambert, P.F., 2010. A mouse model for human anal cancer. Cancer Prev. Res. (Phila) 3 (12), 1534–1541.

Stephen, C., Johnson, M., Bell, A., 1994. First reported cases of hantavirus pulmonary syndrome in Canada. Can. Commun. Dis. Rep. 20 (15), 121–125.

Stittelaar, K.J., Neyts, J., Naesens, L., van Amerongen, G., van Lavieren, R.F., Holy, A., et al., 2006. Antiviral treatment is more effective than smallpox vaccination upon lethal monkeypox virus infection. Nature 439 (7077), 745–748.

Stittelaar, K.J., Tisdale, M., van Amerongen, G., van Lavieren, R.F., Pistoor, F., Simon, J., Osterhaus, A.D., 2008. Evaluation of intravenous zanamivir against experimental influenza A (H5N1) virus infection in cynomolgus macaques. Antiviral Res. 80 (2), 225–228.

Stittelaar, K.J., de Waal, L., van Amerongen, G., Veldhuis Kroeze, E.J., Fraaij, P.L., van Baalen, C.A., et al., 2016. Ferrets as a novel animal model for studying human respiratory syncytial virus infections in immunocompetent and immunocompromised hosts. Viruses 8 (6.).

Stokes, K.L., Chi, M.H., Sakamoto, K., Newcomb, D.C., Currier, M.G., Huckabee, M.M., et al., 2011. Differential pathogenesis of respiratory syncytial virus clinical isolates in BALB/c mice. J. Virol. 85 (12), 5782–5793.

Stone, M., Ma, Z.M., Genesca, M., Fritts, L., Blozois, S., McChesney, M.B., Miller, C.J., 2009. Limited dissemination of pathogenic SIV after vaginal challenge of rhesus monkeys immunized with a live, attenuated lentivirus. Virology 392 (2), 260–270.

Suen, W.W., Uddin, M.J., Wang, W., Brown, V., Adney, D.R., Broad, N., et al., 2015. Experimental West Nile virus infection in rabbits: an alternative model for studying induction of disease and virus control. Pathogens 4 (3), 529–558.

Summers, J., Smolec, J.M., Snyder, R., 1978. A virus similar to human hepatitis B virus associated with hepatitis and hepatoma in woodchucks. Proc. Natl. Acad. Sci. USA 75 (9), 4533–4537.

Sutton, T.C., Subbarao, K., 2015. Development of animal models against emerging coronaviruses: from SARS to MERS coronavirus. Virology 479–480, 247–258.

Svitek, N., Rudd, P.A., Obojes, K., Pillet, S., von Messling, V., 2008. Severe seasonal influenza in ferrets correlates with reduced interferon and increased IL-6 induction. Virology 376 (1), 53–59.

Swanepoel, R., Gill, D.E., Shepherd, A.J., Leman, P.A., Mynhardt, J.H., Harvey, S., 1989. The clinical pathology of Crimean-Congo hemorrhagic fever. Rev. Infect. Dis. 11 (Suppl. 4), S794–S800.

Tacket, C.O., Mason, H.S., Losonsky, G., Estes, M.K., Levine, M.M., Arntzen, C.J., 2000. Human immune responses to a novel Norwalk virus vaccine delivered in transgenic potatoes. J. Infect. Dis. 182 (1), 302–305.

Tan, C.T., Chua, K.B., 2008. Nipah virus encephalitis. Curr. Infect. Dis. Rep. 10 (4), 315–320.

Tan, Y.J., Goh, P.Y., Fielding, B.C., Shen, S., Chou, C.F., Fu, J.L., et al., 2004. Profiles of antibody responses against severe acute respiratory syndrome coronavirus recombinant proteins and their potential use as diagnostic markers. Clin. Diagn. Lab. Immunol. 11 (2), 362–371.

Tanimura, N., Imada, T., Kashiwazaki, Y., Sharifah, S.H., 2006. Distribution of viral antigens and development of lesions in chicken embryos inoculated with Nipah virus. J. Comp. Pathol. 135 (2–3), 74–82.

Tao, X., Garron, T., Agrawal, A.S., Algaissi, A., Peng, B.H., Wakamiya, M., et al., 2016. Characterization and demonstration of the value of a lethal mouse model of Middle East respiratory syndrome coronavirus infection and disease. J. Virol. 90 (1), 57–67.

Taubenberger, J.K., 2006. The origin and virulence of the 1918 "Spanish" influenza virus. Proc. Am. Philos. Soc. 150 (1), 86–112.

Taubenberger, J.K., Morens, D.M., 2008. The pathology of influenza virus infections. Annu. Rev. Pathol. 3, 499–522.

Taylor, R.M., Hurlbut, H.S., Dressler, H.R., Spangler, E.W., Thrasher, D., 1953. Isolation of West Nile virus from *Culex* mosquitoes. J. Egypt Med. Assoc. 36 (3), 199–208.

Teng, M.N., Whitehead, S.S., Bermingham, A., St Claire, M., Elkins, W.R., Murphy, B.R., Collins, P.L., 2000. Recombinant respiratory syncytial virus that does not express the NS1 or M2-2 protein is highly attenuated and immunogenic in chimpanzees. J. Virol. 74 (19), 9317–9321.

Tennant, B.C., 2001. Animal models of hepadnavirus-associated hepatocellular carcinoma. Clin. Liver Dis. 5 (1), 43–68.

Teo, T.H., Lum, F.M., Lee, W.W., Ng, L.F., 2012. Mouse models for Chikungunya virus: deciphering immune mechanisms responsible for disease and pathology. Immunol. Res. 53, 136–147.

ter Meulen, J., Bakker, A.B., van den Brink, E.N., Weverling, G.J., Martina, B.E., Haagmans, B.L., et al., 2004. Human monoclonal antibody as prophylaxis for SARS coronavirus infection in ferrets. Lancet 363 (9427), 2139–2141.

Tesh, R.B., Watts, D.M., Sbrana, E., Siirin, M., Popov, V.L., Xiao, S.Y., 2004. Experimental infection of ground squirrels (*Spermophilus tridecemlineatus*) with monkeypox virus. Emerg. Infect. Dis. 10 (9), 1563–1567.

Tesh, R.B., Siirin, M., Guzman, H., Travassos da Rosa, A.P., Wu, X., Duan, T., et al., 2005. Persistent West Nile virus infection in the golden hamster: studies on its mechanism and possible implications for other flavivirus infections. J. Infect. Dis. 192 (2), 287–295.

Thein, S., Aung, M.M., Shwe, T.N., Aye, M., Zaw, A., Aye, K., et al., 1997. Risk factors in dengue shock syndrome. Am. J. Trop. Med. Hyg. 56 (5), 566–572.

Thippeshappa, R., Ruan, H., Kimata, J.T., 2012. Breaking Barriers to an AIDS Model with Macaque-Tropic HIV-1 Derivatives. Biology (Basel) 1 (2), 134–164.

Thomas, M.K., Pitot, H.C., Liem, A., Lambert, P.F., 2011. Dominant role of HPV16 E7 in anal carcinogenesis. Virology 421 (2), 114–118.

Tignor, G.H., Hanham, C.A., 1993. Ribavirin efficacy in an in vivo model of Crimean-Congo hemorrhagic fever virus (CCHF) infection. Antiviral Res. 22 (4), 309–325.

Torres-Velez, F.J., Shieh, W.J., Rollin, P.E., Morken, T., Brown, C., Ksiazek, T.G., Zaki, S.R., 2008. Histopathologic and immunohistochemical characterization of Nipah virus infection in the guinea pig. Vet. Pathol. 45 (4), 576–585.

Tree, J.A., Hall, G., Pearson, G., Rayner, E., Graham, V.A., Steeds, K., et al., 2015. Sequence of pathogenic events in cynomolgus macaques infected with aerosolized monkeypox virus. J. Virol. 89 (8), 4335–4344.

Tseng, C.T., Huang, C., Newman, P., Wang, N., Narayanan, K., Watts, D.M., et al., 2007. Severe acute respiratory syndrome coronavirus infection of mice transgenic for the human Angiotensin-converting enzyme 2 virus receptor. J. Virol. 81 (3), 1162–1173.

Tseng, C.T., Sbrana, E., Iwata-Yoshikawa, N., Newman, P.C., Garron, T., Atmar, R.L., et al., 2012. Immunization with SARS coronavirus vaccines leads to pulmonary immunopathology on challenge with the SARS virus. PLoS One 7 (4), e35421.

Tsuda, Y., Safronetz, D., Brown, K., LaCasse, R., Marzi, A., Ebihara, H., et al., 2011. Protective efficacy of a bivalent recombinant vesicular stomatitis virus vaccine in the Syrian hamster model of lethal Ebola virus infection. J. Infect. Dis. 204 (Suppl. 3), S1090–S1097.

Tung-Thompson, G., Gentry-Shields, J., Fraser, A., Jaykus, L.A., 2015. Persistence of human norovirus RT-qPCR signals in simulated gastric fluid. Food Environ. Virol. 7 (1), 32–40.

Turcios-Ruiz, R.M., Axelrod, P., St John, K., Bullitt, E., Donahue, J., Robinson, N., Friss, H.E., 2008. Outbreak of necrotizing enterocolitis caused by norovirus in a neonatal intensive care unit. J. Pediatr. 153 (3), 339–344.

Twenhafel, N.A., Mattix, M.E., Johnson, J.C., Robinson, C.G., Pratt, W.D., Cashman, K.A., et al., 2013. Pathology of experimental aerosol *Zaire ebolavirus* infection in rhesus macaques. Vet. Pathol. 50 (3), 514–529.

Twenhafel, N.A., Shaia, C.I., Bunton, T.E., Shamblin, J.D., Wollen, S.E., Pitt, L.M., et al., 2015. Experimental aerosolized guinea pig-adapted *Zaire ebolavirus* (variant: Mayinga) causes lethal pneumonia in guinea pigs. Vet. Pathol. 52 (1), 21–25.

Uberla, K., Stahl-Hennig, C., Bottiger, D., Matz-Rensing, K., Kaup, F.J., Li, J., et al., 1995. Animal model for the therapy of acquired immunodeficiency syndrome with reverse transcriptase inhibitors. Proc. Natl. Acad. Sci. USA 92 (18), 8210–8214.

Valbuena, G., Halliday, H., Borisevich, V., Goez, Y., Rockx, B., 2014. A human lung xenograft mouse model of Nipah virus infection. PLoS Pathog. 10 (4), e1004063.

van der Hoek, L., Pyrc, K., Berkhout, B., 2006. Human coronavirus NL63, a new respiratory virus. FEMS Microbiol. Rev. 30 (5), 760–773.

van der Laan, J.W., Herberts, C., Lambkin-Williams, R., Boyers, A., Mann, A.J., Oxford, J., 2008. Animal models in influenza vaccine testing. Expert Rev. Vaccines 7 (6), 783–793.

van der Vries, E., Stittelaar, K.J., van Amerongen, G., Veldhuis Kroeze, E.J., de Waal, L., Fraaij, P.L., et al., 2013. Prolonged influenza virus shedding and emergence of antiviral resistance in immunocompromised patients and ferrets. PLoS Pathog. 9 (5), e1003343.

van Riel, D., Munster, V.J., de Wit, E., Rimmelzwaan, G.F., Fouchier, R.A., Osterhaus, A.D., Kuiken, T., 2007. Human and avian influenza viruses target different cells in the lower respiratory tract of humans and other mammals. Am. J. Pathol. 171 (4), 1215–1223.

Van Rompay, K.K., Matthews, T.B., Higgins, J., Canfield, D.R., Tarara, R.P., Wainberg, M.A., et al., 2002. Virulence and reduced fitness of simian immunodeficiency virus with the M184V mutation in reverse transcriptase. J. Virol. 76 (12), 6083–6092.

Van Rompay, K.K., Durand-Gasselin, L., Brignolo, L.L., Ray, A.S., Abel, K., Cihlar, T., et al., 2008. Chronic administration of tenofovir to rhesus macaques from infancy through adulthood and pregnancy: summary of pharmacokinetics and biological and virological effects. Antimicrob. Agents Chemother. 52 (9), 3144–3160.

van Schaik, S.M., Enhorning, G., Vargas, I., Welliver, R.C., 1998. Respiratory syncytial virus affects pulmonary function in BALB/c mice. J. Infect. Dis. 177 (2), 269–276.

Veazey, R.S., Klasse, P.J., Ketas, T.J., Reeves, J.D., Piatak, Jr., M., Kunstman, K., et al., 2003. Use of a small molecule CCR5 inhibitor in macaques to treat simian immunodeficiency virus infection or prevent simian-human immunodeficiency virus infection. J. Exp. Med. 198 (10), 1551–1562.

Verstrepen, B.E., Fagrouch, Z., van Heteren, M., Buitendijk, H., Haaksma, T., Beenhakker, N., et al., 2014. Experimental infection of rhesus macaques and common marmosets with a European strain of West Nile virus. PLoS Negl. Trop. Dis. 8 (4), e2797.

Vinzon, S.E., Braspenning-Wesch, I., Muller, M., Geissler, E.K., Nindl, I., Grone, H.J., et al., 2014. Protective vaccination against papillomavirus-induced skin tumors under immunocompetent and immunosuppressive conditions: a preclinical study using a natural outbred animal model. PLoS Pathog. 10 (2), e1003924.

Vishwanathan, S.A., Burgener, A., Bosinger, S.E., Tharp, G.K., Guenthner, P.C., Patel, N.B., et al., 2015. Cataloguing of potential HIV susceptibility factors during the menstrual cycle of pig-tailed macaques by using a systems biology approach. J. Virol. 89 (18), 9167–9177.

Wahl-Jensen, V., Chapman, J., Asher, L., Fisher, R., Zimmerman, M., Larsen, T., Hooper, J.W., 2007. Temporal analysis of Andes virus and Sin Nombre virus infections of Syrian hamsters. J. Virol. 81 (14), 7449–7462.

Walker, J.A., Beck, G.A., Campbell, J.H., Miller, A.D., Burdo, T.H., Williams, K.C., 2015. Anti-alpha4 integrin antibody blocks monocyte/macrophage traffic to the heart and decreases cardiac pathology in a SIV infection model of AIDS. J. Am. Heart Assoc. 4 (7).

Wang, J.T., Sheng, W.H., Fang, C.T., Chen, Y.C., Wang, J.L., Yu, C.J., et al., 2004. Clinical manifestations, laboratory findings, and treatment outcomes of SARS patients. Emerg. Infect. Dis. 10 (5), 818–824.

Wang, Q.H., Souza, M., Funk, J.A., Zhang, W., Saif, L.J., 2006. Prevalence of noroviruses and sapoviruses in swine of various ages determined by reverse transcription-PCR and microwell hybridization assays. J. Clin. Microbiol. 44 (6), 2057–2062.

Wang, Q.H., Costantini, V., Saif, L.J., 2007. Porcine enteric caliciviruses: genetic and antigenic relatedness to human caliciviruses, diagnosis and epidemiology. Vaccine 25 (30), 5453–5466.

Wang, Z., Loh, L., Kedzierski, L., Kedzierska, K., 2016. Avian influenza viruses, inflammation, and CD8(+) T cell Immunity. Front. Immunol. 7, 60.

Warfield, K.L., Alves, D.A., Bradfute, S.B., Reed, D.K., VanTongeren, S., Kalina, W.V., et al., 2007. Development of a model for marburgvirus based on severe-combined immunodeficiency mice. Virol. J. 4, 108.

Warfield, K.L., Bradfute, S.B., Wells, J., Lofts, L., Cooper, M.T., Alves, D.A., et al., 2009. Development and characterization of a mouse model for Marburg hemorrhagic fever. J. Virol. 83 (13), 6404–6415.

Warren, T.K., Trefry, J.C., Marko, S.T., Chance, T.B., Wells, J.B., Pratt, W.D., et al., 2014. Euthanasia assessment in ebola virus infected nonhuman primates. Viruses 6 (11), 4666–4682.

Watanabe, S., Terashima, K., Ohta, S., Horibata, S., Yajima, M., Shiozawa, Y., et al., 2007. Hematopoietic stem cell-engrafted NOD/SCID/IL2Rgamma null mice develop human lymphoid systems and induce long-lasting HIV-1 infection with specific humoral immune responses. Blood 109 (1), 212–218.

Watanabe, S., Tan, K.H., Rathore, A.P., Rozen-Gagnon, K., Shuai, W., Ruedl, C., Vasudevan, S.G., 2012. The magnitude of dengue virus NS1 protein secretion is strain dependent and does not correlate with severe pathologies in the mouse infection model. J. Virol. 86 (10), 5508–5514.

Wauquier, N., Becquart, P., Padilla, C., Baize, S., Leroy, E.M., 2010. Human fatal Zaire ebolavirus infection is associated with an aberrant innate immunity and with massive lymphocyte apoptosis. PLoS Negl. Trop. Dis. 4 (10), 1–10.

Weingartl, H., Czub, M., Czub, S., Neufeld, J., Marszal, P., Gren, J., et al., 2004. Immunization with modified vaccinia virus Ankara-based recombinant vaccine against severe acute respiratory syndrome is associated with enhanced hepatitis in ferrets. J. Virol. 78 (22), 12672–12676.

Weingartl, H., Czub, S., Copps, J., Berhane, Y., Middleton, D., Marszal, P., et al., 2005. Invasion of the central nervous system by Nipah virus in a porcine host. J. Virol. 79 (12), 7528–7534.

Weingartl, H.M., Miller, M., Nfon, C., Wilson, W.C., 2014. Development of a Rift Valley fever virus viremia challenge model in sheep and goats. Vaccine 32 (20), 2337–2344.

Weiss, R.C., Scott, F.W., 1981. Antibody-mediated enhancement of disease in feline infectious peritonitis: comparisons with dengue hemorrhagic fever. Comp. Immunol. Microbiol. Infect. Dis. 4 (2), 175–189.

Wells, R.M., Sosa Estani, S., Yadon, Z.E., Enria, D., Padula, P., Pini, N., et al., 1997. An unusual hantavirus outbreak in southern Argentina: person-to-person transmission? Hantavirus Pulmonary Syndrome Study Group for Patagonia. Emerg. Infect. Dis. 3 (2), 171–174.

Westbury, H.A., Hooper, P.T., Selleck, P.W., Murray, P.K., 1995. Equine morbillivirus pneumonia: susceptibility of laboratory animals to the virus. Aust. Vet. J. 72 (7), 278–279.

Westbury, H.A., Hooper, P.T., Brouwer, S.L., Selleck, P.W., 1996. Susceptibility of cats to equine morbillivirus. Aust. Vet. J. 74 (2), 132–134.

Wichmann, D., Grone, H.J., Frese, M., Pavlovic, J., Anheier, B., Haller, O., et al., 2002. Hantaan virus infection causes an acute neurological disease that is fatal in adult laboratory mice. J. Virol. 76 (17), 8890–8899.

Williams, G.D., Pinto, A.K., Doll, B., Boon, A.C., 2016. A North American H7N3 influenza virus supports reassortment with 2009 pandemic H1N1 and induces disease in mice without prior adaptation. J. Virol. 90 (9), 4796–4806.

Williamson, M.M., Hooper, P.T., Selleck, P.W., Gleeson, L.J., Daniels, P.W., Westbury, H.A., Murray, P.K., 1998. Transmission studies of Hendra virus (equine morbillivirus) in fruit bats, horses and cats. Aust. Vet. J. 76 (12), 813–818.

Williamson, M.M., Hooper, P.T., Selleck, P.W., Westbury, H.A., Slocombe, R.F., 2001. A guinea-pig model of Hendra virus encephalitis. J. Comp. Pathol. 124 (4), 273–279.

Witvrouw, M., Pannecouque, C., Switzer, W.M., Folks, T.M., De Clercq, E., Heneine, W., 2004. Susceptibility of HIV-2, SIV and SHIV to various anti-HIV-1 compounds: implications for treatment and postexposure prophylaxis. Antivir. Ther. 9 (1), 57–65.

Wong, K.T., Grosjean, I., Brisson, C., Blanquier, B., Fevre-Montange, M., Bernard, A., et al., 2003. A golden hamster model for human acute Nipah virus infection. Am. J. Pathol. 163 (5), 2127–2137.

Wong, G., Qiu, X., Richardson, J.S., Cutts, T., Collignon, B., Gren, J., et al., 2015a. Ebola virus transmission in guinea pigs. J. Virol. 89 (2), 1314–1323.

Wong, G., Richardson, J.S., Cutts, T., Qiu, X., Kobinger, G.P., 2015b. Intranasal immunization with an adenovirus vaccine protects guinea pigs from Ebola virus transmission by infected animals. Antiviral Res. 116, 17–19.

Wood, C.E., Chen, Z., Cline, J.M., Miller, B.E., Burk, R.D., 2007. Characterization and experimental transmission of an oncogenic papillomavirus in female macaques. J. Virol. 81 (12), 6339–6345.

World Health Organization, 1997. Dengue Haemorrhagic Fever: Diagnosis, Treatment, Prevention and Control, second ed. World Health Organization, Geneva.

World Health Organization, 2003. The World Health Report 2003—Shaping the Future.

Wright, T.L., Lau, J.Y., 1993. Clinical aspects of hepatitis B virus infection. Lancet 342 (8883), 1340–1344.

Wu, D., Tu, C., Xin, C., Xuan, H., Meng, Q., Liu, Y., et al., 2005. Civets are equally susceptible to experimental infection by two different severe acute respiratory syndrome coronavirus isolates. J. Virol. 79 (4), 2620–2625.

Wu, P., Dupont, W.D., Griffin, M.R., Carroll, K.N., Mitchel, E.F., Gebretsadik, T., Hartert, T.V., 2008. Evidence of a causal role of winter virus infection during infancy in early childhood asthma. Am. J. Respir. Crit. Care Med. 178 (11), 1123–1129.

Wu, K.Y., Zuo, G.L., Li, X.F., Ye, Q., Deng, Y.Q., Huang, X.Y., et al., 2016. Vertical transmission of Zika virus targeting the radial glial cells affects cortex development of offspring mice. Cell Res. 26 (6), 645–654.

Wyckoff, R.W., 1939. Encephalomyelitis in monkeys. Science 89 (2319), 542–543.

Wyde, P.R., Ambrose, M.W., Meyerson, L.R., Gilbert, B.E., 1993. The antiviral activity of SP-303, a natural polyphenolic polymer, against respiratory syncytial and parainfluenza type 3 viruses in cotton rats. Antiviral Res. 20 (2), 145–154.

Xiao, S.Y., Sbrana, E., Watts, D.M., Siirin, M., da Rosa, A.P., Tesh, R.B., 2005. Experimental infection of prairie dogs with monkeypox virus. Emerg. Infect. Dis. 11 (4), 539–545.

Xu, Z.Y., Guo, C.S., Wu, Y.L., Zhang, X.W., Liu, K., 1985. Epidemiological studies of hemorrhagic fever with renal syndrome: analysis of risk factors and mode of transmission. J. Infect. Dis. 152 (1), 137–144.

Yang, P.L., Althage, A., Chung, J., Chisari, F.V., 2002. Hydrodynamic injection of viral DNA: a mouse model of acute hepatitis B virus infection. Proc. Natl. Acad. Sci. U S A 99 (21), 13825–13830.

Yang, X.H., Deng, W., Tong, Z., Liu, Y.X., Zhang, L.F., Zhu, H., et al., 2007. Mice transgenic for human angiotensin-converting enzyme 2 provide a model for SARS coronavirus infection. Comp. Med. 57 (5), 450–459.

Yao, Y., Bao, L., Deng, W., Xu, L., Li, F., Lv, Q., et al., 2014. An animal model of MERS produced by infection of rhesus macaques with MERS coronavirus. J. Infect. Dis. 209 (2), 236–242.

Yauch, L.E., Zellweger, R.M., Kotturi, M.F., Qutubuddin, A., Sidney, J., Peters, B., et al., 2009. A protective role for dengue virus-specific CD8+ T cells. J. Immunol. 182 (8), 4865–4873.

Young, J.C., Hansen, G.R., Graves, T.K., Deasy, M.P., Humphreys, J.G., Fritz, C.L., et al., 2000. The incubation period of hantavirus pulmonary syndrome. Am. J. Trop. Med. Hyg. 62 (6), 714–717.

Yun, N.E., Ronca, S., Tamura, A., Koma, T., Seregin, A.V., Dineley, K.T., et al., 2015. Animal model of sensorineural hearing loss associated with Lassa virus infection. J. Virol. 90 (6), 2920–2927.

Yusuf, S., Piedimonte, G., Auais, A., Demmler, G., Krishnan, S., Van Caeseele, P., et al., 2007. The relationship of meteorological conditions to the epidemic activity of respiratory syncytial virus. Epidemiol. Infect. 135 (7), 1077–1090.

Zaki, S.R., Greer, P.W., Coffield, L.M., Goldsmith, C.S., Nolte, K.B., Foucar, K., et al., 1995. Hantavirus pulmonary syndrome. Pathogenesis of an emerging infectious disease. Am. J. Pathol. 146 (3), 552–579.

Zaucha, G.M., Jahrling, P.B., Geisbert, T.W., Swearengen, J.R., Hensley, L., 2001. The pathology of experimental aerosolized monkeypox virus infection in cynomolgus monkeys (Macaca fascicularis). Lab Invest. 81 (12), 1581–1600.

Zhang, L., Kovalev, G.I., Su, L., 2007. HIV-1 infection and pathogenesis in a novel humanized mouse model. Blood 109 (7), 2978–2981.

Zhang, Q., Shi, J., Deng, G., Guo, J., Zeng, X., He, X., et al., 2013. H7N9 influenza viruses are transmissible in ferrets by respiratory droplet. Science 341 (6144), 410–414.

Zhao, H., Jiang, T., Zhou, X.Z., Deng, Y.Q., Li, X.F., Chen, S.P., et al., 2014a. Induction of neutralizing antibodies against four serotypes of dengue viruses by MixBiEDIII, a tetravalent dengue vaccine. PLoS One 9 (1), e86573.

Zhao, J., Li, K., Wohlford-Lenane, C., Agnihothram, S.S., Fett, C., Zhao, J., et al., 2014b. Rapid generation of a mouse model for Middle East respiratory syndrome. Proc. Natl. Acad. Sci. USA 111 (13), 4970–4975.

Ziegler, S.A., Lu, L., da Rosa, A.P., Xiao, S.Y., Tesh, R.B., 2008. An animal model for studying the pathogenesis of chikungunya virus infection. Am. J. Trop. Med. Hyg. 79 (1), 133–139.

Zitzow, L.A., Rowe, T., Morken, T., Shieh, W.J., Zaki, S., Katz, J.M., 2002. Pathogenesis of avian influenza A (H5N1) viruses in ferrets. J. Virol. 76 (9), 4420–4429.

Zivcec, M., Safronetz, D., Scott, D., Robertson, S., Ebihara, H., Feldmann, H., 2013. Lethal Crimean-Congo hemorrhagic fever virus infection in interferon alpha/beta receptor knockout mice is associated with high viral loads, proinflammatory responses, and coagulopathy. J. Infect. Dis. 207 (12), 1909–1921.

Zlotnik, I., Peacock, S., Grant, D.P., Batter-Hatton, D., 1972. The pathogenesis of Western equine encephalitis virus (W.E.E.) in adult hamsters with special reference to the long and short term effects on the C.N.S. of the attenuated clone 15 variant. Br. J. Exp. Pathol. 53 (1), 59–77.

Zumbrun, E.E., Abdeltawab, N.F., Bloomfield, H.A., Chance, T.B., Nichols, D.K., Kotb, M., Nalca, A., 2012a. Development of a murine model for aerosolized filovirus infection using a panel of BXD recombinant inbred mice. Viruses 4 (12), 3468–3493.

Zumbrun, E.E., Bloomfield, H.A., Dye, J.M., Hunter, T.C., Dabisch, P.A., Garza, N.L., et al., 2012b. A characterization of aerosolized Sudan ebolavirus infection in African green monkeys, cynomolgus macaques, and rhesus macaques. Viruses 4 (10), 2115–2136.

Zumbrun, E.E., Bloomfield, H.A., Frederick, S., Yeager, J., Williams, R.D., Baker, R.J., et al., 2012. Characterization of disease and pathogenesis following airborne exposure of guinea pigs to filoviruses Manuscripts in preparation.

Page left intentionally blank

CANCER

Page left intentionally blank

34

Modeling Cancer Using CRISPR-Cas9 Technology

Sandra Rodriguez-Perales, Marta Martinez-Lage, Raul Torres-Ruiz

Spanish National Cancer Research Centre—CNIO, Madrid, Spain

1 INTRODUCTION

1.1 Why Use Cancer Models?

Cancer is a collection of more than 100 distinct but related diseases that involve multiple genetic and epigenetic alterations owing to dynamic changes in the genome (Hanahan and Weinberg, 2000). These alterations mainly affect genes involved in the control of cell growth and division, including oncogenes and tumor-suppressor genes (TSGs) (Futreal et al., 2004). Large-scale sequencing of numerous types of cancer has provided us with a long list of genetic alterations that are present in human tumors, for example, point mutations, chromosomal rearrangements (translocations, inversions, or deletions), and genome amplifications (Sabatello and Appelbaum, 2016). Alterations, such as passenger mutations do not affect tumorigenesis, whereas many others, such as driver mutations, promote activation of oncogenes and/or inactivation of TSGs, leading to the transformation of normal cells into cancer cells (Easton et al., 2007; Lawrence et al., 2013). The huge amount of cancer genetic alteration data recorded to date must now be processed for use in clinical practice. Hence, genetically modified cell and animal models are essential tools for studying the genes and processes involved in cancer and for investigating the factors underlying malignant transformation, invasion, and metastasis. Such models can also be used to examine the response to therapy.

1.2 Evolution of Cancer Modeling

The development of cancer models has gone through several increasingly complex phases, including human tumors-derived cell lines (Giard et al., 1973), xenograft tumors (Braakhuis et al., 1984), use of carcinogens, and genetically engineered cellular and animal models (Frese and Tuveson, 2007). The in vitro culture of human tumors made it possible to establish cell lines that retained the properties of the cancers of origin and paved the way toward a better understanding of the molecular pathogenesis of cancer. However, while a significant step, in vitro cell cultures were prone to genotypic and phenotypic drift during culture. The various disadvantages of this cancer model prevent us from studying processes,

such as angiogenesis and metastasis, thus necessitating more complex and accurate models to reproduce cancer biology.

Xenograft models enabled in vivo tumor research by the transplantation of human tumor cells into immuno-compromised mice, either under the skin or into the organ in which the tumor originated. The key advantage of xenograft models is that they address the complexity of genetic and epigenetic abnormalities in the tumor, which can be used to aid in the development of individualized molecular therapeutic approaches (Hidalgo et al., 2014; Siolas and Hannon, 2013). The limitation of xenograft models in immunocompromised mice is that they generate loss of the lymphocyte-mediated response to the tumor in the mouse host. The consequent change in tumor architecture alters the tumor microenvironment, thus preventing the study of the initial steps of carcinogenesis (Frese and Tuveson, 2007).

Environmentally induced cancer animal models develop specific tumors after exposure to a given carcinogen, such as chemicals, radiation, or even physical impact resulting in alterations and mutations that lead to uncontrolled cell growth (Kleinstreuer et al., 2013; Parsa, 2012; Rivina et al., 2014). The main limitation of these models is that they are restricted to a small number of cancer types and have incomplete penetrance.

The next complex stage in cancer modeling was the development of techniques that enabled stable modification of the genome, thus facilitating propagation through subsequent generations and the eventual creation of stable animal models. The most noteworthy techniques are transgenesis and gene targeting. Transgenesis is based on the introduction of foreign DNA into the host genome (Smith and Muller, 2013). The transgene is incorporated at a very early stage of embryogenesis so that cells of the entire organism contain the foreign DNA. There are several ways to introduce transgenes. Microinjection into the fertilized embryo is one of the most widely used and is typically applied to overexpress a gene. The main disadvantage of this technique is that it is impossible to control the insertion site and the number of copies that are inserted. In transgenesis, the transgene has to produce a dominant effect over the endogenous gene before it can manifest a phenotype. Gene targeting, on the other hand, alters the endogenous DNA sequence at a previously selected point. Originally, gene targeting was based on the use of a targeting construct containing target gene sequences to induce homologous recombination (HR) and specific modification, resulting in the introduction, inactivation, or mutation of a specific gene of interest (Thomas et al., 1986). This technique is more technically difficult than transgenesis and takes longer to perform. It is used to generate knockout (inactivation of a gene) and knockin (insertion or substitution of a DNA sequence).

1.3 Genome Engineering Technologies

Genome engineering technologies were first developed some decades ago. Using this approach, we can modify precise DNA sequences to study gene function and regulation of the genes involved in cancer through the generation of in vitro and in vivo models. As mentioned in the previous Section 1.2, traditional genome-engineered cancer models were generated using transgenes or HR in murine embryonic stem cells (mESCs) (Van Dyke and Jacks, 2002). In the early 1980s, specific genes were introduced into mESCs, which were then implanted into wild-type blastocysts, thus enabling transmission of genome modifications into the mouse germline to generate transgenic mouse models (Brinster et al., 1981; Harbers et al., 1981; Wagner et al., 1981). The first transgenic cancer models appeared in 1984, when brain tumors were reproduced by delivering the SV40 T-antigen viral oncogene into mouse eggs (Brinster et al., 1984). The second type of induced tumors were tumors resembling human breast cancer, which were created by replacing the mouse *Myc* gene promoter with a hormonally inducible mouse mammary tumor virus promoter (Stewart et al., 1984). In 1986, Capecchi and Smithies, the pioneers of gene modification, developed the technology to modify the genome of mESCs by HR (Smithies et al., 1985; Thomas and Capecchi, 1986; Thomas et al., 1986). This development paved the way for various genome-engineered mouse models (GEMMs) of cancer by inducing precise alterations, leading to gain-of-function (GOF) mutations in oncogenes, and loss-of-function (LOF) mutations in TSGs. The generation of transgenic mice by HR was limited by the need for complex targeting, low efficiency, and the time required for the generation of a mouse with the desired modification (Frese and Tuveson, 2007).

Subsequent HR technology merged with site-specific recombinases (Cre and Flp), resulting in the generation of conditional alleles of numerous cancer genes (Orban et al., 1992; Shibata et al., 1997; Smith et al., 1995). Cre recombinase recognizes two pairs of *loxP* sites, whereas Flp recognizes *FRT* sites, thus leading to reciprocal recombination of specific DNA sequences. On the other hand, numerous transgenic mouse models have been generated by overexpression of cDNA or gene knockdown by RNA interference (RNAi). RNAi technology was used widely for over a decade because it is an easy, rapid, and inexpensive approach to silencing genes (Tavernarakis et al., 2000). However, it is limited by its potential aberrant and artifactual effects, which in turn generate off-target effects (Jackson et al., 2003). Gene knockdown is usually partial and temporary.

Methods that artificially increased gene targeting were developed. These methods were based on the observation that the occurrence of a double-strand break (DSB) in the targeted region dramatically increases

gene-targeting efficiency (Jasin, 1996; Rouet et al., 1994). First, in the mid-1990s, restriction endonuclease I-SceI from *Saccharomyces cerevisiae* was used to induce breaks, thus demonstrating that the generation of controlled DSBs increases targeted HR (Choulika et al., 1995). Subsequently, tools for genome engineering based on site-specific endonucleases were developed; these included zinc-finger nucleases (ZFN) (Bibikova et al., 2003), transcriptor activator-like effector nucleases (TALENs) (Christian et al., 2010), and clustered regularly interspaced short palindromic repeats (CRISPRs) (Jinek et al., 2012). All three methods, which are described in detail later, have revolutionized the study of cancer biology, especially cancer modeling (Torres-Ruiz and Rodriguez Perales, 2015). The use of ZFN and TALEN technologies is limited owing to their problematic design and elevated cost; however, the development of CRISPR systems offers a rapid and easy method for modification of single or multiple loci that overcomes the limitations of previous genome engineering tools, thus facilitating the rapid generation of cancer models.

1.4 Site-Specific Endonuclease Techniques

Genome engineering tools make it possible to edit target genome sequences by adding, replacing, or removing DNA bases. Genome editing relies on the creation of DSBs in DNA, which cells attempt to repair via the homology-directed repair (HDR) pathway or by the error-prone nonhomologous-end joining (NHEJ) (Fig. 34.1A). The NHEJ pathway involves the alignment of one to a few (at most) complementary bases for the religation of two ends to repair the break without a homologous template. This step leads to small insertions and/or deletions (indels) at the repaired locus and therefore generates frameshift mutations that often result in gene disruption and inactivation (Honma et al., 2007). Alternatively, and less frequently, the break can be repaired through the HDR pathway, which is a more accurate mechanism that requires a homologous donor DNA template to guide repair. The HDR pathway has higher fidelity, because the DNA template assists in the repair process, which can be exploited to introduce a precise mutation into the damaged DNA when genetically modified DNA templates are used (Kim and Kim, 2014).

Gene editing methods that exploit the repair mechanism of the cell (ZNFs, TALENs, and CRISPRs) make it possible to directly manipulate the genome of many different species, including bacteria, plants, fishes, and mammals.

1.4.1 ZFNs and TALENs

ZFNs were the first genome-editing tool to use customizable endonucleases. A ZFN is a heterodimer composed of a zinc finger (ZF) domain that binds to DNA and is fused with a cleavage domain (FokI) (Wood et al., 2011). ZF domains are protein modules that recognize sequences of three nucleotides and can be manipulated modularly and designed to direct binding to a specific DNA sequence. Fusion of ZF with FokI nuclease can bind specific sequences and produce the DSB (Fig. 34.1B). Initially, this protein assembly module recognized an 18-bp sequence that was unique in the genome. This base was subsequently modified to recognize sequences measuring 24 bp and longer (Kim et al., 2009). Although ZFN technology allows scientists to make changes at a specific genomic locus, it is difficult to use, and the targeting of new genomic sites requires the creation of new ZF proteins, which is time consuming and expensive.

TALEN technology was developed 15 years after the discovery of ZFNs. TALENs are dimeric nucleases that were originally characterized in *Xanthomonas* bacteria (Richter et al., 2016). Custom sequences of TALENs can be generated to recognize unique genomic sequences and generate cohesive-ended DSBs. The principal difference between ZNFs and TALENs is that TALENs contain an array of conserved protein motifs (33 or 34 amino acids) that differ only at positions 12 and 13, the so-called repeat variable diresidues, which define the DNA-binding specificity of each TALEN module (Fig. 34.1B). Like ZFNs, modular TALEN repeats are linked together to recognize a specific DNA target sequence. The discovery of the DNA recognition code facilitated the prediction and assembly of TALEN DNA-binding domains and led this method to be more widely used by researchers than ZFN (Li et al., 2011). However, although TALENs represented a significant improvement over ZFNs, the modular nature of TALEN techniques makes working with them complicated and difficult.

The ZFN and TALEN platforms enabled us to control gene expression in a more refined way than simple knockdown (Boettcher and McManus, 2015) and have facilitated efficient modification in transformed and primary cells, as well as in animal models that were previously thought to be beyond the scope of such targeted genetic manipulation (Cui et al., 2011; Frank et al., 2013; Hisamatsu et al., 2015; Ochiai et al., 2010). However, both systems present difficulties and practical limitations, namely, laborious protein engineering and the need for selectable markers, which affect targeting efficiency. The newer CRISPR-Cas9 platform overcomes these limitations by providing a simple way to engineer target DNA breaks.

1.4.2 CRISPR-Cas9 System

CRISPRs are short repetitions of DNA sequences present in many microorganisms, such as bacteria and Archaea. The CRISPR-Cas system is composed of CRISPR repeats and its associated Cas genes. It functions as an
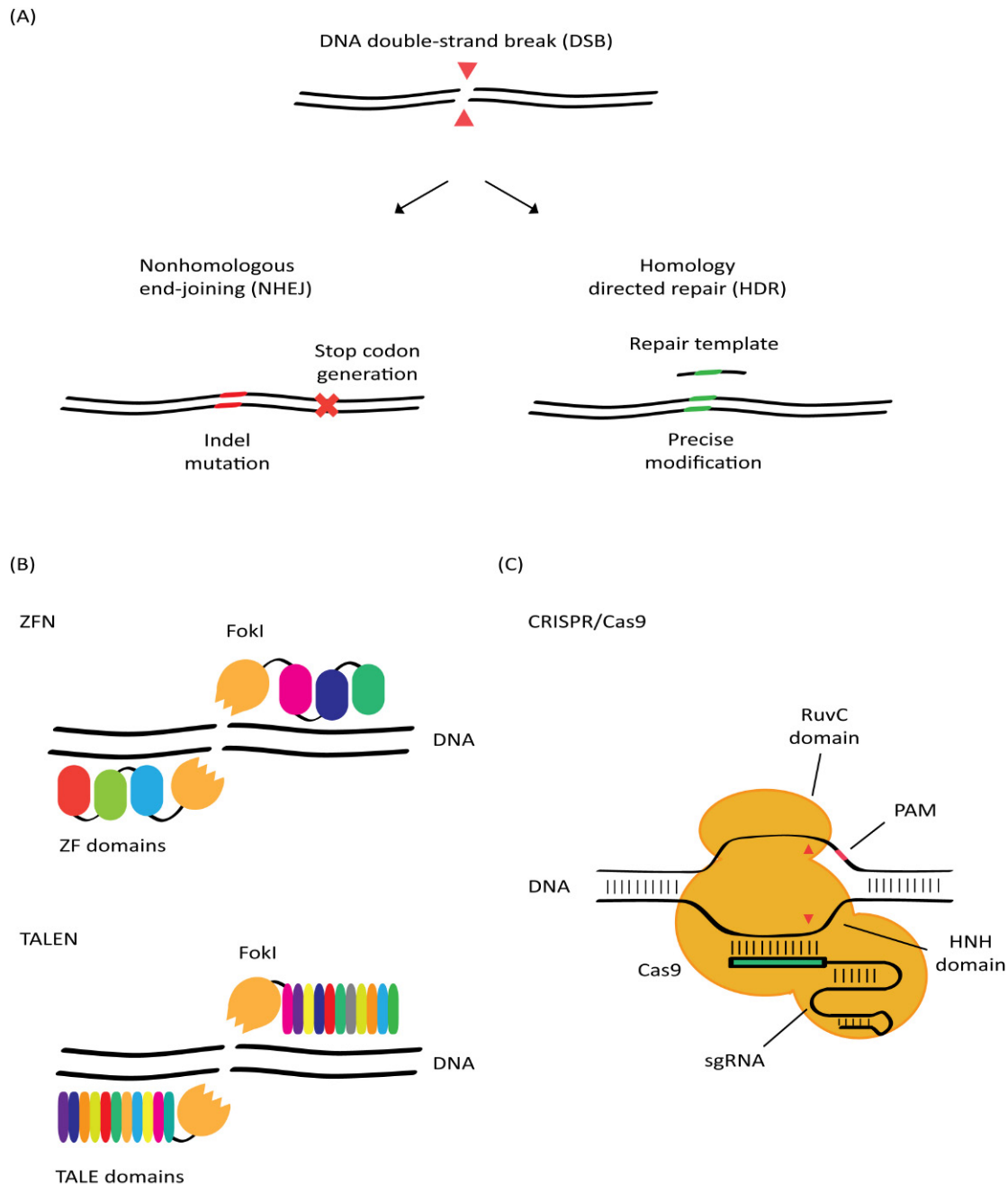
FIGURE 34.1 **Double-strand break *(DSB)* repair machinery and its use by programmable nucleases.** (A) Endogenous DNA repair machinery uses two pathways to repair DSBs: nonhomologous end-joining *(NHEJ)* and homology-directed repair *(HDR)*. (B) Zinc-finger nuclease *(ZFN)* and transcription activator-like effector nuclease *(TALENs)* are DNA-binding domains (colored boxes) that can be assembled as modules to recognize specific sequences (each module recognized 3 bp in the case of ZFNs and 1 bp in the case of TALENs). (C) The CRISPR-Cas9 system is composed of a nuclease (Cas9, orange), which targets specific DNA sequences through the guidance of an sgRNA (green box and linked loops) thanks to the recognition of a PAM sequence (red box). The Cas9 nuclease has two active domains, namely, RuvC and HNH.

adaptive immune system in prokaryotes through the use of RNA-guided nucleases (Cas proteins) and recognizes and targets invasive genetic elements (Barrangou et al., 2007). Once this phase is complete, the ssRNA-Cas ribonucleoprotein complex (RNP) binds to the foreign DNA to produce a DSB that marks this DNA for degradation (Doudna and Charpentier, 2014; Sashital et al., 2012). Recently, the bacterial CRISPR-Cas system was used to create new genome engineering technology, namely, CRISPR-Cas9, which is now a widely used genome-editing tool owing to is simplicity, efficiency, and multiple applications.

The CRISPR-Cas9 system consists of two principal elements, a short synthetic single guide RNA (sgRNA) that fuses crRNA (CRISPR RNA) and tracrRNA (*trans*-activating crRNA) and the Cas9 protein. crRNA contains the named protospacer element (which gives the system the ability to target a specific genomic location) (Jinek et al., 2012), tracrRNA (which acts as a linker between the crRNA and the nuclease to fuse both elements and activate the system) (Jinek et al., 2012), and the Cas9 protein (which behaves like a nuclease producing the DSB at the DNA level) (Marraffini and Sontheimer, 2010) (Fig. 34.1C). The activated RNP complex is directed by the sgRNA to a specific genomic location of interest upstream from a protospacer adjacent motif (PAM) sequence, which consists of an NGG or NAG trinucleotide [the general PAM sequence for *Streptococcus pyogenes* although this may differ depending on the Cas9 species being used (Chylinski et al., 2013)]. By designing an sgRNA we can target a specific DNA region. Once in the cell, the sgRNA forms a complex with the Cas9 endonuclease and guides the complex to the target region. Cas9 nuclease generates blunt-ended DSB three nucleotides upstream of the PAM sequence, thus stimulating activation of the cell repair machinery (NHEJ and/or HDR pathways).

The advantage of the CRISPR-Cas9 system over ZFNs and TALENs is that CRISPR does not depend on protein engineering and requires no more than an accurately designed sgRNA that binds correctly to the target DNA directed by the Cas9 protein. New loci can be targeted by designing and synthesizing 20 new nucleotides of sgRNA that bind to the sequence of interest. Therefore, CRISPR-Cas9 is a genome-editing tool that is able to generate easy, fast, and effective cancer models (Sánchez-Rivera and Jacks, 2015; Torres-Ruiz and Rodriguez Perales, 2015).

1.4.3 CRISPR Applications

Several CRISPR-Cas9 system modifications have been adopted in genome-editing protocols. These include nickase Cas9 (Cas9D10A or Cas9H840A), dead Cas9 (dCas9), sgRNA scaffolds, RNA-targeting Cas9 (RCas9), and dead RCas9 (dRCas9), all of which are applied differently in cancer modeling (Wen et al., 2016).

1.4.3.1 DUAL NICKASE Cas9 SYSTEM

Native or wild-type Cas9 nuclease is composed of two catalytic domains, HNH and RuvC, each of which cuts a strand of the target DNA. Cong et al. (2013) developed a Cas9 mutant nickase form (Cas9D10A and Cas9H840A) that only contains one active catalytic domain. Cas9 nickases still bind DNA based on sgRNA specificity but are only able to cleave one DNA strand (to produce nicks). DNA nicks are usually repaired by the HDR pathway using an intact complementary DNA strand as a

template (either endogenous or supplied exogenously). This CRISPR variant dramatically increases target specificity and reduces off-target effects, thus making it the tool of choice for specific gene editing approaches (Liu et al., 2016).

1.4.3.2 DEAD Cas9 (DCas9)

The Cas9 variant dCas9 is generated by inactivation of both catalytic domains (D10A for HNH and H840A for RuvC in *S. pyogenes* Cas9) so that it still binds to DNA based on sgRNA specificity but is not able to cleave the DNA (Maeder et al., 2013). This variant has several applications, such as regulation of endogenous gene expression by the fusion of dCas9 with effector domains either to activate or to repress gene expression. When dCas9 is fused to a repressor domain, the approach is called CRISPRi (gene silencing), and when it is fused to an activation domain, it is called CRISPRa (gene activation) (Dominguez et al., 2016). dCas9 is also used as an epigenetic modulator through the fusion of dCas9 with epigenetic modifiers (Panda et al., 2013; Thakore et al., 2016). dCas9 can even be used for in vivo imaging when fused to a fluorescent protein and in live cells for targeting specific genomic loci (Chen et al., 2013; Deng et al., 2015). The aforementioned variants make it possible to study specific genes through their activation and repression in cancer models or even variations in architecture during tumorigenesis (Falahi et al., 2015).

1.4.3.3 sgRNA SCAFFOLD (scRNA)

sgRNA scaffolds consist of amplification of the 3′ end of the sgRNA with modular RNA domains that recruit RNA-binding proteins. The function of this variant is to physically link DNA binding and protein recruitment through scRNA. sgRNA scaffolds enable multidirectional regulation and simultaneous repression and activation of several target genes as part of the same regulatory program (Zalatan et al., 2015). Combining scRNA with dCas9 increases the efficiency of regulation, thus making it a good tool for functional investigation at genome level. It can also be applied for screening studies and has proven very useful for the study of regulation in cancer epigenetics (Konermann et al., 2015).

1.4.3.4 RCas9 AND DRCas9

CRISPR-Cas9 recognizes target DNA through sgRNA although the presence of the PAM sequence on the opposite strand is necessary. An alternative strategy that is also able to target a single strand has been generated to enable targeting of RNAs. This approach consists of an exogenous strand of nucleotides containing the PAM sequence, which acts as an opposite strand. Thus, the CRISPR-Cas9 system has been modified so that it can be used as a tool for cleavage of ssRNA (RCas9) (O'Connell et al., 2014). Similar to dCas9, the RCas9 protein has also
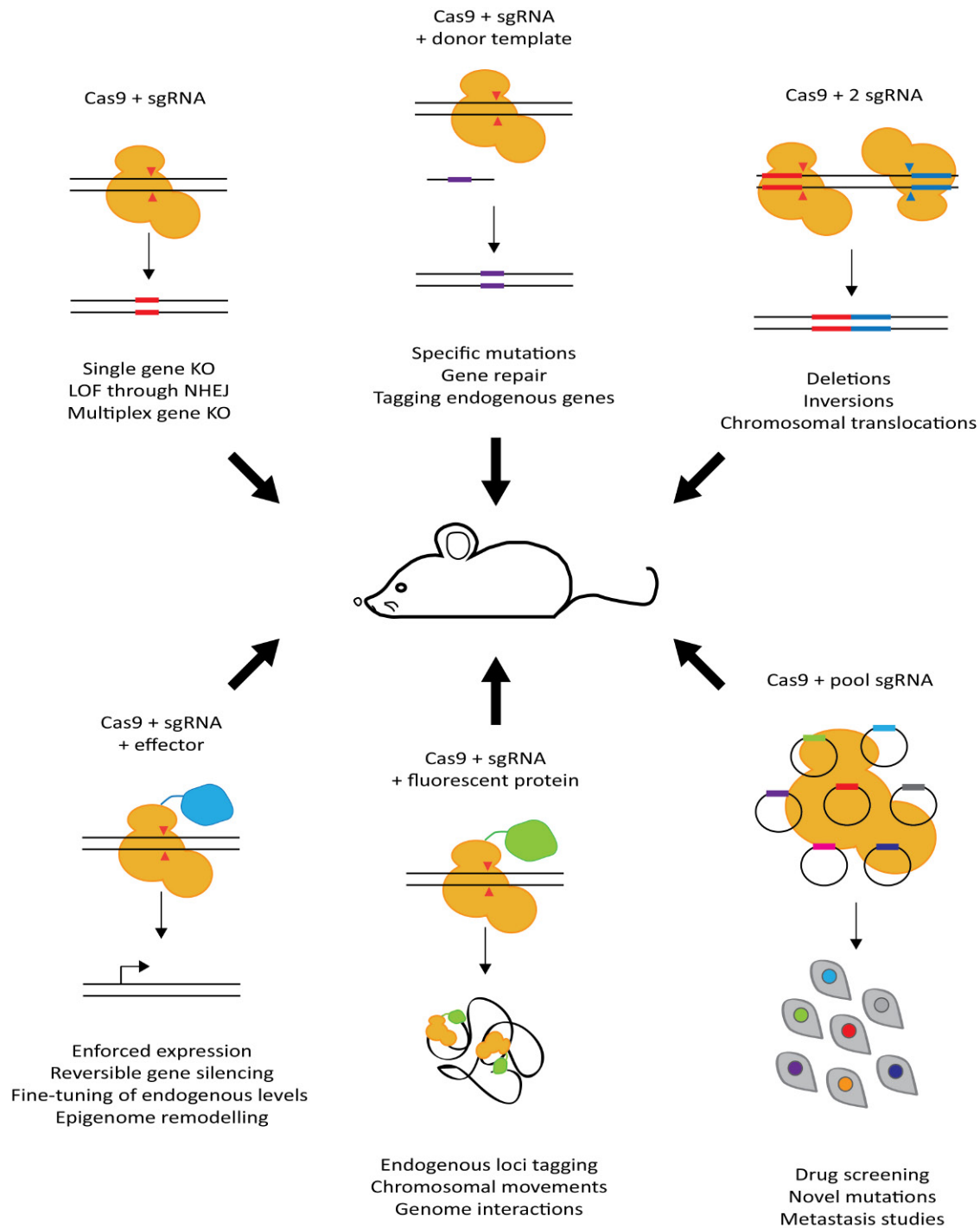
FIGURE 34.2   **Main applications of CRISPR-Cas9 in animal cancer models.**

been modified by inactivating its catalytic domain to obtain dRCas9, which can also be fused to effectors. This approach is useful for the study of splicing regulation and the cancer transcriptome.

The CRISPR-Cas9 system enables any desired modification when we want to model or interrogate a specific cancer system, from genome editing (using the wild-type or nickase variants) to the more complex modulation of transcription levels (dCas9 fused to KRAB or VP64 domains) or even for visualization through various cellular stages during development, malignization, or differentiation (dCas9-eGFP). This methodology is not restricted to modeling, but has also been considered in clinical scenarios (Valletta et al., 2015) (Fig. 34.2).

2 GENERATION OF CRISPR CANCER MODELS

The vast majority of cancers rely on a precise scenario that is not only dependent on a specific genomic alteration, but that also needs to take place in a particular context, that is, in a specific cell type or developmental stage or in combination with several other alterations (Hutmacher et al., 2009; Thakur et al., 2014). As explained in the previous section, many different approaches have been applied to model this complex scenario, with different success rates. During the last 4 years, the CRISPR-Cas9 system has revolutionized the field because of its high efficiency, ease of use, and fast and streamlined applicability. Therefore, it has replaced previously available tools in routine laboratory work, and its application in clinical practice is now becoming a reality (Yin et al., 2016). Consequently, it is the best choice for experts and nonspecialists alike.

2.1 In Vitro Cancer Models

All cancers share a common feature, that is, the generation of de novo genome alterations. These changes are not only restricted to specific point mutations but can also be small deletions, inversions, and duplications, and even large chromosomal rearrangements. The alterations lead to activation of oncogenes, inactivation of TSGs, and alteration of genes involved in DNA repair mechanisms (Krogan et al., 2015). In this section, we summarize the CRISPR-Cas9-based in vitro cancer models generated during the past few years.

2.1.1 Modeling Targeted Mutations In Vitro

Advances in genome sequencing technologies (Girotti et al., 2016) have enabled the discovery of a huge number of specific genetic alterations in human tumors (Vogelstein et al., 2013). To translate all this knowledge into clinical practice, functional studies must be carried out to analyze the role of the alterations in cancer biology. Several groups have edited specific genes, either in cells and animals through the multiple available applications of the versatile CRISPR-Cas9 system, which uses DNA plasmid, viral vectors, mRNA, or protein–RNA complexes to introduce the CRISPR components into the target cell (Kouranova et al., 2016; Liang et al., 2015; Lin et al., 2014; Malina et al., 2013; Nelson and Gersbach, 2016).

One of the first studies to induce targeted genome modification in somatic cells used the CRISPR-Cas9 system in combination with a classic short hairpin RNA (shRNA) approach for the study of leukemogenesis involving a deletion in the long arm of chromosome (7q) (Chen et al., 2014). Disruption in mouse hematopoietic stem cells (mHSPC) of the Mll3 gene, localized in the chromosome 7q, in a specific background (defective for ΔNf1 and Δp53) revealed that this disruption was able to induce a leukemogenic process and also that leukemic cells were heterozygous for the Mll3 gene alteration (thus indicating an unseen mechanism). The authors demonstrated that Mll3 inactivation is tolerated in leukemia cells only when present in a partial dosage, therefore the authors hypothesized that Mll3 is a haploinsufficient TSG acting as a second hit in many acute myeloid leukemia (AML) processes.

Shortly after this initial study, Antal et al. (2015) modified a previously established concept through the use of CRISPR-Cas9, demonstrating that mutations in protein kinase C (*PKC*) genes function as TSGs, thus leading to a switch in therapies from inhibition of PKC activity to restoration of PKC activity. In this case, the authors reestablished the function of the *PKC* gene in a patient-derived colon cancer cell line (DLD1) using genome engineering (via CRISPR-Cas9) in combination with single-stranded oligodeoxynucleotides (ssODNs). The effect of the correction was plausible in a xenograft model, where the tumor size was reduced after the function of the protein was restored, thus demonstrating that the *PKC* mutation confers an anchorage-independent growth advantage in this specific tumor environment and that it has a tumor-suppressive function.

One of the main characteristics of the CRISPR-Cas9 system is its multiplexing ability, which enables it to target several genes in one experiment. Consequently, primary healthy cells, patient-derived cell lines, and well-established cancer cell lines could be modified to carry several mutations. This fundamental advantage of the CRISPR system is of special interest in cancer modeling, since it enables the induction of multiple cooperating mutations, including driving and secondary events. It also facilitates analysis of several combinations of parameters, thus enriching potential results and even leading to the discovery of new variants that shed light on drug discovery screenings. One of the first studies that reported this use was from Ebert and colleagues (Heckl et al., 2014), who took advantage of the viral delivery of the CRISPR components into mHSPC to modify in a single step eight genes (*Tet2, Runx1, Dnmt3, Ezh2, Nf1, Smc3, p53*, and *Asxl1*) frequently affected in patients with AML in combination with an *Flt3* internal tandem duplication (ITD). The *Flt3*-ITD, which is found in many types of leukemia, is insufficient to drive tumorigenesis by itself. The authors demonstrated that mimicking the genetic combinations led to myeloid clonal expansion and transformation to AML, as reported for AML patients. Another major study that took advantage of the system's multiplexing ability was that of Sato and colleagues (Matano et al., 2015), who used a cellular model of human intestinal organoids to mimic colorectal cancer. The authors modeled five mutations both in oncogenes (*KRAS* and *PIK3CA*) and in TSGs (*SMAD4, TP53*, and

APC), which promote niche signal independence. They created LOF mutations in the TSGs, in combination with a knockin strategy using ssODNs to generate specific mutations in *KRAS* (G12V) and in *PIK3CA* (E545K). The desired mutant organoids were obtained using a selection procedure based on an independent growth advantage in culture media lacking specific required factors (for human normal colon cells) (Sato et al., 2011). This system enabled the authors to obtain single cell clones with a different mutational background that recapitulated the transition to adenocarcinoma.

2.1.2 Chromosomal Rearrangements Generated In Vitro

Many tumors are characterized by the presence of specific and recurrent chromosomal rearrangements (deletions, inversions, and translocations). These alterations are often the event that triggers tumorigenesis. The feature common to genome rearrangements is that is that they arise from the cooccurrence of two DSBs in the genomic DNA of a cell. As explained previously, once the DSBs are generated, the cell tries to repair the broken ends using either NHEJ or HDR repair mechanisms. However, the incorrect repair can sometimes spontaneously generate a chromosomal rearrangement (Stratton et al., 2009). Historically, the study of chromosomal rearrangements relied on the use of transgenes or cell lines from patients harboring the mutation/alteration, which, while of invaluable importance, are not the most accurate systems. Genome engineering tools in general, and the CRISPR-Cas9 system in particular, provide us with the opportunity to modify a healthy cell to generate an isogenic counterpart (Liu et al., 2005; Torrance et al., 2001) that differs only in the specific alteration generated and is not affected by possible variegation or positional effects or by the number of copies inserted (Voigt et al., 2008). Consequently, several groups rapidly adapted the system to mimic large rearrangements (including translocations, inversions, and deletions) in cellular models with the aim of recapitulating the primary oncogenic event in a more physiological environment (Torres et al., 2014; Torres-Ruiz and Rodriguez Perales, 2015).

The induction of chromosomal rearrangements requires two different sgRNAs that target both loci involved in the rearrangement to induce two DSBs, which would subsequently be repaired by the NHEJ cell pathway, thus sometimes creating the desired rearrangement. However, the efficiency of this approach varies greatly, mainly because various sgRNAs are used and these target several genomic locations with varying 3D genome structures and accessibility (Jiang et al., 2016). In their pioneering study, Torres et al. (2014) reproduced the t(11;22)(q24;q12) chromosomal translocation, which is characteristic of Ewing sarcoma and leads to the generation of the *EWSR1–FLI1* fusion gene. The authors

were able to induce the t(11;22) translocation in two different cell models, namely, human embryonic kidney cell line (HEK293) and human primary mesenchymal stem cells (hMSC). The newly generated chimeric transcription factor *EWSR1-FLI1* was able to transactivate specific genes described as downstream targets of the fusion protein in human tumors (Cidre-Aranaz and Alonso, 2015), thus confirming that the activity of the fusion protein generated by the CRISPR system was similar to that observed in the patient's cancer cells. The authors also demonstrated the universalization of the approach by recapitulating the AML characteristic t(8;21)(q22;q22)/RUNX1-ETO chromosomal translocation in HEK293 and CD34+ human hematopoietic stem progenitor cells (hHSPCs). Choi and Meyerson (2014) described the recreation of three chromosomal rearrangements in human lung cancer. The three alterations—the t(5;6)(q32;q22)/CD74/ROS1 chromosomal translocations, the inv(2)(p21;p23)/EML4/ALK paracentric inversion, and the inv(10)(p11;q11)/KIF5B/RET pericentric inversion—were generated in HEK293 and in nontransformed immortalized lung epithelial (AALE) cells. Taken together, the results of both studies demonstrated that CRISPR is a feasible tool for recreating chromosomal rearrangements; however, further refinement is necessary to facilitate appropriate recreation of the desired rearrangement. This issue is of critical importance when the cells that acquire the alteration do not possess any selective advantage with respect to their counterpart. Alternative selection approaches that could be used to enrich the target cells include the use of a specific membrane marker activated by the oncogenic protein, selection of cells based on changes in cellular morphology, and any other procedure that could lead to a specific trackable change.

Beyond chromosomal translocations and inversions, specific deletions had been carried out in noncoding regions, enhancers (Avellino et al., 2016), and promoter sequences (Chiba et al., 2015). Genome engineering is a feasible tool for recreating chromosomal rearrangements although this ability is dependent on the localization of the breakpoints, thus demonstrating that efficiency decreases as distance increases (Coppoolse et al., 2005; Schildkraut et al., 2005). Chiba et al. (2015) used two sgRNAs flanking the TERT promoter to model cancer-associated deletions in human embryonic stem cells (hESCs). The deletion induced by CRISPR leads to permanent expression of the telomerase gene, thus mimicking the levels observed in cancer cells and the length of the telomeres.

2.1.3 CRISPR-Cas9 In Vitro High-Throughput Genetic Screens

Functional genomics is an indispensable approach in the identification of gene function, especially when

genome-wide interrogation leads to changes in cellular phenotypes. One of the essential advantages of the CRISPR-Cas9 system is the option of interrogating gene function on a genome-wide scale. The simplicity of programming the CRISPR-Cas9 system suggested a new way to interrogate gene function on a genome-wide scale by the construction of large-scale oligosynthesis of sgRNA sequences. In 2014, Zhang et al. (Sanjana et al., 2014; Shalem et al., 2014) showed that lentiviral delivery of the genome-scale CRISPR knockout (GeCKO) library targeting 18,080 human genes can be used to interrogate gene function on a genome-wide scale, thus facilitating both positive and negative LOF screening in mammalian cells. Taken together with the need to validate drug targets in the drug screening process, this option made CRISPR-Cas9 a promising application in the field of cancer (Agrotis and Ketteler, 2015; Kasap et al., 2014). Through the generation of mutations that confer loss of function, Zhang et al. (Shalem et al., 2014) identified the involvement of several human genes in resistance to vemurafenib, a B-RAF enzyme inhibitor for the treatment of late-stage melanoma that promotes programmed cell death (Sala et al., 2008). The GeCKO library makes it possible to validate both previously reported genes and nonreported genes. In another study, Zhang et al. (Konermann et al., 2015) used a specific variation of the previous library. This variation consisted of GOF through synergistic activation mediators targeting all human coding genes to screen for genes that, upon activation, confer resistance to vemurafenib. As with the previous study, the authors were able to identify novel candidate genes that confer resistance to the drug.

Furthermore, this strategy has been used to interrogate genes involved in metastatic progression. Zhang and Sharp (Chen et al., 2015b) used the GeCKO library to systematically screen genes involved in metastasis in a murine nonmetastatic nonsmall-cell lung cancer cell line. The mutant cell pools were transplanted into mice and generated tumors. After deep sequencing of the metastatic tumors, a set of genes consistently represented in all of the tumors produced was found to be involved in tumor growth and metastasis.

2.2 In Vivo Cancer Models

Cancer displays a wide range of genetic and genomic modifications. Thus, research requires a variety of genomically complex animal models. Numerous GEMMs and nongermline GEMMs (nGEMMs) harboring precise mutations in TSGs and oncogenes have been generated. These models provide the scientific community with invaluable tools to study the biology of cancer and to decipher critical aspects of initiation, maintenance, and progression of the disease. They are also excellent tools for the study of drug resistance (Chen et al., 2012;

Engelman et al., 2008) and for testing new compounds and treatment approaches. Traditional approaches to generate GEMMs require complex molecular protocols, manipulation, and extensive animal husbandry. They are therefore laborious, time consuming, and expensive. nGEMMs can simplify this process because traditional approaches are not able to simultaneously introduce several genetic modifications in adult animals or mESCs (Table 34.1).

Until the advent of CRISPR-based precise genome editing, mouse models of malignancies were based on a limited number of mutations or genes (Guerra et al., 2003; Jackson et al., 2001). The CRISPR-Cas9 system enabled the systematic generation of models harboring alterations in multiple genes, thus making it possible to study collaborative effects in tumor progression or therapeutic resistance or response. The system thus facilitated the combined rapid analysis of multiple mutations in human patients and the subsequent generation of GEMMs and nGEMMs. In 2013, two studies demonstrated the ease, speed, and flexibility with which it was possible to generate multiple GOF or LOF mutations in mice using the CRISPR-Cas9 system, thus considerably increasing the speed and precision with which distinct genotypes can be generated in animals to model human cancer. Taking advantage of the potential for multiplexed genome editing of the CRISPR system, Jaenisch et al. (Wang et al., 2013) demonstrated simultaneous one-step generation of double *Tet1* and *Tet2* knockout mice with a 80% of efficiency. Cas9 mRNAs and sgRNAs were coinjected to target *Tet1* and *Tet2* in mouse zygotes, obtaining mutations in those alleles in mice. The authors also coinjected Cas9 mRNA, sgRNAs, and an ssODN into mouse zygotes to engineer double HDR-mediated edition of two endogenous genes (*Tet1* and *Tet2*) in mouse models. The same group subsequently used CRISPR components and a DNA template to generate mice carrying a tag or a fluorescent reporter construct in the *Nanog*, *Sox2*, and *Oct4* genes, as well as in *Mecp2* conditional mutant mice. The authors also used a pair of sgRNAs to generate mice carrying small Mecp2 gene deletions (Yang et al., 2013).

The CRISPR-Cas9 system can also be used to refine existing models of cancer. It enables reedition of previously established GEMMs to induce additional modifications and study the cooperative effects of several candidate target genes in vivo (Dow and Lowe, 2012). This new model better represents the genetic heterogeneity of human cancer. In the near future, it will be possible to generate in vivo models capable of reproducing the specific alterations found in an individual patient that can be used as a platform to select the most effective therapy. With CRISPR-Cas9 technology, the time necessary to generate genetically engineered mice is reduced from about a year to several weeks.

TABLE 34.1 Overview of the Use of the CRISPR-Cas9 System in the Context of Cancer Modeling

References	PMID	Type of alteration	Target cell	disease	Gene	Delivery
Annunziato et al. (2016)	27340177	Loss-of-function	Breast cells (mouse)	Lobular breast carcinoma	*Pten*	Injection of LV
Maresch et al (2016)	26916719	Loss-of-function and deletions	Pacreatic cells (mouse)	Pancreatic cancer	*Multiplex 13 TSGs*	Injection and electroporation
Guernet et al. (2016)	27453044	Loss-of-function and directed mutation	Various cancer cell models	Lung cancer	*EGFR, KRAS, ALK, TP53, APC*	Nucleofection
Muniyan et al. (2016)	27382435	Loss-of-function	Human PDAC cancer cell lines (orthotopic implantation)	PDAC	*MUC16*	Transfection
Schokrpur et al. (2016)	27358011	Loss-of-function	RENCA cells (mouse)	Metastatic renal cell carcinoma	*VHL*	LV
Ear et al. (2016)	27216296	Loss-of-function	HSPCs (zebrafish)	5q-myelodisplasic syndrome	*RPS14*	RNA injection
Weber et al. (2015)	26508638	Loss-of-function	Hepatic cells (mouse)	HCC	*Multiplex*	Injection
Chiou et al. (2015)	26178787	Loss-of-function	Somatic pancreatic cells (mouse)	PDAC	*Lkb1*	LV and AdV
Dow et al. (2015)	25690852	Loss-of-function	mESCs cells (mouse)	Colon cancer	*Pten, Apc, p53*	Plasmid DNA
Aubrey et al. (2015)	25732831	Loss-of-function	Fetal-liver (ex vivo)	BL	*Mcl-1, p53*	LV
Platt et al. (2014)	25263330	Loss-of-function and directed mutation	Neurons, immune and endothelial cells (mouse)	Lung adenocarcinoma	*Kras, p53, Lkb1*	AAV, LV & particle mediated delivery
Xue et al. (2014)	25119044	Loss-of-function and directed mutation	Liver cells (mouse)	Liver cancer	*Pten, p53*	Injection
Blasco et al. (2014)	25456124	Chromosomal rearrangement	Lung cells (mouse)	NSCLC	*Eml-Alk*	LV
Maddalo et al. (2014)	25378762	Chromosomal rearrangement	Lung cells (mouse)	NSCLC	*Eml-Alk*	AdV
Chen et al. (2014)	24794707	Loss-of-function	HSPCs (ex vivo)	Acute myeloid leukemia (AML)	*Mll3*	DNA electroporation
Sanchez-Rivera et al. (2014)	25337879	Loss-of-function	Lung cells (mouse)	Lung adenocarcinoma	*Kras*, *p53*, and *Lkb1*	LV
Heckl et al. (2014)	24952903	Loss-of-function	HSPCs (ex vivo)	AML	*TET2, DNMT3A, RUNX1, NF1, EZH2*	LV
Wang et al. (2013)	23643243	Loss-of-function and directed mutation	mESCs and zygotes (mouse)	na	*Tet1, Tet2, Tet3, Sry, Uty*	Injection
Xiao et al. (2013)	23748566	Chromosomal rearrangement	Embryo (zebrafish)	na	*mir-126a*	Injection
Malina et al. (2013)	24298059	Loss-of-function	Lymphoma cells (ex vivo)	Lymphoma	*p53*	RV

AML, Acute myeloid leukemia; BL, burkitt lymphoma; HCC, hepatocellular carcinoma; HSPCs, hematopoietic stem progenitor cells; mESC, mouse embryonic stem cells; na, not applicable; NSCLC, nonsmall cell lung cancer; PDAC, pancreatic ductal adenocarcinoma; RENCA, murine renal cancer.

Annunziato, S., Kas, S. M., Nethe, M., Yücel, H., Del Bravo, J., Pritchard, C., et al., 2016. Modeling invasive lobular breast carcinoma by CRISPR/Cas9-mediated somatic genome editing of the mammary gland. Genes Dev. 30 (12), 1470–1480.
Maresch, R., Mueller, S., Veltkamp, C., Öllinger, R., Friedrich, M., Heid, I., et al., 2016. Multiplexed pancreatic genome engineering and cancer induction by transfection-based CRISPR/Cas9 delivery in mice. Nat. Commun. 7, 10770.
Guernet, A., Mungamuri, S. K., Cartier, D., Sachidanandam, R., Jayaprakash, A., Adriouch, S., et al., 2016. CRISPR-barcoding for intratumor genetic heterogeneity modeling and functional analysis of oncogenic driver mutations. Mol. Cell.
Muniyan, S., Haridas, D., Chugh, S., Rachagani, S., Lakshmanan, I., Gupta, S., et al., 2016. MUC16 contributes to the metastasis of pancreatic ductal adenocarcinoma through focal adhesion mediated signaling mechanism. Genes Cancer 7(3-4), 110–124.
Schokrpur, S., Hu, J., Moughon, D. L., Liu, P., Lin, L. C., Hermann, K., et al., 2016. CRISPR-Mediated VHL knockout generates an improved model for metastatic renal cell carcinoma. Sci. Rep. 6, 29032.
Ear, J., Hsueh, J., Nguyen, M., Zhang, Q., Sung, V., Chopra, R., et al., 2016. A Zebrafish model of 5q-syndrome using CRISPR/Cas9 targeting RPS14 reveals a p53-independent and p53-dependent mechanism of erythroid failure. J. Genet. Genomics 43 (5), 307–318.
Chiou, S.H., Winters, I.P., Wang, J., Naranjo, S., Dudgeon, C., Tamburini, F.B., et al., 2015. Pancreatic cancer modeling using retrograde viral vector delivery and in vivo CRISPR/Cas9-mediated somatic genome editing. Genes Dev. 29(14), 1576–1585.
Aubrey, B.J., Kelly, G.L., Kueh, A.J., Brennan, M.S., O'Connor, L., Milla, L., et al., 2015. An inducible lentiviral guide RNA platform enables the identification of tumor-essential genes and tumor-promoting mutations in vivo. Cell Rep. 10(8), 1422–1432.
Xiao, A., Wang, Z., Hu, Y., Wu, Y., Luo, Z., Yang, Z., et al., 2013. Chromosomal deletions and inversions mediated by TALENs and CRISPR/Cas in zebrafish. Nucleic Acids Res. 41(14), e141.

2.2.1 Manipulating Germlines to Generate Transgenic Animal Models

CRISPR-Cas9-based technologies can be used to manipulate germline for generation of transgenic animal models (Wang et al., 2013; Yang et al., 2013). Moreover, the two components of CRISPR-Cas9 (Cas9 nuclease and sgRNA) can be used separately to generate transgenic animal models. Platt et al. (2014) constructed Cre-dependent Cas9 knockin mice by targeting the Cas9 gene driven by the CAG promoter interrupted by the *loxP*-stop-*loxP* (LSL) cassette, which had been introduced at the *Rosa26* locus in mESC. Crossing this mouse line with a constitutive Cre driver or tissue-specific Cre driver strain can generate offspring with constitutive or tissue-specific Cas9 expression, respectively. Using this mouse, Jacks et al. (Sánchez-Rivera et al., 2014) were able to model lung adenocarcinoma thanks to the mutation of three different genes implicated in human pathogenesis (*Kras*, *p53*, and *Lkb1*), thus demonstrating the synergistic power of cancer mouse models based on the CRISPR-Cas9 system.

2.2.2 In Vivo Somatic Genome Engineering

Besides generating animal models through germline manipulation, the CRISPR-Cas9 system has the unprecedented ability to engineer the genome of adult animal models through somatic edition, thus enabling it to sidestep germline manipulation and animal crossbreeding. Somatic gene transfer approaches make it possible to restrict the induction of genomic alterations to tumor-forming cells, resulting in a tumor that closely resembles that of the patient. To date, several alternatives have been explored for delivery of CRISPR-Cas9 tools to a target organ. The methodological features of the delivery approaches should be taken into consideration to achieve effective cancer modeling. Some of these delivery approaches are presented in subsequent sections.

2.2.2.1 HYDRODYNAMIC GENE TRANSFER

The first cancer model based on in vivo somatic mutations was reported by Jacks (Xue et al., 2014), who used hydrodynamic gene transfer to engineer *Pten* and *Trp53* in mouse hepatocytes, thus creating LOF mutations in hepatocytes of adult wild-type mice. This in vivo gene-targeting approach uses rapid injection of controlled hydrodynamic pressure into the capillaries of a relatively large volume of DNA solution to enhance endothelial and parenchymal cell permeability. Carcinogenic CC14-induced liver tumors combined with edition of *Pten* and *Trp53* by the injection of a plasmid to express sgRNAs and Cas9 nuclease in the livers of mice made it possible to reproduce the characteristics of other models generated using classic approaches, thus indicating the feasibility of this approach. In vivo functional validation of liver cancer TSGs was achieved by

exploiting the efficacy of hydrodynamic gene transfer for the liver (Weber et al., 2015). Based on a multiplex combination of sgRNAs to target several TSGs discovered by deep sequencing of human tumors, the authors of the study used Alb-Cre/Kras$^{LSL-G12D/+}$ tumor-prone mice to analyze whether the putative TSGs play a role in the development of liver tumors. A GOF mutation in the β-catenin gene has also been obtained in the livers of adult wild-type mice. Xue et al. (2014) constructed a plasmid containing Cas9, sgRNA targeting β-catenin, and an ssODN donor bearing GOF mutations for the β-catenin gene. The plasmid was delivered into adult mice via hydrodynamic tail-vein injection, leading to accumulation of β-catenin in the nuclei of liver cells. Thus, hydrodynamic gene transfer, although potentially resulting in delivery to many organs (Liu et al., 1999), is a simple, efficient, and versatile method for delivering liver tumor cells.

2.2.2.2 VIRAL DELIVERY OF CRISPR-Cas9 COMPONENTS

The development of the CRISPR-Cas9 system as a genome engineering tool for biotechnological use was quickly followed by the development of viral vectors for delivery of CRISPR components, initially as single modification tools (Ebina et al., 2013; Malina et al., 2013) and subsequently with the aim of generating genome-wide screening (as reported in the Section 2.1.3) (Kabadi et al., 2014; Koike-Yusa et al., 2014; Shalem et al., 2014; Wang et al., 2014; Zhou et al., 2014). Although Cas9 is a large gene (4.1 kb), it can be packed efficiently into lentiviral particles (Holkers et al., 2013); however, it barely fits into recombinant adeno-associated virus (AAV) particles. While viral delivery of CRISPR components paved the way for the edition of poorly transfectable cells in vitro, a more important aspect of this approach is its ability to render somatic gene transfer accessible for in vivo edition experiments.

The applicability of delivering CRISPR components by viral vectors was first demonstrated by Zhang and Sharp (Platt et al., 2014), who developed a Cre-inducible Cas9 mouse based on a Lox-Stop-Lox (LSL)-Cas9 knockin strategy. First, the authors demonstrated that constitutive expression of the Cas9 nuclease using a ubiquitous promoter did not produce abnormalities. Platt et al. used AAVs to mediate expression of Cre recombinase together with an sgRNA targeting the *Rbfox3* gene by injection in the cortex of LSL-Cas9 mice. Three weeks later, deep sequencing of the *Rbfox3* gene revealed formation of indels in the injected region, and Western blot showed depletion of the protein. Zhang and Sharp (Platt et al., 2014) generated the first cancer disease model based on intratracheal delivery of AAVs encoding the CRISPR components to generate *Lkb1* and *Trp53* LOF mutations, specific activating mutation

in *Kras*, and Cre recombinase in LSL-Cas9 mice. Two months after inoculation, the simultaneous pulmonary delivery of AAVs carrying a multicistronic cassette led to deep penetrating lung adenocarcinoma in adult mice. Simultaneous disruption of *Lkb1* and *Trp53* and edition of *Kras* was achieved in a single step. As expected, the authors reported a high frequency of indels at the *Lkb1* and *Trp53* loci although *Kras* displayed an inefficient mutation rate.

Lentivirus delivery has also been used to show the ability of CRISPR-Cas9 to induce oncogenic chromosomal rearrangements in adult mice. Maddalo et al. (2014) and Blasco et al. (2014) reported the successful induction in vivo of Eml4-Alk inversion that is frequently found in human lung cancer. Blasco et al. used lentiviral somatic gene transfer by intrapulmonary inoculation into *Trp53*$^{+/-}$ or *Trp53*$^{-/-}$ murine lungs and generation of inversion rearrangements, thus creating the Emlk4-Alk fusion gene and forming lung tumors in all the mice. The authors demonstrated that intratracheal or intrapulmonary inoculation of lentiviruses was able to induce the *Eml4-Alk* rearrangement in lung cells in vivo.

Jacks (Sánchez-Rivera et al., 2014) used a lentivirus-based vector to express sgRNA together with Cas9 and Cre recombinase in p53$^{fl/fl}$ mice. The authors targeted *Nkx2.1* and *Pten* and found that not all of the lung tumors displayed complete loss of expression of the targeted genes.

Adenoviruses have been used to model large oncogenic chromosomal rearrangements (Maddalo et al., 2014; Shaw et al., 2013; Soda et al., 2007). In contrast to lentiviral vectors, which are integrated in the genome, adenoviruses only lead to transient expression. The use of adenoviral vectors to express CRISPR components reduces the probability of potential off-site cleavage associated with continuous expression. Maddalo et al. used adenoviral delivery of dual expression cassettes encoding both Cas9 and sgRNAs to induce *Eml4-Alk* gene fusion via intrachromosomal inversion. Eight weeks later, all the mice developed lung cancer with features similar to those of ALK+ lung cancer in human patients.

The results of these reports demonstrate the utility and illustrate the variety of currently available approaches, which range from all-in-one vector systems to single or multiple sgRNA delivery by AAVs. The examples presented previously demonstrate that CRISPR-Cas9 is an accurate and efficient platform for inducing combinational or sequential gene edition in adult mice, thus making it possible to model the complex scenario of the cancer process defined by the multistep and somatic nature of oncogenic mutations. Various aspects need to be taken into account before choosing the CRISPR delivery system, including limits in vector packaging size, distribution throughout the tissue (Kumar et al., 2001; Parr-Brownlie et al., 2015; Wu et al., 2010), and choice of serotype for promotion of preferential transduction of specific cell populations (Michelfelder and Trepel, 2009).

2.2.2.3 NONVIRAL DELIVERY OF CRISPR-Cas9 COMPONENTS

Among the nonviral techniques for gene transfer, in vivo electroporation of plasmid DNA enables the introduction of DNA with a high efficiency in specific regions of the mouse brain in utero. Genes can be focally transfected into specific regions of the brain, such as the spinal cord (Saba et al., 2003), hindbrain (Kawauchi et al., 2006), cerebellum (Kawauchi and Saito, 2008; Konishi et al., 2004), diencephalon (Shimogori and Ogawa, 2008), and retina (Matsuda and Cepko, 2004). This approach provides the opportunity to induce different types of brain tumors at specific locations. In vivo electroporation has made it possible to deliver CRISPR components to the mouse brain in utero for cancer modeling (Chen et al., 2015a; Maresch et al., 2016; Zuckermann et al., 2015). In vivo electroporation of Cas9 and an sgRNA targeting *Ptch1* in the embryonic cerebellum was able to cause medulloblastoma (Zuckermann et al., 2015). In utero electroporation of the cerebral cortex to simultaneously deliver sgRNAs targeting *Trp53*, *Nf1*, and *Pten* induced mutations of all three genes and subsequently formation of glioblastoma (Zuckermann et al., 2015). The key issues in cancer modeling based on in utero electroporation include the limited number of transfected cells and the lack of specificity of the targeted cell types. Electroporation-based CRISPR gene editing has also been applied in abdominal organs to generate pancreatic cancer using multiplexed sgRNAs combined with constitutive activation of Kras signaling (Dean et al., 2003; Liu and Huang, 2002; Maresch et al., 2016). This approach offers the advantage of targeting specific regions within an organ, which could result in several different tumor types (Swartling et al., 2012; Zhao et al., 2015).

Nonviral delivery by cationic lipid has been used to deliver Cas9-sgRNAs RNPs (Platt et al., 2014; Zuris et al., 2015). Zuris et al. reported that common cationic lipid nucleic acid transfection reagents can deliver Cas9:sgRNA nuclease complexes into cultured human cells. Delivery of unmodified Cas9:sgRNA complexes resulted in highly efficient genome modification. Interestingly, the complex Cas9:sgRNA delivery approach is substantially more specific than DNA transfection.

These studies demonstrate the potential of rapidly generating mouse models of cancer via somatic genome engineering through different approaches for delivery of CRISPR components to a target organ. Future advances in delivery methods will allow highly efficient in vivo somatic genome engineering.

3 CHALLENGES AND SOLUTIONS

CRISPR-Cas9 has proven successful for modeling cancer. However, the approach is subject to technical limitations. One of the main challenges, both in vivo and in vitro, is delivery to the target cell, tissue, or animal. Many efforts have been made to make delivery more efficient and to broaden its applicability. The various animal models generated include plasmid microinjection (Horii et al., 2014; Mashiko et al., 2013), injection of mRNA into zygotes (Hashimoto and Takemoto, 2015), or porcine oocytes (Sato et al., 2015), and Cas9 RNP (Chen et al., 2016). Recent studies indicate that the RNP approach seems to be the best alternative when no vector trace is required and when the objective is to introduce mutations or generate edition in poorly transfectable cells (Kim et al., 2014). However, this approach is not adequate for delivery to target cells in a living organism or for generating tissue-specific in vivo models, basically owing to the limited efficiency for reaching the target cells. Therefore, a plausible alternative is the use of viral vectors (Chen and Gonçalves, 2016). Currently, the most attractive gene delivery vectors are AAVs, which are nonpathogenic human viruses that enable long-term transgene expression without genomic integration (Smith, 2008). Given the nature of their DNA, they can serve as a vehicle for Cas9 and also for template DNA to repair target cells (Platt et al., 2014; Swiech et al., 2015).

Initially, the main drawback of the CRISPR-Cas9 system was the induction of off-target mutations at sites that are highly homologous to on-target sites (Cho et al., 2014; Hsu et al., 2013; Wu et al., 2014). Off-target DNA cleavage can cause unwanted genetic changes and/or chromosomal rearrangements with unpredictable consequences (Cho et al., 2014). This limitation, which is a major concern in original in vitro studies, seems less relevant in vivo and has almost no importance in the generation of mouse models (Iyer et al., 2015). Nevertheless, the alternatives that have been developed to overcome these drawbacks include the following: (1) acting on sgRNA to modify its specificity by truncating sgRNA (trugRNA) (Fu et al., 2014) or optimizing the structure to increase efficiency and reduce mutagenesis at nontarget sites (Dang et al., 2015), (2) nickases, which cleave on only one strand and must be used in pairs, can be abolished off-target without comprising on-target cleavage (Ran et al., 2013), (3) regulation of the time at which the components are delivered (Dow et al., 2015; Lin et al., 2014) in order to reduce their availability and hence their duration of action. This approach can decrease the probability of generating nondesired DSBs (a seemingly trivial aspect is, however, of critical importance), (4) the quantity of CRISPR components delivered (some of the off-target effects have been shown to be due to the high quantity used) (Hsu et al., 2013; Kuscu et al., 2014; Pattanayak et al., 2013). This issue proved critical in the efficient generation of animal models and was addressed using an appropriate optimization procedure based on appropriate quantities in specific experimental settings (Ren et al., 2014). An additional way to minimize the CRISPR drawbacks is to realize an accurate design of the sgRNA/s. Several web-tools have been developed to that aim, facilitating the design and reducing the probability of undesired off-target effects (Table 34.2).

TABLE 34.2 Descriptions of Some of the Most Representative sgRNA Web-Design Tools

Name	Links	On-target score	Off-target score	PAM type	Organism check	References
CRISPRdirect	http://crispr.dbcls.jp/	No	Yes	Any of 3 nucleotides	Several	Naito, Y., Hino, K., Bono, H., Ui-Tei, K., 2014. CRISPRdirect: software for designing CRISPR/Cas guide RNA with reduced off-target sites. Bioinformatics 31 (7), 1120–1123.
CCTOP	http://crispr.cos.uni-heidelberg.de/	No	Yes	Several species	Several	Stemmer, M., Thumberger, T., Keyer, M.D., Wittbrodt, J., Mateo, J.L., 2015. CCTop: an intuitive, flexible and reliable CRISPR/Cas9 target prediction tool. PLoS One 10 (4), e0124633.
Cas-OFFinder	http://www.rgenome.net/cas-offinder/	No	Yes	Several species	Several	Bae, S., Park, J., Kim, J., 2014. Cas-OFFinder: a fast and versatile algorithm that searches for potential off-target sites of Cas9 RNA-guided endonucleases. Bioinformatics, 30 (10), 1473–1475.

(Continued)

TABLE 34.2 Descriptions of Some of the Most Representative sgRNA Web-Design Tools (*cont.*)

Name	Links	On-target score	Off-target score	PAM type	Organism check	References
CRISPR design	http://crispr.mit.edu/	No	Yes	NGG	Several	Hsu, P.D., Scott, D.A., Weinstein, J.A., Ran, F.A., Konermann, S., Agarwala, V., et al., 2013. DNA targeting specificity of RNA-guided Cas9 nucleases. Nat. Biotechnol. Nat. Biotechnol. 31 (9), 827–832.
CRISPR-ERA	http://crispr-era.stanford.edu/	Yes	Yes	NGG and NAG	Nine	Liu, H., Wei, Z., Dominguez, A., Li, Y., Wang, X., Qi, L.S., 2015. CRISPR-ERA: a comprehensive design tool for CRISPR-mediated gene editing, repression and activation: Fig. 1. Bioinformatics 31 (22), 3676–3678.
CRISPR MultiTargeter	http://www.multicrispr.net/basic_input.html	No	No	NGG or customize	Twelve	Prykhozhij, S.V., Rajan, V., Gaston, D., Berman, J.N., 2015. CRISPR MultiTargeter: a web tool to find common and unique CRISPR single guide RNA Targets in a set of similar sequences. PLoS One 10 (3), e0119372
E-CRISP	http://www.e-crisp.org/E-CRISP/designcrispr.html	No	Yes	NGG and NAG	Several	Heigwer, F., Kerr, G., Boutros, M., 2014. E-CRISP: fast CRISPR target site identification. Nat. Methods 11 (2), 122–123.
flyCRISPR	http://tools.flycrispr.molbio.wisc.edu/targetFinder/	No	Yes	NGG	Insect species	Gratz, S.J., Ukken, F.P., Rubinstein, C.D., Thiede, G., Donohue, L.K., Cummings, A.M., O'connor-Giles, K.M., 2014. Highly specific and efficient CRISPR/Cas9-catalyzed homology-directed repair in *Drosophila.* Genetics 196 (4), 961–971.
WGE	http://www.sanger.ac.uk/htgt/wge/	No	Yes	NGG	Human or mouse	Hodgkins, A., Farne, A., Perera, S., Grego, T., Parry-Smith, D.J., Skarnes, W.C., Iyer, V., 2015. WGE: a CRISPR database for genome engineering: Fig. 1. Bioinformatics 31 (18), 3078–3080.
CHOPCHOP	http://chopchop.cbu.uib.no/	No	Yes	NGG	Several	Labun, K., Montague, T.G., Gagnon, J.A., Thyme, S.B., Valen, E., 2016. CHOPCHOP v2: a web tool for the next generation of CRISPR genome engineering. Nucleic Acids Res. 44 (W1), W272–W276.
sgRNA design	http://portals.broadinstitute.org/gpp/public/analysis-tools/sgrna-design	Yes	Yes	NGG	Human or mouse	Doench, J.G., Fusi, N., Sullender, M., Hegde, M., Vaimberg, E.W., Donovan, K.F., et al., 2016. Optimized sgRNA design to maximize activity and minimize off-target effects of CRISPR-Cas9. Nat. Biotechnol. 34 (2), 184–191.
WU-CRISPR	http://crispr.wustl.edu/	No	Yes	NGG	Human or mouse	Wong, N., Liu, W., Wang, X., 2015. WU-CRISPR: characteristics of functional guide RNAs for the CRISPR/Cas9 system. Genome Biol. 16, 218.
Breaking-Cas	http://bioinfogp.cnb.csic.es/tools/breakingcas/		Yes	Several	ENSEMBL genomes	Oliveros, J.C., Franch, M., Tabas-Madrid, D., San-León, D., Montoliu, L., Cubas, P., Pazos, F., 2016. Breaking-cas—interactive design of guide RNAs for CRISPR-Cas experiments for ENSEMBL genomes. Nucleic Acids Res. 44 (W1), W267-W271.
SSC	http://crispr.dfci.harvard.edu/SSC/	No	Yes	NGG	Human or mouse	Xu, H., Xiao, T., Chen, C., Li, W., Meyer, C.A., Wu, Q., et al., 2015. Sequence determinants of improved CRISPR sgRNA design. Genome Res. 25 (8), 1147–1157.

Name—name of the web-tool; off-target score—prediction of off-target cutting; on-target score—prediction of cutting on-target site; organism check—genomes that could be checked to predict on-target and/or off-target scores; PAM, protospacer adjacent motif.

4 CONCLUDING REMARKS

An experiment based on the CRISPR-Cas9 system can be performed using only a plasmid to express the Cas9 nuclease and an sgRNA targeting a predefined locus. The CRISPR plasmid now costs around €60 or less, can be ordered online, and requires little specialist training. CRISPR enables researchers to engineer more animals in more complex ways and in a wider range of species. Jiahao Sha and colleagues (Niu et al., 2014) demonstrated how far human disease modeling can be taken: the authors used cynomolgus monkeys as a model species for studying human diseases. Until that moment, the application of monkeys in biomedical researches has been significantly hindered by the difficulties in producing animals that have been genetically modified at the desired target sites. The authors induced simultaneous disruption of two target genes (*Ppar-γ* and *Rag1*) using coinjection of Cas9 mRNA and sgRNAs into one-cell-stage embryos.

Although the application of CRISPR-Cas9 in cancer modeling to date has focused on edition of the genome, recreation of epigenetic and transcriptome aberrations could constitute a major approach for cancer modeling in the future. Researchers are hoping to integrate the new CRISPR-Cas9 tools to precisely manipulate the genome and epigenome in animal models. This approach could make it possible to reproduce and analyze—at least partially—the complexity of human cancer. For example, "epi-modeling" of cancer could be performed using epigenetic modifiers fused to dead Cas9 or recruited by scRNA. Such tools will reach the locus of interest and subsequently change the methylation state or mediate histone modification in a site-specific manner. These new approaches will not only improve our understanding of cancer biology, but could also facilitate translational biomedical science. CRISPR could pave the way for new therapeutic approaches and drug screening assays both in vitro and in vivo (Shi et al., 2015).

The rapid advances in CRISPR-Cas9 systems toward application for treatment of human diseases have given rise to the discussion of the ethical implications of this technology (Keener, 2015). In 2015, the first study on the use of CRISPR-Cas9 in human zygotes was published. Although these zygotes were unable to develop into viable embryos because they have one oocyte nucleus and two sperm nuclei, the study raised ethical alarms and led to a worldwide moratorium on genomic engineering of human germlines by both biologists and ethicists (Hurlbut, 2015). It was proposed that, instead of imposing a moratorium on the development of such a promising technology, dynamic guidelines involving society as a whole should be developed to run in parallel with scientific advances so that they can be established progressively (Committee on Science, Technology, and Law; Policy and Global Affairs; National Academies of Sciences, Engineering, and Medicine; and Olson, 2016). Before human germlines can be genetically engineered, appropriate control models are warranted for testing efficacy and safety to minimize collateral effects. Such models would include more accurate and sensitive tools to assess off-target events and mosaicism (Chan et al., 2015).

CRISPR-Cas9 is a groundbreaking technology. It heralds an era of changes, with potential application in therapeutics, disease modeling, and genetic studies. Efforts are already under way to develop CRISPR-Cas9-based treatments for cancers of all levels of genetic complexity. The challenge facing researchers today is to develop innovative technologies and improve the safety and efficacy of the new tools. CRISPR cancer models are revealing factors with wide-ranging implications for human cancers. The combination of such approaches with next-generation sequencing data provides us with an unprecedented opportunity to create powerful and more informative cellular and animal genetic models that enhance our understanding of human cancer. We believe that many of the applications of CRISPR-based genome engineering technology will help to decipher both intrinsic and microenvironmental cellular elements that play a role in oncogenesis, cancer progression, and metastasis and may even enable a cure for some cancers.

Glossary

Chromosomal rearrangements Chromosomal abnormalities where a chromosome's structure is reorganized through deletions, inversions, translocations, or duplications. Usually is produced by a break in both helices of the DNA followed by a rejoining of the ends of the broken area, leading to new genes.

Conditional alleles Alleles that are engineered to be expressed only in the presence of a second component.

Driver and passenger mutations Mutations that differ in the fact that driver mutations give a selective advantage to the cells to grow more than the neighboring cells, increasing its survival or reproduction. In cancer cells, there are a reduced number of driver mutations, while passenger mutations appear in large number in most of tumors and do not confer selective advantage to the cells.

DSB Cleaved generated in both strands of DNA that can be repaired by HR or NHEJ pathways.

GEMMs Transgenic models of mouse used as a tool in biomedical research. They are usually engineered to mutate cancer genes.

GOF mutations Mutations that generate a new function.

HDR A mechanism in cells to repair double-strand DNA breaks (DSBs) that uses a homology sequence to the break to repair the DNA. It can be used to modify the genome of different organism by inserting a DNA with the mutation.

Indels Mutations generated by the insertion or deletion of bases in the genome of an organism.

Knockin A genetically modified organism which has replaced a normal gene by an altered gene with a specific mutation

Knockout (KO) A genetically modified organism that lacks the expression of a particular gene.

LOF Mutations that generate the lost or reduction of a function.

NHEJ pathway process of DNA reparation without the need of a homologous template. It consists in the fact that after the generation of

the DSB, a nuclease processed the ends by its junction and ligation causing generally the lost and introduction of some bases.

Oncogene A gene that had the potential to cause cancer. These genes are abnormally activated by a mutation responsible for the transformation of a normal cell into cancer cells. These genes, before mutate are involved in normal growth and division of cells

Organoid Also known as miniorgan. It is a three-dimensional culture grows in vitro to mimics organ structure and function.

PAM A sequence of three nucleotides downstream of the DNA sequence targeted by Cas9 nuclease.

sgRNA A noncoding RNA composed of a region of 20 nt complementary to the genome, and a Cas9-binding region that guides the protein to perform the cut at a specific locus. sgRNA is a condensation of the crRNA y tracrRNA

ssODNs A set of nucleotides complementary to the target site used as template for the DSB repair by HDR. It presents homology arms on either side of the cut site.

TALENs An engineered restriction enzymes that can cut specific sequences of DNA. It is composed of a transcription activator-like proteins and FokI nuclease.

Transgenesis The introduction of foreign DNA into a genome, so that it remains stable hereditary and affects all cells.

TSG A gene involved in cell growth inhibiting excessive cell proliferation. Mutation in these genes can lead to cancer. It is also known as antioncogene.

Xenograft (also referred as patient-derived xenograft, PDX) A tissue graft or organ implantation of a species into a different one. For example, implantation of human tumor cells in a mouse.

ZFNs An engineered restriction enzymes composed of a ZF DNA-binding domain and a DNA cleavage domain (FockI). The ZF domain can be designed to join a specific region of genome. It facilitates targeted editing of the genome by creating DSBs.

Acknowledgments

References

Agrotis, A., Ketteler, R., 2015. A new age in functional genomics using CRISPR/Cas9 in arrayed library screening. Front. Genet. 6, 300.

Antal, C.E., Hudson, A.M., Kang, E., Zanca, C., Wirth, C., Stephenson, N.L., et al., 2015. Cancer-associated protein kinase C mutations reveal kinase's role as tumor suppressor. Cell 160 (3), 489–502.

Avellino, R., Havermans, M., Erpelinck, C., Sanders, M.A., Hoogenboezem, R., van de Werken, H.J.G., et al., 2016. An autonomous CEBPA enhancer specific for myeloid-lineage priming and neutrophilic differentiation. Blood 127 (24), 2991–3003.

Barrangou, R., Fremaux, C., Deveau, H., Richards, M., Boyaval, P., Moineau, S., et al., 2007. CRISPR provides acquired resistance against viruses in prokaryotes. Science 315 (5819), 1709–1712.

Bibikova, M., Beumer, K., Trautman, J.K., Carroll, D., 2003. Enhancing gene targeting with designed zinc finger nucleases. Science 300 (5620), 764.

Blasco, R.B., Karaca, E., Ambrogio, C., Cheong, T.-C., Karayol, E., Minero, V.G., et al., 2014. Simple and rapid in vivo generation of chromosomal rearrangements using CRISPR/Cas9 technology. Cell Rep. 9 (4), 1219–1227.

Boettcher, M., McManus, M.T., 2015. Choosing the right tool for the Job: RNAi, TALEN, or CRISPR. Mol. Cell 58 (4), 575–585.

Braakhuis, B.J., Sneeuwloper, G., Snow, G.B., 1984. The potential of the nude mouse xenograft model for the study of head and neck cancer. Arch. Otorhinolaryngol. 239 (1), 69–79.

Brinster, R.L., Chen, H.Y., Trumbauer, M., Senear, A.W., Warren, R., Palmiter, R.D., 1981. Somatic expression of herpes thymidine kinase in mice following injection of a fusion gene into eggs. Cell 27 (1 Pt 2), 223–231.

Brinster, R.L., Chen, H.Y., Messing, A., van Dyke, T., Levine, A.J., Palmiter, R.D., 1984. Transgenic mice harboring SV40 T-antigen genes develop characteristic brain tumors. Cell 37 (2), 367–379.

Chan, S., Donovan, P.J., Douglas, T., Gyngell, C., Harris, J., Lovell-Badge, R., et al., 2015. Genome editing technologies and human germline genetic modification: the Hinxton Group Consensus Statement. Am. J. Bioeth. 15 (12), 42–47.

Chen, X., Gonçalves, M.A.F.V., 2016. Engineered viruses as genome editing devices. Mol. Ther. 24 (3), 447–457.

Chen, Z., Cheng, K., Walton, Z., Wang, Y., Ebi, H., Shimamura, T., et al., 2012. A murine lung cancer co-clinical trial identifies genetic modifiers of therapeutic response. Nature 483 (7391), 613–617.

Chen, B., Gilbert, L.A., Cimini, B.A., Schnitzbauer, J., Zhang, W., Li, G.-W., et al., 2013. Dynamic imaging of genomic loci in living human cells by an optimized CRISPR/Cas system. Cell 155 (7), 1479–1491.

Chen, C., Liu, Y., Rappaport, A.R., Kitzing, T., Schultz, N., Zhao, Z., et al., 2014. MLL3 is a haploinsufficient 7q tumor suppressor in acute myeloid leukemia. Cancer Cell 25 (5), 652–665.

Chen, F., Rosiene, J., Che, A., Becker, A., LoTurco, J., 2015a. Tracking and transforming neocortical progenitors by CRISPR/Cas9 gene targeting and piggyBac transposase lineage labeling. Development 142 (20), 3601–3611.

Chen, S., Sanjana, N.E., Zheng, K., Shalem, O., Lee, K., Shi, X., et al., 2015b. Genome-wide CRISPR screen in a mouse model of tumor growth and metastasis. Cell 160 (6), 1246–1260.

Chen, S., Lee, B., Lee, A.Y.-F., Modzelewski, A.J., He, L., 2016. Highly efficient mouse genome editing by CRISPR ribonucleoprotein electroporation of zygotes. J. Biol. Chem. 291 (28), 14457–14467.

Chiba, K., Johnson, J.Z., Vogan, J.M., Wagner, T., Boyle, J.M., Hockemeyer, D., 2015. Cancer-associated TERT promoter mutations abrogate telomerase silencing. eLife 4, e07918.

Cho, S.W., Kim, S., Kim, Y., Kweon, J., Kim, H.S., Bae, S., Kim, J.-S., 2014. Analysis of off-target effects of CRISPR/Cas-derived RNA-guided endonucleases and nickases. Genome Res. 24 (1), 132–141.

Choi, P.S., Meyerson, M., 2014. Targeted genomic rearrangements using CRISPR/Cas technology. Nat. Commun. 5, 3728.

Choulika, A., Perrin, A., Dujon, B., Nicolas, J.F., 1995. Induction of homologous recombination in mammalian chromosomes by using the I-SceI system of *Saccharomyces cerevisiae*. Mol. Cell. Biol. 15 (4), 1968–1973.

Christian, M., Cermak, T., Doyle, E.L., Schmidt, C., Zhang, F., Hummel, A., et al., 2010. Targeting DNA double-strand breaks with TAL effector nucleases. Genetics 186 (2), 757–761.

Chylinski, K., Le Rhun, A., Charpentier, E., 2013. The tracrRNA and Cas9 families of type II CRISPR-Cas immunity systems. RNA Biol. 10 (5), 726–737.

Cidre-Aranaz, F., Alonso, J., 2015. EWS/FLI1 target genes and therapeutic opportunities in ewing sarcoma. Front. Oncol. 5, 162.

Committee on Science, Technology, and Law; Policy and Global Affairs; National Academies of Sciences, Engineering, and Medicine; Olson, S., 2016. International Summit on Human Gene Editing: A Global Discussion. Available from: http://doi.org/10.17226/21913.

Cong, L., Ran, F.A., Cox, D., Lin, S., Barretto, R., Habib, N., et al., 2013. Multiplex genome engineering using CRISPR/Cas systems. Science 339 (6121), 819–823.

Coppoolse, E.R., de Vroomen, M.J., van Gennip, F., Hersmus, B.J.M., van Haaren, M.J.J., 2005. Size does matter: cre-mediated somatic deletion efficiency depends on the distance between the target loxsites. Plant Mol. Biol. 58 (5), 687–698.

Cui, X., Ji, D., Fisher, D.A., Wu, Y., Briner, D.M., Weinstein, E.J., 2011. Targeted integration in rat and mouse embryos with zinc-finger nucleases. Nat. Biotechnol. 29 (1), 64–67.

Dang, Y., Jia, G., Choi, J., Ma, H., Anaya, E., Ye, C., et al., 2015. Optimizing sgRNA structure to improve CRISPR-Cas9 knockout efficiency. Genome Biol. 16, 280.

Dean, D.A., Machado-Aranda, D., Blair-Parks, K., Yeldandi, A.V., Young, J.L., 2003. Electroporation as a method for high-level nonviral gene transfer to the lung. Gene Ther. 10 (18), 1608–1615.

Deng, W., Shi, X., Tjian, R., Lionnet, T., Singer, R.H., 2015. CASFISH: CRISPR/Cas9-mediated in situ labeling of genomic loci in fixed cells. Proc. Natl. Acad. Sci. USA 112 (38), 11870–11875.

Dominguez, A.A., Lim, W.A., Qi, L.S., 2016. Beyond editing: repurposing CRISPR-Cas9 for precision genome regulation and interrogation. Nat. Rev. Mol. Cell Biol. 17 (1), 5–15.

Doudna, J.A., Charpentier, E., 2014. Genome editing. The new frontier of genome engineering with CRISPR-Cas9. Science 346 (6213), 1258096.

Dow, L.E., Lowe, S.W., 2012. Life in the fast lane: mammalian disease models in the genomics era. Cell 148 (6), 1099–1109.

Dow, L.E., Fisher, J., O'Rourke, K.P., Muley, A., Kastenhuber, E.R., Livshits, G., et al., 2015. Inducible in vivo genome editing with CRISPR-Cas9. Nat. Biotechnol. 33 (4), 390–394.

Easton, D.F., Pooley, K.A., Dunning, A.M., Pharoah, P.D.P., Thompson, D., Ballinger, D.G., et al., 2007. Genome-wide association study identifies novel breast cancer susceptibility loci. Nature 447 (7148), 1087–1093.

Ebina, H., Misawa, N., Kanemura, Y., Koyanagi, Y., 2013. Harnessing the CRISPR/Cas9 system to disrupt latent HIV-1 provirus. Sci. Rep. 3, 2510.

Engelman, J.A., Chen, L., Tan, X., Crosby, K., Guimaraes, A.R., Upadhyay, R., et al., 2008. Effective use of PI3K and MEK inhibitors to treat mutant Kras G12D and PIK3CA H1047R murine lung cancers. Nat. Med. 14 (12), 1351–1356.

Falahi, F., Sgro, A., Blancafort, P., 2015. Epigenome engineering in cancer: fairytale or a realistic path to the clinic? Front. Oncol. 5, 22.

Frank, S., Skryabin, B.V., Greber, B., 2013. A modified TALEN-based system for robust generation of knock-out human pluripotent stem cell lines and disease models. BMC Genomics 14, 773.

Frese, K.K., Tuveson, D.A., 2007. Maximizing mouse cancer models. Nat. Rev. Cancer 7 (9), 645–658.

Fu, Y., Sander, J.D., Reyon, D., Cascio, V.M., Joung, J.K., 2014. Improving CRISPR-Cas nuclease specificity using truncated guide RNAs. Nat. Biotechnol. 32 (3), 279–284.

Futreal, P.A., Coin, L., Marshall, M., Down, T., Hubbard, T., Wooster, R., et al., 2004. A census of human cancer genes. Nat. Rev. Cancer 4 (3), 177–183.

Giard, D.J., Aaronson, S.A., Todaro, G.J., Arnstein, P., Kersey, J.H., Dosik, H., Parks, W.P., 1973. In vitro cultivation of human tumors: establishment of cell lines derived from a series of solid tumors. J. Natl. Cancer Inst. 51 (5), 1417–1423.

Girotti, M.R., Gremel, G., Lee, R., Galvani, E., Rothwell, D., Viros, A., et al., 2016. Application of sequencing, liquid biopsies, and patient-derived xenografts for personalized medicine in melanoma. Cancer Discov. 6 (3), 286–299.

Guerra, C., Mijimolle, N., Dhawahir, A., Dubus, P., Barradas, M., Serrano, M., et al., 2003. Tumor induction by an endogenous K-ras oncogene is highly dependent on cellular context. Cancer Cell 4 (2), 111–120.

Hanahan, D., Weinberg, R.A., 2000. The hallmarks of cancer. Cell 100 (1), 57–70.

Harbers, K., Jähner, D., Jaenisch, R., 1981. Microinjection of cloned retroviral genomes into mouse zygotes: integration and expression in the animal. Nature 293 (5833), 540–542.

Hashimoto, M., Takemoto, T., 2015. Electroporation enables the efficient mRNA delivery into the mouse zygotes and facilitates CRISPR/Cas9-based genome editing. Sci. Rep. 5, 11315.

Heckl, D., Kowalczyk, M.S., Yudovich, D., Belizaire, R., Puram, R.V., McConkey, M.E., et al., 2014. Generation of mouse models of myeloid malignancy with combinatorial genetic lesions using CRISPR-Cas9 genome editing. Nat. Biotechnol. 32 (9), 941–946.

Hidalgo, M., Amant, F., Biankin, A.V., Budinská, E., Byrne, A.T., Caldas, C., et al., 2014. Patient-derived xenograft models: an emerging platform for translational cancer research. Cancer Discov. 4 (9), 998–1013.

Hisamatsu, S., Sakaue, M., Takizawa, A., Kato, T., Kamoshita, M., Ito, J., Kashiwazaki, N., 2015. Knockout of targeted gene in porcine somatic cells using zinc-finger nuclease. Anim. Sci. J. 86 (2), 132–137.

Holkers, M., Maggio, I., Liu, J., Janssen, J.M., Miselli, F., Mussolino, C., et al., 2013. Differential integrity of TALE nuclease genes following adenoviral and lentiviral vector gene transfer into human cells. Nucleic Acids Res. 41 (5), e63.

Honma, M., Sakuraba, M., Koizumi, T., Takashima, Y., Sakamoto, H., Hayashi, M., 2007. Non-homologous end-joining for repairing I-SceI-induced DNA double strand breaks in human cells. DNA Repair 6 (6), 781–788.

Horii, T., Arai, Y., Yamazaki, M., Morita, S., Kimura, M., Itoh, M., et al., 2014. Validation of microinjection methods for generating knockout mice by CRISPR/Cas-mediated genome engineering. Sci. Rep. 4, 4513.

Hsu, P.D., Scott, D.A., Weinstein, J.A., Ran, F.A., Konermann, S., Agarwala, V., et al., 2013. DNA targeting specificity of RNA-guided Cas9 nucleases. Nat. Biotechnol. 31 (9), 827–832.

Hurlbut, J.B., 2015. Limits of responsibility: genome editing, Asilomar, and the politics of deliberation. Hastings Cent. Rep. 45 (5), 11–14.

Hutmacher, D.W., Horch, R.E., Loessner, D., Rizzi, S., Sieh, S., Reichert, J.C., et al., 2009. Translating tissue engineering technology platforms into cancer research. J. Cell. Mol. Med. 13 (8A), 1417–1427.

Iyer, V., Shen, B., Zhang, W., Hodgkins, A., Keane, T., Huang, X., Skarnes, W.C., 2015. Off-target mutations are rare in Cas9-modified mice. Nat. Methods 12 (6), 479.

Jackson, E.L., Willis, N., Mercer, K., Bronson, R.T., Crowley, D., Montoya, R., et al., 2001. Analysis of lung tumor initiation and progression using conditional expression of oncogenic K-ras. Genes Devel. 15 (24), 3243–3248.

Jackson, A.L., Bartz, S.R., Schelter, J., Kobayashi, S.V., Burchard, J., Mao, M., et al., 2003. Expression profiling reveals off-target gene regulation by RNAi. Nat. Biotechnol. 21 (6), 635–637.

Jasin, M., 1996. Genetic manipulation of genomes with rare-cutting endonucleases. Trends Genet. 12 (6), 224–228.

Jiang, J., Zhang, L., Zhou, X., Chen, X., Huang, G., Li, F., et al., 2016. Induction of site-specific chromosomal translocations in embryonic stem cells by CRISPR/Cas9. Sci. Rep. 6, 21918.

Jinek, M., Chylinski, K., Fonfara, I., Hauer, M., Doudna, J.A., Charpentier, E., 2012. A programmable dual-RNA-guided DNA endonuclease in adaptive bacterial immunity. Science 337 (6096), 816–821.

Kabadi, A.M., Ousterout, D.G., Hilton, I.B., Gersbach, C.A., 2014. Multiplex CRISPR/Cas9-based genome engineering from a single lentiviral vector. Nucleic Acids Res. 42 (19), e147.

Kasap, C., Elemento, O., Kapoor, T.M., 2014. DrugTargetSeqR: a genomics- and CRISPR-Cas9-based method to analyze drug targets. Nat. Chem. Biol. 10 (8), 626–628.

Kawauchi, D., Saito, T., 2008. Transcriptional cascade from Math1 to Mbh1 and Mbh2 is required for cerebellar granule cell differentiation. Dev. Biol. 322 (2), 345–354.

Kawauchi, D., Taniguchi, H., Watanabe, H., Saito, T., Murakami, F., 2006. Direct visualization of nucleogenesis by precerebellar neurons: involvement of ventricle-directed, radial fibre-associated migration. Development 133 (6), 1113–1123.

Keener, A.B., 2015. Delivering the goods: scientists seek a way to make CRISPR-Cas gene editing more targeted. Nat. Med. 21, 1239–1241.

Kim, H., Kim, J.S., 2014. A guide to genome engineering with programmable nucleases. Nat. Rev. Genet. 15, 321–334.

Kim, H.J., Lee, H.J., Kim, H., Cho, S.W., Kim, J.-S., 2009. Targeted genome editing in human cells with zinc finger nucleases constructed via modular assembly. Genome Res. 19 (7), 1279–1288.

Kim, S., Kim, D., Cho, S.W., Kim, J., Kim, J.-S., 2014. Highly efficient RNA-guided genome editing in human cells via delivery of purified Cas9 ribonucleoproteins. Genome Res. 24 (6), 1012–1019.

Kleinstreuer, N.C., Dix, D.J., Houck, K.A., Kavlock, R.J., Knudsen, T.B., Martin, M.T., et al., 2013. In vitro perturbations of targets in cancer hallmark processes predict rodent chemical carcinogenesis. Toxicol. Sci. 131 (1), 40–55.

Koike-Yusa, H., Li, Y., Tan, E.-P., Velasco-Herrera, M.D.C., Yusa, K., 2014. Genome-wide recessive genetic screening in mammalian cells with a lentiviral CRISPR-guide RNA library. Nat. Biotechnol. 32 (3), 267–273.

Konermann, S., Brigham, M.D., Trevino, A.E., Joung, J., Abudayyeh, O.O., Barcena, C., et al., 2015. Genome-scale transcriptional activation by an engineered CRISPR-Cas9 complex. Nature 517 (7536), 583–588.

Konishi, Y., Stegmüller, J., Matsuda, T., Bonni, S., Bonni, A., 2004. Cdh1-APC controls axonal growth and patterning in the mammalian brain. Science 303 (5660), 1026–1030.

Kouranova, E., Forbes, K., Zhao, G., Warren, J., Bartels, A., Wu, Y., Cui, X., 2016. CRISPRs for optimal targeting: delivery of CRISPR components as DNA, RNA, and protein into cultured cells and single-cell embryos. Hum. Gene Ther. 27 (6), 464–475.

Krogan, N.J., Lippman, S., Agard, D.A., Ashworth, A., Ideker, T., 2015. The cancer cell map initiative: defining the hallmark networks of cancer. Mol. Cell 58 (4), 690–698.

Kumar, M., Keller, B., Makalou, N., Sutton, R.E., 2001. Systematic determination of the packaging limit of lentiviral vectors. Hum. Gene Ther. 12 (15), 1893–1905.

Kuscu, C., Arslan, S., Singh, R., Thorpe, J., Adli, M., 2014. Genome-wide analysis reveals characteristics of off-target sites bound by the Cas9 endonuclease. Nat. Biotechnol. 32 (7), 677–683.

Lawrence, M.S., Stojanov, P., Polak, P., Kryukov, G.V., Cibulskis, K., Sivachenko, A., et al., 2013. Mutational heterogeneity in cancer and the search for new cancer-associated genes. Nature 499 (7457), 214–218.

Li, T., Huang, S., Jiang, W.Z., Wright, D., Spalding, M.H., Weeks, D.P., Yang, B., 2011. TAL nucleases (TALNs): hybrid proteins composed of TAL effectors and FokI DNA-cleavage domain. Nucleic Acids Res. 39 (1), 359–372.

Liang, X., Potter, J., Kumar, S., Zou, Y., Quintanilla, R., Sridharan, M., et al., 2015. Rapid and highly efficient mammalian cell engineering via Cas9 protein transfection. J. Biotechnol. 208, 44–53.

Lin, S., Staahl, B.T., Alla, R.K., Doudna, J.A., 2014. Enhanced homology-directed human genome engineering by controlled timing of CRISPR/Cas9 delivery. eLife 3, e04766.

Liu, F., Huang, L., 2002. Electric gene transfer to the liver following systemic administration of plasmid DNA. Gene Ther. 9 (16), 1116–1119.

Liu, F., Song, Y., Liu, D., 1999. Hydrodynamics-based transfection in animals by systemic administration of plasmid DNA. Gene Ther. 6 (7), 1258–1266.

Liu, P.-Q., Tan, S., Mendel, M.C., Murrills, R.J., Bhat, B.M., Schlag, B., et al., 2005. Isogenic human cell lines for drug discovery: regulation of target gene expression by engineered zinc-finger protein transcription factors. J. Biomol. Screen. 10 (4), 304–313.

Liu, Z., Cheng, T.T.K., Shi, Z., Liu, Z., Lei, Y., Wang, C., et al., 2016. Efficient genome editing of genes involved in neural crest development using the CRISPR/Cas9 system in Xenopus embryos. Cell Biosci. 6, 22.

Maddalo, D., Manchado, E., Concepcion, C.P., Bonetti, C., Vidigal, J.A., Han, Y.-C., et al., 2014. In vivo engineering of oncogenic chromosomal rearrangements with the CRISPR/Cas9 system. Nature 516 (7531), 423–427.

Maeder, M.L., Linder, S.J., Cascio, V.M., Fu, Y., Ho, Q.H., Joung, J.K., 2013. CRISPR RNA-guided activation of endogenous human genes. Nat. Methods 10 (10), 977–979.

Malina, A., Mills, J.R., Cencic, R., Yan, Y., Fraser, J., Schippers, L.M., et al., 2013. Repurposing CRISPR/Cas9 for in situ functional assays. Genes Dev. 27 (23), 2602–2614.

Maresch, R., Mueller, S., Veltkamp, C., Öllinger, R., Friedrich, M., Heid, I., et al., 2016. Multiplexed pancreatic genome engineering and cancer induction by transfection-based CRISPR/Cas9 delivery in mice. Nat. Commun. 7, 10770.

Marraffini, L.A., Sontheimer, E.J., 2010. Self versus non-self discrimination during CRISPR RNA-directed immunity. Nature 463 (7280), 568–571.

Mashiko, D., Fujihara, Y., Satouh, Y., Miyata, H., Isotani, A., Ikawa, M., 2013. Generation of mutant mice by pronuclear injection of circular plasmid expressing Cas9 and single guided RNA. Sci. Rep. 3, 3355.

Matano, M., Date, S., Shimokawa, M., Takano, A., Fujii, M., Ohta, Y., et al., 2015. Modeling colorectal cancer using CRISPR-Cas9-mediated engineering of human intestinal organoids. Nat. Med. 21 (3), 256–262.

Matsuda, T., Cepko, C.L., 2004. Electroporation and RNA interference in the rodent retina in vivo and in vitro. Proc. Natl. Acad. Sci. USA 101 (1), 16–22.

Michelfelder, S., Trepel, M., 2009. Adeno-associated viral vectors and their redirection to cell-type specific receptors. Adv. Genet. 67, 29–60.

Nelson, C.E., Gersbach, C.A., 2016. Engineering delivery vehicles for genome editing. Annu. Rev. Chem. Biomol. Eng. 7, 637–662.

Niu, Y., Shen, B., Cui, Y., Chen, Y., Wang, J., Wang, L., et al., 2014. Generation of gene-modified cynomolgus monkey via Cas9/RNA-mediated gene targeting in one-cell embryos. Cell 156 (4), 836–843.

Ochiai, H., Fujita, K., Suzuki, K.-I., Nishikawa, M., Shibata, T., Sakamoto, N., Yamamoto, T., 2010. Targeted mutagenesis in the sea urchin embryo using zinc-finger nucleases. Genes Cells 15 (8), 875–885.

O'Connell, M.R., Oakes, B.L., Sternberg, S.H., East-Seletsky, A., Kaplan, M., Doudna, J.A., 2014. Programmable RNA recognition and cleavage by CRISPR/Cas9. Nature 516 (7530), 263–266.

Orban, P.C., Chui, D., Marth, J.D., 1992. Tissue- and site-specific DNA recombination in transgenic mice. Proc. Natl. Acad. Sci. USA 89 (15), 6861–6865.

Panda, D., Sharma, A., Shukla, N.K., Jaiswal, R., Dwivedi, S., Raina, V., et al., 2013. Gall bladder cancer and the role of dietary and lifestyle factors: a case-control study in a North Indian population. Eur. J. Cancer Prev. 22 (5), 431–437.

Parr-Brownlie, L.C., Bosch-Bouju, C., Schoderboeck, L., Sizemore, R.J., Abraham, W.C., Hughes, S.M., 2015. Lentiviral vectors as tools to understand central nervous system biology in mammalian model organisms. Front. Mol. Neurosci. 8, 14.

Parsa, N., 2012. Environmental factors inducing human cancers. Iran. J. Public Health 41 (11), 1–9.

Pattanayak, V., Lin, S., Guilinger, J.P., Ma, E., Doudna, J.A., Liu, D.R., 2013. High-throughput profiling of off-target DNA cleavage reveals RNA-programmed Cas9 nuclease specificity. Nat. Biotechnol. 31 (9), 839–843.

Platt, R.J., Chen, S., Zhou, Y., Yim, M.J., Swiech, L., Kempton, H.R., et al., 2014. CRISPR-Cas9 knockin mice for genome editing and cancer modeling. Cell 159 (2), 440–455.

Ran, F.A., Hsu, P.D., Lin, C.-Y., Gootenberg, J.S., Konermann, S., Trevino, A.E., et al., 2013. Double nicking by RNA-guided CRISPR Cas9 for enhanced genome editing specificity. Cell 154 (6), 1380–1389.

Ren, X., Yang, Z., Xu, J., Sun, J., Mao, D., Hu, Y., et al., 2014. Enhanced specificity and efficiency of the CRISPR/Cas9 system with optimized sgRNA parameters in *Drosophila*. Cell Rep. 9 (3), 1151–1162.

Richter, A., Streubel, J., Boch, J., 2016. TAL effector DNA-binding principles and specificity. Methods Mol. Biol. 1338, 9–25.

Rivina, L., Davoren, M., Schiestl, R.H., 2014. Radiation-induced myeloid leukemia in murine models. Hum. Genomics 8, 13.

Rouet, P., Smih, F., Jasin, M., 1994. Introduction of double-strand breaks into the genome of mouse cells by expression of a rare-cutting endonuclease. Mol. Cell. Biol. 14 (12), 8096–8106.

Saba, R., Nakatsuji, N., Saito, T., 2003. Mammalian BarH1 confers commissural neuron identity on dorsal cells in the spinal cord. J. Neurosci. 23 (6), 1987–1991.

Sabatello, M., Appelbaum, P.S., 2016. Raising genomic citizens: adolescents and the return of secondary genomic findings. J. Law Med. Ethics 44 (2), 292–308.

Sala, E., Mologni, L., Truffa, S., Gaetano, C., Bollag, G.E., Gambacorti-Passerini, C., 2008. BRAF silencing by short hairpin RNA or chemical blockade by PLX4032 leads to different responses in melanoma and thyroid carcinoma cells. Mol. Cancer Res. 6 (5), 751–759.

Sánchez-Rivera, F.J., Jacks, T., 2015. Applications of the CRISPR-Cas9 system in cancer biology. Nat. Rev. Cancer 15 (7), 387–395.

Sánchez-Rivera, F.J., Papagiannakopoulos, T., Romero, R., Tammela, T., Bauer, M.R., Bhutkar, A., et al., 2014. Rapid modelling of cooperating genetic events in cancer through somatic genome editing. Nature 516 (7531), 428–431.

Sanjana, N.E., Shalem, O., Zhang, F., 2014. Improved vectors and genome-wide libraries for CRISPR screening. Nat. Methods 11 (8), 783–784.

Sashital, D.G., Wiedenheft, B., Doudna, J.A., 2012. Mechanism of foreign DNA selection in a bacterial adaptive immune system. Mol. Cell 46 (5), 606–615.

Sato, T., Stange, D.E., Ferrante, M., Vries, R.G.J., Van Es, J.H., Van den Brink, S., et al., 2011. Long-term expansion of epithelial organoids from human colon, adenoma, adenocarcinoma, and Barrett's epithelium. Gastroenterology 141 (5), 1762–1772.

Sato, M., Koriyama, M., Watanabe, S., Ohtsuka, M., Sakurai, T., Inada, E., et al., 2015. Direct injection of CRISPR/Cas9-related mRNA into cytoplasm of parthenogenetically activated porcine oocytes causes frequent mosaicism for indel mutations. Int. J. Mol. Sci. 16 (8), 17838–17856.

Schildkraut, E., Miller, C.A., Nickoloff, J.A., 2005. Gene conversion and deletion frequencies during double-strand break repair in human cells are controlled by the distance between direct repeats. Nucleic Acids Res. 33 (5), 1574–1580.

Shalem, O., Sanjana, N.E., Hartenian, E., Shi, X., Scott, D.A., Mikkelsen, T.S., et al., 2014. Genome-scale CRISPR-Cas9 knockout screening in human cells. Science 343 (6166), 84–87.

Shaw, A.T., Kim, D.-W., Nakagawa, K., Seto, T., Crinó, L., Ahn, M.-J., et al., 2013. Crizotinib versus chemotherapy in advanced ALK-positive lung cancer. N. Engl. J. Med. 368 (25), 2385–2394.

Shi, J., Wang, E., Milazzo, J.P., Wang, Z., Kinney, J.B., Vakoc, C.R., 2015. Discovery of cancer drug targets by CRISPR-Cas9 screening of protein domains. Nat. Biotechnol. 33 (6), 661–667.

Shibata, H., Toyama, K., Shioya, H., Ito, M., Hirota, M., Hasegawa, S., et al., 1997. Rapid colorectal adenoma formation initiated by conditional targeting of the Apc gene. Science 278 (5335), 120–123.

Shimogori, T., Ogawa, M., 2008. Gene application with in utero electroporation in mouse embryonic brain. Dev. Growth Diff. 50 (6), 499–506.

Siolas, D., Hannon, G.J., 2013. Patient-derived tumor xenografts: transforming clinical samples into mouse models. Cancer Res. 73 (17), 5315–5319.

Smith, R.H., 2008. Adeno-associated virus integration: virus versus vector. Gene Ther. 15 (11), 817–822.

Smith, H.W., Muller, W.J., 2013. Transgenic mouse models—a seminal breakthrough in oncogene research. Cold Spring Harb. Protoc. 2013 (12), 1099–1108.

Smith, A.J., De Sousa, M.A., Kwabi-Addo, B., Heppell-Parton, A., Impey, H., Rabbitts, P., 1995. A site-directed chromosomal translocation induced in embryonic stem cells by Cre-loxP recombination. Nat. Genet. 9 (4), 376–385.

Smithies, O., Gregg, R.G., Boggs, S.S., Koralewski, M.A., Kucherlapati, R.S., 1985. Insertion of DNA sequences into the human chromosomal beta-globin locus by homologous recombination. Nature 317 (6034), 230–234.

Soda, M., Choi, Y.L., Enomoto, M., Takada, S., Yamashita, Y., Ishikawa, S., et al., 2007. Identification of the transforming EML4-ALK fusion gene in non-small-cell lung cancer. Nature 448 (7153), 561–566.

Stewart, T.A., Pattengale, P.K., Leder, P., 1984. Spontaneous mammary adenocarcinomas in transgenic mice that carry and express MTV/myc fusion genes. Cell 38 (3), 627–637.

Stratton, M.R., Campbell, P.J., Futreal, P.A., 2009. The cancer genome. Nature 458 (7239), 719–724.

Swartling, F.J., Savov, V., Persson, A.I., Chen, J., Hackett, C.S., Northcott, P.A., et al., 2012. Distinct neural stem cell populations give rise to disparate brain tumors in response to N-MYC. Cancer Cell 21 (5), 601–613.

Swiech, L., Heidenreich, M., Banerjee, A., Habib, N., Li, Y., Trombetta, J., et al., 2015. In vivo interrogation of gene function in the mammalian brain using CRISPR-Cas9. Nat. Biotechnol. 33 (1), 102–106.

Tavernarakis, N., Wang, S.L., Dorovkov, M., Ryazanov, A., Driscoll, M., 2000. Heritable and inducible genetic interference by double-stranded RNA encoded by transgenes. Nat. Genet. 24 (2), 180–183.

Thakore, P.I., Black, J.B., Hilton, I.B., Gersbach, C.A., 2016. Editing the epigenome: technologies for programmable transcription and epigenetic modulation. Nat. Methods 13 (2), 127–137.

Thakur, Das, M., Pryer, N.K., Singh, M., 2014. Mouse tumour models to guide drug development and identify resistance mechanisms. J. Pathol. 232 (2), 103–111.

Thomas, K.R., Capecchi, M.R., 1986. Introduction of homologous DNA sequences into mammalian cells induces mutations in the cognate gene. Nature 324 (6092), 34–38.

Thomas, K.R., Folger, K.R., Capecchi, M.R., 1986. High frequency targeting of genes to specific sites in the mammalian genome. Cell 44 (3), 419–428.

Torrance, C.J., Agrawal, V., Vogelstein, B., Kinzler, K.W., 2001. Use of isogenic human cancer cells for high-throughput screening and drug discovery. Nat. Biotechnol. 19 (10), 940–945.

Torres, R., Martin, M.C., Garcia, A., Cigudosa, J.C., Ramirez, J.C., Rodriguez-Perales, S., 2014. Engineering human tumour-associated chromosomal translocations with the RNA-guided CRISPR-Cas9 system. Nat. Commun. 5, 3964.

Torres-Ruiz, R., Rodriguez Perales, S., 2015. CRISPR-Cas9: a revolutionary tool for cancer modelling. Int. J. Mol. Sci. 16 (9), 22151–22168.

Valletta, S., Dolatshad, H., Bartenstein, M., Yip, B.H., Bello, E., Gordon, S., et al., 2015. ASXL1 mutation correction by CRISPR/Cas9 restores gene function in leukemia cells and increases survival in mouse xenografts. Oncotarget 6 (42), 44061–44071.

Van Dyke, T., Jacks, T., 2002. Cancer modeling in the modern era: progress and challenges. Cell 108 (2), 135–144.

Vogelstein, B., Papadopoulos, N., Velculescu, V.E., Zhou, S., Diaz, L.A., Kinzler, K.W., 2013. Cancer genome landscapes. Science 339 (6127), 1546–1558.

Voigt, K., Izsvák, Z., Ivics, Z., 2008. Targeted gene insertion for molecular medicine. J. Mol. Med. 86 (11), 1205–1219.

Wagner, E.F., Stewart, T.A., Mintz, B., 1981. The human beta-globin gene and a functional viral thymidine kinase gene in developing mice. Proc. Natl. Acad. Sci. USA 78 (8), 5016–5020.

Wang, H., Yang, H., Shivalila, C.S., Dawlaty, M.M., Cheng, A.W., Zhang, F., Jaenisch, R., 2013. One-step generation of mice carrying mutations in multiple genes by CRISPR/Cas-mediated genome engineering. Cell 153 (4), 910–918.

Wang, T., Wei, J.J., Sabatini, D.M., Lander, E.S., 2014. Genetic screens in human cells using the CRISPR-Cas9 system. Science 343 (6166), 80–84.

Weber, J., Öllinger, R., Friedrich, M., Ehmer, U., Barenboim, M., Steiger, K., et al., 2015. CRISPR/Cas9 somatic multiplex-mutagenesis for high-throughput functional cancer genomics in mice. Proc. Natl. Acad. Sci. USA 112 (45), 13982–13987.

Wen, W.-S., Yuan, Z.-M., Ma, S.-J., Xu, J., Yuan, D.-T., 2016. CRISPR-Cas9 systems: versatile cancer modelling platforms and promising therapeutic strategies. Int. J. Cancer 138 (6), 1328–1336.

Wood, A.J., Lo, T.-W., Zeitler, B., Pickle, C.S., Ralston, E.J., Lee, A.H., et al., 2011. Targeted genome editing across species using ZFNs and TALENs. Science 333 (6040), 307.

Wu, Z., Yang, H., Colosi, P., 2010. Effect of genome size on AAV vector packaging. Mol. Ther. 18 (1), 80–86.

Wu, X., Scott, D.A., Kriz, A.J., Chiu, A.C., Hsu, P.D., Dadon, D.B., et al., 2014. Genome-wide binding of the CRISPR endonuclease Cas9 in mammalian cells. Nat. Biotechnol. 32 (7), 670–676.

Xue, W., Chen, S., Yin, H., Tammela, T., Papagiannakopoulos, T., Joshi, N.S., et al., 2014. CRISPR-mediated direct mutation of cancer genes in the mouse liver. Nature 514 (7522), 380–384.

Yang, Hui, Wang, H., Shivalila, C.S., Cheng, A.W., Shi, L., Jaenisch, R., 2013. One-step generation of mice carrying reporter and conditional alleles by CRISPR/Cas-mediated genome engineering. Cell 154 (6), 1370–1379.

Yin, H., Song, C.-Q., Dorkin, J.R., Zhu, L.J., Li, Y., Wu, Q., et al., 2016. Therapeutic genome editing by combined viral and non-viral delivery of CRISPR system components in vivo. Nat. Biotechnol. 34 (3), 328–333.

Zalatan, J.G., Lee, M.E., Almeida, R., Gilbert, L.A., Whitehead, E.H., La Russa, M., et al., 2015. Engineering complex synthetic transcriptional programs with CRISPR RNA scaffolds. Cell 160 (1–2), 339–350.

Zhao, Z., Condomines, M., van der Stegen, S.J.C., Perna, F., Kloss, C.C., Gunset, G., et al., 2015. Structural design of engineered costimulation determines tumor rejection kinetics and persistence of CAR T cells. Cancer Cell 28 (4), 415–428.

Zhou, Y., Zhu, S., Cai, C., Yuan, P., Li, C., Huang, Y., Wei, W., 2014. High-throughput screening of a CRISPR/Cas9 library for functional genomics in human cells. Nature 509, 487–491.

Zuckermann, M., Hovestadt, V., Knobbe-Thomsen, C.B., Zapatka, M., Northcott, P.A., Schramm, K., et al., 2015. Somatic CRISPR/Cas9-mediated tumour suppressor disruption enables versatile brain tumour modelling. Nat. Commun. 6, 7391.

Zuris, J.A., Thompson, D.B., Shu, Y., Guilinger, J.P., Bessen, J.L., Hu, J.H., et al., 2015. Cationic lipid-mediated delivery of proteins enables efficient protein-based genome editing in vitro and in vivo. Nat. Biotechnol. 33 (1), 73–80.

Modeling Breast Cancer in Animals—Considerations for Prevention and Treatment Studies

JoEllen Welsh

Cancer Research Center, University at Albany, Albany, NY, United States

1 INTRODUCTION TO ANIMAL MODELS OF BREAST CANCER

In vivo models have long been an integral component of cancer research, with a long history of use in identifying carcinogens, testing preventive agents, and screening therapeutics. This chapter specifically focuses on animal models of breast cancer with a major emphasis on rodent models. Although neither mice nor rats spontaneously develop cancer at high frequency, numerous mutations (naturally occurring, chemically induced and/or genetically engineered) increase cancer incidence in specific strains (Anisimov et al., 2005; Cheon and Orsulic, 2011). Furthermore, immunodeficient rodents can serve as hosts for human cancer cells as xenografts, a model widely used for testing tumorigenicity and evaluating new therapeutics (Clarke, 1996; Mollard et al., 2011). Additional models include virally transmitted cancers, UV or ionizing radiation induced tumors, and cancers promoted by chronic hormone treatments. Each model has advantages and disadvantages, and the specific choice will depend on the type of breast cancer being studied, as well as the specific questions being addressed by the research. Most of the models discussed have been well characterized and are widely available. In the case of heterogeneous cancers like breast, certain models more closely mimic specific subtypes or stages of the human disease. To provide a basis for understanding these diverse models, the biology and heterogeneity of human breast cancer are briefly reviewed prior to discussion of the specific experimental approaches.

2 CONCEPTS OF BREAST CANCER BIOLOGY

2.1 Incidence and Risk Factors

According to the American Cancer Society's most recent statistics (American Cancer Society, 2015), breast cancer is the most commonly diagnosed malignancy in US women, with over 230,000 cases in 2015. The majority of women are diagnosed with invasive cancers and are at high risk for development of deadly metastases. Like many of the solid tumors common in populations living in industrialized countries, the incidence and mortality of breast cancer increases with age. In fact, 80% of diagnoses and almost 90% of deaths from breast cancer are in women over the age of 50. Between 1990 and 2007, the mortality rate from breast cancer has slowly declined (approximately 2.2% per year), an effect deemed to be due to strategies aimed at prevention and treatment, as well as to earlier diagnosis due to widespread screening. Despite these improvements, breast cancer kills over 40,000 women yearly in the United States. Thus, it is clear that additional strategies for treatment and prevention of breast cancer are needed, and research progress in both of these directions often rely on animal models of breast cancer.

Risk factors and etiologic agents associated with breast cancer include those related to reproductive history (age at menarche, age at menopause, nulliparity, parity after age 30, hormone replacement therapy), family history, genetics, and radiation exposure. Tumor suppressor genes associated with breast cancer include the breast cancer susceptibility genes BRCA1 and BRCA2, p53, and ATM; however, it is estimated that only about 10% of breast cancer can be attributed to loss of function mutations in these genes. The vast majority of breast cancer cases are sporadic in nature, although as described later in the chapter several characteristic molecular changes have been linked with disease pathology and prognosis.

2.2 Subtypes and Prognosis

The term "breast cancer" collectively refers to many types of neoplastic diseases that arise in the mammary gland. Although the gland is composed of multiple cell types (epithelial cells, stromal fibroblasts, adipocytes, immune cells), the clinically relevant breast cancers typically derive from the epithelial cells and are thus termed carcinomas. The breast epithelium is a bilayer composed of luminal cells and basal (myoepithelial) cells arranged in ducts and lobules, and cancers can arise from both cell types in either location (Bombonati and Sgroi, 2011). Ductal carcinoma is the most commonly diagnosed type of human breast cancer (accounting for approximately 85% of all breast cancers). In general, the disease continuum begins with ductal hyperplasia and progresses to ductal carcinoma in situ (DCIS, a noninvasive lesion), which gives rise to invasive carcinoma if not removed (Vargo-Gogola and Rosen, 2007). A detailed evaluation of DCIS incidence and risk factors in the United States was recently compiled by the American Cancer Society (American Cancer Society, 2015). Development of invasive cancer from precursor lesions is driven by genetic and epigenetic changes within the epithelial cells and alterations in the complex communications between the epithelial cells and their microenvironment. The resulting carcinomas are highly heterogeneous, and distinct subtypes have been identified based on histopathology, putative cell of origin, genomic profiling, and clinical outcomes. Estrogen receptor-alpha-positive (ER+) and progesterone receptor-positive (PR+) breast cancers account for 60%–70% of the breast cancer cases diagnosed in humans (Anderson et al., 2002). While less common, tumors lacking ER or PR, and those with high expression of the growth factor receptor HER2, are generally more aggressive. As discussed in this chapter, distinct approaches are available to model the various histopathological subtypes of breast cancer in laboratory animals.

Despite continued research, breast cancer is associated with a 20% mortality rate within the first 5 years after diagnosis. The severity of the disease reflects many factors including metastatic potential, hormone independence, drug resistance, and histological heterogeneity. Sites of breast cancer metastasis include regional lymph nodes, lung, liver, brain, and bone. Median survival of patients with metastases is 2–3 years. Development of bone metastases is particularly common (~80% of patients with metastases have skeletal involvement) and is currently incurable. Mechanistic aspects of breast cancer cells homing to bone to induce osteolytic lesions are poorly understood. Animal models that mimic the unique sites of metastases of human breast cancer would be extremely valuable, but currently such models are limited.

Treatment of breast cancer is based on histopathological features (grade, stage, and hormone/growth factor receptor status) of newly diagnosed tumors. Early stage lesions (DCIS) are routinely treated by surgical removal (lumpectomy or mastectomy) followed by radiation therapy and in some cases antiestrogen therapies. For invasive breast cancers, surgery is followed by adjuvant systemic therapy depending on the specific stage and molecular aspects of the primary tumor. Patients with ER+ and/or PR+ tumors will receive hormone therapy; those whose tumors overexpress the growth factor receptor HER2 will receive the targeted therapy trastuzumab, usually in combination with chemotherapy. Patients whose tumors lack hormone and growth factor receptors (so called triple negative or basal-like tumors) will be treated with systemic chemotherapeutic regimens. Newly identified molecular features and the presence of distinct oncogenic pathways are continuously emerging as significant therapeutic targets as well.

Complications arising from current therapies for breast cancer include development of drug resistance, as well as side effects, such as thinking and memory problems (chemobrain), cardiac toxicity, and osteoporosis (with estrogen deprivation therapies). Animal models are increasingly being used to test strategies for prevention of drug resistance and therapeutic side effects.

2.3 Molecular Heterogeneity

Intensive genomic profiling of tumors, and resulting publically available datasets, such as The Cancer Genome Atlas (TCGA), has highlighted the heterogeneity of human breast cancer and facilitated the identification of molecular subtypes (Kreike et al., 2007; Perou et al., 2000; Sorlie et al., 2001; Strehl et al., 2011; Weigelt et al., 2008). Several major subtypes with characteristic gene expression profiles have been identified, which represent about 80% of all breast cancers. Invasive

ductal carcinomas were originally characterized into five major molecular subtypes: luminal A, luminal B, basal/triple negative, HER2 positive, and normal breast-like (Perou et al., 2000). Each subtype exhibits distinct profiles of hormone and growth factor receptors (ER, PR, HER2), cytokeratins, and proliferation markers. Most importantly, each tumor subtype has a characteristic prognostic outcome, with luminal A tumors (which are ER+, PR+, and HER2- and usually express functional p53) typically having much better prognosis than the other types. Luminal B tumors tend to be ER+, PR+, and HER2+ and are usually larger and of higher grade with more frequent p53 mutations than luminal A tumors. HER2 tumors highly express the HER2 growth factor receptor (usually due to genomic amplification), are negative for ER and PR and usually of high tumor grade. Basal/triple negative tumors are predominantly ER- PR- and HER2- but often express HER1 and/or cytokeratin 5/6 proteins and p53 mutations. Most breast cancers that develop in women with loss of function mutations in BRCA1 or BRCA2 are basal/triple negative. Molecular profiling (Lehmann et al., 2011) has confirmed heterogeneity of the basal/triple negative tumors leading to the identification of six subtypes with unique gene expression profiles and ontologies (2 basal-like, 1 mesenchymal, 1 mesenchymal stem-like, 1 immunomodulatory, and 1 luminal androgen receptor subtype). Other less common molecular subtypes have been described including normal breast-like, claudin-low type, and apocrine molecular type. As detailed further in the chapter, recent studies have focused on comparative genomic profiling of human and mouse breast tumors to ascertain whether similarities exist with respect to expression of these well-characterized human breast cancer subtype biomarkers. When possible, it is important to choose an animal model of breast cancer that best mimics the specific subtype of human breast cancer being addressed by the research.

2.4 Breast Cancer Cells of Origin

It has been suggested that the molecular heterogeneity of breast tumors might reflect distinct cells of origin (Lindeman and Visvader, 2010). Thus, the initial target for transformation could be a mammary stem cell, a committed progenitor cell, or a mature breast epithelial cell, all of which would give rise to tumors with distinct features. Another emerging related issue is the recognition that human breast cancers contain "cancer stem cells" or "tumor initiating cells" that drive tumor initiation and/or progression. Advances in techniques to identify and isolate mammary stem cells support the concept that stem cell populations exist in human breast tumors and that analogous populations can be identified in certain murine tumors and human xenografts.

3 MODELING BREAST CANCER IN RODENTS

3.1 General Approaches

Given the reality of species differences and the known diversity of human breast cancer, major challenges exist in modeling breast cancer in animals. No single model is capable of mimicking the heterogeneity characteristic of human breast carcinoma or the natural progression of the disease (particularly the metastatic process). However, molecular comparison of human breast cancers and experimental murine tumors has demonstrated that certain models are highly useful for studying specific disease subtypes. Unfortunately, models are severely limited for some of the rarer types of breast cancers (whose origin and molecular features are often poorly understood). An example is inflammatory breast cancer, which arises more often in younger women, is highly aggressive, and frequently misdiagnosed. Available models of inflammatory breast cancer are limited to a few cell lines that can be grown in immune compromised mice but fail to recapitulate the unique biology of the disease.

Because of these and other limitations, multiple in vivo breast cancer models have been developed and standardized, primarily in mice. Ideally multiple approaches should be used in a complementary fashion to fully address research questions. In addition to the study of carcinogenesis in intact animals (i.e., spontaneous, induced, or transgenic tumor models on wild-type or various knockout backgrounds), the murine mammary gland is amenable to organ culture and transplantation techniques, which have greatly facilitated our understanding of normal glandular development, mammary stem cells, and epithelial–stromal interactions. Although the anatomy and histology of the murine gland is quite distinct from that of the human gland, the epithelial structures, developmental processes, and hormonal controls are similar. The following sections will highlight the most commonly used models in terms of advantages and disadvantages for research purposes with an emphasis on comparative aspects of human versus rodent systems.

3.2 Issues to Consider When Choosing an Animal Model

There are a few key considerations that impact the choice of animal model for breast cancer studies. These include (but are not limited to) the genetic background of the mouse strain, whether an intact immune system is important, whether the research question is focused on treatment or prevention, and whether modeling of metastasis is desired. Inbred mouse strains vary widely in their sensitivity to tumorigenesis, and in some cases this is tissue-specific. In general, mice on the BALB/c, FVB,

and C3H backgrounds are highly susceptible to mammary tumorigenesis whereas those on the C57BL background are quite resistant (Medina, 2010). This has become problematic for many researchers since the C57BL background is frequently used for the generation of knockout mice. Testing carcinogen sensitivity or crossing of knockout mice on the C57Bl background with transgenic models of mammary cancer often requires initial backcrossing to the appropriate background, a laborious and costly process. Another consideration which is particularly important with xenograft studies is whether genetic defects in the immune system of host mice will adversely impact the results or their interpretation (more details on specific immunodeficient mouse strains are provided in Section 5.4). When studying breast cancer prevention, approaches are needed that focus on normal tissue or early stages of disease, whereas new therapeutic approaches are more appropriately evaluated in established tumors and/or models of metastatic disease.

4 SPONTANEOUS AND INDUCED MAMMARY TUMORIGENESIS IN RODENTS

4.1 Spontaneous Mammary Tumors

Most laboratory rodent strains spontaneously develop mammary tumors as they age, but the incidence and tumor pathology varies. In a pathological survey of spontaneous mammary tumors in various mouse strains, papillary adenocarcinomas, glandular adenocarcinomas, microacinar adenocarcinomas, type P tumors, adenomyoepitheliomas, and adenosquamous carcinomas were identified (Mikaelian et al., 2004). The papillary carcinomas that developed in BALB/cJ mice were found to be highly similar to the most common subtype of human breast cancer as they were exclusively composed of cells with a luminal phenotype. Other similarities between spontaneous mammary cancers in mice and human breast cancer are the age dependence, gender differences, hormonal influences, and circadian patterns (Anisimov et al., 2005). However, important species differences include the overall tumor spectrum, the number of genetic events thought to be required for tumor formation, the common occurrence of spontaneous regression in mouse tumors but not human tumors, and differences in dietary responses and metabolism.

4.2 Virally Induced Mammary Tumors

It has long been known that some strains of mice (C3H, GR) with high rates of spontaneous mammary tumors harbor a dominantly expressed, genetically transmitted proviral genome that encodes a highly infectious virus, the mouse mammary tumor virus or MMTV (Callahan

and Smith, 2000). Different strains of MMTV have been isolated from various mouse lines, and these vary in their infectious potency and ability to induce mammary tumors (Dudley et al., 2016). In addition to germline transmission, MMTV is shed in milk of infected females and can be transmitted to pups during lactation. Further details on the life cycle of exogenous MMTV in various murine strains, including the role of the gut microflora in viral transmission, are provided in a recent review (Dudley et al., 2016).

MMTV induces mammary tumors with relatively long latency (6–12 months). Like the majority of human breast cancers, MMTV-induced tumors are dependent on ovarian hormonal cycles. Parous females of strains carrying MMTV in their germline develop mammary tumors that arise from preneoplastic hyperplastic alveolar nodules. The incidence of tumors increases with additional pregnancy/lactation cycles. Analysis of MMTV tumors has demonstrated that they are clonal in nature and result from multiple mutations events. Mechanistically, MMTV is a retrovirus that induces tumors through insertional mutagenesis, a process whereby viral sequences integrate into the host genome and deregulate the expression of critical growth control genes. Initial analysis of viral integration sites in MMTV tumors established that the virus commonly integrates near genes involved in Wnt signaling, mechanistically linking this pathway to mammary tumorigenesis. More recently, high-throughput analysis of MMTV integration sites has been used to identify and validate additional novel mammary oncogenes including those involved in Fgf and map kinase signaling, as well as several unknown genes (Kim et al., 2011; Theodorou et al., 2007). Since it is likely that mutations induced by MMTV and genes identified at integration sites participate in signaling pathways that are relevant to human oncogenesis, the MMTV tumor model has reemerged as an important approach for identification of additional genes that contribute to breast cancer etiology and pathogenesis. In addition, recent studies have identified mammary tumor virus-like particles in samples of human milk and breast cancer suggesting the intriguing possibility that a human mammary tumor virus (HMTV) might be linked to a subset of human breast cancers (Cedro-Tanda et al., 2014; Nartey et al., 2014). If confirmed, the MMTV mouse model will become even more relevant as a research tool.

4.3 Identification of Mammary Carcinogens in Rodents

In addition to tumors that arise spontaneously or in association with MMTV infection, mammary carcinomas can be induced in rodents by various agents including chemical carcinogens, hormonal agents, and ionizing radiation. By far the most commonly used research models employ rats and mice exposed to chemical carcinogens.

Aside from research use, however, another major application of rodent models is screening of environmental, industrial, and other chemicals for carcinogenic potential. The National Toxicology Program (NTP, http://ntp.niehs.nih.gov/) has established standardized long-term carcinogenesis bioassays in rats (Harlan Sprague Dawley) and mice (B6C3F1 hybrid). These protocols employ three exposure concentrations of each test agent, plus untreated controls, in groups of 50 animals with a 2-year monitoring period. NTP maintains a publically accessible, searchable database that catalogs bioassay results. Agents that test positive in this program, which has been in place since 1978, are categorized as potential human carcinogens and further evaluated for public health relevance.

In the case of mammary tumors, the NTP protocol utilizes both male and female animals and employs various routes of administration (i.e., gavage, injection, inhalation) depending on the specific agent. Generally the route of administration is chosen that best mimics the route by which humans would be exposed. The NTP database lists 39 agents that have tested positive for site-specific induction of mammary cancer in either mice or rats (http://ntp.niehs.nih.gov/?objectid=E1D18034-123F-7908-7B2C2AE41B1F3778), including a number of endocrine disruptors. These agents should be considered *potential* carcinogens for the human breast, since it is clear that the species differences between rodents and humans limit direct extrapolation of these bioassays. Furthermore, it should be noted that the existing NTP screening protocols do not take into account important issues, such as the impact of exposure windows (e.g., in utero, puberty, pregnancy), age, or menopausal status, which are all known to be strong modifiers of breast cancer risk in humans. Although this screening program is not focused on research applications, the protocols, technical information, and results are a valuable research resource and can provide the basis for more relevant in vivo studies on environmental chemicals and breast cancer.

4.4 Standardized Protocols for Induction of Mammary Tumors by Chemical Carcinogens

Historically, the rat has been extensively used to study mechanisms of chemically induced mammary tumorigenesis (Huggins et al., 1961; Sydnor et al., 1962). Specific carcinogens that induce mammary tumors in rats include the polycyclic hydrocarbon 7,12-dimethylbenzanthracene (DMBA) and the alkylating agents methylnitrosourea (MNU) and ethylnitrosourea (ENU). The general approach involves gavage treatment of young adult virgin female Sprague Dawley rats with one or multiple doses of carcinogen (e.g., 20 mg DMBA in peanut oil) and monitoring of tumor development over periods of 2–6 months. Monitoring for tumor development is generally by weekly palpation of each mammary fat

pad with quantitation of final tumor weights at necropsy. The data outcomes for these types of studies include: time to tumor detection (latency), percentage of animals developing tumors (incidence), number of tumors per animal (multiplicity), final tumor size (volume and/or weight), and pathology. Typical mammary tumor incidence with these protocols is approximately 50% and individual animals may develop multiple tumors. The low incidence and biological variability in the induction of tumorigenicity and the rate of tumor growth in these protocols somewhat limits their suitability for prevention and therapy studies, as large cohorts of animals are required for statistical validity. However, these techniques have been used to examine the effects of dietary modifications and putative chemopreventive agents on mammary tumorigenesis.

Histologically, the mammary tumors induced in female rats by carcinogens, such as DMBA or MNU are predominantly adenocarcinomas and they generally express ER and PR. Most importantly, the incidence, multiplicity, and latency of these tumors has been shown to be modulated by age, reproductive history, and hormonal status of the rat at the time of carcinogen exposure indicating that their onset is hormone dependent (Russo and Russo, 1996). A major advantage of these rat models is that the resulting tumors are usually hormone dependent, a common feature of human breast tumors. These protocols have thus been useful for dissecting the initiation, promotion, and progression steps of mammary carcinogenesis in relation to endocrine status. A recent report characterized MNU-induced mammary tumors in male rats as a potential model for male breast cancer

(Yoshizawa et al., 2016). In contrast to human male breast cancers which are usually ER positive, however, mammary tumors induced by MNU in male rats weakly expressed ER and were negative for PR, suggesting different pathogenesis in the two species.

A major drawback of the rat chemically induced carcinogenesis model is the limited potential for these tumors to metastasize. And, although the histology and many features of these rat mammary tumors are similar to that of human breast tumors, the specific chemical agents used in these protocols are not considered relevant to the etiology of the human disease.

More recently, the rat protocols have been modified for use in mice in order to examine the impact of various knockout and transgenic manipulations on the sensitivity of the mammary gland to transformation (Medina, 2010). In mice, tumorigenesis is highly strain dependent (DBA2f, BALB/c, and Sencar mice are sensitive whereas C57BL mice are fairly resistant). As a rule, tumorigenesis in mice requires multiple doses of carcinogens, particularly for the less sensitive strains. As in the rat model, administration of exogenous hormones (particularly progestins) enhances tumor incidence and reduces latency of chemically induced murine tumors. A typical protocol for the induction of mammary tumors in C57Bl6 mice using DMBA as carcinogen and the synthetic progestin medroxyprogesterone acetate (MPA) as promoter is shown in Fig. 35.1. With this protocol, tumors appear within 4 months of DMBA administration and an overall incidence rate of approximately 75% is observed by 6 months. Histologically, the tumors that develop in response to DMBA are predominantly squamous or
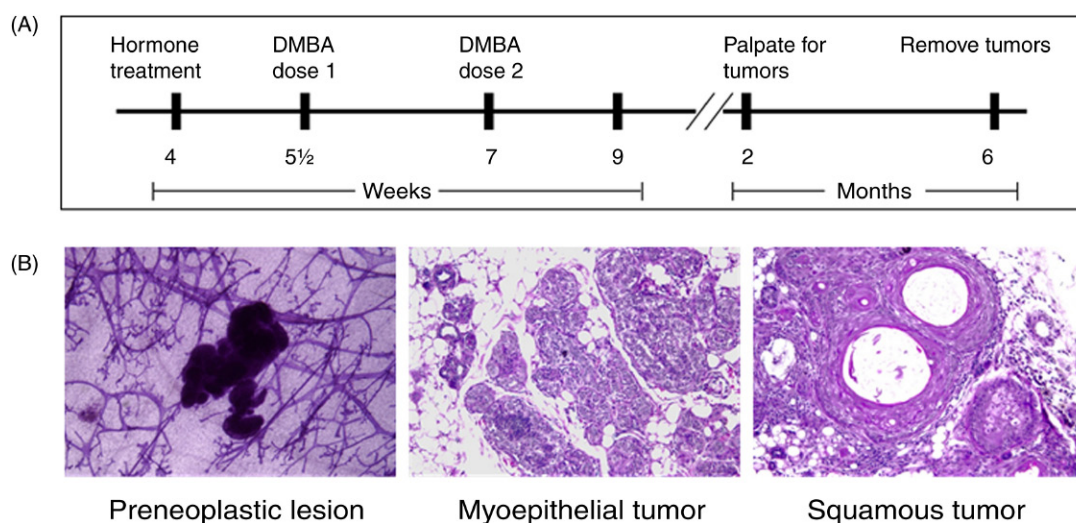
FIGURE 35.1   **General scheme for chemically induced carcinogenesis in mice.** (A) In a typical protocol, prepubertal mice are administered medroxyprogesterone acetate *(MPA)* to stimulate proliferation of the mammary epithelium prior to administration of two doses of dimethylbenzanthracene *(DMBA)* by gavage. Tumor development is monitored by palpation of all 10 mammary glands beginning 2 months after the last dose of DMBA. (B) Whole mounts of mammary glands stained with carmine can be used to visualize preneoplastic lesions. Histological sections fixed in formalin, paraffin embedded, and stained with hematoxylin and eosin are used to examine tumor pathology. Depending on the genetic background, both myoepithelial (pilar-type) and squamous tumors can be induced with these protocols.

adenosquamous carcinomas; however, pilar tumors, scirrhous tubular, spindle cell, and papillary carcinomas are also seen. In contrast to chemically induced mammary tumors in the rat, the tumor types that develop in the murine mammary gland are not usually ER+ or hormone responsive.

One of the important applications of chemically induced mammary tumorigenesis protocols in rodents is for studying the effects of pregnancy on tumor development. In humans, a full-term pregnancy exerts long-term protective effects against breast cancer; however, the mechanisms of this protection are largely unknown (Balogh et al., 2006; Britt et al., 2007; Russo et al., 2006). Pregnancy protects against subsequent chemical carcinogen-induced breast cancer in both rats and mice. For example, the incidence of tumors in virgin rats treated with DMBA was greater than 70%, whereas age-matched animals that had completed a full-term pregnancy prior to carcinogen exposure displayed only 14% incidence. This dramatic difference in tumor development in the rodent models has been exploited in studies designed to identify the mechanisms underlying pregnancy-induced protection against breast cancer. These studies have demonstrated multiple factors that may contribute to this protection including altered hormone status, maturation of the gland, changes in stem cell populations, and altered estrogen responsiveness (Britt et al., 2007; Russo et al., 2006).

A technical problem inherent in use of the mouse model is that the commonly used carcinogens are not specific for mammary cells, and tumors at other sites (i.e., lymph, lung, stomach, and ovary) contribute to the observed morbidity and mortality. The tumor spectrum is strain and dose dependent, however, and various protocols have been developed that optimize formation of mammary tumors, somewhat alleviating this concern (Medina, 2010).

A complementary approach to the whole animal carcinogenesis protocols discussed earlier involves the use of mouse mammary gland whole organ culture (MMOC, Fig. 35.2). The MMOC technique has been extensively used for studies on mammary gland development and epithelial–stromal interactions but can also be applied to carcinogenesis studies (Mehta et al., 2008). The standard
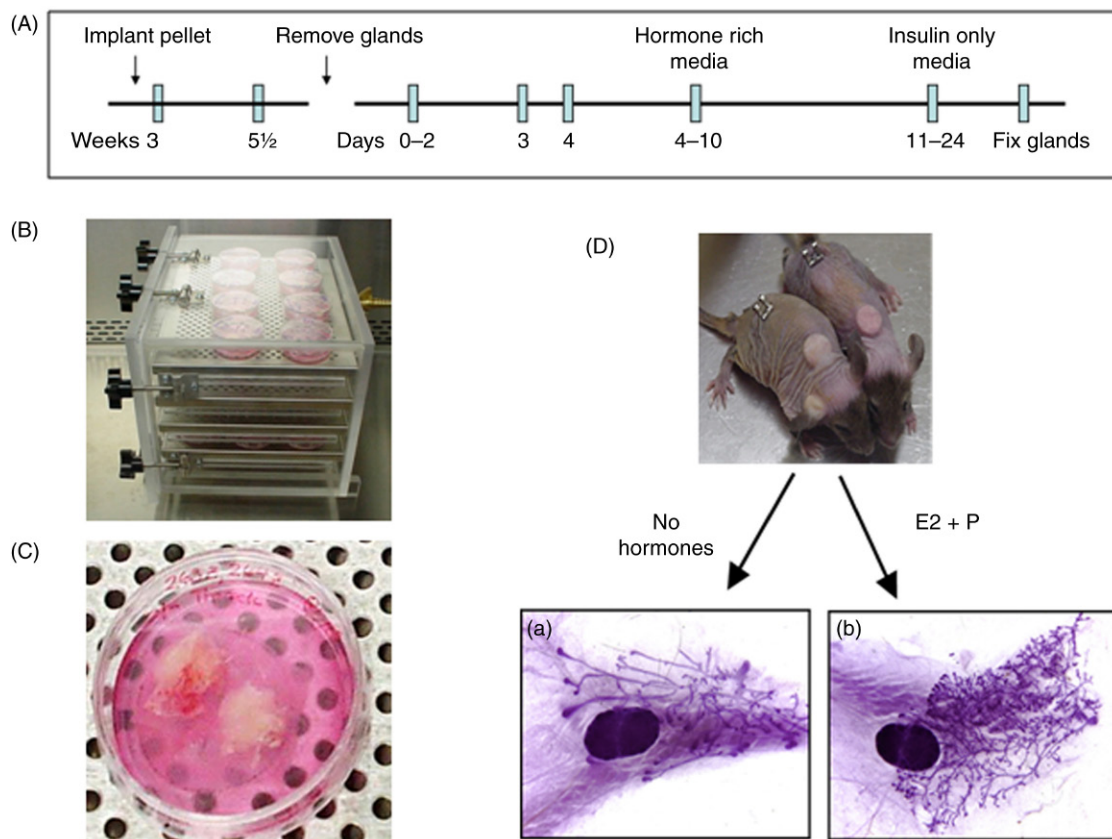
FIGURE 35.2 **Outline of the mouse mammary organ culture procedure.** (A) Prepubertal mice are supplemented with estrogen and progesterone to stimulate glandular growth and facilitate adaptation of the whole organ to culture. Glands are dissected under sterile conditions and placed in culture with media containing specific hormone cocktails and DMBA for induction of alveolar or ductal lesions. (B) Sealed apparatus for organ culture accommodates 24 culture dishes (35 mm diameter). (C) One whole mammary gland is cultured per dish. (D) Subcutaneously implanted hormone pellets facilitate growth of glands in culture. Compared are glands removed from nonsupplemented (a) and hormone supplemented (b) mice after culture.

technique involves pretreatment of 4-week-old BALB/c female mice with 1 μg of estradiol and 1 mg of progesterone for 9 days to prime the glands for culture, followed by removal to serum-free hormone supplemented media. Under the appropriate hormonal conditions, glands undergo lobulo-alveolar development in culture and when hormones are removed these structures regress. It has been demonstrated that inclusion of carcinogens including DMBA and NMU in the culture leads to the induction of preneoplastic lesions in the MMOC system. Furthermore, the prevailing hormonal conditions in the culture modulate the type of lesion produced. Under conditions of estrogen and progesterone stimulation, mammary ductal lesions develop whereas in the absence of these hormones alveolar lesions develop. In MMOC, precancerous lesions can be triggered in response to a 24 h exposure to DMBA and can be detected within 14 days of carcinogen exposure. Suppression of the incidence and multiplicity of these lesions by a variety of natural and synthetic chemicals has been demonstrated (Mehta et al., 2008) indicating the usefulness of this technique as a screening bioassay for chemopreventive agents. Incorporation of chemopreventive agents prior to or after DMBA exposure can provide insight into stage-specific preventive mechanisms. The MMOC is also a valuable approach to rapidly test the impact of specific genes on mammary carcinogenesis using glands from transgenic or knockout mice. However, the procedure requires optimization for mice on backgrounds other than BALB/c, particularly in the length of time animals are treated with hormones prior to harvesting of the glands and the doses of carcinogens employed in cultures.

4.5 Other Mammary Tumor Inducing Agents in Rodents

Although chemical carcinogens in rodents are frequently used to study mammary tumorigenesis, they are not considered to be relevant etiologic agents for human breast cancer. In addition to genetic predisposition, major risk factors for human breast cancer include reproductive history (pregnancy, lactation, hormone use) and exposure to ionizing radiation. Of note, both chronic hormonal stimulation and exposure to radiation have been shown to induce mammary tumors in rodents. Ovarian steroids are necessary for the development of the mammary gland and as such their presence is permissive for growth and survival of the epithelial cells which are the targets for transformation. As noted earlier, estrogen and progesterone supplementation enhance the sensitivity of the mammary gland to spontaneous and chemically induced carcinogenesis. In BALB/c female mice, chronic, continuous administration of the synthetic progestin MPA induces mammary ductal carcinomas with a mean latency of 52 weeks and an incidence

of about 80% (Lanari et al., 2009). In contrast to spontaneous, chemical, or MMTV-induced tumors in mice (which are typically hormone receptor negative), more than 60% of the MPA tumors express ER, PR, and prolactin receptors. In addition, lymph node and lung metastases develop in some cases. As observed for other models, the carcinogenic effect of MPA is strain-specific, with lower incidence in C3H mice than BALB/c mice and no tumor development in C57BL/6 mice.

Several rodent models have been developed for studying the effects of ionizing radiation on mammary tumor development (Medina, 2010). In general, whole body radiation exposure (γ rays or neutrons) induces ductal hyperplasias and adenocarcinomas in female BALB/c mice at low incidence (20%–45%) and with long latency (Storer et al., 1979; Ullrich et al., 1977). The high susceptibility of Balb/c mice to radiation-induced tumors has been attributed to a polymorphism in the Pkrdc gene which codes for a DNA repair enzyme (Rivina et al., 2016). Not unexpectedly, cells derived from murine tumors induced by radiation exposure are characterized by chromosomal instability (a feature not seen in cells from chemically induced tumors). Furthermore, mammary tumors in mice exposed to radiation are hormone independent and metastasize to lung. These features suggest that the protocols used for radiation-induced mammary tumors in mice are highly appropriate for modeling radiation-induced human breast tumors.

5 GRAFTING AND TRANSPLANTATION APPROACHES

5.1 General Issues

The most commonly utilized models of breast cancer for screening therapeutics are those in which transformed cells or whole tissues are grafted into compatible host animals. There are many variations of these techniques, with different cells or tissues (animal, human), hosts (syngeneic, nonsyngeneic), and grafting sites (subcutaneous, orthotopic, systemic). These models are all based on the well-documented premise that only transformed cells are able to survive and grow into tumors in a host animal. In fact, a major use of these models is as a gold-standard test for cellular transformation (Ince et al., 2007) (Fig. 35.3).

The advantages of graft models of breast cancer are that they are technically easy, fairly reproducible, relatively inexpensive, can be applied to transfected/knockout cells and can be used to study freshly isolated human cancer tissue. Furthermore, in contrast to the majority of chemically induced and transgenic models, many human breast cancer cell-line derived xenografts are ER+ and demonstrate hormone dependence in vivo. These
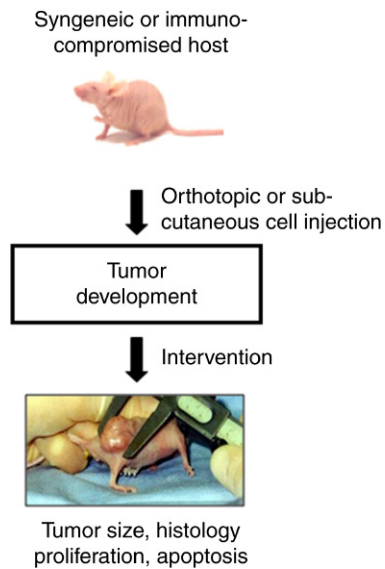
FIGURE 35.3 Flowchart of typical graft experiment. Similar approaches are used for syngeneic (mouse cells into host mice of same genetic background) and nonsyngeneic (human cells into immune-deficient host mice) protocols. Hosts are injected with tumor cells (often mixed with extracellular matrix preparations) at either subcutaneous or orthotopic (mammary fat pad) sites. Depending on the aggressiveness of the injected cells, palpable tumors may develop within 2 weeks. Therapeutic interventions are usually initiated once tumors reach a measurable size ($\sim$200 cm^3) as monitored by calipers. End points of these studies generally include tumor growth rate, size, and weight. Tumor cell proliferation, apoptosis, angiogenesis, and specific biomarkers of interest are usually determined histologically on tumor sections. For modeling of metastasis, cells with metastatic potential are injected directly into the circulation via tail vein, portal vein, or cardiac route and disseminated cells are monitored in lung, liver, bone, and other sites. Variations include the use of freshly obtained biopsy tissue (tumorgrafts), use of tagged cells for noninvasive imaging of tumor growth and dissemination, and intraductal cell injection for modeling of ductal carcinoma in situ.

models have been particularly useful in the identification of environmental estrogens, phytoestrogens, and synthetic ligands that act as agonists or antagonists of ER to modulate tumor growth.

There are several general limitations of graft approaches that should be noted. First, they are not appropriate for studies of primary tumor prevention since the cell lines utilized are already transformed prior to implantation. Interventions that alter tumor development (i.e., the appearance of a solid tumor after implantation of cells) do not "prevent" tumorigenesis, rather they impact on the ability of the already transformed cells to adhere, survive, and proliferate in vivo. Another limitation of graft approaches is that the critical interactions that evolve between epithelial cells and the microenvironment during tumor initiation are not recapitulated. Crosstalk between neoplastic epithelial cells and fibroblasts, immune cells, and endothelial cells is extremely important in the evolution of tumors yet in grafting models transformed cells are introduced into a normal host microenvironment. In addition, and likely related to the lack of a suitable tumor microenvironment, most human xenografts do not spontaneously metastasize in murine hosts, and those that do tend to metastasize to organ sites that are not clinically relevant for human breast cancer. Metastasis can be achieved in xenograft systems via direct injection of breast cancer cells with metastatic potential into the circulation, but these approaches mimic only part of the metastatic cascade. Another important limitation is that immune-deficient hosts must be used for human cells, precluding studies on the influence of the immune system on tumor growth or response to experimental therapies. Finally, the biggest disadvantage of graft models of cancer is that the therapeutic efficacy of drugs against xenografts is not highly predictive of clinical response. Specifically, the majority of drugs that are effective in xenograft studies fail to show similar efficacy in clinical trials. The lack of efficacy likely relates to the rapid growth rate of experimental tumors and their homogeneity compared to human breast tumors. Newer models using patient-derived material for grafting may somewhat overcome this issue (see later). Because of the great variety of models and approaches in the literature, only a few representative models and approaches will be described here. Additional information can be found in recent reviews on in vivo modeling of breast cancer (Holliday and Speirs, 2011; Jenkins et al., 2005; Khanna and Hunter, 2005; Mollard et al., 2011; Troiani et al., 2008).

5.2 Technical Issues

Site of tumor cell administration. As noted previously, during endogenous breast tumor development, complex interactions evolve between the neoplastic epithelial cells and the accessory cells (fibroblasts, adipocytes, vascular, and immune cells) in the tissue microenvironment (Hanahan and Coussens, 2012). Accessory cells secrete growth factors, hormones, and cytokines that modulate the behavior of the epithelial tumor cells, and conversely, tumor cells secrete factors that modulate cells in the microenvironment. These epithelial–stromal interactions contribute to tumor progression via promotion of cell survival, remodeling of the extracellular matrix, and chronic inflammation. Furthermore, crosstalk between tumor cells and endothelial cells is critical for driving angiogenic processes necessary for metastatic spread. Since these events can only be superficially studied in vitro (e.g., with coculture systems), in vivo systems are essential for modeling this aspect of tumor biology. Initially, breast tumor grafts were implanted or injected subcutaneously, a site that does not provide the appropriate extracellular matrix or tissue microenvironment for breast carcinogenesis. Although subcutaneous grafts are easy to establish and monitor, some breast cancer cell lines fail to form tumors when grafted this way. To address these issues, adaptations,

such as the coadministration of extracellular matrix proteins (either purified single proteins or complex biological mixtures, such as Matrigel) or viable fibroblasts with the breast cancer cells have facilitated tumor take -in some cases, however, these methods still do not closely mimic the natural microenvironment of breast tumors. Newer alternative approaches include orthotopic xenografts (injection or implantation of cells directly into the tissue of origin). For breast cancer, orthotopic injections are made into the mammary fat pad or directly into the milk ducts via the nipple (Sflomos et al., 2016; Valdez et al., 2011). As described later in more detail, orthotopic grafts are more clinically relevant and predict drug efficacy better than subcutaneous grafts.

Monitoring tumor growth rates and disease spread. Regardless of the site of grafting or cell/tissue type, procedures for monitoring tumor take and growth rates are required. Once detected by palpation, the size of subcutaneous grafts can be monitored noninvasively by caliper measurement. Inexpensive calibers with digital readout can be connected to a computer for automatic data collection (Worzalla et al., 1990). With calipers, tumor diameter is generally measured in two directions and the height of the mass is measured at its maximum. Tumor volume is calculated as an ellipsoid. For fast-growing tumors, measurements are typically collected once or twice per week over the course of the study. Since the majority of subcutaneous grafts do not infiltrate the muscle and remain in the subcutaneous space, caliper measurements are quite accurate in reflecting tumor size. However, due to considerable operator variability it is recommended that one individual perform all measurements for a particular study. When tumors are growing orthotopically, measurements are still feasible, although technically more challenging depending on the site of tumor engraftment. For these, the most accurate measurements will be at the end of the experiment when tumors are excised and directly measured by calipers and weighing. The use of specialized imaging techniques capable of whole animal fluorescence detection (for use with cells stably tagged with fluorescent markers), as well as micro computed tomography (CT) and positron emission tomography (PET) imaging is becoming more common for noninvasive monitoring of tumor growth and progression in vivo. While technically challenging and requiring specialized equipment, noninvasive monitoring has greatly facilitated the study of both primary tumors and metastatic disease (Jenkins et al., 2005; Manning et al., 2016; Mollard et al., 2011)

5.3 Syngeneic Graft Models of Breast Cancer

Syngeneic graft approaches utilize cancer cells and host mice from a common genetic background and thus avoid the need for immunocompromised host animals, allowing for study of the role of the immune system in tumor growth and metastasis. Another major advantage of syngeneic models is that the tumor cells, microenvironment (stroma, immune cells, extracellular matrix), and host are from the same species. A disadvantage of syngeneic tumor models is their limited similarity to human tumor biology as the commonly used cell lines are driven by mutations that do not mimic those found in human breast cancer. Complementary studies in human xenograft models are recommended to confirm that observations from syngeneic tumor models are relevant to human cancer.

Rodent cell lines that grow in syngeneic hosts have been isolated from spontaneous and chemically induced tumors, as well as from transgenic animal tumors. The well-characterized 4T1 series of cell lines (Aslakson and Miller, 1992) includes five isogenic tumorigenic lines (67NR, 168FARN, 4TO7, 66cl4, and 4T1) that originated from one spontaneous tumor in a BALB/cfC3H mouse. Each cell line displays unique tumorigenic and metastatic capabilities. For example, when introduced orthotopically, the 4T1 line grows rapidly at the primary site and forms metastases in lungs, liver, bone, and brain over a period of 3–6 weeks. When introduced via the tail vein or arterially, metastases are apparent in these same organs after 1–2 weeks. The rapid, efficient, and reproducible metastasis to the same organs that are affected in human breast cancer makes the 4T1 model ideal for the study of metastatic progression of breast cancer in humans. Another interesting property of this model is the availability of sublines with distinct metastatic potential. Sublines 67, 168FAR, and 4T07 are highly tumorigenic, but fail to metastasize at different steps. The nonmetastatic 67 cells fail to leave the primary graft site; 168FAR cells reach the regional lymph nodes but do not produce nodules or spread from the nodes; and the 4T07 cells are found in the circulation and colonize the lungs without advancing into visible metastases. Thus, this comprehensive set of sublines offers the potential to correlate genetic alterations with specific steps in the metastatic process, as well as to test antimetastatic therapies for their ability to interfere with known stages of the process. More recently, stable bioluminescent 4T1 cell lines expressing enhanced firefly luciferase (luc2) have been generated, which are sensitive enough for noninvasive detection of micrometastases in vivo. In addition, genomic and metabolomic profiles of 4T1 and its variant cell lines have been reported (Eckhardt et al., 2005; Lu et al., 2010).

A new syngeneic mouse model with similarities to basal and claudin-low subtypes of human breast cancer has been developed from tumors driven by the Wnt1 oncogene (Dunlap et al., 2012). In this model, two distinct cell lines isolated from Wnt1-driven mammary tumors generated in C57Bl6 mice were characterized with respect to genomic profiles and stem cell enrichment.

The mesenchymal-like M-Wnt cells were enriched for tumor-initiating cells (CD44^{high}/CD24^{low}) compared to the epithelial-like E-Wnt cells. Furthermore, M-Wnt cells demonstrated enhanced epithelial-to-mesenchymal transition (EMT) marker expression, mammosphere-forming ability, migration, invasion, and tumorigenicity relative to E-Wnt cells. Genomic clustering based on microarray profiling indicated that M-Wnt cells mimicked claudin-low breast tumors whereas E-Wnt cells clustered with basal-like tumors. When orthotopically transplanted into ovariectomized C57BL/6 mice, tumors from these two cell lines recapitulated these tumor subtypes. Thus, this model provides a unique and valuable approach to study two of the human breast cancer subtypes associated with poor prognosis in an immune-competent in vivo environment. Because these and other Wnt1-derived cells are capable of syngeneic grafting, they are amenable to study in existing transgenic and knockout mouse strains on the C57Bl6 genetic background as recently described (Zheng et al., 2012).

5.4 Nonsyngeneic (Xenograft) Models

Definition and characteristics. "Non-syngeneic" refers to the transplantation of human tumor cells or tissue fragments into hosts of another species (usually mice). Successful growth of xenografted tumors will only occur if the host animal is immune-deficient to prevent immune rejection of the foreign cells. Although these models have some advantages, they do not replicate many of the histological properties of breast cancers in human patients. Most cell lines grown as tumors consist largely of homogenous, rapidly proliferating epithelial cells with limited stromal infiltration. This is in contrast to the heterogeneity and reactive stroma that are characteristically present in human breast cancers. It is also important to recognize that xenografted tumors are a mosaic of human epithelial tumor cells growing within a murine microenvironment. Thus, all of the accessory cells that are known to infiltrate tumors (fibroblasts, immune cells, endothelial cells, adipocytes) are derived from the host mouse. In some cases, species differences in pathways and signaling (i.e., ligand-receptor complexes, gene regulation, cytokine signaling) will limit cross talk between these murine cell populations and the human breast cancer cells. A related issue is that the normal stromal compartments of the murine and human mammary glands are quite different—whereas mouse stroma primarily consists of adipocytes, human stroma is largely populated by fibroblasts.

As noted previously, recognition of the importance of the microenvironment in tumor growth has prompted investigators to compare various modes and sites of xenografting. Initial studies were conducted almost entirely with cells injected subcutaneously, which facilitates visualization and monitoring of tumor growth but does not mimic the natural environment of a developing breast tumor. To better model developing breast tumors, implantation of cells or tissue fragments into orthotopic sites is increasingly utilized. Of the 10 mammary glands in the mouse, the inguinal and thoracic glands are most commonly used. Fleming et al. (2010) demonstrated that xenografts growing in the inguinal (abdominal) mammary gland had increased tumor take rates, decreased latency, and larger final volumes compared to those growing in the thoracic gland, suggesting that the specific orthotopic site can alter tumor biology.

In a comparative study (Fleming et al., 2010), tumor incidence, latency, and volume were greater for MCF-7 cells grown in the mammary fat pad compared to those grown subcutaneously. Furthermore, estrogen sensitivity and vascularization were enhanced in orthotopic tumors compared to subcutaneous tumors. When introduced into the mammary ducts, MCF-7 cells grew slowly and exhibited desmoplasia and microcalcifications that were not present when cells were implanted in the fat pad (Sflomos et al., 2016). These studies also indicated that the intraductal microenvironment favored maintenance of the luminal gene expression profile in MCF-7 cells. Thus, it is apparent that the microenvironment, governed by the chosen implantation site, dramatically alters both genotype and phenotype of breast cancer xenografts.

Use of surgery-derived tissue for xenografting. To better mimic clinical behavior and clonal evolution of breast cancers, tumor cells or tissue fragments obtained from biopsy material (rather than established cell lines) have been utilized for xenografting (Decaudin, 2011; Ding et al., 2010; Eirew et al., 2015; Garcia-Garcia et al., 2012; Kabos et al., 2012; Kanaya et al., 2016; Marangoni et al., 2007). These so-called patient-derived xenografts (PDX) display high concordance in gene expression, chromosomal alterations, and histology when compared back to the patient's original tumor tissue. Furthermore, patient-derived ER+ luminal breast tumor models have been used to study tumor hormone and receptor action. In one model (Kabos et al., 2012) human breast tumor samples obtained at surgery and immediately transplanted into estrogen supplemented immunodeficient mice were used to select transplantable ER+ breast cancer xenografts derived from both primary and metastatic cases. Xenografts were found to morphologically resemble the tumors of origin, with similar expression of ER and PR, over multiple passages. Four of the tumor xenografts were estrogen dependent, expressed estrogen-regulated genes, and were sensitive to the antiestrogen tamoxifen, a clinically relevant drug. In a related approach, investigators introduced patient-derived cells directly into the mammary ducts to generate slow-growing ER+ tumors that metastasized to clinically relevant

sites (Sflomos et al., 2016). These studies suggest that ER+ tumorgrafts may provide a relevant model of estrogen responsive breast cancer for studies on heterogeneity, metastasis, and drug development.

An extensive panel of tumorgrafts established by Marangoni et al. (2007) includes 15 triple-negative, one ER+, and two HER2+ tumors. Interestingly, tumor take was higher in fragments from high grade, ER− tumors than low grade, ER+ tumors. The histology and genetics of these xenografts also recapitulated the tumors of origin, with common alterations in p53, Rb, and PTEN, and a few samples with amplification of HER2. Of 17 tumorgrafts, 3 demonstrated high propensity for spontaneous lung metastasis. Chemosensitivity screening indicated that 88% of tumorgrafts responded to adriamycin-cyclophosphamide, and the two HER2 amplified tumors responded to the anti-HER2 antibody trastuzumab. The IOWA-1T is another unique PDX that exhibits local spread and skin erosion with a basal molecular profile (Bogachek et al., 2015). These reports demonstrate the feasibility and promise of the tumorgraft approach for screening therapeutic efficacy. Protocols for establishing and passaging xenografts from clinically available tumor tissue have been published (de Plater et al., 2010; Kabos et al., 2012; Marangoni et al., 2007; Morton and Houghton, 2007; Sflomos et al., 2016).

Commonly used immune-deficient mouse strains. In contrast to syngeneic models, successful establishment of xenograft tumors relies on host animals with compromised immunity. Since it is well known that both innate and adaptive immune cells play a major role in cancer progression and eradication, the dependence on animal hosts with defective immunity is a major limitation of xenograft models. Human breast tumors commonly have immune cell infiltration which will not be accurately mimicked in an immune-deficient murine host. Furthermore, many therapies exploit the immune system either by bolstering antitumor immunity or neutralizing inflammation that promotes cancer progression. Screening therapeutics that potentially mediate their effects through immune mechanisms in xenograft models therefore could be misleading.

There are multiple genetic loci in mice that produce immunocompromised phenotypes, but the most commonly used models for xenograft studies are the nu (nude), scid (severe combined immunodeficient), and bg (beige) mouse strains. Although few studies have done direct comparisons, most established breast cancer cell lines appear to grow equally well in all stains. Growth of fresh tumor fragments and metastatic progression may be better in the more immune-compromised strains. Nude mice (homozygous for the nu mutation) are athymic and therefore their major defect is a lack of T cells (Pelleitier and Montplaisir, 1975). Nude mice do have B cells (albeit immature) and retain activity of natural killer (NK) cells and macrophages, which are thought to contribute to the low rates of metastasis of most human xenografts in this model (Clarke, 1996). Nude mice are also hairless, which is an advantage for visualization and measurement of subcutaneous xenografts. The scid mutation results in failure to rearrange the genes encoding antigen-specific receptors of T and B cells. Subsequently, scid mice have small lymphoid organs, lack both immature and mature B cells, and have defective T cells. Scid mice (Bosma and Carroll, 1991) retain NK cells, macrophages, and dendritic cells, all of which might influence tumorigenicity and metastasis. The beige mutation is associated with a severe deficiency of NK cells, defective bactericidal activity of granulocytes, and defective cytotoxic T-cell responses (Baca and Mowat, 1989). Studies of xenografts in both nude and scid mice crossed onto the beige background support a role for NK cells in tumor rejection (Clarke, 1996). The scid/bg mouse and other immune-deficient strains are commercially available and each has specific husbandry requirements due to their immune deficiencies, as well as other associated phenotypes. Currently, strains carrying the nude and scid single mutations remain the most commonly used mouse hosts for human breast cancer xenografts.

5.5 Detailed Characteristics of Human Breast Cancer Cell Lines Used for Xenografting

Introduction to breast cancer cell lines. Since 1958, when the first human breast cancer line BT-20 was established, upward of 50 lines have been isolated from patients with various subtypes of tumors. Most of the long-established breast cancer cell lines in current use were derived from tumor metastases, especially aspirates or pleural effusions, rather than from primary breast tumors. The majority of the patients from which these tumors were removed had completed and often failed multiple courses of therapy (radiation, chemotherapeutics, and/or antihormone). Thus, it is not surprising that most of the available breast cancer cell lines are highly proliferative, aneuploid, poorly differentiated, and drug resistant. Unfortunately, the clinical details on the donors are quite limited for most of the established breast cancer cell lines.

It is important to recognize that established cell lines undergo both genotypic and phenotypic drift when continuously cultured. For example, studies have demonstrated that MCF-7 clones obtained from different sources display differences in growth rate, estrogen responsiveness, karyotype, and clonogenicity (Osborne et al., 1987). These differences most likely represent the selection of distinct subpopulations over time under different laboratory conditions. It stands to reason that xenografts derived from different subclones would display different properties in vivo as well, although this has not been rigorously examined.

Due to their adaptation to continuous culture, most breast cancer cell lines form xenografts that exhibit rapid growth even in subcutaneous sites, precluding the development of metastases before the size of the primary tumor requires ethical sacrifice of the host. Therefore, much of the preclinical research with xenografts is biased toward tumors with high mitotic rates (which are generally rare in humans) rather than slower growing tumors at the early stage. More recently, a series of cell lines (SUM cells) have been generated by Steve Ethier's group at the University of Michigan and are commercially available from Asterand. Some of these cells were isolated from primary tumors of patients prior to initiation of any therapies. Each SUM cell line has been well characterized with respect to known oncogenes, gene expression data, and biomolecular markers, such as ER and HER2. Orthotopic xenografts grown from these cell lines display a range of histologies more reminiscent of the original tumors from which they were derived (with more stromal involvement) than earlier cell lines (Kao et al., 2009).

Recently there has been an interest in determining how well the existing established breast cancer cell lines reflect the known heterogeneity of human breast tumors. Molecular and cellular analysis of a large panel of human breast cancer cell lines has been performed to determine how well their genomic profiles and protein expression patterns mimic primary human breast tumors (Kao et al., 2009; Keller et al., 2010; Neve et al., 2006). As summarized in Table 35.1, the available cell lines can be categorized on the basis of protein biomarkers, genomic analysis, cell surface markers, and breast cancer-associated mutations into groups that model all subtypes of human breast cancer. This list was compiled from recent literature (Herschkowitz et al., 2007; Hollestelle et al., 2010; Kao et al., 2009; Keller et al., 2010; Neve et al., 2006; Riaz et al., 2009) where original data and more specific details are available. Here we will briefly discuss the most commonly used cell lines for modeling each subtype of the human disease, with the caveat that not all cell lines discussed have been thoroughly characterized as xenografts. Additional resources related to human breast cancer cell lines suitable for xenografting include ATCC (http://www.atcc.org/), Asterand (http://www.asterand.com/Asterand/), and the Lawrence Berkeley laboratory breast cancer cell database (http://icbp.lbl.gov/ccc/celllines.php). A comprehensive comparison of morphology, growth, and biomarker expression of 16 human breast cancer cell lines and their xenografts has been published (Keller et al., 2010).

Models for early stage disease. The MCF-7 cell line, which was established from a pleural effusion at the Michigan Cancer Foundation in 1973, is by far the most commonly used xenograft model of breast cancer. Despite its origin from the metastases of an advanced tumor, the cell line is noninvasive and represents a model of early stage disease due to the presence of functional ER and estrogen dependence for growth both in vitro and in vivo. In microarray profiles, the MCF-7 geneset clusters with the luminal subtype of breast cancer (Kao et al., 2009). MCF-7 xenografts express wild-type p53 and remain localized when implanted subcutaneously or into the mammary fat pad but metastasize to bone, lung, brain, and other sites when introduced into the milk duct (Sflomos et al., 2016). This model has been particularly valuable in preclinical testing of antiestrogen therapies (such as tamoxifen and aromatase inhibitors) and identification of mechanisms of resistance to such drugs. Another commonly used ER+ cell line of the luminal subtype is T47D, which was also isolated from a pleural effusion of a patient with invasive ductal carcinoma. Due to their high expression of PR, T47D cells are commonly used to study progesterone signaling in breast cancer and therapeutic efficacy of antiprogestins. Unlike MCF-7 cells, T47D cells express a mutated, nonfunctional form of the tumor suppressor p53. From the SUM series of cell lines, SUM44PE cells (isolated from a pleural effusion) are the best model of the luminal subtype as they express ER. However, they lack PR and have mutated p53 and there is limited information on the biology of xenografts of this cell line. Other luminal breast cancer cell lines that can be used to study early stage disease are listed in Table 35.1.

Models for invasive disease. The MDA-MB-231 cell line (isolated at M D Anderson from a pleural effusion of a patient with invasive ductal carcinoma) is commonly used to model late stage breast cancer. This cell line is ER, PR, and E-cadherin negative and expresses mutated p53. In microarray profiling, the MDA-MB-231 cell genome clusters with the basal subtype of breast cancer. Since the cells also lack the growth factor receptor HER2, they represent a model of triple-negative breast cancer. MDA-MB-231 cells are invasive in vitro and when implanted orthotopically produce xenografts that spontaneously metastasize to lymph nodes. Variants of MDA-MB-231 cells with unique metastatic properties have been selected from the parental cell line (Kang et al., 2003). Bone-seeking (MDA-231BO) and brain-seeking (MDA-231BR) clones were selected by repeated passaging in nude mice and in vitro culture of metastatic cells obtained from bone and brain metastases (Yoneda et al., 2001). When tested in experimental metastasis models, these variants showed preferential homing to bone and brain following intracardiac injection. Stable incorporation of luciferase tags in specific MDA-MB-231 subclones has enabled noninvasive in vivo imaging of experimental metastasis (Jenkins et al., 2005).

Triple-negative breast cancers (TNBC) have been further divided into three major subtypes based on gene expression profiling (Lehmann et al., 2011), and established cell lines have been identified to model each

TABLE 35.1   Appropriate Models for Study of Breast Cancer Stages and Subtypes

Application	Model	Appropriate approaches	Comments
Normal development and carcinogenesis	Mouse mammary gland organ culture	Whole gland ± hormones, DMBA	• Strain dependent (BALB/c preferred) • Suitable for screening preventive agents • Can be performed with tissue from transgenics and knockouts
DCIS	Orthotopic xenografts	MCF10DCIS.COM, SUM-225	• Intraductal cell injection via nipple
Luminal subtype	Orthotopic xenografts	*Wild-type p53*: MCF-7, CAMA1, ZR75-1 *Mutant (m) or negative (−) p53*: T47D(m), BT483(−), SUM44PE(−), HCC202(−), HCC1428(−)	• All except HCC202 are ER+ • MCF7, T47D, HCC1428, CAMA1, ZR75-1, SUM44PE are PR+ • All show little-no invasive activity in Boyden chamber assays
	Transgenic	MMTV-Neu, MMTV-PyVMT, TgWAP-Myc	• Tumors in transgenic mice show weak luminal phenotype and lack ER
	Induced	Chronic MPA treatment-mice NMU—rats	• Both protocols induce ER+ tumors
HER2+	Orthotopic xenografts	*Luminal*: BT474, MDA-MB-361, SK-BR-3, SK-BR-5, UACC812, ZR75-30 *Basal A*: HCC1569, HCC1954, HCC202, SUM190PT	• MDA361, ZR75-30 are ER+ • BT474, SK-BR-3, SK-BR-5, UACC812, HCC1569, HCC1954, HCC202, SUM190PT are ER-
	Transgenic	MMTV-Neu	• Useful for testing anti-Her2 therapies • Genomic profiles show limited conservation between MMTV-Neu tumors and human Her2+ breast cancers
Basal B/triple negative	Orthotopic xenografts	*Wild-type p53*: BT20, HBL100, SUM149PT *Mutant (m) or negative (−) p53*: MDA-MB-231 (m), MDA-MB-435 (m), BT549 (m), SUM159PT (−)	• All except BT20 are invasive in Boyden chamber assays
	Transgenic	Conditional BRCA1 and BRCA2 deletion on p53$^{+/-}$ background, MMTV-Wnt1	• MMTV-Wnt1 tumors show mixed luminal and basal phenotype
	Chemically induced	MPA-DMBA model	• Phenotype strongly influenced by genetic background; genomic clustering based on FVB tumors
Hereditary syndromes	Orthotopic xenografts	MX-1(BRCA1,BRCA2), HCC1937 (BRCA1), HBCx-17(BRCA2)	• Not well-characterized in vivo
	Knockout	Conditional BRCA1 and BRCA2 deletion/ mutation on p53$^{+/-}$ background	• Tumors are triple negative
Metastatic disease	Orthotopic grafts	MDA-MB-231, MDA-MB-453 [4T1] series	• Some luminescent clones are available • [4T1] is syngeneic in BALB/c mice
Inflammatory breast cancer	Orthotopic xenografts	SUM149PT, SUM190PT MARY-X (transplantable)	• Not well-characterized in vivo

TNBC subtype. These cell lines include HCC1806 and MDA-MB-468 (basal-like); CAL-51 and SUM159PT (mesenchymal-like); and SUM185PE and CAL-148 (luminal-androgen receptor). Xenograft studies with these six cell lines indicated subtype-specific drug sensitivity in vivo that matched predictions based on specific genomic alterations.

Models of familial breast cancer. Loss of function mutations in the breast cancer susceptibility genes BRCA1 and BRCA2 are strongly linked to hereditary breast cancer. Although many cell lines exhibit mutations in these tumor suppressor genes, the majority are sporadic mutations that developed either during tumor progression or during cell line establishment. The exception is the few cell lines that have been isolated from tumors of individuals with known BRCA germline mutations. Only one such breast cancer cell line is readily available: HCC1937 cells, which were initiated from a Stage IIB primary ductal carcinoma of a 23-year-old Caucasian female from a family with a known deleterious BRCA1 mutation. HCC1937 cells are homozygous for the BRCA1 5382C mutation, whereas lymphoblastoid cells derived from the same patient are heterozygous for this mutation, indicating loss of heterozygosity in the tumor

cells. This mutation encodes a truncated BRCA1 protein lacking the C-terminus BRCT domain required for repair of DNA damage and regulation of the cell cycle. The tumor-derived cells are ER- and PR-, express mutated p53, and exhibit homozygous deletion of the PTEN gene. HCC1937 cells are highly transformed with a modal chromosome number of 100 (Tomlinson et al., 1998). These cells have been utilized in xenograft models to examine the role of BRCA1 in sensitivity to DNA damaging agents, such as cisplatin in vivo (Tassone et al., 2009). Three additional cell lines with BRCA1 mutations were identified (Elstrodt et al., 2006) in a screen of 41 established breast cancer cell lines: MDA-MB-436 (adenocarcinoma/age 39), SUM149PT (inflammatory breast cancer/age 35), and SUM1315MO2 (invasive ductal carcinoma/age of onset unknown). Another line, HCC3153, which is homozygous for the BRCA1 943ns10 mutation that causes a frameshift leading to a stop at codon 289 in exon 11, was identified during molecular profiling of 52 breast cancer cell lines (Kao et al., 2009). Since mutation analysis was not conducted at the time of isolation of these three BRCA1 mutant cell lines, it is unclear whether the BRCA1 mutations represent germline events (although at least two donors had early onset breast cancer and thus could be bona fide BRCA1 carriers). Furthermore, there is little to no information on the pathology or biology of xenografts derived from these cells. Despite these caveats, these cell lines are suitable for studying BRCA1 functions in the context of breast cancer. In contrast to BRCA1, no established cell lines have been derived from breast tumors of known BRCA2 mutation carriers.

Two xenograft models of BRCA-associated breast cancer (MX-1 and HBCx-17) have been reported to date. The MX-1 breast xenograft which carries mutations in both BRCA1 and BRCA2 has been used to test the antitumor efficacy of PARP inhibitors (Donawho et al., 2007), a class of drugs that targets cells with defects in homologous recombination. Other than its use to screen therapeutics for activity against tumors with mutations in the BRCA genes, the molecular and pathological features of MX-1 xenografts have not been well characterized. The HBCx-17 xenograft model was generated from an infiltrating ductal carcinoma of a woman carrying a germline c.6033_6034delTT BRCA2 mutation (de Plater et al., 2010). Within 1 month after fresh tumor fragments were grafted into the interscapular fat pad of a female nude mouse, a basal-like triple-negative xenograft developed which accurately reflected both the genotype (BRCA mutation, chromosomal changes) and the phenotype (especially with respect to drug sensitivity and resistance) of the primary tumor from which it was derived. These studies demonstrate the feasibility of this approach and support the concept that tumor grafts represent a valuable and relevant complementary approach to traditional cell-line based xenografts for studying molecular aspects of human breast cancer, as well as for testing therapies.

Models of inflammatory breast cancer. Although inflammatory breast cancer accounts for a small (1–5) percentage of all breast cancers, it is a very aggressive disease with high mortality. Inflammatory breast cancers represent a unique subtype of invasive ductal carcinomas that form and grow as emboli which accumulate in and block lymphatic ducts in the dermis. Inflammatory breast cancers are usually diagnosed at an advanced stage and progress rapidly, accounting for their high mortality. Two established cell lines are known to be derived from inflammatory breast cancer patients: SUM149 and SUM190. SUM149 cells were isolated from a pleural effusion, are triple negative, and cluster with the basal subtype of breast cancers. SUM190 cells were isolated from a primary tumor, are ER-, PR-, and HER2+ and cluster with the luminal subtype of breast cancers. When xenografted into immunocompromised mice, both cell lines grow as solid tumors, thus it is unclear how well they model the unique growth characteristics of inflammatory breast cancers in patients (Wang et al., 2009).

Another model of inflammatory breast cancer (MARY-X) has been developed by the Barsky lab (Alpaugh et al., 1999). The MARY-X xenograft is a stable, serial transplantable tumor that was established directly from a 45-year-old patient with inflammatory carcinoma and dermal lymphatic invasion. In scid/nude mice, MARY-X tumor cells grow exclusively within the lymphatics and blood vessels, providing a model highly reminiscent of the human disease. MARY-X tumors are triple negative, lack functional p53, and overexpress E-cadherin and MUC1 similar to cases of human inflammatory breast cancer. There are technical challenges in continuously passaging the MARY-X tumor cells, which must be separated from the associated murine cells, and the model is not widely available. At this point, the paucity of relevant animal models that mimic the unique characteristics of inflammatory breast cancers severely limits progress into this devastating form of breast cancer.

Models of DCIS. Ductal carcinoma in situ (DCIS) is the most common type (80%) of noninvasive breast lesion and is considered a precursor of invasive ductal carcinoma (Bombonati and Sgroi, 2011; Muggerud et al., 2010). While the vast majority of women will not recur after removal of DCIS, there are no validated biomarkers to stratify the subset of patients who will, from those who will not. Thus, in most cases, DCIS is treated conservatively (with surgery, radiation, and/or hormonal therapies) to reduce the risk of recurrence. Further insight into the evolution and progression of DCIS would benefit greatly from relevant animal models, which could be used to develop biomarkers and screen for agents that prevent progression of the disease. Experimental models of noninvasive breast tumors are limited, and the existing

in vivo models do not mimic the known heterogeneity of human DCIS. Within the last few years, a new model of DCIS based on human cell lines and biopsy tissue xenografted into immunocompromised mice has been developed (Behbod et al., 2009; Valdez et al., 2011). This unique approach involves injection of human DCIS cell lines (MCF10DCIS.COM, SUM225) or cells derived from human DCIS biopsies directly into the murine mammary ducts via the nipple. With this method, MCF10D-CIS.COM cells developed into a basal-like DCIS model, whereas SUM225 cells represented a model for HER2+ DCIS. The xenografted tissues initially grew within the mammary ducts, forming single and multilayered epithelium after 8 weeks with stromal invasion in some cases. The grafts recapitulated the patient's original DCIS with respect to heterogeneity and expression of biomarkers, such as human cytokeratins, ER, and HER2. These studies demonstrate that DCIS xenografts can retain the unique pathology and heterogeneity of the human lesions and provide a new tool for probing the cellular and molecular events associated with DCIS progression.

6 GENETICALLY ENGINEERED MOUSE MODELS OF BREAST CANCER

6.1 General Overview

In the early 1980s technology for generating mouse lines carrying cloned genes was developed and at about the same time viral and cellular oncogenes were identified in animal and human cancers. Merging of these two advances in the mid-1980s led to the development of the first transgenic mice carrying activated oncogenes. Some of these mice were found to display heritable predisposition to tumor development. In 1988, the "oncomouse"—a line expressing the c-Myc oncogene specifically in mammary epithelial tissue was developed and patented (Hanahan et al., 2007). This transgenic line spontaneously developed mammary carcinomas in a delayed and asynchronous fashion. As specific genetic events associated with human breast cancers were identified, mice carrying genetic alterations that mimic mutations found in patients were generated. Many of the transgenic models were created with selective oncogene expression in mammary tissue through the use of promoters that are highly active in breast cells. The most commonly used of these promoters are the MMTV-derived long terminal repeat (MMTV-LTR), the whey acidic protein (WAP), and the β-lactoglobin (BLG), which are all active in the luminal epithelial cells of the mouse mammary gland. Activity of these promoters is hormone dependent to some degree, but generally they are highly efficient at driving mammary specific expression beginning at puberty (MMTV) or pregnancy (WAP, BLG). Less frequently used is the keratin 14 (K14) promoter which is expressed in basal and myoepithelial cells but not in luminal cells, allowing for targeting of oncogenes to a different cell of breast cancer origin in the gland. Although selective for mammary tissue, none of these promoters are completely specific, and transgene expression is often detected at low levels in lungs, kidney, prostate, seminal vesicles, salivary glands, and other tissues. Extramammary transgene expression can create problems in interpretation of tumor phenotypes if it results in systemic changes that secondarily affect mammary gland development.

To complement the oncogenic models, mice in which tumor suppressor genes are ablated were generated and many of these lines display increased susceptibility to spontaneous or induced mammary carcinoma (Deng, 2014). To date, thousands of murine models of breast cancer have been generated, using more advanced technologies including inducible promoters, such as the tetracycline regulators and conditional ablation techniques, such as the cre/lox system (Borowsky, 2011; Menezes et al., 2014). Furthermore, many of these mouse lines have been crossed to investigate synergy, or bred onto different background to explore genetic susceptibility. Thus, there are a myriad of models to choose from for studying breast cancer in genetically engineered mice (GEM). It should be remembered that the specific initiating oncogene, the cell of origin that is targeted by the chosen promoter and the developmental timing of oncogene expression will all impact the tumor phenotype of these GEM models. In depth discussion of these approaches and technologies is outside the scope of this chapter, but many reviews are available on the strategies and applications (Borowsky, 2011; Cheon and Orsulic, 2011). A few of the more commonly used models will be briefly described here, including a short comparison of the resulting tumors from some of these mice, and how well they model the pathology and molecular heterogeneity characteristic of human breast tumors.

6.2 Examples of GEM Mammary Tumor Models With Activation of Oncogenes

By definition, an oncogene is a gene whose gain of function (whether by amplification, mutation, or overexpression) increases the risk of carcinogenic transformation for the cell in which it is active. In GEM models of mammary cancer, oncogene activation is mimicked by transgenic overexpression of a normal or mutated version of the gene of interest usually driven by mammary-specific promoters. The most commonly used models are those in which strong oncogenes (Myc, Ras, Wnt, TGFα, and ErbB2) are selectively driven in mammary luminal epithelial cells by the MMTV or WAP promoters. However, new models are routinely being developed and characterized (Borowsky, 2011; Greenow and Smalley, 2015).

The first transgenic model of breast cancer was the MMTV-Myc mouse strain, which developed spontaneous mammary adenocarcinomas by 4–8 months of age (Stewart et al., 1984). When Myc is expressed under the transcriptional control of the WAP promoter, 80% of female transgenics developed multiple tumors affecting single or multiple glands after two pregnancies as early as 2 months of age. The heterogeneity of MMTV-Myc induced mammary tumors was recently evaluated in mice expressing either wild-type Myc or the constitutively active mutant T85A (Andrechek et al., 2009). While the majority of tumors in MMTV-Myc mice were microacinar (composed of cuboidal cells arranged in acini with basal myoepithelial cells), those in mice expressing T85A Myc were predominantly papillary (composed of fibrovascular stalks lined by columnar cells that form gland like spaces). Other tumor types included squamous carcinomas, adenocarcinomas, and those defined as epithelial-mesenchymal transition (EMT)—type tumors. Genomic analysis indicated that these histological subtypes reflected different signaling pathways including β-catenin and Stat3 activities. In addition, activating mutations in the Ras oncogene were particularly prevalent in the EMT-type tumors (Leung et al., 2012). Collectively, these mouse models demonstrated that Myc is a mammary oncogene, but the focal nature of the lesions, the asynchrony and heterogeneity of tumor development, and the prolonged time course indicated that additional molecular events cooperate with Myc to drive carcinogenesis (Hutchinson and Muller, 2000).

Using a similar approach, MMTV-Ras mice were created and characterized by the Leder group (Sinn et al., 1987). In contrast to MMTV-Myc mice, in which only females develop mammary adenocarcinomas, both male and female MMTV-Ras mice exhibited mammary and salivary gland neoplasms within 5 weeks of age. The tumors that developed in MMTV-Ras mice were primarily papillary adenocarcinomas. When MMTV-Myc and MMTV-Ras mice were crossed, the kinetics with which tumors developed was considerably accelerated (Sinn et al., 1987). Comparative aspects of the myc, ras, and bigenic mammary tumors, which are all ER-, have been described (Pattengale et al., 1989).

The MMTV-Neu models (Andrechek et al., 2000; Muller et al., 1996, 1988) were designed to mimic the 20%–30% of human breast cancers that overexpress the growth factor receptor HER2. Human HER2 positive breast cancers are characterized by amplification of the region on chromosome 17 (17q21-q22) which encodes the ERBB2 gene, causing marked upregulation of the HER2 growth factor receptor in tumors. The presence of HER2 amplification in human tumors is associated with aggressive disease that has a high rate of recurrence and poor prognosis. In MMTV-Neu mice, the wild-type form of the rat gene Neu (the homolog of the ErbB2 gene) is expressed from the MMTV promoter. In this model, both virgin and nonvirgin female mice exhibited mammary hyperplasia with a 50% incidence of focal adenocarcinomas by 205 days of age. Lung metastases were detected in 72% of tumor-bearing mice that lived 8 months or longer. Transgenic expression of a constitutively active form of Neu (containing a point mutation that facilitates receptor oligomerization and ligand-independent activation) in the mammary gland markedly accelerated the onset of tumors (Muller et al., 1988; Pattengale et al., 1989). Tumors that developed in MMTV-neu mice were solid nodular adenocarcinomas with some evidence of lumen formation and weak to no detectable expression of ER.

Related to the MMTV-Neu model is the MMTV-PyVMT model, which expresses the polyoma virus middle T antigen under the control of MMTV (Guy et al., 1992). The PyVMT encodes a membrane spanning protein that potently activates pathways downstream of growth factors including ERBB2, including SRC and phosphatidylinositol 3-kinase (PI3K) (Dilworth, 2002). Female MMTV-PyVMT mice developed highly aggressive multifocal ER negative mammary tumors involving the entire fat pad with 100% incidence and an average latency of 35 days. Tumors developed in both virgin and parous females, as well as in males. Tumor-bearing mice developed spontaneous lung metastases within ~90 days (85% penetrance).

Other models in which growth factor pathways are deregulated in association with mammary tumor formation include mice expressing the EGFR ligand TGFα (Lee and Muller, 2010; Pattengale et al., 1989). In three different models, overexpression of TGFα in the mammary epithelium was associated with hyperplasia of alveoli and terminal ducts in virgin female and pregnant transgenic mice. A range of morphologic abnormalities including lobular hyperplasia, cystic hyperplasia, adenoma, and adenocarcinoma were seen in the mammary tissue of transgenic females. With multiple pregnancies and increasing age, up to 40% of multiparous animals developed tumors by 16 months of age (Halter et al., 1992; Matsui et al., 1990). Bigenic mice carrying both WAP-TGFα and WAP-Myc displayed a dramatic acceleration of tumor development, with 100% of bigenic mice developing synchronous mammary tumors at a mean age of 66 days. Of note, when TGFα was driven by the Neu-related lipocalin (NRL) promoter, the hyperplasias, cystic and solid tumors that developed all expressed ER (Rose-Hellekant et al., 2007). These tumors were also hormone dependent as ovariectomy decreased tumor incidence. Thus, this model represents a good choice for studying the formation of ER+ mammary tumors.

6.3 Examples of GEM Mammary Tumor Models With Inactivation of Tumor Suppressor Genes

By definition, tumor suppressor genes are those whose loss of function increases the risk of cancer. Since in general, both alleles of a tumor suppressor gene must be inactivated for cancer to develop, most GEM models of breast cancer have utilized homozygous knockout mice. There are some examples where engineered loss of function or dominant negative mutations have been constructed. Since many tumor suppressor genes have critical roles in development, conditional deletion/mutation is often necessary to avoid embryonic or perinatal lethality or associated disturbances in tissues other than the mammary gland.

The best-characterized tumor suppressor gene is p53, a transcription factor with essential roles in cell cycle and apoptosis control, DNA damage signaling, and metabolism. p53 is commonly mutated in sporadic breast tumors and its germline loss of function increases the risk for development of breast cancer in individuals with Li–Fraumeni syndrome. Not surprisingly, mice lacking p53 develop tumors in multiple tissues (primarily sarcomas and lymphomas) and early mortality from these malignancies precludes the development of mammary tumors (Donehower et al., 1992; Jacks et al., 1994). Thus, other approaches, such as transplantation of p53 null tissue into syngeneic mice (Medina, 2010), use of p53 heterozygous (+/−) mice (Kuperwasser et al., 2000), expression of dominant negative alleles (Wijnhoven et al., 2005), or conditional p53 deletion with cre/lox technology (Lin et al., 2004) have been necessary for studying the role of p53 in mammary tumorigenesis in vivo. Notably, tumor spectrum is altered in p53 deficient mice on the BALB/c genetic background, with preferential development of mammary tumors in p53$^{+/-}$ mice. Median survival was 15 weeks for BALB/c-p53$^{-/-}$ mice compared to 54 weeks for BALB/c-p53$^{+/-}$ mice. Although sarcomas and lymphomas were the most frequent tumor types in BALB/c-p53$^{-/-}$ mice, 55% of the female BALB/c-p53$^{+/-}$ mice developed mammary carcinomas. The mammary tumors in p53$^{+/-}$ mice were highly aneuploidy with frequent loss of the remaining wild-type p53 allele. Transplantation of p53$^{-/-}$ epithelium into syngeneic hosts resulted in 75% tumor formation indicating that complete loss of p53$^{-/-}$ also favors mammary carcinogenesis (Kuperwasser et al., 2000). Using the Cre/loxP system, p53 inactivation with a constitutively active WAP-Cre, but not with MMTV-Cre, led to the development of ER+ mammary tumors (Lin et al., 2004) with genetic alterations, such as Myc amplification and Her2 activation and a high rate of metastasis. Thus, there are multiple p53-deficient GEM models to choose from that recapitulate many aspects of human breast cancer.

The best-characterized mammary-specific tumor suppressor genes in humans are BRCA1 and BRCA2. Germline deletion of either BRCA1 or BRCA2 is embryonic lethal, and mice heterozygous for BRCA1 or BRCA2 do not have increased spontaneous tumor development (Borowsky, 2011). Conditional alleles of both BRCA genes have been created with various promoters (MMTV, WAP, BLG, K14) and in most of these, females indeed developed mammary tumors of diverse types, albeit with long (greater than 1 year) latency (Evers and Jonkers, 2006; Ludwig et al., 2001; Xu et al., 1999). When conditional BRCA models have been crossed with p53$^{+/-}$ mice, synergistic acceleration of spontaneous mammary tumor development was observed. Tumors from MMTV-Cre;Brca1$^{Co/Co}$;p53$^{+/-}$ mice were triple negative, basal-like, and displayed gross genomic instability (Brodie et al., 2001). In K14-Cre;Brca1$^{F5-13/F5-13}$;p53$^{F2-10/F2-10}$ mice, tumors were also highly aneuploid solid carcinomas with basal-like characteristics, including high-proliferation index, poor differentiation, and lack of ER expression (Liu et al., 2007). Tumors from BRCA2 conditional mice displayed aneuploidy and chromosomal aberrations, were usually ER- and HER2-negative with high cyclin D1 expression. Combined tissue-specific inactivation of both Brca2 and p53 resulted in highly efficient mammary tumor formation in K14-Cre;Brca2$^{F11/F11}$;p53$^{F2-10/F2-10}$ female mice (Jonkers et al., 2001). Although there was some heterogeneity in tumor types, most did not express ER, PR, or ErbB2 and were positive for basal cell cytokeratins. Thus, these tumors resembled the human BRCA1-associated cancers, which are triple negative, but not the BRCA2-associated human cancers which are typically ER positive.

Additional GEM models of mammary tumorigenesis involving tumor suppressor genes include Stat1 (mimics human ER positive luminal breast cancers and synergizes with MMTV-Neu driven tumorigenesis) and E-cadherin (mimics human lobular carcinoma in association with p53 deletion) (Derksen et al., 2011). Additional details on mouse models and their relevance to human breast cancer are available in several reviews (Borowsky, 2011; Lee and Muller, 2010; Manning et al., 2016; Menezes et al., 2014; Mohibi et al., 2011; Vargo-Gogola and Rosen, 2007).

7 COMPARATIVE PATHOLOGY AND GENOMICS: MOUSE MAMMARY TUMORS VERSUS HUMAN BREAST CANCER

A consensus report on the comparative pathology of 39 breast cancer GEM models and human breast cancer was generated in 1999 (Cardiff et al., 2000). The conclusion from that analysis was that the overall histology of the available GEM tumors did not resemble the common types of human breast cancer. However, GEM tumors were deemed valuable since genes known

to be associated with human breast cancer did cause cancers in mice and the more heterogeneous tumors did contain regions reminiscent of human breast cancer histology. Notable differences in most mouse tumors compared to human tumors included the lack of fibrosis and inflammation, the limited metastasis, and the hormone independence. Other than xenografts, the rat chemically induced mammary tumorigenesis model was noted as the best model for studying hormone independence. As described in this chapter and recent reviews (Borowsky, 2011; Lee and Muller, 2010; Mohibi et al., 2011) there are considerably more GEM models now, with unique phenotypes including ER positive luminal-type tumors. Furthermore, many of these models have yet to be characterized with respect to sensitivity to induced carcinogenesis (i.e., chemical, hormone, or radiation paradigms). Still lacking, too, are models of the less-frequent tumor types (such as mucinous, tubular, medullary, and inflammatory breast cancers) and those that truly mimic the metastatic patterns characteristic of human breast cancers.

Genomic profiling has provided another approach to assess how well murine tumors model human breast cancers. Profiles of 10 distinct mouse mammary tumor models were conducted to characterize their diversity with an emphasis on the similarities to human breast tumors (Herschkowitz et al., 2007). This analysis indicated that while some mouse models (including WAP-Myc, MMTV-Neu, MMTV-PyVMT) developed tumors with consistent, model-specific patterns of gene expression, others (DMBA-induced models, BRCA/p53$^{+/-}$) displayed much more diversity. In addition, murine tumors clustered into 10 groups which could be subdivided into four main categories (normal, mesenchymal, basal/myoepithelial, and luminal). Based on these genomic profiles, four of the GEM models (WAP-Myc, MMTV-Neu, MMTV-PyVMT, and Wap-Int3) developed luminal-like tumors with the important caveat that the murine tumors lacked ER and thus did not express core ER regulated genes found in the human luminal cluster. Several models, including the Brca1-deficient and DMBA-initiated tumors, showed genomic profiles consistent with human basal-like tumors. Another study applied comparative genomics of p53 null tumors in mouse and basal breast cancers in humans to identify common aberrations (Pfefferle et al., 2016). This study reported five potential drug target genes that were amplified in both murine and human basal-like tumors: *Cul4a*, *Lamp1*, *Met*, *Pnpla6*, and *Tubgcp3*. Collectively, these studies and other publically available comparative genomic analyses provide exceptional resources for choosing the most appropriate mouse model for study of distinct breast cancer subtypes (Usary et al., 2016).

8 STUDYING METASTASIS IN MICE WITH AN EMPHASIS ON NEW MODELS

In general, the patterns of breast cancer dissemination in the available animal models do not recapitulate those observed in human breast cancer. Although several of the GEM models progress to distant metastases, the incidence is relatively low and disease spread to clinically relevant sites, such as brain and bone, is rare. Despite this caveat, both xenograft and GEM approaches have been utilized to study specific aspects of breast cancer metastasis, yielding insights into mechanisms, as well as providing evidence of circulating tumors cells and metastasis suppressor genes in these models (Bohl et al., 2014; Kabeer et al., 2016; Simmons et al., 2015).

Better models of bone metastasis are of particular interest due to the frequency and clinical impact of skeletal spread in patients. Typically, studies of bone metastasis have relied on direct injection of tumor cells (ideally expressing luciferase or other traceable tag) into the tail vein, the left cardiac ventricle, or the bone (tibia, femur, calvaria) of immunocompromised mice. The most frequently used syngeneic model utilizes the 4T1 series of cell lines derived from the BALB/c strain, which when transplanted directly into the bone invade and generate osteolytic lesions with morphologic and genomic similarities to that observed in the human bone–tumor interface (Futakuchi and Singh, 2013). With respect to use of human breast cancer cells in xenograft models, several lines have been identified with propensity for growth in bone, including MDA-MB-435 and certain sublines of MDA-MB-231 cells (Jenkins et al., 2005). However, these also require direct inoculation into the circulation or ectopic implantation into bone for reliable metastases. Advantages, limitations, and specific details are available in recent reviews (Hibberd et al., 2013; Horas et al., 2015; Simmons et al., 2015).

Other approaches involve implantation of neonatal mouse vertebrae or fragments of fetal human bone into the host mice to provide a substrate for cancer cell spread. Rosenblatt (2012) created an "all human" model of breast cancer metastasis to adult bone. In this approach, ER/PR negative, HER2 positive SUM1315 cells injected into the mammary fat pad of immunodeficient mice migrated to previously implanted adult human bone fragments obtained at biopsy (Moreau et al., 2007). The team also created 3D bone-like scaffolds seeded with mesenchymal stromal cells and demonstrated that SUM1315 cells metastasized from the fat pad to both the tissue-engineered scaffolds and native human bone implants. The use of engineered scaffolds as homing sites for breast cancer metastasis from an orthotopic site may provide new opportunities to manipulate the bone microenvironment for mechanistic studies.

9 EMERGING NONRODENT MODELS OF BREAST CANCER

In recent years, efforts have been made to identify nontraditional models of breast cancer through characterization of spontaneous tumors in cats and dogs, induced cancers in primates, and modeling of metastasis in zebrafish. These emerging models are briefly discussed here with an eye to the future. Spontaneous mammary cancers develop in both dogs and cats and are often highly malignant. Dogs develop invasive mammary carcinomas with epidemiological and biological similarities to human breast cancers including a high prevalence of the triple-negative subtype (Rasotto et al., 2014). Interestingly, overexpression of the insulin-like growth factor Type 1 receptor (IGFR1) is common in canine invasive mammary carcinoma (as in human breast cancer) and is associated with aggressive features including lymphovascular invasion, high grade and the triple negative phenotype. IGFR1 overexpression in canine triple-negative tumors is associated with shorter overall and specific survival and shorter disease free index (Jaillardon et al., 2015). Thus spontaneous canine mammary cancer offers a relevant model for preclinical studies on new therapies targeting IGF1R and related pathways in triple-negative breast cancer. Guidelines for characterizing immunohistochemical biomarkers (ER, PR, HER2) and pathology (epithelial vs. myoepithelial, invasion, and micrometastases) of canine mammary tumors have been published to ensure reproducibility and comparison of various studies (Pena et al., 2014).

Feline mammary adenocarcinomas are also highly aggressive with strong similarities in clinical behavior to human basal-like breast cancers (Wiese et al., 2013). Molecular classification of feline mammary carcinomas indicated that the luminal B/HER2-negative subtype was the most common (30%), followed by luminal B/HER2-positive subtype (20%), triple negative basal-like (17%), luminal A (15%), triple negative normal-like (13%), and finally, HER2-positive subtype (7%). Highest survival was observed in cats with the Luminal A subtype while lowest survival was in animals with triple negative basal-like subtypes (Hassan et al., 2016; Soares et al., 2016). Lung was the most frequent site of metastasis. Interestingly, cats with multiple primary tumors showed different molecular subtypes in each carcinoma indicating considerable heterogeneity in etiology. Studies on feline mammary cancer are facilitated by the availability of cell lines (Borges et al., 2016; Hassan et al., 2016), some of which have been characterized for growth and metastasis in nude mice. When inoculated subcutaneously, feline carcinoma cells did not metastasize, but lung, brain, liver, kidney, eye, and bone metastases were confirmed following intratibial and intracardiac injection. Genomic analysis identified upregulation of genes encoding growth factors in the PDGF, EGF, and VEGF families in metastatic lesions. Collectively, these reports provide evidence that both spontaneous and experimental feline mammary carcinomas represent additional models for human breast cancer.

Zebrafish represent a powerful genetic model that is amenable to engraftment approaches and is highly suitable for studies of angiogenesis and metastasis (Moore and Langenau, 2016; Tulotta et al., 2016). Cancer cells can be transplanted into embryonic zebrafish prior to development of a functional immune system or into adult zebrafish with genetic or induced ablation of the immune system. Breast cancer cells of diverse malignant potential exhibit invasive and metastatic properties within embryonic zebrafish that correlate with their tumorigenicity in mouse models (Drabsch et al., 2013). Furthermore, blocking known mediators of metastasis (TGF-β, Smad4, matrixmetalloproteinases) reduces invasion and metastasis in the zebrafish xenograft model and closely mimics results from mouse metastasis models (Drabsch et al., 2013). Combined with sensitive imaging techniques, this model allows for cost-effective and rapid screening of potential inhibitors of angiogenesis and metastasis.

A unique model of breast cancer has been developed in tree shrews, a small primate that is easy to manipulate, maintain, and propagate. While breast cancer can be induced in tree shrews with chemical carcinogens, the incidence is low (50%) and the latency is long (7 months). In a novel approach, mammary tumors were induced within 3 weeks after injection of a lentivirus driving expression of the polyoma middle T oncogene into the mammary ducts (Ge et al., 2016). All injected animals developed tumors and one case showed metastasis to lymph node and lung. Tumor growth was significantly inhibited by established chemotherapeutics (cisplatin and epidoxorubicin). Once fully characterized, this primate model could represent a clinically relevant model suitable for screening of breast cancer therapeutics due to its high efficiency and short latency.

10 CONCLUSIONS

Advances in prevention and treatment for breast cancer rely heavily on the use of animal models. As described in this chapter, rodent models provide good surrogates for human breast tumors and are particularly useful for identification and testing of therapeutics. More efficient use of published data may benefit from sharing of archived resources between labs, a goal of the new web-based tool SEARCHBreast (https://searchbreast.org/), a searchable database, and online collaborative network of breast cancer researchers with experience with in vivo, in vitro, and in silico models of breast cancer. The

aim of this web-based resource is to reduce duplicative research by sharing data and archived materials, thereby accelerating discoveries (Blyth et al., 2016). As emerging models in other species become better characterized and shared, appropriate models for addressing clinical and molecular research questions relevant to human breast cancer can easily be identified.

References

Alpaugh, M.L., Tomlinson, J.S., Shao, Z.M., Barsky, S.H., 1999. A novel human xenograft model of inflammatory breast cancer. Cancer Res. 59 (20), 5079–5084.

American Cancer Society, 2015. Cancer Facts & Figures.

Anderson, W.F., Chatterjee, N., Ershler, W.B., Brawley, O.W., 2002. Estrogen receptor breast cancer phenotypes in the surveillance, epidemiology, and end results database. Breast Cancer Res. Treat. 76 (1), 27–36.

Andrechek, E.R., Cardiff, R.D., Chang, J.T., Gatza, M.L., Acharya, C.R., Potti, A., et al., 2009. Genetic heterogeneity of Myc-induced mammary tumors reflecting diverse phenotypes including metastatic potential [Research Support, N.I.H., Extramural Research Support, Non-U.S. Gov't]. Proc. Natl. Acad. Sci. USA 106 (38), 16387–16392.

Andrechek, E.R., Hardy, W.R., Siegel, P.M., Rudnicki, M.A., Cardiff, R.D., Muller, W.J., 2000. Amplification of the neu/erbB-2 oncogene in a mouse model of mammary tumorigenesis. Proc. Natl. Acad. Sci. USA 97 (7), 3444–3449.

Anisimov, V.N., Ukraintseva, S.V., Yashin, A.I., 2005. Cancer in rodents: does it tell us about cancer in humans? [Research Support, N.I.H., Extramural Research Support, Non-U.S. Gov't Research Support, U.S. Gov't, P.H.S. Review]. Nat. Rev. Cancer 5 (10), 807–819.

Aslakson, C.J., Miller, F.R., 1992. Selective events in the metastatic process defined by analysis of the sequential dissemination of subpopulations of a mouse mammary tumor [Research Support, Non-U.S. Gov't Research Support, U.S. Gov't, P.H.S.]. Cancer Res. 52 (6), 1399–1405.

Baca, M.E., Mowat, A.M., 1989. Immunological studies of NK cell-deficient beige mice. I. Defective ability of beige lymphocytes to mediate local and systemic graft-versus-host reactions. Immunology 66 (1), 125–130.

Balogh, G.A., Heulings, R., Mailo, D.A., Russo, P.A., Sheriff, F., Russo, I.H., et al., 2006. Genomic signature induced by pregnancy in the human breast [Research Support, N.I.H., Extramural]. Int. J. Oncol. 28 (2), 399–410.

Behbod, F., Kittrell, F.S., LaMarca, H., Edwards, D., Kerbawy, S., Heestand, J.C., et al., 2009. An intraductal human-in-mouse transplantation model mimics the subtypes of ductal carcinoma in situ. Breast Cancer Res. 11 (5), R66.

Blyth, K., Carter, P., Morrissey, B., Chelala, C., Jones, L., Holen, I., et al., 2016. SEARCHBreast: a new resource to locate and share surplus archival material from breast cancer animal models to help address the 3Rs. Breast Cancer Res. Treat. 156 (3), 447–452.

Bogachek, M.V., Park, J.M., De Andrade, J.P., Kulak, M.V., White, J.R., Wu, T., et al., 2015. A novel animal model for locally advanced breast cancer. Ann. Surg. Oncol. 22 (3), 866–873.

Bohl, C.R., Harihar, S., Denning, W.L., Sharma, R., Welch, D.R., 2014. Metastasis suppressors in breast cancers: mechanistic insights and clinical potential. J. Mol. Med. (Berl.) 92 (1), 13–30.

Bombonati, A., Sgroi, D.C., 2011. The molecular pathology of breast cancer progression [Research Support, N.I.H., Extramural Research Support, Non-U.S. Gov't Research Support, U.S. Gov't, Non-P.H.S. Review]. J. Pathol. 223 (2), 307–317.

Borges, A., Adega, F., Chaves, R., 2016. Establishment and characterization of a new feline mammary cancer cell line, FkMTp. Cytotechnology 68, 1529–1543.

Borowsky, A.D., 2011. Choosing a mouse model: experimental biology in context—the utility and limitations of mouse models of breast cancer. Cold Spring Harb. Perspect. Biol. 3 (9), a009670.

Bosma, M.J., Carroll, A.M., 1991. The SCID mouse mutant: definition, characterization, and potential uses. Annu. Rev. Immunol. 9, 323–350.

Britt, K., Ashworth, A., Smalley, M., 2007. Pregnancy and the risk of breast cancer [Research Support, Non-U.S. Gov't Review]. Endocr. Relat. Cancer 14 (4), 907–933.

Brodie, S.G., Xu, X., Qiao, W., Li, W.M., Cao, L., Deng, C.X., 2001. Multiple genetic changes are associated with mammary tumorigenesis in Brca1 conditional knockout mice [Research Support, U S Gov't, P H S]. Oncogene 20 (51), 7514–7523.

Callahan, R., Smith, G.H., 2000. MMTV-induced mammary tumorigenesis: gene discovery, progression to malignancy and cellular pathways [Review]. Oncogene 19 (8), 992–1001.

Cardiff, R.D., Anver, M.R., Gusterson, B.A., Hennighausen, L., Jensen, R.A., Merino, M.J., et al., 2000. The mammary pathology of genetically engineered mice: the consensus report and recommendations from the Annapolis meeting. Oncogene 19 (8), 968–988.

Cedro-Tanda, A., Cordova-Solis, A., Juarez-Cedillo, T., Pina-Jimenez, E., Hernandez-Caballero, M.E., Moctezuma-Meza, C., et al., 2014. Prevalence of HMTV in breast carcinomas and unaffected tissue from Mexican women. BMC Cancer 14, 942.

Cheon, D.J., Orsulic, S., 2011. Mouse models of cancer [Research Support, N.I.H., Extramural Research Support, Non-U.S. Gov't Review]. Annu. Rev. Pathol. 6, 95–119.

Clarke, R., 1996. Human breast cancer cell line xenografts as models of breast cancer. The immunobiologies of recipient mice and the characteristics of several tumorigenic cell lines [Research Support, Non-U.S. Gov't Research Support, U.S. Gov't, P.H.S. Review]. Breast Cancer Res. Treat. 39 (1), 69–86.

de Plater, L., Lauge, A., Guyader, C., Poupon, M.F., Assayag, F., de Cremoux, P., et al., 2010. Establishment and characterisation of a new breast cancer xenograft obtained from a woman carrying a germline BRCA2 mutation. Br. J. Cancer 103 (8), 1192–1200.

Decaudin, D., 2011. Primary human tumor xenografted models ('tumorgrafts') for good management of patients with cancer. Anticancer Drugs 22 (9), 827–841.

Deng, C.X., 2014. Conditional knockout mouse models of cancer. Cold Spring Harb. Protoc. 2014 (12), 1217–1233.

Derksen, P.W., Braumuller, T.M., van der Burg, E., Hornsveld, M., Mesman, E., Wesseling, J., et al., 2011. Mammary-specific inactivation of E-cadherin and p53 impairs functional gland development and leads to pleomorphic invasive lobular carcinoma in mice [Research Support, Non-U S Gov't]. Dis. Model Mech. 4 (3), 347–358.

Dilworth, S.M., 2002. Polyoma virus middle T antigen and its role in identifying cancer-related molecules. Nat. Rev. Cancer 2 (12), 951–956.

Ding, L., Ellis, M.J., Li, S., Larson, D.E., Chen, K., Wallis, J.W., et al., 2010. Genome remodelling in a basal-like breast cancer metastasis and xenograft. Nature 464 (7291), 999–1005.

Donawho, C.K., Luo, Y., Luo, Y., Penning, T.D., Bauch, J.L., Bouska, J.J., et al., 2007. ABT-888, an orally active poly(ADP-ribose) polymerase inhibitor that potentiates DNA-damaging agents in preclinical tumor models. Clin. Cancer Res. 13 (9), 2728–2737.

Donehower, L.A., Harvey, M., Slagle, B.L., McArthur, M.J., Montgomery, Jr., C.A., Butel, J.S., et al., 1992. Mice deficient for p53 are developmentally normal but susceptible to spontaneous tumours [Research Support, Non-U S Gov't]. Nature 356 (6366), 215–221.

Drabsch, Y., He, S., Zhang, L., Snaar-Jagalska, B.E., ten Dijke, P., 2013. Transforming growth factor-beta signalling controls human breast cancer metastasis in a zebrafish xenograft model. Breast Cancer Res. 15 (6), R106.

Dudley, J.P., Golovkina, T.V., Ross, S.R., 2016. Lessons learned from mouse mammary tumor virus in animal models. ILAR J. 57 (1), 12–23.

Dunlap, S.M., Chiao, L.J., Nogueira, L., Usary, J., Perou, C.M., Varti-covski, L., et al., 2012. Dietary energy balance modulates epithe-lial-to-mesenchymal transition and tumor progression in murine claudin-low and basal-like mammary tumor models. Cancer Prev. Res. (Phila.) 5 (7), 930–942.

Eckhardt, B.L., Parker, B.S., van Laar, R.K., Restall, C.M., Natoli, A.L., Tavaria, M.D., et al., 2005. Genomic analysis of a spontaneous model of breast cancer metastasis to bone reveals a role for the ex-tracellular matrix [Research Support, N.I.H., Extramural Research Support, Non-U.S. Gov't Research Support, U.S. Gov't, Non-P.H.S. Research Support, U.S. Gov't, P.H.S.]. Mol. Cancer Res. 3 (1), 1–13.

Eirew, P., Steif, A., Khattra, J., Ha, G., Yap, D., Farahani, H., et al., 2015. Dynamics of genomic clones in breast cancer patient xenografts at single-cell resolution. Nature 518 (7539), 422–426.

Elstrodt, F., Hollestelle, A., Nagel, J.H., Gorin, M., Wasielewski, M., van den Ouweland, A., et al., 2006. BRCA1 mutation analysis of 41 hu-man breast cancer cell lines reveals three new deleterious mutants. Cancer Res. 66 (1), 41–45.

Evers, B., Jonkers, J., 2006. Mouse models of BRCA1 and BRCA2 de-ficiency: past lessons, current understanding and future prospects [Research Support, Non-U S Gov't Review]. Oncogene 25 (43), 5885–5897.

Fleming, J.M., Miller, T.C., Meyer, M.J., Ginsburg, E., Vonderhaar, B.K., 2010. Local regulation of human breast xenograft models [Research Support, N.I.H., Extramural Research Support, Non-U.S. Gov't]. J. Cell Physiol. 224 (3), 795–806.

Futakuchi, M., Singh, R.K., 2013. Animal model for mammary tu-mor growth in the bone microenvironment. Breast Cancer 20 (3), 195–203.

Garcia-Garcia, C., Ibrahim, Y.H., Serra, V., Calvo, M.T., Guzman, M., Grueso, J., et al., 2012. Dual mTORC1/2 and HER2 blockade results in antitumor activity in preclinical models of breast cancer resistant to anti-HER2 therapy. Clin. Cancer Res. 18 (9), 2603–2612.

Ge, G.Z., Xia, H.J., He, B.L., Zhang, H.L., Liu, W.J., Shao, M., et al., 2016. Generation and characterization of a breast carcinoma model by PyMT overexpression in mammary epithelial cells of tree shrew, an animal close to primates in evolution. Int. J. Cancer 138 (3), 642–651.

Greenow, K.R., Smalley, M.J., 2015. Overview of genetically engineered mouse models of breast cancer used in translational biology and drug development. Curr. Protoc. Pharmacol. 70, 14.36.11–14.36.14.

Guy, C.T., Cardiff, R.D., Muller, W.J., 1992. Induction of mammary tu-mors by expression of polyomavirus middle T oncogene: a trans-genic mouse model for metastatic disease. Mol. Cell Biol. 12 (3), 954–961.

Halter, S.A., Dempsey, P., Matsui, Y., Stokes, M.K., Graves-Deal, R., Hogan, B.L., et al., 1992. Distinctive patterns of hyperplasia in transgenic mice with mouse mammary tumor virus transforming growth factor-alpha. Characterization of mammary gland and skin proliferations. Am. J. Pathol. 140 (5), 1131–1146.

Hanahan, D., Coussens, L.M., 2012. Accessories to the crime: functions of cells recruited to the tumor microenvironment [Review]. Cancer Cell 21 (3), 309–322.

Hanahan, D., Wagner, E.F., Palmiter, R.D., 2007. The origins of oncom-ice: a history of the first transgenic mice genetically engineered to develop cancer. Genes Dev. 21 (18), 2258–2270.

Hassan, B.B., Elshafae, S.M., Supsavhad, W., Simmons, J.K., Dirksen, W.P., Sokkar, S.M., et al., 2016. Feline mammary cancer: novel nude mouse model and molecular characterization of invasion and me-tastasis genes. Vet. Pathol. 54, 32–43.

Herschkowitz, J.I., Simin, K., Weigman, V.J., Mikaelian, I., Usary, J., Hu, Z., et al., 2007. Identification of conserved gene expression features between murine mammary carcinoma models and human breast tumors [Comparative Study Research Support, N.I.H., Extramural Research Support, Non-U.S. Gov't]. Genome Biol. 8 (5), R76.

Hibberd, C., Cossigny, D.A., Quan, G.M., 2013. Animal cancer models of skeletal metastasis. Cancer Growth Metastasis 6, 23–34.

Hollestelle, A., Nagel, J.H., Smid, M., Lam, S., Elstrodt, F., Wasielewski, M., et al., 2010. Distinct gene mutation profiles among luminal-type and basal-type breast cancer cell lines [Research Support, U.S. Gov't, Non-P.H.S.]. Breast Cancer Res. Treat. 121 (1), 53–64.

Holliday, D.L., Speirs, V., 2011. Choosing the right cell line for breast cancer research [Research Support, Non-U.S. Gov't]. Breast Cancer Res. 13 (4), 215.

Horas, K., Zheng, Y., Zhou, H., Seibel, M.J., 2015. Animal models for breast cancer metastasis to bone: opportunities and limitations. Cancer Invest. 33 (9), 459–468.

Huggins, C., Grand, L.C., Brillantes, F.P., 1961. Mammary cancer in-duced by a single feeding of polymucular hydrocarbons, and its suppression. Nature 189, 204–207.

Hutchinson, J.N., Muller, W.J., 2000. Transgenic mouse models of hu-man breast cancer. Oncogene 19 (53), 6130–6137.

Ince, T.A., Richardson, A.L., Bell, G.W., Saitoh, M., Godar, S., Karnoub, A.E., et al., 2007. Transformation of different human breast epithe-lial cell types leads to distinct tumor phenotypes [Comparative Study Research Support, N.I.H., Extramural Research Support, Non-U.S. Gov't]. Cancer Cell 12 (2), 160–170.

Jacks, T., Remington, L., Williams, B.O., Schmitt, E.M., Halachmi, S., Bronson, R.T., et al., 1994. Tumor spectrum analysis in p53-mutant mice [Research Support, Non-U S Gov't Research Support, U S Gov't, P H S]. Curr. Biol. 4 (1), 1–7.

Jaillardon, L., Abadie, J., Godard, T., Campone, M., Loussouarn, D., Siliart, B., et al., 2015. The dog as a naturally-occurring model for insulin-like growth factor type 1 receptor-overexpressing breast cancer: an observational cohort study. BMC Cancer 15, 664.

Jenkins, D.E., Hornig, Y.S., Oei, Y., Dusich, J., Purchio, T., 2005. Biolumi-nescent human breast cancer cell lines that permit rapid and sensi-tive in vivo detection of mammary tumors and multiple metastases in immune deficient mice. Breast Cancer Res. 7 (4), R444–R454.

Jonkers, J., Meuwissen, R., van der Gulden, H., Peterse, H., van der Valk, M., Berns, A., 2001. Synergistic tumor suppressor activity of BRCA2 and p53 in a conditional mouse model for breast cancer [Re-search Support, Non-U S Gov't]. Nat. Genet. 29 (4), 418–425.

Kabeer, F., Beverly, L.J., Darrasse-Jeze, G., Podsypanina, K., 2016. Meth-ods to study metastasis in genetically modified mice. Cold Spring Harb. Protoc. 2016 (2), pdb.top069948.

Kabos, P., Finlay-Schultz, J., Li, C., Kline, E., Finlayson, C., Wisell, J., et al., 2012. Patient-derived luminal breast cancer xenografts retain hormone receptor heterogeneity and help define unique estrogen-dependent gene signatures. Breast Cancer Res. Treat. 135, 415–432.

Kanaya, N., Somlo, G., Wu, J., Frankel, P., Kai, M., Liu, X., et al., 2016. Characterization of patient-derived tumor xenografts (PDXs) as models for estrogen receptor positive (ER + HER2- and ER + HER2 +) breast cancers. J. Steroid. Biochem. Mol. Biol., doi: http://dx.doi.org/10.1016/j.jsbmb.2016.05.001.

Kang, Y., Siegel, P.M., Shu, W., Drobnjak, M., Kakonen, S.M., Cordon-Cardo, C., et al., 2003. A multigenic program mediating breast cancer metastasis to bone [Comparative Study Research Support, Non-U.S. Gov't Research Support, U.S. Gov't, P.H.S.]. Cancer Cell 3 (6), 537–549.

Kao, J., Salari, K., Bocanegra, M., Choi, Y.L., Girard, L., Gandhi, J., et al., 2009. Molecular profiling of breast cancer cell lines defines relevant tumor models and provides a resource for cancer gene discovery [Research Support, N.I.H., Extramural Research Support, Non-U.S. Gov't]. PLoS One 4 (7), e6146.

Keller, P.J., Lin, A.F., Arendt, L.M., Klebba, I., Jones, A.D., Rudnick, J.A., et al., 2010. Mapping the cellular and molecular heterogeneity of normal and malignant breast tissues and cultured cell lines. Breast Cancer Res. 12 (5), R87.

Khanna, C., Hunter, K., 2005. Modeling metastasis in vivo [Review]. Carcinogenesis 26 (3), 513–523.

Kim, H.H., van den Heuvel, A.P., Schmidt, J.W., Ross, S.R., 2011. Nov-el common integration sites targeted by mouse mammary tumor

virus insertion in mammary tumors have oncogenic activity [Research Support, N.I.H., Extramural]. PLoS One 6 (11), e27425.

Kreike, B., van Kouwenhove, M., Horlings, H., Weigelt, B., Peterse, H., Bartelink, H., et al., 2007. Gene expression profiling and histopathological characterization of triple-negative/basal-like breast carcinomas [Research Support, Non-U.S. Gov't]. Breast Cancer Res. 9 (5), R65.

Kuperwasser, C., Hurlbut, G.D., Kittrell, F.S., Dickinson, E.S., Laucirica, R., Medina, D., et al., 2000. Development of spontaneous mammary tumors in BALB/c p53 heterozygous mice. A model for Li-Fraumeni syndrome [Research Support, Non-U.S. Gov't Research Support, U.S. Gov't, Non-P.H.S. Research Support, U.S. Gov't, P.H.S.]. Am. J. Pathol. 157 (6), 2151–2159.

Lanari, C., Lamb, C.A., Fabris, V.T., Helguero, L.A., Soldati, R., Bottino, M.C., et al., 2009. The MPA mouse breast cancer model: evidence for a role of progesterone receptors in breast cancer [Research Support, N.I.H., Intramural Research Support, Non-U.S. Gov't Review]. Endocr. Relat. Cancer 16 (2), 333–350.

Lee, E.Y., Muller, W.J., 2010. Oncogenes and tumor suppressor genes [Review]. Cold Spring Harb. Perspect. Biol. 2 (10), a003236.

Lehmann, B.D., Bauer, J.A., Chen, X., Sanders, M.E., Chakravarthy, A.B., Shyr, Y., et al., 2011. Identification of human triple-negative breast cancer subtypes and preclinical models for selection of targeted therapies. J. Clin. Invest. 121 (7), 2750–2767.

Leung, J.Y., Andrechek, E.R., Cardiff, R.D., Nevins, J.R., 2012. Heterogeneity in MYC-induced mammary tumors contributes to escape from oncogene dependence [Research Support, N.I.H., Extramural]. Oncogene 31 (20), 2545–2554.

Lin, S.C., Lee, K.F., Nikitin, A.Y., Hilsenbeck, S.G., Cardiff, R.D., Li, A., et al., 2004. Somatic mutation of p53 leads to estrogen receptor alpha-positive and -negative mouse mammary tumors with high frequency of metastasis [Research Support, Non-U S Gov't Research Support, U S Gov't, Non-P H S Research Support, U S Gov't, P H S]. Cancer Res. 64 (10), 3525–3532.

Lindeman, G.J., Visvader, J.E., 2010. Insights into the cell of origin in breast cancer and breast cancer stem cells [Research Support, Non-U.S. Gov't Review]. Asia Pac. J. Clin. Oncol. 6 (2), 89–97.

Liu, X., Holstege, H., van der Gulden, H., Treur-Mulder, M., Zevenhoven, J., Velds, A., et al., 2007. Somatic loss of BRCA1 and p53 in mice induces mammary tumors with features of human BRCA1-mutated basal-like breast cancer [Research Support, Non-U S Gov't]. Proc. Natl. Acad. Sci. USA 104 (29), 12111–12116.

Lu, X., Bennet, B., Mu, E., Rabinowitz, J., Kang, Y., 2010. Metabolomic changes accompanying transformation and acquisition of metastatic potential in a syngeneic mouse mammary tumor model [Research Support, N.I.H., Extramural Research Support, Non-U.S. Gov't Research Support, U.S. Gov't, Non-P.H.S.]. J. Biol. Chem. 285 (13), 9317–9321.

Ludwig, T., Fisher, P., Murty, V., Efstratiadis, A., 2001. Development of mammary adenocarcinomas by tissue-specific knockout of Brca2 in mice [Comparative Study Research Support, Non-U S Gov't Research Support, U S Gov't, P H S]. Oncogene 20 (30), 3937–3948.

Manning, H.C., Buck, J.R., Cook, R.S., 2016. Mouse models of breast cancer: platforms for discovering precision imaging diagnostics and future cancer medicine. J. Nucl. Med. 57 (Suppl. 1), 60s–68s.

Marangoni, E., Vincent-Salomon, A., Auger, N., Degeorges, A., Assayag, F., de Cremoux, P., et al., 2007. A new model of patient tumor-derived breast cancer xenografts for preclinical assays. Clin. Cancer Res. 13 (13), 3989–3998.

Matsui, Y., Halter, S.A., Holt, J.T., Hogan, B.L., Coffey, R.J., 1990. Development of mammary hyperplasia and neoplasia in MMTV-TGF alpha transgenic mice. Cell 61 (6), 1147–1155.

Medina, D., 2010. Of mice and women: a short history of mouse mammary cancer research with an emphasis on the paradigms inspired by the transplantation method [Review]. Cold Spring Harb. Perspect. Biol. 2 (10), a004523.

Mehta, R.G., Naithani, R., Huma, L., Hawthorne, M., Moriarty, R.M., McCormick, D.L., et al., 2008. Efficacy of chemopreventive agents in mouse mammary gland organ culture (MMOC) model: a comprehensive review [Research Support, N.I.H., Extramural Review]. Curr. Med. Chem. 15 (27), 2785–2825.

Menezes, M.E., Das, S.K., Emdad, L., Windle, J.J., Wang, X.Y., Sarkar, D., et al., 2014. Genetically engineered mice as experimental tools to dissect the critical events in breast cancer. Adv. Cancer Res. 121, 331–382.

Mikaelian, I., Blades, N., Churchill, G.A., Fancher, K., Knowles, B.B., Eppig, J.T., et al., 2004. Proteotypic classification of spontaneous and transgenic mammary neoplasms [Research Support, U.S. Gov't, P.H.S.]. Breast Cancer Res. 6 (6), R668–R679.

Mohibi, S., Mirza, S., Band, H., Band, V., 2011. Mouse models of estrogen receptor-positive breast cancer. J. Carcinog. 10 (35), 22.

Mollard, S., Mousseau, Y., Baaj, Y., Richard, L., Cook-Moreau, J., Monteil, J., et al., 2011. How can grafted breast cancer models be optimized? [Review]. Cancer Biol. Ther. 12 (10), 855–864.

Moore, J.C., Langenau, D.M., 2016. Allograft cancer cell transplantation in zebrafish. Adv. Exp. Med. Biol. 916, 265–287.

Moreau, J., Anderson, K.M., Mauney, J.R., Kaplan, D., Rosenblatt, M., 2007. Studies of osteotropism on both sides of the breast cancer-bone interaction. Ann. N Y Acad. Sci. 1117, 328–344.

Morton, C.L., Houghton, P.J., 2007. Establishment of human tumor xenografts in immunodeficient mice. Nat. Protoc. 2 (2), 247–250.

Muggerud, A.A., Hallett, M., Johnsen, H., Kleivi, K., Zhou, W., Tahmasebpoor, S., et al., 2010. Molecular diversity in ductal carcinoma in situ (DCIS) and early invasive breast cancer [Research Support, Non-U S Gov't]. Mol. Oncol. 4 (4), 357–368.

Muller, W.J., Arteaga, C.L., Muthuswamy, S.K., Siegel, P.M., Webster, M.A., Cardiff, R.D., et al., 1996. Synergistic interaction of the Neu proto-oncogene product and transforming growth factor alpha in the mammary epithelium of transgenic mice [Research Support, Non-U.S. Gov't Research Support, U.S. Gov't, Non-P.H.S. Research Support, U.S. Gov't, P.H.S.]. Mol. Cell Biol. 16 (10), 5726–5736.

Muller, W.J., Sinn, E., Pattengale, P.K., Wallace, R., Leder, P., Guy, C.T., et al., 1988. Single-step induction of mammary adenocarcinoma in transgenic mice bearing the activated c-neu oncogene expression of the neu protooncogene in the mammary epithelium of transgenic mice induces metastatic disease [Research Support, Non-U.S. Gov't Research Support, U.S. Gov't, P.H.S.]. Cell 54 (1), 105–115.

Nartey, T., Moran, H., Marin, T., Arcaro, K.F., Anderton, D.L., Etkind, P., et al., 2014. Human mammary tumor virus (HMTV) sequences in human milk. Infect. Agent Cancer 9, 20.

Neve, R.M., Chin, K., Fridlyand, J., Yeh, J., Baehner, F.L., Fevr, T., et al., 2006. A collection of breast cancer cell lines for the study of functionally distinct cancer subtypes [Research Support, N.I.H., Extramural Research Support, Non-U.S. Gov't Research Support, U.S. Gov't, Non-P.H.S.]. Cancer Cell 10 (6), 515–527.

Osborne, C.K., Hobbs, K., Trent, J.M., 1987. Biological differences among MCF-7 human breast cancer cell lines from different laboratories [Comparative Study Research Support, U S Gov't, P H S]. Breast Cancer Res. Treat. 9 (2), 111–121.

Pattengale, P.K., Stewart, T.A., Leder, A., Sinn, E., Muller, W., Tepler, I., et al., 1989. Animal models of human disease. Pathology and molecular biology of spontaneous neoplasms occurring in transgenic mice carrying and expressing activated cellular oncogenes. Am. J. Pathol. 135 (1), 39–61.

Pelleitier, M., Montplaisir, S., 1975. The nude mouse: a model of deficient T-cell function. Methods Achiev. Exp. Pathol. 7, 149–166.

Pena, L., Gama, A., Goldschmidt, M.H., Abadie, J., Benazzi, C., Castagnaro, M., et al., 2014. Canine mammary tumors: a review and consensus of standard guidelines on epithelial and myoepithelial phenotype markers, HER2, and hormone receptor assessment using immunohistochemistry. Vet. Pathol. 51 (1), 127–145.

Perou, C.M., Sorlie, T., Eisen, M.B., van de Rijn, M., Jeffrey, S.S., Rees, C.A., et al., 2000. Molecular portraits of human breast tumours

[Research Support, Non-U.S. Gov't Research Support, U.S. Gov't, P.H.S.]. Nature 406 (6797), 747–752.

Pfefferle, A.D., Agrawal, Y.N., Koboldt, D.C., Kanchi, K.L., Herschkowitz, J.I., Mardis, E.R., et al., 2016. Genomic profiling of murine mammary tumors identifies potential personalized drug targets for p53 deficient mammary cancers. Dis. Model Mech. 9, 749–757.

Rasotto, R., Goldschmidt, M.H., Castagnaro, M., Carnier, P., Caliari, D., Zappulli, V., 2014. The dog as a natural animal model for study of the mammary myoepithelial basal cell lineage and its role in mammary carcinogenesis. J. Comp. Pathol. 151 (2–3), 166–180.

Riaz, M., Elstrodt, F., Hollestelle, A., Dehghan, A., Klijn, J., Schutte, M., 2009. Low-risk susceptibility alleles in 40 human breast cancer cell lines. BMC Cancer 9 (1), 236.

Rivina, L., Davoren, M.J., Schiestl, R.H., 2016. Mouse models for radiation-induced cancers. Mutagenesis 31, 491–509.

Rose-Hellekant, T.A., Schroeder, M.D., Brockman, J.L., Zhdankin, O., Bolstad, R., Chen, K.S., et al., 2007. Estrogen receptor-positive mammary tumorigenesis in TGFalpha transgenic mice progresses with progesterone receptor loss. Oncogene 26 (36), 5238–5246.

Rosenblatt, M., 2012. A tale of mice and (wo)men: development of and insights from an "all human" animal model of breast cancer metastasis to bone. Trans. Am. Clin. Climatol. Assoc. 123, 135–150, discussion 150–131.

Russo, J., Balogh, G.A., Heulings, R., Mailo, D.A., Moral, R., Russo, P.A., et al., 2006. Molecular basis of pregnancy-induced breast cancer protection [Comparative Study Research Support, N.I.H., Extramural Review]. Eur. J. Cancer Prev. 15 (4), 306–342.

Russo, J., Russo, I.H., 1996. Experimentally induced mammary tumors in rats [Review]. Breast Cancer Res. Treat. 39 (1), 7–20.

Sflomos, G., Dormoy, V., Metsalu, T., Jeitziner, R., Battista, L., Scabia, V., et al., 2016. A preclinical model for eralpha-positive breast cancer points to the epithelial microenvironment as determinant of luminal phenotype and hormone response. Cancer Cell 29 (3), 407–422.

Simmons, J.K., Hildreth, III, B.E., Supsavhad, W., Elshafae, S.M., Hassan, B.B., Dirksen, W.P., et al., 2015. Animal models of bone metastasis. Vet. Pathol. 52 (5), 827–841.

Sinn, E., Muller, W., Pattengale, P., Tepler, I., Wallace, R., Leder, P., 1987. Coexpression of MMTV/v-Ha-ras and MMTV/c-myc genes in transgenic mice: synergistic action of oncogenes in vivo. Cell 49 (4), 465–475.

Soares, M., Correia, J., Peleteiro, M.C., Ferreira, F., 2016. St Gallen molecular subtypes in feline mammary carcinoma and paired metastases-disease progression and clinical implications from a 3-year follow-up study. Tumour Biol. 37 (3), 4053–4064.

Sorlie, T., Perou, C.M., Tibshirani, R., Aas, T., Geisler, S., Johnsen, H., et al., 2001. Gene expression patterns of breast carcinomas distinguish tumor subclasses with clinical implications [Research Support, Non-U.S. Gov't Research Support, U.S. Gov't, P.H.S.]. Proc. Natl. Acad. Sci. USA 98 (19), 10869–10874.

Stewart, T.A., Pattengale, P.K., Leder, P., 1984. Spontaneous mammary adenocarcinomas in transgenic mice that carry and express MTV/myc fusion genes. Cell 38 (3), 627–637.

Storer, J.B., Serrano, L.J., Darden, Jr., E.B., Jernigan, M.C., Ullrich, R.L., 1979. Life shortening in RFM and BALB/c mice as a function of radiation quality, dose, and dose rate [Research Support, U.S. Gov't, Non-P.H.S.]. Radiat. Res. 78 (1), 122–161.

Strehl, J.D., Wachter, D.L., Fasching, P.A., Beckmann, M.W., Hartmann, A., 2011. Invasive breast cancer: recognition of molecular subtypes. Breast Care (Basel) 6 (4), 258–264.

Sydnor, K.L., Butenandt, O., Brillantes, F.P., Huggins, C., 1962. Race-strain factor related to hydrocarbon-induced mammary cancer in rats. J. Natl. Cancer Inst. 29, 805–814.

Tassone, P., Di Martino, M.T., Ventura, M., Pietragalla, A., Cucinotto, I., Calimeri, T., et al., 2009. Loss of BRCA1 function increases the antitumor activity of cisplatin against human breast cancer xenografts in vivo. Cancer Biol. Ther. 8 (7), 648–653.

Theodorou, V., Kimm, M.A., Boer, M., Wessels, L., Theelen, W., Jonkers, J., et al., 2007. MMTV insertional mutagenesis identifies genes, gene families and pathways involved in mammary cancer [Research Support, Non-U.S. Gov't]. Nat. Genet. 39 (6), 759–769.

Tomlinson, G.E., Chen, T.T., Stastny, V.A., Virmani, A.K., Spillman, M.A., Tonk, V., et al., 1998. Characterization of a breast cancer cell line derived from a germ-line BRCA1 mutation carrier. Cancer Res. 58 (15), 3237–3242.

Troiani, T., Schettino, C., Martinelli, E., Morgillo, F., Tortora, G., Ciardiello, F., 2008. The use of xenograft models for the selection of cancer treatments with the EGFR as an example. Crit. Rev. Oncol. Hematol. 65 (3), 200–211.

Tulotta, C., He, S., van der Ent, W., Chen, L., Groenewoud, A., Spaink, H.P., et al., 2016. Imaging cancer angiogenesis and metastasis in a zebrafish embryo model. Adv. Exp. Med. Biol. 916, 239–263.

Ullrich, R.L., Jernigan, M.C., Storer, J.B., 1977. Neutron carcinogenesis. Dose and dose-rate effects in BALB/c mice. Radiat. Res. 72 (3), 487–498.

Usary, J., Darr, D.B., Pfefferle, A.D., Perou, C.M., 2016. Overview of genetically engineered mouse models of distinct breast cancer subtypes. Curr. Protoc. Pharmacol. 72, 14.38.11.

Valdez, K.E., Fan, F., Smith, W., Allred, D.C., Medina, D., Behbod, F., 2011. Human primary ductal carcinoma in situ (DCIS) subtype-specific pathology is preserved in a mouse intraductal (MIND) xenograft model. J. Pathol. 225 (4), 565–573.

Vargo-Gogola, T., Rosen, J.M., 2007. Modelling breast cancer: one size does not fit all [Research Support, N.I.H., Extramural Review]. Nat. Rev. Cancer 7 (9), 659–672.

Wang, Y., Liu, X., Chen, L., Cheng, D., Rusckowski, M., Hnatowich, D.J., 2009. Tumor delivery of antisense oligomer using trastuzumab within a streptavidin nanoparticle. Eur. J. Nucl. Med. Mol. Imaging 36 (12), 1977–1986.

Weigelt, B., Horlings, H.M., Kreike, B., Hayes, M.M., Hauptmann, M., Wessels, L.F., et al., 2008. Refinement of breast cancer classification by molecular characterization of histological special types [Research Support, Non-U.S. Gov't]. J. Pathol. 216 (2), 141–150.

Wiese, D.A., Thaiwong, T., Yuzbasiyan-Gurkan, V., Kiupel, M., 2013. Feline mammary basal-like adenocarcinomas: a potential model for human triple-negative breast cancer (TNBC) with basal-like subtype. BMC Cancer 13, 403.

Wijnhoven, S.W., Zwart, E., Speksnijder, E.N., Beems, R.B., Olive, K.P., Tuveson, D.A., et al., 2005. Mice expressing a mammary gland-specific R270H mutation in the p53 tumor suppressor gene mimic human breast cancer development [Research Support, N I H, Extramural Research Support, Non-U S Gov't Research Support, U S Gov't, P H S]. Cancer Res. 65 (18), 8166–8173.

Worzalla, J.F., Bewley, J.R., Grindey, G.B., 1990. Automated measurement of transplantable solid tumors using digital electronic calipers interfaced to a microcomputer. Invest. New Drugs 8 (3), 241–251.

Xu, X., Wagner, K.U., Larson, D., Weaver, Z., Li, C., Ried, T., et al., 1999. Conditional mutation of Brca1 in mammary epithelial cells results in blunted ductal morphogenesis and tumour formation [Research Support, Non-U S Gov't]. Nat. Genet. 22 (1), 37–43.

Yoneda, T., Williams, P.J., Hiraga, T., Niewolna, M., Nishimura, R., 2001. A bone-seeking clone exhibits different biological properties from the MDA-MB-231 parental human breast cancer cells and a brain-seeking clone in vivo and in vitro. J. Bone Miner. Res. 16 (8), 1486–1495.

Yoshizawa, K., Yuki, M., Kinoshita, Y., Emoto, Y., Yuri, T., Shikata, N., et al., 2016. Characterization of mammary adenocarcinomas in male rats after N-methyl-N-nitrosourea exposure-potential for human male breast cancer model. Exp. Toxicol. Pathol. 68 (5), 263–270.

Zheng, Q., Hursting, S.D., Reizes, O., 2012. Leptin regulates cyclin D1 in luminal epithelial cells of mouse MMTV-Wnt-1 mammary tumors. J. Cancer Res. Clin. Oncol. 138, 1607–1612.

SCLEROSIS

Page left intentionally blank

36

Animal Models of Systemic Sclerosis

Toshiyuki Yamamoto

Fukushima Medical University, Fukushima, Japan

1 INTRODUCTION

Systemic sclerosis (SSc) is a connective tissue disease which shows fibrogenesis and vasculogenesis. Although the pathogenesis of SSc has not been fully elucidated yet, it is characterized by the excessive accumulation of extracellular matrix (ECM) proteins in the skin and various internal organs, vascular injury, and immunological abnormalities (Yamamoto, 2009). In early stages of SSc, activated fibroblasts in the affected areas produce high amounts of collagen. Histological analysis of the initial stage of scleroderma reveals perivascular infiltrates of mononuclear cells in the dermis, which is associated with increased collagen synthesis in the surrounding fibroblasts. A number of studies have demonstrated the crucial role of several fibrogenic cytokines released from immunocytes in initiating the sequence of events leading to fibrosis.

Animal models are useful in providing clues for the study of various human diseases and for the exploration of new treatments. Although animal models which exhibit all the aspects of SSc are not currently available, several experimental animal models, such as tight skin (Tsk) mice, Tsk2 mice, bleomycin-induced murine scleroderma, sclerodermatous graft-versus-host disease (Scl-GvHD) mice, exogenous injections of transforming growth factor-β (TGF-β)/connective tissue growth factor (CTGF)-induced murine fibrosis model, Friend leukemia integration-1 (Fli1)-deficient mice, and UCD-200 chicken, etc., as well as several transgenic or knockout mice, have been examined so far (Yamamoto, 2010). In this review, recent insights into the pathogenesis and therapeutic interventions gained from use of animal models of SSc are discussed.

2 BLEOMYCIN-INDUCED MURINE SCLERODERMA

Bleomycin was originally isolated from the fungus *Streptomyces verticillus*, and is frequently used as an antitumor agent for the treatment of various kinds of malignancy. In addition, bleomycin is used by dermatologists as a treatment for recalcitrant warts, hypertrophic scars, and keloid (Yamamoto, 2006a). Bleomycin hydrolase inactivates bleomycin by hydrolyzing the amide bond in the β-aminoalanineamide moiety. Due to the deficiency of the enzyme in the lungs and the skin, bleomycin-induced toxicity occurs predominantly in these organs. Pulmonary fibrosis is a well-known adverse effect of bleomycin, and bleomycin-induced lung injury in rodents is an established model for human pulmonary fibrosis. Mountz et al. (1983) reported that rats injected repeatedly with sublethal doses of bleomycin over a 58-week period developed severe dermal fibrosis similar to those found in human scleroderma with structural abnormalities of collagen fibers; however, histological features were not shown in their paper. On the other hand, we established bleomycin-induced murine scleroderma model by repeated local injections of bleomycin into the shaved back skins, and published in a series of studies (Yamamoto et al., 1999a,b; Yamamoto and Nishioka, 2001; Yamamoto and Nishioka, 2002a; Yamamoto and Nishioka, 2004a; Yamamoto et al., 2000a). Thereafter, this model has been admitted worldwide as a representative scleroderma model, and making use of this model, a number of studies have been performed. Further, modified models have also been reported (Ishikawa et al., 2009; Shibusawa et al., 2008).

Mice at the age of 4–6 weeks are usually chosen. Although dermal sclerosis can be induced by bleomycin in various mice strains, C3H/He, A/J, DBA2, B10.D2, and B10.A, and Balb/c mice develop intense dermal sclerosis, characterized by deposition of homogenous materials and thickened collagen bundles in the dermis. Both males and females can be used, and there are no differences of the degrees in induced fibrosis. Although dermal sclerosis was not very strongly induced in C57BL/6J strain, a frequently used strain as a control wild type in studies using gene-deficient mice, C57BL/6J strain can be used in those experiments. 100 μl of bleomycin at a concentration (higher than 100 μg/mL) is repeatedly injected in the shaved back skin intradermally or subcutaneously. Bleomycin administration is recommended to the superficial areas in the skin to avoid diffusion. Mice are getting thin with weight loss, and easily die if high concentration of bleomycin is given. Bleomycin at a concentration less than 1 mg/mL is usually used.

Histopathological examination revealed definite dermal sclerosis characterized by thickened collagen bundles and deposition of homogenous materials in the thickened dermis with cellular infiltrates, which mimicked human scleroderma. Dermal thickness gradually increased with the onset of the sclerosis. Cellular infiltrates were composed of T cells, monocytes/macrophages, and mast cells, which are supposed to play an important role in the induction of dermal sclerosis. By contrast, dermal sclerosis can be compulsorily induced by bleomycin treatment, even in nude mice, severe combined immunodeficiency (SCID) mice and mast cell-deficient mice (Yamamoto et al., 1999b; Yamamoto and Nishioka, 2001; Yamamoto and Nishioka, 2004a). A study shows that transfer of CD4+ T cells from bleomycin-treated mice induced the same pathological changes and antibody production in untreated Balb/c nude mice (Ishikawa et al., 2009). Mast cells increased in number in tandem with the induction of dermal sclerosis. Also, a marked degranulation was found in particular in the early phase, with elevated plasma histamine levels (Yamamoto et al., 1999a). In some strains, epidermal thickness was also induced as well (Yamamoto et al., 1999b). Further, lung fibrosis showing thickened alveolar walls with cellular infiltrates was also induced early on. Cutaneous changes were generally localized to the area surrounding the injected site, and sclerotic changes were not induced in the remote regions, such as fingers or abdominal skin. After the stoppage of bleomycin injections, sclerotic changes remained at least 6 weeks, suggesting that the induction of dermal sclerosis is not transient but persistent. Thickness of vascular wall in the deep dermis was also observed (Yamamoto and Katayama, 2011). There was some variation among strains in the intensity of the symptoms and the period required to induce dermal sclerosis, and C3H/He, DBA/2, B10.D2, and B10.A strains demonstrated intense dermal sclerosis by bleomycin treatment, suggestive of bleomycin-"susceptible" (Oi et al., 2004; Yamamoto et al., 2000a). Hydroxyproline contents in the bleomycin-treated skin were significantly increased in comparison with those of the PBS-treated skin. Increased production as well as upregulation of mRNA levels of type I collagen was found in the sclerotic skin (Yamamoto et al., 1999a; Yamamoto et al., 2000a). In the bleomycin-induced scleroderma, α-SMA-positive myofibroblasts were observed in the dermis, and gradually increased in tandem with the induction of dermal sclerosis (Yamamoto and Nishioka, 2002a). Interestingly, autoantibodies were detected in the serum after bleomycin treatment (Yamamoto et al., 1999a). Bleomycin hydrolase inactivates bleomycin by hydrolyzing the amide bond in the β-aminoalanineamide moiety. Due to the lack or shortage of this enzyme in the lungs and the skin, bleomycin-induced fibrosis and sclerosis occurs predominantly in these organs. A recent report shows that a one-time injection of bleomycin-poly(L-lactic acid) microspheres can induce dermal sclerosis in mice (Shibusawa et al., 2008); however, this technique is

difficult and can be available in limited institutes. The induction of dermal sclerosis is considered to be, in part, mediated by inflammatory and fibrogenic cytokines, as well as by the direct effect of bleomycin on ECM synthesis in fibroblasts.

Bleomycin exerts various effects on skin-constituted cells, such as fibroblasts, keratinocytes and endothelial cells, as well as immunocytes (Yamamoto, 2006a). In vitro, bleomycin upregulates collagen and TGF-β1 mRNA expression in cultured rat lung (Clark et al., 1980) and human skin fibroblasts (Yamamoto et al., 2000b). Also, bleomycin enhances gene expression of ECM proteins as well as fibrogenic cytokines (Yamamoto et al., 2000b), which may contribute to the induction of fibrosis. Increased TGF-β mRNA transcription is followed by TGF-β mRNA accumulation and TGF-β protein, which causes upregulation of procollagen gene transcription (Breen et al., 1992). It was shown that TGF-β is a mediator of the fibrotic effect of bleomycin at the transcriptional level and that the TGF-β response element is required for bleomycin stimulation of the proα1(I) collagen promoter (King et al., 1994). Endothelial cells have been reported to play an important role in the inflammatory as well as fibrotic process. In vitro studies showed a dose-dependent stimulation of endothelial cell secretion of collagen synthesis by bleomycin (Phan et al., 1991). This stimulatory activity was inhibited by the anti-TGF-β antibody (Phan et al., 1991). TGF-β increases the synthesis of ECM, such as collagen type I and type III, or fibronectin by fibroblasts, modulates cell–matrix adhesion protein receptors, and regulates the production of proteins that can modify the ECM by proteolytic action, such as plasminogen activator, an inhibitor of plasminogen, or procollagenase. In addition, TGF-β is capable of stimulating its own synthesis by fibroblasts through autoinduction. Thus, maintenance of increased TGF-β production may lead to the progressive deposition of ECM, resulting in fibrosis. Actually, TGF-β mRNA is elevated in the lesional skin of SSc, and also shown to colocalize with type I collagen in scleroderma skin (Kulozik et al., 1990). In the bleomycin model, immunohistological analysis showed that TGF-β was detected on the infiltrating cells, which were predominantly composed of macrophages, as well as fibroblasts at sclerotic stages. TGF-β1 and -β2 mRNA expression was also detected in the lesional skin at early phases. Additionally, expression and synthesis of TGF-β1 were increased in bleomycin-"susceptible" mice strains (Oi et al., 2004). CTGF (CCN2) is selectively induced in fibroblasts after activation by active TGF-β, and also regulated by TGF-β accessory receptors (Holmes et al., 2011). CTGF may functionally coordinate the mode of action of TGF-β, such as fibroblast proliferation and ECM production in fibroblasts. High level of CTGF is shown in the lesional skin of bleomycin-induced scleroderma (Liu et al., 2010). Plasminogen activator inhibitor-1 (PAI-1)

is induced by TGF-β, and its promoter contains Smad binding elements. PAI-1 expression was upregulated in the bleomycin-treated skin; however, dermal sclerosis was similarly induced by bleomycin in even PAI-1-deficient mice (Matsushita et al., 2005). PAI-1 plays an important role, but may not be the prerequisite factor, in the development of bleomycin-induced scleroderma. Signaling by TGF-β elicits profibrotic responses in fibroblasts. Upon binding of TGF-β to the type II receptor, the type I receptor becomes activated, and signaling to the nucleus occurs predominantly by phosphorylation of cytoplasmic mediators belonging to the Smad family. Three families of Smads have been identified; receptor-regulated Smad2 and -3 (R-Smads), common partner Smad4 (Co-Smad), and inhibitory Smad6 and -7 (I-Smads). Smad7 has been shown to act as an intracellular antagonist of TGF-β signaling, and an inhibitor of TGF-β-induced transcriptional responses. In scleroderma skin and cultured scleroderma fibroblasts, basal level and TGF-β-inducible expression of Smad7 are selectively decreased, whereas Smad3 expression is increased (Dong et al., 2002). On the other hand, Smad7 expression levels in scleroderma fibroblasts are unclear and disputed (Asano et al., 2004a; Mori et al., 2003). In the bleomycin-treated skin, fibroblasts showed predominantly nuclear localization of Smad3 and intense staining for phospho-Smad2/3 (Takagawa et al., 2003). On the other hand, expression of Smad7 was downregulated, which may account for sustained activation of TGF-β/Smad signaling in the lesional skin. Targeted disruption of Smad3 ameliorated bleomycin-induced scleroderma, unassociated with inflammation (Lakos et al., 2004). Recently, other signaling pathways besides the Smad proteins have also been shown to mediate TGF-β signaling in scleroderma fibroblasts, such as the p38 mitogen-activated protein kinase (MAPK) (Ihn et al., 2005), phosphatidylinositol 3-kinase (PI3K) (Asano et al., 2004b), and Egr-1 (Bhattacharyya et al., 2008) pathways. Other signaling pathways, such as c-abl, Src kinase, and Rac1 are also involved in the induction of scleroderma by bleomycin (Liu et al., 2008; Skhirtladze et al., 2008). Type 2 cytokines, that is, IL-4 and IL-13, have also been suggested to be important in scleroderma. IL-4 is produced by activated memory T cells and mast cells, and promotes fibroblast proliferation, gene expression, and synthesis of ECM proteins, such as collagen and tenascin (Makhluf et al., 1996; Postlethwaite et al., 1992). IL-4 upregulates TGF-β production in eosinophils (Elovic et al., 1998) and T cells (Seder et al., 1998). Increased IL-4 production is detected in the sera or by activated peripheral blood mononuclear cells of patients with SSc (Needlemann et al., 1985). Scleroderma fibroblasts express more IL-4 receptor α and produce more collagen after IL-4 stimulation (Serpier et al., 1997). In the bleomycin model, IL-4 levels in the serum (Yamamoto et al., 1999c) as well as in the

lesional skin (Matsushita et al., 2004) were significantly elevated following bleomycin treatment. Transcription factor T-bet is a master regulator of type 1 immunity, and mice lacking T-bet showed increased sensitivity to bleomycin and exhibited significantly enhanced dermal sclerosis (Aliprantis et al., 2007; Lakos et al., 2006). IL-13 is a potent stimulator of fibroblast proliferation and collagen production (Doucet et al., 1998a; Jinnin et al., 2004; Oriente et al., 2000). The profibrotic effect of IL-13 is postulated to involve irreversible fibroblast activation, triggered either directly (Doucet et al., 1998b) or indirectly through TGF-β (Lee et al., 2001; Oriente et al., 2000). IL-13 transgenic mice show increased lung fibrosis, as well as increased levels of TGF-β1 (Belperio et al., 2002). In the bleomycin model, IL-13 mRNA levels and protein synthesis in the lesional skin were increased, and IL-13 receptor (IL-13R)-α2 expression in the lesional skin was augmented mainly in the infiltrating mononuclear cells and macrophages after bleomycin exposure (Matsushita et al., 2004). Another study showed that IL-13-deficient mice failed to develop an increase in skin sclerosis after bleomycin treatment (Aliprantis et al., 2007). IL-13 may promote the progression of cutaneous fibrosis/sclerosis in the development of bleomycin-induced scleroderma.

Chemokines and chemokine receptors have also been implicated in the pathogenesis of SSc (Yamamoto, 2006b). CCL2/monocyte chemoattractant protein-1 (MCP-1) is a most important chemokine for SSc (Yamamoto, 2008). In vitro studies show that CCL2 upregulates type I collagen mRNA expression in rat fibroblasts, which is indirectly mediated by endogenous upregulation of TGF-β gene expression (Gharaee-Kermani et al., 1996). CCL2 enhances expression of matrix metalloproteinase-1 (MMP-1), MMP-2, as well as TIMP-1 in cultured skin fibroblasts (Yamamoto et al., 2000c). Current studies have demonstrated increased expression of CCL2 in patients with SSc (Distler et al., 2001; Galindo et al., 2001a; Hasegawa et al., 1999; Yamamoto et al., 2001a,b). Scleroderma fibroblasts express increased levels of CCL2 mRNA and protein (Galindo et al., 2001a; Yamamoto et al., 2001a), and stimulation with platelet-derived growth factor (PDGF) resulted in a significant increase in CCL2 mRNA and protein (Distler et al., 2001). Furthermore, the autoinduction of CCL2 was observed in scleroderma fibroblasts, but not in normal fibroblasts (Yamamoto et al., 2001a). CCL2 acts indirectly via IL-1α (Yamamoto et al., 2000c). IL-1α as well as IL-1 receptor levels, in turn, were shown to be significantly increased in scleroderma (Kawaguchi et al., 1999). In addition, IL-1α as well as tumor necrosis factor (TNF)-α are potent inducers of CCL2. Thus, in addition to a direct autocrine stimulatory loop, a mutual induction between IL-1α and CCL2 might lead to a self-perpetuating activation of scleroderma fibroblasts. CCL2 levels may also be increased by IL-13 because IL-13 is a potent stimulator of CCL2 (Zhu et al., 2002). In the

bleomycin model, expression of CCL2 in the infiltrating mononuclear cells was enhanced following bleomycin treatment, and expression of CCL2 in fibroblasts was detected at later stages in the sclerotic skin (Yamamoto and Nishioka, 2003). Expression of CCR-2, a major receptor for CCL2, was also upregulated in the lesional skin at both protein and mRNA levels following bleomycin treatment. Administration of anti-CCL2 neutralizing antibody together with local bleomycin treatment reduced dermal sclerosis, along with collagen content in the skin as well as mRNA expression of type I collagen. These data suggest that CCL2 and CCR-2 signaling plays an important role in the pathogenesis of bleomycin-induced scleroderma. In the CCL2-deficient mice, skin fibrosis was diminished even by the bleomycin treatment (Ferreira et al., 2006). CCL2 may contribute to the induction of dermal sclerosis directly, via its upregulation of mRNA expression of ECM on fibroblasts, as well as indirectly through the mediation of a number of cytokines released from immunocytes recruited into the lesional skin. On the other hand, oxidative stress transiently induces CCL2 mRNA and protein expression in cultured skin fibroblasts (Galindo et al., 2001b), suggesting that ROS may play a regulatory role in inflammation by modulating monocyte chemotactic activity.

Expression of TNF is detectable during the early stages of scleroderma (Hebbar et al., 1996). The serologic level of TNF increases with the clinical severity and biologic activity of the disease (Alecu et al., 1998), or in association with pulmonary fibrosis (Hasegawa et al., 1997). TNF-α targeting therapies are suggested to be effective for reduction of skin fibrosis (Distler et al., 2008). Bleomycin activates human alveolar macrophages to produce TNF-α, and in vivo studies show increased levels of TNF-α protein and mRNA in lungs following bleomycin treatment in mice (Phan and Kunkel, 1992; Piguet et al., 1989). The development of lung fibrosis by bleomycin was prevented by inhibition of TNF signaling through administration of antibodies against TNF-α (Piguet et al., 1989), or in TNF receptor (TNFR)-deficient mice (Ortiz et al., 1999). By contrast, TNFRp55-deficient mice developed severe sclerotic changes of the dermis following bleomycin exposure at extremely earlier time points, as compared with wild-type mice (Murota et al., 2003). Induction of MMP-1 expression was significantly inhibited in the bleomycin-treated skin of TNFRp55-null mice. The authors suggest that signaling mediated by TNFRp55 plays an essential role in MMP-1 expression and a key role in the collagen degradation process in the bleomycin model. The controversial results between skin and lung are also observed in PAI-1 knockout mice (Matsushita et al., 2005). Involvement of the apoptotic process in the pathogenesis of SSc has been investigated. Recent studies have shown that apoptosis of endothelial cells induces resistance to apoptosis in

fibroblasts largely through PI3K-dependent mechanisms (Laplante et al., 2005). Furthermore, fibroblasts exposed to medium conditioned by apoptotic endothelial cells presented myofibroblast changes (Laplante et al., 2005). By contrast, cultured scleroderma fibroblasts were resistant to Fas-induced apoptosis (Jelaska and Korn, 2000; Santiago et al., 2001). Although the effect of TGF-β on apoptosis differs according to cell type, stage of maturation, and other factors, TGF-β1 may play a role in inducing apoptosis-resistant fibroblast populations in SSc (Santiago et al., 2001). In scleroderma fibroblasts, Bcl-2 level was significantly higher, whereas the Bax level significantly decreased (Santiago et al., 2001). On the contrary, alterations in endothelial apoptosis induction were not involved in the development of the disease in either Tsk1/+ or Tsk2/+ mice (Sgonc et al., 1999). In the bleomycin model, TUNEL positivity was prominently detected on keratinocytes and infiltrating mononuclear cells, but not endothelial cells and fibroblasts (Yamamoto and Nishioka, 2004b). DNA fragmentation revealed laddering of the bleomycin-treated skin, and increased expression of Fas and FasL was detected in the lesional skin. mRNA expression as well as activity of caspase-3 was also enhanced after bleomycin treatment. Administration of neutralizing anti-FasL antibody together with local bleomycin treatment reduced the development of dermal sclerosis, in association with the reduction of TUNEL-positive mononuclear cells and with the blockade of apoptosis. Caspase-3 activity was also significantly reduced after anti-FasL treatment. Excessive apoptosis, which cannot be treated by macrophages, may induce proinflammatory cytokines, such as TNF-α or interferons (IFNs), and play a triggering role in the pathogenesis of bleomycin-induced scleroderma. T cells, macrophages, and mast cells are present in increased numbers or in an activated state in the lesional skin of SSc patients, and are thought to play an active role in the pathogenesis of the disease. Additionally, activated peripheral B cells are found in abnormally large numbers in patients with SSc (Sato et al., 2001). B cells contribute not only to antibody production, but also to T cell activation and differentiation and the production of various cytokines. In CD19-deficient mice, induction of dermal and lung fibrosis, cytokine expression and autoantibody production were inhibited (Yoshizaki et al., 2008). They speculate that hyaluronan activates B cells via toll-like receptor (TLR)-4 in this model. Also, expression of TLR-3 is increased in the dermis in this model, which may result in the increase of production of IL-6 and of differentiation into myofibroblasts (Agarwal et al., 2011). Role of innate immunity in SSc has recently been suggested, and TLR stimulation of fibroblasts may trigger cytokine cascades in fibrosis, via activating innate immune system (Fullard and O'Reilly, 2015). In particular, TLR-2, -3, and -4 may play an important role (Fang et al., 2016; Fullard and O'Reilly, 2015; Takahashi et al., 2015). TLR-3 expression was upregulated in SSc, and IFN-α2 induced an upregulation of TLR-3 in human dermal fibroblasts (Agarwal et al., 2011), suggesting an important role of TLRs activation via type I IFNs in fibrosis. Activation of nod-like receptors (NLRs) leads to the activation of inflammasome, and then caspase-1 activation, resulting in the processing and secretion of IL-1β and IL-18. Mice with a deletion of NLR protein 3 were resistant to bleomycin-induced skin fibrosis (Artlett et al., 2011). IL-18 acts as a fibrogenic cytokine, and expression of IL-18 is elevated in SSc (Scala et al., 2004). By contrast, IL-18 downregulated collagen production via the ERK pathway in human dermal fibroblasts (Kim et al., 2010). Thus, role of IL-18 in the development of fibrosis needs further analysis. MicroRNAs (miRNAs) are noncoding small RNAs, and dysregulation of miRNAs is recently shown. miRNA-29a is spontaneously downregulated in scleroderma fibroblasts, and fibrogenic cytokines, such as TGF-β, PDGF-B, and IL-4 reduced the level of miRNA-29a in normal fibroblasts (Maurer et al., 2010). Also, expression of miRNA-29a was reduced in the mouse model of bleomycin-induced scleroderma, suggesting a key regulator of collagen expression in SSc (Maurer et al., 2010). Alternatively, miR-155 was upregulated in scleroderma skin, and miR-155 deficient mice were resistant to bleomycin treatment (Yan et al., 2016). In vitro silencing of miR-155 in fibroblasts inhibited collagen synthesis and signaling pathways of Wnt/β-catenin and Akt. Bleomycin treatment reduced adipose tissues (Ohgo et al., 2013). Myofibroblasts within the fibrotic dermis were derived from intradermal adipocytic cells that had undergone phenotypic transformation, and proposed the term of adipocyte–myofibroblast transition (Marangoni et al., 2015). Cytokines derived from adipose tissues, such as adiponectin and leptin regulate fibroblast proliferation, differentiation, and function, via peroxisome proliferator-activated receptors (PPAR-γ). Leptin is suggested to play a profibrotic by augmentation of TGF-β by reducing PPAR-γ.

Numerous therapeutic approaches have been investigated so far in bleomycin-induced scleroderma model. Systemic administration of anti-TGF-β neutralizing antibody in combination with local bleomycin treatment, suppressed the development of scleroderma (Yamamoto et al., 1999c). This effect was accompanied by the reduction of the number of myofibroblasts, mast cells, and eosinophils. Topical application of a peptide inhibitor of TGF-β has been shown to ameliorate skin fibrosis in bleomycin-induced scleroderma (Santiago et al., 2005). Latency-associated peptide (LAP) is released from latent TGF-β. Local LAP administration along with bleomycin treatment suppressed the induction of dermal sclerosis, as well as collagen and CTGF gene expression, in an ongoing experiment (Wakatsuki-Nakamura

et al., 2012). IFN-γ causes potent inhibition of collagen production in cultured skin fibroblasts. IFN-γ decreased TGF-β-induced α-SMA expression in palatal fibroblasts, as well as changes in morphology (Yokozeki et al., 1999). Moreover, IFN-γ inhibits the TGF-β-induced phosphorylation of Smad3 and the accumulation of Smad3 in the nucleus, whereas induces the expression of Smad7 (Ulloa et al., 1999). In the bleomycin model, systemic administration of IFN-γ together with bleomycin reduced dermal sclerosis, even after the onset of scleroderma (Yamamoto et al., 2000d). Administration of inhibitor of TGF-β/Smad signaling by the activation of nuclear translocation of Y-box binding protein 1 suppressed skin fibrosis in this model (Hasegawa et al., 2009). A small molecule antagonist of CCL2 prevented skin sclerosis induced by bleomycin (Kimura et al., 2007). Bleomycin produces free radicals and induces apoptosis. A reduction of free radical formation may contribute to the decrease of collagen content by inhibition of proline hydroxylation, which leads to the improvement of scleroderma. Lecithinized superoxide dismutase (SOD) with high tissue accumulation and a long half-life in the blood showed an inhibitory effect on bleomycin-induced scleroderma, suggesting that antioxidant therapy may lead to an antifibrotic effect; however, postonset administration of SOD could not attenuate the dermal sclerosis (Yamamoto et al., 1999d). Also, a free radical scavenger, edaravone, inhibited dermal sclerosis (Yoshizaki et al., 2011). Halofuginone has an inhibitory effect on collagen synthesis, and shows antifibrotic effects in a few animal models of scleroderma. By contrast, bleomycin-induced scleroderma was not attenuated by treatment with halofuginone (Yamamoto and Nishioka, 2002b). Halofuginone may not ameliorate dermal sclerosis along with strong inflammation caused by repeated application of bleomycin. Hepatocyte growth factor (HGF) prevented the progression of organ fibrosis. The promoter region of the HGF gene contains a TGF-β inhibitory element. HGF induces proteases which degradate ECM proteins, such as MMPs, membrane type 1-MMP (MT1-MMP), and urokinase-type plasminogen activator (uPA), and also decreases TIMPs (Matsumoto and Nakamura, 2001). Gene transfer of HGF not only prevented the ongoing dermal sclerosis induced by simultaneous local injections of bleomycin, but also ameliorated the previously induced dermal sclerosis (Wu et al., 2004). This effect was mediated by suppressing TGF-β levels. Adenosine is a nucleoside that is generated in response to cellular stresses, such as chronic inflammation and hypoxic conditions. Adenosine A2A receptor-deficient and A2A receptor antagonist-treated mice were protected from developing bleomycin-induced dermal sclerosis (Chan et al., 2006). PPARs are ligand-activated transcription factors that regulate cell proliferation, differentiation, and immune/

inflammation response. PPAR-γ inhibits TGF-β signaling and collagen synthesis (Burgess et al., 2005; Ghosh et al., 2004). Insulin-sensitizing drugs, such as rosiglitazone and pioglitazone, activate PPAR-γ, inhibit TGF-β-induced fibrotic responses. Treatment with PPAR-γ ligand rosiglitazone prevented dermal sclerosis with downregulation of collagen gene expression and myofibroblast accumulation in the lesional skin (Wu et al., 2009). Imatinib mesylate (Gleevec) targets specifically the TGF-β and PDGF signaling pathways by inhibiting the tyrosine kinase activity of c-abl and PDGF receptors. Imatinib reduced dermal thickness, the number of myofibroblasts, and synthesis of ECM proteins in the bleomycin-induced dermal sclerosis (Distler et al., 2007). Further, imatinib induced regression of preexisting ECM accumulation in the skin and decreased dermal thickness (Akhmetshina et al., 2009). Dasatinib and nilotinib, both are dual inhibitor of c-abl and PDGF receptor, potently reduced dermal thickness, the number of myofibroblasts, and collagen content of the skin in the bleomycin model (Akhmetshina et al., 2008). An interaction between CD40 and its ligand CD40L has been suggested as a pathway for immune and inflammatory responses. Cultured scleroderma fibroblasts express CD40 (Fukasawa et al., 2003). In the lesional skin of bleomycin-induced scleroderma, dermal fibroblasts expressed CD40, and mast cells and CD4+ T cells expressed CD40L (Kawai et al., 2008). Anti-CD40L antibody inhibited the induction of skin sclerosis by suppressing fibroblast proliferation and downregulation of CCL2 expression in this model (Kawai et al., 2008). α-Melanocyte-stimulating hormone (α-MSH) has many effects, such as immunomodulation, regulation of exocrine activity and apoptosis, and antifibrotic effect. α-MSH suppresses TGF-β-induced collagen synthesis in vitro. Treatment with α-MSH suppressed bleomycin-induced collagen accumulation in the skin (Kokot et al., 2009). Intravenous immunoglobulin (IVIG) treatment significantly inhibited dermal sclerosis and collagen accumulation, by downregulating TGF-β and CCL2 (Kajii et al., 2011). Lysophosphatidic acid (LPA) is recently implicated to play an important role in fibrosis. LPA receptor inhibitor, a selective LPA1 and LPA3 antagonist, exerted an antifibrotic effect on the bleomycin-induced scleroderma (Ohashi and Yamamoto, 2015). Moreover, a number of new candidates for future treatment have been reported (Avouac et al., 2012; Balistreri et al., 2011; Desallais et al., 2014; Kitaba et al., 2012; Pamuk et al., 2015; Toyama et al., 2016; Ursini et al., 2016).

This model has several advantages, such as easy technique to induce dermal fibrosis, easy handling, short duration until the induction of dermal fibrosis, and high reproducibility independent of mice strains. One of the most useful advantages of this model is that this system can permit to investigate the induction of fibrosis from

prior to, during, and after the development, through the fibrotic process continuously. This great advantage means that the initial event of skin fibrosis can be analyzed. By contrast, skin fibrosis is not diffusely induced, but restricted to the bleomycin-injected sites. Also, many factors, including nonspecific or unessential factors in fibrosis, may be affected by bleomycin treatment.

3 HOCL-INDUCED MURINE SCLERODERMA

Recently, local injections of agents generating various types of ROS induced skin sclerosis in mice. Daily intradermal injections of hypochlorous acid (HOCl) induce skin and lung fibrosis, kidney damages, and serum Topo-I antibody production in Balb/c mice (Servettaz et al., 2009). On the other hand, local injections of agents generating peroxynitrite anions ($ONOO^-$) induced limited skin, but not lung, fibrosis and anti-CENP-B antibody production. As well as bleomycin, those agents capable to produce ROS, which induces phenotypic differentiation into myofibroblasts and enhances production of type I collagen, possibly via the phosphorylation of ERK1/2 and activation of the Ras pathway. In the HOCl-induced fibrosis model, the overproduction of ROS activates ADAM 17, a protease involved in NOTCH cleavage, suggesting that NOTCH pathway is activated (Kavian et al., 2010). In this model system, skin fibrosis is ameliorated by sunitinib (Kavian et al., 2012a) and arsenic trioxide (Kavian et al., 2012b). Some of the agents which induce DNA injury and ROS production exert various effects on endothelial cells and fibroblasts, as well as cause immune imbalance and mediator secretion, leading to dermal sclerosis. As is the same with bleomycin-induced scleroderma, many therapeutic approaches have been reported (Bagnato et al., 2013a,b; Kavian et al., 2015; Marut et al., 2013a,b).

4 TIGHT SKIN MOUSE

4.1 Tsk1 Mouse

Tsk mice are heterozygous for a mutation in the fibrillin-1 gene (Tsk1/+). Fibrillin is a large ECM structural protein and the major component of microfibrils. The most striking feature is the presence of thickened fibrotic skin that is firmly bound to the subcutaneous and deep muscular tissue; however, dermal sclerosis is lacking, and the fibrosis is much deeper in comparison with human SSc. In spite of those differences, there are numerous biochemical and molecular abnormalities that closely resemble those present in patients with SSc. Tsk1/+ mice also display certain visceral changes in the

lungs and hearts; however, vascular involvement has not been reported. The lung abnormalities are present at birth and histologically resemble human emphysema with little fibrosis. Additionally, aged Tsk1/+ mice produce autoantibodies, such as topoisomerase-1 (Topo-1) (Kasturi et al., 1994). mRNA levels of TGF-β, type I, III, and VI collagen in the skin were under temporal and spatial regulation during postnatal growth and development in the Tsk1/+ mice (Pablos et al., 1995). Collagen α1(I) and α1(III) gene-expressing fibroblasts were increased in Tsk1/+ fibrotic lesions. Transient transfections of a series of human α1(I) procollagen promoter constructs into Tsk1/+ fibroblast cultures showed increased transcription rates caused by the lack of the strong inhibitory influence of the regulatory sequence contained in the promoter between -675 and -804 bp (Philips et al., 1995). Additionally, Tsk1/+ nuclear extracts displayed decreased binding to a consensus AP-1 sequence. Transcriptional activation of collagen genes was demonstrated in Tsk1/+ mice in vivo employing reporter transgenes harboring upstream fragments of the 5' flanking region of the mouse α2(I) collagen genes. Wnt signaling stimulated matrix assembly of microfibrillar proteins including fibrillin-1, and increased expression of Wnt2 and SFRP2 in Tsk1/+ mouse skin (Bayle et al., 2008).

In Tsk1/+ mice, mast cells are abundant in the dermis and exhibit prominent degranulation. Mast cell density was dramatically increased in control littermates skin grafted onto Tsk mice, associated with the increase in mRNA levels of TGF-β, stem cell factor, and IL-15 (Wang et al., 2005). In Tsk mice, mast cells are abundant in the thickened dermis and exhibit prominent degranulation (Walker et al., 1987). Mast cells are a rich source of various cytokines, including IL-4 and TGF-β. IL-4 has been shown to induce significant levels of CCL2 production in stromal cells (Kikuchi et al., 1993; Lee et al., 2003). On the other hand, CCL2 upregulates IL-4 mRNA expression and protein production (Lukacs et al., 1997). These observations have led to the hypothesis of the mutual induction of CCL2 and IL-4. IL-4 and TGF-β possibly play important roles in the pathogenesis of fibrosis in Tsk mice. TGF-β was expressed during the rapid postnatal growth of the skin in parallel with high expression of α1(I), α1(III), and α2(VI) collagen genes (Pablos et al., 1995). By contrast, another study did not detect upregulation of TGF-β signaling pathway in Tsk1/+ mice skin (Baxter et al., 2005). Fibroblasts from Tsk1/+ mice are hyperresponsive to IL-4 and TGF-β, displaying increased synthesis of α1(I) collagen mRNA, collagen protein, and activity of a luciferase reporter construct containing α2(I) collagen promoter (MacGaha et al., 2001). After IL-4 stimulation, JAK-1 and JAK-2 were phosphorylated to a greater degree in Tsk1/+ fibroblasts than in C57BL/6 fibroblasts (MacGaha et al., 2003). Targeted mutations in

either the signaling chain of the IL-4 receptor or STAT6 prevents cutaneous hyperplasia in Tsk mice, suggesting the importance of IL-4 (Ong et al., 1999). Smad2 and Smad3 are considered to be the primary signaling molecules involved in the TGF-β signaling transduction pathway. Tsk fibroblasts have elevated Smad3 transcriptional activity compared with normal fibroblasts (MacGaha et al., 2002). This may explain why Tsk fibroblasts are more responsive to TGF-β stimulation. Recent studies have shown that CCL7 is highly overexpressed by neonatal Tsk fibroblasts (Ong et al., 2003). Increased CCL7 protein secretion by Tsk fibroblasts is observed, and CCL7 is abundantly expressed in the dermis of Tsk mice at 10 days and 3 weeks old.

CD4+ T cells have been shown to be required for the excessive accumulation of dermal collagen in Tsk1/+ mice (Wallace et al., 1994). By contrast, the Tsk phenotype fully develops in SCID mice. B cell functional defects caused by the loss of CD19 significantly decreased skin fibrosis in Tsk1/+ mice, suggesting that B cells play an important role (Saito et al., 2002). In Tsk1/+ mice overexpressing CD19, anti-Topo-I antibody levels were significantly increased, although skin thickness was not enhanced (Saito et al., 2002). B cell antigen receptor cross-linking augmented activation of extracellular signal-regulated kinase in Tsk1/+ B cells (Saito et al., 2002). Further, B cell depletion by anti-CD20 antibody significantly suppressed skin fibrosis and autoantibody production in newborn Tsk1/+ mice (Hasegawa et al., 2006). Thus, disrupted B cell signaling may contribute to immunologic abnormalities in Tsk1/+ mice. Endothelial dysfunction has been shown in Tsk1/+ mice (Marie and Beny, 2002). Expression of endothelial nitric oxide synthase (eNOS) protein and gene was significantly reduced in Tsk1/+ skin, and NOS activity was also decreased (Dooley et al., 2008). There is abnormal nitric oxide metabolism in the Tsk1/+ skin, and expression and activity of protective antioxidant enzyme HO-1 was reduced.

Previous studies showed that administration of anti-IL-4 antibody to neonatal Tsk1/+ mice prevented skin fibrosis and dermal collagen content (Ong et al., 1998). Also, shift of a Th2-based immune imbalance in Tsk1/+ mice by treatment with synthetic oligodeoxynucleotides (ODN) containing immunomodulatory CpG motifs prevented the skin fibrosis and thickening (Shen et al., 2005). IVIG therapy decreased splenocyte secretion of IL-4 and TGF-β, resulting in abrogation of fibrogenesis (Blank et al., 2002). A decrease in fibrosis was previously reported by inhibition of mast cell degranulation (Walker et al., 1987), and a recent report showed that intraperitoneal injection of mast cell chymase inhibitor significantly reduced skin fibrosis and the thickness of the subcutaneous fibrous layer (Shiota et al., 2005). Halofuginone has an inhibitory effect on collagen synthesis, and

shows antifibrotic effects in a few animal models of scleroderma. Halofuginone attenuates collagen synthesis as well as collagen gene expression in avian and murine skin fibroblasts (Granot et al., 1993). Halofuginone specifically inhibits α1(I) collagen gene expression without affecting the synthesis of other types of collagen, such as types II and III (Choi et al., 1995; Levi-Schaffer et al., 1996). Halofuginone inhibited TGF-β-induced upregulation of collagen protein and α2(I) promoter activity, as well as phosphorylation and subsequent activation of Smad3 after TGF-β stimulation (McGaha et al., 2002). Dermal application of halofuginone on Tsk1/+ mice for 60 days reduced dermal fibrosis as well as collagen α1(I) gene expression (Pines et al., 2001). Intraperitoneally administered halofuginone also prevented the thickening of the dermis and eliminated the increase of skin collagen in Tsk1/+ model (Choi et al., 1995). Dermal application of halofuginone on Tsk1/+ mice for 60 days reduced dermal fibrosis as well as collagen α1(I) gene expression (Pines et al., 2001). Intraperitoneal administration of anti-CD40L attenuated skin fibrosis and anti-Topo-I antibody production (Komura et al., 2008). HGF gene transfection in Tsk1/+ mice resulted in a marked reduction of hypodermal thickness (Iwasaki et al., 2006). Treatment with imatinib reduced dermal and hypodermal thickening in Tsk1/+ mice (Akhmetshina et al., 2009). Other therapies targeting TGF-β/Smad signaling pathway or SOD are also effective for suppression of skin fibrosis in Tsk mice (Hasegawa et al., 2009; Yoshizaki et al., 2011). A number of new therapies have been tried for cutaneous fibrosis using Tsk mice (Badea et al., 2012; Stenström et al., 2016).

4.2 Tsk2 Mouse

The second murine Tsk mutation was a result of administration of the mutagenic agent, ethylnitrosourea (ENU) (Christner et al., 1995). This mutation has been localized to mouse chromosome 1, is inherited as an autosomal dominant trait, and only heterozygous (Tsk2/+) animals survive. Tsk2/+ mice develop a Tsk phenotype that becomes apparent at 3–4 weeks of age. Histologic examination of the skin revealed marked accumulation of collagen similar to that observed in Tsk1/+ mice. By contrast, a prominent mononuclear cell infiltration is present in the dermis and adipose tissues of Tsk2/+, in contrast to Tsk1/+ mice. Lungs were normal. Biochemical analysis showed that Tsk2/+ skin had 50% more collagen contents than the normal mouse skin, and collagen synthesis in Tsk2/+ cultured dermal fibroblasts was 100% higher compared with normal fibroblasts. Transient transfection experiments with α1(I) collagen promoter constructs demonstrated increased transcriptional activity of the gene, and Sp1 and NF-1 transcriptional factors were involved in the upregulated transcriptional activity of α1(I) collagen promoter in Tsk2/+ fibroblasts

(Christner et al., 1998). Sequences from −96 to +16 bp of the α1(III) collagen promoter play an important role in the upregulated expression in Tsk2/+ fibroblasts (Christner et al., 2003). A recent study has demonstrated that the Tsk2 point mutation is due to a gain-of-function mutation associated with α1(III) (Long et al., 2015). Analysis using a collagen promoter GFP reporter transgene also showed an increase in transgene activity of α1(I) collagen (Barisic-Dujmovic et al., 2008). The presence of antinuclear antibody in the plasma was 92% of the Tsk2/+ mice, and other autoantibodies were also developed (Gentiletti et al., 2005), suggesting the aspects of autoimmunity in this model.

5 SCLERODERMATOUS GRAFT-VERSUS-HOST DISEASE MODEL

Scl-GvHD was produced by transplanting B10.D2 bone marrow and spleen cells into BALB/c mice after lethal gamma irradiation of recipients (Mccormick et al., 1999). Scl-GvHD mice exhibited skin thickening and pulmonary fibrosis by 21 days after bone marrow transplantation. A significant increase of type I collagen mRNA expression and protein synthesis was induced in the dermis. A number of CD11b + 2F8+ monocytes/macrophages and CD3+ T cells of donor origin were seen in the lesional skin. TGF-β1 mRNA levels were upregulated in the lesional skin of Scl-GvHD mice at early phases. Expression of CCL2, CCL3, and CCL5 was increased in the lesional skin prior to skin thickening and infiltration of CD45+ cells (Zhang et al., 2002). Also, allograft inflammatory factor-1 (AIF-1) and IL-6 were significantly expressed in the infiltrating mononuclear cells and fibroblasts in the thickened skin (Yamamoto et al., 2011). Otherwise, DNA microarray analysis showed a number of upregulated genes for CCL2, CCL5, CCL17, IFN-γ-inducible chemokines, PDGF, CTGF, fibroblast growth factor (FGF), epidermal growth factor (EGF), nerve growth factor (NGF), vascular endothelial growth factor (VEGF), and also adhesion molecules in the skin (Zhou et al., 2007). Additionally, Scl-GvHD can be produced by transplanting allogeneic (C57BL/6J) bone marrow and spleen cells into lethally irradiated recipients (LP/J). Onset of GvHD starts at 7 days after transplantation, with epidermal injury and round cells infiltrating in the dermis and subcutis with mononuclear cell exocytosis. By day 14 after bone marrow transplantation, the dermis and subcutis of GvHD mice become sclerotic with compressed and atrophic pilosebaceous units. Extracutaneous involvement includes periportal mononuclear cell infiltrating liver and interstitial round cell influx to lungs and kidneys. Further, a modified model of GvH-induced SSc has been developed (Ruzek et al., 2004). Injection of spleen cells from B10.D2 mice into RAG-

2 knockout mice on the BALB/c background induced dermal thickening, progressive fibrosis of internal organs, and autoantibody generation; however, lung fibrosis was absent.

Neutralization of TGF-β prevented fibrosis in the skin as well as in the lung in this model (Mccormick et al., 1999). LAP treatment prevented skin fibrosis as well as skin thickening in this model (Zhang et al., 2003). Upregulation of mRNA levels of TGF-β and CTGF were also abrogated, while showed no suppressive effects on immune cell activation or recruitment into the skin, which may suggest a more specific target for TGF-β. Intraperitoneally administered halofuginone prevented the thickening of the dermis and eliminated the increase of skin collagen in GvHD model (Choi et al., 1995). Recently, erlotinib prevented dermal fibrosis and organ involvements, as well as reduction of CD4+ T cells infiltration (Morin et al., 2015).

6 SKIN FIBROSIS BY EXOGENOUS INJECTION OF GROWTH FACTORS

TGF-β induces rapid fibrosis and angiogenesis when injected subcutaneously into newborn mice; however, this change was transient. TGF-β-induced subcutaneous fibrosis and subsequent CTGF or basic FGF application caused persistent fibrosis (Mori et al., 1999; Shinozaki et al., 1997). TGF-β caused skin fibrosis after three consecutive days of injection, and serial application of CTGF led to long-term and ECM-rich fibrosis. They suggest that TGF-β play an important role in inducing granulation and fibrotic tissue formation, and CTGF and bFGF are important in maintaining fibrosis, by sustaining α2(I) collagen promoter activation and increasing the number of activated fibroblasts (Takehara, 2003). bFGF induces collagen production by stimulating fibroblasts and CTGF cooperates with bFGF. The mast cell count was significantly but transiently increased in the early phase, while the number of macrophages continued to rise (Chujo et al., 2005). In the lesional skin, serial injections of CTGF after TGF-β increased CCL2 mRNA expression up to 8 times in comparison with only a single injection of TGF-β or CTGF (Chujo et al., 2005). Anti-CTGF reduced skin fibrosis and collagen content (Ikawa et al., 2008). Simultaneous treatment with bFGF and CTGF increased skin fibrosis (Chujo et al., 2009). By contrast, these treatments in CCL2-deficient mice resulted in decreased collagen levels in the skin (Chujo et al., 2009), suggesting an important role of CCL2 for the recruitment of inflammatory cells. In their fibrosis model induced by exogenous injection of growth factors, application of any single growth factor is not sufficient to induce persistent fibrosis, and interaction of CTGF with other growth factors is necessary.

7 UCD-200 CHICKEN

UCD-200 chickens spontaneously develop vascular damage, mononuclear cell infiltrates, fibrosis of the skin and internal organs, and polyarthritis (Van De Water and Gershwin, 1986; Gruschwitz et al., 1991). Additionally, positive AECAs, antinuclear antibodies, anticardiolipin antibodies, and rheumatoid factors are detected in the serum. The disease starts 1–2 weeks after hatching with erythema and swelling of the comb, which subsequently proceeds to a chronic stage characterized by fibrosis with excessive accumulation of collagen. In the inflammatory phase, T cell receptor (TCR)γ/δ+/CD3+/MHC class II$-$T cells prevail in the stratum papillae, while TCR α/β+/CD3+/CD4+/MHC class II+ T cells predominate in the deeper dermis. AECAs can induce apoptosis of endothelial cells through antibody-dependent cell-mediated cytotoxicity via Fas (Sgonc et al., 2000); transfer of AECA-positive sera into healthy chickens induced endothelial cell apoptosis, although this was not followed by skin sclerosis (Worda et al., 2003). These studies demonstrated the in vivo apoptosis-inducing effects of AECAs.

8 TRANSGENIC MOUSE MODELS

8.1 TGF-β Receptor I Transgenic Mouse

Fibroblast-specific TGF-β transgene activation model is an elegant method. Conditional constitutively active TGF-β receptor I transgenic mice offsprings show collagen accumulation in dermis and small pulmonary vessels, epidermal thinning, loss of adipose tissues in subcutis (Denton et al., 2003). By contrast, autoimmune as well as inflammatory aspects are absent in this model.

8.2 Kinase-Deficient Type II TGF-β Receptor Transgenic Mouse

Denton et al. (2005) generated transgenic mice expressing a kinase-deficient type II TGF-β receptor selectively on fibroblasts. These mice develop dermal and pulmonary fibrosis. Transgenic fibroblasts proliferate more rapidly, produced more ECM, and show increased expression of PAI-1, CTGF, Smad3, Smad4, and Smad7. Additionally, transgenic fibroblasts show myofibroblast differentiation.

8.3 Fra-2 Transgenic Mouse

Fos-related antigen-2 (Fra-2) is one of the subfamily of activation protein 1 (AP-1) transcriptional factors. Fra-2 transgenic mice developed severe, proliferative vasculopathy of the lungs resembling pulmonary arterial hypertension (Maurer et al., 2012), suggesting a probable model of SSc-associated pulmonary arterial hypertension. By contrast, a severe loss of small blood vessels is seen in the skin, in parallel with progression of skin fibrosis (Maurer et al., 2009). The reduction in capillary density was preceded by a significant increase in apoptosis in endothelial cells. The most characteristic feature in this model is that Fra-2 transgenic mice exhibit both vasculopathy with capillary loss in the skin and proliferative vasculopathy with arterial hypertension in the lung.

9 KNOCKOUT MOUSE MODELS

9.1 Relaxin Knockout Mouse

Relaxin is a small peptide hormone with antifibrotic and vasodilatory properties. A recent report shows that relaxin-deficient mice present dermal fibrosis characterized by thickening of the skin and increase in collagen content (Samuel et al., 2005). Fibroblasts derived from the skin of the null mice produce higher levels of collagen.

9.2 Fli1 Knockout Mouse

Fli1, a member of Ets transcription factor family, is a potent suppressor of the type I collagen gene, and persistently downregulated in scleroderma fibroblasts (Kubo et al., 2003), in association with increased CTGF and decreased MMP-1 levels (Nakerakanti et al., 2006). Fli1-deficient mice show significant upregulation of collagen (Kubo et al., 2003). Also, expression of Fli1 is greatly reduced in endothelial cells in SSc skin, and endothelial Fli1 deficiency impairs vascular homeostasis, and reduction of pericytes (Asano et al., 2010). Thus, aberrant expression of Fli1 contributes to skin fibrosis and vasculopathy in SSc. c-Abl is an upstream regulator of the PKCδ/phosphor-Fli1 pathway (Bujor et al., 2011). Fli1$^{+/-}$mice developed densely packed collagen bundles, whereas the thickness of the dermis is comparable as wild-type mice. Mice with homozygous targeted deletion of Fli1 carboxyl terminal activation domain partially recapitulate dermal fibrosis, but without dermal thickness. Also, endothelial Fli1 deficiency impairs vascular homeostasis (Asano et al., 2010). Thus, aberrant expression of Fli1 contributes to skin fibrosis and vasculopathy in SSc.

Krüppel-like factor 5 (KLF5) is a member of Sp1/KLF transcription factor family, involved in cardiac and renal fibrosis. Double heterozygous mice for FLI1 and Klf5 spontaneously developed remarkable dermal fibrosis, increased dermal thickness, collagen contents in the skin, and mRNA levels of collagen (Noda et al., 2014). An excellent review regarding a series of Fli1-related scleroderma mice model should be referred (Asano, 2016).
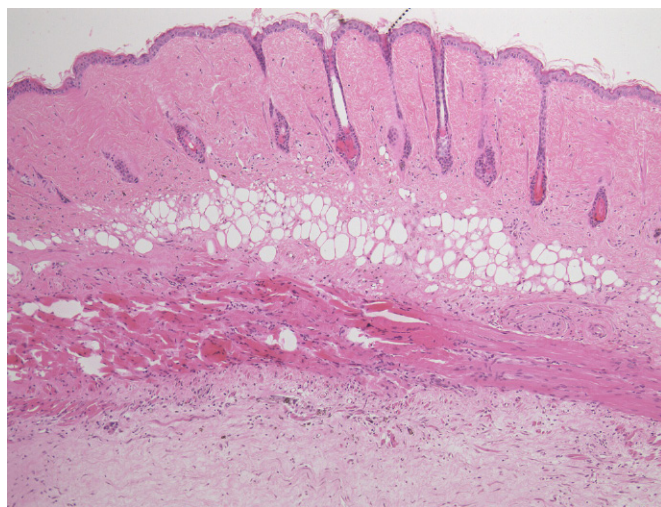
FIGURE 36.1 Histological features of bleomycin-induced scleroderma in C3H/ HeJ strain.

9.3 Caveolin 1 Knockout Mouse

Caveolin 1 regulates TGF-β signaling through internalization of TGF-β receptors. Caveolin 1-deficient mice induced develop skin and lung fibrosis showing increased collagen deposition, and also vascular changes with altered vessel tone and permeability (Castello-Cros et al., 2011).

10 CONCLUSIONS

Complex networks involve cell–cell and cell–matrix interactions via mediators in the induction of cutaneous sclerosis. Activated fibroblasts are a part of the immune system, and modulate immune cell behavior by conditioning the local cellular and cytokine microenvironment. The major characteristic of the bleomycin-induced experimental murine model of scleroderma is the histological mimicry to human scleroderma, which is shown in Fig. 36.1. Since each model has its own advantages, and also disadvantages, researchers are recommended to choose depending on the purpose of studies, that is, to study pathogenesis (fibrogenesis or vasculogenesis), to explore the antifibrotic effect of new drugs, and so on. Transgenic and knockout mice are elegant tools, but not available to anyone, needs special techniques and long periods to be made. It must be mentioned that the animal model is a simplification of the more complex human scleroderma. Nonetheless, the pathogenic mechanism discovered in the animal model may provide novel information, and assist in helping us the better understand the mechanisms underlying human scleroderma. Animal models of scleroderma may also serve as promising tools for the development of new therapies specifically targeting individual cytokines, cytokine antagonists (i.e., antibodies, soluble receptors), cytokine mutants, or of drugs that specifically interfere with the signal transduction pathways involved in the fibrotic process.

Bleomycin-induced murine model has already established a standard model for scleroderma over 15 years, and a number of therapeutic approaches have been tried. However, very few effective drugs are available in the clinical settings. It is greatly and urgently required that new effective antifibrotic therapies will be available for human SSc.

Many studies using knockout mice have demonstrated resistance for skin fibrosis by bleomycin treatment (Akashi et al., 2016; Saigusa et al., 2015; Yang et al., 2012), suggesting several candidate targets of inhibiting cutaneous fibrosis.

References

Agarwal, S.K., Wu, M., Livingston, C.K., et al., 2011. Toll-like receptor 3 upregulation by type I interferon in healthy and scleroderma dermal fibroblasts. Arthritis Res. Ther. 13, R3.

Akashi, K., Saegusa, J., Sendo, S., et al., 2016. Knockout of endothelin type B receptor signaling attenuates bleomycin-induced skin sclerosis in mice. Arthritis Res. Ther. 18, 113.

Akhmetshina, A., Dees, C., Pileckyte, M., et al., 2008. Dual inhibition of c-abl and PDGF receptor signaling by dasatinib and nilotinib for the treatment of dermal fibrosis. FASEB J. 22, 2214–2222.

Akhmetshina, A., Venalis, P., Dees, C., et al., 2009. Treatment with imatinib prevents fibrosis in different preclinical models of systemic sclerosis and induces regression of established fibrosis. Arthritis Rheum. 60, 219–224.

Alecu, M., Geleriu, L., Coman, G., Galatescu, L., 1998. The interleukin-1, interleukin-2, interleukin-6 and tumor necrosis factor α serological levels in localized and systemic sclerosis. Rom. J. Intern. Med. 36, 251–259.

Aliprantis, A.O., Wang, J., Fathman, J.W., et al., 2007. Transcription factor T-bet regulates skin sclerosis through its function in innate immunity and via IL-13. Proc. Natl. Acad. Sci. USA 104, 2827–2830.

Artlett, C.M., Sassi-Gaha, S., Rieger, J.L., et al., 2011. The inflammasome activation caspase 1 mediates fibrosis and myofibroblast differentiation in systemic sclerosis. Arthritis Rheum. 63, 3563–3574.

Asano, Y., 2016. Fli1. In: Takehara, K., Fujimoto, M., Kuwana, M. (Eds.), Systemic Sclerosis: Basic and Translational Research. Springer, New York, pp. 187–209.

Asano, Y., Ihn, H., Yamane, K., Kubo, M., Tamaki, K., 2004a. Impaired Smad7-Smurf-mediated negative regulation of TGF-beta signaling in scleroderma fibroblasts. J. Clin. Invest. 113, 253–264.

Asano, Y., Ihn, H., Yamane, K., Jinnin, M., Mimura, Y., Tamaki, K., 2004b. Phosphatidylinositol 3-kinase is involved in α2(I) collagen gene expression in normal and scleroderma fibroblasts. J. Immunol. 172, 7123–7135.

Asano, Y., Stawski, L., Hant, F., et al., 2010. Endothelial Fli1 deficiency impairs vascular homeostasis. a role in scleroderma vasculopathy. Am. J. Pathol. 176, 1983–1998.

Avouac, J., Palumbo, K., Tomcik, M., et al., 2012. Inhibition of activator protein 1 signaling abrogates transforming growth factor β-mediated activation of fibroblasts and prevents experimental fibrosis. Arthritis Rheum. 64, 1642–1652.

Badea, I., Virtanen, C., Verrall, R.E., Rosenberg, A., Foldvari, M., 2012. Effect of topical interferon-γ gene therapy using gemini nanoparticles on pathophysiological markers of cutaneous scleroderma in Tsk/+ mice. Gene Ther. 19, 978–987.

Bagnato, G., Bitto, A., Irrera, N., et al., 2013a. Propylthiouracil prevents cutaneous and pulmonary fibrosis in the reactive oxygen species murine model of systemic sclerosis. Arthritis Res. Ther. 15, R120.

Bagnato, G., Bitto, A., Pizzino, G., et al., 2013b. Simvastatin attenuates the development of pulmonary and cutaneous fibrosis in a murine model of systemic sclerosis. Rheumatology 52, 1377–1386.

Balistreri, E., Garcia-Gonzalez, E., Selvi, E., et al., 2011. The cannabinoid WIN55, 212-2 abrogates dermal fibrosis in scleroderma bleomycin model. Ann. Rheum. Dis. 70, 695–699.

Barisic-Dujmovic, T., Boban, I., Clark, S.H., 2008. Regulation of collagen gene expression in the Tsk2 mouse. J. Cell Physiol. 215, 464–471.

Baxter, R.M., Crowell, T.P., McCrann, M.E., Frew, E.M., Gardner, H., 2005. Analysis of the tight skin (Tsk1/+) mouse as a model for testing antifibrotic agents. Lab. Invest. 85, 1199–1209.

Bayle, J., Fitch, J., Jacobsen, K., Kumar, R., Lafyatis, R., Lemaire, R., 2008. Increased expression of Wnt2 and SFRP4 in Tsk mouse skin: role of Wnt signaling in altered dermal fibrillin deposition and systemic sclerosis. J. Invest. Dermatol. 128, 871–881.

Belperio, J.A., Dy, M., Burdick, M.D., et al., 2002. Interaction of IL-13 and C10 in the pathogenesis of bleomycin-induced pulmonary fibrosis. Am. J. Respir. Cell Mol. Biol. 27, 419–427.

Bhattacharyya, S., Chen, S.J., Wu, M., et al., 2008. Smad-independent transforming growth factor-beta regulation of early growth response-1 and sustained expression in fibrosis: implications for scleroderma. Am. J. Pathol. 173, 1085–1099.

Blank, M., Levy, Y., Amital, H., Shoenfeld, Y., Pines, M., Genina, O., 2002. The role of intravenous immunoglobulin therapy in mediating skin fibrosis in tight skin mice. Arthritis Rheum. 46, 1689–1690.

Breen, E., Shull, S., Burne, S., et al., 1992. Bleomycin regulation of transforming growth factor-β mRNA in rat lung fibroblasts. Am. J. Respir. Cell Mol. Biol. 6, 146–152.

Bujor, A.M., Asano, Y., Haines, P., Lafyatis, R., Trojanowska, M., 2011. The c-Abl tyrosine kinase controls protein kinase Cδ-induced Fli-1 phosphorylation in human dermal fibroblasts. Arthritis Rheum. 63, 1729–1737.

Burgess, H., Daugherty, L., Thatcher, T., et al., 2005. PPARgamma agonists inhibit TGF-beta induced pulmonary myofibroblast differentiation and collagen production: implications for therapy of lung fibrosis. Am. J. Physiol. 288, L1146–L1153.

Castello-Cros, R., Whitaker-Menezes, D., Molchansky, A., et al., 2011. Scleroderma-like properties of skin from caveolin-1-deficient mice: implications for new treatment strategies in patients with fibrosis and systemic sclerosis. Cell Cycle 10, 2140–2150.

Chan, E.S., Fernandez, P., Merchant, A.A., et al., 2006. Adenosine A2A receptors in diffuse dermal fibrosis: pathogenic role in human dermal fibroblasts and in a murine model of scleroderma. Arthritis Rheum. 54, 2632–2642.

Choi, E.T., Callow, A.D., Sehgal, N.L., Brown, D.M., Ryan, U.S., 1995. Halofuginone, a specific collagen type I inhibitor, reduces anastomotic intima hyperplasia. Arch. Surg. 130, 257–261.

Christner, P.J., Peters, J., Hawkins, D., Siracusa, L.D., Jimenez, S.A., 1995. The tight skin 2 mouse: an animal model of scleroderma displaying cutaneous fibrosis and mononuclear cell infiltration. Arthritis Rheum. 38, 1791–1798.

Christner, P.J., Yufit, Y., Peters, J., MacGrath, R., Jimenez, S.A., 1998. Transcriptional activation of the α1(I) procollagen gene and upregulation of α1(I) and α1(III) procollagen messenger RNA in dermal fibroblasts from tight skin 2 mice. Arthritis Rheum. 41, 2132–2142.

Christner, P.J., Yufit, Y., Peters, J., MacGrath, R., Conway, R.F., Jimenez, S.A., 2003. Transcriptional activation of α1(III) procollagen gene in Tsk2/+ dermal fibroblasts. Biochem. Biophys. Res. Commun. 303, 406–412.

Chujo, S., Shirasaki, F., Kawara, S., et al., 2005. Connective tissue growth factor causes persistent proalpha2(I) collagen gene expression induced by transforming growth factor-beta in a mouse fibrosis model. J. Cell Physiol. 203, 447–456.

Chujo, S., Shirasaki, F., Kondo-Mitazaki, M., Ikawa, Y., Takehara, K., 2009. Role of connective tissue growth factor and its interation with basic fibroblast growth factor and macrophage chemoattractant protein-1 in skin fibrosis. J. Cell Physiol. 220, 189–195.

Clark, J.C., Starcher, B.C., Uitto, J., 1980. Bleomycin-induced synthesis of type I procollagen by human lung skin fibroblasts in culture. Biochim. Biophys. Acta 631, 359–370.

Denton, C.P., Zheng, B., Evans, L.A., et al., 2003. Fibroblast-specific expression of a kinase-deficient type II transforming growth factor β (TGFβ) receptor leads to paradoxical activation of TGFβ signaling pathways with fibrosis in transgenic mice. J. Biol. Chem. 278, 25109–25119.

Denton, C.P., Lindahl, G.E., Khan, K., et al., 2005. Activation of key profibrotic mechanisms in transgenic fibroblasts expressing kinase-deficient type II transforming growth factor-β receptor (TβRIIΔk). J. Biol. Chem. 280, 16053–16065.

Desallais, L., Avouac, J., Fréchet, M., et al., 2014. Targeting IL-6 by both passive or active immunization strategies prevents bleomycin-induced skin fibrosis. Arthritis Res. Ther. 16, R157.

Distler, O., Pap, T., Kowal-Bielecka, O., et al., 2001. Overexpression of monocyte chemoattractant protein 1 in systemic sclerosis: role of platelet-derived growth factor and effects of monocyte chemotaxis and collagen synthesis. Arthritis Rheum. 44, 2665–2678.

Distler, J.H., Jüngel, A., Huber, L.C., et al., 2007. Imatinib mesylate reduces production of extracellular matrix and prevents development of experimental dermal fibrosis. Arthritis Rheum. 56, 311–322.

Distler, J.H.W., Schett, G., Gay, S., Distler, O., 2008. The controversial role of tumor necrosis factor α in fibrotic diseases. Arthritis Rheum. 58, 2228–2235.

Dong, C., Zhu, S., Wang, T., et al., 2002. Deficient Smad7 expression: a putative molecular defect in scleroderma. Proc. Natl. Acad. Sci. USA 99, 3908–3913.

Dooley, A., Low, S.Y., Holmes, A., et al., 2008. Nitric oxide synthase expression and activity in the tight-skin mouse model of fibrosis. Rheumatology 47, 272–280.

Doucet, C., Brouty-Boye, D., Pottin-Clemenceau, C., Canonica, G.W., Jasmin, C., Azzarone, B., 1998a. Interleukin (IL)-4 and IL-13 act on human lung fibroblasts. J. Clin. Invest. 101, 2129–2139.

Doucet, C., Brouty-Boye, D., Pottin-Clemenceau, C., Jasmin, C., Canonica, G.W., Azzarone, B., 1998b. IL-4 and IL-13 specifically increase adhesion molecule and inflammatory cytokine expression in human lung fibroblasts. Int. Immunol. 10, 1421–1433.

Elovic, A.E., Ohyama, H., Sauty, A., et al., 1998. IL-4-dependent regulation of TGF-alpha and TGF-beta1 expression in human eosinophils. J. Immunol. 160, 6121–6127.

Fang, F., Marangoni, R.G., Zhou, X., et al., 2016. Toll-like Receptor 9 Signaling is augmented in systemic sclerosis and elicits transforming growth factor β-dependent fibroblast activation. Arthritis Rheumatol. 68 (8), 1989–2002.

Ferreira, A.M., Takagawa, S., Fresco, R., Zhu, X., Varga, J., DiPietro, L.A., 2006. Diminished induction of skin fibrosis in mice with MCP-1 deficiency. J. Invest. Dermatol. 126, 1900–1908.

Fukasawa, C., Kawaguchi, Y., Harigai, M., et al., 2003. Increased CD40 expression in skin fibroblasts from patients with systemic sclerosis (SSc): role of CD40-CD154 in the phenotype of SSc fibroblasts. Eur. J. Immunol. 33, 2792–2800.

Fullard, N., O'Reilly, S., 2015. Role of innate immune system in systemic sclerosis. Semin. Immunopathol. 37, 511–517.

Galindo, M., Santiago, B., Rivero, M., Rullas, J., Alcami, J., Pablos, J.L., 2001a. Chemokine expression by systemic sclerosis fibroblasts: abnormal regulation of monocyte chemoattractant protein 1 expression. Arthritis Rheum. 44, 1382–1386.

Galindo, M., Santiago, B., Alcami, J., Riyero, M., Martin-Serrano, J., Pablos, J.L., 2001b. Hypoxia induces expression of the chemokines monocyte chemoattractant protein-1 (MCP-1) and IL-8 in human dermal fibroblasts. Clin. Exp. Immunol. 123, 36–41.

Gentiletti, J., McCloskey, L.J., Artlett, C.M., Peters, J., Jimenez, S.A., Christner, P.J., 2005. Demonstration of autoimmunity in the tight skin-2 mouse: a model for scleroderma. J. Immunol. 175, 2418–2426.

Gharaee-Kermani, M., Denholm, E.M., Phan, S.H., 1996. Costimulation of fibroblast collagen and transforming growth factor β1 gene

expression by monocyte chemoattractant protein-1 via specific receptors. J. Biol. Chem. 271, 17779–17784.

Ghosh, A.K., Bhattacharyya, S., Lakos, G., Chen, S.J., Mori, Y., Varga, J., 2004. Disruption of transforming growth factor beta signaling and profibrotic responses in normal skin fibroblasts by peroxisome proliferator-activated receptor gamma. Arthritis Rheum. 50, 1305–1318.

Granot, I., Halevy, O., Hurwitz, S., Pines, M., 1993. Halofuginone: an inhibitor of collagen type I synthesis. Biochim. Biophys. Acta 1156, 107–112.

Gruschwitz, M.S., Moormann, S., Kromer, G., et al., 1991. Phenotypic analysis of skin infiltrates in comparison with peripheral blood lymphocytes, spleen cells and thymocytes in early avian scleroderma. J. Autoimmun. 4, 577–593.

Hasegawa, M., Fujimoto, M., Kikuchi, K., Takehara, K., 1997. Elevated serum tumor necrosis factor-alpha levels in patients with systemic sclerosis: association with pulmonary fibrosis. J. Rheumatol. 24, 663–665.

Hasegawa, M., Sato, S., Takehara, K., 1999. Augmentation of production of chemokines (monocyte chemotactic protein-1 (MCP-1), macrophage inflammatory protein-1α (MIP-1α) and MIP-1β) in patients with systemic sclerosis: MCP-1 and MIP-1α may be involved in the development of pulmonary fibrosis. Clin. Exp. Immunol. 117, 159–165.

Hasegawa, M., Hamaguchi, Y., Yanaba, K., et al., 2006. B-lymphocyte depletion reduces skin fibrosis and autoimmunity in the tight-skin mouse model for systemic sclerosis. Am. J. Pathol 169, 954–966.

Hasegawa, M., Matsushita, Y., Horikawa, M., et al., 2009. A novel inhibitor of Smad-dependent transcriptional activation suppresses tissue fibrosis in mouse models of systemic sclerosis. Arthritis Rheum. 60, 3465–3475.

Hebbar, M., Gillot, J.M., Hachulla, E., et al., 1996. Early expression of E-selectin, tumor necrosis factorα, and mast cell infiltration in the salivary glands of patients with systemic sclerosis. Arthritis Rheum. 39, 1161–1165.

Holmes, A.M., Ponticos, M., Shi-wen, X., Denton, C.P., Abraham, D.J., 2011. Elevated CCN2 expression in scleroderma: a putative role for the TGFβ accessory receptors TGFβIII and endoglin. J. Cell Commun. Signal 5, 173–177.

Ihn, H., Yamane, K., Tamaki, K., 2005. Increased phosphorylation and activation of mitogen-activated protein kinase p38 in scleroderma fibroblasts. J. Invest. Dermatol. 125, 247–255.

Ikawa, Y., Ng, P.S., Endo, K., et al., 2008. Neutralizing monoclonal antibody to human connective tissue growth factor ameliorates transforming growth factor-beta-induced mouse fibrosis. J. Cell Physiol. 216, 680–687.

Ishikawa, H., Takeda, K., Okamoto, A., Matsuo, S.I., Isobe, K.I., 2009. Induction of autoimmunity in a bleomycin-induced murine model of experimental systemic sclerosis: an important role for CD4(+) T cells. J. Invest. Dermatol. 129, 1688–1695.

Iwasaki, T., Imado, T., Kitano, S., Sano, H., 2006. Hepatocyte growth factor ameliorates dermal sclerosis in the tight-skin mouse model of scleroderma. Arthritis Res. Ther. 8, R161.

Jelaska, A., Korn, J.H., 2000. Role of apoptosis and transforming growth factor β1 in fibroblast selection and activation in systemic sclerosis. Arthritis Rheum. 43, 2230–2239.

Jinnin, M., Ihn, H., Yamane, K., Tamaki, K., 2004. Interleukin-13 stimulates the transcription of the human alpha2(I) collagen gene in human dermal fibroblasts. J. Biol. Chem. 279, 41783–41791.

Kajii, M., Suzuki, C., Kashihara, J., et al., 2011. Prevention of excessive collagen accumulation by human intravenous immunoglobulin treatment in a murine model of bleomycin-induced scleroderma. Clin. Exp. Immunol. 163, 235–241.

Kasturi, K.N., Shibata, S., Muryoi, T., Bona, C., 1994. Tight-skin mouse an experimental model for scleroderma. Int. Rev. Immunol. 11, 253–271.

Kavian, N., Servettaz, A., Mongaret, C., et al., 2010. Targeting ADAM-17/notch signaling abrogates the development of systemic sclerosis in a murine model. Arthritis Rheum. 62, 3477–3487.

Kavian, N., Servettaz, A., Marut, W., et al., 2012a. Sunitinib inhibits the phosphorylation of platelet-derived growth factor receptor β in the skin of mice with scleroderma-like features and prevents the development of the disease. Arthritis Rheum. 64, 1990–2000.

Kavian, N., Marut, W., Servettaz, A., et al., 2012b. Reactive oxygen species-mediated killing of activated fibroblasts by arsenic trioxide ameliorates fibrosis in a murine model of systemic sclerosis. Arthritis Rheum. 64, 3430–3440.

Kavian, N., Marut, W., Servettaz, A., et al., 2015. Pantethine prevents murine systemic sclerosis through the inhibition of microparticle shedding. Arthritis Rheumatol. 67, 1881–1890.

Kawaguchi, Y., Hara, M., Wright, T.M., 1999. Endogenous IL-1α from systemic sclerosis fibroblasts induces IL-6 and PDGF-A. J. Clin. Invest. 103, 1253–1260.

Kawai, M., Masuda, A., Kuwana, M., 2008. A CD40-CD154 interaction in tissue fibrosis. Arthritis Rheum. 58, 3562–3573.

Kikuchi, H., Hanazawa, S., Takeshita, A., Nakada, Y., Yamashita, Y., Kitano, S., 1993. Interleukin-4 acts as a potent stimulator for expression of monocyte chemoattractant JE/MCP-1 in mouse peritoneal macrophages. Biochem. Biophys. Res. Commun. 203, 562–569.

Kim, H.J., Song, S.B., Choi, J.M., et al., 2010. IL-18 downregulates collagen production in human dermal fibroblasts via the ERK pathway. J. Invest. Dermatol. 130, 706–715.

Kimura, M., Kawahito, Y., Hamaguchi, M., et al., 2007. SKL-2841, a dual antagonist of MCP-1 and MIP-1 beta, prevents bleomycin-induced sin sclerosis in mice. Biomed. Pharmacother. 61, 222–228.

King, S.L., Lichtler, A.C., Rowe, D.W., et al., 1994. Bleomycin stimulates proα1(I) collagen promoter through transforming growth factor-β response element by intracellular and extracellular signaling. J. Biol. Chem. 269, 13156–13161.

Kitaba, S., Murota, H., Terao, M., et al., 2012. Blockade of interleukin-6 receptor alleviates disease in mouse model of scleroderma. Am. J. Pathol. 180, 165–176.

Kokot, A., Sindrilaru, A., Schiller, M., et al., 2009. α-melanocyte-stimulating hormone suppresses bleomycin-induced collagen synthesis and reduces tissue fibrosis in a mouse model of scleroderma. Arthritis Rheum. 60, 592–603.

Komura, K., Fujimoto, M., Yanaba, K., et al., 2008. Blockade of CD40/CD40 ligand interaction attenuates skin fibrosis and autoimmunity in the tight-skin mouse. Ann. Rheum. Dis. 67, 867–872.

Kubo, M., Czuwara-Ladykowska, J., Moussa, O., et al., 2003. Persistent down-regulation of Fli1, a suppressor of collagen transcription, in fibrotic scleroderma skin. Am. J. Pathol. 163, 571–578.

Kulozik, M., Hogg, A., Lankat-Buttgereit, B., Krieg, T., 1990. Co-localization of transforming growth factor β2 with α1(I) procollagen mRNA in tissue sections of patients with systemic sclerosis. J. Clin. Invest. 86, 917–922.

Lakos, G., Takagawa, S., Chen, S.J., et al., 2004. Targeted disruption of TGF-beta/Smad3 signaling modulates skin fibrosis in a mouse model of scleroderma. Am. J. Pathol. 165, 203–217.

Lakos, G., Melichian, D., Wu, M., Varga, J., 2006. Increased bleomycin-induced skin fibrosis in mice lacking the Th1-specific transcription factor T-bet. Pathobiology 73, 224–237.

Laplante, P., Raymond, M.-A., Gagnon, G., et al., 2005. Novel fibrogenic pathways are activated in response to endothelial apoptosis: Implications in the pathophysiology of systemic sclerosis. J. Immunol. 174, 5740–5749.

Lee, C.G., Homer, R.J., Zhu, Z., et al., 2001. Interleukin-13 induces tissue fibrosis by selectively stimulating and activating transforming growth factor β1. J. Exp. Med. 194, 809–821.

Lee, Y.W., Hennig, B., Toborek, M., 2003. Redox-regulated mechanisms of IL-4-induced MCP-1 expression in human vascular endothelial cells. Am. J. Physiol. Heart Circ. Physiol. 284, H185–H192.

Levi-Schaffer, F., Nagler, A., Slavin, S., Knopov, V., Pines, M., 1996. Inhibition of collagen synthesis and changes in skin morphology in murine graft-versus-host disease and tight skin mice: Effect of halofuginone. J. Invest. Dermatol. 106, 84–88.

Liu, S., Kapoor, M., Shi-wen, X., et al., 2008. Role of Rac1 in a bleomycin-induced scleroderma model using fibroblast-specific Rac1-knockout mice. Arthritis Rheum. 58, 2189–2195.

Liu, S., Taghavi, R., Leask, A., 2010. Connective tissue growth factor is induced in bleomycin-induced skin scleroderma. J. Cell Commun. Signal 4, 25–30.

Long, K.B., Li, Z., Burgwin, C.M., et al., 2015. The Tsk2/+ mouse fibrotic phenotype is due to a gain-of-function mutation in the PIIINP segment of the Col3a1 gene. J. Invest. Dermatol. 135, 718–727.

Lukacs, N.W., Chensue, S.W., Karpus, W.J., et al., 1997. C-C chemokines differentially alter interleukin-4 production from lymphocytes. Am. J. Pathol. 150, 1861–1868.

MacGaha, T.L., Saito, S., Phelps, R.G., et al., 2001. Lack of skin fibrosis in tight skin (TSK) mice with targeted mutation in the interleukin-4Rα and transforming growth factor β genes. J. Invest. Dermatol. 116, 136–143.

MacGaha, T.L., Phelps, R.G., Spiera, H., Bona, C., 2002. Halofuginone, an inhibitor of type-I-collagen synthesis and skin sclerosis, blocks transforming growth factor-beta-mediated Smad3 activation in fibroblasts. J. Invest. Dermatol. 118, 461–470.

MacGaha, T.L., Le, M., Kodera, T., et al., 2003. Molecular mechanisms of interleukin-4-induced up-regulation of type I collagen gene expression in murine fibroblasts. Arthritis Rheum. 48, 2275–2284.

Makhluf, H.A., Stepniakowska, J., Hoffman, S., Smith, E., LeRoy, E.C., Trojanowska, M., 1996. IL-4 upregulates tenascin synthesis in scleroderma and healthy skin fibroblasts. J. Invest. Dermatol. 107, 856–859.

Marangoni, R.G., Korman, B.D., Wei, J., et al., 2015. Myofibroblasts in murine cutaneous fibrosis originate from adiponectin-positive intradermal progenitors. Arthritis Rheumatol. 67, 1062–1073.

Marie, I., Beny, J.L., 2002. Endothelial dysfunction in murine model of systemic sclerosis: tight-skin mouse 1. J. Invest. Dermatol. 119, 1379–1387.

Marut, W., Jamier, V., Kavian, N., et al., 2013a. The natural organosulfur compound dipropyltetrasulfide prevents HOCl-induced systemic sclerosis in the mouse. Arthritis Res. Ther. 15, R167.

Marut, W., Kavian, N., Servettaz, A., et al., 2013b. Amelioration of systemic fibrosis in mice by angiotensin II receptor blockade. Arthritis Rheum. 65, 1367–1377.

Matsumoto, K., Nakamura, T., 2001. Hepatocyte growth factor: renotropic role and potential therapeutics for renal diseases. Kidney Int. 59, 2023–2038.

Matsushita, M., Yamamoto, T., Nishioka, K., 2004. Upregulation of interleukin-13 and its receptor in a murine model of bleomycin-induced scleroderma. Int. Arch. All Immunol. 135, 348–356.

Matsushita, M., Yamamoto, T., Nishioka, K., 2005. Plasminogen activator inhibitor-1 is elevated, but not essential, in the development of bleomycin-induced murine scleroderma. Clin. Exp. Immunol. 139, 429–438.

Maurer, B., Busch, N., Jüngel, A., et al., 2009. Transcription factor fos-related antigen-2 induces progressive peripheral vasculopathy in mice closely resembling human systemic sclerosis. Circulation 120, 2367–2376.

Maurer, B., Stanczyk, J., Jüngel, A., et al., 2010. MicroRNA-29, a key regulator of collagen expression in systemic sclerosis. Arthritis Rheum. 62, 1733–1743.

Maurer, B., Reich, N., Juengel, A., et al., 2012. Fra-2 transgenic mice as a novel model of pulmonary hypertension associated with systemic sclerosis. Ann. Rheum. Dis. 71, 1382–1387.

Mccormick, L.L., Zhang, Y., Tootell, E., Gilliam, A.C., 1999. Anti-TGF-β treatment prevents skin and lung fibrosis in murine sclerodermatous graft-versus-host disease: a model for human scleroderma. J. Immunol. 163, 5693–5699.

McGaha, T.L., Phelps, R.G., Spiera, H., Bona, C., 2002. Halofuginone, an inhibitor of type-I collagen synthesis and skin sclerosis, blocks transforming-growth-factor-β-mediated Smad3 activation in fibroblasts. J. Invest. Dermatol. 118, 461–470.

Mori, T., Kawara, S., Shinozaki, M., et al., 1999. Role and interaction of connective tissue growth factor with transforming growth factor-β in persistent fibrosis. A mouse fibrosis model. J. Cell Physiol. 181, 153–159.

Mori, Y., Chen, S.J., Varga, J., 2003. Expression and regulation of intracellular SMAD signaling in scleroderma skin fibroblasts. Arthritis Rheum. 48, 1964–1978.

Morin, F., Kavian, N., Marut, W., et al., 2015. Inhibition of EGFR tyrosine kinase by erlotinib prevents sclerodermatous graft-versus-host disease in a mouse model. J. Invest. Dermatol. 135, 2385–2393.

Mountz, J.D., Downs Minor, M.B., Turner, R., Thomas, M.B., Richards, F., Pisko, E., 1983. Bleomycin-induced cutaneous toxicity in the rat: analysis of histopathology and ultrastructure compared with progressive systemic sclerosis (scleroderma). Br. J. Dermatol. 108, 679–686.

Murota, H., Hamasaki, Y., Nakashima, T., Yamamoto, K., Katayama, I., Matsuyama, T., 2003. Disruption of tumor necrosis factor receptor p55 impairs collagen turnover in experimentally induced sclerodermic skin fibroblasts. Arthritis Rheum. 48, 1117–1125.

Nakerakanti, S.S., Kapanadze, B., Yamasaki, M., et al., 2006. Fli1 and Ets1 have distinct roles in connective tissue growth factor/CCN2 gene regulation and induction of the profibrotic gene program. J. Biol Chem. 281, 25259–25269.

Needlemann, B.W., Wigley, F.M., Stair, R.W., 1985. Interleukin-1, interleukin-2, interleukin-4, interleukin-6, tumor necrosis factor α, and interferon-γ levels in sera from patients with scleroderma. Arthritis Rheum. 28, 775–780.

Noda, S., Asano, Y., Nishimura, S., et al., 2014. Simultaneous down-regulation of KLF5 and Fli1 is a key feature underlying systemic sclerosis. Nat. Commun. 5, 5797.

Ohashi, T., Yamamoto, T., 2015. Antifibrotic effect of lysophosphatidic acid receptors LPA1 and LPA3 antagonist on experimental murine scleroderma induced by bleomycin. Exp. Dermatol. 24, 698–702.

Ohgo, S., Hasegawa, S., Hasebe, Y., et al., 2013. Bleomycin inhibits adipogenesis and accelerates fibrosis in the subcutaneous adipose layer through TGF-β1. Exp. Dermatol. 22, 769–771.

Oi, M., Yamamoto, T., Nishioka, K., 2004. Increased expression of TGF-β1 in the sclerotic skin in bleomycin-'susceptible' mouse strains. J. Med. Dent. Sci. 51, 7–17.

Ong, D., Wong, C., Roberts, C.R., Teh, H.S., Jirik, F.R., 1998. Anti-IL-4 treatment prevents dermal collagen deposition in the tight-skin mouse model of scleroderma. Eur. J. Immunol. 128, 2619–2629.

Ong, C.J., Ip, S., The, S.J., et al., 1999. A role for T helper 2 cells in mediating skin fibroblasts in tight-skin mice. Cell Immunol. 196, 60–68.

Ong, V.H., Evans, L.A., Shiwen, X., et al., 2003. Monocyte chemoattractant protein 3 as a mediator of fibrosis: overexpression in systemic sclerosis and the type 1 tight-skin mouse. Arthritis Rheum. 48, 1979–1991.

Oriente, A., Fedarko, N.S., Pacocha, S.E., Huang, S.K., Lichtenstein, L.M., Essayan, D.M., 2000. Interleukin-13 modulates collagen homeostasis in human skin and keloid fibroblasts. J. Pharmacol. Exp. Ther. 292, 988–994.

Ortiz, L.A., Lasky, J., Lungarella, G., et al., 1999. Upregulation of the p75 but not the p55 TNF-α receptor mRNA after silica and bleomycin exposure and protection from lung injury in double receptor knockout mice. Am. J. Respir. Cell Mol. Biol. 20, 825–833.

Pablos, J.L., Everett, E.T., Harley, R., LeRoy, E.C., Norris, J.S., 1995. Transforming growth factor-β1 and collagen gene expression during postnatal skin development and fibrosis in the tight-skin mouse. Lab Invest. 72, 180–185.

Pamuk, O.N., Can, G., Ayvaz, S., et al., 2015. Spleen tyrosine kinase (Syk) inhibitor fostamatinib limits tissue damage and fibrosis in a bleomycin-induced scleroderma mouse model. Clin. Exp. Rheumatol. 33 (4 Suppl 91), S15–S22.

Phan, S.H., Kunkel, S.L., 1992. Lung cytokine production in bleomycin-induced pulmonary fibrosis. Exp. Lung Res. 18, 29–43.

Phan, S.H., Gharaee-Kermani, M., Wolber, F., Ryan, U.S., 1991. Stimulation of rat endothelial cell transforming growth factor-β production by bleomycin. J. Clin. Invest. 87, 148–154.

Philips, N., Bashey, R.I., Jimenez, S.A., 1995. Increased α1(I) procollagen gene expression in tight skin (Tsk) mice myocardial fibroblasts is due to a reduced interaction of a negative regulatory sequence with AP-1 transcription factor. J. Biol. Chem. 270, 9313–9321.

Piguet, P.F., Collart, M.A., Gran, G.E., Kapanci, Y., Vassalli, P., 1989. Tumor necrosis factor/cachectin plays a key role in bleomycin-induced pneumopathy and fibrosis. J. Exp. Med. 170, 655–663.

Pines, M., Domb, A., Ohara, M., Inbar, J., Genina, O., Alexiev, R., Nagler, A., 2001. Reduction in dermal fibrosis in the tight-skin (Tsk) mouse after local application of halofuginone. Bichem. Pharmacol. 62, 1221–1227.

Postlethwaite, A.E., Holness, M.A., Katai, H., Raghow, R., 1992. Human fibroblasts synthesize elevated levels of extracellular matrix proteins in response to interleukin 4. J. Clin. Invest. 90, 1479–1485.

Ruzek, M.C., Jha, S., Ledbetter, S., Richards, S.M., Garman, R.D., 2004. A modified model of graft-versus-host induced systemic sclerosis (scleroderma) exhibits all major aspects of the human disease. Arthritis Rheum. 50, 1319–1331.

Saigusa, R., Asano, Y., Taniguchi, T., et al., 2015. Multifaceted contribution of the TLR4-activated IRF5 transcription factor in systemic sclerosis. Proc. Natl. Acad. Sci. USA 112, 15136–15141.

Saito, E., Fujimoto, M., Hasegawa, M., et al., 2002. CD19-dependent B lymphocyte signaling thresholds influence skin fibrosis and autoimmunity in the tight skin mice. J. Clin. Invest. 109, 1453–1462.

Samuel, C.S., Zhao, C., Yang, Q., et al., 2005. The relaxin gene knock-out mouse: a model of progressive scleroderma. J. Invest. Dermatol. 125, 692–699.

Santiago, B., Galindo, M., Rivero, M., Pablos, J.L., 2001. Decreased susceptibility to Fas-induced apoptosis of systemic sclerosis dermal fibroblasts. Arthritis Rheum. 44, 1667–1676.

Santiago, B., Gutierrez-Canas, I., Dotor, J., et al., 2005. Topical application of a peptide inhibitor of transforming growth factor-beta1 ameliorates bleomycin-induced skin fibrosis. J. Invest. Dermatol. 125, 450–455.

Sato, S., Fujimoto, M., Hasegawa, M., Takehara, K., 2001. Altered blood B lymphocyte homeostasis in systemic sclerosis. Expanded naïve B cells and diminished but activated memory B cells. Arthritis Rheum. 50, 1918–1927.

Scala, E., Pallotta, S., Frezzolini, A., et al., 2004. Cytokine and chemokine levels in systemic sclerosis: relationship with cutaneous and internal organ involvement. Clin. Exp. Immunol. 138, 540–546.

Seder, R.A., Marth, T., Sieve, M.C., et al., 1998. Factors involved in the differentiation of TGF-beta-producing cells from naive CD4+ T cells: IL-4 and IFN-gamma have opposite effects, while TGF-beta positively regulates its own production. J. Immunol. 160, 5719–5728.

Serpier, H., Gillery, P., Salmon-Ehr, V., et al., 1997. Antagonistic effect of interferon-gamma and interleukin-4 on fibroblast cultures. J. Invest. Dermatol. 109, 158–162.

Servettaz, A., Goulvestre, C., Kavian, N., et al., 2009. Selective oxidation of DNA topoisomerase 1 induces systemic sclerosis in mice. J. Immunol. 182, 5855–5864.

Sgonc, R., Dietrich, H., Sieberer, C., Wick, G., Christner, P.J., Jimenez, S.A., 1999. Lack of endothelial cell apoptosis in the dermis of tight skin 1 and tight skin 2 mice. Arthritis Rheum. 42, 581–584.

Sgonc, R., Gruschwitz, M.S., Boeck, G., Sepp, N., Gruber, J., Wick, G., 2000. Endothelial cell apoptosis in systemic sclerosis is induced by antibody-dependent cell-mediated cytotoxicity via CD95. Arthritis Rheum. 43, 2550–2562.

Shen, Y., Ichino, M., Nakazawa, M., Minami, M., 2005. CpG oligodeoxynucleotides prevent the development of scleroderma-like syndrome in tight-skin mice by stimulating a Th1 immune response. J. Invest. Dermatol. 124, 1141–1148.

Shibusawa, Y., Negishi, I., Tabata, Y., Ishikawa, O., 2008. Mouse model of dermal fibrosis induced by one-time injection of bleomycin-poly(L-lactic acid) microspheres. Rheumatology 47, 454–457.

Shinozaki, M., Kawara, S., Hayashi, N., Kakinuma, T., Igarashi, A., Takehara, K., 1997. Induction of subcutaneous tissue fibrosis in newborn mice by transforming growth factor-beta-simultaneous application with basic fibroblast growth factor causes persistent fibrosis. Biochem. Biophys. Res. Commun. 237, 292–297.

Shiota, N., Kakizoe, E., Shimoura, K., Tanaka, T., Okunishi, H., 2005. Effect of mast cell chymase inhibitor on the development of scleroderma in tight-skin mice. Br. J. Pharmacol. 145, 424–431.

Skhirtladze, C., Distler, O., Dees, C., et al., 2008. Src kinases in systemic sclerosis: central roles in fibroblast activation and in skin fibrosis. Arthritis Rheum. 58, 1475–1484.

Stenström, M., Nyhlén, H.C., Törngren, M., et al., 2016. Paquinimod reduces skin fibrosis in tight skin 1 mice, an experimental model of systemic sclerosis. J. Dermatol. Sci. 83, 52–59.

Takagawa, S., Lakos, G., Mori, Y., Yamamoto, T., Nishioka, K., Varga, J., 2003. Sustained activation of fibroblast transforming growth factor-β/Smad signaling in a murine model of scleroderma. J. Invest. Dermatol. 121, 41–50.

Takahashi, T., Asano, Y., Ichimura, Y., et al., 2015. Amelioration of tissue fibrosis by toll-like receptor 4 knockout in murine models of systemic sclerosis. Arthritis Rheumatol. 67, 254–265.

Takehara, K., 2003. Pathogenesis of systemic sclerosis. J. Rheumatol. 30, 755–759.

Toyama, T., Asano, Y., Akamata, K., et al., 2016. Tamibarotene ameliorates bleomycin-induced dermal fibrosis by modulating phenotypes of fibroblasts, endothelial cells, and immune cells. J. Invest. Dermatol. 136, 387–398.

Ulloa, L., Doody, J., Massagué, J., 1999. Inhibition of transforming growth factor-β/SMAD signaling by the interferon-γ/STAT pathway. Nature 397, 710–713.

Ursini, F., Grembiale, R.D., D'Antona, L., et al., 2016. Oral metformin ameliorates bleomycin-induced skin fibrosis. J. Invest. Dermatol. 136, 1892–1894.

Van De Water, J., Gershwin, M.E., 1986. Avian scleroderma. An inherited fibrotic disease of White Leghorn chickens resembling progressive systemic sclerosis. Am. J. Pathol. 120, 478–482.

Wakatsuki-Nakamura, T., Oyama, N., Yamamoto, T., 2012. Local injection of latency-associated peptide (LAP), a linker peptide specific for active form of transforming growth factor-beta1 (TGF-β1), inhibits dermal sclerosis in bleomycin-induced murine scleroderma. Exp. Dermatol. 21, 189–194.

Walker, M., Harley, R., LeRoy, E.C., 1987. Inhibition of fibrosis in Tsk mice by blocking mast cell degranulation. J. Rheumatol. 14, 299–301.

Wallace, V.A., Kondo, S., Kono, T., et al., 1994. A role for CD4+ T cells in the pathogenesis of skin fibrosis in tight skin mice. Eur. J. Immunol. 24, 1463–1466.

Wang, H.W., Tedla, N., Hunt, J.E., Wakefield, D., McNeil, H.P., 2005. Mast cell accumulation and cytokine expression in the tight skin mouse model of scleroderma. Exp. Dermatol. 14, 295–302.

Worda, M., Sgonc, R., Dietrich, H., et al., 2003. In vivo analysis of the apoptosis-inducing effect of anti-endothelial cell antibodies in systemic sclerosis by the chorionallantoic membrane assay. Arthritis Rheum. 48, 2605–2614.

Wu, M.-H., Yokozeki, H., Takagawa, S., et al., 2004. Hepatocyte growth factor both prevents and ameliorates the symptoms of dermal sclerosis in a mouse model of scleroderma. Gene Ther. 11, 170–180.

Wu, M., Melichian, D.S., Chang, E., Warner-Blankenship, M., Ghosh, A.K., Varga, J., 2009. Rosiglitazone abrogates bleomycin-induced scleroderma and blocks profibrotic responses through peroxisome proliferator-activated receptor-γ. Am. J. Pathol. 174, 519–533.

Yamamoto, T., 2006a. Bleomycin and the skin. Br. J. Dermatol. 155, 869–875.

Yamamoto, T., 2006b. Chemokines and chemokine receptors in scleroderma. Int. Arch. All Immunol. 140, 345–356.

Yamamoto, T., 2008. Pathogenic role of CCL2/MCP-1 in scleroderma. Front. Biosci. 13, 2686–2695.

Yamamoto, T., 2009. Scleroderma-pathophysiology. Eur. J. Dermatol. 19, 14–24.

Yamamoto, T., 2010. Animal model of systemic sclerosis. J. Dermatol. 37, 26–41.

Yamamoto, T., Katayama, I., 2011. Vascular changes in bleomycin-induced scleroderma. Int. J. Rheumatol. 2011, 270938.

Yamamoto, T., Nishioka, K., 2001. Animal model of sclerotic skin. IV: induction of dermal sclerosis by bleomycin is T cell independent. J. Invest. Dermatol. 117, 999–1001.

Yamamoto, T., Nishioka, K., 2002a. Animal model of sclerotic skin. V: increased expression of α-smooth muscle actin in fibroblastic cells in bleomycin-induced scleroderma. Clin. Immunol. 102, 77–83.

Yamamoto, T., Nishioka, K., 2002b. Analysis of the effect of halofuginone on bleomycin-induced scleroderma. Rheumatology 41, 594–596.

Yamamoto, T., Nishioka, K., 2003. Role of monocyte chemoattractant protein-1 and its receptor, CCR-2, in the pathogenesis of bleomycin-induced scleroderma. J. Invest. Dermatol. 121, 510–516.

Yamamoto, T., Nishioka, K., 2004a. Animal model of sclerotic skin. VI: evaluation of bleomycin-induced skin sclerosis in nude mice. Arch. Dermatol. Res. 295, 453–456.

Yamamoto, T., Nishioka, K., 2004b. Possible role of apoptosis in the pathogenesis of bleomycin-induced scleroderma. J. Invest. Dermatol. 122, 44–50.

Yamamoto, T., Takagawa, S., Katayama, I., et al., 1999a. Animal model of sclerotic skin. I: local injections of bleomycin induce sclerotic skin mimicking scleroderma. J. Invest. Dermatol. 112, 456–462.

Yamamoto, T., Takahashi, Y., Takagawa, S., Katayama, I., Nishioka, K., 1999b. Animal model of sclerotic skin. II: bleomycin induced scleroderma in genetically mast cell deficient WBB6F1-W/Wv mice. J. Rheumatol. 26, 2628–2634.

Yamamoto, T., Takagawa, S., Katayama, I., Nishioka, K., 1999c. Anti-sclerotic effect of anti-transforming growth factor-β antibody in bleomycin-induced scleroderma. Clin. Immunol. 92, 6–13.

Yamamoto, T., Takagawa, S., Mizushima, Y., Nishioka, K., 1999d. Effect of superoxide dismutase on bleomycin-induced dermal sclerosis: implications for the treatment of systemic sclerosis. J. Invest. Dermatol. 113, 843–847.

Yamamoto, T., Kuroda, M., Takagawa, S., Nishioka, K., 2000a. Animal model of sclerotic skin. III: histopathological comparison of bleomycin-induced scleroderma in various mice strains. Arch. Dermatol. Res. 292, 535–541.

Yamamoto, T., Eckes, B., Krieg, T., 2000b. Bleomycin increases steady-state levels of type I collagen, fibronectin and decorin gene expression in human skin fibroblasts. Arch. Dermatol. Res. 292, 556–561.

Yamamoto, T., Eckes, B., Mauch, C., Hartmann, K., Krieg, T., 2000c. Monocyte chemoattractant protein-1 enhances gene expression and synthesis of matrix metalloproteinase-1 in human fibroblasts by an autocrine IL-1α loop. J. Immunol. 164, 6174–6179.

Yamamoto, T., Takagawa, S., Kuroda, M., Nishioka, K., 2000d. Effect of interferon-γ on experimental scleroderma induced by bleomycin. Arch. Dermatol. Res. 292, 362–365.

Yamamoto, T., Eckes, B., Krieg, T., 2001a. High expression and auto-induction of monocyte chemoattractant protein-1 in scleroderma fibroblasts. Eur. J. Immunol. 31, 2936–2941.

Yamamoto, T., Eckes, B., Hartmann, K., Krieg, T., 2001b. Expression of monocyte chemoattractant protein-1 in the lesional skin of systemic sclerosis. J. Dermatol. Sci. 26, 133–139.

Yamamoto, A., Ashihara, E., Nakagawa, Y., et al., 2011. Allograft inflammatory factor-1 is overexpressed and induces fibroblast chemotaxis in the skin of sclerodermatous GVHD in a murine model. Immunol. Lett. 135, 144–150.

Yan, Q., Chen, J., Li, W., et al., 2016. Targeting miR-155 to treat experimental scleroderma. Sci. Rep. 6, 20314.

Yang, L., Serada, S., Fujimoto, M., et al., 2012. Periostin facilitates skin sclerosis via PI3K/Akt dependent mechanism in a mouse model of scleroderma. PLoS One 7, e41994.

Yokozeki, M., Baba, Y., Shimokawa, H., Moriyama, K., Kuroda, T., 1999. Interferon-γ inhibits the myofibroblastic phenotype of rat palatal fibroblasts induced by transforming growth factor-β1 in vitro. FEBS Lett. 442, 61–64.

Yoshizaki, A., Iwata, Y., Mokura, K., et al., 2008. CD19 regulates skin and lung fibrosis via Toll-like receptor signaling in a model of bleomycin-induced scleroderma. Am. J. Pathol. 172, 1650–1663.

Yoshizaki, A., Yanaba, K., Ogawa, A., et al., 2011. The specific free radical scavenger edaravone suppresses fibrosis in the bleomycin-induced and tight skin mouse models of systemic sclerosis. Arthritis Rheum. 63, 3086–3097.

Zhang, Y., Mccormick, L.L., Desai, S.R., Wu, S., Gilliam, A.C., 2002. Murine sclerodermatous graft-versus-host disease, a model for human scleroderma: Cutaneous cytokines, chemokines, and immune cell activation. J. Immunol. 168, 3088–3098.

Zhang, Y., McCormick, L.L., Gilliam, A.C., 2003. Latency-associated peptide prevents skin fibrosis in murine sclerodermatous graft-versus-host disease, a model for human scleroderma. J. Invest. Dermatol. 121, 713–719.

Zhou, L., Askew, D., Wu, C., Gilliam, A.C., 2007. Cutaneous gene expression by DNA microarray in murine sclerodermatous graft-versus-host disease, a model for human scleroderma. J. Invest. Dermatol. 127, 281–292.

Zhu, Z., Ma, B., Zheng, T., et al., 2002. IL-13-induced chemokine responses in the lung: role of CCR2 in the pathogenesis of IL-13-induced inflammation and remodeling. J. Immunol. 168, 2953–2962.

37

Animal Models for the Study of Multiple Sclerosis

Robert H. Miller*, Sharyl Fyffe-Maricich**,
Andrew C. Caprariello[†]

*George Washington University, Washington, DC, United States
**University of Pittsburgh, Rangos Research Center, Pittsburgh, PA, United States
[†]University of Calgary, Hotchkiss Brain Institute, Canada

1 THE COMPLEX BIOLOGY OF MULTIPLE SCLEROSIS

The development of animal models of human diseases has, in general, two main functions. The first function is to generate a greater level of understanding of the basic biology of the disease and the second is to use the models to guide the development of new therapeutic approaches for treatment of the disease. Research into multiple sclerosis (MS) and other demyelinating diseases of the central nervous system (CNS) has followed this path closely over the last 60 years since the first description of an animal model of MS (Rivers et al., 1933). Unfortunate-ly, like many other disease conditions our understanding of the underlying biology of MS has remained quite limited and as a consequence the design of accurate animal models has been challenging and the most frequently utilized models have provided limited insights and effective therapeutics (Furlan et al., 2009).

MS was first described in the 1800s as a malaise that resulted in increasing functional disability. With the advent of histological techniques it became clear that MS was a disease of the CNS that affected regions of the brain and spinal cord. Until quite recently MS was conceived as a white matter disease, largely as a result of the detection of multiple focal areas of demyelination

known as plaques in CNS white matter tracks. This concept is changing with an increasing realization that there are also frequent areas of damage in gray matter suggesting that MS is not simply a disease of white matter (Grothe et al., 2016). The pathology of MS plaques or lesions is characterized by areas of demyelination that often contain a blood vessel at their core and show damage to the myelin sheaths that insulate CNS axons, as well as the formation of an astrocytic response or gliosis contributing to scar formation (Fawcett and Asher, 1999).

The vertebrate CNS contains three major classes of neural cells, Neurons the cells that are electrically active and transmit information throughout the brain and spinal cord extremely rapidly and with a high level of fidelity (Fig. 37.1). Different subpopulations of neurons arise

from distinct regions of the CNS and their characteristics such as neurotransmitter phenotype, morphology and connectivity reflect the interplay of both intrinsic factors and the environment in which the cells develop (Eriksson et al., 1998; Nornes and Das, 1974). The second major class of neural cells is astrocytes (Eng, 1985; Hirano and Goldman, 1988; Miller and Raff, 1984; Montgomery, 1994). These cells, which constitute a heterogenous population of cells, are probably as numerous in the CNS as neurons and perform multiple functions that support both the development and maintenance of the brain and spinal cord (Eng, 1985; Hirano and Goldman, 1988; Miller and Raff, 1984; Montgomery, 1994; Eng and Ghirnikar, 1994). For example, during development radially oriented astrocytes or their precursors
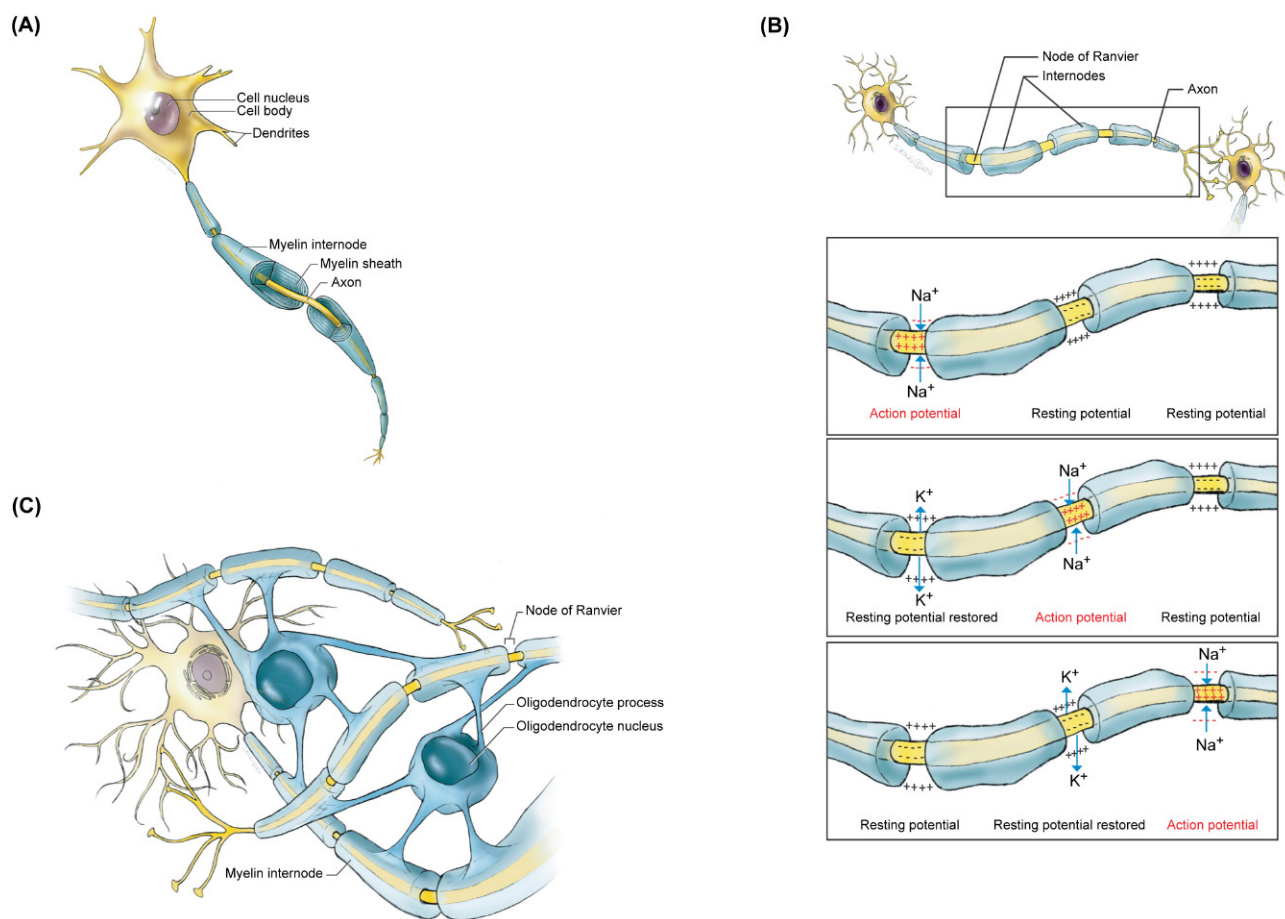
FIGURE 37.1 **Organization of the myelinated axons in the vertebrate CNS.** Myelination, the fatty insulation surrounding axons in the central and peripheral nervous system, facilitates rapid conduction of electrical signals. (A) Neurons are polarized cells that as a general rule receive information onto their dendrites that is processed through the cell body and transmitted to their target along their axons. While most neurons have multiple dendrites they have only a single axon, which is wrapped in myelin. The myelin sheath is composed of spiral wraps of plasma membrane organized into internodes separated by Nodes of Ranvier where the axonal surface is exposed. (B) During the transmission of an action potential along an axon the presence of myelin enhances the velocity of transmission since the signal "jumps" from node to node (see top to bottom). The threshold activity required to fire an action potential is also reduced because the extent of the exposed axon membrane is reduced and the ion channels are more concentrated. During the firing of the action potential sodium flows into the axons resulting in depolarization and the resting potential is subsequently restored through outward transport of potassium channels. (C) Myelin in the CNS is synthesized by oligodendrocytes. One oligodendrocyte can myelinate multiple internodes on multiple different axons. As a result, loss of a relatively small number of oligodendrocytes can have a significant effect on the functioning of multiple axons.

are important as guides for the migration of neuronal cell bodies from their germinal zones to their final destination (Rakic, 1971, 1972). Likewise, astrocytes act as identifiable substrates for the growth of axons toward their appropriate targets (Smith et al., 1986). In the adult CNS, astrocytes play multiple supportive roles including removal of excess neurotransmitters, maintenance of the ionic environment of the CNS and stabilization of the blood–brain barrier (Eng and Ghirnikar, 1994) and potentially promoting regeneration (Miller, 2006). One relatively poorly understood function of astrocytes is the generation of a glial scar in response to CNS injuries (Fitch et al., 1999; Fitch and Silver, 2008; Silver and Miller, 2004). For example, penetrating insults to the brain and spinal cord result in breakdown of the blood brain barrier and provoke hypertrophy and proliferation of astrocytes in the vicinity of the insult (Fitch et al., 1999; Fitch and Silver, 2008; Silver and Miller, 2004). This results in a dense glial scar or gliosis comprised of astrocyte processes and extracellular matrix that is thought to inhibit axonal regeneration (Fitch et al., 1999; Fitch and Silver, 2008; Silver and Miller, 2004). A similar robust glial scar is formed around chronic demyelinating lesions in the absence of a penetrating insult and by analogy has been suggested to block myelin repair (Fuller et al., 2007). The third major class of neural cells in the adult CNS is oligodendrocytes (Miller, 2002) (Fig. 37.1). These cells are derived from progenitors that arise in distinct regions of the CNS and subsequently disperse throughout the CNS (Miller, 2002; Ono et al., 1997; Pringle and Richardson, 1993; Rowitch, 2004). Oligodendrocytes are the primary source of myelin in the adult CNS

(Bunge et al., 1962; Bunge, 1968; Miller, 2002; Raine, 1977). Myelin is a specialized plasma membrane that wraps axons and forms a fatty insulation that promotes the rapid conduction of electrical impulses (Raine, 1977). One primary function of myelin is to provide insulation and protection to axons within the CNS (Morell et al., 1990) and it is composed of multiple layers of modified plasma membrane that acts to increase the conduction velocity of action potential along the axon as well as reduce the threshold for firing axonal action potentials. The bases of this improved conductivity are the nature of the myelin sheath (Fig. 37.1). Myelin sheaths are discontinuous, and the space between adjacent myelin segments is known as the Node of Ranvier. The Node of Ranvier is a highly specialized region comprised of a wide range of unique proteins in both the oligodendrocytes and the axonal membrane including high concentrations of ion channels that are essential for conduction of electrical impulses. This structure is particularly sensitive to damage and disruption of the node results in perturbation of axonal conduction (Fig. 37.2). The composition of the intermodal myelin has been extensively studies. The development of biochemical isolation procedures (Larocca and Norton, 2007; Norton and Poduslo, 1973) identified a number of myelin specific proteins including myelin basic protein that constitutes more than 50% of the myelin sheath, proteolipid protein (PLP) a second major component of CNS myelin and other smaller components such as myelin—associated glycoprotein (MAG), myelin oligodendrocyte protein (MOG), myelin-associated oligodendrocyte basic protein (MOBP) and 2'3' cyclic nucleotide 3'phosphdiesterase (CNP) (Campagnoni, 1988).
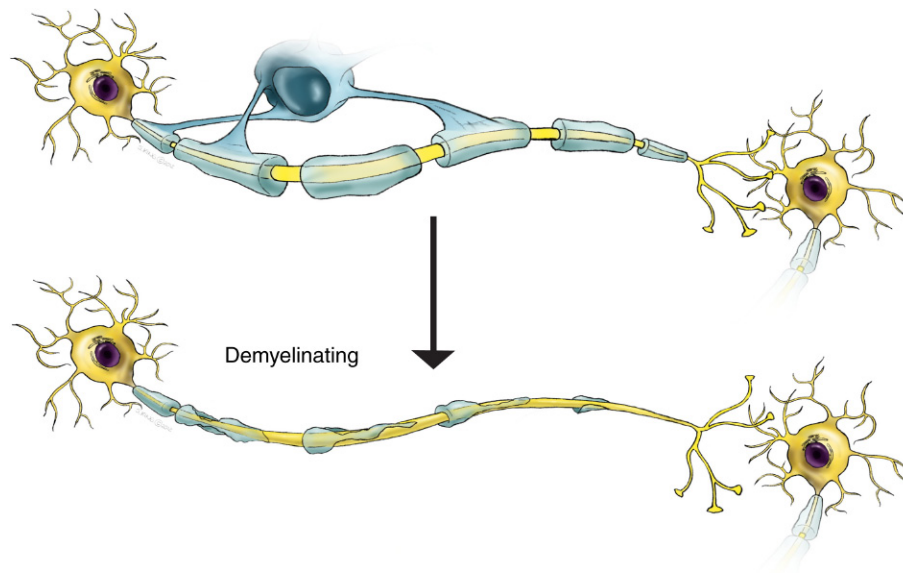
FIGURE 37.2 **Demyelination results in a loss of functional conduction and may result in axonal damage and synapse loss.** Under normal conditions the axon is myelinated along the majority of its length and information flows from one neuronal cell body to the other through action potentials and synapses between the myelinated axon and its target dendrites. As a result of demyelination the myelin covering is destroyed, conduction along the axon is compromised and synaptic connections are lost.

The precise roles for each of these myelin components is unclear although animals with mutations in MBP, such as *shiverer* fail to form compact myelin in the CNS and are not viable (Nave, 1995) while animals lacking PLP appear to develop normally but acquire an axonal pathology later in life (Griffiths et al., 1998; Rosenbluth et al., 2006).

Pathological studies provide strong support for the involvement of neuronal damage in disease progression in MS. For example, considerable axonal loss is observed in areas of demyelination (Trapp et al., 1998) and in some chronic MS patients there is clear brain atrophy as a result of large-scale loss of neuronal cell bodies and axons (Ge et al., 2000; Moore, 1998; Waxman, 1998). The evidence for the role of astrocytes in the pathogenesis of MS is less clear. In regions of demyelination astrocytes undergo a reactive responses that results in an increase in the expression of glial fibrillary acidic protein (GFAP) containing intermediate filaments (Fuller et al., 2007). Whether this represents a protective or pathogenic event is currently unclear (Sofroniew, 2005). The blood brain barrier appears to be a critical entity in the formation of demyelinating lesion in MS and astrocytes have been proposed to play an important role in the maintenance of the blood brain barrier in the adult CNS (Janzer and Raff, 1987).

While there is no conclusive evidence to demonstrate that compromising the integrity of the blood brain barrier leads directly to localized demyelination, a disease variant of MS that preferentially targets the optic nerve known as neuromyelitis opticus (NMO) is thought to result from immune mediated attack on astrocytes and opening of the blood–brain barrier. The evidence for the engagement of oligodendrocytes in the development of MS is strong. First, MS is characterized primarily as a demyelinating disease and since oligodendrocytes are the predominant myelinating cells of the CNS they have long been considered to be the potential target of the disease process (Kerlero et al., 1993; Waxman, 1982).

Currently, it is clear that MS is a complex disease (Moore, 1998; Joy, 2001; Lassmann et al., 2001; Lublin and Reingold, 1996; Lucchinetti et al., 2000; Poser et al., 1983) and MS may in fact reflect a number of distinct but relate diseases all of which share some common characteristics. This diversity of disease is evident in both the presentation of the disease and its pathogenesis (Joy, 2001; Lublin and Reingold, 1996; Lucchinetti et al., 2000; Moore, 1998; Poser et al., 1983). In many cases, MS initially presents as a relapsing remitting disease that frequently progresses over time to a more chronic secondary progressive disease (Fig. 37.3). In a distinct subset of patient the disease
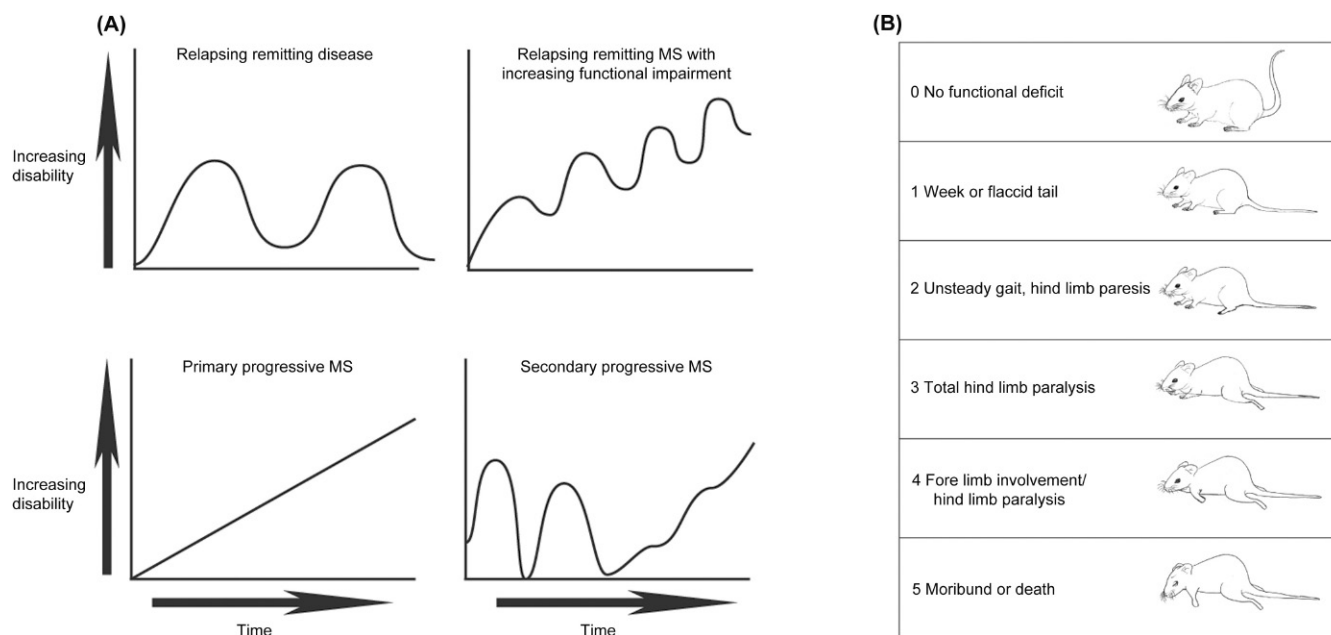
FIGURE 37.3 **Comparison of the progression of disease in the different types of Multiple Sclerosis (MS) and the different models of EAE.** Multiple sclerosis (MS) manifests as several different patterns of functional deficits. Relapsing remitting disease is the most common and often develops into secondary progressive MS. Different stages of MS are functionally mimicked by the animal model EAE. (A) There are general patterns of progression of functional deficits in MS. Early in the disease it manifests as a relapsing-remitting disease in which intervals of functional deficit (relapses) are interspersed with recovery (remission). As disease progresses there is frequently a cumulative functional impairment with each relapse. In a subset of MS patients primary progressive MS results in increasing functional deficit without intervals of remission. Finally, after an extended period of relapsing remitting disease, with or without increasing functional impairment the disease progresses to a secondary progressive pattern. (B) Variations of the EAE model mimic some aspects of disease progression in MS. For example, PLP immunization of SJL mice results in a relapsing remitting disease. The level of functional impairment in EAE animals is scored on the 1–5 scale outlined.

presents as progressive functional impairment from its initial identification known as primary progressive MS (Fig. 37.3), while in other cases the rounds of relapsing–remitting disease slowly accumulate increasing functional impairment (Fig. 37.3).

The diagnosis of MS is relatively complicated (Poser et al., 1983). Currently there is no definitive biomarker that is specific to MS and as a result a diagnosis is dependent on a number of factors rather than a single diagnostic test. Pathological studies demonstrate that regardless of the specifics of presentation virtually all types of MS show white matter regions of demyelination, axonal loss, and gliosis. In the clinic MS is diagnosed through a combination of approaches that includes medical history and clinical examination, as well as imaging and biochemical assessments including both MRI and CSF oligoclonal analyses [reviewed in (Joy, 2001)]. Because the disease is frequently intermittent and has a variable presentation unambiguous diagnosis is often complex. In general, a diagnosis of MS requires clinical evidence of at least two white matter lesions on at least two independent occasions (Lublin and Reingold, 1996; Poser et al., 1983). Such a definition does not include progressive MS, however, the inclusion of MRI analyses is an important aid in the diagnosis. Evidence of neuropathological changes can be detected by MRI in the majority of MS patients although the precise nature of the pathological changes and the specificity for MS is poorly defined since other neuropathological conditions, such as myelopathy can also generate MRI images similar to that seen in with MS. Since demyelination will lead to a slowing or blockade of axonal conduction (Waxman, 1982) some clinical studies have used measurement of axonal conduction through analysis of evoked potentials to assess the level of CNS demyelination although their use has declined in recent years.

Despite intense research efforts the initial stimuli for the onset of MS remains unclear. One hypothesis that has received significant attention is that the trigger for MS is a response to a prior infection or other environmental signal (Correale and Gaitan, 2015). This notion is supported by the findings that MS patients have elevated immunological responses to a variety of pathogens, and may account for some aspects of the epidemiology of MS (Kastrukoff, 1998). The chronic nature of MS and the likelihood that the disease has been ongoing for an extended interval prior to becoming symptomatic makes it extremely difficult to isolate the initial pathogenic signal. A wide range of pathogens have, however, been linked to the onset of MS and these include such diverse entities as spirochetes, Chlamydia and a range of viruses (Joy, 2001). While it may be that multiple pathogens can initiate the disease, or some specific variant of the disease, or that the identification of putative pathogens is non causative it seems likely that the role of the pathogenic insult may

be to enhance susceptibility rather than overtly induce disease. The evidence for a viral link in MS is perhaps the strongest for any pathogen (Das Sarma, 2010; Kakalacheva et al., 2011) and a number of different viruses have been implicated including Epstein–Barr, human herpes virus 6 and human endogenous retroviruses (Das Sarma, 2010; Kakalacheva et al., 2011; Tselis, 2011). Precisely how the viral infection triggers the onset of MS has not been clarified, but it may reflect the initial stimulation of immune responses to viral antigens or the induction of cell death in oligodendrocytes as a result of viral infection.

One aspect of MS that has received extensive interrogation is its genetic linkage (Oksenberg et al., 1996). Several general themes have emerged from these studies. First it is clear that MS is not caused by a gain or loss of function of an individual gene. Rather it appears to be linked to a wide range of genetic associations (Lazzarini, 2004). Several genome wide association studies (GWAS) have identified genes in the major histocompatability locus (MHC) as being associated with MS. In particular it has been proposed that MHC class 11 molecules, such as HLA-DR and HLA-DQ alleles represent risk factors for the disease. Several excellent reviews have been recently written on the genetic linkage of MS and the details will not be discussed further in this review (Baranzini and Nickles, 2012; Gourraud et al., 2012; McElroy and Oksenberg, 2011). It is perhaps not surprising that there would be a detectable linkage to genes that modulate the immune system in MS given the immunological nature of the disease. What is less clear from these studies is the mechanisms by which these genetic changes enhance MS susceptibility. One possibility is that changes in MHC molecules enhance the susceptibility of individuals to mount an autoimmune response following a subacute challenge from an unrelated antigen.

The heterogeneity of MS represents a significant challenge in developing effective animal models that accurately mimic the disease and this has led to the generation of a number of different models each of which share some specific characteristics with a component of the disease (Didonna, 2016). The most long-standing and best-studied models of MS are those that utilize selective stimulation of the peripheral immune system as the major driver of CNS pathogenesis.

2 IMMUNOLOGICAL MODELS FOR CNS DEMYELINATION

One of the characteristics of MS discussed above is the engagement of the immune system. Much of the experimental evidence for a role for the immune system in the pathogenesis comes from animal models that are collectively known as experimental allergic encephalitis (EAE)

(Gold et al., 2006; Mix et al., 2010; Teixeira et al., 2005). In general EAE is an inflammation/demyelinating disease that is induced in host animals through the injection or immunization of the animal with CNS tissue (Krishnamoorthy and Wekerle, 2009). Like MS the presentation of EAE is characterized by functional deficits that are correlated with immune cell infiltration into the brain and spinal cord. The extent of functional deficits is classified on a scale of 1–5 in which 1 represents a flaccid tail, 2 represents hind limb weakness, 3 represents serious hindlimb weakness, 4 represents forelimb engagement and hind limb paralysis and 5 represents death (Fig. 37.3). In most studies the degree of severity is adjusted to between 2.5 and 3.5 that allows for clear determination of increased functional severity or functional recovery.

The utilization of EAE in the study of MS has a long history. The early studies followed the observation that inoculation of rabies infected rabbit CNS tissue into rabies patients induced functional deficits and subsequently involved the injection of spinal cord homogenates derived from human or sheep into rabbits (Stuart, 1928). These treatments resulted in hind limb paralysis and other functional deficits. The initial demonstration of EAE in the primate resulted from immunization of monkeys with spinal cord homogenate derived from rabbit CNS (Rivers et al., 1933). These studies were among the earliest to reveal that the functional deficits were correlated with the pathological accumulation of cells around blood vessels of the brain and spinal cord. Such observations prompted the adoption of the term acute disseminated encephalomyelitis. The term experimental allergic encephalomyelitis was subsequently adopted for multiple variants of this experimental approach. Early studies were somewhat limited since the severity of the disease and even the adoption of pathological conditions was highly variable following injection of spinal cord homogenates. The recognition that EAE had an underlying immunological basis provoked modifications in the experimental protocol to more effectively stimulate the immune system. This was accomplished both by the use of an immune stimulant such as complete Freund's adjuvant (CFA) ultimately combined with pertussis toxin (Munoz et al., 1984). Remarkably, this protocol has changed very little and the majority of modern day EAE experiments still use a combination of CNS derived material delivered in combination with CFA and followed by pertussis toxin.

Although early studies identified important components of the biology of EAE they continued to be challenging due to variability between animals and individual studies. Much early work utilized either guinea pig (Freund et al., 1947) or monkey (Kabat et al., 1947) as the host animal and in efforts to generate more reproducible results investigators explored two avenues. In one case they reproduced the early studies in rats and subsequently mice (Lipton and Freund, 1952; Olitsky and Yager, 1949) in which the individual host variations could be minimized. Second, the relevant immunogenic peptides in the spinal cord and brain homogenates were identified. Perhaps not surprisingly given the demyelinating nature of the model the initial antigenic proteins were predominantly myelin-associated proteins including myelin basic protein (MBP), myelin-oligodendrocyte glycoprotein (MOG) and proteolipid protein (PLP) (Mix et al., 2010). Minor myelin components were also found to be capable of inducing disease when injected into naïve animals suggesting that there was not a tightly restricted repertoire of antigenic proteins that may stimulate an immune attack on the CNS, but rather that most myelin components could act as effective priming antigens. Further refinement of the model resulted from the identification of specific peptides of myelin proteins that provoked a reproducible and consistent disease profile following immunization into genetically defined host populations. As a consequence, several major models of EAE have gained prevalence in the last two decades (Gold et al., 2006; Mix et al., 2010; Teixeira et al., 2005). Among these are the inductions of EAE in the *SJL* mouse genotype following immunization with the PLP $_{139-151}$ peptide. This model generates a relapsing remitting disease that mimics some of the characteristics of relapsing remitting MS. A second commonly used model is that induced in C57/Bl6 mice following immunization with the MOG peptide $_{35-55}$. This model generates a more chronic and progressive disease course that is often used to model later stages of MS. Other models such as the induction of EAE in PL/J mice following immunization with MBP or MOBP (Kaye et al., 2000) and immunization of Biozzi ABH mice with MOG protein (Amor et al., 2005) model selective aspects of MS.

The mechanisms of disease development in the murine models of EAE have been extensively studied and while like MS they are complex, some general concepts have emerged. One central feature is that in many of the models there is a primary role for T cells in the development of the disease. The most compelling demonstration of the pathogenic properties of T cells in CNS demyelination was obtained using an adoptive transfer approach (Ben-Nun et al., 1981; Kojima et al., 1994, 1997). Using rats these investigators showed that T cells specific for an MBP antigen grown in vitro from immunized donor animals were capable of transferring disease to naïve hosts. These studies revealed that while transferred T cells alone were sufficient to induce CNS damage, they did not generate a persistent ongoing disease. Rather the functional deficits were transient, resolving within 1–2 weeks after immunization and more importantly, the pathology generated was not characterized by extensive demyelination. These results suggest the pathology seen

in other models of EAE and in MS itself reflect multiple pathogenic processes in addition to T cell cytotoxicity. One likely candidate to contribute to the pathology of EAE and MS are B cells (Bielekova and Becker, 2010; Cross et al., 2001; Franciotta et al., 2008; Kerlero et al., 1993; Meier et al., 2012). B cells may play multiple roles in the formation of immune mediated pathology in the CNS (Cross et al., 2001). First, they may act as antigen presenting cells, facilitating the activation and expansion of T cell populations within the CNS, as well as enhancing the recruitment of other immune cells into the CNS (Franciotta et al., 2008; Hohlfeld et al., 2008). Perhaps more importantly, B cells act as a source of antibodies directed against myelin antigens. It has been suggested that some subsets of MS lesions are characterized by the expression of antimyelin antibodies and experimental studies implicate MOG as a potential target (Haase et al., 2001). The importance of understanding the roles of B cells in the development of pathology and functional deficits in EAE and MS has increased recently with the demonstration that the therapy Rituximab, which inhibits B cells (Bielekova and Becker, 2010; Hauser et al., 2008) appears to be highly effective in some MS patient populations. One area that has not received extensive attention until relatively recently is the role of the innate immune system in the development of demyelinating pathologies. The activation of microglial cells and their role in myelin clearance has been proposed, and whether they also play a role in antigen presentation along with dendritic cells is currently not well established. It may be that depending on the stage of the disease the prevalent pathological mechanisms are different. For example, while relapsing remitting disease may be largely driven by influx from the peripheral adaptive immune system, progressive disease may be largely a consequence of the innate immune system (Weiner, 2009).

The array of antigens capable of inducing CNS immune responses is extensive and not limited to myelin components. Given that the disease is characterized by demyelination this is somewhat of a surprise. Antigens associated with axons such as the neurofilament triplet and node of Ranvier components such as Contactin/TAG-1and the more ubiquitous S100 are also associated with EAE and MS (Charles et al., 2002). Whether these represent primary targets of the disease such that targeted attack on neurofilaments results in axonal damage, or whether they represent the result of damage to adjacent cells that is secondary to myelin sheath insults is currently unclear. What seems likely, however, is that once the disease has been initiated the destruction of neural tissue that occurs results in a broadening of the pathological basis of the disease and more widespread damage and functional deficits.

The EAE models have a number of characteristics that are extremely useful for understanding the biology of MS and have been the subject of detailed and informative reviews (Gold et al., 2006; Mix et al., 2010). Among the major strengths include the variety of the models and fact that they utilize well-defined antigens in numerous well-developed transgenic animal systems. The engagement of the immune system (Lassmann et al., 1988), the diversity of genetic influences and the distinct pathologies have facilitated the identification of well-defined cytokine/chemokine networks involved in T cell activation and trafficking as well clarification of the role of T cell subsets in regulating disease progression. These models have allowed major contributions to our understanding of the pathobiology of MS and currently serve as the primary tools with which to validate and identify new therapeutic approaches for the treatment of MS.

3 LOCAL INDUCTION OF DEMYELINATION FOLLOWING INJECTION OF MYELIN PEPTIDES

One limitation of the systemic EAE models discussed aforementioned is that like MS, the location and timing of lesions in the CNS is unpredictable. This makes these models difficult to use for directly correlating histologically the loss of myelin with the subsequent functional deficits in any particular axon tract. To address this issue and to facilitate the development of new therapeutic approaches for demyelinating disease investigators have targeted demyelinating lesions to selected CNS regions (Merkler et al., 2006). To achieve targeted immune mediated demyelination, one approach has been to sensitize host animals with subthreshold levels of encephalogenic peptides and subsequently deliver a local injection of a proinflammatory cytokine to stimulate local demyelination. For example, subcutaneous injection of recombinant $_{1-125}$ MOG peptide into the Lewis Rat in combination with incomplete Freund's adjuvant results in a robust anti-MOG immune response that does not generate overt clinical symptoms (Kerschensteiner et al., 2004). After a period of approximately 20 days-localized injection of recombinant rat tumor necrosis factor alpha (TNFα) or interferon-gamma (INF-γ) resulted in localized infiltration of immune cells that was associated with intense local demyelination and axonal damage. The extent of demyelination and the reaction to the injection of proinflammatory cytokines was directly proportional to the level of initial immunization with the immunogenic peptide suggesting that the level of sensitization is a major contributing factor to subsequent myelin loss. Due to the localized nature of the demyelinating lesion, more refined functional studies could be undertaken. Such studies revealed a rapid functional deficit that presumably reflects the damage caused by the intense local immune response. This initial functional deficit was followed by

some degree of functional recovery, even though some structural damage to the targeted axon tract remained.

There are several attractive elements to the model of targeted immune mediated demyelination. These include the ability to assess the long term consequences of a localized immune response on functional outcome and the capability to develop novel therapies that may alleviate not only the initial immunological insult but also promote long-term functional recovery. Such a model, however, also has several weaknesses. This includes the very localized nature of the insult without the engagement of surrounding tissue, such as may occur in MS. A more significant concern is the method of induction of the inflammatory stimuli. The local injection of cytokines results in damage to the blood–brain barrier and the stimulation of a robust astroglial response. The complication of the injection paradigm makes mechanistic interpretation of the outcome of these studies difficult.

Regardless of the exact details of the EAE models there are however a number of important differences between MS and the animal model EAE. Perhaps the most obvious is that MS is a spontaneous occurring disease within human populations while EAE is an induced pathology. By contrast, there are no known spontaneous occurring animal models of MS or EAE and the added complexity of provoking a strong immune response with unrelated antigens may have a significant effect on the ultimate mechanism of the disease and its natural history. As a consequence, therapies developed using the EAE models have not always proven as effective against ongoing MS as predicted.

4 DEVELOPMENT OF MS THERAPIES BASED ON MODELS OF IMMUNE MEDIATED DEMYELINATING DISEASES

The extensive history of research using EAE as a model for MS has resulted in the development of a range potential therapies' for MS and other demyelinating diseases. Given the immunological basis of the model it is not surprising that the majority of these therapies have been oriented toward modulation of the immune response and specifically T cell mediated infiltration and activation in the CNS. While several of these therapies have been quite effective in modulating disease progression in EAE and in controlling MS relapses they have been less effective in promoting long term recovery in MS. Examples of therapies that have been tested in animal models of EAE include Fingolimod otherwise known as FTY720 that is directed against the spingosine-1-phosphate receptor and regulates T and B responses but also appears to directly stimulate remyelination in the CNS (Balatoni et al., 2007; Miron et al., 2010; Miron et al., 2008) and natalizumab that is directed toward adhesion molecules on lymphocytes and blocks the entrance of those cells in the parenchyma of the CNS (Rice et al., 2005; Rose et al., 2008). Such therapies, while modulating relapse activity, have generated unexpected side effects in the setting of clinical applications that have limited their utilization. The development of new therapeutic approaches that likely combine dampening of the immune response with stimulating endogenous myelin repair are likely to be more effective in promoting long-term functional recovery. The development of such combinatorial therapies will be leveraged through the utilization of other animal models of disease.

5 VIRAL MEDIATED MODELS OF DEMYELINATION

Viral infections have been implicated in enhancing susceptibility to MS in a number of studies (Correale and Gaitan, 2015) and a number of effective viral models of demyelination have been developed in order to better understand the pathobiology of MS. Among the most commonly used for the induction of neurological diseases are mouse hepatitis virus (MHV) and Theiler's murine encephalomyelitis virus (TMEV). There are a number of strengths to the viral demyelination models. These include the genetic linkages, the involvement of B cells as well as T cells, the ability to modulate the virus, and alter host responses. Compared to the immunological models of MS, such as EAE the extent of demyelination is substantially greater and the functional deficits longer lasting providing a better opportunity to study the cellular and molecular mechanisms mediating myelin repair. The progression of TMEV induced disease is well established depending on the strain of the virus and the genetics of the host. In some combinations the disease is biphasic in which an early acute phase is followed by more chronic demyelinating disease that usually develops a month or so after infection (Dal Canto and Rabinowitz, 1982). The functional deficits are correlated with extensive demyelination in both the brain and spinal cord. The mechanisms underlying viral induced demyelination have been attributed to two primary pathways. In one case virally infected cells are lysed as a result of the infection and the lysis of oligodendrocytes leads to subsequent demyelination. In the second case the loss of oligodendrocytes and demyelination is a reflection of immune responses to virally infected cells. Several lines of evidence are consistent with a role for the immune system in viral demyelination. These include the finding that passive transfer of anti-TMEV antibody can enhance demyelination in the setting of EAE and demyelination can be stimulated by macrophages infected with TMEV (Tsunoda et al., 1996) and inhibited by macrophage depletion (Rossi et al., 1997). Similar general pathology

and underlying mechanisms have been suggested to mediate disease resulting from MHV infections (Wang et al., 1990). When immune compromised animals are infected with MHV little or no demyelination is seen, however if effective T and B cell functions are restored through transfer of immunocompetent cells then demyelination is seen (Wu et al., 2000). One additional complexity is that the mechanism and extent of demyelination is dependent on both the strain of the virus and the genetics of the host animal since even in some MHV strains, demyelination does not appear to be independent of stimulation of the immune system. To begin to clearly delineate the relative effects of immune stimulation and oligodendrocyte death in the development of demyelinating diseases requires additional animal models that separate these two phenomena.

6 OLIGODENDROCYTE INDUCED CELL DEATH MODELS OF DEMYELINATION

While EAE has provided important insights into the potential role of the immune system in the onset and progression of demyelination in the vertebrate CNS, recent studies suggest that in some conditions the onset of T-cell-mediated inflammation reflects a response to primary CNS damage rather than an initiation of the original insult. Demyelination ultimately reflects damage to oligodendrocytes, the cell responsible for CNS myelin formation. Whether in the complex setting of disease damage to oligodendrocytes is direct (Locatelli et al., 2012) or indirect likely depends on the immediate pathological conditions. An alternative cellular target that may trigger oligodendrocyte damage and demyelination are the axons that are enwrapped in myelin. Indeed, axonal damage is evident in many MS lesions even at early stages of the disease (Trapp et al., 1998), as well as in many of the animal models of immune mediated demyelination (Moreno et al., 2011; Soulika et al., 2009; Traka et al., 2010). Given the complexity of MS and its immune-based animal models, it remains unclear whether axonal degeneration follows myelin loss or whether demyelination is a consequence of axonal damage and degeneration. To distinguish between these possibilities, a new general approach involving the induction of primary oligodendrocyte death is being developed. In these models oligodendrocytes are being targeted by various means to assess whether the loss of oligodendrocytes results in demyelination, how effectively and rapidly remyelination occurs, and whether localized demyelination results in axonal damage. These studies, which compared to the immunological models discussed earlier, are in their infancy, have begun to provide interesting insights and potential model systems for the diversity of pathologies seen in MS. Here we focus on three distinct

methodological approaches for selectively inducing cell death in oligodendrocytes in the adult vertebrate CNS.

6.1 Induction of Oligodendrocyte Cell Death Through the Cell Type Specific Expression of Diphtheria Toxin a (DT-α)

One approach to drive selective death of neural cells that has proven to be effective in the adult CNS involves the selective expression of a toxic molecule targeted to specific cell types (Pohl et al., 2011; Traka et al., 2010). For example, extensive loss of oligodendrocytes has been achieved through the targeted expression of the alpha subunit of the diphtheria toxin (DT-α). Diphtheria toxin (DT) in its natural state is composed of two subunits that have specific functions. While the beta subunit is essential for the entry of the toxin into the cell through interaction with its appropriate receptors the alpha subunit is the cytotoxic component that acts intracellularly.

The cytotoxicity of DT-α is conferred through the inhibition of elongation factor 2 and the subsequent halting of protein translation that in turn results in cell death (Fig. 37.4). In the absence of its "β subunit DT is unable to penetrate cells, limiting the nonspecific induction of cell death in neighboring cells. Targeting the expression of the DT to oligodendrocytes is achieved using Cre/LoxP technology (Fig. 37.4). In this system on one allele, the sequence corresponding to DT-α is knocked-in to the ROSA26 locus while upstream the sequences for
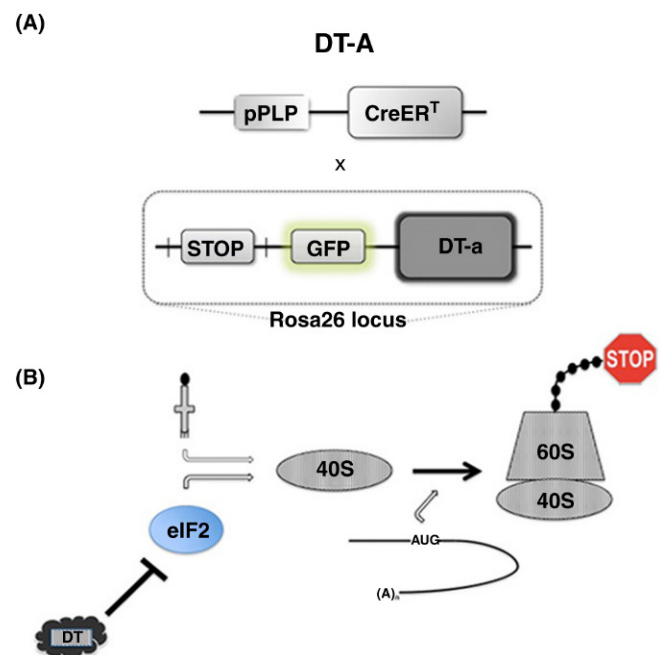
FIGURE 37.4 Schematic showing the overall design for the generation of the DTA mouse. (A) Diagram of the mating scheme used to generate a Tamoxifin responsive DTA mouse. (B) Schematic representation of the functionality of the DTA mouse resulting leading to cell death.

GFP, a Neo cassette, and a strong transcriptional STOP sequence are inserted. On another allele, a cell type specific promoter such as for the proteolipid protein (PLP), a major CNS myelin protein promoter that has repeatedly been shown to target expression to oligodendrocytes and their precursors, drives the expression of a Tamoxifen-inducible CreER^T transgene. In such animals, treatment with Tamoxifen results in experimentally controlled Cre-mediated recombination only in oligodendrocytes (targeted by PLP), excision of the STOP sequence, and selective cell-type expression of cytotoxic DT-α that results in death of the cells in which it is expressed. This approach has a number of major advantages. If CRE recombines efficiently, then a comparatively high number of oligodendrocytes in a given mouse line could potentially express the transgenes and be susceptible to Tamoxifen-mediated cell death. Under such conditions the induction of oligodendrocyte cell death occurs in the absence of any direct insult to the brain or spinal cord and allows accurate assessment of the subsequent CNS responses. Control studies indicate that at low doses Tamoxifen is not selectively toxic to neural cells.

Although only a limited series of studies using the DT-α model of induced oligodendrocyte death have been published there are clearly common themes emerging from this model. For example, independent studies corroborate the observation that severe pathology occurs as a result of the expression of genetically recombined DT-α in oligodendrocytes (Pohl et al., 2011; Traka et al., 2010). One somewhat unexpected outcome of these studies is that following Tamoxifen treatment, while there appeared to be a relatively rapid loss of oligodendrocyte cell bodies as anticipated, there was an apparent retention of myelin and minimal initial functional deficits. After a posttreatment delay of approximately 3 weeks the mice displayed progressive motor deficits associated with significant myelin degradation and vacuolization. The extent of the demyelination was directly correlated with the animals' clinical symptoms suggesting that the functional deficits were a primary consequence of myelin loss. A second somewhat unexpected outcome of these studies was that the widespread loss of oligodendrocytes in this model did not trigger a rapid robust immune response and the clearance of myelin was slow and primarily accomplished by local microglial cells without a significant influx of cells of the peripheral immune system. These studies suggest that oligodendrocyte death alone does not provoke a rapid large-scale immune response. While remyelination was robust in this model, and the animals appeared to recover completely, with longer survival times recovery was compromised. In animals allowed to recover for approximately 30 weeks from the initial demyelination a secondary pathology consisting of demyelination and axonal loss was detected (Traka et al., 2016). This second

phase of demyelination was accompanied by T cell infiltration to the CNS and adoptive transplantation of the T cells into naïve hosts was sufficient to transfer disease. These important findings imply that as a consequence of the priming of the immune system with the first insult the animals develop a long-term autoimmune condition that ultimately leads to CNS demyelination occurring

Not all of the independent studies provide identical results. One important difference between the different analyses is in the area of functional recovery. While clinical recovery was essentially complete in one study, it was completely absent in a parallel report using identical mice, such that the treated mice died only 6 weeks after treatment. Reports of axon health are also conflicting, with clear signs of pathology in one study and no axonal effect in another. Nevertheless, both studies report alterations in evoked potentials in two different sensory modalities suggesting that regardless of the underlying histological abnormalities, the functional outputs of neural networks are similarly perturbed.

As with any animal model of disease, it is important to consider the extent to which specific aspects of human disease are successfully captured by the animal model. In the case of DT-α induced oligodendrocyte cell death, and MS, there are important similarities. A disruption in visual evoked potentials coupled with significant myelin loss, for instance, is reminiscent of the initial symptom in many MS patients. Similarly, newly forming MS lesions, often in normal-appearing white matter, are characterized by the presence of activated microglia but not extensive infiltration of peripheral immune cells (van der Valk and Amor, 2009; van Horssen et al., 2012). A similar cellular profile is observed following oligodendrocyte-targeted expression of DT-α.

The DT-α model also differs from MS in a number of key ways. As discussed previously, MS is not induced but rather is a spontaneous disease with focal lesions separated in time and space. Multiple Sclerosis is also not thought to be toxin-induced although the role of pathogens in its initiation is unclear. In this cell death model there are likely broad, if subtle, effects owing to a toxin that halts cellular protein translation including the de novo production of proteins required for a nonimmunogenic cell suicide and the subsequent recruitment of phagocytic cells. Further, in MS it is thought that the clearance of myelin is relatively rapid following oligodendrocyte death and this accomplished by both CNS-resident and peripheral immune cells. By contrast, the delayed myelin clearance in the DT-α model would suggest either an inhibited or nonexistent rapid stimulation of immune clearance mechanisms. There are concerns with this model surrounding the complete nature of oligodendrocyte loss. If all oligodendrocytes throughout the neuroaxis are lost following Tamoxifen treatment, this differs greatly from the focal loss of oligodendro-

cytes in MS. If, on the other hand, only a portion of cells undergo effective recombination then it is difficult to define the threshold of oligodendrocyte loss that is required for the development of myelin pathology.

6.2 Induction of Oligodendrocyte Cell Death Through Cell Type Specific Expression of the Diphtheria Toxin Receptor

A variation of the model discussed above has also been recently developed (Oluich et al., 2012). In this case specificity of the toxic insult is targeted through the transgenic expression of the appropriate receptor on animals that have a receptor null background. For example, the transgenic expression of the DT receptor (DTR) under the control of an oligodendrocyte specific promoter results in cell type sensitivity to systemically delivered diphtheria toxin. This model has the advantage over the DT-α model in that is somewhat simpler, since it eliminates the need for the Cre/LoxP technology. An example of this approach is the expression of a transgenic DTR under transcriptional control of the promoter for myelin basic protein (MBP), a major oligodendrocyte-specific protein (Oluich et al., 2012) (Fig. 37.5). Intraperitoneal injection of DT then allows selective uptake by transgenic oligodendrocytes expressing the receptor, resulting in the induction of cell death by a mechanism similar to that evoked by DT-α, namely by inhibiting protein synthesis (Fig. 37.5).
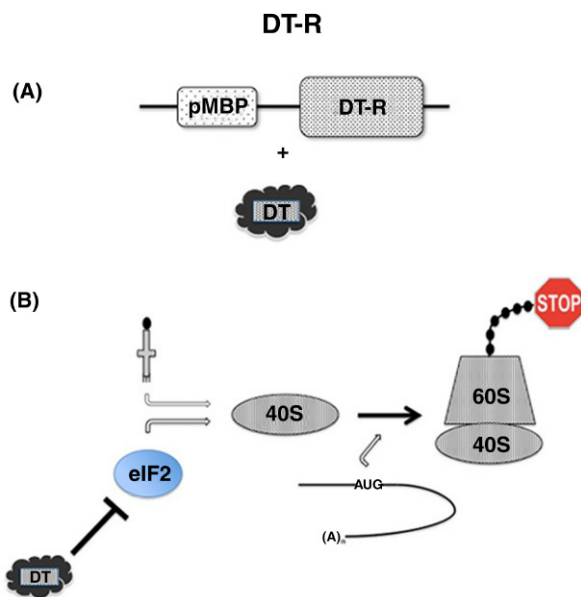
FIGURE 37.5 **Schematic showing the overall design for the generation of the DT-R mouse.** (A) Diagram of the construct used to selectively express DT-R in oligodendrocytes on a background strain that is DT resistant. (B) Schematic representation of the functionality of the DT-R mouse resulting in cell death.

The clinical phenotype following the systemic injection of DT into DTR transgenic mice is similar to that seen in the DT-α mice except that it occurs on a faster time scale and does not show the same delay between initiation of cell death and onset of functional deficits. Neurological symptoms including ataxia, limb paralysis, and tail spasticity appear around 10 days postinjection and progressively develop until euthanasia is required (Oluich et al., 2012). Perturbations in somatosensory evoked potentials together with histological markers of neurodegeneration and abnormal Nodes of Ranvier indicate dysfunctional neural networks. A clear intrathecal immune response is provoked in this model which is reflected in elevated numbers of activated microglia, as well as a wide spread gliotic response characterized by elevated levels GFAP expression in astrocytes (Oluich et al., 2012).

Given the similarities in the targeting and mechanism of cell death, it might be anticipated that the histology and pathology of the DT-α and DTR models would be identical. Somewhat surprisingly this is not the case and while the DT-α mice display severe demyelination, the DTR mice show few if any myelin disturbances. The explanation for such differences is currently unclear. It may be that in the DTR model there is a more extensive engagement of axonal damage that leads to rapid mortality, prior to the development of significantly detectable myelin perturbations. Even if this hypothesis were correct it remains unclear why there would be differential axonal susceptibility in the two models. Possibly, the mode of cell penetration (receptor mediated vs. nonreceptor mediated) regulates the detailed cell death pathways activated in oligodendrocytes. As these models become more established the basis of such differences will likely become resolved.

A potential strength of the DTR model is that it may provide a model system to examine the mechanisms and develop targeted therapies against axonal damage in demyelinating diseases. It is well established that axonopathy is a pathological finding in MS (Trapp et al., 1998), even at early stages of the disease and this axon damage is generally accepted as the biological basis of permanent disability for patients with either primary or secondary progressive MS. Therefore, animal models such as DTR that recapitulate aspects of this pathological feature represent important tools for understanding and manipulating the CNS response to axonopathies. At the current time the DTR model does not appear to provide an accurate representation of the lesions that develop in MS. Indeed, the conspicuous absence of demyelination, a hallmark pathological feature of MS, calls into question its utility as a useful general model of human disease. It may be, however, that on different background strain the degree of demyelination may be greater or the survival of the animals longer. For now, the short sur-

vival time of the oligodendrocyte-DTR mice represents another significant limitation in its ability to model human disease, as MS is not generally associated with a substantially shortened lifespan.

6.3 Induction of Oligodendrocyte Cell Death Through Targeted Activation of the Apoptotic Pathway

Two general pathways mediate cell death. During necrosis, a pathological form of cell death resulting from overwhelming cellular injury, cells swell, membrane integrity is perturbed, and noxious intracellular molecules are released into the extracellular space (Steller, 1995). Apoptosis, on the other hand, is a genetically encoded, noninflammatory means of cellular suicide in which a dying cell fragments into membrane-bound bodies that can be digested by macrophages or neighboring cells. Activated by many different signals that may originate either from within or outside a cell, the controlled dismantling of unwanted cells requires a group of protein degradation enzymes called caspases (Thompson, 1995). An early step in the activation of one arm of the apoptotic cascade is the dimerization of caspase 9 mediated by the molecule APAF1 (Pop et al., 2006; Srinivasula et al., 1998). A model of selective cell ablation has been developed in which a modified, experimentally inducible caspase 9 (iCP9) is introduced into targeted cells using cell type specific promoters. Originally developed to eliminate distinct classes of lymphocytes (Straathof et al., 2005), the iCP9 gene was engineered so that the APAF-1 binding site was replaced with a FK506-like binding site for dimerization by a FK506 analog. Chemically induced dimerization (CID) by the FK506 analog is sufficient to initiate the apoptotic cascade in cells expressing iCP9. An initial study targeted iCP9 to mature oligodendrocytes using the MBP promoter and a lentiviral delivery system. Subsequent injection of the chemical inducer of dimerization (CID) results in the rapid and specific induction of oligodendrocyte death.

In this model, a lentivirus containing iCP9 under transcriptional control of the oligodendrocyte-specific MBP promoter, as well as a reporter expressed from a constitutive, viral promoter was injected into the corpus callosum of adults rats and the animals were allowed to survive for 7–14 days (Fig. 37.6). This resulted in local viral infection of all neural cell types as detected by reporter expression. Intrathecal injection of the CID at a remote site 7–14 days after viral injection resulted in the selective activation of the apoptotic cascade and cell death of oligodendrocytes. Unlike other oligodendrocyte cell death models of demyelination, the iCP9 model resulted in extremely rapid (within 24 h) demyelination, intense localized microglial activation, myelin clearance and localized OPC proliferation in the absence of an initial infiltration of peripheral immune cells including T cells (Caprariello et al., 2012).
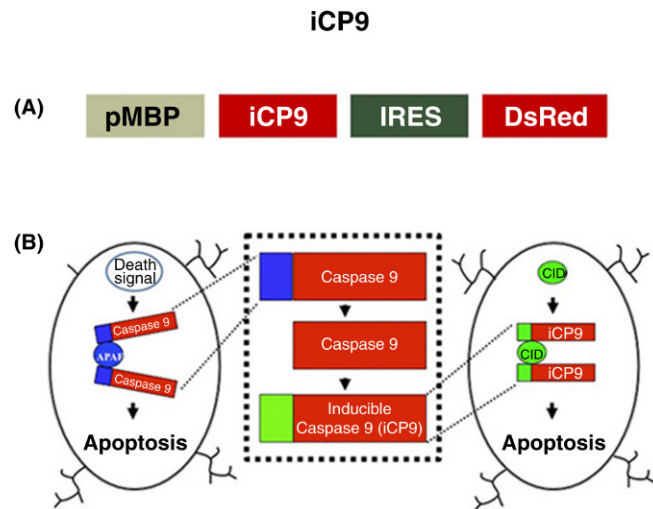
FIGURE 37.6   **Schematic of the overall design and function of the MBP-iCP construct.** (A) Diagram of the construct used to selectively express the modified caspase 9 in oligodendrocytes. (B) Schematic of the mechanisms of inducible oligodendrocytes apoptosis.

Curiously, these effects are not associated with a behavioral phenotype and the histological abnormalities may recover over time. More recently this model has been extended to eliminate the confound of viral delivery. Transgenic animals expressing the iCP9 construct off the MBP promoter have been generated. Local delivery of CID targets oligodendrocyte death specifically. During development delivery of CID to a region of the spinal cord in the first postnatal week, blocks local myelination (Caprariello et al., 2015). Myelination recovers over a subsequent 2-week period and appears to have relatively normal histology. When the treated region of the spinal cord is challenged with a second mechanistically unrelated demyelinating insult in the adult, myelin repair is compromised. While the cellular and molecular bases of these phenomenas are currently poorly defined these studies raise the possibility that insults to the developing CNS compromise the potential for subsequent repair in the adult (Caprariello et al., 2015).

The significance of the iCP9 model to understanding the pathology of MS is still unclear. There are however several aspects of this model that may provide important insights into the development of early MS lesions and perhaps continuing development of the disease in a subset of MS patients. For example, apoptotic oligodendrocytes have been reported in neuropathological specimens from the earliest known lesions (Lucchinetti et al., 2000; Barnett and Prineas, 2004) suggesting this may represent an early event in the generation of an MS plaque. The immunological cell profile of the iCP9 model also mirrored the human condition in certain situations, in which activated microglia but not peripheral immune cells were recruited to the lesion site. Importantly, this pathological profile was reported from

a subset of MS patients (Lucchinetti et al., 2000) but given the heterogeneity of MS is unlikely to accurately represent all patients. It is surprising that rapid histological abnormalities would not generate behavioral abnormalities, however, it is possible that the iCP9 mice display subtle sensory and/or cognitive deficits that have yet to be identified. Additional studies in which oligodendrocyte apoptosis is targeted to critical motor tracts, such as in the spinal cord may reveal such functional deficits. Many rodent models of demyelination are typically associated with complete repair and further studies are needed to assess whether the rapid demyelination seen in the iCP9 model results in a chronic impairment of myelination or undergoes complete repair.

The emergence of new models that selectively target oligodendrocyte death are likely to provide critical new insights into the diversity of demyelinating lesions and the heterogeneity seen in the MS patient population. These models are still in their infancy and whether they will provide a useful platform for the development of therapies for distinct subsets of MS awaits further refinement and analysis.

7 TOXIN MODELS OF DEMYELINATION

The third general approach used to model the biology of demyelination and remyelination in the vertebrate CNS are those utilizing the introduction of a demyelinating toxin.

The use of toxins to induce demyelination is extremely useful for addressing specific questions regarding the biology of the remyelination process given the ability to regulate the generation of the lesions in both time and space. These models are not intended to recapitulate the complex etiology and pathogenesis of MS but instead enable investigators to gain insight into the precise cellular and molecular mechanisms that characterize remyelination in the central nervous system. A major strength of the toxin models is that the location and timing of demyelination and remyelination are distinct. Unlike in the immune mediated demyelinating models where demyelination and remyelination are concurrent, in many of the toxin models the epoch of demyelination is temporally distinct from the epoch of remyelination and this allows for the clear characterization of molecular cues regulating each aspect of lesion generation and repair.

7.1 Focal Toxins

Focal areas of demyelination can be induced by directly injecting chemicals that selectively ablate oligodendrocytes and their myelin. Many different demyelinating agents have been used over the last several

decades including antibodies to oligodendrocyte-related molecules, 6-aminonicotinamide, and diphtheria toxin (see aforementioned), however, those most commonly used include lysolecithin, ethidium bromide, and antibodies against the major sphingolipid component of myelin, galactocerebroside.

7.1.1 Lysolecithin

Lysolecithin (L-α-Lysophosphatidylcholine or LPC) is a potent membrane-dissolving chemical that is typically injected into the white matter as a 1% solution in saline in order to induce focal demyelination (Gregson, 1989). In 1972, Hall was the first to demonstrate the use of LPC to create demyelinating lesions in the white matter of the adult mouse spinal cord (Hall, 1972). Since then, LPC has been used in several additional species including rat (Harrison, 1985), rabbit (Waxman et al., 1979), cat (Blakemore et al., 1977; Gledhill and McDonald, 1977), and monkey (Dousset et al., 1995). The most common locations for the generation of LPC induced lesions include the dorsal or ventral funiculi of the spinal cord typically at the thoracic level, the corpus callosum, the optic nerve, and the caudal cerebellar peduncle. LPC injection results in a rapid loss of myelin and the majority of oligodendrocytes in a focal area. Compared to other models, the loss of oligodendrocytes is somewhat less specific and there is a reduction in astrocytes and some loss of axons although this tends to be limited to the area close to the injection site. One of the remarkable features of the LPC lesions is their ability to recover (Blakemore and Franklin, 2008). In general demyelination occurs rapidly and the lesion area is largely devoid of myelin with 2–3 days after LPC injection (Fig. 37.7). The lesions rapidly become repopulated with oligodendrocyte precursors and after a period of proliferation these cells differentiate into oligodendrocytes and initiate remyelination. In rats and mice, remyelination begins between 7 and 14 days post lesion depending on the location of the lesion and the age of the animal and by 30 days post lesion, remyelination is essentially complete (Fig. 37.9). This reproducible pattern of myelin repair has facilitated the identification of molecular mechanisms that either enhance or inhibit the repair process including the Notch pathway (Zhang et al., 2009), the WNT pathway (Fancy et al., 2009), retinoid X receptor gamma signaling (Huang et al., 2011), growth factors, such as hepatocyte growth factor (Bai et al., 2012), and neuregulin (Penderis et al., 2003a), hormones, such as progesterone (Garay et al., 2011), cell cycle proteins, such as cyclin-dependent kinase (Cdk2) (Caillava et al., 2011), chemokine receptors, such as CXCR2 (Kerstetter et al., 2009), the NOGO receptor LINGO-1 (Mi et al., 2005; Mi et al., 2009), and death receptor 6 (DR6) signaling (Mi et al., 2011), as well as several others. Not all the oligodendrocytes are lost in an LPC lesion. In white matter tracts where there are many large-caliber axons, the myelin generated by the

LFB of LPC lesions overtime
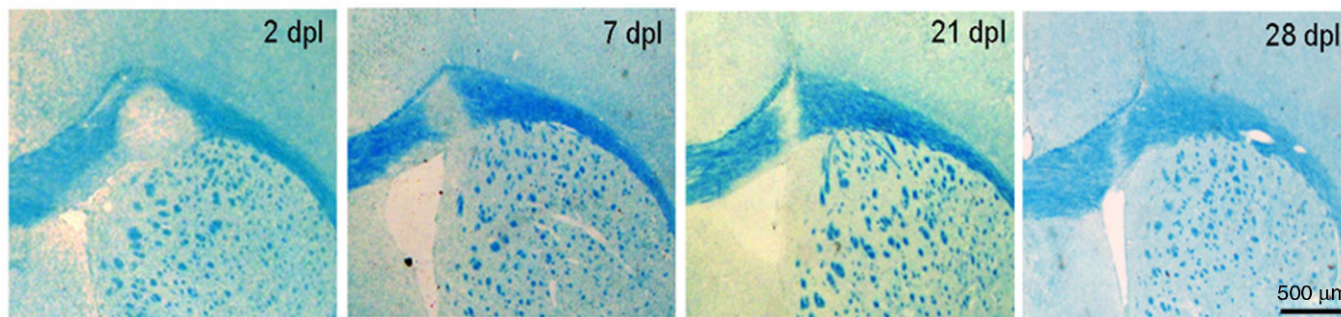
FIGURE 37.7 **Local delivery of the gliotoxin lysolethicin into the corpus callosum of the adult mouse generates a demyelinating lesion that repairs over time.** Two days after stereotactic injection of LPC, coronal sections through the level of the corpus callosum show an area of demyelination following staining with luxol fast blue. The lesion repairs spontaneously beginning at around 7 days post injection and is almost completely repaired by 28 days post lesion as shown by a recovery of luxol fast blue staining in the area.

spared oligodendrocytes can be easily distinguished from newly generated oligodendrocytes by the thickness of the myelin sheaths that they generate. Remyelinated axons are covered by myelin sheaths that are much thinner and have shorter internodes than those generated during development (Figs. 37.8 and 37.9). Remyelination occurs spontaneously in both rats and mice, is quite rapid, and is accomplished mainly by newly generated oligodendrocytes derived from local precursors and not Schwann cells in this model.
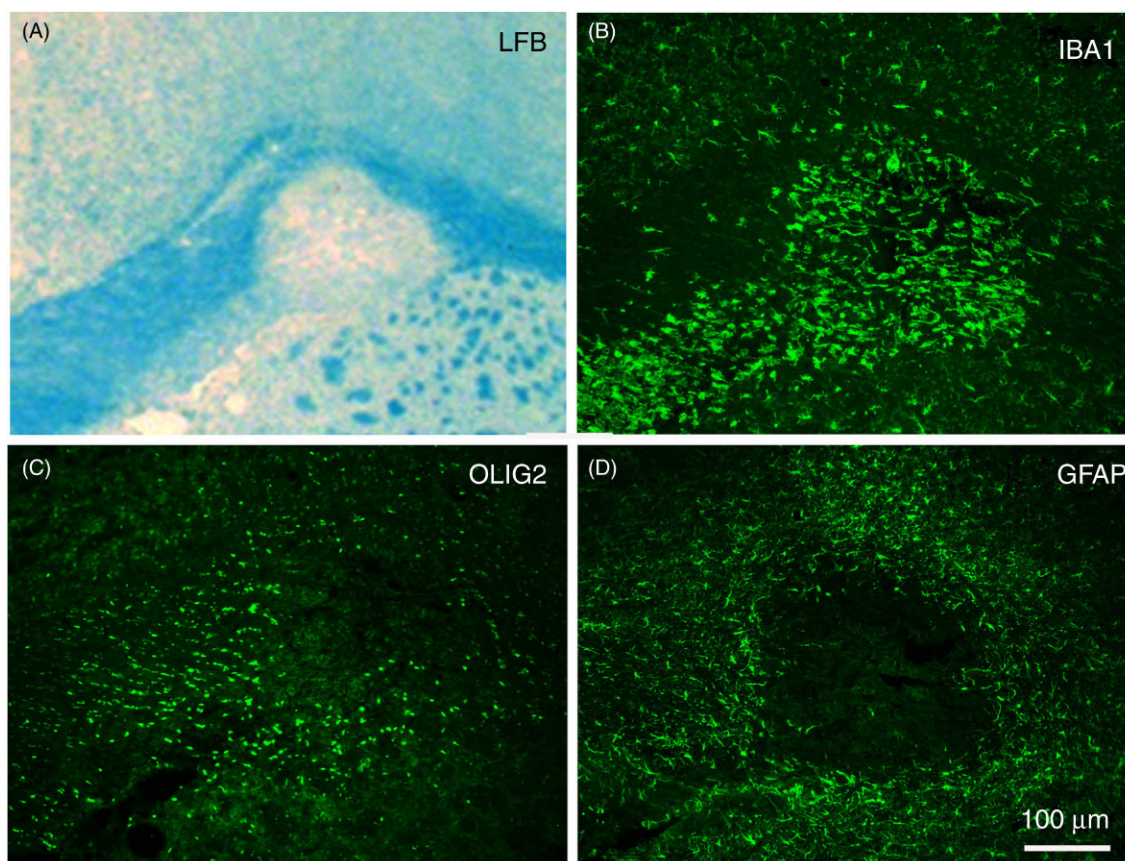
FIGURE 37.8 **Demyelination changes the structure and cellular composition of the lesion area.** In regions of the CNS that are undergoing demyelination as shown by: (A) the reduced staining with the myelin probe Luxol fast blue, there is (B) an increase in the number of activated microglial cells compared to surrounding tissue. This is shown by the upregulation in the density of IBA-1+ microglia following labeling frozen sections with antibodies to IBA-1. (C) The density of Oli2+ oligodendrocyte precursors, the cells that will differentiate into oligodendrocytes is substantially reduced in the lesion area. (D) Demyelination also alters the organization of astrocytes in the lesion area as shown by labeling with antibodies to GFAP. In the middle of the lesion there is a reduction in the number of GFAP+ cells while at the perimeter of the lesion there is an increase in the expression of GFAP as a result of reactive astrocytes that are undergoing gliosis.
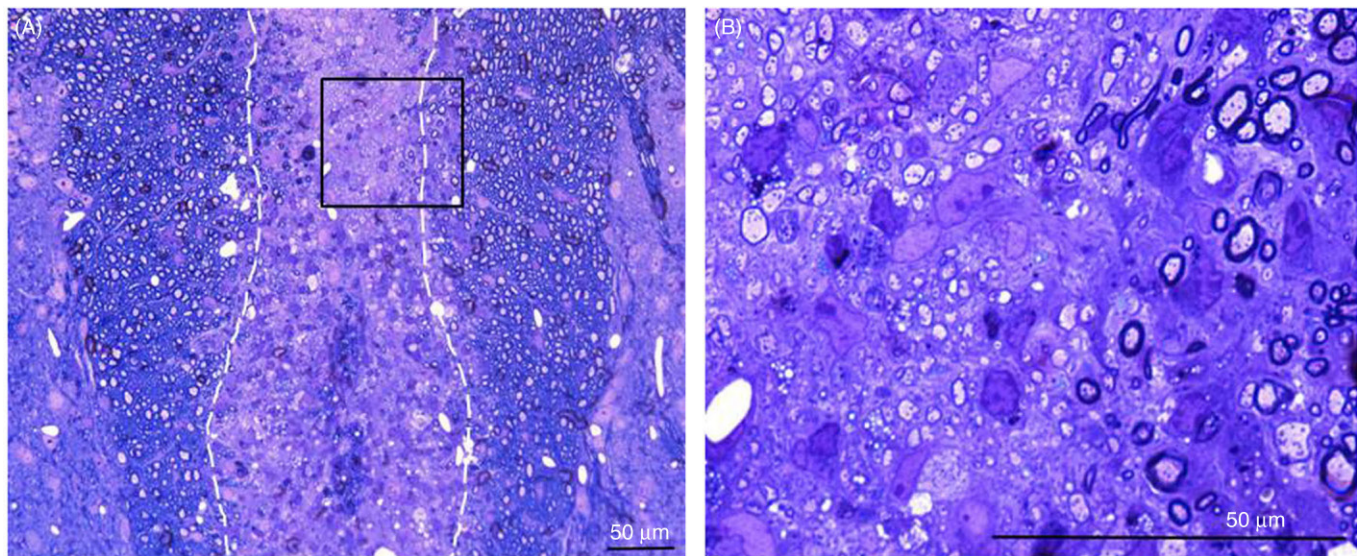
FIGURE 37.9 **Remyelination is characterized by thinly myelinated axons.** Fourteen days after the induction of a local demyelinating lesion by the injection of LPC remyelination is ongoing in the dorsal spinal cord of the 8-week old mouse. Toluidine blue stained 1mm sections clearly show remyelinated axons in the initial lesion when viewed at high power. (A) Low power micrograph with the lesion border clearly delineated (dotted line). (B) Higher power micrograph from the box outlined on a showing thinly remyelinated axons demonstrating myelin repair in the adult spinal cord.

7.1.2 Ethidium Bromide

The toxic effects of ethidium bromide are due to its DNA intercalating properties, therefore all nucleated cells are affected by this agent. The very first experiments that made use of this toxin demonstrated that a direct infusion of ethidium bromide into the cisterna magna resulted in a reproducible acute demyelinating lesion of the rat brain stem (Reynolds and Wilkin, 1993; Yajima and Suzuki, 1979a, 1979b). Over time, the mode of injection has changed, and ethidium bromide is now typically injected directly into white matter tracts as a saline solution that varies from 0.01% or 0.05% to 0.1% depending on the injection site. The lesions following ethidium bromide injections in the dorsal spinal cord tend to be quite large compared to LPC-induced lesions and can involve almost the entire dorsal funiculus, extending up to 8mm longitudinally. The caudal cerebellar peduncles of rats have also been targeted with this approach in order to address critical questions regarding the effects of age, sex, growth factors, and the role of microglia/macrophage activation on remyelination (Penderis et al., 2003a; Li et al., 2005; Li et al., 2006; Zhang et al., 2012; Ibanez et al., 2004; Adamo et al., 2006; Penderis et al., 2003b; Sim et al., 2002).

Although ethidium bromide injections are typically made in either rats or mice, injection into the spinal cords of cats has also been shown to result in large demyelinating lesions (Blakemore, 1982). The early response to ethidium bromide injection involves the destruction of astrocytes, oligodendrocytes, and OPCs while axons are typically spared. Soon after, the initial genera-

tion of the lesions' large numbers of macrophages are found in and around the lesioned area and astrogliosis occurs only around the perimeter of the lesion leaving the center of the lesions essentially devoid of astrocytes (Blakemore, 1982). Following the clearance of myelin debris, remyelination is relatively rapid, although it occurs more slowly than after LPC-induced demyelination. In a comparative study where either LPC or ethidium bromide-induced demyelinating lesions were examined in the caudal cerebellar peduncle of adult rats, extensive oligodendrocyte remyelination was already seen throughout LPC-induced lesions at 6 weeks post injection whereas, a significant proportion of axons remained demyelinated in ethidium bromide-induced lesions. By 3.5 months postinjection, however, almost all axons had remyelinated in ethidium bromide lesions (Woodruff and Franklin, 1999). Interestingly, in contrast to LPC or anti-GalC-induced lesions where most remyelination is mediated by oligodendrocytes a significant amount of remyelination in ethidium bromide-induced lesions are undertaken by Schwann cells (Woodruff and Franklin, 1999; Blakemore, 2005). Remyelinating Schwann cells are typically found in astrocyte-depleted areas of the demyelinated spinal cord and it was initially assumed that they were derived from Schwann cells associated with peripheral nerves or spinal nerve roots in the vicinity (Franklin and Blakemore, 1993). A recent study, however, used in vivo fate mapping to demonstrate that after demyelinating injury, CNS-derived OPCs are able to generate Schwann cells, a surprising finding given that Schwann cells normally develop from the embryonic

neural crest and are restricted to the peripheral nervous system (Zawadzka et al., 2010). One likely hypothesis is that in the absence of astrocyte signaling, cells specified for the oligodendrocyte lineage are diverted to become Schwann cells suggesting the commitment to a myelinating fate over rides the commitment to a specific cell type. The molecular mechanisms responsible for this regulation of cell fate are currently unclear. In MS, when remyelination occurs, it is largely mediated by oligodendrocytes and not Schwann cells thus the significance of the ethidium bromide model for therapeutic development is somewhat limited.

7.1.3 Anti-GalC Antibodies

One approach for selective cell type elimination that has been used in multiple systems is the targeting of the complement cascade though binding to cell type specific, cell surface antibodies (Piddlesden et al., 1993; Raff et al., 1978). In this model the antibody binds to specific cell surface epitopes and addition of complement results in selective cell lysis. This model has been used effectively in vivo using antibodies to galactocerebroside (GalC) the major myelin sphingolipid that marks mature oligodendrocytes as the targeting vector (Raff et al., 1978). Initial studies demonstrated that a single intraspinal injection of complement proteins plus antibodies to GalC resulted in demyelination (Keirstead and Blakemore, 1997). In this model of demyelination in the adult rat spinal cord, some oligodendrocytes survived demyelination enabling the authors to demonstrate that the oligodendrocytes that survive within demyelinated lesions are not induced to divide in the presence of naked axons demonstrating that fully-differentiated oligodendrocytes are postmitotic and do not contribute significantly to remyelination in the adult CNS. Demyelination has also been induced in the rat cerebellar peduncle using this model where axons tend to be spared and remyelination is typically accomplished by oligodendrocytes, not Schwann cells (Woodruff and Franklin, 1999).

7.1.4 Advantages of Focal Toxins

All of these agents produce large areas of demyelination with minimal axonal damage. Focal toxins induce synchronized demyelination in a defined region allowing the investigation of remyelination in the absence of concurrent demyelination. This offers a clear advantage when analyzing molecular changes specific to remyelination since the processes of demyelination and remyelination have temporal separation and spontaneous remyelination follows a highly reproducible time course in rodents. The timing of remyelination has been shown to differ between the three most commonly used focal toxins although all models eventually undergo extensive spontaneous remyelination. After LPC-injection into the cerebellar peduncle of adult rats, remyelination was

evident by 14 days and extensive by 6 weeks whereas, ethidium bromide or anti-GalC induced lesions showed very little remyelination after 14 days although they did show extensive remyelination after 3 months (Woodruff and Franklin, 1999). Finally, unlike immune or viral-mediated models of demyelination, focal toxin-induced lesions have the advantage that they can be induced at any age, in either the brain or the spinal cord, and in any strain or species. The disadvantage of these models is that, particularly in the case of LPC and ethidium bromide the mechanisms of induction of cell death is nonphysiological and if the development of the lesion and the potential repair process is in part dependent on the mechanisms of cell death then it is unclear whether these models will be useful in defining pathogenic processes in MS. Where these models have proven extremely useful is in the development of therapeutics targeted towards remyelination rather than immune regulation. One of the best examples of such therapeutic development is the identification and characterization of anti-LINGO-1 antibodies as a therapy promoting remyelination. A major role of the leucine-rich repeat and Ig domain containing NOGO receptor (LINGO-1) is to inhibit the differentiation of oligodendrocyte progenitor cells (Mi et al., 2005, 2009). LINGO-1 knockout mice show precocious myelination, which suggested that LINGO-1 antagonists might be useful to accelerate myelin repair after demyelination. Using both the LPC and cuprizone models of demyelination, anti-LINGO-1 antibody treatments have been shown to significantly increase the speed of remyelination, a finding that may result in a new therapeutic option for MS patients (Mi et al., 2005, 2009). The anti-LINGO-1 Li81 antibody is the first MS therapy that directly targets myelin repair and is currently being evaluated in clinical trials for MS (Pepinsky et al., 2011). Finally, the use of complement binding antibodies to target oligodendrocyte death may have immediate relevance to MS. It has been suggested that in some MS lesions complement mediated cell lysis contributes to the generation of the pathology and thus this model may directly reflect the generation of lesions in a subset of MS patients.

7.2 Systemic Toxins

One disadvantage of the local toxin models is that they require the injection of the toxin in the parenchyma of the CNS. While this allows for precise localization of the subsequent lesion, it introduces the complexity that any pathology that develops is a consequence of both the injection and the presence of the toxin. An alternative strategy is to utilize a systemic toxin that preferentially targets oligodendrocytes in specific regions of the CNS. The most commonly utilized systemic toxin is Cuprizone.

7.2.1 Cuprizone

Ingestion of the copper chelator cuprizone (biscyclohexanone oxaldihydrazone) results in the reproducible demyelination of specific brain regions in either C57BL/6 or SJL/SVJ mice. The exact mechanism underlying cuprizone-induced demyelination remains unknown but the toxicity is thought to result from a combination of mitochondrial stress and an innate immune response (Linares et al., 2006; Liu et al., 2010; Pasquini et al., 2007). Cuprizone-induced demyelination appears to result from the degeneration of oligodendrocytes rather than a primary attack on the myelin sheaths (Carlton, 1966, 1967; Tansey et al., 1996). Experiments conducted in the late 1960's demonstrated that high doses (0.5%) of cuprizone mixed with basic rodent chow and given to mice early in development resulted in high mortality but that lower doses resulted in demyelinated lesions accompanied by astrogliosis (Carlton, 1967). This model has been refined to the point where mice aged 6–9 weeks are now typically given 0.2%–0.3% cuprizone treatment of for 5–6 weeks which results in acute demyelination of the corpus callosum (Matsushima and Morell, 2001; Stidworthy et al., 2003), as well as the hippocampus (Hoffmann et al., 2008; Koutsoudaki et al., 2009) external capsule (Pott et al., 2009), cerebellar peduncles (Blakemore, 1973; Ludwin, 1978; Torkildsen et al., 2008), cerebellum (Skripuletz et al., 2010; Groebe et al., 2009) cerebral cortex (Skripuletz et al., 2010; Gudi et al., 2009), and striatum (Pott et al., 2009). Far less demyelination is seen in spinal cord suggesting either a differential susceptibility of oligodendrocytes to the toxin or non-uniform penetration of the toxins to the CNS. Distinct gray matter regions have also been shown to be affected in the cortex and hippocampus (Gudi et al., 2009; Norkute et al., 2009), which may reflect death of oligodendrocytes in those regions or a toxic effect of curpizone on other neural cell types. Mice exposed to cuprizone exhibit extensive reactive gliosis, activation of microglia, and significant oligodendrocyte apoptosis. Similar to what is noted with the focal models of demyelination discussed above, acute demyelination is followed by spontaneous remyelination that occurs during the weeks following treatment removal while the mice are fed regular chow. When cuprizone treatment is prolonged to 12 weeks or longer however, remyelination is very sparse resulting in a model of chronic demyelination (Ludwin, 1980).

7.2.2 Advantages of Systemic Toxins

While it is debatable whether the cuprizone model reflects human MS pathology, this reversible demyelination model is useful for studying the biological processes related to both demyelination and remyelination in the CNS. Two major pathological features characteristic of the cuprizone model, however, include primary oligodendrocyte death along with the activation of microglia and these two features are known to occur in a subset of human MS lesions (Barnett and Prineas, 2004). The cuprizone model has been extensively used to examine the potential of various compounds to stimulate myelin repair (Koutsoudaki et al., 2010; Moharregh-Khiabani et al., 2010). A significant advantage of this model is that demyelination can be induced in a reproducible manner in both space and time and mechanisms specific to both demyelination and remyelination, which are not specific to primary inflammatory events, can be investigated. Because the time-course of cuprizone treatment is so long, demyelination is progressive in this model and remyelination begins while demyelination is still taking place. The reappearance of myelin protein expression and partial remyelination has been shown to occur during the late stages of acute demyelination (after 3 weeks) while the mice are still undergoing cuprizone treatment (Jurevics et al., 2001; Lindner et al., 2008; Norkute et al., 2009). This temporal overlap presents a challenge when trying to understand the mechanisms specific to either demyelination or remyelination, however, it does model the human condition more closely since demyelination and remyelination occur concurrently in patients with MS. Recent studies have shown that when Cuprizone treatment is combined with rapamycin treatment which blocks mTor signaling, the spontaneous remyelination is dramatically reduced thereby allowing better quantification of repair processes. A significant advantage of the cuprizone model over other approaches is the relative simplicity of the experimental paradigm. Cuprizone is simply added to regular mouse chow that is fed to the animals each day in contrast to the focal toxin models, which call for potentially technically challenging surgeries involving the use of a stereotactic apparatus to direct the focal lesions to specific areas. Despite the apparent simplicity of this model there are a number of confounding features. First the use of cuprizone is generally limited to mice (although recent studies have reported its use in rat (Adamo et al., 2006; Silvestroff et al., 2012) and there is a clear genetic linkage to the susceptibility for cuprizone toxicity. The basis for such strain difference is unknown. Likewise there are significant differences in susceptibility between gender and age that are poorly understood (Kipp et al., 2009). This lack of clarity is likely a reflection of the lack of understanding about the mechanism mediating Cuprizone toxicity, however proof of principle studies have indicated that signals known from in vitro studies to stimulate oligodendrocyte differentiation such as thyroid hormone (T3) promote remyelination in the cuprizone model (Franco et al., 2008).

8 CONCLUSIONS AND COMMENTS

The heterogeneity of the demyelinating disease MS is well established and this is readily reflected in the wide range of models that mimic a wide range of different attributes of the disease. While some of the models, such as EAE have been established for many years and have formed the basis of a range of current therapies used to treat the disease, other models, such as those that target oligodendrocyte cell death to particular regions of the CNS are recent additions to the arsenal of understanding the pathology of the disease. Each of the model systems discussed in this review has particular merit for developing our understanding of some specific aspect of the disease. For example while EAE models have been very effective at furthering our insights of the immunological basis of the CNS demyelination and particularly the role of T cells in MS, the use of gliotoxins, such as LPC or ethidium bromide have been particularly useful in developing our understanding of the cellular and molecular mechanisms of remyelination.

References

Adamo, A.M., Paez, P.M., Escobar Cabrera, O.E., et al., 2006. Remyelination after cuprizone-induced demyelination in the rat is stimulated by apotransferrin. Experiment. Neurol. 198 (2), 519–529.

Amor, S., Smith, P.A., Hart, B., Baker, D., 2005. Biozzi mice: of mice and human neurological diseases. J. Neuroimmunol. 165 (1–2), 1–10.

Bai, L., Lennon, D.P., Caplan, A.I., et al., 2012. Hepatocyte growth factor mediates mesenchymal stem cell-induced recovery in multiple sclerosis models. Nat. Neurosci. 15 (6), 862–870.

Balatoni, B., Storch, M.K., Swoboda, E.M., et al., 2007. FTY720 sustains and restores neuronal function in the DA rat model of MOG-induced experimental autoimmune encephalomyelitis. Brain Res. Bull. 74 (5), 307–316.

Baranzini, S.E., Nickles, D., 2012. Genetics of multiple sclerosis: swimming in an ocean of data. Curr. Opin. Neurol. 25 (3), 239–245.

Barnett, M.H., Prineas, J.W., 2004. Relapsing and remitting multiple sclerosis: pathology of the newly forming lesion. Ann. Neurol. 55 (4), 458–468.

Ben-Nun, A., Wekerle, H., Cohen, I.R., 1981. The rapid isolation of clonable antigen-specific T lymphocyte lines capable of mediating autoimmune encephalomyelitis. Eur. J. Immunol. 11 (3), 195–199.

Bielekova, B., Becker, B.L., 2010. Monoclonal antibodies in MS: mechanisms of action. Neurology 74 (Suppl. 1), S31–S40.

Blakemore, W.F., 1973. Remyelination of the superior cerebellar peduncle in the mouse following demyelination induced by feeding cuprizone. J. Neurol. Sci. 20 (1), 73–83.

Blakemore, W.F., 1982. Ethidium bromide induced demyelination in the spinal cord of the cat. Neuropathol. Appl. Neurobiol. 8 (5), 365–375.

Blakemore, W.F., 2005. The case for a central nervous system (CNS) origin for the Schwann cells that remyelinate CNS axons following concurrent loss of oligodendrocytes and astrocytes. Neuropathol. Appl. Neurobiol. 31 (1), 1–10.

Blakemore, W.F., Franklin, R.J., 2008. Remyelination in experimental models of toxin-induced demyelination. Curr. Top Microbiol. Immunol. 318, 193–212.

Blakemore, W.F., Eames, R.A., Smith, K.J., McDonald, W.I., 1977. Remyelination in the spinal cord of the cat following intraspinal injections of lysolecithin. J. Neurol. Sci. 33 (1–2), 31–43.

Bunge, R.P., 1968. Glial cells and the central myelin sheath. Physiol Rev 48, 197–251.

Bunge, M.P., Bunge, R.P., Pappas, G.D., 1962. Electron microscopic demonstrations of connections between glia and myelin sheaths in the developing mammalian central nervous system. J. Cell Biol. 12, 448–453.

Caillava, C., Vandenbosch, R., Jablonska, B., et al., 2011. Cdk2 loss accelerates precursor differentiation and remyelination in the adult central nervous system. J. Cell Biol. 193 (2), 397–407.

Campagnoni, A.T., 1988. Molecular biology of myelin proteins from the central nervous system. J. Neurochem. 51, 1–14.

Caprariello, A.V., Mangla, S., Miller, R.H., Selkirk, S.M., 2012. Apoptosis of oligodendrocytes in the central nervous system results in rapid focal demyelination. Ann. Neurol. 72 (3), 395–405.

Caprariello, A.V., Batt, C.E., Zippe, I., Romito-DiGiacomo, R.R., Karl, M., Miller, R.H., 2015. Apoptosis of oligodendrocytes during early development delays myelination and impairs subsequent responses to demyelination. J. Neurosci. 35 (41), 14031–14041.

Carlton, W.W., 1966. Response of mice to the chelating agents sodium diethyldithiocarbamate, alpha-benzoinoxime, and biscyclohexanone oxaldihydrazone. Toxicol. Appl. Pharmacol. 8 (3), 512–521.

Carlton, W.W., 1967. Studies on the induction of hydrocephalus and spongy degeneration by cuprizone feeding and attempts to antidote the toxicity. Life Sci. 6 (1), 11–19.

Charles, P., Reynolds, R., Seilhean, D., et al., 2002. Re-expression of PSA-NCAM by demyelinated axons: an inhibitor of remyelination in multiple sclerosis? Brain 125 (Pt 9), 1972–1979.

Correale, J., Gaitan, M.I., 2015. Multiple sclerosis and environmental factors: the role of vitamin D, parasites, and Epstein-Barr virus infection. Acta Neurol. Scand. 132 (199), 46–55.

Cross, A.H., Trotter, J.L., Lyons, J., 2001. B cells and antibodies in CNS demyelinating disease. J. Neuroimmunol. 112 (1–2), 1–14.

Dal Canto, M.C., Rabinowitz, S.G., 1982. Experimental models of virus-induced demyelination of the central nervous system. Ann. Neurol. 11 (2), 109–127.

Das Sarma, J., 2010. A mechanism of virus-induced demyelination. Interdisc. Perspect. Infect. Dis. 2010, 109239.

Didonna, A., 2016. Preclinical models of multiple sclerosis: advantages and limitations towards better therapies. Curr. Med. Chem. 23 (14), 1442–1459.

Dousset, V., Brochet, B., Vital, A., et al., 1995. Lysolecithin-induced demyelination in primates: preliminary in vivo study with MR and magnetization transfer. AJNR Am. J. Neuroradiol. 16 (2), 225–231.

Eng, L.F., 1985. Glial fibrillary acidic protein (GFAP): the major protein of glial intermediate filaments in differentiated astrocytes. J. Neuroimmunol. 8 (4–6), 203–214.

Eng, L.F., Ghirnikar, R.S., 1994. GFAP and astrogliosis. Brain Pathol. 4 (3), 229–237.

Eriksson, P.S., Perfiliea, E., Bjorn- Erikksson, T., et al., 1998. Neurogenesis in the adult human hippocampus. Nat. Med. 4, 1313–1317.

Fancy, S.P., Baranzini, S.E., Zhao, C., et al., 2009. Dysregulation of the Wnt pathway inhibits timely myelination and remyelination in the mammalian CNS. Genes Dev. 23 (13), 1571–1585.

Fawcett, J.W., Asher, R.A., 1999. The glial scar and central nervous system repair. Brain Res. Bull. 49 (6), 377–391.

Fitch, M.T., Silver, J., 2008. CNS injury, glial scars, and inflammation: Inhibitory extracellular matrices and regeneration failure. Experiment. Neurol. 209 (2), 294–301.

Fitch, M.T., Doller, C., Combs, C.K., Landreth, G.E., Silver, J., 1999. Cellular and molecular mechanisms of glial scarring and progressive cavitation: in vivo and in vitro analysis of inflammation-induced secondary injury after CNS trauma. J. Neurosci. 19 (19), 8182–8198.

Franciotta, D., Salvetti, M., Lolli, F., Serafini, B., Aloisi, F., 2008. B cells and multiple sclerosis. Lancet Neurol. 7 (9), 852–858.

Franco, P.G., Silvestroff, L., Soto, E.F., Pasquini, J.M., 2008. Thyroid hormones promote differentiation of oligodendrocyte progenitor cells and improve remyelination after cuprizone-induced demyelination. Experiment. Neurol. 212 (2), 458–467.

Franklin, R.J., Blakemore, W.F., 1993. Requirements for Schwann cell migration within CNS environments: a viewpoint. Int. J. Dev. Neurosci. 11 (5), 641–649.

Freund, J., Stern, E.R., Pisani, T.M., 1947. Isoallergic encephalomyelitis and radiculitis in guinea pigs after one injection of brain and Mycobacteria in water-in-oil emulsion. J. Immunol. 57 (2), 179–194.

Fuller, M.L., DeChant, A.K., Rothstein, B., et al., 2007. Bone morphogenetic proteins promote gliosis in demyelinating spinal cord lesions. Ann. Neurol. 62 (3), 288–300.

Furlan, R., Cuomo, C., Martino, G., 2009. Animal models of multiple sclerosis. Methods Mol. Biol. 549, 157–173.

Garay, L., Tungler, V., Deniselle, M.C., Lima, A., Roig, P., De Nicola, A.F., 2011. Progesterone attenuates demyelination and microglial reaction in the lysolecithin-injured spinal cord. Neuroscience 192, 588–597.

Ge, Y., Grossman, R.I., Udupa, J.K., et al., 2000. Brain atrophy in relapsing-remitting multiple sclerosis and secondary progressive multiple sclerosis: longitudinal quantitative analysis. Radiology 214 (3), 665–670.

Gledhill, R.F., McDonald, W.I., 1977. Morphological characteristics of central demyelination and remyelination: a single-fiber study. Ann. Neurol. 1 (6), 552–560.

Gold, R., Linington, C., Lassmann, H., 2006. Understanding pathogenesis and therapy of multiple sclerosis via animal models: 70 years of merits and culprits in experimental autoimmune encephalomyelitis research. Brain 129 (Pt 8), 1953–1971.

Gourraud, P.A., Harbo, H.F., Hauser, S.L., Baranzini, S.E., 2012. The genetics of multiple sclerosis: an up-to-date review. Immunol. Rev. 248 (1), 87–103.

Gregson, N.A., 1989. Lysolipids and membrane damage: lysolecithin and its interaction with myelin. Biochem. Soc. Trans. 17 (2), 280–283.

Griffiths, I., Klugmann, M., Anderson, T., et al., 1998. Axonal swellings and degeneration in mice lacking the major proteolipid of myelin. Science 280 (5369), 1610–1613.

Groebe, A., Clarner, T., Baumgartner, W., Dang, J., Beyer, C., Kipp, M., 2009. Cuprizone treatment induces distinct demyelination, astrocytosis, and microglia cell invasion or proliferation in the mouse cerebellum. Cerebellum 8 (3), 163–174.

Grothe, M., Lotze, M., Langner, S., Dressel, A., 2016. The role of global and regional gray matter volume decrease in multiple sclerosis. J. Neurol. 263 (6), 1137–1145.

Gudi, V., Moharregh-Khiabani, D., Skripuletz, T., et al., 2009. Regional differences between grey and white matter in cuprizone induced demyelination. Brain Res. 1283, 127–138.

Haase, C.G., Guggenmos, J., Brehm, U., et al., 2001. The fine specificity of the myelin oligodendrocyte glycoprotein autoantibody response in patients with multiple sclerosis and normal healthy controls. J. Neuroimmunol. 114 (1–2), 220–225.

Hall, S.M., 1972. The effect of injections of lysophosphatidyl choline into white matter of the adult mouse spinal cord. J. Cell Sci. 10 (2), 535–546.

Harrison, B., 1985. Schwann cell and oligodendrocyte remyelination in lysolecithin-induced lesions in irradiated rat spinal cord. J. Neurol. Sci. 67 (2), 143–159.

Hauser, S.L., Waubant, E., Arnold, D.L., et al., 2008. B-cell depletion with rituximab in relapsing-remitting multiple sclerosis. N. Eng. J. Med. 358 (7), 676–688.

Hirano, M., Goldman, J.E., 1988. Gliogenesis in rat spinal cord: evidence for origin of astrocytes and oligodendrocytes from radial precursors. J. Neurosci. Res. 21 (2–4), 155–167.

Hoffmann, K., Lindner, M., Groticke, I., Stangel, M., Loscher, W., 2008. Epileptic seizures and hippocampal damage after cuprizone-induced demyelination in C57BL/6 mice. Experiment. Neurol. 210 (2), 308–321.

Hohlfeld, R., Meinl, E., Dornmair, K., 2008. B- and T-cell responses in multiple sclerosis: novel approaches offer new insights. J. Neurol. Sci. 274 (1–2), 5–8.

Huang, J.K., Jarjour, A.A., Nait Oumesmar, B., et al., 2011. Retinoid X receptor gamma signaling accelerates CNS remyelination. Nat. Neurosci. 14 (1), 45–53.

Ibanez, C., Shields, S.A., El-Etr, M., Baulieu, E.E., Schumacher, M., Franklin, R.J., 2004. Systemic progesterone administration results in a partial reversal of the age-associated decline in CNS remyelination following toxin-induced demyelination in male rats. Neuropathol. Appl. Neurobiol. 30 (1), 80–89.

Janzer, R.C., Raff, M.C., 1987. Astrocytes induce blood-brain barrier properties in endothelial cells. Nature 325 (6101), 253–257.

Joy, Jr., J.E.J.R., 2001. Multiple Sclerosis: Current Status and Strategies for the Future. National Academy Press, Washington DC.

Jurevics, H., Hostettler, J., Muse, E.D., et al., 2001. Cerebroside synthesis as a measure of the rate of remyelination following cuprizone-induced demyelination in brain. J. Neurochem. 77 (4), 1067–1076.

Kabat, E.A., Wolf, A., Bezer, A.E., 1947. The rapid production of acute disseminated encephalomyelitis in rhesus monkeys by injection of heterologous and homologous brain tissue with adjuvants. J. Exp. Med. 85 (1), 117–130.

Kakalacheva, K., Munz, C., Lunemann, J.D., 2011. Viral triggers of multiple sclerosis. Biochim. Biophys. Acta 1812 (2), 132–140.

Kastrukoff, L.F.R.G., 1998. Virology. F.A. Davis Company, Philadelphia.

Kaye, J.F., Kerlero de Rosbo, N., Mendel, I., et al., 2000. The central nervous system-specific myelin oligodendrocytic basic protein (MOBP) is encephalitogenic and a potential target antigen in multiple sclerosis (MS). J. Neuroimmunol. 102 (2), 189–198.

Keirstead, H.S., Blakemore, W.F., 1997. Identification of post-mitotic oligodendrocytes incapable of remyelination within the demyelinated adult spinal cord. J. Neuropathol. Exp. Neurol. 56 (11), 1191–1201.

Kerlero, dRN., Milo, R., Lees, M.B., Burger, D., Bernard, C.C., Ben, N.A., 1993. Reactivity to myelin antigens in multiple sclerosis. Peripheral blood lymphocytes respond predominantly to myelin oligodendrocyte glycoprotein. J. Clin. Invest. 92 (6), 2602–2608.

Kerschensteiner, M., Stadelmann, C., Buddeberg, B.S., et al., 2004. Targeting experimental autoimmune encephalomyelitis lesions to a predetermined axonal tract system allows for refined behavioral testing in an animal model of multiple sclerosis. Am. J. Pathol. 164 (4), 1455–1469.

Kerstetter, A.E., Padovani-Claudio, D.A., Bai, L., Miller, R.H., 2009. Inhibition of CXCR2 signaling promotes recovery in models of multiple sclerosis. Experiment. Neurol. 220 (1), 44–56.

Kipp, M., Clarner, T., Dang, J., Copray, S., Beyer, C., 2009. The cuprizone animal model: new insights into an old story. Acta Neuropathol. 118 (6), 723–736.

Kojima, K., Berger, T., Lassmann, H., et al., 1994. Experimental autoimmune panencephalitis and uveoretinitis transferred to the Lewis rat by T lymphocytes specific for the S100 beta molecule, a calcium binding protein of astroglia. J. Exp. Med. 180 (3), 817–829.

Kojima, K., Wekerle, H., Lassmann, H., Berger, T., Linington, C., 1997. Induction of experimental autoimmune encephalomyelitis by CD4+ T cells specific for an astrocyte protein, S100 beta. J. Neural. Transm. Suppl. 49, 43–51.

Koutsoudaki, P.N., Skripuletz, T., Gudi, V., et al., 2009. Demyelination of the hippocampus is prominent in the cuprizone model. Neurosci. Lett. 451 (1), 83–88.

Koutsoudaki, P.N., Hildebrandt, H., Gudi, V., Skripuletz, T., Skuljec, J., Stangel, M., 2010. Remyelination after cuprizone induced demyelination is accelerated in mice deficient in the polysialic acid synthesizing enzyme St8siaIV. Neuroscience 171 (1), 235–244.

Krishnamoorthy, G., Wekerle, H., 2009. EAE: an immunologist's magic eye. Eur. J. Immunol. 39 (8), 2031–2035.

Larocca, J.N., Norton, W.T., 2007. Isolation of myelin. Curr. Protoc. Cell Biol., Chapter 3: Unit3.25, 3.25.1–3.25.19.

Lassmann, H., Brunner, C., Bradl, M., Linington, C., 1988. Experimental allergic encephalomyelitis: the balance between encephalitogenic T lymphocytes and demyelinating antibodies determines size and structure of demyelinated lesions. Acta Neuropathol. 75 (6), 566–576.

Lassmann, H., Bruck, W., Lucchinetti, C., 2001. Heterogeneity of multiple sclerosis pathogenesis: implications for diagnosis and therapy. Trends Mol. Med. 7 (3), 115–121.

Lazzarini, R.A., 2004. Myelin Biology and Disorders, second ed. Elsevier Academic Press, London, UK.

Li, W.W., Setzu, A., Zhao, C., Franklin, R.J., 2005. Minocycline-mediated inhibition of microglia activation impairs oligodendrocyte progenitor cell responses and remyelination in a non-immune model of demyelination. J. Neuroimmunol. 158 (1–2), 58–66.

Li, W.W., Penderis, J., Zhao, C., Schumacher, M., Franklin, R.J., 2006. Females remyelinate more efficiently than males following demyelination in the aged but not young adult CNS. Experiment. Neurol. 202 (1), 250–254.

Linares, D., Taconis, M., Mana, P., et al., 2006. Neuronal nitric oxide synthase plays a key role in CNS demyelination. J. Neurosci. 26 (49), 12672–12681.

Lindner, M., Heine, S., Haastert, K., et al., 2008. Sequential myelin protein expression during remyelination reveals fast and efficient repair after central nervous system demyelination. Neuropathol. Appl. Neurobiol. 34 (1), 105–114.

Lipton, M.M., Freund, J., 1952. Encephalomyelitis in the rat following intracutaneous injection of central nervous system tissue with adjuvant. Proc. Soc. Exp. Biol. Med. 81 (1), 260–261.

Liu, L., Belkadi, A., Darnall, L., et al., 2010. CXCR2-positive neutrophils are essential for cuprizone-induced demyelination: relevance to multiple sclerosis. Nat. Neurosci. 13 (3), 319–326.

Locatelli, G., Wortge, S., Buch, T., et al., 2012. Primary oligodendrocyte death does not elicit anti-CNS immunity. Nat. Neurosci. 15 (4), 543–550.

Lublin, F.D., Reingold, S.C., 1996. Defining the clinical course of multiple sclerosis: results of an international survey. National Multiple Sclerosis Society (USA) Advisory Committee on Clinical Trials of New Agents in Multiple Sclerosis. Neurology 46 (4), 907–911.

Lucchinetti, C., Bruck, W., Parisi, J., Scheithauer, B., Rodriguez, M., Lassmann, H., 2000. Heterogeneity of multiple sclerosis lesions: implications for the pathogenesis of demyelination. Ann. Neurol. 47 (6), 707–717.

Ludwin, S.K., 1978. Central nervous system demyelination and remyelination in the mouse: an ultrastructural study of cuprizone toxicity. Lab Invest 39 (6), 597–612.

Ludwin, S.K., 1980. Chronic demyelination inhibits remyelination in the central nervous system. An analysis of contributing factors. Lab Invest 43 (4), 382–387.

Matsushima, G.K., Morell, P., 2001. The neurotoxicant, cuprizone, as a model to study demyelination and remyelination in the central nervous system. Brain Pathol. 11 (1), 107–116.

McElroy, J.P., Oksenberg, J.R., 2011. Multiple sclerosis genetics 2010. Neurol. Clin. 29 (2), 219–231.

Meier, U.C., Giovannoni, G., Tzartos, J.S., Khan, G., 2012. Translational mini-review series on B cell subsets in disease. B cells in multiple sclerosis: drivers of disease pathogenesis and Trojan horse for Epstein-Barr virus entry to the central nervous system? Clin. Exp. Immunol. 167 (1), 1–6.

Merkler, D., Ernsting, T., Kerschensteiner, M., Bruck, W., Stadelmann, C., 2006. A new focal EAE model of cortical demyelination: multiple sclerosis-like lesions with rapid resolution of inflammation and extensive remyelination. Brain 129 (Pt 8), 1972–1983.

Mi, S., Miller, R.H., Lee, X., et al., 2005. LINGO-1 negatively regulates myelination by oligodendrocytes. Nat. Neurosci. 8 (6), 745–751.

Mi, S., Miller, R.H., Tang, W., et al., 2009. Promotion of central nervous system remyelination by induced differentiation of oligodendrocyte precursor cells. Ann. Neurol. 65 (3), 304–315.

Mi, S., Lee, X., Hu, Y., et al., 2011. Death receptor 6 negatively regulates oligodendrocyte survival, maturation and myelination. Nat. Med. 17 (7), 816–821.

Miller, R.H., 2002. Regulation of oligodendrocyte development in the vertebrate CNS. Prog. Neurobiol. 67, 451–467.

Miller, R.H., 2006. Building bridges with astrocytes for spinal cord repair. J. Biol. 5 (3), 6.

Miller, R.H., Raff, M.C., 1984. Fibrous and protoplasmic astrocytes are biochemically and developmentally distinct. J. Neurosci. 4 (2), 585–592.

Miron, V.E., Schubart, A., Antel, J.P., 2008. Central nervous system-directed effects of FTY720 (fingolimod). J. Neurol. Sci. 274 (1–2), 13–17.

Miron, V.E., Ludwin, S.K., Darlington, P.J., et al., 2010. Fingolimod (FTY720) enhances remyelination following demyelination of organotypic cerebellar slices. Am. J. Pathol. 176 (6), 2682–2694.

Mix, E., Meyer-Rienecker, H., Hartung, H.P., Zettl, U.K., 2010. Animal models of multiple sclerosis—potentials and limitations. Progr. Neurobiol. 92 (3), 386–404.

Moharregh-Khiabani, D., Blank, A., Skripuletz, T., et al., 2010. Effects of fumaric acids on cuprizone induced central nervous system de- and remyelination in the mouse. PLoS One 5 (7), e11769.

Montgomery, D.L., 1994. Astrocytes: form, functions, and roles in disease. Vet. Pathol. 31 (2), 145–167.

Moore, G.R.W., 1998. Neuropathology and Pathophysiology of the Multiple Sclerosis Lesion. F.A. Davis Company, Philadelphia.

Morell, P., Roberson, M., Meissner, G., Toews, A.D., 1990. Myelin:from electrical insulator to ion, channels., Dynamic Interactions of Myelin Proteins. Wiley-Liss, Inc, New York, 1–24.

Moreno, B., Jukes, J.P., Vergara-Irigaray, N., et al., 2011. Systemic inflammation induces axon injury during brain inflammation. Ann. Neurol. 70 (6), 932–942.

Munoz, J.J., Bernard, C.C., Mackay, I.R., 1984. Elicitation of experimental allergic encephalomyelitis (EAE) in mice with the aid of pertussigen. Cell Immunol. 83 (1), 92–100.

Nave, K.-A., 1995. Neurological mouse mutants: a molecular-genetic analysis of myelin proteins. In: Kettnmann, H., Ransom, B. (Eds.), Neuroglia. Oxford University Press, New York, pp. 571–587.

Norkute, A., Hieble, A., Braun, A., et al., 2009. Cuprizone treatment induces demyelination and astrocytosis in the mouse hippocampus. J. Neurosci. Res. 87 (6), 1343–1355.

Nornes, H.O., Das, G.D., 1974. Temporal pattern of neurogenesis in spinal cord of rat. Time and sites of origin and migration and settling pattern of neuroblasts. Brain Res. 73, 121–138.

Norton, W.T., Poduslo, S.E., 1973. Myelination in rat brain: method of myelin isolation. J. Neurochem. 21, 749–757.

Oksenberg, J.R., Seboun, E., Hauser, S.L., 1996. Genetics of demyelinating diseases. Brain Pathol. 6 (3), 289–302.

Olitsky, P.K., Yager, R.H., 1949. Experimental disseminated encephalomyelitis in white mice. J. Exp. Med. 90 (3), 213–224.

Oluich, L.J., Stratton, J.A., Xing, Y.L., et al., 2012. Targeted ablation of oligodendrocytes induces axonal pathology independent of overt demyelination. J. Neurosci. 32 (24), 8317–8330.

Ono, K., Yasui, Y., Rutishauser, U., Miller, R.H., 1997. Focal ventricular origin and migration of oligodendrocyte precursors into the chick optic nerve. Neuron 19, 1–20.

Pasquini, L.A., Calatayud, C.A., Bertone Una, A.L., Millet, V., Pasquini, J.M., Soto, E.F., 2007. The neurotoxic effect of cuprizone on oligodendrocytes depends on the presence of pro-inflammatory cytokines secreted by microglia. Neurochem. Res. 32 (2), 279–292.

Penderis, J., Woodruff, R.H., Lakatos, A., et al., 2003a. Increasing local levels of neuregulin (glial growth factor-2) by direct infusion into areas of demyelination does not alter remyelination in the rat CNS. Eur. J. Neurosci. 18 (8), 2253–2264.

Penderis, J., Shields, S.A., Franklin, R.J., 2003b. Impaired remyelination and depletion of oligodendrocyte progenitors does not occur following repeated episodes of focal demyelination in the rat central nervous system. Brain 126 (Pt 6), 1382–1391.

Pepinsky, R.B., Shao, Z., Ji, B., et al., 2011. Exposure levels of anti-LIN-GO-1 Li81 antibody in the central nervous system and dose-efficacy relationships in rat spinal cord remyelination models after systemic administration. J. Pharmacol. Exp. Ther. 339 (2), 519–529.

Piddlesden, S.J., Lassmann, H., Zimprich, F., Morgan, B.P., Linington, C., 1993. The demyelinating potential of antibodies to myelin oligodendrocyte glycoprotein is related to their ability to fix complement. Am. J. Pathol. 143 (2), 555–564.

Pohl, H.B., Porcheri, C., Mueggler, T., et al., 2011. Genetically induced adult oligodendrocyte cell death is associated with poor myelin clearance, reduced remyelination, and axonal damage. J. Neurosci. 31 (3), 1069–1080.

Pop, C., Timmer, J., Sperandio, S., Salvesen, G.S., 2006. The apoptosome activates caspase-9 by dimerization. Mol. Cell 22 (2), 269–275.

Poser, C.M., Paty, D.W., Scheinberg, L., et al., 1983. New diagnostic criteria for multiple sclerosis: guidelines for research protocols. Ann. Neurol. 13 (3), 227–231.

Pott, F., Gingele, S., Clarner, T., et al., 2009. Cuprizone effect on myelination, astrogliosis and microglia attraction in the mouse basal ganglia. Brain Res. 1305, 137–149.

Pringle, N.P., Richardson, W.D., 1993. A singularity of PDGF alpha-receptor expression in the dorsoventral axis of the neural tube may define the origin of the oligodendrocyte lineage. Development 117 (2), 525–533.

Raff, M.C., Mirsky, R., Fields, K.L., et al., 1978. Galactocerebroside is a specific cell-surface antigenic marker for oligodendrocytes in culture. Nature 274 (5673), 813–816.

Raine, C.S., 1977. Morphological aspects of myelin and myelination. In: Morell, P. (Ed.), Myelin. Plenum Press, New York and London, pp. 1–49.

Rakic, P., 1971. Neuron-glia relationship during granule cell migration in developing cerebellar cortex. A Golgi and electronmicroscopic study in Macacus Rhesus. J. Comp. Neurol. 141 (3), 283–312.

Rakic, P., 1972. Mode of cell migration to the superficial layers of fetal monkey neocortex. J. Compar. Neurol. 145, 61–84.

Reynolds, R., Wilkin, G.P., 1993. Cellular reaction to an acute demyelinating/remyelinating lesion of the rat brain stem: localisation of GD3 ganglioside immunoreactivity. J. Neurosci. Res. 36 (4), 405–422.

Rice, G.P., Hartung, H.P., Calabresi, P.A., 2005. Anti-alpha4 integrin therapy for multiple sclerosis: mechanisms and rationale. Neurology 64 (8), 1336–1342.

Rivers, T.M., Sprunt, D.H., Berry, G.P., 1933. Observations on attempts to produce acute disseminated encephalomyelitis in monkeys. J. Exp. Med. 58 (1), 39–53.

Rose, J.W., Foley, J., Carlson, N., 2008. Monoclonal antibody treatments for multiple sclerosis. Curr. Neurol. Neurosci. Rep. 8 (5), 419–426.

Rosenbluth, J., Nave, K.A., Mierzwa, A., Schiff, R., 2006. Subtle myelin defects in PLP-null mice. Glia 54 (3), 172–182.

Rossi, C.P., Delcroix, M., Huitinga, I., et al., 1997. Role of macrophages during Theiler's virus infection. J. Virol. 71 (4), 3336–3340.

Rowitch, D., 2004. Glial specification in the vertebrate neural tube. Nat. Rev. Neurosci. 5, 409–419.

Silver, J., Miller, J.H., 2004. Regeneration beyond the glial scar. Nat. Rev. Neurosci. 5 (2), 1393–1397.

Silvestroff, L., Bartucci, S., Pasquini, J., Franco, P., 2012. Cuprizone-induced demyelination in the rat cerebral cortex and thyroid hormone effects on cortical remyelination. Experiment. Neurol. 235 (1), 357–367.

Sim, F.J., Zhao, C., Penderis, J., Franklin, R.J., 2002. The age-related decrease in CNS remyelination efficiency is attributable to an impairment of both oligodendrocyte progenitor recruitment and differentiation. J. Neurosci. 22 (7), 2451–2459.

Skripuletz, T., Bussmann, J.H., Gudi, V., et al., 2010. Cerebellar cortical demyelination in the murine cuprizone model. Brain Pathol. 20 (2), 301–312.

Smith, G.M., Miller, R.H., Silver, J., 1986. Changing role of forebrain astrocytes during development, regenerative failure, and induced regeneration upon transplantation. J. Comp. Neurol. 251 (1), 23–43.

Sofroniew, M.V., 2005. Reactive astrocytes in neural repair and protection. Neuroscientist 11 (5), 400–407.

Soulika, A.M., Lee, E., McCauley, E., Miers, L., Bannerman, P., Pleasure, D., 2009. Initiation and progression of axonopathy in experimental autoimmune encephalomyelitis. J. Neurosci. 29 (47), 14965–14979.

Srinivasula, S.M., Ahmad, M., Fernandes-Alnemri, T., Alnemri, E.S., 1998. Autoactivation of procaspase-9 by Apaf-1-mediated oligomerization. Mol. Cell 1 (7), 949–957.

Steller, H., 1995. Mechanisms and genes of cellular suicide. Science 267 (5203), 1445–1449.

Stidworthy, M.F., Genoud, S., Suter, U., Mantei, N., Franklin, R.J., 2003. Quantifying the early stages of remyelination following cuprizone-induced demyelination. Brain Pathol. 13 (3), 329–339.

Straathof, K.C., Pule, M.A., Yotnda, P., et al., 2005. An inducible caspase 9 safety switch for T-cell therapy. Blood 105 (11), 4247–4254.

Stuart, G.K.K., 1928. The neuro-paralytic accidents of anti-rabies treatment. Ann. Trop. Med. 22, 327–377.

Tansey, F.A., Zhang, H., Cammer, W., 1996. Expression of carbonic anhydrase II mRNA and protein in oligodendrocytes during toxic demyelination in the young adult mouse. Neurochem. Res. 21 (4), 411–416.

Teixeira, S.A.V.A., Bolonheis, S.M., Muscara, M.N., 2005. EAE: A heterogenous group of animal models to study human multiple sclerosis. Drug Discov. Today Disease Models 2 (2), 127–134.

Thompson, C.B., 1995. Apoptosis in the pathogenesis and treatment of disease. Science 267 (5203), 1456–1462.

Torkildsen, O., Brunborg, L.A., Myhr, K.M., Bo, L., 2008. The cuprizone model for demyelination. Acta Neurol. Scand. Suppl. 188, 72–76.

Traka, M., Arasi, K., Avila, R.L., et al., 2010. A genetic mouse model of adult-onset, pervasive central nervous system demyelination with robust remyelination. Brain 133 (10), 3017–3029.

Traka, M., Podojil, J.R., McCarthy, D.P., Miller, S.D., Popko, B., 2016. Oligodendrocyte death results in immune-mediated CNS demyelination. Nat. Neurosci. 19 (1), 65–74.

Trapp, B.D., Peterson, J., Ransohoff, R.M., Rudick, R., Mork, S., Bo, L., 1998. Axonal transection in the lesions of multiple sclerosis. N. Eng. J. Med. 338, 278–285.

Tselis, A., 2011. Evidence for viral etiology of multiple sclerosis. Semin. Neurol. 31 (3), 307–316.

Tsunoda, I., Iwasaki, Y., Terunuma, H., Sako, K., Ohara, Y., 1996. A comparative study of acute and chronic diseases induced by two subgroups of Theiler's murine encephalomyelitis virus. Acta Neuropathol. 91 (6), 595–602.

van der Valk, P., Amor, S., 2009. Preactive lesions in multiple sclerosis. Curr. Opin. Neurol. 22 (3), 207–213.

van Horssen, J., Singh, S., van der Pol, S., et al., 2012. Clusters of activated microglia in normal-appearing white matter show signs of innate immune activation. J. Neuroinflam. 9, 156.

Wang, F.I., Stohlman, S.A., Fleming, J.O., 1990. Demyelination induced by murine hepatitis virus JHM strain (MHV-4) is immunologically mediated. J. Neuroimmunol. 30 (1), 31–41.

Waxman, S.G., 1982. Membranes, myelin, and the pathophysiology of multiple sclerosis. N. E. J. Med. 306 (25), 1529–1533.

Waxman, S.G., 1998. Demyelinating diseases—new pathological insights, new therapeutic targets. N. Eng. J. Med. 338 (5), 323–325.

Waxman, S.G., Kocsis, J.D., Nitta, K.C., 1979. Lysophosphatidyl cho-line-induced focal demyelination in the rabbit corpus callosum. Light-microscopic observations. J. Neurol. Sci. 44 (1), 45–53.

Weiner, H.L., 2009. The challenge of multiple sclerosis: how do we cure a chronic heterogeneous disease? Ann. Neurol. 65 (3), 239–248.

Woodruff, R.H., Franklin, R.J., 1999. Demyelination and remyelination of the caudal cerebellar peduncle of adult rats following stereotaxic injections of lysolecithin, ethidium bromide, and complement/anti-galactocerebroside: a comparative study. Glia 25 (3), 216–228.

Wu, G.F., Dandekar, A.A., Pewe, L., Perlman, S., 2000. CD4 and CD8 T cells have redundant but not identical roles in virus-induced demy-elination. J. Immunol. 165 (4), 2278–2286.

Yajima, K., Suzuki, K., 1979a. Demyelination and remyelination in the rat central nervous system following ethidium bromide injection. Lab Invest. 41 (5), 385–392.

Yajima, K., Suzuki, K., 1979b. Ultrastructural changes of oligodendrog-lia and myelin sheaths induced by ethidium bromide. Neuropathol. Appl. Neurobiol. 5 (1), 49–62.

Zawadzka, M., Rivers, L.E., Fancy, S.P., et al., 2010. CNS-resident glial progenitor/stem cells produce Schwann cells as well as oligoden-drocytes during repair of CNS demyelination. Cell Stem Cell 6 (6), 578–590.

Zhang, Y., Argaw, A.T., Gurfein, B.T., et al., 2009. Notch1 signaling plays a role in regulating precursor differentiation during CNS re-myelination. Proc. Natl. Acad. Sci. USA 106 (45), 19162–19167.

Zhang, Y.J., Zhang, W., Lin, C.G., et al., 2012. Neurotrophin-3 gene modified mesenchymal stem cells promote remyelination and func-tional recovery in the demyelinated spinal cord of rats. J. Neurol. Sci. 313 (1–2), 64–74.

PSYCHIATRIC AND NEUROLOGICAL DISEASE

Page left intentionally blank

38

Animal Models of Mood Disorders: Focus on Bipolar Disorder and Depression

Samira S. Valvassori*, Roger B. Varela*, João Quevedo*,**

*University of Southern Santa Catarina (UNESC), Criciúma, Santa Catarina, Brazil
**Center for Experimental Models in Psychiatry, The University of Texas Medical School at Houston, Houston, TX, United States

1 INTRODUCTION

Mood disorders are a severe mental health condition with a high incidence and comorbid medical problems. According to the Diagnostic and Statistical Manual of Mental Disorders Fifth Edition (DSM-5), the two major mood disorders are major depression (MD) and bipolar disorder (BD). Mood disorders are characterized by extreme and inappropriate mood alteration with significant social, cognitive, and functional impairment. MD is characterized by persistent sadness, fatigue, eating disturbances, sleep disturbances, suicidal thoughts, guilt, and social withdrawal. BD is characterized by episodes of mania and depression with euthymic or normal mood states between the episodes. Manic episodes can consist of hyperactivity, elevated mood or

agitation, racing thoughts, reckless behavior, little need for sleep, and, sometimes, psychosis. Several pharmacological compounds are validated as effective for mood disorders. The most common medications used to treat BD are lithium, anticonvulsants (valproate, carbamazepine, and lamotrigine), and atypical (e.g., clozapine, olanzapine, and risperidone) and typical (haloperidol and chlorpromazine) antipsychotics. MD is generally treated with antidepressants, including tricyclics (e.g., desipramine and imipramine), selective serotonin reuptake inhibitors (SSRIs; fluoxetine and paroxetine), and monoamine oxidase inhibitors (MAOIs; phenelzine and tranylcypromine).

Despite receiving adequate treatment, most patients continue to have recurrent mood episodes, residual symptoms, functional impairment, psychosocial

disability, and significant medical and psychiatric comorbidities. In addition, many patients do not adequately respond to the available medications and cannot tolerate the side effects of these drugs. Research for developing new drugs for mood disorders has focused on specific targets, which could offer more effective and safe treatments. However, a better understanding of the pathophysiologic mechanisms of these disorders is important for designing new drugs and implementing them in clinical practice. The advances in genetic, neurobiological, and pharmacological methodologies have helped in the development of animal models, and these models have been an important tool for investigating new intracellular systems that may be involved in the specific pathophysiology of psychiatric disorders.

However, it is important to emphasize that no animal model developed to date can fully mimic its "corresponding" human psychiatric disorder. Given that BD is a complex mood disorder with recurrent mood swings, including manic, depressive, and mixed episodes, the development of an adequate animal model for this disorder is a challenge. Ellenbroek and Cools (1990) have proposed that valid animal models in psychiatric disorders should demonstrate the following three major criteria: face validity, construct validity, and predictive validity. Face validity indicates how similarly the model can mimic the symptoms of a given illness. Construct validity is related to the ability of the model to reproduce some pathophysiological aspects of the illness. Finally, predictive validity evaluates whether the therapeutic agents used in treating this illness can reverse the symptoms in the animal model.

This chapter seeks to provide a comprehensive overview of traditional and recent animal models for mania and depression, recapitulating their different features, and the possible pathophysiology of mood disorders emulated by those models.

2 ANIMAL MODELS OF MAJOR DEPRESSION

2.1 Environmental Models of Major Depression

The relationship between environmental stress and the incidence of MD in humans is widely described in the scientific literature. Different stress stimuli at different life stages can affect neurodevelopment, decreasing stress resilience in the long run, which increases the odds of developing MD. These stressful situations include intrauterine adversities, child abuse, drugs, life pressure, material and emotional losses, and hardships of modern life.

Based on these clinical observations, the main animal models of depression involve exposing the animals to different stressor stimuli at specific developmental stages, mimicking the human triggers to developing MD. Chronic mild stress (CMS) and maternal deprivation are well-established environmental models of MD that meet the criteria for the aforementioned three validities. These models are able to induce depressive-like behavior, as well as monoaminergic and neuroendocrine alterations in adult animals, and these alterations can be reversed by treatment with classical antidepressants. Further, we will discuss these and other environmental models of MD.

2.1.1 Animal Model of Depression Induced by Maternal Deprivation

It is widely described in the literature that early life adversities, including childhood maltreatment and trauma, can lead to a depressive condition in adult life, and this relationship can occur via several pathways, such as monoaminergic alterations, immune-inflammatory system changes, and neuroplasticity impairment. Among these childhood adversities, we can cite physical violence, sexual abuse, neglect, and loss of the primary caregiver.

Parental care is a strongly established behavior in rodents that is essential for the healthy development of offspring. The animal model of depression induced by maternal deprivation is based on this behavior and induces depressive-like behavior in adult animals after an early life stressor stimulus, mimetizing the incidence of MD following this trigger. In fact, this animal model is very effective and fulfills all three validities, and it has been one of the most frequently described models for MD.

Several studies have consistently demonstrated that adult animals exposed to maternal deprivation in early life show a wide range of depressive-like behaviors, such as increasing immobile time on the tail suspension and a forced swimming test, more dramatically decreased sweet food consumption and anxious-like behaviors. In addition to face validity, maternal deprivation can reproduce several biochemical alterations that are implicated in the pathophysiology of depression, such as impairment in mitochondrial metabolism via the tricarboxylic acid cycle and mitochondrial chain complex activity; increased oxidative stress; decreased dopaminergic, serotoninergic, and GABAergic systems; immune system dysregulation and decreased neurotrophic factor levels. The face validity of this model is well established. Several studies have demonstrated that treatment with a classical antidepressant, imipramine, as well as ketamine and tianeptine can reverse these behavioral and biochemical alterations induced by maternal deprivation, supporting its predictive validity.

This animal model was first described by Levine (1967) in which the animals were maternally deprived for a period of 24 h. This protocol has undergone some adaptations in the deprivation period, which is more commonly 3–4 h of separation per day between the 1st and 20th postnatal day (the duration of the protocol ranges from the authors). This separation consists of removing the mother from the cage for 3–4 h, leaving the progeny alone with only wood shavings and the mother's smell. After the deprivation period, which may vary, the animals go through normal care and are weaned at a regular age. At the adult stage, these animals present with depressive-like behavior. This model can also be used to study the neurobiology of depression and the effects of classical or new candidate therapeutic agents. For this, the animals must undergo a treatment protocol—which can be acute, repeated, or chronic administrations—when the animals reach adulthood, which is at approximately 60 days of age. After the end of the treatment protocol, the depressive-like behavior can be measured with the behavior tests that are described at the end of this section.

The main limitation of the animal model for depression induced by maternal deprivation is its methodological complexity. The entire process must to be carefully monitored because the matrices copulate until the end of the deprivation protocol. Because one litter, in most cases, does not generate sufficient offspring for a complete study, a schedule must be arranged to work with different litters with different dates in the same project.

2.1.2 Animal Model of Depression Induced by Chronic Mild Stress

The modern life style involves several stress events, such as long working journeys, excess responsibilities, noise and visual pollution, violence, insecurity, and others. There is a clinical relationship between stress and the development of MD; patients suffering intense acute stressful situations or chronic stress have a greater vulnerability to developing this disorder. Recently, several studies have demonstrated that stress can interact with DNA expression by a mechanism called epigenetics. These social stress-induced alterations are most evident in specific genes that are related to the neurobiology of MD, including glucocorticoid receptors, neurotrophic factors, and serotonin transporters, strengthening the role of stress in the etiology of depression.

The animal model of depression induced by CMS uses this premise to induce depressive-like behaviors in rodents. Long-term exposure to environmentally stressful situations can cause several behavioral alterations, such as increased immobility on the tail suspension and forced swimming tests, decreased body

licking on the splash test, and decreased consumption of sweet food, supporting the face validity of this model. Classic depressive neurobiological alterations are also observed in rats that are treated with this protocol; these include increasing oxidative stress, mitochondrial alterations, increasing corticosterone levels, decreasing neurotrophins levels, and immune-system alterations. All behavioral and biochemical changes induced by CMS respond positively to treatment with antidepressants, such as imipramine, tianeptine, and ketamine. This finding shows that exposure to stressful situations during adulthood can induce depressive-like behavior and pathophysiological alterations in rodents that are similar to the effects of maternal deprivation. Treatment with classical antidepressants can reverse these alterations, demonstrating the three validities for this model.

Katz (1981) was the first author to describe a protocol based on chronic stress stimuli in rodents that induce anhedonic-like behavior in rats. However, this protocol consisted of a very invasive stimulus, such as cold water swimming and electric shocks, to induce increased corticosterone levels and reduce sucrose consumption. This protocol was adapted to a minor invasive version by Willner et al. (1987) using different and more realistic stimuli that induce depressive-like behavior, and it has been used up through the present. In this protocol, the adult animals are exposed to different stressful situations daily over 40 days. These situations include food deprivation, water deprivation, space containment, space containment at 4°C, exposure to strobe light, social isolation, cage tilting (30 degrees), and damp bedding. The situations are randomly applied during the 40 days and at different periods to avoid predictability. Each stressor has a specific duration, as shown in the table below.

Stressor type	Duration
Food deprivation	24 h
Water deprivation	24 h
Space containment	1–3 h
Space containment at 4°C	1.5–2 h
Strobe light	120–210 min
Social isolation	3 days
Cage tilting	4 h
Damp bedding	4 h

Twenty-four hours after the final stressor, the depressive-like behavior can be measured by the behavioral tests described in this section. As well as the animal model induced by maternal deprivation, this model can be a tool for studying the neurobiological mechanisms of MD and can offer an important approach for investigating novel and classic therapeutic agent targets. For this, acute, repeated, or chronic treatment with

antidepressants or candidate drugs may be started after the last day of the chronic stress protocol.

2.2 Surgical Model of Depression

Surgical animal models are based on anatomic alterations or deletions of specific brain structures, resulting in behavior and biochemical alterations that are similar to the clinical manifestations. The rat sense of smell is a highly evolved, important sense for a series of social behaviors. Pheromones, chemical signals, carry information about the animal's behavior and physiological status, and pheromone detection by other rats modulates several processes, such as reproduction, gender recognition, social dominance, and aggressive and avoidance behaviors. The brain structure responsible for recognizing these pheromones is the olfactory bulb.

Considering the importance of this brain region in the social behaviors of rodents, Jancsar and Leonard (1981) first reported that bilateral olfactory bulbectomy induced irritability in rats, and this behavior was reversed by amitriptyline treatment. Afterward, several other studies demonstrated that this procedure can induce anhedonic and other depressive-like behaviors, such as anorexic manifestations, decreased sexual activity, impairment of social interaction, and reduced sweet food consumption. In addition, the animal model of depression induced by bilateral olfactory bulbectomy caused spatial learning damage in rats. The olfactory bulb has connections with other brain structures that are responsible for mood modulation, such as the amygdala, nucleus accumbens, caudate putamen, and hypothalamus. Disruption of these connections triggers depressive-like biochemical alterations, decreased noradrenergic and serotoninergic activities, increased acetylcholine levels, decreased BDNF levels, and increased TNF-α and IL-1β levels in rat brains. Chronic treatment with clinically effective antidepressants agents—imipramine, sertraline, amitriptyline, fluoxetine, and others—after bilateral olfactory bulbectomy can reverse, partially or completely, these alterations, supporting their predictive validity.

The olfactory bulbectomy surgery was standardized by Kelly et al. (1997) and it consists of a midline frontal incision in the skin on the skull of an animal that was previously anaesthetized with ketamine and xylazine. After skull exposure, 2 burrs are drilled at points 7 mm anterior to the bregma and 2 mm lateral to the bregma. Both olfactory bulbs are aspirated, paying attention to avoid damaging the frontal cortex, and the dead space is filled with a hemostatic sponge to prevent blood loss. The skin above the lesion is closed with suture material and the antibacterial agent is applied. After the surgical procedure, the animals must recover for 14 days; then, depressive-like behavior can be measured or antidepressant treatment can be initiated.

2.3 Genetic Models of Depression

MD has a multifactorial etiology, and genetic and environmental factors interact with each other to determine the pathophysiology and pathogenesis of this disorder. The growing body of genetic study data provides substantial knowledge of specific genes that are related to MD, and these can help with the development of potential animal models for studying this condition. The genetic model of depression consists of inducing rodent DNA alterations in genes that correspond to the human genes in MD.

This class of models is relatively recent, but it has helped provide significant, powerful information on the neurobiology and therapeutic approaches for MD. In this section, we will discuss the main candidate genes for developing animal models of depression.

2.3.1 Tph2 Gene

Monoaminergic dysfunction is one of the first and most described theories of depression pathophysiology. The role of serotoninergic signalization impairment in this disorder is widely evaluated in the clinical literature, and its modulation is a target of several antidepressant agents. Based on the serotoninergic hypothesis, a genetic modified mouse strain was created, showing reduced expression of tryptophan hydroxylase 2 (Tph2), an enzyme that participates in serotonin synthesis. This genetic modification triggers to a decrease in the brain serotonin levels, which is similar to the alterations observed in humans. In addition, animals with this genetic alteration had increased immobility time in the forced swimming test, reinforcing its face validity (Beaulieu et al., 2008). This animal model has great potential to mimic all aspects of depression; however, the data in the literature are scarce, making it necessary to perform more studies with face, construct, and predictive validity.

2.3.2 CB1 Gene

Endocannabinoids play an important role in mood regulation, and several preclinical and clinical studies have demonstrated that alterations in the cannabinoid system can be involved in the pathophysiology of several mental diseases, such as schizophrenia, anxiety, BD, and MD. This role is so evident that endocannabinoid modulation is a new target for pharmacological approaches. Therefore, genetic alteration of cannabinoid receptor 1 (CB1) expression has been proposed for use in an animal model of depression. In fact, CB1 knockout mice demonstrate anxious and depressive-like behavior beyond increased corticosterone in the serum and decreased BDNF levels in the hippocampus. Other notable alterations include

altered serotoninergic alteration, suggesting there is a relationship between these two systems.

2.3.3 BDNF and TrkB Genes

Beyond the neurotransmitter systems, a growing body of evidence has indicated a strong relationship between neurotrophins and mood disorders, especially BDNF. Several animal models of depression can induce a reduction in the brain BDNF levels. In humans, a polymorphism of the BDNF gene denoted Val66met and epigenetic alterations on this DNA region seem to be related to MD. In addition, BDNF upregulation is one of the mechanisms of action for several antidepressant drugs, highlighting the involvement of this protein in depression neurobiology. Because of this role, genetic modifications in BDNF expression in rats have been considered in an animal model of depression.

However, beyond mood modulation, BDNF plays a pivotal role in neurodevelopment, and knockout mice have serious neural damage and perinatal lethality. Conversely, Chan et al. (2006) produced a heterozygote conditional knockout mouse, which only presents with adulthood reductions in BDNF levels. These animals showed depressive-like behavior on the tail-suspension test with an antidepressant phenotype in the forced swimming test. In another study, Saarelainen et al. (2003) showed that a strain of mice expressing nonfunctional versions of TrkB, the main BDNF receptor, was resistant to the effect of antidepressants, indicating the importance of this receptor for depressive-like behavior and the response to treatment.

These results suggest that genes related to BDNF pathway signaling are important for the development of genetic animal models of depression; however, as a protein with different functions in the nervous system, its modulation needs to be enhanced.

2.4 How Can Depressive-Like Behavior be Evaluated in Laboratory Animals?

Mood disorders have a highly complex clinical manifestation. By not having a specific biomarker, these disorders are exclusively diagnosed by behavioral symptoms. MD has a wide range of symptoms because changes in the physiological alteration, such as anorexic behavior, lead to decreased self-esteem.

Mimic symptoms are part of the triad to animal model validations; however, a depressive episode in humans involves such a complex core of behaviors that cannot be evaluated in rodents, including decreased self-esteem, suicidal thinking, low mood, and feelings of guilt. Nevertheless, a selective class of behavioral manifestations can be measured in animals, reflecting human symptoms. One such set of behaviors is called anhedonia, which consists of a loss of interest in pleasurable activities. Other classes of behavior that can be observed in animals include hopelessness, which is a classical manifestation in depressive humans.

As the animals do not present with all behavior criteria for a depressive state, it is not possible to claim that the animal is depressed; as a result, the animal models of depression intend to induce some depressive-like behavior in these animals. There are some tests to evaluate these depressive-like behaviors in rodents, and the primary tests will be described later in the chapter.

2.4.1 Forced Swimming Test

This behavior test aims to evaluate a hopelessness state in rodents by forcing the animal to swim in a water cylinder without a method of escape. After an initial period of motor agitation, the animals naturally tend to adopt a motionless posture, performing movements only to keep their heads out of water, indicating the animal had learned that escape is impossible. This behavior can be anthropomorphically interpreted as if the animals had lost hope in this stressful situation.

In fact, animals submitted to models of depression adopt this immobile posture earlier and longer than control groups. Another interesting fact is that classical antidepressant drug administration per se can reduce the immobile time in healthy control animals, and this test is an important tool for investigating antidepressant effects of new drugs without subjecting the animals to depressive behavior induction protocols.

The forced swimming test is one of the most commonly used approaches for evaluating depressive behavior in animals, and it was first described by Porsolt et al. (1977). It consists of a very simple test without a very sophisticated apparatus and has two versions, one for rats and another for mice. In this section, we will present both protocols.

For rats, the test is divided into two sessions, denoted the training and test sessions, which are separated by 24 h. In the training session, the rat is forced to swim for 15 min in a narrow cylinder that is full of water at $25 \pm 2°C$ and sufficiently deep that the rat cannot touch the bottom and keep its head above water at the same time. No behavior is evaluated in this session, which is only aimed to habituate the animal to the apparatus so that it can learn that there is no way to escape. At the test session, the animal is forced to swim in the same apparatus for 5 min, and the following behavior parameters can be measured (Fig. 38.1):

Swimming: Time that the animal moves around in the water. This behavior tends to reduce over time until the end of the test.

Climbing: Time that the animal tries to climb to the cylinder wall to escape the water. This behavior is decreased in animals that are submitted to models of depression. The walls must be high enough to prevent animal escape.
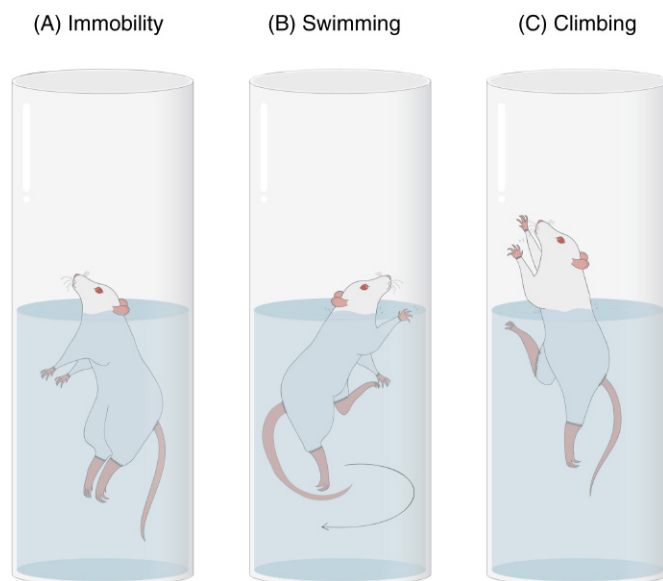
FIGURE 38.1 **Forced swimming test.** Representation of (A) immobility, (B) swimming, and (C) climbing parameters.

Immobility: Time the animal spends with no movements, or moves to keep its head out of water while not intending to move around the apparatus.

It is important to note that the training and test sessions must be as similar as possible, with the same applicator and location in the room, and the apparatus must be identical in the two sessions.

The forced swimming test for mice is even simpler than for rats. The apparatus is the same, which is proportional to the different sizes of the two species; the only difference is that mice do not need two separate sessions for the training and test. Mice demonstrate a significant, stable level of immobility after a single exposure session; then, this test lasts for 6 min. The first 2 min are used for the training time and the last 4 min are spent on immobility, climbing, and swimming evaluations.

2.4.2 Tail Suspension

Tail suspension is an alternative method that was designed by Steru et al. (1985) to be a "dry forced swimming test." This test is also based on hopelessness behavior; however, the immobility is induced by suspending the animal upside down by the tail. As in the forced swimming test in mice, this test has a single 6-min session and, in the first minutes, mice will try to escape from this stressful situation by performing vigorous movements (Fig. 38.2). Afterward, they become immobile. Antidepressant drugs also act on this behavior, decreasing the immobility time.

This test has several advantages compared to the forced swimming test for both the applicator and animal. Tail suspension is a more comfortable position than forced swimming for the animal; in addition, this test does not present the risk of hypothermia at completion.

This test can be performed in a simple box and the animal can be suspended while tied to a hook or taped to the ceiling of the apparatus, not requiring a very large space or handling of substantial equipment.

2.4.3 Sweet Food Consumption

This behavioral test evaluates anhedonic behavior in rats, which is based on the intake of palatable sweet food after repeated training sessions. This protocol, which was originally described by Gamaro et al. (2003) and adapted by some other authors (such as, Lucca et al., 2009), is performed in an open-field apparatus with a sweet cereal pellet in each quadrant of the open-field floor. The animals are submitted to five training sessions during which the animals are placed, once daily for 3 min, in an open-field arena with sweet cereals for the animal to habituate to the food and apparatus. After the training sessions, the animals are submitted to two test sessions of 3 min each, once daily, wherein the number of ingested pellets is counted. Some studies standardize the protocol so that when the animal eats part of the pellet (1/4, 1/3, or 1/2), the fraction is also considered (Fig. 38.3).

It is important to note that animals must be deprived of food for 22 h before all five training sessions and the first test sessions. This deprivation aims to stimulate the animals to consume the sweet pellets, and they are easily habituated to this food. For the last test session, the animals must have ad libitum access to food in the prior 24 h; as a result, the consumption will not be as a food necessity but a search for a pleasurable activity.

The ability of this test to detect depressive-like behavior is well established in the literature, and it is a powerful tool to validate animal models for testing the antidepressant effects of specific drugs. However, by including an extensive protocol and involving a period of stressful situations, such as food deprivation, which can interfere with some protocols, this test is not widely used.

2.4.4 Splash Test

The splash test protocol discussed in this section was described by Ducottet and Belzung (2004) and simultaneously evaluated depressive-like behavior based on two different motivations, anhedonia as sucrose consumption and self-care. This simple test does not require a special apparatus and can be performed in the murine home cage. The splash test consists of spraying a 10% sucrose solution twice on the back of the animal. Because of the solution viscosity, the sucrose dirties the murine fur, inducing a body-licking behavior, called grooming. The sucrose solution acts as a releaser and palatability, permitting persistent grooming. The frequency and total time of grooming within 5 min after sucrose solution application are recorded. Several preclinical studies have demonstrated the sensitivity of the splash test for evaluating depressive-like behavior in different animal

FIGURE 38.2   **Tail suspension test.** Representation of (A) immobility and (B) mobility parameters.
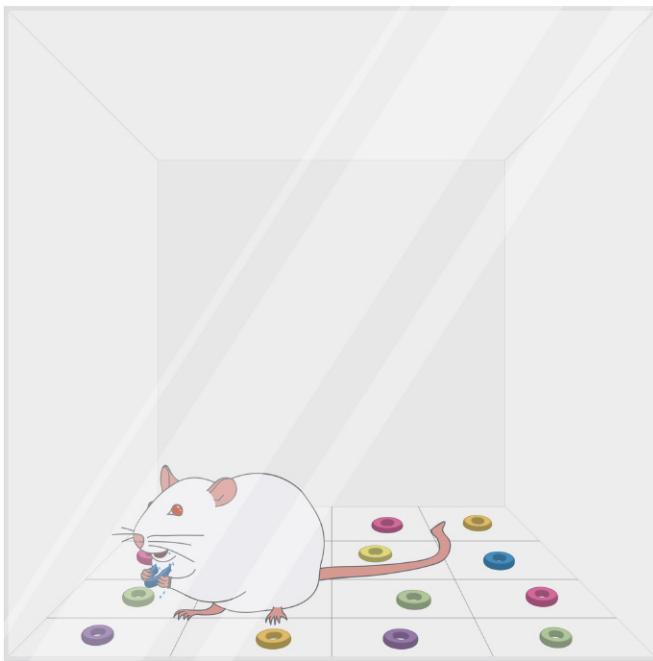
FIGURE 38.3   **Sweet food consumption test.** Representation of apparatus with sweet cereal.

models of depression, as well as the effect of antidepressant treatment in these models. However, this test should be evaluated with other, well-described models, including the forced swimming or tail suspension test.

3 ANIMAL MODELS OF MANIA

As described previously, BD presents a complex, alternating clinical course, with recurrent mood swings including manic and depressive episodes, making the development of an adequate animal model a challenge.

At this time, there is no animal model mimicking both manic and depressive episodes in the same animal. However, the clinical hallmark in diagnosing BD is the presence of manic symptoms, thus an adequate animal model of BD should resemble some features of a manic episode, such as euphoria, irritability, aggressiveness, hyperactivity, insomnia, hypersexuality (an increase in mounting behavior), risk-taking behavior, and/or increased stereotypy (sniffing and grooming) (face validity). Some pharmacological and environmental rodent models of bipolar mania are described later in the chapter.

3.1 Animal Model of Mania Induced by Amphetamine

A number of animal models of mania have used hyperlocomotion induced by psychostimulants. In fact, the most useful model to study BD is the animal model of mania induced by amphetamine (AMPH). Intraperitoneal injection of AMPH in rats induces manic-like behaviors, including hyperactivity, risk-taking behavior, aggressive behavior, and hypersexuality (face validity). Therefore, the manic-like behavior induced by repeated AMPH administration (14 days) in rats is considered a good animal model of mania (Frey et al., 2006). In medical clinic, to be characterized as a manic episode, the subject must demonstrate at least 1 week or more of manic symptoms. In addition, repeated intermittent exposure to stimulants, such as AMPH progressively increases the drug's effect—this phenomenon is called sensitization. Several studies have strongly indicated the presence of behavioral sensitization in patients with BD as an explanation for the progressive behavioral dysfunction observed in this mood disorder.

AMPHs are central nervous system stimulants and act by increasing dopamine (DA) efflux, inhibit the

uptake of DA and inhibit monoamine oxidase. These sympathomimetic substances are chemically related to betaphenylethylamines (the core structure for catecolamines), such as dextroamphetamine (d-AMPH) and methamphetamine (m-AMPH). It is interesting that dopaminergic drugs, such as AMPH, are able to induce manic symptoms in both normal human volunteers and BD subjects (Strakowski and Sax, 1998). It was demonstrated that emergence of manic symptoms is associated with higher urinary DA levels (Joyce et al., 1995). In addition, studies have demonstrated DA receptor changes in BD patients (Pantazopoulos et al., 2004; Vogel et al., 2004; Zhao et al., 2015). Therefore, the construct validity of the animal model of AMPH-induced mania is based on the fact that this drug alters the dopaminergic system, mimicking the pathophysiology of BD.

Mood stabilizing drugs, particularly lithium and valproate, are considered first line agents for both acute mania and maintenance treatment. Therefore, considering the construct validity of the model, lithium and valproate are able to reverse the manic-like behaviors induced by AMPH in rats, such as hyperactivity and risk-taking behavior. Several studies have suggested that the neuroprotective effects of lithium and valproate may be responsible for their therapeutic effects. Indeed, some studies have demonstrated that lithium and valproate are able to protect the brain of rats against AMPH-induced oxidative stress and mitochondrial alterations (Valvassori et al., 2010), which are also observed in brain and blood of BD patients (Andreazza and Young, 2014; Gama et al., 2013). Several biochemical targets of lithium and valproate have been identified, such as the neurotrophin signaling pathway, glycogen synthase kinase-3 (GSK-3), and protein kinase C (PKC). It is interesting that alterations in these molecules elicited by AMPH in rats can be reverted by lithium and tamoxifen (Cechinel-Recco et al., 2012). The animal model of mania induced by AMPH has been important in investigating new intracellular systems that may be involved in BD, while also being a good tool for testing new drugs.

3.2 Animal Model of Mania Induced by Ouabain

The animal model of mania induced by intracerebroventricular (ICV) administration of ouabain was described firstly by Li et al. (1997). However, in the last years, other groups have better characterized the model. The ICV injection of ouabain acutely induces hyperactivity in rats (face validity), which is normalized by the treatment with lithium, carbamazepine, and haloperidol (predictive validity). Interestingly, Ruktanonchai et al. (1998) observed a persistent hyperactivity response 9 days following a single ICV injection of ouabain in rats. In fact, bipolar illness is a recurrent and chronic condition, thus a model of mania which mimics some of these

aspects is a useful tool to investigate the underlying pathophysiological mechanism of BD.

Ouabain is a digitalis-like compound (DLC) that inhibits the sodium- and potassium-activated adenosine triphosphatase (Na + K + ATPase) activity. It is known that inhibition of the Na + K + -ATPase induces depolarization and subsequent neuronal excitation that leads to increased intracellular Ca^{2+} levels and neurotransmitter release, which are related to increases in locomotor activity in rats and manic episodes in bipolar patients. It is interesting that DLC-like compound levels in the parietal cortex from bipolar patients were significantly higher than in normal individuals and depressed patients (Goldstein et al., 2006). These endogenous DCL-like compounds in the brain regulate Na + K + -ATPase activity of the neuron. Additionally, the Na + K + -ATPase activity is reduced in manic and depressed bipolar patients (Looney and El-Mallakh, 1997), pointing the constructs validity of this animal of mania induced by ouabain.

Studies with this animal model have shown that the manic-like hyperactivity induced by ouabain is accompanied by severe brain damage due to an increased formation of lipid and protein oxidation products (Jornada et al., 2011) and a decrease of neurotrophins (Jornada et al., 2010) levels—also observed in BD patients. It was demonstrated that mood stabilizers, lithium and valproate, are able to reverse this brain damage. An increase in oxidative stress has been associated with decreases in the activity of the Na + K + -ATPase in bipolar patients. A recent study has demonstrated that BD patients have impaired Na + K + -ATPase activity and increased lipid peroxidation in serum. In addition, the authors demonstrated that Li induced improvement in the enzyme activity, which was associated with a significant reduction in lipid peroxidation (Banerjee et al., 2012). It is interesting that a recent study from Valvassori group showed that BDNF ICV administration was unable to reverse the ouabain-induced hyperactivity and risk-taking behavior. Nevertheless, BDNF treatment increased BDNF levels, modulated the antioxidant enzymes, and protected the ouabain-induced oxidative damage in the brain of rats. These results suggest that BDNF alteration observed in BD patients may be associated with oxidative damage, both seen in this disorder. Together, these studies suggest that the present model fulfills adequate face, construct, and predictive validity as an animal model of mania; therefore, an important tool to investigating new intracellular systems that may be involved in BD.

3.3 Animal Model of Mania Induced by Sleep Deprivation

The paradoxal sleep deprivation (PSD) protocol is performed in a cage (38 × 31 × 17 cm). The mice are placed 5 per cage, each cage containing 12 platforms (3.5 cm

diameter). In the same box is placed a volume of water 1 in. deep, obligating the animals to stay on platforms. It is important that mice can freely move from one platform to another (Armani et al., 2012; Tufik et al., 2009). Thus, when animals entered the paradoxical phase of sleep, due to muscle atonia, they were awoken by falling into the water. Food and water should be available ad libitum. The period of 36 h of PSD induces the manic-like behaviors in mice (Armani et al., 2012). The mice in the control group should be exposed to the same conditions, except there was no water in the bottom of the box.

PSD in mice has been considered a good animal model of mania because it induces some aspects of a manic episode, such as hyperactivity, hypersexuality, and aggressive behavior (face validity). Indeed, PSD can induce mania in healthy subjects and exacerbates manic attacks or leads to a switch from depression to mania in bipolar patients. Interestingly, PSD has been considered as a rapid-acting antidepressant strategy, improving severe depressive symptoms in major depressive patients. In addition, circadian rhythms and the genes that make up the molecular clock have long been implicated in BD.

Regarding predictive validity, rats treated with lithium and haloperidol demonstrated a decreased latency to fall asleep relative to vehicle-treated animals, which is interpreted as a reduction in manic-like insomnia induced by SD. In addition, the hyperactivity induced by SD is also reversed by lithium and haloperidol. Thus, differently of the pharmacological models of mania, SD induces a range of behavioral alteration beyond simple hyperactivity and this model is responsive to mood-stabilizing drugs treatment, making it perhaps more effective in mimicking the human bipolar mania.

Some studies have suggested that manic states and sleep deprivation could contribute to the pathophysiology of BD through protein kinase C (PKC) signaling abnormalities. Indeed, rodents submitted to the sleep deprivation showed an increase of phosphorylation of MARCKS, a marker for PKC activity in vivo, in the frontal cortex (Szabo et al., 2009). A clinical study demonstrated an increase of PKC activity in platelets from bipolar patients during a manic episode, while lithium and valproate treatments attenuated the activity of this enzyme (Hahn et al., 2005). It is well described in the literature that lithium and valproate directly inhibited PKC, while promanic psychostimulants activate this enzyme, suggesting that PKC modulation plays a critical role in the treatment of mania. PKC plays an important role in regulating neuronal excitability, neurotransmitter release, gene expression, and plasticity, which are systems that modulate mood. Indeed, PKC overactivity has been associated with hyperactivity, risk-taking behavior, and excessive hedonic drive, all of which are symptoms of mania. Together, these studies indicate that animal model of mania induced by SD may have construct validity in the neurobiological alterations that may induce manic-like behaviors.

3.4 How Can Manic-Like Behaviors be Evaluated in Laboratory Animals?

3.4.1 Open-Field Test

The open-field test is used to provide a qualitative and quantitative measurement of exploratory and locomotor activity in rodents. The apparatus consists of an arena surrounded by high walls, to prevent escape, and the floor of the open field is divided into squares. In the test session, the number of square crossings, rearing, and time spent moving are used to assess the activity of the rodent. Automatic open-field apparatuses, which have software-linked infrared beams or video cameras to make the process easier and more accurate, are currently available. Manic-like behaviors, such as hyperactivity, risk-taking behavior, and/or increased stereotypy is easily measured in rats or mice using the open-field test (Fig. 38.4).

Hyperactivity is evaluated in the open-field apparatus through crossings and rearings behaviors. Crossings refer to the total number of square crossings during the test period, used to provide measurement of locomotor activity of the animals. Rearings are the total number of erect postures, adopted by the rodent with the intention of exploring, during the test period. Risk-taking behavior is evaluated through the measurement of total number of visits to the center of open-field. Increased exploration in the center of the open-field by the rodents is
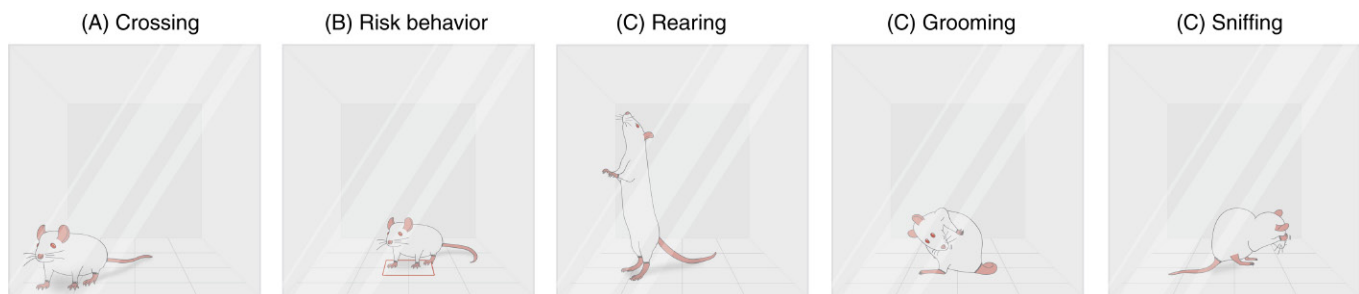
FIGURE 38.4 **Open-field test.** Representation of (A) crossing, (B) risk behavior, (C) rearing, (D) grooming, and (E) sniffing parameters.

interpreted as a tendency for novelty-seeking and risk-taking behavior. Increased novelty seeking/risk taking has been associated with predisposition to rewarding and addictive behaviors

Stereotypy refers to repetitive behaviors in animals, which occur mainly in animals with brain alterations. It can be evaluated by grooming and sniffing behaviors. Grooming refers to the measurement of the total time of grooming behavior during the test period and sniffing is the total time of sniffing behavior during the test period. The stereotypy is a behavioral pattern in which various motor activities are characterized by their repetitiveness and intensity, generally decreasing the locomotion. In other words, the overlap of the two behaviors may lead to false negative results. For example, low dose of AMPH induces increased number of crossings and rearing in rats, while higher doses of this drug induce stereotypy. Therefore, it would be important to assess hyperactivity and stereotypy in the animal models of mania.

3.4.2 Aggressive Behavior

In BD some symptoms, such as violent aggression, anger, and irritability contribute considerably to the diagnostic of this disorder. The aggressive behavior in rodents is evaluated by the resident-intruder test. In this paradigm, the rodents were placed individually in an observation cage for 30 min to habituation. The test is conducted by introducing a male intruder, weighing at least 10 g less than the resident, in this cage. During the test, the latency and duration of social interaction (nose–nose interactions) is measured, as well as the latency to attack, the number of attacks, and the duration of crawl over behavior. Each intruder male should be used only once and then returned to its cage, and the resident should make part of the experimental groups.

3.4.3 Sexual Behavior

It is well described in the literature that the sexual behavior increased in adults with BD during hypomanic or manic episodes. In laboratory rodents it can be evaluated because these animals belong to the internally fertilizing species that require sexual behavior for reproduction. The evaluation protocol of sexual behavior in rodents is given as follows:

Before sexual behavior test, the rats acquired sexual experience through training. The training is important because sexually inexperienced male rats can display low performance. In the test period, a male rat is introduced into the arena 5 min before a female rat. Sexual receptivity in the female rats is established by subcutaneous administration of estradiol benzoate and progesterone before testing sexual behavior. During test of sexual behavior, the following variables are recorded: time to first mount; intromission and ejaculation latencies; total numbers of mounts (i.e., mounts with pelvic thrusting); intromissions (mounts with pelvic thrusting and penile insertion); and ejaculations.

In rodents, sexual behavior can be evaluated indirectly by penile erection and ejaculation. Penile erection can be counted when the rat stood on its hind limbs, bent its body forward, bent its head down to reach the genital area, held and licked its penis in full erection, and displayed hip movements. The erect penis is always visible. In this paradigm ejaculation is scored by the number of ejaculatory plugs. The frequency of penile erection and ejaculation (total number of genital reflexes divided by the number of rats) and latency (time elapsed between the injection to the first genital reflex) is assessed for 60 min.

4 CONCLUSIONS

This chapter has described multiple animal models of MD and BD, and how these models can help our understanding about the pathophysiology of these psychiatric disorders. It is a fact that no animal model developed to date can fully mimic the "corresponding" human psychiatric disorder. However, the available animal models of BD and MD are able to reproduce a large number of symptoms which resemble the human disorder. Despite all limitations, animal models are an important tool for investigation of the neurobiological mechanisms underlying psychiatric disorders, and for preclinical screening of mood-stabilizing and antidepressant drugs.

References

Andreazza, A.C., Young, L.T., 2014. The neurobiology of bipolar disorder: identifying targets for specific agents and synergies for combination treatment. Int. J. Neuropsychopharmacol. 17 (7), 1039–1052.

Armani, F., Andersen, M.L., Andreatini, R., Frussa-Filho, R., Tufik, S., Galduróz, J.C., 2012. Successful combined therapy with tamoxifen and lithium in a paradoxical sleep deprivation-induced mania model. CNS Neurosci. Ther. 18 (2), 119–125.

Banerjee, U., Dasgupta, A., Rout, J.K., Singh, O.P., 2012. Effects of lithium therapy on Na + -K + -ATPase activity and lipid peroxidation in bipolar disorder. Prog. Neuropsychopharmacol. Biol. Psychiatry 37 (1), 56–61.

Beaulieu, J.M., Zhang, X., Rodriguiz, R.M., Sotnikova, T.D., Cools, M.J., Wetsel, W.C., Gainetdinov, R.R., Caron, M.G., 2008. Role of GSK3 beta in behavioral abnormalities induced by serotonin deficiency. Proc. Natl. Acad. Sci. USA 105 (4), 1333–1338.

Cechinel-Recco, K., Valvassori, S.S., Varela, R.B., Resende, W.R., Arent, C.O., Vitto, M.F., Luz, G., de Souza, C.T., Quevedo, J., 2012. Lithium and tamoxifen modulate cellular plasticity cascades in animal model of mania. J. Psychopharmacol. 26 (12), 1594–1604.

Chan, J.P., Unger, T.J., Byrnes, J., Rios, M., 2006. Examination of behavioral deficits triggered by targeting Bdnf in fetal or postnatal brains of mice. Neuroscience 142, 49–58.

Ducottet, C., Belzung, C., 2004. Behaviour in the elevated plus-maze predicts coping after subchronic mild stress in mice. Physiol. Behav. 81 (3), 417–426.

Ellenbroek, B.A., Cools, A.R., 1990. Animal models with construct validity for schizophrenia. Behav. Pharmacol. 1 (6), 469–490.

Frey, B.N., Andreazza, A.C., Cserér, K.M., Martins, M.R., Valvassori, S.S., Réus, G.Z., Quevedo, J., Kapczinski, F., 2006. Effects of mood stabilizers on hippocampus BDNF levels in an animal model of mania. Life Sci. 79 (3), 281–286.

Gama, C.S., Kunz, M., Magalhães, P.V., Kapczinski, F., 2013. Staging and neuroprogression in bipolar disorder: a systematic review of the literature. Rev. Bras Psiquiatr. 35 (1), 70–74.

Gamaro, G.D., Manoli, L.P., Torres, I.L., Silveira, R., Dalmaz, C., 2003. Effects of chronic variate stress on feeding behavior and on monoamine levels in different rat brain structures. Neurochem. Int. 42 (2), 107–114.

Goldstein, I., Levy, T., Galili, D., Ovadia, H., Yirmiya, R., Rosen, H., Lichtstein, D., 2006. Involvement of Na(+), K(+)-ATPase and endogenous digitalis-like compounds in depressive disorders. Biol. Psychiatry 60 (5), 491–499.

Hahn, C.G., Wang, H.Y., Koneru, R., Levinson, D.F., Friedman, E., 2005. Lithium and valproic acid treatments reduce PKC activation and receptor-G protein coupling in platelets of bipolar manic patients. J. Psychiatr. Res. 39 (4), 355–363.

Jancsar, S., Leonard, B.E., 1981. The effect of antidepressants on conditioned taste aversion learning in the olfactory bulbectomized rat. Neuropharmacology 20, 1314–1315.

Jornada, L.K., Moretti, M., Valvassori, S.S., Ferreira, C.L., Padilha, P.T., Arent, C.O., Fries, G.R., Kapczinski, F., Quevedo, J., 2010. Effects of mood stabilizers on hippocampus and amygdala BDNF levels in an animal model of mania induced by ouabain. J. Psychiatr. Res. 44 (8), 506–510.

Jornada, L.K., Valvassori, S.S., Steckert, A.V., Moretti, M., Mina, F., Ferreira, C.L., Arent, C.O., Dal-Pizzol, F., Quevedo, J., 2011. Lithium and valproate modulate antioxidant enzymes and prevent ouabain-induced oxidative damage in an animal model of mania. J. Psychiatr. Res. 45 (2), 162–168.

Joyce, P.R., Fergusson, D.M., Woollard, G., Abbott, R.M., Horwood, L.J., Upton, J., 1995. Urinary catecholamines and plasma hormones predict mood state in rapid cycling bipolar affective disorder. J. Affect. Disord. 33 (4), 233–243.

Katz, R.J., 1981. Animal models and human depressive disorders. Neurosci. Behav. Rev. 5, 231–246.

Kelly, J.P., Wrynn, A., Leonard, B.E., 1997. The olfactory bulbectomized rat as a model of depression: an update. Pharmacol. Ther. 74, 299–316.

Levine, S., 1967. Maternal and environmental influences on the adrenocortical response to stress in weanling rats. Science 156, 258–260.

Li, R., el-Mallakh, R.S., Harrison, L., Changaris, D.G., Levy, R.S., 1997. Lithium prevents ouabain-induced behavioral changes. Toward an animal model for manic depression. Mol. Chem. Neuropathol. 31 (1), 65–72.

Looney, S.W., El-Mallakh, R.S., 1997. Meta-analysis of erythrocyte Na, K-ATPase activity in bipolar illness. Depress. Anxiety 5, 53–65.

Lucca, G., Comim, C.M., Valvassori, S.S., Réus, G.Z., Vuolo, F., Petronilho, F., Dal-Pizzol, F., Gavioli, E.C., Quevedo, J., 2009. Effects of chronic mild stress on the oxidative parameters in the rat brain. Neurochem. Int. 54 (5–6), 358–362.

Pantazopoulos, H., Stone, D., Walsh, J., Benes, F.M., 2004. Differences in the cellular distribution of D1 receptor mRNA in the hippocampus of bipolars and schizophrenics. Synapse 54 (3), 147–155.

Porsolt, R.D., Pichon, M., Jalfre, M., 1977. Depression: a new animal model sensitive to antidepressant treatments. Nature 266, 730.

Ruktanonchai, D.J., El-Mallakh, R.S., Li, R., Levy, R.S., 1998. Persistent hyperactivity following a single intracerebroventricular dose of ouabain. Physiol. Behav. 63 (3), 403–406.

Saarelainen, T., Hendolin, P., Lucas, G., Koponen, E., Sairanen, M., MacDonald, E., Agerman, K., Haapasalo, A., Nawa, H., Aloyz, R., Ernfors, P., Castren, E., 2003. Activation of the TrkB neurotrophin receptor is induced by antidepressant drugs and is required for antidepressantinduced behavioral effects. J. Neurosci. 23, 349–357.

Strakowski, S.M., Sax, K.W., 1998. Progressive behavioral response to repeated d-amphetamine challenge: further evidence for sensitization in humans. Biol. Psychiatry 44 (11), 1171–1177.

Steru, L., Chermat, R., Thierry, B., Simon, P., 1985. The tail suspension test: a new method for screening antidepressants in mice. Psychopharmacology (Berl.) 85, 367–370.

Szabo, S.T., Machado-Vieira, R., Yuan, P., Wang, Y., Wei, Y., Falke, C., Cirelli, C., Tononi, G., Manji, H.K., Du, J., 2009. Glutamate receptors as targets of protein kinase C in the pathophysiology and treatment of animal models of mania. Neuropharmacology 56 (1), 47–55.

Tufik, S., Andersen, M.L., Bittencourt, L.R., Mello, M.T., 2009. Paradoxical sleep deprivation: neurochemical, hormonal and behavioral alterations. Evidence from 30 years of research. An Acad. Bras. Cienc. 81 (3), 521–538.

Valvassori, S.S., Rezin, G.T., Ferreira, C.L., Moretti, M., Gonçalves, C.L., Cardoso, M.R., Streck, E.L., Kapczinski, F., Quevedo, J., 2010. Effects of mood stabilizers on mitochondrial respiratory chain activity in brain of rats treated with d-amphetamine. J. Psychiatr. Res. 44 (14), 903–909.

Vogel, M., Pfeifer, S., Schaub, R.T., Grabe, H.J., Barnow, S., Freyberger, H.J., Cascorbi, I., 2004. Decreased levels of dopamine D3 receptor mRNA in schizophrenic and bipolar patients. Neuropsychobiology 50 (4), 305–310.

Willner, P., Towell, A., Sampson, D., Sophokleous, S., Muscat, R., 1987. Reduction of sucrose preference by chronic unpredictable mild stress, and its restoration by a tricyclic antidepressant. Psychopharmacology (Berl.) 93 (3), 358–364.

Zhao, L., Lin, Y., Lao, G., Wang, Y., Guan, L., Wei, J., Yang, Z., Ni, P., Li, X., Jiang, Z., Li, T., Hao, X., Lin, D., Cao, L., Ma, X., 2015. Association study of dopamine receptor genes polymorphism with cognitive functions in bipolar I disorder patients. J. Affect. Disord. 170, 85–90.

Further Reading

Riegel, R.E., Valvassori, S.S., Elias, G., Réus, G.Z., Steckert, A.V., de Souza, B., Petronilho, F., Gavioli, E.C., Dal-Pizzol, F., Quevedo, J., 2009. Animal model of mania induced by ouabain: evidence of oxidative stress in submitochondrial particles of the rat brain. Neurochem. Int. 55 (7), 491–495.

Page left intentionally blank

Pigs as Model Species to Investigate Effects of Early Life Events on Later Behavioral and Neurological Functions

Rebecca E. Nordquist, Ellen Meijer,
Franz J. van der Staay, Saskia S. Arndt

Utrecht University, Utrecht, The Netherlands

1 INTRODUCTION

Animal models are used to study causes of disease, search for and test potential treatments, and to study fundamental processes. They are often used to study human disease, but animal models can also be used in veterinary or animal sciences, in which an animal can serve as a model for another species, or indeed for its own species. The use of large animal models is discussed in depth in Chapter 3 of this volume.

The importance of early (or even prenatal) life on later functioning in an organism has long been recognized. In humans, early life experience is often seen as influencing predisposition to develop a vast array of physical and mental diseases (Roseboom et al., 2006), including diabetes (Beyerlein et al., 2016), cardiovascular diseases (Barker and Martyn, 1992; Elford et al., 1992), schizophrenia (Matheson et al., 2013), and cognitive deficits (Rooij et al., 2010). Clearly, human studies are based on correlations, not on studies in which early life is manipulated experimentally (which would be unethical). This is an area of research where animal models can play an important role in aiding understanding of underlying mechanisms of effects of conditions during early life, and potential treatment of diseases and disorders resulting from maladaptive early life experiences.

It is increasingly recognized that pigs bear strong resemblance to humans perinatally and during early life, with respect to brain development, physiology, diet, and gastrointestinal function (Gieling et al., 2011a,b,c). This is in strong contrast to rodents, which constitute the most common animal model species at present, but which are vastly different from young humans in terms of development around birth (Gieling et al., 2011c). This implies that young pigs could be useful as models for young humans, and indeed, there are piglet animal models in use for neonatal processes including traumatic injury, neonatal nutrition, and effects of low birth weight (Gieling et al., 2011c).

In farming, management practices in early life can affect the ability of an animal to adapt to its circumstances later in life, and thus its welfare state (Ohl and van der Staay, 2012). Pigs are kept on farms, in some cases for years, as is the case for breeding sows and boars. Fattening pigs are kept until slaughter weight, usually at around 8–12 months of age. This is well past puberty, and in that sense these animals are young adults. Examining effects of management practices during early life on pig development, can give us information about the welfare of these animals and potential compromises to their welfare. In this case, the experimental pig can serve as a model for its own species on farms.

A number of tests have been developed to study the behavior and neurological state of pigs. In this chapter, these tests will be discussed, particularly with respect to their suitability for testing young animals. The potential implications of testing for pig welfare, and particularly the practical aspects herein, are reflected upon in the final section of this chapter.

2 OPERANT TASKS FOR TESTING COGNITIVE FUNCTIONING

In operant tasks, a subject is required to provide a response to elicit a specific outcome. Operant tasks can be very simple, as widely used in feeding stations in group housed pigs; in this type of housing, pigs learn to stand in front of a feeder, which reads a chip in its ear and then provides the pig's daily ration of food. Complex tasks are also possible, which can measure various forms of memory, behavioral flexibility, or internal state of an animal. Several operant tasks which have been developed and used in pigs are described further in the chapter.

2.1 The Holeboard Task

Spatial learning and memory tasks can be highly useful and suitable for testing pigs at both young and older ages. In these types of tasks, animals must learn to search for rewards within either an alley, with fixed starting positions and a single correct route to find all rewards, or within a "free choice" maze (Crannell, 1942; Lachman and Brown, 1957; van der Staay and Bouger, 2005). In the latter, animals are allowed to explore arenas in which rewards can be found in various places. Animals are free to determine in which order they search for rewards, and whether to return to a previously visited location or not. The most efficient strategy is to only visit locations containing rewards, and to visit the rewarded locations only once. The fact that pigs are mobile essentially from birth facilitates the use of spatial learning tasks in piglets, though it is important that the animals have the maturity to be able to learn the task at the age tested. For the full Pig Holeboard, this appears (in our hands) to be from about 6 weeks of age (Antonides et al., 2015b and informal observations).

In spatial memory tasks, an animal must remember where it has already been in order to avoid unrewarded revisits. This list of locations already visited is temporarily held in working memory (Olton and Samuelson, 1976). The information held in working memory is relevant only within a specific trial, as it reflects where an animal has been and already either consumed the rewards, or realized that a location is not baited. Reference memory (Olton and Samuelson, 1976) holds trial-independent information about, for example, the locations where the food reward can be found. One advantage of free choice mazes is that working memory and reference memory can be assessed simultaneously within the same test.

In the pig holeboard test, modeled after the rodent holeboard task, a fixed number of locations within a larger field is baited, for instance 4 locations of a possible 16 (so 1 in 4). For rodents, this test apparatus usually consists of literally a board with holes, some of which contain bait, and some of which do not. For pigs, various constructions suited to the pigs' size and strength have been used, including buckets affixed to the floor (Arts et al., 2009; Bolhuis et al., 2013; Clouard et al., 2016; Haagensen et al., 2013). In our lab, we use a setup in which plastic dog dishes are affixed to a slatted floor, covered by plastic balls. These plastic balls can be nosed
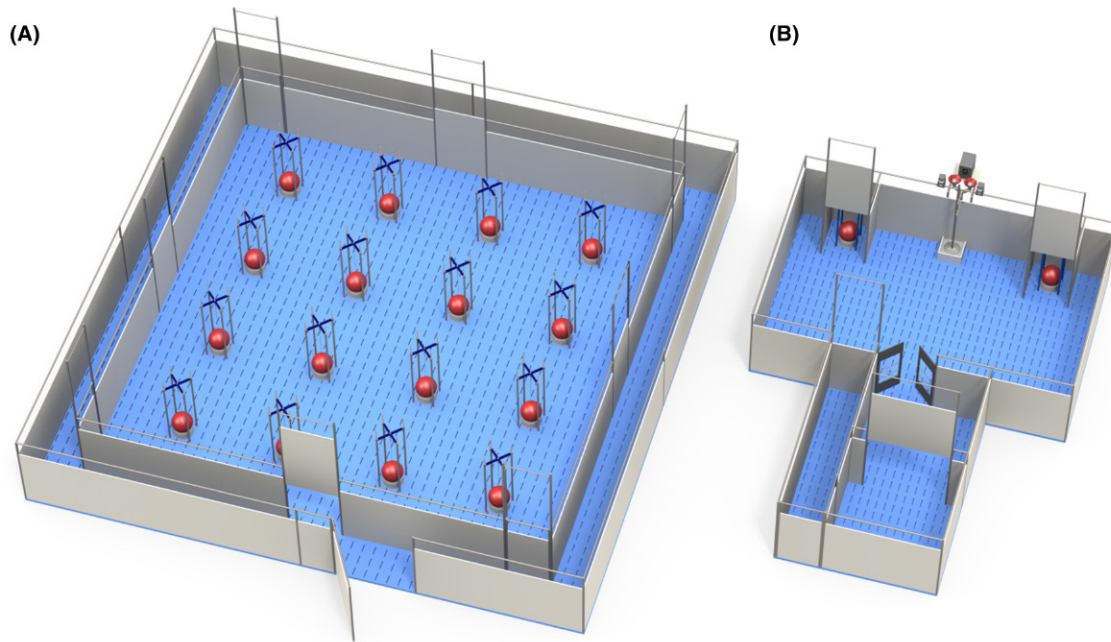
FIGURE 39.1   Holeboard apparatus to assess spatial discrimination learning in pigs (A), and an apparatus for assessing judgment bias and decision-making behavior in pigs (B). (A) In the holeboard task, rewards are hidden underneath hard plastic balls that the animal can raise using its snout. (B) In the gambling task and decision-making apparatus for pigs, the experimental animal enters the testing arena via an antechamber. Each goal-box contains a large hard-plastic ball which can be raised as operant response. Reward (usually M&M's) can be found in a central food trough. The accessibility of the bait in the trough is controlled by the experimenter operating a lid that covers the food trough. *Source: Modified from Antonides et al. (2015a), according to Open Access terms and used with permission from Murphy, E., Kraak, L., van den Broek, J, Nordquist, R.E., van der Staay, F.J., 2015. Decision-making under risk and ambiguity in low-birth-weight pigs. Anim. Cogn. 18(2), 561–572.*

aside to uncover the dishes, which may contain rewards. In our setup, scoring is automated using magnets and sensors installed in the balls and food dishes (Figs. 39.1 and 39.2), which are connected to a computer via an interface. We had specialized software compiled to register time stamps of visits to each bowl, and to calculate various measures, including, among others, working memory, reference memory, latency time to first visits, and order of visits.

The pig holeboard has been shown to produce highly reproducible results when comparing between studies. Independent experiments have used the pig holeboard to compare holeboard performance of low birth weight and normal birth weight animals (Antonides et al., 2015a; Gieling et al., 2012b), animals from large or small litters (Fijn et al., 2016), effects of pharmacological intervention with the M1R blocker biperidin (Gieling et al., 2013), effects of enriched housing (Bolhuis et al., 2013; Grimberg-Henrici et al., 2016), effects of overnight social isolation (van der Staay et al., 2016), and effects of iron deficiency during early life (Antonides et al., 2015b) show highly similar performance between control groups, indicating replicability of the test between studies. The test also shows sensitivity for deficits in performance (Antonides et al., 2015b; Gieling et al., 2013), as well as enhanced performance (Antonides et al., 2015a; Grimberg-Henrici et al., 2016), although the latter will reach ceiling-level

FIGURE 39.2   **Details of the "holes" used in both the pig holeboard setup and the active choice setup used in judgement bias and decision making.** Plastic balls are fitted with magnets and hung from a stainless steel wire in between four stainless steel rods. The balls lay in plastic dishes which contain sensors that can detect movement of the magnet. When the animal displaces the ball, either to gain access to a reward or as an operant response, the sensor detects movement of the magnet, and sends a pulse through the interface to a computer running registration software. *Source: Modified from Antonides et al. (2015a), according to Open Access terms.*

performance relatively quickly as normal animals reach near-perfect performance, particularly on working memory.

Behavioral tests can give valuable information, provided that the tests used are valid and reliable. Validity can be defined as the degree to which a test measures what it is supposed to measure. Reliability on the other hand is defined as the repeatability of scores, obtained from unchanged patients (humans or animals), under diverse scoring conditions (Mokkink et al., 2009). Four different types of reliability are defined: tests-retest, internal consistency, interrater and intrarater reliability. In simpler terms, a test that is valid, gives "right" results while one that is reliable, gives "good" results (Martin and Bateson, 2007). Behavioral tests for pigs are not frequently tested for reliability, which is a major hindrance to the development of the pig as a model species for cognition testing.

We have tested intrarater and interrater reliability in the pig holeboard test, calculating intrarater reliability by comparing data obtained from live video scoring against data obtained from scoring the video recordings of the same trials. We also tested interrater reliability by comparing the results of working and reference memory of the computer program used to register hole visits, the results of working and reference memory as visually scored by the observer. Results from this study showed high interrater reliability when comparing manual scoring to scoring by the specialized software, which points to high reliability of the test setup. The study also showed, however, that for manual observation, experience may play an important role in interrater reliability; interrater reliability was low, possibly due to a learning curve in the observer (Meléndez Suárez, 2014). See Box 39.1 for a detailed description of the methods and results of this reliability study.

BOX 39.1

METHODS AND RESULTS OF A VALIDATION STUDY OF THE PIG HOLEBOARD TASK

Originally reported in Meléndez Suárez (2014).

Procedure: Twenty average weight piglets [(Terra × Finnish landrace) × Duroc], 10 males, and 10 females, from the farm at Utrecht University were selected at 3 weeks of age from 10 different litters. Males and females were housed separately in enriched pens with straw and a ball. The holeboard training started when the piglets were 41 days old. The animals were habituated to the experimenters for a period of 2 weeks, during which they were fed M&M's to get them used to the bait. Each pig was assigned randomly to one of the four configurations, with different locations of the baited bowls. Males and females were divided into two subgroups, with a total of four groups consisting of five pigs each. The four groups were tested randomly using the ABBA and BAAB testing orders on alternate days, where letter A represented the female group and letter B the males. The pigs within the subgroups were tested in a random order as they presented themselves to the door. Each pig was tested twice during a day, one trial right after the other (massed trials).

Intrarater Reliability: On day 18 of training, a veterinarian, with no previous experience at scoring animal behavior, live scored the visits to the bowls for 20 pigs, two trials each. Live scoring was done using a monitor that was connected to a camera located above the Holeboard. Trials were recorded for a second evaluation. The visits to the bowls were scored using a computer with JWatcher Version 1.0 installed. One week after the live scoring, the same

observer scored the video recording, in order to compare both files and obtain the intrarater reliability. JWatcher Version 1.0 was used to calculate the percent of agreement and the kappa coefficient.

Interrater Reliability: Based on the results obtained from the intrarater reliability the working and reference memory of the 40 trials were calculated using the formulas:

$$\text{WM}: \frac{\textit{Number of rewarded visits}}{\textit{Number of visits and revisits to the rewarded set of holes}}$$

$$\text{RM}: \frac{\textit{Number of visits and revisits to the rewarded set of holes}}{\textit{Number of visits and revisits to all holes}}$$

The results obtained for working and reference memory from the computer were compared to those obtained by the observer.

Statistical Analysis: For the intrarater reliability kappa statistics were used to obtain the percentage of agreement and the kappa coefficient.

For the interrater reliability a Wilcoxon *t*-test and a Pearson correlation test were used to see the association between the results from the computer program against the observer, for reference and working memory of the two scoring procedures (automatic vs. observer). All statistical analyses were carried out using a SPSS for Windows (version 16.0) computer program (SPSS Inc., IL, USA).

Results: The kappa coefficient values obtained from the 40 trials are shown in Table 39.1. The highest kappa coefficient score has a value of 1 and represents that the two scoring procedures that are compared have the same sequence of key codes. In this table, we can see that there are several scores with a value of 1, but there are also many low values. The average kappa coefficient for the 40 trials is 0.8.

Table 39.2 contains Pearson correlations from the two data sets and the *P*-values of the correlations. The data sets are highly correlated.

TABLE 39.1   Intrarater Reliability Results (Kappa Coefficient)

Pig	A	B	C	D	E	F	G	H	I	J	K	L	M	N	O	P	Q	R	S	T
RT1	0.73	0.84	1	1	0.49	1	1	1	1	0.25	1	0.32	1	1	1	0.47	1	0.64	0.75	0.75
RT2	0.08	1	1	1	0.26	0.68	1	1	1	1	1	1	1	1	1	1	1	1	1	0.18

The animals were identified with letters from A to T. The reliability of trail 1 and trail 2 were calculated (RT).

TABLE 39.2   Pearson's Correlation for Working Memory (WM) and Reference Memory (RM) of Trial 1 and 2

	Pearson correlation	Pearson correlation (*P*-value)
WM T1	0.995[a]	<0.0001[b]
T2	0.928[a]	<0.0001[b]
RM T1	0.964[a]	<0.0001[b]
T2	0.971[a]	<0.0001[b]

[a] *Correlation is significant at the 0.01 level.*
[b] *P-value is significant <0.05.*

2.2 Judgement Bias

Judgement bias tests (JBTs) measure behavioral responses to ambiguous stimuli after animals have been trained to discriminate between a stimulus (or set of stimuli) predicting a positive consequence (S⁺; reward) and another stimulus (or set of stimuli) predicting a negative consequence (S⁻; punishment or lower-value reward). The "quality" of the ambiguous stimulus lies somewhere between S⁺ and S⁻ (Fig. 39.3). Go/Go and Go/No-go tasks form the two different classes of JBTs in which Go/No-go entails the suppression of the response at S⁻, whereas Go/Go entails that the animal responds to both stimuli types with an active response (Murphy et al., 2013a). JBTs provide a cognitive measure of optimism and/or pessimism since a negative emotional state is expected to cause a negative (pessimistic) judgement of an ambiguous stimulus, whereas a positive emotional state is expected to cause a positive (optimistic) judgement of the same ambiguous stimulus (Boleij et al., 2012; Roelofs et al., 2016).

The pig is one of the species in which JBTs became a frequently used tool to assess emotional states (Brajon et al., 2015; Roelofs et al., in press; Roelofs et al., 2016). Fig. 39.4 shows the JBT used, for example, by Murphy et al. (2013b) for pigs. Since it is known that early life experiences (e.g., stress) can have consequences for later emotional functioning (Pechtel and Pizzagalli, 2011), JBTs might be a useful tool to investigate, especially, the effects of early life experiences. Murphy et al. (2015) succeeded in showing that effects of low birth weight in piglets can be detected in a JBT. Table 39.3 summarizes points to consider when testing pigs in a JBT.

2.3 The Pig Gambling Task—A Variant of the Iowa Gambling Task

Strategies in animal decision-making may relate to differences in early life experiences as suggested by Potenza (2009) for environmental factors in general, by Andrews et al. (2015) for rodents and birds, or by Murphy et al. (2015) for birth weight in pigs. Negative (early life) experiences can induce negative mood states later in life (Mendl et al., 2010), which can consequently affect decision-making when outcomes are uncertain (Mendl et al., 2009). Studying decision-making strategies might thus allow drawing conclusions on emotional states. Decisions have to be made when conditions are uncertain (Kacelnik and Bateson, 1997) and might involve a risk (with a known probability of each outcome) or ambiguity (with an unknown outcome) (Bechara, 2005; Krain et al., 2006).

A common test to study decision making is the Iowa Gambling Task (IGT; Bechara et al., 1994). Animals have
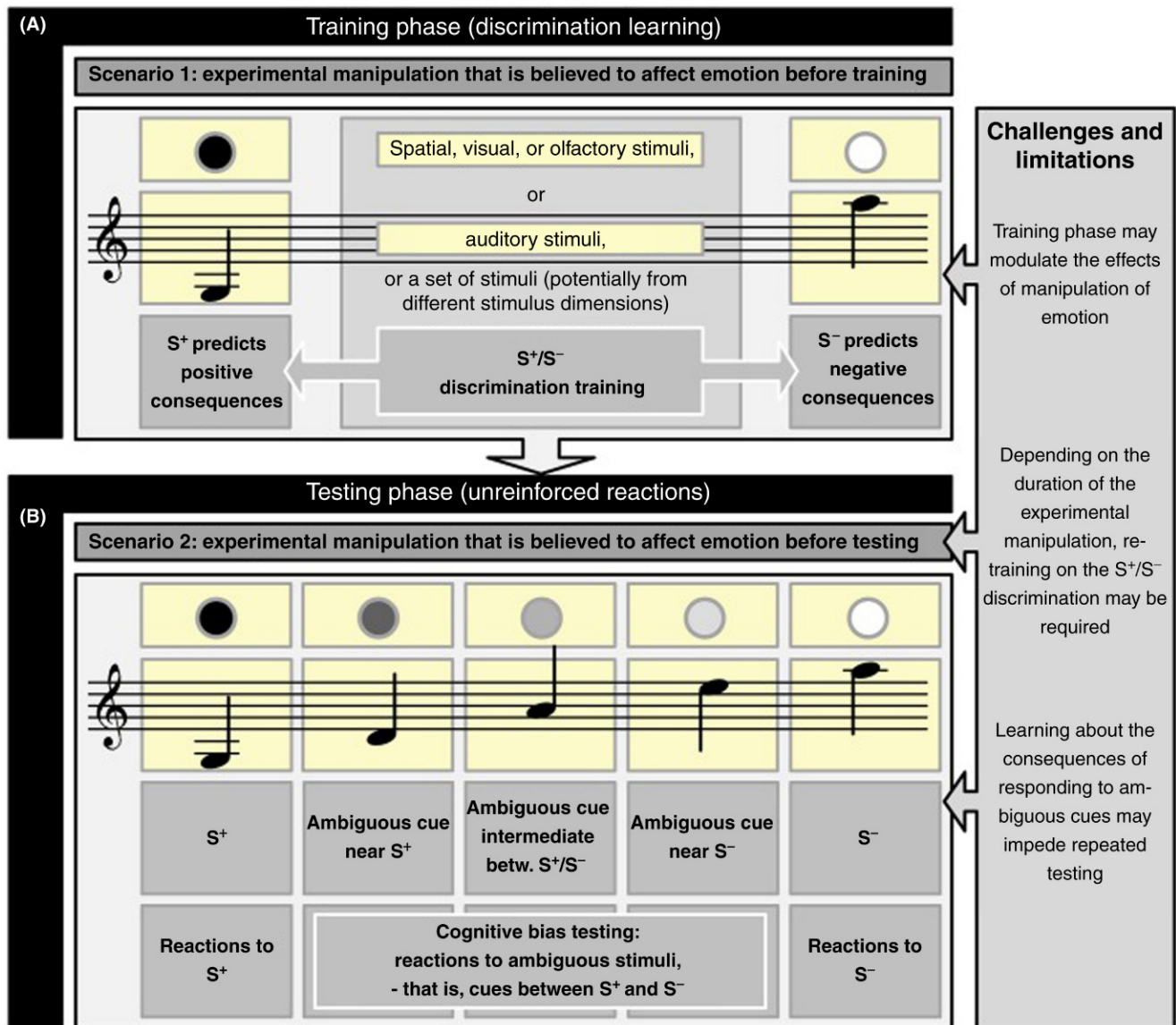
FIGURE 39.3   **Schematic representation of judgment bias training and testing using visual, olfactory, spatial, or auditory cues, or a combination of cues from different stimulus dimensions.** The experimental manipulation that is believed to affect emotion precedes the training phase (A; Scenario 1) or the testing phase (B; Scenario 2). Refreshment of the discrimination acquired during the training phase may be necessary, if the experimental manipulation preceding phase (B) lasts for a longer time period. An example of scenario 1 is studying the effects of growing up in different housing systems, whereas scenario 2 may be applied in a study assessing the effects of shorter lasting experimental manipulations, such as confinement, on emotion. Phase (B) may be repeated multiple times (Douglas et al., 2012) to test the effects of different experimental manipulations in the same animal. Specific challenges and limitations may be connected to the different phases. See Fig. 39.3 for an example of the specific contingencies connected with responding to S⁺, S⁻, and ambiguous cues. *Source: Reprinted from Roelofs, S., Boleij, H., Nordquist, R.E., van der Staay, F.J., 2016. Making decisions under ambiguity: judgment bias tasks for assessing emotional state in animals. Front. Behav. Neurosci. 10, 119, according to Open Access terms.*

to choose between two options: a "safe" or "risky" one. Risk is manipulated by varying the amount of reward, the probability of reward occurrence, or time delay until rewards are delivered (Murphy et al., 2015). Risk-prone individuals have been found to prefer risky options, while risk-averse individuals prefer safe options (Mazur, 1988). Anxiety led to increased risk-prone behavior in humans, as well as in rodents (Miu et al., 2008; de

Visser et al., 2011). Positive mood on the other hand, led to earlier choices for safe options (de Vries et al., 2008).

Murphy et al. (2015) developed the Pig Gambling Task (PGT; see Figs. 39.1 and 39.5), inspired by the IGT. This two-choice probabilistic decision-making task allows studying decision-making under risk, in which the safe, or advantageous option yields greater overall gain. In the setup used by Murphy and coworkers an
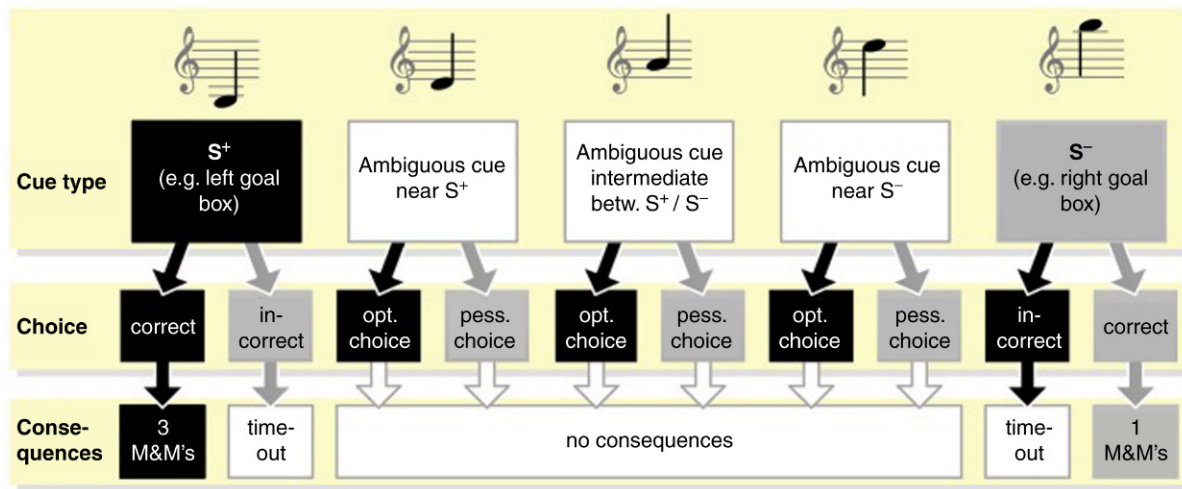
FIGURE 39.4 **Example of the exact contingencies connected with responding to the different cues presented during the testing phase (Fig. 39.1B) in a judgment bias tasks (JBT; programmed consequences of choices as used in Murphy et al. (2013b).** *Source: Reprinted from Roelofs, S., Boleij, H., Nordquist, R.E., van der Staay, F.J., 2016. Making decisions under ambiguity: judgment bias tasks for assessing emotional state in animals. Front. Behav. Neurosci. 10, 119, according to Open Access terms.*

TABLE 39.3 Points to Take Into Consideration When Testing Pigs in a Judgement Bias Task (JBT)

Effects of training/testing on emotional state	Procedural pitfalls
• Training within JBTs might be seen as cognitive enrichment, *improving the welfare* of the study subjects and affecting its emotional state (Carlstead and Sheperdson, 2000; Guldimann et al., 2015; Pomerantz and Terkel, 2009; Puppe et al., 2007; Zebunke et al., 2011).	• Pigs need *extensive habituation* before training and testing of individual animals can take place (Murphy et al., 2013b, 2015). • Initially ambiguous stimuli might *lose their ambiguity* within repeated testing (Roelofs et al., 2016). • Animals might *fail in reaching a required criterion* during training (Brajon et al., 2015).

FIGURE 39.5 **When tested for decision-making strategies, for example, in the PGT, pigs can decide on an advantageous or disadvantageous side.** Rewards used here were chocolate M&M's (Mars Nederland b.v., Veghel, The Netherlands). To illustrate, 8 rewarded trials per series of 10 trials (each yielding 2 M&M's as reward) (advantageous choice) are presented against 3 rewarded trials per series of 10 trials (each yielding 4 M&M's as reward) (disadvantageous choice). The number of rewards used might be varied. Advantageous choices yield, in the long run the largest number of rewards (here 16). *Source: Reprinted from van der Staay, F.J., Schoonderwoerd, A.J., Stadhouders, B., Nordquist, R.E., 2015. Overnight social isolation in pigs decreases salivary cortisol but does not impair spatial learning and memory or performance in a decision-making task. Front. Vet. Sci. 2, 81, according to Open Access terms.*

advantageous option was characterized by small but frequent rewards, whereas a disadvantageous option was characterized by large but infrequent rewards. The advantageous option thus led to greater overall gain in the long run (see also Fig. 39.5). Table 39.4 summarizes some of the considerations when testing pigs in the PGT

2.4 Discrimination Learning

Discrimination learning can be used as a part of training for more difficult tasks, including the judgement bias tasks and Iowa gambling task described earlier in the chapter. It can, however, also be used as a task in and of itself, to determine the ability of animals to discriminate between two stimuli and the capacity of animals to learn and perform tasks based on discrimination in different modalities.

TABLE 39.4 Points to Take Into Consideration When Testing Pigs in a Pig Gambling Task (PGT)

Effects or training/testing on emotional state	Procedural pitfalls
• Training within JBTs might be seen as cognitive enrichment, *improving the welfare* of the study subjects and affecting its emotional state (Carlstead and Sheperdson, 2000; Guldimann et al., 2015; Pomerantz and Terkel, 2009; Puppe et al., 2007; Zebunke et al., 2011)	• Pigs need extensive habituation before training and testing of individual animals can take place (Murphy et al., 2013b, 2015). • Means by which risks are manipulated can influence preferences (Kacelnik and Bateson, 1997). • It is unknown whether pigs can assess maximum number of rewards or minimum number of punishment. They might decide on the option that provides reward in the majority of trials (van der Staay et al., 2016) . • It is unknown how many trials are needed to train pigs to consistently make advantageous choices (van der Staay et al., 2016).

Visual discrimination is frequently used in discrimination learning in various species. This can entail the use of lights, including discrimination between light color, intensity, or frequency of flashing lights. Visual stimuli can also include the use of pictures or patterns. Pigs have visual acuity which is inferior to humans, sheep, and cattle (Entsu et al., 1992; Tanaka et al., 1995; Zonderland et al., 2008) but which should, in theory, be quite sufficient for learning visual discriminations. In practice, however, discrimination based on visual stimuli in pigs has proven quite difficult, requiring lengthy training to show operant responses to distinct 2D shapes (Gieling et al., 2012a; Graf, 1976; Haagensen et al., 2013). Discrimination of conspecifics based on photographs, which has been demonstrated in domestic sheep (Ferreira et al., 2004) and cows (Coulon et al., 2009) did not seem to be possible in pigs (Gieling et al., 2012a).

Discrimination tasks based on auditory stimuli have been more successful, with pigs showing distinct operant responses to auditory stimuli of different frequencies (Murphy et al., 2013a). Other modalities, such as odor cues or tactile cues, have yet to be tested in pigs. Given their strong olfactory and tactile abilities (the snout is particularly sensitive), this may be an interesting avenue to explore to improve discrimination learning.

2.5 Practical Aspects of Training in Operant Tasks

Operant tasks, such as the pig holeboard, judgement bias, or gambling task, are work-intensive in terms of extensive time needed to habituate the animals to being alone in the setup, and because the animals need to be moved from the home pen to a test setup each time testing occurs. The latter can be partly offset by providing a waiting area where animals can stay for up to several hours between trials (thus with at the very least access to water). Training, while relatively fast in terms of learning tasks, still takes several weeks of daily training. On the other hand, the pig holeboard provides a number of measures of spatial memory and motivation within a single test, which can save time relative to conducting multiple sequential behavioral tests.

Training of very young animals in an operant conditioning task needs to be carried out keeping their cognitive, emotional, and physical abilities in mind. One manuscript reporting an attempt to train very young piglets (starting at 17 days of age) in a visual discrimination task reports that attempts at visual discrimination were suspended, as the first response of inserting the snout into a hole to be rewarded with milk was already quite difficult for unimpaired piglets (Andersen et al., 2016). In our hands, we found that piglets before the age of 4–6 weeks had difficulty habituating to being alone in the holeboard setup, and had difficulty learning

the operant response of lifting a ball to gain a reward. This may reflect too high demands of the emotional and cognitive maturity of the animal before these ages to successfully perform an operant response.

For any task in pigs that involves intensive training, there will be a number of practical considerations having to do with the size of the animals. One of these is habituation of the animals to allow movement of the animals from a home pen to a test setup, and testing with as little interference from stress as possible. Even juvenile pigs are quite strong, and within a few weeks after birth it is very difficult to fixate or restrain piglets. If the animals can be fixated, this certainly will lead to stress in the piglets, with all of the welfare implications and potential for confounding the experimental result that this entails. To avoid this, extensive habituation to human contact, handling, and the test setup are highly desired before embarking on cognitive training. For holeboard testing, this entails daily habituation for 2–4 weeks (Fijn et al., 2016; Gieling et al., 2014a). The time involved in habituation of animals will, of necessity, increase the age at which animals can be tested. This may be a hindrance to the use of the holeboard test for testing very young animals. For testing of very young (preweaning) animals, one might consider the use of test setups that can be used either in the presence of or very near the sow and/or siblings. The 8-arm radial maze and the T-maze have been successfully used in very young animals (Dilger and Johnson, 2010; Elmore et al., 2012; Naim et al., 2010). If space allows these apparatus could be placed in the same room as the sow and littermates, allowing auditory and olfactory contact, which may reduce habituation time needed.

For any operant task, the type of reinforcer used will need consideration. Given that the animals need to be repeatedly trained and that the size of the animals requires that they voluntarily enter a test setup, it is advisable to work with a reward rather than an aversive stimulus. We have successfully used M&M's chocolate candies, which are easy to dose and highly palatable to pigs. For very young animals, M&M's have proven to be difficult to chew. In that case, we used small marshmallows. Other groups have used chocolate-covered raisins (Arts et al., 2009; Bolhuis et al., 2013), fruit, and for preweaning animals, milk replacers (Dilger and Johnson, 2010; Elmore et al., 2012) or applesauce (Bertholle et al., 2016; Meijer et al., 2014a).

Automation is also an important consideration in measuring any animal behavior. There are a few obvious advantages to at least some level of automation. First, automatic detection of responses can lead to much more detailed and fine-grained data, particularly regarding time (latency times, total time on task, etc.). This can be nearly impossible to score by hand for fast or repeated behaviors, or when more than one behavior is being scored, but can be relatively easily built into

software. Second, automation can vastly reduce the effects of the experimenter, allowing multiple experimenters to work on a single test and produce similar results. As the experimenter will always have contact with the animals, even if just to move them from the home pen to the experimental setup, there will always be some effects of the experimenter. Different experimenters will be more or less gentle or patient with the animals, and some combinations of personalities of animals and experimenters may provide for either positive or negative interactions, that may differ for a single experimenter with individual animals. Moreover, automatic registration of behavior will reduce the observer bias (Bello et al., 2014).

There are some challenges to automation. For pigs specifically, experimental setups need to be built extremely robustly. Automation involves sensors and wires, which certainly can be built to withstand pigs, but this is (1) specialized work that is frequently not included in standard setups built for automation of behavioral measures, (2) can become quite costly, and (3) needs to be extremely well thought through if flexibility in the setup is required, that is, for disassembling and reassembling a setup if a space is to be used for multiple purposes. Stable builders who are experienced in building pig dwellings can be instrumental in building robust, automated setups.

An important aspect for implementing automation, is that one must know exactly what one wishes to measure in order to operationalize the measures in sensors and software. This can be an issue in pigs, where there is much less data on behavioral responses in tasks or to stimuli than, for instance, the vast amount of data available for rodents. It is highly advisable when introducing a new task, to first observe the animals closely in the task to determine which behaviors and which parameters should be scored. Once the automated setup has been built, the data should be validated (usually by comparing with hand-scored data, see Box 39.1 on validation of the pig holeboard). Raw data should be carefully examined after each experiment, to ensure that no malfunctions are taking place (i.e., dirty or old sensors, loose wires, software bugs, and so on) that can influence results. Some behaviors or parameters will not be easy or possible to detect automatically,as discussed further in the section gait scoring, for example, determining which foot produced a certain footfall. Advances in automation techniques, particularly in sensor development, make automation of more and more parameters possible.

3 NONOPERANT BEHAVIORAL TESTS

Behavior can also be tested in tasks which do not require extensive training, as operant tasks generally do. This may provide an advantage when one wishes to test very young animals; clearly one cannot test a 2-week-old piglet in a task that requires 4 weeks of training. Operant tasks can often give detailed information on cognitive functioning, but for specific questions on cognition or neurological function, nonoperant behavioral tests may provide more useful data. A number of tasks have been developed and used in pigs.

3.1 Measuring Motivation

Motivation is the process within the brain controlling which behaviors and physiological changes occur and when (Fraser et al., 1990). It is a reflection of the inner state of an animal. The inputs for this process may arise both from internal and external sources. For example, the decision to start foraging for food may be based on both internal cues, such as blood glucose level or gut distension and external cues, such as the presence of predators. Changes in motivational state can give rise to changes in appetitive behavior (i.e., searching for stimuli) or consummatory behavior.

Measuring the motivation of an animal to perform a certain behavior may provide information on the relative importance of that behavior for the animal. Captive animals, such as farm animals, may be restricted from performing some behavior. For example, nest-building in prepartum sows is impossible in many of the barren farrowing pens that are used in modern pig farming. Knowledge on the strength of motivation to perform behavior may help to understand the welfare implications of husbandry systems that restrict that behavior.

The motivation of pigs can be assessed in several ways. Perhaps the simplest method is to assess how often or how long an animal performs a behavior. For example, pigs that are food-restricted spend more time performing foraging behavior than nonrestricted animals (Day et al., 1995). Runways or obstacle courses have been used to assess the effect of feed composition on feeding motivation (Souza da Silva et al., 2012) and the difference between low-birthweight and normal-birthweight pigs on feeding motivation (van Eck et al., 2016). In the latter experiment, novel objects were added as obstacles to the runway in order to increase the difficulty of the task.

In operant conditioning, the animal is taught to perform a certain task in order to obtain access to a resource that allows them to perform a particular behavior. The "cost" of the resource can be manipulated by increasing the difficulty of the task (e.g., by increasing the amount of weight an animal needs to displace) or by increasing the number of times an animal needs to perform the task in order to get rewarded (e.g., increasing the number of times a lever needs to be pressed). Operant conditioning tasks have been used in pigs to assess motivation for, for example, food (Lawrence and Illius, 1989; Souza

da Silva et al., 2012; van Eck et al., 2016), illumination (Baldwin and Start, 1985), straw (Pedersen et al., 2002), and heat (Baldwin and Ingram, 1967) and to get away from ammonia or draught (Baldwin and Ingram, 1967; Jones et al., 1998). Operant responses in a food-motivation task using nosewheel turning showed large interindividual variation (Souza da Silva et al., 2012), therefore within-subject designs should be considered when designing experiments using this task. Another parameter that may influence the performance in this test is social context: demand curves for food differ between pigs that are tested alone or together with another pig (Pedersen et al., 2002).

Other tasks may be used to assess motivation as well. The spatial holeboard task (see earlier for more information) includes parameters, such as trial duration and intervisit-interval (reflecting the speed of searching for bait) that can be used as measures for food motivation (Antonides et al., 2015b).

3.2 Mirror Use

The ability to use a mirror to guide movement or decision making has long been considered an indicator of complex cognitive ability. Instrumental use of mirrors (as opposed to the use of mirrors to show self-awareness) has been indicated in some types of primates (Anderson and Gallup, 2011; Heschl and Burkart, 2006; Menzel et al., 1985), dolphins, birds (Medina et al., 2011; Pepperberg et al., 1995), and elephants (Povinelli, 1989).

A paper by Broom et al. (2009) described a study in which pigs appeared to use a mirror to navigate an obstacle to gain access to food, indicating use of high cognitive functioning to solve a spatial problem. This would be an important finding, influencing our perception of pigs and their cognitive abilities. A later study failed to replicate the finding by Broom and coworkers (Gieling et al., 2014b). This indicates that mirror use is not universal in pigs, and may be at the periphery of their cognitive ability.

3.3 Open Field Test

The open field test, originally developed as a test for emotionality in rodents, has been used in pigs since the 1960s (Beilharz and Cox, 1967). It is generally performed in an unfamiliar square, rectangular, or circular arena. The pig is placed in the arena for a certain amount of time, usually between 4 and 10 min, and the behavior of the pig is recorded. Several categories of behaviors can be scored, such as locomotion and exploration (Andersen et al., 2000; Beattie et al., 1995; Donald et al., 2011; Fijn et al., 2016; Fraser, 1974; Gieling et al., 2014a; Meijer et al., 2015; van der Staay et al., 2009), location within

the open field (Andersen et al., 2000; Donald et al., 2011; Fijn et al., 2016), vocalizations (Beattie et al., 1995; Donald et al., 2011; Fijn et al., 2016; Fraser, 1974; Gieling et al., 2014a), elimination (Andersen et al., 2000; Fijn et al., 2016; Fraser, 1974; Gieling et al., 2014a), and escape attempts (Fijn et al., 2016; Meijer et al., 2015).

The open field test is often used as a test for anxiety, exploration, and locomotion. Since it is known from several animal studies, as well as from human studies that stressful experiences in early life can modulate adult behavior (Taylor, 2010), the open field test may be useful to study these early life effects on anxiety later in life. Moreover, in a recent study in pigs, open field test locomotor activity was used as part of behavioral profiling in order to explain differences in learning abilities (Brajon et al., 2016) and it may therefore be a helpful tool when designing experiments.

Although the open field test is often used as a test for anxiety, there are some considerations that need to be taken into account. In general, the open field test may cause anxiety to animals due to social isolation and due to fear of novel environments and open spaces. Social isolation has been linked to indicators for stress by several studies (Kanitz et al., 2009; Poletto et al., 2006; Ruis et al., 2001). However, unlike rodents which show a tendency to remain close to the walls in unfamiliar surroundings, no evidence for this "wall-hugging behavior" in pigs has been found. Treatment with anxiolytics, such as diazepam (Andersen et al., 2000) and azaperone (Donald et al., 2011; Prut and Belzung, 2003), did not result in an increased time spent in the center of the open field. Location within the open field may therefore not be an ethologically valid indicator of anxiety in pigs (Fijn et al., 2016; Murphy et al., 2014).

When designing experiments using open field tests, the behavioral responses that are scored and their interpretation should be carefully considered (Forkman et al., 2007; Murphy et al., 2014). Scoring of the behavioral parameters can either be performed directly while observing the pigs, or from video recordings, or using video-tracking devices (van der Staay et al., 2009). The advantage of using video recordings is that the arena can be divided into several areas without physically having to place lines on the floor of the pen, which may influence the locomotor behavior of the pig. In a study looking at several behavioral parameters scored by two observers and both directly or from video, interrater reliability was ≥0.73 and intrarater reliability was ≥0.78 (Fijn et al., 2016). Open field behavior is generally repeatable over time (Fraser, 1974; Jensen et al., 1995), although repeated exposure within a short period of time will decrease the novelty of the open field and may influence activity and vocalizations (Donald et al., 2011).

3.4 Clinical Examination of Central Nervous System Function

The clinical examination of the central nervous system in pigs has been extensively described in the setting of veterinary medicine, and is still the cornerstone in diagnosing neurologic disease in pigs (Radostits et al., 2007). In research settings, the clinical examination can also provide valuable insight into the functioning of the central nervous system. Some neurological conditions, presenting with one or several well-described symptoms, may be assessed by clinical examination alone. In other cases, the clinical examination may help to narrow down the possible localizations of the problem and may therefore help to limit the necessary ancillary techniques (such as imaging), saving both time and resources and limiting invasive and stressful procedures for the animal. The development of the central nervous system in young animals may be followed by using functional tests (Fox, 1964a,b; Muir, 2000), and may therefore be useful to study the effect of early life influences on development and functioning of the central nervous system later in life.

The clinical examination can be performed by any veterinarian, and with some training biomedical researchers, lab technicians, or students will be able to perform the clinical examination reliably as well. No specialized equipment is needed, and it is therefore an inexpensive technique. An additional advantage is that it is minimally invasive, and therefore may have minimal impact on the welfare of the experimental animals.

There are, however, also some drawbacks to using the results from the clinical examination as outcome parameters in experiments. Adult pigs are large and may be aggressive. This may limit the possibilities to perform some parts of the clinical examination, for example, tests that require the animal to lie down. Another drawback is that the clinical examination only provides functional information but no information on the underlying structural characteristics of the dysfunction.

3.5 Components of the Clinical Neurologic Examination

The components that are described further are for a large part derived from veterinary diagnostic protocols (Hajer et al., 2000). Not every component may be needed for each experiment, and some experiments may benefit from modified or additional tests. Table 39.5 provides an overview of common components of the neurologic examination, how to perform the test, and the expected response from the animal. It is important to perform the tests in an order that causes the least stress to the animal. Tests that require little or no fixation should be performed before more invasive tests and tests that require fixation.

3.6 Proprioception

Proprioception, the awareness of deep pressure and the position and movement of limbs, is mediated through receptors in muscles, tendons, and joints. They relay information to the spinal cord and brain via large Aα and Aβ myelinated fibers. Proprioceptive information is used to adapt body position and gait, and defects in the proprioceptive system may lead to ataxia. The lack of position sense in a limb may be demonstrated by placing the limb in an abnormal position. Unimpaired animals will correct this abnormal position directly. Commonly used tests are dorsal placement of the feet (Fig. 39.6A, Table 39.5) and crossing of limbs (Fig. 39.6B, Table 39.5).

3.7 Cranial Nerve Function

Many cranial nerve deficits can be identified by careful inspection of the head and neck. An abnormal position of the eye may be indicative of lesions to either the oculomotor nerve (divergent strabismus, often accompanied by a drooping eyelid and dilated pupil), trochlear nerve (rotated eyeball), or abducens nerve (converging strabismus). Abnormalities in the motor component of the trigeminal nerve may lead to a drooping lower jaw, facial nerve paralysis may present as a drooping ear, lip, and nose and an inability to close the eye. Atrophy of the neck muscles may be caused by accessory nerve dysfunction, and a paralysed tongue hanging from the mouth may be due to hypoglossus nerve dysfunction.

Several tests specific for certain cranial nerves are possible to perform in pigs (Fig. 39.6C, Table 39.5), although they require a relaxed animal. They may be difficult to perform in very young animals, either because the response is difficult to see (pupillary light reflex) or because animals only develop the adult-like response over time (menace response) (Enzerink, 1998).

3.8 Motor Function

Muscle tone and muscle strength as indicators of motor function may be assessed by observing the gait of the animal. Passive movement of the extremities, when the size of the animal permits, may give a more accurate impression of muscle tone.

3.9 Spinal Reflexes

A spinal reflex requires an intact reflex arc (muscle receptors, sensory axons within a peripheral nerve and dorsal root, lower motor neuron and its axon, muscle). No central input is required for a spinal reflex. However, sensory information may also be relayed to the brain and may result in additional behaviors. An example is the withdrawal reflex (Fig. 39.6D), in which stimulation
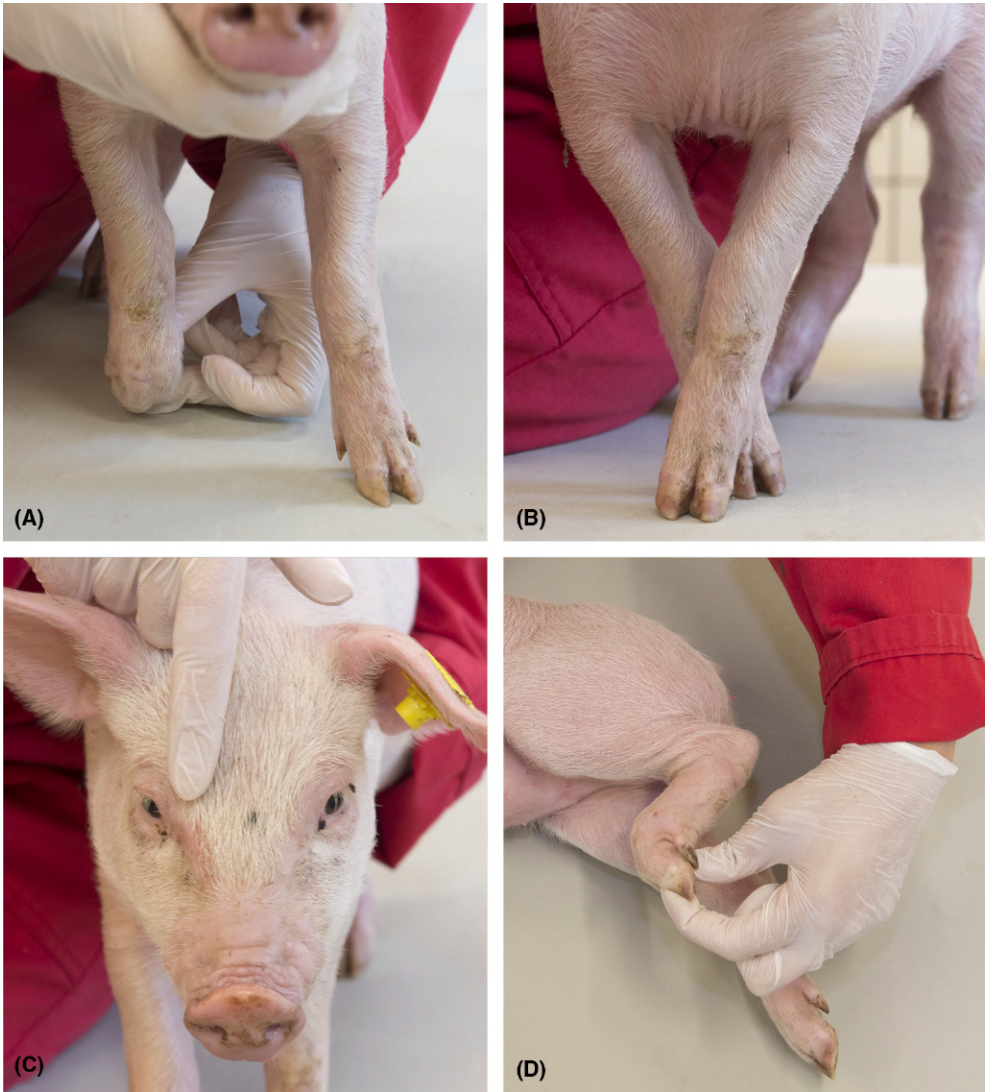
FIGURE 39.6   **Neurologic tests in pigs.** (A) Dorsal placement of foot, (B) crossing of limb, (C) Palpebral blink reflex, (D) withdrawal reflex.

TABLE 39.5   Common Components of the Clinical Examination of the Nervous System

Test	Action	Expected response
Dorsal placement of feet (Fig. 39.6A)	Placing dorsal side of foot in ground surface	Animal corrects abnormal position
Crossing of limbs (Fig. 39.6B)	Crossing the legs of the animal and let the animal put weight on it	Animal corrects abnormal position
Menace response	Moving an object fast in the direction of the eyes	Animal closes eyes
Pupillary light reflex	Shining into the eye with a flashlight	Pupil constricts
Palpebral blink reflex (Fig. 39.6C)	Tactile stimulation of the skin between the eyes	Animal blinks
Patellar reflex	Tapping the patella tendon with a reflex hammer	Flexion of the knee
Withdrawal reflex (Fig. 39.6D)	Pinching the skin between the claws	Flexion of the limb

This overview describes how the test is performed and the expected response from the animal.

of the skin between the claws results in flexing of the limb. Usually light stimulation of the skin is sufficient for the reflex to occur, but when stronger stimuli are needed, pain may be relayed to the brain and may result in guarding behavior or aggression.

In normal animals, central modulation of some reflexes is possible. In some conditions, such as complete transections of the spinal cord, this central modulation is not possible anymore, resulting in so-called "pathological responses." An example is the crossed extensor reflex. When performing the withdrawal reflex, the limb opposite the one being examined is extended. Another example is the occurrence of a massive response or repeated responses after performing the patellar reflex.

3.10 Gait Analysis

The ability to move from one place to another is an important ability for many species, including pigs. Locomotion is achieved through gait, "a complex and strictly coordinated, rhythmic and automatic movement of the limbs and the entire body of the animal, which results in the production of progressive movements" (Back and Clayton, 2013a). In order to produce gait, the integrated efforts of nervous tissue, muscles, bones, joints, tendons, and specialized skin are required. Many parts of the nervous system are involved in healthy gait.

3.11 Why Measure Gait in Neurological Research in Pigs?

Since the nervous system is so heavily involved in locomotion, problems in this system may produce a variety of gait disorders. Therefore, the analysis of gait may yield important information on the functioning of the nervous system. Several aspects of gait may be affected.

Strength may be affected when lower motor neuron function is impaired, resulting in weakness, paresis, or paralysis. Conditions affecting lower motor neurons may be limited to one muscle group, one limb, or may affect several or all limbs (e.g., in polyneuropathic conditions). Muscle tone is usually decreased, and weight bearing or propulsion may be affected, resulting in gait deficits.

Automated rhythmic movement is produced in the so-called spinal pattern generators. Although the presence of spinal pattern generators for limb movement has not been conclusively demonstrated in pigs, it has been shown in several other species, such as cats (Duysens and Van de Crommert, 1998). Due to the presence of these spinal pattern generators, even animals with complete transections of the spinal cord are able to produce rhythmic stepping movements. However, adaptation to the environment is only possible with additional input.

Coordination and adaptation are achieved through the integration of information from the visual, proprio-

ceptive, and vestibular system. Integration and coordination take place in the brainstem, cerebellum, frontal cortex, and spinal cord (Nielsen, 2003; Sahyoun et al., 2004). Lesions in these systems may lead to ataxia, inability to correct for variations in the walking surface, deviations to one side, and hypermetric gait.

3.12 What Aspects of Gait are Important?

In the previous section some gait abnormalities resulting from neurologic impairment have been described. In order to determine the presence and severity of neurologic impairment, several aspects of gait may therefore be assessed.

Kinetic parameters assess the forces that affect motion. Examples of kinetic parameters are the amount of weight that is put on a limb, or the propulsive force that is used to produce forward motion. Kinetic parameters are therefore mainly indicative of the strength of a limb. Additionally, large step-to-step variations in the forces on a limb may be indicative of ataxia. There are of course other factors that may influence the forces involved in locomotion, such as mechanic impairments or pain resulting in voluntary modification of weight bearing.

Temporospatial parameters describe gait in terms of time and space. The timing of footfalls relative to each other, the distance that is bridged in one step or the deviations in the center of gravity are examples of temporospatial parameters. Rhythmicity may be assessed by looking at the consistency of timing parameters (Vrinten and Hamers, 2003). Ataxia may result in large variability in both temporal and spatial parameters and adaptations to neurological impairments, such as decreased balance that may result in wide-based gait (Givon et al., 2009; Gordon-Evans et al., 2009; Ishihara et al., 2009; Stolze et al., 2001).

3.13 How Can we Measure These Aspects of Gait?

There are several methods to measure the aspects of gait that we mentioned earlier in pigs. The most important ones, along with their advantages and drawbacks are described in short further in the chapter (Table 39.6).

3.14 Visual Assessment

Traditionally, visual assessment of gait is the technique that is used most often in research using pigs. Protocols specifically aimed at gait analysis in pigs do exist (Grégoire et al., 2013; Main et al., 2000; Mustonen et al., 2011; Van Steenbergen, 1989), but usually these protocols are geared toward recognizing orthopedic problems rather than neurologic dysfunction. Visual gait

TABLE 39.6 Advantages and Disadvantages of the Use of Pressure Mat Analysis of Pig Gait

Advantages	Drawbacks
Measurements can be performed fast and are minimally invasive	Expensive compared to visual scoring protocols
Several aspects of gait (both kinetic and temporospatial) are collected in one run	Assigning footfalls to the correct claw manually is time-consuming
Objective and repeatable, in contrast to visual scoring protocols	
Several footfalls can be recorded in one run, in contrast to force plate analysis	

assessment does not require costly or elaborate setups and is therefore fast and cheap. There are, however, several drawbacks to visual assessment of gait. It has only moderate interobserver agreement (D'Eath, 2012; Keegan, 2007; Main et al., 2000; Petersen et al., 2004), although the use of experienced observers increases the repeatability of results (Main et al., 2000), and it is inherently subjective (Arkell et al., 2006). Furthermore, since pigs are prey animals they tend to hide signs of disease, complicating the detection of abnormalities (Weary et al., 2008).

3.15 Kinematics

Kinematic analysis is performed by tracking body segments, either by following markers that are placed on anatomical landmarks, or by "markerless" tracking using dedicated software. The temporal and spatial characteristics of gait, along with angles between body segments can be analyzed. Kinematics in pigs have mainly been used to quantify gait abnormalities associated with orthopedic problems (Conte et al., 2014; Stavrakakis et al., 2015a; Thorup et al., 2007). Kinematic setups are usually elaborate and expensive, although efforts to develop simpler and more cost-efficient methods for use in pigs are underway (Stavrakakis et al., 2015b). Another drawback is the possibility of skin movement artifacts. Markers are placed on the skin over bony anatomical landmarks, but during movement skin slides over bones and markers may be displaced so they do not correctly represent the landmarks anymore.

3.16 Force Plates

Force plates are platforms that translate the magnitude and direction of forces exerted onto them (ground reaction forces) into electrical signals using either piezoelectrical transducers or strain gauges. They have been used since the late 1960s and are still considered the "gold standard" for kinetic gait analysis. A large body

of knowledge on the use of force plates in quadrupeds exists, and they have been used, for example, in experiments on the effect of flooring on gait of healthy pigs (Thorup et al., 2008; Von Wachenfelt et al., 2009a,b, 2010) and to assess static weight distribution in standing sows (Karriker et al., 2013; Pluym et al., 2013; Sun et al., 2011). Force plates are able to measure forces in three dimensions and may therefore not only be suitable to assess weight distribution, but also the strength of propulsion which may in turn be an indication for overall strength.

An important drawback of force plates is that they cannot distinguish between feet that are placed simultaneously on the plate. Measurements in which two feet are on the plate simultaneously have to be discarded. This means that the optimal size of the plate is different for animals of different sizes, and that many trials may be needed in order to collect sufficient valid measurements. This may be a drawback in studies that follow growing animals over a longer period of time, for example, in studies investigating the effect of influences early in life on motor function in older animals. Also, there may be large variations between measurements, especially since velocity has a large influence on the ground reaction forces. In species, such as dogs and horses, which can be easily led by a collar or halter, this problem may be solved by setting strict limits for velocity and guiding the animal over the force plate at the required pace. In pigs, this is much more difficult since they resist to being led by a collar. A solution might be to use either an instrumented treadmill or several force plates in a row (Back and Clayton, 2013b), however, this setup has not been used in pigs to this date.

3.17 Pressure Mats

Pressure mats (also called pressure plates or pressure-sensing walkways) contain a dense array of sensors, each of them individually measuring the magnitude and the duration of the force exerted on them. When measurements of all sensors under one claw are combined, a pressure profile for each limb, but also for specific regions, such as the inner or outer claw can be constructed. Unlike force plates, pressure mats only measure vertical forces under the claw.

There are multiple pressure mat systems available, some of which are large enough to capture several footfalls in one measurement. In contrast to force plates, pressure mats allow to distinguish between individual footfalls. This opens up the possibility to eliminate influencing between-run factors, such as velocity, and to collect additional temporospatial parameters, such as step length, stance time, and base of support. These temporospatial parameters may be particularly interesting in the assessment of neurological causes of gait deficits.

In pigs, pressure mats have been used to assess pressure distribution under the claws of healthy sows

(Carvalho et al., 2009), to quantify experimentally induced lameness (Karriker et al., 2013), to assess the effect of pain medication on lameness (Meijer et al., 2015; Pairis-Garcia et al., 2015), to follow the development of normal gait in growing piglets (Meijer et al., 2014a), and to identify lameness due to several orthopedic conditions (Bertholle et al., 2016; Meijer et al., 2014b).

3.18 Pressure Mat Analysis in Pigs

Since pressure mats are able to collect both kinetic and temporospatial information and are fairly straightforward to use in pigs, their potential as a research tool to detect and quantify neurological gait abnormalities will be discussed in more detail.

When a pig steps on the pressure mat, several pressure sensors will be triggered. The frequency with which the sensors measure the force exerted on them can be set manually and usually varies between 63 and 126 Hz. On each timepoint, a certain force will be recorded under the sensor. All forces of the sensors belonging to one footfall are grouped, creating an outline of each footfall with corresponding force-time curves (Fig. 39.7). From these force-time curves several parameters can be derived (Figs 39.7 and 39.8), the most common of which are:

Peak vertical force: the highest peak in the time-force curve.
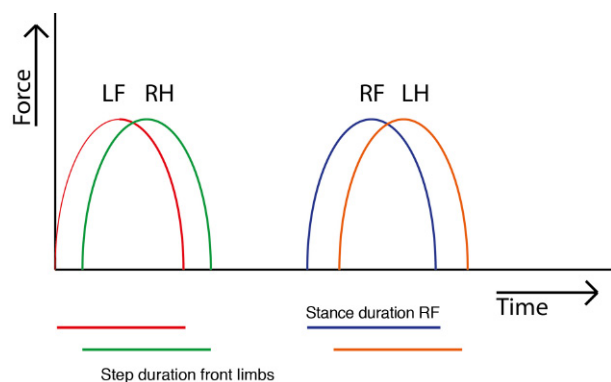
FIGURE 39.7 **Schematic representation of footfall outlines with associated force-time curves.** Outlines and their associated force-time curves have the same color. The temporal parameters Step Duration and Stance Duration in association with the force-time curves are shown in the upper part of the figure. The spatial parameter Step Length in association with the footfall pattern is shown in the lower part of the figure. *LF*, Left front; *LH*, left hind; *RF*, right front; *RH*, right hind.
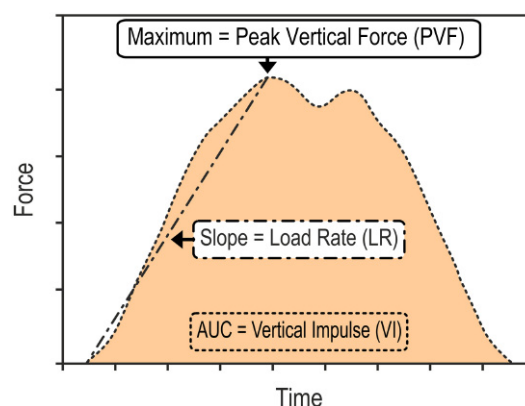
FIGURE 39.8 **Force-time curve of one footfall with associated kinetic parameters.** Peak vertical force *(PVF)*: The highest peak in the force-time curve. Load rate *(LR)*: The slope of the imaginary straight line from the start of the stance phase to the peak of the force-time curve. Vertical impulse *(VI)*: The area under the force-time curve.

Load rate: The slope of the imaginary straight line from the start of the stance phase to the peak of the time-force curve.

Vertical impulse: The area under the time-force curve.

Peak vertical pressure: The highest peak in the time-pressure curve, in which pressure is defined as the force at a timepoint divided by the contact area at that timepoint.

Stance duration: The time the limb is in contact with the ground surface.

Step length: Travelled distance between left and right limb.

Step duration: Time needed for one Step Length to be completed.

Stance percentage: Ratio between the time a limb is in contact with the ground and the duration of the swing phase of that limb.

Additionally, pressures can be visualized by color-coding pressure under each sensor, together creating an outline of each claw. Additional spatial parameters, such as Step Length can be derived from these footprints.

Pressure mat parameters may be influenced by several variables. Velocity has an important effect on most pressure mat parameters. In a study in growing pigs aged 5–15 weeks, velocity influenced Peak Vertical Force, Load Rate, and Peak Vertical Pressure, but not Vertical Impulse (Meijer et al., 2014a). Although no information is available on the influence of velocity on temporospatial parameters in pigs, it is known from horses (McLaughin et al., 1996; Khumsap et al., 2002) that velocity does in fact have a substantial influence on these parameters. Most quadruped species, including pigs, carry about 60% of their weight on their front limbs and the remaining 40% on the hindlimbs (Fernihough et al., 2004; Meijer et al., 2014a; Oosterlinck et al., 2011; Weishaupt, 2008).

It is therefore difficult to directly compare front- and hindlimb-kinetic parameters to each other. Depending on the experimental setup, there may be additional influences on pressure mat parameters, for example, measurement session and variations in body composition between animals or over time (Meijer et al., 2014a; Mölsä et al., 2010; Nordquist et al., 2011).

In order to deal with these influences, asymmetry indices (ASIs) may be used. Symmetry is considered as an important feature of normal locomotion. When one or more limbs of an animal are affected by neurological conditions, the symmetry of the gait may be affected. In kinetic, as well as kinematic gait analysis, this asymmetry may be quantified by comparing parameters of healthy and affected limbs to each other using ASIs. ASIs can be calculated in several ways (Budsberg et al., 1993), but they are most useful when limbs from an animal within one run are compared to each other. This minimizes the effect of interrun variations that may be caused by, for example, velocity differences. In pigs from 5 to 15 weeks old, time did not influence ASIs, which makes them particularly suitable for experiments that follow animals over time (Meijer et al., 2014a).

Perfect symmetry theoretically indicates that an animal is sound. The assumption that a sound animal moves perfectly symmetrically, however, has to be used with caution. In humans, symmetry indices of up to 7.6 (with 0 indicating perfect symmetry and 100 indicating complete lack of weight-bearing on one limb) for PVF were found in clinically healthy subjects (Herzog et al., 1989). Limb dominance and functional differentiation between limbs has been proposed as a reason for the frequently observed gait asymmetry in healthy humans (Sadeghi et al., 2000). Limb dominance has been shown in dogs (Colborne et al., 2011, 2008) and horses (Oosterlinck et al., 2011) and may also be present in pigs. In neurological conditions that affect all four limbs, ASIs may not be useful and other outcomes, such as coefficients of variation, may be more suitable (Hausdorff et al., 1998).

3.19 Obtaining Valid Runs Efficiently

As discussed previously, in order to obtain meaningful results, pigs need to ambulate in a straight line, at a constant velocity, and looking straight ahead. Data collection can be greatly facilitated by using a suitable setup, by habituating the piglets to the test apparatus and by training the animals to perform the desired behavior.

In order to facilitate that the pigs walk in a straight line over the pressure mat, borders on each side of the pressure mat should be placed to guide the pigs over the mat. Older, heavy pigs have a tendency to lean into walls when walking, influencing pressure distribution between limbs. This can be prevented by making the sides of the runway slightly inclined away from the pig.

Furthermore, there should be enough space before and after the actual mat for the pigs to accelerate and decelerate, so that they cross the pressure mat at a constant velocity. The pressure mat should be level with the rest of the runway, and the pigs should not be able to see the borders of the mat. This can easily be achieved by placing a rubber mat over the entire runway including the pressure mat, but the mat should be recalibrated after the rubber mat has been placed. Manufacturers are usually able to provide advice on optimal properties for the rubber mat. Since pigs are curious animals and will chew on anything they find interesting, distractions in the runway (such as cables, screws, changes in color of the floor or borders), as well as in the environment should be removed. An example of an experimental setup is shown in Fig. 39.9. The effect of sudden noises can be minimalized by having a radio playing during the measurements, as long as the pigs are used to the sound of the radio.

Gradually habituating pigs to the test apparatus, social isolation, and the presence of humans increases the efficiency of data collection and decreases the amount of stress an animal experiences. Pigs are social animals and isolation of an animal is known to cause stress (Herskin and Jensen, 2000; Kanitz et al., 2009), which in turn may negatively affect cognitive functioning and thus make training of the animals more difficult (Mendl, 1999; Schwabe and Wolf, 2010). Fear of the experimenter may cause hesitation while crossing the runway and will disrupt the normal gait pattern.

Pigs are easily trainable and they can be taught to cross the runway at a predetermined gait (walk, trot, or canter). We have good experiences with operant conditioning using a secondary reinforcer (clicker training) and with food rewards, such as M&M chocolates (Mars, Incorporated), as the primary reinforcer. Although training is time-consuming, it greatly facilitates data collection. This is particularly important when animals are used that have painful or debilitating conditions, as prolonged testing that may be required in untrained animals to obtain reliable runs may seriously impair their welfare. Also, experimental setups where animals are followed over time and measurements are performed more often may benefit from properly trained animals.

3.20 Conclusions

Gait analysis in pigs may be interesting as an outcome measure for neurological impairment. Several techniques are available. Pressure mat analysis is a promising tool that allows collection of several gait characteristics and multiple footfalls in one run. Some advantages and drawbacks of the technique are summed up in Table 39.6. A suitable setup of the testing apparatus and training of pigs greatly facilitates data collection and may improve the quality of the recorded data.
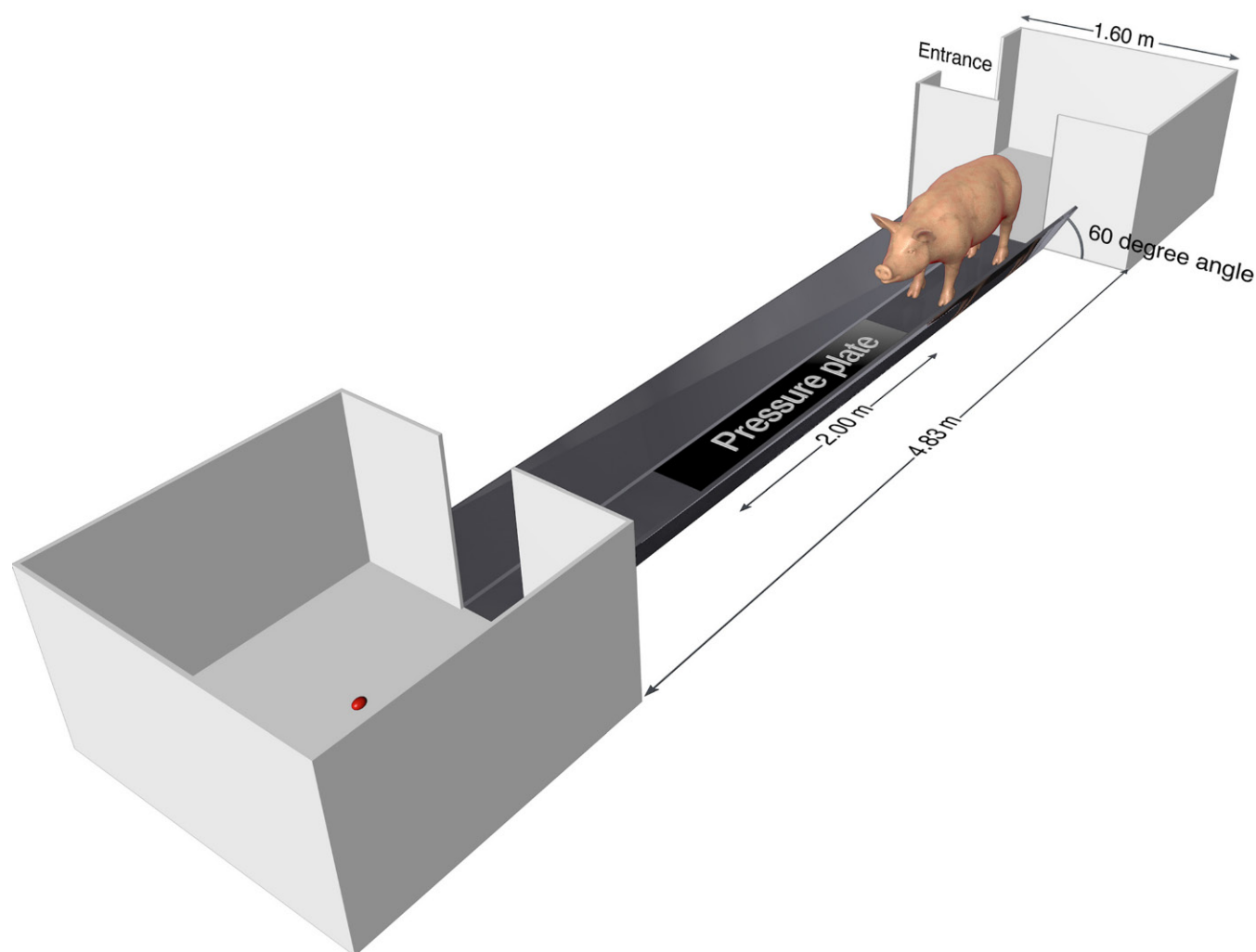
FIGURE 39.9 **Example of an experimental setup for collecting pressure mat data in pigs up to 60 kg of weight.** Walls of the runway are inclined to prevent pigs from leaning into them. Holding pens are situated at both ends of the runway. The pressure mat is built in level with the runway and the entire runway is then covered with a rubber mat (not shown).

4 WELFARE ASPECTS IN THE USE OF PIGS AS MODEL SPECIES

Minimizing unnecessary suffering and increasing the welfare of animals in general is imperative from a legal and ethical point of view. Regardless of the species of interest it is widely accepted that better welfare is inherent to better science. Poole (1997) was one of the first to state that "physiological and behavioral responses to avoidable suffering can act as experimental confounds…."

However, before elaborating on welfare aspects regarding the pig as model animal species we have to clarify some general questions.

4.1 Animal Welfare

The concept of animal welfare is poorly defined and, especially regarding farm animals like the pig, often based on the principle of the "five freedoms", which demand freedom from: (1) thirst, hunger, malnutrition; (2) suffering; (3) pain, injury, disease; (4) the freedom to express normal behavior; and (5) freedom from fear and distress (Newman, 1994) in order to safeguard welfare. The five freedoms, however, do not translate immediately into "measures" for animal welfare (Barnard, 2007; Cuthill, 2007; Ng, 1995; Terranova and Laviola, 2004; Weed and Raber, 2005) and have been criticized, for example, by Korte et al. (2007). Welfare of animals in their view is not at stake as long as the animal has the ability to meet environmental challenges. Other concepts of animal welfare, such as the concept of evolutionary salient welfare (Barnard and Hurst, 1996) are based on the idea that welfare is not at stake as long as the animal is able to fulfill its adaptive needs and is able to make its own decision. Ohl and van der Staay (2012) suggest a dynamic concept of animal welfare, taking the animal's ability

to cope with environmental challenges, the relevance of positive emotions, and the importance of so-called "negative" emotions into consideration. They state that "An individual is in a positive welfare state when it has the freedom adequately to react to hunger, thirst or incorrect food; thermal and physical discomfort; injuries or diseases; fear and chronic stress, and thus, the freedom to display normal behavioral patterns that allow the animal to adapt to the demands of the prevailing environmental circumstances and enable it to reach a state that it perceives as positive." (Ohl and van der Staay, 2012). This appears to represent one of the most appropriate concepts.

Irrespective of which welfare concept is favored, welfare criteria based on scientific evidence are needed, for example, in order to estimate animal suffering. However, identification and validation of welfare-related measures, the prerequisite to improve animal welfare, remains a major challenge and is subject to several studies (Boissy et al., 2007; Duncan, 2005; Yeates and Main, 2008).

4.1.1 Assessment of Welfare

The question remains how to assess welfare of animals. The animals' perception of its inner, thus emotional state is central to present concepts of "animal welfare" (Fraser and Duncan, 1998; Nordenfelt, 2011; Ohl and Putman, 2014; Ohl and van der Staay, 2012; Taylor and Mills, 2007; Webster, 2011). This perception can be inferred indirectly using behavioral and physiological measures. Those measures form the (biological) basis of animal welfare, since they allow to define target values (for welfare states), based on the demands (needs) and behavior of the animal [note that the fact, that those target values are influenced by moral concepts will not be discussed here. For an elaboration see, Ohl and van der Staay (2012)].

4.1.2 Pig Welfare

Chapter 3 elaborates on the relevance of large animal models and large animal model species, such as pigs, for research related to productivity, animal health, and for translational biomedical research. One should, however, not forget another important role of pigs: they are well suited to serve as models in pig-welfare related studies (Renggaman et al., 2015), since using the same species as model offers the highest amount of the external validity (generalizability) (van der Staay et al., 2009).

It is inherent to experimental work that welfare of the study subjects might be impaired. Thus, welfare needs to be taken into consideration at any stage of a study and any attempt must be made to avoid unnecessary impairment of welfare. Since the conceptual and assessment related assertions above are species-transcending, they are applicable to pigs as well. Concerns regarding the welfare of pigs have been raised. However, attention is mainly paid to pigs in (industrial) farming. Many of these concerns are also applicable to pigs used in research. However, the latter are frequently exposed to additional situations or procedures potentially affecting their welfare even more.

Better welfare of pigs and better science with pigs "go hand in hand" (Hawkins et al., 2014). Next to investigating factors that might lead to an impairment of welfare it is of outmost importance to gain more knowledge regarding indicators of positive pig welfare states.

Especially young animals are prone to the effects of environmental factors and handling (Hargreaves and Hutson, 1990) but experiences, like exposure to testing and training have potential consequences for emotional responses and thus the welfare of adult animals as well (Boissy et al., 2007). It is important to realize that stimulation and experiences have a high potential to modulate emotional responses.

4.2 Assessment and Improvement of Pig Welfare

4.2.1 Health of Pigs

As stated earlier, good health is essential for animal welfare. Clinical evaluation needs to be the first step when attempting to assess welfare of pigs. Clinical signs of injury or disease provide a first indication that welfare might be affected. Body condition scoring tools [MAFF (Ministry of Agriculture, Fisheries and Food (1998)], cardiovascular responses, and stress-related hormone measurements might especially be helpful in gaining such first indications of affected welfare. It is obvious that impaired health is inherent to certain experimental manipulations performed on pigs, however, unintended health impairments need to be detected and solved to forestall welfare impairments.

4.2.2 Needs of Pigs—General Remarks

In order to allow pigs to fulfil their needs and/or to provide them with the necessary resources, we need to gain knowledge about their needs. Broom and Johnson (1993) defined needs as "a requirement, which is a consequence of the biology of the animal, to obtain a particular resource or respond to a particular environment or bodily stimulus." Needs furthermore (very likely) vary with factors, such as age, sex, and genetic background and previous experiences. However, the needs of recently created genetically manipulated pigs (Søndergaard and Herskin, 2012) are almost unknown. Comprehensive knowledge about the actual needs of pigs is urgently needed.

The animal's perception of its emotional (welfare) state might be derived by the use of behavioral and physiologicalmeasures. This chapter describes a series of behavioral tests, allowing to gain information on pigs emotional perception and thus, being also useful for

gaining information about the effects of early life events on later emotional functioning.

We suggest that the assessment of welfare, regardless for which purpose an animal is used, should focus on the question whether an animal has the freedom and the capacity to adapt to environmental challenges, including those intrinsically tied to the experimental procedures applied in biomedical experiments.

4.2.3 Behavior in General

A prerequisite for conclusions on the adaptive capacity of an animal is knowledge of the normal/natural behavioral repertoire of the animal species in question (ethograms). Detailed information about the normal behavioral repertoire and the behavioral needs of farm animals is urgently needed. As early as 1978, Kilgour (1978) pointed to the exigency to obtain this basic information: "The ethogram of farm animals should have a high priority for current animal science goals and the farming system must be designed to fit the animal" (Kilgour, 1978, p. 1481).

For pigs, comprehensive ethograms are missing (although at least some ethograms for specific behavioral domains are available). To fall back on ethograms for the wild ancestor, the wild boar (*Sus scrofa*), is only an option under the assumption that domestication and selection on performance characteristics did not alter behavior. However, one needs to realize that the behavior of domesticated pigs is rooted in the wild pig (Baxter et al., 2011; D'Eath and Turner, 2009). Thus, certain behaviors seen in wild pigs might be important for the welfare of domesticated pigs as well.

4.2.4 Aggressive Behavior

Since 2013 sows on farms in the European Union must be housed in groups due to European legislation (DIRECTIVE 2008/120/EC) with the intention to improve welfare. Pigs are indeed socially living animals (Estevez et al., 2007) and individual housing of pigs is thus, generally speaking, a potential risk for welfare (see also Chapter 3). However, as discussed, for example, by Mendl et al. (1992) and Nicholson et al. (1993), aggression, as seen in group housed pigs, might result in an impairment of welfare since stress and injuries are very common consequences. Thus, several studies focus on measures of aggression [like, e.g., skin injuries (Meyer-Hamme et al., 2016)] in order to judge the effects on welfare. However, one has to realize that aggression is adaptive in nature and necessary for resource competition, offspring protection, defense and hierarchy-establishment (Koolhaas and Bohus, 1992). Thus, aggression might form a risk to welfare when its adaptive value is exceeded and consequences like stress and injuries (in receivers of aggression) are excessively present.

Several attempts have been made to reduce aggression among pigs to a minimum. Fredriksen et al. (2008) and Rydhmer et al. (2013), for example, recommend to socialize pigs early and to keep them in (sibling) groups. According to Day et al. (2002) the provision of rooting material (to distract the animals from penmates) successfully reduces aggression.

Dedicated mixing pens are recommended by Verdon et al. (2015). The authors, however, point out that the effects of housing in such mixing pens, on aggression (and stress), have not been investigated yet. Importantly, they point out that a secure development of a hierarchy may lead to less aggression when animals are mixed later in life with unfamiliar females and that such a secure development of a hierarchy might be realized by socialization of juvenile gilts (i.e., young female pig not yet mated, or not yet farrowed) to sows. In general, mixing sows that have been housed together earlier might help to reduce aggression as well (Verdon et al., 2015). The same authors furthermore mention hunger as a possible reason for aggressive behavior and recommend full-body length feeding stalls to reduce aggression (and stress). It is important to note that hunger as a transient state does not negatively affect welfare, because it represents a motivational state that triggers foraging and eating (Phillips et al., 2016). Thus, hunger is essential for the animal to protect its own welfare.

4.2.5 Affiliative Behavior

Pigs have been found to maintain preferential relationships (friendships) with other pigs (Stolba and Wood-Gush, 1984). Affiliative behavior may thus be essential for pig welfare. It is, however, important to identify valid measures of affiliation. Boissy et al. (2007) mention the risk of using proximity between individuals as a measure of affiliation. Proximity might simply be a result of limited space. Allogrooming belongs to the class of affiliative interactions and is believed to be part of pigs natural behavioral repertoire (Meynhardt, 1990), inducing relaxation in groomed pigs (Hansen and Von Borell, 1998). Nevertheless, pigs might experience disturbance due to being (excessively) groomed. Also here, more research is needed to verify the relevance for welfare.

4.2.6 Stereotypic Behavior

Stereotypic behavior has been investigated in pigs (Meunier-Salaün et al., 2001). However, whether the display of behavior reflects an impairment of welfare might be questioned, since, for example, Koolhaas et al. (1999) suggested that stereotypic behavior rather reflects a coping style.

4.2.7 Nest-Building Behavior

Damm et al. (2003) and Thodberg et al. (1999) found nest-building behavior to be essential for sows (at least approximately 1½ day before farrowing). Thus the provision of nesting material is essential for those sows (see also Baxter et al., 2011).

4.2.8 Anticipatory Behavior

Positive anticipation has been suggested to be useful in assessing positive emotional states (welfare) in animals (Boissy et al., 2007). Pigs indeed show increased locomotor activity and frequent behavioral transitions when anticipating food rewards (Dudink et al., 2006). The usefulness of anticipatory behavior in an attempt to draw conclusions on welfare must, however, be judged with care. If pigs do not show such reactions they might simply be fully satisfied or anhedonic (Boissy et al., 2007) or might not be able to learn to anticipate the delivery of feed at fixed time points of a day.

4.2.9 Emotions in General

The emotions discussed in the following can be inherent to certain experimental procedures, as discussed earlier in this chapter, and can thus affect the further life of the animal in question. Especially young pigs experiencing these emotions (unintended; excessively and thus adaptability-exceeding) might perform aberrant in experiments performed later in life (their welfare might have been affected, leading to long-term adverse consequences).

4.2.10 Fear and Anxiety

Fear and anxiety, investigated commonly in pigs (Forkman et al., 2007; Donald et al., 2011), are not negative by nature but trigger important adaptive responses (Ohl et al., 2008), and are not per se indicators of negatively affected welfare. Factors causing undesired, inappropriate, or prolonged anxiety (pathological anxiety; Ohl et al., 2008) need to be identified in order to remove or at least reduce them.

4.2.11 Pain

Like the emotions mentioned earlier, pain is an adaptive response, important for welfare (Ohl and van der Staay, 2012) and survival since it elicits protective vegetative and motor reactions, resulting in learned avoidance. The assessment of pain in animals is still a major challenge. There are some attempts to measure pain in pigs by investigating behavior (Meijer et al., 2015; Sutherland et al., 2012) and/or physiology [clinical and neuroendocrine approaches; Lonardi et al. (2015)]. However, pain is an individual sensation and thus, difficult to measure and compare among animals (Sneddon and Gentle, 2000).

Behavioral changes in general have been suggested to allow for the assessment of overall pain and discomfort by Hay et al. (2003), Moya et al. (2008), and Sutherland et al. (2012). Meijer et al. (2015) suggested locomotion asymmetry and spontaneous locomotor activity as potential indicators of pain associated with lameness in pigs. Classical physiological parameters used, probably indicative of pain, are clinical indicators, such as respiratory rate, blood pressure, rectal temperature, and heart rate in restrained awake piglets (White et al., 1995). A promising tool in assessing pain in pigs are changes in eye temperature due to sympatic and parasympathic systems variations (Lonardi et al., 2015).

All mentioned parameters potentially indicative for pain in pigs need, however, further validation. It is essential to take additional potentially confounding factors into consideration. Prunier et al. (2005), for example, made the important annotation that handling may interfere with physiological and behavioral responses of pigs.

Until valid measures of pain in pigs are available, one should, in particular, rely on the assumption that everything that causes pain in humans potentially causes pain in animals as well (Barnard and Hurst, 1996).

4.2.12 Stress

Stress is not negative by nature but an adaptive response. As outlined earlier, animals need to be able to adapt in order to safeguard welfare. In case the animal's adaptive capacity is reduced, the animal will experience chronic stress when adaptation to the environment is needed (Weiss, 1971) and welfare might be at stake (Korte et al., 2005; McEwen, 1998).

Unfortunately, valid measures for detecting when adaptive stress turns into distress (Holden, 2000) do not yet exist. Lack of control has been suggested to result in chronic stress (Heldt et al., 2002) and controllability has been suggested as being essential for animal welfare (Boissy et al., 2007). Thus, a controllable, or predictable environment is of high importance.

Fredriksen et al. (2008) suggested to socialize pigs early and to keep them in groups in order to reduce stress (Rydhmer et al., 2013). Furthermore, environmental enrichment might be helpful in preventing stress. Next to the fact that enrichment always needs to be decided on, taking the animals' biological needs into consideration, van der Staay et al. (see Chapter 3) made the important annotation that pigs need to be given the opportunity to learn to use enrichment. They furthermore elaborated on stressful situations for pigs on intensive farms. The majority of the discussed situations are applicable to pigs used as model animals in research: changes in housing systems, equipment, types of feed, introduction into groups of unfamiliar pigs, and the role of the human handlers. Thus, pigs in research need to be subjected to housing and experimental conditions with care, keeping possible consequences for welfare in mind.

4.2.13 Housing/Management Procedures

Welfare of pigs might be affected by several housing-related factors, such as space allowance, nutrition, group size, static and dynamic groups, mixing pens (Verdon et al., 2015).

Animals are highly motivated to perform behaviors that lead to the experience of positive emotional states. Housing or management procedures that allow the animals to perform those behaviors promote positive emotional states/welfare.

Pigs are highly motivated to play (Zupan et al., 2016). The degree of expression of this behavior has been considered to be indicative of good welfare (Lawrence and Appleby, 1996; Muller-Schwarze et al., 1982; Newberry et al., 1988; Siviy and Panksepp, 1985; Spinka et al., 2001). Furthermore, play seems to be essential for the development of social and cognitive abilities of many animal species (Fagen et al., 1981; Smith, 1982; Spinka et al., 2001) and of high importance especially during the neonatal period (Spinka et al., 2001). As summarized nicely by Martin et al. (2015) pigs show the whole spectrum of play behavior—including object-, social-, and locomotor play—and point out that play in pigs appears to be sex and age dependent and might form a training for the future.

Play behavior (in pigs) might thus be used as an indicator of welfare and should be stimulated whenever possible. The, probably, most important factor in promoting play is the environment since it can either stimulate or restrict (Martin et al., 2015).

If we intend to stimulate a certain behavior, such as play, we need to familiarize ourselves with the characteristics of the different categories of play (which holds true for all ethological readout parameters). The literature provides several ethograms for play in pigs (Martin et al., 2015; Zupan et al., 2016). As soon as we know what we are looking for we can test play-stimulating procedures/conditions.

Giving pigs the opportunity to play during neonatal development is essential, especially when exposed to behavioral testing later in life. Martin et al. (2015) observed that piglets kept in enriched, thus play-stimulating, environments develop greater sociocognitive abilities.

4.2.14 Space Allowance

Space is essential to pigs since they need to be able to move, assess resources, and to interact with each other and to explore (Verdon et al., 2015).

This factor becomes highly important within farrowing crates in which the execution of the behaviors listed earlier is severely restricted (Chidgey et al., 2016).

4.2.15 Enrichment

Enrichment is believed to improve animal welfare (van der Staay et al., 2009) allows, as stated (Ferguson, 2014) for pigs, the animal to fulfill its needs and to adapt to its environment. Based on these considerations, chains and bite sticks (Scott et al., 2006) and/or rooting material (Studnitz et al., 2007) are frequently given to pigs.

In order to decide on certain forms of enrichment, it is essential to take the animal's biological (behavioral) needs into consideration. The enrichment should be useful for the animal, as inappropriate enrichment can even lead to fear, anxiety, or stress. Pigs may lose interest in biologically nonrelevant enrichment quickly (Newberry, 1995; Van de Perre et al., 2011).

As pointed out by van der Staay et al. (Chapter 3) (cognitive) enrichment might be provided unintended: when testing animals, prior training is often required. This training and testing itself might act as (cognitively) enriching. Thus, while "unintended" enrichment might improve welfare on one side, at the same time it might mask the effects of experimental manipulations (Grimberg-Henrici et al., 2016; Westlund, 2014) In an attempt to make use of the (at least potentially) welfare increasing nature of such cognitive enrichment, the potentially experimental result-confounding characteristics need to be identified first.

4.2.16 Lighting Conditions

Operant preference tests in pigs revealed that they have a preference for lower light intensities (Roelofs et al., in press). This finding might be implemented in housing of pigs in general but also in experimental setups. Carrying out experiments under low light intensities does very likely correspond to the animal's needs and might thus improve welfare during testing.

4.2.17 Handling

Early life experiences, such as handling are quite influential as described earlier in this chapter and pigs have been found to be less fearful later in life when (positive) handling started early in life (Hemsworth et al., 1989).

4.2.18 Testing

Welfare might be at stake at different stages in a pig's life. This is especially important to realize when pigs are intended to be used as animal model species. Early welfare-impairing life experiences have a great potential to affect experimental results (e.g., during cognitive testing). But, when pigs are exposed to experimental studies their welfare might be at stake as well. Thus, within the test- and model evaluation process, the possible consequences of testing on the animals need to be investigated. Otherwise, the validity of the gained test results might be at stake (van der Staay et al., 2009).

Van der Staay and coworkers (see Chapter 3) raised another welfare-related concern within experimental animal work, applicable of course to pigs as well: widely accepted and implemented actions are taken in order to reduce the number of animals being used. This entails sometimes excessive reuse of animals. What does that mean for the welfare of those animals? It is of course desirable to reduce the number of experimental animals

(while still guaranteeing the validity and thus quality of research). However, we urgently need to investigate the possible welfare consequences of reusing pigs in subsequent, additional tests or additional studies.

4.2.19 The 3Rs

Russell et al. (1959) introduced the principle of the 3Rs (refinement, reduction, replacement) to the research community. It is inherent to "replacement" that welfare is not at stake since living animals are not used anymore. "Reduction" might entail welfare consequences if animals are excessively reused. "Refinement" appears to be the most important "R" when it comes to animal welfare since it represents the attempt to reduce negative effects on the animal's welfare by refining husbandry and experimental procedures (Nuffield Council on Bioethics, 2005). Adherence to the principles of the 3Rs is legally required in many countries. Research on the potentially welfare-improving qualities of certain refinement procedures can benefit pigs being used as model species but at the same time pigs used on farms. This becomes even clearer when one realizes that research with pigs is for the largest part carried out on farms and that thus experimental and farm animals are for a major part exposed to the same (e.g., housing and handling) procedures.

4.2.20 Humane Endpoints

A humane endpoint represents the very moment in an experiment at which pain and/or distress, experienced by the animal itself is alleviated or ended by means of discontinuing a procedure or humane killing of the animal in question (see e.g., "Humane endpoints in laboratory animal experimentation"; https://www.humane-endpoints.info/en).

There is ample literature dealing with humane endpoints in general, but almost no literature on humane endpoints for pigs exists. However, Ellegaard et al. (2010) elaborated on possible humane endpoints for the minipig based on the consideration that pain, distress, and discomfort are fundamental for the development and implementation of humane endpoints. The authors list the following signs as a potential basis for determining humane endpoints:

- decrease in bodyweight,
- locomotor or obvious signs of discomfort,
- not wagging the tail or the tail is held between the legs (look for tail bites),
- the animal crouches in a corner (and does not react to people entering),
- ears and head are hanging,
- lacks normal curiosity, and
- change in the normal vocalization pattern upon touch.

—*Ellegaard et al. (2010, p. 174)*

Next to the potential indicators of pain, stress, and discomfort described in this chapter these signs might be useful in determining humane endpoints for pigs.

5 CONCLUSIONS

Recent years have seen an increase in the use of pigs, particularly young pigs, in experimental animal models. While it seems clear that pigs have strong potential as models for young humans, and that examining effects of early life management practices on later life will give us insight into farm pig welfare, the utility of pig-based models can only be tested and validated with the use of reliable and valid tests. The reliability and validity of the tests described in the current chapter have to some extent been determined, but concerted efforts from groups involved in pig research should be undertaken to further develop tools for testing effects of early life events on behavior and welfare in pigs.

References

Andersen, A.D., Sangild, P.T., Munch, S.L., van der Beek, E.M., Renes, I.B., Ginneken, C.V., et al., 2016. Delayed growth, motor function and learning in preterm pigs during early postnatal life. Am. J. Physiol. 310, R481–R491.

Andersen, I.L., Færevik, G., Bøe, K.E., Janczak, A.M., Bakken, M., 2000. Effects of diazepam on the behaviour of weaned pigs in three putative models of anxiety. Appl. Anim. Behav. Sci. 68 (2), 121–130.

Anderson, J.R., Gallup, G.G., 2011. Which primates recognize themselves in mirrors? PLoS Biol. 9 (3), e1001024.

Andrews, C., Viviani, J., Egan, E., Bedford, T., Brilot, B., Nettle, D., Bateson, M., 2015. Early life adversity increases foraging and information gathering in European starlings, *Sturnus vulgaris*. Anim. Behav. 109, 123–132.

Antonides, A., Schoonderwoerd, A.C., Nordquist, R.E., van der Staay, F.J., 2015a. Very low birth weight piglets show improved cognitive performance in the spatial cognitive holeboard task. Front. Behav. Neurosci. 9, 43.

Antonides, A., Schoonderwoerd, A.C., Scholz, G., Berg, B.M., Nordquist, R.E., van der Staay, F.J., 2015b. Pre-weaning dietary iron deficiency impairs spatial learning and memory in the cognitive holeboard task in piglets. Front. Behav. Neurosci. 9, 291.

Arkell, M., Archer, R.M., Guitian, F.J., May, S.A., 2006. Evidence of bias affecting the interpretation of the results of local anaesthetic nerve blocks when assessing lameness in horses. Vet. Record 159 (11), 346–348.

Arts, J.W.M., van der Staay, F.J., Ekkel, E.D., 2009. Working and reference memory of pigs in the spatial holeboard discrimination task. Behav. Brain Res. 205 (1), 303–306.

Back, W., Clayton, H.M., 2013a. Gaits and interlimb coordination. In: Equine Locomotion, second ed. Saunders, St. Louis, USA., p. 85.

Back, W., Clayton, H.M., 2013b. Measurement techniques for gait analysis. In: Equine Locomotion, second ed. Saunders, St. Louis, USA.

Baldwin, B.A., Ingram, D.L., 1967. Behavioural thermoregulation in pigs. Physiol. Behav. 2 (1), 15–16.

Baldwin, B.A., Start, I.B., 1985. Illumination preferences of pigs. Appl. Anim. Behav. Sci. 14 (3), 233–243.

Barker, D.J., Martyn, C.N., 1992. The maternal and fetal origins of cardiovascular disease. J. Epidemiol. Commun. Health 46 (1), 8–11.

Barnard, C., 2007. Ethical regulation and animal science: why animal behaviour is special. Anim. Behav. 74, 5–13.

Barnard, C.J., Hurst, J.L., 1996. Welfare by design: the natural selection of welfare criteria. Anim. Welfare 5, 405–433.

Baxter, E.M., Lawrence, A.B., Edwards, S.A., 2011. Alternative farrowing systems: design criteria for farrowing systems based on the biological needs of sows and piglets. Animal 5 (4), 580–600.

Beattie, V.E., Walker, N., Sneddon, I.A., 1995. Effect of rearing environment and change of environment on the behaviour of gilts. Appl. Anim. Behav. Sci. 46 (1), 57–65.

Bechara, A., 2005. Decision making, impulse control and loss of willpower to resist drugs: a neurocognitive perspective. Nat. Neurosci. 8 (11), 1458–1463.

Bechara, A., Damasio, A.R., Damasio, H., Anderson, S.W., 1994. Insensitivity to future consequences following damage to human prefrontal cortex. Cognition 50 (1–3), 7–15.

Beilharz, R.G., Cox, D.F., 1967. Genetic analysis of open field behavior in swine. J. Anim. Sci. 26 (5), 988.

Bello, S., Krogsboll, L.T., Gruber, J., Zhao, Z.J., Fischer, D., Hrobjartsson, A., 2014. Lack of blinding of outcome assessors in animal model experiments implies risk of observer bias. J. Clin. Epidemiol. 67 (9), 973–983.

Bertholle, C.P., Meijer, E., Back, W., Stegeman, A., van Weeren, P.R., van Nes, A., 2016. A longitudinal study on the performance of in vivo methods to determine the osteochondrotic status of young pigs. BMC Vet. Res. 12, 62.

Beyerlein, A., Donnachie, E., Jergens, S., Ziegler, A., 2016. INfections in early life and development of type 1 diabetes. JAMA 315 (17), 1899–1901.

Boissy, A., Manteuffel, G., Jensen, M.B., Moe, R.O., Spruijt, B., Keeling, L.J., et al., 2007. Assessment of positive emotions in animals to improve their welfare. Physiol. Behav. 92 (3), 375–397.

Boleij, H., van't Klooster, J., Lavrijsen, M., Kirchhoff, S., Arndt, S.S., Ohl, F., 2012. A test to identify judgement bias in mice. Behav. Brain Res. 233 (1), 45–54.

Bolhuis, J.E., Oostindjer, M., Hoeks, C.W.F., de Haas, E.N., Bartels, A.C., Ooms, M., Kemp, B., 2013. Working and reference memory of pigs (Sus scrofa domesticus) in a holeboard spatial discrimination task: the influence of environmental enrichment. Anim. Cogn. 16 (5), 845–850.

Brajon, S., Laforest, J.-P., Schmitt, O., Devillers, N., 2015. The way humans behave modulates the emotional state of piglets. PloS One 10 (8), e0133408.

Brajon, S., Laforest, J.-P., Schmitt, O., Devillers, N., 2016. A preliminary study of the effects of individual response to challenge tests and stress induced by humans on learning performance of weaned piglets (Sus scrofa). Behav. Process. 129, 27–36.

Broom, D.M., Johnson, K.G., 1993. Stress and Animal Welfare. Springer, Netherlands.

Broom, D.M., Sena, H., Moynihan, K.L., 2009. Pigs learn what a mirror image represents and use it to obtain information. Anim. Behav. 78 (5), 1037–1041.

Budsberg, S.C., Jevens, D.J., Brown, J., Foutz, T.L., DeCamp, C.E., Reece, L., 1993. Evaluation of limb symmetry indices, using ground reaction forces in healthy dogs. Am. J. Vet. Res. 54 (10), 1569–1574.

Carlstead, K., Sheperdson, D., 2000. Alleviating stress in zoo animals with environmental enrichment. In: Moberg, G.P., Mench, J.A. (Eds.), The Biology of Animal Stress: Basic Principles and Implications for Animal Welfare. CABI, Wallingford, Oxon, UK, pp. 337–354.

Carvalho, V.C.de., de Alencar Nääs, I., Mollo Neto, M., Souza, S.R.L.de., 2009. Measurement of pig claw pressure distribution. Biosyst. Eng. 103 (3), 357–363.

Chidgey, K.L., Morel, P.C.H., Stafford, K.J., Barugh, I.W., 2016. Observations of sows and piglets housed in farrowing pens with temporary crating or farrowing crates on a commercial farm (vol. 176, p. 12, 2016). Appl. Anim. Behav. Sci. 179, 103.

Clouard, C., Kemp, B., Val-Laillet, D., Gerrits, W.J.J., Bartels, A.C., Bolhuis, J.E., 2016. Prenatal, but not early postnatal, exposure to a Western diet improves spatial memory of pigs later in life and is paired with changes in maternal prepartum blood lipid levels. FASEB J. 30 (7), 2466–2475.

Colborne, G.R., Good, L., Cozens, L.E., Kirk, L.S., 2011. Symmetry of hind limb mechanics in orthopedically normal trotting labrador retrievers. Am. J. Vet. Res. 72 (3), 336–344.

Colborne, G.R., Poma, R., Chambers, H., da Costa, R.C., Konyer, N.B., Nykamp, S., et al., 2008. Are sound dogs mechanically symmetric at trot? No, actually. Vet. Comp. Orthop. Traumatol. 21 (3), 294–301.

Conte, S., Bergeron, R., Gonyou, H., Brown, J., Rioja-Lang, F.C., Connor, L., Devillers, N., 2014. Measure and characterization of lameness in gestating sows using force plate, kinematic, and accelerometer methods. J. Anim. Sci. 92 (12), 5693–5703.

Coulon, M., Deputte, B.L., Heyman, Y., Baudoin, C., 2009. Individual recognition in domestic cattle (Bos taurus): evidence from 2D-images of heads from different breeds. PLoS One 4 (2), e4441.

Crannell, C.W., 1942. The choice point behavior of rats in a multiple path elimination problem. J. Psychol. 13 (2), 201–222.

Cuthill, I.C., 2007. Ethical regulation and animal science: why animal behaviour is not so special. Anim. Behav. 74 (1), 15–22.

D'Eath, R., 2012. Repeated locomotion scoring of a sow herd to measure lameness: consistency over time, the effect of sow characteristics and inter-observer reliability. Anim. Welfare 21 (2), 219–231.

D'Eath, R., Turner, S., 2009. The natural behaviour of the pig. In: Marchant-Forde, J., (Ed.) The Welfare of Pigs. Springer Science and Business Media, Dordrecht, Netherlands, pp. 13–45.

Damm, B.I., Lisborg, L., Vestergaard, K.S., Vanicek, J., 2003. Nestbuilding, behavioural disturbances and heart rate in farrowing sows kept in crates and Schmid pens. Livestock Prod. Sci. 80 (3), 175–187.

Day, J.E., Burfoot, A., Docking, C., Whittaker, X., Spoolder, H.A., Edwards, S., 2002. The effects of prior experience of straw and the level of straw provision on the behaviour of growing pigs. Appl. Anim. Behav. Sci. 76 (3), 189–202.

Day, J.E.L., Kyriazakis, I., Lawrence, A.B., 1995. The effect of food deprivation on the expression of foraging and exploratory behaviour in the growing pig. Appl. Anim. Behav. Sci. 42 (3), 193–206.

de Visser, L., Baars, A.M., Lavrijsen, M., van der Weerd, C.M.M., van den Bos, R., 2011. Decision-making performance is related to levels of anxiety and differential recruitment of frontostriatal areas in male rats. Neuroscience 184, 97–106.

de Vries, M., Holland, R., Witteman, C., 2008. In the winning mood: affect in the Iowa gambling task. Judgment Decision Making 3 (1), 42–50.

Dilger, R.N., Johnson, R.W., 2010. Behavioral assessment of cognitive function using a translational neonatal piglet model. Brain Behav. Immun. 24 (7), 1156–1165.

Donald, R.D., Healy, S.D., Lawrence, A.B., Rutherford, K.M.D., 2011. Emotionality in growing pigs: is the open field a valid test? Physiol. Behav. 104 (5), 906–913.

Douglas, C., Bateson, M., Walsh, C., Bédué, A., Edwards, S.A., 2012. Environmental enrichment induces optimistic cognitive biases in pigs. Appl. Anim. Behav. Sci. 139 (1–2), 65–73.

Dudink, S., Simonse, H., Marks, I., de Jonge, F.H., Spruijt, B.M., 2006. Announcing the arrival of enrichment increases play behaviour and reduces weaning-stress-induced behaviours of piglets directly after weaning. Appl. Anim. Behav. Sci. 101 (1–2), 86–101.

Duncan, I.J.H., 2005. Science-based assessment of animal welfare: farm animals. Rev. Sci. Tech. (Int. Off. Epizootics) 24 (2), 483–492.

Duysens, J., Van de Crommert, H.W.A.A., 1998. Neural control of locomotion; Part 1: the central pattern generator from cats to humans. Gait Posture 7 (2), 131–141.

Elford, J., Shaper, A.G., Whincup, P., 1992. Early life experience and cardiovascular disease—ecological studies. J. Epidemiol. Commun. Health 46 (1), 1–8.

Ellegaard, L., Cunningham, A., Edwards, S., Grand, N., Nevalainen, T., Prescott, M., Schuurman, T., 2010. Welfare of the minipig with special reference to use in regulatory toxicology studies. J. Pharmacol. Toxicol. Methods 62 (3), 167–183.

Elmore, M.R.P., Dilger, R.N., Johnson, R.W., 2012. Place and direction learning in a spatial T-maze task by neonatal piglets. Anim. Cogn. 15 (4), 667–676.

Entsu, S., Dohi, H., Yamada, A., 1992. Visual acuity of cattle determined by the method of discrimination learning. Appl. Anim. Behav. Sci. 34 (1), 1–10.

Enzerink, E., 1998. The menace response and pupillary light reflex in neonatal foals. Equine Vet. J. 30 (6), 546–548.

Estevez, I., Andersen, I.-L., Nævdal, E., 2007. Group size, density and social dynamics in farm animals. Too many, too few: the effects of group size and density in captive animals. Appl. Anim. Behav. Sci. 103 (3–4), 185–204.

Fagen, J., Yengo, L., Roveecollier, C., Enright, M., 1981. Reactivation of a visual-discrimination in early infancy. Dev. Psychol. 17 (3), 266–274.

Ferguson, D.M., 2014. Key features of "environmental fit" that promote good animal welfare in different husbandry systems. Rev. Sci. Tech. (Int. Off. Epizootics) 33 (1), 161–169.

Fernihough, J., Gentry, C., Malcangio, M., Fox, A., Rediske, J., Pellas, T., et al., 2004. Pain related behaviour in two models of osteoarthritis in the rat knee. Pain 112 (1–2), 83–93.

Ferreira, G., Keller, M., Saint-Dizier, H., Perrin, G., Lévy, F., 2004. Transfer between views of conspecific faces at different ages or in different orientations by sheep. Behav. Process. 67 (3), 491–499.

Fijn, L., Antonides, A., Aalderink, D., Nordquist, R.E., van der Staay, F.J., 2016. Does litter size affect emotionality, spatial learning and memory in piglets? Appl. Anim. Behav. Sci. 178, 23–31.

Forkman, B., Boissy, A., Meunier-Salaün, M.-C., Canali, E., Jones, R.B., 2007. A critical review of fear tests used on cattle, pigs, sheep, poultry and horses. Physiol. Behav. 92 (3), 340–374.

Fox, M.W., 1964a. A phylogenetic analysis of behavioral neuro-ontogeny in precocial and nonprecocial mammals. Can. J. Comp. Med. Vet. Sci. 28 (8), 197–202.

Fox, M.W., 1964b. The ontogeny of behaviour and neurologic responses in the dog. Anim. Behav. 12 (2), 301–310.

Fraser, D., 1974. The vocalizations and other behaviour of growing pigs in an "open field" test. Appl. Anim. Ethol. 1 (1), 3–16.

Fraser, D., Duncan, I.J.C., 1998. "Pleasure" "pains" and animal welfare: toward a natural history of affect. Anim. Welfare 7, 383–396.

Fraser, A.F., Broom, D.M., et al., 1990. Farm Animal Behaviour and Welfare. Ballière Tindall, London, UK.

Fredriksen, B., Lium, B.M., Marka, C.H., Mosveen, B., Nafstad, O., 2008. Entire male pigs in farrow-to-finish pens—effects on animal welfare. Appl. Anim. Behav. Sci. 110 (3–4), 258–268.

Gieling, E.T., Nordquist, R.E., van der Staay, F.J., 2011a. Assessing learning and memory in pigs. Anim. Cogn. 14 (2), 151–173.

Gieling, E.T., Schuurman, T., Nordquist, R.E., van der Staay, F.J., 2011b. The pig as a model animal for studying cognition and neurobehavioral disorders. Hagan, J.J. (Ed.), Molecular and Functional Models in Neuropsychiatry, 7, Springer Berlin Heidelberg, Berlin, Heidelberg, pp. 359–383.

Gieling, E.T., Schuurman, T., Nordquist, R.E., van der Staay, F.J., 2011c. The pig as a model animal for studying cognition and neurobehavioral disorders. Curr. Topics Behav. Neurosci. 7, 359–383.

Gieling, E.T., Musschenga, M.A., Nordquist, R.E., van der Staay, F.J., 2012a. Juvenile pigs use simple geometric 2D shapes but not portrait photographs of conspecifics as visual discriminative stimuli. Appl. Anim. Behav. Sci. 142 (3–4), 142–153.

Gieling, E.T., Park, S.Y., Nordquist, R.E., van der Staay, F.J., 2012b. Cognitive performance of low- and normal-birth-weight piglets in a spatial hole-board discrimination task. Pediatric Res. 71 (1), 71–76.

Gieling, E.T., Wehkamp, W., Willigenburg, R., Nordquist, R.E., Ganderup, N.-C., van der Staay, F.J., 2013. Performance of conventional pigs and Gottingen miniature pigs in a spatial holeboard task: effects of the putative muscarinic cognition impairer Biperiden. Behav. Brain Funct. 9, 4.

Gieling, E.T., Antonides, A., Fink-Gremmels, J., ter Haar, K., Kuller, W.I., Meijer, E., et al., 2014a. Chronic allopurinol treatment during the last trimester of pregnancy in sows: effects on low and normal birth weight offspring. Plos One 9 (1), e86396.

Gieling, E.T., Mijdam, E., van der Staay, F.J., Nordquist, R.E., 2014b. Lack of mirror use by pigs to locate food. Appl. Anim. Behav. Sci. 154, 22–29.

Givon, U., Zeilig, G., Achiron, A., 2009. Gait analysis in multiple sclerosis: characterization of temporal–spatial parameters using GAITRite functional ambulation system. Gait Posture 29 (1), 138–142.

Gordon-Evans, W.J., Evans, R.B., Conzemius, M.G., 2009. Accuracy of spatiotemporal variables in gait analysis of neurologic dogs. J. Neurotrauma 26 (7), 1055–1060.

Graf, R., 1976. Visual orientation in pigs in relation to the level of lighting. Rapporten Instituut voor Veeteeltkundig Onderzoek Schoonoord (Netherlands). no B 124. Available from: http://agris.fao.org/agris-search/search.do?recordID=NL19760123144

Grégoire, J., Bergeron, R., D'Allaire, S., Meunier-Salaün, M.-C., Devillers, N., 2013. Assessment of lameness in sows using gait, footprints, postural behaviour and foot lesion analysis. Animal 7 (7), 1163–1173.

Grimberg-Henrici, C.G.E., Vermaak, P., Bolhuis, J.E., Nordquist, R.E., van der Staay, F.J., 2016. Effects of environmental enrichment on cognitive performance of pigs in a spatial holeboard discrimination task. Anim. Cogn. 19 (2), 271–283.

Guldimann, K., Voegeli, S., Wolf, M., Wechsler, B., Gygax, L., 2015. Frontal brain deactivation during a non-verbal cognitive judgement bias test in sheep. Brain Cogn. 93, 35–41.

Haagensen, A.M.J., Grand, N., Klastrup, S., Skytte, C., Sørensen, D.B., 2013. Spatial discrimination and visual discrimination: two methods evaluating learning and memory in juvenile Göttingen minipigs. Behav. Pharmacol. 24 (3), 172–179.

Hajer, R., Hendrikse, J., Rutgers, L.J.E., Sloet van Oldruitenborgh-Oosterbaan, M.M., Weyden, G., 2000. Het klinisch onderzoek bij paard en landbouwhuisdieren. fourth ed. Elsevier gezondheidszorg, Maarssen.

Hansen, S., Von Borell, E., 1998. Impact of pig grouping on sympathovagal balance as measured by heart rate variability. Proceedings of the 32nd Congress of the ISAE, Clermont- Ferrand, France, p. 97.

Hargreaves, A.L., Hutson, G.D., 1990. Changes in heart rate, plasma cortisol and haematocrit of sheep during a shearing procedure. Appl. Anim. Behav. Sci. 26 (1), 91–101.

Hausdorff, J.M., Cudkowicz, M.E., Firtion, R., Wei, J.Y., Goldberger, A.L., 1998. Gait variability and basal ganglia disorders: Stride-to-stride variations of gait cycle timing in parkinson's disease and Huntington's disease. Mov. Disord. 13 (3), 428–437.

Hawkins, P., Clutton, R.E., Dennison, N., Guesgen, M., Leach, M., Sharpe, F., et al., 2014. Report of an RSPCA/AHVLA meeting on the welfare of agricultural animals in research: cattle, goats, pigs and sheep. Presented at the Animal Technology and Welfare.

Hay, M., Vulin, A., Genin, S., Sales, P., Prunier, A., 2003. Assessment of pain induced by castration in piglets: behavioral and physiological responses over the subsequent 5 days. Appl. Anim. Behav. Sci. 82 (3), 201–218.

Heldt, T., Shim, E.B., Kamm, R.D., Mark, R.G., 2002. Computational modeling of cardiovascular response to orthostatic stress. J. Appl. Physiol. 92 (3), 1239–1254.

Hemsworth, P.H., Barnett, J.L., Coleman, G.J., Hansen, C., 1989. A study of the relationships between the attitudinal and behavioural profiles of stockpersons and the level of fear of humans and reproductive performance of commercial pigs. Appl. Anim. Behav. Sci. 23 (4), 301–314.

Herskin, M.S., Jensen, K.H., 2000. Effects of different degrees of social isolation on the behaviour of weaned piglets kept for experimental purposes. Anim. Welfare 9 (3), 237–249.

Herzog, W., Nigg, B.M., Read, L.J., Olsson, E., 1989. Asymmetries in ground reaction force patterns in normal human gait. Med. Sci. Sports Exerc. 21 (1), 110–114.

Heschl, A., Burkart, J., 2006. A new mark test for mirror self-recognition in non-human primates. Primates 47 (3), 187–198.

Holden, C., 2000. Laboratory animals. Researchers pained by effort to define distress precisely. Science (New York, N.Y.) 290 (5496), 1474–1475.

Ishihara, A., Reed, S.M., Rajala-Schultz, P.J., Robertson, J.T., Bertone, A.L., 2009. Use of kinetic gait analysis for detection, quantification, and differentiation of hind limb lameness and spinal ataxia in horses. J. Am. Vet. Med. Assoc. 234 (5), 644–651.

Jensen, P., Forkman, B., Thodberg, K., Köster, E., 1995. Individual variation and consistency in piglet behaviour. Appl. Anim. Behav. Sci. 45 (1), 43–52.

Jones, J.B., Wathes, C.M., Webster, A.J.F., 1998. Operant responses of pigs to atmospheric ammonia. Appl. Anim. Behav. Sci. 58 (1–2), 35–47.

Kacelnik, A., Bateson, M., 1997. Risk-sensitivity: crossroads for theories of decision-making. Trends Cogn. Sci. 1 (8), 304–309.

Kanitz, E., Puppe, B., Tuchscherer, M., Heberer, M., Viergutz, T., Tuchscherer, A., 2009. A single exposure to social isolation in domestic piglets activates behavioural arousal, neuroendocrine stress hormones, and stress-related gene expression in the brain. Physiol. Behav. 98 (1–2), 176–185.

Karriker, L., Abell, C., Pairis-Garcia, M., Holt, W., Sun, G., Coetzee, J., et al., 2013. Validation of a lameness model in sows using physiological and mechanical measurements. J. Anim. Sci. 91 (1), 130–136.

Keegan, K.G., 2007. Evidence-based lameness detection and quantification. Vet. Clin. North Am. Equine Pract. 23 (2), 403–423.

Khumsap, S., Clayton, H.M., Lanovaz, J.L., Bouchey, M., 2002. Effect of walking velocity on forelimb kinematics and kinetics. Equine Vet. J. 34 (S34), 325–329.

Kilgour, R., 1978. The application of animal behavior and the humane care of farm animals. J. Anim. Sci. 46 (5), 1478–1486.

Koolhaas, J.M., Bohus, B., 1992. Animal models of human aggression. In: Boulton, A.A., Baker, G.B., Martin-Iverson, M.T. (Eds.), Animal Models in Psychiatry, II. Humana Press, Totowa, NJ, pp. 249–271.

Koolhaas, J.M., Korte, S.M., De Boer, S.F., van der, V., Van Reenen, C.G., Hopster, H., et al., 1999. Coping styles in animals: current status in behavior and stress-physiology. Neurosci. Biobehav. Rev. 23, 925–935.

Korte, S.M., Koolhaas, J.M., Wingfield, J.C., McEwen, B.S., 2005. The Darwinian concept of stress: benefits of allostasis and costs of allostatic load and the trade-offs in health and disease. Neurosci. Biobehav. Rev. 29 (1), 3–38.

Korte, S.M., Olivier, B., Koolhaas, J.M., 2007. A new animal welfare concept based on allostasis. Physiol. Behav. 92 (3), 422–428.

Krain, A.L., Wilson, A.M., Arbuckle, R., Castellanos, F.X., Milham, M.P., 2006. Distinct neural mechanisms of risk and ambiguity: a meta-analysis of decision-making. NeuroImage 32 (1), 477–484.

Lachman, S.J., Brown, C.R., 1957. Behavior in a free choice multiple path elimination problem. J. Psychol. 43 (1), 27–40.

Lawrence, A.B., Appleby, M.C., 1996. Behaviour and welfare of extensively farmed animals welfare of extensively farmed animals: principles and practice. Appl. Anim. Behav. Sci. 49 (1), 1–8.

Lawrence, A.B., Illius, A.W., 1989. Methodology for measuring hunger and food needs using operant conditioning in the pig. Appl. Anim. Behav. Sci. 24 (4), 273–285.

Lonardi, C., Scollo, A., Normando, S., Brscic, M., Gottardo, F., 2015. Can novel methods be useful for pain assessment of castrated piglets? Animal 9 (5), 871–877.

MAFF (Ministry of Agriculture, Fisheries and Food), 1998. Condition Scoring of Pigs. Ministry of Agriculture, Fisheries and Food, London.

Main, D.C.J., Clegg, J., Spatz, A., Green, L.E., 2000. Repeatability of a lameness scoring system for finishing pigs. Vet. Record 147 (20), 574–576.

Martin, P., Bateson, P., 2007. Measuring Behaviour: An Introductory Guide, third ed. Cambridge University Press, Cambridge.

Martin, J.E., Ison, S.H., Baxter, E.M., 2015. The influence of neonatal environment on piglet play behaviour and post-weaning social and cognitive development. Appl. Anim. Behav. Sci. 163, 69–79.

Matheson, S.L., Shepherd, A.M., Pinchbeck, R.M., Laurens, K.R., Carr, V.J., 2013. Childhood adversity in schizophrenia: a systematic meta-analysis. Psychol. Med. 43 (2), 225–238.

Mazur, J.E., 1988. Choice between small certain and large uncertain reinforcers. Anim. Learn. Behav. 16 (2), 199–205.

McEwen, B.S., 1998. Stress, adaptation, and disease—allostasis and allostatic load. McCann, S.M., Lipton, J.M., Sternberg, E.M., Chrousos, G.P., Gold, P.W., Smith, C.C. (Eds.), Neuroimmunomodulation: Molecular Aspects, Integrative Systems, and Clinical Advances, 840, New York Acad Sciences, New York, pp. 33–44.

McLaughin, Jr., R.M., Gaughan, E.M., Roush, J.K., Skaggs, C.L., 1996. Effects of subject velocity on ground reaction force measurements and stance times in clinically normal horses at the walk and trot. Am. J. Vet. Res. 57 (1), 7–11.

Medina, F.S., Taylor, A.H., Hunt, G.R., Gray, R.D., 2011. New Caledonian crows' responses to mirrors. Anim. Behav. 82 (5), 981–993.

Meijer, E., Oosterlinck, M., van Nes, A., Back, W., van der Staay, F.J., 2014a. Pressure mat analysis of naturally occurring lameness in young pigs after weaning. BMC Vet. Res. 10, 193.

Meijer, E., Bertholle, C.P., Oosterlinck, M., Van Der Staay, F.J., Back, W., Van Nes, A., 2014b. Pressure mat analysis of the longitudinal development of pig locomotion in growing pigs after weaning. BMC Vet. Res. 10 (1), 37.

Meijer, E., van Nes, A., Back, W., van der Staay, F.J., 2015. Clinical effects of buprenorphine on open field behaviour and gait symmetry in healthy and lame weaned piglets. Vet. J. 206 (3), 298–303.

Meléndez Suárez, D., 2014. Injection of vincristine into the dorsal hippocampus causes cognitive deficits in Long Evans rats. Utrecht University, Utrecht, the Netherlands (Unpublished Masters Thesis).

Mendl, M., 1999. Performing under pressure: stress and cognitive function. Appl. Anim. Behav. Sci. 65 (3), 221–244.

Mendl, M., Burman, O.H.P., Parker, R.M.A., Paul, E.S., 2009. Cognitive bias as an indicator of animal emotion and welfare: emerging evidence and underlying mechanisms. Special Issue: Anim. Suffer. Welfare 118 (3–4), 161–181.

Mendl, M., Burman, O.H.P., Paul, E.S., 2010. An integrative and functional framework for the study of animal emotion and mood. Proceedings of the Royal Society B: Biological Sciences 277, 2895–2904.

Mendl, M., Zanella, A.J., Broom, D.M., 1992. Physiological and reproductive correlates of behavioural strategies in female domestic pigs. Anim. Behav. 44 (6), 1107–1121.

Menzel, E.W., Savage-Rumbaugh, E.S., Lawson, J., 1985. Chimpanzee (*Pan troglodytes*) spatial problem solving with the use of mirrors and televised equivalents of mirrors. J. Comp. Psychol. 99 (2), 211–217.

Meunier-Salaün, M.C., Edwards, S.A., Robert, S., 2001. Effect of dietary fibre on the behaviour and health of the restricted fed sow. Anim. Feed Sci. Technol. 90 (1–2), 53–69.

Meyer-Hamme, S.E.K., Lambertz, C., Gauly, M., 2016. Does group size have an impact on welfare indicators in fattening pigs? Animal 10 (1), 142–149.

Meynhardt, H., 1990. Schwarzwild-Report: Mein Leben Unter Wildschweinen. Neumann, Melsungen.

Miu, A.C., Heilman, R.M., Houser, D., 2008. Anxiety impairs decision-making: psychophysiological evidence from an Iowa Gambling Task. Biol. Psychol. 77 (3), 353–358.

Mokkink, L.B., Terwee, C.B., Stratford, P.W., Alonso, J., Patrick, D.L., Riphagen, I., et al., 2009. Evaluation of the methodological quality

of systematic reviews of health status measurement instruments. Qual. Life Res. 18 (3), 313–333.

Mölsä, S.H., Hielm-Björkman, A.K., Laitinen-Vapaavuori, O.M., 2010. Force platform analysis in clinically healthy rottweilers: comparison with labrador retrievers. Vet. Surg. 39 (6), 701–707.

Moya, S.L., Boyle, L.A., Lynch, P.B., Arkins, S., 2008. Effect of surgical castration on the behavioural and acute phase responses of 5-day-old piglets. Appl. Anim. Behav. Sci. 111 (1–2), 133–145.

Muir, G.D., 2000. Early ontogeny of locomotor behaviour: a comparison between altricial and precocial animals. Brain Res. Bull. 53 (5), 719–726.

Muller-Schwarze, D., Stagge, B., Muller-Schwarze, C., 1982. Play behavior: persistence, decrease, and energetic compensation during food shortage in deer fawns. Science (New York, N.Y.) 215 (4528), 85–87.

Murphy, E., Kraak, L., Nordquist, R.E., van der Staay, F.J., 2013a. Successive and conditional discrimination learning in pigs. Anim. Cogn. 16 (6), 883–893.

Murphy, E., Kraak, L., van den Broek, J., Nordquist, R.E., van der Staay, F.J., 2015. Decision-making under risk and ambiguity in low-birth-weight pigs. Anim. Cogn. 18 (2), 561–572.

Murphy, E., Nordquist, R.E., van der Staay, F.J., 2013b. Responses of conventional pigs and Gottingen miniature pigs in an active choice judgement bias task. Appl. Anim. Behav. Sci. 148 (1–2), 64–76.

Murphy, E., Nordquist, R.E., van der Staay, F.J., 2014. A review of behavioural methods to study emotion and mood in pigs, *Sus scrofa*. Appl. Anim. Behav. Sci. 159, 9–28.

Mustonen, K., Ala-Kurikka, E., Orro, T., Peltoniemi, O., Raekallio, M., Vainio, O., Heinonen, M., 2011. Oral ketoprofen is effective in the treatment of non-infectious lameness in sows. Vet. J. 190 (1), 55–59.

Naim, M.Y., Friess, S., Smith, C., Ralston, J., Ryall, K., Helfaer, M.A., Margulies, S.S., 2010. Folic acid enhances early functional recovery in a piglet model of pediatric head injury. Dev. Neurosci. 32 (5–6), 454–467.

Newberry, R., 1995. Environmental enrichment—increasing the biological relevance of captive environments. Appl. Anim. Behav. Sci. 44 (2–4), 229–243.

Newberry, R.C., Wood-Gush, D.G.M., Hall, J.W., 1988. Playful behaviour of piglets. Behav. Process. 17 (3), 205–216.

Newman, S., 1994. Quantitative- and molecular-genetic effects on animal well-being: adaptive mechanisms. J. Anim. Sci. 72 (6), 1641–1653.

Ng, Y.-K., 1995. Towards welfare biology: evolutionary economics of animal consciousness and suffering. Biol. Philos. 10 (3), 255–285.

Nicholson, R.I., McGlone, J.J., Norman, R.L., 1993. Quantification of stress in sows: comparison of individual housing versus social penning. J. Anim. Sci. 71 (Suppl. 1), 112.

Nielsen, J.B., 2003. How we walk: central control of muscle activity during human walking. Neuroscientist 9 (3), 195–204.

Nordenfelt, L., 2011. Health and welfare in animals and humans. Acta Biotheoret. 59, 139–152.

Nordquist, B., Fischer, J., Kim, S.Y., Stover, S.M., Garcia-Nolen, T., Hayashi, K., et al., 2011. Effects of trial repetition, limb side, intra-day and inter-week variation on vertical and craniocaudal ground reaction forces in clinically normal labrador retrievers. Vet. Comp. Orthopaedics Traumatol. 24 (6), 435–444.

Nuffield Council on Bioethics, 2005. The Ethics of Research Involving Animals. London. Available from: http://www.nuffieldbioethics.org/

Ohl, F., Arndt, S.S., van der Staay, F.J., 2008. Pathological anxiety in animals. Vet. J. 175 (1), 18–26.

Ohl, F., Putman, R.J., 2014. Animal welfare at the group level: more than the sum of individual welfare? Acta Biotheoret. 62, 35–45.

Ohl, F., van der Staay, F.J., 2012. Animal welfare: at the interface between science and society. Vet. J. 192 (1), 13–19.

Olton, D.S., Samuelson, R.J., 1976. Remembrance of places passed: spatial memory in rats. J. Exp. Psychol. Anim. Behav. Process. 2 (2), 97–116.

Oosterlinck, M., Pille, F., Back, W., Dewulf, J., Gasthuys, F., 2011. A pressure plate study on fore and hindlimb loading and the association with hoof contact area in sound ponies at the walk and trot. Vet. J. 190 (1), 71–76.

Pairis-Garcia, M., Johnson, A., Abell, C., Coetzee, J., Karriker, L., Millman, S., Stalder, K., 2015. Measuring the efficacy of flunixin meglumine and meloxicam for lame sows using a GAITFour pressure mat and an embedded microcomputer-based force plate system. J. Anim. Sci. 93 (5), 2100.

Pechtel, P., Pizzagalli, D.A., 2011. Effects of early life stress on cognitive and affective function: an integrated review of human literature. Psychopharmacology 214 (1), 55–70.

Pedersen, L.J., Jensen, M.B., Hansen, S.W., Munksgaard, L., Ladewig, J., Matthews, L., 2002. Social isolation affects the motivation to work for food and straw in pigs as measured by operant conditioning techniques. Appl. Anim. Behav. Sci. 77 (4), 295–309.

Pepperberg, I.M., Garcia, S.E., Jackson, E.C., Marconi, S., 1995. Mirror use by African Grey parrots (*Psittacus erithacus*). J. Comp. Psychol. 109 (2), 182–195.

Petersen, H.H., Enøe, C., Nielsen, E.O., 2004. Observer agreement on pen level prevalence of clinical signs in finishing pigs. Prev. Vet. Med. 64 (2), 147–156.

Phillips , C.J.C. (Ed.), Tolkamp, B.J., D'Eath, R.B., 2016. Hunger associated with restricted feeding systems. In: Nutrition and the Welfare of Farm Animals. Springer International Publishing, pp. 11–27.

Pluym, L., Maes, D., Vangeyte, J., Mertens, K., Baert, J., Van Weyenberg, S., et al., 2013. Development of a system for automatic measurements of force and visual stance variables for objective lameness detection in sows: SowSIS. Biosyst. Eng. 116 (1), 64–74.

Poletto, R., Siegford, J.M., Steibel, J.P., Coussens, P.M., Zanella, A.J., 2006. Investigation of changes in global gene expression in the frontal cortex of early-weaned and socially isolated piglets using micro-array and quantitative real-time RT-PCR. Brain Res. 1068 (1), 7–15.

Pomerantz, O., Terkel, J., 2009. Effects of positive reinforcement training techniques on the psychological welfare of zoo-housed chimpanzees (*Pan troglodytes*). Am. J. Primatol. 71 (8), 687–695.

Poole, T., 1997. Happy animals make good science. Lab. Anim. 31 (2), 116–124.

Potenza, M.N., 2009. The importance of animal models of decision-making, gambling and related behaviors: implications for translational research in addiction. Neuropsychopharmacology 34 (13), 2623–2624.

Povinelli, D.J., 1989. Failure to find self-recognition in Asian elephants (*Elephas maximus*) in contrast to their use of mirror cues to discover hidden food. J. Comp. Psychol. 103 (2), 122–131.

Prunier, A., Mounier, A.M., Hay, M., 2005. Effects of castration, tooth resection, or tail docking on plasma metabolites and stress hormones in young pigs. J. Anim. Sci. 83 (1), 216–222.

Prut, L., Belzung, C., 2003. The open field as a paradigm to measure the effects of drugs on anxiety-like behaviors: a review. Eur. J. Pharmacol. 463 (1–3), 3–33.

Puppe, B., Ernst, K., Schoen, P.C., Manteuffel, G., 2007. Cognitive enrichment affects behavioural reactivity in domestic pigs. Appl. Anim. Behav. Sci. 105 (1–3), 75–86.

Radostits, O.M., Gay, C.C., Hinchcliff, K.W., Constable, P.D., 2007. Veterinary Medicine, tenth ed. Saunders Elsevier, Edinbrugh, UK.

Renggaman, A., Choi, H.L., Sudiarto, S.I., Alasaarela, L., Nam, O.S., 2015. Development of pig welfare assessment protocol integrating animal-, environment-, and management-based measures. J. Anim. Sci. Technol. 57 (1), 1–11.

Roelofs, S., Boleij, H., Nordquist, R.E., van der Staay, F.J., 2016. Making decisions under ambiguity: judgment bias tasks for assessing emotional state in animals. Front. Behav. Neurosci. 10, 119.

Roelofs, S., Murphy, E., Ni, H., Gieling, E.T., Nordquist, R.E. and van der Staay, F.J., Judgement bias in pigs is independent from performance in a spatial holeboard task and conditional discrimination learning. Anim. Cogn. in press

Rooij, S.R., de, Wouters, H., Yonker, J.E., Painter, R.C., Roseboom, T.J., 2010. Prenatal undernutrition and cognitive function in late adulthood. Proc. Natl. Acad. Sci. 107 (39), 16881–16886.

Roseboom, T., de Rooij, S., Painter, R., 2006. The Dutch famine and its long-term consequences for adult health. Early Hum. Dev. 82 (8), 485–491.

Ruis, M.A.W., te Brake, J.H.A., Engel, B., Buist, W.G., Blokhuis, H.J., Koolhaas, J.M., 2001. Adaptation to social isolation: acute and long-term stress responses of growing gilts with different coping characteristics. Physiol. Behav. 73 (4), 541–551.

Russell, W.M. S., Burch, R.L., Hume, C.W., 1959. The Principles of Humane Experimental Technique. Available from: http://altweb.jhsph.edu/pubs/books/humane_exp/addendum.

Rydhmer, L., Hansson, M., Lundstrom, K., Brunius, C., Andersson, K., 2013. Welfare of entire male pigs is improved by socialising piglets and keeping intact groups until slaughter. Animal 7 (9), 1532–1541.

Sadeghi, H., Allard, P., Prince, F., Labelle, H., 2000. Symmetry and limb dominance in able-bodied gait: a review. Gait Posture 12 (1), 34–45.

Sahyoun, C., Floyer-Lea, A., Johansen-Berg, H., Matthews, P.M., 2004. Towards an understanding of gait control: brain activation during the anticipation, preparation and execution of foot movements. NeuroImage 21 (2), 568–575.

Schwabe, L., Wolf, O.T., 2010. Learning under stress impairs memory formation. Neurobiol. Learn. Memory 93 (2), 183–188.

Scott, K., Taylor, L., Gill, B.P., Edwards, S.A., 2006. Influence of different types of environmental enrichment on the behaviour of finishing pigs housing in two different systems—1. Hanging toy versus rootable substrate. Appl. Anim. Behav. Sci. 99 (3–4), 222–229.

Siviy, S.M., Panksepp, J., 1985. Energy balance and play in juvenile rats. Physiol. Behav. 35 (3), 435–441.

Smith, E.O., 1982. Animal play behavior. By Robert Fagen. New York: Oxford University Press. 1981. XVIII + 684 pp., figures, tables, references, indices. $19. 95 (paper). Am. J. Phys. Anthropol. 58 (1), 117.

Sneddon, L.U., Gentle, M.J., 2000. Pain in farm animals. Presented at the Workshop 5 on Sustainable Animal Production, Mariensee, Germany

Søndergaard, L.V., Herskin, 2012. Does size matter—considerations of importance for choice of animal species in a transgenic model for Alzheimer's disease. Graue Reihe 51, 84–99.

Souza da Silva, C., van den Borne, J.J.G.C., Gerrits, W.J.J., Kemp, B., Bolhuis, J.E., 2012. Effects of dietary fibers with different physicochemical properties on feeding motivation in adult female pigs. Physiol. Behav. 107 (2), 218–230.

Spinka, M., Newberry, R.C., Bekoff, M., 2001. Mammalian play: training for the unexpected. Quart. Rev. Biol. 76 (2), 141–168.

Stavrakakis, S., Guy, J.H., Syranidis, I., Johnson, G.R., Edwards, S.A., 2015a. Pre-clinical and clinical walking kinematics in female breeding pigs with lameness: a nested case-control cohort study. Vet. J. 205 (1), 38–43.

Stavrakakis, S., Li, W., Guy, J.H., Morgan, G., Ushaw, G., Johnson, G.R., Edwards, S.A., 2015b. Validity of the Microsoft Kinect sensor for assessment of normal walking patterns in pigs. Comp. Electron. Agric. 117, 1–7.

Stolba, A., Wood-Gush, D.G., 1984. The identification of behavioural key features and their incorporation into a housing design for pigs. Ann. Vet. Res. 15 (2), 287–299.

Stolze, H., Kuhtz-Buschbeck, J.P., Drücke, H., Jöhnk, K., Illert, M., Deuschl, G., 2001. Comparative analysis of the gait disorder of normal pressure hydrocephalus and Parkinson's disease. J. Neurol. Neurosurg. Psychiatry 70 (3), 289–297.

Studnitz, M., Jensen, M.B., Pedersen, L.J., 2007. Why do pigs root and in what will they root?: A review on the exploratory behaviour of pigs in relation to environmental enrichment. Appl. Anim. Behav. Sci. 107 (3–4), 183–197.

Sun, G., Fitzgerald, R., Stalder, K., Karriker, L., Johnson, A., Hoff, S., 2011. Development of an embedded microcomputer-based force plate system for measuring sow weight distribution and detection of lameness. Appl. Eng. Agric. 27 (3), 475.

Sutherland, M.A., Davis, B.L., Brooks, T.A., Coetzee, J.F., 2012. The physiological and behavioral response of pigs castrated with and without anesthesia or analgesia. J. Anim. Sci. 90 (7), 2211–2221.

Tanaka, T., Hashimoto, A., Tanida, H., Yoshimoto, T., 1995. Studies on the visual acuity of sheep using shape discrimination learning. J. Ethol. 13(1), 69–75.

Taylor, S.E., 2010. Mechanisms linking early life stress to adult health outcomes. Proc. Natl. Acad. Sci. 107 (19), 8507–8512.

Taylor, K.D., Mills, D.S., 2007. Is quality of life a useful concept for companion animals? Anim. Welfare 16 (S), 55–66.

Terranova, M.L., Laviola, G., 2004. Health-promoting factors and animal welfare. Annali dell'Istituto Superiore Di Sanita 40 (2), 187–193.

Thodberg, K., Jensen, K.H., Herskin, M.S., Jørgensen, E., 1999. Influence of environmental stimuli on nest building and farrowing behaviour in domestic sows. Appl. Anim. Behav. Sci. 63 (2), 131–144.

Thorup, V.M., Tøgersen, F.A., Jørgensen, B., Jensen, B.R., 2007. Biomechanical gait analysis of pigs walking on solid concrete floor. Animal 1, 708–715.

Thorup, V.M., Laursen, B., Jensen, B.R., 2008. Net joint kinetics in the limbs of pigs walking on concrete floor in dry and contaminated conditions. J. Anim. Sci. 86 (4), 992–998.

Van de Perre, V., Driessen, B., Van Thielen, J., Verbeke, G., Geers, R., 2011. Comparison of pig behaviour when given a sequence of enrichment objects or a chain continuously 20, 641–649.

van der Staay, F.J., Arndt, S.S., Nordquist, R.E., 2009. Evaluation of animal models of neurobehavioral disorders. Behav. Brain Funct. 5, 11.

van der Staay, F.J., Bouger, P.C., 2005. Effects of the cholinesterase inhibitors donepezil and metrifonate on scopolamine-induced impairments in the spatial cone field orientation task in rats. Behav. Brain Res. 156 (1), 1–10.

van der Staay, F.J., Schoonderwoerd, A.J., Stadhouders, B., Nordquist, R.E., 2016. Overnight social isolation in pigs decreases salivary cortisol but does not impair spatial learning and memory or performance in a decision-making task. Anim. Behav. Welfare 2, 81.

van Eck, L.M., Antonides, A., Nordquist, R.E., van der Staay, F.J., 2016. Testing post-weaning food motivation in low and normal birth weight pigs in a runway and operant conditioning task. Appl. Anim. Behav. Sci. 181, 83–90.

Van Steenbergen, E.J., 1989. Description and evaluation of a linear scoring system for exterior traits in pigs. Livestock Prod. Sci. 23 (1), 163–181.

Verdon, M., Hansen, C.F., Rault, J.-L., Jongman, E., Hansen, L.U., Plush, K., Hemsworth, P.H., 2015. Effects of group housing on sow welfare: a review. J. Anim. Sci. 93 (5), 1999–2017.

Von Wachenfelt, H., Pinzke, S., Nilsson, C., 2009a. Gait and force analysis of provoked pig gait on clean and fouled concrete surfaces. Biosyst. Eng. 104 (4), 534–544.

Von Wachenfelt, H., Pinzke, S., Nilsson, C., Olsson, O., Ehlorsson, C.-J., 2009b. Force analysis of unprovoked pig gait on clean and fouled concrete surfaces. Biosyst. Eng. 104 (2), 250–257.

Von Wachenfelt, H., Nilsson, C., Pinzke, S., 2010. Gait and force analysis of provoked pig gait on clean and fouled rubber mat surfaces. Biosyst. Eng. 106 (1), 86–96.

Vrinten, D.H., Hamers, F.F., 2003. 'CatWalk' automated quantitative gait analysis as a novel method to assess mechanical allodynia in the rat; a comparison with von Frey testing. Pain 102 (1), 203–209.

Weary, D.M., Huzzey, J.M., von Keyserlingk, M.A.G., 2008. BOARD-INVITED REVIEW: using behavior to predict and identify ill health in animals. J. Anim. Sci. 87 (2), 770–777.

Webster, J., 2011. Zoomorphism and anthropomorphism: fruitful fallacies? Anim. Welfare 20, 29–36.

Weed, J.L., Raber, J.M., 2005. Balancing animal research with animal well-being: establishment of goals and harmonization of approaches. ILAR J./Natl. Res. Council, Inst. Lab. Anim. Resour. 46 (2), 118–128.

Weishaupt, M.A., 2008. Adaptation strategies of horses with lameness. Vet. Clin. North Am. Equine Pract. 24 (1), 79–100.

Weiss, J.M., 1971. Effects of coping behavior in different warning signal conditions on stress pathology in rats. J. Comp. Physiol. Psychol. 77 (1), 1–13.

Westlund, K., 2014. Training is enrichment—and beyond. Appl. Anim. Behav. Sci. 152, 1–6.

White, R.G., DeShazer, J.A., Tressler, C.J., Borcher, G.M., Davey, S., Waninge, A., et al., 1995. Vocalization and physiological response of pigs during castration with or without a local anesthetic. J. Anim. Sci. 73 (2), 381–386.

Yeates, J.W., Main, D.C.J., 2008. Assessment of positive welfare: a review. Vet. J. (London, England: 1997) 175 (3), 293–300.

Zebunke, M., Langbein, J., Manteuffel, G., Puppe, B., 2011. Autonomic reactions indicating positive affect during acoustic reward learning in domestic pigs. Anim. Behav. 81 (2), 481–489.

Zonderland, J.J., Cornelissen, L., Wolthuis-Fillerup, M., Spoolder, H.A.M., 2008. Visual acuity of pigs at different light intensities. Appl. Anim. Behav. Sci. 111 (1), 28–37.

Zupan, M., Rehn, T., de Oliveira, D., Keeling, L.J., 2016. Promoting positive states: the effect of early human handling on play and exploratory behaviour in pigs. Animal 10 (1), 135–141.

40

Animal Models of Alzheimer's Disease

Morgan Newman*, Doris Kretzschmar**, Imran Khan[†,‡,§],
Mengqi Chen[¶], Giuseppe Verdile[†,‡,§], Michael Lardelli*

*University of Adelaide, Adelaide, SA, Australia
**Oregon Institute of Occupational Health Sciences,
Oregon Health & Sciences University, Portland, OR, United States
[†]Curtin Health Innovation Research Institute—Biosciences, Curtin University,
Bentley, WA, Australia
[‡]The University of Western Australia, Crawley, WA, Australia
[§]Hollywood Medical Centre, Nedlands, WA, Australia
[¶]Centre of Excellence for Alzheimer's Disease Research and Care, Edith Cowan University,
Joondalup, WA, Australia

1 INTRODUCTION

Alzheimer's disease is the most common form of human neurodegenerative disease. Worldwide, around 36 million people are known to suffer from dementia and the majority of these have Alzheimer's disease (World Alzheimer Report 2010: The Global Impact of Dementia, 2010). Total worldwide costs of dementia exceeded US $600 billion in 2010 equaling about 1% of world GDP and these costs are projected to rise as the average age of the world's population increases (World Alzheimer Report 2010: The Global Impact of Dementia, 2010). The ability to delay the average age of onset of Alzheimer's disease by even relative short periods could result in large budgetary savings for national health systems (Barnes and Yaffe, 2011; Ltd., 2004). Therefore, research into understanding the pathogenesis of Alzheimer's disease is well motivated.

Alzheimer's disease is broadly classified into two forms. A rare, familial early-onset form (FAD) accounts

for less than 1% of Alzheimer's disease cases (Cruchaga et al., 2012). It is defined as occurring before 65 years of age and is commonly caused by dominant mutations in one of three genes, the *PRESENILIN1* (*PSEN1*), *PRESENILIN2* (*PSEN2*), and *AMYLOID BETA A4 PRECURSOR PROTEIN* (*APP*) genes. The common, late-onset form of Alzheimer's disease occurs from 65 years of age and is frequently regarded as "sporadic" (SAD) without obvious familial inheritance. Nevertheless, it is now evident that mutations in the three genes mentioned earlier can increase the risk of late-onset Alzheimer's disease (Cruchaga et al., 2012). Polymorphisms at a number of other genetic loci have been identified as contributing to the risk of late-onset Alzheimer's disease. The most prominent locus is the gene *APOLIPOPROTEIN E* [*APOE*, (Saunders et al., 1993)] but genome-wide association studies (GWAS) have suggested roles in Alzheimer's disease pathogenesis for numerous other loci [reviewed in Moraes et al. (2012)].

Clinically, Alzheimer's disease is characterized by progressive deterioration of memory and thinking ability and changes in behavior, such as increased mood swings and aggression before eventual withdrawal from communication and interpersonal relationships ultimately leading to death (Neugroschl and Wang, 2011). Confirmation of Alzheimer's disease diagnosis requires postmortem histopathological examination of the brain to demonstrate the characteristic presence of extracellular deposits (plaques) of amyloidβ peptide (a proteolytic product of APP) and intracellular aggregations of the tau protein [derived from the gene *MICROTUBULE-ASSOCIATED PROTEIN TAU* (*MAPT*) (Goedert et al., 1988)] in the hippocampus and neocortex. Alzheimer's disease histopathology also commonly includes reactive gliosis (Serrano-Pozo et al., 2011) and the inappropriate reentry of neurons into a cell cycle that they cannot complete [cell-cycle events (Busser et al., 1998)]. Oxidative stress is also an early marker of Alzheimer's disease pathology and it is now widely understood that the pathological process leading to Alzheimer's disease begins decades before overt symptoms become evident (Nunomura et al., 2001).

Alzheimer's disease was first defined as a distinctive form of dementia by Alois Alzheimer over 100 years ago (Cipriani et al., 2011). By mid-2016 the scientific literature had accumulated over 117,000 papers addressing the disease but there is still no consensus regarding its cause(s) or the molecular mechanisms that underlie the disease process. Tens of hypotheses for the pathological mechanisms underlying Alzheimer's disease have been proposed. Some of the main hypotheses are summarized in Table 40.1.

It is important to remember this diversity of hypotheses when attempting to model Alzheimer's disease in whole organisms since assumptions regarding the disease process will always influence experimental design and the interpretation of experimental results. The widespread dissatisfaction with transgenic mouse models of Alzheimer's disease (Hargis and Blalock, 2016; Robakis, 2011; Zahs and Ashe, 2010 and described later in this review) and the failure in humans of numerous drugs that appeared potent in animal trials (Smith, 2010) are graphic illustrations of this.

It is also important to remember that the early-onset familial forms of Alzheimer's disease and sporadic Alzheimer's disease may have quite distinct pathological mechanisms. Importantly, the GWAS studies of late-onset sporadic Alzheimer's disease did not reveal associations with polymorphisms at *PSEN1*, *PSEN2*, or *APP* [Table 40.1 (Moraes et al., 2012)].

In broad terms, there are two ways to use animal models to investigate human disease. The normal function of genes/proteins involved in the disease can be investigated, mainly through investigating loss-of-function phenotypes, for example, in gene knockout models. Alternatively, when disease-causing mutations are dominant, the motivation is to engineer the human mutations into the animal's genome in an attempt to create a pathological state resembling the human disease. Since mutations causing early-onset Alzheimer's disease are gain-of-function/dominant the majority of animal modeling of Alzheimer's disease has focused on attempts to generate Alzheimer's disease-like neurodegeneration in the highly manipulable, mammalian mouse. However, as we will discuss later, it now appears that genes involved in early-onset Alzheimer's disease are evolving particularly rapidly in the mouse (and rat) relative to most other mammals including other rodents, such as the guinea pig (Sharman et al., 2013). This may explain the overall failure of mouse models to enlighten us greatly regarding Alzheimer's disease pathogenesis. This also highlights the necessity of investigating alternative in vivo models for Alzheimer's disease.

2 INVERTEBRATE MODELS OF ALZHEIMER'S DISEASE

2.1 Invertebrate Models and Their Advantages and Disadvantages for Disease Modeling

Over the last 2 decades, invertebrates have become increasingly popular as models for human neurodegenerative (Alexander et al., 2014; Fernandez-Funez et al., 2015; Jaiswal et al., 2012; Li and Le, 2013; Wentzell and Kretzschmar, 2010). Favored models have been *Drosophila melanogaster* and *Caenorhabditis elegans*, which are well-established model systems that have long been used to address fundamental biological questions. In addition, these models are inexpensive and easy to maintain, produce large numbers of progeny, and have a relatively short life span which allows to study age-dependent degenerative

TABLE 40.1 An Incomplete List of Hypotheses of the Mechanism(s) Underlying Alzheimer's Disease Pathogenesis

Hypothesis	Brief description	References
Amyloid cascade	Accumulation of Aβ peptide by overproduction from APP or by failure of clearance leads to formation of oligomers that have numerous toxic effects	Fjell and Walhovd (2012), Karran et al. (2011)
APP	Changes in other aspects of APP function (e.g., signaling by the intracellular domain or release of the extracellular domain) are important	Ghosal et al. (2009), Israel et al. (2012), Pimplikar et al. (2010)
Axonal transport dysfunction	Changes in active transport in axons lead to neuronal dysfunction	Muresan and Muresan (2011)
Calcium	Changes in calcium are correlated with neurodegeneration	Fedrizzi and Carafoli (2011), Tu et al. (2006)
Cholinergic	AD is due to reduced acetylcholine production	Craig et al. (2011), Francis et al. (1999)
Cholinergic vasculature	Cholinergic deficit decreases cholinergic innervation of cortical neurons and blood vessels causing cerebral hypoperfusion, which contributes to neurodegeneration	Claassen and Jansen (2006)
Hypoxia	Hypoxia initiates AD pathology, for example, by increasing Aβ synthesis	Moussavi Nik et al. (2012), Oresic et al. (2011)
Inflammation	AD is due to long-term inflammatory responses in the brain. This may relate to Aβ accumulation or an autoimmune response	Zotova et al. (2010)
Metal ions	Dysregulation of metal ion transport/accumulation underlies AD pathology	Duce and Bush (2010)
Mitochondria	Pathological changes in mitochondrial function cause AD, for example, by affecting axonal transport	Selfridge et al. (2013)
Mitochondria-associated ER membranes (MAM)	AD is a disorder of ER–mitochondrial communication via MAM dysfunction	Schon and Area-Gomez (2013)
Notch and Aβ	Changes in Notch signaling and Aβ production affect blood vessel density/development	Ethell (2010)
Oxidative stress	Oxidative stress initiates pathological changes that eventually lead to AD pathology	Nunomura et al. (2001)
Pathogens	Herpes simplex virus type-1 and other pathogens initiate AD	Miklossy (2011)
Presenilin (autophagy)	The Presenilins' role in autophagy is central to AD (e.g., through failure to clear aggregated Aβ)	Lee et al. (2010), Yang et al. (2011)
Presenilin (holoprotein)	Presenilin mutations generate mutant Presenilin holoproteins that multimerize with wild-type holoprotein and dominantly interfere with AD-critical functions	Jayne et al. (2016)
Presenilin (γ-secretase)	Changes in γ-secretase activity other than changes in Aβ peptide production contribute to AD	Shen and Kelleher (2007)
Prion-like	Prion-like pathological forms of Aβ and/or tau move between neurons to spread AD pathology in the brain	Guo and Lee (2011), Jucker and Walker (2011)
Synapse	Changes in synapse function are critical, possibly caused by oligomeric Aβ	Pozueta et al. (2013)
Tauopathy spectrum	AD is part of a spectrum of neurodegenerative disorders founded in tau pathology	Dermaut et al. (2005)

(Continued)

TABLE 40.1   An Incomplete List of Hypotheses of the Mechanism(s) Underlying Alzheimer's Disease Pathogenesis (*cont.*)

Hypothesis	Brief description	References
"Two-hit"	Brains showing increased oxidative stress combined with inappropriate cell cycle entry by neurons (cell-cycle events) develop AD pathology	Zhu et al. (2007)
"Two-hit vascular"	Pathological changes in brain vasculature (hit one) induce early neuronal injury and increase brain Aβ (hit two), which amplifies neuronal injury and accelerates neurodegeneration	Zlokovic (2011)
Vascular	AD is due to pathological changes in cerebral vasculature	Marchesi (2011), Stone (2008)

Most hypotheses have numerous variants. Relationships can be seen between many of these ideas. Many of the hypotheses probably encompass elements of the truth. References are given as examples and coverage is certainly incomplete. Refer to "current hypotheses" for more information.

Claassen, J.A., Jansen, R.W., 2006. Cholinergically mediated augmentation of cerebral perfusion in Alzheimer's disease and related cognitive disorders: the cholinergic-vascular hypothesis. J. Gerontol. A Biol. Sci. Med. Sci. 61 (3), 267–271.

Craig, L.A., Hong, N.S., McDonald, R.J., 2011. Revisiting the cholinergic hypothesis in the development of Alzheimer's disease. Neurosci. Biobehav. Rev. 35 (6), 1397–1409.

Dermaut, B., Kumar-Singh, S., Rademakers, R., Theuns, J., Cruts, M., Van Broeckhoven, C., 2005. Tau is central in the genetic Alzheimer-frontotemporal dementia spectrum. Trends Genet. 21 (12), 664–672.

Duce, J.A., Bush, A.I., 2010. Biological metals and Alzheimer's disease: implications for therapeutics and diagnostics. Prog. Neurobiol. 92 (1), 1–18.

Ethell, D.W., 2010. An amyloid-notch hypothesis for Alzheimer's disease. Neuroscientist 16 (6), 614–617.

Fedrizzi, L., Carafoli, E., 2011. Ca²⁺ dysfunction in neurodegenerative disorders: Alzheimer's disease. Biofactors 37 (3), 189–196.

Fjell, A.M., Walhovd, K.B., 2012. Neuroimaging results impose new views on Alzheimer's disease-the role of amyloid revised. Mol. Neurobiol. 45 (1), 153–172.

Francis, P.T., Palmer, A.M., Snape, M., Wilcock, G.K., 1999. The cholinergic hypothesis of Alzheimer's disease: a review of progress. J. Neurol. Neurosurg. Psychiatry 66 (2), 137–147.

Ghosal, K., Vogt, D.L., Liang, M., Shen, Y., Lamb, B.T., Pimplikar, S.W., 2009. Alzheimer's disease-like pathological features in transgenic mice expressing the APP intracellular domain. Proc. Natl. Acad. Sci. USA 106 (43), 18367–18372.

Guo, J.L., Lee, V.M., 2011. Seeding of normal Tau by pathological Tau conformers drives pathogenesis of Alzheimer-like tangles. J. Biol. Chem. 286 (17), 15317–15331.

Israel, M.A., Yuan, S.H., Bardy, C., Reyna, S.M., Mu, Y., Herrera, C., et al., 2012. Probing sporadic and familial Alzheimer's disease using induced pluripotent stem cells. Nature 482 (7384), 216–220.

Jayne, T., Newman, M., Verdile, G., Sutherland, G., Münch, G., Musgrave, I., et al., 2016. Evidence for and against a pathogenic role of reduced gamma-secretase activity in familial Alzheimer's disease. J. Alzheimers Dis. 52, 781–799.

Jucker, M., Walker, L.C., 2011. Pathogenic protein seeding in Alzheimer disease and other neurodegenerative disorders. Ann. Neurol. 70 (4), 532–540.

Karran, E., Mercken, M., De Strooper, B., 2011. The amyloid cascade hypothesis for Alzheimer's disease: an appraisal for the development of therapeutics. Nat. Rev. Drug Discov. 10 (9), 698–712.

Lee, J.H., Yu, W.H., Kumar, A., Lee, S., Mohan, P.S., Peterhoff, C.M., et al., 2010. Lysosomal proteolysis and autophagy require presenilin 1 and are disrupted by Alzheimer-related PS1 mutations. Cell 141 (7), 1146–1158.

Marchesi, V.T., 2011. Alzheimer's dementia begins as a disease of small blood vessels, damaged by oxidative-induced inflammation and dysregulated amyloid metabolism: implications for early detection and therapy. FASEB J. 25 (1), 5–13.

Miklossy, J., 2011. Emerging roles of pathogens in Alzheimer disease. Expert Rev. Mol. Med. 13, e30.

Moussavi Nik, S.H., Wilson, L., Newman, M., Croft, K., Mori, T.A., Musgrave, I., et al., 2012. The BACE1-PSEN-AbetaPP regulatory axis has an ancient role in response to low oxygen/oxidative stress. J. Alzheimers Dis. 28 (3), 515–530.

Muresan, V., Muresan, Z., 2011. A persistent stress response to impeded axonal transport leads to accumulation of amyloid-beta in the endoplasmic reticulum, and is a probable cause of sporadic Alzheimer's disease. Neurodegener. Dis. 10, 10–63.

Nunomura, A., Perry, G., Aliev, G., Hirai, K., Takeda, A., Balraj, E.K., et al., 2001. Oxidative damage is the earliest event in Alzheimer disease. J. Neuropathol. Exp. Neurol. 60 (8), 759–767.

Oresic, M., Hyotylainen, T., Herukka, S.K., Sysi-Aho, M., Mattila, I., Seppanan-Laakso, T., et al., 2011. Metabolome in progression to Alzheimer's disease. Transl. Psychiatry, 1, e57 (Comparative Study Research Support, Non-US Gov't).

Pimplikar, S.W., Nixon, R.A., Robakis, N.K., Shen, J., Tsai, L.H., 2010. Amyloid-independent mechanisms in Alzheimer's disease pathogenesis. J. Neurosci. 30 (45), 14946–14954.

Pozueta, J., Lefort, R., Shelanski, M., 2013. Synaptic changes in Alzheimer's disease and its models. Neuroscience 251, 51–65.

Schon, E.A., Area-Gomez, E., 2013. Mitochondria-associated ER membranes in Alzheimer disease. Mol Cell Neurosci. 55, 26–36.

Selfridge, J.E., E, L., Lu, J., Swerdlow, R.H., 2012. Role of mitochondrial homeostasis and dynamics in Alzheimer's disease. Neurobiol. Dis. 51, 3–12.

Shen, J., Kelleher, R.J., 3rd., 2007. The presenilin hypothesis of Alzheimer's disease: evidence for a loss-of-function pathogenic mechanism. Proc. Natl. Acad. Sci. USA 104 (2), 403–409.

Stone, J., 2008. What initiates the formation of senile plaques? The origin of Alzheimer-like dementias in capillary haemorrhages. Med. Hypotheses 71 (3), 347–359.

Tu, H., Nelson, O., Bezprozvanny, A., Wang, Z., Lee, S.F., Hao, Y.H., et al., 2006. Presenilins form ER Ca²⁺ leak channels, a function disrupted by familial Alzheimer's disease-linked mutations. Cell 126 (5), 981–993 (Research Support, NIH, Extramural Research Support, Non-US Gov't).

Yang, D.S., Stavrides, P., Mohan, P.S., Kaushik, S., Kumar, A., Ohno, M., et al., 2011. Reversal of autophagy dysfunction in the TgCRND8 mouse model of Alzheimer's disease ameliorates amyloid pathologies and memory deficits. Brain 134 (Pt 1), 258–277.

Zhu, X., Lee, H.G., Perry, G., Smith, M.A., 2007. Alzheimer disease, the two-hit hypothesis: an update. Biochim. Biophys. Acta, 1772 (4), 494–502.

Zlokovic, B.V., 2011. Neurovascular pathways to neurodegeneration in Alzheimer's disease and other disorders. Nat. Rev. Neurosci. 12 (12), 723–738.

Zotova, E., Nicoll, J.A., Kalaria, R., Holmes, C., Boche, D., 2010. Inflammation in Alzheimer's disease: relevance to pathogenesis and therapy. Alzheimers Res. Ther. 2 (1), 1.

processes after a couple of weeks instead of month. Furthermore, a plethora of molecular methods and techniques are available in these systems and their development and anatomy is well described. Most importantly, these models allow unbiased large-scale genetic screens, making them potent tools for investigating the genetic mechanisms and pathways underlying neurodegenerative diseases like Alzheimer's disease and for identifying possible risk factors.

The nematode *C. elegans* has a generation time of approximately 3 days and a life span of about 3 weeks (Brenner, 1974). Its nervous system consists of 302 neurons in hermaphrodites, and the position and synaptic connections of each neuron have been mapped and are reproducible from animal to animal (White et al., 1986). Due to its transparent body, cells and proteins can be easily visualized using fluorescently tagged proteins; a feature that greatly facilitates the analyses of protein trafficking and cellular degeneration in living animals. Transgenic lines can be created by fusing a *C. elegans* promoter to a cDNA of interest and injecting it into the gonad or by introducing bacterial artificial chromosomes (BACs) (Gama et al., 2002; Teschendorf and Link, 2009). A major advantage of this model for genetic screens is that RNAi-based knockdowns can be performed by simply feeding animals with bacteria expressing double-stranded RNA libraries (Kamath et al., 2001). In addition, worms can be used for a fairly high throughput drug screen (Lublin and Link, 2013). However, *C. elegans* has a very simple nervous system with a nerve ring in the head region but not a compartmentalized brain. In addition, assays to address cognitive decline in this model are quite limited.

By comparison, *Drosophila* has quite a complex nervous system with approximately 200,000 neurons (Zars et al., 2000). In addition, their brain is organized into distinct regions that control specific functions equivalent to vertebrate brain nuclei, like the antennal lobes that receive olfactory input and that are comparable to the olfactory bulb in mammals. Also similar to the mammalian brain, the fly brain contains several types of morphologically distinguishable glial cells, including some that form a "blood–brain barrier" (Hartenstein, 2011; Parker and Auld, 2006) or astrocyte-like glial cells (Freeman, 2015). Although flies do not have a vascular system like mammals, they also have to supply their brain with oxygen and other gases which is achieved by an air filled tubular network, the tracheal system (Metzger and Krasnow, 1999). At room temperature, the development of *Drosophila* takes about 10 days and adult flies have a live span of 60–80 days (Greenspan, 2004). Although a variety of unique tools have been developed for *Drosophila*, one of the most important technical advantage is based on the use of P-elements, transposable elements that allow stable integration into the genome (Rubin and Spradling, 1982). Initially, this system was used to insert genomic DNA or promoter-gene fusion constructs

into the fly genome but it has also been used to disrupt genes or to insert marker genes into promoter regions to identify expression patterns (Ryder and Russell, 2003). Subsequently, a binary expression system was developed (Brand and Perrimon, 1993), in which individual fly promoters were fused to the yeast transcription factor GAL4, whereas genes of interest were cloned downstream of the UAS sequence (the yeast GAL4-binding region). This method allows a particular responder sequence to be combined with a variety of promoter constructs by a simple genetic cross, resulting, for example, in the expression of a gene of interest in specific cell populations or the labeling of specific cell populations by inducing fluorescent responders like UAS-GFP. In addition, hormone- or heat shock-inducible GAL4s can be used to achieve temporal control of expression, whereas UAS-RNAi lines (which are available at various *Drosophila* stock centers) can be used to knockdown genes in a spatial or temporal fashion. The P-element-based FLP/FRT site-specific recombination system allows the creation of genetic mosaics and site-specific mutagenesis (Bischof and Basler, 2008), and more recently the CRISPR (clustered regularly interspaced short palindromic repeats)/CAS9 system has been added as a powerful tool to manipulate the fly genome (Bassett et al., 2013; Gratz et al., 2013; Yu et al., 2013). Furthermore, several genetic tools are available to study neuronal circuits and functions, including "sensors" to measure PKA activity or Ca^{2+} levels, the light-inducible channelrhodopsin, and genetically engineered neuronal channels (Riemensperger et al., 2012; Stortkuhl and Fiala, 2011; Wachowiak and Knopfel, 2009). Finally, additional binary expression systems have been developed, the Q and LexA system (Lai and Lee, 2006; Potter et al., 2010) that now allow to manipulate several genes independently. Although *Drosophila* provides an excellent model for studying neurodegenerative diseases due to this wealth of available tools, the high level of gene conservation (Wangler and Yamamoto, 2015), and the availability of learning and memory assays, this system has its limitations. Compared to the human brain, the fly brain is less complex and their behavioral repertoire is comparatively small. As mentioned before, flies do not have a blood-carrying vascular system which prevents studying vascular effects of Alzheimer's disease and while *Drosophila* has a conserved innate immune systems, flies lack conventional adaptive immune responses (Hoffmann, 2003).

2.2 Aβ-Based Models and Their Neurotoxic Effects

The amyloid cascade hypothesis, formulated by Hardy and Higgins (1992), has been one of the favored models to explain the pathogenic mechanisms leading to Alzheimer's disease. It is based on the fact that Aβ accumulation

is a key factor in Alzheimer's disease (Glenner and Wong, 1984; Wong et al., 1985) and it gained considerable support with the discovery that mutations associated with familial Alzheimer's disease lead to increased Aβ production (Chartier-Harlin et al., 1991; Goate et al., 1991; Levy-Lahad et al., 1995; Sherrington et al., 1996).

To address whether Aβ peptides are indeed sufficient to induce an Alzheimer's disease-like pathology, several transgenic fly and worm models have been developed that express different forms of human Aβ (Crowther et al., 2005; Finelli et al., 2004; Iijima et al., 2004; Link, 1995; Link et al., 2003). In the first *C. elegans* model the 42 amino acid residue form of Aβ, $Aβ_{42}$ was constitutively expressed in muscles, which caused a progressive paralysis and the accumulation of intracellular amyloid deposits (Link, 1995). This finding was confirmed in an inducible model, which, due to higher expression levels, showed a more severe and rapid paralysis (Link et al., 2003). Later models focused on the expression of $Aβ_{42}$ in neurons and this resulted in deficits in odor preference learning (Dosanjh et al., 2010) and neuronal degeneration (Treusch et al., 2011). Using this model, several modifiers of the neurodegenerative phenotype could be identified that were associated with cytoskeletal genes. When using the locomotion deficits as a screening phenotype, genes involved in protein folding, degradation, and insulin signaling were shown to ameliorate or aggravate this phenotype (Cohen et al., 2006; Fonte et al., 2002, 2008; Hassan et al., 2009). Another study identified a protective effect of mitochondrial thioredoxin in $Aβ_{42}$-expressing transgenic worms (Cacho-Valadez et al., 2012), connecting mitochondrial functions to Alzheimer's disease.

In *Drosophila*, transgenic animals have been created that express full-length APP_{695}, $Aβ_{40}$, $Aβ_{42}$, or mutant forms of APP_{695} and Aβ associated with familial forms of Alzheimer's disease, using the GAL4/UAS system (Cao et al., 2008; Crowther et al., 2005; Fossgreen et al., 1998; Gunawardena and Goldstein, 2001; Iijima et al., 2004). Several studies in mammals have suggested that an increase in $Aβ_{42}$ levels (or an increase in the ratio of $Aβ_{42}$ to $Aβ_{40}$) is an important factor in Alzheimer's disease (Findeis, 2007), although both Aβ peptides are known to accumulate in amyloid plaques in Alzheimer's disease patients. The increased toxicity of $Aβ_{42}$ was confirmed in *Drosophila* because only the induction of $Aβ_{42}$ caused progressive degeneration and plaque formation in *Drosophila*, whereas $Aβ_{40}$ did not (Crowther et al., 2005; Finelli et al., 2004; Iijima et al., 2004). Unexpectedly, however, expression of either peptide resulted in age-dependent decline in olfactory learning, with no significant difference in progression or severity detected between flies expressing $Aβ_{40}$ versus $Aβ_{42}$ (Iijima et al., 2004). That plaque formation is not prerequisite for behavioral deficits was also shown in a climbing assay, which revealed a decline in performance before the appearance of overt Aβ deposits although in this case only

$Aβ_{42}$ was tested (Crowther et al., 2005). Interestingly, this study also showed that the decrease in climbing ability correlated with the accumulation of intracellular Aβ, and a following study showed that the toxicity correlated with the levels of soluble $Aβ_{42}$ oligomers (Speretta et al., 2012). The importance of oligomer formation in pathogenicity was further underscored by generating mutant Aβ constructs that were predicted to affect aggregation. Analyzing 14 mutant $Aβ_{42}$ constructs expressed in flies, Crowther and coworkers found a strong correlation between the propensity to form protofibrils and toxicity (Luheshi et al., 2007). Furthermore, a mutation in $Aβ_{40}$ (E3R) that increased its ability to form soluble aggregates became neurotoxic while a mutation in $Aβ_{42}^{Arctic}$ (I31E) that reduced its propensity to form prefibrillary aggregates decreased its toxic effects (Brorsson et al., 2010). In addition, a mutation that decreased the oligomerization of $Aβ_{42}$ (in this case L17P) reduced its deleterious effects on life span and locomotion (Iijima et al., 2008). Surprisingly, however, the propensity of the different peptides to form oligomers did not correlate with their effects on short-term memory because the L17P mutation caused an even earlier onset of the memory deficits than the more efficiently aggregating Arctic mutation. Intriguingly, pan-neuronal expression of the different Aβ isoforms also induced distinct region-specific neurodegenerative effects, with the Arctic mutation mostly affecting cell bodies and the L17P mutation mostly affecting neurites (Iijima et al., 2008). These findings strongly support evidence obtained from mammalian models that intracellular oligomers of Aβ constitute the toxic species, rather than extracellular plaques (Finder and Glockshuber, 2007; Lublin and Gandy, 2010). Furthermore, these results suggest that oligomer formation and neurotoxicity do not correlate with behavioral deficits and that the formation of Aβ oligomers in specific subcellular compartments induces different pathological phenotypes.

In addition to degeneration and behavioral deficits, $Aβ_{42}$ expression induced several other phenotypes in flies. This includes synaptic deficits, supporting results in mammals that Aβ impairs neuronal transmission and synaptic plasticity (Jang and Chung, 2016; Tampellini, 2015; Zhang et al., 2016). This was first demonstrated at the larval neuromuscular junction where $Aβ_{42}$ induction reduced neurotransmitter release (Chiang et al., 2009). This was later confirmed in the adult nervous system by expression of $Aβ_{42}$ in the giant fiber system, and the projection neurons of the olfactory system which resulted in reduced synaptic activity (Lin et al., 2014b; Zhao et al., 2010). In addition, Huang et al. (2013) described a reduced number of synaptic vesicles, calcium channels, and active zones in these flies which is probably the underlying cause for the defects in synaptic transmission. Recently, it was described that $Aβ_{42}$ expression can also lead to neuronal hyperactivity by degrading K_v4 channels and that, this may be part of the

pathogenicity, was suggested by the finding that over-expression of K_v4 ameliorated the locomotion deficits in expressing $A\beta_{42}$ flies (Ping et al., 2015). Iijima et al. found a change in the localization of mitochondria in $A\beta_{42}$-expressing flies, with fewer mitochondria in axons and dendrites and an accumulation in neuronal somata (Iijima-Ando et al., 2009). Furthermore, interfering with mitochondrial transport by genetic means enhanced the locomotion deficits of $A\beta_{42}$-expressing flies, and even caused age-dependent defects in locomotion in the absence of $A\beta_{42}$, suggesting that changes in mitochondrial distribution are due to transport defects. The resulting depletion of mitochondria at synaptic terminals (Iijima-Ando et al., 2009; Zhao et al., 2010) may further contribute to the observed synaptic dysfunctions. Although the expression of $A\beta$ in these models certainly does not completely recapitulate Alzheimer's disease pathology, these studies nevertheless clearly demonstrate that $A\beta$ peptides alone can have neurotoxic and behavioral effects, providing support for the amyloid cascade hypothesis.

Based on the foregoing evidence that $A\beta$ peptides induce various disease-related phenotypes ranging from synaptic deficits to disrupted behaviors, this model has subsequently been used to identify factors that ameliorate $A\beta$ toxicity by genetic interaction tests. For the purpose of this overview, we will focus on a few of these interacting factors although many more have been described. The suppression of $A\beta_{42}$-induced neuronal degeneration by inhibition of c-Jun amino-terminal kinase (JNK) reveals a role of the JNK pathway in $A\beta_{42}$-induced cell death (Tare et al., 2011) while reducing PI3k-Akt signaling suppressed the memory deficits (Chiang et al., 2010). Another pathway that has been identified to affect $A\beta$ toxicity in flies is ER stress and Ca^{2+} dysregulation because Casas-Tinto et al. (2011) identified X-box-binding protein 1 (XBP1), a protein involved in ER stress responses as neuroprotective in the fly $A\beta_{42}$ model. They also showed that this protein prevented Ca^{2+} release from intracellular stores, supporting data linking calcium homeostasis with Alzheimer's disease (Fedrizzi and Carafoli, 2011). Consistent with the proposed involvement of copper and iron in Alzheimer's disease (Prakash et al., 2016), overexpression of the iron-binding protein ferritin or the MTF-1 transcription factor, which is involved in metal detoxification (Hua et al., 2011; Rival et al., 2009), suppressed deleterious phenotypes caused by $A\beta_{42}$. In contrast, a mutation in the copper transporter Atox1 enhanced $A\beta$ toxicity (Sanokawa-Akakura et al., 2010). The *Drosophila* $A\beta$ model has also been used to investigate the role of the innate immune system in Alzheimer's disease. Immune factors in the Toll pathway were upregulated in $A\beta_{42}$-expressing flies and mutations in Toll and its downstream targets decreased the retinal degeneration observed after $A\beta_{42}$ expression (Tan et al., 2008), suggesting a deleterious effect of immune responses. However, another group using

an $A\beta_{42}{}^{Arctic}$ fly model and microarray-based analyses did not observe an upregulation of genes in the Toll pathway (Favrin et al., 2013).

Lastly, this model has been used to test pharmacological interventions and these studies have identified several protective natural products, like curcumin or traditional Chinese extracts (Caesar et al., 2012; Hou et al., 2014; Ng et al., 2013; Park et al., 2013; Wang et al., 2015), as well as synthetic compounds and peptides (Luheshi et al., 2010; Nerelius et al., 2009; Pratim Bose et al., 2009; Wacker et al., 2014). The relative simplicity with which pharmacological compounds can be tested in *Drosophila* (and in *C. elegans*) will hopefully eventually lead to the discovery of therapeutic strategies that can ameliorate the toxic effects of $A\beta$.

2.3 APP-Based Models and Disruptions of APP Functions

In addition to $A\beta$-based models, transgenic flies have been generated that express wild-type full-length APP_{695} or APP_{695} carrying the Swedish or London mutation associated with familial forms of Alzheimer's disease (Fossgreen et al., 1998; Gunawardena and Goldstein, 2001; Singh and Mahoney, 2011). Inducing these constructs in the larval nervous system induced apoptotic cell death that was more severe when using the FAD mutations (Gunawardena and Goldstein, 2001). Expressing APP_{695} in the eye also caused neuronal degeneration (Fig. 40.1) that was accompanied by amyloid deposit formation and both were enhanced when promoting amyloidogenic cleavage by coexpressing BACE1 or PSN (Greeve
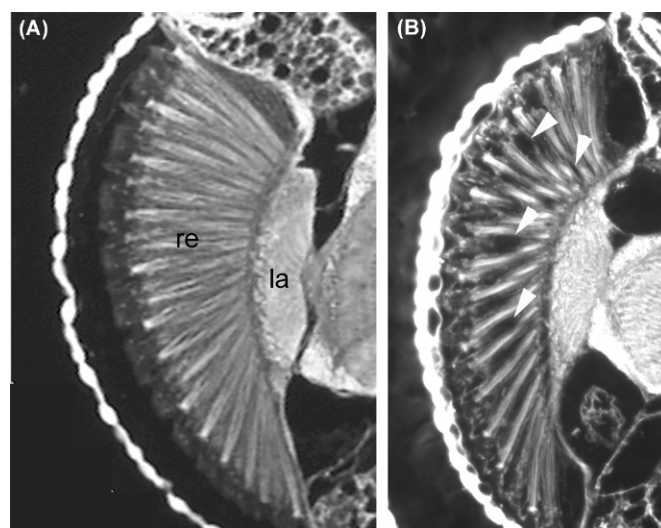
FIGURE 40.1 **Degeneration in the retina after APP_{695} expression in the *Drosophila* eye.** (A) A 30-day-old control fly shows an intact retina *(re)* and lamina *(la)*. (B) In contrast, numerous vacuoles (some indicated by *arrowheads*) have developed in a 30-day-old fly expressing APP_{695} in the eye using GMR-GAL4.

et al., 2004). In addition, APP expression caused axonal transport defects and synaptic alterations, as well as locomotion and learning deficits (Mhatre et al., 2014; Peng et al., 2015; Rodin et al., 2015; Sarantseva et al., 2009). These phenotypes are similar to what has been described after expression of Aβ and together with the finding that an Aβ fragment can be cleaved from APP$_{695}$ by the endogenous *Drosophila* secretases (Greeve et al., 2004); it is possible that these effects are due to the generation of Aβ. Therefore, this model can possibly be used to study the toxicity of the Aβ peptide and to identify factors that affect its generation. Consequently, APP$_{695}$-expressing flies have been used for testing of β- and γ-secretase inhibitors (Chakraborty et al., 2011; Greeve et al., 2004; Groth et al., 2010; Wang et al., 2009). Similarly, this model has been employed to identify genetic factors that impact secretase activity, for example, proteins involved in phospholipid synthesis and membrane composition that have been demonstrated to interfere with γ-secretase activity (Michaki et al., 2012; Nesic et al., 2012).

Although a large body of evidence supports a central role for Aβ in Alzheimer's disease pathology (including the studies in invertebrates described previously), it is still an open question whether disruptions of physiological functions of APP contribute to Alzheimer's disease. In contrast to mammals, which have three APP family members (APP, APPL1, and APPL2), worms and flies have only one APP protein, facilitating loss-of-function studies. Like their mammalian orthologs, the invertebrate APP proteins are membrane-spanning proteins with a large N-terminal extracellular domain and small C-terminal intracellular domain (Luo et al., 1990). Several studies in cell culture have linked the extracellular fragments released by secretase cleavage of APP with functions as cell proliferation, survival, and adhesion (Turner et al., 2003). In contrast, the small intracellular domain (AICD), which is released by γ-secretase cleavage, has been proposed to function as a transcriptional regulator (Beckett et al., 2012). Interestingly, the AICD has the highest degree of sequence conservation when comparing APP proteins from invertebrates and mammals.

Like the mammalian protein, the *C. elegans* APP protein (APL-1) is expressed in a variety of cells, including neurons, muscles, and hypodermal cells (Hornsten et al., 2007). Loss of APL-1 results in lethality during development, which can be rescued by expression of the soluble N-terminal fragment alone, suggesting that the N-terminus is sufficient for the vital function of APL-1 (Hornsten et al., 2007). In contrast, expression of the *Drosophila* APP protein (APPL) appears restricted to neurons, and flies lacking APPL are viable (Luo et al., 1990) although they have a shorter life span and a weak degenerative phenotype when aged (Wentzell et al., 2012). In addition, they show defects in neurite outgrowth (Leyssen et al., 2005; Li et al., 2004; Soldano et al., 2013), axonal transport (Gunawardena and Goldstein, 2001),

and synaptic morphology (Torroja et al., 1999), which are accompanied by changes in neuronal excitability (Ashley et al., 2005; Li et al., 2004). Furthermore, loss of APPL results in memory defects (Bourdet et al., 2015; Goguel et al., 2011). This indicates that disruption of the normal physiological functions of APP may also play a role in the synaptic changes and memory impairment described in Alzheimer's disease (Wang et al., 2012). Like human APP, APPL has been shown to be cleaved by α-, β-, and γ-secretase activity (Carmine-Simmen et al., 2009; Stempfle et al., 2010) and interestingly this also creates a toxic Aβ-like peptide (Carmine-Simmen et al., 2009). Using several fly mutants that develop neurodegenerative phenotypes, Wentzell et al. (2012) showed that expression of the full-length APPL as well as the α-cleaved N-terminal fragment could ameliorate their degenerative phenotype, whereas β-cleavage aggravated the neurodegeneration. Therefore, disease-associated changes in the processing pattern of APP could result in a decrease of the protective α-cleaved N-terminus and an increase of the deleterious β-cleaved form, thereby contributing to the pathology of Alzheimer's disease. Lastly, induction of the AICD fragment of APPL induces changes in the sleep/activity pattern in flies (Blake et al., 2015), indicating that changes in the function of the AICD that occur in Alzheimer's disease could be responsible for the disruptions of the sleep pattern and other daily rhythms that are very common in Alzheimer's disease patients (Guarnieri and Sorbi, 2015; Hastings and Goedert, 2013; Kondratova and Kondratov, 2012; Reddy and O'Neill, 2010; Van Someren and Riemersma-Van Der Lek, 2007).

2.4 Tau and the Role of Phosphorylation

Another hallmark of Alzheimer's disease is the formation of neurofibrillary tangles (NFTs) and in fact NFT accumulation correlates better with the severity of the disease than plaque formation (Arriagada et al., 1992). A major component of NFTs is hyperphosphorylated tau, a protein which like other microtubule-associated proteins binds and stabilizes microtubules (Lee et al., 2001). NFTs not only occur in Alzheimer's disease but in a variety of diseases together called tauopathies that include frontotemporal dementia (FTD) with Parkinsonism linked to chromosome 17 (FTDP-17), Pick's disease, corticobasal degeneration, and progressive supranuclear palsy (Iqbal et al., 2010). Although no mutations have been found in tau that cause Alzheimer's disease, there are mutations that lead to FTDP-17 (Hutton et al., 1998; Spillantini et al., 1998). Some of these mutations have been shown to increase tau phosphorylation (Gendron and Petrucelli, 2009; Iqbal et al., 2009) which in turn has been shown to increases its propensity to form NFTs (Alonso et al., 2008).

Surprisingly both, the expression of wild-type human tau or mutant tau, containing the FTDP-17-associated tau mutations P301L or V337M, in *C. elegans* neurons

induced insoluble aggregate formation, axonal degeneration, and uncoordinated movement (Kraemer et al., 2003). However, the lines expressing mutant tau showed a more rapid accumulation of aggregates and more severe locomotion defects. Analyzing their phosphorylation pattern revealed that not only the mutant forms were hyperphosphorylated but also the wild-type form, which probably accounts for its toxicity. Using the uncoordinated phenotype of these models as a screenable assay, Kraemer et al. (2006) performed a genome-wide RNAi-based interaction screen and in support of the role of hyperphosphorylation in tau neurotoxicity, the RNAi-based knockdown of the PP2A phosphatase enhanced the phenotype. Surprisingly, however, the knockdown of several kinases involved in tau phosphorylation, including glycogen synthase-3 (GSK-3β), also enhanced the locomotion defects. These conflicting findings show that genetic interaction studies in vivo can sometimes be difficult to interpret and one complicating factor could be compensatory mechanisms involving other interacting genes and proteins. Alternatively, the enhancing effect of the kinase knockdowns could be due to increased aggregate formation because experiments in vitro have shown that tau phosphorylation can in some contexts actually inhibit tau aggregation and NFT formation (Schneider et al., 1999). Nevertheless, the value of this interaction test was confirmed by the isolation of other candidate genes, including several chaperones and proteins involved in ubiquitination that, when knocked down, enhanced tau toxicity, presumably by increasing the stability or aggregation of tau (Kraemer et al., 2006).

The first transgenic fly models for tau were published in 2001 by Feany and coworkers (Wittmann et al., 2001) and since then over 30 different tau *Drosophila* models have been established. Similar to what has been described in the *C. elegans* model, expression of wild-type or mutant human tau (R406W and V337M) pan-neuronally in *Drosophila* generated abnormally phosphorylated tau and caused progressive degeneration, whereby the mutant forms had more severe effects (Wittmann et al., 2001). In contrast to *C. elegans*, however, no aggregates could be detected when either the wild-type or the mutant tau variants were expressed in the nervous system, suggesting that the formation of NFTs is not necessary for tau toxicity. Interestingly, NFT-like aggregates were detected when tau was coexpressed with GSK-3β (Jackson et al., 2002), supporting the role of phosphorylation in tau pathology. The link between phosphorylation and neurotoxicity was further investigated by creating mutations in several of the more than 80 predicted phosphorylation sites of tau (Sergeant et al., 2008). Confirming that phosphorylation of tau is a crucial step in acquiring toxic function, mutating 14 known proline-phosphorylation sites did indeed abolish its deleterious effects, whereas single or double mutations had no effect (Steinhilb et al., 2007a,b). In contrast, transgenic flies expressing a tau construct that was pseudophosphorylated at these 14 sites showed enhanced degeneration, compared to flies expressing the wild-type form (Khurana et al., 2006). Surprisingly, the loss of 11 of these sites in a different tau isoform (2N4R) did not have an effect on toxicity (Chatterjee et al., 2009), which indicates that either the critical residues were not mutated in this construct or there is an isoform-specific effect. The latter is supported by the finding that S262 and S356 were shown to be required for subsequent phosphorylation by GSK-3β in one tau isoform (Kosmidis et al., 2010; Nishimura et al., 2004) but when mutated in another tau isoform this had no effect on GSK-3β-mediated phosphorylation (Chatterjee et al., 2009). Tau can be phosphorylated by several kinases besides GSK-3β, including microtubule-affinity regulating kinase (MARK), cdk5, and protein kinase A (Lee et al., 2001). To determine the role of specific kinases in tau toxicity, several groups have performed genetic interaction tests with tau transgenic flies overexpressing specific kinases. Coexpression of either cdk5 or Shaggy (SGG; the *Drosophila* ortholog of GSK-3β) with wild-type human tau increased its phosphorylation and enhanced the degenerative phenotype (Chau et al., 2006; Jackson et al., 2002). Furthermore, these flies now also exhibited detectable tau aggregates, suggesting that phosphorylation by these kinases is an important factor in tau neurotoxicity. However, although phosphorylation by SGG can aggravate tau toxicity, it appears not to be required because as mentioned previously the tau variant with 11 SGG phosphorylation sites mutated was not phosphorylated by SGG but it still caused degeneration (Chatterjee et al., 2009). In contrast, phosphorylation of tau by PAR-1, the fly MARK, seems to be required for tau toxicity because mutating the PAR-1 sites abolished toxicity, whereas overexpressing PAR-1 aggravated the toxicity (Chatterjee et al., 2009; Nishimura et al., 2004). Phosphorylation by PAR-1 could also regulate phosphorylation by other kinases, although this model is still controversial; whereas Nishimura et al. described that phosphorylation by PAR-1 is a prerequisite for phosphorylation by cdk5 and SGG, Jackson et al. detected phosphorylation at the SGG sites even when the PAR-1 sites were mutated (Chatterjee et al., 2009). Further complicating matters, which sites within tau are actually phosphorylated in vivo (and in which sequence) may ultimately depend on the cell type: when tau was expressed in photoreceptors, there was little or no phosphorylation at the SGG sites, whereas these sites were phosphorylated when tau was expressed in CNS neurons (Grammenoudi et al., 2006). The same group also showed that some patterns of tau phosphorylation caused neuronal degeneration, whereas phosphorylation events at other sites were associated with neuronal dysfunction but not degeneration (Kosmidis et al., 2010). Such cell-specific phosphorylation patterns and effects could explain why some neurons are more susceptible to the toxic effects of tau than others, an issue that can be addressed in the

fly model by using neuronal subtype-specific promoter constructs. Lastly, genetic interaction screens have also identified several kinases and phosphatases as modifiers of the tau-induced retinal degeneration (Ambegaokar and Jackson, 2010; Karsten et al., 2006; Shulman and Feany, 2003). Surprisingly, in one of these interaction screens PAR-1 overexpression suppressed the degenerative phenotype in the eye (Shulman and Feany, 2003), in contrast to the PAR-1 overexpression studies described previously which resulted in an enhancing effect. This may indicate that under certain circumstances phosphorylation of tau can actually reduce its toxicity whereas in other contexts it is deleterious. Such a scenario is also supported by the findings that GSK-3β-mediated phosphorylation can be protective, as described previously in the *C. elegans* model (Kraemer et al., 2006) and by Povellato et al. (2014) in *Drosophila*. However, what factors determine when tau phosphorylation has a protective effect versus an enhancing effect still needs to be determined. Nevertheless, these results suggest that phosphorylation of tau is an important aspect for its toxic function, whereby the combined action of several kinases might be more critical than the phosphorylation by one specific kinase or phosphorylation at a single site. In addition, determining the effects of phosphorylation on tau toxicity is further complicated by the finding that the phosphorylation at specific sites and in a specific order affects different tau-associated phenotypes differently (Papanikolopoulou and Skoulakis, 2015). Lastly, it should be noted that tau undergoes many other posttranslational modifications, including glycation, deamination, and acetylation, and only a few studies have addressed their effects on pathogenicity. One recent study using the fly model to address other modifications has reported increased toxicity by pseudoacetylation of tau (Gorsky et al., 2016).

2.5 Effects of Tau Manipulations on Cellular Functions

Genetic interaction tests using flies expressing human tau have also identified proteins involved in many other cellular processes as modifiers of tau toxicity, including cytoskeletal proteins and proteins involved in cell cycling (Ambegaokar and Jackson, 2010; Blard et al., 2006; Butzlaff et al., 2015; Shulman and Feany, 2003). Feany and coworkers showed that expression of Cyclin A, Cyclin B, or Cyclin D enhanced the degenerative phenotype caused by tau, whereas blocking cell-cycle progression by expressing Retinoblastoma factor 1 or the cdk2 inhibitor Dacapo decreased it (Khurana et al., 2006). In addition, this group showed an abnormal activation of the cell cycle in tau-expressing flies and a recent publication demonstrated that microtubule-bound tau inhibits cell mitosis (Bouge and Parmentier, 2016). Maybe not surprisingly, several studies connected cellular defense

pathways with tau toxicity; tau activated the ER stress factor XBP1 and the loss of XBP1 enhanced tau-induced phenotypes (Loewen and Feany, 2010). Similarly, promoting antioxidative pathways suppressed tau toxicity whereas inducing oxidative stress enhanced it (Dias-Santagata et al., 2007). Tau was also shown to affect the cytoskeleton, especially filamentous (F)-actin; tau^{R406W} expression resulted in an accumulation of F-actin and actin-rich rods that resemble the Hirano bodies found in patients with Alzheimer's disease or Pick's disease (Fulga et al., 2007). By interfering with actin dynamics, it also caused a mislocalization of the mitochondrial fission factor DRP1, resulting in mitochondrial abnormalities (DuBoff et al., 2012). Interestingly, changes in mitochondrial distribution and trafficking were also observed in a *C. elegans* model expressing tau^{A152T}, although no insoluble tau aggregates were found (Pir et al., 2016). Nevertheless, these worms showed uncoordinated behavior and a reduced life span, supporting findings in flies that tau toxicity does not depend on aggregate formation. More recently, the Feany group also showed effects of tau^{R406W} on chromatin structure, with a loss of heterochromatin and increased gene expression (Frost et al., 2014), and on lamin and the nucleoskeleton, which plays a role in anchoring heterochromatin (Frost et al., 2016). These studies in the invertebrate model suggest that tau is involved in many more cellular processes than previously anticipated but whether and to what degree a loss of these functions plays a role in Alzheimer's disease or tauopathy pathology still needs to be determined.

The well-known function of tau in binding and stabilizing microtubule has been suggested to play a role in Alzheimer's disease (Trojanowski and Lee, 2005). Phosphorylation releases tau from microtubules, and it has therefore been hypothesized that the toxicity of hyperphosphorylated tau could be due to a loss of its microtubule-interacting function and consequent changes in the cytoskeleton and axonal transport (Yang et al., 2005). This model has gained further support by the discovery that mutations in tau linked with FTDP-17 reduce the ability of tau to bind and promote microtubule stability (Dayanandan et al., 1999; Hasegawa et al., 1998; Hong et al., 1998). When human tau is expressed in *Drosophila*, most of it becomes hyperphosphorylated and localizes to the cytosol, while its microtubule-binding capacity is reduced (Cowan et al., 2010a,b; Feuillette et al., 2010). However, whereas Mudher and coworkers reported that the human tau sequestered endogenous *Drosophila* tau away from microtubules, thereby supporting a loss-of-function mechanism (Cowan et al., 2010a), Lecourtois and coworkers did not observe such an effect (Feuillette et al., 2010). A role of a loss of tau function in neurodegeneration is also supported by the recent findings that a knockdown or a partial deletion of *Drosophila* tau resulted in retinal degeneration and modest degeneration in

the CNS (Bolkan and Kretzschmar, 2014). Furthermore, as mentioned previously, the disruptions of other physiological functions may play a role in Alzheimer's disease. Although future experiments might provide more insights into how disease-related tau modifications affect its physiological functions, tau toxicity might not be due strictly to a gain- or loss-of-function mechanism, but rather to a combination of both.

2.6 Interactions Between tau and Aβ

Several studies have suggested that an interaction between Aβ and tau plays a role in Alzheimer's disease pathogenesis, whereby this might be due to Aβ acting upstream of tau, increasing its phosphorylation, or by synergistic effects of tau and Aβ (Han and Shi, 2016; Small and Duff, 2008). An interaction has also been demonstrated in the *Drosophila* model because coexpression of $Aβ_{42}$ with tau in the eye enhanced the degenerative phenotype (Fulga et al., 2007) and it also exacerbated the axonal transport defects caused by expression of either of these proteins (Folwell et al., 2010). Consequently, several studies have addressed the hypothesis that this interaction is mediated by the effects of APP/Aβ on tau phosphorylation. Iijima and coworkers showed that $Aβ_{42}$ increased the phosphorylation of coexpressed tau, which correlated with enhanced degeneration and increased microtubule-unbound tau but not NFT formation (Ando et al., 2016; Iijima et al., 2010). The changes in phosphorylation appeared to be mediated by the DNA damage-activated Checkpoint kinase 2, suggesting a connection to DNA repair pathways. Coexpression of $Aβ_{42}$ and tau in motorneurons also enhanced tau phosphorylation, in this case probably phosphorylation by GSK-3β (Folwell et al., 2010). Similarly expression of full-length APP increased the phosphorylation of both tau and PAR-1, a process that depended on the LKB-1 kinase (Wang et al., 2007). Interestingly, loss of endogenous tau suppressed the toxicity of Aβ^Arctic expression and although Aβ^Arctic did increase GSK-3β activity, it did not seem to alter tau phosphorylation (Sofola et al., 2010). This supports findings in other models that Aβ can indeed promote tau phosphorylation but also that Tau and Aβ may have other synergistic effects.

Together these studies show that invertebrate models provide a valuable in vivo model to study the physiological and pathogenic functions of APP/Aβ and tau. Although significant advances have been made using these and other models, we are still far away from understanding the pathogenic mechanism leading to Alzheimer's disease. Due to the experimental advantages of these models, together with the low costs, invertebrates provide a system in which complex interactions can be studied, unbiased interaction screens can be performed, and they can be used as a medium-throughput and economical system for drug screening (Table 40.2).

3 NONMAMMALIAN VERTEBRATE MODELS OF ALZHEIMER'S DISEASE

Historically, some nonmammalian vertebrate species have been popular for analysis of the mechanisms controlling embryo development. Typically, the embryos of these species are more accessible and manipulable than those of mammalians. However, being vertebrates, their anatomy and development resemble those of humans more closely than invertebrate embryos.

The three main nonmammalian vertebrate models are the chicken (*Gallus gallus*), the African clawed frog (*Xenopus laevis*), and the zebrafish (*Danio rerio*). Chick embryos develop on the surface of a relatively huge yolk cell and their nearly flat early structure is advantageous for tissue transplantation studies. They have also proven useful for the examination of neuronal differentiation and development, particularly through examination of defined neuronal groups, such as the trigeminal ganglion (Gaik and Farbman, 1973a,b). However, the chicken's long generation time slows genetic analysis and manipulation [but does not make it infeasible (Han, 2009)].

The amphibian *Xenopus* has smaller embryos than the chick and the dividing cells of early cleavage embryos incorporate yolk. *X. laevis* are pseudotetraploid which complicates analysis of gene function due to widespread genetic redundancy (Chain and Evans, 2006). Therefore, a related diploid frog, *Xenopus tropicalis*, has become popular for such studies (Hellsten et al., 2010). Unfertilized *Xenopus* eggs have only low levels of ion channels and other transporter proteins and so forced high-level expression of such proteins in these eggs (e.g., by mRNA injection) has been used to identify and analyze their functions (Sobczak et al., 2010).

The zebrafish has gained considerable popularity in recent years due to its genetic manipulability, the experimentally amenable characteristics of its embryos, and its low cost of maintenance compared to mammals. The use of zebrafish as an experimental model dates back over half a century (Hisaoka, 1958a,b) but in the 1980s it became the first vertebrate model to be used in large-scale mutagenesis screens to detect genes controlling embryo development (see *Development* volume 123 of December 1996). The development of morpholino antisense oligonucleotides made reliable blockage of gene expression feasible in 2000 (Nasevicius and Ekker, 2000). The TILLING (targeting induced local lesions in genomes) methodology allows discovery of point mutations in desired genes (Wienholds et al., 2002). Efficient transposon-based transgenic vectors (Davidson et al., 2003; Kawakami, 2004) and the application of split transgenesis systems, such as Gal4/UAS (Scheer and Campos-Ortega, 1999) have permitted enhancer- and gene-trap screening (Abe et al., 2011). The very rapid development and optical transparency of zebrafish embryos has

TABLE 40.2 *C. elegans* and *Drosophila* Models of Alzheimer's Disease

Construct	Tissue	Phenotypes	References
C. ELEGANS			
$A\beta_{42}$	Muscle	Amyloid deposits Progressive paralysis	Link (1995), Link et al. (2003)
	Neurons	Learning deficits	Dosanjh et al. (2010)
	Glutamatergic neurons	Neuronal degeneration	Treusch et al. (2011)
tau tau[P301L] tau[V337M]	Neurons	Aggregates Neuronal degeneration Uncoordinated movement	Kraemer et al. (2003)
tau[A152T]	Neurons	Uncoordinated movement	Pir et al. (2016)
D. MELANOGASTER			
APP[695]	Retina	Amyloid deposits Retinal degeneration	Greeve et al. (2004)
	Neurons	Amyloid deposits Neuronal degeneration Learning deficits	Sarantseva et al. (2009)
APP[Swedish]	Neurons	Cell death	Gunawardena and Goldstein (2001)
APP[London]	Neurons	Cell death	Gunawardena and Goldstein (2001)
$A\beta_{42}$	Retina	Retinal degeneration	Cao et al. (2008)
$A\beta_{40}$ $A\beta_{42}$ $A\beta_{42}$[Arctic]	Neurons	Amyloid deposits Neuronal degeneration Learning deficits	Crowther et al. (2005), Finelli et al. (2004), Iijima et al. (2004)
tau tau[R406W] tau[V337] tau[P301L]	Retina	Retinal degeneration	Jackson et al. (2002), Karsten et al. (2006), Wittmann et al. (2001), Karsten et al. (2006)
tau tau[R406W]	Neurons	Neuronal defects Learning defects	Kosmidis et al. (2010), Wittmann et al. (2001)

Only disease-associated mutations are included. The phenotypes focus on degeneration, behavioral deficits, and aggregate formation.

Cao, W., Song, H.J., Gangi, T., Kelkar, A., Antani, I., Garza, D., et al., 2008. Identification of novel genes that modify phenotypes induced by Alzheimer's beta-amyloid overexpression in *Drosophila*. Genetics 178 (3), 1457–1471.

Crowther, D.C., Kinghorn, K.J., Miranda, E., Page, R., Curry, J.A., Duthie, F.A., et al., 2005. Intraneuronal Abeta, non-amyloid aggregates and neurodegeneration in a *Drosophila* model of Alzheimer's disease. Neuroscience 132 (1), 123–135.

Dosanjh, L.E., Brown, M.K., Rao, G., Link, C.D., Luo, Y., 2010. Behavioral phenotyping of a transgenic *Caenorhabditis elegans* expressing neuronal amyloid-beta. J. Alzheimers Dis. 19 (2), 681–690.

Finelli, A., Kelkar, A., Song, H.J., Yang, H., Konsolaki, M., 2004. A model for studying Alzheimer's Abeta42-induced toxicity in *Drosophila melanogaster*. Mol. Cell Neurosci. 26 (3), 365–375.

Greeve, I., Kretzschmar, D., Tschape, J.A., Beyn, A., Brellinger, C., Schweizer, M., et al., 2004. Age-dependent neurodegeneration and Alzheimer-amyloid plaque formation in transgenic *Drosophila*. J. Neurosci. 24 (16), 3899–3906.

Gunawardena, S., Goldstein, L.S., 2001. Disruption of axonal transport and neuronal viability by amyloid precursor protein mutations in *Drosophila*. Neuron 32 (3), 389–401.

Iijima, K., Liu, H.P., Chiang, A.S., Hearn, S.A., Konsolaki, M., Zhong, Y., 2004. Dissecting the pathological effects of human Abeta40 and Abeta42 in *Drosophila*: a potential model for Alzheimer's disease. Proc. Natl. Acad. Sci. USA 101 (17), 6623–6628.

Jackson, G.R., Wiedau-Pazos, M., Sang, T.K., Wagle, N., Brown, C.A., Massachi, S., et al. 2002. Human wild-type tau interacts with wingless pathway components and produces neurofibrillary pathology in *Drosophila*. Neuron 34 (4), 509–519.

Karsten, S.L., Sang, T.K., Gehman, L.T., Chatterjee, S., Liu, J., Lawless, G.M., et al., 2006. A genomic screen for modifiers of tauopathy identifies puromycin-sensitive aminopeptidase as an inhibitor of tau-induced neurodegeneration. Neuron 51 (5), 549–560.

Kosmidis, S., Grammenoudi, S., Papanikolopoulou, K., Skoulakis, E.M., 2010. Differential effects of Tau on the integrity and function of neurons essential for learning in *Drosophila*. J. Neurosci. 30 (2), 464–477.

Kraemer, B.C., Zhang, B., Leverenz, J.B., Thomas, J.H., Trojanowski, J.Q., Schellenberg, G.D., 2003. Neurodegeneration and defective neurotransmission in a *Caenorhabditis elegans* model of tauopathy. Proc. Natl. Acad. Sci. USA 100 (17), 9980–9985.

Link, C.D., 1995. Expression of human beta-amyloid peptide in transgenic *Caenorhabditis elegans*. Proc. Natl. Acad. Sci. USA 92 (20), 9368–9372.

Link, C.D., Taft, A., Kapulkin, V., Duke, K., Kim, S., Fei, Q., et al., 2003. Gene expression analysis in a transgenic *Caenorhabditis elegans* Alzheimer's disease model. Neurobiol. Aging 24 (3), 397–413.

Pir, G.J., Choudhary, B., Mandelkow, E., Mandelkow, E.M., 2016. Tau mutant A152T, a risk factor for FTD/PSP, induces neuronal dysfunction and reduced lifespan independently of aggregation in a *C. elegans* Tauopathy model. Mol. Neurodegener. 11, 33.

Sarantseva, S., Timoshenko, S., Bolshakova, O., Karaseva, E., Rodin, D., Schwarzman, A. L., et al., 2009. Apolipoprotein E-mimetics inhibit neurodegeneration and restore cognitive functions in a transgenic *Drosophila* model of Alzheimer's disease. PLoS One 4 (12), e8191.

Treusch, S., Hamamichi, S., Goodman, J.L., Matlack, K.E., Chung, C.Y., Baru, V., et al., 2011. Functional links between Abeta toxicity, endocytic trafficking, and Alzheimer's disease risk factors in yeast. Science 334 (6060), 1241–1245.

Wittmann, C.W., Wszolek, M.F., Shulman, J.M., Salvaterra, P.M., Lewis, J., Hutton, M., et al., 2001. Tauopathy in *Drosophila*: neurodegeneration without neurofibrillary tangles. Science 293 (5530), 711–714.

facilitated labeling of cells with vital dyes and fluorescent proteins for real-time monitoring of experimental effects (Ko et al., 2011). Zebrafish embryos are also very well suited to the application of optogenetics techniques where light is used to modulate and monitor neuronal activity (Del Bene and Wyart, 2012). A previous disadvantage of the zebrafish model relative to mammalian models was the absence of technology available to generate targeted mutations. In recent times, however, zinc finger nucleases (ZFNs), transcription activator-like effector nucleases (TALENS), and the type II prokaryotic CRISPR/Cas systems have been developed for targeted mutagenesis of gene sequences in the zebrafish genome (Ekker, 2008; Hoshijima et al., 2016; Hwang et al., 2013; Sander et al., 2011; Schmid and Haass, 2013).

3.1 Chicken and Frog

Compared to invertebrate or mammalian models relatively little investigation of Alzheimer's disease mechanisms has been performed with nonmammalian vertebrates. The chick embryo expresses the Alzheimer's disease-relevant genes, *APP*, *BACE1*, *BACE2*, *PSEN1*, *PSEN2*, *NCT*, *Neprilysin*, and *ADAM17*. Of particular relevance is that the chick *APP* gene has 96% similarity and the Aβ sequence has 100% similarity to the human sequence (Mileusnic and Rose, 2010). Therefore, the chick is a highly relevant model for the analysis of APP and Aβ peptides. At the biochemical level, the lysozyme that is readily available from chick eggs has been used to analyze the general formation of amyloid protein aggregates (Krebs et al., 2000). A number of studies investigating the properties of Aβ peptides exploiting explanted chick neurons and injection of peptides into chick brains. Membrane-bound and soluble fragments of APP can increase neurite outgrowth (Milward et al., 1992). Small and coworkers have cultured chick sympathetic neurons that are cholinoceptive neurons and so are similar to neurons receiving reduced stimulation in Alzheimer's disease. The neurons are derived from the paravertebral sympathetic ganglia of 11- to 12-day-old chicks. These researchers used cultured chick sympathetic neurons to observe the relationship between APP's stimulation of neurite outgrowth and lipoprotein receptor-related protein (LRP) (Postuma et al., 1998). They also observed how different forms of exogenous human Aβ affect the secretion of the extracellular domain of APP (sAPP) and of endogenous Aβ peptides. Some forms of exogenous Aβ decreased the secretion of sAPP and endogenous Aβ while a calcium ionophore increased sAPP secretion (Mok et al., 2000).

The young chick has been proposed to be suitable model for the analysis of memory consolidation. Together with Gibbs, Small and others have used intracranial injection of Aβ of various sizes and aggregation states into 1-day-old hatchlings to observe how this affected memory. They showed that the ability of Aβ to block consolidation of memory into long-term storage was dependent on its aggregation state. Interestingly, aggregated Aβ only blocked memory consolidation into long-term storage and not short-term/intermediate memory so the action of Aβ on memory in the chick may model the anterograde amnesia seen in Alzheimer's disease (Gibbs et al., 2010). Gibbs et al. have also injected various alternative metabolic substrates into trained and Aβ-injected chicks. This allowed them to show that Aβ's involvement in inhibiting memory consolidation appears to be via a blockage of oxidative metabolism of glucose specifically in astrocytes (Gibbs et al., 2009). Subsequently, a study using cultured chick retinal neurons demonstrated that exogenous soluble $A\beta_{42}$ peptides interfere with the distribution of the glucose transporter, GLUT4 (Oliveira et al., 2015). GLUT4 is the major insulin-responsive glucose transporter and this study provides further support that the $A\beta_{42}$ peptide may interfere with glucose regulation. Primary chicken cell culture models have been employed to examine the contribution of brain cell types to the generation of varying Aβ peptides. Aβ-ELISA followed by subsequent immunoblot analysis revealed that astrocytes and microglia but not neurons preferentially secrete N-terminally truncated Aβ peptides (Oberstein et al., 2015).

Oligomers of Aβ are thought to be toxic possibly via formation of pores in lipid bilayers (Strodel et al., 2010). Alternatively, the oligomers may dysregulate existing signal receptors or membrane channels/transporters, such as the acetylcholine receptors (AChRs) that show reduced activity in Alzheimer's disease. *Xenopus* oocytes have been exploited to investigate these possible activities. Lamb et al. (2005) used expression of various forms of AChR in oocytes and treatment with $A\beta_{42}$ to show that Aβ blocks various subtypes of neuronal nicotinic AChRs but not the α7 subtype. In contrast, Demuro et al. (2011) applied oligomeric $A\beta_{42}$ externally to *Xenopus* oocytes and used patch clamping to show that this treatment creates pores allowing transmembrane Ca^{2+} ion movement. In a follow-up study, quantification of fluorescent time-series data from thousands of individual pores from the *Xenopus* oocytes demonstrated an increased Ca^{2+} flux through the Aβ pores. This disruption to a cell's Ca^{2+} homeostasis would have detrimental implications for cell survival (Ullah et al., 2015).

The *N*-methyl-D-aspartate (NMDA) receptors for glutamate that gate high levels of Ca^{2+} flow are thought to play an important role in synaptic plasticity and memory formation (Bordji et al., 2011). Since NMDA receptor antagonists can, apparently, prevent cell death caused by Aβ oligomers, Texido et al. (2011) expressed NMDA receptors in *Xenopus* oocytes to show that Aβ can activate these receptors and that this effect is suppressed by the

antagonists. One-day-old chicks were used to test the effects of the NMDA receptor antagonist memantine on intact memory function. Through passive avoidance learning tests, Samartgis et al. (2012) was able to demonstrate that memantine (an approved drug for the treatment of cognitive problems in Alzheimer's disease) is capable of facilitating memory consolidation and reconsolidation in 1-day-old chicks.

Xenopus oocytes have also been used to investigate the channel forming/regulating properties of other proteins involved in Alzheimer's disease, such as the Presenilins. Frank LaFerla and coworkers (Leissring et al., 1999b) injected mRNAs encoding normal and mutant forms of PSEN1 to show that the M146V mutation increases the ability of PSEN1 to potentiate the Ca^{2+}-activated Cl^- currents evoked by inositol 1,4,5-trisphosphate (IP3). Similar effects were also observed for PSEN2 (Leissring et al., 1999a). The same laboratory also used *Xenopus* oocytes to investigate the relationship between PSEN1 protein and the calcium transporter sarco-/endoplasmic reticulum Ca^{2+}-ATPase (SERCA) and to show that changes in SERCA activity could affect Aβ production (Green et al., 2008). *Xenopus* oocytes have also been used to explore the function of the APP protein. Suh et al. (1996) showed the injection of a 105 amino acid residue (aa) C-terminal fragment of APP directly into oocytes was, apparently, able to form ion channels.

Reductionist approaches to examining the pathological mechanisms behind Alzheimer's disease (such as those mentioned previously) can reveal a great deal but more holistic approaches will also be necessary for complete understanding. Fascinating work by the laboratory of Ricardo Miledi has shown that cell membranes can be extracted from postmortem Alzheimer's disease brains and then injected into *Xenopus* oocytes (Miledi et al., 2004). These membranes incorporate into the plasma membranes of the oocytes and are then available for measurement of ion channel activities, etc. Brains that have been frozen for many years can, nevertheless, act as a source material for membrane analysis. Miledi and coworkers used this technique to find reduced activity of glutamate receptors in Alzheimer's brains and they were able to show that this was due to relatively decreased expression of glutamate receptors in the diseased brains (Bernareggi et al., 2007).

In large cells, such as the eggs of *Xenopus* or zebrafish (or invertebrates, such as *Drosophila*), the relative volume of cytoplasm is so great that the nucleus is unable to control the cell's biology. Therefore, after fertilization transcription of nuclear genes is not initiated until "midblastoderm transition" when the cytoplasm:nucleus volume ratio is sufficiently small. Before this time, cell division and embryo development are under the control of the RNA and protein products of the maternal genome.

The rapid, successive cleavages that the early embryo undergoes are only possible because large quantities of these products have been deposited in the egg by the mother's ovary. For this reason, *Xenopus* eggs can be used to examine the structural and regulatory molecular machinery involved in the cell cycle. A number of studies have shown aneuploidy in neurons in Alzheimer's disease brains, especially aneuploidy of chromosome 21 on which the APP gene resides (Iourov et al., 2009; Zekanowski and Wojda, 2009). Huntington Potter and coworkers (Borysov et al., 2011) have exploited extracts of *Xenopus* oocytes that can form large numbers of mitotic spindles to examine the effects of Aβ42 on spindle formation and maintenance. They showed that Aβ appears to interfere specifically with interactions between mitotic kinesins and microtubules, and this would likely also lead to aneuploidy in mitotic cells.

The pseudotetraploidy of *X. laevis* illustrates the viability of animals with completely duplicated sets of chromosomes. Whole genome duplication provides the genetic raw material upon which the forces of evolution can act to generate organismal diversity and complexity. There is now considerable evidence that vertebrates underwent two rounds of whole genome duplication early in their evolution such that humans now possess four paralogs of many genes only present as singletons in invertebrate genomes (Furlong and Holland, 2002). One of the advantages of investigating gene function in invertebrate species can be the absence of functional redundancy provided by paralogous genes allowing less ambiguous definition of mutant phenotypes and gene functions.

3.2 Zebrafish

Sequencing of the entire zebrafish genome began in 2001 and has now been through many rounds of assembly (The Danio rerio sequencing project). The genome is extensively annotated and regions of conserved chromosomal synteny between humans and zebrafish have been defined (Catchen et al., 2011). Since the human (tetrapod) and zebrafish (teleost–bony fish) evolutionary lineages separated approximately 450 million years ago (Kumar and Hedges, 1998), it appears that the teleosts probably underwent an additional round of whole genome duplication followed by considerable loss of gene duplicates (Catchen et al., 2011). Thus zebrafish have seven *hox* gene complexes where humans have four and most invertebrates have one (Amores et al., 1998). This can complicate the analysis of human disease genes in zebrafish. In many cases zebrafish genes are identifiable that are clear orthologs of human genes. For example, the Alzheimer's disease-relevant genes *PSEN1* and *PSEN2* have clear zebrafish orthologs *psen1* (Leimer et al., 1999) and *psen2*

(Groth et al., 2002), respectively. However, there are many Alzheimer's disease-relevant genes that have "duplicate orthologs." (Strictly speaking such genes must be described as paralogs since they evolved by duplication within an organism rather than by a speciation event.) Thus, zebrafish possesses the genes *appa* and *appb* that evolved from an ancestral gene that was orthologous to human *APP* (Musa et al., 2001). Similarly, *apoea* and *apoeb* are related to human *APOE* (Babin et al., 1997; Woods et al., 2005) and *mapta* and *maptb* are related to human *MAPT* (tau) (Chen et al., 2009).

The existence of "duplicate orthologs" of human disease genes in zebrafish can present both problems and advantages. Overlapping functions of the duplicates (redundancy) can mean that loss-of-function phenotypes are obscured unless the function of both duplicates is blocked simultaneously. However, if the duplicates have evolved partially nonoverlapping expression patterns then manipulation of the function of only one of the duplicates can result in phenotypes restricted to particular cells or tissues. In some circumstances this may facilitate functional analysis (Blader and Strahle, 1998).

Morpholino antisense oligonucleotides (morpholinos) can rapidly and inexpensively provide information on the function of genes during zebrafish embryogenesis. They are most commonly used to block translation of specific mRNAs (Nasevicius and Ekker, 2000). The morpholinos are injected into recently fertilized eggs before the 4-cell stage at which time they can spread into all cells though cytoplasmic bridges. (Earlier injection is preferable since some translation begins immediately upon fertilization.) Morpholinos can generally be assumed to act potently for the first 48 h of development before hatching and the effect of a morpholino may last longer than 48 h but this must be confirmed for each particular oligonucleotide. However, the effectiveness and specificity of a morpholino should always be thoroughly assessed if this information has not previously been published. (The Zebrafish Model Organism Database, ZFIN, www.zfin.org collates successful morpholino sequences from published articles.) Important controls for work with morpholinos can include examining phenotypes from two or more nonoverlapping morpholinos that target the same mRNA, "rescuing" the morpholino-generated phenotype by injection of an mRNA engineered to lack morpholino complementarity and western blotting to demonstrate loss of translation of the endogenous mRNA (Eisen and Smith, 2008). Recently, technology has been developed for the activation and inactivation of morpholinos by light (Deiters et al., 2010).

The recent availability and feasibility of using genome editing technologies presents an exciting opportunity to develop zebrafish genetic models of neurodegenerative diseases, such as Alzheimer's disease.

ZFNs, TALENs, and CRISP/Rs have been validated for use in the zebrafish and it is inevitable that FAD mutations will be introduced into zebrafish FAD gene orthologs (Hoshijima et al., 2016; Hwang et al., 2013; Schmid and Haass, 2013).

An interesting consequence of the widespread use of morpholinos to investigate gene function in zebrafish was the observation of noncorrespondence between phenotypes produced by morpholino-based interference in gene expression versus endogenous gene mutations. Many genes that show distinct phenotypes when their activity is reduced using morpholinos, (and for which the specificity of the phenotype is validated by rescue experiments in which artificially synthesized mRNA for the gene is injected into embryos), nevertheless, fail to show these phenotypes when supposedly null mutations are introduced into the endogenous gene (Kok et al., 2015). A fascinating paper by Rossi et al. (2015) explained this phenomenon by demonstrating that mutations in endogenous genes—but not morpholino inhibition of gene expression—cause upregulation of related genes that compensate for the loss of expression of the mutated genes. The basis of this difference in response to morpholino- versus mutation-based alterations in gene expression is currently unknown. However, this phenomenon provides the opportunity to identify nonmutated genes that can be upregulated to compensate for particular disease-causing mutations and so may possibly be exploited to alleviate disease in humans (e.g., by identifying drugs that force expression of those nonmutated genes).

3.2.1 Presenilins, γ-Secretase and Manipulation of Gene Splicing

Over the last 20 years there has been extensive research into the normal functions of the genes involved in Alzheimer's disease but our understanding is still quite limited. The majority of genes involved in human disease play roles during embryogenesis so analysis of their loss-of-function phenotypes in zebrafish can be informative. Mutations in the human *PSEN* genes cause the majority of early-onset Alzheimer's disease (mentioned previously). In zebrafish embryos, the *psen1* and *psen2* genes are ubiquitously expressed (Groth et al., 2002; Leimer et al., 1999) as shown by whole mount in situ transcript hybridization (WISH) although higher-level expression of *psen2* was observed in melanocytes (Groth et al., 2002). Lardelli and coworkers have used morpholinos to block the translation in embryos of the Psen1 and Psen2 proteins. Blockage of Psen1 translation (Nornes et al., 2003) causes phenotypes similar to those seen for loss of Psen1 in knockout mice (Shen et al., 1997) that are thought to reflect loss of Notch signaling. However, unlike in mice (Steiner et al., 1999), loss of Psen2 function

also appears to have major effects on Notch (Nornes et al., 2009). The idea that Psen2 shows greater redundancy of function with Psen1 in zebrafish than the orthologs of these genes show in humans/mammals is supported by the fact that zebrafish lacking *psen1* activity is viable (Sundvik et al., 2013) while mice lacking Psen1 activity show an embryonic lethal phenotype similar to loss of Notch signaling (Shen et al., 1997). Zebrafish lacking endogenous Psen1 activity could be manipulated transgenically to express Presenilin proteins that include human Alzheimer's disease mutations. Note, however, that such fish would not strictly model human Alzheimer's disease mutations since the human mutations are always observed in a heterozygous state together with wild-type alleles. Alternatively, the genome editing technologies of TALENs and CRISP/Rs could be utilized to generate Alzheimer's disease-like mutations in the endogenous zebrafish *psen1* gene and these fish could then be studied as heterozygotes.

Relevant to this discussion is the paper by Leimer et al. (1999) in which they expressed zebrafish Psen1 protein in human HEK293 cells and saw an increase in the level of $A\beta_{42}$ produced relative to total cellular $A\beta$. This is similar to observations of $A\beta_{42}$ production in human cells with Alzheimer's disease mutations in PSEN1 [reviewed by Wolfe (2007)]. However, this is not surprising since zebrafish *psen1*, when expressed in human cells, can be regarded as equivalent to a human PSEN1 protein bearing a large number of missense mutations and small in-frame insertions and deletions. Thus, changes in the relative level of $A\beta_{42}$ would be expected.

Interestingly, loss of Psen2 specifically affects the production of a particular type of early neuron in the developing spinal cord—the dorsal longitudinal ascending (DoLA) interneurons. Loss of Psen1 does not affect DoLA numbers while loss of Psen2 does (Nornes et al., 2009). This observation provided the first in vivo bioassay for Psen2 function and was later exploited to show functional interaction between Psen1 and Psen2 [(Nornes et al., 2008) see later].

A fascinating aspect of Alzheimer's disease mutations in the *PSEN* genes is that, almost without exception, none of the over 200 known mutations cause truncation of Presenilin proteins [discussed in Jayne et al. (2016)]. Most of the mutations are missense mutations changing amino acid residues or internal insertions or deletions that preserve the open reading frame (ORF). Even Alzheimer's disease mutations that affect transcript splicing always produce at least one transcript form possessing an ORF that includes C-terminal codons [e.g., Dermaut et al. (2004)]. We previously attempted to model these PSEN splicing mutations in zebrafish embryos by injecting morpholinos targeting splice acceptor sites. The intention was to cause exon skipping to produce transcripts lacking exons 8 or 9 similar to the effects of the human PSEN1

L271V (Kwok et al., 2003) and Δ9 (PerezTur et al., 1995; Prihar et al., 1996) mutations, respectively. By targeting morpholinos to the splice acceptor sites of zebrafish *psen1* exons cognate with human *PSEN1* exons 8 and 9 we hoped to induce exclusion of these exons. However, the predominant products were transcripts that failed to splice out introns 7 and 8, respectively. This led to truncation of the ORF after exons 6 and 7 sequences (Nornes et al., 2008). We have also found that a general characteristic of morpholinos that affect splicing is that they simultaneously appear to inhibit the process of nonsense mediated decay. Thus, aberrant transcripts caused by morpholinos can be translated into truncated protein molecules that commonly have dominant effects on cell biology (Newman et al., 2014). Indeed, for zebrafish *psen1* transcripts we found that truncation of the ORF after exons 6 and 7 resulted in dominant negative effects on Psen1 activity (Nornes et al., 2008). By counting DoLA neurons in developing zebrafish embryos we were also able to observe that these dominant negative effects extended to suppression of Psen2 activity (Nornes et al., 2008).

The effects of interfering with splicing either via mutations or using morpholinos can be complex. For example, the G183V mutation in the splice donor site of exon 6 of human PSEN1 (that appears to cause FTD but not Alzheimer's disease) causes formation of a full-length transcript that includes the G183V missense mutation but also transcripts that lack either exon 6 or exons 6 and 7 (Dermaut et al., 2004). A morpholino binding over the cognate donor site of zebrafish *psen1* transcripts causes inclusion of intron 5 and/or part of intron 6 (it is not known whether these inclusions are simultaneous) (Nornes et al., 2008). Therefore, to validate that dominant effects are due to the ORF of a particular splice product, it can be useful to attempt to replicate the phenotype by injection of an mRNA engineered to encode only that ORF. mRNAs for injection into zebrafish embryos are typically synthesized using the pcGlobin2 vector (Ro et al., 2004) which includes untranslated β-globin sequences that stabilize the transcripts. If the relevant phenotype only occurs after 24 h, this can be difficult to phenocopy using mRNA injection due to the instability of the mRNA (Nornes et al., 2008). In such cases it may be possible to use transient transgenesis with the Tol2 vector and a suitable promoter to drive expression of the mRNA (Kawakami, 2004). Injection of mRNA encoding a *psen1* ORF truncated after exon 7 was able to replicate the early (24 h postfertilization, hpf) but not later (48 hpf) phenotypes seen due to injection of a morpholino that blocked the splice acceptor site of exon 8 (Nornes et al., 2008).

The production of *psen1* transcripts with truncated ORFs is not irrelevant to understanding Alzheimer's disease. Recently, a first ORF-truncating mutation that apparently causes Alzheimer's disease, *K115Efx10*, was

isolated in the human PSEN2 gene (Jayadev et al., 2010). This dinucleotide deletion results in a frameshift and premature stop codon that putatively truncates the PSEN2 protein in its first luminal loop. Interestingly, this truncated protein (if it is expressed) would closely resemble the PS2V isoform of PSEN2 that is generated in neurons under hypoxia and is observed in the brains of people with late onset, sporadic Alzheimer's disease (Sato et al., 1999; Smith et al., 2004). We have used mRNA injection into zebrafish embryos to show that the putative peptide produced by *PSEN2* mutation *K115Efx10* can stimulate γ-secretase activity and suppress the unfolded protein response (UPR) (Moussavi Nik et al., 2015) in a manner similar to that observed for PS2V by Sato et al. (2001). This suggests that the *K115Efx10* mutation that truncates PSEN2 may be pathogenic due to stimulation of Aβ production from APP and supports increased Aβ levels as a common link between *K115Efx10* early-onset Alzheimer's disease and late-onset sporadic Alzheimer's disease. Interestingly, by injecting mRNA coding for PS2V together with morpholinos blocking translation of either endogenous zebrafish Psen1 or Psen2 protein we were able to show that PS2V's action on γ-secretase activity requires Psen1 but not Psen2 activity (Moussavi Nik et al., 2015). In this study we also demonstrated that zebrafish possess a PS2V-like isoform, PS1IV, that is produced from the fish's *PSEN1* rather than *PSEN2* orthologous gene. The molecular mechanism controlling formation of PS2V/PS1IV was probably present in the ancient common ancestor of the *PSEN1* and *PSEN2* genes. Even though human PS2V and zebrafish PS1IV have highly divergent structures we were still able to demonstrate conserved function, in that PS1IV is also able to stimulate γ-secretase activity and suppress the UPR under hypoxia. In a recently published study (Ebrahimie et al., 2016), we used a morpholino to specifically block the induction of PS1IV that normally occurs under hypoxia. Through analysis of the subsequent microarray data we identified gene regulatory networks that are modulated by PS1IV. When PS1IV is absent under hypoxia-like conditions, we observed changes in expression of genes controlling inflammation (particularly sporadic Alzheimer's disease-associated *IL1B* and *CCR5*), vascular development, the UPR, protein synthesis, calcium homeostasis, catecholamine biosynthesis, TOR signaling, and cell proliferation. Our results imply an important role for PS2V in sporadic Alzheimer's disease as a component of a pathological mechanism that includes hypoxia/oxidative stress.

3.2.2 Other Components of γ-Secretase

In humans, γ-secretase complexes include three components other than a PSEN1 or PSEN2 protein. The three components are ANTERIOR PHARYNX DEFECTIVE 1A or 1B encoded by *APH1A* and *APH1B*, respectively;

NICASTRIN encoded by *NCSTN* and PRESENILIN Enhancer 2; *C. ELEGANS*, HOMOLOG OF encoded by *PSENEN* (previously known as *PEN2*). Zebrafish apparently possess orthologous genes *aph1b* (but not *aph1a*) (Francis et al., 2002), *ncstn* (Lim et al., 2015; Strausberg et al., 2002), and *psenen* (Campbell et al., 2006; Francis et al., 2002). Only *psenen* has been subjected to functional investigation of any depth. Xia's laboratory used a morpholino to block translation of Psenen and saw increased destabilization of Psen1 protein, reduced neuron formation and defective somitogenesis as expected for the loss of Notch signaling caused by loss of γ-secretase activity (Campbell et al., 2006). A similar somatic phenotype was seen when translation of Aph1b was blocked (Campbell et al., 2006). Interestingly, blockage of Psenen translation caused much greater induction of apoptosis in developing embryos than blockage of Psen1, Psen2, or Aph1b translation and this apoptosis could be blocked by simultaneous blockage of p53 translation [indicating that induction of the apoptosis was via the p53 pathway (Campbell et al., 2006)]. The same laboratory also used coinjection of Psenen morpholino and Psenen mRNA (engineered to lack the morpholino-binding site) to show that the cytosolic loop domain of Psenen was essential to inhibit the caspase-dependent apoptosis seen when Psenen expression is lost. They also showed that loss of NF-κB function (via blockage of translation of NF-κB component p65) could block this apoptosis (Zetterberg et al., 2006).

3.2.3 Assays for γ-Secretase Activity in Zebrafish

Over 70 proteins are known to be substrates of γ-secretase (Lleo and Saura, 2011) and changes in γ-secretase activity can affect some substrates but not others (Wolfe, 2012). There are, as yet, no published assays in zebrafish that directly observe γ-secretase cleavage activity. To date, analysis of γ-secretase activity in zebrafish has exploited changes in the transcription of genes that are known to be the downstream target of Notch signaling, such as *hairy-related 6* (*her6*) (Arslanova et al., 2010; Bernardos et al., 2005; Campbell et al., 2006) and *neurogenin1* (*neurog1*) (Campbell et al., 2006). However, the transcriptional control of these genes varies in different regions of the embryo (Arslanova et al., 2010; Campbell et al., 2006), so it is not informative to use qPCR on whole embryos to assay their expression in response to factors changing γ-secretase activity. For this reason, changes in the expression of Notch target genes are observed by in situ transcript hybridization in particular tissues (Arslanova et al., 2010; Campbell et al., 2006; Nornes et al., 2008). However, in situ transcript hybridization is a very difficult technique to use quantitatively since the staining of embryos that indicates gene transcription is sensitive to fixation conditions, permeabilization, and incubation times in reagents, etc.

Assessment of γ-secretase cleavage of APP in manipulated zebrafish embryos by monitoring of endogenous Appa cleavage is difficult since the α- or β-secretase cleaved forms of Appa (that are the substrate for γ-secretase cleavage) cannot be detected before 48 hpf. For this reason Wilson and Lardelli (2013) have developed an assay where a modified fragment of Appa (equivalent to the membrane embedded remnant after β-secretase cleavage) fused to GFP is expressed in embryos by mRNA injection or transient Tol2 vector transgenesis. This construct is coexpressed with free GFP and then the ratio of Appa:GFP to free GFP is quantified. Use of this assay system has shown that PSEN2 truncated by the *K115Efx10* mutation boosts APP cleavage in a similar manner to PS2V (Moussavi Nik et al., 2015).

3.2.4 Assays for Autophagy in Zebrafish

Recently, it was discovered that Presenilin proteins apparently play a major role in autophagy since they are required for the acidification of lysosomes (Lee et al., 2010) [although another report disputed this Zhang et al. (2012a)]. FAD mutants of human PSEN1 are defective for this autophagy function. Interestingly, the autophagy function of PSEN1 appears to be dependent on the PSEN1 holoprotein rather than on the endoproteolysed form of PSEN1 that is active in γ-secretase complexes. An inhibitor of γ-secretase also had no effect on autophagy (Lee et al., 2010). He et al. (2009), He and Klionsky (2010) have shown that autophagy can be analyzed in fish by analyzing induction of LC3-II protein (one of the major biochemical markers of autophagy) by immunoblotting using an antibody against human LC3 that cross-reacts with the zebrafish protein. Ganesan et al. (2014) validated the LC3-II immunoblot autophagy assay in the presence of chloroquine (a lysosomal proteolysis inhibitor). He et al. (2009), He and Klionsky (2010) have also developed a transgenic zebrafish expressing GFP coupled to LC3 that can be used in autophagy assays. The ability to manipulate Presenilin protein expression and assay autophagy in zebrafish might rapidly reveal more about the involvement of Presenilins in autophagy and how this relates to their other role in γ-secretase activity (Ganesan et al., 2014).

3.2.5 APP

For the two zebrafish APP paralogs, *appa* and *appb* in situ transcript hybridization analysis detects their expression during embryogenesis after the start of gastrulation. By 24 hpf, their transcripts are found in the developing brain and other tissues with only appb expressed in the spinal cord (Musa et al., 2001). The expression of these genes has also been examined in other ways. Lee and Cole (2007) fused ~8.5 kb of appb sequence upstream of and including the *appb* promoter to GFP and followed this with 5 kb of sequence from the first *appb*

intron. They observed expression in neural and other tissues including in developing vasculature (intersomitic vessels). The observations of vascular expression did not correspond to what had been seen from in situ transcript hybridization other than for expression in the dorsal aorta (Lee and Cole, 2007). Subsequently, Shakes et al. (2008) used GFP-enhancer trapping within a BAC clone of *appb* to analyze transcriptional regulation of this gene. In effect, they generated a series of deletions within the BAC clone and this was then introduced into zebrafish embryos to observe the pattern of GFP expression. They did not mention observation of vascular expression but they found that an enhancer within intron 1 of *appb* also required sequences far upstream of the gene to generate expression resembling that of the endogenous gene.

Recently, Liao et al. (2012) isolated insertions of gene traps containing GFP in the *appa* gene and the related gene *aplp2*. For both genes, the gene traps caused fusions to GFP of the extracellular domains of the proteins they encode. Interestingly, the fusion proteins of both genes were found in vasculature but in situ transcript hybridization could not detect transcription of these genes in endothelial cells of the vasculature. It appears that the proteins are synthesized in neuronal tissue but that their extracellular domains subsequently accumulate in vasculature. This observation suggests that the belief that mammalian APP is transcribed in vasculature may be inaccurate.

Translation-blocking morpholinos and mRNA injection into embryos have also been used to analyze the function of the zebrafish Appa and Appb proteins. Inhibition of Appa translation in developing embryos had little effect. However, it was demonstrated that Appb is required for correct convergent extension cellular movements (Abramsson et al., 2013; Joshi et al., 2009) and normal neural development (Song and Pimplikar, 2012) with axon outgrowth defects corresponding with cytoskeletal organization being observed (Song and Pimplikar, 2012). Coinjection of the morpholino blocking Appb expression with mRNA encoding human APP (that cannot bind the morpholino) rescued the embryonic defects and demonstrated the conservation of function in development between the human and zebrafish proteins (Abramsson et al., 2013; Joshi et al., 2009; Song and Pimplikar, 2012). Interestingly, the convergent extension defects could also be rescued by injection of mRNA encoding only the extracellular domain of human APP usually released by α-secretase cleavage but not by a larger protein including the transmembrane domain but lacking the last 18 C-terminal residues that include the EYNPTY motif or by APP containing the Swedish mutation (APP_{SWE}). Morpholino knockdown studies of *appb* have also demonstrated the importance of Appb in motor neuron patterning and formation (Abramsson et al., 2013), neurogenesis, notch signaling,

and in the formation of a specific cell type, the Mauthner cell, in the developing hindbrain (Banote et al., 2016).

3.2.6 Modeling Aβ Toxicity

The small size of zebrafish embryos and larvae means that individuals can be placed in the wells of microtiter plates and these then used for screening the effects of chemical libraries (Lessman, 2011). This strategy can be used to discover therapeutic compounds for disease states when these states can be modeled in fish. The amyloid hypothesis of Alzheimer's disease supposes that the Aβ peptide or its aggregates can be toxic and so considerable effort has been expended to find compounds to suppress Aβ production or to counter this toxicity. To date, the only published attempt to generate a transgenic model of Aβ toxicity in fish involved expression of $Aβ_{42}$ fused to an optimized secretory signal sequence in the melanin-containing pigment cells of zebrafish (melanophores/melanocytes) using the promoter of the gene *mitfa* (*nacre*) (Newman et al., 2010). It was hoped that this would produce an easily visible but viable phenotype of a disrupted surface pigmentation pattern. Unfortunately, a disrupted pattern only became evident after 16 months by which time the fish were aged adults and effectively sterile.

An alternative strategy for observing Aβ toxicity is simply to expose developing embryos to Aβ in their aqueous support medium. $Aβ_{40}$ (2.5 μM) caused defective development including of the vasculature and accelerated cell senescence (Donnini et al., 2010) as indicated by staining for β-galactosidase activity (Kishi et al., 2008). In their prion protein (PrP) morpholino knockdown model, Sempou et al. (2016) treated 5 hpf embryos with 0.5 μM of oligomeric Aβ. It has been reported that PrP transduces neurotoxic signals from Aβ oligomers in Alzheimer's patients through a not well-defined mechanism (Larson et al., 2012; Um et al., 2012). The treatment of embryos with Aβ oligomers induced biochemical changes consistent with their defined PrP gain-of-function phenotype. More recently, $Aβ_{42}$ peptides were directly injected into the 24 hpf zebrafish brain (Nery et al., 2014). At 5 days postfertilization (dpf), the injected larvae displayed cognitive deficits (demonstrated via a decreased response to avoid an aversive stimulus) and increased Tau phosphorylation. These effects were not accompanied by an increase in apoptosis and could be reversed by lithium treatment. These Aβ toxicity model systems could be useful for future pharmacological screening to alleviate the observed effects.

3.2.7 Hypoxia

Considerable evidence supports that hypoxia may be an important early factor in the etiology of Alzheimer's disease. For example, serum biomarkers of hypoxia can differentiate between people with mild cognitive impairment (MCI) that progress to Alzheimer's disease and those who do not (Oresic et al., 2011), and Aβ levels in serum can be greatly increased after cardiac arrest (Zetterberg et al., 2011). Hypoxia causes the electron transport chain of mitochondria to increase free radical production thus producing oxidative stress (Bell et al., 2007), and cardiovascular risk factors [that are also risk factors for Alzheimer's disease (Kotze and van Rensburg, 2012)] would be expected to affect oxygenation of the brain. Zebrafish are an excellent system for analysis of the biological effects of hypoxia [reviewed by van Rooijen et al. (2011)] and have been proposed as a model for hypoxic–ischemic brain damage (Yu and Li, 2011). Zebrafish embryos and adults can be placed in water depleted of oxygen, and Moussavi Nik et al. (2011) have shown that exposure of embryos and larvae to sodium azide can be used to mimic the effects of hypoxia. Hypoxia produces changes in the splicing of the zebrafish *psen1* gene that are functionally equivalent to human PS2V formation (Moussavi Nik et al., 2015), and Moussavi Nik et al. (2012) showed that, as in humans, the zebrafish *psen1*, *psen2*, *appa*, *appb*, genes as, well as *bace1* (that encodes β-secretase) are upregulated by hypoxia in larvae and adult brain. This supports that production of Aβ is a protective response to hypoxia although Aβ itself has not yet been detected in zebrafish. Interestingly, this study showed that F2-isoprostanes (caused by peroxidation of arachidonic acid) are not suitable as a marker for oxidative stress in zebrafish because of the much lower levels of arachidonic acid in zebrafish compared to mammals. Upregulation of *catalyse* gene expression is an alternative marker of oxidative stress (Jin et al., 2011; Moussavi Nik et al., 2012; Tseng et al., 2011).

3.2.8 APOE

The APOEε4 allele is the main genetic risk factor for late-onset, sporadic Alzheimer's disease. According to Genin et al. (2011), APOE should be considered "a major [Alzheimer's disease] gene with semidominant inheritance." APOE activity is important for clearance of Aβ from the brain [reviewed in Huang and Mucke (2012)] and recent evidence suggests that the pathological ε4 allele may undermine blood–brain barrier integrity (Bell et al., 2012). In zebrafish, the *apoe* genes, *apoea* and *apoeb*, have been analyzed in a variety of contexts. Both *apoea* (Raymond et al., 2006) and *apoeb* (Pujic et al., 2006) show expression in the developing retina and in the yolk syncytial layer of the developing zebrafish. Expression of *apoeb* has also been observed in a variety of other tissues/cell types, such as microglial cells (Veth et al., 2011), developing fins, and epidermis (Monnot et al., 1999; Tingaud-Sequeira et al., 2006), macrophages (Lien et al., 2006), liver, intestine, and ovary (Levi et al., 2012). Expression of *apoeb* has also been observed in regenerating fin tissue

(Monnot et al., 1999). Although little research on APOE function in zebrafish has been performed to date, zebrafish lend themselves to analysis of vascular development and function, for example, through the existence of GFP-labeled vasculature, such as provided by fli1a:EGFP transgenic fish (Lawson and Weinstein, 2002), so we expect to see future work in this area.

3.2.9 MAPT/tau

Alzheimer's disease is classed as a tauopathy and Bai and Burton (2011) have previously discussed the use of zebrafish to analyze this class of diseases. The same laboratory has successfully used the promoter of the *enolase2* gene, *eno2*, to drive expression of a human *MAPT* gene encoding 4 tubulin-binding repeats (R), MAP-Tau4R, in neurons (Bai et al., 2007) at levels eightfold higher than in human brain. Since changes in the ratio of 3R to 4R isoforms of MAPT may be important in some tauopathies (Liu and Gong, 2008), such overexpression of a single isoform might generate pathological states. Another example of MAPT overexpression was the work by Paquet et al. (2009) in which cDNA encoding a mutant form of human MAPT associated with FTD, TAU-P301L, was expressed in zebrafish neurons using a binary and bidirectional transgenic system. A *HuC* promoter was used to drive expression of a Gal4:VP16 fusion protein and this protein then bound to UAS sites in a bidirectional promoter transcribing a fluorescent marker protein gene (DsRed) and the TAU-P301L transgene. This transgenic system is only active in the progeny of fish bearing Gal4:VP16 when these are mated with fish bearing the TAU-P301L transgene. This allows the separate transgenic lines to survive when the combined action of the two transgenes causes a neurodegenerative phenotype. The system is also notable for the fact that the neurons expressing the TAU-P301L transgene could easily be identified due to the coexpression of DsRed in those cells. Paquet et al. were able to use the neurodegenerative phenotype to test the efficacy of inhibitors of GSK-3β that phosphorylate the mutant human TAU in this system. They also exploited the system to investigate whether they could observe any ameliorative effect of the compound methylene blue (van Bebber et al., 2010) that has been proposed to be possibly efficacious in treating Alzheimer's disease [reviewed by Oz et al. (2009)]. They did not observe any ameliorative effects of methylene blue on their transgenic system. Note that, since no comparison was made between the phenotype caused by expression of nonmutant versus mutant MAPT in the fish, it is not certain whether the neurodegenerative phenotype observed is due to the P301L mutation or to overexpression of the human protein, or both. There was also no attempt to quantify the expression of the human protein relative to the expression of the endogenous zebrafish *mapt* genes.

The transient expression of tau-GFP (zebrafish and human) under the control of the HuC promoter in zebrafish embryos also results in high levels of neuronal death (Wu et al., 2016). Treatment of these embryos with either signaling factors (Bcl2-L1, Nrf2, and GDNF) or chemical compounds exhibiting antiapoptotic, antioxidative, or neurotrophic effects can prevent the tau-GFP neuronal cell death. This transient tau-GFP system could be used to discover novel drugs against tauopathies.

GWAS have identified *PICALM* as a locus associated with increased Alzheimer's disease risk. In experiments performed in HeLa cells, Moreau et al. (2014) demonstrated that PICALM modulates autophagy and alters the clearance of tau (a known autophagy substrate). They confirmed this function of PICALM in vivo, using zebrafish transgenic tau models. In their first model, they generated an expression construct comprising a green-red photoconvertible fluorescent protein fused to human tau that was mosaically expressed in the epithelial and muscle cells of the zebrafish. Mosaic tau zebrafish were imaged before and after photoconversion to determine the clearance of the photoconverted red fluorescently tagged tau protein. They confirmed that tau clearance is predominantly mediated by autophagy (through immunoblotting for LC3 levels). Subsequent overexpression of PICALM in the mosaic zebrafish reduced clearance of Tau through inhibition of autophagy. In their second model, they examined the effect of PICALM overexpression on tau toxicity in transgenic zebrafish expressing EGFP-tagged human tau under the control of the rhodopsin promoter that drives expression in the rod photoreceptors (rho:GFP-tau). Through comparisons to transgenic zebrafish expressing rho:GFP (i.e., no tau), they demonstrated neurodegeneration through an increase in apoptotic cells in the retina of the rho:GFP-tau zebrafish. Overexpression of PICALM specifically in the photoreceptors (through electroporation of PICALM DNA) resulted in an acceleration of the neurodegeneration previously observed and in increased tau phosphorylation in the rho:GFP-tau zebrafish only. Rapamycin treatment of rho:GFP-tau zebrafish was able to rescue photoreceptor degeneration in the unelectroporated eyes but not in the PICALM electroporated eyes suggesting that the effect of PICALM on tau toxicity is autophagy dependent. This study is an excellent example of how the zebrafish model can be utilized to answer specific questions about the mechanisms behind Alzheimer's disease in an in vivo setting. Their zebrafish models provided support for the demonstrated mechanistic link of an Alzheimer's disease GWAS risk factor (PICALM) with tau accumulation and autophagy.

The zebrafish genes *mapta* and *maptb* were identified by Chen et al. (2009) who noted their similar but not completely overlapping patterns of expression in developing embryos. In particular, only *maptb* is strongly

expressed in the trigeminal ganglion and dorsal sensory neurons of the developing spinal cord during embryogenesis. Interestingly, *mapta* is expressed as 4R–6R isoforms while *maptb* is predominantly expressed as 3R isoforms. This suggests that manipulation of the expression of these two genes may be informative for understanding the role of the 3R:4R ratio in tau pathogenesis and this contrasts with the mouse which mainly expresses 3R forms of *Mapt*. In unpublished work, Chen et al. have shown that manipulation of *mapta* and *maptb* expression can cause abnormalities in axonogenesis from the trigeminal ganglion. We have assessed the splicing of transcripts of the *mapt* genes in the adult zebrafish brain under hypoxic conditions. We find that hypoxia causes increases in the *mapta* and *maptb* transcript isoforms, particularly the 6R and 4R isoforms of *mapta* and *maptb*, respectively. Expression of the zebrafish ortholog of human *TRA2B*, *tra2b* (that encodes a protein that binds to *MAPT* transcripts to regulate splicing), was reduced under hypoxic conditions, similar to observations in Alzheimer's disease brain. Overall, these findings indicate that hypoxia can alter splicing of zebrafish *MAPT* coorthologs promoting formation of longer transcripts and possibly generating Mapt proteins more prone to hyperphosphorylation. This supports the use of zebrafish to provide insight into the mechanisms regulating *MAPT* transcript splicing under conditions that promote neuronal dysfunction and degeneration (Moussavi Nik et al., 2014).

3.2.10 The Future for Zebrafish Models

Whether the zebrafish can be employed to model a late-onset disease like Alzheimer's disease is debatable since zebrafish have a profound capacity for regeneration and this must impact on the development of neurodegenerative phenotypes. Neurogenesis in the adult zebrafish brain is much more abundant than is observed in mammals (Kizil et al., 2012), consequently making analysis of neuronal loss difficult. However, zebrafish do have high physiological and genetic homology with humans and a similar central nervous system with many behaviors being evolutionarily conserved between zebrafish and mammals. As discussed by Kalueff et al. (2014), the zebrafish is an emerging model for studying a number of complex brain disorders.

Even though the zebrafish has primarily been used to analyze how genes involved in human disease play roles during early zebrafish development; the zebrafish adult brain is becoming increasingly used to investigate Alzheimer's disease. For example, assessment of embryo lead exposure on latent neurological alterations was analyzed in 12-month-aged zebrafish brains (Lee and Freeman, 2016). Microarray analysis of these brains revealed female-specific gene expression changes in the Alzheimer's disease-related genes *APP*, *APOE*, and *SORL1*. This group also demonstrated gender-specific expression changes in Alzheimer's disease-related genes in untreated zebrafish (Lee et al., 2016). Female adult brains showed an upregulation of *appa*, *appb*, and *psen1*, and a downregulation of *apoea* and *apoeb* in 12-month brains compared to 6-month brains. This was not observed in male adult fish brains. Furthermore, Nada et al. (2016) proposed that they had developed a drug-induced Alzheimer's disease zebrafish model by using okadaic acid. Although these drug exposure models still require further validation, it demonstrates the potential utility of the adult zebrafish.

The zebrafish provides unique advantages for modeling single FAD mutations and for transcriptomic and proteomic analysis of gene expression in mutant brains. Single, whole brains provide sufficient RNA or protein for "omics" analyses. The genetic noise that influences human brain transcriptome analyses due to genetic and environmental variation can be greatly reduced by analyzing multiple inbred sibling zebrafish raised in the same tank. Furthermore, zebrafish larvae are the most versatile available vertebrate model system for the screening of chemical libraries to find candidate drugs to treat disease (Rennekamp and Peterson, 2015). Therefore, the development and subsequent analysis of FAD genetic zebrafish models will potentially reveal underlying causes of Alzheimer's disease and also open up new pathways to the development of anti-Alzheimer's disease drugs.

4 MAMMALIAN MODELS OF ALZHEIMER'S DISEASE

Invertebrates provide us with excellent opportunities to decipher the biochemical roles of genes and the implications of genetic mutations in a minimalistic system. Nonmammalian vertebrates enable deciphering of the roles of these genes in disease pathogenesis in relatively simplistic and highly manipulable systems. However, neurodegeneration related to specific human diseases is not a global event and initiates in specific brain compartments. For example, FTD is characterized by prominent neurodegeneration in temporal and/or frontal lobes of the brain (Rabinovici and Miller, 2010), while neurodegeneration in Alzheimer's disease is located to hippocampus, forebrain, and cortex (Bilbul and Schipper, 2011). Thus nonmammalian vertebrates with simpler brain structures cannot faithfully emulate the neurodegeneration observed in human disease. Furthermore, although studies of the cognitive abilities of nonmammalian vertebrates have gained traction in recent years (Marder, 2002), they are yet not very well established. Thus, in some situations, higher order vertebrates with greater homology to human physiological processes and

anatomical structures can be more appropriate for neurodegenerative disease modeling.

The obvious choice to model human neurodegeneration would be the genetically proximal and anatomically similar nonhuman primates (NHP). NHPs have similar brains, cellular metabolomics, and share many of the physiological and behavioral characteristics of humans (Chan, 2004; Lane, 2000). In addition, NHPs show similar age-related cognitive impairment (Joly et al., 2014; Nagahara et al., 2010) and cerebral pathology as observed in human aging (Heuer et al., 2012; Ndung'u et al., 2012), thus NHPs can serve as a model for spontaneous disease development. However, the high costs associated with maintenance of NHPs make large-scale studies prohibitive. In addition, currently it is difficult to generate transgenic NHPs, limiting the use of NHPs in modeling human neurodegeneration (Chen et al., 2012a). Nevertheless, NHPs have been employed as an intermediary animal model when translating research from rodent models to humans (Verdier et al., 2015) [for a review on NHPs see Camus et al. (2015), Huang et al. (2016)]

In contrast to NHPs, mammalian rodent models are more amenable to transgenic techniques, easier to maintain, cost effective, and have a relatively short life span. Although, in comparison to NHPs, rodents are genetically distant to humans, in terms of evolutionary history they are more closely related to humans than the nonmammalian vertebrates (Jucker, 2010), and they can show gene expression profiles similar to humans (Chan et al., 2009; Strand et al., 2007; Zheng-Bradley et al., 2010).

Mouse models currently are the most popular choice for modeling Alzheimer's disease, as mouse transgenic techniques are well established (Doyle et al., 2012) (enabling easy generation of transgenic mice). Mice also have a shorter life span (enabling quick assessment of experiments), have multiple progeny (enabling quick transgenic family expansion), with a relatively short gestation period of ~21 days (enabling large-scale and generational studies). Their husbandry and maintenance costs are also lower than for other mammals. Thus mouse models can be more suitable and practical for modeling human neurodegeneration (Leung and Jia, 2016). In addition, the cognitive abilities of rodent models have been very well characterized and faithfully emulate neurodegeneration along with associated cognitive and behavioral changes (Webster et al., 2014). Murine models of Alzheimer's disease have played an important role in providing significant insight into mechanisms underlying the amyloid hypothesis and are the most commonly used in vivo tool for screening in preclinical drug trials. However, it must be noted that rodents themselves are poor natural models of Alzheimer's disease and do not exhibit pathological hallmarks of the disease, partly due to differences to human Aβ and tau species and aggregation states of these proteins. Thus, transgenic mice expressing human genes have been employed to study familial Alzheimer's disease-related mutations in genes involved in Aβ metabolism (i.e., APP and/or the PSEN genes) and/or tau (MAPT). These transgenic mice have been generated using both random transgene integration and knock-in techniques. In addition, knockout models have also been used to examine the implications of certain Alzheimer's disease-related genes, such as PSEN1/2, APOE, and BACE (see later) in disease pathogenesis.

While murine models have been assumed to be excellent models of autosomal dominant familial forms of Alzheimer's disease, their relevance to the more common, sporadic, late-onset form of the disease has been more contentious. Although genetic predisposition is associated with sporadic Alzheimer's disease, environmental, metabolic, and lifestyle risk factors are thought to play a more important role in disease pathogenesis (Chakrabarti et al., 2015; Piaceri et al., 2013; Stozicka et al., 2007). Further limitations to murine models of Alzheimer's disease include levels of transgene expression (Epis et al., 2010), variations due to genetic background (Lehman et al., 2003a), and the presence of both human and endogenous murine Aβ and tau confounding the interpretation of results (Howlett and Richardson, 2009). Thus to investigate pathogenesis of sporadic Alzheimer's disease, there is an increasing interest in developing nontransgenic animal models for Alzheimer's disease.

In addition to NHPs, other higher mammalian models have been investigated for Alzheimer's disease research as alternatives to the mouse and rat. Polar bears, dogs, and dolphins have all been reported to exhibit age-related pathological features, such as amyloidosis, neuronal-fibrillary deposition, and cognitive deficits similar to humans (see later). The obvious disadvantages of these animals are difficulty of maintenance and the length of time (years to decades) before pathology is observed. Smaller nontransgenic animal models, such as guinea pigs and rabbits are alternatives. Like mice and rats, guinea pigs and rabbits are experimentally amenable but, unlike mice or rats, they show higher sequence conservation to humans in important Alzheimer's disease-associated genes and their Aβ sequence is identical to that of humans. The subsequent section details the characteristics of the most commonly utilized transgenic mouse models for Alzheimer's disease and relevant knock-in and knockout models. Limitations of these mouse models and the growing interest in utilizing nontransgenic models as a more representative model for sporadic Alzheimer's disease will also be discussed.

4.1 Transgenic Rodent Models

4.1.1 Transgenic Mouse Models

The major attribute that has established the mouse as a mainstream model in Alzheimer's disease research is its ability to be genetically manipulated using well-developed transgenic technologies. Various transgenic techniques have been employed to investigate the role of autosomal dominant Alzheimer's disease mutations in mice. In contrast, although rats are more amenable to surgical interventions and cognitive training and are more relevant to human disease from a neuropsychological perspective, transgenic techniques are still under development.

Both random and targeted transgenic methods have been used to develop Alzheimer's disease transgenic models. In the former case, FAD-associated mutations are introduced to the existing murine genetic background (i.e., with the murine endogenous gene expressing simultaneously), using either small cDNA-based expression constructs or artificial chromosomes. Small cDNA-based transgenic models are most commonly driven by a strong neural-specific promoter, such as the platelet derived growth factor-beta (PDGP) promoter (Hsia et al., 1999; Mucke et al., 2000), hamster prion promoter (PrP) (Borchelt et al., 1996; Chishti et al., 2001; Hsiao et al., 1996), or thymocyte antigen promoter (Thy1.2) (Lewis et al., 2000; Richards et al., 2003) which allow ~3- to 30-fold overexpression of the Alzheimer's disease-associated transgene (depending on the promoter applied and genetic background) (Jankowsky et al., 2005). Regionally restricted promoters, such as the calcium calmodulin kinase II (CamKII) promoter (forebrain-specific expression) have also been used (Jankowsky et al., 2005). The development of artificial chromosome-based technology has allowed the introduction of transgenes incorporating large genomic fragments (including the *cis*-acting elements required to regulate gene expression) into models. The transgenes are thus expressed under the control of "native" promoters and transcriptional effectors, which can recapitulate more closely the normal expression patterns of the endogenous gene.

The development of sophisticated gene-targeting technologies underpinned the use of the transgenic mouse as the dominant organism for modeling Alzheimer's disease. These powerful technologies allowed reproduction of the disease features by engineering of existing endogenous genomic loci rather than introduction of exogenous genes. Knockout models have been generated to examine the null phenotypes of particular Alzheimer's disease-related genes, such as *PSEN1* (Dewachter et al., 2002; Shen et al., 1997), *PSEN2* (Herreman et al., 1999), *APOE* (Piedrahita et al., 1992), and *BACE* (Cai et al., 2001). Chimeric models expressing human Alzheimer's disease-associated mutations have also been generated (Jankowsky et al., 2005; Reaume et al., 1996). In these models, key sequences of Alzheimer's disease-related genes were "humanized" and FAD-associated mutations were introduced by targeted point mutation. In such models, the mouse genome remains mostly unchanged except for one or more mutated amino acids. This form of model avoids potential problems resulting from gene overexpression, disrupted spatial and temporal expression, and coexistence of endogenous orthologous genes as seen in other transgenic models. However, the introduction of multiple simultaneous mutations into a genetic locus can still, potentially, confound analysis. Later, we discuss some of the mouse models that express Alzheimer's disease-relevant genes including APP, PS1, tau, apoE, or BACE.

4.1.2 Transgenic APP Models

Modeling of Alzheimer's disease in transgenic mice has been pursued largely under the influence of the amyloid hypothesis, whereby Aβ aggregation is a pivotal event in the disease pathogenesis driving neurodegeneration. However, initial attempts to recapitulate cerebral amyloid accumulation through overexpression of wild-type APP were of little success. Although a number of strategies were pursued (Fukuchi et al., 1996; Lamb et al., 1993; Neve et al., 1996), overexpression of wild-type APP did not result in cerebral deposition of amyloid plaques and cognitive deficits, or overt neuronal loss. Attention was rapidly redirected into the generation of a mouse model expressing FAD-causing mutations.

4.1.3 cDNA-Based Transgenic APP Models

The first success in developing a transgenic FAD-based model came from Games et al. (1995), who generated the PDAPP mouse. In this model, the APP Indiana mutation (V717F) was driven by a strong neuronal-specific PDGF promoter. Under the regulation of such a highly active promoter, the transgenic APP level was approximately 10-fold higher than that of the endogenous mouse APP. The Indiana mutation results in high Aβ$_{42}$ production and age-dependent accumulation of Aβ. In heterozygous mice, deposition of human Aβ begins at 6–9 months in the hippocampus, corpus callosum, and cerebral cortex. Condensed thioflavin S-positive senile plaques resembling those seen in Alzheimer's disease brains were seen after 9 months. Although widespread neuronal loss was absent, impairments in spatial memory and object recognition in young PDAPP mice were reported (Chen et al., 2000; Dodart et al., 1999; Huitron-Resendiz et al., 2002).

Similarly, the Tg2567 mouse was generated by overexpression of a human APP gene containing the Swedish mutation (KM670, 6711L) transcribed from the PrP promoter. The Swedish mutation is located on the N-terminal flanking region of the Aβ, and results in an increase

in $A\beta_{40}$ and $A\beta_{42}$ (Haass et al., 1995). In the Tg2567 mouse, the expression level of the mutant human APP was elevated more than fivefold above the endogenous mouse APP. In the brains of these mice the $A\beta_{40}$ and $A\beta_{42}$ peptides accumulate in an age-dependent manner. Deposition of amyloid plaques commences at 11–13 months in frontal, temporal cortex, hippocampus, presubiculum, subiculum, and cerebellum in a pattern reminiscent of that seen in human Alzheimer's disease. The mice demonstrated memory impairments and deficits in long-term potentiation typical of neuronal dysfunction. However, neuronal loss was not evident (Hsiao et al., 1996). Additionally, cerebrospinal fluid (CSF) $A\beta_{42}$ levels were reduced with the formation of amyloid plaques (Kawarabayashi et al., 2001), resembling the scenario that occurs in Alzheimer's disease patients (Blennow et al., 2006). Due to these characteristics, the Tg2567 line has been widely used in Alzheimer's disease research and for the preclinical evaluation of potential therapeutics. This mouse model also has been commonly used to cross with other transgenic mice containing mutations in PS1 or tau to accelerate amyloid deposition or generate mice containing both senile plaques and NFTs (discussed further subsequently).

Additional APP transgenic models have been generated using strategies similar to that implemented for generation of the PDAPP and Tg2567 lines, where cDNA-based single or double FAD APP mutants were overexpressed by a neuronal-specific promoter. These models often exhibit high expression of the human FAD APP mutation, $A\beta$ accumulation, and deficits in spatial and learning memory. However, the phenotypic features differed based on different mutations under investigation, the promoter used for expression, and the genetic background of the mouse line. For example, whereas the PDAPP line shows accumulation of $A\beta_{42}$, plaques in the Tg2567 line are mostly comprised of $A\beta_{40}$ (Johnson-Wood et al., 1997; Kawarabayashi et al., 2001). Similarly, in transgenic lines harboring the Dutch (APP^{E693Q}) mutation, more extensive accumulation of $A\beta$ in cerebral blood vessels in the form of cerebral amyloid angiopathy (CAA) and cerebral hemorrhage were reported (Herzig et al., 2004). While it is beyond the scope of this chapter to discuss every model, a brief summary of the characteristics of the more commonly used transgenic lines can be found in Table 40.3.

The cDNA-based transgenic lines provide a valuable system to replicate human cerebral amyloidosis in mice and have demonstrated cognitive deficits associated with accumulated $A\beta$. However, these models do not accurately reflect the pathologic condition of human FAD possibly due to the heterologous regulation and overexpression of APP and FAD mutant APP, which deviate considerably from the human conditions. To overcome these issues, transgenic mice have been created whereby an APP transgene is under the control of a native mouse promoter.

4.1.4 YAC/BAC-Based Models

Yeast artificial chromosomes (YACs) and BACs can accommodate large gene inserts including distant regulatory elements and, unlike cDNA-based expression systems, allow for a more spatial and temporally controlled expression of transgenes. Both YACs (Lamb et al., 1993, 1997) and BACs (Chiocco et al., 2004) have been used to express wild-type and clinical mutants of APP in mice. Using these artificial chromosome technologies, transgenic mice containing either the Swedish (swe) and/or London (lon) mutations were created where a more specific and accurate spatial and temporal expression of mutant APP was observed. In a transgenic mice referred to as J1.96 (containing human APP with both the Swedish and London mutations), a single copy of the *APPswe/lon* mutation was detected and the transcriptional expression of this transgene was similar to that of endogenous mouse *APP*. Expression levels of the full-length APP protein remained steady, but levels of the C-terminal fragment (C99) and $A\beta_{42}$ peptide increased twofold over that generated in a transgenic line expressing human wild-type APP (Py8.9) using the same strategy (Lamb et al., 1997).

In another mouse model containing the human *APPswe* mutation (R1.40), multiple copies of the transgene were identified and resulted in two- to threefold overexpression of the mutant APP. While the expression of full-length APP was constantly threefold above that of endogenous APP, the ratio of β/α-cleaved C-terminal APP fragments was dramatically increased. The levels of both $A\beta_{40}$ and $A\beta_{42}$ were proportionally elevated, providing in vivo evidence that the Swedish mutation facilitates β-site cleavage and that the London mutation is able to shift the γ-site toward the 42 aa form of $A\beta$ (Lamb et al., 1997). Comparisons with the cDNA-based transgenic mouse line Tg2567 revealed that both APP holoprotein expression and $A\beta$ production in the R1.40 line was much lower in the hippocampus. Abundant $A\beta$ deposition in the hippocampus was detected in the Tg2567 line at 13.5 months but not in the R1.40 mouse at the same age. In the cortex, the level of $A\beta_{40}$ was similar in both lines, although a significantly higher level of full-length APP was expressed in Tg2567. In the homozygous R1.40 line, $A\beta$ deposition occurred primarily in the frontal cortex at 13–16 months and spreads into hippocampus with age. Unlike the Tg2567 mouse line, cognitive deficits were not observed in both the J1.96 and R1.40 lines (Lehman et al., 2003b). Overall these results suggest that although the YAC/BAC-based systems allow more specific and accurate spatial and temporal expression of mutant APP, greater amyloid deposition and cognitive deficits are achieved by using heterologous promoters.

TABLE 40.3 Examples of Transgenic Mouse Models

Line	Transgene/promoter	Age of plaque onset (months)	CAA	NFTs	Behavioral phenotype	References
PDAPP	APP717I minigene/PDGF-β	6–8	*	—	Impaired spatial memory (3–4 months) Cued fear conditioning (11 months)	Games et al. (1995)
Tg2576	huAPPswe/hamster PrP	9–11	*	—	Memory deficits (9–10 months)	Hsiao et al. (1996)
TgCRND8	APPSweI/hamster PrP	3	*	—	Impairment in acquisition and reversal learning (3 months)	Chishti et al. (2001)
TgArcSwe	huAPPArcSwe/Thy1	6	*	—	Spatial learning deficits (4–8 months)	Lord et al. (2006)
APPDutch	huAPP751D/Thy1.2	22–25	***	—	nr	Herzig et al. (2004)
R1.40	APPSwe gene/YAC	14	*	—	nr	Lamb et al. (1997)
APPV642IKI	APPL/knock-in	—	—	—	Long-term memory significant deficits. Acquisition of spatial memory slightly affected, short-term working memory preserved	Kawasumi et al. (2004)
TgAPPSwe-KI	humanized Aβ and Swe mutation/knock-in	—	—	—	nr	Reaume et al. (1996)
APPswe2576/ TauJNPL3	APPswe(Tg2576) xTau4RP301L(JNPL3)	9–11	*	***	Motor disturbances (4.5–6.5 months)	Lewis et al. (2001)
5XFAD	huAPPsweFL,PSEN1M146L, L286V/exon2 of mThy1	2	nr	—	Spatial learning deficit (4–5 months)	Oakley et al. (2006)
3XTg	APPSwe/TauP301L/Thy1.2x PS1M146VKI	6	*	***	Cognitive impairment (4 months)	Oddo et al. (2003)

CAA, Cerebral amyloid angiopathy; NFTs, neurofibrillary tangles.

Chishti, M.A., Yang, D.S., Janus, C., Phinney, A.L., Horne, P., Pearson, J., et al., 2001. Early-onset amyloid deposition and cognitive deficits in transgenic mice expressing a double mutant form of amyloid precursor protein 695. J. Biol. Chem. 276 (24), 21562–21570.

Games, D., Adams, D., Alessandrini, R., Barbour, R., Berthelette, P., Blackwell, C., et al. 1995. Alzheimer-type neuropathology in transgenic mice overexpressing V717F beta-amyloid precursor protein. Nature 373 (6514), 523–527.

Herzig, M.C., Winkler, D.T., Burgermeister, P., Pfeifer, M., Kohler, E., Schmidt, S.D., et al., 2004. Abeta is targeted to the vasculature in a mouse model of hereditary cerebral hemorrhage with amyloidosis. Nat. Neurosci. 7 (9), 954–960.

Hsiao, K., Chapman, P., Nilsen, S., Eckman, C., Harigaya, Y., Younkin, S., et al., 1996. Correlative memory deficits, Abeta elevation, and amyloid plaques in transgenic mice. Science 274 (5284), 99–102.

Kawasumi, M., Chiba, T., Yamada, M., Miyamae-Kaneko, M., Matsuoka, M., Nakahara, J., et al., 2004. Targeted introduction of V642I mutation in amyloid precursor protein gene causes functional abnormality resembling early stage of Alzheimer's disease in aged mice. Eur. J. Neurosci. 19 (10), 2826–2838.

Lamb, B.T., Call, L.M., Slunt, H.H., Bardel, K.A., Lawler, A.M., Eckman, C.B., et al., 1997. Altered metabolism of familial Alzheimer's disease-linked amyloid precursor protein variants in yeast artificial chromosome transgenic mice. Hum. Mol. Genet. 6 (9), 1535–1541.

Lewis, J., Dickson, D.W., Lin, W.L., Chisholm, L., Corral, A., Jones, G., et al., 2001. Enhanced neurofibrillary degeneration in transgenic mice expressing mutant tau and APP. Science 293 (5534), 1487–1491.

Lord, A., Kalimo, H., Eckman, C., Zhang, X.Q., Lannfelt, L., Nilsson, L.N., 2006. The Arctic Alzheimer mutation facilitates early intraneuronal Abeta aggregation and senile plaque formation in transgenic mice. Neurobiol. Aging 27 (1), 67–77.

Oakley, H., Cole, S.L., Logan, S., Maus, E., Shao, P., Craft, J., et al., 2006. Intraneuronal beta-amyloid aggregates, neurodegeneration, and neuron loss in transgenic mice with five familial Alzheimer's disease mutations: potential factors in amyloid plaque formation. J. Neurosci. 26 (40), 10129–10140.

Oddo, S., Caccamo, A., Shepherd, J.D., Murphy, M.P., Golde, T.E., Kayed, R., et al., 2003. Triple-transgenic model of Alzheimer's disease with plaques and tangles: intracellular Abeta and synaptic dysfunction. Neuron 39 (3), 409–421 (Comparative Study Research Support, Non-US Gov't Research Support, US Gov't, PHS).

Reaume, A.G., Howland, D.S., Trusko, S.P., Savage, M.J., Lang, D.M., Greenberg, B.D., et al., 1996. Enhanced amyloidogenic processing of the beta-amyloid precursor protein in gene-targeted mice bearing the Swedish familial Alzheimer's disease mutations and a "humanized" Abeta sequence. J. Biol. Chem. 271 (38), 23380–23388.

The reason(s) for the differences in Aβ deposition and cognitive state in these two transgenic lines harboring the same FAD mutations are not clear. One possible explanation may be the region-specific regulation of different promoters and the distinct transcriptional profile of the mutant human APP (i.e., the Tg2567 line only expressed the APP_{695} isoform, but all APP isoforms were present in the R1.40 line) (Lehman et al., 2003a).

4.1.5 Knock-Ins

A more elegant way to mimic the pathology of human FAD mutations and to avoid issues surrounding overexpression using specific promoters is to generate a knock-in model. Andrew et al. established the first human APP-swe knock-in line, termed APP SWE-KI in 1996. In this line, targeted mutagenesis technology was employed to introduce the Swedish mutation and "humanize" the mouse endogenous Aβ peptide by altering the three amino acids that differ from human Aβ. The expression level of the mutant APP was equivalent to that of wild-type, endogenous mouse APP, but generation of the APP β-CTF was greatly enhanced, accompanied by a nine-fold elevation of the level of Aβ (Reaume et al., 1996). However, amyloid pathology and associated cognitive deficits were not prominent, even by 22 months of age (Flood et al., 2002). In another knock-in model carrying the APP London mutation (V642I), an increased level of $Aβ_{42}$ was observed but amyloid plaque deposition was absent. Deterioration of long-term memory was evident in very old mice (27–29 months), while short-term working memory was preserved (Kawasumi et al., 2004).

The major difference between the knock-in model and other transgenic models is the absence of endogenous mouse Aβ. It has been shown that human Aβ can coaggregate with rodent Aβ in vivo with the potential to alter the structural conformation of Aβ plaques (Pype et al., 2003). This notion was supported by the finding that the Aβ peptide generated in the brains of Tg2567 transgenic mice lacks modifications, such as N-terminal degradations and levels were ~tenfold greater than that seen in human brains (Kalback et al., 2002). The knock-in models exclude the potential effect of interactions between human and rodent Aβ peptides on the development of pathology. Nevertheless, such studies have demonstrated that Aβ levels can be significantly elevated solely by the Swedish mutation without overexpression of APP in vivo. However, the absence of further histological pathology and behavioral changes in the knock-in mouse models possibly suggests that the pathology observed in other transgenic mice is due to the overexpression of the mutant transgenes and not to the effects of FAD-associated APP mutations themselves.

More recently, however, an APPKI mouse model has been generated that unlike previous attempts exhibit Alzheimer's disease pathology and cognitive deficits.

The model is referred to as the APP^{NL-F} mouse model and was generated by Takaomi Saido's laboratory from the RIKEN brain institute. The Aβ sequence of mouse APP was humanized and the Swedish mutation (KM670/671NL) and Beyreuther/Iberian mutation (I716F) were introduced into exons 16 and 17 of the mouse APP gene (Saito et al., 2014). These mice exhibited increased levels of $Aβ_{42}$ (with a high $Aβ_{42/40}$) ratio and plaque formation at 6 months of age, with similar pathology to that seen in human Alzheimer's disease brain (Saito et al., 2014). Other hallmarks were also exhibited including neuroinflammation, synaptic alterations, and cognitive impairment was observed at 18 months of age. Inclusion of the Arctic mutation (E693G) into exon 17 of mouse APP (APPNL-G-F), resulted in an accelerated pathology, with plaques. This model circumvents the intrinsic problems associated with APP transgenics [see review Nilsson et al. (2014)] and crossbreeding with other KO, KI mice could provide relevant insights into downstream neurodegenerative pathways.

4.1.6 Presenilin Models and Crosses

The Presenilin proteins (PSEN1 and PSEN2) are considered to be the catalytic components of the γ-secretase enzyme that promotes the final cleavage of APP to generate Aβ. Mice lacking PSEN1 die before birth and the embryos display severe skeletal and brain deformities while heterozygotes exhibit tau hyperphosphorylation, markedly reduced Aβ levels, massive neuron loss, and hemorrhages in the CNS (Rozmahel et al., 2002; Shen et al., 1997). These severe phenotypes due to the lack of PSEN1 have been associated with PSEN1's essential function in facilitating Notch signaling. Mice lacking PSEN2 on the other hand only develop a mild pulmonary fibrosis and hemorrhages with age (Herreman et al., 1999; Steiner et al., 1999), consistent with suggestions that PSEN2 is less efficient at γ-secretase activity than PSEN1 (Acx et al., 2014; Bentahir et al., 2006; Mastrangelo et al., 2005; Meckler and Checler, 2014, 2016).

The majority of FAD-associated mutations are located in the *PSEN1* gene. Most of these are associated with severe amyloid pathology in humans as a result of accumulation of the longer, more pathogenic $Aβ_{42}$ peptide species. As such, mice harboring *PSEN1* mutations have been generated, mainly for the purpose of crossing with APP transgenic mice to accelerate pathology. A few transgenic lines containing FAD-associated *PSEN2* mutations have also been generated. Similar transgenic approaches and promoters (such as the PDGF, PrP, and Thy1.8 promoters) were employed in the construction of PSEN1/2 transgenic lines. Although increases in endogenous murine $Aβ_{42}$ levels have been reported in a few PSEN transgenic lines, these mice do not exhibit an Alzheimer's disease-like neuropathology including

amyloid deposition, most likely due to the lower propensity of the endogenous rodent Aβ to aggregate (Duff et al., 1996; Wen et al., 2002). To promote cerebral amyloid deposition, mice expressing PSEN1/2 have been crossed with APP transgenic lines. These mice show accelerated plaque formation and some exhibit neuronal loss. One example is the model developed by Casas et al. who crossed the APP751SL line (harboring APP London and Swedish mutations), with a knock-in model expressing the PSEN1 mutations M233T and L235P. This model developed amyloid plaques at 6 months and exhibited neuronal loss at 10 months (Casas et al., 2004). Interestingly, the neuron loss observed in this model was not associated with extracellular amyloid plaque load, but closely correlated with the presence of intraneuronal Aβ (Casas et al., 2004).

A more aggressive amyloid pathology has been reproduced in a 5xFAD line, which expresses the APP Swedish, Florida, and London mutations, and the PSEN1 M146L and L286V mutations from a Thy1 promoter (Oakley et al., 2006). The combination of these mutations led to a >25-fold increase in the $A\beta_{42}/A\beta_{40}$ ratio in a 9- to 12-month-old mouse compared to the Tg2576 transgenic at a similar age. The accumulation of Aβ commences as early as 2 months of age (compared to Aβ deposition in the Tg2576 mouse that commences at 9–12 months). Formation of plaques initiated in the deep layer of the cortex and subiculum and spread to extensive areas of the cortex, subiculum, and hippocampus, which is similar to other Thy1 promoter driven APP transgene (Oakley et al., 2006). At 4–6 months of age, impairment in hippocampal-related function was evident (Kimura and Ohno, 2009; Ohno et al., 2004, 2006). At 9 months of age these mice show reduced synaptic function and neuronal loss, which correlates with accumulation of intraneuronal Aβ (Oakley et al., 2006; Youmans et al., 2012a). The 5xFAD mice have also recently been crossed to mice expressing APOEε4 and ε3. These mice develop plaques around 6 months of age and provide the opportunity to assess therapeutics in the presence of the major genetic risk factor for sporadic Alzheimer's disease, APOEε4 (Youmans et al., 2012b). Recently, cerebrovascular pathology, such as cerebral microbleeds and CAA have been shown to be exacerbated in female 5xFAD APOEε4 mice (Cacciottolo et al., 2016). These sex-biased APOEε4 effects on the cerebrovascular system were in contrast to observations in human Alzheimer's disease/dementia clinical cohorts, emphasizing the need for caution when interpreting sex-specific effects on pathology seen in these models.

4.1.7 Triple Transgenic Model (3xTg)

As discussed previously, rodent models expressing FAD-associated APP/PSEN1/PSEN2 single or multiple mutations do not successfully reproduce the tau pathology observed in the brains of Alzheimer's disease patients. Therefore, mice expressing mutations in the tau protein, associated with FTD were crossed with mice expressing FAD-associated mutations to achieve both cerebral amyloid deposition and tau pathology. In the APP2576/TauJNPL3 (P301L) transgenic line, increased tau tangle pathology was observed in the limbic system and olfactory cortex, and extended to the subiculum, hippocampus, and occasionally isocortex (Lewis et al., 2001). These are regions that do not exhibit tau pathology in mice bearing only tau transgenes. However, the presence of the mutated tau did not alter Aβ deposition (Lewis et al., 2001). Similarly, injection of Aβ peptide directly into the brains of transgenic mice possessing tau mutations can exacerbate tau pathology (Gotz, 2001). In a 3xTg mice line (with APPSWE, Tau-P301L, and PSEN1 M146V), selective reduction of early-stage tau pathology was evident when anti-Aβ antibodies were injected into the mice brains. However, later-stage tau pathology seemed to be resistant to this treatment (Oddo et al., 2004). Reduction of levels of the tau pathology also appeared to improve the Aβ-related memory impairment and reduced the susceptibility to excitotoxicity in the PDAPP mouse, without altering the high Aβ level (Roberson et al., 2007). The exact mechanism behind the synergistic toxic effect of Aβ and tau is not yet fully elucidated. However, Götz's laboratory showed that deficiency of tau may reduce Aβ toxicity by disrupting the postsynaptic targeting of Fyn, a kinase that acts on the NMDA receptor (Ittner et al., 2010).

Double or triple transgenic models with tau mutations shown a wider spectrum of pathologies resembling that in Alzheimer's disease and have provided valuable insights into the interaction between Aβ and tau pathology. However, NFTs found in Alzheimer's disease brain consist of hyperphosphorylated wild-type tau protein (not mutant tau) through activation of kinases/phosphatases. Tau pathology in the aforementioned mouse lines is induced by mutations in tau characteristic of other dementias including FTD and thus may not truly reflect the consequences of tau/Aβ pathology in Alzheimer's disease.

4.1.8 Crosses With APOE

Crossing of FAD transgenic mice with mice overexpressing or lacking genetic risk factors for sporadic Alzheimer's disease has provided insight into how risk factors influence cerebral amyloidosis. Another motivation behind generation of FAD mice expressing these genetic risk factors has been to attempt to provide more relevant models for sporadic Alzheimer's disease. The ε4 allele of apolipoprotein E (APOE) is by far the strongest genetic risk factor found in most populations studied and accounts for ~50% of Alzheimer's disease cases (Martins et al., 2009). The three major alleles of APOE gene encode

the three major isoforms of the apoE protein, denoted as apoE2, apoE3, and apoE4, which aid in the transport of triglyceride-rich lipoproteins (chylomicrons and VLDL), phospholipid, and cholesterol into cells. Although studies have shown apoE to mediate Aβ production and toxicity, the interactions of its isoforms with Aβ have been the most widely studied. The apoE4 isoform has been shown to bind Aβ poorly and to impair its clearance (Deane et al., 2008). These are two mechanisms by which it is thought to promote amyloid deposition and contribute to the Alzheimer's disease risk associated with the *APOEε4* allele.

The *APOE* knockout mouse model has been crossed to a number of amyloidogenesis models, such as the APPV717F (Holtzman et al., 1999), PDAPP (Fryer et al., 2003), APPswe (Fryer et al., 2003), and Tg2567 (Fryer et al., 2005) mice. In all of these models, the lack of mouse *APOE* appeared to reduce the level of Aβ, delay amyloid deposition, and prevent the development of CAA. Furthermore, the expression of human *APOE* (either the E4 or E3 isoform) in APPV717F, Tg2576, and APPswe mice delayed the development of amyloid deposition compared to mice expressing endogenous mouse *APOE*. Compared to the APPsw lines expressing *APOE E4*, the expression of *APOE E3* reduced amyloid plaques and prevented the formation of CAA.

A study in the PDAPP/TRE transgenic line [in which *APOE* is humanized (Bales et al., 2009)] suggested *APOE* isoform-dependent clearance of Aβ in brain interstitial fluid (Castellano et al., 2011). In mice expressing human *APOEε4* (*APOEε4*-targeted replacement mice), we have recently shown reduced peripheral clearance and reduced uptake of intravenously injected Aβ by two major organs that clear Aβ from the periphery, the liver, and kidney (Sharman et al., 2010). It was also found that levels of the Aβ degradation enzyme, insulin degradation enzyme (IDE) were reduced in the brain and kidney of mice harboring the *APOEε4* allele. The decreased capacity of apoE ε4 to clear/degrade Aβ from the periphery and the associated lower levels of IDE, particularly in the brain, suggested an explanation for the greater brain Aβ accumulation and Alzheimer's disease pathology in Alzheimer's disease individuals with APOEε4 alleles.

4.1.9 Transgenic Rat Models

Although the mouse model is commonly used, efforts have also been made to develop transgenic rat models. Rats offer an advantage over mice that they are closer to humans in terms of genetics (Gibbs et al., 2004), physiology (Jacob and Kwitek, 2002; Lin, 1995), and neurohistology (Tesson et al., 2005). In addition, rats perform better than mice in behavioral tests and the larger bodies of rats are more amenable to surgical procedures, electrophysiology, and neuroimaging, thus facilitating

easier neurological assessments following interventions (Tesson et al., 2005). Furthermore, and similar to humans, the rat possesses six isoforms of tau protein (Hanes et al., 2009), and rat apoE shares considerable (>73%) homology and biochemical properties with human ApoE protein (McLean et al., 1983; Tran et al., 2013). Thus it appears that rat models of Alzheimer's disease should allow for a more accurate assessment of various Alzheimer's disease pathologies implicated in cognitive decline.

Before the advent of rat transgenics, aged rats were used as a model of Alzheimer's disease. However, they failed to faithfully recapitulate Alzheimer's disease pathologies, such as Aβ deposition (Anderson et al., 1999; Echeverria et al., 2004b; Ruiz-Opazo et al., 2004), pronounced deficits in cholinergic and dopaminergic functions (Gilad and Gilad, 1987), and hippocampal degeneration (Greene and Naranjo, 1987).

Initial hAPP (wt or FAD mutant) transgenic rat models failed to show robust extracellular Aβ deposits. However, in these models the accumulation of intracellular Aβ deposition in the neocortical and cortical neurons and hippocampus triggered tau phosphorylation (Folkesson et al., 2007; Kloskowska et al., 2010) and dysregulation of hippocampal proteins involved in memory and learning (Echeverria et al., 2004a,b; Lopez et al., 2004; Vercauteren et al., 2004) leading overall to cognitive dysfunction. These initial rat studies reaffirmed the role of oligomeric Aβ in Alzheimer's disease pathogenesis [reviewed in Do Carmo and Cuello (2013)].

Flood et al. (2009) were the first to successfully generate a transgenic rat model showing robust amyloid deposition. They coexpressed the APP Swedish and London mutations in rats and this resulted in formation of amyloid deposition at 17–18 months. Amyloid deposition was accelerated by the introduction of a third human mutation, PSEN1 M146V, causing plaque formation to be evident by 7 months (Flood et al., 2009). In addition, this triple transgenic rat model showed impaired long-term potentiation accompanied by deficits in spatial learning and memory and this correlated with the level of Aβ in the hippocampus.

More recently, Leon et al. (2010) reported a novel transgenic rat model that appears to display a wide range of Alzheimer's disease-like pathology caused by a single transgene (hAβPPswe, ind). This mutation of human APP was expressed from the murine neuron-specific Thy1.2 promoter (Leon et al., 2010). Extracellular amyloid deposition was detected from 6 months of age in homozygous lines, starting from subiculum and spreading to the rest of the hippocampus and eventually the neocortex. Cognitive impairment was evident at 3 months of age in homozygous animals and correlated with the level of Aβ oligomers. Although the formation of NFTs has been demonstrated in rats expressing trun-

cated human tau protein (t151-391) (Stozicka et al., 2010; Zilka et al., 2006), a transgenic model that exhibits both amyloid plaques and NFTs is yet to be developed.

4.1.10 Modeling the Impact of Risk Factors in Alzheimer's Disease Pathology in Rodents—Type 2 Diabetes

The aforementioned rodent models are generated through incorporation of human genetic mutations that cause FAD, to induce relevant pathology. However, they have been utilized to provide insight into how risk factors contribute to the more common sporadic cases to promote pathology and Alzheimer's disease onset. Unlike FAD, sporadic Alzheimer's disease is multifactorial involving genetic, environmental, and life-style risk factors. Type 2 diabetes mellitus (T2DM) is one such risk factor, where nontransgenic and transgenic rodent models have been utilized to provide insight into underlying mechanisms as well as to evaluate the potential of antidiabetic medications in the treatment of Alzheimer's disease.

Like sporadic Alzheimer's disease, T2DM occurs more commonly in older age with a high prevalence in people >65 years of age. T2DM is characterized by several metabolic abnormalities, chronic inflammation, and cellular insulin resistance leading to elevated blood glucose levels. Similarly, Alzheimer's disease patients are typically hyperinsulinemic with concomitant reduced insulin sensitivity and reduced insulin receptor expression (Carro and Torres-Aleman, 2004a,b; De Felice, 2013a,b; de la Monte, 2012a,b; de la Monte et al., 2012; Steen et al., 2005; Talbot et al., 2012), metabolic stress and inflammation (Verdile et al., 2015). High glucose levels increase the risk of Alzheimer's disease (Crane et al., 2013) and Alzheimer's disease patients show severe dysregulation of glucose metabolism (Abolhassani et al., 2016; Arrieta-Cruz and Gutierrez-Juarez, 2016; Calsolaro and Edison, 2016; Carbonell et al., 2016; Chen and Zhong, 2013; Daulatzai, 2016; Jimenez-Bonilla et al., 2016; Li et al., 2016; Liguori et al., 2016; Minoshima et al., 1997; Morris et al., 2016; Mosconi, 2005; Mosconi et al., 2005, 2006; Oh et al., 2016; Tramutola et al., 2016). Brain imaging studies in T2DM cohorts have shown that diabetes is associated with brain atrophy (Moran et al., 2015) and cerebral glucose hypometabolism (Roberts et al., 2014; Thambisetty et al., 2013). One cross-sectional study of normal, nondiabetics has shown that higher insulin resistance is associated with increases in brain amyloid as measured by the amyloid radiotracer, C11PIB-PET (Willette et al., 2015). This is in contrast to the aforementioned studies in T2DM cohorts (which show no such associations). In human studies there is not yet a coherent explanation regarding how T2DM may promote the progression of Alzheimer's disease pathology. Amyloid deposition may be associated with early stages of insulin resistance whereas, with

the onset of T2DM, cerebral hypometabolism and neuronal dysfunction are main features. Larger, longitudinal studies with other biomarkers of disease are required to provide further insight. However, studies in various models of diabetes and, more recently, models of diabetes and Alzheimer's disease have provided insight into potential mechanisms.

Nontransgenic T2DM rodent (rat) animal models on a high fat/high sugar diet show hyperglycemia, whole body insulin resistance, hepatic steatosis, and defects in lipid and glucose metabolism (Buettner et al., 2006). These T2DM models also present brain inflammation (Pistell et al., 2010) with concomitant reduction in hippocampal brain-derived neurotrophic factor leading to reduced neuronal plasticity (Molteni et al., 2002) and cognitive impairment (Winocur and Greenwood, 2005; Winocur et al., 2005) and increased brain Aβ levels (Pedrini et al., 2009). In addition, a high fat/high sugar diet exacerbates Alzheimer's disease pathology in transgenic mice (Barron et al., 2013; Julien et al., 2010; Kadish et al., 2016; Knight et al., 2014; Kohjima et al., 2010; Ma et al., 2009; Martin et al., 2014; Petrov et al., 2015; Sajan et al., 2016; Shie et al., 2002; Tang et al., 2015; Vandal et al., 2014), either through altering APP processing (Refolo et al., 2001) or by reducing the activity of enzymes that degrade Aβ (Leissring et al., 2003). In these models reduction in brain insulin and insulin signaling are also features which can promote Aβ accumulation and tau hyperphosphorylation [recently reviewed in Verdile et al. (2015)].

The aforementioned studies induce an acute diabetic phenotype with diet manipulation in rodent models, but some researchers model the phenotype chemically, through administering streptozotocin (STZ) which induces islet β-cell failure (Wang et al., 2010) and thus failure to secrete insulin resulting in a type 1 diabetes phenotype. However, intracerebroventricular (ICV) injections of STZ in wistar rats can induce impairments in brain glucose metabolism (hyperglycemia) (Chen et al., 2012b; Heo et al., 2011; Lee et al., 2014) and glucose uptake (Heo et al., 2011) resulting in cognitive deficits (learning and memory loss) (Knezovic et al., 2015; Lannert and Hoyer, 1998; Mehla et al., 2014; Peng et al., 2013; Rodrigues et al., 2010; Shingo et al., 2012; Shonesy et al., 2012), reduced acetyl-CoA media neuronal transmission (Terwel et al., 1995) reduction in neuronal growth function (Duelli et al., 1994; Grunblatt et al., 2006), neuronal loss (Shingo et al., 2013), increased and hyperphosphorylation of tau (Chu and Qian, 2005; Peng et al., 2013), increased phosphorylated GSK-3β (Plaschke and Kopitz, 2015), reduced O-glycanation, increase APP secretases (Park et al., 2015), increased aggregated Aβ (Deng et al., 2009; Lin et al., 2014a; Salkovic-Petrisic et al., 2006), increased neuroinflammation (Chen et al., 2013), mitochondrial dysfunction (Correia

et al., 2013; Paidi et al., 2015), cerebral vascular amyloidosis (Salkovic-Petrisic et al., 2011), and increased oxidative stress (Mehla et al., 2012; Tahirovic et al., 2007a,b) [for more information see Correia et al. (2011), Salkovic-Petrisic and Hoyer (2007), Salkovic-Petrisic et al. (2013), Wang et al. (2014)]. Similarly, ICV administration of STZ in classical Alzheimer's disease transgenic animals, such as those described previously exacerbates Alzheimer's disease pathology (Chen et al., 2012b; Chen et al., 2013, 2014; Plaschke et al., 2010).

These models of diabetes, however, do not reflect the chronic nature of T2DM since they do not take into account the factors that promote progression to overt diabetes in subjects with insulin resistance, which occurs in a majority of type 2 diabetics. Islet amyloid formation and subsequent β-cell destruction has an important role in the progressive decline in insulin secretion and rising blood glucose levels typical of T2DM (Hoppener et al., 1999; Kahn et al., 1999). Islet amyloid is a characteristic pathologic feature of the pancreas in T2DM where >95% of patients have visible islet amyloid at autopsy which correlates with disease severity (Westermark, 1972).

A more chronic model of insulin resistance and hyperglycemia is the homozygous "obese" mouse (ob/ob). These mice develop insulin resistance and diabetes due to a mutation of the leptin gene and, when crossed with Alzheimer's disease (APP23) transgenic mice, Alzheimer's disease pathology and associated cognitive deficits are enhanced (Takeda et al., 2010). However, ob/ob mice still do not model all the pathological conditions of chronic T2DM, as rodent IAPP does not aggregate and thus islet amyloid does not accumulate and no β-cell death is observed (Hoppener et al., 1999).

Accumulation of islet amyloid, islet β-cell failure, and the resulting hyperglycemic conditions can be achieved in mice overexpressing human islet amyloid polypeptide (hIAPP, also called amylin) in pancreatic islet cells (Hoppener et al., 1999; Verchere et al., 1996). These features of the IAPP transgenic mouse model make it a more relevant model to mimic the human chronic condition. A mouse model with overlapping Alzheimer's disease and T2DM pathologies would be useful in providing insight into not only how T2DM accelerates Alzheimer's disease pathology but also how Alzheimer's disease pathology may impact on the diabetes, for which there is growing evidence (Zhang et al., 2012b; Zhang et al., 2013). Such an animal model would also be important as a preclinical model to assess the efficacy of current/novel antidiabetic drugs at slowing down/preventing the progression of Alzheimer's disease in the presence of comorbidities, such as diabetes [reviewed in Verdile et al. (2015)].

4.1.11 Limitations of the Transgenic Rodent Models

The transgenic rodent models of Alzheimer's disease have played an important role in providing significant insight into mechanisms consistent with the amyloid hypothesis and are still currently the most commonly used in vivo tool for screening in preclinical drug trials. Although there are a wide variety of Alzheimer's disease transgenic models, all are based on the presence of single or multiple (up to five) FAD-causing mutations. In reality, Alzheimer's disease patients never inherit multiple pathogenic mutations in *APP*, *PSEN1*, or *tau*. Thus none of the transgenic mice fully mimic the genetics of familial Alzheimer's disease. The relevance of these models to the more common later onset forms of Alzheimer's disease where a heterogeneous etiology occurs is questionable. The results to date indicate limitations of using mice and rats to model a human disease that takes several decades to develop. Furthermore, discrepancies in neuropathology and behavior between transgenic mouse models and human disease suggest caution when interpreting results. These discrepancies include plaque loads greater in older transgenic mice than those found in human Alzheimer's disease brains simultaneous with neurodegenerative effects that are smaller than seen in post mortem brains (Arendash et al., 2001; Kelly et al., 2003). The real question is whether these mice mimic Alzheimer's disease or are models of amyloid deposition and a recent paper by Hargis and Blalock suggests that only the latter may be the case. These researchers examined the concordance between brain gene expression changes seen in transcriptomic data from humans and rodents during normal ageing and in human Alzheimer's disease and in five distinct transgenic mouse models of this disease. Good concordance was seen for ageing in these organisms with very different life spans and between individual cases of sporadic Alzheimer's disease. However, there was little concordance between human Alzheimer's disease and the mouse models or even between the various mouse models themselves (Hargis and Blalock, 2016). This casts doubt over the relevance to sporadic Alzheimer's disease of these transgenic mouse models.

As one might expect from the comparisons of transcriptomic data described previously, another problem with many transgenic rodent models is that they do not encompass the full spectrum of Alzheimer's disease pathology. An example is one of the models discussed previously, the commonly used mouse transgenic line Tg2576 expressing the *APPswe* mutation. Although Aβ deposition is prominent and widespread in this transgenic line, NFT formation and overt neurodegeneration is absent (Hsiao et al., 1996). In more aggressive models in which multiple FAD mutations are coexpressed, neuron loss can be detected (although not to the extent seen in an Alzheimer's disease brain) (Casas et al., 2004; Oakley et al., 2006). In addition, the deposition of amyloid plaques and the decline of cognitive function appear to be highly dependent on the extraordinarily high

expression level of mutant APP, while phenotypic amyloidogenesis and cognitive deficits are not prominent in models expressing a physiological level of the same APP mutation (Flood et al., 2002). Transgenic models that exhibit both amyloid deposition and accumulation of NFTs can only be generated through coexpression of FAD-causing mutations together with tau mutations that cause tauopathies, such as FTD. However, tau mutations do not occur in the human Alzheimer's disease condition where, instead, tangle formation is triggered by the hyperphosphorylation of native tau isoforms. Thus, once again the relevance of these transgenic models to the human Alzheimer's disease condition is questionable.

Although FAD-associated mutations are known to cause Alzheimer's disease, there is no evidence that the proteins from these mutant genes are overexpressed in humans. In addition, it is difficult to separate the contributions of transgenes and normal aging to the cognitive deficits seen in these mice. Furthermore, transgene expression or gene deletions may affect behavior of the animals. Other confounding factors, such as genetic background [see next Owen et al. (1997)] linkage disequilibrium (Crusio, 1996; Gerlai, 1996) and the role of disease modifier genes (Kent et al., 1997) should also be taken into account. The use of nontransgenic littermates is required to better discern any pathogenic effects of mutations over those due to transgene overexpression. Furthermore, most transgenic systems use heterologous promoters. Consequently, the resulting pathology follows the spatial and temporal pattern of the expression of the transgene, which is often different to the progression of pathology seen in humans (Epis et al., 2010).

The expression of the transgene also influences experimental design. For example, insufficient randomization or numbers among experimental groups can lead to false-positive/-negative results, since the expression levels of transgenes can vary greatly between individual animals due to the differences in gender, generation, and genetic background. Loss of transgene copies can occur over generations and this can ameliorate the phenotype of later generations. Outbreeding with mice of different genetic backgrounds can also alter the susceptibility of a line to the transgene. These variables add further complexity to experimental design but cannot be ignored.

The genetic background of transgenic mice may also influence pathology and behavior, as became evident with some of the first transgenic lines which were created on a FVB/N background. This background was later discovered to be unsuitable for learning experiments due to their background visual and learning impairments. This necessitated crossing the transgene into other wild-type backgrounds (i.e., C57Bl6) or generating transgenic mice in genetic strains more suitable for behavioral assessments (Chapman et al., 1999; Johnstone et al., 1991; Moechars et al., 1999).

Overexpressing the APP Swedish mutation in mice of different genetic background has been shown to result in different levels of APP-CTF and Aβ levels, despite similar levels of the APP holoprotein. This indicates that genetic background significantly influences Aβ metabolism (Lehman et al., 2003a). Here, it should be considered that transgenic mice contain endogenous APP and APP-processing enzymes that may interfere with the production of different Aβ species. Another example is the R1.40 transgenic mouse that expresses the APPswe mutation. Despite similar levels of the APP holoprotein, the levels of APP C-terminal fragments and Aβ were found to be altered in the R1.40 mouse when it was backcrossed into three different inbred strains. As a result, the age at which Aβ deposition occurs varies between these three lines (Lehman et al., 2003a). The effect of genetic background on the onset of cerebral amyloidosis has also been reported in other transgenic lines, including Tg2567 (Carlson et al., 1997) and TgCRND8 (Chishti et al., 2001). Genetic background has also been reported to affect vulnerability to excitotoxins, which may contribute to observed variations in pathology onset and development (Schauwecker, 2002; Shuttleworth and Connor, 2001).

Another example of the complexity involved with interpretation of mouse models of Alzheimer's disease is the interaction between rodent and human forms of Aβ accumulating in transgenic animals overexpressing human mutant APP and a PSEN1 transgene (van Groen et al., 2006). Rodent Aβ was associated with human Aβ with its localization in dystrophic neurons surrounding plaques containing human Aβ. Why this occurs is uncertain and it may reflect a situation in which human Aβ acts as a seed for aggregation of rodent Aβ, or increased human Aβ saturates the clearance mechanisms for human (and rodent) Aβ leading to accumulation of both (Howlett and Richardson, 2009). However, the potential problems associated with the presence of endogenous APP and Aβ is somewhat negated with the recent creation of APP KI mice (Saito et al., 2014).

Problems have also occurred with replication of data where experimental results using the same transgenic lines cannot be replicated between different labs. For example, two independent groups, Chen et al. (2000) and Dodart et al. (1999), have characterized the behavior of PDAPP mice. Although both groups observed age-independent behavioral impairments, Dodart et al. (1999) reported impairment of object recognition memory performance, which was not observed by Chen et al. (2000) even in old aged mice. These differences in results may occur due to the genetic background of the mice used or the design of the particular behavioral assessments.

The complexity that occurs with the majority of mouse models and their questionable relevance to Alzheimer's disease, (particularly the sporadic forms where there

is mixed etiology) has prompted investigation of possible nontransgenic mammalian models of Alzheimer's disease.

4.2 Nontransgenic Animal Models

Alzheimer's disease studies using most nontransgenic mammalian models are focused on the highly conserved human APP sequence and, in particular, the complete sequence identity that humans and many other mammals show within their Aβ domains (Beck et al., 1997). Mammals as diverged as polar bears and dolphins share sequence identity with human Aβ but NHPs, dogs, rabbits, and guinea pigs are more commonly used in Alzheimer's disease research. Later, we outline the literature that describes the characterization of Alzheimer's disease pathology in these nontransgenic animals. We examine their role in providing insight into Alzheimer's disease pathogenesis and, in particular, how they may provide better models for sporadic Alzheimer's disease than transgenic rodents (Lecanu and Papadopoulos, 2013; Sarasa and Pesini, 2009; Stephan and Phillips, 2005).

4.2.1 Nonhuman Primates

NHPs have great value in Alzheimer's disease research since they share relatively close common ancestry (and thus genetics) with humans. Therefore, they have comparable brain structures and cognitive capabilities. Age-related cerebral amyloidosis has been demonstrated in a few species of monkey and great ape (Beck et al., 1997; Gearing et al., 1994, 1997; Price et al., 1991; Selkoe et al., 1987). In aged great apes, Aβ deposition can be detected in cerebral blood vessels (as CAA), and in cortex and hippocampus (as diffuse plaques), resembling the pathology observed at early stages of the human Alzheimer's disease condition (Gearing et al., 1994). Dense neuritic amyloid plaques are seldom seen but have been reported in old rhesus monkeys (Gearing et al., 1994). As in humans, the deposition of Aβ within plaques colocalizes with APOE. However, the deposition of various Aβ species (Aβ$_{40}$ and Aβ$_{42}$) within plaques is notably distinct between humans and other primates. For example, in the human Alzheimer's disease brain, Aβ$_{42}$ is the predominant component of amyloid plaques, and is deposited early, while deposition of Aβ$_{40}$ protein occurs at later stages of the disease. In aged orangutans, chimpanzees, and rhesus monkeys, Aβ$_{40}$ is the major species even from a relatively early stage of cerebral amyloidosis to form diffuse plaques (Gearing et al., 1994, 1997). The reason for the differences in Aβ species profile in plaques observed in aged primates and humans is not clear. One possibility may relate to APOE-Aβ metabolism. In both rhesus monkey and chimpanzee, the *APOE* gene is ε4-like (Gearing et al., 1994; Morelli et al., 1996; Poduri et al., 1994). Genetic-association studies have shown that

APOE4 may contribute to the increase of Aβ$_{40}$-positive plaques (Gearing et al., 1996; Schmechel et al., 1993).

Tau hyperphosphorylation and formation of NFTs has only been detected in a few species of NHPs, despite the high homology of their *MAPT* gene with that of humans (e.g., 100% identity in chimpanzees, 99.5% in gorillas, and 96.7% in rhesus monkey). Formation of tau paired helical filaments has been reported in one 41-year-old chimpanzee, but their distribution was mainly within cortical neurons and only rarely in hippocampus, which is distinct from the pattern observed in human Alzheimer's disease (Rosen et al., 2008). Additionally, tau pathologies have also been observed in baboons in neurons and glial cells (Schultz et al., 2000). Similar to amyloid deposition, accumulation of tau is age related, increasing from 31% at 11–20 years to 91% in 26- to 30-year-old baboons (Schultz et al., 2000). In grey mouse lemurs, Alzheimer's disease-like tau pathology was observed in association with brain atrophy, abundant amyloid plaque deposition, and cholinergic neurons loss (Kiatipattanasakul et al., 2000).

Consistent with the age-related cognitive and memory impairment observed in aged humans, aged NHPs exhibit deficits in visuospatial learning (Petrides and Iversen, 1979), recognition memory (Herndon et al., 1997; Moss et al., 1988; Presty et al., 1987), and cognitive processes, such as reversal learning (Bachevalier et al., 1991; Lai et al., 1995; Rapp and Amaral, 1989), working memory, and set-shifting (Moore et al., 2003, 2006). These impairments indicate a decline in function of the frontal cortex and hippocampus and are associated with pathology present in these regions, similar to that shown in human Alzheimer's disease brain (Braak and Braak, 1997; Braak et al., 1998).

The evidence to date indicates that NHPs may represent the closest natural animal model for human Alzheimer's disease. Although they have been utilized in Alzheimer's disease studies, particularly in the evaluation of anti-Alzheimer's disease drugs [reviewed in De Felice and Munoz (2016)], the high cost of maintaining NHPs, their relatively long life span, and limited access to these experimental animals restrict their wider use as Alzheimer's disease models.

4.2.2 Dogs

Similar to NHPs, aged dogs have proven to be useful models for human Alzheimer's disease since they show age-related cognitive decline and amyloid plaques. However, dogs are much more widely available, cheaper, and easier to maintain than primates. The relevance of aged dogs to modeling of sporadic, late-onset human Alzheimer's disease, makes them useful to assess nonpharmacological strategies, dietary and environmental risk factors, and for validating the efficacy of pharmacological treatments.

The most commonly used dog in laboratories is the beagle, which has a median life span of 12–14 years and is considered aged when older than 9 years (equivalent to >68 years in a human (Albert et al., 1994; Lowseth et al., 1990; Patronek et al., 1997). Similar to humans, the cognitive function of aged beagles varies significantly between individuals and can be categorized into "successful aging," "mildly impaired," and "severely impaired," equivalent to cognitively normal, MCI, and dementia in humans (Adams et al., 2000a,b). Similar to humans, the visuospatial (Chan et al., 2002; Studzinski et al., 2006) and executive functions (Callahan et al., 2000; Milgram et al., 2002; Tapp et al., 2003) of dogs are most vulnerable in age-related cognitive decline, while, simple rule-based learning and procedural learning are largely preserved (Milgram et al., 1994).

The Aβ sequence of dog is identical to that of humans (Johnstone et al., 1991; Selkoe et al., 1987), and the pattern of amyloidosis during aging is similar (but not exactly same) to that observed in the human Alzheimer's disease brain, where accumulation of Aβ is initiated in the prefrontal cortex and spreads to the entorhinal and parietal cortices. (Cummings et al., 1996a; Head et al., 2000). The amyloid deposits are predominantly the diffused subtype composed mainly of $A\beta_{42}$ (Cummings et al., 1996b) (and so are distinct from those seen in NHPs where, as mentioned previously, the major Aβ species is $A\beta_{40}$). Accumulation of Aβ within the cerebral blood vessels in the form of CAA has also been observed (Ishihara et al., 1991; Uchida et al., 1990; Yoshino et al., 1996) and is distributed in a similar spatial pattern to that seen in the Alzheimer's disease brain (Attems et al., 2005). In addition, in aged dogs accumulation of cerebral Aβ correlates with cortical atrophy (Gonzalez-Soriano et al., 2001; Kimotsuki et al., 2005), reduced cortex volume (Tapp et al., 2004), neuronal loss (Siwak-Tapp et al., 2008), and cognitive decline (Colle et al., 2000; Cummings et al., 1996a; Head et al., 1998) similar to the human Alzheimer's disease brain.

Aged dogs model sporadic Alzheimer's disease-like pathology and thus have been a valuable model in assessing nonpharmacological and pharmacological interventions for Alzheimer's disease. Being more genetically and physiologically similar to humans than mice and rats, dogs appeared to be better predictors for negative outcomes in preclinical trials. For example, the potential Alzheimer's disease drugs, amapkine (an AMPA receptor), and selegiline (an irreversible monoamine oxidase B inhibitor) showed beneficial effects on cognitive function in rodent models. However, evaluating these agents in dogs revealed similar findings to those in human clinical trials for Alzheimer's disease, where cognitive functioning was not significantly improved. (Studzinski et al., 2005). Furthermore, the outcomes of active immunization trials in dogs were similar to those in human

clinical trials. Despite immunization therapy having success in improving learning and memory in transgenic mouse models exhibiting amyloid pathology (Dodart et al., 2002; Hartman et al., 2005; Kotilinek et al., 2002) improvements were not observed when Aβ immunization was administered to dogs. In aged dogs (8.4–12.4 years old), no improvements in complex learning, spatial memory, and attention were detected in response to the Aβ immunization treatment, although Aβ plaque load was reduced (Head et al., 2008). On the basis of the benefits shown with active immunization in mouse models, commencement of the first human trials (AN1792) showed some now well-documented unwanted side effects, such as increased CAA, serious signs of CNS inflammation including increased T lymphocyte infiltration in the brain and leukoencephalopathy in 18 of 300 patients (6%) which led to the termination of phase II trials [Gilman et al. (2005), reviewed in Foster et al. (2009)]. Twelve of the patients recovered, while 6 suffered from disabling cognitive and neurological deficits. However, as with the mouse models, dogs also failed to reveal the adverse autoimmune responses that occurred in human patients (Head et al., 2008). Aged dogs have also been useful for assessing the impact of nonpharmacological interventions including the benefits of dietary antioxidants and behavioral enrichment in delaying cognitive decline and dementia (Milgram et al., 2002, 2004, 2005; Nippak et al., 2007; Opii et al., 2008; Siwak et al., 2005).

4.2.3 Sheep

Sheep have also been used in studies of neuropathology including the neurodegenerative prion disease scrapie (Hunter, 2007) and as a model for the effect of traumatic brain injury on APP expression (Anderson et al., 2003). Sheep are one of the few animals that, during normal aging, develop NFTs closely resembling those seen in the Alzheimer's disease brain (Braak et al., 1994; Nelson and Saper, 1995; Nelson et al., 1993, 1994). This makes them useful for the study of tau neuropathology. Additionally, there is high homology between sheep and human forms of apolipoprotein (APOE) (Komatsu et al., 1998), unlike rodent APOE. In humans, polymorphisms of APOE are recognized as an important risk factor for the development of Alzheimer's disease (Corder et al., 1993). Whereas no similar polymorphisms have been found in sheep APOE (Komatsu et al., 1998), the high homology between sheep and human APOE makes research easier to translate between the species. In addition, the sheep Aβ sequence is identical to that of humans (Johnstone et al., 1991). ThioS-positive neuritic plaques have been identified in the brains of sheep (Nelson et al., 1994) and soluble levels can be detected by ELISA (Barron et al., 2009).

Similarities between sheep reproduction and human reproduction have provided the opportunity to assess

the impact on Alzheimer's disease-related pathology of the Alzheimer's disease risk factor age and the related reductions in sex hormones. Sheep have proven very useful as a model for human reproduction and metabolism due to similarities in estrus periodicity, breeding, and metabolic rate. The sheep estrus cycle lasts approximately 17 days, more closely approximating the length of the human menstrual cycle than rodents, which have an estrus cycle lasting approximately 4 days. Furthermore, sheep, like humans, are generally limited to one or two offspring, unlike other mammals, such as rodents or dogs that are prolific breeders. As such, sheep are thought to better reflect hormonal regulatory mechanisms of ovulation than prolific breeders. Ovariectomy of sheep has been a very successful model for the study of menopausal symptoms and conditions including hot flushes (MacLeay et al., 2003), heart disease (Gaynor et al., 2000), bone density loss (Newton et al., 2004), and arthritic changes (Cake et al., 2005). On the basis that ovariectomized sheep are a relevant model of human menopause, a study investigated the impact of estrogen depletion and supplementation on Aβ accumulation and oxidative stress in sheep brain (Barron et al., 2009). Neither depletion nor supplementation of estrogen impacted on levels of Aβ or oxidative stress. Evidence from rodent animal studies indicate that, under certain conditions, treatment with supraphysiological concentrations of estrogen can modulate Aβ levels (Levin-Allerhand et al., 2002; Zheng et al., 2002). However, the circumstances necessary to elicit these effects and their relevance to the clinical setting remain unclear.

4.2.4 Guinea Pigs and Rabbits

Guinea pigs and rabbits are small-sized mammalian models that show greater conservation in important Alzheimer's disease-related genes than mice or rats. They are also experimentally more amenable compared to large-sized mammal models, such as primates and dogs. Guinea pig APP protein is 97% identical to human APP and exhibits a similar pattern of transcriptional splicing (Beck et al., 1997). Notably, the Aβ sequence of guinea pigs is identical to that of human (Beck et al., 1997; Sharman et al., 2013). Furthermore, guinea pig Aβ has a demonstrated capacity to form higher order molecular structures, such as oligomers, widely considered to be the principal contributor to neurotoxicity in Alzheimer's disease pathogenesis (Beck et al., 2000). Guinea pigs also share sequence similarities with other Alzheimer's disease-related human genes, such as the presenilins. Indeed, the formation of the PSEN2 truncation, PS2V, which is upregulated in human Alzheimer's disease brains and in neurons under hypoxic conditions, was identified in guinea pig brain and shown to be upregulated in brains from cholesterol-fed animals (Sharman et al., 2013). Intriguingly, the PS2V isoform is not

produced by the PSEN genes of mice or rats (Moussavi Nik et al., 2015). In addition, similar to normal aging in humans, aging in wild-type guinea pigs leads to hyperphosphorylation of Tau in discreet brain regions including the hippocampus. Traumatic brain injury increases the vulnerability of the hippocampus and dysregulation of Alzheimer's disease-related proteins, similar to what is observed in humans (Bates et al., 2014).

Guinea pigs are the only small animal model known to mimic closely human lipoprotein and cholesterol metabolism (Fernandez, 2001) (see later). As such they have been demonstrated to be an excellent nontransgenic model for studies attempting to elucidate the effect of cardiovascular risk factors and drug interventions on the development of Alzheimer's disease. They are also an excellent model for evaluation of dietary interventions as they show aortic plaque accumulation when challenged with a hypercholesterolemic diet (Sharman et al., 2008; Torres-Gonzalez et al., 2008).

High-cholesterol diets have been shown to increase the risk of Alzheimer's disease and the correlation between cholesterol metabolism and amyloidogenesis has been explored in transgenic and nontransgenic animal models (George et al., 2004; Refolo et al., 2000; Sparks et al., 1994; Umeda et al., 2012). However, most of the commonly used rodents and other species have distinct cholesterol profiles compared to humans. For example, rabbits are deficient in hepatic lipase and carry the majority of their cholesterol as VLDL (Badimon et al., 1990). Rats and mice lack plasma cholesterol ester transfer protein and use HDL as the major cholesterol carrier (Moghadasian, 2002). In comparison, the majority of cholesterol in guinea pigs is transported via LDL as in humans (Fernandez, 2001). Therefore, guinea pigs may be a more appropriate model compared to other rodents to study the relationship between cholesterol metabolism and Alzheimer's disease in a physiological context. It is therefore rather surprising that the guinea pig has not been widely used to assess the impact of such dietary interventions on Alzheimer's disease-related pathology, such as Aβ accumulation. Recent failures of drugs in clinical trials indicate that further studies using more appropriate animal models are warranted (De Strooper and Chavez Gutierrez, 2015). Thus, in recent years, the guinea pig has been used to test the efficacy of numerous Alzheimer's disease drug due to its genetic similarity to humans (Brodney et al., 2011; Davtyan et al., 2013; Eketjall et al., 2013; O'Hare et al., 2014; Pohanka et al., 2012; Portelius et al., 2014).

Of course, guinea pigs also have limitations as an Alzheimer's disease model. Compared to rats and mice, guinea pigs are considered to be less suitable to perform learning and memory tasks (Beck et al., 1997). However, a few groups have had success in undertaking behavioral assessments, such as the Morris water

TABLE 40.4 Comparison of Mammalian Models

Model organisms	Husbandry cost	Anatomical similarity to humans	Molecular and genetic similarity to humans	Similarity of pathology to humans	Transgenic technology	Feasibility of large-scale experiments	Affordability of large-scale studies	Availability of antibody reagents
Mouse	$	*	*	*	****	***	**	****
Rat	$	*	*	*	***	***	**	**
Nonhuman primates	$$$	****	****	****	*	*	*	**
Dog	$$	**	***	****	*	*	*	*
Guinea pig	$	*	**	**	*	**	**	*
Rabbit	$	*	**	**	*	**	**	*

*, Least optimal; **, less optimal; ***, optimal; ****, most optimal.

maze with guinea pigs (Dringenberg et al., 2001; Lewejohann et al., 2010). Other limitations associated with the use of guinea pig as a potential model include that breeding and maintenance costs remain relatively high compared to rats and mice and that less-developed gene and protein identification databases are available compared to those for the commonly used rodents. In addition, whether or not guinea pigs can model NFT formation remains to be determined. There is a distinct lack of knowledge of what tau (MAPT) isoforms exist in guinea pigs and whether they are hyperphosphorylated. Only one published study has investigated tau isoforms in guinea pig brain tissue. Takuma et al. (2003) applied an antibody produced against human tau to examine tau isoforms in guinea pig brain and only detected the 1N isoform. They also identified differences in amino-terminal inserts in tau between mice and rats where 1N and 2N insert types are dominant in rats, while 0N and 1N are dominant in mice. The reasons for these species differences in tau amino-terminal isoforms (and indeed the function of these isoforms) remain unclear. However, the dominance of the 1N isoform in humans, mice, rats, and guinea pigs suggest a conserved role for tau containing this particular N-terminal insert.

Like guinea pigs, rabbits do not develop amyloid deposition with age. However, Alzheimer's disease-like pathologies, such as cortical Aβ deposition, loss of neurons in frontal cortex, hippocampus, and cerebellum, and impairments in learning complex tasks, can be induced by a combination of a trace amount of copper and a high-cholesterol diet in rabbits (Sparks and Schreurs, 2003; Woodruff-Pak et al., 2007). This Alzheimer's disease-like pathology can be ameliorated by removing cholesterol from the diet or by cholesterol-lowering treatment (Sparks, 2008). These results indicate that rabbits are suitable models for assessing copper and high-cholesterol intake as risk factors for Alzheimer's disease. Unlike guinea pigs, Alzheimer's disease-like NFT pathology has been identified in rabbits, but only under cholesterol-fed

conditions. One study showed that administering 1% cholesterol for 7 months resulted in Aβ deposition and NFT-like changes in female rabbits (Ghribi et al., 2006). A more recent study showed that total plasma tau levels were increased in cholesterol-fed rabbits and that NFT-like pathology was greatest in cholesterol-fed animals administered distilled water (Sparks et al., 2011). Interestingly, NFT-like pathology was reduced in cholesterol-fed rabbits administered water containing copper (0.12 ppm) and an even greater reduction was observed with tap water (estimated to contain 0.2 ppm copper). The inverse was observed for Aβ pathology, indicating separate mechanisms by which metals in water alter Alzheimer's disease pathology (Table 40.4).

4.2.5 Hibernating Mammals Provide Insight Into tau Phosphorylation in Alzheimer's Disease

Hibernating mammals, such as the Arctic ground squirrel, Syrian hamster, and black bear are interesting animal models for investigating tau pathology in Alzheimer's disease. Hyperphosphorylation of tau protein and formation of NFTs are found in these animals during hibernation and can be reversed after euthermia (Arendt et al., 2003; Hartig et al., 2007; Su et al., 2008). The level of tau phosphorylation in these animals seems to be related both to body temperature and hibernation status (Stieler et al., 2011). Higher degrees of phosphorylation were demonstrated in animals with lower body temperature during hibernation, with the inverse observed under euthermia (Stieler et al., 2011).

Phosphorylation of tau induced by hibernation mostly occurs during early stages of torpor and does not proceed further during the course of torpor. Partial dephosphorylation of tau protein has been observed in aroused Arctic ground squirrels under conditions of sporadic euthermic arousals, but complete dephosphorylation only occurred after euthermy (Su et al., 2008). In hibernating animals, phosphorylation of tau occurs at similar residues as seen for human tau in Alzheimer's disease

patients (T231/S235, T212/S214/T217, S396/404). However, the kinases involved in hibernation and the development of Alzheimer's disease pathology appeared to be distinct. Alzheimer's disease-associated hyperactivation of GSK-3β and SAPK/JNK was not observed in hibernation. In contrast, GSK-3β and SAPK/JNK was largely deactivated due to the low body temperature during hibernation, while, cdk5 and ERK1 seemed to play a vital role in hyperphosphorylation of tau during hibernation (Stieler et al., 2011).

The hyperphosphorylation of tau during hibernation has been proposed to be a protective mechanism to reduce the demand for energy to maintain basic cellular functions during famine (Arendt et al., 2003). Similar hyperphosphorylation of tau was reported in animals under starvation, anesthesia, and cold water stress (Okawa et al., 2003). Under hibernation, tau hyperphosphorylation has been shown to be isolated to the cholinergic neurons in the basal forebrain projection system, but not the gamma-aminobutyric acid (GABA)-ergic neurons, a pattern that is similar to that seen in Alzheimer's disease brain (Hartig et al., 2007).

Neuronal hypometabolism is a feature of Alzheimer's disease and other dementias. It has been suggested to occur early in Alzheimer's disease, possibly prior to the onset of symptoms (Reiman et al., 1996, 2004; Small et al., 2000) and can be a possible predictor of cognitive dysfunction (Devous, 2002; Kim et al., 2005). Stieler et al. (2011) have hypothesized that hyperphosphorylation of tau may represent a physiological response to hypometabolism, occurring in the early stages of Alzheimer's disease pathogenesis. However, due to the persistence of the hypometabolic state of the Alzheimer's disease brain, tau hyperphosphorylation continues resulting in the formation of tangles and eventual neuronal death (Stieler et al., 2011). Animals that hibernate may provide a valuable platform to investigate the physiological functions, molecular pathways, and mechanisms of tau hyperphosphorylation, and its relevance to Alzheimer's disease pathogenesis under conditions of neuronal inactivity.

5 CONCLUSIONS

An animal model can never reflect completely the pathology of a human disease. This applies particularly to modeling of Alzheimer's disease since this condition affects the most complex biological structure in existence—the human brain. Nevertheless, investigating Alzheimer's disease in animal models, including animals highly diverged from humans, such as the invertebrates, is very worthwhile because the discovery of conserved normal and pathological processes in widely diverged organisms indicates the fundamental importance of those processes.

The current uncertainty about the cause(s) and progression of Alzheimer's disease means that we must be particularly cautious in how we interpret information we obtain from modeling this condition. A huge amount of data has been collected regarding the genes, cellular processes, and neurophysiological events that may be involved in development of Alzheimer's disease but no consistent, unifying mechanistic explanation has yet emerged. The reason for this may lie, in part, in the dominant use of mice and rats for Alzheimer's disease modeling and the relatively rapid evolution of Alzheimer's disease-related genes in these rodents (family Muridae) compared to other rodents and mammals. Alternatively, the hypotheses we currently use to guide our experimentation in this area may be inappropriate to a greater or lesser degree. We must also remember that, despite their apparent common histopathology, the inherited and sporadic forms of this disease may be fundamentally different. Since sporadic, late-onset Alzheimer's disease is overwhelmingly more common than the inherited, early-onset form; there should be a greater focus on analyzing Alzheimer's disease-like pathologies and Alzheimer's disease risk factors in nontransgenic mammals. Also, the functions of the genes/proteins identified as associated with sporadic Alzheimer's disease (e.g., by GWAS) should be analyzed in genetically manipulable model organisms including non-Muridae mammals, vertebrates, and invertebrates. Hopefully, these and other strategies will mean that the coming decade produces greater advances in understanding, ameliorating, and preventing Alzheimer's disease than the last.

References

Abe, G., Suster, M.L., Kawakami, K., 2011. Tol2-mediated transgenesis, gene trapping, enhancer trapping, and the Ga14-UAS system. Methods Cell Biol. 104, 23–49.

Abolhassani, N., Leon, J., Sheng, Z., Oka, S., Hamasaki, H., Iwaki, T., et al., 2016. Molecular pathophysiology of impaired glucose metabolism, mitochondrial dysfunction, and oxidative DNA damage in Alzheimer's disease brain. Mech. Ageing Dev 161 (Pt. A), 95–104.

Abramsson, A., Kettunen, P., Banote, R.K., Lott, E., Li, M., Arner, A., et al., 2013. The zebrafish amyloid precursor protein-b is required for motor neuron guidance and synapse formation. Dev. Biol. 381 (2), 377–388.

Acx, H., Chavez-Gutierrez, L., Serneels, L., Lismont, S., Benurwar, M., Elad, N., et al., 2014. Signature amyloid beta profiles are produced by different gamma-secretase complexes. J. Biol. Chem. 289 (7), 4346–4355.

Adams, B., Chan, A., Callahan, H., Milgram, N.W., 2000a. The canine as a model of human cognitive aging: recent developments. Prog. Neuropsychopharmacol. Biol. Psychiatry 24 (5), 675–692.

Adams, B., Chan, A., Callahan, H., Siwak, C., Tapp, D., Ikeda-Douglas, C., et al., 2000b. Use of a delayed non-matching to position task to model age-dependent cognitive decline in the dog. Behav. Brain Res. 108 (1), 47–56.

Albert, R.E., Benjamin, S.A., Shukla, R., 1994. Life span and cancer mortality in the beagle dog and humans. Mech. Ageing Dev. 74 (3), 149–159.

Alexander, A.G., Marfil, V., Li, C., 2014. Use of *Caenorhabditis elegans* as a model to study Alzheimer's disease and other neurodegenerative diseases. Front. Genet. 5, 279.

Alonso, A.C., Li, B., Grundke-Iqbal, I., Iqbal, K., 2008. Mechanism of tau-induced neurodegeneration in Alzheimer disease and related tauopathies. Curr. Alzheimer Res. 5 (4), 375–384.

Ambegaokar, S.S., Jackson, G.R., 2010. Functional genomic screen and network analysis reveal novel modifiers of tauopathy dissociated from tau phosphorylation. Hum. Mol. Genet. 20 (24), 4947–4977.

Amores, A., Force, A., Yan, Y.L., Joly, L., Amemiya, C., Fritz, A., et al., 1998. Zebrafish hox clusters and vertebrate genome evolution. Science 282 (5394), 1711–1714.

Anderson, J.J., Holtz, G., Baskin, P.P., Wang, R., Mazzarelli, L., Wagner, S.L., et al., 1999. Reduced cerebrospinal fluid levels of alpha-secretase-cleaved amyloid precursor protein in aged rats: correlation with spatial memory deficits. Neuroscience 93, 1409–1420.

Anderson, R.W., Brown, C.J., Blumbergs, P.C., McLean, A.J., Jones, N.R., 2003. Impact mechanics and axonal injury in a sheep model. J. Neurotrauma 20 (10), 961–974.

Ando, K., Maruko-Otake, A., Ohtake, Y., Hayashishita, M., Sekiya, M., Iijima, K.M., 2016. Stabilization of microtubule-unbound Tau via Tau phosphorylation at Ser262/356 by Par-1/MARK contributes to augmentation of AD-related phosphorylation and Abeta42-induced Tau toxicity. PLoS Genet. 12 (3), e1005917.

Arendash, G.W., King, D.L., Gordon, M.N., Morgan, D., Hatcher, J.M., Hope, C.E., et al., 2001. Progressive, age-related behavioral impairments in transgenic mice carrying both mutant amyloid precursor protein and presenilin-1 transgenes. Brain Res. 891 (1–2), 42–53.

Arendt, T., Stieler, J., Strijkstra, A.M., Hut, R.A., Rudiger, J., Van der Zee, E.A., et al., 2003. Reversible paired helical filament-like phosphorylation of tau is an adaptive process associated with neuronal plasticity in hibernating animals. J. Neurosci. 23 (18), 6972–6981.

Arriagada, P.V., Growdon, J.H., Hedley-Whyte, E.T., Hyman, B.T., 1992. Neurofibrillary tangles but not senile plaques parallel duration and severity of Alzheimer's disease. Neurology 42 (3 Pt 1), 631–639.

Arrieta-Cruz, I., Gutierrez-Juarez, R., 2016. The role of insulin resistance and glucose metabolism dysregulation in the development of Alzheimer s disease. Rev. Invest. Clin. 68 (2), 53–58.

Arslanova, D., Yang, T., Xu, X.Y., Wong, S.T., Augelli-Szafran, C.E., Xia, W.M., 2010. Phenotypic analysis of images of zebrafish treated with Alzheimer's gamma-secretase inhibitors. BMC Biotechnol. 10, 24.

Ashley, J., Packard, M., Ataman, B., Budnik, V., 2005. Fasciclin II signals new synapse formation through amyloid precursor protein and the scaffolding protein dX11/Mint. J. Neurosci. 25 (25), 5943–5955.

Attems, J., Jellinger, K.A., Lintner, F., 2005. Alzheimer's disease pathology influences severity and topographical distribution of cerebral amyloid angiopathy. Acta Neuropathol. 110 (3), 222–231.

Babin, P.J., Thisse, C., Durliat, M., Andre, M., Akimenko, M.A., Thisse, B., 1997. Both apolipoprotein E and A-I genes are present in a non-mammalian vertebrate and are highly expressed during embryonic development. Proc. Natl Acad. Sci. USA 94 (16), 8622–8627.

Bachevalier, J., Landis, L.S., Walker, L.C., Brickson, M., Mishkin, M., Price, D.L., et al., 1991. Aged monkeys exhibit behavioral deficits indicative of widespread cerebral dysfunction. Neurobiol. Aging 12 (2), 99–111.

Badimon, J.J., Badimon, L., Fuster, V., 1990. Regression of atherosclerotic lesions by high density lipoprotein plasma fraction in the cholesterol-fed rabbit. J. Clin. Invest. 85 (4), 1234–1241.

Bai, Q., Burton, E.A., 2011. Zebrafish models of Tauopathy. Biochim. Biophys. Acta 1812 (3), 353–363.

Bai, Q., Garver, J.A., Hukriede, N.A., Burton, E.A., 2007. Generation of a transgenic zebrafish model of Tauopathy using a novel promoter element derived from the zebrafish eno2 gene. Nucleic Acids Res. 35 (19), 6501–6516.

Bales, K.R., Liu, F., Wu, S., Lin, S., Koger, D., DeLong, C., et al., 2009. Human APOE isoform-dependent effects on brain beta-amyloid levels in PDAPP transgenic mice. J. Neurosci. 29 (21), 6771–6779.

Banote, R.K., Edling, M., Eliassen, F., Kettunen, P., Zetterberg, H., Abramsson, A., 2016. beta-Amyloid precursor protein-b is essential for Mauthner cell development in the zebrafish in a Notch-dependent manner. Dev. Biol. 413 (1), 26–38.

Barnes, D.E., Yaffe, K., 2011. The projected effect of risk factor reduction on Alzheimer's disease prevalence. Lancet Neurol. 10 (9), 819–828.

Barron, A.M., Cake, M., Verdile, G., Martins, R.N., 2009. Ovariectomy and 17beta-estradiol replacement do not alter beta-amyloid levels in sheep brain. Endocrinology 150 (7), 3228–3236.

Barron, A.M., Rosario, E.R., Elteriefi, R., Pike, C.J., 2013. Sex-specific effects of high fat diet on indices of metabolic syndrome in 3xTg-AD mice: implications for Alzheimer's disease. PLoS One 8 (10), e78554.

Bassett, A.R., Tibbit, C., Ponting, C.P., Liu, J.L., 2013. Highly efficient targeted mutagenesis of *Drosophila* with the CRISPR/Cas9 system. Cell Rep. 4 (1), 220–228.

Bates, K., Vink, R., Martins, R., Harvey, A., 2014. Aging, cortical injury and Alzheimer's disease-like pathology in the guinea pig brain. Neurobiol. Aging 35 (6), 1345–1351.

Beck, M., Muller, D., Bigl, V., 1997. Amyloid precursor protein in guinea pigs—complete cDNA sequence and alternative splicing. Biochim. Biophys. Acta 1351 (1–2), 17–21.

Beck, M., Bruckner, M.K., Holzer, M., Kaap, S., Pannicke, T., Arendt, T., et al., 2000. Guinea-pig primary cell cultures provide a model to study expression and amyloidogenic processing of endogenous amyloid precursor protein. Neuroscience 95 (1), 243–254.

Beckett, C., Nalivaeva, N.N., Belyaev, N.D., Turner, A.J., 2012. Nuclear signalling by membrane protein intracellular domains: the AICD enigma. Cell Signal 24 (2), 402–409.

Bell, E.L., Klimova, T.A., Eisenbart, J., Moraes, C.T., Murphy, M.P., Budinger, G.R., et al., 2007. The Qo site of the mitochondrial complex III is required for the transduction of hypoxic signaling via reactive oxygen species production. J. Cell Biol. 177 (6), 1029–1036.

Bell, R.D., Winkler, E.A., Singh, I., Sagare, A.P., Deane, R., Wu, Z., et al., 2012. Apolipoprotein E controls cerebrovascular integrity via cyclophilin A. Nature 485 (7399), 512–516.

Bentahir, M., Nyabi, O., Verhamme, J., Tolia, A., Horre, K., Wiltfang, J., et al., 2006. Presenilin clinical mutations can affect gamma-secretase activity by different mechanisms. J. Neurochem. 96 (3), 732–742.

Bernardos, R.L., Lentz, S.I., Wolfe, M.S., Raymond, P.A., 2005. Notch-Delta signaling is required for spatial patterning and Muller glia differentiation in the zebrafish retina. Dev. Biol. 278 (2), 381–395.

Bernareggi, A., Duenas, Z., Reyes-Ruiz, J.M., Ruzzier, F., Miledi, R., 2007. Properties of glutamate receptors of Alzheimer's disease brain transplanted to frog oocytes. Proc. Natl. Acad. Sci. USA 104 (8), 2956–2960.

Bilbul, M., Schipper, H.M., 2011. Risk profiles of Alzheimer disease. Can. J. Neurol. Sci. 38 (4), 580–592.

Bischof, J., Basler, K., 2008. Recombinases and their use in gene activation, gene inactivation, and transgenesis. Methods Mol. Biol. 420, 175–195.

Blader, P., Strahle, U., 1998. Developmental biology—casting an eye over cyclopia. Nature 395 (6698), 112–113.

Blake, M.R., Holbrook, S.D., Kotwica-Rolinska, J., Chow, E.S., Kretzschmar, D., Giebultowicz, J.M., 2015. Manipulations of amyloid precursor protein cleavage disrupt the circadian clock in aging *Drosophila*. Neurobiol. Dis. 77, 117–126.

Blard, O., Frebourg, T., Campion, D., Lecourtois, M., 2006. Inhibition of proteasome and Shaggy/Glycogen synthase kinase-3beta kinase prevents clearance of phosphorylated tau in *Drosophila*. J. Neurosci. Res. 84 (5), 1107–1115.

Blennow, K., de Leon, M.J., Zetterberg, H., 2006. Alzheimer's disease. Lancet 368 (9533), 387–403.

Bolkan, B.J., Kretzschmar, D., 2014. Loss of Tau results in defects in photoreceptor development and progressive neuronal degeneration in *Drosophila*. Dev. Neurobiol. 74 (12), 1210–1225.

Borchelt, D.R., Thinakaran, G., Eckman, C.B., Lee, M.K., Davenport, F., Ratovitsky, T., et al., 1996. Familial Alzheimer's disease-linked presenilin 1 variants elevate A beta 1-42/1-40 ratio in vitro and in vivo. Neuron 17 (5), 1005–1013.

Bordji, K., Becerril-Ortega, J., Buisson, A., 2011. Synapses, NMDA receptor activity and neuronal Abeta production in Alzheimer's disease. Rev. Neurosci. 22 (3), 285–294.

Borysov, S.I., Granic, A., Padmanabhan, J., Walczak, C.E., Potter, H., 2011. Alzheimer Abeta disrupts the mitotic spindle and directly inhibits mitotic microtubule motors. Cell Cycle 10 (9), 1397–1410.

Bouge, A.L., Parmentier, M.L., 2016. Tau excess impairs mitosis and kinesin-5 function, leading to aneuploidy and cell death. Dis. Model Mech. 9 (3), 307–319.

Bourdet, I., Preat, T., Goguel, V., 2015. The full-length form of the *Drosophila* amyloid precursor protein is involved in memory formation. J. Neurosci. 35 (3), 1043–1051.

Braak, H., Braak, E., 1997. Diagnostic criteria for neuropathologic assessment of Alzheimer's disease. Neurobiol. Aging 18 (4 Suppl.), S85–S88.

Braak, H., Braak, E., Strothjohann, M., 1994. Abnormally phosphorylated tau protein related to the formation of neurofibrillary tangles and neuropil threads in the cerebral cortex of sheep and goat. Neurosci. Lett. 171 (1–2), 1–4.

Braak, H., Braak, E., Bohl, J., Bratzke, H., 1998. Evolution of Alzheimer's disease related cortical lesions. J. Neural. Transm. Suppl. 54, 97–106.

Brand, A.H., Perrimon, N., 1993. Targeted gene expression as a means of altering cell fates and generating dominant phenotypes. Development 118 (2), 401–415.

Brenner, S., 1974. The genetics of *Caenorhabditis elegans*. Genetics 77 (1), 71–94.

Brodney, M.A., Auperin, D.D., Becker, S.L., Bronk, B.S., Brown, T.M., Coffman, K.J., et al., 2011. Diamide amino-imidazoles: a novel series of gamma-secretase inhibitors for the treatment of Alzheimer's disease. Bioorg. Med. Chem. Lett. 21 (9), 2631–2636.

Brorsson, A.C., Bolognesi, B., Tartaglia, G.G., Shammas, S.L., Favrin, G., Watson, I., et al., 2010. Intrinsic determinants of neurotoxic aggregate formation by the amyloid beta peptide. Biophys. J. 98 (8), 1677–1684.

Buettner, R., Parhofer, K.G., Woenckhaus, M., Wrede, C.E., Kunz-Schughart, L.A., Scholmerich, J., et al., 2006. Defining high-fat-diet rat models: metabolic and molecular effects of different fat types. J. Mol. Endocrinol. 36 (3), 485–501.

Busser, J., Geldmacher, D.S., Herrup, K., 1998. Ectopic cell cycle proteins predict the sites of neuronal cell death in Alzheimer's disease brain. J. Neurosci. 18 (8), 2801–2807.

Butzlaff, M., Hannan, S.B., Karsten, P., Lenz, S., Ng, J., Vossfeldt, H., et al., 2015. Impaired retrograde transport by the Dynein/Dynactin complex contributes to Tau-induced toxicity. Hum. Mol. Genet. 24 (13), 3623–3637.

Cacciottolo, M., Christensen, A., Moser, A., Liu, J., Pike, C.J., Smith, C., et al., 2016. The APOE4 allele shows opposite sex bias in microbleeds and Alzheimer's disease of humans and mice. Neurobiol. Aging 37, 47–57.

Cacho-Valadez, B., Munoz-Lobato, F., Pedrajas, J.R., Cabello, J., Fierro-Gonzalez, J.C., Navas, P., et al., 2012. The characterization of the *Caenorhabditis elegans* mitochondrial thioredoxin system uncovers an unexpected protective role of thioredoxin reductase 2 in beta-amyloid peptide toxicity. Antioxid Redox Signal 16, 1384–1400.

Caesar, I., Jonson, M., Nilsson, K.P., Thor, S., Hammarstrom, P., 2012. Curcumin promotes A-beta fibrillation and reduces neurotoxicity in transgenic *Drosophila*. PLoS One 7 (2), e31424.

Cai, H., Wang, Y., McCarthy, D., Wen, H., Borchelt, D.R., Price, D.L., et al., 2001. BACE1 is the major beta-secretase for generation of Abeta peptides by neurons. Nat. Neurosci. 4 (3), 233–234.

Cake, M.A., Appleyard, R.C., Read, R.A., Smith, M.M., Murrell, G.A., Ghosh, P., 2005. Ovariectomy alters the structural and biomechanical properties of ovine femoro-tibial articular cartilage and increases cartilage iNOS. Osteoarthritis Cartilage 13 (12), 1066–1075.

Callahan, H., Ikeda-Douglas, C., Head, E., Cotman, C.W., Milgram, N.W., 2000. Development of a protocol for studying object recognition memory in the dog. Prog. Neuropsychopharmacol. Biol. Psychiatry 24 (5), 693–707.

Calsolaro, V., Edison, P., 2016. Alterations in glucose metabolism in Alzheimer's disease. Recent Pat. Endocr. Metab. Immune Drug Discov. 10, 31–39.

Campbell, W.A., Yang, H., Zetterberg, H., Baulac, S., Sears, J.A., Liu, T.M., et al., 2006. Zebrafish lacking Alzheimer presenilin enhancer 2 (Pen-2) demonstrate excessive p53-dependent apoptosis and neuronal loss. J. Neurochem. 96 (5), 1423–1440.

Camus, S., Ko, W.K., Pioli, E., Bezard, E., 2015. Why bother using non-human primate models of cognitive disorders in translational research? Neurobiol. Learn Mem. 124, 123–129.

Cao, W., Song, H.J., Gangi, T., Kelkar, A., Antani, I., Garza, D., et al., 2008. Identification of novel genes that modify phenotypes induced by Alzheimer's beta-amyloid overexpression in *Drosophila*. Genetics 178 (3), 1457–1471.

Carbonell, F., Zijdenbos, A.P., McLaren, D.G., Iturria-Medina, Y., Bedell, B.J., 2016. Modulation of glucose metabolism and metabolic connectivity by beta-amyloid. J. Cereb. Blood Flow Metab. 36, 2058–2071.

Carlson, G.A., Borchelt, D.R., Dake, A., Turner, S., Danielson, V., Coffin, J.D., et al., 1997. Genetic modification of the phenotypes produced by amyloid precursor protein overexpression in transgenic mice. Hum. Mol. Genet. 6 (11), 1951–1959.

Carmine-Simmen, K., Proctor, T., Tschape, J., Poeck, B., Triphan, T., Strauss, R., et al., 2009. Neurotoxic effects induced by the *Drosophila* amyloid-beta peptide suggest a conserved toxic function. Neurobiol. Dis. 33 (2), 274–281.

Carro, E., Torres-Aleman, I., 2004a. Insulin-like growth factor I and Alzheimer's disease: therapeutic prospects? Expert Rev. Neurother. 4 (1), 79–86.

Carro, E., Torres-Aleman, I., 2004b. The role of insulin and insulin-like growth factor I in the molecular and cellular mechanisms underlying the pathology of Alzheimer's disease. Eur. J. Pharmacol. 490 (1–3), 127–133.

Casas, C., Sergeant, N., Itier, J.M., Blanchard, V., Wirths, O., van der Kolk, N., et al., 2004. Massive CA1/2 neuronal loss with intraneuronal and N-terminal truncated Abeta42 accumulation in a novel Alzheimer transgenic model. Am. J. Pathol. 165 (4), 1289–1300.

Casas-Tinto, S., Zhang, Y., Sanchez-Garcia, J., Gomez-Velazquez, M., Rincon-Limas, D.E., Fernandez-Funez, P., 2011. The ER stress factor XBP1s prevents amyloid-beta neurotoxicity. Hum. Mol. Genet. 20 (11), 2144–2160.

Castellano, J.M., Kim, J., Stewart, F.R., Jiang, H., DeMattos, R.B., Patterson, B.W., et al., 2011. Human apoE isoforms differentially regulate brain amyloid-beta peptide clearance. Sci. Transl. Med. 3 (89), 89ra57.

Catchen, J.M., Braasch, I., Postlethwait, J.H., 2011. Conserved synteny and the zebrafish genome. Methods Cell Biol. 104, 259–285.

Chain, F.J.J., Evans, B.J., 2006. Multiple mechanisms promote the retained expression of gene duplicates in the tetraploid frog *Xenopus laevis*. PLoS Genet. 2 (4), 478–490.

Chakrabarti, S., Khemka, V.K., Banerjee, A., Chatterjee, G., Ganguly, A., Biswas, A., 2015. Metabolic risk factors of sporadic Alzheimer's disease: Implications in the pathology, pathogenesis and treatment. Aging Dis. 6 (4), 282–299.

Chakraborty, R., Vepuri, V., Mhatre, S.D., Paddock, B.E., Miller, S., Michelson, S.J., et al., 2011. Characterization of a *Drosophila* Alzheimer's disease model: pharmacological rescue of cognitive defects. PLoS One 6 (6), e20799.

Chan, A.W., 2004. Transgenic nonhuman primates for neurodegenerative diseases. Reprod. Biol. Endocrinol. 2, 39.

Chan, A.D., Nippak, P.M., Murphey, H., Ikeda-Douglas, C.J., Muggenburg, B., Head, E., et al., 2002. Visuospatial impairments in aged canines (*Canis familiaris*): the role of cognitive-behavioral flexibility. Behav. Neurosci. 116 (3), 443–454.

Chan, E.T., Quon, G.T., Chua, G., Babak, T., Trochesset, M., Zirngibl, R.A., et al., 2009. Conservation of core gene expression in vertebrate tissues. J. Biol. 8 (3), 33.

Chapman, P.F., White, G.L., Jones, M.W., Cooper-Blacketer, D., Marshall, V.J., Irizarry, M., et al., 1999. Impaired synaptic plasticity and learning in aged amyloid precursor protein transgenic mice. Nat. Neurosci. 2 (3), 271–276.

Chartier-Harlin, M.C., Crawford, F., Houlden, H., Warren, A., Hughes, D., Fidani, L., et al., 1991. Early-onset Alzheimer's disease caused by mutations at codon 717 of the beta-amyloid precursor protein gene. Nature 353 (6347), 844–846.

Chatterjee, S., Sang, T.K., Lawless, G.M., Jackson, G.R., 2009. Dissociation of tau toxicity and phosphorylation: role of GSK-3beta, MARK and Cdk5 in a *Drosophila* model. Hum. Mol. Genet. 18 (1), 164–177.

Chau, K.W., Chan, W.Y., Shaw, P.C., Chan, H.Y., 2006. Biochemical investigation of Tau protein phosphorylation status and its solubility properties in *Drosophila*. Biochem. Biophys. Res. Commun. 346 (1), 150–159.

Chen, Z., Zhong, C., 2013. Decoding Alzheimer's disease from perturbed cerebral glucose metabolism: implications for diagnostic and therapeutic strategies. Prog. Neurobiol. 108, 21–43.

Chen, G., Chen, K.S., Knox, J., Inglis, J., Bernard, A., Martin, S.J., et al., 2000. A learning deficit related to age and beta-amyloid plaques in a mouse model of Alzheimer's disease. Nature 408 (6815), 975–979.

Chen, M., Martins, R.N., Lardelli, M., 2009. Complex splicing and neural expression of duplicated tau genes in zebrafish embryos. J. Alzheimers Dis. 18 (2), 305–317.

Chen, Y., Niu, Y., Ji, W., 2012a. Transgenic nonhuman primate models for human diseases: approaches and contributing factors. J. Genet. Genomics 39 (6), 247–251.

Chen, Y., Tian, Z., Liang, Z., Sun, S., Dai, C.L., Lee, M.H., et al., 2012b. Brain gene expression of a sporadic (icv-STZ Mouse) and a familial mouse model (3xTg-AD mouse) of Alzheimer's disease. PLoS One 7 (12), e51432.

Chen, Y., Liang, Z., Blanchard, J., Dai, C.L., Sun, S., Lee, M.H., et al., 2013. A non-transgenic mouse model (icv-STZ mouse) of Alzheimer's disease: similarities to and differences from the transgenic model (3xTg-AD mouse). Mol. Neurobiol. 47 (2), 711–725.

Chen, Y., Liang, Z., Tian, Z., Blanchard, J., Dai, C.L., Chalbot, S., et al., 2014. Intracerebroventricular streptozotocin exacerbates Alzheimer-like changes of 3xTg-AD mice. Mol. Neurobiol. 49 (1), 547–562.

Chiang, H.C., Iijima, K., Hakker, I., Zhong, Y., 2009. Distinctive roles of different beta-amyloid 42 aggregates in modulation of synaptic functions. FASEB J. 23 (6), 1969–1977.

Chiang, H.C., Wang, L., Xie, Z., Yau, A., Zhong, Y., 2010. PI3 kinase signaling is involved in Abeta-induced memory loss in *Drosophila*. Proc. Natl. Acad. Sci. USA 107 (15), 7060–7065.

Chiocco, M.J., Kulnane, L.S., Younkin, L., Younkin, S., Evin, G., Lamb, B.T., 2004. Altered amyloid-beta metabolism and deposition in genomic-based beta-secretase transgenic mice. J. Biol. Chem. 279 (50), 52535–52542.

Chishti, M.A., Yang, D.S., Janus, C., Phinney, A.L., Horne, P., Pearson, J., et al., 2001. Early-onset amyloid deposition and cognitive deficits in transgenic mice expressing a double mutant form of amyloid precursor protein 695. J. Biol. Chem. 276 (24), 21562–21570.

Chu, W.Z., Qian, C.Y., 2005. [Expressions of Abeta1-40, Abeta1-42, tau202, tau396 and tau404 after intracerebroventricular injection of streptozotocin in rats]. Di Yi Jun Yi Da Xue Xue Bao 25 (2), 168–170.

Cipriani, G., Dolciotti, C., Picchi, L., Bonuccelli, U., 2011. Alzheimer and his disease: a brief history. Neurol. Sci. 32 (2), 275–279.

Claassen, J.A., Jansen, R.W., 2006. Cholinergically mediated augmentation of cerebral perfusion in Alzheimer's disease and related cognitive disorders: the cholinergic-vascular hypothesis. J. Gerontol. A Biol. Sci. Med. Sci. 61 (3), 267–271.

Cohen, E., Bieschke, J., Perciavalle, R.M., Kelly, J.W., Dillin, A., 2006. Opposing activities protect against age-onset proteotoxicity. Science 313 (5793), 1604–1610.

Colle, M.A., Hauw, J.J., Crespeau, F., Uchihara, T., Akiyama, H., Checler, F., et al., 2000. Vascular and parenchymal Abeta deposition in the aging dog: correlation with behavior. Neurobiol. Aging 21 (5), 695–704.

Corder, E.H., Saunders, A.M., Strittmatter, W.J., Schmechel, D.E., Gaskell, P.C., Small, G.W., et al., 1993. Gene dose of apolipoprotein E type 4 allele and the risk of Alzheimer's disease in late onset families. Science 261 (5123), 921–923.

Correia, S.C., Santos, R.X., Perry, G., Zhu, X., Moreira, P.I., Smith, M.A., 2011. Insulin-resistant brain state: the culprit in sporadic Alzheimer's disease? Ageing Res. Rev. 10 (2), 264–273.

Correia, S.C., Santos, R.X., Santos, M.S., Casadesus, G., Lamanna, J.C., Perry, G., et al., 2013. Mitochondrial abnormalities in a streptozotocin-induced rat model of sporadic Alzheimer's disease. Curr. Alzheimer Res. 10 (4), 406–419.

Cowan, C.M., Bossing, T., Page, A., Shepherd, D., Mudher, A., 2010a. Soluble hyper-phosphorylated tau causes microtubule breakdown and functionally compromises normal tau in vivo. Acta Neuropathol. 120 (5), 593–604.

Cowan, C.M., Chee, F., Shepherd, D., Mudher, A., 2010b. Disruption of neuronal function by soluble hyperphosphorylated tau in a *Drosophila* model of tauopathy. Biochem. Soc. Trans. 38 (2), 564–570.

Craig, L.A., Hong, N.S., McDonald, R.J., 2011. Revisiting the cholinergic hypothesis in the development of Alzheimer's disease. Neurosci. Biobehav. Rev. 35 (6), 1397–1409.

Crane, P.K., Walker, R., Larson, E.B., 2013. Glucose levels and risk of dementia. N. Engl. J. Med. 369 (19), 1863–1864.

Crowther, D.C., Kinghorn, K.J., Miranda, E., Page, R., Curry, J.A., Duthie, F.A., et al., 2005. Intraneuronal Abeta, non-amyloid aggregates and neurodegeneration in a *Drosophila* model of Alzheimer's disease. Neuroscience 132 (1), 123–135.

Cruchaga, C., Chakraverty, S., Mayo, K., Vallania, F.L., Mitra, R.D., Faber, K., et al., 2012. Rare variants in APP, PSEN1 and PSEN2 increase risk for AD in late-onset Alzheimer's disease families. PLoS One 7 (2), e31039.

Crusio, W.E., 1996. Gene-targeting studies: new methods, old problems. Trends Neurosci. 19 (5), 186–187.

Cummings, B.J., Head, E., Ruehl, W., Milgram, N.W., Cotman, C.W., 1996a. The canine as an animal model of human aging and dementia. Neurobiol. Aging 17 (2), 259–268.

Cummings, B.J., Satou, T., Head, E., Milgram, N.W., Cole, G.M., Savage, M.J., et al., 1996b. Diffuse plaques contain C-terminal A beta 42 and not A beta 40: evidence from cats and dogs. Neurobiol. Aging 17 (4), 653–659.

Daulatzai, M.A., 2016. Cerebral hypoperfusion and glucose hypometabolism: key pathophysiological modulators promote neurodegeneration, cognitive impairment, and Alzheimer's disease. J. Neurosci. Res. 95, 943–972.

Davidson, A.E., Balciunas, D., Mohn, D., Shaffer, J., Hermanson, S., Sivasubbu, S., et al., 2003. Efficient gene delivery and gene expression in zebrafish using the Sleeping Beauty transposon. Dev. Biol. 263 (2), 191–202.

Davtyan, H., Ghochikyan, A., Petrushina, I., Hovakimyan, A., Davtyan, A., Poghosyan, A., et al., 2013. Immunogenicity, efficacy, safety,

and mechanism of action of epitope vaccine (Lu AF20513) for Alzheimer's disease: prelude to a clinical trial. J. Neurosci. 33 (11), 4923–4934.

Dayanandan, R., Van Slegtenhorst, M., Mack, T.G., Ko, L., Yen, S.H., Leroy, K., et al., 1999. Mutations in tau reduce its microtubule binding properties in intact cells and affect its phosphorylation. FEBS Lett. 446 (2–3), 228–232.

De Felice, F.G., 2013a. Alzheimer's disease and insulin resistance: translating basic science into clinical applications. J. Clin. Invest. 123 (2), 531–539.

De Felice, F.G., 2013b. Connecting type 2 diabetes to Alzheimer's disease. Expert Rev. Neurother. 13 (12), 1297–1299.

De Felice, F.G., Munoz, D.P., 2016. Opportunities and challenges in developing relevant animal models for Alzheimer's disease. Ageing Res. Rev. 26, 112–114.

de la Monte, S.M., 2012a. Brain insulin resistance and deficiency as therapeutic targets in Alzheimer's disease. Curr. Alzheimer Res. 9 (1), 35–66.

de la Monte, S.M., 2012b. Contributions of brain insulin resistance and deficiency in amyloid-related neurodegeneration in Alzheimer's disease. Drugs 72 (1), 49–66.

de la Monte, S.M., Re, E., Longato, L., Tong, M., 2012. Dysfunctional pro-ceramide, ER stress, and insulin/IGF signaling networks with progression of Alzheimer's disease. J. Alzheimers Dis. 30 (Suppl. 2), S217–S229.

De Strooper, B., Chavez Gutierrez, L., 2015. Learning by failing: ideas and concepts to tackle gamma-secretases in Alzheimer's disease and beyond. Annu. Rev. Pharmacol. Toxicol. 55, 419–437.

Deane, R., Sagare, A., Hamm, K., Parisi, M., Lane, S., Finn, M.B., et al., 2008. apoE isoform-specific disruption of amyloid beta peptide clearance from mouse brain. J. Clin. Invest. 118 (12), 4002–4013.

Deiters, A., Garner, R.A., Lusic, H., Govan, J.M., Dush, M., Nascone-Yoder, N.M., et al., 2010. Photocaged morpholino oligomers for the light-regulation of gene function in zebrafish and Xenopus embryos. J. Am. Chem. Soc. 132 (44), 15644–15650.

Del Bene, F., Wyart, C., 2012. Optogenetics: A new enlightenment age for zebrafish neurobiology. Dev. Neurobiol. 72 (3), 404–414.

Demuro, A., Smith, M., Parker, I., 2011. Single-channel Ca(2+) imaging implicates Abeta1-42 amyloid pores in Alzheimer's disease pathology. J. Cell Biol. 195 (3), 515–524.

Deng, Y., Li, B., Liu, Y., Iqbal, K., Grundke-Iqbal, I., Gong, C.X., 2009. Dysregulation of insulin signaling, glucose transporters, O-GlcNAcylation, and phosphorylation of tau and neurofilaments in the brain: Implication for Alzheimer's disease. Am. J. Pathol. 175 (5), 2089–2098.

Dermaut, B., Kumar-Singh, S., Engelborghs, S., Theuns, J., Rademakers, R., Sacrens, J., et al., 2004. A novel presenilin 1 mutation associated with Pick's disease but not beta-amyloid plaques. Ann. Neurol. 55 (5), 617–626.

Dermaut, B., Kumar-Singh, S., Rademakers, R., Theuns, J., Cruts, M., Van Broeckhoven, C., 2005. Tau is central in the genetic Alzheimer-frontotemporal dementia spectrum. Trends Genet. 21 (12), 664–672.

Devous, Sr., M.D., 2002. Functional brain imaging in the dementias: role in early detection, differential diagnosis, and longitudinal studies. Eur. J. Nucl. Med. Mol. Imaging 29 (12), 1685–1696.

Dewachter, I., Reverse, D., Caluwaerts, N., Ris, L., Kuiperi, C., Van den Haute, C., et al., 2002. Neuronal deficiency of presenilin 1 inhibits amyloid plaque formation and corrects hippocampal long-term potentiation but not a cognitive defect of amyloid precursor protein [V717I] transgenic mice. J. Neurosci. 22 (9), 3445–3453.

Dias-Santagata, D., Fulga, T.A., Duttaroy, A., Feany, M.B., 2007. Oxidative stress mediates tau-induced neurodegeneration in Drosophila. J. Clin. Invest. 117 (1), 236–245.

Do Carmo, S., Cuello, A.C., 2013. Modeling Alzheimer's disease in transgenic rats. Mol. Neurodegener. 8 (1), 1–11.

Dodart, J.C., Meziane, H., Mathis, C., Bales, K.R., Paul, S.M., Ungerer, A., 1999. Behavioral disturbances in transgenic mice overexpressing the V717F beta-amyloid precursor protein. Behav. Neurosci. 113 (5), 982–990.

Dodart, J.C., Bales, K.R., Gannon, K.S., Greene, S.J., DeMattos, R.B., Mathis, C., et al., 2002. Immunization reverses memory deficits without reducing brain Abeta burden in Alzheimer's disease model. Nat. Neurosci. 5 (5), 452–457.

Donnini, S., Solito, R., Cetti, E., Corti, F., Giachetti, A., Carra, S., et al., 2010. A beta peptides accelerate the senescence of endothelial cells in vitro and in vivo, impairing angiogenesis. FASEB J. 24 (7), 2385–2395.

Dosanjh, L.E., Brown, M.K., Rao, G., Link, C.D., Luo, Y., 2010. Behavioral phenotyping of a transgenic Caenorhabditis elegans expressing neuronal amyloid-beta. J. Alzheimers Dis. 19 (2), 681–690.

Doyle, A., McGarry, M.P., Lee, N.A., Lee, J.J., 2012. The construction of transgenic and gene knockout/knockin mouse models of human disease. Transgenic Res. 21 (2), 327–349.

Dringenberg, H.C., Richardson, D.P., Brien, J.F., Reynolds, J.N., 2001. Spatial learning in the guinea pig: cued versus non-cued learning, sex differences, and comparison with rats. Behav. Brain Res. 124 (1), 97–101.

DuBoff, B., Gotz, J., Feany, M.B., 2012. Tau promotes neurodegeneration via DRP1 mislocalization in vivo. Neuron 75 (4), 618–632.

Duce, J.A., Bush, A.I., 2010. Biological metals and Alzheimer's disease: implications for therapeutics and diagnostics. Prog. Neurobiol. 92 (1), 1–18.

Duelli, R., Schrock, H., Kuschinsky, W., Hoyer, S., 1994. Intracerebroventricular injection of streptozotocin induces discrete local changes in cerebral glucose utilization in rats. Int. J. Dev. Neurosci. 12 (8), 737–741.

Duff, K., Eckman, C., Zehr, C., Yu, X., Prada, C.M., Perez-tur, J., et al., 1996. Increased amyloid-beta42(43) in brains of mice expressing mutant presenilin 1. Nature 383 (6602), 710–713.

Ebrahimie, E., Moussavi Nik, S.H., Newman, M., Van Der Hoek, M., Lardelli, M., 2016. The zebrafish equivalent of Alzheimer's disease-associated PRESENILIN isoform PS2V regulates inflammatory and other responses to hypoxic stress. J. Alzheimers Dis. 52, 581–608.

Echeverria, V., Ducatenzeiler, A., Dowd, E., Jänne, J., Grant, S.M., Szyf, M., et al., 2004a. Altered mitogen-activated protein kinase signaling, tau hyperphosphorylation and mild spatial learning dysfunction in transgenic rats expressing the beta-amyloid peptide intracellularly in hippocampal and cortical neurons. Neuroscience 129, 583–592.

Echeverria, V., Ducatenzeiler, A., Alhonen, L., Janne, J., Grant, S.M., Wandosell, F., et al., 2004b. Rat transgenic models with a phenotype of intracellular Abeta accumulation in hippocampus and cortex. J. Alzheimers Dis. 6 (3), 209–219.

Eisen, J.S., Smith, J.C., 2008. Controlling morpholino experiments: don't stop making antisense. Development 135 (10), 1735–1743.

Eketjall, S., Janson, J., Jeppsson, F., Svanhagen, A., Kolmodin, K., Gustavsson, S., et al., 2013. AZ-4217: a high potency BACE inhibitor displaying acute central efficacy in different in vivo models and reduced amyloid deposition in Tg2576 mice. J. Neurosci. 33 (24), 10075–10084.

Ekker, S.C., 2008. Zinc finger-based knockout punches for zebrafish genes. Zebrafish 5 (2), 121–123.

Epis, R., Gardoni, F., Marcello, E., Genazzani, A., Canonico, P.L., Di Luca, M., 2010. Searching for new animal models of Alzheimer's disease. Eur. J. Pharmacol. 626 (1), 57–63.

Ethell, D.W., 2010. An amyloid-notch hypothesis for Alzheimer's disease. Neuroscientist 16 (6), 614–617.

Favrin, G., Bean, D.M., Bilsland, E., Boyer, H., Fischer, B.E., Russell, S., et al., 2013. Identification of novel modifiers of Abeta toxicity by transcriptomic analysis in the fruitfly. Sci. Rep. 3, 3512.

Fedrizzi, L., Carafoli, E., 2011. Ca^{2+} dysfunction in neurodegenerative disorders: Alzheimer's disease. Biofactors 37 (3), 189–196.

Fernandez, M.L., 2001. Guinea pigs as models for cholesterol and lipoprotein metabolism. J. Nutr. 131 (1), 10–20.

Fernandez-Funez, P., de Mena, L., Rincon-Limas, D.E., 2015. Modeling the complex pathology of Alzheimer's disease in *Drosophila*. Exp. Neurol. 274 (Pt A), 58–71.

Feuillette, S., Miguel, L., Frebourg, T., Campion, D., Lecourtois, M., 2010. *Drosophila* models of human tauopathies indicate that Tau protein toxicity in vivo is mediated by soluble cytosolic phosphorylated forms of the protein. J. Neurochem. 113 (4), 895–903.

Findeis, M.A., 2007. The role of amyloid beta peptide 42 in Alzheimer's disease. Pharmacol. Ther. 116 (2), 266–286.

Finder, V.H., Glockshuber, R., 2007. Amyloid-beta aggregation. Neurodegener. Dis. 4 (1), 13–27.

Finelli, A., Kelkar, A., Song, H.J., Yang, H., Konsolaki, M., 2004. A model for studying Alzheimer's Abeta42-induced toxicity in *Drosophila melanogaster*. Mol. Cell Neurosci. 26 (3), 365–375.

Fjell, A.M., Walhovd, K.B., 2012. Neuroimaging results impose new views on Alzheimer's disease-the role of amyloid revised. Mol. Neurobiol. 45 (1), 153–172.

Flood, D.G., Reaume, A.G., Dorfman, K.S., Lin, Y.G., Lang, D.M., Trusko, S.P., et al., 2002. FAD mutant PS-1 gene-targeted mice: increased A beta 42 and A beta deposition without APP overproduction. Neurobiol. Aging 23 (3), 335–348.

Flood, D.G., Lin, Y.G., Lang, D.M., Trusko, S.P., Hirsch, J.D., Savage, M.J., et al., 2009. A transgenic rat model of Alzheimer's disease with extracellular Abeta deposition. Neurobiol. Aging 30 (7), 1078–1090.

Folkesson, R., Malkiewicz, K., Kloskowska, E., Nilsson, T., Popova, E., Bogdanovic, N., et al., 2007. A transgenic rat expressing human APP with the Swedish Alzheimer's disease mutation. Biochem. Biophys. Res. Commun. 358, 777–782.

Folwell, J., Cowan, C.M., Ubhi, K.K., Shiabh, H., Newman, T.A., Shepherd, D., et al., 2010. Abeta exacerbates the neuronal dysfunction caused by human tau expression in a *Drosophila* model of Alzheimer's disease. Exp. Neurol. 223, 401–409.

Fonte, V., Kapulkin, V., Taft, A., Fluet, A., Friedman, D., Link, C.D., 2002. Interaction of intracellular beta amyloid peptide with chaperone proteins. Proc. Natl. Acad. Sci. USA 99 (14), 9439–9444.

Fonte, V., Kipp, D.R., Yerg, 3rd, J., Merin, D., Forrestal, M., Wagner, E., et al., 2008. Suppression of in vivo beta-amyloid peptide toxicity by overexpression of the HSP-16.2 small chaperone protein. J. Biol. Chem. 283 (2), 784–791.

Fossgreen, A., Bruckner, B., Czech, C., Masters, C.L., Beyreuther, K., Paro, R., 1998. Transgenic *Drosophila* expressing human amyloid precursor protein show gamma-secretase activity and a blistered-wing phenotype. Proc. Natl. Acad. Sci. USA 95 (23), 13703–13708.

Foster, J.K., Verdile, G., Bates, K.A., Martins, R.N., 2009. Immunization in Alzheimer's disease: naive hope or realistic clinical potential? Mol. Psychiatry 14 (3), 239–251.

Francis, P.T., Palmer, A.M., Snape, M., Wilcock, G.K., 1999. The cholinergic hypothesis of Alzheimer's disease: a review of progress. J. Neurol. Neurosurg. Psychiatry 66 (2), 137–147.

Francis, R., McGrath, G., Zhang, J.H., Ruddy, D.A., Sym, M., Apfeld, J., et al., 2002. aph-1 and pen-2 are required for notch pathway signaling, gamma-secretase cleavage of beta APP, and presenilin protein accumulation. Dev. Cell 3 (1), 85–97.

Freeman, M.R., 2015. *Drosophila* central nervous system glia. Cold Spring Harb. Perspect. Biol. 7 (11), pii: a020552.

Frost, B., Hemberg, M., Lewis, J., Feany, M.B., 2014. Tau promotes neurodegeneration through global chromatin relaxation. Nat. Neurosci. 17 (3), 357–366.

Frost, B., Bardai, F.H., Feany, M.B., 2016. Lamin dysfunction mediates neurodegeneration in tauopathies. Curr. Biol. 26 (1), 129–136.

Fryer, J.D., Taylor, J.W., DeMattos, R.B., Bales, K.R., Paul, S.M., Parsadanian, M., et al., 2003. Apolipoprotein E markedly facilitates age-dependent cerebral amyloid angiopathy and spontaneous hemorrhage in amyloid precursor protein transgenic mice. J. Neurosci. 23 (21), 7889–7896.

Fryer, J.D., Simmons, K., Parsadanian, M., Bales, K.R., Paul, S.M., Sullivan, P.M., et al., 2005. Human apolipoprotein E4 alters the amyloid-beta 40:42 ratio and promotes the formation of cerebral amyloid angiopathy in an amyloid precursor protein transgenic model. J. Neurosci. 25 (11), 2803–2810.

Fukuchi, K., Ho, L., Younkin, S.G., Kunkel, D.D., Ogburn, C.E., LeBoeuf, R.C., et al., 1996. High levels of circulating beta-amyloid peptide do not cause cerebral beta-amyloidosis in transgenic mice. Am. J. Pathol. 149 (1), 219–227.

Fulga, T.A., Elson-Schwab, I., Khurana, V., Steinhilb, M.L., Spires, T.L., Hyman, B.T., et al., 2007. Abnormal bundling and accumulation of F-actin mediates tau-induced neuronal degeneration in vivo. Nat. Cell Biol. 9 (2), 139–148.

Furlong, R.F., Holland, P.W., 2002. Were vertebrates octoploid? Philos. Trans. R Soc. Lond. B Biol. Sci. 357 (1420), 531–544.

Gaik, G.C., Farbman, A.I., 1973a. Chicken trigeminal ganglion.1. Anatomical analysis of neuron types in adult. J. Morphol. 141 (1), 43–55.

Gaik, G.C., Farbman, A.I., 1973b. Chicken trigeminal ganglion.2. Fine-structure of neurons during development. J. Morphol. 141 (1), 57–75.

Gama, S.M., De Gasperi, R., Wen, P.H., Gonzalez, E.A., Kelley, K., Lazzarini, R.A., et al., 2002. BAC and PAC DNA for the generation of transgenic animals. Biotechniques 33 (1), 51–53.

Games, D., Adams, D., Alessandrini, R., Barbour, R., Berthelette, P., Blackwell, C., et al., 1995. Alzheimer-type neuropathology in transgenic mice overexpressing V717F beta-amyloid precursor protein. Nature 373 (6514), 523–527.

Ganesan, S., Moussavi Nik, S.H., Newman, M., Lardelli, M., 2014. Identification and expression analysis of the zebrafish orthologues of the mammalian MAP1LC3 gene family. Exp. Cell Res. 328 (1), 228–237.

Gaynor, J.S., Monnet, E., Selzman, C., Parker, D., Kaufman, L., Bryant, H.U., et al., 2000. The effect of raloxifene on coronary arteries in aged ovariectomized ewes. J. Vet. Pharmacol. Ther. 23 (3), 175–179.

Gearing, M., Rebeck, G.W., Hyman, B.T., Tigges, J., Mirra, S.S., 1994. Neuropathology and apolipoprotein E profile of aged chimpanzees: implications for Alzheimer disease. Proc. Natl. Acad. Sci. USA 91 (20), 9382–9386.

Gearing, M., Mori, H., Mirra, S.S., 1996. Abeta-peptide length and apolipoprotein E genotype in Alzheimer's disease. Ann. Neurol. 39 (3), 395–399.

Gearing, M., Tigges, J., Mori, H., Mirra, S.S., 1997. beta-Amyloid (A beta) deposition in the brains of aged orangutans. Neurobiol. Aging 18 (2), 139–146.

Gendron, T.F., Petrucelli, L., 2009. The role of tau in neurodegeneration. Mol. Neurodegener. 4, 13.

Genin, E., Hannequin, D., Wallon, D., Sleegers, K., Hiltunen, M., Combarros, O., et al., 2011. APOE and Alzheimer disease: a major gene with semi-dominant inheritance. Mol. Psychiatry 16 (9), 903–907.

George, A.J., Holsinger, R.M., McLean, C.A., Laughton, K.M., Beyreuther, K., Evin, G., et al., 2004. APP intracellular domain is increased and soluble Abeta is reduced with diet-induced hypercholesterolemia in a transgenic mouse model of Alzheimer disease. Neurobiol. Dis. 16 (1), 124–132.

Gerlai, R., 1996. Gene-targeting studies of mammalian behavior: is it the mutation or the background genotype? Trends Neurosci. 19 (5), 177–181.

Ghosal, K., Vogt, D.L., Liang, M., Shen, Y., Lamb, B.T., Pimplikar, S.W., 2009. Alzheimer's disease-like pathological features in transgenic mice expressing the APP intracellular domain. Proc. Natl. Acad. Sci. USA 106 (43), 18367–18372.

Ghribi, O., Larsen, B., Schrag, M., Herman, M.M., 2006. High cholesterol content in neurons increases BACE, beta-amyloid, and phosphorylated tau levels in rabbit hippocampus. Exp. Neurol. 200 (2), 460–467.

Gibbs, R.A., Weinstock, G.M., Metzker, M.L., Muzny, D.M., Sodergren, E.J., Scherer, S., et al., 2004. Genome sequence of the Brown Norway rat yields insights into mammalian evolution. Nature 428, 493–521.

Gibbs, M.E., Gibbs, Z., Hertz, L., 2009. Rescue of Abeta(1-42)-induced memory impairment in day-old chick by facilitation of astrocytic oxidative metabolism: implications for Alzheimer's disease. J. Neurochem. 109 (Suppl. 1), 230–236.

Gibbs, M.E., Maksel, D., Gibbs, Z., Hou, X., Summers, R.J., Small, D.H., 2010. Memory loss caused by beta-amyloid protein is rescued by a beta(3)-adrenoceptor agonist. Neurobiol. Aging 31 (4), 614–624.

Gilad, G.M., Gilad, V.H., 1987. Age-related reductions in brain cholinergic and dopaminergic indices in two rat strains differing in longevity. Brain Res. 408, 247–250.

Gilman, S., Koller, M., Black, R.S., Jenkins, L., Griffith, S.G., Fox, N.C., et al., 2005. Clinical effects of Abeta immunization (AN1792) in patients with AD in an interrupted trial. Neurology 64 (9), 1553–1562.

Glenner, G.G., Wong, C.W., 1984. Alzheimer's disease: initial report of the purification and characterization of a novel cerebrovascular amyloid protein. Biochem. Biophys. Res. Commun. 120 (3), 885–890.

Goate, A., Chartier-Harlin, M.C., Mullan, M., Brown, J., Crawford, F., Fidani, L., et al., 1991. Segregation of a missense mutation in the amyloid precursor protein gene with familial Alzheimer's disease. Nature 349 (6311), 704–706, (Research Support, Non-US Gov't Research Support, US Gov't, PHS).

Goedert, M., Wischik, C.M., Crowther, R.A., Walker, J.E., Klug, A., 1988. Cloning and sequencing of the cDNA encoding a core protein of the paired helical filament of Alzheimer disease: identification as the microtubule-associated protein tau. Proc. Natl. Acad. Sci. USA 85 (11), 4051–4055.

Goguel, V., Belair, A.L., Ayaz, D., Lampin-Saint-Amaux, A., Scaplehorn, N., Hassan, B.A., et al., 2011. Drosophila amyloid precursor protein-like is required for long-term memory. J. Neurosci. 31 (3), 1032–1037.

Gonzalez-Soriano, J., Marin Garcia, P., Contreras-Rodriguez, J., Martinez-Sainz, P., Rodriguez-Veiga, E., 2001. Age-related changes in the ventricular system of the dog brain. Ann. Anat. 183 (3), 283–291.

Gorsky, M.K., Burnouf, S., Dols, J., Mandelkow, E., Partridge, L., 2016. Acetylation mimic of lysine 280 exacerbates human Tau neurotoxicity in vivo. Sci. Rep. 6, 22685.

Gotz, J., 2001. Tau and transgenic animal models. Brain Res. Brain Res. Rev. 35 (3), 266–286.

Grammenoudi, S., Kosmidis, S., Skoulakis, E.M., 2006. Cell type-specific processing of human Tau proteins in Drosophila. FEBS Lett. 580 (19), 4602–4606.

Gratz, S.J., Cummings, A.M., Nguyen, J.N., Hamm, D.C., Donohue, L.K., Harrison, M.M., et al., 2013. Genome engineering of Drosophila with the CRISPR RNA-guided Cas9 nuclease. Genetics 194 (4), 1029–1035.

Green, K.N., Demuro, A., Akbari, Y., Hitt, B.D., Smith, I.F., Parker, I., et al., 2008. SERCA pump activity is physiologically regulated by presenilin and regulates amyloid beta production. J. Cell Biol. 181 (7), 1107–1116.

Greene, E., Naranjo, J.N., 1987. Degeneration of hippocampal fibers and spatial memory deficits in the aged rat. Neurobiol. Aging 8, 35–43.

Greenspan, R.J., 2004. Fly Pushing; The theory and practice of Drosophila genetics, second ed. Cold Spring Harbor: Cold Spring Harbor Press, NY.

Greeve, I., Kretzschmar, D., Tschape, J.A., Beyn, A., Brellinger, C., Schweizer, M., et al., 2004. Age-dependent neurodegeneration and Alzheimer-amyloid plaque formation in transgenic Drosophila. J. Neurosci. 24 (16), 3899–3906.

Groth, C., Nornes, S., McCarty, R., Tamme, R., Lardelli, M., 2002. Identification of a second presenilin gene in zebrafish with similarity to the human Alzheimer's disease gene presenilin2. Dev. Genes Evol. 212 (10), 486–490.

Groth, C., Alvord, W.G., Quinones, O.A., Fortini, M.E., 2010. Pharmacological analysis of Drosophila melanogaster gamma-secretase with respect to differential proteolysis of Notch and APP. Mol. Pharmacol. 77 (4), 567–574.

Grunblatt, E., Koutsilieri, E., Hoyer, S., Riederer, P., 2006. Gene expression alterations in brain areas of intracerebroventricular streptozotocin treated rat. J. Alzheimer's Dis. 9 (3), 261–271.

Guarnieri, B., Sorbi, S., 2015. Sleep and cognitive decline: a strong bidirectional relationship. it is time for specific recommendations on routine assessment and the management of sleep disorders in patients with mild cognitive impairment and dementia. Eur. Neurol. 74 (1–2), 43–48.

Gunawardena, S., Goldstein, L.S., 2001. Disruption of axonal transport and neuronal viability by amyloid precursor protein mutations in Drosophila. Neuron 32 (3), 389–401.

Guo, J.L., Lee, V.M., 2011. Seeding of normal Tau by pathological Tau conformers drives pathogenesis of Alzheimer-like tangles. J. Biol. Chem. 286 (17), 15317–15331.

Haass, C., Lemere, C.A., Capell, A., Citron, M., Seubert, P., Schenk, D., et al., 1995. The Swedish mutation causes early-onset Alzheimer's disease by beta-secretase cleavage within the secretory pathway. Nat. Med. 1 (12), 1291–1296.

Han, J.Y., 2009. Germ cells and transgenesis in chickens. Comp. Immunol. Microbiol. Infect. Dis. 32 (2), 61–80.

Han, P., Shi, J., 2016. A theoretical analysis of the synergy of amyloid and tau in Alzheimer's disease. J. Alzheimers Dis. 52 (4), 1461–1470.

Hanes, J., Zilka, N., Bartkova, M., Caletkova, M., Dobrota, D., Novak, M., 2009. Rat tau proteome consists of six tau isoforms: implication for animal models of human tauopathies. J. Neurochem. 108, 1167–1176.

Hardy, J.A., Higgins, G.A., 1992. Alzheimer's disease: the amyloid cascade hypothesis. Science 256 (5054), 184–185.

Hargis, K.E., Blalock, E.M., 2016. Transcriptional signatures of brain aging and Alzheimer's disease: what are our rodent models telling us? Behav. Brain Res 322 (Pt. B), 311–328.

Hartenstein, V., 2011. Morphological diversity and development of glia in Drosophila. Glia 59 (9), 1237–1252.

Hartig, W., Stieler, J., Boerema, A.S., Wolf, J., Schmidt, U., Weissfuss, J., et al., 2007. Hibernation model of tau phosphorylation in hamsters: selective vulnerability of cholinergic basal forebrain neurons—implications for Alzheimer's disease. Eur. J. Neurosci. 25 (1), 69–80.

Hartman, R.E., Izumi, Y., Bales, K.R., Paul, S.M., Wozniak, D.F., Holtzman, D.M., 2005. Treatment with an amyloid-beta antibody ameliorates plaque load, learning deficits, and hippocampal long-term potentiation in a mouse model of Alzheimer's disease. J. Neurosci. 25 (26), 6213–6220.

Hasegawa, M., Smith, M.J., Goedert, M., 1998. Tau proteins with FTDP-17 mutations have a reduced ability to promote microtubule assembly. FEBS Lett. 437 (3), 207–210.

Hassan, W.M., Merin, D.A., Fonte, V., Link, C.D., 2009. AIP-1 ameliorates beta-amyloid peptide toxicity in a Caenorhabditis elegans Alzheimer's disease model. Hum. Mol. Genet. 18 (15), 2739–2747.

Hastings, M.H., Goedert, M., 2013. Circadian clocks and neurodegenerative diseases: time to aggregate? Curr. Opin. Neurobiol. 23, 880–887.

He, C., Klionsky, D.J., 2010. Analyzing autophagy in zebrafish. Autophagy 6 (5), 642–644.

He, C., Bartholomew, C.R., Zhou, W., Klionsky, D.J., 2009. Assaying autophagic activity in transgenic GFP-Lc3 and GFP-Gabarap zebrafish embryos. Autophagy 5 (4), 520–526.

Head, E., Callahan, H., Muggenburg, B.A., Cotman, C.W., Milgram, N.W., 1998. Visual-discrimination learning ability and beta-amyloid accumulation in the dog. Neurobiol. Aging 19 (5), 415–425.

Head, E., McCleary, R., Hahn, F.F., Milgram, N.W., Cotman, C.W., 2000. Region-specific age at onset of beta-amyloid in dogs. Neurobiol. Aging 21 (1), 89–96.

Head, E., Pop, V., Vasilevko, V., Hill, M., Saing, T., Sarsoza, F., et al., 2008. A two-year study with fibrillar beta-amyloid (Abeta) immunization

in aged canines: effects on cognitive function and brain Abeta. J. Neurosci. 28 (14), 3555–3566.

Hellsten, U., Harland, R.M., Gilchrist, M.J., Hendrix, D., Jurka, J., Kapitonov, V., et al., 2010. The genome of the western clawed frog *Xenopus tropicalis*. Science 328 (5978), 633–636.

Heo, J.H., Lee, S.R., Lee, S.T., Lee, K.M., Oh, J.H., Jang, D.P., et al., 2011. Spatial distribution of glucose hypometabolism induced by intra-cerebroventricular streptozotocin in monkeys. J. Alzheimers Dis. 25 (3), 517–523.

Herndon, J.G., Moss, M.B., Rosene, D.L., Killiany, R.J., 1997. Patterns of cognitive decline in aged rhesus monkeys. Behav. Brain Res. 87 (1), 25–34.

Herreman, A., Hartmann, D., Annaert, W., Saftig, P., Craessaerts, K., Serneels, L., et al., 1999. Presenilin 2 deficiency causes a mild pulmonary phenotype and no changes in amyloid precursor protein processing but enhances the embryonic lethal phenotype of presenilin 1 deficiency. Proc. Natl. Acad. Sci. USA 96 (21), 11872–11877.

Herzig, M.C., Winkler, D.T., Burgermeister, P., Pfeifer, M., Kohler, E., Schmidt, S.D., et al., 2004. Abeta is targeted to the vasculature in a mouse model of hereditary cerebral hemorrhage with amyloidosis. Nat. Neurosci. 7 (9), 954–960.

Heuer, E., Rosen, R.F., Cintron, A., Walker, L.C., 2012. Nonhuman primate models of Alzheimer-like cerebral proteopathy. Curr. Pharm. Des. 18 (8), 1159–1169.

Hisaoka, K.K., 1958a. Effects of 2-acetylaminofluorene on the embryonic development of the zebrafish. I. morphological studies. Cancer Res. 18 (5), 527–535.

Hisaoka, K.K., 1958b. Effects of 2-acetylaminofluorene on the embryonic development of the zebrafish. II. Histochemical studies. Cancer Res. 18 (6), 664–667.

Hoffmann, J.A., 2003. The immune response of *Drosophila*. Nature 426 (6962), 33–38.

Holtzman, D.M., Bales, K.R., Wu, S., Bhat, P., Parsadanian, M., Fagan, A.M., et al., 1999. Expression of human apolipoprotein E reduces amyloid-beta deposition in a mouse model of Alzheimer's disease. J. Clin. Invest. 103 (6), R15–R21.

Hong, M., Zhukareva, V., Vogelsberg-Ragaglia, V., Wszolek, Z., Reed, L., Miller, B.I., et al., 1998. Mutation-specific functional impairments in distinct tau isoforms of hereditary FTDP-17. Science 282 (5395), 1914–1917.

Hoppener, J.W., Oosterwijk, C., Nieuwenhuis, M.G., Posthuma, G., Thijssen, J.H., Vroom, T.M., et al., 1999. Extensive islet amyloid formation is induced by development of type II diabetes mellitus and contributes to its progression: pathogenesis of diabetes in a mouse model. Diabetologia 42 (4), 427–434.

Hornsten, A., Lieberthal, J., Fadia, S., Malins, R., Ha, L., Xu, X., et al., 2007. APL-1, a *Caenorhabditis elegans* protein related to the human beta-amyloid precursor protein, is essential for viability. Proc. Natl. Acad. Sci. USA 104 (6), 1971–1976.

Hoshijima, K., Jurynec, M.J., Grunwald, D.J., 2016. Precise editing of the zebrafish genome made simple and efficient. Dev. Cell 36 (6), 654–667.

Hou, Y., Wang, Y., Zhao, J., Li, X., Cui, J., Ding, J., et al., 2014. Smart Soup, a traditional Chinese medicine formula, ameliorates amyloid pathology and related cognitive deficits. PLoS One 9 (11), e111215.

Howlett, D.R., Richardson, J.C., 2009. The pathology of APP transgenic mice: a model of Alzheimer's disease or simply overexpression of APP? Histol. Histopathol. 24 (1), 83–100.

Hsia, A.Y., Masliah, E., McConlogue, L., Yu, G.Q., Tatsuno, G., Hu, K., et al., 1999. Plaque-independent disruption of neural circuits in Alzheimer's disease mouse models. Proc. Natl. Acad. Sci. USA 96 (6), 3228–3233.

Hsiao, K., Chapman, P., Nilsen, S., Eckman, C., Harigaya, Y., Younkin, S., et al., 1996. Correlative memory deficits, Abeta elevation, and amyloid plaques in transgenic mice. Science 274 (5284), 99–102.

Hua, H., Munter, L., Harmeier, A., Georgiev, O., Multhaup, G., Schaffner, W., 2011. Toxicity of Alzheimer's disease-associated Abeta peptide is ameliorated in a *Drosophila* model by tight control of zinc and copper availability. Biol. Chem. 392 (10), 919–926.

Huang, Y., Mucke, L., 2012. Alzheimer mechanisms and therapeutic strategies. Cell 148 (6), 1204–1222.

Huang, J.K., Ma, P.L., Ji, S.Y., Zhao, X.L., Tan, J.X., Sun, X.J., et al., 2013. Age-dependent alterations in the presynaptic active zone in a *Drosophila* model of Alzheimer's disease. Neurobiol. Dis. 51, 161–167.

Huang, L., Merson, T.D., Bourne, J.A., 2016. In vivo whole brain, cellular and molecular imaging in nonhuman primate models of neuropathology. Neurosci. Biobehav. Rev. 66, 104–118.

Huitron-Resendiz, S., Sanchez-Alavez, M., Gallegos, R., Berg, G., Crawford, E., Giacchino, J.L., et al., 2002. Age-independent and age-related deficits in visuospatial learning, sleep-wake states, thermoregulation and motor activity in PDAPP mice. Brain Res. 928 (1–2), 126–137.

Hunter, N., 2007. Scrapie: uncertainties, biology and molecular approaches. Biochim. Biophys. Acta 1772 (6), 619–628.

Hutton, M., Lendon, C.L., Rizzu, P., Baker, M., Froelich, S., Houlden, H., et al., 1998. Association of missense and 5'-splice-site mutations in tau with the inherited dementia FTDP-17. Nature 393 (6686), 702–705.

Hwang, W.Y., Fu, Y., Reyon, D., Maeder, M.L., Tsai, S.Q., Sander, J.D., et al., 2013. Efficient genome editing in zebrafish using a CRISPR-Cas system. Nat. Biotechnol. 31 (3), 227–229.

Iijima, K., Liu, H.P., Chiang, A.S., Hearn, S.A., Konsolaki, M., Zhong, Y., 2004. Dissecting the pathological effects of human Abeta40 and Abeta42 in *Drosophila*: a potential model for Alzheimer's disease. Proc. Natl. Acad. Sci. USA 101 (17), 6623–6628.

Iijima, K., Chiang, H.C., Hearn, S.A., Hakker, I., Gatt, A., Shenton, C., et al., 2008. Abeta42 mutants with different aggregation profiles induce distinct pathologies in *Drosophila*. PLoS One 3 (2), e1703.

Iijima, K., Gatt, A., Iijima-Ando, K., 2010. Tau Ser262 phosphorylation is critical for Abeta42-induced tau toxicity in a transgenic *Drosophila* model of Alzheimer's disease. Hum. Mol. Genet. 19 (15), 2947–2957.

Iijima-Ando, K., Hearn, S.A., Shenton, C., Gatt, A., Zhao, L., Iijima, K., 2009. Mitochondrial mislocalization underlies Abeta42-induced neuronal dysfunction in a *Drosophila* model of Alzheimer's disease. PLoS One 4 (12), e8310.

Iourov, I.Y., Vorsanova, S.G., Liehr, T., Yurov, Y.B., 2009. Aneuploidy in the normal, Alzheimer's disease and ataxia-telangiectasia brain: differential expression and pathological meaning. Neurobiol. Dis. 34 (2), 212–220.

Iqbal, K., Liu, F., Gong, C.X., Alonso Adel, C., Grundke-Iqbal, I., 2009. Mechanisms of tau-induced neurodegeneration. Acta Neuropathol. 118 (1), 53–69.

Iqbal, K., Liu, F., Gong, C.-X., Grundke-Iqbal, I., 2010. Tau in Alzheimer disease and related tauopathies. Curr. Alzheimer Res. 7 (8), 656–664.

Ishihara, T., Gondo, T., Takahashi, M., Uchino, F., Ikeda, S., Allsop, D., et al., 1991. Immunohistochemical and immunoelectron microscopical characterization of cerebrovascular and senile plaque amyloid in aged dogs' brains. Brain Res. 548 (1–2), 196–205.

Israel, M.A., Yuan, S.H., Bardy, C., Reyna, S.M., Mu, Y., Herrera, C., et al., 2012. Probing sporadic and familial Alzheimer's disease using induced pluripotent stem cells. Nature 482 (7384), 216–220.

Ittner, L.M., Ke, Y.D., Delerue, F., Bi, M., Gladbach, A., van Eersel, J., et al., 2010. Dendritic function of tau mediates amyloid-beta toxicity in Alzheimer's disease mouse models. Cell 142 (3), 387–397.

Jackson, G.R., Wiedau-Pazos, M., Sang, T.K., Wagle, N., Brown, C.A., Massachi, S., et al., 2002. Human wild-type tau interacts with wingless pathway components and produces neurofibrillary pathology in *Drosophila*. Neuron 34 (4), 509–519.

Jacob, H.J., Kwitek, A.E., 2002. Rat genetics: attaching physiology and pharmacology to the genome. Nat. Rev. Genet. 3, 33–42.

N. PSYCHIATRIC AND NEUROLOGICAL DISEASE

Jaiswal, M., Sandoval, H., Zhang, K., Bayat, V., Bellen, H.J., 2012. Probing mechanisms that underlie human neurodegenerative diseases in *Drosophila*. Annu. Rev. Genet. 46, 371–396.

Jang, S.S., Chung, H.J., 2016. Emerging link between Alzheimer's disease and homeostatic synaptic plasticity. Neural Plast. 2016, 7969272.

Jankowsky, J.L., Slunt, H.H., Gonzales, V., Savonenko, A.V., Wen, J.C., Jenkins, N.A., et al., 2005. Persistent amyloidosis following suppression of Abeta production in a transgenic model of Alzheimer disease. PLoS Med. 2 (12), e355.

Jayadev, S., Leverenz, J.B., Steinbart, E., Stahl, J., Klunk, W., Yu, C.E., et al., 2010. Alzheimer's disease phenotypes and genotypes associated with mutations in presenilin 2. Brain 133, 1143–1154.

Jayne, T., Newman, M., Verdile, G., Sutherland, G., Münch, G., Musgrave, I., et al., 2016. Evidence for and against a pathogenic role of reduced gamma-secretase activity in familial Alzheimer's disease. J. Alzheimer's Dis. 52, 781–799.

Jimenez-Bonilla, J.F., Banzo, I., De Arcocha-Torres, M., Quirce, R., Martinez-Rodriguez, I., Lavado-Perez, C., et al., 2016. Diagnostic role of 11C-Pittsburgh compound B retention patterns and glucose metabolism by fluorine-18-fluorodeoxyglucose PET/CT in amnestic and nonamnestic mild cognitive impairment patients. Nucl. Med. Commun. 37, 1189–1196.

Jin, Y.X., Zheng, S.S., Pu, Y., Shu, L.J., Sun, L.W., Liu, W.P., et al., 2011. Cypermethrin has the potential to induce hepatic oxidative stress, DNA damage and apoptosis in adult zebrafish (*Danio rerio*). Chemosphere 82 (3), 398–404.

Johnson-Wood, K., Lee, M., Motter, R., Hu, K., Gordon, G., Barbour, R., et al., 1997. Amyloid precursor protein processing and A beta42 deposition in a transgenic mouse model of Alzheimer disease. Proc. Natl. Acad. Sci. USA 94 (4), 1550–1555.

Johnstone, E.M., Chaney, M.O., Norris, F.H., Pascual, R., Little, S.P., 1991. Conservation of the sequence of the Alzheimer's disease amyloid peptide in dog, polar bear and five other mammals by cross-species polymerase chain reaction analysis. Brain Res. Mol. Brain Res. 10 (4), 299–305.

Joly, M., Ammersdorfer, S., Schmidtke, D., Zimmermann, E., 2014. Touchscreen-based cognitive tasks reveal age-related impairment in a primate aging model, the grey mouse lemur (*Microcebus murinus*). PLoS One 9 (10), e109393.

Joshi, P., Liang, J.O., DiMonte, K., Sullivan, J., Pimplikar, S.W., 2009. Amyloid precursor protein is required for convergent-extension movements during Zebrafish development. Dev. Biol. 335 (1), 1–11.

Jucker, M., 2010. The benefits and limitations of animal models for translational research in neurodegenerative diseases. Nat. Med. 16 (11), 1210–1214.

Jucker, M., Walker, L.C., 2011. Pathogenic protein seeding in Alzheimer disease and other neurodegenerative disorders. Ann. Neurol. 70 (4), 532–540.

Julien, C., Tremblay, C., Phivilay, A., Berthiaume, L., Emond, V., Julien, P., et al., 2010. High-fat diet aggravates amyloid-beta and tau pathologies in the 3xTg-AD mouse model. Neurobiol. Aging 31 (9), 1516–1531.

Kadish, I., Kumar, A., Beitnere, U., Jennings, E., McGilberry, W., van Groen, T., 2016. Dietary composition affects the development of cognitive deficits in WT and Tg AD model mice. Exp. Gerontol. 86, 39–49.

Kahn, S.E., Andrikopoulos, S., Verchere, C.B., 1999. Islet amyloid: a long-recognized but underappreciated pathological feature of type 2 diabetes. Diabetes 48 (2), 241–253.

Kalback, W., Watson, M.D., Kokjohn, T.A., Kuo, Y.M., Weiss, N., Luehrs, D.C., et al., 2002. APP transgenic mice Tg2576 accumulate Abeta peptides that are distinct from the chemically modified and insoluble peptides deposited in Alzheimer's disease senile plaques. Biochemistry 41 (3), 922–928.

Kalueff, A.V., Stewart, A.M., Gerlai, R., 2014. Zebrafish as an emerging model for studying complex brain disorders. Trends Pharmacol. Sci. 35 (2), 63–75.

Kamath, R.S., Martinez-Campos, M., Zipperlen, P., Fraser, A.G., Ahringer, J., 2001. Effectiveness of specific RNA-mediated interference through ingested double-stranded RNA in *Caenorhabditis elegans*. Genome Biol. 2 (1), RESEARCH0002.

Karran, E., Mercken, M., De Strooper, B., 2011. The amyloid cascade hypothesis for Alzheimer's disease: an appraisal for the development of therapeutics. Nat. Rev. Drug Discov. 10 (9), 698–712.

Karsten, S.L., Sang, T.K., Gehman, L.T., Chatterjee, S., Liu, J., Lawless, G.M., et al., 2006. A genomic screen for modifiers of tauopathy identifies puromycin-sensitive aminopeptidase as an inhibitor of tau-induced neurodegeneration. Neuron 51 (5), 549–560.

Kawakami, K., 2004. Transgenesis and gene trap methods in zebrafish by using the Tol2 transposable element. Zebrafish: Genetics Genomics and Informatics, vol. 77, second ed. Elsevier Academic Press, San Diego, CA, USA, pp. 201–222.

Kawarabayashi, T., Younkin, L.H., Saido, T.C., Shoji, M., Ashe, K.H., Younkin, S.G., 2001. Age-dependent changes in brain, CSF, and plasma amyloid (beta) protein in the Tg2576 transgenic mouse model of Alzheimer's disease. J. Neurosci. 21 (2), 372–381.

Kawasumi, M., Chiba, T., Yamada, M., Miyamae-Kaneko, M., Matsuoka, M., Nakahara, J., et al., 2004. Targeted introduction of V642I mutation in amyloid precursor protein gene causes functional abnormality resembling early stage of Alzheimer's disease in aged mice. Eur. J. Neurosci. 19 (10), 2826–2838.

Kelly, P.H., Bondolfi, L., Hunziker, D., Schlecht, H.P., Carver, K., Maguire, E., et al., 2003. Progressive age-related impairment of cognitive behavior in APP23 transgenic mice. Neurobiol. Aging 24 (2), 365–378.

Kent, G., Iles, R., Bear, C.E., Huan, L.J., Griesenbach, U., McKerlie, C., et al., 1997. Lung disease in mice with cystic fibrosis. J. Clin. Invest. 100 (12), 3060–3069.

Khurana, V., Lu, Y., Steinhilb, M.L., Oldham, S., Shulman, J.M., Feany, M.B., 2006. TOR-mediated cell-cycle activation causes neurodegeneration in a *Drosophila* tauopathy model. Curr. Biol. 16 (3), 230–241.

Kiatipattanasakul, W., Nakayama, H., Yongsiri, S., Chotiapisitkul, S., Nakamura, S., Kojima, H., et al., 2000. Abnormal neuronal and glial argyrophilic fibrillary structures in the brain of an aged albino cynomolgus monkey (*Macaca fascicularis*). Acta Neuropathol. 100 (5), 580–586.

Kim, E.J., Cho, S.S., Jeong, Y., Park, K.C., Kang, S.J., Kang, E., et al., 2005. Glucose metabolism in early onset versus late onset Alzheimer's disease: an SPM analysis of 120 patients. Brain 128 (Pt 8), 1790–1801.

Kimotsuki, T., Nagaoka, T., Yasuda, M., Tamahara, S., Matsuki, N., Ono, K., 2005. Changes of magnetic resonance imaging on the brain in beagle dogs with aging. J. Vet. Med. Sci. 67 (10), 961–967.

Kimura, R., Ohno, M., 2009. Impairments in remote memory stabilization precede hippocampal synaptic and cognitive failures in 5XFAD Alzheimer mouse model. Neurobiol. Dis. 33 (2), 229–235.

Kishi, S., Bayliss, P.E., Uchiyama, J., Koshimizu, E., Qi, J., Nanjappa, P., et al., 2008. The identification of zebrafish mutants showing alterations in senescence-associated biomarkers. PLoS Genet. 4 (8), e1000152.

Kizil, C., Kaslin, J., Kroehne, V., Brand, M., 2012. Adult neurogenesis and brain regeneration in zebrafish. Dev. Neurobiol. 72 (3), 429–461.

Kloskowska, E., Pham, T.M., Nilsson, T., Zhu, S., Oberg, J., Codita, A., et al., 2010. Cognitive impairment in the Tg6590 transgenic rat model of Alzheimer's disease. J. Cell Mol. Med. 14, 1816–1823.

Knezovic, A., Osmanovic-Barilar, J., Curlin, M., Hof, P.R., Simic, G., Riederer, P., et al., 2015. Staging of cognitive deficits and neuropathological and ultrastructural changes in streptozotocin-induced rat model of Alzheimer's disease. J. Neural Transm. (Vienna) 122 (4), 577–592.

Knight, E.M., Martins, I.V., Gumusgoz, S., Allan, S.M., Lawrence, C.B., 2014. High-fat diet-induced memory impairment in triple-transgenic Alzheimer's disease (3xTgAD) mice is independent of changes in amyloid and tau pathology. Neurobiol. Aging 35 (8), 1821–1832.

Ko, S.K., Chen, X., Yoon, J., Shin, I., 2011. Zebrafish as a good vertebrate model for molecular imaging using fluorescent probes. Chem. Soc. Rev. 40 (5), 2120–2130.

Kohjima, M., Sun, Y., Chan, L., 2010. Increased food intake leads to obesity and insulin resistance in the tg2576 Alzheimer's disease mouse model. Endocrinology 151 (4), 1532–1540.

Kok, F.O., Shin, M., Ni, C.W., Gupta, A., Grosse, A.S., van Impel, A., et al., 2015. Reverse genetic screening reveals poor correlation between morpholino-induced and mutant phenotypes in zebrafish. Dev. Cell 32 (1), 97–108.

Komatsu, Y., Horiuchi, M., Ishiguro, N., Matsui, T., Shinagawa, M., 1998. Characterization of the sheep apolipoprotein E (ApoE) gene and allelic variations of the ApoE gene in scrapie Suffolk sheep. Gene 208 (2), 131–138.

Kondratova, A.A., Kondratov, R.V., 2012. The circadian clock and pathology of the ageing brain. Nat. Rev. Neurosci. 13 (5), 325–335.

Kosmidis, S., Grammenoudi, S., Papanikolopoulou, K., Skoulakis, E.M., 2010. Differential effects of Tau on the integrity and function of neurons essential for learning in *Drosophila*. J. Neurosci. 30 (2), 464–477.

Kotilinek, L.A., Bacskai, B., Westerman, M., Kawarabayashi, T., Younkin, L., Hyman, B.T., et al., 2002. Reversible memory loss in a mouse transgenic model of Alzheimer's disease. J. Neurosci. 22 (15), 6331–6335.

Kotze, M.J., van Rensburg, S.J., 2012. Pathology supported genetic testing and treatment of cardiovascular disease in middle age for prevention of Alzheimer's disease. Metab. Brain Dis. 27, 255–266.

Kraemer, B.C., Zhang, B., Leverenz, J.B., Thomas, J.H., Trojanowski, J.Q., Schellenberg, G.D., 2003. Neurodegeneration and defective neurotransmission in a *Caenorhabditis elegans* model of tauopathy. Proc. Natl. Acad. Sci. USA 100 (17), 9980–9985.

Kraemer, B.C., Burgess, J.K., Chen, J.H., Thomas, J.H., Schellenberg, G.D., 2006. Molecular pathways that influence human tau-induced pathology in *Caenorhabditis elegans*. Hum. Mol. Genet. 15 (9), 1483–1496.

Krebs, M.R., Wilkins, D.K., Chung, E.W., Pitkeathly, M.C., Chamberlain, A.K., Zurdo, J., et al., 2000. Formation and seeding of amyloid fibrils from wild-type hen lysozyme and a peptide fragment from the beta-domain. J. Mol. Biol. 300 (3), 541–549.

Kumar, S., Hedges, S.B., 1998. A molecular timescale for vertebrate evolution. Nature 392 (6679), 917–920.

Kwok, J.B.J., Halliday, G.M., Brooks, W.S., Dolios, G., Laudon, H., Murayama, O., et al., 2003. Presenilin-1 mutation L271V results in altered exon 8 splicing and Alzheimer's disease with non-cored plaques and no neuritic dystrophy. J. Biol. Chem. 278 (9), 6748–6754.

Lai, S.L., Lee, T., 2006. Genetic mosaic with dual binary transcriptional systems in *Drosophila*. Nat. Neurosci. 9 (5), 703–709.

Lai, Z.C., Moss, M.B., Killiany, R.J., Rosene, D.L., Herndon, J.G., 1995. Executive system dysfunction in the aged monkey: spatial and object reversal learning. Neurobiol. Aging 16 (6), 947–954.

Lamb, B.T., Sisodia, S.S., Lawler, A.M., Slunt, H.H., Kitt, C.A., Kearns, W.G., et al., 1993. Introduction and expression of the 400 kilobase amyloid precursor protein gene in transgenic mice [corrected]. Nat. Genet. 5 (1), 22–30.

Lamb, B.T., Call, L.M., Slunt, H.H., Bardel, K.A., Lawler, A.M., Eckman, C.B., et al., 1997. Altered metabolism of familial Alzheimer's disease-linked amyloid precursor protein variants in yeast artificial chromosome transgenic mice. Hum. Mol. Genet. 6 (9), 1535–1541.

Lamb, P.W., Melton, M.A., Yakel, J.L., 2005. Inhibition of neuronal nicotinic acetylcholine receptor channels expressed in *Xenopus* oocytes by beta-amyloid1-42 peptide. J. Mol. Neurosci. 27 (1), 13–21.

Lane, M.A., 2000. Nonhuman primate models in biogerontology. Exp. Gerontol. 35 (5), 533–541.

Lannert, H., Hoyer, S., 1998. Intracerebroventricular administration of streptozotocin causes long-term diminutions in learning and memory abilities and in cerebral energy metabolism in adult rats. Behav. Neurosci. 112 (5), 1199–1208.

Larson, M., Sherman, M.A., Amar, F., Nuvolone, M., Schneider, J.A., Bennett, D.A., et al., 2012. The complex PrP(c)-Fyn couples human oligomeric Abeta with pathological tau changes in Alzheimer's disease. J. Neurosci. 32 (47), 16857a–16871a.

Lawson, N.D., Weinstein, B.M., 2002. In vivo imaging of embryonic vascular development using transgenic zebrafish. Dev. Biol. 248 (2), 307–318.

Lecanu, L., Papadopoulos, V., 2013. Modeling Alzheimer's disease with non-transgenic rat models. Alzheimers Res. Ther. 5 (3), 17.

Lee, J.A., Cole, G.J., 2007. Generation of transgenic zebrafish expressing green fluorescent protein under control of zebrafish amyloid precursor protein gene regulatory elements. Zebrafish 4 (4), 277–286.

Lee, J., Freeman, J.L., 2016. Embryonic exposure to 10 mug L^{-1} lead results in female-specific expression changes in genes associated with nervous system development and function and Alzheimer's disease in aged adult zebrafish brain. Metallomics 8, 589–596.

Lee, V.M., Goedert, M., Trojanowski, J.Q., 2001. Neurodegenerative tauopathies. Annu. Rev. Neurosci. 24, 1121–1159.

Lee, J.H., Yu, W.H., Kumar, A., Lee, S., Mohan, P.S., Peterhoff, C.M., et al., 2010. Lysosomal proteolysis and autophagy require presenilin 1 and are disrupted by Alzheimer-related PS1 mutations. Cell 141 (7), 1146–1158.

Lee, Y., Kim, Y.H., Park, S.J., Huh, J.W., Kim, S.H., Kim, S.U., et al., 2014. Insulin/IGF signaling-related gene expression in the brain of a sporadic Alzheimer's disease monkey model induced by intra-cerebroventricular injection of streptozotocin. J. Alzheimers Dis. 38 (2), 251–267.

Lee, J., Peterson, S.M., Freeman, J.L., 2016. Alzheimer's disease risk genes in wild-type adult zebrafish exhibit gender-specific expression changes during aging. Neurogenetics 17, 197–199.

Lehman, E.J., Kulnane, L.S., Gao, Y., Petriello, M.C., Pimpis, K.M., Younkin, L., et al., 2003a. Genetic background regulates beta-amyloid precursor protein processing and beta-amyloid deposition in the mouse. Hum. Mol. Genet. 12 (22), 2949–2956.

Lehman, E.J., Kulnane, L.S., Lamb, B.T., 2003b. Alterations in beta-amyloid production and deposition in brain regions of two transgenic models. Neurobiol. Aging 24 (5), 645–653.

Leimer, U., Lun, K., Romig, H., Walter, J., Grunberg, J., Brand, M., et al., 1999. Zebrafish (*Danio rerio*) presenilin promotes aberrant amyloid beta-peptide production and requires a critical aspartate residue for its function in amyloidogenesis. Biochemistry 38 (41), 13602–13609.

Leissring, M.A., Parker, I., LaFerla, F.M., 1999a. Presenilin-2 mutations modulate amplitude and kinetics of inositol 1,4,5-trisphosphate-mediated calcium signals. J. Biol. Chem. 274 (46), 32535–32538.

Leissring, M.A., Paul, B.A., Parker, I., Cotman, C.W., LaFerla, F.M., 1999b. Alzheimer's presenilin-1 mutation potentiates inositol 1,4,5-trisphosphate-mediated calcium signaling in *Xenopus* oocytes. J. Neurochem. 72 (3), 1061–1068.

Leissring, M.A., Farris, W., Chang, A.Y., Walsh, D.M., Wu, X., Sun, X., et al., 2003. Enhanced proteolysis of beta-amyloid in APP transgenic mice prevents plaque formation, secondary pathology, and premature death. Neuron 40 (6), 1087–1093.

Leon, W.C., Canneva, F., Partridge, V., Allard, S., Ferretti, M.T., DeWilde, A., et al., 2010. A novel transgenic rat model with a full Alzheimer's-like amyloid pathology displays pre-plaque intracellular amyloid-beta-associated cognitive impairment. J. Alzheimers Dis. 20 (1), 113–126.

Lessman, C.A., 2011. The developing zebrafish (*Danio rerio*): a vertebrate model for high-throughput screening of chemical libraries. Birth Defects Res. C Embryo Today 93 (3), 268–280.

Leung, C., Jia, Z., 2016. Mouse genetic models of human brain disorders. Front. Genet. 7, 40.

Levi, L., Ziv, T., Admon, A., Levavi-Sivan, B., Lubzens, E., 2012. Insight into molecular pathways of retinal metabolism, associated with vitellogenesis in zebrafish. Am. J. Physiol. Endocrinol. Metab. 302 (6), E626–644.

Levin-Allerhand, J.A., Lominska, C.E., Wang, J., Smith, J.D., 2002. 17Alpha-estradiol and 17beta-estradiol treatments are effective in lowering cerebral amyloid-beta levels in AbetaPPSWE transgenic mice. J. Alzheimers Dis. 4 (6), 449–457.

Levy-Lahad, E., Wasco, W., Poorkaj, P., Romano, D.M., Oshima, J., Pettingell, W.H., et al., 1995. Candidate gene for the chromosome 1 familial Alzheimer's disease locus. Science 269 (5226), 973–977.

Lewejohann, L., Pickel, T., Sachser, N., Kaiser, S., 2010. Wild genius—domestic fool? Spatial learning abilities of wild and domestic guinea pigs. Front. Zool. 7, 9.

Lewis, P.A., Perez-Tur, J., Golde, T.E., Hardy, J., 2000. The presenilin 1 C92S mutation increases abeta 42 production. Biochem. Biophys. Res. Commun. 277 (1), 261–263.

Lewis, J., Dickson, D.W., Lin, W.L., Chisholm, L., Corral, A., Jones, G., et al., 2001. Enhanced neurofibrillary degeneration in transgenic mice expressing mutant tau and APP. Science 293 (5534), 1487–1491.

Leyssen, M., Ayaz, D., Hebert, S.S., Reeve, S., De Strooper, B., Hassan, B.A., 2005. Amyloid precursor protein promotes post-developmental neurite arborization in the Drosophila brain. EMBO J. 24 (16), 2944–2955.

Li, J., Le, W., 2013. Modeling neurodegenerative diseases in Caenorhabditis elegans. Exp. Neurol. 250, 94–103.

Li, Y., Liu, T., Peng, Y., Yuan, C., Guo, A., 2004. Specific functions of Drosophila amyloid precursor-like protein in the development of nervous system and nonneural tissues. J. Neurobiol. 61 (3), 343–358.

Li, W., Risacher, S.L., Huang, E., Saykin, A.J., 2016. Type 2 diabetes mellitus is associated with brain atrophy and hypometabolism in the ADNI cohort. Neurology 87, 595–600.

Liao, H.K., Wang, Y., Watt, K.E.N., Wen, Q., Breitbach, J., Kemmet, C.K., et al., 2012. Tol2 gene trap integrations in the zebrafish amyloid precursor protein genes appa and aplp2 reveal accumulation of secreted APP at the embryonic veins. Dev. Dyn. 241 (2), 415–425.

Lien, C.L., Schebesta, M., Makino, S., Weber, G.J., Keating, M.T., 2006. Gene expression analysis of zebrafish heart regeneration. PLoS Biol. 4 (8), e260.

Liguori, C., Chiaravalloti, A., Sancesario, G., Stefani, A., Sancesario, G.M., Mercuri, N.B., et al., 2016. Cerebrospinal fluid lactate levels and brain [18F]FDG PET hypometabolism within the default mode network in Alzheimer's disease. Eur. J. Nucl. Med. Mol. Imaging 43, 2040–2049.

Lim, A., Moussavi Nik, S.H., Ebrahimie, E., Lardelli, M., 2015. Analysis of nicastrin gene phylogeny and expression in zebrafish. Dev. Genes Evol. 225 (3), 171–178.

Lin, J.H., 1995. Species similarities and differences in pharmacokinetics. Drug Metab. Dispos. 23, 1008–1021.

Lin, F., Jia, J., Qin, W., 2014a. Enhancement of beta-amyloid oligomer accumulation after intracerebroventricular injection of streptozotocin, which involves central insulin signaling in a transgenic mouse model. Neuroreport 25 (16), 1289–1295.

Lin, J.Y., Wang, W.A., Zhang, X., Liu, H.Y., Zhao, X.L., Huang, F.D., 2014b. Intraneuronal accumulation of Abeta42 induces age-dependent slowing of neuronal transmission in Drosophila. Neurosci. Bull. 30 (2), 185–190.

Link, C.D., 1995. Expression of human beta-amyloid peptide in transgenic Caenorhabditis elegans. Proc. Natl. Acad. Sci. USA 92 (20), 9368–9372.

Link, C.D., Taft, A., Kapulkin, V., Duke, K., Kim, S., Fei, Q., et al., 2003. Gene expression analysis in a transgenic Caenorhabditis elegans Alzheimer's disease model. Neurobiol. Aging 24 (3), 397–413.

Liu, F., Gong, C.X., 2008. Tau exon 10 alternative splicing and tauopathies. Mol. Neurodegener. 3, 8.

Lleo, A., Saura, C.A., 2011. gamma-secretase substrates and their implications for drug development in Alzheimer's disease. Curr. Top. Med. Chem. 11 (12), 1513–1527.

Loewen, C.A., Feany, M.B., 2010. The unfolded protein response protects from tau neurotoxicity in vivo. PLoS One 5 (9), pii: e13084.

Lopez, E.M., Bell, K.F., Ribeiro-da-Silva, A., Cuello, A.C., 2004. Early changes in neurons of the hippocampus and neocortex in transgenic rats expressing intracellular human a-beta. J. Alzheimers Dis. 6, 421–431.

Lord, A., Kalimo, H., Eckman, C., Zhang, X.Q., Lannfelt, L., Nilsson, L.N., 2006. The Arctic Alzheimer mutation facilitates early intraneuronal Abeta aggregation and senile plaque formation in transgenic mice. Neurobiol. Aging 27 (1), 67–77.

Lowseth, L.A., Gillett, N.A., Gerlach, R.F., Muggenburg, B.A., 1990. The effects of aging on hematology and serum chemistry values in the beagle dog. Vet. Clin. Pathol. 19 (1), 13–19.

Ltd., A.E.P., 2004. Delaying the onset of Alzheimer's disease: projections and impacts.

Lublin, A.L., Gandy, S., 2010. Amyloid-beta oligomers: possible roles as key neurotoxins in Alzheimer's disease. Mt. Sinai J. Med. 77 (1), 43–49.

Lublin, A.L., Link, C.D., 2013. Alzheimer's disease drug discovery: in vivo screening using Caenorhabditis elegans as a model for beta-amyloid peptide-induced toxicity. Drug Discov. Today Technol. 10 (1), e115–e119.

Luheshi, L.M., Tartaglia, G.G., Brorsson, A.C., Pawar, A.P., Watson, I.E., Chiti, F., et al., 2007. Systematic in vivo analysis of the intrinsic determinants of amyloid Beta pathogenicity. PLoS Biol. 5 (11), e290.

Luheshi, L.M., Hoyer, W., de Barros, T.P., van Dijk Hard, I., Brorsson, A.C., Macao, B., et al., 2010. Sequestration of the Abeta peptide prevents toxicity and promotes degradation in vivo. PLoS Biol. 8 (3), e1000334.

Luo, L.Q., Martin-Morris, L.E., White, K., 1990. Identification, secretion, and neural expression of APPL, a Drosophila protein similar to human amyloid protein precursor. J. Neurosci. 10 (12), 3849–3861.

Ma, Q.L., Yang, F., Rosario, E.R., Ubeda, O.J., Beech, W., Gant, D.J., et al., 2009. Beta-amyloid oligomers induce phosphorylation of tau and inactivation of insulin receptor substrate via c-Jun N-terminal kinase signaling: suppression by omega-3 fatty acids and curcumin. J. Neurosci. 29 (28), 9078–9089.

MacLeay, J.M., Lehmer, E., Enns, R.M., Mallinckrodt, C., Bryant, H.U., Turner, A.S., 2003. Central and peripheral temperature changes in sheep following ovariectomy. Maturitas 46 (3), 231–238.

Marchesi, V.T., 2011. Alzheimer's dementia begins as a disease of small blood vessels, damaged by oxidative-induced inflammation and dysregulated amyloid metabolism: implications for early detection and therapy. FASEB J. 25 (1), 5–13.

Marder, E., 2002. Non-mammalian models for studying neural development and function. Nature 417 (6886), 318–321.

Martin, S.A.L., Jameson, C.H., Allan, S.M., Lawrence, C.B., 2014. Maternal high-fat diet worsens memory deficits in the triple-transgenic (3xTgAD) mouse model of Alzheimer's disease. PLoS One 9 (6), e99226.

Martins, I.J., Berger, T., Sharman, M.J., Verdile, G., Fuller, S.J., Martins, R.N., 2009. Cholesterol metabolism and transport in the pathogenesis of Alzheimer's disease. J. Neurochem. 111 (6), 1275–1308.

Mastrangelo, P., Mathews, P.M., Chishti, M.A., Schmidt, S.D., Gu, Y., Yang, J., et al., 2005. Dissociated phenotypes in presenilin transgenic mice define functionally distinct gamma-secretases. Proc. Natl. Acad. Sci. USA 102 (25), 8972–8977.

McLean, J.W., Fukazawa, C., Taylor, J.M., 1983. Rat apolipoprotein E mRNA. Cloning and sequencing of double-stranded cDNA. J. Biol. Chem. 258, 8993–9000.

Meckler, X., Checler, F., 2014. Visualization of specific gamma-secretase complexes using bimolecular fluorescence complementation. J. Alzheimers Dis. 40 (1), 161–176.

Meckler, X., Checler, F., 2016. Presenilin 1 and Presenilin 2 target gamma-secretase complexes to distinct cellular compartments. J. Biol. Chem. 291, 12821–12837.

Mehla, J., Pahuja, M., Dethe, S.M., Agarwal, A., Gupta, Y.K., 2012. Amelioration of intracerebroventricular streptozotocin induced cognitive impairment by *Evolvulus alsinoides* in rats: in vitro and in vivo evidence. Neurochem. Int. 61 (7), 1052–1064.

Mehla, J., Chauhan, B.C., Chauhan, N.B., 2014. Experimental induction of type 2 diabetes in aging-accelerated mice triggered Alzheimer-like pathology and memory deficits. J. Alzheimer's Dis. 39 (1), 145–162.

Metzger, R.J., Krasnow, M.A., 1999. Genetic control of branching morphogenesis. Science 284 (5420), 1635–1639.

Mhatre, S.D., Satyasi, V., Killen, M., Paddock, B.E., Moir, R.D., Saunders, A.J., et al., 2014. Synaptic abnormalities in a *Drosophila* model of Alzheimer's disease. Dis. Model Mech. 7 (3), 373–385.

Michaki, V., Guix, F.X., Vennekens, K., Munck, S., Dingwall, C., Davis, J.B., et al., 2012. Down-regulation of the ATP-binding cassette transporter 2 (Abca2) reduces amyloid-beta production by altering Nicastrin maturation and intracellular localization. J. Biol. Chem. 287 (2), 1100–1111.

Miklossy, J., 2011. Emerging roles of pathogens in Alzheimer disease. Expert Rev. Mol. Med. 13, e30.

Miledi, R., Duenas, Z., Martinez-Torres, A., Kawas, C.H., Eusebi, F., 2004. Microtransplantation of functional receptors and channels from the Alzheimer's brain to frog oocytes. Proc. Natl. Acad. Sci. USA 101 (6), 1760–1763.

Mileusnic, R., Rose, S., 2010. The chick as a model for the study of the cellular mechanisms and potential therapies for Alzheimer's disease. Int. J. Alzheimers Dis 2010.

Milgram, N.W., Head, E., Weiner, E., Thomas, E., 1994. Cognitive functions and aging in the dog: acquisition of nonspatial visual tasks. Behav. Neurosci. 108 (1), 57–68.

Milgram, N.W., Head, E., Muggenburg, B., Holowachuk, D., Murphey, H., Estrada, J., et al., 2002. Landmark discrimination learning in the dog: effects of age, an antioxidant fortified food, and cognitive strategy. Neurosci. Biobehav. Rev. 26 (6), 679–695.

Milgram, N.W., Head, E., Zicker, S.C., Ikeda-Douglas, C., Murphey, H., Muggenberg, B.A., et al., 2004. Long-term treatment with antioxidants and a program of behavioral enrichment reduces age-dependent impairment in discrimination and reversal learning in beagle dogs. Exp. Gerontol. 39 (5), 753–765.

Milgram, N.W., Head, E., Zicker, S.C., Ikeda-Douglas, C.J., Murphey, H., Muggenburg, B., et al., 2005. Learning ability in aged beagle dogs is preserved by behavioral enrichment and dietary fortification: a two-year longitudinal study. Neurobiol. Aging 26 (1), 77–90.

Milward, E.A., Papadopoulos, R., Fuller, S.J., Moir, R.D., Small, D., Beyreuther, K., et al., 1992. The amyloid protein precursor of Alzheimer's disease is a mediator of the effects of nerve growth factor on neurite outgrowth. Neuron 9 (1), 129–137.

Minoshima, S., Giordani, B., Berent, S., Frey, K.A., Foster, N.L., Kuhl, D.E., 1997. Metabolic reduction in the posterior cingulate cortex in very early Alzheimer's disease. Ann. Neurol. 42 (1), 85–94.

Moechars, D., Dewachter, I., Lorent, K., Reverse, D., Baekelandt, V., Naidu, A., et al., 1999. Early phenotypic changes in transgenic mice that overexpress different mutants of amyloid precursor protein in brain. J. Biol. Chem. 274 (10), 6483–6492.

Moghadasian, M.H., 2002. Experimental atherosclerosis: a historical overview. Life Sci. 70 (8), 855–865.

Mok, S.S., Clippingdale, A.B., Beyreuther, K., Masters, C.L., Barrow, C.J., Small, D.H., 2000. A beta peptides and calcium influence secretion of the amyloid protein precursor from chick sympathetic neurons in culture. J. Neurosci. Res. 61 (4), 449–457.

Molteni, R., Barnard, R.J., Ying, Z., Roberts, C.K., Gomez-Pinilla, F., 2002. A high-fat, refined sugar diet reduces hippocampal brain-derived neurotrophic factor, neuronal plasticity, and learning. Neuroscience 112 (4), 803–814.

Monnot, M.J., Babin, P.J., Poleo, G., Andre, M., Laforest, L., Ballagny, C., et al., 1999. Epidermal expression of apolipoprotein E gene during fin and scale development and fin regeneration in zebrafish. Dev. Dyn. 214 (3), 207–215.

Moore, T.L., Killiany, R.J., Herndon, J.G., Rosene, D.L., Moss, M.B., 2003. Impairment in abstraction and set shifting in aged rhesus monkeys. Neurobiol. Aging 24 (1), 125–134.

Moore, T.L., Killiany, R.J., Herndon, J.G., Rosene, D.L., Moss, M.B., 2006. Executive system dysfunction occurs as early as middle-age in the rhesus monkey. Neurobiol. Aging 27 (10), 1484–1493.

Moraes, C.F., Lins, T.C., Carmargos, E.F., Naves, J.O., Pereira, R.W., Nobrega, O.T., 2012. Lessons from genome-wide association studies findings in Alzheimer's disease. Psychogeriatrics 12 (1), 62–73.

Moran, C., Beare, R., Phan, T.G., Bruce, D.G., Callisaya, M.L., Srikanth, V., 2015. Type 2 diabetes mellitus and biomarkers of neurodegeneration. Neurology 85 (13), 1123–1130.

Moreau, K., Fleming, A., Imarisio, S., Lopez Ramirez, A., Mercer, J.L., Jimenez-Sanchez, M., et al., 2014. PICALM modulates autophagy activity and tau accumulation. Nat. Commun. 5, 4998.

Morelli, L., Wei, L., Amorim, A., McDermid, J., Abee, C.R., Frangione, B., et al., 1996. Cerebrovascular amyloidosis in squirrel monkeys and rhesus monkeys: apolipoprotein E genotype. FEBS Lett. 379 (2), 132–134.

Morris, J.K., Vidoni, E.D., Wilkins, H.M., Archer, A.E., Burns, N.C., Karcher, R.T., et al., 2016. Impaired fasting glucose is associated with increased regional cerebral amyloid. Neurobiol. Aging 44, 138–142.

Mosconi, L., 2005. Brain glucose metabolism in the early and specific diagnosis of Alzheimer's disease. FDG-PET studies in MCI and AD. Eur. J. Nucl. Med. Mol. Imaging 32 (4), 486–510.

Mosconi, L., Tsui, W.H., De Santi, S., Li, J., Rusinek, H., Convit, A., et al., 2005. Reduced hippocampal metabolism in MCI and AD: automated FDG-PET image analysis. Neurology 64 (11), 1860–1867.

Mosconi, L., De Santi, S., Li, Y., Li, J., Zhan, J., Tsui, W.H., et al., 2006. Visual rating of medial temporal lobe metabolism in mild cognitive impairment and Alzheimer's disease using FDG-PET. Eur. J. Nucl. Med. Mol. Imaging 33 (2), 210–221.

Moss, M.B., Rosene, D.L., Peters, A., 1988. Effects of aging on visual recognition memory in the rhesus monkey. Neurobiol. Aging 9 (5–6), 495–502.

Moussavi Nik, S.H., Newman, M., Lardelli, M., 2011. The response of HMGA1 to changes in oxygen availability is evolutionarily conserved. Exp. Cell Res. 317 (11), 1503–1512.

Moussavi Nik, S.H., Wilson, L., Newman, M., Croft, K., Mori, T.A., Musgrave, I., et al., 2012. The BACE1-PSEN-AbetaPP regulatory axis has an ancient role in response to low oxygen/oxidative stress. J. Alzheimers Dis. 28 (3), 515–530.

Moussavi Nik, S.H., Newman, M., Ganesan, S., Chen, M., Martins, R., Verdile, G., et al., 2014. Hypoxia alters expression of Zebrafish microtubule-associated protein Tau (mapta, maptb) gene transcripts. BMC Res. Notes 7, 767, (Research Support, Non-US Gov't).

Moussavi Nik, S.H., Newman, M., Wilson, L., Ebrahimie, E., Wells, S., Musgrave, I., et al., 2015. Alzheimer's disease-related peptide PS2V plays ancient, conserved roles in suppression of the unfolded protein response under hypoxia and stimulation of gamma-secretase activity. Hum. Mol. Genet. 24 (13), 3662–3678.

Mucke, L., Masliah, E., Yu, G.Q., Mallory, M., Rockenstein, E.M., Tatsuno, G., et al., 2000. High-level neuronal expression of abeta 1-42 in wild-type human amyloid protein precursor transgenic mice: synaptotoxicity without plaque formation. J. Neurosci. 20 (11), 4050–4058.

Muresan, V., Muresan, Z., 2011. A Persistent stress response to impeded axonal transport leads to accumulation of amyloid-beta in the endoplasmic reticulum, and is a probable cause of sporadic Alzheimer's disease. Neurodegener. Dis. 10, 10–63.

Musa, A., Lehrach, H., Russo, V.A., 2001. Distinct expression patterns of two zebrafish homologues of the human APP gene during embryonic development. Dev. Genes Evol. 211 (11), 563–567.

Nada, S.E., Williams, F.E., Shah, Z.A., 2016. Development of a novel and robust pharmacological model of okadaic acid-induced Alzheimer's disease in zebrafish. CNS Neurol. Disord. Drug Targets 15 (1), 86–94.

Nagahara, A.H., Bernot, T., Tuszynski, M.H., 2010. Age-related cognitive deficits in rhesus monkeys mirror human deficits on an automated test battery. Neurobiol. Aging 31 (6), 1020–1031.

Nasevicius, A., Ekker, S.C., 2000. Effective targeted gene 'knockdown' in zebrafish. Nat. Genet. 26 (2), 216–220.

Ndung'u, M., Hartig, W., Wegner, F., Mwenda, J.M., Low, R.W., Akinyemi, R.O., et al., 2012. Cerebral amyloid beta(42) deposits and microvascular pathology in ageing baboons. Neuropathol. Appl. Neurobiol. 38 (5), 487–499.

Nelson, P.T., Saper, C.B., 1995. Ultrastructure of neurofibrillary tangles in the cerebral cortex of sheep. Neurobiol. Aging 16 (3), 315–323.

Nelson, P.T., Marton, L., Saper, C.B., 1993. Alz-50 immunohistochemistry in the normal sheep striatum: a light and electron microscope study. Brain Res. 600 (2), 285–297.

Nelson, P.T., Greenberg, S.G., Saper, C.B., 1994. Neurofibrillary tangles in the cerebral cortex of sheep. Neurosci. Lett. 170 (1), 187–190.

Nerelius, C., Sandegren, A., Sargsyan, H., Raunak, R., Leijonmarck, H., Chatterjee, U., et al., 2009. Alpha-helix targeting reduces amyloid-beta peptide toxicity. Proc. Natl. Acad. Sci. USA 106 (23), 9191–9196.

Nery, L.R., Eltz, N.S., Hackman, C., Fonseca, R., Altenhofen, S., Guerra, H.N., et al., 2014. Brain intraventricular injection of amyloid-beta in zebrafish embryo impairs cognition and increases tau phosphorylation, effects reversed by lithium. PLoS One 9 (9), e105862.

Nesic, I., Guix, F.X., Vennekens, K., Michaki, V., Van Veldhoven, P.P., Feiguin, F., et al., 2012. Alterations in phosphatidylethanolamine levels affect the generation of Abeta. Aging Cell 11 (1), 63–72.

Neugroschl, J., Wang, S., 2011. Alzheimer's disease: diagnosis and treatment across the spectrum of disease severity. Mt. Sinai J. Med. 78 (4), 596–612.

Neve, R.L., Boyce, F.M., McPhie, D.L., Greenan, J., Oster-Granite, M.L., 1996. Transgenic mice expressing APP-C100 in the brain. Neurobiol. Aging 17 (2), 191–203.

Newman, M., Wilson, L., Camp, E., Verdile, G., Martins, R., Lardelli, M., 2010. A zebrafish melanophore model of amyloid beta toxicity. Zebrafish 7 (2), 155–159.

Newman, M., Wilson, L., Verdile, G., Lim, A., Khan, I., Moussavi Nik, S.H., et al., 2014. Differential, dominant activation and inhibition of Notch signalling and APP cleavage by truncations of PSEN1 in human disease. Hum. Mol. Genet. 23 (3), 602–617, (Research Support, Non-US Gov't Research Support, US Gov't, Non-PHS).

Newton, B.I., Cooper, R.C., Gilbert, J.A., Johnson, R.B., Zardiackas, L.D., 2004. The ovariectomized sheep as a model for human bone loss. J. Comp. Pathol. 130 (4), 323–326.

Ng, C.F., Ko, C.H., Koon, C.M., Xian, J.W., Leung, P.C., Fung, K.P., et al., 2013. The aqueous extract of rhizome of Gastrodia elata protected Drosophila and PC12 cells against beta-amyloid-induced neurotoxicity. Evid. Based Complement. Alternat. Med. 2013, 516741.

Nilsson, P., Saito, T., Saido, T.C., 2014. New mouse model of Alzheimer's. ACS Chem. Neurosci. 5 (7), 499–502.

Nippak, P.M., Mendelson, J., Muggenburg, B., Milgram, N.W., 2007. Enhanced spatial ability in aged dogs following dietary and behavioural enrichment. Neurobiol. Learn. Mem. 87 (4), 610–623.

Nishimura, I., Yang, Y., Lu, B., 2004. PAR-1 kinase plays an initiator role in a temporally ordered phosphorylation process that confers tau toxicity in Drosophila. Cell 116 (5), 671–682.

Nornes, S., Groth, C., Camp, E., Ey, P., Lardelli, M., 2003. Developmental control of Presenilin1 expression, endoproteolysis, and interaction in zebrafish embryos. Exp. Cell Res. 289 (1), 124–132.

Nornes, S., Newman, M., Verdile, G., Wells, S., Stoick-Cooper, C.L., Tucker, B., et al., 2008. Interference with splicing of Presenilin transcripts has potent dominant negative effects on Presenilin activity. Hum. Mol. Genet. 17 (3), 402–412, (Research Support, NIH, Extramural. Research Support, Non-US Gov't. Research Support, U.S. Gov't, Non-PHS).

Nornes, S., Newman, M., Wells, S., Verdile, G., Martins, R.N., Lardelli, M., 2009. Independent and cooperative action of Psen2 with Psen1 in zebrafish embryos. Exp. Cell Res. 315 (16), 2791–2801.

Nunomura, A., Perry, G., Aliev, G., Hirai, K., Takeda, A., Balraj, E.K., et al., 2001. Oxidative damage is the earliest event in Alzheimer disease. J. Neuropathol. Exp. Neurol. 60 (8), 759–767.

Oakley, H., Cole, S.L., Logan, S., Maus, E., Shao, P., Craft, J., et al., 2006. Intraneuronal beta-amyloid aggregates, neurodegeneration, and neuron loss in transgenic mice with five familial Alzheimer's disease mutations: potential factors in amyloid plaque formation. J. Neurosci. 26 (40), 10129–10140.

Oberstein, T.J., Spitzer, P., Klafki, H.W., Linning, P., Neff, F., Knolker, H.J., et al., 2015. Astrocytes and microglia but not neurons preferentially generate N-terminally truncated Abeta peptides. Neurobiol. Dis. 73, 24–35.

Oddo, S., Caccamo, A., Shepherd, J.D., Murphy, M.P., Golde, T.E., Kayed, R., et al., 2003. Triple-transgenic model of Alzheimer's disease with plaques and tangles: intracellular Abeta and synaptic dysfunction. Neuron 39 (3), 409–421, (Comparative Study. Research Support, Non-US Gov't. Research Support, US Gov't, PHS).

Oddo, S., Billings, L., Kesslak, J.P., Cribbs, D.H., LaFerla, F.M., 2004. Abeta immunotherapy leads to clearance of early, but not late, hyperphosphorylated tau aggregates via the proteasome. Neuron 43 (3), 321–332.

Oh, H., Madison, C., Baker, S., Rabinovici, G., Jagust, W., 2016. Dynamic relationships between age, amyloid-beta deposition, and glucose metabolism link to the regional vulnerability to Alzheimer's disease. Brain 139, 2275–2289.

O'Hare, E., Scopes, D.I., Kim, E.M., Palmer, P., Spanswick, D., McMahon, B., et al., 2014. Novel 5-aryloxypyrimidine SEN1576 as a candidate for the treatment of Alzheimer's disease. Int. J. Neuropsychopharmacol. 17 (1), 117–126.

Ohno, M., Sametsky, E.A., Younkin, L.H., Oakley, H., Younkin, S.G., Citron, M., et al., 2004. BACE1 deficiency rescues memory deficits and cholinergic dysfunction in a mouse model of Alzheimer's disease. Neuron 41 (1), 27–33.

Ohno, M., Chang, L., Tseng, W., Oakley, H., Citron, M., Klein, W.L., et al., 2006. Temporal memory deficits in Alzheimer's mouse models: rescue by genetic deletion of BACE1. Eur. J. Neurosci. 23 (1), 251–260.

Okawa, Y., Ishiguro, K., Fujita, S.C., 2003. Stress-induced hyperphosphorylation of tau in the mouse brain. FEBS Lett. 535 (1–3), 183–189.

Oliveira, L.T., Leon, G.V., Provance, Jr., D.W., de Mello, F.G., Sorenson, M.M., Salerno, V.P., 2015. Exogenous beta-amyloid peptide interferes with GLUT4 localization in neurons. Brain Res. 1615, 42–50.

Opii, W.O., Joshi, G., Head, E., Milgram, N.W., Muggenburg, B.A., Klein, J.B., et al., 2008. Proteomic identification of brain proteins in the canine model of human aging following a long-term treatment with antioxidants and a program of behavioral enrichment: relevance to Alzheimer's disease. Neurobiol. Aging 29 (1), 51–70.

Oresic, M., Hyotylainen, T., Herukka, S.K., Sysi-Aho, M., Mattila, I., Seppanan-Laakso, T., et al., 2011. Metabolome in progression to Alzheimer's disease. Transl. Psychiatry 1, e57, (Comparative Study. Research Support, Non-US Gov't).

Owen, E.H., Logue, S.F., Rasmussen, D.L., Wehner, J.M., 1997. Assessment of learning by the Morris water task and fear conditioning in inbred mouse strains and F1 hybrids: implications of genetic back-

ground for single gene mutations and quantitative trait loci analyses. Neuroscience 80 (4), 1087–1099.

Oz, M., Lorke, D.E., Petroianu, G.A., 2009. Methylene blue and Alzheimer's disease. Biochem. Pharmacol. 78 (8), 927–932.

Paidi, R.K., Nthenge-Ngumbau, D.N., Singh, R., Kankanala, T., Mehta, H., Mohanakumar, K.P., 2015. Mitochondrial deficits accompany cognitive decline following single bilateral intracerebroventricular streptozotocin. Curr. Alzheimer Res. 12 (8), 785–795.

Papanikolopoulou, K., Skoulakis, E.M., 2015. Temporally distinct phosphorylations differentiate Tau-dependent learning deficits and premature mortality in *Drosophila*. Hum. Mol. Genet. 24 (7), 2065–2077.

Paquet, D., Bhat, R., Sydow, A., Mandelkow, E.M., Berg, S., Hellberg, S., et al., 2009. A zebrafish model of tauopathy allows in vivo imaging of neuronal cell death and drug evaluation. J. Clin. Invest. 119 (5), 1382–1395.

Park, S.H., Lee, S., Hong, Y.K., Hwang, S., Lee, J.H., Bang, S.M., et al., 2013. Suppressive effects of SuHeXiang Wan on amyloid-beta42-induced extracellular signal-regulated kinase hyperactivation and glial cell proliferation in a transgenic *Drosophila* model of Alzheimer's disease. Biol. Pharm. Bull. 36 (3), 390–398.

Park, S.J., Kim, Y.H., Nam, G.H., Choe, S.H., Lee, S.R., Kim, S.U., et al., 2015. Quantitative expression analysis of APP pathway and tau phosphorylation-related genes in the ICV STZ-induced non-human primate model of sporadic Alzheimer's disease. Int. J. Mol. Sci. 16 (2), 2386–2402.

Parker, R.J., Auld, V.J., 2006. Roles of glia in the *Drosophila* nervous system. Semin. Cell Dev. Biol. 17 (1), 66–77.

Patronek, G.J., Waters, D.J., Glickman, L.T., 1997. Comparative longevity of pet dogs and humans: implications for gerontology research. J. Gerontol. A Biol. Sci. Med. Sci. 52 (3), B171–B178.

Pedrini, S., Thomas, C., Brautigam, H., Schmeidler, J., Ho, L., Fraser, P., et al., 2009. Dietary composition modulates brain mass and solubilizable Abeta levels in a mouse model of aggressive Alzheimer's amyloid pathology. Mol. Neurodegener. 4, 40.

Peng, D., Pan, X., Cui, J., Ren, Y., Zhang, J., 2013. Hyperphosphorylation of tau protein in hippocampus of central insulin-resistant rats is associated with cognitive impairment. Cell Physiol. Biochem. 32 (5), 1417–1425.

Peng, F., Zhao, Y., Huang, X., Chen, C., Sun, L., Zhuang, L., et al., 2015. Loss of Polo ameliorates APP-induced Alzheimer's disease-like symptoms in *Drosophila*. Sci. Rep. 5, 16816.

PerezTur, J., Froelich, S., Prihar, G., Crook, R., Baker, M., Duff, K., et al., 1995. A mutation in Alzheimer's disease destroying a splice acceptor site in the presenilin-1 gene. Neuroreport 7 (1), 297–301.

Petrides, M., Iversen, S.D., 1979. Restricted posterior parietal lesions in the rhesus monkey and performance on visuospatial tasks. Brain Res. 161 (1), 63–77.

Petrov, D., Pedros, I., Artiach, G., Sureda, F.X., Barroso, E., Pallas, M., et al., 2015. High-fat diet-induced deregulation of hippocampal insulin signaling and mitochondrial homeostasis deficiencies contribute to Alzheimer disease pathology in rodents. Biochim. Biophys. Acta 1852 (9), 1687–1699.

Piaceri, I., Nacmias, B., Sorbi, S., 2013. Genetics of familial and sporadic Alzheimer's disease. Front. Biosci. (Elite Ed) 5, 167–177.

Piedrahita, J.A., Zhang, S.H., Hagaman, J.R., Oliver, P.M., Maeda, N., 1992. Generation of mice carrying a mutant apolipoprotein E gene inactivated by gene targeting in embryonic stem cells. Proc. Natl. Acad. Sci. USA 89 (10), 4471–4475.

Pimplikar, S.W., Nixon, R.A., Robakis, N.K., Shen, J., Tsai, L.H., 2010. Amyloid-independent mechanisms in Alzheimer's disease pathogenesis. J. Neurosci. 30 (45), 14946–14954.

Ping, Y., Hahm, E.T., Waro, G., Song, Q., Vo-Ba, D.A., Licursi, A., et al., 2015. Linking abeta42-induced hyperexcitability to neurodegeneration, learning and motor deficits, and a shorter lifespan in an Alzheimer's model. PLoS Genet. 11 (3), e1005025.

Pir, G.J., Choudhary, B., Mandelkow, E., Mandelkow, E.M., 2016. Tau mutant A152T, a risk factor for FTD/PSP, induces neuronal dysfunction and reduced lifespan independently of aggregation in a *C. elegans* Tauopathy model. Mol. Neurodegener. 11, 33.

Pistell, P.J., Morrison, C.D., Gupta, S., Knight, A.G., Keller, J.N., Ingram, D.K., et al., 2010. Cognitive impairment following high fat diet consumption is associated with brain inflammation. J. Neuroimmunol. 219 (1–2), 25–32.

Plaschke, K., Kopitz, J., 2015. In vitro streptozotocin model for modeling Alzheimer-like changes: effect on amyloid precursor protein secretases and glycogen synthase kinase-3. J. Neural Transm. (Vienna) 122 (4), 551–557.

Plaschke, K., Kopitz, J., Siegelin, M., Schliebs, R., Salkovic-Petrisic, M., Riederer, P., et al., 2010. Insulin-resistant brain state after intracerebroventricular streptozotocin injection exacerbates Alzheimer-like changes in Tg2576 AbetaPP-overexpressing mice. J. Alzheimers Dis. 19 (2), 691–704.

Poduri, A., Gearing, M., Rebeck, G.W., Mirra, S.S., Tigges, J., Hyman, B.T., 1994. Apolipoprotein E4 and beta amyloid in senile plaques and cerebral blood vessels of aged rhesus monkeys. Am. J. Pathol. 144 (6), 1183–1187.

Pohanka, M., Zemek, F., Bandouchova, H., Pikula, J., 2012. Toxicological scoring of Alzheimer's disease drug huperzine in a guinea pig model. Toxicol. Mech. Methods 22 (3), 231–235.

Portelius, E., Appelkvist, P., Stromberg, K., Hoglund, K., 2014. Characterization of the effect of a novel gamma-secretase modulator on Abeta: a clinically translatable model. Curr. Pharm. Des. 20 (15), 2484–2490.

Postuma, R.B., Martins, R.N., Cappai, R., Beyreuther, K., Masters, C.L., Strickland, D.K., et al., 1998. Effects of the amyloid protein precursor of Alzheimer's disease and other ligands of the LDL receptor-related protein on neurite outgrowth from sympathetic neurons in culture. FEBS Lett. 428 (1–2), 13–16.

Potter, C.J., Tasic, B., Russler, E.V., Liang, L., Luo, L., 2010. The Q system: a repressible binary system for transgene expression, lineage tracing, and mosaic analysis. Cell 141 (3), 536–548.

Povellato, G., Tuxworth, R.I., Hanger, D.P., Tear, G., 2014. Modification of the *Drosophila* model of in vivo Tau toxicity reveals protective phosphorylation by GSK3beta. Biol. Open 3 (1), 1–11.

Pozueta, J., Lefort, R., Shelanski, M., 2013. Synaptic changes in Alzheimer's disease and its models. Neuroscience 251, 51–65.

Prakash, A., Dhaliwal, G.K., Kumar, P., Majeed, A.B., 2016. Brain biometals and Alzheimer's disease—boon or bane? Int. J. Neurosci. 127 (2), 99–108.

Pratim Bose, P., Chatterjee, U., Nerelius, C., Govender, T., Norstrom, T., Gogoll, A., et al., 2009. Poly-*N*-methylated amyloid beta-peptide (Abeta) C-terminal fragments reduce Abeta toxicity in vitro and in *Drosophila melanogaster*. J. Med. Chem. 52 (24), 8002–8009.

Presty, S.K., Bachevalier, J., Walker, L.C., Struble, R.G., Price, D.L., Mishkin, M., et al., 1987. Age differences in recognition memory of the rhesus monkey (*Macaca mulatt*a). Neurobiol. Aging 8 (5), 435–440.

Price, D.L., Martin, L.J., Sisodia, S.S., Wagster, M.V., Koo, E.H., Walker, L.C., et al., 1991. Aged non-human primates: an animal model of age-associated neurodegenerative disease. Brain Pathol. 1 (4), 287–296.

Prihar, G., Fuldner, R.A., PerezTur, J., Lincoln, S., Duff, K., Crook, R., et al., 1996. Structure and alternative splicing of the presenilin-2 gene. Neuroreport 7 (10), 1680–1684.

Pujic, Z., Omori, Y., Tsujikawa, M., Thisse, B., Thisse, C., Malicki, J., 2006. Reverse genetic analysis of neurogenesis in the zebrafish retina. Dev. Biol. 293 (2), 330–347.

Pype, S., Moechars, D., Dillen, L., Mercken, M., 2003. Characterization of amyloid beta peptides from brain extracts of transgenic mice overexpressing the London mutant of human amyloid precursor protein. J. Neurochem. 84 (3), 602–609.

Rabinovici, G.D., Miller, B.L., 2010. Frontotemporal lobar degeneration. CNS Drugs 24 (5), 375–398.

Rapp, P.R., Amaral, D.G., 1989. Evidence for task-dependent memory dysfunction in the aged monkey. J. Neurosci. 9 (10), 3568–3576.

Raymond, P.A., Barthel, L.K., Bernardos, R.L., Perkowski, J.J., 2006. Molecular characterization of retinal stem cells and their niches in adult zebrafish. BMC Dev. Biol. 6, 36.

Reaume, A.G., Howland, D.S., Trusko, S.P., Savage, M.J., Lang, D.M., Greenberg, B.D., et al., 1996. Enhanced amyloidogenic processing of the beta-amyloid precursor protein in gene-targeted mice bearing the Swedish familial Alzheimer's disease mutations and a "humanized" Abeta sequence. J. Biol. Chem. 271 (38), 23380–23388.

Reddy, A.B., O'Neill, J.S., 2010. Healthy clocks, healthy body, healthy mind. Trends Cell Biol. 20 (1), 36–44.

Refolo, L.M., Malester, B., LaFrancois, J., Bryant-Thomas, T., Wang, R., Tint, G.S., et al., 2000. Hypercholesterolemia accelerates the Alzheimer's amyloid pathology in a transgenic mouse model. Neurobiol. Dis. 7 (4), 321–331.

Refolo, L.M., Pappolla, M.A., LaFrancois, J., Malester, B., Schmidt, S.D., Thomas-Bryant, T., et al., 2001. A cholesterol-lowering drug reduces beta-amyloid pathology in a transgenic mouse model of Alzheimer's disease. Neurobiol. Dis. 8 (5), 890–899.

Reiman, E.M., Caselli, R.J., Yun, L.S., Chen, K., Bandy, D., Minoshima, S., et al., 1996. Preclinical evidence of Alzheimer's disease in persons homozygous for the epsilon 4 allele for apolipoprotein E. N. Engl. J. Med. 334 (12), 752–758.

Reiman, E.M., Chen, K., Alexander, G.E., Caselli, R.J., Bandy, D., Osborne, D., et al., 2004. Functional brain abnormalities in young adults at genetic risk for late-onset Alzheimer's dementia. Proc. Natl. Acad. Sci. USA 101 (1), 284–289.

Rennekamp, A.J., Peterson, R.T., 2015. 15 Years of zebrafish chemical screening. Curr. Opin. Chem. Biol. 24, 58–70.

Richards, J.G., Higgins, G.A., Ouagazzal, A.M., Ozmen, L., Kew, J.N., Bohrmann, B., et al., 2003. PS2APP transgenic mice, coexpressing hPS2mut and hAPPswe, show age-related cognitive deficits associated with discrete brain amyloid deposition and inflammation. J. Neurosci. 23 (26), 8989–9003.

Riemensperger, T., Pech, U., Dipt, S., Fiala, A., 2012. Optical calcium imaging in the nervous system of Drosophila melanogaster. Biochim. Biophys. Acta 1820 (8), 1169–1178.

Rival, T., Page, R.M., Chandraratna, D.S., Sendall, T.J., Ryder, E., Liu, B., et al., 2009. Fenton chemistry and oxidative stress mediate the toxicity of the beta-amyloid peptide in a Drosophila model of Alzheimer's disease. Eur. J. Neurosci. 29 (7), 1335–1347.

Ro, H., Soun, K., Kim, E.J., Rhee, M., 2004. Novel vector systems optimized for injecting in vitro-synthesized mRNA into zebrafish embryos. Mol. Cells 17 (2), 373–376.

Robakis, N.K., 2011. Mechanisms of AD neurodegeneration may be independent of Abeta and its derivatives. Neurobiol. Aging 32 (3), 372–379.

Roberson, E.D., Scearce-Levie, K., Palop, J.J., Yan, F., Cheng, I.H., Wu, T., et al., 2007. Reducing endogenous tau ameliorates amyloid beta-induced deficits in an Alzheimer's disease mouse model. Science 316 (5825), 750–754.

Roberts, R.O., Knopman, D.S., Cha, R.H., Mielke, M.M., Pankratz, V.S., Boeve, B.F., et al., 2014. Diabetes and elevated hemoglobin A1c levels are associated with brain hypometabolism but not amyloid accumulation. J. Nucl. Med. 55 (5), 759–764.

Rodin, D.I., Schwarzman, A.L., Sarantseva, S.V., 2015. Expression of human amyloid precursor protein in Drosophila melanogaster nerve cells causes a decrease in presynaptic gene mRNA levels. Genet. Mol. Res. 14 (3), 9225–9232.

Rodrigues, L., Dutra, M.F., Ilha, J., Biasibetti, R., Quincozes-Santos, A., Leite, M.C., et al., 2010. Treadmill training restores spatial cognitive deficits and neurochemical alterations in the hippocampus of rats submitted to an intracerebroventricular administration of streptozotocin. J. Neural Transm. (Vienna) 117 (11), 1295–1305.

Rosen, R.F., Farberg, A.S., Gearing, M., Dooyema, J., Long, P.M., Anderson, D.C., et al., 2008. Tauopathy with paired helical filaments in an aged chimpanzee. J. Comp. Neurol. 509 (3), 259–270.

Rossi, A., Kontarakis, Z., Gerri, C., Nolte, H., Holper, S., Kruger, M., et al., 2015. Genetic compensation induced by deleterious mutations but not gene knockdowns. Nature 524 (7564), 230–233.

Rozmahel, R., Huang, J., Chen, F., Liang, Y., Nguyen, V., Ikeda, M., et al., 2002. Normal brain development in PS1 hypomorphic mice with markedly reduced gamma-secretase cleavage of betaAPP. Neurobiol. Aging 23 (2), 187–194.

Rubin, G.M., Spradling, A.C., 1982. Genetic transformation of Drosophila with transposable element vectors. Science 218 (4570), 348–353.

Ruiz-Opazo, N., Kosik, K.S., Lopez, L.V., Bagamasbad, P., Ponce, L.R., Herrera, V.L., 2004. Attenuated hippocampus-dependent learning and memory decline in transgenic TgAPPswe Fischer-344 rats. Mol. Med. 10 (1–6), 36–44.

Ryder, E., Russell, S., 2003. Transposable elements as tools for genomics and genetics in Drosophila. Brief Funct. Genomic Proteomic 2 (1), 57–71.

Saito, T., Matsuba, Y., Mihira, N., Takano, J., Nilsson, P., Itohara, S., et al., 2014. Single App knock-in mouse models of Alzheimer's disease. Nat. Neurosci. 17 (5), 661–663.

Sajan, M., Hansen, B., Ivey, 3rd, R., Sajan, J., Ari, C., Song, S., et al., 2016. Brain insulin signaling is increased in insulin-resistant states and decreases in FOXOs and PGC-1alpha and increases in Abeta1-40/42 and phospho-Tau may Abet Alzheimer development. Diabetes 65 (7), 1892–1903.

Salkovic-Petrisic, M., Hoyer, S., 2007. Central insulin resistance as a trigger for sporadic Alzheimer-like pathology: an experimental approach. J. Neural Transm. Suppl. (72), 217–233.

Salkovic-Petrisic, M., Tribl, F., Schmidt, M., Hoyer, S., Riederer, P., 2006. Alzheimer-like changes in protein kinase B and glycogen synthase kinase-3 in rat frontal cortex and hippocampus after damage to the insulin signalling pathway. J. Neurochem. 96 (4), 1005–1015.

Salkovic-Petrisic, M., Osmanovic-Barilar, J., Bruckner, M.K., Hoyer, S., Arendt, T., Riederer, P., 2011. Cerebral amyloid angiopathy in streptozotocin rat model of sporadic Alzheimer's disease: a long-term follow up study. J. Neural Transm. (Vienna) 118 (5), 765–772.

Salkovic-Petrisic, M., Knezovic, A., Hoyer, S., Riederer, P., 2013. What have we learned from the streptozotocin-induced animal model of sporadic Alzheimer's disease, about the therapeutic strategies in Alzheimer's research. J. Neural Transm. (Vienna) 120 (1), 233–252.

Samartgis, J.R., Schachte, L., Hazi, A., Crowe, S.F., 2012. Memantine facilitates memory consolidation and reconsolidation in the day-old chick. Neurobiol. Learn. Mem. 97 (4), 380–385.

Sander, J.D., Cade, L., Khayter, C., Reyon, D., Peterson, R.T., Joung, J.K., et al., 2011. Targeted gene disruption in somatic zebrafish cells using engineered TALENs. Nat. Biotechnol. 29 (8), 697–698.

Sanokawa-Akakura, R., Cao, W., Allan, K., Patel, K., Ganesh, A., Heiman, G., et al., 2010. Control of Alzheimer's amyloid beta toxicity by the high molecular weight immunophilin FKBP52 and copper homeostasis in Drosophila. PLoS One 5 (1), e8626.

Sarantseva, S., Timoshenko, S., Bolshakova, O., Karaseva, E., Rodin, D., Schwarzman, A.L., et al., 2009. Apolipoprotein E-mimetics inhibit neurodegeneration and restore cognitive functions in a transgenic Drosophila model of Alzheimer's disease. PLoS One 4 (12), e8191.

Sarasa, M., Pesini, P., 2009. Natural non-trasgenic animal models for research in Alzheimer's disease. Curr. Alzheimer Res. 6 (2), 171–178.

Sato, N., Hori, O., Yamaguchi, A., Lambert, J.C., Chartier-Harlin, M.C., Robinson, P.A., et al., 1999. A novel presenilin-2 splice variant in human Alzheimer's disease brain tissue. J. Neurochem. 72 (6), 2498–2505.

Sato, N., Imaizumi, K., Manabe, T., Taniguchi, M., Hitomi, J., Kataya-ma, T., et al., 2001. Increased production of beta-amyloid and vul-nerability to endoplasmic reticulum stress by an aberrant spliced form of presenilin 2. J. Biol. Chem. 276 (3), 2108–2114.

Saunders, A.M., Strittmatter, W.J., Schmechel, D., George-Hyslop, P.H., Pericak-Vance, M.A., Joo, S.H., et al., 1993. Association of apolipo-protein E allele epsilon 4 with late-onset familial and sporadic Al-zheimer's disease. Neurology 43 (8), 1467–1472.

Schauwecker, P.E., 2002. Modulation of cell death by mouse genotype: differential vulnerability to excitatory amino acid-induced lesions. Exp. Neurol. 178 (2), 219–235.

Scheer, N., Campos-Ortega, J.A., 1999. Use of the Gal4-UAS technique for targeted gene expression in the zebrafish. Mech. Dev. 80 (2), 153–158.

Schmechel, D.E., Saunders, A.M., Strittmatter, W.J., Crain, B.J., Hulette, C.M., Joo, S.H., et al., 1993. Increased amyloid beta-peptide deposi-tion in cerebral cortex as a consequence of apolipoprotein E geno-type in late-onset Alzheimer disease. Proc. Natl. Acad. Sci. USA 90 (20), 9649–9653.

Schmid, B., Haass, C., 2013. Genomic editing opens new avenues for zebrafish as a model for neurodegeneration. J. Neurochem. 127 (4), 461–470.

Schneider, A., Biernat, J., von Bergen, M., Mandelkow, E., Mandelkow, E.M., 1999. Phosphorylation that detaches tau protein from micro-tubules (Ser262, Ser214) also protects it against aggregation into Al-zheimer paired helical filaments. Biochemistry 38 (12), 3549–3558.

Schon, E.A., Area-Gomez, E., 2013. Mitochondria-associated ER mem-branes in Alzheimer disease. Mol. Cell Neurosci. 55, 26–36.

Schultz, C., Hubbard, G.B., Rub, U., Braak, E., Braak, H., 2000. Age-re-lated progression of tau pathology in brains of baboons. Neurobiol. Aging 21 (6), 905–912.

Selfridge, J.E., E, L., Lu, J., Swerdlow, R.H., 2013. Role of mitochondrial homeostasis and dynamics in Alzheimer's disease. Neurobiol. Dis. 51, 3–12.

Selkoe, D.J., Bell, D.S., Podlisny, M.B., Price, D.L., Cork, L.C., 1987. Conservation of brain amyloid proteins in aged mammals and hu-mans with Alzheimer's disease. Science 235 (4791), 873–877.

Sempou, E., Biasini, E., Pinzon-Olejua, A., Harris, D.A., Malaga-Trillo, E., 2016. Activation of zebrafish Src family kinases by the prion pro-tein is an amyloid-beta-sensitive signal that prevents the endocyto-sis and degradation of E-cadherin/beta-catenin complexes in vivo. Mol. Neurodegener. 11, 18.

Sergeant, N., Bretteville, A., Hamdane, M., Caillet-Boudin, M.L., Grog-net, P., Bombois, S., et al., 2008. Biochemistry of Tau in Alzheimer's disease and related neurological disorders. Expert Rev. Proteomics 5 (2), 207–224.

Serrano-Pozo, A., Mielke, M.L., Gomez-Isla, T., Betensky, R.A., Grow-don, J.H., Frosch, M.P., et al., 2011. Reactive glia not only associates with plaques but also parallels tangles in Alzheimer's disease. Am. J. Pathol. 179 (3), 1373–1384.

Shakes, L.A., Malcolm, T.L., Allen, K.L., De, S., Harewood, K.R., Chat-terjee, P.K., 2008. Context dependent function of APPb enhancer identified using enhancer trap-containing BACs as transgenes in zebrafish. Nucleic Acids Res. 36 (19), 6237–6248.

Sharman, M.J., Fernandez, M.L., Zern, T.L., Torres-Gonzalez, M., Krae-mer, W.J., Volek, J.S., 2008. Replacing dietary carbohydrate with protein and fat decreases the concentrations of small LDL and the inflammatory response induced by atherogenic diets in the guinea pig. J. Nutr. Biochem. 19 (11), 732–738.

Sharman, M.J., Morici, M., Hone, E., Berger, T., Taddei, K., Martins, I.J., et al., 2010. APOE genotype results in differential effects on the pe-ripheral clearance of amyloid-beta42 in APOE knock-in and knock-out mice. J. Alzheimers Dis. 21 (2), 403–409.

Sharman, M.J., Moussavi Nik, S.H., Chen, M.M., Ong, D., Wijaya, L., Laws, S.M., et al., 2013. The guinea pig as a model for sporadic Alzheimer's disease (AD): The impact of cholesterol intake on ex-pression of AD-related genes. PLoS One 8 (6), e66235.

Shen, J., Kelleher, 3rd., R.J., 2007. The presenilin hypothesis of Alzheim-er's disease: evidence for a loss-of-function pathogenic mechanism. Proc. Natl. Acad. Sci. USA 104 (2), 403–409.

Shen, J., Bronson, R.T., Chen, D.F., Xia, W., Selkoe, D.J., Tonegawa, S., 1997. Skeletal and CNS defects in Presenilin-1-deficient mice. Cell 89 (4), 629–639.

Sherrington, R., Froelich, S., Sorbi, S., Campion, D., Chi, H., Rogaeva, E.A., et al., 1996. Alzheimer's disease associated with mutations in presenilin 2 is rare and variably penetrant. Hum. Mol. Genet. 5 (7), 985–988.

Shie, F.S., Jin, L.W., Cook, D.G., Leverenz, J.B., LeBoeuf, R.C., 2002. Diet-induced hypercholesterolemia enhances brain A beta accumu-lation in transgenic mice. Neuroreport 13 (4), 455–459.

Shingo, A.S., Kanabayashi, T., Murase, T., Kito, S., 2012. Cognitive decline in STZ-3V rats is largely due to dysfunctional insulin sig-nalling through the dentate gyrus. Behav. Brain Research. 229 (2), 378–383.

Shingo, A.S., Kanabayashi, T., Kito, S., Murase, T., 2013. Intracere-broventricular administration of an insulin analogue recov-ers STZ-induced cognitive decline in rats. Behav. Brain Res. 241, 105–111.

Shonesy, B.C., Thiruchelvam, K., Parameshwaran, K., Rahman, E.A., Karuppagounder, S.S., Huggins, K.W., et al., 2012. Central insulin resistance and synaptic dysfunction in intracerebroventricular-streptozotocin injected rodents. Neurobiol. Aging 33 (2), 430.e5–430.e18.

Shulman, J.M., Feany, M.B., 2003. Genetic modifiers of tauopathy in *Drosophila*. Genetics 165 (3), 1233–1242.

Shuttleworth, C.W., Connor, J.A., 2001. Strain-dependent differences in calcium signaling predict excitotoxicity in murine hippocampal neurons. J. Neurosci. 21 (12), 4225–4236.

Singh, C., Mahoney, M., 2011. Personal communication to FlyBase. Available from: http://flybase.org/reports/FBrf0213105.html

Siwak, C.T., Tapp, P.D., Head, E., Zicker, S.C., Murphey, H.L., Mug-genburg, B.A., et al., 2005. Chronic antioxidant and mitochondrial cofactor administration improves discrimination learning in aged but not young dogs. Prog. Neuropsychopharmacol. Biol. Psychia-try 29 (3), 461–469.

Siwak-Tapp, C.T., Head, E., Muggenburg, B.A., Milgram, N.W., Cot-man, C.W., 2008. Region specific neuron loss in the aged canine hippocampus is reduced by enrichment. Neurobiol. Aging 29 (1), 39–50.

Small, S.A., Duff, K., 2008. Linking Abeta and tau in late-onset Al-zheimer's disease: a dual pathway hypothesis. Neuron 60 (4), 534–542.

Small, G.W., Ercoli, L.M., Silverman, D.H., Huang, S.C., Komo, S., Bookheimer, S.Y., et al., 2000. Cerebral metabolic and cognitive de-cline in persons at genetic risk for Alzheimer's disease. Proc. Natl. Acad. Sci. USA 97 (11), 6037–6042.

Smith, A.D., 2010. Why are drug trials in Alzheimer's disease failing? Lancet 376 (9751), 1466.

Smith, M.J., Sharples, R.A., Evin, G., McLean, C.A., Dean, B., Pavey, G., et al., 2004. Expression of truncated presenilin 2 splice variant in Alzheimer's disease, bipolar disorder, and schizophrenia brain cortex. Mol. Brain Res. 127 (1–2), 128–135.

Sobczak, K., Bangel-Ruland, N., Leier, G., Weber, W.M., 2010. Endog-enous transport systems in the *Xenopus laevis* oocyte plasma mem-brane. Methods 51 (1), 183–189.

Sofola, O., Kerr, F., Rogers, I., Killick, R., Augustin, H., Gandy, C., et al., 2010. Inhibition of GSK-3 ameliorates Abeta pathology in an adult-onset *Drosophila* model of Alzheimer's disease. PLoS Genet. 6 (9), e1001087.

Soldano, A., Okray, Z., Janovska, P., Tmejova, K., Reynaud, E., Claeys, A., et al., 2013. The *Drosophila* homologue of the amyloid precursor protein is a conserved modulator of Wnt PCP signaling. PLoS Biol. 11 (5), e1001562.

Song, P., Pimplikar, S.W., 2012. Knockdown of amyloid precursor protein in zebrafish causes defects in motor axon outgrowth. PLoS One 7 (4), e34209.

Sparks, D.L., 2008. The early and ongoing experience with the cholesterol-fed rabbit as a model of Alzheimer's disease: the old, the new and the pilot. J. Alzheimers Dis. 15 (4), 641–656.

Sparks, D.L., Schreurs, B.G., 2003. Trace amounts of copper in water induce beta-amyloid plaques and learning deficits in a rabbit model of Alzheimer's disease. Proc. Natl. Acad. Sci. USA 100 (19), 11065–11069.

Sparks, D.L., Scheff, S.W., Hunsaker, 3rd, J.C., Liu, H., Landers, T., Gross, D.R., 1994. Induction of Alzheimer-like beta-amyloid immunoreactivity in the brains of rabbits with dietary cholesterol. Exp. Neurol. 126 (1), 88–94.

Sparks, D.L., Ziolkowski, C., Lawmaster, T., Martin, T., 2011. Influence of water quality on cholesterol-induced tau pathology: preliminary data. Int. J. Alzheimers Dis. 2011, 987023.

Speretta, E., Jahn, T.R., Tartaglia, G.G., Favrin, G., Barros, T.P., Imarisio, S., et al., 2012. Expression in *Drosophila* of tandem amyloid beta peptides provides insights into links between aggregation and neurotoxicity. J. Biol. Chem. 287 (24), 20748–20754.

Spillantini, M.G., Murrell, J.R., Goedert, M., Farlow, M.R., Klug, A., Ghetti, B., 1998. Mutation in the tau gene in familial multiple system tauopathy with presenile dementia. Proc. Natl. Acad. Sci. USA 95 (13), 7737–7741.

Steen, E., Terry, B.M., Rivera, E.J., Cannon, J.L., Neely, T.R., Tavares, R., et al., 2005. Impaired insulin and insulin-like growth factor expression and signaling mechanisms in Alzheimer's disease—is this type 3 diabetes? J. Alzheimers Dis. 7 (1), 63–80.

Steiner, H., Duff, K., Capell, A., Romig, H., Grim, M.G., Lincoln, S., et al., 1999. A loss of function mutation of presenilin-2 interferes with amyloid beta-peptide production and notch signaling. J. Biol. Chem. 274 (40), 28669–28673.

Steinhilb, M.L., Dias-Santagata, D., Fulga, T.A., Felch, D.L., Feany, M.B., 2007a. Tau phosphorylation sites work in concert to promote neurotoxicity in vivo. Mol Biol. Cell 18 (12), 5060–5068.

Steinhilb, M.L., Dias-Santagata, D., Mulkearns, E.E., Shulman, J.M., Biernat, J., Mandelkow, E.M., et al., 2007b. S/P and T/P phosphorylation is critical for tau neurotoxicity in *Drosophila*. J. Neurosci. Res. 85 (6), 1271–1278.

Stempfle, D., Kanwar, R., Loewer, A., Fortini, M.E., Merdes, G., 2010. In vivo reconstitution of gamma-secretase in *Drosophila* results in substrate specificity. Mol. Cell Biol. 30 (13), 3165–3175.

Stephan, A., Phillips, A.G., 2005. A case for a non-transgenic animal model of Alzheimer's disease. Genes Brain Behav. 4 (3), 157–172.

Stieler, J.T., Bullmann, T., Kohl, F., Toien, O., Bruckner, M.K., Hartig, W., et al., 2011. The physiological link between metabolic rate depression and tau phosphorylation in mammalian hibernation. PLoS One 6 (1), e14530.

Stone, J., 2008. What initiates the formation of senile plaques? The origin of Alzheimer-like dementias in capillary haemorrhages. Med. Hypotheses 71 (3), 347–359.

Stortkuhl, K.F., Fiala, A., 2011. The smell of blue light: a new approach toward understanding an olfactory neuronal network. Front. Neurosci. 5, 72.

Stozicka, Z., Zilka, N., Novak, M., 2007. Risk and protective factors for sporadic Alzheimer's disease. Acta Virol. 51 (4), 205–222.

Stozicka, Z., Zilka, N., Novak, P., Kovacech, B., Bugos, O., Novak, M., 2010. Genetic background modifies neurodegeneration and neuroinflammation driven by misfolded human tau protein in rat model of tauopathy: implication for immunomodulatory approach to Alzheimer's disease. J. Neuroinflammation 7, 64.

Strand, A.D., Aragaki, A.K., Baquet, Z.C., Hodges, A., Cunningham, P., Holmans, P., et al., 2007. Conservation of regional gene expression in mouse and human brain. PLoS Genet. 3 (4), e59.

Strausberg, R.L., Feingold, E.A., Grouse, L.H., Derge, J.G., Klausner, R.D., Collins, F.S., et al., 2002. Generation and initial analysis of more than 15,000 full-length human and mouse cDNA sequences. Proc. Natl. Acad. Sci. USA 99 (26), 16899–16903.

Strodel, B., Lee, J.W., Whittleston, C.S., Wales, D.J., 2010. Transmembrane structures for Alzheimer's Abeta(1-42) oligomers. J. Am. Chem. Soc. 132 (38), 13300–13312.

Studzinski, C.M., Araujo, J.A., Milgram, N.W., 2005. The canine model of human cognitive aging and dementia: pharmacological validity of the model for assessment of human cognitive-enhancing drugs. Prog. Neuropsychopharmacol. Biol. Psychiatry 29 (3), 489–498.

Studzinski, C.M., Christie, L.A., Araujo, J.A., Burnham, W.M., Head, E., Cotman, C.W., et al., 2006. Visuospatial function in the beagle dog: an early marker of cognitive decline in a model of human aging and dementia. Neurobiol. Learn. Mem. 86 (2), 197–204.

Su, B., Wang, X., Drew, K.L., Perry, G., Smith, M.A., Zhu, X., 2008. Physiological regulation of tau phosphorylation during hibernation. J. Neurochem. 105 (6), 2098–2108.

Suh, Y.H., Chong, Y.H., Kim, S.H., Choi, W., Min, K., Jeong, S.J., et al., 1996. Molecular physiology, biochemistry, and pharmacology of Alzheimer's amyloid precursor protein (APP). Ann. NY Acad. Sci. 786, 169–183.

Sundvik, M., Chen, Y.C., Panula, P., 2013. Presenilin1 regulates histamine neuron development and behavior in zebrafish, *Danio rerio*. J. Neurosci. 33 (4), 1589–1597.

Tahirovic, I., Sofic, E., Sapcanin, A., Gavrankapetanovic, I., Bach-Rojecky, L., Salkovic-Petrisic, M., et al., 2007a. Brain antioxidant capacity in rat models of betacytotoxic-induced experimental sporadic Alzheimer's disease and diabetes mellitus. J. Neural Transm. Suppl. (72), 235–240.

Tahirovic, I., Sofic, E., Sapcanin, A., Gavrankapetanovic, I., Bach-Rojecky, L., Salkovic-Petrisic, M., et al., 2007b. Reduced brain antioxidant capacity in rat models of betacytotoxic-induced experimental sporadic Alzheimer's disease and diabetes mellitus. Neurochem. Res. 32 (10), 1709–1717.

Takeda, S., Sato, N., Uchio-Yamada, K., Sawada, K., Kunieda, T., Takeuchi, D., et al., 2010. Diabetes-accelerated memory dysfunction via cerebrovascular inflammation and Abeta deposition in an Alzheimer mouse model with diabetes. Proc. Natl. Acad. Sci. USA 107 (15), 7036–7041.

Takuma, H., Arawaka, S., Mori, H., 2003. Isoforms changes of tau protein during development in various species. Brain Res. Dev. Brain Res. 142 (2), 121–127.

Talbot, K., Wang, H.Y., Kazi, H., Han, L.Y., Bakshi, K.P., Stucky, A., et al., 2012. Demonstrated brain insulin resistance in Alzheimer's disease patients is associated with IGF-1 resistance, IRS-1 dysregulation, and cognitive decline. J. Clin. Invest. 122 (4), 1316–1338.

Tampellini, D., 2015. Synaptic activity and Alzheimer's disease: a critical update. Front. Neurosci. 9, 423.

Tan, L., Schedl, P., Song, H.J., Garza, D., Konsolaki, M., 2008. The Toll—>NFkappaB signaling pathway mediates the neuropathological effects of the human Alzheimer's Abeta42 polypeptide in *Drosophila*. PLoS One 3 (12), e3966.

Tang, Y., Peng, Y., Liu, J., Shi, L., Wang, Y., Long, J., et al., 2015. Early inflammation-associated factors blunt sterol regulatory element-binding proteins-1-mediated lipogenesis in high-fat diet-fed APPSWE/PSEN1dE9 mouse model of Alzheimer's disease. J. Neurochem. 136, 791–803.

Tapp, P.D., Siwak, C.T., Estrada, J., Head, E., Muggenburg, B.A., Cotman, C.W., et al., 2003. Size and reversal learning in the beagle dog as a measure of executive function and inhibitory control in aging. Learn. Mem. 10 (1), 64–73.

Tapp, P.D., Siwak, C.T., Gao, F.Q., Chiou, J.Y., Black, S.E., Head, E., et al., 2004. Frontal lobe volume, function, and beta-amyloid pathology in a canine model of aging. J. Neurosci. 24 (38), 8205–8213.

Tare, M., Modi, R.M., Nainaparampil, J.J., Puli, O.R., Bedi, S., Fernandez-Funez, P., et al., 2011. Activation of JNK signaling mediates amyloid-ss-dependent cell death. PLoS One 6 (9), e24361.

Terwel, D., Prickaerts, J., Meng, F., Jolles, J., 1995. Brain enzyme activities after intracerebroventricular injection of streptozotocin in rats receiving acetyl-L-carnitine. Eur. J. Pharmacol. 287 (1), 65–71.

Teschendorf, D., Link, C.D., 2009. What have worm models told us about the mechanisms of neuronal dysfunction in human neurodegenerative diseases? Mol. Neurodegener. 4, 38.

Tesson, L., Cozzi, J., Menoret, S., Remy, S., Usal, C., Fraichard, A., et al., 2005. Transgenic modifications of the rat genome. Transgenic Res. 14 (5), 531–546.

Texido, L., Martin-Satue, M., Alberdi, E., Solsona, C., Matute, C., 2011. Amyloid beta peptide oligomers directly activate NMDA receptors. Cell Calcium 49 (3), 184–190.

Thambisetty, M., Jeffrey Metter, E., Yang, A., Dolan, H., Marano, C., Zonderman, A.B., et al., 2013. Glucose intolerance, insulin resistance, and pathological features of Alzheimer disease in the Baltimore Longitudinal Study of Aging. JAMA Neurol. 70 (9), 1167–1172.

The Danio rerio sequencing project, 2016. Available from: http://www.sanger.ac.uk/science/data/zebrafish-genome-project.

Tingaud-Sequeira, A., Forgue, J., Andre, M., Babin, P.J., 2006. Epidermal transient down-regulation of retinol-binding protein 4 and mirror expression of apolipoprotein Eb and estrogen receptor 2a during zebrafish fin and scale development. Dev. Dyn. 235 (11), 3071–3079.

Torres-Gonzalez, M., Volek, J.S., Leite, J.O., Fraser, H., Luz Fernandez, M., 2008. Carbohydrate restriction reduces lipids and inflammation and prevents atherosclerosis in Guinea pigs. J. Atheroscler. Thromb. 15 (5), 235–243.

Torroja, L., Packard, M., Gorczyca, M., White, K., Budnik, V., 1999. The *Drosophila* beta-amyloid precursor protein homolog promotes synapse differentiation at the neuromuscular junction. J. Neurosci. 19 (18), 7793–7803.

Tramutola, A., Lanzillotta, C., Perluigi, M., Butterfield, D.A., 2016. Oxidative stress, protein modification and Alzheimer disease. Brain Res. Bull., (pii: S0361-9230(16)30129-0).

Tran, T.N., Kim, S.H., Gallo, C., Amaya, M., Kyees, J., Narayanaswami, V., 2013. Biochemical and biophysical characterization of recombinant rat apolipoprotein E: similarities to human apolipoprotein E3. Arch. Biochem. Biophys. 529, 18–25.

Treusch, S., Hamamichi, S., Goodman, J.L., Matlack, K.E., Chung, C.Y., Baru, V., et al., 2011. Functional links between Abeta toxicity, endocytic trafficking, and Alzheimer's disease risk factors in yeast. Science 334 (6060), 1241–1245.

Trojanowski, J.Q., Lee, V.M., 2005. Pathological tau: a loss of normal function or a gain in toxicity? Nat. Neurosci. 8 (9), 1136–1137.

Tseng, Y.C., Chen, R.D., Lucassen, M., Schmidt, M.M., Dringen, R., Abele, D., et al., 2011. Exploring uncoupling proteins and antioxidant mechanisms under acute cold exposure in brains of fish. PLoS One 6 (3).

Tu, H., Nelson, O., Bezprozvanny, A., Wang, Z., Lee, S.F., Hao, Y.H., et al., 2006. Presenilins form ER Ca^{2+} leak channels, a function disrupted by familial Alzheimer's disease-linked mutations. Cell 126 (5), 981–993, (Research Support, NIH, Extramural. Research Support, Non-US Gov't).

Turner, P.R., O'Connor, K., Tate, W.P., Abraham, W.C., 2003. Roles of amyloid precursor protein and its fragments in regulating neural activity, plasticity and memory. Prog. Neurobiol. 70 (1), 1–32.

Uchida, K., Miyauchi, Y., Nakayama, H., Goto, N., 1990. Amyloid angiopathy with cerebral hemorrhage and senile plaque in aged dogs. Nihon Juigaku Zasshi 52 (3), 605–611.

Ullah, G., Demuro, A., Parker, I., Pearson, J.E., 2015. Analyzing and modeling the kinetics of amyloid beta pores associated with Alzheimer's disease pathology. PLoS One 10 (9), e0137357.

Um, J.W., Nygaard, H.B., Heiss, J.K., Kostylev, M.A., Stagi, M., Vortmeyer, A., et al., 2012. Alzheimer amyloid-beta oligomer bound to postsynaptic prion protein activates Fyn to impair neurons. Nat. Neurosci. 15 (9), 1227–1235.

Umeda, T., Tomiyama, T., Kitajima, E., Idomoto, T., Nomura, S., Lambert, M.P., et al., 2012. Hypercholesterolemia accelerates intraneuronal accumulation of Abeta oligomers resulting in memory impairment in Alzheimer's disease model mice. Life Sci. 91, 1169–1176.

van Bebber, F., Paquet, D., Hruscha, A., Schmid, B., Haass, C., 2010. Methylene blue fails to inhibit Tau and polyglutamine protein dependent toxicity in zebrafish. Neurobiol. Dis. 39 (3), 265–271.

van Groen, T., Kiliaan, A.J., Kadish, I., 2006. Deposition of mouse amyloid beta in human APP/PS1 double and single AD model transgenic mice. Neurobiol. Dis. 23 (3), 653–662.

van Rooijen, E., Santhakumar, K., Logister, I., Voest, E., Schulte-Merker, S., Giles, R., et al., 2011. A zebrafish model for VHL and hypoxia signaling. Methods Cell Biol. 105, 163–190.

Van Someren, E.J., Riemersma-Van Der Lek, R.F., 2007. Live to the rhythm, slave to the rhythm. Sleep Med. Rev. 11 (6), 465–484.

Vandal, M., White, P.J., Tremblay, C., St-Amour, I., Chevrier, G., Emond, V., et al., 2014. Insulin reverses the high-fat diet-induced increase in brain Abeta and improves memory in an animal model of Alzheimer disease. Diabetes 63 (12), 4291–4301.

Vercauteren, F.G., Clerens, S., Roy, L., Hamel, N., Arckens, L., Vandesande, F., et al., 2004. Early dysregulation of hippocampal proteins in transgenic rats with Alzheimer's disease-linked mutations in amyloid precursor protein and presenilin 1. Brain Res. Mol. Brain Res. 132, 241–259.

Verchere, C.B., D'Alessio, D.A., Palmiter, R.D., Weir, G.C., Bonner-Weir, S., Baskin, D.G., et al., 1996. Islet amyloid formation associated with hyperglycemia in transgenic mice with pancreatic beta cell expression of human islet amyloid polypeptide. Proc. Natl. Acad. Sci. USA 93 (8), 3492–3496.

Verdier, J.M., Acquatella, I., Lautier, C., Devau, G., Trouche, S., Lasbleiz, C., et al., 2015. Lessons from the analysis of nonhuman primates for understanding human aging and neurodegenerative diseases. Front. Neurosci. 9, 64.

Verdile, G., Fuller, S.J., Martins, R.N., 2015. The role of type 2 diabetes in neurodegeneration. Neurobiol. Dis. 84, 22–38.

Veth, K.N., Willer, J.R., Collery, R.F., Gray, M.P., Willer, G.B., Wagner, D.S., et al., 2011. Mutations in zebrafish lrp2 result in adult-onset ocular pathogenesis that models myopia and other risk factors for glaucoma. PLoS Genet. 7 (2), e1001310.

Wachowiak, M., Knopfel, T., 2009. Frontiers in neuroscience optical imaging of brain activity in vivo using genetically encoded probes. In: Frostig, R.D. (Ed.), In Vivo Optical Imaging of Brain Function. CRC Press/Taylor & Francis (Taylor & Francis Group, LLC), Boca Raton (FL).

Wacker, J., Ronicke, R., Westermann, M., Wulff, M., Reymann, K.G., Dobson, C.M., et al., 2014. Oligomer-targeting with a conformational antibody fragment promotes toxicity in Abeta-expressing flies. Acta Neuropathol. Commun. 2, 43.

Wang, J.W., Imai, Y., Lu, B., 2007. Activation of PAR-1 kinase and stimulation of tau phosphorylation by diverse signals require the tumor suppressor protein LKB1. J. Neurosci. 27 (3), 574–581.

Wang, L.F., Zhang, R., Xie, X., 2009. Development of a high-throughput assay for screening of gamma-secretase inhibitor with endogenous human, mouse or *Drosophila* gamma-secretase. Molecules 14 (9), 3589–3599.

Wang, X., Zheng, W., Xie, J.W., Wang, T., Wang, S.L., Teng, W.P., et al., 2010. Insulin deficiency exacerbates cerebral amyloidosis and behavioral deficits in an Alzheimer transgenic mouse model. Mol. Neurodegener. 5, 46.

Wang, Z., Yang, L., Zheng, H., 2011. Role of APP and Abeta in synaptic physiology. Curr. Alzheimer Res. 9, 217–226.

Wang, J.Q., Yin, J., Song, Y.F., Zhang, L., Ren, Y.X., Wang, D.G., et al., 2014. Brain aging and AD-like pathology in streptozotocin-induced diabetic rats. J. Diabetes Res. 2014, 796840.

Wang, Y., Wang, Y., Sui, Y., Yu, H., Shen, X., Chen, S., et al., 2015. The combination of aricept with a traditional Chinese medicine formula, smart soup, may be a novel way to treat Alzheimer's disease. J. Alzheimers Dis. 45 (4), 1185–1195.

Wangler, M.F., Yamamoto, S., 2015. Fruit flies in biomedical research. Genetics 199 (3), 639–653.

Webster, S.J., Bachstetter, A.D., Nelson, P.T., Schmitt, F.A., Van Eldik, L.J., 2014. Using mice to model Alzheimer's dementia: an overview of the clinical disease and the preclinical behavioral changes in 10 mouse models. Front. Genet. 5, 88.

Wen, P.H., Shao, X., Shao, Z., Hof, P.R., Wisniewski, T., Kelley, K., et al., 2002. Overexpression of wild type but not an FAD mutant presenilin-1 promotes neurogenesis in the hippocampus of adult mice. Neurobiol. Dis. 10 (1), 8–19.

Wentzell, J., Kretzschmar, D., 2010. Alzheimer's disease and tauopathy studies in flies and worms. Neurobiol. Dis. 40 (1), 21–28.

Wentzell, J.S., Bolkan, B.J., Carmine-Simmen, K., Swanson, T.L., Musashe, D.T., Kretzschmar, D., 2012. Amyloid precursor proteins are protective in *Drosophila* models of progressive neurodegeneration. Neurobiol. Dis. 46 (1), 78–87.

Westermark, P., 1972. Quantitative studies on amyloid in the islets of Langerhans. Ups. J. Med. Sci. 77 (2), 91–94.

White, J.G., Southgate, E., Thomson, J.N., Brenner, S., 1986. The structure of the nervous system of the nematode *C. elegans*. Philos. Trans. R. Soc. Lond. B Biol. Sci. 314, 1–340.

Wienholds, E., Schulte-Merker, S., Walderich, B., Plasterk, R.H.A., 2002. Target-selected inactivation of the zebrafish rag1 gene. Science 297 (5578), 99–102.

Willette, A.A., Johnson, S.C., Birdsill, A.C., Sager, M.A., Christian, B., Baker, L.D., et al., 2015. Insulin resistance predicts brain amyloid deposition in late middle-aged adults. Alzheimers Dement. 11 (5), 504.e1–510.e1.

Wilson, L., Lardelli, M., 2013. The development of an in vivo gamma-secretase assay using zebrafish embryos. [Research Support, Non-U.S. Gov't]. J. Alzheimers Dis. 36 (3), 521–534.

Winocur, G., Greenwood, C.E., 2005. Studies of the effects of high fat diets on cognitive function in a rat model. Neurobiol. Aging 26 (Suppl. 1), 46–49.

Winocur, G., Greenwood, C.E., Piroli, G.G., Grillo, C.A., Reznikov, L.R., Reagan, L.P., et al., 2005. Memory impairment in obese Zucker rats: an investigation of cognitive function in an animal model of insulin resistance and obesity. Behav. Neurosci. 119 (5), 1389–1395.

Wittmann, C.W., Wszolek, M.F., Shulman, J.M., Salvaterra, P.M., Lewis, J., Hutton, M., et al., 2001. Tauopathy in *Drosophila*: neurodegeneration without neurofibrillary tangles. Science 293 (5530), 711–714.

Wolfe, M.S., 2007. When loss is gain: reduced presenilin proteolytic function leads to increased Abeta42/Abeta40. Talking Point on the role of presenilin mutations in Alzheimer disease. EMBO Rep. 8 (2), 136–140.

Wolfe, M.S., 2012. gamma-Secretase inhibitors and modulators for Alzheimer's disease. J. Neurochem. 120 (Suppl. 1), 89–98.

Wong, C.W., Quaranta, V., Glenner, G.G., 1985. Neuritic plaques and cerebrovascular amyloid in Alzheimer disease are antigenically related. Proc. Natl. Acad. Sci. USA 82 (24), 8729–8732.

Woodruff-Pak, D.S., Agelan, A., Del Valle, L., 2007. A rabbit model of Alzheimer's disease: valid at neuropathological, cognitive, and therapeutic levels. J. Alzheimers Dis. 11 (3), 371–383.

Woods, I.G., Wilson, C., Friedlander, B., Chang, P., Reyes, D.K., Nix, R., et al., 2005. The zebrafish gene map defines ancestral vertebrate chromosomes. Genome Res. 15 (9), 1307–1314.

World Alzheimer Report 2010: The Global Impact of Dementia, 2010. Alzheimer's Disease International.

Wu, B.K., Yuan, R.Y., Lien, H.W., Hung, C.C., Hwang, P.P., Chen, R.P., et al., 2016. Multiple signaling factors and drugs alleviate neuronal death induced by expression of human and zebrafish tau proteins in vivo. J. Biomed. Sci. 23, 25.

Yang, G., Gong, Y.D., Gong, K., Jiang, W.L., Kwon, E., Wang, P., et al., 2005. Reduced synaptic vesicle density and active zone size in mice lacking amyloid precursor protein (APP) and APP-like protein 2. Neurosci. Lett. 384 (1–2), 66–71.

Yang, D.S., Stavrides, P., Mohan, P.S., Kaushik, S., Kumar, A., Ohno, M., et al., 2011. Reversal of autophagy dysfunction in the TgCRND8 mouse model of Alzheimer's disease ameliorates amyloid pathologies and memory deficits. Brain 134 (Pt 1), 258–277.

Yoshino, T., Uchida, K., Tateyama, S., Yamaguchi, R., Nakayama, H., Goto, N., 1996. A retrospective study of canine senile plaques and cerebral amyloid angiopathy. Vet. Pathol. 33 (2), 230–234.

Youmans, K.L., Tai, L.M., Kanekiyo, T., Stine, Jr., W.B., Michon, S.C., Nwabuisi-Heath, E., et al., 2012a. Intraneuronal Abeta detection in 5xFAD mice by a new Abeta-specific antibody. Mol. Neurodegener. 7, 8.

Youmans, K.L., Tai, L.M., Nwabuisi-Heath, E., Jungbauer, L., Kanekiyo, T., Gan, M., et al., 2012b. APOE4-specific changes in Abeta accumulation in a new transgenic mouse model of Alzheimer disease. J. Biol. Chem. 287 (50), 41774–41786.

Yu, X., Li, Y.V., 2011. Zebrafish as an alternative model for hypoxic-ischemic brain damage. Int. J. Physiol. Pathophysiol. Pharmacol. 3 (2), 88–96.

Yu, Z., Ren, M., Wang, Z., Zhang, B., Rong, Y.S., Jiao, R., et al., 2013. Highly efficient genome modifications mediated by CRISPR/Cas9 in *Drosophila*. Genetics 195 (1), 289–291.

Zahs, K.R., Ashe, K.H., 2010. 'Too much good news'—are Alzheimer mouse models trying to tell us how to prevent, not cure, Alzheimer's disease? Trends Neurosci. 33 (8), 381–389.

Zars, T., Wolf, R., Davis, R., Heisenberg, M., 2000. Tissue-specific expression of a type I adenylyl cyclase rescues the *rutabaga* mutant memory defect: in search of the engram. Learn. Mem. 7 (1), 18–31.

Zekanowski, C., Wojda, U., 2009. Aneuploidy, chromosomal missegregation, and cell cycle reentry in Alzheimer's disease. Acta Neurobiol. Exp. (Wars) 69 (2), 232–253.

Zetterberg, H., Campbell, W.A., Yang, H.W., Xia, W.M., 2006. The cytosolic loop of the gamma-secretase component presenilin enhancer 2 protects zebrafish embryos from apoptosis. J. Biol. Chem. 281 (17), 11933–11939.

Zetterberg, H., Mortberg, E., Song, L., Chang, L., Provuncher, G.K., Patel, P.P., et al., 2011. Hypoxia due to cardiac arrest induces a time-dependent increase in serum amyloid beta levels in humans. PLoS One 6 (12), e28263.

Zhang, X., Garbett, K., Veeraraghavalu, K., Wilburn, B., Gilmore, R., Mirnics, K., et al., 2012a. A role for presenilins in autophagy revisited: normal acidification of lysosomes in cells lacking PSEN1 and PSEN2. J. Neurosci. 32 (25), 8633–8648.

Zhang, Y., Zhou, B., Zhang, F., Wu, J., Hu, Y., Liu, Y., et al., 2012b. Amyloid-beta induces hepatic insulin resistance by activating JAK2/STAT3/SOCS-1 signaling pathway. Diabetes 61 (6), 1434–1443.

Zhang, Y., Zhou, B., Deng, B., Zhang, F., Wu, J., Wang, Y., et al., 2013. Amyloid-beta induces hepatic insulin resistance in vivo via JAK2. Diabetes 62 (4), 1159–1166.

Zhang, Y., Li, P., Feng, J., Wu, M., 2016. Dysfunction of NMDA receptors in Alzheimer's disease. Neurol. Sci. 37, 1039–1047.

Zhao, X.L., Wang, W.A., Tan, J.X., Huang, J.K., Zhang, X., Zhang, B.Z., et al., 2010. Expression of beta-amyloid induced age-dependent

presynaptic and axonal changes in *Drosophila*. J. Neurosci. 30 (4), 1512–1522.

Zheng, H., Xu, H., Uljon, S.N., Gross, R., Hardy, K., Gaynor, J., et al., 2002. Modulation of A(beta) peptides by estrogen in mouse models. J. Neurochem. 80 (1), 191–196.

Zheng-Bradley, X., Rung, J., Parkinson, H., Brazma, A., 2010. Large scale comparison of global gene expression patterns in human and mouse. Genome Biol. 11 (12), R124.

Zhu, X., Lee, H.G., Perry, G., Smith, M.A., 2007. Alzheimer disease, the two-hit hypothesis: an update. Biochim. Biophys. Acta 1772 (4), 494–502.

Zilka, N., Filipcik, P., Koson, P., Fialova, L., Skrabana, R., Zilkova, M., et al., 2006. Truncated tau from sporadic Alzheimer's disease suffices to drive neurofibrillary degeneration in vivo. FEBS Lett. 580 (15), 3582–3588.

Zlokovic, B.V., 2011. Neurovascular pathways to neurodegeneration in Alzheimer's disease and other disorders. Nat. Rev. Neurosci. 12 (12), 723–738.

Zotova, E., Nicoll, J.A., Kalaria, R., Holmes, C., Boche, D., 2010. Inflammation in Alzheimer's disease: relevance to pathogenesis and therapy. Alzheimers Res. Ther. 2 (1), 1.

Page left intentionally blank

Neurotoxin 1-Methyl-4-Phenyl-1,2,3,6-Tetrahydropyridine (MPTP)-Induced Animal Models of Parkinson's Disease

Jiro Kasahara, Mohammed E. Choudhury**,
Noriko Nishikawa**, Akie Tanabe*, Ryosuke Tsuji*,
Yu Zhou*, Masatoshi Ogawa*, Hironori Yokoyama*,
Junya Tanaka**, Masahiro Nomoto***

*Institute of Biomedical Sciences, Graduate School of Pharmaceutical Sciences,
Tokushima University, Shoumachi, Tokushima, Japan
**Ehime University Graduate School of Medicine, Shitsukawa, Shitsukawa, Toon-shi, Ehime, Japan

O U T L I N E

Abbreviations

AADC	L-Amino acid decarboxylase
ADL	Activities of daily life
AMPT	α-Methyl p-tyrosine
BBB	Blood–brain barrier
BDNF	Brain-derived neurotrophic factor
Cdk-5	Cyclin-dependent protein kinase 5
[^{11}C]CIT-FP	N-3-Fluoropropyl-2-β-[O-methyl-^{11}C] carbomethoxy-3-β-(4-iodophenyl)-tropane
COMT	Catechol-O-methyl transferase
COX-2	Cyclooxygenase 2
DA	Dopamine
DAT	Dopamine transporter
DARPP-32	Dopamine- and cAMP-regulated neuronal phosphoprotein 32 kDa
DMSO	Dimethylsufoxide
DOPAC	3,4-Dihydroxy-phenylacetic acid
L-dopa	L-3,4-Dihydroxyphenylalanine
[^{18}F]-DTBZ (AV-133)	9-Fluoropropyl-(+)-dihydrotetrabenazine
ER	Endoplasmic reticulum
[^{18}F]FECNT	2β-Carbomethoxy-3β-(4-chlorophenyl)-8-(2-[^{18}F]-fluoroethyl)-nortropane
FGF-2	Basic fibroblast growth factor 2
GDNF	Glial cell line-derived neurotrophic factor
GFAP	Glial fibrillary acidic protein
GPe	External segment of globus pallidus
GPi	Internal segment of globus pallidus
GSH-PX	Glutathione peroxidase
HPLC	High-performance liquid chromatography
HVA	Homovanillic acid
IL-1β	Interleukin 1β
IL-6	Interleukin 6
iNOS	Inducible nitric oxide synthase
JNK	c-Jun N-terminus kinase
LRRK2	Leucine-rich repeat kinase 2
LTF	Latency to fall
MAO-B	Monoamine oxidase B
MDA	Malondialdehyde
MEMRI	Manganese-enhanced magnetic resonance imaging
MPP$^+$	1-Methyl-4-phenyl-pyridinium
MPTP	1-Methyl-4-phenyl-1,2,3,6-tetrahydropyridine
MSNs	Medium spiny neurons
NAT	Noradrenaline transporter
NeuN	Neural nuclei
NF-κB	Nuclear factor-κB
NO	Nitric oxide
6-OHDA	6-Hydroxydopamine
PD	Parkinson's disease
PET	Positron emission tomography
PINK-1	PTEN-induced putative kinase 1
PQ	1,1'-Dimethyl-4-4'-bipyridinium (paraquat)
RNS	Reactive nitrogen species
ROS	Reactive oxygen species
SNpc	Substantia nigra pars compacta
SNr	Substantia nigra pars reticulate
SPECT	Single photon emission computerized tomography
SOD	Superoxide dismutase
STN	Subthalamic nuclei
TH	Tyrosine hydroxylase
TLR2	Toll-like receptor 2
TNF-α	Tumor necrosis factor-α
UPDRS	Unified Parkinson's disease rating scale
VMAT	Vesicle monoamine transporter

1 INTRODUCTION

In 1817, a British clinician James Parkinson described his six patients as showing shaking palsy (Parkinson, 1817), currently known as an extrapyramidal syndrome, and it was the first case report of "Parkinson's disease (PD)" later named by a French neurologist Jean-Martin Charcot (Chacot, 1880). Tretiakoff (1919) showed PD was associated with degeneration of the neurons in substantia nigra pars compacta (SNpc), and Carlsson (1959) showed the neurotransmitter of the nigrostriatal neuron was dopamine (DA). Ehringer and Hornykiewicz (1960) proposed PD was caused by a significant decrease of the striatal dopamine. Thus, PD can be defined as a common neurodegenerative disorder characterized by a slowly progressive motor dysfunction associated with loss of the nigrostriatal dopaminergic neurons resulting in depletion of the striatal dopamine. It was proposed that PD symptoms were expressed when approximately 60% of the dopaminergic neurons in SNpc had died (German et al., 1989), and approximately 70 ~ 80% of dopamine in the striatum had been lost (Jankovic and Marsden, 1988; Ma et al., 2002).

In the striatum, dopaminergic afferent makes synapses to the GABAergic medium spiny neurons (MSNs), which receive dopamine with D_1 or D_2 receptors. The former excites and the latter inhibits the activity of MSNs, respectively. Glutamatergic input from the cortical neurons and cholinergic axons of the striatal interneurons also innervate to MSNs, both of which mainly excite MSNs. In PD, inhibition via D_2 receptor is lost by depletion of dopamine, resulting in hyperactivation of MSNs, which strongly inhibits their target neurons in the external segment of globus pallidus (GPe) (GPe), which are normally innervating to subthalamic nuclei (STN), internal segment of globus pallidus (GPi), and substantia nigra pars reticulata (SNr), respectively (Fig. 41.1). Both STN and GPi are known as targets for the electrodes of deep-brain stimuli therapy in PD (Krack et al., 2010).

For a pharmaceutical treatment of PD, L-3,4-dihydroxyphenylalanine (L-dopa) is most commonly applied as a precursor of dopamine together with an inhibitor for peripheral aromatic L-amino acid decarboxylase (AADC), such as carbidopa. It has been over 40 years since L-dopa in combination with AADC were established as a standard pharmacotherapy of PD (Rascol et al., 2011) Despite some side effects, such as drug-induced dyskinesia (Encarnacion and Hauser, 2008), L-dopa is still a gold standard for PD treatment because of its powerful efficacy on the motor dysfunctions in PD patients. The following drugs are also applicable, although some of them are restricted to
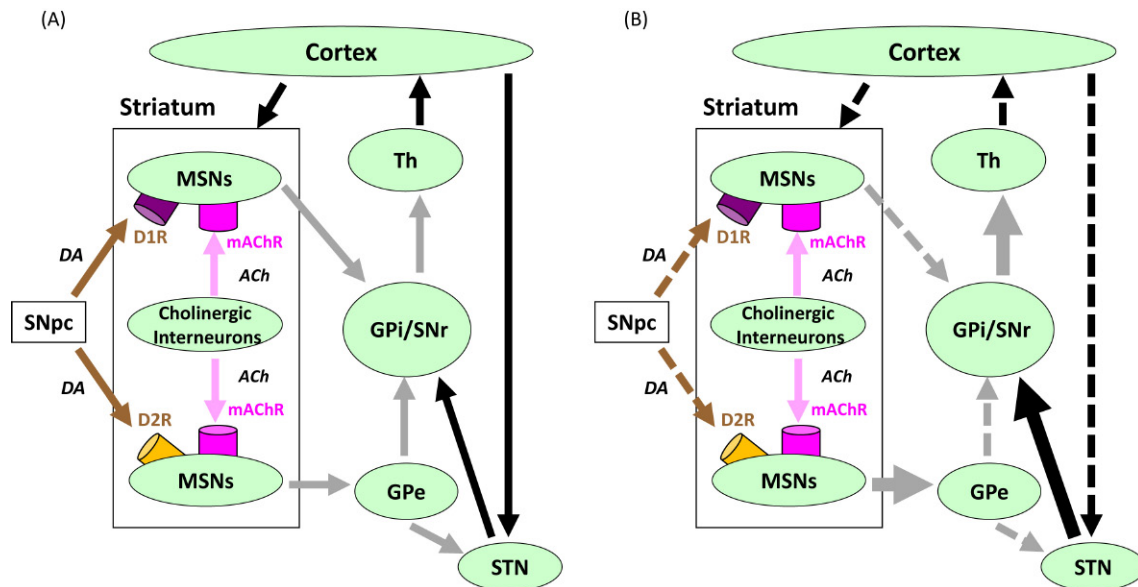
FIGURE 41.1 **Schematic diagrams of the neuronal circuit related to Parkinson's disease (PD).** (A) In normal condition. (B) In PD state. *Arrows* indicate the neurons as follows: *black*, glutamatergic; *gray*, GABAergic; *brown*, dopaminergic; *pink*, cholinergic; broken, decreased; enlarged, hyperactivated, respectively. *ACh*, Acetylcholine; *DA*, dopamine; *GPe*, external section of globus paridus; *GPi*, internal section of globus paridus; *mAChR*, muscarinic acetylcholine receptor; *MSNs*, medium spiny neurons; *SNpc*, substantia nigra pars compacta; *SNr*, substantia nigra pars reticulare; *STN*, subthalamic nuclei; *Th*, thalamus.

apply together with L-dopa: dopamine agonists (mainly for D_2 receptor), such as bromocriptine, pergolide, talipexole, cabergoline, pramipexole, ropinirole, and rotigotine; selegiline, an inhibitor for monoamine oxidase B (MAO-B); entacapone, an inhibitor for catechol-O-methyl transferase (COMT); amantadine, originally developed as an antiinfluenza therapeutic, increases synaptic release of endogenous dopamine and inhibits NMDA receptor; anticholinergic drugs, such as trihexyphenidyl, biperiden, profenamine, and metixene; zonisamide, originally developed as an antiepileptic agent, is proposed to have multiple therapeutic actions; istradefyline, adenosine A2A receptor inhibitor. In Fig. 41.2, we summarize some typical therapeutic agents and their proposed pharmacological targets.

Animal models for PD are essential to understand the detailed pathophysiological mechanisms of PD, and to develop novel therapeutics including pharmaceutical treatments. These models can also be utilized for screening effective substances having therapeutic and/or neuroprotective (disease modifying) effects on PD-related neuronal system, such as the nigrostriatal neurons (Fig. 41.3, based on the molecular pathophysiology of PD discussed later on). In general, favorable animal models should satisfy the following three validities with human PD: face, constructive, and predictive (Trivedi and Jarbe, 2011). Although it is difficult to establish such a model satisfying all of these validities, various animals as PD models have been used to date: nonhuman primates from big monkeys, such as baboons (Kishima et al., 2004)

and macaques (Saiki et al., 2010) to small ones, such as common marmosets (Choudhury et al., 2010), rodents especially rats and mice, rabbits (Ghiribi et al., 2003), dogs (Choi et al., 2011), cats (Schneider and Rothblat, 1991), frogs (Barbeau et al., 1985) and nonvertebrates, such as drosophila (Park et al., 2005) and nematode (Braungert et al., 2004). Among them, nonhuman primates are especially valuable because of their genetic, anatomical, and functional similarities to humans, although there are some difficulties regarding availability, habitation, handling, and experimental techniques. The most frequently used animals are rats and mice as they are readily available and easy to handle. Considering these facts, in this chapter, we focus on the mouse as a rodent and the common marmoset as a nonhuman primate model, respectively, since both of them are relatively easy to handle for their size and availability.

To establish an appropriate animal model, several chemicals/neurotoxins inducing PD-like symptoms are often used, also with increasing use of the transgenic and knockout mice models of specific genes related to familial PD, such as mutated α-synuclein, parkin, PTEN-induced putative kinase 1 (PINK-1), DJ-1, leucine-rich repeat kinase 2 (LRRK2), and so on (Crabtree and Zhang, 2012). Among them, a neurotoxin 1-methyl-4-phenyl-1,2,3,6-tetrahydropyridine (MPTP) is commonly used since it causes a selective loss of dopaminergic neurons and induces typical PD-like symptoms in rodents, amphibians, nonhuman primates, and humans (Barbeau et al., 1985; Blandini and Armentero, 2012; Langston et al., 1983).
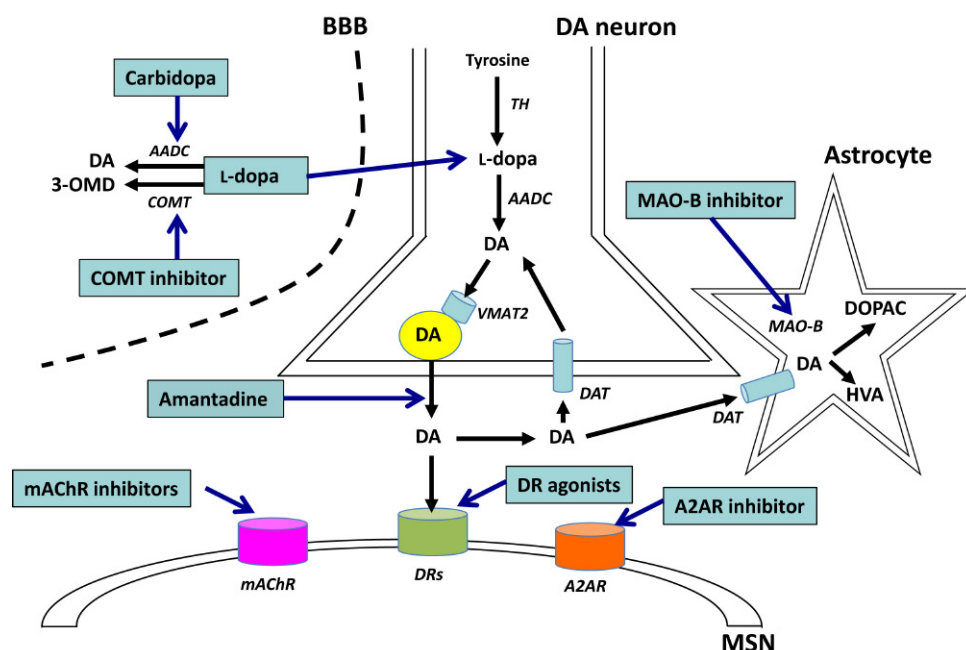
FIGURE 41.2 Schematic diagrams of some typical therapeutic agents for PD and their pharmacological targets. *A2AR*, Adenosine A2A receptor; *AADC*, aromatic amino acid decarboxylase; *BBB*, blood–brain barrier; *COMT*, catechol-O-methyl transferase; *DA*, dopamine; *DAT*, dopamine transporter; *DOPAC*, 3,4-dihydroxyphenylacetic acid; *DRs*, dopamine receptors; *HVA*, homovanillic acid; L-dopa, L-3,4-dihydroxyphe-nylalanine; *mAChR*, muscarinic acetylcholine receptor; *MAO-B*, monoamine oxidase B; *MSN*, medium spiny neuron; *3-OMD*, 3-O-methyldopa; *VMAT2*, vesicle monoamine transporter 2.
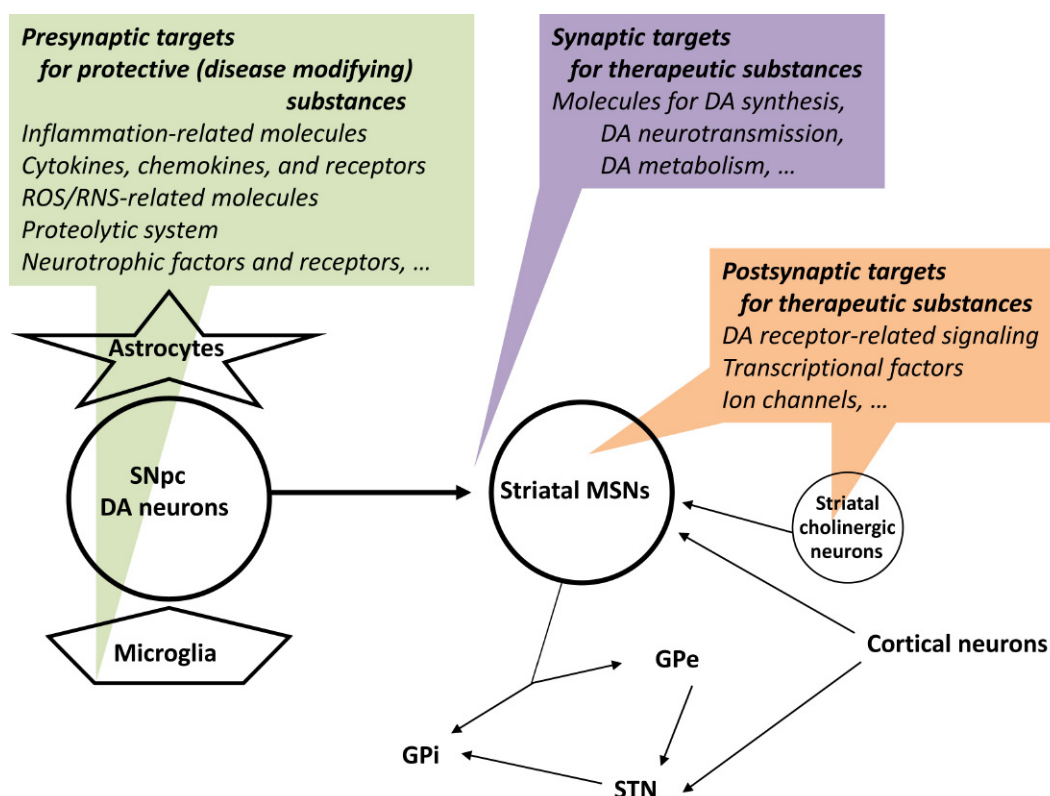
FIGURE 41.3 Possible pharmacological targets in SNpc and the striatum to screen future protective (disease modifying) and therapeutic substances in PD models. *DA*, Dopamine; *GPe*, external section of globus paridus; *GPi*, internal section of globus paridus; *MSNs*, medium spiny neurons; *RNS*, reactive nitrogen species; *ROS*, reactive oxygen species; *SNpc*, substantia nigra pars compacta; *STN*, subthalamic nuclei.

Using MPTP, the authors have studied the molecular details of PD and actions of some therapeutic/neuro-protective drugs in mice and in common marmosets (Araki et al., 2001; Choudhury et al., 2010; Kadoguchi et al., 2014; Kikuta et al., 2015; Muramatsu et al., 2002; Nomoto et al., 1998; Tanabe et al., 2014; Yamamura et al., 2013; Yokoyama et al., 2010a,b).

In this chapter, we first overview the clinical symptoms and characteristics observed in PD patients and in animal models, followed by summarizing the neurotoxins used to establish PD models. Then we describe the practical experimental methods and applications with some results relevant to PD both in mice and in common marmosets.

2 CLINICAL CHARACTERISTICS OF PD AND THEIR RELEVANT SYMPTOMS IN ANIMAL MODELS

To evaluate the animal models of human disease, it is important to understand the clinical characteristics and symptoms of the disease. In this section, we summarize the epidemiological and clinical characteristics of PD briefly, comparing with behavioral and molecular characteristics of animal models for PD.

2.1 Epidemiological Background

PD is the second most common neurodegenerative disorder after Alzheimer's disease (de Lau and Breteler, 2006). The prevalence of PD is about 0.3% of the whole population in first world countries. PD is more common in the elderly and prevalence rises from 1% in those over 60 years of age to 4% of the population over 80 (de Lau and Breteler, 2006). The mean age of onset is around 60 years, although 5%–10% of cases, classified as young onset, begin between the ages of 20 and 50 (Samii et al., 2004). Based on these facts, the use of adult animals rather than juvenile ones for PD models sounds reasonable. Some studies have proposed that PD is more common in men than women, but others failed to detect any differences between the two sexes (de Lau and Breteler, 2006).

Many risk factors and protective factors have been proposed, sometimes in relation to theories concerning possible mechanisms of the disease, however, none have been conclusively related to PD by empirical evidence. When epidemiological studies have been carried out in order to test the relationship between a given factor and PD, they have often been flawed and their results have in some cases been contradictory (de Lau and Breteler, 2006). The most frequently replicated relationships are an increased risk of PD in those exposed to pesticides, such as rotenone, paraquat, and maneb (de Lau and Breteler, 2006). Exposure to these pesticides can double the risk of PD, and indirect measures of exposure, such as living in rural environments, have also been found to increase the risk of PD. As we describe later, in fact, these pesticides are successfully used to produce a PD model in experimental animals.

On the other hand, it was reported that the risk of PD was reduced in smokers down to a third when compared to nonsmokers (de Lau and Breteler, 2006). The basis for this effect is not known, but possibilities include an effect of nicotine as a dopamine stimulant (de Lau and Breteler, 2006; Quik et al., 2009). Tobacco smoke contains compounds that act as MAO inhibitors that also might contribute to this effect (Castagnoli and Murugesan, 2004). Other substances reported to reduce PD risk were caffeine (Bankiewicz et al., 1999), estrogens, antiinflammatory drugs, and so on (de Lau and Breteler, 2006).

2.2 Clinical Stages of PD

Although clinical experts describe symptoms and stages of PD differently, it sometimes is classified based on the daily-life disabilities with three stages as early, moderate, or advanced: Early, the stage when a person has a mild tremor or stiffness but is able to continue work or other normal daily activities. This often refers to a person who has been newly diagnosed with PD; Moderate, the stage when a person begins to experience limited movement. A person with moderate PD may have a mild to moderate tremor with slow movement; Advanced, the stage when a person is significantly limited in his or her activity, despite treatment. Daily fluctuations in symptoms, medicinal side effects that limit treatment, and loss of independence in activities of daily living are common. A person with advanced PD may have significant and frequent changes in posture and movement with speech difficulties.

The severity of PD may also fall into the following five stages known as Hoehn and Yahr's scale: Stage I, symptoms affect only one side of the body; Stage II, both sides of the body are affected, but posture remains normal; Stage III, both sides of the body are affected, and there is a mild imbalance during standing or walking. But the person remains independent; Stage IV, both sides of the body are affected, and there is disabling instability while standing or walking. The person in this stage requires substantial help; Stage V, severe, fully developed disease is present. The person is restricted to a bed or chair. Dementia is also observed in 20 ~ 30% of PD patients, although it only appears in the later stage.

Further detailed ratings established in 1987 known as Unified Parkinson's Disease Rating Scale (UPDRS), a worldwide standard scale of PD, evaluates both motor and nonmotor symptoms subdivided into total 42 subjects, rating each of them with 5 stages. UPDRS consists

of five parts: I, evaluation of mentation, behavior, and mood; II, self evaluation of the activities of daily life (ADL), such as speech, swallowing, handwriting, dressing, hygiene, falling, salivating, turning in bed, walking, cutting food; III, evaluation of motor function scored by clinician; IV, Hoehn and Yahr's scaling of PD severity; V, ADL scaling of Schwab and England. Although it takes time for scoring all the subjects, it is also utilized to evaluate drugs in clinical trial or the result of surgery.

2.3 Clinical Symptoms in PD Patients

The most common symptoms in PD include the following four: (1) bradykinesia which is a slowness of voluntary movement and associated with reduction in automatic movement, such as swinging of the arms during walking, is the most disabling feature. The voice is hypophonic and poorly modulated, which is called monotonous speech. A reduction of the facial muscles movements and blinking lead to the characteristic expressionless masked face; (2) Resting Tremor, the 4–6-Hz "Pill rolling," is typically the most characteristic sign and seen in 60% of the patients with PD. Initially, the tremor may appear in just one arm or leg or only on one side of the body. The tremor may also affect the chin, lips, and tongue. Emotional and physical stresses tend to make the tremor more noticeable. Sleep, complete relaxation, and intentional movement or action usually reduce or diminish the tremor; (3) Rigidity, is defined as an increase in muscle tone of passive movement responding to applied force. PD patients mostly express the lead-pipe type of rigidity and cogwheel type occasionally. Rigidity is used as an indicator to determine the efficacy of the medications; (4) Difficulty with walking (gait disturbance) and balance (postural instability). A person with PD is likely to take small steps and shuffle with his or her feet close together, bend forward slightly at the waist (stooped posture), and have trouble turning around. Balance and posture problems may result in frequent falls. But these problems usually do not develop until later in the course of the disease.

2.4 Symptoms in Nonhuman Primates

Many clinical symptoms described earlier can be reproduced in the experimental nonhuman primates probably because they are in the same species with us. Parameters to be analyzed are: tremor, freezing, locomotion, fine motor skills, akinesia, balance, posture, startle response, gross motor skills, and so on (Bankiewicz et al., 1999). They are usually classified from 0 (normal) to 3 ~ 5 subclasses according to the severity. Alternatively, a scale of clinical rating ranged from 0 to 32 are also applicable (Swanson et al., 2011). In some cases, fine motor skills are evaluated with computerized touch-

panel systems (Swanson et al., 2011). Detailed examples of MPTP-treated common marmoset will be described in the later section.

2.5 Symptoms in Rodents

Although it is well known that rodent models for human diseases are favorable with genetic, biochemical, and anatomical studies, it does not always reflect exact behavioral parameters with symptoms of the disease, because of the differential anatomy, biochemistry, and functions with human. Despite this discrepancy, researchers have developed many useful paradigms to assess motor dysfunctions of rodents as we describe in the later section. It is important to be aware that one experimental paradigm does not always reflect one specific parameter of human exactly. For this reason, multiple paradigms are recommended to examine in each experimental project.

After administrating neurotoxins or chemicals described later, animals show akinesia- and/or bradykinesia-like symptoms, such as freezing, and abnormal movement of limbs with tremor, slowness, rigidity, and so on. Behavioral tasks to analyze these motor dysfunctions will be described later.

3 MOLECULAR PATHOPHYSIOLOGY OF PD

As we mentioned in the previous sections, PD is associated with degeneration of the nigrostriatal dopaminergic neurons. It means a significant reduction of the striatal dopamine with its metabolites and molecular markers for dopaminergic neurons, such as tyrosine hydroxylase (TH) are observed with anatomical and/or biochemical analysis (Nagatsu and Sawada, 2007). It is also known that formation of the acidophilic inclusions called Lewy body with a high amount of α-synuclein and ubiquitin proteins are observed in the cytoplasm of the remaining but degenerated neurons, together with some characteristic small projections called Lewy neurites (Forno, 1996). In fact, increasing evidence suggested impaired proteolytic systems of ubiquitne-proteasome and/or lysosome contributed to the accumulation of α-synuclein, causing endoplasmic reticulum (ER)-stress with progression of the dopaminergic cell death (Cox and Cachón-González, 2012; Wang and Takahashi, 2007). Parkin, a ubiquitin E3 ligase, and its upstream protein kinase PINK1 are known to be involved in the removal of damaged mitochondria by ubiquitinating various substrate proteins in the depolarized mitochondria, and its genetic deficiency is correlated to PD occurrence (Kitada et al., 1998; Matsuda et al., 2010). Parkin is also phosphorylated by c-Abl

tyrosine kinase at tyrosine 143 residue to be inactivated (Ko et al., 2010) and a c-Abl inhibitor nilotinib protected dopaminergic neurons in MPTP mice (Karuppagounder et al., 2014). Thus inhibitors of c-Abl are suggested to be possible disease-modifying agents for PD. Mitochondrial dysfunctions and impaired calcium homeostasis are also related to the apoptotic cell death of dopaminergic neurons (Calí et al., 2011), generating free radicals, reactive oxygen and nitrogen species (ROS/RNS), which in turn cause oxidative stress to neurons. Furthermore, inflammatory and immunological reactions mediated by activated glial cells are strongly suggested to participate in the progression of dopaminergic cell death (Collins et al., 2012). In the activated astrocytes, upregulation of inflammatory cytokines, such as tumor necrosis factor-α (TNF-α) occurs, which triggers the apoptotic signaling of dopaminergic neurons by activation of TNF receptor. In the activated microglia, upregulation of inducible nitric oxide synthase (iNOS) occurs with increasing NO, which also contribute to generate highly toxic radicals, such as $ONOO^-$ (Tieu et al., 2003). Involvement of cyclooxygenase 2 (COX-2) facilitating inflammatory reactions is also known (Minghetti, 2004). Overall, each of these molecular events contributing to aggression of the PD pathology will be a possible protective (disease modifying) and/or therapeutic target of PD (Fig. 41.3), although most of the therapeutic drugs in clinical use today target for the synapse between nigrostriatal dopaminergic neurons and MSNs in the striatum, and none of the protective (disease modifying) drugs inhibiting the progression of PD are practically used yet. In the later section, we discuss the relevancy of these pathophysiological details of human PD and those of MPTP-induced animal model on a molecular level.

4 NEUROTOXINS FOR MAKING PD MODELS

All the agents used to prepare PD models ultimately result in the depletion of the striatal dopamine to express PD-like dysfunctions. In this section, we overview some typical neurotoxins and chemicals for PD models including MPTP in experimental animals.

4.1 6-OHDA

The first neurotoxin for PD model introduced by Ungerstedt (1968) was a hydroxylated analog of DA, 6-hydroxydopamine (6-OHDA). Using Sprague-Dawley rats, he reported a unilateral application of 6-OHDA into the nucleus caudatus putamen or the substantia nigra caused loss of monoaminergic terminals and dopaminergic cell bodies, respectively, with a marked motor asymmetry known as hemi-Parkinsonism, typically characterized by a rotational behavior to the impaired side (Ungerstedt and Arbuthnott, 1970). To date, the 6-OHDA model has been utilized by many researchers to examine pathophysiological hypothesis and possible novel treatment of PD and dyskinesia. Because of low permeability to blood–brain barrier (BBB), however, 6-OHDA must be applied directly into specific region of brain (typically in substantia nigra, medial forebrain bundle, or striatum) using stereotactic apparatus. For this reason, rats are most frequently used and less applied in nonhuman primates (Betarbet et al., 2002). It also requires pretreatment with an inhibitor for noradrenaline transporter (NAT), such as desipramine when selective loss of dopaminergic neurons is desired, because 6-OHDA is effectively incorporated into catecholamine neurons through NAT in addition to dopamine transporter (DAT) (Duty and Jenner, 2011). Furthermore, 6-OHDA can easily be degraded by MAO-B, so pretreatment with an MAO-B inhibitor, such as pargyline is also required to protect 6-OHDA from the oxidative breakdown. Once incorporated into catecholamine neurons, 6-OHDA rapidly gives oxidative stress to form ROS and/or RNS (Duty and Jenner, 2011), and also inhibits mitochondrial respiratory chain by interacting directly with complexes I and IV (Duty and Jenner, 2011). These events are thought to induce the catecholaminergic neurons to die. Although it is one popular experimental model for PD, 6-OHDA does not satisfy all the characteristics of the disease, such as progression of PD and formation of cytoplasmic Lewy body-like inclusions with increased α-synuclein protein (Duty and Jenner, 2011).

4.2 MPTP

The potency of MPTP to utilize in PD-model was found by chance when a synthesized heroin analog meperidine, containing a high amount of MPTP as a by-product, was administrated intravenously by seven individuals. They showed PD-like symptoms, such as akinetic rigidity, and were recovered by L-dopa (Langston et al., 1983). Further studies showed systemic administration of MPTP into nonhuman primates (Langston et al., 1984) and mice (Ricaurte et al., 1987) caused an irreversible and selective degeneration of dopaminergic neurons in the substantia nigra, and elicited PD-like symptoms. Because MPTP is a highly lipophilic molecule, it can easily cross BBB and be converted into the hydrophilic metabolite 1-methyl-4-phenyl-pyridinium (MPP^+) by MAO-B expressed in astrocytes (Figs. 41.4 and 41.5). MPP^+ is selectively incorporated into dopaminergic neurons via DAT, and is taken up into mitochondria, inhibiting complex I of the respiratory electron transfer chain. This leads to impairment of ATP production, elevated intracellular Ca^{2+} levels, and generation of ROS/RNS, eliciting apoptotic cell death of the dopaminergic neurons (Fig. 41.5).
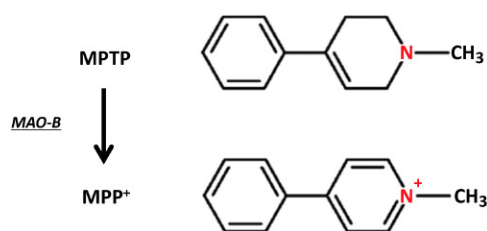
FIGURE 41.4   **Chemical structures of MPTP and its toxic metabolite MPP$^+$.**

Thus, MPP$^+$ is primarily a mitochondrial toxin to specifically disrupt the respiratory system of dopaminergic neurons (Yokoyama et al., 2011a). MPP$^+$ also triggers inflammatory reactions starting from activation and proliferation of astrocyte and microglia (Yokoyama et al., 2011b). It facilitates synthesis and secretion of inflammation-related molecules including cytokines, such as TNF-α, interleukin 1β (IL-1β) and IL-6, chemokines, and prostagrandines. In microglia, upregulation of iNOS also occurs, resulting in increase and release of NO, which attacks neurons with generating toxic ROS and RNS. These events are well consistent with what happened in the brain of PD patients mentioned earlier.

To date, a wide variety of animals including nematodes (Wang et al., 2007), frogs (Barbeau et al., 1985), mice (Sunderström et al., 1990), rats (Laret et al., 2002), rabbits (Ghiribi et al., 2003), cats (Schneider and Rothblat, 1991), dogs (Choi et al., 2011), and nonhuman primates (Nomoto et al., 1998) were demonstrated to have sensitivity to MPTP. Among them, nonhuman primates with the highest MPTP sensitivity are ideal to use, though rodents are still the most widely used because of convenience. Mice are more favorably used than rats because the latter show a relatively high peripheral MAO activity (Kakaria et al., 1987) causing conversion of MPTP to MPP$^+$ before crossing BBB, failing to enter brain. If a researcher prefers to use MPTP in rats, it is necessary to inject MPTP or MPP$^+$ directly into the brain with a stereotactic apparatus as like 6-OHDA (Heikkila et al., 1985). Alternatively, intranasal administration of MPTP has developed recently (Predinger et al., 2012), though its efficiency and specificity should be examined more.

It should be noted that one significant difference of MPTP model with human PD is absence of Lewy body. Even by examining three different schedules of MPTP administration (acute, semichronic, and chronic), none of the obvious Lewy body-like inclusions were found
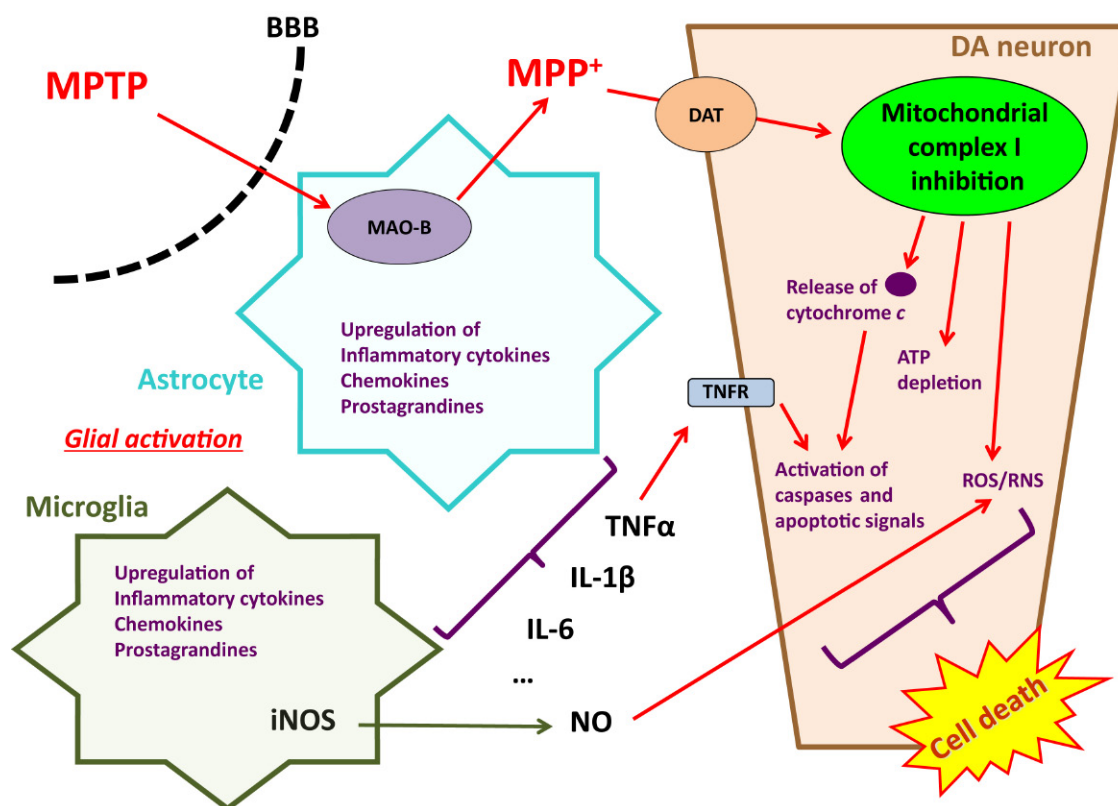
FIGURE 41.5   **Schematic diagram of action of MPTP in SNpc.** *BBB*, Blood–brain barrier; *DAT*, dopamine transporter; *IL*, interleukin; *iNOS*, inducible nitric oxide synthase; *MAO-B*, monoamine oxidase; *NO*, nitric oxide; *ROS*, reactive oxygen species; *RNS*, reactive nitrogen species; *TNF*, tumor necrosis factor.

in mice brain (Shimoji et al., 2005). It was also reported in a study that using two monkeys which survived over 10 years demonstrating severe PD-like symptoms after MPTP treatment in their youth had no Lewy body-like inclusions in brain, even though expression of α-synuclein protein was increased significantly (Halliday et al., 2009). We will discuss this discrepancy in the later section.

4.3 Pesticides

As we described in the previous section, exposure to pesticides, such as rotenone, paraquat, and maneb was shown to have a positive correlation to the risk of PD. Rotenone is one of the lipophilic phenylpropanoid compounds. Because of its selective inhibitory effect on the mitochondrial respiratory complex I similar to MPP⁺ (but have no cell-type specificity), it was expected to be utilized as a chemical for PD model. In fact, chronic, but not acute, systemic administration of rotenone in rats with 2.5 mg/kg/day for 7 ~ 33 days caused a loss of the nigrostriatal dopaminergic neurons, appearance of the cytoplasmic inclusions reminiscent to Lewy body which contained α-synuclein and ubiquitin proteins, and motor dysfunctions including hypokinesis, hunched posture, rigidity, and tremor (Betarbet et al., 2000). This is quite an attractive model with matching face and constructive validities with human PD, however, rotenone also has cardiovascular and other systemic toxicities in addition to the toxicity for central neurons, probably because of its cell-type nonspecific inhibition of mitochondrial complex I, resulting in a relatively high rate of mortality (~30%) where the results tend to vary (Duty and Jenner, 2011).

Different from rotenone, paraquat (1,1′-dimethyl-4-4′-bipyridinium: PQ) does not cross BBB. It is transported into the brain by a neutral amino acid transporter, and incorporated into dopaminergic neurons with a sodium-dependent uptake system (Shimizu et al., 2001). As its chemical structure resembles MPP⁺, it is thought to inhibit mitochondrial respiratory complex I, resulting in a mild loss of the nigrostriatal dopaminergic neurons, although paraquat was reported to have no specificity to DAT (Richardson et al., 2005). On the other hand, however, a recent report showed that paraquat could be incorporated via DAT when it was converted to a monovalent cation PQ(+) rather than a native divalent cation state PQ(2+) (Rappold et al., 2011). This and further studies are expected to clarify a precise mechanism of the selective toxicity of paraquat on dopaminergic neurons.

Manganese ethylene-bis-dithiocarbamate, also called maneb, is known to inhibit mitochondrial respiratory complex III (Zhang et al., 2003). It is frequently used in geographically overlapping areas with paraquat, and it was reported that combined administration of them enhanced the toxicity than the cases of sole use, in fact (Thiruchelvam et al., 2000). In addition, 30 mg/kg of maneb was reported to enhance the neurotoxicity induced by 50 mg/kg MPTP in mice examined with locomotor activities and catalepsy test (Takahashi et al., 1989). Thus, it can be considered that combination of neurotoxins usually enhance the expression and progression of PD-like symptoms with degenerating the nigrostriatal dopaminergic neurons, although an exception was also reported (Aoki et al., 2010).

4.4 Others

Chemicals other than neurotoxins listed earlier—mainly interacting with molecules for dopaminergic neurotransmission, biosynthesis, and metabolism—are also used for PD models, although many of their effects are transient and do not cause a selective degeneration of dopaminergic neurons: Reserpine, an inhibitor for vesicle monoamine transporter (VMAT), resulting in a depletion of synaptic dopamine; Methamphetamine, it also causes a depletion of the striatal dopamine at synaptic terminals; Haloperidol, an inhibitor for D₂ receptor typically causes the antipsychotic drugs-induced extrapyramidal syndrome; α-methyl *p*-tyrosine (AMPT), an inhibitor for TH.

5 MPTP-INDUCED MICE MODEL OF PD

Here we describe practical methods to produce MPTP-induced PD model of mice and how to analyze them with behavioral, immunohistochemical, and biochemical manners. We also discuss the relevance of molecular details between human PD and this model.

5.1 Animal Selection

Among the strains of mice examined in, such as CD-1, C57BL/6, BALB-c, CBA/Ca, NMRI, and Swiss Webster, C57BL/6 is now considered to show the highest sensitivity to MPTP (Filipov et al., 2009; Muthane et al., 1994; Sedelis et al., 2000; Sunderström et al., 1987, 1990). Some researchers tried to explain the reasons for the differential sensitivity among the strains with difference of molecular details, including the activity of MAO-B (Walsh and Wanger, 1989), c-Jun N-terminus kinase (JNK) signaling with COX-2 expression (Boyd et al., 2007), glial functions (Smeyne et al., 2001), and so on, although no conclusive result has been obtained yet.

For the age of mice used, adult ones ranging from 7 ~ 8 weeks to much older—up to ~12 months—are favored, and older animals showed higher MAO-B activity causing their increased sensitivity to MPTP (Walsh and Wanger, 1989).

5.2 Drug Administration

Researchers should carefully handle MPTP in a safety cabinet by wearing gloves, a goggle, and a mask to avoid unexpected inhalation. MPTP can be dissolved in water or saline (150 mM NaCl) with up to 10 mg/mL. It can also be dissolved in dimethyl-sufoxide (DMSO). Subcutaneous or intraperitoneal administration of MPTP is generally performed using a 1 mL disposable syringe. Various schedules and amounts of MPTP administration are reported, it may be roughly classified into three categories: acute, subacute (semichronic), and chronic. Following is the frequently used dosing: 10–20 mg/kg for 4 times with 1 ~ 2-h intervals as an acute model; 30 mg/kg/day for 4 ~ 5 days as a subacute model; 2 times of 25 mg/kg with 250 mg/kg of probenecid in a week for 5 weeks as a chronic model (Shimoji et al., 2005). In fact, various substances including clinically approved ones were successfully evaluated with this model. Some of the typical substances analyzed by us are as follows: L-dopa, cabergoline, perindopril, riluzole, 7-nitroindazole, benzamide, zonisamide, imatinib, nilotinib, mirtazapine, and so on (Araki et al., 2001; Choudhury et al., 2010; Kadoguchi et al., 2014; Kurosaki et al., 2004; Muramatsu et al., 2002; Nomoto et al., 1998; Tanabe et al., 2014; Yamamura et al., 2013; Yokoyama et al., 2010a,b). Acute and subacute models are especially favorable for screening therapeutic substances efficiently with analyzing their molecular details of pharmacology. On the other hand, subacute and chronic administration of MPTP would reflect the processes of PD progression, suitable to analyze its molecular pathophysiology and screening protective (disease modifying) substances. In case of a protective (disease modifying) substance to be applied chronically, subacute (semichronic) protocol of MPTP administration described earlier is also applicable.

It should be noted that differential dosing results in differential effects on behavioral, anatomical, and neurochemical parameters. For example, our previous study (Kuroiwa et al., 2010) with various schedules and dosing of MPTP to 8 weeks old male C57BL/6N mice resulted in differential amounts of the striatal dopamine and its metabolites 3,4-dihydroxy-phenylacetic acid (DOPAC) and homovanillic acid (HVA), even in the cases of the same total 80 mg/kg dosing with four different schedules (Kuroiwa et al., 2010). In this study, we scheduled as follows: (1) 4 × 10 mg/kg/day for 2 consecutive days; (2) 1 × 20 mg/kg/day for 4 consecutive days; (3) 2 × 20 mg/kg/day for 2 consecutive days; (4) 4 × 20 mg/kg in a day. The striata were dissected out in 1, 2, and 3 weeks after MPTP administration. As a result, reduction of the amount of striatal dopamine varied between the four groups: (1) showed a constant reduction to ~40% throughout the periods of examination; (2) only decreased to ~70% in 1 week, then recovered to ~85%; (3) decreased to ~35% in 1 week, but recovered to ~70% after 2 weeks; (4) significantly decreased to ~20%, and the effect was sustained throughout the 3 weeks examined. The magnitude of reduction was (2) < (3) < (1) < (4), showing acute administration with frequent injections resulting in the most effective and prolonged reduction of the striatal dopamine.

5.3 Behavioral Analysis

After administrating MPTP, evaluations of the functional motor coordination and/or balance are usually performed with various behavioral tasks. As we mentioned earlier, multiple tasks are recommended to examine each experimental project.

Generally, behavioral assessments are performed from a few hours to days after MPTP treatment. It should be noted that MPTP sometimes has an acute inhibitory effect on skeletal muscles, probably by inhibiting peripheral nicotinic acetylcholine receptors in the neuromuscular junctions (Hsu et al., 1994). For this reason, it is highly recommended to start the analysis at least with a 24-h interval after the final MPTP treatment, especially when a researcher wants to examine a therapeutic effect of a substance or so. We usually perform behavioral evaluations on or over 3 days after MPTP administration (20 mg/kg × 4 times, total 80 mg/kg with 2-h intervals in a day), when we want to examine the therapeutic effect of a substance, such as L-dopa, because numbers of the nigrostriatal dopaminergic neurons become minimum and those of activated astrocytes and microglia are in maximum (Aoki et al., 2009). Also in our case examining a protective substance, we usually apply MPTP with 10 mg/kg × 4 times with 1-h intervals (total 40 mg/kg) and the substance to be examined is applied 30 min before and 90 min after the first administration of MPTP, then perform behavioral tasks and biochemical examinations on or over the next day of MPTP administration (Yano et al., 2009). Alternatively, MPTP may be administered with 30 mg/kg/day for 4 ~ 5 days, and the substance to be examined would be start to be applied 1 day before starting MPTP administration, followed by daily application until stopping MPTP administration. Another issue is a behavioral recovery despite significant neurodegenerative changes on the nigrostriatal dopaminergic neurons. A study showed, the differential time course of recovery was seen between the different strains of mice (Sedelis et al., 2000). It may also depend on which type of behavioral tasks to apply. Thus, researchers should optimize the schedule of dosing, type of the tasks applied, and the timing to analyze carefully by a pilot experiment. Following behavioral tasks are frequently used to evaluate PD-like motor dysfunctions in mice. We show some pictures of typical experimental apparatuses in Fig. 41.6.
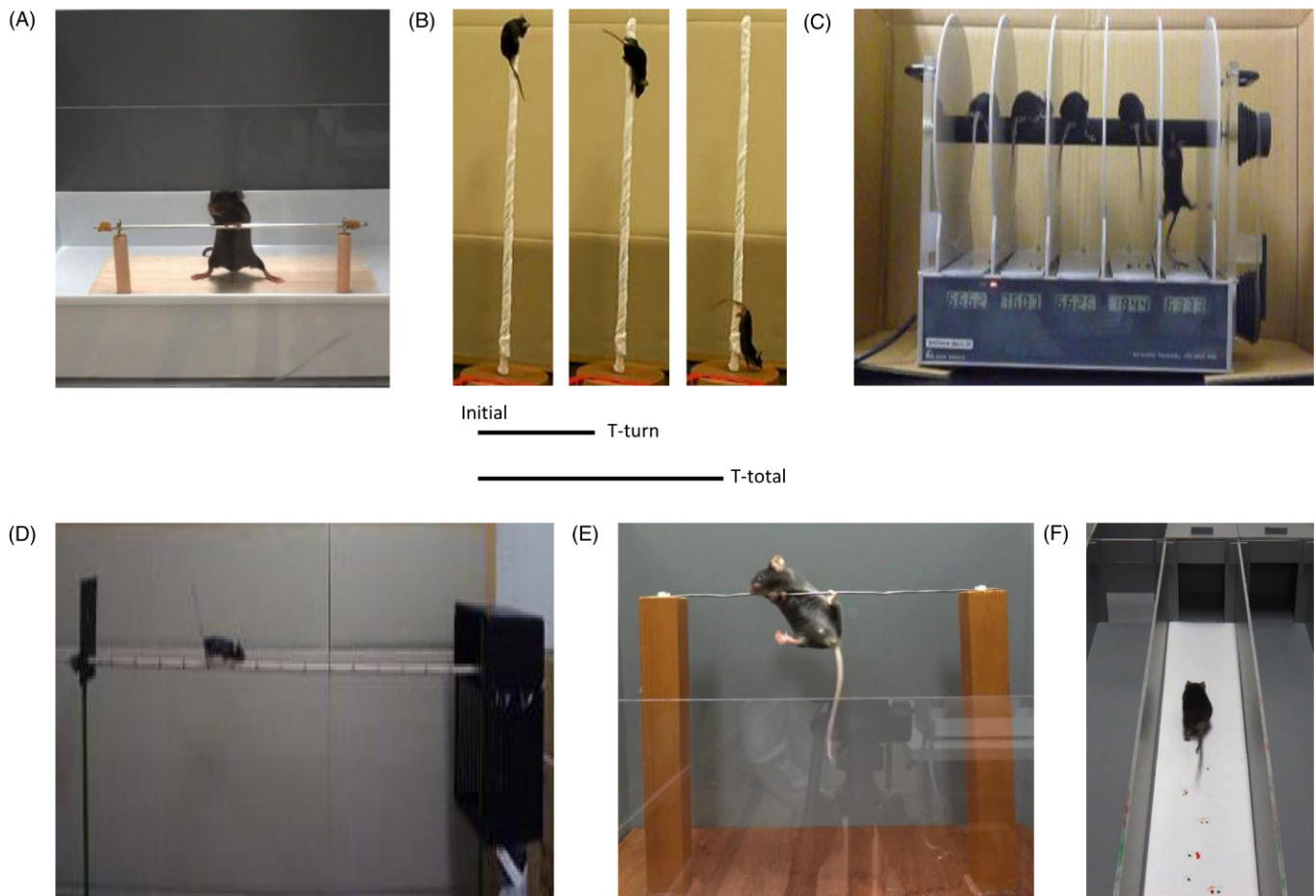
FIGURE 41.6 **Experimental apparatuses to assess motor dysfunctions of mice.** (A) Catalepsy bar test. (B) Pole test. (C) Rota-rod test with a falling mouse on the right. (D) Beam-walking test. (E) Horizontal wire test. (F) Footprint test.

5.4 Catalepsy Bar Test

It requires a relatively simple apparatus consisting of a horizontal bar (typically ranging from 0.2 to 1 cm diameter) made of wood or a stainless steel wire, spanning between two pillars with a typical height of 5–20 cm from the grounding platform (Fig. 41.6A). The period during which the mice keep an immobile posture when putting their forepaws on the bar and hind paws on the ground, known as catalepsy, is recorded until they quit keeping the posture (Watanabe et al., 2008). Similar paradigm called grip test is also applicable (Sedelis et al., 2000). Usually, naive or vehicle-treated animals show a few seconds of catalepsy period, while MPTP-treated mice show a typically prolonged period with three- to five-folds (Watanabe et al., 2008). When the mice quit the immobile posture, some of them may put all their paws on the ground, may lift their hind paws up on the bar and may move on it. The difficulty of this task is a relatively large variation of individuals especially in MPTP-treated animals which cause a failure to detect significance, even though the results show a good tendency. Finally, researchers should also note that catalepsy not only reflects an extrapyramidal syndrome but also psychotic and hypnotic conditions in some cases.

5.5 Pole Test

This paradigm was originally developed to detect MPTP-induced bradykinesia in 1987 (Ogawa et al., 1987), and was also proven to be effective especially for detecting antipsychotic drugs-induced extrapyramidal syndrome with D_2R inhibition (Ohno et al., 1994). The apparatus used consists of a vertical pole fully taped with gauze typically $40 \sim 50$ cm in height standing on a basement platform (Fig. 41.6B). Mice are first settled on the top of the pole with their heads looking upward. Mice then turn their heads downward within a few seconds, and the latency of this is called T-turn. Mice are subsequently moved down along with the pole, and the latency to reach to the ground platform is called T-total. Although both T-turn and T-total can be parameters to evaluate, the latter is more frequently used. MPTP prolongs both of the parameters significantly, such as 2–3 times longer, and is recovered by a therapeutic drug, such as L-dopa (Ogawa et al., 1987).

5.6 Rota-Rod Test

This is a frequently applied paradigm to assess the motor coordination of rodents (Fig. 41.6C) (Kadoguchi et al., 2014; Tanabe et al., 2014; Yokoyama et al., 2010b). The rota-rod apparatus with constant and/or variable speeds can be purchased from many companies selling behavioral apparatuses. It consists of a rotating rod with a few cm of diameter and usually covered by a rubber on its surface, divided into $4 \sim 5$ individual sections so that multiple animals can be assessed in one trial. Mice are put on the rotating rod with a constant speed, typically ranging from 15 to 32 rpm in a trial session, for an appropriate cut off duration, such as 10 min, and the latency to fall on the ground (LTF) is recorded. Alternatively, the rotating speed may be increased during the session, such as from 5 to 30 rpm with a constant increment. A well-trained mouse without drugs can endure to keep walking on the rod for over 10 min even with 32 rpm. MPTP usually shorten the LTF significantly to the extent, such as from half to one-third of the control. It requires some training sessions to minimize the variable of individuals. For this purpose, $1 \sim 2$ training sessions/day for successive $2 \sim 3$ days with a relatively lower speed than the trial session should be performed before MPTP administration.

5.7 Open-Field Test

It is one of the most popular apparatuses to evaluate a locomotor activity and exploratory behavior of rodents in an open box surrounded by walls (Sedelis et al., 2000). The field is usually ~ 2500 cm^2 (50 cm $\times$ 50 cm) divided into 25 areas by drawing lines onto it. There are a wide variety of apparatuses and analysis used, though essentially evaluating the spontaneous activity of the animals with horizontal (distance travelled) and vertical (rearing) directions for various durations. Automated recording systems using an infrared beam and/or video-based tracing are convenient to use. Alternatively, just counting numbers of transition between the divided areas and of rearing frequencies are also acceptable. To minimize the variety of individuals and to exclude an exploratory behavior in a novel field, pretrial habitations may be required. When the effect of MPTP in mice is fully expressed, both horizontal and vertical activities are decreased. This paradigm, however, is highly affected by emotional biases (Belzung and Griebel, 2001), so researchers have to make sure whether the results are caused only by alternation of motor functions.

5.8 Wheel Activity Test

This test allows to evaluate spontaneous locomotor activity during the active cycle of the mouse using an activity wheel (15 cm in diameter). The distance traveled is measured by the total number of wheel rotations completed during an active cycle.

5.9 Elevated Plus Maze

This paradigm is often used for screening anxiolytic drugs, such as benzodiazepines (Belzung and Griebel, 2001). As with open-field test, it can also be used to evaluate spontaneous locomotor and exploratory activities, and is highly affected by emotional biases. The maze is settled with a height, such as 45 cm with pillars standing from the ground floor. The maze consists of four arms of pathways crossing at the center stage with a right angle, and the two paths facing each other have walls, while the other two have no wall. The numbers of arm entry and rearing are convenient indexes of the horizontal and vertical activities, respectively. When the mouse feels anxiety, it tends to remain in the arm with a wall, so the time spent in each arm is also recorded. Frequencies of arm entries decrease in motor impaired mice.

5.10 Beam-Walking Test

The purpose of this test is to measure the traversing speed of mice on the horizontal bar (Fig. 41.6D), evaluating a sensorimotor coordination and the integrity of the vestibular senses (Dean et al., 1981; Sato et al., 2008). The bar with a square or a circular shape, typically $50 \sim 60$ cm in length, is positioned at a height of 50 cm supported by two pillars, having a box at the goal end so that the mice can take rest after traversing. It requires some training sessions (e.g., 3 trials in a day for 2 successive days) before the trial. In the training session, the bar with a relatively large diameter or width, such as $12 \sim 16$ mm is used. In the trial session after MPTP administration, mice are settled at the starting end of the bar with a diameter of $6 \sim 8$ mm, and the time required to reach the box is measured. The traversing speed of MPTP-treated mice tends to delay, and will be recovered by administrating a therapeutic drug, such as L-dopa. It seems to have a higher sensitivity than other paradigms, although some of the mice especially treated with MPTP stop traversing in the middle of the bar (freezing) for several times, which is also considered to reflect one aspect of akinesia.

5.11 Horizontal Wire Test

This test estimates motor coordination and muscle relaxation (Burkard et al., 1985; Vanover et al., 1999). The testing apparatus consists of a solid wire (typically $0.1 \sim 0.2$ cm diameter, $20 \sim 30$ cm length) horizontally stretched $20 \sim 30$ cm above the grounding platform (Fig. 41.6E). Mice are lifted by the tail and allowed to

grasp the wire with their forepaws, and then are released. A mouse passes the task if it grasps the wire with at least one hindpaw within a few (3 ~ 10) seconds. If a mouse takes over the prescribed time to grasp the wire with a hindpaw, or can't grasp the wire, it fails. Mice are trained to pass the task 2 ~ 3 times before MPTP administration. The parameter determines the rate of mice passing the task in each group. The pass rate of control group is approximately over 75%, while the rate of MPTP-treated group decreases to less than half of the control.

5.12 Footprint and Stepping Test

As described earlier in Section 2.3, a PD patient tends to have trouble walking and balancing, taking small steps with his or her feet close together with abnormal balance. Similar symptoms are also observed in MPTP-treated mice. Footprint test and a recently developed stepping test evaluate these abnormalities (Blume et al., 2009; Mohanasundari et al., 2006).

The footprint apparatus consists of a runway, usually 50 ~ 60 cm length, with a dark goal-box at the end (Fig. 41.6F). Mice are trained to walk straight to the gaolbox on the white paper before the trial. After administrating drugs, the forepaws and hindpaws of the mice are painted with different colors (e.g., forepaws with red and hindpaws with green). Then the mice are made to walk on the paper. The footprint patterns are analyzed for three parameters (stride length, stride width, and overlap). Stride length, usually 5 ~ 7 cm, is determined by measuring the distance between each step of the same side of the body. MPTP decrease the length for a half to a third compared to the control mice. Stride width, usually 2 ~ 2.5 cm, is measured as the distance between the right and left footprint, which often increases in MPTP mice. Overlap, usually 0.5 ~ 0.7 cm, is measured as the distance between the center of frontpaw and hindpaw footprints on the same side, which also increase in MPTP mice.

In the stepping test (Blume et al., 2009), a mouse is allowed to settle at one edge of the table with 1.2 m length, typically with all limbs on the table. The experimenter would lift the hind legs up by pulling the tail up with only the forepaws touching on the table. At a steady pace of approximately 1 m in 3 ~ 4 s (for a total distance of 1 m), the experimenter pulled the animal backward by the tail, down toward the other edge of the table, and the number of adjusting steps from both forepaws is computed. A significant decrease in this is observed in MPTP-treated mice when compared to the saline group.

5.13 Immunohistochemical and Biochemical Evaluations With Relevancy to PD

Anatomical and immunohistochemical evaluations can be applied after mice have been fixed with 4% para-

formaldehyde, with preparing paraffin-embed, frozen, or free-float sections, according to researcher's choice.

Most of the anatomical studies are performed in SNpc and in the striatum where dopaminergic neurons with their axons are lost by MPTP treatment. In SNpc, immunostaining with antibodies for TH, DAT, or neural nuclei (NeuN) reliably detect the significant decrease in the number of dopaminergic neurons after MPTP treatment. Our previous study in case of the acute MPTP administration with 4 times of 20 mg/kg with 2-h intervals in a day (total 80 mg/kg) resulted in nearly 60% of TH-positive neurons being lost within 3 days, although around 10% were recovered in 3 weeks after MPTP treatment, probably showing a recovery of TH protein expression in the remaining neurons (Aoki et al., 2009). Similarly in the striatum, the density of TH-positive fibers was decreased significantly, indicating a degeneration of the dopaminergic axons after MPTP administration (Yokoyama et al., 2010b).

The neuronal death in SNpc includes apoptosis because the immunoreactive neurons to the antibody for single-strand DNA, a marker for apoptosis, significantly increased within 5 h till 3 days after MPTP treatment (Aoki et al., 2009). It was also reported in SNpc that MPTP increased the protein expression of cleaved caspase 3, one of the critical executers of apoptosis, and the effects of MPTP were significantly decreased when the gene coding caspase 3 was disrupted (Yamada et al., 2010). Many other studies also reported MPTP-induced apoptosis of the dopaminergic neurons in SNpc, and the apoptotic neurons were also found in SNpc of the postmortem brain of PD patients (Mochizuki et al., 1996), showing a good relevancy between this model and human PD.

MPTP also affects the activation of glial cells. Numbers of both astrocytes detected by antiglial fibrillary acidic protein (GFAP) or S100β antibodies and microglia detected by isolectin B$_4$ or anti-Iba-1 antibody were significantly increased in the same conditions above (Aoki et al., 2009; Himeda et al., 2006; Yokoyama et al., 2010b). These glial cells abundantly express cytokines and chemokines, such as IL-1β, IL-6, and TNF-α, related to inflammatory and immunological reactions, possibly mediating progression of neurodegeneration both in human and this model. Similarity of the time courses of p65 nuclear factor-κB (NF-κB) expression in the reactive astrocytes and ssDNA immunoreactivity in neurons was observed after MPTP treatment (Aoki et al., 2009). Because NF-κB activation was found in both postmortem PD brains and neurotoxin-induced animal models, it is also thought to be a key molecule to induce neuronal apoptosis (Ghosh et al., 2007; Langston, 2002).

MPTP also elicits oxidative stress which is another factor to cause dopaminergic degeneration (Fig. 41.2). In fact, activities of superoxide dismutases (SODs) and glutathione peroxidase (GSH-PX) were decreased, and

malondialdehyde (MDA), the end product of lipid peroxidation, was significantly increased after MPTP administration (Li and Pu, 2011). Further, reduction of lipoamide dehydrogenase and metallothionein in MPTP-treated mice was reported (Dhanasekaran et al., 2008). Involvement of the oxidative stress in PD progression is well known as mentioned previously (Calí et al., 2011), so this is another relevant factor between animal model and human disease, and substances which upregulate these antioxidative proteins would be possible disease modifying agents to slow down PD progression.

As we described in the previous section, formation of Lewy body including accumulated α-synuclein protein oligomers and ubiquitin probably caused by an abnormal ubiquitin-proteasome systems is a characteristic pathology in PD. In contradiction, however, many reports denied the formation of a Lewy body-like inclusion in MPTP-treated mice (Betarbet et al., 2002; Blandini and Armentero, 2012; Halliday et al., 2009; Shimoji et al., 2005; Ungerstedt, 1968). In addition, a proteasome inhibitor failed to induce or enhance neurotoxicity on the nigrostriatal dopaminergic neurons (Kadoguchi et al., 2008a,b). From these results, researchers may suspect MPTP can not mimic the steps of protein degeneration caused by ER-stress in PD. However, MPTP, when administered chronically using osmotic minipump but not with sporadic administration, was reported to form neuronal inclusions containing both increased α-synuclein and ubiquitin proteins (Fornai et al., 2005). Another report also showed that oligolmerization of α-synuclein mediated by fatty acid-binding protein 3 (FABP3) was increased by MPTP treatment with 25 mg/kg for 5 days in mice (Shioda et al., 2014). Though further examinations will be necessary, these reports would open new insight to support the validity of MPTP model reproducing accumulation and oligomerization of α-synuclein, impairment of proteolytic system, and ER-stress elicited in PD.

Many researchers are interested in the protective potency of neurotrophic factors including brain derived neurotrophic factor (BDNF) (Ding et al., 2011; Hung and Lee, 1996; Nagahara and Tuszynski, 2011) and glial cell line-derived neurotrophic factor (GDNF) (Rangasamy et al., 2010) with their receptors. The mesolimbic dopaminergic neurons originated from ventral tegmental area innervated to nucleus accumbens shows less vulnerability to MPTP than the nigrostriatal dopaminergic neurons, and expression of mRNA of BDNF was higher in the former than the latter pathway, possibly explaining the differential sensitivity to the neurotoxin (Hung and Lee, 1996). Furthermore, a study using Fluoro-Jade, a fluorescent detector of neurodegeneration, and other antibodies showed the neurons expressing both TH and TrkB, a receptor of BDNF, were less sensitive to MPTP than other TH-positive neurons in SNpc (Ding

et al., 2011). Mice transplanted bone marrow stem cells expressing recombinant GDNF showed resistance to MPTP on behavioral, immunohistochemical, and biochemical levels (Biju et al., 2010), demonstrating successful delivery of GDNF with macrophage-mediated manner had a protective effect on MPTP neurotoxicity. Nicotine was reported to upregulate both basic fibroblast growth factor 2 (FGF-2) and BDNF in the striatum, with protective effects on MPTP-induced neurotoxicity (Maggio et al., 1998). It suggests the reason why smokers show lower risk of PD mentioned earlier. All of these studies utilized MPTP model, suggesting the possibility of future therapeutics using exogenous or endogenous neurotrophic factors.

In association with loss of nigrostriatal dopaminergic neurons, amounts of the striatal dopamine and its metabolites, DOPAC and HVA, are significantly decreased. They are usually quantified by a high-performance liquid chromatography (HPLC) (Kadoguchi et al., 2014; Kuroiwa et al., 2010; Yokoyama et al., 2010b). Turnover rate of dopamine is expressed with dopamine/(DOPAC + HVA), which can also be regarded as an indirect index of the released dopamine (because it is degraded after released from synaptic vesicles) (Hollerman and Grace, 1990), although inhibition of MAO-B and/or COMT also increases this value. It is also utilized to assess TH activity indirectly. L-dopa could be an indirect index of TH activity under the condition of AADC converting L-dopa to DA is inhibited (Perrin et al., 2004). NSD-1015A, a BBB-permeable AADC, when applied on 30 min prior to sacrifice the mice, can inhibit TH in brain, thus L-dopa is accumulated. The accumulated L-dopa is decreased significantly by MPTP treatment, indicating activity of TH was decreased in association with reduction of TH protein expression (Perrin et al., 2004). HPLC is also combined with a microdialysis to quantitate dopamine and its metabolites in the extracellular fluids of a specific brain region, such as the striatum in living animals, which enables researchers to measure the released dopamine directly (Olive et al., 2000).

Quantification of changes of the protein amount is easily detected by Western blot analysis with higher sensitivity than histochemical methods. It is frequently used to detect the toxicity of MPTP in SNpc and a presynaptic component of the striatum with downregulation of markers for the dopaminergic neurons TH, DAT, and VMAT2, together with upregulation of the glial markers, such as GFAP and Iba-1 (Yokoyama et al., 2010b), although it should be combined with an immunohistochemical analysis when the information of cellular and subcellular localization of the molecule is also necessary. Finding a protein marker reflecting MPTP toxicity in postsynaptic MSNs should also be considered because they will be a good index for the resulting effects of loss of dopamine in the striatum. Moreover, it will be a possible therapeu-

tic target in MSNs (Fig. 41.3). For example, c-Fos protein is one of a product of immediate early genes induced by neuronal activity (Chen et al., 2001). We have recently found a phosphorylated form of cyclin-dependent protein kinase 5 (Cdk5) at tyrosine 15 residue (Cdk5-pTyr15) by c-Abl was abundantly expressed in the striatal matrix compartment (Morigaki et al., 2011), and was negatively regulated by D_2 receptor activation, as well as acute administration of c-Abl inhibitors, such as imatinib (Yamamura et al., 2013) and nilotinib (Tanabe et al., 2014), suggesting the possibility of Cdk5-pTyr15 and its substrate dopamine- and cAMP-regulated neuronal phosphoprotein 32 kDa (DARPP-32) phosphorylated at Thr 75 residue (DARPP32-pThr75) to be pathological protein markers reflecting activity of MSNs. Other reports suggested involvement of of c-Abl in PD progression mentioned earlier (Karuppagounder et al., 2014; Ko et al., 2010). Considering all of these reports, c-Abl inhibitors may be applicable both as PD modifying and as therapeutic agents.

Because MPTP affects both sides of brain hemisphere, researchers can utilize each hemisphere for different purposes: one side for HPLC and the other side for Western blot or RT-PCR, for example.

Thus, MPTP-induced mice model of PD shows most of the pathological characteristics with human PD except for the formation of Lewy body, and has been frequently utilized for drug screening and analysis of pathophysiological and pharmacological mechanisms of PD, its protection and therapeutics.

5.14 Functional Imaging in Mice

Recent advances in imaging technologies have enabled to apply positron emission tomography (PET) to MPTP-treated mice. The first study that applied PET in MPTP mouse was reported in 2001 (Ishiwata et al., 2001), showing decreased presynaptic ligand-DAT binding with N-3-fluoropropyl-2-β-[O-methyl-^{11}C] carbomethoxy-3-β-(4-iodophenyl)-tropane ([^{11}C]CIT-FP) and compensatory upregulation of postsynaptic D_2 receptors with [^{3}H]raclopride after MPTP treatment. Since then, studies using PET have been gradually increasing, especially within the past few years. It has been primarily utilized to visualize the process of progressive degeneration of dopaminergic neurons by MPTP treatment with a DAT ligand 2β-carbomethoxy-3β-(4-chlorophenyl)-8-(2-[^{18}F]-fluoroethyl)-nortropane ([^{18}F] FECNT) (Honer et al., 2006) and a VMAT2 ligand 9-fluoropropyl-(+)-dihydrotetrabenazine ([^{18}F]-DTBZ or AV-133) (Chao et al., 2012; Toomey et al., 2012). Although its application is still limited, PET imaging will be a powerful tool to understand the molecular events of PD and pharmacology of therapeutics in living animals.

A recent study revealed that manganese-enhanced magnetic resonance imaging (MEMRI) was applicable on MPTP mice, showing a correlation between the highly active area in a brain identified with the manganese ion accumulated and severity of nigrostriatal dopaminergic neuronal degeneration quantified with TH immunoreactivity (Kikuta et al., 2015). This may also be applicable for future PD diagnosis.

Microglial activation during and after MPTP treatment had been visualized using bioluminescence in vivo imaging with Toll-like receptor 2-luciferase/green fluorescent protein (TLR2-luc/gfp) reporter mice. This study showed a transient activation of TLR2 signaling during MPTP administration, returned to the basal level within 3 h (Drouin-Ouellet et al., 2011). Using such a cell type specific signaling molecule as a reporter, bioluminescence study will explore further detailed pathophysiological mechanisms of PD in a time-dependent manner in vivo.

6 MPTP-INDUCED COMMON MARMOSET MODEL FOR PD

6.1 General Information to Use Common Marmosets

Common marmoset (*Callithrix jacchus*) is a nonhuman primate belonging to *Cebidae Callitrichinae*, a family of New World monkeys, having a body length of approximately 20 cm with a tail of about 25 cm, and an adult body weight over 240 g. Because of its size, easiness of handling compared to other monkeys, and good reproduction, it is a useful and favorable animal model for human diseases. A recent study of gene expression analysis comparing 26 genes between mice and common marmosets distinguished some shared and different molecules expressed during developmental stages of brain (Mashiko et al., 2012), possibly causing structural and functional differences between them.

6.2 Housing and MPTP Administration

Animals should be purchased from a reliable dealer of experimental animals. In general, both male and female animals with ages 2 ∼ 4 years, 240 ∼ 400 g weight are used for experiments. Usually two animals per cage are housed under controlled temperature (28 ± 1°C) and humidity (50 ± 5%) with a 12-h light/dark cycle. Before starting MPTP treatment, the animals are maintained with free access to food and water. After MPTP treatment, each animal must be fed with milk artificially twice daily when they are unable to voluntarily ingest sufficient food. After MPTP administration, the behavioral studies of Parkinsonism usually are performed by close observation with video camera. MPTP administration is usually done with a variety of doses by a subcutaneous injection. Repeated administration with 24-h

intervals is usually performed. According to the doses injected, the following symptoms are observed.

6.3 Progression of Abnormal Symptoms

The acute effects of MPTP include abnormal movements and alterations of motor behavior and posture. These effects may be observed by the systemic or local administration of MPTP and several dosing regimens (Table 41.1) have been used in many studies (Choudhury et al., 2010; Fox et al., 2002; Jenner et al., 1984; Philippens et al., 2013; Rose et al., 1993). The abnormalities become more striking after each successive dose. They occur within 5 min of drug administration and, initially, may last for 15 ~ 30 min. After four or five doses, some of the acute motor effects may persist. The first motor signs to appear, usually after the third dose, will be intermittent eyelid closure, a decrease in spontaneous movements, including loss of facial expression, and postural tremor. The animals will be awake, however, and may respond to loud noises by opening their eyes, looking at the examiner, and making weak threatening movements. The tremor will be intermittently present, moderate in amplitude, and slow in frequency, and involve the proximal muscles of the extremities. A postural tremor of the head or jaw may be observed in some animals. These acute motor effects may last up to 30 min. Motor signs that appear only after four or five doses include abnormal facial movements and changes in posture, muscle tone, and deglutition. Twitching of the facial muscles and facial grimacing may be prominent effects seen in all of the animals. Extension of the head, rigidity of the upper and lower extremities may be demonstrated by passive range-of-motion testing and may be sustained (turning to one side were observed in some of the animals). Some animals may also have difficulty swallowing, as may be evidenced by drooling and the accumulation of food biscuits in their mouth pouches. Rotatory movements of the eyes may be observed in some animals. In all of the animals, eyelid closure, decreased spontaneous motor activity, rigidity, postural tremor, and difficulty swallowing may persist with a cumulative dose of about 1.7 mg/kg. Abnormal facial movements, head extension, and rotatory eye movements, however, may be observed only during the 30 min immediately after drug administration. After the 5-day period of drug administration, other signs of motor impairment may appear. These include general slowness of movement, a flexed posture, loss of hand dexterity, and "freezing" episodes. The animals remain seated, with marked flexion of the neck, thoracic spine, and upper and lower extremities. There may be evident difficulty in picking up food biscuits, which may be subsequently dropped while being carried to the animal's mouth. Episodes of "freezing" or stopping in the

TABLE 41.1　MPTP Regimens for the Common Marmoset in PD Model

MPTP			
Dose	Duration	Site	References
1 mg/kg	8 days	SC	Philippens et al. (2013)
2 mg/kg	4 days	IP	Jenner et al. (1984)
2 mg/kg	5 days	SC	Fox et al. (2002)
2-2-3-3-3 mg/kg	5 days	IP	Rose et al. (1993)
2.5 mg/kg	3 days	SC	Choudhury et al. (2010)

IP, Intraperitoneal; SC, subcutaneous.

TABLE 41.2　Overview of PD-Related Symptoms of Marmoset With MPTP Treatments

Reference (Ando et al., 2008)	Reference (Pearce et al., 1999)
Staying on the floor	Alertness
Hypoactivity	Reaction
Abnormal limb position	Blinking
Abnormal body position	Checking movement
Bent tail	Posture
Dirty fur	Motility
Excessive eye-blinking	Vocalization
Lack of stimulus tracking	Tremor
No biting	Fur condition
Lack of facial expression	
No squeaking	
Resting tremor	
Moving tremor	
Nonsmooth movement	
Immobility	
Catalepsy	
No food approach	
No food taking	
No food eating	

middle of a motion may be observed in some animals. Motor function deficits may appear to increase during the initial 2-week period after the last dose of the drug (Burns et al., 1983). In Table 41.2, we summarized PD-related symptoms observed in marmosets after MPTP treatment referred from two reports (Ando et al., 2008; Pearce et al., 1999).

When a researcher wants to get a short-term maximal effect of MPTP, it will be administered at a dose of 2.5 mg/kg subcutaneously with 3 times at intervals of

(A)

(B)

Before MPTP
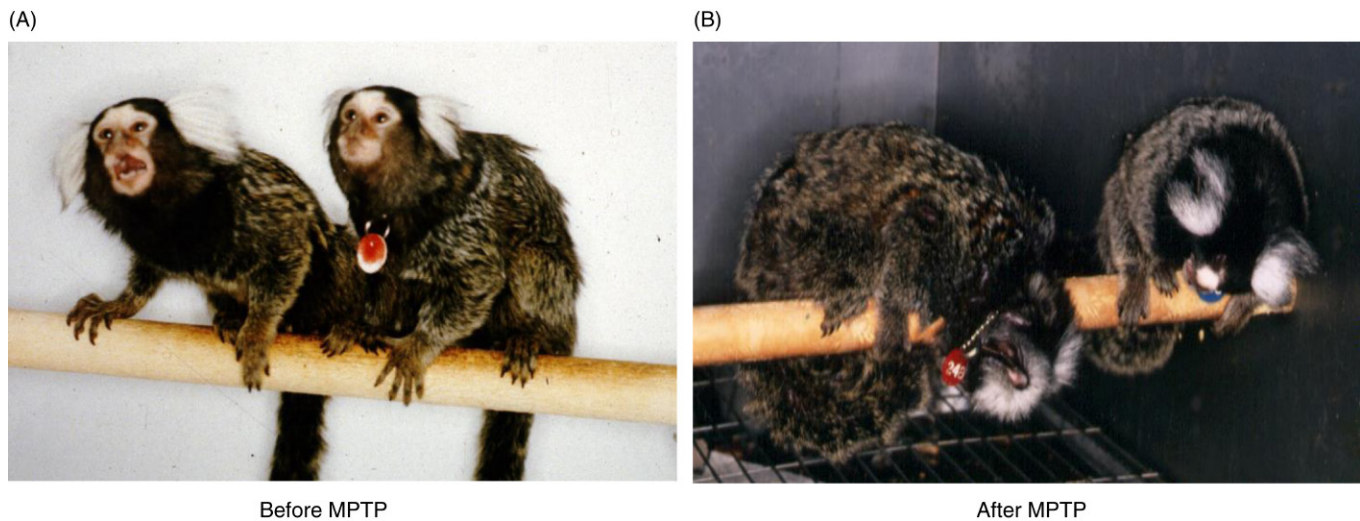
After MPTP

FIGURE 41.7   **Common marmosets.** (A) Normal condition. (B) 14 days after MPTP-treatment at a dose of 2.5 mg/kg subcutaneously with 3 times at intervals of 24 h.

24 h (Choudhury et al., 2010). In Fig. 41.7, we show a picture of normal and MPTP-treated common marmosets.

6.4 Locomotor Activity

Evaluation is usually performed in a monitoring cage unit for locomotor activity with multiple infrared beams covering the inside of the entire cage to automatically detect spontaneous activity of the animal. After a habituation period of ~1 h, an interruption of an infrared beam by a moving marmoset was automatically recorded as a single locomotor count, accumulated over 10 min for up to 8 h.

6.5 Scoring of Severity

The akinesia-like symptom develops, which can be classified with 0 ~ 5: 0 = The animal shows normal behavior; 1 = The animal appears quiet but shows a normal repertoire of movements; 2 = The animal can move freely, but is clumsy when making complicated movements; 3 = The animal makes few slower movements and is obviously clumsy in executing complex movement; 4 = The animal makes few movements unless disturbed, and then movement is slow and limited to a small region of the cage; 5 = The animal is akinetic and does not move even when disturbed (Rose et al., 1993). A well-trained observer scores while the locomotor activity is recorded through a one-way mirror. Besides this, many reports (Annett et al., 1994; Eslamboli et al., 2005; Henderson et al., 1998; Montoya et al., 1990; Palmér et al., 2012; Philippens et al., 2000; Przybyszewski et al., 2006; Roberts et al., 1994; Verhave et al., 2009; Yamane et al., 2010) have been published describing several behavioral tests for this model (Table 41.3).

TABLE 41.3   Overview of Several Behavioral Tests in PD Model

Behavioral test	References
Locomotor activity assessment	Roberts et al. (1994)
Cylinder test	Przybyszewski et al. (2006)
Object retrieval task	Eslamboli et al. (2005)
Tower test	Verhave et al. (2009)
	Palmér et al. (2012)
Bungalow test	Philippens et al. (2000)
Hand-eye coordination test	Philippens et al. (2000)
Fear-potentiated startle response	Philippens et al. (2000)
Rotation test	Annett et al. (1994)
	Henderson et al. (1998)
Conveyor belt test	Annett et al. (1994)
Adhesive labels	Annett et al. (1994)
Reaching into tubes	Annett et al. (1994)
	Henderson et al. (1998)
Staircase	Eslamboli et al. (2005)
	Henderson et al. (1998)
	Montoya et al. (1990)
	Montoya et al. (1990)
Hourglass test	Verhave et al. (2009)
Bar grip power	Yamane et al. (2010)
Treadmill test	Yamane et al. (2010)

6.6 Immunohistochemical, Biochemical Analysis

Basically the same protocols as mice can be applied for immunohistochemical and biochemical analysis. Namely, immunostaining, HPLC, western blot, RT-PCR, and so on.

6.7 Functional Imaging in Common Marmosets

Although PET and single photon emission computed tomography (SPECT) studies using MPTP on nonhuman primates have been reported (Ashkan et al., 2007; Ballanger et al., 2016; Doudet et al., 1989; Eberling et al., 1999; Hantraye et al., 1986), any functional imaging study on MPTP-treated common marmosets has yet to be reported except for the one by Ando et al. (2012). As various radiolabeled analogs interacting with molecules of dopaminergic systems have been developed (Minuzzi et al., 2006), they will be examined in common marmosets in the near future.

7 CONCLUDING REMARKS

Here we have described the characteristics and methodological details of MPTP-induced mouse and common marmoset models of PD. As we have seen, these reliable models have a lot of merits compared to other models with well satisfying the face, constructive, and predictive validities of human PD. As a face validity, bilateral motor dysfunctions related to extrapyramidal syndrome have been well reproduced especially in nonhuman primates including common marmoset, and many behavioral tasks for mice have also been developed. As constructive validities, following characteristics observed in human PD are well reproduced: specific cell death of nigrostriatal dopaminergic neurons; decrease of the striatal dopamine and its metabolites; activation of astrocytes and microglia; oxidative stress caused both by mitochondrial dysfunction and activated glial cells; inflammatory reactions. Although only one exception that does not match to human PD in MPTP model is the formation of Lewy-like inclusion bodies containing α-synuclein and ubiquitin proteins, it may also be reproduced under a certain condition of MPTP administration, probably by continuous delivery with osmotic minipump or by longer administration for at least 5 days. As a predictive validity, many of the drugs in clinical use for PD are also effective in the MPTP model. To understand pathophysiological and pharmacological details, to develop novel therapeutics, and to screen possible substances for protective (disease modifying) and therapeutic drugs of PD, its applications including functional imaging will continue to expand further.

Acknowledgment

References

Ando, K., Maeda, J., Inaji, M., et al., 2008. Neurobehavioral protection by single dose ldeprenyl against MPTP-induced parkinsonism in common marmosets. Psychopharmacology (Berl.) 195, 509–516.

Ando, K., Obayashi, S., Nagai, Y., et al., 2012. PET analysis of dopaminergic neurodegeneration in relation to immobility in the MPTP-treated common marmoset, a model for Parkinson's disease. PLoS One 7, e46371.

Annett, L.E., Martel, F.L., Rogers, D.C., et al., 1994. Behavioral assessment of the effects of embryonic nigral grafts in marmosets with unilateral 6-OHDA lesions of the nigrostriatal pathway. Exp. Neurol. 125, 228–246.

Aoki, E., Yano, R., Yokoyama, H., et al., 2009. Role of nuclear transcription factor kappa B (NF-kappaB) for MPTP (1-methyl-4-phenyl-1,2,3,6-tetrahyropyridine)-induced apoptosis in nigral neurons of mice. Exp. Mol. Pathol. 86, 57–64.

Aoki, E., Yokoyama, H., Kimoto, H., et al., 2010. Chronic administration with rotenone does not enhance MPTP neurotoxicity in C57BL/6 mice. J. Mol. Neurosci. 41, 17–24.

Araki, T., Kumagai, T., Tanaka, K., et al., 2001. Neuroprotective effect of riluzole in MPTP-treated mice. Brain Res. 918, 176–181.

Ashkan, K., Wallace, B.A., Mitrofanis, J., et al., 2007. SPECT imaging, immunohistochemical and behavioural correlations in the primate models of Parkinson's disease. Parkinsonism Relat. Disord. 13, 266–275.

Ballanger, B., Beaudoin-Gobert, M., Neumane, S., et al., 2016. Imaging dopamine and serotonin systems on MPTP monkeys: a longitudinal PET investigation of compensatory mechanisms. J. Neurosci. 36, 1577–1589.

Bankiewicz, K.S., Sanchez-Pernaute, R., Oiwa, Y., et al., 1999. Preclinical models of Parkinson's disease. Curr. Protocol. Neurosci. (Suppl. 9), 9.4.1–9.4.32.

Barbeau, A., Dallaire, L., Buu, N.T., et al., 1985. New amphibian models for the study of 1-methyl-4-phenyl-1,2,3,6-tetrahydropyridine (MPTP). Life Sci. 36, 1125–1134.

Belzung, C., Griebel, G., 2001. Measuring normal and pathological anxiety-like behaviour in mice: a review. Behav. Brain Res. 125, 141–149.

Betarbet, R., Sherer, T.B., Greenamyre, J.T., 2002. Animal models of Parkinson's disease. Bioessays 24, 308–318.

Betarbet, R., Sherer, T.B., MacKenzie, G., et al., 2000. Chronic systemic pesticide exposure reproduces features of Pakinson's disease. Nat. Neurosci. 3, 1301–1306.

Biju, K., Zhou, Q., Li, G., Macrophage-mediated GDNF, et al., 2010. delivery protects against dopaminergic neurodegeneration: a therapeutic strategy for Parkinson's disease. Mol. Ther. 18, 1536–1544.

Blandini, F., Armentero, M.T., 2012. Animal models of Parkinson's disease. FEBS J. 279, 1156–1166.

Blume, S.R., Cass, D.K., Tsueng, K.Y., 2009. Stepping test in mice: a reliable approach in determining forelimb akinesia in MPTP-induced Parkinsonism. Exp. Neurol. 219, 208–211.

Boyd, J.D., Jang, H., Shepherd, K.R., et al., 2007. Response to 1-methyl-4-phenyl-1,2,3,6-tetrahydropyridine (MPTP) differs in mouse strains and reveals a divergence in JNK signaling and COX-2 induction prior to loss of neurons in the substantia nigra pars compacta. Brain Res. 1175, 107–116.

Braungert, E., Gerlach, M., Riederer, P., et al., 2004. *Caenorhabditis elegans* MPP$^+$ model of Parkinson's disease for high-throughput drug screenings. Neurodegener. Dis. 1, 175–183.

Burkard, W.P., Bonetti, E.P., Haefely, W., 1985. The benzodiazepine antagonist Ro 15-1788 reverses the effect of methyl-beta-carboline-3-carboxylate but not of harmaline on cerebellar cGMP and motor performance in mice. Eur. J. Pharmacol. 109, 241–247.

Burns, R.S., Chiueh, C.C., Marley, S.P., et al., 1983. A primate model of parkinsonism: selective destruction of dopaminergic neurons in the pars compacta of the substantia nigra by N-methyl-4-phenyl-1,2,3,6-tetrahydropyridine. Proc. Natl. Acad. Sci. 80, 4546–4550.

Calí, T., Ottolini, D., Brini, M., 2011. Mitochondria, calcium, and endoplasmic reticulum stress in Parkinson's disease. Biofactors 37, 228–240.

Carlsson, A., 1959. The occurrence, distribution and physiological role of catecholamines in the nervous system. Pharmacol. Rev. 11, 490–493.

Castagnoli, K., Murugesan, T., 2004. Tobacco leaf, smoke and smoking, MAO inhibitors, Parkinson's disease and neuroprotection; are there links? Neurotoxicology 25, 279–291.

Chacot, J.M., 1880. Lecon sur les maladies du systeme nerveux, fourth ed. Tome Premier, Paris.

Chao, K.T., Tsao, H.H., Weng, Y.H., et al., 2012. Quantitative analysis of binding sites for 9-fluoropropyl-(+)-dihydrotetrabenazine ([(^{18}F)]AV-133) in a MPTP-lesioned PD mouse model. Synapse 66, 823–831.

Chen, J.Y., Hsu, P.C., Hsu, I.L., et al., 2001. Sequential up-regulation of the c-fos, c-jun and bax genes in the cortex, striatum and cerebellum induced by a single injection of a low dose of 1-methyl-4-phenyl-1,2,3,6-tetrahydropyridine (MPTP) in C57BL/6 mice. Neurosci. Lett. 314, 49–52.

Choi, C.B., Kim, S.Y., Lee, S.H., et al., 2011. Assessment of metabolic changes in the striatum of a MPTP-intoxicated canine model: in vivo ^{1}H-MRS study of an animal model for Parkinson's disease. Magn. Reson. Imag. 29, 32–39.

Choudhury, M.E., Moritoyo, T., Yabe, H., et al., 2010. Zonisamide attenuates MPTP neurotoxicity in marmosets. J. Pharmacol. Sci. 114, 298–303.

Collins, L.M., Toulouse, A., Connor, T.J., et al., 2012. Contributions of central and systemic inflammation to the pathophysiology of Parkinson's disease. Neuropharmacology 62, 2154–2168.

Cox, T., Cachón-González, M.B., 2012. The cellular pathology of lysosomal disease. J. Pathol. 226, 241–254.

Crabtree, D.M., Zhang, J., 2012. Genetically engineered mouse models of Parkinson's disease. Brain Res. Bull. 88, 13–32.

de Lau, L.M., Breteler, M.M., 2006. Epidemiology of Parkinson's disease. Lancet Neurol. 5, 525–535.

Dean, R.L., Scozzafava, J., Goas, J.A., et al., 1981. Age-related differences in behavior across the life span of the C57BL/6J mouse. Exp. Aging Res. 7, 427–451.

Dhanasekaran, M., Albano, C.B., Pellet, L., et al., 2008. Role of lipoamide dehydrogenase and metallothionein on 1-methyl-4-phenyl-1,2,3,6-tetrahydropyridine-induced neurotoxicity. Neurochem. Res. 33, 980–984.

Ding, Y.X., Xia, Y., Jiao, X.Y., et al., 2011. The TrkB-positive dopaminergic neurons are less sensitive to MPTP insult in the substantia nigra of adult C57/BL mice. Neurochem. Res. 36, 1759–1766.

Doudet, D.J., Miyake, H., Finn, R.T., et al., 1989. 6-18F-L-dopa imaging of the dopamine neostriatal system in normal and clinically normal MPTP-treated rhesus monkeys. Exp. Brain Res. 78, 69–80.

Drouin-Ouellet, J., Gibrat, C., Bousquet, C., et al., 2011. The role of the MYD88-dependent pathway in MPTP-induced brain dopaminergic degeneration. J. Neuroinflam. 8, 137.

Duty, S., Jenner, P., 2011. Animal models of Parkinson's disease: a source of novel treatments and clues to the cause of the disease. Br. J. Pharmacol. 164, 1357–1391.

Eberling, J.L., Bankiewicz, K.S., Pivirotto, P., et al., 1999. Dopamine transporter loss and clinical changes in MPTP-lesioned primates. Brain Res. 832, 184–187.

Ehringer, H., Hornykiewicz, O., 1960. Distribution of noradrenaline and dopamine (3-hydroxytyramine) in the human brain and their behavior in diseases of the extrapyramidal system. Klin Wochenshr 38, 1236–1239.

Encarnacion, E.V., Hauser, R.A., 2008. I Levodopa-induced dyskinesias in Parkinson's disease: etiology, impact on quality of life, and treatments. Eur. J. Neurol. 60, 57–66.

Eslamboli, A., Georgievska, B., Ridley, R.M., et al., 2005. Continuous low-level glial cell line-derived neurotrophic factor delivery using recombinant adeno-associated viral vectors provides neuroprotection and induces behavioral recovery in a primate model of Parkinson's disease. J. Neurosci. 25, 769–777.

Filipov, N.M., Norwood, A.B., Sistrunk, S.C., 2009. Strain-specific sensitivity to MPTP of C57BL/6 and BALB/c mice is age dependent. Neuroreport 20, 713–717.

Fornai, F., Schlüter, O.M., Lenzi, P., et al., 2005. Parkinson-like syndrome induced by continuous MPTP infusion: convergent roles of the ubiquitin-proteasome system and alpha-synuclein. Proc. Natl. Acad. Sci. USA 102, 3413–3418.

Forno, L.S., 1996. Neuropathology of Parkinson's disease. J. Neuropathol. Exp. Neurol. 55, 259–272.

Fox, S.H., Henry, B., Hill, M., Crossman, A., Brotchie, J., 2002. Stimulation of cannabinoid receptors reduces levodopa-induced dyskinesia in the MPTP-lesioned nonhuman primate model of Parkinson's disease. Mov. Disord. 17, 1180–1187.

German, D.C., Manaye, K., Smith, W.K., et al., 1989. Midbrain dopaminergic cell loss in Parkinson's disease: computer visualization. Ann. Neurol. 26, 507–514.

Ghiribi, O., Herman, M.M., Pramoonjago, P., et al., 2003. MPP$^+$ induces the endoplasmic reticulum stress response in rabbit brain involving activation of the ATF-6 and NF-kappaB signaling pathways. J. Neuropathol. Exp. Neurol. 62, 1144–1153.

Ghosh, A., Roy, A., Liu, X., Kordower, J.H., et al., 2007. Selective inhibition of NF-kappaB activation prevents dopaminergic neuronal loss in a mouse model of Parkinson's disease. Proc. Natl. Acad. Sci. USA 104, 18754–18759.

Halliday, G., Herrero, M.T., Murphy, K., et al., 2009. No Lewy pathology in monkeys with over 10 years of severe MPTP Parkinsonism. Mov. Disord. 24, 1519–1523.

Hantraye, P., Loc'h, C., Tacke, U., et al., 1986. "In vivo" visualization by positron emission tomography of the progressive striatal dopamine receptor damage occurring in MPTP-intoxicated non-human primates. Life Sci. 39, 1375–1382.

Heikkila, R.E., Niclas, W.J., Duvoisin, R.C., 1985. Dopaminergic toxicity after the stereotaxic administration of the 1-methyl-4-phenylpyridinium ion (MPP+) to rats. Neurosci. Lett. 59, 135–140.

Henderson, J.M., Annett, L.E., Torres, E.M., et al., 1998. Behavioural effects of subthalamic nucleus lesions in the hemiparkinsonian marmoset (*Callithrix jacchus*). Eur. J. Neurosci. 10, 689–698.

Himeda, T., Watanabe, Y., Tounai, H., et al., 2006. Time dependent alterations of co-localization of S100beta and GFAP in the MPTP-treated mice. J. Neural. Transm. 113, 1887–1894.

Hollerman, J.R., Grace, A.A., 1990. The effects of dopamine-depleting brain lesions on the electrophysiological activity of rat substantia nigra dopamine neurons. Brain Res. 533, 203–212.

Honer, M., Hengerer, B., Blagoev, M., et al., 2006. Comparison of [^{18}F]FDOPA, [^{18}F]FMT and [^{18}F]FECNT for imaging dopaminergic neurotransmission in mice. Nucl. Med. Biol. 33, 607–614.

Hsu, K.S., Fu, W.M., Lin-Shiau, S.Y., 1994. Blockade by MPTP of the nicotinic acetylcholine receptor channels in embryonic Xenopus muscle cells. Neuropharmacology 33, 35–41.

Hung, H.C., Lee, E.H., 1996. The mesolimbic dopaminergic pathway is more resistant than the nigrostriatal dopaminergic pathway to

MPTP and MPP+ toxicity: role of BDNF gene expression. Brain Res. Mol. Brain Res. 41, 14–26.

Ishiwata, K., Koyanagi, Y., Abe, K., et al., 2001. Evaluation of neurotoxicity of TIQ and MPTP and of parkinsonism-preventing effect of 1-MeTIQ by in vivo measurement of pre-synaptic dopamine transporters and post-synaptic dopamine D(2) receptors in the mouse striatum. J. Neurochem. 79, 868–876.

Jankovic, J., Marsden, C.D., 1988. Parkinson's Disease and Movement Disorders. Urban/Schwarzenberg, Baltimore.

Jenner, P., Rupniak, N.M., Rose, S., Kelly, E., Kilpatrick, G., Lees, A., Marsden, C.D., 1984. 1-Methyl-4-phenyl-1,2,3,6-tetrahydropyridin-einduced parkinsonism in the common marmoset. Neurosci. Lett. 50, 85–90.

Kadoguchi, N., Umeda, M., Kato, H., et al., 2008a. Proteasome inhibitor does not enhance MPTP neurotoxicity in mice. Cell Mol. Neurobiol. 28, 971–979.

Kadoguchi, N., Kimoto, H., Yano, R., et al., 2008b. Failure of acute administration with proteasome inhibitor to provide a model of Parkinson's disease in mice. Metab. Brain Dis. 23, 147–154.

Kadoguchi, N., Okabe, S., Yamamura, Y., Shono, M., Fukano, T., Tanabe, A., Yokoyama, H., Kasahara, J., 2014. Mirtazapine has a therapeutic potency in 1-methyl-4-phenyl-1,2,3,6-tetrahydropyridine (MPTP)-induced mice model of Parkinson's disease. BMC Neurosci. 15, 79.

Kakaria, R.N., Mitchell, M.H., Harik, S.I., 1987. Correlation of 1-methyl-4-phenyl-1,2,3,6-tetrahydropyridine neurotoxicity with blood-brain barrier monoamine oxidase activity. Proc. Natl. Acad. Sci. USA 84, 3521–3525.

Karuppagounder, S.S., Brahmachari, S., Lee, Y., et al., 2014. The c-Abl inhibitor, Nilotinib, protects dopaminergic neurons in a preclinical animal model of Parkinson's disease. Sci. Rep. 4, 4874.

Kikuta, S., Nakamura, Y., Yamamura, Y., Tamura, A., Homma, N., Yanagawa, Y., Tamura, H., Kasahara, J., Osanai, M., 2015. Quantitative activation-induced manganese-enhanced MRI reveals severity of Parkinson's disease in mice. Sci. Rep. 5, 12800.

Kishima, H., Poyot, T., Bloch, J., et al., 2004. Encapsulated GDNF-producing C2C12 cells for Parkinson's disease: a pre-clinical study in chronic MPTP-treated baboons. Neurobiol. Dis. 16, 428–439.

Kitada, T., Asakawa, S., Hattori, N., et al., 1998. Mutations in the parkin gene cause autosomal recessive juvenile parkinsonism. Nature 392, 605–608.

Ko, H.S., Lee, Y., Shin, J.H., et al., 2010. Phosphorylation by the c-Abl protein tyrosine kinase inhibits parkin's ubiquitination and protective function. Proc. Natl. Acad. Sci. 107, 16691–16696.

Krack, P., Hariz, M.I., Baunez, C., et al., 2010. Deep brain stimulation: from neurology to psychiatry? Trends Neurosci. 33, 474–484.

Kuroiwa, H., Yokoyama, H., Kimoto, H., et al., 2010. Biochemical alterations of the striatum in an MPTP-treated mouse model of Parkinson's disease. Metab. Brain Dis. 25, 177–183.

Kurosaki, R., Muramatsu, Y., Imai, Y., et al., 2004. Neuroprotective effect of the angiotensin-converting enzyme inhibitor perindopril in MPTP-treated mice. Neurol. Res. 26, 644–657.

Langston, J.W., 2002. Parkinson's disease: current and future challenger. Neurotoxicology 23, 443–450.

Langston, J.W., Ballard, P., Terud, J.W., et al., 1983. Chronic Parkinsonism in humans due to a product of meperidine-analog synthesis. Science 219, 979–980.

Langston, J.W., Forno, L.S., Rebert, C.S., et al., 1984. Selective nigral toxicity after systemic administration of 1-methyl-4-phenyl-1,2,3,6-tetrahydropyrine (MPTP) in the squirrel monkey. Brain Res. 292, 390–394.

Laret, M.L., San Millián, J.A., Fabre, E., et al., 2002. Deprenyl protects from MPTP-induced Parkinson-like syndrome and glutathione oxidation in rat striatum. Toxicology 170, 165–171.

Li, S., Pu, X.P., 2011. Neuroprotective effect of kaempferol against 1-methyl-4-phenyl-1,2,3,6-tetrahydropyridine-induced mouse model of Parkinson's disease. Biol. Pharm. Bull. 34, 1291–1296.

Ma, Y., Dhawan, V., Mentis, M., et al., 2002. Parametric mapping of [18F]FPCT binding in early stage Parkinson's disease: a PET study. Synapse 45, 125–133.

Maggio, R., Riva, M., Vaglini, F., et al., 1998. Nicotine prevents experimental parkinsonism in rodents and induces striatal increase of neurotrophic factors. J. Neurochem. 71, 2439–2446.

Mashiko, H., Yoshida, A.C., Kikuchi, S.S., et al., 2012. Comparative anatomy of marmoset and mouse cortex from genomic expression. J. Neurosci. 32, 5039–5053.

Matsuda, N., Sato, S., Shiba, K., et al., 2010. PINK1 stabilized by mitochondrial depolarization recruits Parkin to damaged mitochondria and activates latent Parkin for mitophagy. J. Cell Biol. 189, 211–221.

Minghetti, L., 2004. Cyclooxygenase-2 (COX-2) in inflammatory and degenerative brain diseases. J. Neuropathol. Exp. Neurol. 63, 901–910.

Minuzzi, L., Olsen, A.K., Bender, D., et al., 2006. Quantitative autoradiography of ligands for dopamine receptors and transporters in brain of Göttingen minipig: comparison with results in vivo. Synapse 59, 211–219.

Mochizuki, H., Goto, K., Mori, H., et al., 1996. Histochemical detection of apoptosis in Parkisnon's disease. J. Neurol. Sci. 137, 120–123.

Mohanasundari, M., Srinivasan, M.S., Sethupathy, S., et al., 2006. Enhanced neuroprotective effect by combination of bromocriptine and *Hypericum perforatum* extract against MPTP-induced neurotoxicity in mice. J. Neurol. Sci. 249, 140–144.

Montoya, C.P., Astell, S., Dunnett, S.B., 1990. Effects of nigral and striatal grafts on skilled forelimb use in the rat. Prog. Brain Res. 82, 459–466.

Morigaki, R., Sako, W., Okita, S., et al., 2011. Cyclin-dependent kinase 5 with phosphorylation of tyrosine 15 residue is enriched in striatal matrix compartment in adult mice. Neuroscience 189, 25–31.

Muramatsu, Y., Kurosaki, R., Mikami, T., et al., 2002. Therapeutic effect of neuronal nitric oxide synthase inhibitor (7-nitroindazole) against MPTP neurotoxicity in mice. Metab. Brain Dis. 17, 169–182.

Muthane, U., Ramsay, K.A., Jiang, H., et al., 1994. Differences in nigral neuron number and sensitivity to 1-methyl-4-phenyl-1,2,3,6-tetrahydropyridine in C57/bl and CD-1 mice. Exp. Neurol. 126, 195–204.

Nagahara, A.H., Tuszynski, M.H., 2011. Potential therapeutic uses of BDNF in neurological and psychiatric disorders. Nat. Rev. Drug Discov. 10, 209–219.

Nagatsu, T., Sawada, M., 2007. Biochemistry of postmortem brains in Parkinson's disease: historical overview and future prospects. 2007. J. Neural. Transm. Suppl. 72, 113–120.

Nomoto, M., Kita, S., Iwata, S.I., et al., 1998. Effects of acute or prolonged administration of cabergoline on parkinsonism induced by MPTP in common marmosets. Pharmacol. Biochem. Behav. 59, 717–721.

Ogawa, N., Mizukawa, K., Hirose, Y., et al., 1987. MPTP-induced parkinsonian model in mice: biochemistry, pharmacology and behavior. Eur. Neurol. 26, 16–23.

Ohno, Y., Ishida, K., Ikeda, K., et al., 1994. Evaluation of bradykinesia induction by SM-9018, a novel 5-HT2 and D2 receptor antagonist, using the mouse pole test. Pharmacol. Biochem. Behav. 49, 19–23.

Olive, M.F., Mehmert, K.K., Hodge, C.W., 2000. Microdialysis in the mouse nucleus accumbens: a method for detection of monoamine and amino acid neurotransmitters with simultaneous assessment of locomotor activity. Brain Res. Brain Res. Protoc. 5, 16–24.

Palmér, T., Tamtè, M., Halje, P., et al., 2012. A system for automated tracking of motor components in neurophysiological research. J. Neurosci. Methods 205, 334–344.

Park, J., Kim, S.Y., Cha, G.H., et al., 2005. Drosophila DJ-1 mutants show oxidative stress-sensitive locomotive dysfunction. Gene 361, 133–139.

Parkinson, J., 1817. An Essay on the Shaking Palsy. Sherwood, Neely and Jones, London.

Pearce, R.K., Jackson, M., Britton, D.R., et al., 1999. Actions of the D1 agonists A-77636 and A-86929 on locomotion and dyskinesia in MPTP-treated L-dopa-primed common marmosets. Psychopharmacology (Berl.) 142, 51–60.

Perrin, D., Mamet, J., Scarna, H., et al., 2004. Long-term prenatal hypoxia alters maturation of brain catecholaminergic systems and motor behavior in rats. Synapse 54, 92–101.

Philippens, I.H., Melchers, B.P., Roeling, T.A., et al., 2000. Behavioral test systems in marmoset monkeys. Behav. Res. Methods Instrum. Comput. 32, 173–179.

Philippens, I.H., Wubben, J.A., Finsen, B., 't Hart, B.A., 2013. Oral treatment with the NADPH oxidase antagonist apocynin mitigates clinical and pathological features of parkinsonism in the MPTP marmoset model. J. Neuroimmun. Pharmacol. 8, 715–726.

Predinger, R.D., Nguiar, Jr., A.S., Matheus, F.C., et al., 2012. Intranasal administration of neurotoxicants in animals: support for the olfactory vector hypothesis of Parkinson's disease. Neurotox. Res. 21, 90–116.

Przybyszewski, A.W., Sosale, S., Chaudhuri, A., 2006. Quantification of three-dimensional exploration in the cylinder test by the common marmoset (Callithrix jacchus). Behav. Brain Res. 170, 62–70.

Quik, M., Huang, L.Z., Parameswaran, N., Bordia, T., Campos, C., Perez, X.A., 2009. Multiple roles for nicotine in Parkinson's disease. Biochem. Pharmacol. 78, 677–685.

Rangasamy, S.B., Soderstrom, K., Bakay, R.A., et al., 2010. Neurotrophic factor therapy for Parkinson's disease. Prog. Brain Res. 184, 237–264.

Rappold, P.M., Cui, M., Chesser, A.S., et al., 2011. Paraquat neurotoxicity is mediated by the dopamine transporter and organic cation transporter-3. Proc. Natl. Acad. Sci. USA 108, 20766–20771.

Rascol, O., Lozano, A., Stern, M., et al., 2011. Milestones in Parkinson's disease therapeutics. Mov. Disord. 26, 1072–1082.

Ricaurte, G.A., Irwin, I., Forno, L.S., et al., 1987. Aging and 1-methyl-4-phenyl-1,2,3,6-tetrahydropyrine-induced degeneration of dopaminergic neurons in the substantia nigra. Brain Res. 403, 43–51.

Richardson, J.R., Quan, Y., Sherer, T.B., et al., 2005. Paraquat neurotoxicity is distinct from that of MPTP and rotenone. Toxicol. Sci. 88, 193–201.

Roberts, A.C., De Salvia, M.A., Wilkinson, L.S., et al., 1994. 6-Hydroxy-dopamine lesions of the prefrontal cortex in monkeys enhance performance on an analog of the Wisconsin Card Sort Test: possible interactions with subcortical dopamine. J. Neurosci. 14, 2531–2544.

Rose, S., Nomoto, M., Jackson, E.A., et al., 1993. Age-related effects of 1-methyl-4-phenyl-1,2,3,6-tetrahydropyridine treatment of common marmosets. Eur. J. Pharmacol. 230, 177–185.

Saiki, H., Hayashi, T., Takahashi, R., et al., 2010. Objective and quantitative evaluation of motor function in a monkey model of Parkinson's disease. J. Neurosci. Methods 190, 198–204.

Samii, A., Nutt, J.G., Ransom, B.R., 2004. Parkinson's disease. Lancet 363, 1783–1793.

Sato, K., Sumi-Ichinose, C., Kaji, R., et al., 2008. Differential involvement of striosome and matrix dopamine systems in a transgenic model of dopa-responsive dystonia. Proc. Natl. Acad. Sci. USA 105, 12551–12556.

Schneider, J.S., Rothblat, D.S., 1991. Neurochemical evaluation of the striatum in symptomatic and recovered MPTP-treated cats. Neuroscience 44, 421–429.

Sedelis, M., Hofele, K., Auburger, G.W., et al., 2000. MPTP susceptibility in the mouse: behavioral, neurochemical, and histological analysis of gender and strain differences. Behav. Genet. 30, 171–182.

Shimizu, K., Ohtaki, K., Matsubara, K., et al., 2001. Carrier-mediated processes in blood–brain barrier penetration and neural uptake of paraquat. Brain Res. 906, 135–142.

Shimoji, M., Zhang, L., Mandir, A.S., et al., 2005. Absence of inclusion body formation in the MPTP mouse model of Parkinson's disease. Brain Res. Mol. Brain Res. 134, 103–108.

Shioda, N., Yabuki, Y., Kobayashi, Y., et al., 2014. FABP3 protein promotes α-synuclein oligomerization associated with 1-methyl-1,2,3,6-tetrahydropiridine-induced neurotoxicity. J. Biol. Chem. 289, 18957–18965.

Smeyne, M., Goloubeva, O., Smeyne, R.J., 2001. Strain-dependent susceptibility to MPTP and MPP(+)-induced parkinsonism is determined by glia. Glia 34, 73–80.

Sunderström, E., Fredriksson, A., Archer, T., 1990. Chronic neurochemical and behavioral changes in MPTP-lesioned C57BL/6 mice: a model for Parkinson's disease. Brain Res. 528, 181–188.

Sunderström, E., Strömberg, I., Tsushumi, T., et al., 1987. Studies on the effect of 1-methyl-4-phenyl-1,2,3,6-tetrahydropyridine (MPTP) on central catecholamine neurons in C57BL/6 mice. Comparison with three other strains of mice. Brain Res. 405, 26–38.

Swanson, C.R., Joers, V., Bondarenko, V., et al., 2011. The PPAR-γ agonist pioglitazone modulates inflammation and induces neuroprotection in parkinsonian monkeys. J. Neuroinflammation 8, 91–104.

Takahashi, R.N., Rogerio, R., Zanin, M., 1989. Maneb enhances MPTP neurotoxicity in mice. Res. Commun. Chem. Pathol. Pharmacol. 66, 167–170.

Tanabe, A., Yamamura, Y., Kasahara, J., Morigaki, R., Kaji, R., Goto, S., 2014. A novel tyrosine kinase inhibitor AMN107 (nilotinib) normalizes striatal motor behaviors in a mouse model of Parkinson's disease. Front. Cell Neurosci. 8, 50.

Thiruchelvam, M., Brockel, B.J., Richfield, E.K., et al., 2000. Potentiated and preferential effects of combined paraquat and maneb on nigrostriatal dopamine systems: environmental risk factors for Parkinson's disease? Brain Res. 873, 225–234.

Tieu, K., Ischiropoulos, H., Pzedborski, S., 2003. Nitric oxide and reactive oxygen species in Parkinson's disease. IUBMB Life 55, 329–335.

Toomey, J.S., Bhatia, S., Moon, L.T., et al., 2012. PET Imaging a MPTP-induced mouse model of Parkinson's disease using the fluoropropyl-dihydrotetrabenazine analog [(18)F]-DTBZ (AV-133). PLoS One 7, e39041.

Tretiakoff, C., 1919. Contribution of a l'Etude de l'Anatomie Pathologique du Locus Niger. These de Paris.

Trivedi, M.S., Jarbe, T., 2011. A brief review on recent developments in animal models of schizophrenia. Indian J. Pharmacol. 43, 375–380.

Ungerstedt, U., 1968. 6-Hydroxy-dopamine induced degeneration of central monoamine neurons. Eur. J. Pharmacol. 5, 107–110.

Ungerstedt, U., Arbuthnott, G.W., 1970. Quantitative recording of rotational behavior in rats after 6-hydroxy-dopamine lesions of the nigrostriatal dopamine system. Brain Res. 24, 485–493.

Vanover, K.E., Suruki, M., Robledo, S., et al., 1999. Positive allosteric modulators of the GABA(A) receptor: differential interaction of benzodiazepines and neuroactive steroids with ethanol. Psychopharmacology (Berl.) 141, 77–82.

Verhave, P.S., Vanwersch, R.A., van Helden, H.P., et al., 2009. Two new test methods to quantify motor deficits in a marmoset model for Parkinson's disease. Behav. Brain Res. 200, 214–219.

Walsh, L.S., Wanger, G.C., 1989. Age-dependent effects of 1-methyl-4-phenyl-1,2,3,6-tetrahydropyridine (MPTP): correlation with monoamine oxidase-B. Synapse 3, 308–314.

Wang, H.Q., Takahashi, R., 2007. Expanding insights on the involvement of endoplasmic reticulum stress in Parkinson's disease. Antioxid. Redox. Signal 9, 553–561.

Wang, Y.M., Pu, P., Le, W.D., 2007. ATP depletion is the major cause of MPP+ induced dopamine neuronal death and worm lethality in alpha-synuclein transgenic C. elegans. Neurosci. Bull. 23, 329–335.

Watanabe, Y., Kato, H., Araki, T., 2008. Protective action of neuronal nitric oxide synthase inhibitor in the MPTP mouse model of Parkinson's disease. Metab. Brain Dis. 23, 51–69.

Yamada, M., Kida, K., Amutuhaire, W., et al., 2010. Gene disruption of caspase-3 prevents MPTP-induced Parkinson's disease in mice. Biochem. Biophys. Res. Commun. 402, 312–318.

Yamamura, Y., Morigaki, R., Kasahara, J., Yokoyama, H., Tanabe, A., Okita, S., Koizumi, H., Nagahiro, S., Kaji, R., Goto, S., 2013. Dopamine signaling negatively regulates striatal phosphorylation of Cdk5 at tyrosine 15 in mice. Front. Cell Neurosci. 7, 12.

Yamane, J., Nakamura, M., Iwanami, A., et al., 2010. Transplantation of galectin-1-expressing human neural stem cells into the injured spinal cord of adult common marmosets. J. Neurosci. Res. 88, 1394–1405.

Yano, R., Yokoyama, H., Kuroiwa, H., et al., 2009. A novel anti-Parkinsonian agent, zonisamide, attenuates MPTP-induced neurotoxicity in mice. J. Mol. Neurosci. 39, 211–219.

Yokoyama, H., Kuroiwa, H., Kasahara, J., et al., 2011a. Neuropharmacological approach against MPTP (1-methyl-4-phenyl-1,2,3,6-tetrahydropyrine)-induced mouse model of Parkinson's disease. Acta Neurobiol. Exp. 71, 1–13.

Yokoyama, H., Kuroiwa, H., Tsukada, T., et al., 2010a. Poly(ADP-ribose)polymerase inhibitor can attenuate the neuronal death after 1-methyl-4-phenyl-1,2,3,6-tetrahydropyridine-induced neurotoxicity in mice. J. Neurosci. Res. 88, 1522–1536.

Yokoyama, H., Kuroiwa, H., Yano, R., et al., 2010b. Therapeutic effect of a novel anti-parkinsonian agent zonisamide against MPTP (1-methyl-4-phenyl-1,2,3,6-tetrahydropyridine) neurotoxicity in mice. Metab. Brain Dis. 25, 135–143.

Yokoyama, H., Uchida, H., Kuroiwa, H., et al., 2011b. Role of glial cells in neurotoxin-induced animal models of Parkinson's disease. Neurol. Sci. 32, 1–7.

Zhang, J., Fitsanakis, V.A., Gu, G., et al., 2003. Manganese ethylene-bis dithiocarbamate and selective dopaminergic neurodegeneration in rat: a link through mitochondrial dysfunction. J. Neurochem. 84, 336–346.

42

Animal Models for the Study of Human Neurodegenerative Diseases

Gabriela D. Colpo*, Fabiola M. Ribeiro**, Natalia P. Rocha*, Antônio L. Teixeira*

*University of Texas Health Science Center at Houston, Houston, TX, United States
**Institute of Biological Sciences, Federal University of Minas Gerais (UFMG), Belo Horizonte, MG, Brazil

1 INTRODUCTION

Neurodegenerative diseases are a major cause of disability and premature death among older people worldwide and result from the progressive death of neurons, which over time leads to movement and/or cognitive impairment (Bird et al., 2003; Huisman et al., 2011; Savica et al., 2013). The majority of neurodegenerative diseases are clinically heterogeneous and genetically complex. This is especially true for the two most common neurodegenerative diseases, that is, Alzheimer's disease (AD) and Parkinson's disease (PD), in which >90% of cases are not linked to a single mutation. It is worth mentioning that Huntington's disease (HD) is a purely genetic disorder (Lansbury, 2004).

Despite the diversity of clinical phenotypes, neurodegenerative disorders share common features including clinical course and molecular mechanisms of pathogenesis. Preferential subsets of neurons are affected in neurodegenerative diseases which arise insidiously, progress endlessly, and are frequently age related (Byrne et al., 2011). Neurodegenerative diseases also share some pathological hallmarks: accumulation of characteristic proteins into insoluble aggregates within and/or between neurons along with synaptic loss and neuronal death (Fig. 42.1). These proteins includes α-synuclein (α-syn) of Lewy bodies (LBs) and Lewy neurites in PD, β-amyloid (Aβ) of senile plaques, and tau of neurofibrillary tangles (NFTs) in AD, polyglutamine (polyQ)-rich huntingtin inclusions in HD, TDP-43 aggregates in amyotrophic lateral sclerosis (ALS) and TDP-43 aggregates and tau in frontotemporal dementia (FTD) (Guo and Lee, 2014). Proteins aggregate due to their altered conformation which may result from a primitive
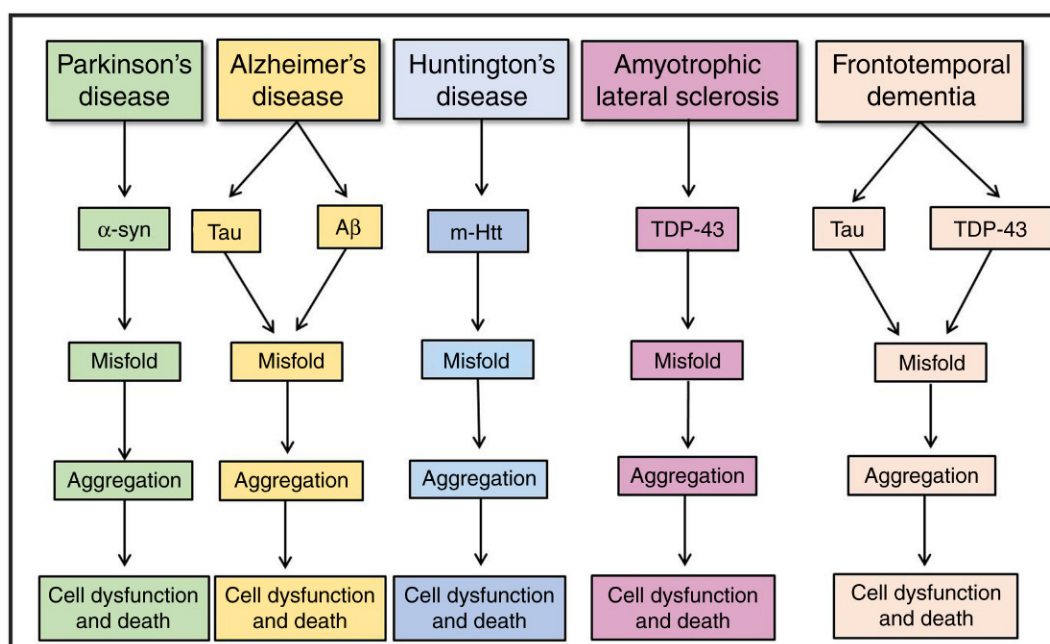
FIGURE 42.1 **Neurodegenerative diseases share common pathological hallmarks: accumulation of characteristic proteins into insoluble aggregates within and/or between neurons, along with cell dysfunction and neuronal death.**

mutation in the coding gene or from an injury as induced, for instance, by excitatory neurotransmitters, cytokines, or environmental toxins (Vidoni et al., 2016). For instance, oxidized protein aggregates may accumulate progressively over time as a consequence of chronic exposure to prooxidative neurotoxins, such as pesticides (e.g., rotenone), herbicides (e.g., paraquat), or recreational drugs (e.g., amphetamine) (Janda et al., 2012, 2015).

So far, there are no treatments capable of modifying the course of neurodegenerative diseases. The identification of effective drugs depends on the understanding of the pathophysiological mechanisms underlying each disease (Ribeiro et al., 2013). One step into this direction depends on the availability of animal models that can mimic the neuropathological and clinical features of each neurodegenerative disease (Duyckaerts et al., 2008). In the current chapter we will provide an overview of the main animal models of AD, PD, HD, ALS, and FTD.

2 PARKINSON'S DISEASE

PD is the second most common neurodegenerative disease and the main cause of parkinsonism, a clinical syndrome characterized by bradykinesia, rigidity, postural instability, and resting tremor. Its prevalence varies from 1% to 4% in people over 60 years (de Rijk et al., 1997; Wright Willis et al., 2010). The neuropathological hallmarks of PD are the loss of dopaminergic neurons in the *substantia nigra pars compacta* (SNpc) and the formation of intraneuronal proteinaceous inclusions called LBs in

affected brain areas. LBs are composed of unbranched α-synuclein (α-syn) filaments and ubiquitin, and most likely result from ineffective protein degradation (Braak et al., 2000, 2003a). *Postmortem* analyses have shown that α-syn inclusions emerge in a predictable order in different parts of the brain and might be linked to the progressive clinical stages of PD (Braak et al., 2004). As the disease advances, neuronal loss is observed in other brain regions, such as the cholinergic nucleus basalis of Meynert, thalamus, amygdala, and the serotoninergic neurons of the raphe nucleus (Braak et al., 2000, 2003b; Jellinger, 1991). Interestingly, clinical studies have shown that nonmotor symptoms may antedate the onset of typical motor signs in PD, stressing the need for understanding the molecular pathways that may trigger the related neurodegenerative process (Obeso et al., 2010).

The etiopathogenesis of PD is rather complex, involving environmental and genetic factors. However, clear genetic factors respond to only a small proportion of cases, the so-called genetic parkinsonism. Point mutations affecting the ubiquitin–proteasome pathway proteins are implicated in these cases (McNaught et al., 2001). Other genetic factors related to mitochondria function and oxidative stress may influence sporadic cases (Palacino et al., 2004; Winklhofer and Haass, 2010). Neuroinflammation is also considered to play a role in PD pathogenesis, and increase levels of inflammatory cytokines are detected in *postmortem* specimens, cerebrospinal fluid, and blood from patients with PD (Mogi et al., 1994; Scalzo et al., 2009).

Therapeutic strategy for PD is based on dopamine analogs, dopamine-degrading enzyme inhibitors, and

deep brain stimulation, all aiming at the improvement of motor symptoms secondary to dopaminergic impairment, but no strategy so far is able to halt the progressive neuronal death (Lees et al., 2009).

2.1 Animal Models of Parkinson's Disease

There are genetic and neurotoxin-based models of PD. Either toxic- or genetic-based models have their own advantages and disadvantages. Indeed, the use of the two in combination would be quite interesting. Accordingly, a multigene modulated transgenic model in combination with a reliable and effective neurotoxin might allow a better modeling PD phenotype. In coming years, we expect to see better models for basic understanding of PD and also for improved high-throughput drug discovery.

2.1.1 Genetic Models

The genetic basis for several forms of PD and related parkinsonian disorders has been elucidated in the past 2 decades. Although the great majority of PD cases cannot be explained by a single mutation, the identification of risk loci, genes, and mutations in PD has provided new insights into disease pathogenesis and indicated new study approaches (Lee et al., 2012).

Genetic models of a disease usually can be made of a mutant gene involved in the development of the disease or a gene that might not be validated in the disease but can recapitulate some key features of the disease in the model system (Jagmag et al., 2015). Five genes are frequently targeted as disease model for PD and they all have been associated with familial PD.

2.1.1.1 α-SYNUCLEIN MODELS

The α-synuclein gene (SNCA gene, designated as PARK1) is linked to a dominant type of familial early-onset PD. The α-syn is the main component of LB observed in the brains of PD patients (Iwatsubo, 2003). Mutations in five locations (A30P, A53T, S129D, S87, E46K) have been identified in familial PD to date. The severity and age of onset of disease depend on the promoter and levels of transgene expression.

Aiming to further investigate the role of α-syn in the pathogenesis of PD, transgenic mice overexpressing human α-syn were generated (Masliah et al., 2000). These models are instructive for studying the molecular mechanisms by which α-syn aggregation as well as neurodegeneration occurs in vivo. However, most of these models failed to show loss of dopaminergic neurons, the key pathological feature of PD, although there are subtle functional abnormalities in the nigrostriatal system and neurodegeneration in other anatomical circuits (Fernagut and Chesselet, 2004; Oliveras-Salva et al., 2013). Also, α-syn transgenic mice overexpressing human α-syn display mitochondrial abnormalities in degenerating neurons (St Martin et al., 2007). The mechanism of α-syn-induced mitochondrial dysfunction might involve sequestration of mitochondrial proteins or yet-unidentified pathways (Olzscha et al., 2011). In addition to mitochondrial dysfunction, a DNA damage response leading to cell death might be one downstream consequence of α-syn aggregation. Although the animal models of PD focused on α-syn are useful and validated, the exact function of this protein is still a matter of debate. Available data suggests that α-syn might be a presynaptic regulator of dopamine release, synthesis, or storage (Maries et al., 2003; Proukakis et al., 2013). Moreover, inflammatory signs were observed in a transgenic mouse overexpressing human α-syn, intracellular accumulation of α-syn within the striatum might induce a different immune response compared to other brain regions (Khandelwal et al., 2010).

As there is no loss of dopaminergic neurons in the substantia nigra of most α-syn transgenic mice, mechanistic studies of dopaminergic neurons death by α-syn have been obtained through the investigation α-syn expression following MPTP (1-methyl-4-phenyl-1,2,3,6-tetrahydropyridine) administration (Nieto et al., 2006; Song and Jung, 2004). Mitochondrial dysfunction appears to be sufficient to induce α-syn aggregation and downstream toxicity for dopaminergic neurons in MPTP mouse models. As expected, dopaminergic neurons of α-syn transgenic mice show more sensitivity for mitochondrial toxins (Nieto et al., 2006).

2.1.1.2 LEUCINE-RICH-REPEAT-KINASE 2 (LRRK2) MODELS

Mutations in the leucine-rich-repeat-kinase 2 (LRRK2) gene (PARK8) are the most common genetic causes of both familial and sporadic PD (Funayama et al., 2002; Paisan-Ruiz et al., 2013). Structurally, LRRK2 is a very interesting protein which has GTPase and kinase domains in addition to leucine-rich repeat domains, forming a large protein kinase. In addition, LRRK2 has several functional motifs and has been implicated in a variety of cellular processes including mitochondrial function, signal transduction, cell death pathways, vesicle trafficking, neurite outgrowth, autophagy, and cytoskeleton assembly (Tsika and Moore, 2012). Several groups have generated LRRK2-related PD mouse models expressing LRRK2 wild-type or PD-associated mutant LRRK2 to simulate aberrant kinase activity (Dawson et al., 2010). Overexpression of wild-type LRRK2 in transgenic mice causes an enhancement of DA release from the striatum and motor hyperactivity owing to this excess DA. On the other hand, overexpression of mutant LRRK2G2019S mice decreases the release and uptake of DA, thereby suggesting a role for LRRK2 in DA transmission (Li et al., 2009). Transgenic mice overexpressing mutant LRRK2R1441G show progressive and age-dependent motor deficits that progress to immobility that can be reversed by levodopa or apomorphine, similar

to what happens in PD (Kumar and Cookson, 2011). Qing Xu et al. generated human bacterial artificial chromosome (BAC)-mediated transgenic mouse models expressing mutant LRRK2 that robustly recapitulate pathological features of PD. These animals develop an age-dependent decrease in motor activity that is progressive and responds to treatment with levodopa. Pathologically, the most salient phenotype is premature axonopathy of nigrostriatal dopaminergic neurons accompanied by hyperphosphorylated tau. These mice also exhibit a consistent dopamine transmission deficit in acute brain slices and live freely moving animals (Xu et al., 2012).

2.1.1.3 PARKIN MODELS

Parkin (*PARK2*) mutations have been seen in cases of familial early-onset PD (autosomal recessive inheritance). Parkin is an integral ligase protein in the ubiquitin–proteasome system and it is widely expressed in most tissues including the brain (Lucking et al., 2000). Most parkin transgenic rodents, that is, *Parkin* KO animals, do not exhibit loss of dopaminergic neurons in the SNpc (Goldberg et al., 2003; Itier et al., 2003; Palacino et al., 2004). Nevertheless, some recently developed transgenic rodent models have demonstrated modest loss of dopaminergic neurons (Dave et al., 2014; Kitada et al., 2009; Van Rompuy et al., 2014). The transgenic parkin mice overexpressing the protein exhibit deficits in behavioral tasks previously shown to be sensitive to nigrostriatal dysfunction. In addition, proteomic studies using parkin-null mice showed marked reduction of mitochondrial respiratory chain proteins and stress response proteins when compared with littermate controls. Surprisingly, MPTP intoxication in parkin-null mice caused a similar level of dopaminergic neuronal toxicity compared with wild-type mice, although parkin overexpression provides protection against MPTP (Paterna et al., 2007; Perez et al., 2005; Thomas et al., 2007). A compensatory remodeling in parkin deficient dopaminergic neurons may have complemented parkin-related protective roles against mitochondrial dysfunction. Moreover, studies have shown that parkin deficiency in mice increases the risk of inflammation and neuronal death loss, suggesting a specific role for parkin in neuroprotection against inflammation-induced degeneration (Frank-Cannon et al., 2008).

2.1.1.4 DJ-1 MODELS

DJ-1 is molecular chaperone that, under an oxidative environment, plays a role in inhibition of α-syn aggregate formation (Shendelman et al., 2004). *DJ-1* (*PARK7*) mutations are linked to autosomal recessive and early-onset PD. *DJ-1* KO models present decreased dopamine release in the striatum but no loss of dopaminergic neurons in the SNpc, and a hypoactivity upon amphetamine challenge (Andres-Mateos et al., 2007; Goldberg et al., 2005). Dopaminergic neurons from *DJ-1* KO mice exhibited elevated mitochondrial oxidant stress due to compromised uncoupling of

mitochondria following basal pacemaker potential (Guzman et al., 2010). In a *Drosophila* homozygous mutant model, severe defects in locomotor ability without loss of dopaminergic neurons were observed, consistent with studies in *DJ-1* KO mice (Goldberg et al., 2005). A new model, the DJ1-C57 mouse, shows promise with significant unilateral loss of dopaminergic (DA) neurons in the SNc that progresses to bilateral degeneration of the nigrostriatal axis with aging and mild motor behavior deficits (Rousseaux et al., 2012). Still, consistent with DJ-1 protective role against stress, dopaminergic neurons with *DJ-1* deletion present increased susceptibility to MPTP toxicity. However, *DJ-1* KO mice do not present increased vulnerability to inflammation-related nigral degeneration (Nguyen et al., 2013).

2.1.1.5 PINK1 MODELS

Mutations in the *PTEN-induced putative kinase 1* (*PINK1*) gene (*PARK6*) result in early-onset PD (autosomal recessive inheritance). PINK1 codes for a mitochondrial kinase which recruits parkin from the cytosol to the mitochondria, increases the ubiquitination activity of parkin, and induces parkin-mediated mitophagy (Lazarou et al., 2013). The phenotypes of *PINK1* and *Parkin* KO mice are very similar as PINK1 and parkin are in the same pathway. Animals present reduced locomotion, but no change on rotarod performance. In addition, neither dopaminergic neurons abnormalities nor LB formation have been observed in *PINK1* KO mice. However, they present mitochondrial functional defects and increased sensitivity to oxidative stress (Kitada et al., 2007). A recently developed *PINK1* KO rat exhibiting dopaminergic neurons loss and motor impairment mimics more closely the PD phenotype (Dave et al., 2014).

2.1.2 Neurotoxic Models

The called neurotoxin-based models of PD are the most effective in reproducing dopamine deficit in primates and rodents. The most widely used compounds for animals models of PD are MPTP, rotenone, and 6-OHDA (6-hydroxy-dopamine).

2.1.2.1 MPTP

MPTP is a neurotoxin precursor of 1-methyl-4-phenylpyridinium (MPP+) which causes damage to the nigrostriatal pathway with a significant loss of dopaminergic neurons in the striatum and SNpc, similar to what it is seen in PD. MPP+ has a high affinity for the membrane dopamine transporter with comparatively lower affinities for the norepinephrine and serotonin transporters (Javitch et al., 1985). Furthermore, MPP+ interacts with the mitochondrial complexes I–III–IV, inhibiting the electron transport chain and inducing ATP depletion and oxidative stress (Bezard and Przedborski, 2011). MPP+ is also linked to impairment of glutamate uptake by astrocytes and neuronal apoptosis (Hazell et al., 1997).

MPTP model on primates presents the most closely pathological features of PD. In this model, motor symptoms are very similar to those observed in humans (bradykinesia, rigidity, and postural abnormalities), except for resting tremor. Although no typical LBs are observed in this model, α-syn immunoreactivity is enhanced in the nigrostriatal system and in other brain areas, such as the striatum and caudate nucleus (Purisai et al., 2005). Symptoms are also reversible by dopaminergic drugs known to be effective in PD. This model has been widely used to investigate new pharmacological treatments for PD as well as strategies to avoid treatment-related dyskinesias.

MPTP is more often used in mice models than in primates largely due to its very high cost in the latter. Primate models are preferred for testing drug treatment protocols just before human studies (Antzoulatos et al., 2010; Verhave et al., 2012). Mice treated with MPTP do not show typical PD behavior; however, motor alterations are observed when significant dopaminergic neuron loss is present (Jackson-Lewis and Przedborski, 2007). Rats have proven to be resistant to MPTP-induced toxicity (Riachi et al., 1990). The reason for this resistance has been speculated to be due to its differential MPP+ sequestration (Schmidt and Ferger, 2001).

MPTP is mainly administered via systemic route through subcutaneous, intravenous, or intracarotid injections. As MPTP is lipophilic, it can cross the blood–brain barrier, allowing greater ease in administration. However, it is very toxic, posing significant concerns with his manipulation and/or administration.

2.1.2.2 ROTENONE

Rotenone is a compound that occurs naturally in several plants and it has been used as abroad spectrum insecticide and pesticide. Rotenone blocks the mitochondrial electron transport chain through the inhibition of complex I, as seen in MPTP. Rotenone is highly lipophilic and easily crosses the blood–brain barrier (Talpade et al., 2000). Rotenone cytotoxicity is based on oxidative stress and reactive oxygen species (ROS) production (Sherer et al., 2003). High doses of rotenone can induce generalized neurodegeneration, so studies have been directed to chronic low-dose regimen in systemic administration of this compound in rodents. In this condition, α-syn positive LBs are observed in the nigrostriatal system (Tieu, 2011). Despite demonstrating slow and specific loss of dopaminergic neurons, this model is difficult to replicate due to the high mortality observed in animals treated with rotenone (Fleming et al., 2004). The route of administration of rotenone can vary. Chronic systemic (intravenous) exposure induces nigrostriatal dopaminergic neurodegeneration. Bilateral stereotaxic injection of rotenone into the medial forebrain bundle of rats causes a depletion of dopamine in the nigrostriatal system with associated rigidity and decreased motor activity, which can be reversed by levodopa therapy (Alam et al., 2004). Rotenone has also been tested in mice through chronic intragastric administration, which is able to induce α-syn accumulation in the enteric nervous system, the dorsal motor nucleus of the vagus, the intermediolateral nucleus of the spinal cord, and the SNpc (Pan-Montojo et al., 2010).

2.1.2.3 6-OHDA

6-OHDA is a selective neurotoxin that was first reported to cause lesions in nigrostriatal dopaminergic neurons in rats (Ungerstedt, 1968), but it has been subsequently shown to work in other animals, such as mice. 6-OHDA does not cross the blood–brain barrier and it needs to be injected into the brain. 6-OHDA is taken up by dopaminergic neurons due to its high affinity to dopamine transporter. Once inside neurons, 6-OHDA is readily oxidized in ROS leading to electron transport chain inhibition and oxidative stress (Mazzio et al., 2004). 6-OHDA is usually injected unilaterally in the SNpc or in the striatum. The unilateral injection causes neuron cell death and molecular changes in the lesion hemisphere compared with the intact hemisphere. In addition, systemic administration of apomorphine or amphetamine-induced rotations in unilateral lesioned in the animals. This model has been used to evaluate motor deficits and behavioral symptoms. However, neither LB nor olfactory deficits were observed in 6-OHDA treated animals (Duty and Jenner, 2011). Furthermore, this model has been useful to study glial involvement in the neurodegenerative process. For instance, studies have shown that microglia activated by overexpression or aberrant expression of α-syn secretes inflammatory cytokines and reactivates oxygen species that contribute to neurodegeneration (Saura et al., 2003). Despite its limitations, the 6-OHDA lesion is a highly reproducible model and has been to test new therapeutic strategies in PD.

3 ALZHEIMER'S DISEASE

AD is the main neurodegenerative disease and the most common cause of dementia, accounting for approximately two thirds of all dementia cases and afflicting more than 35 million individuals worldwide (Querfurth and LaFerla, 2010). AD affects mainly people over 60 years old and its initial presentation is usually memory impairment, but later symptoms include visuospatial, language, and executive dysfunctions (Querfurth and LaFerla, 2010). The vast majority of AD cases is sporadic, and whose causes remain unknown. The histopathological hallmark of AD is the accumulation of NFTs and amyloid plaques in addition to widespread synaptic loss, inflammation, oxidative damage, and neuronal death (Esch et al., 1990; Querfurth and LaFerla, 2010). NFTs are formed by aggregates of hyperphosphorylated tau protein. Extracellular amyloid

plaques are formed from β-amyloid peptides (Aβ), which are fragments formed by cleavage of amyloid precursor protein (APP) (Esch et al., 1990). APP can be processed by α-and γ-secretases, generating a nonamyloidogenic product, or by β- and γ-secretases, generating Aβ peptides, which are amyloidogenic and are likely to form plaques. There is no direct correlation between the number of cortical plaques and cognitive deficit in AD patients, and many individuals have amyloid plaques without cognitive impairment or dementia (Duyckaerts et al., 2009). Furthermore, the quantity and the structure of the senile plaques are not correlated with the severity of dementia, and the amyloid deposition seems to remain stable during the progression of the disease (Jack et al., 2010). While clinical progression of AD symptoms does not correspond to the progression of the amyloid deposition in the human brain, it seems closely related to the progression of tau pathology (Hyman, 2011). Accordingly, factors other than amyloid deposits might have a role in disease progression (Terry et al., 1991). Aβ is a potent mitochondrial poison, especially affecting the synaptic pool (Mungarro-Menchaca et al., 2002). In a transgenic mice model with overexpression of mutant human APP, exposure to Aβ inhibits mitochondrial enzymes in the brain and in isolated mitochondria (Hauptmann et al., 2006; Reddy and Beal, 2008), and cytochrome c oxidase is specifically susceptible (Caspersen et al., 2005). As a consequence, electron transport, ATP production, oxygen consumption, and mitochondrial membrane potential all become impaired.

Although the hypotheses concerning mechanisms underlying AD pathogenesis led to the development of drugs that have been tested in large clinical trials, the results of the trials completed so far are disappointing (Reitz, 2016). At present, there is no effective disease-modifying strategy in AD, and the available drugs are indicated to improve cognitive and behavioral symptoms (Querfurth and LaFerla, 2010).

3.1 Animal Models of Alzheimer's Disease

Animal models have significantly advanced the understanding of AD pathogenesis, but gaps in the knowledge regarding the causes of AD turn difficult to develop a model that recapitulates all aspects of the disease (Ribeiro et al., 2013). To date, animal models used in preclinical studies can be distinguished in: (1) transgenic models of AD consisting in single or multitransgenic animals overexpressing APP, PS (Presenilin) and/or Tau mutations; (2) nontransgenic models obtained by toxins injection in the brain, including direct injection of Aβ or tau, and models of aging (Puzzo et al., 2015).

3.1.1 Transgenic Models

The first transgenic animal built to mimic AD was based on the amyloid hypothesis, thus reproducing the deposits of Aβ in the brain by overexpressing the isoform

β-APP751 (Higgins et al., 1994; Quon et al., 1991). This model is a good model of Aβ hyperproduction, but the animals do not exhibit other features of AD, such as neuronal and/or synaptic loss (Lamb et al., 1993). These are excellent models to better understand the pathophysiologic role of Aβ in AD or to test drugs expected to modulate or reduce Aβ levels.

In 1995, Games et al. created the PDAPP mouse expressing high levels of human APP cDNA with a FAD-associated mutation (substitution of valine at position 717 with phenylalanine). Those animals expressed high levels of APP and developed several characteristics of human AD, such as extracellular amyloid fibrils organized in plaques, apoptosis, dystrophic neuritis subcellular, degenerative changes, synaptic loss, and gliosis that spread progressively from hippocampus to cortex (Games et al., 1995). More importantly, PDAPP mice had memory impairment, the main clinical feature of AD. One year later, Hsiao et al. (1996) created another transgenic mouse model of AD, the Tg2576 line, carrying the double Swedish mutation (K670N and M671L). These mice have increased APP production with consequent overproduction of Aβ40 and Aβ42, and plaques formation in different regions of the brain. Also, hyperphosphorylated tau occurs at old age when animals are around 11–13 months. Conversely, they did not present significant cognitive impairment (King and Arendash, 2002). This model has some advantages that consist in a well-characterized model and the relatively simple management of the colony. The disadvantage is that the AD phenotype occurs late. Indeed, it is usually necessary to wait 2 months to perform experiments to be sure that animals present both synaptic and memory dysfunction (Puzzo et al., 2015).

A model containing three different mutations—3XTg—such as APPSwe, PS1 M146V, and hyperphosphorylated tau (tauP301L) have been generated in mice (Oddo et al., 2003). This model is the only one to exhibit both Aβ and tau pathology that is characteristic of the human form. These animals exhibited Aβ pathology at 6 months of age (increased Aβ40 and Aβ42 levels, intracellular accumulation of Aβ, and amyloid plaques) that preceded tau pathology with NFTs formation at about 1 year old of age. Memory impairment was also evident (Billings et al., 2005; Kazim et al., 2014; Oddo et al., 2003). In addition, this model showed an increase of inflammatory mediators in the hippocampus (Cantarella et al., 2015).

3.1.2 Nontransgenic Models

Nontransgenic models for studying AD are mainly obtained by injecting Aβ or tau directly into the brain via intracerebroventricular (i.c.v.) or intrahippocampal injections (Balducci and Forloni, 2014; Puzzo et al., 2014). The advantages of the use of nontransgenic models include the possibility of (1) investigating Aβ and tau effects in animals different than mice or for which transgenic models are not available, (2) excluding the confounding

effects of overexpression of APP and its fragments, (3) investigating the different role of Aβ and tau species (monomers vs. oligomers vs. insoluble) at different concentrations, (4) investigating the difference between an acute or a chronic administration, and to clarify aspects of the molecular mechanisms underlying Aβ and tau pathology that cannot be investigated using transgenic models (Puzzo et al., 2015). However, acute models do not reproduce the gradual increase in Aβ deposition or tau pathology throughout the years as in humans.

It is worth mentioning that both transgenic and nontransgenic models do not reproduce the entire clinical features of human AD, but we have a number of very interesting tools to study AD. Although with their limitations, both models allow investigating memory, synaptic plasticity, histopathological changes, and molecular mechanisms underlying the disease. They represent an important tool to better understand the pathophysiology of the disease and to establish therapeutic strategies.

4 HUNTINGTON'S DISEASE

HD is an autosomal dominant genetic disorder characterized by progressive motor dysfunction, cognitive decline, and behavioral symptoms (Novak and Tabrizi, 2011; Ready et al., 2008). HD has a prevalence of 5–10 per 100,000 in South America, North America, Australia, and most European countries and countries of European descent, being significantly less prevalent in Africa and Asia with an estimated number of 0.5:100,000 in Japan and China (Walker, 2007). HD affects males and females at the same frequency, and the mean age of onset is around 40 years, although it can be as early as 4 and as late as 80 years of age. In the United States alone, there are about 30,000 patients with HD and there are about 150,000 people at risk of developing the disease (Margolis and Ross, 2003; Walker, 2007).

HD is caused by an expanded CAG repeat in the exon 1 of the *Huntingtin* gene which encodes an expanded polyglutamine stretch near the N-terminus of the 350 kDa huntingtin protein (Htt) (Consortium, 2012). The presence of more than 40 CAGs invariably causes the disease within a normal lifespan, and longer repeats accelerate disease onset (Langbehn et al., 2010). Although the primary factor that determines whether and when a person will develop HD is the length of the expanded CAG tract, the precise clinical manifestations, and onset of the disease are, to some extent, also influenced by environmental and genetic modifiers. While it is commonly acknowledged that the correlation of repeat size accounts for about 70% of the variation in age of onset (Gusella and MacDonald, 2009), there is higher variation in age of onset among patients with repeat lengths below 55 (Myers, 2004).

Mutant Htt is widely expressed, and believed to induce neurodegeneration through abnormal interactions with other proteins. This leads to several cellular alterations, including abnormal vesicle recycling, loss of signaling by brain-derived neurotrophic factor (BDNF), excitotoxicity, perturbation of Ca^{2+} signaling, decrease in intracellular ATP levels, alteration of gene transcription, inhibition of protein clearance pathways, mitochondrial and metabolic disturbances, and ultimately cell death (Zuccato et al., 2010). In addition, microglial activation and the associated neuroinflammation appear to be a prominent pathological feature of HD (Tai et al., 2007). Activated microglia are increased in cortex, striatum, and globus pallidus from patients with HD, and their frequency increases with neuronal loss (Pavese et al., 2006; Sapp et al., 2001). Similarly, the expression of inflammatory mediators is increased specifically in the striatum in HD, presumably in activated microglia, but not in cortex or cerebellum (Silvestroni et al., 2009).

Although the onset of HD is clinically diagnosed on the basis of motor performance, symptoms of psychiatric disorders, such as anxiety, irritability, impulsivity, aggression, apathy, and depressed mood are prevalent among HD gene carriers and patients with HD (Rosenblatt, 2007). Around 40%–50% of patients with HD are found to experience depression (Duff et al., 2007). Also, suicide is four- to sixfold more common in patients with HD than in the general population (Schoenfeld et al., 1984).

Despite the fact that the HD gene was identified over 20 years ago, there is no effective disease-modifying therapy for HD to date. Current pharmacological therapeutics are exclusively symptomatic, aiming at improving motor, cognitive and psychiatric symptoms.

4.1 Animal Models of Huntington's Disease

HD is a genetic disease caused by a single gene mutation. Accordingly, it is highly feasible to develop animal models with genetic manipulations that closely recapitulate HD pathology. Rodents are by far the most commonly used animals for modeling HD. These models include transgenic mice and knock-in (KI) mice. Mouse is the most commonly used mammalian genetic model due to its efficiency, economy, and ease of manipulation. These animal models have been important tools to investigate the pathogenesis of the disease and to try develop therapeutic strategies.

4.1.1 Transgenic Mouse Models

4.1.1.1 R6/1/R6/2

R6/1 (116 CAG repeats) and R6/2 (144 CAG repeats) mice were the first HD mouse models to be developed expressing the exon 1 of human Htt under the control of 1 kb human Htt promoter (Mangiarini et al., 1996). Importantly, all transgenic models also express the two

normal alleles of the murine *Huntingtin* gene. R6/2 is the most extensively studied rodent model of HD, exhibiting a robust phenotype and severe neurological symptoms, including motor deficits, such as lack of motor coordination, abnormal walk, and learning impairment (Carter et al., 1999; Mangiarini et al., 1996). Motor changes start at 4 weeks, and R6/2 mice only survive for 12–13 weeks (Mangiarini et al., 1996). Depression-like behavior has been demonstrated in female R6/2 mice using the forced swimming test (Pang et al., 2009). R6/2 mice also exhibit an increase in anxiety-like behavior (Menalled et al., 2009). Procedural learning deficits have been shown in this model (Cayzac et al., 2011), as well a muscle atrophy (Ribchester et al., 2004). This model is vastly used for drug testing due to its rapid onset. Aggregate formation is very pronounced in this model and intranuclear inclusions are very similar to those observed in biopsy from HD patients and happening prior to the development of symptoms (Davies et al., 1997). However, nuclear Htt aggregates are widely distributed in several brain substrates of R6/2 mice, including the hippocampus and cerebellum, two regions that are relatively spared in HD (Li et al., 2001). Finally, aberrant peripheral immune system activation has been demonstrated in this model. Despite of its robust phenotype, R6/2 mice do not represent a precise model of HD, as this model only expresses the amino-terminal region of the Htt protein, which is mainly composed of polyglutamines. In this regard, R6/2 mice can also be used as a model of polyglutamine diseases including genetic ataxias and spinobulbar muscular atrophy (Ribeiro et al., 2013).

4.1.1.2 YAC128/BACHD

YAC128 and BACHD are transgenic HD mouse models that express full-length human Htt containing 128 and 97 polyglutamines, respectively (Gray et al., 2008; Slow et al., 2003). These mice were created using yeast artificial chromosome (YAC) and BAC technology. BACHD and YAC128 exhibit milder clinical deficit and slower progression compared to R6/2 (Menalled and Chesselet, 2002). Notably, these mice develop selective striatal and cortical atrophy at the age of 12 months, thus recapitulating to some extent the regional selectivity of adult-onset HD. These mice also present electrophysiological abnormalities suggestive of an alteration at glutamatergic synapses (Hodgson et al., 1999). Although BACHD and YAC128 exhibit similar phenotype, there are some differences between them. For instance, the BACHD CAG tract is half CAG and half CAC, providing resistance to polyQ expansions and contractions (Gray et al., 2008). On the other hand, only 7% of the YAC128 CAG tract is CAC (Pouladi et al., 2012b). Moreover, the mRNA levels of DARPP-32, enkephalin, dopamine receptors D1 and D2, and cannabinoid receptor 1 are

significantly decreased in YAC128, but not in BACHD mice (Pouladi et al., 2012b). BACHD mice exhibit reduced levels of Htt aggregates as compared to YAC128 (Gray et al., 2008; Pouladi et al., 2009), but Htt aggregates can be clearly detected in the cortex and striatum of BACHD mice (Gray et al., 2008). BACHD and YAC128 mice develop progressive motor and cognitive and behavioral deficits (Gray et al., 2008; Pouladi et al., 2009; Van Raamsdonk et al., 2005). Deficits in learning and memory have been assessed using a number of sensitive behavioral paradigms, which include tests of procedural learning, spatial learning, associative and nonassociative (habituation) learning, discrimination, episodic learning, and strategy shifting. Deficits in motor learning have been demonstrated during the training phases of the running wheel and rotarod tasks (Pouladi et al., 2012a; Van Raamsdonk et al., 2005). Increases in anxiety-like behavior have been shown in YAC128 and in BACHD mice using the open-field test (Menalled et al., 2009). Furthermore, peripheral immune system activation has been demonstrated in YAC128 mice and impaired macrophage migration has been shown in BACHD mice (Kwan et al., 2012).

4.1.2 HD Knock-In Mouse Models

KI models should be optimal to reproduce human pathology because they are the most faithful reproduction of the genetic mutation and do not overexpress Htt or disrupt endogenous genes by deleterious integrations into the genome (Menalled and Chesselet, 2002). Several KI models with expanded CAG repeats or human mutant Htt exon 1 replacing the corresponding sequences in the endogenous murine Htt gene locus have been generated (Heng et al., 2008; Shelbourne et al., 1999; Wheeler et al., 2000). The most studied mutant Htt-KI models include HdhQ111, CAG140, and HdhQ150 mice, which are suitable for studying HD pathogenesis and testing therapies. All these HD KI mice showed late-onset phenotype and progressive, but mild pathology (Shelbourne et al., 1999; Wheeler et al., 2000). Behavioral abnormalities in this KI model were similar but milder than transgenic mouse models (Woodman et al., 2007). For instance, HdhQ150 mice exhibit late-onset motor changes, including motor task deficit and gait abnormalities (Woodman et al., 2007). These animal present deficits in the novel objection recognition test of episodic memory (Giralt et al., 2012). Depression-like behavior and anxiety-like behavior have also been demonstrated (Orvoen et al., 2012). Although HD KI mice do not develop a phenotypes as robust as those in transgenic mice expressing N-terminal mutant Htt, they recapitulate an important pathological change seen in the brain of the HD patient, which is the preferential accumulation of mutant Htt in striatal neurons (Wheeler et al., 2000).

4.1.3 Transgenic Large Animal Models of HD

Research using large animal models of HD has been very limited. The potential use of large animal models in HD research has been refocused recently with the development of three transgenic large animal models of HD, a nonhuman primate model (rhesus monkey) (*Macaca mulatta*) (Yang et al., 2008), a sheep model (*Ovis aries*) (Jacobsen et al., 2010), and a Tibetan miniature pig model (Yang et al., 2010). The rhesus macaque and pig models were generated using fragments of human *HTT* that included a CAG repeat expansion. By contrast, the sheep model used the full-length human coding sequence of *HTT* that is expressed from a transgene. The symptoms exhibited by each species of HD animal reflect the transgene construct used. HD transgenic monkeys with 84Q can die postnatally, and this early death is associated with the levels of mutant Htt (Yang et al., 2008). Despite their early death, some transgenic monkeys developed key clinical HD features including dystonia, chorea, and seizures (Yang et al., 2008), which have not been replicated by mouse models or other small animal models. Studies of transgenic large animals also showed that smaller N-terminal mutant Htt is more toxic. Transgenic pigs (Baxa et al., 2013) and sheep (Jacobsen et al., 2010) that express much larger Htt fragments develop nondetectable or very mild phenotypes. Thus, even in large animals, expression of small N-terminal mutant Htt fragments appears to be necessary to facilitate disease progression.

5 AMYOTROPHIC LATERAL SCLEROSIS

ALS is a fatal late-onset neurodegenerative disorder that is characterized by a progressive loss of motor neurons of the CNS leading to muscle weakness, wasting, and spasticity (Robberecht and Philips, 2013). Patients with ALS develop progressive muscle weakness along with fasciculation, hyperreflexia, and muscle. Patients with ALS usually die within 3–5 years after the diagnosis (Cudkowicz et al., 1997). For a long time, ALS was regarded as a motor neuron-specific disease. It is now clear that mild cognitive deficits and FTD are common in ALS (Therrien et al., 2016).

There is no familial history of ALS in the majority of cases which are classified as sporadic ALS (sALS). A clear familial history of the disease is present in approximately 10% of patients whose cases are known as familial ALS (fALS). Familial cases of ALS are usually inherited in an autosomal dominant way, although there are some autosomal recessive and X-linked forms. Mutations in more than 10 different genes have been identified to date (Renton et al., 2014). The most common mutations are found in the genes encoding superoxide dismutase 1 (SOD1), fused in sarcoma (FUS), and TDP-43 (TARDBP).

Recently, a hexanucleotide repeat expansion (GGGGCC) in the *C9ORF72* gene was identified as the most frequent cause of fALS (around 40%) in the Western population (DeJesus-Hernandez et al., 2011; Renton et al., 2011). Besides genetic factors, environmental factors seem to play a role in disease pathogenesis, such as toxins, but the evidence comes primarily from experimental models (Ingre et al., 2015).

ALS is a heterogeneous disease not only genetically, but also clinically. The age of onset, the rate of progression, and the presence of cognitive dysfunction are variable. In some patients, neurons in the prefrontal and temporal cortex are affected, leading to cognitive and/or behavioral problems. FTD is present in about 15% of patients with ALS (Lillo and Hodges, 2009; Ringholz et al., 2005). Conversely, 15% of FTD patients show signs of motor neuron disease (Burrell et al., 2011; Lomen-Hoerth et al., 2002).

Different mechanisms have already been suggested to play a role in the pathogenesis of ALS. These include astrocytosis, neuroinflammation, mitochondrial dysfunction, deregulated autophagy, and axonal transport dysfunction and retraction. Modulating these different disease processes could have a positive effect on disease progression, and modifying these pathological mechanisms could be translated into therapeutic strategies.

In 1995, riluzole was approved by the US Food and Drug Administration (FDA) for the treatment of ALS (Bensimon et al., 1994). Two decades later, this drug remains the only approved treatment for ALS. Riluzole increases the life span of the patients by an average of 2–3 months (Miller et al., 2007, 2012). Several preclinical studies have been performed in rodent models of ALS to prevent, reverse, or modulate the disease process. So far, none of these therapeutic strategies has been successfully replicated in clinical trials. As a consequence, besides riluzole, only symptomatic treatments are applied to improve the quality of life of ALS patients.

5.1 Animal Models of Amyotrophic Lateral Sclerosis

The identification of the genetic causes of ALS was critical for advancing the understanding of the pathophysiology of this disorder since these mutations form the basis of the development of experimental models for the disease. There are different mouse models for ALS, such as transgenic and KO mice (Mancuso and Navarro, 2015).

5.1.1 SOD1 Models

Mutations in the *SOD1* gene on chromosome 21 were the first identified causes of autosomal dominant fALS (Rosen, 1993). SOD1 is a ubiquitous cytoplasmic and mitochondrial enzyme which functions in a dimeric state to catalyze the breakdown of damaging ROS, preventing

oxidative stress. Due to the harmful effects of ROS and their association with neurodegenerative diseases, it was originally proposed that pathogenic mutations in SOD1 could cause ALS as a result of a loss of dismutase activity (Rosen, 1993). Subsequent investigation failed to associate mutant SOD1 activity with pathogenicity (Borchelt et al., 1995) and in *SOD1* KO mice do not present motor dysfunction, at least up to 6 months of age (Reaume et al., 1996). More recent characterization of the *SOD1* KO mice has revealed that although they do not exhibit any motor neuron loss, they have significant distal motor axonopathy, indicating a major role of SOD1 in normal neuronal function (Fischer et al., 2011).

Transgenic mouse model (SOD1G93A) of SOD1–ALS was initially developed expressing approximately 20–24 copies of the human coding sequence with the G93A mutation under control of the human *SOD1* promoter (Gurney, 1994). Since the development of this model, over 20 other SOD1 models have been proposed, and SOD1 transgenic mice have been used as the primary rodent models of ALS. Mutant *SOD1* transgenic mice recapitulate many features of ALS, including axonal and mitochondrial dysfunction, progressive neuromuscular dysfunction, gliosis, and motor neuron loss (Bruijn et al., 1997; Chang-Hong et al., 2005; Gurney, 1994). Transgenic SOD1 rodent models may vary the age of disease onset and rates of disease progression. Development of ALS-like symptoms in these mice is known to be mainly dependent of specific factors, including: SOD1 mutation; transgene expression level; gender, and genetic background (Heiman-Patterson et al., 2011; Mancuso et al., 2012).

In order to rule out the possibility that the disease phenotype may be the result of overexpression of SOD1 per se, lines of transgenic mice overexpressing the human wild-type protein have also been created. This so-called wt-hSOD1 mouse model might cause progressive motor neuron degeneration. Homozygous expression of a human wild-type SOD1 transgene resulted in a reduced lifespan, with a median survival of 367 days, accompanied by slow weight gain after birth and more significant weight loss in older male mice (Graffmo et al., 2013). Also, these animals developed an ataxic staggering gait with abnormal hind limb reflexes (Graffmo et al., 2013). Gliosis and misfolded SOD1 were detected in the spinal cord at 100 days of age, as well as signs of vacuolization and axonal damage which are typical of SOD1 overexpression (Jaarsma, 2006; Jaarsma et al., 2000). By end stage, around 40% of motor neurons in the thoracic spinal cord had been lost (Graffmo et al., 2013).

5.1.2 TDP-43 Models

TDP-43 is a 43 kDa nuclear protein originally discovered due to its effects on human immunodeficiency virus transcription (Bento-Abreu et al., 2010). It is encoded by the *TARDBP* gene on chromosome 1, and contains a nuclear-localization signal, two RNA-binding motifs, and a glycine-rich region, which contains a "prion-like" domain and mediates protein and heterogeneous nuclear ribonucleoproteins (hnRNP) interactions. It is within this glycine-rich domain that the majority of pathogenic mutations for ALS have been identified (Kabashi et al., 2008; Sreedharan et al., 2008). In vitro and in vivo studies have identified a variety of aberrant cellular dysfunctions caused by mutant TDP-43, including abnormal neuronal function and synaptic defects (Godena et al., 2011), deleterious effects on mitochondria (Braun et al., 2011; Shan et al., 2010), and proteasome dysfunction. Although it remains unclear how mutations in TARDBP cause ALS, both loss and gain of function mechanisms have been proposed (Tsao et al., 2012). The development of disease phenotypes in the model TDP-43-ALS in rodents is highly dependent upon the promoter used and the level of transgene expression. However, these models display mostly axonal damage with relatively mild motor neuron cell death. In marked contrast to SOD1 transgenic mice, overexpression of human wild-type TDP-43 has been shown to cause significant neurodegeneration (McGoldrick et al., 2013).

5.1.3 FUS Models

FUS was identified because of its oncogenic properties following a chromosomal translocation resulting in the fusion of truncated FUS protein with the transcription factor CHOP (Crozat et al., 1993; Rabbitts et al., 1993). The *FUS* gene is located at 16p11.2 and comprises 15 exons encoding a multifunctional 526 amino-acid protein (Prasad et al., 1994) with a complex domain structure. FUS is ubiquitously expressed in all cells. Some rodent data suggest that expression outside the CNS decreases with age, being absent in mouse skeletal muscle, liver, and kidney from 80 days of age (Huang et al., 2010). FUS binds DNA and RNA, and presents primarily a nuclear localization (Bosco and Landers, 2010; Gal et al., 2011).

Mutations in *FUS* have been described as contributing in similar proportion of fALS cases (FUS-ALS) as TDP-43 mutations. FUS may function downstream TDP-43 and in parallel to other RNA-binding proteins (Kabashi et al., 2011). Developing models of FUS-ALS is essential to clarify the mechanisms by which mutations in this protein cause ALS and how aberrant RNA metabolism may lead to neurodegeneration.

There are four transgenic rodent lines overexpressing FUS: transgenic mice which overexpress HA-tagged human wild-type FUS under control of the mouse prion promoter (Mitchell et al., 2013); somatic brain transgenic mice expressing V5-tagged human wild-type FUS, mutant R521C and FUS lacking its nuclear localization signal (D14) (Verbeeck et al., 2012); transgenic rats which conditionally express human wild-type or mutant FUS under the tetracycline response element system TRE

(Huang et al., 2011); and transgenic rats which express mutant FUS under the CaMKIIa promoter with a TRE (Huang et al., 2012). These models display different phenotypic manifestations ranging from different levels of motor involvement with muscle denervation, axonopathy, and spinal degeneration, to cognitive deficits with memory impairment and hippocampal neuronal death.

5.1.4 C9ORF72 Models

Since the discovery of C9ORF72 hexanucleotide expansions as one of the most frequent causes of ALS, significant efforts has been dedicated for developing animal models based on this mutation. C9ORF72 was modeled in zebra fish by knocking down the zC9ORF72. Loss of function of the zC9ORF72 transcripts causes both behavioral and cellular deficits related to locomotion but without major morphological abnormalities (Ciura et al., 2013). More recently, C9ORF72 transgenic mice have been developed by expressing the abnormal hexanucleotide expansion (G4C2)66, throughout the nervous system by means of somatic brain transgenesis mediated by an adeno-associated virus. Resulting mice presented neuronal nuclear inclusions of poly(Gly-Pro), poly(Gly-Ala), and poly(Gly-Arg) dipeptide repeat proteins, as well as TDP-43 pathology and neuronal loss. Transgenic mice developed behavioral changes resembling those of c9FTD/ALS patients, including hyperactivity, anxiety, antisocial behavior, and motor deficits (Chew et al., 2015).

5.1.5 VCP Models

The identification of mutations in the valosin-containing protein (VCP) as contributing for ALS (Shaw, 2010) and inclusion body myosytis with Paget's disease of bone and frontotemporal lobar degeneration (IBMPFD) (Mehta et al., 2013) has led to the development of mouse models of these diseases (Badadani et al., 2010; Custer et al., 2010). VCP is an AAA-ATPase which has a range of cellular functions (Meyer et al., 2012; Yamanaka et al., 2012). Studies have examined whether KI of the R155H mutation in VCP, which causes ALS (Shaw, 2010), could cause motor neuron degeneration in heterozygosity or homozygosity (Nalbandian et al., 2012; Yin et al., 2012). In heterozygote KI mice, the R155H mutation in VCP did not affect lifespan (Yin et al., 2012). However, these mice developed progressive weakness from 9 months of age and showed significant weight loss by 24 months of age (Yin et al., 2012). Consistent with this motor neuron degeneration, electromyography of hind limb muscles at 24 months of age showed evidence of denervation and neurogenic changes (Yin et al., 2012). Pathological analysis of the spinal cord revealed gliosis, oxidative stress, and cytoplasmic accumulation of mitochondria in motor neurons (Yin et al., 2012). Compared to the heterozygous KI mice, homozygous expression of human mutant VCP resulted in a much more aggressive phenotype, with early lethality and very few pups surviving to 21 days of age (Nalbandian et al., 2012). Although mutations in VCP have complex effects and phenotypes in transgenic mice may not be exclusively due to motor neuron degeneration, study of VCP models has clearly shown the deleterious effects of mutant VCP on motor neuron survival.

6 FRONTOTEMPORAL DEMENTIA

FTD is the third most common form of dementia across all ages, after AD and vascular dementia, and is a leading cause of early-onset dementia. FTD is characterized by progressive deficits in executive function, behavior, and language (Vieira et al., 2013). Due to the similarity of behavioral changes in patients with FDT to those seen in patients with major psychiatric disorders, diagnosis is frequently challenging.

The estimate is that FTD rates will double every 20 years, reaching 115.4 million in 2050. In a metaanalysis of 73 articles of early-onset dementia (patient age <65 years), FTD is the third most prevalent dementia subtype in most studies, with a prevalence ranging from 3% to 26% (Vieira et al., 2013). Also, FTD is still misdiagnosed, and most numbers probably underestimated the true incidence. FTD is classified into three clinical variants: behavioral-variant FTD, which is associated with behavioral and executive deficits; nonfluent variant primary progressive aphasia, with progressive deficits in speech, grammar, and word output; and semantic variant primary progressive aphasia, which is a progressive disorder of semantic knowledge and naming (Gorno-Tempini et al., 2011; Rascovsky et al., 2011). When FTD progresses and the initially focal degeneration becomes more diffuse, affecting larger regions in the frontal and temporal lobes, the symptoms of the three clinical variants can converge. Over time, patients develop global cognitive impairment and motor deficits, and may include parkinsonism and motor neuron disease in some patients. Individuals with end-stage disease have difficulty in eating, moving, and swallowing. Death usually happens about 8 years after the onset and is typically caused by pneumonia or other secondary infections (Bang et al., 2015).

Until 2004, tau was the only molecule known to accumulate in the brain of patients with FTD, and mutations in the *Microtubule Associated Protein Tau (MAPT)* gene were the only known genetic cause of FTD. Since then, two new neuropathological substrates (TDP-43 and FUS) and six new FTD genes (*GRN, C9ORF72, VCP, FUS, CHMP2B,* and *TARDBP,* the gene for TDP-43) have been identified. These advances have created new opportunities to study FTD using rodent models, and to use this important tool for studying pathophysiology of neurodegenerative disorders and new targets for treatment (Roberson, 2011).

No approved disease-modifying drugs are available for the treatment of FTD. Treatment is mainly focused on management of behavioral symptoms. For instance, agitation, aggressiveness, impulsivity, and aberrant eating behavior can improve with the use of selective serotonin reuptake inhibitors (Lebert et al., 2004) and/or low doses of atypical antipsychotics (Asmal et al., 2013). Cholinesterase inhibitors and memantine, drugs use for the treatment of AD, are not beneficial and can even worsen behavioral abnormalities seen in patients with FTD (Mendez et al., 2007).

6.1 Animal Models of Frontotemporal Dementia

Different FTD models have been developed in the past few years. Here, we review recent progress with mouse models based on tau, TDP-43, progranulin, VCP, and CHMP2B.

6.1.1 Tau Models

Tau was the first molecule linked to FTD, both by neuropathology and by genetics. More than 25 lines of transgenic mice have been created that express human tau with mutations linked to FTD. Tau transgenic mice have provided important insights and raised new questions about mechanisms of tau-mediated neurotoxicity.

The first models showed that expressing mutant tau was sufficient to cause both aggregated tau pathology and neuronal death. In both the rTg4510 and hTau lines, neuronal tau aggregates are formed, but neurons without aggregates are more susceptible to death. (Andorfer et al., 2005; Santacruz et al., 2005). Both aggregated tau pathology and neuronal death have been dissociated from the functional deficits in tau mouse models. Another interesting lesson from tau models was that the synapse is not just a target for tau, but a likely site of spreading pathology. It has been proposed that the propensity of neurodegenerative diseases to target large-scale networks is most likely due to transneuronal spread (Zhou et al., 2008).

Not all lineages display the pronounced neurodegeneration seen in the human disease, but among those that do, deficits in synaptic plasticity, and cognitive dysfunction precede neurodegeneration (Yoshiyama et al., 2007). Studies in mice have shown that neurodegeneration and cognitive deficits can be dissociated from neurofibrillary tangle pathology (Santacruz et al., 2005). These findings point to the importance of identifying the species of tau responsible for synaptotoxicity and neurotoxicity in mice and determining whether these tau species also occur in human neurodegenerative diseases.

6.1.2 TDP-43 Models

TDP-43 is connected to FTD by both neuropathology and genetics, but the neuropathologic link is much stronger. TDP-43 is a multifunctional nuclear protein that binds to DNA and RNA (Barmada et al., 2010). Models with deletion of TDP-43 are embryonic lethal early in gestation (Sephton et al., 2010; Wu et al., 2010). Heterozygous mice have normal TDP-43 protein levels and no evident neuropathology, limiting their utility (Sephton et al., 2010; Wu et al., 2010). The first models used heterologous promoters to drive human TDP-43 expression throughout the nervous system developed a sever phenotype marked by significant motor impairment leading to death in weeks to months (Wegorzewska et al., 2009; Wils et al., 2010). In each of these TDP-43 lines, in which brain pathology was examined, frontal cortex was selectively vulnerable to development of ubiquitinated neuronal inclusions, astrogliosis, and neuron loss (Wegorzewska et al., 2009; Wils et al., 2010). Subsequent models were engineered with more restricted promoters to better isolate the forebrain effects of TDP-43 from the motor phenotypes seen in pan-neuronal lines.

Some neuronal populations were more vulnerable than others. In a line expressing wild-type human TDP-43 around 75% of dentate granule neurons were lost, whereas CA1 pyramidal neurons were resistant, and deep cortical layers were more affected than superficial layers (Igaz et al., 2011). When wild-type or mutant TDP-43 was expressed, astrocytosis developed before 5 months of age, and learning/memory and motor deficits developed around 7 months.

6.1.3 Progranulin Models

Mutations in the progranulin gene (GRN) have recently been identified as a cause of about 5% of all FTD, including some sporadic cases. Recent studies using mouse models has defined the expression of PGRN in the brain (Petkau et al., 2010). PGRN is expressed late in neurodevelopment, localizing with markers of mature neurons. PGRN is expressed in neurons in most brain regions, with highest expression in the thalamus, hippocampus, and cortex. Microglia cells also express progranulin, and the level of expression is upregulated by microglial activation.

Around 70 different GRN mutations have been identified in FTD and all reduce progranulin levels or result in loss of progranulin function. Several different lines of progranulin KO mice have been developed. Each had early abnormalities in social behavior without impairment in overall health or motor function (Kayasuga et al., 2007). Evidence for protein mishandling in mice includes accumulation of ubiquitinated protein, lipofuscin, and phosphorylated TDP-43 (Ahmed et al., 2010; Kayasuga et al., 2007). The evidence for neuroinflammation is even stronger with all lines showing high levels of astrogliosis and microgliosis (Ahmed et al., 2010; Kayasuga et al., 2007). The foremost task is to establish the mechanistic basis of the FTD-related behavioral deficits in progranulin-deficient mice, including testing whether the observed protein mishandling or neuroinflammation phenotypes are causally related to neuronal dysfunction, and/or whether other mechanisms are in play.
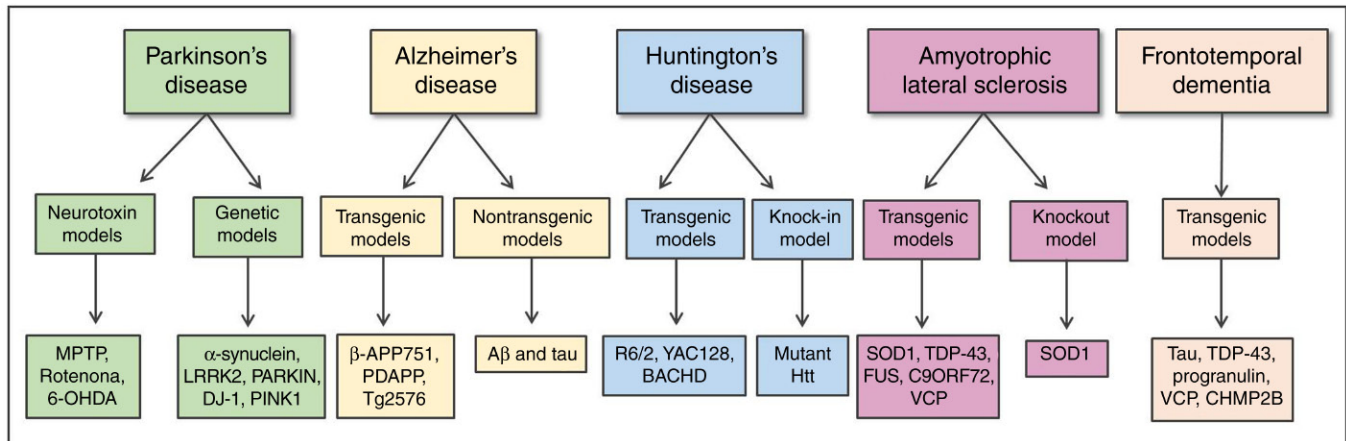
FIGURE 42.2   **Animal models of neurodegenerative diseases.**

6.1.4 VCP Models

Mutations in *VCP* which encodes VCP (VCP in humans or p97 in mouse) can cause pure FTD, but more commonly cause a syndrome with muscle and bone diseases. This rare disorder is called inclusion body myopathy with Paget's disease of bone and frontotemporal dementia (IBMPFD) (Watts et al., 2004). VCP/p97 has numerous functions, including regulating protein degradation through the ubiquitin–proteasome system, endoplasmic reticulum-associated degradation, and autophagy. The clinical presentation of FTD in IBMPFD includes both bvFTD and semantic variant-type progressive aphasia with an age of onset in the mid to late 50s. (Kim et al., 2012; van der Zee et al., 2009). Neuropathologically, FTD caused by VCP mutations is associated with FTLD-TDP type D, a distinct subtype that is not seen in sporadic FTD or with other mutations.

Two transgenic and one KI line are available as models of VCP-related FTD. The transgenic models express human VCP with either the R155H or A232E mutation from a ubiquitous promoter at levels two- to threefold higher than the endogenous gene (Custer et al., 2010). Each of these models exhibits age-dependent muscle, bone, and brain disease related to human. Neuronal dysfunction in the transgenic lines includes increased anxiety-related behavior and impaired novel object recognition (Custer et al., 2010). On *postmortem* examination, all three models had age-dependent gliosis and loss of nuclear TDP-43 with accumulation of ubiquitinated TDP-43 in the cytoplasm (Badadani et al., 2010; Custer et al., 2010).

6.1.5 CHMP2B Models

Mutations in CHMP2B are the rarest cause of FTD, with four proven pathogenic mutations identified in five families to date. In addition, the neuropathology is unique, representing a small cluster of FTD cases with ubiquitinated neuronal cytoplasmic inclusions that do not contain tau, TDP-43, or FUS. (Holm et al., 2009). CHMP2B encodes charged multivesicular protein 2B, which is involved in trafficking endosomes to degradation in lysosomes. Mice expressing CHMP2B Intron promoter develop inclusions of ubiquitinated proteins that are negative for TDP-43 and FUS, as in the FTLD-UPS pathology in patients with CHMP2B mutations (Skibinski et al., 2005). The mice also develop axonal swellings and have reduced survival (Fig. 42.2).

7 CONCLUSIONS

Although the pathophysiology of different neurodegenerative disease shares common mechanisms, especially pathological protein aggregation, these disorders present significant clinical and genetic heterogeneity. Several fundamental issues remain unanswered. What is responsible for triggering the generation of misfolded proteins that initiate disease-related cascades? Why do only certain proteins aggregate in a disease-specific manner if the common final pathway is the impairment of protein homeostasis? What is the factor underlying the selective vulnerability of different brain regions? What is the role played by glial cells in the transmission of protein aggregates? The precise nature of each one of these proteins in the aggregation pathway and their relevance for discrete human diseases require further studies. In this regard, animal models have provided significant contribution to the understanding of the pathophysiology of neurodegenerative diseases. Nevertheless, animal models only recapitulate part of the complex and heterogeneous nature of neurodegenerative diseases. There is still a great challenge ahead to establish new animal models that can truly contribute to the development of preventive and/or disease-modifying therapeutic strategies (Table 42.1).

TABLE 42.1 Main Animal Models of Neurodegenerative Diseases

Disease	Models	Mechanisms	Advantages	Disadvantages
Parkinson's disease	α-Synuclein	*Genetic model*: mutation on A30P, A53T, S129D, S87, E46K in α-*syn* gene and KO model	Decreases in striatal DA. Inclusion bodies. Motor impairments	Not show loss of dopaminergic neurons
	LRRK2	*Genetic model*: mutation on R1441G, G2019S, exon 29, 30 in *LRRK2* gene, KO model	Enhancement of DA release from the striatum. Motor hyperactivity	Different results depending on the mutation used
	PARKIN	*Genetic model*: transgenic overexpression parkin and KO model	Behavioral deficits, mitochondrial dysfunction	Not exhibit loss of dopaminergic neurons
	DJ-1	*Genetic model*: KO model	Defects in locomotor, decreased dopamine release in the striatum	Usually, no loss of dopaminergic neurons in the SNpc
	PINK1	*Genetic model*: KO model	Reduced locomotion, no change on rotarod performance, mitochondrial dysfunction	No dopaminergic neurons abnormalities and LB formation
	MPTP	*Neurotoxic model*: interacts with mitochondrial complexes and increase oxidative stress	Reproduce lesion formation, dopaminergic neuron loss, systemic administration	No LB formation, typical PD behavior not observes, high toxicity
	Rotenone	*Neurotoxic model*: increase oxidative stress and reactive oxygen species production	Reproduce lesion formation, dopaminergic neuron loss, LB formation, systemic administration	Difficult to replicate due to the high mortality
	6-OHDA	*Neurotoxic model*: 6-OHDA is oxidized in reactive oxygen species leading to electron transport chain inhibition and oxidative stress	Reproduce lesion formation, dopaminergic neuron loss	No LB formation. Need inject into the brain
Alzheimer's disease	Transgenic models	*Genetic model*: single or multitransgenic animals overexpressing APP, PS and/or Tau mutations	Usually, mice presented impairment in memory and the main feature of a patient with AD	AD phenotype occurs late. Just in mice
	Nontransgenic models	*Neurotoxic model*: toxins injection in the brain, including Aβ or tau	Use other animals than mice. Investigate the difference between an acute or a chronic administration	Acute models do not reproduce the gradual increase in Aβ occurring in many years in humans
Huntington's disease	R6/1 R6/2	*Genetic model*: R6/1 (116 CAG repeats) and R6/2 (144 CAG repeats) mouse models that were developed, expressing the exon 1 of human Htt under the control of 1 kb human Htt promoter	Severe neurological symptoms, rapid onset, intranuclear inclusions very similar to those observed in biopsy from HD	Only expresses the amino-terminal region of the Htt protein nuclear Htt. Aggregates are widely distributed in several brain substrate
	YAC128/ BACHD	*Genetic model*: mouse express full-length human Htt containing 128 and 97 polyglutamines, respectively	Develop selective striatal and cortical atrophy at the age of 12 months. Progressive motor, cognitive deficits, psychiatric disturbance peripheral immune activation	Milder deficit and slower progression
	HD knock-in	*Genetic model*: models with expanded CAG repeats or human mutant Htt exon l HdhQlll, CAG140, and HdhQ150	Preferential accumulation of mutant Htt in striatal neurons that are mostly affected in HD. Depression-like behavior and increase in anxiety-like behavior	Late-onset phenotype and progressive but mild pathology. Not develop a phenotypes as robust as those in transgenic mice

Amyotrophic lateral sclerosis	SOD1	*Genetic model*: KO model and transgenic SOD1 models	In KO, significant distal motor axonopathy. In transgenic mice many features of ALS, axonal and mitochondrial dysfunction, progressive neuromuscular dysfunction, gliosis, and motor neuron loss	KO does not present motor dysfunction, at least up to 6 months of age. Transgenic have variable ages of disease onset and rates of disease progression
	TDP-43	*Genetic model*: remains unclear which TDP-43 mutations cause ALS	Models display mostly axonal phenotypes with relatively mild motor neuron cell death and significant neurodegeneration	Phenotypes are highly dependent upon the promoter used and the level of transgene expression
	FUS	*Genetic model*: four transgenic rodent lines overexpressing FUS	Motor involvement with muscle denervation, axonopathy and spinal degeneration, cognitive deficits, memory impairment, and hippocampal neurons death	All four models display different phenotypic manifestations
	C9ORF72	*Genetic model*: transgenic mice been expressed abnormal hexanucleotide expansion (G4C2)66 and KO model	Transgenic mice has neuronal nuclear inclusions of poly(Gly-Pro), poly(Gly-Ala), and poly(Gly-Arg) dipeptide repeat protein and neuronal loss	KO mice did not induced degeneration, defects in motor function, or altered survival
	VCP	*Genetic model*: KI of the R155H mutation in VCP	In heterozygosity progressive weakness from 9 months of age and weight loss by 24 months of age. Homozygous resulted in a much more aggressive phenotype, early lethality	Phenotypes in transgenic mice, may not be exclusively due to motor neuron degeneration
Frontotemporal dementia	Tau	*Genetic model*: 25 lines of transgenic mice have been created that express human tau with mutations	Aggregated tau and neuronal death, deficits in synaptic plasticity and cognitive dysfunction and neurodegeneration	Not all lines display the pronounced neurodegeneration seen in the human disease
	TDP-43	*Genetic model*: transgenic and KO model	Astrocytosis developed before 5 months of age, and learning/memory and motor deficits developed around 7 months	None of these features correlates well with the presence of functional deficits across different lines
	Progranulin	*Genetic model*: several different lines of progranulin KO mice	Early abnormalities in social behavior without impairment in overall health or motor function, neuroinflammation	Different results in different lines KO model
	VCP	*Genetic model*: two transgenic and one KI line are available as models of VCP- related	Models exhibit age-dependent muscle, bone, and brain disease related to human	Mutation on VCP can cause pure FTD but more commonly cause a syndrome of FTD with muscle and bone disease
	CHMP2B	*Genetic model*: expressing CHMP2B Intron promoter	Develop axonal swellings and have reduced survival	Neuropathology is unique, representing the small cluster of FTD cases

AD, Alzheimer's disease; ALS, amyotrophic lateral sclerosis; APP, amyloid precursor protein; FTD, frontotemporal dementia; FUS, fused in sarcoma; HD, Huntington's disease; KI, knock-in; LB, Lewy body; LRRK2, leucine-rich-repeat-kinase 2; MPTP, 1-methyl-4-phenyl-1,2,3,6-tetrahydropyridine; 6-OHDA, 6-hydroxy-dopamine; SNpc, substantia nigra pars compacta; SOD1, superoxide dismutase 1; PS, Presenilin; VCP, valosin-containing protein.

References

Ahmed, Z., Sheng, H., Xu, Y.F., Lin, W.L., Innes, A.E., Gass, J., et al., 2010. Accelerated lipofuscinosis and ubiquitination in granulin knockout mice suggest a role for progranulin in successful aging. Am. J. Pathol. 177 (1), 311–324.

Alam, M., Mayerhofer, A., Schmidt, W.J., 2004. The neurobehavioral changes induced by bilateral rotenone lesion in medial forebrain bundle of rats are reversed by L-DOPA. Behav. Brain Res. 151 (1–2), 117–124.

Andorfer, C., Acker, C.M., Kress, Y., Hof, P.R., Duff, K., Davies, P., 2005. Cell-cycle reentry and cell death in transgenic mice expressing non-mutant human tau isoforms. J. Neurosci. 25 (22), 5446–5454.

Andres-Mateos, E., Perier, C., Zhang, L., Blanchard-Fillion, B., Greco, T.M., Thomas, B., et al., 2007. DJ-1 gene deletion reveals that DJ-1 is an atypical peroxiredoxin-like peroxidase. Proc. Natl. Acad. Sci. USA 104 (37), 14807–14812.

Antzoulatos, E., Jakowec, M.W., Petzinger, G.M., Wood, R.I., 2010. Sex differences in motor behavior in the MPTP mouse model of Parkinson's disease. Pharmacol. Biochem. Behav. 95 (4), 466–472.

Asmal, L., Flegar, S.J., Wang, J., Rummel-Kluge, C., Komossa, K., Leucht, S., 2013. Quetiapine versus other atypical antipsychotics for schizophrenia. Cochrane Database Syst. Rev. (11), Article no. CD006625.

Badadani, M., Nalbandian, A., Watts, G.D., Vesa, J., Kitazawa, M., Su, H., et al., 2010. VCP associated inclusion body myopathy and Paget disease of bone knock-in mouse model exhibits tissue pathology typical of human disease. PLoS One 5 (10.), e13183.

Balducci, C., Forloni, G., 2014. In vivo application of beta amyloid oligomers: a simple tool to evaluate mechanisms of action and new therapeutic approaches. Curr. Pharm. Des. 20 (15), 2491–2505.

Bang, J., Spina, S., Miller, B.L., 2015. Frontotemporal dementia. Lancet 386 (10004), 1672–1682.

Barmada, S.J., Skibinski, G., Korb, E., Rao, E.J., Wu, J.Y., Finkbeiner, S., 2010. Cytoplasmic mislocalization of TDP-43 is toxic to neurons and enhanced by a mutation associated with familial amyotrophic lateral sclerosis. J. Neurosci. 30 (2), 639–649.

Baxa, M., Hruska-Plochan, M., Juhas, S., Vodicka, P., Pavlok, A., Juhasova, J., et al., 2013. A transgenic minipig model of Huntington's disease. J. Huntingtons Dis. 2 (1), 47–68.

Bensimon, G., Lacomblez, L., Meininger, V., 1994. A controlled trial of riluzole in amyotrophic lateral sclerosis. ALS/Riluzole Study Group. N. Engl. J. Med. 330 (9), 585–591.

Bento-Abreu, A., Van Damme, P., Van Den Bosch, L., Robberecht, W., 2010. The neurobiology of amyotrophic lateral sclerosis. Eur. J. Neurosci. 31 (12), 2247–2265.

Bezard, E., Przedborski, S., 2011. A tale on animal models of Parkinson's disease. Mov. Disord. 26 (6), 993–1002.

Billings, L.M., Oddo, S., Green, K.N., McGaugh, J.L., LaFerla, F.M., 2005. Intraneuronal Abeta causes the onset of early Alzheimer's disease-related cognitive deficits in transgenic mice. Neuron 45 (5), 675–688.

Bird, T., Knopman, D., VanSwieten, J., Rosso, S., Feldman, H., Tanabe, H., et al., 2003. Epidemiology and genetics of frontotemporal dementia/Pick's disease. Ann. Neurol. 54 (Suppl. 5), S29–S31.

Borchelt, D.R., Guarnieri, M., Wong, P.C., Lee, M.K., Slunt, H.S., Xu, Z.S., et al., 1995. Superoxide dismutase 1 subunits with mutations linked to familial amyotrophic lateral sclerosis do not affect wild-type subunit function. J. Biol. Chem. 270 (7), 3234–3238.

Bosco, D.A., Landers, J.E., 2010. Genetic determinants of amyotrophic lateral sclerosis as therapeutic targets. CNS Neurol. Disord. Drug Targets 9 (6), 779–790.

Braak, H., Rub, U., Sandmann-Keil, D., Gai, W.P., de Vos, R.A., Jansen Steur, E.N., et al., 2000. Parkinson's disease: affection of brain stem nuclei controlling premotor and motor neurons of the somatomotor system. Acta Neuropathol. 99 (5), 489–495.

Braak, H., Del Tredici, K., Rub, U., de Vos, R.A., Jansen Steur, E.N., Braak, E., 2003a. Staging of brain pathology related to sporadic Parkinson's disease. Neurobiol. Aging 24 (2), 197–211.

Braak, H., Rub, U., Gai, W.P., Del Tredici, K., 2003b. Idiopathic Parkinson's disease: possible routes by which vulnerable neuronal types may be subject to neuroinvasion by an unknown pathogen. J. Neural. Transm. (Vienna) 110 (5), 517–536.

Braak, H., Ghebremedhin, E., Rub, U., Bratzke, H., Del Tredici, K., 2004. Stages in the development of Parkinson's disease-related pathology. Cell Tissue Res. 318 (1), 121–134.

Braun, R.J., Sommer, C., Carmona-Gutierrez, D., Khoury, C.M., Ring, J., Buttner, S., Madeo, F., 2011. Neurotoxic 43-kDa TAR DNA-binding protein (TDP-43) triggers mitochondrion-dependent programmed cell death in yeast. J. Biol. Chem. 286 (22), 19958–19972.

Bruijn, L.I., Becher, M.W., Lee, M.K., Anderson, K.L., Jenkins, N.A., Copeland, N.G., et al., 1997. ALS-linked SOD1 mutant G85R mediates damage to astrocytes and promotes rapidly progressive disease with SOD1-containing inclusions. Neuron 18 (2), 327–338.

Burrell, J.R., Vucic, S., Kiernan, M.C., 2011. Isolated bulbar phenotype of amyotrophic lateral sclerosis. Amyotroph. Lateral Scler. 12 (4), 283–289.

Byrne, S.C., Rowland, L.P., Vonsattel, J.P.G., Welzel, A.T., Walsh, D.M., Hardiman, 2011. Common Themes in the Pathogenesis of Neurodegeneration, vol. 1–15, Springer, New York, NY.

Cantarella, G., Di Benedetto, G., Puzzo, D., Privitera, L., Loreto, C., Saccone, S., et al., 2015. Neutralization of TNFSF10 ameliorates functional outcome in a murine model of Alzheimer's disease. Brain 138 (Pt 1), 203–216.

Carter, R.J., Lione, L.A., Humby, T., Mangiarini, L., Mahal, A., Bates, G.P., et al., 1999. Characterization of progressive motor deficits in mice transgenic for the human Huntington's disease mutation. J. Neurosci. 19 (8), 3248–3257.

Caspersen, C., Wang, N., Yao, J., Sosunov, A., Chen, X., Lustbader, J.W., et al., 2005. Mitochondrial Abeta: a potential focal point for neuronal metabolic dysfunction in Alzheimer's disease. FASEB J. 19 (14), 2040–2041.

Cayzac, S., Delcasso, S., Paz, V., Jeantet, Y., Cho, Y.H., 2011. Changes in striatal procedural memory coding correlate with learning deficits in a mouse model of Huntington disease. Proc. Natl. Acad. Sci. USA 108 (22), 9280–9285.

Chang-Hong, R., Wada, M., Koyama, S., Kimura, H., Arawaka, S., Kawanami, T., et al., 2005. Neuroprotective effect of oxidized galectin-1 in a transgenic mouse model of amyotrophic lateral sclerosis. Exp. Neurol. 194 (1), 203–211.

Chew, J., Gendron, T.F., Prudencio, M., Sasaguri, H., Zhang, Y.J., Castanedes-Casey, M., et al., 2015. Neurodegeneration. C9ORF72 repeat expansions in mice cause TDP-43 pathology, neuronal loss, and behavioral deficits. Science 348 (6239), 1151–1154.

Ciura, S., Lattante, S., Le Ber, I., Latouche, M., Tostivint, H., Brice, A., Kabashi, E., 2013. Loss of function of C9orf72 causes motor deficits in a zebrafish model of amyotrophic lateral sclerosis. Ann. Neurol. 74 (2), 180–187.

Consortium, H.D.i., 2012. Induced pluripotent stem cells from patients with Huntington's disease show CAG-repeat-expansion-associated phenotypes. Cell Stem Cell 11 (2), 264–278.

Crozat, A., Aman, P., Mandahl, N., Ron, D., 1993. Fusion of CHOP to a novel RNA-binding protein in human myxoid liposarcoma. Nature 363 (6430), 640–644.

Cudkowicz, M.E., McKenna-Yasek, D., Sapp, P.E., Chin, W., Geller, B., Hayden, D.L., et al., 1997. Epidemiology of mutations in superoxide dismutase in amyotrophic lateral sclerosis. Ann. Neurol. 41 (2), 210–221.

Custer, S.K., Neumann, M., Lu, H., Wright, A.C., Taylor, J.P., 2010. Transgenic mice expressing mutant forms VCP/p97 recapitulate the full spectrum of IBMPFD including degeneration in muscle, brain and bone. Hum. Mol. Genet. 19 (9), 1741–1755.

Dave, K.D., De Silva, S., Sheth, N.P., Ramboz, S., Beck, M.J., Quang, C., et al., 2014. Phenotypic characterization of recessive gene knockout rat models of Parkinson's disease. Neurobiol. Dis. 70, 190–203.

Davies, S.W., Turmaine, M., Cozens, B.A., DiFiglia, M., Sharp, A.H., Ross, C.A., et al., 1997. Formation of neuronal intranuclear inclusions underlies the neurological dysfunction in mice transgenic for the HD mutation. Cell 90 (3), 537–548.

Dawson, T.M., Ko, H.S., Dawson, V.L., 2010. Genetic animal models of Parkinson's disease. Neuron 66 (5), 646–661.

de Rijk, M.C., Tzourio, C., Breteler, M.M., Dartigues, J.F., Amaducci, L., Lopez-Pousa, S., et al., 1997. Prevalence of parkinsonism and Parkinson's disease in Europe: the EUROPARKINSON Collaborative Study. European Community Concerted Action on the Epidemiology of Parkinson's disease. J. Neurol. Neurosurg. Psychiatry 62 (1), 10–15.

DeJesus-Hernandez, M., Mackenzie, I.R., Boeve, B.F., Boxer, A.L., Baker, M., Rutherford, N.J., et al., 2011. Expanded GGGGCC hexanucleotide repeat in noncoding region of C9ORF72 causes chromosome 9p-linked FTD and ALS. Neuron 72 (2), 245–256.

Duff, K., Paulsen, J.S., Beglinger, L.J., Langbehn, D.R., Stout, J.C., Predict, H.D.I.o.t.H.S.G., 2007. Psychiatric symptoms in Huntington's disease before diagnosis: the predict-HD study. Biol. Psychiatry 62 (12), 1341–1346.

Duty, S., Jenner, P., 2011. Animal models of Parkinson's disease: a source of novel treatments and clues to the cause of the disease. Br. J. Pharmacol. 164 (4), 1357–1391.

Duyckaerts, C., Potier, M.C., Delatour, B., 2008. Alzheimer disease models and human neuropathology: similarities and differences. Acta Neuropathol. 115 (1), 5–38.

Duyckaerts, C., Delatour, B., Potier, M.C., 2009. Classification and basic pathology of Alzheimer disease. Acta Neuropathol. 118 (1), 5–36.

Esch, F.S., Keim, P.S., Beattie, E.C., Blacher, R.W., Culwell, A.R., Oltersdorf, T., et al., 1990. Cleavage of amyloid beta peptide during constitutive processing of its precursor. Science 248 (4959), 1122–1124.

Fernagut, P.O., Chesselet, M.F., 2004. Alpha-synuclein and transgenic mouse models. Neurobiol. Dis. 17 (2), 123–130.

Fischer, L.R., Igoudjil, A., Magrane, J., Li, Y., Hansen, J.M., Manfredi, G., Glass, J.D., 2011. SOD1 targeted to the mitochondrial intermembrane space prevents motor neuropathy in the Sod1 knockout mouse. Brain 134 (Pt 1), 196–209.

Fleming, S.M., Zhu, C., Fernagut, P.O., Mehta, A., DiCarlo, C.D., Seaman, R.L., Chesselet, M.F., 2004. Behavioral and immunohistochemical effects of chronic intravenous and subcutaneous infusions of varying doses of rotenone. Exp. Neurol. 187 (2), 418–429.

Frank-Cannon, T.C., Tran, T., Ruhn, K.A., Martinez, T.N., Hong, J., Marvin, M., et al., 2008. Parkin deficiency increases vulnerability to inflammation-related nigral degeneration. J. Neurosci. 28 (43), 10825–10834.

Funayama, M., Hasegawa, K., Kowa, H., Saito, M., Tsuji, S., Obata, F., 2002. A new locus for Parkinson's disease (PARK8) maps to chromosome 12p11.2-q13. 1. Ann. Neurol. 51 (3), 296–301.

Gal, J., Zhang, J., Kwinter, D.M., Zhai, J., Jia, H., Jia, J., Zhu, H., 2011. Nuclear localization sequence of FUS and induction of stress granules by ALS mutants. Neurobiol. Aging 32 (12), 2323.e27–2323.e40.

Games, D., Adams, D., Alessandrini, R., Barbour, R., Berthelette, P., Blackwell, C., et al., 1995. Alzheimer-type neuropathology in transgenic mice overexpressing V717F beta-amyloid precursor protein. Nature 373 (6514), 523–527.

Giralt, A., Saavedra, A., Alberch, J., Perez-Navarro, E., 2012. Cognitive dysfunction in Huntington's disease: humans, mouse models and molecular mechanisms. J. Huntingtons Dis. 1 (2), 155–173.

Godena, V.K., Romano, G., Romano, M., Appocher, C., Klima, R., Buratti, E., et al., 2011. TDP-43 regulates Drosophila neuromuscular junctions growth by modulating Futsch/MAP1B levels and synaptic microtubules organization. PLoS One 6 (3), e17808.

Goldberg, M.S., Fleming, S.M., Palacino, J.J., Cepeda, C., Lam, H.A., Bhatnagar, A., et al., 2003. Parkin-deficient mice exhibit nigrostriatal deficits but not loss of dopaminergic neurons. J. Biol. Chem. 278 (44), 43628–43635.

Goldberg, M.S., Pisani, A., Haburcak, M., Vortherms, T.A., Kitada, T., Costa, C., et al., 2005. Nigrostriatal dopaminergic deficits and hypokinesia caused by inactivation of the familial Parkinsonism-linked gene DJ-1. Neuron 45 (4), 489–496.

Gorno-Tempini, M.L., Hillis, A.E., Weintraub, S., Kertesz, A., Mendez, M., Cappa, S.F., et al., 2011. Classification of primary progressive aphasia and its variants. Neurology 76 (11), 1006–1014.

Graffmo, K.S., Forsberg, K., Bergh, J., Birve, A., Zetterstrom, P., Andersen, P.M., et al., 2013. Expression of wild-type human superoxide dismutase-1 in mice causes amyotrophic lateral sclerosis. Hum. Mol. Genet. 22 (1), 51–60.

Gray, M., Shirasaki, D.I., Cepeda, C., Andre, V.M., Wilburn, B., Lu, X.H., et al., 2008. Full-length human mutant huntingtin with a stable polyglutamine repeat can elicit progressive and selective neuropathogenesis in BACHD mice. J. Neurosci. 28 (24), 6182–6195.

Guo, J.L., Lee, V.M., 2014. Cell-to-cell transmission of pathogenic proteins in neurodegenerative diseases. Nat. Med. 20 (2), 130–138.

Gurney, M.E., 1994. Transgenic-mouse model of amyotrophic lateral sclerosis. N. Engl. J. Med. 331 (25), 1721–1722.

Gusella, J.F., MacDonald, M.E., 2009. Huntington's disease: the case for genetic modifiers. Genome Med. 1 (8), 80.

Guzman, J.N., Sanchez-Padilla, J., Wokosin, D., Kondapalli, J., Ilijic, E., Schumacker, P.T., Surmeier, D.J., 2010. Oxidant stress evoked by pacemaking in dopaminergic neurons is attenuated by DJ-1. Nature 468 (7324), 696–700.

Hauptmann, S., Keil, U., Scherping, I., Bonert, A., Eckert, A., Muller, W.E., 2006. Mitochondrial dysfunction in sporadic and genetic Alzheimer's disease. Exp. Gerontol. 41 (7), 668–673.

Hazell, A.S., Itzhak, Y., Liu, H., Norenberg, M.D., 1997. 1-Methyl-4-phenyl-1,2,3,6-tetrahydropyridine (MPTP) decreases glutamate uptake in cultured astrocytes. J. Neurochem. 68 (5), 2216–2219.

Heiman-Patterson, T.D., Sher, R.B., Blankenhorn, E.A., Alexander, G., Deitch, J.S., Kunst, C.B., et al., 2011. Effect of genetic background on phenotype variability in transgenic mouse models of amyotrophic lateral sclerosis: a window of opportunity in the search for genetic modifiers. Amyotroph. Lateral Scler. 12 (2), 79–86.

Heng, M.Y., Detloff, P.J., Albin, R.L., 2008. Rodent genetic models of Huntington disease. Neurobiol. Dis. 32 (1), 1–9.

Higgins, L.S., Holtzman, D.M., Rabin, J., Mobley, W.C., Cordell, B., 1994. Transgenic mouse brain histopathology resembles early Alzheimer's disease. Ann. Neurol. 35 (5), 598–607.

Hodgson, J.G., Agopyan, N., Gutekunst, C.A., Leavitt, B.R., LePiane, F., Singaraja, R., et al., 1999. A YAC mouse model for Huntington's disease with full-length mutant huntingtin, cytoplasmic toxicity, and selective striatal neurodegeneration. Neuron 23 (1), 181–192.

Holm, I.E., Isaacs, A.M., Mackenzie, I.R., 2009. Absence of FUS-immunoreactive pathology in frontotemporal dementia linked to chromosome 3 (FTD-3) caused by mutation in the CHMP2B gene. Acta Neuropathol. 118 (5), 719–720.

Hsiao, K., Chapman, P., Nilsen, S., Eckman, C., Harigaya, Y., Younkin, S., et al., 1996. Correlative memory deficits, Abeta elevation, and amyloid plaques in transgenic mice. Science 274 (5284), 99–102.

Huang, C., Xia, P.Y., Zhou, H., 2010. Sustained expression of TDP-43 and FUS in motor neurons in rodent's lifetime. Int. J. Biol. Sci. 6 (4), 396–406.

Huang, C., Zhou, H., Tong, J., Chen, H., Liu, Y.J., Wang, D., et al., 2011. FUS transgenic rats develop the phenotypes of amyotrophic lateral sclerosis and frontotemporal lobar degeneration. PLoS Genet. 7 (3), e1002011.

Huang, C., Tong, J., Bi, F., Wu, Q., Huang, B., Zhou, H., Xia, X.G., 2012. Entorhinal cortical neurons are the primary targets of FUS mislocalization and ubiquitin aggregation in FUS transgenic rats. Hum. Mol. Genet. 21 (21), 4602–4614.

Huisman, M.H., de Jong, S.W., van Doormaal, P.T., Weinreich, S.S., Schelhaas, H.J., van der Kooi, A.J., et al., 2011. Population based epidemiology of amyotrophic lateral sclerosis using capture-recapture methodology. J. Neurol. Neurosurg. Psychiatry 82 (10), 1165–1170.

Hyman, B.T., 2011. Amyloid-dependent and amyloid-independent stages of Alzheimer disease. Arch. Neurol. 68 (8), 1062–1064.

Igaz, L.M., Kwong, L.K., Lee, E.B., Chen-Plotkin, A., Swanson, E., Unger, T., et al., 2011. Dysregulation of the ALS-associated gene TDP-43 leads to neuronal death and degeneration in mice. J. Clin. Invest. 121 (2), 726–738.

Ingre, C., Roos, P.M., Piehl, F., Kamel, F., Fang, F., 2015. Risk factors for amyotrophic lateral sclerosis. Clin. Epidemiol. 7, 181–193.

Itier, J.M., Ibanez, P., Mena, M.A., Abbas, N., Cohen-Salmon, C., Bohme, G.A., et al., 2003. Parkin gene inactivation alters behaviour and dopamine neurotransmission in the mouse. Hum. Mol. Genet. 12 (18), 2277–2291.

Iwatsubo, T., 2003. Aggregation of alpha-synuclein in the pathogenesis of Parkinson's disease. J. Neurol. 250 (Suppl. 3), III11–III14.

Jaarsma, D., 2006. Swelling and vacuolisation of mitochondria in transgenic SOD1-ALS mice: a consequence of supranormal SOD1 expression? Mitochondrion 6 (1), 48–49.

Jaarsma, D., Haasdijk, E.D., Grashorn, J.A., Hawkins, R., van Duijn, W., Verspaget, H.W., et al., 2000. Human Cu/Zn superoxide dismutase (SOD1) overexpression in mice causes mitochondrial vacuolization, axonal degeneration, and premature motoneuron death and accelerates motoneuron disease in mice expressing a familial amyotrophic lateral sclerosis mutant SOD1. Neurobiol. Dis. 7 (6 Pt B), 623–643.

Jack, Jr., C.R., Wiste, H.J., Vemuri, P., Weigand, S.D., Senjem, M.L., Zeng, G., et al., 2010. Brain beta-amyloid measures and magnetic resonance imaging atrophy both predict time-to-progression from mild cognitive impairment to Alzheimer's disease. Brain 133 (11), 3336–3348.

Jackson-Lewis, V., Przedborski, S., 2007. Protocol for the MPTP mouse model of Parkinson's disease. Nat. Protoc. 2 (1), 141–151.

Jacobsen, J.C., Bawden, C.S., Rudiger, S.R., McLaughlan, C.J., Reid, S.J., Waldvogel, H.J., et al., 2010. An ovine transgenic Huntington's disease model. Hum. Mol. Genet. 19 (10), 1873–1882.

Jagmag, S.A., Tripathi, N., Shukla, S.D., Maiti, S., Khurana, S., 2015. Evaluation of models of Parkinson's disease. Front. Neurosci. 9, 503.

Janda, E., Isidoro, C., Carresi, C., Mollace, V., 2012. Defective autophagy in Parkinson's disease: role of oxidative stress. Mol. Neurobiol. 46 (3), 639–661.

Janda, E., Lascala, A., Carresi, C., Parafati, M., Aprigliano, S., Russo, V., et al., 2015. Parkinsonian toxin-induced oxidative stress inhibits basal autophagy in astrocytes via NQO2/quinone oxidoreductase 2: implications for neuroprotection. Autophagy 11 (7), 1063–1080.

Javitch, J.A., D'Amato, R.J., Strittmatter, S.M., Snyder, S.H., 1985. Parkinsonism-inducing neurotoxin, N-methyl-4-phenyl-1,2,3,6-tetrahydropyridine: uptake of the metabolite N-methyl-4-phenylpyridine by dopamine neurons explains selective toxicity. Proc. Natl. Acad. Sci. USA 82 (7), 2173–2177.

Jellinger, K.A., 1991. Pathology of Parkinson's disease. Changes other than the nigrostriatal pathway. Mol. Chem. Neuropathol. 14 (3), 153–197.

Kabashi, E., Valdmanis, P.N., Dion, P., Spiegelman, D., McConkey, B.J., Vande Velde, C., et al., 2008. TARDBP mutations in individuals with sporadic and familial amyotrophic lateral sclerosis. Nat. Genet. 40 (5), 572–574.

Kabashi, E., Bercier, V., Lissouba, A., Liao, M., Brustein, E., Rouleau, G.A., Drapeau, P., 2011. FUS and TARDBP but not SOD1 interact in genetic models of amyotrophic lateral sclerosis. PLoS Genet. 7 (8), e1002214.

Kayasuga, Y., Chiba, S., Suzuki, M., Kikusui, T., Matsuwaki, T., Yamanouchi, K., et al., 2007. Alteration of behavioural phenotype in mice by targeted disruption of the progranulin gene. Behav. Brain Res. 185 (2), 110–118.

Kazim, S.F., Blanchard, J., Dai, C.L., Tung, Y.C., LaFerla, F.M., Iqbal, I.G., Iqbal, K., 2014. Disease modifying effect of chronic oral treatment with a neurotrophic peptidergic compound in a triple transgenic mouse model of Alzheimer's disease. Neurobiol. Dis. 71, 110–130.

Khandelwal, P.J., Dumanis, S.B., Feng, L.R., Maguire-Zeiss, K., Rebeck, G., Lashuel, H.A., Moussa, C.E., 2010. Parkinson-related parkin reduces alpha-Synuclein phosphorylation in a gene transfer model. Mol. Neurodegener. 5, 47.

Kim, E.J., Sidhu, M., Gaus, S.E., Huang, E.J., Hof, P.R., Miller, B.L., et al., 2012. Selective frontoinsular von Economo neuron and fork cell loss in early behavioral variant frontotemporal dementia. Cereb. Cortex 22 (2), 251–259.

King, D.L., Arendash, G.W., 2002. Behavioral characterization of the Tg2576 transgenic model of Alzheimer's disease through 19 months. Physiol. Behav. 75 (5), 627–642.

Kitada, T., Pisani, A., Porter, D.R., Yamaguchi, H., Tscherter, A., Martella, G., et al., 2007. Impaired dopamine release and synaptic plasticity in the striatum of PINK1-deficient mice. Proc. Natl. Acad. Sci. USA 104 (27), 11441–11446.

Kitada, T., Tong, Y., Gautier, C.A., Shen, J., 2009. Absence of nigral degeneration in aged parkin/DJ-1/PINK1 triple knockout mice. J. Neurochem. 111 (3), 696–702.

Kumar, A., Cookson, M.R., 2011. Role of LRRK2 kinase dysfunction in Parkinson disease. Expert Rev. Mol. Med. 13, e20.

Kwan, W., Trager, U., Davalos, D., Chou, A., Bouchard, J., Andre, R., et al., 2012. Mutant huntingtin impairs immune cell migration in Huntington disease. J. Clin. Invest. 122 (12), 4737–4747.

Lamb, B.T., Sisodia, S.S., Lawler, A.M., Slunt, H.H., Kitt, C.A., Kearns, W.G., et al., 1993. Introduction and expression of the 400 kilobase amyloid precursor protein gene in transgenic mice [corrected]. Nat. Genet. 5 (1), 22–30.

Langbehn, D.R., Hayden, M.R., Paulsen, J.S., Group, P.-H.I.o.t.H.S., 2010. CAG-repeat length and the age of onset in Huntington disease (HD): a review and validation study of statistical approaches. Am. J. Med. Genet. B Neuropsychiatr. Genet. 153B (2), 397–408.

Lansbury, Jr., P.T., 2004. Back to the future: the 'old-fashioned' way to new medications for neurodegeneration. Nat. Med. 10 (Suppl.), S51–S57.

Lazarou, M., Narendra, D.P., Jin, S.M., Tekle, E., Banerjee, S., Youle, R.J., 2013. PINK1 drives Parkin self-association and HECT-like E3 activity upstream of mitochondrial binding. J. Cell Biol. 200 (2), 163–172.

Lebert, F., Stekke, W., Hasenbroekx, C., Pasquier, F., 2004. Frontotemporal dementia: a randomised, controlled trial with trazodone. Dement. Geriatr. Cogn. Disord. 17 (4), 355–359.

Lee, Y., Dawson, V.L., Dawson, T.M., 2012. Animal models of Parkinson's disease: vertebrate genetics. Cold Spring Harb. Perspect. Med. 2 (10), a009324.

Lees, A.J., Hardy, J., Revesz, T., 2009. Parkinson's disease. Lancet 373 (9680), 2055–2066.

Li, H., Li, S.H., Yu, Z.X., Shelbourne, P., Li, X.J., 2001. Huntingtin aggregate-associated axonal degeneration is an early pathological event in Huntington's disease mice. J. Neurosci. 21 (21), 8473–8481.

Li, Y., Liu, W., Oo, T.F., Wang, L., Tang, Y., Jackson-Lewis, V., et al., 2009. Mutant LRRK2(R1441G) BAC transgenic mice recapitulate cardinal features of Parkinson's disease. Nat. Neurosci. 12 (7), 826–828.

Lillo, P., Hodges, J.R., 2009. Frontotemporal dementia and motor neurone disease: overlapping clinic-pathological disorders. J. Clin. Neurosci. 16 (9), 1131–1135.

Lomen-Hoerth, C., Anderson, T., Miller, B., 2002. The overlap of amyotrophic lateral sclerosis and frontotemporal dementia. Neurology 59 (7), 1077–1079.

Lucking, C.B., Durr, A., Bonifati, V., Vaughan, J., De Michele, G., Gasser, T., et al., 2000. Association between early-onset Parkinson's disease and mutations in the parkin gene. N. Engl. J. Med. 342 (21), 1560–1567.

Mancuso, R., Navarro, X., 2015. Amyotrophic lateral sclerosis: current perspectives from basic research to the clinic. Prog. Neurobiol. 133, 1–26.

Mancuso, R., Olivan, S., Rando, A., Casas, C., Osta, R., Navarro, X., 2012. Sigma-1R agonist improves motor function and motoneuron survival in ALS mice. Neurotherapeutics 9 (4), 814–826.

Mangiarini, L., Sathasivam, K., Seller, M., Cozens, B., Harper, A., Hetherington, C., et al., 1996. Exon 1 of the HD gene with an expanded CAG repeat is sufficient to cause a progressive neurological phenotype in transgenic mice. Cell 87 (3), 493–506.

Margolis, R.L., Ross, C.A., 2003. Diagnosis of Huntington disease. Clin. Chem. 49 (10), 1726–1732.

Maries, E., Dass, B., Collier, T.J., Kordower, J.H., Steece-Collier, K., 2003. The role of alpha-synuclein in Parkinson's disease: insights from animal models. Nat. Rev. Neurosci. 4 (9), 727–738.

Masliah, E., Rockenstein, E., Veinbergs, I., Mallory, M., Hashimoto, M., Takeda, A., et al., 2000. Dopaminergic loss and inclusion body formation in alpha-synuclein mice: implications for neurodegenerative disorders. Science 287 (5456), 1265–1269.

Mazzio, E.A., Reams, R.R., Soliman, K.F., 2004. The role of oxidative stress, impaired glycolysis and mitochondrial respiratory redox failure in the cytotoxic effects of 6-hydroxydopamine in vitro. Brain Res. 1004 (1–2), 29–44.

McGoldrick, P., Joyce, P.I., Fisher, E.M., Greensmith, L., 2013. Rodent models of amyotrophic lateral sclerosis. Biochim. Biophys. Acta 1832 (9), 1421–1436.

McNaught, K.S., Olanow, C.W., Halliwell, B., Isacson, O., Jenner, P., 2001. Failure of the ubiquitin-proteasome system in Parkinson's disease. Nat. Rev. Neurosci. 2 (8), 589–594.

Mehta, S.G., Khare, M., Ramani, R., Watts, G.D., Simon, M., Osann, K.E., et al., 2013. Genotype-phenotype studies of VCP-associated inclusion body myopathy with Paget disease of bone and/or frontotemporal dementia. Clin. Genet. 83 (5), 422–431.

Menalled, L.B., Chesselet, M.F., 2002. Mouse models of Huntington's disease. Trends Pharmacol. Sci. 23 (1), 32–39.

Menalled, L., El-Khodor, B.F., Patry, M., Suarez-Farinas, M., Orenstein, S.J., Zahasky, B., et al., 2009. Systematic behavioral evaluation of Huntington's disease transgenic and knock-in mouse models. Neurobiol. Dis. 35 (3), 319–336.

Mendez, M.F., Shapira, J.S., McMurtray, A., Licht, E., 2007. Preliminary findings: behavioral worsening on donepezil in patients with frontotemporal dementia. Am. J. Geriatr. Psychiatry 15 (1), 84–87.

Meyer, H., Bug, M., Bremer, S., 2012. Emerging functions of the VCP/p97 AAA-ATPase in the ubiquitin system. Nat. Cell Biol. 14 (2), 117–123.

Miller, R.G., Mitchell, J.D., Lyon, M., Moore, D.H., 2007. Riluzole for amyotrophic lateral sclerosis (ALS)/motor neuron disease (MND). Cochrane Database Syst. Rev. (1), Article no. CD001447.

Miller, R.G., Mitchell, J.D., Moore, D.H., 2012. Riluzole for amyotrophic lateral sclerosis (ALS)/motor neuron disease (MND). Cochrane Database Syst. Rev. (3), Article no. CD001447.

Mitchell, J.C., McGoldrick, P., Vance, C., Hortobagyi, T., Sreedharan, J., Rogelj, B., et al., 2013. Overexpression of human wild-type FUS causes progressive motor neuron degeneration in an age- and dose-dependent fashion. Acta Neuropathol. 125 (2), 273–288.

Mogi, M., Harada, M., Riederer, P., Narabayashi, H., Fujita, K., Nagatsu, T., 1994. Tumor necrosis factor-alpha (TNF-alpha) increases both in the brain and in the cerebrospinal fluid from parkinsonian patients. Neurosci. Lett. 165 (1–2), 208–210.

Mungarro-Menchaca, X., Ferrera, P., Moran, J., Arias, C., 2002. beta-Amyloid peptide induces ultrastructural changes in synaptosomes and potentiates mitochondrial dysfunction in the presence of ryanodine. J. Neurosci. Res. 68 (1), 89–96.

Myers, R.H., 2004. Huntington's disease genetics. NeuroRx 1 (2), 255–262.

Nalbandian, A., Llewellyn, K.J., Kitazawa, M., Yin, H.Z., Badadani, M., Khanlou, N., et al., 2012. The homozygote VCP(R(1)(5)(5)H/R(1)(5)(5)H) mouse model exhibits accelerated human VCP-associated disease pathology. PLoS One 7 (9), e46308.

Nguyen, T.A., Frank-Cannon, T., Martinez, T.N., Ruhn, K.A., Marvin, M., Casey, B., et al., 2013. Analysis of inflammation-related nigral degeneration and locomotor function in DJ-1$^{-/-}$ mice. J. Neuroinflammation 10, 50.

Nieto, M., Gil-Bea, F.J., Dalfo, E., Cuadrado, M., Cabodevilla, F., Sanchez, B., et al., 2006. Increased sensitivity to MPTP in human alpha-synuclein A30P transgenic mice. Neurobiol. Aging 27 (6), 848–856.

Novak, M.J., Tabrizi, S.J., 2011. Huntington's disease: clinical presentation and treatment. Int. Rev. Neurobiol. 98, 297–323.

Obeso, J.A., Rodriguez-Oroz, M.C., Goetz, C.G., Marin, C., Kordower, J.H., Rodriguez, M., et al., 2010. Missing pieces in the Parkinson's disease puzzle. Nat. Med. 16 (6), 653–661.

Oddo, S., Caccamo, A., Shepherd, J.D., Murphy, M.P., Golde, T.E., Kayed, R., et al., 2003. Triple-transgenic model of Alzheimer's disease with plaques and tangles: intracellular Abeta and synaptic dysfunction. Neuron 39 (3), 409–421.

Oliveras-Salva, M., Van der Perren, A., Casadei, N., Stroobants, S., Nuber, S., D'Hooge, R., et al., 2013. rAAV2/7 vector-mediated overexpression of alpha-synuclein in mouse substantia nigra induces protein aggregation and progressive dose-dependent neurodegeneration. Mol. Neurodegener. 8, 44.

Olzscha, H., Schermann, S.M., Woerner, A.C., Pinkert, S., Hecht, M.H., Tartaglia, G.G., et al., 2011. Amyloid-like aggregates sequester numerous metastable proteins with essential cellular functions. Cell 144 (1), 67–78.

Orvoen, S., Pla, P., Gardier, A.M., Saudou, F., David, D.J., 2012. Huntington's disease knock-in male mice show specific anxiety-like behaviour and altered neuronal maturation. Neurosci. Lett. 507 (2), 127–132.

Paisan-Ruiz, C., Lewis, P.A., Singleton, A.B., 2013. LRRK2: cause, risk, and mechanism. J. Parkinsons Dis. 3 (2), 85–103.

Palacino, J.J., Sagi, D., Goldberg, M.S., Krauss, S., Motz, C., Wacker, M., et al., 2004. Mitochondrial dysfunction and oxidative damage in parkin-deficient mice. J. Biol. Chem. 279 (18), 18614–18622.

Pang, T.Y., Du, X., Zajac, M.S., Howard, M.L., Hannan, A.J., 2009. Altered serotonin receptor expression is associated with depression-related behavior in the R6/1 transgenic mouse model of Huntington's disease. Hum. Mol. Genet. 18 (4), 753–766.

Pan-Montojo, F., Anichtchik, O., Dening, Y., Knels, L., Pursche, S., Jung, R., et al., 2010. Progression of Parkinson's disease pathology is reproduced by intragastric administration of rotenone in mice. PLoS One 5 (1), e8762.

Paterna, J.C., Leng, A., Weber, E., Feldon, J., Bueler, H., 2007. DJ-1 and Parkin modulate dopamine-dependent behavior and inhibit MPTP-induced nigral dopamine neuron loss in mice. Mol. Ther. 15 (4), 698–704.

Pavese, N., Gerhard, A., Tai, Y.F., Ho, A.K., Turkheimer, F., Barker, R.A., et al., 2006. Microglial activation correlates with severity in Huntington disease: a clinical and PET study. Neurology 66 (11), 1638–1643.

Perez, F.A., Curtis, W.R., Palmiter, R.D., 2005. Parkin-deficient mice are not more sensitive to 6-hydroxydopamine or methamphetamine neurotoxicity. BMC Neurosci. 6, 71.

Petkau, T.L., Neal, S.J., Orban, P.C., MacDonald, J.L., Hill, A.M., Lu, G., et al., 2010. Progranulin expression in the developing and adult murine brain. J. Comp. Neurol. 518 (19), 3931–3947.

Pouladi, M.A., Graham, R.K., Karasinska, J.M., Xie, Y., Santos, R.D., Petersen, A., Hayden, M.R., 2009. Prevention of depressive behaviour in the YAC128 mouse model of Huntington disease by mutation at residue 586 of huntingtin. Brain 132 (Pt 4), 919–932.

Pouladi, M.A., Brillaud, E., Xie, Y., Conforti, P., Graham, R.K., Ehrnhoefer, D.E., et al., 2012a. NP03, a novel low-dose lithium formulation, is neuroprotective in the YAC128 mouse model of Huntington disease. Neurobiol. Dis. 48 (3), 282–289.

Pouladi, M.A., Stanek, L.M., Xie, Y., Franciosi, S., Southwell, A.L., Deng, Y., et al., 2012b. Marked differences in neurochemistry and

aggregates despite similar behavioural and neuropathological features of Huntington disease in the full-length BACHD and YAC128 mice. Hum. Mol. Genet. 21 (10), 2219–2232.

Prasad, D.D., Ouchida, M., Lee, L., Rao, V.N., Reddy, E.S., 1994. TLS/FUS fusion domain of TLS/FUS-erg chimeric protein resulting from the t(16;21) chromosomal translocation in human myeloid leukemia functions as a transcriptional activation domain. Oncogene 9 (12), 3717–3729.

Proukakis, C., Houlden, H., Schapira, A.H., 2013. Somatic alpha-synuclein mutations in Parkinson's disease: hypothesis and preliminary data. Mov. Disord. 28 (6), 705–712.

Purisai, M.G., McCormack, A.L., Langston, W.J., Johnston, L.C., Di Monte, D.A., 2005. Alpha-synuclein expression in the substantia nigra of MPTP-lesioned non-human primates. Neurobiol. Dis. 20 (3), 898–906.

Puzzo, D., Loreto, C., Giunta, S., Musumeci, G., Frasca, G., Podda, M.V., et al., 2014. Effect of phosphodiesterase-5 inhibition on apoptosis and beta amyloid load in aged mice. Neurobiol. Aging 35 (3), 520–531.

Puzzo, D., Gulisano, W., Palmeri, A., Arancio, O., 2015. Rodent models for Alzheimer's disease drug discovery. Expert Opin. Drug Discov. 10 (7), 703–711.

Querfurth, H.W., LaFerla, F.M., 2010. Alzheimer's disease. N. Engl. J. Med. 362 (4), 329–344.

Quon, D., Wang, Y., Catalano, R., Scardina, J.M., Murakami, K., Cordell, B., 1991. Formation of beta-amyloid protein deposits in brains of transgenic mice. Nature 352 (6332), 239–241.

Rabbitts, T.H., Forster, A., Larson, R., Nathan, P., 1993. Fusion of the dominant negative transcription regulator CHOP with a novel gene FUS by translocation t(12;16) in malignant liposarcoma. Nat. Genet. 4 (2), 175–180.

Rascovsky, K., Hodges, J.R., Knopman, D., Mendez, M.F., Kramer, J.H., Neuhaus, J., et al., 2011. Sensitivity of revised diagnostic criteria for the behavioural variant of frontotemporal dementia. Brain 134 (Pt 9), 2456–2477.

Ready, R.E., Mathews, M., Leserman, A., Paulsen, J.S., 2008. Patient and caregiver quality of life in Huntington's disease. Mov. Disord. 23 (5), 721–726.

Reaume, A.G., Elliott, J.L., Hoffman, E.K., Kowall, N.W., Ferrante, R.J., Siwek, D.F., et al., 1996. Motor neurons in Cu/Zn superoxide dismutase-deficient mice develop normally but exhibit enhanced cell death after axonal injury. Nat. Genet. 13 (1), 43–47.

Reddy, P.H., Beal, M.F., 2008. Amyloid beta, mitochondrial dysfunction and synaptic damage: implications for cognitive decline in aging and Alzheimer's disease. Trends Mol. Med. 14 (2), 45–53.

Reitz, C., 2016. Toward precision medicine in Alzheimer's disease. Ann. Transl. Med. 4 (6), 107.

Renton, A.E., Majounie, E., Waite, A., Simon-Sanchez, J., Rollinson, S., Gibbs, J.R., et al., 2011. A hexanucleotide repeat expansion in C9ORF72 is the cause of chromosome 9p21-linked ALS-FTD. Neuron 72 (2), 257–268.

Renton, A.E., Chio, A., Traynor, B.J., 2014. State of play in amyotrophic lateral sclerosis genetics. Nat. Neurosci. 17 (1), 17–23.

Riachi, N.J., Dietrich, W.D., Harik, S.I., 1990. Effects of internal carotid administration of MPTP on rat brain and blood-brain barrier. Brain Res. 533 (1), 6–14.

Ribchester, R.R., Thomson, D., Wood, N.I., Hinks, T., Gillingwater, T.H., Wishart, T.M., et al., 2004. Progressive abnormalities in skeletal muscle and neuromuscular junctions of transgenic mice expressing the Huntington's disease mutation. Eur. J. Neurosci. 20 (11), 3092–3114.

Ribeiro, F.M., Camargos, E.R., de Souza, L.C., Teixeira, A.L., 2013. Animal models of neurodegenerative diseases. Rev. Bras. Psiquiatr. 35 (Suppl 2), S82–S91.

Ringholz, G.M., Appel, S.H., Bradshaw, M., Cooke, N.A., Mosnik, D.M., Schulz, P.E., 2005. Prevalence and patterns of cognitive impairment in sporadic ALS. Neurology 65 (4), 586–590.

Robberecht, W., Philips, T., 2013. The changing scene of amyotrophic lateral sclerosis. Nat. Rev. Neurosci. 14 (4), 248–264.

Roberson, E.D., 2011. Contemporary approaches to Alzheimer's disease and frontotemporal dementia. Methods Mol. Biol. 670, 1–9.

Rosen, D.R., 1993. Mutations in Cu/Zn superoxide dismutase gene are associated with familial amyotrophic lateral sclerosis. Nature 364 (6435), 362.

Rosenblatt, A., 2007. Neuropsychiatry of Huntington's disease. Dialogues Clin. Neurosci. 9 (2), 191–197.

Rousseaux, M.W., Marcogliese, P.C., Qu, D., Hewitt, S.J., Seang, S., Kim, R.H., et al., 2012. Progressive dopaminergic cell loss with unilateral-to-bilateral progression in a genetic model of Parkinson disease. Proc. Natl. Acad. Sci. USA 109 (39), 15918–15923.

Santacruz, K., Lewis, J., Spires, T., Paulson, J., Kotilinek, L., Ingelsson, M., et al., 2005. Tau suppression in a neurodegenerative mouse model improves memory function. Science 309 (5733), 476–481.

Sapp, E., Kegel, K.B., Aronin, N., Hashikawa, T., Uchiyama, Y., Tohyama, K., et al., 2001. Early and progressive accumulation of reactive microglia in the Huntington disease brain. J. Neuropathol. Exp. Neurol. 60 (2), 161–172.

Saura, J., Pares, M., Bove, J., Pezzi, S., Alberch, J., Marin, C., et al., 2003. Intranigral infusion of interleukin-1beta activates astrocytes and protects from subsequent 6-hydroxydopamine neurotoxicity. J. Neurochem. 85 (3), 651–661.

Savica, R., Grossardt, B.R., Bower, J.H., Boeve, B.F., Ahlskog, J.E., Rocca, W.A., 2013. Incidence of dementia with Lewy bodies and Parkinson disease dementia. JAMA Neurol. 70 (11), 1396–1402.

Scalzo, P., Kummer, A., Cardoso, F., Teixeira, A.L., 2009. Increased serum levels of soluble tumor necrosis factor-alpha receptor-1 in patients with Parkinson's disease. J. Neuroimmunol. 216 (1–2), 122–125.

Schmidt, N., Ferger, B., 2001. Neurochemical findings in the MPTP model of Parkinson's disease. J. Neural. Transm. (Vienna) 108 (11), 1263–1282.

Schoenfeld, M., Myers, R.H., Cupples, L.A., Berkman, B., Sax, D.S., Clark, E., 1984. Increased rate of suicide among patients with Huntington's disease. J. Neurol. Neurosurg. Psychiatry 47 (12), 1283–1287.

Sephton, C.F., Good, S.K., Atkin, S., Dewey, C.M., Mayer, P., 3rd, Herz, J., Yu, G., 2010. TDP-43 is a developmentally regulated protein essential for early embryonic development. J. Biol. Chem. 285 (9), 6826–6834.

Shan, X., Chiang, P.M., Price, D.L., Wong, P.C., 2010. Altered distributions of Gemini of coiled bodies and mitochondria in motor neurons of TDP-43 transgenic mice. Proc. Natl. Acad. Sci. USA 107 (37), 16325–16330.

Shaw, C.E., 2010. Capturing VCP: another molecular piece in the ALS jigsaw puzzle. Neuron 68 (5), 812–814.

Shelbourne, P.F., Killeen, N., Hevner, R.F., Johnston, H.M., Tecott, L., Lewandoski, M., et al., 1999. A Huntington's disease CAG expansion at the murine Hdh locus is unstable and associated with behavioural abnormalities in mice. Hum. Mol. Genet. 8 (5), 763–774.

Shendelman, S., Jonason, A., Martinat, C., Leete, T., Abeliovich, A., 2004. DJ-1 is a redox-dependent molecular chaperone that inhibits alpha-synuclein aggregate formation. PLoS Biol. 2 (11), e362.

Sherer, T.B., Betarbet, R., Testa, C.M., Seo, B.B., Richardson, J.R., Kim, J.H., et al., 2003. Mechanism of toxicity in rotenone models of Parkinson's disease. J. Neurosci. 23 (34), 10756–10764.

Silvestroni, A., Faull, R.L., Strand, A.D., Moller, T., 2009. Distinct neuroinflammatory profile in post-mortem human Huntington's disease. Neuroreport 20 (12), 1098–1103.

Skibinski, G., Parkinson, N.J., Brown, J.M., Chakrabarti, L., Lloyd, S.L., Hummerich, H., et al., 2005. Mutations in the endosomal ESCRTIII-complex subunit CHMP2B in frontotemporal dementia. Nat. Genet. 37 (8), 806–808.

Slow, E.J., van Raamsdonk, J., Rogers, D., Coleman, S.H., Graham, R.K., Deng, Y., et al., 2003. Selective striatal neuronal loss in a YAC128 mouse model of Huntington disease. Hum. Mol. Genet. 12 (13), 1555–1567.

Song, S., Jung, Y.K., 2004. Alzheimer's disease meets the ubiquitin-proteasome system. Trends Mol. Med. 10 (11), 565–570.

Sreedharan, J., Blair, I.P., Tripathi, V.B., Hu, X., Vance, C., Rogelj, B., et al., 2008. TDP-43 mutations in familial and sporadic amyotrophic lateral sclerosis. Science 319 (5870), 1668–1672.

St Martin, J.L., Klucken, J., Outeiro, T.F., Nguyen, P., Keller-McGandy, C., Cantuti-Castelvetri, I., et al., 2007. Dopaminergic neuron loss and up-regulation of chaperone protein mRNA induced by targeted over-expression of alpha-synuclein in mouse substantia nigra. J. Neurochem. 100 (6), 1449–1457.

Tai, Y.F., Pavese, N., Gerhard, A., Tabrizi, S.J., Barker, R.A., Brooks, D.J., Piccini, P., 2007. Microglial activation in presymptomatic Huntington's disease gene carriers. Brain 130 (Pt 7), 1759–1766.

Talpade, D.J., Greene, J.G., Higgins, Jr., D.S., Greenamyre, J.T., 2000. In vivo labeling of mitochondrial complex I (NADH:ubiquinone oxidoreductase) in rat brain using [(3)H]dihydrorotenone. J. Neurochem. 75 (6), 2611–2621.

Terry, R.D., Masliah, E., Salmon, D.P., Butters, N., DeTeresa, R., Hill, R., et al., 1991. Physical basis of cognitive alterations in Alzheimer's disease: synapse loss is the major correlate of cognitive impairment. Ann. Neurol. 30 (4), 572–580.

Therrien, M., Dion, P.A., Rouleau, G.A., 2016. ALS: recent developments from genetics studies. Curr. Neurol. Neurosci. Rep. 16 (6), 59.

Thomas, B., von Coelln, R., Mandir, A.S., Trinkaus, D.B., Farah, M.H., Leong Lim, K., et al., 2007. MPTP and DSP-4 susceptibility of substantia nigra and locus coeruleus catecholaminergic neurons in mice is independent of parkin activity. Neurobiol. Dis. 26 (2), 312–322.

Tieu, K., 2011. A guide to neurotoxic animal models of Parkinson's disease. Cold Spring Harb. Perspect. Med. 1 (1), a009316.

Tsao, W., Jeong, Y.H., Lin, S., Ling, J., Price, D.L., Chiang, P.M., Wong, P.C., 2012. Rodent models of TDP-43: recent advances. Brain Res. 1462, 26–39.

Tsika, E., Moore, D.J., 2012. Mechanisms of LRRK2-mediated neurodegeneration. Curr. Neurol. Neurosci. Rep. 12 (3), 251–260.

Ungerstedt, U., 1968. 6-Hydroxy-dopamine induced degeneration of central monoamine neurons. Eur. J. Pharmacol. 5 (1), 107–110.

van der Zee, J., Pirici, D., Van Langenhove, T., Engelborghs, S., Vandenberghe, R., Hoffmann, M., et al., 2009. Clinical heterogeneity in 3 unrelated families linked to VCP p.Arg159His. Neurology 73 (8), 626–632.

Van Raamsdonk, J.M., Pearson, J., Slow, E.J., Hossain, S.M., Leavitt, B.R., Hayden, M.R., 2005. Cognitive dysfunction precedes neuropathology and motor abnormalities in the YAC128 mouse model of Huntington's disease. J. Neurosci. 25 (16), 4169–4180.

Van Rompuy, A.S., Lobbestael, E., Van der Perren, A., Van den Haute, C., Baekelandt, V., 2014. Long-term overexpression of human wild-type and T240R mutant Parkin in rat substantia nigra induces progressive dopaminergic neurodegeneration. J. Neuropathol. Exp. Neurol. 73 (2), 159–174.

Verbeeck, C., Deng, Q., Dejesus-Hernandez, M., Taylor, G., Ceballos-Diaz, C., Kocerha, J., et al., 2012. Expression of Fused in sarcoma mutations in mice recapitulates the neuropathology of FUS proteinopathies and provides insight into disease pathogenesis. Mol. Neurodegener. 7, 53.

Verhave, P.S., Jongsma, M.J., Van Den Berg, R.M., Vanwersch, R.A., Smit, A.B., Philippens, I.H., 2012. Neuroprotective effects of riluzole in early phase Parkinson's disease on clinically relevant parameters in the marmoset MPTP model. Neuropharmacology 62 (4), 1700–1707.

Vidoni, C., Follo, C., Savino, M., Melone, M.A., Isidoro, C., 2016. The role of Cathepsin D in the pathogenesis of human neurodegenerative disorders. Med. Res. Rev. 36, 845–870.

Vieira, R.T., Caixeta, L., Machado, S., Silva, A.C., Nardi, A.E., Arias-Carrion, O., Carta, M.G., 2013. Epidemiology of early-onset dementia: a review of the literature. Clin. Pract. Epidemiol. Ment. Health 9, 88–95.

Walker, F.O., 2007. Huntington's disease. Semin. Neurol. 27 (2), 143–150.

Watts, G.D., Wymer, J., Kovach, M.J., Mehta, S.G., Mumm, S., Darvish, D., et al., 2004. Inclusion body myopathy associated with Paget disease of bone and frontotemporal dementia is caused by mutant valosin-containing protein. Nat. Genet. 36 (4), 377–381.

Wegorzewska, I., Bell, S., Cairns, N.J., Miller, T.M., Baloh, R.H., 2009. TDP-43 mutant transgenic mice develop features of ALS and frontotemporal lobar degeneration. Proc. Natl. Acad. Sci. USA 106 (44), 18809–18814.

Wheeler, V.C., White, J.K., Gutekunst, C.A., Vrbanac, V., Weaver, M., Li, X.J., et al., 2000. Long glutamine tracts cause nuclear localization of a novel form of huntingtin in medium spiny striatal neurons in HdhQ92 and HdhQ111 knock-in mice. Hum. Mol. Genet. 9 (4), 503–513.

Wils, H., Kleinberger, G., Janssens, J., Pereson, S., Joris, G., Cuijt, I., et al., 2010. TDP-43 transgenic mice develop spastic paralysis and neuronal inclusions characteristic of ALS and frontotemporal lobar degeneration. Proc. Natl. Acad. Sci. USA 107 (8), 3858–3863.

Winklhofer, K.F., Haass, C., 2010. Mitochondrial dysfunction in Parkinson's disease. Biochim. Biophys. Acta 1802 (1), 29–44.

Woodman, B., Butler, R., Landles, C., Lupton, M.K., Tse, J., Hockly, E., et al., 2007. The Hdh(Q150/Q150) knock-in mouse model of HD and the R6/2 exon 1 model develop comparable and widespread molecular phenotypes. Brain Res. Bull. 72 (2–3), 83–97.

Wright Willis, A., Evanoff, B.A., Lian, M., Criswell, S.R., Racette, B.A., 2010. Geographic and ethnic variation in Parkinson disease: a population-based study of US Medicare beneficiaries. Neuroepidemiology 34 (3), 143–151.

Wu, L.S., Cheng, W.C., Hou, S.C., Yan, Y.T., Jiang, S.T., Shen, C.K., 2010. TDP-43, a neuro-pathosignature factor, is essential for early mouse embryogenesis. Genesis 48 (1), 56–62.

Xu, Q., Shenoy, S., Li, C., 2012. Mouse models for LRRK2 Parkinson's disease. Parkinsonism Relat. Disord. 18 (Suppl. 1), S186–S189.

Yamanaka, K., Sasagawa, Y., Ogura, T., 2012. Recent advances in p97/VCP/Cdc48 cellular functions. Biochim. Biophys. Acta 1823 (1), 130–137.

Yang, S.H., Cheng, P.H., Banta, H., Piotrowska-Nitsche, K., Yang, J.J., Cheng, E.C., et al., 2008. Towards a transgenic model of Huntington's disease in a non-human primate. Nature 453 (7197), 921–924.

Yang, D., Wang, C.E., Zhao, B., Li, W., Ouyang, Z., Liu, Z., et al., 2010. Expression of Huntington's disease protein results in apoptotic neurons in the brains of cloned transgenic pigs. Hum. Mol. Genet. 19 (20), 3983–3994.

Yin, H.Z., Nalbandian, A., Hsu, C.I., Li, S., Llewellyn, K.J., Mozaffar, T., et al., 2012. Slow development of ALS-like spinal cord pathology in mutant valosin-containing protein gene knock-in mice. Cell Death Dis. 3, e374.

Yoshiyama, Y., Higuchi, M., Zhang, B., Huang, S.M., Iwata, N., Saido, T.C., et al., 2007. Synapse loss and microglial activation precede tangles in a P301S tauopathy mouse model. Neuron 53 (3), 337–351.

Zhou, J., Yu, Q., Zou, T., 2008. Alternative splicing of exon 10 in the tau gene as a target for treatment of tauopathies. BMC Neurosci. 9 (Suppl. 2), S10.

Zuccato, C., Valenza, M., Cattaneo, E., 2010. Molecular mechanisms and potential therapeutic targets in Huntington's disease. Physiol. Rev. 90 (3), 905–981.

Further Reading

Park, J., Kim, S.Y., Cha, G.H., Lee, S.B., Kim, S., Chung, J., 2005. *Drosophila* DJ-1 mutants show oxidative stress-sensitive locomotive dysfunction. Gene 361, 133–139.

Su, L.J., Auluck, P.K., Outeiro, T.F., Yeger-Lotem, E., Kritzer, J.A., Tardiff, D.F., et al., 2010. Compounds from an unbiased chemical screen reverse both ER-to-Golgi trafficking defects and mitochondrial dysfunction in Parkinson's disease models. Dis. Model Mech. 3 (3–4), 194–208.

Page left intentionally blank

Animal Models of Mania: Essential Tools to Better Understand Bipolar Disorder

Aline S. de Miranda*, Roberto Andreatini**,
Antônio L. Teixeira†

*Biological Institute, Federal University of Minas Gerais (UFMG), Belo Horizonte, MG, Brazil
**Federal University of Paraná, Centro Politécnico, Curitiba, PR, Brazil
†University of Texas Health Science Center at Houston,
Houston, TX, United States

1 INTRODUCTION

Bipolar disorder (BD) is a chronic, severe, and disabling psychiatric condition characterized by recurrent mood switches, including mania and depression, which often increase in severity and frequency over time (APA, 2013). The estimated prevalence in general population is 3% with the mean age of first mood episode around 20 years old (Bauer et al., 2010; Perlis et al., 2009). Apart from the core dysfunction in mood regulation, BD is often associated with high rates of medical and psychiatric comorbidities as well as dysfunction in cognition, endocrine, autonomic, and circadian rhythm, all which ultimately related with poor quality of life and

premature mortality (Krishnan, 2005; Sierra et al., 2005; Swartz and Fagiolini, 2012). Increased risk of suicide has been reported in approximately 10%–20% of patients with BD (Novick et al., 2010).

Although depressive symptoms tend to overcome manic and hypomanic episodes in the long-term course of the illness, mania is regarded as the clinical hallmark of BD with the cardinal diagnostic feature being the occurrence of at least one episode of mania and/or hypomania during the lifetime (Angst et al., 2003). Clinically, a manic episode is generally defined by euphoria, hyperactivity, impulsivity, increased risk-taking behavior, increased reward seeking, and decreased need for sleep. The consequences of mania are devastating and include

a significant social and economic burden (APA, 2013). Recurrent episodes of mania might be associated with BD progression, that is, a greater susceptibility for subsequent episodes, treatment resistance, cognitive and functional decline (Fries et al., 2012; Kapczinski et al., 2014). Moreover, there is evidence that effectively treating mania and preventing recurrent manic episodes might minimize depression burden in part by decreasing the risk of postmanic depressive cycling (Sachs and Gardner-Schuster, 2007; Zarate et al., 2001).

Effective treatments as lithium, anticonvulsants, and antipsychotics have improved the prognosis of BD, but a significant number of patients does not respond well to these drugs. These available pharmacological strategies to treat BD were either discovered via serendipity or resulted from testing drugs previously approved for other clinical conditions like the antipsychotics and the anticonvulsants (Gould et al., 2004; Maletic and Raison, 2014). The limited understanding of the cellular and molecular mechanisms involved in BD pathogenesis and physiopathology is a major constraint to the development of effective therapies for the illness. However, a growing body of studies has aimed to unravel the mechanisms underlying the pathophysiology of mania and, ultimately, to identify potential therapeutic targets for BD.

Animal models are valuable tools for the study of underlying neurobiological mechanism of diseases as well as for the assessment of candidate novel strategies in preclinical settings (Lipska and Weinberger, 2000). The development of appropriate animal models of human diseases is a task of major importance and at least three criteria must be met: face, construct, and predictive validities. Face validity is the ability of the model to mimic behavioral changes comparable to those in the human illness, while for the construct validity the pathophysiological alterations must be the same as, or at least similar to, the human condition. Finally, for predictive validity, conventional drugs used to prevent and/or reverse the behavioral problem in humans should be able to do the same in the animal model (Machado-Vieira et al., 2004; Robbins and Sahakian, 1980).

To date, there are no ideal animal models for BD, that is, a model that covers the full spectrum of the disease by mimicking mood/emotional state changes across manic and depressive poles. Current experimental models only allow the independent investigation of manic or depressive-like episodes (Valvassori et al., 2013). Moreover, the available models are not able to emulate the cumulative burden of recurrent spontaneous mood swings, even within the same pole. The lack of valid biomarkers of the illness, uncertainty regarding the mechanisms of action of the existing mood-stabilizing drugs, and the highly complex genetic basis of BD have hampered the development of BD models (Gould and Einat, 2007).

Over the past decades, pharmacological, environmental, and genetic models have been developed in an attempt to unveil mania pathophysiology and to discover future generation of mood-stabilizing compounds. Herein, we will discuss emerging evidence regarding animal models of mania, their contributions, and potential limitations.

2 INSIGHTS FROM PHARMACOLOGICAL ANIMAL MODELS OF MANIA

Pharmacological models of mania are usually easy to induce and, despite their major limitations, have been repetitively employed to investigate mania pathophysiology and novel therapeutic targets with potential mood-stabilizing properties (Einat, 2006; Young et al., 2011). Psychostimulants drugs, especially amphetamines (AMPHs), are the most used pharmacological model to induce mania. However, other compounds with distinct mechanism of actions have also been used to model mania, including Quinpirole, ouabain, GBR 12909, ketamine (Fig. 43.1), and cholera toxin (El-Mallakh et al., 1995; Ghedim et al., 2012; Kofman et al., 1998; Shaldubina et al., 2002; Young et al., 2010). These compounds mimic hyperactivity, one core facet of mania that can be easily measured in behavioral sets. Moreover, psychostimulants may induce reduced sleep and risk-taking behavior that are also important features of mania (Berridge and Stalnaker, 2002; Einat et al., 2003). Cognitive decline was reported following amphetamine and Quinpirole administration, indicating that these models are able to reproduce a different aspect of the illness (Agmo et al., 1997; Einat and Szechtman, 1993; Fries et al., 2015). Other variables that had been included in the behavioral repertoire related to mania are hole exploration by mice (Perry et al., 2009; Souza et al., 2016) and appetitive high frequency ultrasound vocalization (USV) in rats (Pereira et al., 2014).

Other drugs, such as trimethyltin, imidazole, clonidine, testosterone, corticosterone, among others, can induce manic symptoms, such as irritability, aggression, and increased sexual drive. However, their validity as pharmacological models of mania needs to be further addressed (for review see Einat, 2006).

2.1 Psychostimulants—Amphetamines

The hypothesis that dopamine (DA) is involved in the neurobiology of mania proposed in the 1970s (Serra et al., 1979) fostered the development of animal models based on pharmacological changes of the dopaminergic neurotransmission. For instance, BD patients presented modifications in an allele of the DA transporter encoder in the *substantia nigra*, which may contribute to
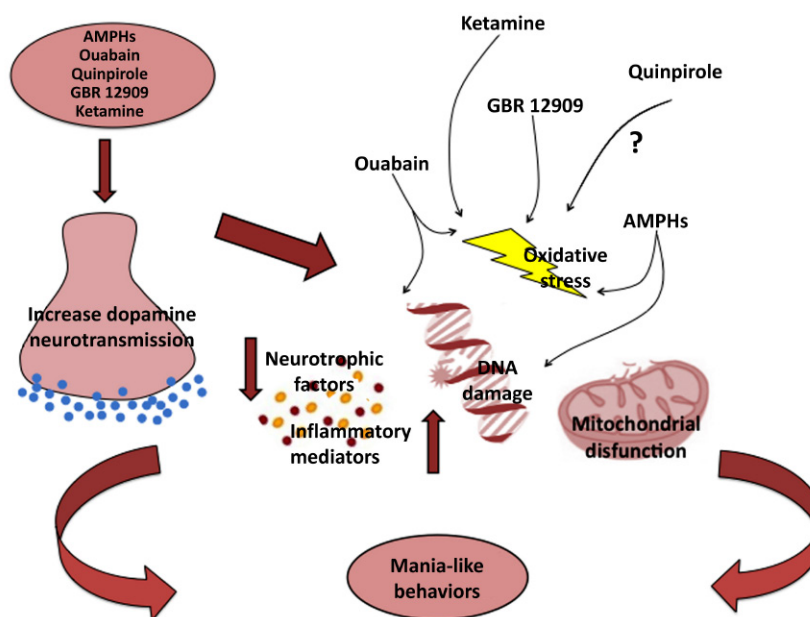
FIGURE 43.1 **Proposed mechanisms of action for pharmacological animal models of mania.** Pharmacological agents that currently present some face, construct, and preditive validities as animal models of mania include: amphetamines *(AMPHs)*, ouabain, GBR 12909, Quinpirole, and ketamine. The administration of these compounds often leads to an increase in the dopaminergic neurotransmission. Dopamine presents a significant redox potential, and high levels of this neurotransmissor have been associated with oxidative damage to proteins, lipids, and DNA in neurons. Besides inducing dopamine release, both AMPHs and ouabain can lead to CNS impairment by increasing oxidative stress, DNA damage, inflammation, mitochondrial dysfunction, and decreasing neurotrophic support, all of which implicated in bipolar disorder (BD) pathophysiology. Oxidative stress has also been demonstrated in GBR 12909 and ketamine models of mania. Evidence regarding the potential of Quinpirole to induce features of BD pathophysiology is still missing, limiting the construct validity of this pharmacological model of mania.

the increase in dopaminergic transmission found in BD (Pinsonneault et al., 2011). A significant increase in the expression of the dopamine receptor D1 was also found in the hippocampus of BD patients, reinforcing the involvement of DA in the pathogenesis of this condition (Pantazopoulos et al., 2004). Psychostimulants act on the central nervous system (CNS) by increasing DA efflux, inhibiting DA reuptake as well as its degradation by the enzyme monoamine oxidase. The result of dopaminergic hyperactivity following the psychostimulants administration in rats is the change in behavior also observed in manic episodes in humans, notably hyperlocomotion (Fiorino and Phillips, 1999).

A diagnostic criterion of DSM-5 for mania is the increased activity presented in nearly all acute manic states (APA, 2013). Although hyperactivity does not reflect the full spectrum of mania, it is an essential component of it. Pharmacological induction of hyperactivity in rodents, usually with psychostimulants such as amphetamine (AMPH) and cocaine, is still the most employed model to study mania since it can be quickly induced, easily measured, and is reliable in its response to the prototypic mood stabilizer lithium (Lerer et al., 1984; Smith, 1981) and valproate (Kuruvilla and Uretsky, 1981; Post and Weiss, 1989; Shaldubina et al., 2002), and antipsychotics (Young et al., 2011). Another important component of mania is cognitive dysfunction, that is, impairment

of attention, memory, and executive functioning that can be easily and reliably rated in laboratory (Burdick et al., 2007). There is consistent evidence that psychostimulants are capable of inducing cognitive impairment in rodents (Fries et al., 2015). In this line, methylphenidate increases hole exploration in mice submitted to holeboard, an effect that was blocked by lithium administration (Souza et al., 2016). Amphetamine also increases high frequency (50 kHz) USV in rats, which is associated with increase in positive affect (Pereira et al., 2014; Rippberger et al., 2015). This effect of amphetamine in 50 kHz USV is blocked by lithium and tamoxifen (Pereira et al., 2014).

Amphetamine (AMPH) is a psychostimulant drug of the phenethylamine class mostly employed and generally accepted in preclinical settings to model mania (O'Donnell and Gould, 2007). AMPH induces release of DA from presynaptic nerve terminals in addition to inhibiting reuptake (Seiden et al., 1993). DA release in response to AMPH occurs by a transporter-mediated release mechanism named reverse transport, which is impulse-independent and has little calcium dependence (Pierce and Kalivas, 1997a; Sulzer et al., 1995). Acute administration of AMPH increases DA levels in striatal slices of rat (Paszti-Gere and Jakus, 2013) and also induces symptoms, such as enhanced mood, racing thoughts, high energy, and restlessness in both

healthy or euthymic BD subjects, supporting the use of those compounds as a model of BD (Anand et al., 2000; Strakowski and Sax, 1998).

In rodent animal models, both AMPH and synthetic compounds with a similar structure, known as amphetamines (AMPHs) including methamphetamine, dextroamphetamine (d-amphetamine), lisdexamfetamine dimesylate (LDX), 3,4-methylenedioxymethamphetamine (MDMA) share a common dopamine-enhancing activity inducing locomotor hyperactivity and psychomotor agitation (Berk et al., 2007; Kara and Einat, 2013). It has been reported that AMPHs-mediated toxicity and behavioral dysfunction involve mesocorticolimbic dopaminergic neurons, which project from the ventral tegmental area (VTA) to the nucleus accumbens (NAc) and prefrontal cortex (PFC) (Pierce and Kalivas, 1997b). For instance, microinjections of D-amphetamine in the NAc and *ventral pallidum* of adult male Sprague–Dawley rats significantly increased locomotor activity and conditioned reward responses (Fletcher et al., 1998). Furthermore, AMPH injected in the NAc also increases 50 kHz USV. The mood stabilizer lithium as well as selective dopamine antagonists, such as haloperidol and chlorpromazine reverse the acute hyperactivity and the increase in 50 kHz USV induced by AMPHs (Gould et al., 2001; Rippberger et al., 2015; Tohen et al., 2003; Vieta and Sanchez-Moreno, 2008).

Apart from increased dopaminergic neurotransmission, oxidative stress, mitochondrial dysfunction, and DNA damage have also been associated with BD pathogenesis (Andreazza et al., 2007, 2008a; Beauvais et al., 2011; Konradi et al., 2004). Considering the redox potential of DA, increased levels of this neurotransmissor lead to oxidative damage to proteins, lipids, and DNA in the neurons (Gluck et al., 2001; Rees et al., 2007). Components of oxidative stress, such as the reactive oxygen species (ROS) are mainly produced in the brain by mitochondrial complexes of the electron transport chain. Thus, an imbalance in the oxidant/antioxidant processes may inhibit electron transport chain complexes, leading to energy metabolism deregulation including decreases in ATP production and ultimately cellular dysfunction (Calabrese et al., 2001; Mattiasson et al., 2003).

In this scenario, Gluck et al. (2001) were the first to show that methamphetamine administration leads to ROS-mediated oxidative stress to proteins and lipid peroxidation, as indicated by a significant increase in the concentration of thiobarbituric acid reactive species (TBARs) and protein carbonyls in the hippocampus and striatum of the methamphetamine-treated mice (Gluck et al., 2001). Similar findings were also reported following acute and repeated exposure to d-amphetamine, which were associated with increased locomotor activity in the open field test (Frey et al., 2006a). Further, they also reported that the oxidative stress induced by acute

or chronic injections of *d*-amphetamine might results of an imbalance between superoxide dismutase (SOD) and catalase (CAT) activities in brain areas like PFC, hippocampus, and striatum, disrupting the antioxidant defense promoted by those enzymes (Frey et al., 2006b). Moreover, an increase of TBARS and superoxide production in submitochondrial particles of the PFC and hippocampus following chronic *d*-amphetamine exposure suggests that AMPHs induce oxidative stress through mitochondrial ROS generation (Frey et al., 2006c). Importantly, the mood stabilizers lithium and valproate reversed and prevented hyperactivity and brain oxidative damage in response to both *d*-amphetamine and methamphetamine administration, supporting a role of oxidative stress in the pathophysiology of BD and the use of these psychostimulant drugs as validity models of mania (Frey et al., 2006d; da-Rosa et al., 2012).

An abnormal cellular energy state affects neuronal function, plasticity, and brain circuit ultimately leading to mood changes (Angst et al., 2003) and cognitive impairment (Quraishi et al., 2009), important features of BD. Mitochondria is the principal source of cellular energy in form of ATP, indicating a potential involvement of this organelle in BD (Kato and Kato, 2000). Acute administration of amphetamine leads to a quickly depletion of ATP levels by 20% in the striatum 1.5 h following the psychoactive drug administration, which were restored within 24 h (Chan et al., 1994). A fast decrease of cytochrome oxidase enzymatic activity, a marker for alterations in mitochondrial function, was also found in rat's striatum (23%–29%) NAc (29%–30%) and *substantia nigra* (31%–43%) 2 h following administration of both methamphetamine and MDMA. Similarly to the Chan et al. (1994) findings, the reduction in cytochrome oxidase activity was transient and returned to control levels within 24 h (Burrows et al., 2000). Significant dysfunction in CNS energy metabolism as indicated by disruption in the activities of Krebs cycle enzymes (citrate synthase and succinate dehydrogenase) and mitochondrial respiratory chain complexes (I–IV) in several brain regions (PFC, amygdala, hippocampus, and striatum) following methamphetamine and *d*-amphetamine exposure was also recently reported (Feier et al., 2012). Accordingly, impairment of mitochondrial complex I activity and oxidative damage to mitochondrial proteins were found in *postmortem* studies of PFC of BD patients (Andreazza et al., 2010). Importantly, mood stabilizers lithium and valproate reversed and prevented AMPHs-induced inhibition of mitochondrial respiratory chain activity and brain energetic metabolism dysfunction (Feier et al., 2013; Valvassori et al., 2010). Altogether, these studies support the hypothesis that disruption in mitochondrial function, possibly in response to an increase in DA levels, is involved in BD pathophysiology.

Oxidative stress and mitochondrial activity impairment may directly damage cellular proteins, DNA, and lipids, thereby compromising cellular function (Gluck et al., 2001; Rees et al., 2007). Indeed, lost in DNA integrity has previously been reported in patients with BD (Andreazza et al., 2007; Frey et al., 2007) in proportion with increased oxidative stress in such patients (Andreazza et al., 2007). Accordingly, rats that received *d*-amphetamine presented both peripheral (blood) and hippocampal DNA damage, which correlated positively with lipid peroxidation. Lithium and valproate treatments restored the oxidative balance and prevented transient damage to the DNA, indicating that AMPHs-induced mania might be an interesting model to investigate the role of DNA impairment in BD (Andreazza et al., 2008b).

Emerging evidence suggests that inflammation underlies BD (Barbosa et al., 2014; van den Ameele et al., 2016). High levels of inflammatory mediators like the cytokines TNF, IL-1β, and IL-6 were found in the serum (Barbosa et al., 2011a; Modabbernia et al., 2013) as well as in the cerebral spinal fluid of BD patients (Söderlund et al., 2011). A role for the immune system in BD was also supported by *postmortem* studies that demonstrated increased expression of the cytokines IL-1β, its receptor (IL-1R), TGF β, as well as astroglial and microglial markers (glial fibrillary acidic protein, inducible nitric oxide synthase, c-fos, and CD11b) in the PFC of BD (Bezchlibnyk et al., 2001; Rao et al., 2010). Apart from enhanced locomotor activity, treatment with *d*-amphetamine increased the levels of the cytokines IL-4, IL-6, IL-10, and TNF in the frontal cortex, striatum, and serum of male Wistar rats. The hyperactivity along with inflammatory alterations was reversed by lithium, supporting the involvement of the immune system in the neurobiology of mania (Valvassori et al., 2015a).

Neurotrophic factors are proteins that mediate neuronal survival, proliferation, and differentiation, being critically involved in mnemonic and emotional processes. Particularly, the Brain-derived neurotrophic factor (BDNF) is abundantly expressed in the hippocampus and cerebral cortex, brain areas thought to be critical for the control of mood, emotion, and cognition (Chao, 2003). There is growing evidence that decreased levels of BDNF are associated with cognitive decline in BD patients (Fernandes et al., 2011). Importantly, significant decrease in BDNF peripheral levels was found during acute episodes of mania, which were prevented by lithium treatment (de Sousa et al., 2011; Tramontina et al., 2009). Altogether these studies provided evidence that peripheral BDNF could be used as a biomarker of mood states and progression of BD.

Resembling the findings in clinical studies with BD patients, a significant decrease in BDNF levels in several brain regions including hippocampus, cortex, amygdala, and *striatum* was also found following *d*-amphetamine

exposure (Cechinel-Recco et al., 2012; Frey et al., 2006e; Macêdo et al., 2012). BDNF reduction as well as hyperactivity induced by *d*-amphetamine was reversed by lithium and valproate (Cechinel-Recco et al., 2012; Frey et al., 2006e). Cognitive impairment associated with BDNF alterations in rat's hippocampus, PFC, and amygdala was also reported following subchronic (7 days) and chronic (35 days) repeated amphetamine injections (Fries et al., 2015). The aforementioned studies support the role of BDNF in mania and reinforce that AMPHs model fulfills adequate face, construct, and predictive validity as an animal model of mania.

Behavioral sensitization, a process whereby repeated intermittent administration of a psychostimulant increases the behavioral response over time, has also been regarded as a classic validated animal model of mania. Repeated intermittent administration of AMPHs in rodents gives rise to the behavioral sensitization phenomena argued to have similarities to the sensitization found in humans (Post, 2007; Robinson and Berridge, 1993). Behavioral sensitization and kindling responses resembling mania along with increased vulnerability to recurrence following successive episodes were initially described by Robert Post following repeated cocaine administration (Post and Weiss, 1989). Further studies confirmed the occurrence of behavioral sensitization following repeated injections of amphetamine and methamphetamine (Cappeliez and Moore, 1990; Kuribara and Uchihashi, 1993; Namima et al., 1999). A potential predictive validity of AMPH sensitization as a behavioral model of mania was proposed as antimanic drugs, such as lithium, valproate, carbamazepine, and lamotrigine were able to reverse *d*-amphetamine sensitization-induced hyperactivity in rodents (Dencker and Husum, 2010). This behavioral sensitization phenomenon has been proposed as a valuable model to explain the chronicity and cyclic course of BD (Post et al., 2001).

Although, psychostimulants are classically employed to model mania in preclinical settings and has provided valuable insights regarding mania pathophysiology and potential therapeutic targets, these pharmacological models have major limitations. Besides not mimicking the full spectrum of the disease, these models are also used as models of drug abuse or addiction and schizophrenia. Moreover, their pathophysiological mechanisms overlap with other major mental disorders, such as schizophrenia and attention deficit hyperactivity disorder, which may compromise their construct validity (Young et al., 2011).

2.2 Amphetamine and Chlordiazepoxide Mixture

The combination of the AMPH psychostimulant *d*-amphetamine with the benzodiazepine derivative chlordiazepoxide (CDP), which presents anxiolytic and

sedative effects, has been proposed as an animal model of mania. Despite the biological mechanisms underlying the potent effects of the AMPH–CDP mixture remain unknown, it results in higher levels of hyperactivity compared to levels triggered by either compound alone, supporting a model face validity (Arban et al., 2005; Aylmer et al., 1987; Kelly et al., 2009).

Some predictive value was also provided by studies showing that acute administration of mood stabilizers, such as lithium and valproate reversed AMPH + CDP-induced hyperactivity (Aylmer et al., 1987; Cao and Peng, 1993). However, the predictive validity of this model is questionable and remains to be fully established. For instance, Arban et al. (2005) conducted a study to investigate the effect of several antimanic drugs, including lamotrigine and carbamazepine, in the hyperactivity caused by AMPH + CDP. Although the antimanic agents successfully decreased hyperactivity, it was unclear whether this effect was due to mood stabilizers action or simply reflected a potentiation of the activity-suppressant effect of CDP by the antimanic drugs (Arban et al., 2005). In an independent study also suggested that the AMPH + CDP might not be an ideal model to investigate novel putative therapies for mania (Kelly et al., 2009). A practical problem with this model is the large number of control groups needed to conclude about the potential antimanic-like effect of experimental drugs (Young et al., 2011).

2.3 Ouabain

In 1983, El-Mallakh first described a potential involvement of the sodium, potassium-activated adenosine triphosphatase (Na$^+$, K$^+$-ATPase) membrane pump in BD pathophysiology. A decrease in the activity of the Na$^+$, K$^+$-ATPase, a major plasma membrane transporter for sodium and potassium that maintains and reestablishes the electrochemical gradient of the neuron, was associated with both phases of BD (El-Mallakh, 1983). Disruptions in Na, K-ATPase activity can lead to both mania and depression by increasing membrane excitability and decreasing neurotransmitter release, affecting neuronal excitability and activity (El-Mallakh and Wyatt, 1995). Accordingly, reduction in Na$^+$, K$^+$-ATPase enzymatic activity in the blood and in the expression of its α2 isoform in the brain temporal cortex of BD patients has been reported (Antia et al., 1995; Huff et al., 2010; Li and El-Mallakh, 2004; Rose et al., 1998).

In this scenario, ouabain (OUA), a potent Na$^+$, K$^+$-ATPase inhibitor, was proposed as a promise pharmacological model of mania. Indeed, intracerebroventricular (ICV) administration of subconvulsive doses of OUA-induced hyperactivity in rodents (El-Mallakh et al., 1995; Li and El-Mallakh, 2004), which were prevented by lithium and valproate, supporting the validity of OUA as a pharmacological model of mania (Jornada et al., 2010a; Li and El-Mallakh, 2004).

Likely psychostimulants, OUA administration also leads to CNS impairment by increasing oxidative stress, DNA damage, inflammation, mitochondrial dysfunction, and decreasing neurotrophic support in several brain regions, including hippocampus, frontal cortex, *striatum*, and amygdala (Freitas et al., 2010; Jornada et al., 2010b; Riegel et al., 2009, 2010; Tonin et al., 2014; Varela et al., 2015). The OUA-induced brain damage was also reversed or prevented by the mood stabilizers lithium and valproate, reinforcing the predictive validity of this model (Banerjee et al., 2012; Freitas et al., 2011; Jornada et al., 2010a, 2011; Valvassori et al., 2015b; Varela et al., 2015).

A recent study showed that ICV injections of OUA impair synaptic plasticity and alter DA release in the rat medial prefrontal cortex (mPFC), a brain area critically involved in cognition. OUA-induced changes in mPFC were prevented by pretreatment with lithium. These findings indicate advantages of this model that, besides inducing behavioral changes, also mimics significant pathophysiological mechanisms of the disease, such as decrease in Na$^+$, K$^+$-ATPase activity and increase in extracellular DA (Sui et al., 2013). Although widely employed to study mania, as a pharmacological model OUA faces some clear limitations. This model cannot fully mimic human BD and to date only one facet of the manic spectrum, hyperlocomotion, was investigated, and future studies are needed to investigate other better behaviors, such as sleep, sexual drive, and aggressivity (Herman et al., 2007).

2.4 Quinpirole

A potential pharmacological model for mimicking mania in animals is the administration of the dopamine D2/D3 receptor agonist, Quinpirole (Einat and Szechtman, 1993; Shaldubina et al., 2002). Increase in locomotor activity as well as cognitive decline following Quinpirole injections has been described (Einat and Szechtman, 1993). Quinpirole induces a biphasic locomotor response, starting with inhibition and followed by excitation, which resembles the oscillating nature of BD (Shaldubina et al., 2002). Mood-stabilizing anticonvulsants, such as valproate, phenytoin, and carbamazepine attenuated Quinpirole-induced hyperactivity without effects on the hypoactive phase (Shaldubina et al., 2002), providing some predictive validity to the model. Since these drugs reversed only the hyperactive state, some authors suggested that the Quinpirole model may not be more advantageous than the AMPHs-induced models (Shaldubina et al., 2002).

In an extended approach of this model, Quinpirole was administered following dopaminergic supersensitivity

induced by chronic treatment with the antidepressant imipramine to mimic the antidepressant-related manic switch. Both lithium and valproate failed to prevent the development of such behavioral supersensitivity, but carbamazepine was effective in preventing imipramine-induced behavioral sensitization (D'Aquila et al., 2000, 2006). Since lithium, carbamazepine, and valproate are all considered poorly effective in the treatment of antidepressant-related mania, the predictive validity of this model is debatable, and cannot be based only on the carbamazepine results (D'Aquila et al., 2001).

2.5 GBR 12909

Manic episodes in BD are associated with increased activation of brain DA systems, which is consistent with genetic linkage studies connecting dopamine transporter (DAT) abnormalities to this disorder (Greenwood et al., 2001; Hayden and Nurnberger, 2006). For instance, genetic modified mice presenting reduced DAT levels exhibited significantly increased extracellular DA activity similarly to BD patients (Vawter et al., 2000; Zhuang et al., 2001). Accordingly, the selective DA transporter reuptake inhibitor, GBR 12909, has been proposed as a potential pharmacological model of mania.

The GBR 12909 administration as a promise candidate of an animal model of mania was also based in a reverse-translational approach. This approach proposed to stratify the complex multifaceted behaviors associated with hyperactivity in animals and translated this response to human. By employing a behavioral pattern monitor (BPM) technique, it was found that BD patients presented motor and exploratory behavior pattern very distinctly from those observed in schizophrenia patients. The striking difference between manic BD and schizophrenia patients in this task highlights the relevance of multivariate assessment of behavior, which may improve the diagnostic differentiation between these two conditions that can be indistinguishable during acute states (Pini et al., 2004; Young et al., 2007). Mice that received AMPH, a mania model criticized for sharing pathophysiological features with schizophrenia models, presented increased motor activity, but reduced exploratory behavior as measured by the BPM (Young et al., 2010). Interestingly, methylphenidate, which also blocked DAT, increased mice hole exploration in the holeboard test (Souza et al., 2016). On the other hand, the administration of GBR 12909 increased activity and exploratory behaviors, a phenotype consistent with the behavior of BD patients in the human BPM (Perry et al., 2009; Young et al., 2010). The selective inhibition of DAT by GBR 12909 was independently of the mice strain and presented a long-lasting (3 h) effect, supporting the face validity of this model.

A recent study found that a single injection of GBR 12909 induced hyperlocomotion and increased exploratory behavior. These behavioral changes were associated with decreased levels of the antioxidant enzyme glutathione (GSH) and increased lipid peroxidation in the hippocampus and striatum, consistent with the oxidative stress role described in BD pathophysiology (Queiroz et al., 2015). Further studies are needed to better address the involvement of inflammation, DNA, and mitochondrial damage, among other factors already reported in pharmacological models and often implicated in BD neurobiology (Fig. 43.1).

Acute administration of valproate and lithium prevented GBR 12909 behavioral and prooxidative alterations (Queiroz et al., 2015). Chronic treatment with valproate partially attenuated the behavior effects of functional decrease of DAT observed in genetic modified mice and following GBR 12909 acute injections (van Enkhuizen et al., 2013). Altogether, these studies provided evidence of the potential predictive validity of this promise model of mania.

In this line, mood stabilizers also blocked methylphenidate-induced hyperlocomotion (Barbosa et al., 2011b; Pereira et al., 2011; Souza et al., 2016; Tonelli et al., 2013) and hole exploration (Souza et al., 2016).

2.6 Ketamine

Ketamine, an antagonist of *N*-methyl-D-aspartate glutamatergic receptor, is also used as a pharmacologically based mania model. Ketamine induced hyperlocomotion in rodents (Gazal et al., 2014, 2015; Ghedim et al., 2012) and there is a case report of manic-like symptoms induced by ketamine (Ricke et al., 2011). Ketamine-induced hyperlocomotion is blocked by lithium and valproate (Gazal et al., 2014, 2015; Ghedim et al., 2012), showing its predictive validity. Moreover, this effect is associated to increase oxidative stress (Gazal et al., 2014, 2015; Ghedim et al., 2012). However, as other psychostimulant models, ketamine challenge is also used to model schizophrenia (Young et al., 2011).

3 INSIGHTS FROM ENVIRONMENTAL MODELS

A significant limitation reported for pharmacological models is that they reflect only one facet of mania, that is, hyperlocomotion, that is also commonly observed in other conditions like schizophrenia and drug abuse (Young et al., 2011). As mania is a complex disorder influenced by environmental and genetic factors, it is reasonable to assume that manipulations of these factors might induce behaviors in animals that resemble human manic states rather than only hyperactivity (Gould and Einat, 2007). Moreover, pharmacological models can give false results (positive or negative) if a significant

pharmacokinetic interaction occurs between induction drug and test drug.

Environmental models of mania in rodents include sleep deprivation, the resident-intruder test, and the dominant–submissive behavior paradigms (Malatynska and Knapp, 2005; McClung, 2011; Miczek et al., 2001). The rodent sleep deprivation model is based in the circadian rhythm changes associated with mania (McClung, 2011). This model presents significant relevance regarding face validity since sleep disruption is one of the hallmarks of mania (Mansell and Pedley, 2008), and sleep deprivation can trigger mania in bipolar patients (Wehr, 1992). Moreover, sleep deprivation reproduces several manic-like behaviors, such as insomnia, hyperactivity, aggressive actions toward other animals, hypersexuality (an increase in mounting behavior), and stereotypy (sniffing and rearing) (Abrial et al., 2015; Fratta et al., 1987; Gessa et al., 1995; Hicks et al., 1979). Increase in protein kinase C (PKC) activity in the PFC of sleep-deprived animals along with changes in glutamatergic signaling supports some construct validity to the model. Furthermore, sleep deprivation increases oxidative stress, which correlated positively with increase in locomotor activity (Kanazawa et al., 2016). Additionally, predictive validity is also suggested since lithium, aripiprazole, and tamoxifen attenuated manic-like behaviors (Abrial et al., 2015; Kanazawa et al., 2016; Szabo et al., 2009).

The resident-intruder test models provocative, intrusive, or aggressive behaviors frequently observed in manic patients (Einat, 2007a). This test consists of introducing an intruder rodent into the home cage of an isolated mouse or rat, and quantifying both the aggressive acts from the resident and the defensive acts and postures exhibited by the intruder (Miczek et al., 2001). Manic-like behaviors, including biting, threatening postures, and tails rattling may be augmented by prolonged isolation or exposure to foot shock applied to the resident rodents (Miczek and O'Donnell, 1978). Although treatment with lithium, valproate, and antipsychotics reduced resident aggression toward intruders (Einat, 2007b; O'Donnell and Gould, 2007), similar effects have been demonstrated following anxiolytics administration (Vassout et al., 2000; Yang et al., 2015), indicating limited predictive validity and specificity to mania.

The dominant–submissive behavior is a more recent proposed environmental model of mania. In this model, subordinate animals, similar to depressed humans, presented increased defensive behavior and reduced activity. On the other hand, dominant animals, similar to manic episodes, exhibited self-confident, assertive and aggressive behavior (Malatynska and Knapp, 2005). Lithium, valproate, and carbamazepine reversed the dominant behavior in a time course similar to that observed in BD patients. For instance, lithium and carbamazepine treatment reduced rodent dominance after 2–3 weeks of treatment (Malatynska and Knapp, 2005; Malatynska et al., 2007). Similar to the resident-intruder test, the dominant–submissive behavior paradigms are also sensitive to the effects of anxiolytic and anxiogenic drugs limiting its construct and predictive validity as a mania model (Vassout et al., 2000).

4 INSIGHTS FROM GENETIC MODELS

BD is a highly heritable disorder that possibly involves multiple genes. In this context, genetic models of mania have been proposed to define specific neurobiological processes and associated behaviors that are involved in the pathways connecting genes and manic symptoms (Gould and Einat, 2007). Due to the possibility of identifying potential behavioral endophenotypes, genetic models might present greater construct validity compared to pharmacological and environmental models (Gould and Einat, 2007; Malkesman et al., 2009).

Rodent genetic models of mania include genes coding for DAT (Ralph-Williams et al., 2003), circadian locomotor output cycle kaput (CLOCK) (Roybal et al., 2007), glutamate receptor 6 (GluR6) (Shaltiel et al., 2008), GSK-3β (Prickaerts et al., 2006), circadian gene D-box binding protein (DBP) (Le-Niculescu et al., 2008), pituitary adenylate cyclase-activating polypeptide (PACAP) (Hattori et al., 2012), extracellular signal-regulated kinase 1 (ERK1) (Engel et al., 2009), postsynaptic density protein (PSD) SHANK3 (Han et al., 2013), inositol-monophosphatase (IMPA)1 (Damri et al., 2015), and B-cell lymphoma 2 (Bcl-2) (Lien et al., 2008). Although genetic models might be promising to understand the neurobiological mechanisms underlying mania and to develop potential therapeutic strategies, further studies are needed to confirm their face and predictive validities (Young et al., 2011).

5 CONCLUSIONS

Pharmacological models of mania have been widely employed to investigate mania pathophysiology and potential therapeutic agents. Apart from their significant limitations, accumulating evidence had supported face, predictive, and construct validities. Moreover, these models had been useful to investigate potential drugs for mania, such as *N*-acetylcysteine plus deferoxamine, curcumin, sulfate magnesium, folic acid, and diphenyl diselenide (Arent et al., 2015; Barbosa et al., 2011b; Brocardo et al., 2010; Brüning et al., 2012; Gazal et al., 2014). It is worth mentioning that many studies investigated the acute effect of antimanic drugs to provide some predictive validity. Although these studies showed positive effects in behavioral pharmacological terms, mania is a

long-term condition that requires chronic therapeutic approaches. Therefore, studies that investigate chronic treatment responses are more likely to exhibit predictive validity for treatment in subjects with BD (Young et al., 2011). Anyway, the pharmacological models of mania aroused interest in this field and may prompt the development of more complex and valid models.

The models based on environmental and genetics manipulations, which are less studied and validated, are promising and apparently overcome some limitations of pharmacologically based models. Finally, new behavioral variables that had been proposed (hole exploration by mice and high frequency USVs in rats) can refine mania models and increase their content validity, making possible the assessment of different facets of the illness.

Acknowledgment

References

Abrial, E., Bétourné, A., Etiévant, A., Lucas, G., Scarna, H., Lambás-Señas, L., Haddjeri, N., 2015. Protein kinase C inhibition rescues manic-like behaviors and hippocampal cell proliferation deficits in the sleep deprivation model of mania. Int. J. Neuropsychopharmacol. 18 (2), 1–11.

Agmo, A., Medrano, A., Garrido, N., Alonso, P., 1997. GABAergic drugs inhibit amphetamine-induced distractibility in the rat. Pharmacol. Biochem. Behav. 58, 119–126.

Anand, A., Verhoeff, P., Seneca, N., Zoghbi, S.S., Seibyl, J.P., Charney, D.S., et al., 2000. Brain SPECT imaging of amphetamine-induced dopamine release in euthymic bipolar disorder patients. Am. J. Psychiatry 157, 1108–1114.

Andreazza, A.C., Frey, B.N., Erdtmann, B., Salvador, M., Rombaldi, F., Santin, A., et al., 2007. DNA damage in bipolar disorder. Psychiatry Res. 153, 27–32.

Andreazza, A.C., Kauer-Sant'anna, M., Frey, B.N., Bond, D.J., Kapczinski, F., Young, L.T., et al., 2008a. Oxidative stress markers in bipolar disorder: a meta-analysis. J. Affect. Disord. 111 (2–3), 135–144.

Andreazza, A.C., Kauer-Sant'Anna, M., Frey, B.N., Stertz, L., Zanotto, C., Ribeiro, L., et al., 2008b. Effects of mood stabilizers on DNA damage in an animal model of mania. J. Psychiatry Neurosci. 33 (6), 516–524.

Andreazza, A.C., Shao, L., Wang, J.F., Young, L.T., 2010. Mitochondrial complex I activity and oxidative damage to mitochondrial proteins in the prefrontal cortex of patients with bipolar disorder. Arch. Gen. Psychiatry 67 (4), 360–368.

Angst, J., Gamma, A., Sellaro, R., Lavori, P.W., Zhang, H., 2003. Recurrence of bipolar disorders and major depression: a life-long perspective. Eur. Arch. Psychiatry Clin. Neurosci. 253 (5), 236–240.

Antia, I.J., Smith, C.E., Wood, A.J., Aronson, J.K., 1995. The upregulation of Na^+, K(+)-ATPase pump numbers in lymphocytes from the first-degree unaffected relatives of patients with manic depressive psychosis in response to in vitro lithium and sodium ethacrynate. J. Affect. Disord. 34, 33–39.

American Psychiatric Association, 2013. Diagnostic and Statistical Manual of Mental Disorders, fifth ed. American Psychiatric Publishing, Washington, DC.

Arban, R., Maraia, G., Brackenborough, K., Winyard, L., Wilson, A., Gerrard, P., et al., 2005. Evaluation of the effects of lamotrigine, valproate and carbamazepine in a rodent model of mania. Behav. Brain Res. 158 (1), 123–132.

Arent, C.O., Valvassori, S.S., Steckert, A.V., Resende, W.R., Dal-Pont, G.C., Lopes-Borges, J., et al., 2015. The effects of n-acetylcysteine and/or deferoxamine on manic-like behavior and brain oxidative damage in mice submitted to the paradoxal sleep deprivation model of mania. J. Psychiatr. Res. 65, 71–79.

Aylmer, C.G., Steinberg, H., Webster, R.A., 1987. Hyperactivity induced by dexamphetamine/chlordiazepoxide mixtures in rats and its attenuation by lithium pretreatment: a role for dopamine? Psychopharmacology (Berl) 91 (2), 198–206.

Banerjee, U., Dasgupta, A., Rout, J.K., Singh, O.P., 2012. Effects of lithium therapy on Na^+-K^+-ATPase activity and lipid peroxidation in bipolar disorder. Prog. Neuropsychopharmacol. Biol. Psychiatry 37 (1), 56–61.

Barbosa, I.G., Huguet, R.B., Mendonça, V.A., Sousa, L.P., Neves, F.S., Bauer, M.E., et al., 2011a. Increased plasma levels of soluble TNF receptor I in patients with bipolar disorder. Eur. Arch. Psychiatry Clin. Neurosci. 261 (2), 139–143.

Barbosa, F.J., Hesse, B., de Almeida, R.B., Baretta, I.P., Boerngen-Lacerda, R., Andreatini, R., 2011b. Magnesium sulfate and sodium valproate block methylphenidate-induced hyperlocomotion, an animal model of mania. Pharmacol. Rep. 63 (1), 64–70.

Barbosa, I.G., Bauer, M.E., Machado-Vieira, R., Teixeira, A.L., 2014. Cytokines in bipolar disorder: paving the way for neuroprogression. Neural Plast. 2014, 1–9.

Bauer, M., Glenn, T., Rasgon, N., Marsh, W., Sagduyu, K., Munoz, R., et al., 2010. Association between age of onset and mood in bipolar disorder: comparison of subgroups identified by cluster analysis and clinical observation. J. Psychiatr. Res. 44, 1170–1175.

Beauvais, G., Atwell, K., Jayanthi, S., Ladenheim, B., Cadet, J.L., 2011. Involvement of dopamine receptors in binge methamphetamine-induced activation of endoplasmic reticulum and mitochondrial stress pathways. PLoS One 6 (12), e28946.

Berk, M., Dodd, S., Kauer-Sant'anna, M., Malhi, G.S., Bourin, M., Kapczinski, F., et al., 2007. Dopamine dysregulation syndrome: implications for a dopamine hypothesis of bipolar disorder. Acta Psychiatr. Scand. Suppl. 434, 41–49.

Berridge, C.W., Stalnaker, T.A., 2002. Relationship between low-dose amphetamine-induced arousal and extracellular norepinephrine and dopamine levels within prefrontal cortex. Synapse 46, 140–149.

Bezchlibnyk, Y.B., Wang, J.F., McQueen, G.M., Young, L.T., 2001. Gene expression differences in bipolar disorder revealed by cDNA array analysis of postmortem frontal cortex. J. Neurochem. 79 (4), 826–834.

Brocardo, P.S., Budni, J., Pavesi, E., Franco, J.L., Uliano-Silva, M., Trevisan, R., et al., 2010. Folic acid administration prevents ouabain-induced hyperlocomotion and alterations in oxidative stress markers in the rat brain. Bipolar Disord. 12 (4), 414–424.

Brüning, C.A., Prigol, M., Luchese, C., Pinton, S., Nogueira, C.W., 2012. Diphenyl diselenide ameliorates behavioral and oxidative parameters in an animal model of mania induced by ouabain. Prog. Neuropsychopharmacol. Biol. Psychiatry 38, 168–174.

Burdick, K.E., Braga, R.J., Goldberg, J.F., Malhotra, A.K., 2007. Cognitive dysfunction in bipolar disorder: future place of pharmacotherapy. CNS Drugs 21, 971–981.

Burrows, K.B., Gudelsky, G., Yamamoto, B.K., 2000. Rapid and transient inhibition of mitochondrial function following methamphetamine or 3,4-methylenedioxymethamphetamine administration. Eur. J. Pharmacol. 398 (1), 11–18.

Calabrese, V., Scapagnini, G., Giuffrida, A.M., Bates, T.E., Clark, J.B., 2001. Mitochondrial involvement in brain function and dysfunction: relevance to aging, neurodegenerative disorders and longevity. Neurochem. Res. 6, 739–764.

Cao, B.J., Peng, N.A., 1993. Magnesium valproate attenuates hyperactivity induced by dexd-amphetamine-chlordiazepoxide mixture in rodents. Eur. J. Pharmacol. 237, 177–181.

Cappeliez, P., Moore, E., 1990. Effects of lithium on an amphetamine animal model of bipolar disorder. Prog. Neuropsychopharmacol. Biol. Psychiatry 14 (3), 347–358.

Cechinel-Recco, K., Valvassori, S.S., Varela, R.B., Resende, W.R., Arent, C.O., Vitto, M.F., et al., 2012. Lithium and tamoxifen modulate cellular plasticity cascades in animal model of mania. J. Psychopharmacol. 26 (12), 1594–1604.

Chan, P., Di Monte, D.A., Luo, J.J., DeLanney, L.E., Irwin, I., Langston, J.W., 1994. Rapid ATP loss caused by methamphetamine in the mouse striatum: relationship between energy impairment and dopaminergic neurotoxicity. J. Neurochem. 62, 2484–2487.

Chao, M.V., 2003. Neurotrophins and their receptors: a convergence point for many signalling pathways. Nat. Rev. Neurosci. 4, 299–309.

Damri, O., Sade, Y., Toker, L., Bersudsky, Y., Belmaker, R.H., Agam, G., et al., 2015. Molecular effects of lithium are partially mimicked by inositol-monophosphatase (IMPA)1 knockout mice in a brain region-dependent manner. Eur. Neuropsychopharmacol. 25 (3), 425–434.

D'Aquila, P.S., Collu, M., Devoto, P., Serra, G., 2000. Chronic lithium chloride fails to prevent imipramine-induced sensitization to the dopamine D2-like receptor agonist quinpirole. Eur. J. Pharmacol. 395 (2), 157–160.

D'Aquila, P.S., Peana, A.T., Tanda, O., Serra, G., 2001. Carbamazepine prevents imipramine-induced behavioural sensitization to the dopamine D2-like receptor agonist quinpirole. Eur. J. Pharmacol. 416, 107–111.

D'Aquila, P.S., Panin, F., Serra, G., 2006. Chronic valproate fails to prevent imipramine-induced behavioural sensitization to the dopamine D2-like receptor agonist quinpirole. Eur. J. Pharmacol. 535, 208–211.

da-Rosa, D.D., Valvassori, S.S., Steckert, A.V., Ornell, F., Ferreira, C.L., Lopes-Borges, J., et al., 2012. Effects of lithium and valproate on oxidative stress and behavioral changes induced by administration of m-AMPH. Psychiatry Res. 198 (3), 521–526.

de Sousa, R.T., van de Bilt, M.T., Diniz, B.S., Ladeira, R.B., Portela, L.V., Souza, D.O., et al., 2011. Lithium increases plasma brain-derived neurotrophic factor in acute bipolar mania: a preliminary 4-week study. Neurosci. Lett. 494 (1), 54–56.

Dencker, D., Husum, H., 2010. Antimanic efficacy of retigabine in a proposed mouse model of bipolar disorder. Behav. Brain Res. 207 (1), 78–83.

Einat, H., 2006. Modelling facets of mania—new directions related to the notion of endophenotypes. J. Psychopharmacol. 20 (5), 714–722.

Einat, H., 2007a. Different behaviors and different strains: potential new ways to model bipolar disorder. Neurosci. Biobehav. Rev. 31, 850–857.

Einat, H., 2007b. Establishment of a battery of simple models for facets of bipolar disorder: a practical approach to achieve increased validity, better screening and possible in-sights into endophenotypes of disease. Behav. Genet. 37, 244–255.

Einat, H., Szechtman, H., 1993. Long-lasting consequences of chronic treatment with the dopamine agonist quinpirole for the undrugged behavior of rats. Behav. Brain Res. 54, 35–41.

Einat, H., Yuan, P., Dogra, S., Manji, H.K., 2003. Does the PKC signaling pathway play a role in the pathophysiology and treatment of bipolar disorder? Biol. Psychiatry 53 (Suppl. 8), S399.

El-Mallakh, R.S., 1983. The Na, K-ATPase hypothesis for manic-depression. I. General considerations. Med. Hypotheses 12, 253–268.

El-Mallakh, R.S., Harrison, L.T., Li, R., Changaris, D.G., Levy, R.S., 1995. An animal model for mania: preliminary results. Prog. Neuropsychopharmacol. Biol. Psychiatry 19 (5), 955–962.

El-Mallakh, R.S., Wyatt, R.J., 1995. The Na,K-ATPase hypothesis for bipolar illness. Biol. Psychiatry 37 (4), 235–244.

Engel, S.R., Creson, T.K., Hao, Y., Shen, Y., Maeng, S., Nekrasova, T., et al., 2009. The extracellular signal-regulated kinase pathway contributes to the control of behavioral excitement. Mol. Psychiatry 14, 448–461.

Feier, G., Valvassori, S.S., Lopes-Borges, J., Varela, R.B., Bavaresco, D.V., Scaini, G., et al., 2012. Behavioral changes and brain energy metabolism dysfunction in rats treated with methamphetamine or dextroamphetamine. Neurosci. Lett. 530 (1), 75–79.

Feier, G., Valvassori, S.S., Varela, R.B., Resende, W.R., Bavaresco, D.V., Morais, M.O., et al., 2013. Lithium and valproate modulate energy metabolism in an animal model of mania induced by methamphetamine. Pharmacol. Biochem. Behav. 103 (3), 589–596.

Fernandes, B.S.1., Gama, C.S., Ceresér, K.M., Yatham, L.N., Fries, G.R., Colpo, G., et al., 2011. Brain-derived neurotrophic factor as a state-marker of mood episodes in bipolar disorders: a systematic review and meta-regression analysis. J. Psychiatr. Res. 45 (8), 995–1004.

Fiorino, D.F., Phillips, A.G., 1999. Facilitation of sexual behavior in male rats following d-amphetamine-induced behavioral sensitization. Psychopharmacology (Berl) 142 (2), 200–208.

Fletcher, P.J., Korth, K.M., Sabijan, M.S., DeSousa, N.J., 1998. Injections of D-amphetamine into the ventral pallidum increase locomotor activity and responding for conditioned reward: a comparison with injections into the nucleus accumbens. Brain Res. 805, 29–40.

Fratta, W., Collu, M., Martellotta, M.C., Pichiri, M., Muntoni, F., Gessa, G.L., 1987. Stress-induced insomnia: opioid-dopamine interactions. Eur. J. Pharmacol. 142, 437–440.

Freitas, T.P., Rezin, G.T., Gonçalves, C.L., Jeremias, G.C., Gomes, L.M., Scaini, G., et al., 2010. Evaluation of citrate synthase activity in brain of rats submitted to an animal model of mania induced by ouabain. Mol. Cell. Biochem. 341 (1–2), 245–249.

Freitas, T.P., Rezin, G.T., Fraga, D.B., Moretti, M., Vieira, J.S., Gomes, L.M., et al., 2011. Mitochondrial respiratory chain activity in an animal model of mania induced by ouabain. Acta Neuropsychiatr. 23 (3), 106–111.

Frey, B.N., Martins, M.R., Petronilho, F.C., Dal-Pizzol, F., Quevedo, J., Kapczinski, F., 2006a. Increased oxidative stress after repeated amphetamine exposure: possible relevance as an animal model of acute mania. Bipolar Disord. 8, 275–280.

Frey, B.N., Valvassori, S.S., Réus, G.Z., Martins, M.R., Petronilho, F.C., Bardini, K., et al., 2006b. Changes in antioxidant defense enzymes after d-amphetamine exposure: implications as an animal model of mania. Neurochem. Res. 31 (5), 699–703.

Frey, B.N., Valvassori, S.S., Gomes, K.M., Martins, M.R., Dal-Pizzol, F., Kapczinski, F., et al., 2006c. Increased oxidative stress in submitochondrial particles after chronic amphetamine exposure. Brain Res. 1097 (1), 224–229.

Frey, B.N., Valvassori, S.S., Réus, G.Z., Martins, M.R., Petronilho, F.C., Bardini, K., et al., 2006d. Effects of lithium and valproate on amphetamine-induced oxidative stress generation in an animal model of mania. J. Psychiatry Neurosci. 31 (5), 326–332.

Frey, B.N., Andreazza, A.C., Ceresér, K.M., Martins, M.R., Valvassori, S.S., Réus, G.Z., et al., 2006e. Effects of mood stabilizers on hippocampus BDNF levels in an animal model of mania. Life Sci. 79 (3), 281–286.

Frey, B.N., Andreazza, A.C., Kunz, M., Gomes, F.A., Quevedo, J., Salvador, M., et al., 2007. Increased oxidative stress and DNA damage in bipolar disorder: a twin-case report. Prog. Neuropsychopharmacol. Biol. Psychiatry 31 (1), 283–285.

Fries, G.R., Pfaffenseller, B., Stertz, L., Paz, A.V., Dargel, A.A., Kunz, M., et al., 2012. Staging and neuroprogression in bipolar disorder. Curr. Psychiatry Rep. 14, 667–675.

Fries, G.R., Valvassori, S.S., Bock, H., Stertz, L., Magalhães, P.V., Mariot, E., et al., 2015. Memory and brain-derived neurotrophic factor after subchronic or chronic amphetamine treatment in an animal model of mania. J. Psychiatr. Res. 68, 329–336.

Gazal, M., Kaufmann, F.N., Acosta, B.A., Oliveira, P.S., Valente, M.R., Ortmann, C.F., 2015. Preventive effect of cecropia pachystachya against ketamine-induced manic behavior and oxidative stress in rats. Neurochem. Res. 40 (7), 1421–1430.

Gazal, M., Valente, M.R., Acosta, B.A., Kaufmann, F.N., Braganhol, E., Lencina, C.L., et al., 2014. Neuroprotective and antioxidant effects of curcumin in a ketamine-induced model of mania in rats. Eur. J. Pharmacol. 724, 132–139.

Gessa, G.L., Pani, L., Fadda, P., Fratta, W., 1995. Sleep deprivation in the rat: an animal model of mania. Eur. Neuropsychopharmacol. 5 (Suppl.), 89–93.

Ghedim, F.V., Fraga Dde, B., Deroza, P.F., Oliveira, M.B., Valvassori, S.S., Steckert, A.V., et al., 2012. Evaluation of behavioral and neurochemical changes induced by ketamine in rats: implications as an animal model of mania. J. Psychiatr. Res. 46, 1569–1575.

Gluck, M.R., Moy, L.Y., Jayatilleke, E., Hogan, K.A., Manzino, L., Sonsalla, P.K., 2001. Parallel increases in lipid and protein oxidative markers in several mouse brain regions after methamphetamine treatment. J. Neurochem. 79, 152–160.

Gould, T.D., Einat, H., 2007. Animal models of bipolar disorder and mood stabilizer efficacy: a critical need for improvement. Neurosci. Biobehav. Rev. 31, 825–831.

Gould, T.J., Keith, R.A., Bhat, R.V., 2001. Differential sensitivity to lithium's reversal of amphetamine-induced open-field activity in two in-bred strains of mice. Behav. Brain Res. 118, 95–105.

Gould, T.D., Quiroz, J.A., Singh, J., Zarate, C.A., Manji, H.K., 2004. Emerging experimental therapeutics for bipolar disorder: insights from the molecular and cellular actions of current mood stabilizers. Mol. Psychiatry 9, 734–755.

Greenwood, T.A., Alexander, M., Keck, P.E., McElroy, S., Sadovnick, A.D., Remick, R.A., et al., 2001. Evidence for linkage disequilibrium between the dopamine transporter and bipolar disorder. Am. J. Med. Genet. 105, 145–151.

Han, K., Holder, Jr., J.L., Schaaf, C.P., Lu, H., Chen, H., Kang, H., et al., 2013. SHANK3 overexpression causes manic-like behaviour with unique pharmacogenetic properties. Nature 503, 72–77.

Hattori, S., Takao, K., Tanda, K., Toyama, K., Shintani, N., Baba, A., 2012. Comprehensive behavioral analysis of pituitary adenylate cyclase-activating polypeptide (PACAP) knockout mice. Front. Behav. Neurosci. 6, 58.

Hayden, E.P., Nurnberger, J.I., 2006. Molecular genetics of bipolar disorder. Genes Brain Behav. 5, 85–95.

Herman, L., Hougland, T., El-Mallakh, R.S., 2007. Mimicking human bipolar ion dysregulation models mania in rats. Neurosci. Biobehav. Rev. 31 (6), 874–881.

Hicks, R.A., Moore, J.D., Hayes, C., Phillips, N., Hawkins, J., 1979. REM sleep deprivation increases aggressiveness in male rats. Physiol. Behav. 22, 1097–1100.

Huff, M.O., Li, X.P., Ginns, E., El-Mallakh, R.S., 2010. Effect of ethacrynic acid on the sodium- and potassium-activated adenosine triphosphatase activity and expression in Old Order Amish bipolar individuals. J. Affect. Disord. 123, 303–307.

Jornada, L.K., Moretti, M., Valvassori, S.S., Ferreira, C.L., Padilha, P.T., Arent, C.O., et al., 2010a. Effects of mood stabilizers on hippocampus and amygdala BDNF levels in an animal model of mania induced by ouabain. J. Psychiatr. Res. 44 (8), 506–510.

Jornada, L.K., Valvassori, S.S., Arent, C.O., Leffa, D., Damiani, A.A., Hainzenreder, G., et al., 2010b. DNA damage after intracerebroventricular injection of ouabain in rats. Neurosci. Lett. 471 (1), 6–9.

Jornada, L.K.1., Valvassori, S.S., Steckert, A.V., Moretti, M., Mina, F., Ferreira, C.L., et al., 2011. Lithium and valproate modulate antioxidant enzymes and prevent ouabain-induced oxidative damage in an animal model of mania. J. Psychiatr. Res. 45 (2), 162–168.

Kanazawa, L.K., Vecchia, D.D., Wendler, E.M., Hocayen, P.A., Dos Reis Lívero, F.A., Stipp, M.C., 2016. Quercetin reduces manic-like behavior and brain oxidative stress induced by paradoxical sleep deprivation in mice. Free Radic. Biol. Med. 99, 79–86.

Kapczinski, F., Magalhaes, P.V., Balanza-Martinez, V., Dias, V.V., Frangou, S., Gama, C.S., et al., 2014. Staging systems in bipolar disorder: an International Society for Bipolar Disorders Task Force Report. Acta Psychiatr. Scand. 130, 354–363.

Kara, N.Z., Einat, H., 2013. Rodent models for mania: practical approaches. Cell Tissue Res. 354, 191–201.

Kato, T., Kato, N., 2000. Mitochondrial dysfunction in bipolar disorder. Bipolar Disord. 2, 180–190.

Kelly, M.P., Logue, S.F., Dwyer, J.M., Beyer, C.E., Majchrowski, H., Cai, Z., et al., 2009. The supra-additive hyperactivity caused by an amphetamine-chlordiazepoxide mixture exhibits an inverted-U dose response: negative implications for the use of a model in screening for mood stabilizers. Pharmacol. Biochem. Behav. 92 (4), 649–654.

Kofman, O., Li, P.P., Warsh, J.J., 1998. Lithium, but not carbamazepine, potentiates hyperactivity induced by intra-accumbens cholera toxin. Pharmacol. Biochem. Behav. 59, 191–200.

Konradi, C., Eaton, M., MacDonald, M.L., Walsh, J., Benes, F.M., Heckers, S., 2004. Molecular evidence for mitochondrial dysfunction in bipolar disorder. Arch. Gen. Psychiatry 61, 300–308.

Krishnan, K.R.R., 2005. Psychiatric and medical comorbidities of bipolar disorder. Psychosom. Med. 67, 1–8.

Kuribara, H., Uchihashi, Y., 1993. Dopamine antagonists can inhibit methamphetamine sensitization, but not cocaine sensitization, when assessed by ambulatory activity in mice. J. Pharm. Pharmacol. 45 (12), 1042–1045.

Kuruvilla, A., Uretsky, N.J., 1981. Effect of sodium valproate on motor function regulated by the activation of GABA receptors. Psychopharmacoly (Berl) 72, 167–172.

Le-Niculescu, H., McFarland, M.J., Ogden, C.A., Balaraman, Y., Patel, S., Tan, J., et al., 2008. Phenomic, convergent functional genomic, and biomarker studies in a stress-reactive genetic animal model of bipolar disorder and co-morbid alcoholism. Am. J. Med. Genet. 147b, 134–166.

Lerer, B., Globus, M., Brik, E., Hamburger, R., Belmaker, R.H., 1984. Effect of treatment and withdrawal from chronic lithium in rats on stimulant-induced responses. Neuropsychobiology 11, 28–32.

Li, R., El-Mallakh, R.S., 2004. Differential response of bipolar and normal control lymphoblastoid cell sodium pump to ethacrynic acid. J. Affect. Disord. 80, 11–17.

Lien, R., Flaisher-Grinberg, S., Cleary, C., Hejny, M., Einat, H., 2008. Behavioral effects of Bcl-2 deficiency: implications for affective disorders. Pharmacol. Rep. 60, 490–498.

Lipska, B.K., Weinberger, D.R., 2000. To model a psychiatric disorder in animals: schizophrenia as a reality test. Neuropsychopharmacology 23, 223–239.

Macêdo, D.S., Medeiros, C.D., Cordeiro, R.C., Sousa, F.C., Santos, J.V., Morais, T.A., et al., 2012. Effects of alpha-lipoic acid in an animal model of mania induced by D-amphetamine. Bipolar Disord. 14 (7), 707–718.

Machado-Vieira, R., Schmidt, A.P., Avila, T.T., Kapczinski, F., Soares, J.C., Souza, D.O., et al., 2004. Increased cerebrospinal fluid levels of S100B protein in rat model of mania induced by ouabain. Life Sci. 76, 805–811.

Malatynska, E., Knapp, R.J., 2005. Dominant-submissive behavior as models of mania and depression. Neurosci. Biobehav. Rev. 29 (4–5), 715–737.

Malatynska, E., Pinhasov, A., Crooke, J.J., Smith-Swintosky, V.L., Brenneman, D.E., 2007. Reduction of dominant or submissive behaviors as models for antimanic or antidepressant drug testing: technical considerations. J. Neurosci. Methods 165, 175–182.

Maletic, V., Raison, C., 2014. Integrated neurobiology of bipolar disorder. Front. Psychiatry 5, 98.

Malkesman, O., Austin, D.R., Chen, G., Manji, H.K., 2009. Reverse translational strategies for developing animal models of bipolar disorder. Dis. Model. Mech. 2, 238–245.

Mansell, W., Pedley, R., 2008. The ascent into mania: a review of psychological processes associated with the development of manic symptoms. Clin. Psychol. Rev. 28, 494–520.

Mattiasson, G., Shamloo, M., Gido, G., Mathi, K., Tomasevic, G., Yi, S., et al., 2003. Uncoupling protein-2 prevents neuronal death and diminishes brain dysfunction after stroke and brain trauma. Nat. Med. 9 (8), 1062–1068.

McClung, C.A., 2011. Circadian rhythms and mood regulation: insights from pre-clinical models. Eur. Neuropsychopharmacology 21 (Suppl. 4), S683–S693.

Miczek, K.A., O'Donnell, J.M., 1978. Intruder-evoked aggression in isolated and nonisolated mice: effects of psychomotor stimulants and L-dopa. Psychopharmacology (Berl) 57, 47–55.

Miczek, K.A., Maxson, S.C., Fish, E.W., Faccidomo, S., 2001. Aggressive behavioral phenotypes in mice. Behav. Brain Res. 125, 167–181.

Modabbernia, A., Taslimi, S., Brietzke, E., Ashrafi, M., 2013. Cytokine alterations in bipolar disorder: a meta-analysis of 30 studies. Biol. Psychiatry 74 (1), 15–25.

Namima, M., Sugihara, K., Watanabe, Y., Sasa, H., Umekage, T., Okamoto, K., 1999. Quantitative analysis of the effects of lithium on the reverse tolerance and the c-Fos expression induced by methamphetamine in mice. Brain Res. Protoc. 4 (1), 11–18.

Novick, D.M., Swartz, H.A., Frank, E., 2010. Suicide attempts in bipolar I and bipolar II disorder: review and meta-analysis of the evidence. Bipolar Disord. 12, 1–9.

O'Donnell, K.C., Gould, T.D., 2007. The behavioral actions of lithium in rodent models: leads to develop novel therapeutics. Neurosci. Biobehav. Rev. 31, 932–962.

Pantazopoulos, H., Stone, D., Walsh, J., Benes, F.M., 2004. Differences in the cellular distribution of D1 receptor mRNA in the hippocampus of bipolars and schizophrenics. Synapse 54, 147–155.

Paszti-Gere, E., Jakus, J., 2013. Protein phosphatases but not reactive oxygen species play functional role in acute amphetamine-mediated dopamine release. Cell Biochem. Biophy. 66, 831–841.

Pereira, M., Martynhak, B.J., Baretta, I.P., Correia, D., Siba, I.P., Andreatini, R., 2011. Antimanic-like effect of tamoxifen is not reproduced by acute or chronic administration of medroxyprogesterone or clomiphene. Neurosci. Lett. 500 (2), 95–98.

Pereira, M., Andreatini, R., Schwarting, R.K., Brenes, J.C., 2014. Amphetamine-induced appetitive 50-kHz calls in rats: a marker of affect in mania? Psychopharmacology 231 (13), 2567–2577.

Perlis, R.H., Dennehy, E.B., Miklowitz, D.J., Delbello, M.P., Ostacher, M., Calabrese, J.R., et al., 2009. Retrospective age at onset of bipolar disorder and outcome during two-year follow-up: results from the STEP-BD study. Bipolar Disord. 11, 391–400.

Perry, W., Minassian, A., Paulus, M.P., Young, J.W., Kincaid, M.J., Ferguson, E.J., et al., 2009. A reverse-translational study of dysfunctional exploration in psychiatric disorders: from mice to men. Arch. Gen. Psychiatry 66 (10), 1072–1080.

Pierce, R.C., Kalivas, P.W., 1997a. A circuitry model of the expression of behavioral sensitization to amphetamine-like psychostimulants. Brain Res. Rev. 25 (2), 192–216.

Pierce, R.C., Kalivas, P.W., 1997b. Repeated cocaine modifies the mechanism by which amphetamine releases dopamine. J. Neurosci. 17, 3254–3262.

Pini, S., de Queiroz, V., Dell'Osso, L., Abelli, M., Mastrocinque, C., Saettoni, M., et al., 2004. Cross-sectional similarities and differences between schizophrenia, schizoaffective disorder and mania or mixed mania with mood-incongruent psychotic features. Eur. Psychiatry 19, 8–14.

Pinsonneault, J.K., Han, D.D., Burdick, K.E., Kataki, M., Bertolino, A., Malhotra, A.K., et al., 2011. Dopamine transporter gene variant affecting expression in human brain is associated with bipolar disorder. Neuropsychopharmacology 36, 1644–1655.

Post, R.M., 2007. Kindling and sensitization as models for affective episode recurrence, cyclicity, and tolerance phenomena. Neurosci. Biobehav. Rev. 31, 858–873.

Post, R.M., Weiss, S.R., 1989. Sensitization, kindling, and anticonvulsants in mania. J. Clin. Psychiatry 50 (Suppl. 23–30), 45–47.

Post, R.M., Weiss, S.R., Leverich, G.S., Smith, M., Zhang, L.X., 2001. Sensitization and kindling-like phenomena in bipolar disorder: implications for psychopharmacology. Clin. Neurosci. Res. 1, 69–81.

Prickaerts, J., Moechars, D., Cryns, K., Lenaerts, I., van Craenendonck, H., Goris, I., et al., 2006. Transgenic mice overexpressing glycogen synthase kinase 3beta: a putative model of hyperactivity and mania. J. Neurosci. 26, 9022–9029.

Queiroz, A.I., de Araújo, M.M., da Silva Araújo, T., de Souza, G.C., Cavalcante, L.M., de Jesus Souza Machado, M., et al., 2015. GBR 12909 administration as an animal model of bipolar mania: time course of behavioral, brain oxidative alterations and effect of mood stabilizing drugs. Metab. Brain Dis. 30 (5), 1207–1215.

Quraishi, S., Walshe, M., McDonald, C., Schulze, K., Kravariti, E., Bramon, E., et al., 2009. Memory functioning in familial bipolar I disorder patients and their relatives. Bipolar Disord. 11 (2), 209–214.

Ralph-Williams, R.J., Paulus, M.P., Zhuang, X., Hen, R., Geyer, M.A., 2003. Valproate attenuates hyperactive and perseverative behaviors in mutant mice with a dysregulated dopamine system. Biol. Psychiatry 53, 352–359.

Rao, J.S., Harry, G.J., Rapoport, S.I., Kim, H.W., 2010. Increased excitotoxicity and neuroinflammatory markers in postmortem frontal cortex from bipolar disorder patients. Mol. Psychiatry 15 (4), 384–392.

Rees, J.N., Florang, V.R., Anderson, D.G., Doorn, J.A., 2007. Lipid peroxidation products inhibit dopamine catabolism yielding aberrant levels of a reactive intermediate. Chem. Res. Toxicol. 20, 1536–1542.

Ricke, A.K., Snook, R.J., Anand, A., 2011. Induction of prolonged mania during ketamine therapy for reflex sympathetic dystrophy. Biol. Psychiatry 70 (4), 13–14.

Riegel, R.E.1., Valvassori, S.S., Elias, G., Réus, G.Z., Steckert, A.V., de Souza, B., et al., 2009. Animal model of mania induced by ouabain: evidence of oxidative stress in submitochondrial particles of the rat brain. Neurochem. Int. 55 (7), 491–495.

Riegel, R.E., Valvassori, S.S., Moretti, M., Ferreira, C.L., Steckert, A.V., de Souza, B., et al., 2010. Intracerebroventricular ouabain administration induces oxidative stress in the rat brain. Int. J. Dev. Neurosci. 28, 233–237.

Rippberger, H., van Gaalen, M.M., Schwarting, R.K.W., Wöhr, M., 2015. Environmental and pharmacological modulation of amphetamine-induced 50-kHz ultrasonic vocalizations in rats. Curr. Neuropharmacol. 13, 220–232.

Robbins, T.W., Sahakian, B.J., 1980. Animal models of mania. In: Bellmaker, R.H., Ban Prang, H.M. (Eds.), Mania: An Evolving Concept. Spectrum, New York, NY, pp. 143–216.

Robinson, T.E., Berridge, K.C., 1993. The neural basis of drug craving: an incentive-sensitization theory of addiction. Brain Res. Rev. 18 (3), 247–291.

Rose, A.M., Mellett, B.J., Valdes, Jr., R., Kleinman, J.E., Herman, M.M., Li, R., et al., 1998. Alpha 2 isoform of the Na, K-adenosine triphosphatase is reduced in temporal cortex of bipolar individuals. Biol. Psychiatry 44, 892–897.

Roybal, K., Theobold, D., Graham, A., DiNieri, J.A., Russo, S.J., Krishnan, V., et al., 2007. Mania-like behavior induced by disruption of CLOCK. Proc. Natl. Acad. Sci. USA 104, 6406–6411.

Sachs, G.S., Gardner-Schuster, E.E., 2007. Adjunctive treatment of acute mania: a clinical overview. Acta Psychiatr. Scand. Suppl. (Suppl. 434), 27–34.

Seiden, L.S., Sabol, K.E., Ricaurte, G.A., 1993. Amphetamine: effects on catecholamine systems and behavior. Annu. Rev. Pharmacol. Toxicol. 32, 639–677.

Serra, G., Argiolas, A., Klimek, V., Fadda, F., Gessa, G.L., 1979. Chronic treatment with antidepressants prevents the inhibitory effect of small doses of apomorphine on dopamine synthesis and motor activity. Life Sci. 25 (5), 415–423.

Shaldubina, A., Einat, H., Szechtman, H., Shimon, H., Belmaker, R.H., 2002. Preliminary evaluation of oral anticonvulsant treatment in the quinpirole model of bipolar disorder. J. Neural Transm. (Vienna) 109 (3), 433–440.

Shaltiel, G., Maeng, S., Malkesman, O., Pearson, B., Schloesser, R.J., Tragon, T., 2008. Evidence for the involvement of the kainate receptor subunit GluR6 (GRIK2) in mediating behavioral displays related to behavioral symptoms of mania. Mol. Psychiatry 13, 858–872.

Sierra, P., Livianos, L., Rojo, L., 2005. Quality of life for patients with bipolar disorder: relationship with clinical and demographic variables. Bipolar Disord. 7 (2), 159–165.

Smith, D.F., 1981. Central and peripheral effects of lithium on amphetamine-induced hyperactivity in rats. Pharmacol. Biochemi. Behav. 14, 439–442.

Söderlund, J., Olsson, S.K., Samuelsson, M., Walther-Jallow, L., Johansson, C., Erhardt, S., et al., 2011. Elevation of cerebrospinal fluid interleukin-1ß in bipolar disorder. J. Psychiatry Neurosci. 36 (2), 114–118.

Souza, L.S., Silva, E.F., Santos, W.B., Asth, L., Lobão-Soares, B., Soares-Rachetti, V.P., 2016. Lithium and valproate prevent methylphenidate-induced mania-like behaviors in the hole board test. Neurosci. Lett. 629, 143–148.

Strakowski, S.M., Sax, K.W., 1998. Progressive behavioral response to repeated d-amphetamine challenge: further evidence for sensitization in humans. Biol. Psychiatry 44, 1171–1177.

Sui, L., Song, X.J., Ren, J., Ju, L.H., Wang, Y., 2013. Intracerebroventricular administration of ouabain alters synaptic plasticity and dopamine release in rat medial prefrontal cortex. J. Neural Transm. (Vienna) 120 (8), 1191–1199.

Sulzer, D., Chen, T.K., Lau, Y.Y., Kristensen, H., Rayport, S., Ewing, A., 1995. Amphetamine redistributes dopamine from synaptic vesicles to the cytosol and promotes reverse transport. J. Neurosci. 15, 4102–4108.

Swartz, H.A., Fagiolini, A., 2012. Cardiovascular disease and bipolar disorder: risk and clinical implications. J. Clin. Psychiatry 73 (12), 1563–1565.

Szabo, S.T., Machado-Vieira, R., Yuan, P., Wang, Y., Wei, Y., Falke, C., et al., 2009. Glutamate receptors as targets of protein kinase C in the pathophysiology and treatment of animal models of mania. Neuropharmacology 56, 47–55.

Tohen, M., Goldberg, J.F., Gonzalez-Pinto Arrillaga, A.M., Azorin, J.M., Vieta, E., Hardy-Bayle, M.C., et al., 2003. A 12-week, double-blind comparison of olanzapine vs haloperidol in the treatment of acute mania. Arch. Gen. Psychiatry 60, 1218–1226.

Tonelli, D.A., Pereira, M., Siba, I.P., Martynhak, B.J., Correia, D., Casarotto, P.C., et al., 2013. The antimanic-like effect of phenytoin and carbamazepine on methylphenidate-induced hyperlocomotion: role of voltage-gated sodium channels. Fundam. Clin. Pharmacol. 27 (6), 650–655.

Tonin, P.T., Valvassori, S.S., Lopes-Borges, J., Mariot, E., Varela, R.B., Teixeira, A.L., et al., 2014. Effects of ouabain on cytokine/chemokine levels in an animal model of mania. J. Neuroimmunol. 276 (1–2), 236–239.

Tramontina, J.F., Andreazza, A.C., Kauer-Sant'anna, M., Stertz, L., Goi, J., Chiarani, F., et al., 2009. Brain-derived neurotrophic factor serum levels before and after treatment for acute mania. Neurosci. Lett. 452 (2), 111–113.

Valvassori, S.S., Rezin, G.T., Ferreira, C.L., Moretti, M., Gonçalves, C.L., Cardoso, M.R., et al., 2010. Effects of mood stabilizers on mitochondrial respiratory chain activity in brain of rats treated with D-amphetamine. J. Psychiatr. Res. 44 (14), 903–909.

Valvassori, S.S., Budni, J., Varela, R.B., Quevedo, J., 2013. Contributions of animal models to the study of mood disorders. Revista Brasileira de Psiquiatria 35 (Suppl. 2), S121–S131.

Valvassori, S.S., Tonin, P.T., Varela, R.B., Carvalho, A.F., Mariot, E., Amboni, R.T., et al., 2015a. Lithium modulates the production of peripheral and cerebral cytokines in an animal model of mania induced by dextroamphetamine. Bipolar Disord. 17 (5), 507–517.

Valvassori, S.S., Resende, W.R., Lopes-Borges, J., Mariot, E., Dal-Pont, G.C., Vitto, M.F., 2015b. Effects of mood stabilizers on oxidative stress-induced cell death signaling pathways in the brains of rats subjected to the ouabain-induced animal model of mania: mood stabilizers exert protective effects against ouabain-induced activation of the cell death pathway. J. Psychiatr. Res. 65, 63–70.

van den Ameele, S., van Diermen, L., Staels, W., Coppens, V., Dumont, G., Sabbe, B., et al., 2016. The effect of mood-stabilizing drugs on cytokine levels in bipolar disorder: a systematic review. J. Affect. Disord. 203, 364–373.

van Enkhuizen, J., Geyer, M.A., Kooistra, K., Young, J.W., 2013. Chronic valproate attenuates some, but not all, facets of mania-like behaviour in mice. Int. J. Neuropsychopharmacol. 16 (5), 1021–1031.

Varela, R.B., Valvassori, S.S., Lopes-Borges, J., Mariot, E., Dal-Pont, G.C., Amboni, R.T., et al., 2015. Sodium butyrate and mood stabilizers block ouabain-induced hyperlocomotion and increase BDNF, NGF and GDNF levels in brain of Wistar rats. J. Psychiatr. Res. 61, 114–121.

Vassout, A., Veenstra, S., Hauser, K., Ofner, S., Brugger, F., Schilling, W., et al., 2000. NKP608: a selective NK-1 receptor antagonist with anxiolytic-like effects in the social interaction and social exploration test in rats. Regul. Pept. 96, 7–16.

Vawter, M.P., Freed, W.J., Kleinman, J.E., 2000. Neuropathology of bipolar disorder. Biol. Psychiatry 48, 486–504.

Vieta, E., Sanchez-Moreno, J., 2008. Acute and long-term treatment of mania. Dialogues Clin. Neurosci. 10, 165–179.

Wehr, T.A., 1992. Improvement of depression and triggering of mania by sleep deprivation. J. Am. Med. Assoc. 267 (4), 548–551.

Yang, C.R., Bai, Y.Y., Ruan, C.S., Zhou, H.F., Liu, D., Wang, X.F., et al., 2015. Enhanced aggressive behaviour in a mouse model of depression. Neurotox. Res. 27, 129–142.

Young, J.W., Minassian, A., Paulus, M.P., Geyer, M.A., Perry, W., 2007. A reverse-translational approach to bipolar disorder: rodent and human studies in the Behavioral Pattern Monitor. Neurosci. Biobehav. Rev. 31 (6), 882–896.

Young, J.W., Goey, A.K., Minassian, A., Perry, W., Paulus, M.P., Geyer, M.A., 2010. GBR 12909 administration as a mouse model of bipolar disorder mania: mimicking quantitative assessment of manic behavior. Psychopharmacology (Berl) 208 (3), 443–454.

Young, J.W., Henry, B.L., Geyer, M.A., 2011. Predictive animal models of mania: hits, misses and future directions. Br. J. Pharmacol. 164, 1263–1284.

Zarate, Jr., C.A., Tohen, M., Fletcher, K., 2001. Cycling into depression from a first episode of mania: a case-comparison study. Am. J. Psychiatry 158 (9), 1524–1526.

Zhuang, X., Oosting, R.S., Jones, S.R., Gainetdinov, R.R., Miller, G.W., Caron, M.G., et al., 2001. Hyperactivity and impaired response habituation in hyperdopaminergic mice. Proce. Natl. Acad. Sci. USA 98, 1982–1987.

Further Reading

Cryan, J.F., Valentino, R.J., Lucki, I., 2005. Assessing substrates underlying the behavioral effects of antidepressants using the modified rat forced swimming test. Neurosci. Biobehav. Rev. 29, 547–569.

Teixeira, A.L., Quevedo, J., 2013. Animal models in psychiatry. Revista Brasileira de Psiquiatria 35 (Suppl. 2), S73–S74.

Page left intentionally blank

Stress Coping and Resilience Modeled in Mice

David M. Lyons, Luis de Lecea, Alan F. Schatzberg

Stanford University, Stanford, CA, United States

1 INTRODUCTION

Severe stress in humans is a risk factor for major depression and anxiety disorders (Charney and Manji, 2004; Duman, 2009; Heim et al., 2010; Krishnan and Nestler, 2008). Consequently, deleterious effects of stress are commonly considered in mental health research. Far fewer studies have addressed the discovery that mild but not minimal nor severe stress exposure promotes subsequent coping and emotion regulation as described by U-shaped functions (Russo et al., 2012; Sapolsky, 2015; Seery et al., 2010). Historical reasons for this imbalance in stress research are discussed by Petticrew and Lee (2011).

In addition to the qualities or intensities of stress exposure, temporal aspects further contribute to the production of stress vulnerability versus resilience (Burchfield, 1979). Prolonged chronic stress leads to vulnerability (Brosschot, 2010), whereas intermittent stress exposures interspersed with undisturbed periods of recovery provide repeated opportunities to learn, practice, and improve coping with subsequent gains in emotion regulation and resilience (Brockhurst et al., 2015; Lee et al., 2014; Lyons et al., 2010a,b). Variously described in studies of humans as inoculating, steeling, or toughening (Dienstbier, 1989; Garmezy et al., 1984; Russo et al., 2012; Rutter, 2006), the notion that learning to cope with stress builds resilience is supported by nonhuman primate research.

In natural and seminatural conditions, squirrel monkey mothers and other group members periodically leave newly weaned offspring beginning at 3–6 months of age to forage for food on their own (Lyons et al., 1998). At this stage of development, offspring are approximately half their adult body size. Initially, brief mother–infant separations studied in controlled experimental conditions elicit distress peep-calls and increase plasma levels of the stress hormone cortisol with partial habituation of these measures observed over repeated separations (Coe et al., 1983; Hennessy, 1986). Later in life, monkeys exposed to intermittent separations show fewer behavioral indications of anxiety, diminished stress-levels of cortisol, and enhanced glucocorticoid feedback regulation of

the hypothalamic–pituitary–adrenal (HPA) axis compared to monkeys not exposed to intermittent separations (Levine and Mody, 2003; Lyons et al., 1999; Lyons et al., 2010b; Parker et al., 2004, 2006). Similar examples have been reported for human children studied in the context of separation stress (Poulton et al., 2001), work-related stress (Mortimer and Staff, 2004), family stress (Hagan et al., 2014), and other diverse stressful life events (Boyce and Chesterman, 1990).

Coping with stress is not, of course, limited to critical or sensitive periods in primate postnatal development. Learning to cope in adult monkeys increases hippocampal neurogenesis and enhances expression of genes involved in cell proliferation and survival (Lyons et al., 2010a). Learning to cope also protects adult monkeys against subsequent stress-induced deficits in behavior on tests of emotionality and diminishes the HPA axis neuroendocrine stress response (Lee et al., 2014). Adult humans who survive earthquakes or floods subsequently respond to natural disasters with diminished anxiety (Norris and Murrell, 1988) and less depressed affect (Knight et al., 2000) compared to inexperienced human survivors.

Here we describe new models of stress coping and resilience in mice (Brockhurst et al., 2015; Lee et al., 2016). Instead of screening for the presence of traits that occur in resilient individuals or the absence of vulnerability to stress (Feder et al., 2009; Russo et al., 2012), we focus on learning to cope with stress and the process of building resilience. Considering resilience as a process implies that it can be modified and improved in humans with or without preexisting psychopathologies (DiCorcia and Tronick, 2011; Masten, 2001; Waugh and Koster, 2015). Humans may more closely resemble various nonhuman primates, but the availability of research tools for dissecting causal pathways that link behavior and brain are far greater in mice compared to monkeys (Gerits and Vanduffel, 2013; Huang and Zeng, 2013). Therefore, mouse models offer essential opportunities to bridge the gap between basic and applied research in psychiatry and behavioral neuroscience.

2 LEARNING TO COPE TRAINING

Adult C57BL/6 male mice weighing ~25 g (range 22–28 g) are maintained in same-sex groups of 2 or 3 animals per cage in climate-controlled rooms with an ambient temperature of 26°C and lights on from 07:00 to 19:00 h (Brockhurst et al., 2015). Food and drinking water are provided *ad libitum*. After 2 weeks of acclimation, mice are randomized to experimental learning to cope sessions of training or a control treatment condition. In the control condition, mice remain undisturbed in their

FIGURE 44.1 **Learning to cope with stress training sessions.** Mice are removed from the home cage every other day for 21 days and individually placed for 15 min behind a mesh-screen barrier in the cage of a larger, same-sex resident mouse breeder. The mesh-screen barrier prevents fighting and physical injury during all 11 training sessions but allows for noncontact interaction. Four C57BL/6 mice are depicted in the home cages of four Swiss Webster resident mouse breeders.

home cage and receive ordinary animal facility care. Age-matched mice in the learning to cope training condition are intermittently exposed to a social stress protocol developed by other investigators (Golden et al., 2011) and modified as follows.

Every other day for 21 days between 2 and 4 h after onset of lights on, mice in the learning to cope condition are removed from their home cage and individually placed for 15 min behind a mesh-screen barrier in the cage of a larger, same-sex, resident Swiss Webster mouse breeder (Fig. 44.1). Each subject is repeatedly exposed to the same resident stranger with different residents used for different subjects to avoid idiosyncratic effects induced by any particular resident. The mesh-screen barrier prevents fighting and physical injury during all 11 training sessions but allows for noncontact interaction. After each training session, mice are immediately returned to their home cage.

3 LEARNING TO COPE IS STRESSFUL

Plasma levels of the stress hormone corticosterone were initially assessed in undisturbed home cage baseline conditions and then immediately after the 1st, 3rd, 7th, and 11th learning to cope training sessions (Brockhurst et al., 2015). Corticosterone levels were also assessed after restraint stress tests conducted 2, 6, and 13 days following completion of learning to cope and control treatment conditions (Brockhurst et al., 2015). Restraint stress tests consisted of confinement for 15 min every other day for seven total sessions in plastic conical 50 mL tubes perforated with ventilation holes. Blood samples for corticosterone measures were collected via the tail vein (refer to http://www.
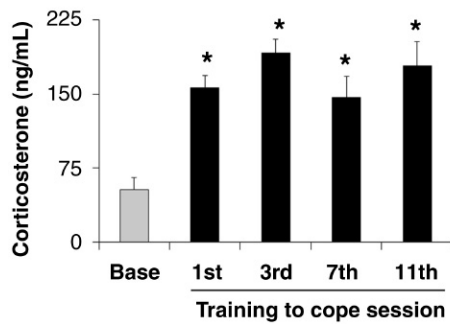
FIGURE 44.2 Repeated tail vein plasma corticosterone levels in undisturbed home cage baseline conditions *(Base)* and immediately after the 1st, 3rd, 7th, and 11th repeated learning to cope training sessions (mean ± SEM, *n* = 8, *P < 0.01 Fishers protected *t*-tests relative to Base following a repeated measures ANOVA described in the text). *Source: From Brockhurst, J., Cheleuitte-Nieves, C., Buckmaster, C.L., Schatzberg, A.F., Lyons, D.M., 2015. Stress inoculation modeled in mice. Transl. Psychiatry 5, e537. Copyright 2015 by Nature Publishing Group.*
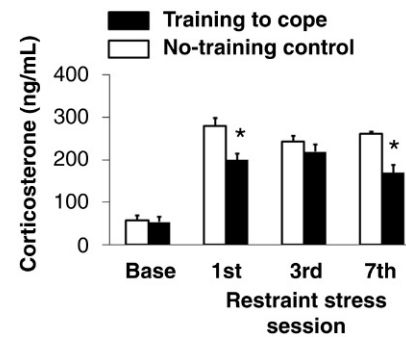
FIGURE 44.3 Repeated tail vein plasma corticosterone levels in undisturbed home cage baseline conditions *(Base)* and immediately after the 1st, 3rd, and 7th repeated restraint stress test sessions (mean ± SEM, *n* = 8, *P < 0.01 Fishers protected *t*-tests following a training treatment-by-sample condition interaction described in the text). *Source: From Brockhurst, J., Cheleuitte-Nieves, C., Buckmaster, C.L., Schatzberg, A.F., Lyons, D.M., 2015. Stress inoculation modeled in mice. Transl. Psychiatry 5, e537. Copyright 2015 by Nature Publishing Group.*

nc3rs.org.uk/mouse-tail-vessel-microsampling-non-surgical) between 2 and 3 h after onset of lights on to control for circadian variation. Plasma extracted from blood samples was assayed in duplicate for corticosterone using a radioimmunoassay without knowledge of the treatment conditions.

Learning to cope training sessions consistently elicited robust corticosterone responses (Fig. 44.2) as discerned by ANOVA (F(4,28) = 13.19, P < 0.001). Learning to cope also diminished subsequent corticosterone responses to restraint (Fig. 44.3) as indicated by a treatment main effect (F1,14) = 15.57, P = 0.001), sample condition main effect (F(3,42) = 91.33, P < 0.001), and treatment-by-sample condition interaction (F(3,42) = 5.33, P = 0.003). Learning to cope has previously been reported to diminish subsequent HPA axis stress hormone responses in juvenile (Parker et al., 2006) and adult (Lee et al., 2014) monkeys. During restraint, we informally noted more struggling and less behavioral immobility in mice trained to cope compared to controls. Follow-up studies were therefore conducted to test this hypothesis in another sample of mice to rule out blood sampling effects on measures of emotional behavior.

4 LEARNING TO COPE REDUCES SUBSEQUENT BEHAVIORAL MEASURES OF EMOTIONALITY

After completion of learning to cope and control treatment conditions, we administered tail-suspension tests counterbalanced with open-field and object-exploration tests to control for test order (Brockhurst et al., 2015). Behavioral tests were conducted 2–13 days after completion of the learning to cope and control treatment conditions between 2 and 3 h after onset of lights on. Video records

were scored by a trained observer using Noldus Observer XT without knowledge of the treatment conditions.

Tail-suspension tests followed a standard protocol (Cryan et al., 2005) with total time spent immobile scored as a measure of behavioral despair. Open-field tests were then conducted repeatedly with each mouse on two consecutive days according to a modified protocol as described by Gould et al. (2009). Mice were individually placed in a white plastic open-field box (40 × 40 × 42 cm) for each daily 10-min test session and the box was cleaned after every test session. Time spent freezing in the open-field box was scored as the absence of all movement except respiration and is considered a measure of anxiety-like behavior in mice (Ahn et al., 2013).

After 2 days of acclimation to the open-field, object-exploration tests were conducted in the same open-field box with a familiar white plastic cap that was continuously maintained in the home cage and a novel black plastic pipe. Both objects were attached to the floor of the open field for each 10-min object-exploration test session. The next day, exploration tests were repeated with the location of objects reversed to control for place preferences. The open-field box and objects were cleaned after every test session. Latencies to explore either of the objects were scored when the animal's head was located within 1 cm of the familiar or novel object.

Mice trained to cope spent significantly less time immobile as a measure of behavioral despair on tail-suspension tests compared to controls (F(1,21) = 6.38, P = 0.021; Fig. 44.4A). Anxiety-like behavior indexed by mean freezing scores from two open-field test sessions was also diminished by learning to cope training compared to controls (F(1,21) = 5.98, P = 0.023; Fig. 44.4B). Learning to cope training has previously been reported
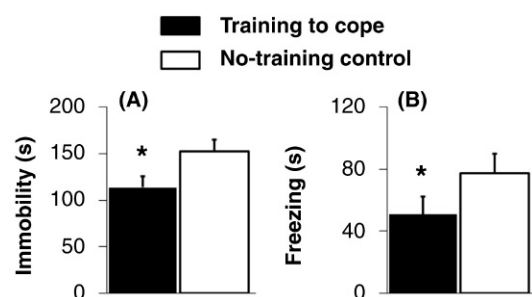
FIGURE 44.4 Learning to cope training subsequently decreases (A) immobility on tail-suspension tests and (B) freezing in the open field (mean ± SEM, *n* = 12, **P* < 0.05 Fishers protected *t*-tests following ANOVAs described in the text). *Note*: different *y*-axis time scales for each graph. *Source: Modified from Brockhurst, J., Cheleuitte-Nieves, C., Buckmaster, C.L., Schatzberg, A.F., Lyons, D.M., 2015. Stress inoculation modeled in mice. Transl. Psychiatry 5, e537. Copyright 2015 by Nature Publishing Group.*
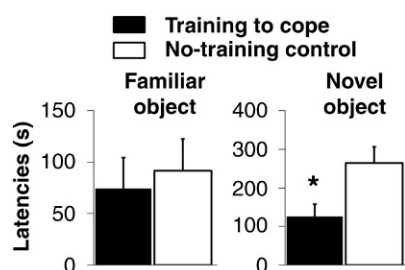
FIGURE 44.5 Learning to cope training subsequently decreases novel but not familiar object-exploration latencies (mean ± SEM, *n* = 12, **P* = 0.017 Fishers protected *t*-test following ANOVAs described in the text). *Note*: different *y*-axis time scales for each graph. *Source: Modified from Brockhurst, J., Cheleuitte-Nieves, C., Buckmaster, C.L., Schatzberg, A.F., Lyons, D.M., 2015. Stress inoculation modeled in mice. Transl. Psychiatry 5, e537. Copyright 2015 by Nature Publishing Group.*

to diminish anxiety-like behavior (Parker et al., 2004) and stress-induced anhedonia (Lee et al., 2014) in monkeys.

During object-exploration tests, object type and treatment main effects were discerned for latency scores as depicted in Fig. 44.5. Shorter exploration latencies were evident for the familiar compared to novel object ($F_{(1,21)}$ = 9.02, *P* = 0.007) and mice trained to cope explored objects faster than controls ($F_{(1,21)}$ = 6.06, *P* = 0.023). Learning to cope training has previously been reported to enhance novel object exploration in monkeys (Parker et al., 2007). Although the object type-by-training treatment interaction was not significant for mice, exploration latencies were significantly diminished by learning to cope training compared to controls for the novel object ($F_{(1,21)}$ = 6.76, *P* = 0.017) but not the familiar object (Fig. 44.5). Shorter exploration latencies were scored on the first compared to the second test day ($F_{(1,21)}$ = 5.06, *P* = 0.035), but the test day-by-training treatment and test day-by-treatment-by-object type interactions were not significant (data not shown).

5 LEARNING TO COPE INCREASES ANTERIOR CINGULATE CORTEX STARGAZIN GENE EXPRESSION

In an unbiased search for neural markers of learning to cope with stress, we discovered increased stargazin (also called TARP gamma-2) gene expression in anterior cingulate cortex of adult monkeys (Lee et al., 2016). Anterior cingulate cortex is involved in learning, memory, cognitive control, emotion, and HPA axis regulation (Etkin et al., 2011; Herman, 2013; Ochsner et al., 2012; Wang et al., 2012; Weible, 2013). Stargazin modulates glutamate receptor signaling via AMPA receptor trafficking (Chen et al., 2000; Jackson and Nicoll, 2011; Vandenberghe et al., 2005) and plays a role in synaptic plasticity (Huganir and Nicoll, 2013) as a mechanism for learning considered functionally in terms of behavior change. Results from monkeys were subsequently tested for reproducibility in mice.

Three days after completion of the behavioral tests described previously, brain tissues from mice were collected after onset of lights on to control for circadian variation (Lee et al., 2016). Responses attributable to behavioral testing were distinguished from prior learning to cope training effects by investigating mice that were and were not behaviorally tested for emotionality after randomization to coping and control treatment conditions. A training treatment main effect ($F_{(1,43)}$ = 6.23, *P* = 0.016) was discerned for anterior cingulate cortex stargazin expression in mice but neither the behavioral testing main effect nor behavioral testing-by-training treatment interaction was significant (Fig. 44.6).

As evidence of learning to cope effects distinct from stress exposures per se, increased anterior cingulate
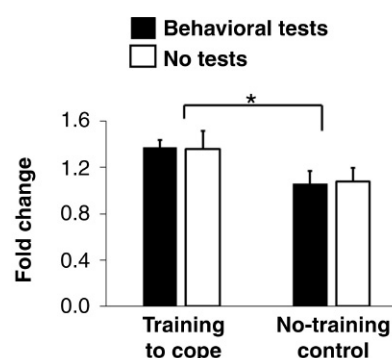
FIGURE 44.6 Anterior cingulate cortex stargazin expression in mice randomized to learning to cope training sessions versus a no-training treatment control. Mice from each training treatment are either exposed or not to subsequent behavioral tests of emotionality (*N* = 11–12 per condition; mean ± SEM; **P* = 0.016). *Source: From Lee, A.G., Capanzana, R., Brockhurst, J., Cheng, M.Y., Buckmaster, C.L., Absher, D., Schatzberg, A.F., Lyons, D.M., 2016. Learning to cope with stress modulates anterior cingulate cortex stargazin expression in monkeys and mice. Neurobiol. Learn. Mem. 131, 95–100. Copyright 2016 by Elsevier.*

cortex stargazin expression correlated inversely with diminished behavioral measures of emotionality in mice. Specifically, increased anterior cingulate cortex stargazin expression correlated with diminished latencies to explore a novel object ($r = -0.53$, df 21, $P = 0.009$) and with diminished immobility on tail-suspension tests ($r = -0.50$, df 21, $P = 0.016$). Increased stargazin expression in anterior cingulate cortex did not correlate with freezing in the open field, and stargazin expression was not measured in mice monitored for corticosterone.

Increased stargazin expression induced by coping in mice was also nearly significant in amygdala ($F(1,21) = 3.09$, $P = 0.093$) but not hippocampus (data not shown). Increased amygdala stargazin expression correlated inversely with diminished tail-suspension immobility ($r = -0.42$, df 21, $P = 0.044$) but not novel object-exploration latencies nor freezing in the open field. Stargazin expression in hippocampus was not correlated with any behavioral measure of emotionality in mice.

6 DISCUSSION

Results demonstrate that learning to cope sessions of training acutely stimulate corticosterone and subsequently enhance active forms of coping behavior in mice. Stargazin gene expression in a brain region involved in learning is increased by coping and stargazin expression correlates inversely with behavioral measures of emotionality. Results in mice parallel our findings from monkeys and support the hypothesis that an aspect of learning to cope with stress is mediated by a common neural mechanism.

Convergence in monkeys and mice reduces the risk of false positive findings and enhances translational relevance (Ciesielski et al., 2014; Lee et al., 2016). Translation has commanded considerable attention because of recent uncertainties about generalization across different species given inevitable biological variation, the use of diverse experimental manipulations, and various ways to operationalize complex outcomes of interest (Institute of Medicine, 2013). Reproducibility across distinct models that utilize different species may help to ensure that observed behavioral and neurobiological effects generalize to broader contexts.

Learning to cope training sessions were designed on the basis of evidence that mild but not minimal nor severe stress exposure provides opportunities to learn, practice, and improve coping as described by U-shaped functions (Russo et al., 2012; Sapolsky, 2015; Seery et al., 2010). Intermittent social separations used in our models of coping in monkeys are described by Lee et al. (2014) and Lyons et al. (2009, 2010a) and a standard social stress protocol was modified to create experimental training conditions for studies of learning to cope in

mice (Brockhurst et al., 2015; Lee et al., 2016). Instead of daily and direct exposure to an aggressive same-sex resident (Golden et al., 2011), learning to cope training sessions for mice were conducted every other day behind a mesh-screen barrier in the cage of a same-sex resident stranger (Fig. 44.1). The mesh-screen barrier prevented fighting and physical injury but allowed for noncontact interaction. Immediately after each training session, subjects were returned to their home cage to allow ample time for recovery and consolidation of learning and memory in familiar undisturbed conditions. Learning to cope training sessions in mice subsequently diminished immobility as a measure of behavioral despair on tail-suspension tests (Fig. 44.4). Learning to cope also subsequently diminished freezing in the open field, decreased novel object-exploration latencies, and reduced corticosterone responses to restraint (Figs. 44.3–44.5).

These results concur with little known studies conducted in the 1950s. Based on Freud's theory that early life stress contributes to the development of subsequent emotional instability, Seymour Levine expected to find that rats exposed to intermittent foot shocks sufficient to elicit evasive movements would show signs of subsequent emotional instability later in life (Levine, 1962; Levine et al., 1956). Levine's findings were not supportive of Freudian theory and he concluded that intermittent exposure to stress "results in the capacity for the organism to respond more effectively when confronted with novel situations or, in other words, to exhibit a diminished emotional response" (Levine, 1962). Levine also found that handling without foot shocks diminished subsequent emotionality in rats and postnatal handling has received considerable research attention in developmental psychobiology (Fernández-Teruel et al., 2002).

Additional indications that stress is not necessarily destructive come from human psychotherapies. Intermittent exposure to mildly stressful situations is a feature of stress inoculation training for people who work in conditions where performance in the face of adversity is required, for example, medical and military personnel, police, firefighters, and rescue workers (Meichenbaum and Novaco, 1985; Saunders et al., 1996; Stetz et al., 2007). Exposure psychotherapies likewise train patients to imagine a graded series of stress inducing situations and encourage interaction with stressors in vivo (McNally, 2007). These procedures promote learning (Craske et al., 2008) and provide opportunities to practice acquired coping skills (Serino et al., 2014).

Animal models of exposure psychotherapies often focus on learned extinction of conditioned fear (Davis et al., 2006; Milad and Quirk, 2012). Extinction occurs when a conditioned stimulus (CS) that was previously paired with an unconditioned stimulus (US) is repeatedly presented on its own. Repeated presentation of the CS alone results in new learning and subsequent inhibition

of the conditioned fear response (Bouton et al., 2006; Milad and Quirk, 2012). Far less researched, but of equal importance, are indications that repeated presentation of the US alone also inhibits conditioned fear responses by devaluing or reducing the impact of the US through a process called US habituation (Rauhut et al., 2001; Rescorla, 1973; Storsve et al., 2010).

Inhibitory effects of CS extinction do not generalize to contexts that differ from those in which CS extinction learning occurred (Bouton, 2002; Harris et al., 2000; Rauhut et al., 2001). Context specificity limits the utility of animal models for exposure psychotherapies based on CS extinction (Craske et al., 2008; McNally, 2007). In contrast, certain models of US habituation are minimally responsive to modulation by contextual cues (Churchill et al., 1987; Evans and Hammond, 1983; Grissom et al., 2007; Hall and Honey, 1989; Jordan et al., 2000; Nyhuis et al., 2010; Rauhut et al., 2001). With respect to minimal modulation by contextual cues, US habituation resembles aspects of learning to cope training for monkeys and mice.

Learning to cope training for mice entails repeated exposure to a larger, same-sex, resident stranger. Training effects then generalize to completely different test contexts as exemplified by diminished immobility during tail suspension, less freezing in the open field, decreased novel object-exploration latencies, and reduced corticosterone responses to restraint (Figs. 44.3–44.5). Learning to cope training effects likewise generalize in studies of monkeys and are minimally responsive to modulation by contextual cues. Intermittent social separations used to train coping in monkeys diminish behavioral and neuroendocrine indications of anxiety and increase novelty seeking behavior in test contexts that differ completely from those in which learning to cope training occurred (Lee et al., 2014; Lyons et al., 2010b; Parker et al., 2007).

Despite similarities in generalization, learning to cope differs from US habituation. Early studies found that habituation during intermittent social separations used to train coping in monkeys occurs much faster for behavioral than glucocorticoid stress hormone responses (Coe et al., 1983; Hennessy, 1986). Learning to cope training likewise acutely increases the primary glucocorticoid stress hormone in mice (i.e., corticosterone) without indications of neuroendocrine habituation over repeated training sessions (Fig. 44.2). Although repeated exposure to homotypic stressors generally results in habituation of the glucocorticoid response in rodents (Herman, 2013), repeated exposure to same-sex social strangers appears to be resistant to neuroendocrine habituation for ten or so sessions in mice (Brockhurst et al., 2015; Warren et al., 2013). Learning to cope training instead has delayed incubation effects (Poulos et al., 2016) insofar as corticosterone responses to subsequent restraint stress

tests are diminished after completion of training compared to no-training controls (Fig. 44.3).

Glucocorticoids are translated into genomic outputs by binding intracellular glucocorticoid receptors that translocate to the nucleus and interact with DNA to regulate the expression of numerous genes (Oakley and Cidlowski, 2013; Zalachoras et al., 2013). Many genes differentially expressed in anterior cingulate cortex of monkeys trained to cope appear to interact with glucocorticoids according to our recent bioinformatics analysis (Lee et al., 2016). Although publicly available data in GEO (http://www.ncbi.nlm.nih.gov/geo/) confirm transcription regulation by glucocorticoids in brain, temporal patterns of glucocorticoid exposure that mimic intermittent sessions of learning to cope are not available for gene expression profiles in GEO. Intermittent versus chronic glucocorticoid exposure differentially regulates the expression of specific genes (Conway-Campbell et al., 2012), and broader profiles of gene expression from diverse brain regions are needed to determine whether differential gene expression profiles explain divergent psychobiological effects of intermittent versus chronic stress.

The gene that encodes stargazin appears to be regulated by glucocorticoids and anterior cingulate cortex stargazin expression is increased by learning to cope in monkeys (Lee et al., 2016). Learning to cope likewise increases anterior cingulate cortex stargazin expression in mice randomized to coping with or without subsequent behavioral tests of emotionality (Fig. 44.6). Increased anterior cingulate cortex stargazin expression induced by coping in mice correlates inversely with behavioral measures of emotionality. Increased stargazin expression induced by coping in mice is also nearly significant in amygdala but not hippocampus.

Although numerous studies confirm that stargazin facilitates synaptic plasticity (Huganir and Nicoll, 2013), few investigations have linked stargazin to learning and memory considered functionally in terms of behavior change. One report indicates that eyeblink conditioning increases stargazin expression in rat cerebellum (Kim and Thompson, 2011), and another study shows that spatial navigational learning increases stargazin expression in rat hippocampus (Blair et al., 2013). We found that learning to cope with stress increases stargazin expression in anterior cingulate cortex of both monkeys and mice (Lee et al., 2016). Stargazin is involved in AMPA receptor trafficking (Chen et al., 2000; Jackson and Nicoll, 2011; Vandenberghe et al., 2005), and pharmacological blockade of AMPA receptors in anterior cingulate cortex impairs assimilation of new information into established mental schemas or associative frameworks (Wang et al., 2012). Nevertheless, all reports connecting stargazin with learning considered functionally in terms of behavior change are

correlational and further studies are needed to establish causal links between learning reflected in behavior and increased stargazin expression in relevant regions of brain. Molecular genetic research tools developed for mice are ideally suited to address this gap in our knowledge.

7 LIMITATIONS

Our findings should be interpreted along with other potential limitations. Results from males may or may not hold true for females. Although learning to cope training sessions enhance subsequent emotion regulation in adult female monkeys (Lee et al., 2014), learning to cope in female mice has not yet been explored. Repeated exposure to a lactating same-sex resident stranger (Jacobson-Pick et al., 2013) may be more effective for training female mice to cope compared to the nonlactating same-sex resident stranger that we used here for males. In home cage conditions, social versus individual housing (Panksepp and Lahvis, 2016) may likewise alter the impact of encounters with a resident stranger for learning to cope training in mice.

Learning to cope training and subsequent tests of emotionality were both conducted shortly after onset of lights on and this schedule may have altered circadian aspects of emotionality. Training and testing also both required transfer of mice from their home cage into new environments. Studies of habituation or extinction during repeated transfers alone are needed but contextual differences between training and testing generally enhance behavioral and neuroendocrine measures of arousal (Bouton et al., 2006; Herman, 2013) instead of producing observed reductions in emotionality. Correlations between behavior and glucocorticoids are not presented because these measures were collected from different mice to control for potential blood sampling effects on behavior. Lastly, the pursuit of convergent evidence in mice and monkeys may minimize false positive findings and enhance translational relevance (Ciesielski et al., 2014), but this approach also increases the risk of falsely disregarding species differences as negative or unimportant results.

8 CONCLUSIONS

Here we describe new mouse models of stress coping and resilience. Learning to cope training sessions acutely increase corticosterone and diminish subsequent immobility on tail-suspension tests. Learning to cope also subsequently diminishes freezing in the open field, decreases novel object-exploration latencies, and reduces corticosterone responses to restraint. Learning to cope increases stargazin expression in anterior cingulate cortex, and stargazin correlates inversely with behavioral measures of emotionality. Stargazin modulates glutamate receptor signaling and plays a role in synaptic plasticity as a mechanism that mediates learning and memory considered functionally in terms of behavior change.

These findings suggest new strategies for research in translational psychiatry and behavioral neuroscience. In addition to investigating how the effects of severe stress damage behavior and brain (Charney and Manji, 2004; Duman, 2009; Nestler, 2014), we propose a complementary approach focused on learning to cope with stress and the process of building of resilience. Mechanisms of learning to cope with stress identified in animal models may provide preventive or therapeutic targets for interventions designed to treat stress disorders in humans. Pharmacological mimicry or facilitation of coping is a novel approach that shifts attention from neuropathology to consider the mechanisms that mediate coping as new targets for programs to build resilience. While not fully complete, this framework supersedes narrower views that regard stress as solely destructive and overlook its broader role in neurobiology, behavior, and human mental health.

Acknowledgments

References

Ahn, S.-H., Jang, E.-H., Choi, J.-H., Lee, H.-R., Bakes, J., Kong, Y.-Y., Kaang, B.-K., 2013. Basal anxiety during an open field test is correlated with individual differences in contextually conditioned fear in mice. Animal Cells Syst. 17 (3), 154–159.

Blair, M.G., Nguyen, N.N., Albani, S.H., L'Etoile, M.M., Andrawis, M.M., Owen, L.M., Oliveira, R.F., Johnson, M.W., Purvis, D.L., Sanders, E.M., Stoneham, E.T., Xu, H., Dumas, T.C., 2013. Developmental changes in structural and functional properties of hippocampal AMPARs parallels the emergence of deliberative spatial navigation in juvenile rats. J. Neurosci. 33 (30), 12218–12228.

Bouton, M.E., 2002. Context, ambiguity, and unlearning: sources of relapse after behavioral extinction. Biol. Psychiatry 52 (10), 976–986.

Bouton, M.E., Westbrook, R.F., Corcoran, K.A., Maren, S., 2006. Contextual and temporal modulation of extinction: behavioral and biological mechanisms. Biol. Psychiatry 60 (4), 352–360.

Boyce, W.T., Chesterman, E., 1990. Life events, social support, and cardiovascular reactivity in adolescence. J. Dev. Behav. Pediatr. 11 (3), 105–111.

Brockhurst, J., Cheleuitte-Nieves, C., Buckmaster, C.L., Schatzberg, A.F., Lyons, D.M., 2015. Stress inoculation modeled in mice. Transl. Psychiatry 5, e537.

Brosschot, J.F., 2010. Markers of chronic stress: prolonged physiological activation and (un)conscious perseverative cognition. Neurosci. Biobehav. Rev. 35 (1), 46–50.

Burchfield, S.R., 1979. The stress response: a new perspective. Psychosom. Med. 41 (8), 661–672.

Charney, D.S., Manji, H.K., 2004. Life stress, genes, and depression: multiple pathways lead to increased risk and new opportunities for intervention. Sci. Signal. 2004 (225), re5.

Chen, L., Chetkovich, D.M., Petralia, R.S., Sweeney, N.T., Kawasaki, Y., Wenthold, R.J., Bredt, D.S., Nicoll, R.A., 2000. Stargazin regulates synaptic targeting of AMPA receptors by two distinct mechanisms. Nature 408 (6815), 936–943.

Churchill, M., Remington, B., Siddle, D.A., 1987. The effects of context change on long-term habituation of the orienting response in humans. Q. J. Exp. Psychol. B 39B, 315–338.

Ciesielski, T.H., Pendergrass, S.A., White, M.J., Kodaman, N., Sobota, R.S., Huang, M., Bartlett, J., Li, L., Pan, Q., Gui, J., Selleck, S.B., Amos, C.I., Richie, M.D., Moore, J.H., Williams, S.M., 2014. Diverse convergent evidence in the genetic analysis of complex disease: coordinating omic, informatic, and experimental evidence to better identify and validate risk factors. BioData Min. 7, 10.

Coe, C.L., Glass, J.C., Wiener, S.G., Levine, S., 1983. Behavioral, but not physiological, adaptation to repeated separation in mother and infant primates. Psychoneuroendocrinology 8 (4), 401–409.

Conway-Campbell, B.L., Pooley, J.R., Hager, G.L., Lightman, S.L., 2012. Molecular dynamics of ultradian glucocorticoid receptor action. Mol. Cell. Endocrinol. 348 (2), 383–393.

Craske, M.G., Kircanski, K., Zelikowsky, M., Mystkowski, J., Chowdhury, N., Baker, A., 2008. Optimizing inhibitory learning during exposure therapy. Behav. Res. Ther. 46 (1), 5–27.

Cryan, J.F., Mombereau, C., Vassout, A., 2005. The tail suspension test as a model for assessing antidepressant activity: review of pharmacological and genetic studies in mice. Neurosci. Biobehav. Rev. 29 (4–5), 571–625.

Davis, M., Ressler, K., Rothbaum, B.O., Richardson, R., 2006. Effects of D-cycloserine on extinction: translation from preclinical to clinical work. Biol. Psychiatry 60 (4), 369–375.

DiCorcia, J.A., Tronick, E., 2011. Quotidian resilience: exploring mechanisms that drive resilience from a perspective of everyday stress and coping. Neurosci. Biobehav. Rev. 35 (7), 1593–1602.

Dienstbier, R.A., 1989. Arousal and physiological toughness: implications for mental and physical health. Psychol. Rev. 96 (1), 84–100.

Duman, R.S., 2009. Neuronal damage and protection in the pathophysiology and treatment of psychiatric illness: stress and depression. Dialogues Clin. Neurosci. 11 (3), 239–255.

Etkin, A., Egner, T., Kalisch, R., 2011. Emotional processing in anterior cingulate and medial prefrontal cortex. Trends Cogn. Sci. 15 (2), 85–93.

Evans, John G., Hammond, Geoffrey R., 1983. Differential generalization of habituation across contexts as a function of stimulus significance. Nov 1983. Anim. Learn. Behav. 11 (4), 431–434.

Feder, A., Nestler, E.J., Charney, D.S., 2009. Psychobiology and molecular genetics of resilience. Nat. Rev. Neurosci. 10 (6), 446–457.

Fernández-Teruel, A., Giménez-Llort, L., Escorihuela, R.M., Gil, L., Aguilar, R., Steimer, T., Tobeña, A., 2002. Early-life handling stimulation and environmental enrichment: are some of their effects mediated by similar neural mechanisms. Pharmacol. Biochem. Behav. 73 (1), 233–245.

Garmezy, N., Masten, A.S., Tellegen, A., 1984. The study of stress and competence in children: a building block for developmental psychopathology. Child Dev. 55 (1), 97–111.

Gerits, A., Vanduffel, W., 2013. Optogenetics in primates: a shining future. Trends Genet. 29 (7), 403–411.

Golden, S.A., Covington, 3rd, H.E., Berton, O., Russo, S.J., 2011. A standardized protocol for repeated social defeat stress in mice. Nat. Protoc. 6 (8), 1183–1191.

Gould, T.D., Dao, D.T., Kovacsics, C.E., 2009. The open field test. Gould, T.D. (Ed.), Mood and Anxiety Related Phenotypes in Mice, Neuromethods, vol. 42, Humana Press, New York, NY, pp. 1–20.

Grissom, N., Iyer, V., Vining, C., Bhatnagar, S., 2007. The physical context of previous stress exposure modifies hypothalamic-pituitary-adrenal responses to a subsequent homotypic stress. Horm. Behav. 51 (1), 95–103.

Hagan, M.J., Roubinov, D.S., Purdom Marreiro, C.L., Luecken, L.J., 2014. Childhood interparental conflict and HPA axis activity in young adulthood: examining nonlinear relations. Dev. Psychobiol. 56 (4), 871–880.

Hall, Geoffrey, Honey, R.C., 1989. Contextual effects in conditioning, latent inhibition, and habituation: associative and retrieval functions of contextual cues. J. Exp. Psychol. Anim. Behav. Process. 15 (3), 232–241.

Harris, J.A., Jones, M.L., Bailey, G.K., Westbrook, R.F., 2000. Contextual control over conditioned responding in an extinction paradigm. J. Exp. Psychol. Anim. Behav. Process. 26 (2), 174–185.

Heim, C., Shugart, M., Craighead, W.E., Nemeroff, C.B., 2010. Neurobiological and psychiatric consequences of child abuse and neglect. Dev. Psychobiol. 52 (7), 671–690.

Hennessy, M.B., 1986. Multiple, brief maternal separations in the squirrel monkey: changes in hormonal and behavioral responsiveness. Physiol. Behav. 36 (2), 245–250.

Herman, J.P., 2013. Neural control of chronic stress adaptation. Front. Behav. Neurosci. 7, 61.

Huang, Z.J., Zeng, H., 2013. Genetic approaches to neural circuits in the mouse. Annu. Rev. Neurosci. 36, 183–215.

Huganir, R.L., Nicoll, R.A., 2013. AMPARs and synaptic plasticity: the last 25 years. Neuron 80 (3), 704–717.

Institute of Medicine, 2013. Improving the Utility and Translation of Animal Models for Nervous System Disorders: Workshop Summary. The National Academies Press, Washington, DC.

Jackson, A.C., Nicoll, R.A., 2011. Stargazin (TARP gamma-2) is required for compartment-specific AMPA receptor trafficking and synaptic plasticity in cerebellar stellate cells. J. Neurosci. 31 (11), 3939–3952.

Jacobson-Pick, S., Audet, M.C., McQuaid, R.J., Kalvapalle, R., Anisman, H., 2013. Social agonistic distress in male and female mice: changes of behavior and brain monoamine functioning in relation to acute and chronic challenges. PLoS One 8 (4), e60133.

Jordan, W.P., Strasser, H.C., McHale, L., 2000. Contextual control of long-term habituation in rats. J. Exp. Psychol. Anim. Behav. Process. 26 (3), 323–339.

Kim, S., Thompson, R.F., 2011. c-Fos, Arc, and stargazin expression in rat eyeblink conditioning. Behav. Neurosci. 125 (1), 117–123.

Knight, Bob G., Margaret, Gatz, Kenneth, Heller, Bengtson, Vern L., 2000. Age and emotional response to the Northridge earthquake: a longitudinal analysis. Psychol. Aging 15 (4), 627–634.

Krishnan, V., Nestler, E.J., 2008. The molecular neurobiology of depression. Nature 455 (7215), 894–902.

Lee, A.G., Buckmaster, C.L., Yi, E., Schatzberg, A.F., Lyons, D.M., 2014. Coping and glucocorticoid receptor regulation by stress inoculation. Psychoneuroendocrinology 49, 272–279.

Lee, A.G., Capanzana, R., Brockhurst, J., Cheng, M.Y., Buckmaster, C.L., Absher, D., Schatzberg, A.F., Lyons, D.M., 2016. Learning to cope with stress modulates anterior cingulate cortex stargazin expression in monkeys and mice. Neurobiol. Learn. Mem. 131, 95–100.

Levine, S., 1962. The effects of infantile experience on adult behavior. In: Bachrach, A.J. (Ed.), Experimental Foundations of Clinical Psychology. Basic Books, New York, NY, pp. 139–169.

Levine, S., Mody, T., 2003. The long-term psychobiological consequences of intermittent postnatal separation in the squirrel monkey. Neurosci. Biobehav. Rev. 27 (1–2), 83–89.

Levine, S., Chevalier, J.A., Korchin, S.J., 1956. The effects of early shock and handling on later avoidance learning. J. Pers. 24 (4), 475–493.

Lyons, D.M., Kim, S., Schatzberg, A.F., Levine, S., 1998. Postnatal foraging demands alter adrenocortical activity and psychosocial development. Dev. Psychobiol. 32 (4), 285–291.

Lyons, D.M., Martel, F.L., Levine, S., Risch, N.J., Schatzberg, A.F., 1999. Postnatal experiences and genetic effects on squirrel monkey social affinities and emotional distress. Horm. Behav. 36 (3), 266–275.

Lyons, D.M., Parker, K.J., Katz, M., Schatzberg, A.F., 2009. Developmental cascades linking stress inoculation, arousal regulation, and resilience. Front. Behav. Neurosci. 3, 32.

Lyons, D.M., Buckmaster, P.S., Lee, A.G., Wu, C., Mitra, R., Duffey, L.M., Buckmaster, C.L., Her, S., Patel, P.D., Schatzberg, A.F., 2010a. Stress coping stimulates hippocampal neurogenesis in adult monkeys. Proc. Natl. Acad. Sci. USA 107 (33), 14823–14827.

Lyons, D.M., Parker, K.J., Schatzberg, A.F., 2010b. Animal models of early life stress: implications for understanding resilience. Dev. Psychobiol. 52 (5), 402–410.

Masten, A.S., 2001. Ordinary magic. Resilience processes in development. Am. Psychol. 56 (3), 227–238.

McNally, R.J., 2007. Mechanisms of exposure therapy: how neuroscience can improve psychological treatments for anxiety disorders. Clin. Psychol. Rev. 27 (6), 750–759.

Meichenbaum, D., Novaco, R., 1985. Stress inoculation: a preventative approach. Issues Ment. Health Nurs. 7 (1–4), 419–435.

Milad, M.R., Quirk, G.J., 2012. Fear extinction as a model for translational neuroscience: ten years of progress. Annu. Rev. Psychol. 63, 129–151.

Mortimer, J.T., Staff, J., 2004. Early work as a source of developmental discontinuity during the transition to adulthood. Dev. Psychopathol. 16 (4), 1047–1070.

Nestler, E.J., 2014. Epigenetic mechanisms of depression. JAMA Psychiatry 71 (4), 454–456.

Norris, Fran H., Murrell, Stanley A., 1988. Prior experience as a moderator of disaster impact on anxiety symptoms in older adults. Am. J. Community Psychol. 16 (5), 665–683.

Nyhuis, T.J., Sasse, S.K., Masini, C.V., Day, H.E., Campeau, S., 2010. Lack of contextual modulation of habituated neuroendocrine responses to repeated audiogenic stress. Behav. Neurosci. 124 (6), 810–820.

Oakley, R.H., Cidlowski, J.A., 2013. The biology of the glucocorticoid receptor: new signaling mechanisms in health and disease. J. Allergy Clin. Immunol. 132 (5), 1033–1044.

Ochsner, K.N., Silvers, J.A., Buhle, J.T., 2012. Functional imaging studies of emotion regulation: a synthetic review and evolving model of the cognitive control of emotion. Ann. NY Acad. Sci. 1251, E1–E24.

Panksepp, J.B., Lahvis, G.P., 2016. Differential influence of social versus isolate housing on vicarious fear learning in adolescent mice. Behav. Neurosci. 130 (2), 206–211.

Parker, K.J., Buckmaster, C.L., Schatzberg, A.F., Lyons, D.M., 2004. Prospective investigation of stress inoculation in young monkeys. Arch. Gen. Psychiatry 61 (9), 933–941.

Parker, K.J., Buckmaster, C.L., Sundlass, K., Schatzberg, A.F., Lyons, D.M., 2006. Maternal mediation, stress inoculation, and the development of neuroendocrine stress resistance in primates. Proc. Natl. Acad. Sci. USA 103 (8), 3000–3005.

Parker, K.J., Rainwater, K.L., Buckmaster, C.L., Schatzberg, A.F., Lindley, S.E., Lyons, D.M., 2007. Early life stress and novelty seeking behavior in adolescent monkeys. Psychoneuroendocrinology 32 (7), 785–792.

Petticrew, M.P., Lee, K., 2011. The "father of stress" meets "big tobacco": Hans Selye and the tobacco industry. Am. J. Public Health 101 (3), 411–418.

Poulos, A.M., Mehta, N., Lu, B., Amir, D., Livingston, B., Santarelli, A., Zhuravka, I., Fanselow, M.S., 2016. Conditioning- and time-dependent increases in context fear and generalization. Learn. Mem. 23 (7), 379–385.

Poulton, R., Milne, B.J., Craske, M.G., Menzies, R.G., 2001. A longitudinal study of the etiology of separation anxiety. Behav. Res. Ther. 39 (12), 1395–1410.

Rauhut, A.S., Thomas, B.L., Ayres, J.J., 2001. Treatments that weaken Pavlovian conditioned fear and thwart its renewal in rats: implications for treating human phobias. J. Exp. Psychol. Anim. Behav. Process. 27 (2), 99–114.

Rescorla, R.A., 1973. Effect of US habituation following conditioning. J. Comp. Physiol. Psychol. 82 (1), 137–143.

Russo, S.J., Murrough, J.W., Han, M.H., Charney, D.S., Nestler, E.J., 2012. Neurobiology of resilience. Nat. Neurosci. 15 (11), 1475–1484.

Rutter, M., 2006. Implications of resilience concepts for scientific understanding. Ann. NY Acad. Sci. 1094, 1–12.

Sapolsky, R.M., 2015. Stress and the brain: individual variability and the inverted-U. Nat. Neurosci. 18 (10), 1344–1346.

Saunders, T., Driskell, J.E., Johnston, J.H., Salas, E., 1996. The effect of stress inoculation training on anxiety and performance. J. Occup. Health Psychol. 1 (2), 170–186.

Seery, M.D., Holman, E.A., Silver, R.C., 2010. Whatever does not kill us: cumulative lifetime adversity, vulnerability, and resilience. J. Pers. Soc. Psychol. 99 (6), 1025–1041.

Serino, S., Triberti, S., Villani, D., Cipresso, P., Gaggioli, A., Riva, G., 2014. Toward a validation of cyber-interventions for stress disorders based on stress inoculation training: a systematic review. Virtual Real. 18 (1), 73–87.

Stetz, M.C., Thomas, M.L., Russo, M.B., Stetz, T.A., Wildzunas, R.M., McDonald, J.J., Weiderhold, B.K., Romano, Jr., J.A., 2007. Stress, mental health, and cognition: a brief review of relationships and countermeasures. Aviat. Space Environ. Med. 78 (5 Suppl.), B252–B260.

Storsve, A.B., McNally, G.P., Richardson, R., 2010. US habituation, like CS extinction, produces a decrement in conditioned fear responding that is NMDA dependent and subject to renewal and reinstatement. Neurobiol. Learn. Mem. 93 (4), 463–471.

Vandenberghe, W., Nicoll, R.A., Bredt, D.S., 2005. Stargazin is an AMPA receptor auxiliary subunit. Proc. Natl. Acad. Sci. USA 102 (2), 485–490.

Wang, S.H., Tse, D., Morris, R.G., 2012. Anterior cingulate cortex in schema assimilation and expression. Learn. Mem. 19 (8), 315–318.

Warren, B.L., Vialou, V.F., Iniguez, S.D., Alcantara, L.F., Wright, K.N., Feng, J., Kennedy, P.J., Laplant, Q., Shen, L., Nestler, E.J., Bolanos-Guzman, C.A., 2013. Neurobiological sequelae of witnessing stressful events in adult mice. Biol. Psychiatry 73 (1), 7–14.

Waugh, C.E., Koster, E.H., 2015. A resilience framework for promoting stable remission from depression. Clin. Psychol. Rev. 41, 49–60.

Weible, A.P., 2013. Remembering to attend: the anterior cingulate cortex and remote memory. Behav. Brain Res. 245, 63–75.

Zalachoras, I., Houtman, R., Meijer, O.C., 2013. Understanding stress-effects in the brain via transcriptional signal transduction pathways. Neuroscience 242, 97–109.

Page left intentionally blank

Index

Page left intentionally blank

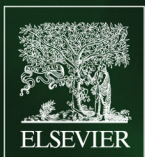# Animal Models for the Study of Human Disease

Edited by **P. Michael Conn**

Second Edition

Animal Models for the Study of Human Disease, second edition identifies important animal models and assesses the advantages and disadvantages of each model for the study of human disease. This new edition provides much needed information on model sharing, animal alternatives, animal ethics, access to databanks of models, and brings together common descriptions of models for busy researchers across biomedical and biological sciences.

Offering easily searchable advantages and disadvantages for each animal model, organized by disease topics, this resource aids researchers in finding the best animal model for research in human disease.

Key Features:

- Organized by disease orientation for ease of searchability

- Provides information on locating resources, animal alternatives, and animal ethics

- Covers a broad range of animal models used in research for human disease

- Contributed by leading experts across the globe

- Expanded coverage of diabetes and neurological diseases